

1N-01
99893
p. 459

AERONAUTICAL ENGINEERING

1995 CUMULATIVE INDEX

(NASA-SP-7037(325))	AERONAUTICAL	N96-18604
ENGINEERING: A CUMULATIVE INDEX TO		
A CONTINUING BIBLIOGRAPHY		
(SUPPLEMENT 325) (NASA) 459 p		Unclas

00/01 0099833



National Aeronautics and
Space Administration

Scientific and Technical
Information Office

The NASA STI Office ... in Profile

Since its founding, NASA has been dedicated to the advancement of aeronautics and space science. The NASA Scientific and Technical Information (STI) Office plays a key part in helping NASA maintain this important role.

The NASA STI Office provides access to the NASA STI Database, the largest collection of aeronautical and space science STI in the world. The STI Office is also NASA's institutional mechanism for disseminating the results of its research and development activities.

Specialized services that help round out the Office's diverse offerings include creating custom thesauri, building customized databases, organizing and publishing research results ... even providing videos.

For more information about the NASA STI Office, you can:

- **Phone** the NASA Access Help Desk at (301) 621-0390
- **Fax** your question to the NASA Access Help Desk at (301) 621-0134
- **E-mail** your question via the **Internet** to help@sti.nasa.gov
- **Write to:**

NASA Access Help Desk
NASA Center for AeroSpace Information
800 Elkridge Landing Road
Linthicum Heights, MD 21090-2934

NASA SP-7037 (325)

December 1995

AERONAUTICAL ENGINEERING

1995 CUMULATIVE INDEX



National Aeronautics and Space Administration
Scientific and Technical Information Program
Washington, DC

1995

SUPPLEMENTS COVERED IN THIS ISSUE

<i>Document</i>	<i>Page Range</i>	<i>Date</i>	<i>Coverage</i>
NASA SP-7037(313)	1-34	January 1995	January 1995
NASA SP-7037(314)	35-64	February 1995	February 1995
NASA SP-7037(315)	65-102	March 1995	March 1995
NASA SP-7037(316)	103-178	April 1995	April 1995
NASA SP-7037(317)	179-218	May 1995	May 1995
NASA SP-7037(318)	219-260	June 1995	June 1995
NASA SP-7037(319)	261-326	July 1995	July 1995
NASA SP-7037(320)	327-364	August 1995	August 1995
NASA SP-7037(321)	365-454	September 1995	September 1995
NASA SP-7037(322)	455-582	October 1995	October 1995
NASA SP-7037(323)	583-682	November 1995	November 1995
NASA SP-7037(324)	683-712	December 1995	December 1995

INTRODUCTION

WHAT THIS CUMULATIVE INDEX IS

This publication is a cumulative index to the abstracts contained in NASA SP-7037 (313) through NASA SP-7037 (324) of *Aeronautical Engineering: A Continuing Bibliography*. NASA SP-7037, and its supplements have been compiled by the Center for AeroSpace Information of the National Aeronautics and Space Administration (NASA). Entries are identified as follows:

1. NASA entries by *STAR* accession numbers N95-10000.
2. Open literature entries by accession numbers A95-60000, A95-70000, and A95-80000.

HOW THIS CUMULATIVE INDEX IS ORGANIZED

This Cumulative Index includes a subject, personal author, corporate source, foreign technology, contract number, report number, and accession number index.

HOW TO USE THE SUBJECT INDEX

Two types of cross-references appear in the subject index:

1. Use (U) references indicate that the subject term is not "postable," i.e., not a valid term, and that the following term or terms are used instead. For example:

AIRCRAFT PROTUBERANCES
U PROTUBERANCES
FLIGHT PERFORMANCE
U FLIGHT CHARACTERISTICS

2. Narrower Term (NT) references refer the user to more specific headings in the same subject area, under which additional material on the subject may be found. For example:

FLOW RESISTANCE
NT AERODYNAMIC DRAG
NT FRICTION DRAG
NT SUPERSONIC DRAG

In addition, a searcher may use the title or title and title extension in the index to narrow further his quest for particular items; this is because subject terms may include documents on different aspects of the same subject term. For example:

AIRLINE OPERATIONS
All-weather operations, including pilot role, instrument landing systems and guidance aids.
Airport congestion as constraint on air travel, considering runway capacity and adjusted demand.

HOW TO USE THE PERSONAL AUTHOR INDEX

All personal authors used in the abstract section citations in the individual supplements appear in the index. Differences in translation schemes may require multiple searching on the index for variants of an author's name. For example:

EMELIANOV, M. D.
and
YEMELYANOV, M. D.

HOW TO USE THE CORPORATE SOURCE INDEX

The corporate source index entries are abridged versions of the corporate sources used in the abstract section citations in the individual supplements. The corporate source supplementary (organizational component) does not appear in the index. For example:

BOEING CO., SEATTLE, WASH. MILITARY AIRCRAFT SYSTEMS DIV. (Source citation entry)
BOEING CO., SEATTLE, WASH. (Source index entry)

HOW TO USE THE FOREIGN TECHNOLOGY INDEX

The foreign technology index identifies research performed outside of the United States. Listings in this index are arranged alphabetically by country of intellectual origin. For example:

CHINA, PEOPLE'S REPUBLIC OF

HOW TO USE THE CONTRACT NUMBER INDEX

All contract numbers that are identified in the abstract section citations in the individual supplements appear in this index. Changes by agencies in the style in which contract numbers are presented may require multiple searching for variants. For example:

AF 33(615)-71-C-1758

F33615-71-C-1758

HOW TO USE THE REPORT NUMBER INDEX

All report numbers that have been assigned by the corporate source, monitoring agency or cataloging activity appear in this index. Variations in cataloging may result in different report number series. For example:

TP-924

ONERA-TP-924

HOW TO USE THE ACCESSION NUMBER INDEX

All documents that were acquired, indexed, and announced in *STAR* during the year which have been assigned a unique identification number appear in this index. For example:

N95-10001

N95-10002

IDENTIFICATION OF DESIRED SUPPLEMENT

The abstract and descriptive cataloging for any accession number selected from the indexes may be found in the appropriate supplement. The page number range of each supplement appears on page ii of this index. Once the range of page numbers containing the selected accession number is located in the second column, the desired supplement number will be found in the first column. For example:

Page 226 will be found in Supplement 318

AVAILABILITY OF DOCUMENTS

Information concerning the availability of documents announced in *Aeronautical Engineering* is found in the Introduction to the most currently issued supplement.

FEDERAL DEPOSITORY LIBRARY PROGRAM

In order to provide the general public with greater access to U.S. Government publications, Congress established the Federal Depository Library Program under the Government Printing Office (GPO), with 53 regional depositories responsible for permanent retention of material, inter-library loan, and reference services. At least one copy of nearly every NASA and NASA-sponsored publication, either in printed or microfiche format, is received and retained by the 53 regional depositories. A list of the regional GPO libraries, arranged alphabetically by state, appears on the inside back cover. These libraries are *not* sales outlets. A local library can contact a Regional Depository to help locate specific reports, or direct contact may be made by an individual.

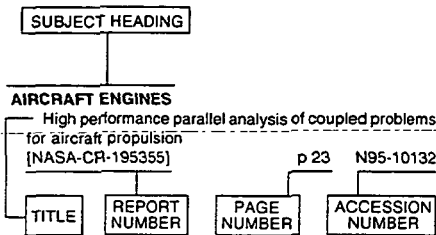
PUBLIC COLLECTIONS OF NASA DOCUMENTS

An extensive collection of NASA and NASA-sponsored publications is maintained by the British Library Lending Division, Boston Spa, Wetherby, Yorkshire, England for public access. The British Library Lending Division also has available many of the non-NASA publications cited in *STAR*. European requesters may purchase facsimile copy or microfiche of NASA and NASA-sponsored documents, those identified by both the symbols # and * from FIZ—Fachinformation Karlsruhe—Bibliographic Service, D-76344 Eggenstein-Leopoldshafen, Germany and TIB—Technische Informationsbibliothek, P.O. Box 60 80, D-30080 Hannover, Germany.

TABLE OF CONTENTS

Subject Index	A-1
Personal Author Index.....	B-1
Corporate Source Index.....	C-1
Foreign Technology Index	D-1
Contract Number Index	E-1
Report Number Index.....	F-1
Accession Number Index	G-1

Typical Subject Index Listing



The subject heading is a key to the subject content of the document. The title is used to provide a description of the subject matter. When the title is insufficiently descriptive of document content, a title extension is added, separated from the title by three hyphens. The accession number and the page number are included in each entry to assist the user in locating the abstract in the abstract section. If applicable, a report number is also included as an aid in identifying the document. Under any one subject heading, the accession numbers are arranged in sequence.

A

A-320 AIRCRAFT

Flying qualities of civil transport aircraft with electrical flight control p 624 N95-32016

A-340 AIRCRAFT

Flying qualities of civil transport aircraft with electrical flight control p 624 N95-32016

A-7 AIRCRAFT

Derived gust spectra for the Macchi MB326H [ARL-TN-3] p 225 N95-21892

ABLATION

On the particular features of dynamic processes in solids with varying boundary during interaction with intensive heat flows [BTN-94-EIX94461408756] p 171 A95-63639

Review of numerical procedures for computational surface thermochemistry [BTN-94-EIX94441386682] p 205 A95-68191

Hypersonic nonequilibrium Navier-Stokes solutions over an ablating graphite nosetip [BTN-95-EIX95152583252] p 305 A95-73553

Ablative thermal management structural material on the hypersonic vehicles [AIAA PAPER 95-6133] p 547 A95-90452

Application of integral methods to ablation charring erosion, a review [BTN-95-EIX95302694460] p 636 A95-94057

Enhancements to integral solutions to ablation and charring [BTN-95-EIX95302694461] p 636 A95-94058

Thermal chemical energy of ablating silica surfaces in air breathing solid rocket engines p 148 N95-16316

ABLATIVE MATERIALS

Trajectory-based heating analysis for the European Space Agency/Rosetta Earth Return Vehicle [BTN-95-EIX95041503787] p 205 A95-69218

Thermal chemical energy of ablating silica surfaces in air breathing solid rocket engines p 148 N95-16316

ABNORMALITIES

Aircraft corrosion study [AD-A279527] p 241 N95-21687

ABRASION

Use of starch based blast media for dry paint stripping [SAE PAPER 932616] p 456 A95-90081

Quality optimization of thermally sprayed coatings produced by the JP-5000 (HVOF) gun using mathematical modeling p 152 N95-19008

ABRASION RESISTANCE

Evaluation of alternate F-14 wing lug coating [AD-A283207] p 129 N95-17631

ABRASIVES

Use of starch based blast media for dry paint stripping [SAE PAPER 932616] p 456 A95-90081

Multilayer anti-erosion coatings p 201 N95-19679

ABSORBERS (EQUIPMENT)

Adaptive tuned vibration absorbers: Tuning laws, tracking agility, sizing, and physical implementations p 25 N95-11280

ABSORPTION SPECTRA

Chemical change in the arctic vortex during AASE 2 [HTN-95-70947] p 352 A95-78012

Latitude variations of stratospheric trace gases [HTN-95-70948] p 352 A95-78013

Empirical corrections of the rigid rotor interaction potential of H₂-H₂ in the attractive region: Dimer features in the FIR absorption spectra [HTN-95-41943] p 361 A95-81690

ABSTRACTS

Bibliography of Doctor Chul Park [NASA-TM-110353] p 527 N95-29351

ABUNDANCE

Comparison of column abundances from three infrared spectrometers during AASE 2 [HTN-95-70946] p 352 A95-78011

Chemical change in the arctic vortex during AASE 2 [HTN-95-70947] p 352 A95-78012

Latitude variations of stratospheric trace gases [HTN-95-70948] p 352 A95-78013

Modeling of plume chemistry of high flying aircraft with H₂ combustion engines p 509 A95-87405

AC GENERATORS

Variations observed in the AC generator signal period of a Sea King helicopter [AD-A284280] p 230 N95-19963

ACCELERATED LIFE TESTS

Micro-measurements of mechanical properties for adhesives and composites using digital imaging technology [NASA-CR-196111] p 22 N95-10231

Hypervelocity Impact Test Facility: A gun for hire [TABES PAPER 94-605] p 86 N95-14639

An artificial corrosion protocol for lap-splices in aircraft skin p 152 N95-19482

Interlaminar shear test method development for long term durability testing of composites p 301 N95-23300

Eddy current detection of pitting corrosion around fastener holes p 315 N95-23507

Test method and test results for environmental assessment of aircraft materials p 302 N95-23509

ACCELERATION (PHYSICS)

Dynamical instability of the aerogravity assist maneuver [BTN-95-EIX95152583282] p 298 A95-73583

The influence of source acceleration on acoustic signals p 577 A95-90136

Prediction of airplane states [BTN-95-EIX0619952748174] p 584 A95-94468

Orbiter rarefied-flow reentry measurements from the OARE on STS-62 [NASA-TM-110182] p 646 N95-30783

ACCELERATION TOLERANCE

Education, training, and human engineering in aerospace; SAE Aerotech '93, Costa Mesa, CA, Sep. 27-30, 1993 [SAE SP-992] p 417 A95-84553

The large radius track centrifuge concept as an acceleration research and simulation device p 379 A95-84560

ACCELEROMETERS

Covariance analysis of strapdown INS considering gyrocompass characteristics [BTN-95-EIX95202637592] p 279 A95-76697

Condition monitoring for helicopters: 3303 Airborne vibration monitoring system [SAE PAPER 931360] p 610 A95-93642

Effects of vibration on inertial wind-tunnel model attitude measurement devices [NASA-TM-109083] p 21 N95-11466

Pressure measurements on an F/A-18 twin vertical tail in buffeting flow. Volume 3: Buffet power spectral densities [AD-A281444] p 36 N95-11829

Test Operation Procedure (TOP): Vibration testing of helicopter equipment [AD-A284433] p 81 N95-15815

Bearing defect signature analysis using advanced nonlinear signal analysis in a controlled environment [NASA-TM-108491] p 441 N95-28364

Results from tests of the Honeywell integrated flight management unit [PB95-211355] p 601 N95-30597

Orbiter rarefied-flow reentry measurements from the OARE on STS-62 [NASA-TM-110182] p 646 N95-30783

A novel instrumentation system for measurement of helicopter rotor motions and loads data, phase 1 [AD-A293309] p 607 N95-30923

ACCEPTABILITY

The air systems controllerate initiatives and policies for the procurement of reliable and maintainable equipment [CONGRESS PAPER C428-6-113] p 549 A95-91682

High-Speed Research: 1994 Sonic Boom Workshop: Atmospheric Propagation and Acceptability Studies [NASA-CP-3279] p 75 N95-14878

The Advanced Avionics Subsystem Technology Demonstration Program p 234 N95-20636

Evaluation of alternative pavement marking materials [AD-A292973] p 626 N95-31468

ACCIDENT INVESTIGATION

Annual review of aircraft accident data: US Air carrier operations, calendar year 1992 [PB95-100319] p 123 N95-17748

ACCIDENT PREVENTION

Aircraft safety evaluation [BTN-94-EIX94511309382] p 103 A95-64608

Fundamentals of catastrophic failure prevention by thrust vectoring [BTN-95-EIX0619952748176] p 606 A95-94470

ASRS problems involving air carrier ground deicing/anti-icing p 611 A95-95194

Modern transport engine experience with environmental ingestion effects p 199 N95-19660

Mishap risk control for advanced aerospace/composite materials p 301 N95-23031

Prevention and control of inlet unstart using an SR-71 simulation p 367 N95-26948

Metascientific problems in safety science [PB95-196408] p 645 N95-30521

SCARLET: DLR rate saturation flight experiment p 598 N95-31068

ACCOMMODATION COEFFICIENT

Unanswered questions concerning the Nocilla gas-surface interaction model [ISBN 1-879921-01-4] p 628 A95-93716

Calculation of satellite drag coefficients [AD-A285118] p 300 N95-23781

ACCUMULATIONS

Control mechanism to prevent correlated message arrivals from degrading signaling no. 7 network performance [BTN-94-EIX94341342286] p 56 A95-60842

A short-term, high-resolution automated snowfall forecasting system p 666 A95-93510

The 1992-3 operational winter forecasting experiment for Stapleton airport p 677 A95-93561

Collection efficiency and ice accretion calculations for a sphere, a swept MS(1)-317 wing, a swept NACA-0012 wing tip, an axisymmetric inlet, and a Boeing 737-300 [NASA-TM-106831] p 123 N95-18582

ACCUMULATORS

Replicator for characterization of cirrus and polar stratospheric cloud particles
[NASA-CR-197785] p 445 N95-26669
175Hp contrarotating homopolar motor design report
[AD-A291138] p 557 N95-30122

ACCURACY

Dryden lectureship in research, a perspective on CFD validation
[AIAA PAPER 93-0002] p 3 A95-60180
Accuracy enhancements for overset grids using a defect correction approach
[AIAA PAPER 94-0523] p 3 A95-60181
Evaluation of the Sparten tight-tolerance AXBT
[HTN-95-40728] p 251 A95-70473
On the choice of appropriate bases for nonlinear dynamic modal analysis
[HTN-95-A0495] p 221 A95-72566
Effects of spatial order of accuracy on the computation of vortical flowfields
[HTN-95-42589] p 459 A95-87219
An investigation of the accuracy of FEM analysis of a graphite epoxy box beam
[SAE PAPER 931221] p 543 A95-88011
Verification of terminal forecasts p 664 A95-93502
Jet stream winds: Comparisons of operational analyses with independent aircraft data at multiple longitudes p 665 A95-93506
Flight test evaluation of the Stanford University/United Airlines differential GPS Category 3 automatic landing system
[NASA-TM-110354] p 593 N95-30788

ACEE PROGRAM

NASA-ACEE/Boeing 737 graphite-epoxy horizontal stabilizer service p 400 N95-28489

ACETYLENE

The Methane-Acetylene Cycle Aerospace Plane: A potential option for inexpensive Earth to orbit transportation
[HTN-95-51845] p 525 A95-87483

ACOUSTIC ATTENUATION

Flyover noise reduction of piston-engine propeller aeroplanes using an active noise control technique
[SAE PAPER 931218] p 509 A95-87466
Modeling lateral attenuation of aircraft flight noise p 570 A95-88464

Active minimization of energy density in three-dimensional enclosures
[NASA-CR-197213] p 172 N95-16848
Effect of atmospheric pressure on measured aircraft noise levels
[PB95-130423] p 232 N95-21425
Suppressor of oscillations in airframe cavities
[AD-D017265] p 388 N95-26507

ACOUSTIC COUPLING

Interaction of jet noise with a nearby panel assembly
[BTN-95-EIX95262694295] p 434 A95-85466
Achievements and tasks for active noise control p 29 N95-11270
The acoustic characteristics of turbomachinery cavities
[NASA-CR-4671] p 476 N95-28720

ACOUSTIC DUCTS

Robust fixed-structure control
[AD-A286515] p 257 N95-22216
Robust fixed-structure control
[AD-A292883] p 679 N95-30961

ACOUSTIC EMISSION

Mach wave emission from a high-temperature supersonic jet
[BTN-95-EIX95152577586] p 264 A95-73496
Mach wave emission from a high-temperature supersonic jet
[HTN-95-42571] p 458 A95-87201
Emerging nondestructive inspection for aging aircraft
[PB95-143053] p 328 N95-25401
Bearing defect signature analysis using advanced nonlinear signal analysis in a controlled environment
[NASA-TM-108491] p 441 N95-28364

ACOUSTIC EXCITATION

Transonic flutter suppression using active acoustic excitations
[BTN-95-EIX95262694310] p 408 A95-85481
Near field of a coaxial jet with and without axial excitation
[HTN-95-42332] p 372 A95-86161
Active open-loop control of particle dispersion in round jets
[HTN-95-42334] p 372 A95-86163
High angle-of-attack airfoil performance improvement by internal acoustic excitation
[HTN-95-42347] p 372 A95-86176
On the differences between the effect of acoustic perturbation and unsteady bleed in controlling flow separation over a cylinder
[SAE PAPER 932573] p 467 A95-90062

A theoretical analysis of airborne sound transfer for a resiliently mounted machine to its foundation p 30 N95-11304

Effect of constraining layer stiffness on performance of damping tile materials using finite element modelling with Rayleigh integral p 30 N95-11306

On the interaction of jet noise with a nearby flexible structure
[NASA-CR-194934] p 57 N95-11812

Impact of Acoustic Loads on Aircraft Structures
[AGARD-CP-549] p 173 N95-19142

Nonlinear dynamic response of aircraft structures to acoustic excitation p 135 N95-19151
Brite-Euram programme: ACOUFAT acoustic fatigue and related damage tolerance of advanced composite and metallic structures p 174 N95-19159

ACOUSTIC FATIGUE

Simulation of Shuttle launch G forces and acoustic loads using the NASA Ames Research Center 20G centrifuge p 86 N95-14089

Impact of Acoustic Loads on Aircraft Structures
[AGARD-CP-549] p 173 N95-19142
Current and future problems in structural acoustic fatigue p 173 N95-19143

High-temperature acoustic test facilities and methods p 174 N95-19149

Nonlinear dynamic response of aircraft structures to acoustic excitation p 135 N95-19151

Acoustic fatigue testing on different materials and skin-stringer elements p 174 N95-19156
Acoustic fatigue characteristics of advanced materials and structures p 174 N95-19157

Brite-Euram programme: ACOUFAT acoustic fatigue and related damage tolerance of advanced composite and metallic structures p 174 N95-19159

Thermo-acoustic fatigue design for hypersonic vehicle skin panels p 162 N95-19161

Application of superplastically formed and diffusion bonded structures in high intensity noise environments p 174 N95-19162

ACOUSTIC IMAGING

Ultrasonic imaging of damages in CRFT-laminates p 578 A95-90828

ACOUSTIC IMPEDANCE

Proceedings of the Sixth International Symposium on Long-Range Sound Propagation
[AD-A290920] p 580 N95-30084

ACOUSTIC MEASUREMENT

Structural acoustic calculations in the low-frequency range
[BTN-95-EIX95152582336] p 323 A95-73538
Disturbance generation in supersonic jets under acoustic excitation
[HTN-95-20926] p 463 A95-88965
Research of the method for evaluating noise caused by sonic boom p 562 A95-91519
Signal processing of noise data from high-speed flyovers
[BTN-95-EIX0619952748178] p 680 A95-94248
Effect of atmospheric pressure on measured aircraft noise levels
[PB95-130423] p 232 N95-21425
Method for extracting forward acoustic wave components from rotating microphone measurements in the inlets of turbofan engines
[NASA-CR-195457] p 616 N95-30779

ACOUSTIC PROPAGATION

Nonreflective boundary conditions for high-order methods
[HTN-95-42328] p 371 A95-86157
High-frequency acoustic radiation from a curved duct of circular cross section p 573 A95-90098
Measurements of atmospheric turbulence effects on tail rotor acoustics p 38 N95-12360
Ducted fan acoustic radiation including the effects of nonuniform mean flow and acoustic treatment
[NASA-CR-197449] p 172 N95-16401

ACOUSTIC PROPERTIES

Experimental investigation of the sources of propeller noise due to the ingestion of turbulence at low speeds
[BTN-95-EIX95262697042] p 569 A95-86859
Wavelet transformations for helicopter identification via acoustic signatures
[AD-A279980] p 257 N95-20963
Active control of fan noise-feasibility study, Volume 1: Flyover system noise studies
[NASA-CR-195392-VOL-1] p 258 N95-21888
Effect of density gradients in confined supersonic shear layers, part 1
[NASA-CR-198029] p 348 N95-24412
Effect of density gradients in confined supersonic shear layers, Part 2: 3-D modes
[NASA-CR-198030] p 349 N95-24413

Photoacoustic chambers for studying solids and gases: Theory and practical examples
[IFTR-39/1994] p 412 N95-26837

The noise reduction potential of dual-stream coaxial rectangular improperly expanded jet flows
[NASA-CR-197820] p 437 N95-26995

Anechoic wind tunnel study of turbulence effects on wind turbine broadband noise p 451 N95-27992
Evaluation of a doubly-swept blade tip for rotorcraft noise reduction
[NASA-CR-189677] p 452 N95-28264

ACOUSTIC SCATTERING

Geometrical acoustics approach for calculating the effects of flow on acoustics scattering
[BTN-94-EIX94321331207] p 61 A95-60790
Atmospheric effects on the risetime and wavenumber of sonic booms p 100 N95-14886
Acoustic scattering from ellipses by the modal element method
[NASA-TM-106935] p 579 N95-29401

ACOUSTIC SIMULATION

The influence of source acceleration on acoustic signals p 577 A95-90136
Design and operation of a thermoacoustic test facility p 147 N95-19150

ACOUSTICS

Rotating Kirchhoff method for three-dimensional transonic blade-vortex interaction hover noise
[BTN-94-EIX94441386601] p 182 A95-67332
Inter-Noise 92: Noise control and the public; International Congress on Noise Control Engineering, Toronto, Ontario, Canada, July 20 - 22, 1992. Vols. 1 & 2
[ISBN 0-931784-25-5] p 559 A95-88457
Rotating Kirchhoff method for three-dimensional transonic blade-vortex interaction hover noise
[HTN-95-20927] p 463 A95-88966
Boundary element analysis of the acoustic field inside three-dimensional regular and irregular ducts p 573 A95-90097
Active control of interior noise in a business jet using piezoceramic actuators p 29 N95-11276
Adaptive tuned vibration absorbers: Tuning laws, tracking agility, sizing, and physical implementations p 25 N95-11280
Modification of the Ames 40- by 80-foot wind tunnel for component acoustic testing for the second generation supersonic transport
[NASA-TM-108850] p 65 N95-13642
Anisotropic heat exchangers/stack configurations for thermoacoustic heat engines
[AD-A280974] p 168 N95-16506
Active minimization of energy density in three-dimensional enclosures
[NASA-CR-197213] p 172 N95-16848
Acoustic climb to cruise test
[NASA-TM-110504] p 230 N95-20155
Acoustic field in unsteady moving media
[NASA-CR-198162] p 438 N95-27179
The acoustic characteristics of turbomachinery cavities
[NASA-CR-4671] p 476 N95-28720

Optical processing and control
[AD-A279157] p 259 N95-21975

Operational parameters and material effects
p 651 N95-32179

Laboratory evaluation of a reactive baffle approach to NOx control
[AD-A283802] p 255 N95-19921

Active control of wake/blade-row interaction noise
[BTN-95-EIX95042474389] p 196 A95-68311
Noise and vibration control
[BTN-95-EIX95042477108] p 179 A95-68351
Smart structures in the control of airframe vibrations
[HTN-95-31014] p 236 A95-71184

Secondary source locations in active noise control: Selection or optimization?
[BTN-94-EIX94381352222] p 257 A95-71738
Grid refinement test of time-periodic flows over bluff bodies
[BTN-94-EIX94401378822] p 307 A95-76491
Summary of an active flexible wing program
[BTN-95-EIX95182619209] p 283 A95-76635
Simulation and model reduction for the active flexible wing program
[BTN-95-EIX95182619211] p 295 A95-76637
Multiple-function digital controller system for active flexible wing wind-tunnel model
[BTN-95-EIX95182619212] p 322 A95-76638
On-line analysis capabilities developed to support the active flexible wing wind-tunnel tests
[BTN-95-EIX95182619213] p 296 A95-76639

Smart structures in the control of airframe vibrations
[HTN-95-31014] p 236 A95-71184

Secondary source locations in active noise control: Selection or optimization?
[BTN-94-EIX94381352222] p 257 A95-71738

Grid refinement test of time-periodic flows over bluff bodies
[BTN-94-EIX94401378822] p 307 A95-76491

Summary of an active flexible wing program
[BTN-95-EIX95182619209] p 283 A95-76635

Simulation and model reduction for the active flexible wing program
[BTN-95-EIX95182619211] p 295 A95-76637

Multiple-function digital controller system for active flexible wing wind-tunnel model
[BTN-95-EIX95182619212] p 322 A95-76638

On-line analysis capabilities developed to support the active flexible wing wind-tunnel tests
[BTN-95-EIX95182619213] p 296 A95-76639

Smart structures in the control of airframe vibrations
[HTN-95-31014] p 236 A95-71184

Secondary source locations in active noise control: Selection or optimization?
[BTN-94-EIX94381352222] p 257 A95-71738

Grid refinement test of time-periodic flows over bluff bodies
[BTN-94-EIX94401378822] p 307 A95-76491

Summary of an active flexible wing program
[BTN-95-EIX95182619209] p 283 A95-76635

Simulation and model reduction for the active flexible wing program
[BTN-95-EIX95182619211] p 295 A95-76637

Multiple-function digital controller system for active flexible wing wind-tunnel model
[BTN-95-EIX95182619212] p 322 A95-76638

On-line analysis capabilities developed to support the active flexible wing wind-tunnel tests
[BTN-95-EIX95182619213] p 296 A95-76639

- Flutter suppression control law design and testing for the active flexible wing
[BTN-95-EIX95182619214] p 292 A95-76640
- Design and multifunction tests of a frequency domain-based active flutter suppression system
[BTN-95-EIX95182619215] p 292 A95-76641
- Rolling maneuver load alleviation using active controls
[BTN-95-EIX95182619217] p 270 A95-76643
- Transonic flutter suppression using active acoustic excitations
[BTN-95-EIX95262694310] p 408 A95-85481
- Active open-loop control of particle dispersion in round jets
[HTN-95-42334] p 372 A95-86163
- Flyover noise reduction of piston-engine propeller aeroplanes using an active noise control technique
[SAE PAPER 931218] p 509 A95-87466
- Aircraft interior sound field analysis in view of active control: Results from the ASANCA project
p 575 A95-90109
- Experimental active control of sound in the ATR 42
p 575 A95-90110
- Preliminary tests of a transonic flutter control wing model
p 499 A95-91566
- ASTOVL Aircraft: Some thoughts on new control strategies
[CONGRESS PAPER C428-5-011] p 517 A95-91680
- Theory and evaluation of active control as a means of reducing helicopter vibration
[CONGRESS PAPER C428-19-124] p 517 A95-91721
- Passive and active vibration control activities in the German helicopter industry
[CONGRESS PAPER C428-19-126] p 517 A95-91722
- Noise Con 1994: Proceedings of the 1994 National Conference on Noise Control Engineering, Progress in Noise Control for Industry
[LC-75-24750] p 28 N95-11259
- Achievements and tasks for active noise control
p 29 N95-11270
- Active control of complex noise problems using a broadband, multichannel controller
p 29 N95-11271
- Active control of turbomachine discrete tones
p 29 N95-11275
- Active control of interior noise in a business jet using piezoceramic actuators
p 29 N95-11276
- Adaptive tuned vibration absorbers: Tuning laws, tracking agility, sizing, and physical implementations
p 25 N95-11280
- Broadband, wide-area active control of sound radiated from vibrating structures using local surface-mounted radiation suppression devices
p 30 N95-11283
- Control of unsteady separated flow associated with the dynamic stall of airfoils
[NASA-CR-197024] p 74 N95-14613
- A computational investigation of wake-induced airfoil flutter in incompressible flow and active flutter control
[AD-A281534] p 142 N95-16109
- Active load control during rolling maneuvers — performed in the Langley Transonic Dynamics Tunnel
[NASA-TP-3455] p 129 N95-17397
- Microgravity isolation system design: A case study
[NASA-TM-106804] p 104 N95-17657
- Helicopter internal noise
p 173 N95-19144
- Active control of fan noise-feasibility study. Volume 1: Flyover system noise studies
[NASA-CR-195392-VOL-1] p 258 N95-21888
- Experimental investigations of on-demand vortex generators
p 250 N95-22451
- Active control of panel vibrations induced by a boundary layer flow
[NASA-CR-197867] p 273 N95-23182
- On-line, adaptive state estimator for active noise control
p 322 N95-23308
- Modeling and control of rotating stall in high speed multi-stage axial compressors
p 513 N95-29244
- Model development for active control of stall phenomena in aircraft gas turbine engines
p 514 N95-29679
- Characterization of stall inception in high-speed single-stage compressors
[AD-A291275] p 514 N95-29934
- Flight Vehicle Integration Panel Workshop on Pilot Induced Oscillations
[AGARD-AR-335] p 597 N95-31061
- Investigating the use of smart acoustically active surfaces for flow separation control in turbomachinery
[AD-A292819] p 648 N95-31443
- Active control technology: Applications and lessons learned
[AGARD-CP-560] p 620 N95-31989
- The role of handling qualities specifications in flight control system design
p 620 N95-31990
- The importance of flying qualities design specifications for active control systems
p 621 N95-31992
- Experiences with ADS-33 helicopter specification testing and contributions to refinement research
p 621 N95-31993
- Model following control for tailoring handling qualities: ACT experience with ATThES
p 622 N95-32000
- Structural aspects of active control technology
p 623 N95-32006
- Flight test results of the F-16 aircraft modified with axisymmetric vectoring exhaust nozzle
p 609 N95-32007
- Experimental Aircraft Programme (EAP): Flight control system design and test
p 623 N95-32010
- Pilot Induced Oscillation: A report on the AGARD Workshop on PIO
p 624 N95-32017
- Vibration reduction in helicopter rotors using an actively controlled partial span trailing edge flap located on the blade
p 624 N95-32111
- ACTIVE SATELLITES**
Effects of satellite bunching on the probability of collision in geosynchronous orbit
[BTN-95-EIX95152583276] p 298 A95-73577
- ACTUATION**
Actuating signals in adaptive control systems
[IFTR-13/1994] p 361 N95-26330
- ACTUATORS**
Smart structures in the control of airframe vibrations
[HTN-95-31014] p 236 A95-71184
- Fundamental mechanisms of aeroelastic control with control surface and strain actuation
[BTN-95-EIX95242670746] p 327 A95-81101
- Torsional actuation with extension-torsion composite coupling and a magnetostrictive actuator
[BTN-95-EIX95262694314] p 435 A95-85485
- Computer aided diagnostic testing of installed flight control servo-actuators
[SAE PAPER 932584] p 494 A95-90068
- Universal electrohydraulic system for the steering gear loading
[CONGRESS PAPER C428-10-106] p 517 A95-91700
- Static shape control for adaptive wings
[HTN-95-A1767] p 627 A95-93330
- ASTRA - A safe, simplex, fly-by-wire aircraft control system
[CONGRESS PAPER C428-37-218] p 610 A95-93634
- Advanced passive cooling for high power electromechanical actuators
[SAE PAPER 931397] p 634 A95-93669
- Power system characteristics for more electric aircraft
[SAE PAPER 931406] p 613 A95-93675
- Adaptive airfoils
[ISBN 1-879921-01-4] p 625 A95-93744
- Panel flutter limit-cycle suppression with piezoelectric actuation
[BTN-95-EIX95302731089] p 618 A95-94208
- Achievements and tasks for active noise control
p 29 N95-11270
- Active control of interior noise in a business jet using piezoceramic actuators
p 29 N95-11276
- Adaptive tuned vibration absorbers: Tuning laws, tracking agility, sizing, and physical implementations
p 25 N95-11280
- The development of a highly reliable power management and distribution system for civil transport aircraft
[NASA-TM-106697] p 50 N95-11867
- Wind-tunnel blockage and actuation systems test of a two-dimensional scramjet inlet unstart model at Mach 6
[NASA-TM-109152] p 97 N95-15898
- Motor drive technologies for the power-by-wire (PBW) program: Options, trends and tradeoffs
[NASA-TM-106885] p 295 N95-23671
- The 1994 Fiber Optic Sensors for Aerospace Technology (FOSAT) Workshop
[NASA-CP-10166] p 337 N95-24207
- Actuating signals in adaptive control systems
[IFTR-13/1994] p 361 N95-26330
- Design and development of a test rig for the high frequency testing of rolling sleeve airsprings
[DSTO-TN-0001] p 411 N95-26378
- Electro-hydrostatic actuator controller design using quantitative feedback theory
[AD-A289220] p 409 N95-26957
- Composite flight-control actuator development
p 410 N95-28281
- Modeling and control of rotating stall in high speed multi-stage axial compressors
p 513 N95-29244
- New adaptive methods for reconfigurable flight control systems, appendix 1
[AD-A292711] p 619 N95-30937
- Investigating the use of smart acoustically active surfaces for flow separation control in turbomachinery
[AD-A292819] p 648 N95-31443
- ADA (PROGRAMMING LANGUAGE)**
A reuse framework for software fault tolerance
[AIAA PAPER 95-1012] p 566 A95-90683
- Accelerated application development for flight software
[AIAA PAPER 95-1031] p 566 A95-90703
- Advanced distributed simulation technology advanced rotary wing aircraft. Software reusability report
[AD-A280434] p 20 N95-10354
- EASY-SIM: A visual simulation system software architecture with an Ada 9X application framework
[AD-A289325] p 448 N95-26895
- Impact of Ada and object-oriented design in the flight dynamics division at Goddard Space Flight Center
[NASA-CR-189412] p 567 N95-28807
- Proceedings of the 12th Annual National Conference on Ada Technology
[AD-A290693] p 569 N95-29644
- The application of Ada and formal methods to a safety critical engine control system
p 710 N95-33142
- ADAPTATION**
Adaptive wind tunnel walls versus wall interference correction methods in 2D flows at high blockage ratios
p 147 N95-19267
- ADAPTIVE CONTROL**
Stabilization of objects with unknown nonstationary parameters, using adaptive nonlinear continuous control systems
[BTN-94-EIX94461407944] p 98 A95-62262
- Using adaptive structures to attenuate rotary wing aeroelastic response
[BTN-95-EIX95062487547] p 192 A95-68361
- Precise navigation using adaptive FIR filtering and time domain spectral estimation
[BTN-95-EIX9514255485] p 227 A95-72888
- Adaptive finite element method for turbulent flow near a propeller
[BTN-95-EIX95142553038] p 305 A95-73460
- On-line learning nonlinear direct neurocontrollers for restructurable control systems
[BTN-95-EIX95242670768] p 359 A95-81079
- Direct adaptive and neural control of wing-rock motion of slender delta wings
[BTN-95-EIX95242670748] p 327 A95-81099
- Neuro-controllers for adaptive helicopter training
[SAE PAPER 932535] p 379 A95-84557
- Application of restructurable flight control system to large transport aircraft
[BTN-95-EIX95282706666] p 515 A95-89639
- Multivariable adaptive control using only input and output measurements for turbojet engines
[BTN-95-EIX95292721165] p 677 A95-92597
- New filtering method for linear weakly coupled stochastic systems
[BTN-95-EIX0608952736485] p 678 A95-92708
- Adaptive airfoils
[ISBN 1-879921-01-4] p 625 A95-93744
- A study of mesh adaption techniques in structured and unstructured meshes
[ISBN 1-879921-01-4] p 678 A95-93757
- Neuro-controllers for adaptive helicopter hover training
[BTN-94-EIX94522407592] p 709 A95-96241
- Active control of complex noise problems using a broadband, multichannel controller
p 29 N95-11271
- Analytical investigation of adaptive control of radiated inlet noise from turbofan engines
p 30 N95-11277
- On the use of controls for subsonic transport performance improvement: Overview and future directions
[NASA-TM-4605] p 10 N95-11408
- Mach number control in the High Speed Wind Tunnel of NLR
[PB94-201670] p 53 N95-13243
- A feedforward control approach to the local navigation problem for autonomous vehicles
[AD-A282787] p 126 N95-17706
- Direct adaptive performance optimization of subsonic transports: A periodic perturbation technique
[NASA-TM-4676] p 284 N95-22829
- Application of neural networks to unsteady aerodynamic control
p 350 N95-25264
- Actuating signals in adaptive control systems
[IFTR-13/1994] p 361 N95-26330
- A gain scheduling optimization method using genetic algorithms
[AD-A289306] p 448 N95-26920
- Flight assessment of the onboard propulsion system model for the Performance Seeking Control algorithm on an F-15 aircraft
[NASA-TM-4705] p 617 N95-31425
- Nonlinear adaptive control of highly maneuverable high performance aircraft
p 710 N95-33712
- A stochastic adaptive control application to flight systems
p 699 N95-34806
- ADAPTIVE FILTERS**
Precise navigation using adaptive FIR filtering and time domain spectral estimation
[BTN-95-EIX9514255485] p 227 A95-72888

Maximum-likelihood spectral estimation and adaptive filtering techniques with application to airborne Doppler weather radar
[NASA-CR-197699] p 316 N95-23670

ADDITIVES

Programmed ignition of metal compounds in a scramjet p 146 N95-10466
Additives in bituminous materials and fuel-resistant sealers
[DOT/FAA/CT-94/78] p 55 N95-12131
Evaluation of an unlighted swinging airport sign
[AD-A284763] p 146 N95-18087
The effect of aviation fuels containing low amounts of static dissipater additive on electrostatic charge generation
[AD-A280075] p 420 N95-28152
Environmentally safe aviation fuels p 631 N95-31768

ADHESION

Micro-measurements of mechanical properties for adhesives and composites using digital imaging technology
[NASA-CR-196111] p 22 N95-10231

ADHESION TESTS

Evaluation of advanced aerospace materials by depth sensing indentation and scratch methods
[BTN-95-EIX95152584678] p 282 A95-73590
Corrosion protection measures for CFC/metal joints of fuel integral tank structures of advanced military aircraft p 303 N95-23510

ADHESIVE BONDING

Evaluation of advanced aerospace materials by depth sensing indentation and scratch methods
[BTN-95-EIX95152584678] p 282 A95-73590
Damage tolerant repair techniques for pressurized aircraft fuselages
[AD-A281982] p 65 N95-14144
Bending effects of unsymmetric adhesively bonded composite repairs on cracked aluminum panels p 92 N95-14456
Ultrasonic techniques for repair of aircraft structures with bonded composite patches p 136 N95-19486
Damage tolerant repair techniques for pressurized aircraft fuselages
[AD-A286298] p 219 N95-22046
Adhesively bonded composite patch repair of cracked aluminum alloy structures p 393 N95-27507
Field repair materials for naval aircraft p 394 N95-27514
The development of an engineering standard for composite repairs p 396 N95-27528

ADHESIVES

Recent developments in nylon superpressure balloons p 385 A95-82512
The key to designing durable adhesively bonded joints
[HTN-95-12033] p 528 A95-88496
Micro-measurements of mechanical properties for adhesives and composites using digital imaging technology
[NASA-CR-196111] p 22 N95-10231
Field repair materials for naval aircraft p 394 N95-27514
Repair of high temperature composite aircraft structure p 395 N95-27520

ADJOINTS

Discrete shape sensitivity equations for aerodynamic problems
[BTN-94-EIX94451393721] p 88 A95-61720

ADJUSTING

Aircraft fuel system lightning protection design and qualification test procedures development
[AD-A288401] p 380 N95-26497

ADSORPTIVITY

Gas chromatography/ion mobility spectrometry as a hyphenated technique for improved explosives detection and analysis p 701 N95-33278

ADVECTION

Fine-scale, poleward transport of tropical air during AASE 2
[HTN-95-70949] p 352 A95-78014
A numerical model to predict the fate of jettisoned aviation fuel
[AD-A289336] p 419 N95-26842

AERIAL RECONNAISSANCE

Joint stars phased array radar antenna
[BTN-95-EIX95042474626] p 209 A95-68280
Tropical cyclone observation and forecasting with and without aircraft reconnaissance
[HTN-95-80701] p 254 A95-72545
Unmanned aerial vehicles
[AD-A286190] p 231 N95-20329
Geophex airborne unmanned survey system
[DE95-007566] p 392 N95-27440

AEROACOUSTICS

Aeroacoustic probe design for microphone to reduce flow-induced self-noise
[AIAA PAPER 93-4343] p 19 A95-60163
An experimental investigation of wing tip turbulence with applications to aerodynamic sound
[AIAA PAPER 86-1918] p 1 A95-60164
Oblique incidence sound absorption of porous materials covered by perforated metal and exposed to tangential airflow
[HTN-94-00681] p 19 A95-60165
On the scaling of small-scale jet noise to large scale
[AIAA PAPER 92-02109] p 27 A95-60166
Recent advances in Euler and Navier-Stokes methods for calculating helicopter rotor aerodynamics and acoustics
[HTN-94-00686] p 2 A95-60169
Study of noise on a small-scale hovering tilt rotor
[HTN-94-00712] p 5 A95-60190
Effect of wind tunnel acoustic modes on linear oscillating cascade aerodynamics
[HTN-94-00760] p 14 A95-60199
Geometrical acoustics approach for calculating the effects of flow on acoustics scattering
[BTN-94-EIX94321331207] p 61 A95-60790
Sound propagation from an arbitrarily oriented multipole placed near a plane, finite impedance surface
[BTN-94-EIX94371338964] p 257 A95-70797
Analysis of a higher harmonic control test to reduce blade vortex interaction noise p 265 A95-73532
Numerical study of sound generation due to a spinning vortex pair
[HTN-95-EIX95182619075] p 307 A95-75760
Aeroacoustic model for weak shock waves based on Burgers equation
[BTN-95-EIX95182619076] p 269 A95-75761
Structure of supersonic jet flow and its radiated sound
[HTN-95-51645] p 431 A95-85027
Screech tones from free and ducted supersonic jets
[HTN-95-51647] p 432 A95-85029
Symposium on Aerodynamics & Aeroacoustics, Tucson, AZ, Mar. 1-2, 1993
[ISBN 981-02-1732-3] p 462 A95-88892
Some aspects of the aeroacoustics of extreme-speed jets p 572 A95-88893
An introduction to generalized functions with some applications in aerodynamics and aeroacoustics p 565 A95-88895
Computing unsteady shock waves for aeroacoustic applications
[HTN-95-20928] p 463 A95-88967
Noise control in aeroacoustics; Proceedings of the 1993 National Conference on Noise Control Engineering, NOISE-CON 93, Williamsburg, VA, May 2-5, 1993
[ISBN 0-931784-26-3] p 573 A95-90088
A large hemi-anechoic enclosure for community-compatible aeroacoustic testing of aircraft propulsion systems p 577 A95-90132
Experimental results of the European HELINOISE aeroacoustic rotor test
[HTN-95-01080] p 578 A95-90266
Empirical refinements to boundary layer transition noise models p 28 N95-11262
On the interaction of jet noise with a nearby flexible structure
[NASA-CR-194934] p 57 N95-11812
En route noise levels from propfan test assessment airplane
[NASA-TP-3451] p 62 N95-12341
Activities of the Institute for Aerospace Studies of Toronto University p 63 N95-12699
Simulation of Shuttle launch G forces and acoustic loads using the NASA Ames Research Center 20G centrifuge p 86 N95-14089
Ultra-high bypass ratio jet noise
[NASA-CR-195394] p 100 N95-14610
Numerical simulation of the SOFIA flowfield
[NASA-CR-197025] p 74 N95-14612
Noise radiation by instability waves in coaxial jets
[NASA-TM-106738] p 100 N95-14618
The aeroacoustics of supersonic coaxial jets
[NASA-TM-106782] p 101 N95-15059
On the Lighthill relationship and sound generation from isotropic turbulence
[NASA-CR-195005] p 159 N95-18191
Aeroacoustic qualification of HERMES shingles p 173 N95-19145
Weapons bay acoustic environment p 173 N95-19146
Impact of noise environment on engine nacelle design p 173 N95-19147
Impact of dynamic loads on propulsion integration p 174 N95-19148
Modelling structurally damaging twin-jet screech p 135 N95-19154

Unsteady aerodynamic analyses for turbomachinery aeroelastic predictions p 141 N95-19381
Active control of fan noise-feasibility study. Volume 1: Flyover system noise studies
[NASA-CR-195392-VOL-1] p 258 N95-21888
Acoustics of laminar boundary layers breakdown p 251 N95-22455
Supersonic jet noise reductions predicted with increased jet spreading rate
[NASA-TM-106872] p 323 N95-23178
Effects of cavity dimensions, boundary layer, and temperature on cavity noise with emphasis on benchmark data to validate computational aeroacoustic codes
[NASA-CR-4653] p 361 N95-24879
Noise impact of advanced high lift systems
[NASA-CR-195028] p 362 N95-26160
Jet mixer noise suppressor using acoustic feedback
[NASA-CASE-LEW-15170-2] p 362 N95-26187
Aircraft noise prediction program theoretical manual: Rotorcraft System Noise Prediction System (ROTONET), part 4
[NASA-TM-83199-PT-4] p 451 N95-26392
Turbomachinery design and tonal acoustics computations
[NASA-CR-197744] p 406 N95-26777
Supersonic coaxial jet noise predictions
[NASA-TM-106917] p 451 N95-26801
A numerical study of fundamental shock noise mechanisms
[NASA-TM-110608] p 451 N95-27908
Anechoic wind tunnel study of turbulence effects on wind turbine broadband noise p 451 N95-27992
Evaluation of a doubly-swept blade tip for rotorcraft noise reduction
[NASA-CR-189677] p 452 N95-28264
Noise exposure reduction of advanced high-lift systems
[NASA-CR-195077] p 452 N95-28670
Response of multi-panel assembly to noise from a jet in forward motion
[NASA-CR-198164] p 442 N95-28673
The spectrum and directivity of turbulent mixing noise from supersonic jets p 579 N95-29415
An extension of the Lighthill theory of jet noise to encompass refraction and shielding
[NASA-TM-110163] p 580 N95-29452
Comparison of spatial numerical operators for duct-nozzle acoustics p 580 N95-30158
The pressure field of a gust interacting with a flat plate p 557 N95-30161
Method for extracting forward acoustic wave components from rotating microphone measurements in the inlets of turbofan engines
[NASA-CR-195457] p 616 N95-30779
Computation of noise radiation from turbofans: A parametric study
[NASA-CR-198359] p 710 N95-32836
Review of combustion-acoustic instabilities
[NASA-TM-107020] p 705 N95-32930
Combustion-acoustic stability analysis for premixed gas turbine combustors
[NASA-TM-107024] p 694 N95-32931
Fan noise prediction assessment
[NASA-CR-195051] p 711 N95-33831

AEROSIST

Science objectives and performance of a radiometer and window design for atmospheric entry experiments p 85 N95-13718
Numerical optimization of synergetic maneuvers
[AD-A283398] p 109 N95-17435

AEROBRAKING

Thermochemical nonequilibrium viscous shock-layer analysis for a Mars aerocapture vehicle
[BTN-95-EIX95082502732] p 239 A95-70139
Minimum-mass design of sandwich aerobrakes for a lunar transfer vehicle
[BTN-95-EIX95212645707] p 299 A95-76759
How 'HITEN's' aerobraking experiments were carried out p 415 A95-82553
Aero-thermodynamic flight environment at HITEN aerobrake experiment p 415 A95-82554
The effect of high lift to drag ratio on aerobraking p 415 A95-85807
Rarefied gas effects on aerobraking/reentry vehicles with wakes
[NASA-CR-196586] p 415 N95-27093

AEROCAPTURE

Thermochemical nonequilibrium viscous shock-layer analysis for a Mars aerocapture vehicle
[BTN-95-EIX95082502732] p 239 A95-70139
Fuel-optimal bank-angle control for lunar-return aerocapture
[BTN-95-EIX95212645706] p 299 A95-76758
The effect of high lift to drag ratio on aerobraking p 415 A95-85807

AERODYNAMIC BALANCE

- Minimum sink-speed in power-off glide
[BTN-95-EIX95062487556] p 193 A95-68370
- Navier-Stokes simulations of Orbiter aerodynamic characteristics including pitch trim and bodyflap
[BTN-95-EIX95041503779] p 204 A95-69210
- Air resonance of hingeless rotor helicopters in trimmed forward flight
[HTN-95-61075] p 369 A95-83659
- Trim conditions for optimal flight performance of hypersonic aircraft p 514 A95-87397
- Handling qualities of hypersonic aircraft and related control requirements p 515 A95-87398
- Tailless aircraft design-recent experiences p 492 A95-88899
- Symmetric steady manoeuvre loads on rigid aircraft of classical configuration at subsonic speeds
[ESDU-94009] p 43 N95-11774
- Free-to-roll tests of X-31 and F-18 subscale models with correlation to flight test results p 69 N95-14237
- Static and dynamic force/moment measurements in the Eidetics water tunnel p 69 N95-14238
- System for determining aerodynamic imbalance
[NASA-CASE-ARC-11913-1] p 311 N95-23377
- Balances for the measurement of multiple components of force in flows of a millisecond duration p 350 N95-25400
- An easy way to analyze longitudinal and lateral-directional trim problems with AEO or OEI p 409 N95-26949
- High- and low-frequency dynamics of isolated blades and rotors with dynamic stall and wake
[AD-A290358] p 503 N95-29322
- AERODYNAMIC BRAKES**
- Minimum-mass design of sandwich aerobrakes for a lunar transfer vehicle
[BTN-95-EIX95212645707] p 299 A95-76759
- Comparative wind tunnel tests of NACA 23024 airfoils with several aileron and spoiler configurations p 376 N95-27976
- Wind turbine trailing edge aerodynamic brakes
[DE95-004061] p 683 N95-32548
- AERODYNAMIC CHARACTERISTICS**
- Waveriders with finlets
[BTN-95-EIX95062487541] p 184 A95-68355
- Two-point transonic airfoil design using optimization for improved off-design performance
[BTN-95-EIX95062487542] p 192 A95-68356
- Aerodynamic effects of delta planform tip sails on wing performance
[BTN-95-EIX95062487544] p 185 A95-68358
- Hypersonic waverider test vehicle: A logical next step
[BTN-95-EIX95041503783] p 193 A95-69214
- Interpretation of waverider performance data using computational fluid dynamics
[BTN-95-EIX95062487534] p 193 A95-69242
- State-space representation of aerodynamic characteristics of an aircraft at high angles of attack
[BTN-95-EIX95062487536] p 187 A95-69244
- Aerodynamic characteristics of strake vortex flaps on a strake-wing configuration
[BTN-95-EIX95062487537] p 187 A95-69245
- Aerodynamic and wake methodology evaluation using Model UH-60A experimental data
[HTN-95-31009] p 220 A95-71179
- New airfoil-design concept with improved aerodynamic characteristics
[PAPER-4384] p 230 A95-72585
- Aerodynamic characteristics of a hypersonic viscous optimized waverider at high altitudes
[BTN-95-EIX95152583251] p 266 A95-73552
- Aerodynamic characteristics of a canard-controlled missile at high angles of attack
[BTN-95-EIX95152583257] p 267 A95-73558
- Aerodynamic characteristics of external store configurations at low speeds
[BTN-95-EIX95182619230] p 271 A95-76656
- The aerodynamic characteristics of cup-like body in supersonic flow p 427 A95-82407
- NAL aerothermodynamic probing and CFD verification mission in OREX experiment p 368 A95-82413
- A concept of a hypersonic flight experiment of a winged vehicle p 414 A95-82477
- T-45A high angle attack testing
[HTN-95-81499] p 386 A95-85213
- Aerodynamic characteristics of truncated airfoils at high angle of attack
[SAE PAPER 931227] p 460 A95-87365
- Verification of engineering methods of aerodynamics for reentry vehicles by DSMC p 525 A95-87386
- Real time for the calculation of the aerodynamic of aircrafts with delta wings p 460 A95-87399
- Low-speed aerodynamic characteristics of a slender wing with vertical fins p 460 A95-87400

- Computational study of boundary layer control for improving airfoil performance
[SAE PAPER 932513] p 466 A95-89186
- Aerodynamic tailoring of the Learjet Model 60 wing
[SAE PAPER 932534] p 492 A95-89194
- Optimization of waverider configurations generated from inclined circular and elliptic cones
[AIAA PAPER 95-6089] p 492 A95-89198
- Aerodynamic off-design behavior of integrated waveriders from take-off up to hypersonic flight
[AIAA PAPER 95-6091] p 466 A95-89200
- Low-speed wind tunnel tests of two waverider configuration models
[AIAA PAPER 95-6093] p 493 A95-89251
- Aerofoil characteristics at low Reynolds number p 472 A95-91507
- A shock tunnel test of a winged hypersonic research vehicle p 474 A95-91538
- A method for calculating mean aerodynamic center and zero-lift moment coefficient of aircraft without tail by using measured flight loads p 474 A95-91552
- A systems for flight data acquisition and analysis for a remotely-piloted research vehicle p 517 A95-91554
- Experimental study of the aerodynamic characteristics of the counter-rotation propellers p 474 - A95-91562
- Preliminary tests of a transonic flutter control wing model p 499 A95-91566
- Supersonic flutter analysis of cantilevered composite plate-wings p 499 A95-91567
- An experimental investigation of forward-swept wings at low Reynolds numbers
[SAE PAPER 931370] p 604 A95-93650
- Prediction of airplane states
[BTN-95-EIX0619952748174] p 584 A95-94468
- Effect of leading- and trailing-edge flaps on clipped delta wings with and without wing camber at supersonic speeds
[NASA-TM-4542] p 5 N95-10028
- An aerodynamic analysis of a mixed flow turbine
[NASA-TM-106674] p 15 N95-10153
- Flow-visualization study of the X-29A aircraft at high angles of attack using a 1/48-scale model
[NASA-TM-104268] p 8 N95-10858
- Gemini: A long-range cargo transport
[NASA-CR-197149] p 45 N95-12626
- The Balsa bullet: A high speed, low-cost general aviation aircraft for Aeroworld
[NASA-CR-197165] p 46 N95-12638
- Experimental aerodynamic characteristics of a generic hypersonic accelerator configuration at Mach numbers 1.5 and 2.0 — conducted in the Langley Unitary Plan Wind Tunnel
[NASA-TM-4413] p 39 N95-12770
- Methodology for sensitivity analysis, approximate analysis, and design optimization in CFD for multidisciplinary applications
[NASA-CR-196981] p 58 N95-13201
- Mach number control in the High Speed Wind Tunnel of NLR
[PB94-201670] p 53 N95-13243
- Numerical simulation of the flow about an F-18 aircraft in the high-alpha regime p 68 N95-14232
- Fourth High Alpha Conference, volume 2
[NASA-CP-10143-VOL-2] p 69 N95-14239
- Building complex simulations rapidly using MATRIX(x): The Space Station redesign
[TABES PAPER 94-632] p 87 N95-14653
- Turbulence: Engineering models, aircraft response p 84 N95-14900
- Low-speed wind tunnel testing of the NPS and NASA Ames Mach 6 optimized waverider
[AD-A283585] p 75 N95-15319
- Joint Proceedings on Aeronautics and Astronautics (JPAA)
[ISBN-7-80-046602-7] p 104 N95-16249
- An approach to aerodynamic characteristics of low radar cross-section fuselages p 106 N95-16251
- FPCAS2D user's guide, version 1.0
[NASA-CR-195413] p 156 N95-16588
- Twin engine afterbody model p 115 N95-17880
- Investigation into the aerodynamic characteristics of a combat aircraft research model fitted with a forward swept wing p 116 N95-17884
- Documentation and archiving of the Space Shuttle wind tunnel test data base. Volume 1: Background and description
[NASA-TM-104806-VOL-1] p 151 N95-19237
- Aerodynamic investigation of the flow field in a 180 deg turn channel with sharp bend p 163 N95-19257
- Interaction of a three strut support on the aerodynamic characteristics of a civil aviation model p 122 N95-19279
- Documentation and archiving of the Space Shuttle wind tunnel test data base. Volume 2: User's Guide to the Archived Data Base
[NASA-TM-104806-VOL-2] p 205 N95-19624

- Evidence that aerodynamic effects, including dynamic stall, dictate HAWT structural loads and power generation in highly transient time frames p 216 N95-19855
- Open Skies project computational fluid dynamic analysis
[AD-A285928] p 223 N95-19991
- Thin tailored composite wing for civil tiltrotor p 285 N95-23317
- Aerodynamic flight control to increase payload capability of future launch vehicles
[NAS-CR-196560] p 300 N95-24032
- Performance of an aerodynamic yaw controller mounted on the space shuttle orbiter body flap at Mach 10
[NASA-TM-109179] p 330 N95-24397
- Experimental study of the effects of Reynolds number on high angle of attack aerodynamic characteristics of forebodies during rotary motion
[NASA-CR-195033] p 330 N95-24443
- Exploratory flow visualization investigation of mast-mounted sights in presence of a rotor
[NASA-TM-4634] p 330 N95-24566
- Low speed aerodynamic characteristics of delta wings with vortex flaps: 60 deg and 70 deg delta wings
[NAL-TR-1245] p 331 N95-25105
- Simulation model of the integrated flight/propulsion control system, displays, and propulsion system for ASTOVL lift-fan aircraft
[NASA-TM-108866] p 405 N95-26412
- Suppressor of oscillations in airframe cavities
[AD-D017265] p 388 N95-26507
- Development and validation of a blade-element mathematical model for the AH-64A Apache helicopter
[NASA-TM-108863] p 367 N95-26710
- AIAA Techfest 20 Proceedings
[NIAR-94-1] p 367 N95-26941
- Modeling of aircraft unsteady aerodynamic characteristics. Part 2: Parameters estimated from wind tunnel data
[NASA-TM-110161] p 410 N95-27839
- Comparative wind tunnel test at high Reynolds numbers of NACA 64 621 airfoils with two aileron configurations
[NASA-CR-377] p 377 N95-27977
- Computational Fluid Dynamics (CFD) analysis of a C-135 aircraft with a side-mounted splitter plate (with comparison to wind tunnel data)
[AD-A292029] p 553 N95-29187
- Transonic, supersonic and hypersonic wind-tunnel tests on aerodynamic characteristics of reentry body with blunted cone configuration
[ISAS-658] p 480 N95-29640
- Experimental studies on boundary-layer transition on a reentry vehicle at transonic and supersonic speeds
[ISAS-659] p 555 N95-29712
- Computational algorithms for aerodynamic analysis and design
[AD-A291084] p 482 N95-29972
- Experimental investigation of aerodynamic devices for wind turbine rotational speed control, phase 1
[DE95-004034] p 564 N95-30016
- Transonic aerodynamic characteristics of a proposed wing-body reusable launch vehicle concept
[NASA-TM-108489] p 592 N95-30712
- Hypervelocity wind tunnel number 9, high Mach number development program
[AD-A289934] p 594 N95-30929
- Unified criteria for ACT aircraft longitudinal dynamics p 607 N95-31065
- Effects of cavity bleed and its configuration on aerodynamic characteristics of supersonic internal flow
[NAL-TR-1247] p 594 N95-31715
- Calculation for aerodynamic characteristics on delta wing with leading-edge separated vortex effect using boundary element method p 684 N95-34524
- Sidewall-effect of the wind tunnel on the estimation of the aerodynamic characteristics of a delta wing p 685 N95-34525
- Numerical simulation of two-dimensional PAR-WIG p 685 N95-34548
- AERODYNAMIC COEFFICIENTS**
- Minimum sink-speed in power-off glide
[BTN-95-EIX95062487556] p 193 A95-68370
- Aerodynamic sensitivity coefficients using the three-dimensional full potential equation
[BTN-95-EIX95062487530] p 186 A95-69238
- Aerodynamic characteristics of strake vortex flaps on a strake-wing configuration
[BTN-95-EIX95062487537] p 187 A95-69245
- Comparison of parameter identification algorithms for flight vehicles
[BTN-94-EIX94371347708] p 219 A95-69967
- Cercignani-Lampis-Lord gas-surface interaction model: Comparisons between theory and simulation
[BTN-95-EIX95041503806] p 242 A95-70131

Flow resolution and domain influence in rarefied hypersonic blunt-body flows
[BTN-95-EIX95082502729] p 220 A95-70136

Navier-Stokes prediction of large-amplitude delta-wing roll oscillations
[BTN-95-EIX95152582329] p 281 A95-73531

Analytic prediction of lift for delta wings with partial leading-edge thrust
[BTN-95-EIX95152582345] p 266 A95-73547

Drag function modeling for air traffic simulation
[BTN-95-EIX95182619154] p 279 A95-76631

Unsteady ground effects on aerodynamic coefficients of finite wings with camber
[BTN-95-EIX95182619233] p 271 A95-76659

Wind-tunnel tests of an inclined cylinder having helical grooves
[BTN-95-EIX95262694306] p 411 A95-85477

Drag coefficients of spherical liquid droplets. Part 1: Quiescent gaseous fields
[BTN-95-EIX95262697040] p 538 A95-86857

Drag coefficients of spherical liquid droplets. Part 2: Turbulent gaseous fields
[BTN-95-EIX95262697041] p 538 A95-86858

Estimation of aerodynamic derivatives: Euler scheme validation and approximate methods for hypersonic configurations
p 460 A95-87385

Aerodynamics of delta wings with application to high-alpha flight mechanics
p 460 A95-87395

Low-speed aerodynamic characteristics of a slender wing with vertical fins
p 460 A95-87400

Separation of winged vehicles in supersonics
[AIAA PAPER 95-6092] p 526 A95-88601

Computational study of a two-slot circulation control airfoil
[SAE PAPER 932531] p 466 A95-89191

Hypersonic waveriders generated from power-law shocks
[AIAA PAPER 95-6160] p 470 A95-90472

Aerodynamic characteristics of supersonic air-intake/aircraft integrated models
p 472 A95-91512

An application of TLS (Total Least Squares) method to estimation of aircraft aerodynamic derivatives
p 517 A95-91551

A method for calculating mean aerodynamic center and zero-lift moment coefficient of aircraft without tail by using measured flight loads
p 474 A95-91552

Wake velocity measurement of counter-rotation propellers
p 474 A95-91563

Momentum and scalar transfer coefficients over aerodynamically smooth Antarctic surfaces
[HTN-95-92932] p 562 A95-91870

Unanswered questions concerning the Nocolia gas-surface interaction model
[ISBN 1-879921-01-4] p 628 A95-93716

A simple analytical aerodynamic model of Langley Winged-Cone Aerospace Plane concept
[NASA-CR-194987] p 54 A95-12175

Dynamic ground effects flight test of an F-15 aircraft
[NASA-TM-4604] p 38 A95-12191

Navier-Stokes predictions of missile aerodynamics
p 74 A95-14451

Low-speed wind tunnel testing of the NPS and NASA Ames Mach 6 optimized waverider
[AD-A283585] p 75 A95-15319

Error propagation equations for estimating the uncertainty in high-speed wind tunnel test results
[DE94-014136] p 145 A95-16509

Measurements on a two-dimensional airfoil with high-lift devices
p 109 A95-17848

Two-dimensional 16.5 percent thick supercritical airfoil NLR 7301
p 110 A95-17854

Sectional prediction of 3D effects for separated flow on rotating blades
[PB94-201696] p 117 A95-18503

Static aerodynamics CFD analysis for 120-mm hypersonic KE projectile design
[ARL-MR-184] p 118 A95-18611

Dynamic Stability Instrumentation System (DSIS). Volume 1: Hardware description
[NASA-TM-109160-VOL-1] p 171 A95-18899

2-D and 3-D oscillating wing aerodynamics for a range of angles of attack including stall
[NASA-TM-4632] p 120 A95-19119

Calculation of satellite drag coefficients
[AD-A285118] p 300 A95-23781

NREL airfoil families for HAWTs
[DE95-000267] p 357 A95-24882

Measurements of longitudinal static aerodynamic coefficients by the cable mount system
[NAL-TR-1226] p 331 A95-25761

User documentation of the CTA program
[AD-A289508] p 375 A95-26854

Wind-tunnel test of the S814 thick root airfoil
[DE95-000268] p 376 A95-27541

Increases in aerofoil lift coefficient at zero angle of attack and in maximum lift coefficient due to deployment of a plain trailing-edge flap, with or without a leading-edge high-lift device, at low speeds
[ESDU-94028] p 477 A95-28885

Wave drag coefficient for axisymmetric forecones at zero incidence (M sub infinity less than or equal to 1.5)
[ESDU-94014] p 552 A95-28903

Increases in aerofoil lift coefficient at zero angle of attack and in maximum lift coefficient due to deployment of a trailing-edge split flap, with or without a leading-edge high-lift device, at low speeds
[ESDU-94029] p 479 A95-29129

Increases in aerofoil lift coefficient at zero angle of attack and in maximum lift coefficient due to deployment of various leading-edge high-lift devices at low speeds
[ESDU-94027] p 481 A95-29898

Introduction to the estimation of the lift coefficients at zero angle of attack and at maximum lift for airfoils with high-lift devices at low speeds
[ESDU-94026] p 481 A95-29899

Dynamic ground effects flight test of the NASA F-15 aircraft
p 692 A95-33024

AERODYNAMIC CONFIGURATIONS

Accuracy enhancements for overset grids using a defect correction approach
[AIAA PAPER 94-0523] p 3 A95-60181

A comparison of turbulence models in computing multi-element airfoil flows
[AIAA PAPER 94-0291] p 4 A95-60185

Study of noise on a small-scale hovering tilt rotor
[HTN-94-00712] p 5 A95-60190

Calculation of geometry of stamps with small allowances for pieces of the aerodynamic profile
[BTN-94-EIX94461408772] p 103 A95-63655

Waveriders with finlets
[BTN-95-EIX95062487541] p 184 A95-68355

Aerodynamically blunt and sharp bodies
[BTN-95-EIX95041503781] p 205 A95-69212

Development of an efficient inverse method for supersonic and hypersonic body design
[BTN-95-EIX95041503784] p 180 A95-69215

Aerodynamic shape optimization using preconditioned conjugate gradient methods
[BTN-95-EIX95142553033] p 263 A95-73465

Base drag prediction on missile configurations
[BTN-95-EIX95152583256] p 266 A95-73557

Aerodynamic characteristics of a canard-controlled missile at high angles of attack
[BTN-95-EIX95152583257] p 267 A95-73558

Techniques for tailoring aircraft stall and post-stall behavior
[SAE PAPER 931226] p 458 A95-87199

Estimation of aerodynamic derivatives: Euler scheme validation and approximate methods for hypersonic configurations
p 460 A95-87385

Aerodynamic design and optimization at Alenia D.V.D.
p 491 A95-87564

Pressure controlled surfaces - a 3D inverse panel method as a design tool
p 491 A95-87565

Improving the efficiency of aerodynamic shape optimization
[HTN-95-61204] p 540 A95-87577

Integration of an hypersonic airbreathing vehicle: Assessment of overall aerodynamic performances and of uncertainties
[AIAA PAPER 95-6100] p 492 A95-88007

Sensitivity derivatives for three dimensional supersonic Euler code using incremental iterative strategy
[HTN-95-20845] p 545 A95-88106

Modeling aerodynamic problems using Smoothed Particle Hydrodynamics (SPH)
[SAE PAPER 932512] p 465 A95-89185

Computational aerodynamic analysis on the Open Skies aircraft
[SAE PAPER 932514] p 466 A95-89187

Aerodynamic tailoring of the Learjet Model 60 wing
[SAE PAPER 932534] p 492 A95-89194

Optimization of waverider configurations generated from inclined circular and elliptic cones
[AIAA PAPER 95-6089] p 492 A95-89198

Accurate drag prediction: A prerequisite for drag reduction research
[SAE PAPER 932571] p 467 A95-90060

A brief survey of wing tip devices for drag reduction
[SAE PAPER 932574] p 467 A95-90063

Aerodynamic simulation on massively parallel systems
p 549 A95-91487

A conceptual design of the SST without horizontal tail
p 498 A95-91520

Conceptual study of next generation high-speed civil transport: A candidate with horizontal tail
p 499 A95-91521

Experimental investigation on aerothermodynamic characteristics of hypersonic transport
p 473 A95-91525

A shock tunnel test of a winged hypersonic research vehicle
p 474 A95-91538

Kinetic heating in hypersonic flight
[CONGRESS PAPER C428-3-056] p 475 A95-91674

A viewpoint on discretization schemes for applied aerodynamic algorithms for complex configurations
p 550 A95-91916

Optimal shape design in hypersonic aerodynamics and electromagnetics
p 639 A95-95397

Navier-Stokes computations around a realistic fighter configuration
p 591 A95-95440

Optimum aerodynamic design via boundary control
[NASA-CR-195882] p 36 A95-11877

Experimental Aerodynamics Division
[NAL-SP-9404] p 35 A95-12166

The FC-1D: The profitable alternative Flying Circus Commercial Aviation Group
[NASA-CR-197152] p 46 A95-12628

Aerodynamic shape optimization of a HSC2 type configuration with improved surface definition
[NASA-CR-197011] p 67 A95-13701

Viper - Design modification
[NASA-CR-197191] p 79 A95-13703

Fatigue evaluation of empennage, forward wing, and winglets/tip fins on part 23 airplanes
[PB94-196813] p 79 A95-13981

A selection of experimental test cases for the validation of CFD codes, volume 1
[AGARD-AR-303-VOL-1] p 91 A95-14201

Computational aerodynamics based on the Euler equations
[AGARD-AG-325] p 72 A95-14264

Optimum Design Methods for Aerodynamics
[AGARD-R-803] p 127 A95-16562

Single-pass method for the solution of inverse potential and rotational problems. Part 1: 2-D and quasi 3-D theory and application
p 107 A95-16563

Single-pass method for the solution of inverse potential and rotational problems. Part 2: Fully 3-D potential theory and applications
p 107 A95-16564

Optimum aerodynamic design via boundary control
p 127 A95-16565

Residual-correction type and related computational methods for aerodynamic design. Part 1: Airfoil and wing design
p 128 A95-16566

Tools for applied engineering optimization
p 128 A95-16570

Automation of reverse engineering process in aircraft modeling and related optimization problems
[NASA-CR-197109] p 129 A95-16899

A selection of experimental test cases for the validation of CFD codes, volume 2
[AGARD-AR-303-VOL-2] p 109 A95-17846

A selection of experimental test cases for the validation of CFD codes. Supplement: Datasets A-E
[AGARD-AR-303-SUPPL] p 117 A95-18539

Documentation and archiving of the Space Shuttle wind tunnel test data base. Volume 1: Background and description
[NASA-TM-104806-VOL-1] p 151 A95-19237

Interference corrections for a centre-line plate mount in a porous-walled transonic wind tunnel
p 122 A95-19280

Panel methods
p 165 A95-19448

Documentation and archiving of the Space Shuttle wind tunnel test data base. Volume 2: User's Guide to the Archived Data Base
[NASA-TM-104806-VOL-2] p 205 A95-19624

The aerodynamic design of an integrated wing lower surface and pylons for reduced drag
[ARA-MEMO-406] p 194 A95-19789

Impeller flow field characterization with a laser two-focus velocimeter
p 313 A95-23440

Aerodynamic shape optimization of wing and wing-body configurations using control theory
[NASA-CR-198024] p 335 A95-25334

Configuration and other differences between Black Hawk and Seahawk helicopters in military service in the USA and Australia
[AR-008-386] p 336 A95-25935

Aeroelasticity of wing and wing-body configurations on parallel computers
[NASA-CR-197756] p 389 A95-26590

Design and testing of low sonic boom configurations and an oblique all-wing supersonic transport
[NASA-CR-197744] p 389 A95-26651

Supersonic civil airplane study and design: Performance and sonic boom
[NASA-CR-197745] p 390 A95-26813

An exploratory application of neural networks for airfoil design
p 448 A95-26943

The noise reduction potential of dual-stream coaxial rectangular improperly expanded jet flows
[NASA-CR-197820] p 437 A95-26995

The lift-fan aircraft: Lessons learned
[NASA-CR-196694] p 392 A95-27143

- NAS Technical Summaries, March 1993 - February 1994
 [NASA-RP-1355] p 453 N95-27367
 Rapid Airplane Parametric Input Design (RAPID)
 p 501 N95-28730
 Automatic blocking for complex three-dimensional configurations p 566 N95-28734
 Block-structured grids for complex aerodynamic configurations: Current status p 551 N95-28736
 A two element laminar flow airfoil optimized for cruise [NASA-CR-198580] p 479 N95-29338
 An experimental investigation of the time-dependent separation of tangent bodies in supersonic flow [AD-A290720] p 480 N95-29500
 Transonic, supersonic and hypersonic wind-tunnel tests on aerodynamic characteristics of reentry body with blunted cone configuration [ISAS-658] p 480 N95-29640
 The 1995 version of the NSWC aeroprediction code. Part 1: Summary of new theoretical methodology [AD-A291518] p 481 N95-29853
 Computational algorithms for aerodynamic analysis and design [AD-A291084] p 482 N95-29972
 A general inverse design procedure for aerodynamic bodies p 606 N95-30497
 Numerical investigation into vortical flow about a delta-wing configuration up to incidences at which vortex breakdown occurs in experiment [PB95-198024] p 593 N95-30837
 Application of multigrid computational fluid dynamics (CFD) methods to rotor analysis [AD-A293012] p 648 N95-31475
 Afterbody/nozzle pressure distributions of a twin-tail twin-engine fighter with axisymmetric nozzles at Mach numbers from 0.6 to 1.2 [NASA-TP-3509] p 594 N95-31984
 The Anglo-French Compact Laser Radar demonstrator programme p 703 N95-32501
 Three-dimensional aerodynamic shape optimization using discrete sensitivity analysis p 691 N95-32904
 Analysis and design methodology for chordwise deformable wings p 692 N95-33311
- AERODYNAMIC DRAG**
 Wing download reduction using vortex trapping plates [HTN-94-00710] p 4 A95-60188
 An assessment of upper surface blowing for the reduction of tilt rotor download [HTN-94-00711] p 5 A95-60189
 Aerodynamic interactions between a rotor and wing in hover [HTN-94-00714] p 5 A95-60192
 Variations of perturbations in perigee height with eccentricity for artificial Earth's satellites due to air drag [HTN-95-40013] p 85 A95-62657
 Interpretation of waverider performance data using computational fluid dynamics [BTN-95-EIX95062487534] p 193 A95-69242
 Cercignani-Lampis-Lord gas-surface interaction model: Comparisons between theory and simulation [BTN-95-EIX95041503806] p 242 A95-70131
 Analytic prediction of lift for delta wings with partial leading-edge thrust [BTN-95-EIX95152582345] p 266 A95-73547
 Base drag prediction on missile configurations [BTN-95-EIX95152583256] p 266 A95-73557
 Improved version of the Naval Surface Warfare Center aeroprediction code (AP93) [BTN-95-EIX95152583260] p 267 A95-73561
 Drag function modeling for air traffic simulation [BTN-95-EIX95182619154] p 279 A95-76631
 Application of Navier-Stokes aerolastic methods to improve fighter wing maneuver performance [BTN-95-EIX95182619218] p 284 A95-76644
 Numerical investigation of supersonic flows around a spiked blunt body [BTN-95-EIX95212645690] p 271 A95-76742
 A comparison of some aerodynamic resistance methods using measurements over cotton and grass from the 1991 California ozone deposition experiment [HTN-95-11295] p 319 A95-77000
 Dynamic stall control for advanced rotorcraft application [BTN-95-EIX95222650793] p 334 A95-79249
 Flow due to an oscillating sphere and an expression for unsteady drag on the sphere at finite Reynolds number [BTN-94-EIX95011441142] p 347 A95-81012
 Flow past a symmetric wedge with forward splitter plate p 427 A95-82406
 Numerical investigation of cylinder wake flow with a rear stagnation jet [HTN-95-51669] p 433 A95-85051
 Effect of Reynolds number and turbulence on airfoil aerodynamics at -90-degree incidence [HTN-95-42320] p 370 A95-86149
- Drag coefficients of spherical liquid droplets. Part 1: Quiescent gaseous fields [BTN-95-EIX95262697040] p 538 A95-86857
 Drag coefficients of spherical liquid droplets. Part 2: Turbulent gaseous fields [BTN-95-EIX95262697041] p 538 A95-86858
 Effects of periodic spanwise blowing on Delta-wing configuration characteristics [HTN-95-81631] p 461 A95-87679
 Parameters of Nocilla gas/surface interaction model from measured accommodation coefficients [HTN-95-81639] p 541 A95-87687
 An overview of static and dynamic airfoil performance [SAE PAPER 931228] p 463 A95-88960
 Aircraft aerodynamic analysis on a personal computer (using the RDS aircraft design software) [SAE PAPER 932530] p 492 A95-89190
 Accurate drag prediction: A prerequisite for drag reduction research [SAE PAPER 932571] p 467 A95-90060
 A brief survey of wing tip devices for drag reduction [SAE PAPER 932574] p 467 A95-90063
 Measurement of drag using a momentum balance [HTN-95-01090] p 468 A95-90276
 Estimation of aerodynamic characteristics for the vortex flaps by the suction analogy p 471 A95-91496
 Application of ACT to unstable motions of an airfoil in ground effect p 471 A95-91500
 High subsonic and high Reynolds number wind tunnel tests of two-dimensional natural-laminar-flow airfoils with suction boundary layer control p 472 A95-91508
 Optimum aerodynamic design of aircraft fuselage using boundary element method p 473 A95-91514
 Experimental study for improving the lift to drag ratio of next generation SST p 473 A95-91524
 A guidance concept for hypersonic aerospacecrafts p 526 A95-91549
 Low speed wind tunnel blockage corrections for airfoils at medium to large angles of attack p 474 A95-91557
 Use of partially open wind tunnel walls for blockage-free separated flows on bodies p 474 A95-91558
 Simultaneous structure/aerodynamic design optimization for a flexible wing structure p 499 A95-91565
 Momentum and scalar transfer coefficients over aerodynamically smooth Antarctic surfaces [HTN-95-92932] p 562 A95-91870
 Supersonic, turbulent flow computation and drag optimization for axisymmetric afterbodies [BTN-95-EIX95302729772] p 637 A95-94134
 Turbulent effects on parachute drag [BTN-95-EIX0619952748193] p 591 A95-94482
 Laminar and turbulent flow over optimal riblets p 639 A95-95383
 Computational flow predictions for hypersonic drag devices p 37 N95-11967
 A simple analytical aerodynamic model of Langley Winged-Cone Aerospace Plane concept [NASA-CR-194987] p 54 N95-12175
 Scale effects on aircraft and weapon aerodynamics [AGARD-AG-323] p 67 N95-14103
 An investigation of the transonic pressure drag coefficient for axis-symmetric bodies [AD-A280990] p 105 N95-15994
 Measurements on a two-dimensional aerofoil with high-lift devices p 109 N95-17848
 Experimental techniques for measuring transonic flow with a three dimensional laser velocimetry system. Application to determining the drag of a fuselage p 163 N95-19258
 An investigation of drag repeatability in half model testing in the ARA Transonic Wind Tunnel [ARA-MEMO-392] p 188 N95-19546
 The aerodynamic design of an integrated wing lower surface and pylons for reduced drag [ARA-MEMO-406] p 194 N95-19789
 Investigation of a thermal buoyancy effect on the drag of half models tested in the ARA Transonic Wind Tunnel [ARA-MEMO-407] p 222 N95-19946
 Research on bluff body vortex wakes [AD-A286319] p 223 N95-20177
 Calculation of satellite drag coefficients [AD-A285118] p 300 N95-23781
 Numerical and experimental study of drag characteristics of two-dimensional HLFC airfoils in high subsonic, high Reynolds number flow [NAL-TR-1244T] p 331 N95-24998
 Thrust measurements of a complete axisymmetric scramjet in an impulse facility p 339 N95-25395
 A theoretical and experimental investigation of the flow over superersonic leading edge wing/body configurations [DRA-TM-AERO-PROP-41] p 331 N95-25649
 Aerodynamic characteristics of the orbital reentry vehicle experimental probe fins in a supersonic flow [NAL-TR-1232] p 342 N95-25664
- Comparative wind tunnel test at high Reynolds numbers of NACA 64 621 airfoils with two aileron configurations p 377 N95-27977
 A hybrid vehicle evaluation code and its application to vehicle design. Revision 1 [DE95-008053] p 441 N95-28029
 A hybrid vehicle evaluation code and its application to vehicle design, revision 2 [DE95-008060] p 441 N95-28139
 Construction and wind tunnel test of a 1/12th scale helicopter model [AD-A288487] p 378 N95-28331
 Study of potential aerodynamic benefits from spanwise blowing at wingtip [NASA-TP-3515] p 378 N95-28669
 Excrescence drag levels on aircraft [ESDU-94044] p 477 N95-28897
 Wave drag coefficient for axisymmetric forecows at zero incidence (M sub infinity less than or equal to 1.5) [ESDU-94014] p 552 N95-28903
 High-and low-frequency dynamics of isolated blades and rotors with dynamic stall and wake [AD-A290358] p 503 N95-29322
 A two element laminar flow airfoil optimized for cruise [NASA-CR-198580] p 479 N95-29338
 Wind turbine trailing edge aerodynamic brakes [DE95-004061] p 683 N95-32548
 Drag measurements of an axisymmetric nacelle mounted on a flat plate at supersonic speeds [NASA-TM-4660] p 684 N95-32821
 Near-limit drop deformation and secondary breakup p 704 N95-32902
- AERODYNAMIC FORCES**
 Adaptive computations of flow around a delta wing with vortex breakdown [BTN-94-EIX94441386631] p 184 A95-68180
 Comparison of electrostatic and aerodynamic forces during parachute opening [BTN-95-EIX95062487532] p 187 A95-69240
 Side forces at high angles of attack. Why, when, how? [BTN-95-EIX95112523809] p 194 A95-69324
 Static aeroelastic characteristics of a composite wing [BTN-95-EIX95152582340] p 282 A95-73542
 Flutter of an infinitely long panel in a duct [BTN-95-EIX95182619087] p 291 A95-75772
 Flow structure in the lee of an inclined 6:1 prolate spheroid [BTN-94-EIX95011441127] p 348 A95-81027
 Aero-thermodynamic flight environment at HITEN aerobrace experiment p 415 A95-82554
 Force and moment on a Joukowski profile in the presence of point vortices [BTN-95-EIX95262694298] p 434 A95-85469
 Wind-tunnel tests of an inclined cylinder having helical grooves [BTN-95-EIX95262694306] p 411 A95-85477
 Aerodynamic characteristics of truncated airfoils at high angle of attack [SAE PAPER 931227] p 460 A95-87365
 Reentry trajectories and their optimization by an evolution algorithm p 525 A95-87394
 Application of artificial neural networks in nonlinear aerodynamics and aircraft design [SAE PAPER 932533] p 492 A95-89193
 Modelling requirements in flight simulation [HTN-95-C0004] p 585 A95-93392
 Flutter analysis of supersonic axial flow cascades using a high resolution Euler solver. Part 1: Formulation and validation [NASA-TM-105798] p 23 N95-10244
 Numerical analysis of tangential slot blowing on a generic chined forebody [NASA-TM-108845] p 37 N95-11927
 Static and dynamic force/moment measurements in the Eidetics water tunnel p 69 N95-14238
 Structural effects of unsteady aerodynamic forces on horizontal-axis wind turbines [DE94-011863] p 157 N95-16939
 Force and pressure data of an ogive-nosed slender body at high angles of attack and different Reynolds numbers p 113 N95-17868
 Subsonic flow around US-orbiter model FALKE in the DNW p 115 N95-17877
 Hydrofoil force balance [AD-D016475] p 160 N95-18461
 Gyroscopic and propeller aerodynamic effects on engine mounts dynamic loads in turbulence conditions p 132 N95-18599
 Transonic aerodynamic characteristics of a proposed wing-body reusable launch vehicle concept [NASA-TM-108489] p 592 N95-30712
 Advanced gust management systems: Lessons learned and perspectives p 622 N95-32002
 SOFIA 2 model telescope wind tunnel test report [NASA-TM-110668] p 683 N95-32764

- Energy absorption device for shock loading
[AD-D017476] p 706 N95-34449
Computations of low speed flow about space-plane
p 685 N95-34544
A simulation of damping process of pendulum motion
due to aerodynamic forces p 711 N95-34551
- AERODYNAMIC HEAT TRANSFER**
On the particular features of dynamic processes in solids
with varying boundary during interaction with intensive heat
flows
[BTN-94-EIX94461408756] p 171 A95-63639
Kinetic theory in aerothermodynamics
[HTN-95-A0002] p 183 A95-67829
Prediction of ice accretion: Comparison between the 2D
and 3D codes
[BTN-94-EIX94441385753] p 213 A95-68217
Approximate method for calculating heating rates on
three-dimensional vehicles
[BTN-95-EIX95041503778] p 210 A95-69209
Ablative thermal management structural material on the
hypersonic vehicles
[AIAA PAPER 95-6133] p 547 A95-90452
Investigation of advanced counterrotation blade
configuration concepts for high speed turbo-prop systems.
Task 8: Cooling flow/heat transfer analysis
[NASA-CR-195359] p 50 N95-11901
Investigation of advanced counterrotation blade
configuration concepts for high speed turbo-prop systems.
Task 8: Cooling flow/heat transfer analysis user's
manual
[NASA-CR-195360] p 50 N95-11951
An analysis code for the Rapid Engineering Estimation
of Momentum and Energy Losses (REMEL)
[NASA-CR-191178] p 108 N95-16887
Documentation and archiving of the Space Shuttle wind
tunnel test data base. Volume 1: Background and
description
[NASA-TM-104806-VOL-1] p 151 N95-19237
Documentation and archiving of the Space Shuttle wind
tunnel test data base. Volume 2: User's Guide to the
Archived Data Base
[NASA-TM-104806-VOL-2] p 205 N95-19624
Numerical computation of aerodynamics and heat
transfer in a turbine cascade and a turn-around duct using
advanced turbulence models p 313 N95-23444
Advanced k-epsilon modeling of heat transfer
[NASA-CR-4679] p 648 N95-31423
- AERODYNAMIC HEATING**
Shock layers and boundary layers in hypersonic flows
[HTN-95-A0003] p 183 A95-67830
Approximate method for calculating heating rates on
three-dimensional vehicles
[BTN-95-EIX95041503778] p 210 A95-69209
Multiblock analysis for Shuttle Orbiter reentry heating
from Mach 24 to Mach 12
[BTN-95-EIX95041503780] p 205 A95-69211
Trajectory-based heating analysis for the European
Space Agency/Rosetta Earth Return Vehicle
[BTN-95-EIX95041503787] p 205 A95-69218
Hypersonic convective heat transfer over 140-deg blunt
cones in different gases
[BTN-95-EIX95152583253] p 306 A95-73554
Convective and radiative heat transfer analysis for the
fire 2 forebody
[BTN-95-EIX95182617460] p 268 A95-75731
Viscoplastic response of structures for intense local
heating
[HTN-95-41540] p 346 A95-77921
Research and development of thermal protection system
of HOPE re-entry vehicle p 413 A95-82358
VSL analysis of hypersonic flows around a reentry
vehicle with equilibrium air chemistry p 413 A95-82400
Hypersonic thermal protection with mass injection at
angle of attack p 414 A95-82414
Numerical simulation of unsteady aerodynamic heating
induced by shock reflections p 428 A95-82418
A study on aerodynamic heating phenomena in
three-dimensional shock wave/turbulent boundary layer
interaction induced by sweptback sharp fins at supersonic
flow p 428 A95-82419
Reentry technology experiment on the first mission of
reentry capsule 'EXPRESS' p 414 A95-82499
Aero-thermodynamic flight environment at HITEN
aerobrace experiment p 415 A95-82554
Studies on gain performance of a combustion driven
CO₂ gas dynamic laser p 428 A95-82679
The effects of wall perturbations on thermo-turbulent
Couette flow
[HTN-95-92255] p 434 A95-85299
Reentry analysis for low Earth orbiting spacecraft
p 415 A95-85774
Computational methods in applied sciences; European
Computational Fluid Dynamics Conference, 1st, Brussels,
Belgium, Sept. 7-11, 1992
[ISBN 0-444-89795-X] p 539 A95-87552
- Numerical simulation of real gas effects and
aerodynamic heating of hypersonic space transportation
vehicles p 540 A95-87558
The effect of wing sweep back upon transition in
hypersonic flow
[AIAA PAPER 95-6090] p 466 A95-89199
The concept of high speed commercial transporter
structure p 498 A95-91517
Kinetic heating in hypersonic flight
[CONGRESS PAPER C428-3-056] p 475 A95-91674
Application of integral methods to ablation charring
erosion, a review
[BTN-95-EIX95302694460] p 636 A95-94057
Enhancements to integral solutions to ablation and
charring
[BTN-95-EIX95302694461] p 636 A95-94058
An axisymmetric analog two-layer convective heating
procedure with application to the evaluation of Space
Shuttle Orbiter wing leading edge and windward surface
heating
[NASA-CR-188343] p 54 N95-11937
Science objectives and performance of a radiometer
and window design for atmospheric entry experiments
[NASA-TM-4637] p 63 N95-12190
Science objectives and performance of a radiometer
and window design for atmospheric entry experiments
p 85 N95-13718
Thermoacoustic environments to simulate reentry
conditions p 86 N95-14096
An engineering code to analyze hypersonic thermal
management systems p 155 N95-16322
Numerical optimization of synergetic maneuvers
[AD-A283398] p 109 N95-17435
A computer code (SKINTEMP) for predicting transient
missile and aircraft heat transfer characteristics
[AD-A286044] p 248 N95-21001
Temperature effects on acoustic interactions between
altitude test facilities and jet engine plumes
[NASA-CR-197638] p 258 N95-21170
Heat transfer measurements in small scale wind
tunnels
[AD-A288689] p 341 N95-26053
Viscous shock-layer analysis on hypersonic flow over
reentry capsule with nonequilibrium chemistry
[ISAS-656] p 436 N95-26739
Rarefied gas effects on aerobreaking/reentry vehicles
with wakes
[NASA-CR-196586] p 415 N95-27093
- AERODYNAMIC INTERFERENCE**
Comprehensive aeromechanics analysis of complex
rotorcraft using 2GCHAS
[HTN-94-00695] p 2 A95-60174
First level release of 2GCHAS for comprehensive
helicopter analysis - a status report
[HTN-94-00697] p 2 A95-60176
Aerodynamic interactions between a rotor and wing in
hover
[HTN-94-00714] p 5 A95-60192
Interference between tanker wing wake with roll-up and
receiver aircraft
[BTN-95-EIX95062487552] p 185 A95-68366
Effect of ground and ceiling planes on shape of
energized wakes
[BTN-95-EIX95062487558] p 186 A95-68372
Numerical simulation of steady and unsteady,
vorticity-dominated aerodynamic interference
[BTN-95-EIX95062487524] p 186 A95-69232
Preliminary assessment of tunnel wall interference in
the NDA cryogenic wind tunnel
[BTN-95-EIX95062487531] p 187 A95-69239
Two-variable method for blockage wall interference in
a circular tunnel
[BTN-95-EIX95062487540] p 187 A95-69248
Wing vertical position effects on wing-body carryover
for noncircular missiles
[BTN-95-EIX95182617462] p 268 A95-75733
Some aspects of the aerodynamics of separating
strap-ons
[BTN-95-EIX95182617464] p 298 A95-75735
Separation of winged vehicles in supersonics
[AIAA PAPER 95-6092] p 526 A95-88601
Aerodynamic interference for supersonic
low-aspect-ratio missiles
[BTN-95-EIX95302694469] p 588 A95-94065
A wall interference assessment and correction system
[NASA-CR-196940] p 58 N95-12228
Lateral jet control for tactical missiles
p 84 N95-14448
Propulsion/airframe interference for ducted propfan
engines with ground effect
[NASA-CR-197110] p 81 N95-14909
Wall-signature methods for high speed wind tunnel wall
interference corrections p 107 N95-16257
2-D aileron effectiveness study p 110 N95-17851
Data from the GARTEur (AD) Action Group 02 airfoil
CAST 7/DOA1 experiments p 111 N95-17856
- Single-engine tail interference model
p 115 N95-17879
Low speed propeller slipstream aerodynamic effects
p 116 N95-17882
Background noise levels measured in the NASA Lewis
9-by-15-foot low-speed wind tunnel
[NASA-TM-106817] p 145 N95-18054
Wall Interference, Support Interference and Flow Field
Measurements
[AGARD-CP-535] p 162 N95-19251
The crucial role of wall interference, support interference
and flow field measurements in the development of
advanced aircraft configurations p 162 N95-19252
Boundary-flow measurement methods for wall
interference assessment and correction: Classification and
review p 163 N95-19262
Estimating wind tunnel interference due to vectored jet
flows p 164 N95-19265
Adaptive wind tunnel walls versus wall interference
correction methods in 2D flows at high blockage ratios
p 167 N95-19267
Interference determination for wind tunnels with slotted
walls p 147 N95-19269
Transonic wind tunnel boundary interference
correction p 147 N95-19271
Calculation of low speed wind tunnel wall interference
from static pressure pipe measurements p 164 N95-19273
The traditional and new methods of accounting for the
factors distorting the flow over a model in large transonic
wind tunnels p 165 N95-19275
Calculation of wall effects of flow on a perforated wall
with a code of surface singularities p 165 N95-19277
Evaluation of combined wall- and support-interference
on wind tunnel models p 122 N95-19278
Interaction of a three strut support on the aerodynamic
characteristics of a civil aviation model p 122 N95-19279
Investigation of a thermal buoyancy effect on the drag
of half models tested in the ARA Transonic Wind Tunnel
[ARA-MEMO-407] p 222 N95-19946
A wall interference assessment/correction system
[NASA-CR-197421] p 309 N95-23183
A method for the modelling of porous and solid wind
tunnel walls in computational fluid dynamics codes
p 523 N95-29795
Unsteady flow simulations about moving boundary
configurations using dynamic domain decomposition
techniques p 649 N95-31837
Numerical analysis around the whole SST
configuration p 693 N95-34541
- AERODYNAMIC LOADS**
Comprehensive aeromechanics analysis of complex
rotorcraft using 2GCHAS
[HTN-94-00695] p 2 A95-60174
First level release of 2GCHAS for comprehensive
helicopter analysis - a status report
[HTN-94-00697] p 2 A95-60176
Numerical simulation of a complete STOVL aircraft in
ground effect
[AIAA PAPER 93-4880] p 4 A95-60187
Engineering methods for the evaluation of transonic
flutter characteristics for aerodynamic control surfaces
[BTN-94-EIX94461408589] p 141 A95-63064
Continuous gust response and sensitivity derivatives
using state-space models
[BTN-95-EIX95062487551] p 203 A95-68365
Brief history of gust models for aircraft design
[BTN-95-EIX95062487557] p 203 A95-68371
State-space representation of aerodynamic
characteristics of an aircraft at high angles of attack
[BTN-95-EIX95062487536] p 187 A95-69244
Aerodynamic and wake methodology evaluation using
Model UH-60A experimental data
[HTN-95-31009] p 220 A95-71179
Advance finite element modeling of rotor blade
aeroelasticity
[HTN-95-31013] p 221 A95-71183
Design constraints in the payload arrangement diagram of
ultrahigh capacity transport airplanes
[BTN-95-EIX95152582319] p 276 A95-73522
Hypersonic rarefied flow past spheres including wake
structure
[BTN-95-EIX95152583250] p 305 A95-73551
Summary of an active flexible wing program
[BTN-95-EIX95182619209] p 283 A95-76635
Rolling maneuver load alleviation using active controls
[BTN-95-EIX95182619217] p 270 A95-76643
Minimum-mass design of sandwich aerobrakes for a
lunar transfer vehicle
[BTN-95-EIX95212645707] p 299 A95-76759
Integrated development of the equations of motion for
elastic hypersonic flight vehicles
[BTN-95-EIX95242670755] p 327 A95-81092
Dynamics and control of a tethered flight vehicle
[BTN-95-EIX95242670754] p 342 A95-81093

- Effects of blade tip shape on dynamics, cost, weight, aerodynamic performance, and aeroelastic response [HTN-95-61074] p 369 A95-83658
- Stability of viscoelastic plate in supersonic flow under random loading [BTN-95-EIX95262694312] p 435 A95-85483
- Stress considerations in reduced-size aeroelastic optimization [BTN-95-EIX95262694313] p 366 A95-85484
- Equivalent beam-column analysis of guyed towers [BTN-95-EIX95262696644] p 435 A95-85519
- Integrated thermal and mechanical analysis of hypersonic vehicles by using adaptive finite element methods p 524 A95-87383
- Navier-Stokes calculations of rotor-airframe interaction in forward flight [HTN-95-01087] p 468 A95-90273
- The concept of high speed commercial transporter structure p 498 A95-91517
- Effects of structural damping on aeroelastic stability of various shaped composite plate wing p 530 A95-91530
- A method for calculating mean aerodynamic center and zero-lift moment coefficient of aircraft without tail by using measured flight loads p 474 A95-91552
- Neural network approach to identification of aerodynamic loads on a wing. 1: Application to cantilevered beam models p 475 A95-91568
- High angle of attack missile aerodynamics [CONGRESS PAPER C428-3-060] p 475 A95-91673
- Test model designs for advanced refractory ceramic materials p 55 N95-11968
- Dynamics of the McDonnell-Douglas Large Scale Dynamic Rig and dynamic calibration of the rotor balance [NASA-TM-108855] p 65 N95-13891
- Fatigue evaluation of empennage, forward wing, and winglets/tip fins on part 23 airplanes [PB94-196813] p 79 N95-13981
- Higher harmonic control analysis for vibration reduction of helicopter rotor systems [NASA-TM-103855] p 66 N95-14419
- Extracting a representative loading spectrum from recorded flight data p 80 N95-14469
- Pressure measurements on an F/A-18 twin vertical tail in buffeting flow. Volume 2: Steady and unsteady RMS pressure data [AD-A281581] p 76 N95-15465
- Prediction of rotor-blade deformations due to unsteady airloads [AD-A284467] p 81 N95-15821
- Residual-correction type and related computational methods for aerodynamic design. Part 2: Multi-point airfoil design p 128 N95-16567
- Optimal shape design for aerodynamics p 128 N95-16568
- Airfoil optimization by the one-shot method p 128 N95-16569
- Aerodynamic shape optimization p 128 N95-16572
- Active load control during rolling maneuvers — performed in the Langley Transonic Dynamics Tunnel [NASA-TP-3455] p 129 N95-17397
- Aircraft Loads due to Turbulence and their Impact on Design and Certification [AGARD-R-798] p 143 N95-18597
- Design limit loads based upon statistical discrete gust methodology p 133 N95-18603
- Pressure measurements on an F/A-18 twin vertical tail in buffeting flow. Volume 4, part 2: Buffet cross spectral densities [AD-A285555] p 143 N95-18641
- Wind turbine blade aerodynamics: The combined experiment [DE94-011866] p 118 N95-18645
- Wind turbine blade aerodynamics: The analysis of field test data [DE94-011867] p 118 N95-18646
- Determination of stores pointing error due to wing flexibility under flight load [NASA-TM-4646] p 134 N95-19044
- The accuracy of parameter estimation in system identification of noisy aircraft load measurement [NASA-CR-197516] p 134 N95-19130
- Brite-Euram programme: ACOUFAT acoustic fatigue and related damage tolerance of advanced composite and metallic structures p 174 N95-19159
- Prediction of fatigue crack growth under flight-simulation loading with the modified CORPUS model p 166 N95-19471
- Development of load spectra for Airbus A330/A340 full scale fatigue tests p 135 N95-19479
- Prediction of rotor-blade deformations due to unsteady airloads [AD-A286593] p 231 N95-20860
- System for determining aerodynamic imbalance [NASA-CASE-ARC-11913-1] p 311 N95-23377
- Review of some results of the author's fatigue investigations with applications in engineering and material science [TAE-698] p 316 N95-23662
- Balances for the measurement of multiple components of force in flows of a millisecond duration p 350 N95-25400
- F/A-18 FOSTP Fatigue test airbag load determination on the vertical and horizontal tails [DSTO-TR-0135] p 388 N95-26389
- Computational analysis of forebody tangential slot blowing on the high alpha research vehicle [NASA-CR-197754] p 389 N95-26591
- Preliminary analysis of dynamic stall effects on a 91-meter wind turbine rotor p 376 N95-27975
- Observed acoustic and aeroelastic spectral responses of a MOD-2 turbine blade to turbulence excitation p 451 N95-27991
- Aeroelasticity and structural optimization of composite helicopter rotor blades with swept tips [NASA-CR-4665] p 397 N95-28262
- Estimation of aerodynamic load distributions on the F/A-18 aircraft using a CFD panel code [DSTO-TR-0147] p 504 N95-29445
- PREDICAT: First order performance calculations of windturbine rotors using the method of the acceleration potential [PB95-206454] p 564 N95-30200
- A novel instrumentation system for measurement of helicopter rotor motions and loads data, phase 1 [AD-A293309] p 607 N95-30923
- Probabilistic reliability modeling of fatigue on the H-46 tie bar [AD-A289926] p 607 N95-30927
- Digital simulation of wind velocities for wind turbine rotors: General considerations [PB95-206447] p 677 N95-31157
- Full-scale hingeless rotor performance and loads [NASA-TM-110356] p 691 N95-32699
- AERODYNAMIC NOISE**
- Comprehensive aeromechanics analysis of complex rotorcraft using 2GCHAS [HTN-94-00695] p 2 A95-60174
- First level release of 2GCHAS for comprehensive helicopter analysis - a status report [HTN-94-00697] p 2 A95-60176
- Active control of wake/blade-row interaction noise [BTN-95-EIX95042474389] p 196 A95-68311
- Vortex shedding noise control in idling circular saws using air ejection at the teeth [BTN-94-EIX94371347214] p 257 A95-69970
- Sound propagation from an arbitrarily oriented multipole placed near a plane, finite impedance surface [BTN-94-EIX94371338964] p 257 A95-70797
- Numerical study of sound generation due to a spinning vortex pair [BTN-95-EIX95182619075] p 307 A95-75760
- Interaction of jet noise with a nearby panel assembly [BTN-95-EIX95262694295] p 434 A95-85466
- An introduction to generalized functions with some applications in aerodynamics and aeroacoustics p 565 A95-88895
- Fan noise reduction from a supersonic inlet during simulated aircraft approach [BTN-95-EIX95292721155] p 572 A95-89894
- Experimental results of the European HELINOISE aeroacoustic rotor test [HTN-95-01080] p 578 A95-90266
- Signal processing of noise data from high-speed flyovers [BTN-95-EIX0619952748178] p 680 A95-94248
- Fan noise research at NASA p 28 N95-11260
- Empirical refinements to boundary layer transition noise models p 28 N95-11262
- Analytical investigation of adaptive control of radiated inlet noise from turbofan engines p 30 N95-11277
- En route noise levels from propfan test assessment airplane [NASA-TP-3451] p 62 N95-12341
- Measurements of atmospheric turbulence effects on tail rotor acoustics [NASA-TM-108843] p 38 N95-12360
- Ducted fan acoustic radiation including the effects of nonuniform mean flow and acoustic treatment [NASA-CR-197449] p 172 N95-16401
- On the Lighthill relationship and sound generation from isotropic turbulence [NASA-CR-195005] p 159 N95-18191
- Active control of fan noise-feasibility study. Volume 1: Flyover system noise studies [NASA-CR-195392-VOL-1] p 258 N95-21888
- Acoustics of laminar boundary layers breakdown p 251 N95-22455
- Supersonic jet noise reductions predicted with increased jet spreading rate [NASA-TM-106872] p 323 N95-23178
- Effects of cavity dimensions, boundary layer, and temperature on cavity noise with emphasis on benchmark data to validate computational aeroacoustic codes [NASA-CR-4653] p 361 N95-24879
- Noise impact of advanced high lift systems [NASA-CR-195028] p 362 N95-26160
- Aircraft noise prediction program theoretical manual: Rotorcraft System Noise Prediction System (ROTONET), part 4 [NASA-TM-83199-PT-4] p 451 N95-26392
- A numerical study of fundamental shock noise mechanisms [NASA-TM-110608] p 451 N95-27908
- Anechoic wind tunnel study of turbulence effects on wind turbine broadband noise p 451 N95-27992
- Noise exposure reduction of advanced high-lift systems [NASA-CR-195077] p 452 N95-28670
- Response of multi-panel assembly to noise from a jet in forward motion [NASA-CR-198164] p 442 N95-28673
- The spectrum and directivity of turbulent mixing noise from supersonic jets p 579 N95-29415
- Turbulent airflow noise production and propagation patterns of a subsonic jet impinging on a flat plate p 580 N95-29502
- Computation of noise radiation from turbofans: A parametric study [NASA-CR-198359] p 710 N95-32836
- Fan noise prediction assessment [NASA-CR-195051] p 711 N95-33831
- Direct analysis of transonic rotor noise with CFD technique p 711 N95-34549
- AERODYNAMIC STABILITY**
- Comprehensive aeromechanics analysis of complex rotorcraft using 2GCHAS [HTN-94-00695] p 2 A95-60174
- First level release of 2GCHAS for comprehensive helicopter analysis - a status report [HTN-94-00697] p 2 A95-60176
- Dynamic stall of an oscillating wing. Part 1: Evaluation of turbulence models [AIAA PAPER 93-3403] p 3 A95-60184
- A generalized algorithm for inverse simulation applied to helicopter maneuvering flight [HTN-95-A0493] p 236 A95-72564
- Air and ground resonance of helicopters with elastically tailored composite rotor blades [HTN-95-A0497] p 222 A95-72568
- Parametric studies for tiltrotor aeroelastic stability in highspeed flight [HTN-95-A0499] p 222 A95-72570
- Analytical study of the neutral stability of a model hypersonic boundary layer [BTN-95-EIX95152577589] p 263 A95-73493
- Navier-Stokes prediction of large-amplitude delta-wing roll oscillations [BTN-95-EIX95152582329] p 281 A95-73531
- Further analysis of high-rate rolling experiments of a 65-deg delta wing [BTN-95-EIX95152582331] p 281 A95-73533
- The influence of alternate inter-blade connections on ground resonance [HTN-95-80859] p 267 A95-75101
- Dynamic investigation of the angular motion of a rotating body-parachute system [BTN-95-EIX95182619220] p 270 A95-76646
- Rotorcraft handling qualities in turbulence [BTN-95-EIX95242670750] p 334 A95-81097
- Direct adaptive and neural control of wing-rock motion of slender delta wings [BTN-95-EIX95242670748] p 327 A95-81099
- Air resonance of hingeless rotor helicopters in trimmed forward flight [HTN-95-61075] p 369 A95-83659
- An analytical model for a nonlinear elastomeric lag damper and its effect on aeromechanical stability in Hover [HTN-95-61076] p 369 A95-83660
- Aerodynamics of delta wings with application to high-alpha flight mechanics p 460 A95-87395
- Measurement of free-flight dynamic stability derivatives of cones in a hypersonic gun tunnel [AIAA PAPER 95-6082] p 519 A95-87411
- Reduced-order nonlinear analysis of aircraft dynamics [BTN-95-EIX95282706665] p 455 A95-89640
- Hubload responses of a rotor in forward flight due to multiple frequency blade pitch variations p 515 A95-91504
- An application of TLS (Total Least Squares) method to estimation of aircraft aerodynamic derivatives p 517 A95-91551
- Some additional stability and performance characteristics of the scissor/pivot wing configurations [SAE PAPER 931383] p 618 A95-93659

- Aeroelastic tailoring research
[PB94-180031] p 6 N95-10135
Add a dimension to your analysis of the helicopter low
airspeed environment
[AD-A283982] p 79 N95-14205
The Aluminum Falcon: A low cost modern commercial
transport
[NASA-CR-197180] p 81 N95-15742
Investigation of dynamic inflow's influence on rotor
control derivatives p 155 N95-16250
A spectrally accurate boundary-layer code for infinite
swept wings
[NASA-CR-195014] p 159 N95-18042
Integrated aerodynamic fin and stowable TVC vane
system
[AD-D016457] p 151 N95-19073
Determination of stability and control derivatives from
the NASA F/A-18 HARV from flight data using the
maximum likelihood method
[NASA-CR-197320] p 204 N95-19576
AIAA Techfest 20 Proceedings
[NIAR-94-1] p 367 N95-26941
An aerodynamic and static-stability analysis of the
Hypersonic Applied Research Technology (HART)
missile
[DA9426923] p 481 N95-29965
Low-speed wind-tunnel investigation of the stability and
control characteristics of a series of flying wings with sweep
angles of 50 deg
[NASA-TM-4640] p 505 N95-30226
Transonic aerodynamic characteristics of a proposed
wing-body reusable launch vehicle concept
[NASA-TM-108489] p 592 N95-30712
Looking for the simple PIO model
p 597 N95-31066
FPCAS3D User's guide: A three dimensional full
potential aeroelastic program, version 1
[NASA-CR-198367] p 651 N95-32205
Full-scale hingeless rotor performance and loads
[NASA-TM-110356] p 691 N95-32699
- AERODYNAMIC STALLING**
Interferometry and computational studies of an
oscillating airfoil compressible dynamic stall flow field
[HTN-94-00703] p 3 A95-60182
Oscillating airfoil compressible dynamic stall studies
[HTN-94-00704] p 3 A95-60183
Dynamic stall of an oscillating wing. Part 1: Evaluation
of turbulence models
[AIAA PAPER 93-3403] p 3 A95-60184
LDV measurements in dynamically separated flows
[ISBN 0-8194-1311-9] p 5 A95-60191
A study of compressibility effects on dynamic stall of
rapidly pitching airfoils
[HTN-94-00715] p 5 A95-60193
Comparison of theory and experiment for non-linear
flutter and stall response of a helicopter blade
[BTN-94-EIX94351108100] p 191 A95-66500
New airfoil-design concept with improved aerodynamic
characteristics
[PAPER-4384] p 230 A95-72585
Computation of the poststall behavior of a circulation
controlled airfoil
[BTN-95-EIX95152582324] p 264 A95-73523
Moving wall effect in relation to other dynamic stall flow
mechanisms
[BTN-95-EIX95152582324] p 265 A95-73527
Dynamic stall control for advanced rotorcraft
application
[BTN-95-EIX95222650793] p 334 A95-79249
Reattachment studies of an oscillating airfoil dynamic
stall flowfield
[HTN-95-51660] p 432 A95-85042
Predicting stall and post-stall behavior of airfoils at low
mach numbers
[BTN-95-EIX95262694297] p 365 A95-85468
Interferometric investigations of compressible dynamic
stall over a transiently pitching airfoil
[HTN-95-42338] p 372 A95-86167
High angle-of-attack airfoil performance improvement by
internal acoustic excitation
[HTN-95-42347] p 372 A95-86176
Techniques for tailoring aircraft stall and post-stall
behavior
[SAE PAPER 931226] p 458 A95-87199
Active boundary-layer control in diffusers
[HTN-95-42580] p 458 A95-87210
Dynamic-stall and structural-modeling effects on
helicopter blade stability with experimental correlation
[HTN-95-81646] p 542 A95-87694
An overview of static and dynamic airfoil performance
[SAE PAPER 931228] p 463 A95-88960
Compressible Navier-Stokes calculations of the flow
over airfoil sections. Comparisons of 1st and 2nd order
turbulence models
[SAE PAPER 932510] p 546 A95-89183
- Collectively variable incidence wingtips for lift control
and reduced gust sensitivity
[HTN-95-92836] p 471 A95-90754
Numerical study of multi-element airfoil aerodynamics
[ISBN 1-879921-01-4] p 587 A95-93750
Control of unsteady separated flow associated with the
dynamic stall of airfoils
[NASA-CR-197024] p 74 N95-14613
Structural effects of unsteady aerodynamic forces on
horizontal-axis wind turbines
[DE94-011863] p 157 N95-16939
Aircraft accident report: Stall and loss of control on final
approach, Atlantic Coast Airlines, Inc./United Express
Flight 6291 Jetstream 4101, N304UE Columbus, OH, 7
January 1994
[PB94-910409] p 123 N95-17646
Numerical simulation of dynamic-stall suppression by
tangential blowing
[AD-A284887] p 120 N95-19110
2-D and 3-D oscillating wing aerodynamics for a range
of angles of attack including stall
[NASA-TM-4632] p 120 N95-19119
Evidence that aerodynamic effects, including dynamic
stall, dictate HAWT structural loads and power generation
in highly transient time frames
[DE94-011865] p 216 N95-19855
Stall precursor study of high frequency data for three
high speed, swept compressor rotors
[AD-A289379] p 406 N95-26878
Horizontal axis wind turbine post stall airfoil
characteristics synthesis
p 376 N95-27974
Preliminary analysis of dynamic stall effects on a
91-meter wind turbine rotor
p 376 N95-27975
Interactions of spanwise and chordwise vorticity
associated with three-dimensional dynamic stall over an
oscillating wing
[AD-A290546] p 477 N95-29091
PIV investigation of compressibility effects on dynamic
stall
p 478 N95-29102
Dynamic stall of a NACA 0012 airfoil in laminar flow
p 479 N95-29243
Pressure based high order TVD methodology for
dynamic stall control
[AD-A290149] p 479 N95-29316
High-and low-frequency dynamics of isolated blades and
rotors with dynamic stall and wake
[AD-A290358] p 503 N95-29322
Validation of the helicopter rotor code HERO
[PB95-198040] p 607 N95-30838
Vorticity dynamics and control of dynamic stall
[AD-A288658] p 620 N95-31400
X-31: A program overview and flight test status
p 609 N95-32013
Control of unsteady separated flow associated with the
dynamic stall of airfoils
[NASA-CR-198972] p 594 N95-32193
Turbulence models in the Navier-Stokes simulation of
airfoil stall
[TRITA-NA-9312] p 705 N95-33059
Numerical simulations of dynamic stall phenomena in
low speed flows
p 685 N95-34546
- AERODYNAMICS**
Turbofan propulsion simulator
[BTN-94-EIX94461290240] p 82 A95-61737
Aircraft model for the AIAA controls design challenge
[BTN-94-EIX9451143921] p 142 A95-64587
Aerodynamic design and calculation of flow around the
plane cascade of turbine
[BTN-94-EIX94481415357] p 104 A95-65347
Behavior of the Johnson-King turbulence model in
axisymmetric supersonic flows
[BTN-94-EIX94441386606] p 183 A95-67337
Powered lift for land and sea
[BTN-95-EIX95041503010] p 192 A95-68313
Aerodynamically blunt and sharp bodies
[BTN-95-EIX95041503781] p 205 A95-69212
Numerical simulation of steady and unsteady,
vorticity-dominated aerodynamic interference
[BTN-95-EIX95062487524] p 186 A95-69232
Numerical simulation of incidence and sweep effects
on delta wing vortex breakdown
[BTN-95-EIX95062487526] p 186 A95-69234
Aerodynamic sensitivity coefficients using the
three-dimensional full potential equation
[BTN-95-EIX95062487530] p 186 A95-69238
Comparison of electrostatic and aerodynamic forces
during parachute opening
[BTN-95-EIX95062487532] p 187 A95-69240
Interpretation of waverider performance data using
computational fluid dynamics
[BTN-95-EIX95062487534] p 193 A95-69242
Aerodynamic characteristics of strake vortex flaps on
a strake-wing configuration
[BTN-95-EIX95062487537] p 187 A95-69245
- Large-scale computational fluid dynamics by the finite
element method
[BTN-94-EIX94381359154] p 243 A95-71744
Mechanical system reliability and risk assessment
[BTN-95-EIX95142553046] p 304 A95-73452
Simulation of turbulent fluctuations
[BTN-95-EIX95142553041] p 304 A95-73457
Laplace interaction law for the computation of viscous
airfoil flow in low- and high-speed aerodynamics
[BTN-95-EIX95142553037] p 263 A95-73461
Preconditioned domain decomposition scheme for
three-dimensional aerodynamic sensitivity analysis
[BTN-95-EIX95152577612] p 321 A95-73471
Shock tunnel measurements of hypervelocity blunted
cone drag
[BTN-95-EIX95152577606] p 305 A95-73477
Eigenanalysis of unsteady flows about airfoils, cascades,
and wings
[BTN-95-EIX95152577597] p 305 A95-73486
Progress in high-lift aerodynamic calculations
[BTN-95-EIX95152582315] p 264 A95-73518
Unstructured grid solutions to a wing/pylon/store
configuration
[BTN-95-EIX95152582322] p 265 A95-73525
Moving wall effect in relation to other dynamic stall flow
mechanisms
[BTN-95-EIX95152582324] p 265 A95-73527
Navier-Stokes prediction of large-amplitude delta-wing
roll oscillations
[BTN-95-EIX95152582329] p 281 A95-73531
Further analysis of high-rate rolling experiments of a
65-deg delta wing
[BTN-95-EIX95152582331] p 281 A95-73533
Pneumatic concept for tip-stall control of cranked-arrow
wings
[BTN-95-EIX95152582335] p 281 A95-73537
Higher-order viscous shock-layer solutions for
high-altitude flows
[BTN-95-EIX95152583255] p 306 A95-73556
Aerodynamic characteristics of a canard-controlled
missile at high angles of attack
[BTN-95-EIX95152583257] p 267 A95-73558
Improved version of the Naval Surface Warfare Center
aeroprediction code (AP93)
[BTN-95-EIX95152583260] p 267 A95-73561
Functional dependence of trajectory dispersion on initial
condition errors
[BTN-95-EIX95152583263] p 298 A95-73564
Supersonic axisymmetric conical flow solutions for
different ratios of specific heats
[BTN-95-EIX95152583283] p 306 A95-73584
Analytical solution for controls, heats, and states of flight
trajectories
[BTN-95-EIX95152583286] p 282 A95-73587
Aerodynamics of the Shuttle Orbiter at high altitudes
[BTN-95-EIX95182617454] p 298 A95-75725
Some aspects of the aerodynamics of separating
strap-ons
[BTN-95-EIX95182617464] p 298 A95-75735
Comparison of linear stability results with flight transition
data
[BTN-95-EIX95182619097] p 283 A95-76582
Aeroelastic vehicle multivariable control synthesis with
analytical robustness evaluation
[BTN-95-EIX95182619115] p 321 A95-76592
Functional agility metrics and optimal trajectory
analysis
[BTN-95-EIX95182619121] p 321 A95-76598
Analytical solution and parameter estimation of projectile
dynamics
[BTN-95-EIX95212645695] p 272 A95-76747
Calculation of wing-alone aerodynamics to high angles
of attack
[BTN-95-EIX95212645713] p 261 A95-76765
Experimental investigation of the flow around a circular
cylinder: Influence of aspect ratio
[BTN-94-EIX95011441120] p 347 A95-80044
Determination of piloting feedback structures for an
altitude tracking task
[BTN-95-EIX95242670770] p 327 A95-81077
Aerodynamic parameters of crop canopies estimated
with a center-of-pressure technique
[HTN-95-41901] p 356 A95-81648
Polar Patrol Balloon system and preliminary
experimental results
p 368 A95-82513
Matrix fraction approach for finite-state aerodynamic
modeling
[BTN-95-EIX95262694311] p 365 A95-85482
Effect of Reynolds number and turbulence on airfoil
aerodynamics at -90-degree incidence
[HTN-95-42320] p 370 A95-86149
Preconditioned domain decomposition scheme for
three-dimensional aerodynamic sensitivity analysis
[HTN-95-42597] p 459 A95-87227

Orbital transport: Technical, meteorological and
 chemical aspects; Aerospace Symposium, 3rd,
 Braunschweig, Germany, Aug. 26-28, 1991
 [ISBN 3-540-563180] p 524 A95-87373
 Design optimization of an airbreathing aerospaceplane
 p 524 A95-87382
 Aerodynamics of delta wings with application to high-
 alpha flight mechanics p 460 A95-87395
 Symposium on Aerodynamics & Aeroacoustics, Tucson,
 AZ, Mar. 1-2, 1993
 [ISBN 981-02-1732-3] p 462 A95-88892
 An introduction to generalized functions with some
 applications in aerodynamics and aeroacoustics
 p 565 A95-88895
 Unsteady aerodynamics of vortical flows: Early and
 recent developments p 462 A95-88896
 Computation of vortex formation over ELAC-1
 configuration using vorticity confinement
 [AIAA PAPER 95-6157] p 470 A95-90469
 Parallel CFD design on network-based computer
 [AIAA PAPER 95-0984] p 565 A95-90656
 Similarity solutions for hypersonic flow past slender
 bodies of revolution at small incidence
 [HTN-95-12195] p 475 A95-91895
 A perspective of rarefied gas flow problems relevant
 to high altitude flight
 [SAE PAPER 931366] p 586 A95-93647
 A design trade study using CFD modeling of reaction
 jets for aerodynamic control
 [SAE PAPER 931384] p 586 A95-93660
 Aerodynamic applications of underexpanded hypersonic
 viscous jets
 [BTN-95-EIX0619952748162] p 589 A95-94456
 Analysis of some interference effects in a transonic wind
 tunnel
 [BTN-95-EIX0619952748166] p 589 A95-94460
 Nonlinear aerodynamic analysis of grid fin
 configurations
 [BTN-95-EIX0619952748172] p 590 A95-94466
 Assessment of technology for aircraft development
 [BTN-95-EIX0619952748181] p 606 A95-94474
 Analysis of low Reynolds number airfoil flows
 [BTN-95-EIX0619952748183] p 590 A95-94476
 Interaction of a weak shock with freestream
 disturbances
 [BTN-95-EIX95332750473] p 638 A95-94687
 Partially implicit method for simulating viscous airfoil
 flows
 [BTN-94-EIX94522406680] p 709 A95-96299
 Computational fluid dynamics uses in fluid
 dynamics/aerodynamics education
 [NASA-TM-108834] p 8 N95-10847
 Potential impacts of advanced aerodynamic technology
 on air transportation system productivity
 [NASA-TM-109154] p 10 N95-11489
 Pressure measurements on an F/A-18 twin vertical tail
 in buffeting flow. Volume 3: Buffet power spectral
 densities
 [AD-A281444] p 36 N95-11829
 Optimum aerodynamic design via boundary control
 [NASA-CR-195882] p 36 N95-11877
 Research in progress in applied mathematics, numerical
 analysis, fluid mechanics, and computer science
 [AD-A284982] p 61 N95-11932
 Flight dynamics of an unmanned aerial vehicle
 [AD-A282259] p 45 N95-12410
 Laws of infrared similitude
 [AD-A282209] p 62 N95-12426
 Activities of the Institute for Aerospace Studies of
 Toronto University p 63 N95-12699
 Mach number control in the High Speed Wind Tunnel
 of NLR
 [PB94-201670] p 53 N95-13243
 A review of 50 years of aerodynamic research with
 NACA/NASA
 [NASA-TM-109163] p 102 N95-13663
 Developments in laser-based diagnostics for wind
 tunnels in the Aeromechanics Division: 1987-1992
 [AD-A283011] p 84 N95-13687
 VUV shock layer radiation in an arc-jet wind tunnel
 experiment p 67 N95-13719
 Scale effects on aircraft and weapon aerodynamics
 [AGARD-AG-323] p 67 N95-14103
 Quality assessment for wind tunnel testing
 [AGARD-AR-304] p 67 N95-14197
 Fourth High Alpha Conference, volume 1
 [NASA-CP-10143-VOL-1] p 67 N95-14229
 Preparations for flight research to evaluate actuated
 forebody strakes on the F-18 high-alpha research
 vehicle p 72 N95-14257
 Computational aerodynamics based on the Euler
 equations
 [AGARD-AG-325] p 72 N95-14264
 Missile Aerodynamics
 [AGARD-R-804] p 73 N95-14445

Aeromechanical design of modern missiles
 p 73 N95-14446
 Engineering Codes for aeroprediction: State-of-the-art
 and new methods p 73 N95-14447
 High angle of attack aerodynamics p 74 N95-14450
 Navier-Stokes predictions of missile aerodynamics
 p 74 N95-14451
 Aero-optics system integration
 [NASA PAPER 94-604] p 100 N95-14638
 The Aluminum Falcon: A low cost modern commercial
 transport p 81 N95-15742
 A workstation based simulator for teaching compressible
 aerodynamics p 170 N95-16906
 Interactive computer graphics applications for
 compressible aerodynamics p 170 N95-17264
 [NASA-TM-106802] p 116 N95-17882
 Low speed propeller slipstream aerodynamic effects
 p 116 N95-17882
 Parachute inflation: A problem in aeroelasticity
 [AD-A284375] p 117 N95-18340
 CFD: Advances and Applications, part 1
 [NAL-SP-9322-PT-1] p 165 N95-19444
 Advanced wind-turbine design studies: Advanced
 conceptual study p 256 N95-20985
 [DE93-000031] p 256 N95-20985
 Aeronautical engineering: A continuing bibliography with
 indexes (supplement 315) p 219 N95-21640
 [NASA-SP-7037(315)] p 219 N95-21640
 Mach 10 computational study of a three-dimensional
 scramjet inlet flow field p 310 N95-23210
 [NASA-TM-4602] p 310 N95-23210
 Aerodynamic design optimization with sensitivity analysis
 and computational fluid dynamics
 [NASA-CR-197419] p 274 N95-23218
 Aerodynamic surface distension system for high angle
 of attack forebody vortex control
 [NASA-CASE-ARC-11979-1] p 286 N95-23390
 Aerodynamic design and analysis of a highly loaded
 turbine exhaust p 312 N95-23435
 Numerical computation of aerodynamics and heat
 transfer in a turbine cascade and a turn-around duct using
 advanced turbulence models p 313 N95-23444
 NTS-spill test facility wind tunnel exhaust plume
 characterization p 297 N95-24019
 [DE95-003630] p 297 N95-24019
 Aeronautical engineering: A continuing bibliography with
 indexes (supplement 316) p 328 N95-24465
 [NASA-SP-7037(316)] p 328 N95-24465
 Aerodynamic parameter estimation via Fourier
 modulating function techniques p 335 N95-24630
 [NASA-CR-4654] p 335 N95-24630
 Using digital filtering techniques as an aid in wind turbine
 data analysis p 357 N95-24853
 [DE94-011862] p 357 N95-24853
 Aeronautical engineering: A continuing bibliography with
 indexes (supplement 317) p 328 N95-25798
 [NASA-SP-7037(317)] p 328 N95-25798
 Cumulative reports and publications through December
 31, 1994 p 361 N95-26085
 [NASA-CR-195043] p 361 N95-26085
 Suppressor of oscillations in airframe cavities
 [AD-D017265] p 388 N95-26507
 Wind-tunnel test of the S814 thick root airfoil
 [DE95-000268] p 376 N95-27541
 Aeronautical engineering: A continuing bibliography with
 indexes (supplement 318) p 367 N95-27543
 [NASA-SP-7037(318)] p 367 N95-27543
 Study of potential aerodynamic benefits from spanwise
 blowing at wingtip p 378 N95-28669
 [NASA-TP-3515] p 378 N95-28669
 A fourth order Euler/Navier-Stokes prediction method
 for the aerodynamics and aeroelasticity of hovering rotor
 blades p 554 N95-29242
 Requirements and trends of computational
 aerodynamics as a tool for aircraft design p 692 N95-34506
 Hypersonic CFD analysis for the aerothermodynamic
 design of HOPE p 684 N95-34520
 Application of CFD technique for HYFLEX aerodynamic
 design p 693 N95-34542
 High order accuracy computational methods in
 aerodynamics using parallel architectures
 [AD-A294167] p 686 N95-34763
AEROELASTIC RESEARCH WINGS
 Structural design optimization with survivability
 dependent constraints application: Primary wing box of a
 multi-role fighter p 398 N95-28440
AEROELASTICITY
 Comprehensive aeromechanics analysis of complex
 rotorcraft using 2GCHAS p 2 A95-60174
 [HTN-94-00695] p 2 A95-60174
 First level release of 2GCHAS for comprehensive
 helicopter analysis - a status report p 2 A95-60176
 [HTN-94-00697] p 2 A95-60176

On the dynamics of aeroelastic oscillators with one
 degree of freedom p 153 A95-64524
 [BTN-94-EIX94501431527] p 153 A95-64524
 Comparison of theory and experiment for non-linear
 flutter and stall response of a helicopter blade
 [BTN-94-EIX94351108100] p 191 A95-66500
 Aeroelastic stability of hingeless rotor blade in hover
 using large deflection theory p 183 A95-67347
 [BTN-94-EIX94441386616] p 183 A95-67347
 Using adaptive structures to attenuate rotary wing
 aeroelastic response p 192 A95-68361
 [BTN-95-EIX95062487547] p 192 A95-68361
 Influence of structural and aerodynamic modeling on
 flutter analysis p 203 A95-68364
 [BTN-95-EIX95062487550] p 203 A95-68364
 Advance finite element modeling of rotor blade
 aeroelasticity p 221 A95-71183
 [HTN-95-31013] p 221 A95-71183
 Air and ground resonance of helicopters with elastically
 tailored composite rotor blades p 222 A95-72568
 [HTN-95-A0497] p 222 A95-72568
 Parametric studies for tiltrotor aeroelastic stability in
 highspeed flight p 222 A95-72570
 [HTN-95-A0499] p 222 A95-72570
 Eigenanalysis of unsteady flows about airfoils, cascades,
 and wings p 305 A95-73486
 [BTN-95-EIX95152577597] p 305 A95-73486
 Efficient sensitivity analysis for rotary-wing
 aeromechanical problems p 264 A95-73497
 [BTN-95-EIX95152577585] p 264 A95-73497
 Limit cycle phenomena in computational transonic
 aeroelasticity p 264 A95-73520
 [BTN-95-EIX95152582317] p 264 A95-73520
 Static aeroelastic characteristics of a composite wing
 [BTN-95-EIX95152582340] p 282 A95-73542
 Flutter of an infinitely long panel in a duct
 [BTN-95-EIX95182619087] p 291 A95-75772
 Aeroelastic vehicle multivariable control synthesis with
 analytical robustness evaluation p 321 A95-76592
 [BTN-95-EIX95182619115] p 321 A95-76592
 Analytical aeropropulsive/aeroelastic
 hypersonic-vehicle model with dynamic analysis
 [BTN-95-EIX95182619138] p 269 A95-76615
 Application of transonic small disturbance theory to the
 active flexible wing model p 270 A95-76636
 [BTN-95-EIX95182619210] p 270 A95-76636
 Application of Navier-Stokes aeroelastic methods to
 improve fighter wing maneuver performance p 284 A95-76644
 [BTN-95-EIX95182619218] p 284 A95-76644
 Multilevel decomposition procedure for efficient design
 optimization of helicopter rotor blades p 334 A95-79240
 [BTN-95-EIX95222650784] p 334 A95-79240
 Fundamental mechanisms of aeroelastic control with
 control surface and strain actuation p 327 A95-81101
 [BTN-95-EIX95242670746] p 327 A95-81101
 Effects of blade tip shape on dynamics, cost, weight,
 aerodynamic performance, and aeroelastic response
 [HTN-95-61074] p 369 A95-83658
 Stress considerations in reduced-size aeroelastic
 optimization p 366 A95-85484
 [BTN-95-EIX95262694313] p 366 A95-85484
 Aeroelastic stability of cascades in turbomachinery
 [HTN-95-61156] p 405 A95-86255
 Aeroelastic response of composite rotor blades
 considering transverse shear and structural damping
 [HTN-95-81647] p 542 A95-87695
 Aeroelastic stability of hingeless rotor blade in hover
 using large deflection theory p 546 A95-88991
 [HTN-95-20952] p 546 A95-88991
 Flight testing of the composite material bearingless rotor
 system for the helicopter p 498 A95-91503
 Hubload responses of a rotor in forward flight due to
 multiple frequency blade pitch variations p 515 A95-91504
 Effects of structural damping on aeroelastic stability of
 various shaped composite plate wing p 530 A95-91530
 [PB94-180031] p 530 A95-91530
 Computer aided static aeroelastic analysis of
 wing/pylon/store combination p 499 A95-91531
 Experiment of the large elastic deformation of biconvex
 wing sections in an air-flow p 475 A95-91564
 Matching fluid and structure meshes for aeroelastic
 computations: a parallel approach p 636 A95-94102
 [BTN-95-EIX95302679864] p 636 A95-94102
 Aeroelastic tailoring research p 6 N95-10135
 [PB94-180049] p 6 N95-10135
 Computations of unsteady aerodynamic loads around
 oscillating wings. Part 1: Formulation p 7 N95-10136
 [PB94-180049] p 7 N95-10136
 Computations of unsteady aerodynamic loads around
 oscillating wings. Part 2: Computed results and
 discussions p 7 N95-10137
 [PB94-180056] p 7 N95-10137

- Flutter analysis of supersonic axial flow cascades using a high resolution Euler solver. Part 1: Formulation and validation
[NASA-TM-105798] p 23 N95-10244
The use of the Regier number in the structural design with flutter constraints
[NASA-TM-109128] p 13 N95-11465
Parallel aeroelastic computations for wing and wing-body configurations
[NASA-CR-196835] p 36 N95-11766
Aeroelastic simulation of higher harmonic control
[NASA-CR-4623] p 37 N95-11911
Studies on the flow induced by an oscillating airfoil in a uniform stream
[PB94-204450] p 40 N95-13250
User's guide for ENSAERO: A multidisciplinary program for fluid/structural/control interaction studies of aircraft (release 1)
[NASA-TM-108853] p 65 N95-13662
Development and application of structural dynamics analysis capabilities
[NASA-CR-197229] p 96 N95-14922
Prediction of rotor-blade deformations due to unsteady airloads
[AD-A284467] p 81 N95-15821
Measurements of unsteady pressure and structural response for an elastic supercritical wing
[NASA-TP-3443] p 104 N95-16560
FPCAS2D user's guide, version 1.0
[NASA-CR-195413] p 156 N95-16588
Parachute inflation: A problem in aeroelasticity
[AD-A284375] p 117 N95-18340
A linear system identification and validation of an AH-64 Apache aeroelastic simulation model
p 146 N95-18903
Unsteady aerodynamic analyses for turbomachinery aeroelastic predictions
p 141 N95-19381
Prediction of rotor-blade deformations due to unsteady airloads
[AD-A286593] p 231 N95-20860
High-performance parallel analysis of coupled problems for aircraft propulsion
[NASA-CR-197440] p 289 N95-23088
Flutter analysis of composite box beams
[NASA-CR-197931] p 294 N95-23392
User's guide for ECAP2D: An Euler unsteady aerodynamic and aeroelastic analysis program for two dimensional oscillating cascades, version 1.0
[NASA-CR-189146] p 316 N95-24189
A non-iterative grid deformation algorithm for computational fluid dynamics for aeroelasticity
[AD-A288298] p 436 N95-26418
Aeroelasticity of wing and wing-body configurations on parallel computers
[NASA-CR-197756] p 389 N95-26590
Aeroelastic stability of wind turbine blade/aileron systems
p 377 N95-27981
Observed acoustic and aeroelastic spectral responses of a MOD-2 turbine blade to turbulence excitation
p 451 N95-27991
Aeroelasticity and structural optimization of composite helicopter rotor blades with swept tips
[NASA-CR-4665] p 397 N95-28262
Unique considerations in the design and experimental evaluation of tailored wings with elastically produced chordwise camber
p 423 N95-28436
Nonlinear dynamics and aeroelasticity of rotorcraft in forward flight
[AD-A291714] p 400 N95-28504
A fourth order Euler/Navier-Stokes prediction method for the aerodynamics and aeroelasticity of hovering rotor blades
p 554 N95-29242
Aeroelastic pilot-in-the-loop oscillations
p 598 N95-31070
Performance improvement of composite wings through aeroelastic tailoring and modern control
[AD-A293689] p 608 N95-31602
Vibration reduction in helicopter rotors using an actively controlled partial span trailing edge flap located on the blade
p 624 N95-32111
FPCAS3D User's guide: A three dimensional full potential aeroelastic program, version 1
[NASA-CR-198367] p 651 N95-32205
Full-scale hingeless rotor performance and loads
[NASA-TM-110356] p 691 N95-32699
Development of a composite tailoring procedure for airplane wing
[NASA-CR-199081] p 691 N95-32928
Analysis and design methodology for chordwise deformable wings
p 692 N95-33311
- AEROMANEUVERING**
Numerical optimization of synergetic maneuvers
[AD-A283398] p 109 N95-17435
- AERONAUTICAL ENGINEERING**
Flight simulation
[BTN-94-EIX94461290242] p 84 A95-61735
- Calculation of geometry of stamps with small allowances for pieces of the aerodynamic profile
[BTN-94-EIX94461408772] p 103 A95-63655
Vortex drift: A historical survey
p 455 A95-88897
Dryden summer 1994 update
[NASA-TM-104305] p 33 N95-10750
Aeronautics and space technology, past, present, and future
p 35 N95-11892
AGARD highlights 94/2
[AGARD-HIGHLIGHTS-94/2] p 102 N95-13640
Artificial intelligence with applications for aircraft
[DOT/FAA/CT-94/41] p 99 N95-13895
Aeronautical engineering: A continuing bibliography with indexes (supplement 315)
[NASA-SP-7037(315)] p 219 N95-21640
Research and Technology, 1994
[NASA-TM-106764] p 262 N95-24025
Aeronautical engineering: A continuing bibliography with indexes (supplement 316)
[NASA-SP-7037(316)] p 328 N95-24465
JPRS report: Science and technology, Central Eurasia
[JPRS-UST-94-027] p 349 N95-24470
JPRS report: Science and technology, Central Eurasia
[JPRS-UST-94-018] p 349 N95-24472
Aeronautical engineering: A continuing bibliography with indexes (supplement 317)
[NASA-SP-7037(317)] p 328 N95-25798
Asian Aeronautics: Technology acquisition drives industry development. Report to Congressional requesters
[GAO/NSIAD-94-140] p 367 N95-26817
The noise reduction potential of dual-stream coaxial rectangular improperly expanded jet flows
[NASA-CR-197820] p 437 N95-26995
Aeronautical engineering: A continuing bibliography with indexes (supplement 318)
[NASA-SP-7037(318)] p 367 N95-27543
A review of Australian and New Zealand investigations on aeronautical fatigue during the period Apr. 1993 - Mar. 1995
[AR-009-202] p 397 N95-27918
JTTC/WTEC annual report and program summary: 1993/94
[NASA-CR-198563] p 454 N95-28038
Role of computational fluid dynamics in aeronautical engineering. Number 12: Formulation and verification of uni-particle upwind schemes for the Euler equations
p 707 N95-34540
- AERONAUTICAL SATELLITES**
Development of aeronautical mobile satellite services over the past thirty years
[BTN-95-EIX95152569458] p 305 A95-73498
- AERONAUTICS**
Proceedings of the FAA Inspection Program Area Review
[AD-A283849] p 77 N95-14350
Research and technology highlights, 1993
[NASA-TM-4575] p 102 N95-15065
NASA video catalog
[NASA-SP-7109(01)] p 363 N95-24238
Aeronautical engineering: A continuing bibliography with indexes (supplement 316)
[NASA-SP-7037(316)] p 328 N95-24465
Research and Technology Objectives and Plans Summary (RTOPS)
[NASA-TM-108574] p 453 N95-28002
Aeronautics and space report of the President
[NASA-TM-110743] p 681 N95-31979
AGARD index of publications: 1992-1994
[AGARD-INDEX-92-94] p 711 N95-33198
- AEROSERVOELASTICITY**
Continuous gust response and sensitivity derivatives using state-space models
[BTN-95-EIX95062487551] p 203 A95-68365
Simulation and model reduction for the active flexible wing program
[BTN-95-EIX95182619211] p 295 A95-76637
Aeroservoelastic aspects of wing/control surface platform shape optimization
[BTN-95-EIX9522650795] p 340 A95-79251
Unsteady aerodynamic effects of trailing edge controls on delta wings
[HTN-95-01099] p 469 A95-90285
Aeroservoelastic coupling on the UF-104 aircraft
p 517 A95-91561
Flight control systems/structural coupling BAe Warton experience in aero-servo elasticity
[CONGRESS PAPER C428-35-059] p 610 A95-93628
- AEROSOLS**
Three-dimensional model interpretation of NO(x) measurements from the lower stratosphere
[HTN-95-90534] p 213 A95-67806
- Performance of a focused cavity aerosol spectrometer for measurements in the stratosphere of particle size in the 0.06-2.0-micrometer-diameter range
[HTN-95-90914] p 253 A95-72423
Microphysical and radiative properties of small cumulus clouds over the sea
[HTN-95-A0526] p 255 A95-73180
On the link between cloud-top radiative properties and sub-cloud aerosol concentrations
[HTN-95-A0527] p 255 A95-73181
Effects on stratospheric ozone from high-speed civil transport: Sensitivity to stratospheric aerosol loading
[HTN-95-91842] p 354 A95-80830
High-speed civil transport impact: Role of sulfate, nitric acid trihydrate, and ice aerosols studied with a two-dimensional model including aerosol physics
[HTN-95-91843] p 354 A95-80831
Potential effects on ozone of future supersonic aircraft/2D simulation
[HTN-95-51282] p 356 A95-80867
Impact on ozone of high-speed stratospheric aircraft: Effects of the emission scenario
[HTN-95-51283] p 356 A95-80868
Effects of a polar stratosphere cloud parameterization on ozone depletion due to stratospheric aircraft in a two-dimensional model
[HTN-95-A1038] p 443 A95-84543
Two dimensional stratospheric aerosol distributions during EASOE
[HTN-95-00726] p 444 A95-86296
Airborne measurements during the Arctic stratospheric experiment: Observation of O3 and NO2
[HTN-95-00748] p 445 A95-86318
Modeling aerosol emissions from the combustion of composite materials
p 301 N95-23038
The atmospheric effects of stratospheric aircraft: A fourth program report
[NASA-RP-1359] p 357 N95-24274
Transport phenomena and interfacial kinetics in multiphase combustion systems
[AD-A288297] p 418 N95-26417
Remote sensing of smoke, clouds, and radiation using AVIRIS during SCAR experiments
p 708 N95-33749
- AEROSPACE ENGINEERING**
AIAA Computing in Aerospace 10, San Antonio, TX, March 28-30, 1995
[ISBN 1-56347-119-1] p 565 A95-90629
Trends in aerospace forgings in the 1990s
[HTN-95-B0408] p 456 A95-90756
Algorithmic trends in CFD in the 1990's for aerospace flow field calculations
p 550 A95-91917
Propulsion education at Carlton University
[SAE PAPER 931391] p 613 A95-93667
Lean manufacturing for lean times
[BTN-95-EIX95302730538] p 583 A95-94036
Activities of Mitsubishi Heavy Industries Ltd.
[PB94-179694] p 22 N95-10085
Aeronautics and space technology, past, present, and future
p 35 N95-11892
Activities of the Institute for Aerospace Studies of Toronto University
p 63 N95-12699
A review of 50 years of aerodynamic research with NACA/NASA
[NASA-TM-109163] p 102 N95-13663
Optimum Design Methods for Aerodynamics
[AGARD-R-803] p 127 N95-16562
Tools for applied engineering optimization
p 128 N95-16570
NASA High Performance Computing and Communications program
[NASA-TM-4653] p 176 N95-18573
NASA Lewis Research Center Workshop on Forced Response in Turbomachinery
[NASA-CP-10147] p 141 N95-19380
Research and Technology, 1994
[NASA-TM-106764] p 262 N95-24025
NASA-UVA light aerospace alloy and structures technology program (LA2ST)
[NASA-CR-198041] p 343 N95-24220
NASA video catalog
[NASA-SP-7109(01)] p 363 N95-24238
High-stakes aviation: US-Japan technology linkages in transport aircraft
[LC-94-65759] p 381 N95-27907
Research and Technology Objectives and Plans Summary (RTOPS)
[NASA-TM-108574] p 453 N95-28002
Probabilistic design of advanced composite structure
p 424 N95-28443
Probabilistic evaluation of fuselage-type composite structures
p 398 N95-28444
Surface Modeling, Grid Generation, and Related Issues in Computational Fluid Dynamic (CFD) Solutions
[NASA-CP-3291] p 476 N95-28723
Requirements for effective use of CFD in aerospace design
p 551 N95-28725

Block-structured grids for complex aerodynamic configurations: Current status p 551 N95-28736

An unstructured-grid software system for solving complex aerodynamic problems p 476 N95-28743

Design, analysis and control of large transports so that control of engine thrust can be used as a back-up of the primary flight controls
[NASA-CR-198958] p 518 N95-30254

Manual for a workstation-based generic flight simulation program (LaRCsim), version 1.4
[NASA-TM-110164] p 518 N95-30327

Developing a workstation-based, real-time simulation for rapid handling qualities evaluations during design
[NASA-CR-198831] p 505 N95-30335

Flight Vehicle Integration Panel Workshop on Pilot Induced Oscillations
[AGARD-AR-335] p 597 N95-31061

AGARD index of publications: 1992-1994
[AGARD-INDEX-92-94] p 711 N95-33198

AEROSPACE INDUSTRY

Overview of AlliedSignal's avionics development in the CIS
[BTN-95-EIX95212641069] p 287 A95-76734

International cooperation in standardization
p 452 A95-82665

A new paradigm: The investment casting cooperative arrangement
[HTN-95-92510] p 539 A95-87330

Changing MRP Systems within the aerospace industry
[CONGRESS PAPER C428-26-051] p 681 A95-93603

A study of software standards used in the avionics industry p 137 N95-16456

The global aircraft shape p 128 N95-16571

Review of the EUROPT Project AERO-0026 p 129 N95-16573

Military aviation maintenance industry in Western Europe: Concentration and internationalization
[PB94-189180] p 104 N95-17451

European aeronautics: Strong government presence in industry structure and research and development support. Report to Congressional Requesters
[GAO/NSIAD-94-71] p 176 N95-18578

Asian Aeronautics: Technology acquisition drives industry development. Report to Congressional requesters
[GAO/NSIAD-94-140] p 367 N95-26817

High-stakes aviation: US-Japan technology linkages in transport aircraft p 381 N95-27907

Surface Modeling, Grid Generation, and Related Issues in Computational Fluid Dynamic (CFD) Solutions
[NASA-CP-3291] p 476 N95-28723

AEROSPACE MEDICINE

The performance of child restraint devices in transport airplane passenger seats
[DOT/FAA/AM-94/19] p 40 N95-12146

A surgical support system for Space Station Freedom p 149 N95-16776

AEROSPACE PLANES

An advanced scramjet propulsion concept for A 350 MG SSTO space plane p 402 A95-82325

Test results on air turbo ramjet engine for a future space plane p 402 A95-82327

R & D on HOPE structure p 413 A95-82355

Research and development of thermal protection system of HOPE re-entry vehicle p 413 A95-82358

Hypersonic trajectory control of aerospace plane with integrated SCRAMJET engine p 413 A95-82384

Air data sensors for atmospheric reentry flight test of winged space vehicle p 413 A95-82412

Hypersonic thermal protection with mass injection at angle of attack p 414 A95-82414

Experiment and analysis on heat transfer of a scramjet leading edge model p 403 A95-82420

Orbital transport: Technical, meteorological and chemical aspects; Aerospace Symposium, 3rd, Braunschweig, Germany, Aug. 26-28, 1991
[ISBN 3-540-563180] p 524 A95-87373

Environmental aspects of Orbital transport: p 559 A95-87377

Design optimization of an airbreathing aerospaceplane p 524 A95-87382

The Methane-Acetylene Cycle Aerospace Plane: A potential option for inexpensive Earth to orbit transportation
[HTN-95-51845] p 525 A95-87483

Numerical simulation of real gas effects and aerodynamic heating of hypersonic space transportation vehicles p 540 A95-87558

The effect of wing sweep back upon transition in hypersonic flow
[AIAA PAPER 95-6090] p 466 A95-89199

Computation of vortex formation over ELAC-1 configuration using vorticity confinement
[AIAA PAPER 95-6157] p 470 A95-90469

Flight test of STS radio controlled scale model p 499 A95-91539

Guidance and control of HOPE and its future technologies p 506 A95-91543

Cooling of aerospace plane using liquid hydrogen and methane
[BTN-95-EIX0619952748171] p 590 A95-94465

Aero-Space Plane: Flexible access to space
[NASA-TM-109904] p 22 N95-10553

A simple analytical aerodynamic model of Langley Winged-Cone Aerospace Plane concept
[NASA-CR-194987] p 54 N95-12175

Thermoacoustic environments to simulate reentry conditions p 86 N95-14096

Air-breathing aerospace plane development essential: Hypersonic propulsion flight tests
[NASA-TM-108857] p 66 N95-14921

Measurements of longitudinal static aerodynamic coefficients by the cable mount system
[NAL-TR-1226] p 331 N95-25761

Computation of the integrated aerodynamic and propulsive flowfields of a generic hypersonic space plane p 481 N95-29788

Computations of low speed flow about space-plane
p 685 N95-34544

AEROSPACE SAFETY

Evolving standards for safety critical software
[CONGRESS PAPER C428-24-142] p 678 A95-93595

Dependable software - the state of the art
[CONGRESS PAPER C428-24-212] p 678 A95-93596

Development of software for safety critical applications for the EH101 Helicopter
[CONGRESS PAPER C428-24-160] p 678 A95-93597

Independent review of Aviation Technology and Research Information Analysis System (ATRIAS) database
[AD-A284049] p 226 N95-21518

AEROSPACE SCIENCES

NASA video catalog
[NASA-SP-7109(01)] p 363 N95-24238

NAS Technical Summaries, March 1993 - February 1994
[NASA-RP-1355] p 453 N95-27367

Research and Technology Objectives and Plans Summary (RTOPS)
[NASA-TM-108574] p 453 N95-28002

Aeronautics and space report of the President
[NASA-TM-110743] p 681 N95-31979

AEROSPACE SYSTEMS

Lightweight, opto-electronic engine control system for aerospace turbine engines
[SAE PAPER 931442] p 614 A95-93692

Activities of the Structures Division, Lewis Research Center
[NASA-TM-108081] p 59 N95-13235

Conference on Aerospace Transparent Materials and Enclosures, volume 1
[AD-A283925] p 133 N95-18677

Design and evaluation of a LQR controller for the bluebird unmanned air vehicle
[AD-A289769] p 504 N95-29457

Computational methods for control and optimal design of aerospace systems
[AD-A292861] p 608 N95-31451

AEROSPACE TECHNOLOGY TRANSFER

Reliability and maintainability
[BTN-95-EIX95042477109] p 179 A95-68350

National AeroSpace Plane: Technology transfer
[BTN-95-EIX95072498879] p 180 A95-68395

AGARD highlights 94/2
[AGARD-HIGHLIGHTS-94/2] p 102 N95-13640

Revitalizing general aviation
[NASA-TM-110113] p 129 N95-16982

AEROSPACE VEHICLES

Application of the multigrid solution technique to hypersonic entry vehicles
[BTN-95-EIX95152583254] p 306 A95-73555

Integrated design of hypersonic waveriders including inlets and tailfins
[BTN-95-EIX95212645692] p 271 A95-76744

GPS modeling for designing aerospace vehicle navigation systems
[BTN-95-EIX95302731223] p 600 A95-94044

Prediction of airplane states
[BTN-95-EIX0619952748174] p 584 A95-94468

Aerodynamic shape optimization of a HSCT type configuration with improved surface definition
[NASA-CR-197011] p 67 N95-13701

Development and application of structural dynamics analysis capabilities
[NASA-CR-197229] p 96 N95-14922

Environmental effects on composite airframes: A study conducted for the ARM UAV Program (Atmospheric Radiation Measurement Unmanned Aerospace Vehicle)
[DE94-015351] p 206 N95-19579

Moving mass trim control for aerospace vehicles
[DE95-002602] p 299 N95-23532

Environmentally regulated aerospace coatings p 631 N95-31775

AEROTHERMOCHEMISTRY

Computation of nonequilibrium viscous flows in arc-jet wind tunnel nozzles
[AIAA PAPER 94-0254] p 2 A95-60173

Improved analytical solution for varying specific heat parallel stream mixing
[BTN-94-EIX94481415349] p 103 A95-65339

Review of numerical procedures for computational surface thermochemistry
[BTN-94-EIX94441386682] p 205 A95-68191

Thermochemical nonequilibrium viscous shock-layer analysis for a Mars aerocapture vehicle
[BTN-95-EIX95082502732] p 239 A95-70139

Hypersonic nonequilibrium Navier-Stokes solutions over an ablating graphite nosetip
[BTN-95-EIX95152583252] p 305 A95-73553

VSL analysis of hypersonic flows around a reentry vehicle with equilibrium air chemistry p 413 A95-82400

NAL aerothermodynamic probing and CFD verification mission in OREX experiment p 368 A95-82413

The aerothermodynamic validation reentry experiment HYPERBA p 524 A95-87380

Surface modeling and grid generation for aeropropulsion CFD p 551 N95-28732

AEROTHERMODYNAMICS

Multiblock analysis for Shuttle Orbiter reentry heating from Mach 24 to Mach 12
[BTN-95-EIX95041503780] p 205 A95-69211

Thermochemical nonequilibrium viscous shock-layer analysis for a Mars aerocapture vehicle
[BTN-95-EIX95082502732] p 239 A95-70139

Adaptive remeshing for convective heat transfer with variable fluid properties
[BTN-95-EIX95082502720] p 243 A95-71033

Hypersonic nonequilibrium Navier-Stokes solutions over an ablating graphite nosetip
[BTN-95-EIX95152583252] p 305 A95-73553

Hypersonic convective heat transfer over 140-deg blunt cones in different gases
[BTN-95-EIX95152583253] p 306 A95-73554

NAL aerothermodynamic probing and CFD verification mission in OREX experiment p 368 A95-82413

An experimental study on radiation from strong shock layer p 368 A95-82421

A conceptual design of hypersonic research vehicle with subscale scramjet engine p 384 A95-82482

Aero-thermodynamic flight environment at HITEN aerobrake experiment p 415 A95-82554

High temperature aspects of the European Hermes programs p 524 A95-87379

The aerothermodynamic validation reentry experiment HYPERBA p 524 A95-87380

Integrated thermal and mechanical analysis of hypersonic vehicles by using adaptive finite element methods p 524 A95-87383

Numerical modeling and simulation of chemically reacting reentry flows p 525 A95-87387

Reentry trajectories and their optimization by an evolution algorithm p 525 A95-87394

Chemical recombination in an expansion tube
[HTN-95-20844] p 544 A95-88105

Experimental investigation on aerothermodynamic characteristics of hypersonic transport p 473 A95-91525

Evaluation of a multigrid-based Navier-Stokes solver for aerothermodynamic computations
[BTN-95-EIX95302694459] p 583 A95-94056

Enhancements to integral solutions to ablation and charring
[BTN-95-EIX95302694461] p 636 A95-94058

Visualization of one-dimensional flow processes in a dual-mode scramjet engine p 15 N95-10465

Test model designs for advanced refractory ceramic materials p 55 N95-11968

Planetary entry experiments
[NASA-CR-194215] p 101 N95-13717

Science objectives and performance of a radiometer and window design for atmospheric entry experiments p 85 N95-13718

Thermoacoustic environments to simulate reentry conditions p 86 N95-14096

An approximate Riemann solver for thermal and chemical nonequilibrium flows
[NASA-CR-195003] p 96 N95-14912

- Laminar and turbulent flow computations of Type 4 shock-shock interference aerothermal loads using unstructured grids
[NASA-CR-195008] p 97 N95-15604
A model for preliminary facility design including simulation issues p 144 N95-16318
Hypersonic wind tunnel test techniques
[AD-A284057] p 118 N95-18663
Design and operation of a thermoacoustic test facility p 147 N95-19150
Thermo-acoustic fatigue design for hypersonic vehicle skin panels p 162 N95-19161
Aero-thermodynamic distortion induced structured dynamic response
[AD-A279931] p 203 N95-19864
Experimental study of vane heat transfer and aerodynamics at elevated levels of turbulence
[NASA-CR-4633] p 244 N95-19912
A computer code (SKINTEMP) for predicting transient missile and aircraft heat transfer characteristics
[AD-A286044] p 248 N95-21001
DSMC calculations for 70-deg blunted cone at 3.2 km/s in nitrogen
[NASA-TM-109181] p 348 N95-24396
Viscous shock-layer analysis on hypersonic flow over reentry capsule with nonequilibrium chemistry
[ISAS-656] p 436 N95-26739
Bibliography of Doctor Chul Park
[NASA-TM-110353] p 527 N95-29351
The 1995 version of the NSWC aeroprediction code. Part 1: Summary of new theoretical methodology
[AD-A291518] p 481 N95-29853
Special publication of National Aerospace Laboratory [NAL-SP-27] p 684 N95-34505
Hypersonic CFD analysis for the aerothermodynamic design of HOPE p 684 N95-34520
- AEROZINE**
Regenerative cooling for liquid propellant rocket thrust chambers
[INPE-5565-TDI/540] p 150 N95-18720
- AFTERBODIES**
Experimental investigation of the flowfield about an upswept afterbody
[BTN-95-EIX95152582321] p 265 A95-73524
Supersonic near-wake afterbody boattailing effects on axisymmetric bodies
[BTN-95-EIX95182617465] p 268 A95-75736
Experimental and numerical analysis of a two-duct nozzle/afterbody model at supersonic Mach numbers [AIAA PAPER 95-6085] p 490 A95-87414
Supersonic, turbulent flow computation and drag optimization for axisymmetric afterbodies
[BTN-95-EIX95302729772] p 637 A95-94134
Supersonic base flow investigation over axisymmetric afterbodies
[PB94-180957] p 39 N95-12578
An investigation of the transonic pressure drag coefficient for axisymmetric bodies
[AD-A280990] p 105 N95-15994
Single-engine tail interference model
p 115 N95-17879
Twin engine afterbody model p 115 N95-17880
Numerical computations of supersonic base flow with special emphasis on turbulence modeling
[AD-A283688] p 119 N95-18670
Transonic and supersonic flowfield measurements about axisymmetric afterbodies for validation of advanced CFD codes p 121 N95-19260
Experimental results for a hypersonic nozzle/afterbody flow field
[NASA-TM-4638] p 274 N95-23250
Validation of a Computational Fluid Dynamics (CFD) code for supersonic axisymmetric base flow p 315 N95-23652
Validation of the NPARC code for nozzle afterbody flows at transonic speeds
[NASA-TM-106971] p 592 N95-30704
Afterbody/nozzle pressure distributions of a twin-tail twin-engine fighter with axisymmetric nozzles at Mach numbers from 0.6 to 1.2
[NASA-TP-3509] p 594 N95-31984
- AFTERBURNING**
Single-engine tail interference model p 115 N95-17879
- AGGLOMERATION**
Agglomeration multigrad for viscous turbulent flows
[AD-A284064] p 8 N95-10848
- AGGREGATES**
Marginal aggregates in flexible pavements: Background survey and experimental plan
[DOT/FAA/CT-94/58] p 53 N95-12216
- AGING (MATERIALS)**
Corrosion prevention and control
[BTN-95-EIX95031502753] p 188 A95-68260
USAF aging aircraft program
[BTN-95-EIX95072498878] p 180 A95-68394
- FAA's Aging Commuter Airplane Program
[SAE PAPER 931248] p 483 A95-89220
Ageing aircraft after ALOHA
[CONGRESS PAPER C428-11-188] p 484 A95-91701
Structural integrity of fuselage panels with multisite damage
[BTN-95-EIX0619952748188] p 637 A95-94250
Additives in bituminous materials and fuel-resistant sealers
[DOT/FAA/CT-94/78] p 55 N95-12131
Hypervelocity Impact Test Facility: A gun for hire
[TABES PAPER 94-605] p 86 N95-14639
Problems with aging wiring in Naval aircraft p 154 N95-16048
Oklahoma City air logistics center (USAF) aging aircraft corrosion program p 262 N95-23519
Proceedings of the 2d USAF Aging Aircraft Conference
[AD-A288217] p 336 N95-25578
- AGREEMENTS**
A new paradigm: The investment casting cooperative arrangement
[HTN-95-92510] p 539 A95-87330
A status report on the development of the Federal Aviation Administration/National Oceanic and Atmospheric Administration Memorandum of Agreement p 652 A95-93447
- AGRICULTURAL AIRCRAFT**
Conversion of production automotive engines for aviation use
[SAE PAPER 932606] p 495 A95-90076
- AGRICULTURE**
MAX-91: Polarimetric SAR results on Montespertoli site p 320 N95-23940
- AH-64 HELICOPTER**
Design optimization of rotor blades for improved performance and vibration
[HTN-95-A0498] p 229 A95-72569
Identification and simulation evaluation of a combat helicopter in hover
[BTN-95-EIX95242670749] p 335 A95-81098
The assessment of the AH-64D, longbow, mast-mounted assembly noise hazard for maintenance personnel
[AD-A284971] p 171 N95-16226
A linear system identification and validation of an AH-64 Apache aeroelastic simulation model p 146 N95-18903
Using the backward transfer paradigm to validate the AH-64 Simulator Training Research Advanced Testbed for Aviation
[AD-A285758] p 238 N95-19931
Development and validation of a blade-element mathematical model for the AH-64A Apache helicopter
[NASA-TM-108863] p 367 N95-26710
Army aviation: Modernization strategy needs to be reassessed. Report to Congressional requestors
[GAO/NSIAD-95-9] p 683 N95-32783
- AILERONS**
Second generation smart actuator
[SAE PAPER 932585] p 505 A95-90069
2-D aileron effectiveness study p 110 N95-17851
Full span flaperons for a biplane p 391 N95-26954
Comparative wind tunnel test at high Reynolds numbers of NACA 64 621 airfoils with two aileron configurations p 377 N95-27977
Aeroelastic stability of wind turbine blade/aileron systems p 377 N95-27981
- AIR**
Ignition analysis of hydrogen/air mixture in supersonic mixing layer p 416 A95-82301
Hypersonic thermal protection with mass injection at angle of attack p 414 A95-82414
Stationary premixed flames in spherical and cylindrical geometries p 418 A95-86165
Flowfield measurements in supersonic film cooling including the effect of shock-wave interaction
[HTN-95-42337] p 405 A95-86166
Linear disturbances in hypersonic, chemically reacting shock layers
[HTN-95-20931] p 464 A95-88970
Airborne rotary air separator study
[NASA-CR-189099] p 290 N95-24053
- AIR BAG RESTRAINT DEVICES**
F/A-18 IPOSTP Fatigue test airbag load determination on the vertical and horizontal tails
[DSTO-TR-0135] p 388 N95-26389
Biodynamic simulation of pilot interaction with a helicopter multi-airbag restraint system
[AD-A290196] p 485 N95-29057
- AIR BREATHING ENGINES**
Computational study of plume-induced separation on a hypersonic powered model
[BTN-95-EIX95152582346] p 266 A95-73548
- Modeling of plume chemistry of high flying aircraft with H2 combustion engines p 509 A95-87405
Testing the hypersonic technology demonstration nozzle: Results from the test campaign 1993/94
[AIAA PAPER 95-6084] p 509 A95-87413
Integration of an hypersonic airbreathing vehicle: Assessment of overall aerodynamic performances and of uncertainties p 492 A95-88007
[AIAA PAPER 95-6100] p 492 A95-88007
Chemically reacting non-equilibrium boundary layers in air breathing propulsion systems p 512 A95-90456
[AIAA PAPER 95-6139] p 512 A95-90456
Application of scramjet engine technology to the design of ram accelerator projectiles p 19 N95-10282
Shock-tunnel combustor testing for hypersonic vehicles
[NASA-CR-196836] p 52 N95-11938
AFOSR Contractors Meeting in Propulsion
[AD-A282729] p 54 N95-12507
A graphical user interface for design and analysis of air breathing propulsion systems p 83 N95-14645
[TABES PAPER 94-616] p 83 N95-14645
Hypersonic air-breathing aer propulsion facility test support requirements p 144 N95-16319
Airborne rotary air separator study
[NASA-CR-189099] p 290 N95-24053
- AIR CARGO**
The effect of rotating loads suspended under a helicopter on their amplitude-frequency characteristics
[BTN-94-EIX94461407959] p 78 A95-62633
Design of a high capacity long range cargo aircraft
[NASA-CR-197176] p 45 N95-12363
Transport aircraft loading and balancing system: Using a CLIPS expert system for military aircraft load planning p 217 N95-19751
Incorporating biplane wing theory into a large, subsonic, all-cargo transport p 391 N95-26956
Enplanement and all cargo activity
[AD-A280074] p 412 N95-28151
- AIR CONDITIONING EQUIPMENT**
Condensing cycle air conditioning system
[SAE PAPER 932056] p 513 A95-91637
- AIR COOLING**
Evaluation of thermal barrier and PS-200 self-lubricating coatings in an air-cooled rotary engine
[NASA-CR-195445] p 289 N95-23222
Static pressure drop by swirling flow of an internal cooling air system through a turbine shaft p 698 N95-34560
- AIR CURRENTS**
Advanced diesel electronic fuel injection and turbocharging
[AD-A279176] p 211 N95-19809
- AIR DATA SYSTEMS**
Air data prediction from surface pressure measurements on guided munitions
[BTN-95-EIX95282706664] p 466 A95-89641
Response of the B-1B air data sensor to simulated dust cloud environments
[AD-A286134] p 235 N95-22036
- AIR DROP OPERATIONS**
Radial reefing method for accelerated and controlled parachute opening
[BTN-95-EIX95062487539] p 187 A95-69247
- AIR DUCTS**
Condensation in jet engine intake ducts during stationary operation
[BTN-95-EIX95292721154] p 612 A95-92590
An investigation of the side-dump dual in-line ramjet combustor p 617 N95-31199
Computation of noise radiation from turbofans: A parametric study
[NASA-CR-198359] p 710 N95-32836
- AIR FILTERS**
Erosion of dust-filtered helicopter turbine engines. Part 2: Erosion reduction
[BTN-95-EIX95182619223] p 289 A95-76649
Life prediction of helicopter engines fitted with dust filters
[BTN-95-EIX95182619224] p 289 A95-76650
Airborne rotary air separator study
[NASA-CR-189099] p 290 N95-24053
- AIR FLOW**
Vortex shedding noise control in idling circular saws using air ejection at the teeth
[BTN-94-EIX94371347214] p 257 A95-69970
Simulation of transverse gas injection in turbulent supersonic air flows p 269 A95-75765
[BTN-95-EIX95182619080] p 269 A95-75765
Tracking of raindrops in flow over an airfoil
[BTN-95-EIX95182619221] p 308 A95-76647
Pressure and temperature distortion testing of a two-stage centrifugal compressor
[BTN-94-EIX95011441250] p 431 A95-84207
Compressible Navier-Stokes computations of multielement airfoil flows using multiblock grids
[HTN-95-42327] p 371 A95-86156

- Nonreflective boundary conditions for high-order methods
[HTN-95-42328] p 371 A95-86157
- General solution procedure for flows in local chemical equilibrium
[HTN-95-42329] p 404 A95-86158
- Structure of a swirl-stabilized, combustor spray
[NASA-TM-106724] p 50 N95-11890
- Impingement flow heat transfer measurements of turbine blades using a jet array
[AD-A283450] p 62 N95-12512
- Transport phenomena in stratified multi-fluid flow in the presence and absence of gravity p 95 N95-14563
- A selection of experimental test cases for the validation of CFD codes, volume 2
[AGARD-AR-303-VOL-2] p 109 N95-17846
- The stability of two-phase flow over a swept-wing
[NASA-CR-194994] p 159 N95-18190
- A selection of experimental test cases for the validation of CFD codes. Supplement: Datasets A-E
[AGARD-AR-303-SUPPL] p 117 N95-18539
- An investigation of drag repeatability in half model testing in the ARA Transonic Wind Tunnel
[ARA-MEMO-392] p 188 N95-19546
- Prediction of wind tunnel effects on the installed F/A-18A inlet flow field at high angles-of-attack
[NASA-CR-195429] p 197 N95-19651
- Vapor generator wand
[NASA-CASE-LAR-15058-1] p 238 N95-20080
- CFD analysis of turbopump volutes p 312 N95-23436
- Phase 2: HGM air flow tests in support of HEX vane investigation p 312 N95-23438
- Flutter clearance flight tests of an OV-10A airplane modified for wake vortex flight experiments
[NASA-TM-109168] p 366 N95-26381
- Linear and nonlinear discrete-time state-space modeling of dynamic systems for control applications p 567 N95-29251
- Turbulent airflow noise production and propagation patterns of a subsonic jet impinging on a flat plate p 580 N95-29502
- Energy absorption device for shock loading
[AD-DO17476] p 706 N95-34449
- AIR INTAKES**
- Some considerations on system design of the hypersonic transport and supersonic air-intakes p 473 A95-91522
- Combustion efficiency in a dual-inlet side-dump ramjet combustor
[AD-A283564] p 83 N95-15329
- Numerical simulation of helicopter engine plume in forward flight
[NASA-CR-197488] p 107 N95-16589
- Data acquisition and processing software for the Low Speed Wind Tunnel tests of the Jindivik auxiliary air intake
[AD-A285455] p 108 N95-17178
- Protective coatings for compressor gas path components p 201 N95-19675
- Three-dimensional Navier-Stokes analysis and redesign of an imbedded bellmouth nozzle in a turbine cascade inlet section p 311 N95-23423
- Air/fuel ratio visualization in a diesel spray p 556 N95-29807
- A pulsed liquid fuel ramjet p 617 N95-31201
- AIR JETS**
- Simulation of transverse gas injection in turbulent supersonic air flows
[BTN-95-EIX95182619080] p 269 A95-75765
- Computational/experimental investigation of staged injection into a Mach 2 flow
[HTN-95-51646] p 432 A95-85028
- Active open-loop control of particle dispersion in round jets
[HTN-95-42334] p 372 A95-86163
- Numerical model of boundary-layer control using air-jet generated vortices
[HTN-95-42581] p 459 A95-87211
- Planar Rayleigh scattering and laser-induced fluorescence for visualization of a hot, Mach 2 annular air jet
[NASA-TM-4576] p 54 N95-13196
- Transport phenomena in stratified multi-fluid flow in the presence and absence of gravity p 95 N95-14563
- An analysis of B-1B extensor jet blast windshield anti-icing performance using pre-cooled compressor bleed air
[AD-A292522] p 485 N95-28811
- A pulsed liquid fuel ramjet p 617 N95-31201
- AIR LAND INTERACTIONS**
- Airborne lidar observation of mountain-wave-induced polar stratospheric clouds during EASOE
[HTN-95-00738] p 444 A95-86308
- AIR LAUNCHING**
- Aerodynamic design of pegasus: Concept to flight with computational fluid dynamics
[BTN-95-EIX95182617463] p 298 A95-75734
- SR-71 may launch targets for missile defense tests
[HTN-95-91872] p 335 A95-81974
- AIR LAW**
- The ICAO CNS/ATM system: New king, new law?
[HTN-95-50218] p 175 A95-64855
- World trends in air transport policies. (Approaching the 21st century)
[HTN-95-50220] p 176 A95-64857
- Operational aviation weather regulations p 652 A95-93446
- A status report on the development of the Federal Aviation Administration/National Oceanic and Atmospheric Administration Memorandum of Agreement p 652 A95-93447
- A study of aircraft post-crash fuel fire mitigation
[AD-A282208] p 40 N95-12499
- Oceanic operations: An authoritative guide to oceanic operations
[FAA-AFS-550] p 277 N95-24065
- AIR MASSES**
- Fine-scale, poleward transport of tropical air during AASE 2
[HTN-95-70949] p 352 A95-78014
- AIR NAVIGATION**
- Commentary on Walton correspondence relating to the ILS glide slope
[BTN-94-EIX94441380856] p 125 A95-64288
- The ICAO CNS/ATM system: New king, new law?
[HTN-95-50218] p 175 A95-64855
- On-the-fly carrier phase ambiguity resolution for precise aircraft landing
[BTN-95-EIX95112522535] p 190 A95-69328
- Development of aeronautical mobile satellite services over the past thirty years
[BTN-95-EIX95152569458] p 305 A95-73498
- Real-time navigation using the global positioning system
[BTN-95-EIX95172595298] p 279 A95-75714
- Describing an attitude p 342 A95-80409
- Ideal proportional navigation p 342 A95-81374
- A market perspective on FANS
[SAE PAPER 932521] p 486 A95-89189
- Introduction of the GPS to civil aviation field p 487 A95-91536
- Status of Enhanced Vision System p 506 A95-91542
- Guidance and control of HOPE and its future technologies p 506 A95-91543
- Performance evaluation test of GPS/DGPS navigation system installed in the NAL Dornier 228: Preliminary ground test results p 487 A95-91575
- Air traffic management: The future challenge
[CONGRESS PAPER C428-7-145] p 488 A95-91686
- Airborne collision avoidance systems - The UK experience
[CONGRESS PAPER C428-7-146] p 488 A95-91687
- Maintenance-free lead acid battery for inertial navigation systems aircraft
[BTN-95-EIX95292721316] p 633 A95-92511
- NEXRAD/ARSR operational comparison p 658 A95-93470
- The use of satellites for aeronautical communications, navigation and surveillance
[CONGRESS PAPER C428-30-159] p 600 A95-93613
- Design and flight evaluation of an integrated navigation and near-terrain helicopter guidance system for night-time and adverse weather operations
[NASA-TM-108837] p 11 N95-10846
- Modular CNI avionics system p 234 N95-20659
- The personal aircraft: Status and issues
[NASA-TM-109174] p 223 N95-20688
- Assessment of a non-dedicated GPS receiver system for precise airborne attitude determination
[DE94-019309] p 229 N95-21520
- A real-time algorithm for integrating differential satellite and inertial navigation information during helicopter approach
[NASA-CR-197409] p 229 N95-21891
- Recommendation on transition from primary/secondary radar to secondary-only radar capability
[AD-A286279] p 249 N95-22005
- Cueing light configuration for aircraft navigation
[NASA-CASE-ARC-11982-1] p 280 N95-23393
- Oceanic operations: An authoritative guide to oceanic operations
[FAA-AFS-550] p 277 N95-24065
- Federal Aviation Administration plan for research, engineering and development, 1995 p 363 N95-24202
- Design and synthesis of a real-time controller for an unmanned air vehicle
[AD-A289134] p 408 N95-26555
- Conceptual design of a map interactive system for military aircraft cockpits
[AD-A289760] p 508 N95-28692
- Flight test of a low-altitude helicopter guidance system with obstacle avoidance capability p 688 N95-32490
- A tactical navigation and routing system for low-level flight p 709 N95-32494
- The Anglo-French Compact Laser Radar demonstrator programme p 703 N95-32501
- AIR POLLUTION**
- Antarctic snow record of southern hemisphere lead pollution
[HTN-95-40359] p 212 A95-66869
- Aircraft engine emission reduction
[BTN-95-EIX95031502750] p 196 A95-68257
- Ozone, skin cancer, and the SST
[BTN-95-EIX95041503011] p 213 A95-68314
- Subsidence of aircraft engine exhaust in the stratosphere: Implications for calculated ozone depletions
[PAPER-93GL03426] p 251 A95-70297
- Volcanic ash forecast transport and dispersion (VAFTAD) model
[HTN-95-80702] p 254 A95-72546
- On the link between cloud-top radiative properties and sub-cloud aerosol concentrations
[HTN-95-A0527] p 255 A95-73181
- In situ observations in aircraft exhaust plumes in the lower stratosphere at midlatitudes
[HTN-95-A0862] p 318 A95-76266
- Transport of exhaust products in the near trail of a jet engine under atmospheric conditions
[HTN-95-91421] p 319 A95-77334
- Vertical transport rates in the stratosphere in 1993 from observations of CO₂, N₂O, and CH₄
[HTN-95-70941] p 351 A95-78006
- An analysis of aircraft exhaust plumes from accidental encounters
[HTN-95-70943] p 351 A95-78008
- Meridional distributions of NO(X), NO(Y), and other species in the lower stratosphere and upper troposphere during AASE 2
[HTN-95-70944] p 352 A95-78009
- Comparison of column abundances from three infrared spectrometers during AASE 2
[HTN-95-70946] p 352 A95-78011
- Chemical change in the arctic vortex during AASE 2
[HTN-95-70947] p 352 A95-78012
- Latitude variations of stratospheric trace gases
[HTN-95-70948] p 352 A95-78013
- Fine-scale, poleward transport of tropical air during AASE 2
[HTN-95-70949] p 352 A95-78014
- North Atlantic air traffic within the lower stratosphere: Cruising times and corresponding emissions
[HTN-95-91841] p 354 A95-80829
- Chemical composition and photochemical reactivity of exhaust from aircraft turbine engines
[HTN-95-51277] p 356 A95-80862
- Potential effects on ozone of future supersonic aircraft/2D simulation
[HTN-95-51282] p 356 A95-80867
- Impact on ozone of high-speed stratospheric aircraft: Effects of the emission scenario
[HTN-95-51283] p 356 A95-80868
- An overview of the EASOE campaign
[HTN-95-00702] p 443 A95-86272
- Aviation and the environment p 657 A95-93464
- Three dimensional model calculations of the global dispersion of high speed aircraft exhaust and implications for stratospheric ozone loss p 26 N95-10657
- Integrating NOISEMAP with the Geographic Resource Analysis Support System (GRASS) to enhance environmental impact assessments and land use compatibility studies p 31 N95-11311
- Regulatory impact analysis and regulatory support document: Control of air pollution; determination of significance for nonroad sources and emission standards for new nonroad compression-ignition engines at or above 37 kilowatts (50 horsepower)
[PB94-194594] p 61 N95-12855
- Atmospheric effects of high-flying subsonic aircraft: A catalogue of perturbing influences
[KNMI-SR-94-03] p 168 N95-18722
- Air pollution mitigation measures for airports and associated activity
[PB94-207610] p 216 N95-19582
- Damage of high temperature components by dust-laden air p 201 N95-19673
- Gas turbine compressor corrosion and erosion in Western Europe
[AD-B196178L] p 201 N95-19678
- Developing an emission factor for hazardous air pollutants for an F-16 using JP-8 fuel
[AD-A284802] p 216 N95-19685
- The atmospheric effects of stratospheric aircraft: A fourth program report
[NASA-RP-1359] p 357 N95-24274

Nitrogen oxide emissions and their control from uninstalled aircraft engines in enclosed test cells: Joint report to Congress on the Environmental Protection Agency - Department of Transportation study [PB95-166237] p 358 N95-26005

AIR PURIFICATION

Laboratory evaluation of a reactive baffle approach to NOx control [AD-A283802] p 255 N95-19921

AIR QUALITY

Nitrogen oxide emissions and their control from uninstalled aircraft engines in enclosed test cells: Joint report to Congress on the Environmental Protection Agency - Department of Transportation study [PB95-166237] p 358 N95-26005

AIR SAMPLING

An air-driven pressure booster pump for aircraft-based air sampling [HTN-95-40689] p 216 A95-69833

Estimates of total organic and inorganic chlorine in the lower stratosphere from in situ and flask measurements during AASE 2 [HTN-95-A0861] p 317 A95-76265

Vertical transport rates in the stratosphere in 1993 from observations of CO₂, N₂O, and CH₄ [HTN-95-70941] p 351 A95-78006

An analysis of aircraft exhaust plumes form accidental encounters [HTN-95-70943] p 351 A95-78008

Meridional distributions of NO(X), NO(Y), and other species in the lower stratosphere and upper troposphere during AASE 2 [HTN-95-70944] p 352 A95-78009

Comparison of column abundances from three infrared spectrometers during AASE 2 [HTN-95-70946] p 352 A95-78011

Chemical change in the arctic vortex during AASE 2 [HTN-95-70947] p 352 A95-78012

Latitude variations of stratospheric trace gases [HTN-95-70948] p 352 A95-78013

Fine-scale, poleward transport of tropical air during AASE 2 [HTN-95-70949] p 352 A95-78014

Chemical composition and photochemical reactivity of exhaust from aircraft turbine engines [HTN-95-51277] p 356 A95-80862

Development of techniques for the in situ observation of OH and HO₂ for studies of the impact of high-altitude supersonic aircraft on the stratosphere [NASA-CR-196759] p 61 N95-12832

Comparison of measured and calculated dynamic loads for the Mod-2 2.5 mW wind turbine system p 440 N95-27983

AIR TO AIR MISSILES

Ideal proportional navigation p 342 A95-81374

AIR TO AIR REFUELING

Interference between tanker wing wake with roll-up and receiver aircraft [BTN-95-EIX95062487552] p 185 A95-68366

AIR TO SURFACE MISSILES

Application of photogrammetry of F-14D store separation [AD-A284154] p 132 N95-18417

AIR TRAFFIC

North Atlantic air traffic within the lower stratosphere: Cruising times and corresponding emissions [HTN-95-91841] p 354 A95-80829

Using ATMS weather products for air traffic strategic planning p 672 A95-93536

Atmospheric effects of high-flying subsonic aircraft: A catalogue of perturbing influences [KNMI-SR-94-03] p 168 N95-18722

On-line handling of air traffic: Management, guidance and control [AGARD-AG-321] p 126 N95-18927

Aviation system capacity improvements through technology [NASA-TM-109165] p 333 N95-24633

Air traffic operational inventory CY 1994 [AD-A288281] p 382 N95-26454

The 1994 updated National Airspace System performance assessment for year 2005 [AD-A288652] p 380 N95-26485

Enplanement and all cargo activity [AD-A280074] p 412 N95-28151

Federal aviation administration plan for research, engineering and development [AD-A290952] p 490 N95-29733

A NASPAC-Based analysis of the delay and cost effects of the western-pacific region preliminary resectorization effort of 1993 [AD-A288696] p 601 N95-31013

Effects of civil titrotor service in the northeast corridor on en route airspace loads [AD-A293586] p 599 N95-31687

Integration of air traffic databases: A case study [AD-A293691] p 602 N95-32022

Fact sheet for Congressional requesters. Airport competition: Essential air service slots at O'Hare International Airport [GAO/RCED-94-118FS] p 699 N95-32759

Report to the Chairman, Subcommittee on Transportation and Related Agencies, Committee on Appropriations, US Senate. Airport Improvement Program: Reliever airport set-aside funds could be redirected [GAO/RCED-94-226] p 699 N95-32786

AIR TRAFFIC CONTROL

The ICAO CNS/ATM system: New king, new law? [HTN-95-50218] p 175 A95-64855

Development of aeronautical mobile satellite services over the past thirty years [BTN-95-EIX95152569458] p 305 A95-73498

Description of a GNSS availability model and its use in developing requirements [BTN-95-EIX95202637603] p 308 A95-76686

Doppler lidar investigation of wake vortex transport between closely spaced parallel runways [HTN-95-81645] p 462 A95-87693

A market perspective on FANS [SAE PAPER 932521] p 486 A95-89189

Analysis of approach paths of two aircraft p 487 A95-91494

Arrival traffic handling for a parallel runway airport p 487 A95-91537

CCLA operation on MLS p 487 A95-91540

Air traffic management: The future challenge [CONGRESS PAPER C428-7-145] p 488 A95-91686

Automatic vehicle location and airfield ground movement [CONGRESS PAPER C428-7-148] p 488 A95-91689

Role of the aviation weather system in providing a real-time ATC volcanic ash advisory system p 663 A95-93494

Analysis of en route controller hazardous weather-related tasks p 665 A95-93503

A new look at aviation meteorology: Integrating aircraft situation display (ASD) with conventional weather displays p 665 A95-93505

Automated aircraft routing through weather-impacted airspace p 666 A95-93512

An echo motion algorithm for air traffic management using a national radar mosaic p 667 A95-93513

The improvement of meteorological data for air traffic management purposes p 668 A95-93518

Using ATMS weather products for air traffic strategic planning p 672 A95-93536

The use of satellites for aeronautical communications, navigation and surveillance [CONGRESS PAPER C428-30-159] p 600 A95-93613

Fundamentals of catastrophic failure prevention by thrust vectoring [BTN-95-EIX0619952748176] p 606 A95-94470

Cooperative problem solving between airline operations control and ATC traffic flow management p 681 A95-95066

Future ATC system integration: Tools for developing a shared vision p 600 A95-95085

Integrated voice and data communications for air traffic service applications p 600 A95-95090

Evaluating the effects of air traffic control automation p 601 A95-95091

Airborne air traffic control: An application of distributed processing in the air traffic control environment [HTN-95-12417] p 611 A95-95210

Atmospheric and wind modeling for ATC [NASA-CR-196786] p 98 N95-13725

Assessment of CTAS ETA prediction capabilities [NASA-CR-197224] p 97 N95-15728

Groundspeed filtering for CTAS [NASA-CR-197223] p 97 N95-15785

Solid state radar demonstration test results at the FAA Technical Center [AD-A281520] p 154 N95-16097

Modeling of Instrument Landing System (ILS) localizer signal on runway 25L at Los Angeles International Airport [NASA-TM-4588] p 125 N95-17384

Helicopter/vertiport MLS precision approaches [AD-A283505] p 126 N95-18059

An analysis of tower (local) controller-pilot voice communications [AD-A283718] p 160 N95-18436

On-line handling of air traffic: Management, guidance and control [AGARD-AG-321] p 126 N95-18927

Crew aiding and automation: A system concept for terminal area operations, and guidelines for automation design [NASA-CR-4631] p 228 N95-19950

Data link terminal DLT document [PB95-110805] p 229 N95-21369

Recommendation on transition from primary/secondary radar to secondary-only radar capability [AD-A286279] p 249 N95-22005

The role of flight progress strips in en route air traffic control: A time-series analysis [DOT/FAA/AM-95/4] p 280 N95-23565

Federal Aviation Administration plan for research, engineering and development, 1995 p 363 N95-24202

Aviation system capacity improvements through technology [NASA-TM-109165] p 333 N95-24633

Weather And Radar Processor (WARP) Test and Evaluation Master Plan (TEMP) [AD-A288280] p 445 N95-26453

Air traffic operational inventory CY 1994 [AD-A288281] p 382 N95-26454

The 1994 updated National Airspace System performance assessment for year 2005 [AD-A288652] p 380 N95-26485

The controller memory guide. Concepts from the field [AD-A289263] p 383 N95-26978

Advanced interactive display formats for terminal area traffic control [NASA-CR-198576] p 384 N95-28188

Development of a coding form for approach control/pilot voice communications [DOT/FAA/AM-95/15] p 384 N95-28540

Proceedings of the AIAA/FAA joint symposium on general aviation systems [AD-A289930] p 368 N95-28610

Automation and cognition in air traffic control: An empirical investigation [AD-A291932] p 488 N95-28790

Conversion of the TRACON operations concepts database into a formal sentence outline job task taxonomy [DOT/FAA/AM-95/16] p 488 N95-28819

MATSurv multisensor air traffic surveillance [AD-A292253] p 489 N95-28887

Terminal area forecasts-fiscal years 1993-2010 [AD-A290835] p 490 N95-29880

Offshore next generation weather radar (NEXRAD) test and evaluation master plan (TEMP) [AD-A291435] p 556 N95-30072

Emerging applications in probability (Sensor management) [AD-A292781] p 601 N95-31433

Initial evaluation of the Oregon State University planetary boundary layer column model for ITWS applications [AD-A293775] p 677 N95-31465

Integrated terminal weather system (ITWS) demonstration and validation operational test and evaluation [AD-A293932] p 602 N95-31521

The ATC operational evaluation of the prototype integrated terminal weather system (ITWS) at Dallas/Fort Worth and Orlando airports (May-September 1993) [AD-A293808] p 677 N95-31587

FAA aviation forecasts: Fiscal year 1995-2006 [AD-A293682] p 584 N95-31598

Controller resource management: What can we learn from aircrews? [DOT/FAA/AM-95/21] p 602 N95-32186

Fact sheet for Congressional Committees. Air traffic control: Status of FAA's modernization program [GAO/RCED-94-167FS] p 603 N95-32197

Report to the Chairman, Subcommittee on Transportation and Related Agencies, Committee on Appropriations, House of Representatives. Air traffic control: Status of FAA's plans to close and contract out low-activity towers [GAO/RCED-94-265] p 603 N95-32199

The DLR research programme on an integrated multi sensor system for surface movement guidance and control p 689 N95-33135

GPS-Squitter interference analysis [AD-A293690] p 689 N95-33480

Human factors certification in the development of future air traffic control systems p 690 N95-34770

AIR TRAFFIC CONTROLLERS (PERSONNEL)

Ground-based wake vortex monitoring, prediction, and ATC interface p 42 N95-13209

An analysis of tower (local) controller-pilot voice communications [AD-A283718] p 160 N95-18436

The role of flight progress strips in en route air traffic control: A time-series analysis [DOT/FAA/AM-95/4] p 280 N95-23565

The controller memory guide. Concepts from the field [AD-A289263] p 383 N95-26978

Development of a coding form for approach control/pilot voice communications [DOT/FAA/AM-95/15] p 384 N95-28540

The ATC operational evaluation of the prototype integrated terminal weather system (ITWS) at Dallas/Fort Worth and Orlando airports (May-September 1993) [AD-A293808] p 677 N95-31587

Controller resource management: What can we learn from aircrews? [DOT/FAA/AM-95/21] p 602 N95-32186

AIR TRANSPORTATION

World trends in air transport policies. (Approaching the 21st century) [HTN-95-50220] p 176 A95-64857

EC Aviation Scene [HTN-95-50223] p 176 A95-64860

Maintenance challenges and trends [BTN-95-EIX95182617808] p 261 A95-75753

The world of regional aircraft - challenges and opportunities [HTN-95-C0002] p 595 A95-93390

A new look at aviation meteorology: Integrating aircraft situation display (ASD) with conventional weather displays p 665 A95-93505

The High Speed Research Program [NASA-TM-109869] p 10 N95-10548

Potential impacts of advanced aerodynamic technology on air transportation system productivity [NASA-TM-109154] p 10 N95-11489

Census US civil aircraft calendar year 1993 [AD-A286309] p 219 N95-20091

Commuter/air taxi ditchings and water-related impacts that occurred from 1979 to 1989 [AD-A285691] p 226 N95-20275

The personal aircraft: Status and issues [NASA-TM-109174] p 223 N95-20688

Report of proceedings: Aviation Accident Investigation Symposium, Volume 2: Participant presentations [PB94-917007] p 277 N95-23598

Oceanic operations: An authoritative guide to oceanic operations [FAA-AFS-550] p 277 N95-24065

Federal Aviation Administration plan for research, engineering and development, 1995 p 363 N95-24202

Aviation system capacity improvements through technology [NASA-TM-109165] p 333 N95-24633

The high speed civil transport and NASA's High Speed Research (HSR) program p 390 N95-26945

Enplanement and all cargo activity [AD-A280074] p 412 N95-28151

Flying ambulances: The approach of a small air force to long distance aeromedical evacuation of critically injured patients p 568 N95-29618

Civil Reserve Air Fleet-Aeromedical Evacuation Ships (CRAF-AESS) p 568 N95-29619

International access to aeromedical evacuation medical equipment assessment data p 569 N95-29622

Federal aviation administration plan for research, engineering and development [AD-A290952] p 490 N95-29733

Aviation capacity enhancement plan 1994 [AD-A292758] p 598 N95-31428

Patient/aircraft forecasting for the strategic aeromedical evacuation lift-bed process [AD-A293902] p 599 N95-31512

Effects of civil tiltrotor service in the northeast corridor on en route airspace loads [AD-A293586] p 599 N95-31687

Report to the Chairman, Subcommittee on Aviation, Committee on Commerce, Science, and Transportation, US Senate. Aviation safety: Data problems threaten FAA strides on safety analysis system [GAO/AIMD-95-27] p 687 N95-32705

Fact sheet for Congressional requesters. Airport competition: Essential air service slots at O'Hare International Airport [GAO/RCD-94-118FS] p 699 N95-32759

Current issues in the design and information content of instrument approach charts [AD-A294752] p 690 N95-34562

AIRBORNE EQUIPMENT

Application of airborne field mill data for use in launch support [HTN-95-50054] p 98 A95-62279

Aircraft-borne, laser-induced fluorescence instrument for the in situ detection of hydroxyl and hydroperoxyl radicals [BTN-95-EIX95072499029] p 253 A95-71908

Data processing and mapping in airborne radiometric surveys [HTN-95-51587] p 442 A95-83591

Mapping of forest fire damages using imaging spectroscopy p 442 A95-83627

External viewing airborne CCTV system [CONGRESS PAPER C428-25-172] p 595 A95-93598

Airborne integrated communications system [CONGRESS PAPER C428-30-162] p 610 A95-93612

Progress and experience with helicopter health and usage monitoring [CONGRESS PAPER C428-31-151] p 603 A95-93615

Remote sensing of turbulence in the clear atmosphere with 2-micron lidars p 59 N95-13213

Extracting a representative loading spectrum from recorded flight data p 80 N95-14469

Generalized method of solving topological optimization problems for electrical airplane equipment systems in computer-aided design p 169 N95-16272

An airborne monitoring system for FOD and erosion faults p 200 N95-19668

Passive range measurement system [AD-D016222] p 258 N95-21100

Assessment of a non-dedicated GPS receiver system for precise airborne attitude determination [DE94-019309] p 229 N95-21520

Hardware cleanliness methodology and certification p 419 N95-27656

Stratospheric Observatory For Infrared Astronomy (SOFIA), Phase A: System concept description [NASA-TM-110669] p 680 N95-32187

In-flight radiometric calibration of AVIRIS in 1994 p 705 N95-33754

Integration of AIRSAR and AVIRIS data for Trail Canyon alluvial fan, Death Valley, California p 709 N95-33760

AIRBORNE LASERS

Computational Fluid Dynamics (CFD) analysis of a C-135 aircraft with a side-mounted splitter plate (with comparison to wind tunnel data) [AD-A292029] p 553 N95-29187

AIRBORNE RADAR

2 micron LIDAR for laser-based remote sensing: Flight demonstration and application survey [BTN-95-EIX95212641072] p 319 A95-76737

Dynamic imaging and RCS measurements of aircraft [BTN-95-EIX95202637582] p 347 A95-78576

The detection and measurement of microburst wind shear by an airborne lidar system p 543 A95-87798

MAX-91: Polarimetric SAR results on Montespertoli site p 320 N95-23940

AIRBORNE/SPACEBORNE COMPUTERS

Guidance and control, 1993; Annual Rocky Mountain Guidance and Control Conference, 16th, Keystone, CO, Feb. 6-10, 1993 [ISBN-0-87703-365-X] p 341 A95-80389

Air data sensors for atmospheric reentry flight test of winged space vehicle p 413 A95-82412

Guidance and control of HOPE and its future technologies p 506 A95-91543

Airborne air traffic control: An application of distributed processing in the air traffic control environment [HTN-95-12417] p 611 A95-95210

Design and flight evaluation of an integrated navigation and near-terrain helicopter guidance system for night-time and adverse weather operations [NASA-TM-108837] p 11 N95-10846

Instructional control and part/whole-task training: A review of the literature and an experimental comparison of strategies applied to instructional simulation [AD-A280860] p 21 N95-10919

An avionics scenario and command model description for Space Generic Open Avionics Architecture (SGOAA) [NASA-CR-188330] p 49 N95-11913

Advanced flight computer. Special study [NASA-CR-198165] p 449 N95-27246

Model following control for tailoring handling qualities: ACT experience with ATTHes p 622 N95-32000

PSC implementation and integration p 695 N95-33014

AIRCRAFT

Fast Floquet theory and trim for multi-bladed rotorcraft [HTN-95-61078] p 370 A95-83662

Polarization diverse ultra-wideband antenna technology p 548 A95-90924

AIRCRAFT ACCIDENT INVESTIGATION

Commentary on Walton correspondence relating to the ILS glide slope [BTN-94-EIX94441380856] p 125 N95-64288

Aircraft accident investigation and airworthiness - A practical example of the interaction of two disciplines with some reflections on possible legal consequences [HTN-95-50219] p 176 A95-64856

Aircraft accident report: Overspeed and loss of power on both engines during descent and power-off emergency, landing Simmons Airlines, Inc., d/b/a, American Eagle Flight 3641, N349SB False River Air Park, New Roads, Louisiana, 1 February 1994 [PB94-910408] p 78 N95-14916

A correlative investigation of simulated occupant motion and accident report in a helicopter crash [AD-A285190] p 123 N95-16404

Aircraft accident report: Stall and loss of control on final approach, Atlantic Coast Airlines, Inc./United Express Flight 6291 Jetstream 4101, N304UE Columbus, OH, 7 January 1994 [PB94-910409] p 123 N95-17646

Spectrogram diagnosis of aircraft disasters p 124 N95-19167

Special investigation report: Maintenance anomaly resulting in dragged engine during landing rollout, Northwest Airlines Flight 18, Boeing 747-251B, N637US, New Tokyo International Airport, Narita, Japan, 1 Mar. 1994 [PB94-917006] p 188 N95-19793

Report of proceedings: Aviation Accident Investigation Symposium, Volume 2: Participant presentations [PB94-917007] p 277 N95-23598

Aircraft accident report. Runway overrun following rejected takeoff. Continental airlines flight 795, McDonnell Douglas MD-82, N18835, LaGuardia Airport, Flushing, NY, 2 March 1994 [PB95-910401] p 277 N95-23609

Aviation Accident Investigation Symposium, Volume 1: Industry recommendations and Safety Board responses [PB94-917005] p 278 N95-24105

Aircraft accident report: Impact with blast fence upon landing rollout Action Air Charters flight 990 Piper PA-31-350, N990RA, Stratford, Connecticut, 27 April 1994 [PB94-910410] p 333 N95-24206

Aircraft accident report: Controlled collision with Terrain Transportes Aereos Ejecutivos, S.A. (TAESA) Learjet 25D, XA-BBA Dulles International Airport Chantilly, Virginia, June 18, 1994 [NTSB/AAR-95/02] p 380 N95-26498

AIRCRAFT ACCIDENTS

Commentary on Walton correspondence relating to the ILS glide slope [BTN-94-EIX94441380856] p 125 A95-64288

Snow-band formation and evolution during the 15 November 1987 aircraft accident at Denver airport [HTN-95-80699] p 254 A95-72543

Real-time decision aiding: Aircraft guidance for wind shear avoidance [BTN-95-EIX95202637575] p 332 A95-78583

The legal status and liability of the copilot, part 2 [HTN-95-A0578] p 452 A95-83158

Ageing aircraft after ALOHA [CONGRESS PAPER C428-11-188] p 484 A95-91701

Explosive sabotage: The potential effects of explosive charges on aircraft [CONGRESS PAPER C428-11-034] p 484 A95-91702

Explanatory factors for the geographic distribution of U.S. Civil aviation mortality [HTN-95-92908] p 484 A95-91846

Deaths and injuries as a result of lightning strikes to aircraft [HTN-95-12213] p 485 A95-91913

Reaction-time response of aircraft crash [BTN-95-EIX95292721296] p 595 A95-92626

Organizational ergonomics and aviation safety p 596 A95-95083

Psycho-social safety perceptions: Helicopters as a case study p 596 A95-95192

ASRS problems involving air carrier ground deicing/anti-icing p 611 A95-95194

General aviation landing incidents and accidents: A review of ASRS and AOPA research findings p 596 A95-95198

EMS helicopter incidents reported to the NASA Aviation Safety Reporting System p 596 A95-95201

The Crash of Flight 232 [NASA-TM-104279] p 11 N95-10737

Plastic hinge modeling of structures [NIAR-94-14] p 24 N95-11168

AGARD highlights 94/2 [AGARD-HIGHLIGHTS-94/2] p 102 N95-13640

Flight in an Adverse Environment [AGARD-LS-197] p 77 N95-14893

Aircraft accident report: Overspeed and loss of power on both engines during descent and power-off emergency, landing Simmons Airlines, Inc., d/b/a, American Eagle Flight 3641, N349SB False River Air Park, New Roads, Louisiana, 1 February 1994 [PB94-910408] p 78 N95-14916

Annual review of aircraft accident data: US air carrier operations, calendar year 1992 [PB95-100319] p 78 N95-15066

Aircraft accident report: Stall and loss of control on final approach, Atlantic Coast Airlines, Inc./United Express Flight 6291 Jetstream 4101, N304UE Columbus, OH, 7 January 1994 [PB94-910409] p 123 N95-17646

Annual review of aircraft accident data: US Air carrier operations, calendar year 1992
 [PB95-100319] p 123 N95-17748
 Spectrogram diagnosis of aircraft disasters p 124 N95-19167
 Special investigation report: Maintenance anomaly resulting in dragged engine during landing rollout. Northwest Airlines Flight 18, Boeing 747-251B, N637US, New Tokyo International Airport, Narita, Japan, 1 Mar. 1994
 [PB94-917006] p 188 N95-19793
 Commuter airplane accident data analysis
 [AD-A286315] p 226 N95-20174
 Commuter/air taxi ditchings and water-related impacts that occurred from 1979 to 1989
 [AD-A285691] p 226 N95-20275
 Analysis of test criteria for specifying foam firefighting agents for aircraft rescue and firefighting
 [AD-A286381] p 227 N95-22352
 Forecasting aircraft mishaps using monthly maintenance reports
 [AD-A286049] p 227 N95-22417
 Mishap risk control for advanced aerospace/composite materials p 301 N95-23031
 Aircraft accident report. Runway overrun following rejected takeoff. Continental Airlines flight 795, McDonnell Douglas MD-82, N18835, LaGuardia Airport, Flushing, NY, 2 March 1994
 [PB95-910401] p 277 N95-23609
 Aircraft fires, smoke toxicity, and survival: An overview
 [DOT/FAA/AM-95/8] p 277 N95-24024
 A review of civil aviation fatal accidents in which lost/disoriented was a cause/factor: 1981-1990
 [DOT/FAA/AM-95/1] p 278 N95-24071
 Aircraft accident report: Impact with blast fence upon landing rollout Action Air Charters flight 990 Piper PA-31-350, N990RA, Stratford, Connecticut, 27 April 1994
 [PB94-910410] p 333 N95-24206
 Aircraft accident report: Controlled collision with Terrain Transportes Aereos Ejecutivos, S.A. (TAESA) Learjet 25D, XA-BBA Dulles International Airport Chantilly, Virginia, June 18, 1994
 [NTSB/AAR-95/02] p 380 N95-26498
 Prevention and control of inlet unstart using an SR-71 simulation p 367 N95-26948
 Mode of human image representation and error checking strategies in complex visual displays
 [AD-A290107] p 485 N95-29210
 The relation of handling qualities ratings to aircraft safety p 597 N95-31067
 SAAB experience with PIO p 598 N95-31069
 Annual review of aircraft accident data: US general aviation calendar year 1993
 [PB95-215828] p 599 N95-31712
 Report to the Chairman, Subcommittee on Aviation, Committee on Commerce, Science, and Transportation, US Senate. Aviation Safety: FAA can better prepare general aviation pilots for mountain flying risks
 [GAO/RCE-94-15] p 687 N95-32784

AIRCRAFT ANTENNAS
 Wind-tunnel tests of an inclined cylinder having helical grooves
 [BTN-95-EIX95262694306] p 411 A95-85477
 Electromagnetic on-aircraft antenna radiation in the presence of composite plates
 [NASA-CR-196126] p 58 N95-12856
 Spiral microstrip antenna with resistance
 [NASA-CASE-LAR-15088-1] p 91 N95-14139
 A VHF/UHF antenna for the Precision Antenna Measurement System (PAMS)
 [AD-A285673] p 156 N95-16621
 Design considerations for an archimedean slot spiral antenna p 211 N95-19798

AIRCRAFT APPROACH SPACING
 Analysis of approach paths of two aircraft p 487 A95-91494
 Guidance and control requirements for high-speed Rollout and Turnoff (ROTO)
 [NASA-CR-195026] p 292 N95-22674
 Characterizing the wake vortex signature for an active line of sight remote sensor
 [NASA-CR-197697] p 333 N95-24391

AIRCRAFT BRAKES
 Surface morphology and structure of carbon-carbon composites in high-energy sliding contact
 [BTN-94-EIX94371347996] p 206 A95-69164
 Aircraft landing gear dynamics present and future
 [SAE PAPER 931400] p 604 A95-93670

AIRCRAFT CARRIERS
 Benefits and limitations of composites in carrier-based aircraft p 422 N95-28422

AIRCRAFT COMMUNICATION
 GateLink highspeed communications with parked aircraft
 [SAE PAPER 932610] p 486 A95-90079

Airborne integrated communications system
 [CONGRESS PAPER C428-30-162] p 610 A95-93612
 The use of satellites for aeronautical communications, navigation and surveillance
 [CONGRESS PAPER C428-30-159] p 600 A95-93613
 Spread spectrum applications in unmanned aerial vehicles
 [AD-A281035] p 156 N95-16448
 Crew aiding and automation: A system concept for terminal area operations, and guidelines for automation design
 [NASA-CR-4631] p 228 N95-19950
 Development of a coding form for approach control/pilot voice communications
 [DOT/FAA/AM-95/15] p 384 N95-28540

AIRCRAFT COMPARTMENTS
 Noise and vibration control
 [BTN-95-EIX95042477108] p 179 A95-68351
 Human factors issues in aircraft cabin design
 [SAE PAPER 932527] p 386 A95-84556
 Development and validation of a numerical acoustic analysis program for aircraft interior noise prediction p 572 A95-88471
 In-flight interior sound field mapping in propeller aircraft p 572 A95-88472
 Numerical and flight measured interior noise characteristics of a twin-engine turboprop general aviation aircraft p 573 A95-90094
 Evaluation of a model for boundary-layer induced noise in aircraft p 574 A95-90102
 Aircraft interior sound field analysis in view of active control: Results from the ASANCA project p 575 A95-90109
 Experimental active control of sound in the ATR 42 p 575 A95-90110
 ASTRYD: A new numerical tool for aircraft cabin and environmental noise prediction p 576 A95-90129
 Prediction of airplane cabin noise due to engine shock cell excitation using statistical energy analysis p 577 A95-90131
 Numerical investigation of sound transmission through double wall cylinders with respect to active noise control p 577 A95-90134
 Condensing cycle air conditioning system
 [SAE PAPER 932056] p 513 A95-91637
 What's next in commercial aircraft environmental control systems?
 [SAE PAPER 932057] p 513 A95-91638
 Development of an aircraft cabin water spray system
 [CONGRESS PAPER C428-25-030] p 595 A95-93599
 Aircraft cabin water spray systems - research and regulatory issues
 [CONGRESS PAPER C428-25-150] p 595 A95-93600
 Transmission loss characteristics of aircraft sidewall systems to control cabin interior noise p 28 N95-11261
 Active control of interior noise in a business jet using piezoceramic actuators p 29 N95-11276
 Broadband, wide-area active control of sound radiated from vibrating structures using local surface-mounted radiation suppression devices p 30 N95-11283
 Viper cabin-fuselage structural design concept with engine installation and wing structural design
 [NASA-CR-197162] p 45 N95-12305
 Cabin fuselage structural design with engine installation and control system
 [NASA-CR-197173] p 47 N95-12639
 Cabin-fuselage-wing structural design concept with engine installation
 [NASA-CR-197172] p 49 N95-12993
 Electromagnetic reverberation characteristics of a large transport aircraft
 [AD-A282923] p 82 N95-15392
 Generalized method of solving topological optimization problems for electrical airplane equipment systems in computer-aided design p 169 N95-16272
 Helicopter internal noise p 173 N95-19144
 Weapons bay acoustic environment p 173 N95-19146
 Noise transmission and reduction in turboprop aircraft p 175 N95-19164
 Aircraft evacuations through Type-3 exits I: Effects of seat placement at the exit
 [DOT/FAA/AM-95/22] p 599 N95-31845

AIRCRAFT CONFIGURATIONS
 Hypersonic waverider test vehicle: A logical next step
 [BTN-95-EIX95041503783] p 193 A95-69214
 Development of an efficient inverse method for supersonic and hypersonic body design
 [BTN-95-EIX95041503784] p 180 A95-69215

Unstructured grid solutions to a wing/pylon/store configuration
 [BTN-95-EIX95152582322] p 265 A95-73525
 Computational fluid dynamics with icing effects
 [SAE PAPER 932532] p 466 A95-89192
 Should large business jets have four under the wing?
 [SAE 931256] p 493 A95-89223
 Aerodynamic simulation on massively parallel systems p 549 A95-91487
 Matching fluid and structure meshes for aeroelastic computations: a parallel approach
 [BTN-95-EIX95302679864] p 636 A95-94102
 Automatic grid generation procedure for complex aircraft configurations
 [BTN-95-EIX95302729765] p 605 A95-94127
 Flow physics of critical states for rolling delta wings
 [BTN-95-EIX0619952748180] p 590 A95-94473
 Computation of vortex breakdown on a rolling delta wing
 [BTN-95-EIX0619952748195] p 591 A95-94484
 X-31 tailless testing
 [NASA-TM-104306] p 13 N95-10751
 A users manual for the method of moments Aircraft Modeling Code (AMC), version 2
 [NASA-CR-196445] p 24 N95-11252
 The present and future of aircraft noise models: A user's perspective p 32 N95-11324
 Potential impacts of advanced aerodynamic technology on air transportation system productivity
 [NASA-TM-109154] p 10 N95-11489
 Impact of agility requirements on configuration synthesis
 [NASA-CR-4627] p 44 N95-11952
 Design of a high capacity long range cargo aircraft
 [NASA-CR-197176] p 45 N95-12363
 Design of a vehicle based system to prevent ozone loss
 [NASA-CR-197199] p 48 N95-12702
 Aerodynamic shape optimization of a HSCAT type configuration with improved surface definition
 [NASA-CR-197011] p 67 N95-13701
 Comparison of full-scale, small-scale, and CFD results for F/A-18 forebody slot blowing p 72 N95-14255
 Portable parallel stochastic optimization for the design of aeropropulsion components
 [NASA-CR-195312] p 154 N95-16072
 STOVL CFD model test case p 115 N95-17881
 Comparison of stochastic and deterministic nonlinear gust analysis methods to meet continuous turbulence criteria p 133 N95-18602
 Panel methods p 165 N95-19448
 Validation and evaluation of the advanced aeronautical CFD system SAUNA: A method developer's view
 [ARA-MEMO-390] p 210 N95-19774
 Verification of the CFD simulation system SAUNA for complex aircraft configurations
 [ARA-MEMO-401] p 211 N95-19776
 Inviscid and viscous flow modelling of complex aircraft configurations using the CFD simulation system sauna
 [ARA-MEMO-403] p 211 N95-19777
 Aerodynamics model for a generic ASTOVL lift-fan aircraft
 [NASA-TM-110347] p 332 N95-26302
 Aeroelasticity of wing and wing-body configurations on parallel computers
 [NASA-CR-197756] p 389 N95-26590
 Comparison of fixed wing aircraft algorithms for JANUS
 [AD-A288503] p 389 N95-26652
 Supersonic civil airplane study and design: Performance and sonic boom
 [NASA-CR-197745] p 390 N95-26813
 A quantitative feedback theory FCS design for the subsonic envelope of the VISTA F-16 including configuration variation
 [AD-A289221] p 409 N95-26958
 Test operations procedure (TOP) 7-3-534 airworthiness testing of fixed wing aircraft: Asymmetric power testing
 [AD-A289458] p 391 N95-26994
 The effects of design details on cost and weight of fuselage structures p 501 N95-28831
 A general inverse design procedure for aerodynamic bodies p 606 N95-30497
 Numerical investigation into vortical flow about a delta-wing configuration up to incidences at which vortex breakdown occurs in experiment
 [PB95-198024] p 593 N95-30837
 Application of multigrid computational fluid dynamics (CFD) methods to rotor analysis
 [AD-A293012] p 648 N95-31475
 Low-Level and Nap-of-the-Earth (NOE) night operations
 [AGARD-CP-563] p 686 N95-32486
 Flight test of a low-altitude helicopter guidance system with obstacle avoidance capability p 688 N95-32490

- Parallel computation of transonic flows about an aircraft configuration using multi-block structured grids p 685 N95-34537
- AIRCRAFT CONSTRUCTION MATERIALS**
- Analytical description of and forecast for stress relaxation of aviation materials under the vibration conditions [BTN-94-EIX94461408751] p 126 A95-63634
- Calculation of geometry of stamps with small allowances for pieces of the aerodynamic profile [BTN-94-EIX94461408772] p 103 A95-63655
- National AeroSpace Plane: Technology transfer [BTN-95-EIX95072498879] p 180 A95-68395
- Prediction of energy absorption capability of composite stiffeners [HTN-95-A0500] p 230 A95-72571
- MIL-HDBK-5 design allowables for fibre/metal laminates: ARALL 2 and ARALL 3 [BTN-94-EIX94371346933] p 300 A95-73345
- Evaluation of advanced aerospace materials by depth sensing indentation and scratch methods [BTN-95-EIX95152584678] p 282 A95-73590
- H-76B fantail demonstrator composite fan blade fabrication [HTN-95-80856] p 283 A95-75098
- Flight simulation fatigue crack growth testing of aluminum alloys [HTN-95-00652] p 418 A95-84731
- Forming and bonding techniques for high-strength aluminum alloys [HTN-95-20605] p 418 A95-84786
- Fatigue of aircraft materials; Specialists' Conference, Delft, Netherlands, 1992 [HTN-95-B0076] p 387 A95-85892
- Fatigue of aircraft materials and structures p 387 A95-85894
- Fibre-Metal laminates p 387 A95-85895
- Applying nanostructured materials to future gas turbine engines [HTN-95-11909] p 404 A95-85990
- Materials and structures for the HSCT [BTN-95-EIX95282711241] p 455 A95-89634
- Mechanical properties of advanced toughened bismaleimide matrix composite p 530 A95-91570
- Intelligent skins development for future military aircraft [CONGRESS PAPER C428-17-189] p 531 A95-91714
- Improving the fire resistance of aircraft structures [CONGRESS PAPER C428-31-152] p 603 A95-93616
- The basis of civil certification and continued airworthiness for composite aircraft structures [CONGRESS PAPER C428-37-173] p 628 A95-93632
- Activities of Mitsubishi Heavy Industries Ltd. [PB94-179694] p 22 N95-10085
- Advanced composites structural concepts and materials technologies for primary aircraft structures. Structural response and failure analysis: ISPAN modules users manual [NASA-CR-4449] p 12 N95-10242
- Advanced composites structural concepts and materials technologies for primary aircraft structures: Design/manufacturing concept assessment [NASA-CR-4447] p 12 N95-10316
- Novel matrix resins for composites for aircraft primary structures, phase 1 [NASA-CR-189657] p 23 N95-10318
- Thermally stable organic polymers [AD-A281380] p 87 N95-14363
- Residual strength of composites with multiple impact damage [AD-A284230] p 87 N95-14409
- The Aluminum Falcon: A low cost modern commercial transport [NASA-CR-197180] p 81 N95-15742
- Shear buckling analysis of a hat-stiffened panel [NASA-TM-4644] p 158 N95-17490
- Conference on Aerospace Transparent Materials and Enclosures. Volume 2: Sessions 5-9 [AD-A283926] p 131 N95-18162
- Conference on Aerospace Transparent Materials and Enclosures, volume 1 [AD-A283925] p 133 N95-18677
- Thermo-acoustic fatigue design for hypersonic vehicle skin panels p 162 N95-19161
- Mishap risk control for advanced aerospace/composite materials p 301 N95-23031
- Technology reinvestment project's focus area: Affordable polymer matrix composites for airframe structures [PB95-136032] p 324 N95-23168
- Development and verification of a resin film infusion/resin transfer molding simulation model for fabrication of advanced textile composites [NASA-CR-197439] p 301 N95-23179
- Test method and test results for environmental assessment of aircraft materials p 302 N95-23509
- US Navy operating experience with new aircraft construction materials p 303 N95-23517
- Review of some results of the author's fatigue investigations with applications in engineering and material science [TAE-698] p 316 N95-23662
- NASA-UVA light aerospace alloy and structures technology program supplement: Aluminum-based materials for high speed aircraft [NASA-CR-4645] p 343 N95-24878
- Jet engine applications for materials with nanometer-scale dimensions p 345 N95-26131
- Static and fatigue testing of full-scale fuselage panels fabricated using a Therm-X(R) process p 420 N95-28270
- ACT/ICAPS: Thermoplastic composite activities p 421 N95-28274
- Development of composite carrythrough bulkhead p 423 N95-28438
- Effects of floor location on response of composite fuselage frames p 423 N95-28439
- Navy composite maintenance and repair experience p 424 N95-28446
- Ninth DOD/NASA/FAA Conference on Fibrous Composites in Structural Design, volume 2 [NASA-CR-198722] p 424 N95-28462
- Overview of the ACT program p 424 N95-28463
- Characterization and manufacture of braided composites for large commercial aircraft structures p 426 N95-28478
- Impact damage resistance of composite fuselage structure, part 1 p 399 N95-28482
- Fundamental concepts in the suppression of delamination buckling by stitching p 426 N95-28486
- Advanced wing design survivability testing and results p 400 N95-28488
- Third NASA Advanced Composites Technology Conference, volume 1, part 2 [NASA-CP-3178-VOL-1-PT-2] p 531 N95-28823
- In situ processing methods for composite fuselage sandwich structures p 531 N95-28826
- Novel cost controlled materials and processing for primary structures p 532 N95-28830
- A weight-efficient design strategy for cutouts in composite transport structures p 533 N95-28843
- Technology integration box beam failure study p 552 N95-28847
- Third NASA Advanced Composites Technology Conference, volume 1, part 1 [NASA-CP-3178-VOL-1-PT-1] p 534 N95-29029
- Challenges and payoff of composites in transport aircraft: 777 empennage and future applications p 534 N95-29031
- Advanced composite fuselage technology p 535 N95-29034
- Cross-stiffened continuous fiber structures p 536 N95-29041
- Development of RTM and powder prepreg resins for subsonic aircraft primary structures p 536 N95-29044
- The effects of aircraft fuel and fluids on the strength properties of Resin Transfer Molded (RTM) composites p 536 N95-29047
- Progress in manufacturing large primary aircraft structures using the stitching/RTM process p 537 N95-29050
- Thermally stable organic polymers [AD-A290755] p 537 N95-29482
- Thermal-mechanical fatigue crack growth in aircraft engine materials [ISBN-0-315-86543-1] p 647 N95-31098
- Development of stitched/RTM primary structures for transport aircraft [NASA-CR-191441] p 630 N95-31421
- Machinability study of Aermet 100 [DE95-011532] p 701 N95-33408
- AIRCRAFT CONTROL**
- Design of a model following, state variable feedback controller for the X-14 VTOL aircraft [HTN-94-00685] p 16 A95-60168
- Aircraft model for the AIAA controls design challenge [BTN-94-EIX94511433921] p 142 A95-64587
- Time-optimal turn to a heading: An analytic solution [BTN-94-EIX94511433940] p 142 A95-64606
- Side forces at high angles of attack. Why, when, how? [BTN-95-EIX95112523809] p 194 A95-69324
- Cypher moves toward autonomous flight [HTN-95-41394] p 283 A95-76390
- Functional agility metrics and optimal trajectory analysis [BTN-95-EIX95182619121] p 321 A95-76598
- Multiaxis pilot ratings for damaged aircraft [BTN-95-EIX95182619128] p 269 A95-76605
- Direct-lift design strategy for longitudinal control of hypersonic aircraft [BTN-95-EIX95182619131] p 291 A95-76608
- Attainable moments for the constrained control allocation problem [BTN-95-EIX95182619149] p 322 A95-76626
- Automatic formation flight control [BTN-95-EIX95182619153] p 292 A95-76630
- Multiple-function digital controller system for active flexible wing wind-tunnel model [BTN-95-EIX95182619212] p 322 A95-76638
- Robustly stable preliminary control systems design for the YF-16 CCV aircraft [BTN-95-EIX95202637608] p 292 A95-76681
- Determination of piloting feedback structures for an altitude tracking task [BTN-95-EIX95242670770] p 327 A95-81077
- On-line learning nonlinear direct neurocontrollers for restructurable control systems [BTN-95-EIX95242670768] p 359 A95-81079
- Robust dynamic inversion for control of highly maneuverable aircraft [BTN-95-EIX95242670747] p 359 A95-81100
- Robust longitudinal axis flight control for an aircraft with thrust vectoring [BTN-95-EIX95122538875] p 408 A95-83000
- Nonlinear decoupling control study for aircraft maneuvering flight [HTN-95-71130] p 408 A95-83491
- T-45A high angle attack testing [HTN-95-81499] p 386 A95-85213
- Application of artificial neural networks in nonlinear aerodynamics and aircraft design [SAE PAPER 932533] p 492 A95-89193
- Aircraft controller synthesis by solving a nonconvex optimization problem [BTN-95-EIX95282706672] p 515 A95-89636
- Application of restructurable flight control system to large transport aircraft [BTN-95-EIX95282706666] p 515 A95-89639
- Computer aided diagnostic testing of installed flight control servo-actuators [SAE PAPER 932584] p 494 A95-90068
- Second generation smart actuator [SAE PAPER 932585] p 505 A95-90069
- Solid state power controller technology [SAE PAPER 931422] p 495 A95-90087
- Aircraft Symposium, 30th, Tsukuba, Japan, Sep. 30 - Oct. 2, 1992 [HTN-95-A1609] p 498 A95-91491
- Guidance and control of HOPE and its future technologies p 506 A95-91543
- An application of TLS (Total Least Squares) method to estimation of aircraft aerodynamic derivatives p 517 A95-91551
- A study of computational difficulty of numerical method in optimal control p 507 A95-91585
- Flight control system design with Multiple Delay Model/Multiple Design Point Approach p 507 A95-91586
- General requirements for the electrohydraulic systems of the aircraft controls loading force on the simulators [CONGRESS PAPER C428-5-138] p 522 A95-91681
- Universal electrohydraulic system for the steering gear loading [CONGRESS PAPER C428-10-106] p 517 A95-91700
- Evolving standards for safety critical software [CONGRESS PAPER C428-24-142] p 678 A95-93595
- Design trends in propulsion control systems [CONGRESS PAPER C428-33-123] p 610 A95-93620
- Surge recovery and compressor working line control using compressor exit mach number measurement [CONGRESS PAPER C428-33-210] p 610 A95-93622
- An advanced vehicle management system [SAE PAPER 931376] p 618 A95-93655
- Experimental performance of a ventral nozzle with pitch and yaw vectoring capability for SSTOVL aircraft [SAE PAPER 931412] p 614 A95-93678
- Fiber optic hardware for transport aircraft [SAE PAPER 931439] p 680 A95-93691
- Fly-By-Light/Power-By-Wire Requirements and Technology Workshop [NASA-CP-10108] p 12 N95-10245
- F-15 Propulsion Controlled Aircraft (PCA) [NASA-TM-104303] p 17 N95-10748
- High-Alpha Research Vehicle (HARV) longitudinal controller: Design, analyses, and simulation results [NASA-TP-3446] p 17 N95-10860
- On the use of controls for subsonic transport performance improvement: Overview and future directions [NASA-TM-4605] p 10 N95-11408

- STOVL Control Integration Program
[NASA-CR-195358] p 18 N95-11487
- Optimum aerodynamic design via boundary control
[NASA-CR-195882] p 36 N95-11877
- Piloted evaluation of an integrated methodology for propulsion and airframe control design
[AD-A290207] p 51 N95-12763
- Fourth High Alpha Conference, volume 1
[NASA-CP-10143-VOL-1] p 67 N95-14229
- Comparison of X-31 flight, wind-tunnel, and water-tunnel yawing moment asymmetries at high angles of attack
p 68 N95-14234
- Parameter identification for X-31A at high angles of attack
p 69 N95-14235
- Fourth High Alpha Conference, volume 2
[NASA-CP-10143-VOL-2] p 69 N95-14239
- X-31 high angle of attack control system performance
p 70 N95-14244
- Flight test results of the F-16 aircraft modified with the axisymmetric vectoring exhaust nozzle
p 70 N95-14245
- Flight validation of ground-based assessment for control power requirements at high angles of attack
p 70 N95-14246
- High angle of attack flying qualities criteria for longitudinal rate command systems
p 70 N95-14247
- Multi-application controls: Robust nonlinear multivariable aerospace controls applications
p 71 N95-14249
- Computing quantitative characteristics of finite-state real-time systems
[AD-A282839] p 83 N95-14343
- A SIMULINK environment for flight dynamics and control analysis: Application to the DHC-2 Beaver. Part 1: Implementation of a model library in SIMULINK. Part 2: Nonlinear analysis of the Beaver autopilot
[NONP-NASA-SUPPL-DK-94-2802] p 84 N95-14815
- Plant and controller optimization by convex methods
[AD-A283700] p 133 N95-18621
- Fiber Optic Control System integration for advanced aircraft. Electro-optic and sensor fabrication, integration, and environmental testing for flight control systems: Laboratory test results
[NASA-CR-195408] p 161 N95-18938
- Fiber Optic Control System integration for advanced aircraft. Electro-optic and sensor fabrication, integration, and environmental testing for flight control systems
[NASA-CR-191194] p 162 N95-19236
- Determination of stability and control derivatives from the NASA F/A-18 HARV from flight data using the maximum likelihood method
[NASA-CR-197320] p 204 N95-19576
- The use of genetic algorithms for flight test and evaluation of artificial intelligence and complex software systems
[AD-A284824] p 217 N95-19688
- Automation of hardware-in-the-loop testing of control systems for unmanned air vehicles
[AD-A284833] p 194 N95-19693
- Airship applications of modern flight test techniques
[AD-A284253] p 194 N95-19731
- Crew aiding and automation: A system concept for terminal area operations, and guidelines for automation design
[NASA-CR-4631] p 228 N95-19950
- Guidance and control requirements for high-speed Rollout and Turnoff (ROTO)
[NASA-CR-195026] p 292 N95-22674
- Nonlinear system guidance in the presence of transmission zero dynamics
[NASA-TM-4661] p 309 N95-22804
- Flight test of the X-29A at high angle of attack: Flight dynamics and controls
[NASA-TP-3537] p 284 N95-22806
- Design of high performance multivariable control systems for supermaneuverable aircraft at high angle of attack
[NASA-CR-197661] p 293 N95-22908
- Stable H(infinity) controller design for the longitudinal dynamics of an aircraft
[NASA-TM-106847] p 293 N95-22954
- Analysis of the longitudinal handling qualities and pilot-induced-oscillation tendencies of the High-Angle-of-Attack Research Vehicle (HARV)
p 293 N95-23297
- Handling qualities of the High Speed Civil Transport
p 294 N95-23325
- Feedback control laws for highly maneuverable aircraft
[NASA-CR-197944] p 295 N95-23410
- Application of neural networks to unsteady aerodynamic control
p 360 N95-25264
- Simulation model of the integrated flight/propulsion control system, displays, and propulsion system for ASTOVL lift-fan aircraft
[NASA-TM-108866] p 405 N95-26412
- Development of a nonlinear simulation for the McDonnell Douglas F-15 Eagle with a longitudinal TECS control-law
[AD-A288610] p 388 N95-26481
- A comparison of the Neal-Smith and omega Tau function, zeta function and tau function flying qualities criteria
[AD-A289503] p 390 N95-26844
- Moving base simulation of an integrated flight and propulsion control system for an ejector-augmentor STOVL aircraft in hover
[NASA-TM-108867] p 606 N95-30646
- Flight Vehicle Integration Panel Workshop on Pilot Induced Oscillations
[AGARD-AR-335] p 597 N95-31061
- The process for addressing the challenges of aircraft pilot coupling
p 597 N95-31063
- Observations on PIO
p 597 N95-31064
- Unified criteria for ACT aircraft longitudinal dynamics
p 607 N95-31065
- Looking for the simple PIO model
p 597 N95-31066
- SAAB experience with PIO
p 598 N95-31069
- Aeroelastic pilot-in-the-loop oscillations
p 598 N95-31070
- Handling qualities analysis on rate limiting elements in flight control systems
p 619 N95-31071
- Calspan experience of PIO and the effects of rate limiting
p 598 N95-31072
- Computational methods for control and optimal design of aerospace systems
[AD-A292861] p 608 N95-31451
- Flight test validation of a frequency-based system identification method on an F-15 aircraft
[NASA-TM-4704] p 620 N95-31846
- The prevention of PIO by design
p 620 N95-31991
- Robust control: A structured approach to solve aircraft flight control problems
p 621 N95-31995
- Evaluation of the techniques of fuzzy control for the piloting an aircraft
p 621 N95-31997
- Control law design using H-infinity and mu-synthesis short-period controller for a tail-airplane
p 622 N95-31999
- Flight demonstration of an advanced pitch control law in the VAAC Harrier aircraft
p 623 N95-32012
- X-31: A program overview and flight test status
p 609 N95-32013
- Flying qualities of civil transport aircraft with electrical flight control
p 624 N95-32016
- Pilot Induced Oscillation: A report on the AGARD Workshop on PIO
p 624 N95-32017
- An Electronic Workshop on the Performance Seeking Control and Propulsion Controlled Aircraft Results of the F-15 Highly Integrated Digital Electronic Control Flight Research Program
[NASA-TM-104276] p 694 N95-33009
- An overview of integrated flight-propulsion controls flight research on the NASA F-15 research airplane
p 694 N95-33010
- Performance seeking control program overview
p 695 N95-33011
- PSC algorithm description
p 695 N95-33013
- PSC implementation and integration
p 695 N95-33014
- Performance seeking control excitation mode
p 696 N95-33019
- Background and principles of throttles-only flight control
p 697 N95-33021
- Propulsion Controlled Aircraft design and development
p 697 N95-33022
- Flight test of a propulsion controlled aircraft system on the NASA F-15 airplane
p 691 N95-33023
- Design challenges encountered in the F-15 PCA flight test program
p 692 N95-33025
- Nonlinear adaptive control of highly maneuverable high performance aircraft
p 710 N95-33712
- A stochastic adaptive control application to flight systems
p 699 N95-34806
- AIRCRAFT DESIGN**
- Flight simulation
[BTN-94-EIX94461290242] p 84 A95-61735
- Maintenance requirements for a supersonic transport
[BTN-95-EIX95031502751] p 179 A95-68258
- Corrosion prevention and control
[BTN-95-EIX95031502753] p 188 A95-68260
- Two-point transonic airfoil design using optimization for improved off-design performance
[BTN-95-EIX95062487542] p 192 A95-68356
- Application of circulation control to advanced subsonic transport aircraft. Part 1: Airfoil development
[BTN-95-EIX95062487545] p 185 A95-68359
- Application of circulation control to advanced subsonic transport aircraft. Part 2: Transport application
[BTN-95-EIX95062487546] p 185 A95-68360
- Coupling equivalent plate and finite element formulations in multiple-method structural analyses
[BTN-95-EIX95062487548] p 192 A95-68362
- Brief history of gust models for aircraft design
[BTN-95-EIX95062487557] p 203 A95-68371
- Future SSTs: A European approach
[BTN-95-EIX95072419883] p 180 A95-68396
- Putting the ACSYNT on aircraft design
[BTN-95-EIX95072419881] p 180 A95-68398
- Hypersonic waverider test vehicle: A logical next step
[BTN-95-EIX95041503783] p 193 A95-69214
- Development of an efficient inverse method for supersonic and hypersonic body design
[BTN-95-EIX95041503784] p 180 A95-69215
- Prediction of energy absorption capability of composite stiffeners
[HTN-95-A0500] p 230 A95-72571
- New airfoil-design concept with improved aerodynamic characteristics
[PAPER-4384] p 230 A95-72585
- Flight-deck displays on the Boeing 777
[BTN-95-EIX95142562402] p 286 A95-73438
- Structural acoustic calculations in the low-frequency range
[BTN-95-EIX95152582336] p 323 A95-73538
- Flow study of supersonic wing-nacelle configuration
[BTN-95-EIX95152582344] p 266 A95-73546
- An analytical and experimental investigation of the response of the curved, composite frame/skin specimens
[HTN-95-80857] p 283 A95-75099
- An unmanned air vehicle concept with tipjet drive
[HTN-95-80858] p 283 A95-75100
- Integrated design of hypersonic waveriders including inlets and tailfins
[BTN-95-EIX95212645692] p 271 A95-76744
- Aeroservoelastic aspects of wing/control surface planform shape optimization
[BTN-95-EIX95222650795] p 340 A95-79251
- An advanced scramjet propulsion concept for A 350 MG SSTO space plane
p 402 A95-82325
- A conceptual design of hypersonic research vehicle with subscale scramjet engine
p 384 A95-82482
- European firms team on supersonic studies
[HTN-95-42215] p 386 A95-84031
- Education, training, and human engineering in aerospace; SAE Aerotech '93, Costa Mesa, CA, Sep. 27-30, 1993
[SAE SP-992] p 417 A95-84553
- Charles Norvin Rinek; an early American pioneer in advanced aviation engines
[SAE PAPER 930485] p 386 A95-84554
- Flying qualities development and flight simulation evaluation of the TW-68 tilt-wing VTOL aircraft
[SAE PAPER 932517] p 386 A95-84555
- Human factors issues in aircraft cabin design
[SAE PAPER 932527] p 386 A95-84556
- Fatigue of aircraft materials and structures
p 387 A95-85894
- Fibre-Metal laminates
p 387 A95-85895
- Elements of structural integrity assurance
p 387 A95-85896
- Damage tolerance capability
p 388 A95-85898
- Concorde: Silver jubilee Mach 2 marks 25 years
[HTN-95-42618] p 483 A95-87248
- Computational methods in applied sciences; European Computational Fluid Dynamics Conference, 1st, Brussels, Belgium, Sept. 7-11, 1992
[ISBN 0-444-89795-X] p 539 A95-87552
- Aerodynamic design and optimization at Alenia D.V.D.
p 491 A95-87564
- Pressure controlled surfaces - a 3D inverse panel method as a design tool
p 491 A95-87565
- A tool for airframe shaping - idea and application
[SAE PAPER 931224] p 491 A95-87568
- Integration of an hypersonic airbreathing vehicle: Assessment of overall aerodynamic performances and of uncertainties
[AIAA PAPER 95-6100] p 492 A95-88007
- Equivalent plate structural modeling for wing shape optimization including transverse shear
[HTN-95-20839] p 492 A95-88100
- The key to designing durable adhesively bonded joints
[HTN-95-12033] p 528 A95-88496
- Symposium on Aerodynamics & Aeroacoustics, Tucson, AZ, Mar. 1-2, 1993
[ISBN 981-02-1732-3] p 462 A95-88892
- Tailless aircraft design-recent experiences
p 492 A95-88899
- Aircraft aerodynamic analysis on a personal computer (using the RDS aircraft design software)
[SAE PAPER 932530] p 492 A95-89190
- Application of artificial neural networks in nonlinear aerodynamics and aircraft design
[SAE PAPER 932533] p 492 A95-89193
- Aerodynamic tailoring of the Learjet Model 60 wing
[SAE PAPER 932534] p 492 A95-89194
- FAA's Aging Commuter Airplane Program
[SAE PAPER 931248] p 483 A95-89220

- Preliminary design of a single engine business jet
[SAE PAPER 931253] p 493 A95-89222
- Should large business jets have four under the wing?
[SAE 931256] p 493 A95-89223
- Electrical power system upgrade methodology for in-service aircraft
[SAE PAPER 932562] p 511 A95-90059
- Integrated Thermal Energy Management (I-TEM): An evaluation tool for aircraft
[SAE PAPER 932577] p 493 A95-90065
- Special purpose landing gear: A survey of historical designs
[SAE PAPER 932579] p 494 A95-90066
- CaRnard: A new roadable aircraft concept
[SAE PAPER 932601] p 494 A95-90071
- Engineering design of Starcar 3
[SAE PAPER 932602] p 494 A95-90072
- Design and styling of an advanced flying automobile
[SAE PAPER 932603] p 494 A95-90073
- Design methodology and infrastructures for flying automobiles
[SAE PAPER 932604] p 495 A95-90074
- Design and analysis of a telescopic wing
[SAE PAPER 932605] p 495 A95-90075
- Engine/airframe installation CFD for commercial transports: An engine manufacturer's perspective
[SAE PAPER 932623] p 495 A95-90084
- Civil aircraft propulsion integration: Current & future
[SAE PAPER 932624] p 495 A95-90085
- ASTRYD: A new numerical tool for aircraft cabin and environmental noise prediction p 576 A95-90129
- Optimum design of composite stiffened wing panels - a parametric study
[HTN-95-01088] p 496 A95-90274
- Functional requirements of an aerospace Design Representation Programming Interface
[AIAA PAPER 95-0967] p 497 A95-90643
- Development and flight testing of the HL-10 lifting body
Aircraft Symposium, 30th, Tsukuba, Japan, Sep. 30 - Oct. 2, 1992
[HTN-95-A1609] p 498 A95-91491
- Numerical design methods for transonic NLF configurations p 471 A95-91498
- Optimum aerodynamic design of aircraft fuselage using boundary element method p 473 A95-91514
- Requirements for next generation supersonic transports p 498 A95-91516
- The concept of high speed commercial transporter structure p 498 A95-91517
- A conceptual design of the SST without horizontal tail p 498 A95-91520
- Conceptual study of next generation high-speed civil transport: A candidate with horizontal tail p 499 A95-91521
- Some considerations on system design of the hypersonic transport and supersonic air-intakes p 473 A95-91522
- Experimental study for improving the lift to drag ratio of next generation SST p 473 A95-91524
- Experimental investigation on aerothermodynamic characteristics of hypersonic transport p 473 A95-91525
- Computer aided static aeroelastic analysis of wing/pylon/store combination p 499 A95-91531
- Guidance and control of HOPE and its future technologies p 506 A95-91543
- A method for calculating mean aerodynamic center and zero-lift moment coefficient of aircraft without tail by using measured flight loads p 474 A95-91552
- Simultaneous structure/aerodynamic design optimization for a flexible wing structure p 499 A95-91565
- Preliminary tests of a transonic flutter control wing model p 499 A95-91566
- Supersonic flutter analysis of cantilevered composite plate-wings p 499 A95-91567
- Some comments on current research and development of civil VTOL aircrafts p 499 A95-91572
- Analysis and scale-model experiment of propeller driving motor for microwave-powered airplane p 487 A95-91576
- Integrated aircraft thermal management and power generation
[SAE PAPER 932055] p 500 A95-91636
- Cost effective small-scale experiments to aid the design of ASTOVL aircraft
[CONGRESS PAPER C428-9-098] p 475 A95-91695
- The Saab-Scania approach to development simulators
[CONGRESS PAPER C428-10-137] p 522 A95-91698
- The use of structural optimisation within aerospace
[CONGRESS PAPER C428-23-008] p 500 A95-91729
- A better than average stress model-photoelastic analysis for airbus design
[CONGRESS PAPER C428-23-005] p 500 A95-91730
- Impact finite element analysis, as an alternative to the testing of windscreens for bird impact
[CONGRESS PAPER C428-23-196] p 500 A95-91732
- Development of an aircraft cabin water spray system
[CONGRESS PAPER C428-25-030] p 595 A95-93599
- Aircraft cabin water spray systems - research and regulatory issues
[CONGRESS PAPER C428-25-150] p 595 A95-93600
- Improving the fire resistance of aircraft structures
[CONGRESS PAPER C428-31-152] p 603 A95-93616
- Variable camber geometry for transport aircraft wings
[CONGRESS PAPER C428-35-061] p 603 A95-93626
- Load alleviation for civil transport aircraft
[CONGRESS PAPER C428-35-057] p 604 A95-93627
- The auxiliary and emergency power supply on the Saab-JAS39 Gripen aircraft
[CONGRESS PAPER C428-36-192] p 612 A95-93631
- Concepts for aircraft subsystem integration
[SAE PAPER 931377] p 604 A95-93656
- SUIT: The integration of aircraft subsystems
[SAE PAPER 931381] p 604 A95-93657
- Aircraft nose gear shimmy studies
[SAE PAPER 931401] p 628 A95-93671
- Modular avionics: Taking today's aircraft into tomorrow
[SAE PAPER 931416] p 610 A95-93681
- Fiber optic hardware for transport aircraft
[SAE PAPER 931439] p 680 A95-93691
- Nonlinear aerodynamic analysis of grid fin configurations
[BTN-95-EIX0619952748172] p 590 A95-94466
- Statistical discrete gust-power spectral density methods overlap-holistic proof and beyond
[BTN-95-EIX0619952748175] p 584 A95-94469
- Assessment of technology for aircraft development
[BTN-95-EIX0619952748181] p 606 A95-94474
- Flight test certification of primary category aircraft using TP101-41E sportplane design standard
[BTN-95-EIX0619952748184] p 606 A95-94477
- Optimal shape design in hypersonic aerodynamics and electromagnetics p 639 A95-95397
- Navier-Stokes computations around a realistic fighter configuration p 591 A95-95440
- High-lift calculations using Navier-Stokes methods p 641 A95-95444
- A modular system for computational fluid dynamics p 641 A95-95446
- An unstructured node centered scheme for the simulation of 3-D inviscid flows p 642 A95-95463
- SAUNA: A system for grid generation and flow simulation using hybrid structured/unstructured grids p 642 A95-95470
- Activities of Mitsubishi Heavy Industries Ltd.
[PB94-179694] p 22 N95-10085
- High speed civil transport: Sonic boom softening and aerodynamic optimization
[NASA-CR-196397] p 28 N95-11192
- ACSNT inner loop flight control design study
[NASA-CR-196316] p 17 N95-11223
- General Aviation Task Force report
[NASA-TM-109950] p 1 N95-11463
- The use of the Regier number in the structural design with flutter constraints
[NASA-TM-109128] p 13 N95-11465
- Symmetric steady manoeuvre loads on rigid aircraft of classical configuration at subsonic speeds
[ESDU-94009] p 43 N95-11774
- Effects of mass on aircraft sidearm controller characteristics
[NASA-TM-104277] p 51 N95-11868
- Optimum aerodynamic design via boundary control
[NASA-CR-195882] p 36 N95-11877
- Impact of agility requirements on configuration synthesis
[NASA-CR-4627] p 44 N95-11952
- Conceptual design of the AE481 Demon Remotely Piloted Vehicle (RPV)
[NASA-CR-197164] p 44 N95-12294
- Viper cabin-fuselage structural design concept with engine installation and wing structural design
[NASA-CR-197162] p 45 N95-12305
- Design of a high capacity long range cargo aircraft
[NASA-CR-197176] p 45 N95-12363
- The Elite: A high speed, low-cost general aviation aircraft for Aeroworld
[NASA-CR-197161] p 45 N95-12530
- Icarus Rewaxed: A high speed, low-cost general aviation aircraft for Aeroworld
[NASA-CR-197155] p 45 N95-12609
- Gemini: A long-range cargo transport
[NASA-CR-197149] p 45 N95-12626
- The FC-1D: The profitable alternative Flying Circus Commercial Aviation Group
[NASA-CR-197152] p 46 N95-12628
- Triton 2 (1B)
[NASA-CR-197188] p 46 N95-12636
- The OFP-6M transport jet
[NASA-CR-197159] p 46 N95-12637
- The Balsa bullet: A high speed, low-cost general aviation aircraft for Aeroworld
[NASA-CR-197165] p 46 N95-12638
- Central coast designs: The Eightball Express. Taking off with convention, cruising with improvements and landing with absolute success
[NASA-CR-197181] p 47 N95-12643
- LCX: Proposal for a low-cost commercial transport
[NASA-CR-197186] p 47 N95-12645
- A preliminary design proposal for a maritime patrol strike aircraft: MPS-2000 Condor
[NASA-CR-197182] p 47 N95-12689
- Design and construction of a remote piloted flying wing
[NASA-CR-197195] p 47 N95-12695
- Activities of the Institute for Aerospace Studies of Toronto University p 63 N95-12699
- Integrated design and manufacturing for the high speed civil transport
[NASA-CR-197183] p 48 N95-12700
- Design and testing of an oblique all-wing supersonic transport
[NASA-CR-196394] p 48 N95-12785
- Cabin-fuselage-wing structural design concept with engine installation
[NASA-CR-197172] p 49 N95-12993
- Aerodynamic shape optimization of a HsCT type configuration with improved surface definition
[NASA-CR-197011] p 67 N95-13701
- Viper - Design modification
[NASA-CR-197191] p 79 N95-13703
- Identification of dynamic systems. Volume 3: Applications to aircraft. Part 2: Nonlinear analysis and manoeuvre design
[AGARD-AG-300-VOL-3-PT-2] p 79 N95-14102
- Probabilistic inspection strategies for minimizing service failures p 93 N95-14461
- Computational predictive methods for fracture and fatigue p 93 N95-14466
- Analysis of small crack behavior for airframe applications p 95 N95-14484
- Full-scale testing and analysis of fuselage structure p 95 N95-14485
- Graphical user interface for the NASA FLOPS aircraft performance and sizing code
[NASA-TM-106649] p 80 N95-14604
- A SIMULINK environment for flight dynamics and control analysis: Application to the DHC-2 Beaver. Part 1: Implementation of a model library in SIMULINK. Part 2: Nonlinear analysis of the Beaver autopilot
[NONP-NASA-SUPPL-DK-94-2802] p 84 N95-14815
- Artificial neural network modeling of damaged aircraft
[AD-A283227] p 80 N95-14849
- Research and technology highlights, 1993
[NASA-TM-4575] p 102 N95-15065
- More supportable T-38A enhancement study
[AD-A283671] p 66 N95-15331
- The F-16 multinational staged improvement program: A case study of risk assessment and risk management
[AD-A281706] p 81 N95-15451
- The Aluminum Falcon: A low cost modern commercial transport
[NASA-CR-197180] p 81 N95-15742
- Joint Proceedings on Aeronautics and Astronautics (JPAA)
[ISBN-7-80-046602-7] p 104 N95-16249
- An improved method of airfoil design p 106 N95-16252
- Development of strength analysis methods and design model for aircraft constructions in Kazan Aviation Institute p 127 N95-16264
- Evaluation of the dynamic stability characteristics of the NAL Light Transport Aircraft
[NAL-PD-CA-9217] p 142 N95-16392
- Optimum Design Methods for Aerodynamics
[AGARD-R-803] p 127 N95-16562
- Optimum aerodynamic design via boundary control p 127 N95-16565
- Residual-correction type and related computational methods for aerodynamic design. Part 1: Airfoil and wing design p 128 N95-16566
- Residual-correction type and related computational methods for aerodynamic design. Part 2: Multi-point airfoil design p 128 N95-16567

Optimal shape design for aerodynamics p 128 N95-16568

Airfoil optimization by the one-shot method p 128 N95-16569

Tools for applied engineering optimization p 128 N95-16570

The global aircraft shape p 128 N95-16571

Applications of automatic differentiation in CFD [NASA-TM-109948] p 157 N95-16828

Multi-lab comparison on R-curve methodologies: Alloy 2024-T3 [NASA-CR-195004] p 151 N95-16860

Automation of reverse engineering process in aircraft modeling and related optimization problems [NASA-CR-197109] p 129 N95-16899

Cooperative control theory and integrated flight and propulsion control [NASA-CR-197493] p 142 N95-17404

OAT15A airfoil data p 111 N95-17857

Measurements of the flow over a low aspect-ratio wing in the Mach number range 0.6 to 0.87 for the purpose of validation of computational methods. Part 1: Wing design, model construction, surface flow. Part 2: Mean flow in the boundary layer and wake, 4 test cases p 112 N95-17860

Investigation into the aerodynamic characteristics of a combat aircraft research model fitted with a forward swept wing p 116 N95-17884

Wing design for a civil tiltrotor transport aircraft [NASA-CR-197523] p 130 N95-18090

Aircraft Loads due to Turbulence and their Impact on Design and Certification [AGARD-R-798] p 143 N95-18597

Design limit loads based upon statistical discrete gust methodology p 133 N95-18603

A review of gust load calculation methods at de Havilland p 118 N95-18604

Ageing nuclear power plant management: An aeronautical viewpoint [NAL-PD-SN-9306] p 105 N95-18606

Course module for AA201: Wing structural design project [AD-A283618] p 133 N95-18616

Plant and controller optimization by convex methods [AD-A283700] p 133 N95-18621

E-6A hardness assurance, maintenance and surveillance program [AD-A283994] p 134 N95-19067

Impact of noise environment on engine nacelle design p 173 N95-19147

Modelling structurally damaging twin-jet screech p 135 N95-19154

Proceedings of the USAF Structural Integrity Program Conference [AD-A285684] p 194 N95-19517

The Computer Aided Aircraft-design Package (CAAP) p 217 N95-19759

The aerodynamic design of an integrated wing lower surface and pylons for reduced drag [ARA-MEMO-406] p 194 N95-19789

F-16XL interview with Marta Bohn-Meyer [NASA-TM-110505] p 223 N95-19996

Parallel calculation of sensitivity derivatives for aircraft design using automatic differentiation [NASA-TM-110103] p 231 N95-20370

Why do airlines want and use thrust reversers? A compilation of airline industry responses to a survey regarding the use of thrust reversers on commercial transport airplanes [NASA-TM-109158] p 226 N95-20706

Euler Technology Assessment program for preliminary aircraft design employing SPLITFLOW code with Cartesian unstructured grid method [NASA-CR-4649] p 273 N95-22917

Euler technology assessment for preliminary aircraft design employing OVERFLOW code with multiblock structured-grid method [NASA-CR-4651] p 273 N95-23095

Control of flow separation in airfoil/wing design applications p 274 N95-23294

Thin tailored composite wing for civil tiltrotor p 285 N95-23317

NASA video catalog [NASA-SP-7109(01)] p 363 N95-24238

Advanced subsonic airplane design and economic studies [NASA-CR-195443] p 338 N95-24304

A crew-centered flight deck design philosophy for High-Speed Civil Transport (HSCT) aircraft [NASA-TM-109171] p 335 N95-24582

Geometric analysis of wing sections [NASA-TM-110346] p 335 N95-24629

Aerodynamic shape optimization of wing and wing-body configurations using control theory [NASA-CR-198024] p 335 N95-25334

The coupling of fluids, dynamics, and controls on advanced architecture computers [NASA-CR-197727] p 360 N95-25797

A quiet STOL Research Aircraft Development program [NAL-TR-1223] p 336 N95-25862

Noise impact of advanced high lift systems [NASA-CR-195028] p 362 N95-26160

Aerodynamics model for a generic ASTOVL lift-fan aircraft [NASA-TM-110347] p 332 N95-26302

Aircraft fuel system lightning protection design and qualification test procedures development [AD-A288401] p 380 N95-26497

Balanced on air aircraft [AD-D017251] p 389 N95-26537

Aeroelasticity of wing and wing-body configurations on parallel computers [NASA-CR-197756] p 389 N95-26590

Supersonic civil airplane study and design: Performance and sonic boom [NASA-CR-197745] p 390 N95-26813

AIAA Techfest 20 Proceedings [NIAR-94-1] p 367 N95-26941

Preliminary design problems and solutions for a supersonic oblique all-wing transport aircraft p 390 N95-26942

An exploratory application of neural networks for airfoil design p 448 N95-26943

Creating an alternative parameter optimization method (APO) p 375 N95-26946

Design of a high altitude long endurance aircraft with manufacturing considerations p 391 N95-26947

Incorporating biplane wing theory into a large, subsonic, all-cargo transport p 391 N95-26956

The lift-fan aircraft: Lessons learned [NASA-CR-196694] p 392 N95-27143

Rapid repair of large area damage to contoured aircraft structures p 394 N95-27516

Wind-tunnel test of the S814 thick root airfoil [DE95-000268] p 376 N95-27541

JPRS report: Science and technology. Central Eurasia [JPRS-UST-94-022] p 438 N95-27699

Propulsion system assessment for very high UAV under ERAT [NASA-CR-195469] p 406 N95-27866

Evaluation of all-electric secondary power for transport aircraft [NASA-CR-189077] p 441 N95-27999

Performance study for inlet installations [NASA-CR-189714] p 406 N95-28227

Ninth DOD/NASA/FAA Conference on Fibrous Composites in Structural Design, volume 3 [NASA-CR-198718] p 420 N95-28266

Ninth DOD/NASA/FAA Conference on Fibrous Composites in Structural Design, volume 1 [NASA-CR-198723] p 421 N95-28420

Benefits and limitations of composites in carrier-based aircraft p 422 N95-28422

Development of composite carrythrough bulkhead p 423 N95-28438

Structural design optimization with survivability dependent constraints application: Primary wing box of a multi-role fighter p 398 N95-28440

Probabilistic design of advanced composite structure p 424 N95-28443

Probabilistic evaluation of fuselage-type composite structures p 398 N95-28444

Ninth DOD/NASA/FAA Conference on Fibrous Composites in Structural Design, volume 2 [NASA-CR-198722] p 424 N95-28462

Overview of the ACT program p 424 N95-28463

Designers' unified cost model p 424 N95-28464

COINS: A composites information database system p 453 N95-28465

Structural testing of the technology integration box beam p 441 N95-28467

Technology integration box beam failure study p 441 N95-28468

Recent progress in NASA Langley textile reinforced composites program p 425 N95-28475

Advanced textile applications for primary aircraft structures p 399 N95-28476

Applications of a damage tolerance analysis methodology in aircraft design and production p 426 N95-28483

Advanced wing design survivability testing and results p 400 N95-28488

Rapid Airplane Parametric Input Design (RAPID) p 501 N95-28730

A grid generation system for multi-disciplinary design optimization p 567 N95-28763

The effects of design details on cost and weight of fuselage structures p 501 N95-28831

Global cost and weight evaluation of fuselage keel design concepts p 501 N95-28840

Cost model relationships between textile manufacturing processes and design details for transport fuselage elements p 536 N95-29043

A two element laminar flow airfoil optimized for cruise [NASA-CR-198580] p 479 N95-29338

Design, analysis and control of large transports so that control of engine thrust can be used as a back-up of the primary flight controls [NASA-CR-198958] p 518 N95-30254

Developing a workstation-based, real-time simulation for rapid handling qualities evaluations during design [NASA-CR-198831] p 505 N95-30335

A general inverse design procedure for aerodynamic bodies p 606 N95-30497

The process for addressing the challenges of aircraft pilot coupling p 597 N95-31063

The relation of handling qualities ratings to aircraft safety p 597 N95-31067

Handling qualities analysis on rate limiting elements in flight control systems p 619 N95-31071

Development of stitched/RTM primary structures for transport aircraft [NASA-CR-191441] p 630 N95-31421

Geometric modeling for computer aided design [NASA-CR-198828] p 679 N95-31982

Catapult-launching of the RAFALE design and experimentation p 609 N95-32008

Three-dimensional aerodynamic shape optimization using discrete sensitivity analysis p 691 N95-32904

Propulsion Controlled Aircraft design and development p 697 N95-33022

Special publication of National Aerospace Laboratory [NAL-SP-27] p 684 N95-34505

Requirements and trends of computational aerodynamics as a tool for aircraft design p 692 N95-34506

Numerical analysis around the whole SST configuration p 693 N95-34541

Application of CFD technique for HYFLEX aerodynamic design p 693 N95-34542

An LDV investigation of support structure influence on the flow field near the wingtip of a STOVL configuration in hover [AD-A294126] p 686 N95-34750

AIRCRAFT DETECTION

Visual contrast detection thresholds for aircraft contrails [AD-A288618] p 328 N95-25607

Orientation determination of aircraft using visual 3D matching and radar. Case study 2 [PB95-165791] p 350 N95-25749

Aircraft IR/acoustic detection evaluation. Volume 2: Development of a ground-based acoustic sensor system for the detection of subsonic jet-powered aircraft [NASA-CR-189705-VOL-2] p 452 N95-28073

Performance study for inlet installations [NASA-CR-189714] p 406 N95-28227

AIRCRAFT ENGINES

Trent engine development [BTN-94-EIX94461290507] p 82 A95-61727

On profiling a cam of an axial aviation diesel engine by periodic splines [BTN-94-EIX94461407946] p 82 A95-62264

On introduction of artificial intelligence elements to heat power engineering [BTN-94-EIX94461407961] p 100 A95-62635

Gas-turbine engines with increased efficiency of two circuits, due to the use of the utilizing steam-turbine circuit [BTN-94-EIX94461408755] p 153 A95-63638

On a program-information system TDsoft [BTN-94-EIX94461408773] p 175 A95-63656

Design optimization of aircraft engine-mount systems. [BTN-94-EIX94351143325] p 195 A95-67298

Aircraft engine emission reduction [BTN-95-EIX95031502750] p 196 A95-68257

Starter/generator testing [BTN-95-EIX95072498877] p 210 A95-68393

Ply layout optimization and micromechanics tailoring of composite aircraft engine structures [BTN-95-EIX95112524206] p 196 A95-69302

Engine life measurement and diagnostics [BTN-95-EIX95041505024] p 235 A95-70133

Subsidence of aircraft engine exhaust in the stratosphere: Implications for calculated ozone depletions [PAPER-93GL03426] p 251 A95-70297

Artificial intelligence for turboprop engine maintenance [BTN-95-EIX95182617812] p 288 A95-75757

Lycoming to test new engine core [HTN-95-41393] p 288 A95-76389

A new type of simulator for simulating the flow-field distortion of engine inlet [BTN-95-EIX95202638963] p 289 A95-76673

- Theoretical and experimental studies of fretting-initiated fatigue failure of aeroengine compressor discs
[BTN-94-EIX9442137285] p 343 A95-78467
- Nitrous oxide and methane emissions from aero engines
[HTN-95-21363] p 353 A95-78678
- Impact of present aircraft emissions of nitrogen oxides on tropospheric ozone and climate forcing
[HTN-95-21364] p 353 A95-78679
- Aircraft gas turbine emissions challenge
[BTN-94-EIX95011441239] p 403 A95-84196
- Nitrogen oxide emissions characteristics of augmented turbofan engines
[BTN-94-EIX95011441240] p 403 A95-84197
- Flex cycle combustor development and demonstration
[BTN-94-EIX95011441245] p 417 A95-84202
- Development of an aeroderivative gas turbine dry low emissions combustion system
[BTN-94-EIX95011441246] p 417 A95-84203
- Charles Norvin Rinek, an early American pioneer in advanced aviation engines
[SAE PAPER 930485] p 386 A95-84554
- NASA-Lewis tests Allison ASTOVL nozzle
[HTN-95-20603] p 404 A95-84784
- Applying nanostructured materials to future gas turbine engines
[HTN-95-11909] p 404 A95-85990
- Flyover noise reduction of piston-engine propeller aeroplanes using an active noise control technique
[SAE PAPER 931218] p 509 A95-87466
- Broadband noise characteristics of a model counter-rotating shrouded propfan
[SAE PAPER 931218] p 572 A95-88470
- Determination of minimum fuel octane number piston aircraft engines
[SAE PAPER 931230] p 528 A95-88961
- Vapor lock studies for gasolines with ethers
[SAE PAPER 931233] p 529 A95-88962
- Ongoing research into high octane unleaded avgas
[SAE PAPER 931234] p 529 A95-88963
- Structural composites in civil gas turbine aero engines
[HTN-95-B0258] p 529 A95-89202
- Preliminary design of a single engine business jet
[SAE PAPER 931253] p 493 A95-89222
- Should large business jets have four under the wing?
[SAE 931256] p 493 A95-89223
- Advances in the application of laser cutting, drilling, and welding aerospace parts
[SAE PAPER 932544] p 547 A95-90052
- A switched reluctance machine rotor position estimator: A neural network application
[SAE PAPER 932560] p 511 A95-90057
- Conversion of production automotive engines for aviation use
[SAE PAPER 932606] p 495 A95-90076
- High bypass separate flow exhaust system improved thrust efficiency by modifying the aft centerbody
[SAE PAPER 932622] p 511 A95-90083
- Engine/airframe installation CFD for commercial transports: An engine manufacturer's perspective
[SAE PAPER 932623] p 495 A95-90084
- Aeronautical technology - recent advances and future prospects
[HTN-95-01097] p 496 A95-90283
- Aircraft Symposium, 30th, Tsukuba, Japan, Sep. 30 - Oct. 2, 1992
[HTN-95-A1609] p 498 A95-91491
- A detailed Euler flow analysis of TPS and fanjet engine
[SAE PAPER 932622] p 473 A95-91515
- Overview of feasibility study on propulsion concepts for high speed civil transport
[SAE PAPER 932623] p 498 A95-91518
- Analysis and scale-model experiment of propeller driving motor for microwave-powered airplane
[CONGRESS PAPER C428-15-094] p 487 A95-91576
- Rolling bearing failure and wear debris detection
[CONGRESS PAPER C428-15-094] p 457 A95-91711
- Simultaneous engineering in aero gas turbine design and manufacture
[CONGRESS PAPER C428-20-204] p 581 A95-91723
- An example of airborne vibration monitoring improving flight safety in the Soloviev D-30-KU engine
[CONGRESS PAPER C428-21-141] p 508 A95-91728
- Applicability of electrically driven accessories for turbohaft engines
[BTN-95-EIX95292721153] p 612 A95-92589
- Manufacture technology
[CONGRESS PAPER C428-27-088] p 612 A95-93605
- The role of material behaviour modelling in stressing and life assessment of modern Aero-engine components
[CONGRESS PAPER C428-27-127] p 612 A95-93606
- Laser processing aircraft and turbine engine parts
[SAE PAPER 931356] p 634 A95-93640
- Concepts for aircraft subsystem integration
[SAE PAPER 931377] p 604 A95-93656
- SUIT: The integration of aircraft subsystems
[SAE PAPER 931381] p 604 A95-93657
- A subsystem integration technology concept
[SAE PAPER 931382] p 604 A95-93658
- A detailed power inverter design for a 250 kW switched reluctance aircraft engine starter/generator
[SAE PAPER 931388] p 613 A95-93664
- Detailed design of a 250-kW switched reluctance starter/generator for an aircraft engine
[SAE PAPER 931389] p 613 A95-93665
- Numerical simulation of the 3D turbulent flow around the combustor dome of an aircraft engine
[SAE PAPER 931389] p 640 A95-95423
- High performance parallel analysis of coupled problems for aircraft propulsion
[NASA-CR-195355] p 23 N95-10132
- NASA Lewis Propulsion Systems Laboratory customer guide manual
[NASA-TM-106569] p 21 N95-10822
- JPRS report: Science and technology. Central Eurasia: Engineering and equipment. Gas dynamics of supersonic shortened nozzles
[JPRS-UST-94-003-L] p 22 N95-10931
- Noise Con 1994: Proceedings of the 1994 National Conference on Noise Control Engineering. Progress in Noise Control for Industry
[LC-75-24750] p 28 N95-11259
- Radiant energy measurements from a scaled jet engine axisymmetric exhaust nozzle for a baseline code validation case
[NASA-TM-106686] p 25 N95-11409
- NASA's Hypersonic Research Engine Project: A review
[NASA-TM-107759] p 50 N95-12860
- Activities of the Structures Division, Lewis Research Center
[NASA-TM-108081] p 59 N95-13235
- Evaluation of alternative in-flight fire suppressants for full-scale testing in simulated aircraft engine nacelles and dry bays
[PB94-203403] p 42 N95-13247
- The development of the F100-PW-220 and F110-GE-100 engines: A case study of risk assessment and risk management
[AD-A282467] p 51 N95-13289
- AGARD highlights 94/2
[AGARD-HIGHLIGHTS-94/2] p 102 N95-13640
- Viper - Design modification
[NASA-CR-197191] p 79 N95-13703
- Turbomachinery Design Using CFD
[AGARD-LS-195] p 89 N95-14127
- Computational methods for preliminary design and geometry definition in turbomachinery
[AGARD-LS-195] p 89 N95-14128
- Elements of a modern turbomachinery design system
[AGARD-LS-195] p 90 N95-14129
- Designing in three dimensions
[AGARD-LS-195] p 90 N95-14130
- The industrial use of CFD in the design of turbomachinery
[AGARD-LS-195] p 90 N95-14133
- New methods, new methodology: Advanced CFD in the Sncma turbomachinery design process
[AGARD-LS-195] p 90 N95-14134
- The role of CFD in the design process
[AGARD-LS-195] p 90 N95-14135
- Aero design of turbomachinery components: CFD in complex systems
[AGARD-LS-195] p 90 N95-14136
- Portable parallel stochastic optimization for the design of aeropropulsion components
[NASA-CR-195312] p 154 N95-16072
- Theoretical fundamentals of the aircraft GTE tests
[NASA-CR-195312] p 138 N95-16265
- Hypersonic air-breathing aeropropulsion facility test support requirements
[NASA-CR-195312] p 144 N95-16319
- The global aircraft shape
[NASA-CR-195312] p 128 N95-16571
- Gyroscopic and propeller aerodynamic effects on engine mounts dynamic loads in turbulence conditions
[NASA-CR-195312] p 132 N95-18599
- Wave cycle design for wave rotor engines with limited nitrogen oxide emissions
[NASA-CR-195312] p 161 N95-18901
- Quality optimization of thermally sprayed coatings produced by the JP-5000 (HVOF) gun using mathematical modeling
[NASA-CR-195312] p 152 N95-19008
- Mathematical Models of Gas Turbine Engines and their Components
[AGARD-LS-198] p 139 N95-19017
- Proceedings of the USAF Structural Integrity Program Conference
[AD-A285684] p 194 N95-19517
- Air pollution mitigation measures for airports and associated activity
[PB94-207610] p 216 N95-19582
- Erosion, Corrosion and Foreign Object Damage Effects in Gas Turbines
[AGARD-CP-558] p 197 N95-19653
- Out of area experiences with the RB199 in Toronto
[CONGRESS PAPER C428-15-094] p 198 N95-19654
- The operation of gas turbine engines in hot and sandy conditions: Royal Air Force experiences in the Gulf conflict
[CONGRESS PAPER C428-15-094] p 198 N95-19655
- Navy foreign object damage and its impact on future gas turbine engine low pressure compression systems
[CONGRESS PAPER C428-15-094] p 198 N95-19658
- Scandinavian Airlines Systems experience on erosion, corrosion and foreign object damage effects on gas turbines
[CONGRESS PAPER C428-15-094] p 198 N95-19659
- Modern transport engine experience with environmental ingestion effects
[CONGRESS PAPER C428-15-094] p 199 N95-19660
- Design of fan blades subjected to bird impact
[CONGRESS PAPER C428-15-094] p 200 N95-19669
- Testing considerations for military aircraft engines in corrosive environments (a Navy perspective)
[CONGRESS PAPER C428-15-094] p 202 N95-19684
- Developing an emission factor for hazardous air pollutants for an F-16 using JP-8 fuel
[AD-A284802] p 216 N95-19685
- Turbine design and application volumes 1, 2, and 3
[E-5666-Vol-1-3] p 236 N95-22341
- High-performance parallel analysis of coupled problems for aircraft propulsion
[NASA-CR-197440] p 289 N95-23088
- Engines-only flight control system
[NASA-CASE-ARC-11944-1] p 294 N95-23389
- The effect of altitude conditions on the particle emissions of a J85-GE-5L turbojet engine
[NASA-TM-106669] p 339 N95-24561
- Bird ingestion into large turbofan engines
[DOT/FAA/CT-93/14] p 333 N95-24631
- Nitrogen oxide emissions and their control from uninstalled aircraft engines in enclosed test cells: Joint report to Congress on the Environmental Protection Agency - Department of Transportation study
[PB95-166237] p 358 N95-26005
- Thermal Barrier Coating Workshop
[NASA-CP-10170] p 344 N95-26119
- Thermal barrier coatings for aircraft engines: History and directions
[NASA-CP-10170] p 344 N95-26121
- Thermal barrier coatings issues in advanced land-based gas turbines
[NASA-CP-10170] p 344 N95-26122
- PVD TBC experience on GE aircraft engines
[NASA-CP-10170] p 345 N95-26126
- Thermal barrier coating life modeling in aircraft gas turbine engines
[NASA-CP-10170] p 346 N95-26140
- Design of a high altitude long endurance aircraft with manufacturing considerations
[NASA-CP-10170] p 391 N95-26947
- Prevention and control of inlet unstart using an SR-71 simulation
[NASA-CP-10170] p 367 N95-26948
- Analysis of aircraft engine blade subject to ice impact
[NASA-CP-10170] p 407 N95-28277
- Application of fiber-reinforced bismaleimide materials to aircraft nacelle structures
[NASA-CP-10170] p 397 N95-28278
- Surface modeling and grid generation for aeropropulsion CFD
[NASA-CP-10170] p 551 N95-28732
- Model development for active control of stall phenomena in aircraft gas turbine engines
[NASA-CP-10170] p 514 N95-29679
- Characterization of stall inception in high-speed single-stage compressors
[AD-A291275] p 514 N95-29934
- Thermal-mechanical fatigue crack growth in aircraft engine materials
[ISBN-0-315-86543-1] p 647 N95-31098
- Icing simulation in the aeropropulsion systems test facility propulsion development test cell C-2
[AD-A293039] p 599 N95-31667
- F-15 propulsion system
[AD-A293039] p 695 N95-33012
- Minimum fan turbine inlet temperature mode evaluation
[AD-A293039] p 696 N95-33016
- The application of Ada and formal methods to a safety critical engine control system
[AD-A293039] p 710 N95-33142
- AIRCRAFT EQUIPMENT**
- Starter/generator testing
[BTN-95-EIX95072498877] p 210 A95-68393
- Lightning protection technology for small general aviation composite material aircraft
[SAE PAPER 931241] p 483 A95-88964
- Performance evaluation test of GPS/DGPS navigation system installed in the NAL Dornier 228: Preliminary ground test results
[CONGRESS PAPER C428-6-113] p 487 A95-91575
- The air systems controllerate initiatives and policies for the procurement of reliable and maintainable equipment
[CONGRESS PAPER C428-6-113] p 549 A95-91682
- The impact of new technology on reliability of avionic equipment
[CONGRESS PAPER C428-6-114] p 549 A95-91683
- The avionics integrity programme (AVIP)
[CONGRESS PAPER C428-6-115] p 549 A95-91684
- Airborne collision avoidance systems - The UK experience
[CONGRESS PAPER C428-7-146] p 488 A95-91687

- Maintenance-free lead acid battery for inertial navigation systems aircraft
[BTN-95-EIX95292721316] p 633 A95-92511
- A subsystem integration technology concept
[SAE PAPER 931382] p 604 A95-93658
- Fatigue design of axially loaded semicircular lugs
[BTN-95-EIX0619952748190] p 637 A95-94252
- Bicarbonate of soda blasting technology for aircraft wheel depainting
[PB94-193323] p 104 N95-17466
- Preliminary evaluation of the F/A-18 quantity/multiple envelope expansion
[AD-A284119] p 132 N95-18407
- FASTPACK: Optimized solutions for modular avionics derived from a parametric study, Part 1: Platform features
p 233 N95-20634
- Immersion/two phase cooling
p 246 N95-20648
- Composite cases for airborne electronic equipment: A technology study and EMC
p 241 N95-20655
- Lightweight electronic enclosures using composite materials
p 241 N95-20656
- Modular supplies for a distributed architecture — avionics packaging
p 234 N95-20657
- Modular CNI avionics system
p 234 N95-20659
- TIM-SCT cable testing protocol
[AD-A286633] p 231 N95-20772
- Design of a controller for a flexible pointing system using H(infinity) synthesis
[AD-A286572] p 256 N95-20828
- Analysis of warping effects on the static and dynamic response of a seat-type structure
[NIAR-94-12] p 348 N95-24211
- Aircraft nosewheel steering simulation
p 412 N95-26944
- Helicopter life substantiation: Review of some USA and UK initiatives
[AD-A290045] p 502 N95-28851
- Development of LaRC (TM): IA thermoplastic polyimide coated aerospace wiring
[NASA-CR-195048] p 537 N95-30252
- Apparent size passive range method
[AD-D017360] p 611 N95-31180
- AIRCRAFT FUEL SYSTEMS**
- Ongoing research into high octane unleaded avgas
[SAE PAPER 931234] p 529 A95-88963
- Aircraft fuel system lightning protection design and qualification test procedures development
[AD-A288401] p 380 N95-26497
- AIRCRAFT FUELS**
- Trajectory modeling of emissions from lower stratospheric aircraft
[HTN-95-41219] p 317 A95-75031
- In situ observations in aircraft exhaust plumes in the lower stratosphere at midlatitudes
[HTN-95-A0862] p 318 A95-76266
- Sensitivity of two-dimensional model predictions of ozone response to stratospheric aircraft: An update
[HTN-95-A0863] p 318 A95-76267
- Modeling student knowledge with self-organizing feature maps
[BTN-95-EIX95262697073] p 564 A95-86862
- Determination of minimum fuel octane number piston aircraft engines
[SAE PAPER 931230] p 528 A95-88961
- Vapor lock studies for gasolines wwith ethers
[SAE PAPER 931233] p 529 A95-88962
- Ongoing research into high octane unleaded avgas
[SAE PAPER 931234] p 529 A95-88963
- Damage to composite aircraft structures from lightning strike attachment to unprotected CFC and internal sparking causing fuel injection
[CONGRESS PAPER C428-4-026] p 531 A95-91675
- Programmed ignition of metal compounds in a scramjet
p 16 N95-10466
- A study of aircraft post-crash fire fuel mitigation
[AD-A282208] p 40 N95-12499
- Analysis of test criteria for specifying foam firefighting agents for aircraft rescue and firefighting
[AD-A286381] p 227 N95-22352
- A numerical model to predict the fate of jettisoned aviation fuel
[AD-A289336] p 419 N95-26842
- The effect of aviation fuels containing low amounts of static dissipative additive on electrostatic charge generation
[AD-A280075] p 420 N95-28152
- The effects of aircraft fuel and fluids on the strength properties of Resin Transfer Molded (RTM) composites
p 536 N95-29047
- Evaluation of commercial water-in-fuel test kits
[AD-A292135] p 537 N95-29572
- Environmentally safe aviation fuels
p 631 N95-31768

AIRCRAFT GUIDANCE

- Analytical solution for controls, heats, and states of flight trajectories
[BTN-95-EIX95152583286] p 282 A95-73587
- Real-time decision aiding: Aircraft guidance for wind shear avoidance
[BTN-95-EIX95202637575] p 332 A95-78583
- Techniques and control of HOPE and its future technologies
p 506 A95-91543
- Airborne collision avoidance systems - The UK experience
[CONGRESS PAPER C428-7-146] p 488 A95-91687
- Research on an autonomous vision-guided helicopter
[AIAA PAPER 94-1240-CP] p 18 N95-11510
- Modeling of Instrument Landing System (ILS) localizer signal on runway 25L at Los Angeles International Airport
[NASA-TM-4588] p 125 N95-17384
- On-line handling of air traffic: Management, guidance and control
[AGARD-AG-321] p 126 N95-18927
- Research requirements for future visual guidance systems
[AD-A279188] p 191 N95-19810
- Guidance and control requirements for high-speed Rollout and Turnoff (ROTO)
[NASA-CR-195026] p 292 N95-22674
- Nonlinear system guidance in the presence of transmission zero dynamics
[NASA-TM-4661] p 309 N95-22804
- How to fly an aircraft with control theory and splines
p 360 N95-25805
- Flight evaluation of GPS/DGPS sensor systems installed in NAL Do228
[NAL-TR-1230] p 382 N95-26585
- Wide Area Differential GPS (WADGPS)
p 489 N95-29107
- Analytical investigations in aircraft and spacecraft trajectory optimization and optimal guidance
[NASA-CR-4672] p 526 N95-29339
- An investigation into the use of satellite-based positioning systems for flight reference/autoland operations
p 489 N95-29542

AIRCRAFT HAZARDS

- Aircraft icing measurements in East Coast winter storms
[HTN-95-60505] p 214 A95-68756
- Thundercloud electric field modeling for the ionosphere-Earth region. 1: Dependence on cloud charge distribution
[HTN-95-41223] p 317 A95-75035
- Identification of aviation weather hazards based on the integration of radar and lightning data
[HTN-95-51323] p 356 A95-80908
- The rain erosion of PEEK (polyetheretherketone)
[CONGRESS PAPER C428-4-039] p 531 A95-91676
- Lee waves benign and malignant
p 595 A95-93554
- Airborne Windshear Detection and Warning Systems. Fifth and Final Combined Manufacturers' and Technologists' Conference, part 2
[NASA-CF-10139-PT-2] p 41 N95-13203
- Certification methodology applied to the NASA experimental radar system
p 41 N95-13205
- Characteristics of civil aviation atmospheric hazards
p 42 N95-13208
- Doppler radar detection of vortex hazard indicators
p 42 N95-13212
- Icing: Accretion, detection, protection
p 77 N95-14897
- Heavy rain effects
p 78 N95-14899
- Aircraft accident report: Overspeed and loss of power on both engines during descent and power-off emergency, landing Simmons Airlines, Inc., d/b/a, American Eagle Flight 3641, N349SB False River Air Park, New Roads, Louisiana, 1 February 1994
[PB94-910408] p 78 N95-14916
- Characterizing the wake vortex signature for an active line of sight remote sensor
[NASA-CR-197697] p 333 N95-24391
- Consistent approach to describing aircraft HIRF protection
[NASA-CR-195067] p 334 N95-25341
- Further investigations of icing effects on an advanced high-lift multi-element airfoil
[NASA-TM-106947] p 381 N95-27762
- A review of falconry as a bird control technique with recommendations for use at the Shuttle Landing Facility, John F. Kennedy Space Center, Florida, USA
[NASA-TM-110142] p 381 N95-27859
- AIRCRAFT HYDRAULIC SYSTEMS**
- Hydraulic system diagnostic sensors
[BTN-95-EIX95031502752] p 209 A95-68259
- Computer aided diagnostic testing of installed flight control servo-actuators
[SAE PAPER 932584] p 494 A95-90068
- Second generation smart actuator
[SAE PAPER 932585] p 505 A95-90069
- New sensor technology for aircraft hydraulic system diagnostics
[SAE PAPER 932586] p 494 A95-90070
- Fault Diagnosis for condition monitoring applied to hydraulic circuits
[CONGRESS PAPER C428-12-165] p 456 A95-91703

AIRCRAFT ICING

- Prediction of ice accretion: Comparison between the 2D and 3D codes
[BTN-94-EIX94441385753] p 213 A95-68217
- Aircraft icing measurements in East Coast winter storms
[HTN-95-60505] p 214 A95-68756
- Conditions associated with large-drop regions
[HTN-95-10688] p 214 A95-68845
- Ice accretion on aircraft wings
[BTN-95-EIX95082502224] p 225 A95-71021
- Potential applications of the SSM/I cloud liquid water parameter to the estimation of marine aircraft icing
[HTN-95-80651] p 254 A95-72495
- Snow-band formation and evolution during the 15 November 1987 aircraft accident at Denver airport
[HTN-95-80699] p 254 A95-72543
- Effect of curvature in the numerical simulation of an electrothermal de-icer pad
[BTN-95-EIX95182619219] p 276 A95-76645
- Aerodynamics of a finite wing with simulated ice
[BTN-95-EIX95182619227] p 270 A95-76653
- Computational fluid dynamics with icing effects
[SAE PAPER 932532] p 466 A95-89192
- International Conference on Aviation Weather Systems, 5th, Vienna, VA, Aug. 2-6, 1993. Preprint Volume
[HTN-95-92940] p 652 A95-93441
- Preliminary comparisons between MM5 NCAR/Penn State model generated icing forecasts and observations
p 655 A95-93458
- Knowing our users -- A challenge for meteorologists at the National Aviation Weather Advisory Unit
p 655 A95-93459
- An in-situ system for warning of icing conditions
p 660 A95-93481
- The aviation gridded forecast system verification program - A description of aviation-impact-variable evaluation plans
p 664 A95-93498
- Use of pilot reports for verification of aircraft icing diagnoses and forecasts
p 666 A95-93508
- Examination of conditions in the proximity of pilot reports of aircraft icing during storm-fest
p 666 A95-93509
- The improvement of meteorological data for air traffic management purposes
p 668 A95-93518
- User involvement in the development of an advanced icing product for use in aviation
p 672 A95-93537
- Creating a global climatology of freezing rain using numerical model output
p 673 A95-93541
- The production of supercooled liquid water by a secondary cold front
p 673 A95-93542
- An application of some cloud modeling techniques to a regional model simulation of an icing event
p 673 A95-93543
- Airplane icing research at the Boeing Company: Participation in the second Canadian Atlantic Storms Program
p 674 A95-93544
- Aircraft icing: Meteorological effects on aircraft performance
p 674 A95-93545
- Preliminary studies of ice formation in upslope clouds
p 674 A95-93546
- The development of an aircraft icing forecast technique using data from maps
p 675 A95-93549
- User's manual for the NASA Lewis ice accretion/heat transfer prediction code with electrothermal deicer input
[NASA-CR-4530] p 57 N95-11888
- Role of wind tunnels and computer codes in the certification and qualification of rotorcraft for flight in forecast icing
[NASA-TM-106747] p 39 N95-13197
- Icing: Accretion, detection, protection
p 77 N95-14897
- Collection efficiency and ice accretion calculations for a sphere, a swept MS(1)-317 wing, a swept NACA-0012 wing tip, an axisymmetric inlet, and a Boeing 737-300
[NASA-TM-106831] p 123 N95-18582
- Methods for scaling icing test conditions
[NASA-TM-106827] p 124 N95-19284
- Additional improvements to the NASA Lewis ice accretion code LEWICE
[NASA-TM-106849] p 309 N95-22669
- Collaborative research on aircraft icing and charging processes in ice
[AD-A285102] p 276 N95-23201
- An analysis of B-1B exterior jet blast windshield anti-icing performance using pre-cooled compressor bleed air
[AD-A292522] p 485 N95-28811

- Users manual for the improved NASA Lewis ice accretion code LEWICE 1.6
[NASA-CR-198355] p 485 N95-29132
- Icing simulation in the aeropropulsion systems test facility propulsion development test cell C-2
[AD-A293039] p 599 N95-31667
- Investigation of water droplet trajectories within the NASA icing research tunnel
[NASA-TM-107023] p 684 N95-32769
- AIRCRAFT INDUSTRY**
- Fatigue resistance of peened 7050-T7451 aluminium alloy: Repair and re-treatment of a component surface
[BTN-94-EIX94371347838] p 206 A95-69131
- Selecting and management of fire fighter aircraft
[BTN-95-EIX95062487538] p 193 A95-69246
- Evaluation and management of research and development in aeronautics
[CONGRESS PAPER C428-8-102] p 581 A95-91691
- Airplane icing research at the Boeing Company: Participation in the second Canadian Atlantic Storms Program
p 674 A95-93544
- Design and construction of a remote piloted flying wing
[NASA-CR-197195] p 47 N95-12695
- The industrial use of CFD in the design of turbomachinery
p 90 N95-14133
- Development of processes, means, and theoretical principles of thin-walled detail plastic forming at Kazan Aviation Institute
p 155 N95-16281
- Public-sector aviation issues: Graduate research award papers, 1992-1993
[PB94-217478] p 219 N95-19967
- Report of proceedings: Aviation Accident Investigation Symposium. Volume 2: Participant presentations
[PB94-917007] p 277 N95-23598
- Strategy in the commercial aircraft industry in the United States: A comparison of decisionmaking by McDonnell-Douglas and Boeing aircraft companies from 1977-1983
p 366 N95-26409
- Surviving the peace. Lessons learned from the aircraft industry in the 1920s and 1930s
[AD-A288284] p 366 N95-26455
- AIRCRAFT INSTRUMENTS**
- Flight-deck displays on the Boeing 777
[BTN-95-EIX95142562402] p 286 A95-73438
- Flight test evaluation of a 35 GHz forward looking altimeter for terrain avoidance
[BTN-95-EIX95212641071] p 287 A95-76736
- An intercomparison of aircraft instrumentation for tropospheric measurements of sulfur dioxide
[HTN-95-91855] p 354 A95-80843
- An intercomparison of aircraft instrumentation for tropospheric measurements of carbonyl sulfide, hydrogen sulfide, and carbon disulfide
[HTN-95-91856] p 355 A95-80844
- An intercomparison of instrumentation for tropospheric measurements of dimethyl sulfide: Aircraft results for concentrations at the parts-per-trillion level
[HTN-95-91857] p 355 A95-80845
- Status of Enhanced Vision System
p 506 A95-91542
- Pitot/static leak testing
[CONGRESS PAPER C428-9-035] p 508 A95-91696
- Design of a modern pitch pointing control system
[BTN-95-EIX95302731226] p 618 A95-94045
- Operational and research aspects of a radio-controlled model flight test program
[BTN-95-EIX0619952748177] p 606 A95-94471
- Airborne air traffic control: An application of distributed processing in the air traffic control environment
[HTN-95-12417] p 611 A95-95210
- Flight test of takeoff performance monitoring system
[NASA-TP-3403] p 51 N95-12664
- Flight parameters monitoring system for tracking structural integrity of rotary-wing aircraft
p 135 N95-19469
- Flight evaluation of GPS/DGPS sensor systems installed in NAL Do228
[NAL-TR-1230] p 382 N95-26585
- Guidelines for the design of GPS and LORAN receiver controls and displays
[AD-A293753] p 602 N95-31572
- Integrated special mission flight management for a flight inspection aircraft
p 692 N95-33145
- AIRCRAFT LANDING**
- High accuracy navigation and landing system using GPS/IMU system integration
[BTN-94-EIX94441386129] p 189 A95-68185
- On-the-fly carrier phase ambiguity resolution for precise aircraft landing
[BTN-95-EIX95112522535] p 190 A95-69328
- Comments on effect of wet snow on the null-reference ILS system
[BTN-95-EIX95142555488] p 227 A95-72885
- Progress in high-lift aerodynamic calculations
[BTN-95-EIX95152582315] p 264 A95-73518
- Fan noise reduction from a supersonic inlet during simulated aircraft approach
[BTN-95-EIX95292721155] p 572 A95-89894
- NASA evaluation of Type 2 chemical depositions — effects of deicer deposition on aircraft tire friction performance
[SAE PAPER 932582] p 495 A95-90086
- Arrival traffic handling for a parallel runway airport
p 487 A95-91537
- CCLA operation on MLS
p 487 A95-91540
- Analysis of an MLS automatic landing control law for the NAL experimental research aircraft D0-228. 2: Curved approach and landing
p 508 A95-91588
- Passive millimeter wave camera for aircraft landing in low visibility conditions
[BTN-95-EIX95292721321] p 609 A95-92513
- Operational and research aspects of a radio-controlled model flight test program
[BTN-95-EIX0619952748177] p 606 A95-94471
- General aviation landing incidents and accidents: A review of ASRS and AOPA research findings
p 596 A95-95198
- Evaluation of F-18A approach and landing flying qualities using an in-flight simulator
[CALSPAN-6241-F-1] p 12 N95-10442
- Dynamic ground effects flight test of an F-15 aircraft
[NASA-TM-4604] p 38 N95-12191
- Passive MMW camera for low visibility landings
p 59 N95-13215
- Airplane takeoff and landing performance monitoring system
[NASA-CASE-LAR-14745-2-SB] p 85 N95-14415
- Assessment of CTAS ETA prediction capabilities
[NASA-CR-197224] p 97 N95-15728
- Application of GPS/SINS/RA integrated system to aircraft approach landing
p 125 N95-16277
- Super-heavy aircraft study
[AD-A279602] p 238 N95-19955
- F-15 resource tape
[NASA-TM-110502] p 230 N95-19994
- Minima reduction simulation test results
[AD-A285626] p 228 N95-21148
- Aircraft accident report: Impact with blast fence upon landing rollout Action Air Charters flight 990 Piper PA-31-350, N990RA, Stratford, Connecticut, 27 April 1994
[PB94-910410] p 333 N95-24206
- Characterizing the wake vortex signature for an active line of sight remote sensor
[NASA-CR-197697] p 333 N95-24391
- Flightpath synthesis and HUD scaling for V/STOL terminal area operations
[NASA-TM-110348] p 383 N95-26587
- An integrated GPS/INS/BARO and radar altimeter system for aircraft precision approach landings
[AD-A289280] p 383 N95-26985
- An investigation into the use of satellite-based positioning systems for flight reference/autoland operations
p 489 N95-29542
- Flight test evaluation of the Stanford University/United Airlines differential GPS Category 3 automatic landing system
[NASA-TM-110354] p 593 N95-30788
- Dynamic ground effects flight test of the NASA F-15 aircraft
p 692 N95-33024
- Design challenges encountered in the F-15 PCA flight test program
p 692 N95-33025
- Machinability study of Aermet 100
[DE95-011532] p 701 N95-33408
- AIRCRAFT MAINTENANCE**
- On-board avionics maintenance
[BTN-94-EIX94461047054] p 82 A95-61741
- Aircraft accident investigation and airworthiness — A practical example of the interaction of two disciplines with some reflections on possible legal consequences
[HTN-95-50219] p 176 A95-64856
- Computerized maintenance aid
[BTN-95-EIX95031502749] p 217 A95-68256
- Maintenance requirements for a supersonic transport
[BTN-95-EIX95031502751] p 179 A95-68258
- Hydraulic system diagnostic sensors
[BTN-95-EIX95031502752] p 209 A95-68259
- Corrosion prevention and control
[BTN-95-EIX95031502753] p 188 A95-68260
- USAF aging aircraft program
[BTN-95-EIX95072498878] p 180 A95-68394
- Service life extensions for the C-141
[BTN-95-EIX95112530749] p 193 A95-69295
- Bonded composite repair of cracked load-bearing holes
[BTN-94-EIX94401360553] p 243 A95-71867
- Maintenance challenges and trends
[BTN-95-EIX95182617808] p 261 A95-75753
- Maintenance programs
[BTN-95-EIX95182617809] p 261 A95-75754
- Aircraft stripping and painting
[BTN-95-EIX95182617810] p 300 A95-75755
- Condition monitoring and diagnostics
[BTN-95-EIX95182617811] p 261 A95-75756
- Artificial intelligence for turboprop engine maintenance
[BTN-95-EIX95182617812] p 288 A95-75757
- Maintenance programs
[HTN-95-92310] p 365 A95-85354
- Artificial intelligence for turboprop engine maintenance
[HTN-95-92313] p 404 A95-85357
- Elements of structural integrity assurance
p 387 A95-85896
- Verification of the damage tolerance of a fighter aircraft
p 388 A95-85897
- FAA's Aging Commuter Airplane Program
[SAE PAPER 931248] p 483 A95-89220
- New sensor technology for aircraft hydraulic system diagnostics
[SAE PAPER 932586] p 494 A95-90070
- GateLink highspeed communications with parked aircraft
[SAE PAPER 932610] p 486 A95-90079
- Aircraft wiring maintenance: Development of a computerized maintenance aid
[SAE PAPER 932615] p 456 A95-90080
- Use of starch based blast media for dry paint stripping
[SAE PAPER 932616] p 456 A95-90081
- Maintenance training to cope with high-tech innovations
[SAE PAPER 932619] p 456 A95-90082
- Ultrasonic imaging of damages in CRFT-laminates
p 578 A95-90828
- Experience of aircraft manufacturer for paint removal using dry stripping method
p 456 A95-91501
- Repairs to composite structure on military aircraft
[CONGRESS PAPER C428-4-067] p 531 A95-91677
- Ageing aircraft after ALOHA
[CONGRESS PAPER C428-11-188] p 484 A95-91701
- Health monitoring and cost implications for an airline operator
[CONGRESS PAPER C428-12-166] p 457 A95-91704
- Gas path debris monitoring
[CONGRESS PAPER C428-15-031] p 508 A95-91710
- Rolling bearing failure and wear debris detection
[CONGRESS PAPER C428-15-094] p 457 A95-91711
- Aircraft gear train diagnostics using the irregular rotation of the external shafts
[CONGRESS PAPER C428-15-097] p 508 A95-91712
- Developments in wear particle analysis using computerised procedures
[CONGRESS PAPER C428-15-216] p 457 A95-91713
- The use of math-dynamic models to aid the development of integrated health and usage monitoring systems
[CONGRESS PAPER C428-19-079] p 457 A95-91720
- Integrated test system single point control of aircraft checkout
[SAE PAPER 931417] p 583 A95-93682
- A generic telerobotics architecture for C-5 industrial processes
[AIAA PAPER 94-1264-CP] p 27 N95-11529
- Damage tolerant repair techniques for pressurized aircraft fuselages
[AD-A281982] p 65 N95-14144
- Proceedings of the FAA Inspection Program Area Review
[AD-A283849] p 77 N95-14350
- More supportable T-38A enhancement study
[AD-A283671] p 66 N95-15331
- Problems with aging wiring in Naval aircraft
p 154 N95-16048
- Military aviation maintenance industry in Western Europe: Concentration and internationalization
[PB94-189180] p 104 N95-17451
- Ultrasonic techniques for repair of aircraft structures with bonded composite patches
p 136 N95-19486
- Air pollution mitigation measures for airports and associated activity
[PB94-207610] p 216 N95-19582
- Erosion, Corrosion and Foreign Object Damage Effects in Gas Turbines
[AGARD-CP-558] p 197 N95-19653
- Out of area experiences with the RB199 in Toronto
p 198 N95-19654
- The operation of gas turbine engines in hot and sandy conditions: Royal Air Force experiences in the Gulf conflict
p 198 N95-19655

- Navy foreign object damage and its impact on future gas turbine engine low pressure compression systems p 198 N95-19658
- Scandinavian Airlines Systems experience on erosion, corrosion and foreign object damage effects on gas turbines p 198 N95-19659
- Special investigation report: Maintenance anomaly resulting in dragged engine during landing rollout. Northwest Airlines Flight 18, Boeing 747-251B, N637US, New Tokyo International Airport, Narita, Japan, 1 Mar. 1994 [PB94-917006] p 188 N95-19793
- Why do airlines want and use thrust reversers? A compilation of airline industry responses to a survey regarding the use of thrust reversers on commercial transport airplanes [NASA-TM-109158] p 226 N95-20706
- Damage tolerant repair techniques for pressurized aircraft fuselages [AD-A286298] p 219 N95-22046
- Forecasting aircraft mishaps using monthly maintenance reports [AD-A286049] p 227 N95-22417
- POD assessment of NDI procedures using a round robin test [AGARD-R-809] p 315 N95-23602
- Enhancement of F/A-18 operational flight measurements: Data report for phase I [DSTO-TR-0049] p 286 N95-23666
- An overview of Health and Usage Monitoring Systems (HUMS) for military helicopters [DSTO-TR-0061] p 327 N95-24200
- Helicopter life substantiation: Review of some USA and UK initiatives [DSTO-TR-0062] p 328 N95-24201
- Estimate of probability of crack detection from service difficulty report data [PB95-149381] p 328 N95-24295
- Emerging nondestructive inspection for aging aircraft [PB95-143053] p 328 N95-25401
- Proceedings of the 2d USAF Aging Aircraft Conference [AD-A288217] p 336 N95-25578
- Survey and implementation of commercial manual controllers for a generic telerobotics architecture [AD-A289215] p 449 N95-26990
- AH-1F COBRA rewire program MANPRINT analysis [AD-A289190] p 391 N95-27018
- Composite Repair of Military Aircraft Structures [AGARD-CP-550] p 392 N95-27504
- Bonded composite repair of metallic aircraft components: Overview of Australian activities p 392 N95-27505
- Status of bonded boron/epoxy doublers for military and commercial aircraft structures p 393 N95-27506
- Adhesively bonded composite patch repair of cracked aluminum alloy structures p 393 N95-27507
- Composite repair of metallic airframe: Twenty years of experience p 393 N95-27508
- Bonded composite repair of thin metallic materials: Variable load amplitude and temperature cycling effects p 393 N95-27509
- Design and structural validation of CF116 upper wing skin boron doubler p 393 N95-27510
- A FEAM based methodology for analyzing composite patch repairs of metallic structures p 394 N95-27511
- Structural modification and repair of C-130 wing structure using bonded composites p 394 N95-27512
- Evaluation of patch effectiveness in repairing aircraft components p 394 N95-27513
- Field repair materials for naval aircraft p 394 N95-27514
- On aircraft repair verification of a fighter A/C integrally stiffened fuselage skin p 394 N95-27515
- Rapid repair of large area damage to contoured aircraft structures p 394 N95-27516
- Composite repair of a CF18: Vertical stabilizer leading edge p 395 N95-27517
- Composite repair issues on the CF-18 aircraft p 395 N95-27518
- Repair technology for thermoplastic aircraft structures p 395 N95-27519
- Repair of high temperature composite aircraft structure p 395 N95-27520
- Composite repair of composite structures p 395 N95-27521
- External patch repair of CFRP/honeycomb sandwich p 395 N95-27522
- Scarf joint technique with cocured and precured patches for composite repair p 396 N95-27524
- Composite or metallic bolted repairs on self-stiffened carbon wing panel of the commuter ATR72 design criteria, analysis, verification by test p 396 N95-27525
- Damage occurrence on composites during testing and fleet service: Repair of Airbus aircraft p 396 N95-27526
- Repairs of CFC primary structures p 396 N95-27527
- The development of an engineering standard for composite repairs p 396 N95-27528
- Proceedings of the AIAA/FAA joint symposium on general aviation systems [AD-A289830] p 368 N95-28610
- The use of electrochemistry and ellipsometry for identifying and evaluating corrosion on aircraft [AD-A290249] p 504 N95-29426
- AGARD flight test techniques series. Volume 13: Reliability and maintainability [AGARD-AG-300-VOL-13] p 504 N95-29503
- Bicarbonate of soda paint stripping process validation and material characterization p 631 N95-31778
- Environmentally Safe and Effective Processes for Paint Removal [AGARD-LS-201] p 650 N95-32165
- Process evaluation p 651 N95-32180
- Standardization work p 651 N95-32181
- AIRCRAFT MANEUVERS**
- Time-optimal turn to a heading: An analytic solution [BTN-94-EIX94511433940] p 142 A95-64606
- Functional agility metrics and optimal trajectory analysis [BTN-95-EIX95182619121] p 321 A95-76598
- Kinematics and aerodynamics of velocity-vector roll [BTN-95-EIX95182619126] p 291 A95-76603
- Optimal lateral-escape maneuvers for microburst encounters during flight approach [BTN-95-EIX95182619127] p 276 A95-76604
- Multiaxis pilot ratings for damaged aircraft [BTN-95-EIX95182619128] p 269 A95-76605
- Automatic formation flight control [BTN-95-EIX95182619153] p 292 A95-76630
- Rolling maneuver load alleviation using active controls [BTN-95-EIX95182619217] p 270 A95-76643
- Application of Navier-Stokes aeroelastic methods to improve fighter wing maneuver performance [BTN-95-EIX95182619218] p 284 A95-76644
- Load alleviation maneuvers for a launch vehicle p 342 A95-81360
- Nonlinear decoupling control study for aircraft maneuvering flight [HTN-95-71130] p 408 A95-83491
- Part-task simulator evaluations of advanced terrain displays [SAE PAPER 932570] p 401 A95-84567
- Application of artificial neural networks in nonlinear aerodynamics and aircraft design [SAE PAPER 932533] p 492 A95-89193
- High-angle-of-attack yawing moment asymmetry of the X-31 aircraft from flight test [NASA-CR-186030] p 13 N95-11410
- Examples of flight path optimization using a multivariate gradient-search method. Addendum A: Variation of optimum flight profile parameters with range [ESDU-94016-ADD-A] p 44 N95-11794
- Comparison of X-31 flight, wind-tunnel, and water-tunnel yawing moment asymmetries at high angles of attack p 68 N95-14234
- X-31 post-stall envelope expansion and tactical utility testing p 70 N95-14242
- X-31 high angle of attack control system performance p 70 N95-14244
- F-15 resource tape [NASA-TM-110502] p 230 N95-19994
- Evaluation of proposed agility metrics using X-31 vs. F/A-18 flight data [AD-A292573] p 502 N95-28977
- AIRCRAFT MODELS**
- Aircraft model for the AIAA controls design challenge [BTN-94-EIX94511433921] p 142 A95-64587
- Flight experience with lightweight, low-power miniaturized instrumentation systems [BTN-95-EIX95062487522] p 180 A95-69230
- RCS measurements, transformations, and comparisons under cylindrical and plane wave illumination [BTN-94-EIX94371347126] p 242 A95-69976
- SEM representation of the early and late time fields scattered from wire targets [BTN-94-EIX94381353142] p 306 A95-74496
- Some aspects of the aerodynamics of separating strap-ons [BTN-95-EIX95182617464] p 298 A95-75735
- Aeroelastic vehicle multivariable control synthesis with analytical robustness evaluation [BTN-95-EIX95182619115] p 321 A95-76592
- Drag function modeling for air traffic simulation [BTN-95-EIX95182619154] p 279 A95-76631
- A tool for airframe shaping - idea and application [SAE PAPER 931224] p 491 A95-87568
- Aerodynamic tailoring of the Learjet Model 60 wing [SAE PAPER 932534] p 492 A95-89194
- CaRnard: A new roadable aircraft concept [SAE PAPER 932601] p 494 A95-90071
- Numerical investigation of sound transmission through double wall cylinders with respect to active noise control p 577 A95-90134
- Aerodynamic characteristics of supersonic air-intake/aircraft integrated models p 472 A95-91512
- Flight test of STS radio controlled scale model p 499 A95-91539
- Analysis and scale-model experiment of propeller driving motor for microwave-powered airplane p 487 A95-91576
- Modelling requirements in flight simulation [HTN-95-C0004] p 585 A95-93392
- Statistical discrete gust-power spectral density methods overlap-holistic proof and beyond [BTN-95-EIX0619952748175] p 584 A95-94469
- Operational and research aspects of a radio-controlled model flight test program [BTN-95-EIX0619952748177] p 606 A95-94471
- Optimal trajectories for an unmanned air-vehicle in the horizontal plane [BTN-95-EIX0619952748191] p 606 A95-94480
- Effect of leading-edge extension fences on the vortex wake of an F/A-18 model [BTN-95-EIX0619952748192] p 591 A95-94481
- Advanced distributed simulation technology advanced rotary wing aircraft. System/segment specification. Volume 5: Simulation system module AH-64D kit [AD-A280433] p 20 N95-10353
- Radio controlled for research [NASA-TM-104292] p 17 N95-10717
- Computer-aided light sheet flow visualization using photogrammetry [NASA-TP-3416] p 26 N95-10859
- The present and future of aircraft noise models: A user's perspective p 32 N95-11324
- STOVL Control Integration Program [NASA-CR-195358] p 18 N95-11487
- Pressure measurements on an F/A-18 twin vertical tail in buffeting flow. Volume 3: Buffet power spectral densities [AD-A281444] p 36 N95-11829
- Icarus Rewaxed: A high speed, low-cost general aviation aircraft for Aeroworld [NASA-CR-197155] p 45 N95-12609
- Electromagnetic on-aircraft antenna radiation in the presence of composite plates [NASA-CR-196126] p 58 N95-12856
- Advanced distributed simulation technology advanced rotary wing aircraft. Study comparing approaches to modeling the ARWA main rotor [AD-A280824] p 79 N95-14306
- Linear prediction data extrapolation superresolution radar imaging p 155 N95-16268
- Automation of reverse engineering process in aircraft modeling and related optimization problems [NASA-CR-197109] p 129 N95-16899
- Measurements on a two-dimensional aerofoil with high-lift devices p 109 N95-17848
- Two-dimensional 16.5 percent thick supercritical airfoil NLR 7301 p 110 N95-17854
- Low-speed surface pressure and boundary layer measurement data for the NLR 7301 airfoil section with trailing edge flap p 111 N95-17855
- Data from the GARTEUR (AD) Action Group 02 airfoil CAST 7/DOA1 experiments p 111 N95-17856
- A supercritical airfoil experiment p 111 N95-17858
- Two-dimensional high-lift airfoil data for CFD code validation p 112 N95-17859
- Measurements of the flow over a low aspect-ratio wing in the Mach number range 0.6 to 0.87 for the purpose of validation of computational methods. Part 1: Wing design, model construction, surface flow. Part 2: Mean flow in the boundary layer and wake, 4 test cases p 112 N95-17860
- Detailed study at supersonic speeds of the flow around delta wings p 112 N95-17861
- Investigation into the aerodynamic characteristics of a combat aircraft research model fitted with a forward swept wing p 116 N95-17884
- Interaction, bursting and control of vortices of a cropped double-delta wing at high angle of attack [AD-A283656] p 119 N95-18669
- Estimating wind tunnel interference due to vectored jet flows p 164 N95-19265
- Effects of yaw and pitch motion on model attitude measurements [NASA-TM-4641] p 250 N95-22109
- An investigation of helicopter dynamic coupling using an analytical model [NASA-CR-197420] p 285 N95-23217
- Inner loop flight control for the High-Speed Civil Transport p 293 N95-23314
- Aspect estimation of an aircraft using library model silhouettes [PB95-141834] p 360 N95-25894

- Airfoil modification effects on subsonic and transonic pressure distributions and performance for the EA-6B airplane
[NASA-TP-3516] p 373 N95-26382
- Simulation model of the integrated flight/propulsion control system, displays, and propulsion system for ASTOVL lift-fan aircraft
[NASA-TM-108866] p 405 N95-26412
- Experimental investigation of static and dynamic ground effect on HOPE ALFLEX vehicle
[NAL-TR-1236] p 388 N95-26525
- Comparison of fixed wing aircraft algorithms for JANUS
[AD-A288503] p 389 N95-26652
- A verification procedure for MSC/NASTRAN Finite Element Models
[NASA-CR-4675] p 392 N95-27371
- Modeling of aircraft unsteady aerodynamic characteristics. Part 2: Parameters estimated from wind tunnel data
[NASA-TM-110161] p 410 N95-27839
- Application of optimization technique to control system design for departure prevention and aircraft model estimation through dynamic inversion.
p 517 N95-29156
- Design and evaluation of a LQR controller for the bluebird unmanned air vehicle*
[AD-A289769] p 504 N95-29457
- Low-order nonlinear dynamic model of IC engine-variable pitch propeller system for general aviation aircraft
[NASA-TM-107006] p 694 N95-32916
- AIRCRAFT NOISE**
- Assessment of helicopter noise annoyance: A comparison between noise from helicopters and from jet aircraft
[BTN-94-EIX94341341967] p 62 A95-60867
- The effects of aircraft (B-52) overflights on ancient structures
[BTN-94-EIX94341340070] p 171 A95-63522
- Noise and vibration control
[BTN-95-EIX95042477108] p 179 A95-68351
- Possible guidelines for helicopter noise assessment
[HTN-95-92535] p 558 A95-87355
- The effects and prediction of rotary wing aircraft noise on the community
[HTN-95-92536] p 558 A95-87356
- Environmental noise monitoring - source identification
[HTN-95-92537] p 558 A95-87357
- The use of the Equivalent Continuous Sound Level (L(sub eq)) as an aircraft noise index
[HTN-95-92542] p 558 A95-87362
- Aircraft noise and sleep disturbance: A field study
[HTN-95-92543] p 558 A95-87363
- Noise levels of helicopters performing elevated pad take-off and landing procedures
[HTN-95-92544] p 559 A95-87364
- Long distance propagation model and its application to aircraft en route noise prediction
[HTN-95-61221] p 491 A95-87594
- Monitoring noise from aircraft operations in the vicinity of airports
p 570 A95-88462
- Nordic Standards for measurement of aircraft noise immersion in residential areas and noise reduction of dwellings
p 570 A95-88463
- Modeling lateral attenuation of aircraft flight noise
p 570 A95-88464
- Time-average aircraft noise descriptors: Confusion with no benefit
p 559 A95-88474
- Aircraft noise zoning in Norway
p 581 A95-88476
- Criticism of the Leq as an index for aircraft noise and other discontinuous noise sources
p 559 A95-88477
- Criticism of the Leq as an index for aircraft noise and other discontinuous noise sources
p 559 A95-88478
- Noise control in aeroacoustics: Proceedings of the 1993 National Conference on Noise Control Engineering, NOISE-CON 93, Williamsburg, VA, May 2-5, 1993
[ISBN 0-931784-26-3] p 573 A95-90088
- Past and present UK research on aircraft noise effects
p 560 A95-90090
- Standardization of aircraft noise insulation measures without compromising results
p 561 A95-90115
- The effect of onset rate on annoyance to military aircraft noise
p 561 A95-90119
- Development and field test of the Beta version of the USAF Assessment System for Aircraft Noise (ASAN)
p 561 A95-90121
- Environmental noise research using the Human Response Monitor (HRM). Phase 1: System development
p 562 A95-90122
- Improvement of the predicted aural detection code ICHIN (I Can Hear It Now)
p 576 A95-90123
- Identification of noise events as aircraft
p 576 A95-90126
- Noise and vibration control in aircraft: A global approach
p 576 A95-90128
- The influence of source acceleration on acoustic signals
p 577 A95-90136
- Effects of signal analysis parameters and noise removal on measured aircraft spectra
p 578 A95-90137
- Incorporation of topography effects in aircraft noise modeling
p 578 A95-90140
- Noise Con 1994: Proceedings of the 1994 National Conference on Noise Control Engineering. Progress in Noise Control for Industry
[LC-75-24750] p 28 N95-11259
- Transmission loss characteristics of aircraft sidewall systems to control cabin interior noise
p 28 N95-11261
- Achievements and tasks for active noise control
p 29 N95-11270
- Active control of turbomachine discrete tones
p 29 N95-11275
- Active control of interior noise in a business jet using piezoceramic actuators
p 29 N95-11276
- Analytical investigation of adaptive control of radiated inlet noise from turbofan engines
p 30 N95-11277
- Adaptive tuned vibration absorbers: Tuning laws, tracking agility, sizing, and physical implementations
p 25 N95-11280
- A theoretical analysis of airborne sound transfer for a resiliently mounted machine to its foundation
p 30 N95-11304
- Effect of constraining layer stiffness on performance of damping tile materials using finite element modelling with Rayleigh integral
p 30 N95-11306
- 25 years of airport sound insulation programs
p 31 N95-11307
- Assessing effects of military aircraft noise on residential property values near airbases
p 31 N95-11310
- Integrating NOISEMAP with the Geographic Resource Analysis Support System (GRASS) to enhance environmental impact assessments and land use compatibility studies
p 31 N95-11311
- At Istanbul-Ataturk Airport measurement and analysis of noise in due of take-off time
p 31 N95-11319
- Determining the effects of alternative departure cutback altitudes and power settings: A case study, John Wayne Airport
p 31 N95-11320
- INM contour validation: A case study
p 31 N95-11321
- MOAMAP: A model that combines several different kinds of aircraft operations
p 32 N95-11323
- The present and future of aircraft noise models: A user's perspective
p 32 N95-11324
- Potential impacts of advanced aerodynamic technology on air transportation system productivity
[NASA-TM-109154] p 10 N95-11489
- En route noise levels from propfan test assessment airplane
[NASA-TP-3451] p 62 N95-12341
- The assessment of the AH-64D, longbow, mast-mounted assembly noise hazard for maintenance personnel
[AD-A284971] p 171 N95-16226
- Helicopter internal noise
p 173 N95-19144
- Impact of noise environment on engine nacelle design
p 173 N95-19147
- Modelling structurally damaging twin-jet screech
p 135 N95-19154
- An overall approach of cockpit noise verification in a military aircraft
p 175 N95-19163
- Noise transmission and reduction in turboprop aircraft
p 175 N95-19164
- Acoustic climb to cruise test
[NASA-TM-110504] p 230 N95-20155
- Effect of atmospheric pressure on measured aircraft noise levels
[PB95-130423] p 232 N95-21425
- The use of cowl camber and taper to reduce rotor/stator interaction noise
[NASA-CR-195421] p 323 N95-22675
- Aviation system capacity improvements through technology
[NASA-TM-109165] p 333 N95-24633
- Aircraft noise prediction program theoretical manual: Rotorcraft System Noise Prediction System (ROTONET), part 4
[NASA-TM-83199-PT-4] p 451 N95-26392
- Evaluation of a doubly-swept blade tip for rotorcraft noise reduction
[NASA-CR-189677] p 452 N95-28264
- Noise exposure reduction of advanced high-lift systems
[NASA-CR-195077] p 452 N95-28670
- Influence of tooth profile modification on spur gear dynamic tooth strain
[NASA-TM-106952] p 553 N95-29112
- Direct analysis of transonic rotor noise with CFD technique
p 711 N95-34549
- AIRCRAFT PARTS**
- Advances in the application of laser cutting, drilling, and welding aerospace parts
[SAE PAPER 932544] p 547 A95-90052
- Fatigue design of axially loaded semicircular lugs
[BTN-95-EIX0619952748190] p 637 A95-94252
- Advanced method and processing technology for complicated shape airframe part forming
p 80 N95-14486
- Automation of reverse engineering process in aircraft modeling and related optimization problems
[NASA-CR-197109] p 129 N95-16899
- Electrochemical impedance pattern recognition for detection of hidden chemical corrosion on aircraft components
[AD-A285998] p 241 N95-20716
- Review of some results of the author's fatigue investigations with applications in engineering and material science
[TAE-698] p 316 N95-23662
- JPRS Report: Science and technology. Central Eurasia [JPRS-UST-95-011] p 335 N95-24541
- Bicarbonate of soda paint stripping process validation and material characterization
p 631 N95-31778
- AIRCRAFT PERFORMANCE**
- An unmanned air vehicle concept with tipjet drive
[HTN-95-80858] p 283 A95-75100
- Multiaxis pilot ratings for damaged aircraft
[BTN-95-EIX95182619128] p 269 A95-76605
- Drag function modeling for air traffic simulation
[BTN-95-EIX95182619154] p 279 A95-76631
- Application of Navier-Stokes aeroelastic methods to improve fighter wing maneuver performance
[BTN-95-EIX95182619218] p 284 A95-76644
- Tracking of raindrops in flow over an airfoil
[BTN-95-EIX95182619221] p 308 A95-76647
- Pilot rating scale for aircraft handling qualities
[HTN-95-42269] p 380 A95-84963
- Note on prediction of aerodynamic lift/drag ratio of WIG (Wing-In-Ground) at cruise
[BTN-95-EIX95282705925] p 467 A95-89665
- Sensitivity of engine-integrated waverider performance to static margin constraint
[AIAA PAPER 95-6142] p 496 A95-90458
- Report to the aerospace profession: SETP Symposium, 37th, Beverly Hills, CA, USA, September 1993
[HTN-95-12142] p 497 A95-90866
- Earthwinds Hilton III: Balloon project
p 497 A95-90871
- Requirements for next generation supersonic transports
p 498 A95-91516
- Flight test of STS radio controlled scale model
p 499 A95-91539
- Improving aircraft impact assessment with the integrated terminal weather system microburst detection algorithm
p 654 A95-93453
- Aircraft icing: Meteorological effects on aircraft performance
p 674 A95-93545
- Jet transport response to a horizontal wind vortex
[BTN-95-EIX0619952748163] p 619 A95-94457
- Extended cooperative control synthesis
[NASA-TM-4561] p 17 N95-10220
- On the use of controls for subsonic transport performance improvement: Overview and future directions
[NASA-TM-4605] p 10 N95-11408
- An application of virtual prototyping to the flight test and evaluation of an unmanned air vehicle
[AD-A281749] p 14 N95-11595
- Examples of flight path optimisation using a multivariate gradient-search method. Addendum A: Variation of optimum flight profile parameters with range
[ESDU-94016-ADD-A] p 44 N95-11794
- Flight investigation of the use of a nose gear jump strut to reduce takeoff ground roll distance of STOL aircraft
[NASA-TM-108819] p 44 N95-12225
- Design of a high capacity long range cargo aircraft
[NASA-CR-197176] p 45 N95-12363
- The FC-1D: The profitable alternative Flying Circus Commercial Aviation Group
[NASA-CR-197152] p 46 N95-12628
- Flight test of takeoff performance monitoring system
[NASA-TP-3403] p 51 N95-12664
- Viper - Design modification
[NASA-CR-197191] p 79 N95-13703
- Scale effects on aircraft and weapon aerodynamics
[AGARD-AG-323] p 67 N95-14103
- High Alpha Technology Program (HATP) ground test to flight comparisons
p 68 N95-14230
- Numerical simulation of the flow about an F-18 aircraft in the high-alpha regime
p 68 N95-14232
- Comparison of X-31 flight, wind-tunnel, and water-tunnel yawing moment asymmetries at high angles of attack
p 68 N95-14234

Flight validation of ground-based assessment for control power requirements at high angles of attack p 70 N95-14246

High angle of attack flying qualities criteria for longitudinal rate command systems p 70 N95-14247

Airplane takeoff and landing performance monitoring system [NASA-CASE-LAR-14745-2-SB] p 85 N95-14415

Aircraft maneuver envelope warning system [NASA-CASE-ARC-11953-1] p 82 N95-14518

Graphical user interface for the NASA FLOPS aircraft performance and sizing code [NASA-TM-106649] p 80 N95-14604

Flight in an Adverse Environment [AGARD-LS-197] p 77 N95-14893

Wind shear and its effects on aircraft p 77 N95-14898

Heavy rain effects p 78 N95-14899

Turbulence: Engineering models, aircraft response p 84 N95-14900

Six degree of freedom flight dynamic and performance simulation of a remotely-piloted vehicle [AERO-TN-9301] p 131 N95-18097

Design limit loads based upon statistical discrete gust methodology p 133 N95-18603

F-15 resource tape [NASA-TM-110502] p 230 N95-19994

Naval aviation: F-14 upgrades are not adequately justified. Report to Congressional Committees [AD-A286338] p 231 N95-20212

Why do airlines want and use thrust reversers? A compilation of airline industry responses to a survey regarding the use of thrust reversers on commercial transport airplanes [NASA-TM-109158] p 226 N95-20706

Guidance and control requirements for high-speed Rollout and Turnoff (ROTO) [NASA-CR-195026] p 292 N95-22674

Direct adaptive performance optimization of subsonic transports: A periodic perturbation technique [NASA-TM-4676] p 284 N95-22829

Design of high performance multivariable control systems for supermaneuverable aircraft at high angle of attack [NASA-CR-197661] p 293 N95-22908

Supersonic civil airplane study and design: Performance and sonic boom [NASA-CR-197745] p 390 N95-26813

A comparison of the Neal-Smith and omega Tau function, zeta function and tau function flying qualities criteria [AD-A289503] p 390 N95-26844

Performance study for inlet installations [NASA-CR-189714] p 406 N95-28227

Benefits and limitations of composites in carrier-based aircraft p 422 N95-28422

Evaluation of proposed agility metrics using X-31 vs. F/A-18 flight data [AD-A292573] p 502 N95-28977

Flight assessment of the onboard propulsion system model for the Performance Seeking Control algorithm on an F-15 aircraft [NASA-TM-4705] p 617 N95-31425

Performance improvement of composite wings through aerelastic tailoring and modern control [AD-A293689] p 608 N95-31602

Flight test validation of a frequency-based system identification method on an F-15 aircraft [NASA-TM-4704] p 620 N95-31846

Report to the Chairman, Legislation and National Security Subcommittee, Committee on Government Operations, House of Representatives. Tactical aircraft: F-15 replacement is premature as currently planned [GAO/NSIAD-94-118] p 679 N95-31987

Lavi flight control system: Design requirements, development and flight test results p 621 N95-31994

Report to the Chairman, Legislation and National Security Subcommittee, Committee on Government Operations, House of Representatives. Unmanned aerial vehicles: Performance of short-range system still in question [GAO/NSIAD-94-65] p 609 N95-32196

Performance seeking control excitation mode p 696 N95-33019

Flight test of a propulsion controlled aircraft system on the NASA F-15 airplane p 691 N95-33023

AIRCRAFT PILOTS

Determination of piloting feedback structures for an altitude tracking task [BTN-95-EIX95242670770] p 327 A95-81077

The legal status and liability of the copilot, part 2 [HTN-95-A0578] p 452 A95-83158

Aviation weather education and the University of North Dakota aviation weather survey p 656 A95-93462

Pilot training initiatives for the '90s p 657 A95-93463

Aviation meteorology education in an AB initio setting p 657 A95-93466

Use of pilot reports for verification of aircraft icing diagnoses and forecasts p 666 A95-93508

Examination of conditions in the proximity of pilot reports of aircraft icing during storm-fest p 666 A95-93509

Design of head-up display symbology for recovery from unusual attitudes p 611 A95-95044

A correlative investigation of simulated occupant motion and accident report in a helicopter crash [AD-A285190] p 123 N95-16404

Visual contrast detection thresholds for aircraft contrails [AD-A288618] p 328 N95-25607

Biodynamic simulation of pilot interaction with a helicopter multi-airbag restraint system [AD-A290196] p 485 N95-29057

A rose by any other name: Certification seen as process rather than content p 688 N95-34766

AIRCRAFT POWER SUPPLIES

Auxiliary Power Unit evolution: Meeting tomorrow's challenges [SAE PAPER 932541] p 510 A95-89195

System design considerations for an APU starter-generator [SAE PAPER 932559] p 511 A95-90056

MIL-STD-461/MIL-STD-704 investigation [SAE PAPER 932561] p 505 A95-90058

Electrical power system upgrade methodology for in-service aircraft [SAE PAPER 932562] p 511 A95-90059

Solid state power controller technology [SAE PAPER 931422] p 495 A95-90087

Secondary power system study for the Iytech RA3 flight test vehicle [AIAA PAPER 95-6158] p 512 A95-90470

Integrated aircraft thermal management and power generation [SAE PAPER 932055] p 500 A95-91636

What's next in commercial aircraft environmental control systems? [SAE PAPER 932057] p 513 A95-91638

The A340 electrical power generation system [CONGRESS PAPER C428-36-193] p 625 A95-93630

The auxiliary and emergency power supply on the Saab JAS39 Gripen aircraft [CONGRESS PAPER C428-36-192] p 612 A95-93631

Concepts for aircraft subsystem integration [SAE PAPER 931377] p 604 A95-93656

SUIT: The integration of aircraft subsystems [SAE PAPER 931381] p 604 A95-93657

Power system characteristics for more electric aircraft [SAE PAPER 931406] p 613 A95-93675

The computer analysis of the prediction of aircraft electrical power supply system reliability p 155 N95-16278

Photovoltaic electric power applied to Unmanned Aerial Vehicles (UAV) p 245 N95-20530

Motor drive technologies for the power-by-wire (PBW) program: Options, trends and tradeoffs [NASA-TM-106885] p 295 N95-23671

Evaluation of all-electric secondary power for transport aircraft [NASA-CR-189077] p 441 N95-27999

AIRCRAFT PRODUCTION

Automatic riveting cell for commercial aircraft floor grid assembly [BTN-95-EIX95182617807] p 261 A95-75752

The analysis of the processing increased weight for pilot production of F-X aircraft [HTN-95-71133] p 385 A95-83494

Automatic riveting cell for commercial aircraft floor grid assembly [HTN-95-92309] p 365 A95-85353

The world of regional aircraft - challenges and opportunities [HTN-95-C0002] p 595 A95-93390

The mini-business approach at Chadderton [CONGRESS PAPER C428-26-037] p 681 A95-93602

Changing MRP Systems within the aerospace industry [CONGRESS PAPER C428-26-051] p 681 A95-93603

Non-contact calibration of a CNC riveting machine [CONGRESS PAPER C428-32-075] p 583 A95-93618

Tooling - a source of productivity [CONGRESS PAPER C428-32-017] p 583 A95-93619

Integrated design and manufacturing for the high speed civil transport [NASA-CR-197183] p 48 N95-12700

Low rate initial production in Army Aviation systems development [AD-A281871] p 127 N95-16356

Composite chronicles: A study of the lessons learned in the development, production, and service of composite structures [NASA-CR-4620] p 151 N95-16859

Report to Congressional Committees. Tactical Aircraft: Concurrence in development and production of F-22 aircraft should be reduced [GAO/NSIAD-95-59] p 336 N95-26338

Overview of the ACT program p 424 N95-28463

Report to the Chairman, Legislation and National Security Subcommittee, Committee on Government Operations, House of Representatives. Tactical aircraft: F-15 replacement is premature as currently planned [GAO/NSIAD-94-118] p 679 N95-31987

AIRCRAFT PRODUCTION COSTS

Designers' unified cost model p 424 N95-28464

COINS: A composites information database system p 453 N95-28465

Composite fuselage crown panel manufacturing technology p 399 N95-28474

AIRCRAFT RELIABILITY

Aircraft safety evaluation [BTN-94-EIX94511309382] p 103 A95-64608

Aircraft accident investigation and airworthiness -- A practical example of the interaction of two disciplines with some reflections on possible legal consequences [HTN-95-50219] p 176 A95-64856

Reliability and maintainability [BTN-95-EIX95042477109] p 179 A95-68350

USAF aging aircraft program [BTN-95-EIX95072498878] p 180 A95-68394

Service life extensions for the C-141 [BTN-95-EIX95112530749] p 193 A95-69295

Labs behind Boeing's new 777 [BTN-95-EIX95142562403] p 280 A95-73437

Fatigue of aircraft materials; Specialists' Conference, Delft, Netherlands, 1992 [HTN-95-B0076] p 387 A95-85892

FAA's Aging Commuter Airplane Program [SAE PAPER 931248] p 483 A95-89220

Fatigue life estimation program for Part 23 airplanes, 'AFS.FOR' [SAE PAPER 931249] p 565 A95-89221

Electrical power system upgrade methodology for in-service aircraft [SAE PAPER 932562] p 511 A95-90059

The rain erosion of PEEK (polyetheretherketone) [CONGRESS PAPER C428-4-039] p 531 A95-91676

The air systems controllerate initiatives and policies for the procurement of reliable and maintainable equipment [CONGRESS PAPER C428-6-113] p 549 A95-91682

The impact of new technology on reliability of avionic equipment [CONGRESS PAPER C428-6-114] p 549 A95-91683

The avionics integrity programme (AVIP) [CONGRESS PAPER C428-6-115] p 549 A95-91684

Ageing aircraft after ALOHA [CONGRESS PAPER C428-11-188] p 484 A95-91701

Fault Diagnosis for condition monitoring applied to hydraulic circuits [CONGRESS PAPER C428-12-165] p 456 A95-91703

Health monitoring and cost implications for an airline operator [CONGRESS PAPER C428-12-166] p 457 A95-91704

Gas path debris monitoring [CONGRESS PAPER C428-15-031] p 508 A95-91710

The use of math-dynamic models to aid the development of integrated health and usage monitoring systems [CONGRESS PAPER C428-19-079] p 457 A95-91720

An example of airborne vibration monitoring improving flight safety in the Soloviev D-30-KU engine [CONGRESS PAPER C428-21-141] p 508 A95-91728

External viewing airborne CCTV system [CONGRESS PAPER C428-25-172] p 595 A95-93598

Progress and experience with helicopter health and usage monitoring [CONGRESS PAPER C428-31-151] p 603 A95-93615

The certification of composite structures for military aircraft [CONGRESS PAPER C428-37-198] p 628 A95-93633

A method of calculating the safe fatigue life of compact, highly-stressed components p 93 N95-14464

Residual life and strength estimates of aircraft structural components with MSD/MED p 136 N95-19485

- Oklahoma City air logistics center (USAF) aging aircraft corrosion program p 262 N95-23519
- Test operations procedure (TOP) 7-3-534 airworthiness testing of fixed wing aircraft: Asymmetric power testing [AD-A289458] p 391 N95-26994
- Composite or metallic bolted repairs on self-stiffened carbon wing panel of the commuter ATR72 design criteria, analysis, verification by test p 396 N95-27525
- AGARD flight test techniques series. Volume 13: Reliability and maintainability [AGARD-AG-300-VOL-13] p 504 N95-29503
- International access to aeromedical evacuation medical equipment assessment data p 569 N95-29622
- AIRCRAFT SAFETY**
- Aircraft safety evaluation [BTN-94-EIX94511309382] p 103 A95-64608
- Ice accretion on aircraft wings [BTN-95-EIX95082502224] p 225 A95-71021
- Potential applications of the SSM/I cloud liquid water parameter to the estimation of marine aircraft icing [HTN-95-80651] p 254 A95-72495
- Volcanic ash forecast transport and dispersion (VAFTAD) model [HTN-95-80702] p 254 A95-72546
- Maintenance programs [BTN-95-EIX95182617809] p 261 A95-75754
- Real-time decision aiding: Aircraft guidance for wind shear avoidance [BTN-95-EIX95202637575] p 332 A95-78583
- Fibre-metal laminates p 387 A95-85895
- Elements of structural integrity assurance p 387 A95-85896
- Damage tolerance capability p 388 A95-85898
- Lightning protection technology for small general aviation composite material aircraft [SAE PAPER 931241] p 483 A95-88964
- Test and evaluation crew resource management p 483 A95-90867
- Airborne collision avoidance systems - The UK experience [CONGRESS PAPER C428-7-146] p 488 A95-91687
- Developments in airfield lighting [CONGRESS PAPER C428-7-147] p 488 A95-91688
- Automatic vehicle location and airfield ground movement [CONGRESS PAPER C428-7-148] p 488 A95-91689
- Ageing aircraft after ALOHA [CONGRESS PAPER C428-11-188] p 484 A95-91701
- Explosive sabotage: The potential effects of explosive charges on aircraft [CONGRESS PAPER C428-11-034] p 484 A95-91702
- RAF ejections - historical perspectives and future requirements [CONGRESS PAPER C428-18-168] p 484 A95-91717
- An example of airborne vibration monitoring improving flight safety in the Soloviev D-30-KU engine [CONGRESS PAPER C428-21-141] p 508 A95-91728
- Passive millimeter wave camera for aircraft landing in low visibility conditions [BTN-95-EIX95292721321] p 609 A95-92513
- Development of an aircraft cabin water spray system [CONGRESS PAPER C428-25-030] p 595 A95-93599
- Aircraft cabin water spray systems - research and regulatory issues [CONGRESS PAPER C428-25-150] p 595 A95-93600
- Civil aircraft performance - developments for improved safety [CONGRESS PAPER C428-25-175] p 596 A95-93601
- Improving the fire resistance of aircraft structures [CONGRESS PAPER C428-31-152] p 603 A95-93616
- Psycho-social safety perceptions: Helicopters as a case study p 596 A95-95192
- ASRS problems involving air carrier ground deicing/anti-icing p 611 A95-95194
- EMS helicopter incidents reported to the NASA Aviation Safety Reporting System p 596 A95-95201
- A study of aircraft post-crash fuel fire mitigation [AD-A282208] p 40 N95-12499
- Evaluation of alternative in-flight fire suppressants for full-scale testing in simulated aircraft engine nacelles and dry bays [PB94-203403] p 42 N95-13247
- AGARD highlights 94/2 [AGARD-HIGHLIGHTS-94/2] p 102 N95-13640
- Risk analysis for the fire safety of airline passengers [PB94-194065] p 77 N95-14179
- The principles of flight test assessment of flight-safety-critical systems in helicopters [AGARD-AG-300-VOL-12] p 77 N95-14199
- Flight in an Adverse Environment [AGARD-LS-197] p 77 N95-14893
- Heavy rain effects p 78 N95-14899
- Aircraft accident report: Overspeed and loss of power on both engines during descent and power-off emergency, landing Simmons Airlines, Inc., d/b/a, American Eagle Flight 3641, N349SB False River Air Park, New Roads, Louisiana, 1 February 1994 [PB94-910408] p 78 N95-14916
- TDWR scan strategy implementation [AD-A284877] p 98 N95-15749
- Aircraft accident report: Stall and loss of control on final approach, Atlantic Coast Airlines, Inc./United Express Flight 6291 Jetstream 4101, N304UE Columbus, OH, 7 January 1994 [PB94-910409] p 123 N95-17646
- A study of the effect of store unsteady aerodynamics on gust and turbulence loads p 133 N95-18601
- Ageing nuclear power plant management: An aeronautical viewpoint [NAL-PD-SN-9306] p 105 N95-18606
- On-line handling of air traffic: Management, guidance and control [AGARD-AG-321] p 126 N95-18927
- Safety study: Commuter airline safety [PB94-917004] p 124 N95-19132
- Modern transport engine experience with environmental ingestion effects p 199 N95-19660
- Special investigation report: Maintenance anomaly resulting in dragged engine during landing rollout. Northwest Airlines Flight 18, Boeing 747-251B, N637US, New Tokyo International Airport, Narita, Japan, 1 Mar. 1994 [PB94-917006] p 188 N95-19793
- Commuter airplane accident data analysis [AD-A286315] p 226 N95-20174
- Commuter/air taxi ditchings and water-related impacts that occurred from 1979 to 1989 [AD-A285691] p 226 N95-20275
- Fuselage burnthrough from large exterior fuel fires [AD-A286295] p 226 N95-22318
- Forecasting aircraft mishaps using monthly maintenance reports [AD-A286049] p 227 N95-22417
- Additional improvements to the NASA Lewis ice accretion code LEWICE [NASA-TM-106849] p 309 N95-22669
- Handling qualities of the High Speed Civil Transport p 294 N95-23325
- Report of proceedings: Aviation Accident Investigation Symposium. Volume 2: Participant presentations [PB94-917007] p 277 N95-23598
- Aircraft fires, smoke toxicity, and survival: An overview [DOT/FAA/AM-95/8] p 277 N95-24024
- A multibody/finite element analysis approach for modeling of crash dynamic responses [NIAR-94-3] p 277 N95-24050
- Aviation Accident Investigation Symposium. Volume 1: Industry recommendations and Safety Board responses [PB94-917005] p 278 N95-24105
- Federal Aviation Administration plan for research, engineering and development, 1995 p 363 N95-24202
- Development of an intervention program to encourage shoulder harness use and aircraft retrofit in general aviation aircraft, phases 1 and 2 [DOT/FAA/AM-95/2] p 333 N95-24384
- Quantity-distance requirements for earth-bermed aircraft shelters [AD-A279692] p 341 N95-24424
- Bird ingestion into large turbofan engines [DOT/FAA/CT-93/14] p 333 N95-24631
- WINCLR: A computer code for heat transfer and clearance calculation in a compressor [NASA-CR-195436] p 366 N95-26363
- Aircraft accident report: Controlled collision with Terrain Transportes Aereos Ejecutivos, S.A. (TAESA) Learjet 25D, XA-BBA Dulles International Airport Chantilly, Virginia, June 18, 1994 [NTSB/AAR-95/02] p 380 N95-26498
- AIAA Techfest 20 Proceedings [NIAR-94-1] p 367 N95-26941
- Prevention and control of inlet unstart using an SR-71 simulation p 367 N95-26948
- Precision landing system mathematical modeling study report for Andrews Air Force Base, runway 19L, Camp Springs, MD [AD-A289015] p 384 N95-27903
- Biodynamic simulation of pilot interaction with a helicopter multi-airbag restraint system [AD-A290196] p 485 N95-29057
- The effect of wear on fire-blocking layer material effectiveness [AD-A291520] p 485 N95-29855
- Development of an intervention program to encourage shoulder harness use and aircraft retrofit in general aviation aircraft: Phases 1 and 2 [AD-A290966] p 485 N95-29873
- Electrical short circuit and current overload tests on aircraft wiring [AD-A293308] p 646 N95-30922
- The relation of handling qualities ratings to aircraft safety p 597 N95-31067
- Chemical options to halons for aircraft use [AD-A293741] p 599 N95-31569
- Aircraft evacuations through Type-3 exits I: Effects of seat placement at the exit [DOT/FAA/AM-95/22] p 599 N95-31845
- Report to the Chairman, Subcommittee on Aviation, Committee on Commerce, Science, and Transportation, US Senate. Aviation safety: Data problems threaten FAA strides on safety analysis system [GAO/AIMD-95-27] p 687 N95-32705
- Report to the Chairman, Subcommittee on Aviation, Committee on Commerce, Science, and Transportation, US Senate. Aviation Safety: FAA can better prepare general aviation pilots for mountain flying risks [GAO/RCED-94-15] p 687 N95-32784
- Aviation security: Development of new security technology has not met expectations. Report to Congressional requesters [GAO/RCED-94-142] p 687 N95-32885
- Current issues in the design and information content of instrument approach charts [AD-A294752] p 690 N95-34562
- The effects of display location and dimensionality on taxiway navigation [AD-A294878] p 690 N95-34570
- Corrosion of fire-damaged aircraft [AD-A294968] p 693 N95-34583
- A rose by any other name: Certification seen as process rather than content p 688 N95-34766
- User type certification for advanced flight control systems p 699 N95-34772
- AIRCRAFT SPECIFICATIONS**
- Integrated flight/pro propulsion control for helicopters [HTN-95-80854] p 290 A95-75096
- MIL-STD-461/MIL-STD-704 investigation [SAE PAPER 932561] p 505 A95-90058
- Six degree of freedom flight dynamic and performance simulation of a remotely-piloted vehicle [AERO-TN-9301] p 131 N95-18097
- Analysis of test criteria for specifying foam firefighting agents for aircraft rescue and firefighting [AD-A286381] p 227 N95-22352
- Experiences with ADS-33 helicopter specification testing and contributions to refinement research p 621 N95-31993
- Lavi flight control system: Design requirements, development and flight test results p 621 N95-31994
- The control system design methodology of the STOL and maneuver technology demonstrator p 621 N95-31998
- Control law design using H-infinity and mu-synthesis short-period controller for a tail-airplane p 622 N95-31999
- AIRCRAFT SPIN**
- T-45A high angle attack testing [HTN-95-81499] p 386 A95-85213
- Techniques for tailoring aircraft stall and post-stall behavior [SAE PAPER 931226] p 458 A95-87199
- AIRCRAFT STABILITY**
- Offset thrust axes and pitch stability [BTN-95-EIX95062487553] p 203 A95-68367
- Postinstability behavior of a two-dimensional airfoil with a structural nonlinearity [BTN-95-EIX95152582337] p 266 A95-73539
- Method for the prediction of the onset of wing rock [BTN-95-EIX95152582342] p 282 A95-73544
- Effect of leeward flow dividers on the wing rock of a delta wing [BTN-95-EIX95152582347] p 282 A95-73549
- Rotocraft handling qualities in turbulence [BTN-95-EIX95242670750] p 334 A95-81097
- Identification and simulation evaluation of a combat helicopter in hover [BTN-95-EIX95242670749] p 335 A95-81098
- Robust longitudinal axis flight control for an aircraft with thrust vectoring [BTN-95-EIX95122538875] p 408 A95-83000
- Dynamic-stall and structural-modeling effects on helicopter blade stability with experimental correlation [HTN-95-81646] p 542 A95-87694
- Reduced-order nonlinear analysis of aircraft dynamics [BTN-95-EIX95282706665] p 455 A95-89640

- Automatic identification of modal damping from Floquet analysis
[HTN-95-01084] p 506 A95-90270
- Sensitivity of engine-integrated waverider performance to static margin constraint
[AIAA PAPER 95-6142] p 496 A95-90458
Aircraft Symposium, 30th, Tsukuba, Japan, Sep. 30 - Oct. 2, 1992
- [HTN-95-A1609] p 498 A95-91491
Aeroseuroelastic coupling on the UF-104 aircraft
p 517 A95-91561
- Determining the accuracy of maximum likelihood parameter estimates with colored residuals
[NASA-CR-194893] p 51 N95-11869
- Static and dynamic force/moment measurements in the Eidetics water tunnel p 69 N95-14238
- System for determining aerodynamic imbalance
[NASA-CASE-ARC-11913-1] p 311 N95-23377
- Aerodynamic flight control to increase payload capability of future launch vehicles
[NAS-CR-196560] p 300 N95-24032
- An easy way to analyze longitudinal and lateral-directional trim problems with AEO or OEI
p 409 N95-26949
- Flight Vehicle Integration Panel Workshop on Pilot Induced Oscillations
[AGARD-AR-335] p 597 N95-31061
- Unified criteria for ACT aircraft longitudinal dynamics p 607 N95-31065
- Looking for the simple PIO model p 597 N95-31066
- Aeroelastic pilot-in-the-loop oscillations
p 598 N95-31070
- The prevention of PIO by design p 620 N95-31991
- Pilot Induced Oscillation: A report on the AGARD Workshop on PIO p 624 N95-32017
- AIRCRAFT STRUCTURES**
- Launcher wing-leading-edge design
[BTN-95-EIX95042477110] p 192 A95-68349
- Coupling equivalent plate and finite element formulations in multiple-method structural analyses
[BTN-95-EIX95062487548] p 192 A95-68362
- Influence of structural and aerodynamic modeling on flutter analysis
[BTN-95-EIX95062487550] p 203 A95-68364
- Continuous gust response and sensitivity derivatives using state-space models
[BTN-95-EIX95062487551] p 203 A95-68365
- Ply layup optimization and micromechanics tailoring of composite aircraft engine structures
[BTN-95-EIX95112524206] p 196 A95-69302
- MIL-HDBK-5 design allowables for fibre/metal laminates: ARALL 2 and ARALL 3
[BTN-94-EIX94371346933] p 300 A95-73345
- Experimental evaluation of a box beam specifically tailored for chordwise deformation
[BTN-95-EIX95182619088] p 283 A95-75773
- Viscoplastic response of structures for intense local heating
[HTN-95-41540] p 346 A95-77921
- Forming and bonding techniques for high-strength aluminum alloys
[HTN-95-20605] p 418 A95-84786
- Automatic riveting cell for commercial aircraft floor grid assembly
[HTN-95-92309] p 365 A95-85353
- Aircraft stripping and painting
[HTN-95-92311] p 365 A95-85355
- Fatigue of aircraft materials; Specialists' Conference, Delft, Netherlands, 1992
[HTN-95-B0076] p 387 A95-85892
- Status and prospects for aluminium-lithium alloys in aircraft structures p 387 A95-85893
- Fatigue of aircraft materials and structures p 387 A95-85894
- Fibre-Metal laminates p 387 A95-85895
- Elements of structural integrity assurance p 387 A95-85896
- Verification of the damage tolerance of a fighter aircraft p 388 A95-85897
- Damage tolerance capability p 388 A95-85898
- Concorde: Silver jubilee Mach 2 marks 25 years
[HTN-95-42618] p 483 A95-87248
- Rapid prototyping of composite aircraft structures
[SAE PAPER 931219] p 539 A95-87530
- The key to designing durable adhesively bonded joints
[HTN-95-12033] p 528 A95-88496
- A method for disbond detection in thermal tomography by domain decomposition method p 545 A95-88955
- Ultrasonic imaging of damages in CRFT-laminates p 578 A95-90828
- Damage to composite aircraft structures from lightning strike attachment to unprotected CFC and internal sparking causing fuel injection
[CONGRESS PAPER C428-4-026] p 531 A95-91675
- Health monitoring and cost implications for an airline operator
[CONGRESS PAPER C428-12-166] p 457 A95-91704
- Improving the fire resistance of aircraft structures
[CONGRESS PAPER C428-31-152] p 603 A95-93616
- The basis of civil certification and continued airworthiness for composite aircraft structures
[CONGRESS PAPER C428-37-173] p 628 A95-93632
- New experimental approach to determine initial fatigue quality with fastener holes
[BTN-94-EIX94522406136] p 701 A95-96273
- Effect of passive venting on static pressure distributions in cavities at subsonic and transonic speeds
[NASA-TM-4549] p 6 N95-10029
- Activities of Mitsubishi Heavy Industries Ltd.
[PB94-179694] p 22 N95-10085
- Advanced composites structural concepts and materials technologies for primary aircraft structures: Structural response and failure analysis
[NASA-CR-4448] p 11 N95-10240
- Advanced composites structural concepts and materials technologies for primary aircraft structures. Structural response and failure analysis: ISPAN modules users manual
[NASA-CR-4449] p 12 N95-10242
- Advanced composites structural concepts and materials technologies for primary aircraft structures: Design/manufacturing concept assessment
[NASA-CR-4447] p 12 N95-10316
- Novel matrix resins for composites for aircraft primary structures, phase 1
[NASA-CR-189657] p 23 N95-10318
- Broadband, wide-area active control of sound radiated from vibrating structures using local surface-mounted radiation suppression devices p 30 N95-11283
- Comments on the use of structureborne noise analysis for large commercial airplanes p 30 N95-11287
- Effect of constraining layer stiffness on performance of damping tile materials using finite element modelling with Rayleigh integral p 30 N95-11306
- Potential impacts of advanced aerodynamic technology on air transportation system productivity
[NASA-TM-109154] p 10 N95-11489
- On the interaction of jet noise with a nearby flexible structure
[NASA-CR-194934] p 57 N95-11812
- Development of an Automated Nondestructive Inspection (ANDI) system for commercial aircraft, phase 1
[AD-A283500] p 40 N95-12623
- Triton 2 (1B)
[NASA-CR-197188] p 46 N95-12636
- FAA/NASA International Symposium on Advanced Structural Integrity Methods for Airframe Durability and Damage Tolerance
[NASA-CP-3274-PT-1] p 92 N95-14453
- Elastic-plastic models for multi-site damage p 92 N95-14454
- Bending effects of unsymmetric adhesively bonded composite repairs on cracked aluminum panels p 92 N95-14456
- Evaluation of bonded boron/epoxy doublers for commercial aircraft aluminum structures p 92 N95-14457
- Inspecting for widespread fatigue damage: Is partial debonding the key? p 93 N95-14458
- Testing and analysis of flat and curved panels with multiple cracks p 93 N95-14460
- Probabilistic inspection strategies for minimizing service failures p 93 N95-14461
- A method of calculating the safe fatigue life of compact, highly-stressed components p 93 N95-14464
- Computational predictive methods for fracture and fatigue p 93 N95-14466
- Influence of crack history on the stable tearing behavior of a thin-sheet material with multiple cracks p 93 N95-14467
- Extracting a representative loading spectrum from recorded flight data p 80 N95-14469
- The role of fretting corrosion and fretting fatigue in aircraft rivet hole cracking p 94 N95-14470
- Fatigue reliability method with in-service inspections p 94 N95-14475
- Nonlinear bulging factor based on R-curve data p 94 N95-14476
- Fracture mechanics validity limits p 95 N95-14480
- Challenges for the aircraft structural integrity program p 80 N95-14481
- The effects of pitting on fatigue crack nucleation in 7075-T6 aluminum alloy p 88 N95-14482
- Large amplitude nonlinear response of flat aluminum, and carbon fiber plastic beams and plates
[AD-A282440] p 96 N95-15547
- Development of strength analysis methods and design model for aircraft constructions in Kazan Aviation Institute p 127 N95-16264
- Development of processes, means, and theoretical principles of thin-walled detail plastic forming at Kazan Aviation Institute p 155 N95-16281
- The use of electrochemistry and ellipsometry for identifying and evaluating corrosion on aircraft
[AD-A285323] p 151 N95-16371
- Rapid solution of large-scale systems of equations p 169 N95-16458
- Composite chronicles: A study of the lessons learned in the development, production, and service of composite structures p 151 N95-16859
- [NASA-CR-4620] p 151 N95-16859
- Course module for AA201: Wing structural design project
[AD-A283618] p 133 N95-18616
- Pressure measurements on an F/A-18 twin vertical tail in buffeting flow. Volume 4, part 2: Buffet cross spectral densities
[AD-A285555] p 143 N95-18641
- The accuracy of parameter estimation in system identification of noisy aircraft load measurement
[NASA-CR-197516] p 134 N95-19130
- Impact of Acoustic Loads on Aircraft Structures
[AGARD-CP-549] p 173 N95-19142
- Current and future problems in structural acoustic fatigue p 173 N95-19143
- Impact of noise environment on engine nacelle design p 173 N95-19147
- High-temperature acoustic test facilities and methods p 174 N95-19149
- Nonlinear dynamic response of aircraft structures to acoustic excitation p 135 N95-19151
- Acoustic fatigue testing on different materials and skin-stringer elements p 174 N95-19156
- Acoustic fatigue characteristics of advanced materials and structures p 174 N95-19157
- Application of superplastically formed and diffusion bonded structures in high intensity noise environments p 174 N95-19162
- FAA/NASA International Symposium on Advanced Structural Integrity Methods for Airframe Durability and Damage Tolerance, part 2
[NASA-CP-3274-PT-2] p 124 N95-19468
- Discrete crack growth analysis methodology for through cracks in pressurized fuselage structures p 166 N95-19473
- Aircraft stress sequence development: A complex engineering process made simple p 136 N95-19480
- Residual life and strength estimates of aircraft structural components with MSD/MED p 136 N95-19485
- Ultrasonic techniques for repair of aircraft structures with bonded composite patches p 136 N95-19486
- Widespread fatigue damage monitoring: Issues and concerns p 136 N95-19488
- Aircraft fatigue and crack growth considering loads by structural component p 137 N95-19497
- Proceedings of the USAF Structural Integrity Program Conference
[AD-A285684] p 194 N95-19517
- Corrosion of aircraft materials: Correlation between nanometer scale and macroscopic structural damage parameters
[AD-A285930] p 241 N95-20299
- Eddy current for detecting second-layer cracks under installed fasteners
[AD-A279871] p 244 N95-20414
- Electrochemical impedance pattern recognition for detection of hidden chemical corrosion on aircraft components
[AD-A284998] p 241 N95-20481
- Review of aeronautical fatigue investigation in the Netherlands during the period March 1991-March 1993
[PB95-139184] p 285 N95-23161
- Double pass retroreflection for corrosion detection in aircraft structures p 323 N95-23503
- Non-destructive detection of corrosion for life management p 314 N95-23505
- Health and usage monitoring systems: Corrosion surveillance p 262 N95-23506
- New nondestructive techniques for the detection and quantification of corrosion in aircraft structures p 315 N95-23512
- Organic coating technology for the protection of aircraft against corrosion p 303 N95-23513
- Corrosion detection and monitoring of aircraft structures: An overview p 303 N95-23515
- Experience of in-service corrosion on military aircraft p 303 N95-23516
- US Navy operating experience with new aircraft construction materials p 303 N95-23517
- Oklahoma City air logistics center (USAF) aging aircraft corrosion program p 262 N95-23519

- NASA-UVA light aerospace alloy and structures technology program (LA2ST)
[NASA-CR-198041] p 343 N95-24220
- JPRS report: Science and technology, Central Eurasia
[JPRS-UST-95-011] p 335 N95-24541
- Proceedings of the 2d USAF Aging Aircraft Conference
[AD-A288217] p 336 N95-25578
- Design and evaluation of a foam-filled hat-stiffened panel concept for aircraft primary structural applications
[NASA-TM-109175] p 346 N95-26251
- A verification procedure for MSC/NASTRAN Finite Element Models
[NASA-CR-4675] p 392 N95-27371
- Composite Repair of Military Aircraft Structures
[AGARD-CP-550] p 392 N95-27504
- Bonded composite repair of metallic aircraft components: Overview of Australian activities
p 392 N95-27505
- Status of bonded boron/epoxy doublers for military and commercial aircraft structures
p 393 N95-27506
- Adhesively bonded composite patch repair of cracked aluminum alloy structures
p 393 N95-27507
- Design and structural validation of CF116 upper wing skin boron doubler
p 393 N95-27510
- A FEAM based methodology for analyzing composite patch repairs of metallic structures
p 394 N95-27511
- Structural modification and repair of C-130 wing structure using bonded composites
p 394 N95-27512
- Evaluation of patch effectiveness in repairing aircraft components
p 394 N95-27513
- Rapid repair of large area damage to contoured aircraft structures
p 394 N95-27516
- Repair technology for thermoplastic aircraft structures
p 395 N95-27519
- Repair of high temperature composite aircraft structure
p 395 N95-27520
- External patch repair of CFRP/honeycomb sandwich
p 395 N95-27522
- Scarf joint technique with cocured and precured patches for composite repair
p 396 N95-27524
- Damage occurrence on composites during testing and fleet service: Repair of Airbus aircraft
p 396 N95-27526
- Repairs of CFC primary structures
p 396 N95-27527
- The development of an engineering standard for composite repairs
p 396 N95-27528
- Ninth DOD/NASA/FAA Conference on Fibrous Composites in Structural Design, volume 3
[NASA-CR-198718] p 420 N95-28266
- Process and control systems for composites manufacturing
p 420 N95-28267
- Advanced tow placement of composite fuselage structure
p 420 N95-28271
- Through-the Thickness(R) braided composites for aircraft applications
p 421 N95-28273
- Resin transfer molding of textile preforms for aircraft structural applications
p 421 N95-28276
- Application of fiber-reinforced bismaleimide materials to aircraft nacelle structures
p 421 N95-28278
- Analysis techniques for the prediction of springback in formed and bonded composite components
p 421 N95-28289
- The effect of material heterogeneity in curved composite beams for use in aircraft structures
p 422 N95-28426
- Vibrational behavior of adaptive aircraft wing structures modelled as composite thin-walled beams
p 423 N95-28435
- Development of composite carrythrough bulkhead
p 423 N95-28438
- Probabilistic design of advanced composite structure
p 424 N95-28443
- Probabilistic evaluation of fuselage-type composite structures
p 398 N95-28444
- Navy composite maintenance and repair experience
p 424 N95-28446
- Ninth DOD/NASA/FAA Conference on Fibrous Composites in Structural Design, volume 2
[NASA-CR-198722] p 424 N95-28462
- Overview of the ACT program
p 424 N95-28463
- COINS: A composites information database system
p 453 N95-28465
- Composite fuselage shell structures research at NASA Langley Research Center
p 425 N95-28466
- Technology integration box beam failure study
p 441 N95-28468
- Development of stitched/RTM composite primary structures
p 425 N95-28469
- Recent progress in NASA Langley textile reinforced composites program
p 425 N95-28475
- Advanced textile applications for primary aircraft structures
p 399 N95-28476
- Comparison of resin film infusion, resin transfer molding, and consolidation of textile preforms for primary aircraft structure
p 425 N95-28477
- Characterization and manufacture of braided composites for large commercial aircraft structures
p 426 N95-28478
- Application of damage tolerance methodology in certification of the Piaggio P-180 Avanti
p 399 N95-28480
- Effect of low-speed impact damage and damage location on behavior of composite panels
p 426 N95-28481
- Third NASA Advanced Composites Technology Conference, volume 1, part 2
[NASA-CP-3178-VOL-1-PT-2] p 531 N95-28823
- Novel cost controlled materials and processing for primary structures
p 532 N95-28830
- Automated fiber placement: Evolution and current demonstrations
p 532 N95-28832
- Dimensional stability of curved panels with cocured stiffeners and cobonded frames
p 532 N95-28836
- Design and evaluation of a foam-filled hat-stiffened panel concept for aircraft primary structural applications
p 502 N95-28841
- A weight-efficient design strategy for cutouts in composite transport structures
p 533 N95-28843
- Buckling analysis of curved composite sandwich panels subjected to inplane loadings
p 533 N95-28845
- Technology integration box beam failure study
p 552 N95-28847
- Advanced composite structural concepts and materials technologies for primary aircraft structures: Advanced material concepts
[NASA-CR-4485] p 503 N95-29027
- Third NASA Advanced Composites Technology Conference, volume 1, part 1
[NASA-CP-3178-VOL-1-PT-1] p 534 N95-29029
- Impact of composites on future transport aircraft
p 534 N95-29030
- Challenges and payoff of composites in transport aircraft: 777 empennage and future applications
p 534 N95-29031
- Weavability of dry polymer powder towpreg
p 535 N95-29036
- Mechanical characterization of 2D, 2D stitched, and 3D braided/RTM materials
p 535 N95-29038
- Performance of resin transfer molded multiaxial warp knit composites
p 535 N95-29039
- Cost model relationships between textile manufacturing processes and design details for transport fuselage elements
p 536 N95-29043
- Development of RTM and powder prepreg resins for subsonic aircraft primary structures
p 536 N95-29044
- Progress in manufacturing large primary aircraft structures using the stitching/RTM process
p 537 N95-29050
- Innovative processing of composites for ultra-high temperature applications, book 1
[AD-A290889] p 537 N95-29842
- A comparison of coating alternatives for US Coast Guard aircraft
[AD-A293270] p 629 N95-31124
- Failure analysis for polycarbonate transparencies
[AD-A292992] p 630 N95-31471
- Performance improvement of composite wings through aeroelastic tailoring and modern control
[AD-A293689] p 608 N95-31602
- The FCS-structural coupling problem and its solution
p 623 N95-32005
- Mapping hidden aircraft defects with dual-band infrared computed tomography
[DE95-011531] p 584 N95-32164
- Selective chemical stripping
p 650 N95-32175
- Development of a composite tailoring procedure for airplane wing
[NASA-CR-199081] p 691 N95-32928
- AIRCRAFT SURVIVABILITY**
- Advanced distributed simulation technology advanced rotary wing aircraft. System/segment specification. Volume 5: Simulation system module AH-64D kit
[AD-A280433] p 20 N95-10353
- Composite waveform generation for EMP and lightning direct-drive testing
[AD-A284159] p 92 N95-14405
- Assessing aircraft survivability to high frequency transient threats
[AD-A283999] p 134 N95-18726
- Commuter airplane accident data analysis
[AD-A286315] p 226 N95-20174
- Commuter/air taxi ditchings and water-related impacts that occurred from 1979 to 1989
[AD-A285691] p 226 N95-20275
- Structural design optimization with survivability dependent constraints application: Primary wing box of a multi-role fighter
p 398 N95-28440
- Advanced wing design survivability testing and results
p 400 N95-28488
- Aviation security: Development of new security technology has not met expectations. Report to Congressional requesters
[GAO/RCED-94-142] p 687 N95-32885
- AIRCRAFT TIRES**
- Critical speed analysis of a non-linear strain ring dynamical model for aircraft tires
[SAE PAPER 932580] p 494 A95-90067
- NASA evaluation of Type 2 chemical depositions — effects of deicer deposition on aircraft tire friction performance
[SAE PAPER 932582] p 495 A95-90086
- Aircraft landing gear dynamics present and future
[SAE PAPER 931400] p 604 A95-93670
- Modelling and analysis of a dual-wheel nosegear: Shimmy instability and impact motions
[SAE PAPER 931402] p 605 A95-93672
- Aircraft nosewheel steering simulation
p 412 N95-26944
- AIRCRAFT WAKES**
- Interference between tanker wing wake with roll-up and receiver aircraft
[BTN-95-EIX95062487552] p 185 A95-68366
- Unsteady ground effects on aerodynamic coefficients of finite wings with camber
[BTN-95-EIX95182619233] p 271 A95-76659
- Doppler lidar investigation of wake vortex transport between closely spaced parallel runways
[HTN-95-81645] p 462 A95-87693
- On controlling the tip vortex flow of a lifting wing
[ISBN 1-879921-01-4] p 587 A95-93736
- Airborne Windshear Detection and Warning Systems. Fifth and Final Combined Manufacturers' and Technologists' Conference, part 1
[NASA-CP-10139-PT-1] p 10 N95-10566
- Potential impacts of advanced aerodynamic technology on air transportation system productivity
[NASA-TM-109154] p 10 N95-11489
- 3D visualization of unsteady 2D airplane wake vortices
[AD-A284745] p 27 N95-11593
- Airborne Windshear Detection and Warning Systems. Fifth and Final Combined Manufacturers' and Technologists' Conference, part 2
[NASA-CP-10139-PT-2] p 41 N95-13203
- Aircraft wake RCS measurement
p 59 N95-13210
- Wake vortex detection at Denver Stapleton Airport with a pulsed 2-micron coherent lidar
p 42 N95-13211
- Doppler radar detection of vortex hazard indicators
p 42 N95-13212
- Remote sensing of turbulence in the clear atmosphere with 2-micron lidars
p 59 N95-13213
- Wake turbulence
p 75 N95-14894
- Aircraft wake vortex takeoff tests at O'Hara International Airport
[AD-A283828] p 118 N95-18624
- Three-dimensional interaction of wake/boundary-layer and vortex/boundary-layer data report
[CUED/A-AEREO/TR-23] p 329 N95-24210
- Characterizing the wake vortex signature for an active line of sight remote sensor
[NASA-CR-197697] p 333 N95-24391
- A numerical method for modelling wings with sharp edges maneuvering at high angles of attack
p 503 N95-29122
- Hot jet/wake turbulent structure and laser propagation. Part 3: Laser propagation measurements and modeling
p 647 N95-30992
- AIRDROPS**
- The performance of cargo airdrop systems using g-12E parachutes: Statistical determination of minimum altitude
[AD-A291666] p 381 N95-28454
- AIRFIELD SURFACE MOVEMENTS**
- Arrival traffic handling for a parallel runway airport
p 487 A95-91537
- Developments in airfield lighting
[CONGRESS PAPER C428-7-147] p 488 A95-91688
- Automatic vehicle location and airfield ground movement
[CONGRESS PAPER C428-7-148] p 488 A95-91689
- Development of an Automated Airfield Dynamic Cone Penetrometer (AADCP) prototype and the evaluation of unsurfaced airfield seismic surveying using Spectral Analysis of Surface Waves (SASW) technology
[AD-A281985] p 145 N95-17444
- Automation technology using Geographic Information System (GIS)
p 324 N95-23284
- The effects of display location and dimensionality on taxiway navigation
[AD-A294878] p 690 N95-34570
- AIRFOIL FENCES**
- Vortical flow structure near the F/A-18 LEX at high incidence
[BTN-95-EIX95062487555] p 186 A95-68369

AIRFOIL OSCILLATIONS

Interferometry and computational studies of an oscillating airfoil compressible dynamic stall flow field [HTN-94-00703] p 3 A95-60182

Oscillating airfoil compressible dynamic stall studies [HTN-94-00704] p 3 A95-60183

LDV measurements in dynamically separated flows [ISBN 0-8194-1311-9] p 5 A95-60191

A study of compressibility effects on dynamic stall of rapidly pitching airfoils [HTN-94-00715] p 5 A95-60193

Effect of wind tunnel acoustic modes on linear oscillating cascade aerodynamics [HTN-94-00760] p 14 A95-60199

Computation of oscillating airfoil flows with one- and two-equation turbulence models [BTN-95-EIX95152577588] p 263 A95-73494

Reattachment studies of an oscillating airfoil dynamic stall flowfield [HTN-95-51660] p 432 A95-85042

Explicit Kutta condition for an unsteady two-dimensional constant potential panel method [HTN-95-51679] p 433 A95-85061

Application of artificial neural networks in nonlinear aerodynamics and aircraft design [SAE PAPER 932533] p 492 A95-89193

Unsteady flow testing in a passive low-correction wind tunnel p 147 N95-19272

Nonlinear dynamics and aeroelasticity of rotorcraft in forward flight [AD-A291714] p 400 N95-28504

Dynamic stall of a NACA 0012 airfoil in laminar flow p 479 N95-29243

Compressibility effects on and control of dynamic stall of oscillating airfoil [AD-A291804] p 480 N95-29428

Control of unsteady separated flow associated with the dynamic stall of airfoils [NASA-CR-198972] p 594 N95-32193

AIRFOIL PROFILES

Forebody flow control on a full-scale F/A-18 aircraft [BTN-95-EIX95152582333] p 281 A95-73535

Effect of curvature in the numerical simulation of an electrothermal de-icer pad [BTN-95-EIX95182619219] p 276 A95-76645

Precision requirement for potential-based panel methods [HTN-95-51666] p 433 A95-85048

Force and moment on a Joukowski profile in the presence of point vortices [BTN-95-EIX95262694298] p 434 A95-85469

Effect of leading-edge extension fences on the vortex wake of an F/A-18 model [BTN-95-EIX0619952748192] p 591 A95-94481

Application of two procedures for dual-point design of transonic airfoils [NASA-TP-3466] p 38 N95-12176

Measurements on a two-dimensional aerofoil with high-lift devices p 109 N95-17848

Investigation of the flow over a series of 14 percent-thick supercritical aerofoils with significant rear camber p 109 N95-17849

Surface pressure and wake drag measurements on the Boeing A4 airfoil in the IAR 1.5X1.5m Wind Tunnel Facility p 110 N95-17850

Low-speed surface pressure and boundary layer measurement data for the NLR 7301 airfoil section with trailing edge flap p 111 N95-17855

In-flight lift-drag characteristics for a forward-swept wing aircraft and comparisons with contemporary aircraft [NASA-TP-3414] p 117 N95-18565

Protective coatings for compressor gas path components p 201 N95-19675

Control of flow separation in airfoil/wing design applications p 274 N95-23294

Geometric analysis of wing sections [NASA-TM-110346] p 335 N95-24629

An exploratory application of neural networks for airfoil design p 448 N95-26943

Comparative wind tunnel tests of NACA 23024 airfoils with several aileron and spoiler configurations p 376 N95-27976

Comparative wind tunnel test at high Reynolds numbers of NACA 64 621 airfoils with two aileron configurations p 377 N95-27977

Numerical study to assess sulfur hexafluoride as a medium for testing multielement airfoils [NASA-TP-3496] p 378 N95-28674

A fourth order Euler/Navier-Stokes prediction method for the aerodynamics and aeroelasticity of hovering rotor blades p 554 N95-29242

Introduction to the estimation of the lift coefficients at zero angle of attack and at maximum lift for aerofoils with high-lift devices at low speeds [ESDU-94026] p 481 N95-29899

Control of unsteady separated flow associated with the dynamic stall of airfoils [NASA-CR-198972] p 594 N95-32193

AIRFOILS

Accuracy enhancements for overset grids using a defect correction approach [AIAA PAPER 94-0523] p 3 A95-60181

A comparison of turbulence models in computing multi-element airfoil flows [AIAA PAPER 94-0291] p 4 A95-60185

Solution-adaptive structured-unstructured grid method for unsteady turbomachinery analysis. Part I: Methodology [BTN-94-EIX94441380983] p 208 A95-67329

Two-point transonic airfoil design using optimization for improved off-design performance [BTN-95-EIX95062487542] p 192 A95-68356

Aerodynamic effects of delta planform tip sails on wing performance [BTN-95-EIX95062487544] p 185 A95-68358

Analysis of an oscillating Joukowski airfoil with surface suction and moving vortices [BTN-95-EIX95062487527] p 186 A95-69235

Aerodynamic sensitivity coefficients using the three-dimensional full potential equation [BTN-95-EIX95062487530] p 186 A95-69238

Preliminary assessment of tunnel wall interference in the NDA cryogenic wind tunnel [BTN-95-EIX95062487531] p 187 A95-69239

Ground effect calculation of two-dimensional airfoil [BTN-94-EIX94371347710] p 219 A95-69969

Ice accretion on aircraft wings [BTN-95-EIX95082502224] p 225 A95-71021

Effects of leading and trailing edge flaps on the aerodynamics of airfoil/vortex interactions [HTN-95-31011] p 221 A95-71181

New airfoil-design concept with improved aerodynamic characteristics [PAPER-4384] p 230 A95-72585

Two-equation turbulence model for unsteady separated flows around airfoils [BTN-95-EIX95142553054] p 262 A95-73444

Laplace interaction law for the computation of viscous airfoil flow in low- and high-speed aerodynamics [BTN-95-EIX95142553037] p 263 A95-73461

Aerodynamic shape optimization using preconditioned conjugate gradient methods [BTN-95-EIX95142553033] p 263 A95-73465

Eigenanalysis of unsteady flows about airfoils, cascades, and wings [BTN-95-EIX95152577597] p 305 A95-73486

Computation of oscillating airfoil flows with one- and two-equation turbulence models [BTN-95-EIX95152577588] p 263 A95-73494

Flow visualization studies on sidewall effects in two-dimensional transonic airfoil testing [BTN-95-EIX95152582313] p 264 A95-73516

Progress in high-lift aerodynamic calculations [BTN-95-EIX95152582315] p 264 A95-73518

Computation of the poststall behavior of a circulation controlled airfoil [BTN-95-EIX95152582320] p 264 A95-73523

Separation control on high-lift airfoils via micro-vortex generators [BTN-95-EIX95152582326] p 265 A95-73529

Study of an airfoil with a flap and spoiler [BTN-95-EIX95152582327] p 265 A95-73530

Effect of underwing frost on a transport aircraft airfoil at flight Reynolds number [BTN-95-EIX95152582334] p 276 A95-73536

Postinstability behavior of a two-dimensional airfoil with a structural nonlinearity [BTN-95-EIX95152582337] p 266 A95-73539

Turbulent transonic airfoil flow simulation using a pressure-based algorithm [BTN-95-EIX95182619078] p 269 A95-75763

Viscous-inviscid interaction method for unsteady low-speed airfoil flows [BTN-95-EIX95182619093] p 269 A95-75778

Tracking of raindrops in flow over an airfoil [BTN-95-EIX95182619221] p 308 A95-76647

Response of a nonrotating rotor blade to lateral turbulence. Part 2: Experiment [BTN-95-EIX95182619229] p 284 A95-76655

On the role of the outer region in the turbulent-boundary-layer bursting process [BTN-94-EIX95011441078] p 348 A95-81056

Direct boundary integral equations method to subsonic flow with circulation past thin airfoils in ground effect [BTN-95-EIX95242673940] p 365 A95-82224

On the influence of time-varying flow velocity on unsteady aerodynamics [HTN-95-61073] p 369 A95-83657

Precision requirement for potential-based panel methods [HTN-95-51666] p 433 A95-85048

Explicit Kutta condition for an unsteady two-dimensional constant potential panel method [HTN-95-51679] p 433 A95-85061

Predicting stall and post-stall behavior of airfoils at low mach numbers [BTN-95-EIX95262694297] p 365 A95-85468

Computational analysis of buffet alleviation in viscous transonic flow over a porous airfoil [BTN-95-EIX95262694321] p 366 A95-85492

Effect of Reynolds number and turbulence on airfoil aerodynamics at -90-degree incidence [HTN-95-42320] p 370 A95-86149

Reduction of blade-vortex interaction noise through porous leading edge [HTN-95-42324] p 371 A95-86153

Compressible Navier-Stokes computations of multielement airfoil flows using multiblock grids [HTN-95-42327] p 371 A95-86156

Interferometric investigations of compressible dynamic stall over a transiently pitching airfoil [HTN-95-42338] p 372 A95-86167

High angle-of-attack airfoil performance improvement by internal acoustic excitation [HTN-95-42347] p 372 A95-86176

Eigenanalysis of unsteady flows about airfoils, cascades, and wings [HTN-95-42582] p 459 A95-87212

Aerodynamic characteristics of truncated airfoils at high angle of attack [SAE PAPER 931227] p 460 A95-87365

Drag and lift in nonadiabatic transonic flow [HTN-95-61208] p 540 A95-87581

Pressure measurements on a pitching airfoil in a water channel [HTN-95-61209] p 541 A95-87582

Two-dimensional unsteady leading-edge separation on a pitching airfoil [HTN-95-81628] p 461 A95-87676

Automated adaptive time-discontinuous finite element method for unsteady compressible airfoil aerodynamics [HTN-95-81637] p 541 A95-87685

Multipoint inverse design of an infinite cascade of airfoils [HTN-95-81640] p 541 A95-87688

Airfoil pressure measurements during oblique shock-wave/vortex interaction in a Mach 3 stream [HTN-95-81641] p 542 A95-87689

Role of Kutta waves on oscillatory shock motion on an airfoil [HTN-95-81642] p 542 A95-87690

Effects of time scales on lift of airfoils in an unsteady stream [HTN-95-81643] p 542 A95-87691

Low-dimensional description of the dynamics in separated flow past thick airfoils [HTN-95-20832] p 544 A95-88093

Effect of annealing and desulfurization on oxide spallation of turbine airfoil material [BTN-95-EIX95282707024] p 528 A95-88264

An overview of static and dynamic airfoil performance [SAE PAPER 931228] p 463 A95-88960

Lift analysis of a variable camber foil using the discrete vortex-blob method [HTN-95-20940] p 545 A95-88979

Compressible Navier-Stokes calculations of the flow over airfoil sections. Comparisons of 1st and 2nd order turbulence models [SAE PAPER 932510] p 546 A95-89183

Computational study of boundary layer control for improving airfoil performance [SAE PAPER 932513] p 466 A95-89186

Computational fluid dynamics with icing effects [SAE PAPER 932532] p 466 A95-89192

Materials and structures for the HSCT [BTN-95-EIX95282711241] p 455 A95-89634

Preliminary study on the fixed transition technique for a shock tube transonic airfoil flow [BTN-95-EIX95282705928] p 455 A95-89663

Low Reynolds number laminar separation bubble control using a backward facing step [SAE PAPER 932572] p 467 A95-90061

Solution of the Navier-Stokes equations on a massively parallel transputer system p 549 A95-91490

Numerical design methods for transonic NLF configurations p 471 A95-91498

Application of ACT to unstable motions of an airfoil in ground effect p 471 A95-91500

Aerofoil characteristics at low Reynolds number p 472 A95-91507

High subsonic and high Reynolds number wind tunnel tests of two-dimensional natural-laminar-flow airfoils with suction boundary layer control p 472 A95-91508

Fixed transition for shock tube transonic flow p 472 A95-91509

A singularity method for a two dimensional stratified shear flow p 473 A95-91513

- Low speed wind tunnel blockage corrections for airfoils at medium to large angles of attack p 474 A95-91557
- Effects of free-stream turbulence intensity on a boundary layer recovering from concave curvature effects [BTN-95-EIX95282710058] p 632 A95-92471
- Comparison of coordinate-invariant and coordinate-aligned upwinding for the Euler equations [HTN-95-A1753] p 633 A95-93316
- Modelling 2D separation from a high lift airfoil with a non-linear eddy-viscosity model and second-moment closure [HTN-95-C0005] p 585 A95-93393
- Primary and secondary vortex structures over accelerated-decelerated airfoils at high angles of attack [SAE PAPER 931368] p 586 A95-93649
- Adaptive airfoils [ISBN 1-879921-01-4] p 625 A95-93744
- Numerical study of multi-element airfoil aerodynamics [ISBN 1-879921-01-4] p 587 A95-93750
- A Kutta condition conscious perturbation stream function boundary element algorithm for 2-D potential aerodynamics [ISBN 1-879921-01-4] p 587 A95-93751
- A study of mesh adaption techniques in structured and unstructured meshes [ISBN 1-879921-01-4] p 678 A95-93757
- Airfoil leading-edge suction and energy conservation for compressible flow [BTN-95-EIX95302730589] p 637 A95-94197
- Comparison of the predictive capabilities of several turbulence models [BTN-95-EIX0619952748167] p 589 A95-94461
- Navier-Stokes applications to high-lift airfoil analysis [BTN-95-EIX0619952748182] p 590 A95-94475
- Analysis of low Reynolds number airfoil flows [BTN-95-EIX0619952748183] p 590 A95-94476
- Lift-enhancing tabs on multielement airfoils [BTN-95-EIX0619952748187] p 591 A95-94479
- A robust inverse inviscid method for airfoil design p 640 A95-95431
- Permeable wall boundary conditions for transonic airfoil design p 641 A95-95445
- Navier-Stokes simulations of WECS airfoil flowfields [DE94-013341] p 7 N95-10226
- Optimum aerodynamic design via boundary control [NASA-CR-195882] p 36 N95-11877
- Control theory based airfoil design using the Euler equations [NASA-CR-196360] p 36 N95-11884
- User's manual for the NASA Lewis ice accretion/heat transfer prediction code with electrothermal deicer input [NASA-CR-4530] p 57 N95-11888
- Application of two procedures for dual-point design of transonic airfoils [NASA-TP-3466] p 38 N95-12176
- Studies on the flow induced by an oscillating airfoil in a uniform stream [PB94-204450] p 40 N95-13250
- A selection of experimental test cases for the validation of CFD codes, volume 1 [AGARD-AR-303-VOL-1] p 91 N95-14201
- Computational aerodynamics based on the Euler equations [AGARD-AG-325] p 72 N95-14264
- Control of unsteady separated flow associated with the dynamic stall of airfoils [NASA-CR-197024] p 74 N95-14613
- Spectral analysis of vortex/free-surface interaction [AD-A283210] p 96 N95-14658
- A computational investigation of wake-induced airfoil flutter in incompressible flow and active flutter control [AD-A281534] p 142 N95-16109
- An improved method of airfoil design p 106 N95-16252
- Residual-correction type and related computational methods for aerodynamic design. Part 1: Airfoil and wing design p 128 N95-16566
- Residual-correction type and related computational methods for aerodynamic design. Part 2: Multi-point airfoil design p 128 N95-16567
- Optimal shape design for aerodynamics p 128 N95-16568
- Airfoil optimization by the one-shot method p 128 N95-16569
- Review of the EUROPT Project AERO-0026 p 129 N95-16573
- 2-D airfoil tests including side wall boundary layer measurements p 158 N95-17847
- Measurements on a two-dimensional airfoil with high-lift devices p 109 N95-17848
- Surface pressure and wake drag measurements on the Boeing A4 airfoil in the IAR 1.5X1.5m Wind Tunnel Facility p 110 N95-17850
- Investigation of an NLF(1)-0416 airfoil in compressible subsonic flow p 110 N95-17852
- Experiments in the trailing edge flow of an NLR 7702 airfoil p 110 N95-17853
- Two-dimensional 16.5 percent thick supercritical airfoil NLR 7301 p 110 N95-17854
- Data from the GARTEur (AD) Action Group 02 airfoil CAST 7/DOA1 experiments p 111 N95-17856
- OAT15A airfoil data p 111 N95-17857
- Two-dimensional high-lift airfoil data for CFD code validation p 112 N95-17859
- Fatigue in single crystal nickel superalloys [AD-A285727] p 152 N95-18068
- Hydrofoil force balance [AD-D016475] p 160 N95-18461
- Solution of full potential equation on an airfoil by multigrid technique [NAL-TM-CSS-9303] p 119 N95-18904
- Numerical simulation of dynamic-stall suppression by tangential blowing [AD-A284887] p 120 N95-19110
- 2-D and 3-D oscillating wing aerodynamics for a range of angles of attack including stall [NASA-TM-4632] p 120 N95-19119
- Development of pneumatic test techniques for subsonic high-lift and in-ground-effect wind tunnel investigations p 121 N95-19268
- Analysis of test section sidewall effects on a two dimensional airfoil: Experimental and numerical investigations p 165 N95-19276
- Ice accretion with varying surface tension [NASA-TM-106826] p 124 N95-19285
- Public-sector aviation issues: Graduate research award papers, 1992-1993 [PB94-217478] p 219 N95-19967
- F-16XL interview with Marta Bohn-Meyer [NASA-TM-110505] p 223 N95-19996
- Computation of transonic flow on composite overlapping grids in 2 D [PB95-131348] p 248 N95-21132
- Unstructured-grid large-eddy simulation of flow over an airfoil p 225 N95-22448
- NREL airfoil families for HAWTs [DE95-000267] p 357 N95-24882
- Wind technology development: Large and small turbines [DE95-000286] p 358 N95-26090
- Thermal barrier coatings for aircraft engines: History and directions p 344 N95-26121
- Airfoil modification effects on subsonic and transonic pressure distributions and performance for the EA-6B airplane [NASA-TP-3516] p 373 N95-26382
- Computational fluid dynamics and transonic flow [AD-A288962] p 436 N95-26405
- An exploratory application of neural networks for airfoil design p 448 N95-26943
- Creating an alternative parameter optimization method (APO) p 375 N95-26946
- The near-wake flow behavior of an oscillating airfoil with modified trailing edge p 375 N95-26953
- Wind-tunnel test of the S814 thick root airfoil [DE95-000268] p 376 N95-27541
- Further investigations of icing effects on an advanced high-lift multi-element airfoil [NASA-TM-106947] p 381 N95-27762
- Horizontal axis wind turbine post stall airfoil characteristics synthesis p 376 N95-27974
- Increments in aerfoil lift coefficient at zero angle of attack and in maximum lift coefficient due to deployment of a plain trailing-edge flap, with or without a leading-edge high-lift device, at low speeds [ESDU-94028] p 477 N95-28885
- PIV investigation of compressibility effects on dynamic stall p 478 N95-29102
- Finite element vorticity-based methods for the solution of the incompressible and compressible Navier-Stokes equations p 553 N95-29119
- Increments in aerfoil lift coefficient at zero angle of attack and in maximum lift coefficient due to deployment of a trailing-edge split flap, with or without a leading-edge high-lift device, at low speeds [ESDU-94029] p 479 N95-29129
- Dynamic stall of a NACA 0012 airfoil in laminar flow p 479 N95-29243
- Acoustic scattering from ellipses by the modal element method [NASA-TM-106935] p 579 N95-29401
- The decay of longitudinal vortices shed from airfoil vortex generators [NASA-CR-198356] p 480 N95-29402
- Compressibility effects on and control of dynamic stall of oscillating airfoil [AD-A291804] p 480 N95-29428
- Increments in aerfoil lift coefficient at zero angle of attack and in maximum lift coefficient due to deployment of various leading-edge high-lift devices at low speeds [ESDU-94027] p 481 N95-29898
- Introduction to the estimation of the lift coefficients at zero angle of attack and at maximum lift for aerofoils with high-lift devices at low speeds [ESDU-94026] p 481 N95-29899
- An interacting boundary layer method for unsteady compressible flows p 557 N95-30290
- Growth and development of roughness-induced stationary crossflow vortices p 482 N95-30294
- Axial loads on yawed rotors [PB95-214193] p 592 N95-30638
- Multigrid convergence acceleration for the 2D Euler equations applied to high-lift systems [PB95-198081] p 593 N95-30814
- A laser-based ice shape profilometer for use in icing wind tunnels [NASA-TM-106936] p 646 N95-30851
- Allison engine testing CMSX-4(reg sign) single crystal turbine blades and vanes [DE95-010308] p 694 N95-32636
- Turbulence models in the Navier-Stokes simulation of airfoil stall [TRITA-NA-9312] p 705 N95-33059
- Special publication of National Aerospace Laboratory [NAL-SP-27] p 684 N95-34505
- Numerical solutions of inviscid and viscous flows about airfoils by TVD method p 684 N95-34521
- Numerical simulations of dynamic stall phenomena in low speed flows p 685 N95-34546
- Numerical simulation of unsteady viscous flow around an airfoil with oscillating spoiler p 685 N95-34547
- Grid generation around airfoil with a flap using boundary element method p 686 N95-34552
- Nonlinear stability of unsteady viscous flow [AD-A294931] p 707 N95-34597

AIRFRAME MATERIALS

Aeronautical technology - recent advances and future prospects

- [HTN-95-01097] p 496 A95-90283
- The panel oxidation and erosion test (POET) facility [AIAA PAPER 95-6151] p 521 A95-90465
- Repairs to composite structure on military aircraft [CONGRESS PAPER C428-4-067] p 531 A95-91677
- Aerospace applications of new materials [CONGRESS PAPER C428-17-135] p 531 A95-91716

The certification of composite structures for military aircraft [CONGRESS PAPER C428-37-198] p 628 A95-93633

Static and dynamic friction behavior of candidate high temperature airframe seal materials [NASA-TM-106571] p 152 N95-16905

- Acoustic fatigue testing on different materials and skin-stringer elements p 174 N95-19156
- Acoustic fatigue characteristics of advanced materials and structures p 174 N95-19157

Environmental effects on composite airframes: A study conducted for the ARM UAV Program (Atmospheric Radiation Measurement Unmanned Aerospace Vehicle) [DE94-015351] p 206 N95-19579

Technology reinvestment project's focus area: Affordable polymer matrix composites for airframe structures [PB95-136032] p 324 N95-23168

Corrosion detection and management of advanced airframe materials [AGARD-CP-565] p 302 N95-23496

The corrosion and protection of advanced aluminum - lithium airframe alloys p 302 N95-23497

Non-destructive detection of corrosion for life management p 314 N95-23505

New nondestructive techniques for the detection and quantification of corrosion in aircraft structures p 315 N95-23512

AIRFRAMES

Maintenance requirements for a supersonic transport [BTN-95-EIX95031502751] p 179 A95-68258

Simplified analysis of general instability of stiffened shells with cutouts in pure bending [BTN-95-EIX95042474418] p 209 A95-68282

Smart structures in the control of airframe vibrations [HTN-95-31014] p 236 A95-71184

An analytical and experimental investigation of the response of the curved, composite frame/skin specimens [HTN-95-80857] p 283 A95-75099

Integrated design of hypersonic waveriders including inlets and tailfins [BTN-95-EIX95212645692] p 271 A95-76744

Hypersonic trajectory control of aerospace plane with integrated SCRAMJET engine p 413 A95-82384

A tool for airframe shaping - idea and application [SAE PAPER 931224] p 491 A95-87568

Analytical developments in support of the NASA aging aircraft program with an application to crack growth from rivets
 [SAE PAPER 931223] p 545 A95-88789
 Lightning protection technology for small general aviation composite material aircraft
 [SAE PAPER 931241] p 483 A95-88964
 Application of restructurable flight control system to large transport aircraft
 [BTN-95-EIX95282706666] p 515 A95-89639
 Intermetallic and titanium matrix composite materials for hypersonic applications
 [AIAA PAPER 95-6132] p 530 A95-90451
 The panel oxidation and erosion test (POET) facility
 [AIAA PAPER 95-6151] p 521 A95-90465
 Tooling - a source of productivity
 [CONGRESS PAPER C428-32-017] p 583 A95-93619
 Evaluation of bonded boron/epoxy doublers for commercial aircraft aluminum structures
 p 92 N95-14457
 Corrosion and corrosion fatigue of airframe aluminum alloys
 p 87 N95-14465
 Development of the NASA/FLAGRO computer program for analysis of airframe structures
 p 94 N95-14473
 Analysis of small crack behavior for airframe applications
 p 95 N95-14484
 Advanced method and processing technology for complicated shape airframe part forming
 p 80 N95-14486
 Cooperative control theory and integrated flight and propulsion control
 [NASA-CR-197493] p 142 N95-17404
 Experimental data on the aerodynamic interactions between a helicopter rotor and an airframe
 p 116 N95-17883
 The generic simulation executive at Manned Flight Simulator
 [AD-A283997] p 146 N95-18724
 FAA/NASA International Symposium on Advanced Structural Integrity Methods for Airframe Durability and Damage Tolerance, part 2
 [NASA-CP-3274-PT-2] p 124 N95-19468
 Development of load spectra for Airbus A330/A340 full scale fatigue tests
 p 135 N95-19479
 Proceedings of the USAF Structural Integrity Program Conference
 [AD-A285684] p 194 N95-19517
 Lift enhancement device
 [AD-D016522] p 224 N95-21864
 Oklahoma City air logistics center (USAF) aging aircraft corrosion program
 p 262 N95-23519
 Advanced subsonic airplane design and economic studies
 [NASA-CR-195443] p 338 N95-24304
 Suppressor of oscillations in airframe cavities
 [AD-D017265] p 388 N95-26507
 Composite repair of metallic airframe: Twenty years of experience
 p 393 N95-27508
 Resin transfer molding of textile preforms for aircraft structural applications
 p 421 N95-28276
 Applications of a damage tolerance analysis methodology in aircraft design and production
 p 426 N95-28483
 NASA-ACEE/Boeing 737 graphite-epoxy horizontal stabilizer service
 p 400 N95-28489
 Rotorcraft crashworthy airframe and fuel system technology development program
 [AD-A289886] p 382 N95-28630
 Cross-stiffened continuous fiber structures
 p 536 N95-29041
 Development of stitched/RTM primary structures for transport aircraft
 [NASA-CR-191441] p 630 N95-31421
 The FCS-structural coupling problem and its solution
 p 623 N95-32005

AIRLINE OPERATIONS

Reliability and maintainability
 [BTN-95-EIX95042477109] p 179 A95-68350
 Development of aeronautical mobile satellite services over the past thirty years
 [BTN-95-EIX95152569458] p 305 A95-73498
 Containing military autotest cost growth through the use of commercial standard equipment architectures
 [BTN-95-EIX95172595295] p 287 A95-75717
 Maintenance challenges and trends
 [BTN-95-EIX95182617808] p 261 A95-75753
 Maintenance programs
 [BTN-95-EIX95182617809] p 261 A95-75754
 Maintenance programs
 [HTN-95-92310] p 365 A95-85354
 Northwest Airlines atmospheric hazards advisory & avoidance system
 p 672 A95-93539
 Assessment of the benefits for improved terminal weather information
 p 673 A95-93540

Cooperative problem solving between airline operations control and ATC traffic flow management
 p 681 A95-95066
 Safety in airport ground handling
 p 626 A95-95193
 Reanalysis of European flight loads data
 [AD-A282052] p 9 N95-11179
 Potential impacts of advanced aerodynamic technology on air transportation system productivity
 [NASA-TM-109154] p 10 N95-11489
 The FC-1D: The profitable alternative Flying Circus Commercial Aviation Group
 [NASA-CR-197152] p 46 N95-12628
 The OPF-6M transport jet
 [NASA-CR-197159] p 46 N95-12637
 Risk analysis for the fire safety of airline passengers
 [PB94-194065] p 77 N95-14179
 Aircraft accident report: Stall and loss of control on final approach, Atlantic Coast Airlines, Inc./United Express Flight 6291 Jetstream 4101, N304UE Columbus, OH, 7 January 1994
 [PB94-910409] p 123 N95-17646
 Safety study: Commuter airline safety
 [PB94-917004] p 124 N95-19132
 Air pollution mitigation measures for airports and associated activity
 [PB94-207610] p 216 N95-19582
 Public-sector aviation issues: Graduate research award papers, 1992-1993
 [PB94-217478] p 219 N95-19967
 Test and evaluation report for the Manual Domestic Passive Profiling System (MDPPS)
 [AD-A286312] p 225 N95-20093
 Aircraft accident report. Runway overrun following rejected takeoff. Continental airlines flight 795, McDonnell Douglas MD-82, N18835, LaGuardia Airport, Flushing, NY, 2 March 1994
 [PB95-910401] p 277 N95-23609
 The airline quality report, 1994
 [NIAR-94-11] p 277 N95-24012
 An integrated GPS/INS/BARO and radar altimeter system for aircraft precision approach landings
 [AD-A289280] p 383 N95-26985
 Development of advanced approach and departure procedures. Failure scenarios
 [PB95-198123] p 601 N95-30815
 A NASPAC-Based analysis of the delay and cost effects of the western-pacific region preliminary resectorization effort of 1993
 [AD-A288696] p 601 N95-31013
 Integrated terminal weather system (ITWS) demonstration and validation operational test and evaluation
 [AD-A293932] p 602 N95-31521
 Analysis and modeling of an airport departure process
 [AD-A293782] p 602 N95-31581
 Fact sheet for Congressional requesters. Airport competition: Essential air service slots at O'Hare International Airport
 [GAO/RCED-94-118FS] p 699 N95-32759

AIRPORT PLANNING

Aircraft noise at a West Coast airport in the next century
 p 560 A95-90095

AIRPORT SECURITY

Test and evaluation report for the Manual Domestic Passive Profiling System (MDPPS)
 [AD-A286312] p 225 N95-20093
 Federal Aviation Administration plan for research, engineering and development, 1995
 p 363 N95-24202
 Aviation security: Development of new security technology has not met expectations. Report to Congressional requesters
 [GAO/RCED-94-142] p 687 N95-32885

AIRPORT TOWERS

Final results of the weather testing component of the Terminal Doppler Weather Radar operational test and evaluation
 p 658 A95-93471
 Air traffic operational inventory CY 1994
 [AD-A288281] p 382 N95-26454
 Terminal area forecasts-fiscal years 1993-2010
 [AD-A290835] p 490 N95-29880
 FAA aviation forecasts: Fiscal year 1995-2006
 [AD-A293682] p 584 N95-31598
 Report to the Chairman, Subcommittee on Transportation and Related Agencies, Committee on Appropriations, House of Representatives. Air traffic control: Status of FAA's plans to close and contract out low-activity towers
 [GAO/RCED-94-265] p 603 N95-32199

AIRPORTS

Aircraft noise and sleep disturbance: A field study
 [HTN-95-92543] p 558 A95-87363
 Monitoring noise from aircraft operations in the vicinity of airports
 p 570 A95-88462

Nordic Standards for measurement of aircraft noise immission in residential areas and noise reduction of dwellings
 p 570 A95-88463
 Modeling lateral attenuation of aircraft flight noise
 p 570 A95-88464
 Factors affecting measured aircraft sound levels in the vicinity of start-of-takeoff roll
 p 571 A95-88465
 Meteorological impacts on airport noise prediction by the 'Integrated Noise Model' application based on Hamiltonian Ray-Tracing program and measurements
 p 571 A95-88467
 Time-average aircraft noise descriptors: Confusion with no benefit
 p 559 A95-88474
 Noise metrics and aviation noise control: The case for DNL
 p 559 A95-88475
 Aircraft noise zoning in Norway
 p 581 A95-88476
 Criticism of the Leq as an index for aircraft noise and other discontinuous noise sources
 p 559 A95-88477
 The evolution of airport noise monitoring systems: Recent achievements and further needs
 p 562 A95-90125

Features of Massport's new noise monitoring system
 p 562 A95-90127

Air traffic management: The future challenge
 [CONGRESS PAPER C428-7-145] p 488 A95-91686
 On designing and engineering the integrated terminal weather system
 p 653 A95-93449
 Status of the terminal Doppler weather radar with deployment underway
 p 653 A95-93450
 The Integrated Terminal Weather System (ITWS) storm cell information and weather impacted airspace detection algorithm
 p 654 A95-93452
 Improving aircraft impact assessment with the integrated terminal weather system microburst detection algorithm
 p 654 A95-93453
 p 654 A95-93455

ITWS gridded analysis
 p 654 A95-93455

The ITWS microburst prediction algorithm
 p 655 A95-93456

Stratus' tephigram as a training/forecasting tool
 p 657 A95-93465

A comparative performance study of TDWR/LLWAS 3 integration algorithms for wind shear detection
 p 658 A95-93468

Investigation of outflow strength variability in Florida downburst-producing storms
 p 659 A95-93476

Preliminary results of high resolution measurements of snowfall at Stapleton International Airport during the winter of 1992-93
 p 661 A95-93484

Automation of observations in the Netherlands
 p 661 A95-93485

Use of high resolution lightning detection and localization sensors for hazardous aviation weather nowcasting
 p 661 A95-93486

The use of radar wind profiles to remove TDWR gust front algorithm false alarms caused by vertical wind shear
 p 661 A95-93488

Terminal Doppler Weather Radar point target filter threshold selection
 p 662 A95-93490

Test results of a low cost airport weather radar
 p 662 A95-93492

Development of a climatology for possible microburst occurrence in Canada
 p 664 A95-93497

Comprehensive verification of terminal forecast ceiling and visibility
 p 664 A95-93500

Objective verification of an enhanced terminal forecast experiment at Denver, Colorado
 p 664 A95-93501

Verification of terminal forecasts
 p 664 A95-93502

MEMFOG - The Memphis fog algorithm
 p 668 A95-93516

FTGEN - An automated FT production system
 p 668 A95-93519

Aviation terminal forecasts based on automated observations (FTAUTO)
 p 668 A95-93520

Nortaf: Computer generated aerodrome forecasts
 p 668 A95-93521

The combination of forecasts in an automated aviation weather forecasting system
 p 669 A95-93522

Aviation weather forecasting automated methods in the RAFC Moscow and the Airport Vnukovo
 p 669 A95-93523

A poor man's expert system for aviation VSRF in complex terrain
 p 669 A95-93524

Dissemination of terminal weather products to the flight deck via data link
 p 669 A95-93525

Windshear detection: TDWR and LLWAS operational experience in Denver 1988-1992
 p 670 A95-93528

Assessment of the benefits for improved terminal weather information
 p 673 A95-93540

The 1992-3 operational winter forecasting experiment for Stapleton airport
 p 677 A95-93561

Safety in airport ground handling
 p 626 A95-95193

25 years of airport sound insulation programs
 p 31 N95-11307

At Istanbul-Ataturk Airport measurement and analysis of noise in due of take-off time
 p 31 N95-11319

- Determining the effects of alternative departure cutback altitudes and power settings: A case study, John Wayne Airport p 31 N95-11320
 INM contour validation: A case study p 31 N95-11321
 Noise modeling for MOAs and ranges p 32 N95-11322
 Moisture induced pressures in concrete airfield pavements [AD-A281974] p 52 N95-11789
 Gemini: A long-range cargo transport [NASA-CR-197149] p 45 N95-12626
 The Balsa bullet: A high speed, low-cost general aviation aircraft for Aeroworld [NASA-CR-197165] p 46 N95-12638
 Certification of windshear performance with RTCA class D radomes p 41 N95-13206
 Airport surveillance using a solid state coherent lidar p 41 N95-13207
 Ground-based wake vortex monitoring, prediction, and ATC interface p 42 N95-13209
 Wake vortex detection at Denver Stapleton Airport with a pulsed 2-micron coherent lidar p 42 N95-13211
 Response to noise around Vaernes and Bodoe airports [PB94-207065] p 62 N95-13575
 Modeling of Instrument Landing System (ILS) localizer signal on runway 25L at Los Angeles International Airport [NASA-TM-4588] p 125 N95-17384
 Evaluation of an unlighted swinging airport sign [AD-A284763] p 146 N95-18087
 Aircraft wake vortex takeoff tests at O'Hara International Airport [AD-A283828] p 118 N95-18624
 On-line handling of air traffic: Management, guidance and control [AGARD-AG-321] p 126 N95-18927
 Air pollution mitigation measures for airports and associated activity [PB94-207610] p 216 N95-19582
 Research requirements for future visual guidance systems [AD-A279188] p 191 N95-19810
 Test and Evaluation Plan (TEP) for Improved Explosive Device Screening Systems (IEDSS) [AD-A286382] p 227 N95-22319
 Analysis of test criteria for specifying foam firefighting agents for aircraft rescue and firefighting [AD-A286381] p 227 N95-22352
 Evaluation of neutron techniques for illicit substance detection [DE95-002988] p 300 N95-22764
 Automation technology using Geographic Information System (GIS) p 324 N95-23284
 Federal Aviation Administration plan for research, engineering and development, 1995 p 363 N95-24202
 Aviation system capacity improvements through technology [NASA-TM-109165] p 333 N95-24633
 The 1994 updated National Airspace System performance assessment for year 2005 [AD-A288652] p 380 N95-26485
 Terminal area forecasts-fiscal years 1993-2010 [AD-A290835] p 490 N95-29880
 Evaluation of retro-reflective beads in airport pavement markings [AD-A291065] p 523 N95-29967
 Prototype stop bar system evaluation at Seattle-Tacoma International Airport [AD-A290136] p 490 N95-30031
 Development of advanced approach and departure procedures. Failure scenarios [PB95-198123] p 601 N95-30815
 A NASPAC-Based analysis of the delay and cost effects of the western-pacific region preliminary resectorization effort of 1993 [AD-A288696] p 601 N95-31013
 Aviation capacity enhancement plan 1994 [AD-A292758] p 598 N95-31428
 Evaluation of alternative pavement marking materials [AD-A292973] p 626 N95-31468
 Integrated terminal weather system (ITWS) demonstration and validation operational test and evaluation [AD-A293932] p 602 N95-31521
 Analysis and modeling of an airport departure process [AD-A293782] p 602 N95-31581
 The ATC operational evaluation of the prototype integrated terminal weather system (ITWS) at Dallas/Fort Worth and Orlando airports (May-September 1993) [AD-A293808] p 677 N95-31587
 FAA aviation forecasts: Fiscal year 1995-2006 [AD-A293682] p 584 N95-31598
 Integration of air traffic databases: A case study [AD-A293691] p 602 N95-32022
 Fact sheet for Congressional Committees. Air traffic control: Status of FAA's modernization program [GAO/RCED-94-167FS] p 603 N95-32197
 Fact sheet for Congressional requesters. Airport competition: Essential air service slots at O'Hare International Airport [GAO/RCED-94-118FS] p 699 N95-32759
 Report to the Chairman, Subcommittee on Transportation and Related Agencies, Committee on Appropriations, US Senate. Airport Improvement Program: Reliever airport set-aside funds could be redirected [GAO/RCED-94-226] p 699 N95-32786
 Report to the Chairman, Subcommittee on Transportation and Related Agencies, Committee on Appropriations, US Senate. Airport Improvement Program: The Military Airport Program has not achieved intended impact [GAO/RCED-94-209] p 700 N95-32888
AIRSHIPS
 The scientific ballooning in Russia p 191 A95-66302
 A program for scientific and applied investigations using aerostat complexes p 182 A95-66304
 Airship applications of modern flight test techniques [AD-A284253] p 194 N95-19731
 CALIOPE and TAISIR airborne experiment platform [DE94-018328] p 250 N95-22299
 Long endurance stratospheric solar powered airship [PB95-178729] p 336 N95-26009
AIRSPACE
 Noise modeling for MOAs and ranges p 32 N95-11322
 Oceanic operations: An authoritative guide to oceanic operations [FAA-AFS-550] p 277 N95-24065
 Aviation system capacity improvements through technology [NASA-TM-109165] p 333 N95-24633
 The 1994 updated National Airspace System performance assessment for year 2005 [AD-A288652] p 380 N95-26485
 Unmanned aerial vehicles, 1994 master plan [AD-A291628] p 398 N95-28411
 Three-D weather displays for aircraft cockpits [AD-A289759] p 508 N95-28691
 Effects of civil tiltrotor service in the northeast corridor on en route airspace loads [AD-A293586] p 599 N95-31687
AIRSPEED
 Minimum sink-speed in power-off glide [BTN-95-EIX95062487556] p 193 A95-68370
 A gust alleviation method by the response feedback p 506 A95-91493
 Development of a pilot tube with multi-hole pyramidal head. 2: A five-hole yaw probe of engineering model p 522 A95-91577
 Flight dynamics of an unmanned aerial vehicle [AD-A282259] p 45 N95-12410
 Remote sensing of turbulence in the clear atmosphere with 2-micron lidars p 59 N95-13213
 Add a dimension to your analysis of the helicopter low airspeed environment [AD-A283982] p 79 N95-14205
 Groundspeed filtering for CTAS [NASA-CR-197223] p 97 N95-15785
 A real-time algorithm for integrating differential satellite and inertial navigation information during helicopter approach [NASA-CR-197409] p 229 N95-21891
 Advanced formation flight control [AD-A289271] p 409 N95-26981
 Experimental and computational investigation of the tip clearance flow in a transonic axial compressor rotor [NASA-TM-106711] p 649 N95-31738
ALASKA
 An integrated system to improve aviation weather forecasts for the Alaska Range p 656 A95-93460
 Alaska's volcanic ash warning system p 663 A95-93495
ALBEDO
 Microphysical and radiative properties of small cumulus clouds over the sea [HTN-95-A0526] p 255 A95-73180
 On the link between cloud-top radiative properties and sub-cloud aerosol concentrations [HTN-95-A0527] p 255 A95-73181
 Air truth validation of cloud albedo estimated from NOAA advanced very high resolution radiometer data [HTN-95-A1021] p 443 A95-84526
ALGORITHMS
 A comparison of three-dimensional nonequilibrium solution algorithms applied to hypersonic flows with stiff chemical source terms [AIAA PAPER 93-2861] p 4 A95-60186
 A grid generation and flow solution method for the Euler equations on unstructured grids [HTN-95-20003] p 153 A95-63201
 Parallel implicit unstructured grid Euler solvers [BTN-95-EIX95042474393] p 217 A95-68307
 Active control of wake/blade-row interaction noise [BTN-95-EIX95042474389] p 196 A95-68311
 Integrated GPS/Glonass navigation: Algorithms and results [BTN-95-EIX95112522531] p 190 A95-69332
 Comparison of parameter identification algorithms for flight vehicles [BTN-94-EIX94371347708] p 219 A95-69967
 Behavior of an inversion-based precipitation retrieval algorithm with high-resolution AMPPR measurements including a low-frequency 10.7-GHz channel [HTN-95-70134] p 252 A95-70656
 Comments on 'correction of inertial navigation with Lorán C on NOAA's P-3 aircraft' [HTN-95-70149] p 227 A95-70671
 Large-scale computational fluid dynamics by the finite element method [BTN-94-EIX94381359154] p 243 A95-71744
 An algorithm for forecasting mountain wave-related turbulence in the stratosphere [HTN-95-80656] p 254 A95-72500
 A generalized algorithm for inverse simulation applied to helicopter maneuvering flight [HTN-95-A0493] p 236 A95-72564
 Buckling and vibration analysis of laminated panels using VICONOPT [PAPER-1746] p 230 A95-72580
 Efficient sensitivity analysis for rotary-wing aeromechanical problems [BTN-95-EIX95152577585] p 264 A95-73497
 Application of the multigrid solution technique to hypersonic entry vehicles [BTN-95-EIX95152583254] p 306 A95-73555
 Functional dependence of trajectory dispersion on initial condition errors [BTN-95-EIX95152583263] p 298 A95-73564
 Optimization of contoured hypersonic scramjet inlets with a least-squares parabolized Navier-Stokes procedure [HTN-95-20976] p 261 A95-74042
 Real-time estimation of atmospheric turbulence severity from in-situ aircraft measurements [BTN-95-EIX95182619231] p 319 A95-76657
 On-line learning nonlinear direct neurocontrollers for restructurable control systems [BTN-95-EIX95242670768] p 359 A95-81079
 Accuracy and efficiency assessments for a weak statement CFD algorithm for high-speed aerodynamics [BTN-94-EIX95011441238] p 370 A95-84195
 Compressible Navier-Stokes computations of multielement airfoil flows using multiblock grids [HTN-95-42327] p 371 A95-86156
 Using the Liou-Steffen algorithm for the Euler and Navier-Stokes equations [HTN-95-42348] p 373 A95-86177
 Quality estimates and stretched meshes based on Delaunay triangulations [HTN-95-42575] p 564 A95-87205
 Reentry trajectories and their optimization by an evolution algorithm p 525 A95-87394
 Meteorological impacts on airport noise prediction by the 'Integrated Noise Model' application based on Hamiltonian Ray-Tracing program and measurements p 571 A95-88467
 Study of strapdown navigation attitude algorithms [BTN-95-EIX95282706655] p 486 A95-89649
 Analyzing fault tolerance using DREDD [AIAA PAPER 95-0952] p 565 A95-90631
 Algorithmic trends in computational fluid dynamics; The Institute for Computer Applications in Science and Engineering (ICASE)/LaRC Workshop, NASA Langley Research Center, Hampton, VA, US, Sep. 15-17, 1991 [ISBN 0-387-94014-6] p 550 A95-91915
 A viewpoint on discretization schemes for applied aerodynamic algorithms for complex configurations p 550 A95-91916
 Algorithmic trends in CFD in the 1990's for aerospace flow field calculations p 550 A95-91917
 Implicit multiblock Euler and Navier-Stokes calculations [HTN-95-A1755] p 634 A95-93318
 On designing and engineering the integrated terminal weather system p 653 A95-93449
 The Integrated Terminal Weather System (ITWS) storm cell information and weather impacted airspace detection algorithm p 654 A95-93452
 Improving aircraft impact assessment with the integrated terminal weather system microburst detection algorithm p 654 A95-93453
 The ITWS microburst prediction algorithm p 655 A95-93456

- Preliminary comparisons between MM5 NCAR/Penn State model generated icing forecasts and observations p 655 A95-93458
- A comparative performance study of TDWR/LLWAS 3 integration algorithms for wind shear detection p 658 A95-93468
- Use of WSR-88D data in the FAA's weather impacted aerospace product p 658 A95-93469
- Flying with automated surface observations p 659 A95-93472
- Estimation of atmospheric turbulence severity from in-situ aircraft measurements p 659 A95-93479
- The use of radar wind profiles to remove TDWR gust front algorithm false alarms caused by vertical wind shear p 661 A95-93488
- LLWAS 2 and LLWAS 3 performance evaluation p 662 A95-93491
- Use of pilot reports for verification of aircraft icing diagnoses and forecasts p 666 A95-93508
- An echo motion algorithm for air traffic management using a national radar mosaic p 667 A95-93513
- Testing of TKE parameterizations in numerical models for clear-air turbulence forecasting p 667 A95-93515
- MEMFOG - The Memphis fog algorithm p 668 A95-93516
- A study of the savings in time and fuel to aviation through the use of upper-air wind forecasts p 672 A95-93538
- Creating a global climatology of freezing rain using numerical model output p 673 A95-93541
- A northern hemisphere clear air turbulence climatology p 674 A95-93547
- An evaluation of clear-air turbulence indices p 674 A95-93548
- The development of an aircraft icing forecast technique using data from maps p 675 A95-93549
- Matching fluid and structure meshes for aeroelastic computations: a parallel approach [BTN-95-EIX95302679864] p 636 A95-94102
- Supersonic, turbulent flow computation and drag optimization for axisymmetric afterbodies [BTN-95-EIX95302729772] p 637 A95-94134
- Modelling wear at intermittently slipping high speed interfaces [BTN-94-EIX94511433698] p 701 A95-96655
- Methodology for sensitivity analysis, approximate analysis, and design optimization in CFD for multidisciplinary applications [NASA-CR-196981] p 58 A95-13201
- Numerical time dependent sheet cavitation simulations using a higher order panel method [PB94-204435] p 59 A95-13249
- Computational aerodynamics based on the Euler equations [AGARD-AG-325] p 72 A95-14264
- Computing quantitative characteristics of finite-state real-time systems [AD-A282839] p 83 A95-14343
- Generalized method of solving topological optimization problems for electrical airplane equipment systems in computer-aided design p 169 A95-16272
- Optimum Design Methods for Aerodynamics [AGARD-R-803] p 127 A95-16562
- FPCAS2D user's guide, version 1.0 [NASA-CR-195413] p 156 A95-16588
- Algorithms for bilevel optimization [NASA-CR-194980] p 170 A95-16897
- Eddy current for detecting second layer cracks under installed fasteners [AD-A282412] p 158 A95-17507
- A platform independent application of Lux illumination prediction algorithms [AD-A283669] p 170 A95-18018
- Minimal time detection algorithms and applications to flight systems [TR-2-FSRC-93] p 171 A95-18564
- Mesh quality control for multiply-refined tetrahedral grids [NASA-CR-197595] p 160 A95-18737
- An assessment of the adaptive unstructured tetrahedral grid, Euler Flow Solver Code FELISA [NASA-TP-3526] p 119 A95-19041
- Application of three-dimensional hybrid structured/unstructured grids to land, sea and air vehicles [ARA-MEMO-399] p 210 A95-19775
- Verification of the CFD simulation system SAUNA for complex aircraft configurations [ARA-MEMO-401] p 211 A95-19776
- Computing methods for the approximate solution of time dependent problems [AD-A286007] p 256 A95-20719
- A real-time algorithm for integrating differential satellite and inertial navigation information during helicopter approach [NASA-CR-197409] p 229 A95-21891
- Direct numerical simulations of on-demand vortex generators: Mathematical formulation p 251 A95-22452
- Aerodynamic design optimization with sensitivity analysis and computational fluid dynamics [NASA-CR-197419] p 274 A95-23218
- On-line, adaptive state estimator for active noise control p 322 A95-23308
- Empirical results on scheduling and dynamic backtracking p 299 A95-23761
- Aerodynamic parameter estimation via Fourier modulating function techniques [NASA-CR-4654] p 335 A95-24630
- A non-iterative grid deformation algorithm for computational fluid dynamics for aeroelasticity [AD-A288298] p 436 A95-26418
- Flightpath synthesis and HUD scaling for V/STOL terminal area operations [NASA-TM-110348] p 383 A95-26587
- Comparison of fixed wing aircraft algorithms for JANUS [AD-A288503] p 389 A95-26652
- Development of an upwind, finite-volume code with finite-rate chemistry [NASA-CR-197747] p 374 A95-26760
- Implementation and demonstration of a multiple model adaptive estimation failure detection system for the F-16 [AD-A289301] p 391 A95-27042
- Modeling of aircraft unsteady aerodynamic characteristics. Part 2: Parameters estimated from wind tunnel data [NASA-TM-110161] p 410 A95-27839
- The applicability of turbulence models to aerodynamic and propulsion flowfields at McDonnell-Douglas Aerospace p 439 A95-27886
- Local design optimization for composite transport fuselage crown panels p 398 A95-28473
- Algorithms for high aspect ratio oriented triangulations p 476 A95-28731
- Optimizing cockpit display configurations with a genetic algorithm system [AD-A289799] p 508 A95-29123
- Acoustic scattering from ellipses by the modal element method [NASA-TM-106935] p 579 A95-29401
- Computational algorithms for aerodynamic analysis and design [AD-A291084] p 482 A95-29972
- New adaptive methods for reconfigurable flight control systems, appendix 1 [AD-A292711] p 619 A95-30937
- Flight assessment of the onboard propulsion system model for the Performance Seeking Control algorithm on an F-15 aircraft [NASA-TM-4705] p 617 A95-31425
- Improved modeling of unsteady heat transfer (The first step) [AD-A292777] p 648 A95-31432
- Integrated terminal weather system (ITWS) demonstration and validation operational test and evaluation [AD-A293932] p 602 A95-31521
- Image representation using fast algorithms based on the Zak transform [AD-A293416] p 679 A95-31684
- PSC algorithm description p 695 A95-33013
- ALL-WEATHER AIR NAVIGATION**
- Comments on effect of wet snow on the null-reference ILS system [BTN-95-EIX95142555488] p 227 A95-72885
- A PC-based interactive simulation of the F-111C Pavé Tack system and related sensor, avionics and aircraft aspects [AD-A285500] p 129 A95-16969
- ALLUVIUM**
- Integration of AIRSAR and AVIRIS data for Trail Canyon alluvial fan, Death Valley, California p 709 A95-33760
- ALPS MOUNTAINS (EUROPE)**
- Data processing and mapping in airborne radiometric surveys [HTN-95-51587] p 442 A95-83591
- A poor man's expert system for aviation VSRF in complex terrain p 669 A95-93524
- ALTERNATING CURRENT**
- The use of electrochemistry and ellipsometry for identifying and evaluating corrosion on aircraft [AD-A285323] p 151 A95-16371
- ALTERNATING DIRECTION IMPLICIT METHODS**
- Convergence acceleration of implicit schemes in the presence of high aspect ratio grid cells p 313 A95-23446
- ALTERNATIVES**
- Life cycle costs of alternatives for F-16 printed circuit board diagnosis equipment [AD-A288744] p 401 A95-28586
- A comparison of coating alternatives for US Coast Guard aircraft [AD-A293270] p 629 A95-31124
- Alternatives to ozone depleting refrigerants in test equipment p 630 A95-31767
- Process evaluation p 651 A95-32180
- ALTIMETERS**
- Validation of empirical orbit error corrections using crossover difference differences [HTN-94-00912] p 25 A95-60227
- Assimilation of altimeter data in a quasi-geostrophic model of the Gulf Stream system: A dynamical perspective [NASA-CR-196313] p 320 A95-23766
- An in situ evaluation of TOPEX/Poseidon altimetric measurements versus measurements made by moorings and inverted echo sounders for sea surface height [NASA-CR-198621] p 447 A95-27805
- ALTIMETRY**
- Geoid lineations of 1000 km wavelength over the central Pacific [HTN-95-11304] p 319 A95-77009
- An in situ evaluation of TOPEX/Poseidon altimetric measurements versus measurements made by moorings and inverted echo sounders for sea surface height [NASA-CR-198621] p 447 A95-27805
- ALTITUDE**
- Ascent wind model for launch vehicle design [BTN-95-EIX95041503799] p 239 A95-70124
- NASA Lewis Propulsion Systems Laboratory customer guide manual [NASA-TM-106569] p 21 A95-10822
- Evaluation of an autopilot based multimodelling [PB94-190725] p 142 A95-17454
- Investigation and characterization of SEU effects and hardening strategies in avionics [AD-A291058] p 509 A95-29950
- Sea wave parameters, small altitudes and distances measurers design for movement control systems of ships, wing-in-surface effect crafts and seaplanes p 708 A95-33141
- ALTITUDE CONTROL**
- Selection of optimal parameters for a system, controlling the flight height, when information about the state vector is incomplete [BTN-94-EIX94461408753] p 168 A95-63636
- Altitude cuing effectiveness of terrain texture characteristics in simulated low-altitude flight [AD-A294369] p 700 A95-34362
- ALTITUDE SIMULATION**
- Icing simulation in the aeropropulsion systems test facility propulsion development test cell C-2 [AD-A293039] p 599 A95-31667
- ALTITUDE TESTS**
- Temperature effects on acoustic interactions between altitude test facilities and jet engine plumes [NASA-CR-197638] p 258 A95-21170
- The effect of altitude conditions on the particle emissions of a J85-GE-5L turbojet engine [NASA-TM-106669] p 339 A95-24561
- ALUMINIDES**
- Ordered intermetallic alloys, part 3: Gamma titanium aluminides [HTN-95-B0396] p 530 A95-90477
- New Trends in coatings developments for turbine blades: Materials processing and repair p 201 A95-19676
- The effect of interface properties on nickel base alloy composites [NASA-CR-198363] p 629 A95-30787
- ALUMINIUM**
- Composite propeller system for Domier 328 [BTN-94-EIX94461290506] p 66 A95-61728
- Low frequency ultrasonic nondestructive inspection of aluminum/adhesive fuselage lap splices [DE94-014242] p 24 A95-11135
- Low-speed wind tunnel testing of the NPS and NASA Ames Mach 6 optimized waverider [AD-A283585] p 75 A95-15319
- Large amplitude nonlinear response of flat aluminum, and carbon fiber plastic beams and plates [AD-A282440] p 96 A95-15547
- Corrosion of aircraft materials: Correlation between nanometer scale and macroscopic structural damage parameters [AD-A285930] p 241 A95-20299
- Corrosion protection measures for CFC/metal joints of fuel integral tank structures of advanced military aircraft p 303 A95-23510
- ALUMINIUM ALLOYS**
- Fatigue resistance of peened 7050-T7451 aluminium alloy: Repair and re-treatment of a component surface [BTN-94-EIX94371347838] p 206 A95-69131
- Flight simulation fatigue crack growth testing of aluminum alloys [HTN-95-00652] p 418 A95-84731

- Forming and bonding techniques for high-strength aluminum alloys [HTN-95-20605] p 418 A95-84786
- Aerospace applications of new materials [CONGRESS PAPER C428-17-135] p 531 A95-91716
- Corrosion and corrosion fatigue of airframe aluminum alloys p 87 N95-14465
- Influence of crack history on the stable tearing behavior of a thin-sheet material with multiple cracks p 93 N95-14467
- The effects of pitting on fatigue crack nucleation in 7075-T6 aluminum alloy p 88 N95-14482
- Multi-lab comparison on R-curve methodologies: Alloy 2024-T3 [NASA-CR-195004] p 151 N95-16860
- The application of Newman crack-closure model to predicting fatigue crack growth p 167 N95-19483
- Fatigue crack growth in 2024-T3 aluminum under tensile and transverse shear stresses p 153 N95-19490
- Prediction of R-curves from small coupon tests p 167 N95-19496
- Electrochemical impedance pattern recognition for detection of hidden chemical corrosion on aircraft components [AD-A284998] p 241 N95-20481
- Electrochemical impedance pattern recognition for detection of hidden chemical corrosion on aircraft components [AD-A285998] p 241 N95-20716
- Aircraft corrosion study [AD-A279527] p 241 N95-21687
- Test method and test results for environmental assessment of aircraft materials p 302 N95-23509
- NASA-UVA light aerospace alloy and structures technology program supplement: Aluminum-based materials for high speed aircraft [NASA-CR-4645] p 343 N95-24878
- The use of electrochemistry and ellipsometry for identifying and evaluating corrosion on aircraft [AD-A290249] p 504 N95-29426
- The mm-wave resonant methods for the detection of corrosion, phase 1 [AD-A291315] p 556 N95-29941
- Electrochemical impedance pattern recognition for detection of hidden chemical corrosion on aircraft components, phase 1 [AD-A291345] p 556 N95-29946
- ALUMINIUM-LITHIUM ALLOYS**
- Status and prospects for aluminium-lithium alloys in aircraft structures p 387 A95-85893
- The corrosion and protection of advanced aluminium - lithium airframe alloys p 302 N95-23497
- AMBIENT TEMPERATURE**
- Similarity rule for jet-temperature effects on transonic base pressure [BTN-95-EIX95222650791] p 329 A95-79247
- AMBULANCES**
- Inadequacy of visual alarms in helicopter air medical transport [HTN-95-01218] p 484 A95-91450
- Flying ambulances: The approach of a small air force to long distance aeromedical evacuation of critically injured patients p 568 N95-29618
- AMMONIUM SULFATES**
- Gas turbine compressor corrosion and erosion in Western Europe [AD-B196178L] p 201 N95-19678
- AMORPHOUS MATERIALS**
- Repair technology for thermoplastic aircraft structures p 395 N95-27519
- AMOUNT**
- Analysis of test criteria for specifying foam firefighting agents for aircraft rescue and firefighting [AD-A286381] p 227 N95-22352
- AMPHIBIOUS AIRCRAFT**
- Selecting and management of fire fighter aircraft [BTN-95-EIX95062487538] p 193 A95-69246
- AMPHIBIOUS VEHICLES**
- Air cushioned landing craft (LCAC) based ship to shore movement simulation: A decision aid for the amphibious commander. A (SMMAT) application [AD-A289635] p 436 N95-26722
- AMPLIFICATION**
- Amplification and breaking of atmospheric gravity waves p 675 A95-93552
- AMPLITUDES**
- Handling qualities analysis on rate limiting elements in flight control systems p 619 N95-31071
- ANALOG CIRCUITS**
- Broadband, wide-area active control of sound radiated from vibrating structures using local surface-mounted radiation suppression devices p 30 N95-11283
- ANALYSIS (MATHEMATICS)**
- Non-linear analysis provides new insights into impact damage of composite structures [HTN-95-42368] p 418 A95-86197
- Computational analysis of forebody tangential slot blowing p 71 N95-14253
- ANALYSIS OF VARIANCE**
- Dynamic stiffness and damping of foil bearings for gas turbine engines [SAE PAPER 931449] p 635 A95-93698
- Modeling F/A-18 flight hour program costs using regression analysis [AD-A293771] p 608 N95-31579
- ANECHOIC CHAMBERS**
- A large hemi-anechoic enclosure for community-compatible aeroacoustic testing of aircraft propulsion systems p 577 A95-90132
- Modification of the Ames 40- by 80-foot wind tunnel for component acoustic testing for the second generation supersonic transport [NASA-TM-108850] p 65 N95-13642
- Background noise levels measured in the NASA Lewis 9- by 15-foot low-speed wind tunnel [NASA-TM-106817] p 145 N95-18054
- Anechoic wind tunnel study of turbulence effects on wind turbine broadband noise p 451 N95-27992
- Anechoic chamber upgrade [AD-A294375] p 700 N95-34342
- ANEMOMETERS**
- Aircraft wake vortex takeoff tests at O'Hara International Airport [AD-A283828] p 118 N95-18624
- ANGLE OF ATTACK**
- An experimental investigation of wing tip turbulence with applications to aerosound p 1 A95-60164
- [AIAA PAPER 86-1918] p 1 A95-60164
- Oscillating airfoil compressible dynamic stall studies [HTN-94-00704] p 3 A95-60183
- A comparison of turbulence models in computing multi-element airfoil flows [AIAA PAPER 94-0291] p 4 A95-60185
- LDV measurements in dynamically separated flows [ISBN 0-8194-1311-9] p 5 A95-60191
- X-29 high-angle-of-attack [BTN-94-EIX94511305383] p 127 A95-64609
- Vortex cutting by a blade. Part II: Computations of vortex response [BTN-94-EIX94441386611] p 208 A95-67342
- Elliptic tip effects on the vortex wake of an axisymmetric body at incidence [BTN-94-EIX94441386612] p 208 A95-67343
- Adaptive computations of flow around a delta wing with vortex breakdown [BTN-94-EIX94441386631] p 184 A95-68180
- Approximate method for calculating heating rates on three-dimensional vehicles [BTN-95-EIX95041503778] p 210 A95-69209
- State-space representation of aerodynamic characteristics of an aircraft at high angles of attack [BTN-95-EIX95062487536] p 187 A95-69244
- F/A-18 inlet calculations at 60-deg angle of attack and 10-deg sideslip [BTN-95-EIX95112524199] p 195 A95-69309
- Side forces at high angles of attack. Why, when, how? [BTN-95-EIX95112523809] p 194 A95-69324
- Aerodynamic characteristics of a canard-controlled missile at high angles of attack [BTN-95-EIX95152583257] p 267 A95-73558
- Improved version of the Naval Surface Warfare Center aeroprediction code (AP93) [BTN-95-EIX95152583260] p 267 A95-73561
- Transient structure of vortex breakdown on a delta wing [BTN-95-EIX95182619073] p 268 A95-75758
- Kinematics and aerodynamics of velocity-vector roll [BTN-95-EIX95182619126] p 291 A95-76603
- Review and development of base pressure and base heating correlations in supersonic flow [BTN-95-EIX95212645688] p 271 A95-76740
- Numerical investigation of supersonic flows around a spiked blunt body [BTN-95-EIX95212645690] p 271 A95-76742
- Calculation of wing-alone aerodynamics to high angles of attack [BTN-95-EIX95212645713] p 261 A95-76765
- Flow structure in the lee of an inclined 6:1 prolate spheroid [BTN-94-EIX95011441127] p 348 A95-81027
- Robust dynamic inversion for control of highly maneuverable aircraft [BTN-95-EIX95242670747] p 359 A95-81100
- Air data sensors for atmospheric reentry flight test of winged space vehicle p 413 A95-82412
- Hypersonic thermal protection with mass injection at angle of attack p 414 A95-82414
- Transition correlations in three-dimensional boundary layers [HTN-95-51648] p 432 A95-85030
- Reattachment studies of an oscillating airfoil dynamic stall flowfield [HTN-95-51660] p 432 A95-85042
- T-45A high angle attack testing [HTN-95-81499] p 386 A95-85213
- Predicting stall and post-stall behavior of airfoils at low mach numbers [BTN-95-EIX95262694297] p 365 A95-85468
- Wind-tunnel tests of an inclined cylinder having helical grooves [BTN-95-EIX95262694306] p 411 A95-85477
- High angle-of-attack airfoil performance improvement by internal acoustic excitation [HTN-95-42347] p 372 A95-86176
- Aerodynamic characteristics of truncated airfoils at high angle of attack [SAE PAPER 931227] p 460 A95-87365
- Aerodynamics of delta wings with application to high-alpha flight mechanics p 460 A95-87395
- Swirl control in an S-duct at high angle of attack [HTN-95-20846] p 545 A95-88107
- Trajectory optimization using parallel shooting method on parallel computer [BTN-95-EIX95282706670] p 564 A95-88175
- Vortex cutting by a blade, Part 2: Computations of vortex response [HTN-95-20937] p 464 A95-88976
- Compressible Navier-Stokes calculations of the flow over airfoil sections. Comparisons of 1st and 2nd order turbulence models [SAE PAPER 932510] p 546 A95-89183
- Reduced-order nonlinear analysis of aircraft dynamics [BTN-95-EIX95282706665] p 455 A95-89640
- Criteria for location of vortex breakdown over delta wings [HTN-95-01092] p 468 A95-90278
- Viscous contribution to the high Mach number damping in pitch of blunt slender cones at small angles of attack [HTN-95-01096] p 469 A95-90282
- A gust alleviation method by the response feedback p 506 A95-91493
- Low speed wind tunnel blockage corrections for airfoils at medium to large angles of attack p 474 A95-91557
- High angle of attack missile aerodynamics [CONGRESS PAPER C428-3-060] p 475 A95-91673
- Similarity solutions for hypersonic flow past slender bodies of revolution at small incidence [HTN-95-12195] p 475 A95-91895
- X-29 high AOA flight test results: An overview [SAE PAPER 931367] p 586 A95-93648
- Primary and secondary vortex structures over accelerated-decelerated airfoils at high angles of attack [SAE PAPER 931368] p 586 A95-93649
- Numerical investigation of high incidence flow over a double-delta wing [BTN-95-EIX0619952748160] p 588 A95-94454
- Quantifiable vortex features of F-106B aircraft at subsonic speeds [BTN-95-EIX0619952748161] p 588 A95-94455
- Aerodynamic applications of underexpanded hypersonic viscous jets [BTN-95-EIX0619952748162] p 589 A95-94456
- Computation of delta-wing roll maneuvers [BTN-95-EIX0619952748164] p 605 A95-94458
- Nonlinear aerodynamic analysis of grid fin configurations [BTN-95-EIX0619952748172] p 590 A95-94466
- Directional control at high angles of attack using blowing through a chined forebody [BTN-95-EIX0619952748179] p 619 A95-94472
- LDV measurements in separated flow on an elliptic wing mounted at an angle of attack on a wall [BTN-94-EIX94441380518] p 702 A95-96559
- Effect of leading- and trailing-edge flaps on clipped delta wings with and without wing camber at supersonic speeds [NASA-TM-4542] p 5 N95-10028
- Aeroelastic tailoring research [PB94-180031] p 6 N95-10135
- Navier-Stokes simulations of WECS airfoil flowfields [DE94-013341] p 7 N95-10226
- F-18 HARV presentation for industry [NASA-TM-104283] p 13 N95-10711
- Flow-visualization study of the X-29A aircraft at high angles of attack using a 1/48-scale model [NASA-TM-104268] p 8 N95-10858
- Numerical simulation of the flow about the F-18 HARV at high angle of attack [NASA-CR-196396] p 9 N95-10940
- Computational analysis of forebody tangential slot blowing on the high alpha research vehicle [NASA-CR-196750] p 10 N95-11367

High-angle-of-attack yawing moment asymmetry of the X-31 aircraft from flight test
 [NASA-CR-186030] p 13 N95-11410

Effects of vibration on inertial wind-tunnel model attitude measurement devices
 [NASA-TM-109083] p 21 N95-11466

Pressure measurements on an F/A-18 twin vertical tail in buffeting flow. Volume 3: Buffet power spectral densities
 [AD-A281444] p 36 N95-11829

Water tunnel flow visualization study of a 4.4 percent scale X-31 forebody
 [NASA-TM-104276] p 36 N95-11898

A simple analytical aerodynamic model of Langley Winged-Cone Aerospace Plane concept
 [NASA-CR-194987] p 54 N95-12175

Fourth High Alpha Conference, volume 1
 [NASA-CP-10143-VOL-1] p 67 N95-14229

High Alpha Technology Program (HATP) ground test to flight comparisons
 p 68 N95-14230

Flight and full-scale wind-tunnel comparison of pressure distributions from an F-18 aircraft at high angles of attack — Conducted in NASA Ames Research Center's 80 by 120 ft wind tunnel
 p 68 N95-14231

Numerical simulation of the flow about an F-18 aircraft in the high-alpha regime
 p 68 N95-14232

Hybrid structured/unstructured grid computations for the F/A-18 at high angle of attack
 p 68 N95-14233

Comparison of X-31 flight, wind-tunnel, and water-tunnel yawing moment asymmetries at high angles of attack
 p 68 N95-14234

Parameter identification for X-31A at high angles of attack
 p 69 N95-14235

Validation of the NASA Dryden X-31 simulation and evaluation of mechanization techniques
 p 69 N95-14236

Fourth High Alpha Conference, volume 2
 [NASA-CP-10143-VOL-2] p 69 N95-14239

F-18 high alpha research vehicle: Lessons learned
 p 69 N95-14240

X-31 high angle of attack control system performance
 p 70 N95-14244

Flight validation of ground-based assessment for control power requirements at high angles of attack
 p 70 N95-14246

High angle of attack flying qualities criteria for longitudinal rate command systems
 p 70 N95-14247

Vista/F-16 Multi-Axis Thrust Vectoring (MATV) control law design and evaluation
 p 71 N95-14248

Multi-application controls: Robust nonlinear multivariable aerospace controls applications
 p 71 N95-14249

Fourth High Alpha Conference, volume 3
 [NASA-CP-10143-VOL-3] p 71 N95-14251

Navy and the HARV: High angle of attack tactical utility issues
 p 71 N95-14252

F/A-18 and F-16 forebody vortex control, static and rotary-balance results
 p 72 N95-14254

Comparison of full-scale, small-scale, and CFD results for F/A-18 forebody slot blowing
 p 72 N95-14255

Low-energy pneumatic control of forebody vortices
 p 72 N95-14256

Preparations for flight research to evaluate actuated forebody strakes on the F-18 high-alpha research vehicle
 p 72 N95-14257

Integration of a mechanical forebody vortex control system into the F-15
 p 72 N95-14258

Engineering Codes for aeroprediction: State-of-the-art and new methods
 p 73 N95-14447

High angle of attack aerodynamics
 p 74 N95-14450

Numerical simulation of the flow about the F-18 HARV at high angle of attack
 [NASA-CR-197023] p 74 N95-14614

An approach to aerodynamic characteristics of low radar cross-section fuselages
 p 106 N95-16251

An improved method of airfoil design
 p 106 N95-16252

Residual-correction type and related computational methods for aerodynamic design. Part 2: Multi-point airfoil design
 p 128 N95-16567

Numerical simulation of transient vortex breakdown above a pitching delta wing
 [AD-A281075] p 107 N95-16808

DLR-F4 wing body configuration
 p 130 N95-17863

DLR-F5: Test wing for CFD and applied aerodynamics
 p 113 N95-17864

Low aspect ratio wing experiment
 p 113 N95-17865

Wind tunnel investigations of the appearance of shocks in the windward region of bodies with circular cross section at angle of attack
 p 113 N95-17866

Three-dimensional boundary layer and flow field data of an inclined prolate spheroid
 p 158 N95-17867

Force and pressure data of an ogive-nosed slender body at high angles of attack and different Reynolds numbers
 p 113 N95-17868

Ellipsoid-cylinder model p 158 N95-17869

Wind tunnel performance comparative test results of a circular cylinder and 50 percent ellipse tailboom for circulation control antitorque applications
 [AD-A283335] p 130 N95-18008

Interaction, bursting and control of vortices of a cropped double-delta wing at high angle of attack
 [AD-A283656] p 119 N95-18669

2-D and 3-D oscillating wing aerodynamics for a range of angles of attack including stall
 [NASA-TM-4632] p 120 N95-19119

Velocity measurements with hot-wires in a vortex-dominated flowfield
 p 121 N95-19261

Prediction of wind tunnel effects on the installed F/A-18A inlet flow field at high angles-of-attack
 [NASA-CR-195429] p 197 N95-19651

T-45A High Angle of Attack Testing: US Naval Test Pilot School 46th Annual Reunion and Symposium
 [AD-A284000] p 231 N95-20466

Pressure measurements on an F/A-18 twin vertical tail in buffeting flow. Volume 1: Wind tunnel test summary
 [AD-A279126] p 225 N95-21877

Effect of juncture fillets on double-delta wings undergoing sideslip at high angles of attack
 [AD-A286165] p 232 N95-22039

Wing pressure distributions from subsonic tests of a high-wing transport model — in the Langley 14- by 22-Foot Subsonic Wind Tunnel
 [NASA-TM-4583] p 272 N95-22802

Flight test of the X-29A at high angle of attack: Flight dynamics and controls
 [NASA-TP-3537] p 284 N95-22806

An assessment of viscous effects in computational simulation of benign and burst vortex flows on generic fighter wind-tunnel models using TEAM code
 [NASA-CR-4650] p 273 N95-23185

Aerodynamic surface distortion system for high angle of attack forebody vortex control
 [NASA-CASE-ARC-11979-1] p 286 N95-23390

Experimental study of the effects of Reynolds number on high angle of attack aerodynamic characteristics of forebodies during rotary motion
 [NASA-CR-195039] p 330 N95-24443

Numerical simulation of the flow about the F-18 HARV at high angle of attack
 [NASA-CR-197755] p 374 N95-26735

A nonintrusive method of quantifying flow visualization data in vortex flow fields
 [AD-A289802] p 552 N95-28948

A numerical method for modelling wings with sharp edges maneuvering at high angles of attack
 p 503 N95-29122

The 1995 version of the NSWC aeroprediction code. Part 1: Summary of new theoretical methodology
 [AD-A291518] p 481 N95-29853

Low-speed wind-tunnel investigation of the stability and control characteristics of a series of flying wings with sweep angles of 50 deg
 [NASA-TM-4640] p 505 N95-30226

Transonic aerodynamic characteristics of a proposed wing-body reusable launch vehicle concept
 [NASA-TM-108489] p 592 N95-30712

Multigrid convergence acceleration for the 2D Euler equations applied to high-lift systems
 [PB95-198081] p 593 N95-30814

Unsteady transonic wind tunnel test on a semispan straked delta wing, oscillating in pitch. Part 1: Description of the model, test setup, data acquisition, and data processing
 [AD-A293113] p 593 N95-30885

X-31: A program overview and flight test status
 p 609 N95-32013

Techniques for the determination of local dynamic pressure and angle of attack on a horizontal axial wind turbine
 [DE95-009204] p 707 N95-32685

A nonlinear vortex lattice method for unsteady flow with separated vortex
 [DLR-FB-94-32] p 704 N95-32787

ANGLES (GEOMETRY)

Numerical investigation of high incidence flow over a double-delta wing
 [BTN-95-EIX0619952748160] p 588 A95-94454

ANGULAR CORRELATION

Angular displacement measuring device
 [NASA-CASE-ARC-11937-1] p 362 N95-26015

ANGULAR VELOCITY

Hypersonic Gas-Surface Energy Accommodation Test Facility
 [DE94-014468] p 39 N95-12652

Effects of yaw and pitch motion on model attitude measurements
 [NASA-TM-4641] p 250 N95-22109

Electro-hydrostatic actuator controller design using quantitative feedback theory
 [AD-A289220] p 409 N95-26957

Preliminary analysis of dynamic stall effects on a 91-meter wind turbine rotor
 p 376 N95-27975

ANISOTROPY

Severe edge effects and simple complimentary interior solutions for thin-walled anisotropic and composite structures
 [AD-A290645] p 555 N95-29562

Airborne passive polarimetric measurements of sea surface anisotropy at 92 GHz
 [NASA-CR-197288] p 707 N95-32823

ANNEALING

Effect of annealing and desulfurization on oxide spallation of turbine airfoil material
 [BTN-95-EIX95282707024] p 528 A95-88264

ANNUAL VARIATIONS

Possible effects of CO2 increase on the high-speed civil transport impact on ozone
 [HTN-95-60779] p 317 A95-75976

Development of a climatological data base to help forecast cloud cover conditions for shuttle landings at the Kennedy Space Center
 p 670 A95-93529

A northern hemisphere clear air turbulence climatology
 p 674 A95-93547

ANNULAR FLOW

Design and operation of a supersonic annular flow facility
 [BTN-94-EIX94441386624] p 183 A95-68173

Near field of a coaxial jet with and without axial excitation
 [HTN-95-42332] p 372 A95-86161

Design and operation of a supersonic annular flow facility
 [HTN-95-20941] p 465 A95-88980

Characterization of annular two-phase gas-liquid flows in microgravity
 p 95 N95-14556

Measurement of gust response on a turbine cascade
 [NASA-TM-106776] p 117 N95-18457

ANODIZING

Aircraft corrosion study
 [AD-A279527] p 241 N95-21687

ANOMALIES

Geophex airborne unmanned survey system
 [DE95-007566] p 392 N95-27440

ANTARCTIC REGIONS

Antarctic snow record of southern hemisphere lead pollution
 [HTN-95-40359] p 212 A95-66869

Momentum and scalar transfer coefficients over aerodynamically smooth Antarctic surfaces
 [HTN-95-92932] p 562 A95-91870

ANTENNA ARRAYS

Joint stars phased array radar antenna
 [BTN-95-EIX95042474626] p 209 A95-68280

Scattering and radiation from cylindrically conformal antennas
 p 645 N95-30669

ANTENNA DESIGN

Joint stars phased array radar antenna
 [BTN-95-EIX95042474626] p 209 A95-68280

A VHF/UHF antenna for the Precision Antenna Measurement System (PAMS)
 [AD-A285673] p 156 N95-16621

Field verification of the wind tunnel coefficients
 p 109 N95-17291

Design considerations for an archimedean slot spiral antenna
 p 211 N95-19798

ANTENNA FEEDS

Inband radar cross section of phased arrays with parallel feeds
 [AD-A284249] p 210 N95-19730

Design considerations for an archimedean slot spiral antenna
 p 211 N95-19798

Simulation of patch and slot antennas using FEM with prismatic elements and investigations of artificial absorber mesh termination schemes
 [NASA-CR-198974] p 704 N95-32822

ANTENNA RADIATION PATTERNS

Comments on effect of wet snow on the null-reference ILS system
 [BTN-95-EIX95142555488] p 227 A95-72885

Geodesic constant method: A novel approach to analytical surface-ray tracing on convex conducting bodies
 [BTN-95-EIX95302731054] p 637 A95-94205

Airborne imaging radiometer scan simulation
 [BTN-95-EIX95332753018] p 638 A95-94793

A users manual for the method of moments Aircraft Modeling Code (AMC), version 2
 [NASA-CR-196445] p 24 N95-11252

Electromagnetic on-aircraft antenna radiation in the presence of composite plates
 [NASA-CR-196126] p 58 N95-12856

A VHF/UHF antenna for the Precision Antenna Measurement System (PAMS)
 [AD-A285673] p 156 N95-16621

Scattering and radiation from cylindrically conformal antennas
 p 645 N95-30669

- Simulation of patch and slot antennas using FEM with prismatic elements and investigations of artificial absorber mesh termination schemes
[NASA-CR-198974] p 704 N95-32822
- Anechoic chamber upgrade
[AD-A294375] p 700 N95-34342
- ANTENNAS**
- Attitude determination using dedicated and nondedicated multi-antenna GPS sensors
[BTN-95-EIX95142555482] p 228 A95-72891
- Impulse radiating antennas p 548 A95-90920
- Polarization diverse ultra-wideband antenna technology p 548 A95-90924
- Airborne imaging radiometer scan simulation
[BTN-95-EIX95332753018] p 638 A95-94793
- ANTI-AIRCRAFT MISSILES**
- Switched bias proportional navigation for homing guidance against highly maneuvering targets
[BTN-95-EIX95182619145] p 279 A95-76622
- ANTICLING ADDITIVES**
- NASA evaluation of Type 2 chemical depositions — effects of deicer deposition on aircraft tire friction performance
[SAE PAPER 932582] p 495 A95-90086
- ASRS problems involving air carrier ground deicing/anti-icing p 611 A95-95194
- ANTIMISSILE DEFENSE**
- SR-71 may launch targets for missile defense tests
[HTN-95-91872] p 335 A95-81974
- ANTISHIP MISSILES**
- Results from tests of the Kearfott T16-B Inertial Measurement Unit
[PB95-212031] p 644 N95-30502
- Results from tests of the Honeywell integrated flight management unit
[PB95-211355] p 601 N95-30597
- APPLICATIONS OF MATHEMATICS**
- Computing methods for the approximate solution of time dependent problems
[AD-A286007] p 256 N95-20719
- Preparation of course materials: Elementary mathematics of powered flight p 324 N95-23320
- Cumulative reports and publications through December 31, 1994
[NASA-CR-195043] p 361 N95-26085
- APPLICATIONS PROGRAMS (COMPUTERS)**
- Dryden lectureship in research, a perspective on CFD validation
[AIAA PAPER 93-0002] p 3 A95-60180
- Putting the ACSYNT on aircraft design
[BTN-95-EIX95072419881] p 180 A95-68398
- Two-variable method for blockage wall interference in a circular tunnel
[BTN-95-EIX95062487540] p 187 A95-69248
- GETRAN: A generic, modularly structured computer code for simulation of dynamic behavior of aero- and power generation gas turbine engines
[BTN-94-EIX95011441241] p 431 A95-84198
- A tool for airframe shaping - idea and application
[SAE PAPER 931224] p 491 A95-87568
- Fatigue life estimation program for Part 23 airplanes, 'AFS, FOR'
[SAE PAPER 931249] p 565 A95-89221
- AlAA Computing in Aerospace 10, San Antonio, TX, March 28-30, 1995
[ISBN 1-56347-119-1] p 565 A95-90629
- Accelerated application development for flight software
[AIAA PAPER 95-1031] p 566 A95-90703
- 3-D Navier-Stokes analysis of crossing glancing shocks/turbulent boundary layer interactions
[BTN-95-EIX95302729768] p 636 A95-94130
- Advanced composites structural concepts and materials technologies for primary aircraft structures. Structural response and failure analysis: ISPAN modules users manual
[NASA-CR-4449] p 12 N95-10242
- Modeling improvements and users manual for axial-flow turbine off-design computer code AXOD
[NASA-CR-195370] p 8 N95-10853
- ACSYNT inner loop flight control design study
[NASA-CR-196316] p 17 N95-11223
- A users manual for the method of moments Aircraft Modeling Code (AMC), version 2
[NASA-CR-196445] p 24 N95-11252
- Application of multivariate optimization techniques to determination of optimum flight path trajectories
[ESDU-94012] p 44 N95-11793
- Efficient and effective handling of cycle slips in global positioning system data p 43 N95-12230
- HLLV avionics requirements study and electronic filing system database development
[NASA-CR-193993] p 49 N95-13027
- Role of wind tunnels and computer codes in the certification and qualification of rotorcraft for flight in forecast icing
[NASA-TM-106747] p 39 N95-13197
- Methodology for sensitivity analysis, approximate analysis, and design optimization in CFD for multidisciplinary applications
[NASA-CR-196981] p 58 N95-13201
- Earth Observing System (EOS)/Advanced Microwave Sounding Unit-A (AMSU-A) software assurance plan
[NASA-CR-196059] p 98 N95-13885
- Evolutionary Telemetry and Command Processor (TCP) architecture p 86 N95-14162
- Development of the NASA/FLAGRO computer program for analysis of airframe structures p 94 N95-14473
- A SIMULINK environment for flight dynamics and control analysis: Application to the DHC-2 Beaver. Part 1: Implementation of a model library in SIMULINK. Part 2: Nonlinear analysis of the Beaver autopilot
[NONP-NASA-SUPPL-DK-94-2802] p 84 N95-14815
- Assessment of CTAS ETA prediction capabilities
[NASA-CR-197224] p 97 N95-15728
- Enhanced capabilities and updated users manual for axial-flow turbine preliminary sizing code TURBAN
[NASA-CR-195405] p 76 N95-15912
- Applications of automatic differentiation in computational fluid dynamics p 156 N95-16461
- Matlab as a robust control design tool p 169 N95-16474
- Tools for applied engineering optimization p 128 N95-16570
- An analysis code for the Rapid Engineering Estimation of Momentum and Energy Losses (REMEL)
[NASA-CR-191178] p 108 N95-16887
- Interactive computer graphics applications for compressible aerodynamics
[NASA-TM-106802] p 170 N95-17264
- A platform independent application of Lux illumination prediction algorithms
[AD-A283669] p 170 N95-18018
- Universal wind tunnel data acquisition and reduction software
[AD-A283897] p 171 N95-18365
- The generic simulation executive at Manned Flight Simulator
[AD-A283997] p 146 N95-18724
- Enhanced capabilities and modified users manual for axial-flow compressor conceptual design code CSPAN
[NASA-TM-106833] p 119 N95-18933
- Aircraft stress sequence development: A complex engineering process made simple p 136 N95-19480
- Statistical analysis of Turbine Engine Diagnostic (TED) field test data
[AD-A283032] p 248 N95-20998
- A computer code (SKINTEMP) for predicting transient missile and aircraft heat transfer characteristics
[AD-A286044] p 248 N95-21001
- Investigation of shear layer transition using various turbulence models p 248 N95-21096
- A user's guide to LUGSAN 1.1: A computer program to calculate and archive lug and sway brace loads for aircraft-carried stores
[DE95-001919] p 232 N95-21730
- The navigation toolkit
[NASA-CR-197290] p 229 N95-22161
- Thermohydrodynamic analysis of cryogenic liquid turbulent fluid film bearings, phase 2
[NASA-CR-197412] p 349 N95-24461
- An evaluation of the Software Through Pictures/T Tool (STP/T) for the Software Support Activity (SSA)
[AD-A288822] p 447 N95-26348
- WINCLR: A computer code for heat transfer and clearance calculation in a compressor
[NASA-CR-195436] p 366 N95-26363
- User documentation of the CTA program
[AD-A289508] p 375 N95-26854
- EASY-SIM: A visual simulation system software architecture with an Ada 9X application framework
[AD-A289325] p 448 N95-26895
- An exploratory application of neural networks for airfoil design p 448 N95-26943
- Determining GPS average performance metrics p 383 N95-27791
- Development of a TECS control-law for the lateral directional axis of the McDonnell Douglas F-15 Eagle
[AD-A289771] p 410 N95-28598
- Ejectors and jet pumps: Computer program for design and performance for steam/gas flow
[ESDU-94046] p 500 N95-28704
- Computer program for estimation of leading-edge suction distribution for plane thin wings at subsonic speeds
[ESDU-94038] p 476 N95-28708
- A procedure for automating CFD simulations of an inlet-bleed problem p 552 N95-28768
- Impact of Ada and object-oriented design in the flight dynamics division at Goddard Space Flight Center
[NASA-CR-189412] p 567 N95-28807
- ISPAN (Interactive Stiffened Panel Analysis): A tool for quick concept evaluation and design trade studies p 533 N95-28846
- MATSurv multisensor air traffic surveillance
[AD-A292253] p 489 N95-28887
- Application of parallel processing technology in complex helicopter analysis. Phase 1
[NASA-CR-197850] p 502 N95-28928
- Development of a rotary wing Navier-Stokes CFD code based on TLNS3D code p 554 N95-29387
- Design and evaluation of a LQR controller for the bluebird unmanned air vehicle
[AD-A289769] p 504 N95-29457
- Linear matrix inequalities for the problem of absolute stability of control systems p 518 N95-29680
- The 1995 version of the NSWC aeroprediction code. Part 1: Summary of new theoretical methodology
[AD-A291518] p 481 N95-29853
- A PC program for estimating measurement uncertainty for aeronautics test instrumentation
[NASA-CR-198361] p 523 N95-30067
- Object-oriented approach for gas turbine engine simulation
[NASA-TM-106970] p 615 N95-30594
- Validation of the NPARC code for nozzle afterbody flows at transonic speeds
[NASA-TM-106971] p 592 N95-30704
- Acceleration potential models
PREDICAT/PREDICDYN applied for calculation of axisymmetric dynamic inflow cases
[PB95-207015] p 647 N95-30957
- Experimental and computational investigation of the tip clearance flow in a transonic axial compressor rotor
[NASA-TM-106711] p 649 N95-31738
- Geometric modeling for computer aided design
[NASA-CR-198828] p 679 N95-31982
- Practical experiences in control systems design using the NCR Bell 205 Airborne Simulator p 624 N95-32015
- FPCAS3D User's guide: A three dimensional full potential aeroelastic program, version 1
[NASA-CR-198367] p 651 N95-32205
- Advanced data visualization and sensor fusion: Conversion of techniques from medical imaging to Earth science p 711 N95-34236
- APPROACH**
- Simulation and flight test evaluation of head-up-display guidance for harrier approach transitions
[BTN-95-EIX95062487533] p 194 A95-69241
- Optimal lateral-escape maneuvers for microburst encounters during final approach
[BTN-95-EIX95182619127] p 276 A95-76604
- Analysis of approach paths of two aircraft p 487 A95-91494
- Arrival traffic handling for a parallel runway airport p 487 A95-91537
- Heliport/vertiport MLS precision approaches
[AD-A283505] p 126 N95-18059
- A real-time algorithm for integrating differential satellite and inertial navigation information during helicopter approach
[NASA-CR-197409] p 229 N95-21891
- APPROACH CONTROL**
- Analysis of approach paths of two aircraft p 487 A95-91494
- CCLA operation on MLS p 487 A95-91540
- Analysis of an MLS automatic landing control law for the NAL experimental research aircraft D0-228. 2: Curved approach and landing p 508 A95-91588
- Developments in airfield lighting
[CONGRESS PAPER C428-7-147] p 488 A95-91688
- Assessment of CTAS ETA prediction capabilities
[NASA-CR-197224] p 97 N95-15728
- Modeling of Instrument Landing System (ILS) localizer signal on runway 25L at Los Angeles International Airport
[NASA-TM-4588] p 125 N95-17384
- Crew aiding and automation: A system concept for terminal area operations, and guidelines for automation design
[NASA-CR-4631] p 228 N95-19950
- Development of a coding form for approach control/pilot voice communications
[DOT/FAA/AM-95/15] p 384 N95-28540
- APPROACH INDICATORS**
- Spatial awareness comparisons between large-screen, integrated pictorial displays and conventional EFIS displays during simulated landing approaches
[NASA-TP-3467] p 80 N95-14852
- Minima reduction simulation test results
[AD-A285626] p 228 N95-21148

- Flight reference display for powered-lift STOL aircraft [NAL-TR-1251] p 337 N95-25005
- Flight test evaluation of the Stanford University/United Airlines differential GPS Category 3 automatic landing system [NASA-TM-110354] p 593 N95-30788
- APPROXIMATION**
- Novel similarity solutions of the sonic small-disturbance equation with applications to airfoil transonic aerodynamics [BTN-94-EIX94341340316] p 35 A95-60852
- Approximate method for calculating heating rates on three-dimensional vehicles [BTN-95-EIX95041503778] p 210 A95-69209
- Adaptive finite element method for turbulent flow near a propeller [BTN-95-EIX95142553038] p 305 A95-73460
- Application of the multigrad solution technique to hypersonic entry vehicles [BTN-95-EIX95152583254] p 306 A95-73555
- Multiple site fatigue damage in fuselage skin splices: Experimental simulation and theoretical prediction [BTN-95-EIX95152584676] p 276 A95-73588
- Application of a control-volume-based finite-element formulation to the shock tube problem [BTN-95-EIX95182619093] p 295 A95-76584
- Contribution of thermal radiation to the temperature profile of ceramic composite materials [BTN-94-EIX95011441252] p 417 A95-84209
- Analysis of low Reynolds number airfoil flows [BTN-95-EIX0619952748183] p 590 A95-94476
- Computing methods for the approximate solution of time dependent problems [AD-A286007] p 256 N95-20719
- PREDICAT: First order performance calculations of windturbine rotors using the method of the acceleration potential [PB95-206454] p 564 N95-30200**
- ARAMID FIBER COMPOSITES**
- MIL-HDBK-5 design allowables for fibre/metal laminates: ARALL 2 and ARALL 3 [BTN-94-EIX94371346933] p 300 A95-73345
- Proof test methodology for composites p 424 N95-28445
- ARC JET ENGINES**
- Life evaluation of a low power arcjet thruster p 403 A95-82337
- AFOSR Contractors Meeting in Propulsion [AD-A282729] p 54 N95-12507
- Arcjet thruster research and technology, phase 2 [NASA-CR-182276] p 105 N95-18044
- ARCHAEOLOGY**
- The effects of aircraft (B-52) overflights on ancient structures [BTN-94-EIX94341340070] p 171 A95-63522
- ARCHITECTURE (COMPUTERS)**
- New commercial off-the-shelf testers are automatic and intelligent [BTN-95-EIX95172595292] p 287 A95-75720
- A new guidance and flight control system for the DELTA 2 launch vehicle — Abstract only p 342 A95-80427
- Determination of flight simulator time delay p 522 A95-91553
- The impact of new technology on reliability of avionic equipment [CONGRESS PAPER C428-6-114] p 549 A95-91683
- Advanced distributed simulation technology advanced rotary wing aircraft. Software reusability report [AD-A280434] p 20 N95-10354
- Formal design and verification of a reliable computing platform for real-time control (phase 3 results) [NASA-TM-109140] p 33 N95-10873
- Parallel methods for the flight simulation model [DE94-013330] p 52 N95-11752
- An avionics scenario and command model description for Space Generic Open Avionics Architecture (SGOAA) [NASA-CR-188330] p 49 N95-11913
- Overview of NASREM: The NASA/NBS standard reference model for teleoperator control system architecture [PB94-194560] p 58 N95-12854
- Methodology for sensitivity analysis, approximate analysis, and design optimization in CFD for multidisciplinary applications [NASA-CR-196981] p 58 N95-13201
- Elements of a modern turbomachinery design system p 90 N95-14129
- Generic architectures for future flight systems p 99 N95-14159
- Space Generic Open Avionics Architecture (SGOAA): Overview p 99 N95-14161
- Evolutionary Telemetry and Command Processor (TCP) architecture p 86 N95-14162
- Automated test environment for a real-time control system [TABES PAPER 94-631] p 99 N95-14652
- Portable parallel stochastic optimization for the design of aeropropulsion components [NASA-CR-195312] p 154 N95-16072
- NASA High Performance Computing and Communications program [NASA-TM-4653] p 176 N95-18573
- The impact of advanced packaging technology on modular avionics architectures p 233 N95-20632
- Standard Hardware Acquisition and Reliability Program (SHARP) advanced SEM-E packaging p 233 N95-20633
- The IEEE scalable coherent interface: An approach for a unified avionics network p 234 N95-20650
- Optical backplane for modular avionics p 257 N95-20652
- High performance backplane components for modular avionics p 247 N95-20653
- The opportunities for and challenges of common integrated electronics [AD-A279991] p 248 N95-20966
- EASY-SIM: A visual simulation system software architecture with an Ada 9X application framework [AD-A289325] p 448 N95-26895
- An exploratory application of neural networks for airfoil design p 448 N95-26943
- Advanced flight computer. Special study [NASA-CR-198165] p 449 N95-27246
- Design of a real-time wind turbine simulator using a custom parallel architecture p 449 N95-27979
- Foundations of technology for constructing highly reliable distributed realtime systems [AD-A293254] p 678 N95-30892
- A highly reliable, high performance open avionics architecture for real time Nap-of-the-Earth operations p 693 N95-32497
- Development and flight testing of an Obstacle Avoidance System for US Army helicopters p 687 N95-32500
- High order accuracy computational methods in aerodynamics using parallel architectures [AD-A294167] p 686 N95-34763
- ARCTIC REGIONS**
- Research aircraft observations of a polar low at the east Greenland ice edge [HTN-95-A0175] p 215 A95-69766
- An algorithm for forecasting mountain wave-related turbulence in the stratosphere [HTN-95-80656] p 254 A95-72500
- Analysis of the physical state of one Arctic polar stratospheric cloud based on observations [HTN-95-70917] p 351 A95-77982
- Comparison of column abundances from three infrared spectrometers during AASE 2 [HTN-95-70946] p 352 A95-78011
- Chemical change in the arctic vortex during AASE 2 [HTN-95-70947] p 352 A95-78012
- An overview of the EASOE campaign [HTN-95-00702] p 443 A95-86272
- Aircraft measurements of CLO and HCL during EASOE 1991/92 [HTN-95-00721] p 444 A95-86291
- An overview of millimeter-wave spectroscopic measurements of chlorine monoxide at Thule, Greenland, February-March, 1992: Vertical profiles, diurnal variation, and longer-term trends [HTN-95-00722] p 444 A95-86292
- Two dimensional stratospheric aerosol distributions during EASOE [HTN-95-00726] p 444 A95-86296
- Airborne measurements during the European Arctic Stratospheric Ozone Experiment column amounts of HNO3 and O3 derived from FTIR emission sounding [HTN-95-00742] p 445 A95-86312
- Airborne measurements during the European Arctic Stratospheric Ozone Experiment: Observation of OCIO [HTN-95-00745] p 445 A95-86315
- Airborne measurements during the Arctic stratospheric experiment: Observation of O3 and NO2 [HTN-95-00748] p 445 A95-86318
- AREA NAVIGATION**
- Crew aiding and automation: A system concept for terminal area operations, and guidelines for automation design [NASA-CR-4631] p 228 N95-19950
- ARGON**
- Hypersonic convective heat transfer over 140-deg blunt cones in different gases [BTN-95-EIX95152583253] p 306 A95-73554
- ARMED FORCES (UNITED STATES)**
- The simulator training research advance testbed for aviation (STRATA): A simulation research facility for army aviation p 626 A95-95161
- Bomber force 2000: Operational concepts for long-range combat aircraft [AD-A279378] p 230 N95-20181
- Utilization of composite materials by the US Army: A look ahead p 421 N95-28421
- Army aviation: Modernization strategy needs to be reassessed. Report to Congressional requestors [GAO/NSIAD-95-9] p 683 N95-32783
- ARTIFICIAL GRAVITY**
- Study on a scheme for the prolongation of microgravity time of balloon-borne drop capsule p 414 A95-82515
- ARTIFICIAL INTELLIGENCE**
- On introduction of artificial intelligence elements to heat power engineering [BTN-94-EIX94461407961] p 100 A95-62635
- Engine life measurement and diagnostics [BTN-95-EIX95041505024] p 235 A95-70133
- New commercial off-the-shelf testers are automatic and intelligent [BTN-95-EIX95172595292] p 287 A95-75720
- Artificial intelligence for turboprop engine maintenance [BTN-95-EIX95182617812] p 288 A95-75757
- Real-time decision aiding: Aircraft guidance for wind shear avoidance [BTN-95-EIX95202637575] p 332 A95-78583
- Intelligent flight trainer for initial rotary wing training [SAE PAPER 932536] p 386 A95-84558
- Artificial intelligence for turboprop engine maintenance [HTN-95-92313] p 404 A95-85357
- AIAA Computing in Aerospace 10, San Antonio, TX, March 28-30, 1995 [ISBN 1-56347-119-1] p 565 A95-90629
- Intelligent tutoring system: F-16 flight simulation p 521 A95-90649
- An intelligent tutoring system for civil aviation flight training p 521 A95-91535
- The 4-D approach to visual control of autonomous systems [AIAA PAPER 94-1243-CP] p 27 N95-11513
- Thunderstorm hypothesis reasoner [AD-A282664] p 60 N95-12805
- Knowledge-based processing for aircraft flight control [NASA-CR-194976] p 99 N95-13727
- Artificial intelligence with applications for aircraft [DOT/FAA/CT-94/41] p 99 N95-13895
- Artificial neural network modeling of damaged aircraft [AD-A283227] p 80 N95-14849
- Workshop on Formal Models for Intelligent Control [AD-A281399] p 169 N95-16864
- Identification of Artificial Intelligence (AI) applications for maintenance, monitoring, and control of airway facilities [AD-A28479] p 125 N95-17373
- The use of genetic algorithms for flight test and evaluation of artificial intelligence and complex software systems [AD-A284824] p 217 N95-19688
- Collected papers of the Soar/IFOR project, Spring 1994 [AD-A280063] p 238 N95-20624
- Design and synthesis of a real-time controller for an unmanned air vehicle [AD-A289134] p 408 N95-26555
- Digital systems validation. Chapter 20 Artificial Intelligence with applications for aircraft. Handbook, volume 2 [AD-A288492] p 448 N95-26638
- Operator modeling in commercial aviation: Cognitive models, intelligent displays, and pilot's assistants [NASA-CR-198609] p 401 N95-28203
- Artificial intelligence techniques for flight test planning, phase 1 [AD-A293962] p 608 N95-31525
- Expert systems and artificial intelligence applications in engineering design and inspection p 710 N95-33008
- ARTIFICIAL SATELLITES**
- Calculation of satellite drag coefficients [AD-A285118] p 300 N95-23781
- Thermal design of returnable satellites [AD-A294113] p 701 N95-34500
- ASCENT**
- Variational principles for ascent shapes of large scientific balloons [BTN-95-EIX95262694320] p 387 A95-85491
- Matlab as a robust control design tool p 169 N95-16474
- ASCENT PROPULSION SYSTEMS**
- Fourth-generation Mars vehicle concepts [BTN-95-EIX95152583267] p 298 A95-73568
- ASCENT TRAJECTORIES**
- Dynamical instability of the aerogravity assist maneuver [BTN-95-EIX95152583282] p 298 A95-73583
- Optimal separation and ascent of lifting upper stages p 525 A95-87396
- Effects of small changes on rate of climb [ESDU-94039] p 501 N95-28707
- ASHES**
- Volcanic ash forecast transport and dispersion (VAFTAD) model [HTN-95-80702] p 254 A95-72546

Role of the aviation weather system in providing a real-time ATC volcanic ash advisory system p 663 A95-93494

Alaska's volcanic ash warning system p 663 A95-93495

ASIA

Jet stream winds: Comparisons of operational analyses with independent aircraft data at multiple longitudes p 665 A95-93506

Asian Aeronautics: Technology acquisition drives industry development. Report to Congressional requesters [GAO/NSIAD-94-140] p 367 N95-26817

ASPECT RATIO

Calculation of wing-alone aerodynamics to high angles of attack [BTN-95-EIX95212645713] p 261 A95-76765

Experimental investigation of the flow around a circular cylinder. Influence of aspect ratio [BTN-94-EIX95011441120] p 347 A95-80044

Note on prediction of aerodynamic lift/drag ratio of WIG (Wing-In-Ground) at cruise [BTN-95-EIX95282705925] p 467 A95-89665

Aerodynamic interference for supersonic low-aspect-ratio missiles [BTN-95-EIX95302694469] p 588 A95-94065

Measurements of the flow over a low aspect-ratio wing in the Mach number range 0.6 to 0.87 for the purpose of validation of computational methods. Part 1: Wing design, model construction, surface flow. Part 2: Mean flow in the boundary layer and wake, 4 test cases p 112 N95-17860

Low-speed wind-tunnel investigation of the stability and control characteristics of a series of flying wings with sweep angles of 50 deg [NASA-TM-4640] p 505 N95-30226

ASPHALT

Additives in bituminous materials and fuel-resistant sealers [DOT/FAA/CT-94/78] p 55 N95-12131

Marginal aggregates in flexible pavements: Background survey and experimental plan [DOT/FAA/CT-94/58] p 53 N95-12216

ASSEMBLING

Advancements in automatic fastening technology [BTN-94-EIX94461290277] p 65 A95-61734

ASSESSMENTS

Possible guidelines for helicopter noise assessment [HTN-95-92535] p 558 A95-67355

Maintenance-free lead acid battery for inertial navigation systems aircraft [BTN-95-EIX95292721316] p 633 A95-92511

The F-16 multinational staged improvement program: A case study of risk assessment and risk management [AD-A281706] p 81 N95-15451

ASSIMILATION

Assimilation of altimeter data in a quasi-geostrophic model of the Gulf Stream system: A dynamical perspective [NASA-CR-196313] p 320 N95-23766

ASTRONAUTICS

NASA video catalog [NASA-SP-7109(01)] p 363 N95-24238

Aeronautical engineering: A continuing bibliography with indexes (supplement 318) [NASA-SP-7037(318)] p 367 N95-27543

ASTRONOMICAL COORDINATES

A platform independent application of Lux illumination prediction algorithms [AD-A283669] p 170 N95-18018

ASTRONOMY

NASA video catalog [NASA-SP-7109(01)] p 363 N95-24238

ASTROPHYSICS

Airborne geophysics and precise positioning: Scientific issues and future directions [LC-94-68678] p 446 N95-27156

ASYMMETRY

Elliptic tip effects on the vortex wake of an axisymmetric body at incidence [BTN-94-EIX94441386612] p 208 A95-67343

Suppression of vortex asymmetry and side force on a circular cone [BTN-95-EIX95042474413] p 209 A95-68287

High-angle-of-attack yawing moment asymmetry of the X-31 aircraft from flight test [NASA-CR-186030] p 13 N95-11410

Water tunnel flow visualization study of a 4.4 percent scale X-31 forebody [NASA-TM-104276] p 36 N95-11898

Low-energy pneumatic control of forebody vortices p 72 N95-14256

Compression strength of composite primary structural components [NASA-CR-197554] p 160 N95-18388

Large-eddy simulation of flow through a plane, asymmetric diffuser p 250 N95-22449

ASYMPTOTIC METHODS

Nonlinear asymptotic theory of hypersonic flow past a circular cone [HTN-95-92599] p 461 A95-87415

Severe edge effects and simple complementary interior solutions for thin-walled anisotropic and composite structures [AD-A290645] p 555 N95-29562

ASYMPTOTIC SERIES

Studies on high pressure and unsteady flame phenomena [AD-A284126] p 152 N95-18410

PREDICAT: First order performance calculations of windturbine rotors using the method of the acceleration potential [PB95-206454] p 564 N95-30200

ATLANTIC OCEAN

Aircraft icing measurements in East Coast winter storms [HTN-95-60505] p 214 A95-68756

Mesoscale structure of precipitation bands in a North Atlantic winter storm [HTN-95-40659] p 215 A95-69803

North Atlantic air traffic within the lower stratosphere: Cruising times and corresponding emissions [HTN-95-91841] p 354 A95-80829

Fractal properties of whitecaps [HTN-95-92121] p 443 A95-83827

A study of the savings in time and fuel to aviation through the use of upper-air wind forecasts p 672 A95-93538

Airplane icing research at the Boeing Company: Participation in the second Canadian Atlantic Storms Program p 674 A95-93544

Oceanic operations: An authoritative guide to oceanic operations [FAA-AFS-550] p 277 N95-24065

ATMOSPHERIC BOUNDARY LAYER

Comparison of wind profiler and aircraft wind measurements at Chebogue Point, Nova Scotia [HTN-95-41833] p 353 A95-80559

ATMOSPHERIC CHEMISTRY

Three-dimensional model interpretation of NO(x) measurements from the lower stratosphere [HTN-95-90534] p 213 A95-67806

Possible effects of CO₂ increase on the high-speed civil transport impact on ozone p 317 A95-75976

The distribution of hydrogen, nitrogen, and chlorine radicals in the lower stratosphere: Implications for changes in O₃ due to emission of NO(y) from supersonic aircraft [HTN-95-70935] p 351 A95-78000

Vertical transport rates in the stratosphere in 1993 from observations of CO₂, N₂O, and CH₄ [HTN-95-70941] p 351 A95-78006

Meridional distributions of NO(x), NO(y), and other species in the lower stratosphere and upper troposphere during AASE 2 [HTN-95-70944] p 352 A95-78009

Comparison of column abundances from three infrared spectrometers during AASE 2 [HTN-95-70946] p 352 A95-78011

Chemical change in the arctic vortex during AASE 2 [HTN-95-70947] p 352 A95-78012

Latitude variations of stratospheric trace gases [HTN-95-70948] p 352 A95-78013

Fine-scale, poleward transport of tropical air during AASE 2 [HTN-95-70949] p 352 A95-78014

High-speed civil transport impact: Role of sulfate, nitric acid trihydrate, and ice aerosols studied with a two-dimensional model including aerosol physics [HTN-95-91843] p 354 A95-80831

An overview of the EASOE campaign [HTN-95-00702] p 443 A95-86272

Aircraft measurements of ClO and HCL during EASOE 1991/92 [HTN-95-00721] p 444 A95-86291

Airborne measurements during the European Arctic Stratospheric Ozone Experiment column amounts of HNO₃ and O₃ derived from FTIR emission sounding [HTN-95-00742] p 445 A95-86312

Airborne measurements during the European Arctic Stratospheric Ozone Experiment: Observation of ClO [HTN-95-00745] p 445 A95-86315

Environmental aspects of Orbital transport p 559 A95-87377

Three dimensional model calculations of the global dispersion of high speed aircraft exhaust and implications for stratospheric ozone loss p 26 N95-10657

Development of techniques for the in situ observation of OH and HO₂ for studies of the impact of high-altitude supersonic aircraft on the stratosphere [NASA-CR-196759] p 61 N95-12832

An Echelle Grating Spectrometer (EGS) for mid-IR remote chemical detection [DE94-019310] p 249 N95-21478

Compendium of NASA data base for the Global Tropospheric Experiment's Pacific Exploratory Mission West-A (PEM West-A) [NASA-TM-109177] p 320 N95-23009

In situ measurements of ClO and implications for the chemistry of inorganic chlorine in the lower stratosphere p 563 N95-29830

ATMOSPHERIC CIRCULATION

Three-dimensional model interpretation of NO(x) measurements from the lower stratosphere [HTN-95-90534] p 213 A95-67806

Potential applications of the SSM/I cloud liquid water parameter to the estimation of marine aircraft icing [HTN-95-80651] p 254 A95-72495

Volcanic ash forecast transport and dispersion (VAFTAD) model [HTN-95-80702] p 254 A95-72546

Meridional distributions of NO(x), NO(y), and other species in the lower stratosphere and upper troposphere during AASE 2 [HTN-95-70944] p 352 A95-78009

Chemical change in the arctic vortex during AASE 2 [HTN-95-70947] p 352 A95-78012

Fine-scale, poleward transport of tropical air during AASE 2 [HTN-95-70949] p 352 A95-78014

Tracer transport for realistic aircraft emission scenarios calculated using a three-dimensional model [HTN-95-41799] p 353 A95-80525

Two dimensional stratospheric aerosol distributions during EASOE [HTN-95-00726] p 444 A95-86296

Atmospheric and wind modeling for ATC [NASA-CR-196786] p 98 N95-13725

ATMOSPHERIC COMPOSITION

Antarctic snow record of southern hemisphere lead pollution [HTN-95-40359] p 212 A95-66689

Three-dimensional model interpretation of NO(x) measurements from the lower stratosphere [HTN-95-90534] p 213 A95-67806

Subsidence of aircraft engine exhaust in the stratosphere: Implications for calculated ozone depletions [PAPER-93GL03426] p 251 A95-70297

Aircraft-borne, laser-induced fluorescence instrument for the in situ detection of hydroxyl and hydroperoxy radicals [BTN-95-EIX95072499029] p 253 A95-71908

Possible effects of CO₂ increase on the high-speed civil transport impact on ozone [HTN-95-60779] p 317 A95-75976

Effects on stratospheric ozone from high-speed civil transport: Sensitivity to stratospheric aerosol loading [HTN-95-91842] p 354 A95-80830

An intercomparison of aircraft instrumentation for tropospheric measurements of sulfur dioxide [HTN-95-91855] p 354 A95-80843

An intercomparison of aircraft instrumentation for tropospheric measurements of carbonyl sulfide, hydrogen sulfide, and carbon disulfide [HTN-95-91856] p 355 A95-80844

An intercomparison of instrumentation for tropospheric measurements of dimethyl sulfide: Aircraft results for concentrations at the parts-per-trillion level [HTN-95-91857] p 355 A95-80845

Three dimensional model calculations of the global dispersion of high speed aircraft exhaust and implications for stratospheric ozone loss p 26 N95-10657

Compendium of NASA data base for the Global Tropospheric Experiment's Pacific Exploratory Mission West-A (PEM West-A) [NASA-TM-109177] p 320 N95-23009

Preliminary analysis of University of North Dakota aircraft data from the FIRE Cirrus IFO-2 [NASA-CR-198038] p 357 N95-24219

In situ measurements of ClO and implications for the chemistry of inorganic chlorine in the lower stratosphere p 563 N95-29830

ATMOSPHERIC CONDUCTIVITY

Fine-scale, poleward transport of tropical air during AASE 2 [HTN-95-70949] p 352 A95-78014

ATMOSPHERIC CORRECTION

Validation of empirical orbit error corrections using crossover difference differences [HTN-94-00912] p 25 A95-60227

Using IRI for the computation of ionospheric corrections for altimeter data analysis p 212 A95-66949

Correction of thin cirrus effects in AVIRIS images using the sensitive 1.375-micron cirrus detecting channel p 708 N95-33748

ATMOSPHERIC DIFFUSION

Computational methods in applied sciences; European Computational Fluid Dynamics Conference, 1st, Brussels, Belgium, Sept. 7-11, 1992
[ISBN 0-444-89795-X] p 539 A95-87552

ATMOSPHERIC EFFECTS

The distribution of hydrogen, nitrogen, and chlorine radicals in the lower stratosphere: Implications for changes in O₃ due to emission of NO_x from supersonic aircraft [HTN-95-70935] p 351 A95-78000
Dynamics of aircraft exhaust plumes in the jet-regime [HTN-95-51275] p 355 A95-80860
Aviation and the environment p 657 A95-93464
High-Speed Research: 1994 Sonic Boom Workshop: Atmospheric Propagation and Acceptability Studies [NASA-CP-3279] p 75 N95-14878
Atmospheric effects on the risetime and waveshape of sonic booms p 100 N95-14886
Matlab as a robust control design tool p 169 N95-16474
Atmospheric effects of high-flying subsonic aircraft: A catalogue of perturbing influences [KNMI-SR-94-03] p 168 N95-18722
Test method and test results for environmental assessment of aircraft materials p 302 N95-23509
Analysis and design methodology for chordwise deformable wings p 692 N95-33311
Correction of thin cirrus effects in AVIRIS images using the sensitive 1.375-micron cirrus detecting channel p 708 N95-33748

ATMOSPHERIC ELECTRICITY

Application of airborne field mill data for use in launch support [HTN-95-50054] p 98 A95-62279

ATMOSPHERIC ENTRY

Trajectory-based heating analysis for the European Space Agency/Rosetta Earth Return Vehicle [BTN-95-EIX95041503787] p 205 A95-69218
Powerful bolide explosion over North Italy [HTN-95-80564] p 218 A95-69658
Application of the multigrid solution technique to hypersonic entry vehicles [BTN-95-EIX95152583254] p 306 A95-73555
Research and development of thermal protection system of HOPE re-entry vehicle p 413 A95-82358
Studies on gain performance of a combustion driven CO₂ gas dynamic laser p 428 A95-82679
Science objectives and performance of a radiometer and window design for atmospheric entry experiments [NASA-TM-4637] p 63 N95-12190
Planetary entry experiments [NASA-CR-194215] p 101 N95-13717
Science objectives and performance of a radiometer and window design for atmospheric entry experiments p 85 N95-13718
Measured and calculated spectral radiation from a blunt body shock layer in an arc-jet wind tunnel [AIAA PAPER 94-0086] p 67 N95-13720

ATMOSPHERIC MODELS

Three-dimensional model interpretation of NO_x measurements from the lower stratosphere [HTN-95-90534] p 213 A95-67806
Microwave and infrared simulations of an intense convective system and comparison with aircraft observations [HTN-95-60511] p 214 A95-68762
Forecasting for a large field program: STORM-FEST [HTN-95-90694] p 215 A95-69721
Ascent wind model for launch vehicle design [BTN-95-EIX95041503799] p 239 A95-70124
Water vapor continuum absorption in mid-latitudes: Aircraft measurements and model comparisons [HTN-95-40756] p 252 A95-71186
Aircraft measurements of water vapour continuum absorption at millimetre wavelengths [HTN-95-90884] p 253 A95-72393
Potential applications of the SSM/I cloud liquid water parameter to the estimation of marine aircraft icing [HTN-95-80651] p 254 A95-72495
An algorithm for forecasting mountain wave-related turbulence in the stratosphere [HTN-95-80656] p 254 A95-72500
Snow-band formation and evolution during the 15 November 1987 aircraft accident at Denver airport [HTN-95-80699] p 254 A95-72543
Volcanic ash forecast transport and dispersion (VAFTAD) model [HTN-95-80702] p 254 A95-72546
Hypersonic convective heat transfer over 140-deg blunt cones in different gases [BTN-95-EIX95152583253] p 306 A95-73554
Thundercloud electric field modeling for the ionosphere-Earth region. 1: Dependence on cloud charge distribution [HTN-95-41223] p 317 A95-75035

Possible effects of CO₂ increase on the high-speed civil transport impact on ozone [HTN-95-60779] p 317 A95-75976

Estimates of total organic and inorganic chlorine in the lower stratosphere from in situ and flask measurements during AASE 2 [HTN-95-A0861] p 317 A95-76265

Sensitivity of two-dimensional model predictions of ozone response to stratospheric aircraft: An update [HTN-95-A0863] p 318 A95-76267

Diurnal variation of lee vortices in Taiwan and the surrounding area [HTN-95-91363] p 318 A95-76394

Sensitivity of supersonic aircraft modelling studies to HNO₃ photolysis rate [HTN-95-11475] p 353 A95-79453

Tracer transport for realistic aircraft emission scenarios calculated using a three-dimensional model [HTN-95-41799] p 353 A95-80525

Effects on stratospheric ozone from high-speed civil transport: Sensitivity to stratospheric aerosol loading [HTN-95-91842] p 354 A95-80830

Potential effects on ozone of future supersonic aircraft/2D simulation [HTN-95-51282] p 356 A95-80867

Impact on ozone of high-speed stratospheric aircraft: Effects of the emission scenario [HTN-95-51283] p 356 A95-80868

Operational multi-scale environment model with grid adaptivity (OMEGA) application to aviation weather p 676 A95-93556

An overview of issues encountered in parallelizing high-resolution weather prediction models p 676 A95-93560

Atmospheric and wind modeling for ATC [NASA-CR-196786] p 98 N95-13725

Microburst vertical wind estimation from horizontal wind measurements [NASA-TP-3460] p 131 N95-18198

Assimilation of altimeter data in a quasi-geostrophic model of the Gulf Stream system: A dynamical perspective [NASA-CR-196313] p 320 N95-23766

A mathematical analysis of the Janus combat simulation weather effects models and sensitivity analysis of sky-to-ground brightness ratio on target detection [AD-A289629] p 446 N95-26858

Manual for a workstation-based generic flight simulation program (LaRCsim), version 1.4 [NASA-TM-110164] p 518 N95-30327

Initial evaluation of the Oregon State University planetary boundary layer column model for ITWS applications [AD-A293775] p 677 N95-31465

ATMOSPHERIC MOISTURE

Observations of fluxes and inland breezes over a heterogeneous surface [HTN-95-80258] p 212 A95-66315

Momentum and scalar transfer coefficients over aerodynamically smooth Antarctic surfaces [HTN-95-92932] p 562 A95-91870

Condensation in jet engine intake ducts during stationary operation [BTN-95-EIX95292721154] p 612 A95-92590

Preliminary comparisons between MM5 NCAR/Penn State model generated icing forecasts and observations p 655 A95-93458

The production of supercooled liquid water by a secondary cold front p 673 A95-93542

Airplane icing research at the Boeing Company: Participation in the second Canadian Atlantic Storms Program p 674 A95-93544

Aircraft icing: Meteorological effects on aircraft performance p 674 A95-93545
Preliminary studies of ice formation in upslope clouds p 674 A95-93546

Response of the B-1B air data sensor to simulated dust cloud environments [AD-A286134] p 235 N95-22036

ATMOSPHERIC PRESSURE

Comparison of column abundances from three infrared spectrometers during AASE 2 [HTN-95-70946] p 352 A95-78011

Aerodynamic parameters of crop canopies estimated with a center-of-pressure technique [HTN-95-41901] p 356 A95-81648

Studies on high pressure and unsteady flame phenomena [AD-A284126] p 152 N95-18410

Effect of atmospheric pressure on measured aircraft noise levels [PB95-130423] p 232 N95-21425

ATMOSPHERIC RADIATION

Possible near-IR channels for remote sensing precipitable water vapor from geostationary satellite platforms [HTN-95-70139] p 214 A95-69431

Aircraft measurements of water vapour continuum absorption at millimetre wavelengths [HTN-95-90884] p 253 A95-72393

ATMOSPHERIC SOUNDING

Application of airborne field mill data for use in launch support [HTN-95-50054] p 98 A95-62279

Comparison of wind profiler and aircraft wind measurements at Chebogue Point, Nova Scotia [HTN-95-41833] p 353 A95-80559

Investigation of outflow strength variability in Florida downburst-producing storms p 659 A95-93476

Examination of conditions in the proximity of pilot reports of aircraft icing during storm-fest p 666 A95-93509

ATMOSPHERIC TEMPERATURE

Potential applications of the SSM/I cloud liquid water parameter to the estimation of marine aircraft icing [HTN-95-80651] p 254 A95-72495

Comparison of column abundances from three infrared spectrometers during AASE 2 [HTN-95-70946] p 352 A95-78011

Effects of a polar stratosphere cloud parameterization on ozone depletion due to stratospheric aircraft in a two-dimensional model [HTN-95-A1038] p 443 A95-84543

Two dimensional stratospheric aerosol distributions during EASOE [HTN-95-00726] p 444 A95-86296

Airborne lidar observation of mountain-wave-induced polar stratospheric clouds during EASOE [HTN-95-00738] p 444 A95-86308

Preliminary comparisons between MM5 NCAR/Penn State model generated icing forecasts and observations p 655 A95-93458

Stratus' tephigram as a training/forecasting tool p 657 A95-93465

An in-situ system for warming of icing conditions p 660 A95-93481

Aircraft icing: Meteorological effects on aircraft performance p 674 A95-93545

Preliminary studies of ice formation in upslope clouds p 674 A95-93546

ATMOSPHERIC TURBULENCE

Brief history of gust models for aircraft design [BTN-95-EIX95062487557] p 203 A95-68371

Response of a nonrotating rotor blade to lateral turbulence. Part 2: Experiment [BTN-95-EIX95182619229] p 284 A95-76655

Real-time estimation of atmospheric turbulence severity from in-situ aircraft measurements [BTN-95-EIX95182619231] p 319 A95-76657

Comparison of wind profiler and aircraft wind measurements at Chebogue Point, Nova Scotia [HTN-95-41833] p 353 A95-80559

Aerodynamic parameters of crop canopies estimated with a center-of-pressure technique [HTN-95-41901] p 356 A95-81648

Real time for the calculation of the aerodynamic of aircrafts with delta wings p 460 A95-87399

Estimation of atmospheric turbulence severity from in-situ aircraft measurements p 659 A95-93479

Preliminary results of turbulence predictions for use in aviation weather forecasting p 675 A95-93551

Turbulence near thunderstorm tops p 675 A95-93553

Atmospheric effects on the risetime and waveshape of sonic booms p 100 N95-14886

The effect of aircraft speed on the penetration of sonic boom noise into a flat ocean p 100 N95-14887

Turbulence: Engineering models, aircraft response p 84 N95-14900

Aircraft Loads due to Turbulence and their Impact on Design and Certification [AGARD-R-798] p 143 N95-18597

The impact of non-linear flight control systems on the prediction of aircraft loads due to turbulence p 143 N95-18598

Gyroscopic and propeller aerodynamic effects on engine mounts dynamic loads in turbulence conditions p 132 N95-18599

Treatment of non-linear systems by timeplane-transformed CT methods: The spectral gust method p 143 N95-18600

A study of the effect of store unsteady aerodynamics on gust and turbulence loads p 133 N95-18601

Comparison of stochastic and deterministic nonlinear gust analysis methods to meet continuous turbulence criteria p 133 N95-18602

Special effects of gust loads on military aircraft p 133 N95-18605

Influence of turbulence parameters, Reynolds number, and body shape on stagnation-region heat transfer [NASA-TP-3487] p 550 N95-28719

Digital simulation of wind velocities for wind turbine rotors: General considerations [PB95-206447] p 677 N95-31157

ATOMIC CLOCKS

Effect of broadcast and precise ephemerides on estimates of the frequency stability of GPS Navstar clocks
[BTN-95-EIX95112522530] p 190 A95-69333

ATOMIC SPECTRA

Measured and calculated spectral radiation from a blunt body shock layer in an arc-jet wind tunnel
[AIAA PAPER 94-0086] p 67 N95-13720

ATOMIZERS

Structure of a swirl-stabilized, combustor spray
[NASA-TM-106724] p 50 N95-11890
Combustion efficiency in a dual-inlet side-dump ramjet combustor
[AD-A283564] p 83 N95-15329

ATOMIZING

Near-limit drop deformation and secondary breakup
p 704 N95-32902

ATTACK AIRCRAFT

A preliminary design proposal for a maritime patrol strike aircraft: MPS-2000 Condor
[NASA-CR-197182] p 47 N95-12689

Naval aviation: F-14 upgrades are not adequately justified. Report to Congressional Committees
[AD-A286338] p 231 N95-20212

Design of a controller for a flexible pointing system using H(infinity) synthesis
[AD-A286572] p 256 N95-20828

AH-1F COBRA rewire program MANPRINT analysis
[AD-A289190] p 391 N95-27018

ATTITUDE (INCLINATION)

Attitude determination using dedicated and nondedicated multi-antenna GPS sensors
[BTN-95-EIX95142555482] p 228 A95-72891

Describing an attitude
Computer simulation of ejection seat motion
[CONGRESS PAPER C428-18-169] p 484 A95-91718

Building complex simulations rapidly using MATRIX(x): The Space Station redesign
[TABES PAPER 94-632] p 87 N95-14653

Dynamic response tests of inertial and optical wind-tunnel model attitude measurement devices
[NASA-TM-109182] p 296 N95-23011

Whirl plus tilt
[DE95-007948] p 452 N95-28108

Synthetic Terrain Imagery for Helmet-Mounted Display, volume 1
[AD-A293612] p 612 N95-31656

ATTITUDE CONTROL

The Cassini spacecraft: Object oriented flight control software
p 359 A95-80405

Study of strapdown navigation attitude algorithms
[BTN-95-EIX95282706655] p 486 A95-89649

Moving mass trim control for aerospace vehicles
[DE95-002602] p 299 N95-23532

Practical experiences in control systems design using the NCR Bell 205 Airborne Simulator
p 624 N95-32015

ATTITUDE INDICATORS

Design of head-up display symbology for recovery from unusual attitudes
p 611 A95-95044

Assessment of a non-dedicated GPS receiver system for precise airborne attitude determination
[DE94-019309] p 229 N95-21520

Dynamic response tests of inertial and optical wind-tunnel model attitude measurement devices
[NASA-TM-109182] p 296 N95-23011

Flight reference display for powered-lift STOL aircraft
[NAL-TR-1251] p 337 N95-25005

AUDITORY PERCEPTION

Improvement of the predicted aural detection code ICHIN (I Can Hear It Now)
p 576 A95-90123

AUGMENTATION

Objective verification of an enhanced terminal forecast experiment at Denver, Colorado
p 664 A95-93501

Aeromechanics technology, volume 1. Task 1: Three-dimensional Euler/Navier-Stokes Aerodynamic Method (TEAM) enhancements
[AD-A285713] p 132 N95-18483

Evaluation of retro-reflective beads in airport pavement markings
[AD-A291065] p 523 N95-29967

The 25th International Symposium on Combustion
[AD-A286825] p 630 N95-31268

Aviation capacity enhancement plan 1994
[AD-A292758] p 598 N95-31428

AUSTRALIA

AIRSAR deployment in Australia, September 1993: Management and objectives
p 321 N95-23948

Comparison of fixed wing aircraft algorithms for JANUS
[AD-A288503] p 389 N95-26652

A review of Australian and New Zealand investigations on aeronautical fatigue during the period Apr. 1993 - Mar. 1995
[AR-009-202] p 397 N95-27918

AUSTRIA

A poor man's expert system for aviation VSRF in complex terrain
p 669 A95-93524

AUTOCLAVES

ACT/ICAPS: Thermoplastic composite activities
p 421 N95-28274

AUTOCLAVING

Rapid prototyping of composite aircraft structures
[SAE PAPER 931219] p 539 A95-87530

AUTOCORRELATION

Prediction of fatigue crack growth under constant amplitude and random loading using specimens with multiple cracks
[AD-A291614] p 397 N95-28409

AUTOGYROS

Wind tunnel tests of a 42 inch diameter self-starting autogyro rotor
[AD-A279922] p 188 N95-19863

AUTOMATA THEORY

GPS-Scuttler capacity analysis
[AD-A280037] p 245 N95-20599

Grid generation and surface modeling for CFD
p 551 N95-28726

AUTOMATED PILOT ADVISORY SYSTEM

Differential GPS and system integration of the Low Visibility Landing and Surface Operations (LVLASO) demonstration
p 280 N95-23318

AUTOMATIC CONTROL

Optimum full-scale subsonic wind tunnel
[AIAA PAPER 86-0732] p 18 A95-60161

Automatic riveting cell for commercial aircraft floor grid assembly
[BTN-95-EIX95182617807] p 261 A95-75752

Cypher moves toward autonomous flight
[HTN-95-41394] p 283 A95-76390

Automatic guidance and control for helicopter obstacle avoidance
[BTN-95-EIX95182619130] p 291 A95-76607

Automatic riveting cell for commercial aircraft floor grid assembly
[HTN-95-92309] p 365 A95-85353

Aircraft stripping and painting
[HTN-95-92311] p 365 A95-85355

Automated aircraft routing through weather-impacted airspace
Operational and research aspects of a radio-controlled model flight test program
[BTN-95-EIX0619952748177] p 606 A95-94471

Operational And Supportability Implementation System (OASIS) test and evaluation master plan
[AD-A284765] p 126 N95-18088

VSTOL Systems Research Aircraft (VSRA) Harrier
[NASA-TM-110117] p 126 N95-18347

NASA develops new digital flight control system
[NASA-NEWS-RELEASE-94-47] p 144 N95-19029

Nonlinear system guidance in the presence of transmission zero dynamics
[NASA-TM-4661] p 309 N95-22804

Performance of the 0.3-meter transonic cryogenic tunnel with air, nitrogen, and sulfur hexafluoride media under closed loop automatic control
[NASA-CR-195052] p 310 N95-23257

Partial camera automation in a simulated Unmanned Air Vehicle
[AD-A288786] p 337 N95-26190

Operator modeling in commercial aviation: Cognitive models, intelligent displays, and pilot's assistants
[NASA-CR-198609] p 401 N95-28203

New adaptive methods for reconfigurable flight control systems, appendix 1
[AD-A292711] p 619 N95-30937

A tactical navigation and routing system for low-level flight
p 709 N95-32494

AUTOMATIC FLIGHT CONTROL

Automatic formation flight control
[BTN-95-EIX95182619153] p 292 A95-76630

Air data sensors for atmospheric reentry flight test of winged space vehicle
Ducted fan VTOL and its flight control system
p 500 A95-91573

Analysis of an MLS automatic landing control law for the NAL experimental research aircraft D0-228. 2: Curved approach and landing
p 508 A95-91588

Development of a TECS control-law for the lateral directional axis of the McDonnell Douglas F-15 Eagle
[AD-A289771] p 410 N95-28598

Design and evaluation of a LQR controller for the bluebird unmanned air vehicle
[AD-A289769] p 504 N95-29457

Automatic flight control system for an unmanned helicopter system design and flight test results
p 622 N95-32004

AUTOMATIC LANDING CONTROL

CCLA operation on MLS
p 487 A95-91540

Flight test evaluation of the Stanford University/United Airlines differential GPS Category 3 automatic landing system
[NASA-TM-110354] p 593 N95-30788

AUTOMATIC PILOTS

Automatic guidance and control for helicopter obstacle avoidance
[BTN-95-EIX95182619130] p 291 A95-76607

Automatic formation flight control
[BTN-95-EIX95182619153] p 292 A95-76630

High-performance, robust, bank-to-turn missile autopilot design
[BTN-95-EIX95242670751] p 336 A95-81096

Load alleviation maneuvers for a launch vehicle
p 342 A95-81360

Air data prediction from surface pressure measurements on guided munitions
[BTN-95-EIX95282706664] p 466 A95-89641

Predictive algorithms for the roll control autopilot of a jet fighter aircraft
[HTN-95-21047] p 515 A95-90424

A design of a robust scheduled autopilot
p 516 A95-91532

A design of a self-learning robust scheduled autopilot
p 516 A95-91533

Missile autopilot designs using full state feedback
p 507 A95-91587

A SIMULINK environment for flight dynamics and control analysis: Application to the DHC-2 Beaver. Part 1: Implementation of a model library in SIMULINK. Part 2: Nonlinear analysis of the Beaver autopilot
[NONP-NASA-SUPPL-DK-94-2802] p 84 N95-14815

Evaluation of an autopilot based multimodelling
[PB94-190725] p 142 N95-17454

Collected papers of the Soar/IFOR project, Spring 1994
[AD-A280063] p 238 N95-20624

Advanced formation flight control
[AD-A289271] p 409 N95-26981

Digital autopilot design for combat aircraft in ALENIA
p 623 N95-32009

Integrated special mission flight management for a flight inspection aircraft
p 692 N95-33145

AUTOMATIC TEST EQUIPMENT

CASS: Design for supportability
[BTN-95-EIX95172595296] p 287 A95-75716

Containing military autotest cost growth through the use of commercial standard equipment architectures
[BTN-95-EIX95172595295] p 287 A95-75717

ATE enabling technologies
[BTN-95-EIX95172595294] p 287 A95-75718

New commercial off-the-shelf testers are automatic and intelligent
[BTN-95-EIX95172595292] p 287 A95-75720

Integrated test system single point control of aircraft checkout
[SAE PAPER 931417] p 583 A95-93682

Life cycle costs of alternatives for F-16 printed circuit board diagnosis equipment
[AD-A288744] p 401 N95-28586

AUTOMATIC WEATHER STATIONS

International Conference on Aviation Weather Systems, 5th, Vienna, VA, Aug. 2-6, 1993. Preprint Volume
[HTN-95-92940] p 652 A95-93441

Flying with automated surface observations
p 659 A95-93472

Representativeness and responsiveness of automated weather systems
p 660 A95-93482

The inference of aviation weather hazards based on the integration of radar and lightning data
p 660 A95-93483

Automation of observations in the Netherlands
p 661 A95-93485

Aviation terminal forecasts based on automated observations (FTAUTO)
p 668 A95-93520

Aviation weather forecasting automated methods in the RAFC Moscow and the Airport Vnukovo
p 669 A95-93523

AUTOMATION

Advancements in automatic fastening technology
[BTN-94-EIX94461290277] p 65 A95-61734

New commercial off-the-shelf testers are automatic and intelligent
[BTN-95-EIX95172595292] p 287 A95-75720

Towards improving the NMC aircraft data base
p 660 A95-93480

Aviation weather forecasting automated methods in the RAFC Moscow and the Airport Vnukovo
p 669 A95-93523

Evaluating the effects of air traffic control automation
p 601 A95-95091

The role of flight progress strips in en route air traffic control: A time-series analysis
[DOT/FAA/AM-95/4] p 280 N95-23565

Automatic blocking for complex three-dimensional configurations p 566 N95-28734

AUTOMOBILE ENGINES

Conversion of production automotive engines for aviation use [SAE PAPER 932606] p 495 A95-90076

AUTOMOBILES

CaRnard: A new roadable aircraft concept [SAE PAPER 932601] p 494 A95-90071

Engineering design of Starcar 3 [SAE PAPER 932602] p 494 A95-90072

Design and styling of an advanced flying automobile [SAE PAPER 932603] p 494 A95-90073

Design methodology and infrastructures for flying automobiles [SAE PAPER 932604] p 495 A95-90074

Design and analysis of a telescopic wing [SAE PAPER 932605] p 495 A95-90075

Application of three-dimensional hybrid structured/unstructured grids to land, sea and air vehicles [ARA-MEMO-399] p 210 N95-19775

Severe edge effects and simple complimentary interior solutions for thin-walled anisotropic and composite structures [AD-A290645] p 555 N95-29562

AUTONOMOUS NAVIGATION

Cypher moves toward autonomous flight [HTN-95-41394] p 283 A95-76390

Application of GPS and Fuzzy Theory to a helicopter p 516 A95-91505

Research on an autonomous vision-guided helicopter [AIAA PAPER 94-1240-CP] p 18 N95-11510

A feedforward control approach to the local navigation problem for autonomous vehicles [AD-A282787] p 126 N95-17706

Interfacing a digital compass to a remote-controlled helicopter [PB95-164927] p 340 N95-24260

AUTOROTATION

Helicopter: A rotating antenna synthetic aperture radar for helicopter allweather operations p 705 N95-33137

AUXILIARY POWER SOURCES

Auxiliary power unit noise of Boeing B737 and B747 aircraft p 571 A95-88468

Auxiliary Power Unit evolution: Meeting tomorrow's challenges [SAE PAPER 932541] p 510 A95-89195

System design considerations for an APU starter-generator [SAE PAPER 932559] p 511 A95-90056

Secondary power system study for the htex RA3 flight test vehicle [AIAA PAPER 95-6158] p 512 A95-90470

The A340 electrical power generation system [CONGRESS PAPER C428-36-193] p 625 A95-93630

The auxiliary and emergency power supply on the Saab JAS39 Gripen aircraft [CONGRESS PAPER C428-36-192] p 612 A95-93631

Moisture induced pressures in concrete airfield pavements [AD-A281974] p 52 N95-11789

Motor drive technologies for the power-by-wire (PBW) program: Options, trends and tradeoffs [NASA-TM-106885] p 295 N95-23671

AUXILIARY PROPULSION

A vehicle health monitoring system for the Space Shuttle Reaction Control System during reentry [NASA-CR-188370] p 527 N95-29447

AVIATION METEOROLOGY

International Conference on Aviation Weather Systems, 5th, Vienna, VA, Aug, 2-6, 1993. Preprint Volume [HTN-95-92940] p 652 A95-93441

An overview of FAA-sponsored aviation weather research and development p 652 A95-93442

The forecast systems laboratory's role in the FAA's aviation weather development program p 652 A95-93443

National aviation weather program plan p 652 A95-93445

Operational aviation weather regulations p 652 A95-93446

A status report on the development of the Federal Aviation Administration/National Oceanic and Atmospheric Administration Memorandum of Agreement p 652 A95-93447

An approach to weather requirements management p 653 A95-93448

On designing and engineering the integrated terminal weather system p 653 A95-93449

Status of the terminal Doppler weather radar with deployment underway p 653 A95-93450

The Integrated Terminal Weather System (ITWS) storm cell information and weather impacted airspace detection algorithm p 654 A95-93452

Improving aircraft impact assessment with the integrated terminal weather system microburst detection algorithm p 654 A95-93453

ITWS ceiling and visibility products p 654 A95-93454

ITWS gridded analysis p 654 A95-93455

The ITWS microburst prediction algorithm p 655 A95-93456

The real-time analysis and prediction of storms program p 655 A95-93457

Preliminary comparisons between MM5 NCAR/Penn State model generated icing forecasts and observations p 655 A95-93458

Knowing our users - A challenge for meteorologists at the National Aviation Weather Advisory Unit p 655 A95-93459

An integrated system to improve aviation weather forecasts for the Alaska Range p 656 A95-93460

Transitioning to the aviation routine weather report (METAR) and the International Aerodrome Forecast (TAF) within the Federal Aviation Administration p 656 A95-93461

Aviation weather education and the University of North Dakota aviation weather survey p 656 A95-93462

Pilot training initiatives for the '90s p 657 A95-93463

Stratus' tephigram as a training/forecasting tool p 657 A95-93465

Aviation meteorology education in an AB initio setting p 657 A95-93466

Sensing thunderstorm microphysics with multiparameter radar: Application for aviation p 657 A95-93467

A comparative performance study of TDWR/LLWAS 3 integration algorithms for wind shear detection p 658 A95-93468

Use of WSR-88D data in the FAA's weather impacted aerospace product p 658 A95-93469

NEXRAD/ARSR operational comparison p 658 A95-93470

Final results of the weather testing component of the Terminal Doppler Weather Radar operational test and evaluation p 658 A95-93471

Flying with automated surface observations p 659 A95-93472

Investigation of outflow strength variability in Florida downburst-producing storms p 659 A95-93476

Transport Canada proposed R&D program for the development of a multi-parameter dual X-Ka band Doppler radar for aviation meteorology applications p 659 A95-93477

Estimation of atmospheric turbulence severity from in-situ aircraft measurements p 659 A95-93479

Towards improving the NMC aircraft data base p 660 A95-93480

An in-situ system for warning of icing conditions p 660 A95-93481

Representativeness and responsiveness of automated weather systems p 660 A95-93482

The inference of aviation weather hazards based on the integration of radar and lightning data p 660 A95-93483

Preliminary results of high resolution measurements of snowfall at Stapleton International Airport during the winter of 1992-93 p 661 A95-93484

Automation of observations in the Netherlands p 661 A95-93485

Use of high resolution lightning detection and localization sensors for hazardous aviation weather nowcasting p 661 A95-93486

The use of radar wind profiles to remove TDWR gust front algorithm false alarms caused by vertical wind shear p 661 A95-93488

The performance of forward scatter visibility sensors for application in autostations and runway visual range in snow and freezing precipitation events p 662 A95-93489

Terminal Doppler Weather Radar point target filter threshold selection p 662 A95-93490

LLWAS 2 and LLWAS 3 performance evaluation p 662 A95-93491

Test results of a low cost airport weather radar p 662 A95-93492

Criteria of forecasting low level wind shear over Qatar p 663 A95-93493

Role of the aviation weather system in providing a real-time ATC volcanic ash advisory system p 663 A95-93494

Alaska's volcanic ash warning system p 663 A95-93495

Development of a climatology for possible microburst occurrence in Canada p 664 A95-93497

The aviation gridded forecast system verification program - A description of aviation-impact-variable evaluation plans p 664 A95-93498

Comprehensive verification of terminal forecast ceiling and visibility p 664 A95-93500

Objective verification of an enhanced terminal forecast experiment at Denver, Colorado p 664 A95-93501

Verification of terminal forecasts p 664 A95-93502

Analysis of en route controller hazardous weather-related tasks p 665 A95-93503

The data link flight information service application p 665 A95-93504

A new look at aviation meteorology: Integrating aircraft situation display (ASD) with conventional weather displays p 665 A95-93505

Jet stream winds: Comparisons of operational analyses with independent aircraft data at multiple longitudes p 665 A95-93506

Use of pilot reports for verification of aircraft icing diagnoses and forecasts p 666 A95-93508

Examination of conditions in the proximity of pilot reports of aircraft icing during storm-fest p 666 A95-93509

A short-term, high-resolution automated snowfall forecasting system p 666 A95-93510

Automated aircraft routing through weather-impacted airspace p 666 A95-93512

An echo motion algorithm for air traffic management using a national radar mosaic p 667 A95-93513

Developing thunderstorm forecast rules utilizing first detectable cloud radar-echoes p 667 A95-93514

Testing of TKE parameterizations in numerical models for clear-air turbulence forecasting p 667 A95-93515

MEMFOG - The Memphis fog algorithm p 668 A95-93516

MDCRS: Aircraft observations collection and uses p 668 A95-93517

The improvement of meteorological data for air traffic management purposes p 668 A95-93518

FTGEN - An automated FT production system p 668 A95-93519

Aviation terminal forecasts based on automated observations (FTAUTO) p 668 A95-93520

Nortaf: Computer generated aerodrome forecasts p 668 A95-93521

The combination of forecasts in an automated aviation weather forecasting system p 669 A95-93522

Aviation weather forecasting automated methods in the RAFC Moscow and the Airport Vnukovo p 669 A95-93523

A poor man's expert system for aviation VSRF in complex terrain p 669 A95-93524

Dissemination of terminal weather products to the flight deck via data link p 669 A95-93525

Dissemination of weather products p 670 A95-93526

Weather products for aviation from WAFC Bracknell p 670 A95-93527

Development of a climatological data base to help forecast cloud cover conditions for shuttle landings at the Kennedy Space Center p 670 A95-93529

Analysis of rapidly developing fog at the Kennedy Space Center p 671 A95-93531

Developing the Aviation Gridded Forecast System p 671 A95-93532

Developing and testing decision-making products for center weather service unit meteorologists p 671 A95-93533

The prototype aviation weather products generator a vehicle to assess user needs p 671 A95-93534

Aviation value-added products and services from the NEXRAD Information Dissemination Service (NIDS) p 671 A95-93535

Using ATMS weather products for air traffic strategic planning p 672 A95-93536

User involvement in the development of an advanced icing product for use in aviation p 672 A95-93537

A study of the savings in time and fuel to aviation through the use of upper-air wind forecasts p 672 A95-93538

Northwest Airlines atmospheric hazards advisory & avoidance system p 672 A95-93539

Assessment of the benefits for improved terminal weather information p 673 A95-93540

Creating a global climatology of freezing rain using numerical model output p 673 A95-93541

The production of supercooled liquid water by a secondary cold front p 673 A95-93542

An application of some cloud modeling techniques to a regional model simulation of an icing event p 673 A95-93543

Airplane icing research at the Boeing Company: Participation in the second Canadian Atlantic Storms Program p 674 A95-93544

Aircraft icing: Meteorological effects on aircraft performance p 674 A95-93545

Preliminary studies of ice formation in upslope clouds p 674 A95-93546

A northern hemisphere clear air turbulence climatology p 674 A95-93547

- An evaluation of clear-air turbulence indices p 674 A95-93548
- The development of an aircraft icing forecast technique using data from maps p 675 A95-93549
- Preliminary results of turbulence predictions for use in aviation weather forecasting p 675 A95-93551
- Amplification and breaking of atmospheric gravity waves p 675 A95-93552
- Turbulence near thunderstorm tops p 675 A95-93553
- A prototype for displaying aviation forecast variables using Eta numerical model output p 676 A95-93555
- Operational multi-scale environment model with grid adaptivity (OMEGA) application to aviation weather p 676 A95-93556
- An overview of issues encountered in parallelizing high-resolution weather prediction models p 676 A95-93560
- The 1992-3 operational winter forecasting experiment for Stapleton airport p 677 A95-93561
- Airborne Windshear Detection and Warning Systems. Fifth and Final Combined Manufacturers' and Technologists' Conference, part 1 [NASA-CP-10139-PT-1] p 10 N95-10566
- Characteristics of a dry, pulsating microburst at Denver Stapleton Airport p 26 N95-10568
- Future enhancements to ground-based microburst detection p 11 N95-10570
- Terminal Doppler Weather Radar Build 5A Operational Test and Evaluation (OT/E) integration and OT/E operational test plan [AD-A283052] p 61 N95-12996
- Flight in an Adverse Environment [AGARD-LS-197] p 77 N95-14893
- Microburst vertical wind estimation from horizontal wind measurements [NASA-TP-3460] p 131 N95-18198
- AVIATION PSYCHOLOGY**
- The selective use of functional optical variables in the control of forward speed [NASA-TM-108849] p 35 N95-12227
- Controller resource management: What can we learn from aircrews? [DOT/FAA/AM-95/21] p 602 N95-32186
- AVIONICS**
- On-board avionics maintenance [BTN-94-EIX94461047054] p 82 A95-61741
- Integrated IR sensors [BTN-95-EIX95041505023] p 242 A95-70132
- Foliage transmission measurements using a ground-based ultrawide band (300-1300 MHz) SAR system [BTN-94-EIX94381351617] p 252 A95-70950
- Labs behind Boeing's new 777 [BTN-95-EIX95142562403] p 280 A95-73437
- CASS: Design for supportability [BTN-95-EIX95172595296] p 287 A95-75716
- Containing military autotest cost growth through the use of commercial standard equipment architectures [BTN-95-EIX95172595295] p 287 A95-75717
- ATE enabling technologies [BTN-95-EIX95172595294] p 287 A95-75718
- New commercial off-the-shelf testers are automatic and intelligent [BTN-95-EIX95172595292] p 287 A95-75720
- Overview of AlliedSignal's avionics development in the CIS [BTN-95-EIX95212641069] p 287 A95-76734
- Design of wide angle head up displays for synthetic vision [BTN-95-EIX95212641070] p 287 A95-76735
- Flight Simulators: Better than the real thing? [HTN-95-42619] p 518 A95-87249
- Commercial applications for military laser radars p 543 A95-87794
- 'Global avionics in the future' report from the 10th annual battery conference [BTN-95-EIX95282706404] p 545 A95-88184
- MIL-STD-461/MIL-STD-704 investigation [SAE PAPER 932561] p 505 A95-90058
- AIAA Computing in Aerospace 10, San Antonio, TX, March 28-30, 1995 [ISBN 1-56347-119-1] p 565 A95-90629
- Integrated performance and reliability specification for digital avionics systems [AIAA PAPER 95-0953] p 506 A95-90632
- Technology-insertion life-cycle-cost model [AIAA PAPER 95-0961] p 581 A95-90638
- The role of simulations in 777 FSEU development [AIAA PAPER 95-0995] p 506 A95-90665
- The ADAGE avionics reference architecture [AIAA PAPER 95-1021] p 566 A95-90693
- Development of Fly-By-Wire system for BK117 p 516 A95-91506
- Status of Enhanced Vision System p 506 A95-91542
- Guidance and control of HOPE and its future technologies p 506 A95-91543
- The impact of new technology on reliability of avionic equipment [CONGRESS PAPER C428-6-114] p 549 A95-91683
- The avionics integrity programme (AVIP) [CONGRESS PAPER C428-6-115] p 549 A95-91684
- Dependable software - the state of the art [CONGRESS PAPER C428-24-212] p 678 A95-93596
- Development of software for safety critical applications for the EH101 Helicopter [CONGRESS PAPER C428-24-160] p 678 A95-93597
- Airborne integrated communications system [CONGRESS PAPER C428-30-162] p 610 A95-93612
- Electromagnetic compatibility - A general overview [CONGRESS PAPER C428-38-084] p 634 A95-93637
- Modular avionics: Taking today's aircraft into tomorrow [SAE PAPER 931416] p 610 A95-93681
- Fly-By-Light/Power-By-Wire Requirements and Technology Workshop [NASA-CR-10108] p 12 N95-10245
- Design and flight evaluation of an integrated navigation and near-terrain helicopter guidance system for night-time and adverse weather operations [NASA-TM-108837] p 11 N95-10846
- The development of a highly reliable power management and distribution system for civil transport aircraft [NASA-TM-106697] p 50 N95-11867
- An avionics scenario and command model description for Space Generic Open Avionics Architecture (SGOAA) [NASA-CR-188330] p 49 N95-11913
- Cabin fuselage structural design with engine installation and control system [NASA-CR-197173] p 47 N95-12639
- HLLV avionics requirements study and electronic filing system database development [NASA-CR-193993] p 49 N95-13027
- Artificial intelligence with applications for aircraft [DOT/FAA/CT-94/41] p 99 N95-13895
- Space Generic Open Avionics Architecture (SGOAA): Overview p 99 N95-14161
- Electromagnetic reverberation characteristics of a large transport aircraft [AD-A282923] p 82 N95-15392
- The computer analysis of the prediction of aircraft electrical power supply system reliability p 155 N95-16278
- A study of software standards used in the avionics industry p 137 N95-16456
- New technologies for space avionics [NASA-CR-197574] p 150 N95-18196
- KC-135 cockpit modernization study. Phase 1: Equipment evaluation [AD-A284099] p 131 N95-18398
- Strategic avionics technology definition studies. Subtask 3-1A3: Electrical Actuation (ELA) Systems Test Facility [NASA-CR-188360] p 143 N95-18567
- Advanced Packaging Concepts for Digital Avionics [AGARD-CP-562] p 233 N95-20631
- The impact of advanced packaging technology on modular avionics architectures p 233 N95-20632
- Standard Hardware Acquisition and Reliability Program (SHARP) advanced SEM-E packaging p 233 N95-20633
- FASTPACK: Optimized solutions for modular avionics derived from a parametric study. Part 1: Platform features p 233 N95-20634
- FASTPACK: Optimized solutions for modular avionics derived from a parametric study. Part 2: Avionics p 233 N95-20635
- The Advanced Avionics Subsystem Technology Demonstration Program p 234 N95-20636
- Ultra-Reliable Digital Avionics (URDA) processor p 245 N95-20638
- MCMS for avionics: Technology selection and intermodule interconnection p 234 N95-20641
- High density monolithic packaging technology for digital/microwave avionics p 240 N95-20646
- High performance backplane components for modular avionics p 247 N95-20653
- Composite cases for airborne electronic equipment: A technology study and EMC p 241 N95-20655
- Modular supplies for a distributed architecture - avionics packaging p 234 N95-20657
- Modular CNI avionics system p 234 N95-20659
- The opportunities for and challenges of common integrated electronics [AD-A279991] p 248 N95-20966
- Systems engineering design and technical analyses for Strategic Avionics Crew-station Design Evaluation Facility (SACDEF) [AD-A286239] p 235 N95-22024
- Evaluation of the Haworth-Newman avionics Display Readability Scale [AD-A286127] p 235 N95-22232
- Assessment of avionics technology in European aerospace organizations [NASA-CR-189201] p 337 N95-24624
- Preload release mechanism [NASA-CASE-MS-C-22327-1] p 350 N95-25592
- Configuration and other differences between Black Hawk and Seahawk helicopters in military service in the USA and Australia [AR-008-386] p 336 N95-25935
- Micro-time stress measurement device development [AD-A289511] p 448 N95-26845
- An analysis of the KC-135 three-person cockpit [AD-A289540] p 390 N95-26873
- Nonlinear calibration of an infrared radiometer [AD-A292436] p 579 N95-28996
- Investigation and characterization of SEU effects and hardening strategies in avionics [AD-A291058] p 509 N95-29950
- Foundations of technology for constructing highly reliable distributed-realtime systems [AD-A293254] p 678 N95-30892
- Experimental Aircraft Programme (EAP): Flight control system design and test p 623 N95-32010
- A highly reliable, high performance open avionics architecture for real time Nap-of-the-Earth operations p 693 N95-32497
- AVOIDANCE**
- Northwest Airlines atmospheric hazards advisory & avoidance system p 672 A95-93539
- Turbulence near thunderstorm tops p 675 A95-93553
- AXES OF ROTATION**
- Horizontal axis wind turbine post stall airfoil characteristics synthesis p 376 N95-27974
- A NASTRAN-based computer program for structural dynamic analysis of Horizontal Axis Wind Turbines p 439 N95-27980
- Measurement and prediction of broadband noise from large horizontal axis wind turbine generators p 451 N95-27990
- AXIAL FLOW**
- Investigation of heat transfer in a rotating ring gap with the axial flow of a coolant during the rotation of the central shaft [BTN-94-EIX94461407951] p 89 A95-62625
- Rotor whirl forces induced by the tip clearance effect in axial flow compressors [BTN-94-EIX94351143331] p 207 A95-67304
- Vortex cutting by a blade. Part II: Computations of vortex response [BTN-94-EIX94441386611] p 208 A95-67342
- Aeroelastic stability of cascades in turbomachinery [HTN-95-61156] p 405 A95-86255
- Flutter analysis of supersonic axial flow cascades using a high resolution Euler solver. Part 1: Formulation and validation [NASA-TM-105798] p 23 N95-10244
- A general theory of two- and three-dimensional rotational flow in subsonic and transonic turbomachines [NASA-CR-4496] p 377 N95-28003
- Unsteady pressure and inflow velocity on a pitching rotor blade in hover p 480 N95-29771
- Laser doppler velocimeter system for subsonic jet mixer nozzle testing at the NASA Lewis Aeroacoustic Propulsion Lab [NASA-TM-106984] p 457 N95-30229
- Development of a linearized unsteady Euler analysis for turbomachinery blade rows [NASA-CR-4677] p 592 N95-30611
- AXIAL FLOW TURBINES**
- Modeling improvements and users manual for axial-flow turbine off-design computer code AXOD [NASA-CR-195370] p 8 N95-10853
- Enhanced capabilities and updated users manual for axial-flow turbine preliminary sizing code TURBAN [NASA-CR-195405] p 76 N95-15912
- AXIAL LOADS**
- Validation of an effective flat cruciform-shaped specimen to study CFRP composite laminate laminates under biaxial loading [BTN-95-EIX95152584677] p 282 A95-73589
- A Lifting Ball Valve for cryogenic fluid applications p 156 N95-16349
- Results of uniaxial and biaxial tests on riveted fuselage lap joint specimens p 136 N95-19491
- Axial loads on yawed rotors [PB95-214193] p 592 N95-30638
- AXIAL MODES**
- Combustion-acoustic stability analysis for premixed gas turbine combustors [NASA-TM-107024] p 694 N95-32931

AXIAL STRESS

Thrust measurement in a 2-D scramjet nozzle
p 339 N95-25397

AXISYMMETRIC BODIES

Elliptic tip effects on the vortex wake of an axisymmetric body at incidence
[BTN-94-EIX94441386612] p 208 A95-67343

Passive porosity with free and fixed separation on a tangent-ogive forebody
[BTN-95-EIX95062487554] p 185 A95-68368

Development of an efficient inverse method for supersonic and hypersonic body design
[BTN-95-EIX95041503784] p 180 A95-69215

Minimum-drag axisymmetric bodies in the supersonic/hypersonic flow regimes
[BTN-95-EIX95041503785] p 180 A95-69216

Supersonic near-wake afterbody boattailing effects on axisymmetric bodies
[BTN-95-EIX95182617465] p 268 A95-75736

Supersonic, turbulent flow computation and drag optimization for axisymmetric afterbodies
[BTN-95-EIX95302729772] p 637 A95-94134

Evaluation of energy-sink stability criteria for dual-spin spacecraft
[AD-A283228] p 87 N95-14850

An investigation of the transonic pressure drag coefficient for axis-symmetric bodies
[AD-A280990] p 105 N95-15994

Pressure distributions on research wing W4 mounted on an axisymmetric body
p 112 N95-17862

Ellipsoid-cylinder model
p 158 N95-17869

AXISYMMETRIC FLOW

Behavior of the Johnson-King turbulence model in axisymmetric supersonic flows
[BTN-94-EIX94441386606] p 183 A95-67337

Supersonic axisymmetric conical flow solutions for different ratios of specific heats
[BTN-95-EIX95152583283] p 306 A95-73584

Behavior of the Johnson-King turbulence model in Axisymmetric supersonic flows
[HTN-95-20932] p 464 A95-88971

Elliptic tip effects on the vortex wake of an axisymmetric body at incidence
[HTN-95-20938] p 464 A95-88977

Hypersonic waveriders generated from power-law shocks
[AIAA PAPER 95-6160] p 470 A95-90472

Numerical studies of Mach reflection with air chemistry
p 548 A95-90575

Optimal shape design in hypersonic aerodynamics and electromagnetics
p 639 A95-95397

Supersonic jet noise reductions predicted with increased jet spreading rate
[NASA-TM-106872] p 323 N95-23178

TIGER: A user-friendly interactive grid generation system for complicated turbomachinery and axis-symmetric configurations
p 322 N95-23419

Validation of a Computational Fluid Dynamics (CFD) code for supersonic axisymmetric base flow
p 315 N95-23652

Inlet flow test calibration for a small axial compressor rig. Part 2: CFD compared with experimental results
[NASA-TM-106999] p 514 N95-30007

Numerical simulations of the flow in the HYPULSE expansion tube
[NASA-TM-110357] p 523 N95-30228

Acceleration potential models
PREDICHT/PREDICDYN applied for calculation of axisymmetric dynamic inflow cases
[PB95-207015] p 647 N95-30957

AZIMUTH

Add a dimension to your analysis of the helicopter low airspeed environment
[AD-A283982] p 79 N95-14205

Apparent size passive range method
[AD-D017360] p 611 N95-31180

B

B-1 AIRCRAFT

Moisture induced pressures in concrete airfield pavements
[AD-A281974] p 52 N95-11789

Case study of risk management in the USAF B-1B bomber program
[AD-A282371] p 62 N95-11944

An analysis of B-1B exterior jet blast windshield anti-icing performance using pre-cooled compressor bleed air
[AD-A292522] p 485 N95-28811

B-2 AIRCRAFT

Integrated test system single point control of aircraft checkout
[SAE PAPER 931417] p 583 A95-93682

B-52 AIRCRAFT

The effects of aircraft (B-52) overflights on ancient structures
[BTN-94-EIX94341340070] p 171 A95-63522

Scattering of short em-pulses by simple and complex targets using impulse radar
p 486 A95-90953

BACKGROUND NOISE

Aeroacoustic probe design for microphone to reduce flow-induced self-noise
[AIAA PAPER 93-4343] p 19 A95-60163

Background noise levels measured in the NASA Lewis 9- by 15-foot low-speed wind tunnel
[NASA-TM-106817] p 145 N95-18054

BACKSCATTERING

Electromagnetic backscattering from a helicopter rotor in the decametric wave band regime
[BTN-94-EIX94381353130] p 243 A95-72648

Analysis of backscattering from wing and fuselage joints
[HTN-95-71134] p 430 A95-83495

BACKUPS

Design, analysis and control of large transports so that control of engine thrust can be used as a back-up of the primary flight controls
[NASA-CR-198958] p 518 N95-30254

BACKWARD DIFFERENCING

A spectrally accurate boundary-layer code for infinite swept wings
[NASA-CR-195014] p 159 N95-18042

BACKWARD FACING STEPS

Low Reynolds number laminar separation bubble control using a backward facing step
[SAE PAPER 932572] p 467 A95-90061

Turbulence characteristics of supersonic boundary layer past a backward facing step
[AIAA PAPER 95-6126] p 470 A95-90447

BACKWASH

Sidewash on the vertical tail in subsonic and supersonic flows
[BTN-95-EIX95152582316] p 264 A95-73519

BAFFLES

Coupled FEM-BEM approach for mean flow effects on vibro-acoustic behavior of planar structures
[BTN-95-EIX95152577587] p 263 A95-73495

BAGGAGE

Test and Evaluation Plan (TEP) for Improvised Explosive Device Screening Systems (IEDSS)
[AD-A286382] p 227 N95-22319

BALLOUT

RAF ejections - historical perspectives and future requirements
[CONGRESS PAPER C428-18-168] p 484 A95-91717

Computer simulation of ejection seat motion
[CONGRESS PAPER C428-18-169] p 484 A95-91718

BALANCE

Helicopter Performance Evaluation (HELPE) computer model
[AD-A284319] p 131 N95-18381

Hydrofoil force balance
[AD-D016475] p 160 N95-18461

BALANCING

Transport aircraft loading and balancing system: Using a CLIPS expert system for military aircraft load planning
p 217 N95-19751

Balanced on air aircraft
[AD-D017251] p 389 N95-26537

BALL BEARINGS

A Lifting Ball Valve for cryogenic fluid applications
p 156 N95-16349

BALLISTIC RANGES

An experimental study on radiation from strong shock layer
p 368 A95-82421

Hypersonic aerodynamics test facility using the external propulsion accelerator
[AIAA PAPER 95-6138] p 470 A95-90455

BALLISTIC TRAJECTORIES

Trajectory-based heating analysis for the European Space Agency/Rosetta Earth Return Vehicle
[BTN-95-EIX95041503787] p 205 A95-69218

Analytical solution and parameter estimation of projectile dynamics
[BTN-95-EIX95212645695] p 272 A95-76747

BALLISTIC VEHICLES

Moving mass trim control for aerospace vehicles
[DE95-002602] p 299 N95-23532

BALLISTICS

Analytical solution and parameter estimation of projectile dynamics
[BTN-95-EIX95212645695] p 272 A95-76747

BALLOON FLIGHT

Balloon technology and observations; Symposium P3 of the COSPAR Plenary Meeting, 29th, Washington, DC, Aug. 28-Sept. 5, 1992
[HTN-95-70250] p 181 A95-66276

French contribution to new balloon designs and materials
p 181 A95-66277

Status of the NASA balloon program
p 181 A95-66296

Overview of the NASA balloon R&D program
p 181 A95-66297

Recent trends in balloon flights from TIFR's National Balloon Facility, Hyderabad
p 191 A95-66300

Balloon flights in France and in Europe
p 204 A95-66301

The scientific ballooning in Russia
p 191 A95-66302

The joint Russian-Brasil research on balloons
p 182 A95-66303

A program for scientific and applied investigations using aerostat complexes
p 182 A95-66304

Long duration balloons
p 191 A95-66305

Polar Patrol Balloon
[BTN-95-EIX95152582318] p 316 A95-73521

Variational principles for ascent shapes of large scientific balloons
[BTN-95-EIX95262694320] p 387 A95-85491

Earthwinds Hilton III: Balloon project
p 497 A95-90871

Comparison of meteorological data with fitted values extracted from projectile trajectory
[AD-A285921] p 255 N95-19989

BALLOON SOUNDING

Balloon technology and observations; Symposium P3 of the COSPAR Plenary Meeting, 29th, Washington, DC, Aug. 28-Sept. 5, 1992
[HTN-95-70250] p 181 A95-66276

Balloon flights in France and in Europe
p 204 A95-66301

Scientific balloons
[NASA-TM-109907] p 7 N95-10556

BALLOON-BORNE INSTRUMENTS

The joint Russian-Brasil research on balloons
p 182 A95-66303

Application of fuzzy logic to optimize placement of an acquisition, tracking, and pointing experiment
p 341 A95-80390

Study on a scheme for the prolongation of microgravity time of balloon-borne drop capsule
p 414 A95-82515

CALIOPE and TAISIR airborne experiment platform
[DE94-018328] p 250 N95-22299

BALLOONS

French contribution to new balloon designs and materials
p 181 A95-66277

A comparative study of internally and externally capped balloons using small scale test balloons
p 181 A95-66285

Status of the NASA balloon program
p 181 A95-66296

Overview of the NASA balloon R&D program
p 181 A95-66297

BALLUTES

Computational flow predictions for hypersonic drag devices
p 37 N95-11967

BALSA

The Balsa bullet: A high speed, low-cost general aviation aircraft for Aeroworld
[NASA-CR-197165] p 46 N95-12638

BANDWIDTH

Foliage transmission measurements using a ground-based ultrawide band (300-1300 MHz) SAR system
[BTN-94-EIX94381351617] p 252 A95-70950

Identification of higher order helicopter dynamics using linear modeling methods
[HTN-95-80851] p 290 A95-75093

Investigation of the effects of bandwidth and time delay on helicopter roll-axis handling qualities
[HTN-95-80853] p 290 A95-75095

BARIUM OXIDES

Phonon characteristics of high (T sub c) superconductors from neutron Doppler broadening measurements
[DE95-003703] p 324 N95-24076

BAROCLINITY

Radar studies of aviation hazards
[AD-A285845] p 226 N95-21831

BARRIER LAYERS

The effect of wear on fire-blocking layer material effectiveness
[AD-A291520] p 485 N95-29855

BARRIERS

Hangars as noise barriers for helicopter noise
p 560 A95-90111

BASE FLOW

Numerical computations of supersonic base flow with special emphasis on turbulence modeling
[BTN-94-EIX94441386632] p 179 A95-68181

Base drag prediction on missile configurations
[BTN-95-EIX95152583256] p 266 A95-73557

- Study of subsonic base cavity flowfield structure using particle image velocimetry
[BTN-95-EIX95222650781] p 327 A95-79237
- Numerical computations of supersonic base flow with special emphasis on turbulence modeling
[HTN-95-20949] p 546 A95-88988
- Supersonic base flow investigation over axisymmetric afterbodies
[PB94-180957] p 39 N95-12578
- Base passive porosity for drag reduction
[NASA-CASE-LAR-15246-1] p 91 N95-14183
- Numerical computations of supersonic base flow with special emphasis on turbulence modeling
[AD-A293688] p 119 N95-18670
- Validation of a Computational Fluid Dynamics (CFD) code for supersonic axisymmetric base flow
p 315 N95-23652
- Navier-Stokes solution of wing wake structure and its perturbation
p 479 N95-29121
- The effects of three dimensional imposed disturbances on bluff body near wake flows
[AD-A290824] p 555 N95-29654
- BASE HEATING**
- Review and development of base pressure and base heating correlations in supersonic flow
[BTN-95-EIX95212645688] p 271 A95-76740
- BASE PRESSURE**
- Review and development of base pressure and base heating correlations in supersonic flow
[BTN-95-EIX95212645688] p 271 A95-76740
- Similarity rule for jet-temperature effects on transonic base pressure
[BTN-95-EIX95222650791] p 329 A95-79247
- Investigation of the flow development on a highly swept canard/wing research model with segmented leading- and trailing-edge flaps
p 114 N95-17876
- BAYS (STRUCTURAL UNITS)**
- Weapons bay acoustic environment
p 173 N95-19146
- BAYS (TOPOGRAPHIC FEATURES)**
- Evaluation of alternative in-flight fire suppressants for full-scale testing in simulated aircraft engine nacelles and dry bays
[PB94-203403] p 42 N95-13247
- BEACONS**
- Cueing light configuration for aircraft navigation
[NASA-CASE-ARC-11982-1] p 280 N95-23393
- BEADS**
- Active open-loop control of particle dispersion in round jets
[HTN-95-42334] p 372 A95-86163
- Evaluation of retro-reflective beads in airport pavement markings
[AD-A291065] p 523 N95-29967
- BEAMS (SUPPORTS)**
- Vibration measurements on rotating machinery using laser Doppler velocimetry
[BTN-94-EIX95011440597] p 429 A95-82986
- Equivalent beam-column analysis of guyed towers
[BTN-95-EIX95262696644] p 435 A95-85519
- Exact dynamic responses of periodic multi-span beams under convected pressure fields
p 25 N95-11288
- Large amplitude nonlinear response of flat aluminum, and carbon fiber plastic beams and plates
[AD-A282440] p 96 N95-15547
- Vibrational behavior of adaptive aircraft wing structures modelled as composite thin-walled beams
p 423 N95-28435
- BEARINGLESS ROTORS**
- Dynamic analysis of bearingless tail rotor blades based on nonlinear shell modes
[BTN-95-EIX95152582338] p 281 A95-73540
- BEARINGS**
- New strategy combining backward inference with forward inference in monitoring and diagnosing techniques for hydrodynamic bearing-rotor systems
[BTN-94-EIX94331336949] p 88 A95-61795
- Finite element model for a flexible non-symmetric rotor on distributed bearing: A stability study
[BTN-94-EIX94381352212] p 306 A95-74612
- The effects of wall perturbations on thermo-turbulent Couette flow
[HTN-95-92255] p 434 A95-85299
- High-speed seal and bearing test facility
p 53 N95-13601
- Bearing defect signature analysis using advanced nonlinear signal analysis in a controlled environment
[NASA-TM-108491] p 441 N95-28364
- BEDS (PROCESS ENGINEERING)**
- Analysis of flow channeling near the wall in packed beds
[HTN-94-00698] p 2 A95-60177
- BELL AIRCRAFT**
- Improving prediction: The incorporation of simplified rotor dynamics in a mathematical model of the bell 412HP
[BTN-95-EIX95152584679] p 282 A95-73591
- Ten-year ground exposure of composite materials used on the Bell Model 206L helicopter flight service program
[NASA-TP-3468] p 55 N95-12357
- Rotorcraft crashworthy airframe and fuel system technology development program
[AD-A289986] p 382 N95-28630
- Bell Helicopter Advanced Rotocraft Transmission (ART) program
[NASA-CR-195479] p 555 N95-29538
- Practical experiences in control systems design using the NCR Bell 205 Airborne Simulator
p 624 N95-32015
- BEND TESTS**
- Experimental evaluation of a box beam specifically tailored for chordwise deformation
[BTN-95-EIX95182619088] p 283 A95-75773
- Failure behaviour of carbon fiber/epoxy composites in pin-ended buckling and bending tests
[HTN-95-71388] p 528 A95-87606
- On aircraft repair verification of a fighter A/C integrally stiffened fuselage skin
p 394 N95-27515
- BENDING**
- Vortex cutting by a blade. Part II: Computations of vortex response
[BTN-94-EIX94441386611] p 208 A95-67342
- Simplified analysis of general instability of stiffened shells with cutouts in pure bending
[BTN-95-EIX95042474418] p 209 A95-68282
- Experimental evaluation of a box beam specifically tailored for chordwise deformation
[BTN-95-EIX95182619088] p 283 A95-75773
- Modal characteristics of rotors using a conical shaft finite element
[BTN-94-EIX94401359745] p 346 A95-77379
- Load alleviation maneuvers for a launch vehicle
p 342 A95-81360
- The dynamic nature of rotor thermal bending due to unsteady lubricant shearing within a bearing
[HTN-95-42091] p 430 A95-83857
- Vortex cutting by a blade, Part 2: Computations of vortex response
[HTN-95-20937] p 464 A95-88976
- Bending effects of unsymmetric adhesively bonded composite repairs on cracked aluminum panels
p 92 N95-14456
- Discrete crack growth analysis methodology for through cracks in pressurized fuselage structures
p 166 N95-19473
- Analysis of composite structures with delaminations under combined bending and compression
p 422 N95-28429
- Design and evaluation of a foam-filled hat-stiffened panel concept for aircraft primary structural applications
p 502 N95-28841
- Technology integration box beam failure study
p 552 N95-28847
- Analysis and design methodology for chordwise deformable wings
p 692 N95-33311
- BENDING FATIGUE**
- Detecting gear tooth fracture in a high contact ratio face gear mesh
[NASA-TM-106822] p 162 N95-19125
- Thrust measurement in a 2-D scramjet nozzle
p 339 N95-25397
- BENDING MOMENTS**
- Optimum design of composite stiffened wing panels - a parametric study
[HTN-95-01088] p 496 A95-90274
- Gemini: A long-range cargo transport
[NASA-CR-197149] p 45 N95-12626
- Investigation of dynamic inflow's influence on rotor control derivatives
p 155 N95-16250
- Technology integration box beam failure study
p 441 N95-28468
- Shear force, bending moment and torque of rigid aircraft in symmetric steady maneuvering flight
[ESDU-94045] p 502 N95-28896
- BERNOULLI THEOREM**
- Acoustic radiation damping of flat rectangular plates subjected to subsonic flows
p 172 N95-18542
- BIAS**
- An intercomparison of instrumentation for tropospheric measurements of dimethyl sulfide: Aircraft results for concentrations at the parts-per-trillion level
[HTN-95-91857] p 355 A95-80845
- BIBLIOGRAPHIES**
- FAA vertical flight bibliography
[DOT/FAA/RD-94/17] p 14 N95-11684
- NASA's Hypersonic Research Engine Project: A review
[NASA-TM-107759] p 50 N95-12860
- Documentation and archiving of the Space Shuttle wind tunnel test data base. Volume 1: Background and description
[NASA-TM-104806-VOL-1] p 151 N95-19237
- Aeronautical engineering: A continuing bibliography with indexes (supplement 315)
[NASA-SP-7037(315)] p 219 N95-21640
- NASA video catalog
[NASA-SP-7109(01)] p 363 N95-24238
- Aeronautical engineering: A continuing bibliography with indexes (supplement 316)
[NASA-SP-7037(316)] p 328 N95-24465
- Aeronautical engineering: A continuing bibliography with indexes (supplement 317)
[NASA-SP-7037(317)] p 328 N95-25798
- Cumulative reports and publications through December 31, 1994
[NASA-CR-195043] p 361 N95-26085
- Aeronautical engineering: A continuing bibliography with indexes (supplement 318)
[NASA-SP-7037(318)] p 367 N95-27543
- Bibliography of Doctor Chul Park
[NASA-TM-110353] p 527 N95-29351
- AGARD index of publications: 1992-1994
[AGARD-INDEX-92-94] p 711 N95-33198
- BINARY STARS**
- Period evolution of PSR B1259-63: Evidence for propeller-torque spindown
[HTN-95-80194] p 581 A95-87903
- BINOCLULAR VISION**
- Factors affecting the perception of tuning in monocular regions of partial binocular overlap displays
[AD-A286287] p 259 N95-22044
- BINOCLARIS**
- Factors affecting the visual fragmentation of the field-of-view in partial binocular overlap displays
[AD-A283081] p 172 N95-17334
- BIODYNAMICS**
- Biodynamic simulation of pilot interaction with a helicopter multi-airbag restraint system
[AD-A290196] p 485 N95-29057
- BIONICS**
- Human factors issues in aircraft cabin design
[SAE PAPER 932527] p 386 A95-84556
- BIOTECHNOLOGY**
- JPRS Report: Science and technology. Central Eurasia
[JPRS-UST-94-032] p 350 N95-24759
- JTEC/WTEC annual report and program summary: 1993/94
[NASA-CR-198563] p 454 N95-28038
- BIPLANES**
- Gemini: A long-range cargo transport
[NASA-CR-197149] p 45 N95-12626
- Full span flaperons for a biplane
p 391 N95-26954
- Incorporating biplane wing theory into a large, subsonic, all-cargo transport
p 391 N95-26956
- BIPOLARITY**
- Development of a bipolar lead/acid battery for the more electric aircraft
[AD-A284050] p 160 N95-18660
- BIRD-AIRCRAFT COLLISIONS**
- Impact finite element analysis, as an alternative to the testing of windscreens for bird impact
[CONGRESS PAPER C428-23-196] p 500 A95-91732
- Design of fan blades subjected to bird impact
p 200 N95-19669
- Bird ingestion into large turbofan engines
[DOT/FAA/CT-93/14] p 333 N95-24631
- Development of repair processes and sources for C/KC-135 aircraft windows/windshields
[AD-A288348] p 367 N95-26629
- A review of falconry as a bird control technique with recommendations for use at the Shuttle Landing Facility, John F. Kennedy Space Center, Florida, USA
[NASA-TM-110142] p 381 N95-27859
- BIRDS**
- Bird ingestion into large turbofan engines
[DOT/FAA/CT-93/14] p 333 N95-24631
- A review of falconry as a bird control technique with recommendations for use at the Shuttle Landing Facility, John F. Kennedy Space Center, Florida, USA
[NASA-TM-110142] p 381 N95-27859
- BISMALIMIDE**
- Mechanical properties of advanced toughened bismaleimide matrix composite
p 530 A95-91570
- Application of fiber-reinforced bismaleimide materials to aircraft nacelle structures
p 397 N95-28278
- BITUMENS**
- Additives in bituminous materials and fuel-resistant sealers
[DOT/FAA/CT-94/78] p 55 N95-12131

BLADE SLAP NOISE

- Sensitivity of acoustic predictions to variation of input parameters
[HTN-95-80855] p 267 A95-75097
- The effects and prediction of rotary wing aircraft noise on the community
[HTN-95-92536] p 558 A95-87356
- Studies of blade-vortex interaction noise reduction by rotor blade modification
[NASA-CR-198590] p 377 N95-28193
- Flow structure generated by perpendicular blade vortex interaction and implications for helicopter noise predictions
[NASA-CR-198590] p 377 N95-28193
- Evaluation of a doubly-swept blade tip for rotorcraft noise reduction
[NASA-CR-189677] p 452 N95-28264
- UHB engine fan broadband noise reduction study
[NASA-CR-198357] p 580 N95-29641
- BLADE TIPS**
- Unsteady lift on a swept blade tip
[BTN-94-EIX95011441154] p 329 A95-80030
- Effects of blade tip shape on dynamics, cost, weight, aerodynamic performance, and aeroelastic response
[HTN-95-61074] p 369 A95-83658
- Blade-by-blade tip clearance measurement system for gas turbine applications
[BTN-95-EIX95292721167] p 546 A95-89899
- Performance deterioration of axial compressors due to blade defects
[NASA-CR-198590] p 377 N95-28193
- Erosion of T56 5th stage rotor blades due to bleed hole overtip flow
[NASA-CR-198590] p 377 N95-28193
- Supersonic flow and shock formation in turbine tip gaps
[NASA-CR-198590] p 377 N95-28193
- Evaluation of a doubly-swept blade tip for rotorcraft noise reduction
[NASA-CR-189677] p 452 N95-28264
- Application of multigrid computational fluid dynamics (CFD) methods to rotor analysis
[AD-A293012] p 648 N95-31475
- Experimental and computational investigation of the tip clearance flow in a transonic axial compressor rotor
[NASA-TM-106711] p 649 N95-31738
- BLADE-VORTEX INTERACTION**
- Validation of the dynamic response of a blade-element UH-60 simulation model in hovering flight
[HTN-94-00663] p 18 A95-60155
- Study of noise on a small-scale hovering tilt rotor
[HTN-94-00712] p 5 A95-60190
- Rotating Kirchhoff method for three-dimensional transonic blade-vortex interaction hover noise
[BTN-94-EIX94441386601] p 182 A95-67332
- Active control of wake/blade-row interaction noise
[BTN-95-EIX95042474389] p 196 A95-68311
- Recent studies of rotorcraft blade-vortex interaction noise
[BTN-95-EIX95062487521] p 218 A95-69229
- Aerodynamic and wake methodology evaluation using Model UH-60A experimental data
[HTN-95-31009] p 220 A95-71179
- Effects of leading and trailing edge flaps on the aerodynamics of airfoil/vortex interactions
[HTN-95-31011] p 221 A95-71181
- Analysis of a higher harmonic control test to reduce blade vortex interaction noise
[BTN-95-EIX95152582330] p 265 A95-73532
- Unsteady lift on a swept blade tip
[BTN-94-EIX95011441154] p 329 A95-80030
- A higher harmonic control test in the DNW to reduce impulsive BVI noise
[HTN-95-61071] p 385 A95-83655
- Reduction of blade-vortex interaction noise through porous leading edge
[HTN-95-42324] p 371 A95-86153
- Dynamic-stall and structural-modeling effects on helicopter blade stability with experimental correlation
[HTN-95-81646] p 542 A95-87694
- Vortex cutting by a blade, part 1: General theory and a simple solution
[HTN-95-20822] p 543 A95-88083
- Rotating Kirchhoff method for three-dimensional transonic blade-vortex interaction hover noise
[HTN-95-20927] p 463 A95-88966
- Vortex cutting by a blade, Part 2: Computations of vortex response
[HTN-95-20937] p 464 A95-88976
- Studies of blade-vortex interaction noise reduction by rotor blade modification
[NASA-CR-198590] p 377 N95-28193
- Experimental results of the European HELINOISE aeroacoustic rotor test
[HTN-95-01080] p 578 A95-90266
- Laser velocimetry and blade pressure measurements of a blade-vortex interaction
[HTN-95-01081] p 547 A95-90267
- Rotor-wake-induced flow separation on a lifting surface
[HTN-95-01082] p 468 A95-90268

- The verification of a theoretical helicopter rotor blade sailing method by means of windtunnel testing
[HTN-95-01093] p 468 A95-90279
- Preliminary results from a particle image velocimetry study of blade-vortex interaction
[HTN-95-01098] p 547 A95-90284
- An innovative algorithm to accurately solve the Euler equations for rotary wing flow
[NASA-CR-198590] p 377 N95-28193
- Prediction of rotor-blade deformations due to unsteady airloads
[AD-A284467] p 81 N95-15821
- Comparative performance tests on the Mod-2, 2.5-mW wind turbine with and without vortex generators
[NASA-CR-198590] p 377 N95-27978
- Measurement and prediction of broadband noise from large horizontal axis wind turbine generators
[NASA-CR-198590] p 377 N95-28193
- Flow structure generated by perpendicular blade vortex interaction and implications for helicopter noise predictions
[NASA-CR-198590] p 377 N95-28193
- Evaluation of a doubly-swept blade tip for rotorcraft noise reduction
[NASA-CR-189677] p 452 N95-28264
- Development of a rotary wing Navier-Stokes CFD code based on TLNS3D code
[AD-A290421] p 554 N95-29387
- Experimental and computational investigation of the tip clearance flow in a transonic axial compressor rotor
[NASA-TM-106711] p 649 N95-31738
- BLANKETS (FUSION REACTORS)**
- MHD-flow in slotted channels with conducting walls
[DE94-018370] p 258 N95-21388
- BLAST LOADS**
- Quantity-distance requirements for earth-bermed aircraft shelters
[AD-A279692] p 341 N95-24424
- Facilities used for plastic media blasting
[NASA-CR-198590] p 377 N95-28193
- Operational parameters and material effects
[NASA-CR-198590] p 377 N95-28193
- BLEEDING**
- On supersonic-inlet boundary-layer bleed flow
[NASA-CR-195426] p 202 N95-19769
- BLOCK COPOLYMERS**
- Additives in bituminous materials and fuel-resistant sealers
[DOT/FAA/CT-94/778] p 55 N95-12131
- BLOCKING**
- Vapor lock studies for gasolines wwith ethers
[SAE PAPER 931233] p 529 A95-88962
- Low speed wind tunnel blockage corrections for airfoils at medium to large angles of attack
[NASA-CR-198590] p 377 N95-28193
- Use of partially open wind tunnel walls for blockage-free separated flows on bodies
[NASA-CR-198590] p 377 N95-28193
- Wind-tunnel blockage and actuation systems test of a two-dimensional scramjet inlet unstart model at Mach 6
[NASA-TM-109152] p 97 N95-15898
- Adaptive wind tunnel walls versus wall interference correction methods in 2D flows at high blockage ratios
[NASA-CR-198590] p 377 N95-28193
- Precision landing system mathematical modeling study report for Andrews Air Force Base, runway 19L, Camp Springs, MD
[AD-A289015] p 384 N95-27903
- Grid generation and surface modeling for CFD
[NASA-CR-198590] p 377 N95-28193
- Automatic blocking for complex three-dimensional configurations
[NASA-CR-198590] p 377 N95-28193
- Block-structured grids for complex aerodynamic configurations: Current status
[NASA-CR-198590] p 377 N95-28193
- BLOCKS**
- Implicit multiblock Euler and Navier-Stokes calculations
[HTN-95-A1755] p 634 A95-93318
- BLOWDOWN WIND TUNNELS**
- Free-jet testing at Mach 3.44 in GASL's aero/thermo test facility
[NASA-CR-198590] p 377 N95-28193
- Operating capability and current status of the reactivated NASA Lewis Research Center Hypersonic Tunnel Facility
[NASA-TM-106808] p 148 N95-19286
- The dynamic approach to rotor blade research: ARA's oscillatory test facility
[ARA-MEMO-405] p 223 N95-20758
- BLOWERS**
- Integration of a mechanical forebody vortex control system into the F-15
[NASA-CR-198590] p 377 N95-28193
- BLOWING**
- Application of circulation control to advanced subsonic transport aircraft. Part 1: Airfoil development
[BTN-95-EIX95062487545] p 185 A95-68359
- Application of circulation control to advanced subsonic transport aircraft. Part 2: Transport application
[BTN-95-EIX95062487546] p 185 A95-68360

- Forebody flow control on a full-scale F/A-18 aircraft
[BTN-95-EIX95152582333] p 281 A95-73535
- Pneumatic concept for tip-stall control of cranked-arrow wings
[BTN-95-EIX95152582335] p 281 A95-73537
- Effects of periodic spanwise blowing on Delta-wing configuration characteristics
[HTN-95-81631] p 461 A95-87679
- Numerical model for circulation-control flows
[HTN-95-81632] p 461 A95-87680
- Computational analysis of forebody tangential slot blowing on the high alpha research vehicle
[NASA-CR-196750] p 10 N95-11367
- Numerical analysis of tangential slot blowing on a generic chined forebody
[NASA-TM-108845] p 37 N95-11927
- Computational analysis of forebody tangential slot blowing
[NASA-CR-198590] p 377 N95-28193
- Comparison of full-scale, small-scale, and CFD results for F/A-18 forebody slot blowing
[NASA-CR-198590] p 377 N95-28193
- Low-energy pneumatic control of forebody vortices
[NASA-CR-198590] p 377 N95-28193
- Computational analysis of forebody tangential slot blowing on the high alpha research vehicle
[NASA-CR-197754] p 389 N95-26591
- Performance characterization of a highly-offset diffuser with and without blowing vortex generator jets
[AD-A289334] p 375 N95-26901
- Pressure based high order TVD methodology for dynamic stall control
[AD-A290149] p 479 N95-29316
- BLUFF BODIES**
- Grid refinement test of time-periodic flows over bluff bodies
[BTN-94-EIX94401378822] p 307 A95-76491
- Research on bluff body vortex wakes
[AD-A286319] p 223 N95-20177
- Effects of three-dimensional imposed 3-D disturbances on bluff-body near wake flows
[AD-A289553] p 374 N95-26757
- The effects of three-dimensional imposed disturbances on bluff body near wake flows: Effects of taper and splitter plates on the near wake characteristics of a circular cylinder in uniform and shear flow
[AD-A292113] p 477 N95-28921
- BLUNT BODIES**
- Approximate method for calculating heating rates on three-dimensional vehicles
[BTN-95-EIX95041503778] p 210 A95-69209
- Aerodynamically blunt and sharp bodies
[BTN-95-EIX95041503781] p 205 A95-69212
- Flow resolution and domain influence in rarefied hypersonic blunt-body flows
[BTN-95-EIX95082502729] p 220 A95-70136
- Shock tunnel measurements of hypervelocity blunted cone drag
[BTN-95-EIX95152577606] p 305 A95-73477
- Zonally decoupled direct simulation Monte Carlo solutions of hypersonic blunt-body wake flows
[BTN-95-EIX95182617458] p 268 A95-75729
- Numerical investigation of supersonic flows around a spiked blunt body
[BTN-95-EIX95212645690] p 271 A95-76742
- Shock tunnel measurements of hypervelocity blunted cone drag
[HTN-95-42591] p 459 A95-87221
- Numerical modeling and simulation of chemically reacting reentry flows
[NASA-CR-198590] p 377 N95-28193
- Experimental investigation of hypersonic flow over a wing-body combination
[AIAA PAPER 95-6083] p 460 A95-87412
- Numerical simulation of three-dimensional hypersonic reacting flows over blunt bodies with catalytic surface
[HTN-95-61184] p 539 A95-87557
- Viscous contribution to the high Mach number damping in pitch of blunt slender cones at small angles of attack
[HTN-95-01096] p 469 A95-90282
- A numerical investigation of flow around a square-section cylinder mounted with a splitter plate
[NASA-CR-198590] p 377 N95-28193
- Ellipsoid-cylinder model
[NASA-CR-198590] p 377 N95-28193
- Shock wave interactions in hypervelocity flow
[AD-A286507] p 250 N95-22212
- DSMC calculations for 70-deg blunted cone at 3.2 km/s in nitrogen
[NASA-TM-109181] p 348 N95-24396
- Experimental and theoretical studies of wakes in stratified flows
[AD-A290203] p 553 N95-29060
- Transonic, supersonic and hypersonic wind-tunnel tests on aerodynamic characteristics of reentry body with blunted cone configuration
[ISAS-658] p 480 N95-29640

- Analysis of planar laser-induced fluorescence images obtained during shakedown testing of the AEDC impulse facility
[AD-A293237] p 646 N95-30906
- The 25th International Symposium on Combustion
[AD-A286825] p 630 N95-31268
- BLUNT TRAILING EDGES**
The effects of three dimensional imposed disturbances on bluff body near wake flows
[AD-A290824] p 555 N95-29654
- BO-105 HELICOPTER**
A generalized algorithm for inverse simulation applied to helicopter maneuvering flight
[HTN-95-A0493] p 236 A95-72564
- Analysis of a higher harmonic control test to reduce blade vortex interaction noise
[BTN-95-EIX95152582330] p 265 A95-73532
- Experimental results of the European HELINOISE aeroacoustic rotor test
[HTN-95-01080] p 578 A95-90266
- Full-scale hingeless rotor performance and loads
[NASA-TM-110356] p 691 N95-32699
- BODIES OF REVOLUTION**
Two-variable method for blockage wall interference in a circular tunnel
[BTN-95-EIX95062487540] p 187 A95-69248
- CFD optimization of a theoretical minimum-drag body
[BTN-95-EIX95182619234] p 308 A95-76660
- Crossflow topology of vortical flows
[HTN-95-51664] p 432 A95-85046
- Geodesic constant method: A novel approach to analytical surface-ray tracing on convex conducting bodies
[BTN-95-EIX95302731054] p 637 A95-94205
- BODY-WING AND TAIL CONFIGURATIONS**
Shear force, bending moment and torque of rigid aircraft in symmetric steady maneuvering flight
[ESDU-94045] p 502 N95-28896
- BODY-WING CONFIGURATIONS**
Time-resolved surface heat flux measurements in the wing/body junction vortex
[BTN-95-EIX95082502716] p 220 A95-71029
- Improved version of the Naval Surface Warfare Center aeroprediction code (AP93)
[BTN-95-EIX95152583260] p 267 A95-73561
- Wing vertical position effects on wing-body carryover for noncircular missiles
[BTN-95-EIX95182617462] p 268 A95-75733
- Some additional stability and performance characteristics of the scissor/pivot wing configurations
[SAE PAPER 931383] p 618 A95-93659
- Parallel aeroelastic computations for wing and wing-body configurations
[NASA-CR-196835] p 36 N95-11766
- Symmetric steady manoeuvre loads on rigid aircraft of classical configuration at subsonic speeds
[ESDU-94009] p 43 N95-11774
- Integrated design and manufacturing for the high speed civil transport
[NASA-CR-197183] p 48 N95-12700
- Cabin-fuselage-wing structural design concept with engine installation
[NASA-CR-197172] p 49 N95-12993
- Wing-body juncture flows
[AD-A281526] p 106 N95-16099
- Aerodynamic shape optimization
p 128 N95-16572
- Review of the EUROPT Project AERO-0026
p 129 N95-16573
- Pressure distributions on research wing W4 mounted on an axisymmetric body
p 112 N95-17862
- DLR-F4 wing body configuration
p 130 N95-17863
- The aerodynamic design of an integrated wing lower surface and pylons for reduced drag
[ARA-MEMO-406] p 194 N95-19789
- Open Skies project computational fluid dynamic analysis
[AD-A285928] p 223 N95-19991
- Aerodynamic shape optimization of wing and wing-body configurations using control theory
[NASA-CR-198024] p 335 N95-25334
- A theoretical and experimental investigation of the flow over supersonic leading edge wing/body configurations
[DRA-TM-AERO-PROP-41] p 331 N95-25649
- Aeroelasticity of wing and wing-body configurations on parallel computers
[NASA-CR-197756] p 389 N95-26590
- Preliminary design problems and solutions for a supersonic oblique all-wing transport aircraft
p 390 N95-26942
- Demonstration of an automated CFD system for three-dimensional flow simulations
p 551 N95-28767
- The 1995 version of the NSWC aeroprediction code. Part 1: Summary of new theoretical methodology
[AD-A291518] p 481 N95-29853
- A numerical study of the small scale wing-body junction problem
p 482 N95-30235
- Transonic aerodynamic characteristics of a proposed wing-body reusable launch vehicle concept
[NASA-TM-108489] p 592 N95-30712
- Numerical investigation into vortical flow about a delta-wing configuration up to incidences at which vortex breakdown occurs in experiment
[PB95-198024] p 593 N95-30837
- BOEING AIRCRAFT**
H-76B fantail demonstrator composite fan blade fabrication
[HTN-95-80856] p 283 A95-75098
- Aerospace applications of beta titanium alloys
[HTN-95-B0394] p 530 A95-90475
- The role of simulations in 777 FSEU development
[AIAA PAPER 95-0995] p 506 A95-90665
- Numerical study of multi-element airfoil aerodynamics
[ISBN 1-879921-01-4] p 587 A95-93750
- Low frequency ultrasonic nondestructive inspection of aluminum/adhesive fuselage lap splices
[DE94-014242] p 24 N95-11135
- Strategy in the commercial aircraft industry in the United States: A comparison of decisionmaking by McDonnell-Douglas and Boeing aircraft companies from 1977-1983
[AD-A288289] p 366 N95-26409
- Report to Congressional Committees. Comanche Helicopter: Testing needs to be completed prior to production decisions
[GAO/NSIAD-95-112] p 397 N95-27910
- Development of advanced approach and departure procedures. Failure scenarios
[PB95-198123] p 601 N95-30815
- BOEING 707 AIRCRAFT**
Electromagnetic reverberation characteristics of a large transport aircraft
[AD-A282923] p 82 N95-15392
- BOEING 737 AIRCRAFT**
Auxiliary power unit noise of Boeing B737 and B747 aircraft
p 571 A95-88468
- Differential GPS and system integration of the Low Visibility Landing and Surface Operations (LVLASO) demonstration
p 280 N95-23318
- NASA-ACEE/Boeing 737 graphite-epoxy horizontal stabilizer service
p 400 N95-28489
- BOEING 747 AIRCRAFT**
Dynamics of aircraft exhaust plumes in the jet-regime
[HTN-95-51275] p 355 A95-80860
- Modeling of aircraft exhaust emissions and infrared spectra for remote measurement of nitrogen oxides
[HTN-95-51276] p 355 A95-80861
- SOFIA: Stratospheric Observatory for Infrared Astronomy
p 363 A95-81583
- Auxiliary power unit noise of Boeing B737 and B747 aircraft
p 571 A95-88468
- Numerical simulation of the SOFIA flowfield
[NASA-CR-197025] p 74 N95-14612
- Special investigation report: Maintenance anomaly resulting in dragged engine during landing rollout. Northwest Airlines Flight 18, Boeing 747-251B, N637US, New Tokyo International Airport, Narita, Japan, 1 Mar. 1994
[PB94-917006] p 188 N95-19793
- Numerical simulation of the SOFIA flow field
[NASA-CR-197757] p 436 N95-26589
- SOFIA 2 model telescope wind tunnel test report
[NASA-TM-110668] p 683 N95-32764
- BOEING 767 AIRCRAFT**
Civil Reserve Air Fleet-Aeromedical Evacuation Shipset (CRAF-AESS)
p 568 N95-29619
- BOEING 777 AIRCRAFT**
Labs behind Boeing's new 777
[BTN-95-EIX95142562403] p 280 A95-73437
- Flight-deck displays on the Boeing 777
[BTN-95-EIX95142562402] p 286 A95-73438
- Challenges and payoff of composites in transport aircraft: 777 empennage and future applications
p 534 N95-29031
- BOILING**
Low gravity quenching of hot tubes with cryogenics
[ISBN 1-879921-01-4] p 635 A95-93728
- BOLDES**
Powerful bolide explosion over North Italy
[HTN-95-80564] p 218 A95-69658
- BOMBER AIRCRAFT**
Bomber force 2000: Operational concepts for long-range combat aircraft
[AD-A279378] p 230 N95-20181
- Systems engineering design and technical analyses for Strategic Avionics Crew-station Design Evaluation Facility (SACDEF)
[AD-A286239] p 235 N95-22024
- Performance study for inlet installations
[NASA-CR-189714] p 406 N95-28227
- BOMBS (ORDNANCE)**
Aerodynamic characteristics of external store configurations at low speeds
[BTN-95-EIX95182619230] p 271 A95-76656
- BONDED JOINTS**
Bonded composite repair of cracked load-bearing holes
[BTN-94-EIX94401360553] p 243 A95-71867
- Application of superplastically formed and diffusion bonded structures in high intensity noise environments
p 174 N95-19162
- Design and structural validation of CF116 upper wing skin boron doubler
p 393 N95-27510
- Composite repair issues on the CF-18 aircraft
p 395 N95-27518
- The development of an engineering standard for composite repairs
p 396 N95-27528
- Aircraft advanced materials research and development program plan
[AD-A290542] p 505 N95-29565
- BONDING**
The key to designing durable adhesively bonded joints
[HTN-95-12033] p 528 A95-88496
- Reliability assessment of Multichip Module technologies via the Triservice/NASA RELTECH program
p 245 N95-20643
- Assuring Known Good Die (KGD) for reliable, cost effective MCMs
p 246 N95-20644
- Status of bonded boron/epoxy doublers for military and commercial aircraft structures
p 393 N95-27506
- Evaluation of patch effectiveness in repairing aircraft components
p 394 N95-27513
- Repair technology for thermoplastic aircraft structures
p 395 N95-27519
- The effect of interface properties on nickel base alloy composites
[NASA-CR-198363] p 629 N95-30787
- BOOSTER ROCKET ENGINES**
Aerodynamic design of pegasus: Concept to flight with computational fluid dynamics
[BTN-95-EIX95182617463] p 298 A95-75734
- Some aspects of the aerodynamics of separating strap-ons
[BTN-95-EIX95182617464] p 298 A95-75735
- The 1993 JANNAF Propulsion Meeting, volume 1
[CPA-PUBL-602-VOL-1] p 148 N95-16312
- BORON FIBERS**
Composite repair of metallic airframe: Twenty years of experience
p 393 N95-27508
- BORON REINFORCED MATERIALS**
Adhesively bonded composite patch repair of cracked aluminum alloy structures
p 393 N95-27507
- Bonded composite repair of thin metallic materials: Variable load amplitude and temperature cycling effects
p 393 N95-27509
- BORON-EPOXY COMPOSITES**
Evaluation of bonded boron/epoxy doublers for commercial aircraft aluminum structures
p 92 N95-14457
- Ultrasonic techniques for repair of aircraft structures with bonded composite patches
p 136 N95-19486
- Bonded composite repair of metallic aircraft components: Overview of Australian activities
p 392 N95-27505
- Status of bonded boron/epoxy doublers for military and commercial aircraft structures
p 393 N95-27506
- Bonded composite repair of thin metallic materials: Variable load amplitude and temperature cycling effects
p 393 N95-27509
- Design and structural validation of CF116 upper wing skin boron doubler
p 393 N95-27510
- Structural modification and repair of C-130 wing structure using bonded composites
p 394 N95-27512
- BOUNDARIES**
Aeroelastic stability of hingeless rotor blade in hover using large deflection theory
[BTN-94-EIX94441386616] p 183 A95-67347
- Unsteady aerodynamics of vortical flows: Early and recent developments
p 462 A95-88896
- Automatic grid generation procedure for complex aircraft configurations
[BTN-95-EIX95302729765] p 605 A95-94127
- Waveform bounding and combination techniques for direct drive testing
[AD-A284075] p 161 N95-19035
- Boundary-flow measurement methods for wall interference assessment and correction: Classification and review
p 163 N95-19262
- Transonic wind tunnel boundary interference correction
p 147 N95-19271
- A non-iterative grid deformation algorithm for computational fluid dynamics for aeroelasticity
[AD-A288298] p 436 N95-26418

BOUNDARY CONDITIONS

- Discrete shape sensitivity equations for aerodynamic problems
[BTN-94-EIX94451393721] p 88 A95-61720
- Kinetic theory in aerothermodynamics
[HTN-95-A0002] p 183 A95-67829
- Shock layers and boundary layers in hypersonic flows
[HTN-95-A0003] p 183 A95-67830
- Determination of wall boundary conditions for high-speed-ratio direct simulation Monte Carlo calculations
[BTN-95-EIX95182617457] p 267 A95-75728
- Observations on using experimental data as boundary conditions for computations
[BTN-95-EIX95182619103] p 321 A95-76588
- Nonreflective boundary conditions for high-order methods
[HTN-95-42328] p 371 A95-86157
- Boundary conditions for unsteady supersonic inlet analyses
[HTN-95-20829] p 544 A95-88090
- Operation of the adaptive-wall wind tunnel of TsAGI, Moscow
p 519 A95-88901
- Efficient mapping topology for turbine combustors with inclined slots/staggered holes
[BTN-95-EIX0616952745805] p 614 A95-94485
- A modular system for computational fluid dynamics
p 641 A95-95446
- A wall interference assessment and correction system
[NASA-CR-196940] p 58 N95-12228
- Laws of infrared similitude
[AD-A282209] p 62 N95-12426
- Studies on the flow induced by an oscillating airfoil in a uniform stream
[PB94-204450] p 40 N95-13250
- Computational aerodynamics based on the Euler equations
[AGARD-AG-325] p 72 N95-14264
- 2-D airfoil tests including side wall boundary layer measurements
p 158 N95-17847
- Data from the GARTEur (AD) Action Group 02 airfoil CAST 7/DOA1 experiments
p 111 N95-17856
- Low aspect ratio wing experiment
p 113 N95-17865
- A spectrally accurate boundary-layer code for infinite swept wings
[NASA-CR-195014] p 159 N95-18042
- Wall correction method with measured boundary conditions for low speed wind tunnels
p 164 N95-19263
- Determination of solid/porous wall boundary conditions from wind tunnel data for computational fluid dynamics codes
p 164 N95-19266
- Analysis of test section sidewall effects on a two dimensional airfoil: Experimental and numerical investigations
p 165 N95-19276
- On supersonic-inlet boundary-layer bleed flow
[NASA-CR-195426] p 202 N95-19769
- Sensitivity of combustion-acoustic instabilities to boundary conditions for premixed gas turbine combustors
[NASA-TM-106890] p 289 N95-23550
- Solution of the Navier-Stokes equations on locally refined Cartesian meshes using state-vector splitting
p 553 N95-29197
- Development of a rotary wing Navier-Stokes CFD code based on TLNS3D code
[AD-A290421] p 554 N95-29387
- Grid resolution and turbulent inflow boundary condition recommendations for NPARC calculations
[NASA-TM-106959] p 482 N95-30253
- Probabilistic reliability modeling of fatigue on the H-46 tie bar
[AD-A289926] p 607 N95-30927
- Review of combustion-acoustic instabilities
[NASA-TM-107020] p 705 N95-32930
- BOUNDARY ELEMENT METHOD**
- Linear instability waves in supersonic jets confined in circular and non-circular ducts
[BTN-94-EIX94341340068] p 103 A95-63520
- Coupled FEM-BEM approach for mean flow effects on vibro-acoustic behavior of planar structures
[BTN-95-EIX95152577587] p 263 A95-73495
- Computational methods in applied sciences; European Computational Fluid Dynamics Conference, 1st, Brussels, Belgium, Sept. 7-11, 1992
[ISBN 0-444-89795-X] p 539 A95-87552
- Optimum aerodynamic design of aircraft fuselage using boundary element method
p 473 A95-91514
- Calculation for aerodynamic characteristics on delta wing with leading-edge separated vortex effect using boundary element method
p 684 N95-34524
- Grid generation around airfoil with a flap using boundary element method
p 686 N95-34552

BOUNDARY INTEGRAL METHOD

- Direct boundary integral equations method to subsonic flow with circulation past thin airfoils in ground effect
[BTN-95-EIX95242673940] p 365 A95-82224
- BOUNDARY LAYER COMBUSTION**
- Numerical simulation of three-dimensional hypersonic reacting flows over blunt bodies with catalytic surface
[HTN-95-61184] p 539 A95-87557
- Propulsion research concerning SFRJ-motors
[PB94-179520] p 14 N95-10083
- Service and physical properties of liquid-jet fuels
p 151 N95-16256
- BOUNDARY LAYER CONTROL**
- Lag model for turbulent boundary layers over rough bleed surfaces
[BTN-94-EIX944413860981] p 208 A95-68165
- Flow structure in the wake of a wishbone vortex generator
[BTN-95-EIX95142553044] p 304 A95-73454
- Separation control on high-lift airfoils via micro-vortex generators
[BTN-95-EIX95152582326] p 265 A95-73529
- Forebody flow control on a full-scale F/A-18 aircraft
[BTN-95-EIX95152582333] p 281 A95-73535
- Flow structure in the lee of an inclined 6:1 prolate spheroid
[BTN-94-EIX95011441127] p 348 A95-81027
- Active boundary-layer control in diffusers
[HTN-95-42580] p 458 A95-87210
- Numerical model of boundary-layer control using air-jet generated vortices
[HTN-95-42581] p 459 A95-87211
- Computational study of boundary layer control for improving airfoil performance
[SAE PAPER 932513] p 466 A95-89186
- Low Reynolds number laminar separation bubble control using a backward facing step
[SAE PAPER 932572] p 467 A95-90061
- On the differences between the effect of acoustic perturbation and unsteady bleed in controlling flow separation over a cylinder
[SAE PAPER 932573] p 467 A95-90062
- Buffeting tests in a cryogenic windtunnel
[HTN-95-92833] p 470 A95-90751
- High subsonic and high Reynolds number wind tunnel tests of two-dimensional natural-laminar-flow airfoils with suction boundary layer control
p 472 A95-91508
- An experimental study on supersonic laminar flow control
p 473 A95-91523
- Hybrid laminar flow over wings enhanced by continuous boundary layer suction
[SAE PAPER 931386] p 587 A95-93662
- Control of unsteady separated flow associated with the dynamic stall of airfoils
[NASA-CR-197024] p 74 N95-14613
- Optimum aerodynamic design via boundary control
p 127 N95-16565
- Parametric study on laminar flow for finite wings at supersonic speeds
[NASA-TM-108852] p 116 N95-18101
- On supersonic-inlet boundary-layer bleed flow
[NASA-CR-195426] p 202 N95-19769
- Flow coefficient behavior for boundary layer bleed holes and slots
[NASA-TM-106846] p 244 N95-19953
- Supersonic laminar flow control research
[NASA-CR-196049] p 249 N95-21340
- Experimental investigations of on-demand vortex generators
p 250 N95-22451
- Performance characterization of a highly-offset diffuser with and without blowing vortex generator jets
[AD-A289334] p 375 N95-26901
- Comparative performance tests on the Mod-2, 2.5-mW wind turbine with and without vortex generators
p 377 N95-27978
- A procedure for automating CFD simulations of an inlet-bleed problem
p 552 N95-28768
- Pressure based high order TVD methodology for dynamic stall control
[AD-A290149] p 479 N95-29316
- Effects of cavity bleed and its configuration on aerodynamic characteristics of supersonic internal flow
[NAL-TR-1247] p 594 N95-31715
- Control of unsteady separated flow associated with the dynamic stall of airfoils
[NASA-CR-198972] p 594 N95-32193
- Numerical simulation of supersonic flow using a new analytical bleed boundary condition
[NASA-CR-198368] p 697 N95-33208
- BOUNDARY LAYER EQUATIONS**
- Predicting stall and post-stall behavior of airfoils at low mach numbers
[BTN-95-EIX95262694297] p 365 A95-85468
- A spectrally accurate boundary-layer code for infinite swept wings
[NASA-CR-195014] p 159 N95-18042

- An approximate theoretical method for modeling the static thrust performance of non-axisymmetric two-dimensional convergent-divergent nozzles
[NASA-CR-195050] p 273 N95-23193
- Supersonic quiet-tunnel development for laminar-turbulent transition research
[NASA-CR-198040] p 340 N95-24302
- Supersonic coaxial jet noise predictions
[NASA-TM-106917] p 451 N95-26801
- BOUNDARY LAYER FLOW**
- Supersonic and hypersonic shock/boundary-layer interaction database
[BTN-94-EIX94441386604] p 182 A95-67335
- Design and operation of a supersonic annular flow facility
[BTN-94-EIX94441386624] p 183 A95-68173
- Aerodynamic mechanism of galloping
[BTN-94-EIX94371347709] p 219 A95-69968
- Analytical study of the neutral stability of a model hypersonic boundary layer
[BTN-95-EIX95152577589] p 263 A95-73493
- Flow visualization studies on sidewall effects in two-dimensional transonic airfoil testing
[BTN-95-EIX95152582313] p 264 A95-73516
- Flow study of supersonic wing-nacelle configuration
[BTN-95-EIX95152582344] p 266 A95-73546
- Instability of three-dimensional boundary layers due to streamline curvature
[HTN-95-61070] p 430 A95-83654
- Free convection past a uniform flux surface inclined at a small angle to the horizontal
[HTN-95-42213] p 430 A95-84029
- Transition correlations in three-dimensional boundary layers
[HTN-95-51648] p 432 A95-85030
- Boundary layer studies over an S-blade
[HTN-95-92261] p 434 A95-85305
- Predicting stall and post-stall behavior of airfoils at low mach numbers
[BTN-95-EIX95262694297] p 365 A95-85468
- High angle-of-attack airfoil performance improvement by internal acoustic excitation
[HTN-95-42347] p 372 A95-86176
- Adaptive wall technology for minimization of wind tunnel boundary interferences - where are we now?
p 519 A95-88903
- Compressible Navier-Stokes calculations of the flow over airfoil sections. Comparisons of 1st and 2nd order turbulence models
[SAE PAPER 932510] p 546 A95-89183
- Nonlinear analysis of the Gortler instability
[BTN-95-EIX95282705926] p 455 A95-89664
- Evaluation of a model for boundary-layer induced noise in aircraft
p 574 A95-90102
- Turbulence characteristics of supersonic boundary layer past a backward facing step
[AIAA PAPER 95-6126] p 470 A95-90447
- Chemically reacting non-equilibrium boundary layers in air breathing propulsion systems
[AIAA PAPER 95-6139] p 512 A95-90456
- Measurement in laminar and transitional boundary-layer flows on concave surface
[BTN-95-EIX95282711333] p 632 A95-92408
- Effects of free-stream turbulence intensity on a boundary layer recovering from concave curvature effects
[BTN-95-EIX95282710058] p 632 A95-92471
- 3-D Navier-Stokes analysis of crossing glancing shocks/turbulent boundary layer interactions
[BTN-95-EIX95302729768] p 636 A95-94130
- Analysis of low Reynolds number airfoil flows
[BTN-95-EIX0619952748183] p 590 A95-94476
- Computational analysis in support of the SSTO flowpath test
[NASA-TM-106757] p 89 N95-13665
- Mach number, flow angle, and loss measurements downstream of a transonic fan-blade cascade
[AD-A280907] p 108 N95-16824
- Experiments in the trailing edge flow of an NLR 7702 airfoil
p 110 N95-17853
- Data from the GARTEur (AD) Action Group 02 airfoil CAST 7/DOA1 experiments
p 111 N95-17856
- The stability of two-phase flow over a swept-wing
[NASA-CR-194994] p 159 N95-18190
- Effect of crossflow on Goertler instability in incompressible boundary layers
[NASA-CR-195007] p 159 N95-18193
- Solution of Navier-Stokes equations using high accuracy monotone schemes
p 161 N95-19019
- Boundary-flow measurement methods for wall interference assessment and correction: Classification and review
p 163 N95-19262
- Viscous flow past aerofoils axisymmetric bodies and wings
p 123 N95-19457
- On supersonic-inlet boundary-layer bleed flow
[NASA-CR-195426] p 202 N95-19769

- Experiments on the flow field physics of confluent boundary layers for high-lift systems
[NASA-CR-197318] p 224 N95-21343
- Acoustics of laminar boundary layers breakdown
p 251 N95-22455
- Active control of panel vibrations induced by a boundary layer flow
[NASA-CR-197867] p 273 N95-23182
- Response of multi-panel assembly to noise from a jet in forward motion
[NASA-CR-198164] p 442 N95-28673
- The effects of three-dimensional imposed disturbances on bluff body near wake flows: Effects of taper and splitter plates on the near wake characteristics of a circular cylinder in uniform and shear flow
[AD-A292113] p 477 N95-28921
- Effects of elevated free-stream turbulence and streamwise acceleration on flow and thermal structures in transitional boundary layers p 556 N95-29729
- Numerical simulations of the flow in the HYPULSE expansion tube
[NASA-TM-110357] p 523 N95-30228
- A numerical study of the small scale wing-body junction problem p 482 N95-30235
- An interacting boundary layer method for unsteady compressible flows p 557 N95-30290
- Advanced k-epsilon modeling of heat transfer
[NASA-CR-4679] p 648 N95-31423
- BOUNDARY LAYER SEPARATION**
- An experimental investigation of wing tip turbulence with applications to aerodynamic
[AIAA PAPER 86-1918] p 1 A95-60164
- Oscillating airfoil compressible dynamic stall studies
[HTN-94-00704] p 3 A95-60183
- Elliptic tip effects on the vortex wake of an axisymmetric body at incidence
[BTN-94-EIX94441386612] p 208 A95-67343
- Experimental study of three-dimensional separation
[BTN-94-EIX94441385752] p 179 A95-68216
- Computation of the poststall behavior of a circulation controlled airfoil
[BTN-95-EIX95152582320] p 264 A95-73523
- Experimental investigation of the flowfield about an upswep afterbody
[BTN-95-EIX95152582321] p 265 A95-73524
- Separation control on high-lift airfoils via micro-vortex generators
[BTN-95-EIX95152582326] p 265 A95-73529
- Study of an airfoil with a flap and spoiler
[BTN-95-EIX95152582327] p 265 A95-73530
- Computational study of plume-induced separation on a hypersonic powered model
[BTN-95-EIX95152582346] p 266 A95-73548
- Scaling of incipient separation in supersonic/transonic speed laminar flows
[BTN-95-EIX95182619104] p 269 A95-76589
- Aerodynamics of a finite wing with simulated ice
[BTN-95-EIX95182619227] p 270 A95-76653
- Experimental study of flow separation on an oscillating flap at Mach 2.4
[BTN-95-EIX95222650792] p 329 A95-79248
- Two-dimensional unsteady leading-edge separation on a pitching airfoil
[HTN-95-81628] p 461 A95-87676
- Effects of time scales on lift of airfoils in an unsteady stream
[HTN-95-81643] p 542 A95-87691
- Fluctuating wall pressures near separation in highly swept turbulent interactions
[HTN-95-20823] p 543 A95-88084
- Symposium on Aerodynamics & Aeroacoustics, Tucson, AZ, Mar. 1-2, 1993
[ISBN 981-02-1732-3] p 462 A95-88892
- Determining unsteady 2D AND 3D boundary layer separation p 462 A95-88898
- An overview of static and dynamic airfoil performance
[SAE PAPER 931228] p 463 A95-88960
- On the differences between the effect of acoustic perturbation and unsteady bleed in controlling flow separation over a cylinder
[SAE PAPER 932573] p 467 A95-90062
- Numerical design methods for transonic NLF configurations p 471 A95-91498
- Vortex lattice method simulation of unsteady flow due to wing/external store combination p 471 A95-91499
- Modelling 2D separation from a high lift airfoil with a non-linear eddy-viscosity model and second-moment closure
[HTN-95-C0005] p 585 A95-93393
- An educational introduction to transonic compressor stage design principles
[SAE PAPER 931393] p 613 A95-93668
- The application of potential CFD methods to helicopter hover flows
[ISBN 1-879921-01-4] p 587 A95-93747
- 2-D and 3-D numerical simulation of a supersonic inlet flowfield p 641 A95-95457
- Wing-body juncture flows
[AD-A281526] p 106 N95-16099
- Time accurate computation of unsteady inlet flows with a dynamic flow adaptive mesh
[AD-A285498] p 157 N95-16736
- Mach number, flow angle, and loss measurements downstream of a transonic fan-blade cascade
[AD-A280907] p 108 N95-16824
- Low-speed surface pressure and boundary layer measurement data for the NLR 7301 airfoil section with trailing edge flap p 111 N95-17855
- Three-dimensional boundary layer and flow field data of an inclined prolate spheroid p 158 N95-17867
- Ellipsoid-cylinder model p 158 N95-17869
- Supersonic vortex flow around a missile body p 114 N95-17870
- Test data on a non-circular body for subsonic, transonic and supersonic Mach numbers p 158 N95-17871
- Experimental investigation of the vortex flow over a 76/60-deg double delta wing p 114 N95-17874
- Wind tunnel test on a 65 deg delta wing with rounded leading edges: The International Vortex Flow Experiment p 114 N95-17875
- Subsonic flow around US-orbiter model FALKE in the DNW p 115 N95-17877
- Sectional prediction of 3D effects for separated flow on rotating blades p 117 N95-18503
- Theoretical investigations of shock/boundary layer interactions on a $Ma(\infty) = 8$ waverider
[DLR-FB-94-12] p 119 N95-18910
- Control of flow separation in airfoil/wing design applications p 274 N95-23294
- Performance characterization of a highly-offset diffuser with and without blowing vortex generator jets
[AD-A289334] p 375 N95-26901
- A procedure for automating CFD simulations of an inlet-bleed problem p 552 N95-28768
- Unsteadiness of shock-induced turbulent boundary layer separation. An inherent feature of turbulent flow or solely a wind tunnel phenomenon p 554 N95-29228
- [AD-A290367] p 554 N95-29228
- Vorticity dynamics and control of dynamic stall
[AD-A286858] p 620 N95-31400
- Investigating the use of smart acoustically active surfaces for flow separation control in turbomachinery
[AD-A292819] p 648 N95-31443
- Control of unsteady separated flow associated with the dynamic stall of airfoils
[NASA-CR-198972] p 594 N95-32193
- Calculation for aerodynamic characteristics on delta wing with leading-edge separated vortex effect using boundary element method p 684 N95-34524
- BOUNDARY LAYER STABILITY**
- Instability of three-dimensional boundary layers due to streamline curvature
[HTN-95-61070] p 430 A95-83654
- Quiet-flow Ludwig tube for high-speed transition research
[BTN-95-EIX95262694309] p 370 A95-85480
- Nonlinear analysis of the Gortler instability
[BTN-95-EIX95282705926] p 455 A95-89664
- Effects of free-stream turbulence intensity on a boundary layer recovering from concave curvature effects
[BTN-95-EIX95282710058] p 632 A95-92471
- Numerical study of Gortler instability: Application to the design of a quiet supersonic wind tunnel
[PB94-184801] p 21 N95-10844
- Parametric study on laminar flow for finite wings at supersonic speeds
[NASA-TM-108852] p 116 N95-18101
- Effect of crossflow on Goertler instability in incompressible boundary layers
[NASA-CR-195007] p 159 N95-18193
- Computational studies of laminar to turbulence transition
[AD-A285622] p 248 N95-21146
- Supersonic laminar flow control research
[NASA-CR-196049] p 249 N95-21340
- Unsteadiness of shock-induced turbulent boundary layer separation. An inherent feature of turbulent flow or solely a wind tunnel phenomenon
[AD-A290367] p 554 N95-29228
- BOUNDARY LAYER TRANSITION**
- Shock layers and boundary layers in hypersonic flows
[HTN-95-A0003] p 183 A95-67830
- Flight experience with lightweight, low-power miniaturized instrumentation systems
[BTN-95-EIX95062487522] p 180 A95-69230
- Hypersonic rarefied flow past spheres including wake structure
[BTN-95-EIX95152583250] p 305 A95-73551
- Scaling of incipient separation in supersonic/transonic speed laminar flows
[BTN-95-EIX95182619104] p 269 A95-76589
- Multiple instabilities of three-dimensional boundary layers along a concave wall
[HTN-95-71126] p 429 A95-83487
- Transition correlations in three-dimensional boundary layers
[HTN-95-51648] p 432 A95-85030
- Surface interference in Rayleigh scattering measurements near forebodies
[HTN-95-51670] p 433 A95-85052
- Quiet-flow Ludwig tube for high-speed transition research
[BTN-95-EIX95262694309] p 370 A95-85480
- Computational study of boundary layer control for improving airfoil performance
[SAE PAPER 932513] p 466 A95-89186
- Nonlinear analysis of swept wing transitional boundary layers
[SAE PAPER 932515] p 466 A95-89188
- Preliminary study on the fixed transition technique for a shock tube transonic airfoil flow
[BTN-95-EIX95282705928] p 455 A95-89663
- Boundary-layer--transition--and--global--skin--friction measurement with an oil-fringe imaging technique
[SAE PAPER 932550] p 547 A95-90054
- Drag reduction in a rectangular duct using riblets
[HTN-95-01091] p 468 A95-90277
- Effect of spherical roughness elements upon transition of a 3-D boundary layer
[HTN-95-92835] p 471 A95-90753
- The use of hot film for the investigation of boundary-layer transition
[CONGRESS PAPER C428-9-199] p 475 A95-91697
- Measurement in laminar and transitional boundary-layer flows on concave surface
[BTN-95-EIX95282711333] p 632 A95-92408
- Transonic flight test of a laminar flow leading edge with surface excrescences
[NASA-TM-4597] p 9 N95-11158
- Empirical refinements to boundary layer transition noise models p 28 N95-11262
- Wind tunnel test on a 65 deg delta wing with a sharp or rounded leading edge: The international vortex flow experiment p 114 N95-17872
- Hypersonic wind tunnel test techniques
[AD-A284057] p 118 N95-18663
- Application of Direct and Large Eddy Simulation to Transition and Turbulence
[AGARD-CP-551] p 248 N95-21061
- Investigation of shear layer transition using various turbulence models p 248 N95-21096
- Computational studies of laminar to turbulence transition
[AD-A285622] p 248 N95-21146
- Acoustic receptivity due to weak surface inhomogeneities in adverse pressure gradient boundary layers
[NASA-TM-4577] p 249 N95-21258
- Supersonic laminar flow control research
[NASA-CR-196049] p 249 N95-21340
- Acoustics of laminar boundary layers breakdown p 251 N95-22455
- Crossflow instability control on a swept-wing: Preliminary studies p 274 N95-23283
- High-lift flow-physics flight experiments on a subsonic civil transport aircraft (B737-100) p 275 N95-23333
- Supersonic quiet-tunnel development for laminar-turbulent transition research
[NASA-CR-198040] p 340 N95-24302
- Experimental studies on boundary-layer transition on a reentry vehicle at transonic and supersonic speeds
[ISAS-659] p 555 N95-29712
- Effects of elevated free-stream turbulence and streamwise acceleration on flow and thermal structures in transitional boundary layers p 556 N95-29729
- Boundary-layer transition and global skin friction measurement with an oil-fringe imaging technique
[NASA-CR-198814] p 557 N95-30224
- BOUNDARY LAYERS**
- Observations of fluxes and inland breezes over a heterogeneous surface
[HTN-95-80258] p 212 A95-66315
- Supersonic and hypersonic shock/boundary-layer interaction database
[BTN-94-EIX94441386604] p 182 A95-67335
- Laplace interaction law for the computation of viscous airfoil flow in low- and high-speed aerodynamics
[BTN-95-EIX95142553037] p 263 A95-73461
- Simulating heat addition via mass addition in constant area compressible flows
[BTN-95-EIX95182619100] p 307 A95-76585
- Scaling of incipient separation in supersonic/transonic speed laminar flows
[BTN-95-EIX95182619104] p 269 A95-76589

- Symposium on Aerodynamics & Aeroacoustics, Tucson, AZ, Mar. 1-2, 1993
 [ISBN 981-02-1732-3] p 462 A95-88892
 Supersonic and hypersonic shock/boundary-layer interaction database p 463 A95-88969
 Kinetic heating in hypersonic flight
 [CONGRESS PAPER C428-3-056] p 475 A95-91674
 Experimental investigation of the flow in diffusers behind an axial flow compressor p 632 A95-92472
 Hybrid laminar flow over wings enhanced by continuous boundary layer suction p 587 A95-93662
 Leading-edge sweepback and shape effects on fin-induced fluctuating pressures p 636 A95-94067
 Application of scramjet engine technology to the design of ram accelerator projectiles p 19 N95-10282
 Aerodynamic shape optimization p 128 N95-16572
 2-D airfoil tests including side wall boundary layer measurements p 158 N95-17847
 Low-speed surface pressure and boundary layer measurement data for the NLR 7301 airfoil section with trailing edge flap p 111 N95-17855
 Measurements of the flow over a low aspect-ratio wing in the Mach number range 0.6 to 0.87 for the purpose of validation of computational methods. Part 1: Wing design, model construction, surface flow. Part 2: Mean flow in the boundary layer and wake, 4 test cases p 112 N95-17860
 Open Skies project computational fluid dynamic analysis [AD-A285928] p 223 N95-19991
 Optimized design of a hypersonic nozzle p 297 N95-23304
 Three-dimensional interaction of wake/boundary-layer and vortex/boundary-layer data report [CUED/A-AEREO/TR-23] p 329 N95-24210
 Transport phenomena and interfacial kinetics in multiphase combustion systems [AD-A288297] p 418 N95-26417
 Dynamic stall of a NACA 0012 airfoil in laminar flow p 479 N95-29243
 Grid resolution and turbulent inflow boundary condition recommendations for NPARC calculations [NASA-TM-106959] p 482 N95-30253
 A numerical study of the starting process in a hypersonic shock tunnel p 626 N95-30493
- BOUNDARY LUBRICATION**
 Lubricant evaluation and performance, 2 [AD-A279144] p 242 N95-21969
- BOUNDARY VALUE PROBLEMS**
 Discrete shape sensitivity equations for aerodynamic problems [BTN-94-EIX94451393721] p 88 A95-61720
 Quality estimates and stretched meshes based on Delaunay triangulations [HTN-95-42575] p 564 A95-87205
 Effect of initial conditions on the response of nonlinear dynamical systems with the application to helicopter rotor dynamics [ISBN 1-879921-01-4] p 605 A95-93731
 PREDICHTAT: First order performance calculations of windturbine rotors using the method of the acceleration potential [PB95-206454] p 564 N95-30200
- BOW WAVES**
 Measurement by coherent anti-Stokes Raman scattering in the R5Ch hypersonic wind tunnel [BTN-95-EIX95112523811] p 188 A95-69322
 An extension of the continuum model by Grad's thirteen moment equations for hypersonic rarefied flows p 478 N95-29118
 Analysis of planar laser-induced fluorescence images obtained during shakedown testing of the AEDC impulse facility [AD-A293237] p 646 N95-30906
- BOX BEAMS**
 Twisting smartly in the wind [BTN-95-EIX95041503093] p 184 A95-68353
 Experimental evaluation of a box beam specifically tailored for chordwise deformation [BTN-95-EIX95182619088] p 283 A95-75773
 An investigation of the accuracy of FEM analysis of a graphite epoxy box beam [SAE PAPER 931221] p 543 A95-88011
 Flutter analysis of composite box beams [NASA-CR-197931] p 294 N95-23392
 C-130 Advanced Technology Center wing box conceptual design/cost study p 423 N95-28437
 Structural testing of the technology integration box beam p 441 N95-28467
 Technology integration box beam failure study p 441 N95-28468
- Technology integration box beam failure study p 552 N95-28847
 Development of a composite tailoring procedure for airplane wing [NASA-CR-199081] p 691 N95-32928
- BRAGG CELLS**
 A three-dimensional orthogonal laser velocimeter for the NASA Ames 7- by 10-foot wind tunnel [NASA-TM-108864] p 249 N95-21323
- BRAIDED COMPOSITES**
 Through-the Thickness(R) braided composites for aircraft applications p 421 N95-28273
 Characterization and manufacture of braided composites for large commercial aircraft structures p 426 N95-28478
 Mechanical characterization of 2D, 2D stitched, and 3D braided/RTM materials p 535 N95-29038
- BRAKES (FOR ARRESTING MOTION)**
 Computational flow predictions for hypersonic drag devices p 37 N95-11967
- BRAKING**
 NASA evaluation of Type 2 chemical depositions --- effects of deicer deposition on aircraft tire friction performance [SAE PAPER 932582] p 495 A95-90086
- BRANCHING (MATHEMATICS)**
 Assessment of technology for aircraft development [BTN-95-EIX0619952748181] p 606 A95-94474
- BRAZING**
 Braze repair possibilities for hot section gas turbine parts p 201 N95-19677
- BREADBOARD MODELS**
 Eddy current for detecting second layer cracks under installed fasteners [AD-A282412] p 158 N95-17507
 Eddy current for detecting second-layer cracks under installed fasteners [AD-A279871] p 244 N95-20414
 Characterization of corrosion and development of a breadboard of a D sight aircraft inspection system, phase 1 [AD-A288347] p 380 N95-26527
 Integrated X-ray testing of the electro-optical breadboard model for the XMM reflection grating spectrometer [DE95-008829] p 644 N95-30507
 A highly reliable, high performance open avionics architecture for real time Nap-of-the-Earth operations p 693 N95-32497
- BREAKING**
 Amplification and breaking of atmospheric gravity waves p 675 A95-93552
- BRIGHTNESS TEMPERATURE**
 Behavior of an inversion-based precipitation retrieval algorithm with high-resolution AMPR measurements including a low-frequency 10.7-GHz channel [HTN-95-70134] p 252 A95-70656
 Water vapor continuum absorption in mid-latitudes: Aircraft measurements and model comparisons [HTN-95-40756] p 252 A95-71186
 Aircraft measurements of water vapour continuum absorption at millimetre wavelengths [HTN-95-90884] p 253 A95-72393
 Airborne imaging radiometer scan simulation [BTN-95-EIX95332753018] p 638 A95-94793
 TIMS observations of surface emissivity in HAPEX-Sahel p 709 N95-33799
- BRISTOL-SIDDELEY BS 53 ENGINE**
 An analysis of the costs and benefits in improving F402-RR-406A High Pressure Turbine, second stage blades under the aircraft engine Component Improvement Program (CIP) [AD-A285127] p 197 N95-19595
- BROADBAND**
 A prediction method for broadband shock associated noise from supersonic rectangular jets p 574 A95-90100
 Impulse radiating antennas p 548 A95-90920
 Polarization diverse ultra-wideband antenna technology p 548 A95-90924
 Scattering of short em-pulses by simple and complex targets using impulse radar p 486 A95-90953
 Ultra-wideband electromagnetic target identification p 486 A95-90955
 Broadband polarization-transfer experiments for rotating solids [GTN-95-0009261494012091-58] p 579 A95-92319
 Active control of complex noise problems using a broadband, multichannel controller p 29 N95-11271
 Broadband, wide-area active control of sound radiated from vibrating structures using local surface-mounted radiation suppression devices p 30 N95-11283
 Measurement and prediction of broadband noise from large horizontal axis wind turbine generators p 451 N95-27990
 Anechoic wind tunnel study of turbulence effects on wind turbine broadband noise p 451 N95-27992
- UHB engine fan broadband noise reduction study [NASA-CR-198357] p 580 N95-29641
- BROADCASTING**
 Effect of broadcast and precise ephemerides on estimates of the frequency stability of GPS Navstar clocks [BTN-95-EIX95112522530] p 190 A95-69333
 GPS-Squitter interference analysis [AD-A293690] p 689 N95-33480
- BRUSH SEALS**
 Brush seal performance and durability issues based on T-700 engine test results [NASA-TM-106502] p 22 N95-11483
 Brush seals for turbine engine fuel conservation p 59 N95-13595
 Air Force seal activities p 60 N95-13600
- BUBBLES**
 Low Reynolds number laminar separation bubble control using a backward facing step [SAE PAPER 932572] p 467 A95-90061
 Low-speed surface pressure and boundary layer measurement data for the NLR 7301 airfoil section with trailing edge flap p 111 N95-17855
- BUCKLING**
 Buckling and vibration analysis of laminated panels using VICONOPT [PAPER-1746] p 230 A95-72580
 Shear buckling response of tailored composite plates [HTN-95-51680] p 418 A95-85062
 Buckling and postbuckling of composite structures [HTN-95-71387] p 528 A95-87605
 Failure behaviour of carbon fiber/epoxy composites in pin-ended buckling and bending tests [HTN-95-71388] p 528 A95-87606
 Optimum design of composite stiffened wing panels - a parametric study [HTN-95-01088] p 496 A95-90274
 Cabin-fuselage-wing structural design concept with engine installation [NASA-CR-197172] p 49 N95-12993
 Shear buckling analysis of a hat-stiffened panel [NASA-TM-4644] p 158 N95-17490
 Design and evaluation of a foam-filled hat-stiffened panel concept for aircraft primary structural applications [NASA-TM-109175] p 346 N95-26251
 Effect of low-speed impact damage and damage location on behavior of composite panels p 426 N95-28481
 Fundamental concepts in the suppression of delamination buckling by stitching p 426 N95-28486
 Damage tolerance of a geodesically stiffened advanced composite structural concept for aircraft structural applications p 399 N95-28487
 Buckling analysis of curved composite sandwich panels subjected to inplane loadings p 533 N95-28845
 ISPAN (Interactive Stiffened Panel Analysis): A tool for quick concept evaluation and design trade studies p 533 N95-28846
 Severe edge effects and simple complimentary interior solutions for thin-walled anisotropic and composite structures [AD-A290645] p 555 N95-29562
- BUDGETING**
 Cuts endanger airborne research --- NASA Ames Research Center Reorganization [HTN-95-20602] p 443 A95-84783
- BUFFETING**
 Interaction of a streamwise vortex with a thin plate: A source of turbulent buffeting [BTN-95-EIX95042474398] p 209 A95-68302
 Computational analysis of buffet alleviation in viscous transonic flow over a porous airfoil [BTN-95-EIX95262694321] p 366 A95-85492
 Buffeting tests in a cryogenic windtunnel [HTN-95-92833] p 470 A95-90751
 Computations of unsteady aerodynamic loads around oscillating wings. Part 1: Formulation [PB94-180049] p 7 N95-10136
 Computations of unsteady aerodynamic loads around oscillating wings. Part 2: Computed results and discussions [PB94-180056] p 7 N95-10137
 Flow-visualization study of the X-29A aircraft at high angles of attack using a 1/48-scale model [NASA-TM-104268] p 8 N95-10858
 Pressure measurements on an F/A-18 twin vertical tail in buffeting flow. Volume 3: Buffet power spectral densities [AD-A281444] p 36 N95-11829
 Pressure measurements on an F/A-18 twin vertical tail in buffeting flow. Volume 2: Steady and unsteady RMS pressure data [AD-A281581] p 76 N95-15465
 Pressure measurements on an F/A-18 twin vertical tail in buffeting flow. Volume 4, part 2: Buffet cross spectral densities [AD-A285555] p 143 N95-18641

- Pressure measurements on an F/A-18 twin vertical tail in buffeting flow. Volume 4, part 1: Buffet cross spectral densities
[AD-A285593] p 237 N95-21214
- Pressure measurements on an F/A-18 twin vertical tail in buffeting flow. Volume 1: Wind tunnel test summary
[AD-A279126] p 225 N95-21877
- Preliminary identification of buffet problems in high speed civil transport p 294 N95-23319
- BULGING**
Nonlinear bulging factor based on R-curve data p 94 N95-14476
- BULKHEADS**
Development of composite carrythrough bulkhead p 423 N95-28438
- BUNCHING**
Effects of satellite bunching on the probability of collision in geosynchronous orbit
[BTN-95-EIX95152583276] p 298 A95-73577
- BUNDLES**
Fiber-optic rotary joint with bundle collimator assemblies
[AD-D016504] p 258 N95-21673
- BUOYANCY**
Stationary premixed flames in spherical and cylindrical geometries
[HTN-95-42336] p 418 A95-86165
- Activated buoyancy propulsion = Paradox Power (tm)
[TABES PAPER 94-619] p 74 N95-14646
- Investigation of a thermal buoyancy effect on the drag of half models tested in the ARA Transonic Wind Tunnel (ARA-MEMO-407) p 222 N95-19946
- BURGER EQUATION**
Aeroacoustic model for weak shock waves based on Burgers equation
[BTN-95-EIX95182619076] p 269 A95-75761
- Effect of stratification and geometrical spreading on sonic boom rise time p 75 N95-14880
- BURN-IN**
Assuring Known Good Die (KGD) for reliable, cost effective MCMs p 246 N95-20644
- BURNING RATE**
Gas turbine preburner-combustor performance during operation with air-water mixture
[DOT/FAA/CT-93/52] p 83 N95-15683
- Studies on high pressure and unsteady flame phenomena
[AD-A284126] p 152 N95-18410
- BUSHINGS**
Dynamic modelling and response characteristics of a magnetic bearing rotor system with auxiliary bearings p 703 N95-32692
- BY-PRODUCTS**
Laboratory evaluation of a reactive baffle approach to NOx control
[AD-A283802] p 255 N95-19921
- BYPASS RATIO**
High bypass separate flow exhaust system improved thrust efficiency by modifying the aft centerbody
[SAE PAPER 932622] p 511 A95-90083
- Fan noise research at NASA p 28 N95-11260
- Ultra-high bypass ratio jet noise
[NASA-CR-195394] p 100 N95-14610
- Wave rotor-enhanced gas turbine engines
[NASA-TM-106998] p 615 N95-30517
- BYPASSES**
A full Navier-Stokes analysis of subsonic diffuser of a bifurcated 70/30 supersonic inlet for high speed civil transport application
[NASA-TM-106637] p 8 N95-10820
- C**
- C (PROGRAMMING LANGUAGE)**
Noise modeling for MOAs and ranges p 32 N95-11322
- C BAND**
Final results of the weather testing component of the Terminal Doppler Weather Radar operational test and evaluation p 658 A95-93471
- C++ (PROGRAMMING LANGUAGE)**
The navigation toolkit
[NASA-CR-197290] p 229 N95-22161
- C-130 AIRCRAFT**
Scattering of short em-pulses by simple and complex targets using impulse radar p 486 A95-90953
- C-130 Advanced Technology Center wing box conceptual design/cost study p 423 N95-28437
- Technology integration box beam failure study p 552 N95-28847
- Flying ambulances: The approach of a small air force to long distance aeromedical evacuation of critically injured patients p 568 N95-29618
- C-135 AIRCRAFT**
Dynamic imaging and RCS measurements of aircraft
[BTN-95-EIX95202637582] p 347 A95-78576
- Computational aerodynamic analysis on the Open Skies aircraft
[SAE PAPER 932514] p 466 A95-89187
- KC-135 cockpit modernization study. Phase 1: Equipment evaluation
[AD-A284099] p 131 N95-18398
- An artificial corrosion protocol for lap-splices in aircraft skin p 152 N95-19482
- Development of repair processes and sources for C/KC-135 aircraft windows/windshields
[AD-A288348] p 367 N95-26629
- An analysis of the KC-135 three-person cockpit
[AD-A289540] p 390 N95-26873
- Two-phase flow research using the learjet apparatus
[NASA-TM-106814] p 438 N95-27854
- Computational Fluid Dynamics (CFD) analysis of a C-135 aircraft with a side-mounted splitter plate (with comparison to wind tunnel data)
[AD-A292029] p 553 N95-29187
- C-141 AIRCRAFT**
Service life extensions for the C-141
[BTN-95-EIX95112530749] p 193 A95-69295
- C-5 AIRCRAFT**
A generic telerobotics architecture for C-5 industrial processes
[AIAA PAPER 94-1264-CP] p 27 N95-11529
- Aircraft wake RCS measurement p 59 N95-13210
- CABIN ATMOSPHERES**
Condensing cycle air conditioning system
[SAE PAPER 932056] p 513 A95-91637
- What's next in commercial aircraft environmental control systems?
[SAE PAPER 932057] p 513 A95-91638
- CABLES (ROPES)**
Measurements of longitudinal static aerodynamic coefficients by the cable mount system
[NAL-TR-1226] p 331 N95-25761
- CADMIUM**
Cadmium plating replacements p 631 N95-31773
- CALCULUS OF VARIATIONS**
A brief survey of constrained mechanics and variational problems in terms of differential forms p 360 N95-25803
- CALIBRATING**
Aircraft electric field measurements: Calibration and ambient field retrieval
[HTN-95-90508] p 213 A95-67780
- Precise orbit determination with a short-arc technique — Abstract only p 240 A95-70543
- Pitot/static leak testing
[CONGRESS PAPER C428-9-035] p 508 A95-91696
- A short-term, high-resolution automated snowfall forecasting system p 666 A95-93510
- Non-contact calibration of a CNC riveting machine
[CONGRESS PAPER C428-32-075] p 583 A95-93618
- Inlet flow test calibration for a small axial compressor facility. Part 1: Design and experimental results
[NASA-TM-106719] p 16 N95-11005
- A new algorithm for five-hole probe calibration, data reduction, and uncertainty analysis
[NASA-TM-106458] p 38 N95-12378
- Strain gage selection in loads equations using a genetic algorithm
[NASA-CR-4597] p 48 N95-12831
- Dynamics of the McDonnell-Douglas Large Scale Dynamic Rig and dynamic calibration of the rotor balance
[NASA-TM-108855] p 65 N95-13891
- An investigation of polynomial calibrations methods for wind tunnel balances p 144 N95-16258
- Aeromechanics technology, volume 1. Task 1: Three-dimensional Euler/Navier-Stokes Aerodynamic Method (TEAM) enhancements
[AD-A285713] p 132 N95-18483
- Applications of the five-hole probe technique for flow field surveys at the Institute for Aerospace Research p 163 N95-19255
- 16-foot transonic tunnel test section flowfield survey
[NASA-TM-109157] p 238 N95-20669
- Design of a variable area diffuser for a 15-inch Mach 6 open-jet tunnel p 297 N95-23309
- Aircraft fuel system lightning protection design and qualification test procedures development
[AD-A288401] p 380 N95-26497
- Nonlinear calibration of an infrared radiometer
[AD-A292436] p 579 N95-28996
- A hybrid electronically scanned pressure module for cryogenic environments
[NASA-TM-110146] p 554 N95-29453
- Inlet flow test calibration for a small axial compressor rig. Part 2: CFD compared with experimental results
[NASA-TM-106999] p 514 N95-30007
- Integrated X-ray testing of the electro-optical breadboard model for the XMM reflection grating spectrometer
[DE95-008829] p 644 N95-30507
- Standardization of surface contamination analysis systems p 631 N95-31798
- In-flight radiometric calibration of AVIRIS in 1994 p 705 N95-33754
- CALIFORNIA**
A comparison of some aerodynamic resistance methods using measurements over cotton and grass from the 1991 California ozone deposition experiment
[HTN-95-11295] p 319 A95-77000
- CAMBER**
Investigation of the flow over a series of 14 percent-thick supercritical aerofoils with significant rear camber p 109 N95-17849
- The use of cowl camber and taper to reduce rotor/stator interaction noise
[NASA-CR-195421] p 323 N95-22675
- CAMBERED WINGS**
Lift analysis of a variable camber foil using the discrete vortex-blob method
[BTN-94-EIX94441386623] p 179 A95-68172
- Unsteady ground effects on aerodynamic coefficients of finite wings with camber
[BTN-95-EIX95182619233] p 271 A95-76659
- Variable camber geometry for transport aircraft wings
[CONGRESS PAPER C428-35-061] p 603 A95-93626
- CAMERAS**
Passive millimeter wave camera for aircraft landing in low visibility conditions
[BTN-95-EIX95292721321] p 609 A95-92513
- Computer-aided light sheet flow visualization using photogrammetry
[NASA-TP-3416] p 26 N95-10859
- Passive MMW camera for low visibility landings p 59 N95-13215
- Passive range measurement system
[AD-D016222] p 258 N95-21100
- Partial camera automation in a simulated Unmanned Air Vehicle
[AD-A288786] p 337 N95-26190
- CAMS**
On profiling a cam of an axial aviation diesel engine by periodic splines
[BTN-94-EIX94461407946] p 82 A95-62264
- CANADA**
Transport Canada proposed R&D program for the development of a multi-parameter dual X-Ka band Doppler radar for aviation meteorology applications p 659 A95-93477
- Development of a climatology for possible microburst occurrence in Canada p 664 A95-93497
- Aviation terminal forecasts based on automated observations (FTAUTO) p 668 A95-93520
- Characterization of corrosion and development of a breadboard of a D sight aircraft inspection system, phase 1
[AD-A288347] p 380 N95-26527
- CANADIAN AIRCRAFT**
Selecting and management of fire fighter aircraft
[BTN-95-EIX95062487538] p 193 A95-69246
- CANARD CONFIGURATIONS**
Numerical simulation of steady and unsteady, vorticity-dominated aerodynamic interference
[BTN-95-EIX95062487524] p 186 A95-69232
- Aerodynamic characteristics of a canard-controlled missile at high angles of attack
[BTN-95-EIX95152583257] p 267 A95-73558
- CaNard: A new roadable aircraft concept
[SAE PAPER 932601] p 494 A95-90071
- Experimental aerodynamic characteristics of a generic hypersonic accelerator configuration at Mach numbers 1.5 and 2.0 — conducted in the Langley Unitary Plan Wind Tunnel
[NASA-TM-4413] p 39 N95-12770
- Fatigue evaluation of empennage, forward wing, and winglets/tip fins on part 23 airplanes
[PB94-196813] p 79 N95-13981
- Experimental study at low supersonic speeds of a missile concept having opposing wraparound tails
[NASA-TM-4582] p 106 N95-16069
- Wind tunnel test on a 65 deg delta wing with a sharp or rounded leading edge: The international vortex flow experiment p 114 N95-17872
- Wind tunnel test on a 65 deg delta wing with rounded leading edges: The International Vortex Flow Experiment p 114 N95-17875
- Investigation of the flow development on a highly swept canard/wing research model with segmented leading- and trailing-edge flaps p 114 N95-17876
- Velocity measurements with hot-wires in a vortex-dominated flowfield p 121 N95-19261
- Inner loop flight control for the High-Speed Civil Transport p 293 N95-23314

- Design and testing of low sonic boom configurations and an oblique all-wing supersonic transport
[NASA-CR-197744] p 389 N95-26651
- Catapult-launching of the RAFALE design and experimentation p 609 N95-32008
- CANOPIES**
Radial reefing method for accelerated and controlled parachute opening
[BTN-95-EIX95062487539] p 187 A95-69247
Failure analysis for polycarbonate transparencies
[AD-A292992] p 630 N95-31471
- CANOPIES (VEGETATION)**
Aerodynamic parameters of crop canopies estimated with a center-of-pressure technique
[HTN-95-41901] p 356 A95-81648
- CANTILEVER BEAMS**
Corrosion behavior of landing gear steels
[AD-A285862] p 242 N95-22132
- CANYONS**
Integration of AIRSAR and CALIRIS data for Trail Canyon alluvial fan, Death Valley, California p 709 N95-33760
- CAPACITORS**
Hypervelocity Impact Test Facility: A gun for hire
[TABES PAPER 94-605] p 86 N95-14639
A hybrid vehicle evaluation code and its application to vehicle design. Revision 1
[DE95-008053] p 441 N95-28029
- CAPE KENNEDY LAUNCH COMPLEX**
Development of a climatological data base to help forecast cloud cover conditions for shuttle landings at the Kennedy Space Center p 670 A95-93529
Analysis of rapidly developing fog at the Kennedy Space Center p 671 A95-93531
A review of falconry as a bird control technique with recommendations for use at the Shuttle Landing Facility, John F. Kennedy Space Center, Florida, USA
[NASA-TM-110142] p 381 N95-27859
- CAPTURE EFFECT**
Floating shock fitting via Lagrangian adaptive meshes
[AD-A289758] p 170 N95-18110
- CARBIDES**
Machinability study of Aermet 100
[DE95-011532] p 701 N95-33408
- CARBON DIOXIDE**
Hypersonic convective heat transfer over 140-deg blunt cones in different gases
[BTN-95-EIX95152583253] p 306 A95-73554
Possible effects of CO₂ increase on the high-speed civil transport impact on ozone
[HTN-95-60779] p 317 A95-75976
Vertical transport rates in the stratosphere in 1993 from observations of CO₂, N₂O, and CH₄
[HTN-95-70941] p 351 A95-78006
Stationary premixed flames in spherical and cylindrical geometries
[HTN-95-42336] p 418 A95-86165
Aviation and the environment p 657 A95-93464
- CARBON DIOXIDE LASERS**
Studies on gain performance of a combustion driven CO₂ gas dynamic laser p 428 A95-82679
Laser based obstacle warning sensors for helicopters p 686 N95-32499
The Anglo-French Compact Laser Radar demonstrator programme p 703 N95-32501
- CARBON DISULFIDE**
An intercomparison of aircraft instrumentation for tropospheric measurements of carbonyl sulfide, hydrogen sulfide, and carbon disulfide
[HTN-95-91856] p 355 A95-80844
- CARBON FIBER REINFORCED PLASTICS**
Aeronautical technology - recent advances and future prospects
[HTN-95-01097] p 496 A95-90283
Ultrasonic imaging of damages in CRFT-laminates p 578 A95-90828
Damage to composite aircraft structures from lightning strike attachment to unprotected CFC and internal sparking causing fuel injection
[CONGRESS PAPER C428-4-026] p 531 A95-91675
Repairs to composite structure on military aircraft
[CONGRESS PAPER C428-4-067] p 531 A95-91677
Aerospace applications of new materials
[CONGRESS PAPER C428-17-135] p 531 A95-91716
The basis of civil certification and continued airworthiness for composite aircraft structures
[CONGRESS PAPER C428-37-173] p 628 A95-93632
Residual strength of composites with multiple impact damage
[BTN-94-EIX94511433967] p 701 A95-96664
Large amplitude nonlinear response of flat aluminum, and carbon fiber plastic beams and plates
[AD-A282440] p 96 N95-15547
- Brite-Euram programme: ACOUFAT acoustic fatigue and related damage tolerance of advanced composite and metallic structures p 174 N95-19159
Mishap risk control for advanced aerospace/composite materials p 301 N95-23031
Study on tensile fatigue testing method of unidirectional fiber-resin matrix composites
[NAL-TR-1241] p 343 N95-24989
Adhesively bonded composite patch repair of cracked aluminum alloy structures p 393 N95-27507
External patch repair of CFRP/honeycomb sandwich p 395 N95-27522
Weavability of dry polymer powder towpreg p 535 N95-29036
- CARBON FIBERS**
Buckling and postbuckling of composite structures
[HTN-95-71387] p 528 A95-87605
Failure behaviour of carbon fiber/epoxy composites in pin-ended buckling and bending tests
[HTN-95-71388] p 528 A95-87606
Corrosion protection measures for CFC/metal joints of fuel integral tank structures of advanced military aircraft p 303 N95-23510
Composite or metallic bolted repairs on self-stiffened carbon wing panel of the commuter ATR72 design criteria, analysis, verification by test p 396 N95-27525
- CARBON ISOTOPES**
An air-driven pressure booster pump for aircraft-based air sampling
[HTN-95-40689] p 216 A95-69833
- CARBON MONOXIDE**
An air-driven pressure booster pump for aircraft-based air sampling
[HTN-95-40689] p 216 A95-69833
Laboratory evaluation of a reactive baffle approach to NOx control
[AD-A283802] p 255 N95-19921
- CARBON STEELS**
In-situ detection of surface passivation or activation and of localized corrosion: Experiences and prospects in aircraft p 302 N95-23508
- CARBON-CARBON COMPOSITES**
Surface morphology and structure of carbon-carbon composites in high-energy sliding contact
[BTN-94-EIX94371347996] p 206 A95-69164
R & D on HOPE structure p 413 A95-82355
- CARBON-PHENOLIC COMPOSITES**
Trajectory-based heating analysis for the European Space Agency/Rosetta Earth Return Vehicle
[BTN-95-EIX95041503787] p 205 A95-69218
- CARBONATES**
Evaluation of alternative in-flight fire suppressants for full-scale testing in simulated aircraft engine nacelles and dry bays
[PB94-203403] p 42 N95-13247
Bicarbonate of soda blasting technology for aircraft wheel repainting
[PB94-193323] p 104 N95-17466
Bicarbonate of soda paint stripping process validation and material characterization p 631 N95-31778
- CARBONYL COMPOUNDS**
An intercomparison of aircraft instrumentation for tropospheric measurements of carbonyl sulfide, hydrogen sulfide, and carbon disulfide
[HTN-95-91856] p 355 A95-80844
- CARET WINGS**
Sensitivity of engine-integrated wavender performance to static margin constraint
[AIAA PAPER 95-6142] p 496 A95-90458
- CARGO**
Evaluation of neutron techniques for illicit substance detection
[DE95-002988] p 300 N95-22764
The performance of cargo airdrop systems using g-12E parachutes: Statistical determination of minimum altitude
[AD-A291666] p 381 N95-28454
- CARGO AIRCRAFT**
Design of a high capacity long range cargo aircraft
[NASA-CR-197176] p 45 N95-12363
Gemini: A long-range cargo transport
[NASA-CR-197149] p 45 N95-12626
The OFP-6M transport jet
[NASA-CR-197159] p 46 N95-12637
Incorporating biplane wing theory into a large, subsonic, all-cargo transport p 391 N95-26956
Report to Congressional Committees. Military airlift: C-17 settlement is not a good deal
[GAO/NSIAD-94-141] p 585 N95-32198
- CARIBBEAN REGION**
Oceanic operations: An authoritative guide to oceanic operations
[FAA-AFS-550] p 277 N95-24065
- CARRIAGES**
A user's guide to LUGSAN 1.1: A computer program to calculate and archive lug and sway brace loads for aircraft-carried stores
[DE95-001919] p 232 N95-21730
- CARTESIAN COORDINATES**
A Cartesian, cell-based approach for adaptively-refined solutions of the Euler and Navier-Stokes equations
[NASA-TM-106786] p 73 N95-14297
User documentation of the CTA program
[AD-A289508] p 375 N95-26854
Surface Modeling, Grid Generation, and Related Issues in Computational Fluid Dynamic (CFD) Solutions
[NASA-CP-3291] p 476 N95-28723
Solution of the Navier-Stokes equations on locally refined Cartesian meshes using state-vector splitting p 553 N95-29197
- CASCADE FLOW**
Effect of wind tunnel acoustic modes on linear oscillating cascade aerodynamics
[HTN-94-00760] p 14 A95-60199
Heat transfer in the flow-through part of axial compressors
[BTN-94-EIX94461407949] p 89 A95-62267
Aerodynamic design and calculation of flow around the plane cascade of turbine
[BTN-94-EIX94481415357] p 104 A95-65347
Eigenanalysis of unsteady flows about airfoils, cascades, and wings
[BTN-95-EIX95152577597] p 305 A95-73486
Aeroelastic stability of cascades in turbomachinery
[HTN-95-61156] p 405 A95-86255
Eigenanalysis of unsteady flows about airfoils, cascades, and wings
[HTN-95-42582] p 459 A95-87212
Multipoint inverse design of an infinite cascade of airfoils
[HTN-95-81640] p 541 A95-87688
Numerical calculations of the turbulent flow through a controlled diffusion compressor cascade
[BTN-95-EIX95282710056] p 632 A95-92473
Flutter analysis of supersonic axial flow cascades using a high resolution Euler solver. Part 1: Formulation and validation
[NASA-TM-105798] p 23 N95-10244
Measurements of pressure and thermal wakes in a transonic turbine cascade
[AD-A283464] p 38 N95-12548
Mach number, flow angle, and loss measurements downstream of a transonic fan-blade cascade
[AD-A280907] p 108 N95-16824
Measurement of gust response on a turbine cascade
[NASA-TM-106776] p 117 N95-18457
Enhanced capabilities and modified users manual for axial-flow compressor conceptual design code CSPAN
[NASA-TM-106833] p 119 N95-18933
Simulation of steady and unsteady viscous flows in turbomachinery p 140 N95-19023
Experimental study of vane heat transfer and aerodynamics at elevated levels of turbulence
[NASA-CR-4633] p 244 N95-19912
Numerical computation of aerodynamics and heat transfer in a turbine cascade and a turn-around duct using advanced turbulence models p 313 N95-23444
User's guide for ECAP2D: An Euler unsteady aerodynamic and aeroelastic analysis program for two dimensional oscillating cascades, version 1.0
[NASA-CR-189146] p 316 N95-24189
Improved modeling of unsteady heat transfer (The first step)
[AD-A292777] p 648 N95-31432
Design of secondary flow control cascade using numerical simulation p 698 N95-34507
A study on the convergence of a 3-D Euler code for cascade flow calculations p 706 N95-34508
Verification of turbine cascade flow with tip clearance p 698 N95-34511
- CASES (CONTAINERS)**
Composite cases for airborne electronic equipment: A technology study and EMC p 241 N95-20655
NASA low-speed axial compressor for fundamental research
[NASA-TM-4635] p 296 N95-23192
Composite intermediate case manufacturing scale-up for advanced engines p 406 N95-28275
- CASSINI MISSION**
The Cassini spacecraft: Object oriented flight control software p 359 A95-80405
- CASUALTIES**
Reentry analysis for low Earth orbiting spacecraft p 415 A95-85774
- CATALOGS (PUBLICATIONS)**
NASA video catalog
[NASA-SP-7109(01)] p 363 N95-24238

CATAPULTS

Catapult-launching of the RAFALE design and experimentation p 609 N95-32008

CATHODE RAY TUBES

An evaluation of aircraft CRT and dot-matrix display legibility requirements [AD-A283933] p 138 N95-18164

CAUCHY PROBLEM

Practical formulation of a positively conservative scheme [HTN-95-51668] p 433 A95-85050

CAVITATION FLOW

Numerical time dependent sheet cavitation simulations using a higher order panel method [PB94-204435] p 59 N95-13249
Cavitation modeling in Euler and Navier-Stokes codes p 315 N95-23630

CAVITIES

Hybrid finite element-modal analysis of jet engine inlet scattering [BTN-95-EIX95242673665] p 427 A95-82259

Hypersonic flow past open cavities [HTN-95-42577] p 458 A95-87207

Effect of passive venting on static pressure distributions in cavities at subsonic and transonic speeds [NASA-TM-4549] p 6 N95-10029

Measurements of shielding effectiveness and cavity characteristics of airplanes [PB94-210051] p 244 N95-20191

Cavitation modeling in Euler and Navier-Stokes codes p 315 N95-23630

Effects of cavity dimensions, boundary layer, and temperature on cavity noise with emphasis on benchmark data to validate computational aeroacoustic codes [NASA-CR-4653] p 361 N95-24879

Suppressor of oscillations in airframe cavities [AD-D017265] p 388 N95-26507

Numerical simulation of the SOFIA flow field [NASA-CR-197757] p 436 N95-26589

Comparison of numerical results and multicavity purge and rim seal data with extensions to dynamics [NASA-TM-106685] p 416 N95-27434

Measurements of store forces and moments and cavity pressures for a generic store in and near a box cavity at subsonic and transonic speeds [NASA-TM-4611] p 378 N95-28241

The acoustic characteristics of turbomachinery cavities [NASA-CR-4671] p 476 N95-28720

Recirculating cavity casing treatment failure [AD-A289330] p 513 N95-28908

Effects of cavity bleed and its configuration on aerodynamic characteristics of supersonic internal flow [NAL-TR-1247] p 594 N95-31715

CAVITY FLOW

Observations on using experimental data as boundary conditions for computations [BTN-95-EIX95182619103] p 321 A95-76588

Study of subsonic base cavity flowfield structure using particle image velocimetry [BTN-95-EIX95222650781] p 327 A95-79237

Weapons bay acoustic environment p 173 N95-19146

A time-accurate finite volume method valid at all flow velocities p 314 N95-23447

Effects of cavity dimensions, boundary layer, and temperature on cavity noise with emphasis on benchmark data to validate computational aeroacoustic codes [NASA-CR-4653] p 361 N95-24879

Calculation of three-dimensional (3-D) internal flow by means of the velocity-vorticity formulation on a staggered grid [NASA-TM-110352] p 376 N95-27258

Numerical analysis of intra-cavity and power-stream flow interaction in multiple gas-turbine disk-cavities [NASA-TM-106886] p 407 N95-28344

The acoustic characteristics of turbomachinery cavities [NASA-CR-4671] p 476 N95-28720

CAVITY RESONATORS

Hybrid finite element-modal analysis of jet engine inlet scattering [BTN-95-EIX95242673665] p 427 A95-82259

CEILINGS (METEOROLOGY)

International Conference on Aviation Weather Systems, 5th, Vienna, VA, Aug. 2-6, 1993. Preprint Volume [HTN-95-92940] p 652 A95-93441

ITWS ceiling and visibility products p 654 A95-93454

Flying with automated surface observations p 659 A95-93472

Transport Canada proposed R&D program for the development of a multi-parameter dual X-Ka band Doppler radar for aviation meteorology applications p 659 A95-93477

The aviation gridded forecast system verification program - A description of aviation-impact-variable evaluation plans p 664 A95-93498

Comprehensive verification of terminal forecast ceiling and visibility p 664 A95-93500

Verification of terminal forecasts p 664 A95-93502

Development of a climatological data base to help forecast cloud cover conditions for shuttle landings at the Kennedy Space Center p 670 A95-93529

CELESTIAL MECHANICS

Period evolution of PSR B1259-63: Evidence for propeller-torque spindown [HTN-95-B0194] p 581 A95-87903

CENSUS

Census US civil aircraft calendar year 1993 [AD-A286309] p 219 N95-20091

CENTER OF GRAVITY

The analysis of the processing increased weight for pilot production of F-X aircraft [HTN-95-71133] p 385 A95-83494

Fatigue evaluation of empennage, forward wing, and winglets/tip fins on part 23 airplanes [PB94-196813] p 79 N95-13981

A quantitative feedback theory FCS design for the subsonic "envelope" of the VISTA F-16 including configuration variation [AD-A289221] p 409 N95-26958

CENTER OF PRESSURE

Aerodynamic parameters of crop canopies estimated with a center-of-pressure technique [HTN-95-41901] p 356 A95-81648

CENTERBODIES

High bypass separate flow exhaust system improved thrust efficiency by modifying the aft centerbody [SAE PAPER 932622] p 511 A95-90083

CENTRAL ATLANTIC REGION (US)

The inference of aviation weather hazards based on the integration of radar and lightning data p 660 A95-93483

CENTRAL PROCESSING UNITS

Trajectory optimization using parallel shooting method on parallel computer [BTN-95-EIX95282706670] p 564 A95-88175

Parallel block implicit integration technique for trajectory parallelism [AD-A289891] p 450 N95-28335

CENTRIFUGAL COMPRESSORS

On calculated models for impellers of centrifugal compressors [BTN-94-EIX94461407947] p 88 A95-62265

Pressure and temperature distortion testing of a two-stage centrifugal compressor [BTN-94-EIX95011441250] p 431 A95-84207

Thermo-hydrodynamic solution of floating ring seals for high pressure compressors using the finite-element method [HTN-95-92246] p 433 A95-85290

Simulation of the unsteady interaction of a centrifugal impeller with its vaned diffuser: flow analysis [BTN-95-EIX95282710055] p 633 A95-92474

Design and development of an advanced two-stage centrifugal compressor [BTN-95-EIX95282710054] p 633 A95-92475

Unsteady flow phenomena in discrete passage diffusers for centrifugal compressors [AD-A281412] p 155 N95-16163

Laser anemometer measurements of the three-dimensional rotor flow field in the NASA low-speed centrifugal compressor [NASA-TP-3527] p 618 N95-31985

An unsteady simulation of a centrifugal compressor stage using the NWT p 707 N95-34536

CENTRIFUGES

Simulation of Shuttle launch G forces and acoustic loads using the NASA Ames Research Center 20G centrifuge p 86 N95-14089

CERAMIC COATINGS

Compliant interlayer [BTN-95-EIX95142562401] p 304 A95-73439

Protective coatings for compressor gas path components p 201 N95-19675

Thermal testing of high performance thermal barrier coatings for turbine blades p 202 N95-19681

PVD TBC experience on GE aircraft engines p 345 N95-26126

Thermal fracture mechanisms in ceramic thermal barrier coatings p 346 N95-26138

Thermal barrier coating life modeling in aircraft gas turbine engines p 346 N95-26140

CERAMIC FIBERS

Development of hypersonic engine seals: Flow effects of preload and engine pressures [BTN-95-EIX95112524204] p 196 A95-69304

Innovative processing of composites for ultra-high temperature applications, book 1 [AD-A290889] p 537 N95-29842

CERAMIC MATRIX COMPOSITES

Launcher wing-leading-edge design [BTN-94-EIX9504277110] p 192 A95-68349

Contribution of thermal radiation to the temperature profile of ceramic composite materials [BTN-94-EIX95011441252] p 417 A95-84209

Ceramic composite attachments for transmission of high-torque loads [BTN-94-EIX95011441256] p 417 A95-84213

The potential for CMCs to replace superalloys in engine exhaust ducts [HTN-95-42298] p 418 A95-84992

Aerospace applications of new materials [CONGRESS PAPER C428-17-135] p 531 A95-91716

A CMC database for use in the next generation launch vehicles (rockets) p 150 N95-18993

Toughened Silcomp composites for gas turbine engine applications [DE95-002851] p 235 N95-21243

Ceramic composite combustor cans for expendable turbine engines [AD-A289551] p 407 N95-28646

Innovative processing of composites for ultra-high temperature applications, book 1 [AD-A290889] p 537 N95-29842

CERAMICS

Ceramic blanket reduces maintenance costs [BTN-94-EIX94461290278] p 77 A95-61733

Compliant interlayer [BTN-95-EIX95142562401] p 304 A95-73439

Test model designs for advanced refractory ceramic materials p 55 N95-11968

Ceramic manufacturing: Optimizing a multivariable system [DE94-015016] p 56 N95-13184

Advanced Turbine Technology Applications Project (ATTAP) [NASA-CR-195393] p 101 N95-15743

Resistance of silicon nitride turbine components to erosion and hot corrosion/oxidation attack p 202 N95-19683

Reliability assessment of Multichip Module technologies via the Triservice/NASA RELTECH program p 245 N95-20643

CERMETS

High velocity oxygen fuel spraying of erosion and wear resistant coatings on jet engine parts p 202 N95-19680

CERTIFICATION

Progress and experience with helicopter health and usage monitoring [CONGRESS PAPER C428-31-151] p 603 A95-93615

The basis of civil certification and continued airworthiness for composite aircraft structures [CONGRESS PAPER C428-37-173] p 628 A95-93632

The certification of composite structures for military aircraft [CONGRESS PAPER C428-37-198] p 628 A95-93633

Role of wind tunnels and computer codes in the certification and qualification of rotorcraft for flight in forecast icing [NASA-TM-106747] p 39 N95-13197

Windshear certification data base for forward-look detection systems p 41 N95-13204

Certification methodology applied to the NASA experimental radar system p 41 N95-13205

Aircraft and sub-system certification by piloted simulation [AGARD-AR-278] p 145 N95-17388

An evaluation of Automatic Terminal Information Service (ATIS) flight deck display presentation options [AD-A280100] p 228 N95-21020

Consistent approach to describing aircraft HIRF protection [NASA-CR-195067] p 334 N95-25341

Bonded composite repair of metallic aircraft components: Overview of Australian activities p 392 N95-27505

Hardware cleanliness methodology and certification p 419 N95-27656

Application of damage tolerance methodology in certification of the Piaggio P-180 Avanti p 399 N95-28480

Flight test evaluation of the Stanford University/United Airlines differential GPS Category 3 automatic landing system [NASA-TM-110354] p 593 N95-30788

- Report to the Chairman, Subcommittee on Aviation, Committee on Commerce, Science, and Transportation, US Senate. Aviation safety: Data problems threaten FAA strides on safety analysis system
[GAC/AIMD-95-27] p 687 N95-32705
- A rose by any other name: Certification seen as process rather than content p 688 N95-34766
- Human factors certification in the development of future air traffic control systems p 690 N95-34770
- Quality assurance and risk management: Perspectives on Human Factors Certification of Advanced Aviation Systems p 690 N95-34771
- User type certification for advanced flight control systems p 699 N95-34772
- CH-47 HELICOPTER**
- Design and flight test of a simplified control system for a transport helicopter p 144 N95-18902
- CHARGE DETECTION**
- Real-time estimation of atmospheric turbulence severity from in-situ aircraft measurements
[BTN-95-EIX95182619231] p 319 A95-76657
- Minimal time detection algorithms and applications to flight systems
[TR-2-FSRC-93] p 171 N95-18564
- CHANNEL FLOW**
- Analysis of flow channeling near the wall in packed beds
[HTN-94-00698] p 2 A95-60177
- Kinetic theory in aerothermodynamics
[HTN-95-A0002] p 183 A95-67829
- Pressure measurements on a pitching airfoil in a water channel
[HTN-95-61209] p 541 A95-87582
- Aerodynamic investigation of the flow field in a 180 deg turn channel with sharp bend p 163 N95-19257
- Large-eddy simulation of flow through a plane, asymmetric diffuser p 250 N95-22449
- A fixed time performance evaluation of parallel CFD applications
[DE94-014240] p 436 N95-26445
- CHANNELS (DATA TRANSMISSION)**
- New filtering method for linear weakly coupled stochastic systems
[BTN-95-EIX0608952736485] p 678 A95-92708
- Optical backplane for modular avionics p 257 N95-20652
- CHARACTERIZATION**
- Characterization of a hot-film probe for hypersonic flow
[AIAA PAPER 95-6110] p 511 A95-90440
- CHARGE COUPLED DEVICES**
- Research instrumentation for polytechnic university's supersonic wind tunnel facility
[AD-A290232] p 523 N95-29468
- CHARGE DISTRIBUTION**
- Thundercloud electric field modeling for the ionosphere-Earth region. 1: Dependence on cloud charge distribution
[HTN-95-41223] p 317 A95-75035
- CHARGE TRANSFER**
- Broadband polarization-transfer experiments for rotating solids
[GTN-95-0009261494012091-58] p 579 A95-92319
- Collaborative research on aircraft icing and charging processes in ice
[AD-A285102] p 276 N95-23201
- CHARTS**
- An exploratory survey of information requirements for instrument approach charts
[AD-A293882] p 601 N95-31520
- Current issues in the design and information content of instrument approach charts
[AD-A294752] p 690 N95-34562
- Resource document for the design of electronic instrument approach procedure displays
[AD-A295108] p 691 N95-34797
- CHEBYSHEV APPROXIMATION**
- Statistical discrete gust-power spectral density methods overlap-holistic proof and beyond
[BTN-95-EIX0619952748175] p 584 A95-94469
- CHECKOUT**
- Integrated test system single point control of aircraft checkout
[SAE PAPER 931417] p 583 A95-93682
- CHEMICAL ANALYSIS**
- An intercomparison of aircraft instrumentation for tropospheric measurements of sulfur dioxide
[HTN-95-91855] p 354 A95-80843
- An intercomparison of aircraft instrumentation for tropospheric measurements of carbonyl sulfide, hydrogen sulfide, and carbon disulfide
[HTN-95-91856] p 355 A95-80844
- An intercomparison of instrumentation for tropospheric measurements of dimethyl sulfide: Aircraft results for concentrations at the parts-per-trillion level
[HTN-95-91857] p 355 A95-80845
- An Echelle Grating Spectrometer (EGS) for mid-IR remote chemical detection
[DE94-019310] p 249 N95-21478
- The effect of wear on fire-blocking layer material effectiveness
[AD-A291520] p 485 N95-29855
- Standardization of surface contamination analysis systems p 631 N95-31798
- CHEMICAL CLEANING**
- Parts washing-alternatives study: United States Coast Guard. Project summary and report
[PB95-166146] p 343 N95-26004
- CHEMICAL COMPOSITION**
- Possible effects of CO₂ increase on the high-speed civil transport impact on ozone
[HTN-95-60779] p 317 A95-75976
- Analysis of the physical state of one Arctic polar stratospheric cloud based on observations
[HTN-95-70917] p 351 A95-77982
- Effects on stratospheric ozone from high-speed civil transport: Sensitivity to stratospheric aerosol loading
[HTN-95-91842] p 354 A95-80830
- An intercomparison of aircraft instrumentation for tropospheric measurements of sulfur dioxide
[HTN-95-91855] p 354 A95-80843
- An intercomparison of aircraft instrumentation for tropospheric measurements of carbonyl sulfide, hydrogen sulfide, and carbon disulfide
[HTN-95-91856] p 355 A95-80844
- An intercomparison of instrumentation for tropospheric measurements of dimethyl sulfide: Aircraft results for concentrations at the parts-per-trillion level
[HTN-95-91857] p 355 A95-80845
- Chemical composition and photochemical reactivity of exhaust from aircraft turbine engines
[HTN-95-51277] p 356 A95-80862
- Modeling of plume chemistry of high flying aircraft with H₂ combustion engines p 509 A95-87405
- Solid fuel ramjet composition
[AD-D016458] p 152 N95-19090
- Replicator for characterization of cirrus and polar stratospheric cloud particles
[NASA-CR-197785] p 445 N95-26669
- Electrochemical impedance pattern recognition for detection of hidden chemical corrosion on aircraft components, phase 1
[AD-A291345] p 556 N95-29946
- CHEMICAL EQUILIBRIUM**
- Linear disturbances in hypersonic, chemically reacting shock layers
[BTN-94-EIX94441386605] p 182 A95-67336
- Thermochemical nonequilibrium viscous shock-layer analysis for a Mars aerocapture vehicle
[BTN-95-EIX95082502732] p 239 A95-70139
- General solution procedure for flows in local chemical equilibrium
[HTN-95-42329] p 404 A95-86158
- Linear disturbances in hypersonic, chemically reacting shock layers
[HTN-95-20931] p 464 A95-88970
- Numerical studies of Mach reflection with air chemistry p 548 A95-90575
- Broadband polarization-transfer experiments for rotating solids
[GTN-95-0009261494012091-58] p 579 A95-92319
- CHEMICAL EXPLOSIONS**
- Evaluation of neutron techniques for illicit substance detection
[DE95-002988] p 300 N95-22764
- CHEMICAL LASERS**
- The 25th International Symposium on Combustion
[AD-A286825] p 630 N95-31268
- CHEMICAL PROPERTIES**
- Photoacoustic chambers for studying solids and gases: Theory and practical examples
[IFTR-39/1994] p 412 N95-26837
- CHEMICAL REACTIONS**
- Linear disturbances in hypersonic, chemically reacting shock layers
[BTN-94-EIX94441386605] p 182 A95-67336
- Linear disturbances in hypersonic, chemically reacting shock layers
[HTN-95-20931] p 464 A95-88970
- A one-dimensional inviscid nonequilibrium flow solver
[ISBN 1-879921-01-4] p 588 A95-93752
- Effects of the chemical reaction model on calculations of supersonic combustion flows
[BTN-95-EIX0616952745802] p 638 A95-94487
- The use of electrochemistry and ellipsometry for identifying and evaluating corrosion on aircraft
[AD-A288536] p 381 N95-27186
- CHEMICAL TESTS**
- Chemical composition and photochemical reactivity of exhaust from aircraft turbine engines
[HTN-95-51277] p 356 A95-80862
- CHEMICAL VAPOR INFILTRATION**
- Scale-up and modeling of forced chemical vapor infiltration
[DE94-017769] p 247 N95-20781
- Ceramic composite combustor cans for expendable turbine engines
[AD-A289551] p 407 N95-28646
- Innovative processing of composites for ultra-high temperature applications, book 1
[AD-A290889] p 537 N95-29842
- CHEMILUMINESCENCE**
- Developments in laser-based diagnostics for wind tunnels in the Aeromechanics Division: 1987-1992
[AD-A283011] p 84 N95-13687
- CHILDREN**
- The performance of child restraint devices in transport airplane passenger seats
[DOT/FAA/AM-94/19] p 40 N95-12146
- CHINA**
- Thermal design of returnable satellites
[AD-A294113] p 701 N95-34500
- CHINESE AIRCRAFT**
- The analysis of the processing increased weight for pilot production of F-X aircraft
[HTN-95-71133] p 385 A95-83494
- CHIPS**
- MCMs for avionics: Technology selection and intermodule interconnection p 234 N95-20641
- Reliability assessment of Multichip Module technologies via the Triservice/NASA RELTECH program p 245 N95-20643
- Assuring Known Good Die (KGD) for reliable, cost effective MCMs p 246 N95-20644
- CHIPS (ELECTRONICS)**
- Intelligent finite element submodeling of multichip modules for reliability analysis
[AD-A292911] p 679 N95-31455
- CHLORINE**
- The distribution of hydrogen, nitrogen, and chlorine radicals in the lower stratosphere: Implications for changes in O₃ due to emission of NO_y from supersonic aircraft
[HTN-95-70935] p 351 A95-78000
- Impact on ozone of high-speed stratospheric aircraft: Effects of the emission scenario
[HTN-95-51283] p 356 A95-80868
- CHLORINE COMPOUNDS**
- Estimates of total organic and inorganic chlorine in the lower stratosphere from in situ and flask measurements during AASE 2
[HTN-95-A0861] p 317 A95-76265
- CHLORINE OXIDES**
- Aircraft measurements of ClO and HCl during EASOE 1991/92
[HTN-95-00721] p 444 A95-86291
- An overview of millimeter-wave spectroscopic measurements of chlorine monoxide at Thule, Greenland, February-March, 1992: Vertical profiles, diurnal variation, and longer-term trends
[HTN-95-00722] p 444 A95-86292
- Airborne measurements during the European Arctic Stratospheric Ozone Experiment: Observation of OCIO
[HTN-95-00745] p 445 A95-86315
- In situ measurements of ClO and implications for the chemistry of inorganic chlorine in the lower stratosphere p 563 N95-29830
- CHOKED FLOW**
- Investigation of starting and ignition transients in the thermally choked ram accelerator p 698 N95-34805
- CHORDS (GEOMETRY)**
- Effect of leading-edge extension fences on the vortex wake of an F/A-18 model
[BTN-95-EIX0619952748192] p 591 A95-94481
- CIRCUIT BOARDS**
- Electromagnetic reverberation characteristics of a large transport aircraft
[AD-A282923] p 82 N95-15392
- CAE for thermal management of aerospace electronic boards using the BETAsoft program p 438 N95-27354
- Life cycle costs of alternatives for F-16 printed circuit board diagnosis equipment
[AD-A288744] p 401 N95-28586
- CIRCUIT BREAKERS**
- Partial discharge testing of high voltage wiring harness for airborne displays
[AD-A289150] p 401 N95-27003
- Electrical short circuit and current overload tests on aircraft wiring
[AD-A293308] p 646 N95-30922
- CIRCUITS**
- A time stepping coupled finite element-state space modeling environment for synchronous machine performance and design analysis in the ABC frame of reference p 649 N95-31948

CIRCULAR CONES

- Elliptic tip effects on the vortex wake of an axisymmetric body at incidence
[BTN-94-EIX94441386612] p 208 A95-67343
- Suppression of vortex asymmetry and side force on a circular cone
[BTN-95-EIX95042474413] p 209 A95-68287
- Quantitative comparison between interferometric measurements and Euler computations for supersonic cone flows
[BTN-95-EIX95222650782] p 358 A95-79238
- The aerodynamic characteristics of cup-like body in supersonic flow
p 427 A95-82407
- Measurement of free-flight dynamic stability derivatives of cones in a hypersonic gun tunnel
[AIAA PAPER 95-6082] p 519 A95-87411
- Nonlinear asymptotic theory of hypersonic flow past a circular cone
[HTN-95-92599] p 461 A95-87415

CIRCULAR CYLINDERS

- Vortex cutting by a blade. Part II: Computations of vortex response
[BTN-94-EIX94441386611] p 208 A95-67342
- Experimental investigation of the flow around a circular cylinder: Influence of aspect ratio
[BTN-94-EIX95011441120] p 347 A95-80044
- Observation of traveling waves in the three-dimensional boundary layer along a yawed cylinder
[HTN-95-61064] p 430 A95-83648
- On the differences between the effect of acoustic perturbation and unsteady bleed in controlling flow separation over a cylinder
[SAE PAPER 932573] p 467 A95-90062
- Wind tunnel investigations of the appearance of shocks in the windward region of bodies with circular cross section at angle of attack
p 113 N95-17866
- Force and pressure data of an ogive-nosed slender body at high angles of attack and different Reynolds numbers
p 113 N95-17868
- Wind tunnel performance comparative test results of a circular cylinder and 50 percent ellipse tailboom for circulation control antitorque applications
[AD-A283335] p 130 N95-18008
- Research on bluff body vortex wakes
[AD-A286319] p 223 N95-20177
- The effects of three-dimensional imposed disturbances on bluff body near wake flows: Effects of taper and splitter plates on the near wake characteristics of a circular cylinder in uniform and shear flow
[AD-A292113] p 477 N95-28921
- A simulation of damping process of pendulum motion due to aerodynamic forces
p 711 N95-34551
- CIRCULAR PLATES**
- Experimental investigation of the flow around a circular cylinder: Influence of aspect ratio
[BTN-94-EIX95011441120] p 347 A95-80044
- CIRCULAR TUBES**
- High-frequency acoustic radiation from a curved duct of circular cross section
p 573 A95-90098

CIRCULATION

- Recirculating cavity casing treatment failure
[AD-A289330] p 513 N95-28908

CIRCULATION CONTROL AIRFOILS

- Application of circulation control to advanced subsonic transport aircraft. Part 1: Airfoil development
[BTN-95-EIX95062487545] p 185 A95-68359
- Application of circulation control to advanced subsonic transport aircraft. Part 2: Transport application
[BTN-95-EIX95062487546] p 185 A95-68360
- Numerical model for circulation-control flows
[HTN-95-81632] p 461 A95-87680
- Computational study of a two-slot circulation control airfoil
[SAE PAPER 932531] p 466 A95-89191
- Wind tunnel performance comparative test results of a circular cylinder and 50 percent ellipse tailboom for circulation control antitorque applications
[AD-A283335] p 130 N95-18008

CIRRUS CLOUDS

- Preliminary analysis of University of North Dakota aircraft data from the FIRE Cirrus IFO-2
[NASA-CR-198038] p 357 N95-24219
- Replicator for characterization of cirrus and polar stratospheric cloud particles
[NASA-CR-197785] p 445 N95-26669
- Correction of thin cirrus effects in AVIRIS images using the sensitive 1.375-micron cirrus detecting channel
p 708 N95-33748

CISLUNAR SPACE

- How 'HITEN's' aerobraking experiments were carried out
p 415 A95-82553

CIVIL AVIATION

- The ICAO CNS/ATM system: New king, new law?
[HTN-95-50218] p 175 A95-64855

- Aircraft accident investigation and airworthiness -- A practical example of the interaction of two disciplines with some reflections on possible legal consequences
[HTN-95-50219] p 176 A95-64856
- World trends in air transport policies. (Approaching the 21st century)
[HTN-95-50220] p 176 A95-64857
- EC Aviation Scene
[HTN-95-50223] p 176 A95-64860
- Development of aeronautical mobile satellite services over the past thirty years
[BTN-95-EIX95152569458] p 305 A95-73498
- Containing military autotest cost growth through the use of commercial standard equipment architectures
[BTN-95-EIX95172595295] p 287 A95-75717
- Maintenance challenges and trends
[BTN-95-EIX95182617808] p 261 A95-75753
- Maintenance programs
[BTN-95-EIX95182617809] p 261 A95-75754
- Possible effects of CO2 increase on the high-speed civil transport impact on ozone
[HTN-95-60779] p 317 A95-75976
- Structural composites in civil gas turbine aero engines
[HTN-95-60258] p 529 A95-89202
- Materials and structures for the HSCT
[BTN-95-EIX95282711241] p 455 A95-89634
- An intelligent tutoring system for civil aviation flight training
p 521 A95-91535
- Introduction of the GPS to civil aviation field
p 487 A95-91536
- Some comments on current research and development of civil VTOL aircrafts
p 499 A95-91572
- Explanatory factors for the geographic distribution of U.S. Civil aviation mortality
[HTN-95-92908] p 484 A95-91846
- Aviation and the environment
p 657 A95-93464
- Automation of observations in the Netherlands
p 661 A95-93485
- Northwest Airlines atmospheric hazards advisory & avoidance system
p 672 A95-93539
- Civil aircraft performance - developments for improved safety
[CONGRESS PAPER C428-25-175] p 596 A95-93601
- Signal processing of noise data from high-speed flyovers
[BTN-95-EIX0619952748178] p 680 A95-94248
- Micro-measurements of mechanical properties for adhesives and composites using digital imaging technology
[NASA-CR-196111] p 22 N95-10231
- A full Navier-Stokes analysis of subsonic diffuser of a bifurcated 70/30 supersonic inlet for high speed civil transport application
[NASA-TM-106637] p 8 N95-10820
- High speed civil transport: Sonic boom softening and aerodynamic optimization
[NASA-CR-196397] p 28 N95-11192
- High speed civil transport aerodynamic optimization
[NASA-CR-196960] p 38 N95-12389
- Integrated design and manufacturing for the high speed civil transport
[NASA-CR-197183] p 48 N95-12700
- Evaluation of alternative in-flight fire suppressants for full-scale testing in simulated aircraft engine nacelles and dry bays
[PB94-203403] p 42 N95-13247
- Aircraft accident report: Overspeed and loss of power on both engines during descent and power-off emergency, landing Simmons Airlines, Inc., d/b/a, American Eagle Flight 3641, N349SB False River Air Park, New Roads, Louisiana, 1 February 1994
[PB94-910408] p 78 N95-14916
- Research and technology highlights, 1993
[NASA-TM-4575] p 102 N95-15065
- European aeronautics: Strong government presence in industry structure and research and development support. Report to Congressional Requesters
[GAO/NSIAD-94-71] p 176 N95-18578
- Federal aviation regulations, part 91. General operating and flight rules. Change 8
[PB94-217445] p 188 N95-19720
- Application of three-dimensional hybrid structured/unstructured grids to land, sea and air vehicles
[ARA-MEMO-399] p 210 N95-19775
- Census US civil aircraft calendar year 1993
[AD-A286309] p 219 N95-20091
- Test and evaluation report for the Manual Domestic Passive Profiling System (MDPPS)
[AD-A286312] p 225 N95-20093
- Inner loop flight control for the High-Speed Civil Transport
p 293 N95-23314
- Handling qualities of the High Speed Civil Transport
p 294 N95-23325

- The airline quality report, 1994
[NIAR-94-11] p 277 N95-24012
- Oceanic operations: An authoritative guide to oceanic operations
[FAA-AFS-550] p 277 N95-24065
- A review of civil aviation fatal accidents in which lost/disoriented was a cause/factor: 1981-1990
[DOT/FAA/AM-95/1] p 278 N95-24071
- CFD research, parallel computation and aerodynamic optimization
[NASA-CR-197748] p 373 N95-26649
- The high speed civil transport and NASA's High Speed Research (HSR) program
p 390 N95-26945
- An integrated GPS/INS/BARO and radar altimeter system for aircraft precision approach landings
[AD-A289280] p 383 N95-26985
- A review of Australian and New Zealand investigations on aeronautical fatigue during the period Apr. 1993 - Mar. 1995
[AR-009-202] p 397 N95-27918
- Rotorcraft crashworthy airframe and fuel system technology development program
[AD-A289986] p 382 N95-28630
- Effects of cabin pressure on climb and descent rates
[ESDU-94040] p 503 N95-29016
- The effect of wear on fire-blocking layer material effectiveness
[AD-A291520] p 485 N95-29855
- Development of advanced approach and departure procedures. Failure scenarios
[PB95-198123] p 601 N95-30815
- Effects of civil tiltrotor service in the northeast corridor on en route airspace loads
[AD-A293586] p 599 N95-31687
- Integration of air traffic databases: A case study
[AD-A293691] p 602 N95-32022
- Report to the Chairman, Subcommittee on Aviation, Committee on Commerce, Science, and Transportation, US Senate. Aviation safety: Data problems threaten FAA strides on safety analysis system
[GAO/AIMD-95-27] p 687 N95-32705
- Fact sheet for Congressional requesters. Airport competition: Essential air service slots at O'Hare International Airport
[GAO/RCED-94-118FS] p 699 N95-32759
- Report to the Chairman, Subcommittee on Transportation and Related Agencies, Committee on Appropriations, US Senate. Airport Improvement Program: Reliever airport set-aside funds could be redirected
[GAO/RCED-94-226] p 699 N95-32786
- Report to the Chairman, Subcommittee on Transportation and Related Agencies, Committee on Appropriations, US Senate. Airport Improvement Program: The Military Airport Program has not achieved intended impact
[GAO/RCED-94-209] p 700 N95-32888
- Human factors certification in the development of future air traffic control systems
p 690 N95-34770
- CIVIL DEFENSE**
- Fundamentals of catastrophic failure prevention by thrust vectoring
[BTN-95-EIX0619952748176] p 606 A95-94470
- CLASSIFICATIONS**
- Initial exploration of the ASRS database
p 681 A95-95204
- Hypersonic flow-field measurements: Intrusive and nonintrusive
[AD-A283867] p 119 N95-18674
- Fuel-type classification and parameters prediction by Gas Liquid Chromatography analysis
[AD-A293442] p 630 N95-91368
- CLEAN ENERGY**
- Activated buoyancy propulsion = Paradox Power (tm)
[TABES PAPER 94-619] p 74 N95-14646
- CLEAN ROOMS**
- Measurement of particle emissions from clean room gas-handling components
[BTN-94-EIX94381359040] p 295 A95-74554
- Measurement of moisture and total hydrocarbon contributions by valves used in clean room gas-delivery systems
[BTN-94-EIX94381359041] p 295 A95-74629
- CLEANERS**
- Parts washing alternatives study: United States Coast Guard. Project summary and report
[PB95-166146] p 343 N95-26004
- CLEANING**
- Hardware cleanliness methodology and certification
p 419 N95-27656
- Bicarbonate of soda paint stripping process validation and material characterization
p 631 N95-31778
- Environmentally Safe and Effective Processes for Paint Removal
[AGARD-LS-201] p 650 N95-32165
- Water blasting paint removal methods
p 650 N95-32170

- Selective chemical stripping p 650 N95-32175
 Facilities used for plastic media blasting p 627 N95-32176
- Operational parameters and material effects p 651 N95-32179
 Standardization work p 651 N95-32181
- CLEANLINESS**
 Hardware cleanliness methodology and certification p 419 N95-27656
- CLEAR AIR TURBULENCE**
 International Conference on Aviation Weather Systems, 5th, Vienna, VA, Aug, 2-6, 1993. Preprint Volume [HTN-95-92940] p 652 A95-93441
 Testing of TKE parameterizations in numerical models for clear-air turbulence forecasting p 667 A95-93515
 Northwest Airlines atmospheric hazards advisory & avoidance system p 672 A95-93539
 A northern hemisphere clear air turbulence climatology p 674 A95-93547
 An evaluation of clear-air turbulence indices p 674 A95-93548
 Airborne Windshear Detection and Warning Systems. Fifth and Final Combined 'Manufacturers' and Technologists' Conference, part 2 [NASA-CP-10139-PT-2] p 41 N95-13203
 Characteristics of civil aviation atmospheric hazards p 42 N95-13208
 Aircraft wake RCS measurement p 59 N95-13210
 Doppler radar detection of vortex hazard indicators p 42 N95-13212
 Remote sensing of turbulence in the clear atmosphere with 2-micron lidars p 59 N95-13213
- CLEARANCES**
 Dynamic behavior of valves with pneumatic chamber for reciprocating compressors [BTN-94-EIX94351143311] p 207 A95-65845
 Aircraft and sub-system certification by piloted simulation [AGARD-AR-278] p 145 N95-17388
 WINCLR: A computer code for heat transfer and clearance calculation in a compressor p 366 N95-26363
 Verification of turbine cascade flow with tip clearance p 698 N95-34511
- CLIMATOLOGY**
 Development of a climatological data base to help forecast cloud cover conditions for shuttle landings at the Kennedy Space Center p 670 A95-93529
 Preliminary analysis of University of North Dakota aircraft data from the FIRE Cirrus IFO-2 [NASA-CR-198038] p 357 N95-24219
 Evaluation of alternative pavement marking materials [AD-A292973] p 626 N95-31468
- CLIMBING FLIGHT**
 Acoustic climb to cruise test [NASA-TM-110504] p 230 N95-20155
 Effects of small changes on rate of climb [ESDU-94039] p 501 N95-28707
 Effects of cabin pressure on climb and descent rates [ESDU-94040] p 503 N95-29016
- CLOSED CIRCUIT TELEVISION**
 External viewing airborne CCTV system [CONGRESS PAPER C428-25-172] p 595 A95-93598
- CLOSED CYCLES**
 Ultimate characteristics of a rocket engine with a turbo-pump supply system [BTN-94-EIX94461408757] p 148 A95-63640
- CLOSURE LAW**
 Modelling 2D separation from a high lift aerofoil with a non-linear eddy-viscosity model and second-moment closure [HTN-95-C0005] p 585 A95-93393
 Preliminary results of turbulence predictions for use in aviation weather forecasting p 675 A95-93551
- CLOSURES**
 New end tube closure system for the ram accelerator [BTN-94-EIX94441380974] p 195 A95-68158
- CLOUD COVER**
 Diurnal variation of lee vortices in Taiwan and the surrounding area [HTN-95-91363] p 318 A95-76394
 Analysis of the physical state of one Arctic polar stratospheric cloud based on observations [HTN-95-70917] p 351 A95-77982
 Flying with automated surface observations p 659 A95-93472
 Transport Canada proposed R&D program for the development of a multi-parameter dual X-Ka band Doppler radar for aviation meteorology applications p 659 A95-93477
 The aviation gridded forecast system verification program - A description of aviation-impact-variable evaluation plans p 664 A95-93498
 Comprehensive verification of terminal forecast ceiling and visibility p 664 A95-93500

- Nortat: Computer generated aerodome forecasts p 668 A95-93521
 Development of a climatological data base to help forecast cloud cover conditions for shuttle landings at the Kennedy Space Center p 670 A95-93529
 Preliminary analysis of University of North Dakota aircraft data from the FIRE Cirrus IFO-2 [NASA-CR-198038] p 357 N95-24219
- CLOUD GLACIATION**
 Preliminary comparisons between MM5 NCAR/Penn State model generated icing forecasts and observations p 655 A95-93458
 The production of supercooled liquid water by a secondary cold front p 673 A95-93542
 An application of some cloud modeling techniques to a regional model simulation of an icing event p 673 A95-93543
 Preliminary studies of ice formation in upslope clouds p 674 A95-93546
 Replicator for characterization of cirrus and polar stratospheric cloud particles [NASA-CR-197785] p 445 N95-26669
- CLOUD HEIGHT INDICATORS**
 ITWS ceiling and visibility products p 654 A95-93454
 Transport Canada proposed R&D program for the development of a multi-parameter dual X-Ka band Doppler radar for aviation meteorology applications p 659 A95-93477
- CLOUD PHYSICS**
 Aircraft icing measurements in East Coast winter storms [HTN-95-60505] p 214 A95-68756
 Microwave and infrared simulations of an intense convective system and comparison with aircraft observations [HTN-95-60511] p 214 A95-68762
 Conditions associated with large-drop regions [HTN-95-10686] p 214 A95-68845
 High-resolution imaging of rain systems with the advanced microwave precipitation radiometer [HTN-95-70133] p 252 A95-70655
 Behavior of an inversion-based precipitation retrieval algorithm with high-resolution AMPR measurements including a low-frequency 10.7-GHz channel [HTN-95-70134] p 252 A95-70656
 Potential applications of the SSM/I cloud liquid water parameter to the estimation of marine aircraft icing [HTN-95-80651] p 254 A95-72495
 Microphysical and radiative properties of small cumulus clouds over the sea [HTN-95-A0526] p 255 A95-73180
 On the link between cloud-top radiative properties and sub-cloud aerosol concentrations [HTN-95-A0527] p 255 A95-73181
 An application of some cloud modeling techniques to a regional model simulation of an icing event p 673 A95-93543
 Preliminary analysis of University of North Dakota aircraft data from the FIRE Cirrus IFO-2 [NASA-CR-198038] p 357 N95-24219
 Remote sensing of smoke, clouds, and radiation using AVIRIS during SCAR experiments p 708 N95-33749
- CLOUD SEEDING**
 A new generation of instruments for flying laboratories [BTN-94-EIX94401363947] p 317 A95-75532
- CLOUDS**
 Analysis of the physical state of one Arctic polar stratospheric cloud based on observations [HTN-95-70917] p 351 A95-77982
- CLOUDS (METEOROLOGY)**
 Microwave and infrared simulations of an intense convective system and comparison with aircraft observations [HTN-95-60511] p 214 A95-68762
 High-resolution imaging of rain systems with the advanced microwave precipitation radiometer [HTN-95-70133] p 252 A95-70655
 Behavior of an inversion-based precipitation retrieval algorithm with high-resolution AMPR measurements including a low-frequency 10.7-GHz channel [HTN-95-70134] p 252 A95-70656
 Effects of a polar stratosphere cloud parameterization on ozone depletion due to stratospheric aircraft in a two-dimensional model p 443 A95-84543
 Airborne lidar observation of mountain-wave-induced polar stratospheric clouds during EASOE [HTN-95-00738] p 444 A95-86308
 The production of supercooled liquid water by a secondary cold front p 673 A95-93542
 An application of some cloud modeling techniques to a regional model simulation of an icing event p 673 A95-93543

CLUTTER

- Terminal Doppler Weather Radar point target filter threshold selection p 662 A95-93490
 Maximum-likelihood spectral estimation and adaptive filtering techniques with application to airborne Doppler weather radar [NASA-CR-197699] p 316 N95-23670
 Resource document for the design of electronic instrument approach procedure displays [AD-A295108] p 691 N95-34797
- COANDA EFFECT**
 Wind tunnel performance comparative test results of a circular cylinder and 50 percent ellipse tailboom for circulation control antitorque applications [AD-A283335] p 130 N95-18008
 Static investigation of two fluidic thrust-vectoring concepts on a two-dimensional convergent-divergent nozzle [NASA-TM-4574] p 120 N95-19042
 Static investigation of two fluidic thrust-vectoring concepts on a two-dimensional convergent-divergent nozzle [NASA-TM-4574] p 222 N95-19913
- COASTS**
 Aircraft icing measurements in East Coast winter storms [HTN-95-60505] p 214 A95-68756
- COATING**
 High velocity oxygen fuel spraying of erosion and wear resistant coatings on jet engine parts p 202 N95-19680
 Aircraft corrosion study [AD-A279527] p 241 N95-21687
 Organic coating technology for the protection of aircraft against corrosion p 303 N95-23513
 Corrosion in service experience with aircraft in France p 303 N95-23518
 A comparison of coating alternatives for US Coast Guard aircraft [AD-A293270] p 629 N95-31124
- COATINGS**
 Aircraft corrosion study [AD-A279527] p 241 N95-21687
 Mechanism of deposit formation on fuel-wetted hot metal surfaces [AD-A289847] p 426 N95-28621
 The effect of adding roughness and thickness to a transonic axial compressor rotor [NASA-TM-106958] p 645 N95-30524
 Machinability study of Aermet 100 [DE95-011532] p 701 N95-33408
- COAXIAL FLOW**
 Near field of a coaxial jet with and without axial excitation [HTN-95-42332] p 372 A95-86161
 Noise radiation by instability waves in coaxial jets [NASA-TM-106738] p 100 N95-14618
 The aeroustics of supersonic coaxial jets [NASA-TM-106782] p 101 N95-15059
 Supersonic coaxial jet noise predictions [NASA-TM-106917] p 451 N95-26801
- COAXIAL NOZZLES**
 Noise radiation by instability waves in coaxial jets [NASA-TM-106738] p 100 N95-14618
 The noise reduction potential of dual-stream coaxial rectangular improperly expanded jet flows [NASA-CR-197820] p 437 N95-26995
- COCKPIT SIMULATORS**
 Programmable cockpit research simulator [AD-A279219] p 204 N95-19848
 The photo-realistic AFIT virtual cockpit [AD-A289376] p 390 N95-26876
- COCKPITS**
 Flight-deck displays on the Boeing 777 [BTN-95-EIX95142562402] p 286 A95-73438
 Application of FEM/SEA for prediction of aircraft cockpit noise p 576 A95-90130
 Draft standard for color active matrix liquid crystal displays (AMLCDs) in US Military aircraft. Recommended best practices [AD-A282950] p 49 N95-12591
 Electromagnetic reverberation characteristics of a large transport aircraft [AD-A282923] p 82 N95-15392
 Industry review of a crew-centered cockpit design process and toolset [AD-A282966] p 130 N95-17661
 KC-135 cockpit modernization study. Phase 1: Equipment evaluation [AD-A284099] p 131 N95-18398
 The generic simulation executive at Manned Flight Simulator [AD-A283997] p 146 N95-18724
 An overall approach of cockpit noise verification in a military aircraft p 175 N95-19163

- Programmable cockpit research simulator
[AD-A279219] p 204 N95-19848
- Differential GPS and system integration of the Low Visibility Landing and Surface Operations (LVLASO) demonstration p 280 N95-23318
- A crew-centered flight deck design philosophy for High-Speed Civil Transport (HSCT) aircraft
[NASA-TM-109171] p 335 N95-24582
- Integrated mission precision attack cockpit technology (IMPACT). Phase 1: Identifying technologies for air-to-ground fighter integration
[AD-A289562] p 389 N95-26684
- An analysis of the KC-135 three-person cockpit
[AD-A289540] p 390 N95-26873
- The photo-realistic AFIT virtual cockpit
[AD-A289376] p 390 N95-26876
- Operator modeling in commercial aviation: Cognitive models, intelligent displays, and pilot's assistants
[NASA-CR-198609] p 401 N95-28203
- Three-D weather displays for aircraft cockpits
[AD-A289759] p 508 N95-28691
- Conceptual design of a map interactive system for military aircraft cockpits
[AD-A289760] p 508 N95-28692
- Optimizing cockpit display configurations with a genetic algorithm system
[AD-A289799] p 508 N95-29123
- CODING**
- Modeling helicopter blade dynamics using a modified Myklestad-Prohl transfer matrix method
[AD-A289891] p 400 N95-28626
- COEFFICIENT OF FRICTION**
- The effects of wall perturbations on thermo-turbulent Couette flow
[HTN-95-92255] p 434 A95-85299
- The role of fretting corrosion and fretting fatigue in aircraft rivet hole cracking p 94 N95-14470
- COGENERATION**
- Small gas turbine component evaluation study
[PB95-147542] p 338 N95-24293
- COGNITION**
- Intelligent tutoring system: F-16 flight simulation p 521 A95-90649
- Operator modeling in commercial aviation: Cognitive models, intelligent displays, and pilot's assistants
[NASA-CR-198609] p 401 N95-28203
- Automation and cognition in air traffic control: An empirical investigation
[AD-A291932] p 488 N95-28790
- COGNITIVE PSYCHOLOGY**
- Automation and cognition in air traffic control: An empirical investigation
[AD-A291932] p 488 N95-28790
- Resource document for the design of electronic instrument approach procedure displays
[AD-A295108] p 691 N95-34797
- COHERENT RADAR**
- Wake vortex detection at Denver Stapleton Airport with a pulsed 2-micron coherent lidar p 42 N95-13211
- COLD FRONTS**
- Nonhydrostatic simulation of frontogenesis in a moist atmosphere. Part 3: Thermal wind imbalance and rainbands
[HTN-95-90356] p 212 A95-66429
- Mesoscale structure of precipitation bands in a North Atlantic winter storm
[HTN-95-40659] p 215 A95-69803
- The production of supercooled liquid water by a secondary cold front p 673 A95-93542
- COLLIMATION**
- RCS measurements, transformations, and comparisons under cylindrical and plane wave illumination
[BTN-94-EIX94371347126] p 242 A95-69976
- COLLIMATORS**
- Fiber-optic rotary joint with bundle collimator assemblies
[AD-DO16504] p 258 N95-21673
- COLLISION AVOIDANCE**
- Automatic guidance and control for helicopter obstacle avoidance
[BTN-95-EIX95182619130] p 291 A95-76607
- Flight test evaluation of a 35 GHz forward looking altimeter for terrain avoidance
[BTN-95-EIX95212641071] p 287 A95-76736
- Airborne collision avoidance systems - The UK experience
[CONGRESS PAPER C428-7-146] p 488 A95-91687
- A tactical navigation and routing system for low-level flight p 709 N95-32494
- Laser based obstacle warning sensors for helicopters p 686 N95-32499
- COLLISIONS**
- Effects of satellite bunching on the probability of collision in geosynchronous orbit
[BTN-95-EIX95152583276] p 298 A95-73577
- A model for temperature-dependent collisional quenching of OH A(sup 2) Sigma(sup +)
[HTN-95-42308] p 450 A95-85002
- Aircraft accident report: Impact with blast fence upon landing rollout Action Air Charters flight 990 Piper PA-31-350, N990RA, Stratford, Connecticut, 27 April 1994
[PB94-910410] p 333 N95-24206
- COLOR**
- Color control in a multichannel simulator display: The display for advanced research and training
[AD-A279717] p 239 N95-20992
- Test and Evaluation Plan (TEP) for Improvised Explosive Device Screening Systems (IEDSS)
[AD-A286382] p 227 N95-22319
- Evaluation of alternative pavement marking materials
[AD-A292973] p 626 N95-31468
- COLORADO**
- Snow-band formation and evolution during the 15 November 1987 aircraft accident at Denver airport
[HTN-95-80699] p 254 A95-72543
- The real-time analysis and prediction of storms program p 655 A95-93457
- Preliminary results of high resolution measurements of snowfall at Stapleton International Airport during the winter of 1992-93 p 661 A95-93484
- Objective verification of an enhanced terminal forecast experiment at Denver, Colorado p 664 A95-93501
- Windshear detection: TDWR and LLWAS operational experience in Denver 1988-1992 p 670 A95-93528
- The production of supercooled liquid water by a secondary cold front p 673 A95-93542
- Preliminary studies of ice formation in upslope clouds p 674 A95-93546
- The development of an aircraft icing forecast technique using data from maps p 675 A95-93549
- The 1992-3 operational winter forecasting experiment for Stapleton airport p 677 A95-93561
- COLUMNS (SUPPORTS)**
- Equivalent beam-column analysis of guyed towers
[BTN-95-EIX95262696644] p 435 A95-85519
- COMBAT**
- Aircraft maneuver envelope warning system
[NASA-CASE-ARC-11953-1] p 82 N95-14518
- Bomber force 2000: Operational concepts for long-range combat aircraft
[AD-A279378] p 230 N95-20181
- A mathematical analysis of the Janus combat simulation weather effects models and sensitivity analysis of sky-to-ground brightness ratio on target detection
[AD-A289629] p 446 N95-26858
- COMBINATORIAL ANALYSIS**
- Passive MMW camera for low visibility landings p 59 N95-13215
- COMBUSTIBLE FLOW**
- Pulsed jet ignition modeling with a full chemistry p 538 A95-87184
- Intrinsic transport and chemistry coupling in combustion phenomena p 538 A95-87191
- Prediction of NO(x) emission index of turbulent diffusion flame p 538 A95-87195
- Influence of the flight trajectory on the exhaust gas composition of a H2-fueled air-breathing ramjet engine p 509 A95-87404
- Multidimensional calculation of spark flame initiation by adopting a generic hydrocarbon kinetic scheme p 528 A95-87566
- Effects of the chemical reaction model on calculations of supersonic combustion flows
[BTN-95-EIX0616952745802] p 638 A95-94487
- Shock tube investigations of combustion phenomena in supersonic flows
[PB94-175262] p 55 N95-11796
- Two-dimensional imaging of OH in a lean burning high pressure combustor
[NASA-TM-106854] p 236 N95-21383
- Numerical simulation of combustion flow around a flame holder with hydrogen injection
[NAL-TR-1233] p 419 N95-26523
- A laboratory scale supersonic combustive flow system
[DE95-006347] p 420 N95-27851
- An investigation of the side-dump dual in-line ramjet combustor p 617 N95-31199
- A pulsed liquid fuel ramjet p 617 N95-31201
- Combustion-acoustic stability analysis for premixed gas turbine combustors
[NASA-TM-107024] p 694 N95-32931
- Calculation of supersonic combustion in SCRAMJET engines p 698 N95-34513
- COMBUSTION**
- Studies on gain performance of a combustion driven CO2 gas dynamic laser p 428 A95-82679
- Two-dimensional imaging of OH in a lean burning high pressure combustor
[NASA-TM-106854] p 236 N95-21383
- Modeling aerosol emissions from the combustion of composite materials p 301 N95-23038
- Workshop report: Measurement techniques in highly transient, spectrally rich combustion environments
[AD-A288395] p 350 N95-25606
- Transport phenomena and interfacial kinetics in multiphase combustion systems
[AD-A288297] p 418 N95-26417
- Numerical simulation of combustion flow around a flame holder with hydrogen injection
[NAL-TR-1233] p 419 N95-26523
- NASA Lewis Research Center's preheated combustor and materials test facility
[NASA-TM-106676] p 626 N95-30592
- The 25th International Symposium on Combustion
[AD-A286825] p 630 N95-31268
- COMBUSTION CHAMBERS**
- Experimental and analytical investigations of wave enhanced supersonic combustors
[AIAA PAPER 89-2787] p 14 A95-60172
- Development and application of the double V type flame stabilizer
[BTN-94-EIX94481415355] p 154 A95-65345
- Aircraft engine emission reduction
[BTN-95-EIX95031502750] p 196 A95-68257
- Simulating heat addition via mass addition in constant area compressible flows
[BTN-95-EIX95182619100] p 307 A95-76585
- Prediction of pre-combustion shock in scramjet combustors: A new method p 402 A95-82323
- Experiment of rocket-ram annular combustor p 412 A95-82324
- Test results on air turbo-ramjet engine for a future space plane p 402 A95-82327
- Studies on plasma jet igniters p 403 A95-82680
- Control requirements for the RB 211 low-emission combustion system p 416 A95-84201
- [BTN-94-EIX95011441244] p 416 A95-84201
- Flex cycle combustor development and demonstration
[BTN-94-EIX95011441245] p 417 A95-84202
- Development of an aeroderivative gas turbine dry low emissions combustion system p 417 A95-84203
- [BTN-94-EIX95011441246] p 417 A95-84203
- Influence of the flight trajectory on the exhaust gas composition of a H2-fueled air-breathing ramjet engine p 509 A95-87404
- Scramjet combustor design in France
[AIAA PAPER 95-6094] p 510 A95-88002
- Conceptual studies of high speed combustors for mixing enhancement mechanisms
[AIAA PAPER 95-6095] p 510 A95-88003
- Modeling three-dimensional gas-turbine combustor model flow using second-moment closure
[HTN-95-20935] p 464 A95-88974
- The DCAF: A high-enthalpy long-duration, direct-connect scramjet test facility
[AIAA PAPER 95-6130] p 512 A95-90450
- An assessment of ground-test facility capabilities for measurement of hypervelocity scramjet performance
[AIAA PAPER 95-6148] p 512 A95-90462
- Aero-engine R&D efforts for environmental protection p 512 A95-91502
- Controlling mechanisms of ignition of solid fuel in a sudden-expansion combustor
[BTN-95-EIX0616952745791] p 628 A95-94255
- Efficient mapping topology for turbine combustors with inclined slots/staggered holes
[BTN-95-EIX0616952745805] p 614 A95-94485
- Evaluation of the transient operation of advanced gas turbine combustors
[BTN-95-EIX0616952745793] p 614 A95-94495
- Vortex generation and mixing in three-dimensional supersonic combustors
[BTN-95-EIX0616952745783] p 614 A95-94503
- Investigation of scramjet injection strategies for high mach number flows
[BTN-95-EIX0616952745782] p 614 A95-94504
- Numerical simulation of the 3D turbulent flow around the combustor dome of an aircraft engine p 640 A95-95423
- Propulsion research concerning SFRJ-motors
[PB94-179520] p 14 N95-10083
- Hydrocarbon-fueled ramjet/scramjet technology program, phase 2 extension
[NASA-CR-189659] p 15 N95-10319
- Visualization of one-dimensional flow processes in a dual-mode scramjet engine p 15 N95-10465
- Engine structures analysis software: Component Specific Modeling (COSMO)
[NASA-CR-195378] p 57 N95-11711
- Shock-tunnel combustor testing for hypersonic vehicles
[NASA-CR-196836] p 52 N95-11938
- Combustion efficiency in a dual-inlet side-dump ramjet combustor
[AD-A283564] p 83 N95-15329

Gas turbine prediffuser-combustor performance during operation with air-water mixture
 [DOT/FAA/CT-93/52] p 83 N95-15683
 A model for preliminary facility design including simulation issues p 144 N95-16318
 Sensitivity of combustion-acoustic instabilities to boundary conditions for premixed gas turbine combustors
 [NASA-TM-106890] p 289 N95-23550
 Effect of density gradients in confined supersonic shear layers, part 1
 [NASA-CR-198029] p 348 N95-24412
 Effect of density gradients in confined supersonic shear layers. Part 2: 3-D modes
 [NASA-CR-198030] p 349 N95-24413
 Experiment on a rectangular cross section scramjet combustor. 2: Effects of fuel injector geometry
 [NAL-TR-1220] p 405 N95-26600
 NASA Lewis Research Center's combustor test facilities and capabilities
 [NASA-TM-106903] p 412 N95-27176
 Combustion system CFD modeling at GE Aircraft Engines p 439 N95-27889
 Experimental investigation of inlet-combustor isolators for a dual-mode scramjet at a Mach number of 4
 [NASA-TP-3502] p 407 N95-28343
 Ceramic composite combustor cans for expendable turbine engines
 [AD-A289551] p 407 N95-28646
 NASA Lewis Research Center's preheated combustor and materials test facility
 [NASA-TM-106676] p 626 N95-30592
 Jet mixing and emission characteristics of transverse jets in annular and cylindrical confined crossflow
 [NASA-TM-106976] p 616 N95-30698
 Jet mixing in a reacting cylindrical crossflow
 [NASA-TM-106975] p 616 N95-30853
 Experimental investigation of turbulent particle dispersion in swirling flows
 [DLR-FB-94-20] p 647 N95-31355
 Combustion-acoustic stability analysis for premixed gas turbine combustors
 [NASA-TM-107024] p 694 N95-32931
 Water model tests on the Allison T56 series 3 combustion system
 [DSTO-TR-0139] p 697 N95-33250
 A study of supersonic mixing flow field with ramp injector p 706 N95-34512

COMBUSTION CHEMISTRY
 Pulsed jet ignition modeling with a full chemistry p 538 N95-87184
 Intrinsic transport and chemistry coupling in combustion phenomena p 538 N95-87191
 Transport phenomena and interfacial kinetics in multiphase combustion systems
 [AD-A288297] p 418 N95-26417
 The 25th International Symposium on Combustion
 [AD-A286825] p 630 N95-31268

COMBUSTION EFFICIENCY
 Scramjet combustor design in France
 [AIAA PAPER 95-6094] p 510 N95-88002
 Injection studies in the French hypersonic technology program
 [AIAA PAPER 95-6096] p 510 N95-88004
 Combustion efficiency in a dual-inlet side-dump ramjet combustor
 [AD-A283564] p 83 N95-15329
 Combustor kinetic energy efficiency analysis of the hypersonic research engine data p 148 N95-16321
 Experimental and analytical methods for the determination of connected-pipe ramjet and ducted rocket internal performance
 [AGARD-AR-323] p 149 N95-17278
 Sensitivity of combustion-acoustic instabilities to boundary conditions for premixed gas turbine combustors
 [NASA-TM-106890] p 289 N95-23550
 Experiment on a rectangular cross section scramjet combustor. 2: Effects of fuel injector geometry
 [NAL-TR-1220] p 405 N95-26600

COMBUSTION PHYSICS
 Studies on plasma jet igniters p 403 N95-82680
 High pressure vaporization and burning of methanol droplets in reduced gravity p 527 N95-87285
 Shock tube investigations of combustion phenomena in supersonic flows
 [PB94-175262] p 55 N95-11796
 Workshop report: Measurement techniques in highly transient, spectrally rich combustion environments
 [AD-A288395] p 350 N95-25606
 Workshop report: Measurement techniques in highly transient, spectrally rich combustion environments
 p 629 N95-31208
 The 25th International Symposium on Combustion
 [AD-A286825] p 630 N95-31268

Review of combustion-acoustic instabilities
 [NASA-TM-107020] p 705 N95-32930

COMBUSTION PRODUCTS
 Aircraft engine emission reduction
 [BTN-95-EIX95031502750] p 196 N95-68257
 Prediction of NO(x) emission index of turbulent diffusion flame p 538 N95-87195
 Numerical study of contaminant effects on combustion of hydrogen, ethane, and methane in air
 [AIAA PAPER 95-6097] p 510 N95-88005
 Wave cycle design for wave rotor engines with limited nitrogen oxide emissions p 161 N95-18901
 Developing an emission factor for hazardous air pollutants for an F-16 using JP-8 fuel
 [AD-A284802] p 216 N95-19685
 Laboratory evaluation of a reactive baffle approach to NOx control
 [AD-A283802] p 255 N95-19921
 Aircraft fires, smoke toxicity, and survival: An overview
 [DOT/FAA/AM-95/8] p 277 N95-24024
 Measurements of ions formed in jet engine exhaust plumes
 [AD-A290940] p 514 N95-29764

COMBUSTION STABILITY
 Sensitivity of combustion-acoustic instabilities to boundary conditions for premixed gas turbine combustors
 [NASA-TM-106890] p 289 N95-23550
 Review of combustion-acoustic instabilities
 [NASA-TM-107020] p 705 N95-32930
 Combustion-acoustic stability analysis for premixed gas turbine combustors
 [NASA-TM-107024] p 694 N95-32931

COMBUSTION TEMPERATURE
 Ultimate characteristics of a rocket engine with a turbo-pump supply system
 [BTN-94-EIX94461408757] p 148 N95-63640
 NASA Lewis Research Center's combustor test facilities and capabilities
 [NASA-TM-106903] p 412 N95-27176
 NASA Lewis Research Center's preheated combustor and materials test facility
 [NASA-TM-106676] p 626 N95-30592

COMBUSTION WIND TUNNELS
 The DCAF: A high-enthalpy long-duration, direct-connect scramjet test facility
 [AIAA PAPER 95-6130] p 512 N95-90450

COMFORT
 Human factors issues in aircraft cabin design
 [SAE PAPER 932527] p 386 N95-84556

COMMAND AND CONTROL
 Evolutionary Telemetry and Command Processor (TCP) architecture p 86 N95-14162
 Spread spectrum applications in unmanned aerial vehicles
 [AD-A281035] p 156 N95-16448
 Workshop on Formal Models for Intelligent Control
 [AD-A281399] p 169 N95-16864
 Packet utilisation definitions for the ESA XMM mission p 150 N95-17596
 The controller memory guide. Concepts from the field
 [AD-A289263] p 383 N95-26978
 The DLR research programme on an integrated multi sensor system for surface movement guidance and control p 689 N95-33135

COMMAND GUIDANCE
 Safety aspects of spacecraft commanding p 149 N95-17248
 Low-level data fusion for landing runways detection p 689 N95-33136

COMMAND LANGUAGES
 A users manual for the method of moments Aircraft Modeling Code (AMC), version 2
 [NASA-CR-196445] p 24 N95-11252

COMMERCE
 Effects of the specific military aspects of satellite navigation on the civil use of GPS/GLONASS p 688 N95-33134

COMMERCIAL AIRCRAFT
 Automatic riveting cell for commercial aircraft floor grid assembly
 [BTN-95-EIX95182617807] p 261 N95-75752
 Maintenance challenges and trends
 [BTN-95-EIX95182617808] p 261 N95-75753
 Maintenance programs
 [BTN-95-EIX95182617809] p 261 N95-75754
 Application of direct transcription to commercial aircraft trajectory optimization
 [BTN-95-EIX95242670766] p 359 N95-81081
 FAA's Aging Commuter Airplane Program
 [SAE PAPER 931248] p 483 N95-89220
 The FAA regional/commuter aircraft flight loads data collection program
 [SAE PAPER 931258] p 493 N95-89224

Engine/airframe installation CFD for commercial transports: An engine manufacturer's perspective
 [SAE PAPER 932623] p 495 N95-90084
 Civil aircraft propulsion integration: Current & future
 [SAE PAPER 932624] p 495 N95-90085
 Twenty-first century commercial transport engines
 p 512 N95-91495
 Some comments on current research and development of civil VTOL aircrafts p 499 N95-91572
 Condensing cycle air conditioning system
 [SAE PAPER 932056] p 513 N95-91637
 What's next in commercial aircraft environmental control systems?
 [SAE PAPER 932057] p 513 N95-91638
 Deaths and injuries as a result of lightning strikes to aircraft
 [HTN-95-12213] p 485 N95-91913
 Estimation of atmospheric turbulence severity from in-situ aircraft measurements p 659 N95-93479
 The basis of civil certification and continued airworthiness for composite aircraft structures
 [CONGRESS PAPER C428-37-173] p 628 N95-93632
 Reanalysis of European flight loads data
 [AD-A282052] p 9 N95-11179
 Comments on the use of structureborne noise analysis for large commercial airplanes p 30 N95-11287
 General Aviation Task Force report
 [NASA-TM-109950] p 1 N95-11463
 The performance of child restraint devices in transport airplane passenger seats
 [DOT/FAA/AM-94/19] p 40 N95-12146
 The FC-1D: The profitable alternative Flying Circus Commercial Aviation Group
 [NASA-CR-197152] p 46 N95-12628
 Central coast designs: The Eightball Express. Taking off with convention, cruising with improvements and landing with absolute success
 [NASA-CR-197181] p 47 N95-12643
 LCX: Proposal for a low-cost commercial transport
 [NASA-CR-197186] p 47 N95-12645
 Proceedings of the FAA Inspection Program Area Review
 [AD-A283849] p 77 N95-14350
 Evaluation of bonded boron/epoxy doublers for commercial aircraft aluminum structures
 p 92 N95-14457
 Annual review of aircraft accident data: US air carrier operations, calendar year 1992
 [PB95-100319] p 78 N95-15066
 The Aluminum Falcon: A low cost modern commercial transport
 [NASA-CR-197180] p 81 N95-15742
 Annual review of aircraft accident data: US Air carrier operations, calendar year 1992
 [PB95-100319] p 123 N95-17748
 DLR-F4 wing body configuration p 130 N95-17863
 Census US civil aircraft calendar year 1993
 [AD-A286309] p 219 N95-20091
 Commuter/air taxi ditchings and water-related impacts that occurred from 1979 to 1989
 [AD-A285691] p 226 N95-20275
 Why do airlines want and use thrust reversers? A compilation of airline industry responses to a survey regarding the use of thrust reversers on commercial transport airplanes
 [NASA-TM-109158] p 226 N95-20706
 Preparation of course materials: Elementary mathematics of powered flight p 324 N95-23320
 Aircraft accident report. Runway overrun following rejected takeoff. Continental airlines flight 795, McDonnell Douglas MD-82, N18835, LaGuardia Airport, Flushing, NY, 2 March 1994
 [PB95-910401] p 277 N95-23609
 Consistent approach to describing aircraft HIRF protection
 [NASA-CR-195067] p 334 N95-25341
 Emerging nondestructive inspection for aging aircraft
 [PB95-143053] p 328 N95-25401
 Strategy in the commercial aircraft industry in the United States: A comparison of decisionmaking by McDonnell-Douglas and Boeing aircraft companies from 1977-1983
 [AD-A288289] p 366 N95-26409
 Radiation safety aspects of commercial high-speed flight transportation
 [NASA-TP-3524] p 453 N95-26427
 An integrated GPS/INS/BARO and radar altimeter system for aircraft precision approach landings
 [AD-A289280] p 383 N95-26985
 Study of potential aerodynamic benefits from spanwise blowing at wingtip
 [NASA-TP-3515] p 378 N95-28669
 In situ processing methods for composite fuselage sandwich structures p 531 N95-28826

- The effect of wear on fire-blocking layer material effectiveness
[AD-A291520] p 485 N95-29855
- Electrochemical impedance pattern recognition for detection of hidden chemical corrosion on aircraft components, phase 1
[AD-A291345] p 556 N95-29946
- Electrical short circuit and current overload tests on aircraft wiring
[AD-A293308] p 646 N95-30922
- Integration of air traffic databases: A case study
[AD-A293691] p 602 N95-32022
- Standardization work
p 651 N95-32181
- Report to the Chairman, Subcommittee on Aviation, Committee on Commerce, Science, and Transportation, US Senate. Aviation safety: Data problems threaten FAA strides on safety analysis system
[GAO/AIMD-95-27] p 687 N95-32705
- COMMONALITY**
- The opportunities for and challenges of common integrated electronics
[AD-A279991] p 248 N95-20966
- COMMONWEALTH OF INDEPENDENT STATES**
- Overview of AlliedSignal's avionics development in the CIS
[BTN-95-EIX95212641069] p 287 A95-76734
- COMMUNICATION**
- Pilot rating scale for aircraft handling qualities
[HTN-95-42269] p 380 A95-84963
- Independent review of Aviation Technology and Research Information Analysis System (ATRIAS) database
[AD-A284049] p 226 N95-21518
- COMMUNICATION EQUIPMENT**
- Airborne integrated communications system
[CONGRESS PAPER C428-30-162] p 610 A95-93612
- COMMUNICATION NETWORKS**
- Use of MOBITEK wireless wide area networks as a solution to land-based positioning and navigation
[BTN-94-EIX94441386132] p 189 A95-68188
- GateLink highspeed communications with parked aircraft
[SAE PAPER 932610] p 486 A95-90079
- Aeronautical satellite communications using the ETS-5 satellite
p 487 A95-91541
- Optical backplane for modular avionics
p 257 N95-20652
- COMMUNITIES**
- The effects and prediction of rotary wing aircraft noise on the community
[HTN-95-92536] p 558 A95-87356
- COMMUTATION**
- Dynamically timed electric motor
[NASA-CASE-MFS-28958-1] p 437 N95-26890
- COMMUTER AIRCRAFT**
- Fatigue evaluation of empennage, forward wing, and winglets/tip fins on part 23 airplanes
[PB94-196813] p 79 N95-13981
- Safety study: Commuter airline safety
[PB94-917004] p 124 N95-19132
- Commuter airplane accident data analysis
[AD-A286315] p 226 N95-20174
- Emerging nondestructive inspection for aging aircraft
[PB95-143053] p 328 N95-25401
- COMPARISON**
- Small gas turbines in the 21st century
[BTN-94-EIX94461290241] p 82 A95-61736
- Comparison of wind profiler and aircraft wind measurements at Chebogue Point, Nova Scotia
[HTN-95-41833] p 353 A95-80559
- An intercomparison of aircraft instrumentation for tropospheric measurements of sulfur dioxide
[HTN-95-91855] p 354 A95-80843
- An intercomparison of aircraft instrumentation for tropospheric measurements of carbonyl sulfide, hydrogen sulfide, and carbon disulfide
[HTN-95-91856] p 355 A95-80844
- An intercomparison of instrumentation for tropospheric measurements of dimethyl sulfide: Aircraft results for concentrations at the parts-per-trillion level
[HTN-95-91857] p 355 A95-80845
- Estimation of aerodynamic derivatives: Euler scheme validation and approximate methods for hypersonic configurations
p 460 A95-87385
- Compressible Navier-Stokes calculations of the flow over airfoil sections. Comparisons of 1st and 2nd order turbulence models
[SAE PAPER 932510] p 546 A95-89183
- Preliminary comparisons between MM5 NCAR/Penn State model generated icing forecasts and observations
p 655 A95-93458
- NEXRAD/ARSR operational comparison
p 658 A95-93470
- The performance of forward scatter visibility sensors for application in autostations and runway visual range in snow and freezing precipitation events
p 662 A95-93489
- Flight and full-scale wind-tunnel comparison of pressure distributions from an F-18 aircraft at high angles of attack — Conducted in NASA Ames Research Center's 80 by 120 ft wind tunnel
p 68 N95-14231
- An in situ evaluation of TOPEX/Poseidon altimetric measurements versus measurements made by moorings and inverted echo sounders for sea surface height
[NASA-CR-198621] p 447 N95-27805
- COMPARTMENTS**
- Laws of infrared similitude
[AD-A282209] p 62 N95-12426
- Facilities used for plastic media blasting
p 627 N95-32176
- COMPASSES**
- Interfacing a digital compass to a remote-controlled helicopter
[PB95-164927] p 340 N95-24260
- COMPENSATORS**
- Modeling and control of rotating stall in high speed multi-stage axial compressors
p 513 N95-29244
- COMPLEX SYSTEMS**
- Integrated test system single point control of aircraft checkout
[SAE PAPER 931417] p 583 A95-93682
- Laws of infrared similitude
[AD-A282209] p 62 N95-12426
- Aero design of turbomachinery components: CFD in complex systems
p 90 N95-14136
- Algorithms for bilevel optimization
[NASA-CR-194980] p 170 N95-16897
- Digital systems validation. Chapter 20 Artificial Intelligence with applications for aircraft. Handbook, volume 2
[AD-A288492] p 448 N95-26638
- The controller memory guide. Concepts from the field
[AD-A289263] p 383 N95-26978
- A rose by any other name: Certification seen as process rather than content
p 688 N95-34766
- Human factors certification in the development of future air traffic control systems
p 690 N95-34770
- Quality assurance and risk management: Perspectives on Human Factors Certification of Advanced Aviation Systems
p 690 N95-34771
- COMPLEX VARIABLES**
- Unbalance response of a dual rotor system: Theory and experiment
[BTN-94-EIX94351143320] p 195 A95-65854
- Study of multiple cracks in airplane fuselage by micromechanics and complex variables
p 94 N95-14468
- COMPONENT RELIABILITY**
- Mechanical system reliability and risk assessment
[BTN-95-EIX95142553046] p 304 A95-73452
- Dependability issues in the reuse of standard components in open architectures
[AIAA PAPER 95-1006] p 566 A95-90678
- The air systems controllerate initiatives and policies for the procurement of reliable and maintainable equipment
[CONGRESS PAPER C428-6-113] p 549 A95-91682
- The impact of new technology on reliability of avionic equipment
[CONGRESS PAPER C428-6-114] p 549 A95-91683
- The avionics integrity programme (AVIP)
[CONGRESS PAPER C428-6-115] p 549 A95-91684
- Residual life and strength estimates of aircraft structural components with MSD/MED
p 136 N95-19485
- COMPOSITE MATERIALS**
- Composite propeller system for Domier 328
[BTN-94-EIX94461290506] p 66 A95-61728
- Numerical modelling of transverse impact on composite coupons
[HTN-95-EIX95082502225] p 240 A95-71022
- Aircraft Symposium, 30th, Tsukuba, Japan, Sep. 30 - Oct. 2, 1992
[HTN-95-A1609] p 498 A95-91491
- Computer aided static aeroelastic analysis of wing/pylon/store combination
p 499 A95-91531
- Repairs to composite structure on military aircraft
[CONGRESS PAPER C428-4-067] p 531 A95-91677
- Intelligent skins development for future military aircraft
[CONGRESS PAPER C428-17-189] p 531 A95-91714
- Stability analysis for elastically tailored rotor blades
[ISBN 1-879921-01-4] p 635 A95-93703
- Application of integral methods to ablation charring erosion, a review
[BTN-95-EIX95302694460] p 636 A95-94057
- Advanced composites structural concepts and materials technologies for primary aircraft structures. Structural response and failure analysis: ISPAN modules users manual
[NASA-CR-4449] p 12 N95-10242
- Ten-year ground exposure of composite materials used on the Bell Model 206L helicopter flight service program
[NASA-TP-3468] p 55 N95-12357
- Development of a composite repair and the associated inspection intervals for the F-111C stiffener runout region
p 66 N95-14477
- Fatigue in single crystal nickel superalloys
[AD-A285727] p 152 N95-18068
- Conference on Aerospace Transparent Materials and Enclosures, Volume 2: Sessions 5-9
[AD-A283926] p 131 N95-18162
- Conference on Aerospace Transparent Materials and Enclosures, volume 1
[AD-A283925] p 133 N95-18677
- Environmental effects on composite airframes: A study conducted for the ARM UAV Program (Atmospheric Radiation Measurement Unmanned Aerospace Vehicle)
[DE94-015351] p 206 N95-19579
- Composite cases for airborne electronic equipment: A technology study and EMC
p 241 N95-20655
- Lightweight electronic enclosures using composite materials
p 241 N95-20656
- Modeling aerosol emissions from the combustion of composite materials
p 301 N95-23038
- Review of aeronautical fatigue investigation in the Netherlands during the period March 1991-March 1993
[PB95-139184] p 285 N95-23161
- NASA-UVA light aerospace alloy and structures technology program (LA2ST)
[NASA-CR-198041] p 343 N95-24220
- JPRS report: Science and technology. Central Eurasia
[JPRS-UST-94-018] p 349 N95-24472
- A FEAM based methodology for analyzing composite patch repairs of metallic structures
p 394 N95-27511
- Rapid repair of large area damage to contoured aircraft structures
p 394 N95-27516
- Repair of high temperature composite aircraft structures
p 395 N95-27520
- Composite repair of composite structures
p 395 N95-27521
- Damage occurrence on composites during testing and fleet service: Repair of Airbus aircraft
p 396 N95-27526
- The development of an engineering standard for composite repairs
p 396 N95-27528
- Process and control systems for composites manufacturing
p 420 N95-28267
- Advanced tow placement of composite fuselage structure
p 420 N95-28271
- ACT/ICAPS: Thermoplastic composite activities
p 421 N95-28274
- Resin transfer molding of textile preforms for aircraft structural applications
p 421 N95-28276
- Analysis techniques for the prediction of springback in formed and bonded composite components
p 421 N95-28289
- Utilization of composite materials by the US Army: A look ahead
p 421 N95-28421
- Benefits and limitations of composites in carrier-based aircraft
p 422 N95-28422
- Development of composite carrythrough bulkhead
p 423 N95-28438
- Reliability analysis of composite structures
p 423 N95-28441
- Navy composite maintenance and repair experience
p 424 N95-28446
- Overview of the ACT program
p 424 N95-28463
- Technology integration box beam failure study
p 441 N95-28468
- Tension fracture of laminates for transport fuselage. Part 1: Material screening
p 398 N95-28471
- Recent progress in NASA Langley textile reinforced composites program
p 425 N95-28475
- Impact damage resistance of composite fuselage structure, part 1
p 399 N95-28482
- Applications of a damage tolerance analysis methodology in aircraft design and production
p 426 N95-28483
- The effects of design details on cost and weight of fuselage structures
p 501 N95-28831
- Impact damage resistance of composite fuselage structure, part 2
p 533 N95-28838
- ISPAN (Interactive Stiffened Panel Analysis): A tool for quick concept evaluation and design trade studies
p 533 N95-28846
- Technology integration box beam failure study
p 552 N95-28847
- IPACS (Integrated Probabilistic Assessment of Composite Structures): Code development and applications
p 534 N95-28849
- Third NASA Advanced Composites Technology Conference, volume 1, part 1
[NASA-CP-3178-VOL-1-PT-1] p 534 N95-29029
- Advanced composites technology program
p 534 N95-29032

- Textile composite fuselage structures development p 534 N95-29033
- Advanced composite fuselage technology p 535 N95-29034
- Performance of resin transfer molded multiaxial warp knit composites p 535 N95-29039
- Aircraft advanced materials research and development program plan [AD-A290542] p 505 N95-29565
- The effect of interface properties on nickel base alloy composites [NASA-CR-198363] p 629 N95-30787
- Development of stitched/RTM primary structures for transport aircraft [NASA-CR-191441] p 630 N95-31421
- COMPOSITE STRUCTURES**
- Finite element time domain - modal formulation for nonlinear flutter of composite panels [BTN-95-EIX95042474401] p 203 A95-68299
- Twisting smartly in the wind [BTN-95-EIX95041503093] p 184 A95-68353
- Bonded composite repair of cracked load-bearing holes [BTN-94-EIX94401360553] p 243 A95-71867
- Air and ground resonance of helicopters with elastically tailored composite rotor blades [HTN-95-A0497] p 222 A95-72568
- Nonlinear angle of twist of advanced composite wing boxes under pure torsion [BTN-95-EIX95152582323] p 281 A95-73526
- Static aeroelastic characteristics of a composite wing [BTN-95-EIX95152582340] p 282 A95-73542
- H-76B fantail demonstrator composite fan blade fabrication [HTN-95-80856] p 283 A95-75098
- Experimental evaluation of a box beam specifically tailored for chordwise deformation [BTN-95-EIX95182619088] p 283 A95-75773
- Shear buckling response of tailored composite plates [HTN-95-51680] p 418 A95-85062
- Torsional actuation with extension-torsion composite coupling and a magnetostrictive actuator [BTN-95-EIX95262694314] p 435 A95-85485
- Non-linear analysis provides new insights into impact damage of composite structures [HTN-95-42368] p 418 A95-86197
- Rapid prototyping of composite aircraft structures [SAE PAPER 931219] p 539 A95-87530
- Buckling and postbuckling of composite structures [HTN-95-71387] p 528 A95-87605
- Aeroelastic response of composite rotor blades considering transverse shear and structural damping [HTN-95-81647] p 542 A95-87695
- An investigation of the accuracy of FEM analysis of a graphite epoxy box beam [SAE PAPER 931221] p 543 A95-88011
- Lightning protection technology for small general aviation composite material aircraft [SAE PAPER 931241] p 483 A95-88964
- Structural composites in civil gas turbine aero engines [HTN-95-B0258] p 529 A95-89202
- Optimum design of composite stiffened wing panels - a parametric study [HTN-95-01088] p 496 A95-90274
- Effects of structural damping on aeroelastic stability of various shaped composite plate wing p 530 A95-91530
- Supersonic flutter analysis of cantilevered composite plate-wings p 499 A95-91567
- Damage to composite aircraft structures from lightning strike attachment to unprotected CFC and internal sparking causing fuel injection [CONGRESS PAPER C428-4-026] p 531 A95-91675
- The basis of civil certification and continued airworthiness for composite aircraft structures [CONGRESS PAPER C428-37-173] p 628 A95-93632
- The certification of composite structures for military aircraft [CONGRESS PAPER C428-37-198] p 628 A95-93633
- Damage tolerance certification of a fighter horizontal stabilizer [BTN-95-EIX0619952748186] p 637 A95-94478
- Residual strength of composites with multiple impact damage [BTN-94-EIX94511433967] p 701 A95-96664
- Aeroelastic tailoring research [PB94-180031] p 6 N95-10135
- Advanced composites structural concepts and materials technologies for primary aircraft structures: Structural response and failure analysis: ISPAN modules users manual [NASA-CR-4449] p 12 N95-10242
- Advanced composites structural concepts and materials technologies for primary aircraft structures: Design/manufacturing concept assessment [NASA-CR-4447] p 12 N95-10316
- Novel matrix resins for composites for aircraft primary structures, phase 1 [NASA-CR-189657] p 23 N95-10318
- Electromagnetic on-aircraft antenna radiation in the presence of composite plates [NASA-CR-196126] p 58 N95-12856
- Residual strength of composites with multiple impact damage [AD-A284230] p 87 N95-14409
- Service and physical properties of liquid-jet fuels p 151 N95-16256
- Composite chronicles: A study of the lessons learned in the development, production, and service of composite structures [NASA-CR-4620] p 151 N95-16859
- Optimization of adaptive intraply hybrid fiber composites with reliability considerations [NASA-TM-106632] p 157 N95-16911
- Wing design for a civil tiltrotor transport aircraft [NASA-CR-197523] p 130 N95-18090
- Compression strength of composite primary structural components [NASA-CR-197554] p 160 N95-18388
- Impact of Acoustic Loads on Aircraft Structures [AGARD-CP-549] p 173 N95-19142
- Mishap risk control for advanced aerospace/composite materials p 301 N95-23031
- Development and verification of a resin film infusion/resin transfer molding simulation model for fabrication of advanced textile composites [NASA-CR-197439] p 301 N95-23179
- Thin tailored composite wing for civil tiltrotor p 285 N95-23317
- US Navy operating experience with new aircraft construction materials p 303 N95-23517
- Composite Repair of Military Aircraft Structures [AGARD-CP-550] p 392 N95-27504
- Bonded composite repair of metallic aircraft components: Overview of Australian activities p 392 N95-27505
- Composite repair of metallic airframe: Twenty years of experience p 393 N95-27508
- A FEAM based methodology for analyzing composite patch repairs of metallic structures p 394 N95-27511
- Structural modification and repair of C-130 wing structure using bonded composites p 394 N95-27512
- Field repair materials for naval aircraft p 394 N95-27514
- Rapid repair of large area damage to contoured aircraft structures p 394 N95-27516
- Composite repair of a CF18: Vertical stabilizer leading edge p 395 N95-27517
- Composite repair issues on the CF-18 aircraft p 395 N95-27518
- Repair technology for thermoplastic aircraft structures p 395 N95-27519
- Repair of high temperature composite aircraft structure p 395 N95-27520
- Composite repair of composite structures p 395 N95-27521
- Scarf joint technique with cocured and precured patches for composite repair p 396 N95-27524
- Damage occurrence on composites during testing and fleet service: Repair of Airbus aircraft p 396 N95-27526
- Repairs of CFC primary structures p 396 N95-27527
- The development of an engineering standard for composite repairs p 396 N95-27528
- Load transfer in the stiffener-to-skin joints of a pressurized fuselage [NASA-CR-198810] p 439 N95-27865
- Aeroelasticity and structural optimization of composite helicopter rotor blades with swept tips [NASA-CR-4665] p 397 N95-28262
- Static and fatigue testing of full-scale fuselage panels fabricated using a Therm-X(R) process p 420 N95-28270
- Advanced tow placement of composite fuselage structure p 420 N95-28271
- ACT/ICAPS: Thermoplastic composite activities p 421 N95-28274
- Composite intermediate case manufacturing scale-up for advanced engines p 406 N95-28275
- Resin transfer molding of textile preforms for aircraft structural applications p 421 N95-28276
- Analysis of aircraft engine blade subject to ice impact p 407 N95-28277
- Application of fiber-reinforced bismaleimide materials to aircraft nacelle structures p 397 N95-28278
- Composite flight-control actuator development p 410 N95-28281
- Analysis techniques for the prediction of springback in formed and bonded composite components p 421 N95-28289
- Ninth DOD/NASA/FAA Conference on Fibrous Composites in Structural Design, volume 1 [NASA-CR-198723] p 421 N95-28420
- The effect of material heterogeneity in curved composite beams for use in aircraft structures p 422 N95-28426
- Analysis of composite structures with delaminations under combined bending and compression p 422 N95-28429
- Application of advanced material systems to composite frame elements p 422 N95-28432
- Unique considerations in the design and experimental evaluation of tailored wings with elastically produced chordwise camber p 423 N95-28436
- Effects of floor location on response of composite fuselage frames p 423 N95-28439
- Structural design optimization with survivability dependent constraints application: Primary wing box of a multi-role fighter p 398 N95-28440
- Reliability analysis of composite structures p 423 N95-28441
- Probabilistic design of advanced composite structure p 424 N95-28443
- Navy composite maintenance and repair experience p 424 N95-28446
- Ninth DOD/NASA/FAA Conference on Fibrous Composites in Structural Design, volume 2 [NASA-CR-198722] p 424 N95-28462
- Overview of the ACT program p 424 N95-28463
- COINS: A composites information database system p 453 N95-28465
- Composite fuselage shell structures research at NASA Langley Research Center p 425 N95-28466
- Structural testing of the technology integration box beam p 441 N95-28467
- Technology integration box beam failure study p 441 N95-28468
- Development of stitched/RTM composite primary structures p 425 N95-28469
- Test and analysis results for composite transport fuselage and wing structures p 398 N95-28470
- Local design optimization for composite transport fuselage crown panels p 398 N95-28473
- Composite fuselage crown panel manufacturing technology p 399 N95-28474
- Recent progress in NASA Langley textile reinforced composites program p 425 N95-28475
- Advanced textile applications for primary aircraft structures p 399 N95-28476
- Characterization and manufacture of braided composites for large commercial aircraft structures p 426 N95-28478
- Application of damage tolerance methodology in certification of the Piaggio P-180 Avanti p 399 N95-28480
- Compressive strength of damaged and repaired composite plates p 442 N95-28484
- Damage tolerance of a geodesically stiffened advanced composite structural concept for aircraft structural applications p 399 N95-28487
- Advanced wing design survivability testing and results p 400 N95-28488
- NASA-ACEE/Boeing 737 graphite-epoxy horizontal stabilizer service p 400 N95-28489
- SMART materials: Surfaces, transforms and interfaces. The commensurate engineering dimension [AD-A289598] p 442 N95-28649
- Third NASA Advanced Composites Technology Conference, volume 1, part 2 [NASA-CP-3178-VOL-1-PT-2] p 531 N95-28823
- In situ processing methods for composite fuselage sandwich structures p 531 N95-28826
- The effects of design details on cost and weight of fuselage structures p 501 N95-28831
- Automated fiber placement: Evolution and current demonstrations p 532 N95-28832
- Manufacturing scale-up of composite fuselage crown panels p 532 N95-28835
- Design, analysis, and fabrication of a pressure box test fixture for tension damage tolerance testing of curved fuselage panels p 533 N95-28839
- Global cost and weight evaluation of fuselage keel design concepts p 501 N95-28840
- A weight-efficient design strategy for cutouts in composite transport structures p 533 N95-28843
- Buckling analysis of curved composite sandwich panels subjected to inplane loadings p 533 N95-28845

- ISpan (Interactive Stiffened Panel Analysis): A tool for quick concept evaluation and design trade studies p 533 N95-28846
- Technology integration box beam failure study p 552 N95-28847
- A global/local analysis method for treating details in structural design p 552 N95-28848
- IPACS (Integrated Probabilistic Assessment of Composite Structures): Code development and applications p 534 N95-28849
- Advanced composite structural concepts and materials technologies for primary aircraft structures: Advanced material concepts [NASA-CR-4485] p 503 N95-29027
- Third NASA Advanced Composites Technology Conference, volume 1, part 1 [NASA-CP-3178-VOL-1-PT-1] p 534 N95-29029
- Impact of composites on future transport aircraft p 534 N95-29030
- Challenges and payoff of composites in transport aircraft: 777 empennage and future applications p 534 N95-29031
- Advanced composites technology program p 534 N95-29032
- Textile composite fuselage structures development p 534 N95-29033
- Advanced composite fuselage technology p 535 N95-29034
- Advanced resin systems and 3D textile preforms for low cost composite structures p 535 N95-29035
- Performance of resin transfer molded multiaxial warp knit composites p 535 N95-29039
- Cost model relationships between textile manufacturing processes and design details for transport fuselage elements p 536 N95-29043
- Development of RTM and powder prepreg resins for subsonic aircraft primary structures p 536 N95-29044
- Progress in manufacturing large primary aircraft structures using the stitching/RTM process p 537 N95-29050
- Test results from large wing and fuselage panels p 537 N95-29051
- Severe edge effects and simple complimentary interior solutions for thin-walled anisotropic and composite structures [AD-A290645] p 555 N95-29562
- Composite structure forming a wear surface [AD-D017462] p 629 N95-30749
- Development of stitched/RTM primary structures for transport aircraft [NASA-CR-191441] p 630 N95-31421
- Performance improvement of composite wings through aeroelastic tailoring and modern control [AD-A293689] p 608 N95-31602
- Mapping hidden aircraft defects with dual-band infrared computed tomography [DE95-011531] p 584 N95-32164
- A probabilistic design method applied to smart composite structures [NASA-TM-106715] p 651 N95-32206
- COMPOSITION (PROPERTY)**
- Controlling mechanisms of ignition of solid fuel in a sudden-expansion combustor [BTN-95-EIX0616952745791] p 628 A95-94255
- COMPRESSIBILITY**
- Investigation of an NLF(1)-0416 airfoil in compressible subsonic flow p 110 N95-17852
- COMPRESSIBILITY EFFECTS**
- A study of compressibility effects on dynamic stall of rapidly pitching airfoils [HTN-94-00715] p 5 A95-60193
- Compressible inviscid vortex flow of a sharp edge delta wing [BTN-95-EIX95262694308] p 370 A95-85479
- PIV investigation of compressibility effects on dynamic stall p 478 N95-29102
- Compressibility effects on and control of dynamic stall of oscillating airfoil [AD-A291804] p 480 N95-29428
- Numerical simulation and analysis of the hypersonic turbulent flow past a blunt-fin/ramp configuration [DLR-FB-94-19] p 483 N95-30349
- COMPRESSIBLE BOUNDARY LAYER**
- Effects of expansions on a supersonic boundary layer: Surface pressure measurements [BTN-95-EIX95142553036] p 263 A95-73462
- Noise radiation by instability waves in coaxial jets [NASA-TM-106738] p 100 N95-14618
- A spectrally accurate boundary-layer code for infinite swept wings [NASA-CR-195014] p 159 N95-18042
- An interacting boundary layer method for unsteady compressible flows
- COMPRESSIBLE FLOW**
- Interferometry and computational studies of an oscillating airfoil compressible dynamic stall flow field [HTN-94-00703] p 3 A95-60182
- Oscillating airfoil compressible dynamic stall studies [HTN-94-00704] p 3 A95-60183
- LDV measurements in dynamically separated flows [ISBN 0-8194-1311-9] p 5 A95-60191
- A study of compressibility effects on dynamic stall of rapidly pitching airfoils [HTN-94-00715] p 5 A95-60193
- Construction of nearly orthogonal multiblock grids for compressible flow simulation [BTN-94-EIX94361133526] p 207 A95-65981
- Aspects of vortex breakdown [HTN-95-A0001] p 183 A95-67828
- Model for compressible turbulence in hypersonic wall boundary and high-speed mixing layers [BTN-94-EIX94441386625] p 184 A95-68174
- Computation of oscillating airfoil flows with one- and two-equation turbulence models [BTN-95-EIX95152577588] p 263 A95-73494
- Supersonic axisymmetric conical flow solutions for different ratios of specific heats [BTN-95-EIX95152583283] p 306 A95-73584
- Multigrid solution of compressible turbulent flow on unstructured meshes using a two-equation model [BTN-94-EIX94401378794] p 307 A95-76484
- Comparison of linear stability results with flight transition data [BTN-95-EIX95182619097] p 283 A95-76582
- Application of a control-volume-based finite-element formulation to the shock tube problem [BTN-95-EIX95182619099] p 295 A95-76584
- Direct boundary integral equations method to subsonic flow with circulation past thin airfoils in ground effect [BTN-95-EIX95242673940] p 365 A95-82224
- Predicting stall and post-stall behavior of airfoils at low mach numbers [BTN-95-EIX95262694297] p 365 A95-85468
- Dynamic unstructured method for flows past multiple objects in relative motion [BTN-95-EIX95262694303] p 435 A95-85474
- Compressible Navier-Stokes computations of multielement airfoil flows using multiblock grids [HTN-95-42327] p 371 A95-86156
- Interferometric investigations of compressible dynamic stall over a transiently pitching airfoil [HTN-95-42338] p 372 A95-86167
- Differencing of density in compressible flow for a pressure-based approach [HTN-95-42349] p 373 A95-86178
- A review of the hot-wire technique in 2-D compressible flow [HTN-95-61157] p 373 A95-86256
- Mesh generation and adaptivity for the solution of compressible viscous high speed flows [BTN-95-EIX95262697157] p 538 A95-86893
- Two-dimensional unsteady leading-edge separation on a pitching airfoil [HTN-95-81628] p 461 A95-87676
- Compressible Navier-Stokes calculations of the flow over airfoil sections. Comparisons of 1st and 2nd order turbulence models [SAE PAPER 932510] p 546 A95-89183
- Modeling aerodynamic problems using Smoothed Particle Hydrodynamics (SPH) [SAE PAPER 932512] p 465 A95-89185
- A detailed Euler flow analysis of TPS and fanjet engine p 473 A95-91515
- Algorithmic trends in computational fluid dynamics; The Institute for Computer Applications in Science and Engineering (ICASE)/LaRC Workshop, NASA Langley Research Center, Hampton, VA, US, Sep. 15-17, 1991 [ISBN 0-387-94014-6] p 550 A95-91915
- An educational introduction to transonic compressor stage design principles [SAE PAPER 931393] p 613 A95-93668
- Supersonic, turbulent flow computation and drag optimization for axisymmetric afterbodies [BTN-95-EIX95302729772] p 637 A95-94134
- Airfoil leading-edge suction and energy conservation for compressible flow [BTN-95-EIX95302730589] p 637 A95-94197
- Navier-Stokes applications to high-lift airfoil analysis [BTN-95-EIX0619952748182] p 590 A95-94475
- Computational fluid dynamics '92; Proceedings of the European Computational Fluid Dynamics Conference, 1st, Brussels, Belgium, Sep. 7-11, 1992. Vols. 1 & 2 [ISBN 0-444-89793-3] p 638 A95-95357
- Numerical solution of Euler and Navier-Stokes equations for 2D transonic problems p 638 A95-95366
- A robust inverse inviscid method for airfoil design p 640 A95-95431
- On the prediction of transonic unsteady flows using second order time accuracy p 641 A95-95448
- A 2D parallel multiblock Navier-Stokes solver with applications on shared- and disturbed memory machines p 643 A95-95475
- Partially implicit method for simulating viscous aerofoil flows [BTN-94-EIX94522406680] p 709 A95-96299
- High performance parallel analysis of coupled problems for aircraft propulsion [NASA-CR-195355] p 23 N95-10132
- Computer code for determination of thermally perfect gas properties [NASA-TP-3447] p 37 N95-11995
- Numerical study of the effects of icing on viscous flow over wings [NASA-CR-197102] p 75 N95-14803
- A workstation based simulator for teaching compressible aerodynamics [NASA-TM-106799] p 170 N95-16906
- Three dimensional compressible turbulent flow computations for a diffusing S-duct with/without vortex generators [NASA-CR-195390] p 138 N95-17402
- Investigation of an NLF(1)-0416 airfoil in compressible subsonic flow p 110 N95-17852
- Floating shock fitting via Lagrangian adaptive meshes [AD-A289758] p 170 N95-18110
- Numerical simulation of dynamic-stall suppression by tangential blowing [AD-A284887] p 120 N95-19110
- On supersonic-inlet boundary-layer bleed flow [NASA-CR-195426] p 202 N95-19769
- Validation and evaluation of the advanced aeronautical CFD system SAUNA: A method developer's view [ARA-MEMO-390] p 210 N95-19774
- Investigation of shear layer transition using various turbulence models p 248 N95-21096
- An approximate theoretical method for modeling the static thrust performance of non-axisymmetric two-dimensional convergent-divergent nozzles [NASA-CR-195050] p 273 N95-23193
- Study of compressible flow through a rectangular-to-semiannular transition duct [NASA-CR-4660] p 338 N95-24392
- Effect of density gradients in confined supersonic shear layers, part 1 [NASA-CR-198029] p 348 N95-24412
- TranAir: A full-potential, solution-adaptive, rectangular grid code for predicting subsonic, transonic, and supersonic flows about arbitrary configurations. User's manual [NASA-CR-4349] p 377 N95-28230
- Wave drag coefficient for axisymmetric forecones at zero incidence (M sub infinity less than or equal to 1.5) [ESDU-94014] p 552 N95-28903
- Surface pressure coefficient distributions for axisymmetric forecones at zero incidence (M sub infinity less than or equal to 1.5) [ESDU-94015] p 477 N95-28904
- Solution of the Navier-Stokes equations on locally refined Cartesian meshes using state-vector splitting p 553 N95-29197
- Modeling and control of rotating stall in high speed multi-stage axial compressors p 513 N95-29244
- Survey of CFD applications for high speed inlets [AD-A291365] p 557 N95-30087
- COMPRESSIBLE FLUIDS**
- A three-dimensional Navier-Stokes/full-potential coupled analysis for rotor blades [ISBN 1-879921-01-4] p 587 A95-93748
- Interactive computer graphics applications for compressible aerodynamics [NASA-TM-106802] p 170 N95-17264
- Pressure updating methods for the steady-state fluid equations [NASA-CR-198163] p 569 N95-30353
- COMPRESSION LOADS**
- Buckling and postbuckling of composite structures [HTN-95-71387] p 528 A95-87605
- Shear buckling analysis of a hat-stiffened panel [NASA-TM-4644] p 158 N95-17490
- Composite repair issues on the CF-18 aircraft p 395 N95-27518
- Analysis of composite structures with delaminations under combined bending and compression p 422 N95-28429
- COMPRESSION TESTS**
- External patch repair of CFRP/honeycomb sandwich p 395 N95-27522
- Test and analysis results for composite transport fuselage and wing structures p 398 N95-28470
- COMPRESSIVE STRENGTH**
- Buckling and postbuckling of composite structures [HTN-95-71387] p 528 A95-87605
- Novel matrix resins for composites for aircraft primary structures, phase 1 [NASA-CR-189657] p 23 N95-10318

- Development of an Automated Airfield Dynamic Cone Penetrometer (AADCP) prototype and the evaluation of unsurfaced airfield seismic surveying using Spectral Analysis of Surface Waves (SASW) technology
[AD-A281985] p 145 N95-17444
- Compression strength of composite primary structural components
[NASA-CR-197554] p 160 N95-18388
- Investigation of static and cyclic bearing failure mechanisms for GR/EP laminates p 422 N95-28427
- Compressive strength of damaged and repaired composite plates p 442 N95-28484
- COMPRESSOR BLADES**
- Heat transfer in the flow-through part of axial compressors
[BTN-94-EIX94461407949] p 89 A95-62267
- Profiling of the working surface of electrodes-tools for circle electrochemical dimensional treatment of compressor blades
[BTN-94-EIX94461407964] p 83 A95-62638
- The effects of surface modification on fretting fatigue in Ti alloy turbine components
[HTN-95-61145] p 404 A95-84909
- Elements of a modern turbomachinery design system
p 90 N95-14129
- Designing in three dimensions p 90 N95-14130
- The industrial use of CFD in the design of turbomachinery p 90 N95-14133
- New methods, new methodology: Advanced CFD in the Sncema turbomachinery design process p 90 N95-14134
- Experimental/analytical approach to understanding mistuning in a transonic wind tunnel compressor
[NASA-TM-108833] p 95 N95-14617
- Performance deterioration of axial compressors due to blade defects p 199 N95-19665
- Erosion of T56 5th stage rotor blades due to bleed hole overtip flow p 200 N95-19666
- High velocity oxygen fuel spraying of erosion and wear resistant coatings on jet engine parts p 202 N95-19680
- NASA low-speed axial compressor for fundamental research
[NASA-TM-4635] p 296 N95-23192
- The effect of adding roughness and thickness to a transonic axial compressor rotor
[NASA-TM-106958] p 645 N95-30524
- Investigating the use of smart acoustically active surfaces for flow separation control in turbomachinery
[AD-A292819] p 648 N95-31443
- COMPRESSOR EFFICIENCY**
- Performance deterioration of axial compressors due to blade defects p 199 N95-19665
- The effect of adding roughness and thickness to a transonic axial compressor rotor
[NASA-TM-106958] p 645 N95-30524
- COMPRESSOR ROTORS**
- Rotor whirl forces induced by the tip clearance effect in axial flow compressors
[BTN-94-EIX94351143331] p 207 A95-67304
- The calculation of erosion in a gas turbine compressor rotor p 199 N95-19664
- Stall precursor study of high frequency data for three high speed, swept compressor rotors
[AD-A289379] p 406 N95-26878
- A general theory of two- and three-dimensional rotational flow in subsonic and transonic turbomachines
[NASA-CR-4496] p 377 N95-28003
- The effect of adding roughness and thickness to a transonic axial compressor rotor
[NASA-TM-106958] p 645 N95-30524
- Experimental and computational investigation of the tip clearance flow in a transonic axial compressor rotor
[NASA-TM-106711] p 649 N95-31738
- COMPRESSORS**
- Dynamic behavior of valves with pneumatic chamber for reciprocating compressors
[BTN-94-EIX94351143311] p 207 A95-65845
- Rotor whirl forces induced by the tip clearance effect in axial flow compressors
[BTN-94-EIX94351143331] p 207 A95-67304
- Static pressure distribution in the inlet of a helicopter turbine compressor p 266 A95-73541
- Theoretical and experimental studies of fretting-initiated fatigue failure of aeroengine compressor discs
[BTN-94-EIX94421372285] p 343 A95-78467
- Active control of fan noise from a turbofan engine
[HTN-95-61198] p 570 A95-87571
- Numerical calculations of the turbulent flow through a controlled diffusion compressor cascade
[BTN-95-EIX95282710056] p 632 A95-92473
- Surge recovery and compressor working line control using compressor exit mach number measurement
[CONGRESS PAPER C428-33-210] p 610 A95-93622
- Brush seal performance and durability issues based on T-700 engine test results
[NASA-TM-106502] p 22 N95-11483
- Object-oriented technology for compressor simulation
[NASA-TM-106723] p 49 N95-11864
- Compressor discharge film riding face seals p 60 N95-13599
- Experimental/analytical approach to understanding mistuning in a transonic wind tunnel compressor
[NASA-TM-108833] p 95 N95-14617
- Gas turbine prediffuser-combustor performance during operation with air-water mixture
[DOT/FAA/CT-93/52] p 83 N95-15683
- Damage of high temperature components by dust-laden air p 201 N95-19673
- Protective coatings for compressor gas path components p 201 N95-19675
- Gas turbine compressor corrosion and erosion in Western Europe
[AD-B196178L] p 201 N95-19678
- Multilayer anti-erosion coatings p 201 N95-19679
- Malone-brayton cycle engine/heat pump
[AD-D016573] p 244 N95-20295
- Recirculating cavity casing treatment failure
[AD-A289330] p 513 N95-28908
- Composite structure forming a wear surface
[AD-D017462] p 629 N95-30749
- Reducing process noise in superconducting helium liquid level probes
[DE95-008956] p 629 N95-30765
- Linear Motor Free Piston Compressor
[AD-A293452] p 647 N95-31374
- Design of secondary flow control cascade using numerical simulation p 698 N95-34507
- COMPTON EFFECT**
- Induced Compton scattering by relativistic electrons in magnetized astrophysical plasmas p 563 N95-29885
- COMPUTATION**
- Improving the efficiency of aerodynamic shape optimization
[HTN-95-61204] p 540 A95-87577
- Enhancements to integral solutions to ablation and charring
[BTN-95-EIX95302694461] p 636 A95-94058
- CFD research, parallel computation and aerodynamic optimization
[NASA-CR-197748] p 373 N95-26649
- A study of workstation computational performance for real-time flight simulation
[NASA-TM-109184] p 449 N95-27241
- COMPUTATIONAL ELECTROMAGNETICS**
- Geodesic constant method: A novel approach to analytical surface-ray tracing on convex conducting bodies
[BTN-95-EIX95302731054] p 637 A95-94205
- Assessment of technology for aircraft development
[BTN-95-EIX0619952748181] p 606 A95-94474
- Scattering and radiation from cylindrically conformal antennas p 645 N95-30669
- Simulation of patch and slot antennas using FEM with prismatic elements and investigations of artificial absorber mesh termination schemes p 704 N95-32822
- COMPUTATIONAL FLUID DYNAMICS**
- Navier-Stokes simulation of rotor-body flowfield in hover using overset grids
[PAPER C15] p 1 A95-60160
- Recent advances in Euler and Navier-Stokes methods for calculating helicopter rotor aerodynamics and acoustics
[HTN-94-00686] p 2 A95-60169
- Numerical simulation of powered-lift flows
[HTN-94-00700] p 3 A95-60179
- Dryden lectureship in research, a perspective on CFD validation
[AIAA PAPER 93-0002] p 3 A95-60180
- Accuracy enhancements for overset grids using a defect correction approach
[AIAA PAPER 94-0523] p 3 A95-60181
- A comparison of turbulence models in computing multi-element airfoil flows
[AIAA PAPER 94-0291] p 4 A95-60185
- Numerical simulation of a complete STOVL aircraft in ground effect
[AIAA PAPER 93-4880] p 4 A95-60187
- Discrete shape sensitivity equations for aerodynamic problems
[BTN-94-EIX94451393721] p 88 A95-61720
- A grid generation and flow solution method for the Euler equations on unstructured grids
[HTN-95-20003] p 153 A95-63201
- Improved analytical solution for varying specific heat parallel stream mixing
[BTN-94-EIX94481415349] p 103 A95-65339
- Rotating Kirchhoff method for three-dimensional transonic blade-vortex interaction hover noise
[BTN-94-EIX94441386601] p 182 A95-67332
- Three-dimensional analysis of scramjet nozzle flows
[BTN-94-EIX94441380978] p 196 A95-68162
- Lag model for turbulent boundary layers over rough bleed surfaces
[BTN-94-EIX94441380981] p 208 A95-68165
- Lift analysis of a variable camber foil using the discrete vortex-blob method
[BTN-94-EIX94441386623] p 179 A95-68172
- Model for compressible turbulence in hypersonic wall boundary and high-speed mixing layers
[BTN-94-EIX94441386625] p 184 A95-68174
- Adaptive computations of flow around a delta wing with vortex breakdown
[BTN-94-EIX94441386631] p 184 A95-68180
- Numerical computations of supersonic base flow with special emphasis on turbulence modeling
[BTN-94-EIX94441386632] p 179 A95-68181
- Review of numerical procedures for computational surface thermochemistry
[BTN-94-EIX94441386682] p 205 A95-68191
- Prediction of ice accretion: Comparison between the 2D and 3D codes
[BTN-94-EIX94441385753] p 213 A95-68217
- Parallel implicit unstructured grid Euler solvers
[BTN-95-EIX95042474393] p 217 A95-68307
- Navier-Stokes simulations of Orbiter aerodynamic characteristics including pitch trim and bodyflap
[BTN-95-EIX95041503779] p 204 A95-69210
- Interpretation of waverider performance data using computational fluid dynamics
[BTN-95-EIX95062487534] p 193 A95-69242
- Two-variable method for blockage wall interference in a circular tunnel
[BTN-95-EIX95062487540] p 187 A95-69248
- Measurement around a rotor blade excited in pitch. Part 1: Dynamic inflow
[HTN-95-31007] p 220 A95-71177
- Measurement around a rotor blade excited in pitch. Part 2: Unsteady surface pressure
[HTN-95-31008] p 220 A95-71178
- Aerodynamic and wake methodology evaluation using Model UH-60A experimental data
[HTN-95-31009] p 220 A95-71179
- Vorticity concentration at the edge of the inboard vortex sheet
[HTN-95-31010] p 221 A95-71180
- Effects of leading and trailing edge flaps on the aerodynamics of airfoil/vortex interactions
[HTN-95-31011] p 221 A95-71181
- Large-scale computational fluid dynamics by the finite element method
[BTN-94-EIX94381359154] p 243 A95-71744
- A generalized algorithm for inverse simulation applied to helicopter maneuvering flight
[HTN-95-A0493] p 236 A95-72564
- High-order state space simulation models of helicopter flight mechanics
[HTN-95-A0494] p 237 A95-72565
- On the choice of appropriate bases for nonlinear dynamic modal analysis
[HTN-95-A0495] p 221 A95-72566
- Flap-lag damping in hover and forward flight with a three-dimensional wake
[HTN-95-A0496] p 221 A95-72567
- Air and ground resonance of helicopters with elastically tailored composite rotor blades
[HTN-95-A0497] p 222 A95-72568
- Design optimization of rotor blades for improved performance and vibration
[HTN-95-A0498] p 229 A95-72569
- Parametric studies for tiltrotor aeroelastic stability in highspeed flight
[HTN-95-A0499] p 222 A95-72570
- Adaptive finite element method for turbulent flow near a propeller
[BTN-95-EIX95142553038] p 305 A95-73460
- Laplace interaction law for the computation of viscous airfoil flow in low- and high-speed aerodynamics
[BTN-95-EIX95142553037] p 263 A95-73461
- Effects of spatial order of accuracy on the computation of vortical flowfields
[BTN-95-EIX95152577604] p 305 A95-73479
- Eigenanalysis of unsteady flows about airfoils, cascades, and wings
[BTN-95-EIX95152577597] p 305 A95-73486
- Progress in high-lift aerodynamic calculations
[BTN-95-EIX95152582315] p 264 A95-73518
- Higher-order viscous shock-layer solutions for high-altitude flows
[BTN-95-EIX95152583255] p 306 A95-73556
- Base drag prediction on missile configurations
[BTN-95-EIX95152583256] p 266 A95-73557

- Predicting exhaust plume boundaries with supersonic external flows
[BTN-95-EIX95152583258] p 297 A95-73559
- Three-dimensional structure of a supersonic jet impinging on an inclined plate
[BTN-95-EIX95152583259] p 267 A95-73560
- Optimization of contoured hypersonic scramjet inlets with a least-squares parabolized Navier-Stokes procedure
[HTN-95-20976] p 261 A95-74042
- Zonally decoupled direct simulation Monte Carlo solutions of hypersonic blunt-body wake flows
[BTN-95-EIX95182617458] p 268 A95-75729
- Convective and radiative heat transfer analysis for the fire 2 forebody
[BTN-95-EIX95182617460] p 268 A95-75731
- Aerodynamic design of pegasus: Concept to flight with computational fluid dynamics
[BTN-95-EIX95182617463] p 298 A95-75734
- Application of wall functions to generalized nonorthogonal curvilinear coordinate systems
[BTN-95-EIX95182619077] p 307 A95-75762
- Turbulent transonic airfoil flow simulation using a pressure-based algorithm
[BTN-95-EIX95182619078] p 269 A95-75763
- Simulation of transverse gas injection in turbulent supersonic air flows
[BTN-95-EIX95182619080] p 269 A95-75765
- Viscous-inviscid interaction method for unsteady low-speed airfoil flows
[BTN-95-EIX95182619093] p 269 A95-75778
- Multigrid solution of compressible turbulent flow on unstructured meshes using a two-equation model
[BTN-94-EIX94401378794] p 307 A95-76484
- Grid refinement test of time-periodic flows over bluff bodies
[BTN-94-EIX94401378822] p 307 A95-76491
- Comparison of linear stability results with flight transition data
[BTN-95-EIX95182619097] p 283 A95-76582
- Application of a control-volume-based finite-element formulation to the shock tube problem
[BTN-95-EIX95182619099] p 295 A95-76584
- CFD optimization of a theoretical minimum-drag body
[BTN-95-EIX95182619234] p 308 A95-76660
- Simulation on the 3-D turbulent flow in the passages of finocyl grain
[BTN-95-EIX95202638962] p 279 A95-76674
- Direct boundary integral equations method to subsonic flow with circulation past thin airfoils in ground effect
[BTN-95-EIX95242673940] p 365 A95-82224
- Rarefied gas numerical wind tunnel: OREX and HOPE
p 427 A95-82391
- VSL analysis of hypersonic flows around a reentry vehicle with equilibrium air chemistry
p 413 A95-82400
- NAL aerothermodynamic probing and CFD verification mission in OREX experiment
p 368 A95-82413
- Numerical simulation of unsteady aerodynamic heating induced by shock reflections
p 428 A95-82418
- Instability of three-dimensional boundary layers due to streamline curvature
[HTN-95-61070] p 430 A95-83654
- Instability of three-dimensional boundary layers due to streamline curvature
[HTN-95-61070] p 430 A95-83654
- Accuracy and efficiency assessments for a weak statement CFD algorithm for high-speed aerodynamics
[BTN-94-EIX9501141238] p 370 A95-84195
- Computational/experimental investigation of staged injection into a Mach 2 flow
[HTN-95-51646] p 432 A95-85028
- Dynamic unstructured method for flows past multiple objects in relative motion
[BTN-95-EIX95262694303] p 435 A95-85474
- Computational analysis of buffet alleviation in viscous transonic flow over a porous airfoil
[BTN-95-EIX95262694321] p 366 A95-85492
- Using the Liou-Steffen algorithm for the Euler and Navier-Stokes equations
[HTN-95-42348] p 373 A95-86177
- Differencing of density in compressible flow for a pressure-based approach
[HTN-95-42349] p 373 A95-86178
- Computational methods in applied sciences; European Computational Fluid Dynamics Conference, 1st, Brussels, Belgium, Sept. 7-11, 1992
[ISBN 0-444-89795-X] p 539 A95-87552
- Numerical simulation of three-dimensional hypersonic reacting flows over blunt bodies with catalytic surface
[HTN-95-61184] p 539 A95-87557
- Numerical simulation of real gas effects and aerodynamic heating of hypersonic space transportation vehicles
p 540 A95-87558
- High-speed reacting flow simulation using USA-series codes
p 540 A95-87559
- Aerodynamic design and optimization at Alenia D.V.D.
p 491 A95-87564
- Improving the efficiency of aerodynamic shape optimization
[HTN-95-61204] p 540 A95-87577
- Simple numerical criterion for vortex breakdown
[HTN-95-61210] p 541 A95-87583
- Automated adaptive time-discontinuous finite element method for unsteady compressible airfoil aerodynamics
[HTN-95-81637] p 541 A95-87685
- Conceptual studies of high speed combustors for mixing enhancement mechanisms
[AIAA PAPER 95-6095] p 510 A95-88003
- Three-dimensional adaptive grid-embedding Euler technique
[HTN-95-20825] p 543 A95-88086
- Sensitivity derivatives for three dimensional supersonic Euler code using incremental iterative strategy
[HTN-95-20845] p 545 A95-88106
- Supersonic and hypersonic shock/boundary-layer interaction database
[HTN-95-20930] p 463 A95-88969
- Adaptive computations of flow around a delta wing with vortex breakdown
[HTN-95-20948] p 465 A95-88987
- Modeling aerodynamic problems using Smoothed Particle Hydrodynamics (SPH)
[SAE PAPER 932512] p 465 A95-89185
- Computational aerodynamic analysis on the Open Skies aircraft
[SAE PAPER 932514] p 466 A95-89187
- Computational study of a two-slot circulation control airfoil
[SAE PAPER 932531] p 466 A95-89191
- Computational fluid dynamics with icing effects
[SAE PAPER 932532] p 466 A95-89192
- Accurate drag prediction: A prerequisite for drag reduction research
[SAE PAPER 932571] p 467 A95-90060
- Engine/airframe installation CFD for commercial transports: An engine manufacturer's perspective
[SAE PAPER 932623] p 495 A95-90084
- Civil aircraft propulsion integration: Current & future
[SAE PAPER 932624] p 495 A95-90085
- Central-difference and upwind-biased schemes for steady and unsteady Euler aerfoil computations
[HTN-95-01094] p 469 A95-90280
- Parallel CFD design on network-based computer
[AIAA PAPER 95-0984] p 565 A95-90656
- Parallel computational fluid dynamics '91; Conference Proceedings, Stuttgart, Germany, Jun. 10-12, 1991
[ISBN 0-444-89363-6] p 548 A95-91479
- Implicit multi-domain method for unsteady compressible inviscid fluid flows around 3D projectiles
[HTN-95-01094] p 548 A95-91482
- Aerodynamic simulation on massively parallel systems
p 549 A95-91487
- Solution of the Navier-Stokes equations on a massively parallel transputer system
p 549 A95-91490
- Aircraft Symposium, 30th, Tsukuba, Japan, Sep. 30 - Oct. 2, 1992
[HTN-95-A1609] p 498 A95-91491
- Numerical experiments on aerodynamic heating mechanism in shock reflection processes
p 471 A95-91497
- Numerical design methods for transonic NLF configurations
p 471 A95-91498
- Vortex lattice method simulation of unsteady flow due to wing/external store combination
p 471 A95-91499
- A detailed Euler flow analysis of TPS and fanjet engine
p 473 A95-91515
- Algorithmic trends in computational fluid dynamics; The Institute for Computer Applications in Science and Engineering (ICASE)/LaRC Workshop, NASA Langley Research Center, Hampton, VA, US, Sep. 15-17, 1991
[ISBN 0-387-94014-6] p 550 A95-91915
- A viewpoint on discretization schemes for applied aerodynamic algorithms for complex configurations
p 550 A95-91916
- Algorithmic trends in CFD in the 1990's for aerospace flow field calculations
p 550 A95-91917
- Beyond the Riemann problem, part 1
p 550 A95-91925
- Numerical calculations of the turbulent flow through a controlled diffusion compressor cascade
[BTN-95-EIX95282710056] p 632 A95-92473
- Comparison of coordinate-invariant and coordinate-aligned upwinding for the Euler equations
[HTN-95-A1753] p 633 A95-93316
- Turbulent flow measurements with a triple-split hot-film probe
[HTN-95-A1774] p 634 A95-93337
- Amplification and breaking of atmospheric gravity waves
p 675 A95-93552
- Operational multi-scale environment model with grid adaptivity (OMEGA) application to aviation weather
p 676 A95-93556
- A design trade study using CFD modeling of reaction jets for aerodynamic control
[SAE PAPER 931384] p 586 A95-93660
- The application of potential CFD methods to helicopter hover flows
[ISBN 1-879921-01-4] p 587 A95-93747
- Evaluation of a multigrid-based Navier-Stokes solver for aerothermodynamic computations
[BTN-95-EIX95302694459] p 583 A95-94056
- 3-D Navier-Stokes analysis of crossing glancing shocks/turbulent boundary layer interactions
[BTN-95-EIX95302729768] p 636 A95-94130
- Supersonic, turbulent flow computation and drag optimization for axisymmetric afterbodies
[BTN-95-EIX95302729772] p 637 A95-94134
- In-flight pressure measurements on a subsonic transport high-lift wing section
[BTN-95-EIX0619952748170] p 589 A95-94464
- Computational fluid dynamics '92; Proceedings of the European Computational Fluid Dynamics Conference, 1st, Brussels, Belgium, Sep. 7-11, 1992. Vols. 1 & 2
[ISBN 0-444-89793-3] p 638 A95-95357
- Discretization of the parabolized Navier-Stokes equations
p 638 A95-95362
- Numerical solution of Euler and Navier-Stokes equations for 2D transonic problems
p 638 A95-95366
- Laminar and turbulent flow over optimal riblets
p 639 A95-95383
- Heat transfer on bent-noise biconic in hypersonic flow
p 639 A95-95394
- Optimal shape design in hypersonic aerodynamics and electromagnetics
p 639 A95-95397
- A numerical investigation of flow around a square-section cylinder mounted with a splitter plate
p 639 A95-95401
- Effects of splitter plate on wake formation from a circular cylinder: A discrete vortex simulation
p 639 A95-95404
- An efficient discrete vortex method for low Reynolds number incompressible flows
p 639 A95-95407
- Viscous flow simulation using the discrete vortex diffusion velocity method
p 639 A95-95421
- Numerical simulation of the 3D turbulent flow around the combustor dome of an aircraft engine
p 640 A95-95423
- A robust inverse inviscid method for airfoil design
p 640 A95-95431
- An improved finite element method for the solution of the compressible Euler and Navier-Stokes equations
p 640 A95-95439
- Navier-Stokes computations around a realistic fighter configuration
p 591 A95-95440
- Implicit multidomain calculation of viscous transonic flows without artificial viscosity or upwinding
p 640 A95-95443
- High-lift calculations using Navier-Stokes methods
p 641 A95-95444
- Permeable wall boundary conditions for transonic airfoil design
p 641 A95-95445
- A modular system for computational fluid dynamics
p 641 A95-95446
- On the prediction of transonic unsteady flows using second order time accuracy
p 641 A95-95448
- Multigrid/multiblock method for transonic potential flow around wing/body/nacelle configurations including a slipstream
p 591 A95-95451
- Implicit upwind-Euler solution algorithms for unstructured-grid applications
p 641 A95-95454
- 2-D and 3-D numerical simulation of a supersonic inlet flowfield
p 641 A95-95457
- Multigrid solution for the compressible Euler equations by an implicit characteristic-flux-averaging
p 642 A95-95459
- Transonic vortical flow predicted with a structured multiblock Euler solver
p 642 A95-95462
- An unstructured node centered scheme for the simulation of 3-D inviscid flows
p 642 A95-95463
- An innovative algorithm to accurately solve the Euler equations for rotary wing flow
p 642 A95-95467
- SAUNA: A system for grid generation and flow simulation using hybrid structured/unstructured grids
p 642 A95-95470
- A cartesian grid finite element method for aerodynamics of moving rigid bodies
p 642 A95-95471
- Grid adaptation for problems in computational fluid dynamics
p 643 A95-95472
- Multi-block finite volume calculation of compressible flow past aerodynamic configurations
p 643 A95-95473
- A 2D parallel multiblock Navier-Stokes solver with applications on shared- and distributed memory machines
p 643 A95-95475
- Grid generation: Algebraic and partial differential equations techniques revisited
p 643 A95-95477

- Surface grid generation for multi-block structured grids p 643 A95-95478
- Arbitrary Lagrangian-Eulerian finite element analysis for flow-induced vibration of rigid body p 643 A95-95485
- High performance parallelized implicit Euler solver for the analysis of unsteady aerodynamic flows p 644 A95-95495
- Hypersonic Navier-Stokes computations about complex configurations p 644 A95-95497
- Navier-Stokes simulation of turbulent vortex high-Re-number flows over a delta wing p 644 A95-95507
- Computational fluid dynamics study of the variable-pitch split-blade fan concept [NASA-CR-189206] p 15 N95-10247
- Proceeding towards hypervelocities in ram accelerators p 19 N95-10285
- A full Navier-Stokes analysis of subsonic diffuser of a bifurcated 70/30 supersonic inlet for high speed civil transport application [NASA-TM-106637] p 8 N95-10820
- Numerical study of Gortler instability: Application to the design of a quiet supersonic wind tunnel [PB94-184801] p 21 N95-10844
- Computational fluid dynamics uses in fluid dynamics/aerodynamics education [NASA-TM-108834] p 8 N95-10847
- Numerical simulation of the flow about the F-18 HARV at high angle of attack [NASA-CR-196396] p 9 N95-10940
- High speed civil transport: Sonic boom softening and aerodynamic optimization [NASA-CR-196397] p 28 N95-11192
- Development of an upwind, finite-volume code with finite-rate chemistry [NASA-CR-196749] p 9 N95-11366
- Steady and unsteady three-dimensional transonic flow computations by integral equation method [NASA-CR-196777] p 10 N95-11582
- Parallel aeroelastic computations for wing and wing-body configurations [NASA-CR-196835] p 36 N95-11766
- Object-oriented technology for compressor simulation [NASA-TM-106723] p 49 N95-11864
- Investigation of advanced counterrotation blade configuration concepts for high speed turboprop systems. Task 8: Cooling flow/heat transfer analysis [NASA-CR-195359] p 50 N95-11901
- Research in progress in applied mathematics, numerical analysis, fluid mechanics, and computer science [AD-A284982] p 61 N95-11932
- An axisymmetric analog two-layer convective heating procedure with application to the evaluation of Space Shuttle Orbiter wing leading edge and windward surface heating [NASA-CR-188343] p 54 N95-11937
- Investigation of advanced counterrotation blade configuration concepts for high speed turboprop systems. Task 8: Cooling flow/heat transfer analysis user's manual [NASA-CR-195360] p 50 N95-11951
- Computational flow predictions for hypersonic drag devices p 37 N95-11967
- High speed civil transport aerodynamic optimization [NASA-CR-196960] p 38 N95-12389
- Supersonic base flow investigation over axisymmetric afterbodies [PB94-180957] p 39 N95-12578
- Validation of the RPLUS3D code for supersonic inlet applications involving three-dimensional shock wave-boundary layer interactions [NASA-TM-106579] p 39 N95-13058
- Numerical time dependent sheet cavitation simulations using a higher order panel method [PB94-204435] p 59 N95-13249
- User's guide for ENSAERO: A multidisciplinary program for fluid/structural/control interaction studies of aircraft (release 1) [NASA-TM-108853] p 65 N95-13662
- Developments in laser-based diagnostics for wind tunnels in the Aeromechanics Division: 1987-1992 [AD-A283011] p 84 N95-13687
- Numerical modeling of a cryogenic fluid within a fuel tank [NASA-TM-4651] p 89 N95-13892
- Turbomachinery Design Using CFD [AGARD-LS-195] p 89 N95-14127
- Computational methods for preliminary design and geometry definition in turbomachinery p 89 N95-14128
- Designing in three dimensions p 90 N95-14130
- Unsteady flows in turbines: Impact on design procedure p 90 N95-14132
- The industrial use of CFD in the design of turbomachinery p 90 N95-14133
- New methods, new methodology: Advanced CFD in the Smecha turbomachinery design process p 90 N95-14134
- The role of CFD in the design process p 90 N95-14135
- Aero design of turbomachinery components: CFD in complex systems p 90 N95-14136
- A selection of experimental test cases for the validation of CFD codes, volume 1 [AGARD-AR-303-VOL-1] p 91 N95-14201
- Hybrid structured/unstructured grid computations for the F/A-18 at high angle of attack p 68 N95-14233
- Computational aerodynamics based on the Euler equations [AGARD-AG-325] p 72 N95-14264
- A Cartesian, cell-based approach for adaptively-refined solutions of the Euler and Navier-Stokes equations [NASA-TM-106786] p 73 N95-14297
- Engineering Codes for aeroprediction: State-of-the-art and new methods p 73 N95-14447
- Navier-Stokes predictions of missile aerodynamics p 74 N95-14451
- Computation of supersonic air-intakes p 74 N95-14452
- Numerical simulation of the flow about the F-18 HARV at high angle of attack [NASA-CR-197023] p 74 N95-14614
- Numerical study of the effects of icing on viscous flow over wings [NASA-CR-197102] p 75 N95-14803
- An approximate Riemann solver for thermal and chemical nonequilibrium flows [NASA-CR-195003] p 96 N95-14912
- Development and application of structural dynamics analysis capabilities [NASA-CR-197229] p 96 N95-14922
- Numerical design of advanced multi-element airfoils [NASA-CR-197135] p 76 N95-15762
- An approach for dynamic grids [NASA-TM-106774] p 76 N95-15853
- Numerical simulation of supersonic compression corners and hypersonic inlet flows using the RPLUS2D code [NASA-TM-106580] p 105 N95-16038
- High altitude hypersonic flowfield radiation [AD-A281386] p 106 N95-16160
- Applications of automatic differentiation in computational fluid dynamics p 156 N95-16461
- Optimum Design Methods for Aerodynamics [AGARD-R-803] p 127 N95-16562
- Time accurate computation of unsteady inlet flows with a dynamic flow adaptive mesh [AD-A285498] p 157 N95-16736
- Applications of automatic differentiation in CFD [NASA-TM-109948] p 157 N95-16828
- Interactive computer graphics applications for compressible aerodynamics [NASA-TM-106802] p 170 N95-17264
- Three dimensional compressible turbulent flow computations for a diffusing S-duct with/without vortex generators [NASA-CR-195390] p 138 N95-17402
- A selection of experimental test cases for the validation of CFD codes, volume 2 [AGARD-AR-303-VOL-2] p 109 N95-17846
- Low-speed surface pressure and boundary layer measurement data for the NLR 7301 airfoil section with trailing edge flap p 111 N95-17855
- Data from the GARTEur (AD) Action Group 02 airfoil CAST 7/DOA1 experiments p 111 N95-17856
- A supercritical airfoil experiment p 111 N95-17858
- Two-dimensional high-lift airfoil data for CFD code validation p 112 N95-17859
- Measurements of the flow over a low aspect-ratio wing in the Mach number range 0.6 to 0.87 for the purpose of validation of computational methods. Part 1: Wing design, model construction, surface flow. Part 2: Mean flow in the boundary layer and wake, 4 test cases p 112 N95-17860
- Detailed study at supersonic speeds of the flow around delta wings p 112 N95-17861
- STOVL CFD model test case p 115 N95-17881
- Low speed propeller slipstream aerodynamic effects p 116 N95-17882
- Parachute inflation: A problem in aeroelasticity [AD-A284375] p 117 N95-18340
- Aeromechanics technology, volume 1. Task 1: Three-dimensional Euler/Navier-Stokes Aerodynamic Method (TEAM) enhancements [AD-A285713] p 132 N95-18483
- A selection of experimental test cases for the validation of CFD codes. Supplement: Datasets A-E [AGARD-AR-303-SUPPL] p 117 N95-18539
- NASA High Performance Computing and Communications program [NASA-TM-4653] p 176 N95-18573
- Static aerodynamics CFD analysis for 120-mm hypersonic KE projectile design [ARL-MR-184] p 118 N95-18611
- Numerical computations of supersonic base flow with special emphasis on turbulence modeling [AD-A283688] p 119 N95-18670
- Hypersonic flow-field measurements: Intrusive and nonintrusive [AD-A283867] p 119 N95-18674
- Mesh quality control for multiply-refined tetrahedral grids [NASA-CR-197595] p 160 N95-18737
- Solution of full potential equation on an airfoil by multigrid technique [NAL-TM-CSS-9303] p 119 N95-18904
- Theoretical investigations of shock/boundary layer interactions on a $Ma(\infty) = 8$ waverider [DLR-FB-94-12] p 119 N95-18910
- Flow field investigation in a free jet - free jet core system for the generation of high intensity molecular beams [DLR-FB-94-11] p 172 N95-18912
- Solution of Navier-Stokes equations using high accuracy monotone schemes p 161 N95-19019
- An assessment of the adaptive unstructured tetrahedral grid, Euler Flow Solver Code FELISA [NASA-TM-3526] p 119 N95-19041
- Static investigation of two fluidic thrust-vectoring concepts on a two-dimensional convergent-divergent nozzle [NASA-TM-4574] p 120 N95-19042
- Determination of stores pointing error due to wing flexibility under flight load [NASA-TM-4646] p 134 N95-19044
- Numerical simulation of dynamic-stall suppression by tangential blowing [AD-A284887] p 120 N95-19110
- Navier-Stokes, flight, and wind tunnel flow analysis for the F/A-18 aircraft [NASA-TP-3478] p 120 N95-19114
- Determination of solid/porous wall boundary conditions from wind tunnel data for computational fluid dynamics codes p 164 N95-19266
- Unsteady aerodynamic analyses for turbomachinery aeroelastic predictions p 141 N95-19381
- Steady potential solver for unsteady aerodynamic analyses p 141 N95-19382
- CFD: Advances and Applications, part 1 [NAL-SP-9322-PT-1] p 165 N95-19444
- Computation of inviscid flows: Full potential method p 165 N95-19447
- Panel methods p 165 N95-19448
- Viscous flow past aerofoils axisymmetric bodies and wings p 123 N95-19457
- On supersonic-inlet boundary-layer bleed flow [NASA-CR-195426] p 202 N95-19769
- Validation and evaluation of the advanced aeronautical CFD system SAUNA: A method developer's view [ARA-MEMO-390] p 210 N95-19774
- Application of three-dimensional hybrid structured/unstructured grids to land, sea and air vehicles [ARA-MEMO-399] p 210 N95-19775
- Verification of the CFD simulation system SAUNA for complex aircraft configurations [ARA-MEMO-401] p 211 N95-19776
- Inviscid and viscous flow modelling of complex aircraft configurations using the CFD simulation system sauna [ARA-MEMO-403] p 211 N95-19777
- Open Skies project computational fluid dynamic analysis [AD-A285928] p 223 N95-19991
- Application of Direct and Large Eddy Simulation to Transition and Turbulence [AGARD-CP-551] p 248 N95-21061
- Investigation of shear layer transition using various turbulence models p 248 N95-21096
- Computational studies of laminar to turbulence transition [AD-A285622] p 248 N95-21146
- Application of Navier-Stokes code PAB3D with kappa-epsilon turbulence model to attached and separated flows [NASA-TP-3480] p 224 N95-21338
- Effects of yaw and pitch motion on model attitude measurements [NASA-TM-4641] p 250 N95-22109
- Unstructured-grid large-eddy simulation of flow over an airfoil p 225 N95-22448
- Large-eddy simulation of flow through a plane, asymmetric diffuser p 250 N95-22449
- Direct numerical simulations of on-demand vortex generators: Mathematical formulation p 251 N95-22452
- Particle kinetic simulation of high altitude hypervelocity flight [NASA-CR-197383] p 309 N95-22481

- Euler Technology Assessment program for preliminary aircraft design employing SPLITFLOW code with Cartesian unstructured grid method
[NASA-CR-4649] p 273 N95-22917
- A CFD study of complex missile and store configurations in relative motion
[NASA-CR-197912] p 285 N95-22949
- Mach 10 computational study of a three-dimensional scramjet inlet flow field
[NASA-TM-4602] p 309 N95-23015
- Euler technology assessment for preliminary aircraft design employing OVERFLOW code with multiblock structured-grid method
[NASA-CR-4651] p 273 N95-23095
- An assessment of viscous effects in computational simulation of benign and burst vortex flows on generic fighter wind-tunnel models using TEAM code
[NASA-CR-4650] p 273 N95-23185
- Mach 10 computational study of a three-dimensional scramjet inlet flow field
[NASA-TM-4602] p 310 N95-23210
- Aerodynamic design optimization with sensitivity analysis and computational fluid dynamics
[NASA-CR-197419] p 274 N95-23218
- TIGER: A user-friendly interactive grid generation system for complicated turbomachinery and axis-symmetric configurations
p 322 N95-23419
- Three-dimensional Navier-Stokes analysis and redesign of an imbedded bellmouth nozzle in a turbine cascade inlet section
p 311 N95-23423
- Supersonic flow and shock formation in turbine tip gaps
p 312 N95-23429
- CFD analysis of turbopump volutes
p 312 N95-23436
- Convergence acceleration of implicit schemes in the presence of high aspect ratio grid cells
p 313 N95-23446
- A time-accurate finite volume method valid at all flow velocities
p 314 N95-23447
- A study of the vortex flow over 76/40-deg double-delta wing
[NASA-CR-195032] p 314 N95-23466
- Validation of a Computational Fluid Dynamics (CFD) code for supersonic axisymmetric base flow
p 315 N95-23652
- Verification of computational aerodynamic predictions for complex hypersonic vehicles using the INCA(trademark) code
[DE95-004757] p 330 N95-24308
- Aerodynamic optimization studies on advanced architecture computers
[NASA-CR-198045] p 330 N95-24379
- DSMC calculations for 70-deg blunted cone at 3.2 km/s in nitrogen
[NASA-TM-109181] p 348 N95-24396
- Aerodynamic shape optimization of wing and wing-body configurations using control theory
[NASA-CR-198024] p 335 N95-25334
- The coupling of fluids, dynamics, and controls on advanced architecture computers
[NASA-CR-197727] p 360 N95-25797
- Recent improvements to and validation of the one dimensional NASA wave rotor model
[NASA-TM-106913] p 332 N95-25962
- A combined geometric approach for solving the Navier-Stokes equations on dynamic grids
[NASA-TM-106919] p 332 N95-26075
- Cumulative reports and publications through December 31, 1994
[NASA-CR-195043] p 361 N95-26085
- Computational fluid dynamics and transonic flow
[AD-A288962] p 436 N95-26405
- A non-iterative grid deformation algorithm for computational fluid dynamics for aeroelasticity
[AD-A288298] p 436 N95-26418
- A fixed time performance evaluation of parallel CFD applications
[DE94-014240] p 436 N95-26445
- Numerical simulation of combustion flow around a flame holder with hydrogen injection
[NAL-TR-1233] p 419 N95-26523
- Supersonic transport grid generation, validation, and optimization
[NASA-CR-197752] p 448 N95-26648
- CFD research, parallel computation and aerodynamic optimization
[NASA-CR-197748] p 373 N95-26649
- Numerical simulation of the flow about the F-18 HARV at high angle of attack
[NASA-CR-197755] p 374 N95-26735
- Development of an upwind, finite-volume code with finite-rate chemistry
[NASA-CR-197747] p 374 N95-26760
- Computational support of the laminar flow supersonic wind tunnel, CNSFV code development, Maglev, and grid generation
[NASA-CR-197750] p 411 N95-26775
- Supersonic civil airplane study and design: Performance and sonic boom
[NASA-CR-197745] p 390 N95-26813
- A numerical method for unsteady transonic flow about wings with control surfaces
[AD-A289631] p 375 N95-26859
- Rarefied gas effects on aerobraking/reentry vehicles with wakes
[NASA-CR-196586] p 415 N95-27093
- Application of CFD to the analysis and design of high-speed inlets
[NASA-CR-198574] p 438 N95-27240
- NAS Technical Summaries, March 1993 - February 1994
[NASA-PP-1355] p 453 N95-27367
- Optimization of wave rotors for use as gas turbine engine topping cycles
[NASA-TM-106951] p 406 N95-27860
- Industry-Wide Workshop on Computational Turbulence Modeling
[NASA-CR-10165] p 439 N95-27882
- A summary of computational experience at GE Aircraft Engines for complex turbulent flows in gas turbines
p 439 N95-27885
- The applicability of turbulence models to aerodynamic and propulsion flowfields at McDonnell-Douglas Aerospace
p 439 N95-27886
- Combustion system CFD modeling at GE Aircraft Engines
p 439 N95-27889
- A NASTRAN-based computer program for structural dynamic analysis of Horizontal Axis Wind Turbines
p 439 N95-27980
- TranAir: A full-potential, solution-adaptive, rectangular grid code for predicting subsonic, transonic, and supersonic flows about arbitrary configurations. Theory document
[NASA-CR-4348] p 378 N95-28265
- Numerical analysis of intra-cavity and power-stream flow interaction in multiple gas-turbine disk-cavities
[NASA-TM-106886] p 407 N95-28344
- Numerical study to assess sulfur hexafluoride as a medium for testing multielement airfoils
[NASA-TP-3496] p 378 N95-28674
- Surface Modeling, Grid Generation, and Related Issues in Computational Fluid Dynamic (CFD) Solutions
[NASA-CP-3291] p 476 N95-28723
- Requirements for effective use of CFD in aerospace design
p 551 N95-28725
- Grid generation and surface modeling for CFD
p 551 N95-28726
- Rapid Airplane Parametric Input Design (RAPID)
p 501 N95-28730
- Algorithms for high aspect ratio oriented triangulations
p 476 N95-28731
- Surface modeling and grid generation for aeropropulsion CFD
p 551 N95-28732
- An unstructured-grid software system for solving complex aerodynamic problems
p 476 N95-28743
- Three-dimensional hybrid grid generation using advancing front techniques
p 567 N95-28745
- Demonstration of an automated CFD system for three-dimensional flow simulations
p 551 N95-28767
- A procedure for automating CFD simulations of an inlet-bleed problem
p 552 N95-28768
- A noninvasive method of quantifying flow visualization data in vortex flow fields
[AD-A289802] p 552 N95-28948
- A study of fluid problems requiring a direct particle simulation
[AD-A290212] p 567 N95-29074
- A vorticity-velocity approach for three-dimensional unsteady viscous flow over wings
p 478 N95-29108
- An extension of the continuum model by Grad's thirteen moment equations for hypersonic rarefied flows
p 478 N95-29118
- A numerical method for modelling wings with sharp edges maneuvering at high angles of attack
p 503 N95-29122
- Computational Fluid Dynamics (CFD) analysis of a C-135 aircraft with a side-mounted splitter plate (with comparison to wind tunnel data)
[AD-A292029] p 553 N95-29187
- Solution of the Navier-Stokes equations on locally refined Cartesian meshes using state-vector splitting
p 553 N95-29197
- A fourth order Euler/Navier-Stokes prediction method for the aerodynamics and aeroelasticity of hovering rotor blades
p 554 N95-29242
- High-and low-frequency dynamics of isolated blades and rotors with dynamic stall and wake
[AD-A290358] p 503 N95-29322
- Development of a rotary wing Navier-Stokes CFD code based on TLNS3D code
[AD-A290421] p 554 N95-29387
- Estimation of aerodynamic load distributions on the F/A-18 aircraft using a CFD panel code
[DSTO-TR-0147] p 504 N95-29445
- Computation of the integrated aerodynamic and propulsive flowfields of a generic hypersonic space plane
p 481 N95-29788
- A method for the modelling of porous and solid wind tunnel walls in computational fluid dynamics codes
p 523 N95-29795
- Computational algorithms for aerodynamic analysis and design
[AD-A291084] p 482 N95-29972
- Inlet flow test calibration for a small axial compressor rig. Part 2: CFD compared with experimental results
[NASA-TM-106999] p 514 N95-30007
- Survey of CFD applications for high speed inlets
[AD-A291365] p 557 N95-30087
- Use of the PARC code to estimate the off-design transonic performance of an over/under turboramjet nozzle
[NASA-TM-106924] p 482 N95-30091
- Comparison of spatial numerical operators for duct-nozzle acoustics
p 580 N95-30158
- A numerical study of the small scale wing-body junction problem
p 482 N95-30235
- Pressure updating methods for the steady-state fluid equations
[NASA-CR-198163] p 569 N95-30353
- A numerical study of the starting process in a hypersonic shock tunnel
p 626 N95-30493
- Development of a linearized unsteady Euler analysis for turbomachinery blade rows
[NASA-CR-4677] p 592 N95-30611
- A numerical model for dynamic wave rotor analysis
[NASA-TM-106997] p 615 N95-30617
- Validation of the NPARC code for nozzle afterbody flows at transonic speeds
[NASA-TM-106971] p 592 N95-30704
- Computation of high-altitude hypersonic flow-field radiation
p 593 N95-30843
- Parametrics on 2D Navier-Stokes analysis of a Mach 2.68 bifurcated rectangular mixed-compression inlet
[NASA-TM-107003] p 617 N95-30861
- Acceleration potential models
PREDICHT/PREDICDYN applied for calculation of axisymmetric dynamic inflow cases
[PB95-207015] p 647 N95-30957
- Advanced k-epsilon modeling of heat transfer
[NASA-CR-4679] p 648 N95-31423
- Application of multigrid computational fluid dynamics (CFD) methods to rotor analysis
[AD-A293012] p 648 N95-31475
- Unsteady flow simulations about moving boundary configurations using dynamic domain decomposition techniques
p 649 N95-31837
- Numerical solution of the full potential equation using a chimera grid approach
[NASA-TM-110360] p 594 N95-32188
- Three-dimensional aerodynamic shape optimization using discrete sensitivity analysis
p 691 N95-32904
- Turbulence models in the Navier-Stokes simulation of airfoil stall
[TRITA-NA-9312] p 705 N95-33059
- Numerical simulation of supersonic flow using a new analytical bleed boundary condition
[NASA-CR-198368] p 697 N95-33208
- Numerical studies of turbulent free surface flows and unsteady propeller flows
[AD-A294377] p 706 N95-34343
- Special publication of National Aerospace Laboratory [NAL-SP-27] p 684 N95-34505
- Requirements and trends of computational aerodynamics as a tool for aircraft design
p 692 N95-34506
- A study on the convergence of a 3-D Euler code for cascade flow calculations
p 706 N95-34508
- A study of supersonic mixing flow field with ramp injector
p 706 N95-34512
- Calculation of supersonic combustion in SCRAMJET engines
p 698 N95-34513
- Hypersonic CFD analysis for the aerothermodynamic design of HOPE
p 684 N95-34520
- Numerical solutions of inviscid and viscous flows about airfoils by TVD method
p 684 N95-34521
- Direct numerical simulation of incompressible homogeneous isotropic turbulence using NWT
p 706 N95-34530
- Performance evaluation of the NWT with incompressible NS code
p 707 N95-34533
- Parallel computation of transonic flows about an aircraft configuration using multi-block structured grids
p 685 N95-34537

Vector-parallel simulations of transonic wind tunnel flows about a fully configured model of aircraft p 685 N95-34538

A large scale 3D Navier-Stokes analysis using NAL-NWT p 707 N95-34539

Role of computational fluid dynamics in aeronautical engineering. Number 12: Formulation and verification of uni-particle upwind schemes for the Euler equations p 707 N95-34540

Application of CFD technique for HYFLEX aerodynamic design p 693 N95-34542

Computations of low speed flow about space-plane p 685 N95-34544

Numerical simulations of dynamic stall phenomena in low speed flows p 685 N95-34546

Numerical simulation of unsteady viscous flow around an airfoil with oscillating spoiler p 685 N95-34547

Direct analysis of transonic rotor noise with CFD technique p 711 N95-34549

A simulation of damping process of pendulum motion due to aerodynamic forces p 711 N95-34551

COMPUTATIONAL GEOMETRY

Multidimensional lines 2: Proximity and applications [BTN-94-EIX94341340329] p 61 A95-60865

Aerodynamic shape optimization of a HSCT type configuration with improved surface definition [NASA-CR-197011] p 67 N95-13701

Computational methods for preliminary design and geometry definition in turbomachinery p 89 N95-14128

Three-dimensional hybrid grid generation using advancing front techniques p 567 N95-28745

Users manual for the improved NASA Lewis ice accretion code LEWICE 1.6 [NASA-CR-198355] p 485 N95-29132

Grid orthogonality effects on predicted turbine midspan heat transfer and performance [NASA-TM-106931] p 554 N95-29371

Acoustic scattering from ellipses by the modal element method [NASA-TM-106935] p 579 N95-29401

Geometric modeling for computer aided design [NASA-CR-198828] p 679 N95-31982

COMPUTATIONAL GRIDS

Navier-Stokes simulation of rotor-body flowfield in hover using overset grids [PAPER C15] p 1 A95-60160

Accuracy enhancements for overset grids using a defect correction approach [AIAA PAPER 94-0523] p 3 A95-60181

A grid generation and flow solution method for the Euler equations on unstructured grids [HTN-95-20003] p 153 A95-63201

Solution-adaptive structured-unstructured grid method for unsteady turbomachinery analysis. Part I: Methodology [BTN-94-EIX94441380983] p 208 A95-67329

Parallel implicit unstructured grid Euler solvers [BTN-95-EIX95042474393] p 217 A95-68307

Multiblock analysis for Shuttle Orbiter reentry heating from Mach 24 to Mach 12 [BTN-95-EIX95041503780] p 205 A95-69211

Flow resolution and domain influence in rarefied hypersonic blunt-body flows [BTN-95-EIX95082502729] p 220 A95-70136

Adaptive remeshing for convective heat transfer with variable fluid properties [BTN-95-EIX95082502720] p 243 A95-71033

Large-scale computational fluid dynamics by the finite element method [BTN-94-EIX94381359154] p 243 A95-71744

Adaptive finite element method for turbulent flow near a propeller [BTN-95-EIX95142553038] p 305 A95-73460

Laplace interaction law for the computation of viscous airfoil flow in low- and high-speed aerodynamics [BTN-95-EIX95142553037] p 263 A95-73461

Effects of spatial order of accuracy on the computation of vortical flowfields [BTN-95-EIX95152577604] p 305 A95-73479

Eigenanalysis of unsteady flows about airfoils, cascades, and wings [BTN-95-EIX95152577597] p 305 A95-73486

Progress in high-lift aerodynamic calculations [BTN-95-EIX95152582315] p 264 A95-73518

Unstructured grid solutions to a wing/pylon/store configuration [BTN-95-EIX95152582322] p 265 A95-73525

Navier-Stokes prediction of large-amplitude delta-wing roll oscillations [BTN-95-EIX95152582329] p 281 A95-73531

Application of the multigrid solution technique to hypersonic entry vehicles [BTN-95-EIX95152583254] p 306 A95-73555

Application of wall functions to generalized nonorthogonal curvilinear coordinate systems [BTN-95-EIX95182619077] p 307 A95-75762

Viscous-inviscid interaction method for unsteady low-speed airfoil flows [BTN-95-EIX95182619093] p 269 A95-75778

Grid refinement test of time-periodic flows over bluff bodies [BTN-94-EIX94401378822] p 307 A95-76491

Observations on using experimental data as boundary conditions for computations [BTN-95-EIX95182619103] p 321 A95-76588

CFD optimization of a theoretical minimum-drag body [BTN-95-EIX95182619234] p 308 A95-76660

Numerical simulation of unsteady aerodynamic heating induced by shock reflections p 428 A95-82418

Computational/experimental investigation of staged injection into a Mach 2 flow [HTN-95-51646] p 432 A95-85028

Practical formulation of a positively conservative scheme [HTN-95-51668] p 433 A95-85050

Compressible Navier-Stokes computations of multielement airfoil flows using multiblock grids [HTN-95-42327] p 371 A95-86156

Experimental investigation of the sources of propeller noise due to the ingestion of turbulence at low speeds [BTN-95-EIX95262697042] p 569 A95-86859

Preconditioned domain decomposition scheme for three-dimensional aerodynamic sensitivity analysis [HTN-95-42597] p 459 A95-87227

Two-dimensional unsteady leading-edge separation on a pitching airfoil [HTN-95-81628] p 461 A95-87676

Numerical model for circulation-control flows [HTN-95-81632] p 461 A95-87680

Boundary conditions for unsteady supersonic inlet analyses [HTN-95-20829] p 544 A95-88090

Computational aerodynamic analysis on the Open Skies aircraft [SAE PAPER 932514] p 466 A95-89187

Central-difference and upwind-biased schemes for steady and unsteady Euler aerofoil computations [HTN-95-01094] p 469 A95-90280

A detailed Euler flow analysis of TPS and fanjet engine p 473 A95-91515

Algorithmic trends in computational fluid dynamics; The Institute for Computer Applications in Science and Engineering (ICASE)/LaRC Workshop, NASA Langley Research Center, Hampton, VA, US, Sep. 15-17, 1991 [ISBN 0-387-94014-6] p 550 A95-91915

A viewpoint on discretization schemes for applied aerodynamic algorithms for complex configurations p 550 A95-91916

Algorithmic trends in CFD in the 1990's for aerospace flow field calculations p 550 A95-91917

The forecast systems laboratory's role in the FAA's aviation weather development program p 652 A95-93443

Weather products for aviation from WAFIC Bracknell p 670 A95-93527

Developing the Aviation Gridded Forecast System p 671 A95-93532

Operational multi-scale environment model with grid adaptivity (OMEGA) application to aviation weather p 676 A95-93556

An overview of issues encountered in parallelizing high-resolution weather prediction models p 676 A95-93560

Evaluation of a multigrid-based Navier-Stokes solver for aerothermodynamic computations [BTN-95-EIX95302694459] p 583 A95-94056

Computational fluid dynamics '92; Proceedings of the European Computational Fluid Dynamics Conference, 1st, Brussels, Belgium, Sep. 7-11, 1992. Vols. 1 & 2 [ISBN 0-444-89793-3] p 638 A95-95357

Discretization of the parabolised Navier-Stokes equations p 638 A95-95362

Numerical solution of Euler and Navier-Stokes equations for 2D transonic problems p 638 A95-95366

Laminar and turbulent flow over optimal riblets p 639 A95-95383

Heat transfer on bent-noise biconic in hypersonic flow p 639 A95-95394

Optimal shape design in hypersonic aerodynamics and electromagnetics p 639 A95-95397

A numerical investigation of flow around a square-section cylinder mounted with a splitter plate p 639 A95-95401

Effects of splitter plate on wake formation from a circular cylinder: A discrete vortex simulation p 639 A95-95404

An efficient discrete vortex method for low Reynolds number incompressible flows p 639 A95-95407

Viscous flow simulation using the discrete vortex diffusion velocity method p 639 A95-95421

Numerical simulation of the 3D turbulent flow around the combustor dome of an aircraft engine p 640 A95-95423

A robust inverse inviscid method for airfoil design p 640 A95-95431

An improved finite element method for the solution of the compressible Euler and Navier-Stokes equations p 640 A95-95439

Navier-Stokes computations around a realistic fighter configuration p 591 A95-95440

Implicit multidomain calculation of viscous transonic flows without artificial viscosity or upwinding p 640 A95-95443

High-lift calculations using Navier-Stokes methods p 641 A95-95444

Permeable wall boundary conditions for transonic airfoil design p 641 A95-95445

A modular system for computational fluid dynamics p 641 A95-95446

On the prediction of transonic unsteady flows using second order time accuracy p 641 A95-95448

Multigrid/multiblock method for transonic potential flow around wing/body/nacelle configurations including a slipstream p 591 A95-95451

Implicit upwind-Euler solution algorithms for unstructured-grid applications p 641 A95-95454

2-D and 3-D numerical simulation of a supersonic inlet flowfield p 641 A95-95457

Multigrid solution for the compressible Euler equations by an implicit characteristic-flux-averaging p 642 A95-95459

Transonic vortical flow predicted with a structured multiblock Euler solver p 642 A95-95462

An unstructured node centered scheme for the simulation of 3-D inviscid flows p 642 A95-95463

An innovative algorithm to accurately solve the Euler equations for rotary wing flow p 642 A95-95467

SAUNA: A system for grid generation and flow simulation using hybrid structured/unstructured grids p 642 A95-95470

A cartesian grid finite element method for aerodynamics of moving rigid bodies p 642 A95-95471

Grid adaptation for problems in computational fluid dynamics p 643 A95-95472

Multi-block finite volume calculation of compressible flow past aerodynamic configurations p 643 A95-95473

A 2D parallel multiblock Navier-Stokes solver with applications on shared- and disturbed memory machines p 643 A95-95475

Grid generation: Algebraic and partial differential equations techniques revisited p 643 A95-95477

Surface grid generation for multi-block structured grids p 643 A95-95478

Arbitrary Lagrangian-Eulerian finite element analysis for flow-induced vibration of rigid body p 643 A95-95485

High performance parallelized implicit Euler solver for the analysis of unsteady aerodynamic flows p 644 A95-95495

Hypersonic Navier-Stokes computations about complex configurations p 644 A95-95497

Navier-Stokes simulation of turbulent vortex high-Re-number flows over a delta wing p 644 A95-95507

Numerical simulation of the flow about the F-18 HARV at high angle of attack [NASA-CR-196396] p 9 N95-10940

Turbomachinery Design Using CFD [AGARD-LS-195] p 89 N95-14127

Aero design of turbomachinery components: CFD in complex systems p 90 N95-14136

Hybrid structured/unstructured grid computations for the F/A-18 at high angle of attack p 68 N95-14233

A Cartesian, cell-based approach for adaptively-refined solutions of the Euler and Navier-Stokes equations [NASA-TM-106786] p 73 N95-14297

An approach for dynamic grids [NASA-TM-106774] p 76 N95-15853

Time accurate computation of unsteady inlet flows with a dynamic flow adaptive mesh [AD-A285498] p 157 N95-16736

Floating shock fitting via Lagrangian adaptive meshes [AD-A289758] p 170 N95-18110

Mesh quality control for multiply-refined tetrahedral grids [NASA-CR-197595] p 160 N95-18737

The mathematical models of flow passage for gas turbine engines and their components p 140 N95-19020

Application of multicomponent models to flow passage simulation in multistage turbomachines and whole gas turbine engines p 140 N95-19022

An assessment of the adaptive unstructured tetrahedral grid, Euler Flow Solver Code FELISA [NASA-TP-3526] p 119 N95-19041

- Numerical simulation of dynamic-stall suppression by tangential blowing
[AD-A284887] p 120 N95-19110
- CFD: Advances and Applications, part 1
[NAL-SP-9322-PT-1] p 165 N95-19444
- Design of fan blades subjected to bird impact
p 200 N95-19669
- Ice-impact analysis of blades p 200 N95-19672
- Validation and evaluation of the advanced aeronautical CFD system SAUNA: A method developer's view
[ARA-MEMO-390] p 210 N95-19774
- Application of three-dimensional hybrid structured/unstructured grids to land, sea and air vehicles
[ARA-MEMO-399] p 210 N95-19775
- Verification of the CFD simulation system SAUNA for complex aircraft configurations
[ARA-MEMO-401] p 211 N95-19776
- Unstructured-grid large-eddy simulation of flow over an airfoil p 225 N95-22448
- A CFD study of complex missile and store configurations in relative motion
[NASA-CR-197912] p 285 N95-22949
- Mach 10 computational study of a three-dimensional scramjet inlet flow field
[NASA-TM-4602] p 310 N95-23210
- TIGER: A user-friendly interactive grid generation system for complicated turbomachinery and axis-symmetric configurations p 322 N95-23419
- CFD analysis of turbopump volutes p 312 N95-23436
- Convergence acceleration of implicit schemes in the presence of high aspect ratio grid cells p 313 N95-23446
- A combined geometric approach for solving the Navier-Stokes equations on dynamic grids
[NASA-TM-106919] p 332 N95-26075
- Computational analysis of forebody tangential slot blowing on the high alpha research vehicle
[NASA-CR-197754] p 389 N95-26591
- Global flowfield about the V-22 Tiltrotor Aircraft
[NASA-CR-198603] p 375 N95-27248
- Calculation of three-dimensional (3-D) internal flow by means of the velocity-vorticity formulation on a staggered grid
[NASA-TM-110352] p 376 N95-27258
- TranAir: A full-potential, solution-adaptive, rectangular grid code for predicting subsonic, transonic, and supersonic flows about arbitrary configurations. User's manual
[NASA-CR-4349] p 377 N95-28230
- TranAir: A full-potential, solution-adaptive, rectangular grid code for predicting subsonic, transonic, and supersonic flows about arbitrary configurations. Theory document
[NASA-CR-4348] p 378 N95-28265
- A grid generation system for multi-disciplinary design optimization p 567 N95-28763
- A global/local analysis method for treating details in structural design p 552 N95-28848
- Navier-Stokes solution of wing wake structure and its perturbation p 479 N95-29121
- Solution of the Navier-Stokes equations on locally refined Cartesian meshes using state-vector splitting p 553 N95-29197
- Grid orthogonality effects on predicted turbine midspan heat transfer and performance
[NASA-TM-106931] p 554 N95-29371
- Survey of CFD applications for high speed inlets
[AD-A291365] p 557 N95-30087
- Grid resolution and turbulent inflow boundary condition recommendations for NPARC calculations
[NASA-TM-106959] p 482 N95-30253
- Parameters on 2D Navier-Stokes analysis of a Mach 2.68 bifurcated rectangular mixed-compression inlet
[NASA-TM-107003] p 617 N95-30861
- Simulation of patch and slot antennas using FEM with prismatic elements and investigations of artificial absorber mesh termination schemes
[NASA-CR-198974] p 704 N95-32822
- Hypersonic CFD analysis for the aerothermodynamic design of HOPE p 684 N95-34520
- Direct numerical simulation of incompressible homogeneous isotropic turbulence using NWT p 706 N95-34530
- Performance evaluation of the NWT with incompressible NS code p 707 N95-34533
- Vector-parallel simulations of transonic wind tunnel flows about a fully configured model of aircraft p 685 N95-34538
- Role of computational fluid dynamics in aeronautical engineering. Number 12: Formulation and verification of uni-particle upwind schemes for the Euler equations p 707 N95-34540
- Numerical simulations of dynamic stall phenomena in low speed flows p 685 N95-34546
- Grid generation around airfoil with a flap using boundary element method p 686 N95-34552
- ### COMPUTER AIDED DESIGN
- Advancements in automatic fastening technology
[BTN-94-EIX94461290277] p 65 A95-61734
- Computerized maintenance aid
[BTN-95-EIX95031502749] p 217 A95-68256
- Two-point transonic airfoil design using optimization for improved off-design performance
[BTN-95-EIX95062487542] p 192 A95-68356
- Putting the ACSYNT on aircraft design
[BTN-95-EIX95072419881] p 180 A95-68398
- Development of an efficient inverse method for supersonic and hypersonic body design
[BTN-95-EIX95041503784] p 180 A95-69215
- Design decisions from the history of the EUVE science payload
[HTN-95-60545] p 205 A95-69854
- Design optimization of rotor blades for improved performance and vibration
[HTN-95-A0498] p 229 A95-72569
- Buckling and vibration analysis of laminated panels using VICONOPT
[PAPER-1746] p 230 A95-72580
- Functional agility metrics and optimal trajectory analysis
[BTN-95-EIX95182619121] p 321 A95-76598
- Modeling of aircraft exhaust emissions and infrared spectra for remote measurement of nitrogen oxides
[HTN-95-51276] p 355 A95-80861
- Estimation of aerodynamic derivatives: Euler scheme validation and approximate methods for hypersonic configurations p 460 A95-87385
- Aerodynamic design and optimization at Alenia D.V.D. p 491 A95-87564
- A tool for airframe shaping - idea and application
[SAE PAPER 931224] p 491 A95-87568
- Aircraft aerodynamic analysis on a personal computer (using the RDS aircraft design software)
[SAE PAPER 932530] p 492 A95-89190
- Aerodynamic tailoring of the Learjet Model 60 wing
[SAE PAPER 932534] p 492 A95-89194
- Integrated Thermal Energy Management (I-TEM): An evaluation tool for aircraft
[SAE PAPER 932577] p 493 A95-90065
- Integrated performance and reliability specification for digital avionics systems
[AIAA PAPER 95-0953] p 506 A95-90632
- Functional requirements of an aerospace Design Representation Programming Interface
[AIAA PAPER 95-0967] p 497 A95-90643
- A computational environment for exhaust nozzle design
[AIAA PAPER 95-1016] p 566 A95-90688
- Computer aided static aeroelastic analysis of wing/pylon/store combination p 499 A95-91531
- Simultaneous engineering in aero gas turbine design and manufacture
[CONGRESS PAPER C428-20-204] p 581 A95-91723
- The use of structural optimisation within aerospace
[CONGRESS PAPER C428-23-008] p 500 A95-91729
- ### Manufacture technology
- [CONGRESS PAPER C428-27-088] p 612 A95-93605
- The role of material behaviour modelling in stressing and life assessment of modern Aero-engine components
[CONGRESS PAPER C428-27-127] p 612 A95-93606
- ### Nonlinear aerodynamic analysis of grid fin configurations
- [BTN-95-EIX0619952748172] p 590 A95-94466
- Assessment of technology for aircraft development
[BTN-95-EIX0619952748181] p 606 A95-94474
- Advanced composites structural concepts and materials technologies for primary aircraft structures. Structural response and failure analysis: ISPAN modules users manual
[NASA-CR-4449] p 12 N95-10242
- High speed civil transport: Sonic boom softening and aerodynamic optimization
[NASA-CR-196397] p 28 N95-11192
- ACSYNT inner loop flight control design study
[NASA-CR-196316] p 17 N95-11223
- The potential of genetic algorithms for conceptual design of rotor systems
[NASA-CR-196813] p 43 N95-11699
- Application of two procedures for dual-point design of transonic airfoils
[NASA-TP-3466] p 38 N95-12176
- High speed civil transport aerodynamic optimization
[NASA-CR-196960] p 38 N95-12389
- Techniques for designing rotorcraft control systems
[NASA-CR-196192] p 52 N95-12791
- Aerodynamic shape optimization of a HSCT type configuration with improved surface definition
[NASA-CR-197011] p 67 N95-13701
- ### Turbomachinery Design Using CFD
- [AGARD-LS-195] p 89 N95-14127
- Designing in three dimensions p 90 N95-14130
- New methods, new methodology: Advanced CFD in the Snecma turbomachinery design process p 90 N95-14134
- Aero design of turbomachinery components: CFD in complex systems p 90 N95-14136
- A SIMULINK environment for flight dynamics and control analysis: Application to the DHC-2 Beaver. Part 1: Implementation of a model library in SIMULINK. Part 2: Nonlinear analysis of the Beaver autopilot
[NONP-NASA-SUPPL-DK-94-2802] p 84 N95-14815
- Generalized method of solving topological optimization problems for electrical airplane equipment systems in computer-aided design p 169 N95-16272
- An engineering code to analyze hypersonic thermal management systems p 155 N95-16322
- Applications of automatic differentiation in CFD
[NASA-TM-109948] p 157 N95-16828
- Wing design for a civil tiltrotor transport aircraft
[NASA-CR-197523] p 130 N95-18090
- Enhanced capabilities and modified users manual for axial-flow compressor conceptual design code CSPAN
[NASA-TM-106833] p 119 N95-18933
- Application of multidisciplinary models to the cooled turbine rotor design p 140 N95-19024
- Perspective problems of gas turbine engines simulation p 140 N95-19026
- Modelling structurally damaging twin-jet screech p 135 N95-19154
- Design of fan blades subjected to bird impact p 200 N95-19669
- Ice-impact analysis of blades p 200 N95-19672
- The Computer Aided Aircraft-design Package (CAAP)
[NASA-CR-197523] p 217 N95-19759
- PalymSys (TM): An extended version of CLIPS for construction and reasoning using blackboards p 217 N95-19767
- Parallel calculation of sensitivity derivatives for aircraft design using automatic differentiation
[NASA-TM-110103] p 231 N95-20370
- Development of quiet-flow supersonic wind tunnels for laminar-turbulent transition research
[NASA-CR-197286] p 239 N95-21436
- Euler Technology Assessment program for preliminary aircraft design employing SPLITFLOW code with Cartesian unstructured grid method
[NASA-CR-4649] p 273 N95-22917
- Euler technology assessment for preliminary aircraft design employing OVERFLOW code with multiblock structured-grid method
[NASA-CR-4651] p 273 N95-23095
- Control of flow separation in airfoil/wing design applications p 274 N95-23294
- Thin tailored composite wing for civil tiltrotor p 285 N95-23317
- CFD analysis of turbopump volutes p 312 N95-23436
- Aerodynamic optimization studies on advanced architecture computers
[NASA-CR-198045] p 330 N95-24379
- Aspect estimation of an aircraft using library model silhouettes
[PB95-141834] p 360 N95-25894
- Aerolasticity of wing and wing-body configurations on parallel computers
[NASA-CR-197756] p 389 N95-26590
- Turbomachinery design and tonal acoustics computations
[NASA-CR-197749] p 406 N95-26777
- Supersonic civil airplane study and design: Performance and sonic boom
[NASA-CR-197745] p 390 N95-26813
- Naval Aviation System TEAM mapping, charting, and geodesy handbook
[AD-A288590] p 446 N95-26841
- Creating an alternative parameter optimization method (APO) p 375 N95-26946
- STEP: A future vision, today
[NONP-NASA-VT-95-49121] p 452 N95-27209
- Application of CFD to the analysis and design of high-speed inlets
[NASA-CR-198574] p 438 N95-27240
- Advanced flight computer. Special study
[NASA-CR-198165] p 449 N95-27246
- CAE for thermal management of aerospace electronic boards using the BETAsoft program p 438 N95-27354
- A NASTRAN-based computer program for structural dynamic analysis of Horizontal Axis Wind Turbines p 439 N95-27980
- Designers' unified cost model p 424 N95-28464

- COINS: A composites information database system
p 453 N95-28465
- Surface Modeling, Grid Generation, and Related Issues in Computational Fluid Dynamic (CFD) Solutions
[NASA-CP-3291] p 476 N95-28723
- Requirements for effective use of CFD in aerospace design
p 551 N95-28725
- Grid generation and surface modeling for CFD
p 551 N95-28726
- Rapid Airplane Parametric Input Design (RAPID)
p 501 N95-28730
- Surface modeling and grid generation for aeropropulsion CFD
p 551 N95-28732
- Automatic blocking for complex three-dimensional configurations
p 566 N95-28734
- Block-structured grids for complex aerodynamic configurations: Current status
p 551 N95-28736
- An unstructured-grid software system for solving complex aerodynamic problems
p 476 N95-28743
- Three-dimensional hybrid grid generation using advancing front techniques
p 567 N95-28745
- Developing a workstation-based, real-time simulation for rapid handling qualities evaluations during design
[NASA-CR-198831] p 505 N95-30335
- A general inverse design procedure for aerodynamic bodies
p 606 N95-30497
- Structural design using equilibrium programming formulations
[NASA-TM-110175] p 645 N95-30682
- Geometric modeling for computer aided design
[NASA-CR-198828] p 679 N95-31982
- Three-dimensional aerodynamic shape optimization using discrete sensitivity analysis
p 691 N95-32904
- Expert systems and artificial intelligence applications in engineering design and inspection
p 710 N95-33008
- COMPUTER AIDED MANUFACTURING**
- Rapid prototyping of composite aircraft structures
[SAE PAPER 931219] p 539 A95-87530
- Manufacture technology
[CONGRESS PAPER C428-27-088] p 612 A95-93605
- Development of an intelligent tool-condition monitoring system for FMS
[CONGRESS PAPER C428-32-012] p 583 A95-93617
- Non-contact calibration of a CNC riveting machine
[CONGRESS PAPER C428-32-075] p 583 A95-93618
- Tooling - a source of productivity
[CONGRESS PAPER C428-32-017] p 583 A95-93619
- COMPUTER AIDED TOMOGRAPHY**
- Mapping hidden aircraft defects with dual-band infrared computed tomography
[DE95-011531] p 584 N95-32164
- COMPUTER ANIMATION**
- New computer delivered training systems to support technical crew training programmes
[CONGRESS PAPER C428-5-036] p 522 A95-91678
- COMPUTER ASSISTED INSTRUCTION**
- The CBT alternative for aviation training: Is it meeting the need?
[SAE PAPER 932596] p 379 A95-84568
- Integrated flight crew transition training for the advanced flight deck aircraft
[SAE PAPER 932599] p 380 A95-84571
- New tools for creating instruction and simulations
[SAE PAPER 932600] p 380 A95-84572
- Maintenance training to cope with high-tech innovations
[SAE PAPER 932619] p 456 A95-90082
- Intelligent tutoring system: F-16 flight simulation
p 521 A95-90649
- An intelligent tutoring system for civil aviation flight training
p 521 A95-91535
- The development of computer-based instructional simulations for the airline industry
p 625 A95-95159
- A workstation based simulator for teaching compressible aerodynamics
[NASA-TM-106799] p 170 N95-16906
- A computer-based multimedia prototype for night vision goggles
[AD-A286208] p 258 N95-21882
- The value of simulation for training
[AD-A289174] p 411 N95-26556
- COMPUTER DESIGN**
- Advanced flight computer. Special study
[NASA-CR-198165] p 449 N95-27246
- COMPUTER GRAPHICS**
- Pilot Weather Advisor system
[BTN-95-EIX95152582314] p 316 A95-73517
- The CBT alternative for aviation training: Is it meeting the need?
[SAE PAPER 932596] p 379 A95-84568
- Automation of observations in the Netherlands
p 661 A95-93485
- Nortaf: Computer generated aerodrome forecasts
p 668 A95-93521
- Dissemination of weather products
p 670 A95-93526
- Developing the Aviation Gridded Forecast System
p 671 A95-93532
- Computer-aided light sheet flow visualization using photogrammetry
[NASA-TP-3416] p 26 N95-10859
- Flight test of takeoff performance monitoring system
[NASA-TP-3403] p 51 N95-12664
- The role of CFD in the design process
p 90 N95-14135
- Spatial awareness comparisons between large-screen, integrated pictorial displays and conventional EFIS displays during simulated landing approaches
[NASA-TP-3467] p 80 N95-14852
- Interactive computer graphics applications for compressible aerodynamics
[NASA-TM-106802] p 170 N95-17264
- An evaluation of aircraft CRT and dot-matrix display legibility requirements
[AD-A283933] p 138 N95-18164
- An evaluation of the Software Through Pictures/T Tool (STP/T) for the Software Support Activity (SSA)
[AD-A288822] p 447 N95-26348
- EASY-SIM: A visual simulation system software architecture with an Ada 9X application framework
[AD-A289325] p 448 N95-26895
- Design and evaluation of a LQR controller for the bluebird unmanned air vehicle
[AD-A289769] p 504 N95-29457
- COMPUTER NETWORKS**
- Parallel CFD design on network-based computer
[AIAA PAPER 95-0984] p 565 A95-90656
- The Saab-Scania approach to development simulators
[CONGRESS PAPER C428-10-137] p 522 A95-91698
- Event correlation for networked simulators
[BTN-95-EIX0619952748168] p 625 A95-94462
- The IEEE scalable coherent interface: An approach for a unified avionics network
p 234 N95-20650
- High performance backbone components for modular avionics
p 247 N95-20653
- The coupling of fluids, dynamics, and controls on advanced architecture computers
[NASA-CR-197727] p 360 N95-25797
- COMPUTER PROGRAM INTEGRITY**
- Earth Observing System (EOS)/Advanced Microwave Sounding Unit-A (AMSU-A) software assurance plan
[NASA-CR-196059] p 98 N95-13885
- Automated test environment for a real-time control system
[TABES PAPER 94-631] p 99 N95-14652
- A study of software standards used in the avionics industry
p 137 N95-16456
- Proceedings of the 12th Annual National Conference on Ada Technology
[AD-A290693] p 569 N95-29644
- COMPUTER PROGRAMMING**
- Knowledge-based processing for aircraft flight control
[NASA-CR-194976] p 99 N95-13727
- Earth Observing System (EOS)/Advanced Microwave Sounding Unit-A (AMSU-A) software assurance plan
[NASA-CR-196059] p 98 N95-13885
- Elements of a modern turbomachinery design system
p 90 N95-14129
- New methods, new methodology: Advanced CFD in the Snecma turbomachinery design process
p 90 N95-14134
- ADST ARWA visual system module software design document
[AD-A283874] p 99 N95-14357
- A study of software standards used in the avionics industry
p 137 N95-16456
- Applications of automatic differentiation in computational fluid dynamics
p 156 N95-16461
- Cumulative reports and publications through December 31, 1994
[NASA-CR-195043] p 361 N95-26085
- STEP: A future revision, today
[NONP-NASA-VT-95-49121] p 452 N95-27209
- Control system design for the MOD-5A 7.3 mW wind turbine generator
p 440 N95-27985
- Software process improvement in the NASA software engineering laboratory
[AD-A289912] p 450 N95-28627
- Proceedings of the 12th Annual National Conference on Ada Technology
[AD-A290693] p 569 N95-29644
- Computational methods for control and optimal design of aerospace systems
[AD-A292861] p 608 N95-31451
- COMPUTER PROGRAMS**
- On a program-information system TDsoft
[BTN-94-EIX94461408773] p 175 A95-63656
- Computerized maintenance aid
[BTN-95-EIX95031502749] p 217 A95-68256
- Flight experience with lightweight, low-power miniaturized instrumentation systems
[BTN-95-EIX95062487522] p 180 A95-69230
- Buckling and vibration analysis of laminated panels using VICONOPT
[PAPER-1746] p 230 A95-72580
- Unstructured grid solutions to a wing/pylon/store configuration
[BTN-95-EIX95152582322] p 265 A95-73525
- Improved version of the Naval Surface Warfare Center aeroprediction code (AP93)
[BTN-95-EIX95152583260] p 267 A95-73561
- Multiple site fatigue damage in fuselage skin splices: Experimental simulation and theoretical prediction
[BTN-95-EIX95152584676] p 276 A95-73588
- Aerodynamic design of pegasus: Concept to flight with computational fluid dynamics
[BTN-95-EIX95182617463] p 298 A95-75734
- CFD optimization of a theoretical minimum-drag body
[BTN-95-EIX95182619234] p 308 A95-76660
- The Cassini spacecraft: Object oriented flight control software
p 359 A95-80405
- The ADAGE avionics reference architecture
[AIAA PAPER 95-1021] p 566 A95-90693
- Accelerated application development for flight software
[AIAA PAPER 95-1031] p 566 A95-90703
- An overview of issues encountered in parallelizing high-resolution weather prediction models
p 676 A95-93560
- F-15 Propulsion Controlled Aircraft (PCA)
[NASA-TM-104303] p 17 N95-10748
- Modeling improvements and users manual for axial-flow turbine off-design computer code AXOD
[NASA-CR-195370] p 8 N95-10853
- Radiant energy measurements from a scaled jet engine axisymmetric exhaust nozzle for a baseline code validation case
[NASA-TM-106686] p 25 N95-11409
- Object-oriented technology for compressor simulation
[NASA-TM-106723] p 49 N95-11864
- Computer code for determination of thermally perfect gas properties
[NASA-TP-3447] p 37 N95-11995
- Flight test of takeoff performance monitoring system
[NASA-TP-3403] p 51 N95-12664
- Overview of NASREM: The NASA/NBS standard reference model for telerobot control system architecture re
[PB94-194560] p 58 N95-12854
- Validation of the RPLUS3D code for supersonic inlet applications involving three-dimensional shock wave-boundary layer interactions
[NASA-TM-106579] p 39 N95-13058
- Numerical time dependent sheet cavitation simulations using a higher order panel method
[PB94-204435] p 59 N95-13249
- The role of CFD in the design process
p 90 N95-14135
- Aero design of turbomachinery components: CFD in complex systems
p 90 N95-14136
- Generic architectures for future flight systems
p 99 N95-14159
- Artificial neural network modeling of damaged aircraft
[AD-A283227] p 80 N95-14849
- USAF single-event sonic boom prediction model: PCBoom3
p 101 N95-14889
- Evaluation of the dynamic stability characteristics of the NAL Light Transport Aircraft
[NAL-PD-CA-9217] p 142 N95-16392
- A study of software standards used in the avionics industry
p 137 N95-16456
- FPCAS2D user's guide, version 1.0
[NASA-CR-195413] p 156 N95-16588
- Demonstration of the Dynamic Flowgraph Methodology using the Titan 2 Space Launch Vehicle Digital Flight Control System
[NASA-CR-197517] p 150 N95-17493
- Data from the GARTEUR (AD) Action Group 02 airfoil CAST 7/DOA1 experiments
p 111 N95-17856
- OAT15A airfoil data
p 111 N95-17857
- Two-dimensional high-lift airfoil data for CFD code validation
p 112 N95-17859
- A platform independent application of Lux illumination prediction algorithms
[AD-A283669] p 170 N95-18018
- Operational And Supportability Implementation System (OASIS) test and evaluation master plan
[AD-A284765] p 126 N95-18088
- Regenerative cooling for liquid propellant rocket thrust chambers
[INPE-5565-TDI/540] p 150 N95-18720
- Hypersonic flight testing
[AD-A283981] p 134 N95-18891

- An assessment of the adaptive unstructured tetrahedral grid, Euler Flow Solver Code FELISA [NASA-TP-3526] p 119 N95-19041
- Evaluation of scanners for C-scan imaging in nondestructive inspection of aircraft [DE94-012473] p 152 N95-19100
- Unsteady aerodynamic analyses for turbomachinery aeroelastic predictions p 141 N95-19381
- Technology Benefit Estimator (T/BEST): User's manual [NASA-TM-106785] p 167 N95-19501
- Design of fan blades subjected to bird impact p 200 N95-19669
- Prediction of rotor-blade deformations due to unsteady airloads [AD-A286593] p 231 N95-20860
- The opportunities for and challenges of common integrated electronics [AD-A279991] p 248 N95-20966
- Data link terminal DLT document [PB95-110805] p 229 N95-21369
- Additional improvements to the NASA Lewis ice accretion code LEWICE [NASA-TM-106849] p 309 N95-22669
- Automation technology using Geographic Information System (GIS) p 324 N95-23284
- Residual strength of thin panels with cracks p 311 N95-23311
- CFD analysis of turbopump volutes p 312 N95-23436
- Enhanced analysis and users manual for radial-inflow turbine conceptual design code RTD [NASA-CR-195454] p 275 N95-23462
- User's guide for ECAP2D: An Euler unsteady aerodynamic and aeroelastic analysis program for two dimensional oscillating cascades, version 1.0 [NASA-CR-189146] p 316 N95-24189
- Verification of computational aerodynamic predictions for complex hypersonic vehicles using the INCA(trademark) code [DE95-004757] p 330 N95-24308
- A non-iterative grid deformation algorithm for computational fluid dynamics for aeroelasticity [AD-A288298] p 436 N95-26418
- Design and synthesis of a real-time controller for an unmanned air vehicle [AD-A289134] p 408 N95-26555
- Comparison of fixed wing aircraft algorithms for JANUS [AD-A288503] p 389 N95-26652
- Development of an upwind, finite-volume code with finite-rate chemistry [NASA-CR-197747] p 374 N95-26760
- STEP: A future vision, today [NONP-NASA-VT-95-49121] p 452 N95-27209
- Application of CFD to the analysis and design of high-speed inlets [NASA-CR-198574] p 438 N95-27240
- Global flowfield about the V-22 Tiltrotor Aircraft [NASA-CR-198603] p 375 N95-27248
- CAE for thermal management of aerospace electronic boards using the BETASoft program p 438 N95-27354
- Flight Mechanics/Estimation Theory Symposium 1995 [NASA-CP-3299] p 416 N95-27763
- A NASTRAN-based computer program for structural dynamic analysis of Horizontal Axis Wind Turbines p 439 N95-27980
- Aeroelastic stability of wind turbine blade/aileron systems p 377 N95-27981
- Calculation of design load for the MOD-5A 7.3 mW wind turbine system p 440 N95-27982
- Control system design for the MOD-5A 7.3 mW wind turbine generator p 440 N95-27985
- Operator modeling in commercial aviation: Cognitive models, intelligent displays, and pilot's assistants [NASA-CR-198609] p 401 N95-28203
- TranAir: A full-potential, solution-adaptive, rectangular grid code for predicting subsonic, transonic, and supersonic flows about arbitrary configurations. User's manual [NASA-CR-4349] p 377 N95-28230
- TranAir: A full-potential, solution-adaptive, rectangular grid code for predicting subsonic, transonic, and supersonic flows about arbitrary configurations. Theory document [NASA-CR-4348] p 378 N95-28265
- Probabilistic evaluation of fuselage-type composite structures p 398 N95-28444
- Software process improvement in the NASA software engineering laboratory [AD-A289912] p 450 N95-28627
- Rapid Airplane Parametric Input Design (RAPID) p 501 N95-28730
- Block-structured grids for complex aerodynamic configurations: Current status p 551 N95-28736
- An unstructured-grid software system for solving complex aerodynamic problems p 476 N95-28743
- Leading-edge suction distribution for plane thin wings at subsonic speeds [ESDU-94037] p 477 N95-28800
- IPACS (Integrated Probabilistic Assessment of Composite Structures): Code development and applications p 534 N95-28849
- Leading edge film cooling effects on turbine blade heat transfer [NASA-TM-106955] p 513 N95-29115
- Optimizing cockpit display configurations with a genetic algorithm system [AD-A289799] p 508 N95-29123
- Mode of human image representation and error checking strategies in complex visual displays [AD-A290107] p 485 N95-29210
- Grid orthogonality effects on predicted turbine midspan heat transfer and performance [NASA-TM-106931] p 554 N95-29371
- Research instrumentation for polytechnic university's supersonic wind tunnel facility [AD-A290232] p 523 N95-29468
- Grid resolution and turbulent inflow boundary condition recommendations for NPARC calculations [NASA-TM-106959] p 482 N95-30253
- Developing a workstation-based, real-time simulation for rapid handling qualities evaluations during design [NASA-CR-198831] p 505 N95-30335
- Fuel-type classification and parameters prediction by Gas Liquid Chromatography analysis [AD-A293442] p 630 N95-31368
- Anechoic chamber upgrade [AD-A294375] p 700 N95-34342
- A study on the convergence of a 3-D Euler code for cascade flow calculations p 706 N95-34508
- Verification of turbine cascade flow with tip clearance p 698 N95-34511
- A study of supersonic mixing flow field with ramp injector p 706 N95-34512
- Calculation of supersonic combustion in SCRAMJET engines p 698 N95-34513
- Numerical solutions of inviscid and viscous flows about airfoils by TVD method p 684 N95-34521
- Performance evaluation of the NWT with incompressible NS code p 707 N95-34533
- Application of CFD technique for HYFLEX aerodynamic design p 693 N95-34542
- COMPUTER SYSTEMS DESIGN**
- Design decisions from the history of the EUVE science payload [HTN-95-60545] p 205 A95-69854
- CASS: Design for supportability [BTN-95-EIX95172595296] p 287 A95-75716
- Containing military autotest cost growth through the use of commercial standard equipment architectures [BTN-95-EIX95172595295] p 287 A95-75717
- ATE enabling technologies [BTN-95-EIX95172595294] p 287 A95-75718
- New commercial off-the-shelf testers are automatic and intelligent [BTN-95-EIX95172595292] p 287 A95-75720
- An overview of issues encountered in parallelizing high-resolution weather prediction models p 676 A95-93560
- An avionics scenario and command model description for Space Generic Open Avionics Architecture (SGOAA) [NASA-CR-188330] p 49 N95-11913
- Overview of NASREM: The NASA/NBS standard reference model for telerobot control system architecture [PB94-194560] p 58 N95-12854
- The Advanced Avionics Subsystem Technology Demonstration Program p 234 N95-20636
- The IEEE scalable coherent interface: An approach for a unified avionics network p 234 N95-20650
- Independent review of Aviation Technology and Research Information Analysis System (ATRIAS) database [AD-A284049] p 226 N95-21518
- The navigation toolkit [NASA-CR-197290] p 229 N95-22161
- On-line, adaptive state estimator for active noise control p 322 N95-23308
- Advanced flight computer. Special study [NASA-CR-198165] p 449 N95-27246
- Design of a real-time wind turbine simulator using a custom parallel architecture p 449 N95-27979
- Foundations of technology for constructing highly reliable distributed realtime systems [AD-A293254] p 678 N95-30892
- A highly reliable, high performance open avionics architecture for real time Nap-of-the-Earth operations p 693 N95-32497
- Development and flight testing of an Obstacle Avoidance System for US Army helicopters p 687 N95-32500
- COMPUTER SYSTEMS PERFORMANCE**
- The ICAO CNS/ATM system: New king, new law? [HTN-95-50218] p 175 A95-64855
- CASS: Design for supportability [BTN-95-EIX95172595296] p 287 A95-75716
- Analyzing fault tolerance using DREDD [AIAA PAPER 95-0952] p 565 A95-90631
- Steady and unsteady three-dimensional transonic flow computations by integral equation method [NASA-CR-196777] p 10 N95-11582
- Earth Observing System (EOS)/Advanced Microwave Sounding Unit-A (AMSU-A) software assurance plan [NASA-CR-196059] p 98 N95-13885
- Generic architectures for future flight systems p 99 N95-14159
- Space Generic Open Avionics Architecture (SGOAA): Overview p 99 N95-14161
- Evolutionary Telemetry and Command Processor (TCP) architecture p 86 N95-14162
- Computing quantitative characteristics of finite-state real-time systems [AD-A282839] p 83 N95-14343
- Digital systems validation. Chapter 20 Artificial Intelligence with applications for aircraft: Handbook, volume 2 [AD-A288492] p 448 N95-26638
- Control system design for the MOD-5A 7.3 mW wind turbine generator p 440 N95-27985
- Modeling spatio-temporal databases to measure the performance of the GPS satellite constellation p 489 N95-29596
- COMPUTER SYSTEMS PROGRAMS**
- FTGEN - An automated FT production system p 668 A95-93519
- A prototype for displaying aviation forecast variables using Eta numerical model output p 676 A95-93555
- The generic simulation executive at Manned Flight Simulator [AD-A283997] p 146 N95-18724
- Technology Benefit Estimator (T/BEST): User's manual [NASA-TM-106785] p 167 N95-19501
- Formal verification of an avionics microprocessor [NASA-CR-4682] p 710 N95-33396
- COMPUTER TECHNIQUES**
- On introduction of artificial intelligence elements to heat power engineering [BTN-94-EIX94461407961] p 100 A95-62635
- Computer aided diagnostic testing of installed flight control servo-actuators [SAE PAPER 932584] p 494 A95-90068
- New sensor technology for aircraft hydraulic system diagnostics [SAE PAPER 932586] p 494 A95-90070
- Aircraft wiring maintenance: Development of a computerized maintenance aid [SAE PAPER 932615] p 456 A95-90080
- Computer-aided light sheet flow visualization using photogrammetry [NASA-TP-3416] p 26 N95-10859
- Parallel methods for the flight simulation model [DE94-013330] p 52 N95-11752
- Research in progress in applied mathematics, numerical analysis, fluid mechanics, and computer science [AD-A284982] p 61 N95-11932
- Study of multiple cracks in airplane fuselage by micromechanics and complex variables p 94 N95-14468
- Extracting a representative loading spectrum from recorded flight data p 80 N95-14469
- A graphical user interface for design and analysis of air breathing propulsion systems [TABES PAPER 94-616] p 83 N95-14645
- Building complex simulations rapidly using MATRIX(x): The Space Station redesign [TABES PAPER 94-632] p 87 N95-14653
- Enhanced capabilities and updated users manual for axial-flow turbine preliminary sizing code TURBAN [NASA-CR-195405] p 76 N95-15912
- Portable parallel stochastic optimization for the design of aeropropulsion components [NASA-CR-195312] p 154 N95-16072
- Joint Proceedings on Aeronautics and Astronautics (JPAA) [ISBN-7-80-046602-7] p 104 N95-16249
- The computer analysis of the prediction of aircraft electrical power supply system reliability p 155 N95-16278
- Rapid solution of large-scale systems of equations p 169 N95-16458
- Interactive computer graphics applications for compressible aerodynamics [NASA-TM-106802] p 170 N95-17264
- Identification of Artificial Intelligence (AI) applications for maintenance, monitoring, and control of airway facilities [AD-A282479] p 125 N95-17373

A platform independent application of Lux illumination prediction algorithms
[AD-A283669] p 170 N95-18018

Transport aircraft loading and balancing system: Using a CLIPS expert system for military aircraft load planning
p 217 N95-19751

The Computer Aided Aircraft-design Package (CAAP)
p 217 N95-19759

PalymSys (TM): An extended version of CLIPS for construction and reasoning using blackboards
p 217 N95-19767

The IEEE scalable coherent interface: An approach for a unified avionics network
p 234 N95-20650

COMPUTER VISION

Research on an autonomous vision-guided helicopter
[AIAA PAPER 94-1240-CP] p 18 N95-11510

The 4-D approach to visual control of autonomous systems
[AIAA PAPER 94-1243-CP] p 27 N95-11513

Aspect estimation of an aircraft using library model silhouettes
[PB95-141834] p 360 N95-25894

EASY-SIM: A visual simulation system software architecture with an Ada 9X application framework
[AD-A289325] p 448 N95-26895

Cost effective, dual-purpose machine vision-based detectors for (1) smoke and flame detection, and (2) engine overhead/burn-through and flame detection
[AD-A292284] p 579 N95-28870

COMPUTERIZED SIMULATION

Nonhydrostatic simulation of frontogenesis in a moist atmosphere. Part 3: Thermal wind imbalance and rainbands
[HTN-95-90356] p 212 A95-66429

Aircraft electric field measurements: Calibration and ambient field retrieval
[HTN-95-90508] p 213 A95-67780

Nonlinear dynamic simulation of single- and multispool core engines, part 1: Computational method
[BTN-95-EIX95112524200] p 210 A95-69308

Numerical modelling of transverse impact on composite coupons
[BTN-95-EIX95082502225] p 240 A95-71022

High-order state space simulation models of helicopter flight mechanics
[HTN-95-A0494] p 237 A95-72565

Navier-Stokes prediction of large-amplitude delta-wing roll oscillations
[BTN-95-EIX95152582329] p 281 A95-73531

Aerodynamic characteristics of a hypersonic viscous optimized waverider at high altitudes
[BTN-95-EIX95152583251] p 266 A95-73552

Hypersonic convective heat transfer over 140-deg blunt cones in different gases
[BTN-95-EIX95152583253] p 306 A95-73554

Predicting exhaust plume boundaries with supersonic external flows
[BTN-95-EIX95152583258] p 297 A95-73559

Improving prediction: The incorporation of simplified rotor dynamics in a mathematical model of the bell 412HP
[BTN-95-EIX95152584679] p 282 A95-73591

New commercial off-the-shelf testers are automatic and intelligent
[BTN-95-EIX95172595292] p 287 A95-75720

Determination of wall boundary conditions for high-speed-ratio direct simulation Monte Carlo calculations
[BTN-95-EIX95182617457] p 267 A95-75728

Zonally decoupled direct simulation Monte Carlo solutions of hypersonic blunt-body wake flows
[BTN-95-EIX95182617458] p 268 A95-75729

Simulating heat addition via mass addition in constant area compressible flows
[BTN-95-EIX95182619100] p 307 A95-76585

Functional agility metrics and optimal trajectory analysis
[BTN-95-EIX95182619121] p 321 A95-76598

Response of a nonrotating rotor blade to lateral turbulence. Part 2: Experiment
[BTN-95-EIX95182619229] p 284 A95-76655

Unsteady ground effects on aerodynamic coefficients of finite wings with camber
[BTN-95-EIX95182619233] p 271 A95-76659

Modeling of aircraft exhaust emissions and infrared spectra for remote measurement of nitrogen oxides
[HTN-95-51276] p 355 A95-80861

GETRAN: A generic, modularly structured computer code for simulation of dynamic behavior of aero- and power generation gas turbine engines
[BTN-94-EIX95011441241] p 431 A95-84198

Effects of a polar stratosphere cloud parameterization on ozone depletion due to stratospheric aircraft in a two-dimensional model
[HTN-95-A1038] p 443 A95-84543

General solution procedure for flows in local chemical equilibrium
[HTN-95-42329] p 404 A95-86158

A new paradigm: The investment casting cooperative arrangement
[HTN-95-92510] p 539 A95-87330

Verification of engineering methods of aerodynamics for reentry vehicles by DSMC
p 525 A95-87386

Numerical studies of Mach reflection with air chemistry
p 548 A95-90575

New computer delivered training systems to support technical crew training programmes
[CONGRESS PAPER C428-5-036] p 522 A95-91678

Developments in wear particle analysis using computerised procedures
[CONGRESS PAPER C428-15-216] p 457 A95-91713

Computer simulation of ejection seat motion
[CONGRESS PAPER C428-18-169] p 484 A95-91718

Discrete crack growth analysis methodology for through cracks in pressurized fuselage structures
[BTN-95-EIX0608952737538] p 633 A95-92751

Preliminary comparisons between MM5 NCAR/Penn State model generated icing forecasts and observations
p 655 A95-93458

Investigation of outflow strength variability in Florida downburst-producing storms
p 659 A95-93476

An application of some cloud modeling techniques to a regional model simulation of an icing event
p 673 A95-93543

Amplification and breaking of atmospheric gravity waves
p 675 A95-93552

Prediction of airplane states
[BTN-95-EIX0619952748174] p 584 A95-94468

Airborne imaging radiometer scan simulation
[BTN-95-EIX95332753018] p 638 A95-94793

Future ATC system integration: Tools for developing a shared vision
p 600 A95-95085

The development of computer-based instructional simulations for the airline industry
p 625 A95-95159

Partially implicit method for simulating viscous aerofoil flows
[BTN-94-EIX94522406680] p 709 A95-96299

Advanced distributed simulation technology advanced rotary wing aircraft. Strawman verification and validation plan for the ARWA simulator system
[AD-A280237] p 19 N95-10349

Advanced distributed simulation technology advanced rotary wing aircraft. System/segment specification. Volume 1: Simulation system module
[AD-A280238] p 20 N95-10350

Advanced distributed simulation technology advanced rotary wing aircraft. System/segment specification. Volume 3: Visual system module
[AD-A280239] p 20 N95-10351

Advanced distributed simulation technology advanced rotary wing aircraft. System/segment specification. Volume 5: Simulation system module AH-64K
[AD-A280433] p 20 N95-10353

Advanced distributed simulation technology advanced rotary wing aircraft. Software reusability report
[AD-A280434] p 20 N95-10354

Computational fluid dynamics uses in fluid dynamics/aerodynamics education
[NASA-TM-108834] p 8 N95-10847

Numerical simulation of the flow about the F-18 HARV at high angle of attack
[NASA-CR-196396] p 9 N95-10940

Parallel methods for the flight simulation model
[DE94-013330] p 52 N95-11752

TKKMOD: A computer simulation program for an integrated wind diesel system. Version 1.0: Document and user guide
[PB94-179090] p 60 N95-11798

Windshear certification data base for forward-look detection systems
p 41 N95-13204

Certification methodology applied to the NASA experimental radar system
p 41 N95-13205

Certification of windshear performance with RTCA class D radomes
p 41 N95-13206

Mach number control in the High Speed Wind Tunnel of NLR
[PB94-201670] p 53 N95-13243

The role of CFD in the design process
p 90 N95-14135

ADST ARWA visual system module software design document
[AD-A283874] p 99 N95-14357

Development of the NASA/FLAGRO computer program for analysis of airframe structures
p 94 N95-14473

Fatigue reliability method with in-service inspections
p 94 N95-14475

Numerical simulation of the SOFIA flowfield
[NASA-CR-197025] p 74 N95-14612

A graphical user interface for design and analysis of air breathing propulsion systems
[TABES PAPER 94-616] p 83 N95-14645

Automated test environment for a real-time control system
[TABES PAPER 94-631] p 99 N95-14652

Building complex simulations rapidly using MATRIX(x): The Space Station redesign
[TABES PAPER 94-632] p 87 N95-14653

A SIMULINK environment for flight dynamics and control analysis: Application to the DHC-2 Beaver. Part 1: Implementation of a model library in SIMULINK. Part 2: Nonlinear analysis of the Beaver autopilot
[NONP-NASA-SUPPL-DK-94-2802] p 84 N95-14815

Evaluation of energy-sink stability criteria for dual-spin spacecraft
[AD-A283228] p 87 N95-14850

Development and application of structural dynamics analysis capabilities
[NASA-CR-197229] p 96 N95-14922

Matlab as a robust control design tool
p 169 N95-16474

Numerical simulation of helicopter engine plume in forward flight
[NASA-CR-197488] p 107 N95-16589

Applications of automatic differentiation in CFD
[NASA-TM-109948] p 157 N95-16828

A workstation based simulator for teaching compressible aerodynamics
[NASA-TM-106799] p 170 N95-16906

A PC-based interactive simulation of the F-111C Pavé Tack system and related sensor, avionics and aircraft aspects
[AD-A285500] p 129 N95-16969

Interactive computer graphics applications for compressible aerodynamics
[NASA-TM-106802] p 170 N95-17264

Demonstration of the Dynamic Flowgraph Methodology using the Titan 2 Space Launch Vehicle Digital Flight Control System
[NASA-CR-197517] p 150 N95-17493

Low-speed surface pressure and boundary layer measurement data for the NLR 7301 airfoil section with trailing edge flap
p 111 N95-17855

Data from the GARTEur (AD) Action Group 02 airfoil CAST 7/DOA1 experiments
p 111 N95-17856

OAT15A airfoil data
p 111 N95-17857

A supercritical airfoil experiment
p 111 N95-17858

Two-dimensional high-lift airfoil data for CFD code validation
p 112 N95-17859

Six degree of freedom flight dynamic and performance simulation of a remotely-piloted vehicle
[AERO-TN-9301] p 131 N95-18097

Helicopter Performance Evaluation (HELPE) computer model
[AD-A284319] p 131 N95-18381

Studies on high pressure and unsteady flame phenomena
[AD-A284126] p 152 N95-18410

Aeromechanics technology, volume 1. Task 1: Three-dimensional Euler/Navier-Stokes Aerodynamic Method (TEAM) enhancements
[AD-A285713] p 132 N95-18483

NASA High Performance Computing and Communications program
[NASA-TM-4653] p 176 N95-18573

The generic simulation executive at Manned Flight Simulator
[AD-A283997] p 146 N95-18724

Perspective problems of gas turbine engines simulation
p 140 N95-19026

Fatigue loads spectra derivation for the Space Shuttle: Second cycle
p 166 N95-19470

Design of fan blades subjected to bird impact
p 200 N95-19669

Ice-impact analysis of blades
p 200 N95-19672

Collected papers of the Soar/IFOR project, Spring 1994
[AD-A280063] p 238 N95-20624

Application of Direct and Large Eddy Simulation to Transition and Turbulence
[AGARD-CP-551] p 248 N95-21061

Simulation of rotor blade element turbulence
[NASA-TM-108862] p 232 N95-21186

A preliminary study of the airwake model used in an existing SH-60B/FFG-7 helicopter/ship simulation program
[DSTO-TR-0015] p 224 N95-21659

Unstructured-grid large-eddy simulation of flow over an airfoil
p 225 N95-22448

Large-eddy simulation of flow through a plane, asymmetric diffuser
p 250 N95-22449

Direct numerical simulations of on-demand vortex generators: Mathematical formulation
p 251 N95-22452

- Particle kinetic simulation of high altitude hypervelocity flight
[NASA-CR-197383] p 309 N95-22481
- High-performance parallel analysis of coupled problems for aircraft propulsion
[NASA-CR-197440] p 289 N95-23088
- Development and verification of a resin film infusion/resin transfer molding simulation model for fabrication of advanced textile composites
[NASA-CR-197439] p 301 N95-23179
- A wall interference assessment/correction system
[AD-A291421] p 309 N95-23183
- Design of a variable area diffuser for a 15-inch Mach 6 open-jet tunnel
p 297 N95-23309
- Development of qualification guidelines for personal computer-based aviation training devices
[DOT/FAA/AM-95/6] p 323 N95-23603
- Estimate of probability of crack detection from service difficulty report data
[PB95-149381] p 328 N95-24295
- The coupling of fluids, dynamics, and controls on advanced architecture computers
[NASA-CR-197727] p 360 N95-25797
- The 1994 updated National Airspace System performance assessment for year 2005
[AD-A288652] p 380 N95-26485
- Numerical simulation of combustion flow around a flame holder with hydrogen injection
[NAL-TR-1233] p 419 N95-26523
- The value of simulation for training
[AD-A289174] p 411 N95-26556
- Comparison of fixed wing aircraft algorithms for JANUS
[AD-A288503] p 389 N95-26652
- Numerical simulation of the flow about the F-18 HARV at high angle of attack
[NASA-CR-197755] p 374 N95-26735
- A numerical model to predict the fate of jettisoned aviation fuel
[AD-A289336] p 419 N95-26842
- A mathematical analysis of the Janus combat simulation weather effects models and sensitivity analysis of sky-to-ground brightness ratio on target detection
[AD-A289629] p 446 N95-26858
- The photo-realistic AFIT virtual cockpit
[AD-A289376] p 390 N95-26876
- EASY-SIM: A visual simulation system software architecture with an Ada 9X application framework
[AD-A289325] p 448 N95-26895
- Analysis and simulation of narrowband GPS jamming using digital excision temporal filtering
[AD-A289328] p 383 N95-26898
- Aircraft nosewheel steering simulation
p 412 N95-26944
- Implementation and demonstration of a multiple model adaptive estimation failure detection system for the F-16
[AD-A289301] p 391 N95-27042
- CAE for thermal management of aerospace electronic boards using the BETASoft program
p 438 N95-27354
- NAS Technical Summaries, March 1993 - February 1994
[NASA-RP-1355] p 453 N95-27367
- Precision landing system mathematical modeling study report for Andrews Air Force Base, runway 19L, Camp Springs, MD
[AD-A289015] p 384 N95-27903
- A NASTRAN-based computer program for structural dynamic analysis of Horizontal Axis Wind Turbines
p 439 N95-27980
- Aeroelastic stability of wind turbine blade/aileron systems
p 377 N95-27981
- A hybrid vehicle evaluation code and its application to vehicle design. Revision 1
[DE95-008053] p 441 N95-28029
- A hybrid vehicle evaluation code and its application to vehicle design, revision 2
[DE95-008060] p 441 N95-28139
- Analysis of aircraft engine blade subject to ice impact
p 407 N95-28277
- Unmanned aerial vehicles, 1994 master plan
[AD-A291628] p 398 N95-28411
- Numerical simulation of crack growth in pressurized fuselages
[PB95-192415] p 400 N95-28636
- Surface Modeling, Grid Generation, and Related Issues in Computational Fluid Dynamic (CFD) Solutions
[NASA-CP-3291] p 476 N95-28723
- Rapid Airplane Parametric Input Design (RAPID)
p 501 N95-28730
- Demonstration of an automated CFD system for three-dimensional flow simulations
p 551 N95-28767
- Users manual for the improved NASA Lewis ice accretion code LEWICE 1.6
[NASA-CR-198355] p 485 N95-29132
- A fourth order Euler/Navier-Stokes prediction method for the aerodynamics and aeroelasticity of hovering rotor blades
p 554 N95-29242
- Applications of digital video and synthetic environments to unmanned aerial vehicles
[AD-A291875] p 504 N95-29437
- Transport delays associated with NASA Langley Flight Simulation Facility
[NASA-TM-110150] p 568 N95-29454
- Design and evaluation of a LQR controller for the bluebird unmanned air vehicle
[AD-A289769] p 504 N95-29457
- Numerical simulations of the flow in the HYPULSE expansion tube
[NASA-TM-110357] p 523 N95-30228
- Teletext media resource tape
[NASA-TM-110648] p 569 N95-30248
- Manual for a workstation-based generic flight simulation program (LaRCsim), version 1.4
[NASA-TM-110164] p 518 N95-30327
- Numerical simulation and analysis of the hypersonic turbulent flow past a blunt-fin/ramp configuration
[DLR-FB-94-19] p 483 N95-30349
- Object-oriented approach for gas turbine engine simulation
[NASA-TM-106970] p 615 N95-30594
- A novel instrumentation system for measurement of helicopter rotor motions and loads data, phase 1
[AD-A293309] p 607 N95-30923
- Calspan experience of PIO and the effects of rate limiting
p 598 N95-31072
- Computer model to simulate testing at the National Transonic Simulation Facility
[NASA-TM-4664] p 627 N95-32217
- The application of helicopter mission simulation to Nap-of-the-Earth operations
p 710 N95-32496
- Requirements and trends of computational aerodynamics as a tool for aircraft design
p 692 N95-34506
- Design of secondary flow control cascade using numerical simulation
p 698 N95-34507
- Calculation of supersonic combustion in SCRAMJET engines
p 698 N95-34513
- Direct numerical simulation of incompressible homogeneous isotropic turbulence using NWT
p 706 N95-34530
- Application of CFD technique for HYFLEX aerodynamic design
p 693 N95-34542
- Numerical simulation of unsteady viscous flow around an airfoil with oscillating spoiler
p 685 N95-34547
- Numerical simulation of two-dimensional PAR-WIG
p 685 N95-34548
- High order accuracy computational methods in aerodynamics using parallel architectures
[AD-A294167] p 686 N95-34763
- COMPUTERS**
- AIAA Computing in Aerospace 10, San Antonio, TX, March 28-30, 1995
[ISBN 1-56347-119-1] p 565 N95-90629
- Evaluation of scanners for C-scan imaging in nondestructive inspection of aircraft
[DE94-012473] p 152 N95-19100
- The opportunities for and challenges of common integrated electronics
[AD-A297991] p 248 N95-20966
- CONCAVITY**
- Multiple instabilities of three-dimensional boundary layers along a concave wall
[HTN-95-71126] p 429 N95-83487
- CONCENTRATION (COMPOSITION)**
- Antarctic snow record of southern hemisphere lead pollution
[HTN-95-40359] p 212 N95-66869
- Time-of-flight mass spectrometer for impulse facilities
[BTN-95-EIX95142553057] p 262 N95-73441
- Erosion of dust-filtered helicopter turbine engines. Part 1: Basic theoretical considerations
[BTN-95-EIX95182619222] p 288 N95-76648
- Evolution of the concentrations of trace species in an aircraft plume: Trajectory study
[HTN-95-A1044] p 443 N95-84549
- CONCORDE AIRCRAFT**
- Maintenance requirements for a supersonic transport
[BTN-95-EIX95031502751] p 179 N95-68258
- Concorde: Silver jubilee Mach 2 marks 25 years
[HTN-95-42618] p 483 N95-87248
- Preliminary identification of buffet problems in high speed civil transport
p 294 N95-23319
- CONCRETES**
- Moisture induced pressures in concrete airfield pavements
[AD-A281974] p 52 N95-11789
- Marginal aggregates in flexible pavements: Background survey and experimental plan
[DOT/FAA/CT-94/58] p 53 N95-12216
- CONCURRENT ENGINEERING**
- Lean manufacturing for lean times
[BTN-95-EIX95302730538] p 583 N95-94036
- Integrated design and manufacturing for the high speed civil transport
[NASA-CR-197183] p 48 N95-12700
- New technologies for space avionics
[NASA-CR-197574] p 150 N95-18196
- STEP: A future vision, today
[NONP-NASA-VT-95-49121] p 452 N95-27209
- CONDENSATION NUCLEI**
- On the link between cloud-top radiative properties and sub-cloud aerosol concentrations
[HTN-95-A0527] p 255 N95-73181
- CONDENSING**
- Condensing cycle air conditioning system
[SAE PAPER 932056] p 513 N95-91637
- CONDUCTIVE HEAT TRANSFER**
- Effect of curvature in the numerical simulation of an electrothermal de-icer pad
[BTN-95-EIX95182619219] p 276 N95-76645
- User's manual for the NASA Lewis ice accretion/heat transfer prediction code with electrothermal deicer input
[NASA-CR-4530] p 57 N95-11888
- CAE for thermal management of aerospace electronic boards using the BETASoft program
p 438 N95-27354
- CONDUCTIVITY**
- The effect of aviation fuels containing low amounts of static dissipater additive on electrostatic charge generation
[AD-A280075] p 420 N95-28152
- CONES**
- Transition correlations in three-dimensional boundary layers
[HTN-95-51648] p 432 N95-85030
- Shock tunnel measurements of hypervelocity blunted cone drag
[HTN-95-42591] p 459 N95-87221
- CONFERENCES**
- Balloon technology and observations; Symposium P3 of the COSPAR Plenary Meeting, 29th, Washington, DC, Aug. 28-Sept. 5, 1992
[HTN-95-70250] p 181 N95-66276
- Guidance and control, 1993; Annual Rocky Mountain Guidance and Control Conference, 16th, Keystone, CO, Feb. 6-10, 1993
[ISBN 0-87703-365-X] p 341 N95-80389
- Education, training, and human engineering in aerospace; SAE Aerotech '93, Costa Mesa, CA, Sep. 27-30, 1993
[SAE SP-992] p 417 N95-84553
- Fatigue of aircraft materials; Specialists' Conference, Delft, Netherlands, 1992
[HTN-95-B0076] p 387 N95-85892
- Orbital transport: Technical, meteorological and chemical aspects; Aerospace Symposium, 3rd, Braunschweig, Germany, Aug. 26-28, 1991
[ISBN 3-540-563180] p 524 N95-87373
- Computational methods in applied sciences; European Computational Fluid Dynamics Conference, 1st, Brussels, Belgium, Sept. 7-11, 1992
[ISBN 0-444-89795-X] p 539 N95-87552
- Inter-Noise 92: Noise control and the public; International Congress on Noise Control Engineering, Toronto, Ontario, Canada, July 20 - 22, 1992. Vols. 1 & 2
[ISBN 0-931784-25-5] p 559 N95-88457
- Symposium on Aerodynamics & Aeroacoustics, Tucson, AZ, Mar. 1-2, 1993
[ISBN 981-02-1732-3] p 462 N95-88892
- Noise control in aeroacoustics; Proceedings of the 1993 National Conference on Noise Control Engineering, NOISE-CON 93, Williamsburg, VA, May 2-5, 1993
[ISBN 0-931784-26-3] p 573 N95-90088
- AIAA Computing in Aerospace 10, San Antonio, TX, March 28-30, 1995
[ISBN 1-56347-119-1] p 565 N95-90629
- Report to the aerospace profession; SETP Symposium, 37th, Beverly Hills, CA, USA, September 1993
[HTN-95-12142] p 497 N95-90866
- Algorithmic trends in computational fluid dynamics; The Institute for Computer Applications in Science and Engineering (ICASE)/LaRC Workshop, NASA Langley Research Center, Hampton, VA, US, Sep. 15-17, 1991
[ISBN 0-387-94014-6] p 550 N95-91915
- International Conference on Aviation Weather Systems, 5th, Vienna, VA, Aug. 2-6, 1993. Preprint Volume
[HTN-95-92940] p 652 N95-93441
- Computational fluid dynamics '92; Proceedings of the European Computational Fluid Dynamics Conference, 1st, Brussels, Belgium, Sep. 7-11, 1992. Vols. 1 & 2
[ISBN 0-444-89793-3] p 638 N95-95357
- Fly-By-Light/Power-By-Wire Requirements and Technology Workshop
[NASA-CP-10108] p 12 N95-10245

Airborne Windshear Detection and Warning Systems. Fifth and Final Combined Manufacturers' and Technologists' Conference, part 1 [NASA-CP-10139-PT-1] p 10 N95-10566
 Noise Con 1994: Proceedings of the 1994 National Conference on Noise Control Engineering. Progress in Noise Control for Industry [LC-75-24750] p 28 N95-11259
 Fourth High Alpha Conference, volume 1 [NASA-CP-10143-VOL-1] p 67 N95-14229
 Fourth High Alpha Conference, volume 2 [NASA-CP-10143-VOL-2] p 69 N95-14239
 Fourth High Alpha Conference, volume 3 [NASA-CP-10143-VOL-3] p 71 N95-14251
 Proceedings of the FAA Inspection Program Area Review [AD-A283849] p 77 N95-14350
 FAA/NASA International Symposium on Advanced Structural Integrity Methods for Airframe Durability and Damage Tolerance [NASA-CP-3274-PT-1] p 92 N95-14453
 High-Speed Research: 1994 Sonic Boom Workshop: Atmospheric Propagation and Acceptability Studies [NASA-CP-3279] p 75 N95-14878
 The 1993 JANNAP Propulsion Meeting, volume 1 [CPIA-PUBL-602-VOL-1] p 148 N95-16312
 Workshop on Formal Models for Intelligent Control [AD-A281399] p 169 N95-16864
 Conference on Aerospace Transparent Materials and Enclosures. Volume 2: Sessions 5-9 [AD-A283926] p 131 N95-18162
 Aircraft Loads due to Turbulence and their Impact on Design and Certification [AGARD-R-798] p 143 N95-18597
 Conference on Aerospace Transparent Materials and Enclosures, volume 1 [AD-A283925] p 133 N95-18677
 Mathematical Models of Gas Turbine Engines and their Components [AGARD-LS-198] p 139 N95-19017
 Wall Interference, Support Interference and Flow Field Measurements [AGARD-CP-535] p 162 N95-19251
 NASA Lewis Research Center Workshop on Forced Response in Turbomachinery [NASA-CP-10147] p 141 N95-19380
 FAA/NASA International Symposium on Advanced Structural Integrity Methods for Airframe Durability and Damage Tolerance, part 2 [NASA-CP-3274-PT-2] p 124 N95-19468
 Proceedings of the USAF Structural Integrity Program Conference [AD-A285684] p 194 N95-19517
 Erosion, Corrosion and Foreign Object Damage Effects in Gas Turbines [AGARD-CP-558] p 197 N95-19653
 T-45A High Angle of Attack Testing: US Naval Test Pilot School 46th Annual Reunion and Symposium [AD-A284000] p 231 N95-20466
 Advanced Packaging Concepts for Digital Avionics [AGARD-CP-562] p 233 N95-20631
 Application of Direct and Large Eddy Simulation to Transition and Turbulence [AGARD-CP-551] p 248 N95-21061
 Corrosion detection and management of advanced airframe materials [AGARD-CP-565] p 302 N95-23496
 Report of proceedings: Aviation Accident Investigation Symposium. Volume 2: Participant presentations [PB94-917007] p 277 N95-23598
 Aviation Accident Investigation Symposium. Volume 1: Industry recommendations and Safety Board responses [PB94-917005] p 278 N95-24105
 The 1994 Fiber Optic Sensors for Aerospace Technology (FOSAT) Workshop [NASA-CP-10166] p 337 N95-24207
 Proceedings of the 2d USAF Aging Aircraft Conference [AD-A288217] p 336 N95-25578
 Thermal Barrier Coating Workshop [NASA-CP-10170] p 344 N95-26119
 AIAA Techfest 20 Proceedings [NIAR-94-1] p 367 N95-26941
 Composite Repair of Military Aircraft Structures [AGARD-CP-550] p 392 N95-27504
 Flight Mechanics/Estimation Theory Symposium 1995 [NASA-CP-3299] p 416 N95-27763
 Industry-Wide Workshop on Computational Turbulence Modeling [NASA-CP-10165] p 439 N95-27882
 Ninth DOD/NASA/FAA Conference on Fibrous Composites in Structural Design, volume 3 [NASA-CR-198718] p 420 N95-28266
 Ninth DOD/NASA/FAA Conference on Fibrous Composites in Structural Design, volume 1 [NASA-CR-198723] p 421 N95-28420

Ninth DOD/NASA/FAA Conference on Fibrous Composites in Structural Design, volume 2 [NASA-CR-198722] p 424 N95-28462
 Proceedings of the AIAA/FAA joint symposium on general aviation systems [AD-A289830] p 368 N95-28610
 Surface Modeling, Grid Generation, and Related Issues in Computational Fluid Dynamic (CFD) Solutions [NASA-CP-3291] p 476 N95-28723
 Third NASA Advanced Composites Technology Conference, volume 1, part 2 [NASA-CP-3178-VOL-1-PT-2] p 531 N95-28823
 Third NASA Advanced Composites Technology Conference, volume 1, part 1 [NASA-CP-3178-VOL-1-PT-1] p 534 N95-29029
 Intelligent turbine engines for Army applications [AD-A290532] p 514 N95-29496
 Proceedings of the 12th Annual National Conference on Ada Technology [AD-A290693] p 569 N95-29644
 Proceedings of the Sixth International Symposium on Long-Range Sound Propagation [AD-A290920] p 580 N95-30084
 Flight Vehicle Integration Panel Workshop on Pilot Induced Oscillations [AGARD-AR-335] p 597 N95-31061
 The 25th International Symposium on Combustion [AD-A286825] p 630 N95-31268
 Active control technology: Applications and lessons learned [AGARD-CP-560] p 620 N95-31989
 Environmentally Safe and Effective Processes for Paint Removal [AGARD-LS-201] p 650 N95-32165
 Low-Level and Nap-of-the-Earth (NOE) night operations [AGARD-CP-563] p 686 N95-32486
 Special publication of National Aerospace Laboratory [NAL-SP-27] p 684 N95-34505

CONFIDENCE LIMITS

Reaction-time response of aircraft crash [BTN-95-EIX95292721296] p 595 A95-92626
 En route noise levels from propfan test assessment airplane [NASA-TP-3451] p 62 N95-12341

CONFIGURATION MANAGEMENT

Accelerated application development for flight software [AIAA PAPER 95-1031] p 566 A95-90703
 Report to Congressional Committees. Comanche Helicopter: Testing needs to be completed prior to production decisions [GAO/NSIAD-95-112] p 397 N95-27910

CONFINEMENT

Numerical mixing calculations of confined reacting jet flows in a cylindrical duct [NASA-TM-106736] p 139 N95-18133
 Dynamics of phase ordering of nematics in a pore [DE95-607662] p 362 N95-25978

CONFORMAL MAPPING

Optimum aerodynamic design via boundary control p 127 N95-16565

CONGRESSIONAL REPORTS

Naval aviation: F-14 upgrades are not adequately justified. Report to Congressional Committees [AD-A286338] p 231 N95-20212
 Report to the Secretary of Defense. Unmanned aerial vehicles: No more Hunter systems should be bought until problems are fixed [GAO/NSIAD-95-52] p 286 N95-24091
 Nitrogen oxide emissions and their control from uninstalled aircraft engines in enclosed test cells: Joint report to Congress on the Environmental Protection Agency - Department of Transportation study [PB95-166237] p 358 N95-26005
 Report to Congressional Committees. Tactical Aircraft: Concurrence in development and production of F-22 aircraft should be reduced [GAO/NSIAD-95-59] p 336 N95-26338
 Report to Congressional Committees. Comanche Helicopter: Testing needs to be completed prior to production decisions [GAO/NSIAD-95-112] p 397 N95-27910
 Report to the Chairman, Legislation and National Security Subcommittee, Committee on Government Operations, House of Representatives. Tactical aircraft: F-15 replacement is premature as currently planned [GAO/NSIAD-94-118] p 679 N95-31987
 Report to the Chairman, Legislation and National Security Subcommittee, Committee on Government Operations, House of Representatives. Unmanned aerial vehicles: Performance of short-range system still in question [GAO/NSIAD-94-65] p 609 N95-32196

Report to Congressional Committees. Military airlift: C-17 settlement is not a good deal [GAO/NSIAD-94-141] p 585 N95-32198
 Report to the Chairman, Subcommittee on Transportation and Related Agencies, Committee on Appropriations, House of Representatives. Air traffic control: Status of FAA's plans to close and contract out low-activity towers [GAO/RCED-94-265] p 603 N95-32199
 Report to the Chairman, Subcommittee on Aviation, Committee on Commerce, Science, and Transportation, US Senate. Aviation safety: Data problems threaten FAA strides on safety analysis system [GAO/AIMD-95-27] p 687 N95-32705
 Fact sheet for Congressional requesters. Airport competition: Essential air service slots at O'Hare International Airport [GAO/RCED-94-118FS] p 699 N95-32759
 Army aviation: Modernization strategy needs to be reassessed. Report to Congressional requesters [GAO/NSIAD-95-9] p 683 N95-32783
 Report to the Chairman, Subcommittee on Aviation, Committee on Commerce, Science, and Transportation, US Senate. Aviation Safety: FAA can better prepare general aviation pilots for mountain flying risks [GAO/RCED-94-15] p 687 N95-32784
 Report to the Chairman, Subcommittee on Transportation and Related Agencies, Committee on Appropriations, US Senate. Airport Improvement Program: Reliever airport set-aside funds could be redirected [GAO/RCED-94-226] p 699 N95-32786
 Aviation security: Development of new security technology has not met expectations. Report to Congressional requesters [GAO/RCED-94-142] p 687 N95-32885
 Report to the Chairman, Subcommittee on Transportation and Related Agencies, Committee on Appropriations, US Senate. Airport Improvement Program: The Military Airport Program has not achieved intended impact [GAO/RCED-94-209] p 700 N95-32888

CONICAL BODIES

DSMC calculations for 70-deg blunted cone at 3.2 km/s in nitrogen [NASA-TM-109181] p 348 N95-24396
 The 25th International Symposium on Combustion [AD-A286825] p 630 N95-31268

CONICAL FLOW

Interpretation of waverider performance data using computational fluid dynamics [BTN-95-EIX95062487534] p 193 A95-69242
 Supersonic axisymmetric conical flow solutions for different ratios of specific heats [BTN-95-EIX95152583283] p 306 A95-73584
 Nonlinear asymptotic theory of hypersonic flow past a circular cone [HTN-95-92599] p 461 A95-87415
 Optimization of waverider configurations generated from inclined circular and elliptic cones [AIAA PAPER 95-6089] p 492 A95-89198
 Heat transfer on bent-noise biconic in hypersonic flow p 639 A95-95394
 Low-speed wind tunnel testing of the NPS and NASA Ames Mach 6 optimized waverider [AD-A283585] p 75 N95-15319

CONJUGATE GRADIENT METHOD

Aerodynamic sensitivity coefficients using the three-dimensional full potential equation [BTN-95-EIX95062487530] p 186 A95-69238
 Aerodynamic shape optimization using preconditioned conjugate gradient methods [BTN-95-EIX95142553033] p 263 A95-73465

CONSERVATION EQUATIONS

Modeling aerodynamic problems using Smoothed Particle Hydrodynamics (SPH) [SAE PAPER 932512] p 465 A95-89185

CONSERVATION LAWS

CFD: Advances and Applications, part 1 [NAL-SP-9322-PT-1] p 165 N95-19444
 A time-accurate finite volume method valid at all flow velocities p 314 N95-23447
 Computational methods for control and optimal design of aerospace systems [AD-A292861] p 608 N95-31451

CONSTITUTIVE EQUATIONS

Non-linear viscoelastic-plastic constitutive relations for an aeronautical PMMA [HTN-95-71132] p 385 A95-83493

CONSTRAINTS

The performance of child restraint devices in transport airplane passenger seats [DOT/FAA/AM-94/19] p 40 N95-12146
 Empirical results on scheduling and dynamic backtracking p 299 N95-23761

- A brief survey of constrained mechanics and variational problems in terms of differential forms p 360 N95-25803
- CONSTRUCTION**
Aeronautical engineering: A continuing bibliography with indexes (supplement 315) [NASA-SP-7037(315)] p 219 N95-21640
- CONSTRUCTION INDUSTRY**
Expert systems and artificial intelligence applications in engineering design and inspection p 710 N95-33008
- CONTAINMENT**
Severe edge effects and simple complimentary interior solutions for thin-walled anisotropic and composite structures [AD-A290645] p 555 N95-29562
- CONTAMINANTS**
Aircraft gas turbine emissions challenge [BTN-94-EIX95011441239] p 403 A95-84196
Nitrogen oxide emissions characteristics of augmented turbofan engines [BTN-94-EIX95011441240] p 403 A95-84197
Numerical study of contaminant effects on combustion of hydrogen, ethane, and methane in air [AIAA PAPER 95-6097] p 510 A95-88005
Three dimensional model calculations of the global dispersion of high speed aircraft exhaust and implications for stratospheric ozone loss p 26 N95-10657
Bicarbonate of soda blasting technology for aircraft wheel deicing [PB94-193323] p 104 N95-17466
Future directions in helicopter protection system configuration p 198 N95-19657
- CONTAMINATION**
Measurement of moisture and total hydrocarbon contributions by valves used in clean room gas-delivery systems [BTN-94-EIX94381359041] p 295 A95-74629
An assessment of ground-test facility capabilities for measurement of hypervelocity scramjet performance [AIAA PAPER 95-6148] p 512 A95-90462
Out of area experiences with the RB199 in Toronto p 198 N95-19654
Community relations plan: Galena Airport and Camp ion Air Force Station, Alaska [AD-A286722] p 446 N95-27234
Hardware cleanliness methodology and certification p 419 N95-27656
Evaluation of commercial water-in-fuel test kits [AD-A292135] p 537 N95-29572
Standardization of surface contamination analysis systems p 631 N95-31798
- CONTINGENCY**
Patient/aircraft forecasting for the strategic aeromedical evacuation lift-bed process [AD-A293902] p 599 N95-31512
- CONTINUITY EQUATION**
Acoustic radiation damping of flat rectangular plates subjected to subsonic flows p 172 N95-18542
- CONTINUOUS NOISE**
Comments on the use of structureborne noise analysis for large commercial airplanes p 30 N95-11287
- CONTINUOUS SPECTRA**
Aircraft measurements of water vapour continuum absorption at millimetre wavelengths [HTN-95-90884] p 253 A95-72393
- CONTINUOUS WAVE LASERS**
The 25th International Symposium on Combustion [AD-A286825] p 630 N95-31268
- CONTINUUM FLOW**
Hypersonic rarefied flow past spheres including wake structure [BTN-95-EIX95152583250] p 305 A95-73551
Hypersonic wind tunnel test techniques [AD-A284057] p 118 N95-18663
Flow field investigation in a free jet - free jet core system for the generation of high intensity molecular beams [DLR-FB-94-11] p 172 N95-18912
- CONTINUUM MECHANICS**
The aerothermodynamic validation reentry experiment HYPERBA p 524 A95-87380
Computational methods in applied sciences; European Computational Fluid Dynamics Conference, 1st, Brussels, Belgium, Sept. 7-11, 1992 [IS8N 0-444-89795-X] p 539 A95-87552
- CONTINUUM MODELING**
The aerothermodynamic validation reentry experiment HYPERBA p 524 A95-87380
Damage tolerant repair techniques for pressurized aircraft fuselages [AD-A281982] p 65 N95-14144
An extension of the continuum model by Grad's thirteen moment equations for hypersonic rarefied flows p 478 N95-29118
- CONTOURS**
New approach to geometric profiling of the design elements of the passage part in turbo-machines [BTN-94-EIX94461408769] p 153 A95-63652
An approach to aerodynamic characteristics of low radar cross-section fuselages p 106 N95-16251
- CONTRACT MANAGEMENT**
Report to Congressional Committees. Military airlift: C-17 settlement is not a good deal [GAO/NSIAD-94-141] p 585 N95-32198
- CONTRACT NEGOTIATION**
Report to Congressional Committees. Military airlift: C-17 settlement is not a good deal [GAO/NSIAD-94-141] p 585 N95-32198
- CONTRAILS**
Transport of exhaust products in the near trail of a jet engine under atmospheric conditions [HTN-95-91421] p 319 A95-77334
Visual contrast detection thresholds for aircraft contrails [AD-A288618] p 328 N95-25607
- CONTRAROTATING PROPELLERS**
Experimental study of the aerodynamic characteristics of the counter-rotation propellers p 474 A95-91562
Wake velocity measurement of counter-rotation propellers p 474 A95-91563
Effects of a forward-swept front rotor on the flowfield of a counterrotation propeller [NASA-TM-106671] p 7 N95-10148
- CONTROL**
Knowledge-based processing for aircraft flight control [NASA-CR-194976] p 99 N95-13727
Strategic avionics technology definition studies. Subtask 3-1A3: Electrical Actuation (ELA) Systems Test Facility [NASA-CR-188360] p 143 N95-18567
- CONTROL BOARDS**
On-line handling of air traffic: Management, guidance and control [AGARD-AG-321] p 126 N95-18927
- CONTROL EQUIPMENT**
Aerodynamic characteristics of strake vortex flaps on a strake-wing configuration [BTN-95-EIX95062487537] p 187 A95-69245
Design of an effective controller via disturbance accommodating left eigenstructure assignment [BTN-95-EIX95282706663] p 565 A95-88178
Computer aided diagnostic testing of installed flight control servo-actuators [SAE PAPER 932584] p 494 A95-90068
Operating capability and current status of the reactivated NASA Lewis Research Center hypersonic tunnel facility [AIAA PAPER 95-6146] p 521 A95-90461
Nonlinear aerodynamic analysis of grid fin configurations [BTN-95-EIX0619952748172] p 590 A95-94466
Broadband, wide-area active control of sound radiated from vibrating structures using local surface-mounted radiation suppression devices p 30 N95-11283
Comments on the use of structureborne noise analysis for large commercial airplanes p 30 N95-11287
Comparison of full-scale, small-scale, and CFD results for F/A-18 forebody slot blowing p 72 N95-14255
Engines-only flight control system [NASA-CASE-ARC-11944-1] p 294 N95-23389
Simulation model of the integrated flight/proulsion control system, displays, and propulsion system for ASTOVL lift-fan aircraft [NASA-TM-108866] p 405 N95-26412
Plate manipulators [AD-A289601] p 374 N95-26719
Experimental investigation of aerodynamic devices for wind turbine rotational speed control, phase 1 [DE95-004034] p 564 N95-30016
- CONTROL ROCKETS**
A vehicle health monitoring system for the Space Shuttle Reaction Control System during reentry [NASA-CR-188370] p 527 N95-29447
- CONTROL SIMULATION**
Investigation of the effects of bandwidth and time delay on helicopter roll-axis handling qualities [HTN-95-80853] p 290 A95-75095
The Saab-Scania approach to development simulators [CONGRESS PAPER C428-10-137] p 522 A95-91698
Instructional control and part/whole-task training: A review of the literature and an experimental comparison of strategies applied to instructional simulation [AD-A280860] p 21 N95-10919
Analytical investigation of adaptive control of radiated inlet noise from turbofan engines p 30 N95-11277
Piloted evaluation of an integrated methodology for propulsion and airframe control design [AD-A290207] p 51 N95-12763
Automation of hardware-in-the-loop testing of control systems for unmanned air vehicles [AD-A284833] p 194 N95-19693
- Development of a nonlinear simulation for the McDonnell Douglas F-15 Eagle with a longitudinal TECS control-law [AD-A288610] p 388 N95-26481
- CONTROL STABILITY**
Stabilization of objects with unknown nonstationary parameters, using adaptive nonlinear continuous control systems [BTN-94-EIX94461407944] p 98 A95-62262
Multivariable stability and robustness of sequentially designed feedback systems [BTN-95-EIX95182619125] p 322 A95-76602
Robustly stable preliminary control systems design for the YF-16 CCV aircraft [BTN-95-EIX95202637608] p 292 A95-76681
Air data prediction from surface pressure measurements on guided munitions [BTN-95-EIX95282706664] p 466 A95-89641
Predictive algorithms for the roll control autopilot of a jet fighter aircraft [HTN-95-21047] p 515 A95-90424
MIMO H-infinity control design method combined with exact model matching p 506 A95-91492
A gust alleviation method by the response feedback p 506 A95-91493
Exact solution of stability margin for the MIMO control system p 507 A95-91582
Effect of coupling term on stability for the two input control system p 507 A95-91583
Comparison of the method of analyzing stability margin by using Minus Inverse Vector Locus with classical method p 507 A95-91584
Multi-application controls: Robust nonlinear multivariable aerospace controls applications p 71 N95-14249
Stable H(infinity) controller design for the longitudinal dynamics of an aircraft [NASA-TM-106847] p 293 N95-22954
Use of blade pitch control to provide power train damping for the Mod-2, 2.5-mW wind turbine p 440 N95-27986
An investigation of pilot induced oscillation phenomena in digital-flight control systems p 623 N95-32011
- CONTROL SURFACES**
Engineering methods for the evaluation of transonic flutter characteristics for aerodynamic control surfaces [BTN-94-EIX94461408589] p 141 A95-83064
Modelling for optimal operations of line milling of aerodynamic surfaces [BTN-94-EIX94461408774] p 138 A95-63657
Comparison of linear stability results with flight transition data [BTN-95-EIX95182619097] p 283 A95-76582
Attainable moments for the constrained control allocation problem [BTN-95-EIX95182619149] p 322 A95-76626
Rolling maneuver load alleviation using active controls [BTN-95-EIX95182619217] p 270 A95-76643
Aeroservoelastic aspects of wing/control surface planform shape optimization [BTN-95-EIX95222650795] p 340 A95-79251
On-line learning nonlinear direct neurocontrollers for restructurable control systems [BTN-95-EIX95242670768] p 359 A95-81079
Fundamental mechanisms of aeroelastic control with control surface and strain actuation [BTN-95-EIX95242670746] p 327 A95-81101
Pressure controlled surfaces - a 3D inverse panel method as a design tool p 491 A95-87565
Application of restructurable flight control system to large transport aircraft [BTN-95-EIX95282706666] p 515 A95-89639
Measurement of drag using a momentum balance [HTN-95-01090] p 468 A95-90276
On controlling the tip vortex flow of a lifting wing [ISBN 1-879921-01-4] p 587 A95-93736
Nonlinear aerodynamic analysis of grid fin configurations [BTN-95-EIX0619952748172] p 590 A95-94466
Free-to-roll tests of X-31 and F-18 subscale models with correlation to flight test results p 69 N95-14237
Multi-application controls: Robust nonlinear multivariable aerospace controls applications p 71 N95-14249
Active load control during rolling maneuvers - performed in the Langley Transonic Dynamics Tunnel [NASA-TP-3455] p 129 N95-17397
Plant and controller optimization by convex methods [AD-A283700] p 133 N95-18621
Aerodynamic surface distension system for high angle of attack forebody vortex control [NASA-CASE-ARC-11979-1] p 286 N95-23390
Plate manipulators [AD-A289601] p 374 N95-26719
A numerical method for unsteady transonic flow about wings with control surfaces [AD-A289631] p 375 N95-26859

- Implementation and demonstration of a multiple model adaptive estimation failure detection system for the F-16 [AD-A289301] p 391 N95-27042
- Transonic aerodynamic characteristics of a proposed wing-body reusable launch vehicle concept [NASA-TM-108489] p 592 N95-30712
- The FCS-structural coupling problem and its solution p 623 N95-32005
- Structural aspects of active control technology p 623 N95-32006

CONTROL SYSTEMS DESIGN

- Flight test development and evaluation of a Kalman filter state estimator for low-altitude flight [HTN-94-00684] p 16 A95-60167
- Design of a model following, state variable feedback controller for the X-14 VTOL aircraft [HTN-94-00685] p 16 A95-60168
- Simulation development of a forward sensor-enhanced low-altitude guidance system [HTN-94-00688] p 17 A95-60170
- Selection of optimal parameters for a system, controlling the flight height, when information about the state vector is incomplete [BTN-94-EIX94461408753] p 168 A95-63636
- Nonsmooth trajectory optimization: An approach using continuous simulated annealing [BTN-94-EIX94511433914] p 168 A95-64580
- H(sup 2)/H(sup INF) controller design for a two-dimensional thin airfoil flutter suppression [BTN-94-EIX94511433918] p 141 A95-64584
- Test bench for rotorcraft hover control [BTN-94-EIX94511433919] p 169 A95-64585
- Aircraft model for the AIAA controls design challenge [BTN-94-EIX94511433921] p 142 A95-64587
- Intelligent control law tuning for AIAA controls design challenge [BTN-94-EIX94511433922] p 169 A95-64588
- Rotorcraft control system design for uncertain vehicle dynamics using quantitative feedback theory [HTN-95-31012] p 236 A95-71182
- Smart structures in the control of airframe vibrations [HTN-95-31014] p 236 A95-71184
- A generalized algorithm for inverse simulation applied to helicopter maneuvering flight [HTN-95-A0493] p 236 A95-72564
- Effects of high order dynamics on helicopter flight control law design [HTN-95-80852] p 290 A95-75094
- Integrated flight/propulsion control for helicopters [HTN-95-80854] p 290 A95-75096
- Multivariable stability and robustness of sequentially designed feedback systems [BTN-95-EIX95182619125] p 322 A95-76602
- H-infinity helicopter flight control law design with and without rotor state feedback [BTN-95-EIX95182619129] p 291 A95-76606
- Direct-lift design strategy for longitudinal control of hypersonic aircraft [BTN-95-EIX95182619131] p 291 A95-76608
- Multirate flutter suppression system design for a model wing [BTN-95-EIX95182619132] p 292 A95-76609
- Derivation of system matrices from nonlinear dynamic simulation of jet engines [BTN-95-EIX95182619139] p 288 A95-76616
- Attainable moments for the constrained control allocation problem [BTN-95-EIX95182619149] p 322 A95-76626
- Automatic formation flight control [BTN-95-EIX95182619153] p 292 A95-76630
- Flutter suppression control law design and testing for the active flexible wing [BTN-95-EIX95182619214] p 292 A95-76640
- Design and multifunction tests of a frequency domain-based active flutter suppression system [BTN-95-EIX95182619215] p 292 A95-76641
- Flutter suppression for the active flexible wing: A classical design [BTN-95-EIX95182619216] p 292 A95-76642
- Rolling maneuver load alleviation using active controls [BTN-95-EIX95182619217] p 270 A95-76643
- Robustly stable preliminary control systems design for the YF-16 CCV aircraft [BTN-95-EIX95202637608] p 292 A95-76681
- Guidance and control, 1993; Annual Rocky Mountain Guidance and Control Conference, 16th, Keystone, CO, Feb. 6-10, 1993 [ISBN-0-87703-365-X] p 341 A95-80389
- The Cassini spacecraft: Object oriented flight control software p 359 A95-80405
- A new guidance and flight control system for the DELTA 2 launch vehicle - Abstract only p 342 A95-80427
- On-line learning nonlinear direct neurocontrollers for restructurable control systems [BTN-95-EIX95242670768] p 359 A95-81079

- Dynamics and control of a tethered flight vehicle [BTN-95-EIX95242670754] p 342 A95-81093
- High-performance, robust, bank-to-turn missile autopilot design [BTN-95-EIX95242670751] p 336 A95-81096
- Direct adaptive and neural control of wing-rock motion of slender delta wings [BTN-95-EIX95242670748] p 327 A95-81099
- Robust dynamic inversion for control of highly maneuverable aircraft [BTN-95-EIX95242670747] p 359 A95-81100
- Nonlinear observer and its application in flight control p 447 A95-82449
- Robust longitudinal axis flight control for an aircraft with thrust vectoring [BTN-95-EIX95122538875] p 408 A95-83000
- Control requirements for the RB 211 low-emission combustion system [BTN-94-EIX95011441244] p 416 A95-84201
- Scheduling of local nonlinear control laws by exogenous signals - an application to flight control [BTN-95-EIX95262694059] p 447 A95-85675
- Aircraft controller synthesis by solving a nonconvex optimization problem [BTN-95-EIX95282706672] p 515 A95-89636
- Application of restructurable flight control system to large transport aircraft [BTN-95-EIX95282706666] p 515 A95-89639
- Second generation smart actuator [SAE PAPER 932585] p 505 A95-90069
- Solid state power controller technology [SAE PAPER 931422] p 495 A95-90087
- A low fin height heat exchanger technology demonstrator for Hermes [SAE PAPER 932119] p 526 A95-90360
- Predictive algorithms for the roll control autopilot of a jet fighter aircraft [HTN-95-21047] p 515 A95-90424
- Aircraft Symposium, 30th, Tsukuba, Japan, Sep. 30 - Oct. 2, 1992 [HTN-95-A1609] p 498 A95-91491
- MIMO H infinity control design method combined with exact model matching p 506 A95-91492
- A gust alleviation method by the response feedback p 506 A95-91493
- Development of Fly-By-Wire system for BK117 p 516 A95-91506
- A design of a robust scheduled autopilot p 516 A95-91532
- A design of a self-learning robust scheduled autopilot p 516 A95-91533
- Design of a flight control system by a new way of pole placement in LQR p 516 A95-91534
- Determination of flight simulator time delay p 522 A95-91553
- On the UF-104 system p 507 A95-91559
- On the flight control system for UF-104 p 507 A95-91560
- Ducted fan VTOL and its flight control system p 500 A95-91573
- A study of computational difficulty of numerical method in optimal control p 507 A95-91585
- Flight control system design with Multiple Delay Model/Multiple Design Point Approach p 507 A95-91586
- Analysis of an MLS automatic landing control law for the NAL experimental research aircraft D0-228. 2: Curved approach and landing p 508 A95-91588
- What's next in commercial aircraft environmental control systems? [SAE PAPER 932057] p 513 A95-91638
- ASTOVL Aircraft: Some thoughts on new control strategies [CONGRESS PAPER C428-5-011] p 517 A95-91680
- Theory and evaluation of active control as a means of reducing helicopter vibration [CONGRESS PAPER C428-19-124] p 517 A95-91721
- Passive and active vibration control activities in the German helicopter industry [CONGRESS PAPER C428-19-126] p 517 A95-91722
- Multivariable adaptive control using only input and output measurements for turbojet engines [BTN-95-EIX95292721165] p 677 A95-92597
- Autonomous helicopter hover positioning by optical tracking [HTN-95-C0006] p 585 A95-93394
- Design trends in propulsion control systems [CONGRESS PAPER C428-33-123] p 610 A95-93620
- Surge recovery and compressor working line control using compressor exit mach number measurement [CONGRESS PAPER C428-33-210] p 610 A95-93622

- ASTRA - A safe, simplex, fly-by-wire aircraft control system [CONGRESS PAPER C428-37-218] p 610 A95-93634
- An advanced vehicle management system [SAE PAPER 931376] p 618 A95-93655
- Calculation of control laws for the digital fuel control unit of a small thrust turbojet [SAE PAPER 931411] p 614 A95-93677
- Lightweight, opto-electronic engine control system for aerospace turbine engines [SAE PAPER 931442] p 614 A95-93692
- Design of a modern pitch pointing control system [BTN-95-EIX95302731226] p 618 A95-94045
- Design and flight evaluation of an integrated navigation and near-terrain helicopter guidance system for night-time and adverse weather operations [NASA-TM-108837] p 11 N95-10846
- High-Alpha Research Vehicle (HARV) longitudinal controller: Design, analyses, and simulation results [NASA-TP-3446] p 17 N95-10860
- Application of an integrated methodology for propulsion and airframe control design to a STOVL aircraft [NASA-TM-106729] p 16 N95-11159
- ACSNT inner loop flight control design study [NASA-CR-196316] p 17 N95-11223
- Noise Con 1994: Proceedings of the 1994 National Conference on Noise Control Engineering. Progress in Noise Control for Industry p 28 N95-11259
- [LC-75-24750] p 28 N95-11259
- Active control of complex noise problems using a broadband, multichannel controller p 29 N95-11271
- Analytical investigation of adaptive control of radiated inlet noise from turbofan engines p 30 N95-11277
- Adaptive tuned vibration absorbers: Tuning laws, tracking agility, sizing, and physical implementations p 25 N95-11280
- Broadband, wide-area active control of sound radiated from vibrating structures using local surface-mounted radiation suppression devices p 30 N95-11283
- Comments on the use of structureborne noise analysis for large commercial airplanes p 30 N95-11287
- On the use of controls for subsonic transport performance improvement: Overview and future directions [NASA-TM-4605] p 10 N95-11408
- STOVL Control Integration Program [NASA-CR-195358] p 18 N95-11487
- Effects of mass on aircraft sidearm controller characteristics [NASA-TM-104277] p 51 N95-11868
- Cabin fuselage structural design with engine installation and control system [NASA-CR-197173] p 47 N95-12639
- Piloted evaluation of an integrated methodology for propulsion and airframe control design [AD-A290207] p 51 N95-12763
- Techniques for designing rotorcraft control systems [NASA-CR-196192] p 52 N95-12791
- Overview of NASREM: The NASA/NBS standard reference model for telerobot control system architecture re [PB94-194560] p 58 N95-12854
- Generic architectures for future flight systems p 99 N95-14159
- Space Generic Open Avionics Architecture (SGOAA): Overview p 99 N95-14161
- X-31 high angle of attack control system performance p 70 N95-14244
- High angle of attack flying qualities criteria for longitudinal rate command systems p 70 N95-14247
- Vista/F-16 Multi-Axis Thrust Vectoring (MATV) control law design and evaluation p 71 N95-14248
- Multi-application controls: Robust nonlinear multivariable aerospace controls applications p 71 N95-14249
- Automated test environment for a real-time control system [TABES PAPER 94-631] p 99 N95-14652
- A SIMULINK environment for flight dynamics and control analysis: Application to the DHC-2 Beaver. Part 1: Implementation of a model library in SIMULINK. Part 2: Nonlinear analysis of the Beaver autopilot [NONP-NASA-SUPPL-DK-94-2802] p 84 N95-14815
- Sensor fault detection and diagnosis simulation of a helicopter engine in an intelligent control framework [AD-A290223] p 137 N95-15970
- Matlab as a robust control design tool p 169 N95-16474
- Workshop on Formal Models for Intelligent Control [AD-A281399] p 169 N95-16864
- Aircraft and sub-system certification by piloted simulation [AGARD-AR-278] p 145 N95-17388

- Cooperative control theory and integrated flight and propulsion control
[NASA-CR-197493] p 142 N95-17404
- Microgravity isolation system design: A case study
[NASA-TM-106804] p 104 N95-17657
- Microgravity isolation system design: A modern control synthesis framework
[NASA-TM-106805] p 105 N95-18197
- Microgravity isolation system design: A modern control analysis framework
[NASA-TM-106803] p 105 N95-18486
- The impact of non-linear flight control systems on the prediction of aircraft loads due to turbulence
p 143 N95-18598
- Plant and controller optimization by convex methods
[AD-A283700] p 133 N95-18621
- Design and flight test of a simplified control system for a transport helicopter
p 144 N95-18902
- Automation of hardware-in-the-loop testing of control systems for unmanned air vehicles
[AD-A284833] p 194 N95-19693
- Improved speed control system for the 87,000 HP wind tunnel drive
[NASA-TM-106840] p 211 N95-19794
- Design of a controller for a flexible pointing system using H(infinity) synthesis
[AD-A286572] p 256 N95-20828
- Design of robust optimal control systems and stability analysis of real structured uncertainties
[AD-A279089] p 256 N95-21913
- Design of high performance multivariable control systems for supermaneuverable aircraft at high angle of attack
[NASA-CR-197661] p 293 N95-22908
- Stable H(infinity) controller design for the longitudinal dynamics of an aircraft
[NASA-TM-106847] p 293 N95-22954
- System identification of the Large-Angle Magnetic Suspension Test Fixture (LAMSTF)
p 296 N95-23299
- Engines-only flight control system
[NASA-CASE-ARC-11944-1] p 294 N95-23389
- Feedback control laws for highly maneuverable aircraft
[NASA-CR-197944] p 295 N95-23410
- Application of neural networks to unsteady aerodynamic control
p 360 N95-25264
- Partial camera automation in a simulated Unmanned Air Vehicle
[AD-A288786] p 337 N95-26190
- Demonstration study of hierarchical control of fluid-dynamic phenomena
[AD-A289341] p 437 N95-26751
- A gain scheduling optimization method using genetic algorithms
[AD-A289306] p 448 N95-26920
- Prevention and control of inlet unstart using an SR-71 simulation
p 367 N95-26948
- Collected papers on wind turbine technology
[NASA-CR-195432] p 447 N95-27970
- Control system design for the MOD-5A 7.3 mW wind turbine generator
p 440 N95-27985
- Use of blade pitch control to provide power train damping for the Mod-2, 2.5-mW wind turbine
p 440 N95-27986
- Variable speed generator application on the MOD-5A 7.3 mW wind turbine generator
p 440 N95-27989
- Development of a TECS control-law for the lateral directional axis of the McDonnell Douglas F-15 Eagle
[AD-A289771] p 410 N95-28598
- Application of optimization technique to control system design for departure prevention and aircraft model estimation through dynamic inversion
p 517 N95-29156
- Design and evaluation of a LQR controller for the bluebird unmanned air vehicle
[AD-A289769] p 504 N95-29457
- Linear matrix inequalities for the problem of absolute stability of control systems
p 518 N95-29680
- Design, analysis and control of large transports so that control of engine thrust can be used as a back-up of the primary flight controls
[NASA-CR-198958] p 518 N95-30254
- Flight Vehicle Integration Panel Workshop on Pilot Induced Oscillations
[AGARD-AR-335] p 597 N95-31061
- SCARLET: DLR rate saturation flight experiment
p 598 N95-31068
- Handling qualities analysis on rate limiting elements in flight control systems
p 619 N95-31071
- Calspan experience of PIO and the effects of rate limiting
p 598 N95-31072
- The role of handling qualities specifications in flight control system design
p 620 N95-31990
- The importance of flying qualities design specifications for active control systems
p 621 N95-31992
- Lavi flight control system: Design requirements, development and flight test results
p 621 N95-31994
- Robust control: A structured approach to solve aircraft flight control problems
p 621 N95-31995
- Dynamic inversion: An evolving methodology for flight control design
p 621 N95-31996
- Evaluation of the techniques of fuzzy control for the piloting an aircraft
p 621 N95-31997
- The control system design methodology of the STOL and maneuver technology demonstrator
p 621 N95-31998
- Control law design using H-infinity and mu-synthesis short-period controller for a tail-airplane
p 622 N95-31999
- Model following control for tailoring handling qualities: ACT experience with ATHeS
p 622 N95-32000
- X-29 flight control system: Lessons learned
p 622 N95-32001
- The FCS-structural coupling problem and its solution
p 623 N95-32005
- Structural aspects of active control technology
p 623 N95-32006
- Flight test results of the F-16 aircraft modified with axisymmetric vectoring exhaust nozzle
p 609 N95-32007
- Digital autopilot design for combat aircraft in ALENIA
p 623 N95-32009
- Experimental Aircraft Programme (EAP): Flight control system design and test
p 623 N95-32010
- An investigation of pilot induced oscillation phenomena in digital-flight control systems
p 623 N95-32011
- Advanced flight control technology achievements at Boeing Helicopters
p 624 N95-32014
- Practical experiences in control systems design using the NCR Bell 205 Airborne Simulator
p 624 N95-32015
- Propulsion Controlled Aircraft design and development
p 697 N95-33022
- Application of advanced safety technique to ring laser gyro inertial navigation system integration
p 689 N95-33140
- Sea wave parameters, small altitudes and distances measurers design for movement control systems of ships, wing-in-surface effect crafts and seaplanes
p 708 N95-33141
- Nonlinear adaptive control of highly maneuverable high performance aircraft
p 710 N95-33712
- Proposed incorporation of mission-oriented flying qualities into MIL-STD-1797A
[AD-A294211] p 698 N95-34306
- CONTROL THEORY**
- Output feedback control under randomly varying distributed delays
[BTN-94-EIX94511433916] p 168 A95-64582
- Design of nonlinear control laws for high-angle-of-attack flight
[BTN-94-EIX94511433920] p 141 A95-64586
- Aircraft model for the AIAA controls design challenge
[BTN-94-EIX94511433921] p 142 A95-64587
- Intelligent control law tuning for AIAA controls design challenge
[BTN-94-EIX94511433922] p 169 A95-64588
- Shuttle entry guidance revisited using nonlinear geometric methods
[BTN-95-EIX95182619144] p 299 A95-76621
- Switched bias proportional navigation for homing guidance against highly maneuvering targets
[BTN-95-EIX95182619145] p 279 A95-76622
- Nonlinear observer and its application in flight control
p 447 A95-82449
- Robust longitudinal axis flight control for an aircraft with thrust vectoring
[BTN-95-EIX95122538875] p 408 A95-83000
- Scheduling of local nonlinear control laws by exogenous signals - an application to flight control
[BTN-95-EIX95262694059] p 447 A95-85675
- Theory and evaluation of active control as a means of reducing helicopter vibration
[CONGRESS PAPER C428-19-124] p 517 A95-91721
- Passive and active vibration control activities in the German helicopter industry
[CONGRESS PAPER C428-19-126] p 517 A95-91722
- Calculation of control laws for the digital fuel control unit of a small thrust turbojet
[SAE PAPER 931411] p 614 A95-93677
- Extended cooperative control synthesis
[NASA-TM-4561] p 17 N95-10220
- Optimum aerodynamic design via boundary control
[NASA-CR-195882] p 36 N95-11877
- Control theory based airfoil design using the Euler equations
[NASA-CR-196360] p 36 N95-11884
- Fourth High Alpha Conference, volume 1
[NASA-CP-10143-VOL-1] p 67 N95-14229
- Fourth High Alpha Conference, volume 3
[NASA-CP-10143-VOL-3] p 71 N95-14251
- Optimum aerodynamic design via boundary control
p 127 N95-16565
- Cooperative control theory and integrated flight and propulsion control
[NASA-CR-197493] p 142 N95-17404
- Summary of a joint program of research into aircraft flight control concepts
[AD-A280012] p 237 N95-20004
- Stable H(infinity) controller design for the longitudinal dynamics of an aircraft
[NASA-TM-106847] p 293 N95-22954
- Aerodynamic shape optimization of wing and wing-body configurations using control theory
[NASA-CR-198024] p 335 N95-25334
- How to fly an aircraft with control theory and splines
p 360 N95-25805
- Actuating signals in adaptive control systems
[IFTR-13/1994] p 361 N95-26330
- Development of a nonlinear simulation for the McDonnell Douglas F-15 Eagle with a longitudinal TECS control-law
[AD-A288610] p 388 N95-26481
- A comparison of the Neal-Smith and omega Tau function, zeta function and tau function flying qualities criteria
[AD-A289503] p 390 N95-26844
- Advanced formation flight control
[AD-A289271] p 409 N95-26981
- Development of a TECS control-law for the lateral directional axis of the McDonnell Douglas F-15 Eagle
[AD-A289771] p 410 N95-28598
- Computational algorithms for aerodynamic analysis and design
[AD-A291084] p 482 N95-29972
- SCARLET: DLR rate saturation flight experiment
p 598 N95-31068
- Flight demonstration of an advanced pitch control law in the VAAC Harrier aircraft
p 623 N95-32012
- Advanced flight control technology achievements at Boeing Helicopters
p 624 N95-32014
- Practical experiences in control systems design using the NCR Bell 205 Airborne Simulator
p 624 N95-32015
- A stochastic adaptive control application to flight systems
p 699 N95-34806
- CONTROL VALVES**
- Dynamic behavior of valves with pneumatic chamber for reciprocating compressors
[BTN-94-EIX94351143311] p 207 A95-65845
- CONTROLLABILITY**
- Side forces at high angles of attack. Why, when, how?
[BTN-95-EIX95112523809] p 194 A95-69324
- Determination of piloting feedback structures for an altitude tracking task
[BTN-95-EIX95242670770] p 327 A95-81077
- Rotorcraft handling qualities in turbulence
[BTN-95-EIX95242670750] p 334 A95-81097
- Pilot rating scale for aircraft handling qualities
[HTN-95-42269] p 380 A95-84963
- Handling qualities of hypersonic aircraft and related control requirements
p 515 A95-87398
- Design of an effective controller via disturbance accommodating left eigenstructure assignment
[BTN-95-EIX95282706663] p 565 A95-88178
- Flight-testing and frequency-domain analysis for rotorcraft handling qualities
[HTN-95-01083] p 515 A95-90269
- Flight test of STS radio controlled scale model
p 499 A95-91539
- Techniques for designing rotorcraft control systems
[NASA-CR-196192] p 52 N95-12791
- Multi-application controls: Robust nonlinear multivariable aerospace controls applications
p 71 N95-14249
- Flight test of the X-29A at high angle of attack: Flight dynamics and controls
[NASA-TP-3537] p 284 N95-22806
- Analysis of the longitudinal handling qualities and pilot-induced-oscillation tendencies of the High-Angle-of-Attack Research Vehicle (HARV)
p 293 N95-23297
- An investigation of the effects of pitch-roll (de)coupling on helicopter handling qualities
[NASA-TM-110349] p 409 N95-26773
- A comparison of the Neal-Smith and omega Tau function, zeta function and tau function flying qualities criteria
[AD-A289503] p 390 N95-26844
- Test operations procedure (TOP) 7-3-534 airworthiness testing of fixed wing aircraft: Asymmetric power testing
[AD-A289458] p 391 N95-26994
- The process for addressing the challenges of aircraft pilot coupling
p 597 N95-31063
- Observations on PIO
p 597 N95-31064
- The relation of handling qualities ratings to aircraft safety
p 597 N95-31067
- SAAB experience with PIO
p 598 N95-31069

CONTROLLERS

- Aeroelastic pilot-in-the-loop oscillations
p 598 N95-31070
- Analysis of heads-up display quickening versus handling qualities
[AD-A293797] p 611 N95-31584
- The role of handling qualities specifications in flight control system design p 620 N95-31990
- Experiences with ADS-33 helicopter specification testing and contributions to refinement research p 621 N95-31993
- Control law design using H-infinity and mu-synthesis short-period controller for a tail-airplane p 622 N95-31999
- Model following control for tailoring handling qualities: ACT experience with ATHeS p 622 N95-32000
- Propulsion Controlled Aircraft design and development p 697 N95-33022
- Design challenges encountered in the F-15 PCA flight test program p 692 N95-33025
- CONTROLLERS**
- Design of a model following, state variable feedback controller for the X-14 VTOL aircraft [HTN-94-00685] p 16 A95-60168
- Control mechanism to prevent correlated message arrivals from degrading signaling no. 7 network performance [BTN-94-EIX94341342286] p 56 A95-60842
- H(sup 2)/H(sup INF) controller design for a two-dimensional thin airfoil flutter suppression [BTN-94-EIX94511433918] p 141 A95-64584
- Test bench for rotorcraft hover control [BTN-94-EIX94511433919] p 169 A95-64585
- Design of nonlinear control laws for high-angle-of-attack flight [BTN-94-EIX94511433920] p 141 A95-64586
- Multiple-function digital controller system for active flexible wing wind-tunnel model [BTN-95-EIX95182619212] p 322 A95-76638
- On-line analysis capabilities developed to support the active flexible wing wind-tunnel tests [BTN-95-EIX95182619213] p 296 A95-76639
- A switched reluctance machine rotor position estimator: A neural network application [SAE PAPER 932560] p 511 A95-90057
- Solid state power controller technology [SAE PAPER 931422] p 495 A95-90087
- Predictive algorithms for the roll control autopilot of a jet fighter aircraft [HTN-95-21047] p 515 A95-90424
- A design of a robust scheduled autopilot p 516 A95-91532
- A design of a self-learning robust scheduled autopilot p 516 A95-91533
- Design of a flight control system by a new way of pole placement in LQR p 516 A95-91534
- An electrorheologically controlled semi-active landing gear [SAE PAPER 931403] p 605 A95-93673
- Calculation of control laws for the digital fuel control unit of a small thrust turbojet [SAE PAPER 931411] p 614 A95-93677
- Extended cooperative control synthesis [NASA-TM-4561] p 17 N95-10220
- High-Alpha Research Vehicle (HARV) longitudinal controller: Design, analyses, and simulation results [NASA-TP-3446] p 17 N95-10860
- Active control of complex noise problems using a broadband, multichannel controller p 29 N95-11271
- Effects of mass on aircraft sidearm controller characteristics [NASA-TM-104277] p 51 N95-11868
- New technologies for space avionics [NASA-CR-197574] p 150 N95-18196
- Microgravity isolation system design: A modern control analysis framework [NASA-TM-106803] p 105 N95-18486
- Plant and controller optimization by convex methods [AD-A283700] p 133 N95-18621
- Design of a controller for a flexible pointing system using H(infinity) synthesis [AD-A286572] p 256 N95-20828
- Robust fixed-structure control [AD-A286515] p 257 N95-22216
- Stable H(infinity) controller design for the longitudinal dynamics of an aircraft [NASA-TM-106847] p 293 N95-22954
- Actuating signals in adaptive control systems [IFTR-13/1994] p 361 N95-26330
- Design and synthesis of a real-time controller for an unmanned air vehicle [AD-A289134] p 408 N95-26555
- Electro-hydrostatic actuator controller design using quantitative feedback theory [AD-A289220] p 409 N95-26957

- Survey and implementation of commercial manual controllers for a generic telerobotics architecture [AD-A289215] p 449 N95-26990
- Flight control design using mixed H2/micron optimization [AD-A289288] p 410 N95-27036
- A hybrid vehicle evaluation code and its application to vehicle design. Revision 1 [DE95-008053] p 441 N95-28029
- Conversion of the TRACON operations concepts database into a formal sentence outline job task taxonomy [DOT/FAA/AM-95/16] p 488 N95-28819
- Analytical investigations in aircraft and spacecraft trajectory optimization and optimal guidance [NASA-CR-4672] p 526 N95-29339
- Design and evaluation of a LQR controller for the bluebird unmanned air vehicle [AD-A289769] p 504 N95-29457
- Robust fixed-structure control [AD-A292883] p 679 N95-30961
- Robust control: A structured approach to solve aircraft flight control problems p 621 N95-31995
- Evaluation of the techniques of fuzzy control for the piloting an aircraft p 621 N95-31997
- Control law design using H-infinity and mu-synthesis short-period controller for a tail-airplane p 622 N95-31999

CONVECTION CELLS

- The Integrated Terminal Weather System (ITWS) storm cell information and weather impacted airspace detection algorithm p 654 A95-93452
- The real-time analysis and prediction of storms program p 655 A95-93457
- An echo motion algorithm for air traffic management using a national radar mosaic p 667 A95-93513
- Dissemination of terminal weather products to the flight deck via data link p 669 A95-93525
- Turbulence near thunderstorm tops p 675 A95-93553

CONVECTION CLOUDS

- Application of airborne field mill data for use in launch support [HTN-95-50054] p 98 A95-62279
- Microwave and infrared simulations of an intense convective system and comparison with aircraft observations [HTN-95-60511] p 214 A95-68762

CONVECTIVE FLOW

- Further analysis of high-rate rolling experiments of a 65-deg delta wing [BTN-95-EIX95152582331] p 281 A95-73533
- Nonreflective boundary conditions for high-order methods [HTN-95-42328] p 371 A95-86157
- Flow physics of critical states for rolling delta wings [BTN-95-EIX0619952748180] p 590 A95-94473

CONVECTIVE HEAT TRANSFER

- Adaptive remeshing for convective heat transfer with variable fluid properties [BTN-95-EIX95082502720] p 243 A95-71033
- Hypersonic convective heat transfer over 140-deg blunt cones in different gases [BTN-95-EIX95152583253] p 306 A95-73554
- Convective and radiative heat transfer analysis for the fire 2 forebody [BTN-95-EIX95182617460] p 268 A95-75731
- Study of heat transfer rates during quenching of a hot tube under microgravity p 428 A95-82641
- Experimental investigation of flow-boiling heat transfer under microgravity p 428 A95-82642
- Free convection past a uniform flux surface inclined at a small angle to the horizontal [HTN-95-42213] p 430 A95-84029
- Constant flux, turbulent convection data using infrared imaging [HTN-95-20731] p 435 A95-86621
- Heat-transfer measurements and computations of swept-shock-wave boundary-layer interactions [HTN-95-81634] p 541 A95-87682
- An axisymmetric analog two-layer convective heating procedure with application to the evaluation of Space Shuttle Orbiter wing leading edge and windward surface heating [NASA-CR-188343] p 54 N95-11937
- Verification of multidisciplinary models for turbomachines p 140 N95-19025
- A computer code (SKINTEMP) for predicting transient missile and aircraft heat transfer characteristics [AD-A286044] p 248 N95-21001
- CAE for thermal management of aerospace electronic boards using the BETAsoft program p 438 N95-27354

CONVERGENCE

- Observations of fluxes and inland breezes over a heterogeneous surface [HTN-95-80258] p 212 A95-66315
- Preconditioned domain decomposition scheme for three-dimensional aerodynamic sensitivity analysis [BTN-95-EIX95152577612] p 321 A95-73471
- Analytical solution for controls, heats, and states of flight trajectories [BTN-95-EIX95152583286] p 282 A95-73587
- Three-dimensional adaptive grid-embedding Euler technique [HTN-95-20825] p 543 A95-88086
- Developing thunderstorm forecast rules utilizing first detectable cloud radar-echoes p 667 A95-93514
- Comparison of the predictive capabilities of several turbulence models [BTN-95-EIX0619952748167] p 589 A95-94461
- Turbulent effects on parachute drag [BTN-95-EIX0619952748193] p 591 A95-94482
- Convergence acceleration of implicit schemes in the presence of high aspect ratio grid cells p 313 N95-23446
- Multigrid convergence acceleration for the 2D Euler equations applied to high-lift systems [PB95-198081] p 593 N95-30814
- A study on the convergence of a 3-D Euler code for cascade flow calculations p 706 N95-34508

CONVERGENT NOZZLES

- Single-engine tail interference model p 115 N95-17879
- CONVERGENT-DIVERGENT NOZZLES**
- Computation of nonequilibrium viscous flows in arc-jet wind tunnel nozzles [AIAA PAPER 94-0254] p 2 A95-60173
- Main features of overexpanded triple jets [BTN-95-EIX95142553040] p 304 A95-73458
- Two-dimensional converging-diverging rippled nozzles at transonic speeds — performed in the Langley 16-Foot Transonic Tunnel [NASA-TP-3444] p 6 N95-10129
- Static investigation of two fluidic thrust-vectoring concepts on a two-dimensional convergent-divergent nozzle [NASA-TM-4574] p 120 N95-19042
- Static investigation of two fluidic thrust-vectoring concepts on a two-dimensional convergent-divergent nozzle [NASA-TM-4574] p 222 N95-19913
- An approximate theoretical method for modeling the static thrust performance of non-axisymmetric two-dimensional convergent-divergent nozzles [NASA-CR-195050] p 273 N95-23193
- Internal performance characteristics of thrust-vectorable axisymmetric ejector nozzles [NASA-TM-4610] p 331 N95-25338

CONVEXITY

- Plant and controller optimization by convex methods [AD-A283700] p 133 N95-18621
- Design of robust optimal control systems and stability analysis of real structured uncertainties [AD-A279089] p 256 N95-21913

COOLANTS

- Investigation of heat transfer in a rotating ring gap with the axial flow of a coolant during the rotation of the central shaft [BTN-94-EIX94461407951] p 89 A95-62625
- Advanced passive cooling for high power electromechanical actuators [SAE PAPER 931397] p 634 A95-93669
- Immersion/two phase cooling p 246 N95-20648
- Effect of film cooling/regenerative cooling on scramjet engine performances [NAL-TR-1242] p 339 N95-24990

COOLING

- Impingement cooling of an isothermally heated surface with a confined slot jet [BTN-94-EIX94421348950] p 347 A95-78494
- Experiment and analysis on heat transfer of a scramjet leading edge model p 403 A95-82420
- Airborne lidar observation of mountain-wave-induced polar stratospheric clouds during EASOE [HTN-95-00738] p 444 A95-86308
- Ablative thermal management structural material on the hypersonic vehicles [AIAA PAPER 95-6133] p 547 A95-90452
- High heat sink fuels for improved aircraft thermal management [SAE PAPER 932084] p 530 A95-91659
- FASTPACK: Optimized solutions for modular avionics derived from a parametric study. Part 2: Avionics p 233 N95-20635
- Immersion/two phase cooling p 246 N95-20648
- Toughened Silcomp composites for gas turbine engine applications [DE95-002851] p 235 N95-21243

- CAE for thermal management of aerospace electronic boards using the BETAsoft program p 438 N95-27354
- COOLING FINNS**
Base drag prediction on missile configurations [BTN-95-EIX95152583256] p 266 A95-73557
Natural convection in central microcavities of vertical, finned enclosures of very high aspect ratios [BTN-95-EIX95282711336] p 632 A95-92405
- COOLING SYSTEMS**
Hypersonic thermal protection with mass injection at angle of attack p 414 A95-82414
Study on the turbine vane and blade for a 1500 C class industrial gas turbine [BTN-94-EIX95011441254] p 431 A95-84211
What's next in commercial aircraft environmental control systems? [SAE PAPER 932057] p 513 A95-91638
A subsystem integration technology concept [SAE PAPER 931382] p 604 A95-93658
Advanced passive cooling for high power electromechanical actuators [SAE PAPER 931397] p 634 A95-93669
Regenerative cooling for liquid propellant rocket thrust chambers [INPE-5565-TDI/540] p 150 N95-18720
Application of multidisciplinary models to the cooled turbine rotor design p 140 N95-19024
Effect of film cooling/regenerative cooling on scramjet engine performances [NAL-TR-1242] p 339 N95-24990
Static pressure drop by swirling flow of an internal cooling air system through a turbine shaft p 698 N95-34560
- COOPERATION**
Cooperative problem solving between airline operations control and ATC traffic flow management p 681 A95-95066
- COORDINATE TRANSFORMATIONS**
Describing an attitude p 342 A95-80409
User documentation of the CTA program [AD-A289508] p 375 N95-26854
- COORDINATES**
On wave-front curvature in linear stability theory [BTN-94-EIX94441385756] p 184 A95-68220
SAR image registration in absolute coordinates using GPS carrier phase position and velocity information. [DE94-018738] p 228 N95-20195
- COPLANARITY**
The coplanar projectile motion problem including the effects of lift and drag [ISBN 1-879921-01-4] p 635 A95-93723
- COPPER**
Permanent magnet electron cyclotron resonance plasma source with remote window [BTN-95-EIX95242674338] p 450 A95-82176
Cu deposition using a permanent magnet electron cyclotron resonance microwave plasma source [DE94-017768] p 304 N95-23981
- COPPER ALLOYS**
NASA-JVA light aerospace alloy and structures technology program supplement: Aluminum-based materials for high speed aircraft [NASA-CR-4645] p 343 N95-24878
- COPPER OXIDES**
Phonon characteristics of high (T sub c) superconductors from neutron Doppler broadening measurements [DE95-003703] p 324 N95-24076
- CORES**
Vortex cutting by a blade. Part II: Computations of vortex response [BTN-94-EIX94441386611] p 208 A95-67342
- CORIOLIS EFFECT**
Integrated development of the equations of motion for elastic hypersonic flight vehicles [BTN-95-EIX95242670755] p 327 A95-81092
- CORNER FLOW**
Numerical simulation of supersonic compression corners and hypersonic inlet flows using the RPLUS2D code [NASA-TM-106580] p 105 N95-16038
Corner vortex suppressor [AD-D016423] p 116 N95-18337
- CORRECTION**
Accuracy enhancements for overSet grids using a defect correction approach [AIAA PAPER 94-0523] p 3 A95-60181
Effects of vibration on inertial wind-tunnel model attitude measurement devices [NASA-TM-109083] p 21 N95-11466
Wall-signature methods for high speed wind tunnel wall interference corrections p 107 N95-16257
Boundary-flow measurement methods for wall interference assessment and correction: Classification and review p 163 N95-19262
Wall correction method with measured boundary conditions for low speed wind tunnels p 164 N95-19263
- Adaptive wind tunnel walls versus wall interference correction methods in 2D flows at high blockage ratios p 147 N95-19267
Transonic wind tunnel boundary interference correction p 147 N95-19271
Calculation of wall effects of flow on a perforated wall with a code of surface singularities p 165 N95-19277
Interference corrections for a centre-line plate mount in a porous-walled transonic wind tunnel p 122 N95-19280
Correction of support influences on measurements with sting mounted wind tunnel models p 122 N95-19281
- CORRELATION**
Precise navigation using adaptive FIR filtering and time domain spectral estimation [BTN-95-EIX95142555485] p 227 A95-72888
Transition correlations in three-dimensional boundary layers [HTN-95-51648] p 432 A95-85030
Event correlation for networked simulators [BTN-95-EIX0619952748168] p 625 A95-94462
Computational methods for preliminary design and geometry definition in turbomachinery p 89 N95-14128
Patterns in the sky: Natural visualization of aircraft flow fields [NASA-SP-514] p 584 N95-31000
- CORROSION**
Modelling of pitting due to corrosion in fuselage lap joints [BTN-95-EIX95082502227] p 240 A95-71024
Effect of surface roughness on local film cooling effectiveness and heat transfer coefficients [AD-A283854] p 91 N95-14351
Corrosion and corrosion fatigue of airframe aluminum alloys The effects of pitting on fatigue crack nucleation in 7075-T6 aluminum alloy p 88 N95-14482
Erosion, Corrosion and Foreign Object Damage Effects in Gas Turbines [AGARD-CP-558] p 197 N95-19653
Out of area experiences with the RB199 in Toronto p 198 N95-19654
Gas turbine compressor corrosion and erosion in Western Europe [AD-B196178L] p 201 N95-19678
Testing considerations for military aircraft engines in corrosive environments (a Navy perspective) p 202 N95-19684
Corrosion of aircraft materials: Correlation between nanometer scale and macroscopic structural damage parameters [AD-A285930] p 241 N95-20299
Electrochemical impedance pattern recognition for detection of hidden chemical corrosion on aircraft components [AD-A284998] p 241 N95-20481
Electrochemical impedance pattern recognition for detection of hidden chemical corrosion on aircraft components [AD-A285998] p 241 N95-20716
Aircraft corrosion study [AD-A279527] p 241 N95-21687
Corrosion detection and management of advanced airframe materials [AGARD-CP-565] p 302 N95-23496
The corrosion and protection of advanced aluminium - lithium airframe alloys p 302 N95-23497
Corrosion of landing gear steels p 302 N95-23500
Double pass retroreflection for corrosion detection in aircraft structures p 323 N95-23503
Non-destructive detection of corrosion for life management p 314 N95-23505
Health and usage monitoring systems: Corrosion surveillance p 262 N95-23506
Eddy current detection of pitting corrosion around fastener holes p 315 N95-23507
In-situ detection of surface passivation or activation and of localized corrosion: Experiences and prospectives in aircraft p 302 N95-23508
Test method and test results for environmental assessment of aircraft materials p 302 N95-23509
New nondestructive techniques for the detection and quantification of corrosion in aircraft structures p 315 N95-23512
Corrosion detection and monitoring of aircraft structures: An overview p 303 N95-23515
Experience of in-service corrosion on military aircraft p 303 N95-23516
US Navy operating experience with new aircraft construction materials p 303 N95-23517
Corrosion in service experience with aircraft in France p 303 N95-23518
Oklahoma City air logistics center (USAF) aging aircraft corrosion program p 262 N95-23519
- Proceedings of the 2d USAF Aging Aircraft Conference [AD-A288217] p 336 N95-25578
The use of electrochemistry and ellipsometry for identifying and evaluating corrosion on aircraft [AD-A288536] p 381 N95-27186
The mm-wave resonant methods for the detection of corrosion, phase 1 [AD-A291315] p 556 N95-29941
Electrochemical impedance pattern recognition for detection of hidden chemical corrosion on aircraft components, phase 1 [AD-A291345] p 556 N95-29946
Corrosion of fire-damaged aircraft [AD-A294968] p 693 N95-34583
- CORROSION PREVENTION**
Corrosion prevention and control [BTN-95-EIX95031502753] p 188 A95-68260
Future directions in helicopter protection system configuration p 198 N95-19657
Corrosion detection and management of advanced airframe materials [AGARD-CP-565] p 302 N95-23496
The corrosion and protection of advanced aluminium - lithium airframe alloys p 302 N95-23497
Corrosion protection measures for CFC/metal joints of fuel integral tank structures of advanced military aircraft p 303 N95-23510
Organic coating technology for the protection of aircraft against corrosion p 303 N95-23513
Corrosion detection and monitoring of aircraft structures: An overview p 303 N95-23515
Experience of in-service corrosion on military aircraft p 303 N95-23516
US Navy operating experience with new aircraft construction materials p 303 N95-23517
Corrosion in service experience with aircraft in France p 303 N95-23518
Characterization of corrosion and development of a breadboard of a D sight aircraft inspection system, phase 1 [AD-A288347] p 380 N95-26527
- CORROSION RESISTANCE**
A CMC database for use in the next generation launch vehicles (rockets) p 150 N95-18993
FAA/NASA International Symposium on Advanced Structural Integrity Methods for Airframe Durability and Damage Tolerance, part 2 [NASA-CP-3274-PT-2] p 124 N95-19468
Resistance of silicon nitride turbine components to erosion and hot corrosion/oxidation attack p 202 N95-19683
In-situ detection of surface passivation or activation and of localized corrosion: Experiences and prospectives in aircraft p 302 N95-23508
Cadmium plating replacements p 631 N95-31773
Environmentally regulated aerospace coatings p 631 N95-31775
- CORROSION TESTS**
Advanced Turbine Technology Applications Project (ATTAP) [NASA-CR-195393] p 101 N95-15743
The use of electrochemistry and ellipsometry for identifying and evaluating corrosion on aircraft [AD-A285323] p 151 N95-16371
An artificial corrosion protocol for lap-splices in aircraft skin p 152 N95-19482
Testing considerations for military aircraft engines in corrosive environments (a Navy perspective) p 202 N95-19684
Corrosion behavior of landing gear steels [AD-A285862] p 242 N95-22132
Corrosion detection and management of advanced airframe materials [AGARD-CP-565] p 302 N95-23496
Corrosion of landing gear steels p 302 N95-23500
Eddy current detection of pitting corrosion around fastener holes p 315 N95-23507
Test method and test results for environmental assessment of aircraft materials p 302 N95-23509
Corrosion protection measures for CFC/metal joints of fuel integral tank structures of advanced military aircraft p 303 N95-23510
New nondestructive techniques for the detection and quantification of corrosion in aircraft structures p 315 N95-23512
US Navy operating experience with new aircraft construction materials p 303 N95-23517
The use of electrochemistry and ellipsometry for identifying and evaluating corrosion on aircraft [AD-A290249] p 504 N95-29426
Bell Helicopter Advanced Rotocraft Transmission (ART) program [NASA-CR-195479] p 555 N95-29538
- COSINE SERIES**
Describing an attitude p 342 A95-80409

COSMIC RAYS

Investigation and characterization of SEU effects and hardening strategies in avionics

[AD-A291058] p 509 N95-29950

COST ANALYSIS

Optimum full-scale subsonic wind tunnel

[AIAA PAPER 86-0732] p 18 A95-60161

Assessing effects of military aircraft noise on residential property values near airbases

p 31 N95-11310

Technology Benefit Estimator (T/BEST): User's manual

[NASA-TM-106785] p 167 N95-19501

An analysis of the costs and benefits in improving F402-RR-406A High Pressure Turbine, second stage blades under the aircraft engine Component Improvement Program (CIP)

[AD-A285127] p 197 N95-19595

The personal aircraft: Status and issues

[NASA-TM-109174] p 223 N95-20688

Small gas turbine component evaluation study

[PB95-147542] p 338 N95-24293

Development of repair processes and sources for C/KC-135 aircraft windows/windshields

[AD-A288348] p 367 N95-26629

An analysis of the KC-135 three-person cockpit

[AD-A289540] p 390 N95-26873

C-130 Advanced Technology Center wing box conceptual design/cost study

p 423 N95-28437

Designers' unified cost model

p 424 N95-28464

Global cost and weight evaluation of fuselage keel design concepts

p 501 N95-28840

Cost model relationships between textile manufacturing processes and design details for transport fuselage elements

p 536 N95-29043

Modeling F/A-18 flight hour program costs using regression analysis

[AD-A293771] p 608 N95-31579

COST EFFECTIVENESS

Assessment of cost and training effectiveness for a candidate training system using the Comparison-Based Prediction model

[SAE PAPER 932598] p 379 A95-84570

Integrated flight crew transition training for the advanced flight deck aircraft

[SAE PAPER 932599] p 380 A95-84571

The potential for CMCs to replace superalloys in engine exhaust ducts

[HTN-95-42298] p 418 A95-84992

Concorde: Silver jubilee Mach 2 marks 25 years

[HTN-95-42618] p 483 A95-87248

Flight Simulators: Better than the real thing?

[HTN-95-42619] p 518 A95-87249

Developments in airfield lighting

[CONGRESS PAPER C428-7-147] p 488 A95-91688

Cost effective small-scale experiments to aid the design of ASTOVL aircraft

[CONGRESS PAPER C428-9-098] p 475 A95-91695

Health monitoring and cost implications for an airline operator

[CONGRESS PAPER C428-12-166] p 457 A95-91704

Optimum Design Methods for Aerodynamics

[AGARD-R-803] p 127 N95-16562

Review of the EUROPT Project AERO-0026

p 129 N95-16573

Naval aviation: F-14 upgrades are not adequately justified. Report to Congressional Committees

[AD-A286338] p 231 N95-20212

Assuring Known Good Die (KGD) for reliable, cost effective MCMS

p 246 N95-20644

Report to Congressional Committees. Comanche Helicopter: Testing needs to be completed prior to production decisions

[GAO/NSIAD-95-112] p 397 N95-27910

COST ESTIMATES

Technology Benefit Estimator (T/BEST): User's manual

[NASA-TM-106785] p 167 N95-19501

Report to Congressional Committees. Comanche Helicopter: Testing needs to be completed prior to production decisions

[GAO/NSIAD-95-112] p 397 N95-27910

COST REDUCTION

Ceramic blanket reduces maintenance costs

[BTN-94-EIX94461290278] p 77 A95-61733

Containing military autotest cost growth through the use of commercial standard equipment architectures

[BTN-95-EIX95172595295] p 287 A95-75717

Maintenance challenges and trends

[BTN-95-EIX95182617808] p 261 A95-75753

Cuts endangerer airborne research — NASA Ames Research Center Reorganization

[HTN-95-20602] p 443 A95-84783

Integrated aircraft thermal management and power generation

[SAE PAPER 932055] p 500 A95-91636

Aerospace applications of new materials

[CONGRESS PAPER C428-17-135] p 531 A95-91716

Design of a high capacity long range cargo aircraft

[NASA-CR-197176] p 45 N95-12363

Central coast designs: The Eightball Express. Taking off with convention, cruising with improvements and landing with absolute success

[NASA-CR-197181] p 47 N95-12643

More supportable T-38A enhancement study

[AD-A283671] p 66 N95-15331

Optimization of adaptive intraply hybrid fiber composites with reliability considerations

[NASA-TM-106632] p 157 N95-16911

Reliability assessment of Multichip Module technologies via the Triservice/NASA RELTECH program

p 245 N95-20643

The opportunities for and challenges of common integrated electronics

[AD-A279991] p 248 N95-20966

C-130 Advanced Technology Center wing box conceptual design/cost study

p 423 N95-28437

Composite fuselage crown panel manufacturing technology

p 399 N95-28474

Impact of composites on future transport aircraft

p 534 N95-29030

Report to the Chairman, Subcommittee on Transportation and Related Agencies, Committee on Appropriations, House of Representatives. Air traffic control: Status of FAA's plans to close and contract out low-activity towers

[GAO/RCD-94-265] p 603 N95-32199

COSTS

Optimal trajectories for hypersonic launch vehicles

[HTN-95-61120] p 415 A95-84884

Aerospace applications of beta titanium alloys

[HTN-95-B0394] p 530 A95-90475

Ceramic manufacturing: Optimizing a multivariable system

[DE94-015016] p 56 N95-13184

Simulation of Shuttle launch G forces and acoustic loads using the NASA Ames Research Center 20G centrifuge

p 86 N95-14089

MCMS for avionics: Technology selection and intermediate interconnection

p 234 N95-20641

An analysis of the impact of ASPA on organizational and depot level maintenance

[AD-A292670] p 457 N95-29414

A NASPAC-Based analysis of the delay and cost effects of the western-pacific region preliminary resectorization effort of 1993

[AD-A288696] p 601 N95-31013

Integration of air traffic databases: A case study

[AD-A293691] p 602 N95-32022

COTTON

A comparison of some aerodynamic resistance methods using measurements over cotton and grass from the 1991 California ozone deposition experiment

[HTN-95-11295] p 319 A95-77000

COUETTE FLOW

The effects of wall perturbations on thermo-turbulent Couette flow

[HTN-95-92255] p 434 A95-85299

Studies in drag reduction

p 478 N95-29094

COUNTER ROTATION

Flow structure in the wake of a wishbone vortex generator

[BTN-95-EIX95142553044] p 304 A95-73454

COUNTERFLOW

Intrinsic transport and chemistry coupling in combustion phenomena

p 538 A95-87191

COUNTERMEASURES

Effect of passive venting on static pressure distributions in cavities at subsonic and transonic speeds

[NASA-TM-4549] p 6 N95-10029

COUPLING

Effect of coupling term on stability for the two input control system

p 507 A95-91583

Flight control systems/structural coupling BAe Warton experience in aero-servo elasticity

[CONGRESS PAPER C428-35-059] p 610 A95-93628

An investigation of the effects of pitch-roll (de)coupling on helicopter handling qualities

[NASA-TM-110349] p 409 N95-26773

COUPLINGS

Demonstration of an elastically coupled twist control concept for tilt rotor blade application

[HTN-95-20959] p 465 A95-88998

COWLINGS

Computational analysis in support of the SSTO flowpath test

[NASA-TM-106757] p 89 N95-13665

Wind-tunnel blockage and actuation systems test of a two-dimensional scramjet inlet unstart model at Mach 6

[NASA-TM-109152] p 97 N95-15898

The use of cowl camber and taper to reduce rotor/stator interaction noise

[NASA-CR-195421] p 323 N95-22675

Wave drag coefficient for axisymmetric forecows at zero incidence (M sub infinity less than or equal to 1.5)

[ESDU-94014] p 552 N95-28903

Surface pressure coefficient distributions for axisymmetric forecows at zero incidence (M sub infinity less than or equal to 1.5)

[ESDU-94015] p 477 N95-28904

CRACK ARREST

Development of the NASA/FLAGRO computer program for analysis of airframe structures

p 94 N95-14473

Axial crack propagation and arrest in pressurized fuselage

p 94 N95-14479

CRACK CLOSURE

Prediction of fatigue crack growth under flight-simulation loading with the modified CORPUS model

p 166 N95-19471

Discrete crack growth analysis methodology for through cracks in pressurized fuselage structures

p 166 N95-19473

The application of Newman crack-closure model to predicting fatigue crack growth

p 167 N95-19483

CRACK GEOMETRY

Corrosion and corrosion fatigue of airframe aluminum alloys

p 87 N95-14465

Study of multiple cracks in airplane fuselage by micromechanics and complex variables

p 94 N95-14468

The role of fretting corrosion and fretting fatigue in aircraft rivet hole cracking

p 94 N95-14470

Fracture mechanics validity limits

p 95 N95-14480

CRACK INITIATION

Inspecting for widespread fatigue damage: Is partial debonding the key?

p 93 N95-14458

The characterization of widespread fatigue damage in fuselage structure

[NASA-TM-109142] p 88 N95-14920

Fatigue in single crystal nickel superalloys

[AD-A282917] p 88 N95-15415

The characterization of widespread fatigue damage in fuselage structure

p 166 N95-19472

Evaluation of the fuselage lap joint fatigue and terminating action repair

p 166 N95-19477

Fatigue life until small cracks in aircraft structures: Durability and damage tolerance

p 135 N95-19478

Results of uniaxial and biaxial tests on riveted fuselage lap joint specimens

p 136 N95-19491

Aircraft fatigue and crack growth considering loads by structural component

p 137 N95-19497

Estimate of probability of crack detection from service difficulty report data

[PB95-149381] p 328 N95-24295

Thermal fracture mechanisms in ceramic thermal barrier coatings

p 346 N95-26138

Failure analysis for polycarbonate transparencies

[AD-A292992] p 630 N95-31471

CRACK OPENING DISPLACEMENT

Fatigue life until small cracks in aircraft structures: Durability and damage tolerance

p 135 N95-19478

CRACK PROPAGATION

Fatigue crack growth in nickel-based superalloys at 500-700 C. 1: Waspaloy

[BTN-94-EIX94371347843] p 206 A95-69136

Bonded composite repair of cracked load-bearing holes

[BTN-94-EIX94401360553] p 243 A95-71867

Growth of multiple cracks and their linkup in a fuselage lap joint

[BTN-95-EIX95142553047] p 286 A95-73451

Multiple site fatigue damage in fuselage skin splices: Experimental simulation and theoretical prediction

[BTN-95-EIX95152584676] p 276 A95-73588

Theoretical and experimental studies of fretting-initiated fatigue failure of aeroengine compressor discs

[BTN-94-EIX94421372285] p 343 A95-78467

Flight simulation fatigue crack growth testing of aluminum alloys

[HTN-95-00652] p 418 A95-84731

Analytical developments in support of the NASA aging aircraft program with an application to crack growth from rivets

[SAE PAPER 931223] p 545 A95-88789

Crack growth characteristics of integrally machined stringer-skin panels

[HTN-95-01095] p 496 A95-90281

Discrete crack growth analysis methodology for through cracks in pressurized fuselage structures

[BTN-95-EIX0608952737538] p 633 A95-92751

FAA/NASA International Symposium on Advanced Structural Integrity Methods for Airframe Durability and Damage Tolerance

[NASA-CP-3274-PT-1] p 92 N95-14453

Elastic-plastic models for multi-site damage

p 92 N95-14454

- Small crack test program for helicopter materials p 92 N95-14455
- Bending effects of unsymmetric adhesively bonded composite repairs on cracked aluminum panels p 92 N95-14456
- Evaluation of bonded boron/epoxy doublers for commercial aircraft aluminum structures p 92 N95-14457
- Inspecting for widespread fatigue damage: Is partial debonding the key? p 93 N95-14458
- Testing and analysis of flat and curved panels with multiple cracks p 93 N95-14460
- Corrosion and corrosion fatigue of airframe aluminum alloys p 87 N95-14465
- Influence of crack history on the stable tearing behavior of a thin-sheet material with multiple cracks p 93 N95-14467
- Study of multiple cracks in airplane fuselage by micromechanics and complex variables p 94 N95-14468
- Development of the NASA/FLAGRO computer program for analysis of airframe structures p 94 N95-14473
- Fatigue reliability method with in-service inspections p 94 N95-14475
- Nonlinear bulging factor based on R-curve data p 94 N95-14476
- Development of a composite repair and the associated inspection intervals for the F-111C stiffener runout region p 66 N95-14477
- Axial crack propagation and arrest in pressurized fuselage p 94 N95-14479
- Fracture mechanics validity limits p 95 N95-14480
- Analysis of small crack behavior for airframe applications p 95 N95-14484
- Full-scale testing and analysis of fuselage structure p 95 N95-14485
- The characterization of widespread fatigue damage in fuselage structure [NASA-TM-109142] p 88 N95-14920
- Fatigue in single crystal nickel superalloys [AD-A282917] p 88 N95-15415
- Multi-lab comparison on R-curve methodologies: Alloy 2024-T3 [NASA-CR-195004] p 151 N95-16860
- Prediction of fatigue crack growth under flight-simulation loading with the modified CORPUS model p 166 N95-19471
- The characterization of widespread fatigue damage in fuselage structure p 166 N95-19472
- Discrete crack growth analysis methodology for through cracks in pressurized fuselage structures p 166 N95-19473
- Evaluation of the fuselage lap joint fatigue and terminating action repair p 166 N95-19477
- Fatigue life until small cracks in aircraft structures: Durability and damage tolerance p 135 N95-19478
- The application of Newman crack-closure model to predicting fatigue crack growth p 167 N95-19483
- Fatigue crack growth in 2024-T3 aluminum under tensile and transverse shear stresses p 153 N95-19490
- Fatigue and residual strength investigation of ARALL(R) -3 and GLARE(R) -2 panels with bonded stringers p 137 N95-19495
- Aircraft fatigue and crack growth considering loads by structural component p 137 N95-19497
- Impact loading of compressor stator vanes by halstone ingestion p 200 N95-19670
- Residual strength of thin panels with cracks p 311 N95-23311
- Estimate of probability of crack detection from service difficulty report data [PB95-149381] p 328 N95-24295
- Adhesively bonded composite patch repair of cracked aluminum alloy structures p 393 N95-27507
- Prediction of fatigue crack growth under constant amplitude and random loading using specimens with multiple cracks [AD-A291614] p 397 N95-28409
- Numerical simulation of crack growth in pressurized fuselages [PB95-192415] p 400 N95-28636
- Tension fracture of laminates for transport fuselage. Part 2: Large notches p 532 N95-28837
- Thermal-mechanical fatigue crack growth in aircraft engine materials [ISBN-0-315-86543-1] p 647 N95-31098
- Failure analysis for polycarbonate transparencies [AD-A292992] p 630 N95-31471
- CRACK TIPS**
- Study of multiple cracks in airplane fuselage by micromechanics and complex variables p 94 N95-14468
- Axial crack propagation and arrest in pressurized fuselage p 94 N95-14479
- Full-scale testing and analysis of fuselage structure p 95 N95-14485
- Discrete crack growth analysis methodology for through cracks in pressurized fuselage structures p 166 N95-19473
- The application of Newman crack-closure model to predicting fatigue crack growth p 167 N95-19483
- Tension fracture of laminates for transport fuselage. Part 2: Large notches p 532 N95-28837
- CRACKING (FRACTURING)**
- Flight simulation fatigue crack growth testing of aluminum alloys [HTN-95-00652] p 418 A95-84731
- Status and prospects for aluminium-lithium alloys in aircraft structures p 387 A95-85893
- Fatigue of aircraft materials and structures p 387 A95-85894
- Fibre-Metal laminates p 387 A95-85895
- Verification of the damage tolerance of a fighter aircraft p 388 A95-85897
- Damage tolerance capability p 388 A95-85898
- Fatigue in single crystal nickel superalloys [AD-A283459] p 56 N95-12546
- Fatigue in single crystal nickel superalloys [AD-A282917] p 88 N95-15415
- Eddy current for detecting second layer cracks under installed fasteners [AD-A282412] p 158 N95-17507
- Evaluation of the fuselage lap joint fatigue and terminating action repair p 166 N95-19477
- Evaluation of patch effectiveness in repairing aircraft components p 394 N95-27513
- Numerical simulation of crack growth in pressurized fuselages [PB95-192415] p 400 N95-28636
- Preparation of S-70A-9 Black Hawk helicopter for flight tests to investigate cause of cracking of inner fuselage panel [AD-A293891] p 608 N95-31544
- CRACKS**
- Growth of multiple cracks and their linkup in a fuselage lap joint [BTN-95-EIX95142553047] p 286 A95-73451
- Multiple site fatigue damage in fuselage skin splices: Experimental simulation and theoretical prediction [BTN-95-EIX95152584676] p 276 A95-73588
- Transient analysis of a cracked rotor passing through critical speed [BTN-94-EIX94401360022] p 306 A95-74702
- Theoretical and experimental studies of fretting-initiated fatigue failure of aeroengine compressor discs [BTN-94-EIX94421372285] p 343 A95-78467
- Discrete crack growth analysis methodology for through cracks in pressurized fuselage structures [BTN-95-EIX0608952737538] p 633 A95-92751
- Structural integrity of fuselage panels with multisite damage [BTN-95-EIX0619952748188] p 637 A95-94250
- New experimental approach to determine initial fatigue quality with fastener holes [BTN-94-EIX94522406136] p 701 A95-96273
- Testing and analysis of flat and curved panels with multiple cracks p 93 N95-14460
- Influence of crack history on the stable tearing behavior of a thin-sheet material with multiple cracks p 93 N95-14467
- Challenges for the aircraft structural integrity program p 80 N95-14481
- Eddy current for detecting second layer cracks under installed fasteners [AD-A282412] p 158 N95-17507
- Evaluation of the fuselage lap joint fatigue and terminating action repair p 166 N95-19477
- Nonlinear analysis of damaged stiffened fuselage shells subjected to combined loads p 137 N95-19499
- Eddy current for detecting second-layer cracks under installed fasteners [AD-A279871] p 244 N95-20414
- Damage tolerant repair techniques for pressurized aircraft fuselages [AD-A286298] p 219 N95-22046
- Residual strength of thin panels with cracks p 311 N95-23311
- Bonded composite repair of metallic aircraft components: Overview of Australian activities p 392 N95-27505
- Design and structural validation of CF116 upper wing skin boron doubler p 393 N95-27510
- Evaluation of patch effectiveness in repairing aircraft components p 394 N95-27513
- Prediction of fatigue crack growth under constant amplitude and random loading using specimens with multiple cracks [AD-A291614] p 397 N95-28409
- The mm-wave resonant methods for the detection of corrosion, phase 1 [AD-A291315] p 556 N95-29941
- Modal identification and its applications to damage detection in vibrating structures p 704 N95-32920
- CRASH INJURIES**
- Biodynamic simulation of pilot interaction with a helicopter multi-airbag restraint system [AD-A290196] p 485 N95-29057
- CRASH LANDING**
- Explanatory factors for the geographic distribution of U.S. Civil aviation mortality [HTN-95-92908] p 484 A95-91846
- The crash of Flight 232 [NASA-TM-104279] p 11 N95-10737
- Aircraft accident report: Overspeed and loss of power on both engines during descent and power-off emergency, landing Simmons Airlines, Inc., d/b/a, American Eagle Flight 3641, N349SB False River Air Park, New Roads, Louisiana, 1 February 1994 [PB94-910408] p 78 N95-14916
- Aircraft accident report: Stall and loss of control on final approach, Atlantic Coast Airlines, Inc./United Express Flight 6291 Jetstream 4101, N304UE Columbus, OH, 7 January 1994 [PB94-910409] p 123 N95-17646
- Commuter/air taxi ditchings and water-related impacts that occurred from 1979 to 1989 [AD-A285691] p 226 N95-20275
- CRASHES**
- Commentary on Walton correspondence relating to the ILS glide slope [BTN-94-EIX94441380856] p 125 A95-64288
- Reaction-time response of aircraft crash [BTN-95-EIX95292721296] p 595 A95-92626
- Plastic hinge modeling of structures [NIAR-94-14] p 24 N95-11168
- A correlative investigation of simulated occupant motion and accident report in a helicopter crash [AD-A285190] p 123 N95-16404
- Commuter airplane accident data analysis [AD-A286315] p 226 N95-20174
- Aircraft fires, smoke toxicity, and survival: An overview [DOT/FAA/AM-95/8] p 277 N95-24024
- A multibody/finite element analysis approach for modeling of crash dynamic responses [NIAR-94-3] p 277 N95-24050
- Rotorcraft crashworthy airframe and fuel system technology development program [AD-A289986] p 382 N95-28630
- CRASHWORTHINESS**
- Prediction of energy absorption capability of composite stiffeners [HTN-95-A0500] p 230 A95-72571
- Triton 2 (1B) [NASA-CR-197188] p 46 N95-12636
- Commuter airplane accident data analysis [AD-A286315] p 226 N95-20174
- Commuter/air taxi ditchings and water-related impacts that occurred from 1979 to 1989 [AD-A285691] p 226 N95-20275
- A multibody/finite element analysis approach for modeling of crash dynamic responses [NIAR-94-3] p 277 N95-24050
- Analysis of warping effects on the static and dynamic response of a seat-type structure [NIAR-94-12] p 348 N95-24211
- Rotorcraft crashworthy airframe and fuel system technology development program [AD-A289986] p 382 N95-28630
- Biodynamic simulation of pilot interaction with a helicopter multi-airbag restraint system [AD-A290196] p 485 N95-29057
- CREEP ANALYSIS**
- Analytical description of and forecast for stress relaxation of aviation materials under the vibration conditions [BTN-94-EIX94461408751] p 126 A95-63634
- The role of material behaviour modelling in stressing and life assessment of modern Aero-engine components [CONGRESS PAPER C428-27-127] p 612 A95-93606
- CREEP PROPERTIES**
- Evolution of oxidation and creep damage mechanisms in HIPed silicon nitride materials [DE95-001360] p 300 N95-22689
- Probabilistic material strength degradation model for Inconel 718 components subjected to high temperature, high-cycle and low-cycle mechanical fatigue, creep and thermal fatigue effects [NASA-CR-197832] p 419 N95-27167
- Scar repairs to graphite/epoxy components p 396 N95-27523
- CREEP TESTS**
- Evolution of oxidation and creep damage mechanisms in HIPed silicon nitride materials [DE95-001360] p 300 N95-22689

CREW PROCEDURES (INFLIGHT)

- Test and evaluation crew resource management p 483 A95-90867
- Federal aviation regulations, part 91. General operating and flight rules. Change 5 [PB94-194883] p 123 N95-17476
- CREW WORKSTATIONS**
- Industry review of a crew-centered cockpit design process and toolset [AD-A282966] p 130 N95-17661
- Systems engineering design and technical analyses for Strategic Avionics Crew-station Design Evaluation Facility (SACDEF) [AD-A286239] p 235 N95-22024
- A crew-centered flight deck design philosophy for High-Speed Civil Transport (HSCT) aircraft [NASA-TM-109171] p 335 N95-24582
- CRITICAL FLOW**
- Hydraulic system diagnostic sensors [BTN-95-EIX95031502752] p 209 A95-68259
- High frequency flow-structural interaction in dense subsonic fluids [NASA-CR-4652] p 330 N95-24217
- CRITICAL LOADING**
- Fatigue loads spectra derivation for the Space Shuttle: Second cycle p 166 N95-19470
- Fundamental concepts in the suppression of delamination buckling by stitching p 426 N95-28486
- CRITICAL PRESSURE**
- Panel flutter limit-cycle suppression with piezoelectric actuation [BTN-95-EIX95302731089] p 618 A95-94208
- CRITICAL VELOCITY**
- Unbalance response of a dual rotor system: Theory and experiment [BTN-94-EIX94351143320] p 195 A95-65854
- Transient analysis of a cracked rotor passing through critical speed [BTN-94-EIX94401360022] p 306 A95-74702
- Critical speed analysis of a non-linear strain ring dynamical model for aircraft tires [SAE PAPER 932580] p 494 A95-90067
- Effect of crossflow on Goertler instability in incompressible boundary layers [NASA-CR-195007] p 159 N95-18193
- Transonic, supersonic and hypersonic wind-tunnel tests on aerodynamic characteristics of reentry body with blunted cone configuration [ISAS-658] p 480 N95-29640
- CROSS COUPLING**
- New eigensolutions and modal analysis for gyroscopic/rotor systems, part 2: perturbation analysis for damped systems [BTN-94-EIX94522410220] p 702 A95-96374
- CROSS FLOW**
- Jet to freestream velocity ratio computations for a jet in a crossflow [AIAA PAPER 93-4860] p 2 A95-60178
- On the dynamics of aeroelastic oscillators with one degree of freedom [BTN-94-EIX94501431527] p 153 A95-64524
- Phenomenological description and simplified modelling of the vortex wake issuing from a jet in a crossflow [BTN-94-EIX94441385754] p 184 A95-68218
- Flow structure in the wake of a wishbone vortex generator [BTN-95-EIX95142553044] p 304 A95-73454
- Experimental investigation of the flowfield about an upstret aftbody [BTN-95-EIX95152582321] p 265 A95-73524
- Observation of traveling waves in the three-dimensional boundary layer along a yawed cylinder [HTN-95-61064] p 430 A95-83648
- Crossflow topology of vortical flows [HTN-95-51664] p 432 A95-85046
- Nonlinear analysis of swept wing transitional boundary layers [SAE PAPER 932515] p 466 A95-89188
- A full Navier-Stokes analysis of subsonic diffuser of a bifurcated 70/30 supersonic inlet for high speed civil transport application [NASA-TM-106637] p 8 N95-10820
- Wall-signature methods for high speed wind tunnel wall interference corrections p 107 N95-16257
- In-flight imaging of transverse gas jets injected into transonic and supersonic crossflows: Design and development [NASA-CR-186031] p 157 N95-17418
- Effect of crossflow on Goertler instability in incompressible boundary layers [NASA-CR-195007] p 159 N95-18193
- Computational studies of laminar to turbulence transition [AD-A285622] p 248 N95-21146
- Crossflow instability control on a swept-wing: Preliminary studies p 274 N95-23283

- Three-dimensional interaction of wake/boundary-layer and vortex/boundary-layer data report [CUED/A-AEREO/TR-23] p 329 N95-24210
- Crossflow mixing of noncircular jets [NASA-TM-106865] p 338 N95-24390
- Effect of density gradients in confined supersonic shear layers. Part 2: 3-D modes [NASA-CR-198030] p 349 N95-24413
- The decay of longitudinal vortices shed from airfoil vortex generators [NASA-CR-198356] p 480 N95-29402
- Growth and development of roughness-induced stationary crossflow vortices p 482 N95-30294
- Effects of initial conditions on a single jet in crossflow [NASA-TM-107002] p 615 N95-30589
- Jet mixing and emission characteristics of transverse jets in annular and cylindrical confined crossflow [NASA-TM-106976] p 616 N95-30698
- Jet mixing in a reacting cylindrical crossflow [NASA-TM-106975] p 616 N95-30853
- CRUISE MISSILES**
- A design trade study using CFD modeling of reaction jets for aerodynamic control [SAE PAPER 931384] p 586 A95-93660
- CRUISING FLIGHT**
- North Atlantic air traffic within the lower stratosphere: Cruising times and corresponding emissions [HTN-95-91841] p 354 A95-80829
- Trim conditions for optimal flight performance of hypersonic aircraft p 514 A95-87397
- Note on prediction of aerodynamic lift/drag ratio of WIG (Wing-In-Ground) at cruise [BTN-95-EIX95282705925] p 467 A95-89665
- A two element laminar flow airfoil optimized for cruise [NASA-CR-198580] p 479 N95-29338
- Minimum fuel mode evaluation p 695 N95-33015
- CRYOGENIC EQUIPMENT**
- A hybrid electronically scanned pressure module for cryogenic environments [NASA-TM-110146] p 554 N95-29453
- Reducing process noise in superconducting helium liquid level probes [DE95-008956] p 629 N95-30765
- CRYOGENIC FLUIDS**
- Low gravity quenching of hot tubes with cryogenics [ISBN 1-879921-01-4] p 635 A95-93728
- Numerical modeling of a cryogenic fluid within a fuel tank [NASA-TM-4651] p 89 N95-13892
- A Lifting Ball Valve for cryogenic fluid applications p 156 N95-16349
- Cavitation modeling in Euler and Navier-Stokes codes p 315 N95-23630
- Thermohydrodynamic analysis of cryogenic liquid turbulent flow fluid film bearings, phase 2 [NASA-CR-197412] p 349 N95-24461
- CRYOGENIC ROCKET PROPELLANTS**
- Airborne rotary separator study [NASA-CR-191045] p 150 N95-18743
- CRYOGENIC TEMPERATURE**
- A hybrid electronically scanned pressure module for cryogenic environments [NASA-TM-110146] p 554 N95-29453
- CRYOGENIC WIND TUNNELS**
- Preliminary assessment of tunnel wall interference in the NDA cryogenic wind tunnel [BTN-95-EIX95062487531] p 187 A95-69239
- Similarity rule for jet-temperature effects on transonic base pressure [BTN-95-EIX9522650791] p 329 A95-79247
- Aerodynamic Investigation with focusing schlieren in a cryogenic wind tunnel [HTN-95-20835] p 544 A95-88096
- Buffeting tests in a cryogenic wind tunnel [HTN-95-92833] p 470 A95-90751
- A hybrid electronically scanned pressure module for cryogenic environments [NASA-TM-110146] p 554 N95-29453
- Computer model to simulate testing at the National Transonic Facility [NASA-TM-4664] p 627 N95-32217
- CRYOGENICS**
- Matrix isolated HF: the high-resolution infrared spectrum of a cryogenically solvated hindered rotor [GTN-95-0301010494002231-16] p 578 A95-92210
- CRYSTAL DISLOCATIONS**
- Fatigue in single crystal nickel superalloys [AD-A282917] p 88 N95-15415
- CRYSTAL FIELD THEORY**
- Matrix isolated HF: the high-resolution infrared spectrum of a cryogenically solvated hindered rotor [GTN-95-0301010494002231-16] p 578 A95-92210
- CRYSTAL LATTICES**
- Matrix isolated HF: the high-resolution infrared spectrum of a cryogenically solvated hindered rotor [GTN-95-0301010494002231-16] p 578 A95-92210

CRYSTAL STRUCTURE

- Fatigue in single crystal nickel superalloys [AD-A283459] p 56 N95-12546
- CRYSTAL SURFACES**
- Fatigue in single crystal nickel superalloys [AD-A282917] p 88 N95-15415
- CUES**
- The advanced flight simulator complex [CONGRESS PAPER C428-5-025] p 522 A95-91679
- CULTURAL RESOURCES**
- The effects of aircraft (B-52) overflights on ancient structures [BTN-94-EIX94341340070] p 171 A95-63522
- CUMULATIVE DAMAGE**
- Computerized maintenance aid [BTN-95-EIX95031502749] p 217 A95-68256
- Fatigue life estimation program for Part 23 airplanes, 'AFS.FOR' [SAE PAPER 931249] p 565 A95-89221
- An artificial corrosion protocol for lap-splices in aircraft skin p 152 N95-19482
- CUMULUS CLOUDS**
- Microphysical and radiative properties of small cumulus clouds over the sea [HTN-95-A0526] p 255 A95-73180
- On the link between cloud-top radiative properties and sub-cloud aerosol concentrations [HTN-95-A0527] p 255 A95-73181
- Developing thunderstorm forecast rules utilizing first detectable cloud radar-echoes p 667 A95-93514
- CURING**
- Ultrasonic techniques for repair of aircraft structures with bonded composite patches p 136 N95-19486
- Development and verification of a resin film infusion/resin transfer molding simulation model for fabrication of advanced textile composites [NASA-CR-197439] p 301 N95-23179
- External patch repair of CFRP/honeycomb sandwich p 395 N95-27522
- CURVATURE**
- Elliptic tip effects on the vortex wake of an axisymmetric body at incidence [BTN-94-EIX94441386612] p 208 A95-67343
- On wave-front curvature in linear stability theory [BTN-94-EIX94441385756] p 184 A95-68220
- Influence of streamwise curvature on longitudinal vortices imbedded in turbulent boundary layers [BTN-94-EIX94401378820] p 307 A95-76489
- Effect of curvature in the numerical simulation of an electrothermal de-icer pad [BTN-95-EIX95182619219] p 276 A95-76645
- Instability of three-dimensional boundary layers due to streamline curvature [HTN-95-61070] p 430 A95-83654
- CURVE FITTING**
- Strain gage selection in loads equations using a genetic algorithm [NASA-CR-4597] p 48 N95-12831
- CURVED BEAMS**
- The effect of material heterogeneity in curved composite beams for use in aircraft structures p 422 N95-28426
- CURVED PANELS**
- Advanced composites structural concepts and materials technologies for primary aircraft structures: Structural response and failure analysis [NASA-CR-4448] p 11 N95-10240
- Testing and analysis of flat and curved panels with multiple cracks p 93 N95-14460
- Nonlinear bulging factor based on R-curve data p 94 N95-14476
- Shear buckling analysis of a hat-stiffened panel [NASA-TM-4644] p 158 N95-17490
- Evaluation of the fuselage lap joint fatigue and terminating action repair p 166 N95-19477
- Rapid repair of large area damage to contoured aircraft structures p 394 N95-27516
- Static and fatigue testing of full-scale fuselage panels fabricated using a Therm-X(R) process p 420 N95-28270
- Dimensional stability of curved panels with cocured stiffeners and cobonded frames p 532 N95-28836
- Design, analysis, and fabrication of a pressure box test fixture for tension damage tolerance testing of curved fuselage panels p 533 N95-28839
- Buckling analysis of curved composite sandwich panels subjected to inplane loadings p 533 N95-28845
- CUSHIONS**
- The effect of wear on fire-blocking layer material effectiveness [AD-A291520] p 485 N95-29855
- CUTTING**
- Modelling for optimal operations of line milling of aerodynamic surfaces [BTN-94-EIX94461408774] p 138 A95-63657

Vortex cutting by a blade. Part II: Computations of vortex response
[BTN-94-EIX94441386611] p 208 A95-67342

Vortex cutting by a blade, Part 2: Computations of vortex response
[HTN-95-20937] p 464 A95-88976

CV-880 AIRCRAFT

Fuselage burnthrough from large exterior fuel fires
[AD-A286295] p 226 N95-22318

CYBERNETICS

Emerging applications in probability (Sensor management)
[AD-A292781] p 601 N95-31433

CYCLES

Corrosion of fire-damaged aircraft
[AD-A294968] p 693 N95-34583

CYCLIC LOADS

Non-linear viscoelastic-plastic constitutive relations for an aeronautical PMMA
[HTN-95-71132] p 385 A95-83493

Fatigue crack growth in 2024-T3 aluminum under tensile and transverse shear stresses p 153 N95-19490

Damage of high temperature components by dust-laden air p 201 N95-19673

Probabilistic material strength degradation model for Inconel 718 components subjected to high temperature, high-cycle and low-cycle mechanical fatigue, creep and thermal fatigue effects
[NASA-CR-197832] p 419 N95-27167

Preliminary analysis of dynamic stall effects on a 91-meter wind turbine rotor p 376 N95-27975

Calculation of design load for the MOD-5A 7.3 mW wind turbine system p 440 N95-27982

Comparison of measured and calculated dynamic loads for the Mod-2 2.5 mW wind turbine system p 440 N95-27983

Investigation of static and cyclic bearing failure mechanisms for GR/EP laminates p 422 N95-28427

CYCLOGENESIS

Research aircraft observations of a polar low at the east Greenland ice edge
[HTN-95-A0175] p 215 A95-69766

Mesoscale structure of precipitation bands in a North Atlantic winter storm
[HTN-95-40659] p 215 A95-69803

Tropical cyclone observation and forecasting with and without aircraft reconnaissance
[HTN-95-80701] p 254 A95-72545

CYCLONES

Research aircraft observations of a polar low at the east Greenland ice edge
[HTN-95-A0175] p 215 A95-69766

Mesoscale structure of precipitation bands in a North Atlantic winter storm
[HTN-95-40659] p 215 A95-69803

CYCLOTRON RADIATION

Permanent magnet electron cyclotron resonance plasma source with remote window
[BTN-95-EIX95242674338] p 450 A95-82176

CYCLOTRON RESONANCE

Permanent magnet electron cyclotron resonance plasma source with remote window
[BTN-95-EIX95242674338] p 450 A95-82176

Cu deposition using a permanent magnet electron cyclotron resonance microwave plasma source
[DE94-017768] p 304 N95-23981

CYLINDERS

Numerical investigation of cylinder wake flow with a rear stagnation jet
[HTN-95-51669] p 433 A95-85051

CYLINDRICAL BODIES

Numerical computations of supersonic base flow with special emphasis on turbulence modeling
[BTN-94-EIX94441386632] p 179 A95-68181

Aerodynamic mechanism of galloping
[BTN-94-EIX94371347709] p 219 A95-69968

Time-resolved surface heat flux measurements in the wing/body junction vortex
[BTN-95-EIX95082502716] p 220 A95-71029

Wind-tunnel tests of an inclined cylinder having helical grooves
[BTN-95-EIX95262694306] p 411 A95-85477

Computation of vortex breakdown on a vortex delta wing
[BTN-95-EIX0619952748195] p 591 A95-94484

Wind tunnel investigations of the appearance of shocks in the windward region of bodies with circular cross section at angle of attack p 113 N95-17866

Force and pressure data of an ogive-nosed slender body at high angles of attack and different Reynolds numbers p 113 N95-17868

Supersonic vortex flow around a missile body p 114 N95-17870

Field and data analysis studies related to the atmospheric environment
[NASA-CR-196543] p 168 N95-18093

Numerical mixing calculations of confined reacting jet flows in a cylindrical duct p 139 N95-18133
[NASA-TM-106736]

Numerical computations of supersonic base flow with special emphasis on turbulence modeling
[AD-A283688] p 119 N95-18670

Effects of three-dimensional imposed 3-D disturbances on bluff-body near wake flows
[AD-A289553] p 374 N95-26757

Experimental and theoretical studies of wakes in stratified flows
[AD-A290203] p 553 N95-29060

CYLINDRICAL SHELLS

Field-consistent element applied to flutter analysis of circular cylindrical shells
[BTN-94-EIX94341341971] p 56 A95-60871

Simplified analysis of general instability of stiffened shells with cutouts in pure bending
[BTN-95-EIX95042474418] p 209 A95-68282

Numerical investigation of sound transmission through double wall cylinders with respect to active noise control p 577 A95-90134

Development of strength analysis methods and design model for aircraft constructions in Kazan Aviation Institute p 127 N95-16264

Compression strength of composite primary structural components
[NASA-CR-197554] p 160 N95-18388

Load transfer in the stiffener-to-skin joints of a pressurized fuselage
[NASA-CR-198610] p 439 N95-27865

CYLINDRICAL WAVES

RCS measurements, transformations, and comparisons under cylindrical and plane wave illumination
[BTN-94-EIX94371347126] p 242 A95-69976

D

DAMAGE

Multiaxis pilot ratings for damaged aircraft
[BTN-95-EIX95182619128] p 269 A95-76605

On-line learning nonlinear direct neurocontrollers for restructurable control systems
[BTN-95-EIX95242670768] p 359 A95-81079

Plaster damage experiments at the BBN Sonic Boom Test Facility p 529 A95-90120

Damage to composite aircraft structures from lightning strike attachment to unprotected CFC and internal sparking causing fuel injection
[CONGRESS PAPER C428-4-026] p 531 A95-91675

Repairs to composite structure on military aircraft
[CONGRESS PAPER C428-4-067] p 531 A95-91677

Elastic-plastic models for multi-site damage p 92 N95-14454

Brite-Euram programme: ACOUFAT acoustic fatigue and related damage tolerance of advanced composite and metallic structures p 174 N95-19159

Widespread fatigue damage monitoring: Issues and concerns p 136 N95-19488

Navy foreign object damage and its impact on future gas turbine engine low pressure compression systems p 198 N95-19658

Scandinavian Airlines Systems experience on erosion, corrosion and foreign object damage effects on gas turbines p 198 N95-19659

Experimental and numerical simulations of the effects of ingested particles in gas turbine engines p 199 N95-19662

Damage of high temperature components by dust-laden air p 201 N95-19673

Rationale for the Modular Air-system Vulnerability Estimation Network (MAVEN) methodology
[AD-A285797] p 284 N95-22510

Residual strength of thin panels with cracks p 311 N95-23311

Double pass retroreflection for corrosion detection in aircraft structures p 323 N95-23503

POD assessment of NDI procedures using a round robin test
[AGARD-R-809] p 315 N95-23602

Bird ingestion into large turbofan engines
[DOT/FAA/CT-93/14] p 333 N95-24631

Scarf repairs to graphite/epoxy components p 396 N95-27523

Damage occurrence on composites during testing and fleet service: Repair of Airbus aircraft p 396 N95-27526

Comparison of resin film infusion, resin transfer molding, and consolidation of textile preforms for primary aircraft structure p 425 N95-28477

Application of damage tolerance methodology in certification of the Piaggio P-180 Avanti p 399 N95-28480

Test results from large wing and fuselage panels p 537 N95-29051

Probabilistic reliability modeling of fatigue on the H-46 tie bar
[AD-A289926] p 607 N95-30927

New adaptive methods for reconfigurable flight control systems, appendix 1
[AD-A292711] p 619 N95-30937

DAMAGE ASSESSMENT

Computerized maintenance aid
[BTN-95-EIX95031502749] p 217 A95-68256

Corrosion prevention and control p 188 A95-68260
[BTN-95-EIX95031502753]

Mechanical system reliability and risk assessment
[BTN-95-EIX95142553046] p 304 A95-73452

Validation of an effective flat cruciform-shaped specimen to study CFRP composite laminates under biaxial loading
[BTN-95-EIX95152584677] p 282 A95-73589

Flight simulation fatigue crack growth testing of aluminum alloys
[HTN-95-00652] p 418 A95-84731

Status and prospects for aluminium-lithium alloys in aircraft structures p 387 A95-85893

Elements of structural integrity assurance p 387 A95-85896

Verification of the damage tolerance of a fighter aircraft p 388 A95-85897

Damage tolerance capability p 388 A95-85898

Ultrasonic imaging of damages in CRFT-laminates p 578 A95-90828

Intelligent skins development for future military aircraft
[CONGRESS PAPER C428-17-189] p 531 A95-91714

Moisture induced pressures in concrete airfield pavements
[AD-A281974] p 52 N95-11789

Inspecting for widespread fatigue damage: Is partial debonding the key? p 93 N95-14458

Probabilistic inspection strategies for minimizing service failures p 93 N95-14461

A method of calculating the safe fatigue life of compact, highly-stressed components p 93 N95-14464

Computational predictive methods for fracture and fatigue p 93 N95-14466

Development of the NASA/FLAGRO computer program for analysis of airframe structures p 94 N95-14473

Challenges for the aircraft structural integrity program p 80 N95-14481

Analysis of small crack behavior for airframe applications p 95 N95-14484

Full-scale testing and analysis of fuselage structure p 95 N95-14485

Artificial neural network modeling of damaged aircraft
[AD-A283227] p 80 N95-14849

POD assessment of NDI procedures using a round robin test
[AGARD-R-809] p 315 N95-23602

Aircraft accident report. Runway overrun following rejected takeoff. Continental airlines flight 795, McDonnell Douglas MD-82, N18835, LaGuardia Airport, Flushing, NY, 2 March 1994
[PB95-910401] p 277 N95-23609

Emerging nondestructive inspection for aging aircraft
[PB95-143053] p 328 N95-25401

Proceedings of the 2d USAF Aging Aircraft Conference
[AD-A288217] p 336 N95-25578

Navy composite maintenance and repair experience p 424 N95-28446

Compressive strength of damaged and repaired composite plates p 442 N95-28484

SMART materials: Surfaces, transforms and interfaces. The commensurate engineering dimension
[AD-A289598] p 442 N95-28649

Mapping hidden aircraft defects with dual-band infrared computed tomography p 584 N95-32164
[DE95-011531]

Modal identification and its applications to damage detection in vibrating structures p 704 N95-32920

DAMPERS

Dynamics of the McDonnell-Douglas Large Scale Dynamic Rig and dynamic calibration of the rotor balance
[NASA-TM-108855] p 65 N95-13891

DAMPING

Lyapunov exponents and stochastic stability of two-dimensional parametrically excited random systems
[BTN-94-EIX94361122401] p 207 A95-65897

Stability of magnetic bearing-rotor systems and the effects of gravity and damping
[BTN-94-EIX94441386619] p 208 A95-68168

Flap-lag damping in hover and forward flight with a three-dimensional wake
[HTN-95-A0496] p 221 A95-72567

Prediction of energy absorption capability of composite stiffeners
[HTN-95-A0500] p 230 A95-72571

- Dynamic-stall and structural-modeling effects on helicopter blade stability with experimental correlation [HTN-95-81646] p 542 A95-87694
- Stability of magnetic bearing-rotor systems and the effects of gravity and damping [HTN-95-20955] p 465 A95-88994
- An electrotheologically controlled semi-active landing gear [SAE PAPER 931403] p 605 A95-93673
- Dynamic stiffness and damping of foil bearings for gas turbine engines [SAE PAPER 931449] p 635 A95-93698
- Van der pol absorber for rotor vibrations [BTN-94-EIX94441385106] p 702 A95-96579
- Use of blade pitch control to provide power train damping for the Mod-2, 2.5-mW wind turbine p 440 A95-27986
- Recirculating cavity casing treatment failure [AD-A289330] p 513 A95-28908
- High-and low-frequency dynamics of isolated blades and rotors with dynamic stall and wake [AD-A290358] p 503 A95-29322
- A simulation of damping process of pendulum motion due to aerodynamic forces p 711 A95-34551

DARKENING

- Factors affecting the perception of luning in monocular regions of partial binocular overlap displays [AD-A286287] p 259 A95-22044

DATA ACQUISITION

- Optimum full-scale subsonic wind tunnel [AIAA PAPER 86-0732] p 18 A95-60161
- Forecasting for a large field program: STORM-FEST [HTN-95-90694] p 215 A95-69721
- Condition monitoring and diagnostics [BTN-95-EIX95182617811] p 261 A95-75756
- The FAA regional/commuter aircraft flight loads data collection program [SAE PAPER 931258] p 493 A95-89224
- A systems for flight data acquisition and analysis for a remotely-piloted research vehicle p 517 A95-91554
- Use of pilot reports for verification of aircraft icing diagnoses and forecasts p 666 A95-93508
- MDCRS: Aircraft observations collection and uses p 668 A95-93517
- Low frequency ultrasonic nondestructive inspection of aluminum/adhesive fuselage lap splices [DE94-014242] p 24 A95-11135
- Development of an experimental facility for analysis of rotor dynamic phenomena [AD-A281897] p 25 A95-11330
- Virtual environment application with partial gravity simulation p 169 A95-15988
- Data acquisition and processing software for the Low Speed Wind Tunnel tests of the Jindivik auxiliary air intake [AD-A285455] p 108 A95-17178
- Universal wind tunnel data acquisition and reduction software [AD-A283897] p 171 A95-18365
- Strategic avionics technology definition studies. Subtask 3-1A3: Electrical Actuation (ELA) Systems Test Facility [NASA-CR-188360] p 143 A95-18567
- Dynamic Stability Instrumentation System (DSIS). Volume 1: Hardware description [NASA-TM-109160-VOL-1] p 171 A95-18899
- Flight parameters monitoring system for tracking structural integrity of rotary-wing aircraft p 135 A95-19469
- Multipoint pressure measurements on continuously moving wind tunnel models [ARA-MEMO-391] p 188 A95-19772
- An Overview of Health and Usage Monitoring Systems (HUMS) for military helicopters [DSTO-TR-0061] p 327 A95-24200
- Weather And Radar Processor (WARP) Test and Evaluation Master Plan (TEMP) [AD-A288280] p 445 A95-26453
- Research instrumentation for polytechnic university's supersonic wind tunnel facility [AD-A290232] p 523 A95-29468
- Electrochemical impedance pattern recognition for detection of hidden chemical corrosion on aircraft components, phase 1 [AD-A291345] p 556 A95-29946
- Offshore next generation weather radar (NEXRAD) OT&E integration and OT&E operational test [AD-A293223] p 646 A95-30902
- Anechoic chamber upgrade [AD-A294375] p 700 A95-34342
- DATA BASE MANAGEMENT SYSTEMS**
- Supersonic and hypersonic shock/boundary-layer interaction database [BTN-94-EIX94441386604] p 182 A95-67335
- DATA BASES**
- Supersonic and hypersonic shock/boundary-layer interaction database [BTN-94-EIX94441386604] p 182 A95-67335

- Computerized maintenance aid [BTN-95-EIX95031502749] p 217 A95-68256
- Modeling student knowledge with self-organizing feature maps [BTN-95-EIX95262697073] p 564 A95-86862
- Supersonic and hypersonic shock/boundary-layer interaction database [HTN-95-20930] p 463 A95-88969
- Towards improving the NMC aircraft data base p 660 A95-93480
- Development of a climatological data base to help forecast cloud cover conditions for shuttle landings at the Kennedy Space Center p 670 A95-93529
- General aviation landing incidents and accidents: A review of ASRS and AOPA research findings p 596 A95-95198
- Initial exploration of the ASRS database p 681 A95-95204
- Advanced distributed simulation technology advanced rotary wing aircraft. System/segment specification. Volume 3: Visual system module [AD-A280239] p 20 A95-10351
- Windshear certification data base for forward-look detection systems p 41 A95-13204
- A selection of experimental test cases for the validation of CFD codes, volume 1 [AGARD-AR-303-VOL-1] p 91 A95-14201
- A supercritical airfoil experiment p 111 A95-17858
- A selection of experimental test cases for the validation of CFD codes. Supplement: Datasets A-E [AGARD-AR-303-SUPPL] p 117 A95-18539
- A CMC database for use in the next generation launch vehicles (rockets) p 150 A95-18993
- Documentation and archiving of the Space Shuttle wind tunnel test data base. Volume 2: User's Guide to the Archived Data Base [NASA-TM-104806-VOL-2] p 205 A95-19624
- Description and flow characterization of hypersonic facilities [AD-A284291] p 223 A95-20248
- Data link terminal DLT document [PB95-110805] p 229 A95-21369
- Independent review of Aviation Technology and Research Information Analysis System (ATRIAS) database [AD-A284049] p 226 A95-21518
- A user's guide to LUGSAN 1.1: A computer program to calculate and archive lug and sway brace loads for aircraft-carried stores [DE95-001919] p 232 A95-21730
- Compendium of NASA data base for the Global Tropospheric Experiment's Pacific Exploratory Mission West-A (PEM West-A) [NASA-TM-109177] p 320 A95-23009
- Impeller flow field characterization with a laser two-focus velocimeter p 313 A95-23440
- NLS Flight Simulation Laboratory (FSL) documentation [NASA-CR-196564] p 363 A95-24439
- AIAA Techfest 20 Proceedings [NIAR-94-1] p 367 A95-26941
- Horizontal axis wind turbine post stall airfoil characteristics synthesis p 376 A95-27974
- Enplanement and all cargo activity [AD-A280074] p 412 A95-28151
- Overview of the ACT program p 424 A95-28463
- COINS: A composites information database system p 453 A95-28465
- Proceedings of the AIAA/FAA joint symposium on general aviation systems [AD-A289830] p 368 A95-28610
- Conversion of the TRACON operations concepts database into a formal sentence outline job task taxonomy [DOT/FAA/AM-95/16] p 488 A95-28819
- Modeling spatio-temporal databases to measure the performance of the GPS satellite constellation p 489 A95-29596
- International access to aeromedical evacuation medical equipment assessment data p 569 A95-29622
- Integration of air traffic databases: A case study [AD-A293691] p 602 A95-32022
- Full-scale hingeless rotor performance and loads [NASA-TM-110356] p 691 A95-32699
- DATA COLLECTION PLATFORMS**
- Aviation terminal forecasts based on automated observations (FTAUTO) p 668 A95-93520
- Long endurance stratospheric solar powered airship [PB95-178729] p 336 A95-26009
- DATA COMPRESSION**
- Fault detection in multiprocessor systems and array processors [BTN-95-EIX95242679097] p 359 A95-81253
- DATA CONVERSION ROUTINES**
- User documentation of the CTA program [AD-A289508] p 375 A95-26854

DATA CORRELATION

- Data from the GARTEur (AD) Action Group 02 airfoil CAST 7/DOA1 experiments p 111 A95-17856
- DATA INTEGRATION**
- MATSurv multisensor air traffic surveillance [AD-A292253] p 489 A95-28887
- DATA LINKS**
- Gatelink highspeed communications with parked aircraft [SAE PAPER 932610] p 486 A95-90079
- An integrated system to improve aviation weather forecasts for the Alaska Range p 656 A95-93460
- The data link flight information service application p 665 A95-93504
- Dissemination of terminal weather products to the flight deck via data link p 669 A95-93525
- Dissemination of weather products p 670 A95-93526
- Weather products for aviation from WAFC Bracknell p 670 A95-93527
- Spread spectrum applications in unmanned aerial vehicles [AD-A281035] p 156 A95-16448
- GPS-Squitter capacity analysis [AD-A280037] p 245 A95-20599
- Data link terminal DLT document [PB95-110805] p 229 A95-21369
- Differential GPS and system integration of the Low Visibility Landing and Surface Operations (LVLASO) demonstration p 280 A95-23318
- DATA MANAGEMENT**
- Gatelink highspeed communications with parked aircraft [SAE PAPER 932610] p 486 A95-90079
- Initial exploration of the ASRS database p 681 A95-95204
- DATA PROCESSING**
- On-line analysis capabilities developed to support the active flexible wing wind-tunnel tests [BTN-95-EIX95182619213] p 296 A95-76639
- Data processing and mapping in airborne radiometric surveys [HTN-95-51587] p 442 A95-83591
- The inference of aviation weather hazards based on the integration of radar and lightning data p 660 A95-93483
- Initial exploration of the ASRS database p 681 A95-95204
- Efficient and effective handling of cycle slips in global positioning system data p 43 A95-12230
- Automation of reverse engineering process in aircraft modeling and related optimization problems [NASA-CR-197109] p 129 A95-16899
- A processing centre for the CNES CE-GPS experimentation p 125 A95-17196
- OAT15A airfoil data p 111 A95-17857
- Flight parameters monitoring system for tracking structural integrity of rotary-wing aircraft p 135 A95-19469
- SAR image registration in absolute coordinates using GPS carrier phase position and velocity information [DE94-018738] p 228 A95-20195
- Optical processing and control [AD-A279157] p 259 A95-21975
- Enhancement of F/A-18 operational flight measurements: Data report for phase 1 [DSTO-TR-0049] p 286 A95-23666
- Calculation of satellite drag coefficients [AD-A285118] p 300 A95-23781
- AVIRIS and TIMS data processing and distribution at the land processes distributed active archive center p 325 A95-23872
- Using digital filtering techniques as an aid in wind turbine data analysis [DE94-011862] p 357 A95-24853
- Weather And Radar Processor (WARP) Test and Evaluation Master Plan (TEMP) [AD-A288280] p 445 A95-26453
- Stall precursor study of high frequency data for three high speed, swept compressor rotors [AD-A293379] p 406 A95-26878
- STEP: A future vision, today [NONP-NASA-VT-95-49121] p 452 A95-27209
- Advanced data visualization and sensor fusion: Conversion of techniques from medical imaging to Earth science p 711 A95-34236
- DATA PROCESSING EQUIPMENT**
- Fault detection in multiprocessor systems and array processors [BTN-95-EIX95242679097] p 359 A95-81253
- Certification of windshear performance with RTCA class D radomes p 41 A95-13206
- The impact of advanced packaging technology on modular avionics architectures p 233 A95-20632

DATA PROCESSING TERMINALS

Evaluation of the Haworth-Newman avionics Display Readability Scale
[AD-A286127] p 235 N95-22232

DATA RECORDERS

Investigation of flight data recorder fire test requirements
[AD-A285832] p 232 N95-20032
Micro-time stress measurement device development
[AD-A289511] p 448 N95-26845
Solid-state data recorder, next development and use
p 705 N95-33143

DATA REDUCTION

Identification of aviation weather hazards based on the integration of radar and lightning data
[HTN-95-51323] p 356 A95-80908

The FAA regional/commuter aircraft flight loads data collection program
[SAE PAPER 931258] p 493 A95-89224

Aviation value-added products and services from the NEXRAD Information Dissemination Service (NIDS)
p 671 A95-93535

Initial exploration of the ASRS database
p 681 A95-95204

Reanalysis of European flight loads data
[AD-A282052] p 9 N95-11179

Efficient and effective handling of cycle slips in global positioning system data
p 43 N95-12230

A new algorithm for five-hole probe calibration, data reduction, and uncertainty analysis
[NASA-TM-106458] p 38 N95-12378

SAR image registration in absolute coordinates using GPS carrier phase position and velocity information
[DE94-018738] p 228 N95-20195

Using digital filtering techniques as an aid in wind turbine data analysis
[DE94-011862] p 357 N95-24853

Artificial intelligence techniques for flight test planning, phase 1
[AD-A293962] p 608 N95-31525

DATA RETRIEVAL

HLLV avionics requirements study and electronic filing system database development
[NASA-CR-193993] p 49 N95-13027

DATA SMOOTHING

New methods, new methodology: Advanced CFD in the Snecma turbomachinery design process
p 90 N95-14134

A brief survey of constrained mechanics and variational problems in terms of differential forms
p 360 N95-25803

DATA STORAGE

Holographic interferometric tomography for reconstructing flow fields
p 310 N95-23287

AVIRIS and TIMS data processing and distribution at the land processes distributed active archive center
p 325 N95-23872

DATA STRUCTURES

Determination of piloting feedback structures for an altitude tracking task
[BTN-95-EIX95242670770] p 327 A95-81077

Matching fluid and structure meshes for aeroelastic computations: a parallel approach
[BTN-95-EIX95302679864] p 636 A95-94102

Knowledge-based processing for aircraft flight control
[NASA-CR-194976] p 99 N95-13727

Computing methods for the approximate solution of time dependent problems
[AD-A286007] p 256 N95-20719

DATA SYSTEMS

Development of an Automated Nondestructive Inspection (ANDI) system for commercial aircraft, phase 1
[AD-A283500] p 40 N95-12623

DATA TRANSFER (COMPUTERS)

AVIRIS and TIMS data processing and distribution at the land processes distributed active archive center
p 325 N95-23872

STEP: A future revision, today
[NONP-NASA-VT-95-49121] p 452 N95-27209

DATA TRANSMISSION

Flight Test Monitoring System using X-window
p 500 A95-91574

Electromagnetic compatibility effects of advanced packaging configurations
p 247 N95-20658

DC 10 AIRCRAFT

The crash of Flight 232
[NASA-TM-104279] p 11 N95-10737

DC 8 AIRCRAFT

Aircraft wake vortex takeoff tests at O'Hara International Airport
[AD-A283828] p 118 N95-18624

Fuselage burnthrough from large exterior fuel fires
[AD-A286295] p 226 N95-22318

Investigation of wing upper surface flow-field disturbance due to NASA DC-8-72 in-flight inboard thrust-reverser deployment
[NASA-TM-110351] p 457 N95-28816

DC 9 AIRCRAFT

Users guide for NASA Lewis Research Center DC-9 Reduced-Gravity Aircraft Program
[NASA-TM-106755] p 146 N95-18586

DEACTIVATION

Recommendation on transition from primary/secondary radar to secondary-only radar capability
[AD-A286279] p 249 N95-22005

DEAD RECKONING

Event correlation for networked simulators
[BTN-95-EIX0619952748168] p 625 A95-94462

DEATH VALLEY (CA)

Integration of AIRSAR and AVIRIS data for Trail Canyon alluvial fan, Death Valley, California
p 709 N95-33760

DEBONDING (MATERIALS)

A method for disbond detection in thermal tomography by domain decomposition technique
p 545 A95-88955

Inspecting for widespread fatigue damage: Is partial debonding the key?
p 93 N95-14458

Evaluation of patch effectiveness in repairing aircraft components
p 394 N95-27513

Composite repair issues on the CF-18 aircraft
p 395 N95-27518

DEBRIS

Gas path debris monitoring
[CONGRESS PAPER C428-15-031] p 508 A95-91710

Rolling bearing failure and wear debris detection
[CONGRESS PAPER C428-15-094] p 457 A95-91711

Developments in wear particle analysis using computerised procedures
[CONGRESS PAPER C428-15-216] p 457 A95-91713

Scandinavian Airlines Systems experience on erosion, corrosion and foreign object damage effects on gas turbines
p 198 N95-19659

Quantity-distance requirements for earth-bermed aircraft shelters
[AD-A279692] p 341 N95-24424

DECATRIC WAVES

Electromagnetic backscattering from a helicopter rotor in the decametric wave band regime
[BTN-94-EIX94381353130] p 243 A95-72648

DECLERATION

Primary and secondary vortex structures over accelerated-decelerated airfoils at high angles of attack
[SAE PAPER 931368] p 586 A95-93649

Rapid deceleration mode evaluation
p 696 N95-33018

DECISION MAKING

Output feedback control under randomly varying distributed delays
[BTN-94-EIX94511433916] p 168 A95-64582

Real-time decision aiding: Aircraft guidance for wind shear avoidance
[BTN-95-EIX95202637575] p 332 A95-78583

Developing and testing decision-making products for center weather service unit meteorologists
p 671 A95-93533

Cooperative problem solving between airline operations control and ATC traffic flow management
p 681 A95-95066

Risk analysis for the fire safety of airline passengers
[PB94-194065] p 77 N95-14179

On-line handling of air traffic: Management, guidance and control
[AGARD-AG-321] p 126 N95-18927

Strategy in the commercial aircraft industry in the United States: A comparison of decisionmaking by McDonnell-Douglas and Boeing aircraft companies from 1977-1983
[AD-A288289] p 366 N95-26409

Community relations plan: Galena Airport and Camp ion Air Force Station, Alaska
[AD-A286722] p 446 N95-27234

Report to the Chairman, Subcommittee on Aviation, Committee on Commerce, Science, and Transportation, US Senate. Aviation safety: Data problems threaten FAA strides on safety analysis system
[GAO/AIMD-95-27] p 687 N95-32705

DECISION THEORY

Classification of ultra high range resolution radar using decision boundary analysis
[AD-A289378] p 437 N95-26877

DECODING

Towards improving the NMC aircraft data base
p 660 A95-93480

DECOMPOSITION

Single-pass method for the solution of inverse potential and rotational problems. Part 1: 2-D and quasi 3-D theory and application
p 107 N95-16563

DECOUPLING

Nonlinear decoupling control study for aircraft maneuvering flight
[HTN-95-71130] p 408 A95-83491

An investigation of the effects of pitch-roll (de)coupling on helicopter handling qualities
[NASA-TM-110349] p 409 N95-26773

New adaptive methods for reconfigurable flight control systems, appendix 1
[AD-A292711] p 619 N95-30937

DEFECTS

Verification of the damage tolerance of a fighter aircraft
p 388 A95-85897

Damage tolerance capability
p 388 A95-85898

Aircraft gear train diagnostics using the irregular rotation of the external shafts
[CONGRESS PAPER C428-15-097] p 508 A95-91712

Performance deterioration of axial compressors due to blade defects
p 199 N95-19665

New nondestructive techniques for the detection and quantification of corrosion in aircraft structures
p 315 N95-23512

Dynamics of phase ordering of nematics in a pore
[DE95-607662] p 362 N95-25978

DEFENSE INDUSTRY

Surviving the peace. Lessons learned from the aircraft industry in the 1920s and 1930s
[AD-A288284] p 366 N95-26455

DEFENSE PROGRAM

Air Force seal activities
p 60 N95-13600

Assessing aircraft survivability to high frequency transient threats
[AD-A283999] p 134 N95-18726

Environmental Compliance Assessment and Management Program
[AD-A279605] p 255 N95-20441

Report to the Secretary of Defense. Unmanned aerial vehicles: No more Hunter systems should be bought until problems are fixed
[GAO/NSIAD-95-52] p 286 N95-24091

An integrated GPS/INS/BARO and radar altimeter system for aircraft precision approach landings
[AD-A289280] p 383 N95-26985

Unmanned aerial vehicles, 1994 master plan
[AD-A291628] p 398 N95-28411

Mode of human image representation and error checking strategies in complex visual displays
[AD-A290107] p 485 N95-29210

Unmanned aerial vehicles, 1994 master plan
p 607 N95-31416

DEFLAGRATION

Preliminary assessment of combustion modes for internal combustion wave rotors
[NASA-TM-107000] p 616 N95-30632

DEFLECTION

Aeroelastic stability of hingeless rotor blade in hover using large deflection theory
[BTN-94-EIX94441386616] p 183 A95-67347

Aeroelastic stability of hingeless rotor blade in hover using large deflection theory
[HTN-95-20952] p 546 A95-88991

Flight dynamics of an unmanned aerial vehicle
[AD-A282259] p 45 N95-12410

Evaluation of an unlighted swinging airport sign
[AD-A284763] p 146 N95-18087

Determination of stores pointing error due to wing flexibility under flight load
[NASA-TM-4646] p 134 N95-19044

Estimating wind tunnel interference due to vectored jet flows
p 164 N95-19265

A non-iterative grid deformation algorithm for computational fluid dynamics for aeroelasticity
[AD-A288298] p 436 N95-26418

DEFORMATION

Modelling of pilowing due to corrosion in fuselage lap joints
[BTN-95-EIX95082502227] p 240 A95-71024

Dynamic analysis of bearingless tail rotor blades based on nonlinear shell modes
[BTN-95-EIX95125282338] p 281 A95-73540

Static aeroelastic characteristics of a composite wing
[BTN-95-EIX95152582340] p 282 A95-73542

Experimental investigation of thermoelastic deformation in turbojet-engine bearings under maintenance inspection
[BTN-95-EIX95292721173] p 546 A95-89904

Prediction of rotor-blade deformations due to unsteady airloads
[AD-A286593] p 231 N95-20860

Analysis of warping effects on the static and dynamic response of a seat-type structure
[NIAR-94-12] p 348 N95-24211

Residual Stress Measurements with Laser Speckle Correlation Interferometry and Local Heat Treating
[DE95-060082] p 349 N95-24598

A non-iterative grid deformation algorithm for computational fluid dynamics for aeroelasticity
[AD-A288298] p 436 N95-26418

Near-limit drop deformation and secondary breakup
p 704 N95-32902

Analysis and design methodology for chordwise deformable wings
p 692 N95-33311

Grid generation around airfoil with a flap using boundary element method
p 686 N95-34552

DEGRADATION

Control mechanism to prevent correlated message arrivals from degrading signaling no. 7 network performance
[BTN-94-EIX94341342286] p 56 A95-60842

Life evaluation of a low power arcjet thruster
p 403 A95-82337

Environmental effects on composite airframes: A study conducted for the ARM UAV Program (Atmospheric Radiation Measurement Unmanned Aerospace Vehicle)
[DE94-015351] p 206 N95-19579

Protective coatings for compressor gas path components
p 201 N95-19675

Multilayer anti-erosion coatings
p 201 N95-19679

Evolution of oxidation and creep damage mechanisms in HiPep silicon nitride materials
[DE95-001360] p 300 N95-22689

Non-destructive detection of corrosion for life management
p 314 N95-23505

In-situ detection of surface passivation or activation and of localized corrosion: Experiences and perspectives in aircraft
p 302 N95-23508

Oklahoma City air logistics center (USAF) aging aircraft corrosion program
p 262 N95-23519

Probabilistic material strength degradation model for Inconel 718 components subjected to high temperature, high-cycle and low-cycle mechanical fatigue, creep and thermal fatigue effects
[NASA-CR-197832] p 419 N95-27167

The effect of interface properties on nickel base alloy composites
[NASA-CR-198363] p 629 N95-30787

Environmentally regulated aerospace coatings
p 631 N95-31775

DEGREES OF FREEDOM

On the dynamics of aeroelastic oscillators with one degree of freedom
[BTN-94-EIX94501431527] p 153 A95-64524

Aerodynamic mechanism of galloping
[BTN-94-EIX94371347709] p 219 A95-69968

High-order state space simulation models of helicopter flight mechanics
[HTN-95-A0494] p 237 A95-72565

Functional dependence of trajectory dispersion on initial condition errors
[BTN-95-EIX95152583263] p 298 A95-73564

Improving prediction: The incorporation of simplified rotor dynamics in a mathematical model of the bell 412HP
[BTN-95-EIX95152584679] p 282 A95-73591

Identification of higher order helicopter dynamics using linear modeling methods
[HTN-95-80851] p 290 A95-75093

Equivalent beam-column analysis of guyed towers
[BTN-95-EIX95262696644] p 435 A95-85519

Low-speed wind tunnel testing of the NPS and NASA Ames Mach 6 optimized waverider
[AD-A283585] p 75 N95-15319

FP-CAS2D user's guide, version 1.0
[NASA-CR-195413] p 156 N95-16588

Six degree of freedom flight dynamic and performance simulation of a remotely-piloted vehicle
[AERC-TN-9301] p 131 N95-18097

Application of photogrammetry of F-14D store separation
[AD-A284154] p 132 N95-18417

Aeroelastic stability of wind turbine blade/aileron systems
p 377 N95-27981

Dynamical systems as models for flow-induced vibrations
[PB95-206991] p 647 N95-30956

DEICERS

Effect of curvature in the numerical simulation of an electrothermal de-icer pad
[BTN-95-EIX95182619219] p 276 A95-76645

NASA evaluation of Type 2 chemical depositions — effects of deicer deposition on aircraft tire friction performance
[SAE PAPER 932582] p 495 A95-90086

User's manual for the NASA Lewis ice accretion/heat transfer prediction code with electrothermal deicer input
[NASA-CR-4530] p 57 N95-11888

Development of anti-icing technology
[PB94-195369] p 78 N95-15439

An analysis of B-1B exterior jet blast windshield anti-icing performance using pre-cooled compressor bleed air
[AD-A292522] p 485 N95-28811

DEICING

Effect of curvature in the numerical simulation of an electrothermal de-icer pad
[BTN-95-EIX95182619219] p 276 A95-76645

Preliminary results of high resolution measurements of snowfall at Stapleton International Airport during the winter of 1992-93
p 661 A95-93484

ASRS problems involving air carrier ground deicing/anti-icing
p 611 A95-95194

User's manual for the NASA Lewis ice accretion/heat transfer prediction code with electrothermal deicer input
[NASA-CR-4530] p 57 N95-11888

Icing: Accretion, detection, protection
p 77 N95-14897

Replicator for characterization of cirrus and polar stratospheric cloud particles
[NASA-CR-197785] p 445 N95-26669

An analysis of B-1B exterior jet blast windshield anti-icing performance using pre-cooled compressor bleed air
[AD-A292522] p 485 N95-28811

User's manual for the improved NASA Lewis ice accretion code LEWICE 1.6
[NASA-CR-198355] p 485 N95-29132

DELAMINATING

Experience of aircraft manufacturer for paint removal using dry stripping method
p 456 A95-91501

Composite repair issues on the CF-18 aircraft
p 395 N95-27518

Repair technology for thermoplastic aircraft structures
p 395 N95-27519

Through-the Thickness(R) braided composites for aircraft applications
p 421 N95-28273

Analysis of composite structures with delaminations under combined bending and compression
p 422 N95-28429

Fundamental concepts in the suppression of delamination buckling by stitching
p 426 N95-28486

DELAY

Control mechanism to prevent correlated message arrivals from degrading signaling no. 7 network performance
[BTN-94-EIX94341342286] p 56 A95-60842

Assessment of the benefits for improved terminal weather information
p 673 A95-93540

Transport delays associated with NASA Langley Flight Simulation Facility
[NASA-TM-110150] p 568 N95-29454

Analysis and modeling of an airport departure process
[AD-A293782] p 602 N95-31581

DELMARVA PENINSULA (DE-MD-VA)

Identification of aviation weather hazards based on the integration of radar and lightning data
[HTN-95-51323] p 356 A95-80908

DELPHI METHOD (FORECASTING)

Aero-optics system integration
[TABES PAPER 94-604] p 100 N95-14638

DELTA LAUNCH VEHICLE

A new guidance and flight control system for the DELTA 2 launch vehicle — Abstract only
p 342 A95-80427

DELTA WINGS

Aspects of vortex breakdown
[HTN-95-A0001] p 183 A95-67828

Adaptive computations of flow around a delta wing with vortex breakdown
[BTN-94-EIX94441386631] p 184 A95-68180

Experimental investigations on limit cycle wing rock of slender wings
[BTN-95-EIX95062487543] p 185 A95-68357

Numerical simulation of incidence and sweep effects on delta wing vortex breakdown
[BTN-95-EIX95062487526] p 186 A95-69234

Effects of spatial order of accuracy on the computation of vortical flowfields
[HTN-95-EIX95152577604] p 305 A95-73479

Unstructured grid solutions to a wing/pylon/store configuration
[BTN-95-EIX95152582322] p 265 A95-73525

Navier-Stokes prediction of large-amplitude delta-wing roll oscillations
[BTN-95-EIX95152582329] p 281 A95-73531

Further analysis of high-rate rolling experiments of a 65-deg delta wing
[BTN-95-EIX95152582331] p 281 A95-73533

Analytic prediction of lift for delta wings with partial leading-edge thrust
[BTN-95-EIX95152582345] p 266 A95-73547

Effect of leeward flow dividers on the wing rock of a delta wing
[BTN-95-EIX95152582347] p 282 A95-73549

Wing vertical position effects on wing-body carryover for noncircular missiles
[BTN-95-EIX95182617462] p 268 A95-75733

Transient structure of vortex breakdown on a delta wing
[BTN-95-EIX95182619073] p 268 A95-75758

Natural laminar flow wing concept for supersonic transports
[BTN-95-EIX95182619226] p 308 A95-76652

Direct adaptive and neural control of wing-rock motion of slender delta wings
[BTN-95-EIX95242670748] p 327 A95-81099

Measurements of vortex pair interaction with a clean or contaminated free surface
[BTN-94-EIX950114410663] p 429 A95-82798

Crossflow topology of vortical flows
[HTN-95-51664] p 432 A95-85046

Compressible inviscid vortex flow of a sharp edge delta wing
[BTN-95-EIX95262694308] p 370 A95-85479

Effects of spatial order of accuracy on the computation of vortical flowfields
[HTN-95-42589] p 459 A95-87219

Aerodynamics of delta wings with application to high-alpha flight mechanics
p 460 A95-87395

Real time for the calculation of the aerodynamic of aircrafts with delta wings
p 460 A95-87399

Low-speed aerodynamic characteristics of a slender wing with vertical fins
p 460 A95-87400

Experimental investigation of hypersonic flow over a wing-body combination
[AIAA PAPER 95-6083] p 460 A95-87412

Simple numerical criterion for vortex breakdown
[HTN-95-61210] p 541 A95-87583

Effects of periodic spanwise blowing on Delta-wing configuration characteristics
[HTN-95-81631] p 461 A95-87679

Dynamic pitch-up of a delta wing
[HTN-95-81633] p 462 A95-87681

Effects of trailing-edge jet entrainment on delta wing vortices
[HTN-95-81644] p 542 A95-87692

Adaptive computations of flow around a delta wing with vortex breakdown
[HTN-95-20948] p 465 A95-88987

Application of artificial neural networks in nonlinear aerodynamics and aircraft design
[SAE PAPER 932533] p 492 A95-89193

The effect of wing sweep back upon transition in hypersonic flow
[AIAA PAPER 95-6090] p 466 A95-89199

Criteria for location of vortex breakdown over delta wings
[HTN-95-01092] p 468 A95-90278

Unsteady aerodynamic effects of trailing edge controls on delta wings
[HTN-95-01099] p 469 A95-90285

Computation of vortex formation over ELAC-1 configuration using vorticity confinement
[AIAA PAPER 95-6157] p 470 A95-90469

Buffering tests in a cryogenic windtunnel
[HTN-95-92833] p 470 A95-90751

Numerical investigation of high incidence flow over a double-delta wing
[BTN-95-EIX0619952748160] p 588 A95-94454

Flow physics of critical states for rolling delta wings
[BTN-95-EIX0619952748180] p 590 A95-94473

Computation of vortex breakdown on a rolling delta wing
[BTN-95-EIX0619952748195] p 591 A95-94484

Navier-Stokes simulation of turbulent vortex high-Re-number flows over a delta wing
p 644 A95-95507

Effect of leading- and trailing-edge flaps on clipped delta wings with and without wing camber at supersonic speeds
[NASA-TM-4542] p 5 N95-10028

Design and construction of a remote piloted flying wing
[NASA-CR-197195] p 47 N95-12695

Experimental aerodynamic characteristics of a generic hypersonic accelerator configuration at Mach numbers 1.5 and 2.0 — conducted in the Langley Unitary Plan Wind Tunnel
[NASA-TM-4413] p 39 N95-12770

A selection of experimental test cases for the validation of CFD codes, volume 1
[AGARD-AR-303-VOL-1] p 91 N95-14201

Numerical simulation of transient vortex breakdown above a pitching delta wing
[AD-A281075] p 107 N95-16808

Transonic Navier-Stokes calculations about a 65 deg delta wing
[NASA-CR-4635] p 108 N95-17273

Detailed study at supersonic speeds of the flow around delta wings
p 112 N95-17861

Wind tunnel test on a 65 deg delta wing with a sharp or rounded leading edge: The international vortex flow experiment
p 114 N95-17872

Delta-wing model
p 114 N95-17873

Experimental investigation of the vortex flow over a 76/60-deg double delta wing
p 114 N95-17874

- Wind tunnel test on a 65 deg delta wing with rounded leading edges: The International Vortex Flow Experiment p 114 N95-17875
- STOVL CFD model test case p 115 N95-17881
- Overview of unsteady transonic wind tunnel test on a semispan straked delta wing oscillating in pitch [AD-A284097] p 117 N95-18380
- Aeromechanics technology, volume 1. Task 1: Three-dimensional Euler/Navier-Stokes Aerodynamic Method (TEAM) enhancements [AD-A285713] p 132 N95-18483
- Interaction, bursting and control of vortices of a cropped double-delta wing at high angle of attack [AD-A283656] p 119 N95-18669
- The utilization of a high speed reflective visualization system in the study of transonic flow over a delta wing p 121 N95-19259
- Velocity measurements with hot-wires in a vortex-dominated flowfield p 121 N95-19261
- Effect of juncture fillets on double-delta wings undergoing sideslip at high angles of attack [AD-A286165] p 232 N95-22039
- A study of the vortex flow over 76/40-deg double-delta wing [NASA-CR-195032] p 314 N95-23466
- Low speed aerodynamic characteristics of delta wings with vortex flaps: 60 deg and 70 deg delta wings [NAL-TR-1245] p 331 N95-25105
- Navier-Stokes solution of wing wake structure and its perturbation p 479 N95-29121
- A numerical method for modelling wings with sharp edges maneuvering at high angles of attack p 503 N95-29122
- Numerical investigation into vortical flow about a delta-wing configuration up to incidences at which vortex breakdown occurs in experiment [PB95-198024] p 593 N95-30837
- Unsteady transonic wind tunnel test on a semispan straked delta wing, oscillating in pitch. Part 1: Description of the model, test setup, data acquisition, and data processing [AD-A293113] p 593 N95-30885
- Calculation for aerodynamic characteristics on delta wing with leading-edge separated vortex effect using boundary element method p 684 N95-34524
- Sidewall-effect of the wind tunnel on the estimation of the aerodynamic characteristics of a delta wing p 685 N95-34525
- DENSIFICATION**
- Ceramic composite combustor cans for expendable turbine engines [AD-A289551] p 407 N95-28646
- DENSITY (MASS/VOLUME)**
- Differencing of density in compressible flow for a pressure-based approach [HTN-95-42349] p 373 N95-86178
- Effect of density gradients in confined supersonic shear layers, part 1 [NASA-CR-198029] p 348 N95-24412
- Effect of density gradients in confined supersonic shear layers. Part 2: 3-D modes [NASA-CR-198030] p 349 N95-24413
- DENSITY DISTRIBUTION**
- Practical formulation of a positively conservative scheme [HTN-95-51668] p 433 N95-85050
- Response of a thin airfoil encountering a strong density discontinuity p 462 N95-88900
- Lee waves benign and malignant p 595 N95-93554
- Aerodynamic characteristics of the orbital reentry vehicle experimental probe fins in a supersonic flow [NAL-TR-1232] p 342 N95-25664
- DENSITY MEASUREMENT**
- Planar air density measurements near model surfaces by ultraviolet Rayleigh/Raman scattering [BTN-94-EIX94441386614] p 213 N95-67345
- Measurement by coherent anti-Stokes Raman scattering in the R5Ch hypersonic wind tunnel [BTN-95-EIX95112523811] p 188 N95-69322
- Planar air density measurements near model surfaces by ultraviolet Rayleigh/Raman scattering [HTN-95-20950] p 546 N95-88989
- DEPENDENT VARIABLES**
- Single-pass method for the solution of inverse potential and rotational problems. Part 2: Fully 3-D potential theory and applications p 107 N95-16564
- DEPLOYMENT**
- EURECA mission control experience and messages for the future p 149 N95-17252
- High strain-rate testing of parachute materials [DE95-009577] p 648 N95-31614
- DEPOLARIZATION**
- Depolarizing trihedral corner reflectors for radar navigation and remote sensing [BTN-95-EIX95302727634] p 636 N95-94108
- DEPOSITION**
- A comparison of some aerodynamic resistance methods using measurements over cotton and grass from the 1991 California ozone deposition experiment [HTN-95-11295] p 319 A95-77000
- NASA evaluation of Type 2 chemical depositions --- effects of deicer deposition on aircraft tire friction performance [SAE PAPER 932582] p 495 A95-90086
- Erosion, Corrosion and Foreign Object Damage Effects in Gas Turbines (AGARD-CP-558) p 197 N95-19653
- Particle deposition in gas turbine blade film cooling holes p 199 N95-19661
- Cu deposition using a permanent magnet electron cyclotron resonance microwave plasma source [DE94-017768] p 304 N95-23981
- DEPOSITS**
- Gas turbine compressor corrosion and erosion in Western Europe [AD-B196178L] p 201 N95-19678
- Mechanism of deposit formation on fuel-wetted hot metal surfaces [AD-A289847] p 426 N95-28621
- DEPTH**
- Evaluation of advanced aerospace materials by depth sensing indentation and scratch methods [BTN-95-EIX95152584678] p 282 A95-73590
- DEPTH MEASUREMENT**
- Evaluation of the Spartan tight-tolerance AXBT [HTN-95-40728] p 251 A95-70473
- DERIVATION**
- Investigation of dynamic inflow's influence on rotor control derivatives p 155 N95-16250
- DESCENT**
- Wind tunnel tests of a 42 inch diameter self-starting autogyro rotor [AD-A279922] p 188 N95-19863
- Effects of cabin pressure on climb and descent rates [ESDU-94040] p 503 N95-29016
- DESCRIPTIVE GEOMETRY**
- Computer-aided light sheet flow visualization using photogrammetry [NASA-TP-3416] p 26 N95-10859
- DESIGN ANALYSIS**
- Foil bearings for gas turbine engines [BTN-94-EIX94461290279] p 82 A95-61732
- Small gas turbines in the 21st century [BTN-94-EIX94461290241] p 82 A95-61736
- Mechanical system reliability and risk assessment [BTN-95-EIX9514253046] p 304 A95-73452
- Efficient sensitivity analysis for rotary-wing aeromechanical problems [BTN-95-EIX95152577585] p 264 A95-73497
- Design constraints in the payload-range diagram of ultrahigh capacity transport airplanes [BTN-95-EIX95152582319] p 276 A95-73522
- Structural acoustic calculations in the low-frequency range [BTN-95-EIX95152582336] p 323 A95-73538
- Aerodynamic design of pegasus: Concept to flight with computational fluid dynamics [BTN-95-EIX95182617463] p 298 A95-75734
- An inverse design method of transonic airfoil and wing [HTN-95-71128] p 385 A95-83489
- Mobile domes for TACTIC telescope p 453 A95-86113
- Design optimization of an airbreathing aerospaceplane p 524 A95-87382
- Integrated thermal and mechanical analysis of hypersonic vehicles by using adaptive finite element methods p 524 A95-87383
- The high enthalpy shock tunnel in Goettingen (HEG) [AD-A283926] p 518 A95-87391
- Design and operation of a supersonic annular flow facility [HTN-95-20941] p 465 A95-88980
- Should large business jets have four under the wing? [SAE 931256] p 493 A95-89223
- A method for calculating mean aerodynamic center and zero-lift moment coefficient of aircraft without tail by using measured flight loads p 474 A95-91552
- The use of structural optimisation within aerospace [CONGRESS PAPER C428-23-008] p 500 A95-91729
- Impact finite element analysis, as an alternative to the testing of windscreens for bird impact [CONGRESS PAPER C428-23-196] p 500 A95-91732
- A design trade study using CFD modeling of reaction jets for aerodynamic control [SAE PAPER 931384] p 586 A95-93660
- A detailed power inverter design for a 250 kW switched reluctance aircraft engine starter/generator [SAE PAPER 931388] p 613 A95-93664
- Detailed design of a 250-kW switched reluctance starter/generator for an aircraft engine [SAE PAPER 931389] p 613 A95-93665
- An educational introduction to transonic compressor stage design principles [SAE PAPER 931393] p 613 A95-93668
- Propulsion simulator for high bypass turbofan performance evaluation [SAE PAPER 931410] p 625 A95-93676
- Lightweight high-temperature fuel metering valves [SAE PAPER 931444] p 635 A95-93693
- A robust inverse inviscid method for airfoil design p 640 A95-95431
- An aerodynamic analysis of a mixed flow turbine [NASA-TM-106674] p 15 N95-10153
- High-Alpha Research Vehicle (HARV) longitudinal controller: Design, analyses, and simulation results [NASA-TP-3446] p 17 N95-10860
- Object-oriented technology for compressor simulation [NASA-TM-106723] p 49 N95-11864
- Triton 2 (1B) p 46 N95-12636
- Optimization of aerospace structures [NASA-CR-196763] p 48 N95-12787
- Methodology for sensitivity analysis, approximate analysis, and design optimization in CFD for multidisciplinary applications [NASA-CR-196981] p 58 N95-13201
- Computational methods for preliminary design and geometry definition in turbomachinery p 89 N95-14128
- The industrial use of CFD in the design of turbomachinery p 90 N95-14133
- The role of CFD in the design process p 90 N95-14135
- Aero design of turbomachinery components: CFD in complex systems p 90 N95-14136
- Building complex simulations rapidly using MATRIX(x): The Space Station redesign [TABES PAPER 94-632] p 87 N95-14653
- Requirements report for SSTO vertical take-off and horizontal landing vehicle [NASA-CR-197029] p 80 N95-14794
- The Aluminum Falcon: A low cost modern commercial transport [NASA-CR-197180] p 81 N95-15742
- Portable parallel stochastic optimization for the design of aeropropulsion components [NASA-CR-195312] p 154 N95-16072
- An improved method of airfoil design p 106 N95-16252
- Small turbojets: Designs and installations p 138 N95-16323
- Rapid solution of large-scale systems of equations p 169 N95-16458
- Matlab as a robust control design tool p 169 N95-16474
- Optimum Design Methods for Aerodynamics [AGARD-R-803] p 127 N95-16562
- Airfoil optimization by the one-shot method p 128 N95-16569
- FPCAS2D user's guide, version 1.0 [NASA-CR-195413] p 156 N95-16588
- Applications of automatic differentiation in CFD [NASA-TM-109948] p 157 N95-16828
- Algorithms for bilevel optimization [NASA-CR-194980] p 170 N95-16897
- Eddy current for detecting second layer cracks under installed fasteners [AD-A282412] p 158 N95-17507
- Conference on Aerospace Transparent Materials and Enclosures. Volume 2: Sessions 5-9 [AD-A283926] p 131 N95-18162
- Microgravity isolation system design: A modern control analysis framework [NASA-TM-106803] p 105 N95-18486
- Strategic avionics technology definition studies. Subtask 3-1A3: Electrical Actuation (ELA) Systems Test Facility [NASA-CR-188360] p 143 N95-18567
- Design limit loads based upon statistical discrete gust methodology p 133 N95-18603
- Conference on Aerospace Transparent Materials and Enclosures, volume 1 [AD-A283925] p 133 N95-18677
- Proceedings of the USAF Structural Integrity Program Conference [AD-A285684] p 194 N95-19517
- Super-heavy aircraft study [AD-A279602] p 238 N95-19955
- Parallel calculation of sensitivity derivatives for aircraft design using automatic differentiation [NASA-TM-110103] p 231 N95-20370
- An evaluation of Automatic Terminal Information Service (ATIS) flight deck display presentation options [AD-A280100] p 228 N95-21020

CALIOPE and TAISIR airborne experiment platform [DE94-018328] p 250 N95-22299

Euler technology assessment for preliminary aircraft design employing OVERFLOW code with multiblock structured-grid method [NASA-CR-4651] p 273 N95-23095

Aerodynamic design optimization with sensitivity analysis and computational fluid dynamics [NASA-CR-197419] p 274 N95-23218

Design of a GaAs/Ge solar array for unmanned aerial vehicles [NASA-TM-106870] p 320 N95-23259

Inner loop flight control for the High-Speed Civil Transport p 293 N95-23314

Enhanced analysis and users manual for radial-inflow turbine conceptual design code RTD [NASA-CR-195454] p 275 N95-23462

Development of a model protection and dynamic response monitoring system for the national transonic facility [NASA-CR-195041] p 340 N95-24388

A crew-centered flight deck design philosophy for High-Speed Civil Transport (HSCT) aircraft [NASA-TM-109171] p 335 N95-24582

Long endurance stratospheric solar powered airship [PB95-178729] p 336 N95-26009

A design perspective on thermal barrier coatings p 344 N95-26120

Supersonic transport grid generation, validation, and optimization [NASA-CR-197752] p 448 N95-26648

CFD research, parallel computation and aerodynamic optimization [NASA-CR-197748] p 373 N95-26649

Design and testing of low sonic boom configurations and an oblique all-wing supersonic transport [NASA-CR-197744] p 389 N95-26651

Preliminary design problems and solutions for a supersonic oblique all-wing transport aircraft p 390 N95-26942

An exploratory application of neural networks for airfoil design p 448 N95-26943

A verification procedure for MSC/NASTRAN Finite Element Models [NASA-CR-4675] p 392 N95-27371

Wind-tunnel test of the S814 thick root airfoil [DE95-000268] p 376 N95-27541

Vibration analysis of a split path gearbox [NASA-TM-106875] p 438 N95-27855

Use of blade pitch control to provide power train damping for the Mod-2, 2.5-mW wind turbine p 440 N95-27986

Variable speed generator application on the MOD-5A 7.3 mW wind turbine generator p 440 N95-27989

Advanced interactive display formats for terminal area traffic control [NASA-CR-198576] p 384 N95-28188

Performance study for inlet installations [NASA-CR-189714] p 406 N95-28227

Unique considerations in the design and experimental evaluation of tailored wings with elastically produced chordwise camber p 423 N95-28436

C-130 Advanced Technology Center wing box conceptual design/cost study p 423 N95-28437

Probabilistic design of advanced composite structure p 424 N95-28443

Nonlinear dynamics and aeroelasticity of rotorcraft in forward flight [AD-A291714] p 400 N95-28504

Grid generation and surface modeling for CFD p 551 N95-28726

Rapid Airplane Parametric Input Design (RAPID) p 501 N95-28730

A grid generation system for multi-disciplinary design optimization p 567 N95-28763

An efficiency study of the simultaneous analysis and design of structures [NASA-TM-110168] p 501 N95-28820

Dimensional stability of curved panels with co-cured stiffeners and cobonded frames p 532 N95-28836

Design, analysis, and fabrication of a pressure box test fixture for tension damage tolerance testing of curved fuselage panels p 533 N95-28839

Global cost and weight evaluation of fuselage keel design concepts p 501 N95-28840

Design and evaluation of a foam-filled hat-stiffened panel concept for aircraft primary structural applications p 502 N95-28841

Influence of tooth profile modification on spur gear dynamic tooth strain [NASA-TM-106952] p 553 N95-29112

Application of optimization technique to control system design for departure prevention and aircraft model estimation through dynamic inversion p 517 N95-29156

Computational algorithms for aerodynamic analysis and design [AD-A291084] p 482 N95-29972

Design, analysis and control of large transports so that control of engine thrust can be used as a back-up of the primary flight controls [NASA-CR-198958] p 518 N95-30254

A novel instrumentation system for measurement of helicopter rotor motions and loads data, phase 1 [AD-A293309] p 607 N95-30923

A time stepping coupled finite element-state space modeling environment for synchronous machine performance and design analysis in the ABC frame of reference p 649 N95-31948

Control law design using H-infinity and mu-synthesis short-period controller for a tail-airplane p 622 N95-31999

Sea wave parameters, small altitudes and distances measurers design for movement control systems of ships, wing-in-surface effect crafts and seaplanes p 708 N95-33141

DESIGN TO COST

The FC-1D: The profitable alternative Flying Circus Commercial Aviation Group [NASA-CR-197152] p 46 N95-12628

The OFP-6M transport jet [NASA-CR-197159] p 46 N95-12637

The effects of design details on cost and weight of fuselage structures p 501 N95-28831

DESULFURIZING

Effect of annealing and desulfurization on oxide spallation of turbine airfoil material [BTN-95-EIX95282707024] p 528 N95-88264

DETECTION

Use of high resolution lightning detection and localization sensors for hazardous aviation weather nowcasting p 661 N95-93486

Analysis of en route controller hazardous weather-related tasks p 665 N95-93503

An evaluation of clear-air turbulence indices p 674 N95-93548

The development of an aircraft icing forecast technique using data from maps p 675 N95-93549

Electrochemical impedance pattern recognition for detection of hidden chemical corrosion on aircraft components [AD-A285998] p 241 N95-20716

Evaluation of neutron techniques for illicit substance detection [DE95-002988] p 300 N95-22764

Health and usage monitoring systems: Corrosion surveillance p 262 N95-23506

In-situ detection of surface passivation or activation and of localized corrosion: Experiences and perspectives in aircraft p 302 N95-23508

New nondestructive techniques for the detection and quantification of corrosion in aircraft structures p 315 N95-23512

Corrosion detection and monitoring of aircraft structures: An overview p 303 N95-23515

Experience of in-service corrosion on military aircraft p 303 N95-23516

The use of electrochemistry and ellipsometry for identifying and evaluating corrosion on aircraft [AD-A290249] p 504 N95-29426

Investigation and characterization of SEU effects and hardening strategies in avionics [AD-A291058] p 509 N95-29950

Low-level data fusion for landing runways detection p 689 N95-33136

Gas chromatography/ion mobility spectrometry as a hyphenated technique for improved explosives detection and analysis p 701 N95-33278

DETERIORATION

Ten-year ground exposure of composite materials used on the Bell Model 206L helicopter flight service program [NASA-TP-3468] p 55 N95-12357

Problems with aging wiring in Naval aircraft p 154 N95-16048

Non-destructive detection of corrosion for life management p 314 N95-23505

An analysis of the impact of ASPA on organizational and depot level maintenance [AD-A292670] p 457 N95-29414

DETONABLE GAS MIXTURES

Investigation of starting and ignition transients in the thermally choked ram accelerator p 698 N95-34805

DETONATION

Determination of minimum fuel octane number piston aircraft engines [SAE PAPER 931230] p 528 N95-88961

Investigation of starting and ignition transients in the thermally choked ram accelerator p 698 N95-34805

DEUTERIUM FLUORIDES

Matrix isolated HF: the high-resolution infrared spectrum of a cryogenically solvated hindered rotor [GTN-95-0301010494002231-16] p 578 N95-92210

DEW POINT

Stratus' tephigram as a training/forecasting tool p 657 N95-93465

DHC 2 AIRCRAFT

A SIMULINK environment for flight dynamics and control analysis: Application to the DHC-2 Beaver. Part 1: Implementation of a model library in SIMULINK. Part 2: Nonlinear analysis of the Beaver autopilot [NONP-NASA-SUPPL-DK-94-2802] p 84 N95-14815

DIAGNOSIS

Condition monitoring and diagnostics [BTN-95-EIX95182617811] p 261 N95-75756

Condition monitoring and diagnostics [HTN-95-92312] p 387 N95-85356

Developments in laser-based diagnostics for wind tunnels in the Aeromechanics Division: 1987-1992 [AD-A283011] p 84 N95-13687

DIAMETERS

Vortex cutting by a blade. Part II: Computations of vortex response [BTN-94-EIX94441386611] p 208 N95-67342

Permanent magnet electron cyclotron resonance plasma source with remote window [BTN-95-EIX95242674338] p 450 N95-82176

DIAMINES

Thermally stable organic polymers [AD-A281380] p 87 N95-14363

DIELECTRICS

Reliability assessment of Multichip Module technologies via the Triservice/NASA RELTECH program p 245 N95-20643

Development of LaRC (TM): IA thermoplastic polyimide coated aerospace wiring [NASA-CR-195048] p 537 N95-30252

DIESEL ENGINES

On profiling a cam of an axial aviation diesel engine by periodic splines [BTN-94-EIX94461407946] p 82 N95-62264

TKKMOD: A computer simulation program for an integrated wind diesel system. Version 1.0: Document and user guide [PB94-179090] p 60 N95-11798

Thermal Barrier Coating Workshop [NASA-CP-10170] p 344 N95-26119

Thermal barrier coatings application in diesel engines p 345 N95-26124

Air/fuel ratio visualization in a diesel spray p 556 N95-29807

DIESEL FUELS

Advanced diesel electronic fuel injection and turbocharging [AD-A279176] p 211 N95-19809

Air/fuel ratio visualization in a diesel spray p 556 N95-29807

DIFFERENCE EQUATIONS

Computation of transonic flow on composite overlapping grids in 2 D [PB95-131348] p 248 N95-21132

DIFFERENTIAL EQUATIONS

Discrete shape sensitivity equations for aerodynamic problems [BTN-94-EIX94451393721] p 88 N95-61720

Solution-adaptive structured-unstructured grid method for unsteady turbomachinery analysis. Part I: Methodology [BTN-94-EIX94441380983] p 208 N95-67329

Three-dimensional structure of a supersonic jet impinging on an inclined plate [BTN-95-EIX95152583259] p 267 N95-73560

Trajectory optimization using parallel shooting method on parallel computer [BTN-95-EIX95282706670] p 564 N95-88175

Computational aerodynamics based on the Euler equations [AGARD-AG-325] p 72 N95-14264

Single-pass method for the solution of inverse potential and rotational problems. Part 2: Fully 3-D potential theory and applications p 107 N95-16564

Optimum aerodynamic design via boundary control p 127 N95-16565

Computation of transonic flow on composite overlapping grids in 2 D [PB95-131348] p 248 N95-21132

Aerodynamic parameter estimation via Fourier modulating function techniques [NASA-CR-4654] p 335 N95-24630

Development of a linearized unsteady Euler analysis for turbomachinery blade rows [NASA-CR-4677] p 592 N95-30611

Multigrad convergence acceleration for the 2D Euler equations applied to high-lift systems [PB95-198081] p 593 N95-30814

DIFFERENTIAL GEOMETRY

Single-pass method for the solution of inverse potential and rotational problems. Part 1: 2-D and quasi 3-D theory and application p 107 N95-16563

DIFFERENTIAL PRESSURE

Hydraulic system diagnostic sensors [BTN-95-EIX95031502752] p 209 A95-68259
 Pressure measurements on an F/A-18 twin vertical tail in buffeting flow. Volume 4, part 2: Buffet cross spectral densities [AD-A285555] p 143 N95-18641
 Effects of cabin pressure on climb and descent rates [ESDU-94040] p 503 N95-29016

DIFFERENTIATION

An introduction to generalized functions with some applications in aerodynamics and aeroacoustics p 565 A95-88895

DIFFRACTION

Compressibility effects on and control of dynamic stall of oscillating airfoil [AD-A291804] p 480 N95-29428

DIFFUSERS

A full Navier-Stokes analysis of subsonic diffuser of a bifurcated 70/30 supersonic inlet for high speed civil transport application [NASA-TM-106637] p 8 N95-10820
 Large-eddy simulation of flow through a plane, asymmetric diffuser p 250 N95-22449

DIFFUSION

Forming and bonding techniques for high-strength aluminum alloys [HTN-95-20605] p 418 A95-84786
 Discretization of the parabolised Navier-Stokes equations p 638 A95-95362
 Viscous flow simulation using the discrete vortex diffusion velocity method p 639 A95-95421
 Agglomeration multigrid for viscous turbulent flows [AD-A284064] p 8 N95-10848

DIFFUSION FLAMES

Prediction of NO(x) emission index of turbulent diffusion flame p 538 A95-87195
 Theories of turbulent combustion in high speed flows [AD-A280933] p 23 N95-10535
 Studies on high pressure and unsteady flame phenomena [AD-A284126] p 152 N95-18410

DIGITAL COMMAND SYSTEMS

Advanced flight computer. Special study [NASA-CR-198165] p 449 N95-27246

DIGITAL COMPUTERS

Formal design and verification of a reliable computing platform for real-time control (phase 3 results) [NASA-TM-109140] p 33 N95-10873
 A PC-based interactive simulation of the F-111C Pave Tack system and related sensor, avionics and aircraft aspects [AD-A285500] p 129 N95-16969

DIGITAL DATA

Certification of windshear performance with RTCA class D radomes p 41 N95-13206
 Using digital filtering techniques as an aid in wind turbine data analysis [DE94-011862] p 357 N95-24853

DIGITAL ELECTRONICS

Calculation of control laws for the digital fuel control unit of a small thrust turbojet [SAE PAPER 931411] p 614 A95-93677
 Formal design and verification of a reliable computing platform for real-time control (phase 3 results) [NASA-TM-109140] p 33 N95-10873
 Advanced Packaging Concepts for Digital Avionics [AGARD-CP-562] p 233 N95-20631
 High density monolithic packaging technology for digital/microwave avionics p 240 N95-20646
 Modular supplies for a distributed architecture — avionics packaging p 234 N95-20657
 Advanced flight computer. Special study [NASA-CR-198165] p 449 N95-27246

DIGITAL FILTERS

Precise navigation using adaptive FIR filtering and time domain spectral estimation [BTN-95-EIX95142555485] p 227 A95-72888
 Using digital filtering techniques as an aid in wind turbine data analysis [DE94-011862] p 357 N95-24853
 Analysis and simulation of narrowband GPS jamming using digital excision temporal filtering [AD-A289328] p 383 N95-26898

DIGITAL NAVIGATION

Precise navigation using adaptive FIR filtering and time domain spectral estimation [BTN-95-EIX95142555485] p 227 A95-72888
 Interfacing a digital compass to a remote-controlled helicopter [PB95-164927] p 340 N95-24260

DIGITAL SIMULATION

Design of a real-time wind turbine simulator using a custom parallel architecture p 449 N95-27979
 Parallel block implicit integration technique for trajectory parallelism [AD-A288961] p 450 N95-28335
 Digital simulation of wind velocities for wind turbine rotors: General considerations [PB95-206447] p 677 N95-31157

DIGITAL SYSTEMS

Evolution of a nose-wheel steering system [BTN-94-EIX94461047056] p 78 A95-61739
 Flight control system mode transitions influence on handling qualities and task performance [BTN-95-EIX95062487525] p 203 A95-69233
 Multiple-function digital controller system for active flexible wing wind-tunnel model [BTN-95-EIX95182619212] p 322 A95-76638
 Impact of near-coincident faults on digital flight control systems [BTN-95-EIX95242670759] p 359 A95-81088
 Integrated performance and reliability specification for digital avionics systems [AIAA PAPER 95-0953] p 506 A95-90632
 ASTRA — A safe, simplex, fly-by-wire aircraft control system [CONGRESS PAPER C428-37-218] p 610 A95-93634

Modeling and analysis for the GPS pseudo-range observable [BTN-95-EIX95302731227] p 600 A95-94046
 Micro-measurements of mechanical properties for adhesives and composites using digital imaging technology [NASA-CR-196111] p 22 N95-10231
 Formal design and verification of a reliable computing platform for real-time control (phase 3 results) [NASA-TM-109140] p 33 N95-10873
 NASA develops new digital flight control system [NASA-NEWS-RELEASE-94-47] p 144 N95-19029
 Ultra-Reliable Digital Avionics (URDA) processor p 245 N95-20638

Digital systems validation. Chapter 20 Artificial Intelligence with applications for aircraft. Handbook, volume 2 [AD-A288492] p 448 N95-26638
 Nonlinear calibration of an infrared radiometer [AD-A292436] p 579 N95-28996
 Design and evaluation of a LQR controller for the bluebird unmanned air vehicle [AD-A289769] p 504 N95-29457

Digital autopilot design for combat aircraft in ALENIA p 623 N95-32009
 An investigation of pilot induced oscillation phenomena in digital-flight control systems p 623 N95-32011
 Advanced flight control technology achievements at Boeing Helicopters p 624 N95-32014
 An Electronic Workshop on the Performance Seeking Control and Propulsion Controlled Aircraft Results of the F-15 Highly Integrated Digital Electronic Control Flight Research Program [NASA-TM-104278] p 694 N95-33009
 An overview of integrated flight-propulsion controls flight research on the NASA F-15 research airplane p 694 N95-33010
 Performance seeking control program overview p 695 N95-33011

Formal verification of an avionics microprocessor [NASA-CR-4682] p 710 N95-33396

DIGITAL TECHNIQUES

Computer-aided light sheet flow visualization using photogrammetry [NASA-TP-3416] p 26 N95-10859

DIGITAL TELEVISION

Applications of digital video and synthetic environments to unmanned aerial vehicles [AD-A291875] p 504 N95-29437

DILUTION

Jet mixing in a reacting cylindrical crossflow [NASA-TM-106975] p 616 N95-30853

DIMENSIONAL ANALYSIS

An aerodynamic analysis of a mixed flow turbine [NASA-TM-106674] p 15 N95-10153
 Nonlinear bulging factor based on R-curve data p 94 N95-14476

DIMENSIONAL MEASUREMENT

Effects of yaw and pitch motion on model attitude measurements [NASA-TM-4641] p 250 N95-22109

DIMENSIONAL STABILITY

Dimensional stability of curved panels with cocured stiffeners and cobonded frames p 532 N95-28836

DIMENSIONLESS NUMBERS

Simple numerical criterion for vortex breakdown [HTN-95-61210] p 541 A95-87583

Near-limit drop deformation and secondary breakup p 704 N95-32902

DIMERIZATION

Empirical corrections of the rigid rotor interaction potential of H2-H2 in the attractive region: Dimer features in the FIR absorption spectra [HTN-95-41943] p 361 A95-81690

DIMETHYL COMPOUNDS

An intercomparison of instrumentation for tropospheric measurements of dimethyl sulfide: Aircraft results for concentrations at the parts-per-trillion level [HTN-95-91857] p 355 A95-80845
 The effects of aircraft fuel and fluids on the strength properties of Resin Transfer Molded (RTM) composites p 536 N95-29047

DIRECT CURRENT

Dynamically timed electric motor [NASA-CASE-MFS-28958-1] p 437 N95-26890
 DC electrostatic gyro suspension system for the Gravity Probe B experiment p 527 N95-29794

DIRECT LIFT CONTROLS

Direct-lift design strategy for longitudinal control of hypersonic aircraft [BTN-95-EIX95182619131] p 291 A95-76608

DIRECTIONAL CONTROL

Exact solution of stability margin for the MIMO control system p 507 A95-91582
 Effect of coupling term on stability for the two input control system p 507 A95-91583
 Comparison of the method of analyzing stability margin by using Minus Inverse Vector Locus with classical method p 507 A95-91584
 Directional control at high angles of attack using blowing through a chined forebody [BTN-95-EIX0619952748179] p 619 A95-94472
 Effect of weak periodic pressure gradient on streamwise vortices near a wall p 29 N95-11263
 Computational analysis of forebody tangential slot blowing on the high alpha research vehicle [NASA-CR-196750] p 10 N95-11367
 Numerical analysis of tangential slot blowing on a generic chined forebody [NASA-TM-108845] p 37 N95-11927
 X-31 quasi-tailless flight demonstration p 70 N95-14243

Feedback control laws for highly maneuverable aircraft [NASA-CR-197944] p 295 N95-23410

Performance of an aerodynamic yaw controller mounted on the space shuttle orbiter body flap at Mach 10 [NASA-TM-109179] p 330 N95-24397

A vehicle health monitoring system for the Space Shuttle Reaction Control System during reentry [NASA-CR-188370] p 527 N95-29447

Sea wave parameters, small altitudes and distances measurers design for movement control systems of ships, wing-in-surface effect crafts and seaplanes p 708 N95-33141

DIRECTIONAL STABILITY

X-31 quasi-tailless flight demonstration p 70 N95-14243

An easy way to analyze longitudinal and lateral-directional trim problems with AEO or OEI p 409 N95-26949

Flight evaluation of forebody vortex control in post-stall flight p 609 N95-32003

DIRECTIVITY

Geometrical acoustics approach for calculating the effects of flow on acoustics scattering [BTN-94-EIX94321331207] p 61 A95-60790
 The spectrum and directivity of turbulent mixing noise from supersonic jets p 579 N95-29415
 Fan noise prediction assessment [NASA-CR-195051] p 711 N95-33831

DISCHARGE COEFFICIENT

Two-dimensional converging-diverging rippled nozzles at transonic speeds — performed in the Langley 16-Foot Transonic Tunnel [NASA-TP-3440] p 6 N95-10129

DISCONNECT DEVICES

Partial discharge testing of high voltage wiring harness for airborne displays [AD-A289150] p 401 N95-27003

DISCONTINUITY

Application of a control-volume-based finite-element formulation to the shock tube problem [BTN-95-EIX95182619099] p 295 A95-76584
 Response of a thin airfoil encountering a strong density discontinuity p 462 A95-88900

DISCRETE COSINE TRANSFORM

Image representation using fast algorithms based on the Zak transform [AD-A293416] p 679 N95-31684

DISCRETE FUNCTIONS

- Statistical discrete gust-power spectral density methods overlap-holistic proof and beyond
[BTN-95-EIX0619952748175] p 584 A95-94469
- Computational aerodynamics based on the Euler equations
[AGARD-AG-325] p 72 N95-14264
- Design limit loads based upon statistical discrete gust methodology p 133 N95-18603
- Linear and nonlinear discrete-time state-space modeling of dynamic systems for control applications p 567 N95-29251
- DISCRIMINANT ANALYSIS (STATISTICS)**
Selecting optimal experiments for feedforward multilayer perceptrons
[AD-A290856] p 678 N95-30406
- DISCRIMINATION**
Sensing thunderstorm microphysics with multiparameter radar: Application for aviation p 657 A95-93467
- DISCUSSION**
Workshop report: Measurement techniques in highly transient, spectrally rich combustion environments p 629 N95-31208
- DISORIENTATION**
Design of head-up display symbology for recovery from unusual attitudes p 611 A95-95044
- A review of civil aviation fatal accidents in which lost/oriented was a cause/factor: 1981-1990
[DOT/FAA/AM-95/1] p 278 N95-24071
- DISPERSING**
A numerical model to predict the fate of jettisoned aviation fuel
[AD-A289336] p 419 N95-26842
- DISPERSIONS**
Functional dependence of trajectory dispersion on initial condition errors
[BTN-95-EIX95152583263] p 298 A95-73564
- Active open-loop control of particle dispersion in round jets
[HTN-95-42334] p 372 A95-86163
- DISPLACEMENT**
Aeroelastic stability of hingeless rotor blade in hover using large deflection theory
[BTN-94-EIX94441386616] p 183 A95-67347
- DISPLACEMENT MEASUREMENT**
Angular displacement measuring device
[NASA-CASE-ARC-11937-1] p 362 N95-26015
- DISPLAY DEVICES**
Simulation and flight test evaluation of head-up-display guidance for harrier approach transitions
[BTN-95-EIX95062487533] p 194 A95-69241
- Flight-deck displays on the Boeing 777
[BTN-95-EIX95142562402] p 286 A95-73438
- Part-task simulator evaluations of advanced terrain displays
[SAE PAPER 932570] p 401 A95-84567
- Inadequacy of visual alarms in helicopter air medical transport
[HTN-95-01218] p 484 A95-91450
- Automatic vehicle location and airfield ground movement
[CONGRESS PAPER C428-7-148] p 488 A95-91689
- The Saab-Scania approach to development simulators
[CONGRESS PAPER C428-10-137] p 522 A95-91698
- A new look at aviation meteorology: Integrating aircraft situation display (ASD) with conventional weather displays p 665 A95-93505
- The prototype aviation weather products generator a vehicle to assess user needs p 671 A95-93534
- A prototype for displaying aviation forecast variables using Eta numerical model output p 676 A95-93555
- Development of software for safety critical applications for the EH101 Helicopter
[CONGRESS PAPER C428-24-160] p 678 A95-93597
- Advanced distributed simulation technology advanced rotary wing aircraft. System/segment specification. Volume 3: Visual system module
[AD-A280239] p 20 N95-10351
- Flight test of takeoff performance monitoring system
[NASA-TP-3403] p 51 N95-12664
- Aircraft maneuver envelope warning system
[NASA-CASE-ARC-11953-1] p 82 N95-14518
- A graphical user interface for design and analysis of air breathing propulsion systems
[TABES PAPER 94-616] p 83 N95-14645
- Spatial awareness comparisons between large-screen, integrated pictorial displays and conventional EFIS displays during simulated landing approaches
[NASA-TP-3467] p 80 N95-14852
- An evaluation of aircraft CRT and dot-matrix display legibility requirements
[AD-A283933] p 138 N95-18164
- The impact of advanced packaging technology on modular avionics architectures p 233 N95-20632

- Color control in a multichannel simulator display: The display for advanced research and training
[AD-A279717] p 239 N95-20992
- Data link terminal DLT document
[PB95-110805] p 229 N95-21369
- Evaluation of the Haworth-Newman avionics Display Readability Scale
[AD-A286127] p 235 N95-22232
- Virtual reality flight control display with six-degree-of-freedom controller and spherical orientation overlay
[NASA-CASE-NPO-18733-1-CU] p 288 N95-22578
- Automation technology using Geographic Information System (GIS) p 324 N95-23284
- Differential GPS and system integration of the Low Visibility Landing and Surface Operations (LVLASO) demonstration p 280 N95-23318
- Preliminary experiments of an optical fiber display
[NAL-TR-1257] p 362 N95-25004
- Advanced interactive display formats for terminal area traffic control
[NASA-CR-198576] p 384 N95-28188
- Operator modeling in commercial aviation: Cognitive models, intelligent displays, and pilot's assistants
[NASA-CR-198609] p 401 N95-28203
- Three-D weather displays for aircraft cockpits
[AD-A289759] p 508 N95-28691
- Conceptual design of a map interactive system for military aircraft cockpits
[AD-A289760] p 508 N95-28692
- Optimizing cockpit display configurations with a genetic algorithm system
[AD-A289799] p 508 N95-29123
- Mode of human image representation and error checking strategies in complex visual displays
[AD-A290107] p 485 N95-29210
- Guidelines for the design of GPS and LORAN receiver controls and displays
[AD-A293753] p 602 N95-31572
- An approach to sensor data fusion for flying and landing aid purpose p 686 N95-32488
- A helmet mounted display for night missions at low altitude p 693 N95-32503
- The effects of display location and dimensionality on taxiway navigation
[AD-A294878] p 690 N95-34570
- Resource document for the design of electronic instrument approach procedure displays
[AD-A295108] p 691 N95-34797
- DISSIPATION**
Estimation of atmospheric turbulence severity from in-situ aircraft measurements p 659 A95-93479
- Automatic grid generation procedure for complex aircraft configurations
[BTN-95-EIX95302729765] p 605 A95-94127
- Wake turbulence p 75 N95-14894
- The effect of aviation fuels containing low amounts of static dissipater additive on electrostatic charge generation
[AD-A280075] p 420 N95-28152
- DISSOLVED GASES**
Dissolved gas - the hidden saboteur
[SAE PAPER 931404] p 628 A95-93674
- DISTANCE**
Earthwinds Hilton III: Balloon project p 497 A95-90871
- Examples of flight path optimization using a multivariate gradient-search method. Addendum A: Variation of optimum flight profile parameters with range
[ESDU-94016-ADD-A] p 44 N95-11794
- Sea wave parameters, small altitudes and distances measurers design for movement control systems of ships, wing-in-surface effect crafts and seaplanes p 708 N95-33141
- DISTANCE MEASURING EQUIPMENT**
Precision landing system mathematical modeling study report for Andrews Air Force Base, runway 19L, Camp Springs, MD
[AD-A289015] p 384 N95-27903
- DISTILLATION**
Airborne rotary air separator study
[NASA-CR-189099] p 290 N95-24053
- DISTORTION**
Pressure and temperature distortion testing of a two-stage centrifugal compressor
[BTN-94-EIX95011441250] p 431 A95-84207
- Aero-thermodynamic distortion induced structured dynamic response
[AD-A279931] p 203 N95-19864
- DISTRIBUTED PROCESSING**
Airborne air traffic control: An application of distributed processing in the air traffic control environment
[HTN-95-12417] p 611 A95-95210
- Rapid solution of large-scale systems of equations p 169 N95-16458

- AVIRIS and TMS data processing and distribution at the land processes distributed active archive center p 325 N95-23872
- The coupling of fluids, dynamics, and controls on advanced architecture computers
[NASA-CR-197727] p 360 N95-25797
- Application of parallel processing technology in complex helicopter analysis. Phase 1
[NASA-CR-197850] p 502 N95-28928
- Selecting optimal experiments for feedforward multilayer perceptrons
[AD-A290856] p 678 N95-30406
- Foundations of technology for constructing highly reliable distributed realtime systems
[AD-A293254] p 678 N95-30892
- DISTRIBUTION FUNCTIONS**
Determination of wall boundary conditions for high-speed-ratio direct simulation Monte Carlo calculations
[AD-A293254] p 267 A95-75278
- DISTURBANCES**
Aircraft noise and sleep disturbance: A field study
[HTN-95-92543] p 558 A95-87363
- DIURNAL VARIATIONS**
Diurnal variation of lee vortices in Taiwan and the surrounding area
[HTN-95-91363] p 318 A95-76394
- A comparison of some aerodynamic resistance methods using measurements over cotton and grass from the 1991 California ozone deposition experiment
[HTN-95-11295] p 319 A95-77000
- An overview of millimeter-wave spectroscopic measurements of chlorine monoxide at Thule, Greenland, February-March, 1992: Vertical profiles, diurnal variation, and longer-term trends
[HTN-95-00722] p 444 A95-86292
- Criteria of forecasting low level wind shear over Qatar p 663 A95-93493
- DIVERGENCE**
Investigation of outflow strength variability in Florida downburst-producing storms p 659 A95-93476
- DIVERGENT NOZZLES**
Single-engine tail interference model p 115 N95-17879
- DIVERTERS**
Computational analysis in support of the SSTO flowpath test
[NASA-TM-106757] p 89 N95-13665
- Drag measurements of an axisymmetric nacelle mounted on a flat plate at supersonic speeds
[NASA-TM-4660] p 684 N95-32821
- DIVIDERS**
Effect of leeward flow dividers on the wing rock of a delta wing
[BTN-95-EIX95152582347] p 282 A95-73549
- DO-328 AIRCRAFT**
Composite propeller system for Dornier 328
[BTN-94-EIX94461290506] p 66 A95-61728
- DOCUMENT STORAGE**
NLS Flight Simulation Laboratory (FSL) documentation
[NASA-CR-196564] p 363 N95-24439
- DOCUMENTATION**
Enhanced capabilities and updated users manual for axial-flow turbine preliminary sizing code TURBAN
[NASA-CR-195405] p 76 N95-15912
- NLS Flight Simulation Laboratory (FSL) documentation
[NASA-CR-196564] p 363 N95-24439
- DOMAINS**
Preconditioned domain decomposition scheme for three-dimensional aerodynamic sensitivity analysis
[HTN-95-42597] p 459 A95-87227
- DOORS**
Aircraft evacuations through Type-3 exits I: Effects of seat placement at the exit
[DOT/FAA/AM-95/22] p 599 N95-31845
- DOPPLER RADAR**
A technique for detecting a tropical cyclone center using a Doppler radar
[HTN-95-20631] p 215 A95-69574
- 2 micron LIDAR for laser-based remote sensing: Flight demonstration and application survey
[BTN-95-EIX95212641072] p 319 A95-76737
- Identification of aviation weather hazards based on the integration of radar and lightning data
[HTN-95-51323] p 356 A95-80908
- Doppler lidar investigation of wake vortex transport between closely spaced parallel runways
[HTN-95-81645] p 462 A95-87693
- International Conference on Aviation Weather Systems, 5th, Vienna, VA, Aug. 2-6, 1993. Preprint Volume
[HTN-95-92940] p 652 A95-93441
- Status of the terminal Doppler weather radar with deployment underway p 653 A95-93450
- ITWS gridded analysis p 654 A95-93455
- The ITWS microburst prediction algorithm p 655 A95-93456

- A comparative performance study of TDWR/LLWAS 3 integration algorithms for wind shear detection p 658 A95-93468
- Use of WSR-88D data in the FAA's weather impacted aerospace product p 658 A95-93469
- NEXRAD/ARSR operational comparison p 658 A95-93470
- Final results of the weather testing component of the Terminal Doppler Weather Radar operational test and evaluation p 658 A95-93471
- Investigation of outflow strength variability in Florida downburst-producing storms p 659 A95-93476
- Transport Canada proposed R&D program for the development of a multi-parameter dual X-Ka band Doppler radar for aviation meteorology applications p 659 A95-93477
- The use of radar wind profiles to remove TDWR gust front algorithm false alarms caused by vertical wind shear p 661 A95-93488
- Terminal Doppler Weather Radar point target filter threshold selection p 662 A95-93490
- Developing thunderstorm forecast rules utilizing first detectable cloud radar-echoes p 667 A95-93514
- Windshear detection: TDWR and LLWAS operational experience in Denver 1988-1992 p 670 A95-93528
- Vertical wind estimation from horizontal wind measurements p 26 N95-10567
- Determining F-factor using ground-based Doppler radar: Validation and results p 11 N95-10571
- Terminal Doppler Weather Radar Build 5A Operational Test and Evaluation (OT/E) integration and OT/E operational test plan p 61 N95-12996
- Airborne Windshear Detection and Warning Systems. Fifth and Final Combined Manufacturers' and Technologists' Conference, part 2 [NASA-CP-10139-PT-2] p 41 N95-13203
- Doppler radar detection of vortex hazard indicators p 42 N95-13212
- TDWR scan strategy implementation [AD-A284877] p 98 N95-15749
- Linear prediction data extrapolation superresolution radar imaging p 155 N95-16268
- Radar studies of aviation hazards [AD-A285845] p 226 N95-21831
- Maximum-likelihood spectral estimation and adaptive filtering techniques with application to airborne Doppler weather radar [NASA-CR-197699] p 316 N95-23670
- Offshore next generation weather radar (NEXRAD) test and evaluation master plan (TEMP) [AD-A291435] p 556 N95-30072
- Offshore next generation weather radar (NEXRAD) OT&E integration and OT&E operational test [AD-A293223] p 646 N95-30902
- Initial evaluation of the Oregon State University planetary boundary layer column model for ITWS applications [AD-A293775] p 677 N95-31465
- DORNIER AIRCRAFT**
- Composite propeller system for Dornier 328 [BTN-94-EIX94461290506] p 66 A95-61728
- DOUGLAS AIRCRAFT**
- Evaluation of all-electric secondary power for transport aircraft [NASA-CR-189077] p 441 N95-27999
- DOWNBURSTS**
- Real time for the calculation of the aerodynamic of aircrafts with delta wings p 460 A95-87399
- Investigation of outflow strength variability in Florida downburst-producing storms p 659 A95-93476
- DOWNTIME**
- Navy foreign object damage and its impact on future gas turbine engine low pressure compression systems p 198 N95-19658
- DOWNWASH**
- Numerical simulation of a complete STOV/L aircraft in ground effect [AIAA PAPER 93-4880] p 4 A95-60187
- Application of ACT to unstable motions of an airfoil in ground effect p 471 A95-91500
- Numerical simulation of helicopter engine plume in forward flight [NASA-CR-197488] p 107 N95-16589
- DRAG**
- Repeatability of ice shapes in the NASA Lewis icing research tunnel [BTN-95-EIX95062487528] p 204 A95-69236
- Shock tunnel measurements of hypervelocity blunt cone drag [BTN-95-EIX95152577606] p 305 A95-73477
- Separation control on high-lift airfoils via micro-vortex generators [BTN-95-EIX95152582326] p 265 A95-73529
- Drag coefficients of spherical liquid droplets. Part 1: Quiescent gaseous fields [BTN-95-EIX95262697040] p 538 A95-86857
- Drag coefficients of spherical liquid droplets. Part 2: Turbulent gaseous fields [BTN-95-EIX95262697041] p 538 A95-86858
- Drag and lift in nonadiabatic transonic flow [HTN-95-61208] p 540 A95-87581
- Numerical computations of supersonic base flow with special emphasis on turbulence modeling [HTN-95-20949] p 546 A95-88988
- The coplanar projectile motion problem including the effects of lift and drag [ISBN 1-879921-01-4] p 635 A95-93723
- Aerodynamic applications of underexpanded hypersonic viscous jets [BTN-95-EIX0619952748162] p 589 A95-94456
- Optimal trajectories for an unmanned air-vehicle in the horizontal plane [BTN-95-EIX0619952748191] p 606 A95-94480
- Turbulent effects on parachute drag [BTN-95-EIX0619952748193] p 591 A95-94482
- Estimation of supersonic leading-edge thrust by a Euler flow model [BTN-95-EIX0619952748194] p 591 A95-94483
- Two-dimensional converging-diverging rippled nozzles at transonic speeds — performed in the Langley 16-Foot Transonic-Tunnel [NASA-TP-3440] p 6 N95-10129
- Control theory based airfoil design using the Euler equations [NASA-CR-196360] p 36 N95-11884
- Investigation of the influence of pylons and stores on the wing lower surface flow p 116 N95-17885
- In-flight lift-drag characteristics for a forward-swept wing aircraft and comparisons with contemporary aircraft [NASA-TP-3414] p 117 N95-18565
- DRAG COEFFICIENTS**
- Navier-Stokes simulations of WECS airfoil flowfields [DE94-013341] p 7 N95-10226
- An investigation of the transonic pressure drag coefficient for axis-symmetric bodies [AD-A280990] p 105 N95-15994
- Static aerodynamics CFD analysis for 120-mm hypersonic KE projectile design [ARL-MR-184] p 118 N95-18611
- DRAG DEVICES**
- Computational flow predictions for hypersonic drag devices p 37 N95-11967
- DRAG MEASUREMENT**
- Repeatability of ice shapes in the NASA Lewis icing research tunnel [BTN-95-EIX95062487528] p 204 A95-69236
- Surface pressure and wake drag measurements on the Boeing A4 airfoil in the IAR 1.5X1.5m Wind Tunnel Facility p 110 N95-17850
- Interference corrections for a centre-line plate mount in a porous-walled transonic wind tunnel p 122 N95-19280
- An investigation of drag repeatability in half model testing in the ARA Transonic Wind Tunnel [ARA-MEMO-392] p 188 N95-19546
- Investigation of a thermal buoyancy effect on the drag of half models tested in the ARA Transonic Wind Tunnel [ARA-MEMO-407] p 222 N95-19946
- Optical processing and control [AD-A279157] p 259 N95-21975
- Excrescence drag levels on aircraft [ESDU-94044] p 477 N95-28897
- DRAG REDUCTION**
- Wing download reduction using vortex trapping plates [HTN-94-00710] p 4 A95-60188
- An assessment of upper surface blowing for the reduction of tilt rotor download [HTN-94-00711] p 5 A95-60189
- Aerodynamic interactions between a rotor and wing in hover [HTN-94-00714] p 5 A95-60192
- Effect of underwing frost on a transport aircraft airfoil at flight Reynolds number [BTN-95-EIX95152582334] p 276 A95-73536
- Numerical investigation of supersonic flows around a spiked blunt body [BTN-95-EIX95212645690] p 271 A95-76742
- Study of subsonic base cavity flowfield structure using particle image velocimetry [BTN-95-EIX95222650781] p 327 A95-79237
- Flow past a symmetric wedge with forward splitter plate p 427 A95-82406
- Flow alteration and drag reduction by riblets in a turbulent boundary layer [HTN-95-61199] p 461 A95-87572
- Accurate drag prediction: A prerequisite for drag reduction research [SAE PAPER 932571] p 467 A95-90060
- A brief survey of wing tip devices for drag reduction [SAE PAPER 932574] p 467 A95-90063
- Drag reduction in a rectangular duct using riblets [HTN-95-01091] p 468 A95-90277
- Laminar and turbulent flow over optimal riblets p 639 A95-95383
- Effect of passive venting on static pressure distributions in cavities at subsonic and transonic speeds [NASA-TM-4549] p 6 N95-10029
- Application of two procedures for dual-point design of transonic airfoils [NASA-TP-3466] p 38 N95-12176
- The FC-1D: The profitable alternative Flying Circus Commercial Aviation Group [NASA-CR-197152] p 46 N95-12628
- Base passive porosity for drag reduction [NASA-CASE-LAR-15246-1] p 91 N95-14183
- An investigation of the transonic pressure drag coefficient for axis-symmetric bodies [AD-A280990] p 105 N95-15994
- The aerodynamic design of an integrated wing lower surface and pylons for reduced drag [ARA-MEMO-406] p 194 N95-19789
- Numerical and experimental study of drag characteristics of two-dimensional HLFC airfoils in high subsonic, high Reynolds number flow [NAL-TR-1244T] p 331 N95-24998
- A theoretical and experimental investigation of the flow over supersonic leading edge wing/body configurations [DRA-TM-AERO-PROP-41] p 331 N95-25649
- Plate manipulators [AD-A289601] p 374 N95-26719
- Studies in drag reduction p 478 N95-29094
- DRAINAGE**
- Numerical modeling of a cryogenic fluid within a fuel tank [NASA-TM-4651] p 89 N95-13892
- DRIFT RATE**
- DC electrostatic gyro suspension system for the Gravity Probe B experiment p 527 N95-29794
- DRONE AIRCRAFT**
- On the UF-104 system p 507 A95-91559
- Aeroservoelastic coupling on the UF-104 aircraft p 517 A95-91561
- DROOPED AIRFOILS**
- Wind tunnel test on a 65 deg delta wing with a sharp or rounded leading edge: The international vortex flow experiment p 114 N95-17872
- DROP SIZE**
- Conditions associated with large-drop regions [HTN-95-10686] p 214 A95-68845
- Study of the droplet spray characteristics of a subsonic wind tunnel [BTN-95-EIX95182619235] p 271 A95-76661
- Aircraft icing: Meteorological effects on aircraft performance p 674 A95-93545
- Structure of a swirl-stabilized, combusting spray [NASA-TM-106724] p 50 N95-11890
- A review of water mist technology for fire suppression [AD-A285738] p 225 N95-20071
- Investigation of water droplet trajectories within the NASA icing research tunnel [NASA-TM-107023] p 684 N95-32769
- Near-limit drop deformation and secondary breakup p 704 N95-32902
- DROPS (LIQUIDS)**
- Study of the droplet spray characteristics of a subsonic wind tunnel [BTN-95-EIX95182619235] p 271 A95-76661
- Drag coefficients of spherical liquid droplets. Part 1: Quiescent gaseous fields [BTN-95-EIX95262697040] p 538 A95-86857
- Drag coefficients of spherical liquid droplets. Part 2: Turbulent gaseous fields [BTN-95-EIX95262697041] p 538 A95-86858
- High pressure vaporization and burning of methanol droplets in reduced gravity p 527 A95-87285
- An in-situ system for warning of icing conditions p 660 A95-93481
- The production of supercooled liquid water by a secondary cold front p 673 A95-93542
- Airplane icing research at the Boeing Company: Participation in the second Canadian Atlantic Storms Program p 674 A95-93544
- Aircraft icing: Meteorological effects on aircraft performance p 674 A95-93545
- Preliminary studies of ice formation in upslope clouds p 674 A95-93546
- The development of an aircraft icing forecast technique using data from maps p 675 A95-93549
- Investigation of water droplet trajectories within the NASA icing research tunnel [NASA-TM-107023] p 684 N95-32769
- Near-limit drop deformation and secondary breakup p 704 N95-32902
- DRUGS**
- Evaluation of neutron techniques for illicit substance detection [DE95-002988] p 300 N95-22764

DUAL SPIN SPACECRAFT

Evaluation of energy-sink stability criteria for dual-spin spacecraft
[AD-A283228] p 87 N95-14850

DUCT GEOMETRY

Linear instability waves in supersonic jets confined in circular and non-circular ducts
[BTN-94-EIX94341340068] p 103 A95-63520

Experimental and numerical analysis of a two-duct nozzle/afterbody model at supersonic Mach numbers
[AIAA PAPER 95-6085] p 490 A95-87414

Three dimensional compressible turbulent flow computations for a diffusing S-duct with/without vortex generators
[NASA-CR-195390] p 138 N95-17402

An investigation of the side-dump dual in-line ramjet combustor
[NASA-CR-197449] p 617 N95-31199

DUCTED FAN ENGINES

Turbofan propulsion simulator
[BTN-94-EIX94461290240] p 82 A95-61737

CaRnard: A new roadable aircraft concept
[SAE PAPER 932601] p 494 A95-90071

Condensation in jet engine intake ducts during stationary operation
[BTN-95-EIX95292721154] p 612 A95-92590

Ducted fan acoustic radiation including the effects of nonuniform mean flow and acoustic treatment
[NASA-CR-197449] p 172 N95-16401

DUCTED FANS

Ducted fan VTOL and its flight control system
[NASA-CR-197110] p 81 N95-14909

Propulsion/airframe interference for ducted propfan engines with ground effect
[NASA-CR-197110] p 81 N95-14909

DUCTED FLOW

Linear instability waves in supersonic jets confined in circular and non-circular ducts
[BTN-94-EIX94341340068] p 103 A95-63520

Design and operation of a supersonic annular flow facility
[BTN-94-EIX94441386624] p 183 A95-68173

Flutter of an infinitely long panel in a duct
[BTN-95-EIX95182619087] p 291 A95-75772

Screech tones from free and ducted supersonic jets
[HTN-95-51647] p 432 A95-85029

Swirl control in an S-duct at high angle of attack
[HTN-95-20846] p 545 A95-88107

Drag reduction in a rectangular duct using riblets
[HTN-95-01091] p 468 A95-90277

An aerodynamic analysis of a mixed flow turbine
[NASA-TM-106674] p 15 N95-10153

Solution of Navier-Stokes equations using high accuracy monotone schemes
[NASA-TM-106913] p 332 N95-25962

Study of compressible flow through a rectangular-to-semiannular transition duct
[NASA-CR-4660] p 338 N95-24392

Recent improvements to and validation of the one dimensional NASA wave rotor model
[NASA-TM-106913] p 332 N95-25962

Comparison of spatial numerical operators for duct-nozzle acoustics
[NASA-CR-4660] p 338 N95-24392

DUCTED ROCKET ENGINES

Experimental and analytical methods for the determination of connected-pipe ramjet and ducted rocket internal performance
[AGARD-AR-323] p 149 N95-17278

DUCTILITY

Multilayer anti-erosion coatings
[NASA-CR-195421] p 323 N95-22675

DUCTS

Boundary element analysis of the acoustic field inside three-dimensional regular and irregular ducts
[NASA-CR-195421] p 323 N95-22675

High-frequency acoustic radiation from a curved duct of circular cross section
[NASA-CR-195421] p 323 N95-22675

Active control of complex noise problems using a broadband, multichannel controller
[NASA-CR-195421] p 323 N95-22675

The use of cowl camber and taper to reduce rotor/stator interaction noise
[NASA-CR-195421] p 323 N95-22675

The acoustic characteristics of turbomachinery cavities
[NASA-CR-4671] p 476 N95-28720

The decay of longitudinal vortices shed from airfoil vortex generators
[NASA-CR-198356] p 480 N95-29402

DUMP COMBUSTORS

An investigation of the side-dump dual in-line ramjet combustor
[NASA-CR-197449] p 617 N95-31199

A pulsed liquid fuel ramjet
[NASA-CR-197449] p 617 N95-31199

DURABILITY

Mathematical modelling concerning the development of a system of similar installations, taking into account their operational intensity (an aircraft-helicopter fleet taken as an example)
[BTN-94-EIX94461408763] p 103 A95-63646

Elements of structural integrity assurance
[NASA-TM-106502] p 22 N95-11483

Brush seal performance and durability issues based on T-700 engine test results
[NASA-TM-106502] p 22 N95-11483

Ten-year ground exposure of composite materials used on the Bell Model 206L helicopter flight service program
[NASA-TP-3468] p 55 N95-12357

FAA/NASA International Symposium on Advanced Structural Integrity Methods for Airframe Durability and Damage Tolerance, part 2
[NASA-CP-3274-PT-2] p 124 N95-19468

Proceedings of the USAF Structural Integrity Program Conference
[AD-A285684] p 194 N95-19517

Interlaminar shear test method development for long term durability testing of composites
[NASA-CP-3274-PT-2] p 124 N95-19468

Development of stitched/RTM composite primary structures
[NASA-CP-3274-PT-2] p 124 N95-19468

Advanced composite structural concepts and materials technologies for primary aircraft structures: Advanced material concepts
[NASA-CR-4485] p 503 N95-29027

Evaluation of retro-reflective beads in airport pavement markings
[AD-A291065] p 523 N95-29967

Evaluation of alternative pavement marking materials
[AD-A292973] p 626 N95-31468

Elements of structural integrity assurance

[NASA-TM-106502] p 22 N95-11483

Brush seal performance and durability issues based on T-700 engine test results
[NASA-TM-106502] p 22 N95-11483

Ten-year ground exposure of composite materials used on the Bell Model 206L helicopter flight service program
[NASA-TP-3468] p 55 N95-12357

FAA/NASA International Symposium on Advanced Structural Integrity Methods for Airframe Durability and Damage Tolerance, part 2
[NASA-CP-3274-PT-2] p 124 N95-19468

Proceedings of the USAF Structural Integrity Program Conference
[AD-A285684] p 194 N95-19517

Interlaminar shear test method development for long term durability testing of composites
[NASA-CP-3274-PT-2] p 124 N95-19468

Development of stitched/RTM composite primary structures
[NASA-CP-3274-PT-2] p 124 N95-19468

Advanced composite structural concepts and materials technologies for primary aircraft structures: Advanced material concepts
[NASA-CR-4485] p 503 N95-29027

Evaluation of retro-reflective beads in airport pavement markings
[AD-A291065] p 523 N95-29967

Evaluation of alternative pavement marking materials
[AD-A292973] p 626 N95-31468

Erosion of dust-filtered helicopter turbine engines. Part 1: Basic theoretical considerations
[BTN-95-EIX95182619222] p 288 A95-76648

Erosion of dust-filtered helicopter turbine engines. Part 2: Erosion reduction
[BTN-95-EIX95182619223] p 289 A95-76649

Life prediction of helicopter engines fitted with dust filters
[BTN-95-EIX95182619224] p 289 A95-76650

Role of the aviation weather system in providing a real-time ATC volcanic ash advisory system
[NASA-CR-197449] p 663 A95-93494

Alaska's volcanic ash warning system
[NASA-CR-197449] p 663 A95-93494

Out of area experiences with the RB199 in Toronto
[NASA-CR-197449] p 663 A95-93494

The operation of gas turbine engines in hot and sandy conditions: Royal Air Force experiences in the Gulf conflict
[NASA-CR-197449] p 663 A95-93494

US Army rotorcraft turboshaft engines sand and dust erosion considerations
[NASA-CR-197449] p 663 A95-93494

Future directions in helicopter protection system configuration
[NASA-CR-197449] p 663 A95-93494

Damage of high temperature components by dust-laden air
[NASA-CR-197449] p 663 A95-93494

Response of the B-1B air data sensor to simulated dust cloud environments
[AD-A286134] p 235 N95-22036

Effects of dust from storage heaters on ignition in scramjets
[NAL-TR-1234] p 405 N95-26706

Erosion of dust-filtered helicopter turbine engines. Part 2: Erosion reduction
[BTN-95-EIX95182619223] p 289 A95-76649

Life prediction of helicopter engines fitted with dust filters
[BTN-95-EIX95182619224] p 289 A95-76650

Particle trajectories in gas turbine engines
[NASA-CR-197449] p 663 A95-93494

Simultaneous three-dimensional velocity and mixing measurements by use of laser Doppler velocimetry and fluorescence probes in a water tunnel
[NASA-TP-3454] p 53 N95-13553

Foil bearings for gas turbine engines
[BTN-94-EIX94461290279] p 82 A95-61732

Dynamic behavior of valves with pneumatic chamber for reciprocating compressors
[BTN-94-EIX94351143311] p 207 A95-65845

Analytical aeropropulsive/aeroelastic hypersonic-vehicle model with dynamic analysis
[BTN-95-EIX95182619138] p 269 A95-76615

GETRAN: A generic, modularly structured computer code for simulation of dynamic behavior of aero- and power generation gas turbine engines
[BTN-94-EIX95011441241] p 431 A95-84198

Dynamic stiffness and damping of foil bearings for gas turbine engines
[SAE PAPER 931449] p 635 A95-93698

Comments on the use of structureborne noise analysis for large commercial airplanes
[NASA-CR-194893] p 51 N95-11869

Determining the accuracy of maximum likelihood parameter estimates with colored residuals
[NASA-CR-194893] p 51 N95-11869

Static and dynamic friction behavior of candidate high temperature airframe seal materials
[NASA-TM-106571] p 152 N95-16905

High frequency flow-structural interaction in dense subsonic fluids
[NASA-CR-4652] p 330 N95-24217

Experimental study of the effects of Reynolds number on high angle of attack aerodynamic characteristics of forebodies during rotary motion
[NASA-CR-195033] p 330 N95-24443

Design of nonlinear control laws for high-angle-of-attack flight
[BTN-94-EIX94511433920] p 141 A95-64586

Demonstration of an elastically coupled twist control concept for tilt rotor blade application
[BTN-94-EIX94441386633] p 196 A95-68182

Using adaptive structures to attenuate rotary wing aerodynamic response
[BTN-95-EIX95062487547] p 192 A95-68361

Flight control systems/structural coupling BAe Warton experience in aero-servo elasticity
[CONGRESS PAPER C428-35-059] p 610 A95-93628

Flight dynamics of an unmanned aerial vehicle
[AD-A282259] p 45 N95-12410

Development of a multicomponent force and moment balance for water tunnel applications, volume 1
[NASA-CR-4642-VOL-1] p 161 N95-18955

A review of falconry as a bird control technique with recommendations for use at the Shuttle Landing Facility, John F. Kennedy Space Center, Florida, USA
[NASA-TM-110142] p 381 N95-27859

Linear and nonlinear discrete-time state-space modeling of dynamic systems for control applications
[NASA-CR-197449] p 567 N95-29251

Computational algorithms for aerodynamic analysis and design
[AD-A291084] p 482 N95-29972

Vorticity dynamics and control of dynamic stall
[AD-A288658] p 620 N95-31400

Ceramic composite attachments for transmission of high-torque loads
[BTN-94-EIX95011441256] p 417 A95-84213

Artificial neural networks for predicting nonlinear dynamic helicopter loads
[HTN-95-51678] p 404 A95-85060

Matlab as a robust control design tool
[NASA-CR-197449] p 663 A95-93494

Gyroscopic and propeller aerodynamic effects on engine mounts dynamic loads in turbulence conditions
[NASA-CR-197449] p 663 A95-93494

Impact of dynamic loads on propulsion integration
[NASA-CR-197449] p 663 A95-93494

Evidence that aerodynamic effects, including dynamic stall, dictate HAWT structural loads and power generation in highly transient time frames
[DE94-011865] p 216 N95-19855

Enhancement of F/A-18 operational flight measurements: Data report for phase 1
[DSTO-TR-0049] p 286 N95-23666

A NASTRAN-based computer program for structural dynamic analysis of Horizontal Axis Wind Turbines
[NASA-TM-106952] p 553 N95-29112

Influence of tooth profile modification on spur gear dynamic tooth strain
[NASA-TM-106952] p 553 N95-29112

Critical speed analysis of a non-linear strain ring dynamical model for aircraft tires
[SAE PAPER 932580] p 494 A95-90067

The use of math-dynamic models to aid the development of integrated health and usage monitoring systems
[CONGRESS PAPER C428-19-079] p 457 A95-91720

Extended cooperative control synthesis
[NASA-TM-4561] p 17 N95-10220

The 4-D approach to visual control of autonomous systems
[AIAA PAPER 94-1243-CP] p 27 N95-11513

An application of virtual prototyping to the flight test and evaluation of an unmanned air vehicle
[AD-A281749] p 14 N95-11595

Analytical and experimental vibration analysis of a faulty gear system
[NASA-TM-106689] p 58 N95-12843

Investigation of dynamic inflow's influence on rotor control derivatives
[NASA-CR-197449] p 663 A95-93494

A review of gust load calculation methods at de Havilland
[NASA-CR-197449] p 663 A95-93494

A linear system identification and validation of an AH-64 Apache aeroelastic simulation model
[NASA-CR-197449] p 663 A95-93494

Large-eddy simulation of flow through a plane, asymmetric diffuser
[NASA-CR-197449] p 663 A95-93494

Large-eddy simulation of flow through a plane, asymmetric diffuser
[NASA-CR-197449] p 663 A95-93494

Large-eddy simulation of flow through a plane, asymmetric diffuser
[NASA-CR-197449] p 663 A95-93494

Large-eddy simulation of flow through a plane, asymmetric diffuser
[NASA-CR-197449] p 663 A95-93494

Large-eddy simulation of flow through a plane, asymmetric diffuser
[NASA-CR-197449] p 663 A95-93494

Large-eddy simulation of flow through a plane, asymmetric diffuser
[NASA-CR-197449] p 663 A95-93494

Large-eddy simulation of flow through a plane, asymmetric diffuser
[NASA-CR-197449] p 663 A95-93494

Large-eddy simulation of flow through a plane, asymmetric diffuser
[NASA-CR-197449] p 663 A95-93494

Large-eddy simulation of flow through a plane, asymmetric diffuser
[NASA-CR-197449] p 663 A95-93494

Large-eddy simulation of flow through a plane, asymmetric diffuser
[NASA-CR-197449] p 663 A95-93494

Large-eddy simulation of flow through a plane, asymmetric diffuser
[NASA-CR-197449] p 663 A95-93494

Large-eddy simulation of flow through a plane, asymmetric diffuser
[NASA-CR-197449] p 663 A95-93494

Large-eddy simulation of flow through a plane, asymmetric diffuser
[NASA-CR-197449] p 663 A95-93494

Large-eddy simulation of flow through a plane, asymmetric diffuser
[NASA-CR-197449] p 663 A95-93494

Large-eddy simulation of flow through a plane, asymmetric diffuser
[NASA-CR-197449] p 663 A95-93494

Large-eddy simulation of flow through a plane, asymmetric diffuser
[NASA-CR-197449] p 663 A95-93494

Large-eddy simulation of flow through a plane, asymmetric diffuser
[NASA-CR-197449] p 663 A95-93494

Large-eddy simulation of flow through a plane, asymmetric diffuser
[NASA-CR-197449] p 663 A95-93494

Large-eddy simulation of flow through a plane, asymmetric diffuser
[NASA-CR-197449] p 663 A95-93494

Large-eddy simulation of flow through a plane, asymmetric diffuser
[NASA-CR-197449] p 663 A95-93494

Large-eddy simulation of flow through a plane, asymmetric diffuser
[NASA-CR-197449] p 663 A95-93494

Large-eddy simulation of flow through a plane, asymmetric diffuser
[NASA-CR-197449] p 663 A95-93494

Large-eddy simulation of flow through a plane, asymmetric diffuser
[NASA-CR-197449] p 663 A95-93494

Large-eddy simulation of flow through a plane, asymmetric diffuser
[NASA-CR-197449] p 663 A95-93494

Large-eddy simulation of flow through a plane, asymmetric diffuser
[NASA-CR-197449] p 663 A95-93494

Large-eddy simulation of flow through a plane, asymmetric diffuser
[NASA-CR-197449] p 663 A95-93494

Large-eddy simulation of flow through a plane, asymmetric diffuser
[NASA-CR-197449] p 663 A95-93494

Large-eddy simulation of flow through a plane, asymmetric diffuser
[NASA-CR-197449] p 663 A95-93494

Large-eddy simulation of flow through a plane, asymmetric diffuser
[NASA-CR-197449] p 663 A95-93494

Large-eddy simulation of flow through a plane, asymmetric diffuser
[NASA-CR-197449] p 663 A95-93494

Large-eddy simulation of flow through a plane, asymmetric diffuser
[NASA-CR-197449] p 663 A95-93494

Large-eddy simulation of flow through a plane, asymmetric diffuser
[NASA-CR-197449] p 663 A95-93494

Large-eddy simulation of flow through a plane, asymmetric diffuser
[NASA-CR-197449] p 663 A95-93494

Large-eddy simulation of flow through a plane, asymmetric diffuser
[NASA-CR-197449] p 663 A95-93494

Large-eddy simulation of flow through a plane, asymmetric diffuser
[NASA-CR-197449] p 663 A95-93494

Large-eddy simulation of flow through a plane, asymmetric diffuser
[NASA-CR-197449] p 663 A95-93494

Large-eddy simulation of flow through a plane, asymmetric diffuser
[NASA-CR-197449] p 663 A95-93494

Large-eddy simulation of flow through a plane, asymmetric diffuser
[NASA-CR-197449] p 663 A95-93494

Large-eddy simulation of flow through a plane, asymmetric diffuser
[NASA-CR-197449] p 663 A95-93494

- Flutter analysis of composite box beams
[NASA-CR-197931] p 294 N95-23392
- Extension to the dynamic modeling of the large angle magnetic suspension test fixture
[NASA-CR-197801] p 411 N95-26768
- Modeling and control of rotating stall in high speed multi-stage axial compressors p 513 N95-29244
- Linear and nonlinear discrete-time state-space modeling of dynamic systems for control applications p 567 N95-29251
- Model development for active control of stall phenomena in aircraft gas turbine engines p 514 N95-29679
- An analytic modeling and system identification study of helicopter dynamics p 505 N95-29787
- Influence of backup bearings and support structure dynamics on the behavior of rotors with active supports [NASA-CR-199080] p 703 N95-32689
- Steady-state dynamic behavior of an auxiliary bearing supported rotor system p 703 N95-32690
- Dynamic behavior of a magnetic bearing supported jet engine rotor with auxiliary bearings p 703 N95-32691
- Dynamic modelling and response characteristics of a magnetic bearing rotor system with auxiliary bearings p 703 N95-32692
- Synchronous dynamics of a coupled shaft/bearing/housing system with auxiliary support from a clearance bearing: Analysis and experiment p 703 N95-32693
- Low-order nonlinear dynamic model of IC engine-variable pitch propeller system for general aviation aircraft [NASA-TM-107006] p 694 N95-32916
- DYNAMIC PRESSURE**
- Panel flutter limit-cycle suppression with piezoelectric actuation [BTN-95-EIX95302731089] p 618 A95-94208
- Pressure measurements on an F/A-18 twin vertical tail in buffeting flow. Volume 3: Buffet power spectral densities [AD-A281444] p 36 N95-11829
- Low-speed wind tunnel testing of the NPS and NASA Ames Mach 6 optimized waverider [AD-A283585] p 75 N95-15319
- Pressure measurements on an F/A-18 twin vertical tail in buffeting flow. Volume 2: Steady and unsteady RMS pressure data [AD-A281581] p 76 N95-15465
- Pressure measurements on an F/A-18 twin vertical tail in buffeting flow. Volume 4, part 2: Buffet cross spectral densities [AD-A285555] p 143 N95-18641
- Pressure measurements on an F/A-18 twin vertical tail in buffeting flow. Volume 1: Wind tunnel test summary [AD-A279126] p 225 N95-21877
- Wind tunnel experiments on wake flow field behind a reentry capsule from a viewpoint of parachute deployment at supersonic speeds [ISAS-655] p 374 N95-26740
- Comparative wind tunnel tests of NACA 23024 airfoils with several aileron and spoiler configurations p 376 N95-27976
- Techniques for the determination of local dynamic pressure and angle of attack on a horizontal axis wind turbine [DE95-009204] p 707 N95-32685
- DYNAMIC RESPONSE**
- Validation of the dynamic response of a blade-element UH-60 simulation model in hovering flight [HTN-94-00663] p 18 A95-60155
- Unbalance response of a dual rotor system: Theory and experiment [BTN-94-EIX94351143320] p 195 A95-65854
- Using adaptive structures to attenuate rotary wing aeroelastic response [BTN-95-EIX95062487547] p 192 A95-68361
- Continuous gust response and sensitivity derivatives using state-space models [BTN-95-EIX95062487551] p 203 A95-68365
- Nonlinear dynamic simulation of single- and multispool core engines, part 1: Computational method [BTN-95-EIX95112524200] p 210 A95-69308
- Effects of AMB parameters on the dynamic stability of the rotor [BTN-94-EIX94381353450] p 323 A95-75494
- Response of a nonrotating rotor blade to lateral turbulence. Part 1: Theory [BTN-95-EIX95182619228] p 284 A95-76654
- Subharmonic and quasi-periodic motions of an eccentric squeeze film damper-mounted rigid rotor [BTN-94-EIX95011440601] p 429 A95-82982
- Dynamic pitch-up of a delta wing [HTN-95-81633] p 462 A95-87681
- Discrete crack growth analysis methodology for through cracks in pressurized fuselage structures [BTN-95-EIX0608952737538] p 633 A95-92751
- Estimation of atmospheric turbulence severity from in-situ aircraft measurements p 659 A95-93479
- Aircraft landing gear dynamics present and future [SAE PAPER 931400] p 604 A95-93670
- Effect of initial conditions on the response of nonlinear dynamical systems with the application to helicopter rotor dynamics [ISBN 1-879921-01-4] p 605 A95-93731
- Jet transport response to a horizontal wind vortex [BTN-95-EIX0619952748163] p 619 A95-94457
- High performance parallel analysis of coupled problems for aircraft propulsion [NASA-CR-195355] p 23 N95-10132
- Exact dynamic responses of periodic multi-span beams under convected pressure fields p 25 N95-11288
- Dynamic response of NASA Rotor Test Apparatus and Sikorsky S-76 hub mounted in the 80- by 120-Foot Wind Tunnel [NASA-TM-108847] p 25 N95-11389
- Flight dynamics of an unmanned aerial vehicle [AD-A282259] p 45 N95-12410
- Turbulence: Engineering models, aircraft response p 84 N95-14900
- Measurements of unsteady pressure and structural response for an elastic supercritical wing [NASA-TP-3443] p 104 N95-16560
- Parachute inflation: A problem in aeroelasticity [AD-A284375] p 117 N95-18340
- A review of gust load calculation methods at de Havilland p 118 N95-18604
- Special effects of gust loads on military aircraft p 133 N95-18605
- Current and future problems in structural acoustic fatigue p 173 N95-19143
- Nonlinear dynamic response of aircraft structures to acoustic excitation p 135 N95-19151
- Forced response of mistuned bladed disks p 141 N95-19383
- Documentation and archiving of the Space Shuttle wind tunnel test data base. Volume 2: User's Guide to the Archived Data Base [NASA-TM-104806-VOL-2] p 205 N95-19624
- Aero-thermodynamic distortion induced structured dynamic response [AD-A279931] p 203 N95-19864
- Effects of yaw and pitch motion on model attitude measurements [NASA-TM-4641] p 250 N95-22109
- Dynamic response tests of inertial and optical wind-tunnel model attitude measurement devices [NASA-TM-109182] p 296 N95-23011
- Influence of backup bearings and support structure dynamics on the behavior of rotors with active supports [NASA-CR-197438] p 310 N95-23190
- A multibody/finite element analysis approach for modeling of crash dynamic responses [NIAR-94-3] p 277 N95-24050
- Analysis of warping effects on the static and dynamic response of a seat-type structure [NIAR-94-12] p 348 N95-24211
- Development of a model protection and dynamic response monitoring system for the national transonic facility [NASA-CR-195041] p 340 N95-24388
- Observed acoustic and aeroelastic spectral responses of a MOD-2 turbine blade to turbulence excitation p 451 N95-27991
- Aeroelasticity and structural optimization of composite helicopter rotor blades with swept tips [NASA-CR-4665] p 397 N95-28262
- Impact damage resistance of composite fuselage structure, part 1 p 399 N95-28482
- High-and low-frequency dynamics of isolated blades and rotors with dynamic stall and wake [AD-A290358] p 503 N95-29322
- Dynamical systems as models for flow-induced vibrations [PB95-206991] p 647 N95-30956
- Dynamic modelling and response characteristics of a magnetic bearing rotor system with auxiliary bearings p 703 N95-32692
- DYNAMIC STABILITY**
- The effect of rotating loads suspended under a helicopter on their amplitude-frequency characteristics [BTN-94-EIX94461407959] p 78 A95-62633
- Dynamic instability of the aerogravity assist maneuver [BTN-95-EIX95152583282] p 298 A95-73583
- Effects of AMB parameters on the dynamic stability of the rotor [BTN-94-EIX94381353450] p 323 A95-75494
- The verification of a theoretical helicopter rotor blade sailing method by means of windtunnel testing [HTN-95-01093] p 468 A95-90279
- Viscous contribution to the high Mach number damping in pitch of blunt slender cones at small angles of attack [HTN-95-01096] p 469 A95-90282
- High-angle-of-attack yawing moment asymmetry of the X-31 aircraft from flight test [NASA-CR-186030] p 13 N95-11410
- Flight dynamics of an unmanned aerial vehicle [AD-A282259] p 45 N95-12410
- Evaluation of the dynamic stability characteristics of the NAL Light Transport Aircraft [NAL-PD-CA-9217] p 142 N95-16392
- Dynamic Stability Instrumentation System (DSIS). Volume 1: Hardware description [NASA-TM-109160-VOL-1] p 171 N95-18899
- Handling qualities of the High Speed Civil Transport p 294 N95-23325
- Analyzing the stability of floating ice floes [AD-A292149] p 563 N95-29160
- Design and evaluation of a LQR controller for the bluebird unmanned air vehicle [AD-A289769] p 504 N95-29457
- Results from tests of the Kearsott T16-B Inertial Measurement Unit [PB95-212031] p 644 N95-30502
- DYNAMIC STRUCTURAL ANALYSIS**
- Lyapunov exponents and stochastic stability of two-dimensional parametrically excited random systems [BTN-94-EIX94361122401] p 207 A95-65897
- Coupling equivalent plate and finite element formulations in multiple-method structural analyses [BTN-95-EIX95062487548] p 192 A95-68362
- Continuous gust response and sensitivity derivatives using state-space models [BTN-95-EIX95062487551] p 203 A95-68365
- Postinstability behavior of a two-dimensional airfoil with a structural nonlinearity [BTN-95-EIX95152582337] p 266 A95-73539
- Modal characteristics of rotors using a conical shaft finite element [BTN-94-EIX94401359745] p 346 A95-77379
- Ceramic composite attachments for transmission of high-torque loads [BTN-94-EIX95011441256] p 417 A95-84213
- Flutter analysis of supersonic axial flow cascades using a high resolution Euler solver. Part 1: Formulation and validation [NASA-TM-105798] p 23 N95-10244
- Plastic hinge modeling of structures [NIAR-94-14] p 24 N95-11168
- Engine structures analysis software: Component Specific Modeling (COSMO) [NASA-CR-195378] p 57 N95-11711
- Analytical and experimental vibration analysis of a faulty gear system [NASA-TM-106689] p 58 N95-12843
- Activities of the Structures Division, Lewis Research Center [NASA-TM-108081] p 59 N95-13235
- User's guide for ENSAERO: A multidisciplinary program for fluid/structural/control interaction studies of aircraft (release 1) [NASA-TM-108853] p 65 N95-13662
- Development and application of structural dynamics analysis capabilities [NASA-CR-197229] p 96 N95-14922
- Prediction of rotor-blade deformations due to unsteady airloads [AD-A284467] p 81 N95-15821
- Parachute inflation: A problem in aeroelasticity [AD-A284375] p 117 N95-18340
- Documentation and archiving of the Space Shuttle wind tunnel test data base. Volume 2: User's Guide to the Archived Data Base [NASA-TM-104806-VOL-2] p 205 N95-19624
- Integrated aerodynamic/dynamic/structural optimization of helicopter rotor blades using multilevel decomposition [NASA-TP-3465] p 285 N95-22953
- Thin tailored composite wing for civil titrotor p 285 N95-23317
- Flutter analysis of composite box beams [NASA-CR-197931] p 294 N95-23392
- Vibration analysis of a split path gearbox [NASA-TM-106875] p 438 N95-27855
- Collected papers on wind turbine technology [NASA-CR-195432] p 447 N95-29790
- A NASTRAN-based computer program for structural dynamic analysis of Horizontal Axis Wind Turbines p 439 N95-29780
- Structural design optimization with survivability dependent constraints application: Primary wing box of a multi-role fighter p 398 N95-28440
- Reliability analysis of composite structures p 423 N95-28441
- Technology integration box beam failure study p 441 N95-28468

An analytic modeling and system identification study of helicopter dynamics p 505 N95-29787
 Influence of backup bearings and support structure dynamics on the behavior of rotors with active supports [NASA-CR-199080] p 703 N95-32689
 Synchronous dynamics of a coupled shaft/bearing/housing system with auxiliary support from a clearance bearing: Analysis and experiment p 703 N95-32693

Development of a composite tailoring procedure for airplane wing [NASA-CR-199081] p 691 N95-32928

DYNAMIC TESTS

Measurement of particle emissions from clean room gas-handling components [BTN-94-EIX94381359040] p 295 A95-74554
 Large amplitude nonlinear response of flat aluminum, and carbon fiber plastic beams and plates [AD-A282440] p 96 N95-15547

Investigation of dynamic inflow's influence on rotor control derivatives p 155 N95-16250

Development of a multicomponent force and moment balance for water tunnel applications, volume 2 [NASA-CR-4642-VOL-2] p 161 N95-18956

Calculation of support interference in dynamic wind-tunnel tests p 122 N95-19282

Effect of atmospheric pressure on measured aircraft noise levels [PB95-130423] p 232 N95-21425

Analysis of warping effects on the static and dynamic response of a seat-type structure [NIAR-94-12] p 348 N95-24211

Experimental investigation of static and dynamic ground effect on HOPE ALFLEX vehicle [NAL-TR-1236] p 388 N95-26525

DYNAMICAL SYSTEMS

Reduced-order nonlinear analysis of aircraft dynamics [BTN-95-EIX95282706665] p 455 A95-89640

Identification of dynamic systems. Volume 3: Applications to aircraft. Part 2: Nonlinear analysis and manoeuvre design [AGARD-AG-300-VOL-3-PT-2] p 79 N95-14102

Nonlinear system guidance in the presence of transmission zero dynamics [NASA-TM-4661] p 309 N95-22804

Actuating signals in adaptive control systems [IFTR-13/1994] p 361 N95-26330

Dynamical systems as models for flow-induced vibrations [PB95-206991] p 647 N95-30956

DYNAMICS

Modeling rotating shafts using axisymmetric solid finite elements with matrix reduction [BTN-94-EIX94351143328] p 207 A95-67301

E**EARTH (PLANET)**

Conversion of Earth-centered Earth-fixed coordinates to geodetic coordinates [BTN-94-EIX94441380862] p 125 A95-64294

EARTH ATMOSPHERE

Variations of perturbations in perigee height with eccentricity for artificial Earth's satellites due to air drag [HTN-95-40013] p 85 A95-62657

Powerful bolide explosion over North Italy [HTN-95-80564] p 218 A95-69658

Overview of remote sensing laser development and semiconductor laser technology [DE94-019103] p 256 N95-21552

EARTH IONOSPHERE

Using IRI for the computation of ionospheric corrections for altimeter data analysis p 212 A95-66949

EARTH OBSERVING SYSTEM (EOS)

Earth Observing System (EOS)/Advanced Microwave Sounding Unit-A (AMSU-A) software assurance plan [NASA-CR-196059] p 98 N95-13885

EARTH ORBITAL RENDEZVOUS

EURECA mission control experience and messages for the future p 149 N95-17252

EARTH ORBITS

Variations of perturbations in perigee height with eccentricity for artificial Earth's satellites due to air drag [HTN-95-40013] p 85 A95-62657

Effects of satellite bunching on the probability of collision in geosynchronous orbit [BTN-95-EIX95152583276] p 298 A95-73577

EARTH RESOURCES PROGRAM

Cuts endanger airborne research --- NASA Ames Research Center Reorganization [HTN-95-20602] p 443 A95-84783

EARTH SCIENCES

Cuts endanger airborne research --- NASA Ames Research Center Reorganization [HTN-95-20602] p 443 A95-84783

JPRS report: Science and technology. Central Eurasia [JPRS-UST-94-018] p 349 N95-24472

Airborne geophysics and precise positioning: Scientific issues and future directions [LC-94-68678] p 446 N95-27156

Advanced data visualization and sensor fusion: Conversion of techniques from medical imaging to Earth science p 711 N95-34236

EARTH SURFACE

Thundercloud electric field modeling for the ionosphere-Earth region. 1: Dependence on cloud charge distribution [HTN-95-41223] p 317 A95-75035

MAX-91: Polarimetric SAR results on Montepertoli site p 320 N95-23940

Naval Aviation System TEAM mapping, charting, and geodesy handbook [AD-A288590] p 446 N95-26841

EAST GERMANY

The DLR research programme on an integrated multi sensor system for surface movement guidance and control p 689 N95-33135

ECCENTRIC ORBITS

Variations of perturbations in perigee height with eccentricity for artificial Earth's satellites due to air drag [HTN-95-40013] p 85 A95-62657

ECCENTRICITY

Period evolution of PSR B1259-63: Evidence for propeller-torque spindown [HTN-95-B0194] p 581 A95-87903

Acoustic scattering from ellipses by the modal element method [NASA-TM-106935] p 579 N95-29401

ECHELLE GRATINGS

An Echelle Grating Spectrometer (EGS) for mid-IR remote chemical detection [DE94-019310] p 249 N95-21478

ECONOMIC ANALYSIS

Design constraints in the payload-range diagram of ultrahigh capacity transport airplanes [BTN-95-EIX95152582319] p 276 A95-73522

The high speed civil transport: A technology challenge p 496 A95-90089

Evaluation and management of research and development in aeronautics [CONGRESS PAPER C428-8-102] p 581 A95-91691

Small gas turbine component evaluation study [PB95-147542] p 338 N95-24293

Advanced subsonic airplane design and economic studies [NASA-CR-195443] p 338 N95-24304

ECONOMICS

Trends in aerospace forgings in the 1990s [HTN-95-B0408] p 456 A95-90756

The world of regional aircraft - challenges and opportunities [HTN-95-C0002] p 595 A95-93390

EDDY CURRENTS

Development of an Automated Nondestructive Inspection (ANDI) system for commercial aircraft, phase 1 [AD-A283500] p 40 N95-12623

Eddy current for detecting second layer cracks under installed fasteners [AD-A282412] p 158 N95-17507

Evaluation of scanners for C-scan imaging in nondestructive inspection of aircraft [DE94-012473] p 152 N95-19100

Eddy current for detecting second-layer cracks under installed fasteners [AD-A279871] p 244 N95-20414

Eddy current detection of pitting corrosion around fastener holes p 315 N95-23507

Emerging nondestructive inspection for aging aircraft [PB95-143053] p 328 N95-25401

Extension to the dynamic modeling of the large angle magnetic suspension test fixture [NASA-CR-197801] p 411 N95-26768

EDDY VISCOSITY

Lag model for turbulent boundary layers over rough bleed surfaces [BTN-94-EIX94441380981] p 208 A95-68165

Adaptive finite element method for turbulent flow near a propeller [BTN-95-EIX95142553038] p 305 A95-73460

Modelling 2D separation from a high lift airfoil with a non-linear eddy-viscosity model and second-moment closure [HTN-95-C0005] p 585 A95-93393

Computational analysis of forebody tangential slot blowing on the high alpha research vehicle [NASA-CR-197754] p 389 N95-26591

Advanced k-epsilon modeling of heat transfer [NASA-CR-4679] p 648 N95-31423

EDGE DETECTION

A tactical navigation and routing system for low-level flight p 709 N95-32494

EDITING

Efficient and effective handling of cycle slips in global positioning system data p 43 N95-12230

EDITING ROUTINES (COMPUTERS)

Stratus' tephigram as a training/forecasting tool p 657 A95-93465

Efficient and effective handling of cycle slips in global positioning system data p 43 N95-12230

EDUCATION

ATE enabling technologies [BTN-95-EIX95172595294] p 287 A95-75718

The NASA-sponsored Maryland center for hypersonic education and research [AIAA PAPER 95-6105] p 519 A95-88010

Maintenance training to cope with high-tech innovations [SAE PAPER 932619] p 456 A95-90082

The NASA/UTA Center for hypersonic research [AIAA PAPER 95-6106] p 520 A95-90438

Research and educational initiatives at the Syracuse University Center for Hypersonics [AIAA PAPER 95-6107] p 520 A95-90439

Aviation weather education and the University of North Dakota aviation weather survey p 656 A95-93462

Pilot training initiatives for the '90s p 657 A95-93463

Aviation meteorology education in an AB initio setting p 657 A95-93466

Propulsion education at Carlton University [SAE PAPER 931391] p 613 A95-93667

An educational introduction to transonic compressor stage design principles [SAE PAPER 931393] p 613 A95-93668

Dryden overview for schools [NASA-TM-104282] p 21 N95-10710

Dryden overview for schools [NASA-TM-104302] p 21 N95-10747

Computational fluid dynamics uses in fluid dynamics/aerodynamics education [NASA-TM-108834] p 8 N95-10847

Activities of the Institute for Aerospace Studies of Toronto University p 63 N95-12699

A graphical user interface for design and analysis of air breathing propulsion systems [TABES PAPER 94-616] p 83 N95-14645

A workstation based simulator for teaching compressible aerodynamics [NASA-TM-106799] p 170 N95-16906

1994 NASA-HU American Society for Engineering Education (ASEE) Summer Faculty Fellowship Program [NASA-CR-194972] p 325 N95-23276

Preparation of course materials: Elementary mathematics of powered flight p 324 N95-23320

EFFECTIVE PERCEIVED NOISE LEVELS

Effect of atmospheric pressure on measured aircraft noise levels [PB95-130423] p 232 N95-21425

Active control of fan noise-feasibility study. Volume 1: Flyover system noise studies [NASA-CR-195392-VOL-1] p 258 N95-21888

EFFICIENCY

Small gas turbines in the 21st century [BTN-94-EIX94461290241] p 82 A95-61736

Electrorheologically controlled landing gear [BTN-94-EIX94461047055] p 78 A95-61740

Computing quantitative characteristics of finite-state real-time systems [AD-A282839] p 83 N95-14343

EFFLUENTS

Potential effects on ozone of future supersonic aircraft/2D simulation [HTN-95-51282] p 356 A95-80867

Development of techniques for the in situ observation of OH and HO2 for studies of the impact of high-altitude supersonic aircraft on the stratosphere [NASA-CR-196759] p 61 N95-12832

Measurements of ions formed in jet engine exhaust plumes [AD-A290940] p 514 N95-29764

EGRESS

Aircraft evacuations through Type-3 exits I: Effects of seat placement at the exit [DOT/FAA/AM-95/72] p 599 N95-31845

EIGENVALUES

Eigenanalysis of unsteady flows about airfoils, cascades, and wings [BTN-95-EIX9515257597] p 305 A95-73486

Design of an effective controller via disturbance accommodating left eigenstructure assignment [BTN-95-EIX95282706663] p 565 A95-88178

New eigensolutions and modal analysis for gyroscopic/rotor systems, part 1: undamped systems [BTN-94-EIX94522410219] p 702 A95-96373

- New eigensolutions and modal analysis for gyroscopic/rotor systems, part 2: perturbation analysis for damped systems
[BTN-94-EIX94522410220] p 702 A95-96374
- Aeroelastic stability of wind turbine blade/aileron systems p 377 N95-27981
- EIGENVECTORS**
Design of an effective controller via disturbance accommodating left eigenstructure assignment
[BTN-95-EIX95282706663] p 565 A95-88178
- New eigensolutions and modal analysis for gyroscopic/rotor systems, part 1: undamped systems
[BTN-94-EIX94522410219] p 702 A95-96373
- New eigensolutions and modal analysis for gyroscopic/rotor systems, part 2: perturbation analysis for damped systems
[BTN-94-EIX94522410220] p 702 A95-96374
- EJECTION**
Computer simulation of ejection seat motion
[CONGRESS PAPER C428-18-169] p 484 A95-91718
- EJECTION SEATS**
RAF ejections - historical perspectives and future requirements
[CONGRESS PAPER C428-18-168] p 484 A95-91717
- Computer simulation of ejection seat motion
[CONGRESS PAPER C428-18-169] p 484 A95-91718
- Preliminary evaluation of the F/A-18 quantity/multiple envelope expansion
[AD-A284119] p 132 N95-18407
- EJECTORS**
Internal performance characteristics of thrust-vectoring axisymmetric ejector nozzles
[NASA-TM-4610] p 331 N95-25338
- Ejectors and jet pumps: Computer program for design and performance for steam/gas flow
[ESDU-94046] p 500 N95-28704
- ELASTIC BENDING**
Residual strength of thin panels with cracks p 311 N95-23311
- Thin tailored composite wing for civil tiltrotor p 285 N95-23317
- ELASTIC DAMPING**
An analytical model for a nonlinear elastomeric lag damper and its effect on aeromechanical stability in Hover
[HTN-95-61076] p 369 A95-83660
- ELASTIC DEFORMATION**
Integrated development of the equations of motion for elastic hypersonic flight vehicles
[BTN-95-EIX95242670755] p 327 A95-81092
- Experiment of the large elastic deformation of biconvex wing sections in an air-flow p 475 A95-91564
- Prediction of rotor-blade deformations due to unsteady airloads
[AD-A284467] p 81 N95-15821
- Determination of stores pointing error due to wing flexibility under flight load
[NASA-TM-4646] p 134 N95-19044
- Impact loading of compressor stator vanes by hailstone ingestion p 200 N95-19670
- Load transfer in the stiffener-to-skin joints of a pressurized fuselage
[NASA-CR-198610] p 439 N95-27865
- Unique considerations in the design and experimental evaluation of tailored wings with elastically produced chordwise camber p 423 N95-28436
- ELASTIC PROPERTIES**
Lyapunov exponents and stochastic stability of two-dimensional parametrically excited random systems
[BTN-94-EIX94361122401] p 207 A95-85897
- Elastic-plastic models for multi-site damage p 92 N95-14454
- ELASTIC WAVES**
Aerodynamic interference for supersonic low-aspect-ratio missiles
[BTN-95-EIX95302694469] p 588 A95-94065
- ELASTOMERS**
Development of a low-cost, modified resin transfer molding process using elastomeric tooling and automated preform fabrication p 420 N95-28268
- ELECTRIC BATTERIES**
'Global avionics in the future' report from the 10th annual battery conference
[BTN-95-EIX95282706404] p 545 A95-88184
- Development of a bipolar lead/acid battery for the more electric aircraft
[AD-A284050] p 160 N95-18660
- ELECTRIC CONDUCTORS**
175Hp contrarotating homopolar motor design report
[AD-A291138] p 557 N95-30122
- ELECTRIC CONNECTORS**
Preload release mechanism
[NASA-CASE-MSC-22327-1] p 350 N95-25592
- Partial discharge testing of high voltage wiring harness for airborne displays
[AD-A289150] p 401 N95-27003
- ELECTRIC CONTROL**
General requirements for the electrohydraulic systems of the aircraft controls loading force on the simulators
[CONGRESS PAPER C428-5-138] p 522 A95-91681
- Flying qualities of civil transport aircraft with electrical flight control p 624 N95-32016
- ELECTRIC CORONA**
Aircraft electric field measurements: Calibration and ambient field retrieval
[HTN-95-90508] p 213 A95-67780
- ELECTRIC DISCHARGES**
Partial discharge testing of high voltage wiring harness for airborne displays
[AD-A289150] p 401 N95-27003
- ELECTRIC EQUIPMENT**
Generalized method of solving topological optimization problems for electrical airplane equipment systems in computer-aided design p 169 N95-16272
- ELECTRIC EQUIPMENT TESTS**
Starter/generator testing
[BTN-95-EIX95072498877] p 210 A95-68393
- Ceramic composite attachments for transmission of high-torque loads
[BTN-94-EIX95011441256] p 417 A95-84213
- Fault detection techniques for complex cable shield topologies
[AD-A286632] p 247 N95-20771
- Partial discharge testing of high voltage wiring harness for airborne displays
[AD-A289150] p 401 N95-27003
- ELECTRIC FIELD STRENGTH**
Application of airborne field mill data for use in launch support p 98 A95-62279
- ELECTRIC FIELDS**
Application of airborne field mill data for use in launch support
[HTN-95-50054] p 98 A95-62279
- Aircraft electric field measurements: Calibration and ambient field retrieval
[HTN-95-90508] p 213 A95-67780
- Thundercloud electric field modeling for the ionosphere-Earth region. 1: Dependence on cloud charge distribution
[HTN-95-41223] p 317 A95-75035
- ELECTRIC GENERATORS**
Starter/generator testing
[BTN-95-EIX95072498877] p 210 A95-68393
- Development of 70MW class superconducting generators
[BTN-94-EIX95011440854] p 429 A95-82905
- System design considerations for an APU starter-generator
[SAE PAPER 932559] p 511 A95-90056
- Electrical power system upgrade methodology for in-service aircraft
[SAE PAPER 932562] p 511 A95-90059
- Secondary power system study for the hytex RA3 flight test vehicle
[AIAA PAPER 95-6158] p 512 A95-90470
- Applicability of electrically driven accessories for turbohaft engines
[BTN-95-EIX95292721153] p 612 A95-92589
- A detailed power inverter design for a 250 kW switched reluctance aircraft engine starter/generator
[SAE PAPER 931388] p 613 A95-93664
- Detailed design of a 250-kW switched reluctance starter/generator for an aircraft engine
[SAE PAPER 931389] p 613 A95-93665
- Wind technology development: Large and small turbines
[DE95-000286] p 358 N95-26090
- A hybrid vehicle evaluation code and its application to vehicle design. Revision 1
[DE95-008053] p 441 N95-28029
- 175Hp contrarotating homopolar motor design report
[AD-A291138] p 557 N95-30122
- A time stepping coupled finite element-state space modeling environment for synchronous machine performance and design analysis in the ABC frame of reference p 649 N95-31948
- ELECTRIC MOTOR VEHICLES**
'Global avionics in the future' report from the 10th annual battery conference
[BTN-95-EIX95282706404] p 545 A95-88184
- ELECTRIC MOTORS**
A switched reluctance machine rotor position estimator. A neural network application
[SAE PAPER 932560] p 511 A95-90057
- Analysis and scale-model experiment of propeller driving motor for microwave-powered airplane p 487 A95-91576
- Power system characteristics for more electric aircraft
[SAE PAPER 931406] p 613 A95-93675
- Motor drive technologies for the power-by-wire (PBW) program: Options, trends and tradeoffs
[NASA-TM-106885] p 295 N95-23671
- Dynamically timed electric motor
[NASA-CASE-MFS-28958-1] p 437 N95-26890
- ELECTRIC NETWORKS**
Modeling resonance in waveguide-to-microstrip junctions by unilateral fin line resonators
[BTN-94-EIX94381323445] p 242 A95-70844
- ELECTRIC POTENTIAL**
Micro-time stress measurement device development
[AD-A289511] p 448 N95-26845
- Mechanism of deposit formation on fuel-wetted hot metal surfaces
[AD-A289847] p 426 N95-28621
- 175Hp contrarotating homopolar motor design report
[AD-A291138] p 557 N95-30122
- ELECTRIC POWER SUPPLIES**
'Global avionics in the future' report from the 10th annual battery conference
[BTN-95-EIX95282706404] p 545 A95-88184
- Evaluation of all-electric secondary power for transport aircraft
[NASA-CR-189077] p 441 N95-27999
- ELECTRIC POWER TRANSMISSION**
Ceramic composite attachments for transmission of high-torque loads
[BTN-94-EIX95011441256] p 417 A95-84213
- ELECTRIC PROPULSION**
Arcjet thruster research and technology, phase 2
[NASA-CR-182276] p 105 N95-18044
- ELECTRIC WIRE**
Computerized maintenance aid
[BTN-95-EIX95031502749] p 217 A95-68256
- Aircraft wiring maintenance: Development of a computerized maintenance aid
[SAE PAPER 932615] p 456 A95-90080
- Problems with aging wiring in Naval aircraft p 154 N95-16048
- Development of LaRC (TM): IA thermoplastic polyimide coated aerospace wiring
[NASA-CR-195048] p 537 N95-30252
- Electrical short circuit and current overload tests on aircraft wiring
[AD-A293308] p 646 N95-30922
- ELECTRICAL ENGINEERING**
Development of 70MW class superconducting generators
[BTN-94-EIX95011440854] p 429 A95-82905
- JPRS report: Science and technology. Central Eurasia
[JPRS-UST-94-027] p 349 N95-24470
- JPRS report: Science and technology. Central Eurasia
[JPRS-UST-94-018] p 349 N95-24472
- FBI report: Science and technology. Central Eurasia
[FBI-UST-95-029] p 649 N95-31728
- ELECTRICAL FAULTS**
Fault detection techniques for complex cable shield topologies
[AD-A286632] p 247 N95-20771
- ELECTRICAL IMPEDANCE**
Electromagnetic on-aircraft antenna radiation in the presence of composite plates
[NASA-CR-196126] p 58 N95-12856
- Scattering and radiation from cylindrically conformal antennas p 645 N95-30669
- ELECTRICAL INSULATION**
Problems with aging wiring in Naval aircraft p 154 N95-16048
- Development of LaRC (TM): IA thermoplastic polyimide coated aerospace wiring
[NASA-CR-195048] p 537 N95-30252
- ELECTRICAL MEASUREMENT**
Application of airborne field mill data for use in launch support
[HTN-95-50054] p 98 A95-62279
- Micro-time stress measurement device development
[AD-A289511] p 448 N95-26845
- ELECTRIFICATION**
Field and data analysis studies related to the atmospheric environment
[NASA-CR-196543] p 168 N95-18093
- Collaborative research on aircraft icing and charging processes in ice
[AD-A285102] p 276 N95-23201
- ELECTRO-OPTICS**
Electro-optic characterization of ultrafast photodetectors using adiabatically compressed soliton pulses
[BTN-94-EIX94381359637] p 257 A95-72675
- Fiber Optic Control System integration for advanced aircraft. Electro-optic and sensor fabrication, integration, and environmental testing for flight control systems
[NASA-CR-191194] p 162 N95-19236

Integrated X-ray testing of the electro-optical breadboard model for the XMM reflection grating spectrometer [DE95-008829] p 644 N95-30507
Low-level data fusion for landing runways detection p 689 N95-33136

ELECTROACOUSTIC TRANSDUCERS

Investigating the use of smart acoustically active surfaces for flow separation control in turbomachinery [AD-A292819] p 648 N95-31443

ELECTROCHEMICAL CORROSION

The use of electrochemistry and ellipsometry for identifying and evaluating corrosion on aircraft [AD-A285323] p 151 N95-16371
Corrosion protection measures for CFC/metal joints of fuel integral tank structures of advanced military aircraft p 303 N95-23510

The use of electrochemistry and ellipsometry for identifying and evaluating corrosion on aircraft [AD-A290249] p 504 N95-29426

ELECTROCHEMICAL MACHINING

Profiling of the working surface of electrodes-tools for circle electrochemical dimensional treatment of compressor blades [BTN-94-EIX94461407964] p 83 A95-62638

ELECTROCHEMISTRY

The use of electrochemistry and ellipsometry for identifying and evaluating corrosion on aircraft [AD-A285323] p 151 N95-16371

Electrochemical impedance pattern recognition for detection of hidden chemical corrosion on aircraft components [AD-A285998] p 241 N95-20716

Health and usage monitoring systems: Corrosion surveillance p 262 N95-23506

In-situ detection of surface passivation or activation and of localized corrosion: Experiences and prospectives in aircraft p 302 N95-23508

Test method and test results for environmental assessment of aircraft materials p 302 N95-23509

The use of electrochemistry and ellipsometry for identifying and evaluating corrosion on aircraft [AD-A288536] p 381 N95-27186

The use of electrochemistry and ellipsometry for identifying and evaluating corrosion on aircraft [AD-A290249] p 504 N95-29426

ELECTRODES

Profiling of the working surface of electrodes-tools for circle electrochemical dimensional treatment of compressor blades [BTN-94-EIX94461407964] p 83 A95-62638

ELECTROHYDRAULIC FORMING

Universal electrohydraulic system for the steering gear loading [CONGRESS PAPER C428-10-106] p 517 A95-91700

ELECTROMAGNETIC COMPATIBILITY

MIL-STD-461/MIL-STD-704 investigation [SAE PAPER 932561] p 505 A95-90058

Electromagnetic compatibility - A general overview [CONGRESS PAPER C428-38-084] p 634 A95-93637

Power system characteristics for more electric aircraft [SAE PAPER 931406] p 613 A95-93675

Electromagnetic reverberation characteristics of a large transport aircraft [AD-A282923] p 82 N95-15392

FASTPACK: Optimized solutions for modular avionics derived from a parametric study. Part 2: Avionics p 233 N95-20635

Composite cases for airborne electronic equipment: A technology study and EMC p 241 N95-20655

Electromagnetic compatibility effects of advanced packaging configurations p 247 N95-20658

ELECTROMAGNETIC FIELDS

Optimal shape design in hypersonic aerodynamics and electromagnetics p 639 A95-95397

Measurements of shielding effectiveness and cavity characteristics of airplanes [PB94-210051] p 244 N95-20191

Consistent approach to describing aircraft HIRF protection [NASA-CR-195067] p 334 N95-25341

ELECTROMAGNETIC INTERACTIONS

A Lifting Ball Valve for cryogenic fluid applications p 156 N95-16349

ELECTROMAGNETIC INTERFERENCE

MIL-STD-461/MIL-STD-704 investigation [SAE PAPER 932561] p 505 A95-90058

Formal design and verification of a reliable computing platform for real-time control (phase 3 results) [NASA-TM-109140] p 33 N95-10873

The development of a highly reliable power management and distribution system for civil transport aircraft [NASA-TM-106697] p 50 N95-11867

Measurements of shielding effectiveness and cavity characteristics of airplanes [PB94-210051] p 244 N95-20191

US Navy operating experience with new aircraft construction materials p 303 N95-23517

ELECTROMAGNETIC MEASUREMENT

Measurements of shielding effectiveness and cavity characteristics of airplanes [PB94-210051] p 244 N95-20191

ELECTROMAGNETIC NOISE MEASUREMENT

Electromagnetic reverberation characteristics of a large transport aircraft [AD-A282923] p 82 N95-15392

ELECTROMAGNETIC PULSES

Composite waveform generation for EMP and lightning direct-drive testing [AD-A284159] p 92 N95-14405

Assessing aircraft survivability to high frequency transient threats [AD-A283999] p 134 N95-18726

Waveform bounding and combination techniques for direct drive testing [AD-A284057] p 161 N95-19035

E-6A hardness assurance, maintenance and surveillance program [AD-A283994] p 134 N95-19067

ELECTROMAGNETIC RADIATION

RCS measurements, transformations, and comparisons under cylindrical and plane wave illumination [BTN-94-EIX94371347126] p 242 A95-69976

Comments on effect of wet snow on the null-reference ILS system [BTN-95-EIX9514255488] p 227 A95-72885

Impulse radiating antennas p 548 A95-90920

Scattering of short em-pulses by simple and complex targets using impulse radar p 486 A95-90953

Ultra-wideband electromagnetic target identification p 486 A95-90955

Electromagnetic on-aircraft antenna radiation in the presence of composite plates [NASA-CR-196126] p 58 N95-12856

Hypersonic wind tunnel test techniques [AD-A284057] p 118 N95-18663

ELECTROMAGNETIC SCATTERING

Hybrid finite element-modal analysis of jet engine inlet scattering [BTN-95-EIX95242673665] p 427 A95-82259

Analysis of backscattering from wing and fuselage joints [HTN-95-71134] p 430 A95-83495

A users manual for the method of moments Aircraft Modeling Code (AMC), version 2 [NASA-CR-196445] p 24 N95-11252

Electromagnetic on-aircraft antenna radiation in the presence of composite plates [NASA-CR-196126] p 58 N95-12856

Inband radar cross section of phased arrays with parallel feeds [AD-A284249] p 210 N95-19730

Induced Compton scattering by relativistic electrons in magnetized astrophysical plasmas p 563 N95-29885

Scattering and radiation from cylindrically conformal antennas p 645 N95-30669

ELECTROMAGNETIC SHIELDING

Measurements of shielding effectiveness and cavity characteristics of airplanes [PB94-210051] p 244 N95-20191

Composite cases for airborne electronic equipment: A technology study and EMC p 241 N95-20655

Lightweight electronic enclosures using composite materials p 241 N95-20656

Fault detection techniques for complex cable shield topologies [AD-A286632] p 247 N95-20771

TIM-SCT cable testing protocol [AD-A286633] p 231 N95-20772

ELECTROMAGNETIC WAVE TRANSMISSION

Measurements of shielding effectiveness and cavity characteristics of airplanes [PB94-210051] p 244 N95-20191

Hypersonic wind tunnel test techniques [AD-A284057] p 118 N95-18663

Cu deposition using a permanent magnet electron cyclotron resonance microwave plasma source [DE94-017768] p 304 N95-23981

Extension to the dynamic modeling of the large angle magnetic suspension test fixture [NASA-CR-197801] p 411 N95-26768

ELECTROMECHANICAL DEVICES

Blade-by-blade tip clearance measurement system for gas turbine applications [BTN-95-EIX95292721167] p 546 A95-89899

Advanced passive cooling for high power electromechanical actuators [SAE PAPER 931397] p 634 A95-93669

Power system characteristics for more electric aircraft [SAE PAPER 931406] p 613 A95-93675

ELECTROMECHANICS

High density monolithic packaging technology for digital/microwave avionics p 240 N95-20646

ELECTRON ENERGY

Measurement and analysis of nitric oxide radiation in an arcjet flow [BTN-95-EIX95082502727] p 243 A95-71040

A survey of bidirectional greater than or equal to MeV ion flows during the Helios 1 and Helios 2 mission: Observations from the Goddard Space Flight Center instruments [HTN-95-70542] p 237 A95-71656

ELECTRON MICROSCOPY

Standardization of surface contamination analysis systems p 631 N95-31798

ELECTRON TRANSFER

A model for temperature-dependent collisional quenching of OH A(sup 2) Sigma(sup +) [HTN-95-42308] p 450 A95-85002

ELECTRONIC AIRCRAFT

Conceptual design of the AE481 Demon Remotely Piloted Vehicle (RPV) [NASA-CR-197164] p 44 N95-12294

E-6A hardness assurance, maintenance and surveillance program [AD-A283994] p 134 N95-19067

ELECTRONIC CONTROL

Second generation smart actuator [SAE PAPER 932585] p 505 A95-90069

Design trends in propulsion control systems [CONGRESS PAPER C428-33-123] p 610 A95-93620

Chinook goes FADEC [CONGRESS PAPER C428-33-078] p 610 A95-93621

An electrorheologically controlled semi-active landing gear [SAE PAPER 931403] p 605 A95-93673

A programmable heater control circuit for spacecraft [NASA-TM-108459] p 9 N95-11157

Advanced diesel electronic fuel injection and turbocharging [AD-A279176] p 211 N95-19809

Wind technology development: Large and small turbines [DE95-000286] p 358 N95-26090

ELECTRONIC EQUIPMENT

Real-time decision aiding: Aircraft guidance for wind shear avoidance [BTN-95-EIX95202637575] p 332 A95-78583

Electromagnetic compatibility - A general overview [CONGRESS PAPER C428-38-084] p 634 A95-93637

Composite cases for airborne electronic equipment: A technology study and EMC p 241 N95-20655

Lightweight electronic enclosures using composite materials p 241 N95-20656

Differential GPS and system integration of the Low Visibility Landing and Surface Operations (LVLASO) demonstration p 280 N95-23318

CAE for thermal management of aerospace electronic boards using the BETAsoft program p 438 N95-27354

Solid-state data recorder, next development and use p 705 N95-33143

ELECTRONIC EQUIPMENT TESTS

CASS: Design for supportability [BTN-95-EIX95172595296] p 287 A95-75716

Fault detection in multiprocessor systems and array processors [BTN-95-EIX95242679097] p 359 A95-81253

Assessment of a non-dedicated GPS receiver system for precise airborne attitude determination [DE94-019309] p 229 N95-21520

ELECTRONIC MODULES

MCMs for avionics: Technology selection and intermodule interconnection p 234 N95-20641

Liquid flow-through cooling of electronic modules p 246 N95-20647

Immersion/two phase cooling p 246 N95-20648

ELECTRONIC PACKAGING

High density monolithic packaging technology for digital/microwave avionics p 240 N95-20646

Liquid flow-through cooling of electronic modules p 246 N95-20647

Electromagnetic compatibility effects of advanced packaging configurations p 247 N95-20658

ELECTRONIC WARFARE

Wind tunnel tests of a 42 inch diameter self-starting autogyro rotor [AD-A279922] p 188 N95-19863

- Systems engineering design and technical analyses for Strategic Avionics Crew-station Design Evaluation Facility (SACDEF)
[AD-A286239] p 235 N95-22024
- ELECTORHEOLOGICAL FLUIDS**
Electrorheologically controlled landing gear
[BTN-94-EIX94461047055] p 78 A95-61740
- ELECTROSTATIC CHARGE**
The effect of aviation fuels containing low amounts of static dissipater additive on electrostatic charge generation
[AD-A280075] p 420 N95-28152
- ELECTROSTATICS**
Comparison of electrostatic and aerodynamic forces during parachute opening
[BTN-95-EIX95062487532] p 187 A95-69240
- ELEVATION**
Synthetic Terrain Imagery for Helmet-Mounted Display, volume 1
[AD-A293612] p 612 N95-31656
- ELEVATION ANGLE**
Apparent size passive range method
[AD-D017360] p 611 N95-31180
- ELEVONS**
Unsteady aerodynamic effects of trailing edge controls on delta wings
[HTN-95-01099] p 469 A95-90285
- ELLIPSES**
Elliptic tip effects on the vortex wake of an axisymmetric body at incidence
[HTN-95-20938] p 464 A95-88977
Acoustic scattering from ellipses by the modal element method
[NASA-TM-106935] p 579 N95-29401
- ELLIPSOmetry**
The use of electrochemistry and ellipsometry for identifying and evaluating corrosion on aircraft
[AD-A285323] p 151 N95-16371
The use of electrochemistry and ellipsometry for identifying and evaluating corrosion on aircraft
[AD-A288536] p 381 N95-27186
The use of electrochemistry and ellipsometry for identifying and evaluating corrosion on aircraft
[AD-A290249] p 504 N95-29426
Standardization of surface contamination analysis systems
p 631 N95-31798
- ELLIPTIC DIFFERENTIAL EQUATIONS**
Automatic multi-block grid generation for high-lift configuration wings
p 567 N95-28764
- ELLIPTIC FUNCTIONS**
Study of strapdown navigation attitude algorithms
[BTN-95-EIX95282706655] p 486 A95-89649
- ELLIPTICAL CYLINDERS**
Ellipsoid-cylinder model
p 158 N95-17869
- EMERGENCIES**
Inadequacy of visual alarms in helicopter air medical transport
[HTN-95-01218] p 484 A95-91450
EMS helicopter incidents reported to the NASA Aviation Safety Reporting System
p 596 A95-95201
Emergency medical service (EMS): A unique flight environment
p 596 A95-95203
Background and principles of throttles-only flight control
p 697 N95-33021
- EMERGENCY LOCATOR TRANSMITTERS**
Federal aviation regulations, part 91. General operating and flight rules. Change 8
[PB94-217445] p 188 N95-19720
- EMISSION**
Nitrous oxide and methane emissions from aero engines
[HTN-95-21363] p 353 A95-78678
- EMISSION SPECTRA**
Analysis of the physical state of one Arctic polar stratospheric cloud based on observations
[HTN-95-70917] p 351 A95-77982
An analysis of aircraft exhaust plumes form accidental encounters
[HTN-95-70943] p 351 A95-78008
Comparison of column abundances from three infrared spectrometers during AASE 2
[HTN-95-70946] p 352 A95-78011
Two-dimensional imaging of OH in a lean burning high pressure combustor
[NASA-TM-106854] p 236 N95-21383
Correction of thin cirrus effects in AVIRIS images using the sensitive 1.375-micron cirrus detecting channel
p 708 N95-33748
- EMISSIVITY**
TIMS observations of surface emissivity in HAPEX-Sahel
p 709 N95-33799
- EMITTANCE**
Measurement and analysis of nitric oxide radiation in an arcjet flow
[BTN-95-EIX95082502727] p 243 A95-71040
- EMOTIONAL FACTORS**
Characteristics of civil aviation atmospheric hazards
p 42 N95-13208
- ENCLOSURE**
Active minimization of energy density in three-dimensional enclosures
[NASA-CR-197213] p 172 N95-16848
- ENCLOSURES**
Facilities used for plastic media blasting
p 627 N95-32176
- ENERGY ABSORPTION**
Prediction of energy absorption capability of composite stiffeners
[HTN-95-A0500] p 230 A95-72571
An electroreologically controlled semi-active landing gear
[SAE PAPER 931403] p 605 A95-93673
Dissolved gas - the hidden saboteur
[SAE PAPER 931404] p 628 A95-93674
Landing gear energy absorption system
[NASA-CASE-MSC-22277-1] p 96 N95-15306
Energy absorption device for shock loading
[AD-D017476] p 706 N95-34449
- ENERGY BUDGETS**
Diurnal variation of lee vortices in Taiwan and the surrounding area
[HTN-95-91363] p 318 A95-76394
User's manual for the NASA Lewis ice accretion/heat transfer prediction code with electrothermal deicer input
[NASA-CR-4530] p 57 N95-11888
Helicopter Performance Evaluation (HELPE) computer model
[AD-A284319] p 131 N95-18381
- ENERGY CONSERVATION**
Drag coefficients of spherical liquid droplets. Part 1: Quiescent gaseous fields
[BTN-95-EIX95262697040] p 538 A95-86857
A study of the savings in time and fuel to aviation through the use of upper-air wind forecasts
p 672 A95-93538
Airfoil leading-edge suction and energy conservation for compressible flow
[BTN-95-EIX95302730589] p 637 A95-94197
Rarefied gas effects on aerobreaking/reentry vehicles with wakes
[NASA-CR-196586] p 415 N95-27093
- ENERGY CONVERSION EFFICIENCY**
Gas-turbine engines with increased efficiency of two circuits, due to the use of the utilizing steam-turbine circuit
[BTN-94-EIX94461408755] p 153 A95-63638
NREL airfoil families for HAWTs
[DE95-000267] p 357 N95-24882
- ENERGY DISSIPATION**
The effects of wall perturbations on thermo-turbulent Couette flow
[HTN-95-92255] p 434 A95-85299
Evaluation of energy-sink stability criteria for dual-spin spacecraft
[AD-A283228] p 87 N95-14850
An analysis code for the Rapid Engineering Estimation of Momentum and Energy Losses (REMEL)
[NASA-CR-191178] p 108 N95-16887
Photoacoustic chambers for studying solids and gases: Theory and practical examples
[IFTR-39/1994] p 412 N95-26837
- ENERGY POLICY**
Wind technology development: Large and small turbines
[DE95-000286] p 358 N95-26090
- ENERGY STORAGE**
TKKMOD: A computer simulation program for an integrated wind diesel system. Version 1.0: Document and user guide
[PB94-179090] p 60 N95-11798
Unitized Regenerative Fuel Cells for solar rechargeable aircraft and zero emission vehicles
[DE95-010684] p 708 N95-33642
- ENERGY TRANSFER**
Contribution of thermal radiation to the temperature profile of ceramic composite materials
[BTN-94-EIX95011441252] p 417 A95-84209
Impact loading of compressor stator vanes by hailstone ingestion
p 200 N95-19670
State-to-state collisional dynamics of atmospheric species
[AD-A285053] p 245 N95-20484
- ENGINE AIRFRAME INTEGRATION**
Flow study of supersonic wing-nacelle configuration
[BTN-95-EIX95152582344] p 266 A95-73546
Integrated flight/propulsion control for helicopters
[HTN-95-80854] p 290 A95-75096
Experimental and numerical analysis of a two-duct nozzle/afterbody model at supersonic Mach numbers
[AIAA PAPER 95-6085] p 490 A95-87414
- Integration of an hypersonic airbreathing vehicle: Assessment of overall aerodynamic performances and of uncertainties
[AIAA PAPER 95-6100] p 492 A95-88007
Engine/airframe installation CFD for commercial transports: An engine manufacturer's perspective
[SAE PAPER 932623] p 495 A95-90084
Civil aircraft propulsion integration: Current & future
[SAE PAPER 932624] p 495 A95-90085
Sensitivity of engine-integrated waverider performance to static margin constraint
[AIAA PAPER 95-6142] p 496 A95-90458
Cabin-fuselage-wing structural design concept with engine installation
[NASA-CR-197172] p 49 N95-12993
Propulsion/airframe interference for ducted propfan engines with ground effect
[NASA-CR-197110] p 81 N95-14909
Cooperative control theory and integrated flight and propulsion control
[NASA-CR-197493] p 142 N95-17404
Impact of dynamic loads on propulsion integration
p 174 N95-19148
Advanced subsonic airplane design and economic studies
[NASA-CR-195443] p 338 N95-24304
Development of an upwind, finite-volume code with finite-rate chemistry
[NASA-CR-197747] p 374 N95-26760
Performance study for inlet installations
[NASA-CR-189714] p 406 N95-28227
- ENGINE ANALYZERS**
Gearbox vibration diagnostic analyzer
[NASA-CR-189141] p 316 N95-23792
- ENGINE CONTROL**
A switched reluctance machine rotor position estimator: A neural network application
[SAE PAPER 932560] p 511 A95-90057
Applicability of electrically driven accessories for turboshaft engines
[BTN-95-EIX95292721153] p 612 A95-92589
Design trends in propulsion control systems
[CONGRESS PAPER C428-33-123] p 610 A95-93620
Chinook goes FADEC
[CONGRESS PAPER C428-33-078] p 610 A95-93621
Surge recovery and compressor working line control using compressor exit mach number measurement
[CONGRESS PAPER C428-33-210] p 610 A95-93622
An advanced vehicle management system
[SAE PAPER 931376] p 618 A95-93655
SUIT: The integration of aircraft subsystems
[SAE PAPER 931381] p 604 A95-93657
Lightweight, opto-electronic engine control system for aerospace turbine engines
[SAE PAPER 931442] p 614 A95-93692
STOVL Control Integration Program
[NASA-CR-195358] p 18 N95-11487
Cooperative control theory and integrated flight and propulsion control
[NASA-CR-197493] p 142 N95-17404
Advanced diesel electronic fuel injection and turbocharging
[AD-A279176] p 211 N95-19809
Prevention and control of inlet unstart using an SR-71 simulation
p 367 N95-26948
Flight test validation of a frequency-based system identification method on an F-15 aircraft
[NASA-TM-4704] p 620 N95-31846
PSC implementation and integration
p 695 N95-33014
The application of Ada and formal methods to a safety critical engine control system
p 710 N95-33142
- ENGINE COOLANTS**
High heat sink fuels for improved aircraft thermal management
[SAE PAPER 932084] p 530 A95-91659
- ENGINE DESIGN**
Trent engine development
[BTN-94-EIX94461290507] p 82 A95-61727
Foil bearings for gas turbine engines
[BTN-94-EIX94461290279] p 82 A95-61732
Small gas turbines in the 21st century
[BTN-94-EIX94461290241] p 82 A95-61736
Gas-turbine engines with increased efficiency of two circuits, due to the use of the utilizing steam-turbine circuit
[BTN-94-EIX94461408755] p 153 A95-63638
Two projects of V. M. Myasishchev
[HTN-95-50269] p 176 A95-65764
Aircraft engine emission reduction
[BTN-95-EIX95031502750] p 196 A95-68257

- Ply layup optimization and micromechanics tailoring of composite aircraft engine structures [BTN-95-EIX95112524206] p 196 A95-69302
- Lycoming to test new engine core [HTN-95-41393] p 288 A95-76389
- Design features of the NAL ramjet engine test facility p 410 A95-82319
- Aircraft gas turbine emissions challenge [BTN-94-EIX95011441239] p 403 A95-84196
- Control requirements for the RB 211 low-emission combustion system [BTN-94-EIX95011441244] p 416 A95-84201
- Flex cycle combustor development and demonstration [BTN-94-EIX95011441245] p 417 A95-84202
- Development of an aeroderivative gas turbine dry low emissions combustion system [BTN-94-EIX95011441246] p 417 A95-84203
- Charles Norvin Rineck, an early American pioneer in advanced aviation engines [SAE PAPER 930485] p 386 A95-84554
- Auxiliary Power Unit evolution: Meeting tomorrow's challenges [SAE PAPER 932541] p 510 A95-89195
- Structural composites in civil gas turbine aero engines [HTN-95-B0258] p 529 A95-89202
- System design considerations for an APU starter-generator [SAE PAPER 932559] p 511 A95-90056
- Conversion of production automotive engines for aviation use [SAE PAPER 932606] p 495 A95-90076
- High bypass separate flow exhaust system improved thrust efficiency by modifying the aft centerbody [SAE PAPER 932622] p 511 A95-90083
- Engine/airframe installation CFD for commercial transports: An engine manufacturer's perspective [SAE PAPER 932623] p 495 A95-90084
- The high speed civil transport: A technology challenge p 496 A95-90089
- Design and development of an advanced two-stage centrifugal compressor [BTN-95-EIX95282710054] p 633 A95-92475
- Propulsion education at Carlton University [SAE PAPER 931391] p 613 A95-93667
- Application of scramjet engine technology to the design of ram accelerator projectiles p 19 A95-10282
- NASA Lewis Propulsion Systems Laboratory customer guide manual [NASA-TM-106569] p 21 A95-10822
- A theoretical analysis of airborne sound transfer for a resiliently mounted machine to its foundation p 30 A95-11304
- Viper cabin-fuselage structural design concept with engine installation and wing structural design [NASA-CR-197162] p 45 A95-12305
- Regulatory impact analysis and regulatory support document: Control of air pollution; determination of significance for nonroad sources and emission standards for new nonroad compression-ignition engines at or above 37 kilowatts (50 horsepower) [PB94-194594] p 61 A95-12855
- NASA's Hypersonic Research Engine Project: A review [NASA-TM-107759] p 50 A95-12860
- Turbomachinery Design Using CFD [AGARD-LS-195] p 89 A95-14127
- Computational methods for preliminary design and geometry definition in turbomachinery p 89 A95-14128
- Elements of a modern turbomachinery design system p 90 A95-14129
- Designing in three dimensions p 90 A95-14130
- Unsteady flows in turbines: Impact on design procedure p 90 A95-14132
- New methods, new methodology: Advanced CFD in the Snecma turbomachinery design process p 90 A95-14134
- Aero design of turbomachinery components: CFD in complex systems p 90 A95-14136
- Computational predictive methods for fracture and fatigue p 93 A95-14466
- The Aluminum Falcon: A low cost modern commercial transport [NASA-CR-197180] p 81 A95-15742
- Advanced Turbine Technology Applications Project (ATTAP) [NASA-CR-195393] p 101 A95-15743
- Small turbojets: Designs and installations p 138 A95-16323
- Experimental and analytical methods for the determination of connected-pipe ramjet and ducted rocket internal performance [AGARD-AR-323] p 149 A95-17278
- Wave cycle design for wave rotor engines with limited nitrogen oxide emissions p 161 A95-18901
- Application of multidisciplinary models to the cooled turbine rotor design p 140 A95-19024
- Perspective problems of gas turbine engines simulation p 140 A95-19026
- Future directions in helicopter protection system configuration p 198 A95-19657
- Navy foreign object damage and its impact on future gas turbine engine low pressure compression systems p 198 A95-19658
- Design of fan blades subjected to bird impact p 200 A95-19669
- Turbine design and application volumes 1, 2, and 3 [E-5666-Vol-1-3] p 236 A95-22341
- Aerodynamic design and analysis of a highly loaded turbine exhaust p 312 A95-23435
- Phase 2: HGM air flow tests in support of HEX vane investigation p 312 A95-23438
- Small gas turbine component evaluation study [PB95-147542] p 338 A95-24293
- Experiment on a rectangular cross section scramjet combustor. 2: Effects of fuel injector geometry [NAL-TR-1220] p 405 A95-26600
- Prevention and control of inlet unstart using an SR-71 simulation p 367 A95-26948
- Preliminary results and research capabilities of a new jet facility at the University of Kansas p 412 A95-26951
- Application of CFD to the analysis and design of high-speed inlets [NASA-CR-198574] p 438 A95-27240
- Comparison of numerical results and multicavity purge and rim seal data with extensions to dynamics [NASA-TM-106685] p 416 A95-27434
- Composite intermediate case manufacturing scale-up for advanced engines p 406 A95-28275
- Surface modeling and grid generation for aeropropulsion CFD p 551 A95-28732
- Wave rotor-enhanced gas turbine engines [NASA-TM-106998] p 615 A95-30517
- An investigation of the side-dump dual in-line ramjet combustor p 617 A95-31199
- A pulsed liquid fuel ramjet p 617 A95-31201
- Design of secondary flow control cascade using numerical simulation p 698 A95-34507
- ENGINE FAILURE**
- Active boundary-layer control in diffusers [HTN-95-42580] p 458 A95-87210
- Vapor lock studies for gasolines wwith ethers [SAE PAPER 931233] p 529 A95-88962
- An investigation of piloting strategies for engine failures during takeoff from offshore platforms [HTN-95-92834] p 497 A95-90752
- Modern transport engine experience with environmental ingestion effects p 199 A95-19660
- ENGINE INLETS**
- F/A-18 inlet calculations at 60-deg angle of attack and 10-deg sideslip [BTN-95-EIX95112524199] p 195 A95-69309
- Numerical study of the performance of swept, curved compression surface scramjet inlets [BTN-95-EIX95112524198] p 197 A95-69310
- A new type of simulator for simulating the flow-field distortion of engine inlet [BTN-95-EIX95202638963] p 289 A95-76673
- Integrated design of hypersonic waveriders including inlets and tailfins [BTN-95-EIX95212645692] p 271 A95-76744
- Prediction of supersonic inlet unstart caused by freestream disturbances [BTN-95-EIX95222650790] p 329 A95-79246
- Hybrid finite element-modal analysis of jet engine inlet scattering [BTN-95-EIX95242673665] p 427 A95-82259
- Hypersonic wind tunnel test of sidewall compression type scramjet inlet p 410 A95-82320
- Sensitivity of engine-integrated waverider performance to static margin constraint [AIAA PAPER 95-6142] p 496 A95-90458
- Aerodynamic characteristics of supersonic air-intake/aircraft integrated models p 472 A95-91512
- Some considerations on system design of the hypersonic transport and supersonic air-intakes p 473 A95-91522
- Application of scramjet engine technology to the design of ram accelerator projectiles p 19 A95-10282
- NASA Lewis Propulsion Systems Laboratory customer guide manual [NASA-TM-106569] p 21 A95-10822
- Analytical investigation of adaptive control of radiated inlet noise from turbofan engines p 30 A95-11277
- Computational analysis in support of the SSTO flowpath test [NASA-TM-106757] p 89 A95-13665
- Computation of supersonic air-intakes p 74 A95-14452
- Wind-tunnel blockage and actuation systems test of a two-dimensional scramjet inlet unstart model at Mach 6 [NASA-TM-109152] p 97 A95-15898
- Two-dimensional scramjet inlet unstart model: Wind-tunnel blockage and actuation systems test [NASA-TM-109984] p 97 A95-15899
- Three dimensional compressible turbulent flow computations for a diffusing S-duct with/without vortex generators [NASA-CR-195390] p 138 A95-17402
- Collection efficiency and ice accretion calculations for a sphere, a swept MS(1)-317 wing, a swept NACA-0012 wing tip, an axisymmetric inlet, and a Boeing 737-300 [NASA-TM-106831] p 123 A95-18582
- Prediction of wind tunnel effects on the installed F/A-18A inlet flow field at high angles-of-attack [NASA-CR-195429] p 197 A95-19651
- Active control of fan noise-feasibility study. Volume 1: Flyover system noise studies [NASA-CR-195392-VOL-1] p 258 A95-21888
- Study of compressible flow through a rectangular-to-semiannular transition duct [NASA-CR-4660] p 338 A95-24392
- Characteristics of the turbine inlet temperature sensing circuit for the T56 turbo-prop engine [DSTO-TR-0095] p 405 A95-26424
- Performance characterization of a highly-offset diffuser with and without blowing vortex generator jets [AD-A289334] p 375 A95-26901
- Prevention and control of inlet unstart using an SR-71 simulation p 367 A95-26948
- Application of CFD to the analysis and design of high-speed inlets [NASA-CR-198574] p 438 A95-27240
- Performance study for inlet installations [NASA-CR-189714] p 406 A95-28227
- Experimental investigation of inlet-combustor isolators for a dual-mode scramjet at a Mach number of 4 [NASA-TP-3502] p 407 A95-28343
- A procedure for automating CFD simulations of an inlet-bleed problem p 552 A95-28768
- Effects of initial conditions on a single jet in crossflow [NASA-TM-107002] p 615 A95-30589
- Method for extracting forward acoustic wave components from rotating microphone measurements in the inlets of turbofan engines [NASA-CR-195457] p 616 A95-30779
- F-15 propulsion system p 695 A95-33012
- Minimum fan turbine inlet temperature mode evaluation p 696 A95-33016
- Fan noise prediction assessment [NASA-CR-195051] p 711 A95-33831
- Subscale study of engine bellmouth inlet vortices in test cell R1D [AD-A294993] p 707 A95-34818
- ENGINE MONITORING INSTRUMENTS**
- Engine life measurement and diagnostics [BTN-95-EIX95041505024] p 235 A95-70133
- High temperature strain gage technology for gas turbine engines [NASA-CR-191177] p 57 A95-11996
- An artificial neural network system for diagnosing gas turbine engine fuel faults [DE94-013960] p 138 A95-17371
- An airborne monitoring system for FOD and erosion faults p 200 A95-19668
- Gearbox vibration diagnostic analyzer [NASA-CR-189141] p 316 A95-23792
- Characteristics of the turbine inlet temperature sensing circuit for the T56 turbo-prop engine [DSTO-TR-0095] p 405 A95-26424
- Cost effective, dual-purpose machine vision-based detectors for (1) smoke and flame detection, and (2) engine overhead/burn-through and flame detection [AD-A292284] p 579 A95-28870
- Method for extracting forward acoustic wave components from rotating microphone measurements in the inlets of turbofan engines [NASA-CR-195457] p 616 A95-30779
- ENGINE NOISE**
- On the scaling of small-scale jet noise to large scale [AIAA PAPER 92-02109] p 27 A95-60166
- Flyover noise reduction of piston-engine propeller aeroplanes using an active noise control technique [SAE PAPER 931218] p 509 A95-87466
- Twenty-first century commercial transport engines p 512 A95-91495
- Aero-engine R&D efforts for environmental protection p 512 A95-91502
- Overview of feasibility study on propulsion concepts for high speed civil transport p 498 A95-91518
- Near field noise prediction requirements [ISVR-TR-234] p 27 A95-11166

Noise Con 1994: Proceedings of the 1994 National Conference on Noise Control Engineering. Progress in Noise Control for Industry [LC-75-24750] p 28 N95-11259

Fan noise research at NASA p 28 N95-11260

Active control of turbomachine discrete tones p 29 N95-11275

Analytical investigation of adaptive control of radiated inlet noise from turbofan engines p 30 N95-11277

A theoretical analysis of airborne sound transfer for a resiliently mounted machine to its foundation p 30 N95-11304

At Istanbul-Ataturk Airport measurement and analysis of noise in due of take-off time p 31 N95-11319

Active control of fan noise-feasibility study. Volume 1: Flyover system noise studies [NASA-CR-195392-VOL-1] p 258 N95-21888

The use of cowl camber and taper to reduce rotor/stator interaction noise [NASA-CR-195421] p 323 N95-22675

Supersonic jet noise reductions predicted with increased jet spreading rate [NASA-TM-106872] p 323 N95-23178

Noise impact of advanced high lift systems [NASA-CR-195028] p 352 N95-26160

Jet mixer noise suppressor using acoustic feedback [NASA-CASE-LEW-15170-2] p 362 N95-26187

Aircraft noise prediction program theoretical manual: Rotorcraft System Noise Prediction System (ROTONET), part 4 [NASA-TM-83199-PT-4] p 451 N95-26392

UHB engine fan broadband noise reduction study [NASA-CR-198357] p 580 N95-29641

An active liner system for jet engine exhaust silencers, phase 1 [AD-A293277] p 617 N95-31191

Computation of noise radiation from turbofans: A parametric study [NASA-CR-198359] p 710 N95-32836

Fan noise prediction assessment [NASA-CR-195051] p 711 N95-33831

ENGINE PARTS

Ply layout optimization and micromechanics tailoring of composite aircraft engine structures [BTN-95-EIX95112524206] p 196 A95-69302

Development of hypersonic engine seals: Flow effects of preload and engine pressures [BTN-95-EIX95112524204] p 196 A95-69304

Nonlinear dynamic simulation of single- and multispool core engines, part 1: Computational method [BTN-95-EIX95112524200] p 210 A95-69308

Compliant interlayer [BTN-95-EIX95142562401] p 304 A95-73439

Advances in the application of laser cutting, drilling, and welding aerospace parts [SAE PAPER 932544] p 547 A95-90052

Laser processing aircraft and turbine engine parts [SAE PAPER 931356] p 634 A95-93640

Brush seals for turbine engine fuel conservation p 59 N95-13595

Air Force seal activities p 60 N95-13600

Hypersonic engine seal development at NASA Lewis Research Center p 60 N95-13602

Quality optimization of thermally sprayed coatings produced by the JP-5000 (HVOF) gun using mathematical modeling p 152 N95-19008

Mathematical Models of Gas Turbine Engines and their Components [AGARD-LS-198] p 139 N95-19017

Toughened Silcomp composites for gas turbine engine applications [DE95-002851] p 235 N95-21243

Influence of backup bearings and support structure dynamics on the behavior of rotors with active supports [NASA-CR-197438] p 310 N95-23190

Evaluation of thermal barrier and PS-200 self-lubricating coatings in an air-cooled rotary engine [NASA-CR-195445] p 289 N95-23222

Small gas turbine component evaluation study [PB95-147542] p 338 N95-24293

Composite intermediate case manufacturing scale-up for advanced engines p 406 N95-28275

Application of fiber-reinforced bismaleimide materials to aircraft nacelle structures p 397 N95-28278

Bicarbonate of soda paint stripping process validation and material characterization p 631 N95-31778

ENGINE STARTERS

Starter/generator testing [BTN-95-EIX95072498877] p 210 A95-68393

System design considerations for an APU starter-generator [SAE PAPER 932559] p 511 A95-90056

A switched reluctance machine rotor position estimator: A neural network application [SAE PAPER 932560] p 511 A95-90057

A detailed power inverter design for a 250 kW switched reluctance aircraft engine starter/generator [SAE PAPER 931388] p 613 A95-93664

Detailed design of a 250-kW switched reluctance starter/generator for an aircraft engine [SAE PAPER 931389] p 613 A95-93665

ENGINE TESTING LABORATORIES

A large hemi-anechoic enclosure for community-compatible aeroacoustic testing of aircraft propulsion systems p 577 A95-90132

Review of new French facilities for PREPHA program [AIAA PAPER 95-6128] p 520 A95-90449

Inlet flow test calibration for a small axial compressor rig. Part 2: CFD compared with experimental results [NASA-TM-106999] p 514 N95-30007

ENGINE TESTS

Design features of the NAL ramjet engine test facility p 410 A95-82319

Experiment of rocket-ram annular combustor p 412 A95-82324

Life evaluation of a low power arcjet thruster p 403 A95-82337

Flex cycle combustor development and demonstration [BTN-94-EIX95011441245] p 417 A95-84202

Scramjet combustor design in France [AIAA PAPER 95-6094] p 510 A95-88002

Determination of minimum fuel octane number piston aircraft engines [SAE PAPER 931230] p 528 A95-88961

Vapor lock studies for gasolines with ethers [SAE PAPER 931233] p 529 A95-88962

Ongoing research into high octane unleaded avgas [SAE PAPER 931234] p 529 A95-88963

Reducing low frequency noise emissions from a Langley Air Force Base Hush-House p 561 A95-90112

Review of new French facilities for PREPHA program [AIAA PAPER 95-6128] p 520 A95-90449

The DCAF: A high-enthalpy long-duration, direct-connect scramjet test facility [AIAA PAPER 95-6130] p 512 A95-90450

Lightweight high-temperature fuel metering valves [SAE PAPER 931444] p 635 A95-93693

Hydrocarbon-fueled ramjet/scramjet technology program, phase 2 extension [NASA-CR-189659] p 15 N95-10319

NASA Lewis Propulsion Systems Laboratory test article systems criteria [NASA-TM-106589] p 20 N95-10446

NASA Lewis Propulsion Systems Laboratory customer guide manual [NASA-TM-106569] p 21 N95-10822

Brush seal performance and durability issues based on T-700 engine test results [NASA-TM-106502] p 22 N95-11483

Shock-tunnel combustor testing for hypersonic vehicles [NASA-CR-196836] p 52 N95-11938

NASA's Hypersonic Research Engine Project: A review [NASA-TM-107759] p 50 N95-12860

Advanced Turbine Technology Applications Project (ATTAP) [NASA-CR-195393] p 101 N95-15743

Theoretical fundamentals of the aircraft GTE tests p 138 N95-16265

Scramjet testing guidelines p 138 N95-16317

Hypersonic air-breathing aer propulsion facility test support requirements p 144 N95-16319

Free-jet testing at Mach 3.44 in GASL's aero/thermo test facility p 145 N95-16320

Unmanned aerial vehicle heavy fuel engine test [AD-A284332] p 139 N95-18383

Airborne rotary separator study [NASA-CR-191045] p 150 N95-18743

Damage of high temperature components by dust-laden air p 201 N95-19673

Testing considerations for military aircraft engines in corrosive environments (a Navy perspective) p 202 N95-19684

Statistical analysis of Turbine Engine Diagnostic (TED) field test data [AD-A286032] p 248 N95-20998

Portable static test facility for small, expendable, turbojet engines, phase 1 [AD-A286337] p 239 N95-21719

Phase 2: HGM air flow tests in support of HEX vane investigation p 312 N95-23438

Impeller flow field characterization with a laser two-focus velocimeter p 313 N95-23440

Turbine-engine applications of thermographic-phosphor temperature measurements [DE95-003625] p 358 N95-25110

Assessment of overhaul surge margin tests applied to the T53 engines in ADF troquois helicopters [AR-008-389] p 339 N95-25936

Nitrogen oxide emissions and their control from uninstalled aircraft engines in enclosed test cells: Joint report to Congress on the Environmental Protection Agency - Department of Transportation study [PB95-166237] p 358 N95-26005

Perspective on thermal barrier coatings for industrial gas turbine applications p 345 N95-26128

Effects of dust from storage heaters on ignition in scramjets [NAL-TR-1234] p 405 N95-26706

Prevention and control of inlet unstart using an SR-71 simulation p 367 N95-26948

UHB engine fan broadband noise reduction study [NASA-CR-198357] p 580 N95-29641

An active liner system for jet engine exhaust silencers, phase 1 [AD-A293277] p 617 N95-31191

A pulsed liquid fuel ramjet p 617 N95-31201

Icing simulation in the aer propulsion systems test facility propulsion development test cell C-2 [AD-A293039] p 599 N95-31667

Allison engine testing CMSX-4 (reg sign) single crystal turbine blades and vanes [DE95-010308] p 694 N95-32636

Maximum thrust mode evaluation p 696 N95-33017

ENGINEERING

1994 NASA-HU American Society for Engineering Education (ASEE) Summer Faculty Fellowship Program [NASA-CR-194972] p 325 N95-23276

ENGINEERING DRAWINGS

Automatic riveting cell for commercial aircraft floor grid assembly [HTN-95-92309] p 365 A95-85353

ENGINEERING MANAGEMENT

NASA Lewis Propulsion Systems Laboratory test article systems criteria [NASA-TM-106589] p 20 N95-10446

Federal aviation administration plan for research, engineering and development [AD-A290952] p 490 N95-29733

ENGINEERS

Charles Norvin Rinek; an early American pioneer in advanced aviation engines [SAE PAPER 930485] p 386 A95-84554

Pilot rating scale for aircraft handling qualities [HTN-95-42269] p 380 A95-84963

Development of strength analysis methods and design model for aircraft constructions in Kazan Aviation Institute p 127 N95-16264

ENTHALPY

Shock layers and boundary layers in hypersonic flows [HTN-95-A0003] p 183 A95-67830

Shock tunnel measurements of hypervelocity blunted cone drag [BTN-95-EIX95152577606] p 305 A95-73477

Effects of the chemical reaction model on calculations of supersonic combustion flows [BTN-95-EIX0618952745802] p 638 A95-94487

Vortex generation and mixing in three-dimensional supersonic combustors [BTN-95-EIX0618952745783] p 614 A95-94503

Numerical study of mixing in a high and low enthalpy supersonic test facility p 7 N95-10467

The Superoorbital Expansion Tube concept, experiment and analysis p 341 N95-25399

Numerical simulation of high enthalpy shock tunnel p 700 N95-34514

ENTRAINMENT

Entrainment and acoustic variations in a round jet from introduced streamwise vorticity [BTN-95-EIX95042474409] p 209 A95-68291

Effects of trailing-edge jet entrainment on delta wing vortices [HTN-95-81644] p 542 A95-87692

ENTRY GUIDANCE (STS)

Shuttle entry guidance revisited using nonlinear geometric methods [BTN-95-EIX95182619144] p 299 A95-76621

ENVIRONMENT EFFECTS

Ozone, skin cancer, and the SST [BTN-95-EIX95041503011] p 213 A95-68314

Impact of present aircraft emissions of nitrogen oxides on tropospheric ozone and climate forcing [HTN-95-21364] p 353 A95-78679

Environmental aspects of Orbital transport: p 559 A95-87377

The high speed civil transport: A technology challenge p 496 A95-90089

Development and field test of the Beta version of the USAF Assessment System for Aircraft Noise (ASAN) p 561 A95-90121

Overview of feasibility study on propulsion concepts for high speed civil transport p 488 A95-91518

Aviation and the environment p 657 A95-93464

Integrating NOISEMAP with the Geographic Resource Analysis Support System (GRASS) to enhance environmental impact assessments and land use compatibility studies p 31 N95-11311

The effect of aircraft speed on the penetration of sonic boom noise into a flat ocean p 100 N95-14887

Modern transport engine experience with environmental ingestion effects p 199 N95-19660

Corrosion of aircraft materials: Correlation between nanometer scale and macroscopic structural damage parameters [AD-A285930] p 241 N95-20299

Modeling aerosol emissions from the combustion of composite materials p 301 N95-23038

The atmospheric effects of stratospheric aircraft: A fourth program report [NASA-RP-1359] p 357 N95-24274

Parts washing alternatives study: United States Coast Guard. Project summary and report [PB95-166146] p 343 N95-26004

Environmentally Safe and Effective Processes for Paint Removal [AGARD-LS-201] p 650 N95-32165

ENVIRONMENT MANAGEMENT

Noise modeling for MOAs and ranges p 32 N95-11322

Environmental Compliance Assessment and Management Program [AD-A279605] p 255 N95-20441

ENVIRONMENT MODELS

Modelling requirements in flight simulation [HTN-95-C0004] p 585 A95-93392

Operational multi-scale environment model with grid adaptivity (OMEGA) application to aviation weather p 676 A95-93556

ENVIRONMENT POLLUTION

Environmental Compliance Assessment and Management Program [AD-A279605] p 255 N95-20441

ENVIRONMENT PROTECTION

Aircraft stripping and painting [BTN-95-EIX95182617810] p 300 A95-75755

Aero-engine R&D efforts for environmental protection p 512 A95-91502

Requirements for next generation supersonic transports p 498 A95-91516

A study of aircraft post-crash fuel fire mitigation [AD-A282208] p 40 N95-12499

Design of a vehicle based system to prevent ozone loss [NASA-CR-197199] p 48 N95-12702

Environmental Compliance Assessment and Management Program [AD-A279605] p 255 N95-20441

Corrosion in service experience with aircraft in France p 303 N95-23518

Nitrogen oxide emissions and their control from uninstalled aircraft engines in enclosed test cells: Joint report to Congress on the Environmental Protection Agency - Department of Transportation study [PB95-166237] p 358 N95-26005

Community relations plan: Galena Airport and Camp ion Air Force Station, Alaska [AD-A286722] p 446 N95-27234

Environmentally safe aviation fuels p 631 N95-31768

Environmentally regulated aerospace coatings p 603 N95-31775

ENVIRONMENT SIMULATION

Hypersonic convective heat transfer over 140-deg blunt cones in different gases [BTN-95-EIX95152583253] p 306 A95-73554

Applications of digital video and synthetic environments to unmanned aerial vehicles [AD-A291875] p 504 N95-29437

ENVIRONMENT SIMULATORS

The value of simulation for training [AD-A289174] p 411 N95-26556

ENVIRONMENTAL CONTROL

Condensing cycle air conditioning system [SAE PAPER 932056] p 513 A95-91637

What's next in commercial aircraft environmental control systems? [SAE PAPER 932057] p 513 A95-91638

ENVIRONMENTAL MONITORING

Commercial applications for military laser radars p 543 A95-87794

A review of Air Force policy and noise models pertaining to the noise environment under low-altitude, high-speed training areas p 561 A95-90118

Environmental noise research using the Human Response Monitor (HRM). Phase 1: System development p 562 A95-90122

Selecting optimum sonic boom monitoring sites in a special-use airspace p 576 A95-90124

The evolution of airport noise monitoring systems: Recent achievements and further needs p 562 A95-90125

Features of Massport's new noise monitoring system p 562 A95-90127

Environmental Compliance Assessment and Management Program [AD-A279605] p 255 N95-20441

ENVIRONMENTAL QUALITY

Development and field test of the Beta version of the USAF Assessment System for Aircraft Noise (ASAN) p 561 A95-90121

ENVIRONMENTAL SURVEYS

Integrating NOISEMAP with the Geographic Resource Analysis Support System (GRASS) to enhance environmental impact assessments and land use compatibility studies p 31 N95-11311

Noise modeling for MOAs and ranges p 32 N95-11322

The effect of aircraft speed on the penetration of sonic boom noise into a flat ocean p 100 N95-14887

ENVIRONMENTAL TESTS

Pressure and temperature distortion testing of a two-stage centrifugal compressor [BTN-94-EIX95011441250] p 431 A95-84207

High-temperature acoustic test facilities and methods p 174 N95-19149

Design and operation of a thermoacoustic test facility p 147 N95-19150

ENVIRONMENTS

Emergency medical service (EMS): A unique flight environment p 596 A95-95203

EPHEMERIDES

Effect of broadcast and precise ephemerides on estimates of the frequency stability of GPS Navstar clocks [BTN-95-EIX95112522530] p 190 A95-69333

EPOXY MATRIX COMPOSITES

Failure behaviour of carbon fiber/epoxy composites in pin-ended buckling and bending tests [HTN-95-71388] p 528 A95-87606

Challenges and payoff of composites in transport aircraft: 777 empennage and future applications p 534 N95-29031

EPOXY RESINS

Novel matrix resins for composites for aircraft primary structures, phase 1 [NASA-CR-189657] p 23 N95-10318

Scarf joint technique with cocured and precured patches for composite repair p 396 N95-27524

In situ processing methods for composite fuselage sandwich structures p 531 N95-28826

Advanced resin systems and 3D textile preforms for low cost composite structures p 535 N95-29035

Evaluation of alternative pavement marking materials [AD-A292973] p 626 N95-31468

EQUATIONS OF MOTION

Solution-adaptive structured-unstructured grid method for unsteady turbomachinery analysis. Part I: Methodology [BTN-94-EIX94441380983] p 208 A95-67329

Aeroelastic stability of hingeless rotor blade in hover using large deflection theory [BTN-94-EIX94441386616] p 183 A95-67347

Functional dependence of trajectory dispersion on initial condition errors [BTN-95-EIX95152583263] p 298 A95-73564

Analytical solution and parameter estimation of projectile dynamics [BTN-95-EIX95212645695] p 272 A95-76747

Integrated development of the equations of motion for elastic hypersonic flight vehicles [BTN-95-EIX95242670755] p 327 A95-81092

Optimal trajectories for an unmanned air-vehicle in the horizontal plane [BTN-95-EIX0619952748191] p 606 A95-94480

Partially implicit method for simulating viscous aerofoil flows [BTN-94-EIX94522406680] p 709 A95-96299

High performance parallel analysis of coupled problems for aircraft propulsion [NASA-CR-195355] p 23 N95-10132

Effect of weak periodic pressure gradient on streamwise vortices near a wall p 29 N95-11263

Evaluation of the dynamic stability characteristics of the NAL Light Transport Aircraft [NAL-PD-CA-9217] p 142 N95-16392

Particle trajectories in gas turbine engines p 199 N95-19663

Comparison of meteorological data with fitted values extracted from projectile trajectory [AD-A285921] p 255 N95-19989

Direct numerical simulations of on-demand vortex generators: Mathematical formulation p 251 N95-22452

Moving mass trim control for aerospace vehicles [DE95-002602] p 299 N95-23532

Linear and nonlinear discrete-time state-space modeling of dynamic systems for control applications p 567 N95-29251

EQUATIONS OF STATE

Shock layers and boundary layers in hypersonic flows [HTN-95-A0003] p 183 A95-67830

Application of a control-volume-based finite-element formulation to the shock tube problem [BTN-95-EIX95182619099] p 295 A95-76584

Determination of stability and control derivatives from the NASA F/A-18 HARV from flight data using the maximum likelihood method [NASA-CR-197320] p 204 N95-19576

On-line, adaptive state estimator for active noise control p 322 N95-23308

Linear and nonlinear discrete-time state-space modeling of dynamic systems for control applications p 567 N95-29251

Pressure updating methods for the steady-state fluid equations [NASA-CR-198163] p 569 N95-30353

EQUILIBRIUM FLOW

Numerical studies of Mach reflection with air chemistry p 548 A95-90575

EQUIPMENT SPECIFICATIONS

An air-driven pressure booster pump for aircraft-based air sampling [HTN-95-40689] p 216 A95-69833

An integrated system to improve aviation weather forecasts for the Alaska Range p 656 A95-93480

An in-situ system for warning of icing conditions p 660 A95-93481

Automation of observations in the Netherlands p 661 A95-93485

The performance of forward scatter visibility sensors for application in autostations and runway visual range in snow and freezing precipitation events p 662 A95-93489

Aviation terminal forecasts based on automated observations (FTAUTO) p 668 A95-93520

A poor man's expert system for aviation VSRF in complex terrain p 669 A95-93524

The development of a model specification for ground support equipment [CONGRESS PAPER C428-38-095] p 625 A95-93636

Dynamically timed electric motor [NASA-CASE-MFS-28958-1] p 437 N95-26890

EROSION

Erosion of dust-filtered helicopter turbine engines. Part 1: Basic theoretical considerations [BTN-95-EIX95182619222] p 288 A95-76648

Erosion of dust-filtered helicopter turbine engines. Part 2: Erosion reduction [BTN-95-EIX95182619223] p 289 A95-76649

Life prediction of helicopter engines fitted with dust filters [BTN-95-EIX95182619224] p 289 A95-76650

Life evaluation of a low power arcjet thruster p 403 A95-82337

The panel oxidation and erosion test (POET) facility [AIAA PAPER 95-6151] p 521 A95-90465

The rain erosion of PEEK (polyetheretherketone) [CONGRESS PAPER C428-4-039] p 531 A95-91676

Application of integral methods to ablation charring erosion, a review [BTN-95-EIX95302694460] p 636 A95-94057

Moisture induced pressures in concrete airfield pavements [AD-A281974] p 52 N95-11789

Erosion, Corrosion and Foreign Object Damage Effects in Gas Turbines [AGARD-CP-558] p 197 N95-19653

The operation of gas turbine engines in hot and sandy conditions: Royal Air Force experiences in the Gulf conflict p 198 N95-19655

US Army rotorcraft turboshaft engines sand and dust erosion considerations p 198 N95-19656

Experimental and numerical simulations of the effects of ingested particles in gas turbine engines p 199 N95-19662

Particle trajectories in gas turbine engines p 199 N95-19663

The calculation of erosion in a gas turbine compressor rotor p 199 N95-19664

Erosion of T56 5th stage rotor blades due to bleed hole overtip flow p 200 N95-19666

An airborne monitoring system for FOD and erosion faults p 200 N95-19668

Gas turbine compressor corrosion and erosion in Western Europe [AD-B196178L] p 201 N95-19678

High velocity oxygen fuel spraying of erosion and wear resistant coatings on jet engine parts p 202 N95-19680

- Resistance of silicon nitride turbine components to erosion and hot corrosion/oxidation attack p 202 N95-19683
- Aircraft corrosion study [AD-A279527] p 241 N95-21687
- Water model tests on the Allison T56 series 3 combustion system [DSTO-TR-0139] p 697 N95-33250
- ERROR ANALYSIS**
- Validation of empirical orbit error corrections using crossover difference differences [HTN-94-00912] p 25 A95-60227
- Possible near-IR channels for remote sensing precipitable water vapor from geostationary satellite platforms [HTN-95-70139] p 214 A95-69431
- Enhancing filter robustness in cascaded GPS-INS integrations [BTN-95-EIX9512555475] p 278 A95-73435
- Covariance analysis of strapdown INS considering gyrocompass characteristics [BTN-95-EIX95202637592] p 279 A95-76697
- Precision requirement for potential-based panel methods [HTN-95-51666] p 433 A95-85048
- Jet stream winds: Comparisons of operational analyses with independent aircraft data at multiple longitudes p 665 A95-93506
- A new algorithm for five-hole probe calibration, data reduction, and uncertainty analysis [NASA-TM-106458] p 38 N95-12378
- Quality assessment for wind tunnel testing [AGARD-AR-304] p 67 N95-14197
- Error propagation equations for estimating the uncertainty in high-speed wind tunnel test results [DE94-014136] p 145 N95-16509
- Field verification of the wind tunnel coefficients p 109 N95-17291
- An analysis of tower (local) controller-pilot voice communications [AD-A283718] p 160 N95-18436
- Optical surface pressure measurements: Accuracy and application field evaluation p 175 N95-19274
- Bearing defect signature analysis using advanced nonlinear signal analysis in a controlled environment [NASA-TM-108491] p 441 N95-28364
- Error modeling for differential GPS [NASA-CR-188367] p 488 N95-28716
- Mode of human image representation and error checking strategies in complex visual displays [AD-A290107] p 485 N95-29210
- A PC program for estimating measurement uncertainty for aeronautics test instrumentation [NASA-CR-198361] p 523 N95-30067
- ERROR CORRECTING CODES**
- Improved version of the Naval Surface Warfare Center aeroprediction code (AP93) [BTN-95-EIX95152583260] p 267 A95-73561
- ERROR CORRECTING DEVICES**
- Hydraulic system diagnostic sensors [BTN-95-EIX95031502752] p 209 A95-68259
- ERRORS**
- A study of computational difficulty of numerical method in optimal control p 507 A95-91585
- Determination of stores pointing error due to wing flexibility under flight load [NASA-TM-4646] p 134 N95-19044
- Development of pneumatic test techniques for subsonic high-lift and in-ground-effect wind tunnel investigations p 121 N95-19268
- Aspect estimation of an aircraft using library model silhouettes [PB95-141834] p 360 N95-25894
- ESCAPE SYSTEMS**
- RAF ejections - historical perspectives and future requirements [CONGRESS PAPER C428-18-168] p 484 A95-91717
- ESSENTIALLY NON-OSCILLATORY SCHEMES**
- Algorithmic trends in computational fluid dynamics; The Institute for Computer Applications in Science and Engineering (ICASE)/LaRC Workshop, NASA Langley Research Center, Hampton, VA, US, Sep. 15-17, 1991 [ISBN 0-387-94014-6] p 550 A95-91915
- ESTIMATES**
- Fatigue reliability method with in-service inspections p 94 N95-14475
- ESTIMATING**
- Improving prediction: The incorporation of simplified rotor dynamics in a mathematical model of the bell 412HP [BTN-95-EIX95152584679] p 282 A95-73591
- Real-time estimation of atmospheric turbulence severity from in-situ aircraft measurements [BTN-95-EIX95182619231] p 319 A95-76657
- Fatigue life estimation program for Part 23 airplanes, 'AFS.FOR' [SAE PAPER 931249] p 565 A95-89221
- The accuracy of parameter estimation in system identification of noisy aircraft load measurement [NASA-CR-197516] p 134 N95-19130
- Estimating wind tunnel interference due to vectored jet flows p 164 N95-19265
- Rationale for the Modular Air-system Vulnerability Estimation Network (MAVEN) methodology [AD-A285797] p 284 N95-22510
- Aerodynamic parameter estimation via Fourier modulating function techniques [NASA-CR-4654] p 335 N95-24630
- Excrescence drag levels on aircraft [ESDU-94044] p 477 N95-28897
- A PC program for estimating measurement uncertainty for aeronautics test instrumentation [NASA-CR-198361] p 523 N95-30067
- ETHANE**
- Numerical study of contaminant effects on combustion of hydrogen, ethane, and methane in air [AIAA PAPER 95-6097] p 510 A95-88005
- ETHERS**
- Vapor-lock studies for gasolines wwith ethers [SAE PAPER 931233] p 529 A95-88962
- ETHYLENE COMPOUNDS**
- Additives in bituminous materials and fuel-resistant sealers [DOT/FAA/CT-94/78] p 55 N95-12131
- EUCLEDEAN GEOMETRY**
- Single-pass method for the solution of inverse potential and rotational problems. Part 2: Fully 3-D potential theory and applications p 107 N95-16564
- EULER EQUATIONS OF MOTION**
- Recent advances in Euler and Navier-Stokes methods for calculating helicopter rotor aerodynamics and acoustics [HTN-94-00686] p 2 A95-60169
- A grid generation and flow solution method for the Euler equations on unstructured grids [HTN-95-20003] p 153 A95-63201
- Parallel implicit unstructured grid Euler solvers [BTN-95-EIX95042474393] p 217 A95-68307
- Ground effect calculation of two-dimensional airfoil [BTN-94-EIX94371347710] p 219 A95-69969
- Limit cycle phenomena in computational transonic aeroelasticity [BTN-95-EIX95152582317] p 264 A95-73520
- Aeroacoustic model for weak shock waves based on Burgers equation [BTN-95-EIX95182619076] p 269 A95-75761
- Quantitative comparison between interferometric measurements and Euler computations for supersonic cone flows [BTN-95-EIX95222650782] p 358 A95-79238
- Practical formulation of a positively conservative scheme [HTN-95-51668] p 433 A95-85050
- Dynamic unstructured method for flows past multiple objects in relative motion [BTN-95-EIX95262694303] p 435 A95-85474
- Nonreflective boundary conditions for high-order methods [HTN-95-42328] p 371 A95-86157
- Using the Liou-Steffen algorithm for the Euler and Navier-Stokes equations [HTN-95-42348] p 373 A95-86177
- Computational methods in applied sciences; European Computational Fluid Dynamics Conference, 1st, Brussels, Belgium, Sept. 7-11, 1992 [ISBN 0-444-89795-X] p 539 A95-87552
- Three-dimensional adaptive grid-embedding Euler technique [HTN-95-20825] p 543 A95-88086
- Sensitivity derivatives for three dimensional supersonic Euler code using incremental iterative strategy [HTN-95-20845] p 545 A95-88106
- Accurate drag prediction: A prerequisite for drag reduction research [SAE PAPER 932571] p 467 A95-90060
- Central-difference and upwind-biased schemes for steady and unsteady Euler aerofoil computations [HTN-95-01094] p 469 A95-90280
- Parallel computational fluid dynamics '91: Conference Proceedings, Stuttgart, Germany, Jun. 10-12, 1991 [ISBN 0-444-89363-6] p 548 A95-91479
- Implicit multi-domain method for unsteady compressible inviscid fluid flows around 3D projectiles p 548 A95-91482
- A detailed Euler flow analysis of TPS and fanjet engine p 473 A95-91515
- Comparison of coordinate-invariant and coordinate-aligned upwinding for the Euler equations [HTN-95-A1753] p 633 A95-93316
- Implicit multiblock Euler and Navier-Stokes calculations [HTN-95-A1755] p 634 A95-93318
- Aerodynamic interference for supersonic low-aspect-ratio missiles [BTN-95-EIX95302694469] p 588 A95-94065
- Estimation of supersonic leading-edge thrust by a Euler flow model [BTN-95-EIX0619952748194] p 591 A95-94483
- Computational fluid dynamics '92; Proceedings of the European Computational Fluid Dynamics Conference, 1st, Brussels, Belgium, Sep. 7-11, 1992. Vols. 1 & 2 [ISBN 0-444-89793-3] p 638 A95-95357
- Numerical solution of Euler and Navier-Stokes equations for 2D transonic problems p 638 A95-95366
- Optimal shape design in hypersonic aerodynamics and electromagnetics p 639 A95-95397
- An improved finite element method for the solution of the compressible Euler and Navier-Stokes equations p 640 A95-95439
- Navier-Stokes computations around a realistic fighter configuration p 591 A95-95440
- Permeable wall boundary conditions for transonic airfoil design p 641 A95-95445
- Multigrid/multiblock method for transonic potential flow around wing/body/nacelle configurations including a slipstream p 591 A95-95451
- Implicit upwind-Euler solution algorithms for unstructured-grid applications p 641 A95-95454
- Multigrid solution for the compressible Euler equations by an implicit characteristic-flux-averaging p 642 A95-95459
- Transonic vortical flow predicted with a structured multiblock Euler solver p 642 A95-95462
- An unstructured node centered scheme for the simulation of 3-D inviscid flows p 642 A95-95463
- An innovative algorithm to accurately solve the Euler equations for rotary wing flow p 642 A95-95467
- Multi-block finite volume calculation of compressible flow past aerodynamic configurations p 643 A95-95473
- Surface grid generation for multi-block structured grids p 643 A95-95478
- High performance parallelized implicit Euler solver for the analysis of unsteady aerodynamic flows p 644 A95-95495
- Effects of a forward-swept front rotor on the flowfield of a counterrotation propeller [NASA-TM-106671] p 7 N95-10148
- Agglomeration multigrid for viscous turbulent flows [AD-A284064] p 8 N95-10848
- Control theory based airfoil design using the Euler equations [NASA-CR-196360] p 36 N95-11884
- User's guide for ENSAERO: A multidisciplinary program for fluid/structural/control interaction studies of aircraft (release 1) [NASA-TM-108853] p 65 N95-13662
- The role of CFD in the design process p 90 N95-14135
- Computational aerodynamics based on the Euler equations [AGARD-AG-325] p 72 N95-14264
- A Cartesian, cell-based approach for adaptively-refined solutions of the Euler and Navier-Stokes equations [NASA-TM-106786] p 73 N95-14297
- Theoretical investigations of shock/boundary layer interactions on a $Ma(\infty) = 8$ waverider [DLR-FB-94-12] p 119 N95-18910
- The mathematical models of flow passage for gas turbine engines and their components p 140 N95-19020
- An assessment of the adaptive unstructured tetrahedral grid, Euler Flow Solver Code FELISA [NASA-TP-3526] p 119 N95-19041
- Validation and evaluation of the advanced aeronautical CFD system SAUNA: A method developer's view [ARA-MEMO-390] p 210 N95-19774
- Verification of the CFD simulation system SAUNA for complex aircraft configurations [ARA-MEMO-401] p 211 N95-19776
- Euler Technology Assessment program for preliminary aircraft design employing SPLITFLOW code with Cartesian unstructured grid method [NASA-CR-4649] p 273 N95-22917
- Euler technology assessment for preliminary aircraft design employing OVERFLOW code with multiblock structured-grid method [NASA-CR-4651] p 273 N95-23095
- An assessment of viscous effects in computational simulation of benign and burst vortex flows on generic fighter wind-tunnel models using TEAM code [NASA-CR-4650] p 273 N95-23185
- Convergence acceleration of implicit schemes in the presence of high aspect ratio grid cells p 313 N95-23446
- Cavitation modeling in Euler and Navier-Stokes codes p 315 N95-23630

- User's guide for ECAP2D: An Euler unsteady aerodynamic and aeroelastic analysis program for two dimensional oscillating cascades, version 1.0 [NASA-CR-189146] p 316 N95-24189
- Effect of density gradients in confined supersonic shear layers, part 1 [NASA-CR-198029] p 348 N95-24412
- Computational fluid dynamics and transonic flow [AD-A288962] p 436 N95-26405
- A fixed time performance evaluation of parallel CFD applications [DE94-014240] p 436 N95-26445
- Evaluation of a doubly-swept blade tip for rotorcraft noise reduction [NASA-CR-189677] p 452 N95-28264
- A fourth order Euler/Navier-Stokes prediction method for the aerodynamics and aeroelasticity of hovering rotor blades p 554 N95-29242
- Pressure updating methods for the steady-state fluid equations [NASA-CR-198163] p 569 N95-30353
- Development of a linearized unsteady Euler analysis for turbomachinery blade rows [NASA-CR-4677] p 592 N95-30611
- Multigrid convergence acceleration for the 2D Euler equations applied to high-lift systems [PB95-198081] p 593 N95-30814
- Special publication of National Aerospace Laboratory [NAL-SP-27] p 684 N95-34505
- A study on the convergence of a 3-D Euler code for cascade flow calculations p 706 N95-34508
- Role of computational fluid dynamics in aeronautical engineering. Number 12: Formulation and verification of ulti-particle upwind schemes for the Euler equations p 707 N95-34540
- Numerical analysis around the whole SST configuration p 693 N95-34541
- Direct analysis of transonic rotor noise with CFD technique p 711 N95-34549
- EULER-LAGRANGE EQUATION**
- Arbitrary Lagrangian-Eulerian finite element analysis for flow-induced vibration of rigid body p 643 A95-95485
- An approach for dynamic grids [NASA-TM-106774] p 76 N95-15853
- EUROCA (ESA)**
- EUROCA mission control experience and messages for the future p 149 N95-17252
- EUROPE**
- EC Aviation Scene [HTN-95-50223] p 176 A95-64860
- An overview of the EASOE campaign [HTN-95-00702] p 443 A95-86272
- Euro-noise '92, London, UK, Sept. 14-18, 1992. Bks. 1-3 [ISBN 1-873082-39-8] p 558 A95-87354
- Assessment of avionics technology in European aerospace organizations [NASA-CR-189201] p 337 N95-24624
- EUROPEAN AIRBUS**
- Automatic riveting cell for commercial aircraft floor grid assembly [BTN-95-EIX95182617807] p 261 A95-75752
- Aeronautical technology - recent advances and future prospects [HTN-95-01097] p 496 A95-90283
- A better than average stress model-photoelastic analysis for Airbus design [CONGRESS PAPER C428-23-005] p 500 A95-91730
- The mini-business approach at Chadderton [CONGRESS PAPER C428-26-037] p 681 A95-93602
- Load alleviation for civil transport aircraft [CONGRESS PAPER C428-35-057] p 604 A95-93627
- The A340 electrical power generation system [CONGRESS PAPER C428-36-193] p 625 A95-93630
- EUROPEAN SPACE AGENCY**
- Integrated X-ray testing of the electro-optical breadboard model for the XMM reflection grating spectrometer [DE95-008829] p 644 N95-30507
- EVACUATING (TRANSPORTATION)**
- Flying ambulances: The approach of a small air force to long distance aeromedical evacuation of critically injured patients p 568 N95-29618
- Civil Reserve Air Fleet-Aeromedical Evacuation Shipset (CRAF-AESS) p 568 N95-29619
- First medical test of the UH-60Q and equipment for use in US Army medevac helicopters p 568 N95-29620
- International access to aeromedical evacuation medical equipment assessment data p 569 N95-29622
- Patient/aircraft forecasting for the strategic aeromedical evacuation lift-bed process [AD-A293902] p 599 N95-31512
- Aircraft evacuations through Type-3 exits I: Effects of seat placement on the exit [DOT/FAA/AM-95/22] p 599 N95-31845
- EVOLUTION**
- Part-task simulator evaluations of advanced terrain displays [SAE PAPER 932570] p 401 A95-84567
- Assessment of cost and training effectiveness for a candidate training system using the Comparison-Based Prediction model [SAE PAPER 932598] p 379 A95-84570
- Test and evaluation crew resource management p 483 A95-90867
- An integrated system to improve aviation weather forecasts for the Alaska Range p 656 A95-93460
- Final results of the weather testing component of the Terminal Doppler Weather Radar operational test and evaluation p 658 A95-93471
- LLWAS 2 and LLWAS 3 performance evaluation p 662 A95-93491
- An echo motion algorithm for air traffic management using a national radar mosaic p 667 A95-93513
- Evaluating the effects of air traffic control automation p 601 A95-95091
- Helicopter Performance Evaluation (HELPE) computer model [AD-A284319] p 131 N95-18381
- Evaluation of scanners for C-scan imaging in nondestructive inspection of aircraft [DE94-012473] p 152 N95-19100
- EVAPORATION**
- Effects of activated reactive evaporation process parameters on the microhardness of polycrystalline silicon carbide thin films [GTN-95-00406090-4621] p 680 A95-93965
- A numerical model to predict the fate of jettisoned aviation fuel [AD-A289336] p 419 N95-26842
- EXCITATION**
- Comparison of NO and OH planar fluorescence temperature measurements in scramjet model flowfields [BTN-95-EIX95042474388] p 209 A95-68312
- Aerodynamic mechanism of galloping [BTN-94-EIX94371347709] p 219 A95-69968
- Measurement around a rotor blade excited in pitch. Part 1: Dynamic inflow [HTN-95-31007] p 220 A95-71177
- Measurement around a rotor blade excited in pitch. Part 2: Unsteady surface pressure [HTN-95-31008] p 220 A95-71178
- SEM representation of the early and late time fields scattered from wire targets [BTN-94-EIX94381353142] p 306 A95-74496
- Research excitation system flight testing [NASA-TM-104289] p 13 N95-10715
- EXHAUST DIFFUSERS**
- Active boundary-layer control in diffusers [HTN-95-42580] p 458 A95-87210
- Experimental investigation of the flow in diffusers behind an axial flow compressor [BTN-95-EIX95282710057] p 632 A95-92472
- Simulation of the unsteady interaction of a centrifugal impeller with its vaned diffuser: flow analysis [BTN-95-EIX95282710055] p 633 A95-92474
- Unsteady flow phenomena in discrete passage diffusers for centrifugal compressors [AD-A281412] p 155 N95-16163
- Design of a variable area diffuser for a 15-inch Mach 6 open-jet tunnel p 297 N95-23309
- Performance characterization of a highly-offset diffuser with and without blowing vortex generator jets [AD-A289334] p 375 N95-26901
- EXHAUST EMISSION**
- Antarctic snow record of southern hemisphere lead pollution [HTN-95-40359] p 212 A95-66869
- Aircraft engine emission reduction [BTN-95-EIX95031502750] p 196 A95-68257
- Subsidence of aircraft engine exhaust in the stratosphere: Implications for calculated ozone depletions [PAPER-93GL03426] p 251 A95-70297
- Trajectory modeling of emissions from lower stratospheric aircraft [HTN-95-41219] p 317 A95-75031
- The distribution of hydrogen, nitrogen, and chlorine radicals in the lower stratosphere: Implications for changes in O₃ due to emission of NO_y from supersonic aircraft [HTN-95-70935] p 351 A95-78000
- An analysis of aircraft exhaust plumes form accidental encounters [HTN-95-70943] p 351 A95-78008
- Chemical change in the arctic vortex during AASE 2 [HTN-95-70947] p 352 A95-78012
- Impact of present aircraft emissions of nitrogen oxides on tropospheric ozone and climate forcing [HTN-95-21364] p 353 A95-78679
- Sensitivity of supersonic aircraft modelling studies to HNO₃ photolysis rate [HTN-95-11475] p 353 A95-79453
- Tracer transport for realistic aircraft emission scenarios calculated using a three-dimensional model [HTN-95-41799] p 353 A95-80525
- Modeling of aircraft exhaust emissions and infrared spectra for remote measurement of nitrogen oxides [HTN-95-51276] p 355 A95-80861
- Chemical composition and photochemical reactivity of exhaust from aircraft turbine engines [HTN-95-51277] p 356 A95-80862
- Impact on ozone of high-speed stratospheric aircraft: Effects of the emission scenario [HTN-95-51283] p 356 A95-80868
- Aircraft gas turbine emissions challenge [BTN-94-EIX95011441239] p 403 A95-84196
- Nitrogen oxide emissions characteristics of augmented turbofan engines [BTN-94-EIX95011441240] p 403 A95-84197
- Development of an aeroderivative gas turbine dry low emissions combustion system [BTN-94-EIX95011441246] p 417 A95-84203
- Three dimensional model calculations of the global dispersion of high speed aircraft exhaust and implications for stratospheric ozone loss p 26 N95-10657
- Regulatory impact analysis and regulatory support document: Control of air pollution; determination of significance for nonroad sources and emission standards for new nonroad compression-ignition engines at or above 37 kilowatts (50 horsepower) [PB94-194594] p 61 N95-12855
- Aircraft wake RCS measurement p 59 N95-13210
- Atmospheric effects of high-flying subsonic aircraft: A catalogue of perturbing influences [KNMI-SR-94-03] p 168 N95-18722
- Wave cycle design for wave rotor engines with limited nitrogen oxide emissions p 161 N95-18901
- Air pollution mitigation measures for airports and associated activity [PB94-207610] p 216 N95-19582
- Developing an emission factor for hazardous air pollutants for an F-16 using JP-8 fuel [AD-A284802] p 216 N95-19685
- Advanced diesel electronic fuel injection and turbocharging [AD-A279176] p 211 N95-19809
- Two-dimensional imaging of OH in a lean burning high pressure combustor [NASA-TM-106854] p 236 N95-21383
- Small gas turbine component evaluation study [PB95-147542] p 338 N95-24293
- The effect of altitude conditions on the particle emissions of a J85-GE-5L turbojet engine [NASA-TM-106669] p 339 N95-24561
- Jet mixing and emission characteristics of transverse jets in annular and cylindrical confined crossflow [NASA-TM-106976] p 616 N95-30698
- EXHAUST FLOW SIMULATION**
- An experimental investigation of scramjet nozzle flow p 402 A95-82322
- EXHAUST GASES**
- Aircraft engine emission reduction [BTN-95-EIX95031502750] p 196 A95-68257
- Predicting exhaust plume boundaries with supersonic external flows [BTN-95-EIX95152583258] p 297 A95-73559
- In situ observations in aircraft exhaust plumes in the lower stratosphere at midlatitudes [HTN-95-A0862] p 318 A95-76266
- Sensitivity of two-dimensional model predictions of ozone response to stratospheric aircraft: An update [HTN-95-A0863] p 318 A95-76267
- North Atlantic air traffic within the lower stratosphere: Cruising times and corresponding emissions [HTN-95-91841] p 354 A95-80829
- Effects on stratospheric ozone from high-speed civil transport: Sensitivity to stratospheric aerosol loading [HTN-95-91842] p 354 A95-80830
- Nitrogen oxide emissions characteristics of augmented turbofan engines [BTN-94-EIX95011441240] p 403 A95-84197
- Evolution of the concentrations of trace species in an aircraft plume: Trajectory study [HTN-95-A1044] p 443 A95-84549
- Prediction of NO(x) emission index of turbulent diffusion flame p 538 A95-87195
- Influence of the flight trajectory on the exhaust gas composition of a H₂-fueled air-breathing ramjet engine p 509 A95-87404
- Control-nonlinear-nonstationary structural response and radiation near a supersonic jet [HTN-95-20929] p 463 A95-88968

- Regulatory impact analysis and regulatory support document: Control of air pollution; determination of significance for nonroad sources and emission standards for new nonroad compression-ignition engines at or above 37 kilowatts (50 horsepower)
[PB94-194594] p 61 N95-12855
- Numerical simulation of helicopter engine plume in forward flight
[NASA-CR-197488] p 107 N95-16589
- Atmospheric effects of high-flying subsonic aircraft: A catalogue of perturbing influences
[KNMI-SR-94-03] p 168 N95-18722
- Impact of dynamic loads on propulsion integration
p 174 N95-19148
- Developing an emission factor for hazardous air pollutants for an F-16 using JP-8 fuel
[AD-A284802] p 216 N95-19685
- NTS-spill test facility wind tunnel exhaust plume characterization
[DE95-003630] p 297 N95-24019
- The atmospheric effects of stratospheric aircraft: A fourth program report
[NASA-PP-1359] p 357 N95-24274
- Measurements of ions formed in jet engine exhaust plumes
[AD-A290940] p 514 N95-29764
- Laser doppler velocimeter system for subsonic jet mixer nozzle testing at the NASA Lewis Aeroacoustic Propulsion Lab
[NASA-TM-106984] p 457 N95-30229
- EXHAUST NOZZLES**
- An experimental investigation of scramjet nozzle flow
p 402 A95-82322
- Influence of the flight trajectory on the exhaust gas composition of a H₂-fueled air-breathing ramjet engine
p 509 A95-87404
- A computational environment for exhaust nozzle design
[AIAA PAPER 95-1016] p 566 A95-90688
- Efficient mapping topology for turbine combustors with inclined slots/staggered holes
[BTN-95-EIX0616952745805] p 614 A95-94485
- Evaluation of the transient operation of advanced gas turbine combustors
[BTN-95-EIX0616952745793] p 614 A95-94495
- Application of scramjet engine technology to the design of ram accelerator projectiles
p 19 N95-10282
- Radiant energy measurements from a scaled jet engine axisymmetric exhaust nozzle for a baseline code validation case
[NASA-TM-106686] p 25 N95-11409
- Ultra-high bypass ratio jet noise
[NASA-CR-195394] p 100 N95-14610
- Small turbojets: Designs and installations
p 138 N95-16323
- Internal performance characteristics of thrust-vectoring axisymmetric ejector nozzles
[NASA-TM-4610] p 331 N95-25338
- Preliminary results and research capabilities of a new jet facility at the University of Kansas
p 412 N95-26951
- Flight test results of the F-16 aircraft modified with axisymmetric vectoring exhaust nozzle
p 609 N95-32007
- EXHAUST SYSTEMS**
- High bypass separate flow exhaust system improved thrust efficiency by modifying the aft centerbody
[SAE PAPER 932622] p 511 A95-90083
- Operating capability and current status of the reactivated NASA Lewis Research Center hypersonic tunnel facility
[AIAA PAPER 95-6146] p 521 A95-90461
- Advanced diesel electronic fuel injection and turbocharging
[AD-A279176] p 211 N95-19809
- Active control of fan noise-feasibility study. Volume 1: Flyover system noise studies
[NASA-CR-195392-VOL-1] p 258 N95-21888
- Aerodynamic design and analysis of a highly loaded turbine exhaust
p 312 N95-23435
- EXHAUST VELOCITY**
- Aerodynamic design and analysis of a highly loaded turbine exhaust
p 312 N95-23435
- EXPANSION**
- Effects of expansions on a supersonic boundary layer: Surface pressure measurements
[BTN-95-EIX95142553036] p 263 A95-73462
- EXPENDABLE STAGES (SPACECRAFT)**
- Program test objectives milestone 3 -- Integrated Propulsion Technology Demonstrator
[NASA-CR-197030] p 127 N95-15971
- EXPERIMENT DESIGN**
- SOFIA: Stratospheric Observatory for Infrared Astronomy
p 363 A95-81583
- Simulation of Shuttle launch G forces and acoustic loads using the NASA Ames Research Center 20G centrifuge
p 86 N95-14089
- A study of software standards used in the avionics industry
p 137 N95-16456
- Experimental and analytical methods for the determination of connected-pipe ramjet and ducted rocket internal performance
[AGARD-AR-323] p 149 N95-17278
- Statistical analysis of Turbine Engine Diagnostic (TED) field test data
[AD-A286032] p 248 N95-20998
- Balanced on air aircraft
[AD-D017251] p 389 N95-26537
- Selecting optimal experiments for feedforward multilayer perceptrons
[AD-A290856] p 678 N95-30406
- EXPERIMENTATION**
- Estimation of aerodynamic derivatives: Euler scheme validation and approximate methods for hypersonic configurations
p 460 A95-87385
- EXPERT SYSTEMS**
- Artificial intelligence for turboprop engine maintenance
[BTN-95-EIX95182617812] p 288 A95-75757
- Artificial intelligence for turboprop engine maintenance
[HTN-95-92313] p 404 A95-85357
- Integrated Thermal Energy Management (I-TEM): An evaluation tool for aircraft
[SAE PAPER 932577] p 493 A95-90065
- An intelligent tutoring system for civil aviation flight training
p 521 A95-91535
- Fault Diagnosis for condition monitoring applied to hydraulic circuits
[CONGRESS PAPER C428-12-165] p 456 A95-91703
- Thunderstorm hypothesis reasoner
[AD-A282664] p 60 N95-12805
- Knowledge-based processing for aircraft flight control
[NASA-CR-194976] p 99 N95-13727
- Artificial intelligence with applications for aircraft
[DOT/FAA/CT-94/41] p 99 N95-13895
- Identification of Artificial Intelligence (AI) applications for maintenance, monitoring, and control of airway facilities
[AD-A282479] p 125 N95-17373
- The use of genetic algorithms for flight test and evaluation of artificial intelligence and complex software systems
[AD-A284824] p 217 N95-19688
- Transport aircraft loading and balancing system: Using a CLIPS expert system for military aircraft load planning
p 217 N95-19751
- The Computer Aided Aircraft-design Package (CAAP)
p 217 N95-19759
- PalymSys (TM): An extended version of CLIPS for construction and reasoning using blackboards
p 217 N95-19767
- Digital systems validation. Chapter 20 Artificial Intelligence with applications for aircraft. Handbook, volume 2
[AD-A288492] p 448 N95-26638
- Expert systems and artificial intelligence applications in engineering design and inspection
p 710 N95-33008
- EXPLOSIONS**
- Explosive sabotage: The potential effects of explosive charges on aircraft
[CONGRESS PAPER C428-11-034] p 484 A95-91702
- Quantity-distance requirements for earth-bermed aircraft shelters
[AD-A279692] p 341 N95-24424
- EXPLOSIVE DEVICES**
- Test and Evaluation Plan (TEP) for Improvised Explosive Device Screening Systems (IEDSS)
[AD-A286382] p 227 N95-22319
- EXPLOSIVES**
- Aviation security: Development of new security technology has not met expectations. Report to Congressional requesters
[GAO/RCE-94-142] p 687 N95-32885
- EXPOSURE**
- The use of the Equivalent Continuous Sound Level (L(sub eq)) as an aircraft noise index
[HTN-95-92542] p 558 A95-87362
- Ten-year ground exposure of composite materials used on the Bell Model 206L helicopter flight service program
[NASA-TP-3468] p 55 N95-12357
- The corrosion and protection of advanced aluminum-lithium airframe alloys
p 302 N95-23497
- Corrosion protection measures for CFC/metal joints of fuel integral tank structures of advanced military aircraft
p 303 N95-23510
- Adhesively bonded composite patch repair of cracked aluminum alloy structures
p 393 N95-27507
- EXTERNAL STORE SEPARATION**
- Dynamic unstructured method for flows past multiple objects in relative motion
[BTN-95-EIX95262694303] p 435 A95-85474
- A cartesian grid finite element method for aerodynamics of moving rigid bodies
p 642 A95-95471
- A CFD study of complex missile and store configurations in relative motion
[NASA-CR-197912] p 285 N95-22949
- An experimental investigation of the time-dependent separation of tangent bodies in supersonic flow
[AD-A290720] p 480 N95-29500
- EXTERNAL STORES**
- The effect of rotating loads suspended under a helicopter on their amplitude-frequency characteristics
[BTN-94-EIX94461407959] p 78 A95-62633
- Aerodynamic characteristics of external store configurations at low speeds
[BTN-95-EIX95182619230] p 271 A95-76656
- Flight testing high lateral asymmetries on highly augmented Fighter/Attack aircraft
[AD-A284206] p 130 N95-17953
- A study of the effect of store unsteady aerodynamics on gust and turbulence loads
p 133 N95-18601
- EXTERNAL SURFACE CURRENTS**
- Dynamic stall of a NACA 0012 airfoil in laminar flow
p 479 N95-29243
- EXTINGUISHING**
- A review of water mist technology for fire suppression
[AD-A285738] p 225 N95-20071
- EXTRACTION**
- On-line, adaptive state estimator for active noise control
p 322 N95-23308
- The mm-wave resonant methods for the detection of corrosion, phase 1
[AD-A291315] p 556 N95-29941
- EXTRAPOLATION**
- High speed civil transport: Sonic boom softening and aerodynamic optimization
[NASA-CR-196397] p 28 N95-11192
- Linear prediction data extrapolation superresolution radar imaging
p 155 N95-16268
- Hypersonic flight testing
[AD-A283981] p 134 N95-18891
- EXTRATERRESTRIAL ENVIRONMENTS**
- Aero-thermodynamic flight environment at HITEN aerobrace experiment
p 415 A95-82554
- Fatigue loads spectra derivation for the Space Shuttle: Second cycle
p 166 N95-19470
- EXTRAVEHICULAR ACTIVITY**
- Education, training, and human engineering in aerospace; SAE Aerotech '93, Costa Mesa, CA, Sep. 27-30, 1993
[SAE SP-992] p 417 A95-84553
- EXTREME ULTRAVIOLET EXPLORER SATELLITE**
- Design decisions from the history of the EUVE science payload
[HTN-95-60545] p 205 A95-69854
- EXTREMELY HIGH FREQUENCIES**
- Flight test evaluation of a 35 GHz forward looking altimeter for terrain avoidance
[BTN-95-EIX95212641071] p 287 A95-76736
- Transport Canada proposed R&D program for the development of a multi-parameter dual X-Ka band Doppler radar for aviation meteorology applications
p 659 A95-93477

F

F-104 AIRCRAFT

- F-104 resource tape
[NASA-TM-104296] p 13 N95-10741

F-106 AIRCRAFT

- Quantifiable vortex features of F-106B aircraft at subsonic speeds
[BTN-95-EIX0619952748161] p 588 A95-94455

F-111 AIRCRAFT

- Development of a composite repair and the associated inspection intervals for the F-111C stiffener runout region
p 66 N95-14477
- A PC-based interactive simulation of the F-111C Pavé Tack system and related sensor, avionics and aircraft aspects
[AD-A285500] p 129 N95-16969

F-14 AIRCRAFT

- Evaluation of alternate F-14 wing lug coating
[AD-A283207] p 129 N95-17631
- Application of photogrammetry of F-14D store separation
[AD-A284154] p 132 N95-18417
- Naval aviation: F-14 upgrades are not adequately justified. Report to Congressional Committees
[AD-A286338] p 231 N95-20212
- Navy composite maintenance and repair experience
p 424 N95-28446

F-15 AIRCRAFT

- Aircraft wiring maintenance: Development of a computerized maintenance aid
[SAE PAPER 932615] p 456 A95-90080
- Propulsion controlled aircraft research
p 497 A95-90869

F-15 835 (HIDEC) resource tape
 [NASA-TM-104297] p 13 N95-10742
 F-15 Propulsion Controlled Aircraft (PCA)
 [NASA-TM-104303] p 17 N95-10748
 On the use of controls for subsonic transport
 performance improvement: Overview and future
 directions p 10 N95-11408
 [NASA-TM-4605] p 10 N95-11408
 Dynamic ground effects flight test of an F-15 aircraft
 [NASA-TM-4604] p 38 N95-12191
 The development of the F100-PW-220 and
 F110-GE-100 engines: A case study of risk assessment
 and risk management p 51 N95-13289
 [AD-A282467] p 51 N95-13289
 Integration of a mechanical forebody vortex control
 system into the F-15 p 72 N95-14258
 Flight evaluation of pneumatic forebody vortex control
 in post-stall flight p 72 N95-14259
 Development of a low-aspect ratio fin for flight research
 experiments p 108 N95-16858
 [NASA-TM-4596] p 108 N95-16858
 F-15 resource tape p 230 N95-19994
 [NASA-TM-110502] p 230 N95-19994
 Development of a nonlinear simulation for the McDonnell
 Douglas F-15 Eagle with a longitudinal TECS control-law
 [AD-A288610] p 388 N95-26481
 Development of a TECS control-law for the lateral
 directional axis of the McDonnell Douglas F-15 Eagle
 [AD-A289771] p 410 N95-28598
 Measurements of ions formed in jet engine exhaust
 plumes p 514 N95-29764
 [AD-A290940] p 514 N95-29764
 Flight assessment of the onboard propulsion system
 model for the Performance Seeking Control algorithm on
 an F-15 aircraft p 617 N95-31425
 [NASA-TM-4705] p 617 N95-31425
 Flight test validation of a frequency-based system
 identification method on an F-15 aircraft p 620 N95-31846
 [NASA-TM-4704] p 620 N95-31846
 Report to the Chairman, Legislation and National
 Security Subcommittee, Committee on Government
 Operations, House of Representatives. Tactical aircraft:
 F-15 replacement is premature as currently planned
 [GAO/NSIAD-94-118] p 679 N95-31987
 An Electronic Workshop on the Performance Seeking
 Control and Propulsion Controlled Aircraft Results of the
 F-15 Highly Integrated Digital Electronic Control Flight
 Research Program p 694 N95-33009
 [NASA-TM-104278] p 694 N95-33009
 An overview of integrated flight-propulsion controls flight
 research on the NASA F-15 research airplane p 694 N95-33010
 Performance seeking control program overview p 695 N95-33011
 F-15 propulsion system p 695 N95-33012
 PSC algorithm description p 695 N95-33013
 PSC implementation and integration p 695 N95-33014
 Minimum fuel mode evaluation p 695 N95-33015
 Minimum fan turbine inlet temperature mode
 evaluation p 696 N95-33016
 Maximum thrust mode evaluation p 696 N95-33017
 Performance seeking control excitation mode p 696 N95-33019
 Performance seeking control (PSC) for the F-15 highly
 integrated digital electronic control (HIDEC) aircraft p 697 N95-33020
 Propulsion Controlled Aircraft design and development p 697 N95-33022
 Flight test of a propulsion controlled aircraft system on
 the NASA F-15 airplane p 691 N95-33023
 Dynamic ground effects flight test of the NASA F-15
 aircraft p 692 N95-33024
 Design challenges encountered in the F-15 PCA flight
 test program p 692 N95-33025

F-16 AIRCRAFT
 Robustly stable preliminary control systems design for
 the YF-16 CCV aircraft [BTN-95-EIX95202637608] p 292 A95-76681
 Intelligent tutoring system: F-16 flight simulation p 521 A95-90649
 Research excitation system flight testing [NASA-TM-104289] p 13 N95-10715
 F-16XL resource tape [NASA-TM-104298] p 13 N95-10743
 The development of the F100-PW-220 and
 F110-GE-100 engines: A case study of risk assessment
 and risk management p 51 N95-13289
 [AD-A282467] p 51 N95-13289
 Flight test results of the F-16 aircraft modified with the
 axisymmetric vectoring exhaust nozzle p 70 N95-14245
 Vista/F-16 Multi-Axis Thrust Vectoring (MATV) control
 law design and evaluation p 71 N95-14248
 F/A-18 and F-16 forebody vortex control, static and
 rotary-balance results p 72 N95-14254

The F-16 multinational staged improvement program:
 A case study of risk assessment and risk management
 [AD-A281706] p 81 N95-15451
 Developing an emission factor for hazardous air
 pollutants for an F-16 using JP-8 fuel [AD-A284802] p 216 N95-19685
 F-16XL interview with Marta Bohn-Meyer
 [NASA-TM-110505] p 223 N95-19996
 A quantitative feedback theory FCS design for the
 subsonic envelope of the VISTA F-16 including
 configuration variation [AD-A289221] p 409 N95-26958
 Flight control design using mixed H2/micron
 optimization [AD-A289288] p 410 N95-27036
 Implementation and demonstration of a multiple model
 adaptive estimation failure detection system for the F-16
 [AD-A289301] p 391 N95-27042
 Life cycle costs of alternatives for F-16 printed circuit
 board diagnosis equipment [AD-A288744] p 401 N95-28586
 Application of optimization technique to control system
 design for departure prevention and aircraft model
 estimation through dynamic inversion p 517 N95-29156
 Looking for the simple PIO model p 597 N95-31066
 Flight test results of the F-16 aircraft modified with
 axisymmetric vectoring exhaust nozzle p 609 N95-32007
 Application of advanced safety technique to ring laser
 gyro inertial navigation system integration p 689 N95-33140

F-18 AIRCRAFT

Vortical flow structure near the F/A-18 LEX at high
 incidence [BTN-95-EIX95062487555] p 186 A95-68369
 F/A-18 inlet calculations at 60-deg angle of attack and
 10-deg sideslip [BTN-95-EIX95112524199] p 195 A95-69309
 Forebody flow control on a full-scale F/A-18 aircraft
 [BTN-95-EIX95152582333] p 281 A95-73535
 Robust longitudinal axis flight control for an aircraft with
 thrust vectoring [BTN-95-EIX95122538875] p 408 A95-83000
 Second generation smart actuator [SAE PAPER 932585] p 505 A95-90069
 Actuated forebody strake controls for the F-18
 High-Alpha Research Vehicle [BTN-95-EIX0619952748173] p 619 A95-94467
 Evaluation of F-18A approach and landing flying qualities
 using an in-flight simulator [CALSPAN-6241-F-1] p 12 N95-10442
 F-18 HARV presentation for industry [NASA-TM-104283] p 13 N95-10711
 F-18 high alpha research vehicle resource tape [NASA-TM-104299] p 13 N95-10744
 Numerical simulation of the flow about the F-18 HARV
 at high angle of attack [NASA-CR-196396] p 9 N95-10940
 Computational analysis of forebody tangential slot
 blowing on the high alpha research vehicle [NASA-CR-196750] p 10 N95-11367
 Flight and full-scale wind-tunnel comparison of pressure
 distributions from an F-18 aircraft at high angles of attack
 — Conducted in NASA Ames Research Center's 80 by
 120 ft wind tunnel p 68 N95-14231
 Numerical simulation of the flow about an F-18 aircraft
 in the high-alpha regime p 68 N95-14232
 Hybrid structured/unstructured grid computations for the
 F/A-18 at high angle of attack p 68 N95-14233
 Free-to-roll tests of X-31 and F-18 subscale models with
 correlation to flight test results p 69 N95-14237
 F-18 high alpha research vehicle: Lessons learned p 69 N95-14240
 Design and development of an F/A-18 inlet distortion
 rake: A cost and time saving solution p 69 N95-14241
 Flight validation of ground-based assessment for control
 power requirements at high angles of attack p 70 N95-14246
 Navy and the HARV: High angle of attack tactical utility
 issues p 71 N95-14252
 Preparations for flight research to evaluate actuated
 forebody strakes on the F-18 high-alpha research
 vehicle p 72 N95-14257
 Numerical simulation of the flow about the F-18 HARV
 at high angle of attack [NASA-CR-197023] p 74 N95-14614
 Pressure measurements on an F/A-18 twin vertical tail
 in buffeting flow. Volume 2: Steady and unsteady RMS
 pressure data [AD-A281581] p 76 N95-15465
 Flight testing high lateral asymmetries on highly
 augmented Fighter/Attack aircraft [AD-A264206] p 130 N95-17953

Pressure measurements on an F/A-18 twin vertical tail
 in buffeting flow. Volume 4, part 2: Buffet cross spectral
 densities [AD-A285555] p 143 N95-18641
 Fiber Optic Control System integration for advanced
 aircraft. Electro-optic and sensor fabrication, integration,
 and environmental testing for flight control systems:
 Laboratory test results [NASA-CR-195408] p 161 N95-18938
 Navier-Stokes, flight, and wind tunnel flow analysis for
 the F/A-18 aircraft [NASA-TP-3478] p 120 N95-19114
 Prediction of wind tunnel effects on the installed F/A-18A
 inlet flow field at high angles-of-attack [NASA-CR-195429] p 197 N95-19651
 Pressure measurements on an F/A-18 twin vertical tail
 in buffeting flow. Volume 1: Wind tunnel test summary
 [AD-A279126] p 225 N95-21877
 Analysis of the longitudinal handling qualities and
 pilot-induced-oscillation tendencies of the
 High-Angle-of-Attack Research Vehicle (HARV) p 293 N95-23297
 Enhancement of F/A-18 operational flight
 measurements: Data report for phase 1 [DSTO-TR-0049] p 286 N95-23666
 F/A-18 IFOSTP Fatigue test airbag load determination
 on the vertical and horizontal tails [DSTO-TR-0135] p 388 N95-26389
 Numerical simulation of the flow about the F-18 HARV
 at high angle of attack [NASA-CR-197755] p 374 N95-26735
 Composite repair of a CF18: Vertical stabilizer leading
 edge p 395 N95-27517
 Composite flight-control actuator development p 410 N95-28281
 Evaluation of proposed agility metrics using X-31 vs.
 F/A-18 flight data [AD-A292573] p 502 N95-28977
 Estimation of aerodynamic load distributions on the
 F/A-18 aircraft using a CFD panel code [DSTO-TR-0147] p 504 N95-29445
 Modeling F/A-18 flight hour program costs using
 regression analysis [AD-A293771] p 608 N95-31579

F-22 AIRCRAFT
 Report to Congressional Committees. Tactical Aircraft:
 Concurrence in development and production of F-22
 aircraft should be reduced [GAO/NSIAD-95-59] p 336 N95-26338
 Report to the Chairman, Legislation and National
 Security Subcommittee, Committee on Government
 Operations, House of Representatives. Tactical aircraft:
 F-15 replacement is premature as currently planned
 [GAO/NSIAD-94-118] p 679 N95-31987

F-4 AIRCRAFT
 Application of photogrammetry of F-14D store
 separation [AD-A284154] p 132 N95-18417

F-8 AIRCRAFT
 Dryden and transonic research [NASA-TM-104281] p 1 N95-10709

FABRICATION
 R & D on HOPE structure p 413 A95-82355
 Rapid prototyping of composite aircraft structures
 [SAE PAPER 931219] p 539 A95-87530
 Advanced Turbine Technology Applications Project
 (ATTAP) [NASA-CR-195393] p 101 N95-15743
 Optimization of adaptive intraply hybrid fiber composites
 with reliability considerations [NASA-TM-106632] p 157 N95-16911
 Scale-up and modeling of forced chemical vapor
 infiltration [DE94-017769] p 247 N95-20781
 Idealized textile composites for experimental/analytical
 correlation p 301 N95-23277
 Development of a low-cost, modified resin transfer
 molding process using elastomeric tooling and automated
 preform fabrication p 420 N95-28268
 Static and fatigue testing of full-scale fuselage panels
 fabricated using a Therm-X(R) process p 420 N95-28270
 Advanced tow placement of composite fuselage
 structure p 420 N95-28271
 Resin transfer molding of textile preforms for aircraft
 structural applications p 421 N95-28276
 In situ processing methods for composite fuselage
 sandwich structures p 531 N95-28826
 Design, analysis, and fabrication of a pressure box test
 fixture for tension damage tolerance testing of curved
 fuselage panels p 533 N95-28839
 Cost model relationships between textile manufacturing
 processes and design details for transport fuselage
 elements p 536 N95-29043

FABRICS

- Failure behaviour of carbon fiber/epoxy composites in pin-ended buckling and bending tests
[HTN-95-71388] p 528 A95-87606
- High strain-rate testing of parachute materials
[DE95-009577] p 648 N95-31614

FABRY-PEROT INTERFEROMETERS

- Fabry-Perot interferometer measurement of static temperature and velocity for ASTOVL model tests
[NASA-TM-107014] p 645 N95-30587

FACILITIES

- Development of an experimental facility for analysis of rotorodynamic phenomena
[AD-A281897] p 25 N95-11330

FACSIMILE COMMUNICATION

- Dissemination of weather products
p 670 A95-93526

FACTORIZATION

- Dynamic stiffness and damping of foil bearings for gas turbine engines
[SAE PAPER 931449] p 635 A95-93698

FAIL-SAFE SYSTEMS

- Residual strength of thin panels with cracks
p 311 N95-23311

FAILURE

- Theoretical and experimental studies of fretting-initiated fatigue failure of aeroengine compressor discs
[BTN-94-EIX94421372285] p 343 A95-78467
- Residual strength of composites with multiple impact damage
[BTN-94-EIX94511433967] p 701 A95-96664
- Development of advanced approach and departure procedures. Failure scenarios
[PB95-198123] p 601 N95-30815
- New adaptive methods for reconfigurable flight control systems, appendix 1
[AD-A292711] p 619 N95-30937
- Transmittance characteristics of US Army rotary-wing aircraft transparencies
[AD-A295035] p 693 N95-34793
- Resource document for the design of electronic instrument approach procedure displays
[AD-A295108] p 691 N95-34797

FAILURE ANALYSIS

- Modelling of pilowing due to corrosion in fuselage lap joints
[BTN-95-EIX95082502227] p 240 A95-71024
- New failure detection approach and its application to GPS autonomous integrity monitoring
[BTN-95-EIX95202637613] p 279 A95-76676
- Fault detection in multiprocessor systems and array processors
[BTN-95-EIX95242679097] p 359 A95-81253
- Buckling and postbuckling of composite structures
[HTN-95-71387] p 528 A95-87605
- Advanced composites structural concepts and materials technologies for primary aircraft structures: Structural response and failure analysis
[NASA-CR-4448] p 11 N95-10240
- Brush seal performance and durability issues based on T-700 engine test results
[NASA-TM-106502] p 22 N95-11483
- Moisture induced pressures in concrete airfield pavements
[AD-A281974] p 52 N95-11789
- Influence of crack history on the stable tearing behavior of a thin-sheet material with multiple cracks
p 93 N95-14467
- A study of software standards used in the avionics industry
p 137 N95-16456
- Handling qualities of the High Speed Civil Transport
p 294 N95-23325
- Implementation and demonstration of a multiple model adaptive estimation failure detection system for the F-16
[AD-A289301] p 391 N95-27042
- Bearing defect signature analysis using advanced nonlinear signal analysis in a controlled environment
[NASA-TM-108491] p 441 N95-28364
- Technology integration box beam failure study
p 441 N95-28468
- Tension fracture of laminates for transport fuselage. Part 1: Material screening
p 398 N95-28471
- Application of damage tolerance methodology in certification of the Piaggio P-180 Avanti
p 399 N95-28480
- Tension fracture of laminates for transport fuselage. Part 2: Large notches
p 532 N95-28837
- Technology integration box beam failure study
p 552 N95-28847
- Recirculating cavity casing treatment failure
[AD-A289330] p 513 N95-28908
- Test results from large wing and fuselage panels
p 537 N95-29051
- Failure analysis for polycarbonate transparencies
[AD-A292992] p 630 N95-31471

FAILURE MODES

- Mechanical system reliability and risk assessment
[BTN-95-EIX95142553046] p 304 A95-73452
- Analytical and experimental vibration analysis of a faulty gear system
[NASA-TM-106689] p 58 N95-12843
- FAA/NASA International Symposium on Advanced Structural Integrity Methods for Airframe Durability and Damage Tolerance
[NASA-CP-3274-PT-1] p 92 N95-14453
- Probabilistic inspection strategies for minimizing service failures
p 93 N95-14461
- A Lifting Ball Valve for cryogenic fluid applications
p 156 N95-16349
- Detecting gear tooth fracture in a high contact ratio face gear mesh
[NASA-TM-106822] p 162 N95-19125
- Soft body impact on titanium fan blades
p 200 N95-19671
- Damage of high temperature components by dust-laden air
p 201 N95-19673
- Advanced Packaging Concepts for Digital Avionics
[AGARD-CP-562] p 233 N95-20631
- Residual strength of thin panels with cracks
p 311 N95-23311
- Static and fatigue testing of full-scale fuselage panels fabricated using a Therm-X(R) process
p 420 N95-28270
- Proof test methodology for composites
p 424 N95-28445
- Numerical simulation of crack growth in pressurized fuselages
[PB95-192415] p 400 N95-28636
- Machinability study of Aermot 100
[DE95-011532] p 701 N95-33408

FALKNER-SKAN EQUATION

- Acoustic receptivity due to weak surface inhomogeneities in adverse pressure gradient boundary layers
[NASA-TM-4577] p 249 N95-21258

FALLING

- Study on a scheme for the prolongation of microgravity time of balloon-borne drop capsule
p 414 A95-82515

FALSE ALARMS

- The use of radar wind profiles to remove TDWR gust front algorithm false alarms caused by vertical wind shear
p 661 A95-93488

FAN BLADES

- H-76B fantail demonstrator composite fan blade fabrication
[HTN-95-80856] p 283 A95-75098
- The effects of surface modification on fretting fatigue in Ti alloy turbine components
[HTN-95-61145] p 404 A95-84909
- Fan noise reduction from a supersonic inlet during simulated aircraft approach
[BTN-95-EIX95292721155] p 572 A95-89894
- Computational fluid dynamics study of the variable-pitch split-blade fan concept
[NASA-CR-189206] p 15 N95-10247
- Fan noise research at NASA
p 28 N95-11260
- Analytical investigation of adaptive control of radiated inlet noise from turbofan engines
p 30 N95-11277
- Ducted fan acoustic radiation including the effects of nonuniform mean flow and acoustic treatment
[NASA-CR-197449] p 172 N95-16401
- Mach number, flow angle, and loss measurements downstream of a transonic fan-blade cascade
[AD-A280907] p 108 N95-16824
- Design of fan blades subjected to bird impact
p 200 N95-19669
- Soft body impact on titanium fan blades
p 200 N95-19671
- UHB engine fan broadband noise reduction study
[NASA-CR-198357] p 580 N95-29641

FANS

- Fan noise reduction from a supersonic inlet during simulated aircraft approach
[BTN-95-EIX95292721155] p 572 A95-89894
- Concepts for the control of rotor noise
p 573 A95-90092

FAR FIELDS

- Novel similarity solutions of the sonic small-disturbance equation with applications to airfoil transonic aerodynamics
[BTN-94-EIX94341340316] p 35 A95-60852
- Analytical investigation of adaptive control of radiated inlet noise from turbofan engines
p 30 N95-11277
- Single crystal nickel superalloys
Exact dynamic responses of periodic multi-span beams under convected pressure fields
p 25 N95-11288
- Ducted fan acoustic radiation including the effects of nonuniform mean flow and acoustic treatment
[NASA-CR-197449] p 172 N95-16401
- Correction of support influences on measurements with sting mounted wind tunnel models
p 122 N95-19281

- Computation of noise radiation from turbofans: A parametric study
[NASA-CR-198359] p 710 N95-32836

FAR INFRARED RADIATION

- Empirical corrections of the rigid rotor interaction potential of H₂-H₂ in the attractive region: Dimer features in the FIR absorption spectra
[HTN-95-41943] p 361 A95-81690

FAR ULTRAVIOLET RADIATION

- Planetary entry experiments
[NASA-CR-194215] p 101 N95-13717
- VUV shock layer radiation in an arc-jet wind tunnel experiment
p 67 N95-13719

FAST FOURIER TRANSFORMATIONS

- Linear prediction data extrapolation superresolution radar imaging
p 155 N95-16268
- Waveform bounding and combination techniques for direct drive testing
[AD-A284075] p 161 N95-19035
- Electrochemical impedance pattern recognition for detection of hidden chemical corrosion on aircraft components
[AD-A284998] p 241 N95-20481
- Image representation using fast algorithms based on the Zak transform
[AD-A293416] p 679 N95-31684

FAST NEUTRONS

- Evaluation of neutron techniques for illicit substance detection
[DE95-002988] p 300 N95-22764

FASTENERS

- New experimental approach to determine initial fatigue quality with fastener holes
[BTN-94-EIX94522406136] p 701 A95-96273
- Eddy current for detecting second layer cracks under installed fasteners
[AD-A282412] p 158 N95-17507
- Eddy current for detecting second-layer cracks under installed fasteners
[AD-A279871] p 244 N95-20414
- Eddy current detection of pitting corrosion around fastener holes
p 315 N95-23507

FATIGUE (MATERIALS)

- Corrosion prevention and control
[BTN-95-EIX95031502753] p 188 A95-68260
- Fatigue resistance of peened 7050-T7451 aluminium alloy: Repair and re-treatment of a component surface
[BTN-94-EIX94371347838] p 206 A95-69131
- Fatigue crack growth in nickel-based superalloys at 500-700 C. 1: Waspaloy
[BTN-94-EIX94371347843] p 206 A95-69136
- Service life extensions for the C-141
[BTN-95-EIX95112530749] p 193 A95-69295
- Growth of multiple cracks and their linkup in a fuselage lap joint
[BTN-95-EIX95142553047] p 286 A95-73451
- Validation of an effective flat cruciform-shaped specimen to study CFRP composite laminates under biaxial loading
[BTN-95-EIX95152584677] p 282 A95-73589
- Evaluation of advanced aerospace materials by depth sensing indentation and scratch methods
[BTN-95-EIX95152584678] p 282 A95-73590
- Theoretical and experimental studies of fretting-initiated fatigue failure of aeroengine compressor discs
[BTN-94-EIX94421372285] p 343 A95-78467
- Ceramic composite attachments for transmission of high-torque loads
[BTN-94-EIX95011441256] p 417 A95-84213
- The effects of surface modification on fretting fatigue in Ti alloy turbine components
[HTN-95-61145] p 404 A95-84909
- Fatigue of aircraft materials; Specialists' Conference, Delft, Netherlands, 1992
[HTN-95-B0076] p 387 A95-85892
- Fatigue of aircraft materials and structures
p 387 A95-85894
- Structural integrity of fuselage panels with multisite damage
[BTN-95-EIX0619952748188] p 637 A95-94250
- Fatigue design of axially loaded semicircular lugs
[BTN-95-EIX0619952748190] p 637 A95-94252
- Damage tolerance certification of a fighter horizontal stabilizer
[BTN-95-EIX0619952748186] p 637 A95-94478
- New experimental approach to determine initial fatigue quality with fastener holes
[BTN-94-EIX94522406136] p 701 A95-96273
- Fatigue in single crystal nickel superalloys
[AD-A283459] p 56 N95-12546
- FAA/NASA International Symposium on Advanced Structural Integrity Methods for Airframe Durability and Damage Tolerance
[NASA-CP-3274-PT-1] p 92 N95-14453
- Inspecting for widespread fatigue damage: Is partial debonding the key?
p 93 N95-14458

- Study of multiple cracks in airplane fuselage by micromechanics and complex variables p 94 N95-14468
- The effects of pitting on fatigue crack nucleation in 7075-T6 aluminum alloy p 88 N95-14482
- Analysis of small crack behavior for airframe applications p 95 N95-14484
- The characterization of widespread fatigue damage in fuselage structure [NASA-TM-109142] p 88 N95-14920
- Fatigue in single crystal nickel superalloys [AD-A285727] p 152 N95-18068
- FAA/NASA International Symposium on Advanced Structural Integrity Methods for Airframe Durability and Damage Tolerance, part 2 [NASA-CP-3274-PT-2] p 124 N95-19468
- Fatigue loads spectra derivation for the Space Shuttle: Second cycle p 166 N95-19470
- Prediction of fatigue crack growth under flight-simulation loading with the modified CORPUS model p 166 N95-19471
- The characterization of widespread fatigue damage in fuselage structure p 166 N95-19472
- Residual life and strength estimates of aircraft structural components with MSD/MED p 136 N95-19485
- Widespread fatigue damage monitoring: Issues and concerns p 136 N95-19488
- Fatigue crack growth in 2024-T3 aluminum under tensile and transverse shear stresses p 153 N95-19490
- Fatigue and residual strength investigation of ARALL(R) -3 and GLARE(R) -2 panels with bonded stringers p 137 N95-19495
- Aircraft fatigue and crack growth considering loads by structural component p 137 N95-19497
- Derived gust spectra for the Macchi MB326H [ARL-TN-3] p 225 N95-21892
- Review of aeronautical fatigue investigation in the Netherlands during the period March 1991-March 1993 [PB95-139184] p 285 N95-23161
- Review of some results of the author's fatigue investigations with applications in engineering and material science [TAE-698] p 316 N95-23662
- A review of Australian and New Zealand investigations on aeronautical fatigue during the period Apr. 1993 - Mar. 1995 [AR-009-202] p 397 N95-27918
- Comparison of measured and calculated dynamic loads for the Mod-2 2.5 mW wind turbine system p 440 N95-27983
- Prediction of fatigue crack growth under constant amplitude and random loading using specimens with multiple cracks [AD-A291614] p 397 N95-28409
- Investigation of static and cyclic bearing failure mechanisms for GR/EP laminates p 422 N95-28427
- Applications of a damage tolerance analysis methodology in aircraft design and production p 426 N95-28483
- Probabilistic reliability modeling of fatigue on the H-46 tie bar [AD-A289926] p 607 N95-30927
- Failure analysis for polycarbonate transparencies [AD-A292992] p 630 N95-31471
- FATIGUE LIFE**
- Growth of multiple cracks and their linkup in a fuselage lap joint [BTN-95-EIX95142553047] p 286 A95-73451
- Flight simulation fatigue crack growth testing of aluminum alloys [HTN-95-00652] p 418 A95-84731
- The effects of surface modification on fretting fatigue in Ti alloy turbine components [HTN-95-61145] p 404 A95-84909
- Artificial neural networks for predicting nonlinear dynamic helicopter loads [HTN-95-51678] p 404 A95-85060
- Fatigue life estimation program for Part 23 airplanes, 'AFS.FOR' [SAE PAPER 931249] p 565 A95-89221
- The FAA regional/commuter aircraft flight loads data collection program [SAE PAPER 931258] p 493 A95-89224
- The avionics integrity programme (AVIP) [CONGRESS PAPER C428-6-115] p 549 A95-91684
- Modeling and life prediction methodology for Titanium Matrix Composites subjected to mission profiles [NASA-TM-109148] p 55 N95-11915
- Cabin-fuselage-wing structural design concept with engine installation [NASA-CR-197172] p 49 N95-12993
- Inspecting for widespread fatigue damage: Is partial debonding the key? p 93 N95-14458
- Probabilistic inspection strategies for minimizing service failures p 93 N95-14461
- A method of calculating the safe fatigue life of compact, highly-stressed components p 93 N95-14464
- Corrosion and corrosion fatigue of airframe aluminum alloys p 87 N95-14465
- Computational predictive methods for fracture and fatigue p 93 N95-14466
- Influence of crack history on the stable tearing behavior of a thin-sheet material with multiple cracks p 93 N95-14467
- Extracting a representative loading spectrum from recorded flight data p 80 N95-14469
- The role of fretting corrosion and fretting fatigue in aircraft rivet hole cracking p 94 N95-14470
- Fatigue reliability method with in-service inspections p 94 N95-14475
- The effects of pitting on fatigue crack nucleation in 7075-T6 aluminum alloy p 88 N95-14482
- Analysis of small crack behavior for airframe applications p 95 N95-14484
- Full-scale testing and analysis of fuselage structure p 95 N95-14485
- Advanced method and processing technology for complicated shape airframe part forming p 80 N95-14486
- Current and future problems in structural acoustic fatigue p 173 N95-19143
- Brite-Euram programme: ACOUFAT acoustic fatigue and related damage tolerance of advanced composite and metallic structures p 174 N95-19159
- Prediction of fatigue crack growth under flight-simulation loading with the modified CORPUS model p 166 N95-19471
- Discrete crack growth analysis methodology for through cracks in pressurized fuselage structures p 166 N95-19473
- Fatigue life until small cracks in aircraft structures: Durability and damage tolerance p 135 N95-19478
- The application of Newman crack-closure model to predicting fatigue crack growth p 167 N95-19483
- Residual life and strength estimates of aircraft structural components with MSD/MED p 136 N95-19485
- Review of some results of the author's fatigue investigations with applications in engineering and material science [TAE-698] p 316 N95-23662
- Helicopter life substantiation: Review of some USA and UK initiatives [DSTO-TR-0062] p 328 N95-24201
- Proceedings of the 2d USAF Aging Aircraft Conference [AD-A288217] p 336 N95-25578
- Helicopter life substantiation: Review of some USA and UK initiatives [AD-A290045] p 502 N95-28851
- FATIGUE TESTS**
- Bonded composite repair of cracked load-bearing holes [BTN-94-EIX94401360553] p 243 A95-71867
- Growth of multiple cracks and their linkup in a fuselage lap joint [BTN-95-EIX95142553047] p 286 A95-73451
- Validation of an effective flat cruciform-shaped specimen to study CFRP composite laminates under biaxial loading [BTN-95-EIX95152584677] p 282 A95-73589
- Evaluation of advanced aerospace materials by depth sensing indentation and scratch methods [BTN-95-EIX95152584678] p 282 A95-73590
- Fatigue strength of high-temperature alloys under conditions of cyclic temperature variation. Communication 1: Experimental procedure and results [BTN-94-EIX94401363884] p 307 A95-75516
- Flight simulation fatigue crack growth testing of aluminum alloys [HTN-95-00652] p 418 A95-84731
- Status and prospects for aluminium-lithium alloys in aircraft structures p 387 A95-85893
- Fibre-Metal laminates p 387 A95-85895
- Elements of structural integrity assurance p 387 A95-85896
- High temperature strain gage technology for gas turbine engines [NASA-CR-191177] p 57 N95-11996
- Analytical and experimental vibration analysis of a faulty gear system [NASA-TM-106689] p 58 N95-12843
- The characterization of widespread fatigue damage in fuselage structure [NASA-TM-109142] p 88 N95-14920
- Fatigue in single crystal nickel superalloys [AD-A282917] p 88 N95-15415
- Detecting gear tooth fracture in a high contact ratio face gear mesh [NASA-TM-106822] p 162 N95-19125
- High-temperature acoustic test facilities and methods p 174 N95-19149
- Acoustic fatigue testing on different materials and skin-stringer elements p 174 N95-19156
- Brite-Euram programme: ACOUFAT acoustic fatigue and related damage tolerance of advanced composite and metallic structures p 174 N95-19159
- Prediction of fatigue crack growth under flight-simulation loading with the modified CORPUS model p 166 N95-19471
- Evaluation of the fuselage lap joint fatigue and terminating action repair p 166 N95-19477
- Development of load spectra for Airbus A330/A340 full scale fatigue tests p 135 N95-19479
- An artificial corrosion protocol for lap-splices in aircraft skin p 152 N95-19482
- Ultrasonic techniques for repair of aircraft structures with bonded composite patches p 136 N95-19486
- Results of uniaxial and biaxial tests on riveted fuselage lap joint specimens p 136 N95-19491
- Lubricant evaluation and performance, 2 [AD-A279144] p 242 N95-21969
- Study on tensile fatigue testing method of unidirectional fiber-resin matrix composites [NAL-TR-1241] p 343 N95-24989
- Design and development of a test rig for the high frequency testing of rolling sleeve airsprings [DSTO-TN-0001] p 411 N95-26378
- F/A-18 IFOSTP Fatigue test airbag load determination on the vertical and horizontal tails [DSTO-TR-0195] p 388 N95-26389
- Composite repair of metallic airframe: Twenty years of experience p 393 N95-27508
- External patch repair of CFRP/honeycomb sandwich p 395 N95-27522
- Damage occurrence on composites during testing and fleet service: Repair of Airbus aircraft p 396 N95-27526
- Static and fatigue testing of full-scale fuselage panels fabricated using a Therm-X(R) process p 420 N95-28270
- Proof test methodology for composites p 424 N95-28445
- Applications of a damage tolerance analysis methodology in aircraft design and production p 426 N95-28483
- Bell Helicopter Advanced Rotocraft Transmission (ART) program [NASA-CR-195479] p 555 N95-29538
- Thermal-mechanical fatigue crack growth in aircraft engine materials [ISBN-0-315-86543-1] p 647 N95-31098
- FAULT DETECTION**
- Engine life measurement and diagnostics [BTN-95-EIX95041505024] p 235 A95-70133
- Evaluation of advanced aerospace materials by depth sensing indentation and scratch methods [BTN-95-EIX95152584678] p 282 A95-73590
- ATE enabling technologies [BTN-95-EIX95172595294] p 287 A95-75718
- Condition monitoring and diagnostics [BTN-95-EIX95182617811] p 261 A95-75756
- New failure detection approach and its application to GPS autonomous integrity monitoring [BTN-95-EIX95202637613] p 279 A95-76676
- Impact of near-coincident faults on digital flight control systems [BTN-95-EIX95242670759] p 359 A95-81088
- Fault detection in multiprocessor systems and array processors [BTN-95-EIX95242679097] p 359 A95-81253
- Condition monitoring and diagnostics [HTN-95-92312] p 387 A95-85356
- Failure detection and isolation structure for global positioning system autonomous integrity monitoring [BTN-95-EIX95282706656] p 486 A95-89648
- Pitot/static leak testing [CONGRESS PAPER C428-9-035] p 508 A95-91696
- Fault Diagnosis for condition monitoring applied to hydraulic circuits [CONGRESS PAPER C428-12-165] p 456 A95-91703
- Health monitoring and cost implications for an airline operator [CONGRESS PAPER C428-12-166] p 457 A95-91704
- Gas path debris monitoring [CONGRESS PAPER C428-15-031] p 508 A95-91710
- Rolling bearing failure and wear debris detection [CONGRESS PAPER C428-15-094] p 457 A95-91711
- Aircraft gear train diagnostics using the irregular rotation of the external shafts [CONGRESS PAPER C428-15-097] p 508 A95-91712

- Developments in wear particle analysis using computerized procedures
[CONGRESS PAPER C428-15-216] p 457 A95-91713
- The use of math-dynamic models to aid the development of integrated health and usage monitoring systems
[CONGRESS PAPER C428-19-079] p 457 A95-91720
- An example of airborne vibration monitoring improving flight safety in the Soloviev D-30-KU engine
[CONGRESS PAPER C428-21-141] p 508 A95-91728
- Progress and experience with helicopter health and usage monitoring
[CONGRESS PAPER C428-31-151] p 603 A95-93615
- Development of an intelligent tool-condition monitoring system for FMS
[CONGRESS PAPER C428-32-012] p 583 A95-93617
- Analytical and experimental vibration analysis of a faulty gear system
[NASA-TM-106689] p 58 A95-12843
- Sensor fault detection and diagnosis simulation of a helicopter engine in an intelligent control framework
[AD-A290223] p 137 N95-15970
- An artificial neural network system for diagnosing gas turbine engine fuel faults
[DE94-013960] p 138 N95-17371
- Eddy current for detecting second layer cracks under installed fasteners
[AD-A282412] p 158 N95-17507
- Detecting gear tooth fracture in a high contact ratio face gear mesh
[NASA-TM-106822] p 162 N95-19125
- An airborne monitoring system for FOD and erosion faults
p 200 N95-19668
- Fault detection techniques for complex cable shield topologies
[AD-A286632] p 247 N95-20771
- A portable transmission vibration analysis system for the S-70A-9 Black Hawk helicopter
[DSTO-TR-0072] p 348 N95-24203
- SMART materials: Surfaces, transforms and interfaces. The commensurate engineering dimension
[AD-A289598] p 442 N95-28649
- Modal identification and its applications to damage detection in vibrating structures p 704 N95-32920
- FAULT TOLERANCE**
- Impact of near-coincident faults on digital flight control systems
[BTN-95-EIX95242670759] p 359 A95-81088
- Application of restructurable flight control system to large transport aircraft
[BTN-95-EIX95282706666] p 515 A95-89639
- Analyzing fault tolerance using DREDD
[AIAA PAPER 95-0952] p 565 A95-90631
- A reuse framework for software fault tolerance
[AIAA PAPER 95-1012] p 566 A95-90683
- Fly-By-Light/Power-By-Wire Requirements and Technology Workshop
[NASA-CP-10108] p 12 N95-10245
- Formal design and verification of a reliable computing platform for real-time control (phase 3 results)
[NASA-TM-109140] p 33 N95-10873
- Challenges for the aircraft structural integrity program p 80 N95-14481
- The Advanced Avionics Subsystem Technology Demonstration Program p 234 N95-20636
- A highly reliable, high performance open avionics architecture for real time Nap-of-the-Earth operations p 693 N95-32497
- FAULT TREES**
- Rationale for the Modular Air-system Vulnerability Estimation Network (MAVEN) methodology
[AD-A285797] p 284 N95-22510
- FEASIBILITY ANALYSIS**
- Modeling of aircraft exhaust emissions and infrared spectra for remote measurement of nitrogen oxides
[HTN-95-51276] p 355 A95-80861
- Overview of feasibility study on propulsion concepts for high speed civil transport p 498 A95-91518
- The personal aircraft: Status and issues
[NASA-TM-109174] p 223 N95-20688
- Inner loop flight control for the High-Speed Civil Transport p 293 N95-23314
- FEATHERING**
- Wind tunnel tests of a 42 inch diameter self-starting autogyro rotor
[AD-A279922] p 188 N95-19863
- FEDERAL BUDGETS**
- Report to the Chairman, Subcommittee on Transportation and Related Agencies, Committee on Appropriations, House of Representatives. Air traffic control: Status of FAA's plans to close and contract out low-activity towers
[GAO/RCED-94-265] p 603 N95-32199
- Army aviation: Modernization strategy needs to be reassessed. Report to Congressional requestors
[GAO/NSIAD-95-9] p 683 N95-32783
- Report to the Chairman, Subcommittee on Transportation and Related Agencies, Committee on Appropriations, US Senate. Airport Improvement Program: Reliever airport set-aside funds could be redirected
[GAO/RCED-94-226] p 699 N95-32786
- Report to the Chairman, Subcommittee on Transportation and Related Agencies, Committee on Appropriations, US Senate. Airport Improvement Program: The Military Airport Program has not achieved intended impact
[GAO/RCED-94-209] p 700 N95-32888
- FEEDBACK**
- Determination of piloting feedback structures for an altitude tracking task
[BTN-95-EIX95242670770] p 327 A95-81077
- Navy and the HARV: High angle of attack tactical utility issues p 71 N95-14252
- Electro-hydrostatic actuator controller design using quantitative feedback theory
[AD-A289220] p 409 N95-26957
- A quantitative feedback theory FCS design for the subsonic envelope of the VISTA F-16 including configuration variation
[AD-A289221] p 409 N95-26958
- FEEDBACK CONTROL**
- Design of a model following, state variable feedback controller for the X-14 VTOL aircraft
[HTN-94-00685] p 16 A95-60168
- Local-optimal control of a flying vehicle, with final state optimized
[BTN-94-EIX94461407957] p 83 A95-62631
- Output feedback control under randomly varying distributed delays
[BTN-94-EIX94511433916] p 168 A95-64582
- H(sup 2)/H(sup INF) controller design for a two-dimensional thin airfoil flutter suppression
[BTN-94-EIX94511433918] p 141 A95-64584
- Time-optimal turn to a heading: An analytic solution
[BTN-94-EIX94511433940] p 142 A95-64606
- Rotorcraft control system design for uncertain vehicle dynamics using quantitative feedback theory
[HTN-95-31012] p 236 A95-71182
- Dynamical instability of the aerogravity assist maneuver
[BTN-95-EIX95152583282] p 298 A95-73583
- Analytical solution for controls, heats, and states of flight trajectories
[BTN-95-EIX95152583286] p 282 A95-73587
- Real-time navigation using the global positioning system
[BTN-95-EIX95172595298] p 279 A95-75714
- Aeroelastic vehicle multivariable control synthesis with analytical robustness evaluation
[BTN-95-EIX95182619115] p 321 A95-76592
- Multivariable stability and robustness of sequentially designed feedback systems
[BTN-95-EIX95182619125] p 322 A95-76602
- H-infinity helicopter flight control law design with and without rotor state feedback
[BTN-95-EIX95182619129] p 291 A95-76606
- Load alleviation maneuvers for a launch vehicle
p 342 A95-81360
- Transonic flutter suppression using active acoustic excitations
[BTN-95-EIX95262694310] p 408 A95-85481
- Scheduling of local nonlinear control laws by exogenous signals - an application to flight control
[BTN-95-EIX95262694059] p 447 A95-85675
- Application of restructurable flight control system to large transport aircraft
[BTN-95-EIX95282706666] p 515 A95-89639
- A gust alleviation method by the response feedback p 506 A95-91493
- Missile autopilot designs using full state feedback p 507 A95-91587
- Extended cooperative control synthesis
[NASA-TM-4561] p 17 N95-10220
- High-Alpha Research Vehicle (HARV) longitudinal controller: Design, analyses, and simulation results
[NASA-TP-3446] p 17 N95-10860
- ACS/NT inner loop flight control design study
[NASA-CR-196316] p 17 N95-11223
- Cooperative control theory and integrated flight and propulsion control p 142 N95-17404
- Microgravity isolation system design: A case study
[NASA-TM-106804] p 104 N95-17657
- Simulation investigation on system identification of gas turbine
[PB95-104238] p 139 N95-17749
- Microgravity isolation system design: A modern control analysis framework
[NASA-TM-106803] p 105 N95-18486
- Plant and controller optimization by convex methods
[AD-A283700] p 133 N95-18621
- Design of robust optimal control systems and stability analysis of real structured uncertainties
[AD-A279089] p 256 N95-21913
- Performance of the 0.3-meter transonic cryogenic tunnel with air, nitrogen, and sulfur hexafluoride media under closed loop automatic control
[NASA-CR-195052] p 310 N95-23257
- System identification of the Large-Angle Magnetic Suspension Test Fixture (LAMSTF) p 296 N95-23299
- On-line, adaptive state estimator for active noise control p 322 N95-23308
- Feedback control laws for highly maneuverable aircraft
[NASA-CR-197944] p 295 N95-23410
- Application of neural networks to unsteady aerodynamic control p 360 N95-25264
- A gain scheduling optimization method using genetic algorithms
[AD-A289306] p 448 N95-26920
- Advanced formation flight control
[AD-A289271] p 409 N95-26981
- Application of optimization technique to control system design for departure prevention and aircraft model estimation through dynamic inversion p 517 N95-29156
- A novel instrumentation system for measurement of helicopter rotor motions and loads data, phase 1
[AD-A293309] p 607 N95-30923
- Structural aspects of active control technology p 623 N95-32006
- Nonlinear adaptive control of highly maneuverable high performance aircraft p 710 N95-33712
- FEEDFORWARD CONTROL**
- Active control of fan noise from a turbofan engine
[HTN-95-61198] p 570 A95-87571
- Application of restructurable flight control system to large transport aircraft
[BTN-95-EIX95282706666] p 515 A95-89639
- High-Alpha Research Vehicle (HARV) longitudinal controller: Design, analyses, and simulation results
[NASA-TP-3446] p 17 N95-10860
- Analytical investigation of adaptive control of radiated inlet noise from turbofan engines p 30 N95-11277
- A feedforward control approach to the local navigation problem for autonomous vehicles
[AD-A282787] p 126 N95-17706
- A neural expert approach to self designing flight control systems
[AD-A279965] p 237 N95-21122
- Selecting optimal experiments for feedforward multilayer perceptrons
[AD-A290856] p 678 N95-30406
- FENCES (BARRIERS)**
- Aircraft accident report: Impact with blast fence upon landing rollout Action Air Charters flight 990 Piper PA-31-350, N990RA, Stratford, Connecticut, 27 April 1994
[PB94-910410] p 333 N95-24206
- FIBER COMPOSITES**
- Twisting smartly in the wind
[BTN-95-EIX95041503093] p 184 A95-68353
- Validation of an effective flat cruciform-shaped specimen to study CFRP composite laminates under biaxial loading
[BTN-95-EIX95152584677] p 282 A95-73589
- Shear buckling response of tailored composite plates
[HTN-95-51680] p 418 A95-85062
- Fatigue of aircraft materials: Specialists' Conference, Delft, Netherlands, 1992
[HTN-95-80076] p 387 A95-85892
- Fibre-Metal laminates p 387 A95-85895
- Buckling and postbuckling of composite structures
[HTN-95-71387] p 528 A95-87605
- Advanced composites structural concepts and materials technologies for primary aircraft structures: Design/manufacturing concept assessment
[NASA-CR-4447] p 12 N95-10316
- Optimization of adaptive intraply hybrid fiber composites with reliability considerations
[NASA-TM-106632] p 157 N95-16911
- A CMC database for use in the next generation launch vehicles (rockets) p 150 N95-18993
- Toughened Silcomp composites for gas turbine engine applications
[DE95-002851] p 235 N95-21243

Corrosion protection measures for CFC/metal joints of fuel integral tank structures of advanced military aircraft p 303 N95-23510

On aircraft repair verification of a fighter A/C integrally stiffened fuselage skin p 394 N95-27515

Composite repair of a CF18: Vertical stabilizer leading edge p 395 N95-27517

Scarf joint technique with cocured and precured patches for composite repair p 396 N95-27524

Composite or metallic bolted repairs on self-stiffened carbon wing panel of the commuter ATR72 design criteria, analysis, verification by test p 396 N95-27525

Repairs of CFC primary structures p 396 N95-27527

Ninth DOD/NASA/FAA Conference on Fibrous Composites in Structural Design, volume 3 [NASA-CR-198718] p 420 N95-28266

Analysis of aircraft engine blade subject to ice impact p 407 N95-28277

Application of fiber-reinforced bismaleimide materials to aircraft nacelle structures p 397 N95-28278

Ninth DOD/NASA/FAA Conference on Fibrous Composites in Structural Design, volume 1 [NASA-CR-198723] p 421 N95-28420

Application of advanced material systems to composite frame elements p 422 N95-28432

Ninth DOD/NASA/FAA Conference on Fibrous Composites in Structural Design, volume 2 [NASA-CR-198722] p 424 N95-28462

Advanced wing design survivability testing and results p 400 N95-28488

Ceramic composite combustor cans for expendable turbine engines [AD-A289551] p 407 N95-28646

Third NASA Advanced Composites Technology Conference, volume 1, part 2 [NASA-CP-3178-VOL-1-PT-2] p 531 N95-28823

Automated fiber placement: Evolution and current demonstrations p 532 N95-28832

Severe edge effects and simple complimentary interior solutions for thin-walled anisotropic and composite structures [AD-A290645] p 555 N95-29562

FIBER OPTICS

Fiber-optic technology for transport aircraft [BTN-94-EIX94511309384] p 103 A95-64610

Intelligent skins development for future military aircraft [CONGRESS PAPER C428-17-189] p 531 A95-91714

Novel implements of optical diagnostic techniques for aerospace applications [CONGRESS PAPER C428-21-081] p 550 A95-91726

Fiber optic hardware for transport aircraft [SAE PAPER 931439] p 680 A95-93691

Activities of the Institute for Aerospace Studies of Toronto University p 63 N95-12699

Fiber Optic Control System integration for advanced aircraft. Electro-optic and sensor fabrication, integration, and environmental testing for flight control systems: Laboratory test results [NASA-CR-195408] p 161 N95-18938

Fiber Optic Control System integration for advanced aircraft. Electro-optic and sensor fabrication, integration, and environmental testing for flight control systems [NASA-CR-191194] p 162 N95-19236

Optical backplane for modular avionics p 257 N95-20652

High performance backplane components for modular avionics p 247 N95-20653

A three-dimensional orthogonal laser velocimeter for the NASA Ames 7- by 10-foot wind tunnel [NASA-TM-108864] p 249 N95-21323

Fiber-optic rotary joint with bundle collimator assemblies [AD-D016504] p 258 N95-21673

Optical processing and control [AD-A279157] p 259 N95-21975

The 1994 Fiber Optic Sensors for Aerospace Technology (FOSAT) Workshop [NASA-CP-10166] p 337 N95-24207

Workshop report: Measurement techniques in highly transient, spectrally rich combustion environments [AD-A288395] p 350 N95-25606

SMART materials: Surfaces, transforms and interfaces. The commensurate engineering dimension [AD-A289598] p 442 N95-28649

Cost effective, dual-purpose machine vision-based detectors for (1) smoke and flame detection, and (2) engine overheat/burn-through and flame detection [AD-A292284] p 579 N95-28870

FIBER ORIENTATION

Theoretical and actual performance of a long duration superpressure balloon made from a biaxially oriented nylon-6 film p 181 A95-66282

Shear buckling response of tailored composite plates [HTN-95-51680] p 418 A95-85062

Automated fiber placement: Evolution and current demonstrations p 532 N95-28832

FIBER STRENGTH

The effect of interface properties on nickel base alloy composites [NASA-CR-198363] p 629 N95-30787

FIBER-MATRIX INTERFACES

The effect of interface properties on nickel base alloy composites [NASA-CR-198363] p 629 N95-30787

FIELD OF VIEW

Design of wide angle head up displays for synthetic vision [BTN-95-EIX95212641070] p 287 A95-76735

Factors affecting the visual fragmentation of the field-of-view in partial binocular overlap displays [AD-A283081] p 172 N95-17334

Factors affecting the perception of luring in monocular regions of partial binocular overlap displays [AD-A286287] p 259 N95-22044

Preliminary experiments of an optical fiber display [NAL-TR-1257] p 362 N95-25004

FIGHTER AIRCRAFT

Design of nonlinear control laws for high-angle-of-attack flight [BTN-94-EIX94511433920] p 141 A95-64586

Powered lift for land and sea [BTN-95-EIX95041503010] p 192 A95-68313

Integrated IR sensors [BTN-95-EIX95041505023] p 242 A95-70132

Method for the prediction of the onset of wing rock [BTN-95-EIX95152582342] p 282 A95-73544

Design and multifunction tests of a frequency domain-based active flutter suppression system [BTN-95-EIX95182619215] p 292 A95-76641

Application of Navier-Stokes aeroelastic methods to improve fighter wing maneuver performance [BTN-95-EIX95182619218] p 284 A95-76644

T-45A high angle attack testing [HTN-95-81499] p 386 A95-85213

Techniques for tailoring aircraft stall and post-stall behavior [SAE PAPER 931226] p 458 A95-87199

Predictive algorithms for the roll control autopilot of a jet fighter aircraft [HTN-95-21047] p 515 A95-90424

Integrated aircraft thermal management and power generation [SAE PAPER 932055] p 500 A95-91636

High heat sink fuels for improved aircraft thermal management [SAE PAPER 932084] p 530 A95-91659

An advanced vehicle management system [SAE PAPER 931376] p 618 A95-93655

Modular avionics: Taking today's aircraft into tomorrow [SAE PAPER 931416] p 610 A95-93681

Design of a modern pitch pointing control system [BTN-95-EIX95302731226] p 618 A95-94045

Fundamentals of catastrophic failure prevention by thrust vectoring [BTN-95-EIX0619952748176] p 606 A95-94470

Directional control at high angles of attack using blowing through a chined forebody [BTN-95-EIX0619952748179] p 619 A95-94472

Damage tolerance certification of a fighter horizontal stabilizer [BTN-95-EIX0619952748186] p 637 A95-94478

Navier-Stokes computations around a realistic fighter configuration p 591 A95-95440

Impact of agility requirements on configuration synthesis [NASA-CR-4627] p 44 N95-11952

High angle of attack flying qualities criteria for longitudinal rate command systems p 70 N95-14247

Comparison of full-scale, small-scale, and CFD results for F/A-18 forebody slot blowing p 72 N95-14255

Investigation into the aerodynamic characteristics of a combat aircraft research model fitted with a forward swept wing p 116 N95-17884

Application of photogrammetry of F-14D store separation [AD-A284154] p 132 N95-18417

Aircraft stress sequence development: A complex engineering process made simple p 136 N95-19480

Proceedings of the USAF Structural Integrity Program Conference [AD-A285684] p 194 N95-19517

An assessment of viscous effects in computational simulation of benign and burst vortex flows on generic fighter wind-tunnel models using TEAM code [NASA-CR-4650] p 273 N95-23185

Integrated mission precision attack cockpit technology (IMPACT). Phase 1: Identifying technologies for air-to-ground fighter integration [AD-A289562] p 389 N95-26684

Performance study for inlet installations [NASA-CR-189714] p 406 N95-28227

Structural design optimization with survivability dependent constraints application: Primary wing box of a multi-role fighter p 398 N95-28440

Numerical investigation into vortical flow about a delta-wing configuration up to incidences at which vortex breakdown occurs in experiment [PB95-198024] p 593 N95-30837

New adaptive methods for reconfigurable flight control systems, appendix 1 [AD-A292711] p 619 N95-30937

Lavi flight control system: Design requirements, development and flight test results p 621 N95-31994

Digital autopilot design for combat aircraft in ALENIA p 623 N95-32009

Experimental Aircraft Programme (EAP): Flight control system design and test p 623 N95-32010

FILAMENT WINDING

Recent advances in graphite/epoxy motor cases p 149 N95-16333

FILLERS

Design and evaluation of a foam-filled hat-stiffened panel concept for aircraft primary structural applications p 502 N95-28841

FILLETS

Effect of juncture fillets on double-delta wings undergoing sideslip at high angles of attack [AD-A286165] p 232 N95-22039

FILM BOILING

Study of heat transfer rates during quenching of a hot tube under microgravity p 428 A95-82641

Experimental investigation of flow-boiling heat transfer under microgravity p 428 A95-82642

FILM COOLING

Influence of injectant Mach number and temperature on supersonic film cooling [BTN-94-EIX94441386686] p 184 A95-68195

Study on the turbine vane and blade for a 1500 C class industrial gas turbine [BTN-94-EIX95011441254] p 431 A95-84211

Flowfield measurements in supersonic film cooling including the effect of shock-wave interaction [HTN-95-42337] p 405 A95-86166

Investigation of advanced counterrotation blade configuration concepts for high speed turbo-prop systems. Task 8: Cooling flow/heat transfer analysis [NASA-CR-195359] p 50 N95-11901

Effect of surface roughness on local film cooling effectiveness and heat transfer coefficients [AD-A283854] p 91 N95-14351

Particle deposition in gas turbine blade film cooling holes p 199 N95-19661

Effect of film cooling/regenerative cooling on scramjet engine performances [NAL-TR-1242] p 339 N95-24990

A summary of computational experience at GE Aircraft Engines for complex turbulent flows in gas turbines p 439 N95-27885

Leading edge film cooling effects on turbine blade heat transfer [NASA-TM-106955] p 513 N95-29115

Effect of velocity and temperature distribution at the hole exit on film cooling of turbine blades [NASA-TM-106954] p 616 N95-30702

FILM THICKNESS

A comparative study of internally and externally capped balloons using small scale test balloons p 181 A95-66285

Characterization of annular two-phase gas-liquid flows in microgravity p 95 N95-14556

FILTRATION

Precise navigation using adaptive FIR filtering and time domain spectral estimation [BTN-95-EIX95142555485] p 227 A95-72888

Erosion of dust-filtered helicopter turbine engines. Part 1: Basic theoretical considerations [BTN-95-EIX95182619222] p 288 A95-76648

Erosion of dust-filtered helicopter turbine engines. Part 2: Erosion reduction [BTN-95-EIX95182619223] p 289 A95-76649

Life prediction of helicopter engines fitted with dust filters [BTN-95-EIX95182619224] p 289 A95-76650

FINITE DIFFERENCE THEORY

Effects of leading and trailing edge flaps on the aerodynamics of airfoil/vortex interactions [HTN-95-31011] p 221 A95-71181

Higher-order viscous shock-layer solutions for high-altitude flows [BTN-95-EIX95152583255] p 306 A95-73556

- Aeroacoustic model for weak shock waves based on Burgers equation
[BTN-95-EIX95182619076] p 269 A95-75761
- Central-difference and upwind-biased schemes for steady and unsteady Euler aerofoil computations
[HTN-95-01094] p 469 A95-90280
- Parallel computational fluid dynamics '91; Conference Proceedings, Stuttgart, Germany, Jun. 10-12, 1991
[ISBN 0-444-89363-6] p 548 A95-91479
- Solution of the Navier-Stokes equations on a massively parallel transputer system
p 549 A95-91490
- A viewpoint on discretization schemes for applied aerodynamic algorithms for complex configurations
p 550 A95-91916
- Computational fluid dynamics '92; Proceedings of the European Computational Fluid Dynamics Conference, 1st, Brussels, Belgium, Sep. 7-11, 1992. Vols. 1 & 2
[ISBN 0-444-89793-3] p 638 A95-95357
- Discretization of the parabolised Navier-Stokes equations
p 638 A95-95362
- Parallel aeroelastic computations for wing and wing-body configurations
[NASA-CR-196835] p 36 N95-11766
- Numerical modeling of a cryogenic fluid within a fuel tank
[NASA-TM-4651] p 89 N95-13892
- An approach for dynamic grids
[NASA-TM-106774] p 76 N95-15853
- Static aerodynamics CFD analysis for 120-mm hypersonic KE projectile design
[ARL-MR-184] p 118 N95-18611
- Computation of inviscid flows: Full potential method
p 165 N95-19447
- A computer code (SKINTEMP) for predicting transient missile and aircraft heat transfer characteristics
[AD-A286044] p 248 N95-21001
- Computation of transonic flow on composite overlapping grids in 2 D
[PB95-131348] p 248 N95-21132
- Development of an upwind, finite-volume code with finite-rate chemistry
[NASA-CR-197747] p 374 N95-26760
- A numerical method for unsteady transonic flow about wings with control surfaces
[AD-A289631] p 375 N95-26859
- Wave drag coefficient for axisymmetric forecows at zero incidence (M sub infinity less than or equal to 1.5)
[ESDU-94014] p 552 N95-28903
- Surface pressure coefficient distributions for axisymmetric forecows at zero incidence (M sub infinity less than or equal to 1.5)
[ESDU-94015] p 477 N95-28904
- Grid orthogonality effects on predicted turbine midspan heat transfer and performance
[NASA-TM-106931] p 554 N95-29371
- Numerical simulation and analysis of the hypersonic turbulent flow past a blunt-fin/ramp configuration
[DLR-FB-94-19] p 483 N95-30349
- Direct analysis of transonic rotor noise with CFD technique
p 711 N95-34549
- A simulation of damping process of pendulum motion due to aerodynamic forces
p 711 N95-34551
- High order accuracy computational methods in aerodynamics using parallel architectures
[AD-A294167] p 686 N95-34763
- FINITE ELEMENT METHOD**
- Design optimization of aircraft engine-mount systems.
[BTN-94-EIX94351143325] p 195 A95-67298
- Modeling rotating shafts using axisymmetric solid finite elements with matrix reduction
[BTN-94-EIX94351143328] p 207 A95-67301
- Aeroelastic stability of hingeless rotor blade in hover using large deflection theory
[BTN-94-EIX94441386616] p 183 A95-67347
- Finite element time domain - modal formulation for nonlinear flutter of composite panels
[BTN-95-EIX95042474401] p 203 A95-68299
- Bi-linear formulation applied to the response and stability of helicopter rotor blade
[BTN-95-EIX95042474400] p 192 A95-68300
- Coupling equivalent plate and finite element formulations in multiple-method structural analyses
[BTN-95-EIX95062487548] p 192 A95-68362
- Influence of structural and aerodynamic modeling on flutter analysis
[BTN-95-EIX95062487550] p 203 A95-68364
- Numerical modelling of transverse impact on composite coupons
[BTN-95-EIX95082502225] p 240 A95-71022
- Modelling of pillowing due to corrosion in fuselage lap joints
[BTN-95-EIX95082502227] p 240 A95-71024
- Adaptive remeshing for convective heat transfer with variable fluid properties
[BTN-95-EIX95082502720] p 243 A95-71033
- Advance finite element modeling of rotor blade aeroelasticity
[HTN-95-31013] p 221 A95-71183
- Large-scale computational fluid dynamics by the finite element method
[BTN-94-EIX94381359154] p 243 A95-71744
- On the choice of appropriate bases for nonlinear dynamic modal analysis
[HTN-95-A0495] p 221 A95-72566
- Parametric studies for titrotor aeroelastic stability in highspeed flight
[HTN-95-A0499] p 222 A95-72570
- Adaptive finite element method for turbulent flow near a propeller
[BTN-95-EIX95142553038] p 305 A95-73460
- Coupled FEM-BEM approach for mean flow effects on vibro-acoustic behavior of planar structures
[BTN-95-EIX95152577587] p 263 A95-73495
- Static aeroelastic characteristics of a composite wing
[BTN-95-EIX95152582340] p 282 A95-73542
- Thermal force modeling for global positioning system satellites using the finite element method
[BTN-95-EIX95152583270] p 278 A95-73571
- Finite element model for a flexible non-symmetric rotor on distributed bearing: A stability study
[BTN-94-EIX94381352212] p 306 A95-74612
- Application of a control-volume-based finite-element formulation to the shock tube problem
[BTN-95-EIX95182619099] p 295 A95-76584
- Effect of curvature in the numerical simulation of an electrothermal de-icer pad
[BTN-95-EIX95182619219] p 276 A95-76645
- Modal characteristics of rotors using a conical shaft finite element
[BTN-94-EIX94401359745] p 346 A95-77379
- Viscoplastic response of structures for intense local heating
[HTN-95-41540] p 346 A95-77921
- Theoretical and experimental studies of fretting-initiated fatigue failure of aeroengine compressor discs
[BTN-94-EIX94421372285] p 343 A95-78467
- Hybrid finite element-modal analysis of jet engine inlet scattering
[BTN-95-EIX95242673665] p 427 A95-82259
- Accuracy and efficiency assessments for a weak statement CFD algorithm for high-speed aerodynamics
[BTN-94-EIX95011441238] p 370 A95-84195
- Thermo-hydrodynamic solution of floating ring seals for high pressure compressors using the finite-element method
[HTN-95-92246] p 433 A95-85290
- Computational methods in applied sciences; European Computational Fluid Dynamics Conference, 1st, Brussels, Belgium, Sept. 7-11, 1992
[ISBN 0-444-89795-X] p 539 A95-87552
- High-speed reacting flow simulation using USA-series codes
p 540 A95-87559
- Automated adaptive time-discontinuous finite element method for unsteady compressible airfoil aerodynamics
[HTN-95-81637] p 541 A95-87685
- Aeroelastic response of composite rotor blades considering transverse shear and structural damping
[HTN-95-81647] p 542 A95-87695
- An investigation of the accuracy of FEM analysis of a graphite epoxy box beam
[SAE PAPER 931221] p 543 A95-88011
- Analytical developments in support of the NASA aging aircraft program with an application to crack growth from rivets
[SAE PAPER 931223] p 545 A95-88789
- Aeroelastic stability of hingeless rotor blade in hover using large deflection theory
[HTN-95-20952] p 546 A95-88991
- Critical speed analysis of a non-linear strain ring dynamical model for aircraft tires
[SAE PAPER 932580] p 494 A95-90067
- Effects of structural damping on aeroelastic stability of various shaped composite plate wing
p 530 A95-91530
- Computer aided static aeroelastic analysis of wing/pylon/store combination
p 499 A95-91531
- Multiojective trajectory optimization by goal programming with fuzzy decision
p 526 A95-91544
- Simultaneous structure/aerodynamic design optimization for a flexible wing structure
p 499 A95-91565
- Impact finite element analysis, as an alternative to the testing of windscreens for bird impact
[CONGRESS PAPER C428-23-196] p 500 A95-91732
- A viewpoint on discretization schemes for applied aerodynamic algorithms for complex configurations
p 550 A95-91916
- Static shape control for adaptive wings
[HTN-95-A1767] p 627 A95-93330
- Fatigue design of axially loaded semicircular lugs
[BTN-95-EIX0619952748190] p 637 A95-94252
- Computational fluid dynamics '92; Proceedings of the European Computational Fluid Dynamics Conference, 1st, Brussels, Belgium, Sep. 7-11, 1992. Vols. 1 & 2
[ISBN 0-444-89793-3] p 638 A95-95357
- Numerical simulation of the 3D turbulent flow around the combustor dome of an aircraft engine
p 640 A95-95423
- An improved finite element method for the solution of the compressible Euler and Navier-Stokes equations
p 640 A95-95439
- A cartesian grid finite element method for aerodynamics of moving rigid bodies
p 642 A95-95471
- Arbitrary Lagrangian-Eulerian finite element analysis for flow-induced vibration of rigid body
p 643 A95-95485
- Navier-Stokes simulation of turbulent vortex high-Re-number flows over a delta wing
p 644 A95-95507
- Modal parameters for cracked rotors: models and comparisons
[BTN-94-EIX94522410226] p 702 A95-96378
- Modelling wear at intermittently slipping high-speed interfaces
[BTN-94-EIX94511433698] p 701 A95-96655
- Advanced composites structural concepts and materials technologies for primary aircraft structures: Structural response and failure analysis
[NASA-CR-4448] p 11 N95-10240
- Advanced composites structural concepts and materials technologies for primary aircraft structures. Structural response and failure analysis: ISPAN modules users manual
[NASA-CR-4449] p 12 N95-10242
- Effect of constraining layer stiffness on performance of damping tile materials using finite element modelling with Rayleigh integral
p 30 N95-11306
- Parallel aeroelastic computations for wing and wing-body configurations
[NASA-CR-196835] p 36 N95-11766
- Accurate interlaminar stress recovery from finite element analysis
[NASA-TM-109149] p 57 N95-11815
- Higher harmonic control analysis for vibration reduction of helicopter rotor systems
[NASA-TM-103855] p 66 N95-14419
- Elastic-plastic models for multi-site damage
p 92 N95-14454
- Bending effects of unsymmetric adhesively bonded composite repairs on cracked aluminum panels
p 92 N95-14456
- Influence of crack history on the stable tearing behavior of a thin-sheet material with multiple cracks
p 93 N95-14467
- Full-scale testing and analysis of fuselage structure
p 95 N95-14485
- Shear buckling analysis of a hat-stiffened panel
[NASA-TM-4644] p 158 N95-17490
- A review of gust load calculation methods at de Havilland
p 118 N95-18604
- Simulation of multidisciplinary problems for the thermostress state of cooled high temperature turbines
p 140 N95-19021
- Discrete crack growth analysis methodology for through cracks in pressurized fuselage structures
p 166 N95-19473
- Widespread fatigue damage monitoring: Issues and concerns
p 136 N95-19488
- Fatigue crack growth in 2024-T3 aluminum under tensile and transverse shear stresses
p 153 N95-19490
- Prediction of R-curves from small coupon tests
p 167 N95-19496
- Soft body impact on titanium fan blades
p 200 N95-19671
- Ice-impact analysis of blades
p 200 N95-19672
- Unstructured-grid large-eddy simulation of flow over an airfoil
p 225 N95-22448
- Idealized textile composites for experimental/analytical correlation
p 301 N95-23277
- Residual strength of thin panels with cracks
p 311 N95-23311
- A multibody/finite element analysis approach for modeling of crash dynamic responses
[NIAR-94-3] p 277 N95-24050
- Dynamic behavior of a magnetic bearing supported jet engine rotor with auxiliary bearings
[NASA-CR-197860] p 338 N95-24213
- A verification procedure for MSC/NASTRAN Finite Element Models
[NASA-CR-4675] p 392 N95-27371
- A FEAM based methodology for analyzing composite patch repairs of metallic structures
p 394 N95-27511
- Scarf repairs to graphite/epoxy components
p 396 N95-27523

- A NASTRAN-based computer program for structural dynamic analysis of Horizontal Axis Wind Turbines
p 439 N95-27980
- Aeroelasticity and structural optimization of composite helicopter rotor blades with swept tips
[NASA-CR-4665] p 397 N95-28262
- TranAir: A full-potential, solution-adaptive, rectangular grid code for predicting subsonic, transonic, and supersonic flows about arbitrary configurations. Theory document
[NASA-CR-4348] p 378 N95-28265
- Analysis techniques for the prediction of springback in formed and bonded composite components
p 421 N95-28289
- Dimensional stability of curved panels with cocured stiffeners and cobonded frames
p 532 N95-28836
- A weight-efficient design strategy for cutouts in composite transport structures
p 533 N95-28843
- Buckling analysis of curved composite sandwich panels subjected to inplane loadings
p 533 N95-28845
- ISPAN (Interactive Stiffened Panel Analysis): A tool for quick concept evaluation and design trade studies
p 533 N95-28846
- A global/local analysis method for treating details in structural design
p 552 N95-28848
- Test results from large wing and fuselage panels
p 537 N95-29051
- Finite element vorticity-based methods for the solution of the incompressible and compressible Navier-Stokes equations
p 553 N95-29119
- Acoustic scattering from ellipses by the modal element method
[NASA-TM-106935] p 579 N95-29401
- Scattering and radiation from cylindrically conformal antennas
p 645 N95-30669
- Intelligent finite element submodeling of multichip modules for reliability analysis
[AD-A292911] p 679 N95-31455
- A time stepping coupled finite element-state space modeling environment for synchronous machine performance and design analysis in the ABC frame of reference
p 649 N95-31948
- FPCAS3D User's guide: A three dimensional full potential aeroelastic program, version 1
[NASA-CR-198367] p 651 N95-32205
- Simulation of patch and slot antennas using FEM with prismatic elements and investigations of artificial absorber mesh termination schemes
[NASA-CR-198974] p 704 N95-32822
- Computation of noise radiation from turbofans: A parametric study
[NASA-CR-198359] p 710 N95-32836
- Fan noise prediction assessment
[NASA-CR-195051] p 711 N95-33831
- High order accuracy computational methods in aerodynamics using parallel architectures
[AD-A294167] p 686 N95-34763
- FINITE VOLUME METHOD**
- Parallel computational fluid dynamics '91: Conference Proceedings, Stuttgart, Germany, Jun. 10-12, 1991
[ISBN 0-444-89363-6] p 548 N95-91479
- Implicit multi-domain method for unsteady compressible inviscid fluid flows around 3D projectiles
p 548 N95-91482
- A detailed Euler flow analysis of TPS and fanjet engine
p 473 N95-91515
- Beyond the Riemann problem, part 1
p 550 N95-91925
- Discretization of the parabolised Navier-Stokes equations
p 638 N95-95362
- Numerical solution of Euler and Navier-Stokes equations for 2D transonic problems
p 638 N95-95366
- Implicit multidomain calculation of viscous transonic flows without artificial viscosity or upwinding
p 640 N95-95443
- Multigrad solution for the compressible Euler equations by an implicit characteristic-flux-averaging
p 642 N95-95459
- An unstructured node centered scheme for the simulation of 3-D inviscid flows
p 642 N95-95463
- An innovative algorithm to accurately solve the Euler equations for rotary wing flow
p 642 N95-95467
- A 2D parallel multiblock Navier-Stokes solver with applications on shared- and disturbed memory machines
p 643 N95-95475
- Development of an upwind, finite-volume code with finite-rate chemistry
[NASA-CR-196749] p 9 N95-11366
- Control theory based airfoil design using the Euler equations
[NASA-CR-196360] p 36 N95-11884
- Validation of the RPLUS3D code for supersonic inlet applications involving three-dimensional shock wave-boundary layer interactions
[NASA-TM-106579] p 39 N95-13058
- Three dimensional compressible turbulent flow computations for a diffusing S-duct with/without vortex generators
[NASA-CR-195390] p 138 N95-17402
- A time-accurate finite volume method valid at all flow velocities
p 314 N95-23447
- Numerical investigation to S-inlet flows (Numerical simulation study of S-inlet flows)
[AD-A289590] p 374 N95-26713
- Leading edge film cooling effects on turbine blade heat transfer
[NASA-TM-106955] p 513 N95-29115
- Solution of the Navier-Stokes equations on locally refined Cartesian meshes using state-vector splitting
p 553 N95-29197
- Grid orthogonality effects on predicted turbine midspan heat transfer and performance
[NASA-TM-106931] p 554 N95-29371
- Turbulence models in the Navier-Stokes simulation of airfoil stall
[TRITA-NA-9312] p 705 N95-33059
- Numerical simulation of two-dimensional PAR-WIG
p 685 N95-34548
- A simulation of damping process of pendulum motion due to aerodynamic forces
p 711 N95-34551
- FINNED BODIES**
- Natural convection in central microcavities of vertical, finned enclosures of very high aspect ratios
[BTN-95-EIX95282711336] p 632 A95-92405
- FINS**
- Modelling for optimal operations of line milling of aerodynamic surfaces
[BTN-94-EIX94461408774] p 138 A95-63657
- Suppression of vortex asymmetry and side force on a circular cone
[BTN-95-EIX95042474413] p 209 A95-68287
- Waveriders with finlets
[BTN-95-EIX95062487541] p 184 A95-68355
- Modeling resonance in waveguide-to-microstrip junctions by unilateral fin line resonators
[BTN-94-EIX94381323445] p 242 A95-70844
- Integrated design of hypersonic waveriders including inlets and tailfins
[BTN-95-EIX95212645692] p 271 A95-76744
- Structure of a double-fin turbulent interaction at high speed
[BTN-95-EIX95222650780] p 347 A95-79236
- A study on aerodynamic heating phenomena in three-dimensional shock wave/turbulent boundary layer interaction induced by sweptback sharp fins at supersonic flow
p 428 A95-82419
- Low-speed aerodynamic characteristics of a slender wing with vertical fins
p 460 A95-87400
- A low fin height heat exchanger technology demonstrator for Hermes
[SAE PAPER 932119] p 526 A95-90360
- Leading-edge sweepback and shape effects on fin-induced fluctuating pressures
[BTN-95-EIX95302694471] p 636 A95-94067
- Depolarizing trihedral corner reflectors for radar navigation and remote sensing
[BTN-95-EIX95302727634] p 636 A95-94108
- Fatigue evaluation of empennage, forward wing, and winglets/tip fins on part 23 airplanes
[PB94-196813] p 79 N95-13981
- Development of a low-aspect ratio fin for flight research experiments
[NASA-TM-4596] p 108 N95-16858
- Integrated aerodynamic fin and stowable TVC vane system
[AD-D016457] p 151 N95-19073
- Aerodynamic characteristics of the orbital reentry vehicle experimental probe fins in a supersonic flow
[NAL-TR-1232] p 342 N95-25664
- Fundamental wind tunnel experiments on low-speed flutter of a tip-fin configuration wing
[NAL-TR-1228] p 332 N95-25762
- Application of damage tolerance methodology in certification of the Piaggio P-180 Avanti
p 399 N95-28480
- Estimation of aerodynamic load distributions on the F/A-18 aircraft using a CFD panel code
[DSTO-TR-0147] p 504 N95-29445
- FIR FILTERS**
- Precise navigation using adaptive FIR filtering and time domain spectral estimation
[BTN-95-EIX95142555485] p 227 A95-72888
- FIRE (CLIMATOLOGY)**
- Preliminary analysis of University of North Dakota aircraft data from the FIRE Cirrus IFO-2
[NASA-CR-198038] p 357 N95-24219
- FIRE CONTROL**
- Evaluation of alternative in-flight fire suppressants for full-scale testing in simulated aircraft engine nacelles and dry bays
[PB94-203403] p 42 N95-13247
- FIRE DAMAGE**
- Mapping of forest fire damages using imaging spectroscopy
p 442 A95-83627
- FIRE EXTINGUISHERS**
- Development of an aircraft cabin water spray system
[CONGRESS PAPER C428-25-030] p 595 A95-93599
- Aircraft cabin water spray systems - research and regulatory issues
[CONGRESS PAPER C428-25-150] p 595 A95-93600
- A review of water mist technology for fire suppression
[AD-A285738] p 225 N95-20071
- FIRE FIGHTING**
- Selecting and management of fire fighter aircraft
[BTN-95-EIX95062487538] p 193 A95-69246
- A review of water mist technology for fire suppression
[AD-A285738] p 225 N95-20071
- Analysis of test criteria for specifying foam firefighting agents for aircraft rescue and firefighting
[AD-A286381] p 227 N95-22352
- Chemical options to halons for aircraft use
[AD-A293741] p 599 N95-31569
- FIRE PREVENTION**
- Ceramic blanket reduces maintenance costs
[BTN-94-EIX94461290278] p 77 A95-61733
- Risk analysis for the fire safety of airline passengers
[PB94-194065] p 77 N95-14179
- FIREPROOFING**
- The effect of wear on fire-blocking layer material effectiveness
[AD-A291520] p 485 N95-29855
- FIRES**
- Improving the fire resistance of aircraft structures
[CONGRESS PAPER C428-31-152] p 603 A95-93616
- Investigation of flight data recorder fire test requirements
[AD-A285832] p 232 N95-20032
- Fuselage burnthrough from large exterior fuel fires
[AD-A286295] p 226 N95-22318
- Rationale for the Modular Air-system Vulnerability Estimation Network (MAVEN) methodology
[AD-A285797] p 284 N95-22510
- Aircraft fires, smoke toxicity, and survival: An overview
[DOT/FAA/AM-95/8] p 277 N95-24024
- Cost effective, dual-purpose machine vision-based detectors for (1) smoke and flame detection, and (2) engine overheat/burn-through and flame detection
[AD-A292284] p 579 N95-28870
- Electrical short circuit and current overload tests on aircraft wiring
[AD-A293308] p 646 N95-30922
- Remote sensing of smoke, clouds, and radiation using AVIRIS during SCAR experiments
p 708 N95-33749
- Corrosion of fire-damaged aircraft
[AD-A294968] p 693 N95-34583
- FITTING**
- Floating shock fitting via Lagrangian adaptive meshes
[AD-A289758] p 170 N95-18110
- FIXED WINGS**
- The present and future of aircraft noise models: A user's perspective
p 32 N95-11324
- Flight dynamics of an unmanned aerial vehicle
[AD-A282259] p 45 N95-12410
- Comparison of fixed wing aircraft algorithms for JANUS
[AD-A288503] p 389 N95-26652
- Test operations procedure (TOP) 7-3-534 airworthiness testing of fixed wing aircraft: Asymmetric power testing
[AD-A289458] p 391 N95-26994
- FIXING**
- Compressive strength of damaged and repaired composite plates
p 442 N95-28484
- FIXTURES**
- Extension to the dynamic modeling of the large angle magnetic suspension test fixture
[NASA-CR-197801] p 411 N95-26768
- Prototype stop bar system evaluation at Seattle-Tacoma International Airport
[AD-A290136] p 490 N95-30031
- FLAME HOLDERS**
- Computation of vortex breakdown
p 165 N95-19462
- Numerical simulation of combustion flow around a flame holder with hydrogen injection
[NAL-TR-1233] p 419 N95-26523
- FLAME PROPAGATION**
- Stationary premixed flames in spherical and cylindrical geometries
[HTN-95-42336] p 418 A95-86165
- Pulsed jet ignition modeling with a full chemistry
p 538 A95-87184
- Prediction of NO(x) emission index of turbulent diffusion flame
p 538 A95-87195

- Multidimensional calculation of spark flame initiation by adopting a generic hydrocarbon kinetic scheme p 528 A95-87566
- Flame-spreading phenomena in the fin-slot region of a solid rocket motor p 23 N95-10296
- A study of aircraft post-crash fuel fire mitigation [AD-A282208] p 40 N95-12499
- AFOSR Contractors Meeting in Propulsion [AD-A282729] p 54 N95-12507
- Fuselage burnthrough from large exterior fuel fires [AD-A286295] p 226 N95-22318
- FLAME RETARDANTS**
- Chemical options to halons for aircraft use [AD-A293741] p 599 N95-31569
- FLAME STABILITY**
- Development and application of the double V type flame stabilizer [BTN-94-EIX94481415355] p 154 A95-65345
- Conceptual studies of high speed combustors for mixing enhancement mechanisms [AIAA PAPER 95-6095] p 510 A95-88003
- FLAMEOUT**
- Gas turbine-prediffuser-combustor performance during operation with air-water mixture [DOT/FAA/CT-93/52] p 83 N95-15683
- FLAMES**
- Development and application of the double V type flame stabilizer [BTN-94-EIX94481415355] p 154 A95-65345
- Cost effective, dual-purpose machine vision-based detectors for (1) smoke and flame detection, and (2) engine overhead/burn-through and flame detection [AD-A292284] p 579 N95-28870
- FLAMMABILITY**
- Improving the fire resistance of aircraft structures [CONGRESS PAPER C428-31-152] p 603 A95-93616
- Programmed ignition of metal compounds in a scramjet p 16 N95-10466
- Investigation of flight data recorder fire test requirements [AD-A285832] p 232 N95-20032
- Fuselage burnthrough from large exterior fuel fires [AD-A286295] p 226 N95-22318
- The effect of wear on fire-blocking layer material effectiveness [AD-A291520] p 485 N95-29855
- FLAMMABLE GASES**
- Stationary premixed flames in spherical and cylindrical geometries [HTN-95-42336] p 418 A95-86165
- FLANGES**
- Application of advanced material systems to composite frame elements p 422 N95-28432
- FLAPERONS**
- Full span flaperons for a biplane p 391 N95-26954
- FLAPPING**
- Wind tunnel tests of a 42 inch diameter self-starting autogyro rotor [AD-A279922] p 188 N95-19863
- Visualization of the multiple supersonic jet oscillations by swept focused strobed schlieren technique p 367 N95-26952
- Full span flaperons for a biplane p 391 N95-26954
- FLAPS (CONTROL SURFACES)**
- Navier-Stokes simulations of Orbiter aerodynamic characteristics including pitch trim and bodyflap [BTN-95-EIX95041503779] p 204 A95-69210
- Study of an airfoil with a flap and spoiler [BTN-95-EIX95152582327] p 265 A95-73530
- Experimental study of flow separation on an oscillating flap at Mach 2.4 [BTN-95-EIX95222650792] p 329 A95-79248
- An overview of static and dynamic airfoil performance [SAE PAPER 931228] p 463 A95-88960
- Performance of an aerodynamic yaw controller mounted on the space shuttle orbiter body flap at Mach 10 [NASA-TM-109179] p 330 N95-24397
- Comparative wind tunnel tests of NACA 23024 airfoils with several aileron and spoiler configurations p 376 N95-27976
- High-and low-frequency dynamics of isolated blades and rotors with dynamic stall and wake [AD-A290358] p 503 N95-29322
- Grid generation around airfoil with a flap using boundary element method p 686 N95-34552
- FLAT PANEL DISPLAYS**
- Draft standard for color active matrix liquid crystal displays (AMLCDs) in US Military aircraft. Recommended best practices [AD-A282950] p 49 N95-12591
- FLAT PLATES**
- Time-resolved surface heat flux measurements in the wing/body junction vortex [BTN-95-EIX95082502716] p 220 A95-71029
- Coupled FEM-BEM approach for mean flow effects on vibro-acoustic behavior of planar structures [BTN-95-EIX95152577587] p 263 A95-73495
- Three-dimensional structure of a supersonic jet impinging on an inclined plate [BTN-95-EIX95152583259] p 267 A95-73560
- Flow past a symmetric wedge with forward splitter plate p 427 A95-82406
- Two-dimensional viscous flow past a flat plate [HTN-95-42210] p 430 A95-84026
- Free convection past a uniform flux surface inclined at a small angle to the horizontal [HTN-95-42213] p 430 A95-84029
- Shear buckling response of tailored composite plates [HTN-95-51680] p 418 A95-85062
- The use of hot film for the investigation of boundary-layer transition [CONGRESS PAPER C428-9-199] p 475 A95-91697
- Primary and secondary vortex structures over accelerated-decelerated airfoils at high angles of attack [SAE PAPER 931368] p 586 A95-93649
- Hybrid laminar flow over wings enhanced by continuous boundary layer suction [SAE PAPER 931386] p 587 A95-93662
- Lift-enhancing tabs on multielement airfoils [BTN-95-EIX0619952748187] p 591 A95-94479
- Validation of the RPLUS3D code for supersonic inlet applications involving three-dimensional shock wave-boundary layer interactions [NASA-TM-106579] p 39 N95-13058
- The stability of two-phase flow over a swept-wing [NASA-CR-194994] p 159 N95-18190
- Acoustic radiation damping of flat rectangular plates subjected to subsonic flows p 172 N95-18542
- Crossflow instability control on a swept-wing: Preliminary studies p 274 N95-23283
- Plate manipulators [AD-A289601] p 374 N95-26719
- Measurements of store forces and moments and cavity pressures for a generic store in and near a box cavity at subsonic and transonic speeds [NASA-TM-4611] p 378 N95-28241
- Construction and wind tunnel test of a 1/12th scale helicopter model [AD-A288487] p 378 N95-28331
- A procedure for automating CFD simulations of an inlet-bleed problem p 552 N95-28768
- Turbulent airflow noise production and propagation patterns of a subsonic jet impinging on a flat plate p 580 N95-29502
- Effects of elevated free-stream turbulence and streamwise acceleration on flow and thermal structures in transitional boundary layers p 556 N95-29729
- The pressure field of a gust interacting with a flat plate p 557 N95-30161
- FLAT SURFACES**
- Validation of an effective flat cruciform-shaped specimen to study CFRP composite laminates under biaxial loading [BTN-95-EIX95152584677] p 282 A95-73589
- FLEXIBILITY**
- Determination of stores pointing error due to wing flexibility under flight load [NASA-TM-4646] p 134 N95-19044
- FLEXIBLE BODIES**
- Static shape control for adaptive wings [HTN-95-A1767] p 627 A95-93330
- FLEXIBLE WINGS**
- Experimental evaluation of a box beam specifically tailored for chordwise deformation [BTN-95-EIX95182619088] p 283 A95-75773
- Summary of an active flexible wing program [BTN-95-EIX95182619209] p 283 A95-76635
- Application of transonic small disturbance theory to the active flexible wing model [BTN-95-EIX95182619210] p 270 A95-76636
- Simulation and model reduction for the active flexible wing program [BTN-95-EIX95182619211] p 295 A95-76637
- Multiple-function digital controller system for active flexible wing wind-tunnel model [BTN-95-EIX95182619212] p 322 A95-76638
- On-line analysis capabilities developed to support the active flexible wing wind-tunnel tests [BTN-95-EIX95182619213] p 296 A95-76639
- Flutter suppression control law design and testing for the active flexible wing [BTN-95-EIX95182619214] p 292 A95-76640
- Flutter suppression for the active flexible wing: A classical design [BTN-95-EIX95182619216] p 292 A95-76642
- Rolling maneuver load alleviation using active controls [BTN-95-EIX95182619217] p 270 A95-76643
- Response of a nonrotating rotor blade to lateral turbulence. Part 1: Theory [BTN-95-EIX95182619228] p 284 A95-76654
- Simultaneous structure/aerodynamic design optimization for a flexible wing structure p 499 A95-91565
- Active load control during rolling maneuvers — performed in the Langley Transonic Dynamics Tunnel [NASA-TP-3455] p 129 N95-17397
- Flutter analysis of composite box beams [NASA-CR-197931] p 294 N95-23392
- FLEXING**
- Hydrofoil force balance [AD-D016475] p 160 N95-18461
- FLIGHT ALTITUDE**
- Selection of optimal parameters for a system, controlling the flight height, when information about the state vector is incomplete [BTN-94-EIX94461408753] p 168 A95-63636
- Aerodynamic characteristics of a hypersonic viscous optimized waverider at high altitudes [BTN-95-EIX95152583251] p 266 A95-73552
- Determining the effects of alternative departure cutback altitudes and power settings: A case study, John Wayne Airport p 31 N95-11320
- Atmospheric effects of high-flying subsonic aircraft: A catalogue of perturbing influences [KNMI-SR-94-03] p 168 N95-18722
- FLIGHT CHARACTERISTICS**
- Design of nonlinear control laws for high-angle-of-attack flight [BTN-94-EIX94511433920] p 141 A95-64586
- State-space representation of aerodynamic characteristics of an aircraft at high angles of attack [BTN-95-EIX95062487536] p 187 A95-69244
- Polar Patrol Balloon [BTN-95-EIX95152582318] p 316 A95-73521
- Analytical solution for controls, heats, and states of flight trajectories [BTN-95-EIX95152583286] p 282 A95-73587
- Real-time estimation of atmospheric turbulence severity from in-situ aircraft measurements [BTN-95-EIX95182619231] p 319 A95-76657
- Determination of piloting feedback structures for an altitude tracking task [BTN-95-EIX95242670770] p 327 A95-81077
- Rotorcraft handling qualities in turbulence [BTN-95-EIX95242670750] p 334 A95-81097
- Atmospheric reentry flight test of winged space vehicle p 414 A95-82483
- Flying qualities development and flight simulation evaluation of the TW-68 tilt-wing VTOL aircraft [SAE PAPER 932517] p 386 A95-84555
- Condition monitoring and diagnostics [HTN-95-92312] p 387 A95-85356
- Techniques for tailoring aircraft stall and post-stall behavior [SAE PAPER 931226] p 458 A95-87199
- Trim conditions for optimal flight performance of hypersonic aircraft p 514 A95-87397
- Aerodynamic off-design behavior of integrated waveriders from take-off up to hypersonic flight [AIAA PAPER 95-6091] p 466 A95-89200
- Low-speed wind tunnel tests of two waverider configuration models [AIAA PAPER 95-6093] p 493 A95-89251
- Flight-testing and frequency-domain analysis for rotorcraft handling qualities [HTN-95-01083] p 515 A95-90269
- A flying qualities study of longitudinal long-term dynamics of hypersonic planes [AIAA PAPER 95-6150] p 521 A95-90464
- Flight testing of the composite material bearingless rotor system for the helicopter p 498 A95-91503
- Flight test of STS radio controlled scale model p 499 A95-91539
- An application of TLS (Total Least Squares) method to estimation of aircraft aerodynamic derivatives p 517 A95-91551
- Jet transport response to a horizontal wind vortex [BTN-95-EIX0619952748163] p 619 A95-94457
- Extended cooperative control synthesis [NASA-TM-4561] p 17 N95-10220
- Evaluation of F-18A approach and landing flying qualities using an in-flight simulator [CALSPAN-6241-F-1] p 12 N95-10442
- High-angle-of-attack yawing moment asymmetry of the X-31 aircraft from flight test [NASA-CR-186030] p 13 N95-11410
- STOVL Control Integration Program [NASA-CR-195358] p 18 N95-11487
- An application of virtual prototyping to the flight test and evaluation of an unmanned air vehicle [AD-A281749] p 14 N95-11595
- Parallel methods for the flight simulation model [DE94-013330] p 52 N95-11752
- Parameter identification for X-31A at high angles of attack p 69 N95-14235

Validation of the NASA Dryden X-31 simulation and evaluation of mechanization techniques p 69 N95-14236

Free-to-roll tests of X-31 and F-18 subscale models with correlation to flight test results p 69 N95-14237

High angle of attack flying qualities criteria for longitudinal rate command systems p 70 N95-14247

Fourth High Alpha Conference, volume 3 [NASA-CP-10143-VOL-3] p 71 N95-14251

Flight in an Adverse Environment [AGARD-LS-197] p 77 N95-14893

Turbulence: Engineering models, aircraft response p 84 N95-14900

Evaluation of the dynamic stability characteristics of the NAL Light Transport Aircraft [NAL-PD-CA-9217] p 142 N95-16392

STOVL CFD model test case p 115 N95-17881

Six degree of freedom flight dynamic and performance simulation of a remotely-piloted vehicle [AERO-TN-9301] p 131 N95-18097

Flight parameters monitoring system for tracking structural integrity of rotary-wing aircraft p 135 N95-19469

Airship applications of modern flight test techniques [AD-A284253] p 194 N95-19731

T-45A High Angle of Attack Testing: US Naval Test Pilot School 46th Annual Reunion and Symposium [AD-A284000] p 231 N95-20466

Flight test of the X-29A at high angle of attack: Flight dynamics and controls p 284 N95-22806

Analysis of the longitudinal handling qualities and pilot-induced-oscillation tendencies of the High-Angle-of-Attack Research Vehicle (HARV) p 293 N95-23297

Preparation of course materials: Elementary mathematics of powered flight p 324 N95-23320

Handling qualities of the High Speed Civil Transport p 294 N95-23325

Aerodynamic characteristics of the orbital reentry vehicle experimental probe fins in a supersonic flow [NAL-TR-1232] p 342 N95-25664

Simulation model of the integrated flight/propulsion control system, displays, and propulsion system for ASTOVL lift-fan aircraft [NASA-TM-108866] p 405 N95-26412

A comparison of the Neal-Smith and omega Tau function, zeta function and tau function flying qualities criteria [AD-A289503] p 390 N95-26844

Manual for a workstation-based generic flight simulation program (LaRCsim), version 1.4 [NASA-TM-110164] p 518 N95-30327

Aeroelastic pilot-in-the-loop oscillations p 598 N95-31070

Proposed incorporation of mission-oriented flying qualities into MIL-STD-1797A [AD-A294211] p 698 N95-34306

FLIGHT CONDITIONS

Hydrocarbon-fueled ramjet/scramjet technology program, phase 2 extension [NASA-CR-189659] p 15 N95-10319

Role of wind tunnels and computer codes in the certification and qualification of rotorcraft for flight in forecast icing [NASA-TM-106747] p 39 N95-13197

Flight in an Adverse Environment [AGARD-LS-197] p 77 N95-14893

Icing: Accretion, detection, protection p 77 N95-14897

Wind shear and its effects on aircraft p 77 N95-14898

Numerical simulation of helicopter engine plume in forward flight [NASA-CR-197488] p 107 N95-16589

Helicopter Performance Evaluation (HELPE) computer model [AD-A284319] p 131 N95-18381

Comparison of frequency response and perturbation methods to extract linear models from a nonlinear simulation [AD-A284115] p 146 N95-18405

Flight parameters monitoring system for tracking structural integrity of rotary-wing aircraft p 135 N95-19469

Derived gust spectra for the Macchi MB326H [ARL-TN-3] p 225 N95-21892

Direct adaptive performance optimization of subsonic transports: A periodic perturbation technique [NASA-TM-4676] p 284 N95-22829

Control of flow separation in airfoil/wing design applications p 274 N95-23294

Electro-hydrostatic actuator controller design using quantitative feedback theory [AD-A289220] p 409 N95-26957

Construction and wind tunnel test of a 1/12th scale helicopter model [AD-A288487] p 378 N95-28331

Computational Fluid Dynamics (CFD) analysis of a C-135 aircraft with a side-mounted splitter plate (with comparison to wind tunnel data) p 553 N95-29187

Integrated terminal weather system (ITWS) demonstration and validation operational test and evaluation [AD-A293932] p 602 N95-31521

Icing simulation in the aeropropulsion systems test facility propulsion development test cell C-2 [AD-A293039] p 599 N95-31667

FLIGHT CONTROL

Flight test development and evaluation of a Kalman filter state estimator for low-altitude flight [HTN-94-00684] p 16 A95-60167

Simulation development of a forward sensor-enhanced low-altitude guidance system [HTN-94-00688] p 17 A95-60170

Stabilization of objects with unknown nonstationary parameters, using adaptive nonlinear continuous control systems [BTN-94-EIX94461407944] p 98 A95-62262

Local-optimal control of a flying vehicle, with final state optimized [BTN-94-EIX94461407957] p 83 A95-62631

Selection of optimal parameters for a system, controlling the flight height, when information about the state vector is incomplete [BTN-94-EIX94461408753] p 168 A95-63636

Output feedback control under randomly varying distributed delays [BTN-94-EIX94511433916] p 168 A95-64582

Design of nonlinear control laws for high-angle-of-attack flight [BTN-94-EIX94511433920] p 141 A95-64586

Time-optimal turn to a heading: An analytic solution [BTN-94-EIX94511433940] p 142 A95-64606

Flight control system mode transitions influence on handling qualities and task performance [BTN-95-EIX95062487525] p 203 A95-69233

Development and flight test of a deployable precision landing system [BTN-95-EIX95062487535] p 190 A95-69243

Rotorcraft control system design for uncertain vehicle dynamics using quantitative feedback theory [HTN-95-31012] p 236 A95-71182

A generalized algorithm for inverse simulation applied to helicopter maneuvering flight [HTN-95-A0493] p 236 A95-72564

Dynamical instability of the aerogravity assist maneuver [BTN-95-EIX95152583282] p 298 A95-73583

Identification of higher order helicopter dynamics using linear modeling methods [HTN-95-80851] p 290 A95-75093

Effects of high order dynamics on helicopter flight control law design [HTN-95-80852] p 290 A95-75094

Investigation of the effects of bandwidth and time delay on helicopter roll-axis handling qualities [HTN-95-80853] p 290 A95-75095

Integrated flight/propulsion control for helicopters [HTN-95-80854] p 290 A95-75096

Cypher moves toward autonomous flight [HTN-95-41394] p 283 A95-76390

Functional agility metrics and optimal trajectory analysis [BTN-95-EIX95182619121] p 321 A95-76598

H-infinity helicopter flight control law design with and without rotor state feedback [BTN-95-EIX95182619129] p 291 A95-76606

Automatic guidance and control for helicopter obstacle avoidance [BTN-95-EIX95182619130] p 291 A95-76607

Direct-lift design strategy for longitudinal control of hypersonic aircraft [BTN-95-EIX95182619131] p 291 A95-76608

Shuttle entry guidance revisited using nonlinear geometric methods [BTN-95-EIX95182619144] p 299 A95-76621

Attainable moments for the constrained control allocation problem [BTN-95-EIX95182619149] p 322 A95-76626

Application of Navier-Stokes aeroelastic methods to improve fighter wing maneuver performance [BTN-95-EIX95182619218] p 284 A95-76644

Robustly stable preliminary control systems design for the YF-16 CGV aircraft [BTN-95-EIX95202637608] p 292 A95-76681

Dynamic imaging and RCS measurements of aircraft [BTN-95-EIX95202637582] p 347 A95-78576

Dynamic stall control for advanced rotorcraft application [BTN-95-EIX95222650793] p 334 A95-79249

Guidance and control, 1993; Annual Rocky Mountain Guidance and Control Conference, 16th, Keystone, CO, Feb. 6-10, 1993 [ISBN-0-87703-365-X] p 341 A95-80389

The Cassini spacecraft: Object oriented flight control software p 359 A95-80405

A new guidance and flight control system for the DELTA 2 launch vehicle - Abstract only p 342 A95-80427

On-line learning nonlinear direct neurocontrollers for restructurable control systems [BTN-95-EIX95242670768] p 359 A95-81079

Impact of near-coincident faults on digital flight control systems [BTN-95-EIX95242670759] p 359 A95-81088

Dynamics and control of a tethered flight vehicle [BTN-95-EIX95242670754] p 342 A95-81093

High-performance, robust, bank-to-turn missile autopilot design [BTN-95-EIX95242670751] p 336 A95-81096

Robust dynamic inversion for control of highly maneuverable aircraft [BTN-95-EIX95242670747] p 359 A95-81100

Nonlinear observer and its application in flight control p 447 A95-82449

Atmospheric reentry flight test of winged space vehicle p 414 A95-82483

Scheduling of local nonlinear control laws by exogenous signals - an application to flight control [BTN-95-EIX95262694059] p 447 A95-85675

Flight Simulators: Better than the real thing? [HTN-95-42619] p 518 A95-87249

Handling qualities of hypersonic aircraft and related control requirements p 515 A95-87398

Application of artificial neural networks in nonlinear aerodynamics and aircraft design [SAE PAPER 932533] p 492 A95-89193

Application of restructurable flight control system to large transport aircraft [BTN-95-EIX95282706666] p 515 A95-89639

Computer aided diagnostic testing of installed flight control servo-actuators [SAE PAPER 932584] p 494 A95-90068

Second generation smart actuator [SAE PAPER 932585] p 505 A95-90069

Unsteady aerodynamic effects of trailing edge controls on delta wings [HTN-95-01099] p 469 A95-90285

Accelerated application development for flight software [AIAA PAPER 95-1031] p 566 A95-90703

Report to the aerospace profession; SETP Symposium, 37th, Beverly Hills, CA, USA, September 1993 [HTN-95-12142] p 497 A95-90866

Propulsion controlled aircraft research p 497 A95-90869

Aircraft Symposium, 30th, Tsukuba, Japan, Sep. 30 - Oct. 2, 1992 [HTN-95-A1609] p 498 A95-91491

MIMO H infinity control design method combined with exact model matching p 506 A95-91492

A gust alleviation method by the response feedback p 506 A95-91493

A design of a robust scheduled autopilot p 516 A95-91532

A design of a self-learning robust scheduled autopilot p 516 A95-91533

Design of a flight control system by a new way of pole placement in LQR p 516 A95-91534

On the flight control system for UF-104 p 507 A95-91560

Aeroservoelastic coupling on the UF-104 aircraft p 517 A95-91561

Exact solution of stability margin for the MIMO control system p 507 A95-91582

Effect of coupling term on stability for the two input control system p 507 A95-91583

Comparison of the method of analyzing stability margin by using Minus Inverse Vector Locus with classical method p 507 A95-91584

A study of computational difficulty of numerical method in optimal control p 507 A95-91585

Flight control system design with Multiple Delay Model/Multiple Design Point Approach p 507 A95-91586

Development of software for safety critical applications for the EH101 Helicopter [CONGRESS PAPER C428-24-160] p 678 A95-93597

Flight control systems/structural coupling BAe Warton experience in aero-servo elasticity [CONGRESS PAPER C428-35-059] p 610 A95-93628

- An advanced vehicle management system
[SAE PAPER 931376] p 618 A95-93655
- Fiber optic hardware for transport aircraft
[SAE PAPER 931439] p 680 A95-93691
- Operational and research aspects of a radio-controlled model flight test program
[BTN-95-EI0619952748177] p 606 A95-94471
- Evaluation of F-18A approach and landing flying qualities using an in-flight simulator
[CALSPAN-6241-F-1] p 12 N95-10442
- F-15 835 (HIDEC) resource tape
[NASA-TM-104297] p 13 N95-10742
- F-15 Propulsion Controlled Aircraft (PCA)
[NASA-TM-104303] p 17 N95-10748
- Formal design and verification of a reliable computing platform for real-time control (phase 3 results)
[NASA-TM-109140] p 33 N95-10873
- Application of an integrated methodology for propulsion and airframe control design to a STOVL aircraft
[NASA-TM-106729] p 16 N95-11159
- ACSINT inner loop flight control design study
[NASA-CR-196316] p 17 N95-11223
- STOVL Control Integration Program
[NASA-CR-195358] p 18 N95-11487
- Research on an autonomous vision-guided helicopter
[AIAA PAPER 94-1240-CP] p 18 N95-11510
- The development of a highly reliable power management and distribution system for civil transport aircraft
[NASA-TM-106697] p 50 N95-11867
- Optimum aerodynamic design via boundary control
[NASA-CR-195882] p 36 N95-11877
- Dynamic ground effects flight test of an F-15 aircraft
[NASA-TM-4604] p 38 N95-12191
- Flight dynamics of an unmanned aerial vehicle
[AD-A282259] p 45 N95-12410
- Triton 2 (1B)
[NASA-CR-197188] p 46 N95-12636
- Piloted evaluation of an integrated methodology for propulsion and airframe control design
[AD-A290207] p 51 N95-12763
- Techniques for designing rotorcraft control systems
[NASA-CR-196192] p 52 N95-12791
- Overview of NASREM: The NASA/NBS standard reference model for teletrotor control system architecture
[PB94-194560] p 58 N95-12854
- Evolutionary Telemetry and Command Processor (TCP) architecture
p 86 N95-14162
- The principles of flight test assessment of flight-safety-critical systems in helicopters
[AGARD-AG-300-VOL-12] p 77 N95-14199
- Add a dimension to your analysis of the helicopter low airspeed environment
[AD-A283982] p 79 N95-14205
- Matlab as a robust control design tool
p 169 N95-16474
- Workshop on Formal Models for Intelligent Control
[AD-A281399] p 169 N95-16864
- EURECA mission control experience and messages for the future
p 149 N95-17252
- Aircraft and sub-system certification by piloted simulation
[AGARD-AR-278] p 145 N95-17388
- Packet utilisation definitions for the ESA XMM mission
p 150 N95-17596
- Flight testing high lateral asymmetries on highly augmented Fighter/Attack aircraft
[AD-A284206] p 130 N95-17953
- VSTOL Systems Research Aircraft (VSRA) Harrier
[NASA-TM-110117] p 126 N95-18347
- The impact of non-linear flight control systems on the prediction of aircraft loads due to turbulence
p 143 N95-18598
- Treatment of non-linear systems by timeplane-transformed CT methods: The spectral gust method
p 143 N95-18600
- Design and flight test of a simplified control system for a transport helicopter
p 144 N95-18902
- Integrated aerodynamic fin and stowable TVC vane system
[AD-D016457] p 151 N95-19073
- The use of genetic algorithms for flight test and evaluation of artificial intelligence and complex software systems
[AD-A284824] p 217 N95-19688
- Automation of hardware-in-the-loop testing of control systems for unmanned air vehicles
[AD-A284833] p 194 N95-19693
- Summary of a joint program of research into aircraft flight control concepts
[AD-A280012] p 237 N95-20004
- A neural expert approach to self designing flight control systems
[AD-A279965] p 237 N95-21122
- Virtual reality flight control display with six-degree-of-freedom controller and spherical orientation overlay
[NASA-CASE-NPO-18733-1-CU] p 288 N95-22578
- Flight test of the X-29A at high angle of attack: Flight dynamics and controls
[NASA-TP-3537] p 284 N95-22806
- Analysis of the longitudinal handling qualities and pilot-induced-oscillation tendencies of the High-Angle-of-Attack Research Vehicle (HARV)
p 293 N95-23297
- Inner loop flight control for the High-Speed Civil Transport
p 293 N95-23314
- Differential GPS and system integration of the Low Visibility Landing and Surface Operations (LVLASO) demonstration
p 280 N95-23318
- Engines-only flight control system
[NASA-CASE-ARC-11944-1] p 294 N95-23389
- Aerodynamic surface distension system for high angle of attack forebody vortex control
[NASA-CASE-ARC-11979-1] p 286 N95-23390
- Feedback control laws for highly maneuverable aircraft
[NASA-CR-197944] p 295 N95-23410
- Aerodynamic flight control to increase payload capability of future launch vehicles
[NAS-CR-196560] p 300 N95-24032
- Assessment of avionics technology in European aerospace organizations
[NASA-CR-189201] p 337 N95-24624
- Development of a nonlinear simulation for the McDonnell Douglas F-15 Eagle with a longitudinal TECS control-law
[AD-A288610] p 388 N95-26481
- Design and synthesis of a real-time controller for an unmanned air vehicle
[AD-A289134] p 408 N95-26555
- An investigation of the effects of pitch-roll (de)coupling on helicopter handling qualities
[NASA-TM-110349] p 409 N95-26773
- A comparison of the Neal-Smith and omega Tau function, zeta function and tau function flying qualities criteria
[AD-A289503] p 390 N95-26844
- Electro-hydrostatic actuator controller design using quantitative feedback theory
[AD-A289220] p 409 N95-26957
- A quantitative feedback theory FCS design for the subsonic envelope of the VISTA F-16 including configuration variation
[AD-A289221] p 409 N95-26958
- Advanced formation flight control
[AD-A289271] p 409 N95-26981
- Flight control design using mixed H2/micron optimization
[AD-A289288] p 410 N95-27036
- Advanced flight computer. Special study
[NASA-CR-198165] p 449 N95-27246
- JPRS report: Science and technology. Central Eurasia
[JPRS-UST-94-022] p 438 N95-27699
- Operator modeling in commercial aviation: Cognitive models, intelligent displays, and pilot's assistants
[NASA-CR-198609] p 401 N95-28203
- Composite flight-control actuator development
p 410 N95-28281
- An investigation into the use of satellite-based positioning systems for flight reference/autoland operations
p 489 N95-29542
- Low-speed wind-tunnel investigation of the stability and control characteristics of a series of flying wings with sweep angles of 50 deg
[NASA-TM-4640] p 505 N95-30226
- Design, analysis and control of large transports so that control of engine thrust can be used as a back-up of the primary flight controls
[NASA-CR-198958] p 518 N95-30254
- Developing a workstation-based, real-time simulation for rapid handling qualities evaluations during design
[NASA-CR-198831] p 505 N95-30335
- Moving base simulation of an integrated flight and propulsion control system for an ejector-augmentor STOVL aircraft in hover
[NASA-TM-108867] p 606 N95-30646
- New adaptive methods for reconfigurable flight control systems, appendix 1
[AD-A292711] p 619 N95-30937
- Flight Vehicle Integration Panel Workshop on Pilot Induced Oscillations
[AGARD-AR-335] p 597 N95-31061
- The process for addressing the challenges of aircraft pilot coupling
p 597 N95-31063
- Observations on PIO
p 597 N95-31064
- SAAB experience with PIO
p 598 N95-31069
- Handling qualities analysis on rate limiting elements in flight control systems
p 619 N95-31071
- Calspan experience of PIO and the effects of rate limiting
p 598 N95-31072
- Active control technology: Applications and lessons learned
[AGARD-CP-560] p 620 N95-31989
- The role of handling qualities specifications in flight control system design
p 620 N95-31990
- The prevention of PIO by design
p 620 N95-31991
- The importance of flying qualities design specifications for active control systems
p 621 N95-31992
- Experiences with ADS-33 helicopter specification testing and contributions to refinement research
p 621 N95-31993
- Lavi flight control system: Design requirements, development and flight test results
p 621 N95-31994
- Robust control: A structured approach to solve aircraft flight control problems
p 621 N95-31995
- Dynamic inversion: An evolving methodology for flight control design
p 621 N95-31996
- Evaluation of the techniques of fuzzy control for the piloting an aircraft
p 621 N95-31997
- The control system design methodology of the STOL and maneuver technology demonstrator
p 621 N95-31998
- Control law design using H-infinity, and mu-synthesis short-period controller for a tail-airplane
p 622 N95-31999
- Model following control for tailoring handling qualities: ACT experience with ATThES
p 622 N95-32000
- X-29 flight control system: Lessons learned
p 622 N95-32001
- The FCS-structural coupling problem and its solution
p 623 N95-32005
- Flight test results of the F-16 aircraft modified with axisymmetric vectoring exhaust nozzle
p 609 N95-32007
- Catapult-launching of the RAFALE design and experimentation
p 609 N95-32008
- Digital autopilot design for combat aircraft in ALENIA
p 623 N95-32009
- Experimental Aircraft Programme (EAP): Flight control system design and test
p 623 N95-32010
- An investigation of pilot induced oscillation phenomena in digital-flight control systems
p 623 N95-32011
- Flight demonstration of an advanced pitch control law in the VAAC Harrier aircraft
p 623 N95-32012
- Advanced flight control technology achievements at Boeing Helicopters
p 624 N95-32014
- Flying qualities of civil transport aircraft with electrical flight control
p 624 N95-32016
- Pilot Induced Oscillation: A report on the AGARD Workshop on PIO
p 624 N95-32017
- A highly reliable, high performance open avionics architecture for real time Nap-of-the-Earth operations
p 693 N95-32497
- An Electronic Workshop on the Performance Seeking Control and Propulsion Controlled Aircraft Results of the F-15 Highly Integrated Digital Electronic Control Flight Research Program
[NASA-TM-104278] p 694 N95-33009
- An overview of integrated flight-propulsion controls flight research on the NASA F-15 research airplane
p 694 N95-33010
- Performance seeking control program overview
p 695 N95-33011
- PSC implementation and integration
p 695 N95-33014
- Background and principles of throttles-only flight control
p 697 N95-33021
- Propulsion Controlled Aircraft design and development
p 697 N95-33022
- Flight test of a propulsion controlled aircraft system on the NASA F-15 airplane
p 691 N95-33023
- Design challenges encountered in the F-15 PCA flight test program
p 692 N95-33025
- Proposed incorporation of mission-oriented flying qualities into MIL-STD-1797A
[AD-A294211] p 698 N95-34306
- Thermal design of returnable satellites
[AD-A294113] p 701 N95-34500
- User type certification for advanced flight control systems
p 699 N95-34772
- A stochastic adaptive control application to flight systems
p 699 N95-34806

FLIGHT CREWS

- Integrated flight crew transition training for the advanced flight deck aircraft
[SAE PAPER 932599] p 380 A95-84571
- Intelligent tutoring system: F-16 flight simulation
p 521 A95-90649
- Report to the aerospace profession; SETP Symposium, 37th, Beverly Hills, CA, USA, September 1993
[HTN-95-12142] p 497 A95-90866
- Test and evaluation crew resource management
p 483 A95-90867
- The development of computer-based instructional simulations for the airline industry
p 625 A95-95159

Aircraft accident report. Runway overrun following rejected takeoff. Continental airlines flight 795, McDonnell Douglas MD-82, N18835, LaGuardia Airport, Flushing, NY, 2 March 1994
 [PB95-910401] p 277 N95-23609
 A crew-centered flight deck design philosophy for High-Speed Civil Transport (HSCT) aircraft
 [NASA-TM-109171] p 335 N95-24582
 An analysis of the KC-135 three-person cockpit
 [AD-A289540] p 390 N95-26873
 Controller resource management: What can we learn from aircrews?
 [DOT/FAA/AM-95/21] p 602 N95-32186
 User type certification for advanced flight control systems
 p 699 N95-34772

FLIGHT ENVELOPES

Robust longitudinal axis flight control for an aircraft with thrust vectoring
 [BTN-95-EIX95122538875] p 408 A95-83000
 X-31 post-stall envelope expansion and tactical utility testing
 p 70 N95-14242
 Flight test results of the F-16 aircraft modified with the axisymmetric vectoring exhaust nozzle
 p 70 N95-14245
 Composite waveform generation for EMP and lightning direct-drive testing
 [AD-A284159] p 92 N95-14405
 Aircraft and sub-system certification by piloted simulation
 [AGARD-AR-278] p 145 N95-17388
 Flight testing high lateral asymmetries on highly augmented Fighter/Attack aircraft
 [AD-A284206] p 130 N95-17953
 Course module for AA201: Wing structural design project
 [AD-A283618] p 133 N95-18616
 Flutter clearance flight tests of an OV-10A airplane modified for wake vortex flight experiments
 [NASA-TM-109168] p 366 N95-26381
 A quantitative feedback theory FCS design for the subsonic envelope of the VISTA F-16 including configuration variation
 [AD-A289221] p 409 N95-26958

FLIGHT HAZARDS

WINDEX -- A new index for forecasting microburst potential
 [HTN-95-90690] p 215 A95-69717
 Thundercloud electric field modeling for the ionosphere-Earth region. 1: Dependence on cloud charge distribution
 [HTN-95-41223] p 317 A95-75035
 Optimal lateral-escape maneuvers for microburst encounters during final approach
 [BTN-95-EIX95182619127] p 276 A95-76604
 International Conference on Aviation Weather Systems, 5th, Vienna, VA, Aug. 2-6, 1993. Preprint Volume
 [HTN-95-92940] p 652 A95-93441
 An integrated system to improve aviation weather forecasts for the Alaska Range
 p 656 A95-93460
 Use of WSR-88D data in the FAA's weather impacted aerospace product
 p 658 A95-93469
 An in-situ system for warning of icing conditions
 p 660 A95-93481
 The inference of aviation weather hazards based on the integration of radar and lightning data
 p 660 A95-93483
 LLWAS 2 and LLWAS 3 performance evaluation
 p 662 A95-93491
 Test results of a low cost airport weather radar
 p 662 A95-93492
 Role of the aviation weather system in providing a real-time ATC volcanic ash advisory system
 p 663 A95-93494
 Alaska's volcanic ash warning system
 p 663 A95-93495
 The aviation gridded forecast system verification program - A description of aviation-impact-variable evaluation plans
 p 664 A95-93498
 Analysis of en route controller hazardous weather-related tasks
 p 665 A95-93503
 The data link flight information service application
 p 665 A95-93504
 Automated aircraft routing through weather-impacted airspace
 p 666 A95-93512
 An echo motion algorithm for air traffic management using a national radar mosaic
 p 667 A95-93513
 A poor man's expert system for aviation VSRF in complex terrain
 p 669 A95-93524
 Windshear detection: TDWR and LLWAS operational experience in Denver 1988-1992
 p 670 A95-93528
 Analysis of rapidly developing fog at the Kennedy Space Center
 p 671 A95-93531
 Northwest Airlines atmospheric hazards advisory & avoidance system
 p 672 A95-93539
 Assessment of the benefits for improved terminal weather information
 p 673 A95-93540

Creating a global climatology of freezing rain using numerical model output
 p 673 A95-93541
 Aircraft icing: Meteorological effects on aircraft performance
 p 674 A95-93545
 A northern hemisphere clear air turbulence climatology
 p 674 A95-93547
 An evaluation of clear-air turbulence indices
 p 674 A95-93548
 Preliminary results of turbulence predictions for use in aviation weather forecasting
 p 675 A95-93551
 Turbulence near thunderstorm tops
 p 675 A95-93553
 A prototype for displaying aviation forecast variables using Eta numerical model output
 p 676 A95-93555
 Airborne Windshear Detection and Warning Systems. Fifth and Final Combined Manufacturers' and Technologists' Conference, part 1
 [NASA-CP-10139-PT-1] p 10 N95-10566
 Vertical wind estimation from horizontal wind measurements
 p 26 N95-10567
 Characteristics of a dry, pulsating microburst at Denver Stapleton Airport
 p 26 N95-10568
 Future enhancements to ground-based microburst detection
 p 11 N95-10570
 Determining F-factor using ground-based Doppler radar: Validation and results
 p 11 N95-10571
 Potential impacts of advanced aerodynamic technology on air transportation system productivity
 [NASA-TM-109154] p 10 N95-11489
 Windshear certification data base for forward-look detection systems
 p 41 N95-13204
 Characteristics of civil aviation atmospheric hazards
 p 42 N95-13208
 Aircraft maneuver envelope warning system
 [NASA-CASE-ARC-11953-1] p 82 N95-14518
 Flight in an Adverse Environment
 [AGARD-LS-197] p 77 N95-14893
 Wake turbulence
 p 75 N95-14894
 Icing: Accretion, detection, protection
 p 77 N95-14897
 Heavy rain effects
 p 78 N95-14899
 Waveform bounding and combination techniques for direct drive testing
 [AD-A284075] p 161 N95-19035
 Bird ingestion into large turbofan engines
 [DOT/FAA/CT-93/14] p 333 N95-24631
 A review of falconry as a bird control technique with recommendations for use at the Shuttle Landing Facility, John F. Kennedy Space Center, Florida, USA
 [NASA-TM-110142] p 381 N95-27859
 Experiments on microbursts
 p 562 N95-29110
 Report to the Chairman, Subcommittee on Aviation, Committee on Commerce, Science, and Transportation, US Senate. Aviation Safety: FAA can better prepare general aviation pilots for mountain flying risks
 [GAO/RCED-94-15] p 687 N95-32784

FLIGHT INSTRUMENTS

Flight experience with lightweight, low-power miniaturized instrumentation systems
 [BTN-95-EIX95062487522] p 180 A95-69230
 Design of wide angle head up displays for synthetic vision
 [BTN-95-EIX95212641070] p 287 A95-76735
 TRISTAR 1: Evaluation methods for testing head-up display (HUD) flight symbology
 [NASA-TM-4665] p 288 N95-24030
 Hardware cleanliness methodology and certification
 p 419 N95-27656
 The effects of display location and dimensionality on taxiway navigation
 [AD-A294878] p 690 N95-34570

FLIGHT LOAD RECORDERS

The FAA regional/commuter aircraft flight loads data collection program
 [SAE PAPER 931258] p 493 A95-89224

FLIGHT MANAGEMENT SYSTEMS

Pilot Weather Advisor system
 [BTN-95-EIX95152582314] p 316 A95-73517
 The CBT alternative for aviation training: Is it meeting the need?
 [SAE PAPER 932596] p 379 A95-84568
 Automated aircraft routing through weather-impacted airspace
 p 666 A95-93512
 Airborne Windshear Detection and Warning Systems. Fifth and Final Combined Manufacturers' and Technologists' Conference, part 2
 [NASA-CP-10139-PT-2] p 41 N95-13203
 The principles of flight test assessment of flight-safety-critical systems in helicopters
 [AGARD-AG-300-VOL-12] p 77 N95-14199
 Airplane takeoff and landing performance monitoring system
 [NASA-CASE-LAR-14745-2-SB] p 85 N95-14415

Crew aiding and automation: A system concept for terminal area operations, and guidelines for automation design
 [NASA-CR-4631] p 228 N95-19950
 Operator modeling in commercial aviation: Cognitive models, intelligent displays, and pilot's assistants
 [NASA-CR-198609] p 401 N95-28203
 Results from tests of the Honeywell integrated flight management unit
 [PB95-211355] p 601 N95-30597
 Integrated special mission flight management for a flight inspection aircraft
 p 692 N95-33145

FLIGHT MECHANICS

High-order state space simulation models of helicopter flight mechanics
 [HTN-95-A0494] p 237 A95-72565
 Functional dependence of trajectory dispersion on initial condition errors
 [BTN-95-EIX9512583263] p 298 A95-73564
 Aerodynamics of the Shuttle Orbiter at high altitudes
 [BTN-95-EIX95182617454] p 298 A95-75725
 Kinematics and aerodynamics of velocity-vector roll
 [BTN-95-EIX95182619126] p 291 A95-76603
 The CBT alternative for aviation training: Is it meeting the need?
 [SAE PAPER 932596] p 379 A95-84568
 Aerodynamics of delta wings with application to high-alpha flight mechanics
 p 460 A95-87395
 Aircraft Symposium, 30th, Tsukuba, Japan, Sep. 30 - Oct. 2, 1992
 [HTN-95-A1609] p 498 A95-91491
 Optimality of the steady-state flight for hypersonic aircraft
 p 526 A95-91550
 A study of computational difficulty of numerical method in optimal control
 p 507 A95-91585
 Flight control system design with Multiple Delay Model/Multiple Design Point Approach
 p 507 A95-91586
 Multivariable adaptive control using only input and output measurements for turbojet engines
 [BTN-95-EIX95292721165] p 677 A95-92597
 Activities of the Institute for Aerospace Studies of Toronto University
 p 63 N95-12699
 NASA-UVA light aerospace alloy and structures technology program (LA2ST)
 [NASA-CR-198041] p 343 N95-24220
 Flight Mechanics/Estimation Theory Symposium 1995
 [NASA-CP-3299] p 416 N95-27763
 Flight Vehicle Integration Panel Workshop on Pilot Induced Oscillations
 [AGARD-AR-335] p 597 N95-31061

FLIGHT OPERATIONS

Pilot Weather Advisor system
 [BTN-95-EIX95152582314] p 316 A95-73517
 Noise modeling for MOAs and ranges
 p 32 N95-11322
 MOAMAP: A model that combines several different kinds of aircraft operations
 p 32 N95-11323
 The present and future of aircraft noise models: A user's perspective
 p 32 N95-11324
 Guidance and control requirements for high-speed Rollout and Turnoff (ROTO)
 [NASA-CR-195026] p 292 N95-22674
 Oceanic operations: An authoritative guide to oceanic operations
 [FAA-AFS-550] p 277 N95-24065
 Advanced gust management systems: Lessons learned and perspectives
 p 622 N95-32002
 Low-Level and Nap-of-the-Earth (NOE) night operations
 [AGARD-CP-563] p 686 N95-32486

FLIGHT OPTIMIZATION

Optimal separation and ascent of lifting upper stages
 p 525 A95-87396
 Trim conditions for optimal flight performance of hypersonic aircraft
 p 514 A95-87397
 Sensitivity of engine-integrated waverider performance to static margin constraint
 [AIAA PAPER 95-6142] p 496 A95-90458
 A study of the savings in time and fuel to aviation through the use of upper-air wind forecasts
 p 672 A95-93538
 Application of multivariate optimization techniques to determination of optimum flight path trajectories
 [ESDU-94012] p 44 N95-11793
 Examples of flight path optimization using a multivariate gradient-search method. Addendum A: Variation of optimum flight profile parameters with range
 [ESDU-94016-ADD-A] p 44 N95-11794

FLIGHT PATHS

Trajectory modeling of emissions from lower stratospheric aircraft
 [HTN-95-41219] p 317 A95-75031
 Optimal lateral-escape maneuvers for microburst encounters during final approach
 [BTN-95-EIX95182619127] p 276 A95-76604

- Analytical solution and parameter estimation of projectile dynamics
[BTN-95-EIX95212645695] p 272 A95-76747
- Dynamic imaging and RCS measurements of aircraft
[BTN-95-EIX95202637582] p 347 A95-78576
- Application of direct transcription to commercial aircraft trajectory optimization
[BTN-95-EIX95242670766] p 359 A95-81081
- Polar Patrol Balloon system and preliminary experimental results
p 368 A95-82513
- An investigation of piloting strategies for engine failures during takeoff from offshore platforms
[HTN-95-92834] p 497 A95-90752
- Analysis of approach paths of two aircraft
p 487 A95-91494
- Multiobjective trajectory optimization by goal programming with fuzzy decision
p 526 A95-91544
- Towards improving the NMC aircraft data base
p 660 A95-93480
- Prediction of airplane states
[BTN-95-EIX0619952748174] p 584 A95-94468
- Application of multivariate optimisation techniques to determination of optimum flight path trajectories
[ESDU-94012] p 44 N95-11793
- Examples of flight path optimisation using a multivariate gradient-search method. Addendum A: Variation of optimum flight profile parameters with range
[ESDU-94016-ADD-A] p 44 N95-11794
- Airborne Windshear Detection and Warning Systems. Fifth and Final Combined Manufacturers' and Technologists' Conference, part 2
[NASA-CP-10139-PT-2] p 41 N95-13203
- Ground-based wake vortex monitoring, prediction, and ATC interface
p 42 N95-13209
- Doppler radar detection of vortex hazard indicators
p 42 N95-13212
- Identification of dynamic systems. Volume 3: Applications to aircraft. Part 2: Nonlinear analysis and manoeuvre design
[AGARD-AG-300-VOL-3-PT-2] p 79 N95-14102
- Assessment of CTAS ETA prediction capabilities
[NASA-CR-197224] p 97 N95-15728
- Comparison of meteorological data with fitted values extracted from projectile trajectory
[AD-A285921] p 255 N95-19989
- Nonlinear system guidance in the presence of transmission zero dynamics
[NASA-TM-4661] p 309 N95-22804
- Engines-only flight control system
[NASA-CASE-ARC-11944-1] p 294 N95-23389
- Flightpath synthesis and HUD scaling for V/STOL terminal area operations
[NASA-TM-110348] p 383 N95-26587
- Analytical investigations in aircraft and spacecraft trajectory optimization and optimal guidance
[NASA-CR-4672] p 526 N95-29339
- Apparatus and method for producing three-dimensional images
[AD-D017455] p 646 N95-30727
- Analysis of heads-up display quickening versus handling qualities
[AD-A293797] p 611 N95-31584
- Low-Level and Nap-of-the-Earth (NOE) night operations
[AGARD-CP-563] p 686 N95-32486
- A tactical navigation and routing system for low-level flight
p 709 N95-32494
- FLIGHT PLANS**
- National aviation weather program plan
p 652 A95-93445
- Low-Level and Nap-of-the-Earth (NOE) night operations
[AGARD-CP-563] p 686 N95-32486
- FLIGHT RECORDERS**
- Investigation of flight data recorder fire test requirements
[AD-A285832] p 232 N95-20032
- The role of flight progress strips in en route air traffic control: A time-series analysis
[DOT/FAA/AM-95/4] p 280 N95-23565
- FLIGHT SAFETY**
- Automatic guidance and control for helicopter obstacle avoidance
[BTN-95-EIX95182619130] p 291 A95-76607
- Lightning protection technology for small general aviation composite material aircraft
[SAE PAPER 931241] p 483 A95-88964
- FAA's Aging Commuter Airplane Program
[SAE PAPER 931248] p 483 A95-89220
- Fundamentals of catastrophic failure prevention by thrust vectoring
[BTN-95-EIX0619952748176] p 606 A95-94470
- Organizational ergonomics and aviation safety
p 596 A95-95083
- Psycho-social safety perceptions: Helicopters as a case study
p 596 A95-95192
- ASRS problems involving air carrier ground deicing/anti-icing
p 611 A95-95194
- General aviation landing incidents and accidents: A review of ASRS and AOPA research findings
p 596 A95-95198
- EMS helicopter incidents reported to the NASA Aviation Safety Reporting System
p 596 A95-95201
- Emergency medical service (EMS): A unique flight environment
p 596 A95-95203
- Initial exploration of the ASRS database
p 681 A95-95204
- Role of wind tunnels and computer codes in the certification and qualification of rotorcraft for flight in forecast icing
[NASA-TM-106747] p 39 N95-13197
- The principles of flight test assessment of flight-safety-critical systems in helicopters
[AGARD-AG-300-VOL-12] p 77 N95-14199
- Flight in an Adverse Environment
[AGARD-LS-197] p 77 N95-14893
- Wind shear and its effects on aircraft
p 77 N95-14898
- Annual review of aircraft accident data: US air carrier operations, calendar year 1992
[PB95-100319] p 78 N95-15066
- TDWR scan strategy implementation
[AD-A284877] p 98 N95-15749
- Federal aviation regulations, part 91. General operating and flight rules. Change 5
[PB94-194883] p 123 N95-17476
- Annual review of aircraft accident data: US Air carrier operations, calendar year 1992
[PB95-100319] p 123 N95-17748
- Users guide for NASA Lewis Research Center DC-9 Reduced-Gravity Aircraft Program
[NASA-TM-106755] p 146 N95-18586
- A study of the effect of store unsteady aerodynamics on gust and turbulence loads
p 133 N95-18601
- On-line handling of air traffic: Management, guidance and control
[AGARD-AG-321] p 126 N95-18927
- Safety study: Commuter airline safety
[PB94-917004] p 124 N95-19132
- Federal aviation regulations, part 91. General operating and flight rules. Change 8
[PB94-217445] p 188 N95-19720
- Commuter/air taxi ditchings and water-related impacts that occurred from 1979 to 1989
[AD-A285691] p 226 N95-20275
- Forecasting aircraft mishaps using monthly maintenance reports
[AD-A286049] p 227 N95-22417
- Additional improvements to the NASA Lewis ice accretion code LEWICE
[NASA-TM-106849] p 309 N95-22669
- Oklahoma City air logistics center (USAF) aging aircraft corrosion program
p 262 N95-23519
- A multibody/finite element analysis approach for modeling of crash dynamic responses
[NIAR-94-3] p 277 N95-24050
- The 1994 updated National Aerospace System performance assessment for year 2005
[AD-A288652] p 380 N95-26485
- The effect of aviation fuels containing low amounts of static dissipater additive on electrostatic charge generation
[AD-A280075] p 420 N95-28152
- The relation of handling qualities ratings to aircraft safety
p 597 N95-31067
- Environmental support of naval aviation
[AD-A292873] p 598 N95-31454
- Report to the Chairman, Subcommittee on Aviation, Committee on Commerce, Science, and Transportation, US Senate. Aviation safety: Data problems threaten FAA strides on safety analysis system
[GAO/AIMD-95-27] p 687 N95-32705
- Report to the Chairman, Subcommittee on Aviation, Committee on Commerce, Science, and Transportation, US Senate. Aviation Safety: FAA can better prepare general aviation pilots for mountain flying risks
[GAO/RCED-94-15] p 687 N95-32784
- Application of advanced safety technique to ring laser gyro inertial navigation system integration
p 689 N95-33140
- The application of Ada and formal methods to a safety critical engine control system
p 710 N95-33142
- FLIGHT SIMULATION**
- Validation of the dynamic response of a blade-element UH-60 simulation model in hovering flight
[HTN-94-00663] p 18 A95-60155
- Simulation development of a forward sensor-enhanced low-altitude guidance system
[HTN-94-00688] p 17 A95-60170
- Flight simulation
[BTN-94-EIX94461290242] p 84 A95-61735
- Simulation and flight test evaluation of head-up-display guidance for harrier approach transitions
[BTN-95-EIX95062487533] p 194 A95-69241
- Comparison of parameter identification algorithms for flight vehicles
[BTN-94-EIX94371347708] p 219 A95-69967
- A generalized algorithm for inverse simulation applied to helicopter maneuvering flight
[HTN-95-A0493] p 236 A95-72564
- High-order state space simulation models of helicopter flight mechanics
[HTN-95-A0494] p 237 A95-72565
- Identification and simulation evaluation of a combat helicopter in hover
[BTN-95-EIX95242670749] p 335 A95-81098
- Design features of the NAL ramjet engine test facility
p 410 A95-82319
- Education, training, and human engineering in aerospace; SAE Aerotech '93, Costa Mesa, CA, Sep. 27-30, 1993
[SAE SP-992] p 417 A95-84553
- Flying qualities development and flight simulation evaluation of the TW-68 tilt-wing VTOL aircraft
[SAE PAPER 932517] p 386 A95-84555
- Integrated flight crew transition training for the advanced flight deck aircraft
[SAE PAPER 932599] p 380 A95-84571
- New tools for creating instruction and simulations
[SAE PAPER 932600] p 380 A95-84572
- Flight simulation fatigue crack growth testing of aluminum alloys
[HTN-95-00652] p 418 A95-84731
- Verification of the damage tolerance of a fighter aircraft
p 388 A95-85897
- Intelligent tutoring system: F-16 flight simulation
p 521 A95-90649
- An investigation of piloting strategies for engine failures during takeoff from offshore platforms
[HTN-95-92834] p 497 A95-90752
- Aircraft Symposium, 30th, Tsukuba, Japan, Sep. 30 - Oct. 2, 1992
[HTN-95-A1609] p 498 A95-91491
- Analysis of an MLS automatic landing control law for the NAL experimental research aircraft D0-228. 2: Curved approach and landing
p 508 A95-91588
- Operational aviation weather regulations
p 652 A95-93446
- The development of computer-based instructional simulations for the airline industry
p 625 A95-95159
- NASA Lewis Propulsion Systems Laboratory customer guide manual
[NASA-TM-106569] p 21 N95-10822
- Instructional control and part/whole-task training: A review of the literature and an experimental comparison of strategies applied to instructional simulation
[AD-A280860] p 21 N95-10919
- STOVL Control Integration Program
[NASA-CR-195358] p 18 N95-11487
- Parallel methods for the flight simulation model
[DE94-013330] p 52 N95-11752
- Activities of the Institute for Aerospace Studies of Toronto University
p 63 N95-12699
- Piloted evaluation of an integrated methodology for propulsion and airframe control design
[AD-A290207] p 51 N95-12763
- Validation of the NASA Dryden X-31 simulation and evaluation of mechanization techniques
p 69 N95-14236
- High angle of attack flying qualities criteria for longitudinal rate command systems
p 70 N95-14247
- Vista/F-18 Multi-Axis Thrust Vectoring (MATV) control law design and evaluation
p 71 N95-14248
- Advanced distributed simulation technology advanced rotary wing aircraft. Study comparing approaches to modeling the ARWA main rotor
[AD-A280824] p 79 N95-14306
- Hypervelocity Impact Test Facility: A gun for hire
[TABES PAPER 94-605] p 86 N95-14639
- Turbulence: Engineering models, aircraft response
p 84 N95-14900
- Six degree of freedom flight dynamic and performance simulation of a remotely-piloted vehicle
[AERO-TN-9301] p 131 N95-18097
- KC-135 cockpit modernization study. Phase 1: Equipment evaluation
[AD-A284099] p 131 N95-18398
- Comparison of frequency response and perturbation methods to extract linear models from a nonlinear simulation
[AD-A284115] p 146 N95-18405
- Development of load spectra for Airbus A330/A340 full scale fatigue tests
p 135 N95-19479
- Summary of a joint program of research into aircraft flight control concepts
[AD-A280012] p 237 N95-20004

Collected papers of the Soar/IFOR project, Spring 1994
 [AD-A280063] p 238 N95-20624
 Minima reduction simulation test results
 [AD-A285626] p 228 N95-21148
 A preliminary study of the airwake model used in an existing SH-60B/FFG-7 helicopter/ship simulation program
 [DSTO-TR-0015] p 224 N95-21659
 Virtual reality flight control display with six-degree-of-freedom controller and spherical orientation overlay
 [NASA-CASE-NPO-18733-1-CU] p 288 N95-22578
 Direct adaptive performance optimization of subsonic transports: A periodic perturbation technique
 [NASA-TM-4676] p 284 N95-22829
 Review of aeronautical fatigue investigation in the Netherlands during the period March 1991-March 1993 [PB95-139184] p 388 N95-23161
 Development of qualification guidelines for personal computer-based aviation training devices
 [DOT/FAA/AM-95/6] p 323 N95-23603
 NLS Flight Simulation Laboratory (FSL) documentation
 [NASA-CR-196564] p 363 N95-24439
 Flight reference display for powered-lift STOL aircraft
 [NAL-TR-1251] p 337 N95-25005
 Simulation model of the integrated flight/propulsion control system, displays, and propulsion system for ASTOVL lift-fan aircraft
 [NASA-TM-108866] p 405 N95-26412
 Development of a nonlinear simulation for the McDonnell Douglas F-15 Eagle with a longitudinal TECS control-law
 [AD-A288610] p 388 N95-26481
 Integrated mission precision attack cockpit technology (IMPACT). Phase 1: Identifying technologies for air-to-ground fighter integration
 [AD-A289562] p 389 N95-26684
 The photo-realistic AFIT virtual cockpit
 [AD-A289376] p 390 N95-26876
 Implementation and demonstration of a multiple model adaptive estimation failure detection system for the F-16
 [AD-A289301] p 391 N95-27042
 The lift-fan aircraft: Lessons learned
 [NASA-CR-196694] p 392 N95-27143
 A study of workstation computational performance for real-time flight simulation
 [NASA-TM-109184] p 449 N95-27241
 Transport delays associated with NASA Langley Flight Simulation Facility
 [NASA-TM-110150] p 568 N95-29454
 Manual for a workstation-based generic flight simulation program (LaRCsim), version 1.4
 [NASA-TM-110164] p 518 N95-30327
 Developing a workstation-based, real-time simulation for rapid handling qualities evaluations during design
 [NASA-CR-198831] p 505 N95-30335
 Moving base simulation of an integrated flight and propulsion control system for an ejector-augmentor STOVL aircraft in hover
 [NASA-TM-108867] p 606 N95-30646
 SCARLET: DLR rate saturation flight experiment
 p 598 N95-31068
 Model following control for tailoring handling qualities: ACT experience with ATTHeS
 p 622 N95-32000
 The application of helicopter mission simulation to Nap-of-the-Earth operations
 p 710 N95-32496
 Low-order nonlinear dynamic model of IC engine-variable pitch propeller system for general aviation aircraft
 [NASA-TM-107006] p 694 N95-32916
 Altitude cuing effectiveness of terrain texture characteristics in simulated low-altitude flight
 [AD-A294369] p 700 N95-34362

FLIGHT SIMULATORS
 Evaluation of simulation motion fidelity criteria in the vertical and directional axes
 [HTN-94-00666] p 18 A95-60156
 Flight simulation
 [BTN-94-EIX94461290242] p 84 A95-61735
 Flight experience with lightweight, low-power miniaturized instrumentation systems
 [BTN-95-EIX95062487522] p 180 A95-69230
 Flight control system mode transitions influence on handling qualities and task performance
 [BTN-95-EIX95062487525] p 203 A95-69233
 Simulation of turbulent fluctuations
 [BTN-95-EIX95142553041] p 304 A95-73457
 The large radius track centrifuge concept as an acceleration research and simulation device
 p 379 A95-84560
 Part-task simulator evaluations of advanced terrain displays
 [SAE PAPER 932570] p 401 A95-84567
 Flight Simulators: Better than the real thing?
 [HTN-95-42619] p 518 A95-87249

A flying qualities study of longitudinal long-term dynamics of hypersonic planes
 [AIAA PAPER 95-6150] p 521 A95-90464
 Determination of flight simulator time delay
 p 522 A95-91553
 Functions of NAL fixed base simulator for helicopter research
 p 522 A95-91555
 A simulator study about effects of visibility upon helicopter pilot performance
 p 522 A95-91556
 New computer delivered training systems to support technical crew training programmes
 [CONGRESS PAPER C428-5-036] p 522 A95-91678
 The advanced flight simulator complex
 [CONGRESS PAPER C428-5-025] p 522 A95-91679
 General requirements for the electrohydraulic systems of the aircraft controls loading force on the simulators
 [CONGRESS PAPER C428-5-138] p 522 A95-91681
 The Saab-Scania approach to development simulators
 [CONGRESS PAPER C428-10-137] p 522 A95-91698
 Modelling requirements in flight simulation
 [HTN-95-C0004] p 585 A95-93392
 Event correlation for networked simulators
 [BTN-95-EIX0619952748168] p 625 A95-94462
 Damage tolerance certification of a fighter horizontal stabilizer
 [BTN-95-EIX0619952748186] p 637 A95-94478
 The simulator training research advance testbed for aviation (STRATA): A simulation research facility for army aviation
 p 626 A95-95161
 Advanced distributed simulation technology advanced rotary wing aircraft. Strawman verification and validation plan for the ARWA simulator system
 [AD-A280237] p 19 N95-10349
 Advanced distributed simulation technology advanced rotary wing aircraft. System/segment specification. Volume 1: Simulation system module
 [AD-A280238] p 20 N95-10350
 Advanced distributed simulation technology advanced rotary wing aircraft. System/segment specification. Volume 3: Visual system module
 [AD-A280239] p 20 N95-10351
 Advanced distributed simulation technology advanced rotary wing aircraft. System/segment specification. Volume 2: Flight station module
 [AD-A280432] p 20 N95-10352
 Advanced distributed simulation technology advanced rotary wing aircraft. System/segment specification. Volume 5: Simulation system module AH-64D kit
 [AD-A280433] p 20 N95-10353
 Instructional control and part/whole-task training: A review of the literature and an experimental comparison of strategies applied to instructional simulation
 [AD-A280860] p 21 N95-10919
 Effects of mass on aircraft sidarm controller characteristics
 [NASA-TM-104277] p 51 N95-11868
 Vertical flight terminal operational procedures. A summary of FAA research and development
 [AD-A283550] p 85 N95-15328
 ADST system test report for the rotary wing aircraft aimed aeromodel and weapon model merge with the ATAC 2 baseline
 [AD-A281580] p 127 N95-16171
 Aircraft and sub-system certification by piloted simulation
 [AGARD-AR-278] p 145 N95-17388
 Comparison of frequency response and perturbation methods to extract linear models from a nonlinear simulation
 [AD-A284115] p 146 N95-18405
 The generic simulation executive at Manned Flight Simulator
 [AD-A283997] p 146 N95-18724
 Helicopter in-flight simulation development and use in test pilot training
 [AD-A283998] p 146 N95-18725
 Assessing aircraft survivability to high frequency transient threats
 [AD-A283999] p 134 N95-18726
 A linear system identification and validation of an AH-64 Apache aeroelastic simulation model
 p 146 N95-18903
 Using the backward transfer paradigm to validate the AH-64 Simulator Training Research Advanced Testbed for Aviation
 [AD-A285758] p 238 N95-19931
 Summary of a joint program of research into aircraft flight control concepts
 [AD-A280012] p 237 N95-20004
 Preliminary experiments of an optical fiber display
 [NAL-TR-1257] p 362 N95-25004
 Visual contrast detection thresholds for aircraft contrails
 [AD-A288618] p 328 N95-25607

The photo-realistic AFIT virtual cockpit
 [AD-A289376] p 390 N95-26876
 The effects of UH-1 experience on UH-60 simulator performance: A preliminary study
 [AD-A289457] p 391 N95-26993
 Flight control design using mixed H2/micron optimization
 [AD-A289288] p 410 N95-27036
 Applications of digital video and synthetic environments to unmanned aerial vehicles
 [AD-A291875] p 504 N95-29437
 Transport delays associated with NASA Langley Flight Simulation Facility
 [NASA-TM-110150] p 568 N95-29454
 UHB engine fan broadband noise reduction study
 [NASA-CR-198357] p 580 N95-29641
 Moving base simulation of an integrated flight and propulsion control system for an ejector-augmentor STOVL aircraft in hover
 [NASA-TM-108867] p 606 N95-30646
 Development of advanced approach and departure procedures. Failure scenarios
 [PB95-198123] p 601 N95-30815
 Image representation using fast algorithms based on the Zak transform
 [AD-A293416] p 679 N95-31684
 Experiences with ADS-33 helicopter specification testing and contributions to refinement research
 p 621 N95-31993
 Model following control for tailoring handling qualities: ACT experience with ATTHeS
 p 622 N95-32000
 Practical experiences in control systems design using the NCR Bell 205 Airborne Simulator
 p 624 N95-32015
 Perceptual dimensions of simulated scenes relevant for visual low-altitude flight
 [AD-A294385] p 700 N95-34344

FLIGHT STABILITY TESTS
 Low-speed wind-tunnel investigation of the stability and control characteristics of a series of flying wings with sweep angles of 50 deg
 [NASA-TM-4640] p 505 N95-30226
 Practical experiences in control systems design using the NCR Bell 205 Airborne Simulator
 p 624 N95-32015

FLIGHT TEST INSTRUMENTS
 External viewing airborne CCTV system
 [CONGRESS PAPER C428-25-172] p 595 A95-93598
 Identification of dynamic systems. Volume 3: Applications to aircraft. Part 2: Nonlinear analysis and manoeuvre design
 [AGARD-AG-300-VOL-3-PT-2] p 79 N95-14102
 Preparation of S-70A-9 Black Hawk helicopter for flight tests to investigate cause of cracking of inner fuselage panel
 [AD-A293891] p 608 N95-31544

FLIGHT TEST VEHICLES
 Hypersonic waverider test vehicle: A logical next step
 [BTN-94-EIX95041503783] p 193 A95-69214
 Development of a low-aspect ratio fin for flight research experiments
 [NASA-TM-4596] p 108 N95-16858
 In-flight imaging of transverse gas jets injected into transonic and supersonic crossflows: Design and development
 [NASA-CR-186031] p 157 N95-17418
 Reentry guidance for hypersonic Flight Experiment (HYFLEX) vehicle
 [NAL-TR-1235] p 334 N95-25764

FLIGHT TESTS
 Flight test development and evaluation of a Kalman filter state estimator for low-altitude flight
 [HTN-94-00684] p 16 A95-60167
 X-29 high-angle-of-attack
 [BTN-94-EIX94511309383] p 127 A95-64609
 Overview of the NASA balloon R&D program
 p 181 A95-66297
 High accuracy navigation and landing system using GPS/IMU system integration
 [BTN-94-EIX94441386129] p 189 A95-68185
 Simulation and flight test evaluation of head-up-display guidance for harrier approach transitions
 [BTN-95-EIX95062487533] p 194 A95-69241
 Development and flight test of a deployable precision landing system
 [BTN-95-EIX95062487535] p 190 A95-69243
 Space flight tests of attitude determination using GPS
 [BTN-95-EIX95112522529] p 190 A95-69334
 Flight test evaluation of a 35 GHz forward looking altimeter for terrain avoidance
 [BTN-95-EIX95212641071] p 287 A95-76736
 2 micron LIDAR for laser-based remote sensing: Flight demonstration and application survey
 [BTN-95-EIX95212641072] p 319 A95-76737

- Air data sensors for atmospheric reentry flight test of winged space vehicle p 413 A95-82412
- Flight evaluation of DGPS and DGPS-INS navigation systems p 382 A95-82462
- A concept of a hypersonic flight experiment of a winged vehicle p 414 A95-82477
- A conceptual design of hypersonic research vehicle with subscale scramjet engine p 384 A95-82482
- Atmospheric reentry flight test of winged space vehicle p 414 A95-82483
- Development and flight results of fiber reinforced balloon p 384 A95-82511
- Recent developments in nylon superpressure balloons p 385 A95-82512
- Polar Patrol Balloon system and preliminary experimental results p 368 A95-82513
- The short range attack missile/light weight exo-atmospheric projectile (SRAM/LEAP) missile tests program
- [HTN-95-81498] p 386 A95-85212
- Evaluation of prediction methods for fluctuating pressures under attached turbulent boundary layers using flight test data p 574 A95-90103
- Flight-testing and frequency-domain analysis for rotorcraft handling qualities
- [HTN-95-01083] p 515 A95-90269
- Report to the aerospace profession; SETP Symposium, 37th, Beverly Hills, CA, USA, September 1993
- [HTN-95-12142] p 497 A95-90866
- Development and flight testing of the HL-10 lifting body p 498 A95-90872
- A gust alleviation method by the response feedback p 506 A95-91493
- Flight testing of the composite material bearingless rotor system for the helicopter p 498 A95-91503
- Flight test of STS radio controlled scale model p 499 A95-91539
- Aeronautical satellite communications using the ETS-5 satellite p 487 A95-91541
- An application of TLS (Total Least Squares) method to estimation of aircraft aerodynamic derivatives p 517 A95-91551
- A systems for flight data acquisition and analysis for a remotely-piloted research vehicle p 517 A95-91554
- On the flight control system for UF-104 p 507 A95-91560
- Flight Test Monitoring System using X-window p 500 A95-91574
- A perspective of rarefied gas flow problems relevant to high altitude flight
- [SAE PAPER 931366] p 586 A95-93647
- X-29 high AOA flight test results: An overview
- [SAE PAPER 931367] p 586 A95-93648
- Actuated forebody strake controls for the F-18 High-Alpha Research Vehicle
- [BTN-95-EIX0619952748173] p 619 A95-94467
- Operational and research aspects of a radio-controlled model flight test program
- [BTN-95-EIX0619952748177] p 606 A95-94471
- Flight test certification of primary category aircraft using TP101-41E sportplane design standard
- [BTN-95-EIX0619952748184] p 606 A95-94477
- Optimal trajectories for an unmanned air-vehicle in the horizontal plane
- [BTN-95-EIX0619952748191] p 606 A95-94480
- Evaluation of F-18A approach and landing flying qualities using an in-flight simulator
- [CALSPAN-6241-F-1] p 12 N95-10442
- Research excitation system flight testing
- [NASA-TM-104289] p 13 N95-10715
- NASA and the SR-71: Back to the future
- [NASA-TM-104290] p 13 N95-10716
- Radio controlled for research
- [NASA-TM-104292] p 17 N95-10717
- Design and flight evaluation of an integrated navigation and near-terrain helicopter guidance system for night-time and adverse weather operations
- [NASA-TM-108837] p 11 N95-10846
- Flow-visualization study of the X-29A aircraft at high angles of attack using a 1/48-scale model
- [NASA-TM-104268] p 8 N95-10858
- Transonic flight test of a laminar flow leading edge with surface excrescences
- [NASA-TM-4597] p 9 N95-11158
- High-angle-of-attack yawing moment asymmetry of the X-31 aircraft from flight test
- [NASA-CR-186030] p 13 N95-11410
- An application of virtual prototyping to the flight test and evaluation of an unmanned air vehicle
- [AD-A281749] p 14 N95-11595
- Dynamic ground effects flight test of an F-15 aircraft
- [NASA-TM-4604] p 38 N95-12191
- Flight investigation of the use of a nose gear jump strut to reduce takeoff ground roll distance of STOL aircraft
- [NASA-TM-108819] p 44 N95-12225
- Flight dynamics of an unmanned aerial vehicle
- [AD-A282259] p 45 N95-12410
- Flight test of takeoff performance monitoring system
- [NASA-TP-3403] p 51 N95-12664
- Identification of dynamic systems. Volume 3: Applications to aircraft. Part 2: Nonlinear analysis and manoeuvre design
- [AGARD-AG-300-VOL-3-PT-2] p 79 N95-14102
- The principles of flight test assessment of flight-safety-critical systems in helicopters
- [AGARD-AG-300-VOL-12] p 77 N95-14199
- Flight and full-scale wind-tunnel comparison of pressure distributions from an F-18 aircraft at high angles of attack
- Conducted in NASA Ames Research Center's 80 by 120 ft wind tunnel p 68 N95-14231
- Comparison of X-31 flight, wind-tunnel, and water-tunnel yawing moment asymmetries at high angles of attack
- p 68 N95-14234
- Parameter identification for X-31A at high angles of attack
- p 69 N95-14235
- Free-to-roll tests of X-31 and F-18 subscale models with correlation to flight test results p 69 N95-14237
- Fourth High Alpha Conference, volume 2
- [NASA-CP-10143-VOL-2] p 69 N95-14239
- F-18 high alpha research vehicle: Lessons learned
- p 69 N95-14240
- X-31 post-stall envelope expansion and tactical utility testing p 70 N95-14242
- X-31 quasi-tailless flight demonstration p 70 N95-14243
- Flight test results of the F-16 aircraft modified with the axisymmetric vectoring exhaust nozzle p 70 N95-14245
- Flight validation of ground-based assessment for control power requirements at high angles of attack
- p 70 N95-14246
- Vista/F-16 Multi-Axis Thrust Vectoring (MATV) control law design and evaluation p 71 N95-14248
- Preparations for flight research to evaluate actuated forebody strakes on the F-18 high-alpha research vehicle p 72 N95-14257
- Flight evaluation of pneumatic forebody vortex control in post-stall flight p 72 N95-14259
- An optical technique for examining aircraft shock wave structures in flight p 96 N95-14879
- Flight in an Adverse Environment
- [AGARD-LS-197] p 77 N95-14893
- Air-breathing aerospace plane development essential: Hypersonic propulsion flight tests
- [NASA-TM-108857] p 66 N95-14921
- Test Operation Procedure (TOP): Vibration testing of helicopter equipment
- [AD-A284433] p 81 N95-15815
- A VHF/UHF antenna for the Precision Antenna Measurement System (PAMS)
- [AD-A285673] p 156 N95-16621
- Development of a low-aspect ratio fin for flight research experiments
- [NASA-TM-4596] p 108 N95-16858
- Modeling of Instrument Landing System (ILS) localizer signal on runway 25L at Los Angeles International Airport
- [NASA-TM-4588] p 125 N95-17384
- Flight testing high lateral asymmetries on highly augmented Fighter/Attack aircraft
- [AD-A284206] p 130 N95-17953
- KC-135 cockpit modernization study. Phase 1: Equipment evaluation
- [AD-A284099] p 131 N95-18398
- Preliminary evaluation of the F/A-18 quantity/multiple envelope expansion
- [AD-A284119] p 132 N95-18407
- Tilt Rotor Unmanned Air Vehicle System (TRUS) demonstrator flight test program
- [AD-A284151] p 132 N95-18415
- Helicopter in-flight simulation development and use in test pilot training
- [AD-A283998] p 146 N95-18725
- Hypersonic flight testing
- [AD-A283981] p 134 N95-18891
- Design and flight test of a simplified control system for a transport helicopter p 144 N95-18902
- Navier-Stokes, flight, and wind tunnel flow analysis for the F/A-18 aircraft
- [NASA-TP-3478] p 120 N95-19114
- Fiber Optic Control System integration for advanced aircraft. Electro-optic and sensor fabrication, integration, and environmental testing for flight control systems
- [NASA-CR-191194] p 162 N95-19236
- The use of genetic algorithms for flight test and evaluation of artificial intelligence and complex software systems
- [AD-A284824] p 217 N95-19688
- Airship applications of modern flight test techniques
- [AD-A284253] p 194 N95-19731
- Open Skies project computational fluid dynamic analysis
- [AD-A285928] p 223 N95-19991
- F-15 resource tape
- [NASA-TM-110502] p 230 N95-19994
- Acoustic climb to cruise test
- [NASA-TM-110504] p 230 N95-20155
- SAR image registration in absolute coordinates using GPS carrier phase position and velocity information
- [DE94-018738] p 228 N95-20195
- Assessment of a non-dedicated GPS receiver system for precise airborne attitude determination
- [DE94-019309] p 229 N95-21520
- Flight test of the X-29A at high angle of attack: Flight dynamics and controls
- [NASA-TP-3537] p 284 N95-22806
- High-lift flow-physics flight experiments on a subsonic civil transport aircraft (B737-100) p 275 N95-23333
- TRISTAR 1: Evaluation methods for testing head-up display (HUD) flight symbology
- [NASA-TM-4665] p 288 N95-24030
- Flight reference display for powered-lift STOL aircraft
- [NAL-TR-1251] p 337 N95-25005
- Flutter clearance flight tests of an OV-10A airplane modified for wake vortex flight experiments
- [NASA-TM-109168] p 366 N95-26381
- Flight evaluation of GPS/DGPS sensor systems installed in NAL Do228
- [NAL-TR-1230] p 382 N95-26585
- The effects of UH-1 experience on UH-60 simulator performance: A preliminary study
- [AD-A289457] p 391 N95-26993
- Test operations procedure (TOP) 7-3-534 airworthiness testing of fixed wing aircraft: Asymmetric power testing
- [AD-A289458] p 391 N95-26994
- Status of bonded boron/epoxy doublers for military and commercial aircraft structures p 393 N95-27506
- Unmanned aerial vehicles, 1994 master plan
- [AD-A291628] p 398 N95-28411
- Proceedings of the AIAA/FAA joint symposium on general aviation systems
- [AD-A289830] p 368 N95-28610
- Investigation of wing upper surface flow-field disturbance due to NASA DC-8-72 in-flight inboard thrust-reverser deployment
- [NASA-TM-110351] p 457 N95-28816
- A nonintrusive method of quantifying flow visualization data in vortex field fields
- [AD-A289802] p 552 N95-28948
- Evaluation of proposed agility metrics using X-31 vs. F/A-18 flight data
- [AD-A292573] p 502 N95-28977
- Computational Fluid Dynamics (CFD) analysis of a C-135 aircraft with a side-mounted splitter plate (with comparison to wind tunnel data)
- [AD-A292029] p 553 N95-29187
- AGARD flight test techniques series. Volume 13: Reliability and maintainability
- [AGARD-AG-300-VOL-13] p 504 N95-29503
- Flight test evaluation of the Stanford University/United Airlines differential GPS Category 3 automatic landing system
- [NASA-TM-110354] p 593 N95-30788
- SCARLET: DLR rate saturation flight experiment
- p 598 N95-31068
- Flight assessment of the onboard propulsion system model for the Performance Seeking Control algorithm on an F-15 aircraft
- [NASA-TM-4705] p 617 N95-31425
- Artificial intelligence techniques for flight test planning, phase 1
- [AD-A293962] p 608 N95-31525
- Preparation of S-70A-9 Black Hawk helicopter for flight tests to investigate cause of cracking of inner fuselage panel
- [AD-A293891] p 608 N95-31544
- Flight test validation of a frequency-based system identification method on an F-15 aircraft
- [NASA-TM-4704] p 620 N95-31846
- Lavi flight control system: Design requirements, development and flight test results p 621 N95-31994
- The control system design methodology of the STOL and maneuver technology demonstrator
- p 621 N95-31998
- X-29 flight control system: Lessons learned
- p 622 N95-32001
- Advanced gust management systems: Lessons learned and perspectives
- p 622 N95-32002
- Flight evaluation of forebody vortex control in post-stall flight
- p 609 N95-32003
- Automatic flight control system for an unmanned helicopter system design and flight test results
- p 622 N95-32004
- Flight test results of the F-16 aircraft modified with axisymmetric vectoring exhaust nozzle
- p 609 N95-32007

- Experimental Aircraft Programme (EAP): Flight control system design and test p 623 N95-32010
- Flight demonstration of an advanced pitch control law in the VAAC Harrier aircraft p 623 N95-32012
- X-31: A program overview and flight test status p 609 N95-32013
- Report to the Chairman, Legislation and National Security Subcommittee, Committee on Government Operations, House of Representatives. Unmanned aerial vehicles: Performance of short-range system still in question [GAO/NSIAD-94-65] p 609 N95-32196
- Flight test of a low-altitude helicopter guidance system with obstacle avoidance capability p 688 N95-32490
- Development and flight testing of an Obstacle Avoidance System for US Army helicopters p 687 N95-32500
- An Electronic Workshop on the Performance Seeking Control and Propulsion Controlled Aircraft Results of the F-15 Highly Integrated Digital Electronic Control Flight Research Program [NASA-TM-104278] p 694 N95-33009
- An overview of integrated flight-propulsion controls flight research on the NASA F-15 research airplane p 694 N95-33010
- Performance seeking control program overview p 695 N95-33011
- Minimum fuel mode evaluation p 695 N95-33015
- Minimum fan turbine inlet temperature mode evaluation p 696 N95-33016
- Maximum thrust mode evaluation p 696 N95-33017
- Performance seeking control excitation mode p 696 N95-33019
- Flight test of a propulsion controlled aircraft system on the NASA F-15 airplane p 691 N95-33023
- Dynamic ground effects flight test of the NASA F-15 aircraft p 692 N95-33024
- Design challenges encountered in the F-15 PCA flight test program p 692 N95-33025
- Integrated special mission flight management for a flight inspection aircraft p 692 N95-33145
- Remote sensing of smoke, clouds, and radiation using AVIRIS during SCAR experiments p 708 N95-33749
- FLIGHT TIME**
- North Atlantic air traffic within the lower stratosphere: Cruising times and corresponding emissions [HTN-95-91841] p 354 A95-90829
- A study of the savings in time and fuel to aviation through the use of upper-air wind forecasts p 672 A95-93538
- An analysis of the impact of ASPA on organizational and depot level maintenance [AD-A292670] p 457 N95-29414
- Modeling F/A-18 flight hour program costs using regression analysis [AD-A293771] p 608 N95-31579
- FLIGHT TRAINING**
- Education, training, and human engineering in aerospace; SAE Aerotech '93, Costa Mesa, CA, Sep. 27-30, 1993 [SAE SP-992] p 417 A95-84553
- Intelligent flight trainer for initial rotary wing training [SAE PAPER 932536] p 386 A95-84558
- Automated hover training: An empirical evaluation [SAE PAPER 932536] p 379 A95-84559
- The CBT alternative for aviation training: Is it meeting the need? [SAE PAPER 932596] p 379 A95-84568
- Assessment of cost and training effectiveness for a candidate training system using the Comparison-Based Prediction model [SAE PAPER 932598] p 379 A95-84570
- Integrated flight crew transition training for the advanced flight deck aircraft [SAE PAPER 932599] p 380 A95-84571
- New computer delivered training systems to support technical crew training programmes [CONGRESS PAPER C428-5-036] p 522 A95-91678
- The advanced flight simulator complex [CONGRESS PAPER C428-5-025] p 522 A95-91679
- The simulator training research advance testbed for aviation (STRATA): A simulation research facility for army aviation p 626 A95-95161
- Public-sector aviation issues: Graduate research award papers, 1992-1993 [PB94-217478] p 219 N95-19967
- T-45A High Angle of Attack Testing: US Naval Test Pilot School 46th Annual Reunion and Symposium [AD-A284000] p 231 N95-20466
- A computer-based multimedia prototype for night vision goggles [AD-A286208] p 258 N95-21882
- Development of qualification guidelines for personal computer-based aviation training devices [DOT/FAA/AM-95/6] p 323 N95-23603
- The value of simulation for training [AD-A289174] p 411 N95-26556
- Controller resource management: What can we learn from aircrews? [DOT/FAA/AM-95/21] p 602 N95-32186
- Altitude cuing effectiveness of terrain texture characteristics in simulated low-altitude flight [AD-A294369] p 700 N95-34362
- FLIR DETECTORS**
- Nonlinear calibration of an infrared radiometer [AD-A292436] p 579 N95-28996
- A helmet mounted display for night missions at low altitude p 693 N95-32503
- FLOATING**
- Analyzing the stability of floating ice floes [AD-A292149] p 563 N95-29160
- FLOORS**
- Automatic riveting cell for commercial aircraft floor grid assembly [BTN-95-EIX95182617807] p 261 A95-75752
- Automatic riveting cell for commercial aircraft floor grid assembly [HTN-95-92309] p 365 A95-85353
- Effects of floor location on response of composite fuselage frames p 423 N95-28439
- FLOUQUET THEOREM**
- Fast Floquet theory and trim for multi-bladed rotorcraft [HTN-95-61078] p 370 A95-83662
- Automatic identification of modal damping from Floquet analysis [HTN-95-01084] p 506 A95-90270
- Aeroelasticity and structural optimization of composite helicopter rotor blades with swept tips [NASA-CR-4665] p 397 N95-28262
- High-and low-frequency dynamics of isolated blades and rotors with dynamic stall and wake [AD-A290358] p 503 N95-29322
- FLORIDA**
- ITWS gridded analysis p 654 A95-93455
- Investigation of outflow strength variability in Florida downburst-producing storms p 659 A95-93476
- Use of high resolution lightning detection and localization sensors for hazardous aviation weather nowcasting p 661 A95-93486
- FLOW CHARACTERISTICS**
- Passive porosity with free and fixed separation on a tangent-ogive forebody [BTN-95-EIX95062487554] p 185 A95-68368
- Vortical flow structure near the F/A-18 LEX at high incidence [BTN-95-EIX95062487555] p 186 A95-68369
- In-flight pressure measurements on a subsonic transport high-lift wing section [BTN-95-EIX0619952748170] p 589 A95-94464
- The NASA Langley 8-foot Transonic Pressure Tunnel calibration [NASA-TP-3437] p 8 N95-10739
- Numerical study of Gortler instability: Application to the design of a quiet supersonic wind tunnel [PB94-184801] p 21 N95-10844
- Unsteady flows in turbines: Impact on design procedure p 90 N95-14132
- The industrial use of CFD in the design of turbomachinery p 90 N95-14133
- A selection of experimental test cases for the validation of CFD codes, volume 2 [AGARD-AR-303-VOL-2] p 109 N95-17846
- Experiments in the trailing edge flow of an NLR 7702 airfoil p 110 N95-17853
- Delta-wing model p 114 N95-17873
- STOVL CFD model test case p 115 N95-17881
- Numerical mixing calculations of confined reacting jet flows in a cylindrical duct [NASA-TM-106736] p 139 N95-18133
- A selection of experimental test cases for the validation of CFD codes. Supplement: Datasets A-E [AGARD-AR-303-SUPPL] p 117 N95-18539
- Navier-Stokes, flight, and wind tunnel flow analysis for the F/A-18 aircraft [NASA-TP-3478] p 120 N95-19114
- Impeller flow field characterization with a laser two-focus velocimeter p 313 N95-23440
- Supersonic quiet-tunnel development for laminar-turbulent transition research [NASA-CR-198040] p 340 N95-24302
- Aerodynamic characteristics of the orbital reentry vehicle experimental probe fins in a supersonic flow [NAL-TR-1232] p 342 N95-25664
- Viscous shock-layer analysis on hypersonic flow over reentry capsule with nonequilibrium chemistry [ISAS-656] p 436 N95-26739
- Wind tunnel experiments on wake flow field behind a reentry capsule from a viewpoint of parachute deployment at supersonic speeds [ISAS-655] p 374 N95-26740
- The effects of three-dimensional imposed disturbances on bluff body near wake flows: Effects of taper and splitter plates on the near wake characteristics of a circular cylinder in uniform and shear flow [AD-A292113] p 477 N95-28921
- Air/fuel ratio visualization in a diesel spray p 556 N95-29807
- Flow quality improvements in the NASA Lewis Research Center 9- by 15-foot Low Speed Wind Tunnel [NASA-CR-195439] p 627 N95-31653
- FLOW COEFFICIENTS**
- Comparison of full-scale, small-scale, and CFD results for F/A-18 forebody slot blowing p 72 N95-14255
- Flow coefficient behavior for boundary layer bleed holes and slots [NASA-TM-106846] p 244 N95-19953
- FLOW DEFLECTION**
- Static investigation of two fluidic thrust-vectoring concepts on a two-dimensional convergent-divergent nozzle [NASA-TM-4574] p 222 N95-19913
- FLOW DISTORTION**
- F/A-18 inlet calculations at 60-deg angle of attack and 10-deg sideslip [BTN-95-EIX95112524199] p 195 A95-69309
- Numerical study of the performance of swept, curved compression surface scramjet inlets [BTN-95-EIX95112524198] p 197 A95-69310
- A new type of simulator for simulating the flow-field distortion of engine inlet [BTN-95-EIX95202638963] p 289 A95-76673
- A full Navier-Stokes analysis of subsonic diffuser of a bifurcated 70/30 supersonic inlet for high speed civil transport application [NASA-TM-106637] p 8 N95-10820
- The traditional and new methods of accounting for the factors distorting the flow over a model in large transonic wind tunnels p 165 N95-19275
- FLOW DISTRIBUTION**
- Interferometry and computational studies of an oscillating airfoil compressible dynamic stall flow field [HTN-94-00703] p 3 A95-60182
- Marangoni-Benard convection in a low-aspect-ratio liquid layer p 56 A95-61544
- Experimental and computational results for the external flowfield of a scramjet inlet [BTN-94-EIX94441380977] p 195 A95-68161
- Experimental investigations on limit cycle wing rock of slender wings [BTN-95-EIX95062487543] p 185 A95-68357
- Experimental investigation of the flowfield about an upswept afterbody [BTN-95-EIX95152582321] p 265 A95-73524
- Convective and radiative heat transfer analysis for the fire 2 forebody [BTN-95-EIX95182617460] p 268 A95-75731
- Supersonic near-wake afterbody boattailing effects on axisymmetric bodies [BTN-95-EIX95182617465] p 268 A95-75736
- Transient structure of vortex breakdown on a delta wing [BTN-95-EIX95182619073] p 268 A95-75758
- Observations on using experimental data as boundary conditions for computations [BTN-95-EIX95182619103] p 321 A95-76588
- Simple method of supersonic flow visualization using watertable [BTN-95-EIX95182619105] p 269 A95-76590
- Tracking of raindrops in flow over an airfoil [BTN-95-EIX95182619221] p 308 A95-76647
- Aerodynamics of a finite wing with simulated ice [BTN-95-EIX95182619227] p 270 A95-76653
- Neural network prediction of three-dimensional unsteady separated flowfields [BTN-95-EIX95182619232] p 308 A95-76658
- An experimental investigation of scramjet nozzle flow p 402 A95-82322
- Numerical analysis of flow field around gas rudder p 407 A95-82333
- Rarefied gas numerical wind tunnel: OREX and HOPE p 427 A95-82391
- VSL analysis of hypersonic flows around a reentry vehicle with equilibrium air chemistry p 413 A95-82400
- Flow past a symmetric wedge with forward splitter plate p 427 A95-82406
- A study on aerodynamic heating phenomena in three-dimensional shock wave/turbulent boundary layer interaction induced by sweptback sharp fins at supersonic flow p 428 A95-82419
- Studies on gain performance of a combustion driven CO2 gas dynamic laser p 428 A95-82679
- Measurements of vortex pair interaction with a clean or contaminated free surface [BTN-94-EIX95011441063] p 429 A95-82798

- Two-dimensional viscous flow past a flat plate
[HTN-95-42210] p 430 A95-84026
- Structure of supersonic jet flow and its radiated sound
[HTN-95-51645] p 431 A95-85027
- Computational/experimental investigation of staged injection into a Mach 2 flow
[HTN-95-51646] p 432 A95-85028
- Reattachment studies of an oscillating airfoil dynamic stall flowfield
[HTN-95-51660] p 432 A95-85042
- Crossflow topology of vortical flows
[HTN-95-51664] p 432 A95-85046
- Practical formulation of a positively conservative scheme
[HTN-95-51668] p 433 A95-85050
- Numerical investigation of cylinder wake flow with a rear stagnation jet
[HTN-95-51669] p 433 A95-85051
- Flowfield measurements in supersonic film cooling including the effect of shock-wave interaction
[HTN-95-42337] p 405 A95-86166
- Interferometric investigations of compressible dynamic stall over a transiently pitching airfoil
[HTN-95-42338] p 372 A95-86167
- Effects of spatial order of accuracy on the computation of vortical flowfields
[HTN-95-42589] p 459 A95-87219
- A flow pattern map for two-phase liquid-gas flow under reduced gravity conditions
p 539 A95-87280
- Low-speed aerodynamic characteristics of a slender wing with vertical fins
p 460 A95-87400
- Experimental and numerical analysis of a two-duct nozzle/afterbody model at supersonic Mach numbers
[AIAA PAPER 95-6085] p 490 A95-87414
- Unsteady panel method for flows with multiple bodies moving along various paths
[HTN-95-61203] p 540 A95-87576
- Numerical model for circulation-control flows
[HTN-95-81632] p 461 A95-87680
- Dynamic pitch-up of a delta wing
[HTN-95-81633] p 462 A95-87681
- Automated adaptive time-discontinuous finite element method for unsteady compressible airfoil aerodynamics
[HTN-95-81637] p 541 A95-87685
- Airfoil pressure measurements during oblique shock-wave/vortex interaction in a Mach 3 stream
[HTN-95-81641] p 542 A95-87689
- Computational fluid dynamics with icing effects
[SAE PAPER 932532] p 466 A95-89192
- Accurate drag prediction: A prerequisite for drag reduction research
[SAE PAPER 932571] p 467 A95-90060
- Laser velocimetry and blade pressure measurements of a blade-vortex interaction
[HTN-95-01081] p 547 A95-90267
- Rotor-wake-induced flow separation on a lifting surface
[HTN-95-01082] p 468 A95-90268
- Viscous contribution to the high Mach number damping in pitch of blunt slender cones at small angles of attack
[HTN-95-01096] p 469 A95-90282
- Preliminary results from a particle image velocimetry study of blade-vortex interaction
[HTN-95-01098] p 547 A95-90284
- Algorithmic trends in computational fluid dynamics; The Institute for Computer Applications in Science and Engineering (ICASE)/LaRC Workshop, NASA Langley Research Center, Hampton, VA, US, Sep. 15-17, 1991
[ISBN 0-387-94014-6] p 550 A95-91915
- Algorithmic trends in CFD in the 1990's for aerospace flow field calculations
p 550 A95-91917
- Lee waves benign and malignant
p 595 A95-93554
- Laser velocimetry in the supersonic regime: Advancements, limitations, and outlook
[SAE PAPER 931365] p 634 A95-93646
- X-29 high AOA flight test results: An overview
[SAE PAPER 931367] p 586 A95-93648
- 3-D Navier-Stokes analysis of crossing glancing shocks/turbulent boundary layer interactions
[BTN-95-EI195302729768] p 636 A95-94130
- Effect of passive venting on static pressure distributions in cavities at subsonic and transonic speeds
[NASA-TM-4549] p 6 N95-10029
- Effects of a forward-swept front rotor on the flowfield of a counterrotation propeller
[NASA-TM-106671] p 7 N95-10148
- Navier-Stokes simulations of WECS airfoil flowfields
[DE94-013341] p 7 N95-10226
- Application of scramjet engine technology to the design of ram accelerator projectiles
p 19 N95-10282
- Inlet flow test calibration for a small axial compressor facility. Part 1: Design and experimental results
[NASA-TM-106719] p 16 N95-11005
- A shadowgraph study of the National Launch System's 1 1/2 stage vehicle configuration and Heavy Lift Launch Vehicle configuration — Using the Marshall Space Flight Center's 14-Inch Trisonic Wind Tunnel
[NASA-RP-1347] p 35 N95-11710
- Structure of a swirl-stabilized, combustor spray
[NASA-TM-106724] p 50 N95-11890
- Numerical analysis of tangential slot blowing on a generic chined forebody
[NASA-TM-108845] p 37 N95-11927
- Computational flow predictions for hypersonic drag devices
p 37 N95-11967
- Test model designs for advanced refractory ceramic materials
p 55 N95-11968
- Experimental Aerodynamics Division
[NAL-SP-9404] p 35 N95-12166
- Supersonic base flow investigation over axisymmetric afterbodies
[PB94-180957] p 39 N95-12578
- Numerical time dependent sheet cavitation simulations using a higher order panel method
[PB94-204435] p 59 N95-13249
- The industrial use of CFD in the design of turbomachinery
p 90 N95-14133
- Numerical simulation of the flow about an F-18 aircraft in the high-alpha regime
p 68 N95-14232
- Hybrid structured/unstructured grid computations for the F/A-18 at high angle of attack
p 68 N95-14233
- Axis switching and spreading of an asymmetric jet: Role of vorticity dynamics
[NASA-TM-106385] p 73 N95-14418
- Computation of supersonic air-intakes
p 74 N95-14452
- Numerical simulation of the SOFIA flowfield
[NASA-CR-197025] p 74 N95-14612
- An optical technique for examining aircraft shock wave structures in flight
p 96 N95-14879
- Propulsion/airframe interference for ducted propfan engines with ground effect
[NASA-CR-197110] p 81 N95-14909
- Gas turbine prediffuser-combustor performance during operation with air-water mixture
[DOT/FAA/CT-93/52] p 83 N95-15683
- Two-dimensional scramjet inlet unstart model: Wind-tunnel blockage and actuation systems test
[NASA-TM-109984] p 97 N95-15899
- Residual-correction type and related computational methods for aerodynamic design. Part 1: Airfoil and wing design
p 128 N95-16566
- Airfoil optimization by the one-shot method
p 128 N95-16569
- Numerical simulation of helicopter engine plume in forward flight
[NASA-CR-197488] p 107 N95-16589
- Numerical simulation of transient vortex breakdown above a pitching delta wing
[AD-A281075] p 107 N95-16808
- Three-dimensional boundary layer and flow field data of an inclined prolate spheroid
p 158 N95-17867
- Force and pressure data of an ogive-nosed slender body at high angles of attack and different Reynolds numbers
p 113 N95-17868
- Pressure distribution measurements on an isolated TPS 441 nacelle
p 115 N95-17878
- Low speed propeller slipstream aerodynamic effects
p 116 N95-17882
- Floating shock fitting via Lagrangian adaptive meshes
[AD-A289758] p 170 N95-18110
- Numerical mixing calculations of confined reacting jet flows in a cylindrical duct
[NASA-TM-106736] p 139 N95-18133
- Hypersonic flow-field measurements: Intrusive and nonintrusive
[AD-A283867] p 119 N95-18674
- The crucial role of wall interference, support interference and flow field measurements in the development of advanced aircraft configurations
p 162 N95-19252
- Applications of the five-hole probe technique for flow field surveys at the Institute for Aerospace Research
p 163 N95-19255
- Aerodynamic investigation of the flow field in a 180 deg turn channel with sharp bend
p 163 N95-19257
- The utilization of a high speed reflective visualization system in the study of transonic flow over a delta wing
p 121 N95-19259
- Transonic and supersonic flowfield measurements about axisymmetric afterbodies for validation of advanced CFD codes
p 121 N95-19260
- Velocity measurements with hot-wires in a vortex-dominated flowfield
p 121 N95-19261
- Determination of solid/porous wall boundary conditions from wind tunnel data for computational fluid dynamics codes
p 164 N95-19266
- Calculation of low speed wind tunnel wall interference from static pressure pipe measurements
p 164 N95-19273
- Parabolized Navier-Stokes solution of supersonic/hypersonic flows
p 123 N95-19464
- Prediction of wind tunnel effects on the installed F/A-18A inlet flow field at high angles-of-attack
[NASA-CR-195429] p 197 N95-19651
- 16-foot transonic tunnel test section flowfield survey
[NASA-TM-109157] p 238 N95-20669
- Wake measurements in a strong adverse pressure gradient
[NASA-CR-197272] p 224 N95-21031
- Application of Navier-Stokes code PAB3D with kappa-epsilon turbulence model to attached and separated flows
[NASA-TP-3480] p 224 N95-21338
- Experiments on the flow field physics of confluent boundary layers for high-lift systems
[NASA-CR-197318] p 224 N95-21343
- Flow visualization studies of VTOL aircraft models during Hover in ground effect
[NASA-TM-108860] p 272 N95-22666
- A CFD study of complex missile and store configurations in relative motion
[NASA-CR-197912] p 285 N95-22949
- Mach 10 computational study of a three-dimensional scramjet inlet flow field
[NASA-TM-4602] p 309 N95-23015
- Experimental results for a hypersonic nozzle/afterbody flow field
[NASA-TM-4638] p 274 N95-23250
- Holographic interferometric tomography for reconstructing flow fields
p 310 N95-23287
- Three-dimensional unsteady flow calculations in an advanced gas generator turbine
p 312 N95-23425
- A study of the vortex flow over 76/40-deg double-delta wing
[NASA-CR-195032] p 314 N95-23466
- Validation of a Computational Fluid Dynamics (CFD) code for supersonic axisymmetric base flow
p 315 N95-23652
- Exploratory flow visualization investigation of mast-mounted sights in presence of a rotor
[NASA-TM-4634] p 330 N95-24566
- Low speed aerodynamic characteristics of delta wings with vortex flaps: 60 deg and 70 deg delta wings
[NAL-TR-1245] p 331 N95-25105
- Numerical simulation of the SOFIA flow field
[NASA-CR-197757] p 436 N95-26589
- CFD research, parallel computation and aerodynamic optimization
[NASA-CR-197748] p 373 N95-26649
- Wind tunnel experiments on wake flow field behind a reentry capsule from a viewpoint of parachute deployment at supersonic speeds
[ISAS-655] p 374 N95-26740
- Rarefied gas effects on aerobraking/reentry vehicles with wakes
[NASA-CR-196586] p 415 N95-27093
- Global flowfield about the V-22 Tiltrotor Aircraft
[NASA-CR-198803] p 375 N95-27248
- Measurements of store forces and moments and cavity pressures for a generic store in and near a box cavity at subsonic and transonic speeds
[NASA-TM-4611] p 378 N95-28241
- TranAir: A full-potential, solution-adaptive, rectangular grid code for predicting subsonic, transonic, and supersonic flows about arbitrary configurations. Theory document
[NASA-CR-4348] p 378 N95-28265
- Numerical analysis of intra-cavity and power-stream flow interaction in multiple gas-turbine disk-cavities
[NASA-TM-106886] p 407 N95-28344
- Surface modeling and grid generation for aeropropulsion CFD
p 551 N95-28732
- Investigation of wing upper surface flow-field disturbance due to NASA DC-8-72 in-flight inboard thrust-reverser deployment
[NASA-TM-110351] p 457 N95-28816
- A nonintrusive method of quantifying flow field visualization data in vortex flow fields
[AD-A289802] p 552 N95-28948
- Development of a rotary wing Navier-Stokes CFD code based on TLNS3D code
[AD-A290421] p 554 N95-29387
- Effects of elevated free-stream turbulence and streamwise acceleration on flow and thermal structures in transitional boundary layers
p 556 N95-29729
- Computation of the integrated aerodynamic and propulsive flowfields of a generic hypersonic space plane
p 481 N95-29788
- Comparison of spatial numerical operators for duct-nozzle acoustics
p 580 N95-30158
- Numerical simulations of the flow in the HYPULSE expansion tube
[NASA-TM-110357] p 523 N95-30228
- Axial loads on yawed rotors
[PB95-214193] p 592 N95-30638

- Computation of high-altitude hypersonic flow-field radiation p 593 N95-30843
- Acceleration potential models
PREDICAT/PREDICDYN applied for calculation of axisymmetric dynamic inflow cases
[PB95-207015] p 647 N95-30957
- Patterns in the sky: Natural visualization of aircraft flow fields
[NASA-SP-514] p 584 N95-31000
- Numerical simulation of ram accelerator performance including transient effects during initiation of combustion and sensitivity studies p 629 N95-31203
- Investigating the use of smart acoustically active surfaces for flow separation control in turbomachinery
[AD-A292819] p 648 N95-31443
- Laser anemometer measurements of the three-dimensional rotor flow field in the NASA low-speed centrifugal compressor
[NASA-TP-3527] p 618 N95-31985
- A nonlinear vortex lattice method for unsteady flow with separated vortex
[DLR-FB-94-32] p 704 N95-32787
- Numerical simulation of supersonic flow using a new analytical bleed boundary condition
[NASA-CR-198368] p 697 N95-33208
- Water model tests on the Allison T56 series 3 combustion system
[DSTO-TR-0139] p 697 N95-33250
- A study of supersonic mixing flow field with ramp injector p 706 N95-34512
- Calculation of supersonic combustion in SCRAMJET engines p 698 N95-34513
- An LDV investigation of support structure influence on the flow field near the wingtip of a STOLV configuration in hover
[AD-A294126] p 686 N95-34750
- Subscale study of engine bellmouth inlet vortices in test cell R1D
[AD-A294993] p 707 N95-34818

FLOW EQUATIONS

- Analysis of flow channeling near the wall in packed beds
[HTN-94-00698] p 2 A95-60177
- Novel similarity solutions of the sonic small-disturbance equation with applications to airfoil transonic aerodynamics
[BTN-94-EIX94341340316] p 35 A95-60852
- High performance parallel analysis of coupled problems for aircraft propulsion
[NASA-CR-195355] p 23 N95-10132
- Control theory based airfoil design using the Euler equations
[NASA-CR-196360] p 36 N95-11884
- Steady potential solver for unsteady aerodynamic analyses p 141 N95-19382
- Application of Navier-Stokes code PAB3D with kappa-epsilon turbulence model to attached and separated flows
[NASA-TP-3480] p 224 N95-21338
- Model development for active control of stall phenomena in aircraft gas turbine engines p 514 N95-29679

FLOW GEOMETRY

- A survey of bidirectional greater than or equal to MeV ion flows during the Helios 1 and Helios 2 mission: Observations from the Goddard Space Flight Center instruments
[HTN-95-70542] p 237 A95-71656
- Numerical simulation of the flow about the F-18 HARV at high angle of attack
[NASA-CR-196396] p 9 N95-10940
- Elements of a modern turbomachinery design system p 90 N95-14129
- Application of multicomponent models to flow passage simulation in multistage turbomachines and whole gas turbine engines p 140 N95-19022

FLOW MEASUREMENT

- Oscillating airfoil compressible dynamic stall studies
[HTN-94-00704] p 3 A95-60183
- Measurement by coherent anti-Stokes Raman scattering in the R5Ch hypersonic wind tunnel
[BTN-95-EIX95112523811] p 188 A95-69322
- Vorticity concentration at the edge of the inboard vortex sheet
[HTN-95-31010] p 221 A95-71180
- Time-of-flight mass spectrometer for impulse facilities
[BTN-95-EIX95142553057] p 262 A95-73441
- Flow structure in the wake of a wishbone vortex generator
[BTN-95-EIX95142553044] p 304 A95-73454
- Real-time estimation of atmospheric turbulence severity from in-situ aircraft measurements
[BTN-95-EIX95182619231] p 319 A95-76657
- Quantitative comparison between interferometric measurements and Euler computations for supersonic cone flows
[BTN-95-EIX9522650782] p 358 A95-79238

- Observation of traveling waves in the three-dimensional boundary layer along a yawed cylinder
[HTN-95-61064] p 430 A95-83648
- Drag coefficients of spherical liquid droplets. Part 1: Quiescent gaseous fields
[BTN-95-EIX95262697040] p 538 A95-86857
- A review of free-stream flow fluctuation and steady-state flow quality measurements in the AEDC/VKF Supersonic Tunnel A and Hypersonic Tunnel B
[AIAA PAPER 95-6137] p 520 A95-90454
- The use of hot film for the investigation of boundary-layer transition
[CONGRESS PAPER C428-9-199] p 475 A95-91697
- Measurement in laminar and transitional boundary-layer flows on concave surface
[BTN-95-EIX95282711333] p 632 A95-92408
- Turbulent flow measurements with a triple-split hot-film probe
[HTN-95-A1774] p 634 A95-93337
- Laser velocimetry in the supersonic regime: Advancements, limitations, and outlook
[SAE PAPER 931365] p 634 A95-93646
- A new algorithm for five-hole probe calibration, data reduction, and uncertainty analysis
[NASA-TM-106458] p 38 N95-12378
- Impingement flow heat transfer measurements of turbine blades using a jet array
[AD-A283450] p 62 N95-12512
- Planar Rayleigh scattering and laser-induced fluorescence for visualization of a hot, Mach 2 annular air jet
[NASA-TM-4576] p 54 N95-13196
- Simultaneous three-dimensional velocity and mixing measurements by use of laser Doppler velocimetry and fluorescence probes in a water tunnel
[NASA-TP-3454] p 53 N95-13553
- Quality assessment for wind tunnel testing
[AGARD-AR-304] p 67 N95-14197
- Design and development of an F/A-18 inlet distortion rake: A cost and time saving solution p 69 N95-14241
- Mach number, flow angle, and loss measurements downstream of a transonic fan-blade cascade
[AD-A280907] p 108 N95-16824
- Detailed study at supersonic speeds of the flow around delta wings p 112 N95-17861
- Wall interference, Support Interference and Flow Field Measurements
[AGARD-CP-535] p 162 N95-19251
- The crucial role of wall interference, support interference and flow field measurements in the development of advanced aircraft configurations p 162 N95-19252
- Applications of the five-hole probe technique for flow field surveys at the Institute for Aerospace Research p 163 N95-19255
- Aerodynamic investigation of the flow field in a 180 deg turn channel with sharp bend p 163 N95-19257
- Experimental techniques for measuring transonic flow with a three dimensional laser velocimetry system. Application to determining the drag of a fuselage p 163 N95-19258
- Transonic and supersonic flowfield measurements about axisymmetric afterbodies for validation of advanced CFD codes p 121 N95-19260
- Transverse vorticity measurements in the NASA Ames 80 x 120 wind tunnel boundary layer p 251 N95-22457
- Impeller flow field characterization with a laser two-focus velocimeter p 313 N95-23440
- Supersonic quiet-tunnel development for laminar-turbulent transition research
[NASA-CR-198040] p 340 N95-24302
- Experiments on microbursts p 562 N95-29110
- Laser doppler velocimeter system for subsonic jet mixer nozzle testing at the NASA Lewis Aeroacoustic Propulsion Lab
[NASA-TM-106984] p 457 N95-30229
- Spatially-resolved velocity measurements in steady, high-speed, reacting flows using laser-induced OH fluorescence p 650 N95-32109

FLOW STABILITY

- Linear instability waves in supersonic jets confined in circular and non-circular ducts
[BTN-94-EIX94341340068] p 103 A95-63520
- Aspects of vortex breakdown
[HTN-95-A0001] p 183 A95-67828
- Tip vortex on a swept wing. Mean flow and unsteady phenomena
[BTN-94-EIX94441385755] p 184 A95-68219
- Numerical simulation of steady and unsteady, vorticity-dominated aerodynamic interference
[BTN-95-EIX95062487524] p 186 A95-69232
- Multiple instabilities of three-dimensional boundary layers along a concave wall p 429 A95-83487

- Screech tones from free and ducted supersonic jets
[HTN-95-51647] p 432 A95-85029
- Transition correlations in three-dimensional boundary layers
[HTN-95-51648] p 432 A95-85030
- Vortex cutting by a blade, part 1: General theory and a simple solution
[HTN-95-20822] p 543 A95-88083
- Nonlinear analysis of swept wing transitional boundary layers
[SAE PAPER 932515] p 466 A95-89188
- Instabilities originating from suction holes used for Laminar Flow Control (LFC)
[NASA-CR-196395] p 6 N95-10131
- Noise radiation by instability waves in coaxial jets
[NASA-TM-106738] p 100 N95-14618
- The stability of two-phase flow over a swept-wing
[NASA-CR-194994] p 159 N95-18190
- A time-accurate finite volume method valid at all flow velocities p 314 N95-23447
- Growth and development of roughness-induced stationary crossflow vortices p 482 N95-30294
- Nonlinear stability of unsteady viscous flow
[AD-A294931] p 707 N95-34597

FLOW THEORY

- Hypersonic flow simulation with thermoelectric effect p 368 A95-82669
- Robust fixed-structure control
[AD-A286515] p 257 N95-22216
- Robust fixed-structure control
[AD-A292883] p 679 N95-30961
- FLOW VELOCITY**
- Flow structure in the wake of a wishbone vortex generator
[BTN-95-EIX95142553044] p 304 A95-73454
- Simulation of turbulent fluctuations
[BTN-95-EIX95142553041] p 304 A95-73457
- Effects of expansions on a supersonic boundary layer: Surface pressure measurements
[BTN-95-EIX95142553036] p 263 A95-73462
- Supersonic axisymmetric conical flow solutions for different ratios of specific heats p 306 A95-73584
- Real-time estimation of atmospheric turbulence severity from in-situ aircraft measurements
[BTN-95-EIX95182619231] p 319 A95-76657
- On the influence of time-varying flow velocity on unsteady aerodynamics p 369 A95-83657
- Numerical investigation of cylinder wake flow with a rear stagnation jet
[HTN-95-51669] p 433 A95-85051
- Development of a large-aspect-ratio rectangular turbulent free jet
[HTN-95-42333] p 372 A95-86162
- Laser velocimetry in the supersonic regime: Advancements, limitations, and outlook
[SAE PAPER 931365] p 634 A95-93646
- Controlling mechanisms of ignition of solid fuel in a sudden-expansion combustor
[BTN-95-EIX0616952745791] p 628 A95-94255
- Numerical investigation of high incidence flow over a double-delta wing
[BTN-95-EIX0619952748160] p 588 A95-94454
- Quantifiable vortex features of F-106B aircraft at subsonic speeds
[BTN-95-EIX0619952748161] p 588 A95-94455
- Spectral mapping of quasiperiodic structures in a vortex flow
[BTN-95-EIX0619952748165] p 589 A95-94459
- Correlation of unsteady pressure and inflow velocity fields of a pitching rotor blade
[BTN-95-EIX0619952748169] p 589 A95-94463
- Evaluation of the transient operation of advanced gas turbine combustors
[BTN-95-EIX0616952745793] p 614 A95-94495
- Simultaneous three-dimensional velocity and mixing measurements by use of laser Doppler velocimetry and fluorescence probes in a water tunnel
[NASA-TP-3454] p 53 N95-13553
- Phase 2: HGM air flow tests in support of HEX vane investigation p 312 N95-23438
- Impeller flow field characterization with a laser two-focus velocimeter p 313 N95-23440
- A time-accurate finite volume method valid at all flow velocities p 314 N95-23447
- An investigation of the AFIT 2-inch shock tube as a flow source for supersonic testing
[AD-A289246] p 412 N95-26966
- NASA Dryden flow visualization facility
[NASA-TM-4631] p 449 N95-27914
- Navier-Stokes solution of wing wake structure and its perturbation p 479 N95-29121
- The decay of longitudinal vortices shed from airfoil vortex generators
[NASA-CR-198356] p 480 N95-29402

- Unsteady pressure and inflow velocity on a pitching rotor blade in hover p 480 N95-29771
- Laser anemometer measurements of the three-dimensional rotor flow field in the NASA low-speed centrifugal compressor [NASA-TP-3527] p 618 N95-31985
- FLOW VISUALIZATION**
- Suppression of vortex asymmetry and side force on a circular cone [BTN-95-EIX95042474413] p 209 A95-68287
- Vorticity concentration at the edge of the inboard vortex sheet [HTN-95-31010] p 221 A95-71180
- Flow visualization studies on sidewall effects in two-dimensional transonic airfoil testing [BTN-95-EIX95152582313] p 264 A95-73516
- Experimental investigation of the flowfield about an upswep afterbody [BTN-95-EIX95152582321] p 265 A95-73524
- Simple method of supersonic flow visualization using watertable [BTN-95-EIX95182619105] p 269 A95-76590
- Aerodynamic characteristics of external store configurations at low speeds [BTN-95-EIX95182619230] p 271 A95-76656
- Hypersonic wind tunnel test of sidewall compression type scramjet inlet p 410 A95-82320
- Measurements of vortex pair interaction with a clean or contaminated free surface [BTN-94-EIX95011441063] p 429 A95-82798
- Effects of time scales on lift of airfoils in an unsteady stream [HTN-95-81643] p 542 A95-87691
- Aerodynamic investigation with focusing schlieren in a cryogenic wind tunnel [HTN-95-20835] p 544 A95-88096
- A note on the interpretation of mini-tuft photographs [HTN-95-01089] p 468 A95-90275
- Preliminary results from a particle image velocimetry study of blade-vortex interaction [HTN-95-01098] p 547 A95-90284
- An experimental investigation of forward-swept wings at low Reynolds numbers [SAE PAPER 931370] p 604 A95-93650
- Directional control at high angles of attack using blowing through a chined forebody [BTN-95-EIX0619952748179] p 619 A95-94472
- Performance variation of scramjet nozzle at various nozzle pressure ratios [BTN-95-EIX0616952745781] p 615 A95-94505
- LDV measurements in separated flow on an elliptic wing mounted at an angle of attack on a wall [BTN-94-EIX94441380518] p 702 A95-96559
- Proceeding towards hypervelocities in ram accelerators p 19 N95-10285
- Control of wind tunnel operations using neural net interpretation of flow visualization records [NASA-TM-106683] p 24 N95-10854
- Flow-visualization study of the X-29A aircraft at high angles of attack using a 1/48-scale model [NASA-TM-104268] p 8 N95-10858
- Computer-aided light sheet flow visualization using photogrammetry [NASA-TP-3416] p 26 N95-10859
- A shadowgraph study of the National Launch System's 1 1/2 stage vehicle configuration and Heavy Lift Launch Vehicle configuration — Using the Marshall Space Flight Center's 14-Inch Trisonic Wind Tunnel [NASA-RP-1347] p 35 N95-11710
- Water tunnel flow visualization study of a 4.4 percent scale X-31 forebody [NASA-TM-104276] p 36 N95-11898
- Planar Rayleigh scattering and laser-induced fluorescence for visualization of a hot, Mach 2 annular air jet [NASA-TM-4576] p 54 N95-13196
- Simultaneous three-dimensional velocity and mixing measurements by use of laser Doppler velocimetry and fluorescence probes in a water tunnel [NASA-TP-3454] p 53 N95-13553
- Numerical simulation of the flow about an F-18 aircraft in the high-alpha regime p 68 N95-14232
- Free-to-roll tests of X-31 and F-18 subscale models with correlation to flight test results p 69 N95-14237
- An optical technique for examining aircraft shock wave structures in flight p 96 N95-14879
- Gas turbine prediffuser-combustor performance during operation with air-water mixture [DOT/FAA/CT-93/52] p 83 N95-15683
- Two-dimensional scramjet inlet unstart model: Wind-tunnel blockage and actuation systems test [NASA-TM-109984] p 97 N95-15899
- In-flight imaging of transverse gas jets injected into transonic and supersonic crossflows: Design and development [NASA-CR-186031] p 157 N95-17418
- Subsonic flow around US-orbiter model FALKE in the DNW p 115 N95-17877
- Overview of unsteady transonic wind tunnel test on a semispan straked delta wing oscillating in pitch [AD-A284097] p 117 N95-18380
- Hypersonic flow-field measurements: Intrusive and nonintrusive [AD-A283867] p 119 N95-18674
- Static investigation of two fluidic thrust-vectoring concepts on a two-dimensional convergent-divergent nozzle [NASA-TM-4574] p 120 N95-19042
- The crucial role of wall interference, support interference and flow field measurements in the development of advanced aircraft configurations p 162 N95-19252
- The utilization of a high speed reflective visualization system in the study of transonic flow over a delta wing p 121 N95-19259
- Effect of juncture fillets on double-delta wings undergoing sideslip at high angles of attack [AD-A286165] p 232 N95-22039
- Experimental investigations of on-demand vortex generators p 250 N95-22451
- Flow visualization studies of VTOL aircraft models during Hover in ground effect [NASA-TM-108860] p 272 N95-22666
- Experimental results for a hypersonic nozzle/afterbody flow field [NASA-TM-4638] p 274 N95-23250
- Exploratory flow visualization investigation of mast-mounted sights in presence of a rotor [NASA-TM-4634] p 330 N95-24566
- Plate manipulators [AD-A289601] p 374 N95-26719
- Visualization of the multiple supersonic jet oscillations by swept focused strobed schlieren technique p 367 N95-26952
- NASA Dryden flow visualization facility [NASA-TM-4631] p 449 N95-27914
- Measurements of store forces and moments and cavity pressures for a generic store in and near a box cavity at subsonic and transonic speeds [NASA-TM-4611] p 378 N95-28241
- Demonstration of an automated CFD system for three-dimensional flow simulations p 551 N95-28767
- Investigation of wing upper surface flow-field disturbance due to NASA DC-8-72 in-flight inboard thrust-reverser deployment [NASA-TM-110351] p 457 N95-28816
- A nonintrusive method of quantifying flow visualization data in vortex flow fields [AD-A289802] p 552 N95-28948
- Experiments on microbursts p 562 N95-29110
- Research instrumentation for polytechnic university's supersonic wind tunnel facility [AD-A290232] p 523 N95-29468
- Air/fuel ratio visualization in a diesel spray p 556 N95-29807
- Analysis of planar laser-induced fluorescence images obtained during shakedown testing of the AEDC impulse facility [AD-A293237] p 646 N95-30906
- Patterns in the sky: Natural visualization of aircraft flow fields [NASA-SP-514] p 584 N95-31000
- An investigation of the side-dump dual in-line ramjet combustor p 617 N95-31199
- Subscale study of engine bellmouth inlet vortices in test cell R1D [AD-A294993] p 707 N95-34818
- FLOWMETERS**
- New sensor technology for aircraft hydraulic system diagnostics [SAE PAPER 932586] p 494 A95-90070
- Lightweight high-temperature fuel metering valves [SAE PAPER 931444] p 635 A95-93693
- FLUID BOUNDARIES**
- Predicting exhaust plume boundaries with supersonic external flows [BTN-95-EIX95152583258] p 297 A95-73559
- FLUID DYNAMICS**
- Solution-adaptive structured-unstructured grid method for unsteady turbomachinery analysis. Part I: Methodology [BTN-94-EIX94441380983] p 208 A95-67329
- Rotating Kirchhoff method for three-dimensional transonic blade-vortex interaction hover noise [BTN-94-EIX94441386601] p 182 A95-67332
- Supersonic and hypersonic shock/boundary-layer interaction database [BTN-94-EIX94441386604] p 182 A95-67335
- Possible effects of CO2 increase on the high-speed civil transport impact on ozone [HTN-95-60779] p 317 A95-75976
- Transport of exhaust products in the near trail of a jet engine under atmospheric conditions [HTN-95-91421] p 319 A95-77334
- Numerical analysis of flow field around gas rudder p 407 A95-82333
- Rarefied gas numerical wind tunnel: OREX and HOPE p 427 A95-82391
- A study on aerodynamic heating phenomena in three-dimensional shock wave/turbulent boundary layer interaction induced by sweptback sharp fins at supersonic flow p 428 A95-82419
- Force and moment on a Joukowski profile in the presence of point vortices [BTN-95-EIX95262694298] p 434 A95-85469
- Determining unsteady 2D AND 3D boundary layer separation p 462 A95-88898
- Theories of turbulent combustion in high speed flows [AD-A280933] p 23 N95-10535
- Agglomeration multigrid for viscous turbulent flows [AD-A284064] p 8 N95-10848
- Evaluation of alternative in-flight fire suppressants for full-scale testing in simulated aircraft engine nacelles and dry bays [PB94-203403] p 42 N95-13247
- Unsteady flow phenomena in discrete passage diffusers for centrifugal compressors [AD-A281412] p 155 N95-16163
- An analysis code for the Rapid Engineering Estimation of Momentum and Energy Losses (REMEL) [NASA-CR-191178] p 108 N95-16887
- Computation of vortex breakdown p 165 N95-19462
- Description and flow characterization of hypersonic facilities [AD-A284291] p 223 N95-20248
- Turbine design and application volumes 1, 2, and 3 [E-5666-Vol-1-3] p 236 N95-22341
- High-lift flow-physics flight experiments on a subsonic civil transport aircraft (B737-100) p 275 N95-23333
- A non-iterative grid deformation algorithm for computational fluid dynamics for aeroelasticity [AD-A288298] p 436 N95-26418
- Demonstration study of hierarchical control of fluid-dynamic phenomena [AD-A289341] p 437 N95-26751
- Basic studies in turbulent shear flows [AD-A289145] p 437 N95-26998
- Analyzing the stability of floating ice floes [AD-A292149] p 563 N95-29160
- FLUID FILMS**
- Characterization of annular two-phase gas-liquid flows in microgravity p 95 N95-14556
- Wormgear geometry adopted for implementing hydrostatic lubrication and formulation of the lubrication problem [AD-A290331] p 210 N95-19567
- Thermohydrodynamic analysis of cryogenic liquid turbulent flow fluid film bearings, phase 2 [NASA-CR-197412] p 349 N95-24461
- Transport phenomena and interfacial kinetics in multiphase combustion systems [AD-A288297] p 418 N95-26417
- FLUID FILTERS**
- Hydraulic system diagnostic sensors [BTN-95-EIX95031502752] p 209 A95-68259
- Gas chromatography/ion mobility spectrometry as a hyphenated technique for improved explosives detection and analysis p 701 N95-33278
- FLUID FLOW**
- New approach to geometric profiling of the design elements of the passage part in turbo-machines [BTN-94-EIX94461408769] p 153 A95-63652
- Experimental investigation of the flow around a circular cylinder: Influence of aspect ratio [BTN-94-EIX95011441120] p 347 A95-80044
- Experimental investigation of composite channel heat pipe operation in micro-gravity environment p 428 A95-82645
- Pressure and temperature distortion testing of a two-stage centrifugal compressor [BTN-94-EIX95011441250] p 431 A95-84207
- Condensation in jet engine intake ducts during stationary operation [BTN-95-EIX95292721154] p 612 A95-92590
- Numerical investigation of high incidence flow over a double-delta wing [BTN-95-EIX0619952748160] p 588 A95-94454
- Efficient mapping topology for turbine combustors with inclined slots/staggered holes [BTN-95-EIX0616952745805] p 614 A95-94485
- High performance parallel analysis of coupled problems for aircraft propulsion [NASA-CR-195355] p 23 N95-10132
- Hydrofoil force balance [AD-D016475] p 160 N95-18461

- Computation of vortex breakdown
 Application of Direct and Large Eddy Simulation to Transition and Turbulence [AGARD-CP-551] p 165 N95-19462
 Holographic interferometric tomography for reconstructing flow fields Phase 2: HGM air flow tests in support of HEX vane investigation A time-accurate finite volume method valid at all flow velocities The acoustic characteristics of turbomachinery cavities [NASA-CR-4671] p 248 N95-21061 p 310 N95-23287 p 312 N95-23438 p 314 N95-23447 p 476 N95-28720 p 476 N95-28743 p 556 N95-29807
 Computational methods for control and optimal design of aerospace systems [AD-A292861] p 608 N95-31451
- FLUID JETS**
 Jet mixing in a reacting cylindrical crossflow [NASA-TM-106975] p 616 N95-30853
- FLUID MECHANICS**
 Fundamental investigation of composite channel heat pipe operation in micro-gravity environment An introduction to generalized functions with some applications in aerodynamics and aeroacoustics Laws of infrared similitude Activities of the Institute for Aerospace Studies of Toronto University Aeromechanics technology, volume 1. Task 1: Three-dimensional Euler/Navier-Stokes Aerodynamic Method (TEAM) enhancements [AD-A285713] NASA-UVA light aerospace alloy and structures technology program (LA2ST) [NASA-CR-198041] JPRS report: Science and technology, Central Eurasia [JPRS-UST-94-018] p 428 A95-82645 p 565 A95-88895 p 62 N95-12426 p 63 N95-12699 p 132 N95-18483 p 343 N95-24220 p 349 N95-24472
- FLUID PRESSURE**
 Hydraulic system diagnostic sensors Two-dimensional viscous flow past a flat plate Analyzing the stability of floating ice floes [AD-A292149] [BTN-95-EIX95031502752] [HTN-95-42210] p 209 A95-68259 p 430 A95-84026 p 563 N95-29160
- FLUID-SOLID INTERACTIONS**
 Review of numerical procedures for computational surface thermochemistry Interaction of a streamwise vortex with a thin plate: A source of turbulent buffeting Structural acoustic calculations in the low-frequency range On the role of the outer region in the turbulent-boundary-layer bursting process Parameters of Nocilla gas/surface interaction model from measured accommodation coefficients High frequency flow-structural interaction in dense subsonic fluids [NASA-CR-4652] [BTN-94-EIX94441386682] [BTN-95-EIX95042474398] [HTN-95-EIX95152582336] [BTN-94-EIX95011441078] [HTN-95-81639] [NASA-CR-197756] [NASA-CR-198367] p 205 A95-68191 p 209 A95-68302 p 323 A95-73538 p 348 A95-81056 p 541 A95-87687 p 330 N95-24217
- FLUIDICS**
 Static investigation of two fluidic thrust-vectoring concepts on a two-dimensional convergent-divergent nozzle Static investigation of two fluidic thrust-vectoring concepts on a two-dimensional convergent-divergent nozzle [NASA-TM-4574] p 120 N95-19042 p 222 N95-19913
- FLUORESCENCE**
 Simultaneous three-dimensional velocity and mixing measurements by use of laser Doppler velocimetry and fluorescence probes in a water tunnel [NASA-TP-3454] p 53 N95-13553
- FLUOROCARBONS**
 Evaluation of alternative in-flight fire suppressants for full-scale testing in simulated aircraft engine nacelles and dry bays [PB94-203403] p 42 N95-13247
- FLUTTER**
 H(sup 2)/H(sup INF) controller design for a two-dimensional thin airfoil flutter suppression [BTN-94-EIX94511433918] Comparison of theory and experiment for non-linear flutter and stall response of a helicopter blade [BTN-94-EIX94351108100] p 141 A95-64584 p 191 A95-66500
- Influence of structural and aerodynamic modeling on flutter analysis [BTN-95-EIX95062487550] Postinstability behavior of a two-dimensional airfoil with a structural nonlinearity [BTN-95-EIX95152582337] Flutter of an infinitely long panel in a duct [BTN-95-EIX95182619087] Multirate flutter suppression system design for a model wing [BTN-95-EIX95182619132] Summary of an active flexible wing program [BTN-95-EIX95182619209] Multiple-function digital controller system for active flexible wing wind-tunnel model [BTN-95-EIX95182619212] Flutter suppression control law design and testing for the active flexible wing [BTN-95-EIX95182619214] Flutter suppression for the active flexible wing: A classical design [BTN-95-EIX95182619216] Aeroelastic stability of hingeless rotor blade in hover using large deflection theory [HTN-95-20952] Buffeting tests in a cryogenic windtunnel [HTN-95-92833] Effects of structural damping on aeroelastic stability of various shaped composite plate wing Aeroservoelastic coupling on the UF-104 aircraft Preliminary tests of a transonic flutter control wing model Supersonic flutter analysis of cantilevered composite plate-wings Experience control systems/structural coupling BAe Warton flight in aero-servo elasticity [CONGRESS PAPER C428-35-059] The use of the Regier number in the structural design with flutter constraints [NASA-TM-109128] A computational investigation of wake-induced airfoil flutter in incompressible flow and active flutter control [AD-A281534] Flutter analysis of composite box beams [NASA-CR-197931] Aeroelasticity of wing and wing-body configurations on parallel computers [NASA-CR-197756] Nonlinear dynamics and aeroelasticity of rotorcraft in forward flight [AD-A291714] FPCAS3D User's guide: A three dimensional full potential aeroelastic program, version 1 [NASA-CR-198367] p 203 A95-68364 p 266 A95-73539 p 291 A95-75772 p 292 A95-76609 p 283 A95-76635 p 322 A95-76638 p 292 A95-76640 p 292 A95-76642 p 546 A95-88991 p 470 A95-90751 p 530 A95-91530 p 517 A95-91561 p 499 A95-91566 p 499 A95-91567 p 610 A95-93628 p 13 N95-11465 p 142 N95-16109 p 294 N95-23392 p 389 N95-26590 p 400 N95-28504 p 651 N95-32205
- FLUTTER ANALYSIS**
 Field-consistent element applied to flutter analysis of circular cylindrical shells [BTN-94-EIX94341341971] Engineering methods for the evaluation of transonic flutter characteristics for aerodynamic control surfaces [BTN-94-EIX94461408589] Finite element time domain - modal formulation for nonlinear flutter of composite panels [BTN-95-EIX95042474401] Influence of structural and aerodynamic modeling on flutter analysis [BTN-95-EIX95062487550] Application of transonic small disturbance theory to the active flexible wing model [BTN-95-EIX95182619210] Aeroelastic stability of cascades in turbomachinery [HTN-95-61156] Eigenanalysis of unsteady flows about airfoils, cascades, and wings [HTN-95-42582] Flutter analysis of supersonic axial flow cascades using a high resolution Euler solver. Part 1: Formulation and validation [NASA-TM-105798] A computational investigation of wake-induced airfoil flutter in incompressible flow and active flutter control [AD-A281534] Flutter analysis of composite box beams [NASA-CR-197931] Fundamental wind tunnel experiments on low-speed flutter of a tip-fin configuration wing [NAL-TR-1228] Flutter clearance flight tests of an OV-10A airplane modified for wake vortex flight experiments [NASA-TM-109168] FPCAS3D User's guide: A three dimensional full potential aeroelastic program, version 1 [NASA-CR-198367] p 56 A95-60871 p 141 A95-63064 p 203 A95-68299 p 203 A95-68364 p 270 A95-76636 p 405 A95-86255 p 459 A95-87212 p 23 N95-10244 p 142 N95-16109 p 332 N95-25762 p 366 N95-26381 p 651 N95-32205
- FLUX DENSITY**
 Multigrad solution for the compressible Euler equations by an implicit characteristic-flux-averaging Active minimization of energy density in three-dimensional enclosures [NASA-CR-197213] p 642 A95-95459 p 172 N95-16848
- FLUX DIFFERENCE SPLITTING**
 An aerodynamic and static-stability analysis of the Hypersonic Applied Research Technology (HART) missile [DA9426923] Role of computational fluid dynamics in aeronautical engineering, Number 12: Formulation and verification of uni-particle upwind schemes for the Euler equations p 481 N95-29965 p 707 N95-34540
- FLUX VECTOR SPLITTING**
 Implicit upwind-Euler solution algorithms for unstructured-grid applications p 641 A95-95454
- FLY BY LIGHT CONTROL**
 Fiber-optic technology for transport aircraft [BTN-94-EIX94511309384] Fly-By-Light/Power-By-Wire Requirements and Technology Workshop [NASA-CP-10108] Fiber Optic Control System integration for advanced aircraft. Electro-optic and sensor fabrication, integration, and environmental testing for flight control systems: Laboratory test results [NASA-CR-195408] Fiber Optic Control System integration for advanced aircraft. Electro-optic and sensor fabrication, integration, and environmental testing for flight control systems [NASA-CR-191194] p 103 A95-64610 p 12 N95-10245 p 162 N95-19236
- FLY BY WIRE CONTROL**
 Flight control system mode transitions influence on handling qualities and task performance [BTN-95-EIX95062487525] Development of Fly-By-Wire system for BK117 Load alleviation for civil transport aircraft [CONGRESS PAPER C428-35-057] ASTRA - A safe, simplex, fly-by-wire aircraft control system [CONGRESS PAPER C428-37-218] Dryden and transonic research [NASA-TM-104281] The development of a highly reliable power management and distribution system for civil transport aircraft [NASA-TM-106897] Development of a bipolar lead/acid battery for the more electric aircraft [AD-A284050] NASA develops new digital flight control system [NASA-NEWS-RELEASE-94-47] Evaluation of all-electric secondary power for transport aircraft [NASA-CR-189077] SCARLET: DLR rate saturation flight experiment Model following control for tailoring handling qualities: ACT experience with ATHeS Digital autopilot design for combat aircraft in ALENIA Advanced flight control technology achievements at Boeing Helicopters [NASA-TM-106897] p 203 A95-69233 p 516 A95-91506 p 604 A95-93627 p 610 A95-93634 p 1 N95-10709 p 50 N95-11867 p 160 N95-18660 p 144 N95-19029 p 441 N95-27999 p 598 N95-31068 p 622 N95-32000 p 623 N95-32009 p 624 N95-32014
- FLYING PLATFORMS**
 CALIOPE and TAISIR airborne experiment platform [DE94-018328] p 250 N95-22299
- FLYWHEELS**
 A hybrid vehicle evaluation code and its application to vehicle design. Revision 1 [DE95-008053] p 441 N95-28029
- FOAMS**
 Analysis of test criteria for specifying foam firefighting agents for aircraft rescue and firefighting [AD-A286381] Design and evaluation of a foam-filled hat-stiffened panel concept for aircraft primary structural applications [NASA-TM-109175] The effect of wear on fire-blocking layer material effectiveness [AD-A291520] p 227 N95-22352 p 346 N95-26251 p 485 N95-29855
- FOG**
 MEMFOG - The Memphis fog algorithm Analysis of rapidly developing fog at the Kennedy Space Center Assessment of the benefits for improved terminal weather information The mm-wave resonant methods for the detection of corrosion, phase 1 [AD-A291315] p 668 A95-93516 p 671 A95-93531 p 673 A95-93540 p 556 N95-29941

FOIL BEARINGS

- Foil bearings for gas turbine engines
[BTN-94-EIX94461290279] p 82 A95-61732
- Dynamic stiffness and damping of foil bearings for gas turbine engines
[SAE PAPER 931449] p 635 A95-93698
- Influence of backup bearings and support structure dynamics on the behavior of rotors with active supports
[NASA-CR-197438] p 310 N95-23190

FOLDING STRUCTURES

- Design and analysis of a telescopic wing
[SAE PAPER 932605] p 495 A95-90075

FOLIAGE

- Foliage transmission measurements using a ground-based ultrawide band (300-1300 MHz) SAR system
[BTN-94-EIX94381351617] p 252 A95-70950

FORCE DISTRIBUTION

- Free-to-roll tests of X-31 and F-18 subscale models with correlation to flight test results p 69 N95-14237
- 2-D aileron effectiveness study p 110 N95-17851
- Hydrofoil force balance
[AD-D016475] p 160 N95-18461
- Thrust measurements of a complete axisymmetric scramjet in an impulse facility p 339 N95-25395
- Balances for the measurement of multiple components of force in flows of a millisecond duration p 350 N95-25400

FORCED CONVECTION

- Convection heat transfer distributions over plates with square ribs from infrared thermography measurements
[HTN-95-20713] p 435 A95-86603
- A computer code (SKINTEMP) for predicting transient missile and aircraft heat transfer characteristics
[AD-A286044] p 248 N95-21001

FORCED VIBRATION

- Forced response of mistuned bladed disks p 141 N95-19383
- Dynamical systems as models for flow-induced vibrations
[PB95-206991] p 647 N95-30956

FOREBODIES

- Aeroacoustic probe design for microphone to reduce flow-induced self-noise
[AIAA PAPER 93-4343] p 19 A95-60163
- Experimental and computational results for the external flowfield of a scramjet inlet
[BTN-94-EIX94441380977] p 195 A95-68161
- Passive porosity with free and fixed separation on a tangent-ogive forebody
[BTN-95-EIX95062487554] p 185 A95-68368
- Aerodynamically blunt and sharp bodies
[BTN-95-EIX95041503781] p 205 A95-69212
- Forebody flow control on a full-scale F/A-18 aircraft
[BTN-95-EIX95152582333] p 281 A95-73535
- Convective and radiative heat transfer analysis for the fire 2 forebody
[BTN-95-EIX95182617460] p 268 A95-75731
- Review and development of base pressure and base heating correlations in supersonic flow
[BTN-95-EIX95212645688] p 271 A95-76740
- Surface interference in Rayleigh scattering measurements near forebodies
[HTN-95-51670] p 433 A95-85052
- Actuated forebody strake controls for the F-18 High-Alpha Research Vehicle
[BTN-95-EIX0619952748173] p 619 A95-94467
- Computational analysis of forebody tangential slot blowing on the high alpha research vehicle
[NASA-CR-196750] p 10 N95-11367
- High-angle-of-attack yawing moment asymmetry of the X-31 aircraft from flight test
[NASA-CR-186030] p 13 N95-11410
- Water tunnel flow visualization study of a 4.4 percent scale X-31 forebody
[NASA-TM-104276] p 36 N95-11898
- Numerical analysis of tangential slot blowing on a generic chined forebody
[NASA-TM-108845] p 37 N95-11927
- High Alpha Technology Program (HATP) ground test to flight comparisons p 68 N95-14230
- Fourth High Alpha Conference, volume 3
[NASA-CP-10143-VOL-3] p 71 N95-14251
- Computational analysis of forebody tangential slot blowing p 71 N95-14253
- F/A-18 and F-16 forebody vortex control, static and rotary-balance results p 72 N95-14254
- Comparison of full-scale, small-scale, and CFD results for F/A-18 forebody slot blowing p 72 N95-14255
- Low-energy pneumatic control of forebody vortices p 72 N95-14256
- Preparations for flight research to evaluate actuated forebody strakes on the F-18 high-alpha research vehicle p 72 N95-14257
- Integration of a mechanical forebody vortex control system into the F-15 p 72 N95-14258

- Flight evaluation of pneumatic forebody vortex control in post-stall flight p 72 N95-14259
- Aerodynamic surface distension system for high angle of attack forebody vortex control
[NASA-CASE-ARC-11979-1] p 286 N95-23390
- Experimental study of the effects of Reynolds number on high angle of attack aerodynamic characteristics of forebodies during rotary motion
[NASA-CR-195033] p 330 N95-24443
- Computational analysis of forebody tangential slot blowing on the high alpha research vehicle
[NASA-CR-197754] p 389 N95-26591
- Computational methods for control and optimal design of aerospace systems p 608 N95-31451
- Flight evaluation of forebody vortex control in post-stall flight p 609 N95-32003

FORECASTING

- Radar studies of aviation hazards
[AD-A285845] p 226 N95-21831
- Patient/aircraft forecasting for the strategic aeromedical evacuation lift-bed process
[AD-A293902] p 599 N95-31512
- FAA aviation forecasts: Fiscal year 1995-2006
[AD-A293682] p 584 N95-31598

FOREIGN BODIES

- Erosion, Corrosion and Foreign Object Damage Effects in Gas Turbines
[AGARD-CP-558] p 197 N95-19653

FOREST FIRES

- Mapping of forest fire damages using imaging spectroscopy p 442 A95-83627

FORESTS

- Foliage transmission measurements using a ground-based ultrawide band (300-1300 MHz) SAR system
[BTN-94-EIX94381351617] p 252 A95-70950

FORGING

- Trends in aerospace forgings in the 1990s
[HTN-95-B0408] p 456 A95-90756

FORM FACTORS

- Nonlinear bulging factor based on R-curve data p 94 N95-14476
- Ultra-Reliable Digital Avionics (URDA) processor p 245 N95-20638

FORMAT

- Programmable cockpit research simulator
[AD-A279219] p 204 N95-19848
- FASTPACK: Optimized solutions for modular avionics derived from a parametric study. Part 2: Avionics p 233 N95-20635
- An evaluation of Automatic Terminal Information Service (ATIS) flight deck display presentation options
[AD-A280100] p 228 N95-21020

FORMING TECHNIQUES

- Forming and bonding techniques for high-strength aluminum alloys
[HTN-95-20605] p 418 A95-84786
- Advanced method and processing technology for complicated shape airframe part forming p 80 N95-14486

FORTRAN

- Buckling and vibration analysis of laminated panels using VICONOPT
[PAPER-1746] p 230 A95-72580
- Applications of automatic differentiation in computational fluid dynamics p 156 N95-16461

FORWARD SCATTERING

- The performance of forward scatter visibility sensors for application in autostations and runway visual range in snow and freezing precipitation events p 662 A95-93489

FOURIER ANALYSIS

- Aerodynamic parameter estimation via Fourier modulating function techniques
[NASA-CR-4654] p 335 N95-24630

FOURIER SERIES

- Compression strength of composite primary structural components
[NASA-CR-197554] p 160 N95-18388
- Load transfer in the stiffener-to-skin joints of a pressurized fuselage
[NASA-CR-198610] p 439 N95-27865

FOURIER TRANSFORMATION

- Two-variable method for blockage wall interference in a circular tunnel
[BTN-95-EIX95062487540] p 187 A95-69248
- Electrochemical impedance pattern recognition for detection of hidden chemical corrosion on aircraft components, phase 1
[AD-A291345] p 556 N95-29946
- Standardization of surface contamination analysis systems p 631 N95-31798

FOURIER-BESSEL TRANSFORMATIONS

- Apparatus and method for producing three-dimensional images
[AD-D017455] p 646 N95-30727

FRACTALS

- Fractal properties of whitecaps
[HTN-95-92121] p 443 A95-83827

FRACTOGRAPHY

- The characterization of widespread fatigue damage in fuselage structure p 166 N95-19472
- Thermal-mechanical fatigue crack growth in aircraft engine materials
[ISBN-0-315-86543-1] p 647 N95-31098

FRACTURE MECHANICS

- Analytical developments in support of the NASA aging aircraft program with an application to crack growth from rivets
[SAE PAPER 931223] p 545 A95-88789
- The role of material behaviour modelling in stressing and life assessment of modern Aero-engine components
[CONGRESS PAPER C428-27-127] p 612 A95-93606

- Structural integrity of fuselage panels with multisite damage
[BTN-95-EIX0619952748188] p 637 A95-94250
- Modeling and life prediction methodology for Titanium Matrix Composites subjected to mission profiles
[NASA-TM-109148] p 55 N95-11915

- Fatigue in single crystal nickel superalloys
[AD-A283459] p 56 N95-12546
- Computational predictive methods for fracture and fatigue p 93 N95-14466

- Influence of crack history on the stable tearing behavior of a thin-sheet material with multiple cracks p 93 N95-14467

- Development of the NASA/FLAGRO computer program for analysis of airframe structures p 94 N95-14473
- Fracture mechanics validity limits p 95 N95-14480
- Challenges for the aircraft structural integrity program p 80 N95-14481

- Fatigue in single crystal nickel superalloys
[AD-A282917] p 88 N95-15415

- FAA/NASA International Symposium on Advanced Structural Integrity Methods for Airframe Durability and Damage Tolerance, part 2 p 124 N95-19468

- The application of Newman crack-closure model to predicting fatigue crack growth p 167 N95-19483
- Tension fracture of laminates for transport fuselage. Part 2: Large notches p 532 N95-28837

FRACTURE STRENGTH

- Fatigue resistance of peened 7050-T7451 aluminium alloy: Repair and re-treatment of a component surface
[BTN-94-EIX94371347838] p 206 A95-69131
- Status and prospects for aluminium-lithium alloys in aircraft structures p 387 A95-85893

- Multi-lab comparison on R-curve methodologies: Alloy 2024-T3 p 151 N95-16860

- A CMC database for use in the next generation launch vehicles (rockets) p 150 N95-18993

- Prediction of R-curves from small coupon tests p 167 N95-19496

FRACTURES (MATERIALS)

- Detecting gear tooth fracture in a high contact ratio face gear mesh
[NASA-TM-106822] p 162 N95-19125

FRACTURING

- Multi-lab comparison on R-curve methodologies: Alloy 2024-T3 p 151 N95-16860

- Thermal fracture mechanisms in ceramic thermal barrier coatings p 346 N95-26138

- Tension fracture of laminates for transport fuselage. Part 1: Material screening p 398 N95-28471

- Design, analysis, and fabrication of a pressure box test fixture for tension damage tolerance testing of curved fuselage panels p 533 N95-28839

- Failure analysis for polycarbonate transparencies
[AD-A292992] p 630 N95-31471

FRAGMENTATION

- Quantity-distance requirements for earth-bermed aircraft shelters
[AD-A279692] p 341 N95-24424

FRAGMENTS

- Rationale for the Modular Air-system Vulnerability Estimation Network (MAVEN) methodology
[AD-A285797] p 284 N95-22510

FRAMES

- Analysis of warping effects on the static and dynamic response of a seat-type structure
[NIAR-94-12] p 348 N95-24211

- Application of advanced material systems to composite frame elements p 422 N95-28432

- Effects of floor location on response of composite fuselage frames p 423 N95-28439

FREE CONVECTION

- Natural convection in central microcavities of vertical, finned enclosures of very high aspect ratios
[BTN-95-EIX95282711336] p 632 A95-92405

FREE FALL

- Hailstone heat and mass transfer measurements
[ISBN-0-315-86304-8] p 563 N95-29797
- FREE FLIGHT TEST APPARATUS**
The aerothermodynamic validation reentry experiment
HYPERBA p 524 A95-87380
Measurement of free-flight dynamic stability derivatives of cones in a hypersonic gun tunnel
[AIAA PAPER 95-6082] p 519 A95-87411
- FREE FLOW**
Jet to freestream velocity ratio computations for a jet in a crossflow
[AIAA PAPER 93-4860] p 2 A95-60178
Aerodynamic shape optimization using preconditioned conjugate gradient methods
[BTN-95-EIX95142553033] p 263 A95-73465
Unstructured grid solutions to a wing/pylon/store configuration
[BTN-95-EIX95152582322] p 265 A95-73525
Hypersonic nonequilibrium Navier-Stokes solutions over an ablating graphite nosetip
[BTN-95-EIX95152583252] p 305 A95-73553
Comparison of linear stability results with flight transition data
[BTN-95-EIX95182619097] p 283 A95-76582
On the influence of time-varying flow velocity on unsteady aerodynamics
[HTN-95-61073] p 369 A95-83657
Experimental investigation of the sources of propeller noise due to the ingestion of turbulence at low speeds
[BTN-95-EIX95262697042] p 569 A95-86859
Low Reynolds number laminar separation bubble control using a backward facing step
[SAE PAPER 932572] p 467 A95-90061
A review of free-stream flow fluctuation and steady-state flow quality measurements in the AEDC/VKF Supersonic Tunnel A and Hypersonic Tunnel B
[AIAA PAPER 95-6137] p 520 A95-90454
Turbulent effects on parachute drag
[BTN-95-EIX0619952748193] p 591 A95-94482
Interaction of a weak shock with freestream disturbances
[BTN-95-EIX95332750473] p 638 A95-94687
Measurements of pressure and thermal wakes in a transonic turbine cascade
[AD-A283464] p 38 N95-12548
Two-dimensional scramjet inlet unstart model: Wind-tunnel blockage and actuation systems test
[NASA-TM-109984] p 97 N95-15899
Investigation of the flow over a series of 14 percent-thick supercritical aerofoils with significant rear camber
p 109 N95-17849
OAT15A airfoil data p 111 N95-17857
Two-dimensional high-lift airfoil data for CFD code validation p 112 N95-17859
Exploratory flow visualization investigation of mast-mounted sights in presence of a rotor
[NASA-TM-4634] p 330 N95-24566
Influence of turbulence parameters, Reynolds number, and body shape on stagnation-region heat transfer
[NASA-TP-3487] p 550 N95-28719
Comparison of spatial numerical operators for duct-nozzle acoustics p 580 N95-30158
Numerical studies of turbulent free surface flows and unsteady propeller flows
[AD-A294377] p 706 N95-34343
- FREE JETS**
Main features of overexpanded triple jets
[BTN-95-EIX95142553040] p 304 A95-73458
Screech tones from free and ducted supersonic jets
[HTN-95-51647] p 432 A95-85029
Stochastic approach to noise modeling for free turbulent flows
[HTN-95-42321] p 371 A95-86150
Development of a large-aspect-ratio rectangular turbulent free jet
[HTN-95-42333] p 372 A95-86162
Axis switching and spreading of an asymmetric jet: Role of vorticity dynamics
[NASA-TM-106385] p 73 N95-14418
Flow field investigation in a free jet - free jet core system for the generation of high intensity molecular beams
[DLR-FB-94-11] p 172 N95-18912
Temperature effects on acoustic interactions between altitude test facilities and jet engine plumes
[NASA-CR-197638] p 258 N95-21170
Preliminary results and research capabilities of a new jet facility at the University of Kansas p 412 N95-26951
- FREE MOLECULAR FLOW**
Cercignani-Lampis-Lord gas-surface interaction model: Comparisons between theory and simulation
[BTN-95-EIX95041503806] p 242 A95-70131

FREE VIBRATION

- Influence of structural and aerodynamic modeling on flutter analysis
[BTN-95-EIX95062487550] p 203 A95-68364
- FREEZING**
Creating a global climatology of freezing rain using numerical model output p 673 A95-93541
- FREIGHT COSTS**
Design of a high capacity long range cargo aircraft
[NASA-CR-197176] p 45 N95-12363
- FREQUENCIES**
Fatigue crack growth in nickel-based superalloys at 500-700 C. 1: Waspaloy
[BTN-94-EIX94371347843] p 206 A95-69136
Foliage transmission measurements using a ground-based ultrawide band (300-1300 MHz) SAR system
[BTN-94-EIX94381351617] p 252 A95-70950
Rotorcraft control system design for uncertain vehicle dynamics using quantitative feedback theory
[HTN-95-31012] p 236 A95-71182
Experimental investigation of the sources of propeller noise due to the ingestion of turbulence at low speeds
[BTN-95-EIX95262697042] p 569 A95-86859
Flight-testing and frequency-domain analysis for rotorcraft handling qualities
[HTN-95-01083] p 515 A95-90269
Automatic identification of modal damping from Floquet analysis
[HTN-95-01084] p 506 A95-90270
Experimental study of the helicopter-mobile radioelectrical channel and possible extension to the satellite-mobile channel p 247 N95-20945
Prediction of fatigue crack growth under constant amplitude and random loading using specimens with multiple cracks
[AD-A291614] p 397 N95-28409
PIO: A historical perspective p 597 N95-31062
- FREQUENCY MODULATION**
Electromagnetic backscattering from a helicopter rotor in the decametric wave band regime
[BTN-94-EIX94381353130] p 243 A95-72648
- FREQUENCY RANGES**
Handling qualities analysis on rate limiting elements in flight control systems p 619 N95-31071
- FREQUENCY RESPONSE**
Precise navigation using adaptive FIR filtering and time domain spectral estimation
[BTN-95-EIX9514255485] p 227 A95-72888
Real-time navigation using the global positioning system
[BTN-95-EIX95172595298] p 279 A95-75714
Comparison of frequency response and perturbation methods to extract linear models from a nonlinear simulation
[AD-A284115] p 146 N95-18405
Comparison of stochastic and deterministic nonlinear gust analysis methods to meet continuous turbulence criteria p 133 N95-18602
Handling qualities analysis on rate limiting elements in flight control systems p 619 N95-31071
Calspan experience of PIO and the effects of rate limiting p 598 N95-31072
- FREQUENCY STABILITY**
Effect of broadcast and precise ephemerides on estimates of the frequency stability of GPS Navstar clocks
[BTN-95-EIX95112522530] p 190 A95-69333
Sensitivity of combustion-acoustic instabilities to boundary conditions for premixed gas turbine combustors
[NASA-TM-106890] p 289 N95-23550
- FRETTING**
The effects of surface modification on fretting fatigue in Ti alloy turbine components
[HTN-95-61145] p 404 A95-84909
The role of fretting corrosion and fretting fatigue in aircraft rivet hole cracking p 94 N95-14470
- FRETTING CORROSION**
The role of fretting corrosion and fretting fatigue in aircraft rivet hole cracking p 94 N95-14470
- FRICTION**
Impact, friction, and wear testing of microsamples of polycrystalline silicon p 361 A95-79988
Evaluation of retro-reflective beads in airport pavement markings
[AD-A291065] p 523 N95-29967
Evaluation of alternative pavement marking materials
[AD-A292973] p 626 N95-31468
- FRICTION DRAG**
Studies in drag reduction p 478 N95-29094
- FRICTION FACTOR**
Static and dynamic friction behavior of candidate high temperature airframe seal materials
[NASA-TM-106571] p 152 N95-16905
Studies in drag reduction p 478 N95-29094

FRICTION MEASUREMENT

- Boundary-layer transition and global skin friction measurement with an oil-fringe imaging technique
[SAE PAPER 932550] p 547 A95-90054
Boundary-layer transition and global skin friction measurement with an oil-fringe imaging technique
[NASA-CR-198814] p 557 N95-30224
- FRONTS (METEOROLOGY)**
Observations of fluxes and inland breezes over a heterogeneous surface p 212 A95-66315
Mesoscale structure of precipitation bands in a North Atlantic winter storm
[HTN-95-40659] p 215 A95-69803
Final results of the weather testing component of the Terminal Doppler Weather Radar operational test and evaluation p 658 A95-93471
The use of radar wind profiles to remove TDWR gust front algorithm false alarms caused by vertical wind shear p 661 A95-93488
- FROST**
Effect of underwing frost on a transport aircraft airfoil at flight Reynolds number
[BTN-95-EIX95152582334] p 276 A95-73536
- FUEL COMBUSTION**
Aircraft engine emission reduction
[BTN-95-EIX95031502750] p 196 A95-68257
Pressure and temperature distortion testing of a two-stage centrifugal compressor
[BTN-94-EIX95011441250] p 431 A95-84207
Pulsed jet ignition modeling with a full chemistry
p 538 A95-87184
Intrinsic transport and chemistry coupling in combustion phenomena p 538 A95-87191
Prediction of NO(x) emission index of turbulent diffusion flame p 538 A95-87195
Determination of minimum fuel octane number piston aircraft engines
[SAE PAPER 931230] p 528 A95-88961
Programmed ignition of metal compounds in a scramjet p 16 N95-10466
Structure of a swirl-stabilized, combustor spray
[NASA-TM-106724] p 50 N95-11890
Combustor kinetic energy efficiency analysis of the hypersonic research engine data p 148 N95-16321
Fuselage burnthrough from large exterior fuel fires
[AD-A286295] p 226 N95-22318
Shock tunnel studies of scramjet phenomena 1993
[NASA-CR-195038] p 350 N95-25394
Air/fuel ratio visualization in a diesel spray p 556 N95-29807
Preliminary assessment of combustion modes for internal combustion wave rotors
[NASA-TM-107000] p 616 N95-30632
An investigation of the side-dump dual in-line ramjet combustor p 617 N95-31199
A pulsed liquid fuel ramjet p 617 N95-31201
Numerical simulation of ram accelerator performance including transient effects during initiation of combustion and sensitivity studies p 629 N95-31203
Combustion-acoustic stability analysis for premixed gas turbine combustors
[NASA-TM-107024] p 694 N95-32931
- FUEL CONSUMPTION**
Aircraft engine emission reduction
[BTN-95-EIX95031502750] p 196 A95-68257
Fuel-optimal bank-angle control for lunar-return aerocapture
[BTN-95-EIX95212645706] p 299 A95-76758
Twenty-first century commercial transport engines
p 512 A95-91495
Optimality of the steady-state flight for hypersonic aircraft p 526 A95-91550
A study of the savings in time and fuel to aviation through the use of upper-air wind forecasts p 672 A95-93538
Examples of flight path optimization using a multivariate gradient-search method. Addendum A: Variation of optimum flight profile parameters with range
[ESDU-94016-ADD-A] p 44 N95-11794
Protective coatings for compressor gas path components p 201 N95-19675
Small gas turbine component evaluation study
[PB95-147542] p 338 N95-24293
Wave rotor-enhanced gas turbine engines
[NASA-TM-106998] p 615 N95-30517
Minimum fuel mode evaluation p 695 N95-33015
- FUEL CONTROL**
Ultimate characteristics of a rocket engine with a turbo-pump supply system
[BTN-94-EIX94461408757] p 148 A95-63640
Calculation of control laws for the digital fuel control unit of a small thrust turbojet
[SAE PAPER 931411] p 614 A95-93677
Viper cabin-fuselage structural design concept with engine installation and wing structural design
[NASA-CR-197162] p 45 N95-12305

- New technologies for space avionics
[NASA-CR-197574] p 150 N95-18196
- FUEL CORROSION**
Characterization of corrosion and development of a breadboard of a D sight aircraft inspection system, phase 1
[AD-A288347] p 380 N95-26527
- FUEL FLOW**
Vapor lock studies for gasolines wwith ethers
[SAE PAPER 931233] p 529 A95-88962
Aviation and the environment p 657 A95-93464
Evaluation of the transient operation of advanced gas turbine combustors
[BTN-95-EIX0616952745793] p 614 A95-94495
- FUEL INJECTION**
Experimental and analytical investigations of wave enhanced supersonic combustors
[AIAA PAPER 89-2787] p 14 A95-60172
Scramjet combustor design in France
[AIAA PAPER 95-6094] p 510 A95-88002
Injection studies in the French hypersonic technology program
[AIAA PAPER 95-6096] p 510 A95-88004
Hydrocarbon-fueled ramjet/scramjet technology program, phase 2 extension
[NASA-CR-189659] p 15 N95-10319
Advanced diesel electronic fuel injection and turbocharging
[AD-A279176] p 211 N95-19809
Shock tunnel studies of scramjet phenomena 1993
[NASA-CR-195038] p 350 N95-25394
Scramjet thrust measurement in a shock tunnel
p 339 N95-25396
Numerical simulation of combustion flow around a flame holder with hydrogen injection
[NAL-TR-1233] p 419 N95-26523
Experiment on a rectangular cross section scramjet combustor. 2: Effects of fuel injector geometry
[NAL-TR-1220] p 405 N95-26600
Air/fuel ratio visualization in a diesel spray
p 556 N95-29807
An investigation of the side-dump dual in-line ramjet combustor
p 617 N95-31199
A pulsed liquid fuel ramjet
p 617 N95-31201
Numerical simulation of ram accelerator performance including transient effects during initiation of combustion and sensitivity studies
p 629 N95-31203
- FUEL SPRAYS**
Structure of a swirl-stabilized, combustng spray
[NASA-TM-106724] p 50 N95-11890
Air/fuel ratio visualization in a diesel spray
p 556 N95-29807
Experimental investigation of turbulent particle dispersion in swirling flows
[DLR-FB-94-20] p 647 N95-31355
- FUEL SYSTEMS**
Development of an aeroderivative gas turbine dry low emissions combustion system
[BTN-94-EIX95011441246] p 417 A95-84203
A subsystem integration technology concept
[SAE PAPER 931382] p 604 A95-93658
Advanced distributed simulation technology advanced rotary wing aircraft. System/segment specification. Volume 2: Flight station module
[AD-A280432] p 20 N95-10352
Rotorcraft crashworthy airframe and fuel system technology development program
[AD-A289886] p 382 N95-28630
- FUEL TANKS**
Numerical modeling of a cryogenic fluid within a fuel tank
[NASA-TM-4651] p 89 N95-13892
- FUEL TESTS**
Determination of minimum fuel octane number piston aircraft engines
[SAE PAPER 931230] p 528 A95-88961
Vapor lock studies for gasolines wwith ethers
[SAE PAPER 931233] p 529 A95-88962
Ongoing research into high octane unleaded avgas
[SAE PAPER 931234] p 529 A95-88963
Unmanned aerial vehicle heavy fuel engine test
[AD-A284332] p 139 N95-18383
- FUEL VALVES**
Lightweight high-temperature fuel metering valves
[SAE PAPER 931444] p 635 A95-93693
A Lifting Ball Valve for cryogenic fluid applications
p 156 N95-16349
- FUEL-AIR RATIO**
Air/fuel ratio visualization in a diesel spray
p 556 N95-29807
- FUELS**
Controlling mechanisms of ignition of solid fuel in a sudden-expansion combustor
[BTN-95-EIX0616952745791] p 628 A95-94255
Unmanned aerial vehicle heavy fuel engine test
[AD-A284332] p 139 N95-18383
- Transport phenomena and interfacial kinetics in multiphase combustion systems
[AD-A288297] p 418 N95-26417
Proceedings of the AIAA/FAA joint symposium on general aviation systems
[AD-A289830] p 368 N95-28610
Fuel-type classification and parameters prediction by Gas Liquid Chromatography analysis
[AD-A293442] p 630 N95-31368
- FULL SCALE TESTS**
NASA Lewis Propulsion Systems Laboratory test article systems criteria
[NASA-TM-106589] p 20 N95-10446
Computational analysis of forebody tangential slot blowing
p 71 N95-14253
Testing and analysis of flat and curved panels with multiple cracks
p 93 N95-14460
Wall interaction effects for a full-scale helicopter rotor in the NASA Ames 80- by 120-foot wind tunnel
p 121 N95-19270
Evaluation of the fuselage lap joint fatigue and terminating action repair
p 166 N95-19477
Development of load spectra for Airbus A330/A340 full scale fatigue tests
p 135 N95-19479
Testing considerations for military aircraft engines in corrosive environments (a Navy perspective)
p 202 N95-19684
Structural modification and repair of C-130 wing structure using bonded composites
p 394 N95-27512
Report to Congressional Committees. Comanche Helicopter. Testing needs to be completed prior to production decisions
[GAO/NSIAD-95-112] p 397 N95-27910
Comparative wind tunnel tests of NACA 23024 airfoils with several aileron and spoiler configurations
p 376 N95-27976
Full-scale hingeless rotor performance and loads
[NASA-TM-110356] p 691 N95-32699
- FUNCTIONAL DESIGN SPECIFICATIONS**
New approach to geometric profiling of the design elements of the passage part in turbo-machines
[BTN-94-EIX94461408769] p 153 A95-63652
SOFIA: Stratospheric Observatory for Infrared Astronomy
p 363 A95-81583
Mobile domes for TACTIC telescope
p 453 A95-86113
Secondary power system study for the hytex RA3 flight test vehicle
[AIAA PAPER 95-6158] p 512 A95-90470
Advanced distributed simulation technology advanced rotary wing aircraft. Strawman verification and validation plan for the ARWA simulator system
[AD-A280237] p 19 N95-10349
Advanced distributed simulation technology advanced rotary wing aircraft. System/segment specification. Volume 1: Simulation system module
[AD-A280238] p 20 N95-10350
Advanced distributed simulation technology advanced rotary wing aircraft. System/segment specification. Volume 3: Visual system module
[AD-A280239] p 20 N95-10351
Advanced distributed simulation technology advanced rotary wing aircraft. System/segment specification. Volume 2: Flight station module
[AD-A280432] p 20 N95-10352
Advanced distributed simulation technology advanced rotary wing aircraft. System/segment specification. Volume 5: Simulation system module AH-64D kit
[AD-A280433] p 20 N95-10353
Generalized method of solving topological optimization problems for electrical airplane equipment systems in computer-aided design
p 169 N95-16272
The impact of non-linear flight control systems on the prediction of aircraft loads due to turbulence
p 143 N95-18598
Design limit loads based upon statistical discrete gust methodology
p 133 N95-18603
- FUNCTIONS (MATHEMATICS)**
An introduction to generalized functions with some applications in aerodynamics and aerocoustics
p 565 A95-88895
- FUSELAGES**
Simplified analysis of general instability of stiffened shells with cutouts in pure bending
[BTN-95-EIX95042474418] p 209 A95-68282
Modelling of pilloowing due to corrosion in fuselage lap joints
[BTN-95-EIX95082502227] p 240 A95-71024
Design optimization of rotor blades for improved performance and vibration
[HTN-95-A0498] p 229 A95-72569
Growth of multiple cracks and their linkup in a fuselage lap joint
[BTN-95-EIX95142553047] p 286 A95-73451
- Efficient sensitivity analysis for rotary-wing aeromechanical problems
[BTN-95-EIX95152577585] p 264 A95-73497
Experimental investigation of the flowfield about an upswept afterbody
[BTN-95-EIX95152582321] p 265 A95-73524
Multiple site fatigue damage in fuselage skin splices: Experimental simulation and theoretical prediction
[BTN-95-EIX95152584676] p 276 A95-73588
An analytical and experimental investigation of the response of the curved, composite frame/skin specimens
[HTN-95-80857] p 283 A95-75099
Analysis of backscattering from wing and fuselage joints
[HTN-95-71134] p 430 A95-83495
Considerations in the development of the coupled rotor fuselage model
[HTN-95-61077] p 370 A95-83661
Materials and structures for the HSCT
[BTN-95-EIX95282711241] p 455 A95-89634
Optimum aerodynamic design of aircraft fuselage using boundary element method
p 473 A95-91514
Explosive sabotage: The potential effects of explosive charges on aircraft
[CONGRESS PAPER C428-11-034] p 484 A95-91702
Discrete crack growth analysis methodology for through cracks in pressurized fuselage structures
[BTN-95-EIX0608952737538] p 633 A95-92751
Analysis and testing of a graphite-epoxy sandwich shell fuselage test structure
[ISBN 1-879921-01-4] p 605 A95-93746
Structural integrity of fuselage panels with multisite damage
[BTN-95-EIX0619952748188] p 637 A95-94250
Advanced composites structural concepts and materials technologies for primary aircraft structures: Structural response and failure analysis
[NASA-CR-4448] p 11 N95-10240
Advanced composites structural concepts and materials technologies for primary aircraft structures: Design/manufacturing concept assessment
[NASA-CR-4447] p 12 N95-10316
Comments on the use of structureborne noise analysis for large commercial airplanes
p 30 N95-11287
Symmetric steady manoeuvre loads on rigid aircraft of classical configuration at subsonic speeds
[ESDU-94009] p 43 N95-11774
Cabin fuselage structural design with engine installation and control system
[NASA-CR-197173] p 47 N95-12639
Cabin-fuselage-wing structural design concept with engine installation
[NASA-CR-197172] p 49 N95-12993
Damage tolerant repair techniques for pressurized aircraft fuselages
[AD-A281982] p 65 N95-14144
Study of multiple cracks in airplane fuselage by micromechanics and complex variables
p 94 N95-14468
Axial crack propagation and arrest in pressurized fuselage
p 94 N95-14479
Full-scale testing and analysis of fuselage structure
p 95 N95-14485
The characterization of widespread fatigue damage in fuselage structure
[NASA-TM-109142] p 88 N95-14920
An approach to aerodynamic characteristics of low radar cross-section fuselages
p 106 N95-16251
Numerical simulation of helicopter engine plume in forward flight
[NASA-CR-197488] p 107 N95-16589
Wind tunnel investigations of the appearance of shocks in the windward region of bodies with circular cross section at angle of attack
p 113 N95-17866
STOVL CFD model test case
p 115 N95-17881
Investigation of the influence of pylons and stores on the wing lower surface flow
p 116 N95-17885
Application of photogrammetry of F-14D store separation
[AD-A284154] p 132 N95-18417
Experimental techniques for measuring transonic flow with a three dimensional laser velocimetry system. Application to determining the drag of a fuselage
p 163 N95-19258
The characterization of widespread fatigue damage in fuselage structure
p 166 N95-19472
Discrete crack growth analysis methodology for through cracks in pressurized fuselage structures
p 166 N95-19473
Evaluation of the fuselage lap joint fatigue and terminating action repair
p 166 N95-19477
Development of load spectra for Airbus A330/A340 full scale fatigue tests
p 135 N95-19479

Results of uniaxial and biaxial tests on riveted fuselage lap joint specimens p 136 N95-19491
 Prediction of R-curves from small coupon tests p 167 N95-19496
 Nonlinear analysis of damaged stiffened fuselage shells subjected to combined loads p 137 N95-19499
 Damage tolerant repair techniques for pressurized aircraft fuselages p 219 N95-22046
 [AD-A286298]
 Fuselage burnthrough from large exterior fuel fires [AD-A286295] p 226 N95-22318
 Residual strength of thin panels with cracks p 311 N95-23311
 Estimate of probability of crack detection from service difficulty report data [PB95-149381] p 328 N95-24295
 Characterization of corrosion and development of a breadboard of a D sight aircraft inspection system, phase 1 [AD-A288347] p 380 N95-26527
 On aircraft repair verification of a fighter A/C integrally stiffened fuselage skin p 394 N95-27515
 Load transfer in the stiffener-to-skin joints of a pressurized fuselage [NASA-CR-198610] p 439 N95-27865
 Static and fatigue testing of full-scale fuselage panels fabricated using a Therm-X(R) process p 420 N95-28270
 Advanced tow placement of composite fuselage structure p 420 N95-28271
 ACT/ICAPS: Thermoplastic composite activities p 421 N95-28274
 The effect of material heterogeneity in curved composite beams for use in aircraft structures p 422 N95-28426
 Effects of floor location on response of composite fuselage frames p 423 N95-28439
 Probabilistic evaluation of fuselage-type composite structures p 398 N95-28444
 Composite fuselage shell structures research at NASA Langley Research Center p 425 N95-28466
 Test and analysis results for composite transport fuselage and wing structures p 398 N95-28470
 Tension fracture of laminates for transport fuselage. Part 1: Material screening p 398 N95-28471
 Local design optimization for composite transport fuselage crown panels p 398 N95-28473
 Composite fuselage crown panel manufacturing technology p 399 N95-28474
 Advanced textile applications for primary aircraft structures p 399 N95-28476
 Characterization and manufacture of braided composites for large commercial aircraft structures p 426 N95-28478
 Impact damage resistance of composite fuselage structure, part 1 p 399 N95-28482
 Damage tolerance of a geodesically stiffened advanced composite structural concept for aircraft structural applications p 399 N95-28487
 Rotorcraft crashworthy airframe and fuel system technology development program [AD-A28986] p 382 N95-28630
 Numerical simulation of crack growth in pressurized fuselages [PB95-192415] p 400 N95-28636
 In situ processing methods for composite fuselage sandwich structures p 531 N95-28826
 The effects of design details on cost and weight of fuselage structures p 501 N95-28831
 Manufacturing scale-up of composite fuselage crown panels p 532 N95-28835
 Tension fracture of laminates for transport fuselage. Part 2: Large notches p 532 N95-28837
 Impact damage resistance of composite fuselage structure, part 2 p 533 N95-28838
 Design, analysis, and fabrication of a pressure box test fixture for tension damage tolerance testing of curved fuselage panels p 533 N95-28839
 Global cost and weight evaluation of fuselage keel design concepts p 501 N95-28840
 Advanced composites technology program p 534 N95-29032
 Textile composite fuselage structures development p 534 N95-29033
 Advanced composite fuselage technology p 535 N95-29034
 Advanced resin systems and 3D textile preforms for low cost composite structures p 535 N95-29035
 Cross-stiffened continuous fiber structures p 536 N95-29041
 Cost model relationships between textile manufacturing processes and design details for transport fuselage elements p 536 N95-29043
 Test results from large wing and fuselage panels p 537 N95-29051

Estimation of aerodynamic load distributions on the F/A-18 aircraft using a CFD panel code [DSTO-TR-0147] p 504 N95-29445
 Development of stitched/RTM primary structures for transport aircraft [NASA-CR-191441] p 630 N95-31421
 Preparation of S-70A-9 Black Hawk helicopter for flight tests to investigate cause of cracking of inner fuselage panel [AD-A293891] p 608 N95-31544

FUSION WELDING

JPRS report: Science and technology. Central Eurasia [JPRS-UST-95-011] p 335 N95-24541

FUZZY SETS

Application of fuzzy logic to optimize placement of an acquisition, tracking, and pointing experiment p 341 A95-80390

FUZZY SYSTEMS

Application of fuzzy logic to optimize placement of an acquisition, tracking, and pointing experiment p 341 A95-80390

Application of GPS and Fuzzy Theory to a helicopter p 516 A95-91505

A design of a self-learning robust scheduled autopilot p 516 A95-91533

Multiobjective trajectory optimization by goal programming with fuzzy decision p 526 A95-91544

Artificial intelligence with applications for aircraft [DOT/FAA/CT-94/41] p 99 N95-13895

Workshop on Formal Models for Intelligent Control [AD-A281399] p 169 N95-16864

Digital systems validation. Chapter 20 Artificial Intelligence with applications for aircraft. Handbook, volume 2 [AD-A288492] p 448 N95-26638

Evaluation of the techniques of fuzzy control for the piloting an aircraft p 621 N95-31997

G**GALERKIN METHOD**

An improved finite element method for the solution of the compressible Euler and Navier-Stokes equations p 640 A95-95439

Agglomeration multigrid for viscous turbulent flows [AD-A284064] p 8 N95-10848

Numerical study to assess sulfur hexafluoride as a medium for testing multielement airfoils [NASA-TP-3496] p 378 N95-28674

Finite element vorticity-based methods for the solution of the incompressible and compressible Navier-Stokes equations p 553 N95-29119

GALLIUM ARSENIDES

Photovoltaic electric power applied to Unmanned Aerial Vehicles (UAV) p 245 N95-20530

Design of a GaAs/Ge solar array for unmanned aerial vehicles [NASA-TM-106870] p 320 N95-23259

Laser based obstacle warning sensors for helicopters p 686 N95-32499

GAME THEORY

Structural design using equilibrium programming formulations [NASA-TM-110175] p 645 N95-30682

GAMMA RAY TELESCOPES

Mobile domes for TACTIC telescope p 453 A95-86113

GAS ANALYSIS

Fuel-type classification and parameters prediction by Gas Liquid Chromatography analysis [AD-A293442] p 630 N95-31368

GAS CHROMATOGRAPHY

Fuel-type classification and parameters prediction by Gas Liquid Chromatography analysis [AD-A293442] p 630 N95-31368

Gas chromatography/ion mobility spectrometry as a hyphenated technique for improved explosives detection and analysis p 701 N95-33278

GAS DENSITY

Planar air density measurements near model surfaces by ultraviolet Rayleigh/Raman scattering [HTN-95-20950] p 546 A95-88989

GAS DETECTORS

Aircraft-borne, laser-induced fluorescence instrument for the in situ detection of hydroxyl and hydroperoxy radicals [BTN-95-EIX95072499029] p 253 A95-71908

GAS DYNAMICS

Kinetic theory in aerothermodynamics [HTN-95-A0002] p 183 A95-67829

Measurement of particle emissions from clean room gas-handling components [BTN-94-EIX94431359040] p 295 A95-74554

Measurement of moisture and total hydrocarbon contributions by valves used in clean room gas-delivery systems p 295 A95-74629

[BTN-94-EIX94381359041] p 295 A95-74629
 Studies on gain performance of a combustion driven CO₂ gas dynamic laser p 428 A95-82679

JPRS report: Science and technology. Central Eurasia: Engineering and equipment. Gas dynamics of supersonic shortened nozzles [JPRS-UST-94-003-L] p 22 N95-10931

Activities of the institute for Aerospace Studies of Toronto University p 63 N95-12699

Simulation of multidisciplinary problems for the thermostress state of cooled high temperature turbines p 140 N95-19021

Application of multidisciplinary models to the cooled turbine rotor design p 140 N95-19024

State-to-state collisional dynamics of atmospheric species [AD-A285053] p 245 N95-20484

High-performance parallel analysis of coupled problems for aircraft propulsion [NASA-CR-197440] p 289 N95-23088

Acoustic scattering from ellipses by the modal element method [NASA-TM-106935] p 579 N95-29401

Numerical simulation of ram accelerator performance including transient effects during initiation of combustion and sensitivity studies p 629 N95-31203

GAS EXPANSION

Experiment of rocket-ram annular combustor p 412 A95-82324

The noise reduction potential of dual-stream coaxial rectangular improperly expanded jet flows [NASA-CR-197820] p 437 N95-26995

Numerical simulations of the flow in the HYPULSE expansion tube [NASA-TM-110357] p 523 N95-30228

GAS FLOW

Numerical analysis of flow field around gas rudder p 407 A95-82333

Rarefied gas numerical wind tunnel: OREX and HOPE p 427 A95-82391

Intrinsic transport and chemistry coupling in combustion phenomena p 538 A95-87191

A flow pattern map for two-phase liquid-gas flow under reduced gravity conditions p 539 A95-87280

Numerical simulation of three-dimensional hypersonic reacting flows over blunt bodies with catalytic surface [HTN-95-61184] p 539 A95-87557

A perspective of rarefied gas flow problems relevant to high altitude flight [SAE PAPER 931366] p 586 A95-93647

An approximate Riemann solver for thermal and chemical nonequilibrium flows [NASA-CR-195003] p 96 N95-14912

Flow field investigation in a free jet - free jet core system for the generation of high intensity molecular beams [DLR-FB-94-11] p 172 N95-18912

Mathematical Models of Gas Turbine Engines and their Components [AGARD-LS-198] p 139 N95-19017

The mathematical models of flow passage for gas turbine engines and their components p 140 N95-19020

Application of multicomponent models to flow passage simulation in multistage turbomachines and whole gas turbine engines p 140 N95-19022

Application of multidisciplinary models to the cooled turbine rotor design p 140 N95-19024

Parabolized Navier-Stokes solution of supersonic/hypersonic flows p 123 N95-19464

High-performance parallel analysis of coupled problems for aircraft propulsion [NASA-CR-197440] p 289 N95-23088

GAS GENERATORS

Evaluation of scramjet nozzle performance p 402 A95-82321

Integral rocket ramjets [AD-A285135] p 240 N95-20906

Three-dimensional unsteady flow calculations in an advanced gas generator turbine p 312 N95-23425

A numerical model for dynamic wave rotor analysis [NASA-TM-106997] p 615 N95-30617

Preliminary assessment of combustion modes for internal combustion wave rotors [NASA-TM-107000] p 616 N95-30632

GAS HEATING

Hypersonic nonequilibrium Navier-Stokes solutions over an ablating graphite nosetip [BTN-95-EIX95152583252] p 305 A95-73553

GAS INJECTION

Influence of injectant Mach number and temperature on supersonic film cooling [BTN-94-EIX94441386686] p 184 A95-68195

- Simulation of transverse gas injection in turbulent supersonic air flows
[BTN-95-EIX95182619080] p 269 A95-75765
- High-speed civil transport impact: Role of sulfate, nitric acid trihydrate, and ice aerosols studied with a two-dimensional model including aerosol physics
[HTN-95-91843] p 354 A95-80831
- Hypersonic thermal protection with mass injection at angle of attack
p 414 A95-82414
- Computational/experimental investigation of staged injection into a Mach 2 flow
[HTN-95-51646] p 432 A95-85028
- Quantitative investigation of compressible mixing: Staged transverse injection into Mach 2 flow
[HTN-95-42330] p 404 A95-86159
- Flowfield measurements in supersonic film cooling including the effect of shock-wave interaction
[HTN-95-42337] p 405 A95-86166
- Numerical study of mixing in a high and low enthalpy supersonic test facility
p 7 N95-10467
- In-flight imaging of transverse gas jets injected into transonic and supersonic crossflows: Design and development
[NASA-CR-186031] p 157 N95-17418
- GAS JETS**
- Linear instability waves in supersonic jets confined in circular and non-circular ducts
[BTN-94-EIX9431340068] p 103 A95-63520
- Mach wave emission from a high-temperature supersonic jet
[BTN-95-EIX95152577586] p 264 A95-73496
- Similarity rule for jet-temperature effects on transonic base pressure
[BTN-95-EIX95222650791] p 329 A95-79247
- Mach wave emission from a high-temperature supersonic jet
[HTN-95-42571] p 458 A95-87201
- The aeroacoustics of supersonic coaxial jets
[NASA-TM-106782] p 101 N95-15059
- Resonant interaction of a linear array of supersonic rectangular jets: An experimental study
[NASA-CR-195398] p 76 N95-15852
- The spectrum and directivity of turbulent mixing noise from supersonic jets
p 579 N95-29415
- Turbulent airflow noise production and propagation patterns of a subsonic jet impinging on a flat plate
p 580 N95-29502
- Laser doppler velocimeter system for subsonic jet mixer nozzle testing at the NASA Lewis Aeroacoustic Propulsion Lab
[NASA-TM-106984] p 457 N95-30229
- GAS MIXTURES**
- Hypersonic convective heat transfer over 140-deg blunt cones in different gases
[BTN-95-EIX95152583253] p 306 A95-73554
- General solution procedure for flows in local chemical equilibrium
[HTN-95-42329] p 404 A95-86158
- GAS PRESSURE**
- An investigation of the AFIT 2-inch shock tube as a flow source for supersonic testing
[AD-A289246] p 412 N95-26966
- GAS STREAMS**
- Experimental results for a hypersonic nozzle/afterbody flow field
[NASA-TM-4638] p 274 N95-23250
- GAS TEMPERATURE**
- Ultimate characteristics of a rocket engine with a turbo-pump supply system
[BTN-94-EIX94461408757] p 148 A95-63640
- Aerodynamic characteristics of the orbital reentry vehicle experimental probe fins in a supersonic flow
[NAL-TR-1232] p 342 N95-25664
- GAS TURBINE ENGINES**
- Effect of wind tunnel acoustic modes on linear oscillating cascade aerodynamics
[HTN-94-00760] p 14 A95-60199
- Foil bearings for gas turbine engines
[BTN-94-EIX94461290279] p 82 A95-61732
- Small gas turbines in the 21st century
[BTN-94-EIX94461290241] p 82 A95-61736
- Mechanism and technological particular features of thermomagnetic hardening
[BTN-94-EIX94461407953] p 89 A95-62627
- Profiling of the working surface of electrodes-tools for circle electrochemical dimensional treatment of compressor blades
[BTN-94-EIX94461407964] p 83 A95-62638
- Gas-turbine engines with increased efficiency of two circuits, due to the use of the utilizing steam-turbine circuit
[BTN-94-EIX94461408755] p 153 A95-63638
- Modelling for optimal operations of line milling of aerodynamic surfaces
[BTN-94-EIX94461408774] p 138 A95-63657
- Fatigue crack growth in nickel-based superalloys at 500-700 C. 1: Waspaloy
[BTN-94-EIX94371347843] p 206 A95-69136
- Nonlinear dynamic simulation of single- and multispool core engines, part 1: Computational method
[BTN-95-EIX95112524200] p 210 A95-69308
- Engine life measurement and diagnostics
[BTN-95-EIX95041505024] p 235 A95-70133
- Fatigue strength of high-temperature alloys under conditions of cyclic temperature variation. Communication 1: Experimental procedure and results
[BTN-94-EIX94401363884] p 307 A95-75516
- Erosion of dust-filtered helicopter turbine engines. Part 2: Erosion reduction
[BTN-95-EIX95182619223] p 289 A95-76649
- GETRAN: A generic, modularly structured computer code for simulation of dynamic behavior of aero- and power generation gas turbine engines
[BTN-94-EIX95011441241] p 431 A95-84198
- Flex cycle combustor development and demonstration
[BTN-94-EIX95011441245] p 417 A95-84202
- Development of an aeroderivative gas turbine dry low emissions combustion system
[BTN-94-EIX95011441246] p 417 A95-84203
- Study on the turbine vane and blade for a 1500 C class industrial gas turbine
[BTN-94-EIX95011441254] p 431 A95-84211
- The effects of surface modification on fretting fatigue in Ti alloy turbine components
[HTN-95-61145] p 404 A95-84909
- Applying nanostructured materials to future gas turbine engines
[HTN-95-11909] p 404 A95-85990
- A new paradigm: The investment casting cooperative arrangement
[HTN-95-92510] p 539 A95-87330
- Auxiliary Power Unit evolution: Meeting tomorrow's challenges
[SAE PAPER 932541] p 510 A95-89195
- Structural composites in civil gas turbine aero engines
[HTN-95-B0258] p 529 A95-89202
- System design considerations for an APU starter-generator
[SAE PAPER 932559] p 511 A95-90056
- A switched reluctance machine rotor position estimator: A neural network application
[SAE PAPER 932560] p 511 A95-90057
- Gas path debris monitoring
[CONGRESS PAPER C428-15-031] p 508 A95-91710
- Simultaneous engineering in aero gas turbine design and manufacture
[CONGRESS PAPER C428-20-204] p 581 A95-91723
- Design and development of an advanced two-stage centrifugal compressor
[BTN-95-EIX95282710054] p 633 A95-92475
- Manufacture technology
[CONGRESS PAPER C428-27-088] p 612 A95-93605
- The role of material behaviour modelling in stressing and life assessment of modern Aero-engine components
[CONGRESS PAPER C428-27-127] p 612 A95-93606
- Laser processing aircraft and turbine engine parts
[SAE PAPER 931356] p 634 A95-93640
- Lightweight high-temperature fuel metering valves
[SAE PAPER 931444] p 635 A95-93693
- Dynamic stiffness and damping of foil bearings for gas turbine engines
[SAE PAPER 931449] p 635 A95-93698
- NASA Lewis Propulsion Systems Laboratory customer guide manual
[NASA-TM-106569] p 21 N95-10822
- Modeling improvements and users manual for axial-flow turbine off-design computer code AXOD
[NASA-CR-195370] p 8 N95-10853
- Brush seal performance and durability issues based on T-700 engine test results
[NASA-TM-106502] p 22 N95-11483
- High temperature strain gage technology for gas turbine engines
[NASA-CR-191177] p 57 N95-11996
- Impingement flow heat transfer measurements of turbine blades using a jet array
[AD-A283450] p 62 N95-12512
- Effect of surface roughness on local film cooling effectiveness and heat transfer coefficients
[AD-A283854] p 91 N95-14351
- Gas turbine prediffuser-combustor performance during operation with air-water mixture
[DOT/FAA/CT-93/52] p 83 N95-15683
- Advanced Turbine Technology Applications Project (ATTAP)
[NASA-CR-195393] p 101 N95-15743
- Theoretical fundamentals of the aircraft GTE tests
p 138 N95-16265
- An artificial neural network system for diagnosing gas turbine engine fuel faults
[DE94-013960] p 138 N95-17371
- Simulation investigation on system identification of gas turbine
[PB95-104238] p 139 N95-17749
- Wave cycle design for wave rotor engines with limited nitrogen oxide emissions
p 161 N95-18901
- Mathematical Models of Gas Turbine Engines and their Components
[AGARD-LS-198] p 139 N95-19017
- The mathematical models of flow passage for gas turbine engines and their components
p 140 N95-19020
- Application of multicomponent models to flow passage simulation in multistage turbomachines and whole gas turbine engines
p 140 N95-19022
- Proceedings of the USAF Structural Integrity Program Conference
[AD-A285684] p 194 N95-19517
- Erosion, Corrosion and Foreign Object Damage Effects in Gas Turbines
[AGARD-CP-558] p 197 N95-19653
- Out of area experiences with the RB199 in Toronto
p 198 N95-19654
- The operation of gas turbine engines in hot and sandy conditions: Royal Air Force experiences in the Gulf conflict
p 198 N95-19655
- US Army rotorcraft turboshaft engines sand and dust erosion considerations
p 198 N95-19656
- Navy foreign object damage and its impact on future gas turbine engine low pressure compression systems
p 198 N95-19658
- Experimental and numerical simulations of the effects of ingested particles in gas turbine engines
p 199 N95-19662
- Particle trajectories in gas turbine engines
p 199 N95-19663
- An airborne monitoring system for FOD and erosion faults
p 200 N95-19668
- Aero-thermodynamic distortion induced structured dynamic response
[AD-A279931] p 203 N95-19864
- Experimental study of vane heat transfer and aerodynamics at elevated levels of turbulence
[NASA-CR-4633] p 244 N95-19912
- Toughened Silcomp composites for gas turbine engine applications
[DE95-002851] p 235 N95-21243
- Evolution of oxidation and creep damage mechanisms in HIPed silicon nitride materials
[DE95-001360] p 300 N95-22689
- Small gas turbine component evaluation study
[PB95-147542] p 338 N95-24293
- Thermal barrier coatings for aircraft engines: History and directions
p 344 N95-26121
- Thermal barrier coatings application in diesel engines
p 345 N95-26124
- Thermal barrier coating experience in the gas turbine engine
p 345 N95-26125
- PVD TBC experience on GE aircraft engines
p 345 N95-26126
- Perspective on thermal barrier coatings for industrial gas turbine applications
p 345 N95-26128
- Jet engine applications for materials with nanometer-scale dimensions
p 345 N95-26131
- Thermal conductivity of zirconia thermal barrier coatings
p 345 N95-26133
- Thermal barrier coating life modeling in aircraft gas turbine engines
p 346 N95-26140
- Transport phenomena and interfacial kinetics in multiphase combustion systems
[AD-A288297] p 418 N95-26417
- Optimization of wave rotors for use as gas turbine engine topping cycles
[NASA-TM-106951] p 406 N95-27860
- A summary of computational experience at GE Aircraft Engines for complex turbulent flows in gas turbines
p 439 N95-27885
- Composite intermediate case manufacturing scale-up for advanced engines
p 406 N95-28275
- Intelligent turbine engines for Army applications
[AD-A290532] p 514 N95-29496
- Model development for active control of stall phenomena in aircraft gas turbine engines
p 514 N95-29679
- Characterization of stall inception in high-speed single-stage compressors
[AD-A291275] p 514 N95-29934
- The fluid mechanics of a high aspect ratio slot with an impressed pressure gradient and secondary injection
p 557 N95-30304
- Wave rotor-enhanced gas turbine engines
[NASA-TM-106998] p 615 N95-30517

- Object-oriented approach for gas turbine engine simulation
[NASA-TM-106970] p 615 N95-30594
- A numerical model for dynamic wave rotor analysis
[NASA-TM-106997] p 615 N95-30617
- Preliminary assessment of combustion modes for internal combustion wave rotors
[NASA-TM-107000] p 616 N95-30632
- Jet mixing and emission characteristics of transverse jets in annular and cylindrical confined crossflow
[NASA-TM-106976] p 616 N95-30698
- Thermal-mechanical fatigue crack growth in aircraft engine materials
[ISBN-0-315-86543-1] p 647 N95-31098
- Advanced turbine systems program conceptual design and product development
[DE95-000088] p 650 N95-32163
- Combustion-acoustic stability analysis for premixed gas turbine combustors
[NASA-TM-107024] p 694 N95-32931
- The application of Ada and formal methods to a safety critical engine control system p 710 N95-33142
- GAS TURBINES**
- Rotor whirl forces induced by the tip clearance effect in axial flow compressors
[BTN-94-EIX94351143331] p 207 A95-67304
- Aircraft engine emission reduction
[BTN-95-EIX95031502750] p 196 A95-68257
- Modeling three-dimensional gas-turbine combustor model flow using second-moment closure
[HTN-95-20935] p 464 A95-88974
- Blade-by-blade tip clearance measurement system for gas turbine applications
[BTN-95-EIX95292721167] p 546 A95-89899
- Applicability of electrically driven accessories for turboshaft engines
[BTN-95-EIX95292721153] p 612 A95-92589
- Efficient mapping topology for turbine combustors with inclined slots/staggered holes
[BTN-95-EIX0616952745805] p 614 A95-94485
- Evaluation of the transient operation of advanced gas turbine combustors
[BTN-95-EIX0616952745793] p 614 A95-94495
- Modeling improvements and users manual for axial-flow turbine off-design computer code AXOD
[NASA-CR-195370] p 8 N95-10853
- Turbomachinery Design Using CFD
[AGARD-LS-195] p 89 N95-14127
- Fatigue in single crystal nickel superalloys
[AD-A285727] p 152 N95-18068
- Numerical mixing calculations of confined reacting jet flows in a cylindrical duct
[NASA-TM-106736] p 139 N95-18133
- Scandinavian Airlines Systems experience on erosion, corrosion and foreign object damage effects on gas turbines
p 198 N95-19659
- Particle deposition in gas turbine blade film cooling holes
p 199 N95-19661
- The calculation of erosion in a gas turbine compressor rotor
p 199 N95-19664
- Erosion of T56 5th stage rotor blades due to bleed hole overtip flow
p 200 N95-19666
- Protective coatings for compressor gas path components
p 201 N95-19675
- Braze repair possibilities for hot section gas turbine parts
p 201 N95-19677
- Gas turbine compressor corrosion and erosion in Western Europe
[AD-B196178L] p 201 N95-19678
- Multilayer anti-erosion coatings
p 201 N95-19679
- Toughened Silcomp composites for gas turbine engine applications
[DE95-002851] p 235 N95-21243
- Sensitivity of combustion-acoustic instabilities to boundary conditions for premixed gas turbine combustors
[NASA-TM-106890] p 289 N95-23550
- Thermal Barrier Coating Workshop
[NASA-CP-10170] p 344 N95-26119
- Thermal barrier coatings issues in advanced land-based gas turbines
p 344 N95-26122
- Numerical analysis of intra-cavity and power-stream flow interaction in multiple gas-turbine disk-cavities
[NASA-TM-106886] p 407 N95-28344
- Intelligent turbine engines for Army applications
[AD-A290532] p 514 N95-29496
- Jet mixing in a reacting cylindrical crossflow
[NASA-TM-106975] p 616 N95-30853
- Static pressure drop by swirling flow of an internal cooling air system through a turbine shaft p 698 N95-34560
- Subscale study of engine bellmouth inlet vortices in test cell R1D
[AD-A294993] p 707 N95-34818
- GAS-LIQUID INTERACTIONS**
- Characterization of annular two-phase gas-liquid flows in microgravity p 95 N95-14556
- GAS-SOLID INTERACTIONS**
- On the particular features of dynamic processes in solids with varying boundary during interaction with intensive heat flows
[BTN-94-EIX94461408756] p 171 A95-63639
- Cercignani-Lampis-Lord gas-surface interaction model: Comparisons between theory and simulation
[BTN-95-EIX95041503806] p 242 A95-70131
- Three-dimensional structure of a supersonic jet impinging on an inclined plate
[BTN-95-EIX95152583259] p 267 A95-73560
- Numerical studies of turbulent free surface flows and unsteady propeller flows
[AD-A294377] p 706 N95-34343
- GAS-SOLID INTERFACES**
- On the particular features of dynamic processes in solids with varying boundary during interaction with intensive heat flows
[BTN-94-EIX94461408756] p 171 A95-63639
- GASEOUS DIFFUSION**
- Vertical transport rates in the stratosphere in 1993 from observations of CO₂, N₂O, and CH₄
[HTN-95-70941] p 351 A95-78006
- GASES**
- Development of an upwind, finite-volume code with finite-rate chemistry
[NASA-CR-197747] p 374 N95-26760
- Photoacoustic chambers for studying solids and gases: Theory and practical examples
[IFTR-39/1994] p 412 N95-26837
- GASOLINE**
- Vapor lock studies for gasolines wwith ethers
[SAE PAPER 931233] p 529 A95-88962
- Ongoing research into high octane unleaded avgas
[SAE PAPER 931234] p 529 A95-88963
- A hybrid vehicle evaluation code and its application to vehicle design. Revision 1
[DE95-008053] p 441 N95-28029
- GATES (CIRCUITS)**
- Optical processing and control
[AD-A279157] p 259 N95-21975
- GAUSSIAN ELIMINATION**
- Large-scale computational fluid dynamics by the finite element method
[BTN-94-EIX94381359154] p 243 A95-71744
- GEAR TEETH**
- Analytical and experimental vibration analysis of a faulty gear system
[NASA-TM-106689] p 58 N95-12843
- Detecting gear tooth fracture in a high contact ratio face gear mesh
[NASA-TM-106822] p 162 N95-19125
- Wormgear geometry adopted for implementing hydrostatic lubrication and formulation of the lubrication problem
[AD-A290331] p 210 N95-19567
- Influence of tooth profile modification on spur gear dynamic tooth strain
[NASA-TM-106952] p 553 N95-29112
- GEARS**
- Aircraft gear train diagnostics using the irregular rotation of the external shafts
[CONGRESS PAPER C428-15-097] p 508 A95-91712
- Analytical and experimental vibration analysis of a faulty gear system
[NASA-TM-106689] p 58 N95-12843
- Detecting gear tooth fracture in a high contact ratio face gear mesh
[NASA-TM-106822] p 162 N95-19125
- Wormgear geometry adopted for implementing hydrostatic lubrication and formulation of the lubrication problem
[AD-A290331] p 210 N95-19567
- Gearbox vibration diagnostic analyzer
[NASA-CR-189141] p 316 N95-23792
- Vibration analysis of a split path gearbox
[NASA-TM-106875] p 438 N95-27855
- Influence of tooth profile modification on spur gear dynamic tooth strain
[NASA-TM-106952] p 553 N95-29112
- GENERAL AVIATION AIRCRAFT**
- Techniques for tailoring aircraft stall and post-stall behavior
[SAE PAPER 931226] p 458 A95-87199
- Lightning protection technology for small general aviation composite material aircraft
[SAE PAPER 931241] p 483 A95-88964
- Fatigue life estimation program for Part 23 airplanes, 'AFS.FOR'
[SAE PAPER 931249] p 565 A95-89221
- Preliminary design of a single engine business jet
[SAE PAPER 931253] p 493 A95-89222
- Should large business jets have four under the wing?
[SAE 931256] p 493 A95-89223
- The FAA regional/commuter aircraft flight loads data collection program
[SAE PAPER 931258] p 493 A95-89224
- CaNard: A new roadable aircraft concept
[SAE PAPER 932601] p 494 A95-90071
- Engineering design of Starcar 3
[SAE PAPER 932602] p 494 A95-90072
- Design and styling of an advanced flying automobile
[SAE PAPER 932603] p 494 A95-90073
- Design methodology and infrastructures for flying automobiles
[SAE PAPER 932604] p 495 A95-90074
- Design and analysis of a telescopic wing
[SAE PAPER 932605] p 495 A95-90075
- Conversion of production automotive engines for aviation use
[SAE PAPER 932606] p 495 A95-90076
- Civil aircraft propulsion integration: Current & future
[SAE PAPER 932624] p 495 A95-90085
- Deaths and injuries as a result of lightning strikes to aircraft
[HTN-95-12213] p 485 A95-91913
- General aviation landing incidents and accidents: A review of ASRS and AOPA research findings
p 596 A95-95198
- General Aviation Task Force report
[NASA-TM-109950] p 1 N95-11463
- The Elite: A high speed, low-cost general aviation aircraft for Aeroworld
[NASA-CR-197161] p 45 N95-12530
- Icarus Rewaxed: A high speed, low-cost general aviation aircraft for Aeroworld
[NASA-CR-197155] p 45 N95-12609
- The Balsa bullet: A high speed, low-cost general aviation aircraft for Aeroworld
[NASA-CR-197165] p 46 N95-12638
- Revitalizing general aviation
[NASA-TM-110113] p 129 N95-16982
- Annual review of aircraft accident data: US Air carrier operations, calendar year 1992
[PB95-100319] p 123 N95-17748
- Census US civil aircraft calendar year 1993
[AD-A286309] p 219 N95-20091
- The personal aircraft: Status and issues
[NASA-TM-109174] p 223 N95-20688
- Development of an intervention program to encourage shoulder harness use and aircraft retrofit in general aviation aircraft, phases 1 and 2
[DOT/FAA/AM-95/2] p 333 N95-24384
- Proceedings of the AIAA/FAA joint symposium on general aviation systems
[AD-A289830] p 368 N95-28610
- Development of an intervention program to encourage shoulder harness use and aircraft retrofit in general aviation aircraft: Phases 1 and 2
[AD-A290966] p 485 N95-29873
- Terminal area forecasts-fiscal years 1993-2010
[AD-A290835] p 490 N95-29880
- Annual review of aircraft accident data: US general aviation calendar year 1993
[PB95-215828] p 599 N95-31712
- Report to the Chairman, Subcommittee on Aviation, Committee on Commerce, Science, and Transportation, US Senate. Aviation Safety: FAA can better prepare general aviation pilots for mountain flying risks
[GAO/RCED-94-15] p 687 N95-32784
- Report to the Chairman, Subcommittee on Transportation and Related Agencies, Committee on Appropriations, US Senate. Airport Improvement Program: Reliever airport set-aside funds could be redirected
[GAO/RCED-94-226] p 699 N95-32786
- Low-order nonlinear dynamic model of IC engine-variable pitch propeller system for general aviation aircraft
[NASA-TM-107006] p 694 N95-32916
- GENERAL OVERVIEWS**
- Dryden overview for schools
[NASA-TM-104282] p 21 N95-10710
- Dryden tour tape, 1994
[NASA-TM-104288] p 21 N95-10714
- A review of 50 years of aerodynamic research with NACA/NASA
[NASA-TM-109163] p 102 N95-13663
- Composite chronicles: A study of the lessons learned in the development, production, and service of composite structures
[NASA-CR-4620] p 151 N95-16859
- Aircraft fires, smoke toxicity, and survival: An overview
[DOT/FAA/AM-95/8] p 277 N95-24024
- Review of combustion-acoustic instabilities
[NASA-TM-107020] p 705 N95-32930
- Performance seeking control (PSC) for the F-15 highly integrated digital electronic control (HIDEC) aircraft
p 697 N95-33020

GENETIC ALGORITHMS

- The potential of genetic algorithms for conceptual design of rotor systems
[NASA-CR-196813] p 43 N95-11699
- Strain gage selection in loads equations using a genetic algorithm
[NASA-CR-4597] p 48 N95-12831
- Review of the EUROPT Project AERO-0026
p 129 N95-16573
- The use of genetic algorithms for flight test and evaluation of artificial intelligence and complex software systems
[AD-A284824] p 217 N95-19688
- A gain scheduling optimization method using genetic algorithms
[AD-A289306] p 448 N95-26920

GEODESIC LINES

- Damage tolerance of a geodesically stiffened advanced composite structural concept for aircraft structural applications
p 399 N95-28487

GEODESY

- Conversion of Earth-centered Earth-fixed coordinates to geodetic coordinates
[BTN-94-EIX94441380862] p 125 A95-64294
- Efficient and effective handling of cycle slips in global positioning system data
p 43 N95-12230
- Naval Aviation System TEAM mapping, charting, and geodesy handbook
[AD-A288590] p 446 N95-26841

GEODETIC COORDINATES

- Conversion of Earth-centered Earth-fixed coordinates to geodetic coordinates
[BTN-94-EIX94441380862] p 125 A95-64294

GEOGRAPHIC INFORMATION SYSTEMS

- Pilot Weather Advisor system
[BTN-95-EIX95152582314] p 316 A95-73517
- Integrating NOISEMAP with the Geographic Resource Analysis Support System (GRASS) to enhance environmental impact assessments and land use compatibility studies
p 31 N95-11311
- Automation technology using Geographic Information System (GIS)
p 324 N95-23284

GEOGRAPHY

- Explanatory factors for the geographic distribution of U.S. Civil aviation mortality
[HTN-95-92908] p 484 A95-91846

GEODES

- Geoid lineations of 1000 km wavelength over the central Pacific
[HTN-95-11304] p 319 A95-77009

GEOMETRIC DILUTION OF PRECISION

- On the exact solutions of pseudorange equations
[BTN-95-EIX95142555477] p 278 A95-73433
- Determining GPS average performance metrics
p 383 N95-27791

GEOMETRICAL ACOUSTICS

- Geometrical acoustics approach for calculating the effects of flow on acoustics scattering
[BTN-94-EIX94321331207] p 61 A95-60790

GEOMETRICAL OPTICS

- Airborne passive polarimetric measurements of sea surface anisotropy at 92 GHz
[NASA-CR-197288] p 707 N95-32823

GEOPHYSICS

- Data processing and mapping in airborne radiometric surveys
[HTN-95-51587] p 442 A95-83591
- Airborne geophysics and precise positioning: Scientific issues and future directions
[LC-94-68678] p 446 N95-27156
- Geophex airborne unmanned survey system
[DE95-007566] p 392 N95-27440
- Integration of AIRSAR and AVIRIS data for Trail Canyon alluvial fan, Death Valley, California
p 709 N95-33760

GEOSYNCHRONOUS ORBITS

- Effects of satellite bunching on the probability of collision in geosynchronous orbit
[BTN-95-EIX95152583276] p 298 A95-73577

GERMANIUM ALLOYS

- Design of a GaAs/Ge solar array for unmanned aerial vehicles
[NASA-TM-106870] p 320 N95-23259

GLARE

- An evaluation of aircraft CRT and dot-matrix display legibility requirements
[AD-A283933] p 138 N95-18164

GLASS

- Evaluation of retro-reflective beads in airport pavement markings
[AD-A291065] p 523 N95-29967

GLASS FIBER REINFORCED PLASTICS

- Study on tensile fatigue testing method of unidirectional fiber-resin matrix composites
[NAL-TR-1241] p 343 N95-24989

GLASS FIBERS

- Scarf joint technique with cocured and precured patches for composite repair
p 396 N95-27524
- Utilization of composite materials by the US Army: A look ahead
p 421 N95-28421

GLIDE LANDINGS

- Local-optimal control of a flying vehicle, with final state optimized
[BTN-94-EIX94461407957] p 83 A95-62631

GLIDE PATHS

- Commentary on Walton correspondence relating to the ILS glide slope
[BTN-94-EIX94441380856] p 125 A95-64288
- Application of GPS/SINS/RA integrated system to aircraft approach landing
p 125 N95-16277

GLIDERS

- Flight experience with lightweight, low-power miniaturized instrumentation systems
[BTN-95-EIX95062487522] p 180 A95-69230
- Sailplane glide performance and control using fixed and articulating winglets
[NASA-CR-198579] p 392 N95-27180

GLIDING

- Local-optimal control of a flying vehicle, with final state optimized
[BTN-94-EIX94461407957] p 83 A95-62631
- Minimum sink-speed in power-off glide
[BTN-95-EIX95062487556] p 193 A95-68370
- Sailplane glide performance and control using fixed and articulating winglets
[NASA-CR-198579] p 392 N95-27180
- GLOBAL AIR POLLUTION**
- Nitrous oxide and methane emissions from aero engines
[HTN-95-21363] p 353 A95-78678
- Impact of present aircraft emissions of nitrogen oxides on tropospheric ozone and climate forcing
[HTN-95-21364] p 353 A95-78679
- Environmental aspects of Orbital transport:
Aero-engine R&D efforts for environmental protection
p 559 A95-87377
p 512 A95-91502

GLOBAL POSITIONING SYSTEM

- High accuracy navigation and landing system using GPS/IMU system integration
[BTN-94-EIX94441386129] p 189 A95-68185
- GPS/GLONASS/INS test program
[BTN-94-EIX94441386131] p 189 A95-68187
- Use of MOBITEK wireless wide area networks as a solution to land-based positioning and navigation
[BTN-94-EIX94441386132] p 189 A95-68188
- Evaluation of the radio frequency susceptibility of commercial GPS receivers
[BTN-95-EIX95042474624] p 189 A95-68278
- On-the-fly carrier phase ambiguity resolution for precise aircraft landing
[BTN-95-EIX95112522535] p 190 A95-69328
- Results and performance of multi-site reference station differential GPS
[BTN-95-EIX95112522534] p 190 A95-69329
- Integrated GPS/Glonass navigation: Algorithms and results
[BTN-95-EIX95112522531] p 190 A95-69332
- Effect of broadcast and precise ephemerides on estimates of the frequency stability of GPS Navstar clocks
[BTN-95-EIX95112522530] p 190 A95-69333
- Space flight tests of attitude determination using GPS
[BTN-95-EIX95112522529] p 190 A95-69334
- Attitude determination using dedicated and nondedicated multi-antenna GPS sensors
[BTN-95-EIX95142555482] p 228 A95-72891
- On the exact solutions of pseudorange equations
[BTN-95-EIX95142555477] p 278 A95-73433
- Enhancing filter robustness in cascaded GPS-INS integrations
[BTN-95-EIX95142555475] p 278 A95-73435
- Thermal force modeling for global positioning system satellites using the finite element method
[BTN-95-EIX95152583270] p 278 A95-73571
- Real-time navigation using the global positioning system
[BTN-95-EIX95172595298] p 279 A95-75714
- New failure detection approach and its application to GPS autonomous integrity monitoring
[BTN-95-EIX95202637613] p 279 A95-76676
- Description of a GNSS availability model and its use in developing requirements
[BTN-95-EIX95202637603] p 308 A95-76686
- Flight evaluation of DGPS and DGPS-INS navigation systems
p 382 A95-82462
- Orbital transport: Technical, meteorological and chemical aspects; Aerospace Symposium, 3rd, Braunschweig, Germany, Aug. 26-28, 1991
[ISBN 3-540-563180] p 524 A95-87373

- Failure detection and isolation structure for global positioning system autonomous integrity monitoring
[BTN-95-EIX95282706656] p 486 A95-89648
- Application of GPS and Fuzzy Theory to a helicopter
p 516 A95-91505
- Introduction of the GPS to civil aviation field
p 487 A95-91536
- Performance evaluation test of GPS/DGPS navigation system installed in the NAL Dornier 228: Preliminary ground test results
p 487 A95-91575
- GPS modeling for designing aerospace vehicle navigation systems
[BTN-95-EIX95302731223] p 600 A95-94044
- Modeling and analysis for the GPS pseudo-range observable
[BTN-95-EIX95302731227] p 600 A95-94046
- Efficient and effective handling of cycle slips in global positioning system data
p 43 N95-12230
- Application of GPS/SINS/RA integrated system to aircraft approach landing
p 125 N95-16277
- A processing centre for the CNES CE-GPS experimentation
p 125 N95-17196
- Helicopter/vertipod MLS precision approaches
[AD-A283505] p 126 N95-18059
- GPS-Squitter capacity analysis
[AD-A280037] p 245 N95-20599
- Assessment of a non-dedicated GPS receiver system for precise airborne attitude determination
[DE94-019309] p 229 N95-21520
- Differential GPS and system integration of the Low Visibility Landing and Surface Operations (LVLASO) demonstration
p 280 N95-23318
- Real-time testing and demonstration of the US Army Corps of Engineers' Real-Time On-The-Fly positioning system
[AD-A288624] p 334 N95-25609
- Flight evaluation of GPS/DGPS sensor systems installed in NAL Do228
[NAL-TR-1230] p 382 N95-26585
- Analysis and simulation of narrowband GPS jamming using digital excision temporal filtering
[AD-A289328] p 383 N95-26898
- Flight Mechanics/Estimation Theory Symposium 1995
[NASA-CP-3299] p 416 N95-27763
- Determining GPS average performance metrics
p 383 N95-27791
- Error modeling for differential GPS
[NASA-CR-188367] p 488 N95-28716
- Wide Area Differential GPS (WADGPS)
p 489 N95-29107
- An investigation into the use of satellite-based positioning systems for flight reference/autoland operations
p 489 N95-29542
- Modeling spatio-temporal databases to measure the performance of the GPS satellite constellation
p 489 N95-29596
- Flight test evaluation of the Stanford University/United Airlines differential GPS Category 3 automatic landing system
[NASA-TM-110354] p 593 N95-30788
- Guidelines for the design of GPS and LORAN receiver controls and displays
[AD-A293753] p 602 N95-31572
- A tactical navigation and routing system for low-level flight
p 709 N95-32494
- Effects of the specific military aspects of satellite navigation on the civil use of GPS/GLONASS
p 688 N95-33134
- GPS-Squitter interference analysis
[AD-A293690] p 689 N95-33480
- GLONASS**
- GPS/GLONASS/INS test program
[BTN-94-EIX94441386131] p 189 A95-68187
- Integrated GPS/Glonass navigation: Algorithms and results
[BTN-95-EIX95112522531] p 190 A95-69332
- Effects of the specific military aspects of satellite navigation on the civil use of GPS/GLONASS
p 688 N95-33134
- GLOW DISCHARGES**
- Effect of annealing and desulfurization on oxide spallation of turbine airfoil material
[BTN-95-EIX95282707024] p 528 A95-88264
- GOERTLER INSTABILITY**
- Instability of three-dimensional boundary layers due to streamline curvature
[HTN-95-61070] p 430 A95-83654
- Nonlinear analysis of the Gortler instability
[BTN-95-EIX95282705926] p 455 A95-89664
- Numerical study of Gortler instability: Application to the design of a quiet supersonic wind tunnel
[PB94-184801] p 21 N95-10844
- Effect of crossflow on Goertler instability in incompressible boundary layers
[NASA-CR-195007] p 159 N95-18193

- Computational studies of laminar to turbulence transition
[AD-A285622] p 248 N95-21146
- GOES SATELLITES**
Flight Mechanics/Estimation Theory Symposium 1995
[NASA-CP-3299] p 416 N95-27763
- GOGGLES**
A computer-based multimedia prototype for night vision goggles
[AD-A286208] p 258 N95-21882
- GOVERNMENT PROCUREMENT**
Case study of risk management in the USAF B-1B bomber program
[AD-A282371] p 62 N95-11944
Report to Congressional Committees. Tactical Aircraft: Concurrence in development and production of F-22 aircraft should be reduced
[GAC/NSIAD-95-59] p 336 N95-26338
Surviving the peace. Lessons learned from the aircraft industry in the 1920s and 1930s
[AD-A288284] p 366 N95-26455
A case study of the teaming concept in the procurement of the V-22 aircraft
[AD-A293770] p 608 N95-31578
Report to Congressional Committees. Military airlift: C-17 settlement is not a good deal
[GAC/NSIAD-94-141] p 585 N95-32198
Army aviation: Modernization strategy needs to be reassessed. Report to Congressional requesters
[GAC/NSIAD-95-9] p 683 N95-32783
- GOVERNMENT/INDUSTRY RELATIONS**
EC Aviation Scene
[HTN-95-50223] p 176 A95-64860
General Aviation Task Force report
[NASA-TM-109950] p 1 N95-11463
Airborne Windshear Detection and Warning Systems. Fifth and Final Combined Manufacturers' and Technologists' Conference, part 2
[NASA-CP-10139-PT-2] p 41 N95-13203
Windshear certification data base for forward-look detection systems
[GAC/NSIAD-94-71] p 176 N95-18578
Environmental Compliance Assessment and Management Program
[AD-A279605] p 255 N95-20441
STEP: A future vision, today
[NONP-NASA-VT-95-49121] p 452 N95-27209
Collected papers on wind turbine technology
[NASA-CR-195432] p 447 N95-27970
A case study of the teaming concept in the procurement of the V-22 aircraft
[AD-A293770] p 608 N95-31578
- GRAPHICAL USER INTERFACE**
Noise modeling for MOAs and ranges
[AD-A283669] p 170 N95-18018
HLLV avionics requirements study and electronic filing system database development
[NASA-CR-193993] p 49 N95-13027
Graphical user interface for the NASA FLOPS aircraft performance and sizing code
[NASA-TM-106649] p 80 N95-14604
A graphical user interface for design and analysis of air breathing propulsion systems
[TABES PAPER 94-616] p 83 N95-14645
A workstation based simulator for teaching compressible aerodynamics
[NASA-TM-106799] p 170 N95-16906
A platform independent application of Lux illumination prediction algorithms
[AD-A283669] p 170 N95-18018
TIGER: A user-friendly interactive grid generation system for complicated turbomachinery and axis-symmetric configurations
[NASA-CR-198828] p 679 N95-31982
- GRAPHITE**
Hypersonic nonequilibrium Navier-Stokes solutions over an ablating graphite nosetip
[BTN-95-EIX95152583252] p 305 A95-73553
Mechanical characterization of 2D, 2D stitched, and 3D braided/RTM materials
[AD-A283669] p 170 N95-18018
- GRAPHITE-EPOXY COMPOSITES**
Prediction of energy absorption capability of composite stiffeners
[HTN-95-A0500] p 230 A95-72571
An analytical and experimental investigation of the response of the curved, composite frame/skin specimens
[HTN-95-80857] p 283 A95-75099
- Failure behaviour of carbon fiber/epoxy composites in pin-ended buckling and bending tests
[HTN-95-71388] p 528 A95-87606
An investigation of the accuracy of FEM analysis of a graphite epoxy box beam
[SAE PAPER 931221] p 543 A95-88011
Optimal design of composite helicopter power transmission shafts with axially varying fiber layup
[HTN-95-01086] p 529 A95-90272
Analysis and testing of a graphite-epoxy sandwich shell fuselage test structure
[ISBN 1-879921-01-4] p 605 A95-93746
Residual strength of composites with multiple impact damage
[AD-A284230] p 87 N95-14409
Recent advances in graphite/epoxy motor cases
p 149 N95-16333
Structural modification and repair of C-130 wing structure using bonded composites
p 394 A95-27512
Scar repairs to graphite/epoxy components
p 396 N95-27523
Load transfer in the stiffener-to-skin joints of a pressurized fuselage
[NASA-CR-198610] p 439 N95-27865
Investigation of static and cyclic bearing failure mechanisms for GR/EP laminates
p 422 N95-28427
Effects of floor location on response of composite fuselage frames
p 423 N95-28439
Structural testing of the technology integration box beam
p 441 N95-28467
Effect of low-speed impact damage and damage location on behavior of composite panels
p 426 N95-28481
Compressive strength of damaged and repaired composite plates
p 442 N95-28484
Fundamental concepts in the suppression of delamination buckling by stitching
p 426 N95-28486
NASA-ACEE/Boeing 737 graphite-epoxy horizontal stabilizer service
p 400 N95-28489
Novel cost controlled materials and processing for primary structures
p 532 N95-28830
Cross-stiffened continuous fiber structures
p 536 N95-29041
The effects of aircraft fuel and fluids on the strength properties of Resin Transfer Molded (RTM) composites
p 536 N95-29047
- GRAPHITE-POLYIMIDE COMPOSITES**
R & D on HOPE structure
p 413 A95-82355
- GRAPHS (CHARTS)**
Naval Aviation System TEAM mapping, charting, and geodesy handbook
[AD-A288590] p 446 N95-26841
- GRASSLANDS**
A comparison of some aerodynamic resistance methods using measurements over cotton and grass from the 1991 California ozone deposition experiment
[HTN-95-11295] p 319 A95-77000
- GRATINGS (SPECTRA)**
Integrated X-ray testing of the electro-optical breadboard model for the XMM reflection grating spectrometer
[DE95-008829] p 644 N95-30507
- GRAUPEL**
Microwave and infrared simulations of an intense convective system and comparison with aircraft observations
[HTN-95-60511] p 214 A95-68762
High-resolution imaging of rain systems with the advanced microwave precipitation radiometer
[HTN-95-70133] p 252 A95-70655
Sensing thunderstorm microphysics with multiparameter radar: Application for aviation
p 657 A95-93467
- GRAVELS**
Marginal aggregates in flexible pavements: Background survey and experimental plan
[DOT/FAA/CT-94/58] p 53 N95-12216
- GRAVIMETERS**
Navigational technology of dual usage
p 688 N95-33131
- GRAVITATION**
Transport phenomena in stratified multi-fluid flow in the presence and absence of gravity
p 95 N95-14563
- GRAVITATIONAL EFFECTS**
Validation of empirical orbit error corrections using crossover difference differences
[HTN-94-00912] p 25 A95-60227
Stability of magnetic bearing-rotor systems and the effects of gravity and damping
[BTN-94-EIX94441386619] p 208 A95-68168
Stability of magnetic bearing-rotor systems and the effects of gravity and damping
[HTN-95-20955] p 465 A95-88994
Low gravity quenching of hot tubes with cryogens
[ISBN 1-879921-01-4] p 635 A95-93728
Airborne rotary air separator study
[NASA-CR-189099] p 290 N95-24053
- GRAVITATIONAL FIELDS**
Validation of empirical orbit error corrections using crossover difference differences
[HTN-94-00912] p 25 A95-60227
- GRAVITATIONAL PHYSIOLOGY**
Virtual environment application with partial gravity simulation
p 169 N95-15988
A surgical support system for Space Station Freedom
p 149 N95-16776
- GRAVITY PROBE B**
DC electrostatic gyro suspension system for the Gravity Probe B experiment
p 527 N95-29794
- GRAVITY WAVES**
An algorithm for forecasting mountain wave-related turbulence in the stratosphere
[HTN-95-80656] p 254 A95-72500
Amplification and breaking of atmospheric gravity waves
p 675 A95-93552
Turbulence near thunderstorm tops
p 675 A95-93553
Lee waves benign and malignant
p 595 A95-93554
- GRAY GAS**
Contribution of thermal radiation to the temperature profile of ceramic composite materials
[BTN-94-EIX95011441252] p 417 A95-84209
- GREEN'S FUNCTIONS**
Numerical time dependent sheet cavitation simulations using a higher order panel method
[PB94-204435] p 59 N95-13249
Studies on the flow induced by an oscillating airfoil in a uniform stream
[PB94-204450] p 40 N95-13250
- GREENLAND**
An overview of millimeter-wave spectroscopic measurements of chlorine monoxide at Thule, Greenland, February-March, 1992: Vertical profiles, diurnal variation, and longer-term trends
[HTN-95-00722] p 444 A95-86292
- GRID GENERATION (MATHEMATICS)**
A grid generation and flow solution method for the Euler equations on unstructured grids
[HTN-95-20003] p 153 A95-63201
Adaptive computations of flow around a delta wing with vortex breakdown
[BTN-94-EIX94441386631] p 184 A95-68180
CFD optimization of a theoretical minimum-drag body
[BTN-95-EIX95182619234] p 308 A95-76660
Computational/experimental investigation of staged injection into a Mach 2 flow
[HTN-95-51646] p 432 A95-85028
Practical formulation of a positively conservative scheme
[HTN-95-51668] p 433 A95-85050
Mesh generation and adaptivity for the solution of compressible viscous high speed flows
[BTN-95-EIX95262697157] p 538 A95-86893
Quality estimates and stretched meshes based on Delaunay triangulations
[HTN-95-42575] p 564 A95-87205
Three-dimensional adaptive grid-embedding Euler technique
[HTN-95-20825] p 543 A95-88086
Computational aerodynamic analysis on the Open Skies aircraft
[SAE PAPER 932514] p 466 A95-89187
Implicit multi-domain method for unsteady compressible inviscid fluid flows around 3D projectiles
p 548 A95-91482
Aerodynamic simulation on massively parallel systems
p 549 A95-91487
Solution of the Navier-Stokes equations on a massively parallel transputer system
p 549 A95-91490
Numerical experiments on aerodynamic heating mechanism in shock reflection processes
p 471 A95-91497
Automated aircraft routing through weather-impacted airspace
p 666 A95-93512
Operational multi-scale environment model with grid adaptivity (OMEGA) application to aviation weather
p 676 A95-93556
A study of mesh adaption techniques in structured and unstructured meshes
[ISBN 1-879921-01-4] p 678 A95-93757
Automatic grid generation procedure for complex aircraft configurations
[BTN-95-EIX95302729765] p 605 A95-94127
Nonlinear aerodynamic analysis of grid fin configurations
[BTN-95-EIX0619952748172] p 590 A95-94466
Computational fluid dynamics '92: Proceedings of the European Computational Fluid Dynamics Conference, 1st, Brussels, Belgium, Sep. 7-11, 1992. Vols. 1 & 2
[ISBN 0-444-89793-3] p 638 A95-95357
Discretization of the parabolised Navier-Stokes equations
p 638 A95-95362

- A numerical investigation of flow around a square-section cylinder mounted with a splitter plate p 639 A95-95401
- A robust inverse inviscid method for airfoil design p 640 A95-95431
- High-lift calculations using Navier-Stokes methods p 641 A95-95444
- Permeable wall boundary conditions for transonic airfoil design p 641 A95-95445
- A modular system for computational fluid dynamics p 641 A95-95446
- On the prediction of transonic unsteady flows using second order time accuracy p 641 A95-95448
- SAUNA: A system for grid generation and flow simulation using hybrid structured/unstructured grids p 642 A95-95470
- Grid adaptation for problems in computational fluid dynamics p 643 A95-95472
- A 2D parallel multiblock Navier-Stokes solver with applications on shared- and distributed memory machines p 643 A95-95475
- Grid generation: Algebraic and partial differential equations techniques revisited p 643 A95-95477
- Surface grid generation for multi-block structured grids p 643 A95-95478
- High performance parallelized implicit Euler solver for the analysis of unsteady aerodynamic flows p 644 A95-95495
- Numerical simulation of the flow about the F-18 HARV at high angle of attack p 9 N95-10940 [NASA-CR-196396]
- Aerodynamic shape optimization of a HSCT type configuration with improved surface definition [NASA-CR-197011] p 67 N95-13701
- The role of CFD in the design process p 90 N95-14135
- Computational aerodynamics based on the Euler equations [AGARD-AG-325] p 72 N95-14264
- A Cartesian, cell-based approach for adaptively-refined solutions of the Euler and Navier-Stokes equations [NASA-TM-106786] p 73 N95-14297
- An approach for dynamic grids [NASA-TM-106774] p 76 N95-15853
- Mesh quality control for multiply-refined tetrahedral grids [NASA-CR-197595] p 160 N95-18737
- Simulation of multidisciplinary problems for the thermostress state of cooled high temperature turbines p 140 N95-19021
- An assessment of the adaptive unstructured tetrahedral grid, Euler Flow Solver Code FELISA [NASA-TP-3526] p 119 N95-19041
- CFD: Advances and Applications, part 1 [NAL-SP-9322-PT-1] p 165 N95-19444
- Validation and evaluation of the advanced aeronautical CFD system SAUNA: A method developer's view [ARA-MEMO-390] p 210 N95-19774
- Application of three-dimensional hybrid structured/unstructured grids to land, sea and air vehicles [ARA-MEMO-399] p 210 N95-19775
- Venification of the CFD simulation system SAUNA for complex aircraft configurations [ARA-MEMO-401] p 211 N95-19776
- Inviscid and viscous flow modelling of complex aircraft configurations using the CFD simulation system sauna [ARA-MEMO-403] p 211 N95-19777
- Open Skies project computational fluid dynamic analysis [AD-A285928] p 223 N95-19991
- Unstructured-grid large-eddy simulation of flow over an airfoil p 225 N95-22448
- Euler Technology Assessment program for preliminary aircraft design employing SPLITFLOW code with Cartesian unstructured grid method [NASA-CR-4649] p 273 N95-22917
- A CFD study of complex missile and store configurations in relative motion [NASA-CR-197912] p 285 N95-22949
- High-performance parallel analysis of coupled problems for aircraft propulsion [NASA-CR-197440] p 289 N95-23088
- Euler technology assessment for preliminary aircraft design employing OVERFLOW code with multiblock structured-grid method [NASA-CR-4651] p 273 N95-23095
- TIGER: A user-friendly interactive grid generation system for complicated turbomachinery and axis-symmetric configurations p 322 N95-23419
- CFD analysis of turbopump volutes p 312 N95-23436
- Aerodynamic shape optimization of wing and wing-body configurations using control theory [NASA-CR-198024] p 335 N95-25334
- A combined geometric approach for solving the Navier-Stokes equations on dynamic grids [NASA-TM-106919] p 332 N95-26075
- Supersonic transport grid generation, validation, and optimization [NASA-CR-197752] p 448 N95-26648
- Numerical simulation of the flow about the F-18 HARV at high angle of attack [NASA-CR-197755] p 374 N95-26735
- Computational support of the laminar flow supersonic wind tunnel, CNSFV code development, Maglev, and grid generation [NASA-CR-197750] p 411 N95-26775
- Global flowfield about the V-22 Tiltrotor Aircraft [NASA-CR-198603] p 375 N95-27248
- Calculation of three-dimensional (3-D) internal flow by means of the velocity-vorticity formulation on a staggered grid [NASA-TM-110352] p 376 N95-27258
- TranAir: A full-potential, solution-adaptive, rectangular grid code for predicting subsonic, transonic, and supersonic flows about arbitrary configurations. Theory document [NASA-CR-4348] p 378 N95-28265
- Surface Modeling, Grid Generation, and Related Issues in Computational Fluid Dynamic (CFD) Solutions [NASA-CP-3291] p 476 N95-28723
- Grid generation and surface modeling for CFD p 551 N95-28726
- Rapid Airplane Parametric Input Design (RAPID) p 501 N95-28730
- Algorithms for high aspect ratio oriented triangulations p 476 N95-28731
- Surface modeling and grid generation for aeropropulsion CFD p 551 N95-28732
- Block-structured grids for complex aerodynamic configurations: Current status p 551 N95-28736
- An unstructured-grid software system for solving complex aerodynamic problems p 476 N95-28743
- Three-dimensional hybrid grid generation using advancing front techniques p 567 N95-28745
- A grid generation system for multi-disciplinary design optimization p 567 N95-28763
- Automatic multi-block grid generation for high-lift configuration wings p 567 N95-28764
- Demonstration of an automated CFD system for three-dimensional flow simulations p 551 N95-28767
- Solution of the Navier-Stokes equations on locally refined Cartesian meshes using state-vector splitting p 553 N95-29197
- Grid orthogonality effects on predicted turbine midspan heat transfer and performance [NASA-TM-106931] p 554 N95-29371
- Grid resolution and turbulent inflow boundary condition recommendations for NPARC calculations [NASA-TM-106959] p 482 N95-30253
- Numerical solution of the full potential equation using a chimera grid approach [NASA-TM-110360] p 594 N95-32188
- Simulation of patch and slot antennas using FEM with prismatic elements and investigations of artificial absorber mesh termination schemes [NASA-CR-198974] p 704 N95-32822
- Grid generation around airfoil with a flap using boundary element method p 686 N95-34552
- GROOVES**
- Wind-tunnel tests of an inclined cylinder having helical grooves [BTN-95-EIX95262694306] p 411 A95-85477
- GROUND BASED CONTROL**
- EURECA mission control experience and messages for the future p 149 N95-17252
- Air traffic operational inventory CY 1994 [AD-A288281] p 382 N95-26454
- FAA aviation forecasts: Fiscal year 1995-2006 [AD-A293682] p 584 N95-31598
- GROUND CREWS**
- Pilot rating scale for aircraft handling qualities [HTN-95-42269] p 380 A95-84963
- GROUND EFFECT (AERODYNAMICS)**
- Numerical simulation of powered-lift flows [HTN-94-00700] p 3 A95-60179
- Numerical simulation of a complete STOVL aircraft in ground effect [AIAA PAPER 93-4880] p 4 A95-60187
- Effect of ground and ceiling planes on shape of energized wakes [BTN-95-EIX95062487558] p 186 A95-68372
- Ground effect calculation of two-dimensional airfoil [BTN-94-EIX94371347710] p 219 A95-69969
- Air and ground resonance of helicopters with elastically tailored composite rotor blades [HTN-95-A0497] p 222 A95-72568
- The influence of alternate inter-blade connections on ground resonance [HTN-95-80859] p 267 A95-75101
- Stability derivatives of a flapped plate in unsteady ground effect [BTN-95-EIX95182619225] p 270 A95-76651
- Unsteady ground effects on aerodynamic coefficients of finite wings with camber [BTN-95-EIX95182619233] p 271 A95-76659
- Direct boundary integral equations method to subsonic flow with circulation past thin airfoils in ground effect [BTN-95-EIX95242673940] p 365 A95-82224
- Note on prediction of aerodynamic lift/drag ratio of WIG (Wing-In-Ground) at cruise [BTN-95-EIX95282705925] p 467 A95-89665
- Application of ACT to unstable motions of an airfoil in ground effect p 471 A95-91500
- Recent research in ASTOVL aircraft ground environment [CONGRESS PAPER C428-9-040] p 475 A95-91694
- 3D visualization of unsteady 2D airplane wake vortices [AD-A284745] p 27 N95-11593
- Dynamic ground effects flight test of an F-15 aircraft [NASA-TM-4604] p 38 N95-12191
- Propulsion/airframe interference for ducted propfan engines, with ground effect [NASA-CR-197110] p 81 N95-14909
- Tilt Rotor Unmanned Air Vehicle System (TRUS) demonstrator flight test program [AD-A284151] p 132 N95-18415
- Development of pneumatic test techniques for subsonic high-lift and in-ground-effect wind tunnel investigations p 121 N95-19268
- Flow visualization studies of VTOL aircraft models during hover in ground effect [NASA-TM-108860] p 272 N95-22666
- Experimental investigation of static and dynamic ground effect on HOPE ALFLEX vehicle [NAL-TR-1236] p 388 N95-26525
- Dynamic ground effects flight test of the NASA F-15 aircraft p 692 N95-33024
- Numerical simulation of two-dimensional PAR-WIG p 685 N95-34548
- GROUND EFFECT (COMMUNICATIONS)**
- Windshear certification data base for forward-look detection systems p 41 N95-13204
- GROUND EFFECT MACHINES**
- Note on prediction of aerodynamic lift/drag ratio of WIG (Wing-In-Ground) at cruise [BTN-95-EIX95282705925] p 467 A95-89665
- Air cushioned landing craft (LAC) based ship to shore movement simulation: A decision aid for the amphibious commander. A (SMMAT) application [AD-A289635] p 436 N95-26722
- GROUND HANDLING**
- Safety in airport ground handling p 626 A95-95193
- GROUND RESONANCE**
- Air and ground resonance of helicopters with elastically tailored composite rotor blades [HTN-95-A0497] p 222 A95-72568
- The influence of alternate inter-blade connections on ground resonance [HTN-95-80859] p 267 A95-75101
- Dynamic response of NASA Rotor Test Apparatus and Sikorsky S-76 hub mounted in the 80- by 120-Foot Wind Tunnel [NASA-TM-108847] p 25 N95-11389
- GROUND SPEED**
- The selective use of functional optical variables in the control of forward speed [NASA-TM-108849] p 35 N95-12227
- Groundspeed filtering for CTAS [NASA-CR-197223] p 97 N95-15785
- Apparent size passive range method [AD-D017360] p 611 N95-31180
- GROUND STATIONS**
- Results and performance of multi-site reference station differential GPS [BTN-95-EIX95112522534] p 190 A95-69329
- An application of virtual prototyping to the flight test and evaluation of an unmanned air vehicle [AD-A281749] p 14 N95-11595
- A VHF/UHF antenna for the Precision Antenna Measurement System (PAMS) [AD-A285673] p 156 N95-16621
- A processing centre for the CNES CE-GPS experimentation p 125 N95-17196
- GPS-Squitter capacity analysis [AD-A280037] p 245 N95-20599
- Wide Area Differential GPS (WADGPS) p 489 N95-29107
- GROUND SUPPORT EQUIPMENT**
- GateLink highspeed communications with parked aircraft [SAE PAPER 932610] p 486 A95-90079
- The A340 electrical power generation system [CONGRESS PAPER C428-36-193] p 625 A95-93630

- The development of a model specification for ground support equipment
[CONGRESS PAPER C428-38-095] p 625 A95-93636
- GROUND TESTS**
Reducing low frequency noise emissions from a Langley Air Force Base Hush-House p 561 A95-90112
Optimal trajectories for an unmanned air-vehicle in the horizontal plane
[BTN-95-EIX0619952748191] p 606 A95-94480
NASA's Hypersonic Research Engine Project: A review
[NASA-TM-107759] p 50 N95-12860
Simulation of Shuttle launch G forces and acoustic loads using the NASA Ames Research Center 20G centrifuge
p 86 N95-14089
High Alpha Technology Program (HATP) ground test to flight comparisons p 68 N95-14230
A model for preliminary facility design including simulation issues p 144 N95-16318
Hypersonic air-breathing aer propulsion facility test support requirements p 144 N95-16319
Development of a low-aspect ratio fin for flight research experiments p 108 N95-16858
[NASA-TM-4596]
Hypersonic flight testing
[AD-A283981] p 134 N95-18891
Description and flow characterization of hypersonic facilities
[AD-A284291] p 223 N95-20248
The Supersonic Expansion Tube concept, experiment and analysis p 341 N95-25399
Propulsion Controlled Aircraft design and development p 697 N95-33022
- GROUND TRUTH**
Field verification of the wind tunnel coefficients p 109 N95-17291
Flight test evaluation of the Stanford University/United Airlines differential GPS Category 3 automatic landing system
[NASA-TM-110354] p 593 N95-30788
- GROUND WIND**
Observations of fluxes and inland breezes over a heterogeneous surface
[HTN-95-80258] p 212 A95-66315
- GROUND-AIR-GROUND COMMUNICATION**
Integrated voice and data communications for air traffic service applications p 600 A95-95090
- GUIDANCE (MOTION)**
Moving mass trim control for aerospace vehicles
[DE95-002602] p 299 N95-23532
- GUIDANCE SENSORS**
Aero-optics system integration
[TABES PAPER 94-604] p 100 N95-14638
Assessment of a non-dedicated GPS receiver system for precise airborne attitude determination
[DE94-019309] p 229 N95-21520
The DLR research programme on an integrated multi sensor system for surface movement guidance and control p 689 N95-33135
- GUIDE VANES**
Propulsion simulator for high bypass turbofan performance evaluation
[SAE PAPER 931410] p 625 A95-93676
- GULF OF MEXICO**
Oceanic operations: An authoritative guide to oceanic operations
[FAA-AFS-550] p 277 N95-24065
- GULF STREAM**
Orbital velocities induced by surface waves
[HTN-95-90902] p 253 A95-72411
Assimilation of altimeter data in a quasi-geostrophic model of the Gulf Stream system: A dynamical perspective
[NASA-CR-196313] p 320 N95-23766
- GUN PROPELLANTS**
The 1993 JANNAF Propulsion Meeting, volume 1
[CPIA-PUBL-602-VOL-1] p 148 N95-16312
- GUST ALLEVIATORS**
Collectively variable incidence wingtips for lift control and reduced gust sensitivity
[HTN-95-92836] p 471 A95-90754
A gust alleviation method by the response feedback p 506 A95-91493
- GUST LOADS**
Response of a nonrotating rotor blade to lateral turbulence. Part 2: Experiment
[BTN-95-EIX95182619229] p 284 A95-76655
Reanalysis of European flight loads data
[AD-A282052] p 9 N95-11179
The impact of non-linear flight control systems on the prediction of aircraft loads due to turbulence p 143 N95-18598
A study of the effect of store unsteady aerodynamics on gust and turbulence loads p 133 N95-18601
- Comparison of stochastic and deterministic nonlinear gust analysis methods to meet continuous turbulence criteria p 133 N95-18602
A review of gust load calculation methods at de Havilland p 118 N95-18604
Special effects of gust loads on military aircraft p 133 N95-18605
Derived gust spectra for the Macchi MB326H
[ARL-TN-3] p 225 N95-21892
Review of aeronautical fatigue investigation in the Netherlands during the period March 1991-March 1993
[PB95-139184] p 285 N95-23161
Calculation of design load for the MOD-SA 7.3 mW wind turbine system p 440 N95-27982
Comparison of measured and calculated dynamic loads for the Mod-2 2.5 mW wind turbine system p 440 N95-27983
Advanced gust management systems: Lessons learned and perspectives p 622 N95-32002
- GUSTS**
H(sup 2)/H(sup INF) controller design for a two-dimensional thin airfoil flutter suppression
[BTN-94-EIX94511433918] p 141 A95-64584
Continuous gust response and sensitivity derivatives using state-space models
[BTN-95-EIX95062487551] p 203 A95-68365
Brief history of gust models for aircraft design
[BTN-95-EIX95062487557] p 203 A95-68371
Final results of the weather testing component of the Terminal Doppler Weather Radar operational test and evaluation p 658 A95-93471
The use of radar wind profiles to remove TDWR gust front algorithm false alarms caused by vertical wind shear p 661 A95-93488
Statistical discrete gust-power spectral density methods overlap-holistic proof and beyond
[BTN-95-EIX0619952748175] p 584 A95-94469
Reanalysis of European flight loads data
[AD-A282052] p 9 N95-11179
Field verification of the wind tunnel coefficients p 109 N95-17291
Measurement of gust response on a turbine cascade
[NASA-TM-106776] p 117 N95-18457
Treatment of non-linear systems by timeplane-transformed CT methods: The spectral gust method p 143 N95-18600
Design limit loads based upon statistical discrete gust methodology p 133 N95-18603
A review of gust load calculation methods at de Havilland p 118 N95-18604
Special effects of gust loads on military aircraft p 133 N95-18605
Calculation of design load for the MOD-SA 7.3 mW wind turbine system p 440 N95-27982
The pressure field of a gust interacting with a flat plate p 557 N95-30161
- GYROCOMPASSES**
Covariance analysis of strapdown INS considering gyrocompass characteristics
[BTN-95-EIX95202637592] p 279 A95-76697
Results from tests of the Honeywell integrated flight management unit
[PB95-211355] p 601 N95-30597
- GYROSCOPES**
DC electrostatic gyro suspension system for the Gravity Probe B experiment p 527 N95-29794
- GYROSCOPIC STABILITY**
Stability of magnetic bearing-rotor systems and the effects of gravity and damping
[BTN-94-EIX94441386619] p 208 A95-68168
Evaluation of energy-sink stability criteria for dual-spin spacecraft
[AD-A283228] p 87 N95-14850
Gyroscopic and propeller aerodynamic effects on engine mounts dynamic loads in turbulence conditions p 132 N95-18599
DC electrostatic gyro suspension system for the Gravity Probe B experiment p 527 N95-29794
- H**
- H-INFINITY CONTROL**
H-infinity helicopter flight control law design with and without rotor state feedback
[BTN-95-EIX95182619129] p 291 A95-76606
A design of a self-learning robust scheduled autopilot p 516 A95-91533
Automation of hardware-in-the-loop testing of control systems for unmanned air vehicles
[AD-A284833] p 194 N95-19693
Design of robust optimal control systems and stability analysis of real structured uncertainties
[AD-A279089] p 256 N95-21913
- Stable H(infinity) controller design for the longitudinal dynamics of an aircraft
[NASA-TM-106847] p 293 N95-22954
Feedback control laws for highly maneuverable aircraft
[NASA-CR-197944] p 295 N95-23410
- H-60 HELICOPTER**
Configuration and other differences between Black Hawk and Seahawk helicopters in military service in the USA and Australia
[AR-008-386] p 336 N95-25935
- HAIL**
The real-time analysis and prediction of storms program p 655 A95-93457
Sensing thunderstorm microphysics with multiparameter radar: Application for aviation p 657 A95-93467
Impact loading of compressor stator vanes by hailstone ingestion p 200 N95-19670
Hailstone heat and mass transfer measurements
[ISBN-0-315-86304-8] p 563 N95-29797
- HALOCARBONS**
Chemical options to halons for aircraft use
[AD-A293741] p 599 N95-31569
- HAMILTONIAN FUNCTIONS**
Trajectory optimization using parallel shooting method on parallel computer
[BTN-95-EIX95282706670] p 564 A95-88175
Vortex drift: A historical survey p 455 A95-88897
Dynamics of phase ordering of nematics in a pore
[DE95-607662] p 362 N95-25978
Aeroelasticity and structural optimization of composite helicopter rotor blades with swept tips
[NASA-CR-4665] p 397 N95-28262
- HANDBOOKS**
Naval Aviation System TEAM mapping, charting, and geodesy handbook
[AD-A288590] p 446 N95-26841
- HANGARS**
Hangars as noise barriers for helicopter noise p 560 A95-90111
- HARDENING (MATERIALS)**
Mechanism and technological particular features of thermomagnetic hardening
[BTN-94-EIX94461407953] p 89 A95-62627
- HARDNESS**
Evaluation of advanced aerospace materials by depth sensing indentation and scratch methods
[BTN-95-EIX95152584678] p 282 A95-73590
A CMC database for use in the next generation launch vehicles (rockets) p 150 N95-18993
E-6A hardness assurance, maintenance and surveillance program
[AD-A283994] p 134 N95-19067
- HARDWARE**
AIAA Computing in Aerospace 10, San Antonio, TX, March 28-30, 1995
[ISBN 1-56347-119-1] p 565 A95-90629
An overview of issues encountered in parallelizing high-resolution weather prediction models p 676 A95-93560
- HARMONIC CONTROL**
Recent studies of rotorcraft blade-vortex interaction noise
[BTN-95-EIX95062487521] p 218 A95-69229
Analysis of a higher harmonic control test to reduce blade vortex interaction noise
[BTN-95-EIX95152582330] p 265 A95-73532
A higher harmonic control test in the DNW to reduce impulsive BVI noise
[HTN-95-61071] p 385 A95-83655
Hubload responses of a rotor in forward flight due to multiple frequency blade pitch variations p 515 A95-91504
Aeroelastic simulation of higher harmonic control
[NASA-CR-4623] p 37 N95-11911
Higher harmonic control analysis for vibration reduction of helicopter rotor systems
[NASA-TM-103855] p 66 N95-14419
- HARMONIC MOTION**
Subharmonic and quasi-periodic motions of an eccentric squeeze film damper-mounted rigid rotor
[BTN-94-EIX95011440601] p 429 A95-82982
- HARMONIC OSCILLATORS**
Dynamical systems as models for flow-induced vibrations
[PB95-206991] p 647 N95-30956
- HARMONICS**
On the influence of time-varying flow velocity on unsteady aerodynamics
[HTN-95-61073] p 369 A95-83657
Control-nonlinear-nonstationary structural response and radiation near a supersonic jet
[HTN-95-20929] p 463 A95-88968

HARNESSES

- The performance of child restraint devices in transport airplane passenger seats
[DOT/FAA/AM-94/19] p 40 N95-12146
- Development of an intervention program to encourage shoulder harness use and aircraft retrofit in general aviation aircraft, phases 1 and 2
[DOT/FAA/AM-95/2] p 333 N95-24384
- Partial discharge testing of high voltage wiring harness for airborne displays
[AD-A289150] p 401 N95-27003
- Development of an intervention program to encourage shoulder harness use and aircraft retrofit in general aviation aircraft: Phases 1 and 2
[AD-A290966] p 485 N95-29873
- HARRIER AIRCRAFT**
- Simulation and flight test evaluation of head-up-display guidance for harrier approach transitions
[BTN-95-EIX95062487533] p 194 A95-69241
- Moisture induced pressures in concrete airfield pavements
[AD-A281974] p 52 N95-11789
- VSTOL Systems Research Aircraft (VSRA) Harrier
[NASA-TM-110117] p 126 N95-18347
- An analysis of the costs and benefits in improving F402-RR-406A High Pressure Turbine, second stage blades under the aircraft engine Component Improvement Program (CIP)
[AD-A285127] p 197 N95-19595
- Forecasting aircraft mishaps using monthly maintenance reports
[AD-A286049] p 227 N95-22417
- Navy composite maintenance and repair experience
p 424 N95-28446
- Flight demonstration of an advanced pitch control law in the VAAC Harrier aircraft
p 623 N95-32012

HAZARDS

- Radial reefing method for accelerated and controlled parachute opening
[BTN-95-EIX95062487539] p 187 A95-69247
- The assessment of the AH-64D, longbow, mast-mounted assembly noise hazard for maintenance personnel
[AD-A284971] p 171 N95-16226
- Assuring Known Good Die (KGD) for reliable, cost effective MCMs
p 246 N95-20644
- Radar studies of aviation hazards
[AD-A285845] p 226 N95-21831
- Mishap risk control for advanced aerospace/composite materials
p 301 N95-23031
- The effect of aviation fuels containing low amounts of static dissipater additive on electrostatic charge generation
[AD-A280075] p 420 N95-28152
- Environmentally Safe and Effective Processes for Paint Removal
[AGARD-LS-201] p 650 N95-32165

HEAD-UP DISPLAYS

- Design of wide angle head up displays for synthetic vision
[BTN-95-EIX95212641070] p 287 A95-76735
- Status of Enhanced Vision System
p 506 A95-91542
- Design of head-up display symbology for recovery from unusual attitudes
p 611 A95-95044
- Instructional control and part/whole-task training: A review of the literature and an experimental comparison of strategies applied to instructional simulation
[AD-A280860] p 21 N95-10919
- Airplane takeoff and landing performance monitoring system
[NASA-CASE-LAR-14745-2-SB] p 85 N95-14415
- VSTOL Systems Research Aircraft (VSRA) Harrier
[NASA-TM-110117] p 126 N95-18347
- TRISTAR 1: Evaluation methods for testing head-up display (HUD) flight symbology
[NASA-TM-4665] p 288 N95-24030
- Simulation model of the integrated flight/propulsion control system, displays, and propulsion system for ASTOVL lift-fan aircraft
[NASA-TM-108866] p 405 N95-26412
- Analysis of heads-up display quickening versus handling qualities
[AD-A293797] p 611 N95-31584
- The effects of display location and dimensionality on taxiway navigation
[AD-A294878] p 690 N95-34570

HEARING

- The assessment of the AH-64D, longbow, mast-mounted assembly noise hazard for maintenance personnel
[AD-A284971] p 171 N95-16226

HEAT BALANCE

- Enhancements to integral solutions to ablation and charring
[BTN-95-EIX95302694461] p 636 A95-94058

HEAT ENGINES

- On a program-information system TDoft
[BTN-94-EIX94461408773] p 175 A95-63656
- Advanced Turbine Technology Applications Project (ATTAP)
[NASA-CR-195393] p 101 N95-15743
- Anisotropic heat exchangers/stack configurations for thermoacoustic heat engines
[AD-A280974] p 168 N95-16506

HEAT EXCHANGERS

- Base drag prediction on missile configurations
[BTN-95-EIX95152583256] p 266 A95-73557
- A low fin height heat exchanger technology demonstrator for Hermes
[SAE PAPER 932119] p 526 A95-90360
- Oscillating-flow regenerator test rig
[NASA-CR-196982] p 53 N95-13200
- Anisotropic heat exchangers/stack configurations for thermoacoustic heat engines
[AD-A280974] p 168 N95-16506
- Airborne rotary separator study
[NASA-CR-191045] p 150 N95-18743
- Malone-brayton cycle engine/heat pump
[AD-D016573] p 244 N95-20295
- Microchannel heat pipe cooling of modules
p 246 N95-20649
- Phase 2: HGM air flow tests in support of HEX vane investigation
p 312 N95-23438
- Mechanism of deposit formation on fuel-wetted hot metal surfaces
[AD-A289847] p 426 N95-28621

HEAT FLUX

- Kinetic theory in aerothermodynamics
[HTN-95-A0002] p 183 A95-67829
- Time-resolved surface heat flux measurements in the wing/body junction vortex
[BTN-95-EIX95082502716] p 220 A95-71029
- Hypersonic model testing in a shock tunnel
[BTN-95-EIX95222650789] p 329 A95-79245
- Experiment and analysis on heat transfer of a scramjet leading edge model
p 403 A95-82420
- Free convection past a uniform flux surface inclined at a small angle to the horizontal
[HTN-95-42213] p 430 A95-84029
- Contribution of thermal radiation to the temperature profile of ceramic composite materials
[BTN-94-EIX95011441252] p 417 A95-84209
- Constant flux, turbulent convection data using infrared imaging
[HTN-95-20731] p 435 A95-86621
- Corrective term in wall slip equations for Knudsen layer
[BTN-95-EIX95282705070] p 455 A95-89667
- The use of hot film for the investigation of boundary-layer transition
[CONGRESS PAPER C428-9-199] p 475 A95-91697
- Heat transfer on bent-noise biconic in hypersonic flow
p 639 A95-95394
- Hypersonic engine leading edge experiments in a high heat flux, supersonic flow environment
[NASA-TM-106742] p 91 N95-14299
- Turbine-engine applications of thermographic-phosphor temperature measurements
[DE95-003625] p 358 N95-25110
- Influence of turbulence parameters, Reynolds number, and body shape on stagnation-region heat transfer
[NASA-TP-3487] p 550 N95-28719

HEAT GENERATION

- On introduction of artificial intelligence elements to heat power engineering
[BTN-94-EIX94461407961] p 100 A95-62635

HEAT MEASUREMENT

- The use of thermochromic liquid crystals for heat transfer measurements in short duration hypersonic wind tunnel facilities
[AIAA PAPER 95-6115] p 520 A95-90443
- Science objectives and performance of a radiometer and window design for atmospheric entry experiments
[NASA-TM-4637] p 63 N95-12190

HEAT OF SOLUTION

- Analytical solution for controls, heats, and states of flight trajectories
[BTN-95-EIX95152583286] p 282 A95-73587

HEAT PIPES

- Experimental investigation of composite channel heat pipe operation in micro-gravity environment
p 428 A95-82645
- Microchannel heat pipe cooling of modules
p 246 N95-20649

HEAT PUMPS

- Second-law analysis of vapor compression heat pumps with solution circuit
[BTN-94-EIX95011441236] p 431 A95-84193
- Malone-brayton cycle engine/heat pump
[AD-D016573] p 244 N95-20295

HEAT RESISTANT ALLOYS

- National AeroSpace Plane: Technology transfer
[BTN-95-EIX95072498879] p 180 A95-68395
- Fatigue crack growth in nickel-based superalloys at 500-700 C. 1: Waspaloy
[BTN-94-EIX94371347843] p 206 A95-69136
- Fatigue strength of high-temperature alloys under conditions of cyclic temperature variation. Communication 1: Experimental procedure and results
[BTN-94-EIX94401363884] p 307 A95-75516
- Study on the turbine vane and blade for a 1500 C class industrial gas turbine
[BTN-94-EIX95011441254] p 431 A95-84211
- The potential for CMCs to replace superalloys in engine exhaust ducts
[HTN-95-42298] p 418 A95-84992
- Fatigue in single crystal nickel superalloys
[AD-A283459] p 56 N95-12546
- Fatigue in single crystal nickel superalloys
[AD-A282917] p 88 N95-15415
- Fatigue in single crystal nickel superalloys
[AD-A285727] p 152 N95-18068
- New Trends in coatings developments for turbine blades: Materials processing and repair
p 201 N95-19676
- Allison engine testing CMSX-4(reg sign) single crystal turbine blades and vanes
[DE95-010308] p 694 N95-32636

HEAT SHIELDING

- Ablative thermal management structural material on the hypersonic vehicles
[AIAA PAPER 95-6133] p 547 A95-90452
- Application of integral methods to ablation charring erosion, a review
[BTN-95-EIX95302694460] p 636 A95-94057
- Enhancements to integral solutions to ablation and charring
[BTN-95-EIX95302694461] p 636 A95-94058
- Test model designs for advanced refractory ceramic materials
p 55 N95-11968

HEAT SINKS

- High heat sink fuels for improved aircraft thermal management
[SAE PAPER 932084] p 530 A95-91659

HEAT TRANSFER

- Heat transfer in the flow-through part of axial compressors
[BTN-94-EIX94461407949] p 89 A95-62267
- Investigation of heat transfer in a rotating ring gap with the axial flow of a coolant during the rotation of the central shaft
[BTN-94-EIX94461407951] p 89 A95-62625
- Investigation of heat transfer between rotating shafts of transmissions of turbojet engines
[BTN-94-EIX94461408760] p 138 A95-63643
- Nonhydrostatic simulation of frontogenesis in a moist atmosphere. Part 3: Thermal wind imbalance and rainbands
[HTN-95-90356] p 212 A95-66429
- Experimental and computational results for the external flowfield of a scramjet inlet
[BTN-94-EIX94441380977] p 195 A95-68161
- Time-resolved surface heat flux measurements in the wing/body junction vortex
[BTN-95-EIX95082502716] p 220 A95-71029
- Measurement and analysis of nitric oxide radiation in an arcjet flow
[BTN-95-EIX95082502727] p 243 A95-71040
- Comparison of linear stability results with flight transition data
[BTN-95-EIX95182619097] p 283 A95-76582
- Application of a control-volume-based finite-element formulation to the shock tube problem
[BTN-95-EIX95182619099] p 295 A95-76584
- Simulating heat addition via mass addition in constant area compressible flows
[BTN-95-EIX95182619100] p 307 A95-76585
- Impingement cooling of an isothermally heated surface with a confined slot jet
[BTN-94-EIX94421348950] p 347 A95-78494
- Experiment and analysis on heat transfer of a scramjet leading edge model
p 403 A95-82420
- Experimental investigation of composite channel heat pipe operation in micro-gravity environment
p 428 A95-82645
- Convection heat transfer distributions over plates with square ribs from infrared thermography measurements
[HTN-95-20713] p 435 A95-86603
- A flow pattern map for two-phase liquid-gas flow under reduced gravity conditions
p 539 A95-87280
- Experimental study of shock/shock interference heating on a swept cylinder
p 472 A95-91510
- The concept of high speed commercial transporter structure
p 498 A95-91517
- Momentum and scalar transfer coefficients over aerodynamically smooth Antarctic surfaces
[HTN-95-92932] p 562 A95-91870

- Natural convection in central microcavities of vertical, finned enclosures of very high aspect ratios
[BTN-95-EIX95282711336] p 632 A95-92405
- Advanced passive cooling for high power electromechanical actuators
[SAE PAPER 931397] p 634 A95-93669
- Evaluation of a multigrid-based Navier-Stokes solver for aerothermodynamic computations
[BTN-95-EIX95302694459] p 583 A95-94056
- Leading-edge sweepback and shape effects on fin-induced fluctuating pressures
[BTN-95-EIX95302694471] p 636 A95-94067
- Laws of infrared similitude
[AD-A282209] p 62 N95-12426
- Impingement flow heat transfer measurements of turbine blades using a jet array
[AD-A283450] p 62 N95-12512
- Service and physical properties of liquid-jet fuels
p 151 N95-16256
- An engineering code to analyze hypersonic thermal management systems
p 155 N95-16322
- Hypersonic wind tunnel test techniques
[AD-A284057] p 118 N95-18663
- Hypersonic flight testing
[AD-A283981] p 134 N95-18891
- Application of multidisciplinary models to the cooled turbine rotor design
p 140 N95-19024
- An investigation of drag repeatability in half model testing in the ARA Transonic Wind Tunnel
[ARA-MEMO-392] p 188 N95-19546
- Experimental study of vane heat transfer and aerodynamics at elevated levels of turbulence
[NASA-CR-4633] p 244 N95-19912
- Investigation of a thermal buoyancy effect on the drag of half models tested in the ARA Transonic Wind Tunnel
[ARA-MEMO-407] p 222 N95-19946
- Microchannel heat pipe cooling of modules
p 246 N95-20649
- Shock wave interactions in hypervelocity flow
[AD-A286507] p 250 N95-22212
- Development and verification of a resin film infusion/resin transfer molding simulation model for fabrication of advanced textile composites
[NASA-CR-197439] p 301 N95-23179
- WINCLR: A computer code for heat transfer and clearance calculation in a compressor
[NASA-CR-195436] p 366 N95-26363
- Leading edge film cooling effects on turbine blade heat transfer
[NASA-TM-106955] p 513 N95-29115
- Grid orthogonality effects on predicted turbine midspan heat transfer and performance
[NASA-TM-106931] p 554 N95-29371
- Halitstone heat and mass transfer measurements
[ISBN-0-315-86304-8] p 563 N95-29797
- Jet mixing in a reacting cylindrical crossflow
[NASA-TM-106975] p 616 N95-30853
- Review of combustion-acoustic instabilities
[NASA-TM-107020] p 705 N95-32930
- HEAT TRANSFER COEFFICIENTS**
- Effect of surface roughness on local film cooling effectiveness and heat transfer coefficients
[AD-A283854] p 91 N95-14351
- Effect of velocity and temperature distribution at the hole exit on film cooling of turbine blades
[NASA-TM-106954] p 616 N95-30702
- HEAT TRANSMISSION**
- Drag and lift in nonadiabatic transonic flow
[HTN-95-61208] p 540 A95-87581
- HEATING**
- Cabin fuselage structural design with engine installation and control system
[NASA-CR-197173] p 47 N95-12639
- Vapor generator wand
[NASA-CASE-LAR-15058-1] p 238 N95-20080
- Residual Stress Measurements with Laser Speckle Correlation Interferometry and Local Heat Treating
[DE95-060082] p 349 N95-24598
- HEATING EQUIPMENT**
- Second-law analysis of vapor compression heat pumps with solution circuit
[BTN-94-EIX95011441236] p 431 A95-84193
- A programmable heater control circuit for spacecraft
[NASA-TM-108459] p 9 N95-11157
- HEAVY LIFT LAUNCH VEHICLES**
- A shadowgraph study of the National Launch System's 1 1/2 stage vehicle configuration and Heavy Lift Launch Vehicle configuration -- Using the Marshall Space Flight Center's 14-Inch Transonic Wind Tunnel
[NASA-RP-1347] p 35 N95-11710
- HLLV avionics requirements study and electronic filing system database development
[NASA-CR-193993] p 49 N95-13027
- HEIGHT**
- A northern hemisphere clear air turbulence climatology
p 674 A95-93547

HELICOPTER CONTROL

- Test bench for rotorcraft hover control
[BTN-94-EIX94511433919] p 169 A95-64585
- Rotorcraft control system design for uncertain vehicle dynamics using quantitative feedback theory
[HTN-95-31012] p 236 A95-71182
- Smart structures in the control of airframe vibrations
[HTN-95-31014] p 236 A95-71184
- A generalized algorithm for inverse simulation applied to helicopter maneuvering flight
[HTN-95-A0493] p 236 A95-72564
- High-order state space simulation models of helicopter flight mechanics
[HTN-95-A0494] p 237 A95-72565
- Identification of higher order helicopter dynamics using linear modeling methods
[HTN-95-80851] p 290 A95-75093
- Effects of high order dynamics on helicopter flight control law design
[HTN-95-80852] p 290 A95-75094
- Investigation of the effects of bandwidth and time delay on helicopter roll-axis handling qualities
[HTN-95-80853] p 290 A95-75095
- Integrated flight/propulsion control for helicopters
[HTN-95-80854] p 290 A95-75096
- H-infinity helicopter flight control law design with and without rotor state feedback
[BTN-95-EIX95182619129] p 291 A95-76606
- Automatic guidance and control for helicopter obstacle avoidance
[BTN-95-EIX95182619130] p 291 A95-76607
- Neuro-controllers for adaptive helicopter training
[SAE PAPER 932535] p 379 A95-84557
- Automated hover training: An empirical evaluation
[SAE PAPER 932536] p 379 A95-84559
- Torsional actuation with extension-torsion composite coupling and a magnetostrictive actuator
[BTN-95-EIX95262694314] p 435 A95-85485
- Flight-testing and frequency-domain analysis for rotorcraft handling qualities
[HTN-95-01083] p 515 A95-90269
- Automatic identification of modal damping from Floquet analysis
[HTN-95-01084] p 506 A95-90270
- Application of GPS and Fuzzy Theory to a helicopter
p 516 A95-91505
- Development of Fly-By-Wire system for BK117
p 516 A95-91506
- Functions of NAL fixed base simulator for helicopter research
p 522 A95-91555
- A simulator study about effects of visibility upon helicopter pilot performance
p 522 A95-91556
- Theory and evaluation of active control as a means of reducing helicopter vibration
[CONGRESS PAPER C428-19-124] p 517 A95-91721
- Passive and active vibration control activities in the German helicopter industry
[CONGRESS PAPER C428-19-126] p 517 A95-91722
- Development of software for safety critical applications for the EH101 Helicopter
[CONGRESS PAPER C428-24-160] p 678 A95-93597
- Chinook goes FADEC
[CONGRESS PAPER C428-33-078] p 610 A95-93621
- Design and flight evaluation of an integrated navigation and near-terrain helicopter guidance system for night-time and adverse weather operations
[NASA-TM-108837] p 11 N95-10846
- Research on an autonomous vision-guided helicopter
[AIAA PAPER 94-1240-CP] p 18 N95-11510
- Aeroelastic simulation of higher harmonic control
[NASA-CR-4623] p 37 N95-11911
- Techniques for designing rotorcraft control systems
[NASA-CR-196192] p 52 N95-12791
- Design and flight test of a simplified control system for a transport helicopter
p 144 N95-18902
- An investigation of helicopter dynamic coupling using an analytical model
[NASA-CR-197420] p 285 N95-23217
- An investigation of the effects of pitch-roll (de)coupling on helicopter handling qualities
[NASA-TM-110349] p 409 N95-26773
- Experiences with ADS-33 helicopter specification testing and contributions to refinement research
p 621 N95-31993
- Model following control for tailoring handling qualities: ACT experience with ATHeS
p 622 N95-32000
- Practical experiences in control systems design using the NCR Bell 205 Airborne Simulator
p 624 N95-32015

HELICOPTER DESIGN

- Design optimization of rotor blades for improved performance and vibration
[HTN-95-A0498] p 229 A95-72569
- Integrated flight/propulsion control for helicopters
[HTN-95-80854] p 290 A95-75096
- H-76B fantail demonstrator composite fan blade fabrication
[HTN-95-80856] p 283 A95-75098
- Multilevel decomposition procedure for efficient design optimization of helicopter rotor blades
[BTN-95-EIX95222650784] p 334 A95-79240
- Dynamic-stall and structural-modeling effects on helicopter blade stability with experimental correlation
[HTN-95-81646] p 542 A95-87694
- Optimal design of composite helicopter power transmission shafts with axially varying fiber layout
[HTN-95-01086] p 529 A95-90272
- Design and flight evaluation of an integrated navigation and near-terrain helicopter guidance system for night-time and adverse weather operations
[NASA-TM-108837] p 11 N95-10846
- The potential of genetic algorithms for conceptual design of rotor systems
[NASA-CR-196813] p 43 N95-11699
- Construction and wind tunnel test of a 1/12th scale helicopter model
[AD-A288487] p 378 N95-28331
- Modeling helicopter blade dynamics using a modified Myklestad-Prohl transfer matrix method
[AD-A289891] p 400 N95-28626
- A novel instrumentation system for measurement of helicopter rotor motions and loads data, phase 1
[AD-A293309] p 607 N95-30923
- Automatic flight control system for an unmanned helicopter system design and flight test results
p 622 N95-32004
- HELICOPTER ENGINES**
- Erosion of dust-filtered helicopter turbine engines. Part 1: Basic theoretical considerations
[BTN-95-EIX95182619222] p 288 A95-76648
- Erosion of dust-filtered helicopter turbine engines. Part 2: Erosion reduction
[BTN-95-EIX95182619223] p 289 A95-76649
- Life prediction of helicopter engines fitted with dust filters
[BTN-95-EIX95182619224] p 289 A95-76650
- Design and development of an advanced two-stage centrifugal compressor
[BTN-95-EIX95282710054] p 633 A95-92475
- Chinook goes FADEC
[CONGRESS PAPER C428-33-078] p 610 A95-93621
- Sensor fault detection and diagnosis simulation of a helicopter engine in an intelligent control framework
[AD-A290223] p 137 N95-15970
- Numerical simulation of helicopter engine plume in forward flight
[NASA-CR-197488] p 107 N95-16589
- US Army rotorcraft turboshaft engines sand and dust erosion considerations
p 198 N95-19656
- Future directions in helicopter protection system configuration
p 198 N95-19657
- HELICOPTER PERFORMANCE**
- Validation of the dynamic response of a blade-element UH-60 simulation model in hovering flight
[HTN-94-00663] p 18 A95-60155
- The effect of rotating loads suspended under a helicopter on their amplitude-frequency characteristics
[BTN-94-EIX94461407959] p 78 A95-62633
- A generalized algorithm for inverse simulation applied to helicopter maneuvering flight
[HTN-95-A0493] p 236 A95-72564
- High-order state space simulation models of helicopter flight mechanics
[HTN-95-A0494] p 237 A95-72565
- Air and ground resonance of helicopters with elastically tailored composite rotor blades
[HTN-95-A0497] p 222 A95-72568
- Design optimization of rotor blades for improved performance and vibration
[HTN-95-A0498] p 229 A95-72569
- Investigation of the effects of bandwidth and time delay on helicopter roll-axis handling qualities
[HTN-95-80853] p 290 A95-75095
- The influence of alternate inter-blade connections on ground resonance
[HTN-95-80859] p 267 A95-75101
- Dynamic stall control for advanced rotorcraft application
[BTN-95-EIX95222650793] p 334 A95-79249
- Rotorcraft handling qualities in turbulence
[BTN-95-EIX95242670750] p 334 A95-81097
- Condition monitoring and diagnostics
[HTN-95-92312] p 387 A95-85356

- Flight-testing and frequency-domain analysis for rotorcraft handling qualities
[HTN-95-01083] p 515 A95-90269
- An investigation of piloting strategies for engine failures during takeoff from offshore platforms
[HTN-95-92834] p 497 A95-90752
- Flight testing of the composite material bearingless rotor system for the helicopter
p 498 A95-91503
- Hubload responses of a rotor in forward flight due to multiple frequency blade pitch variations
p 515 A95-91504
- Progress and experience with helicopter health and usage monitoring
[CONGRESS PAPER C428-31-151] p 603 A95-93615
- Add a dimension to your analysis of the helicopter low airspeed environment
[AD-A283982] p 79 N95-14205
- Helicopter Performance Evaluation (HELPE) computer model
[AD-A284319] p 131 N95-18381
- An investigation of the effects of pitch-roll (de)coupling on helicopter handling qualities
[NASA-TM-110349] p 409 N95-26773
- An analytic modeling and system identification study of helicopter dynamics
p 505 N95-29787
- HELICOPTER PROPELLER DRIVE**
- Optimal design of composite helicopter power transmission shafts with axially varying fiber layout
[HTN-95-01086] p 529 A95-90272
- Flight testing of the composite material bearingless rotor system for the helicopter
p 498 A95-91503
- Aircraft gear train diagnostics using the irregular rotation of the external shafts
[CONGRESS PAPER C428-15-097] p 508 A95-91712
- Gearbox vibration diagnostic analyzer
[NASA-CR-189141] p 316 N95-23792
- A portable transmission vibration analysis system for the S-70A-9 Black Hawk helicopter
[DSTO-TR-0072] p 348 N95-24203
- Bell Helicopter Advanced Rotorcraft Transmission (ART) program
[NASA-CR-195479] p 555 N95-29538
- HELICOPTER TAIL ROTORS**
- Measurements of atmospheric turbulence effects on tail rotor acoustics
[NASA-TM-108843] p 38 N95-12360
- HELICOPTER WAKES**
- Aerodynamic and wake methodology evaluation using Model UH-60A experimental data
[HTN-95-31009] p 220 A95-71179
- Vorticity concentration at the edge of the inboard vortex sheet
[HTN-95-31010] p 221 A95-71180
- Flap-lag damping in hover and forward flight with a three-dimensional wake
[HTN-95-A0496] p 221 A95-72567
- Vortex methods for the computational analysis of rotor/body interaction
[HTN-95-61072] p 369 A95-83656
- Considerations in the development of the coupled rotor fuselage model
[HTN-95-61077] p 370 A95-83661
- Laser velocimetry and blade pressure measurements of a blade-vortex interaction
[HTN-95-01081] p 547 A95-90267
- Rotor-wake-induced flow separation on a lifting surface
[HTN-95-01082] p 468 A95-90268
- An experimental investigation of helicopter downwash and tailboom interaction at the Wichita State University 7x10 foot wind tunnel
p 375 N95-26955
- High- and low-frequency dynamics of isolated blades and rotors with dynamic stall and wake
[AD-A290358] p 503 N95-29322
- Validation of the helicopter rotor code HERO
[PB95-198040] p 607 N95-30838
- HELICOPTERS**
- Recent advances in Euler and Navier-Stokes methods for calculating helicopter rotor aerodynamics and acoustics
[HTN-94-00686] p 2 A95-60169
- Assessment of helicopter noise annoyance: A comparison between noise from helicopters and from jet aircraft
[BTN-94-EIX94341341967] p 62 A95-60867
- Test bench for rotorcraft hover control
[BTN-94-EIX94511433919] p 169 A95-64585
- Bilinear formulation applied to the response and stability of helicopter rotor blade
[BTN-95-EIX95042474400] p 192 A95-68300
- Flight control system mode transitions influence on handling qualities and task performance
[BTN-95-EIX95062487525] p 203 A95-69233
- Measurement around a rotor blade excited in pitch. Part 2: Unsteady surface pressure
[HTN-95-31008] p 220 A95-71178
- Rotorcraft control system design for uncertain vehicle dynamics using quantitative feedback theory
[HTN-95-31012] p 236 A95-71182
- Advance finite element modeling of rotor blade aeroelasticity
[HTN-95-31013] p 221 A95-71183
- Smart structures in the control of airframe vibrations
[HTN-95-31014] p 236 A95-71184
- Air and ground resonance of helicopters with elastically tailored composite rotor blades
[HTN-95-A0497] p 222 A95-72568
- Static pressure distribution in the inlet of a helicopter turbine compressor
[BTN-95-EIX95152582339] p 266 A95-73541
- Improving prediction: The incorporation of simplified rotor dynamics in a mathematical model of the bell 412HP
[BTN-95-EIX95152584679] p 282 A95-73591
- Sensitivity of acoustic predictions to variation of input parameters
[HTN-95-80855] p 267 A95-75097
- The influence of alternate inter-blade connections on ground resonance
[HTN-95-80859] p 267 A95-75101
- A higher harmonic control test in the DNW to reduce impulsive BVI noise
[HTN-95-61071] p 385 A95-83655
- Vortex methods for the computational analysis of rotor/body interaction
[HTN-95-61072] p 369 A95-83656
- Effects of blade tip shape on dynamics, cost, weight, aerodynamic performance, and aeroelastic response
[HTN-95-61074] p 369 A95-83658
- Air resonance of hingeless rotor helicopters in trimmed forward flight
[HTN-95-61075] p 369 A95-83659
- An analytical model for a nonlinear elastomeric lag damper and its effect on aeromechanical stability in Hover
[HTN-95-61076] p 369 A95-83660
- Considerations in the development of the coupled rotor fuselage model
[HTN-95-61077] p 370 A95-83661
- Artificial neural networks for predicting nonlinear dynamic helicopter loads
[HTN-95-51678] p 404 A95-85060
- Reduction of blade-vortex interaction noise through porous leading edge
[HTN-95-42324] p 371 A95-86153
- Possible guidelines for helicopter noise assessment
[HTN-95-92535] p 558 A95-87355
- The effects and prediction of rotary wing aircraft noise on the community
[HTN-95-92536] p 558 A95-87356
- Noise levels of helicopters performing elevated pad take-off and landing procedures
[HTN-95-92544] p 559 A95-87364
- Prediction level of noise by a helicopter
p 571 A95-88469
- Assessment of helicopter noise annoyance: A comparison between helicopters and jet aircraft
p 560 A95-88480
- Concepts for the control of rotor noise
p 573 A95-90092
- Studies of blade-vortex interaction noise reduction by rotor blade modification
p 573 A95-90093
- Hangars as noise barriers for helicopter noise
p 560 A95-90111
- Aeronautical technology - recent advances and future prospects
[HTN-95-01097] p 496 A95-90283
- Inadequacy of visual alarms in helicopter air medical transport
[HTN-95-01218] p 484 A95-91450
- The use of math-dynamic models to aid the development of integrated health and usage monitoring systems
[CONGRESS PAPER C428-19-079] p 457 A95-91720
- New filtering method for linear weakly coupled stochastic systems
[BTN-95-EIX0608952736485] p 678 A95-92708
- Autonomous helicopter hover positioning by optical tracking
[HTN-95-C0006] p 585 A95-93394
- Condition monitoring for helicopters: 3303 Airborne vibration monitoring system
[SAE PAPER 931380] p 610 A95-93642
- The application of potential CFD methods to helicopter hover flows
[ISBN 1-879921-01-4] p 587 A95-93747
- Psycho-social safety perceptions: Helicopters as a case study
p 596 A95-95192
- EMS helicopter incidents reported to the NASA Aviation Safety Reporting System
p 596 A95-95201
- Neuro-controllers for adaptive helicopter hover training
[BTN-94-EIX94522407592] p 709 A95-96241
- The present and future of aircraft noise models: A user's perspective
p 32 N95-11324
- FAA vertical flight bibliography
[DOT/FAA/RD-94/17] p 14 N95-11684
- Ten-year ground exposure of composite materials used on the Bell Model 206L helicopter flight service program
[NASA-TP-3468] p 55 N95-12357
- Role of wind tunnels and computer codes in the certification and qualification of rotorcraft for flight in forecast icing
[NASA-TM-106747] p 39 N95-13197
- The principles of flight test assessment of flight-safety-critical systems in helicopters
[AGARD-AG-300-VOL-12] p 77 N95-14199
- Higher harmonic control analysis for vibration reduction of helicopter rotor systems
[NASA-TM-103855] p 66 N95-14419
- Small crack test program for helicopter materials
p 92 N95-14455
- A method of calculating the safe fatigue life of compact, highly-stressed components
p 93 N95-14464
- Vertical flight terminal operational procedures. A summary of FAA research and development
[AD-A283550] p 85 N95-15328
- Test Operation Procedure (TOP): Vibration testing of helicopter equipment
[AD-A284433] p 81 N95-15815
- A correlative investigation of simulated occupant motion and accident report in a helicopter crash
[AD-A285190] p 123 N95-16404
- Experimental data on the aerodynamic interactions between a helicopter rotor and an airframe
p 116 N95-17883
- Helicopter/vertiport MLS precision approaches
[AD-A283505] p 126 N95-18059
- Helicopter Performance Evaluation (HELPE) computer model
[AD-A284319] p 131 N95-18381
- Tilt Rotor Unmanned Air Vehicle System (TRUS) demonstrator flight test program
[AD-A284151] p 132 N95-18415
- Helicopter in-flight simulation development and use in test pilot training
[AD-A283998] p 146 N95-18725
- Helicopter internal noise
p 173 N95-19144
- Particle trajectories in gas turbine engines
p 199 N95-19663
- The calculation of erosion in a gas turbine compressor rotor
p 199 N95-19664
- Multilayer anti-erosion coatings
p 201 N95-19679
- The personal aircraft: Status and issues
[NASA-TM-109174] p 223 N95-20688
- Experimental study of the helicopter-mobile radioelectrical channel and possible extension to the satellite-mobile channel
p 247 N95-20945
- Wavelet transformations for helicopter identification via acoustic signatures
[AD-A279980] p 257 N95-20963
- An investigation of helicopter dynamic coupling using an analytical model
[NASA-CR-197420] p 285 N95-23217
- Thin tailored composite wing for civil tiltrotor
p 285 N95-23317
- Interfacing a digital compass to a remote-controlled helicopter
[PB95-164927] p 340 N95-24260
- Aircraft noise prediction program theoretical manual: Rotorcraft System Noise Prediction System (ROTONET), part 4
[NASA-TM-83199-PT-4] p 451 N95-26392
- An investigation of the effects of pitch-roll (de)coupling on helicopter handling qualities
[NASA-TM-110349] p 409 N95-26773
- Flow structure generated by perpendicular blade vortex interaction and implications for helicopter noise predictions
[NASA-CR-198590] p 377 N95-28193
- Aeroelasticity and structural optimization of composite helicopter rotor blades with swept tips
[NASA-CR-4665] p 397 N95-28262
- Construction and wind tunnel test of a 1/12th scale helicopter model
[AD-A288487] p 378 N95-28331
- Modeling helicopter blade dynamics using a modified Myklestad-Prohl transfer matrix method
[AD-A289991] p 400 N95-28626
- Rotorcraft crashworthy airframe and fuel system technology development program
[AD-A289986] p 382 N95-28630
- Application of parallel processing technology in complex helicopter analysis. Phase 1
[NASA-CR-197850] p 502 N95-28928

Biodynamic simulation of pilot interaction with a helicopter multi-airbag restraint system
[AD-A290196] p 485 N95-29057

Bell Helicopter Advanced Rotocraft Transmission (ART) program
[NASA-CR-195479] p 555 N95-29538

Severe edge effects and simple complementary interior solutions for thin-walled anisotropic and composite structures
[AD-A290645] p 555 N95-29562

First medical test of the UH-60Q and equipment for use in US Army medevac helicopters p 568 N95-29620

Probabilistic reliability modeling of fatigue on the H-46 tie bar
[AD-A289926] p 607 N95-30927

Application of multigrid computational fluid dynamics (CFD) methods to rotor analysis
[AD-A293012] p 648 N95-31475

Advanced flight control technology achievements at Boeing Helicopters p 624 N95-32014

Vibration reduction in helicopter rotors using an actively controlled partial span trailing edge flap located on the blade p 624 N95-32111

Flight test of a low-altitude helicopter guidance system with obstacle avoidance capability p 688 N95-32490

Tactical low-level helicopter communications p 702 N95-32492

The application of helicopter mission simulation to Nap-of-the-Earth operations p 710 N95-32496

Development and flight testing of an Obstacle Avoidance System for US Army helicopters p 687 N95-32500

The Anglo-French Compact Laser Radar demonstrator programme p 703 N95-32501

Direct analysis of transonic rotor noise with CFD technique p 711 N95-34549

HELIPORTS

Noise levels of helicopters performing elevated pad take-off and landing procedures
[HTN-95-92544] p 559 A95-87364

FAA vertical flight bibliography
[DOT/FAA/RD-94/17] p 14 N95-11684

Heliport/vertiport MLS precision approaches
[AD-A283505] p 126 N95-18059

HELIUM

Flowfield measurements in supersonic film cooling including the effect of shock-wave interaction
[HTN-95-42337] p 405 A95-86166

Numerical study of mixing in a high and low enthalpy supersonic test facility p 7 N95-10467

Reducing process noise in superconducting helium liquid level probes
[DE95-008956] p 629 N95-30765

HELMET MOUNTED DISPLAYS

Design and flight evaluation of an integrated navigation and near-terrain helicopter guidance system for night-time and adverse weather operations
[NASA-TM-108837] p 11 N95-10846

Factors affecting the visual fragmentation of the field-of-view in partial binocular overlap displays
[AD-A283081] p 172 N95-17334

Factors affecting the perception of luning in monocular regions of partial binocular overlap displays
[AD-A286287] p 259 N95-22044

Partial discharge testing of high voltage wiring harness for airborne displays
[AD-A289150] p 401 N95-27003

Synthetic Terrain Imagery for Helmet-Mounted Display, Volume 2: Software design document
[AD-A293611] p 612 N95-31655

Synthetic Terrain Imagery for Helmet-Mounted Display, volume 1
[AD-A293612] p 612 N95-31656

Flight test of a low-altitude helicopter guidance system with obstacle avoidance capability p 688 N95-32490

A helmet mounted display for night missions at low altitude p 693 N95-32503

HELMETS

Biodynamic simulation of pilot interaction with a helicopter multi-airbag restraint system
[AD-A290196] p 485 N95-29057

HELMHOLTZ VORTICITY EQUATION

Vortex drift: A historical survey p 455 A95-88897

HEPTANES

Structure of a swirl-stabilized, combusting spray
[NASA-TM-106724] p 50 N95-11890

HERMES MANNED SPACEPLANE

High temperature aspects of the European Hermes programs p 524 A95-87379

A low fin height heat exchanger technology demonstrator for Hermes
[SAE PAPER 932119] p 526 A95-90360

Aeroacoustic qualification of HERMES shingles p 173 N95-19145

HERMITIAN POLYNOMIAL

Image representation using fast algorithms based on the Zak transform
[AD-A293416] p 679 N95-31684

HETERODYNING

Laser based obstacle warning sensors for helicopters p 686 N95-32499

HETEROGENEITY

Evolution of the concentrations of trace species in an aircraft plume: Trajectory study
[HTN-95-A1044] p 443 A95-84549

The effect of material heterogeneity in curved composite beams for use in aircraft structures p 422 N95-28426

HEURISTIC METHODS

Automatic guidance and control for helicopter obstacle avoidance
[BTN-95-EIX95182619130] p 291 A95-76607

HIGH ALTITUDE

Aerodynamic characteristics of a hypersonic viscous optimized waverider at high altitudes
[BTN-95-EIX95152583251] p 266 A95-73552

Higher-order viscous shock-layer solutions for high-altitude flows
[BTN-95-EIX95152583255] p 306 A95-73556

Aerodynamics of the Shuttle Orbiter at high altitudes
[BTN-95-EIX95182617454] p 298 A95-75725

Modeling of plume chemistry of high flying aircraft with H2 combustion engines p 509 A95-87405

A perspective of rarefied gas flow problems relevant to high altitude flight
[SAE PAPER 931366] p 586 A95-93647

Development of techniques for the in situ observation of OH and HO2 for studies of the impact of high-altitude supersonic aircraft on the stratosphere
[NASA-CR-196759] p 61 N95-12832

Photovoltaic electric power applied to Unmanned Aerial Vehicles (UAV) p 245 N95-20530

Particle kinetic simulation of high altitude hypervelocity flight
[NASA-CR-197383] p 309 N95-22481

Design of a high altitude long endurance aircraft with manufacturing considerations p 391 N95-26947

Propulsion system assessment for very high UAV under ERAST
[NASA-CR-195469] p 406 N95-27866

Computation of high-altitude hypersonic flow-field radiation p 593 N95-30843

Unitized Regenerative Fuel Cells for solar rechargeable aircraft and zero emission vehicles
[DE95-010684] p 708 N95-33642

HIGH ALTITUDE BALLOONS

Balloon technology and observations; Symposium P3 of the COSPAR Plenary Meeting, 29th, Washington, DC, Aug. 28-Sept. 5, 1992
[HTN-95-70250] p 181 A95-66276

Balloon flights in France and in Europe p 204 A95-66301

The scientific ballooning in Russia p 191 A95-66302

A program for scientific and applied investigations using aerostat complexes p 182 A95-66304

Application of fuzzy logic to optimize placement of an acquisition, tracking, and pointing experiment p 341 A95-80390

Development and flight results of fiber reinforced balloon p 384 A95-82511

Recent developments in nylon superpressure balloons p 385 A95-82512

Polar Patrol Balloon system and preliminary experimental results p 368 A95-82513

Study on a scheme for the prolongation of microgravity time of balloon-borne drop capsule p 414 A95-82515

Variational principles for ascent shapes of large scientific balloons
[BTN-95-EIX95262694320] p 387 A95-85491

Scientific balloons
[NASA-TM-109907] p 7 N95-10556

HIGH ALTITUDE ENVIRONMENTS

An air-driven pressure booster pump for aircraft-based air sampling
[HTN-95-40689] p 216 A95-69833

HIGH ASPECT RATIO

Natural convection in central microcavities of vertical, finned enclosures of very high aspect ratios
[BTN-95-EIX95282711336] p 632 A95-92405

Convergence acceleration of implicit schemes in the presence of high aspect ratio grid cells p 313 N95-23446

Algorithms for high aspect ratio oriented triangulations p 476 N95-28731

The fluid mechanics of a high aspect ratio slot with an impressed pressure gradient and secondary injection p 557 N95-30304

High aspect ratio metal microstructures and method for preparing the same
[AD-D017463] p 629 N95-30750

HIGH ENERGY ELECTRONS

Induced Compton scattering by relativistic electrons in magnetized astrophysical plasmas p 563 N95-29885

HIGH ENERGY FUELS

Solid fuel ramjet composition
[AD-D016458] p 152 N95-19090

HIGH FREQUENCIES

High-frequency acoustic radiation from a curved duct of circular cross section p 573 A95-90098

Assessing aircraft survivability to high frequency transient threats p 134 N95-18726

Design and development of a test rig for the high frequency testing of rolling sleeve airsprings
[DSTO-TN-0001] p 411 N95-26378

HIGH GRAVITY ENVIRONMENTS

The large radius track centrifuge concept as an acceleration research and simulation device p 379 A95-84560

HIGH PRESSURE

Thermo-hydrodynamic solution of floating ring seals for high pressure compressors using the finite-element method
[HTN-95-92246] p 433 A95-85290

High pressure vaporization and burning of methanol droplets in reduced gravity p 527 A95-87285

Effect of surface roughness on local film cooling effectiveness and heat transfer coefficients
[AD-A283854] p 91 N95-14351

Twin engine afterbody model p 115 N95-17880

Studies on high pressure and unsteady flame phenomena
[AD-A284126] p 152 N95-18410

An analysis of the costs and benefits in improving F402-RR-406A High Pressure Turbine, second stage blades under the aircraft engine Component Improvement Program (CIP)
[AD-A285127] p 197 N95-19595

An investigation of the AFIT 2-inch shock tube as a flow source for supersonic testing
[AD-A289246] p 412 N95-26966

NASA Lewis Research Center's combustor test facilities and capabilities
[NASA-TM-106903] p 412 N95-27176

HIGH RESOLUTION

MAX-91: Polarimetric SAR results on Montespertoli site p 320 N95-23940

Classification of ultra high range resolution radar using decision boundary analysis
[AD-A289378] p 437 N95-26877

Computational algorithms for aerodynamic analysis and design
[AD-A291084] p 482 N95-29972

HIGH REYNOLDS NUMBER

Aerodynamic Investigation with focusing schlieren in a cryogenic wind tunnel p 544 A95-88096

High subsonic and high Reynolds number wind tunnel tests of two-dimensional natural-laminar-flow airfoils with suction boundary layer control p 472 A95-91508

Navier-Stokes simulation of turbulent vortex high-Re-number flows over a delta wing p 644 A95-95507

Numerical simulation of the flow about the F-18 HARV at high angle of attack
[NASA-CR-196396] p 9 N95-10940

Numerical simulation of the flow about an F-18 aircraft in the high-alpha regime p 68 N95-14232

Numerical simulation of the flow about the F-18 HARV at high angle of attack
[NASA-CR-197023] p 74 N95-14614

Detailed study at supersonic speeds of the flow around delta wings p 112 N95-17861

On the Lighthill relationship and sound generation from isotropic turbulence
[NASA-CR-195005] p 159 N95-18191

Unsteady aerodynamic analyses for turbomachinery aeroelastic predictions p 141 N95-19381

Numerical and experimental study of drag characteristics of two-dimensional HLFC airfoils in high subsonic, high Reynolds number flow
[NAL-TR-12447] p 331 N95-24998

Comparative wind tunnel test at high Reynolds numbers of NACA 64 621 airfoils with two aileron configurations p 377 N95-27977

HIGH SPEED

Possible effects of CO2 increase on the high-speed civil transport impact on ozone p 317 A95-75976

Impact on ozone of high-speed stratospheric aircraft: Effects of the emission scenario
[HTN-95-51283] p 356 A95-80868

Mesh generation and adaptivity for the solution of compressible viscous high speed flows
[BTN-95-EIX95262697157] p 538 A95-86893

- Conceptual studies of high speed combustors for mixing enhancement mechanisms
[AJAA PAPER 95-6095] p 510 A95-88003
- GateLink highspeed communications with parked aircraft
[SAE PAPER 932610] p 486 A95-90079
- Signal processing of noise data from high-speed flyovers
[BTN-95-EIX0619952748178] p 680 A95-94248
- The High Speed Research Program
[NASA-TM-109869] p 10 N95-10548
- The Elite: A high speed, low-cost general aviation aircraft for Aeroworld
[NASA-CR-197161] p 45 N95-12530
- The Balsa bullet: A high speed, low-cost general aviation aircraft for Aeroworld
[NASA-CR-197165] p 46 N95-12638
- High-Speed Research: 1994 Sonic Boom Workshop: Atmospheric Propagation and Acceptability Studies
[NASA-CP-3279] p 75 N95-14878
- Error propagation equations for estimating the uncertainty in high-speed wind tunnel test results
[DE94-014136] p 145 N95-16509
- Two-dimensional 16.5 percent thick supercritical airfoil NLR 7301
p 110 N95-17854
- Hypersonic flight testing
[AD-A263981] p 134 N95-18891
- Advanced diesel electronic fuel injection and turbocharging
[AD-A279176] p 211 N95-19809
- Inner loop flight control for the High-Speed Civil Transport
p 293 N95-23314
- Application of CFD to the analysis and design of high-speed inlets
[NASA-CR-198574] p 438 N95-27240
- Modeling and control of rotating stall in high speed multi-stage axial compressors
p 513 N95-29244
- Compressibility effects on and control of dynamic stall of oscillating airfoil
[AD-A291804] p 480 N95-29428
- Characterization of stall inception in high-speed single-stage compressors
[AD-A291275] p 514 N95-29934
- HIGH STRENGTH**
Repairs of CFC primary structures
p 396 N95-27527
- HIGH STRENGTH ALLOYS**
Forming and bonding techniques for high-strength aluminum alloys
[HTN-95-20605] p 418 A95-84786
- HIGH STRENGTH STEELS**
Test method and test results for environmental assessment of aircraft materials
p 302 N95-23509
- HIGH TEMPERATURE**
Mach wave emission from a high-temperature supersonic jet
[HTN-95-42571] p 458 A95-87201
- Lightweight high-temperature fuel metering valves
[SAE PAPER 931444] p 635 A95-93693
- Effects of activated reactive evaporation process parameters on the microhardness of polycrystalline silicon carbide thin films
[GTN-95-00406090-4621] p 680 A95-93965
- Brush seal performance and durability issues based on T-700 engine test results
[NASA-TM-106502] p 22 N95-11483
- High temperature strain gage technology for gas turbine engines
[NASA-CR-191177] p 57 N95-11996
- Damage of high temperature components by dust-laden air
p 201 N95-19673
- New Trends in coatings developments for turbine blades: Materials processing and repair
p 201 N95-19676
- Toughened Silcomp composites for gas turbine engine applications
[DE95-002851] p 235 N95-21243
- Evolution of oxidation and creep damage mechanisms in HiPEd silicon nitride materials
[DE95-001360] p 300 N95-22689
- Design of a variable area diffuser for a 15-inch Mach 6 open-jet tunnel
p 297 N95-23309
- Innovative processing of composites for ultra-high temperature applications, book 1
[AD-A290889] p 537 N95-29842
- NASA Lewis Research Center's preheated combustor and materials test facility
[NASA-TM-106676] p 626 N95-30592
- HIGH TEMPERATURE ENVIRONMENTS**
The potential for CMCs to replace superalloys in engine exhaust ducts
[HTN-95-42298] p 418 A95-84992
- Measurements of pressure and thermal wakes in a transonic turbine cascade
[AD-A283464] p 38 N95-12548
- Hypersonic engine leading edge experiments in a high heat flux, supersonic flow environment
[NASA-TM-106742] p 91 N95-14299
- Aerodynamic characteristics of the orbital reentry vehicle experimental probe fins in a supersonic flow
[NAL-TR-1232] p 342 N95-25664
- Advanced composite structural concepts and materials technologies for primary aircraft structures: Advanced material concepts
[NASA-CR-4485] p 503 N95-29027
- Static pressure drop by swirling flow of an internal cooling air system through a turbine shaft
p 698 N95-34560
- HIGH TEMPERATURE FLUIDS**
A one-dimensional inviscid nonequilibrium flow solver
[ISBN 1-879921-01-4] p 588 A95-93752
- HIGH TEMPERATURE GASES**
Mach wave emission from a high-temperature supersonic jet
[BTN-95-EIX95152577586] p 264 A95-73496
- Temperature effects on acoustic interactions between altitude test facilities and jet engine plumes
[NASA-CR-197638] p 258 N95-21170
- Toughened Silcomp composites for gas turbine engine applications
[DE95-002851] p 235 N95-21243
- Phase 2: HGM air flow tests in support of HEX vane investigation
p 312 N95-23438
- High frequency flow-structural interaction in dense subsonic fluids
[NASA-CR-4652] p 330 N95-24217
- Computation of high-altitude hypersonic flow-field radiation
p 593 N95-30843
- HIGH TEMPERATURE SUPERCONDUCTORS**
Phonon characteristics of high (T sub c) superconductors from neutron Doppler broadening measurements
[DE95-003703] p 324 N95-24076
- HIGH TEMPERATURE TESTS**
Contribution of thermal radiation to the temperature profile of ceramic composite materials
[BTN-94-EIX95011441252] p 417 A95-84209
- Study on the turbine vane and blade for a 1500 C class industrial gas turbine
[BTN-94-EIX95011441254] p 431 A95-84211
- High-temperature acoustic test facilities and methods
p 174 N95-19149
- Design and operation of a thermoacoustic test facility
p 147 N95-19150
- Investigation of flight data recorder fire test requirements
[AD-A285832] p 232 N95-20032
- Thermally stable organic polymers
[AD-A290755] p 537 N95-29482
- Bell Helicopter Advanced Rotocraft Transmission (ART) program
[NASA-CR-195479] p 555 N95-29538
- HIGH VOLTAGES**
Partial discharge testing of high voltage wiring harness for airborne displays
[AD-A289150] p 401 N95-27003
- HIGHLY MANEUVERABLE AIRCRAFT**
Robust dynamic inversion for control of highly maneuverable aircraft
[BTN-95-EIX95242670747] p 359 A95-81100
- Impact of agility requirements on configuration synthesis
[NASA-CR-4627] p 44 N95-11952
- Feedback control laws for highly maneuverable aircraft
[NASA-CR-197944] p 295 N95-23410
- Computational methods for control and optimal design of aerospace systems
[AD-A292861] p 608 N95-31451
- Nonlinear adaptive control of highly maneuverable high performance aircraft
p 710 N95-33712
- HILSCH TUBES**
3D visualization of unsteady 2D airplane wake vortices
[AD-A284745] p 27 N95-11593
- HISTORIES**
Design decisions from the history of the EUVE science payload
[HTN-95-60545] p 205 A95-69854
- Development of aeronautical mobile satellite services over the past thirty years
[BTN-95-EIX95152569458] p 305 A95-73498
- Special purpose landing gear: A survey of historical designs
[SAE PAPER 932579] p 494 A95-90066
- What's next in commercial aircraft environmental control systems?
[SAE PAPER 932057] p 513 A95-91638
- Langley overview
[NASA-TM-109891] p 20 N95-10547
- Aeronautics and space technology, past, present, and future
p 35 N95-11892
- NASA's Hypersonic Research Engine Project: A review
[NASA-TM-107759] p 50 N95-12860
- A review of 50 years of aerodynamic research with NACA/NASA
[NASA-TM-109163] p 102 N95-13663
- The personal aircraft: Status and issues
[NASA-TM-109174] p 223 N95-20688
- Application of CFD to the analysis and design of high-speed inlets
[NASA-CR-198574] p 438 N95-27240
- PIO: A historical perspective
p 597 N95-31062
- HL-10 REENTRY VEHICLE**
Development and flight testing of the HL-10 lifting body
p 498 A95-90872
- HL-10 dedication ceremony
[NASA-TM-104295] p 13 N95-10740
- HOLDERS**
Test model designs for advanced refractory ceramic materials
p 55 N95-11968
- Background noise levels measured in the NASA Lewis 9- by 15-foot low-speed wind tunnel
[NASA-TM-106817] p 145 N95-18054
- HOLES**
Erosion of T56 5th stage rotor blades due to bleed hole overtip flow
p 200 N95-19666
- HOLES (MECHANICAL)**
Bonded composite repair of cracked load-bearing holes
[BTN-94-EIX94401360553] p 243 A95-71867
- Analytical developments in support of the NASA aging aircraft program with an application to crack growth from rivets
[SAE PAPER 931223] p 545 A95-88789
- New experimental approach to determine initial fatigue quality with fastener holes
[BTN-94-EIX94522406136] p 701 A95-96273
- Impingement flow heat transfer measurements of turbine blades using a jet array
[AD-A283450] p 62 N95-12512
- Particle deposition in gas turbine blade film cooling holes
p 199 N95-19661
- Eddy current detection of pitting corrosion around fastener holes
p 315 N95-23507
- POD assessment of NDI procedures using a round robin test
[AGARD-R-809] p 315 N95-23602
- Leading edge film cooling effects on turbine blade heat transfer
[NASA-TM-106955] p 513 N95-29115
- HOLOGRAPHIC INTERFEROMETRY**
Quantitative comparison between interferometric measurements and Euler computations for supersonic cone flows
[BTN-95-EIX9522650782] p 358 A95-79238
- Head-on parallel blade-vortex interaction
[HTN-95-61197] p 491 A95-87570
- Developments in laser-based diagnostics for wind tunnels in the Aeromechanics Division: 1987-1992
[AD-A283011] p 84 N95-13687
- Holographic interferometric tomography for reconstructing flow fields
p 310 N95-23287
- HOLOGRAPHY**
Control of wind tunnel operations using neural net interpretation of flow visualization records
[NASA-TM-106683] p 24 N95-10854
- Development and flight testing of an Obstacle Avoidance System for US Army helicopters
p 687 N95-32500
- HOMING**
Switched bias proportional navigation for homing guidance against highly maneuvering targets
[BTN-95-EIX95182619145] p 279 A95-76622
- HOMING DEVICES**
Ideal proportional navigation
p 342 A95-81374
- HOMOGENEOUS TURBULENCE**
Direct numerical simulation of incompressible homogeneous isotropic turbulence using NWT
p 706 N95-34530
- HONEYCOMB STRUCTURES**
Minimum-mass design of sandwich aerobrakes for a lunar transfer vehicle
[BTN-95-EIX95212645707] p 299 A95-76759
- Field repair materials for naval aircraft
p 394 N95-27514
- Composite repair of a CF18: Vertical stabilizer leading edge
p 395 N95-27517
- Composite repair issues on the CF-18 aircraft
p 395 N95-27518
- External patch repair of CFRP/honeycomb sandwich
p 395 N95-27522
- Scarf repairs to graphite/epoxy components
p 396 N95-27523
- HOPE AEROSPACE PLANE**
Rarefied gas numerical wind tunnel: OREX and HOPE
p 427 A95-82391

- Guidance and control of HOPE and its future technologies p 506 A95-91543
 Experimental investigation of static and dynamic ground effect on HOPE ALFLEX vehicle [NAL-TR-1236] p 388 N95-26525
- HORIZONTAL FLIGHT**
 Time-optimal turn to a heading: An analytic solution [BTN-94-EIX94511433940] p 142 A95-64606
 Response of a nonrotating rotor blade to lateral turbulence. Part 1: Theory [BTN-95-EIX95182619228] p 284 A95-76654
 Air resonance of hingeless rotor helicopters in trimmed forward flight [HTN-95-61075] p 369 A95-83659
 Numerical simulation of helicopter engine plume in forward flight [NASA-CR-197488] p 107 N95-16589
- HORIZONTAL ORIENTATION**
 Horizontal axis wind turbine post stall airfoil characteristics synthesis p 376 N95-27974
 A NASTRAN-based computer program for structural dynamic analysis of Horizontal Axis Wind Turbines p 439 N95-27980
 Measurement and prediction of broadband noise from large horizontal axis wind turbine generators p 451 N95-27990
- HORIZONTAL TAIL SURFACES**
 A conceptual design of the SST without horizontal tail p 498 A95-91520
 Conceptual study of next generation high-speed civil transport: A candidate with horizontal tail p 499 A95-91521
 Symmetric steady manoeuvre loads on rigid aircraft of classical configuration at subsonic speeds [ESDU-94009] p 43 N95-11774
- HORSeshOE VORTICES**
 Wing-body juncture flows [AD-A281526] p 106 N95-16099
- HOT CORROSION**
 New Trends in coatings developments for turbine blades: Materials processing and repair p 201 N95-19676
 Resistance of silicon nitride turbine components to erosion and hot corrosion/oxidation attack p 202 N95-19683
- HOT ISOSTATIC PRESSING**
 Evolution of oxidation and creep damage mechanisms in HIPed silicon nitride materials [DE95-001360] p 300 N95-22689
- HOT SURFACES**
 Mechanism of deposit formation on fuel-wetted hot metal surfaces [AD-A289847] p 426 N95-28621
- HOT-FILM ANEMOMETERS**
 Characterization of a hot-film probe for hypersonic flow [AIAA PAPER 95-6110] p 511 A95-90440
 The use of hot film for the investigation of boundary-layer transition [CONGRESS PAPER C428-9-199] p 475 A95-91697
 Turbulent flow measurements with a triple-split hot-film probe [HTN-95-A1774] p 634 A95-93337
 An in-situ system for warning of icing conditions p 660 A95-93481
- HOT-WIRE ANEMOMETERS**
 A review of the hot-wire technique in 2-D compressible flow [HTN-95-61157] p 373 A95-86256
- HOT-WIRE FLOWMETERS**
 Transverse vorticity measurements in the NASA Ames 80 x 120 wind tunnel boundary layer p 251 N95-22457
- HOVERING**
 Validation of the dynamic response of a blade-element UH-60 simulation model in hovering flight [HTN-94-00663] p 18 A95-60155
 Evaluation of simulation motion fidelity criteria in the vertical and directional axes [HTN-94-00666] p 18 A95-60156
 Navier-Stokes simulation of rotor-body flowfield in hover using overset grids [PAPER C15] p 1 A95-60160
 Study of noise on a small-scale hovering tilt rotor [HTN-94-00712] p 5 A95-60190
 Aerodynamic interactions between a rotor and wing in hover [HTN-94-00714] p 5 A95-60192
 Rotating Kirchhoff method for three-dimensional transonic blade-vortex interaction hover noise [BTN-94-EIX94441386601] p 182 A95-67332
 Aeroelastic stability of hingeless rotor blade in hover using large deflection theory [BTN-94-EIX94441386616] p 183 A95-67347
 Simulation and flight test evaluation of head-up-display guidance for hamier approach transitions [BTN-95-EIX95062487533] p 194 A95-69241

- Measurement around a rotor blade excited in pitch. Part 1: Dynamic inflow [HTN-95-31007] p 220 A95-71177
 Measurement around a rotor blade excited in pitch. Part 2: Unsteady surface pressure [HTN-95-31008] p 220 A95-71178
 Rotorcraft control system design for uncertain vehicle dynamics using quantitative feedback theory [HTN-95-31012] p 236 A95-71182
 Flap-lag damping in hover and forward flight with a three-dimensional wake [HTN-95-A0496] p 221 A95-72567
 Air and ground resonance of helicopters with elastically tailored composite rotor blades [HTN-95-A0497] p 222 A95-72568
 H-infinity helicopter flight control law design with and without rotor state feedback [BTN-95-EIX95182619129] p 291 A95-76606
 Identification and simulation evaluation of a combat helicopter in hover [BTN-95-EIX95242670749] p 335 A95-81098
 Neuro-controllers for adaptive helicopter training [SAE PAPER 932535] p 379 A95-84557
 Intelligent flight trainer for initial rotary wing training [SAE PAPER 932536] p 386 A95-84558
 Automated hover training: An empirical evaluation [SAE PAPER 932536] p 379 A95-84559
 Autonomous helicopter hover positioning by optical tracking [HTN-95-C0006] p 585 A95-93394
 Stability analysis for elastically tailored rotor blades [ISBN 1-879921-01-4] p 635 A95-93703
 The application of potential CFD methods to helicopter hover flows [ISBN 1-879921-01-4] p 587 A95-93747
 Flow visualization studies of VTOL aircraft models during Hover in ground effect [NASA-TM-108860] p 272 N95-22666
 An experimental investigation of helicopter downwash and tailboom interaction at the Wichita State University 7x10 foot wind tunnel p 375 N95-26955
 A fourth order Euler/Navier-Stokes prediction method for the aerodynamics and aeroelasticity of hovering rotor blades p 554 N95-29242
 Development of a rotary wing Navier-Stokes CFD code based on TLNS3D code [AD-A290421] p 554 N95-29387
 Unsteady pressure and inflow velocity on a pitching rotor blade in hover p 480 N95-29771
 An analytic modeling and system identification study of helicopter dynamics p 505 N95-29787
 Moving base simulation of an integrated flight and propulsion control system for an ejector-augmentor STOVL aircraft in hover [NASA-TM-108867] p 606 N95-30646
 An LDV investigation of support structure influence on the flow field near the wingtip of a STOVL configuration in hover [AD-A294126] p 686 N95-34750
- HOVERING STABILITY**
 An analytical model for a nonlinear elastomeric lag damper and its effect on aeromechanical stability in Hover [HTN-95-61076] p 369 A95-83660
- HUBBLE SPACE TELESCOPE**
 Guidance and control, 1993; Annual Rocky Mountain Guidance and Control Conference, 16th, Keystone, CO, Feb. 6-10, 1993 [ISBN 0-87703-365-X] p 341 A95-80389
- HUBS**
 Composite propeller system for Domier 328 [BTN-94-EIX94461290506] p 66 A95-61728
 Effects of blade tip shape on dynamics, cost, weight, aerodynamic performance, and aeroelastic response [HTN-95-61074] p 369 A95-83658
 Considerations in the development of the coupled rotor fuselage model [HTN-95-61077] p 370 A95-83661
 Efficient sensitivity analysis for rotary-wing aeromechanical problems [HTN-95-42570] p 458 A95-87200
 Dynamic response of NASA Rotor Test Apparatus and Sikorsky S-76 hub mounted in the 80- by 120-Foot Wind Tunnel [NASA-TM-108847] p 25 N95-11389
 Dynamics of the McDonnell-Douglas Large Scale Dynamic Rig and dynamic calibration of the rotor balance [NASA-TM-108855] p 65 N95-13891
 NASA low-speed axial compressor for fundamental research [NASA-TM-4635] p 296 N95-23192
- HUMAN CENTRIFUGES**
 The large radius track centrifuge concept as an acceleration research and simulation device p 379 A95-84560

HUMAN FACTORS ENGINEERING

- Education, training, and human engineering in aerospace; SAE Aerotech '93, Costa Mesa, CA, Sep. 27-30, 1993 [SAE SP-992] p 417 A95-84553
 Human factors issues in aircraft cabin design [SAE PAPER 932527] p 386 A95-84556
 Inter-Noise 92: Noise control and the public; International Congress on Noise Control Engineering, Toronto, Ontario, Canada, July 20 - 22, 1992. Vols. 1 & 2 [ISBN 0-931784-25-5] p 559 A95-88457
 The mini-business approach at Chadderton [CONGRESS PAPER C428-26-037] p 681 A95-93602
- Organizational ergonomics and aviation safety p 596 A95-95083
 ASRS problems involving air carrier ground deicing/anti-icing p 611 A95-95194
 Emergency medical service (EMS): A unique flight environment p 596 A95-95203
 Neuro-controllers for adaptive helicopter hover training [BTN-94-EIX94522407592] p 709 A95-96241
 Aircraft maneuver envelope warning system [NASA-CASE-ARC-11953-1] p 82 N95-14518
 A graphical user interface for design and analysis of air breathing propulsion systems [TABES PAPER 94-616] p 83 N95-14645
 Industry review of a crew-centered cockpit design process and toolset [AD-A282966] p 130 N95-17661
 Conference on Aerospace Transparent Materials and Enclosures, volume 1 [AD-A283925] p 133 N95-18677
 An overall approach of cockpit noise verification in a military aircraft p 175 N95-19163
 Crew aiding and automation: A system concept for terminal area operations, and guidelines for automation design [NASA-CR-4631] p 228 N95-19950
 An evaluation of Automatic Terminal Information Service (ATIS) flight deck display presentation options [AD-A280100] p 228 N95-21020
 Independent review of Aviation Technology and Research Information Analysis System (ATRIAS) database [AD-A284049] p 226 N95-21518
 Systems engineering design and technical analyses for Strategic Avionics Crew-station Design Evaluation Facility (SACDEF) [AD-A286239] p 235 N95-22024
 TRISTAR 1: Evaluation methods for testing head-up display (HUD) flight symbology [NASA-TM-4665] p 288 N95-24030
 A crew-centered flight deck design philosophy for High-Speed Civil Transport (HSCT) aircraft [NASA-TM-109171] p 335 N95-24582
 Digital systems validation. Chapter 20 Artificial Intelligence with applications for aircraft. Handbook, volume 2 [AD-A288492] p 448 N95-26638
 Integrated mission precision attack cockpit technology (IMPACT). Phase 1: Identifying technologies for air-to-ground fighter integration [AD-A289562] p 389 N95-26684
 Conversion of the TRACON operations concepts database into a formal sentence outline job task taxonomy [DOT/FAA/AM-95/16] p 488 N95-28819
 Guidelines for the design of GPS and LORAN receiver controls and displays [AD-A293753] p 602 N95-31572
 Analysis of heads-up display quickening versus handling qualities [AD-A293797] p 611 N95-31584
 Aircraft evacuations through Type-3 exits I: Effects of seat placement at the exit [DOT/FAA/AM-95/22] p 599 N95-31845
 The application of helicopter mission simulation to Nap-of-the-Earth operations p 710 N95-32496
 A helmet mounted display for night missions at low altitude p 693 N95-32503
 Current issues in the design and information content of instrument approach charts [AD-A294752] p 690 N95-34562
 A rose by any other name: Certification seen as process rather than content p 688 N95-34766
 Human factors certification in the development of future air traffic control systems p 690 N95-34770
 Quality assurance and risk management: Perspectives on Human Factors Certification of Advanced Aviation Systems p 690 N95-34771
- HUMAN PERFORMANCE**
 Flight control system mode transitions influence on handling qualities and task performance [BTN-95-EIX95062487525] p 203 A95-69233

- The simulator training research advance testbed for aviation (STRATA): A simulation research facility for army aviation p 626 A95-95161
- Conversion of the TRACON operations concepts database into a formal sentence outline job task taxonomy [DOT/FAA/AM-95/16] p 488 N95-28819
- Mode of human image representation and error checking strategies in complex visual displays [AD-A290107] p 485 N95-29210
- Quality assurance and risk management: Perspectives on Human Factors Certification of Advanced Aviation Systems p 690 N95-34771
- HUMAN REACTIONS**
- Euro-noise '92, London, UK, Sept. 14-18, 1992. Bks. 1-3 [ISBN 1-873082-39-8] p 558 A95-87354
- The effects and prediction of rotary wing aircraft noise on the community [HTN-95-92536] p 558 A95-87356
- Criticism of the Leq as an index for aircraft noise and other discontinuous noise sources p 559 A95-88477
- Criticism of the Leq as an index for aircraft noise and other discontinuous noise sources p 559 A95-88478
- Assessment of helicopter noise annoyance: A comparison between helicopters and jet aircraft p 560 A95-88480
- Past and present UK research on aircraft noise effects p 560 A95-90090
- Recent laboratory studies of loudness and annoyance to sonic booms p 575 A95-90117
- The effect of onset rate on annoyance to military aircraft noise p 561 A95-90119
- Environmental noise research using the Human Response Monitor (HRM). Phase 1: System development p 562 A95-90122
- Improvement of the predicted aural detection code ICHIN (I Can Hear It Now) p 576 A95-90123
- HUMAN-COMPUTER INTERFACE**
- AIAA Computing in Aerospace 10, San Antonio, TX, March 28-30, 1995 [ISBN 1-56347-119-1] p 565 A95-90629
- A graphical user interface for design and analysis of air breathing propulsion systems [TABES PAPER 94-616] p 83 N95-14645
- Guidelines for the design of GPS and LORAN receiver controls and displays [AD-A293753] p 602 N95-31572
- HUMIDITY**
- Preliminary comparisons between MM5 NCAR/Penn State model generated icing forecasts and observations p 655 A95-93458
- Stratus' tephigram as a training/forecasting tool p 657 A95-93465
- Examination of conditions in the proximity of pilot reports of aircraft icing during storm-fest p 666 A95-93509
- MEMFOG - The Memphis fog algorithm p 668 A95-93516
- Effect of stratification and geometrical spreading on sonic boom rise time p 75 N95-14880
- Corrosion of landing gear steels p 302 N95-23500
- Patterns in the sky: Natural visualization of aircraft flow fields [NASA-SP-514] p 584 N95-31000
- HURRICANES**
- A technique for detecting a tropical cyclone center using a Doppler radar [HTN-95-20631] p 215 A95-69574
- HYBRID CIRCUITS**
- A programmable heater control circuit for spacecraft [NASA-TM-108459] p 9 N95-11157
- HYBRID COMPOSITES**
- Optimization of adaptive intraply hybrid fiber composites with reliability considerations [NASA-TM-106632] p 157 N95-16911
- HYBRID NAVIGATION SYSTEMS**
- Integrated GPS/Glonass navigation: Algorithms and results [BTN-95-EIX95112522531] p 190 A95-69332
- Flight evaluation of DGPS and DGPS-INS navigation systems p 382 A95-82462
- Failure detection and isolation structure for global positioning system autonomous integrity monitoring [BTN-95-EIX95282706656] p 486 A95-89648
- HYBRID STRUCTURES**
- Three-dimensional hybrid grid generation using advancing front techniques p 567 N95-28745
- HYDRATES**
- Analysis of the physical state of one Arctic polar stratospheric cloud based on observations [HTN-95-70917] p 351 A95-77982
- High-speed civil transport impact: Role of sulfate, nitric acid trihydrate, and ice aerosols studied with a two-dimensional model including aerosol physics [HTN-95-91843] p 354 A95-80831
- HYDRAULIC ANALOGIES**
- Simple method of supersonic flow visualization using watertable [BTN-95-EIX95182619105] p 269 A95-76590
- Verification of multidisciplinary models for turbomachines p 140 N95-19025
- HYDRAULIC CONTROL**
- General requirements for the electrohydraulic systems of the aircraft controls loading force on the simulators [CONGRESS PAPER C428-5-138] p 522 A95-91681
- HYDRAULIC EQUIPMENT**
- Dissolved gas - the hidden saboteur [SAE PAPER 931404] p 628 A95-93674
- The development of a highly reliable power management and distribution system for civil transport aircraft [NASA-TM-106697] p 50 N95-11867
- The industrial use of CFD in the design of turbomachinery p 90 N95-14133
- Composite flight-control actuator development p 410 N95-28281
- HYDRAULIC FLUIDS**
- Hydraulic system diagnostic sensors [BTN-95-EIX95031502752] p 209 A95-68259
- Dissolved gas - the hidden saboteur [SAE PAPER 931404] p 628 A95-93674
- The effects of aircraft fuel and fluids on the strength properties of Resin Transfer Molded (RTM) composites p 536 N95-29047
- HYDRAULIC TEST TUNNELS**
- Corner vortex suppressor [AD-DO16423] p 116 N95-18337
- Development of a multicomponent force and moment balance for water tunnel applications, volume 1 [NASA-CR-4642-VOL-1] p 161 N95-18955
- Development of a multicomponent force and moment balance for water tunnel applications, volume 2 [NASA-CR-4642-VOL-2] p 161 N95-18956
- Demonstration study of hierarchical control of fluid-dynamic phenomena [AD-A289341] p 437 N95-26751
- HYDROCARBON COMBUSTION**
- Multidimensional calculation of spark flame initiation by adopting a generic hydrocarbon kinetic scheme p 528 A95-87566
- Hydrocarbon-fueled ramjet/scramjet technology program, phase 2 extension [NASA-CR-189659] p 15 N95-10319
- HYDROCARBON FUELS**
- The Methane-Acetylene Cycle Aerospace Plane: A potential option for inexpensive Earth to orbit transportation [HTN-95-51845] p 525 A95-87483
- Hydrocarbon-fueled ramjet/scramjet technology program, phase 2 extension [NASA-CR-189659] p 15 N95-10319
- A study of aircraft post-crash fuel fire mitigation [AD-A282208] p 40 N95-12499
- Analysis of test criteria for specifying foam firefighting agents for aircraft rescue and firefighting [AD-A286381] p 227 N95-22352
- HYDROCARBONS**
- Measurement of moisture and total hydrocarbon contributions by valves used in clean room gas-delivery systems [BTN-94-EIX94381359041] p 295 A95-74629
- A study of aircraft post-crash fuel fire mitigation [AD-A282208] p 40 N95-12499
- HYDRODYNAMICS**
- New strategy combining backward inference with forward inference in monitoring and diagnosing techniques for hydrodynamic bearing-rotor systems [BTN-94-EIX94331336949] p 88 A95-61795
- Numerical study of sound generation due to a spinning vortex pair [BTN-95-EIX95182619075] p 307 A95-75760
- Thermo-hydrodynamic solution of floating ring seals for high pressure compressors using the finite-element method [HTN-95-92246] p 433 A95-85290
- Modeling aerodynamic problems using Smoothed Particle Hydrodynamics (SPH) [SAE PAPER 932512] p 465 A95-89185
- The acoustic characteristics of turbomachinery cavities [NASA-CR-4671] p 476 N95-28720
- Analyzing the stability of floating ice floes [AD-A292149] p 563 N95-29160
- HYDROFLUORIC ACID**
- Matrix isolated HF: the high-resolution infrared spectrum of a cryogenically solvated hindered rotor [GTN-95-0301010494002231-16] p 578 A95-92210
- HYDROFOILS**
- Lift analysis of a variable camber foil using the discrete vortex-blob method [HTN-95-20940] p 545 A95-88979
- Hydrofoil force balance [AD-DO16475] p 160 N95-18461
- Numerical studies of turbulent free surface flows and unsteady propeller flows [AD-A294377] p 706 N95-34343
- HYDROGEN**
- The distribution of hydrogen, nitrogen, and chlorine radicals in the lower stratosphere: Implications for changes in O3 due to emission of NO(y) from supersonic aircraft [HTN-95-70935] p 351 A95-78000
- Ignition analysis of hydrogen/air mixture in supersonic mixing layer p 416 A95-82301
- General solution procedure for flows in local chemical equilibrium [HTN-95-42329] p 404 A95-86158
- Stationary premixed flames in spherical and cylindrical geometries [HTN-95-42336] p 418 A95-86165
- Intrinsic transport and chemistry coupling in combustion phenomena p 538 A95-87191
- Numerical study of contaminant effects on combustion of hydrogen, ethane, and methane in air [AIAA PAPER 95-6097] p 510 A95-88005
- Cooling of aerospace plane using liquid hydrogen and methane [BTN-95-EIX0619952748171] p 590 A95-94465
- A hybrid vehicle evaluation code and its application to vehicle design. Revision 1 [DE95-008053] p 441 N95-28029
- HYDROGEN CHLORIDES**
- Aircraft measurements of ClO and HCL during EASOE 1991/92 [HTN-95-00721] p 444 A95-86291
- HYDROGEN ENGINES**
- Secondary power system study for the hytex RA3 flight test vehicle [AIAA PAPER 95-6158] p 512 A95-90470
- A hybrid vehicle evaluation code and its application to vehicle design. Revision 1 [DE95-008053] p 441 N95-28029
- A hybrid vehicle evaluation code and its application to vehicle design, revision 2 [DE95-008060] p 441 N95-28139
- HYDROGEN FUELS**
- Studies on plasma jet igniters p 403 A95-82680
- Influence of the flight trajectory on the exhaust gas composition of a H2-fueled air-breathing ramjet engine p 509 A95-87404
- Modeling of plume chemistry of high flying aircraft with H2 combustion engines p 509 A95-87405
- The Methane-Acetylene Cycle Aerospace Plane: A potential option for inexpensive Earth to orbit transportation [HTN-95-51845] p 525 A95-87483
- Scramjet combustor design in France [AIAA PAPER 95-6094] p 510 A95-88002
- Airborne rotary separator study [NASA-CR-191045] p 150 N95-18743
- Shock tunnel studies of scramjet phenomena 1993 [NASA-CR-195038] p 350 N95-25394
- HYDROGEN SULFIDE**
- Analysis of the physical state of one Arctic polar stratospheric cloud based on observations [HTN-95-70917] p 351 A95-77982
- An intercomparison of aircraft instrumentation for tropospheric measurements of carbonyl sulfide, hydrogen sulfide, and carbon disulfide [HTN-95-91856] p 355 A95-80844
- HYDROGRAPHY**
- Assimilation of altimeter data in a quasi-geostrophic model of the Gulf Stream system: A dynamical perspective [NASA-CR-196313] p 320 N95-23766
- Real-time testing and demonstration of the US Army Corps of Engineers' Real-Time On-The-Fly positioning system [AD-A288624] p 334 N95-25609
- HYDROSTATIC PRESSURE**
- Oscillating-flow regenerator test rig [NASA-CR-196982] p 53 N95-13200
- HYDROSTATICS**
- Wormgear geometry adopted for implementing hydrostatic lubrication and formulation of the lubrication problem [AD-A290331] p 210 N95-19567
- Electro-hydrostatic actuator controller design using quantitative feedback theory [AD-A289220] p 409 N95-26957
- HYDROXYL EMISSION**
- Development of techniques for the in situ observation of OH and HO2 for studies of the impact of high-altitude supersonic aircraft on the stratosphere [NASA-CR-196759] p 61 N95-12832
- Two-dimensional imaging of OH in a lean burning high pressure combustor [NASA-TM-106854] p 236 N95-21383

HYDROXYL RADICALS

- Comparison of NO and OH planar fluorescence temperature measurements in scramjet model flowfields [BTN-95-EIX95042474388] p 209 A95-68312
- Aircraft-borne, laser-induced fluorescence instrument for the in situ detection of hydroxyl and hydroperoxy radicals [BTN-95-EIX95072499029] p 253 A95-71908
- A model for temperature-dependent collisional quenching of OH A(sup 2) Sigma(sup +) [HTN-95-42308] p 450 A95-85002
- Two-dimensional imaging of OH in a lean burning high pressure combustor [NASA-TM-106854] p 236 N95-21383
- Spatially-resolved velocity measurements in steady, high-speed, reacting flows using laser-induced OH fluorescence p 650 N95-32109
- HYGROSCOPICITY**
- Gas turbine compressor corrosion and erosion in Western Europe [AD-B196178L] p 201 N95-19678
- HYPERBOLIC DIFFERENTIAL EQUATIONS**
- On the exact solutions of pseudorange equations [BTN-95-EIX9514255477] p 278 A95-73433
- HYPERCUBE MULTIPROCESSORS**
- A fixed time performance evaluation of parallel CFD applications [DE94-014240] p 436 N95-26445
- HYPERSONIC AIRCRAFT**
- Hyperersonic waverider test vehicle: A logical next step [BTN-95-EIX95041503783] p 193 A95-69214
- Development of an efficient inverse method for supersonic and hypersonic body design [BTN-95-EIX95041503784] p 180 A95-69215
- Direct-lift design strategy for longitudinal control of hypersonic aircraft [BTN-95-EIX95182619131] p 291 A95-76608
- An advanced scramjet propulsion concept for A 350 MG SSTO space plane p 402 A95-82325
- A conceptual design of hypersonic research vehicle with subscale scramjet engine p 384 A95-82482
- Optimal trajectories for hypersonic launch vehicles [HTN-95-61120] p 415 A95-84884
- Orbital transport: Technical, meteorological and chemical aspects; Aerospace Symposium, 3rd, Braunschweig, Germany, Aug. 26-28, 1991 [ISBN 3-540-563180] p 524 A95-87373
- Environmental aspects of Orbital transport p 559 A95-87377
- Hyperersonic technology experimental vehicles (The need for flight testing at hypersonic speed) p 490 A95-87378
- Trim conditions for optimal flight performance of hypersonic aircraft p 514 A95-87397
- Handling qualities of hypersonic aircraft and related control requirements p 515 A95-87398
- Real time for the calculation of the aerodynamic of aircrafts with delta wings p 460 A95-87399
- Secondary power system study for the htex RA3 flight test vehicle [AIAA PAPER 95-6158] p 512 A95-90470
- Aircraft Symposium, 30th, Tsukuba, Japan, Sep. 30 - Oct. 2, 1992 [HTN-95-A1609] p 498 A95-91491
- Some considerations on system design of the hypersonic transport and supersonic air-intakes p 473 A95-91522
- Experimental investigation on aerothermodynamic characteristics of hypersonic transport p 473 A95-91525
- A shock tunnel test of a winged hypersonic research vehicle p 474 A95-91538
- Optimality of the steady-state flight for hypersonic aircraft p 526 A95-91550
- Optimal shape design in hypersonic aerodynamics and electromagnetics p 639 A95-95397
- Shock-tunnel combustor testing for hypersonic vehicles [NASA-CR-196836] p 52 N95-11938
- A simple analytical aerodynamic model of Langley Winged-Cone Aerospace Plane concept [NASA-CR-194987] p 54 N95-12175
- Numerical modeling of a cryogenic fluid within a fuel tank [NASA-TM-4651] p 89 N95-13892
- Static and dynamic friction behavior of candidate high temperature airframe seal materials [NASA-TM-106571] p 152 N95-16905
- HYPERSONIC BOUNDARY LAYER**
- Shock layers and boundary layers in hypersonic flows [HTN-95-A0003] p 183 A95-67830
- Model for compressible turbulence in hypersonic wall boundary and high-speed mixing layers [BTN-94-EIX94441386625] p 184 A95-68174
- Analytical study of the neutral stability of a model hypersonic boundary layer [BTN-95-EIX95152577589] p 263 A95-73493

- Structure of a double-fin turbulent interaction at high speed [BTN-95-EIX95222650780] p 347 A95-79236
- Characterization of a hot-film probe for hypersonic flow [AIAA PAPER 95-6110] p 511 A95-90440
- Hyperersonic shock wave/turbulent boundary layer interactions in the vicinity of an expansion corner [AIAA PAPER 95-6125] p 469 A95-90446
- HYPERSONIC FLIGHT**
- Navier-Stokes simulations of Orbiter aerodynamic characteristics including pitch trim and bodyflap [BTN-95-EIX95041503779] p 204 A95-69210
- Multiblock analysis for Shuttle Orbiter reentry heating from Mach 24 to Mach 12 [BTN-95-EIX95041503780] p 205 A95-69211
- Shock tunnel measurements of hypervelocity blunted cone drag [BTN-95-EIX95152577606] p 305 A95-73477
- Analytical solution for controls, heats, and states of flight trajectories [BTN-95-EIX95152583286] p 282 A95-73587
- Direct-lift design strategy for longitudinal control of hypersonic aircraft [BTN-95-EIX95182619131] p 291 A95-76608
- Integrated development of the equations of motion for elastic hypersonic flight vehicles [BTN-95-EIX95242670755] p 327 A95-81092
- Hyperersonic trajectory control of aerospace plane with integrated SCRAMJET engine p 413 A95-82384
- Hyperersonic thermal protection with mass injection at angle of attack p 414 A95-82414
- Hyperersonic technology experimental vehicles (The need for flight testing at hypersonic speed) p 490 A95-87378
- High temperature aspects of the European Hermes programs p 524 A95-87379
- Integrated thermal and mechanical analysis of hypersonic vehicles by using adaptive finite element methods p 524 A95-87383
- Estimation of aerodynamic derivatives: Euler scheme validation and approximate methods for hypersonic configurations p 460 A95-87385
- Numerical simulation of real gas effects and aerodynamic heating of hypersonic space transportation vehicles p 540 A95-87558
- International collaboration in hypersonic technologies - A specific and worthwhile initiative [AIAA PAPER 95-6140] p 581 A95-90457
- A waverider derived hypersonic X-vehicle [AIAA PAPER 95-6162] p 496 A95-90473
- A shock tunnel test of a winged hypersonic research vehicle p 474 A95-91538
- A guidance concept for hypersonic aerospacecrafts p 526 A95-91549
- Optimality of the steady-state flight for hypersonic aircraft p 526 A95-91550
- Kinetic heating in hypersonic flight [CONGRESS PAPER C428-3-056] p 475 A95-91674
- A perspective of rarefied gas flow problems relevant to high altitude flight [SAE PAPER 931366] p 586 A95-93647
- Design and evaluation of candidate pressure ports for the HYFLITE experiment [NASA-TM-109146] p 22 N95-11003
- Hyperersonic engine leading edge experiments in a high heat flux, supersonic flow environment [NASA-TM-106742] p 91 N95-14299
- Air-breathing aerospace plane development essential: Hyperersonic propulsion flight tests [NASA-TM-108857] p 66 N95-14921
- Hyperersonic flight testing [AD-A283981] p 134 N95-18891
- Particle kinetic simulation of high altitude hypervelocity flight [NASA-CR-197383] p 309 N95-22481
- Computation of high-altitude hypersonic flow-field radiation p 593 N95-30843
- Application of CFD technique for HYFLEX aerodynamic design p 693 N95-34542
- HYPERSONIC FLOW**
- Computation of nonequilibrium viscous flows in arc-jet wind tunnel nozzles [AIAA PAPER 94-0254] p 2 A95-60173
- A comparison of three-dimensional nonequilibrium solution algorithms applied to hypersonic flows with stiff chemical source terms [AIAA PAPER 93-2861] p 4 A95-60186
- Shock layers and boundary layers in hypersonic flows [HTN-95-A0003] p 183 A95-67830
- Experimental and computational results for the external flowfield of a scramjet inlet [BTN-94-EIX94441380977] p 195 A95-68161
- Measurement by coherent anti-Stokes Raman scattering in the R5Ch hypersonic wind tunnel [BTN-95-EIX95112523811] p 188 A95-69322

- Flow resolution and domain influence in rarefied hypersonic blunt-body flows [BTN-95-EIX95082502729] p 220 A95-70136
- Time-of-flight mass spectrometer for impulse facilities [BTN-95-EIX95142553057] p 262 A95-73441
- Analytical study of the neutral stability of a model hypersonic boundary layer [BTN-95-EIX95152577589] p 263 A95-73493
- Hyperersonic rarefied flow past spheres including wake structure [BTN-95-EIX95152583250] p 305 A95-73551
- Application of the multigrad solution technique to hypersonic entry vehicles [BTN-95-EIX95152583254] p 306 A95-73555
- Zonally decoupled direct simulation Monte Carlo solutions of hypersonic blunt-body wake flows [BTN-95-EIX95182617458] p 268 A95-75729
- Scaling of incipient separation in supersonic/transonic speed laminar flows [BTN-95-EIX95182619104] p 269 A95-76589
- Review and development of base pressure and base heating correlations in supersonic flow [BTN-95-EIX95212645688] p 271 A95-76740
- Numerical analysis of hypersonic low-density scramjet inlet flow [BTN-95-EIX95212645694] p 272 A95-76746
- Laser velocimetry seed-particle behavior in shear layers at Mach 12 [BTN-95-EIX95212645712] p 272 A95-76764
- Structure of a double-fin turbulent interaction at high speed [BTN-95-EIX95222650780] p 347 A95-79236
- Hyperersonic model testing in a shock tunnel [BTN-95-EIX95222650789] p 329 A95-79245
- Supercooling in hypersonic nitrogen wind tunnels [BTN-94-EIX95011441134] p 340 A95-81020
- VSL analysis of hypersonic flows around a reentry vehicle with equilibrium air chemistry p 413 A95-82400
- Reentry technology experiment on the first mission of reentry capsule 'EXPRESS' p 414 A95-82499
- Hyperersonic flow simulation with thermoelectric effect p 368 A95-82669
- Accuracy and efficiency assessments for a weak statement CFD algorithm for high-speed aerodynamics [BTN-94-EIX95011441238] p 370 A95-84195
- Hyperersonic flow past open cavities [HTN-95-42577] p 458 A95-87207
- Vorticity in an inviscid fluid at hypersonic speeds [HTN-95-42590] p 539 A95-87220
- Numerical modeling and simulation of chemically reacting reentry flows p 525 A95-87387
- The high enthalpy shock tunnel in Goettingen (HEG) p 518 A95-87391
- Thrust modeling for hypersonic engines [AIAA PAPER 95-6081] p 509 A95-87410
- Experimental investigation of hypersonic flow over a wing-body combination [AIAA PAPER 95-6083] p 460 A95-87412
- Nonlinear asymptotic theory of hypersonic flow past a circular cone [HTN-95-92599] p 461 A95-87415
- Computational methods in applied sciences; European Computational Fluid Dynamics Conference, 1st, Brussels, Belgium, Sept. 7-11, 1992 [ISBN 0-444-89795-X] p 539 A95-87552
- Numerical simulation of three-dimensional hypersonic reacting flows over blunt bodies with catalytic surface [HTN-95-61184] p 539 A95-87557
- Numerical simulation of real gas effects and aerodynamic heating of hypersonic space transportation vehicles p 540 A95-87558
- Chemical recombination in an expansion tube [HTN-95-20844] p 544 A95-88105
- Supersonic and hypersonic shock/boundary-layer interaction database [HTN-95-20930] p 463 A95-88969
- Characterization of a hot-film probe for hypersonic flow [AIAA PAPER 95-6110] p 511 A95-90440
- Research activity at the shock tube facility at NASA Ames [HTN-95-20930] p 547 A95-90559
- Numerical studies of Mach reflection with air chemistry p 548 A95-90575
- Similarity solutions for hypersonic flow past slender bodies of revolution at small incidence [HTN-95-12195] p 475 A95-91895
- Application of integral methods to ablation charring erosion, a review [BTN-95-EIX95302694460] p 636 A95-94057
- Aerodynamic applications of underexpanded hypersonic viscous jets [BTN-95-EIX0619952748162] p 589 A95-94456
- Hyperersonic Navier-Stokes computations about complex configurations p 644 A95-95497

- Development of an upwind, finite-volume code with finite-rate chemistry
[NASA-CR-196749] p 9 N95-11366
- Shock-tunnel combustor testing for hypersonic vehicles
[NASA-CR-196836] p 52 N95-11938
- Hypersonic Gas-Surface Energy Accommodation Test Facility
[DE94-014468] p 39 N95-12652
- Thermoacoustic environments to simulate reentry conditions
[NASA-CR-195008] p 86 N95-14096
- Laminar and turbulent flow computations of Type 4 shock-shock interference aerothermal loads using unstructured grids
[NASA-CR-195008] p 97 N95-15604
- High altitude hypersonic flowfield radiation
[AD-A281386] p 106 N95-16160
- In-flight imaging of transverse gas jets injected into transonic and supersonic crossflows: Design and development
[NASA-CR-186031] p 157 N95-17418
- Hypersonic flow-field measurements: Intrusive and nonintrusive
[AD-A283867] p 119 N95-18674
- Theoretical investigations of shock/boundary layer interactions on a $Ma(\infty) = 8$ waverider
[DLR-FB-94-12] p 119 N95-18910
- Parabolized Navier-Stokes solution of supersonic/hypersonic flows
[NASA-TM-106824] p 223 N95-20794
- Application of pressure sensitive paint in hypersonic flows
[AD-A286507] p 250 N95-22212
- Shock wave interactions in hypervelocity flow
[NASA-TM-4638] p 274 N95-23250
- Shock tunnel combustor testing for hypersonic vehicles
[NASA-TM-109181] p 348 N95-24396
- Shock wave interactions in hypervelocity flow
[AD-A286507] p 250 N95-22212
- Experimental results for a hypersonic nozzle/afterbody flow field
[NASA-TM-4638] p 274 N95-23250
- Design of a variable area diffuser for a 15-inch Mach 6 open-jet tunnel
[NASA-TM-109152] p 97 N95-15898
- Verification of computational aerodynamic predictions for complex hypersonic vehicles using the INCA(trademark) code
[DE95-004757] p 330 N95-24308
- DSMC calculations for 70-deg blunt cone at 3.2 km/s in nitrogen
[NASA-TM-109181] p 348 N95-24396
- Design of a variable area diffuser for a 15-inch Mach 6 open-jet tunnel
[NASA-TM-109152] p 97 N95-15898
- Verification of computational aerodynamic predictions for complex hypersonic vehicles using the INCA(trademark) code
[DE95-004757] p 330 N95-24308
- DSMC calculations for 70-deg blunt cone at 3.2 km/s in nitrogen
[NASA-TM-109181] p 348 N95-24396
- Viscous shock-layer analysis on hypersonic flow over reentry capsule with nonequilibrium chemistry
[ISAS-656] p 436 N95-26739
- A study of fluid problems requiring a direct particle simulation
[AD-A290212] p 567 N95-29074
- An extension of the continuum model by Grad's thirteen moment equations for hypersonic rarefied flows
[NASA-TM-106757] p 89 N95-13665
- Numerical simulation and analysis of the hypersonic turbulent flow past a blunt-fin/ramp configuration
[DLR-FB-94-19] p 483 N95-30349
- Flow models for the design of a hypersonic iodine vapor wind tunnel nozzle with chemical and vibrational nonequilibrium effects
[NASA-TM-106924] p 482 N95-30091
- A numerical study of the starting process in a hypersonic shock tunnel
[NASA-TM-106924] p 482 N95-30091
- Computation of high-altitude hypersonic flow-field radiation
[NASA-TM-106924] p 482 N95-30091
- Analysis of planar laser-induced fluorescence images obtained during shakedown testing of the AEDC impulse facility
[AD-A293237] p 646 N95-30906
- Hypersonic CFD analysis for the aerothermodynamic design of HOPE
[NASA-TM-106924] p 482 N95-30091
- HYPERSONIC HEAT TRANSFER**
- Hypersonic convective heat transfer over 140-deg blunt cones in different gases
[BTN-95-EIX95152583253] p 266 A95-73548
- High temperature aspects of the European Hermes programs
[HTN-95-20931] p 464 A95-88970
- Integrated thermal and mechanical analysis of hypersonic vehicles by using adaptive finite element methods
[AIAA PAPER 95-6125] p 469 A95-90446
- Numerical simulation of real gas effects and aerodynamic heating of hypersonic space transportation vehicles
[NASA-TM-106924] p 482 N95-30091
- The use of thermochromic liquid crystals for heat transfer measurements in short duration hypersonic wind tunnel facilities
[AIAA PAPER 95-6115] p 520 A95-90443
- Hypersonic shock wave/turbulent boundary layer interactions in the vicinity of an expansion corner
[AIAA PAPER 95-6125] p 469 A95-90446
- Experimental investigation on aerothermodynamic characteristics of hypersonic transport
[HTN-95-42591] p 459 A95-87221
- Computational fluid dynamics '92; Proceedings of the European Computational Fluid Dynamics Conference, 1st, Brussels, Belgium, Sep. 7-11, 1992. Vols. 1 & 2
[ISBN 0-444-89793-3] p 638 A95-95357
- Heat transfer on bent-noise biconic in hypersonic flow
[NASA-CR-188343] p 54 N95-11937
- An axisymmetric analog two-layer convective heating procedure with application to the evaluation of Space Shuttle Orbiter wing leading edge and windward surface heating
[NASA-TM-106742] p 91 N95-14299
- Hypersonic engine leading edge experiments in a high heat flux, supersonic flow environment
[AD-A288689] p 341 N95-26053
- HYPERSONIC INLETS**
- Experimental and computational results for the external flowfield of a scramjet inlet
[BTN-94-EIX94441380977] p 182 A95-67336
- Optimization of contoured hypersonic scramjet inlets with a least-squares parabolized Navier-Stokes procedure
[HTN-95-20976] p 464 A95-88970
- Numerical analysis of hypersonic low-density scramjet inlet flow
[BTN-95-EIX95212645694] p 272 A95-76746
- Hypersonic shock wave/turbulent boundary layer interactions in the vicinity of an expansion corner
[AIAA PAPER 95-6125] p 469 A95-90446
- 3-D Navier-Stokes analysis of crossing glancing shocks/turbulent boundary layer interactions
[BTN-95-EIX95302729768] p 636 A95-94130
- Shock-tunnel combustor testing for hypersonic vehicles
[NASA-CR-196836] p 52 N95-11938
- Computational analysis in support of the SSTO flowpath test
[NASA-TM-106757] p 89 N95-13665
- Wind-tunnel blockage and actuation systems test of a two-dimensional scramjet inlet unstart model at Mach 6
[NASA-TM-109152] p 97 N95-15898
- Two-dimensional scramjet inlet unstart model: Wind-tunnel blockage and actuation systems test
[NASA-TM-109984] p 97 N95-15899
- Numerical simulation of supersonic compression corners and hypersonic inlet flows using the RPLUS2D code
[NASA-TM-106580] p 105 N95-16038
- HYPERSONIC NOZZLES**
- Testing the hypersonic technology demonstration nozzle: Results from the test campaign 1993/94
[AIAA PAPER 95-6084] p 509 A95-87413
- Chemically reacting non-equilibrium boundary layers in air breathing propulsion systems
[AIAA PAPER 95-6139] p 512 A95-90456
- Optimized design of a hypersonic nozzle
[NASA-TM-106580] p 105 N95-16038
- Use of the PARC code to estimate the off-design transonic performance of an over/under turboramjet nozzle
[NASA-TM-106924] p 482 N95-30091
- HYPERSONIC REENTRY**
- Shock layers and boundary layers in hypersonic flows
[HTN-95-A0003] p 183 A95-67830
- VSL analysis of hypersonic flows around a reentry vehicle with equilibrium air chemistry
[NASA-TM-106924] p 482 N95-30091
- Atmospheric reentry flight test of winged space vehicle
[ISAS-656] p 436 N95-26739
- Viscous shock-layer analysis on hypersonic flow over reentry capsule with nonequilibrium chemistry
[ISAS-656] p 436 N95-26739
- HYPERSONIC SHOCK**
- Linear disturbances in hypersonic, chemically reacting shock layers
[BTN-94-EIX94441386605] p 182 A95-67336
- Linear disturbances in hypersonic, chemically reacting shock layers
[HTN-95-20931] p 464 A95-88970
- Hypersonic shock wave/turbulent boundary layer interactions in the vicinity of an expansion corner
[AIAA PAPER 95-6125] p 469 A95-90446
- HYPERSONIC SPEED**
- Aerodynamically blunt and sharp bodies
[BTN-95-EIX95041503781] p 205 A95-69212
- Navier-Stokes computation of a viscous optimized waverider
[BTN-95-EIX95041503782] p 193 A95-69213
- Minimum-drag axisymmetric bodies in the supersonic/hypersonic flow regimes
[BTN-95-EIX95041503785] p 180 A95-69216
- Shock tunnel measurements of hypervelocity blunted cone drag
[HTN-95-42591] p 459 A95-87221
- Shock-tunnel combustor testing for hypersonic vehicles
[NASA-CR-196836] p 52 N95-11938
- Low-speed wind tunnel testing of the NPS and NASA Ames Mach 6 optimized waverider
[AD-A283585] p 75 N95-15319
- Numerical simulation of supersonic compression corners and hypersonic inlet flows using the RPLUS2D code
[NASA-TM-106580] p 105 N95-16038
- Scramjet testing guidelines
[NASA-TM-4602] p 309 N95-23015
- Mach 10 computational study of a three-dimensional scramjet inlet flow field
[NASA-TM-4602] p 309 N95-23015
- Mach 10 computational study of a three-dimensional scramjet inlet flow field
[NASA-TM-4602] p 309 N95-23015
- Design of a variable area diffuser for a 15-inch Mach 6 open-jet tunnel
[NASA-TM-4602] p 309 N95-23015
- Performance of an aerodynamic yaw controller mounted on the space shuttle orbiter body flap at Mach 10
[NASA-TM-109179] p 330 N95-24397
- Application of CFD to the analysis and design of high-speed inlets
[NASA-CR-198574] p 438 N95-27240
- Unsteadiness of shock-induced turbulent boundary layer separation. An inherent feature of turbulent flow or solely a wind tunnel phenomenon
[AD-A290367] p 554 N95-29228
- Transonic, supersonic and hypersonic wind-tunnel tests on aerodynamic characteristics of reentry body with blunted cone configuration
[ISAS-658] p 480 N95-29640
- HYPERSONIC TEST APPARATUS**
- Measurement of free-flight dynamic stability derivatives of cones in a hypersonic gun tunnel
[AIAA PAPER 95-6082] p 519 A95-87411
- A model for preliminary facility design including simulation issues
[NASA-TM-109179] p 330 N95-24397
- Hypersonic air-breathing aer propulsion facility test support requirements
[NASA-TM-109179] p 330 N95-24397
- HYPERSONIC VEHICLES**
- Navier-Stokes computation of a viscous optimized waverider
[BTN-95-EIX95041503782] p 193 A95-69213
- Interpretation of waverider performance data using computational fluid dynamics
[BTN-95-EIX95062487534] p 193 A95-69242
- Computational study of plume-induced separation on a hypersonic powered model
[BTN-95-EIX95152582346] p 266 A95-73548
- Application of the multigrid solution technique to hypersonic entry vehicles
[BTN-95-EIX95152583254] p 306 A95-73555
- Analytical aeropropulsive/aeroelastic hypersonic-vehicle model with dynamic analysis
[BTN-95-EIX95182619138] p 269 A95-76615
- Integrated design of hypersonic waveriders including inlets and tailfins
[BTN-95-EIX95212645692] p 272 A95-76744
- Integrated development of the equations of motion for elastic hypersonic flight vehicles
[BTN-95-EIX95242670755] p 327 A95-81092
- A concept of a hypersonic flight experiment of a winged vehicle
[AIAA PAPER 95-6083] p 460 A95-87412
- Integrated thermal and mechanical analysis of hypersonic vehicles by using adaptive finite element methods
[AIAA PAPER 95-6085] p 490 A95-87414
- Estimation of aerodynamic derivatives: Euler scheme validation and approximate methods for hypersonic configurations
[AIAA PAPER 95-6132] p 530 A95-90451
- Optimal separation and ascent of lifting upper stages
[AIAA PAPER 95-6132] p 530 A95-90451
- Experimental investigation of hypersonic flow over a wing-body combination
[AIAA PAPER 95-6083] p 460 A95-87412
- Testing the hypersonic technology demonstration nozzle: Results from the test campaign 1993/94
[AIAA PAPER 95-6084] p 509 A95-87413
- Experimental and numerical analysis of a two-duct nozzle/afterbody model at supersonic Mach numbers
[AIAA PAPER 95-6085] p 490 A95-87414
- Integration of an hypersonic airbreathing vehicle: Assessment of overall aerodynamic performances and of uncertainties
[AIAA PAPER 95-6100] p 492 A95-88007
- Intermetallic and titanium matrix composite materials for hypersonic applications
[AIAA PAPER 95-6132] p 530 A95-90451
- Ablative thermal management structural material on the hypersonic vehicles
[AIAA PAPER 95-6133] p 547 A95-90452
- A flying qualities study of longitudinal long-term dynamics of hypersonic planes
[AIAA PAPER 95-6150] p 521 A95-90464
- The panel oxidation and erosion test (POET) facility
[AIAA PAPER 95-6151] p 521 A95-90465

A waverider derived hypersonic X-vehicle
 [AIAA PAPER 95-6162] p 496 A95-90473
 Research activity at the shock tube facility at NASA Ames p 547 A95-90559
 Development of an upwind, finite-volume code with finite-rate chemistry
 [NASA-CR-196749] p 9 N95-11366
 Experimental aerodynamic characteristics of a generic hypersonic accelerator configuration at Mach numbers 1.5 and 2.0 — conducted in the Langley Unitary Plan Wind Tunnel
 [NASA-TM-4413] p 39 N95-12770
 Ultraviolet emissions occurring about hypersonic vehicles in rarefied flows
 [AD-A281452] p 106 N95-16076
 Hypersonic wind tunnel test techniques
 [AD-A284057] p 118 N95-18663
 Thermo-acoustic fatigue design for hypersonic vehicle skin panels p 162 N95-19161
 Description and flow characterization of hypersonic facilities
 [AD-A284291] p 223 N95-20248
 Particle kinetic simulation of high altitude hypervelocity flight
 [NASA-CR-197383] p 309 N95-22481
 Verification of computational aerodynamic predictions for complex hypersonic vehicles using the INCA(trademark) code
 [DE95-004757] p 330 N95-24308
 Reentry guidance for hypersonic Flight Experiment (HYFLEX) vehicle
 [NAL-TR-1235] p 334 N95-25764
 Heat transfer measurements in small scale wind tunnels
 [AD-A288689] p 341 N95-26053
 Application of CFD technique for HYFLEX aerodynamic design p 693 N95-34542

HYPERSONIC WAKES

Zonally decoupled direct simulation Monte Carlo solutions of hypersonic blunt-body wake flows
 [BTN-95-EIX95182617458] p 268 A95-75729

HYPERSONIC WIND TUNNELS

Time-of-flight mass spectrometer for impulse facilities
 [BTN-95-EIX95142553057] p 262 A95-73441
 Supercooling in hypersonic nitrogen wind tunnels
 [BTN-94-EIX95011441134] p 340 A95-81020
 Design features of the NAL ramjet engine test facility p 410 A95-82319
 Hypersonic wind tunnel test of sidewall compression type scramjet inlet p 410 A95-82320
 An experimental investigation of scramjet nozzle flow p 402 A95-82322
 High temperature aspects of the European Hermes programs p 524 A95-87379
 The use of thermochromic liquid crystals for heat transfer measurements in short duration hypersonic wind tunnel facilities
 [AIAA PAPER 95-6115] p 520 A95-90443
 A review of free-stream flow fluctuation and steady-state flow quality measurements in the AEDC/VKF Supersonic Tunnel A and Hypersonic Tunnel B
 [AIAA PAPER 95-6137] p 520 A95-90454
 Operating capability and current status of the reactivated NASA Lewis Research Center hypersonic tunnel facility [AIAA PAPER 95-6146] p 521 A95-90461
 Mach number control in the High Speed Wind Tunnel of NLR
 [PB94-201670] p 53 N95-13243
 Wind-tunnel blockage and actuation systems test of a two-dimensional scramjet inlet unstart model at Mach 6 [NASA-TM-109152] p 97 N95-15898
 Two-dimensional scramjet inlet unstart model: Wind-tunnel blockage and actuation systems test [NASA-TM-109984] p 97 N95-15899
 Wall-signature methods for high speed wind tunnel wall interference corrections p 107 N95-16257
 A model for preliminary facility design including simulation issues p 144 N95-16318
 Hypersonic air-breathing aeropropulsion facility test support requirements p 144 N95-16319
 Hypersonic wind tunnel test techniques
 [AD-A284057] p 118 N95-18663
 Operating capability and current status of the reactivated NASA Lewis Research Center Hypersonic Tunnel Facility
 [NASA-TM-106808] p 148 N95-19286
 Optimized design of a hypersonic nozzle p 297 N95-23304
 Flow models for the design of a hypersonic iodine vapor wind tunnel nozzle with chemical and vibrational nonequilibrium effects p 592 N95-30448

HYPERSONICS

Supersonic and hypersonic shock/boundary-layer interaction database
 [BTN-94-EIX94441386604] p 182 A95-67335

Waveriders with finlets
 [BTN-95-EIX95062487541] p 184 A95-68355
 Computational study of plume-induced separation on a hypersonic powered model
 [BTN-95-EIX95152582346] p 266 A95-73548
 Aerodynamic characteristics of a hypersonic viscous optimized waverider at high altitudes
 [BTN-95-EIX95152583251] p 266 A95-73552
 Hypersonic nonequilibrium Navier-Stokes solutions over an ablating graphite nosetip
 [BTN-95-EIX95152583252] p 305 A95-73553
 Hypersonic model testing in a shock tunnel
 [BTN-95-EIX95222650789] p 329 A95-79245
 Integrated development of the equations of motion for elastic hypersonic flight vehicles
 [BTN-95-EIX95242670755] p 327 A95-81092
 Hypersonic technology experimental vehicles (The need for flight testing at hypersonic speed) p 490 A95-87378
 High temperature aspects of the European Hermes programs p 524 A95-87379
 Measurement of free-flight dynamic stability derivatives of cones in a hypersonic gun tunnel
 [AIAA PAPER 95-6082] p 519 A95-87411
 Experimental investigation of hypersonic flow over a wing-body combination
 [AIAA PAPER 95-6083] p 460 A95-87412
 Experimental and numerical analysis of a two-duct nozzle/afterbody model at supersonic Mach numbers [AIAA PAPER 95-6085] p 490 A95-87414
 Integration of an hypersonic airbreathing vehicle: Assessment of overall aerodynamic performances and of uncertainties
 [AIAA PAPER 95-6100] p 492 A95-88007
 The NASA-sponsored Maryland center for hypersonic education and research p 519 A95-88010
 Optimization of waverider configurations generated from inclined circular and elliptic cones
 [AIAA PAPER 95-6089] p 492 A95-89198
 The effect of wing sweep back upon transition in hypersonic flow
 [AIAA PAPER 95-6090] p 466 A95-89199
 Aerodynamic off-design behavior of integrated waveriders from take-off up to hypersonic flight
 [AIAA PAPER 95-6091] p 466 A95-89200
 The NASA/UTA Center for hypersonic research
 [AIAA PAPER 95-6106] p 520 A95-90438
 Research and educational initiatives at the Syracuse University Center for Hypersonics
 [AIAA PAPER 95-6107] p 520 A95-90439
 Hypersonic shock wave/turbulent boundary layer interactions in the vicinity of an expansion corner
 [AIAA PAPER 95-6125] p 469 A95-90446
 Hypersonic aerodynamics test facility using the external propulsion accelerator
 [AIAA PAPER 95-6138] p 470 A95-90455
 Hypersonic waveriders generated from power-law shocks
 [AIAA PAPER 95-6160] p 470 A95-90472
 A waverider derived hypersonic X-vehicle
 [AIAA PAPER 95-6162] p 496 A95-90473
 A perspective of rarefied gas flow problems relevant to high altitude flight
 [SAE PAPER 931366] p 586 A95-93647
 Cooling of aerospace plane using liquid hydrogen and methane
 [BTN-95-EIX0619952748171] p 590 A95-94465
 Application of scramjet engine technology to the design of ram accelerator projectiles p 19 N95-10282
 Computational flow predictions for hypersonic drag devices p 37 N95-11967
 Experimental aerodynamic characteristics of a generic hypersonic accelerator configuration at Mach numbers 1.5 and 2.0 — conducted in the Langley Unitary Plan Wind Tunnel
 [NASA-TM-4413] p 39 N95-12770
 An approximate Riemann solver for thermal and chemical nonequilibrium flows
 [NASA-CR-195003] p 96 N95-14912
 High altitude hypersonic flowfield radiation
 [AD-A281386] p 106 N95-16160
 An engineering code to analyze hypersonic thermal management systems p 155 N95-16322
 Static aerodynamics CFD analysis for 120-mm hypersonic KE projectile design
 [ARL-MR-184] p 118 N95-18611
 Description and flow characterization of hypersonic facilities
 [AD-A284291] p 223 N95-20248
 Computation of the integrated aerodynamic and propulsive flowfields of a generic hypersonic space plane p 481 N95-29788

An aerodynamic and static-stability analysis of the Hypersonic Applied Research Technology (HART) missile
 [DA9426923] p 481 N95-29965
 Special publication of National Aerospace Laboratory [NAL-SP-27] p 684 N95-34505

HYPERVELOCITY FLOW
 An assessment of ground-test facility capabilities for measurement of hypervelocity scramjet performance
 [AIAA PAPER 95-6148] p 512 A95-90462
 Shock wave interactions in hypervelocity flow
 [AD-A286507] p 250 N95-22212
 Numerical simulation of high enthalpy shock tunnel p 700 N95-34514

HYPERVELOCITY GUNS
 Hypersonic aerodynamics test facility using the external propulsion accelerator
 [AIAA PAPER 95-6138] p 470 A95-90455
 Proceeding towards hypervelocities in ram accelerators p 19 N95-10285

HYPERVELOCITY IMPACT
 Hypervelocity Impact Test Facility: A gun for hire
 [TABES PAPER 94-605] p 86 N95-14639
 Hypervelocity wind tunnel number 9, high Mach number development program
 [AD-A289934] p 594 N95-30929

HYPERVELOCITY LAUNCHERS
 New end tube closure system for the ram accelerator
 [BTN-94-EIX94441380974] p 195 A95-68158

HYPERVELOCITY PROJECTILES
 An experimental study on radiation from strong shock layer p 368 A95-82421
 Numerical simulation of ram accelerator performance including transient effects during initiation of combustion and sensitivity studies p 629 N95-31203

HYPERVELOCITY WIND TUNNELS
 Hypervelocity wind tunnel number 9, high Mach number development program
 [AD-A289934] p 594 N95-30929
 Numerical simulation of high enthalpy shock tunnel p 700 N95-34514

HYSTERESIS
 Computation of oscillating airfoil flows with one- and two-equation turbulence models
 [BTN-95-EIX95152577588] p 263 A95-73494
 An overview of static and dynamic airfoil performance
 [SAE PAPER 931228] p 463 A95-88960
 Numerical study of multi-element airfoil aerodynamics [ISBN 1-879921-01-4] p 587 A95-93750

ICE
 Repeatability of ice shapes in the NASA Lewis icing research tunnel
 [BTN-95-EIX95062487528] p 204 A95-69236
 High-resolution imaging of rain systems with the advanced microwave precipitation radiometer
 [HTN-95-70133] p 252 A95-70655
 Ice accretion on aircraft wings
 [BTN-95-EIX95082502224] p 225 A95-71021
 High-speed civil transport impact: Role of sulfate, nitric acid trihydrate, and ice aerosols studied with a two-dimensional model including aerosol physics
 [HTN-95-91843] p 354 A95-80831
 Momentum and scalar transfer coefficients over aerodynamically smooth Antarctic surfaces
 [HTN-95-92932] p 562 A95-91870
 User's manual for the NASA Lewis ice accretion/heat transfer prediction code with electrothermal deicer input [NASA-CR-4530] p 57 N95-11888
 Ice accretion with varying surface tension
 [NASA-TM-106826] p 124 N95-19285
 Ice-impact analysis of blades p 200 N95-19672
 Collaborative research on aircraft icing and charging processes in ice
 [AD-A285102] p 276 N95-23201
 Analysis of aircraft engine blade subject to ice impact p 407 N95-28277
 A laser-based ice shape profilometer for use in icing wind tunnels
 [NASA-TM-106936] p 646 N95-30851

ICE CLOUDS
 Microwave and infrared simulations of an intense convective system and comparison with aircraft observations
 [HTN-95-60511] p 214 A95-68762
 Replicator for characterization of cirrus and polar stratospheric cloud particles p 445 N95-26669
 [NASA-CR-197785]
 Icing simulation in the aeropropulsion systems test facility propulsion development test cell C-2
 [AD-A293039] p 599 N95-31667

ICE FLOES

- Analyzing the stability of floating ice floes
[AD-A292149] p 563 N95-29160

ICE FORMATION

- Aircraft icing measurements in East Coast winter storms
[HTN-95-60505] p 214 A95-68756
- Conditions associated with large-drop regions
[HTN-95-10686] p 214 A95-68845
- Repeatability of ice shapes in the NASA Lewis icing research tunnel
[BTN-95-EIX95062487528] p 204 A95-69236
- User's manual for the NASA Lewis ice accretion/heat transfer prediction code with electrothermal deicer input
[NASA-CR-4530] p 57 N95-11888
- Ice accretion with varying surface tension
[NASA-TM-106826] p 124 N95-19285
- Replicator for characterization of cirrus and polar stratospheric cloud particles
[NASA-CR-197785] p 445 N95-26669
- Further investigations of icing effects on an advanced high-lift multi-element airfoil
[NASA-TM-106947] p 381 N95-27762
- User's manual for the improved NASA Lewis ice accretion code LEWICE 1.6
[NASA-CR-198355] p 485 N95-29132
- Halstone heat and mass transfer measurements
[ISBN-O-315-86304-8] p 563 N95-29797
- A laser-based ice shape profilometer for use in icing wind tunnels
[NASA-TM-106936] p 646 N95-30851

ICE NUCLEI

- Preliminary studies of ice formation in upslope clouds
p 674 A95-93546

ICE PREVENTION

- User's manual for the NASA Lewis ice accretion/heat transfer prediction code with electrothermal deicer input
[NASA-CR-4530] p 57 N95-11888
- Icing: Accretion, detection, protection
p 77 N95-14897
- Development of anti-icing technology
[PB94-195369] p 78 N95-15439
- An analysis of B-1B exterior jet blast windshield anti-icing performance using pre-cooled compressor bleed air
[AD-A292522] p 485 N95-28811

IDEAL GAS

- Linear disturbances in hypersonic, chemically reacting shock layers
[BTN-94-EIX94441386605] p 182 A95-67336
- General solution procedure for flows in local chemical equilibrium
[HTN-95-42329] p 404 A95-86158
- Research activity at the shock tube facility at NASA Ames
p 547 A95-90559
- Computer code for determination of thermally perfect gas properties
[NASA-TP-3447] p 37 N95-11995
- Shock wave interactions in hypervelocity flow
[AD-A286507] p 250 N95-22212
- Recent improvements to and validation of the one dimensional NASA wave rotor model
[NASA-TM-106913] p 332 N95-25962
- Numerical simulation and analysis of the hypersonic turbulent flow past a blunt-fin/ramp configuration
[DLR-FB-94-19] p 483 N95-30349

IDENTIFYING

- Identification of noise events as aircraft
p 576 A95-90126
- The use of electrochemistry and ellipsometry for identifying and evaluating corrosion on aircraft
[AD-A285323] p 151 N95-16371
- The use of electrochemistry and ellipsometry for identifying and evaluating corrosion on aircraft
[AD-A288536] p 381 N95-27186

IGNITION

- Ignition analysis of hydrogen/air mixture in supersonic mixing layer
p 416 A95-82301
- Studies on plasma jet igniters
p 403 A95-82680
- Intrinsic transport and chemistry coupling in combustion phenomena
p 538 A95-87191
- Injection studies in the French hypersonic technology program
[AIAA PAPER 95-6096] p 510 A95-88004
- Damage to composite aircraft structures from lightning strike attachment to unprotected CFC and internal sparking causing fuel injection
[CONGRESS PAPER C428-4-026] p 531 A95-91675
- Controlling mechanisms of ignition of solid fuel in a sudden-expansion combustor
[BTN-95-EIX0616952745791] p 628 A95-94255
- Programmed ignition of metal compounds in a scramjet
p 16 N95-10466
- Theories of turbulent combustion in high speed flows
[AD-A280933] p 23 N95-10535

- Effects of dust from storage heaters on ignition in scramjets
[NAL-TR-1234] p 405 N95-26706
- Preliminary assessment of combustion modes for internal combustion wave rotors
[NASA-TM-107000] p 616 N95-30632
- The 25th International Symposium on Combustion
[AD-A286825] p 630 N95-31268
- Investigation of starting and ignition transients in the thermally choked ram accelerator
p 698 N95-34805

ILLUMINATION

- Cabin fuselage structural design with engine installation and control system
[NASA-CR-197173] p 47 N95-12639
- Powerful boide explosion over North Italy
[HTN-95-80564] p 218 A95-69658
- A platform independent application of Lux illumination prediction algorithms
[AD-A283669] p 170 N95-18018

IMAGE ANALYSIS

- Scientific and technical photography at NASA Langley Research Center
p 310 N95-23290
- Statistics of multi-look AIRSAR imagery: A comparison of theory with measurements
p 320 N95-23947
- Aspect estimation of an aircraft using library model silhouettes
[PB95-141834] p 360 N95-25894

IMAGE CONVERTERS

- Hypervelocity Impact Test Facility: A gun for hire
[TABES PAPER 94-605] p 86 N95-14639

IMAGE ENHANCEMENT

- Quantifiable vortex features of F-106B aircraft at subsonic speeds
[BTN-95-EIX0619952748161] p 588 A95-94455

IMAGE PROCESSING

- Simple method of supersonic flow visualization using watertable
[BTN-95-EIX95182619105] p 269 A95-76590
- A method for disbond detection in thermal tomography by domain decomposition method
p 545 A95-88955
- Actuated forebody strake controls for the F-18 High-Alpha Research Vehicle
[BTN-95-EIX0619952748173] p 619 A95-94467
- Computer-aided light sheet flow visualization using photogrammetry
[NASA-TP-3416] p 26 N95-10859
- Research on an autonomous vision-guided helicopter
[AIAA PAPER 94-1240-CP] p 18 N95-11510
- Joint Proceedings on Aeronautics and Astronautics (JPAA)
[ISBN-7-80-046602-7] p 104 N95-16249
- SAR image registration in absolute coordinates using GPS carrier phase position and velocity information
[DE94-018738] p 228 N95-20195
- AVIRIS and TIMS data processing and distribution at the land processes distributed active archive center
p 325 N95-23872

- Statistics of multi-look AIRSAR imagery: A comparison of theory with measurements
p 320 N95-23947
- Apparatus and method for producing three-dimensional images
[AD-D017455] p 646 N95-30727

- Analysis of planar laser-induced fluorescence images obtained during shakedown testing of the AEDC impulse facility
[AD-A293237] p 646 N95-30906
- Image representation using fast algorithms based on the Zak transform
[AD-A293416] p 679 N95-31684
- Development and flight testing of an Obstacle Avoidance System for US Army helicopters
p 687 N95-32500

IMAGE RECONSTRUCTION

- Computer-aided light sheet flow visualization using photogrammetry
[NASA-TP-3416] p 26 N95-10859
- Image representation using fast algorithms based on the Zak transform
[AD-A293416] p 679 N95-31684

IMAGERY

- Color control in a multichannel simulator display: The display for advanced research and training
[AD-A279717] p 239 N95-20992
- Synthetic Terrain Imagery for Helmet-Mounted Display, volume 1
[AD-A293612] p 612 N95-31656

IMAGING RADAR

- Foliage transmission measurements using a ground-based ultrawide band (300-1300 MHz) SAR system
[BTN-94-EIX94381351617] p 252 A95-70950
- Linear prediction data extrapolation superresolution radar imaging
p 155 N95-16268

IMAGING SPECTROMETERS

- In-flight radiometric calibration of AVIRIS in 1994
p 705 N95-33754

IMAGING TECHNIQUES

- Dynamic imaging and RCS measurements of aircraft
[BTN-95-EIX95202637582] p 347 A95-78576
- Time-domain imaging of airborne targets using ultra-wideband or short-pulse radar
[BTN-95-EIX95242673673] p 450 A95-82251
- Mapping of forest fire damages using imaging spectroscopy
p 442 A95-83627
- Boundary-layer transition and global skin friction measurement with an oil-fringe imaging technique
[SAE PAPER 932550] p 547 A95-90054
- Airborne imaging radiometer scan simulation
[BTN-95-EIX95332753018] p 638 A95-94793
- Micro-measurements of mechanical properties for adhesives and composites using digital imaging technology
[NASA-CR-196111] p 22 N95-10231
- Linear prediction data extrapolation superresolution radar imaging
p 155 N95-16268
- In-flight imaging of transverse gas jets injected into transonic and supersonic crossflows: Design and development
[NASA-CR-186031] p 157 N95-17418
- Evaluation of scanners for C-scan imaging in nondestructive inspection of aircraft
[DE94-012473] p 152 N95-19100
- Corrosion of aircraft materials: Correlation between nanometer scale and macroscopic structural damage parameters
[AD-A285930] p 241 N95-20299
- Two-dimensional imaging of OH in a lean burning high pressure combustor
[NASA-TM-106854] p 236 N95-21383
- Scientific and technical photography at NASA Langley Research Center
p 310 N95-23290
- AIRSAR deployment in Australia, September 1993: Management and objectives
p 321 N95-23948
- Replicator for characterization of cirrus and polar stratospheric cloud particles
[NASA-CR-197785] p 445 N95-26669
- A nonintrusive method of quantifying flow visualization data in vortex flow fields
[AD-A289802] p 552 N95-28948
- Nonlinear calibration of an infrared radiometer
[AD-A292436] p 579 N95-28996
- Compressibility effects on and control of dynamic stall of oscillating airfoil
[AD-A291804] p 480 N95-29428
- Boundary-layer transition and global skin friction measurement with an oil-fringe imaging technique
[NASA-CR-198814] p 557 N95-30224
- A laser-based ice shape profilometer for use in icing wind tunnels
[NASA-TM-106936] p 646 N95-30851
- Analysis of planar laser-induced fluorescence images obtained during shakedown testing of the AEDC impulse facility
[AD-A293237] p 646 N95-30906
- Advanced data visualization and sensor fusion: Conversion of techniques from medical imaging to Earth science
p 711 N95-34236

IMPACT

- Modelling and analysis of a dual-wheel nosegear: Shimmy instability and impact motions
[SAE PAPER 931402] p 605 A95-93672
- Particle deposition in gas turbine blade cooling holes
p 199 N95-19661

IMPACT DAMAGE

- Numerical modelling of transverse impact on composite coupons
[BTN-95-EIX95082502225] p 240 A95-71022
- Non-linear analysis provides new insights into impact damage of composite structures
[HTN-95-42368] p 418 A95-86197
- Reaction-time response of aircraft crash
[BTN-95-EIX95292721296] p 595 A95-92626
- Residual strength of composites with multiple impact damage
[BTN-94-EIX94511433967] p 701 A95-96664
- Residual strength of composites with multiple impact damage
[AD-A284230] p 87 N95-14409
- An airborne monitoring system for FOD and erosion faults
p 200 N95-19668
- Design of fan blades subjected to bird impact
p 200 N95-19669
- Impact loading of compressor stator vanes by hailstone ingestion
p 200 N95-19670
- Soft body impact on titanium fan blades
p 200 N95-19671
- Ice-impact analysis of blades
p 200 N95-19672
- Analysis of aircraft engine blade subject to ice impact
p 407 N95-28277
- Effect of low-speed impact damage and damage location on behavior of composite panels
p 426 N95-28481

Impact damage resistance of composite fuselage structure, part 1 p 399 N95-28482
 Applications of a damage tolerance analysis methodology in aircraft design and production p 426 N95-28483
 Compressive strength of damaged and repaired composite plates p 442 N95-28484
 Fundamental concepts in the suppression of delamination buckling by stitching p 426 N95-28486
 Damage tolerance of a geodesically stiffened advanced composite structural concept for aircraft structural applications p 399 N95-28487
 Advanced wing design survivability testing and results p 400 N95-28488
 Impact damage resistance of composite fuselage structure, part 2 p 533 N95-28838

IMPACT LOADS

Impact finite element analysis, as an alternative to the testing of windscreens for bird impact [CONGRESS PAPER C428-23-196] p 500 A95-91732
 Impact loading of compressor stator vanes by hailstone ingestion p 200 N95-19670
 Super-heavy aircraft study [AD-A279602] p 238 N95-19955
 Analysis of warping effects on the static and dynamic response of a seat-type structure [NIAR-94-12] p 348 N95-24211
 Effects of floor location on response of composite fuselage frames p 423 N95-28439

IMPACT RESISTANCE

Conference on Aerospace Transparent Materials and Enclosures. Volume 2: Sessions 5-9 [AD-A283926] p 131 N95-18162
 Design and evaluation of a foam-filled hat-stiffened panel concept for aircraft primary structural applications [NASA-TM-109175] p 346 N95-26251

IMPACT STRENGTH

Effects of floor location on response of composite fuselage frames p 423 N95-28439

IMPACT TESTS

Measurement of particle emissions from clean room gas-handling components [BTN-94-EIX94381359040] p 295 A95-74554
 Impact, friction, and wear testing of microsamples of polycrystalline silicon p 361 A95-79988
 Residual strength of composites with multiple impact damage [BTN-94-EIX94511433967] p 701 A95-96664
 The performance of child restraint devices in transport airplane passenger seats [DOT/FAA/AM-94/19] p 40 N95-12146
 Hypervelocity Impact Test Facility: A gun for hire [TABES PAPER 94-605] p 86 N95-14639
 Soft body impact on titanium fan blades p 200 N95-19671
 Development of repair processes and sources for C/KC-135 aircraft windows/windshields [AD-A288348] p 367 N95-26629
 Analysis of aircraft engine blade subject to ice impact p 407 N95-28277
 Effect of low-speed impact damage and damage location on behavior of composite panels p 426 N95-28481
 Impact damage resistance of composite fuselage structure, part 1 p 399 N95-28482
 Applications of a damage tolerance analysis methodology in aircraft design and production p 426 N95-28483
 Damage tolerance of a geodesically stiffened advanced composite structural concept for aircraft structural applications p 399 N95-28487
 Rotorcraft crashworthy airframe and fuel system technology development program [AD-A289986] p 382 N95-28630

IMPACT TOLERANCES

Through-the Thickness(R) braided composites for aircraft applications p 421 N95-28273
 Impact damage resistance of composite fuselage structure, part 2 p 533 N95-28838

IMPEDANCE

Electrochemical impedance pattern recognition for detection of hidden chemical corrosion on aircraft components [AD-A284998] p 241 N95-20481
 The use of electrochemistry and ellipsometry for identifying and evaluating corrosion on aircraft [AD-A290249] p 504 N95-29426
 Electrochemical impedance pattern recognition for detection of hidden chemical corrosion on aircraft components, phase 1 [AD-A291345] p 556 N95-29946

IMPEDANCE MEASUREMENT

The use of electrochemistry and ellipsometry for identifying and evaluating corrosion on aircraft [AD-A285323] p 151 N95-16371

Fault detection techniques for complex cable shield topologies [AD-A286632] p 247 N95-20771
 TIM-SCT cable testing protocol [AD-A286633] p 231 N95-20772

IMPELLERS

On calculated models for impellers of centrifugal compressors [BTN-94-EIX94461407947] p 88 A95-62265
 Simulation of the unsteady interaction of a centrifugal impeller with its vaned diffuser: flow analysis [BTN-95-EIX95282710055] p 633 A95-92474
 Laser anemometer measurements of the three-dimensional rotor flow field in the NASA low-speed centrifugal compressor [NASA-TP-3527] p 618 N95-31985

IMPINGEMENT

Impinging flow heat transfer measurements of turbine blades using a jet array [AD-A283450] p 62 N95-12512
 Shock wave interactions in hypervelocity flow [AD-A286507] p 250 N95-22212

IMPROVEMENT

Electrical power system upgrade methodology for in-service aircraft [SAE PAPER 932562] p 511 A95-90059
 The improvement of meteorological data for air traffic management purposes p 668 A95-93518

IMPULSES

A higher harmonic control test in the DNW to reduce impulsive BVI noise [HTN-95-61071] p 385 A95-83655
 Impulse radiating antennas p 548 A95-90920
 Scattering of short em-pulses by simple and complex targets using impulse radar p 486 A95-90953
 Thrust measurements of a complete axisymmetric scramjet in an impulse facility p 339 N95-25395

IN SITU MEASUREMENT

Application of airborne field mill data for use in launch support [HTN-95-50054] p 98 A95-62279
 In situ observations in aircraft exhaust plumes in the lower stratosphere at midlatitudes [HTN-95-A0862] p 318 A95-76266
 Real-time estimation of atmospheric turbulence severity from in-situ aircraft measurements [BTN-95-EIX95182619231] p 319 A95-76657
 Estimation of atmospheric turbulence severity from in-situ aircraft measurements p 659 A95-93479
 An in-situ system for warning of icing conditions p 660 A95-93481
 Science objectives and performance of a radiometer and window design for atmospheric entry experiments p 85 N95-13718
 Replicator for characterization of cirrus and polar stratospheric cloud particles [NASA-CR-197785] p 445 N95-26669
 In situ measurements of ClO and implications for the chemistry of inorganic chlorine in the lower stratosphere p 563 N95-29830

IN-FLIGHT MONITORING

Condition monitoring and diagnostics [HTN-95-92312] p 387 A95-85356
 New sensor technology for aircraft hydraulic system diagnostics [SAE PAPER 932586] p 494 A95-90070
 Gas path debris monitoring [CONGRESS PAPER C428-15-031] p 508 A95-91710
 An example of airborne vibration monitoring improving flight safety in the Soloviev D-30-KU engine [CONGRESS PAPER C428-21-141] p 508 A95-91728
 External viewing airborne CCTV system [CONGRESS PAPER C428-25-172] p 595 A95-93598
 Progress and experience with helicopter health and usage monitoring [CONGRESS PAPER C428-31-151] p 603 A95-93615
 Design and development of an F/A-18 inlet distortion rake: A cost and time saving solution p 69 N95-14241
 Airplane takeoff and landing performance monitoring system [NASA-CASE-LAR-14745-2-SB] p 85 N95-14415
 Test Operation Procedure (TOP): Vibration testing of helicopter equipment [AD-A284433] p 81 N95-15815
 Flight parameters monitoring system for tracking structural integrity of rotary-wing aircraft p 135 N95-19469
 Enhancement of F/A-18 operational flight measurements: Data report for phase 1 [DSTO-TR-0049] p 286 N95-23666

An overview of Health and Usage Monitoring Systems (HUMS) for military helicopters [DSTO-TR-0061] p 327 N95-24200

INCENDIARY AMMUNITION

Rationale for the Modular Air-system Vulnerability Estimation Network (MAVEN) methodology [AD-A285797] p 284 N95-22510

INCIDENCE

Oblique incidence sound absorption of porous materials covered by perforated metal and exposed to tangential airflow [HTN-94-00681] p 19 A95-60165
 Collectively variable incidence wingtips for lift control and reduced gust sensitivity [HTN-95-92836] p 471 A95-90754
 Numerical investigation of high incidence flow over a double-delta wing [BTN-95-EIX0619952748160] p 588 A95-94454

INCOMPRESSIBLE BOUNDARY LAYER

Effect of crossflow on Goertler instability in incompressible boundary layers [NASA-CR-195007] p 159 N95-18193

INCOMPRESSIBLE FLOW

Aspects of vortex breakdown [HTN-95-A0001] p 183 A95-67828
 Time-resolved surface heat flux measurements in the wing/body junction vortex [BTN-95-EIX95082502716] p 220 A95-71029
 Adaptive remeshing for convective heat transfer with variable fluid properties [BTN-95-EIX95082502720] p 243 A95-71033
 Two-equation turbulence model for unsteady separated flows around airfoils [BTN-95-EIX95142553054] p 262 A95-73444
 Adaptive finite element method for turbulent flow near a propeller [BTN-95-EIX95142553038] p 305 A95-73460
 Eigenanalysis of unsteady flows about airfoils, cascades, and wings [BTN-95-EIX95152577597] p 305 A95-73486
 Progress in high-lift aerodynamic calculations [BTN-95-EIX95152582315] p 264 A95-73518
 Sidewash on the vertical tail in subsonic and supersonic flows [BTN-95-EIX95152582316] p 264 A95-73519
 Postinstability behavior of a two-dimensional airfoil with a structural nonlinearity [BTN-95-EIX95152582337] p 266 A95-73539
 Grid refinement test of time-periodic flows over bluff bodies [BTN-94-EIX94401378822] p 307 A95-76491
 Aerodynamic characteristics of external store configurations at low speeds [BTN-95-EIX95182619230] p 271 A95-76656
 Study of the droplet spray characteristics of a subsonic wind tunnel [BTN-95-EIX95182619235] p 271 A95-76661
 Simulation on the 3-D turbulent flow in the passages of finocyl grain [BTN-95-EIX95202638962] p 279 A95-76674
 Direct boundary integral equations method to subsonic flow with circulation past thin airfoils in ground effect [BTN-95-EIX95242673940] p 365 A95-82224
 On the influence of time-varying flow velocity on unsteady aerodynamics [HTN-95-61073] p 369 A95-83657
 Predicting stall and post-stall behavior of airfoils at low mach numbers [BTN-95-EIX95262694297] p 365 A95-85468
 Prediction of two-dimensional momentumless wake by k-epsilon-gamma model [BTN-95-EIX95262694299] p 434 A95-85470
 Multipoint inverse design of an infinite cascade of airfoils [HTN-95-81640] p 541 A95-87688
 Low-dimensional description of the dynamics in separated flow past thick airfoils [HTN-95-20832] p 544 A95-88093
 Vortex lattice method simulation of unsteady flow due to wing/external store combination p 471 A95-91499
 Optimum aerodynamic design of aircraft fuselage using boundary element method p 473 A95-91514
 Lee waves benign and malignant p 595 A95-93554
 Correlation of unsteady pressure and inflow velocity fields of a pitching rotor blade [BTN-95-EIX0619952748169] p 589 A95-94463
 Computational fluid dynamics '92; Proceedings of the European Computational Fluid Dynamics Conference, 1st, Brussels, Belgium, Sep. 7-11, 1992. Vols. 1 & 2 [ISBN 0-444-89793-3] p 638 A95-95357
 Discretization of the parabolised Navier-Stokes equations p 638 A95-95362
 Numerical solution of Euler and Navier-Stokes equations for 2D transonic problems p 638 A95-95366
 Laminar and turbulent flow over optimal riblets p 639 A95-95383

- A numerical investigation of flow around a square-section cylinder mounted with a splitter plate p 639 A95-95401
- An efficient discrete vortex method for low Reynolds number incompressible flows p 639 A95-95407
- A computational investigation of wake-induced airfoil flutter in incompressible flow and active flutter control [AD-A281534] p 142 N95-16109
- Direct numerical simulations of on-demand vortex generators: Mathematical formulation p 251 N95-22452
- CFD research, parallel computation and aerodynamic optimization [NASA-CR-197748] p 373 N95-26649
- Finite element vorticity-based methods for the solution of the incompressible and compressible Navier-Stokes equations p 553 N95-29119
- Dynamic stall of a NACA 0012 airfoil in laminar flow p 479 N95-29243
- Pressure updating methods for the steady-state fluid equations [NASA-CR-198163] p 569 N95-30353
- Axial loads on yawed rotors [PB95-214193] p 592 N95-30638
- Acceleration potential models PREDICAT/PREDICDYN applied for calculation of axisymmetric dynamic inflow cases [PB95-207015] p 647 N95-30957
- Numerical simulations of dynamic stall phenomena in low speed flows p 685 N95-34546
- Nonlinear stability of unsteady viscous flow [AD-A294931] p 707 N95-34597
- INCOMPRESSIBLE FLUIDS**
- Dynamics of aircraft exhaust plumes in the jet-regime [HTN-95-51275] p 355 A95-80860
- Dissolved gas - the hidden saboteur [SAE PAPER 931404] p 628 A95-93674
- INCONEL (TRADEMARK)**
- Probabilistic material strength degradation model for Inconel 718 components subjected to high temperature, high-cycle and low-cycle mechanical fatigue, creep and thermal fatigue effects [NASA-CR-197832] p 419 N95-27167
- INDENTATION**
- Evaluation of advanced aerospace materials by depth sensing indentation and scratch methods [BTN-95-EIX95152584678] p 282 A95-73590
- The effects of surface modification on fretting fatigue in Ti alloy turbine components [HTN-95-61145] p 404 A95-84909
- INDEXES (DOCUMENTATION)**
- HLLV avionics requirements study and electronic filing system database development [NASA-CR-193993] p 49 N95-13027
- Aeronautical engineering: A continuing bibliography with indexes (supplement 315) [NASA-SP-7037(315)] p 219 N95-21640
- Aeronautical engineering: A continuing bibliography with indexes (supplement 316) [NASA-SP-7037(316)] p 328 N95-24465
- Aeronautical engineering: A continuing bibliography with indexes (supplement 317) [NASA-SP-7037(317)] p 328 N95-25798
- Aeronautical engineering: A continuing bibliography with indexes (supplement 318) [NASA-SP-7037(318)] p 367 N95-27543
- AGARD index of publications: 1992-1994 [AGARD-INDEX-92-94] p 711 N95-33198
- INDEXES (RATIOS)**
- Prediction of NO(x) emission index of turbulent diffusion flame p 538 A95-87195
- The use of the Equivalent Continuous Sound Level (L(sub eq)) as an aircraft noise index [HTN-95-92542] p 558 A95-87362
- INDIA**
- Experimental Aerodynamics Division [NAL-SP-9404] p 35 N95-12166
- INDICATING INSTRUMENTS**
- Directional control at high angles of attack using blowing through a chined forebody [BTN-95-EIX0619952748179] p 619 A95-94472
- INDIUM ARSENIDES**
- An Echelle Grating Spectrometer (EGS) for mid-IR remote chemical detection [DE94-019310] p 249 N95-21478
- INDUCTANCE**
- A time stepping coupled finite element-state space modeling environment for synchronous machine performance and design analysis in the ABC frame of reference p 649 N95-31948
- INDUCTION MOTORS**
- Improved speed control system for the 87,000 HP wind tunnel drive [NASA-TM-106840] p 211 N95-19794
- Motor drive technologies for the power-by-wire (PBW) program: Options, trends and tradeoffs [NASA-TM-106885] p 295 N95-23671
- INDUSTRIAL MANAGEMENT**
- Asian Aeronautics: Technology acquisition drives industry development. Report to Congressional requesters [GAO/NSIAD-94-140] p 367 N95-26817
- INDUSTRIAL PLANTS**
- Noise Con 1994: Proceedings of the 1994 National Conference on Noise Control Engineering. Progress in Noise Control for Industry [LC-75-24750] p 28 N95-11259
- Electro-hydrostatic actuator controller design using quantitative feedback theory [AD-A289220] p 409 N95-26957
- INDUSTRIES**
- Military aviation maintenance industry in Western Europe: Concentration and internationalization [PB94-189180] p 104 N95-17451
- Standard Hardware Acquisition and Reliability Program (SHARP) advanced SEM-E packaging p 233 N95-20633
- INELASTIC COLLISIONS**
- Rarefied gas numerical wind tunnel: OREX and HOPE p 427 A95-82391
- INEQUALITIES**
- Linear matrix inequalities for the problem of absolute stability of control systems p 518 N95-29680
- INERTIAL GUIDANCE**
- Results from tests of the Kearfott T16-B Inertial Measurement Unit [PB95-212031] p 644 N95-30502
- INERTIAL NAVIGATION**
- High accuracy navigation and landing system using GPS/IMU system integration [BTN-94-EIX94441386129] p 189 A95-68185
- GPS/GLONASS/INS test program [BTN-94-EIX94441386131] p 189 A95-68187
- Comments on 'correction of inertial navigation with Loran C on NOAA's P-3 aircraft' [HTN-95-70149] p 227 A95-70671
- Enhancing filter robustness in cascaded GPS-INS integrations [BTN-95-EIX95142555475] p 278 A95-73435
- Covariance analysis of strapdown INS considering gyrocompass characteristics [BTN-95-EIX95202637592] p 279 A95-76697
- Flight evaluation of DGPS and DGPS-INS navigation systems p 382 A95-82462
- Failure detection and isolation structure for global positioning system autonomous integrity monitoring [BTN-95-EIX95282706656] p 486 A95-89648
- Study of strapdown navigation attitude algorithms [BTN-95-EIX95282706655] p 486 A95-89649
- Maintenance-free lead acid battery for inertial navigation systems aircraft [BTN-95-EIX95292721316] p 633 A95-92511
- GPS modeling for designing aerospace vehicle navigation systems [BTN-95-EIX95302731223] p 600 A95-94044
- Application of GPS/SINS/RA integrated system to aircraft approach landing p 125 N95-16277
- Assessment of a non-dedicated GPS receiver system for precise airborne attitude determination [DE94-019309] p 229 N95-21520
- A real-time algorithm for integrating differential satellite and inertial navigation information during helicopter approach [NASA-CR-197409] p 229 N95-21891
- Results from tests of the Honeywell integrated flight management unit [PB95-211355] p 601 N95-30597
- Navigational technology of dual usage p 688 N95-33131
- Application of advanced safety technique to ring laser gyro inertial navigation system integration p 689 N95-33140
- INERTIAL PLATFORMS**
- Dynamic response tests of inertial and optical wind-tunnel model attitude measurement devices [NASA-TM-109182] p 296 N95-23011
- INFERENCE**
- New strategy combining backward inference with forward inference in monitoring and diagnosing techniques for hydrodynamic bearing-rotor systems [BTN-94-EIX94331336949] p 88 A95-61795
- INFILTRATION**
- Development and verification of a resin film infusion/resin transfer molding simulation model for fabrication of advanced textile composites [NASA-CR-197439] p 301 N95-23179
- INFINITE SPAN WINGS**
- Three-dimensional interaction of wake/boundary-layer and vortex/boundary-layer data report [CUED/A-AEREO/TR-23] p 329 N95-24210
- INFORMATION DISSEMINATION**
- An overview of FAA-sponsored aviation weather research and development p 652 A95-93442
- National aviation weather program plan p 652 A95-93445
- Operational aviation weather regulations p 652 A95-93446
- Status of the terminal Doppler weather radar with deployment underway p 653 A95-93450
- Knowing our users - A challenge for meteorologists at the National Aviation Weather Advisory Unit p 655 A95-93459
- An integrated system to improve aviation weather forecasts for the Alaska Range p 656 A95-93460
- Flying with automated surface observations p 659 A95-93472
- Analysis of en route controller hazardous weather-related tasks p 665 A95-93503
- The data link flight information service application p 665 A95-93504
- Aviation value-added products and services from the NEXRAD Information Dissemination Service (NIDS) p 671 A95-93535
- ICASE [NASA-CR-195001] p 170 N95-16898
- INFORMATION FLOW**
- The IEEE scalable coherent interface: An approach for a unified avionics network p 234 N95-20650
- A nonintrusive method of quantifying flow visualization data in vortex flow fields [AD-A289802] p 552 N95-28948
- INFORMATION MANAGEMENT**
- HLLV avionics requirements study and electronic filing system database development [NASA-CR-193993] p 49 N95-13027
- Collected papers of the Soar/IFOR project, Spring 1994 [AD-A280063] p 238 N95-20624
- INFORMATION PROCESSING (BIOLOGY)**
- Automation and cognition in air traffic control: An empirical investigation [AD-A291932] p 488 N95-28790
- INFORMATION RETRIEVAL**
- On a program-information system TDsoft [BTN-94-EIX94461408773] p 175 A95-63656
- HLLV avionics requirements study and electronic filing system database development [NASA-CR-193993] p 49 N95-13027
- INFORMATION SYSTEMS**
- Independent review of Aviation Technology and Research Information Analysis System (ATRIAS) database [AD-A284049] p 226 N95-21518
- Aeronautical engineering: A continuing bibliography with indexes (supplement 315) [NASA-SP-7037(315)] p 219 N95-21640
- Automation technology using Geographic Information System (GIS) p 324 N95-23284
- NLS Flight Simulation Laboratory (FSL) documentation [NASA-CR-196564] p 363 N95-24439
- The ATC operational evaluation of the prototype integrated terminal weather system (ITWS) at Dallas/Fort Worth and Orlando airports (May-September 1993) [AD-A293808] p 677 N95-31587
- INFORMATION TRANSFER**
- Functional requirements of an aerospace Design Representation Programming Interface [AIAA PAPER 95-0967] p 497 A95-90643
- INFRARED ABSORPTION**
- Water vapor continuum absorption in mid-latitudes: Aircraft measurements and model comparisons [HTN-95-40756] p 252 A95-71186
- INFRARED ASTRONOMY**
- SOFIA: Stratospheric Observatory for Infrared Astronomy p 363 A95-81583
- Stratospheric Observatory For Infrared Astronomy (SOFIA). Phase A: System concept description [NASA-TM-110669] p 680 N95-32187
- INFRARED DETECTORS**
- Integrated IR sensors [BTN-95-EIX95041505023] p 242 A95-70132
- State-to-state collisional dynamics of atmospheric species [AD-A285053] p 245 N95-20484
- Cost effective, dual-purpose machine vision-based detectors for (1) smoke and flame detection, and (2) engine overheat/burn-through and flame detection [AD-A292284] p 579 N95-28870
- Apparent size passive range method [AD-D017360] p 611 N95-31180
- INFRARED IMAGERY**
- Numerical simulation of a complete STOV/L aircraft in ground effect [AIAA PAPER 93-4880] p 4 A95-60187

Constant flux, turbulent convection data using infrared imaging
 [HTN-95-20731] p 435 A95-86621
 AVIRIS and TIMS data processing and distribution at the land processes distributed active archive center
 p 325 N95-23872
 Hailstone heat and mass transfer measurements
 [ISBN-0-315-86304-8] p 563 N95-29797
 A helmet mounted display for night missions at low altitude
 p 693 N95-32503
 Correction of thin cirrus effects in AVIRIS images using the sensitive 1.375-micron cirrus detecting channel
 p 708 N95-33748
 Remote sensing of smoke, clouds, and radiation using AVIRIS during SCAR experiments
 p 708 N95-33749

INFRARED INSPECTION
 A method for disbond detection in thermal tomography by domain decomposition method
 p 545 A95-88955

INFRARED INSTRUMENTS
 Aero-optics system integration
 [TABES PAPER 94-604] p 100 N95-14638
 Nonlinear calibration of an infrared radiometer
 [AD-A292436] p 579 N95-28996
 HeliRadar: A rotating antenna synthetic aperture radar for helicopter allweather operations
 p 705 N95-33137

INFRARED LASERS
 2 micron LIDAR for laser-based remote sensing: Flight demonstration and application survey
 [BTN-95-EIX95212641072] p 319 A95-76737
 State-to-state collisional dynamics of atmospheric species
 [AD-A285053] p 245 N95-20484

INFRARED RADIATION
 Laws of infrared similitude
 [AD-A282209] p 62 N95-12426
 Application of photogrammetry of F-14D store separation
 [AD-A284154] p 132 N95-18417
 An Echelle Grating Spectrometer (EGS) for mid-IR remote chemical detection
 [DE94-019310] p 249 N95-21478
 Nonlinear calibration of an infrared radiometer
 [AD-A292436] p 579 N95-28996
 Correction of thin cirrus effects in AVIRIS images using the sensitive 1.375-micron cirrus detecting channel
 p 708 N95-33748

INFRARED RADIOMETERS
 Microwave and infrared simulations of an intense convective system and comparison with aircraft observations
 [HTN-95-60511] p 214 A95-68762
 Nonlinear calibration of an infrared radiometer
 [AD-A292436] p 579 N95-28996

INFRARED SCANNERS
 TIMS observations of surface emissivity in HAPEX-Sahel
 p 709 N95-33799

INFRARED SPECTRA
 Modeling of aircraft exhaust emissions and infrared spectra for remote measurement of nitrogen oxides
 [HTN-95-51276] p 355 A95-80861
 Matrix isolated HF: the high-resolution infrared spectrum of a cryogenically solvated hindered rotor
 [GTN-95-0301010494002231-16] p 578 A95-92210
 AVIRIS and TIMS data processing and distribution at the land processes distributed active archive center
 p 325 N95-23872
 TIMS observations of surface emissivity in HAPEX-Sahel
 p 709 N95-33799

INFRARED SPECTROMETERS
 Possible near-IR channels for remote sensing precipitable water vapor from geostationary satellite platforms
 [HTN-95-70139] p 214 A95-69431
 An Echelle Grating Spectrometer (EGS) for mid-IR remote chemical detection
 [DE94-019310] p 249 N95-21478
 In-flight radiometric calibration of AVIRIS in 1994
 p 705 N95-33754
 Integration of AIRSAR and AVIRIS data for Trail Canyon alluvial fan, Death Valley, California
 p 709 N95-33760

INFRARED SPECTROSCOPY
 Standardization of surface contamination analysis systems
 p 631 N95-31798

INFRARED TELESCOPES
 SOFIA: Stratospheric Observatory for Infrared Astronomy
 p 363 A95-81583
 Stratospheric Observatory For Infrared Astronomy (SOFIA). Phase A: System concept description
 [NASA-TM-110669] p 680 N95-32187
 SOFIA: Aft cavities wind tunnel test
 [NASA-TM-110673] p 683 N95-32682
 SOFIA 2 model telescope wind tunnel test report
 [NASA-TM-110668] p 683 N95-32764

INFRARED TRACKING
 Apparent size passive range method
 [AD-D017360] p 611 N95-31180

INGESTION (ENGINES)
 Erosion of dust-filtered helicopter turbine engines. Part 1: Basic theoretical considerations
 [BTN-95-EIX95182619222] p 288 A95-76648
 Erosion of dust-filtered helicopter turbine engines. Part 2: Erosion reduction
 [BTN-95-EIX95182619223] p 289 A95-76649
 Life prediction of helicopter engines fitted with dust filters
 [BTN-95-EIX95182619224] p 289 A95-76650
 Modern transport engine experience with environmental ingestion effects
 p 199 N95-19660
 Experimental and numerical simulations of the effects of ingested particles in gas turbine engines
 p 199 N95-19662
 Bird ingestion into large turbofan engines
 [DOT/FAA/CT-93/14] p 333 N95-24631
 WINCLR: A computer code for heat transfer and clearance calculation in a compressor
 [NASA-CR-195436] p 366 N95-26363
 Comparison of numerical results and multicavity purge and rim seal data with extensions to dynamics
 [NASA-TM-106685] p 416 N95-27434

INJECTION
 Permanent magnet electron cyclotron resonance plasma source with remote window
 [BTN-95-EIX95242674338] p 450 A95-82176
 Combustion efficiency in a dual-inlet side-dump ramjet combustor
 [AD-A283564] p 83 N95-15329

INJECTORS
 Quantitative investigation of compressible mixing: Staged transverse injection into Mach 2 flow
 [HTN-95-42330] p 404 A95-86159
 Conceptual studies of high speed combustors for mixing enhancement mechanisms
 [AIAA PAPER 95-6095] p 510 A95-88003
 Injection studies in the French hypersonic technology program
 [AIAA PAPER 95-6096] p 510 A95-88004
 The DCAF: A high-enthalpy long-duration, direct-connect scramjet test facility
 [AIAA PAPER 95-6130] p 512 A95-90450
 Investigation of scramjet injection strategies for high mach number flows
 [BTN-95-EIX0616952745782] p 614 A95-94504
 Experiment on a rectangular cross section scramjet combustor. 2: Effects of fuel injector geometry
 [NAL-TR-1220] p 405 N95-26600
 A study of supersonic mixing flow field with ramp injector
 p 706 N95-34512

INJURIES
 RAF ejections - historical perspectives and future requirements
 [CONGRESS PAPER C428-18-168] p 484 A95-91717
 Deaths and injuries as a result of lightning strikes to aircraft
 [HTN-95-12213] p 485 A95-91913

INLET AIRFRAME CONFIGURATIONS
 Sensitivity of engine-integrated waverider performance to static margin constraint
 [AIAA PAPER 95-6142] p 496 A95-90458
 Performance study for inlet installations
 [NASA-CR-189714] p 406 N95-28227

INLET FLOW
 Experimental and computational results for the external flowfield of a scramjet inlet
 [BTN-94-EIX94441380977] p 195 A95-68161
 Lag model for turbulent boundary layers over rough bleed surfaces
 [BTN-94-EIX94441380981] p 208 A95-68165
 Numerical study of the performance of swept, curved compression surface scramjet inlets
 [BTN-95-EIX95112524198] p 197 A95-69310
 Static pressure distribution in the inlet of a helicopter turbine compressor
 [BTN-95-EIX95152582339] p 266 A95-73541
 A new type of simulator for simulating the flow-field distortion of engine inlet
 [BTN-95-EIX95202638963] p 289 A95-76673
 Numerical analysis of hypersonic low-density scramjet inlet flow
 [BTN-95-EIX95212645694] p 272 A95-76746
 Prediction of supersonic inlet unstart caused by freestream disturbances
 [BTN-95-EIX9522650790] p 329 A95-79246
 Boundary conditions for unsteady supersonic inlet analyses
 [HTN-95-20829] p 544 A95-88090
 Aerodynamic characteristics of supersonic air-intake/aircraft integrated models
 p 472 A95-91512
 Some considerations on system design of the hypersonic transport and supersonic air-intakes
 p 473 A95-91522
 2-D and 3-D numerical simulation of a supersonic inlet flowfield
 p 641 A95-95457

A full Navier-Stokes analysis of subsonic diffuser of a bifurcated 70/30 supersonic inlet for high speed civil transport application
 [NASA-TM-106637] p 8 N95-10820
 Numerical simulation of the flow about the F-18 HARV at high angle of attack
 [NASA-CR-196396] p 9 N95-10940
 Inlet flow test calibration for a small axial compressor facility. Part 1: Design and experimental results
 [NASA-TM-106719] p 16 N95-11005
 Computational analysis in support of the SSTO flowpath test
 [NASA-TM-106757] p 89 N95-13665
 Design and development of an F/A-18 inlet distortion rake: A cost and time saving solution
 p 69 N95-14241
 Wind-tunnel blockage and actuation systems test of a two-dimensional scramjet inlet unstart model at Mach 6
 [NASA-TM-109152] p 97 N95-15898
 Two-dimensional scramjet inlet unstart model: Wind-tunnel blockage and actuation systems test
 [NASA-TM-109984] p 97 N95-15899
 Numerical simulation of supersonic compression corners and hypersonic inlet flows using the RPLUS2D code
 [NASA-TM-106580] p 105 N95-16038
 Unsteady flow phenomena in discrete passage diffusers for centrifugal compressors
 [AD-A281412] p 155 N95-16163
 Time accurate computation of unsteady inlet flows with a dynamic flow adaptive mesh
 [AD-A285498] p 157 N95-16736
 Three dimensional compressible turbulent flow computations for a diffusing S-duct with/without vortex generators
 [NASA-CR-195390] p 138 N95-17402
 Wind turbine blade aerodynamics: The combined experiment
 [DE94-011866] p 118 N95-18645
 Wind turbine blade aerodynamics: The analysis of field test data
 [DE94-011867] p 118 N95-18646
 Prediction of wind tunnel effects on the installed F/A-18A inlet flow field at high angles-of-attack
 [NASA-CR-195429] p 197 N95-19651
 Flow visualization studies of VTOL aircraft models during Hover in ground effect
 [NASA-TM-108860] p 272 N95-22666
 Mach 10 computational study of a three-dimensional scramjet inlet flow field
 [NASA-TM-4602] p 309 N95-23015
 Mach 10 computational study of a three-dimensional scramjet inlet flow field
 [NASA-TM-4602] p 310 N95-23210
 Three-dimensional Navier-Stokes analysis and redesign of an imbedded bellmouth nozzle in a turbine cascade inlet section
 p 311 N95-23423
 Supersonic flow and shock formation in turbine tip gaps
 p 312 N95-23429
 Study of compressible flow through a rectangular-to-semiannular transition duct
 [NASA-CR-4660] p 338 N95-24392
 Numerical investigation to S-inlet flows (Numerical simulation study of S-inlet flows)
 [AD-A289590] p 374 N95-26713
 Demonstration of an automated CFD system for three-dimensional flow simulations
 p 551 N95-28767
 A procedure for automating CFD simulations of an inlet-bleed problem
 p 552 N95-28768
 Unsteady pressure and inflow velocity on a pitching rotor blade in hover
 p 480 N95-29771
 Inlet flow test calibration for a small axial compressor rig. Part 2: CFD compared with experimental results
 [NASA-TM-106999] p 514 N95-30007
 Survey of CFD applications for high speed inlets
 [AD-A291365] p 557 N95-30087
 Effects of initial conditions on a single jet in crossflow
 [NASA-TM-107002] p 615 N95-30589
 An investigation of the side-dump dual in-line ramjet combustor
 p 617 N95-31199
 A pulsed liquid fuel ramjet
 p 617 N95-31201

INLET NOZZLES
 Active boundary-layer control in diffusers
 [HTN-95-42580] p 458 A95-87210
 Testing the hypersonic technology demonstration nozzle: Results from the test campaign 1993/94
 [AIAA PAPER 95-6084] p 509 A95-87413
 Experimental and numerical analysis of a two-duct nozzle/afterbody model at supersonic Mach numbers
 [AIAA PAPER 95-6085] p 490 A95-87414
 Shock-tunnel combustor testing for hypersonic vehicles
 [NASA-CR-196836] p 52 N95-11938
 Combustor kinetic energy efficiency analysis of the hypersonic research engine data
 p 148 N95-16321
 Small turbojets: Designs and installations
 p 138 N95-16323

Study of compressible flow through a rectangular-to-semiannular transition duct [NASA-CR-4660] p 338 N95-24392

INLET PRESSURE
F/A-18 inlet calculations at 60-deg angle of attack and 10-deg sideslip [BTN-95-EIX95112524199] p 195 A95-69309

INLET TEMPERATURE
Characteristics of the turbine inlet temperature sensing circuit for the T56 turbo-prop engine [DSTO-TR-0095] p 405 N95-26424
Minimum fan turbine inlet temperature mode evaluation p 696 N95-33016

INMARSAT SATELLITES
A processing centre for the CNES CE-GPS experimentation p 125 N95-17196

INORGANIC COMPOUNDS
Estimates of total organic and inorganic chlorine in the lower stratosphere from in situ and flask measurements during AASE 2 [HTN-95-A0861] p 317 A95-76265

INPUT/OUTPUT ROUTINES
Selecting optimal experiments for feedforward multilayer perceptions [AD-A290856] p 678 N95-30406

INSECTS
Airfoil characteristics at low Reynolds number p 472 A95-91507

INSPECTION
Maintenance programs [HTN-95-92310] p 365 A95-85354
Fibre-Metal laminates p 387 A95-85895
Elements of structural integrity assurance p 387 A95-85896
Verification of the damage tolerance of a fighter aircraft p 388 A95-85897
Damage tolerance capability p 388 A95-85898
Experimental investigation of thermoelastic deformation in turbojet-engine bearings under maintenance inspection [BTN-95-EIX95292721173] p 546 A95-89904
Development of an Automated Nondestructive Inspection (ANDI) system for commercial aircraft, phase 1 [AD-A283500] p 40 N95-12623
Proceedings of the FAA Inspection Program Area Review [AD-A283849] p 77 N95-14350
Probabilistic inspection strategies for minimizing service failures p 93 N95-14461
A method of calculating the safe fatigue life of compact, highly-stressed components p 93 N95-14464
Computational predictive methods for fracture and fatigue p 93 N95-14466
Fatigue reliability method with in-service inspections p 94 N95-14475
Development of a composite repair and the associated inspection intervals for the F-111C stiffener runout region p 66 N95-14477
Full-scale testing and analysis of fuselage structure p 95 N95-14485
Double pass retroreflection for corrosion detection in aircraft structures p 323 N95-23503
Non-destructive detection of corrosion for life management p 314 N95-23505
Health and usage monitoring systems: Corrosion surveillance p 262 N95-23506
Eddy current detection of pitting corrosion around fastener holes p 315 N95-23507
Corrosion detection and monitoring of aircraft structures: An overview p 303 N95-23515
Experience of in-service corrosion on military aircraft p 303 N95-23516
POD assessment of NDI procedures using a round robin test [AGARD-R-809] p 315 N95-23602
Estimate of probability of crack detection from service difficulty report data [PB95-149381] p 328 N95-24295
Characterization of corrosion and development of a breadboard of a D sight aircraft inspection system, phase 1 [AD-A288347] p 380 N95-26527
Report to the Chairman, Subcommittee on Aviation, Committee on Commerce, Science, and Transportation, US Senate. Aviation safety: Data problems threaten FAA strides on safety analysis system [GAC/AIMD-95-27] p 687 N95-32705
Expert systems and artificial intelligence applications in engineering design and inspection p 710 N95-33008
Integrated special mission flight management for a flight inspection aircraft p 692 N95-33145

INSTALLING
Mathematical modelling concerning the development of a system of similar installations, taking into account their operational intensity (an aircraft-helicopter fleet taken as an example) [BTN-94-EIX94461408763] p 103 A95-63646
Engine/airframe installation CFD for commercial transports: An engine manufacturer's perspective [SAE PAPER 932623] p 495 A95-90084
Solid-state data recorder, next development and use p 705 N95-33143

INSTRUMENT APPROACH
Heliport/vertiport MLS precision approaches [AD-A283505] p 126 N95-18059
Aviation capacity enhancement plan 1994 [AD-A292758] p 598 N95-31428
An exploratory survey of information requirements for instrument approach charts [AD-A293882] p 601 N95-31520
Current issues in the design and information content of instrument approach charts [AD-A294752] p 690 N95-34562
Resource document for the design of electronic instrument approach procedure displays [AD-A295108] p 691 N95-34797

INSTRUMENT ERRORS
Effects of vibration on inertial wind-tunnel model attitude measurement devices [NASA-TM-109083] p 21 N95-11466
Flight evaluation of GPS/DGPS sensor systems installed in NAL Do228 [NAL-TR-1230] p 382 N95-26585

INSTRUMENT LANDING SYSTEMS
Commentary on Walton correspondence relating to the ILS glide slope [BTN-94-EIX94441380856] p 125 A95-64288
Comments on effect of wet snow on the null-reference ILS system [BTN-95-EIX95142555488] p 227 A95-72885
Modeling of Instrument Landing System (ILS) localizer signal on runway 25L at Los Angeles International Airport [NASA-TM-4588] p 125 N95-17384
An integrated GPS/INS/BARO and radar altimeter system for aircraft precision approach landings [AD-A289280] p 383 N95-26985
An exploratory survey of information requirements for instrument approach charts [AD-A293882] p 601 N95-31520
Current issues in the design and information content of instrument approach charts [AD-A294752] p 690 N95-34562

INSTRUMENT PACKAGES
Field and data analysis studies related to the atmospheric environment [NASA-CR-196543] p 168 N95-18093

INSULATION
25 years of airport sound insulation programs p 31 N95-11307

INTAKE SYSTEMS
Static pressure distribution in the inlet of a helicopter turbine compressor [BTN-95-EIX95152582339] p 266 A95-73541
Gas path debris monitoring [CONGRESS PAPER C428-15-031] p 508 A95-91710
Condensation in jet engine intake ducts during stationary operation [BTN-95-EIX95292721154] p 612 A95-92590
Prediction of wind tunnel effects on the installed F/A-18A inlet flow field at high angles-of-attack [NASA-CR-195429] p 197 N95-19651

INTEGRAL EQUATIONS
Coupled FEM-BEM approach for mean flow effects on vibro-acoustic behavior of planar structures [BTN-95-EIX95152577587] p 263 A95-73495
Direct boundary integral equations method to subsonic flow with circulation past thin airfoils in ground effect [BTN-95-EIX95242673940] p 365 A95-82224
An inverse design method of transonic airfoil and wing [HTN-95-71128] p 385 A95-83489
Steady and unsteady three-dimensional transonic flow computations by integral equation method [NASA-CR-196777] p 10 N95-11582

INTEGRAL ROCKET RAMJETS
Integral rocket ramjets [AD-A285135] p 240 N95-20906

INTEGRALS
Application of integral methods to ablation charring erosion, a review [BTN-95-EIX95302694460] p 636 A95-94057
Enhancements to integral solutions to ablation and charring [BTN-95-EIX95302694461] p 636 A95-94058

INTEGRATED CIRCUITS
A programmable heater control circuit for spacecraft [NASA-TM-108459] p 9 N95-11157
Ultra-Reliable Digital Avionics (URDA) processor p 245 N95-20638
Assuring Known Good Die (KGD) for reliable, cost effective MCMs p 246 N95-20644
Liquid flow-through cooling of electronic modules p 246 N95-20647
Cu deposition using a permanent magnet electron cyclotron resonance microwave plasma source [DE94-017768] p 304 N95-23981
Intelligent finite element submodeling of multichip modules for reliability analysis [AD-A292911] p 679 N95-31455

INTEGRATED LIBRARY SYSTEMS
AVIRIS and TIMS data processing and distribution at the land processes distributed active archive center p 325 N95-23872

INTEGRATED MISSION CONTROL CENTER
EURECA mission control experience and messages for the future p 149 N95-17252
FAA aviation forecasts: Fiscal year 1995-2006 [AD-A293682] p 584 N95-31598

INTEGRATED OPTICS
Integrated IR sensors [BTN-95-EIX95041505023] p 242 A95-70132

INTERACTIONAL AERODYNAMICS
Interference between tanker wing wake with roll-up and receiver aircraft [BTN-95-EIX95062487552] p 185 A95-68366
Wing vertical position effects on wing-body carryover for noncircular missiles [BTN-95-EIX95182617462] p 268 A95-75733
Structure of a double-fin turbulent interaction at high speed [BTN-95-EIX95222650780] p 347 A95-79236
Interaction of jet noise with a nearby panel assembly [BTN-95-EIX95262694295] p 434 A95-85466
Simulation of the unsteady interaction of a centrifugal impeller with its vaned diffuser: flow analysis [BTN-95-EIX95282710055] p 633 A95-92474
Instabilities originating from suction holes used for Laminar Flow Control (LFC) [NASA-CR-196395] p 6 N95-10131
Wing-body juncture flows [AD-A281526] p 106 N95-16099
A computational investigation of wake-induced airfoil flutter in incompressible flow and active flutter control [AD-A281534] p 142 N95-16109
Single-engine tail interference model p 115 N95-17879
Sectional prediction of 3D effects for separated flow on rotating blades [PB94-201696] p 117 N95-18503
Pressure measurements on an F/A-18 twin vertical tail in buffeting flow. Volume 4, part 2: Buffet cross spectral densities [AD-A285555] p 143 N95-18641
Three-dimensional interaction of wake/boundary-layer and vortex/boundary-layer data report [CUED/A-AEREO/TR-23] p 329 N95-24210
An interacting boundary layer method for unsteady compressible flows p 557 N95-30290
Numerical analysis around the whole SST configuration p 693 N95-34541

INTERFACES
Functional requirements of an aerospace Design Representation Programming Interface [AIAA PAPER 95-0967] p 497 A95-90643
Modelling wear at intermittently slipping high speed interfaces [BTN-94-EIX94511433698] p 701 A95-96655

INTERFACIAL TENSION
Ice accretion with varying surface tension [NASA-TM-106826] p 124 N95-19285

INTERFERENCE
A wall interference assessment and correction system [NASA-CR-196940] p 58 N95-12228

INTERFERENCE DRAG
Single-engine tail interference model p 115 N95-17879

INTERFERENCE FIT
Design and structural validation of CF116 upper wing skin boron doubler p 393 N95-27510

INTERFERENCE IMMUNITY
Electromagnetic compatibility - A general overview [CONGRESS PAPER C428-38-084] p 634 A95-93637

INTERFEROMETERS
Interferometry and computational studies of an oscillating airfoil compressible dynamic stall flow field [HTN-94-00703] p 3 A95-60182

- Laser interferometer skin-friction measurements of crossing-shock-wave/turbulent-boundary-layer ns
[HTN-95-20834] p 544 A95-88095
- INTERFEROMETRY**
Joint stars phased array radar antenna
[BTN-95-EIX95042474626] p 209 A95-68280
Interferometric investigations of compressible dynamic stall over a transiently pitching airfoil
[HTN-95-42338] p 372 A95-86167
Use of high resolution lightning detection and localization sensors for hazardous aviation weather nowcasting
p 661 A95-93486
Emerging nondestructive inspection for aging aircraft
[PB95-143053] p 328 N95-25401
Compressibility effects on and control of dynamic stall of oscillating airfoil
p 480 N95-29428
An investigation into the use of satellite-based positioning systems for flight reference/autoland operations
p 489 N95-29542
- INTERIOR BALLISTICS**
Investigation of starting and ignition transients in the thermally choked ram accelerator p 698 N95-34805
- INTERLAMINAR STRESS**
Accurate interlaminar stress recovery from finite element analysis
[NASA-TM-109149] p 57 N95-11815
- INTERLAYERS**
Compliant interlayer
[BTN-95-EIX95142562401] p 304 A95-73439
- INTERMETALLICS**
Intermetallic and titanium matrix composite materials for hypersonic applications
[AIAA PAPER 95-6132] p 530 A95-90451
Ordered intermetallic alloys, part 3: Gamma titanium aluminides
[HTN-95-B0396] p 530 A95-90477
Brazing repair possibilities for hot section gas turbine parts
p 201 N95-19677
- INTERMOLECULAR FORCES**
Flow resolution and domain influence in rarefied hypersonic blunt-body flows
[BTN-95-EIX95082502729] p 220 A95-70136
- INTERNAL COMBUSTION ENGINES**
A stationary flow of a viscous liquid in radial clearances of rotor bearings in the turbocompressor of an internal combustion engine
[BTN-94-EIX94461408765] p 153 A95-63648
Aircraft engine emission reduction
[BTN-95-EIX95031502750] p 196 A95-68257
Conversion of production automotive engines for aviation use
[SAE PAPER 932606] p 495 A95-90076
A hybrid vehicle evaluation code and its application to vehicle design, Revision 1
[DE95-008053] p 441 N95-28029
A hybrid vehicle evaluation code and its application to vehicle design, revision 2
[DE95-008060] p 441 N95-28139
Low-order nonlinear dynamic model of IC engine-variable pitch propeller system for general aviation aircraft
[NASA-TM-107006] p 694 N95-32916
- INTERNAL ENERGY**
Computation of high-altitude hypersonic flow-field radiation
p 593 N95-30843
- INTERNAL FLOW**
State-space representation of aerodynamic characteristics of an aircraft at high angles of attack
[BTN-95-EIX95062487536] p 187 A95-69244
Main features of overexpanded triple jets
[BTN-95-EIX95142553040] p 304 A95-73458
Determination of solid/porous wall boundary conditions from wind tunnel data for computational fluid dynamics codes
p 164 N95-19266
Experimental study of vane heat transfer and aerodynamics at elevated levels of turbulence
[NASA-CR-4633] p 244 N95-19912
Mach 10 computational study of a three-dimensional scramjet inlet flow field
[NASA-TM-4602] p 309 N95-23015
NASA low-speed axial compressor for fundamental research
[NASA-TM-4635] p 296 N95-23192
CFD analysis of turbopump volutes
p 312 N95-23436
Impeller flow field characterization with a laser two-focus velocimeter
p 313 N95-23440
High frequency flow-structural interaction in dense subsonic fluids
[NASA-CR-4652] p 330 N95-24217
A fixed time performance evaluation of parallel CFD applications
[DE94-014240] p 436 N95-26445

- Calculation of three-dimensional (3-D) internal flow by means of the velocity-vorticity formulation on a staggered grid
[NASA-TM-110352] p 376 N95-27258
Comparison of numerical results and multicavity purge and rim seal data with extensions to dynamics
[NASA-TM-106685] p 416 N95-27434
Ejectors and jet pumps: Computer program for design and performance for steam/gas flow
[ESDU-94046] p 500 N95-28704
The acoustic characteristics of turbomachinery cavities
[NASA-CR-4671] p 476 N95-28720
Finite element vorticity-based methods for the solution of the incompressible and compressible Navier-Stokes equations
p 553 N95-29119
Laser doppler velocimeter system for subsonic jet mixer nozzle testing at the NASA Lewis Aeroacoustic Propulsion Lab
[NASA-TM-106984] p 457 N95-30229
Effects of cavity bleed and its configuration on aerodynamic characteristics of supersonic internal flow
[NAL-TR-1247] p 594 N95-31715
- INTERNAL PRESSURE**
Effects of the chemical reaction model on calculations of supersonic combustion flows
[BTN-95-EIX0616952745802] p 638 A95-94487
Experimental and analytical methods for the determination of connected-pipe ramjet and ducted rocket internal performance
[AGARD-AR-323] p 149 N95-17278
Nonlinear analysis of damaged stiffened fuselage shells subjected to combined loads
p 137 N95-19499
Residual strength of thin panels with cracks
p 311 N95-23311
Composite fuselage shell structures research at NASA Langley Research Center
p 425 N95-28466
Design, analysis, and fabrication of a pressure box test fixture for tension damage tolerance testing of curved fuselage panels
p 533 N95-28839
- INTERNATIONAL COOPERATION**
World trends in air transport policies. (Approaching the 21st century)
[HTN-95-50220] p 176 A95-64857
International cooperation in standardization
p 452 A95-82665
International collaboration in hypersonic technologies - A specific and worthwhile initiative
[AIAA PAPER 95-6140] p 581 A95-90457
Transitioning to the aviation routine weather report (METAR) and the International Aerodrome Forecast (TAF) within the Federal Aviation Administration
p 656 A95-93461
Aircraft and sub-system certification by piloted simulation
[AGARD-AR-278] p 145 N95-17388
Military aviation maintenance industry in Western Europe: Concentration and internationalization
[PB94-189180] p 104 N95-17451
European aeronautics: Strong government presence in industry structure and research and development support. Report to Congressional Requesters
[GAO/NSIAD-94-71] p 176 N95-18578
High-stakes aviation: US-Japan technology linkages in transport aircraft
[LC-94-65759] p 381 N95-27907
JTEC/WTEC annual report and program summary: 1993/94
[NASA-CR-198563] p 454 N95-28038
- INTERNATIONAL SPACE STATION**
Assessment of the Space Station program
p 149 N95-16352
- INTERNATIONAL TRADE**
Overview of AlliedSignal's avionics development in the CIS
[BTN-95-EIX95212641069] p 287 A95-76734
General Aviation Task Force report
[NASA-TM-109950] p 1 N95-11463
- INTERORBITAL TRAJECTORIES**
Numerical optimization of synergetic maneuvers
[AD-A283398] p 109 N95-17435
- INTERPLANETARY DUST**
Hypervelocity Impact Test Facility: A gun for hire
[TABES PAPER 94-605] p 86 N95-14639
- INTERPLANETARY SPACECRAFT**
Fourth-generation Mars vehicle concepts
[BTN-95-EIX95152583267] p 298 A95-73568
- INTERPOLATION**
New approach to geometric profiling of the design elements of the passage part in turbo-machines
[BTN-94-EIX94461408769] p 153 A95-63652
Secondary source locations in active noise control: Selection or optimization?
[BTN-94-EIX94381352222] p 257 A95-71738

- Application of a control-volume-based finite-element formulation to the shock tube problem
[BTN-95-EIX95182619099] p 295 A95-76584
Evaluation of an autopilot based multimodelling
[PB94-190725] p 142 N95-17454
On-line, adaptive state estimator for active noise control
p 322 N95-23308
Leading-edge suction distribution for plane thin wings at subsonic speeds
[ESDU-94037] p 477 N95-28800
- INTERPROCESSOR COMMUNICATION**
PalymSys (TM): An extended version of CLIPS for construction and reasoning using blackboards
p 217 N95-19767
The IEEE scalable coherent interface: An approach for a unified avionics network
p 234 N95-20650
- INVARIANCE**
Comparison of coordinate-invariant and coordinate-aligned upwinding for the Euler equations
[HTN-95-A1753] p 633 A95-93316
- INVENTIONS**
Charles Norvin Rineck; an early American pioneer in advanced aviation engines
[SAE PAPER 930485] p 386 A95-84554
- INVENTORIES**
The generic simulation executive at Manned Flight Simulator
[AD-A283997] p 146 N95-18724
- INVERSE SCATTERING**
Time-domain imaging of airborne targets using ultra-wideband or short-pulse radar
[BTN-95-EIX95242673673] p 450 A95-82251
- INVERSIONS**
Application of optimization technique to control system design for departure prevention and aircraft model estimation through dynamic inversion
p 517 N95-29156
Dynamic inversion: An evolving methodology for flight control design
p 621 N95-31996
- INVERTERS**
A detailed power inverter design for a 250 kW switched reluctance aircraft engine starter/generator
[SAE PAPER 931388] p 613 A95-93664
- INVESTMENT CASTING**
A new paradigm: The investment casting cooperative arrangement
[HTN-95-92510] p 539 A95-87330
- INVISCID FLOW**
Improved analytical solution for varying specific heat parallel stream mixing
[BTN-94-EIX94481415349] p 103 A95-65339
Construction of nearly orthogonal multiblock grids for compressible flow simulation
[BTN-94-EIX94361133526] p 207 A95-65981
Two-variable method for blockage wall interference in a circular tunnel
[BTN-95-EIX95062487540] p 187 A95-69248
Aerodynamic shape optimization using preconditioned conjugate gradient methods
[BTN-95-EIX95142553033] p 263 A95-73465
Effects of spatial order of accuracy on the computation of vortical flowfields
[BTN-95-EIX95152577604] p 305 A95-73479
Sidewash on the vertical tail in subsonic and supersonic flows
[BTN-95-EIX95152582316] p 264 A95-73519
Unstructured grid solutions to a wing/pylon/store configuration
[BTN-95-EIX95152582322] p 265 A95-73525
Three-dimensional structure of a supersonic jet impinging on an inclined plate
[BTN-95-EIX95152583259] p 267 A95-73560
Dynamic unstructured method for flows past multiple objects in relative motion
[BTN-95-EIX95262694303] p 435 A95-85474
Compressible inviscid vortex flow of a sharp edge delta wing
[BTN-95-EIX95262694308] p 370 A95-85479
General solution procedure for flows in local chemical equilibrium
[HTN-95-42329] p 404 A95-86158
Vorticity in an inviscid fluid at hypersonic speeds
[HTN-95-42590] p 539 A95-87220
Modeling aerodynamic problems using Smoothed Particle Hydrodynamics (SPH)
[SAE PAPER 932512] p 465 A95-89185
A note on the Kutta-Joukowski formula
[ISBN 1-879921-01-4] p 635 A95-93735
A one-dimensional inviscid nonequilibrium flow solver
[ISBN 1-879921-01-4] p 588 A95-93752
Effects of splitter plate on wake formation from a circular cylinder: A discrete vortex simulation
p 639 A95-95404
A robust inverse inviscid method for airfoil design
p 640 A95-95431

- An unstructured node centered scheme for the simulation of 3-D inviscid flows p 642 A95-95463
- Computations of unsteady aerodynamic loads around oscillating wings. Part 1: Formulation [PB94-180049] p 7 N95-10136
- Computations of unsteady aerodynamic loads around oscillating wings. Part 2: Computed results and discussions [PB94-180056] p 7 N95-10137
- An axisymmetric analog two-layer convective heating procedure with application to the evaluation of Space Shuttle Orbiter wing leading edge and windward surface heating [NASA-CR-188343] p 54 N95-11937
- An approximate Riemann solver for thermal and chemical nonequilibrium flows [NASA-CR-195003] p 96 N95-14912
- Interactive computer graphics applications for compressible aerodynamics [NASA-TM-106802] p 170 N95-17264
- Computation of inviscid flows: Full potential method p 165 N95-19447
- Viscous flow past aerofoils axisymmetric bodies and wings p 123 N95-19457
- Validation and evaluation of the advanced aeronautical CFD system SAUNA: A method developer's view [ARA-MEMO-390] p 210 N95-19774
- Verification of the CFD simulation system SAUNA for complex aircraft configurations [ARA-MEMO-401] p 211 N95-19776
- Inviscid and viscous flow modelling of complex aircraft configurations using the CFD simulation system sauna [ARA-MEMO-403] p 211 N95-19777
- A fixed time performance evaluation of parallel CFD applications [DE94-014240] p 436 N95-26445
- An unstructured-grid software system for solving complex aerodynamic problems p 476 N95-28743
- Wave drag coefficient for axisymmetric forecones at zero incidence (M sub infinity less than or equal to 1.5) [ESDU-94014] p 552 N95-28903
- Surface pressure coefficient distributions for axisymmetric forecones at zero incidence (M sub infinity less than or equal to 1.5) [ESDU-94015] p 477 N95-28904
- Solution of the Navier-Stokes equations on locally refined Cartesian meshes using state-vector splitting p 553 N95-29197
- Dynamic stall of a NACA 0012 airfoil in laminar flow p 479 N95-29243
- Survey of CFD applications for high speed inlets [AD-A291365] p 557 N95-30087
- Pressure updating methods for the steady-state fluid equations [NASA-CR-198163] p 569 N95-30353
- Development of a linearized unsteady Euler analysis for turbomachinery blade rows [NASA-CR-4677] p 592 N95-30611
- Axial loads on yawed rotors [PB95-214193] p 592 N95-30638
- Parametrics on 2D Navier-Stokes analysis of a Mach 2.68 bifurcated rectangular mixed-compression inlet [NASA-TM-107003] p 617 N95-30861
- Acceleration potential models PREDICAT/PREDICDYN applied for calculation of axisymmetric dynamic inflow cases [PB95-207015] p 647 N95-30957
- Numerical solutions of inviscid and viscous flows about airfoils by TVD method p 684 N95-34521
- Numerical analysis around the whole SST configuration p 693 N95-34541
- IODINE**
- Flow models for the design of a hypersonic iodine vapor wind tunnel nozzle with chemical and vibrational nonequilibrium effects p 592 N95-30448
- ION CONCENTRATION**
- A survey of bidirectional greater than or equal to MeV ion flows during the Helios 1 and Helios 2 mission: Observations from the Goddard Space Flight Center instruments [HTN-95-70542] p 237 A95-71656
- Measurements of ions formed in jet engine exhaust plumes [AD-A290940] p 514 N95-29764
- ION CYCLOTRON RADIATION**
- Cu deposition using a permanent magnet electron cyclotron resonance microwave plasma source [DE94-017768] p 304 N95-23981
- ION MOBILITY SPECTROSCOPY**
- Gas chromatography/ion mobility spectrometry as a hyphenated technique for improved explosives detection and analysis p 701 N95-33278
- IONIZED GASES**
- Aerodynamic characteristics of the orbital reentry vehicle experimental probe fins in a supersonic flow [NAL-TR-1232] p 342 N95-25664
- IONIZING RADIATION**
- The joint Russian-Brazil research on balloons p 182 A95-66303
- Radiation safety aspects of commercial high-speed flight transportation [NASA-TP-3524] p 453 N95-26427
- IONOSPHERES**
- Thundercloud electric field modeling for the ionosphere-Earth region. 1: Dependence on cloud charge distribution - [HTN-95-41223] p 317 A95-75035
- IONOSPHERIC PROPAGATION**
- Using IRI for the computation of ionospheric corrections for altimeter data analysis p 212 A95-66949
- IRON ALLOYS**
- NASA-UVa light aerospace alloy and structures technology program supplement: Aluminum-based materials for high speed aircraft [NASA-CR-4645] p 343 N95-24878
- ISCCP PROJECT**
- Preliminary analysis of University of North Dakota aircraft data from the FIRE Cirrus IFO-2 [NASA-CR-198038] p 357 N95-24219
- ISENTROPIC PROCESSES**
- Trajectory modeling of emissions from lower stratospheric aircraft [HTN-95-41219] p 317 A95-75031
- ISOLATORS**
- Experimental investigation of inlet-combustor isolators for a dual-mode scramjet at a Mach number of 4 [NASA-TP-3502] p 407 N95-28343
- ISOTHERMAL FLOW**
- Crossflow mixing of noncircular jets [NASA-TM-106865] p 338 N95-24390
- ISOTHERMAL PROCESSES**
- Impingement cooling of an isothermally heated surface with a confined slot jet [BTN-94-EIX94421348950] p 347 A95-78494
- ISOTROPIC TURBULENCE**
- On the Lighthill relationship and sound generation from isotropic turbulence [NASA-CR-195005] p 159 N95-18191
- Application of Direct and Large Eddy Simulation to Transition and Turbulence [AGARD-CP-551] p 248 N95-21061
- Special publication of National Aerospace Laboratory [NAL-SP-27] p 684 N95-34505
- Direct numerical simulation of incompressible homogeneous isotropic turbulence using NWT p 706 N95-34530
- ISOTROPY**
- Fatigue in single crystal nickel superalloys [AD-A285727] p 152 N95-18068
- ITERATIVE SOLUTION**
- Preconditioned domain decomposition scheme for three-dimensional aerodynamic sensitivity analysis [BTN-95-EIX95152577612] p 321 A95-73471
- Sensitivity derivatives for three dimensional supersonic Euler code using incremental iterative strategy [HTN-95-20845] p 545 A95-88106
- Aero-optics system integration [TABES PAPER 94-604] p 100 N95-14638
- An easy way to analyze longitudinal and lateral-directional trim problems with AEO or OEI p 409 N95-26949
- J**
- J INTEGRAL**
- Elastic-plastic models for multi-site damage p 92 N95-14454
- Multi-lab comparison on R-curve methodologies: Alloy 2024-T3 [NASA-CR-195004] p 151 N95-16860
- J-85 ENGINE**
- The effect of altitude conditions on the particle emissions of a J85-GE-5L turbojet engine [NASA-TM-106669] p 339 N95-24561
- JAMMING**
- Analysis and simulation of narrowband GPS jamming using digital excision temporal filtering [AD-A289328] p 383 N95-26898
- JAPAN**
- High-stakes aviation: US-Japan technology linkages in transport aircraft [LC-94-65759] p 381 N95-27907
- JTEC/WTEC annual report and program summary: 1993/94 [NASA-CR-198563] p 454 N95-28038
- JAS-39 AIRCRAFT**
- Verification of the damage tolerance of a fighter aircraft p 388 A95-85897
- SAAB experience with PIO p 598 N95-31069
- JET AIRCRAFT**
- Impact on ozone of high-speed stratospheric aircraft: Effects of the emission scenario [HTN-95-51283] p 356 A95-80868
- Aircraft gas turbine emissions challenge [BTN-94-EIX95011441239] p 403 A95-84196
- Preliminary design of a single engine business jet [SAE PAPER 931253] p 493 A95-89222
- Should large business jets have four over the wing? [SAE 931256] p 493 A95-89223
- Signal processing of noise data from high-speed flyovers [BTN-95-EIX0619952748178] p 680 A95-94248
- Jet transport response to a horizontal wind vortex [BTN-95-EIX0619952748163] p 619 A95-94457
- The Aluminum Falcon: A low cost modern commercial transport [NASA-CR-197180] p 81 N95-15742
- Preliminary evaluation of the F/A-18 quantity/multiple envelope expansion [AD-A284119] p 132 N95-18407
- Aircraft IR/acoustic detection evaluation. Volume 2: Development of a ground-based acoustic sensor system for the detection of subsonic jet-powered aircraft [NASA-CR-189705-VOL-2] p 452 N95-28073
- JET AIRCRAFT NOISE**
- On the scaling of small-scale jet noise to large scale [AIAA PAPER 92-02109] p 27 A95-60166
- Structure of supersonic jet flow and its radiated sound [HTN-95-51645] p 431 A95-85027
- Screech tones from free and ducted supersonic jets [HTN-95-51647] p 432 A95-85029
- Interaction of jet noise with a nearby panel assembly [BTN-95-EIX95262694295] p 434 A95-85466
- Factors affecting measured aircraft sound levels in the vicinity of start-of-takeoff roll p 571 A95-88465
- Some aspects of the aeroacoustics of extreme-speed jets p 572 A95-88893
- A prediction method for broadband shock associated noise from supersonic rectangular jets p 574 A95-90100
- Reduction of supersonic jet noise using swirl: A concept revisited p 574 A95-90101
- Research of the method for evaluating noise caused by sonic boom p 562 A95-91519
- Signal processing of noise data from high-speed flyovers [BTN-95-EIX0619952748178] p 680 A95-94248
- Near field noise prediction requirements [ISVR-TR-234] p 27 N95-11166
- Fan noise research at NASA p 28 N95-11260
- Exact dynamic responses of periodic multi-span beams under convected pressure fields p 25 N95-11288
- On the interaction of jet noise with a nearby flexible structure [NASA-CR-194934] p 57 N95-11812
- Ultra-high bypass ratio jet noise [NASA-CR-195394] p 100 N95-14610
- Noise radiation by instability waves in coaxial jets [NASA-TM-106738] p 100 N95-14618
- The aeroacoustics of supersonic coaxial jets [NASA-TM-106782] p 101 N95-15059
- Active control of fan noise-feasibility study. Volume 1: Flyover system noise studies [NASA-CR-195392-VOL-1] p 258 N95-21888
- Supersonic jet noise reductions predicted with increased jet spreading rate [NASA-TM-106872] p 323 N95-23178
- Noise impact of advanced high lift systems [NASA-CR-195028] p 362 N95-26160
- Jet mixer noise suppressor using acoustic feedback [NASA-CASE-LEW-15170-2] p 362 N95-26187
- Supersonic coaxial jet noise predictions [NASA-TM-106917] p 451 N95-26801
- Preliminary results and research capabilities of a new jet facility at the University of Kansas p 412 N95-26951
- Basic studies in turbulent shear flows [AD-A289145] p 437 N95-26998
- A numerical study of fundamental shock noise mechanisms [NASA-TM-110608] p 451 N95-27908
- Response of multi-panel assembly to noise from a jet in forward motion [NASA-CR-198164] p 442 N95-28673
- The spectrum and directivity of turbulent mixing noise from supersonic jets p 579 N95-29415
- Computation of noise radiation from turbofans: A parametric study [NASA-CR-198359] p 710 N95-32836
- JET CONTROL**
- A design trade study using CFD modeling of reaction jets for aerodynamic control [SAE PAPER 931384] p 586 A95-93660
- Lateral jet control for tactical missiles p 84 N95-14448

- New technologies for space avionics
[NASA-CR-197574] p 150 N95-18196
- JET ENGINE FUELS**
- Hydrocarbon-fueled ramjet/scramjet technology program, phase 2 extension
[NASA-CR-189659] p 15 N95-10319
- Programmed ignition of metal compounds in a scramjet
[AD-A289847] p 16 N95-10466
- Service and physical properties of liquid-jet fuels
Investigation of flight data recorder fire test requirements
[AD-A285832] p 232 N95-20032
- Two-dimensional imaging of OH in a lean burning high pressure combustor
[NASA-TM-106854] p 236 N95-21383
- Mechanism of deposit formation on fuel-wetted hot metal surfaces
[AD-A289847] p 426 N95-28621
- JET ENGINES**
- Design optimization of aircraft engine-mount systems.
[BTN-94-EIX94351143325] p 195 A95-67298
- Adaptive modeling of jet engine performance with application to condition monitoring
[BTN-95-EIX95112524205] p 196 A95-69303
- Transport of exhaust products in the near trail of a jet engine under atmospheric conditions
[HTN-95-91421] p 319 A95-77334
- Nitrous oxide and methane emissions from aero engines
[HTN-95-21363] p 353 A95-78678
- North Atlantic air traffic within the lower stratosphere: Cruising times and corresponding emissions
[HTN-95-91841] p 354 A95-80829
- Effects on stratospheric ozone from high-speed civil transport: Sensitivity to stratospheric aerosol loading
[HTN-95-91842] p 354 A95-80830
- Dynamics of aircraft exhaust plumes in the jet-regime
[HTN-95-51275] p 355 A95-80860
- Hybrid finite element-modal analysis of jet engine inlet scattering
[BTN-95-EIX95242673665] p 427 A95-82259
- A computational environment for exhaust nozzle design
[AIAA PAPER 95-1016] p 566 A95-90688
- High heat sink fuels for improved aircraft thermal management
[SAE PAPER 932084] p 530 A95-91659
- Condensation in jet engine intake ducts during stationary operation
[BTN-95-EIX95292721154] p 612 A95-92590
- Radiant energy measurements from a scaled jet engine axisymmetric exhaust nozzle for a baseline code validation case
[NASA-TM-106686] p 25 N95-11409
- Engine structures analysis software: Component Specific Modeling (COSMO)
[NASA-CR-195378] p 57 N95-11711
- The development of the F100-PW-220 and F110-GE-100 engines: A case study of risk assessment and risk management
[AD-A282467] p 51 N95-13289
- Pressure distribution measurements on an isolated TPS 441 nacelle
[AD-A284802] p 115 N95-17878
- Developing an emission factor for hazardous air pollutants for an F-16 using JP-8 fuel
[AD-A284802] p 216 N95-19685
- Temperature effects on acoustic interactions between altitude test facilities and jet engine plumes
[NASA-CR-197638] p 258 N95-21170
- High-performance parallel analysis of coupled problems for aircraft propulsion
[NASA-CR-197440] p 289 N95-23088
- Dynamic behavior of a magnetic bearing supported jet engine rotor with auxiliary bearings
[NASA-CR-197860] p 338 N95-24213
- A design perspective on thermal barrier coatings
[AD-A293277] p 344 N95-26120
- Jet engine applications for materials with nanometer-scale dimensions
[AD-A293277] p 345 N95-26131
- Performance characterization of a highly-offset diffuser with and without blowing vortex generator jets
[AD-A289334] p 375 N95-26901
- Preliminary results and research capabilities of a new jet facility at the University of Kansas
[AD-A293277] p 412 N95-26951
- An active liner system for jet engine exhaust silencers, phase 1
[AD-A293277] p 617 N95-31191
- Influence of backup bearings and support structure dynamics on the behavior of rotors with active supports
[NASA-CR-199080] p 703 N95-32689
- Steady-state dynamic behavior of an auxiliary bearing supported rotor system
[AD-A293277] p 703 N95-32690
- Dynamic behavior of a magnetic bearing supported jet engine rotor with auxiliary bearings
[AD-A293277] p 703 N95-32691

JET EXHAUST

- Transport of exhaust products in the near trail of a jet engine under atmospheric conditions
[HTN-95-91421] p 319 A95-77334
- Sensitivity of supersonic aircraft modelling studies to HNO₃ photolysis rate
[HTN-95-11475] p 353 A95-79453
- Tracer transport for realistic aircraft emission scenarios calculated using a three-dimensional model
[HTN-95-41799] p 353 A95-80525
- North Atlantic air traffic within the lower stratosphere: Cruising times and corresponding emissions
[HTN-95-91841] p 354 A95-80829
- Effects on stratospheric ozone from high-speed civil transport: Sensitivity to stratospheric aerosol loading
[HTN-95-91842] p 354 A95-80830
- Dynamics of aircraft exhaust plumes in the jet-regime
[HTN-95-51275] p 355 A95-80860
- Moisture induced pressures in concrete airfield pavements
[AD-A281974] p 52 N95-11789
- Measurements of ions formed in jet engine exhaust plumes
[AD-A290940] p 514 N95-29764
- Hot jet/wake turbulent structure and laser propagation. Part 3: Laser propagation measurements and modeling
[HTN-95-41799] p 647 N95-30992

JET FLAPS

- The role of simulations in 777 FSEU development
[AIAA PAPER 95-0995] p 506 A95-90665
- A wind tunnel investigation of the effects of micro-vortex generators and Gurney flaps on the high-lift characteristics of a business jet wing
[NASA-TM-110626] p 607 N95-30827

JET FLOW

- Jet to freestream velocity ratio computations for a jet in a crossflow
[AIAA PAPER 93-4860] p 2 A95-60178
- Numerical simulation of powered-lift flows
[HTN-94-00700] p 3 A95-60179
- Phenomenological description and simplified modelling of the vortex wake issuing from a jet in a crossflow
[BTN-94-EIX94441385754] p 184 A95-68218
- Pneumatic concept for tip-stall control of cranked-arrow wings
[BTN-95-EIX95152582335] p 281 A95-73537
- Impingement cooling of an isothermally heated surface with a confined slot jet
[BTN-94-EIX94421348950] p 347 A95-78494
- Dynamics of aircraft exhaust plumes in the jet-regime
[HTN-95-51275] p 355 A95-80860
- Numerical investigation of cylinder wake flow with a rear stagnation jet
[HTN-95-51669] p 433 A95-85051
- Interaction of jet noise with a nearby panel assembly
[BTN-95-EIX95262694295] p 434 A95-85466
- Prediction of two-dimensional momentumless wake by k - ϵ - γ model
[BTN-95-EIX95262694299] p 434 A95-85470
- Mixing enhancement by and noise characteristics of streamwise vortices in an air jet
[HTN-95-42322] p 371 A95-86151
- Intrinsic transport and chemistry coupling in combustion phenomena
[HTN-95-81632] p 538 A95-87191
- Numerical model for circulation-control flows
[HTN-95-81632] p 461 A95-87680
- Cost effective small-scale experiments to aid the design of ASTOVL aircraft
[CONGRESS PAPER C428-9-098] p 475 A95-91695
- Aerodynamic applications of underexpanded hypersonic viscous jets
[BTN-95-EIX0619952748162] p 589 A95-94456
- Investigation of scramjet injection strategies for high mach number flows
[BTN-95-EIX0616952745782] p 614 A95-94504
- On the interaction of jet noise with a nearby flexible structure
[NASA-CR-194934] p 57 N95-11812
- Simultaneous three-dimensional velocity and mixing measurements by use of laser Doppler velocimetry and fluorescence probes in a water tunnel
[NASA-TP-3454] p 53 N95-13553
- Lateral jet control for tactical missiles
[AD-A293277] p 84 N95-14448
- Numerical mixing calculations of confined reacting jet flows in a cylindrical duct
[NASA-TM-106736] p 139 N95-18133
- Flow field investigation in a free jet - free jet core system for the generation of high intensity molecular beams
[DLR-FB-94-11] p 172 N95-18912
- Jet mixer noise suppressor using acoustic feedback
[NASA-CASE-LEW-15170-2] p 362 N95-26187
- The noise reduction potential of dual-stream coaxial rectangular improperly expanded jet flows
[NASA-CR-197820] p 437 N95-26995

- Response of multi-panel assembly to noise from a jet in forward motion
[NASA-CR-198164] p 442 N95-28673
- An extension of the Lighthill theory of jet noise to encompass refraction and shielding
[NASA-TM-110163] p 580 N95-29452
- Effects of initial conditions on a single jet in crossflow
[NASA-TM-107002] p 615 N95-30589
- Hot jet/wake turbulent structure and laser propagation. Part 3: Laser propagation measurements and modeling
[HTN-95-41799] p 647 N95-30992

JET IMPINGEMENT

- Three-dimensional structure of a supersonic jet impinging on an inclined plate
[BTN-95-EIX95152583259] p 267 A95-73560
- Impingement cooling of an isothermally heated surface with a confined slot jet
[BTN-94-EIX94421348950] p 347 A95-78494
- Recent research in ASTOVL aircraft ground environment
[CONGRESS PAPER C428-9-040] p 475 A95-91694
- Cost effective small-scale experiments to aid the design of ASTOVL aircraft
[CONGRESS PAPER C428-9-098] p 475 A95-91695
- Turbulent airflow noise production and propagation patterns of a subsonic jet impinging on a flat plate
[HTN-95-41799] p 580 N95-29502

JET LIFT

- Numerical simulation of powered-lift flows
[HTN-94-00700] p 3 A95-60179
- Recent research in ASTOVL aircraft ground environment
[CONGRESS PAPER C428-9-040] p 475 A95-91694

JET MIXING FLOW

- On the scaling of small-scale jet noise to large scale
[AIAA PAPER 92-02109] p 27 A95-60166
- Experimental and analytical investigations of wave enhanced supersonic combustors
[AIAA PAPER 89-2787] p 14 A95-60172
- Mixing enhancement by and noise characteristics of streamwise vortices in an air jet
[HTN-95-42322] p 371 A95-86151
- Quantitative investigation of compressible mixing: Staged transverse injection into Mach 2 flow
[HTN-95-42330] p 404 A95-86159
- Conceptual studies of high speed combustors for mixing enhancement mechanisms
[AIAA PAPER 95-6095] p 510 A95-88003
- Injection studies in the French hypersonic technology program
[AIAA PAPER 95-6096] p 510 A95-88004
- Numerical study of mixing in a high and low enthalpy supersonic test facility
[ISVR-TR-234] p 7 N95-10467
- Near field noise prediction requirements
[ISVR-TR-234] p 27 N95-11166
- Axis switching and spreading of an asymmetric jet: Role of vorticity dynamics
[NASA-TM-106385] p 73 N95-14418
- Noise radiation by instability waves in coaxial jets
[NASA-TM-106738] p 100 N95-14618
- Experimental investigations of on-demand vortex generators
[NASA-TM-106872] p 250 N95-22451
- Supersonic jet noise reductions predicted with increased jet spreading rate
[NASA-TM-106872] p 323 N95-23178
- Crossflow mixing of noncircular jets
[NASA-TM-106865] p 338 N95-24390
- Jet mixer noise suppressor using acoustic feedback
[NASA-CASE-LEW-15170-2] p 362 N95-26187
- The spectrum and directivity of turbulent mixing noise from supersonic jets
[NASA-TM-107002] p 579 N95-29415
- Effects of initial conditions on a single jet in crossflow
[NASA-TM-107002] p 615 N95-30589
- Jet mixing and emission characteristics of transverse jets in annular and cylindrical confined crossflow
[NASA-TM-106976] p 616 N95-30698
- Jet mixing in a reacting cylindrical crossflow
[NASA-TM-106975] p 616 N95-30853

JET NOZZLES

- Entrainment and acoustic variations in a round jet from introduced streamwise vorticity
[BTN-95-EIX95042474409] p 209 A95-68291
- Performance variation of scramjet nozzle at various nozzle pressure ratios
[BTN-95-EIX0616952745781] p 615 A95-94505
- Visualization of the multiple supersonic jet oscillations by swept focused strobed schlieren technique
[NASA-TM-106984] p 367 N95-26952
- Laser doppler velocimeter system for subsonic jet mixer nozzle testing at the NASA Lewis Aeroacoustic Propulsion Lab
[NASA-TM-106984] p 457 N95-30229
- JET PROPULSION**
- Twin engine afterbody model
[AD-A293277] p 115 N95-17880

- Laser doppler velocimeter system for subsonic jet mixer nozzle testing at the NASA Lewis Aeroacoustic Propulsion Lab [NASA-TM-106984] p 457 N95-30229
- JET PUMPS**
Ejectors and jet pumps: Computer program for design and performance for steam/gas flow [ESDU-94046] p 500 N95-28704
- JET STREAMS (METEOROLOGY)**
Jet stream winds: Comparisons of operational analyses with independent aircraft data at multiple longitudes p 665 A95-93506
Using ATMS weather products for air traffic strategic planning p 672 A95-93536
- JET THRUST**
Directional control at high angles of attack using blowing through a chined forebody [BTN-95-EIX0619952748179] p 619 A95-94472
Static investigation of two fluidic thrust-vectoring concepts on a two-dimensional convergent-divergent nozzle [NASA-TM-4574] p 222 N95-19913
Scramjet thrust measurement in a shock tunnel p 339 A95-25396
- A vehicle health monitoring system for the Space Shuttle Reaction Control System during reentry [NASA-CR-188370] p 527 N95-29447
Design, analysis and control of large transports so that control of engine thrust can be used as a back-up of the primary flight controls [NASA-CR-198958] p 518 N95-30254
Maximum thrust mode evaluation p 696 N95-33017
Rapid deceleration mode evaluation p 696 N95-33018
Background and principles of throttles-only flight control p 697 N95-33021
- JET VANES**
Study on the turbine vane and blade for a 1500 C class industrial gas turbine [BTN-94-EIX95011441254] p 431 A95-84211
Integrated aerodynamic fin and stowable TVC vane system [AD-D016457] p 151 N95-19073
- JETSTREAM AIRCRAFT**
Aircraft accident report: Stall and loss of control on final approach, Atlantic Coast Airlines, Inc./United Express Flight 6291 Jetstream 4101, N304UE Columbus, OH, 7 January 1994 [PB94-910409] p 123 N95-17646
- JETTISONING**
A numerical model to predict the fate of jettisoned aviation fuel [AD-A289336] p 419 N95-26842
- JINDIVJ TARGET AIRCRAFT**
Data acquisition and processing software for the Low Speed Wind Tunnel tests of the Jindivj auxiliary air intake [AD-A285455] p 108 N95-17178
- JOINTS (JUNCTIONS)**
Analysis of backscattering from wing and fuselage joints [HTN-95-71134] p 430 A95-83495
The key to designing durable adhesively bonded joints [HTN-95-12033] p 528 A95-88496
New experimental approach to determine initial fatigue quality with fastener holes [BTN-94-EIX94522406136] p 701 A95-96273
The role of fretting corrosion and fretting fatigue in aircraft rivet hole cracking p 94 N95-14470
Evaluation of scanners for C-scan imaging in nondestructive inspection of aircraft [DE94-012473] p 152 N95-19100
Reliability assessment of Multichip Module technologies via the Triservice/NASA RELTECH program p 245 N95-20643
Fiber-optic rotary joint with bundle collimator assemblies [AD-D016504] p 258 N95-21673
Status of bonded boron/epoxy doublers for military and commercial aircraft structures p 393 N95-27506
Load transfer in the stiffener-to-skin joints of a pressurized fuselage [NASA-CR-198610] p 439 N95-27865
A numerical study of the small scale wing-body junction problem p 482 N95-30235
- JOURNAL BEARINGS**
The dynamic nature of rotor thermal bending due to unsteady lubricant shearing within a bearing [HTN-95-42091] p 430 A95-83857
Effect of squeeze film damper land geometry on damper performance [HTN-95-92247] p 434 A95-85291
Thermohydrodynamic analysis of cryogenic liquid turbulent flow fluid film bearings, phase 2 [NASA-CR-197412] p 349 N95-24461
- JP-4 JET FUEL**
Regenerative cooling for liquid propellant rocket thrust chambers [INPE-5565-TDI/540] p 150 N95-18720
Airborne rotary separator study [NASA-CR-191045] p 150 N95-18743
- JP-5 JET FUEL**
Unmanned aerial vehicle heavy fuel engine test [AD-A284332] p 139 N95-18383
Regenerative cooling for liquid propellant rocket thrust chambers [INPE-5565-TDI/540] p 150 N95-18720
- JP-8 JET FUEL**
High heat sink fuels for improved aircraft thermal management [SAE PAPER 932084] p 530 A95-91659
Unmanned aerial vehicle heavy fuel engine test [AD-A284332] p 139 N95-18383
Developing an emission factor for hazardous air pollutants for an F-16 using JP-8 fuel [AD-A284802] p 216 N95-19685
- K**
- K-EPSILON TURBULENCE MODEL**
Computation of the poststall behavior of a circulation controlled airfoil [BTN-95-EIX95152582320] p 264 A95-73523
Application of wall functions to generalized nonorthogonal curvilinear coordinate systems [BTN-95-EIX95182619077] p 307 A95-75762
Dynamics of aircraft exhaust plumes in the jet-regime [HTN-95-51275] p 355 A95-80860
Prediction of two-dimensional momentumless wake by k-epsilon-gamma model [BTN-95-EIX95262694299] p 434 A95-85470
Computational methods in applied sciences; European Computational Fluid Dynamics Conference, 1st, Brussels, Belgium, Sept. 7-11, 1992 [ISBN 0-444-89795-X] p 539 A95-87552
Heat-transfer measurements and computations of swept-shock-wave boundary-layer interactions [HTN-95-81634] p 541 A95-87682
Computational study of boundary layer control for improving airfoil performance [SAE PAPER 932513] p 466 A95-89186
Modification of the two-equation turbulence model in NPARC to a Chien low Reynolds number k-epsilon formulation [NASA-TM-106710] p 37 N95-11917
Numerical computations of supersonic base flow with special emphasis on turbulence modeling [AD-A283688] p 119 N95-18670
Application of Navier-Stokes code PAB3D with kappa-epsilon turbulence model to attached and separated flows [NASA-TP-3480] p 224 N95-21338
Numerical computation of aerodynamics and heat transfer in a turbine cascade and a turn-around duct using advanced turbulence models p 313 N95-23444
Grid resolution and turbulent inflow boundary condition recommendations for NPARC calculations [NASA-TM-106959] p 482 N95-30253
Advanced k-epsilon modeling of heat transfer [NASA-CR-4679] p 648 N95-31423
- KALMAN FILTERS**
Flight test development and evaluation of a Kalman filter state estimator for low-altitude flight [HTN-94-00684] p 16 A95-60167
Comparison of parameter identification algorithms for flight vehicles [BTN-94-EIX94371347708] p 219 A95-69967
Comments on 'correction of inertial navigation with Loran C on NOAA's P-3 aircraft' [HTN-95-70149] p 227 A95-70671
Enhancing filter robustness in cascaded GPS-INS integrations [BTN-95-EIX95142555475] p 278 A95-73435
Real-time navigation using the global positioning system [BTN-95-EIX95172595298] p 279 A95-75714
New failure detection approach and its application to GPS autonomous integrity monitoring [BTN-95-EIX95202637613] p 279 A95-76676
Failure detection and isolation structure for global positioning system autonomous integrity monitoring [BTN-95-EIX95282706656] p 486 A95-89648
New filtering method for linear weakly coupled stochastic systems [BTN-95-EIX0608952736485] p 678 A95-92708
The combination of forecasts in an automated aviation weather forecasting system p 669 A95-93522
Groundspeed filtering for CTAS [NASA-CR-197223] p 97 N95-15785
- Application of GPS/SINS/RA integrated system to aircraft approach landing p 125 N95-16277
A real-time algorithm for integrating differential satellite and inertial navigation information during helicopter approach [NASA-CR-197409] p 229 N95-21891
A vehicle health monitoring system for the Space Shuttle Reaction Control System during reentry [NASA-CR-188370] p 527 N95-29447
- KAPTON (TRADEMARK)**
Problems with aging wiring in Naval aircraft p 154 N95-16048
- KAWASAKI AIRCRAFT**
A quiet STOL Research Aircraft Development program [NAL-TR-1223] p 336 N95-25862
- KEELS**
Global cost and weight evaluation of fuselage keel design concepts p 501 N95-28840
- KELVIN-HELMHOLTZ INSTABILITY**
Linear instability waves in supersonic jets confined in circular and non-circular ducts [BTN-94-EIX94341340068] p 103 A95-63520
Conditions associated with large-drop regions [HTN-95-10686] p 214 A95-68845
- KEVLAR (TRADEMARK)**
Ten-year ground exposure of composite materials used on the Bell Model 206L helicopter flight service program [NASA-TP-3468] p 55 N95-12357
Utilization of composite materials by the US Army: A look ahead p 421 N95-28421
- KINETIC ENERGY**
Testing of TKE parameterizations in numerical models for clear-air turbulence forecasting p 667 A95-93515
Activated buoyancy propulsion = Paradox Power (tm) [TABES PAPER 94-619] p 74 N95-14646
Spectral analysis of vortex/free-surface interaction [AD-A283210] p 96 N95-14658
Combustor kinetic energy efficiency analysis of the hypersonic research engine data p 148 N95-16321
An analysis code for the Rapid Engineering Estimation of Momentum and Energy Losses (REMEL) [NASA-CR-191178] p 108 N95-16887
Static aerodynamics CFD analysis for 120-mm hypersonic KE projectile design [ARL-MR-184] p 118 N95-18611
- KINETIC EQUATIONS**
Testing of TKE parameterizations in numerical models for clear-air turbulence forecasting p 667 A95-93515
Preliminary results of turbulence predictions for use in aviation weather forecasting p 675 A95-83551
- KINETIC THEORY**
Kinetic theory in aerothermodynamics [HTN-95-A0002] p 183 A95-67829
- KINETICS**
Dynamics of phase ordering of nematics in a pore [DE95-607662] p 362 N95-29578
- KITS**
Evaluation of commercial water-in-fuel test kits [AD-A292135] p 537 N95-29572
- KNOWLEDGE BASED SYSTEMS**
On-board avionics maintenance [BTN-94-EIX94461047054] p 82 A95-61741
New tools for creating instruction and simulations [SAE PAPER 932600] p 380 A95-84572
Selecting optimal experiments for feedforward multilayer perceptrons [AD-A290856] p 678 N95-30406
Evaluation of the techniques of fuzzy control for the piloting an aircraft p 621 N95-31997
- KNOWLEDGE BASES (ARTIFICIAL INTELLIGENCE)**
Thunderstorm hypothesis reasoner [AD-A282664] p 60 N95-12805
Knowledge-based processing for aircraft flight control [NASA-CR-194976] p 99 N95-13727
Digital systems validation. Chapter 20 Artificial Intelligence with applications for aircraft. Handbook, volume 2 [AD-A288492] p 448 N95-26638
- KNOWLEDGE REPRESENTATION**
Modeling student knowledge with self-organizing feature maps [BTN-95-EIX95262697073] p 564 A95-86862
Evaluation of the techniques of fuzzy control for the piloting an aircraft p 621 N95-31997
- KNUDSEN FLOW**
Kinetic theory in aerothermodynamics [HTN-95-A0002] p 183 A95-67829
Hypersonic rarefied flow past spheres including wake structure [BTN-95-EIX95152583250] p 305 A95-73551
Aerodynamic characteristics of a hypersonic viscous optimized waverider at high altitudes [BTN-95-EIX95152583251] p 266 A95-73552
Aerodynamics of the Shuttle Orbiter at high altitudes [BTN-95-EIX95182617454] p 298 A95-75725

- Numerical analysis of hypersonic low-density scramjet inlet flow
[BTN-95-EIX95212645694] p 272 A95-76746
- KOLMOGOROV THEORY**
Sphere wakes at moderate Reynolds numbers in a turbulent environment
[HTN-95-42331] p 372 A95-86160
- KUTTA-JOUKOWSKI CONDITION**
Laplace interaction law for the computation of viscous airfoil flow in low- and high-speed aerodynamics
[BTN-95-EIX95142553037] p 263 A95-73461
Explicit Kutta condition for an unsteady two-dimensional constant potential panel method
[HTN-95-51679] p 433 A95-85061
A note on the Kutta-Joukowski formula
[ISBN 1-879921-01-4] p 635 A95-93735
A Kutta condition conscious perturbation stream function boundary element algorithm for 2-D potential aerodynamics
[ISBN 1-879921-01-4] p 587 A95-93751
Numerical time dependent sheet cavitation simulations using a higher order panel method
[PB94-204435] p 59 N95-13249
- LABOR**
Partial camera automation in a simulated Unmanned Air Vehicle
[AD-A288786] p 337 N95-26190
- LABORATORIES**
Labs behind Boeing's new 777
[BTN-95-EIX95142562403] p 280 A95-73437
Propulsion education at Carleton University
[SAE PAPER 931391] p 613 A95-93667
NLS Flight Simulation Laboratory (FSL) documentation
[NASA-CR-196564] p 363 N95-24439
High strain-rate testing of parachute materials
[DE95-009577] p 648 N95-31614
- LABORATORY EQUIPMENT**
NASA Lewis Propulsion Systems Laboratory test article systems criteria
[NASA-TM-106589] p 20 N95-10446
A laboratory scale supersonic combustive flow system
[DE95-006347] p 420 N95-27851
- LAGRANGE MULTIPLIERS**
Coupling equivalent plate and finite element formulations in multiple-method structural analyses
[BTN-95-EIX95062487548] p 192 A95-68362
Large-scale computational fluid dynamics by the finite element method
[BTN-94-EIX94381359154] p 243 A95-71744
Compression strength of composite primary structural components
[NASA-CR-197554] p 160 N95-18388
A neural expert approach to self designing flight control systems
[AD-A279965] p 237 N95-21122
- LAGRANGIAN FUNCTION**
Modeling aerodynamic problems using Smoothed Particle Hydrodynamics (SPH)
[SAE PAPER 932512] p 465 A95-89185
Amplification and breaking of atmospheric gravity waves
[AD-A289758] p 170 N95-18110
- LAMINAR BOUNDARY LAYER**
Flight experience with lightweight, low-power miniaturized instrumentation systems
[BTN-95-EIX95062487522] p 180 A95-69230
Review and development of base pressure and base heating correlations in supersonic flow
[BTN-95-EIX95212645688] p 271 A95-76740
Quiet-flow Ludweig tube for high-speed transition research
[BTN-95-EIX95262694309] p 370 A95-85480
Nonlinear analysis of swept wing transitional boundary layers
[SAE PAPER 932515] p 466 A95-89188
Nonlinear analysis of the Gortler instability
[BTN-95-EIX95282705926] p 455 A95-89664
Low Reynolds number laminar separation bubble control using a backward facing step
[SAE PAPER 932572] p 467 A95-90061
Measurement in laminar and transitional boundary-layer flows on concave surface
[BTN-95-EIX95282711333] p 632 A95-92408
Instabilities originating from suction holes used for Laminar Flow Control (LFC)
[NASA-CR-196395] p 6 N95-10131
Validation of the RPLUS3D code for supersonic inlet applications involving three-dimensional shock wave-boundary layer interactions
[NASA-TM-106579] p 39 N95-13058

- Three-dimensional boundary layer and flow field data of an inclined prolate spheroid p 158 N95-17867
Parametric study on laminar flow for finite wings at supersonic speeds
[NASA-TM-108852] p 116 N95-18101
Acoustic receptivity due to weak surface inhomogeneities in adverse pressure gradient boundary layers
[NASA-TM-4577] p 249 N95-21258
Supersonic laminar flow control research
[NASA-CR-196049] p 249 N95-21340
Development of quiet-flow supersonic wind tunnels for laminar-turbulent transition research
[NASA-CR-197286] p 239 N95-21436
Acoustics of laminar boundary layers breakdown
[NASA-CR-197286] p 251 N95-22455
- Numerical simulations of the flow in the HYPULSE expansion tube
[NASA-TM-110357] p 523 N95-30228
- LAMINAR FLOW**
Effect of ambient turbulence intensity on sphere wakes at intermediate Reynolds numbers
[BTN-95-EIX95182619101] p 308 A95-76586
Scaling of incipient separation in supersonic/transonic speed laminar flows
[BTN-95-EIX95182619104] p 269 A95-76589
Impingement cooling of an isothermally heated surface with a confined slot jet
[BTN-94-EIX94421348950] p 347 A95-78494
Measurements of vortex pair interaction with a clean or contaminated free surface
[BTN-94-EIX95011441063] p 429 A95-82798
Quiet-flow Ludweig tube for high-speed transition research
[BTN-95-EIX95262694309] p 370 A95-85480
Influence of wing shapes on surface pressure fluctuations at wing-body junctions
[HTN-95-61196] p 491 A95-87569
Two-dimensional unsteady leading-edge separation on a pitching airfoil
[HTN-95-81628] p 461 A95-87676
Unsteady aerodynamics of vortical flows: Early and recent developments p 462 A95-88896
Computational study of boundary layer control for improving airfoil performance
[SAE PAPER 932513] p 466 A95-89186
Hybrid laminar flow over wings enhanced by continuous boundary layer suction
[SAE PAPER 931386] p 587 A95-93662
Laminar and turbulent flow over optimal riblets
[HTN-95-61196] p 639 A95-95383
Transect flight test of a laminar flow leading edge with surface excrescences
[NASA-TM-4597] p 9 N95-11158
Transport phenomena in stratified multi-fluid flow in the presence and absence of gravity p 95 N95-14563
Laminar and turbulent flow computations of Type 4 shock-shock interference aerothermal loads using unstructured grids
[NASA-CR-195008] p 97 N95-15604
Parametric study on laminar flow for finite wings at supersonic speeds
[NASA-TM-108852] p 116 N95-18101
Studies on high pressure and unsteady flame phenomena
[AD-A284126] p 152 N95-18410
Numerical simulation of dynamic-stall suppression by tangential blowing
[AD-A284887] p 120 N95-19110
High-lift flow-physics flight experiments on a subsonic civil transport aircraft (B737-100) p 275 N95-23333
Numerical and experimental study of drag characteristics of two-dimensional HLFC airfoils in high subsonic, high Reynolds number flow
[NAL-TR-1244T] p 331 N95-24998
Computational support of the laminar flow supersonic wind tunnel, CNSFV code development, Maglev, and grid generation
[NASA-CR-197750] p 411 N95-26775
Dynamic stall of a NACA 0012 airfoil in laminar flow
[AD-A281982] p 479 N95-29243
Numerical simulations of the flow in the HYPULSE expansion tube
[NASA-TM-110357] p 523 N95-30228
Vorticity dynamics and control of dynamic stall
[AD-A288658] p 620 N95-31400
- LAMINAR FLOW AIRFOILS**
Natural laminar flow wing concept for supersonic transports
[BTN-95-EIX95182619226] p 308 A95-76652
Viper — Design modification
[NASA-CR-197191] p 79 N95-13703
Numerical and experimental study of drag characteristics of two-dimensional HLFC airfoils in high subsonic, high Reynolds number flow
[NAL-TR-1244T] p 331 N95-24998

- A two element laminar flow airfoil optimized for cruise
[NASA-CR-198580] p 479 N95-29338
- LAMINAR HEAT TRANSFER**
Multiblock analysis for Shuttle Orbiter reentry heating from Mach 24 to Mach 12
[BTN-95-EIX95041503780] p 205 A95-69211
Influence of turbulence parameters, Reynolds number, and body shape on stagnation-region heat transfer
[NASA-TP-3487] p 550 N95-28719
- LAMINAR MIXING**
Ignition analysis of hydrogen/air mixture in supersonic mixing layer p 416 A95-82301
- LAMINAR WAKES**
Effect of ambient turbulence intensity on sphere wakes at intermediate Reynolds numbers
[BTN-95-EIX95182619101] p 308 A95-76586
- LAMINATES**
Field-consistent element applied to flutter analysis of circular cylindrical shells
[BTN-94-EIX94371341971] p 56 A95-60871
Launcher wing-leading-edge design
[BTN-95-EIX95042477110] p 192 A95-68349
Ply layout optimization and micromechanics tailoring of composite aircraft engine structures
[BTN-95-EIX9512524206] p 196 A95-69302
Prediction of energy absorption capability of composite stiffeners
[HTN-95-A0500] p 230 A95-72571
MIL-HDBK-5 design allowables for fibre/metal laminates: ARALL 2 and ARALL 3
[BTN-94-EIX94371346933] p 300 A95-73345
Dynamic analysis of bearingless tail rotor blades based on nonlinear shell modes
[BTN-95-EIX95152582338] p 281 A95-73540
Validation of an effective flat cruciform-shaped specimen to study CFRP composite laminates under biaxial loading
[BTN-95-EIX95152584677] p 282 A95-73589
Fatigue of aircraft materials; Specialists' Conference, Delft, Netherlands, 1992
[HTN-95-B0076] p 387 A95-85892
Fatigue of aircraft materials and structures
[HTN-95-B0076] p 387 A95-85894
Fibre-Metal laminates p 387 A95-85895
Active plate and missile wing development using directionally attached piezoelectric elements
[HTN-95-42340] p 408 A95-86169
Aeroelastic response of composite rotor blades considering transverse shear and structural damping
[HTN-95-81647] p 542 A95-87695
Analytical developments in support of the NASA aging aircraft program with an application to crack growth from rivets
[SAE PAPER 931223] p 545 A95-88789
Ultrasonic imaging of damages in CRFT-laminates
[HTN-95-81647] p 578 A95-90828
Accurate interlaminar stress recovery from finite element analysis
[NASA-TM-109149] p 57 N95-11815
Damage tolerant repair techniques for pressurized aircraft fuselages
[AD-A281982] p 65 N95-14144
Reliability assessment of Multichip Module technologies via the Triservice/NASA RELTECH program
[AD-A281982] p 245 N95-20643
Damage tolerant repair techniques for pressurized aircraft fuselages
[AD-A286298] p 219 N95-22046
Interlaminar shear test method development for long term durability testing of composites
[AD-A286298] p 301 N95-23300
New nondestructive techniques for the detection and quantification of corrosion in aircraft structures
[AD-A286298] p 315 N95-23512
Scarf repairs to graphite/epoxy components
[AD-A286298] p 396 N95-27523
Scarf joint technique with cocured and precured patches for composite repair
[AD-A286298] p 396 N95-27524
Analysis of aircraft engine blade subject to ice impact
[AD-A286298] p 407 N95-28277
Investigation of static and cyclic bearing failure mechanisms for GR/EP laminates p 422 N95-28427
Probabilistic evaluation of fuselage-type composite structures p 398 N95-28444
Development of stitched/RTM composite primary structures p 425 N95-28469
Tension fracture of laminates for transport fuselage. Part 1: Material screening p 398 N95-28471
Effect of low-speed impact damage and damage location on behavior of composite panels p 426 N95-28481
Impact damage resistance of composite fuselage structure, part 1 p 399 N95-28482
Applications of a damage tolerance analysis methodology in aircraft design and production
[AD-A286298] p 426 N95-28483

Fundamental concepts in the suppression of delamination buckling by stitching p 426 N95-28486
 Novel cost controlled materials and processing for primary structures p 532 N95-28830
 Dimensional stability of curved panels with cocured stiffeners and cobonded frames p 532 N95-28836
 Tension fracture of laminates for transport fuselage. Part 2: Large notches p 532 N95-28837
 Impact damage resistance of composite fuselage structure, part 2 p 533 N95-28838
 A weight-efficient design strategy for cutouts in composite transport structures p 533 N95-28843
 A global/local analysis method for treating details in structural design p 552 N95-28848
 IPACS (Integrated Probabilistic Assessment of Composite Structures): Code development and applications p 534 N95-28849
 Thermally stable organic polymers
 [AD-A290755] p 537 N95-29482
 Development of a composite tailoring procedure for airplane wing
 [NASA-CR-199081] p 691 N95-32928

LAND
 Assessing effects of military aircraft noise on residential property values near airbases p 31 N95-11310

LAND USE
 Aircraft noise at a West Coast airport in the next century p 560 A95-90095
 Integrating NOISEMAP with the Geographic Resource Analysis Support System (GRASS) to enhance environmental impact assessments and land use compatibility studies p 31 N95-11311

LANDING
 Full span flaperons for a biplane p 391 N95-26954

LANDING AIDS
 Commentary on Walton correspondence relating to the ILS glide slope
 [BTN-94-EIX94441380856] p 125 A95-64288
 High accuracy navigation and landing system using GPS/IMU system integration
 [BTN-94-EIX94441386129] p 189 A95-68185
 Development and flight test of a deployable precision landing system
 [BTN-95-EIX95062487535] p 190 A95-69243
 On-the-fly carrier phase ambiguity resolution for precise aircraft landing
 [BTN-95-EIX95112522535] p 190 A95-69328
 Assessment of CTAS ETA prediction capabilities
 [NASA-CR-197224] p 97 N95-15728
 Joint Proceedings on Aeronautics and Astronautics (JPAA)
 [ISBN-7-80-046602-7] p 104 N95-16249
 Application of GPS/SINS/RA integrated system to aircraft approach landing p 125 N95-16277
 Guidance and control requirements for high-speed Rollout and Turnoff (ROTO)
 [NASA-CR-195026] p 292 N95-22674
 Precision landing system mathematical modeling study report for Andrews Air Force Base, runway 19L, Camp Springs, MD
 [AD-A289015] p 384 N95-27903
 Automatic flight control system for an unmanned helicopter system design and flight test results p 622 N95-32004
 An approach to sensor data fusion for flying and landing aid purpose p 686 N95-32488

LANDING GEAR
 Electro-rheologically controlled landing gear
 [BTN-94-EIX94461047055] p 78 A95-61740
 Soft landing on the slope surface of a landing vehicle with an air shock-absorber of forced pressurization
 [BTN-94-EIX94461407941] p 85 A95-62259
 Polymer composite applications to aerospace equipment
 [HTN-95-80257] p 529 A95-89201
 Special purpose landing gear: A survey of historical designs
 [SAE PAPER 932579] p 494 A95-90066
 Aircraft landing gear dynamics present and future
 [SAE PAPER 931400] p 604 A95-93670
 Aircraft nose gear shimmy studies
 [SAE PAPER 931401] p 628 A95-93671
 Modelling and analysis of a dual-wheel nosegear: Shimmy instability and impact motions
 [SAE PAPER 931402] p 605 A95-93672
 An electro-rheologically controlled semi-active landing gear
 [SAE PAPER 931403] p 605 A95-93673
 Flight investigation of the use of a nose gear jump strut to reduce takeoff ground roll distance of STOL aircraft
 [NASA-TM-108819] p 44 N95-12225
 Gemini: A long-range cargo transport
 [NASA-CR-197149] p 45 N95-12626
 Landing gear energy absorption system
 [NASA-CASE-MS-C-22277-1] p 96 N95-15306

The Aluminum Falcon: A low cost modern commercial transport
 [NASA-CR-197180] p 81 N95-15742
 Corrosion behavior of landing gear steels
 [AD-A285662] p 242 N95-22132
 Corrosion of landing gear steels p 302 N95-23500
 Aircraft nosewheel steering simulation
 p 412 N95-26944
 Rotorcraft crashworthy airframe and fuel system technology development program
 [AD-A289986] p 382 N95-28630
 Machinability study of Aermot 100
 [DE95-011532] p 701 N95-33408

LANDING LOADS
 Viper cabin-fuselage structural design concept with engine installation and wing structural design
 [NASA-CR-197162] p 45 N95-12305
 Gemini: A long-range cargo transport
 [NASA-CR-197149] p 45 N95-12626
 Landing gear energy absorption system
 [NASA-CASE-MS-C-22277-1] p 96 N95-15306
 Super-heavy aircraft study
 [AD-A279602] p 238 N95-19955

LANDING SIMULATION
 Evaluation of F-18A approach and landing flying qualities using an in-flight simulator
 [CALSPAN-6241-F-1] p 12 N95-10442
 Spatial awareness comparisons between large-screen, integrated pictorial displays and conventional EFIS displays during simulated landing approaches
 [NASA-TP-3467] p 80 N95-14852
 Development of load spectra for Airbus A330/A340 full scale fatigue tests p 135 N95-19479

LANDING SITES
 Noise levels of helicopters performing elevated pad take-off and landing procedures
 [HTN-95-92544] p 559 A95-87364
 Development of a climatological data base to help forecast cloud cover conditions for shuttle landings at the Kennedy Space Center p 670 A95-93529
 Analysis of rapidly developing fog at the Kennedy Space Center p 671 A95-93531
 Development of an Automated Airfield Dynamic Cone Penetrometer (AADCP) prototype and the evaluation of unstaffed airfield seismic surveying using Spectral Analysis of Surface Waves (SASW) technology
 [AD-A281985] p 145 N95-17444

LANDMARKS
 Using landmarks for the vehicle location measurement
 [PB94-184512] p 43 N95-12582

LANGUAGE PROGRAMMING
 The application of Ada and formal methods to a safety critical engine control system p 710 N95-33142

LANTHANUM OXIDES
 Phonon characteristics of high (T sub c) superconductors from neutron Doppler broadening measurements
 [DE95-003703] p 324 N95-24076

LAP JOINTS
 Modelling of pilowing due to corrosion in fuselage lap joints
 [BTN-95-EIX95082502227] p 240 A95-71024
 Growth of multiple cracks and their linkup in a fuselage lap joint
 [BTN-95-EIX95142553047] p 286 A95-73451
 Analytical developments in support of the NASA aging aircraft program with an application to crack growth from rivets
 [SAE PAPER 931223] p 545 A95-88789
 Full-scale testing and analysis of fuselage structure
 p 95 N95-14485
 The characterization of widespread fatigue damage in fuselage structure
 [NASA-TM-109142] p 88 N95-14920
 Evaluation of the fuselage lap joint fatigue and terminating action repair p 166 N95-19477
 Fatigue life until small cracks in aircraft structures: Durability and damage tolerance p 135 N95-19478
 An artificial corrosion protocol for lap-splices in aircraft skin p 152 N95-19482
 Results of uniaxial and biaxial tests on riveted fuselage lap joint specimens p 136 N95-19491
 Nonlinear analysis of damaged stiffened fuselage shells subjected to combined loads p 137 N95-19499
 Estimate of probability of crack detection from service difficulty report data
 [PB95-149381] p 328 N95-24295
 Characterization of corrosion and development of a breadboard of a D sight aircraft inspection system, phase 1
 [AD-A288347] p 380 N95-26527

LAPLACE TRANSFORMATION
 Laplace interaction law for the computation of viscous airfoil flow in low- and high-speed aerodynamics
 [BTN-95-EIX95142553037] p 263 A95-73461

LAPSE RATE
 Stratus' tephigram as a training/forecasting tool
 p 657 A95-93465
 Examination of conditions in the proximity of pilot reports of aircraft icing during storm-fest p 666 A95-93509

LASER ANEMOMETERS
 Transonic and supersonic flowfield measurements about axisymmetric afterbodies for validation of advanced CFD codes p 121 N95-19260
 Experimental and computational investigation of the tip clearance flow in a transonic axial compressor rotor
 [NASA-TM-106711] p 649 N95-31738
 Laser anemometer measurements of the three-dimensional rotor flow field in the NASA low-speed centrifugal compressor
 [NASA-TP-3527] p 618 N95-31985

LASER APPLICATIONS
 2 micron LIDAR for laser-based remote sensing: Flight demonstration and application survey
 [BTN-95-EIX95212641072] p 319 A95-76737
 The detection and measurement of microburst wind shear by an airborne lidar system p 543 A95-87798
 Laser velocimetry in the supersonic regime: Advances, limitations, and outlook
 [SAE PAPER 931365] p 634 A95-93646
 Overview of remote sensing laser development and semiconductor laser technology
 [DE94-019103] p 256 N95-21552
 Residual Stress Measurements with Laser Speckle Correlation Interferometry and Local Heat Treating
 [DE95-060082] p 349 N95-24598
 Structural design optimization with survivability dependent constraints application: Primary wing box of a multi-role fighter p 398 N95-28440
 A laser-based ice shape profilometer for use in icing wind tunnels
 [NASA-TM-106936] p 646 N95-30851
 Hot jet/wake turbulent structure and laser propagation. Part 3: Laser propagation measurements and modeling p 647 N95-30992

LASER CUTTING
 Advances in the application of laser cutting, drilling, and welding aerospace parts
 [SAE PAPER 932544] p 547 A95-90052
 Laser processing aircraft and turbine engine parts
 [SAE PAPER 931356] p 634 A95-93640

LASER DOPPLER VELOCIMETERS
 LDV measurements in dynamically separated flows
 [ISBN 0-8194-1311-9] p 5 A95-60191
 Measurement around a rotor blade excited in pitch. Part 1: Dynamic inflow
 [HTN-95-31007] p 220 A95-71177
 Laser velocimetry seed-particle behavior in shear layers at Mach 12
 [BTN-95-EIX95212645712] p 272 A95-76764
 Vibration measurements on rotating machinery using laser Doppler velocimetry
 [BTN-94-EIX95011440597] p 429 A95-82986
 Laser velocimetry and blade pressure measurements of a blade-vortex interaction
 [HTN-95-01081] p 547 A95-90267
 Novel implements of optical diagnostic techniques for aerospace applications
 [CONGRESS PAPER C428-21-081] p 550 A95-91726
 LDV measurements in separated flow on an elliptic wing mounted at an angle of attack on a wall
 [BTN-94-EIX94441380518] p 702 A95-96559
 Simultaneous three-dimensional velocity and mixing measurements by use of laser Doppler velocimetry and fluorescence probes in a water tunnel
 [NASA-TP-3454] p 53 N95-13553
 Developments in laser-based diagnostics for wind tunnels in the Aeromechanics Division: 1987-1992
 [AD-A283011] p 84 N95-13687
 Aerodynamic investigation of the flow field in a 180 deg turn channel with sharp bend p 163 N95-19257
 Experimental techniques for measuring transonic flow with a three dimensional laser velocimetry system. Application to determining the drag of a fuselage p 163 N95-19258
 Transonic and supersonic flowfield measurements about axisymmetric afterbodies for validation of advanced CFD codes p 121 N95-19260
 A three-dimensional orthogonal laser velocimeter for the NASA Ames 7- by 10-foot wind tunnel
 [NASA-TM-108864] p 249 N95-21323
 Impeller flow field characterization with a laser two-focus velocimeter p 313 N95-23440
 Laser doppler velocimeter system for subsonic jet mixer nozzle testing at the NASA Lewis Aeroacoustic Propulsion Lab
 [NASA-TM-106984] p 457 N95-30229

LASER DRILLING

Advances in the application of laser cutting, drilling, and welding aerospace parts

- [SAE PAPER 932544] p 547 A95-90052
Laser processing aircraft and turbine engine parts
[SAE PAPER 931356] p 634 A95-93640

LASER GUIDANCE

Development and flight testing of an Obstacle Avoidance System for US Army helicopters

- p 687 N95-32500

LASER GYROSCOPES

Optical processing and control

- [AD-A279157] p 259 N95-21975
Results from tests of the Honeywell integrated flight management unit
[PB95-211355] p 601 N95-30597
Application of advanced safety technique to ring laser gyro inertial navigation system integration
p 689 N95-33140

LASER INDUCED FLUORESCENCE

Comparison of NO and OH planar fluorescence temperature measurements in scramjet model flowfields

- [BTN-95-EIX95042474388] p 209 A95-68312
Aircraft-borne, laser-induced fluorescence instrument for the in situ detection of hydroxyl and hydroperoxyl radicals

[BTN-95-EIX95072499029] p 253 A95-71908
Development of techniques for the in situ observation of OH and HO₂ for studies of the impact of high-altitude supersonic aircraft on the stratosphere

[NASA-CR-196759] p 61 N95-12832

Planar Rayleigh scattering and laser-induced fluorescence for visualization of a hot, Mach 2 annular air jet

- [NASA-TM-4576] p 54 N95-13196
Developments in laser-based diagnostics for wind tunnels in the Aeromechanics Division: 1987-1992

[AD-A283011] p 84 N95-13687

Two-dimensional imaging of OH in a lean burning high pressure combustor

[NASA-TM-106854] p 236 N95-21383

Analysis of planar laser-induced fluorescence images obtained during shakedown testing of the AEDC impulse facility

[AD-A293237] p 646 N95-30906

Spatially-resolved velocity measurements in steady, high-speed, reacting flows using laser-induced OH fluorescence

- p 650 N95-32109

LASER INTERFEROMETRY

Laser interferometer skin-friction measurements of crossing-shock-wave/turbulent-boundary-layer

[HTN-95-20834] p 544 A95-88095

LASER RANGE FINDERS

Precision orbit determination of altimetric satellites

- p 86 N95-14282

LASER SPECTROMETERS

AIRSAAR deployment in Australia, September 1993: Management and objectives

- p 321 N95-23948

LASER WELDING

Advances in the application of laser cutting, drilling, and welding aerospace parts

- [SAE PAPER 932544] p 547 A95-90052
Laser processing aircraft and turbine engine parts
[SAE PAPER 931356] p 634 A95-93640

LASERS

Planar air density measurements near model surfaces by ultraviolet Rayleigh/Raman scattering

[BTN-94-EIX94441386614] p 213 A95-67345

Laser device for measuring a vessel's speed

[HTN-95-60992] p 361 A95-80633

Developments in laser-based diagnostics for wind tunnels in the Aeromechanics Division: 1987-1992

[AD-A283011] p 84 N95-13687

Aircraft wake vortex takeoff tests at O'Hara International Airport

[AD-A283828] p 118 N95-18624

A laser-based ice shape profilometer for use in icing wind tunnels

[NASA-TM-106936] p 646 N95-30851

LATERAL CONTROL

Pneumatic concept for tip-stall control of cranked-arrow wings

[BTN-95-EIX95152582335] p 281 A95-73537

H-infinity helicopter flight control law design with and without rotor state feedback

[BTN-95-EIX95182619129] p 291 A95-76606

Fuel-optimal bank-angle control for lunar-return aerocapture

[BTN-95-EIX95212645706] p 299 A95-76758

Low-speed aerodynamic characteristics of a slender wing with vertical fins

p 460 A95-87400

Predictive algorithms for the roll control autopilot of a jet fighter aircraft

[HTN-95-21047] p 515 A95-90424

Exact solution of stability margin for the MIMO control system

- p 507 A95-91582

Effect of coupling term on stability for the two input control system

- p 507 A95-91583

Comparison of the method of analyzing stability margin by using Minus Inverse Vector Locus with classical method

- p 507 A95-91584

Missile autopilot designs using full state feedback

- p 507 A95-91587

Flight evaluation of pneumatic forebody vortex control in post-stall flight

- p 72 N95-14259

Lateral jet control for tactical missiles

- p 84 N95-14448

Evaluation of an autopilot based multimodelling

[PB94-190725] p 142 N95-17454

Determination of stability and control derivatives from the NASA F/A-18 HARV from flight data using the maximum likelihood method

[NASA-CR-197320] p 204 N95-19576

Aerodynamic surface distension system for high angle of attack forebody vortex control

[NASA-CASE-ARC-11979-1] p 286 N95-23390

Feedback control laws for highly maneuverable aircraft

[NASA-CR-197944] p 295 N95-23410

LATERAL STABILITY

Aerodynamic characteristics of strake vortex flaps on a strake-wing configuration

[BTN-95-EIX95062487537] p 187 A95-69245

An easy way to analyze longitudinal and lateral-directional trim problems with AEO or OEI

p 409 N95-26949

Transonic aerodynamic characteristics of a proposed wing-body reusable launch vehicle concept

[NASA-TM-108489] p 592 N95-30712

LATEX

Additives in bituminous materials and fuel-resistant sealers

[DOT/FAA/CT-94/78] p 55 N95-12131

LATITUDE MEASUREMENT

Latitude variations of stratospheric trace gases

[HTN-95-70948] p 352 A95-78013

LAUNCH VEHICLE CONFIGURATIONS

Requirements report for SSTO vertical take-off and horizontal landing vehicle

[NASA-CR-197029] p 80 N95-14794

LAUNCH VEHICLES

Launcher wing-leading-edge design

[BTN-95-EIX95042477110] p 192 A95-68349

Load alleviation maneuvers for a launch vehicle

p 342 A95-81360

Field and data analysis studies related to the atmospheric environment

[NASA-CR-196543] p 168 N95-18093

Aerodynamic flight control to increase payload capability of future launch vehicles

[NASA-CR-196560] p 300 N95-24032

Airborne rotary air separator study

[NASA-CR-189099] p 290 N95-24053

LAUNCHERS

Permanent magnet electron cyclotron resonance plasma source with remote window

[BTN-95-EIX95242674338] p 450 A95-82176

LAUNCHING

Field and data analysis studies related to the atmospheric environment

[NASA-CR-196543] p 168 N95-18093

LAVAL NUMBER

Main features of overexpanded triple jets

[BTN-95-EIX95142553040] p 304 A95-73458

LAW (JURISPRUDENCE)

Aircraft accident investigation and airworthiness - A practical example of the interaction of two disciplines with some reflections on possible legal consequences

[HTN-95-50219] p 176 A95-64856

EC Aviation Scene

[HTN-95-50223] p 176 A95-64860

Environmental Compliance Assessment and Management Program

[AD-A279605] p 255 N95-20441

LAWS

Laws of infrared similitude

[AD-A282209] p 62 N95-12426

LAY-UP

Plly layup optimization and micromechanics tailoring of composite aircraft engine structures

[BTN-95-EIX9511254206] p 196 A95-69302

Optimal design of composite helicopter power transmission shafts with axially varying fiber layup

[HTN-95-01086] p 529 A95-90272

Field repair materials for naval aircraft

p 394 N95-27514

Advanced tow placement of composite fuselage structure

p 420 N95-28271

LAYOUTS

Programmable cockpit research simulator

[AD-A279219] p 204 N95-19848

LEAD (METAL)

Antarctic snow record of southern hemisphere lead pollution

[HTN-95-40359] p 212 A95-66869

LEAD ACID BATTERIES

Maintenance-free lead acid battery for inertial navigation systems aircraft

[BTN-95-EIX95292721316] p 633 A95-92511

TKKMOD: A computer simulation program for an integrated wind diesel system. Version 1.0: Document and user guide

[PB94-179090] p 60 N95-11798

Development of a bipolar lead/acid battery for the more electric aircraft

[AD-A284050] p 160 N95-18660

LEADING EDGE FLAPS

Effects of leading and trailing edge flaps on the aerodynamics of airfoil/vortex interactions

[HTN-95-31011] p 221 A95-71181

Natural laminar flow wing concept for supersonic transports

[BTN-95-EIX95182619226] p 308 A95-76652

Effect of leading- and trailing-edge flaps on clipped delta wings with and without wing camber at supersonic speeds

[NASA-TM-4542] p 5 N95-10028

Numerical simulation of the flow about the F-18 HARV at high angle of attack

[NASA-CR-196396] p 9 N95-10940

Hybrid structured/unstructured grid computations for the F/A-18 at high angle of attack

p 68 N95-14233

Investigation of the flow development on a highly swept canard/wing research model with segmented leading- and trailing-edge flaps

p 114 N95-17876

Wing pressure distributions from subsonic tests of a high-wing transport model - in the Langley 14- by 22-Foot Subsonic Wind Tunnel

[NASA-TM-4583] p 272 N95-22802

Increments in aerofoil lift coefficient at zero angle of attack and in maximum lift coefficient due to deployment of a plain trailing-edge flap, with or without a leading-edge high-lift device, at low speeds

[ESDU-94028] p 477 N95-28885

Pressure based high order TVD methodology for dynamic stall control

[AD-A290149] p 479 N95-29316

Increments in aerofoil lift coefficient at zero angle of attack and in maximum lift coefficient due to deployment of various leading-edge high-lift devices at low speeds

[ESDU-94027] p 481 N95-29898

Low-speed wind-tunnel investigation of the stability and control characteristics of a series of flying wings with sweep angles of 50 deg

[NASA-TM-4640] p 505 N95-30226

LEADING EDGE SLATS

Dynamic stall control for advanced rotorcraft application

[BTN-95-EIX95222650793] p 334 A95-79249

The role of simulations in 777 FSEU development

[AIAA PAPER 95-0995] p 506 A95-90665

Lift enhancing tabs for airfoils

[NASA-CASE-ARC-11990-1] p 286 N95-23395

Three-dimensional interaction of wake/boundary-layer and vortex/boundary-layer data report

[CUE/D/A-AEREO/TR-23] p 329 N95-24210

LEADING EDGE SWEEP

Aerodynamic effects of delta planform tip sails on wing performance

[BTN-95-EIX95062487544] p 185 A95-68358

The effect of wing sweep back upon transition in hypersonic flow

[AIAA PAPER 95-6090] p 466 A95-89199

Sidewall-effect of the wind tunnel on the estimation of the aerodynamic characteristics of a delta wing

p 685 N95-34525

LEADING EDGE THRUST

Analytic prediction of lift for delta wings with partial leading-edge thrust

[BTN-95-EIX95152582345] p 266 A95-73547

Estimation of supersonic leading-edge thrust by a Euler flow model

[BTN-95-EIX0619952748194] p 591 A95-94483

LEADING EDGES

Launcher wing-leading-edge design

[BTN-95-EIX95042477110] p 192 A95-68349

Vertical flow structure near the F/A-18 LEX at high incidence

[BTN-95-EIX95062487555] p 186 A95-68369

Numerical simulation of incidence and sweep effects on delta wing vortex breakdown

[BTN-95-EIX95062487526] p 186 A95-69234

Pneumatic concept for tip-stall control of cranked-arrow wings

[BTN-95-EIX95152582335] p 281 A95-73537

- Dynamic stall control for advanced rotorcraft application
[BTN-95-EIX95222650793] p 334 A95-79249
- Experiment and analysis on heat transfer of a scramjet leading edge model p 403 A95-82420
- Reduction of blade-vortex interaction noise through porous leading edge
[HTN-95-42324] p 371 A95-86153
- Aerodynamics of delta wings with application to high-alpha flight mechanics p 460 A95-87395
- Two-dimensional unsteady leading-edge separation on a pitching airfoil
[HTN-95-81628] p 461 A95-87676
- Dynamic pitch-up of a delta wing
[HTN-95-81633] p 462 A95-87681
- Computational fluid dynamics with icing effects
[SAE PAPER 932532] p 466 A95-89192
- Estimation of aerodynamic characteristics for the vortex flaps by the suction analogy p 471 A95-91496
- An experimental study on supersonic laminar flow control p 473 A95-91523
- Experimental investigation on aerothermodynamic characteristics of hypersonic transport p 473 A95-91525
- Leading-edge sweepback and shape effects on fin-induced fluctuating pressures
[BTN-95-EIX95302694471] p 636 A95-94067
- Airfoil leading-edge suction and energy conservation for compressible flow
[BTN-95-EIX95302730589] p 637 A95-94197
- Flow physics of critical states for rolling delta wings
[BTN-95-EIX0619952748180] p 590 A95-94473
- Effect of leading-edge extension fences on the vortex wake of an F/A-18 model
[BTN-95-EIX0619952748192] p 591 A95-94481
- Transonic flight test of a laminar flow leading edge with surface excrescences
[NASA-TM-4597] p 9 A95-11158
- Impingement flow heat transfer measurements of turbine blades using a jet array
[AD-A283450] p 62 A95-12512
- Hypersonic engine leading edge experiments in a high heat flux, supersonic flow environment
[NASA-TM-106742] p 91 A95-14299
- Control of unsteady separated flow associated with the dynamic stall of airfoils p 74 A95-14613
- Transonic Navier-Stokes calculations about a 65 deg delta wing
[NASA-CR-4635] p 108 A95-17273
- Two-dimensional high-lift airfoil data for CFD code validation p 112 A95-17859
- Wind tunnel test on a 65 deg delta wing with a sharp or rounded leading edge: The international vortex flow experiment p 114 A95-17872
- Wind tunnel test on a 65 deg delta wing with rounded leading edges: The International Vortex Flow Experiment p 114 A95-17875
- Impact loading of compressor stator vanes by hailstone ingestion p 200 A95-19670
- Soft body impact on titanium fan blades p 200 A95-19671
- Ice-impact analysis of blades p 200 A95-19672
- A theoretical and experimental investigation of the flow over supersonic leading edge wing/body configurations
[DRA-TM-AERO-PROP-41] p 331 A95-25649
- Airfoil modification effects on subsonic and transonic pressure distributions and performance for the EA-6B airplane
[NASA-TP-3516] p 373 A95-26382
- Composite repair of a CF18: Vertical stabilizer leading edge p 395 A95-27517
- Wind-tunnel test of the S814 thick root airfoil
[DE95-000268] p 376 A95-27541
- Computer program for estimation of leading-edge suction distribution for plane thin wings at subsonic speeds
[ESDU-94038] p 476 A95-28708
- Leading-edge suction distribution for plane thin wings at subsonic speeds p 477 A95-28800
- A noninvasive method of quantifying flow visualization data in vortex flow fields
[AD-A289802] p 552 A95-28948
- Leading edge film cooling effects on turbine blade heat transfer
[NASA-TM-106955] p 513 A95-29115
- Navier-Stokes solution of wing wake structure and its perturbation p 479 A95-29121
- A numerical method for modelling wings with sharp edges maneuvering at high angles of attack p 503 A95-29122
- A laser-based ice shape profilometer for use in icing wind tunnels
[NASA-TM-106936] p 646 A95-30851
- Vorticity dynamics and control of dynamic stall
[AD-A288658] p 620 A95-31400
- Control of unsteady separated flow associated with the dynamic stall of airfoils
[NASA-CR-198972] p 594 A95-32193
- A nonlinear vortex lattice method for unsteady flow with separated vortex
[DLR-FB-94-32] p 704 A95-32787
- Calculation for aerodynamic characteristics on delta wing with leading-edge separated vortex effect using boundary element method p 684 A95-34524
- Nonlinear stability of unsteady viscous flow
[AD-A294931] p 707 A95-34597
- LEAKAGE**
- Development of hypersonic engine seals: Flow effects of preload and engine pressures
[BTN-95-EIX95112524204] p 196 A95-69304
- Pitot/static leak testing
[CONGRESS PAPER C428-9-035] p 508 A95-91696
- Air Force seal activities p 60 A95-13600
- The fluid mechanics of a high aspect ratio slot with an impressed pressure gradient and secondary injection p 557 A95-30304
- LEARJET AIRCRAFT**
- Application of airborne field mill data for use in launch support
[HTN-95-50054] p 98 A95-62279
- Aerodynamic tailoring of the Learjet Model 60 wing
[SAE PAPER 932534] p 492 A95-89194
- Effects of mass on aircraft sidearm controller characteristics
[NASA-TM-104277] p 51 A95-11868
- Aircraft wake RCS measurement p 59 A95-13210
- Characterization of annular two-phase gas-liquid flows in microgravity p 95 A95-14556
- Aircraft accident report: Controlled collision with Terrain Transportes Aereos Ejecutivos, S.A. (TAESA) Learjet 25D, XA-BBA Dulles International Airport Chantilly, Virginia, June 18, 1994
[NTSB/AAR-95/02] p 380 A95-26498
- Two-phase flow research using the learjet apparatus
[NASA-TM-106814] p 438 A95-27854
- LEARNING**
- Intelligent flight trainer for initial rotary wing training
[SAE PAPER 932536] p 386 A95-84558
- LEARNING CURVES**
- Neuro-controllers for adaptive helicopter hover training
[BTN-94-EIX94522407592] p 709 A95-96241
- LEAST SQUARES METHOD**
- Attitude determination using dedicated and nondedicated multi-antenna GPS sensors
[BTN-95-EIX95142555482] p 228 A95-72891
- Optimization of contoured hypersonic scramjet inlets with a least-squares parabolized Navier-Stokes procedure
[HTN-95-20976] p 261 A95-74042
- Describing an attitude p 342 A95-80409
- Matrix fraction approach for finite-state aerodynamic modeling
[BTN-95-EIX95262694311] p 365 A95-85482
- An application of TLS (Total Least Squares) method to estimation of aircraft aerodynamic derivatives p 517 A95-91551
- The accuracy of parameter estimation in system identification of noisy aircraft load measurement
[NASA-CR-197516] p 134 A95-19130
- Comparison of meteorological data with fitted values extracted from projectile trajectory
[AD-A285921] p 255 A95-19989
- Aerodynamic parameter estimation via Fourier modulating function techniques
[NASA-CR-4654] p 335 A95-24630
- Apparatus and method for producing three-dimensional images
[AD-D017455] p 646 A95-30727
- LEE WAVES**
- Diurnal variation of lee vortices in Taiwan and the surrounding area
[HTN-95-91363] p 318 A95-76394
- Lee waves benign and malignant p 595 A95-93554
- LEGENDRE FUNCTIONS**
- Bilinear formulation applied to the response and stability of helicopter rotor blade
[BTN-95-EIX95042474400] p 192 A95-68300
- LEGIBILITY**
- An evaluation of aircraft CRT and dot-matrix display legibility requirements
[AD-A283933] p 138 A95-18164
- Evaluation of the Haworth-Newman avionics Display Readability Scale
[AD-A286127] p 235 A95-22232
- LENGTH**
- Numerical investigation of supersonic flows around a spiked blunt body
[BTN-95-EIX95212645690] p 271 A95-76742
- LENTICULAR BODIES**
- Test data on a non-circular body for subsonic, transonic and supersonic Mach numbers p 158 A95-17871
- Evolution of oxidation and creep damage mechanisms in HIPed silicon nitride materials
[DE95-001360] p 300 A95-22689
- LIABILITIES**
- The legal status and liability of the copilot, part 2
[HTN-95-A0578] p 452 A95-83158
- LIBRARIES**
- Aspect estimation of an aircraft using library model silhouettes
[PB95-141834] p 360 A95-25894
- LIFE (DURABILITY)**
- Life evaluation of a low power arcjet thruster p 403 A95-82337
- Micro-measurements of mechanical properties for adhesives and composites using digital imaging technology
[NASA-CR-196111] p 22 A95-10231
- Activities of the Structures Division, Lewis Research Center
[NASA-TM-108081] p 59 A95-13235
- Effect of surface roughness on local film cooling effectiveness and heat transfer coefficients
[AD-A283854] p 91 A95-14351
- FAA/NASA International Symposium on Advanced Structural Integrity Methods for Airframe Durability and Damage Tolerance, part 2
[NASA-CP-3274-PT-2] p 124 A95-19468
- Test method and test results for environmental assessment of aircraft materials p 302 A95-23509
- Thermal barrier coating life modeling in aircraft gas turbine engines p 346 A95-26140
- LIFE CYCLE COSTS**
- Technology-insertion life-cycle-cost model
[AIAA PAPER 95-0961] p 581 A95-90638
- Intelligent skins development for future military aircraft
[CONGRESS PAPER C428-17-189] p 531 A95-91714
- Aerospace applications of new materials
[CONGRESS PAPER C428-17-135] p 531 A95-91716
- Generic architectures for future flight systems p 99 A95-14159
- Aerodynamic shape optimization p 128 A95-16572
- Life cycle costs of alternatives for F-16 printed circuit board diagnosis equipment
[AD-A288744] p 401 A95-28586
- Novel cost controlled materials and processing for primary structures p 532 A95-28830
- LIFE SCIENCES**
- NASA video catalog
[NASA-SP-7109(01)] p 363 A95-24238
- JPRS Report: Science and technology, Central Eurasia
[JPRS-UST-94-032] p 350 A95-24759
- JPRS report: Science and technology, Central Eurasia
[JPRS-UST-94-022] p 438 A95-27699
- LIFT**
- Nonhydrostatic simulation of frontogenesis in a moist atmosphere. Part 3: Thermal wind imbalance and rainbands
[HTN-95-90356] p 212 A95-66429
- Lift analysis of a variable camber foil using the discrete vortex-blob method
[BTN-94-EIX94441386623] p 179 A95-68172
- Application of circulation control to advanced subsonic transport aircraft. Part 2: Transport application
[BTN-95-EIX95062487546] p 185 A95-68360
- Minimum sink-speed in power-off glide
[BTN-95-EIX95062487556] p 193 A95-68370
- Numerical simulation of incidence and sweep effects on delta wing vortex breakdown
[BTN-95-EIX95062487526] p 186 A95-69234
- Analysis of an oscillating Joukowski airfoil with surface suction and moving vortices
[BTN-95-EIX95062487527] p 186 A95-69235
- Interpretation of waverider performance data using computational fluid dynamics p 193 A95-69242
- [BTN-95-EIX95062487534] p 193 A95-69242
- Cercignani-Lampis-Lord gas-surface interaction model: Comparisons between theory and simulation
[BTN-95-EIX95041503806] p 242 A95-70131
- New airfoil-design concept with improved aerodynamic characteristics
[PAPER-4384] p 230 A95-72585
- Laplace interaction law for the computation of viscous airfoil flow in low- and high-speed aerodynamics
[BTN-95-EIX95142553037] p 263 A95-73461
- Progress in high-lift aerodynamic calculations
[BTN-95-EIX95152582315] p 264 A95-73518
- Separation control on high-lift airfoils via micro-vortex generators
[BTN-95-EIX95152582326] p 265 A95-73529

- Study of an airfoil with a flap and spoiler
[BTN-95-EIX95152582327] p 265 A95-73530
- Pneumatic concept for tip-stall control of cranked-arrow wings
[BTN-95-EIX95152582335] p 281 A95-73537
- Dynamic stall control for advanced rotorcraft application
[BTN-95-EIX95222650793] p 334 A95-79249
- Unsteady lift on a swept blade tip
[BTN-94-EIX95011441154] p 329 A95-80030
- Drag and lift in nonadiabatic transonic flow
[HTN-95-61208] p 540 A95-87581
- Effects of periodic spanwise blowing on Delta-wing configuration characteristics
[HTN-95-81631] p 461 A95-87679
- Parameters of Nocilla gas/surface interaction model from measured accommodation coefficients
[HTN-95-81639] p 541 A95-87687
- Effects of time scales on lift of airfoils in an unsteady stream
[HTN-95-81643] p 542 A95-87691
- An overview of static and dynamic airfoil performance
[SAE PAPER 931228] p 463 A95-88960
- Lift analysis of a variable camber foil using the discrete vortex-blob method
[HTN-95-20940] p 545 A95-88979
- Aircraft aerodynamic analysis on a personal computer (using the RDS aircraft design software)
[SAE PAPER 932530] p 492 A95-89190
- Rotor-wake-induced flow separation on a lifting surface
[HTN-95-01082] p 468 A95-90268
- The verification of a theoretical helicopter rotor blade sailing method by means of windtunnel testing
[HTN-95-01093] p 468 A95-90279
- Collectively variable incidence wingtips for lift control and reduced gust sensitivity
[HTN-95-92836] p 471 A95-90754
- Estimation of aerodynamic characteristics for the vortex flaps by the suction analogy
p 471 A95-91496
- A singularity method for a two dimensional stratified shear flow
p 473 A95-91513
- A guidance concept for hypersonic aerospacecrafts
p 526 A95-91549
- The coplanar projectile motion problem including the effects of lift and drag
[ISBN 1-879921-01-4] p 635 A95-93723
- A note on the Kutta-Joukowski formula
[ISBN 1-879921-01-4] p 635 A95-93735
- A Kutta condition conscious perturbation stream function boundary element algorithm for 2-D potential aerodynamics
[ISBN 1-879921-01-4] p 587 A95-93751
- Estimation of supersonic leading-edge thrust by a Euler flow model
[BTN-95-EIX0619952748194] p 591 A95-94483
- Navier-Stokes simulations of WECS airfoil flowfields
[DE94-013341] p 7 N95-10226
- A simple analytical aerodynamic model of Langley Winged-Cone Aerospace Plane concept
[NASA-CR-194987] p 54 N95-12175
- Cabin-fuselage-wing structural design concept with engine installation
[NASA-CR-197172] p 49 N95-12993
- Scale effects on aircraft and weapon aerodynamics
[AGARD-AG-323] p 67 N95-14103
- Numerical design of advanced multi-element airfoils
[NASA-CR-197135] p 76 N95-15762
- Measurements on a two-dimensional airfoil with high-lift devices
p 109 N95-17848
- In-flight lift-drag characteristics for a forward-swept wing aircraft and comparisons with contemporary aircraft
[NASA-TP-3414] p 117 N95-18565
- Lift enhancement device
[AD-D016522] p 224 N95-21864
- High-lift flow-physics flight experiments on a subsonic civil transport aircraft (B737-100)
p 275 N95-23333
- Lift enhancing tabs for airfoils
[NASA-CASE-ARC-11990-1] p 286 N95-23395
- NREL airfoil families for HAWTs
[DE95-000267] p 357 N95-24882
- Aerodynamic characteristics of the orbital reentry vehicle experimental probe fins in a supersonic flow
[NAL-TR-1232] p 342 N95-25664
- Noise impact of advanced high lift systems
[NASA-CR-195028] p 362 N95-26160
- Wind-tunnel test of the S814 thick root airfoil
[DE95-000268] p 376 N95-27541
- Study of potential aerodynamic benefits from spanwise blowing at wingtip
[NASA-TP-3515] p 378 N95-28669
- Noise exposure reduction of advanced high-lift systems
[NASA-CR-195077] p 452 N95-28670
- Increments in aerofoil lift coefficient at zero angle of attack and in maximum lift coefficient due to deployment of a plain trailing-edge flap, with or without a leading-edge high-lift device, at low speeds
[ESDU-94028] p 477 N95-28885
- Increments in aerofoil lift coefficient at zero angle of attack and in maximum lift coefficient due to deployment of a trailing-edge split flap, with or without a leading-edge high-lift device, at low speeds
[ESDU-94029] p 479 N95-29129
- A two element laminar flow airfoil optimized for cruise
[NASA-CR-198580] p 479 N95-29338
- Increments in aerofoil lift coefficient at zero angle of attack and in maximum lift coefficient due to deployment of various leading-edge high-lift devices at low speeds
[ESDU-94027] p 481 N95-29898
- Introduction to the estimation of the lift coefficients at zero angle of attack and at maximum lift for aerofoils with high-lift devices at low speeds
[ESDU-94026] p 481 N95-29899
- Multigrad convergence acceleration for the 2D Euler equations applied to high-lift systems
[PB95-198081] p 593 N95-30814
- A wind tunnel investigation of the effects of micro-vortex generators and Gurney flaps on the high-lift characteristics of a business jet wing
[NASA-TM-110626] p 607 N95-30827
- Validation of the helicopter rotor code HERO
[PB95-198040] p 607 N95-30838
- Analysis and design methodology for chordwise deformable wings
p 692 N95-33311
- Numerical simulations of dynamic stall phenomena in low speed flows
p 685 N95-34546
- Numerical simulation of two-dimensional PAR-WIG
p 685 N95-34548
- LIFT AUGMENTATION**
- Experiments on the flow field physics of confluent boundary layers for high-lift systems
[NASA-CR-197318] p 224 N95-21343
- LIFT DEVICES**
- Wake measurements in a strong adverse pressure gradient
[NASA-CR-197272] p 224 N95-21031
- Experiments on the flow field physics of confluent boundary layers for high-lift systems
[NASA-CR-197318] p 224 N95-21343
- Lift enhancement device
[AD-D016522] p 224 N95-21864
- Experimental investigations of on-demand vortex generators
p 250 N95-22451
- Increments in aerofoil lift coefficient at zero angle of attack and in maximum lift coefficient due to deployment of a plain trailing-edge flap, with or without a leading-edge high-lift device, at low speeds
[ESDU-94028] p 477 N95-28885
- Increments in aerofoil lift coefficient at zero angle of attack and in maximum lift coefficient due to deployment of various leading-edge high-lift devices at low speeds
[ESDU-94027] p 481 N95-29898
- Introduction to the estimation of the lift coefficients at zero angle of attack and at maximum lift for aerofoils with high-lift devices at low speeds
[ESDU-94026] p 481 N95-29899
- A wind tunnel investigation of the effects of micro-vortex generators and Gurney flaps on the high-lift characteristics of a business jet wing
[NASA-TM-110626] p 607 N95-30827
- LIFT DRAG RATIO**
- Navier-Stokes computation of a viscous optimized waverider
[BTN-95-EIX95041503782] p 193 A95-69213
- The effect of high lift to drag ratio on aerobraking
p 415 A95-85807
- Note on prediction of aerodynamic lift/drag ratio of WIG (Wing-In-Ground) at cruise
[BTN-95-EIX95282705925] p 467 A95-89665
- Low Reynolds number laminar separation bubble control using a backward facing step
[SAE PAPER 932572] p 467 A95-90061
- Hypersonic waveriders generated from power-law shocks
[AIAA PAPER 95-6160] p 470 A95-90472
- Estimation of aerodynamic characteristics for the vortex flaps by the suction analogy
p 471 A95-91496
- Experimental study for improving the lift to drag ratio of next generation SST
p 473 A95-91524
- The OFP-6M transport jet
[NASA-CR-197159] p 46 N95-12637
- The Balsa bullet: A high speed, low-cost general aviation aircraft for Aeroworld
[NASA-CR-197165] p 46 N95-12638
- An approach to aerodynamic characteristics of low radar cross-section fuselages
p 106 N95-16251
- Residual-correction type and related computational methods for aerodynamic design. Part 2: Multi-point airfoil design
p 128 N95-16567
- The global aircraft shape
p 128 N95-16571
- Aerodynamic shape optimization
p 128 N95-16572
- Low speed aerodynamic characteristics of delta wings with vortex flaps: 60 deg and 70 deg delta wings
[NAL-TR-1245] p 331 N95-25105
- Noise exposure reduction of advanced high-lift systems
[NASA-CR-195077] p 452 N95-28670
- A two element laminar flow airfoil optimized for cruise
[NASA-CR-198580] p 479 N95-29338
- Numerical analysis around the whole SST configuration
p 693 N95-34541
- LIFT FANS**
- Aerodynamics model for a generic ASTOVL lift-fan aircraft
[NASA-TM-110347] p 332 N95-26302
- The lift-fan aircraft: Lessons learned
[NASA-CR-196694] p 392 N95-27143
- LIFTING BODIES**
- Design optimization of an airbreathing aerospaceplane
p 524 A95-87382
- A design trade study using CFD modeling of reaction jets for aerodynamic control
[SAE PAPER 931384] p 586 A95-93660
- HL-10 dedication ceremony
[NASA-TM-104295] p 13 N95-10740
- LIFTING REENTRY VEHICLES**
- A concept of a hypersonic flight experiment of a winged vehicle
p 414 A95-82477
- Atmospheric reentry flight test of winged space vehicle
p 414 A95-82483
- LIFTOFF (LAUNCHING)**
- Fourth-generation Mars vehicle concepts
[BTN-95-EIX95152583267] p 298 A95-73568
- LIGHT AIRCRAFT**
- Flight test certification of primary category aircraft using TP101-41E sportplane design standard
[BTN-95-EIX0619952748184] p 606 A95-94477
- LIGHT ALLOYS**
- NASA-UVA light aerospace alloy and structures technology program (LA2ST)
[NASA-CR-198041] p 343 N95-24220
- LIGHT HELICOPTERS**
- Army aviation: Modernization strategy needs to be reassessed. Report to Congressional requestors
[GAO/NSIAD-95-9] p 683 N95-32783
- LIGHT SCATTERING**
- Fractal properties of whitecaps
[HTN-95-92121] p 443 A95-83827
- LIGHT TRANSPORT AIRCRAFT**
- Evaluation of the dynamic stability characteristics of the NAL Light Transport Aircraft
[NAL-PD-CA-9217] p 142 N95-16392
- LIGHTHILL GAS MODEL**
- Acoustics of laminar boundary layers breakdown
p 251 N95-22455
- LIGHTHILL METHOD**
- On the Lighthill relationship and sound generation from isotropic turbulence
[NASA-CR-195005] p 159 N95-18191
- A numerical study of fundamental shock noise mechanisms
[NASA-TM-110608] p 451 N95-27908
- LIGHTNING EQUIPMENT**
- Altitude cuing effectiveness of terrain texture characteristics in simulated low-altitude flight
[AD-A294369] p 700 N95-34362
- LIGHTNING**
- Application of airborne field mill data for use in launch support
[HTN-95-50054] p 98 A95-62279
- Aircraft electric field measurements: Calibration and ambient field retrieval
[HTN-95-90508] p 213 A95-67780
- Identification of aviation weather hazards based on the integration of radar and lightning data
[HTN-95-51323] p 356 A95-80908
- Lightning protection technology for small general aviation composite material aircraft
[SAE PAPER 931241] p 483 A95-88964
- Damage to composite aircraft structures from lightning strike attachment to unprotected CFC and internal sparking causing fuel injection
[CONGRESS PAPER C428-4-026] p 531 A95-91675
- Deaths and injuries as a result of lightning strikes to aircraft
[HTN-95-12213] p 485 A95-91913
- The inference of aviation weather hazards based on the integration of radar and lightning data
p 660 A95-93483
- Use of high resolution lightning detection and localization sensors for hazardous aviation weather nowcasting
p 661 A95-93486
- Using ATMS weather products for air traffic strategic planning
p 672 A95-93536

- Thunderstorm hypothesis reasoner
[AD-A282664] p 60 N95-12805
- Composite waveform generation for EMP and lightning direct-drive testing
[AD-A284159] p 92 N95-14405
- Field and data analysis studies related to the atmospheric environment
[NASA-CR-196543] p 168 N95-18093
- Aircraft fuel system lightning protection design and qualification test procedures development
[AD-A288401] p 380 N95-26497
- LINE OF SIGHT**
Characterizing the wake vortex signature for an active line of sight remote sensor
[NASA-CR-197697] p 333 N95-24391
- LINE SPECTRA**
VUV shock layer radiation in an arc-jet wind tunnel experiment
p 67 N95-13719
- LINEAR ARRAYS**
Resonant interaction of a linear array of supersonic rectangular jets: An experimental study
[NASA-CR-195398] p 76 N95-15852
- Inband radar cross section of phased arrays with parallel feeds
[AD-A284249] p 210 N95-19730
- LINEAR EQUATIONS**
Analytical study of the neutral stability of a model hypersonic boundary layer
[BTN-95-EIX9515257589] p 263 A95-73493
- Neural network prediction of three-dimensional unsteady separated flowfields
[BTN-95-EIX95182619232] p 308 A95-76658
- Rapid solution of large-scale systems of equations
p 169 N95-16458
- Linear and nonlinear discrete-time state-space modeling of dynamic systems for control applications
p 567 N95-29251
- LINEAR PREDICTION**
Linear prediction data extrapolation superresolution radar imaging
p 155 N95-16268
- LINEAR QUADRATIC GAUSSIAN CONTROL**
Output feedback control under randomly varying distributed delays
[BTN-94-EIX94511433916] p 168 A95-64582
- Effects of high order dynamics on helicopter flight control law design
[HTN-95-80852] p 290 A95-75094
- Flutter suppression control law design and testing for the active flexible wing
[BTN-95-EIX95182619214] p 292 A95-76640
- Application of ACT to unstable motions of an airfoil in ground effect
p 471 A95-91500
- Design and evaluation of a LQR controller for the bluebird unmanned air vehicle
[AD-A289769] p 504 N95-29457
- A stochastic adaptive control application to flight systems
p 699 N95-34806
- LINEAR QUADRATIC REGULATOR**
Aeroelastic vehicle multivariable control synthesis with analytical robustness evaluation
[BTN-95-EIX95182619115] p 321 A95-76592
- Dynamics and control of a tethered flight vehicle
[BTN-95-EIX95242670754] p 342 A95-81093
- Fundamental mechanisms of aeroelastic control with control surface and strain actuation
[BTN-95-EIX95242670746] p 327 A95-81101
- Load alleviation maneuvers for a launch vehicle
p 342 A95-81360
- Application of ACT to unstable motions of an airfoil in ground effect
p 471 A95-91500
- Design of a flight control system by a new way of pole placement in LQR
p 516 A95-91534
- System identification of the Large-Angle Magnetic Suspension Test Fixture (LAMSTF)
p 296 N95-23299
- LINEAR SYSTEMS**
New filtering method for linear weakly coupled stochastic systems
[BTN-95-EIX0608952736485] p 678 A95-92708
- Linear and nonlinear discrete-time state-space modeling of dynamic systems for control applications
p 567 N95-29251
- Design and evaluation of a LQR controller for the bluebird unmanned air vehicle
[AD-A289769] p 504 N95-29457
- Linear matrix inequalities for the problem of absolute stability of control systems
p 518 N95-29680
- Apparatus and method for producing three-dimensional images
[AD-D017455] p 646 N95-30727
- Linear Motor Free Piston Compressor
[AD-A293452] p 647 N95-31374
- LINEAR TRANSFORMATIONS**
Lyapunov exponents and stochastic stability of two-dimensional parametrically excited random systems
[BTN-94-EIX94361122401] p 207 A95-65897
- Robust control: A structured approach to solve aircraft flight control problems
p 621 N95-31995
- LINEAR VIBRATION**
Acoustic radiation damping of flat rectangular plates subjected to subsonic flows
p 172 N95-18542
- Active control of panel vibrations induced by a boundary layer flow
[NASA-CR-197867] p 273 N95-23182
- LINEARITY**
Comparison of linear stability results with flight transition data
[BTN-95-EIX95182619097] p 283 A95-76582
- LINEARIZATION**
Dynamical instability of the aerogravity assist maneuver
[BTN-95-EIX95152583282] p 298 A95-73583
- Design of high performance multivariable control systems for supersonic aircraft at high angle of attack
[NASA-CR-197661] p 293 N95-22908
- Development of a linearized unsteady Euler analysis for turbomachinery blade rows
[NASA-CR-4677] p 592 N95-30611
- LINES (GEOMETRY)**
Multidimensional lines 2: Proximity and applications
[BTN-94-EIX94341340329] p 61 A95-60865
- LININGS**
Oblique incidence sound absorption of porous materials covered by perforated metal and exposed to tangential airflow
[HTN-94-00681] p 19 A95-60165
- Composite structure forming a wear surface
[AD-D017462] p 629 N95-30749
- An active liner system for jet engine exhaust silencers, phase 1
[AD-A293277] p 617 N95-31191
- Water model tests on the Allison T56 series 3 combustion system
[DSTO-TR-0139] p 697 N95-33250
- LINKAGES**
Probabilistic reliability modeling of fatigue on the H-46 tie bar
[AD-A289926] p 607 N95-30927
- LIQUEFIED GASES**
Cooling of aerospace plane using liquid hydrogen and methane
[BTN-95-EIX0619952748171] p 590 A95-94465
- LIQUID CHROMATOGRAPHY**
Fuel-type classification and parameters prediction by Gas Liquid Chromatography analysis
[AD-A293442] p 630 N95-31368
- LIQUID COOLING**
Liquid flow-through cooling of electronic modules
p 246 N95-20647
- Microchannel heat pipe cooling of modules
p 246 N95-20649
- 175Hp contrarotating homopolar motor design report
[AD-A291138] p 557 N95-30122
- LIQUID CRYSTALS**
Flow visualization studies on sidewall effects in two-dimensional transonic airfoil testing
[BTN-95-EIX95152582313] p 264 A95-73516
- The use of thermochromic liquid crystals for heat transfer measurements in short duration hypersonic wind tunnel facilities
[AIAA PAPER 95-6115] p 520 A95-90443
- Draft standard for color active matrix liquid crystal displays (AMLCDs) in US Military aircraft. Recommended best practices
[AD-A282950] p 49 N95-12591
- Dynamics of phase ordering of nematics in a pore
[DE95-607662] p 362 N95-25978
- LIQUID FLOW**
A flow pattern map for two-phase liquid-gas flow under reduced gravity conditions
p 539 A95-87280
- Thermohydrodynamic analysis of cryogenic liquid turbulent flow fluid film bearings, phase 2
[NASA-CR-197412] p 349 N95-24461
- LIQUID FUELS**
Mechanism of deposit formation on fuel-wetted hot metal surfaces
[AD-A289847] p 426 N95-28621
- A pulsed liquid fuel ramjet
p 617 N95-31201
- LIQUID HYDROGEN**
Cooling of aerospace plane using liquid hydrogen and methane
[BTN-95-EIX0619952748171] p 590 A95-94465
- LIQUID LEVELS**
Reducing process noise in superconducting helium liquid level probes
[DE95-008956] p 629 N95-30765
- LIQUID METALS**
MHD-flow in slotted channels with conducting walls
[DE94-018370] p 258 N95-21388
- LIQUID NITROGEN**
Performance of the 0.3-meter transonic cryogenic tunnel with air, nitrogen, and sulfur hexafluoride media under closed loop automatic control
[NASA-CR-195052] p 310 N95-23257
- LIQUID OXYGEN**
Airborne rotary separator study
[NASA-CR-191045] p 150 N95-18743
- LIQUID PROPELLANT ROCKET ENGINES**
Ultimate characteristics of a rocket engine with a turbo-pump supply system
[BTN-94-EIX94461408757] p 148 A95-63640
- Experiment of rocket-ram annular combustor
p 412 A95-82324
- AFOSR Contractors Meeting in Propulsion
[AD-A282729] p 54 N95-12507
- LIQUID ROCKET PROPELLANTS**
Fourth-generation Mars vehicle concepts
[BTN-95-EIX95152583267] p 298 A95-73568
- Workshop report: Measurement techniques in highly transient, spectrally rich combustion environments
p 629 N95-31208
- LIQUID-GAS MIXTURES**
Characterization of annular two-phase gas-liquid flows in microgravity
p 95 N95-14556
- Two-phase flow research using the lejaert apparatus
[NASA-TM-106814] p 438 N95-27854
- LIQUID-LIQUID INTERFACES**
Marangoni-Benard convection in a low-aspect-ratio liquid layer
p 56 A95-61544
- LIQUID-VAPOR INTERFACES**
Flow-visualization study of the X-29A aircraft at high angles of attack using a 1/48-scale model
[NASA-TM-104268] p 8 N95-10858
- Numerical modeling of a cryogenic fluid within a fuel tank
[NASA-TM-4651] p 89 N95-13892
- Characterization of annular two-phase gas-liquid flows in microgravity
p 95 N95-14556
- LISTS**
ICASE
[NASA-CR-195001] p 170 N95-16898
- LITHIUM ALLOYS**
NASA-UVA light aerospace alloy and structures technology program supplement: Aluminum-based materials for high speed aircraft
[NASA-CR-4645] p 343 N95-24878
- LOAD CARRYING CAPACITY**
An analytical and experimental investigation of the response of the curved, composite frame/skin specimens
[HTN-95-80857] p 283 A95-75099
- LOAD DISTRIBUTION (FORCES)**
Shear buckling response of tailored composite plates
[HTN-95-51680] p 418 A95-85062
- Neural network approach to identification of aerodynamic loads on a wing. 1: Application to cantilevered beam models
p 475 A95-91568
- High angle of attack missile aerodynamics
[CONGRESS PAPER C428-3-060] p 475 A95-91673
- Transport aircraft loading and balancing system: Using a CLIPS expert system for military aircraft load planning
p 217 N95-19751
- Estimation of aerodynamic load distributions on the F/A-18 aircraft using a CFD panel code
[DSTO-TR-0147] p 504 N95-29445
- LOAD TESTS**
Experimental evaluation of a box beam specifically tailored for chordwise deformation
[BTN-95-EIX95182619088] p 283 A95-75773
- Universal electrohydraulic system for the steering gear loading
[CONGRESS PAPER C428-10-106] p 517 A95-91700
- Strain gage selection in loads equations using a genetic algorithm
[NASA-CR-4597] p 48 N95-12831
- Development of load spectra for Airbus A330/A340 full scale fatigue tests
p 135 N95-19479
- On aircraft repair verification of a fighter A/C integrally stiffened fuselage skin
p 394 N95-27515
- Comparison of measured and calculated dynamic loads for the Mod-2 2.5 mW wind turbine system
p 440 N95-27983
- Development of composite carrythrough bulkhead
p 423 N95-28438
- Structural testing of the technology integration box beam
p 441 N95-28467
- Technology integration box beam failure study
p 441 N95-28468
- Electrical short circuit and current overload tests on aircraft wiring
[AD-A293308] p 646 N95-30922
- LOADING MOMENTS**
Rolling maneuver load alleviation using active controls
[BTN-95-EIX95182619217] p 270 A95-76643

- Optimization of aerospace structures
[NASA-CR-196763] p 48 N95-12787
- Strain gage selection in loads equations using a genetic algorithm
[NASA-CR-4597] p 48 N95-12831
- LOADING OPERATIONS**
- Damage tolerance certification of a fighter horizontal stabilizer
[BTN-95-EIX0619952748186] p 637 A95-94478
- Transport aircraft loading and balancing system: Using a CLIPS expert system for military aircraft load planning
p 217 N95-19751
- LOADS (FORCES)**
- The effect of rotating loads suspended under a helicopter on their amplitude-frequency characteristics
[BTN-94-EIX94461407959] p 78 A95-62633
- Load alleviation maneuvers for a launch vehicle
p 342 A95-81360
- Efficient sensitivity analysis for rotary-wing aeromechanical problems
[HTN-95-42570] p 458 A95-87200
- General requirements for the electrohydraulic systems of the aircraft controls loading force on the simulators
[CONGRESS PAPER C428-5-138] p 522 A95-91681
- Discrete crack growth analysis methodology for through cracks in pressurized fuselage structures
[BTN-95-EIX0608952737538] p 633 A95-92751
- Fatigue design of axially loaded semicircular lugs
[BTN-95-EIX0619952748190] p 637 A95-94252
- Symmetric steady manoeuvre loads on rigid aircraft of classical configuration at subsonic speeds
[ESDU-94009] p 43 N95-11774
- Cabin fuselage structural design with engine installation and control system
[NASA-CR-197173] p 47 N95-12639
- Fatigue evaluation of empennage, forward wing, and winglets/tip fins on part 23 airplanes
[PB94-196813] p 79 N95-13981
- Simulation of Shuttle launch G forces and acoustic loads using the NASA Ames Research Center 20G centrifuge
p 86 N95-14089
- An investigation of polynomial calibrations methods for wind tunnel balances
p 144 N95-16258
- Field verification of the wind tunnel coefficients
p 109 N95-17291
- Aircraft fatigue and crack growth considering loads by structural component
p 137 N95-19497
- Nonlinear analysis of damaged stiffened fuselage shells subjected to combined loads
p 137 N95-19499
- A user's guide to LUGSAN 1.1: A computer program to calculate and archive lug and sway brace loads for aircraft-carried stores
[DE95-001919] p 232 N95-21730
- A comparison of measured wind park load histories with the WISPER and WISPERX load spectra
[DE95-000295] p 446 N95-27459
- Load transfer in the stiffener-to-skin joints of a pressurized fuselage
[NASA-CR-198610] p 439 N95-27865
- A hybrid vehicle evaluation code and its application to vehicle design, Revision 1
[DE95-008053] p 441 N95-28029
- A hybrid vehicle evaluation code and its application to vehicle design, revision 2
[DE95-008060] p 441 N95-28139
- Local design optimization for composite transport fuselage crown panels
p 398 N95-28473
- Comparison of resin film infusion, resin transfer molding, and consolidation of textile preforms for primary aircraft structure
p 425 N95-28477
- Severe edge effects and simple complimentary interior solutions for thin-walled anisotropic and composite structures
[AD-A290645] p 555 N95-29562
- LOCAL AREA NETWORKS**
- Flight Test Monitoring System using X-window
p 500 A95-91574
- NLS Flight Simulation Laboratory (FSL) documentation
[NASA-CR-196564] p 363 N95-24439
- Applications of digital video and synthetic environments to unmanned aerial vehicles
[AD-A291875] p 504 N95-29437
- LOG PERIODIC ANTENNAS**
- A VHF/UHF antenna for the Precision Antenna Measurement System (PAMS)
[AD-A285673] p 156 N95-16621
- LOGIC DESIGN**
- Workshop on Formal Models for Intelligent Control
[AD-A281399] p 169 N95-16864
- LOGICAL ELEMENTS**
- The development of an aircraft icing forecast technique using data from maps
p 675 A95-93549
- LOGISTICS**
- More supportable T-38A enhancement study
[AD-A283671] p 66 N95-15331
- E-6A hardness assurance, maintenance and surveillance program
[AD-A283994] p 134 N95-19067
- The value of simulation for training
[AD-A289174] p 411 N95-26556
- LOGISTICS MANAGEMENT**
- Fact sheet for Congressional Committees. Air traffic control: Status of FAA's modernization program
[GAO/RCED-94-167FS] p 603 N95-32197
- LONG TERM EFFECTS**
- An overview of millimeter-wave spectroscopic measurements of chlorine monoxide at Thule, Greenland, February-March, 1992: Vertical profiles, diurnal variation, and longer-term trends
[HTN-95-00722] p 444 A95-86292
- Ten-year ground exposure of composite materials used on the Bell Model 206L helicopter flight service program
[NASA-TP-3468] p 55 N95-12357
- LONGITUDINAL CONTROL**
- Rotorcraft control system design for uncertain vehicle dynamics using quantitative feedback theory
[HTN-95-31012] p 236 A95-71182
- H-infinity helicopter flight control law design with and without rotor state feedback
[BTN-95-EIX95182619129] p 291 A95-76606
- Direct-lift design strategy for longitudinal control of hypersonic aircraft
[BTN-95-EIX95182619131] p 291 A95-76608
- Robustly stable preliminary control systems design for the YF-16 CCV aircraft
[BTN-95-EIX95202637608] p 292 A95-76681
- Robust dynamic inversion for control of highly maneuverable aircraft
[BTN-95-EIX95242670747] p 359 A95-81100
- Robust longitudinal axis flight control for an aircraft with thrust vectoring
[BTN-95-EIX95122538875] p 408 A95-83000
- High-Alpha Research Vehicle (HARV) longitudinal controller: Design, analyses, and simulation results
[NASA-TP-3446] p 17 N95-10860
- Comparison of X-31 flight, wind-tunnel, and water-tunnel yawing moment asymmetries at high angles of attack
p 68 N95-14234
- High angle of attack flying qualities criteria for longitudinal rate command systems
p 70 N95-14247
- Determination of stability and control derivatives from the NASA F/A-18 HARV from flight data using the maximum likelihood method
[NASA-CR-197320] p 204 N95-19576
- Analysis of the longitudinal handling qualities and pilot-induced-oscillation tendencies of the High-Angle-of-Attack Research Vehicle (HARV)
p 293 N95-23297
- Aerodynamic surface distension system for high angle of attack forebody vortex control
[NASA-CASE-ARC-11979-1] p 286 N95-23390
- A comparison of the Neal-Smith and omega Tau function, zeta function and tau function flying qualities criteria
[AD-A289503] p 390 N95-26844
- Use of blade pitch control to provide power train damping for the Mod-2, 2.5-mW wind turbine
p 440 N95-27986
- Flight Vehicle Integration Panel Workshop on Pilot Induced Oscillations
[AGARD-AR-335] p 597 N95-31061
- LONGITUDINAL STABILITY**
- Offset thrust axes and pitch stability
[BTN-95-EIX95062487553] p 203 A95-68367
- Navier-Stokes simulations of Orbiter aerodynamic characteristics including pitch trim and bodyflap
[BTN-95-EIX95041503779] p 204 A95-69210
- Tailless aircraft design-recent experiences
p 492 A95-88899
- A flying qualities study of longitudinal long-term dynamics of hypersonic planes
[AIAA PAPER 95-6150] p 521 A95-90464
- An easy way to analyze longitudinal and lateral-directional trim problems with AEO or OEI
p 409 N95-26949
- Transonic aerodynamic characteristics of a proposed wing-body reusable launch vehicle concept
[NASA-TM-108489] p 592 N95-30712
- Unified criteria for ACT aircraft longitudinal dynamics
p 607 N95-31065
- LONGITUDINAL WAVES**
- The decay of longitudinal vortices shed from airfoil vortex generators
[NASA-CR-198356] p 480 N95-29402
- LORAN**
- Guidelines for the design of GPS and LORAN receiver controls and displays
[AD-A293753] p 602 N95-31572
- LORAN C**
- Comments on 'correction of inertial navigation with Loran C on NOAA's P-3 aircraft'
[HTN-95-70149] p 227 A95-70671
- LOSSES**
- Thrust modeling for hypersonic engines
[AIAA PAPER 95-6081] p 509 A95-87410
- LOUDNESS**
- Assessment of helicopter noise annoyance: A comparison between helicopters and jet aircraft
p 560 A95-88480
- LOUDSPEAKERS**
- Broadband, wide-area active control of sound radiated from vibrating structures using local surface-mounted radiation suppression devices
p 30 N95-11283
- LOW ALTITUDE**
- Flight test development and evaluation of a Kalman filter state estimator for low-altitude flight
[HTN-94-00684] p 16 A95-60167
- Simulation development of a forward sensor-enhanced low-altitude guidance system
[HTN-94-00688] p 17 A95-60170
- Design and flight evaluation of an integrated navigation and near-terrain helicopter guidance system for night-time and adverse weather operations
[NASA-TM-108837] p 11 N95-10846
- Multilayer anti-erosion coatings
p 201 N95-19679
- Synthetic Terrain Imagery for Helmet-Mounted Display, volume 1
[AD-A293612] p 612 N95-31656
- Advanced gust management systems: Lessons learned and perspectives
p 622 N95-32002
- Low-Level and Nap-of-the-Earth (NOE) night operations
[AGARD-CP-563] p 686 N95-32486
- Flight test of a low-altitude helicopter guidance system with obstacle avoidance capability
p 688 N95-32490
- Tactical low-level helicopter communications
p 702 N95-32492
- A helmet mounted display for night missions at low altitude
p 693 N95-32503
- Perceptual dimensions of simulated scenes relevant for visual low-altitude flight
[AD-A294385] p 700 N95-34344
- LOW ASPECT RATIO**
- Marangoni-Bernard convection in a low-aspect-ratio liquid layer
p 56 A95-61544
- Development of a low-aspect ratio fin for flight research experiments
[NASA-TM-4596] p 108 N95-16858
- LOW ASPECT RATIO WINGS**
- An approach to aerodynamic characteristics of low radar cross-section fuselages
p 106 N95-16251
- Low aspect ratio wing experiment
p 113 N95-17865
- A nonlinear vortex lattice method for unsteady flow with separated vortex
[DLR-FB-94-32] p 704 N95-32787
- LOW CONDUCTIVITY**
- Quality optimization of thermally sprayed coatings produced by the JP-5000 (HVOF) gun using mathematical modeling
p 152 N95-19008
- LOW COST**
- The Balsa bullet: A high speed, low-cost general aviation aircraft for Aeroworld
[NASA-CR-197165] p 46 N95-12638
- LCX: Proposal for a low-cost commercial transport
[NASA-CR-197186] p 47 N95-12645
- Assessing aircraft survivability to high frequency transient threats
[AD-A283999] p 134 N95-18726
- Programmable cockpit research simulator
[AD-A279219] p 204 N95-19848
- Design of a high altitude long endurance aircraft with manufacturing considerations
p 391 N95-26947
- Development of a low-cost, modified resin transfer molding process using elastomeric tooling and automated preform fabrication
p 420 N95-28268
- LOW DENSITY FLOW**
- Higher-order viscous shock-layer solutions for high-altitude flows
[BTN-95-EIX95152583255] p 306 A95-73556
- Numerical analysis of hypersonic low-density scramjet inlet flow
[BTN-95-EIX95212645694] p 272 A95-76746
- LOW EARTH ORBITS**
- Reentry analysis for low Earth orbiting spacecraft
p 415 A95-85774
- LOW FREQUENCIES**
- Behavior of an inversion-based precipitation retrieval algorithm with high-resolution AMPR measurements including a low-frequency 10.7-GHz channel
[HTN-95-70134] p 252 A95-70656
- Reducing low frequency noise emissions from a Langley Air Force Base Hush-House
p 561 A95-90112
- Low frequency ultrasonic nondestructive inspection of aluminum/adhesive fuselage lap splices
[DE94-014242] p 24 N95-11135

LOW PRESSURE

Research aircraft observations of a polar low at the east Greenland ice edge
[HTN-95-A0175] p 215 A95-69766

LOW REYNOLDS NUMBER

Low Reynolds number laminar separation bubble control using a backward facing step
[SAE PAPER 932572] p 467 A95-90061

A low fin height heat exchanger technology demonstrator for Hermes
[SAE PAPER 932119] p 526 A95-90360

Aerofoil characteristics at low Reynolds number
p 472 A95-91507

An experimental investigation of forward-swept wings at low Reynolds numbers
[SAE PAPER 931370] p 604 A95-93650

An efficient discrete vortex method for low Reynolds number incompressible flows
p 639 A95-95407

Modification of the two-equation turbulence model in NPARC to a Chien low Reynolds number k-epsilon formulation
[NASA-TM-106710] p 37 N95-11917

Advanced k-epsilon modeling of heat transfer
[NASA-CR-4679] p 648 N95-31423

LOW SPEED

Aerodynamic characteristics of a canard-controlled missile at high angles of attack
[BTN-95-EIX95152583257] p 267 A95-73558

Viscous-inviscid interaction method for unsteady low-speed airfoil flows
[BTN-95-EIX95182619093] p 269 A95-75778

Aerodynamic characteristics of external store configurations at low speeds
[BTN-95-EIX95182619230] p 271 A95-76656

Low-speed wind tunnel tests of two waverider configuration models
[AIAA PAPER 95-6093] p 493 A95-89251

Low-speed wind tunnel testing of the NPS and NASA Ames Mach 6 optimized waverider
[AD-A283585] p 75 N95-15319

Two-dimensional 16.5 percent thick supercritical airfoil NLR 7301
p 110 N95-17854

Low-speed surface pressure and boundary layer measurement data for the NLR 7301 airfoil section with trailing edge flap
p 111 N95-17855

Force and pressure data of an ogive-nosed slender body at high angles of attack and different Reynolds numbers
p 113 N95-17868

Low speed propeller slipstream aerodynamic effects
p 116 N95-17882

Velocity measurements with hot-wires in a vortex-dominated flowfield
p 121 N95-19261

NASA low-speed axial compressor for fundamental research
[NASA-TM-4635] p 296 N95-23192

Handling qualities of the High Speed Civil Transport
p 294 N95-23325

Low speed aerodynamic characteristics of delta wings with vortex flaps: 60 deg and 70 deg delta wings
[NAL-TR-1245] p 331 N95-25105

Effect of low-speed impact damage and damage location on behavior of composite panels
p 426 N95-28481

Damage tolerance of a geodesically stiffened advanced composite structural concept for aircraft structural applications
p 399 N95-28487

Low-speed wind-tunnel investigation of the stability and control characteristics of a series of flying wings with sweep angles of 50 deg
[NASA-TM-4640] p 505 N95-30226

LOW SPEED STABILITY

Handling qualities of hypersonic aircraft and related control requirements
p 515 A95-87398

Low-speed aerodynamic characteristics of a slender wing with vertical fins
p 460 A95-87400

LOW SPEED WIND TUNNELS

Low speed wind tunnel blockage corrections for airfoils at medium to large angles of attack
p 474 A95-91557

Data acquisition and processing software for the Low Speed Wind Tunnel tests of the Jindivik auxiliary air intake
[AD-A285455] p 108 N95-17178

Low speed propeller slipstream aerodynamic effects
p 116 N95-17882

Background noise levels measured in the NASA Lewis 9- by 15-foot low-speed wind tunnel
[NASA-TM-106817] p 145 N95-18054

Wall correction method with measured boundary conditions for low speed wind tunnels
p 164 N95-19263

Calculation of low speed wind tunnel wall interference from static pressure pipe measurements
p 164 N95-19273

Vapor generator wand
[NASA-CASE-LAR-15058-1] p 238 N95-20080

Flow quality improvements in the NASA Lewis Research Center 9- by 15-foot Low Speed Wind Tunnel
[NASA-CR-195439] p 627 N95-31653

LOW TEMPERATURE

High density monolithic packaging technology for digital/microwave avionics
p 240 N95-20646

LOW TURBULENCE

Separation control on high-lift airfoils via micro-vortex generators
[BTN-95-EIX95152582326] p 265 A95-73529

LOW VISIBILITY

Passive millimeter wave camera for aircraft landing in low visibility conditions
[BTN-95-EIX95292721321] p 609 A95-92513

Passive MMW camera for low visibility landings
p 59 N95-13215

Differential GPS and system integration of the Low Visibility Landing and Surface Operations (LVLASO) demonstration
p 280 N95-23318

The effects of display location and dimensionality on taxiway navigation
[AD-A294878] p 690 N95-34570

LOWER ATMOSPHERE

Aircraft-borne, laser-induced fluorescence instrument for the in situ detection of hydroxyl and hydroperoxyl radicals
[BTN-95-EIX95072499029] p 253 A95-71908

LUBRICANTS

A stationary flow of a viscous liquid in radial clearances of rotor bearings in the turbocompressor of an internal combustion engine
[BTN-94-EIX94461408765] p 153 A95-63648

The dynamic nature of rotor thermal bending due to unsteady lubricant shearing within a bearing
[HTN-95-42091] p 430 A95-83857

Lubricant evaluation and performance, 2
[AD-A279144] p 242 N95-21969

LUBRICATION

Effect of squeeze film damper land geometry on damper performance
[HTN-95-92247] p 434 A95-85291

Rolling bearing failure and wear debris detection
[CONGRESS PAPER C428-15-094] p 457 A95-91711

Wormgear geometry adopted for implementing hydrostatic lubrication and formulation of the lubrication problem
[AD-A290331] p 210 N95-19567

LUGS

Evaluation of alternate F-14 wing lug coating
[AD-A283207] p 129 N95-17631

A user's guide to LUGSAN 1.1: A computer program to calculate and archive lug and sway brace loads for aircraft-carried stores
[DE95-001919] p 232 N95-21730

LUMBAR REGION

A multibody/finite element analysis approach for modeling of crash dynamic responses
[NIAR-94-3] p 277 N95-24050

LUMINAIRES

Prototype stop bar system evaluation at Seattle-Tacoma International Airport
[AD-A290136] p 490 N95-30031

LUMINANCE

Factors affecting the perception of tuning in monocular regions of partial binocular overlap displays
[AD-A286287] p 259 N95-22044

LUMINESCENCE

Optical surface pressure measurements: Accuracy and application field evaluation
p 175 N95-19274

LUMINOUS INTENSITY

Application of pressure sensitive paint in hypersonic flows
[NASA-TM-106824] p 223 N95-20794

LUNAR ORBITS

How 'HITEN's' aerobraking experiments were carried out
p 415 A95-82553

LUNAR SPACECRAFT

Minimum-mass design of sandwich aerobrakes for a lunar transfer vehicle
[BTN-95-EIX95212645707] p 299 A95-76759

M**MACH NUMBER**

Oscillating airfoil compressible dynamic stall studies
[HTN-94-00704] p 3 A95-60183

A comparison of three-dimensional nonequilibrium solution algorithms applied to hypersonic flows with stiff chemical source terms
[AIAA PAPER 93-2861] p 4 A95-60186

A study of compressibility effects on dynamic stall of rapidly pitching airfoils
[HTN-94-00715] p 5 A95-60193

Supersonic and hypersonic shock/boundary-layer interaction database
[BTN-94-EIX94441386604] p 182 A95-67335

Linear disturbances in hypersonic, chemically reacting shock layers
[BTN-94-EIX94441386605] p 182 A95-67336

Behavior of the Johnson-King turbulence model in axisymmetric supersonic flows
[BTN-94-EIX94441386606] p 183 A95-67337

Influence of an injectant Mach number and temperature on supersonic film cooling
[BTN-94-EIX94441386686] p 184 A95-68195

Multiblock analysis for Shuttle Orbiter reentry heating from Mach 24 to Mach 12
[BTN-95-EIX95041503780] p 205 A95-69211

Navier-Stokes computation of a viscous optimized waverider
[BTN-95-EIX95041503782] p 193 A95-69213

Minimum-drag axisymmetric bodies in the supersonic/hypersonic flow regimes
[BTN-95-EIX95041503785] p 180 A95-69216

Flow resolution and domain influence in rarefied hypersonic blunt-body flows
[BTN-95-EIX95082502729] p 220 A95-70136

Main features of overexpanded triple jets
[BTN-95-EIX95142553040] p 304 A95-73458

Analytical study of the neutral stability of a model hypersonic boundary layer
[BTN-95-EIX95152577589] p 263 A95-73493

Mach wave emission from a high-temperature supersonic jet
[BTN-95-EIX95152577586] p 264 A95-73496

Improved version of the Naval Surface Warfare Center aeroprediction code (AP93)
[BTN-95-EIX95152583260] p 267 A95-73561

Flutter of an infinitely long panel in a duct
[BTN-95-EIX95182619087] p 291 A95-75772

Scaling of incipient separation in supersonic/transonic speed laminar flows
[BTN-95-EIX95182619104] p 269 A95-76589

Natural laminar flow wing concept for supersonic transports
[BTN-95-EIX95182619226] p 308 A95-76652

Numerical investigation of supersonic flows around a spiked blunt body
[BTN-95-EIX95212645690] p 271 A95-76742

Calculation of wing-alone aerodynamics to high angles of attack
[BTN-95-EIX95212645713] p 261 A95-76765

Study of subsonic base cavity flowfield structure using particle image velocimetry
[BTN-95-EIX95222650781] p 327 A95-79237

Predicting stall and post-stall behavior of airfoils at low mach numbers
[BTN-95-EIX95262694297] p 365 A95-85468

Compressible inviscid vortex flow of a sharp edge delta wing
[BTN-95-EIX95262694308] p 370 A95-85479

Condensation in jet engine intake ducts during stationary operation
[BTN-95-EIX95292721154] p 612 A95-92590

Some additional stability and performance characteristics of the scissor/pivot wing configurations
[SAE PAPER 931383] p 618 A95-93659

Airfoil leading-edge suction and energy conservation for compressible flow
[BTN-95-EIX95302730589] p 637 A95-94197

Aerodynamic applications of underexpanded hypersonic viscous jets
[BTN-95-EIX0619952748162] p 589 A95-94456

Analysis of some interference effects in a transonic wind tunnel
[BTN-95-EIX0619952748166] p 589 A95-94460

In-flight pressure measurements on a subsonic transport high-lift wing section
[BTN-95-EIX0619952748170] p 589 A95-94464

Estimation of supersonic leading-edge thrust by a Euler flow model
[BTN-95-EIX0619952748194] p 591 A95-94483

Interaction of a weak shock with freestream disturbances
[BTN-95-EIX95332750473] p 638 A95-94687

Effect of leading- and trailing-edge flaps on clipped delta wings with and without wing camber at supersonic speeds
[NASA-TM-4542] p 5 N95-10028

A shadowgraph study of the National Launch System's 1 1/2 stage vehicle configuration and Heavy Lift Launch Vehicle configuration — Using the Marshall Space Flight Center's 14-Inch Trisonic Wind Tunnel
[NASA-RP-1347] p 35 N95-11710

Shock-tunnel combustor testing for hypersonic vehicles
[NASA-CR-196836] p 52 N95-11938

- A simple analytical aerodynamic model of Langley Winged-Cone Aerospace Plane concept
[NASA-CR-194987] p 54 N95-12175
- Experimental aerodynamic characteristics of a generic hypersonic accelerator configuration at Mach numbers 1.5 and 2.0 — conducted in the Langley Unitary Plan Wind Tunnel
[NASA-TM-4413] p 39 N95-12770
- Mach number control in the High Speed Wind Tunnel of NLR
[PB94-201670] p 53 N95-13243
- Unsteady flow phenomena in discrete passage diffusers for centrifugal compressors
[AD-A281412] p 155 N95-16163
- Scramjet testing guidelines p 138 N95-16317
- Error propagation equations for estimating the uncertainty in high-speed wind tunnel test results
[DE94-014136] p 145 N95-16509
- Mach number, flow angle, and loss measurements downstream of a transonic fan-blade cascade
[AD-A280907] p 108 N95-16824
- Comparison of computational and experimental results for a supercritical airfoil
[NASA-TM-4601] p 108 N95-16908
- 2-D aileron effectiveness study p 110 N95-17851
- Investigation of an NLF(1)-0416 airfoil in compressible subsonic flow p 110 N95-17852
- OAT15A airfoil data p 111 N95-17857
- Measurements of the flow over a low aspect-ratio wing in the Mach number range 0.6 to 0.87 for the purpose of validation of computational methods. Part 1: Wing design, model construction, surface flow. Part 2: Mean flow in the boundary layer and wake, 4 test cases
p 112 N95-17860
- Pressure distributions on research wing W4 mounted on an axisymmetric body p 112 N95-17862
- DLR-F4 wing body configuration p 130 N95-17863
- Low aspect ratio wing experiment p 113 N95-17865
- Measurement of gust response on a turbine cascade
[NASA-TM-106776] p 117 N95-18457
- Flow coefficient behavior for boundary layer bleed holes and slots
[NASA-TM-106846] p 244 N95-19953
- Wing pressure distributions from subsonic tests of a high-wing transport model — in the Langley 14-by-22-Foot Subsonic Wind Tunnel p 272 N95-22802
- [NASA-TM-4583] p 272 N95-22802
- Performance of the 0.3-meter transonic cryogenic tunnel with air, nitrogen, and sulfur hexafluoride media under closed loop automatic control
[NASA-CR-195052] p 310 N95-23257
- Design of a variable area diffuser for a 15-inch Mach 6 open-jet tunnel p 297 N95-23309
- Comparative wind tunnel test at high Reynolds numbers of NACA 64 621 airfoils with two aileron configurations p 377 N95-27977
- Measurements of store forces and moments and cavity pressures for a generic store in and near a box cavity at subsonic and transonic speeds
[NASA-TM-4611] p 378 N95-28241
- An experimental investigation of the time-dependent separation of tangent bodies in supersonic flow
[AD-A290720] p 480 N95-29500
- Transonic, supersonic and hypersonic wind-tunnel tests on aerodynamic characteristics of reentry body with blunted cone configuration
[ISAS-658] p 480 N95-29640
- The 1995 version of the NSWC aeroprediction code. Part 1: Summary of new theoretical methodology
[AD-A291518] p 481 N95-29853
- An aerodynamic and static-stability analysis of the Hypersonic Applied Research Technology (HART) missile
[DA9426923] p 481 N95-29965
- Transonic aerodynamic characteristics of a proposed wing-body reusable launch vehicle concept
[NASA-TM-108489] p 592 N95-30712
- Unsteady transonic wind tunnel test on a semispan straked delta wing, oscillating in pitch. Part 1: Description of the model, test setup, data acquisition, and data processing
[AD-A293113] p 593 N95-30885
- Hypervelocity wind tunnel number 9, high Mach number development program
[AD-A289934] p 594 N95-30929
- Control of unsteady separated flow associated with the dynamic stall of airfoils
[NASA-CR-198972] p 594 N95-32193
- MACH REFLECTION**
- Numerical studies of Mach reflection with air chemistry p 548 A95-90575
- Numerical experiments on aerodynamic heating mechanism in shock reflection processes p 471 A95-91497
- MACHINE LEARNING**
- On-line learning nonlinear direct neurocontrollers for restructurable control systems p 359 A95-81079
[BTN-95-EIX95242670768]
- A neural expert approach to self designing flight control systems
[AD-A279965] p 237 N95-21122
- Selecting optimal experiments for feedforward multilayer perceptrons
[AD-A290856] p 678 N95-30406
- MACHINE TOOLS**
- Automatic riveting cell for commercial aircraft floor grid assembly
[BTN-95-EIX95182617807] p 261 A95-75752
- Development of an intelligent tool-condition monitoring system for FMS
[CONGRESS PAPER C428-32-012] p 583 A95-93617
- Development of processes, means, and theoretical principles of thin-walled detail plastic forming at Kazan Aviation Institute p 155 N95-16281
- MAGNESIUM ALLOYS**
- NASA-UVA light aerospace alloy and structures technology program supplement: Aluminum-based materials for high speed aircraft
[NASA-CR-4645] p 343 N95-24878
- MAGNESIUM CHLORIDES**
- Gas turbine compressor corrosion and erosion in Western Europe
[AD-B196178L] p 201 N95-19678
- MAGNETIC ANOMALIES**
- The joint Russian-Brazil research on balloons p 182 A95-66303
- MAGNETIC BEARINGS**
- Stability of magnetic bearing-rotor systems and the effects of gravity and damping
[BTN-94-EIX94441386619] p 208 A95-68168
- Effects of AMB parameters on the dynamic stability of the rotor
[BTN-94-EIX94381353450] p 323 A95-75494
- Stability of magnetic bearing-rotor systems and the effects of gravity and damping
[HTN-95-20955] p 465 A95-88994
- Influence of backup bearings and support structure dynamics on the behavior of rotors with active supports
[NASA-CR-197438] p 310 N95-23190
- Dynamic behavior of a magnetic bearing supported jet engine rotor with auxiliary bearings
[NASA-CR-197860] p 338 N95-24213
- Whirl plus tilt
[DE95-007948] p 452 N95-28108
- Influence of backup bearings and support structure dynamics on the behavior of rotors with active supports
[NASA-CR-199080] p 703 N95-32689
- Dynamic behavior of a magnetic bearing supported jet engine rotor with auxiliary bearings p 703 N95-32691
- Dynamic modeling and response characteristics of a magnetic bearing rotor system with auxiliary bearings p 703 N95-32692
- Synchronous dynamics of a coupled shaft/bearing/housing system with auxiliary support from a clearance bearing: Analysis and experiment p 703 N95-32693
- MAGNETIC COILS**
- Extension to the dynamic modeling of the large angle magnetic suspension test fixture
[NASA-CR-197801] p 411 N95-26768
- MAGNETIC DISKS**
- A selection of experimental test cases for the validation of CFD codes. Supplement: Datasets A-E
[AGARD-AR-303-SUPPL] p 117 N95-18539
- MAGNETIC EFFECTS**
- Effects of AMB parameters on the dynamic stability of the rotor
[BTN-94-EIX94381353450] p 323 A95-75494
- MAGNETIC FIELDS**
- Mechanism and technological particular features of thermomagnetic hardening
[BTN-94-EIX94461407953] p 89 A95-62627
- Powerful bolide explosion over North Italy
[HTN-95-80564] p 218 A95-69658
- MAGNETIC LEVITATION VEHICLES**
- Computational support of the laminar flow supersonic wind tunnel, CNSFV code development, Maglev, and grid generation
[NASA-CR-197750] p 411 N95-26775
- MAGNETIC SUSPENSION**
- System identification of the Large-Angle Magnetic Suspension Test Fixture (LAMSTF) p 296 N95-23299
- Extension to the dynamic modeling of the large angle magnetic suspension test fixture
[NASA-CR-197801] p 411 N95-26768
- MAGNETOHYDRODYNAMIC FLOW**
- Temperature diagnostics in the hypersonic flow regime: An application to develop a stagnation temperature probe
[AIAA PAPER 95-6114] p 511 A95-90442
- MHD-flow in slotted channels with conducting walls
[DE94-018370] p 258 N95-21388
- MAGNETOHYDRODYNAMICS**
- MHD-flow in slotted channels with conducting walls
[DE94-018370] p 258 N95-21388
- MAGNETOMETERS**
- Flight Mechanics/Estimation Theory Symposium 1995
[NASA-CP-3299] p 416 N95-27763
- MAGNETOSTATIC FIELDS**
- A time stepping coupled finite element-state space modeling environment for synchronous machine performance and design analysis in the ABC frame of reference p 649 N95-31948
- MAGNETOSTRICTION**
- Torsional actuation with extension-torsion composite coupling and a magnetostrictive actuator
[BTN-95-EIX95262694314] p 435 A95-85485
- MAINTAINABILITY**
- Maintenance requirements for a supersonic transport
[BTN-95-EIX95031502751] p 179 A95-68258
- Reliability and maintainability
[BTN-95-EIX9504277109] p 179 A95-68350
- The air systems controllerate initiatives and policies for the procurement of reliable and maintainable equipment
[CONGRESS PAPER C428-6-113] p 549 A95-91682
- KC-135 cockpit modernization study. Phase 1: Equipment evaluation
[AD-A284099] p 131 N95-18398
- Navy foreign object damage and its impact on future gas turbine engine low pressure compression systems p 198 N95-19658
- New Trends in coatings developments for turbine blades: Materials processing and repair p 201 N95-19676
- Design of a high altitude long endurance aircraft with manufacturing considerations p 391 N95-26947
- Report to Congressional Committees. Comanche Helicopter: Testing needs to be completed prior to production decisions
[GAO/NSIAD-95-112] p 397 N95-27910
- MAINTENANCE**
- Ceramic blanket reduces maintenance costs
[BTN-94-EIX94461290278] p 77 A95-61733
- Fatigue resistance of peened 7050-T7451 aluminum alloy: Repair and re-treatment of a component surface
[BTN-94-EIX94371347838] p 206 A95-69131
- Condition monitoring and diagnostics
[HTN-95-92312] p 387 A95-85356
- Cabin fuselage structural design with engine installation and control system
[NASA-CR-197173] p 47 N95-12639
- The assessment of the AH-64D, longbow, mast-mounted assembly noise hazard for maintenance personnel
[AD-A284971] p 171 N95-16226
- Identification of Artificial Intelligence (AI) applications for maintenance, monitoring, and control of airway facilities
[AD-A282479] p 125 N95-17373
- E-6A hardness assurance, maintenance and surveillance program
[AD-A283994] p 134 N95-19067
- Performance deterioration of axial compressors due to blade defects p 199 N95-19665
- An airborne monitoring system for FOD and erosion faults p 200 N95-19668
- Braze repair possibilities for hot section gas turbine parts p 201 N95-19677
- Public-sector aviation issues: Graduate research award papers, 1992-1993
[PB94-217478] p 219 N95-19967
- Life cycle costs of alternatives for F-16 printed circuit board diagnosis equipment
[AD-A288744] p 401 N95-28586
- An analysis of the impact of ASPA on organizational and depot level maintenance
[AD-A292670] p 457 N95-29414
- MAINTENANCE TRAINING**
- The value of simulation for training
[AD-A289174] p 411 N95-26556
- MAN MACHINE SYSTEMS**
- Flight-deck displays on the Boeing 777
[BTN-95-EIX95142562402] p 286 A95-73438
- Human factors issues in aircraft cabin design
[SAE PAPER 932527] p 386 A95-84556
- Automated hover training: An empirical evaluation
[SAE PAPER 932536] p 379 A95-84559
- The advanced flight simulator complex
[CONGRESS PAPER C428-5-025] p 522 A95-91679
- ASTOVL Aircraft: Some thoughts on new control strategies
[CONGRESS PAPER C428-5-011] p 517 A95-91680

- General requirements for the electrohydraulic systems of the aircraft controls loading force on the simulators [CONGRESS PAPER C428-5-138] p 522 A95-91681
- The Saab-Scania approach to development simulators [CONGRESS PAPER C428-10-137] p 522 A95-91698
- Airborne integrated communications system [CONGRESS PAPER C428-30-162] p 610 A95-93612
- Neuro-controllers for adaptive helicopter hover training [BTN-94-EIX94522407592] p 709 A95-96241
- Industry review of a crew-centered cockpit design process and toolset [AD-A282966] p 130 N95-17661
- Crew aiding and automation: A system concept for terminal area operations, and guidelines for automation design [NASA-CR-4631] p 228 N95-19950
- Collected papers of the Soar/IFOR project, Spring 1994 [AD-A280063] p 238 N95-20624
- Systems engineering design and technical analyses for Strategic Avionics Crew-station Design Evaluation Facility (SACDEF) [AD-A286239] p 235 N95-22024
- A crew-centered flight deck design philosophy for High-Speed Civil Transport (HSCT) aircraft [NASA-TM-109171] p 335 N95-24582
- Integrated mission precision attack cockpit technology (IMPACT), Phase 1: Identifying technologies for air-to-ground fighter integration [AD-A289562] p 389 N95-26684
- Survey and implementation of commercial manual controllers for a generic telerobotics architecture [AD-A289215] p 449 N95-26990
- Telepresence media resource tape [NASA-TM-110648] p 569 N95-30248
- The application of helicopter mission simulation to Nap-of-the-Earth operations p 710 N95-32496
- A rose by any other name: Certification seen as process rather than content p 688 N95-34766
- Human factors certification in the development of future air traffic control systems p 690 N95-34770
- Quality assurance and risk management: Perspectives on Human Factors Certification of Advanced Aviation Systems p 690 N95-34771
- User type certification for advanced flight control systems p 699 N95-34772
- MANAGEMENT**
- Test and evaluation crew resource management p 483 A95-90867
- An approach to weather requirements management p 653 A95-93448
- MANAGEMENT INFORMATION SYSTEMS**
- AVIRIS and TIMS data processing and distribution at the land processes distributed active archive center p 325 N95-23872
- MANAGEMENT METHODS**
- Technology Benefit Estimator (T/BEST): User's manual [NASA-TM-106785] p 167 N95-19501
- MANAGEMENT PLANNING**
- Maintenance programs [BTN-95-EIX95182617809] p 261 A95-75754
- The F-16 multinational staged improvement program: A case study of risk assessment and risk management [AD-A281706] p 81 N95-15451
- Air traffic operational inventory CY 1994 [AD-A288281] p 382 N95-26454
- Federal aviation administration plan for research, engineering and development [AD-A290952] p 490 N95-29733
- Unmanned aerial vehicles, 1994 master plan p 607 N95-31416
- MANAGEMENT SYSTEMS**
- Integrated Thermal Energy Management (I-TEM): An evaluation tool for aircraft [SAE PAPER 932577] p 493 A95-90065
- Air traffic management: The future challenge [CONGRESS PAPER C428-7-145] p 488 A95-91686
- The development of a highly reliable power management and distribution system for civil transport aircraft [NASA-TM-106697] p 50 N95-11867
- An engineering code to analyze hypersonic thermal management systems p 155 N95-16322
- Packet utilisation definitions for the ESA XMM mission p 150 N95-17596
- On-line handling of air traffic: Management, guidance and control [AGARD-AG-321] p 126 N95-18927
- MANEUVERABILITY**
- Side forces at high angles of attack. Why, when, how? [BTN-95-EIX95112523809] p 194 A95-69324
- Dynamical instability of the aerogravity assist maneuver [BTN-95-EIX95152583262] p 298 A95-73583
- Multi-axis pilot ratings for damaged aircraft [BTN-95-EIX95182619128] p 269 A95-76605
- Solutions of generalized proportional navigation with maneuvering and nonmaneuvering targets [BTN-95-EIX95202637606] p 279 A95-76683
- Determination of piloting feedback structures for an altitude tracking task [BTN-95-EIX95242670770] p 327 A95-81077
- Rotorcraft handling qualities in turbulence [BTN-95-EIX95242670750] p 334 A95-81097
- Robust dynamic inversion for control of highly maneuverable aircraft [BTN-95-EIX95242670747] p 359 A95-81100
- Computation of delta-wing roll maneuvers [BTN-95-EIX0619952748164] p 605 A95-94458
- Optimal trajectories for an unmanned air-vehicle in the horizontal plane [BTN-95-EIX0619952748191] p 606 A95-94480
- Impact of agility requirements on configuration synthesis [NASA-CR-4627] p 44 N95-11952
- Parameter identification for X-31A at high angles of attack p 69 N95-14235
- Vista/F-16 Multi-Axis Thrust Vectoring (MATV) control law design and evaluation p 71 N95-14248
- Airfoil modification effects on subsonic and transonic pressure distributions and performance for the EA-6B airplane [NASA-TP-3516] p 373 N95-26382
- Dynamic inversion: An evolving methodology for flight control design p 621 N95-31996
- X-31: A program overview and flight test status p 609 N95-32013
- MANEUVERS**
- A generalized algorithm for inverse simulation applied to helicopter maneuvering flight [HTN-95-A0493] p 236 A95-72564
- Symmetric steady manoeuvre loads on rigid aircraft of classical configuration at subsonic speeds [ESDU-94009] p 43 N95-11774
- Aircraft maneuver envelope warning system [NASA-CASE-ARC-11953-1] p 82 N95-14518
- Full span flaperons for a biplane p 391 N95-26954
- Synthetic Terrain Imagery for Helmet-Mounted Display, volume 1 [AD-A293612] p 612 N95-31656
- MANIFOLDS**
- Aerodynamic design and analysis of a highly loaded turbine exhaust p 312 N95-23435
- Phase 2: HGM air flow tests in support of HEX vane investigation p 312 N95-23438
- MANIPULATORS**
- Measurement of drag using a momentum balance [HTN-95-01090] p 468 A95-90276
- Plate manipulators [AD-A289601] p 374 N95-26719
- Survey and implementation of commercial manual controllers for a generic telerobotics architecture [AD-A289215] p 449 N95-26990
- MANNED SPACE FLIGHT**
- Virtual environment application with partial gravity simulation p 169 N95-15988
- NASA video catalog [NASA-SP-7109(01)] p 363 N95-24238
- Aeronautics and space report of the President [NASA-TM-110743] p 681 N95-31979
- MANUALS**
- NASA Lewis Propulsion Systems Laboratory customer guide manual [NASA-TM-106569] p 21 N95-10822
- Enhanced capabilities and updated users manual for axial-flow turbine preliminary sizing code TURBAN [NASA-CR-195405] p 76 N95-15912
- Rationale for the Modular Air-system Vulnerability Estimation Network (MAVEN) methodology [AD-A265797] p 284 N95-22510
- MANUFACTURING**
- Automatic riveting cell for commercial aircraft floor grid assembly [BTN-95-EIX95182617807] p 261 A95-75752
- International cooperation in standardization p 452 A95-82665
- A new paradigm: The investment casting cooperative arrangement [HTN-95-92510] p 539 A95-87330
- Simultaneous engineering in aero gas turbine design and manufacture [CONGRESS PAPER C428-20-204] p 581 A95-91723
- Lean manufacturing for lean times [BTN-95-EIX95302730538] p 583 A95-94036
- European aeronautics: Strong government presence in industry structure and research and development support. Report to Congressional Requesters [GAO/NSIAD-94-71] p 176 N95-18578
- High density monolithic packaging technology for digital/microwave avionics p 240 N95-20646
- Design of a high altitude long endurance aircraft with manufacturing considerations p 391 N95-26947
- Process and control systems for composites manufacturing p 420 N95-28267
- ACT/ICAPS: Thermoplastic composite activities p 421 N95-28274
- Composite intermediate case manufacturing scale-up for advanced engines p 406 N95-28275
- Composite fuselage crown panel manufacturing technology p 399 N95-28474
- Third NASA Advanced Composites Technology Conference, volume 1, part 2 [NASA-CP-3178-VOL-1-PT-2] p 531 N95-28823
- Manufacturing scale-up of composite fuselage crown panels p 532 N95-28835
- Advanced composite fuselage technology p 535 N95-29034
- Progress in manufacturing large primary aircraft structures using the stitching/RTM process p 537 N95-29050
- MANY BODY PROBLEM**
- Unsteady panel method for flows with multiple bodies moving along various paths [HTN-95-61203] p 540 A95-87576
- MAP MATCHING GUIDANCE**
- Simulation development of a forward sensor-enhanced low-altitude guidance system [HTN-94-00688] p 17 A95-60170
- MAPPING**
- Data processing and mapping in airborne radiometric surveys [HTN-95-51587] p 442 A95-83591
- Mapping of forest fire damages using imaging spectroscopy p 442 A95-83627
- In-flight interior sound field mapping in propeller aircraft p 572 A95-88472
- MAPS**
- Automation technology using Geographic Information System (GIS) p 324 N95-23284
- MARANGONI CONVECTION**
- Marangoni-Benard convection in a low-aspect-ratio liquid layer p 56 A95-61544
- MARINE ENVIRONMENTS**
- Aircraft icing measurements in East Coast winter storms [HTN-95-60505] p 214 A95-68756
- Potential applications of the SSM/I cloud liquid water parameter to the estimation of marine aircraft icing [HTN-95-80651] p 254 A95-72495
- An intercomparison of instrumentation for tropospheric measurements of dimethyl sulfide: Aircraft results for concentrations at the parts-per-trillion level [HTN-95-91857] p 355 A95-80845
- The effect of aircraft speed on the penetration of sonic boom noise into a flat ocean p 100 N95-14887
- Transport phenomena and interfacial kinetics in multiphase combustion systems [AD-A288297] p 418 N95-26417
- Benefits and limitations of composites in carrier-based aircraft p 422 N95-28422
- MARINE METEOROLOGY**
- Research aircraft observations of a polar low at the east Greenland ice edge [HTN-95-A0175] p 215 A95-69766
- Microphysical and radiative properties of small cumulus clouds over the sea [HTN-95-A0526] p 255 A95-73180
- On the link between cloud-top radiative properties and sub-cloud aerosol concentrations [HTN-95-A0527] p 255 A95-73181
- MARINE PROPULSION**
- Simulation investigation on system identification of gas turbine [PB95-104238] p 139 N95-17749
- MARINE TECHNOLOGY**
- JTEC/WTEC annual report and program summary: 1993/94 [NASA-CR-198563] p 454 N95-28038
- MARINE TRANSPORTATION**
- Results and performance of multi-site reference station differential GPS [BTN-95-EIX95112522534] p 190 A95-69329
- MARINER MARK 2 SPACECRAFT**
- The Cassini spacecraft: Object oriented flight control software p 359 A95-80405
- MARITIME SATELLITES**
- Development of aeronautical mobile satellite services over the past thirty years [BTN-95-EIX95152569458] p 305 A95-73498
- MARKET RESEARCH**
- A market perspective on FANS [SAE PAPER 932521] p 486 A95-89189

Quality optimization of thermally sprayed coatings produced by the JP-5000 (HVOF) gun using mathematical modeling p 152 N95-19008

The airline quality report, 1994 [NIAR-94-11] p 277 N95-24012

MARKOV PROCESSES

Analysis and modeling of an airport departure process [AD-A293782] p 602 N95-31581

MARS (PLANET)

Fourth-generation Mars vehicle concepts [BTN-95-EIX95152583267] p 298 A95-73568

MARS EXPLORATION

Fourth-generation Mars vehicle concepts [BTN-95-EIX95152583267] p 298 A95-73568

MARS PROBES

Thermochemical nonequilibrium viscous shock-layer analysis for a Mars aerocapture vehicle [BTN-95-EIX95082502732] p 239 A95-70139

MARS SURFACE

Virtual environment application with partial gravity simulation p 169 N95-15988

MARYLAND

The NASA-sponsored Maryland center for hypersonic education and research [AIAA PAPER 95-6105] p 519 A95-88010

MASS

Effects of mass on aircraft sidearm controller characteristics [NASA-TM-104277] p 51 N95-11868

MASS BALANCE

The analysis of the processing increased weight for pilot production of F-X aircraft [HTN-95-71133] p 385 A95-83494

MASS FLOW

Simulating heat addition via mass addition in constant area compressible flows [BTN-95-EIX95182619100] p 307 A95-76585

Adaptive-wall wind-tunnel research at Ames Research Center: A retrospective p 519 A95-88902

A full Navier-Stokes analysis of subsonic diffuser of a bifurcated 70/30 supersonic inlet for high speed civil transport application [NASA-TM-106637] p 8 N95-10820

Comparison of full-scale, small-scale, and CFD results for F/A-18 forebody slot blowing p 72 N95-14255

Simulation of multidisciplinary problems for the thermostress state of cooled high temperature turbines p 140 N95-19021

Leading edge film cooling effects on turbine blade heat transfer [NASA-TM-106955] p 513 N95-29115

MASS FLOW RATE

Characterization of a hot-film probe for hypersonic flow [AIAA PAPER 95-6110] p 511 A95-90440

Condensation in jet engine intake ducts during stationary operation [BTN-95-EIX95292721154] p 612 A95-92590

MASS SPECTROMETERS

Time-of-flight mass spectrometer for impulse facilities [BTN-95-EIX95142553057] p 262 A95-73441

MASS TRANSFER

Passive porosity with free and fixed separation on a tangent-ogive forebody [BTN-95-EIX95062487554] p 185 A95-68368

Simulating heat addition via mass addition in constant area compressible flows [BTN-95-EIX95182619100] p 307 A95-76585

High-speed reacting flow simulation using USA-series codes p 540 A95-87559

A study of aircraft post-crash fuel fire mitigation [AD-A282208] p 40 N95-12499

Hailstone heat and mass transfer measurements [ISBN-0-315-86304-8] p 563 N95-29797

MASSIVELY PARALLEL PROCESSORS

Implicit multiblock Euler and Navier-Stokes calculations [HTN-95-A1755] p 634 A95-93318

Steady and unsteady three-dimensional transonic flow computations by integral equation method [NASA-CR-196777] p 10 N95-11582

Portable parallel stochastic optimization for the design of aeropropulsion components [NASA-CR-195312] p 154 N95-16072

MATCHING

Orientation determination of aircraft using visual 3D matching and radar. Case study 2 [PB95-165791] p 350 N95-25749

MATERIALS HANDLING

Measurement of particle emissions from clean room gas-handling components [BTN-94-EIX94381359040] p 295 A95-74554

MATERIALS SCIENCE

JPRS report: Science and technology. Central Eurasia [JPRS-UST-94-018] p 349 N95-24472

JPRS report: Science and technology. Central Eurasia [JPRS-UST-94-022] p 438 N95-27699

MATERIALS TESTS

Study on the turbine vane and blade for a 1500 C class industrial gas turbine [BTN-94-EIX95011441254] p 431 A95-84211

Test model designs for advanced refractory ceramic materials p 55 N95-11968

Regenerative cooling for liquid propellant rocket thrust chambers [INPE-5565-TDI/540] p 150 N95-18720

Proof test methodology for composites p 424 N95-28445

Impact damage resistance of composite fuselage structure, part 1 p 399 N95-28482

NASA-ACEE/Boeing 737 graphite-epoxy horizontal stabilizer service p 400 N95-28489

Thermally stable organic polymers [AD-A290755] p 537 N95-29482

The effect of wear on fire-blocking layer material effectiveness [AD-A291520] p 485 N95-29855

MATHEMATICAL LOGIC

Application of fuzzy logic to optimize placement of an acquisition, tracking, and pointing experiment p 341 A95-80390

Digital systems validation. Chapter 20 Artificial Intelligence with applications for aircraft. Handbook, volume 2 [AD-A288492] p 448 N95-26638

MATHEMATICAL MODELS

On calculated models for impellers of centrifugal compressors [BTN-94-EIX94461407947] p 88 A95-62265

Mathematical modelling concerning the development of a system of similar installations, taking into account their operational intensity (an aircraft-helicopter fleet taken as an example) [BTN-94-EIX94461408763] p 103 A95-63646

On the dynamics of aeroelastic oscillators with one degree of freedom [BTN-94-EIX94501431527] p 153 A95-64524

Nonsmooth trajectory optimization: An approach using continuous simulated annealing [BTN-94-EIX94511433914] p 168 A95-64580

H^(sup 2)/H^(sup INF) controller design for a two-dimensional thin airfoil flutter suppression [BTN-94-EIX94511433918] p 141 A95-64584

Test bench for rotorcraft hover control [BTN-94-EIX94511433919] p 169 A95-64585

Aircraft model for the AIAA controls design challenge [BTN-94-EIX94511433921] p 142 A95-64587

Phenomenological description and simplified modelling of the vortex wake issuing from a jet in a crossflow [BTN-94-EIX94441385754] p 184 A95-68218

Brief history of gust models for aircraft design [BTN-95-EIX95062487557] p 203 A95-68371

Numerical simulation of steady and unsteady, vorticity-dominated aerodynamic interference [BTN-94-EIX95062487524] p 186 A95-69232

State-space representation of aerodynamic characteristics of an aircraft at high angles of attack [BTN-95-EIX95062487536] p 187 A95-69244

Adaptive modeling of jet engine performance with application to condition monitoring [BTN-95-EIX95112524205] p 196 A95-69303

Ascent wind model for launch vehicle design [BTN-95-EIX95041503799] p 239 A95-70124

Modeling resonance in waveguide-to-microstrip junctions by unilateral fin line resonators [BTN-94-EIX94381323445] p 242 A95-70844

Numerical modelling of transverse impact on composite coupons [BTN-95-EIX95082502225] p 240 A95-71022

Modelling of pillowing due to corrosion in fuselage lap joints [BTN-95-EIX95082502227] p 240 A95-71024

Measurement and analysis of nitric oxide radiation in an arcjet flow [BTN-95-EIX95082502727] p 243 A95-71040

Secondary source locations in active noise control: Selection or optimization? [BTN-94-EIX94381352222] p 257 A95-71738

Large-scale computational fluid dynamics by the finite element method [BTN-94-EIX94381359154] p 243 A95-71744

High-order state space simulation models of helicopter flight mechanics [HTN-95-A0494] p 237 A95-72565

Microphysical and radiative properties of small cumulus clouds over the sea [HTN-95-A0526] p 255 A95-73180

On the exact solutions of pseudorange equations [BTN-95-EIX95142555477] p 278 A95-73433

Mechanical system reliability and risk assessment [BTN-95-EIX95142553046] p 304 A95-73452

Simulation of turbulent fluctuations [BTN-95-EIX95142553041] p 304 A95-73457

Effects of expansions on a supersonic boundary layer: Surface pressure measurements [BTN-95-EIX95142553036] p 263 A95-73462

Aerodynamic shape optimization using preconditioned conjugate gradient methods [BTN-95-EIX95142553033] p 263 A95-73465

Analytical study of the neutral stability of a model hypersonic boundary layer [BTN-95-EIX95152577589] p 263 A95-73493

Efficient sensitivity analysis for rotary-wing aeromechanical problems [BTN-95-EIX95152577585] p 264 A95-73497

Limit cycle phenomena in computational transonic aeroelasticity [BTN-95-EIX95152582317] p 264 A95-73520

Hypersonic rarefied flow past spheres including wake structure [BTN-95-EIX95152583250] p 305 A95-73551

Aerodynamic characteristics of a hypersonic viscous optimized waverider at high altitudes [BTN-95-EIX95152583251] p 266 A95-73552

Hypersonic nonequilibrium Navier-Stokes solutions over an ablating graphite nose tip [BTN-95-EIX95152583252] p 305 A95-73553

Hypersonic convective heat transfer over 140-deg blunt cones in different gases [BTN-95-EIX95152583253] p 306 A95-73554

Application of the multigrid solution technique to hypersonic entry vehicles [BTN-95-EIX95152583254] p 306 A95-73555

Higher-order viscous shock-layer solutions for high-altitude flows [BTN-95-EIX95152583255] p 306 A95-73556

Base drag prediction on missile configurations [BTN-95-EIX95152583256] p 266 A95-73557

Aerodynamic characteristics of a canard-controlled missile at high angles of attack [BTN-95-EIX95152583257] p 267 A95-73558

Predicting exhaust plume boundaries with supersonic external flows [BTN-95-EIX95152583258] p 297 A95-73559

Three-dimensional structure of a supersonic jet impinging on an inclined plate [BTN-95-EIX95152583259] p 267 A95-73560

Functional dependence of trajectory dispersion on initial condition errors [BTN-95-EIX95152583263] p 298 A95-73564

Thermal force modeling for global positioning system satellites using the finite element method [BTN-95-EIX95152583270] p 278 A95-73571

Supersonic axisymmetric conical flow solutions for different ratios of specific heats [BTN-95-EIX95152583283] p 306 A95-73584

Improving prediction: The incorporation of simplified rotor dynamics in a mathematical model of the bell 412HP [BTN-95-EIX95152584679] p 282 A95-73591

Finite element model for a flexible non-symmetric rotor on distributed bearing: A stability study [BTN-94-EIX94381352212] p 306 A95-74612

Flutter of an infinitely long panel in a duct [BTN-95-EIX95182619087] p 291 A95-75772

Observations on using experimental data as boundary conditions for computations [BTN-95-EIX95182619103] p 321 A95-76588

Aeroelastic vehicle multivariable control synthesis with analytical robustness evaluation [BTN-95-EIX95182619115] p 321 A95-76592

Analytical aeropropulsive/aeroelastic hypersonic-vehicle model with dynamic analysis [BTN-95-EIX95182619138] p 269 A95-76615

Drag function modeling for air traffic simulation [BTN-95-EIX95182619154] p 279 A95-76631

Application of transonic small disturbance theory to the active flexible wing model [BTN-95-EIX95182619210] p 270 A95-76636

Simulation and model reduction for the active flexible wing program [BTN-95-EIX95182619211] p 295 A95-76637

Erosion of dust-filtered helicopter turbine engines. Part 1: Basic theoretical considerations [BTN-95-EIX95182619222] p 288 A95-76648

Stability derivatives of a flapped plate in unsteady ground effect [BTN-95-EIX95182619225] p 270 A95-76651

Response of a nonrotating rotor blade to lateral turbulence. Part 1: Theory [BTN-95-EIX95182619228] p 284 A95-76654

Response of a nonrotating rotor blade to lateral turbulence. Part 2: Experiment [BTN-95-EIX95182619229] p 284 A95-76655

Aerodynamic characteristics of external store configurations at low speeds [BTN-95-EIX95182619230] p 271 A95-76656

- Neural network prediction of three-dimensional unsteady separated flowfields
[BTN-95-EIX95182619232] p 308 A95-76658
- Unsteady ground effects on aerodynamic coefficients of finite wings with camber
[BTN-95-EIX95182619233] p 271 A95-76659
- CFD optimization of a theoretical minimum-drag body
[BTN-95-EIX95182619234] p 308 A95-76660
- A comparison of some aerodynamic resistance methods using measurements over cotton and grass from the 1991 California ozone deposition experiment
[HTN-95-11295] p 319 A95-77000
- Viscoplastic response of structures for intense local heating
[HTN-95-41540] p 346 A95-77921
- Theoretical and experimental studies of fretting-initiated fatigue failure of aeroengine compressor discs
[BTN-94-EIX94421372285] p 343 A95-78467
- Modeling of aircraft exhaust emissions and infrared spectra for remote measurement of nitrogen oxides
[HTN-95-51276] p 355 A95-80861
- Chemical composition and photochemical reactivity of exhaust from aircraft turbine engines
[HTN-95-51277] p 356 A95-80862
- Impact of near-coincident faults on digital flight control systems
[BTN-95-EIX95242670759] p 359 A95-81088
- Nonlinear decoupling control study for aircraft maneuvering flight
[HTN-95-71130] p 408 A95-83491
- Flying qualities development and flight simulation evaluation of the TW-68 tilt-wing VTOL aircraft
[SAE PAPER 932517] p 386 A95-84555
- Assessment of cost and training effectiveness for a candidate training system using the Comparison-Based Prediction model
[SAE PAPER 932598] p 379 A95-84570
- A model for temperature-dependent collisional quenching of OH A(sup 2) Sigma(sup +)
[HTN-95-42308] p 450 A95-85002
- Artificial neural networks for predicting nonlinear dynamic helicopter loads
[HTN-95-51678] p 404 A95-85060
- Matrix fraction approach for finite-state aerodynamic modeling
[BTN-95-EIX95262694311] p 365 A95-85482
- Variational principles for ascent shapes of large scientific balloons
[BTN-95-EIX95262694320] p 387 A95-85491
- Equivalent beam-column analysis of guyed towers
[BTN-95-EIX95262696644] p 435 A95-85519
- Stochastic approach to noise modeling for free turbulent flows
[HTN-95-42321] p 371 A95-86150
- Reduction of blade-vortex interaction noise through porous leading edge
[HTN-95-42324] p 371 A95-86153
- Nonreflective boundary conditions for high-order methods
[HTN-95-42328] p 371 A95-86157
- Numerical modeling and simulation of chemically reacting reentry flows
p 525 A95-87387
- Optimal separation and ascent of lifting upper stages
p 525 A95-87396
- Thrust modeling for hypersonic engines
[AIAA PAPER 95-6081] p 509 A95-87410
- Modeling lateral attenuation of aircraft flight noise
p 570 A95-88464
- Factors affecting measured aircraft sound levels in the vicinity of start-of-takeoff roll
p 571 A95-88465
- A prediction model for noise from low-altitude military aircraft
p 571 A95-88466
- Meteorological impacts on airport noise prediction by the 'Integrated Noise Model' application based on Hamiltonian Ray-Tracing program and measurements
p 571 A95-88467
- Development and validation of a numerical acoustic analysis program for aircraft interior noise prediction
p 572 A95-88471
- Response of a thin airfoil encountering a strong density discontinuity
p 462 A95-88900
- Nonlinear analysis of the Gortler instability
[BTN-95-EIX95282705926] p 455 A95-89664
- Boundary element analysis of the acoustic field inside three-dimensional regular and irregular ducts
p 573 A95-90097
- Enroute NASA/FAA low-frequency propfan test in Alabama (October 1987): A versatile atmospheric aircraft long-range noise prediction system
p 573 A95-90099
- Progressive wave equations and algorithms for sonic boom propagation
p 575 A95-90104
- A total variation diminishing finite difference algorithm for sonic boom propagation models
p 575 A95-90105
- A review of Air Force policy and noise models pertaining to the noise environment under low-altitude, high-speed training areas
p 561 A95-90118
- ASTRYD: A new numerical tool for aircraft cabin and environmental noise prediction
p 576 A95-90129
- Application of FEM/SEA for prediction of aircraft cockpit noise
p 576 A95-90130
- Incorporation of topography effects in aircraft noise modeling
p 578 A95-90140
- Technology-insertion life-cycle-cost model
[AIAA PAPER 95-0961] p 581 A95-90638
- Implicit multi-domain method for unsteady compressible inviscid fluid flows around 3D projectiles
p 548 A95-91482
- The use of math-dynamic models to aid the development of integrated health and usage monitoring systems
[CONGRESS PAPER C428-19-079] p 457 A95-91720
- Discrete crack growth analysis methodology for through cracks in pressurized fuselage structures
[BTN-95-EIX0608952737538] p 633 A95-92751
- Static shape control for adaptive wings
[HTN-95-A1767] p 627 A95-93330
- Modelling 2D separation from a high lift aerofoil with a non-linear eddy-viscosity model and second-moment closure
[HTN-95-C0005] p 585 A95-93393
- Examination of conditions in the proximity of pilot reports of aircraft icing during storm-fest
p 666 A95-93509
- Nortat: Computer generated aerodrome forecasts
p 668 A95-93521
- The combination of forecasts in an automated aviation weather forecasting system
p 669 A95-93522
- Weather products for aviation from WAFIC Bracknell
p 670 A95-93527
- Creating a global climatology of freezing rain using numerical model output
p 673 A95-93541
- An application of some cloud modeling techniques to a regional model simulation of an icing event
p 673 A95-93543
- Modelling and analysis of a dual-wheel nosegear: Shimmy instability and impact motions
[SAE PAPER 931402] p 605 A95-93672
- GPS modeling for designing aerospace vehicle navigation systems
[BTN-95-EIX95302731223] p 600 A95-94044
- Modeling and analysis for the GPS pseudo-range observable
[BTN-95-EIX95302731227] p 600 A95-94046
- Application of integral methods to ablation charring erosion, a review
[BTN-95-EIX95302694460] p 636 A95-94057
- Numerical investigation of high incidence flow over a double-delta wing
[BTN-95-EIX0619952748160] p 588 A95-94454
- Analysis of some interference effects in a transonic wind tunnel
[BTN-95-EIX0619952748166] p 589 A95-94460
- Turbulent effects on parachute drag
[BTN-95-EIX0619952748193] p 591 A95-94482
- Estimation of supersonic leading-edge thrust by a Euler flow model
[BTN-95-EIX0619952748194] p 591 A95-94483
- Effects of the chemical reaction model on calculations of supersonic combustion flows
[BTN-95-EIX0616952745802] p 638 A95-94487
- Evaluation of the transient operation of advanced gas turbine combustors
[BTN-95-EIX0616952745793] p 614 A95-94495
- Neuro-controllers for adaptive helicopter hover training
[BTN-94-EIX94522407592] p 709 A95-96241
- Modal parameters for cracked rotors: models and comparisons
[BTN-94-EIX94522410226] p 702 A95-96378
- Modelling wear at intermittently slipping high speed interfaces
[BTN-94-EIX94511433698] p 701 A95-96655
- High performance parallel analysis of coupled problems for aircraft propulsion
[NASA-CR-195355] p 23 N95-10132
- Modeling improvements and users manual for axial-flow turbine off-design computer code AXOD
[NASA-CR-195370] p 8 N95-10853
- Plastic hinge modeling of structures
[NIAR-94-14] p 24 N95-11168
- Empirical refinements to boundary layer transition noise models
p 28 N95-11262
- Integrating NOISEMAP with the Geographic Resource Analysis Support System (GRASS) to enhance environmental impact assessments and land use compatibility studies
p 31 N95-11311
- INM contour validation: A case study
p 31 N95-11321
- Parallel methods for the flight simulation model
[DE94-013330] p 52 N95-11752
- Determining the accuracy of maximum likelihood parameter estimates with colored residuals
[NASA-CR-194893] p 51 N95-11869
- A simple analytical aerodynamic model of Langley Winged-Cone Aerospace Plane concept
[NASA-CR-194987] p 54 N95-12175
- Numerical time dependent sheet cavitation simulations using a higher order panel method
[PB94-204435] p 59 N95-13249
- Studies on the flow induced by an oscillating airfoil in a uniform stream
[PB94-204450] p 40 N95-13250
- Numerical modeling of a cryogenic fluid within a fuel tank
[NASA-TM-4651] p 89 N95-13892
- Unsteady flows in turbines: Impact on design procedure
p 90 N95-14132
- Add a dimension to your analysis of the helicopter low airspeed environment
[AD-A283982] p 79 N95-14205
- Numerical simulation of the flow about an F-18 aircraft in the high-alpha regime
p 68 N95-14232
- Validation of the NASA Dryden X-31 simulation and evaluation of mechanization techniques
p 69 N95-14236
- Higher harmonic control analysis for vibration reduction of helicopter rotor systems
[NASA-TM-103855] p 66 N95-14419
- FAA/NASA International Symposium on Advanced Structural Integrity Methods for Airframe Durability and Damage Tolerance
[NASA-CP-3274-PT-1] p 92 N95-14453
- Elastic-plastic models for multi-site damage
p 92 N95-14454
- Bending effects of unsymmetric adhesively bonded composite repairs on cracked aluminum panels
p 92 N95-14456
- The role of fretting corrosion and fretting fatigue in aircraft rivet hole cracking
p 94 N95-14470
- Development of a composite repair and the associated inspection intervals for the F-111C stiffener runout region
p 66 N95-14477
- Axial crack propagation and arrest in pressurized fuselage
p 94 N95-14479
- Fracture mechanics validity limits
p 95 N95-14480
- Noise radiation by instability waves in coaxial jets
[NASA-TM-106738] p 100 N95-14618
- USAF single-event sonic boom prediction model: PCBoom3
p 101 N95-14889
- Joint Proceedings on Aeronautics and Astronautics (JPAA)
[ISBN-7-80-046602-7] p 104 N95-16249
- An investigation of polynomial calibrations methods for wind tunnel balances
p 144 N95-16258
- Evaluation of the dynamic stability characteristics of the NAL Light Transport Aircraft
[NAL-PD-CA-9217] p 142 N95-16392
- Numerical simulation of helicopter engine plume in forward flight
[NASA-CR-197488] p 107 N95-16589
- Algorithms for bilevel optimization
[NASA-CR-194980] p 170 N95-16897
- Evaluation of an autopilot based multimodelling
[PB94-190725] p 142 N95-17454
- Demonstration of the Dynamic Flowgraph Methodology using the Titan 2 Space Launch Vehicle Digital Flight Control System
[NASA-CR-197517] p 150 N95-17493
- Numerical mixing calculations of confined reacting jet flows in a cylindrical duct
[NASA-TM-106736] p 139 N95-18133
- Compression strength of composite primary structural components
[NASA-CR-197554] p 160 N95-18388
- Aeromechanics technology, volume 1. Task 1: Three-dimensional Euler/Navier-Stokes Aerodynamic Method (TEAM) enhancements
[AD-A285713] p 132 N95-18483
- Minimal time detection algorithms and applications to flight systems
[TR-2-FSRC-93] p 171 N95-18564
- The impact of non-linear flight control systems on the prediction of aircraft loads due to turbulence
p 143 N95-18598
- Regenerative cooling for liquid propellant rocket thrust chambers
[INPE-5565-TDI/540] p 150 N95-18720
- A linear system identification and validation of an AH-64 Apache aeroelastic simulation model
p 146 N95-18903
- Mathematical Models of Gas Turbine Engines and their Components
[AGARD-LS-198] p 139 N95-19017
- The mathematical models of flow passage for gas turbine engines and their components
p 140 N95-19020
- Simulation of multidisciplinary problems for the thermostress state of cooled high temperature turbines
p 140 N95-19021

Application of multicomponent models to flow passage simulation in multistage turbomachines and whole gas turbine engines p 140 N95-19022

Application of multidisciplinary models to the cooled turbine rotor design p 140 N95-19024

Unsteady aerodynamic analyses for turbomachinery aeroelastic predictions p 141 N95-19381

Forced response of mistuned bladed disks p 141 N95-19383

Prediction of fatigue crack growth under flight-simulation loading with the modified CORPUS model p 166 N95-19471

Discrete crack growth analysis methodology for through cracks in pressurized fuselage structures p 166 N95-19473

Particle trajectories in gas turbine engines p 199 N95-19663

The calculation of erosion in a gas turbine compressor rotor p 199 N95-19664

Design of fan blades subjected to bird impact p 200 N95-19669

Soft body impact on titanium fan blades p 200 N95-19671

Ice-impact analysis of blades p 200 N95-19672

Damage of high temperature components by dust-laden air p 201 N95-19673

On supersonic-inlet boundary-layer bleed flow [NASA-CR-195426] p 202 N95-19769

Computing methods for the approximate solution of time dependent problems [AD-A286007] p 256 N95-20719

Scale-up and modeling of forced chemical vapor infiltration [DE94-017769] p 247 N95-20781

Effects of yaw and pitch motion on model attitude measurements [NASA-TM-4641] p 250 N95-22109

Direct numerical simulations of on-demand vortex generators: Mathematical formulation p 251 N95-22452

Particle kinetic simulation of high altitude hypervelocity flight [NASA-CR-197383] p 309 N95-22481

Modeling aerosol emissions from the combustion of composite materials p 301 N95-23038

Supersonic jet noise reductions predicted with increased jet spreading rate [NASA-TM-106872] p 323 N95-23178

Development and verification of a resin film infusion/resin transfer molding simulation model for fabrication of advanced textile composites [NASA-CR-197439] p 301 N95-23179

An approximate theoretical method for modeling the static thrust performance of non-axisymmetric two-dimensional convergent-divergent nozzles [NASA-CR-195050] p 273 N95-23193

An investigation of helicopter dynamic coupling using an analytical model [NASA-CR-197420] p 285 N95-23217

Idealized textile composites for experimental/analytical correlation p 301 N95-23277

Inner loop flight control for the High-Speed Civil Transport p 293 N95-23314

Preparation of course materials: Elementary mathematics of powered flight p 324 N95-23320

Aerodynamic design and analysis of a highly loaded turbine exhaust p 312 N95-23435

Phase 2: HGM air flow tests in support of HEX vane investigation p 312 N95-23438

Moving mass trim control for aerospace vehicles [DE95-002602] p 299 N95-23532

Assimilation of altimeter data in a quasi-geostrophic model of the Gulf Stream system: A dynamical perspective [NASA-CR-196313] p 320 N95-23766

Statistics of multi-look AIRSAR imagery: A comparison of theory with measurements p 320 N95-23947

A multibody/finite element analysis approach for modeling of crash dynamic responses [NIAR-94-3] p 277 N95-24050

Effect of density gradients in confined supersonic shear layers, part 1 [NASA-CR-198029] p 348 N95-24412

Effect of density gradients in confined supersonic shear layers, Part 2: 3-D modes [NASA-CR-198030] p 349 N95-24413

Aerodynamic parameter estimation via Fourier modulating function techniques [NASA-CR-4654] p 335 N95-24630

Recent improvements to and validation of the one dimensional NASA wave rotor model [NASA-TM-106913] p 332 N95-25962

Thermal barrier coating life modeling in aircraft gas turbine engines p 346 N95-26140

Aerodynamics model for a generic ASTOVL lift-fan aircraft [NASA-TM-110347] p 332 N95-26302

Simulation model of the integrated flight/propulsion control system, displays, and propulsion system for ASTOVL lift-fan aircraft [NASA-TM-108866] p 405 N95-26412

Development of a nonlinear simulation for the McDonnell Douglas F-15 Eagle with a longitudinal TECS control-law [AD-A288610] p 388 N95-26481

The 1994 updated National Airspace System performance assessment for year 2005 [AD-A288652] p 380 N95-26485

Development and validation of a blade-element mathematical model for the AH-64A Apache helicopter [NASA-TM-108863] p 367 N95-26710

Numerical investigation to S-inlet flows (Numerical simulation study of S-inlet flows) [AD-A289590] p 374 N95-26713

Numerical simulation of the flow about the F-18 HARV at high angle of attack [NASA-CR-197755] p 374 N95-26735

Photoacoustic chambers for studying solids and gases: Theory and practical examples [IFTR-39/1994] p 412 N95-26837

A numerical model to predict the fate of jettisoned aviation fuel [AD-A289336] p 419 N95-26842

A gain scheduling optimization method using genetic algorithms [AD-A289306] p 448 N95-26920

Aircraft nosewheel steering simulation p 412 N95-26944

Implementation and demonstration of a multiple model adaptive estimation failure detection system for the F-16 [AD-A289301] p 391 N95-27042

Probabilistic material strength degradation model for Inconel 718 components subjected to high temperature, high-cycle and low-cycle mechanical fatigue, creep and thermal fatigue effects [NASA-CR-197832] p 419 N95-27167

A verification procedure for MSC/NASTRAN Finite Element Models [NASA-CR-4675] p 392 N95-27371

Fight Mechanics/Estimation Theory Symposium 1995 [NASA-CP-3299] p 416 N95-27763

Vibration analysis of a split path gearbox [NASA-TM-106875] p 438 N95-27855

Load transfer in the stiffener-to-skin joints of a pressurized fuselage [NASA-CR-198610] p 439 N95-27865

Precision landing system mathematical modeling study report for Andrews Air Force Base, runway 19L, Camp Springs, MD [AD-A289015] p 384 N95-27903

Collected papers on wind turbine technology [NASA-CR-195432] p 447 N95-27970

Preliminary analysis of dynamic stall effects on a 91-meter wind turbine rotor p 376 N95-27975

Comparative wind tunnel tests of NACA 23024 airfoils with several aileron and spoiler configurations p 376 N95-27976

Comparative performance tests on the Mod-2, 2.5-mW wind turbine with and without vortex generators p 377 N95-27978

Design of a real-time wind turbine simulator using a custom parallel architecture p 449 N95-27979

Aeroelastic stability of wind turbine blade/aileron systems p 377 N95-27981

Whirl plus tilt [DE95-007948] p 452 N95-28108

Operator modeling in commercial aviation: Cognitive models, intelligent displays, and pilot's assistants [NASA-CR-198609] p 401 N95-28203

Aeroelasticity and structural optimization of composite helicopter rotor blades with swept tips [NASA-CR-4665] p 397 N95-28262

Analysis of aircraft engine blade subject to ice impact p 407 N95-28277

Structural design optimization with survivability dependent constraints application: Primary wing box of a multi-role fighter p 398 N95-28440

Proof test methodology for composites p 424 N95-28445

Designers' unified cost model p 424 N95-28464

Local design optimization for composite transport fuselage crown panels p 398 N95-28473

Nonlinear dynamics and aeroelasticity of rotorcraft in forward flight [AD-A291714] p 400 N95-28504

Development of a TECS control-law for the lateral directional axis of the McDonnell Douglas F-15 Eagle [AD-A289771] p 410 N95-28598

Ejectors and jet pumps: Computer program for design and performance for steam/gas flow [ESDU-94046] p 500 N95-28704

Effects of small changes on rate of climb [ESDU-94039] p 501 N95-28707

Influence of turbulence parameters, Reynolds number, and body shape on stagnation-region heat transfer [NASA-TP-3487] p 550 N95-28719

Rapid Airplane Parametric Input Design (RAPID) p 501 N95-28730

Surface modeling and grid generation for aeropropulsion CFD p 551 N95-28732

Automatic blocking for complex three-dimensional configurations p 566 N95-28734

Automatic multi-block grid generation for high-lift configuration wings p 567 N95-28764

A global/local analysis method for treating details in structural design p 552 N95-28848

Cost model relationships between textile manufacturing processes and design details for transport fuselage elements p 536 N95-29043

A numerical method for modelling wings with sharp edges maneuvering at high angles of attack p 503 N95-29122

Users manual for the improved NASA Lewis ice accretion code LEWICE 1.6 [NASA-CR-198355] p 485 N95-29132

Application of optimization technique to control system design for departure prevention and aircraft model estimation through dynamic inversion p 517 N95-29156

A fourth order Euler/Navier-Stokes prediction method for the aerodynamics and aeroelasticity of hovering rotor blades p 554 N95-29242

Modeling and control of rotating stall in high speed multi-stage axial compressors p 513 N95-29244

Linear and nonlinear discrete-time state-space modeling of dynamic systems for control applications p 567 N95-29251

Acoustic scattering from ellipses by the modal element method [NASA-TM-106935] p 579 N95-29401

Modeling spatio-temporal databases to measure the performance of the GPS satellite constellation p 489 N95-29596

An analytic modeling and system identification study of helicopter dynamics p 505 N95-29787

Manual for a workstation-based generic flight simulation program (LaRCsim), version 1.4 [NASA-TM-110164] p 518 N95-30327

A numerical model for dynamic wave rotor analysis [NASA-TM-106997] p 615 N95-30617

Axial loads on yawed rotors [PB95-214193] p 592 N95-30638

Computation of high-altitude hypersonic flow-field radiation p 593 N95-30843

Dynamical systems as models for flow-induced vibrations [PB95-206991] p 647 N95-30956

Acceleration potential models PREDICAT/PREDICDYN applied for calculation of axisymmetric dynamic inflow cases [PB95-207015] p 647 N95-30957

Looking for the simple PIO model p 597 N95-31066

Calspan experience of PIO and the effects of rotor limiting p 598 N95-31072

Numerical simulation of ram accelerator performance including transient effects during initiation of combustion and sensitivity studies p 629 N95-31203

The 25th International Symposium on Combustion [AD-A286825] p 630 N95-31268

Analysis and modeling of an airport departure process [AD-A293782] p 602 N95-31581

A time stepping coupled finite element-state space modeling environment for synchronous machine performance and design analysis in the ABC frame of reference p 649 N95-31948

Tactical low-level helicopter communications p 702 N95-32492

A highly reliable, high performance open avionics architecture for real time Nap-of-the-Earth operations p 693 N95-32497

Techniques for the determination of local dynamic pressure and angle of attack on a horizontal axis wind turbine [DE95-009204] p 707 N95-32685

PSC algorithm description p 695 N95-33013

Calculation of supersonic combustion in SCRAMJET engines p 698 N95-34513

MATRICES (MATHEMATICS)

Direct splitting of coefficient matrix for numerical calculation of transonic nozzle flow [BTN-94-EIX94481415356] p 103 A95-65346

Unbalance response of a dual rotor system: Theory and experiment [BTN-94-EIX94351143320] p 195 A95-65854

Describing an attitude p 342 A95-80409

- Matrix fraction approach for finite-state aerodynamic modeling
[BTN-95-EIX95262694311] p 365 A95-85482
- Higher harmonic control analysis for vibration reduction of helicopter rotor systems
[NASA-TM-103855] p 66 N95-14419
- Plant and controller optimization by convex methods
[AD-A283700] p 133 N95-18621
- Modeling helicopter blade dynamics using a modified Myklestad-Prohl transfer matrix method
[AD-A289891] p 400 N95-28626
- Linear matrix inequalities for the problem of absolute stability of control systems p 518 N95-29680
- MATRIX MATERIALS**
- Intermetallic and titanium matrix composite materials for hypersonic applications
[AIAA PAPER 95-6132] p 530 A95-90451
- Novel matrix resins for composites for aircraft primary structures, phase 1
[NASA-CR-189657] p 23 N95-10318
- Thermally stable organic polymers
[AD-A281380] p 87 N95-14363
- US Navy operating experience with new aircraft construction materials p 303 N95-23517
- Advanced composite structural concepts and materials technologies for primary aircraft structures: Advanced material concepts
[NASA-CR-4485] p 503 N95-29027
- Thermally stable organic polymers
[AD-A290755] p 537 N95-29482
- MATRIX METHODS**
- Modeling helicopter blade dynamics using a modified Myklestad-Prohl transfer matrix method
[AD-A289891] p 400 N95-28626
- MATRIX THEORY**
- Matrix fraction approach for finite-state aerodynamic modeling
[BTN-95-EIX95262694311] p 365 A95-85482
- New eigensolutions and modal analysis for gyroscopic/rotor systems, part 1: undamped systems
[BTN-94-EIX94522410219] p 702 A95-96373
- MAXIMUM ENTROPY METHOD**
- Robust fixed-structure control
[AD-A286515] p 257 N95-22216
- Robust fixed-structure control
[AD-A292883] p 679 N95-30961
- MAXIMUM LIKELIHOOD ESTIMATES**
- Comparison of parameter identification algorithms for flight vehicles
[BTN-94-EIX94371347708] p 219 A95-69967
- Determining the accuracy of maximum likelihood parameter estimates with colored residuals
[NASA-CR-194893] p 51 N95-11869
- Minimal time detection algorithms and applications to flight systems
[TR-2-FSRC-93] p 171 N95-18564
- Determination of stability and control derivatives from the NASA F/A-18 HARV from flight data using the maximum likelihood method
[NASA-CR-197320] p 204 N95-19576
- Maximum-likelihood spectral estimation and adaptive filtering techniques with application to airborne Doppler weather radar
[NASA-CR-197699] p 316 N95-23670
- Estimate of probability of crack detection from service difficulty report data
[PB95-149381] p 328 N95-24295
- An analytic modeling and system identification study of helicopter dynamics p 505 N95-29787
- MCDONNELL AIRCRAFT**
- Performance study for inlet installations
[NASA-CR-189714] p 406 N95-28227
- MCDONNELL DOUGLAS AIRCRAFT**
- Evolution of a nose-wheel steering system
[BTN-94-EIX94461047056] p 78 A95-61739
- Fiber-optic technology for transport aircraft
[BTN-94-EIX94511309384] p 103 A95-64610
- Aerospace applications of beta titanium alloys
[HTN-95-B0394] p 530 A95-90475
- Strategy in the commercial aircraft industry in the United States: A comparison of decisionmaking by McDonnell-Douglas and Boeing aircraft companies from 1977-1983
[AD-A288289] p 366 N95-26409
- Report to Congressional Committees, Military airlift: C-17 settlement is not a good deal
[GAO/NSIAD-94-141] p 585 N95-32198
- MD 11 AIRCRAFT**
- Integrated flight crew transition training for the advanced flight deck aircraft
[SAE PAPER 932599] p 380 A95-84571
- MEAN FREE PATH**
- A preliminary study of the airwake model used in an existing SH-60B/FFG-7 helicopter/ship simulation program
[DSTO-TR-0015] p 224 N95-21659
- MEASURE AND INTEGRATION**
- Trajectory optimization using parallel shooting method on parallel computer
[BTN-95-EIX95282706670] p 564 A95-88175
- MEASURING INSTRUMENTS**
- Application of airborne field mill data for use in launch support
[HTN-95-50054] p 98 A95-62279
- An intercomparison of aircraft instrumentation for tropospheric measurements of sulfur dioxide
[HTN-95-91855] p 354 A95-80843
- An intercomparison of aircraft instrumentation for tropospheric measurements of carbonyl sulfide, hydrogen sulfide, and carbon disulfide
[HTN-95-91856] p 355 A95-80844
- An intercomparison of instrumentation for tropospheric measurements of dimethyl sulfide: Aircraft results for concentrations at the parts-per-trillion level
[HTN-95-91857] p 355 A95-80845
- Preliminary results of high resolution measurements of snowfall at Stapleton International Airport during the winter of 1992-93
[AD-A283981] p 134 N95-18891
- A short-term, high-resolution automated snowfall forecasting system p 666 A95-93510
- The 1992-3 operational winter forecasting experiment for Stapleton airport p 677 A95-93561
- Hypersonic flight testing
[AD-A283981] p 134 N95-18891
- Workshop report: Measurement techniques in highly transient, spectrally rich combustion environments
[AD-A288395] p 350 N95-25606
- Flutter clearance flight tests of an OV-10A airplane modified for wake vortex flight experiments
[NASA-TM-109168] p 366 N95-26381
- Research instrumentation for polytechnic university's supersonic wind tunnel facility
[AD-A290232] p 523 N95-29468
- MECHANICAL DEVICES**
- Preload release mechanism
[NASA-CASE-MSC-22327-1] p 350 N95-25592
- MECHANICAL DRIVES**
- Applicability of electrically driven accessories for turboshaft engines
[BTN-95-EIX95292721153] p 612 A95-92589
- Control system design for the MOD-5A 7.3 mW wind turbine generator p 440 N95-27985
- Variable speed generator application on the MOD-5A 7.3 mW wind turbine generator p 440 N95-27989
- MECHANICAL ENGINEERING**
- Ceramic composite attachments for transmission of high-torque loads
[BTN-94-EIX95011441256] p 417 A95-84213
- Strategic avionics technology definition studies, Subtask 3-1A3: Electrical Actuation (ELA) Systems Test Facility
[NASA-CR-188360] p 143 N95-18567
- NASA-UVA light aerospace alloy and structures technology program (LA2ST)
[NASA-CR-198041] p 343 N95-24220
- JPRS report: Science and technology, Central Eurasia
[JPRS-UST-94-027] p 349 N95-24470
- Influence of tooth profile modification on spur gear dynamic tooth strain
[NASA-TM-106952] p 553 N95-29112
- MECHANICAL IMPEDANCE**
- Sound propagation from an arbitrarily oriented multipole placed near a plane, finite impedance surface
[BTN-94-EIX94371338964] p 257 A95-70797
- MECHANICAL MEASUREMENT**
- Design optimization of aircraft engine-mount systems.
[BTN-94-EIX94351143325] p 195 A95-67298
- Blade-by-blade tip clearance measurement system for gas turbine applications
[BTN-95-EIX95292721167] p 546 A95-89899
- MECHANICAL OSCILLATORS**
- On the dynamics of aeroelastic oscillators with one degree of freedom
[BTN-94-EIX94501431527] p 153 A95-64524
- MECHANICAL PROPERTIES**
- Engineering methods for the evaluation of transonic flutter characteristics for aerodynamic control surfaces
[BTN-94-EIX94461408589] p 141 A95-63064
- Residual strength of composites with multiple impact damage
[BTN-94-EIX94511433967] p 701 A95-96664
- Micro-measurements of mechanical properties for adhesives and composites using digital imaging technology
[NASA-CR-196111] p 22 N95-10231
- Course module for AA201: Wing structural design project
[AD-A283618] p 133 N95-18616
- Environmental effects on composite airframes: A study conducted for the ARM UAV Program (Atmospheric Radiation Measurement Unmanned Aerospace Vehicle)
[DE94-015351] p 206 N95-19579
- Corrosion behavior of landing gear steels
[AD-A285862] p 242 N95-22132
- Idealized textile composites for experimental/analytical correlation p 301 N95-23277
- Through-the Thickness(R) braided composites for aircraft applications p 421 N95-28273
- Application of advanced material systems to composite frame elements p 422 N95-28432
- Shear force, bending moment and torque of rigid aircraft in symmetric steady maneuvering flight
[ESDU-94045] p 502 N95-28896
- Mechanical characterization of 2D, 2D stitched, and 3D braided/RTM materials p 535 N95-29038
- The effect of interface properties on nickel base alloy composites
[NASA-CR-198363] p 629 N95-30787
- High strain-rate testing of parachute materials
[DE95-009577] p 648 N95-31614
- MECHANICS (PHYSICS)**
- Laws of infrared similitude
[AD-A282209] p 62 N95-12426
- MECHANIZATION**
- An evaluation of Automatic Terminal Information Service (ATIS) flight deck display presentation options
[AD-A280100] p 228 N95-21020
- MEDICAL EQUIPMENT**
- Inadequacy of visual alarms in helicopter air medical transport
[HTN-95-01218] p 484 A95-91450
- Flying ambulances: The approach of a small air force to long distance aeromedical evacuation of critically injured patients p 568 N95-29618
- Civil Reserve Air Fleet-Aeromedical Evacuation Shipset (CRAF-AESS) p 568 N95-29619
- First medical test of the UH-60Q and equipment for use in US Army medevac helicopters p 568 N95-29620
- International access to aeromedical evacuation medical equipment assessment data p 569 N95-29622
- MEDICAL SCIENCE**
- JPRS Report: Science and technology, Central Eurasia
[JPRS-UST-94-032] p 350 N95-24759
- Advanced data visualization and sensor fusion: Conversion of techniques from medical imaging to Earth science p 711 N95-34236
- MEDICAL SERVICES**
- EMS helicopter incidents reported to the NASA Aviation Safety Reporting System p 596 A95-95201
- Emergency medical service (EMS): A unique flight environment p 596 A95-95203
- A surgical support system for Space Station Freedom
[NASA-CR-196776] p 149 N95-16776
- Flying ambulances: The approach of a small air force to long distance aeromedical evacuation of critically injured patients p 568 N95-29618
- Civil Reserve Air Fleet-Aeromedical Evacuation Shipset (CRAF-AESS) p 568 N95-29619
- First medical test of the UH-60Q and equipment for use in US Army medevac helicopters p 568 N95-29620
- International access to aeromedical evacuation medical equipment assessment data p 569 N95-29622
- Patient/aircraft forecasting for the strategic aeromedical evacuation lift-bed process
[AD-A293902] p 599 N95-31512
- MEMORY**
- Automation and cognition in air traffic control: An empirical investigation
[AD-A291932] p 488 N95-28790
- MEMORY (COMPUTERS)**
- Parallel implicit unstructured grid Euler solvers
[BTN-95-EIX95042474393] p 217 A95-68307
- Parallel methods for the flight simulation model
[DE94-013330] p 52 N95-11752
- Methodology for sensitivity analysis, approximate analysis, and design optimization in CFD for multidisciplinary applications
[NASA-CR-196981] p 58 N95-13201
- Rapid solution of large-scale systems of equations p 169 N95-16458
- MENTAL PERFORMANCE**
- Resource document for the design of electronic instrument approach procedure displays
[AD-A295108] p 691 N95-34797
- MERIDIONAL FLOW**
- Meridional distributions of NO(X), NO(Y), and other species in the lower stratosphere and upper troposphere during AASE 2
[HTN-95-70944] p 352 A95-78009
- MESH**
- Automatic riveting cell for commercial aircraft floor grid assembly
[HTN-95-92309] p 365 A95-85353
- MESOMETEOROLOGY**
- Forecasting for a large field program: STORM-FEST
[HTN-95-90694] p 215 A95-69721

- Snow-band formation and evolution during the 15 November 1987 aircraft accident at Denver airport [HTN-95-80699] p 254 A95-72543
- Diurnal variation of lee vortices in Taiwan and the surrounding area [HTN-95-91363] p 318 A95-76394
- The development of an aircraft icing forecast technique using data from maps p 675 A95-93549
- An overview of issues encountered in parallelizing high-resolution weather prediction models p 676 A95-93560
- MESOSCALE PHENOMENA**
- Observations of fluxes and inland breezes over a heterogeneous surface [HTN-95-80258] p 212 A95-66315
- Research aircraft observations of a polar low at the east Greenland ice edge [HTN-95-A0175] p 215 A95-69766
- MESSAGES**
- Control mechanism to prevent correlated message arrivals from degrading signaling no. 7 network performance [BTN-94-EIX94341342286] p 56 A95-60842
- METAL BONDING**
- Application of superplastically formed and diffusion bonded structures in high intensity noise environments p 174 A95-19162
- METAL COATINGS**
- Experience of aircraft manufacturer for paint removal using dry stripping method p 456 A95-91501
- Cu deposition using a permanent magnet electron cyclotron resonance microwave plasma source [DE94-017768] p 304 A95-23981
- High aspect ratio metal microstructures and method for preparing the same [AD-D017463] p 629 A95-30750
- METAL FATIGUE**
- Fatigue resistance of peened 7050-T7451 aluminum alloy: Repair and re-treatment of a component surface [BTN-94-EIX94371347838] p 206 A95-69131
- Multiple site fatigue damage in fuselage skin splices: Experimental simulation and theoretical prediction [BTN-95-EIX95152584676] p 276 A95-73588
- Fatigue strength of high-temperature alloys under conditions of cyclic temperature variation. Communication 1: Experimental procedure and results [BTN-94-EIX94401363884] p 307 A95-75516
- Status and prospects for aluminum-lithium alloys in aircraft structures p 387 A95-85893
- Fatigue in single crystal nickel superalloys [AD-A282917] p 88 A95-15415
- Evaluation of the fuselage lap joint fatigue and terminating action repair p 166 A95-19477
- The application of Newman crack-closure model to predicting fatigue crack growth p 167 A95-19483
- Proceedings of the 2d USAF Aging Aircraft Conference [AD-A288217] p 336 A95-25578
- Adhesively bonded composite patch repair of cracked aluminum alloy structures p 393 A95-27507
- METAL FIBERS**
- Compliant interlayer [BTN-95-EIX95142562401] p 304 A95-73439
- Damage tolerant repair techniques for pressurized aircraft fuselages [AD-A281982] p 65 A95-14144
- METAL MATRIX COMPOSITES**
- MIL-HDBK-5 design allowables for fibre/metal laminates: ARALL 2 and ARALL 3 [BTN-94-EIX94371346933] p 300 A95-73345
- Intermetallic and titanium matrix composite materials for hypersonic applications [AIAA PAPER 95-6132] p 530 A95-90451
- Modeling and life prediction methodology for Titanium Matrix Composites subjected to mission profiles [NASA-TM-109148] p 55 A95-11915
- NASA-UVA light aerospace alloy and structures technology program supplement: Aluminum-based materials for high speed aircraft [NASA-CR-4645] p 343 A95-24878
- Aircraft advanced materials research and development program plan [AD-A290542] p 505 A95-29565
- Innovative processing of composites for ultra-high temperature applications, book 1 [AD-A290889] p 537 A95-29842
- METAL SHEETS**
- Influence of crack history on the stable tearing behavior of a thin-sheet material with multiple cracks p 93 A95-14467
- Prediction of R-curves from small coupon tests p 167 A95-19496
- METAL SURFACES**
- Planar air density measurements near model surfaces by ultraviolet Rayleigh/Raman scattering [BTN-94-EIX94441386614] p 213 A95-67345
- Mechanism of deposit formation on fuel-wetted hot metal surfaces [AD-A289847] p 426 A95-28621
- Standardization of surface contamination analysis systems p 631 A95-31798
- METAL WORKING**
- Development of processes, means, and theoretical principles of thin-walled detail plastic forming at Kazan Aviation Institute p 155 A95-16281
- METAL-METAL BONDING**
- Forming and bonding techniques for high-strength aluminum alloys [HTN-95-20605] p 418 A95-84786
- METALLIZING**
- High aspect ratio metal microstructures and method for preparing the same [AD-D017463] p 629 A95-30750
- METALLOGRAPHY**
- Fatigue crack growth in nickel-based superalloys at 500-700 C. 1: Waspaloy [BTN-94-EIX94371347843] p 206 A95-69136
- The effects of pitting on fatigue crack nucleation in 7075-T6 aluminum alloy p 88 A95-14482
- METALS**
- Bicarbonate of soda blasting technology for aircraft wheel depainting [PB94-193223] p 104 A95-17466
- METASTABLE STATE**
- Supercooling in hypersonic nitrogen wind tunnels [BTN-94-EIX95011441134] p 340 A95-81020
- METEOROLOGICAL BALLOONS**
- Polar Patrol Balloon [BTN-95-EIX95152582318] p 316 A95-73521
- Comparison of meteorological data with fitted values extracted from projectile trajectory [AD-A285921] p 255 A95-19989
- METEOROLOGICAL CHARTS**
- Weather products for aviation from WAFIC Bracknell p 670 A95-93527
- METEOROLOGICAL INSTRUMENTS**
- A new generation of instruments for flying laboratories [BTN-94-EIX94401363947] p 317 A95-75532
- Aviation terminal forecasts based on automated observations (FTAUTO) p 668 A95-93520
- METEOROLOGICAL PARAMETERS**
- A new look at aviation meteorology: Integrating aircraft situation display (ASD) with conventional weather displays p 665 A95-93505
- The improvement of meteorological data for air traffic management purposes p 668 A95-93518
- A poor man's expert system for aviation VSRF in complex terrain p 669 A95-93524
- Weather products for aviation from WAFIC Bracknell p 670 A95-93527
- A prototype for displaying aviation forecast variables using Eta numerical model output p 676 A95-93555
- Thunderstorm hypothesis reasoner [AD-A282664] p 60 A95-12805
- Wind-shear certification data base for forward-look detection systems p 41 A95-13204
- Certification methodology applied to the NASA experimental radar system p 41 A95-13205
- Airport surveillance using a solid state coherent lidar p 41 A95-13207
- Characteristics of civil aviation atmospheric hazards p 42 A95-13208
- Wake vortex detection at Denver Stapleton Airport with a pulsed 2-micron coherent lidar p 42 A95-13211
- Comparison of meteorological data with fitted values extracted from projectile trajectory [AD-A285921] p 255 A95-19989
- Compendium of NASA data base for the Global Tropospheric Experiment's Pacific Exploratory Mission West-A (PEM West-A) [NASA-TM-109177] p 320 A95-23009
- Weather And Radar Processor (WARP) Test and Evaluation Master Plan (TEMP) [AD-A288280] p 445 A95-26453
- Initial evaluation of the Oregon State University planetary boundary layer column model for ITWS applications [AD-A293775] p 677 A95-31465
- METEOROLOGICAL RADAR**
- The detection and measurement of microburst wind shear by an airborne lidar system p 543 A95-87798
- International Conference on Aviation Weather Systems, 5th, Vienna, VA, Aug. 2-6, 1993. Preprint Volume [HTN-95-92940] p 652 A95-93441
- Status of the terminal Doppler weather radar with deployment underway p 653 A95-93450
- The Integrated Terminal Weather System (ITWS) storm cell information and weather impacted airspace detection algorithm p 654 A95-93452
- Improving aircraft impact assessment with the integrated terminal weather system microburst detection algorithm p 654 A95-93453
- Use of WSR-88D data in the FAA's weather impacted aerospace product p 658 A95-93469
- NEXRAD/ARSR operational comparison p 658 A95-93470
- Final results of the weather testing component of the Terminal Doppler Weather Radar operational test and evaluation p 658 A95-93471
- The use of radar wind profiles to remove TDWR gust front algorithm false alarms caused by vertical wind shear p 661 A95-93488
- Terminal Doppler Weather Radar point target filter threshold selection p 662 A95-93490
- Test results of a low cost airport weather radar p 662 A95-93492
- Dissemination of terminal weather products to the flight deck via data link p 669 A95-93525
- Wind-shear detection: TDWR and LLWAS operational experience in Denver 1988-1992 p 670 A95-93528
- Aviation value-added products and services from the NEXRAD Information Dissemination Service (NIDS) p 671 A95-93535
- Using ATMS weather products for air traffic strategic planning p 672 A95-93536
- Vertical wind estimation from horizontal wind measurements p 26 A95-10567
- Terminal Doppler Weather Radar Build 5A Operational Test and Evaluation (OT/E) integration and OT/E operational test plan [AD-A283052] p 61 A95-12996
- Characteristics of civil aviation atmospheric hazards p 42 A95-13208
- TDWR scan strategy implementation [AD-A284877] p 98 A95-15749
- Radar studies of aviation hazards [AD-A285845] p 226 A95-21831
- Maximum-likelihood spectral estimation and adaptive filtering techniques with application to airborne Doppler weather radar [NASA-CR-197699] p 316 A95-23670
- Weather And Radar Processor (WARP) Test and Evaluation Master Plan (TEMP) [AD-A288280] p 445 A95-26453
- Offshore next generation weather radar (NEXRAD) test and evaluation master plan (TEMP) [AD-A291435] p 556 A95-30072
- Offshore next generation weather radar (NEXRAD) OT&E integration and OT&E operational test [AD-A293223] p 646 A95-30902
- Initial evaluation of the Oregon State University planetary boundary layer column model for ITWS applications [AD-A293775] p 677 A95-31465
- METEOROLOGICAL RESEARCH AIRCRAFT**
- An air-driven pressure booster pump for aircraft-based air sampling [HTN-95-40689] p 216 A95-69833
- Design of a high altitude long endurance aircraft with manufacturing considerations p 391 A95-26947
- METEOROLOGICAL SATELLITES**
- Field and data analysis studies related to the atmospheric environment [NASA-CR-196543] p 168 A95-18093
- Calculation of satellite drag coefficients [AD-A285118] p 300 A95-23781
- METEOROLOGICAL SERVICES**
- An overview of FAA-sponsored aviation weather research and development p 652 A95-93442
- The forecast systems laboratory's role in the FAA's aviation weather development program p 652 A95-93443
- National aviation weather program plan p 652 A95-93445
- Operational aviation weather regulations p 652 A95-93446
- A status report on the development of the Federal Aviation Administration/National Oceanic and Atmospheric Administration Memorandum of Agreement p 652 A95-93447
- An approach to weather requirements management p 653 A95-93448
- On designing and engineering the integrated terminal weather system p 653 A95-93449
- ITWS ceiling and visibility products p 654 A95-93454
- Knowing our users - A challenge for meteorologists at the National Aviation Weather Advisory Unit p 655 A95-93459
- The aviation gridded forecast system verification program - A description of aviation-impact-variable evaluation plans p 664 A95-93498
- Objective verification of an enhanced terminal forecast experiment at Denver, Colorado p 664 A95-93501
- Analysis of en route controller hazardous weather-related tasks p 665 A95-93503
- The data link flight information service application p 665 A95-93504

- MDCRS: Aircraft observations collection and uses p 668 A95-93517
- FTGEN - An automated FT production system p 668 A95-93519
- Nortaf: Computer generated aerodrome forecasts p 668 A95-93521
- The combination of forecasts in an automated aviation weather forecasting system p 669 A95-93522
- Dissemination of terminal weather products to the flight deck via data link p 669 A95-93525
- Dissemination of weather products p 670 A95-93526
- Weather products for aviation from WAFB Bracknell p 670 A95-93527
- Developing and testing decision-making products for center weather service unit meteorologists p 671 A95-93533
- The prototype aviation weather products generator a vehicle to assess user needs p 671 A95-93534
- Aviation value-added products and services from the NEXRAD Information Dissemination Service (NIDS) p 671 A95-93535
- Northwest Airlines atmospheric hazards advisory & avoidance system p 672 A95-93539
- Future enhancements to ground-based microburst detection p 11 N95-10570
- Integrated terminal weather system (ITWS) demonstration and validation operational test and evaluation [AD-A293932] p 602 N95-31521
- The ATC operational evaluation of the prototype integrated terminal weather system (ITWS) at Dallas/Fort Worth and Orlando airports (May-September 1993) [AD-A293808] p 677 N95-31587
- METEOROLOGY**
- Powerful bolide explosion over North Italy [HTN-95-80564] p 218 A95-69658
- A new generation of instruments for flying laboratories [BTN-94-EIX94401363947] p 317 A95-75532
- Vertical transport rates in the stratosphere in 1993 from observations of CO₂, N₂O, and CH₄ [HTN-95-70941] p 351 A95-78006
- Chemical change in the arctic vortex during AASE 2 [HTN-95-70947] p 352 A95-78012
- Environmental aspects of Orbital transport p 559 A95-87377
- Meteorological impacts on airport noise prediction by the "Integrated Noise Model" application based on Hamiltonian Ray-Tracing program and measurements p 571 A95-88467
- Comparison of meteorological data with fitted values extracted from projectile trajectory [AD-A285921] p 255 N95-19989
- METHANE**
- Vertical transport rates in the stratosphere in 1993 from observations of CO₂, N₂O, and CH₄ [HTN-95-70941] p 351 A95-78006
- Nitrous oxide and methane emissions from aero engines [HTN-95-21363] p 353 A95-78678
- Stationary premixed flames in spherical and cylindrical geometries [HTN-95-42336] p 418 A95-86165
- The Methane-Acetylene Cycle Aerospace Plane: A potential option for inexpensive Earth to orbit transportation [HTN-95-51845] p 525 A95-87483
- Numerical study of contaminant effects on combustion of hydrogen, ethane, and methane in air [AIAA PAPER 95-6097] p 510 A95-88005
- Cooling of aerospace plane using liquid hydrogen and methane [BTN-95-EIX0619952748171] p 590 A95-94465
- Airborne rotary separator study [NASA-CR-191045] p 150 N95-18743
- METHOD OF MOMENTS**
- A users manual for the method of moments Aircraft Modeling Code (AMC), version 2 [NASA-CR-196445] p 24 N95-11252
- METHODOLOGY**
- The navigation toolkit [NASA-CR-197290] p 229 N95-22161
- METHYL ALCOHOL**
- High pressure vaporization and burning of methanol droplets in reduced gravity p 527 A95-87285
- MICROBURSTS (METEOROLOGY)**
- WINDEX - A new index for forecasting microburst potential [HTN-95-90690] p 215 A95-69717
- Optimal lateral-escape maneuvers for microburst encounters during final approach [BTN-95-EIX95182619127] p 276 A95-76604
- The detection and measurement of microburst wind shear by an airborne lidar system p 543 A95-87798
- International Conference on Aviation Weather Systems, 5th, Vienna, VA, Aug. 2-6, 1993. Preprint Volume [HTN-95-92940] p 652 A95-93441
- Status of the terminal Doppler weather radar with deployment underway p 653 A95-93450
- Improving aircraft impact assessment with the integrated terminal weather system microburst detection algorithm p 654 A95-93453
- The ITWS microburst prediction algorithm p 655 A95-93456
- Final results of the weather testing component of the Terminal Doppler Weather Radar operational test and evaluation p 658 A95-93471
- LLWAS 2 and LLWAS 3 performance evaluation p 662 A95-93491
- Test results of a low cost airport weather radar p 662 A95-93492
- Development of a climatology for possible microburst occurrence in Canada p 664 A95-93497
- Dissemination of terminal weather products to the flight deck via data link p 669 A95-93525
- Airborne Windshear Detection and Warning Systems. Fifth and Final Combined Manufacturers' and Technologists' Conference, part 1 [NASA-CP-10139-PT-1] p 10-N95-10566
- Vertical wind estimation from horizontal wind measurements p 26 N95-10567
- Characteristics of a dry, pulsating microburst at Denver Stapleton Airport p 26 N95-10568
- Future enhancements to ground-based microburst detection p 11 N95-10570
- Determining F-factor using ground-based Doppler radar: Validation and results p 11 N95-10571
- Airborne Windshear Detection and Warning Systems. Fifth and Final Combined Manufacturers' and Technologists' Conference, part 2 [NASA-CP-10139-PT-2] p 41 N95-13203
- Certification methodology applied to the NASA experimental radar system p 41 N95-13205
- Certification of windshear performance with RTCA class D radomes p 41 N95-13206
- Microburst vertical wind estimation from horizontal wind measurements [NASA-TP-3460] p 131 N95-18198
- Experiments on microbursts p 562 N95-29110
- MICROCHANNELS**
- Microchannel heat pipe cooling of modules p 246 N95-20649
- MICROCOMPUTERS**
- Instructional control and part/whole-task training: A review of the literature and an experimental comparison of strategies applied to instructional simulation [AD-A280860] p 21 N95-10919
- Control system design for the MOD-5A 7.3 mW wind turbine generator p 440 N95-27985
- MICROCRACKS**
- Fatigue in single crystal nickel superalloys [AD-A283459] p 56 N95-12546
- Fatigue life until small cracks in aircraft structures: Durability and damage tolerance p 135 N95-19478
- Impact loading of compressor stator vanes by hailstone ingestion p 200 N95-19670
- MICROELECTRONICS**
- Lightweight electronic enclosures using composite materials p 241 N95-20656
- MICROGRAVITY**
- Study on a scheme for the prolongation of microgravity time of balloon-borne drop capsule p 414 A95-82515
- Study of heat transfer rates during quenching of a hot tube under microgravity p 428 A95-82641
- Experimental investigation of flow-boiling heat transfer under microgravity p 428 A95-82642
- Stationary premixed flames in spherical and cylindrical geometries [HTN-95-42336] p 418 A95-86165
- A flow pattern map for two-phase liquid-gas flow under reduced gravity conditions p 539 A95-87280
- High pressure vaporization and burning of methanol droplets in reduced gravity p 527 A95-87285
- Characterization of annular two-phase gas-liquid flows in microgravity p 95 N95-14556
- Virtual environment application with partial gravity simulation p 169 N95-15988
- A surgical support system for Space Station Freedom p 149 N95-16776
- Microgravity isolation system design: A case study [NASA-TM-106804] p 104 N95-17657
- Microgravity isolation system design: A modern control synthesis framework [NASA-TM-106805] p 105 N95-18197
- Microgravity isolation system design: A modern control analysis framework [NASA-TM-106803] p 105 N95-18486
- Users guide for NASA Lewis Research Center DC-9 Reduced-Gravity Aircraft Program [NASA-TM-106755] p 146 N95-18586
- Two-phase flow research using the learjet apparatus [NASA-TM-106814] p 438 N95-27854
- MICROHARDNESS**
- Effects of activated reactive evaporation process parameters on the microhardness of polycrystalline silicon carbide thin films [GTN-95-00406090-4621] p 680 A95-93965
- MICROMECHANICS**
- Ply layout optimization and micromechanics tailoring of composite aircraft engine structures [BTN-95-EIX95112524206] p 196 A95-69302
- Impact, friction, and wear testing of microsamples of polycrystalline silicon p 361 A95-79988
- Modeling and life prediction methodology for Titanium Matrix Composites subjected to mission profiles [NASA-TM-109148] p 55 N95-11915
- Study of multiple cracks in airplane fuselage by micromechanics and complex variables p 94 N95-14468
- MICROPARTICLES**
- Activated buoyancy propulsion = Paradox Power (tm) [TABES PAPER 94-619] p 74 N95-14646
- MICROPHONES**
- Aeroacoustic probe design for microphone to reduce flow-induced self-noise [AIAA PAPER 93-4343] p 19 A95-60163
- Oblique incidence sound absorption of porous materials covered by perforated metal and exposed to tangential airflow [HTN-94-00681] p 19 A95-60165
- Background noise levels measured in the NASA Lewis 9- by 15-foot low-speed wind tunnel [NASA-TM-106817] p 145 N95-18054
- Method for extracting forward acoustic wave components from rotating microphone measurements in the inlets of turbofan engines [NASA-CR-195457] p 616 N95-30779
- MICROPROCESSORS**
- The role of simulations in 777 FSEU development [AIAA PAPER 95-0995] p 506 A95-90665
- Micro-time stress measurement device development [AD-A289511] p 448 N95-26845
- Formal verification of an avionics microprocessor [NASA-CR-4682] p 710 N95-33396
- MICROSTRIP ANTENNAS**
- Spiral microstrip antenna with resistance [NASA-CASE-LAR-15088-1] p 91 N95-14139
- Scattering and radiation from cylindrically conformal antennas p 645 N95-30669
- MICROSTRIP DEVICES**
- Modeling resonance in waveguide-to-microstrip junctions by unilateral fin line resonators [BTN-94-EIX94381323445] p 242 A95-70844
- MICROSTRUCTURE**
- Surface morphology and structure of carbon-carbon composites in high-energy sliding contact [BTN-94-EIX94371347996] p 206 A95-69164
- Applying nanostructured materials to future gas turbine engines [HTN-95-11909] p 404 A95-85990
- Analysis of small crack behavior for airframe applications p 95 N95-14484
- NASA-UVA light aerospace alloy and structures technology program (LA2ST) [NASA-CR-198041] p 343 N95-24220
- High aspect ratio metal microstructures and method for preparing the same [AD-D017463] p 629 N95-30750
- MICROWAVE ABSORPTION**
- Aircraft measurements of water vapour continuum absorption at millimetre wavelengths [HTN-95-90884] p 253 A95-72393
- MICROWAVE EQUIPMENT**
- Anechoic chamber upgrade [AD-A294375] p 700 N95-34342
- MICROWAVE FREQUENCIES**
- Integration of AIRSAR and AVIRIS data for Trail Canyon alluvial fan, Death Valley, California p 709 N95-33760
- MICROWAVE IMAGERY**
- Passive millimeter wave camera for aircraft landing in low visibility conditions [BTN-95-EIX95292721321] p 609 A95-92513
- Passive MMW camera for low visibility landings p 59 N95-13215
- MICROWAVE LANDING SYSTEMS**
- CCLA operation on MLS p 487 A95-91540
- Analysis of an MLS automatic landing control law for the NAL experimental research aircraft D0-228. 2. Curved approach and landing p 508 A95-91588
- Spatial awareness comparisons between large-screen, integrated pictorial displays and conventional EFIS displays during simulated landing approaches [NASA-TP-3467] p 80 N95-14852
- Heliport/vertiport MLS precision approaches [AD-A283505] p 126 N95-18059

- Minima reduction simulation test results
[AD-A285626] p 228 N95-21148
- An integrated GPS/INS/BARO and radar altimeter system for aircraft precision approach landings
[AD-A289280] p 383 N95-26985
- Precision landing system mathematical modeling study report for Andrews Air Force Base, runway 19L, Camp Springs, MD
[AD-A289015] p 384 N95-27903
- Flight test evaluation of the Stanford University/United Airlines differential GPS Category 3 automatic landing system
[NASA-TM-110354] p 593 N95-30788
- Development of advanced approach and departure procedures. Failure scenarios
[PB95-198123] p 601 N95-30815
- The DLR research programme on an integrated multi sensor system for surface movement guidance and control
p 689 N95-33135

MICROWAVE RADIOMETERS

- Microwave and infrared simulations of an intense convective system and comparison with aircraft observations
[HTN-95-60511] p 214 A95-68762
- High-resolution imaging of rain systems with the advanced microwave precipitation radiometer
[HTN-95-70133] p 252 A95-70655
- Behavior of an inversion-based precipitation retrieval algorithm with high-resolution AMPR measurements including a low-frequency 10.7-GHz channel
[HTN-95-70134] p 252 A95-70656

MICROWAVE SCATTERING

- Precision landing system mathematical modeling study report for Andrews Air Force Base, runway 19L, Camp Springs, MD
[AD-A289015] p 384 N95-27903

MICROWAVE SOUNDING

- Aircraft measurements of water vapour continuum absorption at millimetre wavelengths
[HTN-95-90884] p 253 A95-72393

MICROWAVES

- Permanent magnet electron cyclotron resonance plasma source with remote window
[BTN-95-EIX95242674338] p 450 A95-82176
- Cu deposition using a permanent magnet electron cyclotron resonance microwave plasma source
[DE94-017768] p 304 N95-23981

MIDLATITUDE ATMOSPHERE

- Mesoscale structure of precipitation bands in a North Atlantic winter storm
[HTN-95-40659] p 215 A95-69803

MIE SCATTERING

- Microphysical and radiative properties of small cumulus clouds over the sea
[HTN-95-A0526] p 255 A95-73180
- On the link between cloud-top radiative properties and sub-cloud aerosol concentrations
[HTN-95-A0527] p 255 A95-73181
- Airborne measurements during the Arctic stratospheric experiment: Observation of O3 and NO2
[HTN-95-00748] p 445 A95-86318

MILITARY AIR FACILITIES

- Assessing effects of military aircraft noise on residential property values near airbases
p 31 N95-11310
- Report to the Chairman, Subcommittee on Transportation and Related Agencies, Committee on Appropriations, US Senate. Airport Improvement Program: The Military Airport Program has not achieved intended impact
[GAO/RCED-94-209] p 700 N95-32888

MILITARY AIRCRAFT

- The effects of aircraft (B-52) overflights on ancient structures
[BTN-94-EIX94341340070] p 171 A95-63522
- USAF aging aircraft program
[BTN-95-EIX95072498878] p 180 A95-68394
- A prediction model for noise from low-altitude military aircraft
p 571 A95-88466
- MIL-STD-461/MIL-STD-704 investigation
[SAE PAPER 932561] p 505 A95-90058
- Electrical power system upgrade methodology for in-service aircraft
[SAE PAPER 932562] p 511 A95-90059
- The effect of onset rate on annoyance to military aircraft noise
p 561 A95-90119
- Aeronautical technology - recent advances and future prospects
[HTN-95-01097] p 496 A95-90283
- Unsteady aerodynamic effects of trailing edge controls on delta wings
[HTN-95-01099] p 469 A95-90285
- Repairs to composite structure on military aircraft
[CONGRESS PAPER C428-4-067] p 531 A95-91677
- Intelligent skins development for future military aircraft
[CONGRESS PAPER C428-17-189] p 531 A95-91714

- The auxiliary and emergency power supply on the Saab JAS39 Gripen aircraft
[CONGRESS PAPER C428-36-192] p 612 A95-93631

- The certification of composite structures for military aircraft
[CONGRESS PAPER C428-37-198] p 628 A95-93633

- Proceedings of the FAA Inspection Program Area Review
[AD-A283849] p 77 N95-14350

- Research and technology highlights, 1993
[NASA-TM-4575] p 102 N95-15065

- Military aviation maintenance industry in Western Europe: Concentration and internationalization
[PB94-189180] p 104 N95-17451

- Application of three-dimensional hybrid structured/unstructured grids to land, sea and air vehicles
[ARA-MEMO-399] p 210 N95-19775

- Digital systems validation. Chapter 20 Artificial Intelligence with applications for aircraft. Handbook, volume 2
[AD-A288492] p 448 N95-26638

- Naval Aviation System TEAM mapping, charting, and geodesy handbook
[AD-A288590] p 446 N95-26841

- A review of Australian and New Zealand investigations on aeronautical fatigue during the period Apr. 1993 - Mar. 1995
[AR-009-202] p 397 N95-27918

- Aircraft IR/acoustic detection evaluation. Volume 2: Development of a ground-based acoustic sensor system for the detection of subsonic jet-powered aircraft
[NASA-CR-189705-VOL-2] p 452 N95-28073

- Catapult-launching of the RAFALE design and experimentation
p 609 N95-32008

- Report to the Chairman, Legislation and National Security Subcommittee, Committee on Government Operations, House of Representatives. C-17 Aircraft program: Improvements in initial provisioning process
[GAO/NSIAD-94-63] p 584 N95-32194

MILITARY AVIATION

- Low rate initial production in Army Aviation systems development
[AD-A281871] p 127 N95-16356
- Forecasting aircraft mishaps using monthly maintenance reports
[AD-A286049] p 227 N95-22417
- Environmental support of naval aviation
[AD-A292873] p 598 N95-31454

MILITARY HELICOPTERS

- Rotorcraft handling qualities in turbulence
[BTN-95-EIX95242670750] p 334 A95-81097
- Design and flight evaluation of an integrated navigation and near-terrain helicopter guidance system for night-time and adverse weather operations
[NASA-TM-108837] p 11 N95-10846
- Advanced distributed simulation technology advanced rotary wing aircraft. Study comparing approaches to modeling the ARWA main rotor
[AD-A280824] p 79 N95-14306

- US Army rotorcraft turboshaft engines sand and dust erosion considerations
p 198 N95-19656
- An overview of Health and Usage Monitoring Systems (HUMS) for military helicopters
[DSTO-TR-0061] p 327 N95-24200

- Helicopter life substantiation: Review of some USA and UK initiatives
[DSTO-TR-0062] p 328 N95-24201

- AH-1F COBRA rewire program MANPRINT analysis
[AD-A289190] p 391 N95-27018

- Report to Congressional Committees. Comanche Helicopter: Testing needs to be completed prior to production decisions
[GAO/NSIAD-95-112] p 397 N95-27910

- Construction and wind tunnel test of a 1/12th scale helicopter model
[AD-A288487] p 378 N95-28331

- Tie-down trials involving a Sikorsky S-70B-2 helicopter
[DSTO-TR-0132] p 400 N95-28567

- Helicopter life substantiation: Review of some USA and UK initiatives
[AD-A290045] p 502 N95-28851

- Optimizing cockpit display configurations with a genetic algorithm system
[AD-A289799] p 508 N95-29123

- Preparation of S-70A-9 Black Hawk helicopter for flight tests to investigate cause of cracking of inner fuselage panel
[AD-A293891] p 608 N95-31544

- Army aviation: Modernization strategy needs to be reassessed. Report to Congressional requestors
[GAO/NSIAD-95-9] p 683 N95-32783

- HeliRadar: A rotating antenna synthetic aperture radar for helicopter all-weather operations
p 705 N95-33137

MILITARY OPERATIONS

- Joint stars phased array radar antenna
[BTN-95-EIX9504274626] p 209 A95-68280

- A review of Air Force policy and noise models pertaining to the noise environment under low-altitude, high-speed training areas
p 561 A95-90118

- Design and flight evaluation of an integrated navigation and near-terrain helicopter guidance system for night-time and adverse weather operations
[NASA-TM-108837] p 11 N95-10846

- MOAMAP: A model that combines several different kinds of aircraft operations
p 32 N95-11323

- The present and future of aircraft noise models: A user's perspective
p 32 N95-11324

- Bomber force 2000: Operational concepts for long-range combat aircraft
[AD-A279378] p 230 N95-20181

- The value of simulation for training
[AD-A289174] p 411 N95-26556

- Digital systems validation. Chapter 20 Artificial Intelligence with applications for aircraft. Handbook, volume 2
[AD-A288492] p 448 N95-26638

- Air cushioned landing craft (LCAC) based ship to shore movement simulation: A decision aid for the amphibious commander. A (SMMAT) application
[AD-A289635] p 436 N95-26722

- Applications of digital video and synthetic environments to unmanned aerial vehicles
[AD-A291875] p 504 N95-29437

- Unmanned aerial vehicles. 1994 master plan
p 607 N95-31416

- Effects of the specific military aspects of satellite navigation on the civil use of GPS/GLONASS
p 688 N95-33134

- Proposed incorporation of mission-oriented flying qualities into MIL-STD-1797A
[AD-A294211] p 698 N95-34306

MILITARY TECHNOLOGY

- Reliability and maintainability
[BTN-95-EIX95042477109] p 179 A95-68350

- Commercial applications for military laser radars
p 543 A95-87794

- Assessment of Russian VSTOL technology evaluating the YAK-38 'FORGER' and YAK-141 'FREESTYLE'
p 497 A95-90868

- Unmanned aerial vehicles
[AD-A286190] p 231 N95-20329

- Standard Hardware Acquisition and Reliability Program (SHARP) advanced SEM-E packaging
p 233 N95-20633

- Navigational technology of dual usage
p 688 N95-33131

- The DLR research programme on an integrated multi sensor system for surface movement guidance and control
p 689 N95-33135

- HeliRadar: A rotating antenna synthetic aperture radar for helicopter all-weather operations
p 705 N95-33137

- Application of advanced safety technique to ring laser gyro inertial navigation system integration
p 689 N95-33140

MILLIMETER WAVES

- An overview of millimeter-wave spectroscopic measurements of chlorine monoxide at Thule, Greenland, February-March, 1992: Vertical profiles, diurnal variation, and longer-term trends
[HTN-95-00722] p 444 A95-86292

- Passive millimeter wave camera for aircraft landing in low visibility conditions
[BTN-95-EIX95292721321] p 609 A95-92513

- Passive MMW camera for low visibility landings
p 59 N95-13215

- The mm-wave resonant methods for the detection of corrosion, phase 1
[AD-A291315] p 556 N95-29941

MILLING (MACHINING)

- Modelling for optimal operations of line milling of aerodynamic surfaces
[BTN-94-EIX94461408774] p 138 A95-63657

- Development of an intelligent tool-condition monitoring system for FMS
[CONGRESS PAPER C428-32-012] p 583 A95-93617

- Tooling - a source of productivity
[CONGRESS PAPER C428-32-017] p 583 A95-93619

MIMO (CONTROL SYSTEMS)

- Multirate flutter suppression system design for a model wing
[BTN-95-EIX95182619132] p 292 A95-76609

- Design and multifunction tests of a frequency domain-based active flutter suppression system
[BTN-95-EIX95182619215] p 292 A95-76641

- MIMO H infinity control design method combined with exact model matching
p 506 A95-91492

Exact solution of stability margin for the MIMO control system p 507 A95-91582

MINERALOGY
Integration of AIRSAR and AVIRIS data for Trail Canyon alluvial fan, Death Valley, California p 709 N95-33760

MINIATURE ELECTRONIC EQUIPMENT
A programmable heater control circuit for spacecraft [NASA-TM-108459] p 9 N95-11157

MINIMA
Prediction of fatigue crack growth under constant amplitude and random loading using specimens with multiple cracks [AD-A291614] p 397 N95-28409

MINIMUM DRAG
Minimum-drag axisymmetric bodies in the supersonic/hypersonic flow regimes [BTN-95-EIX95041503785] p 180 A95-69216
CFD optimization of a theoretical minimum-drag body [BTN-95-EIX95182619234] p 308 A95-76660
Control of flow separation in airfoil/wing design applications p 274 N95-23294

MISSILE BODIES
Wing vertical position effects on wing-body carryover for noncircular missiles [BTN-95-EIX95182617462] p 268 A95-75733
Supersonic vortex flow around a missile body p 114 N95-17870

MISSILE COMPONENTS
The 1995 version of the NSWC aeroprediction code. Part 1: Summary of new theoretical methodology [AD-A291518] p 481 N95-29853

MISSILE CONFIGURATIONS
Base drag prediction on missile configurations [BTN-95-EIX95152583256] p 266 A95-73557
Aerodynamic characteristics of a canard-controlled missile at high angles of attack [BTN-95-EIX95152583257] p 267 A95-73558
Implicit multi-domain method for unsteady compressible inviscid fluid flows around 3D projectiles p 548 A95-91482
High angle of attack missile aerodynamics [CONGRESS PAPER C428-3-060] p 475 A95-91673
Experimental Aerodynamics Division [NAL-SP-9404] p 35 N95-12166
A selection of experimental test cases for the validation of CFD codes, volume 1 [AGARD-AR-303-VOL-1] p 91 N95-14201
Missile Aerodynamics [AGARD-R-804] p 73 N95-14445
Engineering Codes for aeroprediction: State-of-the-art and new methods p 73 N95-14447
Navier-Stokes predictions of missile aerodynamics p 74 N95-14451
Experimental study at low supersonic speeds of a missile concept having opposing wraparound tails [NASA-TM-4582] p 106 N95-16069
Evaluation of an autopilot based multimodelling [PB94-190725] p 142 N95-17454
A selection of experimental test cases for the validation of CFD codes, volume 2 [AGARD-AR-303-VOL-2] p 109 N95-17846
A selection of experimental test cases for the validation of CFD codes. Supplement: Datasets A-E [AGARD-AR-303-SUPPL] p 117 N95-18539
Application of three-dimensional hybrid structured/unstructured grids to land, sea and air vehicles [ARA-MEMO-399] p 210 N95-19775
The 1995 version of the NSWC aeroprediction code. Part 1: Summary of new theoretical methodology [AD-A291518] p 481 N95-29853
An aerodynamic and static-stability analysis of the Hypersonic Applied Research Technology (HART) missile [DA9426923] p 481 N95-29965

MISSILE CONTROL
Side forces at high angles of attack. Why, when, how? [BTN-95-EIX95112523809] p 194 A95-69324
Switched bias proportional navigation for homing guidance against highly maneuvering targets [BTN-95-EIX95182619145] p 279 A95-76622
High-performance, robust, bank-to-turn missile autopilot design [BTN-95-EIX95242670751] p 336 A95-81096
Ideal proportional navigation p 342 A95-81374
Numerical analysis of flow field around gas rudder p 407 A95-82333
The short range attack missile/light weight exo-atmospheric projectile (SRAM/LEAP) missile tests program [HTN-95-81498] p 386 A95-85212
Active plate and missile wing development using directionally attached piezoelectric elements [HTN-95-42340] p 408 A95-86169

Air data prediction from surface pressure measurements on guided munitions [BTN-95-EIX95282706664] p 466 A95-89641
Missile autopilot designs using full state feedback p 507 A95-91587
A design trade study using CFD modeling of reaction jets for aerodynamic control [SAE PAPER 931384] p 586 A95-93660
Lateral jet control for tactical missiles p 84 N95-14448
Experimental study at low supersonic speeds of a missile concept having opposing wraparound tails [NASA-TM-4582] p 106 N95-16069
Evaluation of an autopilot based multimodelling [PB94-190725] p 142 N95-17454
Integrated aerodynamic fin and stowable TVC vane system [AD-DO16457] p 151 N95-19073
Moving mass trim control for aerospace vehicles [DE95-002602] p 299 N95-23532
Results from tests of the Kearfott T16-B Inertial Measurement Unit [PB95-212031] p 644 N95-30502
Results from tests of the Honeywell integrated flight management unit [PB95-211355] p 601 N95-30597

MISSILE DEFENSE
The short range attack missile/light weight exo-atmospheric projectile (SRAM/LEAP) missile tests program [HTN-95-81498] p 386 A95-85212

MISSILE DESIGN
The short range attack missile/light weight exo-atmospheric projectile (SRAM/LEAP) missile tests program [HTN-95-81498] p 386 A95-85212
Aeromechanical design of modern missiles p 73 N95-14446

MISSILE LAUNCHERS
SR-71 may launch targets for missile defense tests [HTN-95-91872] p 335 A95-81974

MISSILE STRUCTURES
Development of a low-cost, modified resin transfer molding process using elastomeric tooling and automated preform fabrication p 420 N95-28268

MISSILE SYSTEMS
SR-71 may launch targets for missile defense tests [HTN-95-91872] p 335 A95-81974

MISSILE TRAJECTORIES
Parallel methods for the flight simulation model [DE94-013330] p 52 N95-11752
A CFD study of complex missile and store configurations in relative motion [NASA-CR-197912] p 285 N95-22949
Parallel block implicit integration technique for trajectory parallelism [AD-A288961] p 450 N95-28335

MISSILES
Aerodynamic characteristics of a canard-controlled missile at high angles of attack [BTN-95-EIX95152583257] p 267 A95-73558
Wing vertical position effects on wing-body carryover for noncircular missiles [BTN-95-EIX95182617462] p 268 A95-75733
Supersonic near-wake afterbody boattailing effects on axisymmetric bodies [BTN-95-EIX95182617465] p 268 A95-75736
High-performance, robust, bank-to-turn missile autopilot design [BTN-95-EIX95242670751] p 336 A95-81096
Numerical analysis of flow field around gas rudder p 407 A95-82333
A study of mesh adaption techniques in structured and unstructured meshes [ISBN 1-879921-01-4] p 678 A95-93757
Aerodynamic interference for supersonic low-aspect-ratio missiles [BTN-95-EIX95302694469] p 588 A95-94065
Parallel methods for the flight simulation model [DE94-013330] p 52 N95-11752
Missile Aerodynamics [AGARD-R-804] p 73 N95-14445
Aeromechanical design of modern missiles p 73 N95-14446
Engineering Codes for aeroprediction: State-of-the-art and new methods p 73 N95-14447
High angle of attack aerodynamics p 74 N95-14450
Navier-Stokes predictions of missile aerodynamics p 74 N95-14451
Evaluation of an autopilot based multimodelling [PB94-190725] p 142 N95-17454
Solid fuel ramjet composition [AD-DO16458] p 152 N95-19090
A computer code (SKINTEMP) for predicting transient missile and aircraft heat transfer characteristics [AD-A286044] p 248 N95-21001

User documentation of the CTA program [AD-A289508] p 375 N95-26854
The 1995 version of the NSWC aeroprediction code. Part 1: Summary of new theoretical methodology [AD-A291518] p 481 N95-29853
An aerodynamic and static-stability analysis of the Hypersonic Applied Research Technology (HART) missile [DA9426923] p 481 N95-29965

MISSION PLANNING
Design decisions from the history of the EUVE science payload [HTN-95-60545] p 205 A95-69854
Generic architectures for future flight systems p 99 N95-14159
Space Generic Open Avionics Architecture (SGOAA): Overview p 99 N95-14161
Evolutionary Telemetry and Command Processor (TCP) architecture p 86 N95-14162
EURECA mission control experience and messages for the future p 149 N95-17252
Fatigue loads spectra derivation for the Space Shuttle: Second cycle p 166 N95-19470
Stratospheric Observatory For Infrared Astronomy (SOFIA): Phase A: System concept description [NASA-TM-110669] p 680 N95-32187
Low-Level and Nap-of-the-Earth (NOE) night operations [AGARD-CP-563] p 686 N95-32486

MIST
A review of water mist technology for fire suppression [AD-A285738] p 225 N95-20071

MIXERS
Jet mixer noise suppressor using acoustic feedback [NASA-CASE-LEW-15170-2] p 362 N95-26187
Laser doppler velocimeter system for subsonic jet mixer nozzle testing at the NASA Lewis Aeroacoustic Propulsion Lab [NASA-TM-106984] p 457 N95-30229

MIXING
Comparison of NO and OH planar fluorescence temperature measurements in scramjet model flowfields [BTN-95-EIX95042474388] p 209 A95-68312
Enhanced mixing of multiple supersonic rectangular jets by synchronized screech [HTN-95-42592] p 459 A95-87222
Effects of initial conditions on a single jet in crossflow [NASA-TM-107002] p 615 N95-30589

MIXING LAYERS (FLUIDS)
Model for compressible turbulence in hypersonic wall boundary and high-speed mixing layers [BTN-94-EIX94441386625] p 184 A95-68174
Resonant interaction of a linear array of supersonic rectangular jets: An experimental study [NASA-CR-195398] p 76 N95-15852
Numerical mixing calculations of confined reacting jet flows in a cylindrical duct [NASA-TM-106736] p 139 N95-18133
Studies on high pressure and unsteady flame phenomena [AD-A284126] p 152 N95-18410
Basic studies in turbulent shear flows [AD-A289145] p 437 N95-26998
Grid resolution and turbulent inflow boundary condition recommendations for NPARC calculations [NASA-TM-106959] p 482 N95-30253

MIXING LENGTH FLOW THEORY
Model for compressible turbulence in hypersonic wall boundary and high-speed mixing layers [BTN-94-EIX94441386625] p 184 A95-68174
Supersonic coaxial jet noise predictions [NASA-TM-106917] p 451 N95-26801

MIXING RATIOS
An analysis of aircraft exhaust plumes form accidental encounters [HTN-95-70943] p 351 A95-78008
Preliminary comparisons between MM5 NCAR/Penn State model generated icing forecasts and observations [NASA-TM-106959] p 655 A95-93458

MOBILE COMMUNICATION SYSTEMS
Use of MOBITEK wireless wide area networks as a solution to land-based positioning and navigation [BTN-94-EIX94441386132] p 189 A95-68188
Development of aeronautical mobile satellite services over the past thirty years [BTN-95-EIX95152569458] p 305 A95-73498
Experimental study of the helicopter-mobile radioelectrical channel and possible extension to the satellite-mobile channel p 247 N95-20945

MODAL RESPONSE
On the choice of appropriate bases for nonlinear dynamic modal analysis [HTN-95-A0495] p 221 A95-72566
Automatic identification of modal damping from Floquet analysis [HTN-95-01084] p 506 A95-90270

- Dynamic response of NASA Rotor Test Apparatus and Sikorsky S-76 hub mounted in the 80- by 120-Foot Wind Tunnel
[NASA-TM-108847] p 25 N95-11389
- Dynamics of the McDonnell-Douglas Large Scale Dynamic Rig and dynamic calibration of the rotor balance
[NASA-TM-108855] p 65 N95-13891
- Modal identification and its applications to damage detection in vibrating structures p 704 N95-32920
- MODEL REFERENCE ADAPTIVE CONTROL**
New adaptive methods for reconfigurable flight control systems, appendix 1
[AD-A292711] p 619 N95-30937
- MODELS**
Fan noise reduction from a supersonic inlet during simulated aircraft approach
[BTN-95-EIX95292721155] p 572 A95-89894
- Cost effective small-scale experiments to aid the design of ASTOVL aircraft
[CONGRESS PAPER C428-9-098] p 475 A95-91695
- The effect of interface properties on nickel base alloy composites
[NASA-CR-198363] p 629 N95-30787
- MODES**
Experimental/analytical approach to understanding mistuning in a transonic wind tunnel compressor
[NASA-TM-108833] p 95 N95-14617
- MODES (STANDING WAVES)**
Effect of density gradients in confined supersonic shear layers. Part 2: 3-D modes
[NASA-CR-198030] p 349 N95-24413
- MODULATION**
Propulsion controlled aircraft research
p 497 A95-90869
- Aerodynamic parameter estimation via Fourier modulating function techniques
[NASA-CR-4654] p 335 N95-24630
- Experimental investigation of aerodynamic devices for wind turbine rotational speed control, phase 1
[DE95-004034] p 564 N95-30016
- MODULES**
Modular avionics: Taking today's aircraft into tomorrow
[SAE PAPER 931416] p 610 A95-93681
- Advanced composites structural concepts and materials technologies for primary aircraft structures: Structural response and failure analysis
[NASA-CR-4448] p 11 N95-10240
- FASTPACK: Optimized solutions for modular avionics derived from a parametric study. Part 2: Avionics
p 233 N95-20635
- Ultra-Reliable Digital Avionics (URDA) processor
p 245 N95-20638
- Assuring Known Good Die (KGD) for reliable, cost effective MCMs
p 246 N95-20644
- Modular supplies for a distributed architecture — avionics packaging
p 234 N95-20657
- Intelligent finite element submodeling of multiphase modules for reliability analysis
[AD-A292911] p 679 N95-31455
- MODULUS OF ELASTICITY**
Evaluation of advanced aerospace materials by depth sensing indentation and scratch methods
[BTN-95-EIX95152584678] p 282 A95-73590
- Interlaminar shear test method development for long term durability testing of composites
p 301 N95-23300
- MOISTURE**
Measurement of moisture and total hydrocarbon contributions by valves used in clean room gas-delivery systems
[BTN-94-EIX94381359041] p 295 A95-74629
- Moisture induced pressures in concrete airfield pavements
[AD-A281974] p 52 N95-11789
- Bonded composite repair of thin metallic materials: Variable load amplitude and temperature cycling effects
p 393 N95-27509
- MOISTURE CONTENT**
Study of the droplet spray characteristics of a subsonic wind tunnel
[BTN-95-EIX95182619235] p 271 A95-76661
- Investigation of water droplet trajectories within the NASA icing research tunnel
[NASA-TM-107023] p 684 N95-32769
- MOLECULAR BEAMS**
Unanswered questions concerning the Nocilla gas-surface interaction model
[ISBN 1-879921-01-4] p 628 A95-93716
- Hypersonic Gas-Surface Energy Accommodation Test Facility
[DE94-014468] p 39 N95-12652
- Flow field investigation in a free jet - free jet core system for the generation of high intensity molecular beams
[DLR-FB-94-11] p 172 N95-18912
- State-to-state collisional dynamics of atmospheric species
[AD-A285053] p 245 N95-20484
- MOLECULAR EXCITATION**
Two-dimensional imaging of OH in a lean burning high pressure combustor
[NASA-TM-106854] p 236 N95-21383
- MOLECULAR FLOW**
Kinetic theory in aerothermodynamics
[HTN-95-A0002] p 183 A95-67829
- Parameters of Nocilla gas/surface interaction model from measured accommodation coefficients
[HTN-95-81639] p 541 A95-87687
- A perspective of rarefied gas flow problems relevant to high altitude flight
[SAE PAPER 931366] p 586 A95-93647
- MOLECULAR INTERACTIONS**
Empirical corrections of the rigid rotor interaction potential of H₂-H₂ in the attractive region: Dimer features in the FIR absorption spectra
[HTN-95-41943] p 361 A95-81690
- A perspective of rarefied gas flow problems relevant to high altitude flight
[SAE PAPER 931366] p 586 A95-93647
- MOLECULAR OSCILLATIONS**
Activated buoyancy propulsion = Paradox Power (tm)
[TABES PAPER 94-619] p 74 N95-14646
- MOLECULAR ROTATION**
Measurement by coherent anti-Stokes Raman scattering in the R5Ch hypersonic wind tunnel
[BTN-95-EIX95112523811] p 188 A95-69322
- MOLECULES**
Determination of wall boundary conditions for high-speed-ratio direct simulation Monte Carlo calculations
[BTN-95-EIX95182617457] p 267 A95-75728
- MOMENTS OF INERTIA**
Flight dynamics of an unmanned aerial vehicle
[AD-A282259] p 45 N95-12410
- A quantitative feedback theory FCS design for the subsonic envelope of the VISTA F-16 including configuration variation
[AD-A289221] p 409 N95-26958
- MOMENTUM**
Effects of periodic spanwise blowing on Delta-wing configuration characteristics
[HTN-95-81631] p 461 A95-87679
- Measurement of drag using a momentum balance
[HTN-95-01090] p 468 A95-90276
- MOMENTUM THEORY**
Rarefied gas effects on aerobraking/reentry vehicles with wakes
[NASA-CR-196586] p 415 N95-27093
- MOMENTUM TRANSFER**
Momentum and scalar transfer coefficients over aerodynamically smooth Antarctic surfaces
[HTN-95-92932] p 562 A95-91870
- Activated buoyancy propulsion = Paradox Power (tm)
[TABES PAPER 94-619] p 74 N95-14646
- MONITORS**
Hydraulic system diagnostic sensors
[BTN-95-EIX95031502752] p 209 A95-68259
- Environmental noise monitoring - source identification
[HTN-95-92537] p 558 A95-87357
- Flight Test Monitoring System using X-window
p 500 A95-91574
- Condition monitoring for helicopters: 3303 Airborne vibration monitoring system
[SAE PAPER 931360] p 610 A95-93642
- MONOPLANES**
The Elite: A high speed, low-cost general aviation aircraft for Aeroworld
[NASA-CR-197161] p 45 N95-12530
- Icarus Rewaxed: A high speed, low-cost general aviation aircraft for Aeroworld
[NASA-CR-197155] p 45 N95-12609
- Triton 2 (1B)
[NASA-CR-197188] p 46 N95-12636
- Incorporating biplane wing theory into a large, subsonic, all-cargo transport
p 391 N95-26956
- MONOTONE FUNCTIONS**
Design of robust optimal control systems and stability analysis of real structured uncertainties
[AD-A279089] p 256 N95-21913
- MONTE CARLO METHOD**
Hypersonic rarefied flow past spheres including wake structure
[BTN-95-EIX95152583250] p 305 A95-73551
- Aerodynamic characteristics of a hypersonic viscous optimized waverider at high altitudes
[BTN-95-EIX95152583251] p 266 A95-73552
- Higher-order viscous shock-layer solutions for high-altitude flows
[BTN-95-EIX95152583255] p 306 A95-73556
- Functional dependence of trajectory dispersion on initial condition errors
[BTN-95-EIX95152583263] p 298 A95-73564
- Determination of wall boundary conditions for high-speed-ratio direct simulation Monte Carlo calculations
[BTN-95-EIX95182617457] p 267 A95-75728
- Zonally decoupled direct simulation Monte Carlo solutions of hypersonic blunt-body wake flows
[BTN-95-EIX95182617458] p 268 A95-75729
- Numerical analysis of hypersonic low-density scramjet inlet flow
[BTN-95-EIX95212645694] p 272 A95-76746
- Rarefied gas numerical wind tunnel: OREX and HOPE
p 427 A95-82391
- Parameters of Nocilla gas/surface interaction model from measured accommodation coefficients
[HTN-95-81639] p 541 A95-87687
- Fatigue reliability method with in-service inspections
p 94 N95-14475
- Particle kinetic simulation of high altitude hypervelocity flight
[NASA-CR-197383] p 309 N95-22481
- DSMC calculations for 70-deg blunted cone at 3.2 km/s in nitrogen
[NASA-TM-109181] p 348 N95-24396
- Airborne passive polarimetric measurements of sea surface anisotropy at 92 GHz
[NASA-CR-197288] p 707 N95-32823
- MOON-EARTH TRAJECTORIES**
Fuel-optimal bank-angle control for lunar-return aerocapture
[BTN-95-EIX95212645706] p 299 A95-76758
- MOORING**
An in situ evaluation of TOPEX/Poseidon altimetric measurements versus measurements made by moorings and inverted echo sounders for sea surface height
[NASA-CR-198621] p 447 N95-27805
- MORPHOLOGY**
Integration of AIRSAR and AVIRIS data for Trail Canyon alluvial fan, Death Valley, California
p 709 N95-33760
- MORTALITY**
Explanatory factors for the geographic distribution of U.S. Civil aviation mortality
[HTN-95-92908] p 484 A95-91846
- Deaths and injuries as a result of lightning strikes to aircraft
[HTN-95-12213] p 485 A95-91913
- MOSAICS**
Developing the Aviation Gridded Forecast System
p 671 A95-93532
- Aviation value-added products and services from the NEXRAD Information Dissemination Service (NIDS)
p 671 A95-93535
- The development of an aircraft icing forecast technique using data from maps
p 675 A95-93549
- MOSCOW**
Aviation weather forecasting automated methods in the RAFC Moscow and the Airport Vnukovo
p 669 A95-93523
- MOTION**
Multiport pressure measurements on continuously moving wind tunnel models
[ARA-MEMO-391] p 188 N95-19772
- MOTION PERCEPTION**
The selective use of functional optical variables in the control of forward speed
[NASA-TM-108849] p 35 N95-12227
- MOTION PICTURES**
NASA video catalog
[NASA-SP-7109(01)] p 363 N95-24238
- MOTION SIMULATION**
Evaluation of simulation motion fidelity criteria in the vertical and directional axes
[HTN-94-00666] p 18 A95-60156
- Flight simulation
[BTN-94-EIX94461290242] p 84 A95-61735
- The advanced flight simulator complex
[CONGRESS PAPER C428-5-025] p 522 A95-91679
- Simulation of rotor blade element turbulence
[NASA-TM-108862] p 232 N95-21186
- A preliminary study of the airwake model used in an existing SH-60B/FFG-7 helicopter/ship simulation program
[DSTO-TR-0015] p 224 N95-21659
- Air cushioned landing craft (LCAC) based ship to shore movement simulation: A decision aid for the amphibious commander. A (SMMAT) application
[AD-A289635] p 436 N95-26722
- Telepresence media resource tape
[NASA-TM-110648] p 569 N95-30248
- MOTION SIMULATORS**
Collected papers on wind turbine technology
[NASA-CR-195432] p 447 N95-27970
- Design of a real-time wind turbine simulator using a custom parallel architecture
p 449 N95-27979

MOTION STABILITY

Determination of piloting feedback structures for an altitude tracking task
[BTN-95-EIX95242670770] p 327 A95-81077

MOUNTAINS

An algorithm for forecasting mountain wave-related turbulence in the stratosphere
[HTN-95-80656] p 254 A95-72500

Airborne lidar observation of mountain-wave-induced polar stratospheric clouds during EASOE
[HTN-95-00738] p 444 A95-86308

An integrated system to improve aviation weather forecasts for the Alaska Flange p 656 A95-93460

A poor man's expert system for aviation VSRF in complex terrain p 669 A95-93524

Amplification and breaking of atmospheric gravity waves p 675 A95-93552

Lee waves benign and malignant p 595 A95-93554

Report to the Chairman, Subcommittee on Aviation, Committee on Commerce, Science, and Transportation, US Senate. Aviation Safety: FAA can better prepare general aviation pilots for mountain flying risks
[GAO/RCED-94-15] p 687 N95-32784

MOUNTING

Active plate and missile wing development using directionally attached piezoelectric elements
[HTN-95-42340] p 408 A95-86169

A theoretical analysis of airborne sound transfer for a resiliently mounted machine to its foundation p 30 N95-11304

MRCIA AIRCRAFT

Out of area experiences with the RB199 in Toronto p 198 N95-19654

MULLITES

Innovative processing of composites for ultra-high temperature applications, book 1
[AD-A290889] p 537 N95-29842

MULTIBLOCK GRIDS

Construction of nearly orthogonal multiblock grids for compressible flow simulation
[BTN-94-EIX94361133526] p 207 A95-65981

Automatic multi-block grid generation for high-lift configuration wings p 567 N95-28764

Numerical solution of the full potential equation using a chimera grid approach
[NASA-TM-110360] p 594 N95-32188

Parallel computation of transonic flows about an aircraft configuration using multi-block structured grids p 685 N95-34537

A large scale 3D Navier-Stokes analysis using NAL-NWT p 707 N95-34539

MULTIDISCIPLINARY DESIGN OPTIMIZATION

Ply layup optimization and micromechanics tailoring of composite aircraft engine structures
[BTN-95-EIX95112524206] p 196 A95-69302

Multilevel decomposition procedure for efficient design optimization of helicopter rotor blades
[BTN-95-EIX95222650784] p 334 A95-79240

Aeroseuroelastic aspects of wing/control surface planform shape optimization
[BTN-95-EIX95222650795] p 340 A95-79251

NASA High Performance Computing and Communications program
[NASA-TM-4653] p 176 N95-18573

Aerodynamic optimization studies on advanced architecture computers
[NASA-CR-198045] p 330 N95-24379

Structural design optimization with survivability dependent constraints application: Primary wing box of a multi-role fighter p 398 N95-28440

Surface Modeling, Grid Generation, and Related Issues in Computational Fluid Dynamic (CFD) Solutions
[NASA-CP-3291] p 476 N95-28723

A grid generation system for multi-disciplinary design optimization p 567 N95-28763

MULTIGRID METHODS

Navier-Stokes simulation of rotor-body flowfield in hover using overset grids
[PAPER C15] p 1 A95-60160

Jet to freestream velocity ratio computations for a jet in a crossflow
[AIAA PAPER 93-4860] p 2 A95-60178

Application of the multigrid solution technique to hypersonic entry vehicles
[BTN-95-EIX95152583254] p 306 A95-73555

Three-dimensional adaptive grid-embedding Euler technique
[HTN-95-20825] p 543 A95-88086

Parallel computational fluid dynamics '91: Conference Proceedings, Stuttgart, Germany, Jun. 10-12, 1991
[ISBN 0-444-89363-6] p 548 A95-91479

Computational fluid dynamics '92: Proceedings of the European Computational Fluid Dynamics Conference, 1st, Brussels, Belgium, Sep. 7-11, 1992. Vols. 1 & 2
[ISBN 0-444-89793-3] p 638 A95-95357

Navier-Stokes computations around a realistic fighter configuration p 591 A95-95440

Multigrid solution for the compressible Euler equations by an implicit characteristic-flux-averaging p 642 A95-95459

SAUNA: A system for grid generation and flow simulation using hybrid structured/unstructured grids p 642 A95-95470

Hypersonic Navier-Stokes computations about complex configurations p 644 A95-95497

Agglomeration multigrid for viscous turbulent flows [AD-A284064] p 8 N95-10848

Solution of full potential equation on an airfoil by multigrid technique
[NAL-TM-CSS-9303] p 119 N95-18904

CFD: Advances and Applications, part 1
[NAL-SP-9322-PT-1] p 165 N95-19444

Inviscid and viscous flow modelling of complex aircraft configurations using the CFD simulation system sauna [ARA-MEMO-403] p 211 N95-19777

Surface Modeling, Grid Generation, and Related Issues in Computational Fluid Dynamic (CFD) Solutions
[NASA-CP-3291] p 476 N95-28723

Block-structured grids for complex aerodynamic configurations: Current status p 551 N95-28736

Three-dimensional hybrid grid generation using advancing front techniques p 567 N95-28745

Leading edge film cooling effects on turbine blade heat transfer
[NASA-TM-106955] p 513 N95-29115

Development of a rotary wing Navier-Stokes CFD code based on TLNS3D code
[AD-A290421] p 554 N95-29387

Pressure updating methods for the steady-state fluid equations
[NASA-CR-198163] p 569 N95-30353

Multigrid convergence acceleration for the 2D Euler equations applied to high-lift systems
[PB95-198081] p 593 N95-30814

A simulation of damping process of pendulum motion due to aerodynamic forces p 711 N95-34551

MULTIMEDIA

A computer-based multimedia prototype for night vision goggles
[AD-A286208] p 258 N95-21882

MULTIPATH TRANSMISSION

Active control of complex noise problems using a broadband, multichannel controller p 29 N95-11271

Precision landing system mathematical modeling study report for Andrews Air Force Base, runway 19L, Camp Springs, MD
[AD-A289015] p 384 N95-27903

Tactical low-level helicopter communications p 702 N95-32492

MULTIPHASE FLOW

Effect of ambient turbulence intensity on sphere wakes at intermediate Reynolds numbers
[BTN-95-EIX95182619101] p 308 A95-76586

An aerodynamic analysis of a mixed flow turbine
[NASA-TM-106674] p 15 N95-10153

MULTIPLYING

Fiber Optic Control System integration for advanced aircraft. Electro-optic and sensor fabrication, integration, and environmental testing for flight control systems: Laboratory test results
[NASA-CR-195408] p 161 N95-18938

MULTIPOLES

Sound propagation from an arbitrarily oriented multipole placed near a plane, finite impedance surface
[BTN-94-EIX94371338964] p 257 A95-70797

MULTIPROCESSING (COMPUTERS)

Parallel methods for the flight simulation model
[DE94-013330] p 52 N95-11752

Portable parallel stochastic optimization for the design of aeropropulsion components
[NASA-CR-195312] p 154 N95-16072

MULTISENSOR APPLICATIONS

Low-level data fusion for landing runways detection p 689 N95-33136

Advanced data visualization and sensor fusion: Conversion of techniques from medical imaging to Earth science p 711 N95-34236

MULTISENSOR FUSION

Passive MMW camera for low visibility landings p 59 N95-13215

MATSurv multisensor air traffic surveillance
[AD-A292253] p 489 N95-28887

An approach to sensor data fusion for flying and landing aid purpose p 686 N95-32488

The DLR research programme on an integrated multi sensor system for surface movement guidance and control p 689 N95-33135

Low-level data fusion for landing runways detection p 689 N95-33136

Advanced data visualization and sensor fusion: Conversion of techniques from medical imaging to Earth science p 711 N95-34236

MULTISPECTRAL BAND SCANNERS

TIMS observations of surface emissivity in HAPEX-Sahel p 709 N95-33799

MULTISPECTRAL RADAR

The Anglo-French Compact Laser Radar demonstrator programme p 703 N95-32501

MULTIVARIABLE CONTROL

Aeroelastic vehicle multivariable control synthesis with analytical robustness evaluation
[BTN-95-EIX95182619115] p 321 A95-76592

Multivariable stability and robustness of sequentially designed feedback systems
[BTN-95-EIX95182619125] p 322 A95-76602

Derivation of system matrices from nonlinear dynamic simulation of jet engines
[BTN-95-EIX95182619139] p 288 A95-76616

High-performance, robust, bank-to-turn missile autopilot design
[BTN-95-EIX95242670751] p 336 A95-81096

Multivariable adaptive control using only input and output measurements for turbojet engines p 677 A95-92597

Design of high performance multivariable control systems for supermaneuverable aircraft at high angle of attack
[NASA-CR-197661] p 293 N95-22908

N

NACELLES

Civil aircraft propulsion integration: Current & future
[SAE PAPER 932624] p 495 A95-90085

Evaluation of alternative in-flight fire suppressants for full-scale testing in simulated aircraft engine nacelles and dry bays
[PB94-203403] p 42 N95-13247

Ducted fan acoustic radiation including the effects of nonuniform mean flow and acoustic treatment
[NASA-CR-197449] p 172 N95-16401

Pressure distribution measurements on an isolated TPS 441 nacelle p 115 N95-17878

Low speed propeller slipstream aerodynamic effects p 116 N95-17882

Impact of noise environment on engine nacelle design p 173 N95-19147

Application of fiber-reinforced bismaleimide materials to aircraft nacelle structures p 397 N95-28278

Drag measurements of an axisymmetric nacelle mounted on a flat plate at supersonic speeds
[NASA-TM-4660] p 684 N95-32821

Fan noise prediction assessment
[NASA-CR-195051] p 711 N95-33831

NAP-OF-THE-EARTH NAVIGATION

Automatic guidance and control for helicopter obstacle avoidance
[BTN-95-EIX95182619130] p 291 A95-76607

Low-Level and Nap-of-the-Earth (NOE) night operations
[AGARD-CP-563] p 686 N95-32486

The application of helicopter mission simulation to Nap-of-the-Earth operations p 710 N95-32496

A highly reliable, high performance open avionics architecture for real time Nap-of-the-Earth operations p 693 N95-32497

Laser based obstacle warning sensors for helicopters p 686 N95-32499

NARROWBAND

Analysis and simulation of narrowband GPS jamming using digital excision temporal filtering
[AD-A289328] p 383 N95-26898

NASA PROGRAMS

Status of the NASA balloon program p 181 A95-66296

Overview of the NASA balloon R&D program p 181 A95-66297

The NASA-sponsored Maryland center for hypersonic education and research
[AIAA PAPER 95-6105] p 519 A95-88010

The NASA/UTA center for hypersonic research
[AIAA PAPER 95-6106] p 520 A95-90438

Research and educational initiatives at the Syracuse University Center for Hypersonics
[AIAA PAPER 95-6107] p 520 A95-90439

NASA Lewis Propulsion Systems Laboratory test article systems criteria
[NASA-TM-106589] p 20 N95-10446

Langley overview
[NASA-TM-109891] p 20 N95-10547

Dryden overview for schools
[NASA-TM-104282] p 21 N95-10710

Dryden tour tape, 1994 p 21 N95-10714

[NASA-TM-104288]

- Building the Integrated Test Facility: A foundation for the future
[NASA-TM-104280] p 21 N95-10738
- NASA Lewis Propulsion Systems Laboratory customer guide manual
[NASA-TM-106569] p 21 N95-10822
- General Aviation Task Force report
[NASA-TM-109950] p 1 N95-11463
- Aeronautics and space technology, past, present, and future
p 35 N95-11892
- NASA's Hypersonic Research Engine Project: A review
[NASA-TM-107759] p 50 N95-12860
- A review of 50 years of aerodynamic research with NACA/NASA
[NASA-TM-109163] p 102 N95-13663
- Research and technology highlights, 1993
[NASA-TM-4575] p 102 N95-15065
- Assessment of the Space Station program
p 149 N95-16352
- ICASE
[NASA-CR-195001] p 170 N95-16898
- NASA High Performance Computing and Communications program
[NASA-TM-4653] p 176 N95-18573
- 1994 NASA-HU American Society for Engineering Education (ASEE) Summer Faculty Fellowship Program
[NASA-CR-194972] p 325 N95-23276
- Research and Technology, 1994
[NASA-TM-106764] p 262 N95-24025
- AIAA Techfest 20 Proceedings
[NIAR-94-1] p 367 N95-26941
- The high speed civil transport and NASA's High Speed Research (HSR) program
p 390 N95-26945
- Research and Technology Objectives and Plans Summary (RTOPS)
[NASA-TM-108574] p 453 N95-28002
- Overview of the ACT program
p 424 N95-28463
- Software process improvement in the NASA software engineering laboratory
[AD-A289912] p 450 N95-28627
- NASA SPACE PROGRAMS**
Space Generic Open Avionics Architecture (SGOAA): Overview
p 99 N95-14161
- NASTRAN**
Thin tailored composite wing for civil tiltrotor
p 285 N95-23317
- A NASTRAN-based computer program for structural dynamic analysis of Horizontal Axis Wind Turbines
p 439 N95-27980
- Applications of a damage tolerance analysis methodology in aircraft design and production
p 426 N95-28483
- NATIONAL AEROSPACE PLANE PROGRAM**
National AeroSpace Plane: Technology transfer
[BTN-95-EIX95072498879] p 180 N95-68395
- The Methane-Acetylene Cycle Aerospace Plane: A potential option for inexpensive Earth to orbit transportation
[HTN-95-51845] p 525 N95-87483
- Aero-Space Plane: Flexible access to space
[NASA-TM-109904] p 22 N95-10553
- Hypersonic engine seal development at NASA Lewis Research Center
p 60 N95-13602
- NATIONAL AIRSPACE SYSTEM**
Analysis of en route controller hazardous weather-related tasks
p 665 N95-93503
- Using ATMS weather products for air traffic strategic planning
p 672 N95-93536
- Integrated voice and data communications for air traffic service applications
p 600 N95-95090
- Vertical flight terminal operational procedures. A summary of FAA research and development
[AD-A283550] p 85 N95-15328
- Identification of Artificial Intelligence (AI) applications for maintenance, monitoring, and control of airway facilities
[AD-A282479] p 125 N95-17373
- Operational And Supportability Implementation System (OASIS) test and evaluation master plan
[AD-A284765] p 126 N95-18088
- Federal Aviation Administration plan for research, engineering and development, 1995
p 363 N95-24202
- Aviation system capacity improvements through technology
[NASA-TM-109165] p 333 N95-24633
- The 1994 updated National Airspace System performance assessment for year 2005
[AD-A288652] p 380 N95-26485
- Federal aviation administration plan for research, engineering and development
[AD-A290952] p 490 N95-29733
- A NASPAC-Based analysis of the delay and cost effects of the western-pacific region preliminary resectorization effort of 1993
[AD-A288696] p 601 N95-31013
- Effects of civil tiltrotor service in the northeast corridor on en route airspace loads
[AD-A293686] p 599 N95-31687
- NATIONAL AVIATION SYSTEM**
An approach to weather requirements management
p 653 A95-93448
- FAA aviation forecasts: Fiscal year 1995-2006
[AD-A293682] p 584 N95-31598
- NATIONAL LAUNCH VEHICLE PROGRAM**
A shadowgraph study of the National Launch System's 1 1/2 stage vehicle configuration and Heavy Lift Launch Vehicle configuration — Using the Marshall Space Flight Center's 14-Inch Trisonic Wind Tunnel
[NASA-RP-1347] p 35 N95-11710
- NATURAL LANGUAGE PROCESSING**
Collected papers of the Soar/IFOR project, Spring 1994
[AD-A280063] p 238 N95-20624
- NAVIER-STOKES EQUATION**
Navier-Stokes simulation of rotor-body flowfield in hover using overset grids
[PAPER C15] p 1 A95-60160
- Recent advances in Euler and Navier-Stokes methods for calculating helicopter rotor aerodynamics and acoustics
[HTN-94-00686] p 2 A95-60169
- Solution-adaptive structured-unstructured grid method for unsteady turbomachinery analysis. Part I: Methodology
[BTN-94-EIX94441380983] p 208 A95-67329
- Linear disturbances in hypersonic, chemically reacting shock layers
[BTN-94-EIX94441386605] p 182 A95-67336
- Shock layers and boundary layers in hypersonic flows
[HTN-95-A0003] p 183 A95-67830
- Three-dimensional analysis of scramjet nozzle flows
[BTN-94-EIX94441380978] p 196 A95-68162
- Navier-Stokes computation of a viscous optimized waverider
[BTN-95-EIX95041503782] p 193 A95-69213
- Numerical simulation of incidence and sweep effects on delta wing vortex breakdown
[BTN-95-EIX95062487526] p 186 A95-69234
- Large-scale computational fluid dynamics by the finite element method
[BTN-94-EIX94381359154] p 243 A95-71744
- Preconditioned domain decomposition scheme for three-dimensional aerodynamic sensitivity analysis
[BTN-95-EIX95152577612] p 321 A95-73471
- Effects of spatial order of accuracy on the computation of vortical flowfields
[BTN-95-EIX95152577604] p 305 A95-73479
- Computation of oscillating airfoil flows with one- and two-equation turbulence models
[BTN-95-EIX95152577588] p 263 A95-73494
- Computation of the poststall behavior of a circulation controlled airfoil
[BTN-95-EIX95152582320] p 264 A95-73523
- Navier-Stokes prediction of large-amplitude delta-wing roll oscillations
[BTN-95-EIX95152582329] p 281 A95-73531
- Computational study of plume-induced separation on a hypersonic powered model
[BTN-95-EIX95152582346] p 266 A95-73548
- Hypersonic rarefied flow past spheres including wake structure
[BTN-95-EIX95152583250] p 305 A95-73551
- Hypersonic nonequilibrium Navier-Stokes solutions over an ablating graphite nosetip
[BTN-95-EIX95152583252] p 305 A95-73553
- Hypersonic convective heat transfer over 140-deg blunt cones in different gases
[BTN-95-EIX95152583253] p 306 A95-73554
- Application of the multigrid solution technique to hypersonic entry vehicles
[BTN-95-EIX95152583254] p 306 A95-73555
- Higher-order viscous shock-layer solutions for high-altitude flows
[BTN-95-EIX95152583255] p 306 A95-73556
- Optimization of contoured hypersonic scramjet inlets with a least-squares parabolized Navier-Stokes procedure
[HTN-95-20976] p 261 A95-74042
- Convective and radiative heat transfer analysis for the fire 2 forebody
[BTN-95-EIX95182617460] p 268 A95-75731
- Turbulent transonic airfoil flow simulation using a pressure-based algorithm
[BTN-95-EIX95182619078] p 269 A95-75763
- Simulation of transverse gas injection in turbulent supersonic air flows
[BTN-95-EIX95182619080] p 269 A95-75765
- Viscous-inviscid interaction method for unsteady low-speed airfoil flows
[BTN-95-EIX95182619093] p 269 A95-75778
- Influence of streamwise curvature on longitudinal vortices imbedded in turbulent boundary layers
[BTN-94-EIX94401378820] p 307 A95-76489
- Grid refinement test of time-periodic flows over bluff bodies
[BTN-94-EIX94401378822] p 307 A95-76491
- Numerical investigation of supersonic flows around a spiked blunt body
[BTN-95-EIX95212645690] p 271 A95-76742
- Computational/experimental investigation of staged injection into a Mach 2 flow
[HTN-95-51646] p 432 A95-85028
- Practical formulation of a positively conservative scheme
[HTN-95-51668] p 433 A95-85050
- Compressible Navier-Stokes computations of multielement airfoil flows using multiblock grids
[HTN-95-42327] p 371 A95-86156
- Using the Liou-Steffen algorithm for the Euler and Navier-Stokes equations
[HTN-95-42348] p 373 A95-86177
- Mesh generation and adaptivity for the solution of compressible viscous high speed flows
[BTN-95-EIX95262697157] p 538 A95-86893
- Pulsed jet ignition modeling with a full chemistry
p 538 A95-87184
- Hypersonic flow past open cavities
[HTN-95-42577] p 458 A95-87207
- Computational methods in applied sciences; European Computational Fluid Dynamics Conference, 1st, Brussels, Belgium, Sept. 7-11, 1992
[ISBN 0-444-89795-X] p 539 A95-87552
- Two-dimensional unsteady leading-edge separation on a pitching airfoil
[HTN-95-81628] p 461 A95-87676
- Numerical model for circulation-control flows
[HTN-95-81632] p 461 A95-87680
- Heat-transfer measurements and computations of swept-shock-wave boundary-layer interactions
[HTN-95-81634] p 541 A95-87682
- Low-dimensional description of the dynamics in separated flow past thick airfoils
[HTN-95-20832] p 544 A95-88093
- Compressible Navier-Stokes calculations of the flow over airfoil sections. Comparisons of 1st and 2nd order turbulence models
[SAE PAPER 932510] p 546 A95-89183
- Computational study of boundary layer control for improving airfoil performance
[SAE PAPER 932513] p 466 A95-89186
- Computational aerodynamic analysis on the Open Skies aircraft
[SAE PAPER 932514] p 466 A95-89187
- Computational study of a two-slot circulation control airfoil
[SAE PAPER 932531] p 466 A95-89191
- Computational fluid dynamics with icing effects
[SAE PAPER 932532] p 466 A95-89192
- Navier-Stokes calculations of rotor-airframe interaction in forward flight
[HTN-95-01087] p 468 A95-90273
- Parallel computational fluid dynamics '91; Conference Proceedings, Stuttgart, Germany, Jun. 10-12, 1991
[ISBN 0-444-89363-6] p 548 A95-91479
- Aerodynamic simulation on massively parallel systems
p 549 A95-91487
- Solution of the Navier-Stokes equations on a massively parallel transputer system
p 549 A95-91490
- Numerical experiments on aerodynamic heating mechanism in shock reflection processes
p 471 A95-91497
- Implicit multiblock Euler and Navier-Stokes calculations
[HTN-95-A1755] p 634 A95-93318
- Evaluation of a multigrid-based Navier-Stokes solver for aerothermodynamic computations
[BTN-95-EIX95302694459] p 583 A95-94056
- 3-D Navier-Stokes analysis of crossing glancing shocks/turbulent boundary layer interactions
[BTN-95-EIX95302729768] p 636 A95-94130
- Supersonic, turbulent flow computation and drag optimization for axisymmetric afterbodies
[BTN-95-EIX95302729772] p 637 A95-94134
- Computation of delta-wing roll maneuvers
[BTN-95-EIX0619952748164] p 605 A95-94458
- Navier-Stokes applications to high-lift airfoil analysis
[BTN-95-EIX0619952748182] p 590 A95-94475
- Analysis of low Reynolds number airfoil flows
[BTN-95-EIX0619952748183] p 590 A95-94476
- Computational fluid dynamics '92; Proceedings of the European Computational Fluid Dynamics Conference, 1st, Brussels, Belgium, Sep. 7-11, 1992. Vols. 1 & 2
[ISBN 0-444-89793-3] p 638 A95-95357
- Discretization of the parabolised Navier-Stokes equations
p 638 A95-95362

- Numerical solution of Euler and Navier-Stokes equations for 2D transonic problems p 638 A95-95366
- Laminar and turbulent flow over optimal riblets p 639 A95-95383
- Heat transfer on bent-noise biconic in hypersonic flow p 639 A95-95394
- A numerical investigation of flow around a square-section cylinder mounted with a splitter plate p 639 A95-95401
- An efficient discrete vortex method for low Reynolds number incompressible flows p 639 A95-95407
- Viscous flow simulation using the discrete vortex diffusion velocity method p 639 A95-95421
- An improved finite element method for the solution of the compressible Euler and Navier-Stokes equations p 640 A95-95439
- Navier-Stokes computations around a realistic fighter configuration p 591 A95-95440
- Implicit multidomain calculation of viscous transonic flows without artificial viscosity or upwinding p 640 A95-95443
- High-lift calculations using Navier-Stokes methods p 641 A95-95444
- On the prediction of transonic unsteady flows using second order time accuracy p 641 A95-95448
- 2-D and 3-D numerical simulation of a supersonic inlet flowfield p 641 A95-95457
- A cartesian grid finite element method for aerodynamics of moving rigid bodies p 642 A95-95471
- Multi-block finite volume calculation of compressible flow past aerodynamic configurations p 643 A95-95473
- A 2D parallel multiblock Navier-Stokes solver with applications on shared- and disturbed memory machines p 643 A95-95475
- Surface grid generation for multi-block structured grids p 643 A95-95478
- Hypersonic Navier-Stokes computations about complex configurations p 644 A95-95497
- Navier-Stokes simulation of turbulent vortex high-Re-number flows over a delta wing p 644 A95-95507
- Partially implicit method for simulating viscous aerofoil flows [BTN-94-EIX94522406680] p 709 A95-96299
- Navier-Stokes simulations of WECS airfoil flowfields [DE94-013341] p 7 N95-10226
- A full Navier-Stokes analysis of subsonic diffuser of a bifurcated 70/30 supersonic inlet for high speed civil transport application [NASA-TM-106637] p 8 N95-10820
- Agglomeration multigrid for viscous turbulent flows [AD-A284064] p 8 N95-10848
- Numerical simulation of the flow about the F-18 HARV at high angle of attack [NASA-CR-196396] p 9 N95-10940
- Steady and unsteady three-dimensional transonic flow computations by integral equation method [NASA-CR-196777] p 10 N95-11582
- Investigation of advanced counterrotation blade configuration concepts for high speed turboprop systems. Task 8: Cooling flow/heat transfer analysis [NASA-CR-195359] p 50 N95-11901
- Supersonic base flow investigation over axisymmetric afterbodies [PB94-180957] p 39 N95-12578
- Validation of the RPLUS3D code for supersonic inlet applications involving three-dimensional shock wave-boundary layer interactions [NASA-TM-106579] p 39 N95-13058
- User's guide for ENSAERO: A multidisciplinary program for fluid/structural/control interaction studies of aircraft (release 1) [NASA-TM-108853] p 65 N95-13662
- Numerical modeling of a cryogenic fluid within a fuel tank [NASA-TM-4651] p 89 N95-13892
- The role of CFD in the design process p 90 N95-14135
- Hybrid structured/unstructured grid computations for the F/A-18 at high angle of attack p 68 N95-14233
- A Cartesian, cell-based approach for adaptively-refined solutions of the Euler and Navier-Stokes equations [NASA-TM-106786] p 73 N95-14297
- Navier-Stokes predictions of missile aerodynamics p 74 N95-14451
- Numerical study of the effects of icing on viscous flow over wings [NASA-CR-197102] p 75 N95-14803
- Comparison of computational and experimental results for a supercritical airfoil [NASA-TM-4601] p 108 N95-16908
- Three dimensional compressible turbulent flow computations for a diffusing S-duct with/without vortex generators [NASA-CR-195390] p 138 N95-17402
- Static aerodynamics CFD analysis for 120-mm hypersonic KE projectile design [ARL-MR-184] p 118 N95-18611
- Numerical computations of supersonic base flow with special emphasis on turbulence modeling [AD-A283688] p 119 N95-18670
- Theoretical investigations of shock/boundary layer interactions on a $Ma(\infty) = 8$ waverider [DLR-FB-94-12] p 119 N95-18910
- Solution of Navier-Stokes equations using high accuracy monotone schemes p 161 N95-19019
- Simulation of steady and unsteady viscous flows in turbomachinery p 140 N95-19023
- Numerical simulation of dynamic-stall suppression by tangential blowing [AD-A284887] p 120 N95-19110
- Unsteady aerodynamic analyses for turbomachinery aerodynamic predictions p 141 N95-19381
- Parabolized Navier-Stokes solution of supersonic/hypersonic flows p 123 N95-19464
- Inviscid and viscous flow modelling of complex aircraft configurations using the CFD simulation system sauna [ARA-MEMO-403] p 211 N95-19777
- Open Skies project computational fluid dynamic analysis [AD-A285928] p 223 N95-19991
- Application of Navier-Stokes code PAB3D with kappa-epsilon turbulence model to attached and separated flows [NASA-TP-3480] p 224 N95-21338
- Unstructured-grid large-eddy simulation of flow over an airfoil p 225 N95-22448
- Large-eddy simulation of flow through a plane, asymmetric diffuser p 250 N95-22449
- An assessment of viscous effects in computational simulation of benign and burst vortex flows on generic fighter wind-tunnel models using TEAM code [NASA-CR-4650] p 273 N95-23185
- Mach 10 computational study of a three-dimensional scramjet inlet flow field [NASA-TM-4602] p 310 N95-23210
- Numerical computation of aerodynamics and heat transfer in a turbine cascade and a turn-around duct using advanced turbulence models p 313 N95-23444
- Convergence acceleration of implicit schemes in the presence of high aspect ratio grid cells p 313 N95-23446
- A time-accurate finite volume method valid at all flow velocities p 314 N95-23447
- Cavitation modeling in Euler and Navier-Stokes codes p 315 N95-23630
- Verification of computational aerodynamic predictions for complex hypersonic vehicles using the INCA(trademark) code [DE95-004757] p 330 N95-24308
- A combined geometric approach for solving the Navier-Stokes equations on dynamic grids [NASA-TM-106919] p 332 N95-26075
- Computational analysis of forebody tangential slot blowing on the high alpha research vehicle [NASA-CR-197754] p 389 N95-26591
- Study of potential aerodynamic benefits from spanwise blowing at wingtip [NASA-TP-3515] p 378 N95-28669
- Numerical study to assess sulfur hexafluoride as a medium for testing multielement airfoils [NASA-TP-3496] p 378 N95-28674
- An unstructured-grid software system for solving complex aerodynamic problems p 476 N95-28743
- A vorticity-velocity approach for three-dimensional unsteady viscous flow over wings p 478 N95-29108
- Leading edge film cooling effects on turbine blade heat transfer [NASA-TM-106955] p 513 N95-29115
- An extension of the continuum model by Grad's thirteen moment equations for hypersonic rarefied flows p 478 N95-29118
- Finite element vorticity-based methods for the solution of the incompressible and compressible Navier-Stokes equations p 553 N95-29119
- Navier-Stokes solution of wing wake structure and its perturbation p 479 N95-29121
- Solution of the Navier-Stokes equations on locally refined Cartesian meshes using state-vector splitting p 553 N95-29197
- A fourth order Euler/Navier-Stokes prediction method for the aerodynamics and aeroelasticity of hovering rotor blades p 554 N95-29242
- Grid orthogonality effects on predicted turbine midspan heat transfer and performance [NASA-TM-106931] p 554 N95-29371
- Development of a rotary wing Navier-Stokes CFD code based on TLNS3D code [AD-A290421] p 554 N95-29387
- Computation of the integrated aerodynamic and propulsive flowfields of a generic hypersonic space plane p 481 N95-29788
- Survey of CFD applications for high speed inlets [AD-A291365] p 557 N95-30087
- Use of the PARC code to estimate the off-design transonic performance of an over/under turboramjet nozzle [NASA-TM-106924] p 482 N95-30091
- Computation of high-altitude hypersonic flow-field radiation p 593 N95-30843
- Parametrics on 2D Navier-Stokes analysis of a Mach 2.68 bifurcated rectangular mixed-compression inlet [NASA-TM-107003] p 617 N95-30861
- Numerical simulation of ram accelerator performance including transient effects during initiation of combustion and sensitivity studies p 629 N95-31203
- The 25th International Symposium on Combustion [AD-A286825] p 630 N95-31268
- Unsteady flow simulations about moving boundary configurations using dynamic domain decomposition techniques p 649 N95-31837
- Turbulence models in the Navier-Stokes simulation of airfoil stall [TRITA-NA-9312] p 705 N95-33059
- Numerical studies of turbulent free surface flows and unsteady propeller flows [AD-A294377] p 706 N95-34343
- Calculation of supersonic combustion in SCRAMJET engines p 698 N95-34513
- Hypersonic CFD analysis for the aerothermodynamic design of HOPE p 684 N95-34520
- Numerical solutions of inviscid and viscous flows about airfoils by TVD method p 684 N95-34521
- Direct numerical simulation of incompressible homogeneous isotropic turbulence using NWT p 706 N95-34530
- Performance evaluation of the NWT with incompressible NS code p 707 N95-34533
- Parallel computation of transonic flows about an aircraft configuration using multi-block structured grids p 685 N95-34537
- Vector-parallel simulations of transonic wind tunnel flows about a fully configured model of aircraft p 685 N95-34538
- A large scale 3D Navier-Stokes analysis using NAL-NWT p 707 N95-34539
- Computations of low speed flow about space-plane p 685 N95-34544
- Numerical simulations of dynamic stall phenomena in low speed flows p 685 N95-34546
- Numerical simulation of unsteady viscous flow around an airfoil with oscillating spoiler p 685 N95-34547
- A simulation of damping process of pendulum motion due to aerodynamic forces p 711 N95-34551
- NAVIGATION**
- Development and flight test of a deployable precision landing system [BTN-95-EIX95062487535] p 190 A95-69243
- Switched bias proportional navigation for homing guidance against highly maneuvering targets [BTN-95-EIX95182619145] p 279 A95-76622
- New failure detection approach and its application to GPS autonomous integrity monitoring [BTN-95-EIX95202637613] p 279 A95-76676
- Solutions of generalized proportional navigation with maneuvering and nonmaneuvering targets [BTN-95-EIX95202637606] p 279 A95-76683
- The navigation toolkit [NASA-CR-197290] p 229 N95-22161
- Operator modeling in commercial aviation: Cognitive models, intelligent displays, and pilot's assistants [NASA-CR-198609] p 401 N95-28203
- Qualitative environmental navigation: Theory and practice — robot navigation p 601 N95-30486
- NAVIGATION AIDS**
- Flight test development and evaluation of a Kalman filter state estimator for low-altitude flight [HTN-94-00684] p 16 A95-60167
- Conversion of Earth-centered Earth-fixed coordinates to geodetic coordinates [BTN-94-EIX94441380862] p 125 A95-64294
- On-the-fly carrier phase ambiguity resolution for precise aircraft landing [BTN-95-EIX95112522535] p 190 A95-69328
- Precise navigation using adaptive FIR filtering and time domain spectral estimation [BTN-95-EIX9514255485] p 227 A95-72888
- A market perspective on FANS [SAE PAPER 932521] p 486 A95-89189
- Automatic vehicle location and airfield ground movement [CONGRESS PAPER C428-7-148] p 488 A95-91689

Spatial awareness comparisons between large-screen, integrated pictorial displays and conventional EFIS displays during simulated landing approaches [NASA-TP-3467] p 80 N95-14852

GPS-Scuttler capacity analysis [AD-A280037] p 245 N95-20599

Minima reduction simulation test results [AD-A285626] p 228 N95-21148

Cueing light configuration for aircraft navigation [NASA-CASE-ARC-11982-1] p 280 N95-23393

TRISTAR 1: Evaluation methods for testing head-up display (HUD) flight symbology [NASA-TM-4665] p 288 N95-24030

Conceptual design of a map interactive system for military aircraft cockpits [AD-A289760] p 508 N95-28692

An exploratory survey of information requirements for instrument approach charts [AD-A293882] p 601 N95-31520

An approach to sensor data fusion for landing and aid purpose p 686 N95-32488

Laser based obstacle warning sensors for helicopters p 686 N95-32499

A helmet mounted display for night missions at low altitude p 693 N95-32503

Effects of the specific military aspects of satellite navigation on the civil use of GPS/GLONASS p 688 N95-33134

Current issues in the design and information content of instrument approach charts [AD-A294752] p 690 N95-34562

NAVIGATION INSTRUMENTS

Simulation development of a forward sensor-enhanced low-altitude guidance system [HTN-94-00688] p 17 A95-60170

Comments on effect of wet snow on the null-reference ILS system [BTN-95-EIX9514255488] p 227 A95-72885

Assessment of a non-dedicated GPS receiver system for precise airborne attitude determination [DE94-019309] p 229 N95-21520

Flight evaluation of GPS/DGPS sensor systems installed in NAL Do228 [NAL-TR-1230] p 382 N95-26585

Guidelines for the design of GPS and LORAN receiver controls and displays [AD-A293753] p 602 N95-31572

An approach to sensor data fusion for flying and landing aid purpose p 686 N95-32488

Low-level data fusion for landing runways detection p 689 N95-33136

NAVIGATION SATELLITES

Description of a GNSS availability model and its use in developing requirements [BTN-95-EIX95202637603] p 308 A95-76686

Analysis and simulation of narrowband GPS jamming using digital excision temporal filtering [AD-A289328] p 383 N95-26898

Determining GPS average performance metrics p 383 N95-27791

NAVIGATORS

An analysis of the KC-135 three-person cockpit [AD-A289540] p 390 N95-26873

NAVSTAR SATELLITES

Effect of broadcast and precise ephemerides on estimates of the frequency stability of GPS Navstar clocks [BTN-95-EIX95112522530] p 190 A95-69333

Modeling spatio-temporal databases to measure the performance of the GPS satellite constellation p 489 N95-29596

NAVY

Navy and the HARV: High angle of attack tactical utility issues p 71 N95-14252

Naval Aviation System TEAM mapping, charting, and geodesy handbook [AD-A288590] p 446 N95-26841

Navy composite maintenance and repair experience p 424 N95-28446

Environmental support of naval aviation [AD-A292873] p 598 N95-31454

NEAR FIELDS

Rotating Kirchhoff method for three-dimensional transonic blade-vortex interaction hover noise [BTN-94-EIX94441386601] p 182 A95-67332

Near field of a coaxial jet with and without axial excitation [HTN-95-42332] p 372 A95-86161

Development of a large-aspect-ratio rectangular turbulent free jet [HTN-95-42333] p 372 A95-86162

Active open-loop control of particle dispersion in round jets [HTN-95-42334] p 372 A95-86163

Near field noise prediction requirements [ISVR-TR-234] p 27 N95-11166

Correction of support influences on measurements with sting mounted wind tunnel models p 122 N95-19281

Unsteady pressure and inflow velocity on a pitching rotor blade in hover p 480 N95-29771

NEAR INFRARED RADIATION

Possible near-IR channels for remote sensing precipitable water vapor from geostationary satellite platforms [HTN-95-70139] p 214 A95-69431

2 micron LIDAR for laser-based remote sensing: Flight demonstration and application survey [BTN-95-EIX95212641072] p 319 A95-76737

VUV shock layer radiation in an arc-jet wind tunnel experiment p 67 N95-13719

AVIRIS and TIMS data processing and distribution at the land processes distributed active archive center p 325 N95-23872

NEAR WAKES

Supersonic near-wake afterbody boattailing effects on axisymmetric bodies [BTN-95-EIX95182617465] p 268 A95-75736

Study of subsonic base cavity flowfield structure using particle image velocimetry [BTN-95-EIX95222650781] p 327 A95-79237

Research on bluff body vortex wakes [AD-A286319] p 223 N95-20177

DSMC calculations for 70-deg blunted cone at 3.2 km/s in nitrogen [NASA-TM-109181] p 348 N95-24396

Effects of three-dimensional imposed 3-D disturbances on bluff-body near wake flows [AD-A289553] p 374 N95-26757

The near-wake flow behavior of an oscillating airfoil with modified trailing edge p 375 N95-26953

The effects of three-dimensional imposed disturbances on bluff body near wake flows: Effects of taper and splitter plates on the near wake characteristics of a circular cylinder in uniform and shear flow [AD-A292113] p 477 N95-28921

Navier-Stokes solution of wing wake structure and its perturbation p 479 N95-29121

NETHERLANDS

Automation of observations in the Netherlands p 661 A95-93485

Review of aeronautical fatigue investigation in the Netherlands during the period March 1991-March 1993 [PB95-139184] p 285 N95-23161

Development of advanced approach and departure procedures. Failure scenarios [PB95-198123] p 601 N95-30815

NEURAL NETS

Artificial intelligence for turboprop engine maintenance [BTN-95-EIX95182617812] p 288 A95-75757

Neural network prediction of three-dimensional unsteady separated flowfields [BTN-95-EIX95182619232] p 308 A95-76658

On-line learning nonlinear direct neurocontrollers for restructurable control systems [BTN-95-EIX95242670768] p 359 A95-81079

Direct adaptive and neural control of wing-rock motion of slender delta wings [BTN-95-EIX95242670748] p 327 A95-81099

Neuro-controllers for adaptive helicopter training [SAE PAPER 932535] p 379 A95-84557

Artificial neural networks for predicting nonlinear dynamic helicopter loads [HTN-95-51678] p 404 A95-85060

Artificial intelligence for turboprop engine maintenance [HTN-95-92313] p 404 A95-85357

Modeling student knowledge with self-organizing feature maps [BTN-95-EIX95262697073] p 564 A95-86862

Application of artificial neural networks in nonlinear aerodynamics and aircraft design [SAE PAPER 932533] p 492 A95-89193

A switched reluctance machine rotor position estimator: A neural network application [SAE PAPER 932560] p 511 A95-90057

A design of a self-learning robust scheduled autopilot p 516 A95-91533

Neural network approach to identification of aerodynamic loads on a wing. 1: Application to cantilevered beam models p 475 A95-91568

Neuro-controllers for adaptive helicopter hover training [BTN-94-EIX94522407592] p 709 A95-96241

Control of wind tunnel operations using neural net interpretation of flow visualization records [NASA-TM-106683] p 24 N95-10854

Optimization of aerospace structures [NASA-CR-196763] p 48 N95-12787

Artificial intelligence with applications for aircraft [DOT/FAA/CT-94/41] p 99 N95-13895

Faithful neural network modeling of damaged aircraft [AD-A283227] p 80 N95-14849

An artificial neural network system for diagnosing gas turbine engine fuel faults [DE94-013960] p 138 N95-17371

The accuracy of parameter estimation in system identification of noisy aircraft load measurement [NASA-CR-197516] p 134 N95-19130

A neural expert approach to self designing flight control systems [AD-A279965] p 237 N95-21122

On-line, adaptive state estimator for active noise control p 322 N95-23308

Application of neural networks to unsteady aerodynamic control p 360 N95-25264

Digital systems validation. Chapter 20 Artificial Intelligence with applications for aircraft. Handbook, volume 2 [AD-A288492] p 448 N95-26638

An exploratory application of neural networks for airfoil design p 448 N95-26943

Selecting optimal experiments for feedforward multilayer perceptrons [AD-A290856] p 678 N95-30406

NEUTRAL BUOYANCY SIMULATION

Education, training, and human engineering in aerospace; SAE Aerotech '93, Costa Mesa, CA, Sep. 27-30, 1993 [SAE SP-992] p 417 A95-84553

NEUTRONS

Phonon characteristics of high (T sub c) superconductors from neutron Doppler broadening measurements [DE95-003703] p 324 N95-24076

Investigation and characterization of SEU effects and hardening strategies in avionics [AD-A291058] p 509 N95-29950

NEW YORK

Research and educational initiatives at the Syracuse University Center for Hypersonics [AIAA PAPER 95-6107] p 520 A95-90439

NEW ZEALAND

A review of Australian and New Zealand investigations on aeronautical fatigue during the period Apr. 1993 - Mar. 1995 [AR-009-202] p 397 N95-27918

NEWFOUNDLAND

Aircraft icing measurements in East Coast winter storms [HTN-95-60505] p 214 A95-68756

FTGEN - An automated FT production system p 668 A95-93519

NEWTON METHODS

Trajectory optimization using parallel shooting method on parallel computer [BTN-95-EIX95282706670] p 564 A95-88175

Higher harmonic control analysis for vibration reduction of helicopter rotor systems [NASA-TM-103855] p 66 N95-14419

NEWTON-RAPHSON METHOD

Demonstration of the Dynamic Flowgraph Methodology using the Titan 2 Space Launch Vehicle Digital Flight Control System [NASA-CR-197517] p 150 N95-17493

NICKEL ALLOYS

Fatigue crack growth in nickel-based superalloys at 500-700 C. 1: Waspaloy [BTN-94-EIX94371347843] p 206 A95-69136

Viscoplastic response of structures for intense local heating [HTN-95-41540] p 346 A95-77921

Study on the turbine vane and blade for a 1500 C class industrial gas turbine [BTN-94-EIX95011441254] p 431 A95-84211

Effect of annealing and desulfurization on oxide spallation of turbine airfoil material [BTN-95-EIX95282707024] p 528 A95-88264

Fatigue in single crystal nickel superalloys [AD-A283459] p 56 N95-12546

Fatigue in single crystal nickel superalloys [AD-A282917] p 88 N95-15415

Fatigue in single crystal nickel superalloys [AD-A285727] p 152 N95-18068

The effect of interface properties on nickel base alloy composites [NASA-CR-198363] p 629 N95-30787

Cadmium plating replacements p 631 N95-31773

NICKEL CADMIUM BATTERIES

Maintenance-free lead acid battery for inertial navigation systems aircraft [BTN-95-EIX95292721316] p 633 A95-92511

NIGHT

Low-Level and Nap-of-the-Earth (NOE) night operations [AGARD-CP-563] p 686 N95-32486

An approach to sensor data fusion for flying and landing aid purpose p 686 N95-32488

NIGHT FLIGHTS (AIRCRAFT)

- Aircraft noise and sleep disturbance: A field study
[HTN-95-92543] p 558 A95-87363
- A computer-based multimedia prototype for night vision goggles
[AD-A286208] p 258 N95-21882

NIGHT VISION

- A platform independent application of Lux illumination prediction algorithms
[AD-A283669] p 170 N95-18018
- Ultra-Reliable Digital Avionics (URDA) processor
p 245 N95-20638
- A computer-based multimedia prototype for night vision goggles
[AD-A286208] p 258 N95-21882
- Laser based obstacle warning sensors for helicopters
p 686 N95-32499
- A helmet mounted display for night missions at low altitude
p 693 N95-32503

NITRIC ACID

- Analysis of the physical state of one Arctic polar stratospheric cloud based on observations
[HTN-95-70917] p 351 A95-77982
- Sensitivity of supersonic aircraft modelling studies to HNO₃ photolysis rate
[HTN-95-11475] p 353 A95-79453
- High-speed civil transport impact: Role of sulfate, nitric acid trihydrate, and ice aerosols studied with a two-dimensional model including aerosol physics
[HTN-95-91843] p 354 A95-80831
- Impact on ozone of high-speed stratospheric aircraft: Effects of the emission scenario
[HTN-95-51283] p 356 A95-80868
- Airborne measurements during the European Arctic Stratospheric Ozone Experiment column amounts of HNO₃ and O₃ derived from FTIR emission sounding
[HTN-95-00742] p 445 A95-86312

NITRIC OXIDE

- Comparison of NO and OH planar fluorescence temperature measurements in scramjet model flowfields
[BTN-95-EIX95042474388] p 209 A95-68312
- Measurement and analysis of nitric oxide radiation in an arcjet flow
[BTN-95-EIX95082502727] p 243 A95-71040
- Nitrogen oxide emissions characteristics of augmented turbofan engines
[BTN-94-EIX95011441240] p 403 A95-84197

NITROGEN

- Measurement by coherent anti-Stokes Raman scattering in the R5Ch hypersonic wind tunnel
[BTN-95-EIX95112523811] p 188 A95-69322
- The distribution of hydrogen, nitrogen, and chlorine radicals in the lower stratosphere: Implications for changes in O₃ due to emission of NO(y) from supersonic aircraft
[HTN-95-70935] p 351 A95-78000
- Supercooling in hypersonic nitrogen wind tunnels
[BTN-94-EIX95011441134] p 340 A95-81020
- DSMC calculations for 70-deg blunted cone at 3.2 km/s in nitrogen
[NASA-TM-109181] p 348 N95-24396
- Numerical simulations of the flow in the HYPULSE expansion tube
[NASA-TM-110357] p 523 N95-30228

NITROGEN DIOXIDE

- Three-dimensional model interpretation of NO(x) measurements from the lower stratosphere
[HTN-95-90534] p 213 A95-67806
- Nitrogen oxide emissions characteristics of augmented turbofan engines
[BTN-94-EIX95011441240] p 403 A95-84197
- Airborne measurements during the Arctic stratospheric experiment: Observation of O₃ and NO₂
[HTN-95-00748] p 445 A95-86318

NITROGEN OXIDES

- Three-dimensional model interpretation of NO(x) measurements from the lower stratosphere
[HTN-95-90534] p 213 A95-67806
- Analysis of the physical state of one Arctic polar stratospheric cloud based on observations
[HTN-95-70917] p 351 A95-77982
- The distribution of hydrogen, nitrogen, and chlorine radicals in the lower stratosphere: Implications for changes in O₃ due to emission of NO(y) from supersonic aircraft
[HTN-95-70935] p 351 A95-78000
- Vertical transport rates in the stratosphere in 1993 from observations of CO₂, N₂O, and CH₄
[HTN-95-70941] p 351 A95-78006
- Meridional distributions of NO(x), NO(y), and other species in the lower stratosphere and upper troposphere during AASE 2
[HTN-95-70944] p 352 A95-78009
- Impact of present aircraft emissions of nitrogen oxides on tropospheric ozone and climate forcing
[HTN-95-21364] p 353 A95-78679

- Sensitivity of supersonic aircraft modelling studies to HNO₃ photolysis rate
[HTN-95-11475] p 353 A95-79453
- Tracer transport for realistic aircraft emission scenarios calculated using a three-dimensional model
[HTN-95-41799] p 353 A95-80525
- Modeling of aircraft exhaust emissions and infrared spectra for remote measurement of nitrogen oxides
[HTN-95-51276] p 355 A95-80861
- Potential effects on ozone of future supersonic aircraft/2D simulation
[HTN-95-51282] p 356 A95-80867
- Impact on ozone of high-speed stratospheric aircraft: Effects of the emission scenario
[HTN-95-51283] p 356 A95-80868
- Aircraft gas turbine emissions challenge
[BTN-94-EIX95011441239] p 403 A95-84196
- Evolution of the concentrations of trace species in an aircraft plume: Trajectory study
[HTN-95-A1044] p 443 A95-84549
- Prediction of NO(x) emission index of turbulent diffusion flame
p 538 A95-87195
- Aviation and the environment
p 657 A95-93464
- Numerical mixing calculations of confined reacting jet flows in a cylindrical duct
[NASA-TM-106736] p 139 N95-18133
- Wave cycle design for wave rotor engines with limited nitrogen oxide emissions
p 161 N95-18901
- Laboratory evaluation of a reactive baffle approach to NOx control
[AD-A283802] p 255 N95-19921
- Nitrogen oxide emissions and their control from uninstalled aircraft engines in enclosed test cells: Joint report to Congress on the Environmental Protection Agency - Department of Transportation study
[PB95-166237] p 358 N95-26005

NITROGEN PLASMA

- Temperature diagnostics in the hypersonic flow regime: An application to develop a stagnation temperature probe
[AIAA PAPER 95-6114] p 511 A95-90442

NITROUS OXIDES

- Nitrous oxide and methane emissions from aero engines
[HTN-95-21363] p 353 A95-78678

NOISE

- The accuracy of parameter estimation in system identification of noisy aircraft load measurement
[NASA-CR-197516] p 134 N95-19130

NOISE (SOUND)

- Secondary source locations in active noise control: Selection or optimization?
[BTN-94-EIX94381352222] p 257 A95-71738
- Mach wave emission from a high-temperature supersonic jet
[BTN-95-EIX95152577586] p 264 A95-73496
- A higher harmonic control test in the DNW to reduce impulsive BVI noise
[HTN-95-61071] p 385 A95-83655
- Experimental investigation of the sources of propeller noise due to the ingestion of turbulence at low speeds
[BTN-95-EIX95262697042] p 569 A95-86859
- Euro-noise '92, London, UK, Sept. 14-18, 1992. Bks. 1-3
[ISBN 1-873082-39-8] p 558 A95-87354
- Active control of fan noise from a turbofan engine
[HTN-95-61198] p 570 A95-87571
- Inter-Noise 92: Noise control and the public; International Congress on Noise Control Engineering, Toronto, Ontario, Canada, July 20 - 22, 1992. Vols. 1 & 2
[ISBN 0-931784-25-5] p 559 A95-88457
- Disturbance generation in supersonic jets under acoustic excitation
[HTN-95-20926] p 463 A95-88965
- Noise Con 1994: Proceedings of the 1994 National Conference on Noise Control Engineering. Progress in Noise Control for Industry
[LC-75-24750] p 28 N95-11259
- Comments on the use of structureborne noise analysis for large commercial airplanes
p 30 N95-11287
- 25 years of airport sound insulation programs
p 31 N95-11307
- At Istanbul-Ataturk Airport measurement and analysis of noise in due of take-off time
p 31 N95-11319
- The assessment of the AH-64D, longbow, mast-mounted assembly noise hazard for maintenance personnel
[AD-A284971] p 171 N95-16226
- NOISE GENERATORS**
- Recent studies of rotorcraft blade-vortex interaction noise
[BTN-95-EIX95062487521] p 218 A95-69229
- Unsteady aerodynamics of vortical flows: Early and recent developments
p 462 A95-88896
- Fan noise research at NASA
p 28 N95-11260
- Active control of complex noise problems using a broadband, multichannel controller
p 29 N95-11271
- Noise radiation by instability waves in coaxial jets
[NASA-TM-106738] p 100 N95-14618
- Resonant interaction of a linear array of supersonic rectangular jets: An experimental study
[NASA-CR-195398] p 76 N95-15852
- Ducted fan acoustic radiation including the effects of nonuniform mean flow and acoustic treatment
[NASA-CR-197449] p 172 N95-16401
- Turbulent airflow noise production and propagation patterns of a subsonic jet impinging on a flat plate
p 580 N95-29502
- UHB engine fan broadband noise reduction study
[NASA-CR-198357] p 580 N95-29641
- NOISE INTENSITY**
- The effects and prediction of rotary wing aircraft noise on the community
[HTN-95-92536] p 558 A95-87356
- Empirical refinements to boundary layer transition noise models
p 28 N95-11262
- Integrating NOISEMAP with the Geographic Resource Analysis Support System (GRASS) to enhance environmental impact assessments and land use compatibility studies
p 31 N95-11311
- Noise modeling for MOAs and ranges
p 32 N95-11322
- En route noise levels from propfan test assessment airplane
[NASA-TP-3451] p 62 N95-12341
- Response to noise around Vaernes and Bodoe airports
[PB94-207065] p 62 N95-13575
- Ultra-high bypass ratio jet noise
[NASA-CR-195394] p 100 N95-14610
- The assessment of the AH-64D, longbow, mast-mounted assembly noise hazard for maintenance personnel
[AD-A284971] p 171 N95-16226
- An overall approach of cockpit noise verification in a military aircraft
p 175 N95-19163
- Acoustic climb to cruise test
[NASA-TM-110504] p 230 N95-20155
- Bell Helicopter Advanced Rotorcraft Transmission (ART) program
[NASA-CR-195479] p 555 N95-29538
- NOISE MEASUREMENT**
- A higher harmonic control test in the DNW to reduce impulsive BVI noise
[HTN-95-61071] p 385 A95-83655
- Euro-noise '92, London, UK, Sept. 14-18, 1992. Bks. 1-3
[ISBN 1-873082-39-8] p 558 A95-87354
- Possible guidelines for helicopter noise assessment
[HTN-95-92535] p 558 A95-87355
- Environmental noise monitoring - source identification
[HTN-95-92537] p 558 A95-87357
- The use of the Equivalent Continuous Sound Level (L_{sub eq}) as an aircraft noise index
[HTN-95-92542] p 558 A95-87362
- Aircraft noise and sleep disturbance: A field study
[HTN-95-92543] p 558 A95-87363
- Noise levels of helicopters performing elevated pad take-off and landing procedures
[HTN-95-92544] p 559 A95-87364
- Long distance propagation model and its application to aircraft en route noise prediction
[HTN-95-61221] p 491 A95-87594
- Monitoring noise from aircraft operations in the vicinity of airports
p 570 A95-88462
- Nordic Standards for measurement of aircraft noise emission in residential areas and noise reduction of dwellings
p 570 A95-88463
- A prediction model for noise from low-altitude military aircraft
p 571 A95-88466
- Auxiliary power unit noise of Boeing B737 and B747 aircraft
p 571 A95-88468
- Prediction level of noise by a helicopter
p 571 A95-88469
- Broadband noise characteristics of a model counter-rotating shrouded propfan
p 572 A95-88470
- In-flight interior sound field mapping in propeller aircraft
p 572 A95-88472
- Time-average aircraft noise descriptors: Confusion with no benefit
p 559 A95-88474
- Noise metrics and aviation noise control: The case for DNL
p 559 A95-88475
- Criticism of the Leq as an index for aircraft noise and other discontinuous noise sources
p 559 A95-88477
- Criticism of the Leq as an index for aircraft noise and other discontinuous noise sources
p 559 A95-88478
- Assessment of helicopter noise annoyance: A comparison between helicopters and jet aircraft
p 560 A95-88480
- Past and present UK research on aircraft noise effects
p 560 A95-90090
- Numerical and flight measured interior noise characteristics of a twin-engine turboprop general aviation aircraft
p 573 A95-90094

- Aircraft interior sound field analysis in view of active control: Results from the ASANCA project p 575 A95-90109
- Recent laboratory studies of loudness and annoyance to sonic booms p 575 A95-90117
- The effect of onset rate on annoyance to military aircraft noise p 561 A95-90119
- Development and field test of the Beta version of the USAF Assessment System for Aircraft Noise (ASAN) p 561 A95-90121
- Selecting optimum sonic boom monitoring sites in a special-use airspace p 576 A95-90124
- The evolution of airport noise monitoring systems: Recent achievements and further needs p 562 A95-90125
- Identification of noise events as aircraft p 576 A95-90126
- Features of Massport's new noise monitoring system p 562 A95-90127
- Experimental results of the European HELINOISE aeroacoustic rotor test [HTN-95-01080] p 578 A95-90266
- Signal processing of noise data from high-speed flyovers [BTN-95-EIX0619952748178] p 680 A95-94248
- Near field noise prediction requirements [ISVR-TR-234] p 27 N95-11166
- 25 years of airport sound insulation programs p 31 N95-11307
- At Istanbul-Ataturk Airport measurement and analysis of noise in due of take-off time p 31 N95-11319
- INM contour validation: A case study p 31 N95-11321
- Background noise levels measured in the NASA Lewis 9- by 15-foot low-speed wind tunnel [NASA-TM-106817] p 145 N95-18054
- ### NOISE METERS
- Environmental noise research using the Human Response Monitor (HRM). Phase 1: System development p 562 A95-90122
- ### NOISE POLLUTION
- Criticism of the Leq as an index for aircraft noise and other discontinuous noise sources p 559 A95-88477
- Reducing low frequency noise emissions from a Langley Air Force Base Hush-House p 561 A95-90112
- A review of Air Force policy and noise models pertaining to the noise environment under low-altitude, high-speed training areas p 561 A95-90118
- The effect of onset rate on annoyance to military aircraft noise p 561 A95-90119
- Development and field test of the Beta version of the USAF Assessment System for Aircraft Noise (ASAN) p 561 A95-90121
- Environmental noise research using the Human Response Monitor (HRM). Phase 1: System development p 562 A95-90122
- Research of the method for evaluating noise caused by sonic boom p 562 A95-91519
- Aviation and the environment p 657 A95-93464
- Noise Con 1994: Proceedings of the 1994 National Conference on Noise Control Engineering. Progress in Noise Control for Industry [LC-75-24750] p 28 N95-11259
- Fan noise research at NASA p 28 N95-11260
- Transmission loss characteristics of aircraft sidewall systems to control cabin interior noise p 28 N95-11261
- 25 years of airport sound insulation programs p 31 N95-11307
- Integrating NOISEMAP with the Geographic Resource Analysis Support System (GRASS) to enhance environmental impact assessments and land use compatibility studies p 31 N95-11311
- Determining the effects of alternative departure cutback altitudes and power settings: A case study, John Wayne Airport p 31 N95-11320
- ### NOISE PREDICTION
- Rotating Kirchhoff method for three-dimensional transonic blade-vortex interaction hover noise [BTN-94-EIX94441386601] p 182 A95-67332
- Analysis of a higher harmonic control test to reduce blade vortex interaction noise [BTN-95-EIX95152582330] p 265 A95-73532
- Unsteady lift on a swept blade tip [BTN-94-EIX95011441154] p 329 A95-80030
- Stochastic approach to noise modeling for free turbulent flows [HTN-95-42321] p 371 A95-86150
- The propagation of sound from an arbitrarily oriented dipole over a finite impedance plane p 570 A95-88459
- Improvement of the predicted aural detection code ICHIN (I Can Hear It Now) p 576 A95-90123
- Comments on the use of structureborne noise analysis for large commercial airplanes p 30 N95-11287
- A theoretical analysis of airborne sound transfer for a resiliently mounted machine to its foundation p 30 N95-11304
- MOAMAP: A model that combines several different kinds of aircraft operations p 32 N95-11323
- Noise radiation by instability waves in coaxial jets [NASA-TM-106738] p 100 N95-14618
- On the Lighthill relationship and sound generation from isotropic turbulence [NASA-CR-195005] p 159 N95-18191
- A numerical study of fundamental shock noise mechanisms [NASA-TM-110608] p 451 N95-27908
- Measurement and prediction of broadband noise from large horizontal axis wind turbine generators p 451 N95-27990
- Flow structure generated by perpendicular blade vortex interaction and implications for helicopter noise predictions [NASA-CR-198590] p 377 N95-28193
- Response of multi-panel assembly to noise from a jet in forward motion [NASA-CR-198164] p 442 N95-28673
- An extension of the Lighthill theory of jet noise to encompass refraction and shielding [NASA-TM-110163] p 580 N95-29452
- ### NOISE PREDICTION (AIRCRAFT)
- Structure of supersonic jet flow and its radiated sound [HTN-95-51645] p 431 A95-85027
- Modeling lateral attenuation of aircraft flight noise p 570 A95-88464
- A prediction model for noise from low-altitude military aircraft p 571 A95-88466
- Meteorological impacts on airport noise prediction by the 'Integrated Noise Model' application based on Hamiltonian Ray-Tracing program and measurements p 571 A95-88467
- Prediction level of noise by a helicopter p 571 A95-88469
- Development and validation of a numerical acoustic analysis program for aircraft interior noise prediction p 572 A95-88471
- Aircraft noise at a West Coast airport in the next century p 560 A95-90095
- Enroute NASA/FAA low-frequency propfan test in Alabama (October 1987): A versatile atmospheric aircraft long-range noise prediction system p 573 A95-90099
- A prediction method for broadband shock associated noise from supersonic rectangular jets p 574 A95-90100
- Evaluation of a model for boundary-layer induced noise in aircraft p 574 A95-90102
- Evaluation of prediction methods for fluctuating pressures under attached turbulent boundary layers using flight test data p 574 A95-90103
- ASTRYD: A new numerical tool for aircraft cabin and environmental noise prediction p 576 A95-90129
- Application of FEM/SEA for prediction of aircraft cockpit noise p 576 A95-90130
- Prediction of airplane cabin noise due to engine shock cell excitation using statistical energy analysis p 577 A95-90131
- Incorporation of topography effects in aircraft noise modeling p 578 A95-90140
- Research of the method for evaluating noise caused by sonic boom p 562 A95-91519
- Near field noise prediction requirements [ISVR-TR-234] p 27 N95-11166
- INM contour validation: A case study p 31 N95-11321
- Noise modeling for MOAs and ranges p 32 N95-11322
- The present and future of aircraft noise models: A user's perspective p 32 N95-11324
- Ultra-high bypass ratio jet noise [NASA-CR-195394] p 100 N95-14610
- The aeroacoustics of supersonic coaxial jets [NASA-TM-106782] p 101 N95-15059
- Modelling structurally damaging twin-jet screech p 135 N95-19154
- Supersonic jet noise reductions predicted with increased jet spreading rate [NASA-TM-106872] p 323 N95-23178
- Aircraft noise prediction program theoretical manual: Rotorcraft System Noise Prediction System (ROTONET), part 4 [NASA-TM-83199-PT-4] p 451 N95-26392
- Supersonic coaxial jet noise predictions [NASA-TM-106917] p 451 N95-26801
- Computation of noise radiation from turbofans: A parametric study [NASA-CR-198359] p 710 N95-32836
- Fan noise prediction assessment [NASA-CR-195051] p 711 N95-33831
- ### NOISE PROPAGATION
- Screech tones from free and ducted supersonic jets [HTN-95-51647] p 432 A95-85029
- Inter-Noise 92: Noise control and the public; International Congress on Noise Control Engineering, Toronto, Ontario, Canada, July 20 - 22, 1992. Vols. 1 & 2 [ISBN 0-931784-25-5] p 559 A95-88457
- Modeling lateral attenuation of aircraft flight noise p 570 A95-88464
- Meteorological impacts on airport noise prediction by the 'Integrated Noise Model' application based on Hamiltonian Ray-Tracing program and measurements p 571 A95-88467
- Enroute NASA/FAA low-frequency propfan test in Alabama (October 1987): A versatile atmospheric aircraft long-range noise prediction system p 573 A95-90099
- En route noise levels from propfan test assessment airplane [NASA-TP-3451] p 62 N95-12341
- Noise transmission and reduction in turboprop aircraft p 175 N95-19164
- Effect of atmospheric pressure on measured aircraft noise levels [PB95-130423] p 232 N95-21425
- Turbulent airflow noise production and propagation patterns of a subsonic jet impinging on a flat plate p 580 N95-29502
- ### NOISE REDUCTION
- Aeroacoustic probe design for microphone to reduce flow-induced self-noise [AIAA PAPER 93-4343] p 19 A95-60163
- Oblique incidence sound absorption of porous materials covered by perforated metal and exposed to tangential airflow p 19 A95-60165
- Active control of wake/blade-row interaction noise [BTN-95-EIX95042474389] p 196 A95-68311
- Noise and vibration control [BTN-95-EIX95042477108] p 179 A95-68351
- Vortex shedding noise control in idling circular saws using air ejection at the teeth [BTN-94-EIX94371347214] p 257 A95-69970
- Secondary source locations in active noise control: Selection or optimization? [BTN-94-EIX94381352222] p 257 A95-71738
- Analysis of a higher harmonic control test to reduce blade vortex interaction noise [BTN-95-EIX95152582330] p 265 A95-73532
- A higher harmonic control test in the DNW to reduce impulsive BVI noise [HTN-95-61071] p 385 A95-83655
- Screech tones from free and ducted supersonic jets [HTN-95-51647] p 432 A95-85029
- Mixing enhancement by and noise characteristics of streamwise vortices in an air jet [HTN-95-42322] p 371 A95-86151
- Reduction of blade-vortex interaction noise through porous leading edge [HTN-95-42324] p 371 A95-86153
- Enhanced mixing of multiple supersonic rectangular jets by synchronized screech [HTN-95-42592] p 459 A95-87222
- Euro-noise '92, London, UK, Sept. 14-18, 1992. Bks. 1-3 [ISBN 1-873082-39-8] p 558 A95-87354
- Flyover noise reduction of piston-engine propeller aeroplanes using an active noise control technique [SAE PAPER 931218] p 509 A95-87466
- Inter-Noise 92: Noise control and the public; International Congress on Noise Control Engineering, Toronto, Ontario, Canada, July 20 - 22, 1992. Vols. 1 & 2 [ISBN 0-931784-25-5] p 559 A95-88457
- Inter-Noise 92: Noise control and the public; International Congress on Noise Control Engineering, Toronto, Ontario, Canada, July 20 - 22, 1992. Vols. 1 & 2 [ISBN 0-931784-25-5] p 559 A95-88457
- Modeling lateral attenuation of aircraft flight noise p 570 A95-88464
- Fan noise reduction from a supersonic inlet during simulated aircraft approach [BTN-95-EIX95292721155] p 572 A95-89894
- Noise control in aeroacoustics; Proceedings of the 1993 National Conference on Noise Control Engineering, NOISE-CON 93, Williamsburg, VA, May 2-5, 1993 [ISBN 0-931784-26-3] p 573 A95-90088
- Concepts for the control of rotor noise p 573 A95-90092
- Studies of blade-vortex interaction noise reduction by rotor blade modification p 573 A95-90093
- Reduction of supersonic jet noise using swirl: A concept revisited p 574 A95-90101
- Evaluation of a model for boundary-layer induced noise in aircraft p 574 A95-90102
- Aircraft interior sound field analysis in view of active control: Results from the ASANCA project p 575 A95-90109

- Experimental active control of sound in the ATR 42
p 575 A95-90110
- Hangars as noise barriers for helicopter noise
p 560 A95-90111
- Reducing low frequency noise emissions from a Langley Air Force Base Hush-House
p 561 A95-90112
- Standardization of aircraft noise insulation measures without compromising results
p 561 A95-90115
- Noise and vibration control in aircraft: A global approach
p 576 A95-90128
- Numerical investigation of sound transmission through double wall cylinders with respect to active noise control
p 577 A95-90134
- Effects of signal analysis parameters and noise removal on measured aircraft spectra
p 578 A95-90137
- Electromagnetic compatibility - A general overview [CONGRESS PAPER C428-38-084]
p 634 A95-93637
- Control of wind tunnel operations using neural net interpretation of flow visualization records [NASA-TM-106683]
p 24 N95-10854
- Noise Con 1994: Proceedings of the 1994 National Conference on Noise Control Engineering, Progress in Noise Control for Industry
[LC-75-24750]
p 28 N95-11259
- Fan noise research at NASA
p 28 N95-11260
- Transmission loss characteristics of aircraft sidewall systems to control cabin interior noise
p 28 N95-11261
- Achievements and tasks for active noise control
p 29 N95-11270
- Active control of complex noise problems using a broadband, multichannel controller
p 29 N95-11271
- Active control of turbomachine discrete tones
p 29 N95-11275
- Active control of interior noise in a business jet using piezoceramic actuators
p 29 N95-11276
- Analytical investigation of adaptive control of radiated inlet noise from turbofan engines
p 30 N95-11277
- Adaptive tuned vibration absorbers: Tuning laws, tracking agility, sizing, and physical implementations
p 25 N95-11280
- Broadband, wide-area active control of sound radiated from vibrating structures using local surface-mounted radiation suppression devices
p 30 N95-11283
- Comments on the use of structureborne noise analysis for large commercial airplanes
p 30 N95-11287
- A theoretical analysis of airborne sound transfer for a resiliently mounted machine to its foundation
p 30 N95-11304
- Effect of constraining layer stiffness on performance of damping tile materials using finite element modelling with Rayleigh integral
p 30 N95-11306
- 25 years of airport sound insulation programs
p 31 N95-11307
- Integrating NOISEMAP with the Geographic Resource Analysis Support System (GRASS) to enhance environmental impact assessments and land use compatibility studies
p 31 N95-11311
- Determining the effects of alternative departure cutback altitudes and power settings: A case study, John Wayne Airport
p 31 N95-11320
- Noise modeling for MOAs and ranges
p 32 N95-11322
- Modification of the Ames 40- by 80-foot wind tunnel for component acoustic testing for the second generation supersonic transport
[NASA-TM-108850]
p 65 N95-13642
- Ultra-high bypass ratio jet noise
[NASA-CR-195394]
p 100 N95-14610
- The aeroacoustics of supersonic coaxial jets
[NASA-TM-106782]
p 101 N95-15059
- Resonant interaction of a linear array of supersonic rectangular jets: An experimental study
[NASA-CR-195398]
p 76 N95-15852
- Background noise levels measured in the NASA Lewis 9- by 15-foot low-speed wind tunnel
[NASA-TM-106817]
p 145 N95-18054
- Helicopter internal noise
p 173 N95-19144
- Impact of noise environment on engine nacelle design
p 173 N95-19147
- An overall approach of cockpit noise verification in a military aircraft
p 175 N95-19163
- Noise transmission and reduction in turboprop aircraft
p 175 N95-19164
- Active control of fan noise-feasibility study, Volume 1: Flyover system noise studies
[NASA-CR-195392-VOL-1]
p 258 N95-21888
- The use of cowl camber and taper to reduce rotor/stator interaction noise
[NASA-CR-195421]
p 323 N95-22675
- Supersonic jet noise reductions predicted with increased jet spreading rate
[NASA-TM-106872]
p 323 N95-23178
- On-line, adaptive state estimator for active noise control
p 322 N95-23308
- Noise impact of advanced high lift systems
[NASA-CR-195028]
p 362 N95-26160
- Jet mixer noise suppressor using acoustic feedback
[NASA-CASE-LEW-15170-2]
p 362 N95-26187
- Supersonic coaxial jet noise predictions
[NASA-TM-106917]
p 451 N95-26801
- The noise reduction potential of dual-stream coaxial rectangular improperly expanded jet flows
[NASA-CR-197820]
p 437 N95-26995
- Evaluation of a doubly-swept blade tip for rotorcraft noise reduction
[NASA-CR-189677]
p 452 N95-28264
- Noise exposure reduction of advanced high-lift systems
[NASA-CR-195077]
p 452 N95-28670
- Bell Helicopter Advanced Rotorcraft Transmission (ART) program
[NASA-CR-195479]
p 555 N95-29538
- UHB engine fan broadband noise reduction study
[NASA-CR-198357]
p 580 N95-29641
- Reducing process noise in superconducting helium liquid level probes
[DE95-008956]
p 629 N95-30765
- An active liner system for jet engine exhaust silencers, phase 1
[AD-A293277]
p 617 N95-31191
- NOISE SPECTRA**
- Effects of signal analysis parameters and noise removal on measured aircraft spectra
p 578 A95-90137
- Active control of complex noise problems using a broadband, multichannel controller
p 29 N95-11271
- Measurement and prediction of broadband noise from large horizontal axis wind turbine generators
p 451 N95-27990
- Observed acoustic and aeroelastic spectral responses of a MOD-2 turbine blade to turbulence excitation
p 451 N95-27991
- The spectrum and directivity of turbulent mixing noise from supersonic jets
p 579 N95-29415
- NOISE TOLERANCE**
- Assessment of helicopter noise annoyance: A comparison between noise from helicopters and from jet aircraft
[BTN-94-EIX94341341967]
p 62 A95-60867
- Modeling student knowledge with self-organizing feature maps
[BTN-95-EIX95262697073]
p 564 A95-86862
- Past and present UK research on aircraft noise effects
p 560 A95-90090
- NOMOGRAPHS**
- Development of a climatological data base to help forecast cloud cover conditions for shuttle landings at the Kennedy Space Center
p 670 A95-93529
- NONDESTRUCTIVE TESTS**
- A method for disbond detection in thermal tomography by domain decomposition method
p 545 A95-88955
- Ultrasonic imaging of damages in CRFT-laminates
p 578 A95-90828
- Development of an Automated Nondestructive Inspection (ANDI) system for commercial aircraft, phase 1
[AD-A283500]
p 40 N95-12623
- Analysis of small crack behavior for airframe applications
p 95 N95-14484
- Advanced Turbine Technology Applications Project (ATTAP)
[NASA-CR-195393]
p 101 N95-15743
- Eddy current for detecting second-layer cracks under installed fasteners
[AD-A279871]
p 244 N95-20414
- Double pass retroreflection for corrosion detection in aircraft structures
p 323 N95-23503
- Non-destructive detection of corrosion for life management
p 314 N95-23505
- New nondestructive techniques for the detection and quantification of corrosion in aircraft structures
p 315 N95-23512
- POD assessment of NDI procedures using a round robin test
[AGARD-R-809]
p 315 N95-23602
- Emerging nondestructive inspection for aging aircraft
[PB95-143053]
p 328 N95-25401
- Proceedings of the 2d USAF Aging Aircraft Conference
[AD-A288217]
p 336 N95-25578
- Characterization of corrosion and development of a breadboard of a D sight aircraft inspection system, phase 1
[AD-A288347]
p 380 N95-26527
- The use of electrochemistry and ellipsometry for identifying and evaluating corrosion on aircraft
[AD-A290249]
p 504 N95-29426
- Electrochemical impedance pattern recognition for detection of hidden chemical corrosion on aircraft components, phase 1
[AD-A291345]
p 556 N95-29946
- Mapping hidden aircraft defects with dual-band infrared computed tomography
[DE95-011531]
p 584 N95-32164
- NONEQUILIBRIUM CONDITIONS**
- Research activity at the shock tube facility at NASA Ames
p 547 A95-90559
- NONEQUILIBRIUM FLOW**
- Computation of nonequilibrium viscous flows in arc-jet wind tunnel nozzles
[AIAA PAPER 94-0254]
p 2 A95-60173
- A comparison of three-dimensional nonequilibrium solution algorithms applied to hypersonic flows with stiff chemical source terms
[AIAA PAPER 93-2861]
p 4 A95-60186
- Thermochemical nonequilibrium viscous shock-layer analysis for a Mars aerocapture vehicle
[BTN-95-EIX95082502732]
p 239 A95-70139
- Hypersonic nonequilibrium Navier-Stokes solutions over an ablating graphite nosetip
[BTN-95-EIX95152583252]
p 305 A95-73553
- Higher-order viscous shock-layer solutions for high-altitude flows
[BTN-95-EIX95152583255]
p 306 A95-73556
- Chemically reacting non-equilibrium boundary-layers in air breathing propulsion systems
[AIAA PAPER 95-6139]
p 512 A95-90456
- A one-dimensional inviscid nonequilibrium flow solver
[ISBN 1-879921-01-4]
p 588 A95-93752
- An approximate Riemann solver for thermal and chemical nonequilibrium flows
[NASA-CR-195003]
p 96 N95-14912
- High altitude hypersonic flowfield radiation
[AD-A281386]
p 106 N95-16160
- Viscous shock-layer analysis on hypersonic flow over reentry capsule with nonequilibrium chemistry
[ISAS-656]
p 436 N95-26739
- Flow models for the design of a hypersonic iodine vapor wind tunnel nozzle with chemical and vibrational nonequilibrium effects
p 592 N95-30448
- NONEQUILIBRIUM RADIATION**
- Measurement and analysis of nitric oxide radiation in an arcjet flow
[BTN-95-EIX95082502727]
p 243 A95-71040
- Measured and calculated spectral radiation from a blunt body shock layer in an arc-jet wind tunnel
[AIAA PAPER 94-0086]
p 67 N95-13720
- NONFLAMMABLE MATERIALS**
- The effect of wear on fire-blocking layer material effectiveness
[AD-A291520]
p 485 N95-29855
- NONINTRUSIVE MEASUREMENT**
- Surface interference in Rayleigh scattering measurements near forebodies
[HTN-95-51670]
p 433 A95-85052
- Flame-spreading phenomena in the fin-slot region of a solid rocket motor
p 23 N95-10296
- Planar Rayleigh scattering and laser-induced fluorescence for visualization of a hot, Mach 2 annular air jet
[NASA-TM-4576]
p 54 N95-13196
- Simultaneous three-dimensional velocity and mixing measurements by use of laser Doppler velocimetry and fluorescence probes in a water tunnel
[NASA-TP-3454]
p 53 N95-13553
- Wall Interference, Support Interference and Flow Field Measurements
[AGARD-CP-535]
p 162 N95-19251
- The crucial role of wall interference, support interference and flow field measurements in the development of advanced aircraft configurations
p 162 N95-19252
- Impeller flow field characterization with a laser two-focus velocimeter
p 313 N95-23440
- Research instrumentation for polytechnic university's supersonic wind tunnel facility
[AD-A290232]
p 523 N95-29468
- An investigation of the side-dump dual in-line ramjet combustor
p 617 N95-31199
- Spatially-resolved velocity measurements in steady, high-speed, reacting flows using laser-induced OH fluorescence
p 650 N95-32109
- NONLINEAR EQUATIONS**
- Finite element time domain - modal formulation for nonlinear flutter of composite panels
[BTN-95-EIX95042474401]
p 203 A95-68299
- Neural network prediction of three-dimensional unsteady separated flowfields
[BTN-95-EIX95182619232]
p 308 A95-76658
- Subharmonic and quasi-periodic motions of an eccentric squeeze film damper-mounted rigid rotor
[BTN-94-EIX95011440601]
p 429 A95-82982
- Unsteady aerodynamics of vortical flows: Early and recent developments
p 462 A95-88896
- Nonlinear analysis of swept wing transitional boundary layers
[SAE PAPER 932515]
p 466 A95-89188

Critical speed analysis of a non-linear strain ring dynamical model for aircraft tires
 [SAE PAPER 932580] p 494 A95-90067
 Modelling 2D separation from a high lift aerofoil with a non-linear eddy-viscosity model and second-moment closure
 [HTN-95-C0005] p 585 A95-93393
 Interaction of a weak shock with freestream disturbances
 [BTN-95-EIX95332750473] p 638 A95-94687
 Rapid solution of large-scale systems of equations
 p 169 N95-16458
 Moving mass trim control for aerospace vehicles
 [DE95-002602] p 299 N95-23532
 Development of a nonlinear simulation for the McDonnell Douglas F-15 Eagle with a longitudinal TECS control-law
 [AD-A288610] p 388 N95-26481
 An easy way to analyze longitudinal and lateral-directional trim problems with AEO or OEI
 p 409 N95-26949
 Linear and nonlinear discrete-time state-space modeling of dynamic systems for control applications
 p 567 N95-29251

NONLINEAR FEEDBACK

Design of high performance multivariable control systems for supermaneuverable aircraft at high angle of attack
 [NASA-CR-197661] p 293 N95-22908
 Nonlinear adaptive control of highly maneuverable high performance aircraft
 p 710 N95-33712

NONLINEAR PROGRAMMING

Application of direct transcription to commercial aircraft trajectory optimization
 [BTN-95-EIX95242670766] p 359 A95-81081
 Structural design using equilibrium programming formulations
 [NASA-TM-110175] p 645 N95-30682

NONLINEAR SYSTEMS

Design of nonlinear control laws for high-angle-of-attack flight
 [BTN-94-EIX94511433920] p 141 A95-64586
 Aircraft model for the AIAA controls design challenge
 [BTN-94-EIX94511433921] p 142 A95-64587
 On the choice of appropriate bases for nonlinear dynamic modal analysis
 [HTN-95-A0495] p 221 A95-72566
 Nonlinear observer and its application in flight control
 p 447 A95-82449
 Nonlinear decoupling control study for aircraft maneuvering flight
 [HTN-95-71130] p 408 A95-83491
 GETRAN: A generic, modularly structured computer code for simulation of dynamic behavior of aero- and power generation gas turbine engines
 [BTN-94-EIX95011441241] p 431 A95-84198
 Artificial neural networks for predicting nonlinear dynamic helicopter loads
 [HTN-95-51678] p 404 A95-85060
 Scheduling of local nonlinear control laws by exogenous signals - an application to flight control
 [BTN-95-EIX95262694059] p 447 A95-85675
 Application of artificial neural networks in nonlinear aerodynamics and aircraft design
 [SAE PAPER 932533] p 492 A95-89193
 Vortex lattice method simulation of unsteady flow due to wing/external store combination
 p 471 A95-91499
 Lee waves benign and malignant
 p 595 A95-93554
 Effect of initial conditions on the response of nonlinear dynamical systems with the application to helicopter rotor dynamics
 [ISBN 1-879921-01-4] p 605 A95-93731
 Nonlinear aerodynamic analysis of grid fin configurations
 [BTN-95-EIX0619952748172] p 590 A95-94466
 High-Alpha Research Vehicle (HARV) longitudinal controller: Design, analyses, and simulation results
 [NASA-TP-3446] p 17 N95-10860
 Identification of dynamic systems. Volume 3: Applications to aircraft. Part 2: Nonlinear analysis and manoeuvre design
 [AGARD-AG-300-VOL-3-PT-2] p 79 N95-14102
 2-D aileron effectiveness study
 p 110 N95-17851
 The impact of non-linear flight control systems on the prediction of aircraft loads due to turbulence
 p 143 N95-18598
 Treatment of non-linear systems by timeplane-transformed CT methods: The spectral gust method
 p 143 N95-18600
 Nonlinear dynamic response of aircraft structures to acoustic excitation
 p 135 N95-19151
 A neural expert approach to self designing flight control systems
 [AD-A279965] p 237 N95-21122
 Nonlinear system guidance in the presence of transmission zero dynamics
 [NASA-TM-4661] p 309 N95-22804

A gain scheduling optimization method using genetic algorithms
 [AD-A289306] p 448 N95-26920
 Nonlinear dynamics and aeroelasticity of rotorcraft in forward flight
 [AD-A291714] p 400 N95-28504
 Linear and nonlinear discrete-time state-space modeling of dynamic systems for control applications
 p 567 N95-29251

NONLINEARITY

Aeroelastic stability of hingeless rotor blade in hover using large deflection theory
 [BTN-94-EIX94441386616] p 183 A95-67347
 Analytical solution for controls, heats, and states of flight trajectories
 [BTN-95-EIX95152583286] p 282 A95-73587
 Non-linear analysis provides new insights into impact damage of composite structures
 [HTN-95-42368] p 418 A95-86197
 Fracture mechanics validity limits
 p 95 N95-14480
 Algorithms for bilevel optimization
 [NASA-CR-194980] p 170 N95-16897
 Comparison of stochastic and deterministic nonlinear gust analysis methods to meet continuous turbulence criteria
 p 133 N95-18602
 Unsteady aerodynamic analyses for turbomachinery aeroelastic predictions
 p 141 N95-19381
 Nonlinear analysis of damaged stiffened fuselage shells subjected to combined loads
 p 137 N95-19499
 Robust fixed-structure control
 [AD-A286515] p 257 N95-22216
 Bearing defect signature analysis using advanced nonlinear signal analysis in a controlled environment
 [NASA-TM-108491] p 441 N95-28364
 Nonlinear calibration of an infrared radiometer
 [AD-A292436] p 579 N95-28996
 The 1995 version of the NSWC aeroprediction code. Part 1: Summary of new theoretical methodology
 [AD-A291518] p 481 N95-29853
 New adaptive methods for reconfigurable flight control systems, appendix 1
 [AD-A292711] p 619 N95-30937
 Robust fixed-structure control
 [AD-A292883] p 679 N95-30961
 Computational methods for control and optimal design of aerospace systems
 [AD-A292861] p 608 N95-31451
 Dynamic inversion: An evolving methodology for flight control design
 p 621 N95-31996
 Nonlinear stability of unsteady viscous flow
 [AD-A294931] p 707 N95-34597

NONUNIFORM FLOW

Ducted fan acoustic radiation including the effects of nonuniform mean flow and acoustic treatment
 [NASA-CR-197449] p 172 N95-16401

NONUNIFORMITY

Response of a thin airfoil encountering a strong density discontinuity
 p 462 A95-88900
 Flame-spreading phenomena in the fin-slot region of a solid rocket motor
 p 23 N95-10296

NORMAL DENSITY FUNCTIONS

Statistical discrete gust-power spectral density methods overlap-hoistic proof and beyond
 [BTN-95-EIX0619952748175] p 584 A95-94469

NORMAL SHOCK WAVES

Visualization of one-dimensional flow processes in a dual-mode scramjet engine
 p 15 N95-10465

NORTH AMERICA

Ten-year ground exposure of composite materials used on the Bell Model 206L helicopter flight service program
 [NASA-TP-3468] p 55 N95-12357

NORTH ATLANTIC TREATY ORGANIZATION (NATO)

AGARD index of publications: 1992-1994
 [AGARD-INDEX-92-94] p 711 N95-33198

NORTH DAKOTA

Aviation weather education and the University of North Dakota aviation weather survey
 p 656 A95-93462

NORTHERN HEMISPHERE

Trajectory modeling of emissions from lower stratospheric aircraft
 [HTN-95-41219] p 317 A95-75031
 North Atlantic air traffic within the lower stratosphere: Cruising times and corresponding emissions
 [HTN-95-91841] p 354 A95-80829
 A northern hemisphere clear air turbulence climatology
 p 674 A95-93547

NORWAY

Aircraft noise zoning in Norway
 p 581 A95-88476

NOSE CONES

Shock tunnel measurements of hypervelocity blunted cone drag
 [BTN-95-EIX95152577606] p 305 A95-73477
 Viscous contribution to the high Mach number damping in pitch of blunt slender cones at small angles of attack
 [HTN-95-01096] p 469 A95-90282

Transonic, supersonic and hypersonic wind-tunnel tests on aerodynamic characteristics of reentry body with blunted cone configuration
 [NASA-658] p 480 N95-29640

NOSE TIPS

Hypersonic nonequilibrium Navier-Stokes solutions over an ablating graphite nosetip
 [BTN-95-EIX95152583252] p 305 A95-73553
 Shock tunnel measurements of hypervelocity blunted cone drag
 [HTN-95-42591] p 459 A95-87221

NOSE WHEELS

Evolution of a nose-wheel steering system
 [BTN-94-EIX94461047056] p 78 A95-61739
 Aircraft nose gear shimmy studies
 [SAE PAPER 931401] p 628 A95-93671
 Flight investigation of the use of a nose gear jump strut to reduce takeoff ground roll distance of STOL aircraft
 [NASA-TM-108819] p 44 N95-12225

NOSES (FOREBODIES)

Aircraft nose gear shimmy studies
 [SAE PAPER 931401] p 628 A95-93671
 Modelling and analysis of a dual-wheel nose gear: Shimmy instability and impact motions
 [SAE PAPER 931402] p 605 A95-93672
 Directional control at high angles of attack using blowing through a chined forebody
 [BTN-95-EIX0619952748179] p 619 A95-94472
 Flight evaluation of forebody vortex control in post-stall flight
 p 609 N95-32003

NOTCH SENSITIVITY

Tension fracture of laminates for transport fuselage. Part 1: Material screening
 p 398 N95-28471

NOTCH TESTS

Interlaminar shear test method development for long term durability testing of composites
 p 301 N95-23300
 The effect of interface properties on nickel base alloy composites
 [NASA-CR-198363] p 629 N95-30787

NOTCHES

Tension fracture of laminates for transport fuselage. Part 2: Large notches
 p 532 N95-28837

NOWCASTING

Forecasting for a large field program: STORM-FEST
 [HTN-95-90694] p 215 A95-69721
 The real-time analysis and prediction of storms program
 p 655 A95-93457
 Use of high resolution lightning detection and localization sensors for hazardous aviation weather nowcasting
 p 661 A95-93486
 The 1992-3 operational winter forecasting experiment for Stapleton airport
 p 677 A95-93561

NOZZLE DESIGN

Studies on gain performance of a combustion driven CO2 gas dynamic laser
 p 428 A95-82679
 NASA-Lewis tests Allison ASTOVL nozzle
 [HTN-95-20603] p 404 A95-84784
 Testing the hypersonic technology demonstration nozzle: Results from the test campaign 1993/94
 [AIAA PAPER 95-6084] p 509 A95-87413
 A model for preliminary facility design including simulation issues
 p 144 N95-16318
 Development of quiet-flow supersonic wind tunnels for laminar-turbulent transition research
 [NASA-CR-197286] p 239 N95-21436
 An approximate theoretical method for modeling the static thrust performance of non-axisymmetric two-dimensional convergent-divergent nozzles
 [NASA-CR-195050] p 273 N95-23193
 Optimized design of a hypersonic nozzle
 p 297 N95-23304
 Design of a variable area diffuser for a 15-inch Mach 6 open-jet tunnel
 p 297 N95-23309
 Three-dimensional Navier-Stokes analysis and redesign of an imbedded bellmouth nozzle in a turbine cascade inlet section
 p 311 N95-23423
 Internal performance characteristics of thrust-vectorable axisymmetric ejector nozzles
 [NASA-TM-4610] p 331 N95-25338
 The noise reduction potential of dual-stream coaxial rectangular improperly expanded jet flows
 [NASA-CR-197820] p 437 N95-26995
 Use of the PARC code to estimate the off-design transonic performance of an over/under turboramjet nozzle
 [NASA-TM-106924] p 482 N95-30091
 Laser doppler velocimeter system for subsonic jet mixer nozzle testing at the NASA Lewis Aeroacoustic Propulsion Lab
 [NASA-TM-106984] p 457 N95-30229
 Flow models for the design of a hypersonic iodine vapor wind tunnel nozzle with chemical and vibrational nonequilibrium effects
 p 592 N95-30448

NOZZLE EFFICIENCY

- Experimental performance of a ventral nozzle with pitch and yaw vectoring capability for SSTOVL aircraft [SAE PAPER 931412] p 614 A95-93678
- Combustor kinetic energy efficiency analysis of the hypersonic research engine data p 148 N95-16321
- An approximate theoretical method for modeling the static thrust performance of non-axisymmetric two-dimensional convergent-divergent nozzles [NASA-CR-195050] p 273 N95-23193
- Internal performance characteristics of thrust-vectoring axisymmetric ejector nozzles [NASA-TM-4610] p 331 N95-25338
- Use of the PARC code to estimate the off-design transonic performance of an over/under turboramjet nozzle [NASA-TM-106924] p 482 N95-30091

NOZZLE FLOW

- On the scaling of small-scale jet noise to large scale [AIAA PAPER 92-02109] p 27 A95-60166
- Computation of nonequilibrium viscous flows in arc-jet wind tunnel nozzles [AIAA PAPER 94-0254] p 2 A95-60173
- Direct splitting of coefficient matrix for numerical calculation of transonic nozzle flow [BTN-94-EIX94481415356] p 103 A95-65346
- Three-dimensional analysis of scramjet nozzle flows [BTN-94-EIX94441380978] p 196 A95-68162
- Lag model for turbulent boundary layers over rough bleed surfaces [BTN-94-EIX94441380981] p 208 A95-68165
- Entrainment and acoustic variations in a round jet from introduced streamwise vorticity [BTN-95-EIX95042474409] p 209 A95-68291
- Measurement and analysis of nitric oxide radiation in an arcjet flow [BTN-95-EIX95082502727] p 243 A95-71040
- Predicting exhaust plume boundaries with supersonic external flows [BTN-95-EIX951525683258] p 297 A95-73559
- Simulation on the 3-D turbulent flow in the passages of finocyl grain [BTN-95-EIX95202638962] p 279 A95-76674
- Evaluation of scramjet nozzle performance p 402 A95-82321
- An experimental investigation of scramjet jets p 402 A95-82322
- Enhanced mixing of multiple supersonic rectangular jets by synchronized screech [HTN-95-42592] p 459 A95-87222
- The high enthalpy shock tunnel in Goettingen (HEG) p 518 A95-87391
- Testing the hypersonic technology demonstration nozzle: Results from the test campaign 1993/94 [AIAA PAPER 95-6084] p 509 A95-87413
- Chemically reacting non-equilibrium boundary layers in air breathing propulsion systems [AIAA PAPER 95-6139] p 512 A95-90456
- An experimental study on interacting flow between supersonic flow and secondary flow injected normally through circular nozzle p 472 A95-91511
- Efficient mapping topology for turbine combustors with inclined slots/staggered holes [BTN-95-EIX0616952745805] p 614 A95-94485
- Effects of the chemical reaction model on calculations of supersonic combustion flows [BTN-95-EIX0616952745802] p 638 A95-94487
- Evaluation of the transient operation of advanced gas turbine combustors [BTN-95-EIX0616952745793] p 614 A95-94495
- Performance variation of scramjet nozzle at various nozzle pressure ratios [BTN-95-EIX0616952745781] p 615 A95-94505
- Propulsion research concerning SFRJ-motors [PB94-179520] p 14 N95-10083
- Two-dimensional converging-diverging rippled nozzles at transonic speeds — performed in the Langley 16-Foot Transonic Tunnel [NASA-TP-3440] p 6 N95-10129
- Flow field investigation in a free jet - free jet core system for the generation of high intensity molecular beams [DLR-FB-94-11] p 172 N95-18912
- Static investigation of two fluidic thrust-vectoring concepts on a two-dimensional convergent-divergent nozzle [NASA-TM-4574] p 222 N95-19913
- An approximate theoretical method for modeling the static thrust performance of non-axisymmetric two-dimensional convergent-divergent nozzles [NASA-CR-195050] p 273 N95-23193
- Experimental results for a hypersonic nozzle/afterbody flow field [NASA-TM-4638] p 274 N95-23250
- An investigation of the AFIT 2-inch shock tube as a flow source for supersonic testing [AD-A289246] p 412 N95-26966

- A laboratory scale supersonic combustive flow system [DE95-006347] p 420 N95-27851
- Ejectors and jet pumps: Computer program for design and performance for steam/gas flow [ESDU-94046] p 500 N95-28704
- Use of the PARC code to estimate the off-design transonic performance of an over/under turboramjet nozzle [NASA-TM-106924] p 482 N95-30091
- Comparison of spatial numerical operators for duct-nozzle acoustics p 580 N95-30158
- Flow models for the design of a hypersonic iodine vapor wind tunnel nozzle with chemical and vibrational nonequilibrium effects p 592 N95-30448
- Validation of the NPARC code for nozzle afterbody flows at transonic speeds [NASA-TM-106971] p 592 N95-30704

NOZZLE GEOMETRY

- Testing the hypersonic technology demonstration nozzle: Results from the test campaign 1993/94 [AIAA PAPER 95-6084] p 509 A95-87413
- Two-dimensional converging-diverging rippled nozzles at transonic speeds — performed in the Langley 16-Foot Transonic Tunnel [NASA-TP-3440] p 6 N95-10129
- Radiant energy measurements from a scaled jet engine axisymmetric exhaust nozzle for a baseline code validation case [NASA-TM-106686] p 25 N95-11409
- Ultra-high bypass ratio jet noise [NASA-CR-195394] p 100 N95-14610
- Thrust measurement in a 2-D scramjet nozzle p 339 N95-25397
- Use of the PARC code to estimate the off-design transonic performance of an over/under turboramjet nozzle [NASA-TM-106924] p 482 N95-30091

NOZZLE THRUST COEFFICIENTS

- An assessment of ground-test facility capabilities for measurement of hypervelocity scramjet performance [AIAA PAPER 95-6148] p 512 A95-90462

NOZZLE WALLS

- Supersonic quiet-tunnel development for laminar-turbulent transition research [NASA-CR-198040] p 340 N95-24302

NUCLEAR PHYSICS

- Laws of infrared similitude [AD-A282209] p 62 N95-12426

NUCLEAR POWER PLANTS

- Reaction-time response of aircraft crash [BTN-95-EIX95292721296] p 595 A95-92626

NUCLEAR POWER REACTORS

- Ageing nuclear power plant management: An aeronautical viewpoint [NAL-PD-SN-9306] p 105 N95-18606

NUMERICAL ANALYSIS

- Novel similarity solutions of the sonic small-disturbance equation with applications to airfoil transonic aerodynamics [BTN-94-EIX94341340316] p 35 A95-60852
- On the dynamics of aeroelastic oscillators with one degree of freedom [BTN-94-EIX94501431527] p 153 A95-64524
- Construction of nearly orthogonal multiblock grids for compressible flow simulation [BTN-94-EIX94361133526] p 207 A95-65981
- Solution-adaptive structured-unstructured grid method for unsteady turbomachinery analysis. Part I: Methodology [BTN-94-EIX94441380983] p 208 A95-67329
- Numerical analysis of flow field around gas rudder p 407 A95-82333
- Compressible Navier-Stokes computations of multielement airfoil flows using multiblock grids [HTN-95-42327] p 371 A95-86156
- Effects of spatial order of accuracy on the computation of local flowfields [HTN-95-42589] p 459 A95-87219
- Estimation of aerodynamic derivatives: Euler scheme validation and approximate methods for hypersonic configurations p 460 A95-87385
- Verification of engineering methods of aerodynamics for reentry vehicles by DSMC p 525 A95-87386
- Simple numerical criterion for vortex breakdown [HTN-95-61210] p 541 A95-87583
- New experimental approach to determine initial fatigue quality with fastener holes [BTN-94-EIX94522406136] p 701 A95-96273
- Numerical simulation of the flow about the F-18 HARV at high angle of attack [NASA-CR-196396] p 9 N95-10940
- Optimum Design Methods for Aerodynamics [AGARD-R-803] p 127 N95-16562
- Optimal shape design for aerodynamics p 128 N95-16568

Review of the EUROPT Project AERO-0026

- p 129 N95-16573
- A numerical study of fundamental shock noise mechanisms [NASA-TM-110608] p 451 N95-27908
- Numerical analysis of intra-cavity and power-stream flow interaction in multiple gas-turbine disk-cavities [NASA-TM-106886] p 407 N95-28344

NUMERICAL CONTROL

- Test bench for rotorcraft hover control [BTN-94-EIX94511433919] p 169 A95-64585
- Guidance and control, 1993; Annual Rocky Mountain Guidance and Control Conference, 16th, Keystone, CO, Feb. 6-10, 1993 [ISBN-0-87703-365-X] p 341 A95-80389
- The Cassini spacecraft: Object oriented flight control software p 359 A95-80405
- A new guidance and flight control system for the DELTA 2 launch vehicle — Abstract only p 342 A95-80427
- Non-contact calibration of a CNC riveting machine [CONGRESS PAPER C428-32-075] p 583 A95-93618
- Design and flight evaluation of an integrated navigation and near-terrain helicopter guidance system for night-time and adverse weather operations [NASA-TM-108837] p 11 N95-10846
- Formal design and verification of a reliable computing platform for real-time control (phase 3 results) [NASA-TM-109140] p 33 N95-10873
- Low frequency ultrasonic nondestructive inspection of aluminum/adhesive fuselage lap splices [DE94-014242] p 24 N95-11135
- Improved speed control system for the 87,000 HP wind tunnel drive [NASA-TM-106840] p 211 N95-19794
- Process and control systems for composites manufacturing p 420 N95-28267
- Catapult-launching of the RAFALE design and experimentation p 609 N95-32008

NUMERICAL FLOW VISUALIZATION

- Numerical investigation of cylinder wake flow with a rear stagnation jet [HTN-95-51669] p 433 A95-85051
- Computational methods in applied sciences; European Computational Fluid Dynamics Conference, 1st, Brussels, Belgium, Sept. 7-11, 1992 [ISBN 0-444-89795-X] p 539 A95-87552
- Numerical simulation of real gas effects and aerodynamic heating of hypersonic space transportation vehicles p 540 A95-87558
- Aerodynamic design and optimization at Alenia D.V.D. p 491 A95-87564
- Numerical model for circulation-control flows [HTN-95-81632] p 461 A95-87680
- Multipoint inverse design of an infinite cascade of airfoils [HTN-95-81640] p 541 A95-87688
- Three-dimensional adaptive grid-embedding Euler technique [HTN-95-20825] p 543 A95-88086
- Low-dimensional description of the dynamics in separated flow past thick airfoils [HTN-95-20832] p 544 A95-88093
- Swirl control in an S-duct at high angle of attack [HTN-95-20846] p 545 A95-88107
- Turbulence characteristics of supersonic boundary layer past a backward facing step [AIAA PAPER 95-6126] p 470 A95-90447
- Computational fluid dynamics '92; Proceedings of the European Computational Fluid Dynamics Conference, 1st, Brussels, Belgium, Sep. 7-11, 1992. Vols. 1 & 2 [ISBN 0-444-89793-3] p 638 A95-95357
- Viscous flow simulation using the discrete vortex diffusion velocity method p 639 A95-95421
- Numerical simulation of the 3D turbulent flow around the combustor dome of an aircraft engine p 640 A95-95423
- High-lift calculations using Navier-Stokes methods p 641 A95-95444
- Permeable wall boundary conditions for transonic airfoil design p 641 A95-95445
- A modular system for computational fluid dynamics p 641 A95-95446
- On the prediction of transonic unsteady flows using second order time accuracy p 641 A95-95448
- Multigrid/multiblock method for transonic potential flow around wing/body/nacelle configurations including a slipstream p 591 A95-95451
- Multigrid solution for the compressible Euler equations by an implicit characteristic-flux-averaging p 642 A95-95459
- SAUNA: A system for grid generation and flow simulation using hybrid structured/unstructured grids p 642 A95-95470
- Grid adaptation for problems in computational fluid dynamics p 643 A95-95472

Multi-block finite volume calculation of compressible flow past aerodynamic configurations p 643 A95-95473
 A 2D parallel multiblock Navier-Stokes solver with applications on shared- and disturbed memory machines p 643 A95-95475
 Grid generation: Algebraic and partial differential equations techniques revisited p 643 A95-95477
 Arbitrary Lagrangian-Eulerian finite element analysis for flow-induced vibration of rigid body p 643 A95-95485
 High performance parallelized implicit Euler solver for the analysis of unsteady aerodynamic flows p 644 A95-95495
 Hypersonic Navier-Stokes computations about complex configurations p 644 A95-95497
 Navier-Stokes simulation of turbulent vortex high-Re-number flows over a delta wing p 644 A95-95507
 Visualization of one-dimensional flow processes in a dual-mode scramjet engine p 15 N95-10465
 3D visualization of unsteady 2D airplane wake vortices [AD-A284745] p 27 N95-11593

NUMERICAL WEATHER FORECASTING

WINDEX -- A new index for forecasting microburst potential
 [HTN-95-90690] p 215 A95-69717
 An algorithm for forecasting mountain wave-related turbulence in the stratosphere [HTN-95-80656] p 254 A95-72500
 Preliminary comparisons between MMS NCAR/Penn State model generated icing forecasts and observations p 655 A95-93458
 An integrated system to improve aviation weather forecasts for the Alaska Range p 656 A95-93460
 Jet stream winds: Comparisons of operational analyses with independent aircraft data at multiple longitudes p 665 A95-93506
 Testing of TKE parameterizations in numerical models for clear-air turbulence forecasting p 667 A95-93515
 FTGEN - An automated FT production system p 668 A95-93519
 Nortat: Computer generated aerodome forecasts p 668 A95-93521
 The combination of forecasts in an automated aviation weather forecasting system p 669 A95-93522
 Aviation weather forecasting automated methods in the RAFC Moscow and the Airport Vnukovo p 669 A95-93523

A poor man's expert system for aviation VSRF in complex terrain p 669 A95-93524
 Weather products for aviation from WAFIC Bracknell p 670 A95-93527
 User involvement in the development of an advanced icing product for use in aviation p 672 A95-93537
 Creating a global climatology of freezing rain using numerical model output p 673 A95-93541
 An application of some cloud modeling techniques to a regional model simulation of an icing event p 673 A95-93543

A northern hemisphere clear air turbulence climatology p 674 A95-93547
 Preliminary results of turbulence predictions for use in aviation weather forecasting p 675 A95-93551
 A prototype for displaying aviation forecast variables using Eta numerical model output p 676 A95-93555
 Operational multi-scale environment model with grid adaptivity (OMEGA) application to aviation weather p 676 A95-93556

An overview of issues encountered in parallelizing high-resolution weather prediction models p 676 A95-93560
 Thunderstorm hypothesis reasoner [AD-A282664] p 60 N95-12805

RUSSELL NUMBER

Natural convection in central microcavities of vertical, finned enclosures of very high aspect ratios [BTN-95-EIX95282711336] p 632 A95-92405

NYLON (TRADEMARK)

Theoretical and actual performance of a long duration superpressure balloon made from a biaxially oriented nylon-6 film p 181 A95-66282
 Recent developments in nylon superpressure balloons p 385 A95-82512
 High strain-rate testing of parachute materials [DE95-009577] p 648 N95-31614



OASES

Operational And Supportability Implementation System (OASIS) test and evaluation master plan [AD-A284765] p 126 N95-18088

OBJECT-ORIENTED PROGRAMMING

The Cassini spacecraft: Object oriented flight control software p 359 A95-80405

Education, training, and human engineering in aerospace; SAE Aerotech '93, Costa Mesa, CA, Sep. 27-30, 1993

[SAE SP-992] p 417 A95-84553
 New tools for creating instruction and simulations [SAE PAPER 932600] p 380 A95-84572
 Knowledge-based processing for aircraft flight control [NASA-CR-194976] p 99 N95-13727
 Safety aspects of spacecraft commanding p 149 N95-17248

The navigation toolkit [NASA-CR-197290] p 229 N95-22161
 EASY-SIM: A visual simulation system software architecture with an Ada 9X application framework [AD-A289325] p 448 N95-26895
 Impact of Ada and object-oriented design in the flight dynamics division at Goddard Space Flight Center [NASA-CR-189412] p 567 N95-28807

OBLIQUE SHOCK WAVES

Direct splitting of coefficient matrix for numerical calculation of transonic nozzle flow [BTN-94-EIX94481415356] p 103 A95-65346
 Scaling of incipient separation in supersonic/transonic speed laminar flows [BTN-95-EIX95182619104] p 269 A95-76589
 Structure of a double-fin turbulent interaction at high speed [BTN-95-EIX95222650780] p 347 A95-79236

Visualization of one-dimensional flow processes in a dual-mode scramjet engine p 15 N95-10465
 Shock wave interactions in hypervelocity flow [AD-A286507] p 250 N95-22212
 Supersonic flow and shock formation in turbine tip gaps p 312 N95-23429

Grid resolution and turbulent inflow boundary condition recommendations for NPARC calculations [NASA-TM-106959] p 482 N95-30253
 Numerical simulation of supersonic flow using a new analytical bleed boundary condition [NASA-CR-198368] p 697 N95-33208

OBLIQUE WINGS

Design and testing of an oblique all-wing supersonic transport [NASA-CR-196394] p 48 N95-12785
 Preliminary design problems and solutions for a supersonic oblique all-wing transport aircraft p 390 N95-26942

OBSERVABILITY (SYSTEMS)

Nonlinear observer and its application in flight control p 447 A95-82449

OBSERVATION

Verification of terminal forecasts p 664 A95-93502
 Weather products for aviation from WAFIC Bracknell p 670 A95-93527

OBSTACLE AVOIDANCE

Optimal lateral-escape maneuvers for microburst encounters during final approach [BTN-95-EIX95182619127] p 276 A95-76604
 Automatic guidance and control for helicopter obstacle avoidance [BTN-95-EIX95182619130] p 291 A95-76607
 Flight test of a low-altitude helicopter guidance system with obstacle avoidance capability p 688 N95-32490
 A tactical navigation and routing system for low-level flight p 709 N95-32494
 Development and flight testing of an Obstacle Avoidance System for US Army helicopters p 687 N95-32500

OCEAN BOTTOM

Geoid lineations of 1000 km wavelength over the central Pacific [HTN-95-11304] p 319 A95-77009

OCEAN DATA ACQUISITIONS SYSTEMS

Validation of empirical orbit error corrections using crossover difference differences [HTN-94-00912] p 25 A95-60227

OCEAN DYNAMICS

Airborne passive polarimetric measurements of sea surface anisotropy at 92 GHz [NASA-CR-197288] p 707 N95-32823

OCEAN MODELS

Orbital velocities induced by surface waves [HTN-95-90902] p 253 A95-72411
 Assimilation of altimeter data in a quasi-geostrophic model of the Gulf Stream system: A dynamical perspective [NASA-CR-196313] p 320 N95-23766
 Airborne passive polarimetric measurements of sea surface anisotropy at 92 GHz [NASA-CR-197288] p 707 N95-32823

OCEAN SURFACE

Precision orbit determination of altimetric satellites p 86 N95-14282
 Assimilation of altimeter data in a quasi-geostrophic model of the Gulf Stream system: A dynamical perspective [NASA-CR-196313] p 320 N95-23766

An in situ evaluation of TOPEX/Poseidon altimetric measurements versus measurements made by moorings and inverted echo sounders for sea surface height [NASA-CR-198621] p 447 N95-27805

Airborne passive polarimetric measurements of sea surface anisotropy at 92 GHz [NASA-CR-197288] p 707 N95-32823

OCEAN TEMPERATURE

Evaluation of the Sparton tight-tolerance AXBT [HTN-95-40728] p 251 A95-70473

OCEANOGRAPHY

Validation of empirical orbit error corrections using crossover difference differences [HTN-94-00912] p 25 A95-60227
 Field and data analysis studies related to the atmospheric environment [NASA-CR-196543] p 168 N95-18093
 Airborne geophysics and precise positioning: Scientific issues and future directions [LC-94-68678] p 446 N95-27156

OCTANE NUMBER

Determination of minimum fuel octane number piston aircraft engines [SAE PAPER 931230] p 528 A95-88961
 Ongoing research into high octane unleaded avgas [SAE PAPER 931234] p 529 A95-88963

OCTETS

Control mechanism to prevent correlated message arrivals from degrading signaling no. 7 network performance [BTN-94-EIX94341342286] p 56 A95-60842

OFFSHORE PLATFORMS

An investigation of piloting strategies for engine failures during takeoff from offshore platforms [HTN-95-92834] p 497 A95-90752

OGIVES

Passive porosity with free and fixed separation on a tangent-ogive forebody [BTN-95-EIX95062487554] p 185 A95-68368

OH-58 HELICOPTER

Condition monitoring and diagnostics [HTN-95-92312] p 387 A95-85356

OILS

Boundary-layer transition and global skin friction measurement with an oil-fringe imaging technique [SAE PAPER 932550] p 547 A95-90054
 Bicarbonate of soda blasting technology for aircraft wheel depainting [PB94-19323] p 104 N95-17466
 Boundary-layer transition and global skin friction measurement with an oil-fringe imaging technique [NASA-CR-198814] p 557 N95-30224

OKLAHOMA

Final results of the weather testing component of the Terminal Doppler Weather Radar operational test and evaluation p 658 A95-93471

ON-LINE SYSTEMS

On-line analysis capabilities developed to support the active flexible wing wind-tunnel tests [BTN-95-EIX95182619213] p 296 A95-76639
 Sensor fault detection and diagnosis simulation of a helicopter engine in an intelligent control framework [AD-A290223] p 137 N95-15970
 On-line handling of air traffic: Management, guidance and control [AGARD-AG-321] p 126 N95-18927
 On-line, adaptive state estimator for active noise control p 322 N95-23308
 Electrochemical impedance pattern recognition for detection of hidden chemical corrosion on aircraft components, phase 1 [AD-A291345] p 556 N95-29946

ONBOARD DATA PROCESSING

Design and flight evaluation of an integrated navigation and near-terrain helicopter guidance system for night-time and adverse weather operations [NASA-TM-108837] p 11 N95-10846
 Packet utilisation definitions for the ESA XMM mission p 150 N95-17596

ONE DIMENSIONAL FLOW

Simulating heat addition via mass addition in constant area compressible flows [BTN-95-EIX95182619100] p 307 A95-76585
 Corrective term in wall slip equations for Knudsen layer [BTN-95-EIX95282705070] p 455 A95-89667
 A one-dimensional inviscid nonequilibrium flow solver [ISBN 1-879921-01-4] p 588 A95-93752
 Visualization of one-dimensional flow processes in a dual-mode scramjet engine p 15 N95-10465
 Computer code for determination of thermally perfect gas properties [NASA-TP-3447] p 37 N95-11995
 Recent improvements to and validation of the one dimensional NASA wave rotor model [NASA-TM-106913] p 332 N95-25962

- Model development for active control of stall phenomena in aircraft gas turbine engines p 514 N95-29679
- OPENINGS**
Hypersonic flow past open cavities [HTN-95-42577] p 458 A95-87207
Use of partially open wind tunnel walls for blockage-free separated flows on bodies p 474 A95-91558
- OPERATING COSTS**
Selecting and management of fire fighter aircraft [BTN-95-EIX95062487538] p 193 A95-69246
Design constraints in the payload-range diagram of ultrahigh capacity transport airplanes [BTN-95-EIX95152582319] p 276 A95-73522
Containing military autotest cost growth through the use of commercial standard equipment architectures [BTN-95-EIX95172595295] p 287 A95-75717
The FC-1D: The profitable alternative Flying Circus Commercial Aviation Group [NASA-CR-197152] p 46 N95-12628
The OFF-6M transport jet [NASA-CR-197159] p 46 N95-12637
Central coast designs: The Eightball Express. Taking off with convention, cruising with improvements and landing with absolute success [NASA-CR-197181] p 47 N95-12643
LCX: Proposal for a low-cost commercial transport [NASA-CR-197186] p 47 N95-12645
Protective coatings for compressor gas path components p 201 N95-19675
Impact of composites on future transport aircraft p 534 N95-29030
Modeling F/A-18 flight hour program costs using regression analysis [AD-A293771] p 608 N95-31579
- OPERATING SYSTEMS (COMPUTERS)**
The generic simulation executive at Manned Flight Simulator [AD-A283997] p 146 N95-18724
- OPERATING TEMPERATURE**
Temperature effects on acoustic interactions between altitude test facilities and jet engine plumes [NASA-CR-197638] p 258 N95-21170
- OPERATIONAL HAZARDS**
Erosion, Corrosion and Foreign Object Damage Effects in Gas Turbines [AGARD-CP-558] p 197 N95-19653
The operation of gas turbine engines in hot and sandy conditions: Royal Air Force experiences in the Gulf conflict p 198 N95-19655
Quantity-distance requirements for earth-bermed aircraft shelters [AD-A279692] p 341 N95-24424
- OPERATIONAL PROBLEMS**
Air traffic operational inventory CY 1994 [AD-A288281] p 382 N95-26454
- OPERATIONS RESEARCH**
NASA Lewis Propulsion Systems Laboratory test article systems criteria [NASA-TM-106589] p 20 N95-10446
- OPTICAL COMMUNICATION**
Optical backplane for modular avionics p 257 N95-20652
- OPTICAL COMPUTERS**
High performance backplane components for modular avionics p 247 N95-20653
- OPTICAL FIBERS**
A three-dimensional orthogonal laser velocimeter for the NASA Ames 7- by 10-foot wind tunnel [NASA-TM-108864] p 249 N95-21323
Preliminary experiments of an optical fiber display [NAL-TR-1257] p 382 N95-25004
Standardization of surface contamination analysis systems p 631 N95-31798
- OPTICAL MATERIALS**
Aero-optics system integration [TABES PAPER 94-604] p 100 N95-14638
- OPTICAL MEASUREMENT**
Laser device for measuring a vessel's speed [HTN-95-60992] p 361 A95-80633
Optical surface pressure measurements: Accuracy and application field evaluation p 175 N95-19274
Dynamic response tests of inertial and optical wind-tunnel model attitude measurement devices [NASA-TM-109182] p 296 N95-23011
Angular displacement measuring device [NASA-CASE-ARC-11937-1] p 362 N95-26015
- OPTICAL MEASURING INSTRUMENTS**
Fiber Optic Control System integration for advanced aircraft. Electro-optic and sensor fabrication, integration, and environmental testing for flight control systems [NASA-CR-191194] p 162 N95-19236
State-to-state collisional dynamics of atmospheric species [AD-A285053] p 245 N95-20484
Optical processing and control [AD-A279157] p 259 N95-21975
- The 1994 Fiber Optic Sensors for Aerospace Technology (FOSAT) Workshop [NASA-CP-10166] p 337 N95-24207
HeliRadar: A rotating antenna synthetic aperture radar for helicopter allweather operations p 705 N95-33137
- OPTICAL RADAR**
2 micron LIDAR for laser-based remote sensing: Flight demonstration and application survey [BTN-95-EIX95212641072] p 319 A95-76737
Doppler lidar investigation of wake vortex transport between closely spaced parallel runways [HTN-95-81645] p 462 A95-87693
Commercial applications for military laser radars p 543 A95-87794
The detection and measurement of microburst wind shear by an airborne lidar system p 543 A95-87798
Airborne Windshear Detection and Warning Systems. Fifth and Final Combined Manufacturers' and Technologists' Conference, part 2 [NASA-CP-10139-PT-2] p 41 N95-13203
Airport surveillance using a solid state coherent lidar p 41 N95-13207
Wake vortex detection at Denver Stapleton Airport with a pulsed 2-micron coherent lidar p 42 N95-13211
Remote sensing of turbulence in the clear atmosphere with 2-micron lidars p 59 N95-13213
Flight test of a low-altitude helicopter guidance system with obstacle avoidance capability p 688 N95-32490
Laser based obstacle warning sensors for helicopters p 686 N95-32499
Development and flight testing of an Obstacle Avoidance System for US Army helicopters p 687 N95-32500
The Anglo-French Compact Laser Radar demonstrator programme p 703 N95-32501
- OPTICAL SWITCHING**
Optical processing and control [AD-A279157] p 259 N95-21975
- OPTICAL THICKNESS**
Microphysical and radiative properties of small cumulus clouds over the sea [HTN-95-A0526] p 255 A95-73180
Air truth validation of cloud albedo estimated from NOAA advanced very high resolution radiometer data [HTN-95-A1021] p 443 A95-84526
- OPTICAL TRACKING**
Autonomous helicopter hover positioning by optical tracking [HTN-95-C0006] p 585 A95-93394
Passive range measurement system [AD-D016222] p 258 N95-21100
Orientation determination of aircraft using visual 3D matching and radar. Case study 2 [PB95-165791] p 350 N95-25749
- OPTICS**
JPRS report: Science and technology. Central Eurasia [JPRS-UST-94-018] p 349 N95-24472
- OPTIMAL CONTROL**
Local-optimal control of a flying vehicle, with final state optimized [BTN-94-EIX94461407957] p 83 A95-62631
Selection of optimal parameters for a system, controlling the flight height, when information about the state vector is incomplete [BTN-94-EIX94461408753] p 168 A95-63636
Modelling for optimal operations of line milling of aerodynamic surfaces [BTN-94-EIX94461408774] p 138 A95-63657
Nonsmooth trajectory optimization: An approach using continuous simulated annealing [BTN-94-EIX94511433914] p 168 A95-64560
Time-optimal turn to a heading: An analytic solution [BTN-94-EIX94511433940] p 142 A95-64606
Aeroelastic vehicle multivariable control synthesis with analytical robustness evaluation [BTN-95-EIX95182619115] p 321 A95-76592
Functional agility metrics and optimal trajectory analysis [BTN-95-EIX95182619121] p 321 A95-76598
Design and multifunction tests of a frequency domain-based active flutter suppression system [BTN-95-EIX95182619215] p 292 A95-76641
Fuel-optimal bank-angle control for lunar-return aerocapture [BTN-95-EIX95212645706] p 299 A95-76758
Application of direct transcription to commercial aircraft trajectory optimization [BTN-95-EIX95242670766] p 359 A95-81081
Fundamental mechanisms of aeroelastic control with control surface and strain actuation [BTN-95-EIX95242670746] p 327 A95-81101
Handling qualities of hypersonic aircraft and related control requirements p 515 A95-87398
New filtering method for linear weakly coupled stochastic systems [BTN-95-EIX0608952736485] p 678 A95-92708
- Panel flutter limit-cycle suppression with piezoelectric actuation [BTN-95-EIX95302731089] p 618 A95-94208
Optimal trajectories for an unmanned air-vehicle in the horizontal plane [BTN-95-EIX0619952748191] p 606 A95-94480
Extended cooperative control synthesis [NASA-TM-4561] p 17 N95-10220
On the use of controls for subsonic transport performance improvement: Overview and future directions [NASA-TM-4605] p 10 N95-11408
Techniques for designing rotorcraft control systems [NASA-CR-196192] p 52 N95-12791
Microgravity isolation system design: A case study [NASA-TM-106804] p 104 N95-17657
A feedforward control approach to the local navigation problem for autonomous vehicles [AD-A282787] p 126 N95-17706
Microgravity isolation system design: A modern control synthesis framework [NASA-TM-106805] p 105 N95-18197
Active control of panel vibrations induced by a boundary layer flow [NASA-CR-197867] p 273 N95-23182
Flight control design using mixed H2/micron optimization [AD-A289288] p 410 N95-27036
Modeling and control of rotating stall in high speed multi-stage axial compressors p 513 N95-29244
Analytical investigations in aircraft and spacecraft trajectory optimization and optimal guidance [NASA-CR-4672] p 526 N95-29339
Linear matrix inequalities for the problem of absolute stability of control systems p 518 N95-29680
SCARLET: DLR rate saturation flight experiment p 598 N95-31068
Robust control: A structured approach to solve aircraft flight control problems p 621 N95-31995
Model following control for tailoring handling qualities: ACT experience with ATHeS p 622 N95-32000
An Electronic Workshop on the Performance Seeking Control and Propulsion Controlled Aircraft Results of the F-15 Highly Integrated Digital Electronic Control Flight Research Program [NASA-TM-104278] p 694 N95-33009
An overview of integrated flight-propulsion controls flight research on the NASA F-15 research airplane p 694 N95-33010
Performance seeking control program overview p 695 N95-33011
PSC algorithm description p 695 N95-33013
Performance seeking control excitation mode p 696 N95-33019
Performance seeking control (PSC) for the F-15 highly integrated digital electronic control (HIDEC) aircraft p 697 N95-33020
- OPTIMIZATION**
Intelligent control law tuning for AIAA controls design challenge [BTN-94-EIX94511433922] p 169 A95-64588
Two-point transonic airfoil design using optimization for improved off-design performance [BTN-95-EIX95062487542] p 192 A95-68356
Navier-Stokes computation of a viscous optimized waverider [BTN-95-EIX95041503782] p 193 A95-69213
Secondary source locations in active noise control: Selection or optimization? [BTN-94-EIX94381352222] p 257 A95-71738
Aerodynamic shape optimization using preconditioned conjugate gradient methods [BTN-95-EIX95142553033] p 263 A95-73465
Improved version of the Naval Surface Warfare Center aeroprediction code (AP93) [BTN-95-EIX95152583260] p 267 A95-73561
Optimization of contoured hypersonic scramjet inlets with a least-squares parabolized Navier-Stokes procedure [HTN-95-20976] p 261 A95-74042
CFD optimization of a theoretical minimum-drag body [BTN-95-EIX95182619234] p 308 A95-76660
Optimal trajectories for hypersonic launch vehicles [HTN-95-61120] p 415 A95-84884
Design optimization of an airbreathing aerospaceplane p 524 A95-87382
Aerodynamic design and optimization at Alenia D.V.D. p 491 A95-87564
Improving the efficiency of aerodynamic shape optimization [HTN-95-61204] p 540 A95-87577
Trajectory optimization using parallel shooting method on parallel computer [BTN-95-EIX95282706670] p 564 A95-88175

- Optimization of waverider configurations generated from inclined circular and elliptic cones
[AIAA PAPER 95-6089] p 492 A95-89198
- Aircraft controller synthesis by solving a nonconvex optimization problem
[BTN-95-EIX95282706672] p 515 A95-89636
- Optimal design of composite helicopter power transmission shafts with axially varying fiber layup
[HTN-95-01086] p 529 A95-90272
- Parallel CFD design on network-based computer
[AIAA PAPER 95-0984] p 565 A95-90656
- A computational environment for exhaust nozzle design
[AIAA PAPER 95-1016] p 566 A95-90688
- The use of structural optimization within aerospace
[CONGRESS PAPER C428-23-008] p 500 A95-91729
- A better than average stress model-photoelastic analysis for airbus design
[CONGRESS PAPER C428-23-005] p 500 A95-91730
- Supersonic, turbulent flow computation and drag optimization for axisymmetric afterbodies
[BTN-95-EIX95302729772] p 637 A95-94134
- The use of the Regier number in the structural design with flutter constraints
[NASA-TM-109128] p 13 N95-11465
- Optimization of aerospace structures
[NASA-CR-196763] p 48 N95-12787
- Ceramic manufacturing: Optimizing a multivariable system
[DE94-015016] p 56 N95-13184
- Methodology for sensitivity analysis, approximate analysis, and design optimization in CFD for multidisciplinary applications
[NASA-CR-196981] p 58 N95-13201
- Turbomachinery Design Using CFD
[AGARD-LS-195] p 89 N95-14127
- Computational methods for preliminary design and geometry definition in turbomachinery
p 89 N95-14128
- Elements of a modern turbomachinery design system
p 90 N95-14129
- Portable parallel stochastic optimization for the design of aeropropulsion components
[NASA-CR-195312] p 154 N95-16072
- Optimum Design Methods for Aerodynamics
[AGARD-R-803] p 127 N95-16562
- Optimum aerodynamic design via boundary control
p 127 N95-16565
- Optimal shape design for aerodynamics
p 128 N95-16568
- Airfoil optimization by the one-shot method
p 128 N95-16569
- Tools for applied engineering optimization
p 128 N95-16570
- The global aircraft shape
p 128 N95-16571
- Aerodynamic shape optimization
p 128 N95-16572
- Review of the EUROPT Project AERO-0026
p 129 N95-16573
- Algorithms for bilevel optimization
[NASA-CR-194980] p 170 N95-16897
- Optimization of adaptive intraply hybrid fiber composites with reliability considerations
[NASA-TM-106632] p 157 N95-16911
- Parallel calculation of sensitivity derivatives for aircraft design using automatic differentiation
[NASA-TM-110103] p 231 N95-20370
- Robust fixed-structure control
[AD-A286515] p 257 N95-22216
- Direct adaptive performance optimization of subsonic transports: A periodic perturbation technique
[NASA-TM-4676] p 284 N95-22829
- Integrated aerodynamic/dynamic/structural optimization of helicopter rotor blades using multilevel decomposition
[NASA-TP-3465] p 285 N95-22953
- Aerodynamic design optimization with sensitivity analysis and computational fluid dynamics
[NASA-CR-197419] p 274 N95-23218
- Aerodynamic optimization studies on advanced architecture computers
[NASA-CR-198045] p 330 N95-24379
- Geometric analysis of wing sections
[NASA-TM-110346] p 335 N95-24629
- Aerodynamic shape optimization of wing and wing-body configurations using control theory
[NASA-CR-198024] p 335 N95-25334
- Supersonic transport grid generation, validation, and optimization
[NASA-CR-197752] p 448 N95-26648
- Creating an alternative parameter optimization method (APO)
p 375 N95-26946
- Optimization of wave rotors for use as gas turbine engine topping cycles
[NASA-TM-106951] p 406 N95-27860
- Local design optimization for composite transport fuselage crown panels
p 398 N95-28473
- An efficiency study of the simultaneous analysis and design of structures
[NASA-TM-110168] p 501 N95-28820
- Users manual for the improved NASA Lewis ice accretion code LEWICE 1.6
[NASA-CR-198355] p 485 N95-29132
- A general inverse design procedure for aerodynamic bodies
p 606 N95-30497
- Robust fixed-structure control
[AD-A292883] p 679 N95-30961
- Three-dimensional aerodynamic shape optimization using discrete sensitivity analysis
p 691 N95-32904
- OPTOELECTRONIC DEVICES**
- Integrated IR sensors
[BTN-95-EIX95041505023] p 242 A95-70132
- Lightweight, opto-electronic engine control system for aerospace turbine engines
[SAE PAPER 931442] p 614 A95-93692
- High performance backplane components for modular avionics
p 247 N95-20653
- ORBIT CALCULATION**
- Thermal force modeling for global positioning system satellites using the finite element method
[BTN-95-EIX95152583270] p 278 A95-73571
- Aerodynamics of the Shuttle Orbiter at high altitudes
[BTN-95-EIX95182617454] p 298 A95-75725
- Period evolution of PSR B1259-63: Evidence for propeller-torque spindown
[HTN-95-B0194] p 581 A95-87903
- Precision orbit determination of altimetric satellites
p 86 N95-14282
- Flight Mechanics/Estimation Theory Symposium 1995
[NASA-CP-3299] p 416 N95-27763
- ORBIT INSERTION**
- Optimal separation and ascent of lifting upper stages
p 525 A95-87396
- ORBIT PERTURBATION**
- Thermal force modeling for global positioning system satellites using the finite element method
[BTN-95-EIX95152583270] p 278 A95-73571
- ORBIT TRANSFER VEHICLES**
- Minimum-mass design of sandwich aerobrakes for a lunar transfer vehicle
[BTN-95-EIX95212645707] p 299 A95-76759
- ORBITAL ELEMENTS**
- Period evolution of PSR B1259-63: Evidence for propeller-torque spindown
[HTN-95-B0194] p 581 A95-87903
- ORBITAL MANEUVERS**
- The effect of high lift to drag ratio on aerobraking
p 415 A95-85807
- Numerical optimization of synergetic maneuvers
[AD-A283398] p 109 N95-17435
- ORBITAL MECHANICS**
- Variations of perturbations in perigee height with eccentricity for artificial Earth's satellites due to air drag
[HTN-95-40013] p 85 A95-62657
- ORBITAL VELOCITY**
- Orbital velocities induced by surface waves
[HTN-95-90902] p 253 A95-72411
- The effect of high lift to drag ratio on aerobraking
p 415 A95-85807
- ORDNANCE**
- Air data prediction from surface pressure measurements on guided munitions
[BTN-95-EIX95282706664] p 466 A95-89641
- ORGANIC COMPOUNDS**
- Estimates of total organic and inorganic chlorine in the lower stratosphere from in situ and flask measurements during AASE 2
[HTN-95-A0861] p 317 A95-76265
- ORGANIC MATERIALS**
- Organic coating technology for the protection of aircraft against corrosion
p 303 N95-23513
- ORGANIZATIONS**
- Organizational ergonomics and aviation safety
p 596 A95-95083
- ORIFICES**
- Flow coefficient behavior for boundary layer bleed holes and slots
[NASA-TM-106846] p 244 N95-19953
- ORTHO HYDROGEN**
- Empirical corrections of the rigid rotor interaction potential of H₂-H₂ in the attractive region: Dimer features in the FIR absorption spectra
[HTN-95-41943] p 361 A95-81690
- ORTHOGONALITY**
- Construction of nearly orthogonal multiblock grids for compressible flow simulation
[BTN-94-EIX94361133526] p 207 A95-65981
- Grid orthogonality effects on predicted turbine midspan heat transfer and performance
[NASA-TM-106931] p 554 N95-29371
- OSCILLATING FLOW**
- Experimental study of flow separation on an oscillating flap at Mach 2.4
[BTN-95-EIX95222650792] p 329 A95-79248
- On the role of the outer region in the turbulent-boundary-layer bursting process
[BTN-94-EIX95011441078] p 348 A95-81056
- Role of Kutta waves on oscillatory shock motion on an airfoil
[HTN-95-81642] p 542 A95-87690
- Computations of unsteady aerodynamic loads around oscillating wings. Part 1: Formulation
[PB94-180049] p 7 N95-10136
- Computations of unsteady aerodynamic loads around oscillating wings. Part 2: Computed results and discussions
[PB94-180056] p 7 N95-10137
- Oscillating flow regenerator test rig
[NASA-CR-196982] p 53 N95-13200
- A computational investigation of wake-induced airfoil flutter in incompressible flow and active flutter control
[AD-A281534] p 142 N95-16109
- Interactions of spanwise and chordwise vorticity associated with three-dimensional dynamic stall over an oscillating wing
[AD-A280546] p 477 N95-29091
- Dynamical systems as models for flow-induced vibrations
[PB95-206991] p 647 N95-30956
- OSCILLATION DAMPERS**
- An analytical model for a nonlinear elastomeric lag damper and its effect on aeromechanical stability in Hover
[HTN-95-61076] p 369 A95-83660
- Tuned mass damper for integrally bladed turbine rotor
[NASA-CASE-MFS-28697-1] p 159 N95-18325
- OSCILLATIONS**
- On the dynamics of aeroelastic oscillators with one degree of freedom
[BTN-94-EIX94501431527] p 153 A95-64524
- Linear disturbances in hypersonic, chemically reacting shock layers
[BTN-94-EIX94441386605] p 182 A95-67336
- Analysis of an oscillating Joukowski airfoil with surface suction and moving vortices
[BTN-95-EIX95062487527] p 186 A95-69235
- Measurement around a rotor blade excited in pitch. Part 1: Dynamic inflow
[HTN-95-31007] p 220 A95-71177
- Measurement around a rotor blade excited in pitch. Part 2: Unsteady surface pressure
[HTN-95-31008] p 220 A95-71178
- Smart structures in the control of airframe vibrations
[HTN-95-31014] p 236 A95-71184
- Design optimization of rotor blades for improved performance and vibration
[HTN-95-A0498] p 229 A95-72569
- Further analysis of high-rate rolling experiments of a 65-deg delta wing
[BTN-95-EIX95152582331] p 281 A95-73533
- Postinstability behavior of a two-dimensional airfoil with a structural nonlinearity
[BTN-95-EIX95152582337] p 266 A95-73539
- Flow due to an oscillating sphere and an expression for unsteady drag on the sphere at finite Reynolds number
[BTN-94-EIX95011441142] p 347 A95-81012
- A flying qualities study of longitudinal long-term dynamics of hypersonic planes
[AIAA PAPER 95-6150] p 521 A95-90464
- Modelling and analysis of a dual-wheel nosegear: Shimmy instability and impact motions
[SAE PAPER 931402] p 605 A95-93672
- Numerical study of multi-element airfoil aerodynamics
[ISBN 1-879921-01-4] p 587 A95-93750
- Studies on the flow induced by an oscillating airfoil in a uniform stream
[PB94-204450] p 40 N95-13250
- Overview of unsteady transonic wind tunnel test on a semispan straked delta wing oscillating in pitch
[AD-A284097] p 117 N95-18380
- Development of a multicomponent force and moment balance for water tunnel applications, volume 2
[NASA-CR-4642-VOL-2] p 161 N95-18956
- Robust fixed-structure control
[AD-A286515] p 257 N95-22216
- Suppressor of oscillations in airframe cavities
[AD-D017265] p 388 N95-26507
- Visualization of the multiple supersonic jet oscillations by swept focused strobed schlieren technique
p 367 N95-26952
- The near-wake flow behavior of an oscillating airfoil with modified trailing edge
p 375 N95-26953
- OSCILLATORS**
- A simulation of damping process of pendulum motion due to aerodynamic forces
p 711 N95-34551

OV-10 AIRCRAFT

Flutter clearance flight tests of an OV-10A airplane modified for wake vortex flight experiments
[NASA-TM-109168] p 366 N95-26381

OVER-THE-HORIZON RADAR

An application of virtual prototyping to the flight test and evaluation of an unmanned air vehicle
[AD-A281749] p 14 N95-11595

OXIDATION

The panel oxidation and erosion test (POET) facility
[AIAA PAPER 95-6151] p 521 A95-90465

Effect of surface roughness on local film cooling effectiveness and heat transfer coefficients
[AD-A283854] p 91 N95-14351

Resistance of silicon nitride turbine components to erosion and hot corrosion/oxidation attack
p 202 N95-19683

Evolution of oxidation and creep damage mechanisms in HIPed silicon nitride materials
[DE95-001360] p 300 N95-22689

Mechanism of deposit formation on fuel-wetted hot metal surfaces
[AD-A289847] p 426 N95-28621

Innovative processing of composites for ultra-high temperature applications, book 1
[AD-A290889] p 537 N95-29842

OXIDATION RESISTANCE

Toughened Silcomp composites for gas turbine engine applications
[DE95-002851] p 235 N95-21243

Lubricant evaluation and performance, 2
[AD-A279144] p 242 N95-21969

Thermal barrier coating experience in the gas turbine engine
p 345 N95-26125

OXIDE FILMS

Transport phenomena and interfacial kinetics in multiphase combustion systems
[AD-A288297] p 418 N95-26417

OXIDES

Effect of annealing and desulfurization on oxide spallation of turbine airfoil material
[BTN-95-EIX95282707024] p 528 A95-88264

OXYGEN

Aircraft measurements of water vapour continuum absorption at millimetre wavelengths
[HTN-95-90884] p 253 A95-72393

General solution procedure for flows in local chemical equilibrium
[HTN-95-42329] p 404 A95-86158

Evolution of oxidation and creep damage mechanisms in HIPed silicon nitride materials
[DE95-001360] p 300 N95-22689

Unitized Regenerative Fuel Cells for solar rechargeable aircraft and zero emission vehicles
[DE95-010684] p 708 N95-33642

OZONE

Subsidence of aircraft engine exhaust in the stratosphere: Implications for calculated ozone depletions
[PAPER-93GL03426] p 251 A95-70297

Aircraft-borne, laser-induced fluorescence instrument for the in situ detection of hydroxyl and hydroperoxyl radicals
[BTN-95-EIX95072499029] p 253 A95-71908

Sensitivity of two-dimensional model predictions of ozone response to stratospheric aircraft: An update
[HTN-95-A0863] p 318 A95-76267

A comparison of some aerodynamic resistance methods using measurements over cotton and grass from the 1991 California ozone deposition experiment
[HTN-95-11295] p 319 A95-77000

The distribution of hydrogen, nitrogen, and chlorine radicals in the lower stratosphere: Implications for changes in O₃ due to emission of NO(y) from supersonic aircraft
[HTN-95-70935] p 351 A95-78000

Meridional distributions of NO(X), NO(Y), and other species in the lower stratosphere and upper troposphere during AASE 2
[HTN-95-70944] p 352 A95-78009

Effects on stratospheric ozone from high-speed civil transport: Sensitivity to stratospheric aerosol loading
[HTN-95-91842] p 354 A95-80830

Potential effects on ozone of future supersonic aircraft/2D simulation
[HTN-95-51282] p 356 A95-80867

Impact on ozone of high-speed stratospheric aircraft: Effects of the emission scenario
[HTN-95-51283] p 356 A95-80868

Evolution of the concentrations of trace species in an aircraft plume: Trajectory study
[HTN-95-A1044] p 443 A95-84549

Airborne measurements during the European Arctic Stratospheric Ozone Experiment column amounts of HNO₃ and O₃ derived from FTIR emission sounding
[HTN-95-00742] p 445 A95-86312

Airborne measurements during the Arctic stratospheric experiment: Observation of O₃ and NO₂
[HTN-95-00748] p 445 A95-86318

Three dimensional model calculations of the global dispersion of high speed aircraft exhaust and implications for stratospheric ozone loss
p 26 N95-10657

Compendium of NASA data base for the Global Tropospheric Experiment's Pacific Exploratory Mission West-A (PEM West-A)
[NASA-TM-109177] p 320 N95-23009

The atmospheric effects of stratospheric aircraft: A fourth program report
[NASA-RP-1359] p 357 N95-24274

OZONE DEPLETION

Ozone, skin cancer, and the SST
[BTN-95-EIX95041503011] p 213 A95-68314

Subsidence of aircraft engine exhaust in the stratosphere: Implications for calculated ozone depletions
[PAPER-93GL03426] p 251 A95-70297

Trajectory modeling of emissions from lower stratospheric aircraft
[HTN-95-41219] p 317 A95-75031

Possible effects of CO₂ increase on the high-speed civil transport impact on ozone
[HTN-95-60779] p 317 A95-75976

Estimates of total organic and inorganic chlorine in the lower stratosphere from in situ and flask measurements during AASE 2
[HTN-95-A0861] p 317 A95-76265

In situ observations in aircraft exhaust plumes in the lower stratosphere at midlatitudes
[HTN-95-A0862] p 318 A95-76266

Sensitivity of two-dimensional model predictions of ozone response to stratospheric aircraft: An update
[HTN-95-A0863] p 318 A95-76267

An analysis of aircraft exhaust plumes from accidental encounters
[HTN-95-70943] p 351 A95-78008

Meridional distributions of NO(X), NO(Y), and other species in the lower stratosphere and upper troposphere during AASE 2
[HTN-95-70944] p 352 A95-78009

Sensitivity of supersonic aircraft modelling studies to HNO₃ photolysis rate
[HTN-95-11475] p 353 A95-79453

Effects on stratospheric ozone from high-speed civil transport: Sensitivity to stratospheric aerosol loading
[HTN-95-91842] p 354 A95-80830

High-speed civil transport impact: Role of sulfate, nitric acid trihydrate, and ice aerosols studied with a two-dimensional model including aerosol physics
[HTN-95-91843] p 354 A95-80831

Effects of a polar stratosphere cloud parameterization on ozone depletion due to stratospheric aircraft in a two-dimensional model
[HTN-95-A1038] p 443 A95-84543

An overview of the EASOE campaign
[HTN-95-00702] p 443 A95-86272

Three dimensional model calculations of the global dispersion of high speed aircraft exhaust and implications for stratospheric ozone loss
p 26 N95-10657

Design of a vehicle based system to prevent ozone loss
[NASA-CR-197199] p 48 N95-12702

In situ measurements of ClO and implications for the chemistry of inorganic chlorine in the lower stratosphere
p 563 N95-29830

Alternatives to ozone depleting refrigerants in test equipment
p 630 N95-31767

OZONOMETRY

An overview of the EASOE campaign
[HTN-95-00702] p 443 A95-86272

OZONOSPHERE

Ozone, skin cancer, and the SST
[BTN-95-EIX95041503011] p 213 A95-68314

Impact of present aircraft emissions of nitrogen oxides on tropospheric ozone and climate forcing
[HTN-95-21364] p 353 A95-78679

P

P-N JUNCTIONS

Electro-optic characterization of ultrafast photodetectors using adiabatically compressed soliton pulses
[BTN-94-EIX94381359637] p 257 A95-72675

P-3 AIRCRAFT

Comments on 'correction of inertial navigation with Loran C on NOAA's P-3 aircraft'
[HTN-95-70149] p 227 A95-70671

PACIFIC OCEAN

Geoid lineations of 1000 km wavelength over the central Pacific
[HTN-95-11304] p 319 A95-77009

Oceanic operations: An authoritative guide to oceanic operations
[FAA-AFS-550] p 277 N95-24065

PACKAGING

Advanced Packaging Concepts for Digital Avionics
[AGARD-CP-562] p 233 N95-20631

The impact of advanced packaging technology on modular avionics architectures
p 233 N95-20632

Standard Hardware Acquisition and Reliability Program (SHARP) advanced SEM-E packaging
p 233 N95-20633

FASTPACK: Optimized solutions for modular avionics derived from a parametric study. Part 2: Avionics
p 233 N95-20635

Ultra-Reliable Digital Avionics (URDA) processor
p 245 N95-20638

PACKETS (COMMUNICATION)

Packet utilisation definitions for the ESA XMM mission
p 150 N95-17596

PAINT REMOVAL

Use of starch based blast media for dry paint stripping
[SAE PAPER 932616] p 456 A95-90081

PAINTS

Aircraft stripping and painting
[BTN-95-EIX95182617810] p 300 A95-75755

Aircraft stripping and painting
[HTN-95-92211] p 365 A95-85355

Use of starch based blast media for dry paint stripping
[SAE PAPER 932616] p 456 A95-90081

Bicarbonate of soda blasting technology for aircraft wheel decontamination
[PB94-193323] p 104 N95-17466

Application of pressure sensitive paint in hypersonic flows
[NASA-TM-106824] p 223 N95-20794

A comparison of coating alternatives for US Coast Guard aircraft
[AD-A293270] p 629 N95-31124

Cadmium plating replacements
p 631 N95-31773

Bicarbonate of soda paint stripping process validation and material characterization
p 631 N95-31778

Environmentally Safe and Effective Processes for Paint Removal
[AGARD-LS-201] p 650 N95-32165

Water blasting paint removal methods
p 650 N95-32170

Selective chemical stripping
p 650 N95-32175

Operational parameters and material effects
p 651 N95-32179

Process evaluation
p 651 N95-32180

Standardization work
p 651 N95-32181

PANEL FLUTTER

Finite element time domain - modal formulation for nonlinear flutter of composite panels
[BTN-95-EIX9504274401] p 203 A95-68299

Panel flutter limit-cycle suppression with piezoelectric actuation
[BTN-95-EIX95302731089] p 618 A95-94208

PANEL METHOD (FLUID DYNAMICS)

Vortex cutting by a blade. Part II: Computations of vortex response
[BTN-94-EIX94441386611] p 208 A95-67342

Ice accretion on aircraft wings
[BTN-95-EIX95082502224] p 225 A95-71021

Viscous-inviscid interaction method for unsteady low-speed airflow flows
[BTN-95-EIX95182619093] p 269 A95-75778

Precision requirement for potential-based panel methods
[HTN-95-51666] p 433 A95-85048

Explicit Kutta condition for an unsteady two-dimensional constant potential panel method
[HTN-95-51679] p 433 A95-85061

Pressure controlled surfaces - a 3D inverse panel method as a design tool
p 491 A95-87565

Unsteady panel method for flows with multiple bodies moving along various paths
[HTN-95-61203] p 540 A95-87576

Computational aerodynamic analysis on the Open Skies aircraft
[SAE PAPER 932514] p 466 A95-89187

Computational fluid dynamics with icing effects
[SAE PAPER 932532] p 466 A95-89192

Computer aided static aeroelastic analysis of wing/pylon/store combination
p 499 A95-91531

Steady and unsteady three-dimensional transonic flow computations by integral equation method
[NASA-CR-196777] p 10 N95-11582

Numerical time dependent sheet cavitation simulations using a higher order panel method
[PB94-204435] p 59 N95-13249

Studies on the flow induced by an oscillating airfoil in a uniform stream
[PB94-204450] p 40 N95-13250

A computational investigation of wake-induced airfoil flutter in incompressible flow and active flutter control [AD-A281534] p 142 N95-16109

Course module for AA201: Wing structural design project [AD-A283618] p 133 N95-18616

Calculation of support interference in dynamic wind-tunnel tests p 122 N95-19282

CFD: Advances and Applications, part 1 [NAL-SP-9322-PT-1] p 165 N95-19444

Panel methods p 165 N95-19448

Open Skies project computational fluid dynamic analysis [AD-A285928] p 223 N95-19991

TranAir: A full-potential, solution-adaptive, rectangular grid code for predicting subsonic, transonic, and supersonic flows about arbitrary configurations. Theory document [NASA-CR-4348] p 378 N95-28265

A numerical method for modelling wings with sharp edges maneuvering at high angles of attack p 503 N95-29122

Estimation of aerodynamic load distributions on the F/A-18 aircraft using a CFD panel code [DSTO-TR-0147] p 504 N95-29445

PANELS

Buckling and vibration analysis of laminated panels using VICONOPT [PAPER-1746] p 230 A95-72580

Flutter of an infinitely long panel in a duct [BTN-95-EIX95182619087] p 291 A95-75772

Experiment and analysis on heat transfer of a scramjet leading edge model p 403 A95-82420

Interaction of jet noise with a nearby panel assembly [BTN-95-EIX95262694295] p 434 A95-85466

Structural integrity of fuselage panels with multisite damage [BTN-95-EIX0619952748188] p 637 A95-94250

Bending effects of unsymmetric adhesively bonded composite repairs on cracked aluminum panels p 92 N95-14456

Full-scale testing and analysis of fuselage structure p 95 N95-14485

Advanced method and processing technology for complicated shape airframe part forming p 80 N95-14486

Thermo-acoustic fatigue design for hypersonic vehicle skin panels p 162 N95-19161

Soft body impact on titanium fan blades p 200 N95-19671

Active control of panel vibrations induced by a boundary layer flow [NASA-CR-197867] p 273 N95-23182

Residual strength of thin panels with cracks p 311 N95-23311

Design and evaluation of a foam-filled hat-stiffened panel concept for aircraft primary structural applications [NASA-TM-109175] p 346 N95-26251

Composite fuselage crown panel manufacturing technology p 399 N95-28474

Effect of low-speed impact damage and damage location on behavior of composite panels p 426 N95-28481

Response of multi-panel assembly to noise from a jet in forward motion [NASA-CR-198164] p 442 N95-28673

Manufacturing scale-up of composite fuselage crown panels p 532 N95-28835

Design and evaluation of a foam-filled hat-stiffened panel concept for aircraft primary structural applications p 502 N95-28841

A weight-efficient design strategy for cutouts in composite transport structures p 533 N95-28843

ISPAN (Interactive Stiffened Panel Analysis): A tool for quick concept evaluation and design trade studies p 533 N95-28846

PARA HYDROGEN

Empirical corrections of the rigid rotor interaction potential of H2-H2 in the attractive region: Dimer features in the FIR absorption spectra [HTN-95-41943] p 361 A95-81690

PARABOLAS

Nonlinear stability of unsteady viscous flow [AD-A294931] p 707 N95-34597

PARABOLIC BODIES

Experimental study of the helicopter-mobile radioelectrical channel and possible extension to the satellite-mobile channel p 247 N95-20945

PARABOLIC FLIGHT

A surgical support system for Space Station Freedom p 149 N95-16776

Users guide for NASA Lewis Research Center DC-9 Reduced-Gravity Aircraft Program [NASA-TM-106755] p 146 N95-18586

PARACHUTE DESCENT

Radial reefing method for accelerated and controlled parachute opening [BTN-95-EIX95062487539] p 187 A95-69247

Dynamic investigation of the angular motion of a rotating body-parachute system [BTN-95-EIX95182619220] p 270 A95-76646

PARACHUTE FABRICS

High strain-rate testing of parachute materials [DE95-009577] p 648 N95-31614

PARACHUTES

Comparison of electrostatic and aerodynamic forces during parachute opening [BTN-95-EIX95062487532] p 187 A95-69240

Radial reefing method for accelerated and controlled parachute opening [BTN-95-EIX95062487539] p 187 A95-69247

Dynamic investigation of the angular motion of a rotating body-parachute system [BTN-95-EIX95182619220] p 270 A95-76646

Turbulent effects on parachute drag [BTN-95-EIX0619952748193] p 591 A95-94482

Parachute inflation: A problem in aeroelasticity [AD-A284375] p 117 N95-18340

Wind tunnel experiments on wake flow field behind a reentry capsule from a viewpoint of parachute deployment at supersonic speeds [ISAS-655] p 374 N95-26740

The performance of cargo airdrop systems using g-12E parachutes: Statistical determination of minimum altitude [AD-A291666] p 381 N95-28454

High strain-rate testing of parachute materials [DE95-009577] p 648 N95-31614

Energy absorption device for shock loading [AD-D017476] p 706 N95-34449

PARAFOILS

Development and flight test of a deployable precision landing system [BTN-95-EIX95062487535] p 190 A95-69243

PARALLEL COMPUTERS

Parallel implicit unstructured grid Euler solvers [BTN-95-EIX95042474393] p 217 A95-68307

Fault detection in multiprocessor systems and array processors [BTN-95-EIX95242679097] p 359 A95-81253

Aeroelasticity of wing and wing-body configurations on parallel computers [NASA-CR-197756] p 389 N95-26590

Direct numerical simulation of incompressible homogeneous isotropic turbulence using NWT p 706 N95-34530

High order accuracy computational methods in aerodynamics using parallel architectures [AD-A294167] p 686 N95-34763

PARALLEL PROCESSING (COMPUTERS)

Parallel implicit unstructured grid Euler solvers [BTN-95-EIX95042474393] p 217 A95-68307

Large-scale computational fluid dynamics by the finite element method [BTN-94-EIX94381359154] p 243 A95-71744

Fault detection in multiprocessor systems and array processors [BTN-95-EIX95242679097] p 359 A95-81253

Trajectory optimization using parallel shooting method on parallel computer [BTN-95-EIX95282706670] p 564 A95-88175

Parallel CFD design on network-based computer [AIAA PAPER 95-0984] p 565 A95-90656

Parallel computational fluid dynamics '91; Conference Proceedings, Stuttgart, Germany, Jun. 10-12, 1991 [ISBN 0-444-89363-6] p 548 A95-91479

Implicit multi-domain method for unsteady compressible inviscid fluid flows around 3D projectiles p 548 A95-91482

Aerodynamic simulation on massively parallel systems p 549 A95-91487

Solution of the Navier-Stokes equations on a massively parallel transporter system p 549 A95-91490

An overview of issues encountered in parallelizing high-resolution weather prediction models p 676 A95-93560

High performance parallel analysis of coupled problems for aircraft propulsion [NASA-CR-195355] p 23 N95-10132

Control of wind tunnel operations using neural net interpretation of flow visualization records [NASA-TM-106683] p 24 N95-10854

Parallel methods for the flight simulation model [DE94-013330] p 52 N95-11752

Parallel aeroelastic computations for wing and wing-body configurations [NASA-CR-196835] p 36 N95-11766

High speed civil transport aerodynamic optimization [NASA-CR-196960] p 38 N95-12389

Artificial neural network modeling of damaged aircraft [AD-A283227] p 80 N95-14849

Portable parallel stochastic optimization for the design of aeropropulsion components [NASA-CR-195312] p 154 N95-16072

Rapid solution of large-scale systems of equations p 169 N95-16458

Computing methods for the approximate solution of time dependent problems [AD-A286007] p 256 N95-20719

High-performance parallel analysis of coupled problems for aircraft propulsion [NASA-CR-197440] p 289 N95-23088

Aerodynamic optimization studies on advanced architecture computers [NASA-CR-198045] p 330 N95-24379

The coupling of fluids, dynamics, and controls on advanced architecture computers [NASA-CR-197727] p 360 N95-25797

A fixed time performance evaluation of parallel CFD applications [DE94-014240] p 436 N95-26445

Aeroelasticity of wing and wing-body configurations on parallel computers [NASA-CR-197756] p 389 N95-26590

An exploratory application of neural networks for airfoil design p 448 N95-26943

NAS Technical Summaries, March 1993 - February 1994 [NASA-RP-1355] p 453 N95-27367

Design of a real-time wind turbine simulator using a custom parallel architecture p 449 N95-27979

Parallel block implicit integration technique for trajectory parallelism [AD-A288961] p 450 N95-28335

Application of parallel processing technology in complex helicopter analysis. Phase 1 [NASA-CR-197850] p 502 N95-28928

A study of fluid problems requiring a direct particle simulation [AD-A290212] p 567 N95-29074

An unsteady simulation of a centrifugal compressor stage using the NWT p 707 N95-34536

Parallel computation of transonic flows about an aircraft configuration using multi-block structured grids p 685 N95-34537

Vector-parallel simulations of transonic wind tunnel flows about a fully configured model of aircraft p 685 N95-34538

A large scale 3D Navier-Stokes analysis using NAL-NWT p 707 N95-34539

Computations of low speed flow about space-plane p 685 N95-34544

High order accuracy computational methods in aerodynamics using parallel architectures [AD-A294167] p 686 N95-34763

PARALLEL PROGRAMMING

A 2D parallel multiblock Navier-Stokes solver with applications on shared- and disturbed memory machines p 643 A95-95475

High performance parallelized implicit Euler solver for the analysis of unsteady aerodynamic flows p 644 A95-95495

Portable parallel stochastic optimization for the design of aeropropulsion components [NASA-CR-195312] p 154 N95-16072

NASA High Performance Computing and Communications program [NASA-TM-4653] p 176 N95-18573

Parallel block implicit integration technique for trajectory parallelism [AD-A288961] p 450 N95-28335

PARALLELEPIPEDS

Analyzing the stability of floating ice floes [AD-A292149] p 563 N95-29160

PARAMETER IDENTIFICATION

Comparison of parameter identification algorithms for flight vehicles [BTN-94-EIX94371347708] p 219 A95-69967

Attitude determination using dedicated and nondedicated multiantenna GPS sensors [BTN-95-EIX9514255482] p 228 A95-72891

Improving prediction: The incorporation of simplified rotor dynamics in a mathematical model of the bell 412HP [BTN-95-EIX95152584679] p 282 A95-73591

Analytical solution and parameter estimation of projectile dynamics [BTN-95-EIX95212645695] p 272 A95-76747

Impact of near-coincident faults on digital flight control systems [BTN-95-EIX95242670759] p 359 A95-81088

Identification and simulation evaluation of a combat helicopter in hover [BTN-95-EIX95242670749] p 335 A95-81098

Application of restructurable flight control system to large transport aircraft [BTN-95-EIX95282706666] p 515 A95-89639

- Air data prediction from surface pressure measurements on guided munitions
 [BTN-95-EIX95282706664] p 466 A95-89641
- Design of a modern pitch pointing control system
 [BTN-95-EIX95302731226] p 618 A95-94045
- Modeling and analysis for the GPS pseudo-range observable
 [BTN-95-EIX95302731227] p 600 A95-94046
- Determining the accuracy of maximum likelihood parameter estimates with colored residuals
 [NASA-CR-194893] p 51 N95-11869
- Identification of dynamic systems. Volume 3: Applications to aircraft. Part 2: Nonlinear analysis and manoeuvre design
 [AGARD-AG-300-VOL-3-PT-2] p 79 N95-14102
- Parameter identification for X-31A at high angles of attack
 p 69 N95-14235
- Minimal time detection algorithms and applications to flight systems
 [TR-2-FSRC-93] p 171 N95-18564
- Aerodynamic parameter estimation via Fourier modulating function techniques
 [NASA-CR-4654] p 335 N95-24630
- Actuating signals in adaptive control systems
 [IFTR-13/1994] p 361 N95-26330
- An analytic modeling and system identification study of helicopter dynamics
 p 505 N95-29787
- New adaptive methods for reconfigurable flight control systems, appendix 1
 [AD-A292711] p 619 N95-30937
- Handling qualities analysis on rate limiting elements in flight control systems
 p 619 N95-31071
- PARAMETERIZATION**
- An algorithm for forecasting mountain wave-related turbulence in the stratosphere
 [HTN-95-80656] p 254 A95-72500
- Effects of a polar stratosphere cloud parameterization on ozone depletion due to stratospheric aircraft in a two-dimensional model
 [HTN-95-A1038] p 443 A95-84543
- Testing of TKE parameterizations in numerical models for clear-air turbulence forecasting
 p 667 A95-93515
- An application of some cloud modeling techniques to a regional model simulation of an icing event
 p 673 A95-93543
- PARTIAL DIFFERENTIAL EQUATIONS**
- Instability of three-dimensional boundary layers due to streamline curvature
 [HTN-95-61070] p 430 A95-83654
- PARTICLE COLLISIONS**
- State-to-state collisional dynamics of atmospheric species
 [AD-A285053] p 245 N95-20484
- PARTICLE EMISSION**
- Measurement of particle emissions from clean room gas-handling components
 [BTN-94-EIX94381359040] p 295 A95-74554
- PARTICLE IMAGE VELOCIMETRY**
- Transient structure of vortex breakdown on a delta wing
 [BTN-95-EIX95182619073] p 268 A95-75758
- Laser velocimetry seed-particle behavior in shear layers at Mach 12
 [BTN-95-EIX95212645712] p 272 A95-76764
- Study of subsonic base cavity flowfield structure using particle image velocimetry
 [BTN-95-EIX95222650781] p 327 A95-79237
- Flow structure in the lee of an inclined 6:1 prolate spheroid
 [BTN-94-EIX95011441127] p 348 A95-81027
- Preliminary results from a particle image velocimetry study of blade-vortex interaction
 [HTN-95-01098] p 547 A95-90284
- PIV investigation of compressibility effects on dynamic stall
 p 478 N95-29102
- PARTICLE SIZE DISTRIBUTION**
- Performance of a focused cavity aerosol spectrometer for measurements in the stratosphere of particle size in the 0.06-2.0-micrometer-diameter range
 [HTN-95-90914] p 253 A95-72423
- Microphysical and radiative properties of small cumulus clouds over the sea
 [HTN-95-A0526] p 255 A95-73180
- On the link between cloud-top radiative properties and sub-cloud aerosol concentrations
 [HTN-95-A0527] p 255 A95-73181
- Erosion of dust-filtered helicopter turbine engines. Part 1: Basic theoretical considerations
 [BTN-95-EIX95182619222] p 288 A95-76648
- An in-situ system for warming of icing conditions
 p 660 A95-93481
- Aircraft icing: Meteorological effects on aircraft performance
 p 674 A95-93545
- The calculation of erosion in a gas turbine compressor rotor
 p 199 N95-19664
- The effect of altitude conditions on the particle emissions of a J85-GE-5L turbojet engine
 [NASA-TM-106669] p 339 N95-24561
- Investigation of water droplet trajectories within the NASA icing research tunnel
 [NASA-TM-107023] p 684 N95-32769
- PARTICLE TRAJECTORIES**
- Tracking of raindrops in flow over an airfoil
 [BTN-95-EIX95182619221] p 308 A95-76647
- Study of the droplet spray characteristics of a subsonic wind tunnel
 [BTN-95-EIX95182619235] p 271 A95-76661
- Particle deposition in gas turbine blade film cooling holes
 p 199 N95-19661
- Experimental and numerical simulations of the effects of ingested particles in gas turbine engines
 p 199 N95-19662
- Particle trajectories in gas turbine engines
 p 199 N95-19663
- The calculation of erosion in a gas turbine compressor rotor
 p 199 N95-19664
- Investigation of water droplet trajectories within the NASA icing research tunnel
 [NASA-TM-107023] p 684 N95-32769
- PARTICULATES**
- Laser velocimetry seed-particle behavior in shear layers at Mach 12
 [BTN-95-EIX95212645712] p 272 A95-76764
- Hypervelocity Impact Test Facility: A gun for hire
 [TABES PAPER 94-605] p 86 N95-14639
- PARTITIONS (MATHEMATICS)**
- Implicit multiblock Euler and Navier-Stokes calculations
 [HTN-95-A1755] p 634 A95-93318
- PASSAGEWAYS**
- Aircraft evacuations through Type-3 exits I: Effects of seat placement at the exit
 [DOT/FAA/AM-95/22] p 599 N95-31845
- PASSENGER AIRCRAFT**
- Maintenance requirements for a supersonic transport
 [BTN-95-EIX95031502751] p 179 A95-68258
- FAA's Aging Commuter Airplane Program
 [SAE PAPER 931248] p 483 A95-89220
- Preliminary design of a single engine business jet
 [SAE PAPER 931253] p 493 A95-89222
- Should large business jets have four under the wing?
 [SAE 931256] p 493 A95-89223
- The FAA regional/commuter aircraft flight loads data collection program
 [SAE PAPER 931258] p 493 A95-89224
- Low frequency ultrasonic nondestructive inspection of aluminum/adhesive fuselage lap splices
 [DE94-014242] p 24 N95-11135
- The Elite: A high speed, low-cost general aviation aircraft for Aeroworld
 [NASA-CR-197161] p 45 N95-12530
- Icarus Rewaxed: A high speed, low-cost general aviation aircraft for Aeroworld
 [NASA-CR-197155] p 45 N95-12609
- The OFF-6M transport jet
 [NASA-CR-197159] p 46 N95-12637
- The Balsa bullet: A high speed, low-cost general aviation aircraft for Aeroworld
 [NASA-CR-197165] p 46 N95-12638
- Central coast designs: The Eightball Express. Taking off with convention, cruising with improvements and landing with absolute success
 [NASA-CR-197181] p 47 N95-12643
- LCX: Proposal for a low-cost commercial transport
 [NASA-CR-197186] p 47 N95-12645
- The Aluminum Falcon: A low cost modern commercial transport
 [NASA-CR-197180] p 81 N95-15742
- Commuter/air taxi ditchings and water-related impacts that occurred from 1979 to 1989
 [AD-A285691] p 226 N95-20275
- Noise impact of advanced high lift systems
 [NASA-CR-195028] p 362 N95-26160
- Design, analysis and control of large transports so that control of engine thrust can be used as a back-up of the primary flight controls
 [NASA-CR-198958] p 518 N95-30254
- PASSENGERS**
- The performance of child restraint devices in transport airplane passenger seats
 [DOT/FAA/AM-94/19] p 40 N95-12146
- Characteristics of civil aviation atmospheric hazards
 p 42 N95-13208
- Test and evaluation report for the Manual Domestic Passive Profiling System (MDPPS)
 [AD-A286312] p 225 N95-20093
- A multibody/finite element analysis approach for modeling of crash dynamic responses
 [NIAR-94-3] p 277 N95-24050
- Enplanement and all cargo activity
 [AD-A280074] p 412 N95-28151
- PASSIVITY**
- In-situ detection of surface passivation or activation and of localized corrosion: Experiences and prospectives in aircraft
 p 302 N95-23508
- PATIENTS**
- Patient/aircraft forecasting for the strategic aeromedical evacuation lift-bed process
 [AD-A293902] p 599 N95-31512
- PATTERN RECOGNITION**
- Electrochemical impedance pattern recognition for detection of hidden chemical corrosion on aircraft components
 [AD-A284998] p 241 N95-20481
- Electrochemical impedance pattern recognition for detection of hidden chemical corrosion on aircraft components, phase 1
 [AD-A291345] p 556 N95-29946
- Selecting optimal experiments for feedforward multilayer perceptrons
 [AD-A290856] p 678 N95-30406
- PATTERN REGISTRATION**
- SAR image registration in absolute coordinates using GPS carrier phase position and velocity information
 [DE94-018738] p 228 N95-20195
- PAVEMENTS**
- Moisture induced pressures in concrete airfield pavements
 [AD-A281974] p 52 N95-11789
- Additives in bituminous materials and fuel-resistant sealers
 [DOT/FAA/CT-94/78] p 55 N95-12131
- Marginal aggregates in flexible pavements: Background survey and experimental plan
 [DOT/FAA/CT-94/58] p 53 N95-12216
- Development of anti-icing technology
 [PB94-195369] p 78 N95-15439
- Super-heavy aircraft study
 [AD-A279602] p 238 N95-19955
- Evaluation of retro-reflective beads in airport pavement markings
 [AD-A291065] p 523 N95-29967
- Evaluation of alternative pavement marking materials
 [AD-A292973] p 626 N95-31468
- PAYLOAD MASS RATIO**
- Optimal trajectories for hypersonic launch vehicles
 [HTN-95-61120] p 415 A95-84884
- PAYLOADS**
- Recent trends in balloon flights from TIFR's National Balloon Facility, Hyderabad
 p 191 A95-66300
- Design decisions from the history of the EUVE science payload
 [HTN-95-60545] p 205 A95-69854
- Design constraints in the payload-range diagram of ultrahigh capacity transport airplanes
 [BTN-95-EIX95152582319] p 276 A95-73522
- Dynamic investigation of the angular motion of a rotating body-parachute system
 [BTN-95-EIX95182619220] p 270 A95-76646
- Virtual environment application with partial gravity simulation
 p 169 N95-15988
- Parachute inflation: A problem in aeroelasticity
 [AD-A284375] p 117 N95-18340
- Aerodynamic flight control to increase payload capability of future launch vehicles
 [NAS-CR-196560] p 300 N95-24032
- PEACETIME**
- Surviving the peace. Lessons learned from the aircraft industry in the 1920s and 1930s
 [AD-A288284] p 366 N95-26455
- PEEK**
- The rain erosion of PEEK (polyetheretherketone)
 [CONGRESS PAPER C428-4-039] p 531 A95-91676
- PEELING**
- Experience of aircraft manufacturer for paint removal using dry stripping method
 p 456 A95-91501
- PEENING**
- Fatigue resistance of peened 7050-T7451 aluminum alloy: Repair and re-treatment of a component surface
 [BTN-94-EIX94371347838] p 206 A95-69131
- PENDULUMS**
- On the dynamics of aeroelastic oscillators with one degree of freedom
 [BTN-94-EIX94501431527] p 153 A95-64524
- Dynamical systems as models for flow-induced vibrations
 [PB95-206991] p 647 N95-30956
- PENETRATION**
- Passive MMW camera for low visibility landings
 p 59 N95-13215
- Development of an Automated Airfield Dynamic Cone Penetrometer (AACDP) prototype and the evaluation of unsurfaced airfield seismic surveying using Spectral Analysis of Surface Waves (SASW) technology
 [AD-A281985] p 145 N95-17444

- Rationale for the Modular Air-system Vulnerability Estimation Network (MAVEN) methodology [AD-A285797] p 284 N95-22510
- PENETROMETERS**
Development of an Automated Airfield Dynamic Cone Penetrometer (AADCP) prototype and the evaluation of unsurfaced airfield seismic surveying using Spectral Analysis of Surface Waves (SASW) technology [AD-A281985] p 145 N95-17444
- PERCEPTION**
Psycho-social safety perceptions: Helicopters as a case study p 596 A95-95192
- PERFORMED PLATES**
A global/local analysis method for treating details in structural design p 552 N95-28848
- PERFORMANCE PREDICTION**
Aerodynamic design and calculation of flow around the plane cascade of turbine [BTN-94-EIX94481415357] p 104 A95-65347
Adaptive modeling of jet engine performance with application to condition monitoring [BTN-95-EIX95112524205] p 196 A95-69303
Nonlinear dynamic simulation of single- and multispool core engines, part 1: Computational method [BTN-95-EIX95112524200] p 210 A95-69308
Multiaxis pilot ratings for damaged aircraft [BTN-95-EIX95182619128] p 269 A95-76605
Drag function modeling for air traffic simulation [BTN-95-EIX95182619154] p 279 A95-76631
Life prediction of helicopter engines fitted with dust filters [BTN-95-EIX95182619224] p 289 A95-76650
SOFIA: Stratospheric Observatory for Infrared Astronomy p 363 A95-81583
Prediction of pre-combustion shock in scramjet combustors: A new method p 402 A95-82323
Condition monitoring and diagnostics [HTN-95-92312] p 387 A95-85356
The high enthalpy shock tunnel in Goettingen (HEG) p 518 A95-87391
Integration of an hypersonic airbreathing vehicle: Assessment of overall aerodynamic performances and of uncertainties [AIAA PAPER 95-6100] p 492 A95-88007
Note on prediction of aerodynamic lift/drag ratio of WIG (Wing-In-Ground) at cruise [BTN-95-EIX95282705925] p 467 A95-89665
Integrated performance and reliability specification for digital avionics systems [AIAA PAPER 95-0953] p 506 A95-90632
Assessment of technology for aircraft development [BTN-95-EIX0619952748181] p 606 A95-94474
Navier-Stokes applications to high-lift airfoil analysis [BTN-95-EIX0619952748182] p 590 A95-94475
Modeling improvements and users manual for axial-flow turbine off-design computer code AXOD [NASA-CR-195370] p 8 N95-10853
Object-oriented technology for compressor simulation [NASA-TM-106723] p 49 N95-11864
Airport surveillance using a solid state coherent lidar p 41 N95-13207
The industrial use of CFD in the design of turbomachinery p 90 N95-14133
Airplane takeoff and landing performance monitoring system [NASA-CASE-LAR-14745-2-SB] p 85 N95-14415
The computer analysis of the prediction of aircraft electrical power supply system reliability p 155 N95-16278
Six degree of freedom flight dynamic and performance simulation of a remotely-piloted vehicle [AERO-TN-9301] p 131 N95-18097
Lubricant evaluation and performance, 2 [AD-A279144] p 242 N95-21969
An approximate theoretical method for modeling the static thrust performance of non-axisymmetric two-dimensional convergent-divergent nozzles [NASA-CR-195050] p 273 N95-23193
Effect of film cooling/regenerative cooling on scramjet engine performances [NAL-TR-1242] p 339 N95-24990
Air cushioned landing craft (LCAC) based ship to shore movement simulation: A decision aid for the amphibious commander. A (SMMAT) application [AD-A289635] p 436 N95-26722
A study of workstation computational performance for real-time flight simulation [NASA-TM-109184] p 449 N95-27241
Determining GPS average performance metrics p 383 N95-27791
Horizontal axis wind turbine post stall airfoil characteristics synthesis p 376 N95-27974
Calculation of design load for the MOD-5A 7.3 mW wind turbine system p 440 N95-27982
- AGARD flight test techniques series. Volume 13: Reliability and maintainability [AGARD-AG-300-VOL-13] p 504 N95-29503
Modeling spatio-temporal databases to measure the performance of the GPS satellite constellation p 489 N95-29596
Transonic, supersonic and hypersonic wind-tunnel tests on aerodynamic characteristics of reentry body with blunted cone configuration [ISAS-658] p 480 N95-29640
PREDICHAT: First order performance calculations of windturbine rotors using the method of the acceleration potential [PB95-206454] p 564 N95-30200
Probabilistic reliability modeling of fatigue on the H-46 tie bar [AD-A289926] p 607 N95-30927
Hot jet/wake turbulent structure and laser propagation. Part 3: Laser propagation measurements and modeling p 647 N95-30992
- PERFORMANCE TESTS**
Turbofan propulsion simulator [BTN-94-EIX94461290240] p 82 A95-61737
GPS/GLONASS/INS test program [BTN-94-EIX94441386131] p 189 A95-68187
Space flight tests of attitude determination using GPS [BTN-95-EIX9511252529] p 190 A95-69334
Labs behind Boeing's new 777 [BTN-95-EIX95142562403] p 280 A95-73437
Containing military autotest cost growth through the use of commercial standard equipment architectures [BTN-95-EIX95172595295] p 287 A95-75717
Flight test evaluation of a 35 GHz forward looking altimeter for terrain avoidance [BTN-95-EIX95212641071] p 287 A95-76736
Flex cycle combustor development and demonstration [BTN-94-EIX95011441245] p 417 A95-84202
Pressure and temperature distortion testing of a two-stage centrifugal compressor [BTN-94-EIX95011441250] p 431 A95-84207
NASA-Lewis tests Allison ASTOVL nozzle [HTN-95-20603] p 404 A95-84784
T-45A high angle attack testing [HTN-95-81499] p 386 A95-85213
A low fin height heat exchanger technology demonstrator for Hermes [SAE PAPER 932119] p 526 A95-90360
The DCAF: A high-enthalpy long-duration, direct-connect scramjet test facility [AIAA PAPER 95-6130] p 512 A95-90450
An assessment of ground-test facility capabilities for measurement of hypervelocity scramjet performance [AIAA PAPER 95-6148] p 512 A95-90462
A flying qualities study of longitudinal long-term dynamics of hypersonic planes [AIAA PAPER 95-6150] p 521 A95-90464
Performance evaluation test of GPS/DGPS navigation system installed in the NAL Dornier 228: Preliminary ground test results p 487 A95-91575
The performance of forward scatter visibility sensors for application in autostations and runway visual range in snow and freezing precipitation events p 662 A95-93489
LLWAS 2 and LLWAS 3 performance evaluation p 662 A95-93491
Test results of a low cost airport weather radar p 662 A95-93492
User involvement in the development of an advanced icing product for use in aviation p 672 A95-93537
Operational and research aspects of a radio-controlled model flight test program [BTN-95-EIX0619952748177] p 606 A95-94471
NASA Lewis Propulsion Systems Laboratory test article systems criteria [NASA-TM-106589] p 20 N95-10446
Brush seal performance and durability issues based on T-700 engine test results [NASA-TM-106502] p 22 N95-11483
Terminal Doppler Weather Radar Build 5A Operational Test and Evaluation (OT/E) integration and OT/E operational test plan [AD-A283052] p 61 N95-12996
Brush seals for turbine engine fuel conservation p 59 N95-13595
Compressor discharge film riding face seals p 60 N95-13599
Solid state radar demonstration test results at the FAA Technical Center [AD-A281520] p 154 N95-16097
ADST system test report for the rotary wing aircraft airmat aeromodel and weapon model merge with the ATAC 2 baseline [AD-A281580] p 127 N95-16171
Wind tunnel performance comparative test results of a circular cylinder and 50 percent ellipse tailboom for circulation control antitorque applications [AD-A283335] p 130 N95-18008
- Conference on Aerospace Transparent Materials and Enclosures. Volume 2: Sessions 5-9 [AD-A283926] p 131 N95-18162
Helicopter Performance Evaluation (HELPE) computer model [AD-A284319] p 131 N95-18381
A review of water mist technology for fire suppression [AD-A285738] p 225 N95-20071
GPS-Squitter capacity analysis [AD-A280037] p 245 N95-20599
An Echelle Grating Spectrometer (EGS) for mid-IR remote chemical detection [DE94-019310] p 249 N95-21478
Response of the B-1B air data sensor to simulated dust cloud environments [AD-A286134] p 235 N95-22036
Performance of the 0.3-meter transonic cryogenic tunnel with air, nitrogen, and sulfur hexafluoride media under closed loop automatic control [NASA-CR-195052] p 310 N95-23257
Report to the Secretary of Defense. Unmanned aerial vehicles: No more Hunter systems should be bought until problems are fixed [GAO/NSIAD-95-52] p 286 N95-24091
Flight reference display for powered-lift STOL aircraft [NAL-TR-1251] p 337 N95-25005
Internal performance characteristics of thrust-vectoring axisymmetric ejector nozzles [NASA-TM-4610] p 331 N95-25338
Wind technology development: Large and small turbines [DE95-000286] p 358 N95-26090
Weather And Radar Processor (WARP) Test and Evaluation Master Plan (TEMP) [AD-A288280] p 445 N95-26453
Aircraft fuel system lightning protection design and qualification test procedures development [AD-A288401] p 380 N95-26497
Development of repair processes and sources for C/KC-135 aircraft windows/windshields [AD-A288348] p 367 N95-26629
Design and testing of low sonic boom configurations and an oblique air-wing supersonic transport [NASA-CR-197744] p 389 N95-26651
The effects of UH-1 experience on UH-60 simulator performance: A preliminary study [AD-A289457] p 391 N95-26993
The noise reduction potential of dual-stream coaxial rectangular improperly expanded jet flows [NASA-CR-197820] p 437 N95-26995
Sailplane glide performance and control using fixed and articulating winglets [NASA-CR-198579] p 392 N95-27180
Propulsion system assessment for very high UAV under ERAST [NASA-CR-195469] p 406 N95-27866
Collected papers on wind turbine technology [NASA-CR-195432] p 447 N95-27970
Comparative performance tests on the Mod-2, 2.5-mW wind turbine with and without vortex generators p 377 N95-27978
Experimental investigation of inlet-combustor isolators for a dual-mode scramjet at a Mach number of 4 [NASA-TP-3502] p 407 N95-28343
Influence of tooth profile modification on spur gear dynamic tooth strain [NASA-TM-106952] p 553 N95-29112
Offshore next generation weather radar (NEXRAD) test and evaluation master plan (TEMP) [AD-A291435] p 556 N95-30072
Development of LaRC (TM): IA thermoplastic polyimide coated aerospace wiring [NASA-CR-195048] p 537 N95-30252
Integrated X-ray testing of the electro-optical breadboard model for the XMM reflection grating spectrometer [DE95-008829] p 644 N95-30507
Results from tests of the Honeywell integrated flight management unit [PB95-211355] p 601 N95-30597
A novel instrumentation system for measurement of helicopter rotor motions and loads data, phase 1 [AD-A293309] p 607 N95-30923
Alternatives to ozone depleting refrigerants in test equipment p 630 N95-31767
Environmentally safe aviation fuels p 631 N95-31768
Cadmium plating replacements p 631 N95-31773
Report to the Chairman, Legislation and National Security Subcommittee, Committee on Government Operations, House of Representatives. Unmanned aerial vehicles: Performance of short-range system still in question [GAO/NSIAD-94-65] p 609 N95-32196
Performance evaluation of the NWT with incompressible NS code p 707 N95-34533

PERIGEEES

Variations of perturbations in perigee height with eccentricity for artificial Earth's satellites due to air drag [HTN-95-40013] p 85 A95-62657

PERIODIC FUNCTIONS

On profiling a cam of an axial aviation diesel engine by periodic splines [BTN-94-EIX94461407946] p 82 A95-62264

PERIODIC VARIATIONS

Grid refinement test of time-periodic flows over bluff bodies [HTN-94-EIX94401378822] p 307 A95-76491
Compression strength of composite primary structural components [NASA-CR-197554] p 160 N95-18388
Determining GPS average performance metrics p 383 N95-27791

PERMANENT MAGNETS

Permanent magnet electron cyclotron resonance plasma source with remote window [BTN-95-EIX95242674338] p 450 A95-82176
Cu deposition using a permanent magnet electron cyclotron resonance microwave plasma source [DE94-017768] p 304 N95-23981

PERMEABILITY

Analysis of flow channeling near the wall in packed beds [HTN-94-00698] p 2 A95-60177

PERMITTIVITY

The mm-wave resonant methods for the detection of corrosion, phase 1 [AD-A291315] p 556 N95-29941

PERSONAL COMPUTERS

New commercial off-the-shelf testers are automatic and intelligent [BTN-95-EIX95172595292] p 287 A95-75720
'Global avionics in the future' report from the 10th annual battery conference [BTN-95-EIX95282706404] p 545 A95-88184
Aircraft aerodynamic analysis on a personal computer (using the RDS aircraft design software) [SAE PAPER 932530] p 492 A95-89190
Development of qualification guidelines for personal computer-based aviation training devices [DOT/FAA/AM-95/6] p 323 N95-23603

PERSONNEL

CASS: Design for supportability [BTN-95-EIX95172595296] p 287 A95-75716
ATE enabling technologies [BTN-95-EIX95172595294] p 287 A95-75718

PERSONNEL MANAGEMENT

Development of strength analysis methods and design model for aircraft constructions in Kazan Aviation Institute p 127 N95-16264

PERSPEX (TRADEMARK)

Non-linear viscoelastic-plastic constitutive relations for an aeronautical PMMA [HTN-95-71132] p 385 A95-83493

PERTURBATION

Aeroelastic stability of hingeless rotor blade in hover using large deflection theory [BTN-94-EIX94441386616] p 183 A95-67347

The effects of wall perturbations on thermo-turbulent Couette flow [HTN-95-92255] p 434 A95-85299

On the differences between the effect of acoustic perturbation and unsteady bleed in controlling flow separation over a cylinder [SAE PAPER 932573] p 467 A95-90062

New eigensolutions and modal analysis for gyroscopic/rotor systems, part 2: perturbation analysis for damped systems [BTN-94-EIX94522410220] p 702 A95-96374

Airfoil optimization by the one-shot method p 128 N95-16569

Comparison of frequency response and perturbation methods to extract linear models from a nonlinear simulation [AD-A284115] p 146 N95-18405

Direct adaptive performance optimization of subsonic transports: A periodic perturbation technique [NASA-TM-4676] p 284 N95-22829

Suppressor of oscillations in airframe cavities [AD-D017265] p 388 N95-26507

Navier-Stokes solution of wing wake structure and its perturbation p 479 N95-29121

Performance seeking control excitation mode p 636 N95-33019

PERTURBATION THEORY

Analytical study of the neutral stability of a model hypersonic boundary layer [BTN-95-EIX95152577589] p 263 A95-73493

Application of transonic small disturbance theory to the active flexible wing model [BTN-95-EIX95182619210] p 270 A95-76636

Nonlinear asymptotic theory of hypersonic flow past a circular cone [HTN-95-92599] p 461 A95-87415

PETN Gas chromatography/ion mobility spectrometry as a hyphenated technique for improved explosives detection and analysis p 701 N95-33278

PHASE CHANGE MATERIALS

Advanced passive cooling for high power electromechanical actuators [SAE PAPER 931397] p 634 A95-93669

PHASE LOCKED SYSTEMS

Real-time navigation using the global positioning system [BTN-95-EIX95172595298] p 279 A95-75714

PHASE SHIFT

Real-time navigation using the global positioning system [BTN-95-EIX95172595298] p 279 A95-75714

Developments in laser-based diagnostics for wind tunnels in the Aeromechanics Division: 1987-1992 [AD-A283011] p 84 N95-13687

PHASE SHIFT KEYING

Evaluation of the radio frequency susceptibility of commercial GPS receivers [BTN-95-EIX95042474624] p 189 A95-68278

PHASE TRANSFORMATIONS

Mechanism and technological particular features of thermomagnetic hardening [BTN-95-EIX94461407953] p 89 A95-62627

High-speed civil transport impact: Role of sulfate, nitric acid trihydrate, and ice aerosols studied with a two-dimensional model including aerosol physics [HTN-95-91843] p 354 A95-80831

PHASE VELOCITY

SAR image registration in absolute coordinates using GPS carrier phase position and velocity information [DE94-018738] p 228 N95-20195

PHASED ARRAYS

Joint stars phased array radar antenna [BTN-95-EIX95042474626] p 209 A95-68280

Inband radar cross section of phased arrays with parallel feeds [AD-A284249] p 210 N95-19730

PHILIPPINES

Two dimensional stratospheric aerosol distributions during EASOE [HTN-95-00726] p 444 A95-86296

Airborne measurements during the Arctic stratospheric experiment: Observation of O3 and NO2 [HTN-95-00748] p 445 A95-86318

PHONONS

Phonon characteristics of high (T sub c) superconductors from neutron Doppler broadening measurements [DE95-003703] p 324 N95-24076

PHOSPHORESCENCE

Application of pressure sensitive paint in hypersonic flows [NASA-TM-106824] p 223 N95-20794

PHOTOACOUSTIC SPECTROSCOPY

Photoacoustic chambers for studying solids and gases: Theory and practical examples [IFTR-39/1994] p 412 N95-26837

PHOTOCHEMICAL REACTIONS

Possible effects of CO2 increase on the high-speed civil transport impact on ozone [HTN-95-60779] p 317 A95-75976

Estimates of total organic and inorganic chlorine in the lower stratosphere from in situ and flask measurements during AASE 2 [HTN-95-A0861] p 317 A95-76265

High-speed civil transport impact: Role of sulfate, nitric acid trihydrate, and ice aerosols studied with a two-dimensional model including aerosol physics [HTN-95-91843] p 354 A95-80831

Chemical composition and photochemical reactivity of exhaust from aircraft turbine engines [HTN-95-51277] p 356 A95-80862

Evolution of the concentrations of trace species in an aircraft plume: Trajectory study [HTN-95-A1044] p 443 A95-84549

Development of techniques for the in situ observation of OH and HO2 for studies of the impact of high-altitude supersonic aircraft on the stratosphere [NASA-CR-196759] p 61 N95-12832

The atmospheric effects of stratospheric aircraft: A fourth program report [NASA-RP-1359] p 357 N95-24274

PHOTOCHROMISM

Conference on Aerospace Transparent Materials and Enclosures, volume 1 [AD-A283925] p 133 N95-18677

PHOTOCONDUCTORS

High aspect ratio metal microstructures and method for preparing the same [AD-D017463] p 629 N95-30750

PHOTODIODES

Electro-optic characterization of ultrafast photodetectors using adiabatically compressed soliton pulses [BTN-94-EIX94381359637] p 257 A95-72675

PHOTOELASTIC ANALYSIS

A better than average stress model-photoelastic analysis for airbus design [CONGRESS PAPER C428-23-005] p 500 A95-91730

PHOTOGRAMMETRY

Computer-aided light sheet flow visualization using photogrammetry [NASA-TP-3416] p 26 N95-10859

Application of photogrammetry of F-14D store separation [AD-A284154] p 132 N95-18417

PHOTOGRAPHIC MEASUREMENT

A note on the interpretation of mini-tuft photographs [HTN-95-01089] p 468 A95-90275

Experiments on microbursts p 562 N95-29110

PHOTOGRAPHS

Simple method of supersonic flow visualization using watertable [BTN-95-EIX95182619105] p 269 A95-76590

Scientific and technical photography at NASA Langley Research Center p 310 N95-23290

PHOTOGRAPHY

Scientific and technical photography at NASA Langley Research Center p 310 N95-23290

PHOTOLYSIS

Sensitivity of supersonic aircraft modelling studies to HNO3 photolysis rate [HTN-95-11475] p 353 A95-79453

PHOTOMETERS

Electro-optic characterization of ultrafast photodetectors using adiabatically compressed soliton pulses [BTN-94-EIX94381359637] p 257 A95-72675

Angular displacement measuring device [NASA-CASE-ARC-11937-1] p 362 N95-26015

PHOTONS

The 1994 Fiber Optic Sensors for Aerospace Technology (FOSAT) Workshop [NASA-CP-10166] p 337 N95-24207

PHOTOVOLTAIC CONVERSION

Photovoltaic electric power applied to Unmanned Aerial Vehicles (UAV) p 245 N95-20530

Wind technology development: Large and small turbines [DE95-000286] p 358 N95-26090

PHOTOVOLTAIC EFFECT

Optical processing and control [AD-A279157] p 259 N95-21975

PHYSICAL OPTICS

Time-domain imaging of airborne targets using ultra-wideband or short-pulse radar [BTN-95-EIX95242673673] p 450 A95-82251

PHYSIOLOGICAL EFFECTS

Effects of cabin pressure on climb and descent rates [ESDU-94040] p 503 N95-29016

PIEZOELECTRIC CERAMICS

Active plate and missile wing development using directionally attached piezoelectric elements [HTN-95-42340] p 408 A95-86169

Active control of interior noise in a business jet using piezoceramic actuators p 29 N95-11276

PIEZOELECTRIC TRANSDUCERS

Smart structures in the control of airframe vibrations [HTN-95-31014] p 236 A95-71184

Panel flutter limit-cycle suppression with piezoelectric actuation [BTN-95-EIX95302731089] p 618 A95-94208

Test Operation Procedure (TOP): Vibration testing of helicopter equipment [AD-A284433] p 81 N95-15815

A hybrid electronically scanned pressure module for cryogenic environments [NASA-TM-110146] p 554 N95-29453

PIEZOELECTRICITY

Vibrational behavior of adaptive aircraft wing structures modelled as composite thin-walled beams p 423 N95-28435

PILOT ERROR

Organizational ergonomics and aviation safety p 596 A95-95083

Aircraft accident report: Stall and loss of control on final approach, Atlantic Coast Airlines, Inc./United Express Flight 6291 Jetstream 4101, N304UE Columbus, OH, 7 January 1994 [PB94-910409] p 123 N95-17646

PILOT INDUCED OSCILLATION

Aircraft and sub-system certification by piloted simulation [AGARD-AR-278] p 145 N95-17388

- Analysis of the longitudinal handling qualities and pilot-induced-oscillation tendencies of the High-Angle-of-Attack Research Vehicle (HARV) p 293 N95-23297
- Flight Vehicle Integration Panel Workshop on Pilot Induced Oscillations [AGARD-AR-335] p 597 N95-31061
- PIO: A historical perspective p 597 N95-31062
- The process for addressing the challenges of aircraft pilot coupling p 597 N95-31063
- Observations on PIO p 597 N95-31064
- Unified criteria for ACT aircraft longitudinal dynamics p 607 N95-31065
- Looking for the simple PIO model p 597 N95-31066
- SCARLET: DLR rate saturation flight experiment p 598 N95-31068
- SAAB experience with PIO p 598 N95-31069
- Aeroelastic pilot-in-the-loop oscillations p 598 N95-31070
- Calspan experience of PIO and the effects of rate limiting p 598 N95-31072
- The role of handling qualities specifications in flight control system design p 620 N95-31990
- The prevention of PIO by design p 620 N95-31991
- An investigation of pilot induced oscillation phenomena in digital-flight control systems p 623 N95-32011
- Pilot Induced Oscillation: A report on the AGARD Workshop on PIO p 624 N95-32017
- PILOT PERFORMANCE**
- Simulation and flight test evaluation of head-up-display guidance for harrier approach transitions [BTN-95-EIX95062487533] p 194 A95-69241
- Automated hover training: An empirical evaluation [SAE PAPER 932536] p 379 A95-84559
- Pilot rating scale for aircraft handling qualities [HTN-95-42269] p 380 A95-84963
- A flying qualities study of longitudinal long-term dynamics of hypersonic planes [AIAA PAPER 95-6150] p 521 A95-90464
- An investigation of piloting strategies for engine failures during takeoff from offshore platforms [HTN-95-92834] p 497 A95-90752
- Aircraft Symposium, 30th, Tsukuba, Japan, Sep. 30 - Oct. 2, 1992 [HTN-95-A1609] p 498 A95-91491
- Functions of NAL fixed base simulator for helicopter research p 522 A95-91555
- A simulator study about effects of visibility upon helicopter pilot performance p 522 A95-91556
- Design of head-up display symbology for recovery from unusual attitudes p 611 A95-95044
- EMS helicopter incidents reported to the NASA Aviation Safety Reporting System p 596 A95-95201
- Emergency medical service (EMS): A unique flight environment p 596 A95-95203
- Aircraft and sub-system certification by piloted simulation [AGARD-AR-278] p 145 N95-17388
- Using the backward transfer paradigm to validate the AH-64 Simulator Training Research Advanced Testbed for Aviation [AD-A285758] p 238 N95-19931
- TRISTAR 1: Evaluation methods for testing head-up display (HUD) flight symbology [NASA-TM-4665] p 288 N95-24030
- A review of civil aviation fatal accidents in which lost/disoriented was a cause/factor: 1981-1990 [DOT/FAA/AM-95/1] p 278 N95-24071
- The effects of UH-1 experience on UH-60 simulator performance: A preliminary study [AD-A289457] p 391 N95-26993
- PIO: A historical perspective p 597 N95-31062
- Looking for the simple PIO model p 597 N95-31066
- The effects of display location and dimensionality on taxiway navigation [AD-A294878] p 690 N95-34570
- A rose by any other name: Certification seen as process rather than content p 688 N95-34766
- PILOT TRAINING**
- Evaluation of simulation motion fidelity criteria in the vertical and directional axes [HTN-94-00666] p 18 A95-60156
- Education, training, and human engineering in aerospace: SAE Aerotech '93, Costa Mesa, CA, Sep. 27-30, 1993 [SAE SP-992] p 417 A95-84553
- Neuro-controllers for adaptive helicopter training [SAE PAPER 932535] p 379 A95-84557
- Intelligent flight trainer for initial rotary wing training [SAE PAPER 932536] p 386 A95-84558
- The large radius track centrifuge concept as an acceleration research and simulation device p 379 A95-84560
- The CBT alternative for aviation training: Is it meeting the need? [SAE PAPER 932596] p 379 A95-84568
- Flight Simulators: Better than the real thing? [HTN-95-42619] p 518 A95-87249
- Intelligent tutoring system: F-16 flight simulation p 521 A95-90649
- An intelligent tutoring system for civil aviation flight training p 521 A95-91535
- Functions of NAL fixed base simulator for helicopter research p 522 A95-91555
- New computer delivered training systems to support technical crew training programmes [CONGRESS PAPER C428-5-036] p 522 A95-91678
- The advanced flight simulator complex [CONGRESS PAPER C428-5-025] p 522 A95-91679
- General requirements for the electrohydraulic systems of the aircraft controls loading force on the simulators [CONGRESS PAPER C428-5-138] p 522 A95-91681
- Pilot training initiatives for the '90s p 657 A95-93463
- Aviation meteorology education in an AB initio setting p 657 A95-93466
- The development of computer-based instructional simulations for the airline industry p 625 A95-95159
- Neuro-controllers for adaptive helicopter hover training [BTN-94-EIX94522407592] p 709 A95-96241
- Vertical flight terminal operational procedures. A summary of FAA research and development [AD-A283550] p 85 N95-15328
- Helicopter in-flight simulation development and use in test pilot training [AD-A283998] p 146 N95-18725
- Programmable cockpit research simulator [AD-A279219] p 204 N95-19848
- A computer-based multimedia prototype for night vision goggles [AD-A286208] p 258 N95-21882
- PILOTLESS AIRCRAFT**
- Conceptual design of the AE481 Demon Remotely Piloted Vehicle (RPV) [NASA-CR-197164] p 44 N95-12294
- Spread spectrum applications in unmanned aerial vehicles [AD-A281035] p 156 N95-16448
- Unmanned aerial vehicle heavy fuel engine test [AD-A284332] p 139 N95-18383
- Environmental effects on composite airframes: A study conducted for the ARM UAV Program (Atmospheric Radiation Measurement Unmanned Aerospace Vehicle) [DE94-015351] p 206 N95-19579
- Automation of hardware-in-the-loop testing of control systems for unmanned air vehicles [AD-A284833] p 194 N95-19693
- Unmanned aerial vehicles [AD-A286190] p 231 N95-20329
- Photovoltaic electric power applied to Unmanned Aerial Vehicles (UAV) p 245 N95-20530
- Design of a GaAs/Ge solar array for unmanned aerial vehicles [NASA-TM-106870] p 320 N95-23259
- Report to the Secretary of Defense. Unmanned aerial vehicles: No more Hunter systems should be bought until problems are fixed [GAO/NSIAD-95-52] p 286 N95-24091
- Design and synthesis of a real-time controller for an unmanned air vehicle [AD-A289134] p 408 N95-26555
- Propulsion system assessment for very high UAV under ERAST [NASA-CR-195469] p 406 N95-27866
- Unmanned aerial vehicles, 1994 master plan [AD-A291628] p 398 N95-28411
- Unmanned Aerial Vehicle technology [DSTO-GD-0044] p 503 N95-29362
- Applications of digital video and synthetic environments to unmanned aerial vehicles [AD-A291875] p 504 N95-29437
- Design and evaluation of a LQR controller for the bluebird unmanned air vehicle [AD-A289769] p 504 N95-29457
- Unmanned aerial vehicles, 1994 master plan p 607 N95-31416
- Automatic flight control system for an unmanned helicopter system design and flight test results p 622 N95-32004
- Report to the Chairman, Legislation and National Security Subcommittee, Committee on Government Operations, House of Representatives. Unmanned aerial vehicles: Performance of short-range system still in question [GAO/NSIAD-94-65] p 609 N95-32196
- PILOTS (PERSONNEL)**
- ASTOVFL Aircraft: Some thoughts on new control strategies [CONGRESS PAPER C428-5-011] p 517 A95-91680
- An analysis of tower (local) controller-pilot voice communications [AD-A283718] p 160 N95-18436
- Development of a coding form for approach control/pilot voice communications [DOT/FAA/AM-95/15] p 384 N95-28540
- PIPE FLOW**
- Studies in drag reduction p 478 N95-29094
- PIPER AIRCRAFT**
- Aircraft accident report: Impact with blast fence upon landing rollout Action Air Charters flight 990 Piper PA-31-350, N990RA, Stratford, Connecticut, 27 April 1994 [PB94-910410] p 333 N95-24206
- PIPES (TUBES)**
- Study of heat transfer rates during quenching of a hot tube under microgravity p 428 A95-82641
- Experimental investigation of flow-boiling heat transfer under microgravity p 428 A95-82642
- Low gravity quenching of hot tubes with cryogens [ISBN 1-879921-01-4] p 635 A95-93728
- PISTON ENGINES**
- Flyover noise reduction of piston-engine propeller aeroplanes using an active noise control technique [SAE PAPER 931218] p 509 A95-87466
- Determination of minimum fuel octane number piston aircraft engines [SAE PAPER 931230] p 528 A95-88961
- Conversion of production automotive engines for aviation use [SAE PAPER 932606] p 495 A95-90076
- Linear Motor Free Piston Compressor [AD-A283452] p 647 N95-31374
- PISTON THEORY**
- Finite element time domain - modal formulation for nonlinear flutter of composite panels [BTN-95-EIX95042474401] p 203 A95-68299
- PISTONS**
- The high enthalpy shock tunnel in Goettingen (HEG) High performance parallel analysis of coupled problems for aircraft propulsion [NASA-CR-195355] p 23 N95-10132
- PITCH (INCLINATION)**
- A study of compressibility effects on dynamic stall of rapidly pitching airfoils [HTN-94-00715] p 5 A95-60193
- Offset thrust axes and pitch stability [BTN-95-EIX95062487553] p 203 A95-68367
- Measurement around a rotor blade excited in pitch. Part 1: Dynamic inflow [HTN-95-31007] p 220 A95-71177
- Measurement around a rotor blade excited in pitch. Part 2: Unsteady surface pressure [HTN-95-31008] p 220 A95-71178
- Identification of higher order helicopter dynamics using linear modeling methods [HTN-95-80851] p 290 A95-75093
- Sensitivity of acoustic predictions to variation of input parameters [HTN-95-80855] p 267 A95-75097
- On the influence of time-varying flow velocity on unsteady aerodynamics [HTN-95-61073] p 369 A95-83657
- Interferometric investigations of compressible dynamic stall over a transiently pitching airfoil [HTN-95-42338] p 372 A95-86167
- Two-dimensional unsteady leading-edge separation on a pitching airfoil [HTN-95-81628] p 461 A95-87676
- Dynamic pitch-up of a delta wing [HTN-95-81633] p 462 A95-87681
- Hubload responses of a rotor in forward flight due to multiple frequency blade pitch variations p 515 A95-91504
- Experimental performance of a ventral nozzle with pitch and yaw vectoring capability for SSTOVL aircraft [SAE PAPER 931412] p 614 A95-93678
- Correlation of unsteady pressure and inflow velocity fields of a pitching rotor blade [BTN-95-EIX0619952748169] p 589 A95-94463
- Numerical simulation of transient vortex breakdown above a pitching delta wing [AD-A281075] p 107 N95-16808
- Development of a multicomponent force and moment balance for water tunnel applications, volume 2 [NASA-CR-4642-VOL-2] p 161 N95-18956
- An investigation of the effects of pitch-roll (decoupling) on helicopter handling qualities [NASA-TM-110349] p 409 N95-26773
- PIV investigation of compressibility effects on dynamic stall p 478 N95-29102
- Unsteady pressure and inflow velocity on a pitching rotor blade in hover p 480 N95-29771
- Flight demonstration of an advanced pitch control law in the VAAC Harrier aircraft p 623 N95-32012

PITCHING MOMENTS

Navier-Stokes simulations of Orbiter aerodynamic characteristics including pitch trim and bodyflap [BTN-95-EIX95041503779] p 204 A95-69210
 Kinematics and aerodynamics of velocity-vector roll [BTN-95-EIX95182619126] p 291 A95-76603
 Dynamic stall control for advanced rotorcraft application [BTN-95-EIX95222650793] p 334 A95-79249
 Force and moment on a Joukowski profile in the presence of point vortices [BTN-95-EIX95262694298] p 434 A95-85469
 Aerodynamic characteristics of truncated airfoils at high angle of attack [SAE PAPER 931227] p 460 A95-87365
 A simple analytical aerodynamic model of Langley Winged-Cone Aerospace Plane concept [NASA-CR-194987] p 54 N95-12175
 Static and dynamic force/moment measurements in the Eidetics water tunnel p 69 N95-14238
 Flight evaluation of pneumatic forebody vortex control in post-stall flight p 72 N95-14259
 Measurements on a two-dimensional aerofoil with high-lift devices p 109 N95-17848
 Static aerodynamics - CFD - analysis - for -120-mm hypersonic KE projectile design [ARL-MR-184] p 118 N95-18611
 Development of a multicomponent force and moment balance for water tunnel applications, volume 1 [NASA-CR-4642-VOL-1] p 161 N95-18955
 Effects of yaw and pitch motion on model attitude measurements [NASA-TM-4641] p 250 N95-22109
 A comparison of the Neal-Smith and omega Tau function, zeta function and tau function flying qualities criteria [AD-A289503] p 390 N95-26844
 SOFIA 2 model telescope wind tunnel test report [NASA-TM-110668] p 683 N95-32764

PITOT TUBES

Development of a pilot tube with multi-hole pyramidal head. 2: A five-hole yaw probe of engineering model p 522 A95-91577
 Pitot/static leak testing [CONGRESS PAPER C428-9-035] p 508 A95-91696
 In-flight pressure measurements on a subsonic transport high-lift wing section [BTN-95-EIX0619952748170] p 589 A95-94464
 Hypersonic flow-field measurements: Intrusive and nonintrusive [AD-A283867] p 119 N95-18674
 Response of the B-1B air data sensor to simulated dust cloud environments [AD-A286134] p 235 N95-22036

PITTING

The effects of pitting on fatigue crack nucleation in 7075-T6 aluminum alloy p 88 N95-14482
 Detecting gear tooth fracture in a high contact ratio face gear mesh [NASA-TM-106822] p 162 N95-19125
 Corrosion of aircraft materials: Correlation between nanometer scale and macroscopic structural damage parameters [AD-A285930] p 241 N95-20299
 Eddy current detection of pitting corrosion around fastener holes p 315 N95-23507

PIVOTS

Status of bonded boron/epoxy doublers for military and commercial aircraft structures p 393 N95-27506

PLANAR STRUCTURES

Analysis of planar laser-induced fluorescence images obtained during shakedown testing of the AEDC impulse facility [AD-A293237] p 646 N95-30906

PLANE WAVES

RCS measurements, transformations, and comparisons under cylindrical and plane wave illumination [BTN-94-EIX94371347126] p 242 A95-69976
 Acoustic scattering from ellipses by the modal element method [NASA-TM-106935] p 579 N95-29401

PLANETARY ATMOSPHERES

Planetary entry experiments [NASA-CR-194215] p 101 N95-13717

PLANETARY BOUNDARY LAYER

Initial evaluation of the Oregon State University planetary boundary layer column model for ITWS applications [AD-A293775] p 677 N95-31465

PLANETARY MAPPING

Naval Aviation System TEAM mapping, charting, and geodesy handbook [AD-A288590] p 446 N95-26841

PLATFORMS

Aerodynamic effects of delta platform tip sails on wing performance [BTN-95-EIX95062487544] p 185 A95-68358

A study of the vortex flow over 76/40-deg double-delta wing [NASA-CR-195032] p 314 N95-23466
 Leading-edge suction distribution for plane thin wings at subsonic speeds [ESDU-94037] p 477 N95-28800
 Low-speed wind-tunnel investigation of the stability and control characteristics of a series of flying wings with sweep angles of 50 deg [NASA-TM-4640] p 505 N95-30226

PLANNING

Using ATMS weather products for air traffic strategic planning p 672 A95-93536
 Cooperative problem solving between airline operations control and ATC traffic flow management p 681 A95-95066

PLASMA JET WIND TUNNELS

Computation of nonequilibrium viscous flows in arc-jet wind tunnel nozzles [AIAA PAPER 94-0254] p 2 A95-60173

PLASMA JETS

Studies on plasma jet igniters p 403 A95-82680

PLASMA SPRAYING

Thermal conductivity of zirconia thermal barrier coatings p 345 N95-26133

PLASMAS (PHYSICS)

Permanent magnet electron cyclotron resonance plasma source with remote window [BTN-95-EIX95242674338] p 450 A95-82176
 Cu deposition using a permanent magnet electron cyclotron resonance microwave plasma source [DE94-017768] p 304 N95-23981

PLASTERS

Plaster damage experiments at the BBN Sonic Boom Test Facility p 529 A95-90120

PLASTIC BODIES

Large amplitude nonlinear response of flat aluminum, and carbon fiber plastic beams and plates [AD-A282440] p 96 N95-15547

PLASTIC DEFORMATION

Non-linear viscoelastic-plastic constitutive relations for an aeronautical PMMA [HTN-95-71132] p 385 A95-83493
 Plastic hinge modeling of structures [NIAR-94-14] p 24 N95-11168
 Development of processes, means, and theoretical principles of thin-walled detail plastic forming at Kazan Aviation Institute p 155 N95-16281
 Prediction of fatigue crack growth under flight-simulation loading with the modified CORPUS model p 166 N95-19471
 Impact loading of compressor stator vanes by hailstone ingestion p 200 N95-19670
 Soft body impact on titanium fan blades p 200 N95-19671

PLASTIC PLATES

Large amplitude nonlinear response of flat aluminum, and carbon fiber plastic beams and plates [AD-A282440] p 96 N95-15547

PLASTIC PROPERTIES

Elastic-plastic models for multi-site damage p 92 N95-14454

PLASTICS

Facilities used for plastic media blasting p 627 N95-32176

PLATE THEORY

Coupling equivalent plate and finite element formulations in multiple-method structural analyses [BTN-95-EIX95062487548] p 192 A95-68362
 Equivalent plate structural modeling for wing shape optimization including transverse shear [HTN-95-20839] p 492 A95-88100
 Discrete crack growth analysis methodology for through cracks in pressurized fuselage structures p 166 N95-19473
 Idealized textile composites for experimental/analytical correlation p 301 N95-23277

PLATES (STRUCTURAL MEMBERS)

Stability derivatives of a flapped plate in unsteady ground effect [BTN-95-EIX95182619225] p 270 A95-76651
 Stability of viscoelastic plate in supersonic flow under random loading [BTN-95-EIX95262694312] p 435 A95-85483
 Convection heat transfer distributions over plates with square ribs from infrared thermography measurements [HTN-95-20713] p 435 A95-86603
 Equivalent plate structural modeling for wing shape optimization including transverse shear [HTN-95-20839] p 492 A95-88100
 Electromagnetic on-aircraft antenna radiation in the presence of composite plates [NASA-CR-196126] p 58 N95-12856
 Compressive strength of damaged and repaired composite plates p 442 N95-29484

Fundamental concepts in the suppression of delamination buckling by stitching p 426 N95-28486
 The effects of three-dimensional imposed disturbances on bluff body near wake flows: Effects of taper and splitter plates on the near wake characteristics of a circular cylinder in uniform and shear flow [AD-A292113] p 477 N95-28921

PLATING

Cadmium plating replacements p 631 N95-31773

PLENUM CHAMBERS

Unsteady flow testing in a passive low-correction wind tunnel p 147 N95-19272

PLUMES

Predicting exhaust plume boundaries with supersonic external flows [BTN-95-EIX95152583258] p 297 A95-73559
 In situ observations in aircraft exhaust plumes in the lower stratosphere at midlatitudes [HTN-95-A0862] p 318 A95-76266
 An analysis of aircraft exhaust plumes form accidental encounters [HTN-95-70943] p 351 A95-78008
 Dynamics of aircraft exhaust plumes in the jet-regime [HTN-95-51275] p 355 A95-80860
 Evolution of the concentrations of trace species in an aircraft plume: Trajectory study [HTN-95-A1044] p 443 A95-84549
 Modeling of plume chemistry of high flying aircraft with H2 combustion engines p 509 A95-87405
 Numerical simulation of helicopter engine plume in forward flight [NASA-CR-197488] p 107 N95-16589
 Impact of dynamic loads on propulsion integration p 174 N95-19148
 Estimating wind tunnel interference due to vectored jet flows p 164 N95-19265
 Temperature effects on acoustic interactions between altitude test facilities and jet engine plumes [NASA-CR-197638] p 258 N95-21170
 NTS-spill test facility wind tunnel exhaust plume characterization [DE95-003630] p 297 N95-24019
 The atmospheric effects of stratospheric aircraft: A fourth program report [NASA-RP-1359] p 357 N95-24274
 Measurements of ions formed in jet engine exhaust plumes [AD-A290940] p 514 N95-29764
 Vorticity dynamics and control of dynamic stall [AD-A286658] p 620 N95-31400

PNEUMATIC CONTROL

Forebody flow control on a full-scale F/A-18 aircraft [BTN-95-EIX95152582333] p 281 A95-73535
 Pneumatic concept for tip-stall control of cranked-arrow wings [BTN-95-EIX95152582335] p 281 A95-73537
 Directional control at high angles of attack using blowing through a chined forebody [BTN-95-EIX0619952748179] p 619 A95-94472
 Flight investigation of the use of a nose gear jump strut to reduce takeoff ground roll distance of STOL aircraft [NASA-TM-108819] p 44 N95-12225
 F/A-18 and F-16 forebody vortex control, static and rotary-balance results p 72 N95-14254
 Low-energy pneumatic control of forebody vortices p 72 N95-14256
 Flight evaluation of pneumatic forebody vortex control in post-stall flight p 72 N95-14259

PNEUMATIC EQUIPMENT

Turbofan propulsion simulator [BTN-94-EIX94461290240] p 82 A95-61737
 Design and development of a test rig for the high frequency testing of rolling sleeve airsprings [DSTO-TN-0001] p 411 N95-26378

PNEUMATIC PROBES

A new algorithm for five-hole probe calibration, data reduction, and uncertainty analysis [NASA-TM-106458] p 38 N95-12378

PNEUMATICS

Dynamic behavior of valves with pneumatic chamber for reciprocating compressors [BTN-94-EIX94351143311] p 207 A95-65845
 The development of a highly reliable power management and distribution system for civil transport aircraft [NASA-TM-106697] p 50 N95-11867
 F/A-18 and F-16 forebody vortex control, static and rotary-balance results p 72 N95-14254
 Low-energy pneumatic control of forebody vortices p 72 N95-14256
 Integration of a mechanical forebody vortex control system into the F-15 p 72 N95-14258
 Development of pneumatic test techniques for subsonic high-lift and in-ground-effect wind tunnel investigations p 121 N95-19268

POINTING CONTROL SYSTEMS

- Application of fuzzy logic to optimize placement of an acquisition, tracking, and pointing experiment p 341 A95-80390
- Design of a modern pitch pointing control system [BTN-95-EIX95302731226] p 618 A95-94045
- POISSON EQUATION**
- Steady and unsteady three-dimensional transonic flow computations by integral equation method [NASA-CR-196777] p 10 N95-11582
- POLAR COORDINATES**
- User documentation of the CTA program [AD-A289508] p 375 N95-26854
- POLAR METEOROLOGY**
- Research aircraft observations of a polar low at the east Greenland ice edge [HTN-95-A0175] p 215 A95-69766
- An overview of the EASOE campaign [HTN-95-00702] p 443 A95-86272
- Replicator for characterization of cirrus and polar stratospheric cloud particles [NASA-CR-197785] p 445 N95-26669
- POLAR REGIONS**
- Latitude variations of stratospheric trace gases [HTN-95-70948] p 352 A95-78013
- Fine-scale, poleward transport of tropical air during AASE 2 [HTN-95-70949] p 352 A95-78014
- Polar Patrol Balloon system and preliminary experimental results p 368 A95-82513
- Oceanic operations: An authoritative guide to oceanic operations [FAA-AFS-550] p 277 N95-24065
- POLARIMETRY**
- Foliage transmission measurements using a ground-based ultrawide band (300-1300 MHz) SAR system [BTN-94-EIX94381351617] p 252 A95-70950
- MAX-91: Polarimetric SAR results on Montepertoli site p 320 N95-23940
- Statistics of multi-look AIRSAR imagery: A comparison of theory with measurements p 320 N95-23947
- Airborne passive polarimetric measurements of sea surface anisotropy at 92 GHz [NASA-CR-197288] p 707 N95-32823
- POLARIZATION (SPIN ALIGNMENT)**
- Broadband polarization-transfer experiments for rotating solids [GTN-95-0009261494012091-58] p 579 A95-92319
- POLARIZED LIGHT**
- Angular displacement measuring device [NASA-CASE-ARC-11937-1] p 362 N95-26015
- POLARIZED RADIATION**
- Polarization diverse ultra-wideband antenna technology p 548 A95-90924
- POLICIES**
- A review of Air Force policy and noise models pertaining to the noise environment under low-altitude, high-speed training areas p 561 A95-90118
- Mishap risk control for advanced aerospace/composite materials p 301 N95-23031
- Process evaluation p 651 N95-32180
- Report to the Chairman, Legislation and National Security Subcommittee, Committee on Government Operations, House of Representatives. C-17 Aircraft program: Improvements in initial provisioning process [GAO/NSIAD-94-63] p 584 N95-32194
- POLISHING**
- Fatigue resistance of peened 7050-T7451 aluminum alloy: Repair and re-treatment of a component surface [BTN-94-EIX94371347838] p 206 A95-69131
- POLLUTION**
- Community relations plan: Galena Airport and Camp ion Air Force Station, Alaska [AD-A286722] p 446 N95-27234
- POLLUTION CONTROL**
- Noise Con 1994: Proceedings of the 1994 National Conference on Noise Control Engineering. Progress in Noise Control for Industry [LC-75-24750] p 28 N95-11259
- Fan noise research at NASA p 28 N95-11260
- Transmission loss characteristics of aircraft sidewall systems to control cabin interior noise p 28 N95-11261
- Design of a vehicle based system to prevent ozone loss [NASA-CR-197199] p 48 N95-12702
- Regulatory impact analysis and regulatory support document: Control of air pollution; determination of significance for nonroad sources and emission standards for new nonroad compression-ignition engines at or above 37 kilowatts (50 horsepower) [PB94-194594] p 61 N95-12855
- Air pollution mitigation measures for airports and associated activity [PB94-207610] p 216 N95-19582

- Environmental Compliance Assessment and Management Program [AD-A279605] p 255 N95-20441
- Small gas turbine component evaluation study [PB95-147542] p 338 N95-24293
- Parts washing alternatives study: United States Coast Guard. Project summary and report [PB95-166146] p 343 N95-26004
- Environmentally regulated aerospace coatings p 631 N95-31775
- POLLUTION MONITORING**
- An analysis of aircraft exhaust plumes form accidental encounters [HTN-95-70943] p 351 A95-78008
- Comparison of column abundances from three infrared spectrometers during AASE 2 [HTN-95-70946] p 352 A95-78011
- Chemical change in the arctic vortex during AASE 2 [HTN-95-70947] p 352 A95-78012
- Fine-scale, poleward transport of tropical air during AASE 2 [HTN-95-70949] p 352 A95-78014
- Chemical composition and photochemical reactivity of exhaust from aircraft turbine engines [HTN-95-51277] p 356 A95-80862
- Environmental Compliance Assessment and Management Program [AD-A279605] p 255 N95-20441
- Modeling aerosol emissions from the combustion of composite materials p 301 N95-23038
- Nitrogen oxide emissions and their control from uninstalled aircraft engines in enclosed test cells: Joint report to Congress on the Environmental Protection Agency - Department of Transportation study [PB95-166237] p 358 N95-26005
- POLLUTION TRANSPORT**
- Trajectory modeling of emissions from lower stratospheric aircraft [HTN-95-41219] p 317 A95-75031
- Transport of exhaust products in the near trail of a jet engine under atmospheric conditions [HTN-95-91421] p 319 A95-77334
- Tracer transport for realistic aircraft emission scenarios calculated using a three-dimensional model [HTN-95-41799] p 353 A95-80525
- Effects on stratospheric ozone from high-speed civil transport: Sensitivity to stratospheric aerosol loading [HTN-95-91842] p 354 A95-80830
- Role of the aviation weather system in providing a real-time ATC volcanic ash advisory system p 663 A95-93494
- Alaska's volcanic ash warning system p 663 A95-93495
- Three dimensional model calculations of the global dispersion of high speed aircraft exhaust and implications for stratospheric ozone loss p 26 N95-10657
- POLYBUTADIENE**
- Solid fuel ramjet composition [AD-D016458] p 152 N95-19090
- POLYCARBONATES**
- Failure analysis for polycarbonate transparencies [AD-A292992] p 630 N95-31471
- POLYCHLORINATED BIPHENYLS**
- The impact of advanced packaging technology on modular avionics architectures p 233 N95-20632
- POLYCRYSTALS**
- Impact, friction, and wear testing of microsamples of polycrystalline silicon p 361 A95-79988
- Effects of activated reactive evaporation process parameters on the microhardness of polycrystalline silicon carbide thin films [GTN-95-00406090-4621] p 680 A95-93965
- POLYETHYLENES**
- French contribution to new balloon designs and materials p 181 A95-66277
- Balloon flights in France and in Europe p 204 A95-66301
- Development and flight results of fiber reinforced balloon p 384 A95-82511
- POLYIMIDES**
- Thermally stable organic polymers [AD-A281380] p 87 N95-14363
- Advanced composite structural concepts and materials technologies for primary aircraft structures: Advanced material concepts [NASA-CR-4485] p 503 N95-29027
- Weavability of dry polymer powder towpreg p 535 N95-29036
- Development of LaRC (TM): IA thermoplastic polyimide coated aerospace wiring [NASA-CR-195048] p 537 N95-30252
- POLYMER BLENDS**
- Thermally stable organic polymers [AD-A281380] p 87 N95-14363
- Thermally stable organic polymers [AD-A290755] p 537 N95-29482

POLYMER CHEMISTRY

- Thermally stable organic polymers [AD-A290755] p 537 N95-29482
- POLYMER MATRIX COMPOSITES**
- Validation of an effective flat cruciform-shaped specimen to study CFRP composite laminates under biaxial loading [BTN-95-EIX95152584677] p 282 A95-73589
- Polymer composite applications to aerospace equipment [HTN-95-B0257] p 529 A95-89201
- Materials and structures for the HSCT [BTN-95-EIX95282711241] p 455 A95-89634
- Mechanical properties of advanced toughened bismaleimide matrix composite p 530 A95-91570
- The basis of civil certification and continued airworthiness for composite aircraft structures [CONGRESS PAPER C428-37-173] p 628 A95-93632
- The certification of composite structures for military aircraft [CONGRESS PAPER C428-37-198] p 628 A95-93633
- Micro-measurements of mechanical properties for adhesives and composites using digital imaging technology [NASA-CR-196111] p 22 N95-10231
- Thermally stable organic polymers [AD-A281380] p 87 N95-14363
- Mishap risk control for advanced aerospace/composite materials p 301 N95-23031
- Technology reinvestment project's focus area: Affordable polymer matrix composites for airframe structures [PB95-136032] p 324 N95-23168
- Advanced wing design survivability testing and results p 400 N95-28488
- Advanced composite structural concepts and materials technologies for primary aircraft structures: Advanced material concepts [NASA-CR-4485] p 503 N95-29027
- Advanced composite fuselage technology p 535 N95-29034
- POLYMERIC FILMS**
- Theoretical and actual performance of a long duration superpressure balloon made from a biaxially oriented nylon-6 film p 181 A95-66282
- Recent trends in balloon flights from TIFF's National Balloon Facility, Hyderabad p 191 A95-66300
- Development of LaRC (TM): IA thermoplastic polyimide coated aerospace wiring [NASA-CR-195048] p 537 N95-30252
- POLYMERIZATION**
- Thermally stable organic polymers [AD-A290755] p 537 N95-29482
- POLYMETHYL METHACRYLATE**
- Non-linear viscoelastic-plastic constitutive relations for an aeronautical PMMA [HTN-95-71132] p 385 A95-83493
- POLYNOMIALS**
- Elliptic tip effects on the vortex wake of an axisymmetric body at incidence [BTN-94-EIX94441386612] p 208 A95-67343
- Matrix fraction approach for finite-state aerodynamic modeling [BTN-95-EIX95262694311] p 365 A95-85482
- An investigation of polynomial calibrations methods for wind tunnel balances p 144 N95-16258
- POLYPHENYL ETHER**
- Lubricant evaluation and performance, 2 [AD-A279144] p 242 N95-21969
- POLYURETHANE RESINS**
- Ten-year ground exposure of composite materials used on the Bell Model 206L helicopter flight service program [NASA-TP-3468] p 55 N95-12357
- Evaluation of alternate F-14 wing lug coating [AD-A283207] p 129 N95-17631
- PONTRYAGIN PRINCIPLE**
- Optimal trajectories for an unmanned air-vehicle in the horizontal plane [BTN-95-EIX0619952748191] p 606 A95-94480
- POPULATIONS**
- Effects of satellite bunching on the probability of collision in geosynchronous orbit [BTN-95-EIX95152583276] p 298 A95-73577
- POROSITY**
- Passive porosity with free and fixed separation on a tangent-ogive forebody [BTN-95-EIX95062487554] p 185 A95-68368
- Analysis of some interference effects in a transonic wind tunnel [BTN-95-EIX0619952748166] p 589 A95-94460
- Base passive porosity for drag reduction [NASA-CASE-LAR-15246-1] p 91 N95-14183

POROUS BOUNDARY LAYER CONTROL

- Computational analysis of buffet alleviation in viscous transonic flow over a porous airfoil
[BTN-95-EIX95262694321] p 366 A95-85492
- Reduction of blade-vortex interaction noise through porous leading edge
[HTN-95-42324] p 371 A95-86153
- Instabilities originating from suction holes used for Laminar Flow Control (LFC)
[NASA-CR-196395] p 6 N95-10131

POROUS MATERIALS

- Oblique incidence sound absorption of porous materials covered by perforated metal and exposed to tangential airflow
[HTN-94-00681] p 19 A95-60165
- Analysis of flow channeling near the wall in packed beds
[HTN-94-00698] p 2 A95-60177
- Service and physical properties of liquid-jet fuels
p 151 N95-16256

POROUS PLATES

- The stability of two-phase flow over a swept-wing
[NASA-CR-194994] p 159 N95-18190

POROUS WALLS

- Determination of solid/porous wall boundary conditions from wind tunnel data for computational fluid dynamics codes
p 164 N95-19266
- Calculation of wall effects of flow on a perforated wall with a code of surface singularities
p 165 N95-19277
- A method for the modelling of porous and solid wind tunnel walls in computational fluid dynamics codes
p 523 N95-29795

PORTABLE EQUIPMENT

- Environmental noise monitoring - source identification
[HTN-95-92537] p 558 A95-87357
- A portable transmission vibration analysis system for the S-70A-9 Black Hawk helicopter
[DSTO-TR-0072] p 348 N95-24203

PORTS (OPENINGS)

- Design and evaluation of candidate pressure ports for the HYFLITE experiment
[NASA-TM-109146] p 22 N95-11003

POSITION (LOCATION)

- Secondary source locations in active noise control: Selection or optimization?
[BTN-94-EIX94381352222] p 257 A95-71738
- Description of a GNSS availability model and its use in developing requirements
[BTN-95-EIX95202637603] p 308 A95-76686
- Automatic vehicle location and airfield ground movement
[CONGRESS PAPER C428-7-148] p 488 A95-91689
- Using landmarks for the vehicle location measurement
[PB94-184512] p 43 N95-12582
- Low-energy pneumatic control of forebody vortices
p 72 N95-14256

- SAR image registration in absolute coordinates using GPS carrier phase position and velocity information
[DE94-018738] p 228 N95-20195

- Electro-hydrostatic actuator controller design using quantitative feedback theory
[AD-A289220] p 409 N95-26957

- Effects of floor location on response of composite fuselage frames
p 423 N95-28439

- Conceptual design of a map interactive system for military aircraft cockpits
[AD-A289760] p 508 N95-28692

POSITION ERRORS

- Dynamical instability of the aerogravity assist maneuver
[BTN-95-EIX95152583282] p 298 A95-73583
- CCLA operation on MLS
p 487 A95-91540
- Performance evaluation test of GPS/DGPS navigation system installed in the NAL Dornier 228: Preliminary ground test results
p 487 A95-91575
- Precision orbit determination of altimetric satellites
p 86 N95-14282

- Flight evaluation of GPS/DGPS sensor systems installed in NAL Do228
[NAL-TR-1230] p 382 N95-26585

- Error modeling for differential GPS
[NASA-CR-188367] p 488 N95-28716

- Wide Area Differential GPS (WADGPS)
p 489 N95-29107

POSITION INDICATORS

- A switched reluctance machine rotor position estimator: A neural network application
[SAE PAPER 932560] p 511 A95-90057
- Spatial awareness comparisons between large-screen, integrated pictorial displays and conventional EFIS displays during simulated landing approaches
[NASA-TP-3467] p 80 N95-14852
- TRISTAR 1: Evaluation methods for testing head-up display (HUD) flight symbology
[NASA-TM-4665] p 288 N95-24030

- Real-time testing and demonstration of the US Army Corps of Engineers' Real-Time On-The-Fly positioning system
[AD-A288624] p 334 N95-25609

POSITION SENSING

- DC electrostatic gyro suspension system for the Gravity Probe B experiment
p 527 N95-29794

POSITIONING

- Airborne geophysics and precise positioning: Scientific issues and future directions
[LC-94-68678] p 446 N95-27156
- An investigation into the use of satellite-based positioning systems for flight reference/autoland operations
p 489 N95-29542

POTENTIAL ENERGY

- Empirical corrections of the rigid rotor interaction potential of H₂-H₂ in the attractive region: Dimer features in the FIR absorption spectra
[HTN-95-41943] p 361 A95-81690
- Precision requirement for potential-based panel methods
[HTN-95-51666] p 433 A95-85048
- Explicit Kutta condition for an unsteady two-dimensional constant potential panel method
[HTN-95-51679] p 433--A95-85061

POTENTIAL FLOW

- Novel similarity solutions of the sonic small-disturbance equation with applications to airfoil transonic aerodynamics
[BTN-94-EIX94341340316] p 35 A95-60852
- Effects of leading and trailing edge flaps on the aerodynamics of airfoil/vortex interactions
[HTN-95-31011] p 221 A95-71181
- Viscous-inviscid interaction method for unsteady low-speed airfoil flows
[BTN-95-EIX95182619093] p 269 A95-75778
- Study of the droplet spray characteristics of a subsonic wind tunnel
[BTN-95-EIX95182619235] p 271 A95-76661
- A Kutta condition conscious perturbation stream function boundary element algorithm for 2-D potential aerodynamics
[ISBN 1-879921-01-4] p 587 A95-93751

- Multigrid/multiblock method for transonic potential flow around wing/body/nacelle configurations including a slipstream
p 591 A95-95451
- A cartesian grid finite element method for aerodynamics of moving rigid bodies
p 642 A95-95471

- Control theory based airfoil design using the Euler equations
[NASA-CR-196360] p 36 N95-11884

- Single-pass method for the solution of inverse potential and rotational problems. Part 1: 2-D and quasi 3-D theory and application
p 107 N95-16563
- Solution of full potential equation on an airfoil by multigrid technique
[NAL-TM-CSS-9303] p 119 N95-18904

- CFD: Advances and Applications, part 1
[NAL-SP-9322-PT-1] p 165 N95-19444
- Computation of inviscid flows: Full potential method
p 165 N95-19447

- Viscous flow past aerofoils axisymmetric bodies and wings
p 123 N95-19457
- Computational fluid dynamics and transonic flow
[AD-A288962] p 436 N95-26405

- Computational algorithms for aerodynamic analysis and design
[AD-A291084] p 482 N95-29972

- Axial loads on yawed rotors
[PB95-214193] p 592 N95-30638
- Acceleration potential models
PREDICCHAT/PREDICDYN applied for calculation of axisymmetric dynamic inflow cases
[PB95-207015] p 647 N95-30957

- Numerical solution of the full potential equation using a chimera grid approach
[NASA-TM-110360] p 594 N95-32188

POTENTIAL THEORY

- Single-pass method for the solution of inverse potential and rotational problems. Part 2: Fully 3-D potential theory and applications
p 107 N95-16564

- PREDICCHAT: First order performance calculations of windturbine rotors using the method of the acceleration potential
[PB95-206454] p 564 N95-30200

POWDER (PARTICLES)

- Weavability of dry polymer powder towpreg
p 535 N95-29036
- Thermally stable organic polymers
[AD-A290755] p 537 N95-29482

POWER CONDITIONING

- Electrical power system upgrade methodology for in-service aircraft
[SAE PAPER 932562] p 511 A95-90059
- Solid state power controller technology
[SAE PAPER 931422] p 495 A95-90087

- Strategic avionics technology definition studies. Subtask 3-1A3: Electrical Actuation (ELA) Systems Test Facility
[NASA-CR-188360] p 143 N95-18567

POWER EFFICIENCY

- Wake velocity measurement of counter-rotation propellers
p 474 A95-91563

Adaptive airfoils

- [ISBN 1-879921-01-4] p 625 A95-93744

- Determining the effects of alternative departure outback altitudes and power settings: A case study, John Wayne Airport
p 31 N95-11320

POWER FACTOR CONTROLLERS

- Control system design for the MOD-5A 7.3 mW wind turbine generator
p 440 N95-27985

POWER LINES

- Fault detection techniques for complex cable shield topologies
[AD-A286632] p 247 N95-20771

- TIM-SCT cable testing protocol
[AD-A286633] p 231 N95-20772

POWER LOSS

- Aircraft accident report: Overspeed and loss of power on both engines during descent and power-off emergency, landing-Simmons Airlines, Inc., d/b/a; American Eagle Flight 3641, N349SB False River Air Park, New Roads, Louisiana, 1 February 1994
[PB94-910408] p 78 N95-14916

POWER PLANTS

- Wind technology development: Large and small turbines
[DE95-000286] p 358 N95-26090

POWER SPECTRA

- Statistical discrete gust-power spectral density methods overlap-holistic proof and beyond
[BTN-95-EIX0619952748175] p 584 A95-94469

- A preliminary study of the airwake model used in an existing SH-60B/FFG-7 helicopter/ship simulation program
[DSTO-TR-0015] p 224 N95-21659

- Derived gust spectra for the Macchi MB326H
[ARL-TN-3] p 225 N95-21892

POWER TRANSMISSION

- A theoretical analysis of airborne sound transfer for a resiliently mounted machine to its foundation
p 30 N95-11304

POWERED LIFT AIRCRAFT

- Powered lift for land and sea
[BTN-95-EIX95041503010] p 192 A95-68313

- STOVL CFD model test case
p 115 N95-17881

- Flight reference display for powered-lift STOL aircraft
[NAL-TR-1251] p 337 N95-25005

- A quiet STOL Research Aircraft Development program
[NAL-TR-1223] p 336 N95-25862

- Moving base simulation of an integrated flight and propulsion control system for an ejector-augmentor STOVL aircraft in hover
[NASA-TM-108867] p 606 N95-30646

POWERED MODELS

- Computational study of plume-induced separation on a hypersonic powered model
[BTN-95-EIX95152582346] p 266 A95-73548

- Hypersonic aerodynamics test facility using the external propulsion accelerator
[AIAA PAPER 95-6138] p 470 A95-90455

- An LDV investigation of support structure influence on the flow field near the wingtip of a STOVL configuration in hover
[AD-A294126] p 686 N95-34750

PRECIPITATION (METEOROLOGY)

- Aircraft icing measurements in East Coast winter storms
[HTN-95-60505] p 214 A95-68756

- WINDEX - A new index for forecasting microburst potential
[HTN-95-90690] p 215 A95-69717

- Mesoscale structure of precipitation bands in a North Atlantic winter storm
[HTN-95-40659] p 215 A95-69803

- Diurnal variation of lee vortices in Taiwan and the surrounding area
[HTN-95-91363] p 318 A95-76394

- The aviation gridded forecast system verification program - A description of aviation-impact-variable evaluation plans
p 664 A95-93498

- FTGEN - An automated FT production system
p 668 A95-93519

- Dissemination of terminal weather products to the flight deck via data link
p 669 A95-93525

PRECIPITATION PARTICLE MEASUREMENT

- Sensing thunderstorm microphysics with multiparameter radar: Application for aviation
p 657 A95-93467

PRECISION

- Precision requirement for potential-based panel methods
[HTN-95-51666] p 433 A95-85048

Development of processes, means, and theoretical principles of thin-walled detail plastic forming at Kazan Aviation Institute p 155 N95-16281
 An integrated GPS/INS/BARO and radar altimeter system for aircraft precision approach landings [AD-A289280] p 383 N95-26985

PRECONDITIONING

Large-scale computational fluid dynamics by the finite element method [BTN-95-EIX94381359154] p 243 A95-71744
 Aerodynamic shape optimization using preconditioned conjugate gradient methods [BTN-95-EIX95142553033] p 263 A95-73465

PREDICTION ANALYSIS TECHNIQUES

Analytic prediction of lift for delta wings with partial leading-edge thrust [BTN-95-EIX95152582345] p 266 A95-73547
 Aerodynamic characteristics of a hypersonic viscous optimized waverider at high altitudes [BTN-95-EIX95152583251] p 266 A95-73552
 Base drag prediction on missile configurations [BTN-95-EIX95152583256] p 266 A95-73557
 Aerodynamic characteristics of a canard-controlled missile at high angles of attack [BTN-95-EIX95152583257] p 267 A95-73558
 Predicting exhaust plume boundaries with supersonic external flows [BTN-95-EIX95152583258] p 297 A95-73559

Improved version of the Naval Surface Warfare Center aeroprediction code (AP93) [BTN-95-EIX95152583260] p 267 A95-73561
 Multiple site fatigue damage in fuselage skin splices: Experimental simulation and theoretical prediction [BTN-95-EIX95152584676] p 276 A95-73588
 Improving prediction: The incorporation of simplified rotor dynamics in a mathematical model of the bell 412HP [BTN-95-EIX95152584679] p 282 A95-73591
 Comparison of linear stability results with flight transition data [BTN-95-EIX95182619097] p 283 A95-76582

Real-time estimation of atmospheric turbulence severity from in-situ aircraft measurements [BTN-95-EIX95182619231] p 319 A95-76657
 Neural network prediction of three-dimensional unsteady separated flowfields [BTN-95-EIX95182619232] p 308 A95-76658
 Prediction of pre-combustion shock in scramjet combustors: A new method p 402 A95-82323
 Artificial neural networks for predicting nonlinear dynamic helicopter loads [HTN-95-51678] p 404 A95-85060

Comparison of the predictive capabilities of several turbulence models [BTN-95-EIX0619952748167] p 589 A95-94461
 Prediction of airplane states [BTN-95-EIX0619952748174] p 584 A95-94468
 Micro-measurements of mechanical properties for adhesives and composites using digital imaging technology [NASA-CR-196111] p 22 N95-10231
 A theoretical analysis of airborne sound transfer for a resiliently mounted machine to its foundation p 30 N95-11304

Modeling and life prediction methodology for Titanium Matrix Composites subjected to mission profiles [NASA-TM-109148] p 55 N95-11915
 Computational predictive methods for fracture and fatigue p 93 N95-14466
 USAF single-event sonic boom prediction model: PCBoom3 p 101 N95-14889
 The computer analysis of the prediction of aircraft electrical power supply system reliability p 155 N95-16278

Forced response of mistuned bladed disks p 141 N95-19383

Forecasting aircraft mishaps using monthly maintenance reports [AD-A286049] p 227 N95-22417
 Additional improvements to the NASA Lewis ice accretion code LEWICE [NASA-TM-106849] p 309 N95-22669

Development and verification of a resin film infusion/resin transfer molding simulation model for fabrication of advanced textile composites [NASA-CR-197439] p 301 N95-23179

Aircraft noise prediction program theoretical manual: Rotorcraft System Noise Prediction System (ROTONET), part 4 [NASA-TM-83199-PT-4] p 451 N95-26392

A NASTRAN-based computer program for structural dynamic analysis of Horizontal Axis Wind Turbines p 439 N95-27980
 Calculation of design load for the MOD-5A 7.3 mW wind turbine system p 440 N95-27982

Comparison of measured and calculated dynamic loads for the Mod-2 2.5 mW wind turbine system p 440 N95-27983

Applications of a damage tolerance analysis methodology in aircraft design and production p 426 N95-28483

A fourth order Euler/Navier-Stokes prediction method for the aerodynamics and aeroelasticity of hovering rotor blades p 554 N95-29242

Acceleration potential models
 PREDICAT/PREDICDYN applied for calculation of axisymmetric dynamic inflow cases [PB95-207015] p 647 N95-30957
 Hot jet/wake turbulent structure and laser propagation. Part 3: Laser propagation measurements and modeling p 647 N95-30992

PREDICTIONS

Accurate drag prediction: A prerequisite for drag reduction research [SAE PAPER 932571] p 467 A95-90060
 Predictive algorithms for the roll control autopilot of a jet fighter aircraft [HTN-95-21047] p 515 A95-90424
 Fracture mechanics validity limits p 95 N95-14480
 Aero-optics system integration [TABES PAPER 94-604] p 100 N95-14638
 Wind shear and its effects on aircraft p 77 N95-14898

The use of cowl camber and taper to reduce rotor/stator interaction noise [NASA-CR-195421] p 323 N95-22675
 Failure analysis for polycarbonate transparencies [AD-A292922] p 630 N95-31471

PREDICTOR-CORRECTOR METHODS

Automatic multi-block grid generation for high-lift configuration wings p 567 N95-28764

PREFORMS

Through-the Thickness(R) braided composites for aircraft applications p 421 N95-28273
 Resin transfer molding of textile preforms for aircraft structural applications p 421 N95-28276
 Recent progress in NASA Langley textile reinforced composites program p 425 N95-28475
 Advanced textile applications for primary aircraft structures p 399 N95-28476
 Comparison of resin film infusion, resin transfer molding, and consolidation of textile preforms for primary aircraft structure p 425 N95-28477

PREMIXED FLAMES

Stationary premixed flames in spherical and cylindrical geometries [HTN-95-42336] p 418 A95-86165
 Studies on high pressure and unsteady flame phenomena [AD-A284126] p 152 N95-18410
 Sensitivity of combustion-acoustic instabilities to boundary conditions for premixed gas turbine combustors [NASA-TM-106890] p 289 N95-23550
 Combustion-acoustic stability analysis for premixed gas turbine combustors [NASA-TM-107024] p 694 N95-32931

PREMIXING

Ignition analysis of hydrogen/air mixture in supersonic mixing layer p 416 A95-82301

PREPREGS

Novel matrix resins for composites for aircraft primary structures, phase 1 [NASA-CR-189657] p 23 N95-10318
 Scarf joint technique with cocured and precured patches for composite repair p 396 N95-27524
 Advanced tow placement of composite fuselage structure p 420 N95-28271
 Advanced resin systems and 3D textile preforms for low cost composite structures p 535 N95-29035
 Weavability of dry polymer powder towpreg p 535 N95-29036
 Performance of resin transfer molded multiaxial warp knit composites p 535 N95-29039
 Development of RTM and powder prepreg resins for subsonic aircraft primary structures p 536 N95-29044
 Thermally stable organic polymers [AD-A290755] p 537 N95-29482

PRESIDENTIAL REPORTS

Aeronautics and space report of the President [NASA-TM-110743] p 681 N95-31979

PRESSURE

Effects of expansions on a supersonic boundary layer: Surface pressure measurements [BTN-95-EIX95142553036] p 263 A95-73462
 Neural network prediction of three-dimensional unsteady separated flowfields [BTN-95-EIX95182619232] p 308 A95-76658
 Differentiating of density in compressible flow for a pressure-based approach [HTN-95-42349] p 373 A95-86178

Computation of delta-wing roll maneuvers [BTN-95-EIX0619952748164] p 605 A95-94458

Correlation of unsteady pressure and inflow velocity fields of a pitching rotor blade [BTN-95-EIX0619952748169] p 589 A95-94463

Investigation of the influence of pylons and stores on the wing lower surface flow p 116 N95-17885

Surface pressure coefficient distributions for axisymmetric forecows at zero incidence (M sub infinity less than or equal to 1.5) [ESDU-94015] p 477 N95-28904
 Application of multigrid computational fluid dynamics (CFD) methods to rotor analysis [AD-A293012] p 648 N95-31475

PRESSURE DISTRIBUTION

Experimental and computational results for the external flowfield of a scramjet inlet [BTN-94-EIX94441380977] p 195 A95-68161
 Suppression of vortex asymmetry and side force on a circular cone [BTN-95-EIX95042474413] p 209 A95-68287
 Measurement around a rotor blade excited in pitch. Part 2: Unsteady surface pressure [HTN-95-31008] p 220 A95-71178
 Aerodynamics of a finite wing with simulated ice [BTN-95-EIX95182619227] p 270 A95-76653

Aerodynamic characteristics of external store configurations at low speeds [BTN-95-EIX95182619230] p 271 A95-76656
 Neural network prediction of three-dimensional unsteady separated flowfields [BTN-95-EIX95182619232] p 308 A95-76658
 Hypersonic model testing in a shock tunnel [BTN-95-EIX95222650789] p 329 A95-79245

The aerodynamic characteristics of cup-like body in supersonic flow p 427 A95-82407
 Practical formulation of a positively conservative scheme [HTN-95-51668] p 433 A95-85050

Pressure controlled surfaces - a 3D inverse panel method as a design tool p 491 A95-87565
 Influence of wing shapes on surface pressure fluctuations at wing-body junctions [HTN-95-61196] p 491 A95-87569

Airfoil pressure measurements during oblique shock-wave/vortex interaction in a Mach 3 stream [HTN-95-81641] p 542 A95-87689

Fluctuating wall pressures near separation in highly swept turbulent interactions [HTN-95-20823] p 543 A95-88084

Chemical recombination in an expansion tube [HTN-95-20844] p 544 A95-88105
 Lift analysis of a variable camber foil using the discrete vortex-blob method [HTN-95-20940] p 545 A95-88979

Numerical computations of supersonic base flow with special emphasis on turbulence modeling [HTN-95-20949] p 546 A95-88988

A note on the interpretation of mini-tuft photographs [HTN-95-01089] p 468 A95-90275
 Viscous contribution to the high Mach number damping in pitch of blunt slender cones at small angles of attack [HTN-95-01096] p 469 A95-90282

Optimum aerodynamic design of aircraft fuselage using boundary element method p 473 A95-91514
 Development of a pilot tube with multi-hole pyramidal head. 2: A five-hole yaw probe of engineering model p 522 A95-91577

Leading-edge sweepback and shape effects on fin-induced fluctuating pressures [BTN-95-EIX95302694471] p 636 A95-94067

Effect of passive venting on static pressure distributions in cavities at subsonic and transonic speeds [NASA-TM-4549] p 6 N95-10029

Navier-Stokes simulations of WECS airfoil flowfields [DE94-013341] p 7 N95-10226

Effect of weak periodic pressure gradient on streamwise vortices near a wall p 29 N95-11263

Exact dynamic responses of periodic multi-span beams under convected pressure fields p 25 N95-11288

Application of two procedures for dual-point design of transonic airfoils [NASA-TP-3466] p 38 N95-12176

Base passive porosity for drag reduction [NASA-CASE-LAR-15246-1] p 91 N95-14183
 Flight and full-scale wind-tunnel comparison of pressure distributions from an F-18 aircraft at high angles of attack -- Conducted in NASA Ames Research Center's 80 by 120 ft wind tunnel p 68 N95-14231

Numerical simulation of the SOFIA flowfield [NASA-CR-197025] p 74 N95-14612
 Activated buoyancy propulsion = Paradox Power (tm) [TABES PAPER 94-619] p 74 N95-14646

- Pressure measurements on an F/A-18 twin vertical tail in buffeting flow. Volume 2: Steady and unsteady RMS pressure data
[AD-A281581] p 76 N95-15465
An improved method of airfoil design p 106 N95-16252
- Wall-signature methods for high speed wind tunnel wall interference corrections p 107 N95-16257
- Measurements of unsteady pressure and structural response for an elastic supercritical wing
[NASA-TP-3443] p 104 N95-16560
- Residual-correction type and related computational methods for aerodynamic design. Part 1: Airfoil and wing design p 128 N95-16566
- Aerodynamic shape optimization p 128 N95-16572
- Review of the EUROPT Project AERO-0026 p 129 N95-16573
- 2-D airfoil tests including side wall boundary layer measurements p 158 N95-17847
- Measurements on a two-dimensional airfoil with high-lift devices p 109 N95-17848
- 2-D aileron effectiveness study p 110 N95-17851
- Two-dimensional 16.5 percent thick supercritical airfoil NLR 7301 p 110 N95-17854
- Low-speed surface pressure and boundary layer measurement data for the NLR 7301 airfoil section with trailing edge flap p 111 N95-17855
- Measurements of the flow over a low aspect-ratio wing in the Mach number range 0.6 to 0.87 for the purpose of validation of computational methods. Part 1: Wing design, model construction, surface flow. Part 2: Mean flow in the boundary layer and wake, 4 test cases p 112 N95-17860
- Detailed study at supersonic speeds of the flow around delta wings p 112 N95-17861
- Pressure distributions on research wing W4 mounted on an axisymmetric body p 112 N95-17862
- DLR-F5: Test wing for CFD and applied aerodynamics p 113 N95-17864
- Wind tunnel investigations of the appearance of shocks in the windward region of bodies with circular cross section at angle of attack p 113 N95-17866
- Force and pressure data of an ogive-nosed slender body at high angles of attack and different Reynolds numbers p 113 N95-17868
- Pressure distribution measurements on an isolated TPS 441 nacelle p 115 N95-17878
- Measurement of gust response on a turbine cascade
[NASA-TM-106776] p 117 N95-18457
- Aeromechanics technology, volume 1. Task 1: Three-dimensional Euler/Navier-Stokes Aerodynamic Method (TEAM) enhancements
[AD-A285713] p 132 N95-18483
- 2-D and 3-D oscillating wing aerodynamics for a range of angles of attack including stall
[NASA-TM-4632] p 120 N95-19119
- Analysis of test section sidewall effects on a two dimensional airfoil: Experimental and numerical investigations p 165 N95-19276
- Application of pressure sensitive paint in hypersonic flows
[NASA-TM-106824] p 223 N95-20794
- Wing pressure distributions from subsonic tests of a high-wing transport model — in the Langley 14-by-22-Foot Subsonic Wind Tunnel p 272 N95-22802
- Three-dimensional unsteady flow calculations in an advanced gas generator turbine p 312 N95-23425
- Experimental study of the effects of Reynolds number on high angle of attack aerodynamic characteristics of forebodies during rotary motion
[NASA-CR-195033] p 330 N95-24443
- Airfoil modification effects on subsonic and transonic pressure distributions and performance for the EA-6B airplane
[NASA-TP-3516] p 373 N95-26382
- Wind tunnel experiments on wake flow field behind a reentry capsule from a viewpoint of parachute deployment at supersonic speeds
[ISAS-655] p 374 N95-26740
- Comparative wind tunnel test at high Reynolds numbers of NACA 64 621 airfoils with two aileron configurations p 377 N95-27977
- Measurements of store forces and moments and cavity pressures for a generic store in and near a box cavity at subsonic and transonic speeds
[NASA-TM-4611] p 378 N95-28241
- Computer program for estimation of leading-edge suction distribution for plane thin wings at subsonic speeds
[ESDU-94038] p 476 N95-28708
- The pressure field of a gust interacting with a flat plate p 557 N95-30161
- Afterbody/nozzle pressure distributions of a twin-tail twin-engine fighter with axisymmetric nozzles at Mach numbers from 0.6 to 1.2
[NASA-TP-3509] p 594 N95-31984
- PRESSURE DRAG**
Application of Navier-Stokes aeroelastic methods to improve fighter wing maneuver performance
[BTN-95-EIX95182619218] p 284 A95-76644
- An investigation of the transonic pressure drag coefficient for ax-symmetric bodies
[AD-A280990] p 105 N95-15994
- A theoretical and experimental investigation of the flow over supersonic leading edge wing/body configurations
[DRA-TM-AERO-PROP-41] p 331 N95-25649
- PRESSURE DROP**
Static pressure drop by swirling flow of an internal cooling air system through a turbine shaft p 698 N95-34560
- PRESSURE EFFECTS**
Development of hypersonic engine seals: Flow effects of preload and engine pressures
[BTN-95-EIX95112524204] p 196 A95-69304
- Main features of overexpanded triple jets
[BTN-95-EIX95142553040] p 304 A95-73458
- Effects of expansions on a supersonic boundary layer: Surface pressure measurements
[BTN-95-EIX95142553036] p 263 A95-73462
- Experimental investigation of the flowfield about an upswep afterbody
[BTN-95-EIX95152582321] p 265 A95-73524
- Prediction of supersonic inlet unstart caused by freestream disturbances
[BTN-95-EIX95222650790] p 329 A95-79246
- Pressure and temperature distortion testing of a two-stage centrifugal compressor
[BTN-94-EIX95011441250] p 431 A95-84207
- Performance variation of scramjet nozzle at various nozzle pressure ratios
[BTN-95-EIX0616952745781] p 615 A95-94505
- Interaction of a weak shock with freestream disturbances
[BTN-95-EIX95332750473] p 638 A95-94687
- Effect of weak periodic pressure gradient on streamwise vortices near a wall p 29 N95-11263
- Wake measurements in a strong adverse pressure gradient
[NASA-CR-197272] p 224 N95-21031
- Effect of atmospheric pressure on measured aircraft noise levels
[PB95-130423] p 232 N95-21425
- Load transfer in the stiffener-to-skin joints of a pressurized fuselage
[NASA-CR-198610] p 439 N95-27865
- Composite fuselage shell structures research at NASA Langley Research Center p 425 N95-28466
- Effects of cabin pressure on climb and descent rates
[ESDU-94040] p 503 N95-29016
- Pressure updating methods for the steady-state fluid equations
[NASA-CR-198163] p 569 N95-30353
- PRESSURE GRADIENTS**
Behavior of the Johnson-King turbulence model in axisymmetric supersonic flows
[BTN-94-EIX94441386606] p 183 A95-67337
- Turbulent transonic airfoil flow simulation using a pressure-based algorithm
[BTN-95-EIX95182619078] p 269 A95-75763
- Simulating heat addition via mass addition in constant area compressible flows
[BTN-95-EIX95182619100] p 307 A95-76585
- Effect of weak periodic pressure gradient on streamwise vortices near a wall p 29 N95-11263
- Airfoil optimization by the one-shot method p 128 N95-16569
- Tools for applied engineering optimization p 128 N95-16570
- Mach number, flow angle, and loss measurements downstream of a transonic fan-blade cascade
[AD-A280907] p 108 N95-16824
- Investigation of the flow over a series of 14 percent-thick supercritical airfoils with significant rear camber p 109 N95-17849
- Effect of crossflow on Goertler instability in incompressible boundary layers
[NASA-CR-195007] p 159 N95-18193
- Wake measurements in a strong adverse pressure gradient
[NASA-CR-197272] p 224 N95-21031
- Acoustic receptivity due to weak surface inhomogeneities in adverse pressure gradient boundary layers
[NASA-TM-4577] p 249 N95-21258
- Large-eddy simulation of flow through a plane, asymmetric diffuser p 250 N95-22449
- The fluid mechanics of a high aspect ratio slot with an impressed pressure gradient and secondary injection p 557 N95-30304
- Subscale study of engine bellmouth inlet vortices in test cell R1D
[AD-A294993] p 707 N95-34818
- PRESSURE MEASUREMENT**
Separation control on high-lift airfoils via micro-vortex generators
[BTN-95-EIX95152582326] p 265 A95-73529
- Influence of wing shapahes on surface pressure fluctuations at wing-body junctions
[HTN-95-61196] p 491 A95-87569
- Pressure measurements on a pitching airfoil in a water channel
[HTN-95-61209] p 541 A95-87582
- Air data prediction from surface pressure measurements on guided munitions
[BTN-95-EIX95282706664] p 466 A95-89641
- Laser velocimetry and blade pressure measurements of a blade-vortex interaction
[HTN-95-01081] p 547 A95-90267
- Rotor-wake-induced flow separation on a lifting surface
[HTN-95-01082] p 468 A95-90268
- Development of a pilot tube with multi-hole pyramidal head: 2: A five-hole yaw probe of engineering model p 522 A95-91577
- Cost effective small-scale experiments to aid the design of ASTOVL aircraft
[CONGRESS PAPER C428-9-098] p 475 A95-91695
- Leading-edge sweepback and shape effects on fin-induced fluctuating pressures
[BTN-95-EIX95302694471] p 636 A95-94067
- In-flight pressure measurements on a subsonic transport high-lift wing section
[BTN-95-EIX0619952748170] p 589 A95-94464
- Performance variation of scramjet nozzle at various nozzle pressure ratios
[BTN-95-EIX0616952745781] p 615 A95-94505
- Design and evaluation of candidate pressure ports for the HYFLITE experiment
[NASA-TM-109146] p 22 N95-11003
- Pressure measurements on an F/A-18 twin vertical tail in buffeting flow. Volume 3: Buffet power spectral densities
[AD-A281444] p 36 N95-11829
- A new algorithm for five-hole probe calibration, data reduction, and uncertainty analysis
[NASA-TM-106458] p 38 N95-12378
- Design and development of an F/A-18 inlet distortion rake: A cost and time saving solution p 69 N95-14241
- Pressure measurements on an F/A-18 twin vertical tail in buffeting flow. Volume 2: Steady and unsteady RMS pressure data
[AD-A281581] p 76 N95-15465
- Data acquisition and processing software for the Low Speed Wind Tunnel tests of the Jindivik auxiliary air intake
[AD-A285455] p 108 N95-17178
- Measurements on a two-dimensional aerofoil with high-lift devices p 109 N95-17848
- Surface pressure and wake drag measurements on the Boeing A4 airfoil in the IAR 1.5X1.5m Wind Tunnel Facility p 110 N95-17850
- Pressure distribution measurements on an isolated TPS 441 nacelle p 115 N95-17878
- Applications of the five-hole probe technique for flow field surveys at the Institute for Aerospace Research p 163 N95-19255
- Calculation of low speed wind tunnel wall interference from static pressure pipe measurements p 164 N95-19273
- Optical surface pressure measurements: Accuracy and application field evaluation p 175 N95-19274
- Multipoint pressure measurements on continuously moving wind tunnel models
[ARA-MEMO-391] p 188 N95-19772
- Application of pressure sensitive paint in hypersonic flows
[NASA-TM-106824] p 223 N95-20794
- Pressure measurements on an F/A-18 twin vertical tail in buffeting flow. Volume 4, part 1: Buffet cross spectral densities
[AD-A285593] p 237 N95-21214
- Workshop report: Measurement techniques in highly transient, spectrally rich combustion environments
[AD-A288395] p 350 N95-25606
- Stall precursor study of high frequency data for three high speed, swept compressor rotors
[AD-A289379] p 406 N95-26878
- Interactions of spanwise and chordwise vorticity associated with three-dimensional dynamic stall over an oscillating wing
[AD-A290546] p 477 N95-29091
- Analyzing the stability of floating ice floes
[AD-A292149] p 563 N95-29160

A hybrid electronically scanned pressure module for cryogenic environments
[NASA-TM-110146] p 554 N95-29453

Research instrumentation for polytechnic university's supersonic wind tunnel facility
[AD-A290232] p 523 N95-29468

Unsteady pressure and inflow velocity on a pitching rotor blade in hover p 480 N95-29771

Workshop report: Measurement techniques in highly transient, spectrally rich combustion environments p 629 N95-31208

Subscale study of engine bellmouth inlet vortices in test cell R1D
[AD-A294993] p 707 N95-34818

PRESSURE OSCILLATIONS

Effect of weak periodic pressure gradient on streamwise vortices near a wall p 29 N95-11263

Active control of panel vibrations induced by a boundary layer flow
[NASA-CR-197867] p 273 N95-23182

The acoustic characteristics of turbomachinery cavities
[NASA-CR-4671] p 476 N95-28720

Unsteady pressure and inflow velocity on a pitching rotor blade in hover p 480 N95-29771

PRESSURE PULSES

System for determining aerodynamic imbalance
[NASA-CASE-ARC-11913-1] p 311 N95-23377

A pulsed liquid fuel ramjet p 617 N95-31201

PRESSURE RATIO

Performance variation of scramjet nozzle at various nozzle pressure ratios
[BTN-95-EIX0616952745781] p 615 A95-94505

Pressure measurements on an F/A-18 twin vertical tail in buffeting flow. Volume 3: Buffet power spectral densities
[AD-A281444] p 36 N95-11829

Error propagation equations for estimating the uncertainty in high-speed wind tunnel test results
[DE94-014136] p 145 N95-16509

Internal performance characteristics of thrust-vectoring axisymmetric ejector nozzles
[NASA-TM-4610] p 331 N95-25338

The noise reduction potential of dual-stream coaxial rectangular improperly expanded jet flows
[NASA-CR-197820] p 437 N95-26995

Application of multigrad computational fluid dynamics (CFD) methods to rotor analysis
[AD-A293012] p 648 N95-31475

PRESSURE RECOVERY

F/A-18 inlet calculations at 60-deg angle of attack and 10-deg sideslip
[BTN-95-EIX95112524199] p 195 A95-69309

Numerical study of the performance of swept, curved compression surface scramjet inlets
[BTN-95-EIX95112524198] p 197 A95-69310

Experimental investigation of the flow in diffusers behind an axial flow compressor
[BTN-95-EIX95282710057] p 632 A95-92472

Linear Motor Free Piston Compressor
[AD-A293452] p 647 N95-31374

PRESSURE REDUCTION

Erosion of T56 5th stage rotor blades due to bleed hole overlap flow p 200 N95-19666

MHD-flow in slotted channels with conducting walls
[DE94-018370] p 258 N95-21388

Effects of cavity bleed and its configuration on aerodynamic characteristics of supersonic internal flow
[NAL-TR-1247] p 594 N95-31715

PRESSURE SENSORS

Air data prediction from surface pressure measurements on guided munitions
[BTN-95-EIX95282706664] p 466 A95-89641

New sensor technology for aircraft hydraulic system diagnostics
[SAE PAPER 932586] p 494 A95-90070

Design and evaluation of candidate pressure ports for the HYFLITE experiment
[NASA-TM-109146] p 22 N95-11003

Pressure measurements on an F/A-18 twin vertical tail in buffeting flow. Volume 3: Buffet power spectral densities
[AD-A281444] p 36 N95-11829

A new algorithm for five-hole probe calibration, data reduction, and uncertainty analysis
[NASA-TM-106458] p 38 N95-12378

Design and development of an F/A-18 inlet distortion rake: A cost and time saving solution p 69 N95-14241

Single-engine tail interference model p 115 N95-17879

Overview of unsteady transonic wind tunnel test on a semispan straked delta wing oscillating in pitch
[AD-A284097] p 117 N95-18380

Applications of the five-hole probe technique for flow field surveys at the Institute for Aerospace Research p 163 N95-19255

Optical surface pressure measurements: Accuracy and application field evaluation p 175 N95-19274

Multipoint pressure measurements on continuously moving wind tunnel models
[ARA-MEMO-391] p 188 N95-19772

Response of the B-1B air data sensor to simulated dust cloud environments
[AD-A286134] p 235 N95-22036

Impeller flow field characterization with a laser two-focus velocimeter p 313 N95-23440

Process and control systems for composites manufacturing p 420 N95-28267

A hybrid electronically scanned pressure module for cryogenic environments
[NASA-TM-110146] p 554 N95-29453

Workshop report: Measurement techniques in highly transient, spectrally rich combustion environments p 629 N95-31208

PRESSURE VESSELS

Oscillating-flow regenerator test rig
[NASA-CR-196982] p 53 N95-13200

Compression strength of composite primary structural components
[NASA-CR-197554] p 160 N95-18388

Process and control systems for composites manufacturing p 420 N95-28267

PRESSURIZED CABINS

Global cost and weight evaluation of fuselage keel design concepts p 501 N95-28840

Effects of cabin pressure on climb and descent rates
[ESDU-94040] p 503 N95-29016

PRESSURIZING

Linear Motor Free Piston Compressor
[AD-A293452] p 647 N95-31374

PRESTRESSING

Development of hypersonic engine seals: Flow effects of preload and engine pressures
[BTN-95-EIX95112524204] p 196 A95-69304

PREVENTION

Design of a vehicle based system to prevent ozone loss
[NASA-CR-197199] p 48 N95-12702

The prevention of PIO by design p 620 N95-31991

PRIMERS (COATINGS)

Use of starch based blast media for dry paint stripping
[SAE PAPER 932616] p 456 A95-90081

Organic coating technology for the protection of aircraft against corrosion p 303 N95-23513

PRINTED CIRCUITS

Ultra-Reliable Digital Avionics (URDA) processor p 245 N95-20638

Life cycle costs of alternatives for F-16 printed circuit board diagnosis equipment
[AD-A288744] p 401 N95-28586

PROBABILITY DENSITY FUNCTIONS

Modeling of supersonic turbulent combustion using assumed probability density functions
[BTN-95-EIX95112524190] p 206 A95-69318

MOAMAP: A model that combines several different kinds of aircraft operations p 32 N95-11323

Statistics of multi-look AIRSAR imagery: A comparison of theory with measurements p 320 N95-23947

PROBABILITY DISTRIBUTION FUNCTIONS

Probabilistic evaluation of fuselage-type composite structures p 398 N95-28444

PROBABILITY THEORY

Effects of satellite bunching on the probability of collision in geosynchronous orbit
[BTN-95-EIX95152583276] p 298 A95-73577

Airplane icing research at the Boeing Company: Participation in the second Canadian Atlantic Storms Program p 674 A95-93544

Probabilistic inspection strategies for minimizing service failures p 93 N95-14461

Aircraft wake vortex takeoff tests at O'Hara International Airport
[AD-A283828] p 118 N95-18624

Probabilistic design of advanced composite structure p 424 N95-28443

Proof test methodology for composites p 424 N95-28445

Probabilistic reliability modeling of fatigue on the H-46 tie bar
[AD-A289926] p 607 N95-30927

Emerging applications in probability (Sensor management)
[AD-A292781] p 601 N95-31433

A probabilistic design method applied to smart composite structures
[NASA-TM-106715] p 651 N95-32206

PROBES

Eddy current for detecting second layer cracks under installed fasteners
[AD-A282412] p 158 N95-17507

PROBLEM SOLVING

On the exact solutions of pseudorange equations
[BTN-95-EIX95142555477] p 278 A95-73433

Application of a control-volume-based finite-element formulation to the shock tube problem
[BTN-95-EIX95182619099] p 295 A95-76584

Aircraft controller synthesis by solving a nonconvex optimization problem
[BTN-95-EIX95282706672] p 515 A95-89636

An approach to weather requirements management p 653 A95-93448

Optimum Design Methods for Aerodynamics
[AGARD-R-803] p 127 N95-16562

Review of the EUROPT Project AERO-0026 p 129 N95-16573

PalymSys (TM): An extended version of CLIPS for construction and reasoning using blackboards p 217 N95-19767

Computing methods for the approximate solution of time dependent problems
[AD-A286007] p 256 N95-20719

Empirical results on scheduling and dynamic backtracking p 299 N95-23761

Aerodynamic parameter estimation via Fourier modulating function techniques
[NASA-CR-4654] p 335 N95-24630

An unstructured-grid software system for solving complex aerodynamic problems p 476 N95-28743

A procedure for automating CFD simulations of an inlet-bleed problem p 552 N95-28768

PROCEDURES

Maintenance programs
[HTN-95-92310] p 365 A95-85354

Scientific and technical photography at NASA Langley Research Center p 310 N95-23290

PROCESS CONTROL (INDUSTRY)

STEP: A future revision, today
[NONP-NASA-VT-95-49121] p 452 N95-27209

PROCUREMENT

The Advanced Avionics Subsystem Technology Demonstration Program p 234 N95-20636

PROCUREMENT MANAGEMENT

Case study of risk management in the USAF B-1B bomber program
[AD-A282371] p 62 N95-11944

A case study of the teaming concept in the procurement of the V-22 aircraft
[AD-A293770] p 608 N95-31578

Report to the Chairman, Legislation and National Security Subcommittee, Committee on Government Operations, House of Representatives. C-17 Aircraft program: Improvements in initial provisioning process
[GAO/NSIAD-94-63] p 584 N95-32194

PROCUREMENT POLICY

A status report on the development of the Federal Aviation Administration/National Oceanic and Atmospheric Administration Memorandum of Agreement p 652 A95-93447

Low rate initial production in Army Aviation systems development
[AD-A281871] p 127 N95-16356

PRODUCT DEVELOPMENT

Trent engine development
[BTN-94-EIX94461290507] p 82 A95-61727

New commercial off-the-shelf testers are automatic and intelligent
[BTN-95-EIX95172595292] p 287 A95-75720

Evaluation and management of research and development in aeronautics
[CONGRESS PAPER C428-8-102] p 581 A95-91691

Simultaneous engineering in aero gas turbine design and manufacture
[CONGRESS PAPER C428-20-204] p 581 A95-91723

An overview of FAA-sponsored aviation weather research and development p 652 A95-93442

The forecast systems laboratory's role in the FAA's aviation weather development program p 652 A95-93443

On designing and engineering the integrated terminal weather system p 653 A95-93449

ITWS ceiling and visibility products p 654 A95-93454

Automation of observations in the Netherlands p 661 A95-93485

Developing the Aviation Gridded Forecast System p 671 A95-93532

The prototype aviation weather products generator a vehicle to assess user needs p 671 A95-93534

Aviation value-added products and services from the NEXRAD Information Dissemination Service (NIDS) p 671 A95-93535

User involvement in the development of an advanced icing product for use in aviation p 672 A95-93537

The development of a model specification for ground support equipment [CONGRESS PAPER C428-38-095] p 625 A95-93636

Lean manufacturing for lean times [BTN-95-EIX95302730538] p 583 A95-94036

FAA vertical flight bibliography [DOT/FAA/RD-94/17] p 14 N95-11684

Integrated design and manufacturing for the high speed civil transport [NASA-CR-197183] p 48 N95-12700

Eddy current for detecting second layer cracks under installed fasteners [AD-A282412] p 158 N95-17507

A quiet STOL Research Aircraft Development program [NAL-TR-1223] p 336 N95-25862

Requirements for effective use of CFD in aerospace design p 551 N95-28725

Computational methods for control and optimal design of aerospace systems [AD-A292861] p 608 N95-31451

Initial evaluation of the Oregon State University planetary boundary layer column model for ITWS applications [AD-A293775] p 677 N95-31465

Advanced turbine systems program conceptual design and product development [DE95-000088] p 650 N95-32163

Development and flight testing of an Obstacle Avoidance System for US Army helicopters p 687 N95-32500

PRODUCTION COSTS

Impact of composites on future transport aircraft p 534 N95-29030

Challenges and payoff of composites in transport aircraft: 777 empennage and future applications p 534 N95-29031

PRODUCTION ENGINEERING

Development of an intelligent tool-condition monitoring system for FMS [CONGRESS PAPER C428-32-012] p 583 A95-93617

PRODUCTION MANAGEMENT

Changing MRP Systems within the aerospace industry [CONGRESS PAPER C428-26-051] p 681 A95-93603

PRODUCTIVITY

Modelling for optimal operations of line milling of aerodynamic surfaces [BTN-94-EIX94461408774] p 138 A95-63657

Tooling - a source of productivity [CONGRESS PAPER C428-32-017] p 583 A95-93619

Potential impacts of advanced aerodynamic technology on air transportation system productivity [NASA-TM-109154] p 10 N95-11489

Development of processes, means, and theoretical principles of thin-walled detail plastic forming at Kazan Aviation Institute p 155 N95-16281

The global aircraft shape p 128 N95-16571

PROFILES

Test and evaluation report for the Manual Domestic Passive Profiling System (MDPPS) [AD-A286312] p 225 N95-20093

PROFILOMETERS

On profiling a cam of an axial aviation diesel engine by periodic splines [BTN-94-EIX94461407946] p 82 A95-62264

Profiling of the working surface of electrodes-tools for circle electrochemical dimensional treatment of compressor blades [BTN-94-EIX94461407964] p 83 A95-62638

An integrated system to improve aviation weather forecasts for the Alaska Range p 656 A95-93460

A laser-based ice shape profilometer for use in icing wind tunnels [NASA-TM-106936] p 646 N95-30851

PROGRAM VERIFICATION (COMPUTERS)

Dryden lectureship in research, a perspective on CFD validation [AIAA PAPER 93-0002] p 3 A95-60180

Response of a nonrotating rotor blade to lateral turbulence. Part 2: Experiment [BTN-95-EIX95182619229] p 284 A95-76655

Evolving standards for safety critical software [CONGRESS PAPER C428-24-142] p 678 A95-93595

Formal design and verification of a reliable computing platform for real-time control (phase 3 results) [NASA-TM-109140] p 33 N95-10873

Automated test environment for a real-time control system [TABES PAPER 94-631] p 99 N95-14652

Verification of computational aerodynamic predictions for complex hypersonic vehicles using the INCA(trademark) code [DE95-004757] p 330 N95-24308

An evaluation of the Software Through Pictures/T Tool (STP/T) for the Software Support Activity (SSA) [AD-A288822] p 447 N95-26348

A verification procedure for MSC/NASTRAN Finite Element Models [NASA-CR-4675] p 392 N95-27371

Calculation of design load for the MOD-5A 7.3 mW wind turbine system p 440 N95-27982

An unstructured-grid software system for solving complex aerodynamic problems p 476 N95-28743

Grid resolution and turbulent inflow boundary condition recommendations for NPARC calculations [NASA-TM-106959] p 482 N95-30253

Validation of the NPARC code for nozzle afterbody flows at transonic speeds [NASA-TM-106971] p 592 N95-30704

Formal verification of an avionics microprocessor [NASA-CR-4682] p 710 N95-33396

Verification of turbine cascade flow with tip clearance p 698 N95-34511

PROGRAMMING ENVIRONMENTS

The ADAGE avionics reference architecture [AIAA PAPER 95-1021] p 566 A95-90693

Portable parallel stochastic optimization for the design of aeropropulsion components [NASA-CR-195312] p 154 N95-16072

PROJECT MANAGEMENT

A new paradigm: The investment casting cooperative arrangement [HTN-95-92510] p 539 A95-87330

ITWS ceiling and visibility products p 654 A95-93454

Case study of risk management in the USAF B-1B bomber program [AD-A282371] p 62 N95-11944

The development of the F100-PW-220 and F110-GE-100 engines: A case study of risk assessment and risk management [AD-A282467] p 51 N95-13289

Review of the EUROPT Project AERO-0026 p 129 N95-16573

Unmanned aerial vehicles. 1994 master plan p 607 N95-31416

A case study of the teaming concept in the procurement of the V-22 aircraft [AD-A293770] p 608 N95-31578

PROJECT PLANNING

Aircraft advanced materials research and development program plan [AD-A290542] p 505 N95-29565

PROJECTILES

Implicit multi-domain method for unsteady compressible inviscid fluid flows around 3D projectiles p 548 A95-91482

The coplanar projectile motion problem including the effects of lift and drag [ISBN 1-879921-01-4] p 635 A95-93723

Propulsion research concerning SFRJ-motors [PB94-179520] p 14 N95-10083

Static aerodynamics CFD analysis for 120-mm hypersonic KE projectile design [ARL-MR-184] p 118 N95-18611

Comparison of meteorological data with fitted values extracted from projectile trajectory [AD-A285921] p 255 N95-19989

PROLATE SPHEROIDS

Flow structure in the lee of an inclined 6:1 prolate spheroid [BTN-94-EIX95011441127] p 348 A95-81027

Three-dimensional boundary layer and flow field data of an inclined prolate spheroid p 158 N95-17867

PROP-FAN TECHNOLOGY

Long distance propagation model and its application to aircraft en route noise prediction [HTN-95-61221] p 491 A95-87594

Broadband noise characteristics of a model counter-rotating shrouded propfan p 572 A95-88470

Twenty-first century commercial transport engines p 512 A95-91495

En route noise levels from propfan test assessment airplane [NASA-TP-3451] p 62 N95-12341

Propulsion/airframe interference for ducted propfan engines with ground effect [NASA-CR-197110] p 81 N95-14909

FPCAS2D user's guide, version 1.0 [NASA-CR-195413] p 156 N95-16588

PROPANE

Design of a vehicle based system to prevent ozone loss [NASA-CR-197199] p 48 N95-12702

PROPELLANT COMBUSTION

Application of scramjet engine technology to the design of ram accelerator projectiles p 19 N95-10282

PROPELLANT GRAINS

Simulation on the 3-D turbulent flow in the passages of finocyl grain [BTN-95-EIX95202638962] p 279 A95-76674

PROPELLANT TESTS

Airborne rotary separator study [NASA-CR-191045] p 150 N95-18743

PROPELLER BLADES

Composite propeller system for Dornier 328 [BTN-94-EIX94461290506] p 66 A95-61728

Head-on parallel blade-vortex interaction [HTN-95-61197] p 491 A95-87570

Polymer composite applications to aerospace equipment [HTN-95-80257] p 529 A95-89201

Ice-impact analysis of blades p 200 N95-19672

System for determining aerodynamic imbalance [NASA-CASE-ARC-11913-1] p 311 N95-23377

Development and validation of a blade-element mathematical model for the AH-64A Apache helicopter [NASA-TM-108863] p 367 N95-26710

Analysis of aircraft engine blade subject to ice impact p 407 N95-28277

PROPELLER EFFICIENCY

Experimental study of the aerodynamic characteristics of the counter-rotation propellers p 474 A95-91562

PROPELLER FANS

En route noise levels from propfan test assessment airplane [NASA-TP-3451] p 62 N95-12341

Propulsion/airframe interference for ducted propfan engines with ground effect [NASA-CR-197110] p 81 N95-14909

FPCAS2D user's guide, version 1.0 [NASA-CR-195413] p 156 N95-16588

Ice-impact analysis of blades p 200 N95-19672

PROPELLER NOISE

Experimental investigation of the sources of propeller noise due to the ingestion of turbulence at low speeds [BTN-95-EIX95262697042] p 569 A95-86859

Flyover noise reduction of piston-engine propeller aeroplanes using an active noise control technique [SAE PAPER 931218] p 509 A95-87466

Head-on parallel blade-vortex interaction [HTN-95-61197] p 491 A95-87570

In-flight interior sound field mapping in propeller aircraft p 572 A95-88472

Noise transmission and reduction in turboprop aircraft p 175 N95-19164

PROPELLER SLIPSTREAMS

Wake velocity measurement of counter-rotation propellers p 474 A95-91563

Low speed propeller slipstream aerodynamic effects p 116 N95-17882

PROPELLERS

Composite propeller system for Dornier 328 [BTN-94-EIX94461290506] p 66 A95-61728

Adaptive finite element method for turbulent flow near a propeller [BTN-95-EIX95142553038] p 305 A95-73460

Experimental investigation of the sources of propeller noise due to the ingestion of turbulence at low speeds [BTN-95-EIX95262697042] p 569 A95-86859

Period evolution of PSR B1259-63: Evidence for propeller-torque spindown [HTN-95-B0194] p 581 A95-87903

Analysis and scale-model experiment of propeller driving motor for microwave-powered airplane p 487 A95-91576

Multigrid/multiblock method for transonic potential flow around wing/body/nacelle configurations including a slipstream p 591 A95-95451

Aircraft accident report: Overspeed and loss of power on both engines during descent and power-off emergency, landing Simmons Airlines, Inc., d/b/a, American Eagle Flight 3641, N349SB False River Air Park, New Roads, Louisiana, 1 February 1994 [PB94-910408] p 78 N95-14916

Gyroscopic and propeller aerodynamic effects on engine mounts dynamic loads in turbulence conditions p 132 N95-18599

Numerical studies of turbulent free surface flows and unsteady propeller flows [AD-A294377] p 706 N95-34343

PROPORTIONAL CONTROL

Ideal proportional navigation p 342 A95-81374

PROPULSION

Powered lift for land and sea [BTN-95-EIX95041503010] p 192 A95-68313

Analytical aeropropulsive/aeroelastic hypersonic-vehicle model with dynamic analysis [BTN-95-EIX95182619138] p 269 A95-76615

Activated buoyancy propulsion = Paradox Power (tm) [TAPES PAPER 94-619] p 74 N95-14646
 The 1993 JANNAF Propulsion Meeting, volume 1 [CPIA-PUBL-602-VOL-1] p 148 N95-16312
 Operating capability and current status of the reactivated NASA Lewis Research Center Hypersonic Tunnel Facility [NASA-TM-106808] p 148 N95-19286
 T-45A High Angle of Attack Testing: US Naval Test Pilot School 46th Annual Reunion and Symposium [AD-A284000] p 231 N95-20466
 Airborne rotary air separator study [NASA-CR-189099] p 290 N95-24053
 Advanced subsonic airplane design and economic studies [NASA-CR-195443] p 338 N95-24304
 Workshop report: Measurement techniques in highly transient, spectrally rich combustion environments [AD-A288395] p 350 N95-25606
 The lift-fan aircraft: Lessons learned [NASA-CR-196694] p 392 N95-27143
 NAS Technical Summaries, March 1993 - February 1994 [NASA-RP-1355] p 453 N95-27367
 Catapult-launching of the RAFALE design and experimentation p 609 N95-32008

PROPULSION SYSTEM CONFIGURATIONS

Mechanical system reliability and risk assessment [BTN-95-EIX95142553046] p 304 A95-73452
 Integrated flight/propulsion control for helicopters [HTN-95-80854] p 290 A95-75096
 An unmanned air vehicle concept with tipjet drive [HTN-95-80858] p 283 A95-75100
 An advanced scramjet propulsion concept for A 350 MG SSTO space plane p 402 A95-82325
 Test results on air turbo ramjet engine for a future space plane p 402 A95-82327
 Design optimization of an airbreathing aerospaceplane p 524 A95-87382
 NASA Lewis Propulsion Systems Laboratory test article systems criteria [NASA-TM-106589] p 20 N95-10446
 NASA Lewis Propulsion Systems Laboratory customer guide manual [NASA-TM-106569] p 21 N95-10822
 Shock-tunnel combustor testing for hypersonic vehicles [NASA-CR-196836] p 52 N95-11938
 Design and testing of an oblique all-wing supersonic transport [NASA-CR-196394] p 48 N95-12785
 Activities of the Structures Division, Lewis Research Center [NASA-TM-108081] p 59 N95-13235
 Computational aerodynamics based on the Euler equations [AGARD-AG-325] p 72 N95-14264
 Small turbojets: Designs and installations p 138 N95-16323
 The global aircraft shape p 128 N95-16571
 Technology Benefit Estimator (T/BEST): User's manual [NASA-TM-106785] p 167 N95-19501
 Simulation model of the integrated flight/propulsion control system, displays, and propulsion system for ASTOVL lift-fan aircraft [NASA-TM-108866] p 405 N95-26412
 Propulsion system assessment for very high UAV under ERAST [NASA-CR-195469] p 406 N95-27866
 Surface modeling and grid generation for aeropropulsion CFD p 551 N95-28732
 Design, analysis and control of large transports so that control of engine thrust can be used as a back-up of the primary flight controls [NASA-CR-198958] p 518 N95-30254
 Numerical simulation of ram accelerator performance including transient effects during initiation of combustion and sensitivity studies p 629 N95-31203

PROPULSION SYSTEM PERFORMANCE

Development and application of the double V type flame stabilizer [BTN-94-EIX94481415355] p 154 A95-65345
 Aerodynamic design and calculation of flow around the plane cascade of turbine [BTN-94-EIX94481415357] p 104 A95-65347
 Adaptive modeling of jet engine performance with application to condition monitoring [BTN-95-EIX95112524205] p 196 A95-69303
 Nonlinear dynamic simulation of single- and multispool core engines, part 1: Computational method [BTN-95-EIX95112524200] p 210 A95-69308
 Optimal trajectories for hypersonic launch vehicles [HTN-95-61120] p 415 A95-84884

Design and development of an advanced two-stage centrifugal compressor [BTN-95-EIX95282710054] p 633 A95-92475
 Propulsion simulator for high bypass turbofan performance evaluation [SAE PAPER 931410] p 625 A95-93676
 Computational fluid dynamics study of the variable-pitch split-blade fan concept [NASA-CR-189206] p 15 N95-10247
 NASA Lewis Propulsion Systems Laboratory test article systems criteria [NASA-TM-106589] p 20 N95-10446
 NASA Lewis Propulsion Systems Laboratory customer guide manual [NASA-TM-106569] p 21 N95-10822
 Modeling improvements and users manual for axial-flow turbine off-design computer code AXOD [NASA-CR-195370] p 8 N95-10853
 Shock-tunnel combustor testing for hypersonic vehicles [NASA-CR-196836] p 52 N95-11938
 Design and construction of a remote piloted flying wing [NASA-CR-197195] p 47 N95-12695
 Activities of the Structures Division, Lewis Research Center [NASA-TM-108081] p 59 N95-13235
 Fourth High Alpha Conference, volume 1 [NASA-CP-10143-VOL-1] p 67 N95-14229
 A graphical user interface for design and analysis of air breathing propulsion systems [TAPES PAPER 94-616] p 83 N95-14645
 Gas turbine prediffuser-combustor performance during operation with air-water mixture [DOT/FAA/CT-93/52] p 83 N95-15683
 Joint Proceedings on Aeronautics and Astronautics (JPAA) [ISBN-7-80-046602-7] p 104 N95-16249
 Service and physical properties of liquid-jet fuels p 151 N95-16256
 Theoretical fundamentals of the aircraft GTE tests p 138 N95-16265
 Experimental and analytical methods for the determination of connected-pipe ramjet and ducted rocket internal performance [AGARD-AR-323] p 149 N95-17278
 Cooperative control theory and integrated flight and propulsion control [NASA-CR-197493] p 142 N95-17404
 Airborne rotary separator study [NASA-CR-191045] p 150 N95-18743
 Object-oriented approach for gas turbine engine simulation [NASA-TM-106970] p 615 N95-30594
 Flight assessment of the onboard propulsion system model for the Performance Seeking Control algorithm on an F-15 aircraft [NASA-TM-4705] p 617 N95-31425
 Low-order nonlinear dynamic model of IC engine-variable pitch propeller system for general aviation aircraft [NASA-TM-107006] p 694 N95-32916
 PSC algorithm description p 695 N95-33013
 Performance seeking control (PSC) for the F-15 highly integrated digital electronic control (HIDEC) aircraft p 697 N95-33020
 Subscale study of engine bellmouth inlet vortices in test cell R1D [AD-A294993] p 707 N95-34818

PROPULSION EFFICIENCY

Thrust modeling for hypersonic engines [AIAA PAPER 95-6081] p 509 A95-87410
 High bypass separate flow exhaust system improved thrust efficiency by modifying the aft centerbody [SAE PAPER 932622] p 511 A95-90083
 Propulsion system assessment for very high UAV under ERAST [NASA-CR-195469] p 406 N95-27866

PROTECTION

Lightning protection technology for small general aviation composite material aircraft [SAE PAPER 931241] p 483 A95-88964
 The assessment of the AH-64D, longbow, mast-mounted assembly noise hazard for maintenance personnel [AD-A284971] p 171 N95-16226
 Development of a model protection and dynamic response monitoring system for the national transonic facility [NASA-CR-195041] p 340 N95-24388
 Aircraft fuel system lightning protection design and qualification test procedures development [AD-A288401] p 380 N95-26497

PROTECTIVE COATINGS

Evaluation of advanced aerospace materials by depth sensing indentation and scratch methods [BTN-95-EIX95152584678] p 282 A95-73590

Evaluation of alternate F-14 wing lug coating [AD-A283207] p 129 N95-17631
 Quality optimization of thermally sprayed coatings produced by the JP-5000 (HVOF) gun using mathematical modeling p 152 N95-19008
 Erosion, Corrosion and Foreign Object Damage Effects in Gas Turbines [AGARD-CP-558] p 197 N95-19653
 Protective coatings for compressor gas path components p 201 N95-19675
 New Trends in coatings developments for turbine blades: Materials processing and repair p 201 N95-19676
 High velocity oxygen fuel spraying of erosion and wear resistant coatings on jet engine parts p 202 N95-19680
 Evaluation of thermal barrier and PS-200 self-lubricating coatings in an air-cooled rotary engine [NASA-CR-195445] p 289 N95-23222
 Corrosion protection measures for CFC/metal joints of fuel integral tank structures of advanced military aircraft p 303 N95-23510
 Environmentally regulated aerospace coatings p 631 N95-31775

PROTOCOL (COMPUTERS)

Generic architectures for future flight systems p 99 N95-14159
 Space Generic Open Avionics Architecture (SGOAA): Overview p 99 N95-14161
 Evolutionary Telemetry and Command Processor (TCP) architecture p 86 N95-14162
 High performance backplane components for modular avionics p 247 N95-20653
 Mode of human image representation and error checking strategies in complex visual displays [AD-A290107] p 485 N95-29210

PROTON RESONANCE

Phonon characteristics of high (T sub c) superconductors from neutron Doppler broadening measurements [DE95-003703] p 324 N95-24076

PROTOTYPES

Rapid prototyping of composite aircraft structures [SAE PAPER 931219] p 539 A95-87530
 An integrated system to improve aviation weather forecasts for the Alaska Range p 656 A95-93460
 An in-situ system for warning of icing conditions p 660 A95-93481
 Developing and testing decision-making products for center weather service unit meteorologists p 671 A95-93533
 The prototype aviation weather products generator a vehicle to assess user needs p 671 A95-93534
 User involvement in the development of an advanced icing product for use in aviation p 672 A95-93537
 A prototype for displaying aviation forecast variables using Eta numerical model output p 676 A95-93555
 Low frequency ultrasonic nondestructive inspection of aluminum/adhesive fuselage lap splices [DE94-014242] p 24 N95-11135
 An application of virtual prototyping to the flight test and evaluation of an unmanned air vehicle [AD-A281749] p 14 N95-11595
 A surgical support system for Space Station Freedom p 149 N95-16776

New technologies for space avionics

[NASA-CR-197574] p 150 N95-18196
 Prototype stop bar system evaluation at Seattle-Tacoma International Airport [AD-A290136] p 490 N95-30031
 Catapult-launching of the RAFALE design and experimentation p 609 N95-32008

PROVING

Validation of empirical orbit error corrections using crossover difference differences [HTN-94-00912] p 25 A95-60227
 Verification of engineering methods of aerodynamics for reentry vehicles by DSMC p 525 A95-87386
 The Integrated Terminal Weather System (ITWS) storm cell information and weather impacted airspace detection algorithm p 654 A95-93452
 The aviation gridded forecast system verification program - A description of aviation-impact-variable evaluation plans p 664 A95-93498
 Comprehensive verification of terminal forecast ceiling and visibility p 664 A95-93500
 Objective verification of an enhanced terminal forecast experiment at Denver, Colorado p 664 A95-93501
 Verification of terminal forecasts p 664 A95-93502
 Use of pilot reports for verification of aircraft icing diagnoses and forecasts p 666 A95-93508
 The 1992-3 operational winter forecasting experiment for Stapleton airport p 677 A95-93561
 Supersonic transport grid generation, validation, and optimization [NASA-CR-197752] p 448 N95-26648
 Proof test methodology for composites p 424 N95-28445

PROVISIONING

Report to the Chairman, Legislation and National Security Subcommittee, Committee on Government Operations, House of Representatives. C-17 Aircraft program: Improvements in initial provisioning process [GAO/NSIAD-94-63] p 584 N95-32194

PSYCHOLOGICAL EFFECTS

Ground-based wake vortex monitoring, prediction, and ATC interface p 42 N95-13209

PSYCHOLOGICAL TESTS

The selective use of functional optical variables in the control of forward speed [NASA-TM-108849] p 35 N95-12227

PUBLIC HEALTH

Criticism of the Leq as an Index for aircraft noise and other discontinuous noise sources p 559 A95-88476
JPRS Report: Science and technology. Central Eurasia [JPRS-UST-94-032] p 350 N95-24759

PUBLIC RELATIONS

Community relations plan: Galena Airport and Camp ion Air Force Station, Alaska [AD-A286722] p 446 N95-27234

PULSARS

Period evolution of PSR B1259-63: Evidence for propeller-torque spindown [HTN-95-B0194] p 581 A95-87903

PULSE COMMUNICATION

Integrated voice and data communications for air traffic service applications p 600 A95-95090
Tactical low-level helicopter communications p 702 N95-32492

PULSE DOPPLER RADAR

Certification of windshear performance with RTCA class D radomes p 41 N95-13206

PULSE RADAR

Time-domain imaging of airborne targets using ultra-wideband or short-pulse radar [BTN-95-EIX95242673673] p 450 A95-82251
Impulse radiating antennas p 548 A95-90920
Solid state radar demonstration test results at the FAA Technical Center [AD-A281520] p 154 N95-16097

PULSEJET ENGINES

Pulsed jet ignition modeling with a full chemistry p 538 A95-87184

PUMP IMPELLERS

Impeller flow field characterization with a laser two-focus velocimeter p 313 N95-23440

PUMPS

An air-driven pressure booster pump for aircraft-based air sampling [HTN-95-40689] p 216 A95-69833

PURGING

Comparison of numerical results and multicavity purge and rim seal data with extensions to dynamics [NASA-TM-106685] p 416 N95-27434

PYLONS

Computer aided static aeroelastic analysis of wing/pylon/store combination p 499 A95-91531
Investigation of the influence of pylons and stores on the wing lower surface flow p 116 N95-17885
The aerodynamic design of an integrated wing lower surface and pylons for reduced drag [ARA-MEMO-406] p 194 N95-19789

PYROLYSIS

Propulsion research concerning SFRJ-motors [PB94-179520] p 14 N95-10083

Q

Q FACTORS

Measurements of shielding effectiveness and cavity characteristics of airplanes [PB94-210051] p 244 N95-20191

QATAR

Criteria of forecasting low level wind shear over Qatar p 663 A95-93493

QUADRATIC PROGRAMMING

Application of direct transcription to commercial aircraft trajectory optimization [BTN-95-EIX95242670766] p 359 A95-81081
Automation of reverse engineering process in aircraft modeling and related optimization problems [NASA-CR-197109] p 129 N95-16899

QUADRUPLES

Numerical study of sound generation due to a spinning vortex pair [BTN-95-EIX95182619075] p 307 A95-75760

QUALITY

Quality estimates and stretched meshes based on Delaunay triangulations [HTN-95-42575] p 564 A95-87205
The airline quality report, 1994 [NIAR-94-11] p 277 N95-24012

QUALITY CONTROL

A review of free-stream flow fluctuation and steady-state flow quality measurements in the AEDC/VKF Supersonic Tunnel A and Hypersonic Tunnel B [AIAA PAPER 95-6137] p 520 A95-90454

Lean manufacturing for lean times p 583 A95-94036

Earth Observing System (EOS)/Advanced Microwave Sounding Unit-A (AMSU-A) software assurance plan [NASA-CR-196059] p 98 N95-13885

Mesh quality control for multiply-refined tetrahedral grids [NASA-CR-197595] p 160 N95-18737

STEP: A future vision, today [NONP-NASA-VT-95-49121] p 452 N95-27209

The development of an engineering standard for composite repairs p 396 N95-27528

Conversion of the TRACON operations concepts database into a formal sentence outline job task taxonomy [DOT/FAA/AM-95/16] p 488 N95-28819

AGARD flight test techniques series. Volume 13: Reliability and maintainability [AGARD-AG-300-VOL-13] p 504 N95-29503

Quality assurance and risk management: Perspectives on Human Factors Certification of Advanced Aviation Systems p 690 N95-34771

QUANTITATIVE ANALYSIS

Simple method of supersonic flow visualization using watertable [BTN-95-EIX95182619105] p 269 A95-76590

Evaluation of neutron techniques for illicit substance detection [DE95-002988] p 300 N95-22764

QUANTUM MECHANICS

Broadband polarization-transfer experiments for rotating solids [GTN-95-0009261494012091-58] p 579 A95-92319

QUENCHING (ATOMIC PHYSICS)
A model for temperature-dependent collisional quenching of OH A(sup 2) Sigma(sup +) [HTN-95-42308] p 450 A95-85002

QUENCHING (COOLING)

Study of heat transfer rates during quenching of a hot tube under microgravity p 428 A95-82641

Experimental investigation of flow-boiling heat transfer under microgravity p 428 A95-82642

Low gravity quenching of hot tubes with cryogenes [ISBN 1-879921-01-4] p 635 A95-93728

QUEUING THEORY

Analysis and modeling of an airport departure process [AD-A293782] p 602 N95-31581

R

RABBITS

Advanced formation flight control [AD-A289271] p 409 N95-26981

RADAR

Impulse radiating antennas p 548 A95-90920
Scattering of short em-pulses by simple and complex targets using impulse radar p 486 A95-90953

RADAR ANTENNAS

Joint stars phased array radar antenna [BTN-95-EIX95042474626] p 209 A95-68280

HeliRadar: A rotating antenna synthetic aperture radar for helicopter allweather operations p 705 N95-33137

RADAR APPROACH CONTROL

Terminal area forecasts-fiscal years 1993-2010 [AD-A290835] p 490 N95-29880

Integrated terminal weather system (ITWS) demonstration and validation operational test and evaluation [AD-A293932] p 602 N95-31521

RADAR BEACONS

GPS-Squitter capacity analysis [AD-A280037] p 245 N95-20599

Recommendation on transition from primary/secondary radar to secondary-only radar capability [AD-A286279] p 249 N95-22005

GPS-Squitter interference analysis [AD-A293690] p 689 N95-33480

RADAR CORNER REFLECTORS

Depolarizing trihedral corner reflectors for radar navigation and remote sensing [BTN-95-EIX95302727634] p 636 A95-94108

RADAR CROSS SECTIONS

Electromagnetic backscattering from a helicopter rotor in the decametric wave band regime [BTN-94-EIX94381353130] p 243 A95-72648

Dynamic imaging and RCS measurements of aircraft [BTN-95-EIX95202637582] p 347 A95-78576

Analysis of backscattering from wing and fuselage joints [HTN-95-71134] p 430 A95-83495

Optimal shape design in hypersonic aerodynamics and electromagnetics p 639 A95-95397

An approach to aerodynamic characteristics of low radar cross-section fuselages p 106 N95-16251

Inband radar cross section of phased arrays with parallel feeds [AD-A284249] p 210 N95-19730

RADAR DATA

NEXRAD/ARSR operational comparison p 658 A95-93470

Dissemination of terminal weather products to the flight deck via data link p 669 A95-93525

Aviation value-added products and services from the NEXRAD Information Dissemination Service (NIDS) p 671 A95-93535

Statistics of multi-look AIRSAR imagery: A comparison of theory with measurements p 320 N95-23947

Classification of ultra high range resolution radar using decision boundary analysis [AD-A289378] p 437 N95-26877

Integration of AIRSAR and AVIRIS data for Trail Canyon alluvial fan, Death Valley, California p 709 N95-33760

RADAR DETECTION

Identification of aviation weather hazards based on the integration of radar and lightning data [HTN-95-51323] p 356 A95-80908

The detection and measurement of microburst wind shear by an airborne lidar system p 543 A95-87798

Status of the terminal Doppler weather radar with deployment underway p 653 A95-93450

The Integrated Terminal Weather System (ITWS) storm cell information and weather impacted airspace detection algorithm p 654 A95-93452

Improving aircraft impact assessment with the integrated terminal weather system microburst detection algorithm p 654 A95-93453

The ITWS microburst prediction algorithm p 655 A95-93456

A comparative performance study of TDWR/LLWAS 3 integration algorithms for wind shear detection p 658 A95-93468

Use of WSR-88D data in the FAA's weather impacted aerospace product p 658 A95-93469

Final results of the weather testing component of the Terminal Doppler Weather Radar operational test and evaluation p 658 A95-93471

Transport Canada proposed R&D program for the development of a multi-parameter dual X-Ka band Doppler radar for aviation meteorology applications p 659 A95-93477

The inference of aviation weather hazards based on the integration of radar and lightning data p 660 A95-93483

The use of radar wind profiles to remove TDWR gust front algorithm false alarms caused by vertical wind shear p 661 A95-93488

LLWAS 2 and LLWAS 3 performance evaluation p 662 A95-93491

Test results of a low cost airport weather radar p 662 A95-93492

Alaska's volcanic ash warning system p 663 A95-93495

Development of a climatology for possible microburst occurrence in Canada p 664 A95-93497

An echo motion algorithm for air traffic management using a national radar mosaic p 667 A95-93513

Developing thunderstorm forecast rules utilizing first detectable cloud radar-echoes p 667 A95-93514

Windshear detection: TDWR and LLWAS operational experience in Denver 1988-1992 p 670 A95-93528

Using ATMS weather products for air traffic strategic planning p 672 A95-93536

Airborne Windshear Detection and Warning Systems. Fifth and Final Combined Manufacturers' and Technologists' Conference, part 1 [NASA-CP-10139-PT-1] p 10 N95-10566

Vertical wind estimation from horizontal wind measurements p 26 N95-10567

Future enhancements to ground-based microburst detection p 11 N95-10570

Determining F-factor using ground-based Doppler radar. Validation and results p 11 N95-10571

Airborne Windshear Detection and Warning Systems. Fifth and Final Combined Manufacturers' and Technologists' Conference, part 2 [NASA-CP-10139-PT-2] p 41 N95-13203

Windshear certification data base for forward-look detection systems p 41 N95-13204

Certification methodology applied to the NASA experimental radar system p 41 N95-13205

Certification of windshear performance with RTCA class D radomes p 41 N95-13206

Airport surveillance using a solid state coherent lidar p 41 N95-13207

Ground-based wake vortex monitoring, prediction, and ATC interface p 42 N95-13209

- Aircraft wake RCS measurement p 59 N95-13210
Wake vortex detection at Denver Stapleton Airport with a pulsed 2-micron coherent lidar p 42 N95-13211
Doppler radar detection of vortex hazard indicators p 42 N95-13212
Remote sensing of turbulence in the clear atmosphere with 2-micron lidars p 59 N95-13213
Characterizing the wake vortex signature for an active line of sight remote sensor [NASA-CR-197697] p 333 N95-24391
Laser based obstacle warning sensors for helicopters p 686 N95-32499

RADAR ECHOES

- The Integrated Terminal Weather System (ITWS) storm cell information and weather impacted airspace detection algorithm p 654 A95-93452
Sensing thunderstorm microphysics with multiparameter radar: Application for aviation p 657 A95-93467
Automated aircraft routing through weather-impacted airspace p 666 A95-93512
An echo motion algorithm for air traffic management using a national radar mosaic p 667 A95-93513
Developing thunderstorm forecast rules utilizing first detectable cloud radar-echoes p 667 A95-93514

RADAR EQUIPMENT

- Offshore next generation weather radar (NEXRAD) test and evaluation master plan (TEMP) [AD-A291435] p 556 N95-30072
GPS-Squitter interference analysis [AD-A293690] p 689 N95-33480

RADAR FILTERS

- Terminal Doppler Weather Radar point target filter threshold selection p 662 A95-93490
Groundspeed filtering for CTAS [NASA-CR-197223] p 97 N95-15785

RADAR IMAGERY

- Dynamic imaging and RCS measurements of aircraft [BTN-95-EIX95202637582] p 347 A95-78576
Time-domain imaging of airborne targets using ultra-wideband or short-pulse radar [BTN-95-EIX95242673673] p 450 A95-82251
SAR image registration in absolute coordinates using GPS carrier phase position and velocity information [DE94-018738] p 228 N95-20195
Statistics of multi-look AIRSAR imagery: A comparison of theory with measurements p 320 N95-23947
AIRSAR deployment in Australia, September 1993: Management and objectives p 321 N95-23948
Apparatus and method for producing three-dimensional images [AD-D017455] p 646 N95-30727

RADAR MAPS

- Differential GPS and system integration of the Low Visibility Landing and Surface Operations (LVLASO) demonstration p 280 N95-23318
MAX-91: Polarimetric SAR results on Montespertoli site p 320 N95-23940

RADAR MEASUREMENT

- Dynamic imaging and RCS measurements of aircraft [BTN-95-EIX95202637582] p 347 A95-78576
Sensing thunderstorm microphysics with multiparameter radar: Application for aviation p 657 A95-93467
Preliminary results of high resolution measurements of snowfall at Stapleton International Airport during the winter of 1992-93 p 661 A95-93484
A short-term, high-resolution automated snowfall forecasting system p 666 A95-93510
Certification methodology applied to the NASA experimental radar system p 41 N95-13205
Aircraft wake RCS measurement p 59 N95-13210
Microburst vertical wind estimation from horizontal wind measurements [NASA-TP-3460] p 131 N95-18198

RADAR NAVIGATION

- Depolarizing trihedral corner reflectors for radar navigation and remote sensing [BTN-95-EIX95302727634] p 636 A95-94108
Recommendation on transition from primary/secondary radar to secondary-only radar capability [AD-A286279] p 249 N95-22005

RADAR NETWORKS

- Status of the terminal Doppler weather radar with deployment underway p 653 A95-93450
Use of WSR-88D data in the FAA's weather impacted aerospace product p 658 A95-93469
NEXRAD/ARSR operational comparison p 658 A95-93470
An echo motion algorithm for air traffic management using a national radar mosaic p 667 A95-93513

RADAR SCATTERING

- Hybrid finite element-modal analysis of jet engine inlet scattering [BTN-95-EIX95242673665] p 427 A95-82259
Inband radar cross section of phased arrays with parallel feeds [AD-A284249] p 210 N95-19730

RADAR SIGNATURES

- Aircraft wake RCS measurement p 59 N95-13210
Wake vortex detection at Denver Stapleton Airport with a pulsed 2-micron coherent lidar p 42 N95-13211
Characterizing the wake vortex signature for an active line of sight remote sensor [NASA-CR-197697] p 333 N95-24391

RADAR TARGETS

- Time-domain imaging of airborne targets using ultra-wideband or short-pulse radar [BTN-95-EIX95242673673] p 450 A95-82251
The Anglo-French Compact Laser Radar demonstrator programme p 703 N95-32501

RADAR TRACKING

- Joint stars phased array radar antenna [BTN-95-EIX95042474626] p 209 A95-68280
ITWS gridded analysis p 654 A95-93455
Final results of the weather testing component of the Terminal Doppler Weather Radar operational test and evaluation p 658 A95-93471
Orientation determination of aircraft using visual 3D matching and radar. Case study 2 [PB95-165791] p 350 N95-25749
Aspect estimation of an aircraft using library model silhouettes [PB95-141834] p 360 N95-25894
Classification of ultra high range resolution radar using decision boundary analysis [AD-A289378] p 437 N95-26877

RADAR TRANSMITTERS

- Solid state radar demonstration test results at the FAA Technical Center [AD-A281520] p 154 N95-16097

RADIAL FLOW

- Enhanced analysis and users manual for radial-inflow turbine conceptual design code RTD [NASA-CR-195454] p 275 N95-23462
A general theory of two- and three-dimensional rotational flow in subsonic and transonic turbomachines [NASA-CR-4496] p 377 N95-28003

RADIAL VELOCITY

- Investigation of outflow strength variability in Florida downburst-producing storms p 659 A95-93476

RADIANCE

- Water vapor continuum absorption in mid-latitudes: Aircraft measurements and model comparisons [HTN-95-40756] p 252 A95-71186
In-flight radiometric calibration of AVIRIS in 1994 p 705 N95-33754

RADIANT HEATING

- Science objectives and performance of a radiometer and window design for atmospheric entry experiments p 85 N95-13718
VUV shock layer radiation in an arc-jet wind tunnel experiment p 67 N95-13719

RADIATION EFFECTS

- Contribution of thermal radiation to the temperature profile of ceramic composite materials [BTN-94-EIX95011441252] p 417 A95-84209
Consistent approach to describing aircraft HIRF protection [NASA-CR-195067] p 334 N95-25341

RADIATION MEASUREMENT

- Radiant energy measurements from a scaled jet engine axisymmetric exhaust nozzle for a baseline code validation case [NASA-TM-106686] p 25 N95-11409

RADIATION MEASURING INSTRUMENTS

- A VHF/UHF antenna for the Precision Antenna Measurement System (PAMS) [AD-A285673] p 156 N95-16621

RADIATION PROTECTION

- Consistent approach to describing aircraft HIRF protection [NASA-CR-195067] p 334 N95-25341
Radiation safety aspects of commercial high-speed flight transportation [NASA-TP-3524] p 453 N95-26427

RADIATION SPECTRA

- Science objectives and performance of a radiometer and window design for atmospheric entry experiments p 85 N95-13718
High altitude hypersonic flowfield radiation [AD-A281386] p 106 N95-16160
Computation of high-altitude hypersonic flow-field radiation p 593 N95-30843

RADIATIVE HEAT TRANSFER

- Convective and radiative heat transfer analysis for the fire 2 forebody [BTN-95-EIX95182617460] p 268 A95-75731
Possible effects of CO2 increase on the high-speed civil transport impact on ozone [HTN-95-60779] p 317 A95-75976
An experimental study on radiation from strong shock layer p 368 A95-82421

- Science objectives and performance of a radiometer and window design for atmospheric entry experiments [NASA-TM-4637] p 63 N95-12190
CAE for thermal management of aerospace electronic boards using the BETAsoft program p 438 N95-27354

RADIATIVE TRANSFER

- Microwave and infrared simulations of an intense convective system and comparison with aircraft observations [HTN-95-60511] p 214 A95-68762
Microphysical and radiative properties of small cumulus clouds over the sea [HTN-95-A0526] p 255 A95-73180
On the link between cloud-top radiative properties and sub-cloud aerosol concentrations [HTN-95-A0527] p 255 A95-73181
Contribution of thermal radiation to the temperature profile of ceramic composite materials [BTN-94-EIX95011441252] p 417 A95-84209
Air truth validation of cloud albedo estimated from NOAA advanced very high resolution radiometer data [HTN-95-A1021] p 443 A95-84526

RADICALS

- The distribution of hydrogen, nitrogen, and chlorine radicals in the lower stratosphere: Implications for changes in O3 due to emission of NO(y) from supersonic aircraft [HTN-95-70935] p 351 A95-78000

RADIO ALTIMETERS

- Flight test evaluation of a 35 GHz forward looking altimeter for terrain avoidance [BTN-95-EIX95212641071] p 287 A95-76736
Precision orbit determination of altimetric satellites p 86 N95-14282
Application of GPS/SINS/RA integrated system to aircraft approach landing p 125 N95-16277
An integrated GPS/INS/BARO and radar altimeter system for aircraft precision approach landings [AD-A289280] p 383 N95-26985

RADIO ANTENNAS

- Space flight tests of attitude determination using GPS [BTN-95-EIX95112522529] p 190 A95-69334
Design considerations for an archimedean slot spiral antenna p 211 N95-19798

RADIO COMMUNICATION

- Integrated voice and data communications for air traffic service applications p 600 A95-95090
Modular CNI avionics system p 234 N95-20659
Tactical low-level helicopter communications p 702 N95-32492

RADIO CONTROL

- Operational and research aspects of a radio-controlled model flight test program [BTN-95-EIX0619952748177] p 606 A95-94471
Radio controlled for research [NASA-TM-104292] p 17 N95-10717

RADIO EMISSION

- Induced Compton scattering by relativistic electrons in magnetized astrophysical plasmas p 563 N95-29885

RADIO FREQUENCIES

- CASS: Design for supportability [BTN-95-EIX95172595296] p 287 A95-75716
Low frequency ultrasonic nondestructive inspection of aluminum/adhesive fuselage lap splices [DE94-014242] p 24 N95-11135
Hypersonic wind tunnel test techniques [AD-A284057] p 118 N95-18663
The impact of advanced packaging technology on modular avionics architectures p 233 N95-20632
High density monolithic packaging technology for digital/microwave avionics p 240 N95-20646
Tactical low-level helicopter communications p 702 N95-32492

RADIO FREQUENCY INTERFERENCE

- Evaluation of the radio frequency susceptibility of commercial GPS receivers [BTN-95-EIX95042474624] p 189 A95-68278

RADIO NAVIGATION

- GPS/GLONASS/INS test program [BTN-94-EIX94441386131] p 189 A95-68187
Integrated GPS/Glonass navigation: Algorithms and results [BTN-95-EIX95112522531] p 190 A95-69332
Analysis and simulation of narrowband GPS jamming using digital excision temporal filtering [AD-A289328] p 383 N95-26898
Wide Area Differential GPS (WADGPS) p 489 N95-29107

RADIO RECEIVERS

- Evaluation of the radio frequency susceptibility of commercial GPS receivers [BTN-95-EIX95042474624] p 189 A95-68278
Space flight tests of attitude determination using GPS [BTN-95-EIX95112522529] p 190 A95-69334

Flight evaluation of GPS/DGPS sensor systems installed in NAL Do228 [NAL-TR-1230] p 382 N95-26585
 Guidelines for the design of GPS and LORAN receiver controls and displays [AD-A293753] p 602 N95-31572
 Anechoic chamber upgrade [AD-A294375] p 700 N95-34342

RADIO SPECTRA
 Induced Compton scattering by relativistic electrons in magnetized astrophysical plasmas p 563 N95-29885

RADIOMETERS
 Data processing and mapping in airborne radiometric surveys [HTN-95-51587] p 442 A95-83591
 Airborne imaging radiometer scan simulation [BTN-95-EIX9532753018] p 638 A95-94793
 Science objectives and performance of a radiometer and window design for atmospheric entry experiments [NASA-TM-4637] p 63 N95-12190
 Planetary entry experiments [NASA-CR-194215] p 101 N95-13717
 Science objectives and performance of a radiometer and window design for atmospheric entry experiments p 85 N95-13718
 Nonlinear calibration of an infrared radiometer [AD-A292436] p 579 N95-28996
 Low-level data fusion for landing runways detection p 689 N95-33136

RADOMES
 Mobile domes for TACTIC telescope p 453 A95-86113
 Certification of windshear performance with RTCA class D radomes p 41 N95-13206

RAIL TRANSPORTATION
 Environmental noise monitoring - source identification [HTN-95-92537] p 558 A95-87357
 Navigational technology of dual usage p 688 N95-33131

RAIN
 Nonhydrostatic simulation of frontogenesis in a moist atmosphere. Part 3: Thermal wind imbalance and rainbands [HTN-95-90356] p 212 A95-66429
 Microwave and infrared simulations of an intense convective system and comparison with aircraft observations [HTN-95-60511] p 214 A95-68762
 High-resolution imaging of rain systems with the advanced microwave precipitation radiometer [HTN-95-70133] p 252 A95-70655
 Behavior of an inversion-based precipitation retrieval algorithm with high-resolution AMPR measurements including a low-frequency 10.7-GHz channel [HTN-95-70134] p 252 A95-70656
 Snow-band formation and evolution during the 15 November 1987 aircraft accident at Denver airport [HTN-95-80699] p 254 A95-72543
 The rain erosion of PEEK (polyetheretherketone) [CONGRESS PAPER C428-4-039] p 531 A95-91676
 Sensing thunderstorm microphysics with multiparameter radar: Application for aviation p 657 A95-93467
 Creating a global climatology of freezing rain using numerical model output p 673 A95-93541
 Heavy rain effects p 78 N95-14899

RAINDROPS
 Tracking of raindrops in flow over an airfoil [BTN-95-EIX95182619221] p 308 A95-76647
 Aircraft corrosion study [AD-A279527] p 241 N95-21687

RAM ACCELERATORS
 New end tube closure system for the ram accelerator [BTN-94-EIX94441380974] p 195 A95-68158
 Application of scramjet engine technology to the design of ram accelerator projectiles p 19 N95-10282
 Egin Air Force Base Ram Accelerator Research Facility p 19 N95-10284
 Proceeding towards hypervelocities in ram accelerators p 19 N95-10285
 Numerical simulation of ram accelerator performance including transient effects during initiation of combustion and sensitivity studies p 629 N95-31203
 Investigation of starting and ignition transients in the thermally choked ram accelerator p 698 N95-34805

RAMAN SPECTRA
 Planar air density measurements near model surfaces by ultraviolet Rayleigh/Raman scattering [BTN-94-EIX94441386614] p 213 A95-67345
 Measurement by coherent anti-Stokes Raman scattering in the R5Ch hypersonic wind tunnel [BTN-95-EIX95112523811] p 188 A95-69322
 Planar air density measurements near model surfaces by ultraviolet Rayleigh/Raman scattering [HTN-95-20950] p 546 A95-88989

RAMJET ENGINES
 Development of hypersonic engine seals: Flow effects of preload and engine pressures [BTN-95-EIX95112524204] p 196 A95-69304
 Experiment of rocket-ram annular combustor p 412 A95-82324
 Orbital transport: Technical, meteorological and chemical aspects; Aerospace Symposium, 3rd, Braunschweig, Germany, Aug. 26-28, 1991 [ISBN 3-540-563180] p 524 A95-87373
 Hypersonic technology experimental vehicles (The need for flight testing at hypersonic speed) p 490 A95-87378
 Influence of the flight trajectory on the exhaust gas composition of a H2-fueled air-breathing ramjet engine p 509 A95-87404
 Vortex generation and mixing in three-dimensional supersonic combustors [BTN-95-EIX0616952745783] p 614 A95-94503
 Hydrocarbon-fueled ramjet/scramjet technology program, phase 2 extension [NASA-CR-189659] p 15 N95-10319
 Hypersonic engine seal development at NASA Lewis Research Center p 60 N95-13602
 Combustion efficiency in a dual-inlet side-dump ramjet combustor [AD-A283564] p 83 N95-15329
 The 1993 JANNAF Propulsion Meeting, volume 1 [CPA-PUBL-602-VOL-1] p 148 N95-16312
 Thermal chemical energy of ablating silica surfaces in air breathing solid rocket engines p 148 N95-16316
 Free-jet testing at Mach 3.44 in GASL's aero/thermo test facility p 145 N95-16320
 Experimental and analytical methods for the determination of connected-pipe ramjet and ducted rocket internal performance [AGARD-AR-323] p 149 N95-17278
 Solid fuel ramjet composition [AD-D016458] p 152 N95-19090
 Integral rocket ramjets [AD-A285135] p 240 N95-20906
 Workshop report: Measurement techniques in highly transient, spectrally rich combustion environments [AD-A288395] p 350 N95-25606
 Transport phenomena and interfacial kinetics in multiphase combustion systems [AD-A288297] p 418 N95-26417
 Numerical simulation of combustion flow around a flame holder with hydrogen injection [NAL-TR-1233] p 419 N95-26523
 An investigation of the side-dump dual in-line ramjet combustor p 617 N95-31199
 A pulsed liquid fuel ramjet p 617 N95-31201
 Workshop report: Measurement techniques in highly transient, spectrally rich combustion environments p 629 N95-31208

RAMJET MISSILES
 Computation of supersonic air-intakes p 74 N95-14452

RAMPS (STRUCTURES)
 Safety in airport ground handling p 626 A95-95193

RANDOM ACCESS MEMORY
 Investigation and characterization of SEU effects and hardening strategies in avionics [AD-A291058] p 509 N95-29950

RANDOM ERRORS
 Functional dependence of trajectory dispersion on initial condition errors [BTN-95-EIX95152583263] p 298 A95-73564

RANDOM LOADS
 Stability of viscoelastic plate in supersonic flow under random loading [BTN-95-EIX95262694312] p 435 A95-85483

RANDOM NOISE
 New filtering method for linear weakly coupled stochastic systems [BTN-95-EIX0608952736485] p 678 A95-92708

RANGE (EXTREMES)
 A comparison of measured wind park load histories with the WISPER and WISPERX load spectra [DE95-000295] p 446 N95-27459

RANGEFINDING
 Passive range measurement system [AD-D016222] p 258 N95-21100
 Apparent size passive range method [AD-D017360] p 611 N95-31180

RARE GASES
 Ignition analysis of hydrogen/air mixture in supersonic mixing layer p 416 A95-82301

RAREFIED GAS DYNAMICS
 Cercignani-Lampis-Lord gas-surface interaction model: Comparisons between theory and simulation [BTN-95-EIX95041503806] p 242 A95-70131
 Flow resolution and domain influence in rarefied hypersonic blunt-body flows [BTN-95-EIX95082502729] p 220 A95-70136

Hypersonic rarefied flow past spheres including wake structure [BTN-95-EIX95152583250] p 305 A95-73551
 Verification of engineering methods of aerodynamics for reentry vehicles by DSMC p 525 A95-87386
 Ultraviolet emissions occurring about hypersonic vehicles in rarefied flows [AD-A281452] p 106 N95-16076
 Particle kinetic simulation of high altitude hypervelocity flight [NASA-CR-197383] p 309 N95-22481
 DSMC calculations for 70-deg blunted cone at 3.2 km/s in nitrogen [NASA-TM-109181] p 348 N95-24396
 A study of fluid problems requiring a direct particle simulation [AD-A290212] p 567 N95-29074
 An extension of the continuum model by Grad's thirteen moment equations for hypersonic rarefied flows p 478 N95-29118
 Orbiter rarefied-flow reentry measurements from the OARE on STS-62 [NASA-TM-110182] p 646 N95-30783

RAREFIED GASES
 Rarefied gas numerical wind tunnel: OREX and HOPE p 427 A95-82391
 A perspective of rarefied gas flow problems relevant to high altitude flight [SAE PAPER 931366] p 586 A95-93647
 Rarefied gas effects on aerobraking/reentry vehicles with wakes [NASA-CR-196586] p 415 N95-27093

RATES (PER TIME)
 Vertical transport rates in the stratosphere in 1993 from observations of CO2, N2O, and CH4 [HTN-95-70941] p 351 A95-78006

RATINGS
 Pilot rating scale for aircraft handling qualities [HTN-95-42269] p 380 A95-84963
 Possible guidelines for helicopter noise assessment [HTN-95-92535] p 558 A95-87355
 The airline quality report, 1994 [NIAR-94-11] p 277 N95-24012
 The relation of handling qualities ratings to aircraft safety p 597 N95-31067

RATIOS
 Supersonic axisymmetric conical flow solutions for different ratios of specific heats [BTN-95-EIX95152583283] p 306 A95-73584

RATS
 Simulation of Shuttle launch G forces and acoustic loads using the NASA Ames Research Center 20G centrifuge p 86 N95-14089

RAY TRACING
 Geodesic constant method: A novel approach to analytical surface-ray tracing on convex conducting bodies [BTN-95-EIX95302731054] p 637 A95-94205

RAYLEIGH EQUATIONS
 Mach wave emission from a high-temperature supersonic jet [HTN-95-42571] p 458 A95-87201

RAYLEIGH NUMBER
 Natural convection in central microcavities of vertical, finned enclosures of very high aspect ratios [BTN-95-EIX95282711336] p 632 A95-92405

RAYLEIGH SCATTERING
 Planar air density measurements near model surfaces by ultraviolet Rayleigh/Raman scattering [BTN-94-EIX94441386614] p 213 A95-67345
 Surface interference in Rayleigh scattering measurements near forebodies [HTN-95-51670] p 433 A95-85052
 Planar air density measurements near model surfaces by ultraviolet Rayleigh/Raman scattering [HTN-95-20950] p 546 A95-88989
 Planar Rayleigh scattering and laser-induced fluorescence for visualization of a hot, Mach 2 annular air jet [NASA-TM-4576] p 54 N95-13196
 Developments in laser-based diagnostics for wind tunnels in the Aeromechanics Division: 1987-1992 [AD-A283011] p 84 N95-13687

RAYLEIGH-BENARD CONVECTION
 Marangoni-Benard convection in a low-aspect-ratio liquid layer p 56 A95-61544

RDX
 Gas chromatography/ion mobility spectrometry as a hyphenated technique for improved explosives detection and analysis p 701 N95-33278

REACTING FLOW
 Modeling of supersonic turbulent combustion using assumed probability density functions [BTN-95-EIX95112524190] p 206 A95-69318
 An experimental study on radiation from strong shock layer p 368 A95-82421

- Numerical modeling and simulation of chemically reacting reentry flows p 525 A95-87387
 Computational methods in applied sciences; European Computational Fluid Dynamics Conference, 1st, Brussels, Belgium, Sept. 7-11, 1992
 [ISBN 0-444-89795-X] p 539 A95-87552
 Numerical simulation of three-dimensional hypersonic reacting flows over blunt bodies with catalytic surface [HTN-95-61184] p 539 A95-87557
 High-speed reacting flow simulation using USA-series codes p 540 A95-87559
 Multidimensional calculation of spark flame initiation by adopting a generic hydrocarbon kinetic scheme p 528 A95-87566
 Chemical recombination in an expansion tube [HTN-95-20844] p 544 A95-88105
 Chemically reacting non-equilibrium boundary layers in air breathing propulsion systems [AIAA PAPER 95-6139] p 512 A95-90456
 Theories of turbulent combustion in high speed flows [AD-A280933] p 23 N95-10535
 Development of an upwind, finite-volume code with finite-rate chemistry [NASA-CR-196749] p 9 N95-11366
 Numerical mixing calculations of confined reacting jet flows in a cylindrical duct [NASA-TM-106736] p 139 N95-18133
 Computation of vortex breakdown p 165 N95-19462
 Bibliography of Doctor Chul Park [NASA-TM-110353] p 527 N95-29351
 Computation of the integrated aerodynamic and propulsive flowfields of a generic hypersonic space plane p 481 N95-29788
 Spatially-resolved velocity measurements in steady, high-speed, reacting flows using laser-induced OH fluorescence p 650 N95-32109
- REACTION KINETICS**
 Aircraft engine emission reduction [BTN-95-EIX95031502750] p 196 A95-68257
 Influence of the flight trajectory on the exhaust gas composition of a H2-fueled air-breathing ramjet engine p 509 A95-87404
 Multidimensional calculation of spark flame initiation by adopting a generic hydrocarbon kinetic scheme p 528 A95-87566
 Numerical study of contaminant effects on combustion of hydrogen, ethane, and methane in air [AIAA PAPER 95-6097] p 510 A95-88005
 Sensitivity of combustion-acoustic instabilities to boundary conditions for premixed gas turbine combustors [NASA-TM-106890] p 289 N95-23550
 Transport phenomena and interfacial kinetics in multiphase combustion systems [AD-A288297] p 418 N95-26417
 The 25th International Symposium on Combustion [AD-A286825] p 630 N95-31268
 Combustion-acoustic stability analysis for premixed gas turbine combustors [NASA-TM-107024] p 694 N95-32931
- REACTION TIME**
 Reaction-time response of aircraft crash [BTN-95-EIX95292721296] p 595 A95-92626
- REACTIVITY**
 Laboratory evaluation of a reactive baffle approach to NOx control [AD-A283802] p 255 N95-19921
- REACTOR DESIGN**
 Ageing nuclear power plant management: An aeronautical viewpoint [NAL-PD-SN-9306] p 105 N95-18606
- REACTOR SAFETY**
 Reaction-time response of aircraft crash [BTN-95-EIX95292721296] p 595 A95-92626
 Ageing nuclear power plant management: An aeronautical viewpoint [NAL-PD-SN-9306] p 105 N95-18606
- READING**
 Evaluation of the Haworth-Newman avionics Display Readability Scale [AD-A286127] p 235 N95-22232
- REAL GASES**
 Hypersonic model testing in a shock tunnel [BTN-95-EIX95222650789] p 329 A95-79245
 Numerical simulation of real gas effects and aerodynamic heating of hypersonic space transportation vehicles p 540 A95-87558
 Computer code for determination of thermally perfect gas properties [NASA-TP-3447] p 37 N95-11995
 Numerical simulation of high enthalpy shock tunnel p 700 N95-34514

REAL TIME OPERATION

- High-order state space simulation models of helicopter flight mechanics [HTN-95-A0494] p 237 A95-72565
 Pilot Weather Advisor system [BTN-95-EIX95152582314] p 316 A95-73517
 Real-time navigation using the global positioning system [BTN-95-EIX95172595298] p 279 A95-75714
 Estimates of total organic and inorganic chlorine in the lower stratosphere from in situ and flask measurements during AASE 2 [HTN-95-A0861] p 317 A95-76265
 Real-time estimation of atmospheric turbulence severity from in-situ aircraft measurements [BTN-95-EIX95182619231] p 319 A95-76657
 Real-time decision aiding: Aircraft guidance for wind shear avoidance [BTN-95-EIX95202637575] p 332 A95-78583
 The real-time analysis and prediction of storms program p 655 A95-93457
 Preliminary results of high resolution measurements of snowfall at Stapleton International Airport during the winter of 1992-93 p 661 A95-93484
 Role of the aviation weather system in providing a real-time ATC volcanic ash advisory system p 663 A95-93494
 Formal design and verification of a reliable computing platform for real-time control (phase 3 results) [NASA-TM-109140] p 33 N95-10873
 The 4-D approach to visual control of autonomous systems [AIAA PAPER 94-1243-CP] p 27 N95-11513
 Computing quantitative characteristics of finite-state real-time systems [AD-A282839] p 83 N95-14343
 Airplane takeoff and landing performance monitoring system [NASA-CASE-LAR-14745-2-SB] p 85 N95-14415
 A graphical user interface for design and analysis of air breathing propulsion systems [TABES PAPER 94-616] p 83 N95-14645
 Automated test environment for a real-time control system [TABES PAPER 94-631] p 99 N95-14652
 Sensor fault detection and diagnosis simulation of a helicopter engine in an intelligent control framework [AD-A290223] p 137 N95-15970
 PalymSys (TM): An extended version of CLIPS for construction and reasoning using blackboards p 217 N95-19767
 The impact of advanced packaging technology on modular avionics architectures p 233 N95-20632
 A real-time algorithm for integrating differential satellite and inertial navigation information during helicopter approach [NASA-CR-197409] p 229 N95-21891
 Real-time testing and demonstration of the US Army Corps of Engineers' Real-Time On-The-Fly positioning system [AD-A288624] p 334 N95-25609
 Design and synthesis of a real-time controller for an unmanned air vehicle [AD-A289134] p 408 N95-26555
 A study of workstation computational performance for real-time flight simulation [NASA-TM-109184] p 449 N95-27241
 Geophex airborne unmanned survey system [DE95-007566] p 392 N95-27440
 Design of a real-time wind turbine simulator using a custom parallel architecture p 449 N95-27979
 Control system design for the MOD-5A 7.3 mW wind turbine generator p 440 N95-27985
 Transport delays associated with NASA Langley Flight Simulation Facility [NASA-TM-110150] p 568 N95-29454
 Manual for a workstation-based generic flight simulation program (LaRCsim), version 1.4 [NASA-TM-110164] p 518 N95-30327
 Developing a workstation-based, real-time simulation for rapid handling qualities evaluations during design [NASA-CR-198831] p 505 N95-30335
 Foundations of technology for constructing highly reliable distributed realtime systems [AD-A293254] p 678 N95-30892
 New adaptive methods for reconfigurable flight control systems, appendix 1 [AD-A292711] p 619 N95-30937
 A highly reliable, high performance open avionics architecture for real time Nap-of-the-Earth operations p 693 N95-32497
 The application of Ada and formal methods to a safety critical engine control system p 710 N95-33142

REATTACHED FLOW

- Reattachment studies of an oscillating airfoil dynamic stall flowfield [HTN-95-51660] p 432 A95-85042
 Kinetic heating in hypersonic flight [CONGRESS PAPER C428-3-056] p 475 A95-91674
- RECEIVERS**
 Attitude determination using dedicated and nondedicated multi-antenna GPS sensors [BTN-95-EIX95142555482] p 228 A95-72891
 Modeling and analysis for the GPS pseudo-range observable [BTN-95-EIX95302731227] p 600 A95-94046
 Assessment of a non-dedicated GPS receiver system for precise airborne attitude determination [DE94-019309] p 229 N95-21520
- RECIPROCATION**
 Dynamic behavior of valves with pneumatic chamber for reciprocating compressors [BTN-94-EIX94351143311] p 207 A95-65845
 Linear Motor Free Piston Compressor [AD-A293452] p 647 N95-31374
- RECIRCULATIVE FLUID FLOW**
 Application of Direct and Large Eddy Simulation to Transition and Turbulence [AGARD-CP-551] p 248 N95-21061
- RECOMBINATION REACTIONS**
 Chemical recombination in an expansion tube [HTN-95-20844] p 544 A95-88105
- RECOMMENDATIONS**
 Aviation Accident Investigation Symposium, Volume 1: Industry recommendations and Safety Board responses [PB94-917005] p 278 N95-24105
 High-stakes aviation: US-Japan technology linkages in transport aircraft [LC-94-65759] p 381 N95-27907
 Report to Congressional Committees, Comanche Helicopter: Testing needs to be completed prior to production decisions [GAO/NSIAD-95-112] p 397 N95-27910
- RECONNAISSANCE AIRCRAFT**
 Conceptual design of the AE481 Demon Remotely Piloted Vehicle (RPV) [NASA-CR-197164] p 44 N95-12294
 A preliminary design proposal for a maritime patrol strike aircraft: MPS-2000 Condor [NASA-CR-197182] p 477 N95-12689
 Spread spectrum applications in unmanned aerial vehicles [AD-A281035] p 156 N95-16448
 Unmanned aerial vehicles [AD-A286190] p 231 N95-20329
 Passive range measurement system [AD-D016222] p 258 N95-21100
 Unmanned aerial vehicles, 1994 master plan p 607 N95-31416
 Report to the Chairman, Legislation and National Security Subcommittee, Committee on Government Operations, House of Representatives. Unmanned aerial vehicles: Performance of short-range system still in question [GAO/NSIAD-94-65] p 609 N95-32196
- RECONSTRUCTION**
 Holographic interferometric tomography for reconstructing flow fields p 310 N95-23287
- RECOVERABLE LAUNCH VEHICLES**
 Program test objectives milestone 3 --- Integrated Propulsion Technology Demonstrator [NASA-CR-197030] p 127 N95-15971
- RECOVERY**
 Design of head-up display symbology for recovery from unusual attitudes p 611 A95-95044
- RECTANGULAR PLANFORMS**
 A fourth order Euler/Navier-Stokes prediction method for the aerodynamics and aeroelasticity of hovering rotor blades p 554 N95-29242
- RECTANGULAR PLATES**
 Accurate interlaminar stress recovery from finite element analysis [NASA-TM-109149] p 57 N95-11815
 Acoustic radiation damping of flat rectangular plates subjected to subsonic flows p 172 N95-18542
- RECTANGULAR WIND TUNNELS**
 Corner vortex suppressor [AD-D016423] p 116 N95-18337
- RECTANGULAR WINGS**
 Aerodynamic effects of delta planform tip sails on wing performance [BTN-95-EIX95062487544] p 185 A95-68358
 Aerodynamics of a finite wing with simulated ice [BTN-95-EIX95182619227] p 270 A95-76653
 Steady and unsteady three-dimensional transonic flow computations by integral equation method [NASA-CR-196777] p 10 N95-11582
 Navier-Stokes solution of wing wake structure and its perturbation p 479 N95-29121

REDUNDANCY

- A new guidance and flight control system for the DELTA 2 launch vehicle — Abstract only p 342 A95-80427
 An analysis of the impact of ASPA on organizational and depot level maintenance [AD-A292670] p 457 N95-29414

REDUNDANT COMPONENTS

- Influence of backup bearings and support structure dynamics on the behavior of rotors with active supports [NASA-CR-199080] p 703 N95-32689
 Steady-state dynamic behavior of an auxiliary bearing supported rotor system p 703 N95-32690
 Dynamic behavior of a magnetic bearing supported jet engine rotor with auxiliary bearings p 703 N95-32691
 Dynamic modelling and response characteristics of a magnetic bearing rotor system with auxiliary bearings p 703 N95-32692
 Synchronous dynamics of a coupled shaft/bearing/housing system with auxiliary support from a clearance bearing: Analysis and experiment p 703 N95-32693

REENTRY EFFECTS

- An experimental study on radiation from strong shock layer p 368 A95-82421
 Science objectives and performance of a radiometer and window design for atmospheric entry experiments p 85 N95-13718
 VUV shock layer radiation in an arc-jet wind tunnel experiment p 67 N95-13719

REENTRY GUIDANCE

- A guidance concept for hypersonic aerospacecrafts p 526 A95-91549
 Reentry guidance for hypersonic Flight Experiment (HYFLEX) vehicle [NAL-TR-1235] p 334 N95-25764

REENTRY PHYSICS

- Orbital transport: Technical, meteorological and chemical aspects; Aerospace Symposium, 3rd, Braunschweig, Germany, Aug. 26-28, 1991 [ISBN 3-540-563180] p 524 A95-87373
 The aerothermodynamic validation reentry experiment HYPERBA p 524 A95-87380
 Numerical modeling and simulation of chemically reacting reentry flows p 525 A95-87387
 Reentry trajectories and their optimization by an evolution algorithm p 525 A95-87394

REENTRY RANGE

- Reentry analysis for low Earth orbiting spacecraft p 415 A95-85774

REENTRY SHIELDING

- Trajectory-based heating analysis for the European Space Agency/Rosetta Earth Return Vehicle [BTN-95-EIX95041503787] p 205 A95-69218
 Reentry technology experiment on the first mission of reentry capsule 'EXPRESS' p 414 A95-82499
 Thermoacoustic environments to simulate reentry conditions p 86 N95-14096

REENTRY TRAJECTORIES

- Multiblock analysis for Shuttle Orbiter reentry heating from Mach 24 to Mach 12 [BTN-95-EIX95041503780] p 205 A95-69211
 Shuttle entry guidance revisited using nonlinear geometric methods [BTN-95-EIX95182619144] p 299 A95-76621
 The aerothermodynamic validation reentry experiment HYPERBA p 524 A95-87380
 Reentry trajectories and their optimization by an evolution algorithm p 525 A95-87394

REENTRY VEHICLES

- Trajectory-based heating analysis for the European Space Agency/Rosetta Earth Return Vehicle [BTN-95-EIX95041503787] p 205 A95-69218
 Functional dependence of trajectory dispersion on initial condition errors [BTN-95-EIX95152583263] p 298 A95-73564
 Hypersonic model testing in a shock tunnel [BTN-95-EIX95222650789] p 329 A95-79245
 VSL analysis of hypersonic flows around a reentry vehicle with equilibrium air chemistry p 413 A95-82400
 Reentry technology experiment on the first mission of reentry capsule 'EXPRESS' p 414 A95-82499
 Verification of engineering methods of aerodynamics for reentry vehicles by DSMC p 525 A95-87386
 Numerical modeling and simulation of chemically reacting reentry flows p 525 A95-87387
 Reentry trajectories and their optimization by an evolution algorithm p 525 A95-87394
 Application of integral methods to ablation charring erosion, a review [BTN-95-EIX95302694460] p 636 A95-94057
 Moving mass trim control for aerospace vehicles [DE95-002602] p 299 N95-23532

- Transonic, supersonic and hypersonic wind-tunnel tests on aerodynamic characteristics of reentry body with blunted cone configuration [ISAS-658] p 480 N95-29640
 Experimental studies on boundary-layer transition on a reentry vehicle at transonic and supersonic speeds [ISAS-659] p 555 N95-29712
 Numerical simulation of high enthalpy shock tunnel p 700 N95-34514

REFERENCE ATMOSPHERES

- Using IRI for the computation of ionospheric corrections for altimeter data analysis p 212 A95-66949

REFLECTANCE

- Possible near-IR channels for remote sensing precipitable water vapor from geostationary satellite platforms [HTN-95-70139] p 214 A95-69431
 Preliminary results of high resolution measurements of snowfall at Stapleton International Airport during the winter of 1992-93 p 661 A95-93484
 A short-term, high-resolution automated snowfall forecasting system p 666 A95-93510
 Developing thunderstorm forecast rules utilizing first detectable cloud radar-echoes p 667 A95-93514

REFLECTING TELESCOPES

- Stratospheric Observatory For Infrared Astronomy (SOFIA), Phase A: System concept description [NASA-TM-110669] p 680 N95-32187

REFLECTORS

- Depolarizing trihedral corner reflectors for radar navigation and remote sensing [BTN-95-EIX95302727834] p 636 A95-94108

REFRACTION

- An extension of the Lighthill theory of jet noise to encompass refraction and shielding [NASA-TM-110163] p 580 N95-29452

REFRACTORY MATERIALS

- Compliant interlayer [BTN-95-EIX95142562401] p 304 A95-73439
 Application of integral methods to ablation charring erosion, a review [BTN-95-EIX95302694460] p 636 A95-94057
 Test model designs for advanced refractory ceramic materials p 55 N95-11968
 Thermally stable organic polymers [AD-A281380] p 87 N95-14363
 Static and dynamic friction behavior of candidate high temperature airframe seal materials [NASA-TM-106571] p 152 N95-16905
 Innovative processing of composites for ultra-high temperature applications, book 1 [AD-A290889] p 537 N95-29842
 The mm-wave resonant methods for the detection of corrosion, phase 1 [AD-A291315] p 556 N95-29941
 NASA Lewis Research Center's preheated combustor and materials test facility [NASA-TM-106676] p 626 N95-30592

REFRIGERANTS

- Alternatives to ozone depleting refrigerants in test equipment p 630 N95-31767

REFRIGERATING

- Reducing process noise in superconducting helium liquid level probes [DE95-008956] p 629 N95-30765

REFRIGERATORS

- Reducing process noise in superconducting helium liquid level probes [DE95-008956] p 629 N95-30765

REGENERATIVE COOLING

- Regenerative cooling for liquid propellant rocket thrust chambers [INPE-5565-TDI/540] p 150 N95-18720
 Effect of film cooling/regenerative cooling on scramjet engine performances [NAL-TR-1242] p 339 N95-24990

REGENERATIVE FUEL CELLS

- Unitized Regenerative Fuel Cells for solar rechargeable aircraft and zero emission vehicles [DE95-010684] p 708 N95-33642

REGENERATORS

- Oscillating-flow regenerator test rig [NASA-CR-196982] p 53 N95-13200

REGIONAL PLANNING

- Aircraft noise zoning in Norway p 581 A95-88476
 Aircraft noise at a West Coast airport in the next century p 560 A95-90095

REGRESSION ANALYSIS

- Subharmonic and quasi-periodic motions of an eccentric squeeze film damper-mounted rigid rotor [BTN-94-EIX95011440601] p 429 A95-82982
 Selecting optimal experiments for feedforward multilayer perceptrons [AD-A290856] p 678 N95-30406

- Modeling F/A-18 flight hour program costs using regression analysis [AD-A293771] p 608 N95-31579

REGULATIONS

- Euro-noise '92, London, UK, Sept. 14-18, 1992. Bks. 1-3 [ISBN 1-873082-39-8] p 558 A95-87354
 Aircraft noise zoning in Norway p 581 A95-88476
 A review of Air Force policy and noise models pertaining to the noise environment under low-altitude, high-speed training areas p 561 A95-90118
 Operational aviation weather regulations p 652 A95-93446
 Civil aircraft performance - developments for improved safety [CONGRESS PAPER C428-25-175] p 596 A95-93601

- Fatigue evaluation of empennage, forward wing, and winglets/tip fins on part 23 airplanes [PB94-196813] p 79 N95-13981

- Application of GPS/SINS/RA integrated system to aircraft approach landing p 125 N95-16277
 Evaluation of the dynamic stability characteristics of the NAL Light Transport Aircraft

- [NAL-PD-CA-9217] p 142 N95-16392
 Federal aviation regulations, part 91. General operating and flight rules. Change 5 [PB94-194883] p 123 N95-17476

- Safety study: Commuter airline safety [PB94-917004] p 124 N95-19132

- Federal aviation regulations, part 91. General operating and flight rules. Change 8 [PB94-217445] p 188 N95-19720

- Environmental Compliance Assessment and Management Program [AD-A279605] p 255 N95-20441

- Environmentally regulated aerospace coatings p 631 N95-31775

REINFORCED SHELLS

- Launcher wing-leading-edge design [BTN-95-EIX95042477110] p 192 A95-68349
 Load transfer in the stiffener-to-skin joints of a pressurized fuselage [NASA-CR-198610] p 439 N95-27865

REINFORCEMENT (STRUCTURES)

- Prediction of energy absorption capability of composite stiffeners [HTN-95-A0500] p 230 A95-72571
 Development and flight results of fiber reinforced balloon p 384 A95-82511
 Design and evaluation of a foam-filled hat-stiffened panel concept for aircraft primary structural applications [NASA-TM-109175] p 346 N95-26251
 Recent progress in NASA Langley textile reinforced composites program p 425 N95-28475

REINFORCING FIBERS

- Compliant interlayer [BTN-95-EIX95142562401] p 304 A95-73439
 Development and flight results of fiber reinforced balloon p 384 A95-82511

- Ceramic composite attachments for transmission of high-torque loads [BTN-94-EIX95011441256] p 417 A95-84213

- The rain erosion of PEEK (polyetheretherketone) [CONGRESS PAPER C428-4-039] p 531 A95-91676

- Modeling and life prediction methodology for Titanium Matrix Composites subjected to mission profiles [NASA-TM-109148] p 55 N95-11915

- Composite repair of metallic airframe: Twenty years of experience p 393 N95-27508

- Application of advanced material systems to composite frame elements p 422 N95-28432

- Comparison of resin film infusion, resin transfer molding, and consolidation of textile preforms for primary aircraft structure p 425 N95-28477

- Fundamental concepts in the suppression of delamination buckling by stitching p 426 N95-28486
 The effect of interface properties on nickel base alloy composites [NASA-CR-198363] p 629 N95-30787

REINFORCING MATERIALS

- Recent progress in NASA Langley textile reinforced composites program p 425 N95-28475

RELATIVISTIC PARTICLES

- Induced Compton scattering by relativistic electrons in magnetized astrophysical plasmas p 563 N95-29885

RELAXATION METHOD (MATHEMATICS)

- A comparison of three-dimensional nonequilibrium solution algorithms applied to hypersonic flows with stiff chemical source terms [AIAA PAPER 93-2861] p 4 A95-60186

RELIABILITY

- Introduction of the GPS to civil aviation field p 487 A95-91536

The development of a highly reliable power management and distribution system for civil transport aircraft
[NASA-TM-106697] p 50 N95-11867

Fatigue reliability method with in-service inspections
p 94 N95-14475

Problems with aging wiring in Naval aircraft
p 154 N95-16048

Optimization of adaptive intraply hybrid fiber composites with reliability considerations
[NASA-TM-106632] p 157 N95-16911

Standard Hardware Acquisition and Reliability Program (SHARP) advanced SEM-E packaging
p 233 N95-20633

Reliability assessment of Multichip Module technologies via the Triservice/NASA RELTECH program
p 245 N95-20643

Assuring Known Good Die (KGD) for reliable, cost effective MCMs
p 246 N95-20644

Prototype stop bar system evaluation at Seattle-Tacoma International Airport
[AD-A290136] p 490 N95-30031

RELIABILITY ANALYSIS

Aircraft safety evaluation
[BTN-94-EIX94511309382] p 103 A95-64608

USAF aging aircraft program
[BTN-95-EIX95072498878] p 180 A95-68394

Impact of near-coincident faults on digital flight control systems
[BTN-95-EIX95242670759] p 359 A95-81088

Integrated performance and reliability specification for digital avionics systems
[AIAA PAPER 95-0953] p 506 A95-90632

Dependability issues in the reuse of standard components in open architectures
[AIAA PAPER 95-1006] p 566 A95-90678

The avionics integrity programme (AVIP)
[CONGRESS PAPER C428-6-115] p 549 A95-91684

Evolving standards for safety critical software
[CONGRESS PAPER C428-24-142] p 678 A95-93595

Dependable software - the state of the art
[CONGRESS PAPER C428-24-212] p 678 A95-93596

The computer analysis of the prediction of aircraft electrical power supply system reliability
p 155 N95-16278

Residual life and strength estimates of aircraft structural components with MSD/MED
p 136 N95-19485

The 1994 updated National Airspace System performance assessment for year 2005
[AD-A288652] p 380 N95-26485

Reliability analysis of composite structures
p 423 N95-28441

Proceedings of the 12th Annual National Conference on Ada Technology
[AD-A290693] p 569 N95-29644

A PC program for estimating measurement uncertainty for aeronautics test instrumentation
[NASA-CR-198361] p 523 N95-30067

Probabilistic reliability modeling of fatigue on the H-46 tie bar
[AD-A289926] p 607 N95-30927

A NASPAC-Based analysis of the delay and cost effects of the western-pacific region preliminary resectorization effort of 1993
[AD-A288696] p 601 N95-31013

Intelligent finite element submodeling of multichip modules for reliability analysis
[AD-A292911] p 679 N95-31455

RELIABILITY ENGINEERING

Electrical power system upgrade methodology for in-service aircraft
[SAE PAPER 932562] p 511 A95-90059

Illustrated structural application of universal first-order reliability method
[NASA-TP-3501] p 54 N95-11870

The principles of flight test assessment of flight-safety-critical systems in helicopters
[AGARD-AG-300-VOL-12] p 77 N95-14199

The computer analysis of the prediction of aircraft electrical power supply system reliability
p 155 N95-16278

Reliability analysis of composite structures
p 423 N95-28441

Probabilistic design of advanced composite structure
p 424 N95-28443

Proof test methodology for composites
p 424 N95-28445

RELIEF MAPS

Naval Aviation System TEAM mapping, charting, and geodesy handbook
[AD-A288590] p 446 N95-26841

Flight test of a low-altitude helicopter guidance system with obstacle avoidance capability
p 688 N95-32490

RELUCTANCE

A detailed power inverter design for a 250 kW switched reluctance aircraft engine starter/generator
[SAE PAPER 931388] p 613 A95-93664

Detailed design of a 250-kW switched reluctance starter/generator for an aircraft engine
[SAE PAPER 931389] p 613 A95-93665

REMOTE CONTROL

Cypher moves toward autonomous flight
[HTN-95-41394] p 283 A95-76390

On the UF-104 system
p 507 A95-91559

Interfacing a digital compass to a remote-controlled helicopter
[PB95-164927] p 340 N95-24260

Geophex airborne unmanned survey system
[DE95-007566] p 392 N95-27440

REMOTE SENSING

Possible near-IR channels for remote sensing precipitable water vapor from geostationary satellite platforms
[HTN-95-70139] p 214 A95-69431

High-resolution imaging of rain systems with the advanced microwave precipitation radiometer
[HTN-95-70133] p 252 A95-70655

Laser device for measuring a vessel's speed
[HTN-95-60992] p 361 A95-80633

Modeling of aircraft exhaust emissions and infrared spectra for remote measurement of nitrogen oxides
[HTN-95-51276] p 355 A95-80861

Mapping of forest fire damages using imaging spectroscopy
p 442 A95-83627

Cuts endanger airborne research --- NASA Ames Research Center Reorganization
[HTN-95-20602] p 443 A95-84783

The real-time analysis and prediction of storms program
p 655 A95-93457

Depolarizing trihedral corner reflectors for radar navigation and remote sensing
[BTN-95-EIX95302727634] p 636 A95-94108

Remote sensing of turbulence in the clear atmosphere with 2-micron lidars
p 59 N95-13213

An Echelle Grating Spectrometer (EGS) for mid-IR remote chemical detection
[DE94-019310] p 249 N95-21478

Overview of remote sensing laser development and semiconductor laser technology
[DE94-019103] p 256 N95-21552

AVIRIS and TIMS data processing and distribution at the land processes distributed active archive center
p 325 N95-23872

AIRSAR deployment in Australia, September 1993: Management and objectives
p 321 N95-23948

Preliminary analysis of University of North Dakota aircraft data from the FIRE Cirrus IFO-2
[NASA-CR-199038] p 357 N95-24219

Turbine-engine applications of thermographic-phosphor temperature measurements
[DE95-003625] p 358 N95-25110

Emerging applications in probability (Sensor management)
[AD-A292781] p 601 N95-31433

Laser based obstacle warning sensors for helicopters
p 686 N95-32499

Airborne passive polarimetric measurements of sea surface anisotropy at 92 GHz
[NASA-CR-197288] p 707 N95-32823

Low-level data fusion for landing runways detection
p 689 N95-33136

Correction of thin cirrus effects in AVIRIS images using the sensitive 1.375-micron cirrus detecting channel
p 708 N95-33748

Remote sensing of smoke, clouds, and radiation using AVIRIS during SCAR experiments
p 708 N95-33749

Integration of AIRSAR and AVIRIS data for Trail Canyon alluvial fan, Death Valley, California
p 709 N95-33760

Advanced data visualization and sensor fusion: Conversion of techniques from medical imaging to Earth science
p 711 N95-34236

REMOTE SENSORS

Attitude determination using dedicated and nondedicated multiantenna GPS sensors
[BTN-95-EIX95142555482] p 228 A95-72891

An integrated system to improve aviation weather forecasts for the Alaska Range
p 656 A95-93460

Flying with automated surface observations
p 659 A95-93472

Representativeness and responsiveness of automated weather systems
p 660 A95-93482

The inference of aviation weather hazards based on the integration of radar and lightning data
p 660 A95-93483

Use of high resolution lightning detection and localization sensors for hazardous aviation weather nowcasting
p 661 A95-93486

The performance of forward scatter visibility sensors for application in autostations and runway visual range in snow and freezing precipitation events
p 662 A95-93489

Role of the aviation weather system in providing a real-time ATC volcanic ash advisory system
p 663 A95-93494

Characterizing the wake vortex signature for an active line of sight remote sensor
[NASA-CR-197697] p 333 N95-24391

REMOTELY PILOTED VEHICLES

An unmanned air vehicle concept with tipjet drive
[HTN-95-80858] p 283 A95-75100

Cypher moves toward autonomous flight
[HTN-95-41394] p 283 A95-76390

A systems for flight data acquisition and analysis for a remotely-piloted research vehicle
p 517 A95-91554

On the UF-104 system
p 507 A95-91559

On the flight control system for UF-104
p 507 A95-91560

An application of virtual prototyping to the flight test and evaluation of an unmanned air vehicle
[AD-A281749] p 14 N95-11595

Conceptual design of the AE481 Demon Remotely Piloted Vehicle (RPV)
[NASA-CR-197164] p 44 N95-12294

Design and construction of a remote piloted flying wing
[NASA-CR-197195] p 47 N95-12695

Six degree of freedom flight dynamic and performance simulation of a remotely-piloted vehicle
[AERO-TN-9301] p 131 N95-18097

Unmanned aerial vehicles
[AD-A286190] p 231 N95-20329

Interfacing a digital compass to a remote-controlled helicopter
[PB95-164927] p 340 N95-24260

Design and synthesis of a real-time controller for an unmanned air vehicle
[AD-A289134] p 408 N95-26555

Unmanned aerial vehicles, 1994 master plan
[AD-A291628] p 398 N95-28411

Unmanned Aerial Vehicle technology
[DSTO-GD-0044] p 503 N95-29362

REMOVAL

The use of radar wind profiles to remove TDWR gust front algorithm false alarms caused by vertical wind shear
p 661 A95-93488

Bicarbonate of soda blasting technology for aircraft wheel depainting
[PB94-193323] p 104 N95-17466

Environmentally Safe and Effective Processes for Paint Removal
[AGARD-LS-201] p 650 N95-32165

Water blasting paint removal methods
p 650 N95-32170

Selective chemical stripping
p 650 N95-32175

Process evaluation
p 651 N95-32180

Standardization work
p 651 N95-32181

REPLACING

Application of photogrammetry of F-14D store separation
[AD-A284154] p 132 N95-18417

A comparison of coating alternatives for US Coast Guard aircraft
[AD-A293270] p 629 N95-31124

Environmentally safe aviation fuels
p 631 N95-31768

Cadmium plating replacements
p 631 N95-31773

Bicarbonate of soda paint stripping process validation and material characterization
p 631 N95-31778

Report to the Chairman, Legislation and National Security Subcommittee, Committee on Government Operations, House of Representatives. Tactical aircraft F-15 replacement is premature as currently planned
[GAO/NSIAD-94-118] p 679 N95-31987

Fact sheet for Congressional Committees. Air traffic control: Status of FAA's modernization program
[GAO/RCED-94-167FS] p 603 N95-32197

Proposed incorporation of mission-oriented flying qualities into MIL-STD-1797A
[AD-A294211] p 698 N95-34306

REPORTS

Towards improving the NMC aircraft data base
p 660 A95-93480

Use of pilot reports for verification of aircraft icing diagnoses and forecasts
p 666 A95-93508

Examination of conditions in the proximity of pilot reports of aircraft icing during storm-fest
p 666 A95-93509

ICASE
[NASA-CR-195001] p 170 N95-16898

REPRODUCTION (COPYING)

An analysis of the impact of ASPA on organizational and depot level maintenance
[AD-A292670] p 457 N95-29414

REQUIREMENTS

European firms team on supersonic studies
 [HTN-95-42215] p 386 A95-84031
 Functional requirements of an aerospace Design Representation Programming Interface
 [AIAA PAPER 95-0967] p 497 A95-90643
 The role of simulations in 777 FSEU development
 [AIAA PAPER 95-0995] p 506 A95-90665
 Selective chemical stripping p 650 N95-32175

RESCUE OPERATIONS

Analysis of test criteria for specifying foam firefighting agents for aircraft rescue and firefighting
 [AD-A286381] p 227 N95-22352

RESEARCH

Airplane icing research at the Boeing Company: Participation in the second Canadian Atlantic Storms Program p 674 A95-93544
 Dryden and transonic research
 [NASA-TM-104281] p 1 N95-10709
 Aero-thermodynamic distortion induced structured dynamic response
 [AD-A279931] p 203 N95-19864
 1994 NASA-HU-American Society for Engineering Education (ASEE) Summer Faculty Fellowship Program
 [NASA-CR-194972] p 325 N95-23276
 Research and Technology, 1994
 [NASA-TM-106764] p 262 N95-24025
 The high speed civil transport and NASA's High Speed Research (HSR) program p 390 N95-26945
 Metascientific problems in safety science
 [PB95-196408] p 645 N95-30521

RESEARCH AIRCRAFT

Microwave and infrared simulations of an intense convective system and comparison with aircraft observations
 [HTN-95-60511] p 214 A95-68762
 A conceptual design of hypersonic research vehicle with subscale scramjet engine p 384 A95-82482
 Hypersonic technology experimental vehicles (The need for flight testing at hypersonic speed)
 p 490 A95-87378
 A waverider derived hypersonic X-vehicle
 [AIAA PAPER 95-6162] p 496 A95-90473
 A systems for flight data acquisition and analysis for a remotely-piloted research vehicle p 517 A95-91554
 F-18 HARV presentation for industry
 [NASA-TM-104283] p 13 N95-10711
 Research excitation system flight testing
 [NASA-TM-104289] p 13 N95-10715
 Radio controlled for research
 [NASA-TM-104292] p 17 N95-10717
 F-104 resource tape
 [NASA-TM-104296] p 13 N95-10741
 F-15 835 (HIDEC) resource tape
 [NASA-TM-104297] p 13 N95-10742
 F-16XL resource tape
 [NASA-TM-104298] p 13 N95-10743
 X-31 resource tape
 [NASA-TM-104300] p 13 N95-10745
 NACA/NASA: X-1 through X-31
 [NASA-TM-104304] p 1 N95-10749
 Fan noise research at NASA p 28 N95-11260
 Fourth High Alpha Conference, volume 2
 [NASA-CP-10143-VOL-2] p 69 N95-14239
 F-18 high alpha research vehicle: Lessons learned
 p 69 N95-14240
 Design and development of an F/A-18 inlet distortion rake: A cost and time saving solution
 p 69 N95-14241
 Flight test results of the F-16 aircraft modified with the axisymmetric vectoring exhaust nozzle
 p 70 N95-14245
 Flight validation of ground-based assessment for control power requirements at high angles of attack
 p 70 N95-14246
 Numerical simulation of the flow about the F-18 HARV at high angle of attack
 [NASA-CR-197023] p 74 N95-14614
 VSTOL Systems Research Aircraft (VSRA) Harrier
 [NASA-TM-110117] p 126 N95-18347
 Fiber Optic Control System integration for advanced aircraft. Electro-optic and sensor fabrication, integration, and environmental testing for flight control systems: Laboratory test results
 [NASA-CR-195408] p 161 N95-18938
 Analysis of the longitudinal handling qualities and pilot-induced-oscillation tendencies of the High-Angle-of-Attack Research Vehicle (HARV)
 p 293 N95-23297
 A quiet STOL Research Aircraft Development program
 [NAL-TR-1223] p 336 N95-25862
 Flightpath synthesis and HUD scaling for V/STOL terminal area operations
 [NASA-TM-110348] p 383 N95-26587

An Electronic Workshop on the Performance Seeking Control and Propulsion Controlled Aircraft Results of the F-15 Highly Integrated Digital Electronic Control Flight Research Program
 [NASA-TM-104278] p 694 N95-33009
 An overview of integrated flight-propulsion controls flight research on the NASA F-15 research airplane
 p 694 N95-33010
 Performance seeking control program overview
 p 695 N95-33011
 F-15 propulsion system
 p 695 N95-33012
 PSC algorithm description
 p 695 N95-33013
 PSC implementation and integration
 p 695 N95-33014
 Minimum fuel mode evaluation
 p 695 N95-33015
 Minimum fan turbine inlet temperature mode evaluation
 p 696 N95-33016
 Maximum thrust mode evaluation
 p 696 N95-33017
 Performance seeking control excitation mode
 p 696 N95-33019
 Performance seeking control (PSC) for the F-15 highly integrated digital electronic control (HIDEC) aircraft
 p 697 N95-33020
 Design challenges encountered in the F-15 PCA flight test program
 p 692 N95-33025

RESEARCH AND DEVELOPMENT

Balloon technology and observations; Symposium P3 of the COSPAR Plenary Meeting, 29th, Washington, DC, Aug. 28-Sept. 5, 1992
 [HTN-95-70250] p 181 A95-66276
 Development of 70MW class superconducting generators
 [BTN-94-EIX95011440854] p 429 A95-82905
 International collaboration in hypersonic technologies - A specific and worthwhile initiative
 [AIAA PAPER 95-6140] p 581 A95-90457
 An overview of FAA-sponsored aviation weather research and development
 p 652 A95-93442
 The forecast systems laboratory's role in the FAA's aviation weather development program
 p 652 A95-93443
 Transport Canada proposed R&D program for the development of a multi-parameter dual X-Ka band Doppler radar for aviation meteorology applications
 p 659 A95-93477
 Aviation weather forecasting automated methods in the RAFC Moscow and the Airport Vnukovo
 p 669 A95-93523
 Dryden summer 1994 update
 [NASA-TM-104305] p 33 N95-10750
 JPRS report: Science and technology, Central Eurasia: Engineering and equipment. Gas dynamics of supersonic shortened nozzles
 [JPRS-UST-94-003-L] p 22 N95-10931
 Experimental Aerodynamics Division
 [NAL-SP-9404] p 35 N95-12166
 Air Force seal activities
 p 60 N95-13600
 A review of 50 years of aerodynamic research with NACA/NASA
 [NASA-TM-109163] p 102 N95-13663
 Research and technology highlights, 1993
 [NASA-TM-4575] p 102 N95-15065
 Vertical flight terminal operational procedures. A summary of FAA research and development
 [AD-A283550] p 85 N95-15328
 ICASE
 [NASA-CR-195001] p 170 N95-16898
 NASA High Performance Computing and Communications program
 [NASA-TM-4653] p 176 N95-18573
 European aeronautics: Strong government presence in industry structure and research and development support. Report to Congressional Requesters
 [GAO/NSIAD-94-71] p 176 N95-18578
 Federal Aviation Administration plan for research, engineering and development, 1995
 p 363 N95-24202
 JPRS report: Science and technology, Central Eurasia
 [JPRS-UST-94-027] p 349 N95-24470
 JPRS report: Science and technology, Central Eurasia
 [JPRS-UST-94-018] p 349 N95-24472
 JPRS report: Science and technology, Central Eurasia
 [JPRS-UST-95-011] p 335 N95-24541
 Assessment of avionics technology in European aerospace organizations
 [NASA-CR-189201] p 337 N95-24624
 JPRS Report: Science and technology, Central Eurasia
 [JPRS-UST-94-032] p 350 N95-24759
 JPRS report: Science and technology, Central Eurasia
 [JPRS-UST-94-022] p 438 N95-27699
 Collected papers on wind turbine technology
 [NASA-CR-195432] p 447 N95-27970
 Research and Technology Objectives and Plans Summary (RTOPS)
 [NASA-TM-108574] p 453 N95-28002

JTEC/WTEC annual report and program summary: 1993/94
 [NASA-CR-198563] p 454 N95-28038
 Aircraft advanced materials research and development program plan
 [AD-A290542] p 505 N95-29565
 Federal aviation administration plan for research, engineering and development
 [AD-A290952] p 490 N95-29733
 FBIS report: Science and technology, Central Eurasia
 [FBIS-UST-95-029] p 649 N95-31728
 Aeronautics and space report of the President
 [NASA-TM-110743] p 681 N95-31979

RESEARCH FACILITIES

The NASA-sponsored Maryland center for hypersonic education and research
 [AIAA PAPER 95-6105] p 519 A95-88010
 A large hemi-anechoic enclosure for community-compatible aeroacoustic testing of aircraft propulsion systems
 p 577 A95-90132
 The NASA/UTA Center for hypersonic research
 [AIAA PAPER 95-6106] p 520 A95-90438
 Research and educational initiatives at the Syracuse University Center for Hypersonics
 [AIAA PAPER 95-6107] p 520 A95-90439
 Review of new French facilities for PREPHA program
 [AIAA PAPER 95-6128] p 520 A95-90449
 The simulator training research advance testbed for aviation (STRATA): A simulation research facility for army aviation
 p 626 A95-95161
 Eglin Air Force Base Ram Accelerator Research Facility
 p 19 N95-10284
 Langley overview
 [NASA-TM-109891] p 20 N95-10547
 Dryden overview for schools
 [NASA-TM-104282] p 21 N95-10710
 Dryden tour tape, 1994
 [NASA-TM-104288] p 21 N95-10714
 Dryden overview for schools
 [NASA-TM-104302] p 21 N95-10747
 Activities of the Institute for Aerospace Studies of Toronto University
 p 63 N95-12699
 Simulation of Shuttle launch G forces and acoustic loads using the NASA Ames Research Center 20G centrifuge
 p 86 N95-14089
 Thermoacoustic environments to simulate reentry conditions
 p 86 N95-14096
 Research and technology highlights, 1993
 [NASA-TM-4575] p 102 N95-15065
 Development of strength analysis methods and design model for aircraft constructions in Kazan Aviation Institute
 p 127 N95-16264
 A study of software standards used in the avionics industry
 p 137 N95-16456
 A VHF/UHF antenna for the Precision Antenna Measurement System (PAMS)
 [AD-A285673] p 156 N95-16621
 ICASE
 [NASA-CR-195001] p 170 N95-16898
 Preliminary results and research capabilities of a new jet facility at the University of Kansas
 p 412 N95-26951
 A review of Australian and New Zealand investigations on aeronautical fatigue during the period Apr. 1993 - Mar. 1995
 [AR-009-202] p 397 N95-27918

RESEARCH MANAGEMENT

Evaluation and management of research and development in aeronautics
 [CONGRESS PAPER C428-8-102] p 581 A95-91691
 Research and Technology Objectives and Plans Summary (RTOPS)
 [NASA-TM-108574] p 453 N95-28002
 Federal aviation administration plan for research, engineering and development
 [AD-A290952] p 490 N95-29733
 Emerging applications in probability (Sensor management)
 [AD-A292781] p 601 N95-31433
 Aviation security: Development of new security technology has not met expectations. Report to Congressional requesters
 [GAO/RCED-94-142] p 687 N95-32885

RESEARCH PROJECTS

Future SSTs a European approach
 [BTN-95-EIX95072419883] p 180 A95-68396
 NACA/NASA: X-1 through X-31
 [NASA-TM-104304] p 1 N95-10749
 Dryden summer 1994 update
 [NASA-TM-104305] p 33 N95-10750
 A review of Australian and New Zealand investigations on aeronautical fatigue during the period Apr. 1993 - Mar. 1995
 [AR-009-202] p 397 N95-27918
 Collected papers on wind turbine technology
 [NASA-CR-195432] p 447 N95-27970

- The Anglo-French Compact Laser Radar demonstrator programme p 703 N95-32501
- The DLR research programme on an integrated multi sensor system for surface movement guidance and control p 689 N95-33135
- RESEARCH VEHICLES**
- Actuated forebody strake controls for the F-18 High-Alpha Research Vehicle [BTN-95-EIX0619952748173] p 619 A95-94467
- F-18 high alpha research vehicle resource tape [NASA-TM-104299] p 13 N95-10744
- High-Alpha Research Vehicle (HARV) longitudinal controller: Design, analyses, and simulation results [NASA-TP-3446] p 17 N95-10860
- Experimental aerodynamic characteristics of a generic hypersonic accelerator configuration at Mach numbers 1.5 and 2.0 — conducted in the Langley Unitary Plan Wind Tunnel [NASA-TM-4413] p 39 N95-12770
- Preparations for flight research to evaluate actuated forebody strakes on the F-18 high-alpha research vehicle p 72 N95-14257
- Determination of stability and control derivatives from the NASA F/A-18 HARV from flight data using the maximum likelihood method [NASA-CR-197320] p 204 N95-19576
- Differential GPS and system integration of the Low Visibility Landing and Surface Operations (LVLASO) demonstration p 280 N95-23318
- Computational analysis of forebody tangential slot blowing on the high alpha research vehicle [NASA-CR-197754] p 389 N95-26591
- Numerical simulation of the flow about the F-18 HARV at high angle of attack [NASA-CR-197755] p 374 N95-26735
- A noninvasive method of quantifying flow visualization data in vortex flow fields [AD-A289802] p 552 N95-28948
- RESIDENTIAL AREAS**
- Nordic Standards for measurement of aircraft noise immersion in residential areas and noise reduction of dwellings p 570 A95-88463
- Standardization of aircraft noise insulation measures without compromising results p 561 A95-90115
- RESIDUAL STRENGTH**
- Crack growth characteristics of integrally machined stringer-skin panels [HTN-95-01095] p 496 A95-90281
- Structural integrity of fuselage panels with multisite damage [BTN-95-EIX0619952748188] p 637 A95-94250
- Residual strength of composites with multiple impact damage [BTN-94-EIX94511433967] p 701 A95-96664
- Residual strength of composites with multiple impact damage [AD-A284230] p 87 N95-14409
- Testing and analysis of flat and curved panels with multiple cracks p 93 N95-14460
- Residual life and strength estimates of aircraft structural components with MSD/MED p 136 N95-19485
- Widespread fatigue damage monitoring: Issues and concerns p 136 N95-19488
- Fatigue and residual strength investigation of ARALL(R) -3 and GLARE(R) -2 panels with bonded stringers p 137 N95-19495
- Prediction of R-curves from small coupon tests p 167 N95-19496
- Residual strength of thin panels with cracks p 311 N95-23311
- Investigation of static and cyclic bearing failure mechanisms for GR/EP laminates p 422 N95-28427
- RESIDUAL STRESS**
- The effects of surface modification on fretting fatigue in Ti alloy turbine components [HTN-95-61145] p 404 A95-84909
- Residual strength of composites with multiple impact damage [AD-A284230] p 87 N95-14409
- Advanced method and processing technology for complicated shape airframe part forming p 80 N95-14486
- Residual Stress Measurements with Laser Speckle Correlation Interferometry and Local Heat Treating [DE95-060082] p 349 N95-24598
- RESIDUES**
- Hardware cleanliness methodology and certification p 419 N95-27656
- Gas chromatography/ion mobility spectrometry as a hyphenated technique for improved explosives detection and analysis p 701 N95-33278
- RESIN MATRIX COMPOSITES**
- Novel matrix resins for composites for aircraft primary structures, phase 1 [NASA-CR-189657] p 23 N95-10318
- Thermally stable organic polymers [AD-A281380] p 87 N95-14363
- Advanced resin systems and 3D textile preforms for low cost composite structures p 535 N95-29035
- Mechanical characterization of 2D, 2D stitched, and 3D braided/RTM materials p 537 N95-29038
- Development of RTM and powder prepreg resins for subsonic aircraft primary structures p 536 N95-29044
- Progress in manufacturing large primary aircraft structures using the stitching/RTM process p 537 N95-29050
- Test results from large wing and fuselage panels p 537 N95-29051
- Thermally stable organic polymers [AD-A290755] p 537 N95-29482
- RESIN TRANSFER MOLDING**
- Polymer composite applications to aerospace equipment [HTN-95-B0257] p 529 A95-89201
- Development and verification of a resin film infusion/resin transfer molding simulation model for fabrication of advanced textile composites [NASA-CR-197439] p 301 N95-23179
- Development of a low-cost, modified resin transfer molding process using elastomeric tooling and automated preform fabrication p 420 N95-28268
- Resin transfer molding of textile preforms for aircraft structural applications p 421 N95-28276
- Development of stitched/RTM composite primary structures p 425 N95-28469
- Test and analysis results for composite transport fuselage and wing structures p 398 N95-28470
- Composite fuselage crown panel manufacturing technology p 399 N95-28474
- Advanced textile applications for primary aircraft structures p 399 N95-28476
- Comparison of resin film infusion, resin transfer molding, and consolidation of textile preforms for primary aircraft structure p 425 N95-28477
- Characterization and manufacture of braided composites for large commercial aircraft structures p 426 N95-28478
- Manufacturing scale-up of composite fuselage crown panels p 532 N95-28835
- Third NASA Advanced Composites Technology Conference, volume 1, part 1 [NASA-CP-3178-VOL-1-PT-1] p 534 N95-29029
- Textile composite fuselage structures development p 534 N95-29033
- Advanced resin systems and 3D textile preforms for low cost composite structures p 535 N95-29035
- Performance of resin transfer molded multiaxial warp knit composites p 535 N95-29039
- Cross-stiffened continuous fiber structures p 536 N95-29041
- Cost model relationships between textile manufacturing processes and design details for transport fuselage elements p 536 N95-29043
- Development of RTM and powder prepreg resins for subsonic aircraft primary structures p 536 N95-29044
- The effects of aircraft fuel and fluids on the strength properties of Resin Transfer Molded (RTM) composites p 536 N95-29047
- Progress in manufacturing large primary aircraft structures using the stitching/RTM process p 537 N95-29050
- Test results from large wing and fuselage panels p 537 N95-29051
- Development of stitched/RTM primary structures for transport aircraft [NASA-CR-191441] p 630 N95-31421
- RESINS**
- Composite repair of metallic airframe: Twenty years of experience p 393 N95-27508
- Field repair materials for naval aircraft p 394 N95-27514
- Development of stitched/RTM composite primary structures p 425 N95-28469
- Performance of resin transfer molded multiaxial warp knit composites p 535 N95-29039
- RESISTORS**
- Spiral microstrip antenna with resistance [NASA-CASE-LAR-15088-1] p 91 N95-14139
- RESOLUTION**
- Research requirements for future visual guidance systems [AD-A279188] p 191 N95-19810
- Grid resolution and turbulent inflow boundary condition recommendations for NPARC calculations [NASA-TM-106959] p 482 N95-30253
- RESONANCE**
- Modeling resonance in waveguide-to-microstrip junctions by unilateral fin line resonators [BTN-94-EIX94381323445] p 242 A95-70844
- Air resonance of hingeless rotor helicopters in trimmed forward flight [HTN-95-61075] p 369 A95-83659
- Temperature effects on acoustic interactions between altitude test facilities and jet engine plumes [NASA-CR-197638] p 258 N95-21170
- RESONANT FREQUENCIES**
- On the choice of appropriate bases for nonlinear dynamic modal analysis [HTN-95-A0495] p 221 A95-72566
- Dynamic response of NASA Rotor Test Apparatus and Sikorsky S-76 hub mounted in the 80- by 120-Foot Wind Tunnel [NASA-TM-108847] p 25 N95-11389
- Effects of mass on aircraft sidearm controller characteristics [NASA-TM-104277] p 51 N95-11868
- Experimental/analytical approach to understanding mistuning in a transonic wind tunnel compressor [NASA-TM-108833] p 95 N95-14617
- Phonon characteristics of high (T sub c) superconductors from neutron Doppler broadening measurements [DE95-003703] p 324 N95-24076
- RESONANT VIBRATION**
- Aircraft landing gear dynamics present and future [SAE PAPER 931400] p 604 A95-93670
- Aircraft nose gear shimmy studies [SAE PAPER 931401] p 628 A95-93671
- A theoretical analysis of airborne sound transfer for a resiliently mounted machine to its foundation p 30 N95-11304
- Dynamical systems as models for flow-induced vibrations [PB95-206991] p 647 N95-30956
- RESONATORS**
- Modeling resonance in waveguide-to-microstrip junctions by unilateral fin line resonators [BTN-94-EIX94381323445] p 242 A95-70844
- Anisotropic heat exchangers/stack configurations for thermoacoustic heat engines [AD-A280974] p 168 N95-16506
- RESOURCES MANAGEMENT**
- 'Global avionics in the future' report from the 10th annual battery conference [BTN-95-EIX95282706404] p 545 A95-88184
- Public-sector aviation issues: Graduate research award papers, 1992-1993 [PB94-217478] p 219 N95-19967
- Controller resource management: What can we learn from aircrews? [DOT/FAA/AM-95/21] p 602 N95-32186
- RESPONSE TIME (COMPUTERS)**
- Computing quantitative characteristics of finite-state real-time systems [AD-A282839] p 83 N95-14343
- Modeling spatio-temporal databases to measure the performance of the GPS satellite constellation p 489 N95-29596
- RESPONSES**
- Representativeness and responsiveness of automated weather systems p 660 A95-93482
- RETROFITTING**
- Development of an intervention program to encourage shoulder harness use and aircraft retrofit in general aviation aircraft: Phases 1 and 2 [AD-A290966] p 485 N95-29873
- RETROREFLECTION**
- Double pass retroreflection for corrosion detection in aircraft structures p 323 N95-23503
- REUSABLE LAUNCH VEHICLES**
- Separation of winged vehicles in supersonics [AIAA PAPER 95-6092] p 526 A95-88601
- REUSE**
- Dependability issues in the reuse of standard components in open architectures [AIAA PAPER 95-1006] p 566 A95-90678
- REVERBERATION**
- Electromagnetic reverberation characteristics of a large transport aircraft [AD-A282923] p 82 N95-15392
- REVERBERATION CHAMBERS**
- Design and operation of a thermoacoustic test facility p 147 N95-19150
- Photoacoustic chambers for studying solids and gases: Theory and practical examples [IFTR-39/1994] p 412 N95-26837
- REVERSE ENGINEERING**
- Automation of reverse engineering process in aircraft modeling and related optimization problems [NASA-CR-197109] p 129 N95-16899
- REVERSED FLOW**
- Aerodynamic characteristics of external store configurations at low speeds [BTN-95-EIX95182619230] p 271 A95-76656
- PIV investigation of compressibility effects on dynamic stall p 478 N95-29102

REVIEWING

Boundary-flow measurement methods for wall interference assessment and correction: Classification and review p 163 N95-19262

REVISIONS

Static shape control for adaptive wings [HTN-95-A1767] p 627 A95-93330

REYNOLDS EQUATION

Influence of streamwise curvature on longitudinal vortices imbedded in turbulent boundary layers [BTN-94-EIX94401378820] p 307 A95-76489

Agglomeration multigrid for viscous turbulent flows [AD-A284064] p 8 N95-10848

Computational analysis of forebody tangential slot blowing on the high alpha research vehicle [NASA-CR-197754] p 389 N95-26591

Numerical studies of turbulent free surface flows and unsteady propeller flows [AD-A294377] p 706 N95-34343

REYNOLDS NUMBER

An experimental investigation of wing tip turbulence with applications to aerodynamic p.1. A95-60164 [AIAA PAPER 86-1918]

Accuracy enhancements for overset grids using a defect correction approach [AIAA PAPER 94-0523] p 3 A95-60181

A comparison of turbulence models in computing multi-element airfoil flows [AIAA PAPER 94-0291] p 4 A95-60185

Effect of underwing frost on a transport aircraft airfoil at flight Reynolds number [BTN-95-EIX95152582334] p 276 A95-73536

Effect of ambient turbulence intensity on sphere wakes at intermediate Reynolds numbers [BTN-95-EIX95182619101] p 308 A95-76586

Flow due to an oscillating sphere and an expression for unsteady drag on the sphere at finite Reynolds number [BTN-94-EIX95011441142] p 347 A95-81012

Flow structure in the lee of an inclined 6:1 prolate spheroid [BTN-94-EIX95011441127] p 348 A95-81027

Instability of three-dimensional boundary layers due to streamline curvature [HTN-95-61070] p 430 A95-83654

Predicting stall and post-stall behavior of airfoils at low mach numbers [BTN-95-EIX95262694297] p 365 A95-85468

Effect of Reynolds number and turbulence on airfoil aerodynamics at -90-degree incidence [HTN-95-42320] p 370 A95-86149

Sphere wakes at moderate Reynolds numbers in a turbulent environment [HTN-95-42331] p 372 A95-86160

Drag coefficients of spherical liquid droplets. Part 2: Turbulent gaseous fields [BTN-95-EIX95262697041] p 538 A95-86858

An overview of static and dynamic airfoil performance [SAE PAPER 931228] p 463 A95-88960

Momentum and scalar transfer coefficients over aerodynamically smooth Antarctic surfaces [HTN-95-92932] p 562 A95-91870

Controlling mechanisms of ignition of solid fuel in a sudden-expansion combustor [BTN-95-EIX0616952745791] p 628 A95-94255

Aerodynamic applications of underexpanded hypersonic viscous jets [BTN-95-EIX0619952748162] p 589 A95-94456

Navier-Stokes applications to high-lift airfoil analysis [BTN-95-EIX0619952748182] p 590 A95-94475

Analysis of low Reynolds number airfoil flows [BTN-95-EIX0619952748183] p 590 A95-94476

Lift-enhancing tabs on multielement airfoils [BTN-95-EIX0619952748187] p 591 A95-94479

LDV measurements in separated flow on an elliptic wing mounted at an angle of attack on a wall [BTN-94-EIX94441380518] p 702 A95-96559

Scale effects on aircraft and weapon aerodynamics [AGARD-AG-323] p 67 N95-14103

High Alpha Technology Program (HATP) ground test to flight comparisons p 68 N95-14230

Transonic Navier-Stokes calculations about a 65 deg delta wing [NASA-CR-4635] p 108 N95-17273

2-D airfoil effectiveness study p 110 N95-17851

Two-dimensional 16.5 percent thick supercritical airfoil NLR 7301 p 111 N95-17854

OAT15A airfoil data p 111 N95-17857

Pressure distributions on research wing W4 mounted on an axisymmetric body p 112 N95-17862

Three-dimensional boundary layer and flow field data of an inclined prolate spheroid p 158 N95-17867

Force and pressure data of an ogive-nosed slender body at high angles of attack and different Reynolds numbers p 113 N95-17868

Effect of crossflow on Goertler instability in incompressible boundary layers [NASA-CR-195007] p 159 N95-18193

Hypersonic flow-field measurements: Intrusive and nonintrusive [AD-A263867] p 119 N95-18674

Velocity measurements with hot-wires in a vortex-dominated flowfield p 121 N95-19261

Unsteady flow testing in a passive low-correction wind tunnel p 147 N95-19272

Research on bluff body vortex wakes [AD-A266319] p 223 N95-20177

Acoustic receptivity due to weak surface inhomogeneities in adverse pressure gradient boundary layers [NASA-TM-4577] p 249 N95-21258

Experiments on the flow field physics of confluent boundary layers for high-lift systems [NASA-CR-197318] p 224 N95-21343

Wing pressure distributions from subsonic tests of a high-wing transport model -- in the Langley 14- by 22-Foot Subsonic Wind Tunnel [NASA-TM-4583] p 272 N95-22802

Design of a variable area diffuser for a 15-inch Mach 6 open-jet tunnel p 297 N95-23309

Experimental study of the effects of Reynolds number on high angle of attack aerodynamic characteristics of forebodies during rotary motion [NASA-CR-195033] p 330 N95-24443

Comparative wind tunnel test at high Reynolds numbers of NACA 64 621 airfoils with two aileron configurations p 377 N95-27977

Influence of turbulence parameters, Reynolds number, and body shape on stagnation-region heat transfer [NASA-TP-3487] p 550 N95-28719

The effects of three-dimensional imposed disturbances on bluff body near wake flows: Effects of taper and splitter plates on the near wake characteristics of a circular cylinder in uniform and shear flow [AD-A292113] p 477 N95-28921

Studies in drag reduction p 478 N95-29094

Finite element vorticity-based methods for the solution of the incompressible and compressible Navier-Stokes equations p 553 N95-29119

Control of unsteady separated flow associated with the dynamic stall of airfoils [NASA-CR-198972] p 594 N95-32193

REYNOLDS STRESS

Development of a large-aspect-ratio rectangular turbulent free jet [HTN-95-42333] p 372 A95-86162

RHEOLOGY

Electrorheologically controlled landing gear [BTN-94-EIX94461047055] p 78 A95-61740

An electrorheologically controlled semi-active landing gear [SAE PAPER 931403] p 605 A95-93673

Development of LaRC (TM): IA thermoplastic polyimide coated aerospace wiring [NASA-CR-195048] p 537 N95-30252

RIBLETS

Flow alteration and drag reduction by riblets in a turbulent boundary layer [HTN-95-61199] p 461 A95-87572

Drag reduction in a rectangular duct using riblets [HTN-95-01091] p 468 A95-90277

Laminar and turbulent flow over optimal riblets p 639 A95-95383

Studies in drag reduction p 478 N95-29094

RIBS (SUPPORTS)

Convection heat transfer distributions over plates with square ribs from infrared thermography measurements [HTN-95-20713] p 435 A95-86603

RICCATI EQUATION

Design of robust optimal control systems and stability analysis of real structured uncertainties [AD-A279089] p 256 N95-21913

RICHARDSON NUMBER

An evaluation of clear-air turbulence indices p 674 A95-93548

Amplification and breaking of atmospheric gravity waves p 675 A95-93552

RIEMANN MANIFOLD

Beyond the Riemann problem, part 1 p 550 A95-91925

RIEMANN WAVES

Computational aerodynamics based on the Euler equations [AGARD-AG-325] p 72 N95-14264

RIFLES

Severe edge effects and simple complimentary interior solutions for thin-walled anisotropic and composite structures [AD-A290645] p 555 N95-29562

RIGID ROTORS

Aeroelastic stability of hingeless rotor blade in hover using large deflection theory [BTN-94-EIX94441386616] p 183 A95-67347

Subharmonic and quasi-periodic motions of an eccentric squeeze film damper-mounted rigid rotor [BTN-94-EIX95011440601] p 429 A95-82982

Air resonance of hingeless rotor helicopters in trimmed forward flight [HTN-95-61075] p 369 A95-83659

Effect of squeeze film damper land geometry on damper performance [HTN-95-92247] p 434 A95-85291

Aeroelastic simulation of higher harmonic control [NASA-CR-4623] p 37 N95-11911

Higher harmonic control analysis for vibration reduction of helicopter rotor systems [NASA-TM-103855] p 66 N95-14419

High- and low-frequency dynamics of isolated blades and rotors with dynamic stall and wake [AD-A290358] p 503 N95-29322

Full-scale hingeless rotor performance and loads [NASA-TM-110356] p 691 N95-32699

RIGID STRUCTURES

Prediction of airplane states [BTN-95-EIX0619952748174] p 584 A95-94468

Plastic hinge modeling of structures [NIAR-94-14] p 24 N95-11168

Composite fuselage shell structures research at NASA Langley Research Center p 425 N95-28466

RIMS

Comparison of numerical results and multicavity purge and rim seal data with extensions to dynamics [NASA-TM-106685] p 416 N95-27434

RING LASERS

Optical processing and control [AD-A279157] p 259 N95-21975

Application of advanced safety technique to ring laser gyro inertial navigation system integration p 689 N95-33140

RING STRUCTURES

Thermo-hydrodynamic solution of floating ring seals for high pressure compressors using the finite-element method [HTN-95-92246] p 433 A95-85290

Critical speed analysis of a non-linear strain ring dynamical model for aircraft tires [SAE PAPER 932580] p 494 A95-90067

RIPPLES

Preliminary evaluation of the F/A-18 quantity/multiple envelope expansion [AD-A284119] p 132 N95-18407

RISK

Mechanical system reliability and risk assessment [BTN-95-EIX95142553046] p 304 A95-73452

Psycho-social safety perceptions: Helicopters as a case study p 596 A95-95192

Emergency medical service (EMS): A unique flight environment p 596 A95-95203

Case study of risk management in the USAF B-1B bomber program [AD-A282371] p 62 N95-11944

Characteristics of civil aviation atmospheric hazards p 42 N95-13208

The development of the F100-PW-220 and F110-GE-100 engines: A case study of risk assessment and risk management [AD-A282467] p 51 N95-13289

Risk analysis for the fire safety of airline passengers [PB94-194065] p 77 N95-14179

The F-16 multinational staged improvement program: A case study of risk assessment and risk management [AD-A281706] p 81 N95-15451

Report to Congressional Committees. Tactical Aircraft: Concurrence in development and production of F-22 aircraft should be reduced [GAO/NSIAD-95-59] p 336 N95-26338

RIVETED JOINTS

Growth of multiple cracks and their linkup in a fuselage lap joint [BTN-95-EIX95142553047] p 286 A95-73451

Fatigue of aircraft materials and structures p 387 A95-85894

The characterization of widespread fatigue damage in fuselage structure [NASA-TM-109142] p 88 N95-14920

Fatigue life until small cracks in aircraft structures: Durability and damage tolerance p 135 N95-19478

Results of uniaxial and biaxial tests on riveted fuselage lap joint specimens p 136 N95-19491

Estimate of probability of crack detection from service difficulty report data [PB95-149381] p 328 N95-24295

RIVETING

- Automatic riveting cell for commercial aircraft floor grid assembly
[BTN-95-EIX95182617807] p 261 A95-75752
- Automatic riveting cell for commercial aircraft floor grid assembly
[HTN-95-92309] p 365 A95-85353
- Non-contact calibration of a CNC riveting machine
[CONGRESS PAPER C428-32-075] p 583 A95-93618
- Damage tolerant repair techniques for pressurized aircraft fuselages
[AD-A281982] p 65 N95-14144
- Damage tolerant repair techniques for pressurized aircraft fuselages
[AD-A286298] p 219 N95-22046
- RIVETS**
- Analytical developments in support of the NASA aging aircraft program with an application to crack growth from rivets
[SAE PAPER 931223] p 545 A95-88789
- The role of fretting corrosion and fretting fatigue in aircraft rivet hole cracking p 94 N95-14470
- Evaluation of the fuselage lap joint fatigue and terminating action repair p 166 N95-19477
- The mm-wave resonant methods for the detection of corrosion, phase 1
[AD-A291315] p 556 N95-29941
- ROBOT CONTROL**
- Guidance and control, 1993; Annual Rocky Mountain Guidance and Control Conference, 16th, Keystone, CO, Feb. 6-10, 1993
[ISBN-0-87703-365-X] p 341 A95-80389
- Overview of NASREM: The NASA/NBS standard reference model for telerobot control system architecture re
[PB94-194560] p 58 N95-12854
- Qualitative environmental navigation: Theory and practice — robot navigation p 601 N95-30486
- ROBOT SENSORS**
- Development of an Automated Nondestructive Inspection (ANDI) system for commercial aircraft, phase 1
[AD-A283500] p 40 N95-12623
- ROBOTICS**
- Fourth-generation Mars vehicle concepts
[BTN-95-EIX95152583267] p 298 A95-73568
- A generic telerobotics architecture for C-5 industrial processes
[AIAA PAPER 94-1264-CP] p 27 N95-11529
- Joint Proceedings on Aeronautics and Astronautics (JPAA)
[ISBN-7-80-046602-7] p 104 N95-16249
- A feedforward control approach to the local navigation problem for autonomous vehicles
[AD-A282787] p 126 N95-17706
- Survey and implementation of commercial manual controllers for a generic telerobotics architecture
[AD-A289215] p 449 N95-26990
- Emerging applications in probability (Sensor management)
[AD-A292781] p 601 N95-31433
- ROBOTS**
- Automatic riveting cell for commercial aircraft floor grid assembly
[BTN-95-EIX95182617807] p 261 A95-75752
- Aircraft stripping and painting
[HTN-95-92311] p 365 A95-85355
- Rapid prototyping of composite aircraft structures
[SAE PAPER 931219] p 539 A95-87530
- Overview of NASREM: The NASA/NBS standard reference model for telerobot control system architecture re
[PB94-194560] p 58 N95-12854
- Qualitative environmental navigation: Theory and practice — robot navigation p 601 N95-30486
- ROBUSTNESS (MATHEMATICS)**
- Enhancing filter robustness in cascaded GPS-INS integrations
[BTN-95-EIX9514255475] p 278 A95-73435
- Identification of higher order helicopter dynamics using linear modeling methods
[HTN-95-80851] p 290 A95-75093
- Aeroelastic vehicle multivariable control synthesis with analytical robustness evaluation
[BTN-95-EIX95182619115] p 321 A95-76592
- Multivariable stability and robustness of sequentially designed feedback systems
[BTN-95-EIX95182619125] p 322 A95-76602
- Robustly stable preliminary control systems design for the YF-16 CCV aircraft
[BTN-95-EIX95202637608] p 292 A95-76681
- High-performance, robust, bank-to-turn missile autopilot design
[BTN-95-EIX95242670751] p 336 A95-81096

- Robust dynamic inversion for control of highly maneuverable aircraft
[BTN-95-EIX95242670747] p 359 A95-81100
- MIMO H infinity control design method combined with exact model matching p 506 A95-91492
- A design of a robust scheduled autopilot
p 516 A95-91532
- A design of a self-learning robust scheduled autopilot
p 516 A95-91533
- Missile autopilot designs using full state feedback
p 507 A95-91587
- A robust inverse inviscid method for airfoil design
p 640 A95-95431
- Accurate interlaminar stress recovery from finite element analysis
[NASA-TM-109149] p 57 N95-11815
- Multi-application controls: Robust nonlinear multivariable aerospace controls applications
p 71 N95-14249
- Tools for applied engineering optimization
p 128 N95-16570
- Design of high performance multivariable control systems for supermaneuverable aircraft at high angle of attack
[NASA-CR-197661] p 293 N95-22908
- Robust control: A structured approach to solve aircraft flight control problems p 621 N95-31995
- ROCKET ENGINE CONTROL**
- New technologies for space avionics
[NASA-CR-197574] p 150 N95-18196
- ROCKET ENGINE DESIGN**
- Program test objectives milestone 3 --- Integrated Propulsion Technology Demonstrator
[NASA-CR-197030] p 127 N95-15971
- Arjet thruster research and technology, phase 2
[NASA-CR-182276] p 105 N95-18044
- ROCKET ENGINES**
- Investigation of heat transfer in a rotating ring gap with the axial flow of a coolant during the rotation of the central shaft
[BTN-94-EIX94461407951] p 89 A95-62625
- Fourth-generation Mars vehicle concepts
[BTN-95-EIX95152583267] p 298 A95-73568
- Integrated aerodynamic fin and stowable TVC vane system
[AD-D016457] p 151 N95-19073
- Impeller flow field characterization with a laser two-focus velocimeter p 313 N95-23440
- ROCKET NOZZLES**
- Experiment of rocket-ram annular combustor
p 412 A95-82324
- ROCKET THRUST**
- Regenerative cooling for liquid propellant rocket thrust chambers
[INPE-5565-TDI/540] p 150 N95-18720
- ROLL**
- Navier-Stokes prediction of large-amplitude delta-wing roll oscillations
[BTN-95-EIX95152582329] p 281 A95-73531
- Further analysis of high-rate rolling experiments of a 65-deg delta wing
[BTN-95-EIX95152582331] p 281 A95-73533
- Method for the prediction of the onset of wing rock
[BTN-95-EIX95152582342] p 282 A95-73544
- Investigation of the effects of bandwidth and time delay on helicopter roll-axis handling qualities
[HTN-95-80853] p 290 A95-75095
- Kinematics and aerodynamics of velocity-vector roll
[BTN-95-EIX95182619126] p 291 A95-76603
- Multiple-function digital controller system for active flexible wing wind-tunnel model
[BTN-95-EIX95182619212] p 322 A95-76638
- Rolling maneuver load alleviation using active controls
[BTN-95-EIX95182619217] p 270 A95-76643
- High angle of attack missile aerodynamics
[CONGRESS PAPER C428-3-060] p 475 A95-91673
- Active load control during rolling maneuvers — performed in the Langley Transonic Dynamics Tunnel
[NASA-TP-3455] p 129 N95-17397
- Development of a multicomponent force and moment balance for water tunnel applications, volume 2
[NASA-CR-4642-VOL-2] p 161 N95-18956
- Feedback control laws for highly maneuverable aircraft
[NASA-CR-197944] p 295 N95-23410
- An investigation of the effects of pitch-roll (de)coupling on helicopter handling qualities
[NASA-TM-110349] p 409 N95-26773
- ROLLER BEARINGS**
- Experimental investigation of thermoelastic deformation in turbojet-engine bearings under maintenance inspection
[BTN-95-EIX95292721173] p 546 A95-89904
- Rolling bearing failure and wear debris detection
[CONGRESS PAPER C428-15-094] p 457 A95-91711

- Influence of backup bearings and support structure dynamics on the behavior of rotors with active supports
[NASA-CR-199080] p 703 N95-32689
- Dynamic behavior of a magnetic bearing supported jet engine rotor with auxiliary bearings p 703 N95-32691
- Dynamic modelling and response characteristics of a magnetic bearing rotor system with auxiliary bearings
p 703 N95-32692
- Synchronous dynamics of a coupled shaft/bearing/housing system with auxiliary support from a clearance bearing: Analysis and experiment
p 703 N95-32693
- ROLLING CONTACT LOADS**
- Design and development of a test rig for the high frequency testing of rolling sleeve airsprings
[DSTO-TN-0001] p 411 N95-26378
- ROLLING MOMENTS**
- Interference between tanker wing wake with roll-up and receiver aircraft
[BTN-95-EIX95062487552] p 185 A95-68366
- Effect of leeward flow dividers on the wing rock of a delta wing
[BTN-95-EIX95152582347] p 282 A95-73549
- Kinematics and aerodynamics of velocity-vector roll
[BTN-95-EIX95182619126] p 291 A95-76603
- Flow structure in the lee of an inclined 6:1 prolate spheroid
[BTN-94-EIX95011441127] p 348 A95-81027
- 3D visualization of unsteady 2D airplane wake vortices
[AD-A284745] p 27 N95-11593
- Static and dynamic force/moment measurements in the Eidetics water tunnel p 69 N95-14238
- Experimental study at low supersonic speeds of a missile concept having opposing wraparound tails
[NASA-TM-4582] p 106 N95-16069
- Development of a multicomponent force and moment balance for water tunnel applications, volume 1
[NASA-CR-4642-VOL-1] p 161 N95-18955
- ROSETTA MISSION**
- Trajectory-based heating analysis for the European Space Agency/Rosetta Earth Return Vehicle
[BTN-95-EIX95041503787] p 205 A95-69218
- ROTARY ENGINES**
- Unmanned aerial vehicle heavy fuel engine test
[AD-A284332] p 139 N95-18383
- Evaluation of thermal barrier and PS-200 self-lubricating coatings in an air-cooled rotary engine
[NASA-CR-195445] p 289 N95-23222
- ROTARY STABILITY**
- F/A-18 and F-16 forebody vortex control, static and rotary-balance results p 72 N95-14254
- Experimental study of the effects of Reynolds number on high angle of attack aerodynamic characteristics of forebodies during rotary motion
[NASA-CR-195033] p 330 N95-24443
- Comparison of numerical results and multicavity purge and rim seal data with extensions to dynamics
[NASA-TM-106685] p 416 N95-27434
- Whirl plus tilt
[DE95-007948] p 452 N95-28108
- ROTARY WING AIRCRAFT**
- Recent studies of rotorcraft blade-vortex interaction noise
[BTN-95-EIX95062487521] p 218 A95-69229
- Measurement around a rotor blade excited in pitch. Part 1: Dynamic inflow
[HTN-95-31007] p 220 A95-71177
- An unmanned air vehicle concept with tipjet drive
[HTN-95-80858] p 283 A95-75100
- Cypher moves toward autonomous flight
[HTN-95-41394] p 283 A95-76390
- Dynamic stall control for advanced rotorcraft application
[BTN-95-EIX95222650793] p 334 A95-79249
- Intelligent flight trainer for initial rotary wing training
[SAE PAPER 932536] p 386 A95-84558
- Advanced distributed simulation technology advanced rotary wing aircraft. Strawman verification and validation plan for the ARWA simulator system
[AD-A280237] p 19 N95-10349
- Advanced distributed simulation technology advanced rotary wing aircraft. System/segment specification. Volume 1: Simulation system module
[AD-A280238] p 20 N95-10350
- Advanced distributed simulation technology advanced rotary wing aircraft. System/segment specification. Volume 3: Visual system module
[AD-A280239] p 20 N95-10351
- Advanced distributed simulation technology advanced rotary wing aircraft. System/segment specification. Volume 2: Flight station module
[AD-A280432] p 20 N95-10352
- Advanced distributed simulation technology advanced rotary wing aircraft. System/segment specification. Volume 5: Simulation system module AH-64D kit
[AD-A280433] p 20 N95-10353

- Advanced distributed simulation technology advanced rotary wing aircraft. Software reusability report [AD-A280434] p 20 N95-10354
- Noise modeling for MOAs and ranges p 32 N95-11322
- FAA vertical flight bibliography [DOT/FAA/RD-94/17] p 14 N95-11684
- ADST ARWA visual system module software design document [AD-A283874] p 99 N95-14357
- Vertical flight terminal operational procedures. A summary of FAA research and development [AD-A283550] p 85 N95-15328
- ADST system test report for the rotary wing aircraft airmet aeromodel and weapon model merge with the ATAC 2 baseline [AD-A281580] p 127 N95-16171
- Experimental data on the aerodynamic interactions between a helicopter rotor and an airframe p 116 N95-17883
- Flight parameters monitoring system for tracking structural integrity of rotary-wing aircraft p 135 N95-19469
- Rotorcraft ditchings and water-related impacts that occurred from 1982 to 1989, phase 1 [AD-A279164] p 189 N95-19805
- System for determining aerodynamic imbalance [NASA-CASE-ARC-11913-1] p 311 N95-23377
- Vibration analysis of a split path gearbox [NASA-TM-106875] p 438 N95-27855
- Evaluation of a doubly-swept blade tip for rotorcraft noise reduction [NASA-CR-189677] p 452 N95-28264
- Application of advanced material systems to composite frame elements p 422 N95-28432
- Rotorcraft crashworthy airframe and fuel system technology development program [AD-A289866] p 382 N95-28630
- Low-Level and Nap-of-the-Earth (NOE) night operations [AGARD-CP-563] p 686 N95-32486
- Transmittance characteristics of US Army rotary-wing aircraft transparencies [AD-A295035] p 693 N95-34793
- ROTARY WINGS**
- Validation of the dynamic response of a blade-element UH-60 simulation model in hovering flight [HTN-94-00663] p 18 A95-60155
- Comprehensive aeromechanics analysis of complex rotorcraft using 2GCHAS [HTN-94-00695] p 2 A95-60174
- First level release of 2GCHAS for comprehensive helicopter analysis - a status report [HTN-94-00697] p 2 A95-60176
- Comparison of theory and experiment for non-linear flutter and stall response of a helicopter blade [BTN-94-EIX94351108100] p 191 A95-66500
- Rotating Kirchhoff method for three-dimensional transonic blade-vortex interaction hover noise [BTN-94-EIX94441386601] p 182 A95-67332
- Bilinear formulation applied to the response and stability of helicopter rotor blade [BTN-95-EIX95042474400] p 192 A95-68300
- Using adaptive structures to attenuate rotary wing aeroelastic response [BTN-95-EIX95062487547] p 192 A95-68361
- Measurement around a rotor blade excited in pitch. Part 1: Dynamic inflow [HTN-95-31007] p 220 A95-71177
- Measurement around a rotor blade excited in pitch. Part 2: Unsteady surface pressure p 220 A95-71178
- Aerodynamic and wake methodology evaluation using Model UH-60A experimental data [HTN-95-31009] p 220 A95-71179
- Effects of leading and trailing edge flaps on the aerodynamics of airfoil/vortex interactions [HTN-95-31011] p 221 A95-71181
- Advance finite element modeling of rotor blade aeroelasticity [HTN-95-31013] p 221 A95-71183
- On the choice of appropriate bases for nonlinear dynamic modal analysis [HTN-95-A0495] p 221 A95-72566
- Flap-lag damping in hover and forward flight with a three-dimensional wake [HTN-95-A0496] p 221 A95-72567
- Air and ground resonance of helicopters with elastically tailored composite rotor blades [HTN-95-A0497] p 222 A95-72568
- Design optimization of rotor blades for improved performance and vibration [HTN-95-A0498] p 229 A95-72569
- Electromagnetic backscattering from a helicopter rotor in the decametric wave band regime [BTN-94-EIX94381353130] p 243 A95-72648
- Efficient sensitivity analysis for rotary-wing aeromechanical problems [BTN-95-EIX95152577585] p 264 A95-73497
- Dynamic analysis of bearingless tail rotor blades based on nonlinear shell modes [BTN-95-EIX95152582338] p 281 A95-73540
- Sensitivity of acoustic predictions to variation of input parameters [HTN-95-80855] p 267 A95-75097
- The influence of alternate inter-blade connections on ground resonance [HTN-95-80859] p 267 A95-75101
- Response of a nonrotating rotor blade to lateral turbulence. Part 1: Theory [BTN-95-EIX95182619228] p 284 A95-76654
- Response of a nonrotating rotor blade to lateral turbulence. Part 2: Experiment [BTN-95-EIX95182619229] p 284 A95-76655
- Multilevel decomposition procedure for efficient design optimization of helicopter rotor blades [BTN-95-EIX95222650784] p 334 A95-79240
- Dynamic stall control for advanced rotorcraft application [BTN-95-EIX95222650793] p 334 A95-79249
- A higher harmonic control test in the DNW to reduce impulsive BVI noise [HTN-95-61071] p 385 A95-83655
- Effects of blade tip shape on dynamics, cost, weight, aerodynamic performance, and aeroelastic response [HTN-95-61074] p 369 A95-83658
- An analytical model for a nonlinear elastomeric lag damper and its effect on aeromechanical stability in Hover [HTN-95-61076] p 369 A95-83660
- Considerations in the development of the coupled rotor fuselage model [HTN-95-61077] p 370 A95-83661
- Fast Floquet theory and trim for multi-bladed rotorcraft [HTN-95-61078] p 370 A95-83662
- Fast Floquet theory and trim for multi-bladed rotorcraft [HTN-95-61078] p 370 A95-83662
- Torsional actuation with extension-torsion composite coupling and a magnetostrictive actuator [BTN-95-EIX95262694314] p 435 A95-85485
- Efficient sensitivity analysis for rotary-wing aeromechanical problems [HTN-95-42570] p 458 A95-87200
- Dynamic-stall and structural-modeling effects on helicopter blade stability with experimental correlation [HTN-95-81646] p 542 A95-87694
- Aeroelastic response of composite rotor blades considering transverse shear and structural damping [HTN-95-81647] p 542 A95-87695
- Studies of blade-vortex interaction noise reduction by rotor blade modification p 573 A95-90093
- Experimental results of the European HELINOISE aeroacoustic rotor test [HTN-95-01080] p 578 A95-90266
- Laser velocimetry and blade pressure measurements of a blade-vortex interaction [HTN-95-01081] p 547 A95-90267
- Rotor-wake-induced flow separation on a lifting surface [HTN-95-01082] p 468 A95-90268
- Navier-Stokes calculations of rotor-airframe interaction in forward flight [HTN-95-01087] p 468 A95-90273
- The verification of a theoretical helicopter rotor blade sailing method by means of windtunnel testing [HTN-95-01093] p 468 A95-90279
- Flight testing of the composite material bearingless rotor system for the helicopter p 498 A95-91503
- Hubload responses of a rotor in forward flight due to multiple frequency blade pitch variations p 515 A95-91504
- Theory and evaluation of active control as a means of reducing helicopter vibration [CONGRESS PAPER C428-19-124] p 517 A95-91721
- Effect of initial conditions on the response of nonlinear dynamical systems with the application to helicopter rotor dynamics [ISBN 1-879921-01-4] p 605 A95-93731
- A three-dimensional Navier-Stokes/full-potential coupled analysis for rotor blades [ISBN 1-879921-01-4] p 587 A95-93748
- An innovative algorithm to accurately solve the Euler equations for rotary wing flow p 642 A95-95467
- The potential of genetic algorithms for conceptual design of rotor systems [NASA-CR-196813] p 43 N95-11699
- Advanced distributed simulation technology advanced rotary wing aircraft. Study comparing approaches to modeling the ARWA main rotor [AD-A280824] p 79 N95-14306
- Higher harmonic control analysis for vibration reduction of helicopter rotor systems [NASA-TM-103855] p 66 N95-14419
- Prediction of rotor-blade deformations due to unsteady airloads [AD-A284467] p 81 N95-15821
- Experimental data on the aerodynamic interactions between a helicopter rotor and an airframe p 116 N95-17883
- A linear system identification and validation of an AH-64 Apache aeroelastic simulation model p 146 N95-18903
- 2-D and 3-D oscillating wing aerodynamics for a range of angles of attack including stall [NASA-TM-4632] p 120 N95-19119
- Wall interaction effects for a full-scale helicopter rotor in the NASA Ames 80- by 120-foot wind tunnel p 121 N95-19270
- Prediction of rotor-blade deformations due to unsteady airloads [AD-A286593] p 231 N95-20860
- Simulation of rotor blade element turbulence [NASA-TM-108862] p 232 N95-21186
- Integrated aerodynamic/dynamic/structural optimization of helicopter rotor blades using multilevel decomposition [NASA-TP-3465] p 285 N95-22953
- System for determining aerodynamic imbalance [NASA-CASE-ARC-11913-1] p 311 N95-23377
- An experimental investigation of helicopter downwash and tailboom interaction at the Wichita State University 7x10 foot wind tunnel p 375 N95-26955
- Flow structure generated by perpendicular blade vortex interaction and implications for helicopter noise predictions [NASA-CR-198590] p 377 N95-28193
- Aeroelasticity and structural optimization of composite helicopter rotor blades with swept tips [NASA-CR-4665] p 397 N95-28262
- Evaluation of a doubly-swept blade tip for rotorcraft noise reduction [NASA-CR-189677] p 452 N95-28264
- Nonlinear dynamics and aeroelasticity of rotorcraft in forward flight [AD-A291714] p 400 N95-28504
- Modeling helicopter blade dynamics using a modified Myklestad-Prohl transfer matrix method [AD-A289891] p 400 N95-28626
- Interactions of spanwise and chordwise vorticity associated with three-dimensional dynamic stall over an oscillating wing [AD-A290546] p 477 N95-29091
- A fourth order Euler/Navier-Stokes prediction model for the aerodynamics and aeroelasticity of hovering rotor blades p 554 N95-29242
- High- and low-frequency dynamics of isolated blades and rotors with dynamic stall and wake [AD-A290358] p 503 N95-29322
- Development of a rotary wing Navier-Stokes CFD code based on TLNS3D code [AD-A290421] p 554 N95-29387
- Unsteady pressure and inflow velocity on a pitching rotor blade in hover p 480 N95-29771
- Validation of the helicopter rotor code HERO [PB95-198040] p 607 N95-30838
- A novel instrumentation system for measurement of helicopter rotor motions and loads data, phase 1 [AD-A293309] p 607 N95-30923
- ROTATING BODIES**
- The effect of rotating loads suspended under a helicopter on their amplitude-frequency characteristics [BTN-94-EIX94461407959] p 78 A95-62633
- Dynamic investigation of the angular motion of a rotating body-parachute system [BTN-95-EIX95182619220] p 270 A95-76646
- Vibration measurements on rotating machinery using laser Doppler velocimetry [BTN-94-EIX95011440597] p 429 A95-82986
- Transition correlations in three-dimensional boundary layers [HTN-95-51648] p 432 A95-85030
- Broadband polarization-transfer experiments for rotating solids [GTN-95-0009261494012091-58] p 579 A95-92319
- Building complex simulations rapidly using MATRIX(x): The Space Station redesign [TABES PAPER 94-632] p 87 N95-14653
- A Lifting Ball Valve for cryogenic fluid applications p 156 N95-16349
- Robust fixed-structure control [AD-A286515] p 257 N95-22216
- Robust fixed-structure control [AD-A292883] p 679 N95-30961

ROTATING DISKS

Modal parameters for cracked rotors: models and comparisons
 [BTN-94-EIX94522410226] p 702 A95-96378
 Engine structures analysis software: Component Specific Modeling (COSMO)
 [NASA-CR-195378] p 57 N95-11711

ROTATING SHAFTS

Investigation of heat transfer in a rotating ring gap with the axial flow of a coolant during the rotation of the central shaft
 [BTN-94-EIX94461407951] p 89 A95-62625
 Investigation of heat transfer between rotating shafts of transmissions of turbojet engines
 [BTN-94-EIX94461408760] p 138 A95-63643
 Modeling rotating shafts using axisymmetric solid finite elements with matrix reduction
 [BTN-94-EIX94351143328] p 207 A95-67301
 Transient analysis of a cracked rotor passing through critical speed
 [BTN-94-EIX94401360022] p 306 A95-74702
 Modal characteristics of rotors using a conical shaft finite element
 [BTN-94-EIX94401359745] p 346 A95-77379
 Aircraft gear train diagnostics using the irregular rotation of the external shafts
 [CONGRESS PAPER C428-15-097] p 508 A95-91712
 Use of blade pitch control to provide power train damping for the Mod-2, 2.5-mW wind turbine p 440 N95-27986
 Synchronous dynamics of a coupled shaft/bearing/housing system with auxiliary support from a clearance bearing: Analysis and experiment
 p 703 N95-32693
 Full-scale hingeless rotor performance and loads
 [NASA-TM-110356] p 691 N95-32699

ROTATING STALLS

Unsteady flow phenomena in discrete passage diffusers for centrifugal compressors
 [AD-A281412] p 155 N95-16163
 Modeling and control of rotating stall in high speed multi-stage axial compressors p 513 N95-29244
 Model development for active control of stall phenomena in aircraft gas turbine engines p 514 N95-29679

ROTATION

Rotating Kirchhoff method for three-dimensional transonic blade-vortex interaction hover noise
 [BTN-94-EIX94441386601] p 182 A95-67332
 Aeroelastic stability of hingeless rotor blade in hover using large deflection theory
 [BTN-94-EIX94441386616] p 183 A95-67347
 Dynamic investigation of the angular motion of a rotating body-parachute system
 [BTN-95-EIX95182619220] p 270 A95-76646
 Correlation of unsteady pressure and inflow velocity fields of a pitching rotor blade
 [BTN-95-EIX0619952748169] p 589 A95-94463
 New eigensolutions and modal analysis for gyroscopic/rotor systems, part 1: undamped systems
 [BTN-94-EIX94522410219] p 702 A95-96373
 New eigensolutions and modal analysis for gyroscopic/rotor systems, part 2: perturbation analysis for damped systems
 [BTN-94-EIX94522410220] p 702 A95-96374
 Modal parameters for cracked rotors: models and comparisons
 [BTN-94-EIX94522410226] p 702 A95-96378
 Development of an experimental facility for analysis of rotor dynamic phenomena
 [AD-A281897] p 25 N95-11330
 Experimental/analytical approach to understanding mistuning in a transonic wind tunnel compressor
 [NASA-TM-108833] p 95 N95-14617
 Aspect estimation of an aircraft using library model silhouettes
 [PB95-141834] p 360 N95-25894
 Whirl plus tilt
 [DE95-007948] p 452 N95-28108
 Modeling helicopter blade dynamics using a modified Myklestad-Prohl transfer matrix method
 [AD-A289891] p 400 N95-28626
 Three-D weather displays for aircraft cockpits
 [AD-A289759] p 508 N95-28691
 Composite structure forming a wear surface
 [AD-D017462] p 629 N95-30749
 Validation of the helicopter rotor code HERO
 [PB95-198040] p 607 N95-30838

ROTATIONAL SPECTRA

Matrix isolated HF: the high-resolution infrared spectrum of a cryogenically solvated hindered rotor
 [GTN-95-0301010494002231-16] p 578 A95-92210

ROTATIONAL STATES

Matrix isolated HF: the high-resolution infrared spectrum of a cryogenically solvated hindered rotor
 [GTN-95-0301010494002231-16] p 578 A95-92210

ROTOR AERODYNAMICS

Recent advances in Euler and Navier-Stokes methods for calculating helicopter rotor aerodynamics and acoustics
 [HTN-94-00686] p 2 A95-60169
 Measurement around a rotor blade excited in pitch. Part 1: Dynamic inflow
 [HTN-95-31007] p 220 A95-71177
 Measurement around a rotor blade excited in pitch. Part 2: Unsteady surface pressure
 [HTN-95-31008] p 220 A95-71178
 Vorticity concentration at the edge of the inboard vortex sheet
 [HTN-95-31010] p 221 A95-71180
 Effects of leading and trailing edge flaps on the aerodynamics of airfoil/vortex interactions
 [HTN-95-31011] p 221 A95-71181
 Advance finite element modeling of rotor blade aeroelasticity
 [HTN-95-31013] p 221 A95-71183
 High-order state space simulation models of helicopter flight mechanics
 [HTN-95-A0494] p 237 A95-72565
 On the choice of appropriate bases for nonlinear dynamic modal analysis
 [HTN-95-A0495] p 221 A95-72566
 Flap-lag damping in hover and forward flight with a three-dimensional wake
 [HTN-95-A0496] p 221 A95-72567
 Design optimization of rotor blades for improved performance and vibration
 [HTN-95-A0498] p 229 A95-72569
 Parametric studies for tiltrotor aeroelastic stability in highspeed flight
 [HTN-95-A0499] p 222 A95-72570
 Efficient sensitivity analysis for rotary-wing aeromechanical problems
 [BTN-95-EIX95152577585] p 264 A95-73497
 Effects of high order dynamics on helicopter flight control law design
 [HTN-95-80852] p 290 A95-75094
 Sensitivity of acoustic predictions to variation of input parameters
 [HTN-95-80855] p 267 A95-75097
 The influence of alternate inter-blade connections on ground resonance
 [HTN-95-80859] p 267 A95-75101
 Response of a nonrotating rotor blade to lateral turbulence. Part 2: Experiment
 [BTN-95-EIX95182619229] p 284 A95-76655
 Multilevel decomposition procedure for efficient design optimization of helicopter rotor blades
 [BTN-95-EIX95222650784] p 334 A95-79240
 Vortex methods for the computational analysis of rotor/body interaction
 [HTN-95-61072] p 369 A95-83656
 Considerations in the development of the coupled rotor fuselage model
 [HTN-95-61077] p 370 A95-83661
 Fast Floquet theory and trim for multi-bladed rotorcraft
 [HTN-95-61078] p 370 A95-83662
 On the differences between the effect of acoustic perturbation and unsteady bleed in controlling flow separation over a cylinder
 [SAE PAPER 932573] p 467 A95-90062
 Studies of blade-vortex interaction noise reduction by rotor blade modification
 p 573 A95-90093
 Experimental results of the European HELINOISE aeroacoustic rotor test
 [HTN-95-01080] p 578 A95-90266
 Laser velocimetry and blade pressure measurements of a blade-vortex interaction
 [HTN-95-01081] p 547 A95-90267
 Rotor-wake-induced flow separation on a lifting surface
 [HTN-95-01082] p 468 A95-90268
 Navier-Stokes calculations of rotor-airframe interaction in forward flight
 [HTN-95-01087] p 468 A95-90273
 The verification of a theoretical helicopter rotor blade sailing method by means of windtunnel testing
 [HTN-95-01093] p 468 A95-90279
 A three-dimensional Navier-Stokes/full-potential coupled analysis for rotor blades
 [ISBN 1-879921-01-4] p 587 A95-93748
 An innovative algorithm to accurately solve the Euler equations for rotary wing flow p 642 A95-95467
 Flutter analysis of supersonic axial flow cascades using a high resolution Euler solver. Part 1: Formulation and validation
 [NASA-TM-105798] p 23 N95-10244
 Computational fluid dynamics study of the variable-pitch split-blade fan concept
 [NASA-CR-189206] p 15 N95-10247
 Aeroelastic simulation of higher harmonic control
 [NASA-CR-4623] p 37 N95-11911

Measurements of atmospheric turbulence effects on tail rotor acoustics
 [NASA-TM-108843] p 38 N95-12360
 Dynamics of the McDonnell-Douglas Large Scale Dynamic Rig and dynamic calibration of the rotor balance
 [NASA-TM-108855] p 65 N95-13891
 Investigation of dynamic inflow's influence on rotor control derivatives p 155 N95-16250
 Measurement of gust response on a turbine cascade
 [NASA-TM-106776] p 117 N95-18457
 Sectional prediction of 3D effects for separated flow on rotating blades
 [PB94-201696] p 117 N95-18503
 Wind turbine blade aerodynamics: The combined experiment
 [DE94-011866] p 118 N95-18645
 Wind turbine blade aerodynamics: The analysis of field test data
 [DE94-011867] p 118 N95-18646
 The dynamic approach to rotor blade research: ARA's oscillatory test facility
 [ARA-MEMO-405] p 223 N95-20758
 Recent improvements to and validation of the one dimensional NASA wave rotor model
 [NASA-TM-106913] p 332 N95-25962
 Aircraft noise prediction program theoretical manual: Rotorcraft System Noise Prediction System (ROTONET), part 4
 [NASA-TM-83199-PT-4] p 451 N95-26392
 Development and validation of a blade-element mathematical model for the AH-64A Apache helicopter
 [NASA-TM-108863] p 367 N95-26710
 Preliminary analysis of dynamic stall effects on a 91-meter wind turbine rotor p 376 N95-27975
 A numerical model for dynamic wave rotor analysis
 [NASA-TM-106997] p 615 N95-30617
 Axial loads on yawed rotors
 [PB95-214193] p 592 N95-30638
 A novel instrumentation system for measurement of helicopter rotor motions and loads data, phase 1
 [AD-A293309] p 607 N95-30923
 Digital simulation of wind velocities for wind turbine rotors: General considerations
 [PB95-206447] p 677 N95-31157
 Full-scale hingeless rotor performance and loads
 [NASA-TM-110356] p 691 N95-32699
 Direct analysis of transonic rotor noise with CFD technique p 711 N95-34549

ROTOR BLADES
 Response of a nonrotating rotor blade to lateral turbulence. Part 2: Experiment
 [BTN-95-EIX95182619229] p 284 A95-76655
 Concepts for the control of rotor noise
 p 573 A95-90092
 Studies of blade-vortex interaction noise reduction by rotor blade modification p 573 A95-90093
 Stability analysis for elastically tailored rotor blades
 [ISBN 1-879921-01-4] p 635 A95-93703
 Investigation of dynamic inflow's influence on rotor control derivatives p 155 N95-16250
 A fourth order Euler/Navier-Stokes prediction method for the aerodynamics and aeroelasticity of hovering rotor blades p 554 N95-29242
 Unsteady pressure and inflow velocity on a pitching rotor blade in hover p 480 N95-29771
 Full-scale hingeless rotor performance and loads
 [NASA-TM-110356] p 691 N95-32699

ROTOR BLADES (TURBOMACHINERY)
 Demonstration of an elastically coupled twist control concept for tilt rotor blade application
 [BTN-94-EIX94441386633] p 196 A95-68182
 Efficient sensitivity analysis for rotary-wing aeromechanical problems
 [BTN-95-EIX95152577585] p 264 A95-73497
 Analysis of a higher harmonic control test to reduce blade vortex interaction noise
 [BTN-95-EIX95152582330] p 265 A95-73532
 Aeroelastic stability of hingeless rotor blade in hover using large deflection theory
 [HTN-95-20952] p 546 A95-88991
 Demonstration of an elastically coupled twist control concept for tilt rotor blade application
 [HTN-95-20959] p 465 A95-88998
 Flutter analysis of supersonic axial flow cascades using a high resolution Euler solver. Part 1: Formulation and validation
 [NASA-TM-105798] p 23 N95-10244
 Unsteady flows in turbines: Impact on design procedure p 90 N95-14132
 Tuned mass damper for integrally bladed turbine rotor
 [NASA-CASE-MFS-28697-1] p 159 N95-18325
 Measurement of gust response on a turbine cascade
 [NASA-TM-106776] p 117 N95-18457
 Verification of multidisciplinary models for turbomachines p 140 N95-19025

- Prediction of rotor-blade deformations due to unsteady airloads
[AD-A286593] p 231 N95-20860
- Enhanced analysis and users manual for radial-inflow turbine conceptual design code RTD
[NASA-CR-195454] p 275 N95-23462
- Comparison of numerical results and multicavity purge and rim seal data with extensions to dynamics
[NASA-TM-106685] p 416 N95-27434
- Preliminary analysis of dynamic stall effects on a 91-meter wind turbine rotor
p 376 N95-27975
- Comparative wind tunnel tests of NACA 23024 airfoils with several aileron and spoiler configurations
p 376 N95-27976
- Development of a linearized unsteady Euler analysis for turbomachinery blade rows
[NASA-CR-4677] p 592 N95-30611
- ROTOR BODY INTERACTIONS**
- Navier-Stokes simulation of rotor-body flowfield in hover using overset grids
[PAPER C15] p 1 A95-60160
- Comprehensive aeromechanics analysis of complex rotorcraft using 2GCHAS
[HTN-94-00695] p.2 A95-60174
- First level release of 2GCHAS for comprehensive helicopter analysis - a status report
[HTN-94-00697] p 2 A95-60176
- High-order state space simulation models of helicopter flight mechanics
[HTN-95-A0494] p 237 A95-72565
- Design optimization of rotor blades for improved performance and vibration
[HTN-95-A0498] p 229 A95-72569
- Vortex methods for the computational analysis of rotor/body interaction
[HTN-95-61072] p 369 A95-83656
- Air resonance of hingeless rotor helicopters in trimmed forward flight
[HTN-95-61075] p 369 A95-83659
- Considerations in the development of the coupled rotor fuselage model
[HTN-95-61077] p 370 A95-83661
- Navier-Stokes calculations of rotor-airframe interaction in forward flight
[HTN-95-01087] p 468 A95-90273
- Experimental data on the aerodynamic interactions between a helicopter rotor and an airframe
p 116 N95-17883
- An investigation of helicopter dynamic coupling using an analytical model
[NASA-CR-197420] p 285 N95-23217
- An analytic modeling and system identification study of helicopter dynamics
p 505 N95-29787
- ROTOR DYNAMICS**
- On calculated models for impellers of centrifugal compressors
[BTN-94-EIX94461407947] p 88 A95-62265
- Stability of magnetic bearing-rotor systems and the effects of gravity and damping
[BTN-94-EIX94441386619] p 208 A95-68168
- Demonstration of an elastically coupled twist control concept for tilt rotor blade application
[BTN-94-EIX94441386633] p 196 A95-68182
- Using adaptive structures to attenuate rotary wing aeroelastic response
[BTN-95-EIX95062487547] p 192 A95-68361
- Measurement around a rotor blade excited in pitch. Part 1: Dynamic inflow
[HTN-95-31007] p 220 A95-71177
- Measurement around a rotor blade excited in pitch. Part 2: Unsteady surface pressure
[HTN-95-31008] p 220 A95-71178
- Air and ground resonance of helicopters with elastically tailored composite rotor blades
[HTN-95-A0497] p 222 A95-72568
- Improving prediction: The incorporation of simplified rotor dynamics in a mathematical model of the bell 412HP
[BTN-95-EIX95152584679] p 282 A95-73591
- Transient analysis of a cracked rotor passing through critical speed
[BTN-94-EIX94401360022] p 306 A95-74702
- Identification of higher order helicopter dynamics using linear modeling methods
[HTN-95-80851] p 290 A95-75093
- Effects of high order dynamics on helicopter flight control law design
[HTN-95-80852] p 290 A95-75094
- Integrated flight/propulsion control for helicopters
[HTN-95-80854] p 290 A95-75096
- Effects of AMB parameters on the dynamic stability of the rotor
[BTN-94-EIX94381353450] p 323 A95-75494
- Multilevel decomposition procedure for efficient design optimization of helicopter rotor blades
[BTN-95-EIX95222650784] p 334 A95-79240
- A higher harmonic control test in the DNW to reduce impulsive BVI noise
[HTN-95-61071] p 385 A95-83655
- Vortex methods for the computational analysis of rotor/body interaction
[HTN-95-61072] p 369 A95-83656
- An analytical model for a nonlinear elastomeric lag damper and its effect on aeromechanical stability in Hover
[HTN-95-61076] p 369 A95-83660
- Considerations in the development of the coupled rotor fuselage model
[HTN-95-61077] p 370 A95-83661
- Fast Floquet theory and trim for multi-bladed rotorcraft
[HTN-95-61078] p 370 A95-83662
- The dynamic nature of rotor thermal bending due to unsteady lubricant shearing within a bearing
[HTN-95-42091] p 430 A95-83857
- GETRAN: A generic, modularly structured computer code for simulation of dynamic behavior of aero- and power generation gas turbine engines
[BTN-94-EIX95011441241] p 431 A95-84198
- Navier-Stokes calculations of rotor-airframe interaction in forward flight
[HTN-95-01087] p 468 A95-90273
- Correlation of unsteady pressure and inflow velocity fields of a pitching rotor blade
[BTN-95-EIX0619952748169] p 589 A95-94463
- Development of an experimental facility for analysis of rotor dynamic phenomena
[AD-A281897] p 25 N95-11330
- Dynamic response of NASA Rotor Test Apparatus and Sikorsky S-76 hub mounted in the 80- by 120-Foot Wind Tunnel
[NASA-TM-108847] p 25 N95-11389
- Aeroelastic simulation of higher harmonic control
[NASA-CR-4623] p 37 N95-11911
- Advanced distributed simulation technology advanced rotary wing aircraft. Study comparing approaches to modeling the ARWA main rotor
[AD-A280824] p 79 N95-14306
- Tuned mass damper for integrally bladed turbine rotor
[NASA-CASE-MFS-28697-1] p 159 N95-18325
- A linear system identification and validation of an AH-64 Apache aeroelastic simulation model
p 146 N95-18903
- The dynamic approach to rotor blade research: ARA's oscillatory test facility
[ARA-MEMO-405] p 223 N95-20758
- Influence of backup bearings and support structure dynamics on the behavior of rotors with active supports
[NASA-CR-197438] p 310 N95-23190
- Evaluation of thermal barrier and PS-200 self-lubricating coatings in an air-cooled rotary engine
[NASA-CR-195445] p 289 N95-23222
- Dynamic behavior of a magnetic bearing supported jet engine rotor with auxiliary bearings
[NASA-CR-197860] p 338 N95-24213
- Thermohydrodynamic analysis of cryogenic liquid turbulent flow fluid film bearings, phase 2
[NASA-CR-197412] p 349 N95-24461
- Aircraft noise prediction program theoretical manual: Rotorcraft System Noise Prediction System (ROTONET), part 4
[NASA-TM-83199-PT-4] p 451 N95-26392
- Development and validation of a blade-element mathematical model for the AH-64A Apache helicopter
[NASA-TM-108863] p 367 N95-26710
- Stall precursor study of high frequency data for three high speed, swept compressor rotors
[AD-A289379] p 406 N95-26878
- Whirl plus tilt
[DE95-007948] p 452 N95-28108
- Modeling helicopter blade dynamics using a modified Myklestad-Prohl transfer matrix method
[AD-A289891] p 400 N95-28626
- An analytic modeling and system identification study of helicopter dynamics
p 505 N95-29787
- Vibration reduction in helicopter rotors using an actively controlled partial span trailing edge flap located on the blade
p 624 N95-32111
- Influence of backup bearings and support structure dynamics on the behavior of rotors with active supports
[NASA-CR-199080] p 307 N95-32689
- Steady-state dynamic behavior of an auxiliary bearing supported rotor system
p 703 N95-32690
- Dynamic behavior of a magnetic bearing supported jet engine rotor with auxiliary bearings
p 703 N95-32691
- Dynamic modelling and response characteristics of a magnetic bearing rotor system with auxiliary bearings
p 703 N95-32692
- Synchronous dynamics of a coupled shaft/bearing/housing system with auxiliary support from a clearance bearing: Analysis and experiment
p 703 N95-32693
- ROTOR SPEED**
- Experimental/analytical approach to understanding mistuning in a transonic wind tunnel compressor
[NASA-TM-108833] p 95 N95-14617
- ROTOR STATOR INTERACTIONS**
- The use of cowl camber and taper to reduce rotor/stator interaction noise
[NASA-CR-195421] p 323 N95-22675
- ROTOR SYSTEMS RESEARCH AIRCRAFT**
- H-76B fantail demonstrator composite fan blade fabrication
[HTN-95-80856] p 283 A95-75098
- ROTORS**
- New strategy combining backward inference with forward inference in monitoring and diagnosing techniques for hydrodynamic bearing-rotor systems
[BTN-94-EIX94331336949] p 88 A95-61795
- A stationary flow of a viscous liquid in radial clearances of rotor bearings in the turbocompressor of an internal combustion engine
[BTN-94-EIX94461408765] p 153 A95-63648
- Unbalance response of a dual rotor system: Theory and experiment
[BTN-94-EIX94351143320] p 195 A95-65854
- Modeling rotating shafts using axisymmetric solid finite elements with matrix reduction
[BTN-94-EIX94351143328] p 207 A95-67301
- Stability of magnetic bearing-rotor systems and the effects of gravity and damping
[BTN-94-EIX94441386619] p 208 A95-68168
- Recent studies of rotorcraft blade-vortex interaction noise
[BTN-95-EIX95062487521] p 218 A95-69229
- Finite element model for a flexible non-symmetric rotor on distributed bearing: A stability study
[BTN-94-EIX94381352212] p 306 A95-74612
- Transient analysis of a cracked rotor passing through critical speed
[BTN-94-EIX94401360022] p 306 A95-74702
- Effects of AMB parameters on the dynamic stability of the rotor
[BTN-94-EIX94381353450] p 323 A95-75494
- Modal characteristics of rotors using a conical shaft finite element
[BTN-94-EIX94401359745] p 346 A95-77379
- The dynamic nature of rotor thermal bending due to unsteady lubricant shearing within a bearing
[HTN-95-42091] p 430 A95-83857
- Stability of magnetic bearing-rotor systems and the effects of gravity and damping
[HTN-95-20955] p 465 A95-88994
- A switched reluctance machine rotor position estimator: A neural network application
[SAE PAPER 932560] p 511 A95-90057
- Matrix isolated HF: the high-resolution infrared spectrum of a cryogenically solvated hindered rotor
[GTN-95-0301010494002231-16] p 578 A95-92210
- New eigensolutions and modal analysis for gyroscopic/rotor systems, part 1: undamped systems
[BTN-94-EIX94522410219] p 702 A95-96373
- New eigensolutions and modal analysis for gyroscopic/rotor systems, part 2: perturbation analysis for damped systems
[BTN-94-EIX94522410220] p 702 A95-96374
- Modal parameters for cracked rotors: models and comparisons
[BTN-94-EIX94522410226] p 702 A95-96378
- Van der pol absorber for rotor vibrations
[BTN-94-EIX94441385106] p 702 A95-96579
- Effects of a forward-swept front rotor on the flowfield of a counterrotation propeller
[NASA-TM-106671] p 7 N95-10148
- Development of an experimental facility for analysis of rotor dynamic phenomena
[AD-A281897] p 25 N95-11330
- Dynamic response of NASA Rotor Test Apparatus and Sikorsky S-76 hub mounted in the 80- by 120-Foot Wind Tunnel
[NASA-TM-108847] p 25 N95-11389
- Ceramic manufacturing: Optimizing a multivariable system
[DE94-015016] p 56 N95-13184
- Evaluation of energy-sink stability criteria for dual-spin spacecraft
[AD-A283228] p 87 N95-14850
- A Lifting Ball Valve for cryogenic fluid applications
p 156 N95-16349
- Numerical simulation of helicopter engine plume in forward flight
[NASA-CR-197488] p 107 N95-16589
- Structural effects of unsteady aerodynamic forces on horizontal-axis wind turbines
[DE94-011863] p 157 N95-16939
- Wave cycle design for wave rotor engines with limited nitrogen oxide emissions
p 161 N95-18901

Wind tunnel tests of a 42 inch diameter self-starting autogyro rotor
 [AD-A279922] p 188 N95-19863

Variations observed in the AC generator signal period of a Sea King helicopter
 [AD-A284280] p 230 N95-19963

Scale-up and modeling of forced chemical vapor infiltration
 [DE94-017769] p 247 N95-20781

Advanced wind turbine design studies: Advanced conceptual study
 [DE93-000031] p 256 N95-20985

Influence of backup bearings and support structure dynamics on the behavior of rotors with active supports
 [NASA-CR-197438] p 310 N95-23190

Thin tailored composite wing for civil tiltrotor
 p 285 N95-23317

Dynamic behavior of a magnetic bearing supported jet engine rotor with auxiliary bearings
 [NASA-CR-197860] p 338 N95-24213

Exploratory flow visualization investigation of mast-mounted sights in presence of a rotor
 [NASA-TM-4634] p 330 N95-24566

Recent improvements to and validation of the one dimensional NASA wave rotor model
 [NASA-TM-106913] p 332 N95-25962

Dynamics of phase ordering of nematics in a pore
 [DE95-607662] p 362 N95-25978

Optimization of wave rotors for use as gas turbine engine topping cycles
 [NASA-TM-106951] p 406 N95-27860

Comparative wind tunnel tests of NACA 23024 airfoils with several aileron and spoiler configurations
 p 376 N95-27976

Whirl plus tilt
 [DE95-007948] p 452 N95-28108

PREDICAT: First order performance calculations of windturbine rotors using the method of the acceleration potential
 [PB95-206454] p 564 N95-30200

Wave rotor-enhanced gas turbine engines
 [NASA-TM-106998] p 615 N95-30517

A numerical model for dynamic wave rotor analysis
 [NASA-TM-106997] p 615 N95-30617

Preliminary assessment of combustion modes for internal combustion wave rotors
 [NASA-TM-107000] p 616 N95-30632

Improved modeling of unsteady heat transfer (The first step)
 [AD-A292777] p 648 N95-31432

Application of multigrid computational fluid dynamics (CFD) methods to rotor analysis
 [AD-A293012] p 648 N95-31475

Influence of backup bearings and support structure dynamics on the behavior of rotors with active supports
 [NASA-CR-199080] p 703 N95-32689

Steady-state dynamic behavior of an auxiliary bearing supported rotor system
 p 703 N95-32690

Dynamic behavior of a magnetic bearing supported jet engine rotor with auxiliary bearings
 p 703 N95-32691

Dynamic modelling and response characteristics of a magnetic bearing rotor system with auxiliary bearings
 p 703 N95-32692

Synchronous dynamics of a coupled shaft/bearing/housing system with auxiliary support from a clearance bearing: Analysis and experiment
 p 703 N95-32693

ROUTES

Three-D weather displays for aircraft cockpits
 [AD-A289759] p 508 N95-28691

Conceptual design of a map interactive system for military aircraft cockpits
 [AD-A289760] p 508 N95-28692

FAA aviation forecasts: Fiscal year 1995-2006
 [AD-A293682] p 584 N95-31598

RUBBER

Evaluation of alternative pavement marking materials
 [AD-A292973] p 626 N95-31468

RUDDERS

Numerical analysis of flow field around gas rudder
 p 407 A95-82333

The development of a highly reliable power management and distribution system for civil transport aircraft
 [NASA-TM-106697] p 50 N95-11867

RUGGEDNESS

Depolarizing trihedral corner reflectors for radar navigation and remote sensing
 [BTN-95-EIX95302727634] p 636 A95-94108

RUN TIME (COMPUTERS)

Design of a real-time wind turbine simulator using a custom parallel architecture
 p 449 N95-27979

RUNGE-KUTTA METHOD

Parallel implicit unstructured grid Euler solvers
 [BTN-95-EIX95042474393] p 217 A95-68307

Effects of spatial order of accuracy on the computation of vortical flowfields
 [BTN-95-EIX95152577604] p 305 A95-73479

Accuracy and efficiency assessments for a weak statement CFD algorithm for high-speed aerodynamics
 [BTN-94-EIX95011441238] p 370 A95-84195

Evaluation of a multigrid-based Navier-Stokes solver for aerothermodynamic computations
 [BTN-95-EIX95302694459] p 583 A95-94056

Numerical solution of Euler and Navier-Stokes equations for 2D transonic problems
 p 638 A95-95366

Hypersonic Navier-Stokes computations about complex configurations
 p 644 A95-95497

The role of CFD in the design process
 p 90 N95-14135

Numerical computation of aerodynamics and heat transfer in a turbine cascade and a turn-around duct using advanced turbulence models
 p 313 N95-23444

Parallel block implicit integration technique for trajectory parallelism
 [AD-A288961] p 450 N95-28335

Numerical study to assess sulfur hexafluoride as a medium for testing multielement airfoils
 [NASA-TP-3496] p 378 N95-28674

Development of a rotary wing Navier-Stokes CFD code based on TLNS3D code
 [AD-A290421] p 554 N95-29387

Comparison of spatial numerical operators for duct-nozzle acoustics
 p 580 N95-30158

RUNWAY ALIGNMENT

Arrival traffic handling for a parallel runway airport
 p 487 A95-91537

RUNWAY CONDITIONS

Guidance and control requirements for high-speed Rollout and Turnoff (ROTO)
 [NASA-CR-195026] p 292 N95-22674

RUNWAY LIGHTS

Developments in airfield lighting
 [CONGRESS PAPER C428-7-147] p 488 A95-91688

RUNWAYS

NASA evaluation of Type 2 chemical depositions --- effects of deicer deposition on aircraft tire friction performance
 [SAE PAPER 932582] p 495 A95-90086

The performance of forward scatter visibility sensors for application in autostations and runway visual range in snow and freezing precipitation events
 p 662 A95-93489

Additives in bituminous materials and fuel-resistant sealers
 [DOT/FAA/CT-94/78] p 55 N95-12131

Marginal aggregates in flexible pavements: Background survey and experimental plan
 [DOT/FAA/CT-94/58] p 53 N95-12216

The Balsa bullet: A high speed, low-cost general aviation aircraft for Aeroworld
 [NASA-CR-197165] p 46 N95-12638

Modeling of Instrument Landing System (ILS) localizer signal on runway 25L at Los Angeles International Airport
 [NASA-TM-4588] p 125 N95-17384

Aircraft wake vortex takeoff tests at O'Hara International Airport
 [AD-A283828] p 118 N95-18624

Super-heavy aircraft study
 [AD-A279602] p 238 N95-19955

Aircraft accident report. Runway overrun following rejected takeoff. Continental airlines flight 795, McDonnell Douglas MD-82, N18835, LaGuardia Airport, Flushing, NY, 2 March 1994
 [PB95-910401] p 277 N95-23609

Aircraft accident report: Impact with blast fence upon landing rollout Action Air Charters flight 990 Piper PA-31-350, N990RA, Stratford, Connecticut, 27 April 1994
 [PB94-910410] p 333 N95-24206

Precision landing system mathematical modeling study report for Andrews Air Force Base, runway 19L, Camp Springs, MD
 [AD-A289015] p 384 N95-27903

Evaluation of retro-reflective beads in airport pavement markings
 [AD-A291065] p 523 N95-29967

Prototype stop bar system evaluation at Seattle-Tacoma International Airport
 [AD-A290136] p 490 N95-30031

Low-level data fusion for landing runways detection
 p 689 N95-33136

RUSSIAN FEDERATION

Development of strength analysis methods and design model for aircraft constructions in Kazan Aviation Institute
 p 127 N95-16264

JPRS report: Science and technology. Central Eurasia [JPRS-UST-94-027] p 349 N95-24470

JPRS report: Science and technology. Central Eurasia [JPRS-UST-94-018] p 349 N95-24472

JPRS Report: Science and technology. Central Eurasia
 [JPRS-UST-94-032] p 350 N95-24759

JPRS report: Science and technology. Central Eurasia [JPRS-UST-94-022] p 438 N95-27699

FBIS report: Science and technology. Central Eurasia [FBIS-UST-95-029] p 649 N95-31728

S

S MATRIX THEORY

Hybrid finite element-modal analysis of jet engine inlet scattering
 [BTN-95-EIX95242673665] p 427 A95-82259

S WAVES

Beyond the Riemann problem, part 1
 p 550 A95-91925

SAAB AIRCRAFT

The auxiliary and emergency power supply on the Saab JAS39 Gripen aircraft
 [CONGRESS PAPER C428-36-192] p 612 A95-93631

SABOT PROJECTILES

Analytical solution and parameter estimation of projectile dynamics
 [BTN-95-EIX95212645695] p 272 A95-76747

Hypersonic aerodynamics test facility using the external propulsion accelerator
 [AIAA PAPER 95-6138] p 470 A95-90455

SABOTAGE

Explosive sabotage: The potential effects of explosive charges on aircraft
 [CONGRESS PAPER C428-11-034] p 484 A95-91702

SAFETY

Safety in airport ground handling
 p 626 A95-95193

Cabin fuselage structural design with engine installation and control system
 [NASA-CR-197173] p 47 N95-12639

Mishap risk control for advanced aerospace/composite materials
 p 301 N95-23031

SAFETY DEVICES

Lightning protection technology for small general aviation composite material aircraft
 [SAE PAPER 931241] p 483 A95-88964

Risk analysis for the fire safety of airline passengers
 [PB94-194065] p 77 N95-14179

Aviation security: Development of new security technology has not met expectations. Report to Congressional requesters
 [GAO/RCED-94-142] p 687 N95-32885

SAFETY FACTORS

Aircraft accident investigation and airworthiness -- A practical example of the interaction of two disciplines with some reflections on possible legal consequences
 [HTN-95-50219] p 176 A95-64856

Accelerated application development for flight software
 [AIAA PAPER 95-1031] p 566 A95-90703

Explanatory factors for the geographic distribution of U.S. Civil aviation mortality
 [HTN-95-92908] p 484 A95-91846

Reaction-time response of aircraft crash
 [BTN-95-EIX95292721296] p 595 A95-92626

Illustrated structural application of universal first-order reliability method
 [NASA-TP-3501] p 54 N95-11870

Characteristics of civil aviation atmospheric hazards
 p 42 N95-13208

Generic architectures for future flight systems
 p 99 N95-14159

Wake turbulence
 p 75 N95-14894

The global aircraft shape
 p 128 N95-16571

Safety aspects of spacecraft commanding
 p 149 N95-17248

Aircraft and sub-system certification by piloted simulation
 [AGARD-AR-278] p 145 N95-17388

The personal aircraft: Status and issues
 [NASA-TM-109174] p 223 N95-20688

Analysis of test criteria for specifying foam firefighting agents for aircraft rescue and firefighting
 [AD-A286381] p 227 N95-22352

Corrosion detection and monitoring of aircraft structures: An overview
 p 303 N95-23515

Metascientific problems in safety science
 [PB95-196408] p 645 N95-30521

SAFETY MANAGEMENT

Maintenance programs
 [BTN-95-EIX95182617809] p 261 A95-75754

Human factors issues in aircraft cabin design
 [SAE PAPER 932527] p 386 A95-84556

FAA's Aging Commuter Airplane Program
 [SAE PAPER 931248] p 483 A95-89220

- Safety aspects of spacecraft commanding p 149 N95-17248
- Safety study: Commuter airline safety [PB94-917004] p 124 N95-19132
- Rotorcraft ditchings and water-related impacts that occurred from 1982 to 1989, phase 1 [AD-A279164] p 189 N95-19805
- A review of civil aviation fatal accidents in which loss/disoriented was a cause/factor: 1981-1990 [DOT/FAA/AM-95/1] p 278 N95-24071
- Aviation Accident Investigation Symposium. Volume 1: Industry recommendations and Safety Board responses [PB94-917005] p 278 N95-24105
- Metascientific problems in safety science [PB95-196408] p 645 N95-30521
- Fact sheet for Congressional Committees. Air traffic control: Status of FAA's modernization program [GAO/RCED-94-167FS] p 603 N95-32197
- SALT BATHS**
- Corrosion of landing gear steels p 302 N95-23500
- SALT SPRAY TESTS**
- The effects of pitting on fatigue crack nucleation in 7075-T6 aluminum alloy p 88 N95-14482
- Corrosion of landing gear steels p 302 N95-23500
- SAMPLING**
- Electro-optic characterization of ultrafast photodetectors using adiabatically compressed soliton pulses [BTN-94-EIX94381359637] p 257 A95-72675
- Monitoring noise from aircraft operations in the vicinity of airports p 570 A95-88462
- Nordic Standards for measurement of aircraft noise immersion in residential areas and noise reduction of dwellings p 570 A95-88463
- SANDS**
- Marginal aggregates in flexible pavements: Background survey and experimental plan [DOT/FAA/CT-94/58] p 53 N95-12216
- The operation of gas turbine engines in hot and sandy conditions: Royal Air Force experiences in the Gulf conflict p 198 N95-19655
- US Army rotorcraft turboshaft engines sand and dust erosion considerations p 198 N95-19656
- Future directions in helicopter protection system configuration p 198 N95-19657
- Erosion of T56 5th stage rotor blades due to bleed hole overtip flow p 200 N95-19666
- SANDWICH STRUCTURES**
- Minimum-mass design of sandwich aerobrakes for a lunar transfer vehicle [BTN-95-EIX95212645707] p 299 A95-76759
- An investigation of the accuracy of FEM analysis of a graphite epoxy box beam [SAE PAPER 931221] p 543 A95-88011
- Analysis and testing of a graphite-epoxy sandwich shell fuselage test structure [ISBN 1-879921-01-4] p 605 A95-93746
- Composite repair issues on the CF-18 aircraft p 395 N95-27518
- External patch repair of CFRP/honeycomb sandwich p 395 N95-27522
- Application of fiber-reinforced bismaleimide materials to aircraft nacelle structures p 397 N95-28278
- In situ processing methods for composite fuselage sandwich structures p 531 N95-28826
- The effects of design details on cost and weight of fuselage structures p 501 N95-28831
- Buckling analysis of curved composite sandwich panels subjected to inplane loadings p 533 N95-28845
- SAPPHIRE**
- The effect of interface properties on nickel base alloy composites [NASA-CR-198363] p 629 N95-30787
- SATELLITE ALTIMETRY**
- Using IRI for the computation of ionospheric corrections for altimeter data analysis p 212 A95-66949
- Precise orbit determination with a short-arc technique — Abstract only p 240 A95-70543
- Precision orbit determination of altimetric satellites p 86 N95-14282
- SATELLITE ATTITUDE CONTROL**
- Space flight tests of attitude determination using GPS [BTN-95-EIX95112522529] p 190 A95-69334
- SATELLITE COMMUNICATION**
- Development of aeronautical mobile satellite services over the past thirty years [BTN-95-EIX95152569458] p 305 A95-73498
- Pilot Weather Advisor system [BTN-95-EIX95152582314] p 316 A95-73517
- Aeronautical satellite communications using the ETS-5 satellite p 487 A95-91541
- The use of satellites for aeronautical communications, navigation and surveillance [CONGRESS PAPER C428-30-159] p 600 A95-93613
- Space Generic Open Avionics Architecture (SGOAA): Overview p 99 N95-14161
- SATELLITE CONSTELLATIONS**
- Modeling spatio-temporal databases to measure the performance of the GPS satellite constellation p 489 N95-29596
- SATELLITE CONTROL**
- AIAA Computing in Aerospace 10, San Antonio, TX, March 28-30, 1995 [ISBN 1-56347-119-1] p 565 A95-90629
- SATELLITE DRAG**
- Calculation of satellite drag coefficients [AD-A285118] p 300 N95-23781
- SATELLITE IMAGERY**
- Correction of thin cirrus effects in AVIRIS images using the sensitive 1.375-micron cirrus detecting channel p 708 N95-33748
- SATELLITE NAVIGATION SYSTEMS**
- High accuracy navigation and landing system using GPS/IMU system integration [BTN-94-EIX94441386128] p 189 A95-68185
- Results and performance of multi-site reference station differential GPS [BTN-95-EIX95112522534] p 190 A95-69329
- Failure detection and isolation structure for global positioning system autonomous integrity monitoring [BTN-95-EIX95282706656] p 486 A95-89648
- Generic architectures for future flight systems p 99 N95-14159
- An investigation into the use of satellite-based positioning systems for flight reference/autoland operations p 489 N95-29542
- Effects of the specific military aspects of satellite navigation on the civil use of GPS/GLONASS p 688 N95-33134
- SATELLITE OBSERVATION**
- Possible near-IR channels for remote sensing precipitable water vapor from geostationary satellite platforms [HTN-95-70139] p 214 A95-69431
- Air truth validation of cloud albedo estimated from NOAA advanced very high resolution radiometer data [HTN-95-A1021] p 443 A95-94526
- Alaska's volcanic ash warning system p 663 A95-93495
- An in situ evaluation of TOPEX/Poseidon altimetric measurements versus measurements made by moorings and inverted echo sounders for sea surface height [NASA-CR-198821] p 447 N95-27805
- SATELLITE ORBITS**
- Validation of empirical orbit error corrections using crossover difference differences [HTN-94-00912] p 25 A95-60227
- Variations of perturbations in perigee height with eccentricity for artificial Earth's satellites due to air drag [HTN-95-40013] p 85 A95-62657
- Precise orbit determination with a short-arc technique — Abstract only p 240 A95-70543
- Thermal force modeling for global positioning system satellites using the finite element method [BTN-95-EIX95152583270] p 278 A95-73571
- Precision orbit determination of altimetric satellites p 86 N95-14282
- Determining GPS average performance metrics p 383 N95-27791
- SATELLITE PERTURBATION**
- Variations of perturbations in perigee height with eccentricity for artificial Earth's satellites due to air drag [HTN-95-40013] p 85 A95-62657
- SATELLITE TEMPERATURE**
- Thermal design of returnable satellites [AD-A294113] p 701 N95-34500
- SATELLITE TRACKING**
- Precise orbit determination with a short-arc technique — Abstract only p 240 A95-70543
- Tropical cyclone observation and forecasting with and without aircraft reconnaissance [HTN-95-80701] p 254 A95-72545
- Application of fuzzy logic to optimize placement of an acquisition, tracking, and pointing experiment p 341 A95-80390
- Flight Mechanics/Estimation Theory Symposium 1995 [NASA-CP-3299] p 416 N95-27763
- Determining GPS average performance metrics p 383 N95-27791
- SATELLITE-BORNE INSTRUMENTS**
- Integrated X-ray testing of the electro-optical breadboard model for the XMM reflection grating spectrometer [DE95-008829] p 644 N95-30507
- SAWS**
- Vortex shedding noise control in idling circular saws using air ejection at the teeth [BTN-94-EIX94371347214] p 257 A95-69970
- SCALARS**
- Momentum and scalar transfer coefficients over aerodynamically smooth Antarctic surfaces [HTN-95-92932] p 562 A95-91870
- SCALE EFFECT**
- Scale effects on aircraft and weapon aerodynamics [AGARD-AG-323] p 67 N95-14103
- Methods for scaling icing test conditions [NASA-TM-106827] p 124 N95-19284
- SCALE MODELS**
- Aerodynamic characteristics of a canard-controlled missile at high angles of attack [BTN-95-EIX95152583257] p 267 A95-73558
- The model builders [NASA-TM-109902] p 20 N95-10552
- Radio controlled for research [NASA-TM-104292] p 17 N95-10717
- Flow-visualization study of the X-29A aircraft at high angles of attack using a 1/48-scale model [NASA-TM-104268] p 8 N95-10858
- Pressure measurements on an F/A-18 twin vertical tail in buffeting flow. Volume 3: Buffet power spectral densities [AD-A281444] p 36 N95-11829
- Laws of infrared similitude [AD-A282209] p 62 N95-12426
- Impingement flow heat transfer measurements of turbine blades using a jet array [AD-A283450] p 62 N95-12512
- Design and construction of a remote piloted flying wing [NASA-CR-197195] p 47 N95-12695
- Mach number control in the High Speed Wind Tunnel of NLR [PB94-201670] p 53 N95-13243
- Methods for scaling icing test conditions [NASA-TM-106827] p 124 N95-19284
- Particle deposition in gas turbine blade film cooling holes p 199 N95-19661
- Heat transfer measurements in small scale wind tunnels [AD-A288689] p 341 N95-26053
- Comparative wind tunnel tests of NACA 23024 airfoils with several aileron and spoiler configurations p 376 N95-27976
- Transonic, supersonic and hypersonic wind-tunnel tests on aerodynamic characteristics of reentry body with blunted cone configuration [ISAS-658] p 480 N95-29640
- Subscale study of engine bellmouth inlet vortices in test cell R1D [AD-A294993] p 707 N95-34818
- SCALING LAWS**
- On the scaling of small-scale jet noise to large scale [AIAA PAPER 92-02109] p 27 A95-60166
- Scaling of incipient separation in supersonic/transonic speed laminar flows [BTN-95-EIX95182619104] p 269 A95-76589
- Some aspects of the aeroacoustics of extreme-speed jets p 572 A95-88893
- Methods for scaling icing test conditions [NASA-TM-106827] p 124 N95-19284
- SCANDINAVIA**
- Nordic Standards for measurement of aircraft noise immersion in residential areas and noise reduction of dwellings p 570 A95-88463
- Nortaf: Computer generated aerodome forecasts p 668 A95-93521
- The combination of forecasts in an automated aviation weather forecasting system p 669 A95-93522
- SCANNERS**
- Foliage transmission measurements using a ground-based ultrawide band (300-1300 MHz) SAR system [BTN-94-EIX94381351617] p 252 A95-70950
- TDWR scan strategy implementation [AD-A284877] p 98 N95-15749
- Evaluation of scanners for C-scan imaging in nondestructive inspection of aircraft [DE94-012473] p 152 N95-19100
- Test and Evaluation Plan (TEP) for Improvised Explosive Device Screening Systems (IEDSS) [AD-A286382] p 227 N95-22319
- SCANNING ELECTRON MICROSCOPY**
- SEM representation of the early and late time fields scattered from wire targets [BTN-94-EIX94381353142] p 306 A95-74496
- High aspect ratio metal microstructures and method for preparing the same [AD-D017463] p 629 N95-30750
- SCATTERING**
- Planar air density measurements near model surfaces by ultraviolet Rayleigh/Raman scattering [BTN-94-EIX94441386614] p 213 A95-67345
- Scattering of short em-pulses by simple and complex targets using impulse radar p 486 A95-90953
- Ultra-wideband electromagnetic target identification p 486 A95-90955

- Unanswered questions concerning the Nocilla gas-surface interaction model
[ISBN 1-979921-01-4] p 628 A95-93716
- Apparatus and method for producing three-dimensional images
[AD-D017455] p 646 N95-30727
- SCHEDULES**
- A hybrid vehicle evaluation code and its application to vehicle design. Revision 1
[DE95-008053] p 441 N95-28029
- A hybrid vehicle evaluation code and its application to vehicle design, revision 2
[DE95-008060] p 441 N95-28139
- Patient/aircraft forecasting for the strategic aeromedical evacuation lift-bed process
[AD-A293902] p 599 N95-31512
- SCHEDULING**
- Changing MRP Systems within the aerospace industry [CONGRESS PAPER C428-26-051] p 681 A95-93603
- Empirical results on scheduling and dynamic backtracking p 299 N95-23761
- A gain scheduling optimization method using genetic algorithms
[AD-A289306] p 448 N95-26920
- An analysis of the impact of ASPA on organizational and depot level maintenance
[AD-A292670] p 457 N95-29414
- SCHLIEREN PHOTOGRAPHY**
- A study of compressibility effects on dynamic stall of rapidly pitching airfoils
[HTN-94-00715] p 5 A95-60193
- Aerodynamic investigation with focusing schlieren in a cryogenic wind tunnel
[HTN-95-20835] p 544 A95-88096
- Fixed transition for shock tube transonic flow p 472 A95-91509
- An optical technique for examining aircraft shock wave structures in flight p 96 N95-14879
- Two-dimensional scramjet inlet unstart model: Wind-tunnel blockage and actuation systems test [NASA-TM-109984] p 97 N95-15899
- Wind tunnel investigations of the appearance of shocks in the windward region of bodies with circular cross section at angle of attack p 113 N95-17866
- Visualization of the multiple supersonic jet oscillations by swept focused strobed schlieren technique p 367 N95-26952
- SCHMIDT NUMBER**
- Aerodynamic applications of underexpanded hypersonic viscous jets
[BTN-95-EIX0619952748162] p 589 A95-94456
- SCIENTIFIC VISUALIZATION**
- A prototype for displaying aviation forecast variables using Eta numerical model output p 676 A95-93555
- Advanced data visualization and sensor fusion: Conversion of techniques from medical imaging to Earth science p 711 N95-34236
- SCIENTISTS**
- Two projects of V. M. Myasishchev
[HTN-95-50269] p 176 A95-65764
- ICASE
[NASA-CR-195001] p 170 N95-16898
- SEA LEVEL**
- Precision orbit determination of altimetric satellites p 86 N95-14282
- An in situ evaluation of TOPEX/Poseidon altimetric measurements versus measurements made by moorings and inverted echo sounders for sea surface height [NASA-CR-198621] p 447 N95-27805
- SEALERS**
- Additives in bituminous materials and fuel-resistant sealers
[DOT/FAA/CT-94/78] p 55 N95-12131
- SEALING**
- Hypersonic engine seal development at NASA Lewis Research Center p 60 N95-13602
- SEALS (STOPPERS)**
- Development of hypersonic engine seals: Flow effects of preload and engine pressures
[BTN-95-EIX95112524204] p 196 A95-69304
- Thermo-hydrodynamic solution of floating ring seals for high pressure compressors using the finite-element method
[HTN-95-92246] p 433 A95-85290
- Compressor discharge film riding face seals p 60 N95-13599
- High-speed seal and bearing test facility p 53 N95-13601
- Hypersonic engine seal development at NASA Lewis Research Center p 60 N95-13602
- Comparison of numerical results and multicavity purge and rim seal data with extensions to dynamics [NASA-TM-106685] p 416 N95-27434
- Numerical analysis of intra-cavity and power-stream flow interaction in multiple gas-turbine disk-cavities
[NASA-TM-106886] p 407 N95-28344
- The fluid mechanics of a high aspect ratio slot with an impressed pressure gradient and secondary injection p 557 N95-30304
- SEAPLANES**
- Sea wave parameters, small altitudes and distances measurers design for movement control systems of ships, wing-in-surface effect crafts and seaplanes p 708 N95-33141
- SEAS**
- Prototype stop bar system evaluation at Seattle-Tacoma International Airport
[AD-A290136] p 490 N95-30031
- SEAT BELTS**
- The performance of child restraint devices in transport airplane passenger seats
[DOT/FAA/AM-94/19] p 40 N95-12146
- Development of an intervention program to encourage shoulder harness use and aircraft retrofit in general aviation aircraft, phases 1 and 2
[DOT/FAA/AM-95/2] p 333 N95-24384
- Development of an intervention program to encourage shoulder harness use and aircraft retrofit in general aviation aircraft: Phases 1 and 2
[AD-A290966] p 485 N95-29873
- SEATS**
- Dynamic behavior of valves with pneumatic chamber for reciprocating compressors
[BTN-94-EIX94351143311] p 207 A95-65845
- A correlative investigation of simulated occupant motion and accident report in a helicopter crash
[AD-A285190] p 123 N95-16404
- Analysis of warping effects on the static and dynamic response of a seat-type structure
[NIAR-94-12] p 348 N95-24211
- The effect of wear on fire-blocking layer material effectiveness
[AD-A291520] p 485 N95-29855
- SECONDARY FLOW**
- An experimental study on interacting flow between supersonic flow and secondary flow injected normally through circular nozzle p 472 A95-91511
- Elements of a modern turbomachinery design system p 90 N95-14129
- Static investigation of two fluidic thrust-vectoring concepts on a two-dimensional convergent-divergent nozzle
[NASA-TM-4574] p 120 N95-19042
- Three-dimensional unsteady flow calculations in an advanced gas generator turbine p 312 N95-23425
- Internal performance characteristics of thrust-vectoring axisymmetric ejector nozzles
[NASA-TM-4610] p 331 N95-25338
- Turbomachinery design and tonal acoustics computations
[NASA-CR-197749] p 406 N95-26777
- Numerical analysis of intra-cavity and power-stream flow interaction in multiple gas-turbine disk-cavities
[NASA-TM-106886] p 407 N95-28344
- Design of secondary flow control cascade using numerical simulation p 698 N95-34507
- SECONDARY INJECTION**
- The fluid mechanics of a high aspect ratio slot with an impressed pressure gradient and secondary injection p 557 N95-30304
- SEGMENTS**
- Control mechanism to prevent correlated message arrivals from degrading signaling no. 7 network performance
[BTN-94-EIX94341342286] p 56 A95-60842
- SELECTION**
- MCMs for avionics: Technology selection and intermodule interconnection p 234 N95-20641
- Operational parameters and material effects p 651 N95-32179
- SELECTIVE FADING**
- Experimental study of the helicopter-mobile radioelectrical channel and possible extension to the satellite-mobile channel p 247 N95-20945
- SELF ADAPTIVE CONTROL SYSTEMS**
- A neural expert approach to self designing flight control systems
[AD-A279965] p 237 N95-21122
- SELF EXCITATION**
- Aircraft nose gear shimmy studies
[SAE PAPER 931401] p 628 A95-93671
- Nonlinear dynamics and aeroelasticity of rotorcraft in forward flight
[AD-A291714] p 400 N95-28504
- SEMICONDUCTOR JUNCTIONS**
- Modeling resonance in waveguide-to-microstrip junctions by unilateral fin line resonators
[BTN-94-EIX94381323445] p 242 A95-70844
- SEMICONDUCTOR LASERS**
- Overview of remote sensing laser development and semiconductor laser technology
[DE94-019103] p 256 N95-21552
- SEMISPAN MODELS**
- 2-D and 3-D oscillating wing aerodynamics for a range of angles of attack including stall
[NASA-TM-4632] p 120 N95-19119
- Unsteady transonic wind tunnel test on a semispan straked delta wing, oscillating in pitch. Part 1: Description of the model, test setup, data acquisition, and data processing
[AD-A293113] p 593 N95-30885
- SENSITIVITY**
- Discrete shape sensitivity equations for aerodynamic problems
[BTN-94-EIX94451393721] p 88 A95-61720
- Preconditioned domain decomposition scheme for three-dimensional aerodynamic sensitivity analysis
[BTN-95-EIX95152577612] p 321 A95-73471
- Efficient sensitivity analysis for rotary-wing aeromechanical problems
[BTN-95-EIX95152577585] p 264 A95-73497
- Efficient sensitivity analysis for rotary-wing aeromechanical problems
[HTN-95-42570] p 458 A95-87200
- Preconditioned domain decomposition scheme for three-dimensional aerodynamic sensitivity analysis
[HTN-95-42597] p 459 A95-87227
- Methodology for sensitivity analysis, approximate analysis, and design optimization in CFD for multidisciplinary applications
[NASA-CR-196981] p 58 N95-13201
- Applications of automatic differentiation in computational fluid dynamics p 156 N95-16461
- Numerical simulation of ram accelerator performance including transient effects during initiation of combustion and sensitivity studies p 629 N95-31203
- Correction of thin cirrus effects in AVIRIS images using the sensitive 1.375-micron cirrus detecting channel p 708 N95-33748
- SENSORS**
- Determination of stores pointing error due to wing flexibility under flight load
[NASA-TM-4646] p 134 N95-19044
- The 1994 Fiber Optic Sensors for Aerospace Technology (FOSAT) Workshop
[NASA-CP-10166] p 337 N95-24207
- SENTENCES**
- Conversion of the TRACON operations concepts database into a formal sentence outline job task taxonomy
[DOT/FAA/AM-95/16] p 488 N95-28819
- SEPARATED FLOW**
- LDV measurements in dynamically separated flows [ISBN 0-8194-1311-9] p 5 A95-60191
- State-space representation of aerodynamic characteristics of an aircraft at high angles of attack
[BTN-95-EIX95062487536] p 187 A95-69244
- Two-equation turbulence model for unsteady separated flows around airfoils
[BTN-95-EIX95142553054] p 262 A95-73444
- Computation of oscillating airfoil flows with one- and two-equation turbulence models p 263 A95-73494
- Computational study of plume-induced separation on a hypersonic powered model
[BTN-95-EIX95152582346] p 266 A95-73548
- Simulating heat addition via mass addition in constant area compressible flows p 307 A95-76585
- Scaling of incipient separation in supersonic/transonic speed laminar flows
[BTN-95-EIX95182619104] p 269 A95-76589
- Neural network prediction of three-dimensional unsteady separated flowfields
[BTN-95-EIX95182619232] p 308 A95-76658
- Reattachment studies of an oscillating airfoil dynamic stall flowfield
[HTN-95-51660] p 432 A95-85042
- Crossflow topology of vortical flows
[HTN-95-51664] p 432 A95-85046
- Low-dimensional description of the dynamics in separated flow past thick airfoils
[HTN-95-20832] p 544 A95-88093
- Rotor-wake-induced flow separation on a lifting surface
[HTN-95-01082] p 468 A95-90268
- A note on the interpretation of mini-tuft photographs
[HTN-95-01089] p 468 A95-90275
- Use of partially open wind tunnel walls for blockage-free separated flows on bodies p 474 A95-91558
- High angle of attack missile aerodynamics [CONGRESS PAPER C428-3-060] p 475 A95-91673
- Kinetic heating in hypersonic flight [CONGRESS PAPER C428-3-056] p 475 A95-91674

- Beyond the Riemann problem, part 1
p 550 A95-91925
- Primary and secondary vortex structures over accelerated-decelerated airfoils at high angles of attack [SAE PAPER 931368] p 586 A95-93649
- Heat transfer on bent-noise biconic in hypersonic flow p 639 A95-95394
- LDV measurements in separated flow on an elliptic wing mounted at an angle of attack on a wall [BTN-94-EIX94441380518] p 702 A95-96559
- Control of unsteady separated flow associated with the dynamic stall of airfoils [NASA-CR-197024] p 74 N95-14613
- Numerical simulation of helicopter engine plume in forward flight [NASA-CR-197488] p 107 N95-16589
- Application of Navier-Stokes code PAB3D with kappa-epsilon turbulence model to attached and separated flows [NASA-TP-3480] p 224 N95-21338
- Demonstration study of hierarchical control of fluid-dynamic phenomena [AD-A289341] p 437 N95-26751
- Performance characterization of a highly-offset diffuser with and without blowing vortex generator jets [AD-A289334] p 375 N95-26901
- Unsteadiness of shock-induced turbulent boundary layer separation. An inherent feature of turbulent flow or solely a wind tunnel phenomenon p 554 N95-29228
- Dynamic stall of a NACA 0012 airfoil in laminar flow p 479 N95-29243
- Vorticity dynamics and control of dynamic stall [AD-A288658] p 620 N95-31400
- Investigating the use of smart acoustically active surfaces for flow separation control in turbomachinery [AD-A292819] p 648 N95-31443
- A nonlinear vortex lattice method for unsteady flow with separated vortex [DLR-FB-94-32] p 704 N95-32787
- Calculation for aerodynamic characteristics on delta wing with leading-edge separated vortex effect using boundary element method p 684 N95-34524
- Numerical simulations of dynamic stall phenomena in low speed flows p 685 N95-34546
- SEPARATORS**
- Airborne rotary separator study [NASA-CR-191045] p 150 N95-18743
- Future directions in helicopter protection system configuration p 198 N95-19657
- Reducing process noise in superconducting helium liquid level probes [DE95-008956] p 629 N95-30765
- SEQUENCING**
- A comparison of measured wind park load histories with the WISPER and WISPERX load spectra [DE95-000295] p 446 N95-27459
- SEQUENTIAL ANALYSIS**
- An efficiency study of the simultaneous analysis and design of structures [NASA-TM-110168] p 501 N95-28820
- SERVICE LIFE**
- USAF aging aircraft program [BTN-95-EIX95072498878] p 180 A95-68394
- Service life extensions for the C-141 [BTN-95-EIX95112530749] p 193 A95-69295
- Engine life measurement and diagnostics [BTN-95-EIX95041505024] p 235 A95-70133
- Life prediction of helicopter engines fitted with dust filters [BTN-95-EIX95182619224] p 289 A95-76650
- The FAA regional/commuter aircraft flight loads data collection program [SAE PAPER 931258] p 493 A95-89224
- The avionics integrity programme (AVIP) [CONGRESS PAPER C428-6-115] p 549 A95-91684
- The role of material behaviour modelling in stressing and life assessment of modern Aero-engine components [CONGRESS PAPER C428-27-127] p 612 A95-93606
- Damage tolerance certification of a fighter horizontal stabilizer [BTN-95-EIX0619952748186] p 637 A95-94478
- FAA/NASA International Symposium on Advanced Structural Integrity Methods for Airframe Durability and Damage Tolerance p 92 N95-14453
- [NASA-CP-3274-PT-1] p 93 N95-14461
- Probabilistic inspection strategies for minimizing service failures p 93 N95-14461
- Development of the NASA/FLAGRO computer program for analysis of airframe structures p 94 N95-14473
- Challenges for the aircraft structural integrity program p 80 N95-14481
- Problems with aging wiring in Naval aircraft p 154 N95-16048
- Service and physical properties of liquid-jet fuels p 151 N95-16256
- Oklahoma City air logistics center (USAF) aging aircraft corrosion program p 262 N95-23519
- An overview of Health and Usage Monitoring Systems (HUMS) for military helicopters [DSTO-TR-0061] p 327 N95-24200
- Helicopter life substantiation: Review of some USA and UK initiatives [DSTO-TR-0062] p 328 N95-24201
- Proceedings of the 2d USAF Aging Aircraft Conference [AD-A288217] p 336 N95-25578
- PVD TBC experience on GE aircraft engines p 345 N95-26126
- Helicopter life substantiation: Review of some USA and UK initiatives [AD-A290045] p 502 N95-28851
- Advanced composite structural concepts and materials technologies for primary aircraft structures: Advanced material concepts [NASA-CR-4485] p 503 N95-29027
- SERVOCONTROL**
- Computer aided diagnostic testing of installed flight control servo-actuators [SAE PAPER 932584] p 494 A95-90068
- Second generation smart actuator [SAE PAPER 932585] p 505 A95-90069
- SERVO MECHANISMS**
- Computer aided diagnostic testing of installed flight control servo-actuators [SAE PAPER 932584] p 494 A95-90068
- Second generation smart actuator [SAE PAPER 932585] p 505 A95-90069
- Lightweight, opto-electronic engine control system for aerospace turbine engines [SAE PAPER 931442] p 614 A95-93692
- Design and synthesis of a real-time controller for an unmanned air vehicle [AD-A289134] p 408 N95-26555
- SEWING**
- Development of stitched/RTM composite primary structures p 425 N95-28469
- Test and analysis results for composite transport fuselage and wing structures p 398 N95-28470
- SH-3 HELICOPTER**
- Variations observed in the AC generator signal period of a Sea King helicopter [AD-A284280] p 230 N95-19963
- SHADOWGRAPH PHOTOGRAPHY**
- Simple method of supersonic flow visualization using watertable [BTN-95-EIX95182619105] p 269 A95-76590
- Control of wind tunnel operations using neural net interpretation of flow visualization records [NASA-TM-106683] p 24 N95-10854
- A shadowgraph study of the National Launch System's 1 1/2 stage vehicle configuration and Heavy Lift Launch Vehicle configuration -- Using the Marshall Space Flight Center's 14-inch Trisonic Wind Tunnel [NASA-RP-1347] p 35 N95-11710
- SHAFTS (MACHINE ELEMENTS)**
- Finite element model for a flexible non-symmetric rotor on distributed bearing: A stability study [BTN-94-EIX94381352212] p 306 A95-74612
- Optimal design of composite helicopter power transmission shafts with axially varying fiber layup [HTN-95-01086] p 529 A95-90272
- Wall interaction effects for a full-scale helicopter rotor in the NASA Ames 80- by 120-foot wind tunnel p 121 N95-19270
- Static pressure drop by swirling flow of an internal cooling air system through a turbine shaft p 698 N95-34560
- SHALLOW SHELLS**
- Dynamic analysis of bearingless tail rotor blades based on nonlinear shell modes [BTN-95-EIX95152582338] p 281 A95-73540
- SHAPE CONTROL**
- Static shape control for adaptive wings [HTN-95-A1767] p 627 A95-93330
- Computational algorithms for aerodynamic analysis and design [AD-A291084] p 482 N95-29972
- SHAPE FUNCTIONS**
- Discrete shape sensitivity equations for aerodynamic problems [BTN-94-EIX94451393721] p 88 A95-61720
- Bilinear formulation applied to the response and stability of helicopter rotor blade [BTN-95-EIX95042474400] p 192 A95-68300
- Geometric analysis of wing sections [NASA-TM-110346] p 335 N95-24629
- SHAPE MEMORY ALLOYS**
- Adaptive airfoils [ISBN 1-879921-01-4] p 625 A95-93744
- SMART materials: Surfaces, transforms and interfaces. The commensurate engineering dimension [AD-A289598] p 442 N95-28649
- SHAPES**
- Repeatability of ice shapes in the NASA Lewis icing research tunnel [BTN-95-EIX95062487528] p 204 A95-69236
- Effects of blade tip shape on dynamics, cost, weight, aerodynamic performance, and aeroelastic response [HTN-95-61074] p 369 A95-83658
- Variational principles for ascent shapes of large scientific balloons [BTN-95-EIX95262694320] p 387 A95-85491
- Advanced method and processing technology for complicated shape airframe part forming p 80 N95-14486
- Optimum aerodynamic design via boundary control p 127 N95-16565
- Residual-correction type and related computational methods for aerodynamic design. Part 1: Airfoil and wing design p 128 N95-16566
- Optimal shape design for aerodynamics p 128 N95-16568
- Airfoil optimization by the one-shot method p 128 N95-16569
- The global aircraft shape p 128 N95-16571
- Review of the EUROPT Project AERO-0026 p 129 N95-16573
- Ice accretion with varying surface tension [NASA-TM-106826] p 124 N95-19285
- Influence of turbulence parameters, Reynolds number, and body shape on stagnation-region heat transfer [NASA-TP-3487] p 550 N95-28719
- Computational algorithms for aerodynamic analysis and design [AD-A291084] p 482 N95-29972
- A laser-based ice shape profilometer for use in icing wind tunnels [NASA-TM-106936] p 646 N95-30851
- SHARP LEADING EDGES**
- Compressible inviscid vortex flow of a sharp edge delta wing [BTN-95-EIX95262694308] p 370 A95-85479
- Wind tunnel test on a 65 deg delta wing with a sharp or rounded leading edge: The international vortex flow experiment p 114 N95-17872
- Delta-wing model p 114 N95-17873
- Experimental investigation of the vortex flow over a 76/60-deg double delta wing p 114 N95-17874
- Interaction, bursting and control of vortices of a cropped double-delta wing at high angle of attack [AD-A283656] p 119 N95-18669
- SHEAR**
- Finite element model for a flexible non-symmetric rotor on distributed bearing: A stability study [BTN-94-EIX94381352212] p 306 A95-74612
- SHEAR FLOW**
- Aerodynamic mechanism of galloping [BTN-94-EIX94371347709] p 219 A95-69968
- Adaptive finite element method for turbulent flow near a propeller [BTN-95-EIX95142553038] p 305 A95-73460
- Prediction of two-dimensional momentumless wake by k-epsilon-gamma model [BTN-95-EIX95262694299] p 434 A95-85470
- High angle-of-attack airfoil performance improvement by internal acoustic excitation p 372 A95-86176
- [HTN-95-42347] p 473 A95-91513
- A singularity method for a two dimensional stratified shear flow p 473 A95-91513
- Turbulent flow measurements with a triple-split hot-film probe [HTN-95-A1774] p 634 A95-93337
- An evaluation of clear-air turbulence indices p 674 A95-93548
- Investigation of shear layer transition using various turbulence models p 248 N95-21096
- Basic studies in turbulent shear flows [AD-A289145] p 437 N95-26998
- The effects of three-dimensional imposed disturbances on bluff body near wake flows: Effects of taper and splitter plates on the near wake characteristics of a circular cylinder in uniform and shear flow [AD-A292113] p 477 N95-28921
- SHEAR LAYERS**
- Laser velocimetry seed-particle behavior in shear layers at Mach 12 [BTN-95-EIX95212645712] p 272 A95-76764
- Near field of a coaxial jet with and without axial excitation [HTN-95-42332] p 372 A95-86161
- Vorticity in an inviscid fluid at hypersonic speeds [HTN-95-42590] p 539 A95-87220
- Investigation of shear layer transition using various turbulence models p 248 N95-21096

- Effect of density gradients in confined supersonic shear layers, part 1
[NASA-CR-198029] p 348 N95-24412
- Effect of density gradients in confined supersonic shear layers. Part 2: 3-D modes
[NASA-CR-198030] p 349 N95-24413
- Navier-Stokes solution of wing wake structure and its perturbation
p 479 N95-29121
- Dynamic stall of a NACA 0012 airfoil in laminar flow
p 479 N95-29243
- Grid resolution and turbulent inflow boundary condition recommendations for NPARC calculations
[NASA-TM-106959] p 482 N95-30253
- SHEAR STRAIN**
- Finite element model for a flexible non-symmetric rotor on distributed bearing: A stability study
[BTN-94-EIX9438152212] p 306 A95-74612
- SHEAR STRENGTH**
- Interlaminar shear test method development for long term durability testing of composites
p 301 N95-23300
- Scar joint technique with cocured and precured patches for composite repair
p 396 N95-27524
- SHEAR STRESS**
- Nonlinear angle of twist of advanced composite wing boxes under pure torsion
[BTN-95-EIX95152582323] p 281 A95-73526
- Shear buckling response of tailored composite plates
[HTN-95-51680] p 418 A95-85062
- Aeroelastic response of composite rotor blades considering transverse shear and structural damping
[HTN-95-81647] p 542 A95-87695
- Laser interferometer skin-friction measurements of crossing-shock-wave/turbulent-boundary-layer
ns
[HTN-95-20834] p 544 A95-88095
- Equivalent plate structural modeling for wing shape optimization including transverse shear
[HTN-95-20839] p 492 A95-88100
- Accurate interlaminar stress recovery from finite element analysis
[NASA-TM-109149] p 57 N95-11815
- An analysis code for the Rapid Engineering Estimation of Momentum and Energy Losses (REMEL)
[NASA-CR-191178] p 108 N95-16887
- Shear buckling analysis of a hat-stiffened panel
[NASA-TM-4644] p 158 N95-17490
- Fatigue crack growth in 2024-T3 aluminum under tensile and transverse shear stresses
p 153 N95-19490
- High-lift flow-physics flight experiments on a subsonic civil transport aircraft (B737-100)
p 275 N95-23333
- Buckling analysis of curved composite sandwich panels subjected to inplane loadings
p 533 N95-28845
- Shear force, bending moment and torque of rigid aircraft in symmetric steady maneuvering flight
[ESDU-94045] p 502 N95-28896
- SHELLS (STRUCTURAL FORMS)**
- Analysis and testing of a graphite-epoxy sandwich shell fuselage test structure
[ISBN 1-879921-01-4] p 605 A95-93746
- Composite fuselage shell structures research at NASA Langley Research Center
p 425 N95-28466
- A global/local analysis method for treating details in structural design
p 552 N95-28848
- SHELTERS**
- Quantity-distance requirements for earth-bermed aircraft shelters
[AD-A279692] p 341 N95-24424
- SHIELDING**
- Ceramic blanket reduces maintenance costs
[BTN-94-EIX94461290278] p 77 A95-61733
- An extension of the Lighthill theory of jet noise to encompass refraction and shielding
[NASA-TM-110163] p 580 N95-29452
- SHIPS**
- Tie-down trials involving a Sikorsky S-70B-2 helicopter
[DSTO-TR-0132] p 400 N95-28567
- SHOCK ABSORBERS**
- Soft landing on the slope surface of a landing vehicle with an air shock-absorber of forced pressurization
[BTN-94-EIX94461407941] p 85 A95-62259
- An electrohydraulically controlled semi-active landing gear
[SAE PAPER 931403] p 605 A95-93673
- Landing gear energy absorption system
[NASA-CASE-MSC-22277-1] p 96 N95-15306
- Energy absorption device for shock loading
[AD-D017476] p 706 N95-34449
- SHOCK HEATING**
- Application of the multigrad solution technique to hypersonic entry vehicles
[BTN-95-EIX95152583254] p 306 A95-73555
- Heat-transfer measurements and computations of swept-shock-wave boundary-layer interactions
[HTN-95-81634] p 541 A95-87682
- Numerical experiments on aerodynamic heating mechanism in shock reflection processes
p 471 A95-91497
- Experimental study of shock/shock interference heating on a swept cylinder
p 472 A95-91510
- The Superorbital Expansion Tube concept, experiment and analysis
p 341 N95-25399
- SHOCK LAYERS**
- Linear disturbances in hypersonic, chemically reacting shock layers
[BTN-94-EIX94441386605] p 182 A95-67336
- Thermochemical nonequilibrium viscous shock-layer analysis for a Mars aerocapture vehicle
[BTN-95-EIX95082502732] p 239 A95-70139
- Higher-order viscous shock-layer solutions for high-altitude flows
[BTN-95-EIX95152583255] p 306 A95-73556
- VSL analysis of hypersonic flows around a reentry vehicle with equilibrium air chemistry
p 413 A95-82400
- An experimental study on radiation from strong shock layer
p 368 A95-82421
- Linear disturbances in hypersonic, chemically reacting shock layers
[HTN-95-20931] p 464 A95-88970
- Science objectives and performance of a radiometer and window design for atmospheric entry experiments
p 85 N95-13718
- VUV shock layer radiation in an arc-jet wind tunnel experiment
p 67 N95-13719
- Measured and calculated spectral radiation from a blunt body shock layer in an arc-jet wind tunnel
[AIAA PAPER 94-0086] p 67 N95-13720
- Laminar and turbulent flow computations of Type 4 shock-shock interference aerothermal loads using unstructured grids
[NASA-CR-195008] p 97 N95-15604
- Viscous shock-layer analysis on hypersonic flow over reentry capsule with nonequilibrium chemistry
[ISAS-656] p 436 N95-26739
- SHOCK MEASURING INSTRUMENTS**
- Micro-time stress measurement device development
[AD-A289511] p 448 N95-26845
- SHOCK RESISTANCE**
- Quality optimization of thermally sprayed coatings produced by the JP-5000 (HVOF) gun using mathematical modeling
p 152 N95-19008
- SHOCK TESTS**
- Shock tunnel studies of scramjet phenomena 1993
[NASA-CR-195038] p 350 N95-25394
- The Superorbital Expansion Tube concept, experiment and analysis
p 341 N95-25399
- SHOCK TUBES**
- Application of a control-volume-based finite-element formulation to the shock tube problem
[BTN-95-EIX95182619099] p 295 A95-76584
- Research activity at the shock tube facility at NASA Ames
p 547 A95-90559
- Fixed transition for shock tube transonic flow
p 472 A95-91509
- Shock tube investigations of combustion phenomena in supersonic flows
[PB94-175262] p 55 N95-11796
- The Superorbital Expansion Tube concept, experiment and analysis
p 341 N95-25399
- An investigation of the AFIT 2-inch shock tube as a flow source for supersonic testing
[AD-A289246] p 412 N95-26966
- Numerical simulations of the flow in the HYPULSE expansion tube
[NASA-TM-110357] p 523 N95-30228
- Computation of high-altitude hypersonic flow-field radiation
p 593 N95-30843
- SHOCK TUNNELS**
- Shock tunnel measurements of hypervelocity blunted cone drag
[BTN-95-EIX95152577606] p 305 A95-73477
- Shock tunnel measurements of hypervelocity blunted cone drag
[HTN-95-42591] p 459 A95-87221
- The high enthalpy shock tunnel in Goettingen (HEG)
p 518 A95-87391
- Hypersonic shock wave/turbulent boundary layer interactions in the vicinity of an expansion corner
[AIAA PAPER 95-6125] p 469 A95-90446
- Experimental study of shock/shock interference heating on a swept cylinder
p 472 A95-91510
- A shock tunnel test of a winged hypersonic research vehicle
p 474 A95-91538
- Shock tunnel studies of scramjet phenomena 1993
[NASA-CR-195038] p 350 N95-25394
- Thrust measurements of a complete axisymmetric scramjet in an impulse facility
p 339 N95-25395
- Scramjet thrust measurement in a shock tunnel
p 339 N95-25396
- Balances for the measurement of multiple components of force in flows of a millisecond duration
p 350 N95-25400
- A numerical study of the starting process in a hypersonic shock tunnel
p 626 N95-30493
- Numerical simulation of high enthalpy shock tunnel
p 700 N95-34514
- SHOCK WAVE INTERACTION**
- Aspects of vortex breakdown
[HTN-95-A0001] p 183 A95-67828
- Flow study of supersonic wing-nacelle configuration
[BTN-95-EIX95152582344] p 266 A95-73546
- Scaling of incipient separation in supersonic/transonic speed laminar flows
[BTN-95-EIX95182619104] p 269 A95-76589
- Structure of a double-fin turbulent interaction at high speed
[BTN-95-EIX95222650780] p 347 A95-79236
- A study on aerodynamic heating phenomena in three-dimensional shock wave/turbulent boundary layer interaction induced by sweptback sharp fins at supersonic flow
p 428 A95-82419
- Compressible inviscid vortex flow of a sharp edge delta wing
[BTN-95-EIX95262694308] p 370 A95-85479
- Heat-transfer measurements and computations of swept-shock-wave boundary-layer interactions
[HTN-95-81634] p 541 A95-87682
- Airfoil pressure measurements during oblique shock-wave/vortex interaction in a Mach 3 stream
[HTN-95-81641] p 542 A95-87689
- Experimental study of shock/shock interference heating on a swept cylinder
p 472 A95-91510
- An experimental study on interacting flow between supersonic flow and secondary flow injected normally through circular nozzle
p 472 A95-91511
- 3-D Navier-Stokes analysis of crossing glancing shocks/turbulent boundary layer interactions
[BTN-95-EIX95302729768] p 636 A95-94130
- Application of scramjet engine technology to the design of ram accelerator projectiles
p 19 N95-10282
- Visualization of one-dimensional flow processes in a dual-mode scramjet engine
p 15 N95-10465
- Validation of the RPLUS3D code for supersonic inlet applications involving three-dimensional shock wave-boundary layer interactions
[NASA-TM-106579] p 39 N95-13058
- Atmospheric effects on the risetime and waveshape of sonic booms
p 100 N95-14886
- The effect of aircraft speed on the penetration of sonic boom noise into a flat ocean
p 100 N95-14887
- Laminar and turbulent flow computations of Type 4 shock-shock interference aerothermal loads using unstructured grids
[NASA-CR-195008] p 97 N95-15604
- Wind-tunnel blockage and actuation systems test of a two-dimensional scramjet inlet unstart model at Mach 6
[NASA-TM-109152] p 97 N95-15898
- Numerical simulation of supersonic compression corners and hypersonic inlet flows using the RPLUS2D code
[NASA-TM-106580] p 105 N95-16038
- Mach number, flow angle, and loss measurements downstream of a transonic fan-blade cascade
[AD-A280907] p 108 N95-16824
- Theoretical investigations of shock/boundary layer interactions on a Ma(infinity) = 8 waverider
[DLR-FB-94-12] p 119 N95-18910
- Shock wave interactions in hypervelocity flow
[AD-A286507] p 250 N95-22212
- Mach 10 computational study of a three-dimensional scramjet inlet flow field
[NASA-TM-4602] p 310 N95-23210
- Supersonic flow and shock formation in turbine tip gaps
p 312 N95-23429
- A numerical study of fundamental shock noise mechanisms
[NASA-TM-110608] p 451 N95-27908
- Response of multi-panel assembly to noise from a jet in forward motion
[NASA-CR-198164] p 442 N95-28673
- A procedure for automating CFD simulations of an inlet-bleed problem
p 552 N95-28768
- The 1995 version of the NSWC aeroprediction code. Part 1: Summary of new theoretical methodology
[AD-A291518] p 481 N95-29853
- A numerical study of the starting process in a hypersonic shock tunnel
p 626 N95-30493
- Experimental and computational investigation of the tip clearance flow in a transonic axial compressor rotor
[NASA-TM-106711] p 499 N95-31738
- Numerical simulation of supersonic flow using a new analytical bleed boundary condition
[NASA-CR-198368] p 697 N95-33208
- SHOCK WAVE PROFILES**
- Research activity at the shock tube facility at NASA Ames
p 547 A95-90559

SHOCK WAVE PROPAGATION

Aeroacoustic model for weak shock waves based on Burgers equation
 [BTN-95-EIX95182619076] p 269 A95-75761
 Role of Kutta waves on oscillatory shock motion on an airfoil
 [HTN-95-81642] p 542 A95-87690
 Some aspects of the aeroacoustics of extreme-speed jets
 p 572 A95-88893
 High speed civil transport: Sonic boom softening and aerodynamic optimization
 [NASA-CR-196397] p 28 N95-11192
 USAF single-event sonic boom prediction model: PCBooms3
 p 101 N95-14889
 A numerical study of fundamental shock noise mechanisms
 [NASA-TM-110608] p 451 N95-27908

SHOCK WAVES

Experimental and analytical investigations of wave enhanced supersonic combustors
 [AIAA PAPER 89-2787] p 14 A95-60172
 Aerodynamic design and calculation of flow around the plane cascade of turbine
 [BTN-94-EIX94481415357] p 104 A95-65347
 Supersonic and hypersonic shock boundary-layer interaction database
 [BTN-94-EIX9441386604] p 182 A95-67335
 Shock layers and boundary layers in hypersonic flows
 [HTN-95-A0003] p 183 A95-67830
 Measurement by coherent anti-Stokes Raman scattering in the R5Ch hypersonic wind tunnel
 [BTN-95-EIX95112523811] p 188 A95-69322
 Flow study of supersonic wing-nacelle configuration
 [BTN-95-EIX95152582344] p 266 A95-73546
 Application of the multigrad solution technique to hypersonic entry vehicles
 [BTN-95-EIX95152583254] p 306 A95-73555
 Three-dimensional structure of a supersonic jet impinging on an inclined plate
 [BTN-95-EIX95152583259] p 267 A95-73560
 Supersonic axisymmetric conical flow solutions for different ratios of specific heats
 [BTN-95-EIX95152583283] p 306 A95-73584
 Aeroacoustic model for weak shock waves based on Burgers equation
 [BTN-95-EIX95182619076] p 269 A95-75761
 Observations on using experimental data as boundary conditions for computations
 [BTN-95-EIX95182619103] p 321 A95-76588
 Prediction of pre-combustion shock in scramjet combustors: A new method
 p 402 A95-82323
 The aerodynamic characteristics of cup-like body in supersonic flow
 p 427 A95-82407
 Numerical simulation of unsteady aerodynamic heating induced by shock reflections
 p 428 A95-82418
 A study on aerodynamic heating phenomena in three-dimensional shock wave/turbulent boundary layer interaction induced by sweptback sharp fins at supersonic flow
 p 428 A95-82419
 Hypersonic flow simulation with thermoelectric effect
 p 368 A95-82669
 Flowfield measurements in supersonic film cooling including the effect of shock-wave interaction
 [HTN-95-42337] p 405 A95-86166
 Numerical modeling and simulation of chemically reacting reentry flows
 p 525 A95-87387
 Experimental investigation of hypersonic flow over a wing-body combination
 [AIAA PAPER 95-6083] p 460 A95-87412
 Boundary conditions for unsteady supersonic inlet analyses
 [HTN-95-20829] p 544 A95-88090
 Laser interferometer skin-friction measurements of crossing-shock-wave/turbulent-boundary-layer ns
 [HTN-95-20834] p 544 A95-88095
 Some aspects of the aeroacoustics of extreme-speed jets
 p 572 A95-88893
 Computing unsteady shock waves for aeroacoustic applications
 [HTN-95-20928] p 463 A95-88967
 Computational aerodynamic analysis on the Open Skies aircraft
 [SAE PAPER 932514] p 466 A95-89187
 Preliminary study on the fixed transition technique for a shock tube transonic airfoil flow
 [BTN-95-EIX95282705928] p 455 A95-89663
 Hypersonic waveriders generated from power-law shocks
 [AIAA PAPER 95-6160] p 470 A95-90472
 A detailed Euler flow analysis of TPS and fanjet engine
 p 473 A95-91515
 Similarity solutions for hypersonic flow past slender bodies of revolution at small incidence
 [HTN-95-12195] p 475 A95-91895

Signal processing of noise data from high-speed flyovers
 [BTN-95-EIX0619952748178] p 680 A95-94248
 Interaction of a weak shock with freestream disturbances
 [BTN-95-EIX95332750473] p 638 A95-94687
 Near field noise prediction requirements
 [ISVR-TR-234] p 27 N95-11166
 Activities of the Institute for Aerospace Studies of Toronto University
 p 63 N95-12699
 An optical technique for examining aircraft shock wave structures in flight
 p 96 N95-14879
 Time accurate computation of unsteady inlet flows with a dynamic flow adaptive mesh
 [AD-A285498] p 157 N95-16736
 Investigation of the flow over a series of 14 percent-thick supercritical aerofoils with significant rear camber
 p 109 N95-17849
 Wind tunnel investigations of the appearance of shocks in the windward region of bodies with circular cross section at angle of attack
 p 113 N95-17866
 Aeromechanics technology, volume 1, Task 1: Three-dimensional Euler/Navier-Stokes Aerodynamic Method (TEAM) enhancements
 [AD-A285713] p 132 N95-18483
 Flow field investigation in a free jet - free jet core system for the generation of high intensity molecular beams
 [DLR-FB-94-11] p 172 N95-18912
 Spectrogram diagnosis of aircraft disasters
 p 124 N95-19167
 Shock wave interactions in hypervelocity flow
 [AD-A286507] p 250 N95-22212
 Shock tunnel studies of scramjet phenomena 1993
 [NASA-CR-195038] p 350 N95-25394
 Scramjet thrust measurement in a shock tunnel
 p 339 N95-25396
 An investigation of the AFIT 2-inch shock tube as a flow source for supersonic testing
 [AD-A289246] p 412 N95-26966
 A numerical study of fundamental shock noise mechanisms
 [NASA-TM-110608] p 451 N95-27908
 Wave drag coefficient for axisymmetric forecows at zero incidence (M sub infinity less than or equal to 1.5)
 [ESDU-94014] p 552 N95-28903
 Surface pressure coefficient distributions for axisymmetric forecows at zero incidence (M sub infinity less than or equal to 1.5)
 [ESDU-94015] p 477 N95-28904
 An extension of the continuum model by Grad's thirteen moment equations for hypersonic rarefied flows
 p 478 N95-29118
 Unsteadiness of shock-induced turbulent boundary layer separation. An inherent feature of turbulent flow or solely a wind tunnel phenomenon
 [AD-A290367] p 554 N95-29228
 An experimental investigation of the time-dependent separation of tangent bodies in supersonic flow
 [AD-A290720] p 480 N95-29500
 Survey of CFD applications for high speed inlets
 [AD-A291365] p 557 N95-30087
 Numerical simulation of ram accelerator performance including transient effects during initiation of combustion and sensitivity studies
 p 629 N95-31203
 Effects of cavity bleed and its configuration on aerodynamic characteristics of supersonic internal flow
 [NAL-TR-1247] p 594 N95-31715
 Near-limit drop deformation and secondary breakup
 p 704 N95-32902
 Energy absorption device for shock loading
 [AD-D017476] p 706 N95-34449
 A study of supersonic mixing flow field with ramp injector
 p 706 N95-34512

SHORT CIRCUIT CURRENTS
 Electrical short circuit and current overload tests on aircraft wiring
 [AD-A293308] p 646 N95-30922

SHORT CIRCUITS
 Electrical short circuit and current overload tests on aircraft wiring
 [AD-A293308] p 646 N95-30922

SHORT CRACKS
 Widespread fatigue damage monitoring: Issues and concerns
 p 136 N95-19488

SHORT RANGE BALLISTIC MISSILES
 The short range attack missile/light weight exo-atmospheric projectile (SRAM/LEAP) missile tests program
 [HTN-95-81498] p 386 A95-85212

SHORT TAKEOFF AIRCRAFT
 Recent research in ASTOVL aircraft ground environment
 [CONGRESS PAPER C428-9-040] p 475 A95-91694
 Cost effective small-scale experiments to aid the design of ASTOVL aircraft
 [CONGRESS PAPER C428-9-098] p 475 A95-91695

Flight investigation of the use of a nose gear jump strut to reduce takeoff ground roll distance of STOL aircraft
 [NASA-TM-108819] p 44 N95-12225
 A preliminary design proposal for a maritime patrol strike aircraft: MPS-2000 Condor
 [NASA-CR-197182] p 47 N95-12689
 Flight reference display for powered-lift STOL aircraft
 [NAL-TR-1251] p 337 N95-25005
 A quiet STOL Research Aircraft Development program
 [NAL-TR-1223] p 336 N95-25862
 The control system design methodology of the STOL and maneuver technology demonstrator
 p 621 N95-31998

SHUTTLE IMAGING RADAR
 AIRSAR deployment in Australia, September 1993: Management and objectives
 p 321 N95-23948

SIDE INLETS
 An investigation of the side-dump dual in-line ramjet combustor
 p 617 N95-31199

SIDESLIP
 F/A-18 inlet calculations at 60-deg angle of attack and 10-deg sideslip
 [BTN-95-EIX95112524199] p 195 A95-69309
 Method for the prediction of the onset of wing rock
 [BTN-95-EIX95152582342] p 282 A95-73544
 Effect of leeward flow dividers on the wing rock of a delta wing
 [BTN-95-EIX95152582347] p 282 A95-73549
 Reduced-order nonlinear analysis of aircraft dynamics
 [BTN-95-EIX95282706665] p 455 A95-89640
 Flow-visualization study of the X-29A aircraft at high angles of attack using a 1/48-scale model
 [NASA-TM-104268] p 8 N95-10858
 Flight evaluation of pneumatic forebody vortex control in post-stall flight
 p 72 N95-14259
 Pressure measurements on an F/A-18 twin vertical tail in buffeting flow. Volume 1: Wind tunnel test summary
 [AD-A279126] p 225 N95-21877
 Effect of juncture fillets on double-delta wings undergoing sideslip at high angles of attack
 [AD-A286165] p 232 N95-22039
 Wing pressure distributions from subsonic tests of a high-wing transport model — in the Langley 14- by 22-Foot Subsonic Wind Tunnel
 [NASA-TM-108483] p 272 N95-22802
 Transonic aerodynamic characteristics of a proposed wing-body reusable launch vehicle concept
 [NASA-TM-108489] p 592 N95-30712

SIGNAL ANALYSIS
 Effects of signal analysis parameters and noise removal on measured aircraft spectra
 p 578 A95-90137
 Speech analysis and synthesis based on pitch-synchronous segmentation of the speech waveform
 [AD-A288824] p 435 N95-26349
 Bearing defect signature analysis using advanced nonlinear signal analysis in a controlled environment
 [NASA-TM-108491] p 441 N95-28364

SIGNAL ANALYZERS
 The impact of advanced packaging technology on modular avionics architectures
 p 233 N95-20632

SIGNAL PROCESSING
 Using IRI for the computation of ionospheric corrections for altimeter data analysis
 p 212 A95-66949
 Evaluation of the radio frequency susceptibility of commercial GPS receivers
 [BTN-95-EIX95042474624] p 189 A95-68278
 Precise navigation using adaptive FIR filtering and time domain spectral estimation
 [BTN-95-EIX95142555485] p 227 A95-72888
 Simulation of turbulent fluctuations
 [BTN-95-EIX95142553041] p 304 A95-73457
 Ultra-wideband electromagnetic target identification
 p 486 A95-90955
 The Saab-Scania approach to development simulators
 [CONGRESS PAPER C428-10-137] p 522 A95-91698
 Signal processing of noise data from high-speed flyovers
 [BTN-95-EIX0619952748178] p 680 A95-94248
 Certification of windshear performance with RTCA class D radomes
 p 41 N95-13206
 Joint Proceedings on Aeronautics and Astronautics (JPAA)
 [ISBN-7-80-046602-7] p 104 N95-16249
 Dynamic Stability Instrumentation System (DSIS). Volume 1: Hardware description
 [NASA-TM-109160-VOL-1] p 171 N95-18899
 Waveform bounding and combination techniques for direct drive testing
 [AD-A284075] p 161 N95-19035
 Variations observed in the AC generator signal period of a Sea King helicopter
 [AD-A284280] p 230 N95-19963
 The impact of advanced packaging technology on modular avionics architectures
 p 233 N95-20632

- Wavelet transformations for helicopter identification via acoustic signatures
[AD-A279980] p 257 N95-20963
- Maximum-likelihood spectral estimation and adaptive filtering techniques with application to airborne Doppler weather radar
[NASA-CR-197699] p 316 N95-23670
- A novel instrumentation system for measurement of helicopter rotor motions and loads data, phase 1
[AD-A293309] p 607 N95-30923
- SIGNAL TRANSMISSION**
- Attitude determination using dedicated and nondedicated multi-antenna GPS sensors
[BTN-95-EIX95142555482] p 228 A95-72891
- SIGNAL ANALYSIS**
- Bearing defect signature analysis using advanced nonlinear signal analysis in a controlled environment
[NASA-TM-108491] p 441 N95-28364
- SIGNATURES**
- The use of electrochemistry and ellipsometry for identifying and evaluating corrosion on aircraft
[AD-A285323] p 151 N95-16371
- An assessment of the adaptive unstructured tetrahedral grid, Euler Flow Solver Code FELISA
[NASA-TP-3526] p 119 N95-19041
- Application of wavelet-filtering techniques to intermittent turbulent and wall pressure events. Part 1: Exploratory results
[AD-A286077] p 247 N95-20849
- SIKORSKY AIRCRAFT**
- H-76B fantail demonstrator composite fan blade fabrication
[HTN-95-80856] p 283 A95-75098
- Cypher moves toward autonomous flight
[HTN-95-41394] p 283 A95-76390
- Dynamic response of NASA Rotor Test Apparatus and Sikorsky S-76 hub mounted in the 80- by 120-Foot Wind Tunnel
[NASA-TM-108847] p 25 N95-11389
- Report to Congressional Committees. Comanche Helicopter: Testing needs to be completed prior to production decisions
[GAO/NSIAD-95-112] p 397 N95-27910
- Tie-down trials involving a Sikorsky S-70B-2 helicopter
[DSTO-TR-0132] p 400 N95-28567
- SILENCERS**
- An active liner system for jet engine exhaust silencers, phase 1
[AD-A293277] p 617 N95-31191
- SILICON**
- Cu deposition using a permanent magnet electron cyclotron resonance microwave plasma source
[DE94-017768] p 304 N95-23981
- Synthetic Terrain Imagery for Helmet-Mounted Display. Volume 2: Software design document
[AD-A293611] p 612 N95-31655
- SILICON CARBIDES**
- Launcher wing-leading-edge design
[BTN-95-EIX95042477110] p 192 A95-68349
- Intermetallic and titanium matrix composite materials for hypersonic applications
[AIAA PAPER 95-6132] p 530 A95-90451
- Effects of activated reactive evaporation process parameters on the microhardness of polycrystalline silicon carbide thin films
[GTN-95-00406090-4621] p 680 A95-93965
- Modeling and life prediction methodology for Titanium Matrix Composites subjected to mission profiles
[NASA-TM-109148] p 55 N95-11915
- Innovative processing of composites for ultra-high temperature applications, book 1
[AD-A290889] p 537 N95-29842
- SILICON COMPOUNDS**
- Impact, friction, and wear testing of microsamples of polycrystalline silicon
p 361 A95-79988
- SILICON DIOXIDE**
- Thermal chemical energy of ablating silica surfaces in air breathing solid rocket engines
p 148 N95-16316
- Evaluation of retro-reflective beads in airport pavement markings
[AD-A291065] p 523 N95-29967
- SILICON NITRIDES**
- Advanced Turbine Technology Applications Project (ATTAP)
[NASA-CR-195393] p 101 N95-15743
- Resistance of silicon nitride turbine components to erosion and hot corrosion/oxidation attack
p 202 N95-19683
- Evolution of oxidation and creep damage mechanisms in HIPed silicon nitride materials
[DE95-001360] p 300 N95-22689
- SILICONES**
- Hardware cleanliness methodology and certification
p 419 N95-27656
- SILVER ALLOYS**
- NASA-UVA light aerospace alloy and structures technology program supplement: Aluminum-based materials for high speed aircraft
[NASA-CR-4645] p 343 N95-24878
- SIMILARITY NUMBERS**
- Similarity rule for jet-temperature effects on transonic base pressure
[BTN-95-EIX9522650791] p 329 A95-79247
- SIMULATED ANNEALING**
- Nonsmooth trajectory optimization: An approach using continuous simulated annealing
[BTN-94-EIX94511433914] p 168 A95-64580
- Aircraft controller synthesis by solving a nonconvex optimization problem
[BTN-95-EIX95282706672] p 515 A95-89636
- SIMULATION**
- Unbalance response of a dual rotor system: Theory and experiment
[BTN-94-EIX94351143320] p 195 A95-65854
- Construction of nearly orthogonal multiblock grids for compressible flow simulation
[BTN-94-EIX94361133526] p 207 A95-65981
- Simulation and model reduction for the active flexible wing program
[BTN-95-EIX95182619211] p 295 A95-76637
- Studies on gain performance of a combustion driven CO₂ gas dynamic laser
p 428 A95-82679
- Automated aircraft routing through weather-impacted airspace
p 666 A95-93512
- Object-oriented technology for compressor simulation
[NASA-TM-106723] p 49 N95-11864
- Numerical time dependent sheet cavitation simulations using a higher order panel method
[PB94-204435] p 59 N95-13249
- A correlative investigation of simulated occupant motion and accident report in a helicopter crash
[AD-A285190] p 123 N95-16404
- A surgical support system for Space Station Freedom
p 149 N95-16776
- Simulation of multidisciplinary problems for the theroestress state of cooled high temperature turbines
p 140 N95-19021
- Simulation of steady and unsteady viscous flows in turbomachinery
p 140 N95-19023
- Computational simulations for some tests in transonic wind tunnels
p 164 N95-19264
- Determination of solid/porous wall boundary conditions from wind tunnel data for computational fluid dynamics codes
p 164 N95-19266
- Holographic interferometric tomography for reconstructing flow fields
p 310 N95-23287
- The near-wake flow behavior of an oscillating airfoil with modified trailing edge
p 375 N95-26953
- Advanced formation flight control
[AD-A289271] p 409 N95-26981
- A hybrid vehicle evaluation code and its application to vehicle design, Revision 1
[DE95-008053] p 441 N95-28029
- A hybrid vehicle evaluation code and its application to vehicle design, revision 2
[DE95-008060] p 441 N95-28139
- Numerical simulation of high enthalpy shock tunnel
p 700 N95-34514
- An unsteady simulation of a centrifugal compressor stage using the NWT
p 707 N95-34536
- Vector-parallel simulations of transonic wind tunnel flows about a fully configured model of aircraft
p 685 N95-34538
- A simulation of damping process of pendulum motion due to aerodynamic forces
p 711 N95-34551
- SIMULATORS**
- Turbofan propulsion simulator
[BTN-94-EIX94461290240] p 82 A95-61737
- A new type of simulator for simulating the flow-field distortion of engine inlet
[BTN-95-EIX95202638963] p 289 A95-76673
- Study on a scheme for the prolongation of microgravity time of balloon-borne drop capsule
p 414 A95-82515
- Propulsion simulator for high bypass turbofan performance evaluation
[SAE PAPER 931410] p 625 A95-93676
- Evaluation of alternative in-flight fire suppressants for full-scale testing in simulated aircraft engine nacelles and dry bays
[PB94-203403] p 42 N95-13247
- Color control in a multichannel simulator display: The display for advanced research and training
[AD-A279717] p 239 N95-20992
- An evaluation of Automatic Terminal Information Service (ATIS) flight deck display presentation options
[AD-A280100] p 228 N95-21020
- Computational methods for control and optimal design of aerospace systems
[AD-A292861] p 608 N95-31451
- SIMULTANEOUS EQUATIONS**
- An easy way to analyze longitudinal and lateral-directional trim problems with AEO or OEI
p 409 N95-26949
- An efficiency study of the simultaneous analysis and design of structures
[NASA-TM-110168] p 501 N95-28820
- SINE WAVES**
- Dynamic stall of a NACA 0012 airfoil in laminar flow
p 479 N95-29243
- SINGLE CRYSTALS**
- Fatigue in single crystal nickel superalloys
[AD-A283459] p 56 N95-12546
- Fatigue in single crystal nickel superalloys
[AD-A282917] p 88 N95-15415
- Fatigue in single crystal nickel superalloys
[AD-A285727] p 152 N95-18068
- SINGLE ENGINE AIRCRAFT**
- Preliminary design of a single engine business jet
[SAE PAPER 931253] p 493 A95-89222
- Low-order nonlinear dynamic model of IC engine-variable pitch propeller system for general aviation aircraft
[NASA-TM-107006] p 694 N95-32916
- SINGLE EVENT UPSETS**
- Investigation and characterization of SEU effects and hardening strategies in avionics
[AD-A291058] p 509 N95-29950
- SINGLE STAGE TO ORBIT VEHICLES**
- Requirements report for SSTO vertical take-off and horizontal landing vehicle
[NASA-CR-197029] p 80 N95-14794
- Mattab as a robust control design tool
p 169 N95-16474
- Transonic aerodynamic characteristics of a proposed wing-body reusable launch vehicle concept
[NASA-TM-108489] p 592 N95-30712
- SINGULARITY (MATHEMATICS)**
- A singularity method for a two dimensional stratified shear flow
p 473 A95-91513
- A wall interference assessment and correction system
[NASA-CR-196940] p 58 N95-12228
- Determination of solid/porous wall boundary conditions from wind tunnel data for computational fluid dynamics codes
p 164 N95-19266
- A wall interference assessment/correction system
[NASA-CR-197421] p 309 N95-23183
- SINTERING**
- Ceramic manufacturing: Optimizing a multivariable system
[DE94-015016] p 56 N95-13184
- SITE SELECTION**
- Secondary source locations in active noise control: Selection or optimization?
[BTN-94-EIX94381352222] p 257 A95-71738
- Selecting optimum sonic boom monitoring sites in a special-use airspace
p 576 A95-90124
- SITTING POSITION**
- A multibody/finite element analysis approach for modeling of crash dynamic responses
[NIAR-94-3] p 277 N95-24050
- SIZE (DIMENSIONS)**
- Scale-up and modeling of forced chemical vapor infiltration
[DE94-017769] p 247 N95-20781
- SIZE DISTRIBUTION**
- Combustion efficiency in a dual-inlet side-dump ramjet combustor
[AD-A283564] p 83 N95-15329
- SKIN (STRUCTURAL MEMBER)**
- Multiple site fatigue damage in fuselage skin splices: Experimental simulation and theoretical prediction
[BTN-95-EIX95152584676] p 276 A95-73588
- An analytical and experimental investigation of the response of the curved, composite frame/skin specimens
[HTN-95-80857] p 283 A95-75099
- Equivalent plate structural modeling for wing shape optimization including transverse shear
[HTN-95-20839] p 492 A95-88100
- Crack growth characteristics of integrally machined stringer-skin panels
[HTN-95-01095] p 496 A95-90281
- Damage to composite aircraft structures from lightning strike attachment to unprotected CFC and internal sparking causing fuel injection
[CONGRESS PAPER C428-4-026] p 531 A95-91675
- Intelligent skins development for future military aircraft
[CONGRESS PAPER C428-17-189] p 531 A95-91714
- Acoustic fatigue testing on different materials and skin-stringer elements
p 174 N95-19156
- Thermo-acoustic fatigue design for hypersonic vehicle skin panels
p 162 N95-19161
- An artificial corrosion protocol for lap-splices in aircraft skin
p 152 N95-19482

On aircraft repair verification of a fighter A/C integrally stiffened fuselage skin p 394 A95-27515

SKIN FRICTION
 Behavior of the Johnson-King turbulence model in axisymmetric supersonic flows p 183 A95-67337
 [BTN-94-EIX94441386606]
 Vortical flow structure near the F/A-18 LEX at high incidence p 186 A95-68369
 [BTN-95-EIX95062487555]
 Laser interferometer skin-friction measurements of crossing-shock-wave/turbulent-boundary-layer ns
 [HTN-95-20834] p 544 A95-88095
 Boundary-layer transition and global skin friction measurement with an oil-fringe imaging technique [SAE PAPER 932550] p 547 A95-90054
 An analysis code for the Rapid Engineering Estimation of Momentum and Energy Losses (REMEL) [NASA-CR-191178] p 108 N95-16887
 Application of Navier-Stokes code PAB3D with kappa-epsilon turbulence model to attached and separated flows p 224 N95-21338
 [NASA-TP-3480]
 Boundary-layer transition and global skin friction measurement with an oil-fringe imaging technique [NASA-CR-198814] p 557 N95-30224
 Improved modeling of unsteady heat transfer (The first step) [AD-A292777] p 648 N95-31432

SKY BRIGHTNESS
 A mathematical analysis of the Janus combat simulation weather effects models and sensitivity analysis of sky-to-ground brightness ratio on target detection [AD-A289629] p 446 N95-26858

SLEEP
 Aircraft noise and sleep disturbance: A field study [HTN-95-92543] p 558 A95-87363

SLEEP DEPRIVATION
 Criticism of the Leq as an Index for aircraft noise and other discontinuous noise sources p 559 A95-88478

SLEEVES
 Design and development of a test rig for the high frequency testing of rolling sleeve airsprings [DSTO-TN-0001] p 411 N95-26378

SLENDER BODIES
 Passive porosity with free and fixed separation on a tangent-ogive forebody p 185 A95-68368
 [BTN-95-EIX95062487554]
 Aerodynamically blunt and sharp bodies [BTN-95-EIX95041503781] p 205 A95-69212
 Crossflow topology of vortical flows [HTN-95-51664] p 432 A95-85046
 Similarity solutions for hypersonic flow past slender bodies of revolution at small incidence [HTN-95-12195] p 475 A95-91895
 A selection of experimental test cases for the validation of CFD codes, volume 1 [AGARD-AR-303-VOL-1] p 91 N95-14201
 Force and pressure data of an ogive-nosed slender body at high angles of attack and different Reynolds numbers p 113 N95-17868
 Calculation for aerodynamic characteristics on delta wing with leading-edge separated vortex effect using boundary element method p 684 N95-34524

SLENDER CONES
 Linear disturbances in hypersonic, chemically reacting shock layers p 182 A95-67336
 [BTN-94-EIX94441386605]
 Shock tunnel measurements of hypervelocity blunted cone drag [BTN-95-EIX95152577606] p 305 A95-73477
 Similarity solutions for hypersonic flow past slender bodies of revolution at small incidence [HTN-95-12195] p 475 A95-91895

SLENDER WINGS
 Experimental investigations on limit cycle wing rock of slender wings p 185 A95-68357
 [BTN-95-EIX95062487543]
 Direct adaptive and neural control of wing-rock motion of slender delta wings [BTN-95-EIX95242670748] p 327 A95-81099
 Analysis and design methodology for chordwise deformable wings p 692 N95-33311

SLIDING
 Prediction of fatigue crack growth under constant amplitude and random loading using specimens with multiple cracks [AD-A291614] p 397 N95-28409

SLIDING FRICTION
 Surface morphology and structure of carbon-carbon composites in high-energy sliding contact [BTN-94-EIX94371347996] p 206 A95-69164

SLIP FLOW
 Corrective term in wall slip equations for Knudsen layer [BTN-95-EIX95282705070] p 455 A95-89667

SLOPES
 Elliptic tip effects on the vortex wake of an axisymmetric body at incidence [BTN-94-EIX94441386612] p 208 A95-67343

SLOT ANTENNAS
 Design considerations for an archimedean slot spiral antenna p 211 N95-19798
 Simulation of patch and slot antennas using FEM with prismatic elements and investigations of artificial absorber mesh termination schemes [NASA-CR-198974] p 704 N95-32822

SLOTS
 Forebody flow control on a full-scale F/A-18 aircraft [BTN-95-EIX95152582333] p 281 A95-73535
 Pneumatic concept for tip-stall control of cranked-arrow wings [BTN-95-EIX95152582335] p 281 A95-73537
 Computational analysis of forebody tangential slot blowing on the high alpha research vehicle [NASA-CR-196750] p 10 N95-11367
 Numerical analysis of tangential slot blowing on a generic chined forebody [NASA-TM-108845] p 37 N95-11927
 Computational analysis of forebody tangential slot blowing p 71 N95-14253
 Comparison of full-scale, small-scale, and CFD results for F/A-18 forebody slot blowing p 72 N95-14255
 Interference determination for wind tunnels with slotted walls p 147 N95-19269
 Computational analysis of forebody tangential slot blowing on the high alpha research vehicle [NASA-CR-197754] p 389 N95-26591
 The fluid mechanics of a high aspect ratio slot with an impressed pressure gradient and secondary injection p 557 N95-30304

SLOTTED WIND TUNNELS
 The NASA Langley 8-foot Transonic Pressure Tunnel calibration [NASA-TP-3437] p 8 N95-10739
 Interference determination for wind tunnels with slotted walls p 147 N95-19269

SMART STRUCTURES
 Twisting smartly in the wind [BTN-95-EIX95041503093] p 184 A95-68353
 Smart structures in the control of airframe vibrations [HTN-95-31014] p 236 A95-71184
 Intelligent skins development for future military aircraft [CONGRESS PAPER C428-17-189] p 531 A95-91714
 Collected papers of the Soar//IFOR project, Spring 1994 [AD-A280063] p 238 N95-20624
 SMART materials: Surfaces, transforms and interfaces. The commensurate engineering dimension [AD-A289598] p 442 N95-28649
 Structural aspects of active control technology p 623 N95-32006

SMOKE
 Modeling aerosol emissions from the combustion of composite materials p 301 N95-23038
 Aircraft fires, smoke toxicity, and survival: An overview [DOT/FAA/AM-95/8] p 277 N95-24024
 Remote sensing of smoke, clouds, and radiation using AVIRIS during SCAR experiments p 708 N95-33749
 Corrosion of fire-damaged aircraft [AD-A294968] p 693 N95-34583

SMOKE DETECTORS
 Cost effective, dual-purpose machine vision-based detectors for (1) smoke and flame detection, and (2) engine overhead/burn-through and flame detection [AD-A292284] p 579 N95-28870

SMOOTHING
 Grid generation and surface modeling for CFD p 551 N95-28726

SNOW
 Antarctic snow record of southern hemisphere lead pollution [HTN-95-40359] p 212 A95-66869
 Snow-band formation and evolution during the 15 November 1987 aircraft accident at Denver airport [HTN-95-80699] p 254 A95-72543
 Comments on effect of wet snow on the null-reference ILS system [BTN-95-EIX95142555488] p 227 A95-72885
 Momentum and scalar transfer coefficients over aerodynamically smooth Antarctic surfaces [HTN-95-92932] p 562 A95-91870
 Preliminary results of high resolution measurements of snowfall at Stapleton International Airport during the winter of 1992-93 p 661 A95-93484
 A short-term, high-resolution automated snowfall forecasting system p 666 A95-93510
 The 1992-3 operational winter forecasting experiment for Stapleton airport p 677 A95-93561

SNOWSTORMS
 Snow-band formation and evolution during the 15 November 1987 aircraft accident at Denver airport [HTN-95-80699] p 254 A95-72543
 A short-term, high-resolution automated snowfall forecasting system p 666 A95-93510
 Preliminary studies of ice formation in upslope clouds p 674 A95-93546

SODIUM
 Evaluation of alternative in-flight fire suppressants for full-scale testing in simulated aircraft engine nacelles and dry bays [PB94-203403] p 42 N95-13247

SODIUM CHLORIDES
 Gas turbine compressor corrosion and erosion in Western Europe [AD-B196178L] p 201 N95-19678

SOFIA (AIRBORNE OBSERVATORY)
 SOFIA: Stratospheric Observatory for Infrared Astronomy p 363 A95-81583
 Numerical simulation of the SOFIA flowfield [NASA-CR-197025] p 74 N95-14612
 Numerical simulation of the SOFIA flow field [NASA-CR-197757] p 436 N95-26589
 Stratospheric Observatory For Infrared Astronomy (SOFIA), Phase A: System concept description [NASA-TM-110669] p 680 N95-32187
 SOFIA: Aft cavities wind tunnel test [NASA-TM-110673] p 683 N95-32682
 SOFIA 2 model telescope wind tunnel test report [NASA-TM-110668] p 683 N95-32764

SOFT LANDING
 Soft landing on the slope surface of a landing vehicle with an air shock-absorber of forced pressurization [BTN-94-EIX94461407941] p 85 A95-62259

SOFTWARE DEVELOPMENT TOOLS
 Integrated Thermal Energy Management (I-TEM): An evaluation tool for aircraft [SAE PAPER 932577] p 493 A95-90065
 Automated test environment for a real-time control system [TABES PAPER 94-631] p 99 N95-14652
 Applications of automatic differentiation in computational fluid dynamics p 156 N95-16461
 Data acquisition and processing software for the Low Speed Wind Tunnel tests of the Jindivik auxiliary air intake [AD-A285455] p 108 N95-17178
 An evaluation of the Software Through Pictures/T Tool (STP/T) for the Software Support Activity (SSA) [AD-A288822] p 447 N95-26348
 Developing a workstation-based, real-time simulation for rapid handling qualities evaluations during design [NASA-CR-198831] p 505 N95-30335

SOFTWARE ENGINEERING
 A reuse framework for software fault tolerance [AIAA PAPER 95-1012] p 566 A95-90683
 The ADAGE avionics reference architecture [AIAA PAPER 95-1021] p 566 A95-90693
 Accelerated application development for flight software [AIAA PAPER 95-1031] p 566 A95-90703
 Advanced distributed simulation technology advanced rotary wing aircraft. Software reusability report [AD-A280434] p 20 N95-10354
 Knowledge-based processing for aircraft flight control [NASA-CR-194976] p 99 N95-13727
 Earth Observing System (EOS)/Advanced Microwave Sounding Unit-A (AMSU-A) software assurance plan [NASA-CR-196059] p 98 N95-13885
 Generic architectures for future flight systems p 99 N95-14159
 ADST ARWA visual system module software design document [AD-A283874] p 99 N95-14357
 Automated test environment for a real-time control system [TABES PAPER 94-631] p 99 N95-14652
 A study of software standards used in the avionics industry p 137 N95-16456
 Rapid solution of large-scale systems of equations p 169 N95-16458
 Applications of automatic differentiation in computational fluid dynamics p 156 N95-16461
 Data acquisition and processing software for the Low Speed Wind Tunnel tests of the Jindivik auxiliary air intake [AD-A285455] p 108 N95-17178
 NASA High Performance Computing and Communications program [NASA-TM-4653] p 176 N95-18573
 An evaluation of the Software Through Pictures/T Tool (STP/T) for the Software Support Activity (SSA) [AD-A288822] p 447 N95-26348

- A NASTRAN-based computer program for structural dynamic analysis of Horizontal Axis Wind Turbines
p 439 N95-27980
- Control system design for the MOD-5A 7.3 mW wind turbine generator
p 440 N95-27985
- Operator modeling in commercial aviation: Cognitive models, intelligent displays, and pilot's assistants
[NASA-CR-198609] p 401 N95-28203
- Unmanned aerial vehicles, 1994 master plan
[AD-A291628] p 398 N95-28411
- Software process improvement in the NASA software engineering laboratory
[AD-A289912] p 450 N95-28627
- Surface Modeling, Grid Generation, and Related Issues in Computational Fluid Dynamic (CFD) Solutions
[NASA-CP-3291] p 476 N95-28723
- Requirements for effective use of CFD in aerospace design
p 551 N95-28725
- Rapid Airplane Parametric Input Design (RAPID)
p 501 N95-28730
- Algorithms for high aspect ratio oriented triangulations
p 476 N95-28731
- Surface modeling and grid generation for aeropropulsion CFD
p 551 N95-28732
- Automatic blocking for complex three-dimensional configurations
p 566 N95-28734
- Block-structured grids for complex aerodynamic configurations: Current status
p 551 N95-28736
- An unstructured-grid software system for solving complex aerodynamic problems
p 476 N95-28743
- Three-dimensional hybrid grid generation using advancing front techniques
p 567 N95-28745
- Impact of Ada and object-oriented design in the flight dynamics division at Goddard Space Flight Center
[NASA-CR-189412] p 567 N95-28807
- Modeling spatio-temporal databases to measure the performance of the GPS satellite constellation
p 489 N95-29596
- Proceedings of the 12th Annual National Conference on Ada Technology
[AD-A290693] p 569 N95-29644
- Manual for a workstation-based generic flight simulation program (LARCsim), version 1.4
[NASA-TM-110164] p 518 N95-30327
- Developing a workstation-based, real-time simulation for rapid handling qualities evaluations during design
[NASA-CR-198831] p 505 N95-30335
- Computational methods for control and optimal design of aerospace systems
[AD-A292861] p 608 N95-31451
- Synthetic Terrain Imagery for Helmet-Mounted Display. Volume 2: Software design document
[AD-A293611] p 612 N95-31655
- Anechoic chamber upgrade
[AD-A294375] p 700 N95-34342
- SOFTWARE RELIABILITY**
- A reuse framework for software fault tolerance
[AIAA PAPER 95-1012] p 566 A95-90683
- Evolving standards for safety critical software
[CONGRESS PAPER C428-24-142] p 678 A95-93595
- Dependable software - the state of the art
[CONGRESS PAPER C428-24-212] p 678 A95-93596
- Development of software for safety critical applications for the EH101 Helicopter
[CONGRESS PAPER C428-24-160] p 678 A95-93597
- Space Generic Open Avionics Architecture (SGOAA): Overview
p 99 N95-14161
- Evolutionary Telemetry and Command Processor (TCP) architecture
p 86 N95-14162
- SOFTWARE REUSE**
- A reuse framework for software fault tolerance
[AIAA PAPER 95-1012] p 566 A95-90683
- The ADAGE avionics reference architecture
[AIAA PAPER 95-1021] p 566 A95-90693
- SOIL MAPPING**
- Development of an Automated Airfield Dynamic Cone Penetrometer (AADCP) prototype and the evaluation of unsurfaced airfield seismic surveying using Spectral Analysis of Surface Waves (SASW) technology
[AD-A291985] p 145 N95-17444
- SOLAR ARRAYS**
- Building complex simulations rapidly using MATRIX(x): The Space Station redesign
[TABES PAPER 94-632] p 87 N95-14653
- Design of a GaAs/Ge solar array for unmanned aerial vehicles
[NASA-TM-106870] p 320 N95-23259
- SOLAR CELLS**
- Hypersonic Gas-Surface Energy Accommodation Test Facility
[DE94-014468] p 39 N95-12652
- Photovoltaic electric power applied to Unmanned Aerial Vehicles (UAV)
p 245 N95-20530
- Design of a GaAs/Ge solar array for unmanned aerial vehicles
[NASA-TM-106870] p 320 N95-23259
- SOLAR ELECTRIC PROPULSION**
- CALIOPE and TAISSIR airborne experiment platform
[DE94-018328] p 250 N95-22299
- SOLAR POWERED AIRCRAFT**
- Long endurance stratospheric solar powered airship
[PB95-178729] p 336 N95-26009
- SOLAR RADIATION**
- Remote sensing of smoke, clouds, and radiation using AVIRIS during SCAR experiments
p 708 N95-33749
- SOLAR WIND**
- A survey of bidirectional greater than or equal to MeV ion flows during the Helios 1 and Helios 2 mission: Observations from the Goddard Space Flight Center instruments
[HTN-95-70542] p 237 A95-71656
- SOLID LUBRICANTS**
- Evaluation of thermal barrier and PS-200 self-lubricating coatings in an air-cooled rotary engine
[NASA-CR-195445] p 289 N95-23222
- SOLID MECHANICS**
- Activities of the Institute for Aerospace Studies of Toronto University
p 63 N95-12699
- NASA-UVA light aerospace alloy and structures technology program (LA2ST)
[NASA-CR-198041] p 343 N95-24220
- SOLID PROPELLANT COMBUSTION**
- Propulsion research concerning SFRJ-motors
[PB94-179520] p 14 N95-10083
- Solid fuel ramjet composition
[AD-D016458] p 152 N95-19090
- Workshop report: Measurement techniques in highly transient, spectrally rich combustion environments
p 629 N95-31208
- SOLID PROPELLANT IGNITION**
- Flame-spreading phenomena in the fin-slot region of a solid rocket motor
p 23 N95-10296
- SOLID PROPELLANT ROCKET ENGINES**
- Simulation on the 3-D turbulent flow in the passages of finocyl grain
[BTN-95-EIX95202638962] p 279 A95-76674
- Flame-spreading phenomena in the fin-slot region of a solid rocket motor
p 23 N95-10296
- Computational flow predictions for hypersonic drag devices
p 37 N95-11967
- AFOSR Contractors Meeting in Propulsion
[AD-A282729] p 54 N95-12507
- The 1993 JANNAP Propulsion Meeting, volume 1
[CPIA-PUBL-602-VOL-1] p 148 N95-16312
- Thermal chemical energy of ablating silica surfaces in air breathing solid rocket engines
p 148 N95-16316
- Recent advances in graphite/epoxy motor cases
p 149 N95-16333
- SOLID PROPELLANTS**
- Integral rocket ramjets
[AD-A285135] p 240 N95-20906
- SOLID ROCKET PROPELLANTS**
- Workshop report: Measurement techniques in highly transient, spectrally rich combustion environments
p 629 N95-31208
- SOLID SOLUTIONS**
- Multilayer anti-erosion coatings
p 201 N95-19679
- SOLID STATE**
- Solid-state data recorder, next development and use
p 705 N95-33143
- SOLID STATE DEVICES**
- Solid state power controller technology
[SAE PAPER 931422] p 495 A95-90087
- Airport surveillance using a solid state coherent lidar
p 41 N95-13207
- Solid state radar demonstration test results at the FAA Technical Center
[AD-A281520] p 154 N95-16097
- SOLID STATE LASERS**
- 2 micron LIDAR for laser-based remote sensing: Flight demonstration and application survey
[BTN-95-EIX95212641072] p 319 A95-76737
- Wake vortex detection at Denver Stapleton Airport with a pulsed 2-micron coherent lidar
p 42 N95-13211
- Development and flight testing of an Obstacle Avoidance System for US Army helicopters
p 687 N95-32500
- SOLID SURFACES**
- Surface Modeling, Grid Generation, and Related Issues in Computational Fluid Dynamic (CFD) Solutions
[NASA-CP-3291] p 476 N95-28723
- Grid generation and surface modeling for CFD
p 551 N95-28726
- Surface modeling and grid generation for aeropropulsion CFD
p 551 N95-28732
- SOLID WASTES**
- Bicarbonate of soda blasting technology for aircraft wheel depainting
[PB94-193323] p 104 N95-17466
- SOLIDS**
- On the particular features of dynamic processes in solids with varying boundary during interaction with intensive heat flows
[BTN-94-EIX94461408756] p 171 A95-63639
- Photoacoustic chambers for studying solids and gases: Theory and practical examples
[IFTR-39/1994] p 412 N95-26837
- SOLVATION**
- Matrix isolated HF: the high-resolution infrared spectrum of a cryogenically solvated hindered rotor
[GTN-95-0301010494002231-16] p 578 A95-92210
- SONIC BOOMS**
- Aeroacoustic model for weak shock waves based on Burgers equation
[BTN-95-EIX95182619076] p 269 A95-75761
- Progressive wave equations and algorithms for sonic boom propagation
p 575 A95-90104
- A total variation diminishing finite difference algorithm for sonic boom propagation models
p 575 A95-90105
- Recent laboratory studies of loudness and annoyance to sonic booms
p 575 A95-90117
- Plaster damage experiments at the BBN Sonic Boom Test Facility
p 529 A95-90120
- Selecting optimum sonic boom monitoring sites in a special-use airspace
p 576 A95-90124
- Research of the method for evaluating noise caused by sonic boom
p 562 A95-91519
- High speed civil transport: Sonic boom softening and aerodynamic optimization
[NASA-CR-196397] p 28 N95-11192
- MOAMAP: A model that combines several different kinds of aircraft operations
p 32 N95-11323
- High-Speed Research: 1994 Sonic Boom Workshop: Atmospheric Propagation and Acceptability Studies
[NASA-CP-3279] p 75 N95-14878
- Effect of stratification and geometrical spreading on sonic boom rise time
p 75 N95-14880
- Atmospheric effects on the risetime and waveshape of sonic booms
p 100 N95-14886
- The effect of aircraft speed on the penetration of sonic boom noise into a flat ocean
p 100 N95-14887
- USAF single-event sonic boom prediction model: PCBoom3
p 101 N95-14889
- Floating shock fitting via Lagrangian adaptive meshes
[AD-A289758] p 170 N95-18110
- An assessment of the adaptive unstructured tetrahedral grid, Euler Flow Solver Code FELISA
[NASA-TP-3526] p 119 N95-19041
- Design and testing of low sonic boom configurations and an oblique all-wing supersonic transport
[NASA-CR-197744] p 389 N95-26651
- Supersonic civil airplane study and design: Performance and sonic boom
[NASA-CR-197745] p 390 N95-26813
- SOOT**
- The effect of altitude conditions on the particle emissions of a J85-GE-5L turbojet engine
[NASA-TM-106669] p 339 N95-24561
- SORBENTS**
- Laboratory evaluation of a reactive baffle approach to NOx control
[AD-A283802] p 255 N95-19921
- SOUND AMPLIFICATION**
- Computing unsteady shock waves for aeroacoustic applications
[HTN-95-20928] p 463 A95-88967
- SOUND DETECTING AND RANGING**
- Aircraft IR/acoustic detection evaluation. Volume 2: Development of a ground-based acoustic sensor system for the detection of subsonic jet-powered aircraft
[NASA-CR-189705-VOL-2] p 452 N95-28073
- SOUND FIELDS**
- Rotating Kirchhoff method for three-dimensional transonic blade-vortex interaction hover noise
[BTN-94-EIX94441386601] p 182 A95-67332
- Numerical study of sound generation due to a spinning vortex pair
[BTN-95-EIX95182619075] p 307 A95-75760
- Stochastic approach to noise modeling for free turbulent flows
[HTN-95-42321] p 371 A95-86150
- Achievements and tasks for active noise control
p 29 N95-11270
- Active minimization of energy density in three-dimensional enclosures
[NASA-CR-197213] p 172 N95-16848
- Acoustic field in unsteady moving media
[NASA-CR-198162] p 438 N95-27179
- Method for extracting forward acoustic wave components from rotating microphone measurements in the inlets of turbofan engines
[NASA-CR-195457] p 616 N95-30779

SOUND GENERATORS

Anisotropic heat exchangers/stack configurations for thermoacoustic heat engines
[AD-A280974] p 168 N95-16506

A numerical study of fundamental shock noise mechanisms
[NASA-TM-110608] p 451 N95-27908

SOUND INTENSITY

Factors affecting measured aircraft sound levels in the vicinity of start-of-takeoff roll p 571 A95-88465
Time-average aircraft noise descriptors: Confusion with no benefit p 559 A95-88474
Noise metrics and aviation noise control: The case for DNL p 559 A95-88475

SOUND PRESSURE

Evaluation of prediction methods for fluctuating pressures under attached turbulent boundary layers using flight test data p 574 A95-90103
Numerical simulation of the SOFIA flowfield
[NASA-CR-197025] p 74 N95-14612

Weapons bay acoustic environment p 173 N95-19146
Modelling structurally damaging twin-jet screech p 135 N95-19154
Numerical simulation of the SOFIA flow field
[NASA-CR-197757] p 436 N95-26589

Observed acoustic and aeroelastic spectral responses of a MOD-2 turbine blade to turbulence excitation p 451 N95-27991

Anechoic wind tunnel study of turbulence effects on wind turbine broadband noise p 451 N95-27992

Turbulent airflow noise production and propagation patterns of a subsonic jet impinging on a flat plate p 580 N95-29502

SOUND PROPAGATION

Sound propagation from an arbitrarily oriented multipole placed near a plane, finite impedance surface
[BTN-94-EIX94371338964] p 257 A95-70797

The propagation of sound from an arbitrarily oriented dipole over a finite impedance plane p 570 A95-88459

Progressive wave equations and algorithms for sonic boom propagation p 575 A95-90104

A total variation diminishing finite difference algorithm for sonic boom propagation models p 575 A95-90105

Recent laboratory studies of loudness and annoyance to sonic booms p 575 A95-90117

The influence of source acceleration on acoustic signals p 577 A95-90136

At Istanbul-Ataturk Airport measurement and analysis of noise in due of take-off time p 31 N95-11319

Proceedings of the Sixth International Symposium on Long-Range Sound Propagation
[AD-A290920] p 580 N95-30084

Method for extracting forward acoustic wave components from rotating microphone measurements in the inlets of turbofan engines
[NASA-CR-195457] p 616 N95-30779

SOUND TRANSDUCERS

Aircraft IR/acoustic detection evaluation. Volume 2: Development of a ground-based acoustic sensor system for the detection of subsonic jet-powered aircraft
[NASA-CR-189705-VOL-2] p 452 N95-28073

Investigating the use of smart acoustically active surfaces for flow separation control in turbomachinery
[AD-A292819] p 648 N95-31443

SOUND TRANSMISSION

Oblique incidence sound absorption of porous materials covered by perforated metal and exposed to tangential airflow
[HTN-94-00681] p 19 A95-60165

Numerical investigation of sound transmission through double wall cylinders with respect to active noise control p 577 A95-90134

Transmission loss characteristics of aircraft sidewall systems to control cabin interior noise p 28 N95-11261

A theoretical analysis of airborne sound transfer for a resiliently mounted machine to its foundation p 30 N95-11304

Effect of constraining layer stiffness on performance of damping tile materials using finite element modelling with Rayleigh integral p 30 N95-11306

Proceedings of the Sixth International Symposium on Long-Range Sound Propagation
[AD-A290920] p 580 N95-30084

SOUND WAVES

Sound propagation from an arbitrarily oriented multipole placed near a plane, finite impedance surface
[BTN-94-EIX94371338964] p 257 A95-70797

Coupled FEM-BEM approach for mean flow effects on vibro-acoustic behavior of planar structures
[BTN-95-EIX95152577587] p 263 A95-73495

Mach wave emission from a high-temperature supersonic jet
[BTN-95-EIX95152577586] p 264 A95-73496

Transonic flutter suppression using active acoustic excitations
[BTN-95-EIX95262694310] p 408 A95-85481

Nonreflective boundary conditions for high-order methods
[HTN-95-42328] p 371 A95-86157

Disturbance generation in supersonic jets under acoustic excitation
[HTN-95-20926] p 463 A95-88965

Fan noise reduction from a supersonic inlet during simulated aircraft approach
[BTN-95-EIX95292721155] p 572 A95-89894

Signal processing of noise data from high-speed flyovers
[BTN-95-EIX0619952748178] p 680 A95-94248

Interaction of a weak shock with freestream disturbances
[BTN-95-EIX95332750473] p 638 A95-94687

Empirical refinements to boundary layer transition noise models p 28 N95-11262

Active control of turbomachine discrete tones p 29 N95-11275

En route noise levels from propfan test assessment airplane
[NASA-TP-3451] p 62 N95-12341

Ducted fan acoustic radiation including the effects of nonuniform mean flow and acoustic treatment
[NASA-CR-197449] p 172 N95-16401

Active minimization of energy density in three-dimensional enclosures
[NASA-CR-197213] p 172 N95-16848

Acoustic radiation damping of flat rectangular plates subjected to subsonic flows p 172 N95-18542

Temperature effects on acoustic interactions between altitude test facilities and jet engine plumes
[NASA-CR-197638] p 258 N95-21170

Acoustic receptivity due to weak surface inhomogeneities in adverse pressure gradient boundary layers
[NASA-TM-4577] p 249 N95-21258

Effect of atmospheric pressure on measured aircraft noise levels
[PB95-130423] p 232 N95-21425

Observed acoustic and aeroelastic spectral responses of a MOD-2 turbine blade to turbulence excitation p 451 N95-27991

Anechoic wind tunnel study of turbulence effects on wind turbine broadband noise p 451 N95-27992

The acoustic characteristics of turbomachinery cavities
[NASA-CR-4671] p 476 N95-28720

SOUNDING
An in situ evaluation of TOPEX/Poseidon altimetric measurements versus measurements made by moorings and inverted echo sounders for sea surface height
[NASA-CR-198621] p 447 N95-27805

SOURCES
Environmental noise monitoring - source identification
[HTN-95-92537] p 558 A95-87357

SOUTHERN HEMISPHERE
Antarctic snow record of southern hemisphere lead pollution
[HTN-95-40359] p 212 A95-66869

SPACE DEBRIS
Hypervelocity Impact Test Facility: A gun for hire
[TABES PAPER 94-605] p 86 N95-14639

SPACE ENVIRONMENT SIMULATION
Simulation of Shuttle launch G forces and acoustic loads using the NASA Ames Research Center 20G centrifuge p 86 N95-14089

Thermoacoustic environments to simulate reentry conditions p 86 N95-14096

Hypervelocity Impact Test Facility: A gun for hire
[TABES PAPER 94-605] p 86 N95-14639

Virtual environment application with partial gravity simulation p 169 N95-15988

SPACE EXPLORATION
Aeronautics and space technology, past, present, and future p 35 N95-11892

NASA video catalog
[NASA-SP-7109(01)] p 363 N95-24238

Aeronautics and space report of the President
[NASA-TM-110743] p 681 N95-31979

SPACE LAW
The ICAO CNS/ATM system: New king, new law?
[HTN-95-50218] p 175 A95-64855

World trends in air transport policies. (Approaching the 21st century)
[HTN-95-50220] p 176 A95-64857

SPACE NAVIGATION
Guidance and control, 1993; Annual Rocky Mountain Guidance and Control Conference, 16th, Keystone, CO, Feb. 6-10, 1993
[ISBN-0-87703-365-X] p 341 A95-80389

Describing an attitude p 342 A95-80409

Flight Mechanics/Estimation Theory Symposium 1995
[NASA-CP-3299] p 416 N95-27763

SPACE PERCEPTION
Spatial awareness comparisons between large-screen, integrated pictorial displays and conventional EFIS displays during simulated landing approaches
[NASA-TP-3467] p 80 N95-14852

SPACE PLASMAS
Induced Compton scattering by relativistic electrons in magnetized astrophysical plasmas p 563 N95-29885

SPACE PROCESSING
Fourth-generation Mars vehicle concepts
[BTN-95-EIX95152583267] p 298 A95-73568

Microgravity isolation system design: A modern control analysis framework
[NASA-TM-106803] p 105 N95-18486

SPACE SHUTTLE BOOSTERS
Documentation and archiving of the Space Shuttle wind tunnel test data base. Volume 1: Background and description
[NASA-TM-104806-VOL-1] p 151 N95-19237

SPACE SHUTTLE MAIN ENGINE
Automated test environment for a real-time control system
[TABES PAPER 94-631] p 99 N95-14652

Phase 2: HGM air flow tests in support of HEX vane investigation p 312 N95-23438

SPACE SHUTTLE MISSIONS
Orbiter rarefied-flow reentry measurements from the OARE on STS-62
[NASA-TM-110182] p 646 N95-30783

SPACE SHUTTLE ORBITERS
Navier-Stokes simulations of Orbiter aerodynamic characteristics including pitch trim and bodyflap
[BTN-95-EIX95041503779] p 204 A95-69210

Multiblock analysis for Shuttle Orbiter reentry heating from Mach 24 to Mach 12
[BTN-95-EIX95041503780] p 205 A95-69211

Aerodynamics of the Shuttle Orbiter at high altitudes
[BTN-95-EIX95182617454] p 298 A95-75725

Shuttle entry guidance revisited using nonlinear geometric methods
[BTN-95-EIX95182619144] p 299 A95-76621

An axisymmetric analog two-layer convective heating procedure with application to the evaluation of Space Shuttle Orbiter wing leading edge and windward surface heating
[NASA-CR-188343] p 54 N95-11937

Hypersonic flight testing
[AD-A283981] p 134 N95-18891

Documentation and archiving of the Space Shuttle wind tunnel test data base. Volume 1: Background and description
[NASA-TM-104806-VOL-1] p 151 N95-19237

Performance of an aerodynamic yaw controller mounted on the space shuttle orbiter body flap at Mach 10
[NASA-TM-109179] p 330 N95-24397

A vehicle health monitoring system for the Space Shuttle Reaction Control System during reentry
[NASA-CR-188370] p 527 N95-29447

Orbiter rarefied-flow reentry measurements from the OARE on STS-62
[NASA-TM-110182] p 646 N95-30783

SPACE SHUTTLES
NAL aerothermodynamic probing and CFD verification mission in OREX experiment p 368 A95-82413

Development of a climatological data base to help forecast cloud cover conditions for shuttle landings at the Kennedy Space Center p 670 A95-93529

Analysis of rapidly developing fog at the Kennedy Space Center p 671 A95-93531

Aircraft nose gear shimmy studies
[SAE PAPER 931401] p 628 A95-93671

Ultraviolet emissions occurring about hypersonic vehicles in rarefied flows
[AD-A281452] p 106 N95-16076

Field and data analysis studies related to the atmospheric environment
[NASA-CR-196543] p 168 N95-18093

Hypersonic flight testing
[AD-A283981] p 134 N95-18891

Documentation and archiving of the Space Shuttle wind tunnel test data base. Volume 1: Background and description
[NASA-TM-104806-VOL-1] p 151 N95-19237

Fatigue loads spectra derivation for the Space Shuttle: Second cycle p 166 N95-19470

Documentation and archiving of the Space Shuttle wind tunnel test data base. Volume 2: User's Guide to the Archived Data Base
[NASA-TM-104806-VOL-2] p 205 N95-19624

SPACE STATION FREEDOM
A surgical support system for Space Station Freedom p 149 N95-16776

SPACE STATIONS

- Optimization of aerospace structures
[NASA-CR-196763] p 48 N95-12787
Building complex simulations rapidly using MATRIX(x):
The Space Station redesign
[TABES PAPER 94-632] p 87 N95-14653
SPACE SURVEILLANCE (SPACEBORNE)
The use of satellites for aeronautical communications,
navigation and surveillance
[CONGRESS PAPER C428-30-159] p 600 A95-93613

SPACE TRANSPORTATION

- Air-breathing aerospace plane development essential:
Hypersonic propulsion flight tests
[NASA-TM-108857] p 66 N95-14921

SPACE-TIME FUNCTIONS

- Linear and nonlinear discrete-time state-space modeling
of dynamic systems for control applications
p 567 N95-29251
A time stepping coupled finite element-state space
modeling environment for synchronous machine
performance and design analysis in the ABC frame of
reference p 649 N95-31948

SPACEBORNE EXPERIMENTS

- Microgravity isolation system design: A modern control
synthesis framework
[NASA-TM-106805] p 105 N95-18197

SPACECRAFT

- Polarization diverse ultra-wideband antenna
technology p 548 A95-90924

SPACECRAFT ANTENNAS

- Space flight tests of attitude determination using GPS
[BTN-95-EIX95112522529] p 190 A95-69334

SPACECRAFT BREAKUP

- Reentry analysis for low Earth orbiting spacecraft
p 415 A95-85774

SPACECRAFT CONFIGURATIONS

- Aerodynamic simulation on massively parallel systems
p 549 A95-91487
Fatigue loads spectra derivation for the Space Shuttle:
Second cycle p 166 N95-19470

SPACECRAFT CONSTRUCTION MATERIALS

- Evaluation of advanced aerospace materials by depth
sensing indentation and scratch methods
[BTN-95-EIX95152584678] p 282 A95-73590
R & D on HOPE structure p 413 A95-82355
Activities of Mitsubishi Heavy Industries Ltd.
[PB94-179694] p 22 N95-10085
Modeling and life prediction methodology for Titanium
Matrix Composites subjected to mission profiles
[NASA-TM-109148] p 55 N95-11915
Test model designs for advanced refractory ceramic
materials p 55 N95-11968
Recent advances in graphite/epoxy motor cases
p 149 N95-16333
Conference on Aerospace Transparent Materials and
Enclosures, Volume 2: Sessions 5-9
[AD-A283926] p 131 N95-18162
Conference on Aerospace Transparent Materials and
Enclosures, volume 1
[AD-A283925] p 133 N95-18677
A CMC database for use in the next generation launch
vehicles (rockets) p 150 N95-18993

SPACECRAFT CONTROL

- Fuel-optimal bank-angle control for lunar-return
aerocapture
[BTN-95-EIX95212645706] p 299 A95-76758
Guidance and control, 1993; Annual Rocky Mountain
Guidance and Control Conference, 16th, Keystone, CO,
Feb. 6-10, 1993
[ISBN-0-87703-365-X] p 341 A95-80389
The Cassini spacecraft: Object oriented flight control
software p 359 A95-80405
Air data sensors for atmospheric reentry flight test of
winged space vehicle p 413 A95-82412
A guidance concept for hypersonic aerospacecrafts
p 526 A95-91549
Safety aspects of spacecraft commanding
p 149 N95-17248
Packet utilisation definitions for the ESA XMM mission
p 150 N95-17596
Performance of an aerodynamic yaw controller mounted
on the space shuttle orbiter body flap at Mach 10
[NASA-TM-109179] p 330 N95-24397
A vehicle health monitoring system for the Space Shuttle
Reaction Control System during reentry
[NASA-CR-188370] p 527 N95-29447

SPACECRAFT DESIGN

- Two projects of V. M. Myasishchev
[HTN-95-50269] p 176 A95-65764
Guidance and control, 1993; Annual Rocky Mountain
Guidance and Control Conference, 16th, Keystone, CO,
Feb. 6-10, 1993
[ISBN-0-87703-365-X] p 341 A95-80389
R & D on HOPE structure p 413 A95-82355

- Activities of Mitsubishi Heavy Industries Ltd.
[PB94-179694] p 22 N95-10085
The model builders
[NASA-TM-109902] p 20 N95-10552
Optimization of aerospace structures
[NASA-CR-196763] p 48 N95-12787
Building complex simulations rapidly using MATRIX(x):
The Space Station redesign
[TABES PAPER 94-632] p 87 N95-14653
Requirements report for SSTO vertical take-off and
horizontal landing vehicle p 80 N95-14794
[NASA-CR-197029] p 80 N95-14794
JPRS report: Science and technology, Central Eurasia
[JPRS-UST-94-022] p 438 N95-27699
Geometric modeling for computer aided design
[NASA-CR-198828] p 679 N95-31982

SPACECRAFT ELECTRONIC EQUIPMENT

- An avionics scenario and command model description
for Space Generic Open Avionics Architecture (SGOAA)
[NASA-CR-188330] p 49 N95-11913

SPACECRAFT GLOW

- Ultraviolet emissions occurring about hypersonic
vehicles in rarefied flows
[AD-A281452] p 106 N95-16076

SPACECRAFT GUIDANCE

- Guidance and control, 1993; Annual Rocky Mountain
Guidance and Control Conference, 16th, Keystone, CO,
Feb. 6-10, 1993
[ISBN-0-87703-365-X] p 341 A95-80389
A guidance concept for hypersonic aerospacecrafts
p 526 A95-91549

- Analytical investigations in aircraft and spacecraft
trajectory optimization and optimal guidance
[NASA-CR-4672] p 526 N95-29339
A vehicle health monitoring system for the Space Shuttle
Reaction Control System during reentry
[NASA-CR-188370] p 527 N95-29447

SPACECRAFT INSTRUMENTS

- Guidance and control, 1993; Annual Rocky Mountain
Guidance and Control Conference, 16th, Keystone, CO,
Feb. 6-10, 1993
[ISBN-0-87703-365-X] p 341 A95-80389
Development of techniques for the in situ observation
of OH and HO₂ for studies of the impact of high-altitude
supersonic aircraft on the stratosphere
[NASA-CR-196759] p 61 N95-12832

SPACECRAFT LANDING

- Soft landing on the slope surface of a landing vehicle
with an air shock-absorber of forced pressurization
[BTN-94-EIX94461407941] p 85 A95-62259
Landing gear energy absorption system
[NASA-CASE-MSC-22277-1] p 96 N95-15306

SPACECRAFT LAUNCHING

- Fourth-generation Mars vehicle concepts
[BTN-95-EIX95152583267] p 298 A95-73568
Simulation of Shuttle launch G forces and acoustic loads
using the NASA Ames Research Center 20G centrifuge
p 86 N95-14089
Program test objectives milestone 3 --- Integrated
Propulsion Technology Demonstrator
[NASA-CR-197030] p 127 N95-15971

SPACECRAFT MANEUVERS

- Dynamics and control of a tethered flight vehicle
[BTN-95-EIX95242670754] p 342 A95-81093

SPACECRAFT MODELS

- Thermal force modeling for global positioning system
satellites using the finite element method
[BTN-95-EIX95152583270] p 278 A95-73571
The model builders
[NASA-TM-109902] p 20 N95-10552
Safety aspects of spacecraft commanding
p 149 N95-17248

SPACECRAFT MOTION

- Analytical investigations in aircraft and spacecraft
trajectory optimization and optimal guidance
[NASA-CR-4672] p 526 N95-29339

SPACECRAFT ORBITS

- How 'HITEN's' aerobraking experiments were carried
out p 415 A95-82553

SPACECRAFT PERFORMANCE

- Guidance and control, 1993; Annual Rocky Mountain
Guidance and Control Conference, 16th, Keystone, CO,
Feb. 6-10, 1993
[ISBN-0-87703-365-X] p 341 A95-80389
Safety aspects of spacecraft commanding
p 149 N95-17248

SPACECRAFT PROPULSION

- Arjet thruster research and technology, phase 2
[NASA-CR-182276] p 105 N95-18044
A vehicle health monitoring system for the Space Shuttle
Reaction Control System during reentry
[NASA-CR-188370] p 527 N95-29447

SPACECRAFT RECOVERY

- Development and flight test of a deployable precision
landing system
[BTN-95-EIX95062487535] p 190 A95-69243

SPACECRAFT REENTRY

- Multiblock analysis for Shuttle Orbiter reentry heating
from Mach 24 to Mach 12
[BTN-95-EIX95041503780] p 205 A95-69211
Shuttle entry guidance revisited using nonlinear
geometric methods
[BTN-95-EIX95182619144] p 299 A95-76621
Air data sensors for atmospheric reentry flight test of
winged space vehicle p 413 A95-82412
NAL aerothermodynamic probing and CFD verification
mission in OREX experiment p 368 A95-82413
Hypersonic thermal protection with mass injection at
angle of attack p 414 A95-82414
Hypersonic flow simulation with thermoelectric effect
p 368 A95-82669
Reentry analysis for low Earth orbiting spacecraft
p 415 A95-85774

- Corrective term in wall slip equations for Knudsen
layer
[BTN-95-EIX95282705070] p 455 A95-89667

- The Superorbital Expansion Tube concept, experiment
and analysis p 341 N95-25399
Viscous shock-layer analysis on hypersonic flow over
reentry capsule with nonequilibrium chemistry
[ISAS-656] p 436 N95-26739
Rarefied gas effects on aerobraking/reentry vehicles
with wakes
[NASA-CR-196586] p 415 N95-27093
A vehicle health monitoring system for the Space Shuttle
Reaction Control System during reentry
[NASA-CR-188370] p 527 N95-29447
Orbiter rarefied-flow reentry measurements from the
OARE on STS-62
[NASA-TM-110182] p 646 N95-30783

SPACECRAFT SHIELDING

- Trajectory-based heating analysis for the European
Space Agency/Rosetta Earth Return Vehicle
[BTN-95-EIX95041503787] p 205 A95-69218
Research and development of thermal protection system
of HOPE re-entry vehicle p 413 A95-82358
Test model designs for advanced refractory ceramic
materials p 55 N95-11968

SPACECRAFT STABILITY

- Evaluation of energy-sink stability criteria for dual-spin
spacecraft
[AD-A283228] p 87 N95-14850
Transonic aerodynamic characteristics of a proposed
wing-body reusable launch vehicle concept
[NASA-TM-108489] p 592 N95-30712

SPACECRAFT STRUCTURES

- R & D on HOPE structure p 413 A95-82355
Activities of Mitsubishi Heavy Industries Ltd.
[PB94-179694] p 22 N95-10085
Aerodynamic qualification of HERMES shingles
p 173 N95-19145

SPACECRAFT TEMPERATURE

- A low fin height heat exchanger technology
demonstrator for Hermes
[SAE PAPER 932119] p 526 A95-90360
A programmable heater control circuit for spacecraft
[NASA-TM-108459] p 9 N95-11157

SPACECRAFT TRACKING

- Flight Mechanics/Estimation Theory Symposium 1995
[NASA-CP-3299] p 416 N95-27763

SPACECRAFT TRAJECTORIES

- Effects of satellite bunching on the probability of collision
in geosynchronous orbit
[BTN-95-EIX95152583276] p 298 A95-73577
Analytical investigations in aircraft and spacecraft
trajectory optimization and optimal guidance
[NASA-CR-4672] p 526 N95-29339

SPACECREWS

- Virtual environment application with partial gravity
simulation p 169 N95-15988

SPACING

- Main features of overexpanded triple jets
[BTN-95-EIX95142553040] p 304 A95-73458

SPALLATION

- Phonon characteristics of high (T sub c) superconductors
from neutron Doppler broadening measurements
[DE95-003703] p 324 N95-24076

SPALLING

- Effect of annealing and desulfurization on oxide
spallation of turbine airfoil material
[BTN-95-EIX95282707024] p 528 A95-88264
Aircraft corrosion study
[AD-A279527] p 241 N95-21687
Thermal barrier coating life modeling in aircraft gas
turbine engines p 346 N95-26140

SPANWISE BLOWING

- Study of potential aerodynamic benefits from spanwise
blowing at wingtip
[NASA-TP-3515] p 378 N95-28669
Pressure based high order TVD methodology for
dynamic stall control
[AD-A290149] p 479 N95-29316

SPARE PARTS

Report to the Chairman, Legislation and National Security Subcommittee, Committee on Government Operations, House of Representatives. C-17 Aircraft program: Improvements in initial provisioning process [GAO/NSIAD-94-63] p 584 N95-32194

SPARK IGNITION

Multidimensional calculation of spark flame initiation by adopting a generic hydrocarbon kinetic scheme p 528 A95-87566

Aircraft fuel system lightning protection design and qualification test procedures development [AD-A288401] p 380 N95-26497

SPATIAL DISTRIBUTION

Thundercloud electric field modeling for the ionosphere-Earth region. 1: Dependence on cloud charge distribution [HTN-95-41223] p 317 A95-75035

Fractal properties of whitecaps [HTN-95-92121] p 443 A95-83827

Use of pilot reports for verification of aircraft icing diagnoses and forecasts p 666 A95-93508

Vortex generation and mixing in three-dimensional supersonic combustors [BTN-95-EIX0616952745783] p 614 A95-94503

Investigation of scramjet injection strategies for high mach number flows [BTN-95-EIX0616952745782] p 614 A95-94504

Modeling spatio-temporal databases to measure the performance of the GPS satellite constellation p 489 N95-29596

Image representation using fast algorithms based on the Zak transform [AD-A293416] p 679 N95-31684

SPATIAL FILTERING

Simulation of turbulent fluctuations [BTN-95-EIX95142553041] p 304 A95-73457

Terminal Doppler Weather Radar point target filter threshold selection p 662 A95-93490

SPECIFIC HEAT

Improved analytical solution for varying specific heat parallel stream mixing [BTN-94-EIX94481415349] p 103 A95-65339

Supersonic axisymmetric conical flow solutions for different ratios of specific heats [BTN-95-EIX95152583283] p 306 A95-73584

Review and development of base pressure and base heating correlations in supersonic flow [BTN-95-EIX95212645688] p 271 A95-76740

Similarity rule for jet-temperature effects on transonic base pressure [BTN-95-EIX9522650791] p 329 A95-79247

Computer code for determination of thermally perfect gas properties [NASA-TP-3447] p 37 N95-11995

SPECIFICATIONS

International cooperation in standardization p 452 A95-82665

Computational predictive methods for fracture and fatigue p 93 N95-14466

Handling qualities of the High Speed Civil Transport p 294 N95-23325

SPECKLE INTERFEROMETRY

Novel implements of optical diagnostic techniques for aerospace applications [CONGRESS PAPER C428-21-081] p 550 A95-91726

Residual Stress Measurements with Laser Speckle Correlation Interferometry and Local Heat Treating [DE95-060082] p 349 N95-24598

SPECKLE PATTERNS

Residual Stress Measurements with Laser Speckle Correlation Interferometry and Local Heat Treating [DE95-060082] p 349 N95-24598

SPECTRA

Measured and calculated spectral radiation from a blunt body shock layer in an arc-jet wind tunnel [AIAA PAPER 94-0086] p 67 N95-13720

High order accuracy computational methods in aerodynamics using parallel architectures [AD-A294167] p 686 N95-34763

Transmittance characteristics of US Army rotary-wing aircraft transparencies [AD-A295035] p 693 N95-34793

SPECTRAL METHODS

A spectrally accurate boundary-layer code for infinite swept wings [NASA-CR-195014] p 159 N95-18042

Treatment of non-linear systems by timeplane-transformed CT methods: The spectral gust method p 143 N95-18600

Derived gust spectra for the Macchi MB326H [ARL-TN-3] p 225 N95-21892

SPECTRAL REFLECTANCE

Correction of thin cirrus effects in AVIRIS images using the sensitive 1.375-micron cirrus detecting channel p 708 N95-33748

Remote sensing of smoke, clouds, and radiation using AVIRIS during SCAR experiments p 708 N95-33749

SPECTRAL SENSITIVITY

Sensitivity of acoustic predictions to variation of input parameters [HTN-95-80855] p 267 A95-75097

SPECTROMETERS

Performance of a focused cavity aerosol spectrometer for measurements in the stratosphere of particle size in the 0.06-2.0-micrometer-diameter range [HTN-95-90914] p 253 A95-72423

Integrated X-ray testing of the electro-optical breadboard model for the XMM reflection grating spectrometer [DE95-008829] p 644 N95-30507

SPECTROSCOPIC ANALYSIS

Comparison of diurnal abundances from three infrared spectrometers during AASE 2 [HTN-95-70946] p 352 A95-78011

Chemical change in the arctic vortex during AASE 2 [HTN-95-70947] p 352 A95-78012

Temperature diagnostics in the hypersonic flow regime: An application to develop a stagnation temperature probe [AIAA PAPER 95-6114] p 511 A95-90442

Electrochemical impedance pattern recognition for detection of hidden chemical corrosion on aircraft components [AD-A284998] p 241 N95-20481

Measurements of ions formed in jet engine exhaust plumes [AD-A290940] p 514 N95-29764

SPECTRO ANALYSIS

Measurement around a rotor blade excited in pitch. Part 1: Dynamic inflow [HTN-95-31007] p 220 A95-71177

Precise navigation using adaptive FIR filtering and time domain spectral estimation [BTN-95-EIX95142555485] p 227 A95-72888

An experimental study on radiation from strong shock layer [HTN-95-82421] p 368 A95-82421

Flight-testing and frequency-domain analysis for rotorcraft handling qualities [HTN-95-01083] p 515 A95-90269

Signal processing of noise data from high-speed flyovers [BTN-95-EIX0619952748178] p 680 A95-94248

Spectral mapping of quasiperiodic structures in a vortex flow [BTN-95-EIX0619952748165] p 589 A95-94459

Spectral analysis of vortex/free-surface interaction [AD-A283210] p 96 N95-14658

Development of an Automated Airfield Dynamic Cone Penetrometer (AADCP) prototype and the evaluation of unsurfaced airfield seismic surveying using Spectral Analysis of Surface Waves (SASW) technology [AD-A281985] p 145 N95-17444

Spectrogram diagnosis of aircraft disasters p 124 N95-19167

Phonon characteristics of high (T sub c) superconductors from neutron Doppler broadening measurements [DE95-003703] p 324 N95-24076

Fabry-Perot interferometer measurement of static temperature and velocity for ASTOVL model tests [NASA-TM-107014] p 645 N95-30587

SPEECH RECOGNITION

Speech analysis and synthesis based on pitch-synchronous segmentation of the speech waveform [AD-A288824] p 435 N95-26349

SPEED CONTROL

Scheduling of local nonlinear control laws by exogenous signals - an application to flight control [BTN-95-EIX95262694059] p 447 A95-85675

The selective use of functional optical variables in the control of forward speed [NASA-TM-108849] p 35 N95-12227

Improved speed control system for the 87,000 HP wind tunnel drive [NASA-TM-106840] p 211 N95-19794

Experimental investigation of aerodynamic devices for wind turbine rotational speed control, phase 1 [DE95-004034] p 564 N95-30016

SPEED INDICATORS

In-flight pressure measurements on a subsonic transport high-lift wing section [BTN-95-EIX0619952748170] p 589 A95-94464

Flight dynamics of an unmanned aerial vehicle [AD-A282259] p 45 N95-12410

Flight reference display for powered-lift STOL aircraft [NAL-TR-1251] p 337 N95-25005

SPEED REGULATORS

Simulation investigation on system identification of gas turbine [PB95-104238] p 139 N95-17749

Variable speed generator application on the MOD-5A 7.3 mW wind turbine generator p 440 N95-27989

Wind turbine trailing edge aerodynamic brakes [DE95-004061] p 683 N95-32548

SPHERES

Hypersonic rarefied flow past spheres including wake structure [BTN-95-EIX95152583250] p 305 A95-73551

Flow due to an oscillating sphere and an expression for unsteady drag on the sphere at finite Reynolds number [BTN-94-EIX95011441142] p 347 A95-81012

Sphere wakes at moderate Reynolds numbers in a turbulent environment [HTN-95-42331] p 372 A95-86160

Collection efficiency and ice accretion calculations for a sphere, a swept MS(1)-317 wing, a swept NACA-0012 wing tip, an axisymmetric inlet, and a Boeing 737-300 [NASA-TM-106831] p 123 N95-18582

Experimental and theoretical studies of wakes in stratified flows [AD-A290203] p 553 N95-29060

SPHERICAL COORDINATES

Application of wall functions to generalized nonorthogonal curvilinear coordinate systems [BTN-95-EIX95182619077] p 307 A95-75762

Single-pass method for the solution of inverse potential and rotational problems. Part 2: Fully 3-D potential theory and applications p 107 N95-16564

SPHERICAL WAVES

Effect of ambient turbulence intensity on sphere wakes at intermediate Reynolds numbers [BTN-95-EIX95182619101] p 308 A95-76586

Numerical investigation of supersonic flows around a spiked blunt body [BTN-95-EIX95212645690] p 271 A95-76742

SPIKE

A multibody/finite element analysis approach for modeling of crash dynamic responses [NIAR-94-3] p 277 N95-24050

SPIRAL ANTENNAS

Spiral microstrip antenna with resistance [NASA-CASE-LAR-15088-1] p 91 N95-14139

Design considerations for an archimedean slot spiral antenna p 211 N95-19798

SPLASHING

Tracking of raindrops in flow over an airfoil [BTN-95-EIX95182619221] p 308 A95-76647

Reducing process noise in superconducting helium liquid level probes [DE95-008956] p 629 N95-30765

SPLICING

Multiple site fatigue damage in fuselage skin splices: Experimental simulation and theoretical prediction [BTN-95-EIX95152584676] p 276 A95-73588

SPLINE FUNCTIONS

On profiling a cam of an axial aviation diesel engine by periodic splines [BTN-94-EIX94461407946] p 82 A95-62264

SPLINES

Pressure controlled surfaces - a 3D inverse panel method as a design tool p 491 A95-87565

How to fly an aircraft with control theory and splines p 360 N95-25805

SPLIT FLAPS

Increments in aerofoil lift coefficient at zero angle of attack and in maximum lift coefficient due to deployment of a trailing-edge split flap, with or without a leading-edge high-lift device, at low speeds [ESDU-94029] p 479 N95-29129

SPLITTING

Turbulent flow measurements with a triple-split hot-film probe [HTN-95-A1774] p 634 A95-93337

Solution of the Navier-Stokes equations on locally refined Cartesian meshes using state-vector splitting p 553 N95-29197

SPOILER SLOTAILERONS

Comparative wind tunnel tests of NACA 23024 airfoils with several aileron and spoiler configurations p 376 N95-27976

SPOILERS

Study of an airfoil with a flap and spoiler [BTN-95-EIX95152582327] p 265 A95-73530

Numerical simulation of unsteady viscous flow around an airfoil with oscillating spoiler p 685 N95-34547

SPRAY CHARACTERISTICS

Study of the droplet spray characteristics of a subsonic wind tunnel [BTN-95-EIX95182619235] p 271 A95-76661

SPRAYED COATINGS

Quality optimization of thermally sprayed coatings produced by the JP-5000 (HVOF) gun using mathematical modeling p 152 N95-19008
 High velocity oxygen fuel spraying of erosion and wear resistant coatings on jet engine parts p 202 N95-19680
 [JPRS report: Science and technology. Central Eurasia [JPRS-UST-95-011] p 335 N95-24541

SPRAYERS

Development of an aircraft cabin water spray system [CONGRESS PAPER C428-25-030] p 595 A95-93599
 Aircraft cabin water spray systems - research and regulatory issues [CONGRESS PAPER C428-25-150] p 595 A95-93600
 Structure of a swirl-stabilized, combusting spray [NASA-TM-106724] p 50 N95-11890
 Air/fuel ratio visualization in a diesel spray p 556 N95-29807

SPRAYING

High velocity oxygen fuel spraying of erosion and wear resistant coatings on jet engine parts p 202 N95-19680
 Thermal testing of high performance thermal barrier coatings for turbine blades p 202 N95-19681
 A review of water mist technology for fire suppression [AD-A285738] p 225 N95-20071
 Measurement methods and standards for processing and application of thermal barrier coatings p 344 N95-26123
 Icing simulation in the aeropropulsion systems test facility propulsion development test cell C-2 [AD-A293039] p 599 N95-31667

SPREAD SPECTRUM TRANSMISSION

Spread spectrum applications in unmanned aerial vehicles [AD-A281035] p 156 N95-16448

SPREADING

Effect of stratification and geometrical spreading on sonic boom rise time p 75 N95-14880

SPRINGS (ELASTIC)

An analytical model for a nonlinear elastomeric lag damper and its effect on aeromechanical stability in Hover [HTN-95-61076] p 369 A95-83660
 Analysis techniques for the prediction of springback in formed and bonded composite components p 421 N95-28289

SPUTTERING

Permanent magnet electron cyclotron resonance plasma source with remote window [BTN-95-EIX95242674338] p 450 A95-82176

SQUEEZE FILMS

Subharmonic and quasi-periodic motions of an eccentric squeeze film damper-mounted rigid rotor [BTN-94-EIX95011440601] p 429 A95-82982
 Effect of squeeze film damper land geometry on damper performance [HTN-95-92247] p 434 A95-85291

SR-71 AIRCRAFT

SR-71 may launch targets for missile defense tests [HTN-95-91872] p 335 A95-81974
 NASA and the SR-71: Back to the future [NASA-TM-104290] p 13 N95-10716

STABILITY

Lyapunov exponents and stochastic stability of two-dimensional parametrically excited random systems [BTN-94-EIX94361122401] p 207 A95-65897
 Modeling rotating shafts using axisymmetric solid finite elements with matrix reduction [BTN-94-EIX94351143328] p 207 A95-67301
 Linear disturbances in hypersonic, chemically reacting shock layers [BTN-94-EIX94441386605] p 182 A95-67336
 Aeroelastic stability of hingeless rotor blade in hover using large deflection theory [BTN-94-EIX94441386616] p 183 A95-67347
 Bilinear formulation applied to the response and stability of helicopter rotor blade [BTN-95-EIX95042474400] p 192 A95-68300
 Fatigue resistance of peened 7050-T7451 aluminum alloy: Repair and re-treatment of a component surface [BTN-94-EIX94371347838] p 206 A95-69131
 Comparison of linear stability results with flight transition data [BTN-95-EIX95182619097] p 283 A95-76582
 Observation of traveling waves in the three-dimensional boundary layer along a yawed cylinder [HTN-95-61064] p 430 A95-83648
 Linear disturbances in hypersonic, chemically reacting shock layers [HTN-95-20931] p 464 A95-88970

Aeroelastic stability of hingeless rotor blade in hover using large deflection theory [HTN-95-20952] p 546 A95-88991
 Stability of magnetic bearing-rotor systems and the effects of gravity and damping [HTN-95-20955] p 465 A95-88994
 Stability analysis for elastically tailored rotor blades [ISBN 1-879921-01-4] p 635 A95-93703
 Influence of crack history on the stable tearing behavior of a thin-sheet material with multiple cracks p 93 N95-14467
 Helicopter in-flight simulation development and use in test pilot training [AD-A283998] p 146 N95-18725
 Robust fixed-structure control [AD-A286515] p 257 N95-22216
 Thin tailored composite wing for civil tiltrotor p 285 N95-23317
 Robust fixed-structure control [AD-A292883] p 679 N95-30961
 Nonlinear stability of unsteady viscous flow [AD-A294931] p 707 N95-34597

STABILITY AUGMENTATION

Identification and simulation evaluation of a combat helicopter in hover [BTN-95-EIX95242670749] p 335 A95-81098

STABILITY DERIVATIVES

State-space representation of aerodynamic characteristics of an aircraft at high angles of attack [BTN-95-EIX95062487536] p 187 A95-69244
 Aerodynamic characteristics of strake vortex flaps on a strake-wing configuration [BTN-95-EIX95062487537] p 187 A95-69245
 Attainable moments for the constrained control allocation problem [BTN-95-EIX95182619149] p 322 A95-76626
 Stability derivatives of a flapped plate in unsteady ground effect [BTN-95-EIX95182619225] p 270 A95-76651
 Modelling requirements in flight simulation [HTN-95-C0004] p 585 A95-93392
 Evaluation of the dynamic stability characteristics of the NAL Light Transport Aircraft [NAL-PD-CA-9217] p 142 N95-16392
 Error propagation equations for estimating the uncertainty in high-speed wind tunnel test results [DE94-014136] p 145 N95-16509
 Advanced gust management systems: Lessons learned and perspectives p 622 N95-32002

STABILITY TESTS

Linear disturbances in hypersonic, chemically reacting shock layers [BTN-94-EIX94441386605] p 182 A95-67336
 State-space representation of aerodynamic characteristics of an aircraft at high angles of attack [BTN-95-EIX95062487536] p 187 A95-69244
 Functional dependence of trajectory dispersion on initial condition errors [BTN-95-EIX95152583263] p 298 A95-73564
 FPCAS2D user's guide, version 1.0 [NASA-CR-195413] p 156 N95-16588
 Design of robust optimal control systems and stability analysis of real structured uncertainties [AD-A279089] p 256 N95-21913
 Flight control design using mixed H2/micron optimization [AD-A289288] p 410 N95-27036
 The effects of three-dimensional imposed disturbances on bluff body near wake flows: Effects of taper and splitter plates on the near wake characteristics of a circular cylinder in uniform and shear flow [AD-A292113] p 477 N95-28921

STABILIZATION

The effect of rotating loads suspended under a helicopter on their amplitude-frequency characteristics [BTN-94-EIX94461407959] p 78 A95-62633
 Microgravity isolation system design: A modern control analysis framework [NASA-TM-106803] p 105 N95-18486
 Robust fixed-structure control [AD-A286515] p 257 N95-22216
 Robust fixed-structure control [AD-A292883] p 679 N95-30961

STABILIZERS (FLUID DYNAMICS)

Integrated design of hypersonic waveriders including inlets and tailfins [BTN-95-EIX95212645692] p 271 A95-76744
 Effect of leading-edge extension fences on the vortex wake of an F/A-18 model p 591 A95-94481
 Flow-visualization study of the X-29A aircraft at high angles of attack using a 1/48-scale model [NASA-TM-104268] p 8 N95-10858

Pressure measurements on an F/A-18 twin vertical tail in buffeting flow. Volume 3: Buffet power spectral densities [AD-A281444] p 36 N95-11829
 Experimental aerodynamic characteristics of a generic hypersonic accelerator configuration at Mach numbers 1.5 and 2.0 -- conducted in the Langley Unitary Plan Wind Tunnel [NASA-TM-4413] p 39 N95-12770
 X-31 quasi-tailless flight demonstration p 70 N95-14243
 Pressure measurements on an F/A-18 twin vertical tail in buffeting flow. Volume 2: Steady and unsteady RMS pressure data [AD-A281581] p 76 N95-15465
 Twin engine afterbody model p 115 N95-17880
 Pressure measurements on an F/A-18 twin vertical tail in buffeting flow. Volume 4, part 1: Buffet cross spectral densities [AD-A285593] p 237 N95-21214
 Pressure measurements on an F/A-18 twin vertical tail in buffeting flow. Volume 1: Wind tunnel test summary [AD-A279126] p 225 N95-21877
 Composite repair of a CF18: Vertical stabilizer leading edge p 395 N95-27517
 NASA-ACEE/Boeing 737 graphite-epoxy horizontal stabilizer service p 400 N95-28489
 Estimation of aerodynamic load distributions on the F/A-18 aircraft using a CFD panel code [DSTO-TR-0147] p 504 N95-29445
 Low-speed wind-tunnel investigation of the stability and control characteristics of a series of flying wings with sweep angles of 50 deg [NASA-TM-4640] p 505 N95-30226

STAGE SEPARATION

Optimal separation and ascent of lifting upper stages p 525 A95-87396
 Separation of winged vehicles in supersonics [AIAA PAPER 95-6092] p 526 A95-88601

STAGNATION FLOW

Measurement by coherent anti-Stokes Raman scattering in the R5Ch hypersonic wind tunnel [BTN-95-EIX95112523811] p 188 A95-69322
 Numerical investigation of cylinder wake flow with a rear stagnation jet [HTN-95-51669] p 433 A95-85051
 Influence of turbulence parameters, Reynolds number, and body shape on stagnation-region heat transfer [NASA-TP-3487] p 550 N95-28719

STAGNATION POINT

Influence of wing shapes on surface pressure fluctuations at wing-body junctions [HTN-95-61196] p 491 A95-87569
 Cooling of aerospace plane using liquid hydrogen and methane [BTN-95-EIX0619952748171] p 590 A95-94465
 Science objectives and performance of a radiometer and window design for atmospheric entry experiments [NASA-TM-4637] p 63 N95-12190

STAGNATION PRESSURE

Main features of overexpanded triple jets [BTN-95-EIX9514253040] p 304 A95-73458
 An assessment of ground-test facility capabilities for measurement of hypervelocity scramjet performance [AIAA PAPER 95-6148] p 512 A95-90462
 Condensation in jet engine intake ducts during stationary operation [BTN-95-EIX95292721154] p 612 A95-92590
 Leading edge film cooling effects on turbine blade heat transfer [NASA-TM-106955] p 513 N95-29115
 Modeling and control of rotating stall in high speed multi-stage axial compressors p 513 N95-29244

STAGNATION TEMPERATURE

Temperature diagnostics in the hypersonic flow regime: An application to develop a stagnation temperature probe [AIAA PAPER 95-6114] p 511 A95-90442
 Numerical study of mixing in a high and low enthalpy supersonic test facility p 7 N95-10467
 Leading edge film cooling effects on turbine blade heat transfer [NASA-TM-106955] p 513 N95-29115

STAINLESS STEELS

Mechanism of deposit formation on fuel-wetted hot metal surfaces [AD-A289847] p 426 N95-28621

STALLING

Characterization of stall inception in high-speed single-stage compressors [AD-A291275] p 514 N95-29934

STAMPING

Calculation of geometry of stamps with small allowances for pieces of the aerodynamic profile [BTN-94-EIX94461408772] p 103 A95-63655

STANDARD DEVIATION

Optimization of adaptive intraply hybrid fiber composites with reliability considerations
[NASA-TM-106632] p 157 N95-16911

STANDARDIZATION

International cooperation in standardization
p 452 A95-82665

Dependability issues in the reuse of standard components in open architectures
[AIAA PAPER 95-1006] p 566 A95-90678

Modular avionics: Taking today's aircraft into tomorrow
[SAE PAPER 931416] p 610 A95-93681

Evolutionary Telemetry and Command Processor (TCP) architecture
p 86 N95-14162

TIM-SCT cable testing protocol
[AD-A286633] p 231 N95-20772

A comparison of measured wind park load histories with the WISPER and WISPERX load spectra
[DE95-000295] p 446 N95-27459

The development of an engineering standard for composite repairs
p 396 N95-27528

Standardization of surface contamination analysis systems
p 631 N95-31798

Standardization work
p 651 N95-32181

STANDARDS

Corrosion prevention and control
[BTN-95-EIX95031502753] p 188 A95-68260

International cooperation in standardization
p 452 A95-82665

Euro-noise '92, London, UK, Sept. 14-18, 1992. Bks. 1-3
[ISBN 1-873082-39-8] p 558 A95-87354

Possible guidelines for helicopter noise assessment
[HTN-95-92535] p 558 A95-87355

Nordic Standards for measurement of aircraft noise immission in residential areas and noise reduction of dwellings
p 570 A95-88463

MIL-STD-461/MIL-STD-704 investigation
[SAE PAPER 932561] p 505 A95-90058

Transitioning to the aviation routine weather report (METAR) and the International Aerodrome Forecast (TAF) within the Federal Aviation Administration
p 656 A95-93461

Evolving standards for safety critical software
[CONGRESS PAPER C428-24-142] p 678 A95-93595

Civil aircraft performance - developments for improved safety
[CONGRESS PAPER C428-25-175] p 596 A95-93601

The development of a model specification for ground support equipment
[CONGRESS PAPER C428-38-095] p 625 A95-93636

Flight test certification of primary category aircraft using TP101-41E sportplane design standard
[BTN-95-EIX0619952748184] p 606 A95-94477

Draft standard for color active matrix liquid crystal displays (AMLCDs) in US Military aircraft. Recommended best practices
[AD-A282950] p 49 N95-12591

Regulatory impact analysis and regulatory support document: Control of air pollution; determination of significance for nonroad sources and emission standards for new nonroad compression-ignition engines at or above 37 kilowatts (50 horsepower)
[PB94-194594] p 61 N95-12855

A study of software standards used in the avionics industry
p 137 N95-16456

Field verification of the wind tunnel coefficients
p 109 N95-17291

Aircraft and sub-system certification by piloted simulation
[AGARD-AR-278] p 145 N95-17388

Proposed incorporation of mission-oriented flying qualities into MIL-STD-1797A
[AD-A294211] p 698 N95-34306

STANTON NUMBER

Hypersonic model testing in a shock tunnel
[BTN-95-EIX95222650789] p 329 A95-79245

STARCHES

Use of starch based blast media for dry paint stripping
[SAE PAPER 932616] p 456 A95-90081

STARTING

A numerical study of the starting process in a hypersonic shock tunnel
p 626 N95-30493

Investigation of starting and ignition transients in the thermally choked ram accelerator
p 698 N95-34805

STATE ESTIMATION

New failure detection approach and its application to GPS autonomous integrity monitoring
[BTN-95-EIX95202637613] p 279 A95-76676

STATE VECTORS

Selection of optimal parameters for a system, controlling the flight height, when information about the state vector is incomplete

[BTN-94-EIX94461408753] p 168 A95-63636

Solution of the Navier-Stokes equations on locally refined Cartesian meshes using state-vector splitting

p 553 N95-29197

STATIC AERODYNAMIC CHARACTERISTICS

Engineering Codes for aeroprediction: State-of-the-art and new methods
p 73 N95-14447

Measurements of longitudinal static aerodynamic coefficients by the cable mount system
[NAL-TR-1226] p 331 N95-25761

Reliability analysis of composite structures
p 423 N95-28441

STATIC CHARACTERISTICS

Static aeroelastic characteristics of a composite wing
[BTN-95-EIX95152582340] p 282 A95-73542

Static shape control for adaptive wings
[HTN-95-A1767] p 627 A95-93330

Effects of floor location on response of composite fuselage frames
p 423 N95-28439

STATIC ELECTRICITY

The effect of aviation fuels containing low amounts of static dissipative additive on electrostatic charge generation

[AD-A280075] p 420 N95-28152

STATIC FRICTION

Static and dynamic friction behavior of candidate high temperature airframe seal materials
[NASA-TM-106571] p 152 N95-16905

STATIC LOADS

Course module for AA201: Wing structural design project
[AD-A283618] p 133 N95-18616

Investigation of static and cyclic bearing failure mechanisms for GR/EP laminates
p 422 N95-28427

STATIC MODELS

Verification of multidisciplinary models for turbomachines
p 140 N95-19025

STATIC PRESSURE

Static pressure distribution in the inlet of a helicopter turbine compressor
[BTN-95-EIX95152582339] p 266 A95-73541

Aerodynamic characteristics of external store configurations at low speeds
[BTN-95-EIX95182619230] p 271 A95-76656

Pitot/static leak testing
[CONGRESS PAPER C428-9-035] p 508 A95-91696

Condensation in jet engine intake ducts during stationary operation
[BTN-95-EIX95292721154] p 612 A95-92590

Effect of passive venting on static pressure distributions in cavities at subsonic and transonic speeds
[NASA-TM-4549] p 6 N95-10029

Flight and full-scale wind-tunnel comparison of pressure distributions from an F-18 aircraft at high angles of attack - Conducted in NASA Ames Research Center's 80 by 120 ft wind tunnel
p 68 N95-14231

Hypersonic flow-field measurements: Intrusive and nonintrusive
[AD-A283867] p 119 N95-18674

Calculation of low speed wind tunnel wall interference from static pressure pipe measurements
p 164 N95-19273

Modeling and control of rotating stall in high speed multi-stage axial compressors
p 513 N95-29244

Afterbody/nozzle pressure distributions of a twin-tail twin-engine fighter with axisymmetric nozzles at Mach numbers from 0.6 to 1.2
[NASA-TP-3509] p 594 N95-31984

Static pressure drop by swirling flow of an internal cooling air system through a turbine shaft
p 698 N95-34560

STATIC STABILITY

Offset thrust axes and pitch stability
[BTN-95-EIX95062487553] p 203 A95-68367

Some additional stability and performance characteristics of the scissor/pivot wing configurations
[SAE PAPER 931383] p 618 A95-93659

Flight dynamics of an unmanned aerial vehicle
[AD-A282259] p 45 N95-12410

Plant and controller optimization by convex methods
[AD-A283700] p 133 N95-18621

Hypersonic wind tunnel test techniques
[AD-A284057] p 118 N95-18663

Handling qualities of the High Speed Civil Transport
p 294 N95-23325

An aerodynamic and static-stability analysis of the Hypersonic Applied Research Technology (HART) missile
[DA9426923] p 481 N95-29965

STATIC TESTS

Validation of an effective flat cruciform-shaped specimen to study CFRP composite laminates under biaxial loading

[BTN-95-EIX95152584677] p 282 A95-73589

Development of a composite repair and the associated inspection intervals for the F-111C stiffener runout region
p 66 N95-14477

Development of a multicomponent force and moment balance for water tunnel applications, volume 1
[NASA-CR-4642-VOL-1] p 161 N95-18955

Static investigation of two fluidic thrust-vectoring concepts on a two-dimensional convergent-divergent nozzle
[NASA-TM-4574] p 120 N95-19042

Static investigation of two fluidic thrust-vectoring concepts on a two-dimensional convergent-divergent nozzle
[NASA-TM-4574] p 222 N95-19913

Portable static test facility for small, expendable, turbojet engines, phase 1
[AD-A286337] p 239 N95-21719

Corrosion protection measures for CFC/metal joints of fuel integral tank structures of advanced military aircraft
p 303 N95-23510

Analysis of warping effects on the static and dynamic response of a seat-type structure
[NIAR-94-12] p 348 N95-24211

Experimental investigation of static and dynamic ground effect on HOPE ALFLEX vehicle
[NAL-TR-1236] p 388 N95-26525

On aircraft repair verification of a fighter A/C integrally stiffened fuselage skin
p 394 N95-27515

External patch repair of CFRP/honeycomb sandwich
p 395 N95-27522

Static and fatigue testing of full-scale fuselage panels fabricated using a Therm-X(R) process
p 420 N95-28270

Development of composite carrythrough bulkhead
p 423 N95-28438

STATIC THRUST

An approximate theoretical method for modeling the static thrust performance of non-axisymmetric two-dimensional convergent-divergent nozzles
[NASA-CR-195050] p 273 N95-23193

STATIONKEEPING

Dynamics and control of a tethered flight vehicle
[BTN-95-EIX95242670754] p 342 A95-81093

Building complex simulations rapidly using MATRIX(x): The Space Station redesign
[TABES PAPER 94-632] p 87 N95-14653

Arjet thruster research and technology, phase 2
[NASA-CR-182276] p 105 N95-18044

STATISTICAL ANALYSIS

Effects of satellite bunching on the probability of collision in geosynchronous orbit
[BTN-95-EIX95152583276] p 298 A95-73577

Fluctuating wall pressures near separation in highly swept turbulent interactions
[HTN-95-20823] p 543 A95-88084

Event correlation for networked simulators
[BTN-95-EIX0619952748168] p 625 A95-94462

Statistical discrete gust-power spectral density methods overlap-holistic proof and beyond
[BTN-95-EIX0619952748175] p 584 A95-94469

Statistical analysis of Turbine Engine Diagnostic (TED) field test data
[AD-A286032] p 248 N95-20998

On-line, adaptive state estimator for active noise control
p 322 N95-23308

POD assessment of NDI procedures using a round robin test
[AGARD-R-809] p 315 N95-23602

Probabilistic material strength degradation model for Inconel 718 components subjected to high temperature, high-cycle and low-cycle mechanical fatigue, creep and thermal fatigue effects
[NASA-CR-197832] p 419 N95-27167

Calculation of design load for the MOD-5A 7.3 mW wind turbine system
p 440 N95-27982

Reliability analysis of composite structures
p 423 N95-28441

The performance of cargo airdrop systems using g-12E parachutes: Statistical determination of minimum altitude
[AD-A291666] p 381 N95-28454

STATISTICAL DISTRIBUTIONS

Minimal time detection algorithms and applications to flight systems
[TR-2-FSRC-93] p 171 N95-18564

STATORS

Effect of surface roughness on local film cooling effectiveness and heat transfer coefficients
[AD-A283854] p 91 N95-14351

A Lifting Ball Valve for cryogenic fluid applications
p 156 N95-16349

- Impact loading of compressor stator vanes by hailstone ingestion p 200 N95-19670
Enhanced analysis and users manual for radial-inflow turbine conceptual design code RTD [NASA-CR-195454] p 275 N95-23462

STDN (NETWORK)

- Evolutionary Telemetry and Command Processor (TCP) architecture p 86 N95-14162

STEADY FLOW

- Determining unsteady 2D AND 3D boundary layer separation p 462 A95-88898
Central-difference and upwind-biased schemes for steady and unsteady Euler aerofoil computations [HTN-95-01094] p 469 A95-90280
A review of free-stream flow fluctuation and steady-state flow quality measurements in the AEDC/VKF Supersonic Tunnel A and Hypersonic Tunnel B [AIAA PAPER 95-6137] p 520 A95-90454
Numerical solutions of three dimensional viscous flows [ISBN 1-879921-01-4] p 587 A95-93749
Analytic solution of the thickness problem of a rectangular wing in steady subsonic flow [ISBN 1-879921-01-4] p 588 A95-93758
Steady and unsteady three-dimensional transonic flow computations by integral equation method [NASA-CR-196777] p 10 N95-11582
Acoustic radiation damping of flat rectangular plates subjected to subsonic flows p 172 N95-18542
Simulation of steady and unsteady viscous flows in turbomachinery p 140 N95-19023
Steady potential solver for unsteady aerodynamic analyses p 141 N95-19382
Shock wave interactions in hypervelocity flow [AD-A286507] p 250 N95-22212
Aerodynamic design and analysis of a highly loaded turbine exhaust p 312 N95-23435
Axial loads on yawed rotors [PB95-214193] p 592 N95-30638
Spatially-resolved velocity measurements in steady, high-speed, reacting flows using laser-induced OH fluorescence p 650 N95-32109

STEADY STATE

- Optimality of the steady-state flight for hypersonic aircraft p 526 A95-91550
Experimental/analytical approach to understanding mistuning in a transonic wind tunnel compressor [NASA-TM-108833] p 95 N95-14617
Pressure updating methods for the steady-state fluid equations [NASA-CR-198163] p 569 N95-30353
Steady-state dynamic behavior of an auxiliary bearing supported rotor system p 703 N95-32690
Subscale study of engine bellmouth inlet vortices in test cell R1D [AD-A294993] p 707 N95-34818

STEAM

- Ejectors and jet pumps: Computer program for design and performance for steam/gas flow [ESDU-94046] p 500 N95-28704

STEAM TURBINES

- Gas-turbine engines with increased efficiency of two circuits, due to the use of the utilizing steam-turbine circuit [BTN-94-EIX94461408755] p 153 A95-63638

STEELS

- Corrosion behavior of landing gear steels [AD-A285862] p 242 N95-22132
Corrosion of landing gear steels p 302 N95-23500
JPRS report: Science and technology. Central Eurasia [JPRS-UST-95-011] p 335 N95-24541
The mm-wave resonant methods for the detection of corrosion, phase 1 [AD-A291315] p 556 N95-29941

STEERING

- Evolution of a nose-wheel steering system [BTN-94-EIX94461047056] p 78 A95-61739
Aircraft nosewheel steering simulation p 412 N95-26944

STELLAR ENVELOPES

- Period evolution of PSR B1259-63: Evidence for propeller-torque spindown [HTN-95-B0194] p 581 A95-87903

STELLAR MASS ACCRETION

- Period evolution of PSR B1259-63: Evidence for propeller-torque spindown [HTN-95-B0194] p 581 A95-87903

STELLAR ORBITS

- Period evolution of PSR B1259-63: Evidence for propeller-torque spindown [HTN-95-B0194] p 581 A95-87903

STEPPING MOTORS

- Blade-by-blade tip clearance measurement system for gas turbine applications [BTN-95-EIX95292721167] p 546 A95-89899

STIFFENING

- Prediction of energy absorption capability of composite stiffeners [HTN-95-A0500] p 230 A95-72571
Fatigue of aircraft materials and structures p 387 A95-85894
Optimum design of composite stiffened wing panels - a parametric study [HTN-95-01088] p 496 A95-90274
Compression strength of composite primary structural components [NASA-CR-197554] p 160 N95-18388

STIFFNESS

- Foil bearings for gas turbine engines [BTN-94-EIX94461290279] p 82 A95-61732
Lyapunov exponents and stochastic stability of two-dimensional parametrically excited random systems [BTN-94-EIX94361122401] p 207 A95-65897
Dynamic analysis of bearingless tail rotor blades based on nonlinear shell modes [BTN-95-EIX95152582338] p 281 A95-73540
Finite element model for a flexible non-symmetric rotor on distributed bearing: A stability study [BTN-94-EIX94381352212] p 306 A95-74612
Dynamic stiffness and damping of foil bearings for gas turbine engines [SAE PAPER 931449] p 635 A95-93698
Effect of constraining layer stiffness on performance of damping tile materials using finite element modelling with Rayleigh integral p 30 N95-11306
Cabin-fuselage-wing structural design concept with engine installation [NASA-CR-197172] p 49 N95-12993
Development of a composite repair and the associated inspection intervals for the F-111C stiffener runout region p 66 N95-14477
A CMC database for use in the next generation launch vehicles (rockets) p 150 N95-18993
Integrated aerodynamic/dynamic/structural optimization of helicopter rotor blades using multilevel decomposition [NASA-TP-3465] p 285 N95-22953
Design and evaluation of a foam-filled hat-stiffened panel concept for aircraft primary structural applications [NASA-TM-109175] p 346 N95-26251
Damage tolerance of a geodesically stiffened advanced composite structural concept for aircraft structural applications p 399 N95-28487
Dimensional stability of curved panels with co-cured stiffeners and cobonded frames p 532 N95-28836
Impact damage resistance of composite fuselage structure, part 2 p 533 N95-28838
Design and evaluation of a foam-filled hat-stiffened panel concept for aircraft primary structural applications p 502 N95-28841
ISPAN (Interactive Stiffened Panel Analysis): A tool for quick concept evaluation and design trade studies p 533 N95-28846

STIFFNESS MATRIX

- Equivalent plate structural modeling for wing shape optimization including transverse shear [HTN-95-20839] p 492 A95-88100

STOCHASTIC PROCESSES

- Output feedback control under randomly varying distributed delays [BTN-94-EIX94511433916] p 168 A95-64582
Lyapunov exponents and stochastic stability of two-dimensional parametrically excited random systems [BTN-94-EIX94361122401] p 207 A95-65897
Stochastic approach to noise modeling for free turbulent flows [HTN-95-42321] p 371 A95-86150
Recent research in ASTOVL aircraft ground environment [CONGRESS PAPER C428-9-040] p 475 A95-91694
New filtering method for linear weakly coupled stochastic systems [BTN-95-EIX0608952736485] p 678 A95-92708
MOAMAP: A model that combines several different kinds of aircraft operations p 32 N95-11323
Portable parallel stochastic optimization for the design of aeropropulsion components [NASA-CR-195312] p 154 N95-16072
Comparison of stochastic and deterministic nonlinear gust analysis methods to meet continuous turbulence criteria p 133 N95-18602
Forced response of mistuned bladed disks p 141 N95-19383
A NASTRAN-based computer program for structural dynamic analysis of Horizontal Axis Wind Turbines p 439 N95-27980
A stochastic adaptive control application to flight systems p 699 N95-34806

STORMS (METEOROLOGY)

- Aircraft icing measurements in East Coast winter storms [HTN-95-60505] p 214 A95-68756
Mesoscale structure of precipitation bands in a North Atlantic winter storm [HTN-95-40659] p 215 A95-69803
Aiplane icing research at the Boeing Company: Participation in the second Canadian Atlantic Storms Program p 674 A95-93544
Radar studies of aviation hazards [AD-A285845] p 226 N95-21831

STOVL AIRCRAFT

- Numerical simulation of powered-lift flows [HTN-94-00700] p 3 A95-60179
Numerical simulation of a complete STOVL aircraft in ground effect [AIAA PAPER 93-4880] p 4 A95-60187
Powered lift for land and sea [BTN-95-EIX95041503010] p 192 A95-68313
Simulation and flight test evaluation of head-up-display guidance for harrier approach transitions [BTN-95-EIX95062487533] p 194 A95-69241
Experimental performance of a ventral nozzle with pitch and yaw vectoring capability for SSTOVL aircraft [SAE PAPER 931412] p 614 A95-93678
Application of an integrated methodology for propulsion and airframe control design to a STOVL aircraft [NASA-TM-106729] p 16 N95-11159
STOVL Control Integration Program [NASA-CR-195358] p 18 N95-11487
Piloted evaluation of an integrated methodology for propulsion and airframe control design [AD-A290207] p 51 N95-12763
Aerodynamics model for a generic ASTOVL lift-fan aircraft [NASA-TM-110347] p 332 N95-26302
Simulation model of the integrated flight/propulsion control system, displays, and propulsion system for ASTOVL lift-fan aircraft [NASA-TM-108866] p 405 N95-26412
Moving base simulation of an integrated flight and propulsion control system for an ejector-augmentor STOVL aircraft in hover [NASA-TM-108867] p 606 N95-30646

STOWAGE (ONBOARD EQUIPMENT)

- Tie-down trials involving a Sikorsky S-70B-2 helicopter [DSTO-TR-0132] p 400 N95-28567

STRAIN DISTRIBUTION

- Critical speed analysis of a non-linear strain ring dynamical model for aircraft tires [SAE PAPER 932580] p 494 A95-90067

STRAIN ENERGY METHODS

- Nonlinear bulging factor based on R-curve data p 94 N95-14476
Evaluation of patch effectiveness in repairing aircraft components p 394 N95-27513

STRAIN ENERGY RELEASE RATE

- Bending effects of unsymmetric adhesively bonded composite repairs on cracked aluminum panels p 92 N95-14456
Analysis of composite structures with delaminations under combined bending and compression p 422 N95-28429

STRAIN GAGE BALANCES

- Static and dynamic force/moment measurements in the Eidetics water tunnel p 69 N95-14238
Dynamic Stability Instrumentation System (DSIS). Volume 1: Hardware description [NASA-TM-109160-VOL-1] p 171 N95-18899
Development of a multicomponent force and moment balance for water tunnel applications, volume 1 [NASA-CR-4642-VOL-1] p 161 N95-18955
Development of a multicomponent force and moment balance for water tunnel applications, volume 2 [NASA-CR-4642-VOL-2] p 161 N95-18956

STRAIN GAGES

- High temperature strain gage technology for gas turbine engines [NASA-CR-191177] p 57 N95-11996
Strain gage selection in loads equations using a genetic algorithm [NASA-CR-4597] p 48 N95-12831
Static and dynamic force/moment measurements in the Eidetics water tunnel p 69 N95-14238
Extracting a representative loading spectrum from recorded flight data p 80 N95-14469
Hydrofoil force balance [AD-D016475] p 160 N95-18461
Vapor generator wand [NASA-CASE-LAR-15058-1] p 238 N95-20080
Influence of tooth profile modification on spur gear dynamic tooth strain [NASA-TM-106952] p 553 N95-29112

STRAIN MEASUREMENT

Shock tunnel measurements of hypervelocity blunted cone drag
 [BTN-95-EIX95152577606] p 305 A95-73477
 High temperature strain gage technology for gas turbine engines
 [NASA-CR-191177] p 57 N95-11996
 Static and dynamic force/moment measurements in the Eidetics water tunnel
 p 69 N95-14238
 Scramjet thrust measurement in a shock tunnel
 p 339 N95-25396
 Angular displacement measuring device
 [NASA-CASE-ARC-11937-1] p 362 N95-26015
 SMART materials: Surfaces, transforms and interfaces. The commensurate engineering dimension
 [AD-A289598] p 442 N95-28649

STRAIN RATE

Technology integration box beam failure study
 p 441 N95-28468
 High strain-rate testing of parachute materials
 [DE95-009577] p 648 N95-31614

STRAKES

Aerodynamic characteristics of strake vortex flaps on a strake-wing configuration
 [BTN-95-EIX95062487537] p 187 A95-69245
 Water tunnel flow visualization study of a 4.4 percent scale X-31 forebody
 [NASA-TM-104276] p 36 N95-11898
 Preparations for flight research to evaluate actuated forebody strakes on the F-18 high-alpha research vehicle
 p 72 N95-14257
 Integration of a mechanical forebody vortex control system into the F-15
 p 72 N95-14258
 Experimental investigation of the vortex flow over a 76/60-deg double delta wing
 p 114 N95-18784
 Pressure based high order TVD methodology for dynamic stall control
 [AD-A290149] p 479 N95-29316
 Unsteady transonic wind tunnel test on a semispan straked delta wing, oscillating in pitch. Part 1: Description of the model, test setup, data acquisition, and data processing
 [AD-A293113] p 593 N95-30885

STRAPDOWN INERTIAL GUIDANCE

A new guidance and flight control system for the DELTA 2 launch vehicle — Abstract only
 p 342 A95-80427
 Study of strapdown navigation attitude algorithms
 [BTN-95-EIX95282706655] p 486 A95-89649

STRAPS

Axial crack propagation and arrest in pressurized fuselage
 p 94 N95-14479

STRATEGY

Bomber force 2000: Operational concepts for long-range combat aircraft
 [AD-A279378] p 230 N95-20181

STRATIFICATION

Effect of stratification and geometrical spreading on sonic boom rise time
 p 75 N95-14880

STRATIFIED FLOW

A singularity method for a two dimensional stratified shear flow
 p 473 A95-91513
 Experimental and theoretical studies of wakes in stratified flows
 [AD-A290203] p 553 N95-29060

STRATOCUMULUS CLOUDS

Air truth validation of cloud albedo estimated from NOAA advanced very high resolution radiometer data
 [HTN-95-A1021] p 443 A95-84526

STRATOSPHERE

Recent trends in balloon flights from TIFR's National Balloon Facility, Hyderabad
 p 191 A95-66300
 Long duration balloons
 p 191 A95-66305
 Three-dimensional model interpretation of NO(x) measurements from the lower stratosphere
 [HTN-95-90534] p 213 A95-67806
 Ozone, skin cancer, and the SST
 [BTN-95-EIX95041503011] p 213 A95-68314
 An air-driven pressure booster pump for aircraft-based air sampling
 [HTN-95-40689] p 216 A95-69833
 Subsidence of aircraft engine exhaust in the stratosphere: Implications for calculated ozone depletions
 [PAPER-93GL03426] p 251 A95-70297
 Aircraft-borne, laser-induced fluorescence instrument for the in situ detection of hydroxyl and hydroperoxyl radicals
 [BTN-95-EIX95072499029] p 253 A95-71908
 Performance of a focused cavity aerosol spectrometer for measurements in the stratosphere of particle size in the 0.06-2.0-micrometer-diameter range
 [HTN-95-90914] p 253 A95-72423
 An algorithm for forecasting mountain wave-related turbulence in the stratosphere
 [HTN-95-80656] p 254 A95-72500

Trajectory modeling of emissions from lower stratospheric aircraft
 [HTN-95-41219] p 317 A95-75031
 Possible effects of CO2 increase on the high-speed civil transport impact on ozone
 [HTN-95-60779] p 317 A95-75976
 Estimates of total organic and inorganic chlorine in the lower stratosphere from in situ and flask measurements during AASE 2
 [HTN-95-A0861] p 317 A95-76265
 In situ observations in aircraft exhaust plumes in the lower stratosphere at midlatitudes
 [HTN-95-A0862] p 318 A95-76266
 Sensitivity of two-dimensional model predictions of ozone response to stratospheric aircraft: An update
 [HTN-95-A0863] p 318 A95-76267
 Analysis of the physical state of one Arctic polar stratospheric cloud based on observations
 [HTN-95-70917] p 351 A95-77982
 The distribution of hydrogen, nitrogen, and chlorine radicals in the lower stratosphere: Implications for changes in O3 due to emission of NO(y) from supersonic aircraft
 [HTN-95-70935] p 351 A95-78000
 Vertical transport rates in the stratosphere in 1993 from observations of CO2, N2O, and CH4
 [HTN-95-70941] p 351 A95-78006
 Meridional distributions of NO(x), NO(y), and other species in the lower stratosphere and upper troposphere during AASE 2
 [HTN-95-70944] p 352 A95-78009
 Chemical change in the arctic vortex during AASE 2
 [HTN-95-70947] p 352 A95-78012
 Latitude variations of stratospheric trace gases
 [HTN-95-70948] p 352 A95-78013
 Sensitivity of supersonic aircraft modelling studies to HNO3 photolysis rate
 [HTN-95-11475] p 353 A95-79453
 Tracer transport for realistic aircraft emission scenarios calculated using a three-dimensional model
 [HTN-95-41799] p 353 A95-80525
 North Atlantic air traffic within the lower stratosphere: Cruising times and corresponding emissions
 [HTN-95-91841] p 354 A95-80829
 Effects on stratospheric ozone from high-speed civil transport: Sensitivity to stratospheric aerosol loading
 [HTN-95-91842] p 354 A95-80830
 Potential effects on ozone of future supersonic aircraft/2D simulation
 [HTN-95-51282] p 356 A95-80867
 Impact on ozone of high-speed stratospheric aircraft: Effects of the emission scenario
 [HTN-95-51283] p 356 A95-80868
 Effects of a polar stratosphere cloud parameterization on ozone depletion due to stratospheric aircraft in a two-dimensional model
 [HTN-95-A1038] p 443 A95-84543
 An overview of the EASOE campaign
 [HTN-95-00702] p 443 A95-86272
 Aircraft measurements of CLO and HCL during EASOE 1991/92
 [HTN-95-00721] p 444 A95-86291
 An overview of millimeter-wave spectroscopic measurements of chlorine monoxide at Thule, Greenland, February-March, 1992: Vertical profiles, diurnal variation, and longer-term trends
 [HTN-95-00722] p 444 A95-86292
 Two dimensional stratospheric aerosol distributions during EASOE
 [HTN-95-00726] p 444 A95-86296
 Airborne lidar observation of mountain-wave-induced polar stratospheric clouds during EASOE
 [HTN-95-00738] p 444 A95-86308
 Airborne measurements during the European Arctic Stratospheric Ozone Experiment column amounts of HNO3 and O3 derived from FTIR emission sounding
 [HTN-95-00742] p 445 A95-86312
 Airborne measurements during the European Arctic Stratospheric Ozone Experiment: Observation of OCIO
 [HTN-95-00745] p 445 A95-86315
 Airborne measurements during the Arctic stratospheric experiment: Observation of O3 and NO2
 [HTN-95-00748] p 445 A95-86318
 Orbital transport: Technical, meteorological and chemical aspects; Aerospace Symposium, 3rd, Braunschweig, Germany, Aug. 26-28, 1991
 [ISBN 3-540-563180] p 524 A95-87373
 Environmental aspects of Orbital transport:
 p 559 A95-87377
 Three dimensional model calculations of the global dispersion of high speed aircraft exhaust and implications for stratospheric ozone loss
 p 26 N95-10657
 Development of techniques for the in situ observation of OH and HO2 for studies of the impact of high-altitude supersonic aircraft on the stratosphere
 [NASA-CR-196759] p 61 N95-12832

The atmospheric effects of stratospheric aircraft: A fourth program report
 [NASA-RP-1359] p 357 N95-24274
 Long endurance stratospheric solar powered aircraft
 [PB95-178729] p 336 N95-26009
 Replicator for characterization of cirrus and polar stratospheric cloud particles
 [NASA-CR-197785] p 445 N95-26669
 In situ measurements of ClO and implications for the chemistry of inorganic chlorine in the lower stratosphere
 p 563 N95-29830

STRATUS CLOUDS

Air truth validation of cloud albedo estimated from NOAA advanced very high resolution radiometer data
 [HTN-95-A1021] p 443 A95-84526

STREAM FUNCTIONS (FLUIDS)

Hybrid laminar flow over wings enhanced by continuous boundary layer suction
 [SAE JOURNAL 931386] p 587 A95-93662

STREAMLINING

Determining unsteady 2D AND 3D boundary layer separation
 p 462 A95-88898
 Aero design-of turbomachinery components: CFD in complex systems
 p 90 N95-14136

STRESS ANALYSIS

Analytical description of and forecast for stress relaxation of aviation materials under the vibration conditions
 [BTN-94-EIX94461408751] p 126 A95-63634
 A comparative study of internally and externally capped balloons using small scale test balloons
 p 181 A95-66285
 Theoretical and experimental studies of fretting-initiated fatigue failure of aeroengine compressor discs
 [BTN-94-EIX94421372285] p 343 A95-78467
 Stress considerations in reduced-size aeroelastic optimization
 [BTN-95-EIX95262694313] p 366 A95-85484
 Equivalent plate structural modeling for wing shape optimization including transverse shear
 [HTN-95-20839] p 492 A95-88100
 A better than average stress model-photoelastic analysis for airbus design
 [CONGRESS PAPER C428-23-005] p 500 A95-91730
 Impact finite element analysis, as an alternative to the testing of windscreens for bird impact
 [CONGRESS PAPER C428-23-196] p 500 A95-91732
 The role of material behaviour modelling in stressing and life assessment of modern Aero-engine components
 [CONGRESS PAPER C428-27-127] p 612 A95-93606
 Analysis and testing of a graphite-epoxy sandwich shell fuselage test structure
 [ISBN 1-879921-01-4] p 605 A95-93746
 Optimization of aerospace structures
 [NASA-CR-196763] p 48 N95-12787
 Fatigue evaluation of empennage, forward wing, and winglets/tip fins on part 23 airplanes
 [PB94-196813] p 79 N95-13981
 Composite waveform generation for EMP and lightning direct-drive testing
 [AD-A284159] p 92 N95-14405
 A method of calculating the safe fatigue life of compact, highly-stressed components
 p 93 N95-14464
 Development of a composite repair and the associated inspection intervals for the F-111C stiffener runout region
 p 66 N95-14477
 Aircraft stress sequence development: A complex engineering process made simple
 p 136 N95-19480
 Prediction of R-curves from small coupon tests
 p 167 N95-19496
 Residual Stress Measurements with Laser Speckle Correlation Interferometry and Local Heat Treating
 [DE95-060082] p 349 N95-24598
 Design and structural validation of CF116 upper wing skin boron doubler
 p 393 N95-27510
 Evaluation of patch effectiveness in repairing aircraft components
 p 394 N95-27513
 Repair technology for thermoplastic aircraft structures
 p 395 N95-27519
 Scarf repairs to graphite/epoxy components
 p 396 N95-27523
 Damage occurrence on composites during testing and fleet service: Repair of Airbus aircraft
 p 396 N95-27526
 Reliability analysis of composite structures
 p 423 N95-28441
 Probabilistic reliability modeling of fatigue on the H-46 tie bar
 [AD-A289926] p 607 N95-30927

STRESS CONCENTRATION
 Tension fracture of laminates for transport fuselage. Part 1: Material screening
 p 398 N95-28471

STRESS CORROSION CRACKING

- Corrosion behavior of landing gear steels
[AD-A285862] p 242 N95-22132
The corrosion and protection of advanced aluminum -
lithium airframe alloys p 302 N95-23497
Corrosion of landing gear steels p 302 N95-23500

STRESS DISTRIBUTION

- Accurate interlaminar stress recovery from finite element
analysis
[NASA-TM-109149] p 57 N95-11815
Development of the NASA/FLAGRO computer program
for analysis of airframe structures p 94 N95-14473
Prediction of R-curves from small coupon tests
p 167 N95-19496
Tension fracture of laminates for transport fuselage. Part
1: Material screening p 398 N95-28471

STRESS FUNCTIONS

- Theoretical and actual performance of a long duration
supersurface balloon made from a biaxially oriented
nylon-6 film p 181 A95-66282

STRESS INTENSITY FACTORS

- Fatigue crack growth in nickel-based superalloys at
500-700 C. 1: Waspaloy
[BTN-94-EIX94371347843] p 206 A95-69136
Bonded composite repair of cracked load-bearing
holes
[BTN-94-EIX94401360553] p 243 A95-71867
Multiple site fatigue damage in fuselage skin splices:
Experimental simulation and theoretical prediction
[BTN-95-EIX95152584676] p 276 A95-73588
Crack growth characteristics of integrally machined
stringer-skin panels
[HTN-95-01095] p 496 A95-90281
Fatigue design of axially loaded semicircular lugs
[BTN-95-EIX0619952748190] p 637 A95-94252
FAA/NASA International Symposium on Advanced
Structural Integrity Methods for Airframe Durability and
Damage Tolerance
[NASA-CP-3274-PT-1] p 92 N95-14453
Elastic-plastic models for multi-site damage
p 92 N95-14454
Bending effects of unsymmetric adhesively bonded
composite repairs on cracked aluminum panels
p 92 N95-14456
Inspecting for widespread fatigue damage: Is partial
debonding the key? p 93 N95-14458
Fracture mechanics validity limits p 95 N95-14480
Challenges for the aircraft structural integrity program
p 80 N95-14481
The effects of pitting on fatigue crack nucleation in
7075-T6 aluminum alloy p 88 N95-14482
Multi-lab comparison on R-curve methodologies: Alloy
2024-T3
[NASA-CR-195004] p 151 N95-16860
Discrete crack growth analysis methodology for through
cracks in pressurized fuselage structures
p 166 N95-19473

STRESS MEASUREMENT

- Residual Stress Measurements with Laser Speckle
Correlation Interferometry and Local Heat Treating
[DE95-060082] p 349 N95-24598

STRESS RELAXATION

- Analytical description of and forecast for stress
relaxation of aviation materials under the vibration
conditions
[BTN-94-EIX94461408751] p 126 A95-63634

STRESS WAVES

- Thrust measurement in a 2-D scramjet nozzle
p 339 N95-25397

STRESS-STRAIN DIAGRAMS

- Non-linear viscoelastic-plastic constitutive relations for
an aeronautical PMMA
[HTN-95-71132] p 385 A95-83493

STRESS-STRAIN RELATIONSHIPS

- Critical speed analysis of a non-linear strain ring
dynamical model for aircraft tires
[SAE PAPER 932580] p 494 A95-90067
Modeling and life prediction methodology for Titanium
Matrix Composites subjected to mission profiles
[NASA-TM-109148] p 55 N95-11915
Elastic-plastic models for multi-site damage
p 92 N95-14454
Small crack test program for helicopter materials
p 92 N95-14455
Evaluation of bonded boron/epoxy doublers for
commercial aircraft aluminum structures
p 92 N95-14457
Inspecting for widespread fatigue damage: Is partial
debonding the key? p 93 N95-14458
Corrosion and corrosion fatigue of airframe aluminum
alloys p 87 N95-14465

STRESSED-SKIN STRUCTURES

- An investigation of the accuracy of FEM analysis of a
graphite epoxy box beam
[SAE PAPER 931221] p 543 A95-88011

STRESSES

- Fatigue design of axially loaded semicircular lugs
[BTN-95-EIX0619952748190] p 637 A95-94252

STRETCH FORMING

- Application of advanced material systems to composite
frame elements p 422 N95-28432

STRINGERS

- Crack growth characteristics of integrally machined
stringer-skin panels
[HTN-95-01095] p 496 A95-90281
Effect of constraining layer stiffness on performance of
damping tile materials using finite element modelling with
Rayleigh integral p 30 N95-11306
Acoustic fatigue testing on different materials and
skin-stringer elements p 174 N95-19156
Fatigue and residual strength investigation of ARALL(R)
-3 and GLARE(R) -2 panels with bonded stringers
p 137 N95-19495
Load transfer in the stiffener-to-skin joints of a
pressurized fuselage
[NASA-CR-198610] p 439 N95-27865

STRIPPING

- Aircraft stripping and painting
[BTN-95-EIX95182617810] p 300 A95-75755
Aircraft stripping and painting
[HTN-95-92311] p 365 A95-85355
Use of starch based blast media for dry paint stripping
[SAE PAPER 932616] p 456 A95-90081
Operational parameters and material effects
p 651 N95-32179
Process evaluation p 651 N95-32180

STROUHAL NUMBER

- Experimental investigation of the flow around a circular
cylinder. Influence of aspect ratio
[BTN-94-EIX95011441120] p 347 A95-80044
Flow due to an oscillating sphere and an expression
for unsteady drag on the sphere at finite Reynolds
number
[BTN-94-EIX95011441142] p 347 A95-81012
Spectral mapping of quasiperiodic structures in a vortex
flow
[BTN-95-EIX0619952748165] p 589 A95-94459
The effects of three-dimensional imposed disturbances
on bluff body near wake flows: Effects of taper and splitter
plates on the near wake characteristics of a circular cylinder
in uniform and shear flow
[AD-A292113] p 477 N95-28921

STRUCTURAL ANALYSIS

- A comparative study of internally and externally capped
balloons using small scale test balloons
p 181 A95-66285
Overview of the NASA balloon R&D program
p 181 A95-66297
Computerized maintenance aid
[BTN-95-EIX95031502749] p 217 A95-68256
Simplified analysis of general instability of stiffened
shells with cutouts in pure bending
[BTN-95-EIX95042474418] p 209 A95-68282
Bilinear formulation applied to the response and stability
of helicopter rotor blade
[BTN-95-EIX95042474400] p 192 A95-68300
Numerical modelling of transverse impact on composite
coupons
[BTN-95-EIX95082502225] p 240 A95-71022
Static aeroelastic characteristics of a composite wing
[BTN-95-EIX95152582340] p 282 A95-73542
Aeroservoelastic aspects of wing/control surface
planform shape optimization
[BTN-95-EIX95222650795] p 340 A95-79251
Shear buckling response of tailored composite plates
[HTN-95-51680] p 418 A95-85062
Equivalent beam-column analysis of guyed towers
[BTN-95-EIX95262696644] p 435 A95-85519
An investigation of the accuracy of FEM analysis of a
graphite epoxy box beam
[SAE PAPER 931221] p 543 A95-88011
Equivalent plate structural modeling for wing shape
optimization including transverse shear
[HTN-95-20839] p 492 A95-88100
Computer aided static aeroelastic analysis of
wing/pylon/store combination p 499 A95-91531
The use of structural optimisation within aerospace
[CONGRESS PAPER C428-23-008] p 500 A95-91729
Load alleviation for civil transport aircraft
[CONGRESS PAPER C428-35-057] p 604 A95-93627
Advanced composites structural concepts and materials
technologies for primary aircraft structures. Structural
response and failure analysis: ISPAN modules users
manual
[NASA-CR-4449] p 12 N95-10242
Noise Con 1994: Proceedings of the 1994 National
Conference on Noise Control Engineering. Progress in
Noise Control for Industry
[LC-75-24750] p 28 N95-11259

- Parallel aeroelastic computations for wing and wing-body
configurations
[NASA-CR-196835] p 36 N95-11766
Optimization of aerospace structures
[NASA-CR-196763] p 48 N95-12787
FAA/NASA International Symposium on Advanced
Structural Integrity Methods for Airframe Durability and
Damage Tolerance
[NASA-CP-3274-PT-1] p 92 N95-14453
Elastic-plastic models for multi-site damage
p 92 N95-14454
Small crack test program for helicopter materials
p 92 N95-14455
Bending effects of unsymmetric adhesively bonded
composite repairs on cracked aluminum panels
p 92 N95-14456
Evaluation of bonded boron/epoxy doublers for
commercial aircraft aluminum structures
p 92 N95-14457
Inspecting for widespread fatigue damage: Is partial
debonding the key? p 93 N95-14458
Testing and analysis of flat and curved panels with
multiple cracks p 93 N95-14460
Probabilistic inspection strategies for minimizing service
failures p 93 N95-14461
A method of calculating the safe fatigue life of compact,
highly-stressed components p 93 N95-14464
Corrosion and corrosion fatigue of airframe aluminum
alloys p 87 N95-14465
Computational predictive methods for fracture and
fatigue p 93 N95-14466
Influence of crack history on the stable tearing behavior
of a thin-sheet material with multiple cracks
p 93 N95-14467
Study of multiple cracks in airplane fuselage by
micromechanics and complex variables
p 94 N95-14468
Extracting a representative loading spectrum from
recorded flight data p 80 N95-14469
Development of the NASA/FLAGRO computer program
for analysis of airframe structures p 94 N95-14473
Fatigue reliability method with in-service inspections
p 94 N95-14475
Nonlinear bulging factor based on R-curve data
p 94 N95-14476
Development of a composite repair and the associated
inspection intervals for the F-111C stiffener runout
region p 66 N95-14477
Axial crack propagation and arrest in pressurized
fuselage p 94 N95-14479
Fracture mechanics validity limits p 95 N95-14480
Challenges for the aircraft structural integrity program
p 80 N95-14481
The effects of pitting on fatigue crack nucleation in
7075-T6 aluminum alloy p 88 N95-14482
Analysis of small crack behavior for airframe
applications p 95 N95-14484
Full-scale testing and analysis of fuselage structure
p 95 N95-14485
Advanced method and processing technology for
complicated shape airframe part forming
p 80 N95-14486
FPCAS2D user's guide, version 1.0
[NASA-CR-195413] p 156 N95-16588
Measurements on a two-dimensional aerofoil with
high-lift devices p 109 N95-17848
FAA/NASA International Symposium on Advanced
Structural Integrity Methods for Airframe Durability and
Damage Tolerance, part 2
[NASA-CP-3274-PT-2] p 124 N95-19468
Flight parameters monitoring system for tracking
structural integrity of rotary-wing aircraft
p 135 N95-19469
Technology Benefit Estimator (T/BEST): User's
manual
[NASA-TM-106785] p 167 N95-19501
Proceedings of the USAF Structural Integrity Program
Conference
[AD-A285684] p 194 N95-19517
Super-heavy aircraft study
[AD-A279602] p 238 N95-19955
A non-iterative grid deformation algorithm for
computational fluid dynamics for aeroelasticity
[AD-A288298] p 436 N95-26418
Bonded composite repair of metallic aircraft
components: Overview of Australian activities
p 392 N95-27505
Design and structural validation of CF116 upper wing
skin boron doubler p 393 N95-27510
Load transfer in the stiffener-to-skin joints of a
pressurized fuselage
[NASA-CR-198610] p 439 N95-27865
Aeroelasticity and structural optimization of composite
helicopter rotor blades with swept tips
[NASA-CR-4665] p 397 N95-28262

Static and fatigue testing of full-scale fuselage panels fabricated using a Therm-X(R) process p 420 N95-28270

Analysis techniques for the prediction of springback in formed and bonded composite components p 421 N95-28289

Investigation of static and cyclic bearing failure mechanisms for GR/EP laminates p 422 N95-28427

Analysis of composite structures with delaminations under combined bending and compression p 422 N95-28429

Development of composite carrythrough bulkhead p 423 N95-28438

Probabilistic evaluation of fuselage-type composite structures p 398 N95-28444

Composite fuselage shell structures research at NASA Langley Research Center p 425 N95-28466

Structural testing of the technology integration box beam p 441 N95-28467

Development of stitched/RTM composite primary structures p 425 N95-28469

Test and analysis results for composite transport fuselage and wing structures p 398 N95-28470

An efficiency study of the simultaneous analysis and design of structures [NASA-TM-110168] p 501 N95-28820

Impact damage resistance of composite fuselage structure, part 2 p 533 N95-28838

Buckling analysis of curved composite sandwich panels subjected to inplane loadings p 533 N95-28845

ISPAN (Interactive Stiffened Panel Analysis): A tool for quick concept evaluation and design trade studies p 533 N95-28846

A global/local analysis method for treating details in structural design p 552 N95-28848

IPACS (Integrated Probabilistic Assessment of Composite Structures): Code development and applications p 534 N95-28849

Advanced composites technology program p 534 N95-29032

Test results from large wing and fuselage panels p 537 N95-29051

STRUCTURAL DESIGN

Coupling equivalent plate and finite element formulations in multiple-method structural analyses [BTN-95-EIX95062487548] p 192 A95-68362

Ply layup optimization and micromechanics tailoring of composite aircraft engine structures [BTN-95-EIX95112524206] p 196 A95-69302

Design optimization of rotor blades for improved performance and vibration [HTN-95-A0498] p 229 A95-72569

Minimum-mass design of sandwich aerobrakes for a lunar transfer vehicle [BTN-95-EIX95212645707] p 299 A95-76759

Multilevel decomposition procedure for efficient design optimization of helicopter rotor blades [BTN-95-EIX95222650784] p 334 A95-79240

Recent developments in nylon superpressure balloons p 385 A95-82512

Development of 70MW class superconducting generators [BTN-94-EIX95011440854] p 429 A95-82905

Ceramic composite attachments for transmission of high-torque loads [BTN-94-EIX95011441256] p 417 A95-84213

Shear buckling response of tailored composite plates [HTN-95-51680] p 418 A95-85062

Stress considerations in reduced-size aeroelastic optimization [BTN-95-EIX95262694313] p 366 A95-85484

Materials and structures for the HSCT [BTN-95-EIX95282711241] p 455 A95-89634

Standardization of aircraft noise insulation measures without compromising results p 561 A95-90115

Optimum design of composite stiffened wing panels - a parametric study [HTN-95-01088] p 496 A95-90274

Simultaneous structure/aerodynamic design optimization for a flexible wing structure p 499 A95-91565

Preliminary tests of a transonic flutter control wing model p 499 A95-91566

The use of structural optimisation within aerospace [CONGRESS PAPER C428-23-008] p 500 A95-91729

A better than average stress model-photoelastic analysis for airbus design [CONGRESS PAPER C428-23-005] p 500 A95-91730

Reaction-time response of aircraft crash [BTN-95-EIX95292721296] p 595 A95-92626

Advanced composites structural concepts and materials technologies for primary aircraft structures: Structural response and failure analysis [NASA-CR-4448] p 11 N95-10240

Advanced composites structural concepts and materials technologies for primary aircraft structures: Structural response and failure analysis: ISPAN modules users manual [NASA-CR-4449] p 12 N95-10242

Advanced composites structural concepts and materials technologies for primary aircraft structures: Design/manufacturing concept assessment [NASA-CR-4447] p 12 N95-10316

The use of the Regier number in the structural design with flutter constraints [NASA-TM-109128] p 13 N95-11465

Viper cabin-fuselage structural design concept with engine installation and wing structural design [NASA-CR-197162] p 45 N95-12305

Cabin fuselage structural design with engine installation and control system [NASA-CR-197173] p 47 N95-12639

Cabin-fuselage-wing structural design concept with engine installation [NASA-CR-197172] p 49 N95-12993

FAA/NASA International Symposium on Advanced Structural Integrity Methods for Airframe Durability and Damage Tolerance [NASA-CP-3274-PT-1] p 92 N95-14453

Requirements report for SSTO vertical take-off and horizontal landing vehicle [NASA-CR-197029] p 80 N95-14794

A Lifting Ball Valve for cryogenic fluid applications p 156 N95-16349

Rapid solution of large-scale systems of equations p 169 N95-16458

Wing design for a civil tiltrotor transport aircraft [NASA-CR-197523] p 130 N95-18090

Course module for AA201: Wing structural design project [AD-A283618] p 133 N95-18616

Impact of Acoustic Loads on Aircraft Structures [AGARD-CP-549] p 173 N95-19142

Current and future problems in structural acoustic fatigue p 173 N95-19143

Aeroacoustic qualification of HERMES shingles p 173 N95-19145

Integrated aerodynamic/dynamic/structural optimization of helicopter rotor blades using multilevel decomposition [NASA-TP-3465] p 285 N95-22953

Design and evaluation of a foam-filled hat-stiffened panel concept for aircraft primary structural applications [NASA-TM-109175] p 346 N95-26251

Design and development of a test rig for the high frequency testing of rolling sleeve airsprings [DSTO-TN-0001] p 411 N95-26378

AIAA Techfest 20 Proceedings [NIAR-94-1] p 367 N95-26941

Damage occurrence on composites during testing and fleet service: Repair of Airbus aircraft p 396 N95-27526

Load transfer in the stiffener-to-skin joints of a pressurized fuselage [NASA-CR-198610] p 439 N95-27865

Horizontal axis wind turbine post stall airfoil characteristics synthesisization p 376 N95-27974

Calculation of design load for the MOD-5A 7.3 mW wind turbine system p 440 N95-27982

Whirl plus tilt [DE95-007948] p 452 N95-28108

Ninth DOD/NASA/FAA Conference on Fibrous Composites in Structural Design, volume 3 [NASA-CR-198718] p 420 N95-28266

Development of a low-cost, modified resin transfer molding process using elastomeric tooling and automated preform fabrication p 420 N95-28268

Resin transfer molding of textile preforms for aircraft structural applications p 421 N95-28276

Ninth DOD/NASA/FAA Conference on Fibrous Composites in Structural Design, volume 1 [NASA-CR-198723] p 421 N95-28420

Ninth DOD/NASA/FAA Conference on Fibrous Composites in Structural Design, volume 2 [NASA-CR-198722] p 424 N95-28462

Overview of the ACT program p 424 N95-28463

Development of stitched/RTM composite primary structures p 425 N95-28469

Recent progress in NASA Langley textile reinforced composites program p 425 N95-28475

Damage tolerance of a geodesically stiffened advanced composite structural concept for aircraft structural applications p 399 N95-28487

The effects of design details on cost and weight of fuselage structures p 501 N95-28831

Design and evaluation of a foam-filled hat-stiffened panel concept for aircraft primary structural applications p 502 N95-28841

A weight-efficient design strategy for cutouts in composite transport structures p 533 N95-28843

A global/local analysis method for treating details in structural design p 552 N95-28848

Advanced composite fuselage technology p 535 N95-29034

Structural design using equilibrium programming formulations [NASA-TM-110175] p 645 N95-30682

Failure analysis for polycarbonate transparencies [AD-A292992] p 630 N95-31471

Structural aspects of active control technology p 623 N95-32006

A probabilistic design method applied to smart composite structures [NASA-TM-106715] p 651 N95-32206

Analysis and design methodology for chordwise deformable wings p 692 N95-33311

STRUCTURAL DESIGN CRITERIA

Mobile domes for TACTIC telescope p 453 A95-86113

Integrated thermal and mechanical analysis of hypersonic vehicles by using adaptive finite element methods p 524 A95-87383

Higher harmonic control analysis for vibration reduction of helicopter rotor systems [NASA-TM-103855] p 66 N95-14419

Aircraft Loads due to Turbulence and their Impact on Design and Certification [AGARD-R-798] p 143 N95-18597

An Echelle Grating Spectrometer (EGS) for mid-IR remote chemical detection [DE94-019310] p 249 N95-21478

Structural design optimization with survivability dependent constraints application: Primary wing box of a multi-role fighter p 398 N95-28440

Selecting optimal experiments for feedforward multilayer perceptrons [AD-A290856] p 678 N95-30406

A probabilistic design method applied to smart composite structures [NASA-TM-106715] p 651 N95-32206

STRUCTURAL ENGINEERING

Inter-Noise 92: Noise control and the public; International Congress on Noise Control Engineering, Toronto, Ontario, Canada, July 20 - 22, 1992. Vols. 1 & 2 [ISBN 0-931784-25-5] p 559 A95-88457

NASA Lewis Research Center Workshop on Forced Response in Turbomachinery [NASA-CP-10147] p 141 N95-19380

NASA-UVA light aerospace alloy and structures technology program (LA2ST) [NASA-CR-198041] p 343 N95-24220

JPRS report: Science and technology, Central Eurasia [JPRS-UST-94-027] p 349 N95-24470

Probabilistic evaluation of fuselage-type composite structures p 398 N95-28444

COINS: A composites information database system p 453 N95-28465

Textile composite fuselage structures development p 534 N95-29033

Developing a workstation-based, real-time simulation for rapid handling qualities evaluations during design [NASA-CR-198831] p 505 N95-30335

STRUCTURAL FAILURE

Simplified analysis of general instability of stiffened shells with cutouts in pure bending [BTN-95-EIX95042474418] p 209 A95-68282

Prediction of energy absorption capability of composite stiffeners [HTN-95-A0500] p 230 A95-72571

An analytical and experimental investigation of the response of the curved, composite frame/skin specimens [HTN-95-80857] p 283 A95-75099

Buckling and postbuckling of composite structures [HTN-95-71387] p 528 A95-87605

Ageing aircraft after ALOHA [CONGRESS PAPER C428-11-188] p 484 A95-91701

Explosive sabotage: The potential effects of explosive charges on aircraft [CONGRESS PAPER C428-11-034] p 484 A95-91702

Structural integrity of fuselage panels with multisite damage [BTN-95-EIX0619952748188] p 637 A95-94250

Illustrated structural application of universal first-order reliability method [NASA-TP-3501] p 54 N95-11870

Damage tolerant repair techniques for pressurized aircraft fuselages [AD-A281982] p 65 N95-14144

FAA/NASA International Symposium on Advanced Structural Integrity Methods for Airframe Durability and Damage Tolerance [NASA-CP-3274-PT-1] p 92 N95-14453

- Challenges for the aircraft structural integrity program p 80 N95-14481
- Forced response of mistuned bladed disks p 141 N95-19383
- FAA/NASA International Symposium on Advanced Structural Integrity Methods for Airframe Durability and Damage Tolerance, part 2 p 124 N95-19468
- [NASA-CP-3274-PT-2] Results of uniaxial and biaxial tests on riveted fuselage lap joint specimens p 136 N95-19491
- Proceedings of the USAF Structural Integrity Program Conference [AD-A285684] p 194 N95-19517
- Corrosion of aircraft materials: Correlation between nanometer scale and macroscopic structural damage parameters [AD-A285930] p 241 N95-20299
- Design and structural validation of CF116 upper wing skin boron doubler p 393 N95-27510
- Repair technology for thermoplastic aircraft structures p 395 N95-27519
- Applications of a damage tolerance analysis methodology in aircraft design and production p 426 N95-28483
- Numerical simulation of crack growth in pressurized fuselages [PB95-192415] p 400 N95-28636
- STRUCTURAL MEMBERS**
- Lyapunov exponents and stochastic stability of two-dimensional parametrically excited random systems [BTN-94-EIX94361122401] p 207 A95-65897
- Comparison of resin film infusion, resin transfer molding, and consolidation of textile preforms for primary aircraft structure p 425 N95-28477
- Mechanical characterization of 2D, 2D stitched, and 3D braided/RTM materials p 535 N95-29038
- STRUCTURAL RELIABILITY**
- USAF aging aircraft program [BTN-95-EIX95072498878] p 180 A95-68394
- Analytical developments in support of the NASA aging aircraft program with an application to crack growth from rivets [SAE PAPER 931223] p 545 A95-88789
- Illustrated structural application of universal first-order reliability method [NASA-TP-3501] p 54 N95-11870
- Current and future problems in structural acoustic fatigue p 173 N95-19143
- Reliability analysis of composite structures p 423 N95-28441
- Probabilistic design of advanced composite structure p 424 N95-28443
- A probabilistic design method applied to smart composite structures [NASA-TM-106715] p 651 N95-32206
- STRUCTURAL STABILITY**
- Finite element model for a flexible non-symmetric rotor on distributed bearing: A stability study [BTN-94-EIX94381352212] p 306 A95-74612
- Flutter of an infinitely long panel in a duct [BTN-95-EIX95182619087] p 291 A95-75772
- Stability of viscoelastic plate in supersonic flow under random loading [BTN-95-EIX95262694312] p 435 A95-85483
- Dynamic-stall and structural-modeling effects on helicopter blade stability with experimental correlation [HTN-95-81646] p 542 A95-87694
- Application of superplastically formed and diffusion bonded structures in high intensity noise environments p 174 N95-19162
- Aeroelastic stability of wind turbine blade/aileron systems p 377 N95-27981
- STRUCTURAL STRAIN**
- Dynamic analysis of bearingless tail rotor blades based on nonlinear shell modes [BTN-95-EIX95152582338] p 281 A95-73540
- STRUCTURAL VIBRATION**
- The effects of aircraft (B-52) overflights on ancient structures [BTN-94-EIX94341340070] p 171 A95-63522
- Analytical description of and forecast for stress relaxation of aviation materials under the vibration conditions [BTN-94-EIX94461408751] p 126 A95-63634
- Noise and vibration control [BTN-95-EIX95042477108] p 179 A95-68351
- Coupled FEM-BEM approach for mean flow effects on vibro-acoustic behavior of planar structures [BTN-95-EIX95152577587] p 263 A95-73495
- Transient analysis of a cracked rotor passing through critical speed [BTN-94-EIX94401360022] p 306 A95-74702
- Analytical aeropropulsive/aeroelastic hypersonic-vehicle model with dynamic analysis [BTN-95-EIX95182619138] p 269 A95-76615
- Modal characteristics of rotors using a conical shaft finite element [BTN-94-EIX94401359745] p 346 A95-77379
- Subharmonic and quasi-periodic motions of an eccentric squeeze film damper-mounted rigid rotor [BTN-94-EIX95011440601] p 429 A95-82982
- Vibration measurements on rotating machinery using laser Doppler velocimetry [BTN-94-EIX95011440597] p 429 A95-82986
- Interaction of jet noise with a nearby panel assembly [BTN-95-EIX95262694295] p 434 A95-85466
- Condition monitoring for helicopters: 3303 Airborne vibration monitoring system [SAE PAPER 931360] p 610 A95-93642
- Arbitrary Lagrangian-Eulerian finite element analysis for flow-induced vibration of rigid body p 643 A95-95485
- Noise Con 1994: Proceedings of the 1994 National Conference on Noise Control Engineering. Progress in Noise Control for Industry [LC-75-24750] p 28 N95-11259
- Active control of interior noise in a business jet using piezoceramic actuators p 29 N95-11276
- Adaptive tuned vibration absorbers: Tuning laws, tracking agility, sizing, and physical implementations p 25 N95-11280
- Broadband, wide-area active control of sound radiated from vibrating structures using local surface-mounted radiation suppression devices p 30 N95-11283
- Comments on the use of structureborne noise analysis for large commercial airplanes p 30 N95-11287
- Exact dynamic responses of periodic multi-span beams under convected pressure fields p 25 N95-11288
- A theoretical analysis of airborne sound transfer for a resiliently mounted machine to its foundation p 30 N95-11304
- On the interaction of jet noise with a nearby flexible structure [NASA-CR-194934] p 57 N95-11812
- Large amplitude nonlinear response of flat aluminum, and carbon fiber plastic beams and plates [AD-A282440] p 96 N95-15547
- Pressure measurements on an F/A-18 twin vertical tail in buffeting flow. Volume 4, part 2: Buffet cross spectral densities [AD-A285555] p 143 N95-18641
- Nonlinear dynamic response of aircraft structures to acoustic excitation p 135 N95-19151
- Spectrogram diagnosis of aircraft disasters p 124 N95-19167
- Active control of panel vibrations induced by a boundary layer flow [NASA-CR-197867] p 273 N95-23182
- Gearbox vibration diagnostic analyzer [NASA-CR-189141] p 316 N95-23792
- Vibration analysis of a split path gearbox [NASA-TM-106875] p 438 N95-27855
- Vibration reduction in helicopter rotors using an actively controlled partial span trailing edge flap located on the blade p 624 N95-32111
- Synchronous dynamics of a coupled shaft/bearing/housing system with auxiliary support from a clearance bearing: Analysis and experiment p 703 N95-32693
- Modal identification and its applications to damage detection in vibrating structures p 704 N95-32920
- STRUCTURAL WEIGHT**
- Materials and structures for the HSCT [BTN-95-EIX95282711241] p 455 A95-89634
- Structural design optimization with survivability dependent constraints application: Primary wing box of a multi-role fighter p 398 N95-28440
- The effects of design details on cost and weight of fuselage structures p 501 N95-28831
- STRUCTURED GRIDS (MATHEMATICS)**
- Surface Modeling, Grid Generation, and Related Issues in Computational Fluid Dynamic (CFD) Solutions [NASA-CP-3291] p 476 N95-28723
- Automatic blocking for complex three-dimensional configurations p 566 N95-28734
- Block-structured grids for complex aerodynamic configurations: Current status p 551 N95-28736
- Three-dimensional hybrid grid generation using advancing front techniques p 567 N95-28745
- Parallel computation of transonic flows about an aircraft configuration using multi-block structured grids p 685 N95-34537
- A large scale 3D Navier-Stokes analysis using NAL-NWT p 707 N95-34539
- STRUTS**
- Flight investigation of the use of a nose gear jump strut to reduce takeoff ground roll distance of STOL aircraft [NASA-TM-108819] p 44 N95-12225
- Interaction of a three strut support on the aerodynamic characteristics of a civil aviation model p 122 N95-19279
- STUDENTS**
- A workstation based simulator for teaching compressible aerodynamics [NASA-TM-106799] p 170 N95-16906
- Three-D weather displays for aircraft cockpits [AD-A289759] p 508 N95-28691
- SUBCRITICAL FLOW**
- An improved method of airfoil design p 106 N95-16252
- SUBLIMATION**
- Ablative thermal management structural material on the hypersonic vehicles [AIAA PAPER 95-6133] p 547 A95-90452
- SUBMARINES**
- Application of three-dimensional hybrid structured/unstructured grids to land, sea and air vehicles [ARA-MEMO-399] p 210 N95-19775
- SUBMERGING**
- Immersion/two phase cooling p 246 N95-20648
- SUBROUTINES**
- Demonstration of the Dynamic Flowgraph Methodology using the Titan 2 Space Launch Vehicle Digital Flight Control System [NASA-CR-197517] p 150 N95-17493
- Steady potential solver for unsteady aerodynamic analyses p 141 N95-19382
- A preliminary study of the airwake model used in an existing SH-60B/FFG-7 helicopter/ship simulation program [DSTO-TR-0015] p 224 N95-21659
- SUBSONIC AIRCRAFT**
- An analysis of aircraft exhaust plumes from accidental encounters [HTN-95-70943] p 351 A95-78008
- Atmospheric effects of high-flying subsonic aircraft: A catalogue of perturbing influences [KNMI-SR-94-03] p 168 N95-18722
- Advanced subsonic airplane design and economic studies [NASA-CR-195443] p 338 N95-24304
- Development of RTM and powder prepreg resins for subsonic aircraft primary structures p 536 N95-29044
- SUBSONIC FLOW**
- Jet to freestream velocity ratio computations for a jet in a crossflow [AIAA PAPER 93-4860] p 2 A95-60178
- F/A-18 inlet calculations at 60-deg angle of attack and 10-deg sideslip [BTN-95-EIX95112524199] p 195 A95-69309
- Sidewash on the vertical tail in subsonic and supersonic flows [BTN-95-EIX95152582316] p 264 A95-73519
- Analytic prediction of lift for delta wings with partial leading-edge thrust [BTN-95-EIX95152582345] p 266 A95-73547
- Higher-order viscous shock-layer solutions for high-altitude flows [BTN-95-EIX95152583255] p 306 A95-73556
- Comparison of linear stability results with flight transition data [BTN-95-EIX95182619097] p 283 A95-76582
- Study of the droplet spray characteristics of a subsonic wind tunnel [BTN-95-EIX95182619235] p 271 A95-76661
- Study of subsonic base cavity flowfield structure using particle image velocimetry [BTN-95-EIX95222650781] p 327 A95-79237
- Unsteady lift on a swept blade tip [BTN-94-EIX95011441154] p 329 A95-80030
- Direct boundary integral equations method to subsonic flow with circulation past thin airfoils in ground effect [BTN-95-EIX95242673940] p 365 A95-82224
- Interaction of jet noise with a nearby panel assembly [BTN-95-EIX95262694295] p 434 A95-85466
- Aerodynamic design and optimization at Alenia D.V.D. p 491 A95-87564
- Two-dimensional unsteady leading-edge separation on a pitching airfoil [HTN-95-81628] p 461 A95-87676
- Aerodynamic off-design behavior of integrated waveriders from take-off up to hypersonic flight [AIAA PAPER 95-6091] p 466 A95-89200
- A brief survey of wing tip devices for drag reduction [SAE PAPER 932574] p 467 A95-90063
- Measurement of drag using a momentum balance [HTN-95-01090] p 468 A95-90276
- High subsonic and high Reynolds number wind tunnel tests of two-dimensional natural-laminar-flow airfoils with suction boundary layer control p 472 A95-91508
- Comparison of coordinate-invariant and coordinate-aligned upwinding for the Euler equations [HTN-95-A1753] p 633 A95-93316
- Analytic solution of the thickness problem of a rectangular wing in steady subsonic flow [ISBN 1-879921-01-4] p 588 A95-93758

- Quantifiable vortex features of F-106B aircraft at subsonic speeds
[BTN-95-EIX0619952748161] p 588 A95-94455
- In-flight pressure measurements on a subsonic transport high-lift wing section
[BTN-95-EIX0619952748170] p 589 A95-94464
- Nonlinear aerodynamic analysis of grid fin configurations
[BTN-95-EIX0619952748172] p 590 A95-94466
- Axis switching and spreading of an asymmetric jet: Role of vorticity dynamics
[NASA-TM-106385] p 73 N95-14418
- Three dimensional compressible turbulent flow computations for a diffusing S-duct with/without vortex generators
[NASA-CR-195390] p 138 N95-17402
- Investigation of an NLF(1)-0416 airfoil in compressible subsonic flow
p 110 N95-17852
- Measurements of the flow over a low aspect-ratio wing in the Mach number range 0.6 to 0.87 for the purpose of validation of computational methods. Part 1: Wing design, model construction, surface flow. Part 2: Mean flow in the boundary layer and wake, 4 test cases
p 112 N95-17860
- Pressure distributions on research wing W4 mounted on an axisymmetric body
p 112 N95-17862
- Three-dimensional boundary layer and flow field data of an inclined prolate spheroid
p 158 N95-17867
- Ellipsoid-cylinder model
p 158 N95-17869
- Delta-wing model
p 114 N95-17873
- Wind tunnel test on a 65 deg delta wing with rounded leading edges: The International Vortex Flow Experiment
p 114 N95-17875
- Investigation of the flow development on a highly swept canard/wing research model with segmented leading- and trailing-edge flaps
p 114 N95-17876
- Subsonic flow around US-orbiter model FALKE in the DNW
p 115 N95-17877
- Measurement of gust response on a turbine cascade
[NASA-TM-106776] p 117 N95-18457
- Acoustic radiation damping of flat rectangular plates subjected to subsonic flows
p 172 N95-18542
- Solution of full potential equation on an airfoil by multigrid technique
[NAL-TM-CSS-9303] p 119 N95-18904
- Calculation of support interference in dynamic wind-tunnel tests
p 122 N95-19282
- Wing pressure distributions from subsonic tests of a high-wing transport model -- in the Langley 14-by-22-Foot Subsonic Wind Tunnel
[NASA-TM-4583] p 272 N95-22802
- High frequency flow-structural interaction in dense subsonic fluids
[NASA-CR-4652] p 330 N95-24217
- Effects of cavity dimensions, boundary layer, and temperature on cavity noise with emphasis on benchmark data to validate computational aeroacoustic codes
[NASA-CR-4653] p 361 N95-24879
- Numerical and experimental study of drag characteristics of two-dimensional HLFC airfoils in high subsonic, high Reynolds number flow
[NAL-TR-1244T] p 331 N95-24998
- A fixed time performance evaluation of parallel CFD applications
[DE94-014240] p 436 N95-26445
- TranAir: A full-potential, solution-adaptive, rectangular grid code for predicting subsonic, transonic, and supersonic flows about arbitrary configurations. User's manual
[NASA-CR-4349] p 377 N95-28230
- TranAir: A full-potential, solution-adaptive, rectangular grid code for predicting subsonic, transonic, and supersonic flows about arbitrary configurations. Theory document
[NASA-CR-4348] p 378 N95-28265
- Response of multi-panel assembly to noise from a jet in forward motion
[NASA-CR-198164] p 442 N95-28673
- Finite element vorticity-based methods for the solution of the incompressible and compressible Navier-Stokes equations
p 553 N95-29119
- The pressure field of a gust interacting with a flat plate
p 557 N95-30161
- Laser doppler velocimeter system for subsonic jet mixer nozzle testing at the NASA Lewis Aeroacoustic Propulsion Lab
[NASA-TM-106984] p 457 N95-30229
- Computations of low speed flow about space-plane
p 685 N95-34544
- SUBSONIC FLUTTER**
- Design and multifunction tests of a frequency domain-based active flutter suppression system
[BTN-95-EIX95182619215] p 292 A95-76641
- Fundamental wind tunnel experiments on low-speed flutter of a tip-fin configuration wing
[NAL-TR-1228] p 332 N95-25762
- SUBSONIC SPEED**
- Preliminary assessment of tunnel wall interference in the NDA cryogenic wind tunnel
[BTN-95-EIX95062487531] p 187 A95-69239
- Computation of the poststall behavior of a circulation controlled airfoil
[BTN-95-EIX95152582320] p 264 A95-73523
- Aerodynamic characteristics of a canard-controlled missile at high angles of attack
[BTN-95-EIX95152583257] p 267 A95-73558
- Some aspects of the aeroacoustics of extreme-speed jets
p 572 A95-88893
- Effect of passive venting on static pressure distributions in cavities at subsonic and transonic speeds
[NASA-TM-4549] p 6 N95-10029
- On the use of controls for subsonic transport performance improvement: Overview and future directions
[NASA-TM-4605] p 10 N95-11408
- Symmetric steady manoeuvre loads on rigid aircraft of classical configuration at subsonic speeds
[ESDU-94009] p 43 N95-11774
- The development of a highly reliable power management and distribution system for civil transport aircraft
[NASA-TM-106697] p 50 N95-11867
- Ultra-high bypass ratio jet noise
[NASA-CR-195394] p 100 N95-14610
- Measurements of the flow over a low aspect-ratio wing in the Mach number range 0.6 to 0.87 for the purpose of validation of computational methods. Part 1: Wing design, model construction, surface flow. Part 2: Mean flow in the boundary layer and wake, 4 test cases
p 112 N95-17860
- DLR-F4 wing body configuration
p 130 N95-17863
- Low aspect ratio wing experiment
p 113 N95-17865
- Test data on a non-circular body for subsonic, transonic and supersonic Mach numbers
p 158 N95-17871
- Wind tunnel test on a 65 deg delta wing with a sharp or rounded leading edge: The international vortex flow experiment
p 114 N95-17872
- Inner loop flight control for the High-Speed Civil Transport
p 293 N95-23314
- High-lift flow-physics flight experiments on a subsonic civil transport aircraft (B737-100)
p 275 N95-23333
- Noise impact of advanced high lift systems
[NASA-CR-195028] p 362 N95-26160
- Airfoil modification effects on subsonic and transonic pressure distributions and performance for the EA-6B airplane
[NASA-TP-3516] p 373 N95-26382
- Performance characterization of a highly-offset diffuser with and without blowing vortex generator jets
[AD-A289334] p 375 N95-26901
- A general theory of two- and three-dimensional rotational flow in subsonic and transonic turbomachines
[NASA-CR-4496] p 377 N95-28003
- Measurements of store forces and moments and cavity pressures for a generic store in and near a box cavity at subsonic and transonic speeds
[NASA-TM-4611] p 378 N95-28241
- Study of potential aerodynamic benefits from spanwise blowing at wingtip
[NASA-TP-3515] p 378 N95-28669
- Noise exposure reduction of advanced high-lift systems
[NASA-CR-195077] p 452 N95-28670
- Numerical study to assess sulfur hexafluoride as a medium for testing multielement airfoils
[NASA-TP-3496] p 378 N95-28674
- Computer program for estimation of leading-edge suction distribution for plane thin wings at subsonic speeds
[ESDU-94038] p 476 N95-28708
- Leading-edge suction distribution for plane thin wings at subsonic speeds
[ESDU-94037] p 477 N95-28800
- Increments in aerofoil lift coefficient at zero angle of attack and in maximum lift coefficient due to deployment of a plain trailing-edge flap, with or without a leading-edge high-lift device, at low speeds
[ESDU-94028] p 477 N95-28885
- Increments in aerofoil lift coefficient at zero angle of attack and in maximum lift coefficient due to deployment of a trailing-edge split flap, with or without a leading-edge high-lift device, at low speeds
[ESDU-94029] p 479 N95-29129
- Transonic, supersonic and hypersonic wind-tunnel tests on aerodynamic characteristics of reentry body with blunted cone configuration
[ISAS-658] p 480 N95-29640
- The 1995 version of the NSWC aeroprediction code. Part 1: Summary of new theoretical methodology
[AD-A291518] p 481 N95-29853
- Transonic aerodynamic characteristics of a proposed wing-body reusable launch vehicle concept
[NASA-TM-108489] p 592 N95-30712
- Minimum fuel mode evaluation
p 695 N95-33015
- SUBSONIC WIND TUNNELS**
- Optimum full-scale subsonic wind tunnel
[AIAA PAPER 86-0732] p 18 A95-60161
- Study of the droplet spray characteristics of a subsonic wind tunnel
[BTN-95-EIX95182619235] p 271 A95-76661
- Modification of the Ames 40- by 80-foot wind tunnel for component acoustic testing for the second generation supersonic transport
[NASA-TM-108850] p 65 N95-13642
- Unsteady flow testing in a passive low-correction wind tunnel
p 147 N95-19272
- Evaluation of combined wall- and support-interference on wind tunnel models
p 122 N95-19278
- SUBSTRATES**
- Evaluation of advanced aerospace materials by depth sensing indentation and scratch methods
[BTN-95-EIX95152584678] p 282 A95-73590
- Development of a bipolar lead/acid battery for the more electric aircraft
[AD-A284050] p 160 N95-18660
- High aspect ratio metal microstructures and method for preparing the same
[AD-D017463] p 629 N95-30750
- Operational parameters and material effects
p 651 N95-32179
- SUCTION**
- Analysis of an oscillating Joukowski airfoil with surface suction and moving vortices
[BTN-95-EIX95062487527] p 186 A95-69235
- Analytic prediction of lift for delta wings with partial leading-edge thrust
[BTN-95-EIX95152582345] p 266 A95-73547
- Experimental investigation of the flow around a circular cylinder: Influence of aspect ratio
[BTN-94-EIX95011441120] p 347 A95-80044
- Operation of the adaptive-wall wind tunnel of TsAGI, Moscow
p 519 N95-88901
- High subsonic and high Reynolds number wind tunnel tests of two-dimensional natural-laminar-flow airfoils with suction boundary layer control
p 472 A95-91508
- An experimental study on supersonic laminar flow control
p 473 A95-91523
- Hybrid laminar flow over wings enhanced by continuous boundary layer suction
[SAE PAPER 931386] p 587 A95-93662
- Instabilities originating from suction holes used for Laminar Flow Control (LFC)
[NASA-CR-196395] p 6 N95-10131
- Computer program for estimation of leading-edge suction distribution for plane thin wings at subsonic speeds
[ESDU-94038] p 476 N95-28708
- Leading-edge suction distribution for plane thin wings at subsonic speeds
[ESDU-94037] p 477 N95-28800
- Pressure based high order TVD methodology for dynamic stall control
[AD-A290149] p 479 N95-29316
- SULFATES**
- High-speed civil transport impact: Role of sulfate, nitric acid trihydrate, and ice aerosols studied with a two-dimensional model including aerosol physics
[HTN-95-91843] p 354 A95-80831
- Remote sensing of smoke, clouds, and radiation using AVIRIS during SCAR experiments
p 708 N95-33749
- SULFIDES**
- An intercomparison of instrumentation for tropospheric measurements of dimethyl sulfide: Aircraft results for concentrations at the parts-per-trillion level
[HTN-95-91857] p 355 A95-80845
- SULFUR**
- Compendium of NASA data base for the Global Tropospheric Experiment's Pacific Exploratory Mission West-A (PEM West-A)
[NASA-TM-109177] p 320 N95-23009
- SULFUR DIOXIDES**
- An intercomparison of aircraft instrumentation for tropospheric measurements of sulfur dioxide
[HTN-95-91855] p 354 A95-80843
- Gas turbine compressor corrosion and erosion in Western Europe
[AD-B196178L] p 201 N95-19678
- SULFUR HEXAFLUORIDE**
- Stationary premixed flames in spherical and cylindrical geometries
[HTN-95-42336] p 418 A95-86165
- Performance of the 0.3-meter transonic cryogenic tunnel with air, nitrogen, and sulfur hexafluoride media under closed loop automatic control
[NASA-CR-195052] p 310 N95-23257

- Numerical study to assess sulfur hexafluoride as a medium for testing multielement airfoils
[NASA-TP-3496] p 378 N95-28674
- SULFUR OXIDES**
Evolution of the concentrations of trace species in an aircraft plume: Trajectory study
[HTN-95-A1044] p 443 A95-84549
- SUPERCHARGERS**
Advanced diesel electronic fuel injection and turbocharging
[AD-A279176] p 211 N95-19809
Unitized Regenerative Fuel Cells for solar rechargeable aircraft and zero emission vehicles
[DE95-010684] p 708 N95-33642
- SUPERCOMPUTERS**
NASA High Performance Computing and Communications program
[NASA-TM-4653] p 176 N95-18573
NAS Technical Summaries, March 1993 - February 1994
[NASA-RP-1355] p 453 N95-27367
- SUPERCONDUCTING DEVICES**
Development of 70MW class superconducting generators
[BTN-94-EIX95011440854] p 429 A95-82905
- SUPERCONDUCTING POWER TRANSMISSION**
Development of 70MW class superconducting generators
[BTN-94-EIX95011440854] p 429 A95-82905
- SUPERCONDUCTIVITY**
Reducing process noise in superconducting helium liquid level probes
[DE95-008956] p 629 N95-30765
- SUPERCONDUCTORS (MATERIALS)**
Development of 70MW class superconducting generators
[BTN-94-EIX95011440854] p 429 A95-82905
- SUPERCOOLING**
Supercooling in hypersonic nitrogen wind tunnels
[BTN-94-EIX95011441134] p 340 A95-81020
The production of supercooled liquid water by a secondary cold front
p 673 A95-93542
Airplane icing research at the Boeing Company: Participation in the second Canadian Atlantic Storms Program
p 674 A95-93544
Aircraft icing: Meteorological effects on aircraft performance
p 674 A95-93545
Preliminary studies of ice formation in upslope clouds
p 674 A95-93546
The development of an aircraft icing forecast technique using data from maps
p 675 A95-93549
- SUPERCritical AIRFOILS**
Comparison of computational and experimental results for a supercritical airfoil
[NASA-TM-4601] p 108 N95-16908
A supercritical airfoil experiment
p 111 N95-17858
Control of unsteady separated flow associated with the dynamic stall of airfoils
[NASA-CR-198972] p 594 N95-32193
- SUPERCritical FLOW**
Comparison of coordinate-invariant and coordinate-aligned upwinding for the Euler equations
[HTN-95-A1753] p 633 A95-93316
- SUPERCritical WINGS**
Dryden and transonic research
[NASA-TM-104281] p 1 N95-10709
Measurements of unsteady pressure and structural response for an elastic supercritical wing
[NASA-TP-3443] p 104 N95-16560
- SUPERPLASTIC FORMING**
Application of superplastically formed and diffusion bonded structures in high intensity noise environments
p 174 N95-19162
- SUPERPRESSURE BALLOONS**
Theoretical and actual performance of a long duration superpressure balloon made from a biaxially oriented nylon-6 film
p 181 A95-66282
Long duration balloons
p 191 A95-66305
- SUPERSONIC AIRCRAFT**
Ozone, skin cancer, and the SST
[BTN-95-EIX95041503011] p 213 A95-68314
Development of an efficient inverse method for supersonic and hypersonic body design
[BTN-95-EIX95041503784] p 180 A95-69215
Mach wave emission from a high-temperature supersonic jet
[BTN-95-EIX95152577586] p 264 A95-73496
Flow study of supersonic wing-nacelle configuration
[BTN-95-EIX95152582344] p 266 A95-73546
The distribution of hydrogen, nitrogen, and chlorine radicals in the lower stratosphere: Implications for changes in O₃ due to emission of NO_y from supersonic aircraft
[HTN-95-70935] p 351 A95-78000
Sensitivity of supersonic aircraft modelling studies to HNO₃ photolysis rate
[HTN-95-11475] p 353 A95-79453
- Effects on stratospheric ozone from high-speed civil transport: Sensitivity to stratospheric aerosol loading
[HTN-95-91842] p 354 A95-80830
High-speed civil transport impact: Role of sulfate, nitric acid trihydrate, and ice aerosols studied with a two-dimensional model including aerosol physics
[HTN-95-91843] p 354 A95-80831
Potential effects on ozone of future supersonic aircraft/2D simulation
[HTN-95-51282] p 356 A95-80867
Aircraft gas turbine emissions challenge
[BTN-94-EIX95011441239] p 403 A95-84196
Fan noise reduction from a supersonic inlet during simulated aircraft approach
[BTN-95-EIX95292721155] p 572 A95-89894
A prediction method for broadband shock associated noise from supersonic rectangular jets
p 574 A95-90100
Reduction of supersonic jet noise using swirl: A concept revisited
p 574 A95-90101
A computational environment for exhaust nozzle design
[AIAA PAPER 95-1016] p 566 A95-90688
Experimental performance of a ventral nozzle with pitch and yaw vectoring capability for SSTOVL aircraft
[SAE PAPER 931412] p 614 A95-93678
Estimation of supersonic leading-edge thrust by a Euler flow model
[BTN-95-EIX0619952748194] p 591 A95-94483
Three dimensional model calculations of the global dispersion of high speed aircraft exhaust and implications for stratospheric ozone loss
p 26 N95-10657
The present and future of aircraft noise models: A user's perspective
p 32 N95-11324
STOVL Control Integration Program
[NASA-CR-195358] p 18 N95-11487
Development of techniques for the in situ observation of OH and HO₂ for studies of the impact of high-altitude supersonic aircraft on the stratosphere
[NASA-CR-196759] p 61 N95-12832
A procedure for automating CFD simulations of an inlet-bleed problem
p 552 N95-28768
- SUPERSONIC AIRFOILS**
Natural laminar flow wing concept for supersonic transports
[BTN-95-EIX95182619226] p 308 A95-76652
- SUPERSONIC BOUNDARY LAYERS**
Effects of expansions on a supersonic boundary layer: Surface pressure measurements
[BTN-95-EIX95142553036] p 263 A95-73462
Surface interference in Rayleigh scattering measurements near forebodies
[HTN-95-51670] p 433 A95-85052
Turbulence characteristics of supersonic boundary layer past a backward facing step
[AIAA PAPER 95-6126] p 470 A95-90447
Supersonic laminar flow control research
[NASA-CR-196049] p 249 N95-21340
Numerical simulation of supersonic flow using a new analytical bleed boundary condition
[NASA-CR-198368] p 697 N95-33208
- SUPERSONIC COMBUSTION**
Experimental and analytical investigations of wave enhanced supersonic combustors
[AIAA PAPER 89-2787] p 14 A95-60172
Comparison of NO and OH planar fluorescence temperature measurements in scramjet model flowfields
[BTN-95-EIX95042474388] p 209 A95-68312
Modeling of supersonic turbulent combustion using assumed probability density functions
[BTN-95-EIX95112524190] p 206 A95-69318
Simulating heat addition via mass addition in constant area compressible flows
[BTN-95-EIX95182619100] p 307 A95-76585
Ignition analysis of hydrogen/air mixture in supersonic mixing layer
p 416 A95-82301
Prediction of pre-combustion shock in scramjet combustors: A new method
p 402 A95-82323
Computational methods in applied sciences: European Computational Fluid Dynamics Conference, 1st, Brussels, Belgium, Sept. 7-11, 1992
[ISBN 0-444-89795-X] p 539 A95-87552
High-speed reacting flow simulation using USA-series codes
p 540 A95-87559
Numerical study of contaminant effects on combustion of hydrogen, ethane, and methane in air
[AIAA PAPER 95-6097] p 510 A95-88005
Temperature diagnostics in the hypersonic flow regime: An application to develop a stagnation temperature probe
[AIAA PAPER 95-6114] p 511 A95-90442
Effects of the chemical reaction model on calculations of supersonic combustion flows
[BTN-95-EIX0616952745802] p 638 A95-94487
Propulsion research concerning SFRJ-motors
[PB94-179520] p 14 N95-10083
- Hydrocarbon-fueled ramjet/scramjet technology program, phase 2 extension
[NASA-CR-189659] p 15 N95-10319
Programmed ignition of metal compounds in a scramjet
p 16 N95-10466
Numerical study of mixing in a high and low enthalpy supersonic test facility
p 7 N95-10467
Theories of turbulent combustion in high speed flows
[AD-A280933] p 23 N95-10535
Shock tube investigations of combustion phenomena in supersonic flows
[PB94-175262] p 55 N95-11796
AFOSR Contractors Meeting in Propulsion
[AD-A282729] p 54 N95-12507
Planar Rayleigh scattering and laser-induced fluorescence for visualization of a hot, Mach 2 annular air jet
[NASA-TM-4576] p 54 N95-13196
Studies on high pressure and unsteady flame phenomena
[AD-A284126] p 152 N95-18410
Effect of density gradients in confined supersonic shear layers, part 1
[NASA-CR-198029] p 348 N95-24412
Effect of density gradients in confined supersonic shear layers. Part 2: 3-D modes
[NASA-CR-198030] p 349 N95-24413
Numerical simulation of ram accelerator performance including transient effects during initiation of combustion and sensitivity studies
p 629 N95-31203
The 25th International Symposium on Combustion
[AD-A286825] p 630 N95-31268
Calculation of supersonic combustion in SCRAMJET engines
p 698 N95-34513
- SUPERSONIC COMBUSTION RAMJET ENGINES**
Experimental and analytical investigations of wave enhanced supersonic combustors
[AIAA PAPER 89-2787] p 14 A95-60172
Experimental and computational results for the external flowfield of a scramjet inlet
[BTN-94-EIX94441380977] p 195 A95-68161
Three-dimensional analysis of scramjet nozzle flows
[BTN-94-EIX94441380978] p 196 A95-68162
Comparison of NO and OH planar fluorescence temperature measurements in scramjet model flowfields
[BTN-95-EIX95042474388] p 209 A95-68312
Numerical study of the performance of swept, curved compression surface scramjet inlets
[BTN-95-EIX95112524198] p 197 A95-69310
Computational study of plume-induced separation on a hypersonic powered model
[BTN-95-EIX95152582346] p 266 A95-73548
Optimization of contoured hypersonic scramjet inlets with a least-squares parabolized Navier-Stokes procedure
[HTN-95-20976] p 261 A95-74042
Numerical analysis of hypersonic low-density scramjet inlet flow
[BTN-95-EIX95212645694] p 272 A95-76746
Design features of the NAL ramjet engine test facility
p 410 A95-82319
Hypersonic wind tunnel test of sidewall compression type scramjet inlet
p 410 A95-82320
Evaluation of scramjet nozzle performance
p 402 A95-82321
An experimental investigation of scramjet nozzle flow
p 402 A95-82322
Prediction of pre-combustion shock in scramjet combustors: A new method
p 402 A95-82323
An advanced scramjet propulsion concept for a 350 MG SSTO space plane
p 402 A95-82325
Hypersonic trajectory control of aerospace plane with integrated SCRAMJET engine
p 413 A95-82384
Experiment and analysis on heat transfer of a scramjet leading edge model
p 403 A95-82420
A conceptual design of hypersonic research vehicle with subscale scramjet engine
p 384 A95-82482
Studies on plasma jet igniters
p 403 A95-82680
Thrust modeling for hypersonic engines
[AIAA PAPER 95-6081] p 509 A95-87410
Scramjet combustor design in France
[AIAA PAPER 95-6094] p 510 A95-88002
Injection studies in the French hypersonic technology program
[AIAA PAPER 95-6096] p 510 A95-88004
Review of new French facilities for PREPHA program
[AIAA PAPER 95-6128] p 520 A95-90449
The DCAF: A high-enthalpy long-duration, direct-connect scramjet test facility
[AIAA PAPER 95-6130] p 512 A95-90450
An assessment of ground-test facility capabilities for measurement of hypervelocity scramjet performance
[AIAA PAPER 95-6148] p 512 A95-90462
An experimental study on interacting flow between supersonic flow and secondary flow injected normally through circular nozzle
p 472 A95-91511

- A three-dimensional moving mesh method for the calculation of unsteady transonic flows
[HTN-95-C0007] p 585 A95-93395
- Scramjet thrust measurement in a shock tunnel
[HTN-95-C0008] p 586 A95-93396
- Investigation of scramjet injection strategies for high mach number flows
[BTN-95-EIX0616952745782] p 614 A95-94504
- Performance variation of scramjet nozzle at various nozzle pressure ratios
[BTN-95-EIX0616952745781] p 615 A95-94505
- Propulsion research concerning SFRJ-motors
[PB94-179520] p 14 N95-10083
- Application of scramjet engine technology to the design of ram accelerator projectiles p 19 N95-10282
- Hydrocarbon-fueled ramjet/scramjet technology program, phase 2 extension
[NASA-CR-189659] p 15 N95-10319
- Visualization of one-dimensional flow processes in a dual-mode scramjet engine p 15 N95-10465
- Programmed ignition of metal compounds in a scramjet p 16 N95-10466
- Shock-tunnel combustor testing for hypersonic vehicles
[NASA-CR-196836] p 52 N95-11938
- NASA's Hypersonic Research Engine Project: A review
[NASA-TM-107759] p 50 N95-12860
- Air-breathing aerospace plane development essential: Hypersonic propulsion flight tests
[NASA-TM-108857] p 66 N95-14921
- Wind-tunnel blockage and actuation systems test of a two-dimensional scramjet inlet unstart model at Mach 6
[NASA-TM-109152] p 97 N95-15898
- Two-dimensional scramjet inlet unstart model: Wind-tunnel blockage and actuation systems test
[NASA-TM-109984] p 97 N95-15899
- Scramjet testing guidelines p 138 N95-16317
- Combustor kinetic energy efficiency analysis of the hypersonic research engine data p 148 N95-16321
- Operating capability and current status of the reactivated NASA Lewis Research Center Hypersonic Tunnel Facility
[NASA-TM-106808] p 148 N95-19286
- Mach 10 computational study of a three-dimensional scramjet inlet flow field
[NASA-TM-4602] p 309 N95-23015
- Mach 10 computational study of a three-dimensional scramjet inlet flow field
[NASA-TM-4602] p 310 N95-23210
- Effect of film cooling/regenerative cooling on scramjet engine performances
[NAL-TR-1242] p 339 N95-24990
- Shock tunnel studies of scramjet phenomena 1993
[NASA-CR-195038] p 350 N95-25394
- Thrust measurements of a complete axisymmetric scramjet in an impulse facility p 339 N95-25395
- Scramjet thrust measurement in a shock tunnel p 339 N95-25396
- Thrust measurement in a 2-D scramjet nozzle p 339 N95-25397
- Balances for the measurement of multiple components of force in flows of a millisecond duration p 350 N95-25400
- Experiment on a rectangular cross section scramjet combustor. 2: Effects of fuel injector geometry
[NAL-TR-1220] p 405 N95-26600
- Effects of dust from storage heaters on ignition in scramjets
[NAL-TR-1234] p 405 N95-26706
- Experimental investigation of inlet-combustor isolators for a dual-mode scramjet at a Mach number of 4
[NASA-TP-3502] p 407 N95-28343
- Calculation of supersonic combustion in SCRAMJET engines p 698 N95-34513
- SUPERSONIC COMMERCIAL AIR TRANSPORT**
- European firms team on supersonic studies
[HTN-95-42215] p 386 A95-84031
- The high speed civil transport: A technology challenge p 496 A95-90089
- The concept of high speed commercial transporter structure p 498 A95-91517
- Overview of feasibility study on propulsion concepts for high speed civil transport p 498 A95-91518
- SUPERSONIC COMPRESSORS**
- Boundary conditions for unsteady supersonic inlet analyses
[HTN-95-20829] p 544 A95-88090
- SUPERSONIC CRUISE AIRCRAFT RESEARCH**
- Future SSTs a European approach
[BTN-95-EIX95072419883] p 180 A95-68396
- Conceptual study of next generation high-speed civil transport: A candidate with horizontal tail p 499 A95-91521
- SUPERSONIC DIFFUSERS**
- A full Navier-Stokes analysis of subsonic diffuser of a bifurcated 70/30 supersonic inlet for high speed civil transport application
[NASA-TM-106637] p 8 N95-10820
- Parametrics on 2D Navier-Stokes analysis of a Mach 2.68 bifurcated rectangular mixed-compression inlet
[NASA-TM-107003] p 617 N95-30861
- SUPERSONIC DRAG**
- CFD optimization of a theoretical minimum-drag body
[BTN-95-EIX95182619234] p 308 A95-76660
- SUPERSONIC FLIGHT**
- Supersonic flutter analysis of cantilevered composite plate-wings p 499 A95-91567
- The effect of aircraft speed on the penetration of sonic boom noise into a flat ocean p 100 N95-14887
- SUPERSONIC FLOW**
- Behavior of the Johnson-King turbulence model in axisymmetric supersonic flows p 183 A95-67337
- Design and operation of a supersonic annular flow facility
[BTN-94-EIX94441386624] p 183 A95-68173
- Numerical computations of supersonic base flow with special emphasis on turbulence modeling
[BTN-94-EIX94441386632] p 179 A95-68181
- Influence of injectant Mach number and temperature on supersonic film cooling
[BTN-94-EIX94441386686] p 184 A95-68195
- Numerical study of the performance of swept, curved compression surface scramjet inlets
[BTN-95-EIX95112524198] p 197 A95-69310
- Main features of overexpanded triple jets
[BTN-95-EIX95142553040] p 304 A95-73458
- Sidewash on the vertical tail in subsonic and supersonic flows
[BTN-95-EIX95152582316] p 264 A95-73519
- Predicting exhaust plume boundaries with supersonic external flows
[BTN-95-EIX95152583258] p 297 A95-73559
- Supersonic axisymmetric conical flow solutions for different ratios of specific heats
[BTN-95-EIX95152583283] p 306 A95-73584
- Supersonic near-wake afterbody boattailing effects on axisymmetric bodies
[BTN-95-EIX95182617465] p 268 A95-75736
- Simulating heat addition via mass addition in constant area compressible flows
[BTN-95-EIX95182619100] p 307 A95-76585
- Observations on using experimental data as boundary conditions for computations
[BTN-95-EIX95182619103] p 321 A95-76588
- Scaling of incipient separation in supersonic/transonic speed laminar flows
[BTN-95-EIX95182619104] p 269 A95-76589
- Simple method of supersonic flow visualization using watertable
[BTN-95-EIX95182619105] p 269 A95-76590
- CFD optimization of a theoretical minimum-drag body
[BTN-95-EIX95182619234] p 308 A95-76660
- Review and development of base pressure and base heating correlations in supersonic flow
[BTN-95-EIX95212645688] p 271 A95-76740
- Numerical investigation of supersonic flows around a spiked blunt body
[BTN-95-EIX95212645690] p 271 A95-76742
- Quantitative comparison between interferometric measurements and Euler computations for supersonic cone flows
[BTN-95-EIX9522650782] p 358 A95-79238
- Experimental study of flow separation on an oscillating flap at Mach 2.4
[BTN-95-EIX9522650792] p 329 A95-79248
- Unsteady lift on a swept blade tip
[BTN-94-EIX95011441154] p 329 A95-80030
- The aerodynamic characteristics of cup-like body in supersonic flow p 427 A95-82407
- A study on aerodynamic heating phenomena in three-dimensional shock wave/turbulent boundary layer interaction induced by sweptback sharp fins at supersonic flow p 428 A95-82419
- Accuracy and efficiency assessments for a weak statement CFD algorithm for high-speed aerodynamics
[BTN-94-EIX95011441238] p 370 A95-84195
- Computational/experimental investigation of staged injection into a Mach 2 flow
[HTN-95-51646] p 432 A95-85028
- Stability of viscoelastic plate in supersonic flow under random loading
[BTN-95-EIX95262694312] p 435 A95-85483
- Flowfield measurements in supersonic film cooling including the effect of shock-wave interaction
[HTN-95-42337] p 405 A95-86166
- Aerodynamic design and optimization at Alenia D.V.D. p 491 A95-87564
- Sensitivity derivatives for three dimensional supersonic Euler code using incremental iterative strategy
[HTN-95-20845] p 545 A95-88106
- Supersonic and hypersonic shock/boundary-layer interaction database p 463 A95-88969
- Linear disturbances in hypersonic, chemically reacting shock layers
[HTN-95-20931] p 464 A95-88970
- Behavior of the Johnson-King turbulence model in Axisymmetric supersonic flows p 464 A95-88971
- Design and operation of a supersonic annular flow facility
[HTN-95-20932] p 464 A95-88971
- Numerical computations of supersonic base flow with special emphasis on turbulence modeling
[HTN-95-20949] p 546 A95-88988
- The DCAF: A high-enthalpy long-duration, direct-connect scramjet test facility
[AIAA PAPER 95-6130] p 512 A95-90450
- An experimental study on interacting flow between supersonic flow and secondary flow injected normally through circular nozzle p 472 A95-91511
- An experimental study on supersonic laminar flow control p 473 A95-91523
- Comparison of coordinate-invariant and coordinate-aligned upwinding for the Euler equations
[HTN-95-A1753] p 633 A95-93316
- Laser velocimetry in the supersonic regime: Advancements, limitations, and outlook
[SAE PAPER 931365] p 634 A95-93646
- Supersonic, turbulent flow computation and drag optimization for axisymmetric afterbodies
[BTN-95-EIX95302729772] p 637 A95-94134
- Effects of the chemical reaction model on calculations of supersonic combustion flows
[BTN-95-EIX0616952745802] p 638 A95-94487
- Vortex generation and mixing in three-dimensional supersonic combustors
[BTN-95-EIX0616952745783] p 614 A95-94503
- Investigation of scramjet injection strategies for high mach number flows p 614 A95-94504
- Numerical study of mixing in a high and low enthalpy supersonic test facility p 7 N95-10467
- Theories of turbulent combustion in high speed flows
[AD-A280933] p 23 N95-10535
- Shock tube investigations of combustion phenomena in supersonic flows
[PB94-175262] p 55 N95-11796
- Supersonic base flow investigation over axisymmetric afterbodies p 39 N95-12578
- In-flight imaging of transverse gas jets injected into transonic and supersonic crossflows: Design and development
[NASA-CR-186031] p 157 N95-17418
- Detailed study at supersonic speeds of the flow around delta wings p 112 N95-17861
- Wind tunnel investigations of the appearance of shocks in the windward region of bodies with circular cross section at angle of attack p 113 N95-17866
- Supersonic vortex flow around a missile body p 114 N95-17870
- Numerical computations of supersonic base flow with special emphasis on turbulence modeling
[AD-A283688] p 119 N95-18670
- An assessment of the adaptive unstructured tetrahedral grid, Euler Flow Solver Code FELISA
[NASA-TP-3526] p 119 N95-19041
- Transonic and supersonic flowfield measurements about axisymmetric afterbodies for validation of advanced CFD codes p 121 N95-19260
- Parabolized Navier-Stokes solution of supersonic/hypersonic flows p 123 N95-19464
- Application of Navier-Stokes code PAB3D with kappa-epsilon turbulence model to attached and separated flows
[NASA-TP-3480] p 224 N95-21338
- Shock wave interactions in hypervelocity flow
[AD-A286507] p 250 N95-22212
- Supersonic flow and shock formation in turbine tip gaps p 312 N95-23429
- Validation of a Computational Fluid Dynamics (CFD) code for supersonic axisymmetric base flow p 315 N95-23652
- Effect of film cooling/regenerative cooling on scramjet engine performances
[NAL-TR-1242] p 339 N95-24990
- A theoretical and experimental investigation of the flow over supersonic leading edge wing/body configurations
[DRA-TM-AERO-PROP-41] p 331 N95-25649
- Aerodynamic characteristics of the orbital reentry vehicle experimental probe fins in a supersonic flow
[NAL-TR-1232] p 342 N95-25664

A fixed time performance evaluation of parallel CFD applications [DE94-014240] p 436 N95-26445
 Wind tunnel experiments on wake flow field behind a reentry capsule from a viewpoint of parachute deployment at supersonic speeds [ISAS-655] p 374 N95-26740
 Development of an upwind, finite-volume code with finite-rate chemistry [NASA-CR-197747] p 374 N95-26760
 An investigation of the AFIT 2-inch shock tube as a flow source for supersonic testing [AD-A289246] p 412 N95-26966
 A laboratory scale supersonic combustive flow system [DE95-006347] p 420 N95-27851
 TranAir: A full-potential, solution-adaptive, rectangular grid code for predicting subsonic, transonic, and supersonic flows about arbitrary configurations. User's manual [NASA-CR-4349] p 377 N95-28230
 TranAir: A full-potential, solution-adaptive, rectangular grid code for predicting subsonic, transonic, and supersonic flows about arbitrary configurations. Theory document [NASA-CR-4348] p 378 N95-28265
 Research instrumentation for polytechnic university's supersonic wind tunnel facility [AD-A290232] p 523 N95-29468
 An experimental investigation of the time-dependent separation of tangent bodies in supersonic flow [AD-A290720] p 480 N95-29500
 Survey of CFD applications for high speed inlets [AD-A291365] p 557 N95-30087
 Effects of cavity bleed and its configuration on aerodynamic characteristics of supersonic internal flow [NAL-TR-1247] p 594 N95-31715
 Numerical simulation of supersonic flow using a new analytical bleed boundary condition [NASA-CR-198368] p 697 N95-33208
 A study of supersonic mixing flow field with ramp injector p 706 N95-34512
 Calculation of supersonic combustion in SCRAMJET engines p 698 N95-34513

SUPERSONIC FLUTTER

Field-consistent element applied to flutter analysis of circular cylindrical shells [BTN-94-EIX94341341971] p 56 A95-60871
 Flutter analysis of supersonic axial flow cascades using a high resolution Euler solver. Part 1: Formulation and validation [NASA-TM-105798] p 23 N95-10244

SUPERSONIC INLETS

Lag model for turbulent boundary layers over rough bleed surfaces [BTN-94-EIX94441380981] p 208 A95-68165
 Numerical study of the performance of swept, curved compression surface scramjet inlets [BTN-95-EIX95112524198] p 197 A95-69310
 Prediction of supersonic inlet unstart caused by freestream disturbances [BTN-95-EIX9522650790] p 329 A95-79246
 Boundary conditions for unsteady supersonic inlet analyses [HTN-95-20829] p 544 A95-88090
 2-D and 3-D numerical simulation of a supersonic inlet flowfield p 641 A95-95457
 A full Navier-Stokes analysis of subsonic diffuser of a bifurcated 70/30 supersonic inlet for high speed civil transport application [NASA-TM-106637] p 8 N95-10820
 Validation of the RPLUS3D code for supersonic inlet applications involving three-dimensional shock wave-boundary layer interactions [NASA-TM-106579] p 39 N95-13058
 Computation of supersonic air-intakes p 74 N95-14452
 Time accurate computation of unsteady inlet flows with a dynamic flow adaptive mesh [AD-A285498] p 157 N95-16736
 On supersonic-inlet boundary-layer bleed flow [NASA-CR-195426] p 202 N95-19769
 Mach 10 computational study of a three-dimensional scramjet inlet flow field [NASA-TM-4602] p 310 N95-23210
 Supersonic flow and shock formation in turbine tip gaps p 312 N95-23429
 Survey of CFD applications for high speed inlets [AD-A291365] p 557 N95-30087
 Parametrics on 2D Navier-Stokes analysis of a Mach 2.68 bifurcated rectangular mixed-compression inlet [NASA-TM-107003] p 617 N95-30861
 Drag measurements of an axisymmetric nacelle mounted on a flat plate at supersonic speeds [NASA-TM-4660] p 684 N95-32821

Numerical simulation of supersonic flow using a new analytical bleed boundary condition [NASA-CR-198368] p 697 N95-33208

SUPERSONIC JET FLOW

Linear instability waves in supersonic jets confined in circular and non-circular ducts [BTN-94-EIX94341340068] p 103 A95-63520
 Mach wave emission from a high-temperature supersonic jet [BTN-95-EIX95152577586] p 264 A95-73496
 Three-dimensional structure of a supersonic jet impinging on an inclined plate [BTN-95-EIX95152583259] p 267 A95-73560
 Simulation of transverse gas injection in turbulent supersonic air flows [BTN-95-EIX95182619080] p 269 A95-75765
 Structure of supersonic jet flow and its radiated sound [HTN-95-51645] p 431 A95-85027
 Screech tones from free and ducted supersonic jets [HTN-95-51647] p 432 A95-85029
 Quantitative investigation of compressible mixing: Staged transverse injection into Mach 2 flow [HTN-95-42330] p 404 A95-86159
 Mach wave emission from a high-temperature supersonic jet [HTN-95-42571] p 458 A95-87201
 Enhanced mixing of multiple supersonic rectangular jets by synchronized screech [HTN-95-42592] p 459 A95-87222
 Disturbance generation in supersonic jets under acoustic excitation [HTN-95-20926] p 463 A95-88965
 Computing unsteady shock waves for aeroacoustic applications [HTN-95-20928] p 463 A95-88967
 Control-nonlinear-nonstationary structural response and radiation near a supersonic jet [HTN-95-20929] p 463 A95-88968
 Signal processing of noise data from high-speed flyovers [BTN-95-EIX0619952748178] p 680 A95-94248
 Noise radiation by instability waves in coaxial jets [NASA-TM-106738] p 100 N95-14618
 The aeroacoustics of supersonic coaxial jets [NASA-TM-106782] p 101 N95-15059
 Resonant interaction of a linear array of supersonic rectangular jets: An experimental study [NASA-CR-195398] p 76 N95-15852
 Temperature effects on acoustic interactions between altitude test facilities and jet engine plumes [NASA-CR-197638] p 258 N95-21170
 Supersonic jet noise reductions predicted with increased jet spreading rate [NASA-TM-106872] p 323 N95-23178
 Supersonic coaxial jet noise predictions [NASA-TM-106917] p 451 N95-26801
 Preliminary results and research capabilities of a new jet facility at the University of Kansas p 412 N95-26951
 Visualization of the multiple supersonic jet oscillations by swept focused strobed schlieren technique p 367 N95-26952
 A numerical study of fundamental shock noise mechanisms [NASA-TM-110608] p 451 N95-27908
 The spectrum and directivity of turbulent mixing noise from supersonic jets p 579 N95-29415
 Spatially-resolved velocity measurements in steady, high-speed, reacting flows using laser-induced OH fluorescence p 650 N95-32109

SUPERSONIC NOZZLES
 Three-dimensional analysis of scramjet nozzle flows [BTN-94-EIX94441380978] p 196 A95-68162
 Evaluation of scramjet nozzle performance p 402 A95-82321
 JPRES report: Science and technology, Central Eurasia: Engineering and equipment. Gas dynamics of supersonic shortened nozzles [JPRES-UST-94-003-L] p 22 N95-10931
 Resonant interaction of a linear array of supersonic rectangular jets: An experimental study [NASA-CR-195398] p 76 N95-15852
 Development of quiet-flow supersonic wind tunnels for laminar-turbulent transition research [NASA-CR-197286] p 239 N95-21436

SUPERSONIC SPEED
 Aerodynamically blunt and sharp bodies [BTN-95-EIX95041503781] p 205 A95-69212
 Minimum-drag axisymmetric bodies in the supersonic/hypersonic flow regimes [BTN-95-EIX95041503785] p 180 A95-69216
 Interpretation of waverider performance data using computational fluid dynamics [BTN-95-EIX95062487534] p 193 A95-69242

Simple method of supersonic flow visualization using watertable [BTN-95-EIX95182619105] p 269 A95-76590
 Concorde: Silver jubilee Mach 2 marks 25 years [HTN-95-42618] p 483 A95-87248
 Some aspects of the aeroacoustics of extreme-speed jets p 572 A95-88893
 Effect of leading- and trailing-edge flaps on clipped delta wings with and without wing camber at supersonic speeds [NASA-TM-4542] p 5 N95-10028
 Numerical simulation of supersonic compression corners and hypersonic inlet flows using the RPLUS2D code [NASA-TM-106580] p 105 N95-16038
 Experimental study at low supersonic speeds of a missile concept having opposing wraparound tails [NASA-TM-4582] p 106 N95-16069
 Detailed study at supersonic speeds of the flow around delta wings p 112 N95-17861
 Test data on a non-circular body for subsonic, transonic and supersonic Mach numbers p 158 N95-17871
 Wind tunnel test on a 65 deg delta wing with a sharp or rounded leading edge: The international vortex flow experiment p 114 N95-17872
 Parametric study on laminar flow for finite wings at supersonic speeds [NASA-TM-108852] p 116 N95-18101
 Flow coefficient behavior for boundary layer bleed holes and slots [NASA-TM-106846] p 244 N95-19953
 Effect of density gradients in confined supersonic shear layers, part 1 [NASA-CR-198029] p 348 N95-24412
 An investigation of the AFIT 2-inch shock tube as a flow source for supersonic testing [AD-A289246] p 412 N95-26966
 Experimental investigation of inlet-combustor isolators for a dual-mode scramjet at a Mach number of 4 [NASA-TP-3502] p 407 N95-28343
 Transonic, supersonic and hypersonic wind-tunnel tests on aerodynamic characteristics of reentry body with blunted cone configuration [ISAS-658] p 480 N95-29640
 Experimental studies on boundary-layer transition on a reentry vehicle at transonic and supersonic speeds [ISAS-659] p 555 N95-29712
 The 1995 version of the NSWC aero prediction code. Part 1: Summary of new theoretical methodology [AD-A291518] p 481 N95-29853
 An aerodynamic and static-stability analysis of the Hypersonic Applied Research Technology (HART) missile [DA9426923] p 481 N95-29965
 Spatially-resolved velocity measurements in steady, high-speed, reacting flows using laser-induced OH fluorescence p 650 N95-32109
 Drag measurements of an axisymmetric nacelle mounted on a flat plate at supersonic speeds [NASA-TM-4660] p 684 N95-32821
 Minimum fuel mode evaluation p 695 N95-33015
 Rapid deceleration mode evaluation p 696 N95-33018

SUPERSONIC TRANSPORTS

Future SSTs a European approach [BTN-95-EIX95072419883] p 180 A95-68396
 Natural laminar flow wing concept for supersonic transports [BTN-95-EIX95182619226] p 308 A95-76652
 Materials and structures for the HSCT [BTN-95-EIX95282711241] p 455 A95-89634
 Aeronautical technology - recent advances and future prospects [HTN-95-01097] p 496 A95-90283
 Aircraft Symposium, 30th, Tsukuba, Japan, Sep. 30 - Oct. 2, 1992 [HTN-95-A1609] p 498 A95-91491
 Requirements for next generation supersonic transports p 498 A95-91516
 A conceptual design of the SST without horizontal tail p 498 A95-91520
 Conceptual study of next generation high-speed civil transport: A candidate with horizontal tail p 499 A95-91521
 Experimental study for improving the lift to drag ratio of next generation SST p 473 A95-91524
 Flight test of STS radio controlled scale model p 499 A95-91539
 Mechanical properties of advanced toughened bismaleimide matrix composite p 530 A95-91570
 Signal processing of noise data from high-speed flyovers [BTN-95-EIX0619952748178] p 680 A95-94248
 Micro-measurements of mechanical properties for adhesives and composites using digital imaging technology [NASA-CR-196111] p 22 N95-10231

- The High Speed Research Program
[NASA-TM-109869] p 10 N95-10548
- A full Navier-Stokes analysis of subsonic diffuser of a bifurcated 70/30 supersonic inlet for high speed civil transport application
[NASA-TM-106637] p 8 N95-10820
- High speed civil transport: Sonic boom softening and aerodynamic optimization
[NASA-CR-196397] p 28 N95-11192
- High speed civil transport aerodynamic optimization
[NASA-CR-196960] p 38 N95-12389
- Integrated design and manufacturing for the high speed civil transport
[NASA-CR-197183] p 48 N95-12700
- Design and testing of an oblique all-wing supersonic transport
[NASA-CR-196394] p 48 N95-12785
- Modification of the Ames 40- by 80-foot wind tunnel for component acoustic testing for the second generation supersonic transport
[NASA-TM-108850] p 65 N95-13642
- Aerodynamic shape optimization of a HSCT type configuration with improved surface definition
[NASA-CR-197011] p 67 N95-13701
- Aerodynamic shape optimization
p 128 N95-16572
- Multi-lab comparison on R-curve methodologies: Alloy 2024-T3
[NASA-CR-195004] p 151 N95-16860
- Inner loop flight control for the High-Speed Civil Transport
p 293 N95-23314
- Preliminary identification of buffet problems in high speed civil transport
p 294 N95-23319
- Handling qualities of the High Speed Civil Transport
p 294 N95-23325
- The atmospheric effects of stratospheric aircraft: A fourth program report
[NASA-RP-1359] p 357 N95-24274
- Study of compressible flow through a rectangular-to-semiannular transition duct
[NASA-CR-4660] p 338 N95-24392
- A crew-centered flight deck design philosophy for High-Speed Civil Transport (HSCT) aircraft
[NASA-TM-109171] p 335 N95-24582
- NASA-JV'a light aerospace alloy and structures technology program supplement: Aluminum-based materials for high speed aircraft
[NASA-CR-4645] p 343 N95-24878
- Supersonic transport grid generation, validation, and optimization
[NASA-CR-197752] p 448 N95-26648
- CFD research, parallel computation and aerodynamic optimization
[NASA-CR-197748] p 373 N95-26649
- Design and testing of low sonic boom configurations and an oblique all-wing supersonic transport
[NASA-CR-197744] p 389 N95-26651
- Supersonic civil airplane study and design: Performance and sonic boom
[NASA-CR-197745] p 390 N95-26813
- Preliminary design problems and solutions for a supersonic oblique all-wing transport aircraft
p 390 N95-26942
- The high speed civil transport and NASA's High Speed Research (HSR) program
p 390 N95-26945
- Drag measurements of an axisymmetric nacelle mounted on a flat plate at supersonic speeds
[NASA-TM-4660] p 684 N95-32821
- Numerical analysis around the whole SST configuration
p 693 N95-34541
- SUPERSONIC TURBINES**
- Computational fluid dynamics study of the variable-pitch split-blade fan concept
[NASA-CR-189206] p 15 N95-10247
- Measurements of pressure and thermal wakes in a transonic turbine cascade
[AD-A283464] p 38 N95-12548
- Turbomachinery design and tonal acoustics computations
[NASA-CR-197749] p 406 N95-26777
- SUPERSONIC WAKES**
- Wind tunnel experiments on wake flow field behind a reentry capsule from a viewpoint of parachute deployment at supersonic speeds
[ISAS-655] p 374 N95-26740
- SUPERSONIC WIND TUNNELS**
- Design and operation of a supersonic annular flow facility
[BTN-94-EIX94441386624] p 183 A95-68173
- Quiet-flow Ludweig tube for high-speed transition research
[BTN-95-EIX95262694309] p 370 A95-85480
- Turbulence characteristics of supersonic boundary layer past a backward facing step
[AIAA PAPER 95-6126] p 470 A95-90447
- A review of free-stream flow fluctuation and steady-state flow quality measurements in the AEDC/VKF Supersonic Tunnel A and Hypersonic Tunnel B
[AIAA PAPER 95-6137] p 520 A95-90454
- Numerical study of Gortler instability: Application to the design of a quiet supersonic wind tunnel
[PB94-184801] p 21 N95-10844
- Design and testing of an oblique all-wing supersonic transport
[NASA-CR-196394] p 48 N95-12785
- Mach number control in the High Speed Wind Tunnel of NLR
[PB94-201670] p 53 N95-13243
- Free-jet testing at Mach 3.44 in GASL's aero/thermo test facility
p 145 N95-16320
- Improved speed control system for the 87,000 HP wind tunnel drive
[NASA-TM-106840] p 211 N95-19794
- Supersonic laminar flow control research
[NASA-CR-196049] p 249 N95-21340
- Development of quiet-flow supersonic wind tunnels for laminar-turbulent transition research
[NASA-CR-197286] p 239 N95-21436
- Supersonic quiet-tunnel development for laminar-turbulent transition research
[NASA-CR-198040] p 340 N95-24302
- Computational support of the laminar flow supersonic wind tunnel, CNSFV code development, Maglev, and grid generation
[NASA-CR-197750] p 411 N95-26775
- A laboratory scale supersonic combustive flow system
[DE95-006347] p 420 N95-27851
- Research instrumentation for polytechnic university's supersonic wind tunnel facility
[AD-A290232] p 523 N95-29468
- SUPERSONICS**
- Separation of winged vehicles in supersonics
[AIAA PAPER 95-6092] p 526 A95-88601
- Symposium on Aerodynamics & Aeroacoustics, Tucson, AZ, Mar. 1-2, 1993
[ISBN 981-02-1732-3] p 462 A95-88892
- Modeling aerodynamic problems using Smoothed Particle Hydrodynamics (SPH)
[SAE PAPER 932512] p 465 A95-89185
- Nonlinear analysis of swept wing transitional boundary layers
[SAE PAPER 932515] p 466 A95-89188
- Aerodynamic interference for supersonic low-aspect-ratio missiles
[BTN-95-EIX95302694469] p 588 A95-94065
- Estimation of supersonic leading-edge thrust by a Euler flow model
[BTN-95-EIX0619952748194] p 591 A95-94483
- SUPPORT INTERFERENCE**
- Wall Interference, Support Interference and Flow Field Measurements
[AGARD-CP-535] p 162 N95-19251
- The crucial role of wall interference, support interference and flow field measurements in the development of advanced aircraft configurations
p 162 N95-19252
- Evaluation of combined wall- and support-interference on wind tunnel models
p 122 N95-19278
- Interaction of a three strut support on the aerodynamic characteristics of a civil aviation model
p 122 N95-19279
- Interference corrections for a centre-line plate mount in a porous-walled transonic wind tunnel
p 122 N95-19280
- Correction of support influences on measurements with sting mounted wind tunnel models
p 122 N95-19281
- Calculation of support interference in dynamic wind-tunnel tests
p 122 N95-19282
- SUPPORT SYSTEMS**
- CASS: Design for supportability
[BTN-95-EIX95172595296] p 287 A95-75716
- NASA Lewis Propulsion Systems Laboratory customer guide manual
[NASA-TM-106569] p 21 N95-10822
- Integrating NOISEMAP with the Geographic Resource Analysis Support System (GRASS) to enhance environmental impact assessments and land use compatibility studies
p 31 N95-11311
- A surgical support system for Space Station Freedom
p 149 N95-16776
- SUPPORTS**
- Measurements of longitudinal static aerodynamic coefficients by the cable mount system
[NAL-TR-1226] p 331 N95-25761
- Tie-down trials involving a Sikorsky S-70B-2 helicopter
[DSTO-TR-0132] p 400 N95-28567
- SUPPRESSORS**
- Cornet vortex suppressor
[AD-D016423] p 116 N95-18337
- Jet mixer noise suppressor using acoustic feedback
[NASA-CASE-LEW-15170-2] p 362 N95-26187
- Suppressor of oscillations in airframe cavities
[AD-D017265] p 388 N95-26507
- SURFACE COOLING**
- Cooling of aerospace plane using liquid hydrogen and methane
[BTN-95-EIX0619952748171] p 590 A95-94465
- SURFACE CRACKS**
- Small crack test program for helicopter materials
p 92 N95-14455
- Thermal fracture mechanisms in ceramic thermal barrier coatings
p 346 N95-26138
- SURFACE DIFFUSION**
- Hypersonic Gas-Surface Energy Accommodation Test Facility
[DE94-014468] p 39 N95-12652
- SURFACE DISTORTION**
- Double pass retroreflection for corrosion detection in aircraft structures
p 323 N95-23503
- SURFACE LAYERS**
- Effects of expansions on a supersonic boundary layer: Surface pressure measurements
[BTN-95-EIX95142553036] p 263 A95-73462
- SURFACE NAVIGATION**
- Use of MOBITEX wireless wide area networks as a solution to land-based positioning and navigation
[BTN-94-EIX94441386132] p 189 A95-68188
- Results and performance of multi-site reference station differential GPS
[BTN-95-EIX95112522534] p 190 A95-69329
- Using landmarks for the vehicle location measurement
[PB94-184512] p 43 N95-12582
- The effects of display location and dimensionality on taxiway navigation
[AD-A294878] p 690 N95-34570
- SURFACE NOISE INTERACTIONS**
- Experimental results of the European HELINOISE aeroacoustic rotor test
[HTN-95-01080] p 578 A95-90266
- The pressure field of a gust interacting with a flat plate
p 557 N95-30161
- SURFACE PROPERTIES**
- Observations of fluxes and inland breezes over a heterogeneous surface
[HTN-95-80258] p 212 A95-66315
- Surface morphology and structure of carbon-carbon composites in high-energy sliding contact
[BTN-94-EIX94371347996] p 206 A95-69164
- Possible near-IR channels for remote sensing precipitable water vapor from geostationary satellite platforms
[HTN-95-70139] p 214 A95-69431
- Aerodynamic shape optimization using preconditioned conjugate gradient methods
[BTN-95-EIX95142553033] p 263 A95-73465
- Planar air density measurements near model surfaces by ultraviolet Rayleigh/Raman scattering
[HTN-95-20950] p 546 A95-88989
- Operational multi-scale environment model with grid adaptivity (OMEGA) application to aviation weather
p 676 A95-93556
- Experimental and numerical simulations of the effects of ingested particles in gas turbine engines
p 199 N95-19662
- Guidance and control requirements for high-speed Rollout and Turnoff (ROTO)
[NASA-CR-195026] p 292 N95-22674
- Development of a linearized unsteady Euler analysis for turbomachinery blade rows
[NASA-CR-4677] p 592 N95-30611
- Standardization of surface contamination analysis systems
p 631 N95-31798
- Operational parameters and material effects
p 651 N95-32179
- SURFACE REACTIONS**
- Review of numerical procedures for computational surface thermochemistry
[BTN-94-EIX94441386682] p 205 A95-68191
- Powerful bolide explosion over North Italy
[HTN-95-80564] p 218 A95-69658
- Hypersonic nonequilibrium Navier-Stokes solutions over an ablating graphite nosetip
[BTN-95-EIX95152583252] p 305 A95-73553
- High-speed civil transport impact: Role of sulfate, nitric acid trihydrate, and ice aerosols studied with a two-dimensional model including aerosol physics
[HTN-95-91843] p 354 A95-80831
- Experimental and numerical simulations of the effects of ingested particles in gas turbine engines
p 199 N95-19662
- In-situ detection of surface passivation or activation and of localized corrosion: Experiences and perspectives in aircraft
p 302 N95-23508
- Operational parameters and material effects
p 651 N95-32179

SURFACE ROUGHNESS

- The effects of wall perturbations on thermo-turbulent Couette flow
[HTN-95-92255] p 434 A95-85299
Constant flux, turbulent convection data using infrared imaging
[HTN-95-20731] p 435 A95-86621
Effect of spherical roughness elements upon transition of a 3-D boundary layer
[HTN-95-92835] p 471 A95-90753
Aircraft corrosion study
[AD-A279527] p 241 N95-21687
Proceedings of the Sixth International Symposium on Long-Range Sound Propagation
[AD-A290920] p 580 N95-30084
The effect of adding roughness and thickness to a transonic axial compressor rotor
[NASA-TM-106958] p 645 N95-30524

SURFACE ROUGHNESS EFFECTS

- Effect of surface roughness on local film cooling effectiveness and heat transfer coefficients
[AD-A283854] p 91 N95-14351
Growth and development of roughness-induced stationary crossflow vortices p 482 N95-30294

SURFACE TEMPERATURE

- Flow resolution and domain influence in rarefied hypersonic blunt-body flows
[BTN-95-EIX95082502729] p 220 A95-70136
Impingement flow heat transfer measurements of turbine blades using a jet array
[AD-A283450] p 62 N95-12512
Verification of multidisciplinary models for turbomachines p 140 N95-19025
Particle kinetic simulation of high altitude hypervelocity flight
[NASA-CR-197383] p 309 N95-22481
Hailstone heat and mass transfer measurements
[ISBN-0-315-86304-8] p 563 N95-29797

SURFACE TO AIR MISSILES

- Ideal proportional navigation p 342 A95-81374

SURFACE TREATMENT

- Modelling for optimal operations of line milling of aerodynamic surfaces
[BTN-94-EIX94461408774] p 138 A95-63657
Fatigue resistance of peened 7050-T7451 aluminium alloy: Repair and re-treatment of a component surface
[BTN-94-EIX94371347838] p 206 A95-69131
The effects of surface modification on fretting fatigue in Ti alloy turbine components
[HTN-95-61145] p 404 A95-84909
Aircraft stripping and painting
[HTN-95-92311] p 365 A95-85355
Use of starch based blast media for dry paint stripping
[SAE PAPER 932616] p 456 A95-90081
Aircraft corrosion study
[AD-A279527] p 241 N95-21687
Experience of in-service corrosion on military aircraft p 303 N95-23516

SURFACE VEHICLES

- Base passive porosity for drag reduction
[NASA-CASE-LAR-15246-1] p 91 N95-14183

SURFACE WATER

- Orbital velocities induced by surface waves
[HTN-95-90902] p 253 A95-72411

SURFACE WAVES

- Orbital velocities induced by surface waves
[HTN-95-90902] p 253 A95-72411
Development of an Automated Airfield Dynamic Cone Penetrometer (AADCP) prototype and the evaluation of unsurfaced airfield seismic surveying using Spectral Analysis of Surface Waves (SASW) technology
[AD-A281985] p 145 N95-17444
Sea wave parameters, small altitudes and distances: measurers design for movement control systems of ships, wing-in-surface effect crafts and seaplanes p 708 N95-33141

- Numerical studies of turbulent free surface flows and unsteady propeller flows
[AD-A294377] p 706 N95-34343

SURGERY

- A surgical support system for Space Station Freedom p 149 N95-16776

SURGES

- Surge recovery and compressor working line control using compressor exit mach number measurement
[CONGRESS PAPER C428-33-210] p 610 A95-93622

SURVEILLANCE

- E-6A hardness assurance, maintenance and surveillance program
[AD-A283994] p 134 N95-19067
GPS-Squitter capacity analysis
[AD-A280037] p 245 N95-20599
GPS-Squitter interference analysis
[AD-A293690] p 689 N95-33480

SURVEILLANCE RADAR

- Aviation value-added products and services from the NEXRAD Information Dissemination Service (NIDS)
p 671 A95-93535
Solid state radar demonstration test results at the FAA Technical Center
[AD-A281520] p 154 N95-16097
Recommendation on transition from primary/secondary radar to secondary-only radar capability
[AD-A286279] p 249 N95-22005
MATSurv multisensor air traffic surveillance
[AD-A292253] p 489 N95-28887

SURVEYS

- Aviation weather education and the University of North Dakota aviation weather survey p 656 A95-93462
Developing and testing decision-making products for center weather service unit meteorologists p 671 A95-93533
Response to noise around Vaernes and Bodoe airports
[PB94-207065] p 62 N95-13575
Industry review of a crew-centered cockpit design process and toolset
[AD-A282966] p 130 N95-17661
Development of an intervention program to encourage shoulder harness use and aircraft retrofit in general aviation aircraft, phases 1 and 2
[DOT/FAA/AM-95/2] p 333 N95-24384
Survey and implementation of commercial manual controllers for a generic telerobotics architecture
[AD-A289215] p 449 N95-26990
Geophex airborne unmanned survey system
[DE95-007566] p 392 N95-27440
Development of an intervention program to encourage shoulder harness use and aircraft retrofit in general aviation aircraft: Phases 1 and 2
[AD-A290966] p 485 N95-29873
Transmittance characteristics of US Army rotary-wing aircraft transparencies
[AD-A295035] p 693 N95-34793

SURVIVAL

- Aircraft fires, smoke toxicity, and survival: An overview
[DOT/FAA/AM-95/8] p 277 N95-24024

SWEEP ANGLE

- Aerodynamic effects of delta planform tip sails on wing performance
[BTN-95-EIX95062487544] p 185 A95-68358
Effect of crossflow on Goertler instability in incompressible boundary layers
[NASA-CR-195007] p 159 N95-18193
NUMERICAL SIMULATION OF INCIDENCE AND SWEEP EFFECTS ON DELTA WING VORTEX BREAKDOWN
[BTN-95-EIX95062487526] p 186 A95-69234
Some additional stability and performance characteristics of the scissor/pivot wing configurations
[SAE PAPER 931383] p 618 A95-93659
Evaluation of a doubly-swept blade tip for rotorcraft noise reduction
[NASA-CR-189677] p 452 N95-28264

SWEEPBACK

- A study on aerodynamic heating phenomena in three-dimensional shock wave/turbulent boundary layer interaction induced by sweepback sharp fins at supersonic flow p 428 A95-82419
Criteria for location of vortex breakdown over delta wings
[HTN-95-01092] p 468 A95-90278

SWEEP FORWARD WINGS

- Natural laminar flow wing concept for supersonic transports
[BTN-95-EIX95182619226] p 308 A95-76652
X-29 high AOA flight test results: An overview
[SAE PAPER 931367] p 586 A95-93648
An experimental investigation of forward-swept wings at low Reynolds numbers
[SAE PAPER 931370] p 604 A95-93650
Aeroelastic tailoring research
[PB94-180031] p 6 N95-10135
The Aluminum Falcon: A low cost modern commercial transport
[NASA-CR-197180] p 81 N95-15742
Investigation into the aerodynamic characteristics of a combat aircraft research model fitted with a forward swept wing p 116 N95-17884
In-flight lift-drag characteristics for a forward-swept wing aircraft and comparisons with contemporary aircraft
[NASA-TP-3414] p 117 N95-18565
Flight test of the X-29A at high angle of attack: Flight dynamics and controls p 284 N95-22806
Flight evaluation of forebody vortex control in post-stall flight p 609 N95-32003

SWEEP WINGS

- Tip vortex on a swept wing. Mean flow and unsteady phenomena
[BTN-94-EIX94441385755] p 184 A95-68219
Limit cycle phenomena in computational transonic aerelasticity
[BTN-95-EIX95152582317] p 264 A95-73520
Method for the prediction of the onset of flow rock
[BTN-95-EIX95152582342] p 282 A95-73544
Aerodynamics of a finite wing with simulated ice
[BTN-95-EIX95182619227] p 270 A95-76653
Multiple instabilities of three-dimensional boundary layers along a concave wall
[HTN-95-71126] p 429 A95-83487
Nonlinear analysis of swept wing transitional boundary layers
[SAE PAPER 932515] p 466 A95-89188
A note on the interpretation of mini-tuft photographs
[HTN-95-01089] p 468 A95-90275
Numerical design methods for transonic NLF configurations p 471 A95-91498
An experimental study on supersonic laminar flow control p 473 A95-91523
Supersonic flutter analysis of cantilevered composite plate-wings p 499 A95-91567
Optimum aerodynamic design via boundary control
[NASA-CR-195882] p 36 N95-11877
Investigation of the flow development on a highly swept canard/wing research model with segmented leading- and trailing-edge flaps p 114 N95-17876
A spectrally accurate boundary-layer code for infinite swept wings
[NASA-CR-195014] p 159 N95-18042
Collection efficiency and ice accretion calculations for a sphere, a swept MS(1)-317 wing, a swept NACA-0012 wing tip, an axisymmetric inlet, and a Boeing 737-300
[NASA-TM-106831] p 123 N95-18582
The utilization of a high speed reflective visualization system in the study of transonic flow over a delta wing p 121 N95-19259
Velocity measurements with hot-wires in a vortex-dominated flowfield p 121 N95-19261
Computational simulations for some tests in transonic wind tunnels p 164 N95-19264
Computational studies of laminar to turbulence transition
[AD-A285622] p 248 N95-21146
Lift enhancement device
[AD-D016522] p 224 N95-21864
Crossflow instability control on a swept-wing: Preliminary studies p 274 N95-23283
Three-dimensional interaction of wake/boundary-layer and vortex/boundary-layer data report
[CUED/A-AEREO/TR-23] p 329 N95-24210
Aerodynamic shape optimization of wing and wing-body configurations using control theory
[NASA-CR-198024] p 335 N95-25334
Study of potential aerodynamic benefits from spanwise blowing at wingtip
[NASA-TP-3515] p 378 N95-28669
A large scale 3D Navier-Stokes analysis using NAL-NWT p 707 N95-34539

SWEEPBACK WINGS

- Fluctuating wall pressures near separation in highly swept turbulent interactions
[HTN-95-20823] p 543 A95-88084
Measurements of the flow over a low aspect-ratio wing in the Mach number range 0.6 to 0.87 for the purpose of validation of computational methods. Part 1: Wing design, model construction, surface flow. Part 2: Mean flow in the boundary layer and wake, 4 test cases p 112 N95-17860
Pressure distributions on research wing W4 mounted on an axisymmetric body p 112 N95-17862
DLR-F4 wing body configuration p 130 N95-17863
DLR-F5: Test wing for CFD and applied aerodynamics p 113 N95-17864
Delta-wing model p 114 N95-17873
Wind tunnel test on a 65 deg delta wing with rounded leading edges: The International Vortex Flow Experiment p 114 N95-17875

SWING WINGS

- CaInard: A new roadable aircraft concept
[SAE PAPER 932601] p 494 A95-90071

SWINGBY TECHNIQUE

- How 'HITEN's' aerobraking experiments were carried out p 415 A95-82553

SWIRLING

- Swirl control in an S-duct at high angle of attack
[HTN-95-20846] p 545 A95-88107
Structure of a swirl-stabilized, combustor spray
[NASA-TM-106724] p 50 N95-11890
Aerodynamic design and analysis of a highly loaded turbine exhaust p 312 N95-23435
Effects of initial conditions on a single jet in crossflow
[NASA-TM-107002] p 615 N95-30589

- Experimental investigation of turbulent particle dispersion in swirling flows
[DLR-FB-94-20] p 647 N95-31355
- Static pressure drop by swirling flow of an internal cooling air system through a turbine shaft p 698 N95-34560
- SWITCHES**
- A detailed power inverter design for a 250 kW switched reluctance aircraft engine starter/generator
[SAE PAPER 931388] p 613 A95-93664
- Detailed design of a 250-kW switched reluctance starter/generator for an aircraft engine
[SAE PAPER 931389] p 613 A95-93665
- SWITCHING CIRCUITS**
- A switched reluctance machine rotor position estimator: A neural network application
[SAE PAPER 932560] p 511 A95-90057
- Demonstration of the Dynamic Flowgraph Methodology using the Titan 2 Space Launch Vehicle Digital Flight Control System
[NASA-CR-197517] p 150 N95-17493
- SYMBOLS**
- TRISTAR 1: Evaluation methods for testing head-up display (HUD) flight symbology
[NASA-TM-4665] p 288 N95-24030
- Allison engine testing CMSX-4 (reg sign) single crystal turbine blades and vanes
[DE95-010308] p 694 N95-32636
- SYNCHRONOUS MOTORS**
- Starter/generator testing
[BTN-95-EIX95072498877] p 210 A95-68393
- A time stepping coupled finite element-state space modeling environment for synchronous machine performance and design analysis in the ABC frame of reference p 649 N95-31948
- SYNCHRONOUS SATELLITES**
- Possible near-IR channels for remote sensing precipitable water vapor from geostationary satellite platforms
[HTN-95-70139] p 214 A95-69431
- SYNOPTIC METEOROLOGY**
- Research aircraft observations of a polar low at the east Greenland ice edge
[HTN-95-A0175] p 215 A95-69766
- Mesoscale structure of precipitation bands in a North Atlantic winter storm
[HTN-95-40659] p 215 A95-69803
- Examination of conditions in the proximity of pilot reports of aircraft icing during storm-fest p 666 A95-93509
- Analysis of rapidly developing fog at the Kennedy Space Center p 671 A95-93531
- SYNTAX**
- Object-oriented technology for compressor simulation
[NASA-TM-106723] p 49 N95-11864
- SYNTHETIC APERTURE RADAR**
- Dynamic imaging and RCS measurements of aircraft
[BTN-95-EIX95202637582] p 347 A95-78576
- Linear prediction data extrapolation superresolution radar imaging p 155 N95-16268
- MAX-91: Polarimetric SAR results on Montespertoli site p 320 N95-23940
- Statistics of multi-look AIRSAR imagery: A comparison of theory with measurements p 320 N95-23947
- AIRSAR deployment in Australia, September 1993: Management and objectives p 321 N95-23948
- Apparatus and method for producing three-dimensional images
[AD-D017455] p 646 N95-30727
- HelixRadar: A rotating antenna synthetic aperture radar for helicopter all-weather operations p 705 N95-33137
- SYNTHETIC ARRAYS**
- Apparatus and method for producing three-dimensional images
[AD-D017455] p 646 N95-30727
- SYSTEM EFFECTIVENESS**
- Assessment of cost and training effectiveness for a candidate training system using the Comparison-Based Prediction model
[SAE PAPER 932598] p 379 A95-84570
- Transport delays associated with NASA Langley Flight Simulation Facility
[NASA-TM-110150] p 568 N95-29454
- Federal aviation administration plan for research, engineering and development
[AD-A290952] p 490 N95-29733
- SYSTEM FAILURES**
- Mechanical system reliability and risk assessment
[BTN-95-EIX95142553046] p 304 A95-73452
- The principles of flight test assessment of flight-safety-critical systems in helicopters
[AGARD-AG-300-VOL-12] p 77 N95-14199
- Probabilistic reliability modeling of fatigue on the H-46 tie bar
[AD-A289926] p 607 N95-30927
- SYSTEM IDENTIFICATION**
- Comparison of frequency response and perturbation methods to extract linear models from a nonlinear simulation
[AD-A284115] p 146 N95-18405
- A linear system identification and validation of an AH-64 Apache aeroelastic simulation model
p 146 N95-18903
- The accuracy of parameter estimation in system identification of noisy aircraft load measurement
[NASA-CR-197516] p 134 N95-19130
- Modular CNI avionics system p 234 N95-20659
- System identification of the Large-Angle Magnetic Suspension Test Fixture (LAMSTF) p 296 N95-23299
- An analytic modeling and system identification study of helicopter dynamics p 505 N95-29787
- Flight test validation of a frequency-based system identification method on an F-15 aircraft
[NASA-TM-4704] p 620 N95-31846
- SYSTEMS ANALYSIS**
- GPS/GLONASS/INS test program
[BTN-94-EIX94441386131] p 189 A95-68187
- CASS: Design for supportability
[BTN-95-EIX95172595296] p 287 A95-75716
- Aerodynamic design of pegasus: Concept to flight with computational fluid dynamics
[BTN-95-EIX95182617463] p 298 A95-75734
- Determination of piloting feedback structures for an altitude tracking task
[BTN-95-EIX95242670770] p 327 A95-81077
- Application of direct transcription to commercial aircraft trajectory optimization
[BTN-95-EIX95242670766] p 359 A95-81081
- Analyzing fault tolerance using DREDD
[AIAA PAPER 95-0952] p 565 A95-90631
- Modeling and analysis for the GPS pseudo-range observable
[BTN-95-EIX95302731227] p 600 A95-94046
- Evaluating the effects of air traffic control automation
p 601 A95-95091
- New eigensolutions and modal analysis for gyroscopic/rotor systems, part 1: undamped systems
[BTN-94-EIX94522410219] p 702 A95-96373
- New eigensolutions and modal analysis for gyroscopic/rotor systems, part 2: perturbation analysis for damped systems
[BTN-94-EIX94522410220] p 702 A95-96374
- Demonstration of the Dynamic Flowgraph Methodology using the Titan 2 Space Launch Vehicle Digital Flight Control System
[NASA-CR-197517] p 150 N95-17493
- Comparison of measured and calculated dynamic loads for the Mod-2 2.5 mW wind turbine system
p 440 N95-27983
- Variable speed generator application on the MOD-5A 7.3 mW wind turbine generator p 440 N95-27989
- Application of optimization technique to control system design for departure prevention and aircraft model estimation through dynamic inversion p 517 N95-29156
- Prototype stop bar system evaluation at Seattle-Tacoma International Airport
[AD-A290136] p 490 N95-30031
- Design, analysis and control of large transports so that control of engine thrust can be used as a back-up of the primary flight controls
[NASA-CR-198958] p 518 N95-30254
- SYSTEMS ENGINEERING**
- Mathematical modelling concerning the development of a system of similar installations, taking into account their operational intensity (an aircraft-helicopter fleet taken as an example)
[BTN-94-EIX94461408763] p 103 A95-63646
- Aeroelastic vehicle multivariable control synthesis with analytical robustness evaluation
[BTN-95-EIX95182619115] p 321 A95-76592
- Ceramic composite attachments for transmission of high-torque loads
[BTN-94-EIX95011441256] p 417 A95-84213
- AIAA Computing in Aerospace 10, San Antonio, TX, March 28-30, 1995
[ISBN 1-56347-119-1] p 565 A95-90629
- Dependability issues in the reuse of standard components in open architectures
[AIAA PAPER 95-1006] p 566 A95-90678
- Modular avionics: Taking today's aircraft into tomorrow
[SAE PAPER 931416] p 610 A95-93681
- Integrated test system single point control of aircraft checkout
[SAE PAPER 931417] p 583 A95-93682
- Fiber optic hardware for transport aircraft
[SAE PAPER 931439] p 680 A95-93691
- Future ATC system integration: Tools for developing a shared vision p 600 A95-95085
- Evaluating the effects of air traffic control automation
p 601 A95-95091
- The development of computer-based instructional simulations for the airline industry p 625 A95-95159
- Object-oriented technology for compressor simulation
[NASA-TM-106723] p 49 N95-11864
- Integrated design and manufacturing for the high speed civil transport
[NASA-CR-197183] p 48 N95-12700
- ADST ARWA visual system module software design document
[AD-A283874] p 99 N95-14357
- Aeromechanical design of modern missiles
p 73 N95-14446
- Automated test environment for a real-time control system
[TABES PAPER 94-631] p 99 N95-14652
- Program test objectives milestone 3 --- Integrated Propulsion Technology Demonstrator
[NASA-CR-197030] p 127 N95-15971
- Generalized method of solving topological optimization problems for electrical airplane equipment systems in computer-aided design p 169 N95-16272
- The computer analysis of the prediction of aircraft electrical power supply system reliability
p 155 N95-16278
- Cooperative control theory and integrated flight and propulsion control
[NASA-CR-197493] p 142 N95-17404
- Packet utilisation definitions for the ESA XMM mission
p 150 N95-17596
- Simulation investigation on system identification of gas turbine
[PB95-104238] p 139 N95-17749
- Strategic avionics technology definition studies. Subtask 3-1A3: Electrical Actuation (ELA) Systems Test Facility
[NASA-CR-188360] p 143 N95-18567
- Hypersonic flight testing
[AD-A283981] p 134 N95-18891
- FASTPACK: Optimized solutions for modular avionics derived from a parametric study. Part 1: Platform features
p 233 N95-20634
- Advanced wind turbine design studies: Advanced conceptual study
[DE93-000031] p 256 N95-20985
- Inner loop flight control for the High-Speed Civil Transport p 293 N95-23314
- Aerodynamic design and analysis of a highly loaded turbine exhaust p 312 N95-23435
- Aircraft fuel system lightning protection design and qualification test procedures development
[AD-A288401] p 380 N95-26497
- Design and synthesis of a real-time controller for an unmanned air vehicle
[AD-A289134] p 408 N95-26555
- Calculation of design load for the MOD-5A 7.3 mW wind turbine system p 440 N95-27982
- Unmanned aerial vehicles, 1994 master plan
[AD-A291628] p 398 N95-28411
- Application of optimization technique to control system design for departure prevention and aircraft model estimation through dynamic inversion p 517 N95-29156
- Design and evaluation of a LQR controller for the bluebird unmanned air vehicle
[AD-A289769] p 504 N95-29457
- Modeling spatio-temporal databases to measure the performance of the GPS satellite constellation
p 489 N95-29596
- Design, analysis and control of large transports so that control of engine thrust can be used as a back-up of the primary flight controls
[NASA-CR-198958] p 518 N95-30254
- Automatic flight control system for an unmanned helicopter system design and flight test results
p 622 N95-32004
- Digital autopilot design for combat aircraft in ALENIA
p 623 N95-32009
- Advanced turbine systems program conceptual design and product development
[DE95-000088] p 650 N95-32163
- Stratospheric Observatory For Infrared Astronomy (SOFIA). Phase A: System concept description
[NASA-TM-110669] p 680 N95-32187
- Human factors certification in the development of future air traffic control systems p 690 N95-34770
- Quality assurance and risk management: Perspectives on Human Factors Certification of Advanced Aviation Systems p 690 N95-34771
- SYSTEMS INTEGRATION**
- First level release of 2GCHAS for comprehensive helicopter analysis - a status report
[HTN-94-00697] p 2 A95-60176
- Labs behind Boeing's new 777
[BTN-95-EIX95142562403] p 280 A95-73437
- Integrated Thermal Energy Management (I-TEM): An evaluation tool for aircraft
[SAE PAPER 932577] p 493 A95-90065

- Integrated aircraft thermal management and power generation
[SAE PAPER 932055] p 500 A95-91636
Concepts for aircraft subsystem integration
[SAE PAPER 931377] p 604 A95-93656
SUIT: The integration of aircraft subsystems
[SAE PAPER 931381] p 604 A95-93657
A subsystem integration technology concept
[SAE PAPER 931382] p 604 A95-93658
Integrated test system single point control of aircraft checkout
[SAE PAPER 931417] p 583 A95-93682
Future ATC system integration: Tools for developing a shared vision p 600 A95-95085
Integrated voice and data communications for air traffic service applications p 600 A95-95090
Fly-By-Light/Power-By-Wire Requirements and Technology Workshop
[NASA-CP-10108] p 12 N95-10245
Terminal Doppler Weather Radar Build 5A Operational Test and Evaluation (OT/E) integration and OT/E operational test plan
[AD-A283052] p 61 N95-12996
Aero-optics system integration
[TABES PAPER 94-604] p 100 N95-14638
FASTPACK: Optimized solutions for modular avionics derived from a parametric study. Part 1: Platform features p 233 N95-20634
Automation technology using Geographic Information System (GIS) p 324 N95-23284
Differential GPS and system integration of the Low Visibility Landing and Surface Operations (LVLASO) demonstration p 280 N95-23318
The process for addressing the challenges of aircraft pilot coupling p 597 N95-31063
Experimental Aircraft Programme (EAP): Flight control system design and test p 623 N95-32010
The application of helicopter mission simulation to Nap-of-the-Earth operations p 710 N95-32496
A helmet mounted display for night missions at low altitude p 693 N95-32503
PSC implementation and integration p 695 N95-33014
The DLR research programme on an integrated multi sensor system for surface movement guidance and control p 689 N95-33135
Application of advanced safety technique to ring laser gyro inertial navigation system integration p 689 N95-33140
Integrated special mission flight management for a flight inspection aircraft p 692 N95-33145
Gas chromatography/ion mobility spectrometry as a hyphenated technique for improved explosives detection and analysis p 701 N95-33278
- SYSTEMS SIMULATION**
Derivation of system matrices from nonlinear dynamic simulation of jet engines
[BTN-95-EIX95182619139] p 288 A95-76616
The role of simulations in 777 FSEU development
[AIAA PAPER 95-0995] p 506 A95-90665
Advanced distributed simulation technology advanced rotary wing aircraft. Strawman verification and validation plan for the ARWA simulator system
[AD-A280237] p 19 N95-10349
Advanced distributed simulation technology advanced rotary wing aircraft. System/segment specification. Volume 1: Simulation system module
[AD-A280238] p 20 N95-10350
Advanced distributed simulation technology advanced rotary wing aircraft. System/segment specification. Volume 3: Visual system module
[AD-A280239] p 20 N95-10351
Advanced distributed simulation technology advanced rotary wing aircraft. System/segment specification. Volume 2: Flight station module
[AD-A280432] p 20 N95-10352
Advanced distributed simulation technology advanced rotary wing aircraft. System/segment specification. Volume 5: Simulation system module AH-64D kit
[AD-A280433] p 20 N95-10353
Advanced distributed simulation technology advanced rotary wing aircraft. Software reusability report
[AD-A280434] p 20 N95-10354
Foundations of technology for constructing highly reliable distributed realtime systems
[AD-A293254] p 678 N95-30892
- SYSTEMS STABILITY**
Dynamical instability of the aerogravity assist maneuver
[BTN-95-EIX95152583282] p 298 A95-73583
Development of 70MW class superconducting generators
[BTN-94-EIX95011440854] p 429 A95-82905
Actuating signals in adaptive control systems
[IFTR-13/1994] p 361 N95-26330
- Application of optimization technique to control system design for departure prevention and aircraft model estimation through dynamic inversion p 517 N95-29156
Linear matrix inequalities for the problem of absolute stability of control systems p 518 N95-29680
- T**
- T-38 AIRCRAFT**
More supportable T-38A enhancement study
[AD-A283671] p 66 N95-15331
- T-53 ENGINE**
Assessment of overhaul surge margin tests applied to the T53 engines in ADF Iroquois helicopters
[AR-008-389] p 339 N95-25936
- T-55 ENGINE**
Chinook goes FADEC
[CONGRESS PAPER C428-33-078] p 610 A95-93621
- T-56 ENGINE**
Characteristics of the turbine inlet temperature sensing circuit for the T56 turbo-prop engine
[DSTO-TR-0095] p 405 N95-26424
Water model tests on the Allison T56 series 3 combustion system
[DSTO-TR-0139] p 697 N95-33250
- TABLES (DATA)**
Enplanement and all cargo activity
[AD-A280074] p 412 N95-28151
- TABS (CONTROL SURFACES)**
Aerodynamic characteristics of a canard-controlled missile at high angles of attack
[BTN-95-EIX95152583257] p 267 A95-73558
Lift-enhancing tabs on multielement airfoils
[BTN-95-EIX0619952748187] p 591 A95-94479
Axis switching and spreading of an asymmetric jet: Role of vorticity dynamics
[NASA-TM-106385] p 73 N95-14418
Lift enhancing tabs for airfoils
[NASA-CASE-ARC-11990-1] p 286 N95-23395
- TACHOMETERS**
Variations observed in the AC generator signal period of a Sea King helicopter
[AD-A284280] p 230 N95-19963
Solid-state data recorder, next development and use p 705 N95-33143
- TACTICS**
Tactical low-level helicopter communications p 702 N95-32492
A tactical navigation and routing system for low-level flight p 709 N95-32494
- TAIL ASSEMBLIES**
Sidewash on the vertical tail in subsonic and supersonic flows
[BTN-95-EIX95152582316] p 264 A95-73519
Directional control at high angles of attack using blowing through a chined forebody
[BTN-95-EIX0619952748179] p 619 A95-94472
Effect of leading-edge extension fences on the vortex wake of an F/A-18 model
[BTN-95-EIX0619952748192] p 591 A95-94481
Flow-visualization study of the X-29A aircraft at high angles of attack using a 1/48-scale model
[NASA-TM-104268] p 8 N95-10858
Pressure measurements on an F/A-18 twin vertical tail in buffeting flow. Volume 3: Buffet power spectral densities
[AD-A281444] p 36 N95-11829
Viper cabin-fuselage structural design concept with engine installation and wing structural design
[NASA-CR-197162] p 45 N95-12305
Experimental aerodynamic characteristics of a generic hypersonic accelerator configuration at Mach numbers 1.5 and 2.0 — conducted in the Langley Unitary Plan Wind Tunnel
[NASA-TM-4413] p 39 N95-12770
Fatigue evaluation of empennage, forward wing, and winglets/tip fins on part 23 airplanes
[PB94-196813] p 79 N95-13981
Pressure measurements on an F/A-18 twin vertical tail in buffeting flow. Volume 2: Steady and unsteady RMS pressure data
[AD-A281581] p 76 N95-15465
Single-engine tail interference model p 115 N95-17879
Twin engine afterbody model p 115 N95-17880
Pressure measurements on an F/A-18 twin vertical tail in buffeting flow. Volume 4, part 2: Buffet cross spectral densities
[AD-A285555] p 143 N95-18641
Pressure measurements on an F/A-18 twin vertical tail in buffeting flow. Volume 4, part 1: Buffet cross spectral densities
[AD-A285593] p 237 N95-21214
- Pressure measurements on an F/A-18 twin vertical tail in buffeting flow. Volume 1: Wind tunnel test summary
[AD-A279126] p 225 N95-21877
Preliminary identification of buffet problems in high speed civil transport p 294 N95-23319
F/A-18 IFOSTP Fatigue test airbag load determination on the vertical and horizontal tails
[DSTO-TR-0135] p 388 N95-26389
Numerical simulation of the SOFIA flow field
[NASA-CR-197757] p 436 N95-26589
Application of damage tolerance methodology in certification of the Piaggio P-180 Avanti p 399 N95-28480
Challenges and payoff of composites in transport aircraft: 777 empennage and future applications p 534 N95-29031
Low-speed wind-tunnel investigation of the stability and control characteristics of a series of flying wings with sweep angles of 50 deg
[NASA-TM-4640] p 505 N95-30226
Afterbody/nozzle pressure distributions of a twin-tail twin-engine fighter with axisymmetric nozzles at Mach numbers from 0.6 to 1.2
[NASA-TP-3509] p 594 N95-31984
- TAIL ROTORS**
Dynamic analysis of bearingless tail rotor blades based on nonlinear shell modes
[BTN-95-EIX95152582338] p 281 A95-73540
- TAIL SURFACES**
Effect of leading-edge extension fences on the vortex wake of an F/A-18 model
[BTN-95-EIX0619952748192] p 591 A95-94481
Pressure measurements on an F/A-18 twin vertical tail in buffeting flow. Volume 3: Buffet power spectral densities
[AD-A281444] p 36 N95-11829
Pressure measurements on an F/A-18 twin vertical tail in buffeting flow. Volume 2: Steady and unsteady RMS pressure data
[AD-A281581] p 76 N95-15465
Pressure measurements on an F/A-18 twin vertical tail in buffeting flow. Volume 4, part 1: Buffet cross spectral densities
[AD-A285593] p 237 N95-21214
Pressure measurements on an F/A-18 twin vertical tail in buffeting flow. Volume 1: Wind tunnel test summary
[AD-A279126] p 225 N95-21877
- TAILLESS AIRCRAFT**
Tailless aircraft design-recent experiences p 492 A95-88899
Design and construction of a remote piloted flying wing
[NASA-CR-197195] p 47 N95-12695
X-31 quasi-tailless flight demonstration p 70 N95-14243
- TAIWAN**
Diurnal variation of lee vortices in Taiwan and the surrounding area
[HTN-95-91363] p 318 A95-76394
- TAKEOFF**
Progress in high-lift aerodynamic calculations
[BTN-95-EIX95152582315] p 264 A95-73518
Effect of underwing frost on a transport aircraft airfoil at flight Reynolds number
[BTN-95-EIX95152582334] p 276 A95-73536
Factors affecting measured aircraft sound levels in the vicinity of start-of-takeoff roll p 571 A95-88465
An investigation of piloting strategies for engine failures during takeoff from offshore platforms
[HTN-95-92834] p 497 A95-90752
Determining the effects of alternative departure cutback altitudes and power settings: A case study, John Wayne Airport p 31 N95-11320
Flight investigation of the use of a nose gear jump strut to reduce takeoff ground roll distance of STOL aircraft
[NASA-TM-108819] p 44 N95-12225
The Elite: A high speed, low-cost general aviation aircraft for Aeroworld
[NASA-CR-197161] p 45 N95-12530
The Balsa bullet: A high speed, low-cost general aviation aircraft for Aeroworld
[NASA-CR-197165] p 46 N95-12638
Flight test of takeoff performance monitoring system
[NASA-TP-3403] p 51 N95-12664
Airplane takeoff and landing performance monitoring system
[NASA-CASE-LAR-14745-2-SB] p 85 N95-14415
STOVL CFD model test case p 115 N95-17881
Tilt Rotor Unmanned Air Vehicle System (TRUS) demonstrator flight test program
[AD-A284151] p 132 N95-18415
Aircraft wake vortex takeoff tests at O'Hara International Airport
[AD-A283828] p 118 N95-18624
F-15 resource tape
[NASA-TM-110502] p 230 N95-19994

Aircraft accident report. Runway overrun following rejected takeoff. Continental airlines flight 795, McDonnell Douglas MD-82, N18835, LaGuardia Airport, Flushing, NY, 2 March 1994 [PB95-910401] p 277 N95-23609
 Analysis and modeling of an airport departure process [AD-A293782] p 602 N95-31581
 An LDV investigation of support structure influence on the flow field near the wingtip of a STOVL configuration in hover [AD-A294126] p 686 N95-34750

TAKEOFF RUNS
 Flight investigation of the use of a nose gear jump strut to reduce takeoff ground roll distance of STOL aircraft [NASA-TM-108819] p 44 N95-12225

TANDEM WING AIRCRAFT
 CaRnard: A new roadable aircraft concept [SAE PAPER 932601] p 494 A95-90071

TANKER AIRCRAFT
 KC-135 cockpit modernization study. Phase 1: Equipment evaluation [AD-A284099] p 131 N95-18398

TAPERING
 The use of cowi camber and taper to reduce rotor/stator interaction noise [NASA-CR-195421] p 323 N95-22675
 Leading-edge suction distribution for plane thin wings at subsonic speeds [ESDU-94037] p 477 N95-28800

TARGET ACQUISITION
 Application of fuzzy logic to optimize placement of an acquisition, tracking, and pointing experiment p 341 A95-80390
 A mathematical analysis of the Janus combat simulation weather effects models and sensitivity analysis of sky-to-ground brightness ratio on target detection [AD-A289629] p 446 N95-26858
 Classification of ultra high range resolution radar using decision boundary analysis [AD-A289378] p 437 N95-26877
 Aircraft IR/acoustic detection evaluation. Volume 2: Development of a ground-based acoustic sensor system for the detection of subsonic jet-powered aircraft [NASA-CR-189705-VOL-2] p 452 N95-28073
 MATSurv multisensor air traffic surveillance [AD-A292253] p 489 N95-28887
 Offshore next generation weather radar (NEXRAD) test and evaluation master plan (TEMP) [AD-A291435] p 556 N95-30072
 Apparent size passive range method [AD-DO17360] p 611 N95-31180

TARGET DRONE AIRCRAFT
 SR-71 may launch targets for missile defense tests [HTN-95-91872] p 335 A95-81974
 On the flight control system for UF-104 p 507 A95-91560

TARGET RECOGNITION
 Ultra-wideband electromagnetic target identification p 486 A95-90955
 Classification of ultra high range resolution radar using decision boundary analysis [AD-A289378] p 437 N95-26877

TARGETS
 SEM representation of the early and late time fields scattered from wire targets [BTN-94-EIX94381353142] p 306 A95-74496
 Permanent magnet electron cyclotron resonance plasma source with remote window [BTN-95-EIX95242674338] p 450 A95-82176
 Scattering of short em-pulses by simple and complex targets using impulse radar p 486 A95-90953
 Advanced composites structural concepts and materials technologies for primary aircraft structures: Structural response and failure analysis [NASA-CR-4448] p 11 N95-10240
 Classification of ultra high range resolution radar using decision boundary analysis [AD-A289378] p 437 N95-26877
 Three-D weather displays for aircraft cockpits [AD-A289759] p 508 N95-28691
 Conceptual design of a map interactive system for military aircraft cockpits [AD-A289760] p 508 N95-28692

TASKS
 Conversion of the TRACON operations concepts database into a formal sentence outline job task taxonomy [DOT/FAA/AM-95/16] p 488 N95-28819
 Resource document for the design of electronic instrument approach procedure displays [AD-A295108] p 691 N95-34797

TAXIING
 Developments in airfield lighting [CONGRESS PAPER C428-7-147] p 488 A95-91688

The effects of display location and dimensionality on taxiway navigation [AD-A294878] p 690 N95-34570

TAXONOMY
 Conversion of the TRACON operations concepts database into a formal sentence outline job task taxonomy [DOT/FAA/AM-95/16] p 488 N95-28819

TAYLOR INSTABILITY
 Instability of three-dimensional boundary layers due to streamline curvature [HTN-95-61070] p 430 A95-83654

TDR SATELLITES
 Flight Mechanics/Estimation Theory Symposium 1995 [NASA-CP-3299] p 416 N95-27763

TECHNICAL WRITING
 ICASE [NASA-CR-195001] p 170 N95-16898

TECHNOLOGICAL FORECASTING
 Navigational technology of dual usage p 688 N95-33131
 Solid-state data recorder, next development and use p 705 N95-33143

TECHNOLOGIES
 International collaboration in hypersonic technologies - A specific and worthwhile initiative [AIAA PAPER 95-6140] p 581 A95-90457
 JPRS report: Science and technology. Central Eurasia [JPRS-UST-94-027] p 349 N95-24470
 JPRS report: Science and technology. Central Eurasia [JPRS-UST-94-018] p 349 N95-24472
 JPRS Report: Science and technology. Central Eurasia [JPRS-UST-94-032] p 350 N95-24759
 FBIS report: Science and technology. Central Eurasia [FBIS-UST-95-029] p 649 N95-31728

TECHNOLOGY ASSESSMENT
 Applying nanostructured materials to future gas turbine engines [HTN-95-11909] p 404 A95-85990
 Hypersonic technology experimental vehicles (The need for flight testing at hypersonic speed) p 490 A95-87378
 Auxiliary Power Unit evolution: Meeting tomorrow's challenges [SAE PAPER 932541] p 510 A95-89195
 Aeronautical technology - recent advances and future prospects [HTN-95-01097] p 496 A95-90283
 Secondary power system study for the hytex RA3 flight test vehicle [AIAA PAPER 95-6158] p 512 A95-90470
 Report to the aerospace profession; SETP Symposium, 37th, Beverly Hills, CA, USA, September 1993 [HTN-95-12142] p 497 A95-90866
 Assessment of Russian VSTOL technology evaluating the YAK-38 'FORGER' and YAK-141 'FREESTYLE' p 497 A95-90868
 Assessment of technology for aircraft development [BTN-95-EIX0619952748181] p 606 A95-94474
 Impact of agility requirements on configuration synthesis [NASA-CR-4627] p 44 N95-11952
 Reliability assessment of Multichip Module technologies via the Triservice/NASA RELTECH program p 245 N95-20643
 High density monolithic packaging technology for digital/microwave avionics p 240 N95-20646
 Euler Technology Assessment program for preliminary aircraft design employing SPLITFLOW code with Cartesian unstructured grid method [NASA-CR-4649] p 273 N95-22917
 Euler technology assessment for preliminary aircraft design employing OVERFLOW code with multiblock structured-grid method [NASA-CR-4651] p 273 N95-23095
 Motor drive technologies for the power-by-wire (PBW) program: Options, trends and tradeoffs [NASA-TM-106885] p 295 N95-23671
 Report to the Secretary of Defense. Unmanned aerial vehicles: No more Hunter systems should be bought until problems are fixed [GAO/NSIAD-95-52] p 286 N95-24091
 Assessment of avionics technology in European aerospace organizations [NASA-CR-189201] p 337 N95-24624
 Wind technology development: Large and small turbines [DE95-000286] p 358 N95-26090
 Asian Aeronautics: Technology acquisition drives industry development. Report to Congressional requesters [GAO/NSIAD-94-140] p 367 N95-26817

A review of falconry as a bird control technique with recommendations for use at the Shuttle Landing Facility, John F. Kennedy Space Center, Florida, USA [NASA-TM-110142] p 381 N95-27859
 Propulsion system assessment for very high UAV under ERAST [NASA-CR-195469] p 406 N95-27866
 High-stakes aviation: US-Japan technology linkages in transport aircraft [LC-94-65759] p 381 N95-27907
 JTEC/WTEC annual report and program summary: 1993/94 [NASA-CR-198563] p 454 N95-28038
 Navy composite maintenance and repair experience p 629 N95-28446
 Composite fuselage crown panel manufacturing technology p 399 N95-28474
 Requirements for effective use of CFD in aerospace design p 551 N95-28725
 Block-structured grids for complex aerodynamic configurations: Current status p 551 N95-28736
 Unmanned Aerial Vehicle technology [DSTO-GD-0044] p 503 N95-29362
 The relation of handling qualities ratings to aircraft safety p 597 N95-10667
 Workshop report: Measurement techniques in highly transient, spectrally rich combustion environments p 629 N95-31208
 Active control technology: Applications and lessons learned [AGARD-CP-560] p 620 N95-31989
 Effects of the specific military aspects of satellite navigation on the civil use of GPS/GLONASS p 688 N95-33134
 HeliRadar: A rotating antenna synthetic aperture radar for helicopter allweather operations p 705 N95-33137

TECHNOLOGY TRANSFER
 Commercial applications for military laser radars p 543 A95-87794
 Research and technology highlights, 1993 [NASA-TM-4575] p 102 N95-15065
 Technology reinvestment project's focus area: Affordable polymer matrix composites for airframe structures [PB95-136032] p 324 N95-23168
 Research and Technology, 1994 [NASA-TM-106764] p 262 N95-24025
 High-stakes aviation: US-Japan technology linkages in transport aircraft [LC-94-65759] p 381 N95-27907
 Collected papers on wind turbine technology [NASA-CR-195432] p 447 N95-27970
 Navigational technology of dual usage p 688 N95-33131
 Effects of the specific military aspects of satellite navigation on the civil use of GPS/GLONASS p 688 N95-33134
 Advanced data visualization and sensor fusion: Conversion of techniques from medical imaging to Earth science p 711 N95-34236

TECHNOLOGY UTILIZATION
 ATE enabling technologies [BTN-95-EIX95172595294] p 287 A95-75718
 Technology-insertion life-cycle-cost model [AIAA PAPER 95-0961] p 581 A95-90638
 General Aviation Task Force report [NASA-TM-109950] p 1 N95-11463
 Program test objectives milestone 3 - Integrated Propulsion Technology Demonstrator [NASA-CR-197030] p 127 N95-15971
 Revitalizing general aviation [NASA-TM-110113] p 129 N95-16982
 Independent review of Aviation Technology and Research Information Analysis System (ATRIAS) database [AD-A284049] p 226 N95-21518
 Technology reinvestment project's focus area: Affordable polymer matrix composites for airframe structures [PB95-136032] p 324 N95-23168
 Aviation system capacity improvements through technology [NASA-TM-109165] p 333 N95-24633
 Integrated mission precision attack cockpit technology (IMPACT). Phase 1: Identifying technologies for air-to-ground fighter integration [AD-A289562] p 389 N95-26684
 Utilization of composite materials by the US Army: A look ahead p 421 N95-28421
 Requirements for effective use of CFD in aerospace design p 551 N95-28725
 Unmanned Aerial Vehicle technology [DSTO-GD-0044] p 503 N95-29362
 Structural aspects of active control technology p 623 N95-32006

- Expert systems and artificial intelligence applications in engineering design and inspection p 710 N95-33008
 Navigational technology of dual usage p 688 N95-33131
 The DLR research programme on an integrated multi sensor system for surface movement guidance and control p 689 N95-33135
 Solid-state data recorder, next development and use p 705 N95-33143

TELECOMMUNICATION

- Experimental study of the helicopter-mobile radioelectrical channel and possible extension to the satellite-mobile channel p 247 N95-20945

TELEMETRY

- Evolutionary Telemetry and Command Processor (TCP) architecture p 86 N95-14162
 Packet utilisation definitions for the ESA XMM mission p 150 N95-17596

TELEOPERATORS

- Telepresence media resource tape (NASA-TM-110648) p 569 N95-30248

TELEROBOTICS

- Guidance and control, 1993; Annual Rocky Mountain Guidance and Control Conference, 16th, Keystone, CO, Feb. 6-10, 1993 p 341 A95-80389
 [ISBN-0-87703-365-X]
 A generic telerobotics architecture for C-5 industrial processes [AIAA PAPER 94-1264-CP] p 27 N95-11529
 Overview of NASREM: The NASA/NBS standard reference model for telerobot control system architecture [PB94-194560] p 58 N95-12854
 Survey and implementation of commercial manual controllers for a generic telerobotics architecture [AD-A289215] p 449 N95-26990

TELESCOPES

- Numerical simulation of the SOFIA flow field [NASA-CR-197757] p 436 N95-26589

TEMPERATE REGIONS

- In situ observations in aircraft exhaust plumes in the lower stratosphere at midlatitudes [HTN-95-A0862] p 318 A95-76266

TEMPERATURE

- Controlling mechanisms of ignition of solid fuel in a sudden-expansion combustor [BTN-95-EIX0616952745791] p 628 A95-94255

TEMPERATURE CONTROL

- A low fin height heat exchanger technology demonstrator for Hermes [SAE PAPER 932119] p 526 A95-90360
 Integrated aircraft thermal management and power generation [SAE PAPER 932055] p 500 A95-91636
 High heat sink fuels for improved aircraft thermal management [SAE PAPER 932084] p 530 A95-91659
 Concepts for aircraft subsystem integration [SAE PAPER 931377] p 604 A95-93656
 A subsystem integration technology concept [SAE PAPER 931382] p 604 A95-93658
 A programmable heater control circuit for spacecraft [NASA-TM-108459] p 9 N95-11157
 Transport phenomena in stratified multi-fluid flow in the presence and absence of gravity p 95 N95-14563
 An engineering code to analyze hypersonic thermal management systems p 155 N95-16322
 Liquid flow-through cooling of electronic modules p 246 N95-20647
 Characteristics of the turbine inlet temperature sensing circuit for the T56 turbo-prop engine [DSTO-TR-0095] p 405 N95-26424
 CAE for thermal management of aerospace electronic boards using the BETAsoft program p 438 N95-27354
 Minimum fan turbine inlet temperature mode evaluation p 696 N95-33016
 Thermal design of returnable satellites [AD-A294113] p 701 N95-34500

TEMPERATURE DEPENDENCE

- A model for temperature-dependent collisional quenching of OH A(sup 2) Sigma(sup +) [HTN-95-42308] p 450 A95-85002
 Computer code for determination of thermally perfect gas properties [NASA-TP-3447] p 37 N95-11995

TEMPERATURE DISTRIBUTION

- Convection heat transfer distributions over plates with square ribs from infrared thermography measurements [HTN-95-20713] p 435 A95-86603
 Effect of surface roughness on local film cooling effectiveness and heat transfer coefficients [AD-A283854] p 91 N95-14351
 Simulation of multidisciplinary problems for the thermostress state of cooled high temperature turbines p 140 N95-19021

- Verification of multidisciplinary models for turbomachines p 140 N95-19025
 Effects of elevated free-stream turbulence and streamwise acceleration on flow and thermal structures in transitional boundary layers p 556 N95-29729
 Effect of velocity and temperature distribution at the hole exit on film cooling of turbine blades [NASA-TM-106954] p 616 N95-30702

TEMPERATURE EFFECTS

- Theoretical and actual performance of a long duration superpressure balloon made from a biaxially oriented nylon-6 film p 181 A95-66282
 Influence of injectant Mach number and temperature on supersonic film cooling [BTN-94-EIX94441386686] p 184 A95-68195
 Prediction of supersonic inlet unstart caused by freestream disturbances [BTN-95-EIX95222650790] p 329 A95-79246
 Similarity rule for jet-temperature effects on transonic base pressure [BTN-95-EIX95222650791] p 329 A95-79247
 The dynamic nature of rotor thermal bending due to unsteady lubricant shearing within a bearing [HTN-95-42091] p 430 A95-83857
 Pressure and temperature distortion testing of a two-stage centrifugal compressor [BTN-94-EIX95011441250] p 431 A95-84207
 Advanced Turbine Technology Applications Project (ATTAP) [NASA-CR-195393] p 101 N95-15743
 Static and dynamic friction behavior of candidate high temperature airframe seal materials [NASA-TM-106571] p 152 N95-16905
 An investigation of drag repeatability in half model testing in the ARA Transonic Wind Tunnel [ARA-MEMO-392] p 188 N95-19546
 Investigation of a thermal buoyancy effect on the drag of half models tested in the ARA Transonic Wind Tunnel [ARA-MEMO-407] p 222 N95-19946
 Temperature effects on acoustic interactions between altitude test facilities and jet engine plumes [NASA-CR-197638] p 258 N95-21170
 Effect of atmospheric pressure on measured aircraft noise levels [PB95-130423] p 232 N95-21425
 Effects of cavity dimensions, boundary layer, and temperature on cavity noise with emphasis on benchmark data to validate computational aeroacoustic codes [NASA-CR-4653] p 361 N95-24879
 The noise reduction potential of dual-stream coaxial rectangular improperly expanded jet flows [NASA-CR-197820] p 437 N95-26995
 Probabilistic material strength degradation model for Inconel 718 components subjected to high temperature, high-cycle and low-cycle mechanical fatigue, creep and thermal fatigue effects [NASA-CR-197832] p 419 N95-27167
 Bonded composite repair of thin metallic materials: Variable load amplitude and temperature cycling effects p 393 N95-27509
 Repair of high temperature composite aircraft structure p 395 N95-27520
 Scarf joint technique with cocured and precured patches for composite repair p 396 N95-27524
 Recirculating cavity casing treatment failure [AD-A289330] p 513 N95-28908
 Development of LaRC (TM): IA thermoplastic polyimide coated aerospace wiring [NASA-CR-195048] p 537 N95-30252

TEMPERATURE GRADIENTS

- Marangoni-Benard convection in a low-aspect-ratio liquid layer p 56 A95-61544

TEMPERATURE INVERSIONS

- Criteria of forecasting low level wind shear over Qatar p 663 A95-93493

TEMPERATURE MEASUREMENT

- Comparison of NO and OH planar fluorescence temperature measurements in scramjet model flowfields [BTN-95-EIX95042474388] p 209 A95-68312
 Measurement by coherent anti-Stokes Raman scattering in the R5Ch hypersonic wind tunnel [BTN-95-EIX95112523811] p 188 A95-69322
 Time-resolved surface heat flux measurements in the wing/body junction vortex [BTN-95-EIX95082502716] p 220 A95-71029
 Constant flux, turbulent convection data using infrared imaging [HTN-95-20731] p 435 A95-86621
 Temperature diagnostics in the hypersonic flow regime: An application to develop a stagnation temperature probe [AIAA PAPER 95-6114] p 511 A95-90442
 Airborne imaging radiometer scan simulation [BTN-95-EIX95332753018] p 638 A95-94793

- Measurements of pressure and thermal wakes in a transonic turbine cascade [AD-A283464] p 38 N95-12548
 Turbine-engine applications of thermographic-phosphor temperature measurements [DE95-003625] p 358 N95-25110
 Characteristics of the turbine inlet temperature sensing circuit for the T56 turbo-prop engine [DSTO-TR-0095] p 405 N95-26424
 Fabry-Perot interferometer measurement of static temperature and velocity for ASTOVL model tests [NASA-TM-107014] p 645 N95-30587

TEMPERATURE MEASURING INSTRUMENTS

- Micro-time stress measurement device development [AD-A289511] p 448 N95-26845

TEMPERATURE PROBES

- Temperature diagnostics in the hypersonic flow regime: An application to develop a stagnation temperature probe [AIAA PAPER 95-6114] p 511 A95-90442
 Hypersonic flow-field measurements: Intrusive and nonintrusive [AD-A283867] p 119 N95-18674

TEMPERATURE PROFILES

- Evaluation of the Sparton tight-tolerance AXBT [HTN-95-40728] p 251 A95-70473
 Contribution of thermal radiation to the temperature profile of ceramic composite materials [BTN-94-EIX95011441252] p 417 A95-84209
 Stratus' tephigram as a training/forecasting tool p 657 A95-93465

- The improvement of meteorological data for air traffic management purposes p 668 A95-93518
 Creating a global climatology of freezing rain using numerical model output p 673 A95-93541
 Transport phenomena in stratified multi-fluid flow in the presence and absence of gravity p 95 N95-14563

TEMPERATURE SENSORS

- New sensor technology for aircraft hydraulic system diagnostics [SAE PAPER 932586] p 494 A95-90070
 Characteristics of the turbine inlet temperature sensing circuit for the T56 turbo-prop engine [DSTO-TR-0095] p 405 N95-26424

TEMPORAL DISTRIBUTION

- Use of pilot reports for verification of aircraft icing diagnoses and forecasts p 666 A95-93508
 Modeling spatio-temporal databases to measure the performance of the GPS satellite constellation p 489 N95-29596

TENNESSEE

- MEMFOG - The Memphis fog algorithm p 668 A95-93516

TENSILE CREEP

- Evolution of oxidation and creep damage mechanisms in HIPed silicon nitride materials [DE95-001360] p 300 N95-22689

TENSILE PROPERTIES

- Tension fracture of laminates for transport fuselage. Part 1: Material screening p 398 N95-28471

TENSILE STRENGTH

- Review of some results of the author's fatigue investigations with applications in engineering and material science [TAE-698] p 316 N95-23662
 Study on tensile fatigue testing method of unidirectional fiber-resin matrix composites [NAL-TR-1241] p 343 N95-24989
 Status of bonded boron/epoxy doublers for military and commercial aircraft structures p 393 N95-27506
 The effects of aircraft fuel and fluids on the strength properties of Resin Transfer Molded (RTM) composites p 536 N95-29047

TENSILE STRESS

- Fatigue crack growth in 2024-T3 aluminum under tensile and transverse shear stresses p 153 N95-19490
 Composite repair issues on the CF-18 aircraft p 395 N95-27518

TENSILE TESTS

- Soft body impact on titanium fan blades p 200 N95-19671
 On aircraft repair verification of a fighter A/C integrally stiffened fuselage skin p 394 N95-27515
 Design, analysis, and fabrication of a pressure box test fixture for tension damage tolerance testing of curved fuselage panels p 533 N95-28839

TENSOR ANALYSIS

- Single-pass method for the solution of inverse potential and rotational problems. Part 1: 2-D and quasi 3-D theory and application p 107 N95-16563

TEPHIGRAMS

- Stratus' tephigram as a training/forecasting tool p 657 A95-93465

TERCOM

Simulation development of a forward sensor-enhanced low-altitude guidance system
[HTN-94-00688] p 17 A95-60170

TERMINAL FACILITIES

Arrival traffic handling for a parallel runway airport
p 487 A95-91537
Status of the terminal Doppler weather radar with deployment underway
p 653 A95-93450
TDWR scan strategy implementation
[AD-A284877] p 98 N95-15749
The ATC operational evaluation of the prototype integrated terminal weather system (ITWS) at Dallas/Fort Worth and Orlando airports (May-September 1993)
[AD-A293808] p 677 N95-31587

TERMINAL GUIDANCE

Nonlinear observer and its application in flight control
p 447 A95-82449

TERRAIN

Partial camera automation in a simulated Unmanned Air Vehicle
[AD-A288786] p 337 N95-26190
Synthetic Terrain Imagery for Helmet-Mounted Display. Volume 2: Software design document
[AD-A293611] p 612 N95-31655
Synthetic Terrain Imagery for Helmet-Mounted Display, volume 1
[AD-A293612] p 612 N95-31656
Perceptual dimensions of simulated scenes relevant for visual low-altitude flight
[AD-A294385] p 700 N95-34344
Altitude cuing effectiveness of terrain texture characteristics in simulated low-altitude flight
[AD-A294369] p 700 N95-34362

TERRAIN FOLLOWING

Part-task simulator evaluations of advanced terrain displays
[SAE PAPER 932570] p 401 A95-84567
Flight test of a low-altitude helicopter guidance system with obstacle avoidance capability
p 688 N95-32490
A tactical navigation and routing system for low-level flight
p 709 N95-32494
A highly reliable, high performance open avionics architecture for real time Nap-of-the-Earth operations
p 693 N95-32497

TEST CHAMBERS

Oblique incidence sound absorption of porous materials covered by perforated metal and exposed to tangential airflow
[HTN-94-00681] p 19 A95-60165
Study on a scheme for the prolongation of microgravity time of balloon-borne drop capsule
p 414 A95-82515
Characterization of annular two-phase gas-liquid flows in microgravity
p 95 N95-14556
High-temperature acoustic test facilities and methods
p 174 N95-19149
Development of pneumatic test techniques for subsonic high-lift and in-ground-effect wind tunnel investigations
p 121 N95-19268
Unsteady flow testing in a passive low-correction wind tunnel
p 147 N95-19272
16-foot transonic tunnel test section flowfield survey
[NASA-TM-109157] p 238 N95-20669
Design of a variable area diffuser for a 15-inch Mach 6 open-jet tunnel
p 297 N95-23309
NASA Lewis Research Center's combustor test facilities and capabilities
[NASA-TM-106903] p 412 N95-27176
Two-phase flow research using the learjet apparatus
[NASA-TM-106814] p 438 N95-27854
NASA Dryden flow visualization facility
[NASA-TM-4631] p 449 N95-27914

TEST EQUIPMENT

Computer aided diagnostic testing of installed flight control servo-actuators
[SAE PAPER 932584] p 494 A95-90068
NASA Lewis Propulsion Systems Laboratory test article systems criteria
[NASA-TM-106589] p 20 N95-10446
Small crack test program for helicopter materials
p 92 N95-14455

TEST FACILITIES

Labs behind Boeing's new 777
[BTN-95-EIX95142562403] p 280 A95-73437
The NASA-sponsored Maryland center for hypersonic education and research
[AIAA PAPER 95-6105] p 519 A95-88010
Chemical recombination in an expansion tube
[HTN-95-20844] p 544 A95-88105
Design and operation of a supersonic annular flow facility
[HTN-95-20941] p 465 A95-88980
Plaster damage experiments at the BBN Sonic Boom Test Facility
p 529 A95-90120

A large hemi-anechoic enclosure for community-compatible aeroacoustic testing of aircraft propulsion systems
p 577 A95-90132
The NASA/UTA Center for hypersonic research
[AIAA PAPER 95-6106] p 520 A95-90438
Research and educational initiatives at the Syracuse University Center for Hypersonics
[AIAA PAPER 95-6107] p 520 A95-90439
Hypersonic aerodynamics test facility using the external propulsion accelerator
[AIAA PAPER 95-6138] p 470 A95-90455
An assessment of ground-test facility capabilities for measurement of hypervelocity scramjet performance
[AIAA PAPER 95-6148] p 512 A95-90462
The panel oxidation and erosion test (POET) facility
[AIAA PAPER 95-6151] p 521 A95-90465
Universal electrohydraulic system for the steering gear loading
[CONGRESS PAPER C428-10-106] p 517 A95-91700

Building the Integrated Test Facility: A foundation for the future
[NASA-TM-104280] p 21 N95-10738
The Western Aeronautical Test Range
[NASA-TM-104301] p 21 N95-10746
NASA Lewis Propulsion Systems Laboratory customer guide manual
[NASA-TM-106569] p 21 N95-10822
Inlet flow test calibration for a small axial compressor facility. Part 1: Design and experimental results
[NASA-TM-106719] p 16 N95-11005
Hypersonic Gas-Surface Energy Accommodation Test Facility
[DE94-014468] p 39 N95-12652
High-speed seal and bearing test facility
p 53 N95-13601
Hypervelocity Impact Test Facility: A gun for hire
[TABES PAPER 94-605] p 86 N95-14639
Experimental and analytical methods for the determination of connected-pipe ramjet and ducted rocket internal performance
[AGARD-AR-323] p 149 N95-17278
Strategic avionics technology definition studies. Subtask 3-1A3: Electrical Actuation (ELA) Systems Test Facility
[NASA-CR-188360] p 143 N95-18567
High-temperature acoustic test facilities and methods
p 174 N95-19149
Development of pneumatic test techniques for subsonic high-lift and in-ground-effect wind tunnel investigations
p 121 N95-19268
Operating capability and current status of the reactivated NASA Lewis Research Center Hypersonic Tunnel Facility
[NASA-TM-106808] p 148 N95-19286
Description and flow characterization of hypersonic facilities
[AD-A284291] p 223 N95-20248
Portable static test facility for small, expendable, turbojet engines, phase 1
[AD-A286337] p 239 N95-21719
NASA low-speed axial compressor for fundamental research
[NASA-TM-4635] p 296 N95-23192
System identification of the Large-Angle Magnetic Suspension Test Fixture (LAMSTF)
p 296 N95-23299
The Superorbital Expansion Tube concept, experiment and analysis
p 341 N95-25399
Stall precursor study of high frequency data for three high speed, swept compressor rotors
[AD-A289379] p 406 N95-26878
NASA Lewis Research Center's combustor test facilities and capabilities
[NASA-TM-106903] p 412 N95-27176
NASA Lewis Research Center's preheated combustor and materials test facility
[NASA-TM-106676] p 626 N95-30592
Icing simulation in the aeropropulsion systems test facility propulsion development test cell C-2
[AD-A293039] p 599 N95-31667

TEST FIRING

Program test objectives milestone 3 --- Integrated Propulsion Technology Demonstrator
[NASA-CR-197030] p 127 N95-15971

TEST PILOTS

Pilot rating scale for aircraft handling qualities
[HTN-95-42269] p 380 A95-84963
Preliminary evaluation of the F/A-18 quantity/multiple envelope expansion
[AD-A284119] p 132 N95-18407
Helicopter in-flight simulation development and use in test pilot training
[AD-A283998] p 146 N95-18725
T-45A High Angle of Attack Testing: US Naval Test Pilot School 46th Annual Reunion and Symposium
[AD-A284000] p 231 N95-20466

TEST RANGES

The Western Aeronautical Test Range
[NASA-TM-104301] p 21 N95-10746
X-31 tailless testing
[NASA-TM-104306] p 13 N95-10751

TEST STANDS

Determination of minimum fuel octane number piston aircraft engines
[SAE PAPER 931230] p 528 A95-88961
Oscillating-flow regenerator test rig
[NASA-CR-196982] p 53 N95-13200
NASA High Performance Computing and Communications program
[NASA-TM-4653] p 176 N95-18573
Design and development of a test rig for the high frequency testing of rolling sleeve airsprings
[DSTO-TN-0001] p 411 N95-26378
Inlet flow test calibration for a small axial compressor rig. Part 2: CFD compared with experimental results
[NASA-TM-106999] p 514 N95-30007
NASA Lewis Research Center's preheated combustor and materials test facility
[NASA-TM-106676] p 626 N95-30592

TESTING TIME

Computer model to simulate testing at the National Transonic Facility
[NASA-TM-4664] p 627 N95-32217

TETHERED BALLOONS

CALLOPE and TAISIR airborne experiment platform
[DE94-018328] p 250 N95-22299

TETHERED SATELLITES

Dynamics and control of a tethered flight vehicle
[BTN-95-EIX95242670754] p 342 A95-81093

TETHERING

Dynamics and control of a tethered flight vehicle
[BTN-95-EIX95242670754] p 342 A95-81093

TETRAHEDRONS

Mesh generation and adaptivity for the solution of compressible viscous high speed flows
[BTN-95-EIX95262697157] p 538 A95-86893
Mesh quality control for multiply-refined tetrahedral grids
[NASA-CR-197595] p 160 N95-18737
An assessment of the adaptive unstructured tetrahedral grid, Euler Flow Solver Code FELISA
[NASA-TP-3526] p 119 N95-19041

TEXAS

The NASA/UTA Center for hypersonic research
[AIAA PAPER 95-6106] p 520 A95-90438

TEXTILES

Development and verification of a resin film infusion/resin transfer molding simulation model for fabrication of advanced textile composites
[NASA-CR-197439] p 301 N95-23179
Recent progress in NASA Langley textile reinforced composites program
p 425 N95-28475
Advanced textile applications for primary aircraft structures
p 399 N95-28476
Third NASA Advanced Composites Technology Conference, volume 1, part 2
[NASA-CP-3178-VOL-1-PT-2] p 531 N95-28823
Novel cost controlled materials and processing for primary structures
p 532 N95-28830
Textile composite fuselage structures development
p 534 N95-29033
Advanced resin systems and 3D textile preforms for low cost composite structures
p 535 N95-29035
Performance of resin transfer molded multiaxial warp knit composites
p 535 N95-29039
Cross-stiffened continuous fiber structures
p 536 N95-29041
Cost model relationships between textile manufacturing processes and design details for transport fuselage elements
p 536 N95-29043

TEXTS

The controller memory guide. Concepts from the field
[AD-A289263] p 383 N95-26978

TEXTURES

Perceptual dimensions of simulated scenes relevant for visual low-altitude flight
[AD-A294385] p 700 N95-34344
Altitude cuing effectiveness of terrain texture characteristics in simulated low-altitude flight
[AD-A294369] p 700 N95-34362

THEMATIC MAPPING

AVIRIS and TIMS data processing and distribution at the land processes distributed active archive center
p 325 N95-23872

THEODORSEN TRANSFORMATION

Flutter analysis of composite box beams
[NASA-CR-197931] p 294 N95-23392

THEORIES

Horizontal axis wind turbine post stall airfoil characteristics synthesisization
p 376 N95-27974

THERMAL ANALYSIS

- Multiblock analysis for Shuttle Orbiter reentry heating from Mach 24 to Mach 12
[BTN-95-EIX95041503780] p 205 A95-69211
- Trajectory-based heating analysis for the European Space Agency/Rosetta Earth Return Vehicle
[BTN-95-EIX95041503787] p 205 A95-69218
- Effect of curvature in the numerical simulation of an electrothermal de-icer pad
[BTN-95-EIX95182619219] p 276 A95-76645
- Experiment and analysis on heat transfer of a scramjet leading edge model
p 403 A95-82420
- Integrated Thermal Energy Management (I-TEM): An evaluation tool for aircraft
[SAE PAPER 932577] p 493 A95-90065
- Radiant energy measurements from a scaled jet engine axisymmetric exhaust nozzle for a baseline code validation case
[NASA-TM-106686] p 25 N95-11409
- Investigation of advanced counterrotation blade configuration concepts for high speed turbo-prop systems. Task 8: Cooling flow/heat transfer analysis
[NASA-CR-195359] p 50 N95-11901
- Investigation of advanced counterrotation blade configuration concepts for high speed turbo-prop systems. Task 8: Cooling flow/heat transfer analysis user's manual
[NASA-CR-195360] p 50 N95-11951
- AFOSR Contractors Meeting in Propulsion
[AD-A282729] p 54 N95-12507
- Development of a composite repair and the associated inspection intervals for the F-111C stiffener runout region
p 66 N95-14477
- Thermo-acoustic fatigue design for hypersonic vehicle skin panels
p 162 N95-19161
- Technology Benefit Estimator (T/BEST): User's manual
[NASA-TM-106785] p 167 N95-19501
- Lubricant evaluation and performance, 2
[AD-A279144] p 242 N95-21969
- Thermohydrodynamic analysis of cryogenic liquid turbulent flow fluid film bearings, phase 2
[NASA-CR-197412] p 349 N95-24461
- CAE for thermal management of aerospace electronic boards using the BETAsoft program
p 438 N95-27354
- An analysis of B-1B exterior jet blast windshield anti-icing performance using pre-cooled compressor bleed air
[AD-A292522] p 485 N95-28811
- Intelligent finite element submodeling of multichip modules for reliability analysis
[AD-A292911] p 679 N95-31455
- THERMAL BOUNDARY LAYER**
- Prediction of ice accretion: Comparison between the 2D and 3D codes
[BTN-94-EIX94441385753] p 213 A95-68217
- Effects of elevated free-stream turbulence and streamwise acceleration on flow and thermal structures in transitional boundary layers
p 556 N95-29729
- THERMAL CONDUCTIVITY**
- Evaluation of the Spartan tight-tolerance AXBT
[HTN-95-40728] p 251 A95-70473
- Quality optimization of thermally sprayed coatings produced by the JP-5000 (HVOF) gun using mathematical modeling
p 152 N95-19008
- Thermal conductivity of zirconia thermal barrier coatings
p 345 N95-26133
- THERMAL CONTROL COATINGS**
- Study on the turbine vane and blade for a 1500 C class industrial gas turbine
[BTN-94-EIX95011441254] p 431 A95-84211
- Quality optimization of thermally sprayed coatings produced by the JP-5000 (HVOF) gun using mathematical modeling
p 152 N95-19008
- Thermal testing of high performance thermal barrier coatings for turbine blades
p 202 N95-19681
- Evaluation of thermal barrier and PS-200 self-lubricating coatings in an air-cooled rotary engine
[NASA-CR-195445] p 289 N95-23222
- Thermal Barrier Coating Workshop
[NASA-CP-10170] p 344 N95-26119
- A design perspective on thermal barrier coatings
p 344 N95-26120
- Thermal barrier coatings for aircraft engines: History and directions
p 344 N95-26121
- Thermal barrier coatings issues in advanced land-based gas turbines
p 344 N95-26122
- Measurement methods and standards for processing and application of thermal barrier coatings
p 344 N95-26123
- Thermal barrier coatings application in diesel engines
p 345 N95-26124
- Thermal barrier coating experience in the gas turbine engine
p 345 N95-26125
- PVD TBC experience on GE aircraft engines
p 345 N95-26126

- Perspective on thermal barrier coatings for industrial gas turbine applications
p 345 N95-26128
- Thermal conductivity of zirconia thermal barrier coatings
p 345 N95-26133
- Thermal fracture mechanisms in ceramic thermal barrier coatings
p 346 N95-26138
- Thermal barrier coating life modeling in aircraft gas turbine engines
p 346 N95-26140
- THERMAL CYCLING TESTS**
- Fatigue strength of high-temperature alloys under conditions of cyclic temperature variation. Communication 1: Experimental procedure and results
[BTN-94-EIX94401363884] p 307 A95-75516
- High temperature strain gage technology for gas turbine engines
[NASA-CR-191177] p 57 N95-11996
- Composite repair of metallic airframe: Twenty years of experience
p 393 N95-27508
- Bonded composite repair of thin metallic materials: Variable load amplitude and temperature cycling effects
p 393 N95-27509
- Recirculating cavity casing treatment failure
[AD-A289330] p 513 N95-28908
- THERMAL DIFFUSION**
- Aerodynamic applications of underexpanded hypersonic viscous jets
[BTN-95-EIX0619952748162] p 589 A95-94456
- THERMAL EMISSION**
- AVIRIS and TIMS data processing and distribution at the land processes distributed active archive center
p 325 N95-23872
- Thermal design of returnable satellites
[AD-A294113] p 701 N95-34500
- THERMAL ENERGY**
- Integrated Thermal Energy Management (I-TEM): An evaluation tool for aircraft
[SAE PAPER 932577] p 493 A95-90065
- THERMAL ENVIRONMENTS**
- Thermal force modeling for global positioning system satellites using the finite element method
[BTN-95-EIX95152583270] p 278 A95-73571
- Hypersonic wind tunnel test techniques
[AD-A284057] p 118 N95-18663
- MCMs for avionics: Technology selection and intermodule interconnection
p 234 N95-20641
- A hybrid electronically scanned pressure module for cryogenic environments
[NASA-TM-110146] p 554 N95-29453
- THERMAL FATIGUE**
- Fatigue strength of high-temperature alloys under conditions of cyclic temperature variation. Communication 1: Experimental procedure and results
[BTN-94-EIX94401363884] p 307 A95-75516
- Thermal testing of high performance thermal barrier coatings for turbine blades
p 202 N95-19681
- Probabilistic material strength degradation model for Inconel 718 components subjected to high temperature, high-cycle and low-cycle mechanical fatigue, creep and thermal fatigue effects
[NASA-CR-197832] p 419 N95-27167
- Thermal-mechanical fatigue crack growth in aircraft engine materials
[ISBN-0-315-86543-1] p 647 N95-31098
- THERMAL INSULATION**
- Review of numerical procedures for computational surface thermochemistry
[BTN-94-EIX94441386682] p 205 A95-68191
- Design and evaluation of candidate pressure ports for the HYFLITE experiment
[NASA-TM-109146] p 22 N95-11003
- Thermal chemical energy of ablating silica surfaces in air breathing solid rocket engines
p 148 N95-16316
- Thermal barrier coating experience in the gas turbine engine
p 345 N95-26125
- THERMAL MAPPING**
- Mapping hidden aircraft defects with dual-band infrared computed tomography
[DE95-011531] p 584 N95-32164
- THERMAL PROTECTION**
- Minimum-mass design of sandwich aerobrakes for a lunar transfer vehicle
[BTN-95-EIX95212645707] p 299 A95-76759
- Research and development of thermal protection system of HOPE re-entry vehicle
p 413 A95-82358
- Hypersonic thermal protection with mass injection at angle of attack
p 414 A95-82414
- High temperature aspects of the European Hermes programs
p 524 A95-87379
- Ablative thermal management structural material on the hypersonic vehicles
[AIAA PAPER 95-6133] p 547 A95-90452
- Design and evaluation of candidate pressure ports for the HYFLITE experiment
[NASA-TM-109146] p 22 N95-11003
- Test model designs for advanced refractory ceramic materials
p 55 N95-11968

- Thermoacoustic environments to simulate reentry conditions
p 86 N95-14096
- Requirements report for SSTO vertical take-off and horizontal landing vehicle
[NASA-CR-197029] p 80 N95-14794
- Thermal chemical energy of ablating silica surfaces in air breathing solid rocket engines
p 148 N95-16316
- THERMAL RADIATION**
- Thermal force modeling for global positioning system satellites using the finite element method
[BTN-95-EIX95152583270] p 278 A95-73571
- Contribution of thermal radiation to the temperature profile of ceramic composite materials
[BTN-94-EIX95011441252] p 417 A95-84209
- High altitude hypersonic flowfield radiation
[AD-A281386] p 106 N95-16160
- THERMAL RESISTANCE**
- Effects of activated reactive evaporation process parameters on the microhardness of polycrystalline silicon carbide thin films
[GTN-95-00406090-4621] p 680 A95-93965
- A CMC database for use in the next generation launch vehicles (rockets)
p 150 N95-18993
- THERMAL SHOCK**
- On the particular features of dynamic processes in solids with varying boundary during interaction with intensive heat flows
[BTN-94-EIX94461408756] p 171 A95-63639
- Quality optimization of thermally sprayed coatings produced by the JP-5000 (HVOF) gun using mathematical modeling
p 152 N95-19008
- Thermal testing of high performance thermal barrier coatings for turbine blades
p 202 N95-19681
- THERMAL STABILITY**
- Nonhydrostatic simulation of frontogenesis in a moist atmosphere. Part 3: Thermal wind imbalance and rainbands
[HTN-95-90356] p 212 A95-66429
- Thermally stable organic polymers
[AD-A281380] p 87 N95-14363
- Toughened Silcomp composites for gas turbine engine applications
[DE95-002851] p 235 N95-21243
- Lubricant evaluation and performance, 2
[AD-A279144] p 242 N95-21969
- Field repair materials for naval aircraft
p 394 N95-27514
- Thermally stable organic polymers
[AD-A290755] p 537 N95-29482
- THERMAL STRESSES**
- On the particular features of dynamic processes in solids with varying boundary during interaction with intensive heat flows
[BTN-94-EIX94461408756] p 171 A95-63639
- Finite element time domain - modal formulation for nonlinear flutter of composite panels
[BTN-95-EIX95042474401] p 203 A95-68299
- Minimum-mass design of sandwich aerobrakes for a lunar transfer vehicle
[BTN-95-EIX95212645707] p 299 A95-76759
- The concept of high speed commercial transporter structure
p 498 A95-91517
- The role of material behaviour modelling in stressing and life assessment of modern Aero-engine components
[CONGRESS PAPER C428-27-127] p 612 A95-93606
- Cooling of aerospace plane using liquid hydrogen and methane
[BTN-95-EIX0619952748171] p 590 A95-94465
- Hypersonic engine leading edge experiments in a high heat flux, supersonic flow environment
[NASA-TM-106742] p 91 N95-14299
- Laminar and turbulent flow computations of Type 4 shock-shock interference aerothermal loads using unstructured grids
[NASA-CR-195008] p 97 N95-15604
- Simulation of multidisciplinary problems for the thermostress state of cooled high temperature turbines
p 140 N95-19021
- Application of multidisciplinary models to the cooled turbine rotor design
p 140 N95-19024
- Thermal fracture mechanisms in ceramic thermal barrier coatings
p 346 N95-26138
- Composite repair of metallic airframe: Twenty years of experience
p 393 N95-27508
- Intelligent finite element submodeling of multichip modules for reliability analysis
[AD-A292911] p 679 N95-31455
- THERMAL VACUUM TESTS**
- Thermoacoustic environments to simulate reentry conditions
p 86 N95-14096
- THERMOCHEMISTRY**
- Thermal chemical energy of ablating silica surfaces in air breathing solid rocket engines
p 148 N95-16316

THERMOCHROMATIC MATERIALS

The use of thermochromic liquid crystals for heat transfer measurements in short duration hypersonic wind tunnel facilities
[AIAA PAPER 95-6115] p 520 A95-90443

THERMOCOUPLES

Characteristics of the turbine inlet temperature sensing circuit for the T56 turbo-prop engine
[DSTO-TR-0095] p 405 N95-26424
Process and control systems for composites manufacturing p 420 N95-28267

THERMODYNAMIC CYCLES

Second-law analysis of vapor compression heat pumps with solution circuit
[BTN-94-EIX95011441236] p 431 A95-84193
Wave cycle design for wave rotor engines with limited nitrogen oxide emissions p 161 N95-18901
Malone-brayton cycle engine/heat pump
[AD-DO16573] p 244 N95-20295

THERMODYNAMIC EFFICIENCY

Second-law analysis of vapor compression heat pumps with solution circuit
[BTN-94-EIX95011441236] p 431 A95-84193

THERMODYNAMIC EQUILIBRIUM

Thermochemical nonequilibrium viscous shock-layer analysis for a Mars aerocapture vehicle
[BTN-95-EIX95082502732] p 239 A95-70139
Computation of the integrated aerodynamic and propulsive flowfields of a generic hypersonic space plane p 481 N95-29788

THERMODYNAMIC PROPERTIES

Numerical studies of Mach reflection with air chemistry p 548 A95-90575
Modeling and life prediction methodology for Titanium Matrix Composites subjected to mission profiles
[NASA-TM-109148] p 55 N95-11915
Laws of infrared similitude p 62 N95-12426
Evaluation of alternative in-flight fire suppressants for full-scale testing in simulated aircraft engine nacelles and dry bays
[PB94-203403] p 42 N95-13247
Anisotropic heat exchangers/stack configurations for thermoacoustic heat engines
[AD-A280974] p 168 N95-16506
Single-pass method for the solution of inverse potential and rotational problems. Part 1: 2-D and quasi 3-D theory and application p 107 N95-16563
Single-pass method for the solution of inverse potential and rotational problems. Part 2: Fully 3-D potential theory and applications p 107 N95-16564
Innovative processing of composites for ultra-high temperature applications, book 1
[AD-A290889] p 537 N95-29842
Thermal design of returnable satellites
[AD-A294113] p 701 N95-34500

THERMODYNAMICS

On introduction of artificial intelligence elements to heat power engineering
[BTN-94-EIX94461407961] p 100 A95-62635
On a program-information system TDSOFT
[BTN-94-EIX94461408773] p 175 A95-63656
Thermo-hydrodynamic solution of floating ring seals for high pressure compressors using the finite-element method
[HTN-95-92246] p 433 A95-85290
Chemically reacting non-equilibrium boundary layers in air breathing propulsion systems
[AIAA PAPER 95-6139] p 512 A95-90456
Laws of infrared similitude
[AD-A282209] p 62 N95-12426
Turbine design and application volumes 1, 2, and 3
[E-5666-Vol-1-3] p 236 N95-22341

THERMOELASTICITY

On the particular features of dynamic processes in solids with varying boundary during interaction with intensive heat flows
[BTN-94-EIX94461408756] p 171 A95-63639
Experimental investigation of thermoelastic deformation in turbojet-engine bearings under maintenance inspection
[BTN-95-EIX95292721173] p 546 A95-89904

THERMOELECTRICITY

Hypersonic flow simulation with thermoelectric effect p 368 A95-82669

THERMOGRAPHY

Convection heat transfer distributions over plates with square ribs from infrared thermography measurements
[HTN-95-20713] p 435 A95-86603
A method for disbond detection in thermal tomography by domain decomposition method p 545 A95-88955
Turbine-engine applications of thermographic-phosphor temperature measurements
[DE95-003625] p 358 N95-25110
Emerging nondestructive inspection for aging aircraft
[PB95-143053] p 328 N95-25401

THERMOHYDRAULICS

A low fin height heat exchanger technology demonstrator for Hermes
[SAE PAPER 932119] p 526 A95-90360

THERMOMAGNETIC EFFECTS

Mechanism and technological particular features of thermomagnetic hardening
[BTN-94-EIX94461407953] p 89 A95-62627

THERMOPLASTIC RESINS

Analysis techniques for the prediction of springback in formed and bonded composite components p 421 N95-28289
Characterization and manufacture of braided composites for large commercial aircraft structures p 426 N95-28478
Advanced wing design survivability testing and results p 400 N95-28488

THERMOPLASTICITY

Repair technology for thermoplastic aircraft structures
[NASA-CR-195048] p 395 N95-27519
ACT/ICAPS: Thermoplastic composite activities p 421 N95-28274
Development of LaRC (TM): IA thermoplastic polyimide coated aerospace wiring
[NASA-CR-195048] p 537 N95-30252

THERMOSETTING RESINS

In situ processing methods for composite fuselage sandwich structures p 531 N95-28826
Third NASA Advanced Composites Technology Conference, volume 1, part 1
[NASA-CP-3178-VOL-1-PT-1] p 534 N95-29029

THERMOSPHERE

Calculation of satellite drag coefficients
[AD-A285118] p 300 N95-23781

THESES

Advanced formation flight control
[AD-A289271] p 409 N95-26981

THICKNESS

Aerodynamic characteristics of truncated airfoils at high angle of attack
[SAE PAPER 931227] p 460 A95-87365
Scarf repairs to graphite/epoxy components p 396 N95-27523
The effect of adding roughness and thickness to a transonic axial compressor rotor
[NASA-TM-106958] p 645 N95-30524

THICKNESS RATIO

Introduction to the estimation of the lift coefficients at zero angle of attack and at maximum lift for aerofoils with high-lift devices at low speeds
[ESDU-94026] p 481 N95-29899

THIN AIRFOILS

Novel similarity solutions of the sonic small-disturbance equation with applications to airfoil transonic aerodynamics
[BTN-94-EIX94341340316] p 35 A95-60852
H^(sup)2/H^(sup)INF controller design for a two-dimensional thin airfoil flutter suppression
[BTN-94-EIX94511433918] p 141 A95-64584
Response of a thin airfoil encountering a strong density discontinuity p 462 A95-88900
Wing-body juncture flows
[AD-A281526] p 106 N95-16099

THIN FILMS

Effects of activated reactive evaporation process parameters on the microhardness of polycrystalline silicon carbide thin films
[GTN-95-00406090-4621] p 680 A95-93965
Reliability assessment of Multichip Module technologies via the Triservice/NASA RELTECH program p 245 N95-20643

THIN PLATES

Interaction of a streamwise vortex with a thin plate: A source of turbulent buffeting
[BTN-95-EIX95042474398] p 209 A95-68302
Fatigue crack growth in 2024-T3 aluminum under tensile and transverse shear stresses p 153 N95-19490

THIN WALLED SHELLS

Development of strength analysis methods and design model for aircraft constructions in Kazan Aviation Institute p 127 N95-16264

THIN WALLS

Development of processes, means, and theoretical principles of thin-walled detail plastic forming at Kazan Aviation Institute p 155 N95-16281
Vibrational behavior of adaptive aircraft wing structures modelled as composite thin-walled beams p 423 N95-28435
Severe edge effects and simple complimentary interior solutions for thin-walled anisotropic and composite structures
[AD-A290645] p 555 N95-29562
Development of LaRC (TM): IA thermoplastic polyimide coated aerospace wiring
[NASA-CR-195048] p 537 N95-30252

Performance improvement of composite wings through aeroelastic tailoring and modern control
[AD-A293689] p 608 N95-31602

THIN WINGS

Static aeroelastic characteristics of a composite wing
[BTN-95-EIX95152582340] p 282 A95-73542
Unsteady ground effects on aerodynamic coefficients of finite wings with camber
[BTN-95-EIX95182619233] p 271 A95-76659
The effect of wing sweep back upon transition in hypersonic flow
[AIAA PAPER 95-6090] p 466 A95-89199
Effect of leading- and trailing-edge flaps on clipped delta wings with and without wing camber at supersonic speeds
[NASA-TM-4542] p 5 N95-10028
Thin tailored composite wing for civil tiltrotor p 285 N95-23317
Computer program for estimation of leading-edge suction distribution for plane thin wings at subsonic speeds
[ESDU-94038] p 476 N95-28708
Leading-edge suction distribution for plane thin wings at subsonic speeds
[ESDU-94037] p 477 N95-28800

THREAT EVALUATION

Test and evaluation report for the Manual Domestic Passive Profiling System (MDPPS)
[AD-A286312] p 225 N95-20093
Consistent approach to describing aircraft HIRF protection
[NASA-CR-195067] p 334 N95-25341

THREE DIMENSIONAL BODIES

Rarefied gas numerical wind tunnel: OREX and HOPE p 427 A95-82391
Development of an upwind, finite-volume code with finite-rate chemistry
[NASA-CR-196749] p 9 N95-11366
Development of an upwind, finite-volume code with finite-rate chemistry
[NASA-CR-197747] p 374 N95-26760
A grid generation system for multi-disciplinary design optimization p 567 N95-28763

THREE DIMENSIONAL BOUNDARY LAYER

Experimental study of three-dimensional separation
[BTN-94-EIX94441385752] p 179 A95-68216
Approximate method for calculating heating rates on three-dimensional vehicles
[BTN-95-EIX95041503778] p 210 A95-69209
Multiple instabilities of three-dimensional boundary layers along a concave wall
[HTN-95-71126] p 429 A95-83487
Observation of traveling waves in the three-dimensional boundary layer along a yawed cylinder
[HTN-95-61064] p 430 A95-83648
Instability of three-dimensional boundary layers due to streamline curvature p 430 A95-83654
[HTN-95-61070] p 430 A95-83654
Transition correlations in three-dimensional boundary layers
[HTN-95-51648] p 432 A95-85030
Nonlinear analysis of swept wing transitional boundary layers
[SAE PAPER 932515] p 466 A95-89188
Validation of the RPLUS3D code for supersonic inlet applications involving three-dimensional shock wave-boundary layer interactions
[NASA-TM-106579] p 39 N95-13058
Three-dimensional boundary layer and flow field data of an inclined prolate spheroid p 158 N95-17867
A spectrally accurate boundary-layer code for infinite swept wings
[NASA-CR-195014] p 159 N95-18042
Effect of crossflow on Goertler instability in incompressible boundary layers
[NASA-CR-195007] p 159 N95-18193
Sectional prediction of 3D effects for separated flow on rotating blades
[PB94-201696] p 117 N95-18503

THREE DIMENSIONAL COMPOSITES

Mechanical characterization of 2D, 2D stitched, and 3D braided/RTM materials p 535 N95-29038
Cross-stiffened continuous fiber structures p 536 N95-29041

THREE DIMENSIONAL FLOW

A comparison of three-dimensional nonequilibrium solution algorithms applied to hypersonic flows with stiff chemical source terms
[AIAA PAPER 93-2861] p 4 A95-60186
Three-dimensional analysis of scramjet nozzle flows
[BTN-94-EIX94441380978] p 196 A95-68162
Prediction of ice accretion: Comparison between the 2D and 3D codes
[BTN-94-EIX94441385753] p 213 A95-68217

- Interaction of a streamwise vortex with a thin plate: A source of turbulent buffeting
[BTN-95-EIX95042474398] p 209 A95-68302
- Flap-lag damping in hover and forward flight with a three-dimensional wake
[HTN-95-A0496] p 221 A95-72567
- Effects of spatial order of accuracy on the computation of vertical flowfields
[BTN-95-EIX95152577604] p 305 A95-73479
- Influence of streamwise curvature on longitudinal vortices imbedded in turbulent boundary layers
[BTN-94-EIX94401378820] p 307 A95-76489
- Comparison of linear stability results with flight transition data
[BTN-95-EIX95182619097] p 283 A95-76582
- Neural network prediction of three-dimensional unsteady separated flowfields
[BTN-95-EIX95182619232] p 308 A95-76658
- Unsteady ground effects on aerodynamic coefficients of finite wings with camber
[BTN-95-EIX95182619233] p 271 A95-76659
- Study of the droplet spray characteristics of a subsonic wind tunnel
[BTN-95-EIX95182619235] p 271 A95-76661
- Simulation on the 3-D turbulent flow in the passages of finocyl grain
[BTN-95-EIX95202638962] p 279 A95-76674
- Quantitative comparison between interferometric measurements and Euler computations for supersonic cone flows
[BTN-95-EIX95222650782] p 358 A95-79238
- Computational/experimental investigation of staged injection into a Mach 2 flow
[HTN-95-51646] p 432 A95-85028
- Numerical simulation of three-dimensional hypersonic reacting flows over blunt bodies with catalytic surface
[HTN-95-61184] p 539 A95-87557
- Three-dimensional adaptive grid-embedding Euler technique
[HTN-95-20825] p 543 A95-88086
- Sensitivity derivatives for three dimensional supersonic Euler code using incremental iterative strategy
[HTN-95-20845] p 545 A95-88106
- Determining unsteady 2D AND 3D boundary layer separation
p 462 A95-88898
- Modeling three-dimensional gas-turbine combustor model flow using second-moment closure
[HTN-95-20935] p 464 A95-88974
- Accurate drag prediction: A prerequisite for drag reduction research
[SAE PAPER 932571] p 467 A95-90060
- A note on the interpretation of mini-tuft photographs
[HTN-95-01089] p 468 A95-90275
- Effect of spherical roughness elements upon transition of a 3-D boundary layer
[HTN-95-92835] p 471 A95-90753
- Experimental investigation of the flow in diffusers behind an axial flow compressor
[BTN-95-EIX95282710057] p 632 A95-92472
- Simulation of the unsteady interaction of a centrifugal impeller with its vaned diffuser: flow analysis
[BTN-95-EIX95282710055] p 633 A95-92474
- Numerical solutions of three dimensional viscous flows
[ISBN 1-879921-01-4] p 587 A95-93749
- Analytic solution of the thickness problem of a rectangular wing in steady subsonic flow
[ISBN 1-879921-01-4] p 588 A95-93758
- 3-D Navier-Stokes analysis of crossing glancing shocks/turbulent boundary layer interactions
[BTN-95-EIX95302729768] p 636 A95-94130
- Vortex generation and mixing in three-dimensional supersonic combustors
[BTN-95-EIX0616952745783] p 614 A95-94503
- An aerodynamic analysis of a mixed flow turbine
[NASA-TM-106674] p 15 N95-10153
- Steady and unsteady three-dimensional transonic flow computations by integral equation method
[NASA-CR-196777] p 10 N95-11582
- Numerical time dependent sheet cavitation simulations using a higher order panel method
[PB94-204435] p 59 N95-13249
- Designing in three dimensions p 90 N95-14130
- Unsteady flows in turbines: Impact on design procedure p 90 N95-14132
- Aero design of turbomachinery components: CFD in complex systems p 90 N95-14136
- Numerical design of advanced multi-element airfoils
[NASA-CR-197135] p 76 N95-15762
- Wing-body juncture flows
[AD-A281526] p 106 N95-16099
- Three dimensional compressible turbulent flow computations for a diffusing S-duct with/without vortex generators
[NASA-CR-195390] p 138 N95-17402
- Test data on a non-circular body for subsonic, transonic and supersonic Mach numbers p 158 N95-17871
- Low speed propeller slipstream aerodynamic effects p 116 N95-17882
- Sectional prediction of 3D effects for separated flow on rotating blades p 117 N95-18503
- [PB94-201696]
- An assessment of the adaptive unstructured tetrahedral grid, Euler Flow Solver Code FELISA
[NASA-TP-3526] p 119 N95-19041
- Validation and evaluation of the advanced aeronautical CFD system SAUNA: A method developer's view
[ARA-MEMO-390] p 210 N95-19774
- Application of Direct and Large Eddy Simulation to Transition and Turbulence
[AGARD-CP-551] p 248 N95-21061
- Mach 10 computational study of a three-dimensional scramjet inlet flow field
[NASA-TM-4602] p 309 N95-23015
- Mach 10 computational study of a three-dimensional scramjet inlet flow field p 310 N95-23210
- [NASA-TM-4602]
- Holographic interferometric tomography for reconstructing flow fields p 310 N95-23287
- Three-dimensional unsteady flow calculations in an advanced gas generator turbine p 312 N95-23425
- Phase 2: HGM air flow tests in support of HEX vane investigation p 312 N95-23438
- Three-dimensional interaction of wake/boundary-layer and vortex/boundary-layer data report
[CUE/A-AEREO/TR-23] p 329 N95-24210
- Computational fluid dynamics and transonic flow
[AD-A288962] p 436 N95-26405
- Effects of three-dimensional imposed 3-D disturbances on bluff-body near wake flows
[AD-A289553] p 374 N95-26757
- Turbomachinery design and tonal acoustics computations p 406 N95-26777
- [NASA-CR-197749]
- Global flowfield about the V-22 Tiltrotor Aircraft
[NASA-CR-198603] p 375 N95-27248
- Calculation of three-dimensional (3-D) internal flow by means of the velocity-vorticity formulation on a staggered grid
[NASA-TM-110352] p 376 N95-27258
- A general theory of two- and three-dimensional rotational flow in subsonic and transonic turbomachines
[NASA-CR-4496] p 377 N95-28003
- TranAir: A full-potential, solution-adaptive, rectangular grid code for predicting subsonic, transonic, and supersonic flows about arbitrary configurations. User's manual p 377 N95-28230
- Demonstration of an automated CFD system for three-dimensional flow simulations p 551 N95-28767
- The effects of three-dimensional imposed disturbances on bluff body near wake flows: Effects of taper and splitter plates on the near wake characteristics of a circular cylinder in uniform and shear flow
[AD-A292113] p 477 N95-28921
- A study of fluid problems requiring a direct particle simulation
[AD-A290212] p 567 N95-29074
- Interactions of spanwise and chordwise vorticity associated with three-dimensional dynamic stall over an oscillating wing
[AD-A290546] p 477 N95-29091
- A vorticity-velocity approach for three-dimensional unsteady viscous flow over wings p 478 N95-29108
- Leading edge film cooling effects on turbine blade heat transfer
[NASA-TM-106955] p 513 N95-29115
- Finite element vorticity-based methods for the solution of the incompressible and compressible Navier-Stokes equations p 553 N95-29119
- High-and low-frequency dynamics of isolated blades and rotors with dynamic stall and wake
[AD-A290358] p 503 N95-29322
- The decay of longitudinal vortices shed from airfoil vortex generators
[NASA-CR-198356] p 480 N95-29402
- A numerical study of the small scale wing-body junction problem p 482 N95-30235
- Development of a linearized unsteady Euler analysis for turbomachinery blade rows
[NASA-CR-4677] p 592 N95-30611
- Unsteady flow simulations about moving boundary configurations using dynamic domain decomposition techniques p 649 N95-31837
- Laser anemometer measurements of the three-dimensional rotor flow field in the NASA low-speed centrifugal compressor
[NASA-TP-3527] p 618 N95-31985
- Investigation of water droplet trajectories within the NASA icing research tunnel
[NASA-TM-107023] p 684 N95-32769
- Three-dimensional aerodynamic shape optimization using discrete sensitivity analysis p 691 N95-32904
- Design of secondary flow control cascade using numerical simulation p 698 N95-34507
- A study on the convergence of a 3-D Euler code for cascade flow calculations p 706 N95-34508

THREE DIMENSIONAL MODELS

- Microwave and infrared simulations of an intense convective system and comparison with aircraft observations
[HTN-95-60511] p 214 A95-68762
- Numerical simulation of incidence and sweep effects on delta wing vortex breakdown
[BTN-95-EIX95062487526] p 186 A95-69234
- Three-dimensional structure of a supersonic jet impinging on an inclined plate
[BTN-95-EIX95152583259] p 267 A95-73560
- Neural network prediction of three-dimensional unsteady separated flowfields
[BTN-95-EIX95182619232] p 308 A95-76658
- Tracer transport for realistic aircraft emission scenarios calculated using a three-dimensional model
[HTN-95-41799] p 353 A95-80525
- A tool for airframe shaping - idea and application
[SAE PAPER 931224] p 491 A95-87568
- Long distance propagation model and its application to aircraft en route noise prediction
[HTN-95-61221] p 491 A95-87594
- Adaptive wall technology for minimization of wind tunnel boundary interferences - where are we now?
p 519 A95-88903
- Rotating Kirchhoff method for three-dimensional transonic blade-vortex interaction hover noise
[HTN-95-20927] p 463 A95-88966
- Modeling three-dimensional gas-turbine combustor model flow using second-moment closure
[HTN-95-20935] p 464 A95-88974
- A three-dimensional Navier-Stokes/full-potential coupled analysis for rotor blades
[ISBN 1-879921-01-4] p 587 A95-93748
- Three dimensional model calculations of the global dispersion of high speed aircraft exhaust and implications for stratospheric ozone loss p 26 N95-10657
- Validation of the RPLUS3D code for supersonic inlet applications involving three-dimensional shock wave-boundary layer interactions
[NASA-TM-106579] p 39 N95-13058
- Turbomachinery Design Using CFD
[AGARD-LS-195] p 89 N95-14127
- Designing in three dimensions p 90 N95-14130
- Unsteady flows in turbines: Impact on design procedure p 90 N95-14132
- The role of CFD in the design process p 90 N95-14135
- Add a dimension to your analysis of the helicopter low airspeed environment
[AD-A283982] p 79 N95-14205
- Application of three-dimensional hybrid structured/unstructured grids to land, sea and air vehicles
[ARA-MEMO-399] p 210 N95-19775
- Open Skies project computational fluid dynamic analysis p 223 N95-19991
- Orientation determination of aircraft using visual 3D matching and radar. Case study 2
[PB95-165791] p 350 N95-25749
- Automatic blocking for complex three-dimensional configurations p 566 N95-28734
- Three-dimensional hybrid grid generation using advancing front techniques p 567 N95-28745
- Automatic multi-block grid generation for high-lift configuration wings p 567 N95-28764
- High-and low-frequency dynamics of isolated blades and rotors with dynamic stall and wake
[AD-A290358] p 503 N95-29322
- An unsteady simulation of a centrifugal compressor stage using the NWT p 707 N95-34536
- A large scale 3D Navier-Stokes analysis using NAL-NWT p 707 N95-34539

THREE DIMENSIONAL MOTION

- Aerodynamic sensitivity coefficients using the three-dimensional full potential equation
[BTN-95-EIX95062487530] p 186 A95-69238
- Preconditioned domain decomposition scheme for three-dimensional aerodynamic sensitivity analysis
[BTN-95-EIX95152577612] p 321 A95-73471
- Effect of density gradients in confined supersonic shear layers. Part 2: 3-D modes
[NASA-CR-198030] p 349 N95-24413

THRESHOLDS

- Examination of conditions in the proximity of pilot reports of aircraft icing during storm-fest p 666 A95-93509

THRESHOLDS (PERCEPTION)

- Visual contrast detection thresholds for aircraft contrails
[AD-A288618] p 328 N95-25607

THROATS

Design of a variable area diffuser for a 15-inch Mach 6 open-jet tunnel p 297 N95-23309

THRUST

Offset thrust axes and pitch stability [BTN-95-EIX95062487553] p 203 A95-68367
 Evaluation of scramjet nozzle performance p 402 A95-82321
 Experiment of rocket-ram annular combustor p 412 A95-82324
 Thrust modeling for hypersonic engines [AIAA PAPER 95-6081] p 509 A95-87410
 Propulsion controlled aircraft research p 497 A95-90869
 Two-dimensional converging-diverging rippled nozzles at transonic speeds — performed in the Langley 16-Foot Transonic Tunnel [NASA-TP-3440] p 6 N95-10129
 Thrust measurement in a 2-D scramjet nozzle p 339 N95-25397
 Investigation of wing upper surface flow-field disturbance due to NASA DC-8-72 in-flight inboard thrust-reverser deployment [NASA-TM-110351] p 457 N95-28816

THRUST AUGMENTATION

High bypass separate flow exhaust system improved thrust efficiency by modifying the aft centerbody [SAE PAPER 932622] p 511 A95-90083

THRUST CHAMBERS

Regenerative cooling for liquid propellant rocket thrust chambers [INPE-5565-TDI/540] p 150 N95-18720

THRUST CONTROL

Analytical solution for controls, heats, and states of flight trajectories [BTN-95-EIX95152583286] p 282 A95-73587
 Application of an integrated methodology for propulsion and airframe control design to a STOVL aircraft [NASA-TM-106729] p 16 N95-11159
 Piloted evaluation of an integrated methodology for propulsion and airframe control design [AD-A290207] p 51 N95-12763
 A vehicle health monitoring system for the Space Shuttle Reaction Control System during reentry [NASA-CR-188370] p 527 N95-29447
 Design, analysis and control of large transports so that control of engine thrust can be used as a back-up of the primary flight controls [NASA-CR-198958] p 518 N95-30254
 An Electronic Workshop on the Performance Seeking Control and Propulsion Controlled Aircraft Results of the F-15 Highly Integrated Digital Electronic Control Flight Research Program [NASA-TM-104278] p 694 N95-33009
 An overview of integrated flight-propulsion controls flight research on the NASA F-15 research airplane p 694 N95-33010
 Performance seeking control program overview p 695 N95-33011
 PSC algorithm description p 695 N95-33013
 Maximum thrust mode evaluation p 696 N95-33017
 Rapid deceleration mode evaluation p 696 N95-33018
 Background and principles of throttles-only flight control p 697 N95-33021
 Propulsion Controlled Aircraft design and development p 697 N95-33022
 Flight test of a propulsion controlled aircraft system on the NASA F-15 airplane p 691 N95-33023
 Design challenges encountered in the F-15 PCA flight test program p 692 N95-33025

THRUST MEASUREMENT

A three-dimensional moving mesh method for the calculation of unsteady transonic flows [HTN-95-C0007] p 585 A95-93395
 Scramjet thrust measurement in a shock tunnel [HTN-95-C0008] p 586 A95-93396
 Thrust measurements of a complete axisymmetric scramjet in an impulse facility p 339 N95-25395
 Scramjet thrust measurement in a shock tunnel p 339 N95-25396
 Thrust measurement in a 2-D scramjet nozzle p 339 N95-25397
 Balances for the measurement of multiple components of force in flows of a millisecond duration p 350 N95-25400

THRUST REVERSAL

Why do airlines want and use thrust reversers? A compilation of airline industry responses to a survey regarding the use of thrust reversers on commercial transport airplanes [NASA-TM-109158] p 226 N95-20706
 Investigation of wing upper surface flow-field disturbance due to NASA DC-8-72 in-flight inboard thrust-reverser deployment [NASA-TM-110351] p 457 N95-28816

THRUST VECTOR CONTROL

Robust longitudinal axis flight control for an aircraft with thrust vectoring [BTN-95-EIX95122538875] p 408 A95-83000
 Trim conditions for optimal flight performance of hypersonic aircraft p 514 A95-87397
 Actuated forebody strake controls for the F-18 High-Alpha Research Vehicle [BTN-95-EIX0619952748173] p 619 A95-94467
 Fundamentals of catastrophic failure prevention by thrust vectoring [BTN-95-EIX0619952748176] p 606 A95-94470
 High-Alpha Research Vehicle (HARV) longitudinal controller: Design, analyses, and simulation results [NASA-TP-3446] p 17 N95-10860
 STOVL Control Integration Program [NASA-CR-195358] p 18 N95-11487
 Fourth High Alpha Conference, volume 1 [NASA-CP-10143-VOL-1] p 67 N95-14229
 Parameter identification for X-31A at high angles of attack p 69 N95-14235
 Fourth High Alpha Conference, volume 2 [NASA-CP-10143-VOL-2] p 69 N95-14239
 F-18 high alpha research vehicle: Lessons learned p 69 N95-14240
 X-31 post-stall envelope expansion and tactical utility testing p 70 N95-14242
 X-31 quasi-tailless flight demonstration p 70 N95-14243
 X-31 high angle of attack control system performance p 70 N95-14244
 Flight test results of the F-16 aircraft modified with the axisymmetric vectoring exhaust nozzle p 70 N95-14245
 Vista/F-16 Multi-Axis Thrust Vectoring (MATV) control law design and evaluation p 71 N95-14248
 Multi-application controls: Robust nonlinear multivariable aerospace controls applications p 71 N95-14249
 Navy and the HARV: High angle of attack tactical utility issues p 71 N95-14252
 Preparations for flight research to evaluate actuated forebody strakes on the F-18 high-alpha research vehicle p 72 N95-14257
 VSTOL Systems Research Aircraft (VSRA) Harrier [NASA-TM-110117] p 126 N95-18347
 Static investigation of two fluidic thrust-vectoring concepts on a two-dimensional convergent-divergent nozzle [NASA-TM-4574] p 120 N95-19042
 Integrated aerodynamic fin and stowable TVC vane system [AD-D016457] p 151 N95-19073
 Static investigation of two fluidic thrust-vectoring concepts on a two-dimensional convergent-divergent nozzle [NASA-TM-4574] p 222 N95-19913
 Internal performance characteristics of thrust-vectoring axisymmetric ejector nozzles [NASA-TM-4610] p 331 N95-25338
 Flight demonstration of an advanced pitch control law in the VAAAC Harrier aircraft p 623 N95-32012
 X-31: A program overview and flight test status p 609 N95-32013

THRUST-WEIGHT RATIO

The OFF-GM transport jet [NASA-CR-197159] p 46 N95-12637

THUNDERSTORMS

WINDEX — A new index for forecasting microburst potential [HTN-95-90690] p 215 A95-69717
 Thundercloud electric field modeling for the ionosphere-Earth region. 1: Dependence on cloud charge distribution [HTN-95-41223] p 317 A95-75035
 Identification of aviation weather hazards based on the integration of radar and lightning data [HTN-95-51323] p 356 A95-80908
 The Integrated Terminal Weather System (ITWS) storm cell information and weather impacted airspace detection algorithm p 654 A95-93452
 The ITWS microburst prediction algorithm p 655 A95-93456
 The real-time analysis and prediction of storms program p 655 A95-93457
 Sensing thunderstorm microphysics with multiparameter radar: Application for aviation p 657 A95-93467
 Final results of the weather testing component of the Terminal Doppler Weather Radar operational test and evaluation p 658 A95-93471
 Investigation of outflow strength variability in Florida downburst-producing storms p 659 A95-93476
 The inference of aviation weather hazards based on the integration of radar and lightning data p 660 A95-93483

Use of high resolution lightning detection and localization sensors for hazardous aviation weather nowcasting p 661 A95-93486
 Criteria of forecasting low level wind shear over Qatar p 663 A95-93493
 Developing thunderstorm forecast rules utilizing first detectable cloud radar-echoes p 667 A95-93514
 Northwest Airlines atmospheric hazards advisory & avoidance system p 672 A95-93539
 Assessment of the benefits for improved terminal weather information p 673 A95-93540
 Turbulence near thunderstorm tops p 675 A95-93553
 Thunderstorm hypothesis reasoner [AD-A282664] p 60 N95-12805
 Collaborative research on aircraft icing and charging processes in ice [AD-A285102] p 276 N95-23201

TILES

Effect of constraining layer stiffness on performance of damping tile materials using finite element modelling with Rayleigh integral p 30 N95-11306
 Aeroacoustic qualification of HERMES shingles p 173 N95-19145

TILT ROTOR AIRCRAFT

Wing download reduction using vortex trapping plates [HTN-94-00710] p 4 A95-60188
 Parametric studies for tiltrotor aeroelastic stability in highspeed flight [HTN-95-A0499] p 222 A95-72570
 Demonstration of an elastically coupled twist control concept for tilt rotor blade application [HTN-95-20959] p 465 A95-88998
 FAA vertical flight bibliography [DOT/FAA/RD-94/17] p 14 N95-11684
 Wing design for a civil tiltrotor transport aircraft [NASA-CR-197523] p 130 N95-18090
 Tilt Rotor Unmanned Air Vehicle System (TRUS) demonstrator flight test program [AD-A284151] p 132 N95-18415
 Effects of civil tiltrotor service in the northeast corridor on en route airspace loads [AD-A293586] p 599 N95-31687

TILT WING AIRCRAFT

Flying qualities development and flight simulation evaluation of the TW-68 tilt-wing VTOL aircraft [SAE PAPER 932517] p 386 A95-84555

TILTING ROTORS

Study of noise on a small-scale hovering tilt rotor [HTN-94-00712] p 5 A95-60190
 Aerodynamic interactions between a rotor and wing in hover [HTN-94-00714] p 5 A95-60192
 Demonstration of an elastically coupled twist control concept for tilt rotor blade application [BTN-94-EIX94441386633] p 196 A95-68182
 Parametric studies for tiltrotor aeroelastic stability in highspeed flight [HTN-95-A0499] p 222 A95-72570

TIME CONSTANT

Analysis of heads-up display quickening versus handling qualities [AD-A293797] p 611 N95-31584

TIME DEPENDENCE

Grid refinement test of time-periodic flows over bluff bodies [BTN-94-EIX94401378822] p 307 A95-76491
 Time-average aircraft noise descriptors: Confusion with no benefit p 559 A95-88474
 Noise metrics and aviation noise control: The case for DNL p 559 A95-88475
 Numerical time dependent sheet cavitation simulations using a higher order panel method [PB94-204435] p 59 N95-13249
 An approach for dynamic grids [NASA-TM-106774] p 76 N95-15853
 Demonstration of the Dynamic Flowgraph Methodology using the Titan 2 Space Launch Vehicle Digital Flight Control System [NASA-CR-197517] p 150 N95-17493
 Minimal time detection algorithms and applications to flight systems [TR-2-FSRC-93] p 171 N95-18564
 Velocity measurements with hot-wires in a vortex-dominated flowfield p 121 N95-19261
 Computing methods for the approximate solution of time dependent problems [AD-A286007] p 256 N95-20719
 Dynamics of phase ordering of nematics in a pore [DE95-607662] p 362 N95-25978
 An experimental investigation of the time-dependent separation of tangent bodies in supersonic flow [AD-A290720] p 480 N95-29500
 The prevention of PIO by design p 620 N95-31991

TIME LAG

- Using IRI for the computation of ionospheric corrections for altimeter data analysis p 212 A95-66949
Investigation of the effects of bandwidth and time delay on helicopter roll-axis handling qualities
[HTN-95-80853] p 290 A95-75095
An analytical model for a nonlinear elastomeric lag damper and its effect on aeromechanical stability in Hover
[HTN-95-61076] p 369 A95-83660
Determination of flight simulator time delay p 522 A95-91553
Flow physics of critical states for rolling delta wings
[BTN-95-EIX0619952748180] p 590 A95-94473
F/A-18 and F-16 forebody vortex control, static and rotary-balance results p 72 N95-14254
SCARLET: DLR rate saturation flight experiment p 598 N95-31068
The prevention of PIO by design p 620 N95-31991

TIME MARCHING

- Three-dimensional adaptive grid-embedding Euler technique
[HTN-95-20825] p 543 A95-88086
Numerical solution of Euler and Navier-Stokes equations for 2D transonic problems p 638 A95-95366
Hypersonic Navier-Stokes computations about complex configurations p 644 A95-95497
Numerical computations of supersonic base flow with special emphasis on turbulence modeling
[AD-A283688] p 119 N95-18670
Computation of transonic flow on composite overlapping grids in 2 D
[PB95-131348] p 248 N95-21132
Numerical investigation to S-inlet flows (Numerical simulation study of S-inlet flows)
[AD-A289590] p 374 N95-26713

TIME OF FLIGHT SPECTROMETERS

- Time-of-flight mass spectrometer for impulse facilities
[BTN-95-EIX95142553057] p 262 A95-73441

TIME SERIES ANALYSIS

- Verification of terminal forecasts p 664 A95-93502
The role of flight progress strips in en route air traffic control: A time-series analysis
[DOT/FAA/AM-95/4] p 280 N95-23565

TIN ALLOYS

- Cadmium plating replacements p 631 N95-31773

TIP SPEED

- Experimental and computational investigation of the tip clearance flow in a transonic axial compressor rotor
[NASA-TM-106711] p 649 N95-31738

TIPS

- Elliptic tip effects on the vortex wake of an axisymmetric body at incidence
[HTN-95-20938] p 464 A95-88977

TITANIUM

- Aerospace applications of beta titanium alloys
[HTN-95-B0394] p 530 A95-90475
Modeling and life prediction methodology for Titanium Matrix Composites subjected to mission profiles
[NASA-TM-109148] p 55 N95-11915
Soft body impact on titanium fan blades p 200 N95-19671

TITANIUM ALLOYS

- National AeroSpace Plane: Technology transfer
[BTN-95-EIX95072498879] p 180 A95-68395
Fatigue resistance of peened 7050-T7451 aluminium alloy: Repair and re-treatment of a component surface
[BTN-94-EIX94371347838] p 206 A95-69131
The effects of surface modification on fretting fatigue in Ti alloy turbine components
[HTN-95-61145] p 404 A95-84909
Intermetallic and titanium matrix composite materials for hypersonic applications
[AIAA PAPER 95-6132] p 530 A95-90451
Ordered intermetallic alloys, part 3: Gamma titanium aluminides
[HTN-95-B0396] p 530 A95-90477
Aerospace applications of new materials
[CONGRESS PAPER C428-17-135] p 531 A95-91716
Electrochemical impedance pattern recognition for detection of hidden chemical corrosion on aircraft components
[AD-A284998] p 241 N95-20481
Electrochemical impedance pattern recognition for detection of hidden chemical corrosion on aircraft components
[AD-A285998] p 241 N95-20716
Electrochemical impedance pattern recognition for detection of hidden chemical corrosion on aircraft components, phase 1
[AD-A291345] p 556 N95-29946
- TITANIUM NITRIDES**
Protective coatings for compressor gas path components p 201 N95-19675

TOLERANCES (MECHANICS)

- Corrosion prevention and control
[BTN-95-EIX95031502753] p 188 A95-68260
The analysis of the processing increased weight for pilot production of F-X aircraft
[HTN-95-71133] p 385 A95-83494
Verification of the damage tolerance of a fighter aircraft p 388 A95-85897
Damage tolerance certification of a fighter horizontal stabilizer
[BTN-95-EIX0619952748186] p 637 A95-94478
FAA/NASA International Symposium on Advanced Structural Integrity Methods for Airframe Durability and Damage Tolerance
[NASA-CP-3274-PT-1] p 92 N95-14453
Development of the NASA/FLAGRO computer program for analysis of airframe structures p 94 N95-14473
Brite-Euram programme: ACOUFAT acoustic fatigue and related damage tolerance of advanced composite and metallic structures p 174 N95-19159
FAA/NASA International Symposium on Advanced Structural Integrity Methods for Airframe Durability and Damage Tolerance, part 2
[NASA-CP-3274-PT-2] p 124 N95-19468
Fatigue life until small cracks in aircraft structures: Durability and damage tolerance p 135 N95-19478
Proceedings of the USAF Structural Integrity Program Conference
[AD-A285684] p 194 N95-19517
Toughened Silcomp composites for gas turbine engine applications
[DE95-002851] p 235 N95-21243
Tension fracture of laminates for transport fuselage. Part 1: Material screening p 398 N95-28471
Application of damage tolerance methodology in certification of the Piaggio P-180 Avanti p 399 N95-28480
Applications of a damage tolerance analysis methodology in aircraft design and production p 426 N95-28483
Damage tolerance of a geodesically stiffened advanced composite structural concept for aircraft structural applications p 399 N95-28487
Design, analysis, and fabrication of a pressure box test fixture for tension damage tolerance testing of curved fuselage panels p 533 N95-28839
- TOLLMIEN-SCHLICHTING WAVES**
The use of hot film for the investigation of boundary-layer transition
[CONGRESS PAPER C428-9-199] p 475 A95-91697
Instabilities originating from suction holes used for Laminar Flow Control (LFC)
[NASA-CR-196395] p 6 N95-10131
- TOMOGRAPHY**
A method for disbond detection in thermal tomography by domain decomposition method p 545 A95-88955
Evaluation of neutron techniques for illicit substance detection
[DE95-002988] p 300 N95-22764
Emerging nondestructive inspection for aging aircraft
[PB95-143053] p 328 N95-25401
- TOPOGRAPHY**
Geoid lineations of 1000 km wavelength over the central Pacific
[HTN-95-11304] p 319 A95-77009
Effect of squeeze film damper land geometry on damper performance
[HTN-95-92247] p 434 A95-85291
Incorporation of topography effects in aircraft noise modeling p 578 A95-90140
AVIRIS and TIMS data processing and distribution at the land processes distributed active archive center p 325 N95-23872
Partial camera automation in a simulated Unmanned Air Vehicle
[AD-A288786] p 337 N95-26190
Naval Aviation System TEAM mapping, charting, and geodesy handbook
[AD-A288590] p 446 N95-26841
Airborne geophysics and precise positioning: Scientific issues and future directions
[LC-94-68678] p 446 N95-27156
- TOPOLOGY**
Multidimensional lines 2: Proximity and applications
[BTN-94-EIX94341340329] p 61 A95-60865
Crossflow topology of vortical flows
[HTN-95-51664] p 432 A95-85046
Efficient mapping topology for turbine combustors with inclined slots/staggered holes
[BTN-95-EIX0616952745805] p 614 A95-94485
LDV measurements in separated flow on an elliptic wing mounted at an angle of attack on a wall
[BTN-94-EIX94441380518] p 702 A95-96559
Generalized method of solving topological optimization problems for electrical airplane equipment systems in computer-aided design p 169 N95-16272

CFD analysis of turbopump volutes

- p 312 N95-23436
- TOPPING CYCLE ENGINES**
Optimization of wave rotors for use as gas turbine engine topping cycles
[NASA-TM-106951] p 406 N95-27860
- TORNADOES**
The real-time analysis and prediction of storms program p 655 A95-93457
- TORQUE**
Ceramic composite attachments for transmission of high-torque loads
[BTN-94-EIX95011441256] p 417 A95-84213
Whirl plus tilt
[DE95-007948] p 452 N95-28108
Shear force, bending moment and torque of rigid aircraft in symmetric steady maneuvering flight
[ESDU-94045] p 502 N95-28896
175Hp contrarotating homopolar motor design report
[AD-A291138] p 557 N95-30122
- TORSION**
Nonlinear angle of twist of advanced composite wing boxes under pure torsion
[BTN-95-EIX95152582323] p 281 A95-73526
Modal characteristics of rotors using a conical shaft finite element
[BTN-94-EIX94401359745] p 346 A95-77379
Course module for AA201: Wing structural design project
[AD-A283618] p 133 N95-18616
- TORSIONAL STRESS**
Torsional actuation with extension-torsion composite coupling and a magnetostrictive actuator
[BTN-95-EIX95262694314] p 435 A95-85485
- TORSIONAL VIBRATION**
Application of Navier-Stokes aeroelastic methods to improve fighter wing maneuver performance
[BTN-95-EIX95182619218] p 284 A95-76644
Modelling and analysis of a dual-wheel nosegear: Shimmy instability and impact motions
[SAE PAPER 931402] p 605 A95-93672
- TOTAL ENERGY SYSTEMS**
Development of a TECS control-law for the lateral directional axis of the McDonnell Douglas F-15 Eagle
[AD-A289771] p 410 N95-28598
- TOTAL QUALITY MANAGEMENT**
The mini-business approach at Chadderton
[CONGRESS PAPER C428-26-037] p 681 A95-93602
- TOUCHDOWN**
F-15 resource tape
[NASA-TM-110502] p 230 N95-19994
- TOUGHNESS**
Mechanical properties of advanced toughened bismaleimide matrix composite p 530 A95-91570
- TOWED BODIES**
Wind-tunnel tests of an inclined cylinder having helical grooves
[BTN-95-EIX95262694306] p 411 A95-85477
- TOWERS**
Equivalent beam-column analysis of guyed towers
[BTN-95-EIX95262696644] p 435 A95-85519
An evaluation of Automatic Terminal Information Service (ATIS) flight deck display presentation options
[AD-A280100] p 228 N95-21020
- TOXIC HAZARDS**
Chemical composition and photochemical reactivity of exhaust from aircraft turbine engines
[HTN-95-51277] p 356 A95-80862
Developing an emission factor for hazardous air pollutants for an F-16 using JP-8 fuel
[AD-A284802] p 216 N95-19685
- TOXICITY**
Modeling aerosol emissions from the combustion of composite materials p 301 N95-23038
Aircraft fires, smoke toxicity, and survival: An overview
[DOT/FAA/AM-95/8] p 277 N95-24024
Environmentally Safe and Effective Processes for Paint Removal
[AGARD-LS-201] p 650 N95-32165
- TRACE CONTAMINANTS**
Latitude variations of stratospheric trace gases
[HTN-95-70948] p 352 A95-78013
Tracer transport for realistic aircraft emission scenarios calculated using a three-dimensional model
[HTN-95-41799] p 353 A95-80525
Evolution of the concentrations of trace species in an aircraft plume: Trajectory study
[HTN-95-A1044] p 443 A95-84549
- TRACE ELEMENTS**
Remote sensing of smoke, clouds, and radiation using AVIRIS during SCAR experiments p 708 N95-33749
- TRACKING (POSITION)**
A technique for detecting a tropical cyclone center using a Doppler radar
[HTN-95-20631] p 215 A95-69574

- Tropical cyclone observation and forecasting with and without aircraft reconnaissance
[HTN-95-80701] p 254 A95-72545
- Solutions of generalized proportional navigation with maneuvering and nonmaneuvering targets
[BTN-95-EIX95202637606] p 279 A95-76683
- Determination of piloting feedback structures for an altitude tracking task
[BTN-95-EIX95242670770] p 327 A95-81077
- NEXRAD/ARSR operational comparison
p 658 A95-93470
- Towards improving the NMC aircraft data base
p 660 A95-93480
- Modeling and analysis for the GPS pseudo-range observable
[BTN-95-EIX95302731227] p 600 A95-94046
- MATSurv multisensor air traffic surveillance
[AD-A292253] p 489 N95-28887
- TRACKING RADAR**
- Signal processing of noise data from high-speed flyovers
[BTN-95-EIX0619952748178] p 680 A95-94248
- Doppler radar detection of vortex hazard indicators
p 42 N95-13212
- TRACTION**
- NASA evaluation of Type 2 chemical depositions -- effects of deicer deposition on aircraft tire friction performance
[SAE PAPER 932582] p 495 A95-90086
- TRADEOFFS**
- The application of helicopter mission simulation to Nap-of-the-Earth operations
p 710 N95-32496
- TRAFFIC**
- Control mechanism to prevent correlated message arrivals from degrading signaling no. 7 network performance
[BTN-94-EIX94341342286] p 56 A95-60842
- Environmental noise monitoring - source identification
[HTN-95-92537] p 558 A95-87357
- Response to noise around Vaernes and Bodoe airports
[PB94-207065] p 62 N95-13575
- TRAILING EDGE FLAPS**
- Effects of leading and trailing edge flaps on the aerodynamics of airfoil/vortex interactions
[HTN-95-31011] p 221 A95-71181
- Natural laminar flow wing concept for supersonic transports
[BTN-95-EIX95182619226] p 308 A95-76652
- Torsional actuation with extension-torsion composite coupling and a magnetostrictive actuator
[BTN-95-EIX95262694314] p 435 A95-85485
- Experimental investigation of hypersonic flow over a wing-body combination
[AIAA PAPER 95-6083] p 460 A95-87412
- Effect of leading- and trailing-edge flaps on clipped delta wings with and without wing camber at supersonic speeds
[NASA-TM-4542] p 5 N95-10028
- Low-speed surface pressure and boundary layer measurement data for the NLR 7301 airfoil section with trailing edge flap
p 111 N95-17855
- Two-dimensional high-lift airfoil data for CFD code validation
p 112 N95-17859
- Investigation of the flow development on a highly swept canard/wing research model with segmented leading- and trailing-edge flaps
p 114 N95-17876
- Lift enhancement device
[AD-D016522] p 224 N95-21864
- Wing pressure distributions from subsonic tests of a high-wing transport model -- in the Langley 14-by-22-Foot Subsonic Wind Tunnel
[NASA-TM-4583] p 272 N95-22802
- Increments in aerofoil lift coefficient at zero angle of attack and in maximum lift coefficient due to deployment of a plain trailing-edge flap, with or without a leading-edge high-lift device, at low speeds
[ESDU-94028] p 477 N95-28885
- Increments in aerofoil lift coefficient at zero angle of attack and in maximum lift coefficient due to deployment of a trailing-edge split flap, with or without a leading-edge high-lift device, at low speeds
[ESDU-94029] p 479 N95-29129
- Low-speed wind-tunnel investigation of the stability and control characteristics of a series of flying wings with sweep angles of 50 deg
[NASA-TM-4640] p 505 N95-30226
- Vibration reduction in helicopter rotors using an actively controlled partial span trailing edge flap located on the blade
p 624 N95-32111
- TRAILING EDGES**
- Computation of the poststall behavior of a circulation controlled airfoil
[BTN-95-EIX95152582320] p 264 A95-73523
- Explicit Kutta condition for an unsteady two-dimensional constant potential panel method
[HTN-95-51679] p 433 A95-85061
- Effects of trailing-edge jet entrainment on delta wing vortices
[HTN-95-81644] p 542 A95-87692
- A note on the interpretation of mini-tuft photographs
[HTN-95-01089] p 468 A95-90275
- Unsteady aerodynamic effects of trailing edge controls on delta wings
[HTN-95-01099] p 469 A95-90285
- Vortex lattice method simulation of unsteady flow due to wing/external store combination
p 471 A95-91499
- Flow physics of critical states for rolling delta wings
[BTN-95-EIX0619952748180] p 590 A95-94473
- Two-dimensional converging-diverging rippled nozzles at transonic speeds -- performed in the Langley 16-Foot Transonic Tunnel
[NASA-TP-3440] p 6 N95-10129
- Experiments in the trailing edge flow of an NLR 7702 airfoil
p 110 N95-17852
- Erosion of T56 5th stage rotor blades due to bleed hole overtip flow
p 200 N95-19666
- Lift enhancing tabs for airfoils
[NASA-CASE-ARC-11990-1] p 286 N95-23395
- Airfoil modification effects on subsonic and transonic pressure distributions and performance for the EA-6B airplane
[NASA-TP-3516] p 373 N95-26382
- The near-wake flow behavior of an oscillating airfoil with modified trailing edge
p 375 N95-26953
- Navier-Stokes solution of wing wake structure and its perturbation
p 479 N95-29121
- Experimental investigation of aerodynamic devices for wind turbine rotational speed control, phase 1
[DE95-004034] p 564 N95-30016
- Wind turbine trailing edge aerodynamic brakes
[DE95-004061] p 683 N95-32548
- TRAINING AIRCRAFT**
- A review of Air Force policy and noise models pertaining to the noise environment under low-altitude, high-speed training areas
p 561 A95-90118
- ASTRA - A safe, simplex, fly-by-wire aircraft control system
[CONGRESS PAPER C428-37-218] p 610 A95-93634
- Triton 2 (1B)
[NASA-CR-197188] p 46 N95-12636
- Viper -- Design modification
[NASA-CR-197191] p 79 N95-13703
- Aircraft stress sequence development: A complex engineering process made simple
p 136 N95-19480
- TRAINING ANALYSIS**
- Using the backward transfer paradigm to validate the AH-64 Simulator Training Research Advanced Testbed for Aviation
[AD-A285758] p 238 N95-19931
- TRAINING DEVICES**
- Assessment of cost and training effectiveness for a candidate training system using the Comparison-Based Prediction model
[SAE PAPER 932598] p 379 A95-84570
- New computer delivered training systems to support technical crew training programmes
[CONGRESS PAPER C428-5-036] p 522 A95-91678
- Helicopter in-flight simulation development and use in test pilot training
[AD-A283998] p 146 N95-18725
- Virtual reality flight control display with six-degree-of-freedom controller and spherical orientation overlay
[NASA-CASE-NPO-18733-1-CU] p 288 N95-22578
- Development of qualification guidelines for personal computer-based aviation training devices
[DOT/FAA/AM-95/6] p 323 N95-23603
- Applications of digital video and synthetic environments to unmanned aerial vehicles
[AD-A291875] p 504 N95-29437
- TRAINING EVALUATION**
- Automated hover training: An empirical evaluation
[SAE PAPER 932536] p 379 A95-84559
- Aviation weather education and the University of North Dakota aviation weather survey
p 656 A95-93462
- Pilot training initiatives for the '90s
p 657 A95-93463
- Programmable cockpit research simulator
[AD-A279219] p 204 N95-19848
- Controller resource management: What can we learn from aircrews?
[DOT/FAA/AM-95/21] p 602 N95-32186
- TRAINING SIMULATORS**
- Education, training, and human engineering in aerospace; SAE Aerotech '93, Costa Mesa, CA, Sep. 27-30, 1993
[SAE SP-992] p 417 A95-84553
- Neuro-controllers for adaptive helicopter training
[SAE PAPER 932535] p 379 A95-84557
- Intelligent flight trainer for initial rotary wing training
[SAE PAPER 932536] p 386 A95-84558
- Automated hover training: An empirical evaluation
[SAE PAPER 932536] p 379 A95-84559
- TRAJECTORIES**
- Functional dependence of trajectory dispersion on initial condition errors
[BTN-95-EIX95152583263] p 298 A95-73564
- Optimal trajectories for hypersonic launch vehicles
[HTN-95-61120] p 415 A95-84884
- Influence of the flight trajectory on the exhaust gas composition of a H2-fueled air-breathing ramjet engine
p 509 A95-87404
- Trajectory optimization using parallel shooting method on parallel computer
[BTN-95-EIX95282706670] p 564 A95-88175
- Computer simulation of ejection seat motion
[CONGRESS PAPER C428-18-169] p 484 A95-91718
- Comparison of meteorological data with fitted values extracted from projectile trajectory
[AD-A285921] p 255 N95-19989
- The performance of cargo airdrop systems using g-12E parachutes: Statistical determination of minimum altitude
[AD-A291666] p 381 N95-28454
- A tactical navigation and routing system for low-level flight
p 709 N95-32494
- TRAJECTORY ANALYSIS**
- Trajectory modeling of emissions from lower stratospheric aircraft
[HTN-95-41219] p 317 A95-75031
- Functional agility metrics and optimal trajectory analysis
[BTN-95-EIX95182619121] p 321 A95-76598
- Analytical solution and parameter estimation of projectile dynamics
[BTN-95-EIX95212645695] p 272 A95-76747
- Role of the aviation weather system in providing a real-time ATC volcanic ash advisory system
p 663 A95-93494
- Alaska's volcanic ash warning system
p 663 A95-93495
- Effects of small changes on rate of climb
[ESDU-94039] p 501 N95-28707
- TRAJECTORY CONTROL**
- A generalized algorithm for inverse simulation applied to helicopter maneuvering flight
[HTN-95-A0493] p 236 A95-72564
- Dynamical instability of the aerogravity assist maneuver
[BTN-95-EIX95152583282] p 298 A95-73563
- Analytical solution for controls, heats, and states of flight trajectories
[BTN-95-EIX95152583286] p 282 A95-73587
- Functional agility metrics and optimal trajectory analysis
[BTN-95-EIX95182619121] p 321 A95-76598
- Ideal proportional navigation
p 342 A95-81374
- Hypersonic trajectory control of aerospace plane with integrated SCRAMJET engine
p 413 A95-82384
- An advanced vehicle management system
[SAE PAPER 931376] p 618 A95-93655
- Matlab as a robust control design tool
p 169 N95-16474
- Nonlinear system guidance in the presence of transmission zero dynamics
[NASA-TM-4661] p 309 N95-22804
- TRAJECTORY OPTIMIZATION**
- Nonsmooth trajectory optimization: An approach using continuous simulated annealing
[BTN-94-EIX94511433914] p 168 A95-64580
- Analytical solution for controls, heats, and states of flight trajectories
[BTN-95-EIX95152583286] p 282 A95-73587
- Optimal lateral-escape maneuvers for microburst encounters during final approach
[BTN-95-EIX95182619127] p 276 A95-76604
- Application of direct transcription to commercial aircraft trajectory optimization
[BTN-95-EIX95242670766] p 359 A95-81081
- Reentry trajectories and their optimization by an evolution algorithm
p 525 A95-87394
- Optimal separation and ascent of lifting upper stages
p 525 A95-87396
- Multiobjective trajectory optimization by goal programming with fuzzy decision
p 526 A95-91544
- Application of multivariate optimization techniques to determination of optimum flight path trajectories
[ESDU-94012] p 44 N95-11793
- Numerical optimization of synergetic maneuvers
[AD-A283398] p 109 N95-17435
- Analytical investigations in aircraft and spacecraft trajectory optimization and optimal guidance
[NASA-CR-4672] p 526 N95-29339

TRAJECTORY PLANNING

Qualitative environmental navigation: Theory and practice -- robot navigation p 601 N95-30486

TRANSATMOSPHERIC VEHICLES

Thermo-acoustic fatigue design for hypersonic vehicle skin panels p 162 N95-19161

TRANSDUCERS

Low frequency ultrasonic nondestructive inspection of aluminum/adhesive fuselage lap splices [DE94-014242] p 24 N95-11135

Workshop report: Measurement techniques in highly transient, spectrally rich combustion environments [AD-A288395] p 350 N95-25606

TRANSFER FUNCTIONS

Precise navigation using adaptive FIR filtering and time domain spectral estimation [BTN-95-EIX95142555485] p 227 A95-72888

Broadband, wide-area active control of sound radiated from vibrating structures using local surface-mounted radiation suppression devices p 30 N95-11283

On-line, adaptive state estimator for active noise control p 322 N95-23308

Aerodynamic parameter estimation via Fourier modulating function techniques [NASA-CR-4654] p 335 N95-24630

TRANSFER OF TRAINING

Using the backward transfer paradigm to validate the AH-64 Simulator Training Research Advanced Testbed for Aviation [AD-A285758] p 238 N95-19931

TRANSFER ORBITS

Numerical optimization of synergetic maneuvers [AD-A283398] p 109 N95-17435

TRANSFORMATIONS (MATHEMATICS)

Conversion of Earth-centered Earth-fixed coordinates to geodetic coordinates [BTN-94-EIX94441380862] p 125 A95-64294

An improved method of airfoil design p 106 N95-16252

TRANSIENT OSCILLATIONS

Experimental/analytical approach to understanding mistuning in a transonic wind tunnel compressor [NASA-TM-108833] p 95 N95-14617

TRANSIENT RESPONSE

Transient analysis of a cracked rotor passing through critical speed [BTN-94-EIX94401360022] p 306 A95-74702

Evaluation of the transient operation of advanced gas turbine combustors [BTN-95-EIX0616952745793] p 614 A95-94495

TRANSITION FLIGHT

Application of an integrated methodology for propulsion and airframe control design to a STOVL aircraft [NASA-TM-106729] p 16 N95-11159

STOVL CFD model test case p 115 N95-17881

TRANSITION FLOW

Computation of oscillating airfoil flows with one- and two-equation turbulence models [BTN-95-EIX95152577588] p 263 A95-73494

The effect of wing sweep back upon transition in hypersonic flow [AIAA PAPER 95-6090] p 466 A95-89199

Corrective term in wall slip equations for Knudsen layer [BTN-95-EIX95282705070] p 455 A95-89667

Effect of spherical roughness elements upon transition of a 3-D boundary layer [HTN-95-92835] p 471 A95-90753

Experimental investigation of the vortex flow over a 76/60-deg double delta wing p 114 N95-17874

Application of Direct and Large Eddy Simulation to AGARD and Turbulence [AGARD-CP-551] p 248 N95-21061

Acoustic receptivity due to weak surface inhomogeneities in adverse pressure gradient boundary layers [NASA-TM-4577] p 249 N95-21258

Crossflow instability control on a swept-wing: Preliminary studies p 274 N95-23283

Study of compressible flow through a rectangular-to-semiannular transition duct [NASA-CR-4660] p 338 N95-24392

TRANSITION POINTS

Experimental studies on boundary-layer transition on a reentry vehicle at transonic and supersonic speeds [ISAS-659] p 555 N95-29712

TRANSITION TEMPERATURE

Phonon characteristics of high (T sub c) superconductors from neutron Doppler broadening measurements [DE95-003703] p 324 N95-24076

TRANSLATING

Partial camera automation in a simulated Unmanned Air Vehicle [AD-A288786] p 337 N95-26190

TRANSLATIONAL MOTION

Reduced-order nonlinear analysis of aircraft dynamics [BTN-95-EIX95282706665] p 455 A95-89640

TRANSMISSION EFFICIENCY

Efficient and effective handling of cycle slips in global positioning system data p 43 N95-12230

TRANSMISSION LOSS

Transmission loss characteristics of aircraft sidewall systems to control cabin interior noise p 28 N95-11261

A theoretical analysis of airborne sound transfer for a resiliently mounted machine to its foundation p 30 N95-11304

TRANSMISSION RATE (COMMUNICATIONS)

Aeronautical satellite communications using the ETS-5 satellite p 487 A95-91541

Electromagnetic compatibility effects of advanced packaging configurations p 247 N95-20658

TRANSMISSIONS (MACHINE ELEMENTS)

Investigation of heat transfer between rotating shafts of transmissions of turbojet engines [BTN-94-EIX94461408760] p 138 A95-63643

Optimal design of composite helicopter power transmission shafts with axially varying fiber layup [HTN-95-01086] p 529 A95-90272

A portable transmission vibration analysis system for the S-700A-9 Black Hawk helicopter [DSTO-TR-0072] p 348 N95-24203

Influence of tooth profile modification on spur gear dynamic tooth strain [NASA-TM-106952] p 553 N95-29112

Bell Helicopter Advanced Rotocraft Transmission (ART) program [NASA-CR-195479] p 555 N95-29538

TRANSMITTANCE

Transmittance characteristics of US Army rotary-wing aircraft transparencies [AD-A295035] p 693 N95-34793

TRANSMITTER RECEIVERS

Airborne integrated communications system [CONGRESS PAPER C428-30-162] p 610 A95-93612

High performance backplane components for modular avionics p 247 N95-20653

TRANSMITTERS

Flight dynamics of an unmanned aerial vehicle [AD-A282259] p 45 N95-12410

Apparatus and method for producing three-dimensional images [AD-D017455] p 646 N95-30727

TRANSONIC COMPRESSORS

An educational introduction to transonic compressor stage design principles [SAE PAPER 931393] p 613 A95-93668

A general theory of two- and three-dimensional rotational flow in subsonic and transonic turbomachines [NASA-CR-4496] p 377 N95-28003

The effect of adding roughness and thickness to a transonic axial compressor rotor [NASA-TM-106958] p 645 N95-30524

Experimental and computational investigation of the tip clearance flow in a transonic axial compressor rotor [NASA-TM-106711] p 649 N95-31738

TRANSONIC FLIGHT

Aerodynamic sensitivity coefficients using the three-dimensional full potential equation [BTN-95-EIX95062487530] p 186 A95-69238

Preliminary tests of a transonic flutter control wing model p 499 A95-91566

Transonic flight test of a laminar flow leading edge with surface excrescences [NASA-TM-4597] p 9 N95-11158

Computational analysis of forebody tangential slot blowing on the high alpha research vehicle [NASA-CR-196750] p 10 N95-11367

TRANSONIC FLOW

Novel similarity solutions of the sonic small-disturbance equation with applications to airfoil transonic aerodynamics [BTN-94-EIX94341340316] p 35 A95-60852

Engineering methods for the evaluation of transonic flutter characteristics for aerodynamic control surfaces [BTN-94-EIX94461408589] p 141 A95-63064

Aerodynamic design and calculation of flow around the plane cascade of turbine [BTN-94-EIX94481415357] p 104 A95-65347

Rotating Kirchhoff method for three-dimensional transonic blade-vortex interaction hover noise [BTN-94-EIX94441386601] p 182 A95-67332

Aerodynamic and wake methodology evaluation using Model UH-60A experimental data [HTN-95-31009] p 220 A95-71179

Aerodynamic shape optimization using preconditioned conjugate gradient methods [BTN-95-EIX95142553033] p 263 A95-73465

Flow visualization studies on sidewall effects in two-dimensional transonic airfoil testing [BTN-95-EIX95152582313] p 264 A95-73516

Improved version of the Naval Surface Warfare Center aeroprediction code (AP93) [BTN-95-EIX95152583260] p 267 A95-73561

Turbulent transonic airfoil flow simulation using a pressure-based algorithm [BTN-95-EIX95182619078] p 269 A95-75763

Scaling of incipient separation in supersonic/transonic speed laminar flows [BTN-95-EIX95182619104] p 269 A95-76589

Similarity rule for jet-temperature effects on transonic base pressure [BTN-95-EIX9522650791] p 329 A95-79247

An inverse design method of transonic airfoil and wing [HTN-95-71128] p 385 A95-83489

Transonic flutter suppression using active acoustic excitations [BTN-95-EIX95262694310] p 408 A95-85481

Computational analysis of buffet alleviation in viscous transonic flow over a porous airfoil [BTN-95-EIX95262694321] p 366 A95-85492

Aerodynamic design and optimization at Alenia D.V.D. Drag and lift in nonadiabatic transonic flow [HTN-95-61208] p 540 A95-87581

Dynamic pitch-up of a delta wing [HTN-95-81633] p 462 A95-87681

Automated adaptive time-discontinuous finite element method for unsteady compressible airfoil aerodynamics [HTN-95-81637] p 541 A95-87685

Role of Kutta waves on oscillatory shock motion on an airfoil [HTN-95-81642] p 542 A95-87690

Unsteady aerodynamics of vortical flows: Early and recent developments p 462 A95-88896

Rotating Kirchhoff method for three-dimensional transonic blade-vortex interaction hover noise [HTN-95-20927] p 463 A95-88966

Aerodynamic off-design behavior of integrated waveriders from take-off up to hypersonic flight [AIAA PAPER 95-6091] p 466 A95-89200

Preliminary study on the fixed transition technique for a shock tube transonic airfoil flow [BTN-95-EIX95282705928] p 455 A95-89663

Solution of the Navier-Stokes equations on a massively parallel transputer system p 549 A95-91490

Numerical design methods for transonic NLF configurations p 471 A95-91498

Fixed transition for shock tube transonic flow p 472 A95-91509

Comparison of coordinate-invariant and coordinate-aligned upwinding for the Euler equations [HTN-95-A1753] p 633 A95-93316

Evaluation of a multigrid-based Navier-Stokes solver for aerothermodynamic computations [BTN-95-EIX95302694459] p 583 A95-94056

Leading-edge sweepback and shape effects on fin-induced fluctuating pressures [BTN-95-EIX95302694471] p 636 A95-94067

Aerodynamic applications of underexpanded hypersonic viscous jets [BTN-95-EIX0619952748162] p 589 A95-94456

Analysis of some interference effects in a transonic wind tunnel [BTN-95-EIX0619952748166] p 589 A95-94460

Comparison of the predictive capabilities of several turbulence models [BTN-95-EIX0619952748167] p 589 A95-94461

Estimation of supersonic leading-edge thrust by a Euler flow model [BTN-95-EIX0619952748194] p 591 A95-94483

Interaction of a weak shock with freestream disturbances [BTN-95-EIX95332750473] p 638 A95-94687

Numerical solution of Euler and Navier-Stokes equations for 2D transonic problems p 638 A95-95366

Implicit multidomain calculation of viscous transonic flows without artificial viscosity or upwinding p 640 A95-95443

Permeable wall boundary conditions for transonic airfoil design p 641 A95-95445

On the prediction of transonic unsteady flows using second order time accuracy p 641 A95-95448

Multigrid/multiblock method for transonic potential flow around wing/body/nacelle configurations including a slipstream p 591 A95-95451

Transonic vortical flow predicted with a structured multiblock Euler solver p 642 A95-95462

A cartesian grid finite element method for aerodynamics of moving rigid bodies p 642 A95-95471

Dryden and transonic research [NASA-TM-104281] p 31 N95-10709

- Steady and unsteady three-dimensional transonic flow computations by integral equation method
[NASA-CR-196777] p 10 N95-11582
- An investigation of the transonic pressure drag coefficient for axis-symmetric bodies
[AD-A280990] p 105 N95-15994
- Mach number, flow angle, and loss measurements downstream of a transonic fan-blade cascade
[AD-A280907] p 108 N95-16824
- Comparison of computational and experimental results for a supercritical airfoil
[NASA-TM-4601] p 108 N95-16908
- Transonic Navier-Stokes calculations about a 65 deg delta wing
[NASA-CR-4635] p 108 N95-17273
- 2-D airfoil tests including side wall boundary layer measurements
p 158 N95-17847
- Investigation of an NLF(1)-0416 airfoil in compressible subsonic flow
p 110 N95-17852
- OAT15A airfoil data
p 111 N95-17857
- DLR-F5: Test wing for CFD and applied aerodynamics
p 113 N95-17864
- Wind tunnel test on a 65 deg delta wing with rounded leading edges: The International Vortex Flow Experiment
p 114 N95-17875
- Investigation of the flow development on a highly swept canard/wing research model with segmented leading- and trailing-edge flaps
p 114 N95-17876
- Overview of unsteady transonic wind tunnel test on a semispan straked delta wing oscillating in pitch
[AD-A284097] p 117 N95-18380
- Experimental techniques for measuring transonic flow with a three dimensional laser velocimetry system. Application to determining the drag of a fuselage
p 163 N95-19258
- The utilization of a high speed reflective visualization system in the study of transonic flow over a delta wing
p 121 N95-19259
- Transonic and supersonic flowfield measurements about axisymmetric afterbodies for validation of advanced CFD codes
p 121 N95-19260
- Transonic wind tunnel boundary interference correction
p 147 N95-19271
- Validation and evaluation of the advanced aeronautical CFD system SAUNA: A method developer's view
[ARA-MEMO-390] p 210 N95-19774
- Computation of transonic flow on composite overlapping grids in 2 D
[PB95-131348] p 248 N95-21132
- Computational fluid dynamics and transonic flow
[AD-A288962] p 436 N95-26405
- A numerical method for unsteady transonic flow about wings with control surfaces
[AD-A289631] p 375 N95-26859
- A general theory of two- and three-dimensional rotational flow in subsonic and transonic turbomachines
[NASA-CR-4496] p 377 N95-28003
- TranAir: A full-potential, solution-adaptive, rectangular grid code for predicting subsonic, transonic, and supersonic flows about arbitrary configurations. User's manual
[NASA-CR-4349] p 377 N95-28230
- TranAir: A full-potential, solution-adaptive, rectangular grid code for predicting subsonic, transonic, and supersonic flows about arbitrary configurations. Theory document
[NASA-CR-4348] p 378 N95-28265
- A method for the modelling of porous and solid wind tunnel walls in computational fluid dynamics codes
p 523 N95-29795
- Use of the PARC code to estimate the off-design transonic performance of an over/under turboramjet nozzle
[NASA-TM-106924] p 482 N95-30091
- Numerical solutions of inviscid and viscous flows about airfoils by TVD method
p 684 N95-34521
- Parallel computation of transonic flows about an aircraft configuration using multi-block structured grids
p 685 N95-34537
- Vector-parallel simulations of transonic wind tunnel flows about a fully configured model of aircraft
p 685 N95-34538
- TRANSONIC FLUTTER**
Engineering methods for the evaluation of transonic flutter characteristics for aerodynamic control surfaces
[BTN-94-EIX94461408589] p 141 A95-63064
- Limit cycle phenomena in computational transonic aeroelasticity
[BTN-95-EIX95152582317] p 264 A95-73520
- Application of transonic small disturbance theory to the active flexible wing model
[BTN-95-EIX95182619210] p 270 A95-76636
- Rolling maneuver load alleviation using active controls
[BTN-95-EIX95182619217] p 270 A95-76643
- Transonic flutter suppression using active acoustic excitations
[BTN-95-EIX95262694310] p 408 A95-85481
- Aeroelastic tailoring research
[PB94-180031] p 6 N95-10135
- Computations of unsteady aerodynamic loads around oscillating wings. Part 1: Formulation
[PB94-180049] p 7 N95-10136
- Computations of unsteady aerodynamic loads around oscillating wings. Part 2: Computed results and discussions
[PB94-180056] p 7 N95-10137
- TRANSONIC NOZZLES**
Direct splitting of coefficient matrix for numerical calculation of transonic nozzle flow
[BTN-94-EIX94481415356] p 103 A95-65346
- TRANSONIC SPEED**
Two-point transonic airfoil design using optimization for improved off-design performance
[BTN-95-EIX95062487542] p 192 A95-68356
- Effect of passive venting on static pressure distributions in cavities at subsonic and transonic speeds
[NASA-TM-4549] p 6 N95-10029
- Two-dimensional converging-diverging, rippled nozzles at transonic speeds — performed in the Langley 16-Foot Transonic Tunnel
[NASA-TP-3440] p 6 N95-10129
- Scale effects on aircraft and weapon aerodynamics
[AGAFD-AG-323] p 67 N95-14103
- Measurements of unsteady pressure and structural response for an elastic supercritical wing
[NASA-TP-3443] p 104 N95-16560
- Two-dimensional 16.5 percent thick supercritical airfoil NLR 7301
p 110 N95-17854
- DLR-F4 wing body configuration
p 130 N95-17863
- Low aspect ratio wing experiment
p 113 N95-17865
- Test data on a non-circular body for subsonic, transonic and supersonic Mach numbers
p 158 N95-17871
- Wind tunnel test on a 65 deg delta wing with a sharp or rounded leading edge: The international vortex flow experiment
p 114 N95-17872
- In-flight lift-drag characteristics for a forward-swept wing aircraft and comparisons with contemporary aircraft
[NASA-TP-3414] p 117 N95-18565
- Computational simulations for some tests in transonic wind tunnels
p 164 N95-19264
- Airfoil modification effects on subsonic and transonic pressure distributions and performance for the EA-6B airplane
[NASA-TP-3516] p 373 N95-26382
- Measurements of store forces and moments and cavity pressures for a generic store in and near a box cavity at subsonic and transonic speeds
[NASA-TM-4611] p 378 N95-28241
- Excess drag levels on aircraft
[ESDU-94044] p 477 N95-28897
- Transonic, supersonic and hypersonic wind-tunnel tests on aerodynamic characteristics of reentry body with blunted cone configuration
[ISAS-658] p 480 N95-29640
- Experimental studies on boundary-layer transition on a reentry vehicle at transonic and supersonic speeds
[ISAS-659] p 555 N95-29712
- Validation of the NPARC code for nozzle afterbody flows at transonic speeds
[NASA-TM-106971] p 592 N95-30704
- Transonic aerodynamic characteristics of a proposed wing-body reusable launch vehicle concept
[NASA-TM-108489] p 592 N95-30712
- Unsteady transonic wind tunnel test on a semispan straked delta wing, oscillating in pitch. Part 1: Description of the model, test setup, data acquisition, and data processing
[AD-A293113] p 593 N95-30885
- Afterbody/nozzle pressure distributions of a twin-tail twin-engine fighter with axisymmetric nozzles at Mach numbers from 0.6 to 1.2
[NASA-TP-3509] p 594 N95-31984
- Direct analysis of transonic rotor noise with CFD technique
p 711 N95-34549
- TRANSONIC WIND TUNNELS**
Aerodynamic investigation with focusing schlieren in a cryogenic wind tunnel
[HTN-95-20835] p 544 A95-88096
- Adaptive-wall wind-tunnel research at Ames Research Center: A retrospective
p 519 A95-88902
- Adaptive wall technology for minimization of wind tunnel boundary interferences - where are we now?
p 519 A95-88903
- The NASA Langley 8-foot Transonic Pressure Tunnel calibration
[NASA-TP-3437] p 8 N95-10739
- Mach number control in the High Speed Wind Tunnel of NLR
[PB94-201670] p 53 N95-13243
- Experimental/analytical approach to understanding mistuning in a transonic wind tunnel compressor
[NASA-TM-108833] p 95 N95-14617
- Wall-signature methods for high speed wind tunnel wall interference corrections
p 107 N95-16257
- Comparison of computational and experimental results for a supercritical airfoil
[NASA-TM-4601] p 108 N95-16908
- Single-engine tail interference model
p 115 N95-17879
- Overview of unsteady transonic wind tunnel test on a semispan straked delta wing oscillating in pitch
[AD-A284097] p 117 N95-18380
- Computational simulations for some tests in transonic wind tunnels
p 164 N95-19264
- Interference determination for wind tunnels with slotted walls
p 147 N95-19269
- Transonic wind tunnel boundary interference correction
p 147 N95-19271
- The traditional and new methods of accounting for the factors distorting the flow over a model in large transonic wind tunnels
p 165 N95-19275
- Interference corrections for a centre-line plate mount in a porous-walled transonic wind tunnel
p 122 N95-19280
- An investigation of drag repeatability in half model testing in the ARA Transonic Wind Tunnel
[ARA-MEMO-392] p 188 N95-19546
- Multipoint pressure measurements on continuously moving wind tunnel models
[ARA-MEMO-391] p 188 N95-19772
- Investigation of a thermal buoyancy effect on the drag of half models tested in the ARA Transonic Wind Tunnel
[ARA-MEMO-407] p 222 N95-19946
- 16-foot transonic tunnel test section flowfield survey
[NASA-TM-109157] p 238 N95-20669
- Testing in the ARA Transonic Wind Tunnel
[ARA-MEMO-395] p 239 N95-20799
- Performance of the 0.3-meter transonic cryogenic tunnel with air, nitrogen, and sulfur hexafluoride media under closed loop automatic control
[NASA-CR-195052] p 310 N95-23257
- Three-dimensional Navier-Stokes analysis and redesign of an imbedded bellmouth nozzle in a turbine cascade inlet section
p 311 N95-23423
- Development of a model protection and dynamic response monitoring system for the national transonic facility
[NASA-CR-195041] p 340 N95-24388
- Computer model to simulate testing at the National Transonic Facility
[NASA-TM-4664] p 627 N95-32217
- Vector-parallel simulations of transonic wind tunnel flows about a fully configured model of aircraft
p 685 N95-34538
- TRANSPARENCE**
Conference on Aerospace Transparent Materials and Enclosures. Volume 2: Sessions 5-9
[AD-A283926] p 131 N95-18162
- Conference on Aerospace Transparent Materials and Enclosures, volume 1
[AD-A283925] p 133 N95-18677
- TRANSPONDERS**
Evolutionary Telemetry and Command Processor (TCP) architecture
p 86 N95-14162
- TRANSPORT AIRCRAFT**
Fiber-optic technology for transport aircraft
[BTN-94-EIX94511309384] p 103 A95-64610
- Corrosion prevention and control
[BTN-95-EIX95031502753] p 188 A95-68260
- Ozone, skin cancer, and the SST
[BTN-95-EIX95041503011] p 213 A95-68314
- Application of circulation control to advanced subsonic transport aircraft. Part 1: Airfoil development
[BTN-95-EIX95062487545] p 185 A95-68359
- Application of circulation control to advanced subsonic transport aircraft. Part 2: Transport application
[BTN-95-EIX95062487546] p 185 A95-68360
- Design constraints in the payload-range diagram of ultrahigh capacity transport airplanes
[BTN-95-EIX95152582319] p 276 A95-73522
- Effect of underwing frost on a transport aircraft airfoil at flight Reynolds number
[BTN-95-EIX95152582334] p 276 A95-73536
- Possible effects of CO2 increase on the high-speed civil transport impact on ozone
[HTN-95-60779] p 317 A95-75976
- Effects of a polar stratosphere cloud parameterization on ozone depletion due to stratospheric aircraft in a two-dimensional model
[HTN-95-A1038] p 443 A95-84543
- Evolution of the concentrations of trace species in an aircraft plume: Trajectory study
[HTN-95-A1044] p 443 A95-84549
- Damage tolerance capability
p 388 A95-85898

Non-linear analysis provides new insights into impact damage of composite structures
[HTN-95-42368] p 418 A95-86197

FAA's Aging Commuter Airplane Program
[SAE PAPER 931248] p 483 A95-89220

The FAA regional/commuter aircraft flight loads data collection program
[SAE PAPER 931258] p 493 A95-89224

Application of restructurable flight control system to large transport aircraft
[BTN-95-EIX95282706666] p 515 A95-89639

Engine/airframe installation CFD for commercial transports: An engine manufacturer's perspective
[SAE PAPER 932623] p 495 A95-90084

Twenty-first century commercial transport engines
p 512 A95-91495

Some comments on current research and development of civil VTOL aircrafts
p 499 A95-91572

Estimation of atmospheric turbulence severity from in-situ aircraft measurements
p 659 A95-93479

Towards improving the NMC aircraft data base
p 660 A95-93480

Variable camber geometry for transport aircraft wings
[CONGRESS PAPER C428-35-061] p 603 A95-93626

Load alleviation for civil transport aircraft
[CONGRESS PAPER C428-35-057] p 604 A95-93627

Fiber optic hardware for transport aircraft
[SAE PAPER 931439] p 680 A95-93691

Navier-Stokes applications to high-lift airfoil analysis
[BTN-95-EIX0619952748182] p 590 A95-94475

Flight test certification of primary category aircraft using TP101-41E sportplane design standard
[BTN-95-EIX0619952748184] p 606 A95-94477

Reanalysis of European flight loads data
[AD-A282052] p 9 N95-11179

On the use of controls for subsonic transport performance improvement: Overview and future directions
[NASA-TM-4605] p 10 N95-11408

The development of a highly reliable power management and distribution system for civil transport aircraft
[NASA-TM-106697] p 50 N95-11867

The performance of child restraint devices in transport airplane passenger seats
[DOT/FAA/AM-94/19] p 40 N95-12146

The FC-1D: The profitable alternative Flying Circus Commercial Aviation Group
[NASA-CR-197152] p 46 N95-12628

LCX: Proposal for a low-cost commercial transport
[NASA-CR-197186] p 47 N95-12645

Design and testing of an oblique all-wing supersonic transport
[NASA-CR-196394] p 48 N95-12785

Numerical design of advanced multi-element airfoils
[NASA-CR-197135] p 76 N95-15762

DLR-F4 wing body configuration
p 130 N95-17863

Wing design for a civil tiltrotor transport aircraft
[NASA-CR-197523] p 130 N95-18090

European aeronautics: Strong government presence in industry structure and research and development support. Report to Congressional Requesters
[GAO/NSIAD-94-71] p 176 N95-18578

Proceedings of the USAF Structural Integrity Program Conference
[AD-A285684] p 194 N95-19517

Transport aircraft loading and balancing system: Using a CLIPS expert system for military aircraft load planning
p 217 N95-19751

Why do airlines want and use thrust reversers? A compilation of airline industry responses to a survey regarding the use of thrust reversers on commercial transport airplanes
[NASA-TM-109158] p 226 N95-20706

Wing pressure distributions from subsonic tests of a high-wing transport model — in the Langley 14 by 22-Foot Subsonic Wind Tunnel
[NASA-TM-4583] p 272 N95-22802

Handling qualities of the High Speed Civil Transport
p 294 N95-23325

High-lift flow-physics flight experiments on a subsonic civil transport aircraft (B737-100)
p 275 N95-23333

Emerging nondestructive inspection for aging aircraft
[PB95-143053] p 328 N95-25401

A quiet STOL Research Aircraft Development program
[NAL-TR-1223] p 336 N95-25862

Preliminary design problems and solutions for a supersonic oblique all-wing transport aircraft
p 390 N95-26942

Load transfer in the stiffener-to-skin joints of a pressurized fuselage
[NASA-CR-198610] p 439 N95-27865

High-stakes aviation: US-Japan technology linkages in transport aircraft
[LC-94-65759] p 381 N95-27907

Evaluation of all-electric secondary power for transport aircraft
[NASA-CR-189077] p 441 N95-27999

Overview of the ACT program
p 424 N95-28463

Designers' unified cost model
p 424 N95-28464

COINS: A composites information database system
p 453 N95-28465

Composite fuselage shell structures research at NASA Langley Research Center
p 425 N95-28466

Test and analysis results for composite transport fuselage and wing structures
p 398 N95-28470

Automated fiber placement: Evolution and current demonstrations
p 532 N95-28832

Effects of cabin pressure on climb and descent rates
[ESDU-94040] p 503 N95-29016

Advanced composite structural concepts and materials technologies for primary aircraft structures: Advanced material concepts
[NASA-CR-4485] p 503 N95-29027

Impact of composites on future transport aircraft
p 534 N95-29030

Advanced composites technology program
p 534 N95-29032

Textile composite fuselage structures development
p 534 N95-29033

Cost model relationships between textile manufacturing processes and design details for transport fuselage elements
p 536 N95-29043

Electrical short circuit and current overload tests on aircraft wiring
[AD-A293308] p 646 N95-30922

Report to the Chairman, Legislation and National Security Subcommittee, Committee on Government Operations, House of Representatives. C-17 Aircraft program: Improvements in initial provisioning process
[GAO/NSIAD-94-63] p 584 N95-32194

TRANSPORT PROPERTIES

Kinetic theory in aerothermodynamics
[HTN-95-A0002] p 183 A95-67829

Intrinsic transport and chemistry coupling in combustion phenomena
p 538 A95-87191

Transport phenomena in stratified multi-fluid flow in the presence and absence of gravity
p 95 N95-14563

Transport phenomena and interfacial kinetics in multiphase combustion systems
[AD-A288297] p 418 N95-26417

TRANSPORT THEORY
An introduction to generalized functions with some applications in aerodynamics and aeroacoustics
p 565 A95-88895

TRANSPORT VEHICLES

Solid-state data recorder, next development and use
p 705 N95-33143

TRANSPORTATION

Noise Con 1994: Proceedings of the 1994 National Conference on Noise Control Engineering. Progress in Noise Control for Industry
[LC-75-24750] p 28 N95-11259

Rotorcraft ditchings and water-related impacts that occurred from 1982 to 1989, phase 1
[AD-A279164] p 189 N95-19805

Mode of human image representation and error checking strategies in complex visual displays
[AD-A290107] p 485 N95-29210

TRANSUTERS

Parallel block implicit integration technique for trajectory parallelism
[AD-A288961] p 450 N95-28335

TRANSVERSE OSCILLATION

Coupled FEM-BEM approach for mean flow effects on vibro-acoustic behavior of planar structures
[BTN-95-EIX9515257587] p 263 A95-73495

TRAPPED VORTICES

Analysis of an oscillating Joukowski airfoil with surface suction and moving vortices
[BTN-95-EIX95062487527] p 186 A95-69235

TRAVELING WAVES

Observation of traveling waves in the three-dimensional boundary layer along a yawed cylinder
[HTN-95-61064] p 430 A95-83648

Acoustic scattering from ellipses by the modal element method
[NASA-TM-106935] p 579 N95-29401

TRENDS

Trends in aerospace forgings in the 1990s
[HTN-95-B0408] p 456 A95-90756

Algorithmic trends in computational fluid dynamics; The Institute for Computer Applications in Science and Engineering (ICASE)/LaRC Workshop, NASA Langley Research Center, Hampton, VA, US, Sep. 15-17, 1991
[ISBN 0-387-94014-6] p 550 A95-91915

New Trends in coatings developments for turbine blades: Materials processing and repair
p 201 N95-19676

High-stakes aviation: US-Japan technology linkages in transport aircraft
[LC-94-65759] p 381 N95-27907

TRIANGULATION

Quality estimates and stretched meshes based on Delaunay triangulations
[HTN-95-42575] p 564 A95-87205

Algorithms for high aspect ratio oriented triangulations
p 476 N95-28731

TRIBOLOGY

Surface morphology and structure of carbon-carbon composites in high-energy sliding contact
[BTN-94-EIX94371347996] p 206 A95-69164

Thermo-hydrodynamic solution of floating ring seals for high pressure compressors using the finite-element method
[HTN-95-92246] p 433 A95-85290

Effect of squeeze film damper land geometry on damper performance
[HTN-95-92247] p 434 A95-85291

The effects of wall perturbations on thermo-turbulent Couette flow
[HTN-95-92255] p 434 A95-85299

NASA evaluation of Type 2 chemical depositions — effects of deicer deposition on aircraft tire friction performance
[SAE PAPER 932582] p 495 A95-90086

Brush seal performance and durability issues based on T-700 engine test results
[NASA-TM-106502] p 22 N95-11483

Composite structure forming a wear surface
[AD-D017462] p 629 N95-30749

TRISONIC WIND TUNNELS

Experimental Aerodynamics Division
[NAL-SP-9404] p 35 N95-12166

Interference corrections for a centre-line plate mount in a porous-walled transonic wind tunnel
p 122 N95-19280

TROPICAL METEOROLOGY

Tropical cyclone observation and forecasting with and without aircraft reconnaissance
[HTN-95-80701] p 254 A95-72545

TROPICAL REGIONS

Fine-scale, poleward transport of tropical air during AASE 2
[HTN-95-70949] p 352 A95-78014

Field and data analysis studies related to the atmospheric environment
[NASA-CR-196543] p 168 N95-18093

TROPOSPHERE

Possible near-IR channels for remote sensing precipitable water vapor from geostationary satellite platforms
[HTN-95-70139] p 214 A95-69431

Meridional distributions of NO(X), NO(Y), and other species in the lower stratosphere and upper troposphere during AASE 2
[HTN-95-70944] p 352 A95-78009

Impact of present aircraft emissions of nitrogen oxides on tropospheric ozone and climate forcing
[HTN-95-21364] p 353 A95-78679

An intercomparison of aircraft instrumentation for tropospheric measurements of sulfur dioxide
[HTN-95-91855] p 354 A95-80843

An intercomparison of aircraft instrumentation for tropospheric measurements of carbonyl sulfide, hydrogen sulfide, and carbon disulfide
[HTN-95-91856] p 355 A95-80844

Compendium of NASA data base for the Global Tropospheric Experiment's Pacific Exploratory Mission West-A (PEM West-A)
[NASA-TM-109177] p 320 N95-23009

Excrescence drag levels on aircraft
[ESDU-94044] p 477 N95-28897

TROPOSPHERIC WAVES

Amplification and breaking of atmospheric gravity waves
p 675 A95-93552

TRUNCATION ERRORS

Precision requirement for potential-based panel methods
[HTN-95-51666] p 433 A95-85048

TUNGSTEN CARBIDES

Quality optimization of thermally sprayed coatings produced by the JP-5000 (HVOF) gun using mathematical modeling
p 152 N95-19008

TUNING

Intelligent control law tuning for AIAA controls design challenge
[BTN-94-EIX94511433922] p 169 A95-64588

Adaptive tuned vibration absorbers: Tuning laws, tracking agility, sizing, and physical implementations
p 25 N95-11280

Experimental/analytical approach to understanding mistuning in a transonic wind tunnel compressor
[NASA-TM-108833] p 95 N95-14617

Forced response of mistuned bladed disks
p 141 N95-19383

TURBINE BLADES

- Ultimate characteristics of a rocket engine with a turbo-pump supply system
[BTN-94-EIX94461408757] p 148 A95-63640
- Modelling for optimal operations of line milling of aerodynamic surfaces
[BTN-94-EIX94461408774] p 138 A95-63657
- Fatigue strength of high-temperature alloys under conditions of cyclic temperature variation. Communication 1: Experimental procedure and results
[BTN-94-EIX94401363884] p 307 A95-75516
- Boundary layer studies over an S-blade
[HTN-95-92261] p 434 A95-85305
- Multipoint inverse design of an infinite cascade of airfoils
[HTN-95-81640] p 541 A95-87688
- Engine structures analysis software: Component Specific Modeling (COSMO)
[NASA-CR-195378] p 57 N95-11711
- Investigation of advanced counterrotation blade configuration concepts for high speed turbo-prop systems. Task 8: Cooling flow/heat transfer analysis
[NASA-CR-195359] p 50 N95-11901
- Impingement flow heat transfer measurements of turbine blades using a jet array
[AD-A283450] p 62 N95-12512
- Measurements of pressure and thermal wakes in a transonic turbine cascade
[AD-A283464] p 38 N95-12548
- The industrial use of CFD in the design of turbomachinery
p 90 N95-14133
- New methods, new methodology: Advanced CFD in the Snerca turbomachinery design process
p 90 N95-14134
- Structural effects of unsteady aerodynamic forces on horizontal-axis wind turbines
[DE94-011863] p 157 N95-16939
- Measurement of gust response on a turbine cascade
[NASA-TM-106776] p 117 N95-18457
- Wind turbine blade aerodynamics: The combined experiment
[DE94-011866] p 118 N95-18645
- Wind turbine blade aerodynamics: The analysis of field test data
[DE94-011867] p 118 N95-18646
- Simulation of multidisciplinary problems for the thermosress state of cooled high temperature turbines
p 140 N95-19021
- Application of multidisciplinary models to the cooled turbine rotor design
p 140 N95-19024
- Aerodynamic investigation of the flow field in a 180 deg turn channel with sharp bend
p 163 N95-19257
- An analysis of the costs and benefits in improving F402-RR-406A High Pressure Turbine, second stage blades under the aircraft engine Component Improvement Program (CIP)
[AD-A285127] p 197 N95-19595
- Out of area experiences with the RB199 in Toronto
p 198 N95-19654
- Particle deposition in gas turbine blade film cooling holes
p 199 N95-19661
- Experimental and numerical simulations of the effects of ingested particles in gas turbine engines
p 199 N95-19662
- Damage of high temperature components by dust-laden air
p 201 N95-19673
- New Trends in coatings developments for turbine blades: Materials processing and repair
p 201 N95-19676
- Thermal testing of high performance thermal barrier coatings for turbine blades
p 202 N95-19681
- Resistance of silicon nitride turbine components to erosion and hot corrosion/oxidation attack
p 202 N95-19683
- Evidence that aerodynamic effects, including dynamic stall, dictate HAWT structural loads and power generation in highly transient time frames
[DE94-011865] p 216 N95-19855
- Advanced wind turbine design studies: Advanced conceptual study
[DE93-000031] p 256 N95-20985
- Supersonic flow and shock formation in turbine tip gaps
p 312 N95-23429
- Using digital filtering techniques as an aid in wind turbine data analysis
[DE94-011862] p 357 N95-24853
- NREL airfoil families for HAWTs
[DE95-000267] p 357 N95-24882
- A summary of computational experience at GE Aircraft Engines for complex turbulent flows in gas turbines
p 439 N95-27885
- Comparative performance tests on the Mod-2, 2.5-mW wind turbine with and without vortex generators
p 377 N95-27978
- Aeroelastic stability of wind turbine blade/aileron systems
p 377 N95-27981

- Comparison of measured and calculated dynamic loads for the Mod-2 2.5 mW wind turbine system
p 440 N95-27983
- Use of blade pitch control to provide power train damping for the Mod-2, 2.5-mW wind turbine
p 440 N95-27986
- Observed acoustic and aeroelastic spectral responses of a MOD-2 turbine blade to turbulence excitation
p 451 N95-27991
- Leading edge film cooling effects on turbine blade heat transfer
[NASA-TM-106955] p 513 N95-29115
- Grid orthogonality effects on predicted turbine midspan heat transfer and performance
[NASA-TM-106931] p 554 N95-29371
- Effect of velocity and temperature distribution at the hole exit on film cooling of turbine blades
[NASA-TM-106954] p 616 N95-30702
- Acceleration potential models
PREDICAT/PREDICDYN applied for calculation of axisymmetric dynamic inflow cases
[PB95-207015] p 647 N95-30957
- Advanced turbine systems program conceptual design and product development
[DE95-000088] p 650 N95-32163
- Allison engine testing CMSX-4(reg sign) single crystal turbine blades and vanes
[DE95-010308] p 694 N95-32636

TURBINE ENGINES

- Erosion of dust-filtered helicopter turbine engines. Part 1: Basic theoretical considerations
[BTN-95-EIX95182619222] p 288 A95-76648
- Life prediction of helicopter engines fitted with dust filters
[BTN-95-EIX95182619224] p 289 A95-76650
- Chemical composition and photochemical reactivity of exhaust from aircraft turbine engines
[HTN-95-51277] p 356 A95-80862
- Advances in the application of laser cutting, drilling, and welding aerospace parts
[SAE PAPER 932544] p 547 A95-90052
- Lightweight, opto-electronic engine control system for aerospace turbine engines
[SAE PAPER 931442] p 614 A95-93692
- NASA Lewis Propulsion Systems Laboratory test article systems criteria
[NASA-TM-106589] p 20 N95-10446
- Air Force seal activities
p 60 N95-13600
- Effect of surface roughness on local film cooling effectiveness and heat transfer coefficients
[AD-A283854] p 91 N95-14351
- Modern transport engine experience with environmental ingestion effects
p 199 N95-19660
- Damage of high temperature components by dust-laden air
p 201 N95-19673
- New Trends in coatings developments for turbine blades: Materials processing and repair
p 201 N95-19676
- Statistical analysis of Turbine Engine Diagnostic (TED) field test data
[AD-A286032] p 248 N95-20998
- Turbine design and application volumes 1, 2, and 3
[E-5666-Vol-1-3] p 236 N95-22341
- Turbine-engine applications of thermographic-phosphor temperature measurements
[DE95-003625] p 358 N95-25110
- A design perspective on thermal barrier coatings
p 344 N95-26120
- Ceramic composite combustor cans for expendable turbine engines
[AD-A289551] p 407 N95-28646
- Intelligent turbine engines for Army applications
[AD-A290532] p 514 N95-29496

TURBINE PUMPS

- Ultimate characteristics of a rocket engine with a turbo-pump supply system
[BTN-94-EIX94461408757] p 148 A95-63640
- Boundary layer studies over an S-blade
[HTN-95-92261] p 434 A95-85305
- CFD analysis of turbopump volutes
p 312 N95-23436
- Phase 2: HGM air flow tests in support of HEX vane investigation
p 312 N95-23438
- Comparison of numerical results and multicavity purge and rim seal data with extensions to dynamics
[NASA-TM-106685] p 416 N95-27434

TURBINE WHEELS

- Preliminary analysis of dynamic stall effects on a 91-meter wind turbine rotor
p 376 N95-27975
- Use of blade pitch control to provide power train damping for the Mod-2, 2.5-mW wind turbine
p 440 N95-27986
- Variable speed generator application on the MOD-5A 7.3 mW wind turbine generator
p 440 N95-27989
- UHB engine fan broadband noise reduction study
[NASA-CR-198357] p 580 N95-29641
- Axial loads on yawed rotors
[PB95-214193] p 592 N95-30638

TURBINES

- Aerodynamic design and calculation of flow around the plane cascade of turbine
[BTN-94-EIX94481415357] p 104 A95-65347
- Static pressure distribution in the inlet of a helicopter turbine compressor
[BTN-95-EIX95152582339] p 266 A95-73541
- An aerodynamic analysis of a mixed flow turbine
[NASA-TM-106674] p 15 N95-10153
- Impingement flow heat transfer measurements of turbine blades using a jet array
[AD-A283450] p 62 N95-12512
- Effect of surface roughness on local film cooling effectiveness and heat transfer coefficients
[AD-A283854] p 91 N95-14351
- Simulation of multidisciplinary problems for the thermosress state of cooled high temperature turbines
p 140 N95-19021
- Scale-up and modeling of forced chemical vapor infiltration
[DE94-017769] p 247 N95-20781
- Turbine design and application volumes 1, 2, and 3
[E-5666-Vol-1-3] p 236 N95-22341
- Three-dimensional unsteady flow calculations in an advanced gas generator turbine
p 312 N95-23425
- Aerodynamic design and analysis of a highly loaded turbine exhaust
p 312 N95-23435
- CFD analysis of turbopump volutes
p 312 N95-23436
- Numerical computation of aerodynamics and heat transfer in a turbine cascade and a turn-around duct using advanced turbulence models
p 313 N95-23444
- Enhanced analysis and users manual for radial-inflow turbine conceptual design code RTD
[NASA-CR-195454] p 275 N95-23462
- A comparison of measured wind park load histories with the WISPER and WISPERX load spectra
[DE95-000295] p 446 N95-27459
- Improved modeling of unsteady heat transfer (The first step)
[AD-A292777] p 648 N95-31432
- Advanced turbine systems program conceptual design and product development
[DE95-000088] p 650 N95-32163
- Allison engine testing CMSX-4(reg sign) single crystal turbine blades and vanes
[DE95-010308] p 694 N95-32636
- Verification of turbine cascade flow with tip clearance
p 698 N95-34511

TURBOCOMPRESSORS

- Heat transfer in the flow-through part of axial compressors
[BTN-94-EIX94461407949] p 89 A95-62267
- Investigation of heat transfer in a rotating ring gap with the axial flow of a coolant during the rotation of the central shaft
[BTN-94-EIX94461407951] p 89 A95-62625
- A stationary flow of a viscous liquid in radial clearances of rotor bearings in the turbocompressor of an internal combustion engine
[BTN-94-EIX94461408765] p 153 A95-63648
- Thermo-hydrodynamic solution of floating ring seals for high pressure compressors using the finite-element method
[HTN-95-92246] p 433 A95-85290
- Experimental investigation of the flow in diffusers behind an axial flow compressor
[BTN-95-EIX95282710057] p 632 A95-92472
- Inlet flow test calibration for a small axial compressor facility. Part 1: Design and experimental results
[NASA-TM-106719] p 16 N95-11005
- Ceramic manufacturing: Optimizing a multivariable system
[DE94-015016] p 56 N95-13184
- Computational methods for preliminary design and geometry definition in turbomachinery
p 89 N95-14128
- Elements of a modern turbomachinery design system
p 90 N95-14129
- Enhanced capabilities and modified users manual for axial-flow compressor conceptual design code CSPAN
[NASA-TM-106833] p 119 N95-18933
- Performance deterioration of axial compressors due to blade defects
p 199 N95-19665
- Impact loading of compressor stator vanes by hailstone ingestion
p 200 N95-19670
- Advanced diesel electronic fuel injection and turbocharging
[AD-A279176] p 211 N95-19809
- NASA low-speed axial compressor for fundamental research
[NASA-TM-4635] p 296 N95-23192
- WINCLR: A computer code for heat transfer and clearance calculation in a compressor
[NASA-CR-195436] p 366 N95-26363

- Modeling and control of rotating stall in high speed multi-stage axial compressors p 513 N95-29244
Inlet flow test calibration for a small axial compressor rig. Part 2: CFD compared with experimental results [NASA-TM-106999] p 514 N95-30007
The effect of adding roughness and thickness to a transonic axial compressor rotor [NASA-TM-106958] p 645 N95-30524
Investigating the use of smart acoustically active surfaces for flow separation control in turbomachinery [AD-A292819] p 648 N95-31443
Experimental and computational investigation of the tip clearance flow in a transonic axial compressor rotor [NASA-TM-106711] p 649 N95-31738
- TURBOFAN AIRCRAFT**
A preliminary design proposal for a maritime patrol strike aircraft: MPS-2000 Condor [NASA-CR-197182] p 47 N95-12689
- TURBOFAN ENGINES**
Trent engine development [BTN-94-EIX94461290507] p 82 A95-61727
Turbofan propulsion simulator [BTN-94-EIX94461290240] p 82 A95-61737
Lycoming to test new engine core [HTN-95-41393] p 288 A95-76389
Derivation of system matrices from nonlinear dynamic simulation of jet engines [BTN-95-EIX95182619139] p 288 A95-76616
Nitrogen oxide emissions characteristics of augmented turbofan engines [BTN-94-EIX95011441240] p 403 A95-84197
GETRAN: A generic, modularly structured computer code for simulation of dynamic behavior of aero- and power generation gas turbine engines [BTN-94-EIX95011441241] p 431 A95-84198
Control requirements for the RB 211 low-emission combustion system [BTN-94-EIX95011441244] p 416 A95-84201
Active control of fan noise from a turbofan engine [HTN-95-61198] p 570 A95-87571
Preliminary design of a single engine business jet [SAE PAPER 931253] p 493 A95-89222
Fan noise reduction from a supersonic inlet during simulated aircraft approach [BTN-95-EIX95292721155] p 572 A95-89894
High bypass separate flow exhaust system improved thrust efficiency by modifying the aft centerbody [SAE PAPER 932622] p 511 A95-90083
Civil aircraft propulsion integration: Current & future [SAE PAPER 932624] p 495 A95-90085
Prediction of airplane cabin noise due to engine shock cell excitation using statistical energy analysis p 577 A95-90131
Twenty-first century commercial transport engines p 512 A95-91495
Aero-engine R&D efforts for environmental protection p 512 A95-91502
Design trends in propulsion control systems [CONGRESS PAPER C428-33-123] p 610 A95-93620
Surge recovery and compressor working line control using compressor exit mach number measurement [CONGRESS PAPER C428-33-210] p 610 A95-93622
An educational introduction to transonic compressor stage design principles [SAE PAPER 931393] p 613 A95-93668
Propulsion simulator for high bypass turbofan performance evaluation [SAE PAPER 931410] p 625 A95-93676
Computational fluid dynamics study of the variable-pitch split-blade fan concept [NASA-CR-189206] p 15 N95-10247
Fan noise research at NASA p 28 N95-11260
Active control of turbomachine discrete tones p 29 N95-11275
Analytical investigation of adaptive control of radiated inlet noise from turbofan engines p 30 N95-11277
The OFP-6M transport jet [NASA-CR-197159] p 46 N95-12637
Gas turbine prediffuser-combustor performance during operation with air-water mixture [DOT/FAA/CT-93/52] p 83 N95-15683
Bird ingestion into large turbofan engines [DOT/FAA/CT-93/14] p 333 N95-24631
UHB engine fan broadband noise reduction study [NASA-CR-198357] p 580 N95-29641
Wave rotor-enhanced gas turbine engines [NASA-TM-106998] p 615 N95-30517
Method for extracting forward acoustic wave components from rotating microphone measurements in the inlets of turbofan engines [NASA-CR-195457] p 616 N95-30779
Computation of noise radiation from turbofans: A parametric study [NASA-CR-198359] p 710 N95-32836
- An Electronic Workshop on the Performance Seeking Control and Propulsion Controlled Aircraft Results of the F-15 Highly Integrated Digital Electronic Control Flight Research Program [NASA-TM-104278] p 694 N95-33009
An overview of integrated flight-propulsion controls flight research on the NASA F-15 research airplane p 694 N95-33010
F-15 propulsion system p 695 N95-33012
- TURBOFANS**
Propulsion simulator for high bypass turbofan performance evaluation [SAE PAPER 931410] p 625 A95-93676
Computational fluid dynamics study of the variable-pitch split-blade fan concept [NASA-CR-189206] p 15 N95-10247
Fan noise research at NASA p 28 N95-11260
Recirculating cavity casing treatment failure [AD-A289330] p 513 N95-28908
Computation of noise radiation from turbofans: A parametric study [NASA-CR-198359] p 710 N95-32836
- TURBOJET ENGINE CONTROL**
Derivation of system matrices from nonlinear dynamic simulation of jet engines [BTN-95-EIX95182619139] p 288 A95-76616
Control requirements for the RB 211 low-emission combustion system [BTN-94-EIX95011441244] p 416 A95-84201
Application of an integrated methodology for propulsion and airframe control design to a STOVL aircraft [NASA-TM-106729] p 16 N95-11159
Flight assessment of the onboard propulsion system model for the Performance Seeking Control algorithm on an F-15 aircraft [NASA-TM-4705] p 617 N95-31425
An Electronic Workshop on the Performance Seeking Control and Propulsion Controlled Aircraft Results of the F-15 Highly Integrated Digital Electronic Control Flight Research Program [NASA-TM-104278] p 694 N95-33009
An overview of integrated flight-propulsion controls flight research on the NASA F-15 research airplane p 694 N95-33010
Performance seeking control program overview p 695 N95-33011
PSC algorithm description p 695 N95-33013
Minimum fuel mode evaluation p 695 N95-33015
Minimum fan turbine inlet temperature mode evaluation p 696 N95-33016
Maximum thrust mode evaluation p 696 N95-33017
Rapid deceleration mode evaluation p 696 N95-33018
Performance seeking control excitation mode p 696 N95-33019
Performance seeking control (PSC) for the F-15 highly integrated digital electronic control (HIDEC) aircraft p 697 N95-33020
Propulsion Controlled Aircraft design and development p 697 N95-33022
- TURBOJET ENGINES**
Investigation of heat transfer between rotating shafts of transmissions of turbojet engines [BTN-94-EIX94461408760] p 138 A95-63643
Development and application of the double V type flame stabilizer [BTN-94-EIX94481415355] p 154 A95-65345
Unbalance response of a dual rotor system: Theory and experiment [BTN-94-EIX94351143320] p 195 A95-65854
Aircraft gas turbine emissions challenge [BTN-94-EIX95011441239] p 403 A95-84196
Experimental investigation of thermoelastic deformation in turbojet-engine bearings under maintenance inspection [BTN-95-EIX95292721173] p 546 A95-89904
Multivariable adaptive control using only input and output measurements for turbojet engines [BTN-95-EIX95292721165] p 677 A95-92597
Propulsion education at Carlton University [SAE PAPER 931391] p 613 A95-93667
Calculation of control laws for the digital fuel control unit of a small thrust turbojet [SAE PAPER 931411] p 614 A95-93677
Small turbojets: Designs and installations p 138 N95-16323
Perspective problems of gas turbine engines simulation p 140 N95-19026
Portable static test facility for small, expendable, turbojet engines, phase 1 [AD-A286337] p 239 N95-21719
Comparison of numerical results and multicavity purge and rim seal data with extensions to dynamics [NASA-TM-106685] p 416 N95-27434
- TURBOMACHINE BLADES**
Study on the turbine vane and blade for a 1500 C class industrial gas turbine [BTN-94-EIX95011441254] p 431 A95-84211
Aeroelastic stability of cascades in turbomachinery [HTN-95-61156] p 405 A95-86255
Experimental investigation of the sources of propeller noise due to the ingestion of turbulence at low speeds [BTN-95-EIX95262697042] p 569 A95-86859
Blade-by-blade tip clearance measurement system for gas turbine applications [BTN-95-EIX95292721167] p 546 A95-89899
Correlation of unsteady pressure and inflow velocity fields of a pitching rotor blade [BTN-95-EIX95292748169] p 589 A95-94463
NASA Lewis Research Center Workshop on Forced Response in Turbomachinery [NASA-CP-10147] p 141 N95-19380
Forced response of mistuned bladed disks p 141 N95-19383
Investigation of shear layer transition using various turbulence models p 248 N95-21096
- TURBOMACHINERY**
New approach to geometric profiling of the design elements of the passage part in turbo-machines [BTN-94-EIX94461408769] p 153 A95-63652
Rotor whirl forces induced by the tip clearance effect in axial flow compressors [BTN-94-EIX94351143331] p 207 A95-67304
Solution-adaptive structured-unstructured grid method for unsteady turbomachinery analysis. Part I: Methodology [BTN-94-EIX94441380983] p 208 A95-67329
Aeroelastic stability of cascades in turbomachinery [HTN-95-61156] p 405 A95-86255
Investigation of advanced counterrotation blade configuration concepts for high speed turboprop systems. Task 8: Cooling flow/heat transfer analysis user's manual [NASA-CR-195360] p 50 N95-11951
Turbomachinery Design Using CFD [AGARD-LS-195] p 89 N95-14127
Designing in three dimensions p 90 N95-14130
The industrial use of CFD in the design of turbomachinery p 90 N95-14133
New methods, new methodology: Advanced CFD in the Snecma turbomachinery design process p 90 N95-14134
The role of CFD in the design process p 90 N95-14135
Aero design of turbomachinery components: CFD in complex systems p 90 N95-14136
Application of multicomponent models to flow passage simulation in multistage turbomachines and whole gas turbine engines p 140 N95-19022
Simulation of steady and unsteady viscous flows in turbomachinery p 140 N95-19023
Verification of multidisciplinary models for turbomachines p 140 N95-19025
NASA Lewis Research Center Workshop on Forced Response in Turbomachinery [NASA-CP-10147] p 141 N95-19380
Unsteady aerodynamic analyses for turbomachinery aeroelastic predictions p 141 N95-19381
Steady potential solver for unsteady aerodynamic analyses p 141 N95-19382
Forced response of mistuned bladed disks p 141 N95-19383
A general theory of two- and three-dimensional rotational flow in subsonic and transonic turbomachines [NASA-CR-4496] p 377 N95-28003
Bearing defect signature analysis using advanced nonlinear signal analysis in a controlled environment [NASA-TM-108491] p 441 N95-28364
The acoustic characteristics of turbomachinery cavities [NASA-CR-4671] p 476 N95-28720
Model development for active control of stall phenomena in aircraft gas turbine engines p 514 N95-29679
Investigating the use of smart acoustically active surfaces for flow separation control in turbomachinery [AD-A292819] p 648 N95-31443
- TURBOPROP AIRCRAFT**
Development and validation of a numerical acoustic analysis program for aircraft interior noise prediction p 572 A95-88471
Numerical and flight measured interior noise characteristics of a twin-engine turboprop general aviation aircraft p 573 A95-90094
Enroute NASA/FAA low-frequency propfan test in Alabama (October 1987): A versatile atmospheric aircraft long-range noise prediction system p 573 A95-90099
Experimental active control of sound in the ATR 42 p 575 A95-90110
Noise transmission and reduction in turboprop aircraft p 175 N95-19164

TURBOPROP ENGINES

- Artificial intelligence for turboprop engine maintenance
[BTN-95-EIX95182617812] p 288 A95-75757
- Lycoming to test new engine core
[HTN-95-41393] p 288 A95-76389
- Artificial intelligence for turboprop engine maintenance
[HTN-95-92313] p 404 A95-85357
- Investigation of advanced counterrotation blade configuration concepts for high speed turboprop systems.
Task 8: Cooling flow/heat transfer analysis user's manual
[NASA-CR-195360] p 50 N95-11951
- Brush seals for turbine engine fuel conservation
p 59 N95-13595

TURBORAMJET ENGINES

- Test results on air turbo ramjet engine for a future space plane
p 402 A95-82327
- Use of the PARC code to estimate the off-design transonic performance of an over/under turboramjet nozzle
[NASA-TM-106924] p 482 N95-30091

TURBOSHAFTS

- Lycoming to test new engine core
[HTN-95-41393] p 288 A95-76389
- Applicability of electrically driven accessories for turboshaft engines
[BTN-95-EIX95292721153] p 612 A95-92589
- Sensor fault detection and diagnosis simulation of a helicopter engine in an intelligent control framework
[AD-A290223] p 137 N95-15970
- US Army rotorcraft turboshaft engines sand and dust erosion considerations
p 198 N95-19656
- Future directions in helicopter protection system configuration
p 198 N95-19657
- Wave rotor-enhanced gas turbine engines
[NASA-TM-106998] p 615 N95-30517

TURBULENCE

- An experimental investigation of wing tip turbulence with applications to aerosound
[AIAA PAPER 86-1918] p 1 A95-60164
- Model for compressible turbulence in hypersonic wall boundary and high-speed mixing layers
[BTN-94-EIX94441386625] p 184 A95-68174
- Tip vortex on a swept wing. Mean flow and unsteady phenomena
[BTN-94-EIX94441385755] p 184 A95-68219
- An algorithm for forecasting mountain wave-related turbulence in the stratosphere
[HTN-95-80656] p 254 A95-72500
- Navier-Stokes prediction of large-amplitude delta-wing roll oscillations
[BTN-95-EIX95152582329] p 281 A95-73531
- Flow study of supersonic wing-nacelle configuration
[BTN-95-EIX95152582344] p 266 A95-73546
- Observations on using experimental data as boundary conditions for computations
[BTN-95-EIX95182619103] p 321 A95-76588
- Response of a nonrotating rotor blade to lateral turbulence. Part 1: Theory
[BTN-95-EIX95182619228] p 284 A95-76654
- Structure of a double-fin turbulent interaction at high speed
[BTN-95-EIX95222650780] p 347 A95-79236
- On the role of the outer region in the turbulent-boundary-layer bursting process
[BTN-94-EIX95011441078] p 348 A95-81056
- Prediction of two-dimensional momentumless wake by k-epsilon-gamma model
[BTN-95-EIX95262694299] p 434 A95-85470
- Quantitative investigation of compressible mixing: Staged transverse injection into Mach 2 flow
[HTN-95-42330] p 404 A95-86159
- Drag coefficients of spherical liquid droplets. Part 2: Turbulent gaseous fields
[BTN-95-EIX95262697041] p 538 A95-86858
- Experimental investigation of the sources of propeller noise due to the ingestion of turbulence at low speeds
[BTN-95-EIX95262697042] p 569 A95-86859
- Vortex cutting by a blade, part 1: General theory and a simple solution
[HTN-95-20822] p 543 A95-88083
- Fluctuating wall pressures near separation in highly swept turbulent interactions
[HTN-95-20823] p 543 A95-88084
- Hypersonic shock wave/turbulent boundary layer interactions in the vicinity of an expansion corner
[AIAA PAPER 95-6125] p 469 A95-90446
- Turbulence characteristics of supersonic boundary layer past a backward facing step
[AIAA PAPER 95-6126] p 470 A95-90447
- Measurement in laminar and transitional boundary-layer flows on concave surface
[BTN-95-EIX95282711333] p 632 A95-92408
- Knowing our users - A challenge for meteorologists at the National Aviation Weather Advisory Unit
p 655 A95-93459

- The aviation gridded forecast system verification program - A description of aviation-impact-variable evaluation plans
p 664 A95-93458
- Statistical discrete gust-power spectral density methods overlap-holistic proof and beyond
[BTN-95-EIX0619952748175] p 584 A95-94469
- Turbulent effects on parachute drag
[BTN-95-EIX0619952748193] p 591 A95-94482
- Interaction of a weak shock with freestream disturbances
[BTN-95-EIX95332750473] p 638 A95-94687
- Empirical refinements to boundary layer transition noise models
p 28 N95-11262
- Effect of weak periodic pressure gradient on streamwise vortices near a wall
p 29 N95-11263
- Modification of the two-equation turbulence model in NPARC to a Chien low Reynolds number k-epsilon formulation
[NASA-TM-106710] p 37 N95-11917
- Spectral analysis of vortex/free-surface interaction
[AD-A283210] p 96 N95-14658
- Structural effects of unsteady aerodynamic forces on horizontal-axis wind turbines
[DE94-011863] p 157 N95-16939
- Experiments in the trailing edge flow of an NLR 7702 airfoil
p 110 N95-17853
- Experimental study of vane heat transfer and aerodynamics at elevated levels of turbulence
[NASA-CR-4633] p 244 N95-19912
- Application of wavelet-filtering techniques to intermittent turbulent and wall pressure events. Part 1: Exploratory results
[AD-A286077] p 247 N95-20849
- Experimental investigations of on-demand vortex generators
p 250 N95-22451
- Basic studies in turbulent shear flows
[AD-A289145] p 437 N95-26998
- NAS Technical Summaries, March 1993 - February 1994
[NASA-RP-1355] p 453 N95-27367
- Industry-Wide Workshop on Computational Turbulence Modeling
[NASA-CP-10165] p 439 N95-27882
- Effects of elevated free-stream turbulence and streamwise acceleration on flow and thermal structures in transitional boundary layers
p 556 N95-29729
- Numerical simulation and analysis of the hypersonic turbulent flow past a blunt-fin/ramp configuration
[DLR-FB-94-19] p 483 N95-30349
- Hot jet/wake turbulent structure and laser propagation. Part 3: Laser propagation measurements and modeling
p 647 N95-30992
- Advanced k-epsilon modeling of heat transfer
[NASA-CR-4679] p 648 N95-31423
- Advanced gust management systems: Lessons learned and perspectives
p 622 N95-32002

TURBULENCE EFFECTS

- Effect of ambient turbulence intensity on sphere wakes at intermediate Reynolds numbers
[BTN-95-EIX95182619101] p 308 A95-76586
- Rotorcraft handling qualities in turbulence
[BTN-95-EIX95242670750] p 334 A95-81097
- Effects of free-stream turbulence intensity on a boundary layer recovering from concave curvature effects
[BTN-95-EIX95282710058] p 632 A95-92471
- Assessment of technology for aircraft development
[BTN-95-EIX0619952748181] p 606 A95-94474
- Measurements of atmospheric turbulence effects on tail rotor acoustics
[NASA-TM-108843] p 38 N95-12360
- Measurements of pressure and thermal wakes in a transonic turbine cascade
[AD-A283464] p 38 N95-12548
- Atmospheric effects on the risetime and waveshape of sonic booms
p 100 N95-14886
- The effect of aircraft speed on the penetration of sonic boom noise into a flat ocean
p 100 N95-14887
- Wake turbulence
p 75 N95-14894
- A study of the effect of store unsteady aerodynamics on gust and turbulence loads
p 133 N95-18601
- Comparison of stochastic and deterministic nonlinear gust analysis methods to meet continuous turbulence criteria
p 133 N95-18602
- Design limit loads based upon statistical discrete gust methodology
p 133 N95-18603
- Pressure measurements on an F/A-18 twin vertical tail in buffeting flow. Volume 4, part 2: Buffet cross spectral densities
[AD-A285555] p 143 N95-18641
- Simulation of rotor blade element turbulence
[NASA-TM-108862] p 232 N95-21186
- A preliminary study of the airwake model used in an existing SH-60B/FFG-7 helicopter/ship simulation program
[DSTO-TR-0015] p 224 N95-21659

- Observed acoustic and aeroelastic spectral responses of a MOD-2 turbine blade to turbulence excitation
p 451 N95-27991
- Anechoic wind tunnel study of turbulence effects on wind turbine broadband noise
p 451 N95-27992
- Influence of turbulence parameters, Reynolds number, and body shape on stagnation-region heat transfer
[NASA-TP-3487] p 550 N95-28719
- Turbulent airflow noise production and propagation patterns of a subsonic jet impinging on a flat plate
p 580 N95-29502
- Effects of elevated free-stream turbulence and streamwise acceleration on flow and thermal structures in transitional boundary layers
p 556 N95-29729
- Numerical simulation and analysis of the hypersonic turbulent flow past a blunt-fin/ramp configuration
[DLR-FB-94-19] p 483 N95-30349

TURBULENCE MODELS

- Dynamic stall of an oscillating wing. Part 1: Evaluation of turbulence models
[AIAA PAPER 93-3403] p 3 A95-60184
- A comparison of turbulence models in computing multi-element airfoil flows
[AIAA PAPER 94-0291] p 4 A95-60185
- Supersonic and hypersonic shock/boundary-layer interaction database
[BTN-94-EIX94441386604] p 182 A95-67335
- Behavior of the Johnson-King turbulence model in axisymmetric supersonic flows
[BTN-94-EIX94441386606] p 183 A95-67337
- Shock layers and boundary layers in hypersonic flows
[HTN-A0003] p 183 A95-67830
- Lag model for turbulent boundary layers over rough bleed surfaces
[BTN-94-EIX94441380981] p 208 A95-68165
- Model for compressible turbulence in hypersonic wall boundary and high-speed mixing layers
[BTN-94-EIX94441386625] p 184 A95-68174
- Numerical computations of supersonic base flow with special emphasis on turbulence modeling
[BTN-94-EIX94441386632] p 179 A95-68181
- Numerical simulation of incidence and sweep effects on delta wing vortex breakdown
[BTN-95-EIX95062487526] p 186 A95-69234
- Modeling of supersonic turbulent combustion using assumed probability density functions
[BTN-95-EIX95112524190] p 206 A95-69318
- Two-equation turbulence model for unsteady separated flows around airfoils
[BTN-95-EIX95142553054] p 262 A95-73444
- Flow structure in the wake of a wishbone vortex generator
[BTN-95-EIX95142553044] p 304 A95-73454
- Adaptive finite element method for turbulent flow near a propeller
[BTN-95-EIX95142553038] p 305 A95-73460
- Laplace interaction law for the computation of viscous airfoil flow in low- and high-speed aerodynamics
[BTN-95-EIX95142553037] p 263 A95-73461
- Computation of oscillating airfoil flows with one- and two-equation turbulence models
[BTN-95-EIX95152577588] p 263 A95-73494
- Progress in high-lift aerodynamic calculations
[BTN-95-EIX95142553035] p 264 A95-73518
- Computation of the poststall behavior of a circulation controlled airfoil
[BTN-95-EIX95152582320] p 264 A95-73523
- Transport of exhaust products in the near trail of a jet engine under atmospheric conditions
[HTN-95-91421] p 319 A95-77334
- Structure of a double-fin turbulent interaction at high speed
[BTN-95-EIX95222650780] p 347 A95-79236
- Effect of Reynolds number and turbulence on airfoil aerodynamics at -90-degree incidence
[HTN-95-42320] p 370 A95-86149
- Numerical model for circulation-control flows
[HTN-95-81632] p 461 A95-87680
- Compressible Navier-Stokes calculations of the flow over airfoil sections. Comparisons of 1st and 2nd order turbulence models
[SAE PAPER 932510] p 546 A95-89183
- Computational study of a two-slot circulation control airfoil
[SAE PAPER 932531] p 466 A95-89191
- Turbulent flow measurements with a triple-split hot-film probe
[HTN-95-A1774] p 634 A95-93337
- Estimation of atmospheric turbulence severity from in-situ aircraft measurements
p 659 A95-93479
- Comparison of the predictive capabilities of several turbulence models
[BTN-95-EIX0619952748167] p 589 A95-94461
- Turbulence: Engineering models, aircraft response
p 84 N95-14900

- Laminar and turbulent flow computations of Type 4 shock-shock interference aerothermal loads using unstructured grids
[NASA-CR-195008] p 97 N95-15604
- Transonic Navier-Stokes calculations about a 65 deg delta wing
[NASA-CR-4635] p 108 N95-17273
- A supercritical airfoil experiment p 111 N95-17858
- Aeromechanics technology, volume 1. Task 1: Three-dimensional Euler/Navier-Stokes Aerodynamic Method (TEAM) enhancements
[AD-A285713] p 132 N95-18483
- Solution of Navier-Stokes equations using high accuracy monotone schemes p 161 N95-19019
- Simulation of steady and unsteady viscous flows in turbomachinery p 140 N95-19023
- Inviscid and viscous flow modelling of complex aircraft configurations using the CFD simulation system sauna
[ARA-MEMO-403] p 211 N95-19777
- Open Skies project computational fluid dynamic analysis
[AD-A285928] p 223 N95-19991
- Investigation of shear layer transition using various turbulence models p 248 N95-21096
- Simulation of rotor blade element turbulence
[NASA-TM-108862] p 232 N95-21186
- Large-eddy simulation of flow through a plane, asymmetric diffuser p 250 N95-22449
- Numerical computation of aerodynamics and heat transfer in a turbine cascade and a turn-around duct using advanced turbulence models p 313 N95-23444
- Supersonic coaxial jet noise predictions
[NASA-TM-106917] p 451 N95-26801
- Industry-Wide Workshop on Computational Turbulence Modeling
[NASA-CP-10165] p 439 N95-27882
- A summary of computational experience at GE Aircraft Engines for complex turbulent flows in gas turbines p 439 N95-27885
- The applicability of turbulence models to aerodynamic and propulsion flowfields at McDonnell-Douglas Aerospace p 439 N95-27886
- Combustion system CFD modeling at GE Aircraft Engines p 439 N95-27889
- Measurement and prediction of broadband noise from large horizontal axis wind turbine generators p 451 N95-27990
- Grid orthogonality effects on predicted turbine midspan heat transfer and performance
[NASA-TM-106931] p 554 N95-29371
- The decay of longitudinal vortices shed from airfoil vortex generators
[NASA-CR-198356] p 480 N95-29402
- Computation of the integrated aerodynamic and propulsive flowfields of a generic hypersonic space plane p 481 N95-29788
- An aerodynamic and static-stability analysis of the Hypersonic Applied Research Technology (HART) missile
[DA9426923] p 481 N95-29965
- Numerical simulation and analysis of the hypersonic turbulent flow past a blunt-fin/ramp configuration
[DLR-FB-94-19] p 483 N95-30349
- Validation of the NPARC code for nozzle afterbody flows at transonic speeds
[NASA-TM-106971] p 592 N95-30704
- Parametrics on 2D Navier-Stokes analysis of a Mach 2.68 bifurcated rectangular mixed-compression inlet
[NASA-TM-107003] p 617 N95-30861
- Hot jet/wake turbulent structure and laser propagation. Part 3: Laser propagation measurements and modeling p 647 N95-30992
- Turbulence models in the Navier-Stokes simulation of airfoil stall
[TRITA-NA-9312] p 705 N95-33059
- Numerical studies of turbulent free surface flows and unsteady propeller flows
[AD-A294377] p 706 N95-34343
- Numerical simulation of unsteady viscous flow around an airfoil with oscillating spoiler p 685 N95-34547
- TURBULENT BOUNDARY LAYER**
- Lag model for turbulent boundary layers over rough bleed surfaces
[BTN-94-EIX94441380981] p 208 A95-68165
- Design and operation of a supersonic annular flow facility
[BTN-94-EIX94441386624] p 183 A95-68173
- Experimental study of three-dimensional separation
[BTN-94-EIX94441385752] p 179 A95-68216
- Flow structure in the wake of a wishbone vortex generator
[BTN-95-EIX95142553044] p 304 A95-73454
- Effects of expansions on a supersonic boundary layer. Surface pressure measurements
[BTN-95-EIX95142553036] p 263 A95-73462
- Influence of streamwise curvature on longitudinal vortices imbedded in turbulent boundary layers
[BTN-94-EIX94401378820] p 307 A95-76489
- Review and development of base pressure and base heating correlations in supersonic flow
[BTN-95-EIX95212645688] p 271 A95-76740
- Structure of a double-fin turbulent interaction at high speed
[BTN-95-EIX95222650780] p 347 A95-79236
- Experimental study of flow separation on an oscillating flap at Mach 2.4
[BTN-95-EIX95222650792] p 329 A95-79248
- On the role of the outer region in the turbulent-boundary-layer bursting process
[BTN-94-EIX95011441078] p 348 A95-81056
- A study on aerodynamic heating phenomena in three-dimensional shock wave/turbulent boundary layer interaction induced by sweptback sharp fins at supersonic flow p 428 A95-82419
- Numerical model of boundary-layer control using air-jet generated vortices
[HTN-95-42581] p 459 A95-87211
- Flow alteration and drag reduction by riblets in a turbulent boundary layer
[HTN-95-61199] p 461 A95-87572
- Numerical model for circulation-control flows
[HTN-95-81632] p 461 A95-87680
- Heat-transfer measurements and computations of swept-shock-wave boundary-layer interactions
[HTN-95-81634] p 541 A95-87682
- Laser interferometer skin-friction measurements of crossing-shock-wave/turbulent-boundary-layer ns
[HTN-95-20834] p 544 A95-88095
- Compressible Navier-Stokes calculations of the flow over airfoil sections. Comparisons of 1st and 2nd order turbulence models
[SAE PAPER 932510] p 546 A95-89183
- Evaluation of prediction methods for fluctuating pressures under attached turbulent boundary layers using flight test data p 574 A95-90103
- Drag reduction in a rectangular duct using riblets
[HTN-95-01091] p 468 A95-90277
- Viscous contribution to the high Mach number damping in pitch of blunt slender cones at small angles of attack
[HTN-95-01096] p 469 A95-90282
- An experimental study on interacting flow between supersonic flow and secondary flow injected normally through circular nozzle p 472 A95-91511
- Effects of free-stream turbulence intensity on a boundary layer recovering from concave curvature effects
[BTN-95-EIX95282710058] p 632 A95-92471
- 3-D Navier-Stokes analysis of crossing glancing shocks/turbulent boundary layer interactions
[BTN-95-EIX95302729768] p 636 A95-94130
- Empirical refinements to boundary layer transition noise models p 28 N95-11262
- Exact dynamic responses of periodic multi-span beams under convected pressure fields p 25 N95-11288
- Validation of the RPLUS3D code for supersonic inlet applications involving three-dimensional shock wave-boundary layer interactions
[NASA-TM-106579] p 39 N95-13058
- Atmospheric effects on the risetime and waveshape of sonic booms p 100 N95-14886
- Numerical simulation of supersonic compression corners and hypersonic inlet flows using the RPLUS2D code
[NASA-TM-106580] p 105 N95-16038
- Three-dimensional boundary layer and flow field data of an inclined prolate spheroid p 158 N95-17867
- Sectional prediction of 3D effects for separated flow on rotating blades
[PBS94-201696] p 117 N95-18503
- Theoretical investigations of shock/boundary layer interactions on a $Ma(\infty) = 8$ waverider
[DLR-FB-94-12] p 119 N95-18910
- Flow field investigation in a free jet - free jet core system for the generation of high intensity molecular beams
[DLR-FB-94-11] p 172 N95-18912
- Application of wavelet-filtering techniques to intermittent turbulent and wall pressure events. Part 1: Exploratory results
[AD-A286077] p 247 N95-20849
- Experimental investigations of on-demand vortex generators p 250 N95-22451
- Transverse vorticity measurements in the NASA Ames 80 x 120 wind tunnel boundary layer p 251 N95-22457
- Effects of cavity dimensions, boundary layer, and temperature on cavity noise with emphasis on benchmark data to validate computational aeroacoustic codes
[NASA-CR-4653] p 361 N95-24879
- The near-wake flow behavior of an oscillating airfoil with modified trailing edge p 375 N95-26953
- Measurement and prediction of broadband noise from large horizontal axis wind turbine generators p 451 N95-27990
- Unsteadiness of shock-induced turbulent boundary layer separation. An inherent feature of turbulent flow or solely a wind tunnel phenomenon
[AD-A290367] p 554 N95-29228
- The decay of longitudinal vortices shed from airfoil vortex generators
[NASA-CR-198356] p 480 N95-29402
- Experimental studies on boundary-layer transition on a reentry vehicle at transonic and supersonic speeds
[ISAS-659] p 555 N95-29712
- Numerical simulations of the flow in the HYPULSE expansion tube
[NASA-TM-110357] p 523 N95-30228
- TURBULENT COMBUSTION**
- Modeling of supersonic turbulent combustion using assumed probability density functions
[BTN-95-EIX95112524190] p 206 A95-69318
- Pulsed jet ignition modeling with a full chemistry p 538 A95-87184
- Prediction of NO(x) emission index of turbulent diffusion flame p 538 A95-87195
- Theories of turbulent combustion in high speed flows
[AD-A280933] p 23 N95-10535
- Combustion system CFD modeling at GE Aircraft Engines p 439 N95-27889
- A pulsed liquid fuel ramjet p 617 N95-31201
- TURBULENT DIFFUSION**
- Transport of exhaust products in the near trail of a jet engine under atmospheric conditions
[HTN-95-91421] p 319 A95-77334
- Experimental investigation of turbulent particle dispersion in swirling flows
[DLR-FB-94-20] p 647 N95-31355
- TURBULENT FLOW**
- Observations of fluxes and inland breezes over a heterogeneous surface
[HTN-95-80258] p 212 A95-66315
- Aspects of vortex breakdown
[HTN-95-A0001] p 183 A95-67828
- Design and operation of a supersonic annular flow facility
[BTN-94-EIX94441386624] p 183 A95-68173
- Numerical computations of supersonic base flow with special emphasis on turbulence modeling
[BTN-94-EIX94441386632] p 179 A95-68181
- Interaction of a streamwise vortex with a thin plate: A source of turbulent buffeting
[BTN-95-EIX95042474398] p 209 A95-68302
- Numerical study of the performance of swept, curved compression surface scramjet inlets
[BTN-95-EIX95112524198] p 197 A95-69310
- Time-resolved surface heat flux measurements in the wing/body junction vortex
[BTN-95-EIX95082502716] p 220 A95-71029
- Two-equation turbulence model for unsteady separated flows around airfoils
[BTN-95-EIX95142553054] p 262 A95-73444
- Flow structure in the wake of a wishbone vortex generator
[BTN-95-EIX95142553044] p 304 A95-73454
- Simulation of turbulent fluctuations
[BTN-95-EIX95142553041] p 304 A95-73457
- Adaptive finite element method for turbulent flow near a propeller
[BTN-95-EIX95142553038] p 305 A95-73460
- Laplace interaction law for the computation of viscous airfoil flow in low- and high-speed aerodynamics
[BTN-95-EIX95142553037] p 263 A95-73461
- Effects of expansions on a supersonic boundary layer: Surface pressure measurements
[BTN-95-EIX95142553036] p 263 A95-73462
- Computation of oscillating airfoil flows with one- and two-equation turbulence models
[BTN-95-EIX95152577588] p 263 A95-73494
- Mach wave emission from a high-temperature supersonic jet
[BTN-95-EIX95152577586] p 264 A95-73496
- Base drag prediction on missile configurations
[BTN-95-EIX95152583256] p 266 A95-73557
- Turbulent transonic airfoil flow simulation using a pressure-based algorithm
[BTN-95-EIX95182619078] p 269 A95-75763
- Simulation of transverse gas injection in turbulent supersonic air flows
[BTN-95-EIX95182619080] p 269 A95-75765
- Multigrid solution of compressible turbulent flow on unstructured meshes using a two-equation model
[BTN-94-EIX94401378794] p 307 A95-76484
- Influence of streamwise curvature on longitudinal vortices imbedded in turbulent boundary layers
[BTN-94-EIX94401378820] p 307 A95-76489

- Effect of ambient turbulence intensity on sphere wakes at intermediate Reynolds numbers
[BTN-95-EIX95182619101] p 308 A95-76586
- Real-time estimation of atmospheric turbulence severity from in-situ aircraft measurements
[BTN-95-EIX95182619231] p 319 A95-76657
- Simulation on the 3-D turbulent flow in the passages of finocyl grain
[BTN-95-EIX95202638962] p 279 A95-76674
- On the role of the outer region in the turbulent-boundary-layer bursting process
[BTN-94-EIX95011441078] p 348 A95-81056
- The effects of wall perturbations on thermo-turbulent Couette flow
[HTN-95-92255] p 434 A95-85299
- Boundary layer studies over an S-blade
[HTN-95-92261] p 434 A95-85305
- Stochastic approach to noise modeling for free turbulent flows
[HTN-95-42321] p 371 A95-86150
- Sphere wakes at moderate Reynolds numbers in a turbulent environment
[HTN-95-42331] p 372 A95-86160
- A review of the hot-wire technique in 2-D compressible flow
[HTN-95-61157] p 373 A95-86256
- Drag coefficients of spherical liquid droplets. Part 1: Quiescent gaseous fields
[BTN-95-EIX95262697040] p 538 A95-86857
- Drag coefficients of spherical liquid droplets. Part 2: Turbulent gaseous fields
[BTN-95-EIX95262697041] p 538 A95-86858
- Behavior of the Johnson-King turbulence model in Axisymmetric supersonic flows
[HTN-95-20932] p 464 A95-88971
- Modeling three-dimensional gas-turbine combustor model flow using second-moment closure
[HTN-95-20935] p 464 A95-88974
- Numerical computations of supersonic base flow with special emphasis on turbulence modeling
[HTN-95-20949] p 546 A95-88988
- Computational study of boundary layer control for improving airfoil performance
[SAE PAPER 932513] p 466 A95-89186
- Nonlinear analysis of swept wing transitional boundary layers
[SAE PAPER 932515] p 466 A95-89188
- Drag reduction in a rectangular duct using riblets
[HTN-95-01091] p 468 A95-90277
- Criteria for location of vortex breakdown over delta wings
[HTN-95-01092] p 468 A95-90278
- Algorithmic trends in CFD in the 1990's for aerospace flow field calculations
p 550 A95-91917
- Effects of free-stream turbulence intensity on a boundary layer recovering from concave curvature effects
[BTN-95-EIX95282710058] p 632 A95-92471
- Numerical calculations of the turbulent flow through a controlled diffusion compressor cascade
[BTN-95-EIX95282710056] p 632 A95-92473
- Turbulent flow measurements with a triple-split hot-film probe
[HTN-95-A1774] p 634 A95-93337
- Leading-edge sweepback and shape effects on fin-induced fluctuating pressures
[BTN-95-EIX95302694471] p 636 A95-94067
- Supersonic, turbulent flow computation and drag optimization for axisymmetric afterbodies
[BTN-95-EIX95302729772] p 637 A95-94134
- Comparison of the predictive capabilities of several turbulence models
[BTN-95-EIX0619952748167] p 589 A95-94461
- Assessment of technology for aircraft development
[BTN-95-EIX0619952748181] p 606 A95-94474
- Turbulent effects on parachute drag
[BTN-95-EIX0619952748193] p 591 A95-94482
- Laminar and turbulent flow over optimal riblets
p 639 A95-95383
- Numerical simulation of the 3D turbulent flow around the combustor dome of an aircraft engine
p 640 A95-95423
- Grid adaptation for problems in computational fluid dynamics
p 643 A95-95472
- Navier-Stokes simulation of turbulent vortex high-Re-number flows over a delta wing
p 644 A95-95507
- Agglomeration multigrid for viscous turbulent flows
[AD-A284064] p 8 N95-10848
- Empirical refinements to boundary layer transition noise models
p 28 N95-11262
- Effect of weak periodic pressure gradient on streamwise vortices near a wall
p 29 N95-11263
- Pressure measurements on an F/A-18 twin vertical tail in buffeting flow. Volume 3: Buffet power spectral densities
[AD-A281444] p 36 N95-11829
- Modification of the two-equation turbulence model in NPARC to a Chien low Reynolds number k-epsilon formulation
[NASA-TM-106710] p 37 N95-11917
- Measurements of pressure and thermal wakes in a transonic turbine cascade
[AD-A283464] p 38 N95-12548
- Methodology for sensitivity analysis, approximate analysis, and design optimization in CFD for multidisciplinary applications
[NASA-CR-196981] p 58 N95-13201
- Transport phenomena in stratified multi-fluid flow in the presence and absence of gravity
p 95 N95-14563
- Laminar and turbulent flow computations of Type 4 shock-shock interference aerothermal loads using unstructured grids
[NASA-CR-195008] p 97 N95-15604
- Time accurate computation of unsteady inlet flows with a dynamic flow adaptive mesh
[AD-A285498] p 157 N95-16736
- Three dimensional compressible turbulent flow computations for a diffusing S-duct with/without vortex generators
[NASA-CR-195390] p 138 N95-17402
- Interaction, bursting and control of vortices of a cropped double-delta wing at high angle of attack
[AD-A283656] p 119 N95-18669
- Numerical computations of supersonic base flow with special emphasis on turbulence modeling
[AD-A283688] p 119 N95-18670
- Simulation of steady and unsteady viscous flows in turbomachinery
p 140 N95-19023
- Velocity measurements with hot-wires in a vortex-dominated flowfield
p 121 N95-19261
- Viscous flow past aerofoils axisymmetric bodies and wings
p 123 N95-19457
- Application of wavelet-filtering techniques to intermittent turbulent and wall pressure events. Part 1: Exploratory results
[AD-A286077] p 247 N95-20849
- A computer code (SKINTEMP) for predicting transient missile and aircraft heat transfer characteristics
[AD-A286044] p 248 N95-21001
- Application of Direct and Large Eddy Simulation to Transition and Turbulence
[AGARD-CP-551] p 248 N95-21061
- Large-eddy simulation of flow through a plane, asymmetric diffuser
p 250 N95-22449
- Crossflow instability control on a swept-wing: Preliminary studies
p 274 N95-23283
- High-lift flow-physics flight experiments on a subsonic civil transport aircraft (B737-100)
p 275 N95-23333
- Numerical computation of aerodynamics and heat transfer in a turbine cascade and a turn-around duct using advanced turbulence models
p 313 N95-23444
- Convergence acceleration of implicit schemes in the presence of high aspect ratio grid cells
p 313 N95-23446
- Thermohydrodynamic analysis of cryogenic liquid turbulent flow fluid film bearings, phase 2
[NASA-CR-197412] p 349 N95-24461
- Plate manipulators
[AD-A289601] p 374 N95-26719
- Basic studies in turbulent shear flows
[AD-A289145] p 437 N95-26998
- A summary of computational experience at GE Aircraft Engines for complex turbulent flows in gas turbines
p 439 N95-27885
- Numerical study to assess sulfur hexafluoride as a medium for testing multielement airfoils
[NASA-TP-3496] p 378 N95-28674
- Influence of turbulence parameters, Reynolds number, and body shape on stagnation-region heat transfer
[NASA-TP-3487] p 550 N95-28719
- Studies in drag reduction
p 478 N95-29094
- Unsteadiness of shock-induced turbulent boundary layer separation. An inherent feature of turbulent flow or solely a wind tunnel phenomenon
[AD-A290367] p 554 N95-29228
- Turbulent airflow noise production and propagation patterns of a subsonic jet impinging on a flat plate
p 580 N95-29502
- Experimental studies on boundary-layer transition on a reentry vehicle at transonic and supersonic speeds
[ISA-659] p 555 N95-29712
- Computation of the integrated aerodynamic and propulsive flowfields of a generic hypersonic space plane
p 481 N95-29788
- Survey of CFD applications for high speed inlets
[AD-A291365] p 557 N95-30087
- Numerical simulations of the flow in the HYPULSE expansion tube
[NASA-TM-110357] p 523 N95-30228
- Numerical simulation and analysis of the hypersonic turbulent flow past a blunt-fin/ramp configuration
[DLR-FB-94-19] p 483 N95-30349
- A pulsed liquid fuel ramjet
p 617 N95-31201
- Advanced k-epsilon modeling of heat transfer
[NASA-CR-4679] p 648 N95-31423
- Improved modeling of unsteady heat transfer (The first step)
[AD-A292777] p 648 N95-31432
- Numerical studies of turbulent free surface flows and unsteady propeller flows
[AD-A294377] p 706 N95-34343
- TURBULENT HEAT TRANSFER**
- Constant flux, turbulent convection data using infrared imaging
[HTN-95-20731] p 435 A95-86621
- Improved modeling of unsteady heat transfer (The first step)
[AD-A292777] p 648 N95-31432
- TURBULENT JETS**
- Development of a large-aspect-ratio rectangular turbulent free jet
[HTN-95-42333] p 372 A95-86162
- Planar Rayleigh scattering and laser-induced fluorescence for visualization of a hot, Mach 2 annular air-jet
[NASA-TM-4576] p 54 N95-13196
- Application of Direct and Large Eddy Simulation to Transition and Turbulence
[AGARD-CP-551] p 248 N95-21061
- Crossflow mixing of noncircular jets
[NASA-TM-106865] p 338 N95-24390
- TURBULENT MIXING**
- Development of a large-aspect-ratio rectangular turbulent free jet
[HTN-95-42333] p 372 A95-86162
- Conceptual studies of high speed combustors for mixing enhancement mechanisms
[AIAA PAPER 95-6095] p 510 A95-88003
- The spectrum and directivity of turbulent mixing noise from supersonic jets
p 579 N95-29415
- Experimental investigation of turbulent particle dispersion in swirling flows
[DLR-FB-94-20] p 647 N95-31355
- A study of supersonic mixing flow field with ramp injector
p 706 N95-34512
- TURBULENT WAKES**
- Phenomenological description and simplified modelling of the vortex wake issuing from a jet in a crossflow
[BTN-94-EIX94441385754] p 184 A95-68218
- Flow structure in the wake of a wishbone vortex generator
[BTN-95-EIX95142553044] p 304 A95-73454
- Adaptive finite element method for turbulent flow near a propeller
[BTN-95-EIX95142553038] p 305 A95-73460
- Sphere wakes at moderate Reynolds numbers in a turbulent environment
[HTN-95-42331] p 372 A95-86160
- Reduction of supersonic jet noise using swirl: A concept revisited
p 574 A95-90101
- Measurements of pressure and thermal wakes in a transonic turbine cascade
[AD-A283464] p 38 N95-12548
- A supercritical airfoil experiment
p 111 N95-17858
- Application of Direct and Large Eddy Simulation to Transition and Turbulence
[AGARD-CP-551] p 248 N95-21061
- Experimental and theoretical studies of wakes in stratified flows
[AD-A290203] p 553 N95-29060
- TURNING FLIGHT**
- Time-optimal turn to a heading: An analytic solution
[BTN-94-EIX94511433940] p 142 A95-64606
- Efficient sensitivity analysis for rotary-wing aeromechanical problems
[BTN-95-EIX95152577585] p 264 A95-73497
- Functional agility metrics and optimal trajectory analysis
[BTN-95-EIX95182619121] p 321 A95-76598
- Optimal lateral-escape maneuvers for microburst encounters during final approach
[BTN-95-EIX95182619127] p 276 A95-76604
- TVD SCHEMES**
- Three-dimensional structure of a supersonic jet impinging on an inclined plate
[BTN-95-EIX95152583259] p 267 A95-73560
- Numerical simulation of unsteady aerodynamic heating induced by shock reflections
p 428 A95-82418
- Pulsed jet ignition modeling with a full chemistry
p 538 A95-87184
- A total variation diminishing finite difference algorithm for sonic boom propagation models
p 575 A95-90105
- Numerical studies of Mach reflection with air chemistry
p 548 A95-90575
- Heat transfer on bent-noise biconic in hypersonic flow
p 639 A95-95394

- Development of an upwind, finite-volume code with finite-rate chemistry
[NASA-CR-196749] p 9 N95-11366
- Development of an upwind, finite-volume code with finite-rate chemistry
[NASA-CR-197747] p 374 N95-26760
- Pressure based high order TVD methodology for dynamic stall control
[AD-A290149] p 479 N95-29316
- Improved modeling of unsteady heat transfer (The first step)
[AD-A292777] p 648 N95-31432
- Verification of turbine cascade flow with tip clearance
p 698 N95-34511
- Hypersonic CFD analysis for the aerothermodynamic design of HOPE
p 684 N95-34520
- Numerical solutions of inviscid and viscous flows about airfoils by TVD method
p 684 N95-34521
- Vector-parallel simulations of transonic wind tunnel flows about a fully configured model of aircraft
p 685 N95-34538
- Numerical simulation of unsteady viscous flow around an airfoil with oscillating spoiler
p 685 N95-34547
- Direct analysis of transonic rotor noise with CFD technique
p 711 N95-34549

TWISTED WINGS

- Demonstration of an elastically coupled twist control concept for tilt rotor blade application
[BTN-94-EIX94441386633] p 196 A95-68182
- Nonlinear angle of twist of advanced composite wing boxes under pure torsion
[BTN-95-EIX95152582323] p 281 A95-73526
- Effect of leading- and trailing-edge flaps on clipped delta wings with and without wing camber at supersonic speeds
[NASA-TM-4542] p 5 N95-10028
- Determination of stores pointing error due to wing flexibility under flight load
[NASA-TM-4646] p 134 N95-19044

TWISTING

- Twisting smartly in the wind
[BTN-95-EIX95041503093] p 184 A95-68353
- Application of Navier-Stokes aeroelastic methods to improve fighter wing maneuver performance
[BTN-95-EIX95182619218] p 284 A95-76644
- Demonstration of an elastically coupled twist control concept for tilt rotor blade application
[HTN-95-20959] p 465 A95-88998

TWO DIMENSIONAL BODIES

- Ground effect calculation of two-dimensional airfoil
[BTN-94-EIX94371347710] p 219 A95-69969
- Explicit Kutta condition for an unsteady two-dimensional constant potential panel method
[HTN-95-51679] p 433 A95-85061
- 2-D airfoil tests including side wall boundary layer measurements
p 158 N95-17847
- 2-D airfoil effectiveness study
p 110 N95-17851

TWO DIMENSIONAL BOUNDARY LAYER

- Influence of streamwise curvature on longitudinal vortices imbedded in turbulent boundary layers
[BTN-94-EIX94401378820] p 307 A95-76489
- Nonlinear analysis of the Gortler instability
[BTN-95-EIX95282705926] p 455 A95-89664

TWO DIMENSIONAL FLOW

- Novel similarity solutions of the sonic small-disturbance equation with applications to airfoil transonic aerodynamics
[BTN-94-EIX94341340316] p 35 A95-60852
- A grid generation and flow solution method for the Euler equations on unstructured grids
[HTN-95-20003] p 153 A95-63201
- Prediction of ice accretion: Comparison between the 2D and 3D codes
[BTN-94-EIX94441385753] p 213 A95-68217
- Parallel implicit unstructured grid Euler solvers
[BTN-95-EIX95042474393] p 217 A95-68307
- Effects of leading and trailing edge flaps on the aerodynamics of airfoil/vortex interactions
[HTN-95-31011] p 221 A95-71181
- Predicting exhaust plume boundaries with supersonic external flows
[BTN-95-EIX95152583258] p 297 A95-73559
- Comparison of linear stability results with flight transition data
[BTN-95-EIX95182619097] p 283 A95-76582
- Observations on using experimental data as boundary conditions for computations
[BTN-95-EIX95182619103] p 321 A95-76588
- Study of the droplet spray characteristics of a subsonic wind tunnel
[BTN-95-EIX95182619235] p 271 A95-76661
- Study of subsonic base cavity flowfield structure using particle image velocimetry
[BTN-95-EIX9522650781] p 327 A95-79237
- Numerical analysis of flow field around gas rudder
p 407 A95-82333

- Two-dimensional viscous flow past a flat plate
[HTN-95-42210] p 430 A95-84026
- Prediction of two-dimensional momentumless wake by k-epsilon-gamma model
[BTN-95-EIX95262694299] p 434 A95-85470
- A review of the hot-wire technique in 2-D compressible flow
[HTN-95-61157] p 373 A95-86256
- Two-dimensional unsteady leading-edge separation on a pitching airfoil
[HTN-95-81628] p 461 A95-87676
- Determining unsteady 2D AND 3D boundary layer separation
p 462 A95-88898
- Modelling 2D separation from a high lift airfoil with a non-linear eddy-viscosity model and second-moment closure
[HTN-95-C0005] p 585 A95-93393
- Shock-tunnel combustor testing for hypersonic vehicles
[NASA-CR-196836] p 52 N95-11938
- Numerical time dependent sheet cavitation simulations using a higher order panel method
[PB94-204435] p 59 N95-13249
- Studies on the flow induced by an oscillating airfoil in a uniform stream
[PB94-204450] p 40 N95-13250
- Numerical simulation of supersonic compression corners and hypersonic inlet flows using the RPLUS2D code
[NASA-TM-106580] p 105 N95-16038
- Two-dimensional high-lift airfoil data for CFD code validation
p 112 N95-17859
- Numerical simulation of dynamic-stall suppression by tangential blowing
[AD-A284887] p 120 N95-19110
- Static investigation of two fluidic thrust-vectoring concepts on a two-dimensional convergent-divergent nozzle
[NASA-TM-4574] p 222 N95-19913
- Investigation of shear layer transition using various turbulence models
p 220 N95-21096
- Two-dimensional imaging of OH in a lean burning high pressure combustor
[NASA-TM-106854] p 236 N95-21383
- Shock wave interactions in hypervelocity flow
[AD-A286507] p 250 N95-22212
- Direct numerical simulations of on-demand vortex generators: Mathematical formulation
p 251 N95-22452
- User's guide for ECAP2D: An Euler unsteady aerodynamic and aeroelastic analysis program for two dimensional oscillating cascades, version 1.0
[NASA-CR-189146] p 316 N95-24189
- Thrust measurement in a 2-D scramjet nozzle
p 339 N95-25397
- A combined geometric approach for solving the Navier-Stokes equations on dynamic grids
[NASA-TM-106919] p 332 N95-26075
- Numerical simulation of combustion flow around a flame holder with hydrogen injection
[NAL-TR-1233] p 419 N95-26523
- A general theory of two- and three-dimensional rotational flow in subsonic and transonic turbomachines
[NASA-CR-4496] p 377 N95-28003
- An extension of the continuum model by Grad's thirteen moment equations for hypersonic rarefied flows
p 478 N95-29118
- Finite element vorticity-based methods for the solution of the incompressible and compressible Navier-Stokes equations
p 553 N95-29119
- Modeling and control of rotating stall in high speed multi-stage axial compressors
p 513 N95-29244
- Acoustic scattering from ellipses by the modal element method
[NASA-TM-106935] p 579 N95-29401
- The effects of three dimensional imposed disturbances on bluff body near wake flows
[AD-A290824] p 555 N95-29654
- Multigrid convergence acceleration for the 2D Euler equations applied to high-lift systems
[PB95-198081] p 593 N95-30814
- Parameters on 2D Navier-Stokes analysis of a Mach 2.68 bifurcated rectangular mixed-compression inlet
[NASA-TM-107003] p 617 N95-30861
- Vorticity dynamics and control of dynamic stall
[AD-A288658] p 620 N95-31400
- Numerical solution of the full potential equation using a chimera grid approach
[NASA-TM-110360] p 594 N95-32188

TWO DIMENSIONAL MODELS

- Nonhydrostatic simulation of frontogenesis in a moist atmosphere. Part 3: Thermal wind imbalance and rainbands
[HTN-95-90356] p 212 A95-66429
- Predicting exhaust plume boundaries with supersonic external flows
[BTN-95-EIX95152583258] p 297 A95-73559

- Sensitivity of two-dimensional model predictions of ozone response to stratospheric aircraft: An update
[HTN-95-A0863] p 318 A95-76267
- Observations on using experimental data as boundary conditions for computations
[BTN-95-EIX95182619103] p 321 A95-76588
- High-speed civil transport impact: Role of sulfate, nitric acid trihydrate, and ice aerosols studied with a two-dimensional model including aerosol physics
[HTN-95-91843] p 354 A95-80831
- Dynamics of aircraft exhaust plumes in the jet-regime
[HTN-95-51275] p 355 A95-80860
- Potential effects on ozone of future supersonic aircraft/2D simulation
[HTN-95-51282] p 356 A95-80867
- Impact on ozone of high-speed stratospheric aircraft: Effects of the emission scenario
[HTN-95-51283] p 356 A95-80868
- Effects of a polar stratosphere cloud parameterization on ozone depletion due to stratospheric aircraft in a two-dimensional model
[HTN-95-A1038] p 443 A95-84543
- The propagation of sound from an arbitrarily oriented dipole over a finite impedance plane
p 570 A95-88459
- Analytical developments in support of the NASA aging aircraft program with an application to crack growth from rivets
[SAE PAPER 931223] p 545 A95-88789
- Adaptive wall technology for minimization of wind tunnel boundary interferences - where are we now?
p 519 A95-88903
- A Kutta condition conscious perturbation stream function boundary element algorithm for 2-D potential aerodynamics
[ISBN 1-879921-01-4] p 587 A95-93751
- Measurements on a two-dimensional airfoil with high-lift devices
p 109 N95-17848
- Investigation of the flow over a series of 14 percent-thick supercritical airfoils with significant rear camber
p 109 N95-17849
- Experiments in the trailing edge flow of an NLR 7702 airfoil
p 110 N95-17853
- Two-dimensional 16.5 percent thick supercritical airfoil NLR 7301
p 110 N95-17854
- Low-speed surface pressure and boundary layer measurement data for the NLR 7301 airfoil section with trailing edge flap
p 111 N95-17855
- OAT15A airfoil data
p 111 N95-17857
- A supercritical airfoil experiment
p 111 N95-17858
- Two-dimensional high-lift airfoil data for CFD code validation
p 112 N95-17859
- Static investigation of two fluidic thrust-vectoring concepts on a two-dimensional convergent-divergent nozzle
[NASA-TM-4574] p 120 N95-19042
- Interference determination for wind tunnels with slotted walls
p 147 N95-19269
- Open Skies project computational fluid dynamic analysis
[AD-A285928] p 223 N95-19991
- An Echelle Grating Spectrometer (EGS) for mid-IR remote chemical detection
[DE94-019310] p 249 N95-21478
- Acoustic scattering from ellipses by the modal element method
[NASA-TM-106935] p 579 N95-29401
- Experimental investigation of aerodynamic devices for wind turbine rotational speed control, phase 1
[DE95-004034] p 584 N95-30016

TWO FLUID MODELS

- Static investigation of two fluidic thrust-vectoring concepts on a two-dimensional convergent-divergent nozzle
[NASA-TM-4574] p 120 N95-19042

TWO PHASE FLOW

- Simulation of transverse gas injection in turbulent supersonic air flows
[BTN-95-EIX95182619080] p 269 A95-75765
- Study of heat transfer rates during quenching of a hot tube under microgravity
p 428 A95-82641
- Experimental investigation of flow-boiling heat transfer under microgravity
p 428 A95-82642
- A flow pattern map for two-phase liquid-gas flow under reduced gravity conditions
p 539 A95-87280
- Characterization of annular two-phase gas-liquid flows in microgravity
p 95 N95-14556
- Gas turbine prediffuser-combustor performance during operation with air-water mixture
[DOT/FAA/CT-93/52] p 83 N95-15683
- The stability of two-phase flow over a swept-wing
[NASA-CR-194994] p 159 N95-18190
- Two-phase flow research using the learjet apparatus
[NASA-TM-106814] p 438 N95-27854

- Experimental investigation of turbulent particle dispersion in swirling flows [DLR-FB-94-20] p 647 N95-31355
- U**
- U.S.S.R.**
Assessment of Russian VSTOL technology evaluating the YAK-38 'FORGER' and YAK-141 'FREESTYLE' p 497 A95-90868
- U.S.S.R. SPACE PROGRAM**
Two projects of V. M. Myasishchev [HTN-95-50269] p 176 A95-65764
- U-2 AIRCRAFT**
Field and data analysis studies related to the atmospheric environment [NASA-CR-196543] p 168 N95-18093
- UH-1 HELICOPTER**
Assessment of overhaul surge margin tests applied to the T53 engines in ADF Iroquois helicopters [AR-008-389] p 339 N95-25936
The effects of UH-1 experience on UH-60 simulator performance: A preliminary study [AD-A289457] p 391 N95-26993
- UH-60A HELICOPTER**
Validation of the dynamic response of a blade-element UH-60 simulation model in hovering flight [HTN-94-00663] p 18 A95-60155
Aerodynamic and wake methodology evaluation using Model UH-60A experimental data [HTN-95-31009] p 220 A95-71179
A portable transmission vibration analysis system for the S-70A-9 Black Hawk helicopter [DSTO-TR-0072] p 348 N95-24203
- UKRAINE**
JPRS report: Science and technology. Central Eurasia [JPRS-UST-94-022] p 438 N95-27699
- ULTRAHIGH FREQUENCIES**
Use of high resolution lightning detection and localization sensors for hazardous aviation weather nowcasting p 661 A95-93486
A VHF/UHF antenna for the Precision Antenna Measurement System (PAMS) [AD-A285673] p 156 N95-16621
- ULTRASONIC FLAW DETECTION**
Ultrasonic imaging of damages in CRFT-laminates p 578 A95-90828
- ULTRASONIC TESTS**
Low frequency ultrasonic nondestructive inspection of aluminum/adhesive fuselage lap splices [DE94-014242] p 24 N95-11135
Emerging nondestructive inspection for aging aircraft [PB95-143053] p 328 N95-25401
- ULTRASONICS**
Ultrasonic techniques for repair of aircraft structures with bonded composite patches p 136 N95-19486
- ULTRAVIOLET EMISSION**
Ultraviolet emissions occurring about hypersonic vehicles in rarefied flows [AD-A281452] p 106 N95-16076
- UMBILICAL CONNECTORS**
Microgravity isolation system design: A modern control synthesis framework [NASA-TM-106805] p 105 N95-18197
- UNCAMBERED WINGS**
Effect of leading- and trailing-edge flaps on clipped delta wings with and without wing camber at supersonic speeds [NASA-TM-4542] p 5 N95-10028
- UNDER SURFACE BLOWING**
Wing download reduction using vortex trapping plates [HTN-94-00710] p 4 A95-60188
- UNIFORM FLOW**
Experimental investigation of the flow around a circular cylinder: Influence of aspect ratio [BTN-94-EIX95011441120] p 347 A95-80044
Hybrid laminar flow over wings enhanced by continuous boundary layer suction [SAE PAPER 931386] p 587 A95-93662
Acoustic radiation damping of flat rectangular plates subjected to subsonic flows p 172 N95-18542
The effects of three-dimensional imposed disturbances on bluff body near wake flows: Effects of taper and splitter plates on the near wake characteristics of a circular cylinder in uniform and shear flow [AD-A292113] p 477 N95-28921
Acceleration potential models
PREDICAT/PREDICDYN applied for calculation of axisymmetric dynamic inflow cases [PB95-207015] p 647 N95-30957
- UNITED KINGDOM**
The use of the Equivalent Continuous Sound Level ($L_{sub eq}$) as an aircraft noise index [HTN-95-92542] p 558 A95-87362
- Air traffic management: The future challenge [CONGRESS PAPER C428-7-145] p 488 A95-91686
Airborne collision avoidance systems - The UK experience [CONGRESS PAPER C428-7-146] p 488 A95-91687
Helicopter life substantiation: Review of some USA and UK initiatives [DSTO-TR-0062] p 328 N95-24201
- UNITED STATES**
EC Aviation Scene [HTN-95-50223] p 176 A95-64860
Transitioning to the aviation routine weather report (METAR) and the International Aerodrome Forecast (TAF) within the Federal Aviation Administration p 656 A95-93461
Use of pilot reports for verification of aircraft icing diagnoses and forecasts p 666 A95-93508
Annual review of aircraft accident data: US air carrier operations, calendar year 1992 [PB95-100319] p 78 N95-15066
Annual review of aircraft accident data: US Air carrier operations, calendar year 1992 [PB95-100319] p 123 N95-17748
Census US civil aircraft calendar year 1993 [AD-A286309] p 219 N95-20091
Helicopter life substantiation: Review of some USA and UK initiatives [DSTO-TR-0062] p 328 N95-24201
Strategy in the commercial aircraft industry in the United States: A comparison of decisionmaking by McDonnell-Douglas and Boeing aircraft companies from 1977-1983 [AD-A288289] p 366 N95-26409
Comparison of fixed wing aircraft algorithms for JANUS [AD-A288503] p 389 N95-26652
Annual review of aircraft accident data: US general aviation calendar year 1993 [PB95-215828] p 599 N95-31712
Aeronautics and space report of the President [NASA-TM-110743] p 681 N95-31979
- UNIVERSITIES**
Aviation weather education and the University of North Dakota aviation weather survey p 656 A95-93462
Propulsion education at Carlton University [SAE PAPER 931391] p 613 A95-93667
1994 NASA-HU American Society for Engineering Education (ASEE) Summer Faculty Fellowship Program [NASA-CR-194972] p 325 N95-23276
- UNIVERSITY PROGRAM**
The NASA-sponsored Maryland center for hypersonic education and research [AIAA PAPER 95-6105] p 519 A95-88010
The NASA/UTA Center for hypersonic research [AIAA PAPER 95-6106] p 520 A95-90438
Research and educational initiatives at the Syracuse University Center for Hypersonics [AIAA PAPER 95-6107] p 520 A95-90439
Aviation meteorology education in an AB initio setting p 657 A95-93466
- UNIX (OPERATING SYSTEM)**
Manual for a workstation-based generic flight simulation program (LaRCsim), version 1.4 [NASA-TM-110164] p 518 N95-30327
- UNMANNED SPACECRAFT**
A concept of a hypersonic flight experiment of a winged vehicle p 414 A95-82477
Reentry technology experiment on the first mission of reentry capsule 'EXPRESS' p 414 A95-82499
- UNSTEADY AERODYNAMICS**
Dynamic stall of an oscillating wing. Part 1: Evaluation of turbulence models [AIAA PAPER 93-3403] p 3 A95-60184
Effect of wind tunnel acoustic modes on linear oscillating cascade aerodynamics [HTN-94-00760] p 14 A95-60199
Continuous gust response and sensitivity derivatives using state-space models [BTN-95-EIX95062487551] p 203 A95-68365
State-space representation of aerodynamic characteristics of an aircraft at high angles of attack [BTN-95-EIX95062487536] p 187 A95-69244
Measurement around a rotor blade excited in pitch. Part 2: Unsteady surface pressure [HTN-95-31008] p 220 A95-71178
Aerodynamic and wake methodology evaluation using Model UH-60A experimental data [HTN-95-31009] p 220 A95-71179
Effects of leading and trailing edge flaps on the aerodynamics of airfoil/vortex interactions [HTN-95-31011] p 221 A95-71181
Neural network prediction of three-dimensional unsteady separated flowfields [BTN-95-EIX95182619232] p 308 A95-76658
- Unsteady ground effects on aerodynamic coefficients of finite wings with camber [BTN-95-EIX95182619233] p 271 A95-76659
Aeroservoelastic aspects of wing/control surface planform shape optimization [BTN-95-EIX95222650795] p 340 A95-79251
On the influence of time-varying flow velocity on unsteady aerodynamics [HTN-95-61073] p 369 A95-83657
Explicit Kutta condition for an unsteady two-dimensional constant potential panel method [HTN-95-51679] p 433 A95-85061
On the differences between the effect of acoustic perturbation and unsteady bleed in controlling flow separation over a cylinder [SAE PAPER 932573] p 467 A95-90062
Vortex lattice method simulation of unsteady flow due to wing/external store combination p 471 A95-91499
Flow physics of critical states for rolling delta wings [BTN-95-EIX0619952748180] p 590 A95-94473
High performance parallelized implicit Euler solver for the analysis of unsteady aerodynamic flows p 644 A95-95495
- Computations of unsteady aerodynamic loads around oscillating wings. Part 1: Formulation [PB94-180049] p 7 N95-10136
Computations of unsteady aerodynamic loads around oscillating wings. Part 2: Computed results and discussions [PB94-180056] p 7 N95-10137
Flutter analysis of supersonic axial flow cascades using a high resolution Euler solver. Part 1: Formulation and validation [NASA-TM-105798] p 23 N95-10244
Aeroelastic simulation of higher harmonic control [NASA-CR-4623] p 37 N95-11911
User's guide for ENSAERO: A multidisciplinary program for fluid/structural/control interaction studies of aircraft (release 1) [NASA-TM-108853] p 65 N95-13662
Higher harmonic control analysis for vibration reduction of helicopter rotor systems [NASA-TM-103855] p 66 N95-14419
A computational investigation of wake-induced airfoil flutter in incompressible flow and active flutter control [AD-A281534] p 142 N95-16109
Numerical simulation of transient vortex breakdown above a pitching delta wing [AD-A281075] p 107 N95-16808
Structural effects of unsteady aerodynamic forces on horizontal-axis wind turbines [DE94-011863] p 157 N95-16939
Overview of unsteady transonic wind tunnel test on a semispan straked delta wing oscillating in pitch [AD-A284097] p 117 N95-18380
Sectional prediction of 3D effects for separated flow on rotating blades [PB94-201696] p 117 N95-18503
A study of the effect of store unsteady aerodynamics on gust and turbulence loads p 133 N95-18801
Pressure measurements on an F/A-18 twin vertical tail in buffeting flow. Volume 4, part 2: Buffet cross spectral densities [AD-A285555] p 143 N95-18641
Wind turbine blade aerodynamics: The combined experiment [DE94-011866] p 118 N95-18645
Wind turbine blade aerodynamics: The analysis of field test data [DE94-011867] p 118 N95-18646
Unsteady aerodynamic analyses for turbomachinery aeroelastic predictions p 141 N95-19381
Steady potential solver for unsteady aerodynamic analyses p 141 N95-19382
Evidence that aerodynamic effects, including dynamic stall, dictate HAWT structural loads and power generation in highly transient time frames [DE94-011865] p 216 N95-19855
The dynamic approach to rotor blade research: ARA's oscillatory test facility [ARA-MEMO-405] p 223 N95-20758
Prediction of rotor-blade deformations due to unsteady airloads [AD-A286593] p 231 N95-20860
Pressure measurements on an F/A-18 twin vertical tail in buffeting flow. Volume 4, part 1: Buffet cross spectral densities [AD-A285593] p 237 N95-21214
Pressure measurements on an F/A-18 twin vertical tail in buffeting flow. Volume 1: Wind tunnel test summary [AD-A279126] p 225 N95-21877
Direct numerical simulations of on-demand vortex generators: Mathematical formulation p 251 N95-22452
Flutter analysis of composite box beams [NASA-CR-197931] p 294 N95-23392

- User's guide for ECAP2D: An Euler unsteady aerodynamic and aeroelastic analysis program for two dimensional oscillating cascades, version 1.0 [NASA-CR-189146] p 316 N95-24189
- Application of neural networks to unsteady aerodynamic control p 360 N95-25264
- An experimental investigation of helicopter downwash and tailboom interaction at the Wichita State University 7x10 foot wind tunnel p 375 N95-26955
- Modeling of aircraft unsteady aerodynamic characteristics. Part 2: Parameters estimated from wind tunnel data p 410 N95-27839
- [NASA-TM-110161]
- A numerical study of fundamental shock noise mechanisms p 451 N95-27908
- [NASA-TM-110608]
- Unsteady pressure and inflow velocity on a pitching rotor blade in hover p 480 N95-29771
- Development of a linearized unsteady Euler analysis for turbomachinery blade rows p 592 N95-30611
- [NASA-CR-4677]
- Axial loads on yawed rotors p 592 N95-30638
- [PB95-214193]
- Validation of the helicopter rotor code HERO p 607 N95-30838
- [PB95-198040]
- Unsteady transonic wind tunnel test on a semispan straked delta wing, oscillating in pitch. Part 1: Description of the model, test setup, data acquisition, and data processing p 593 N95-30885
- [AD-A293113]
- Unsteady flow simulations about moving boundary configurations using dynamic domain decomposition techniques p 649 N95-31837
- FP-CAS3D User's guide: A three dimensional full potential aeroelastic program, version 1 [NASA-CR-198367] p 651 N95-32205
- UNSTEADY FLOW**
- Oscillating airfoil compressible dynamic stall studies [HTN-94-00704] p 3 A95-60183
- LDV measurements in dynamically separated flows [ISBN 0-8194-1311-9] p 5 A95-60191
- A study of compressibility effects on dynamic stall of rapidly pitching airfoils p 5 A95-60193
- [HTN-94-00715]
- Solution-adaptive structured-unstructured grid method for unsteady turbomachinery analysis. Part I: Methodology p 208 A95-67329
- [BTN-94-EIX94441380983]
- Rotating Kirchhoff method for three-dimensional transonic blade-vortex interaction hover noise p 182 A95-67332
- [BTN-94-EIX94441386601]
- Lift analysis of a variable camber foil using the discrete vortex-blob method p 179 A95-68172
- [BTN-94-EIX94441386623]
- Tip vortex on a swept wing. Mean flow and unsteady phenomena p 184 A95-68219
- [BTN-94-EIX94441385755]
- Active control of wake/blade-row interaction noise p 196 A95-68311
- [BTN-95-EIX95042474389]
- Two-equation turbulence model for unsteady separated flows around airfoils p 262 A95-73444
- [BTN-95-EIX95142553054]
- Eigenanalysis of unsteady flows about airfoils, cascades, and wings p 305 A95-73486
- [BTN-95-EIX95152577597]
- Computation of oscillating airfoil flows with one- and two-equation turbulence models p 263 A95-73494
- [BTN-95-EIX95152577588]
- Limit cycle phenomena in computational transonic aeroelasticity p 264 A95-73520
- [BTN-95-EIX95152582317]
- Moving wall effect in relation to other dynamic stall flow mechanisms p 265 A95-73527
- [BTN-95-EIX95152582324]
- Numerical study of sound generation due to a spinning vortex pair p 307 A95-75760
- [BTN-95-EIX95182619075]
- Viscous-inviscid interaction method for unsteady low-speed airfoil flows p 269 A95-75778
- [BTN-95-EIX95182619093]
- Stability derivatives of a flapped plate in unsteady ground effect p 270 A95-76651
- [BTN-95-EIX95182619225]
- Response of a nonrotating rotor blade to lateral turbulence. Part 1: Theory p 284 A95-76654
- [BTN-95-EIX95182619228]
- Neural network prediction of three-dimensional unsteady separated flowfields p 308 A95-76658
- [BTN-95-EIX95182619232]
- Unsteady ground effects on aerodynamic coefficients of finite wings with camber p 271 A95-76659
- [BTN-95-EIX95182619233]
- Prediction of supersonic inlet unstart caused by freestream disturbances p 329 A95-79246
- [BTN-95-EIX95222650790]
- Unsteady lift on a swept blade tip p 329 A95-80030
- [BTN-94-EIX95011441154]
- Flow due to an oscillating sphere and an expression for unsteady drag on the sphere at finite Reynolds number p 347 A95-81012
- [BTN-94-EIX95011441142]
- Dynamic unstructured method for flows past multiple objects in relative motion p 435 A95-85474
- [BTN-95-EIX95262694303]
- Eigenanalysis of unsteady flows about airfoils, cascades, and wings p 459 A95-87212
- [HTN-95-42582]
- Unsteady panel method for flows with multiple bodies moving along various paths p 540 A95-87576
- [HTN-95-61203]
- Two-dimensional unsteady leading-edge separation on a pitching airfoil p 461 A95-87676
- [HTN-95-81628]
- Automated adaptive time-discontinuous finite element method for unsteady compressible airfoil aerodynamics p 541 A95-87685
- [HTN-95-81637]
- Effects of time scales on lift of airfoils in an unsteady stream p 542 A95-87691
- [HTN-95-81643]
- Boundary conditions for unsteady supersonic inlet analyses p 544 A95-88090
- [HTN-95-20829]
- Low-dimensional description of the dynamics in separated flow past thick airfoils p 544 A95-88093
- [HTN-95-20832]
- Symposium on Aerodynamics & Aeroacoustics, Tucson, AZ, Mar. 1-2, 1993 p 462 A95-88892
- [ISBN 981-02-1732-3]
- Unsteady aerodynamics of vortical flows: Early and recent developments p 462 A95-88896
- Determining unsteady 2D AND 3D boundary layer separation p 462 A95-88898
- [HTN-95-20928]
- Computing unsteady shock waves for aeroacoustic applications p 463 A95-88967
- [HTN-95-20940]
- Lift analysis of a variable camber foil using the discrete vortex-blob method p 545 A95-88979
- [HTN-95-20940]
- On the differences between the effect of acoustic perturbation and unsteady bleed in controlling flow separation over a cylinder p 467 A95-90062
- [SAE PAPER 932573]
- Implicit multi-domain method for unsteady compressible inviscid fluid flows around 3D projectiles p 548 A95-91482
- [HTN-95-20940]
- Aerofoil characteristics at low Reynolds number p 472 A95-91507
- [HTN-95-20940]
- A viewpoint on discretization schemes for applied aerodynamic algorithms for complex configurations p 550 A95-91916
- [HTN-95-20940]
- Simulation of the unsteady interaction of a centrifugal impeller with its vaned diffuser: flow analysis p 633 A95-92474
- [BTN-95-EIX95282710055]
- Primary and secondary vortex structures over accelerated-decelerated airfoils at high angles of attack [SAE PAPER 931368] p 586 A95-93649
- [SAE PAPER 931368]
- Numerical solutions of three dimensional viscous flows [ISBN 1-879921-01-4] p 587 A95-93749
- [ISBN 1-879921-01-4]
- Computation of delta-wing roll maneuvers p 605 A95-94458
- [BTN-95-EIX0619952748164]
- Correlation of unsteady pressure and inflow velocity fields of a pitching rotor blade p 589 A95-94463
- [BTN-95-EIX0619952748169]
- Flow physics of critical states for rolling delta wings p 590 A95-94473
- [BTN-95-EIX0619952748180]
- On the prediction of transonic unsteady flows using second order time accuracy p 641 A95-95448
- [BTN-95-EIX0619952748180]
- A cartesian grid finite element method for aerodynamics of moving rigid bodies p 642 A95-95471
- [BTN-95-EIX0619952748180]
- Partially implicit method for simulating viscous aerofoil flows p 709 A95-96299
- [BTN-94-EIX94522406680]
- Effects of a forward-swept front rotor on the flowfield of a counterrotation propeller p 7 N95-10148
- [NASA-TM-106671]
- Numerical study of Gortler instability: Application to the design of a quiet supersonic wind tunnel p 21 N95-10844
- [PB94-184801]
- Effect of weak periodic pressure gradient on streamwise vortices near a wall p 29 N95-11263
- [PB94-184801]
- Steady and unsteady three-dimensional transonic flow computations by integral equation method p 10 N95-11582
- [NASA-CR-196777]
- Activities of the Institute for Aerospace Studies of Toronto University p 63 N95-12699
- [NASA-CR-196777]
- Studies on the flow induced by an oscillating airfoil in a uniform stream p 40 N95-13250
- [PB94-204450]
- Unsteady flows in turbines: Impact on design procedure p 90 N95-14132
- [PB94-204450]
- Aero design of turbomachinery components: CFD in complex systems p 90 N95-14136
- [NASA-CR-197024]
- Control of unsteady separated flow associated with the dynamic stall of airfoils p 74 N95-14613
- [NASA-CR-197024]
- Spectral analysis of vortex/tree-surface interaction [AD-A283210] p 96 N95-14658
- [AD-A283210]
- Numerical study of the effects of icing on viscous flow over wings p 75 N95-14803
- [NASA-CR-197102]
- Prediction of rotor-blade deformations due to unsteady airloads p 81 N95-15821
- [AD-A284467]
- Unsteady flow phenomena in discrete passage diffusers for centrifugal compressors p 155 N95-16163
- [AD-A281412]
- Measurements of unsteady pressure and structural response for an elastic supercritical wing p 104 N95-16560
- [NASA-TP-3443]
- Time accurate computation of unsteady inlet flows with a dynamic flow adaptive mesh p 157 N95-16736
- [AD-A285498]
- A supercritical airfoil experiment p 111 N95-17858
- [AD-A285498]
- Overview of unsteady transonic wind tunnel test on a semispan straked delta wing oscillating in pitch p 117 N95-18380
- [AD-A284097]
- Pressure measurements on an F/A-18 twin vertical tail in buffeting flow. Volume 4, part 2: Buffet cross spectral densities p 143 N95-18641
- [AD-A285555]
- Wind turbine blade aerodynamics: The combined experiment p 118 N95-18645
- [DE94-011866]
- Wind turbine blade aerodynamics: The analysis of field test data p 118 N95-18646
- [DE94-011867]
- The mathematical models of flow passage for gas turbine engines and their components p 140 N95-19020
- [DE94-011867]
- Simulation of steady and unsteady viscous flows in turbomachinery p 140 N95-19023
- [DE94-011867]
- Unsteady flow testing in a passive low-correction wind tunnel p 147 N95-19272
- [DE94-011867]
- Calculation of support interference in dynamic wind-tunnel tests p 122 N95-19282
- [DE94-011867]
- Simulation of rotor blade element turbulence p 232 N95-21186
- [NASA-TM-108862]
- Direct numerical simulations of on-demand vortex generators: Mathematical formulation p 251 N95-22452
- [NASA-TM-108862]
- Acoustics of laminar boundary layers breakdown p 251 N95-22455
- [NASA-TM-108862]
- A CFD study of complex missile and store configurations in relative motion p 285 N95-22949
- [NASA-CR-197912]
- Holographic interferometric tomography for reconstructing flow fields p 310 N95-23287
- [NASA-CR-197912]
- Three-dimensional unsteady flow calculations in an advanced gas generator turbine p 312 N95-23425
- [NASA-CR-197912]
- Aerodynamic design and analysis of a highly loaded turbine exhaust p 312 N95-23435
- [NASA-CR-197912]
- A time-accurate finite volume method valid at all flow velocities p 314 N95-23447
- [NASA-CR-197912]
- High frequency flow-structural interaction in dense subsonic fluids p 330 N95-24217
- [NASA-CR-4652]
- Thermohydrodynamic analysis of cryogenic liquid turbulent flow fluid film bearings, phase 2 p 349 N95-24461
- [NASA-CR-197412]
- Recent improvements to and validation of the one dimensional NASA wave rotor model p 332 N95-25962
- [NASA-TM-106913]
- A combined geometric approach for solving the Navier-Stokes equations on dynamic grids p 332 N95-26075
- [NASA-TM-106919]
- Turbomachinery design and tonal acoustics computations p 406 N95-26777
- [NASA-CR-197749]
- A numerical method for unsteady transonic flow about wings with control surfaces p 375 N95-26859
- [AD-A289631]
- Global flowfield about the V-22 Tiltrotor Aircraft p 375 N95-27248
- [NASA-CR-198603]
- Comparison of numerical results and multicavity purge and rim seal data with extensions to dynamics p 416 N95-27434
- [NASA-TM-106685]
- A numerical study of fundamental shock noise mechanisms p 451 N95-27908
- [NASA-TM-110608]
- The acoustic characteristics of turbomachinery cavities p 476 N95-28720
- [NASA-CR-4671]
- Interactions of spanwise and chordwise vorticity associated with three-dimensional dynamic stall over an oscillating wing p 477 N95-29091
- [AD-A290546]

A vorticity-velocity approach for three-dimensional unsteady viscous flow over wings p 478 N95-29108

Unsteadiness of shock-induced turbulent boundary layer separation. An inherent feature of turbulent flow or solely a wind tunnel phenomenon
[AD-A290367] p 554 N95-29228

Research instrumentation for polytechnic university's supersonic wind tunnel facility
[AD-A290232] p 523 N95-29468

An experimental investigation of the time-dependent separation of tangent bodies in supersonic flow
[AD-A290720] p 480 N95-29500

An interacting boundary layer method for unsteady compressible flows p 557 N95-30290

A numerical study of the starting process in a hypersonic shock tunnel p 626 N95-30493

Vorticity dynamics and control of dynamic stall
[AD-A288658] p 620 N95-31400

Unsteady flow simulations about moving boundary configurations using dynamic domain decomposition techniques p 649 N95-31837

Control of unsteady separated flow associated with the dynamic stall of airfoils
[NASA-CR-198972] p 594 N95-32193

A nonlinear vortex lattice method for unsteady flow with separated vortex
[DLR-FB-94-32] p 704 N95-32787

Numerical studies of turbulent free surface flows and unsteady propeller flows
[AD-A294377] p 706 N95-34343

A study on the convergence of a 3-D Euler code for cascade flow calculations p 706 N95-34508

Numerical solutions of inviscid and viscous flows about airfoils by TVD method p 684 N95-34521

An unsteady simulation of a centrifugal compressor stage using the NWT p 707 N95-34536

Numerical simulation of unsteady viscous flow around an airfoil with oscillating spoiler p 685 N95-34547

Nonlinear stability of unsteady viscous flow
[AD-A294931] p 707 N95-34597

UNSTEADY STATE

Acoustic field in unsteady moving media
[NASA-CR-198162] p 438 N95-27179

UNSTRUCTURED GRIDS (MATHEMATICS)

A grid generation and flow solution method for the Euler equations on unstructured grids
[HTN-95-20003] p 153 A95-63201

Dynamic unstructured method for flows past multiple objects in relative motion
[BTN-95-EIX95262694303] p 435 A95-85474

Mesh generation and adaptivity for the solution of compressible viscous high speed flows
[BTN-95-EIX95262697157] p 538 A95-86893

Navier-Stokes applications to high-lift airfoil analysis
[BTN-95-EIX0619952748182] p 590 A95-94475

Laminar and turbulent flow computations of Type 4 shock-shock interference aerothermal loads using unstructured grids
[NASA-CR-195008] p 97 N95-15604

Application of three-dimensional hybrid structured/unstructured grids to land, sea and air vehicles
[ARA-MEMO-399] p 210 N95-19775

Numerical study to assess sulfur hexafluoride as a medium for testing multielement airfoils
[NASA-TP-3496] p 378 N95-28674

Surface Modeling, Grid Generation, and Related Issues in Computational Fluid Dynamic (CFD) Solutions
[NASA-CP-3291] p 476 N95-28723

Grid generation and surface modeling for CFD
p 551 N95-28726

Algorithms for high aspect ratio oriented triangulations
p 476 N95-28731

An unstructured-grid software system for solving complex aerodynamic problems p 476 N95-28743

Three-dimensional hybrid grid generation using advancing front techniques p 567 N95-28745

Demonstration of an automated CFD system for three-dimensional flow simulations p 551 N95-28767

UNSWEPT WINGS

Numerical design of advanced multi-element airfoils
[NASA-CR-197135] p 76 N95-15762

UPGRADING

Technology-insertion life-cycle-cost model
[AIAA PAPER 95-0961] p 581 A95-90638

UPPER ATMOSPHERE

Testing of TKE parameterizations in numerical models for clear-air turbulence forecasting p 667 A95-93515

MDCRS: Aircraft observations collection and uses
p 668 A95-93517

Particle kinetic simulation of high altitude hypervelocity flight
[NASA-CR-197383] p 309 N95-22481

UPPER SURFACE BLOWING

Wing download reduction using vortex trapping plates
[HTN-94-00710] p 4 A95-60188

An assessment of upper surface blowing for the reduction of tilt rotor download
[HTN-94-00711] p 5 A95-60189

Dynamic stall control for advanced rotorcraft application
[BTN-95-EIX95222650793] p 334 A95-79249

Numerical simulation of dynamic-stall suppression by tangential blowing
[AD-A284887] p 120 N95-19110

A quiet STOL Research Aircraft Development program
[NAL-TR-1223] p 336 N95-25862

UPWIND SCHEMES (MATHEMATICS)

Application of the multigrid solution technique to hypersonic entry vehicles
[BTN-95-EIX95152583254] p 306 A95-73555

Central-difference and upwind-biased schemes for steady and unsteady Euler aerofoil computations
[HTN-95-01094] p 469 A95-90280

Parallel computational fluid dynamics '91; Conference Proceedings, Stuttgart, Germany, Jun. 10-12, 1991
[ISBN 0-444-89363-6] p 548 A95-91479

Beyond the Riemann problem, part 1
p 550 A95-91925

Comparison of coordinate-invariant and coordinate-aligned upwinding for the Euler equations
[HTN-95-A1753] p 633 A95-93316

Implicit upwind-Euler solution algorithms for unstructured-grid applications p 641 A95-95454

Hypersonic Navier-Stokes computations about complex configurations p 644 A95-95497

Development of an upwind, finite-volume code with finite-rate chemistry
[NASA-CR-196749] p 9 N95-11366

Computational aerodynamics based on the Euler equations
[AGARD-AG-325] p 72 N95-14264

URBAN TRANSPORTATION

Air pollution mitigation measures for airports and associated activity
[PB94-207610] p 216 N95-19582

USER MANUALS (COMPUTER PROGRAMS)

Fatigue life estimation program for Part 23 airplanes, 'AFS.FOR'
[SAE PAPER 931249] p 565 A95-89221

Advanced composites structural concepts and materials technologies for primary aircraft structures. Structural response and failure analysis: ISPAN modules users manual
[NASA-CR-4449] p 12 N95-10242

Modeling improvements and users manual for axial-flow turbine off-design computer code AXOD
[NASA-CR-195370] p 8 N95-10853

A users manual for the method of moments Aircraft Modeling Code (AMC), version 2
[NASA-CR-196445] p 24 N95-11252

Engine structures analysis software: Component Specific Modeling (COSMO)
[NASA-CR-195378] p 57 N95-11711

TKKMOD: A computer simulation program for an integrated wind diesel system. Version 1.0: Document and user guide
[PB94-179090] p 60 N95-11798

User's manual for the NASA Lewis ice accretion/heat transfer prediction code with electrothermal deicer input
[NASA-CR-4530] p 57 N95-11888

Investigation of advanced counterrotation blade configuration concepts for high speed turboprop systems. Task 8: Cooling flow/heat transfer analysis user's manual
[NASA-CR-195360] p 50 N95-11951

User's guide for ENSAERO: A multidisciplinary program for fluid/structural/control interaction studies of aircraft (release 1)
[NASA-TM-108853] p 65 N95-13662

Graphical user interface for the NASA FLOPS aircraft performance and sizing code
[NASA-TM-106649] p 80 N95-14604

Enhanced capabilities and updated users manual for axial-flow turbine preliminary sizing code TURBAN
[NASA-CR-195405] p 76 N95-15912

FPCAS2D user's guide, version 1.0
[NASA-CR-195413] p 156 N95-16588

Users guide for NASA Lewis Research Center DC-9 Reduced-Gravity Aircraft Program
[NASA-TM-106755] p 146 N95-18586

Enhanced capabilities and modified users manual for axial-flow compressor conceptual design code CSPAN
[NASA-TM-106833] p 119 N95-18933

Technology Benefit Estimator (T/BEST): User's manual
[NASA-TM-106785] p 167 N95-19501

A user's guide to LUGSAN 1.1: A computer program to calculate and archive lug and sway brace loads for aircraft-carried stores
[DE95-001919] p 232 N95-21730

Enhanced analysis and users manual for radial-inflow turbine conceptual design code RTD
[NASA-CR-195454] p 275 N95-23462

User's guide for ECAP2D: An Euler unsteady aerodynamic and aeroelastic analysis program for two dimensional oscillating cascades, version 1.0
[NASA-CR-189146] p 316 N95-24189

WINCLR: A computer code for heat transfer and clearance calculation in a compressor
[NASA-CR-195436] p 366 N95-26363

Aircraft noise prediction program theoretical manual: Rotorcraft System Noise Prediction System (ROTONET), part 4
[NASA-TM-83199-PT-4] p 451 N95-26392

User documentation of the CTA program
[AD-A289508] p 375 N95-26854

TranAir: A full-potential, solution-adaptive, rectangular grid code for predicting subsonic, transonic, and supersonic flows about arbitrary configurations. User's manual
[NASA-CR-4349] p 377 N95-28230

Users manual for the improved NASA Lewis ice accretion code LEWICE 1.6
[NASA-CR-198355] p 485 N95-29132

Manual for a workstation-based generic flight simulation program (LaRCsim), version 1.4
[NASA-TM-110164] p 518 N95-30327

FPCAS3D User's guide: A three dimensional full potential aeroelastic program, version 1
[NASA-CR-198367] p 651 N95-32205

Computer model to simulate testing at the National Transonic Facility
[NASA-TM-4664] p 627 N95-32217

USER REQUIREMENTS

On a program-information system TDsoft
[BTN-94-EIX94461408773] p 175 A95-63656

Real-time navigation using the global positioning system
[BTN-95-EIX95172595298] p 279 A95-75714

An approach to weather requirements management
p 653 A95-93448

On designing and engineering the integrated terminal weather system
p 653 A95-93449

ITWS ceiling and visibility products
p 654 A95-93454

Knowing our users -- A challenge for meteorologists at the National Aviation Weather Advisory Unit
p 655 A95-93459

The improvement of meteorological data for air traffic management purposes
p 668 A95-93518

Developing the Aviation Gridded Forecast System
p 671 A95-93532

The prototype aviation weather products generator a vehicle to assess user needs
p 671 A95-93534

Aviation value-added products and services from the NEXRAD Information Dissemination Service (NIDS)
p 671 A95-93535

Universal wind tunnel data acquisition and reduction software
[AD-A283897] p 171 N95-18365

The value of simulation for training
[AD-A289174] p 411 N95-26556

Requirements for effective use of CFD in aerospace design
p 551 N95-28725

An exploratory survey of information requirements for instrument approach charts
[AD-A293882] p 601 N95-31520

Resource document for the design of electronic instrument approach procedure displays
[AD-A295108] p 691 N95-34797

V

V-22 AIRCRAFT

An assessment of upper surface blowing for the reduction of tilt rotor download
[HTN-94-00711] p 5 A95-60189

Thin tailored composite wing for civil tiltrotor
p 285 N95-23317

Global flowfield about the V-22 Tiltrotor Aircraft
[NASA-CR-198603] p 375 N95-27248

Navy composite maintenance and repair experience
p 424 N95-28446

A case study of the teaming concept in the procurement of the V-22 aircraft
[AD-A293770] p 608 N95-31578

V/STOL AIRCRAFT

ASTOVL Aircraft: Some thoughts on new control strategies
[CONGRESS PAPER C428-5-011] p 517 A95-91680

Cooperative control theory and integrated flight and propulsion control
[NASA-CR-197493] p 142 N95-17404

STOVL CFD model test case
p 115 N95-17881

VSTOL Systems Research Aircraft (VSRA) Hamier [NASA-TM-110117] p 126 N95-18347
 NASA develops new digital flight control system [NASA-NEWS-RELEASE-94-47] p 144 N95-19029
 Flightpath synthesis and HUD scaling for V/STOL terminal area operations [NASA-TM-110348] p 383 N95-26587
 Fabry-Perot interferometer measurement of static temperature and velocity for ASTOVL model tests [NASA-TM-107014] p 645 N95-30587
 An LDV investigation of support structure influence on the flow field near the wingtip of a STOVFL configuration in hover [AD-A294126] p 686 N95-34750

VALIDITY
 Representativeness and responsiveness of automated weather systems p 660 A95-93482
 Fracture mechanics validity limits p 95 N95-14480

VALLEYS
 A poor man's expert system for aviation VSRF in complex terrain p 669 A95-93524

VALUE ENGINEERING
 Evaluation and management of research and development in aeronautics [CONGRESS PAPER C428-8-102] p 581 A95-91691
 An analysis of the KC-135 three-person cockpit [AD-A289540] p 390 N95-26873

VALVES
 Measurement of moisture and total hydrocarbon contributions by valves used in clean room gas-delivery systems [BTN-94-EIX94381359041] p 295 A95-74629

VANELESS DIFFUSERS
 Laser anemometer measurements of the three-dimensional rotor flow field in the NASA low-speed centrifugal compressor [NASA-TP-3527] p 618 N95-31985

VANES
 Simulation of the unsteady interaction of a centrifugal impeller with its vaned diffuser: flow analysis [BTN-95-EIX95262710055] p 633 A95-92474
 Experimental performance of a ventral nozzle with pitch and yaw vectoring capability for SSTOVL aircraft [SAE PAPER 931412] p 614 A95-93678
 Engine structures analysis software: Component Specific Modeling (COSMO) [NASA-CR-195378] p 57 N95-11711
 Effect of surface roughness on local film cooling effectiveness and heat transfer coefficients [AD-A283854] p 91 N95-14351
 Application of multidisciplinary models to the cooled turbine rotor design p 140 N95-19024
 Impact loading of compressor stator vanes by hailstone ingestion p 200 N95-19670
 Protective coatings for compressor gas path components p 201 N95-19675
 Braze repair possibilities for hot section gas turbine parts p 201 N95-19677
 Experimental study of vane heat transfer and aerodynamics at elevated levels of turbulence [NASA-CR-4633] p 244 N95-19912
 Phase 2: HGM air flow tests in support of HEX vane investigation p 312 N95-23438
 Allison engine testing CMSX-4(reg sign) single crystal turbine blades and vanes [DE95-010308] p 694 N95-32636

VAPOR DEPOSITION
 Measurement methods and standards for processing and application of thermal barrier coatings p 344 N95-26123
 PVD TBC experience on GE aircraft engines p 345 N95-26126
 Thermal conductivity of zirconia thermal barrier coatings p 345 N95-26133
 Innovative processing of composites for ultra-high temperature applications, book 1 [AD-A290889] p 537 N95-29842

VAPORIZERS
 Vapor generator wand [NASA-CASE-LAR-15058-1] p 238 N95-20080

VAPORIZING
 High pressure vaporization and burning of methanol droplets in reduced gravity p 527 A95-87285

VAPORS
 Supercooling in hypersonic nitrogen wind tunnels [BTN-94-EIX95011441134] p 340 A95-81020
 Vapor lock studies for gasolines with ethers [SAE PAPER 931233] p 529 A95-88962
 NTS-spill test facility wind tunnel exhaust plume characterization [DE95-003630] p 297 N95-24019

VARIABILITY
 Investigation of outflow strength variability in Florida downburst-producing storms p 659 A95-93476

Ceramic manufacturing: Optimizing a multivariable system [DE94-015016] p 56 N95-13184

VARIABLE AMPLITUDE LOADING
 Fatigue of aircraft materials and structures p 387 A95-85894
 Prediction of fatigue crack growth under flight-simulation loading with the modified CORPUS model p 166 N95-19471
 Bonded composite repair of thin metallic materials: Variable load amplitude and temperature cycling effects p 393 N95-27509

VARIABLE CYCLE ENGINES
 Overview of feasibility study on propulsion concepts for high speed civil transport p 498 A95-91518

VARIABLE PITCH PROPELLERS
 Low-order nonlinear dynamic model of IC engine-variable pitch propeller system for general aviation aircraft [NASA-TM-107006] p 694 N95-32916

VARIABLE SWEEP WINGS
 Some additional stability and performance characteristics of the scissor/pivot wing configurations [SAE PAPER 931383] p 618 A95-93659
 A preliminary design proposal for a maritime patrol strike aircraft: MPS-2000 Condor [NASA-CR-197182] p 47 N95-12689

VARIATIONAL PRINCIPLES
 Variational principles for ascent shapes of large scientific balloons [BTN-95-EIX95262694320] p 387 A95-85491

VARIATIONS
 Variations of perturbations in perigee height with eccentricity for artificial Earth's satellites due to air drag [HTN-95-40013] p 85 A95-62657
 Simulation of turbulent fluctuations [BTN-95-EIX95142553041] p 304 A95-73457
 Latitude variations of stratospheric trace gases [HTN-95-70948] p 352 A95-78013
 A review of free-stream flow fluctuation and steady-state flow quality measurements in the AEDC/VKF Supersonic Tunnel A and Hypersonic Tunnel B [AIAA PAPER 95-6137] p 520 A95-90454

VECTORS (MATHEMATICS)
 Describing an attitude p 342 A95-80409
 Optimal trajectories for an unmanned air-vehicle in the horizontal plane [BTN-95-EIX0619952748191] p 606 A95-94480
 New eigensolutions and modal analysis for gyroscopic/rotor systems, part 1: undamped systems [BTN-94-EIX94522410219] p 702 A95-96373

VELOCITY
 A comparison of some aerodynamic resistance methods using measurements over cotton and grass from the 1991 California ozone deposition experiment [HTN-95-11295] p 319 A95-77000
 Experimental investigation of the sources of propeller noise due to the ingestion of turbulence at low speeds [BTN-95-EIX95262697042] p 569 A95-86859

VELOCITY DISTRIBUTION
 Jet to freestream velocity ratio computations for a jet in a crossflow [AIAA PAPER 93-4860] p 2 A95-60178
 Aspects of vortex breakdown [HTN-95-A0001] p 183 A95-67828
 Determination of wall boundary conditions for high-speed-ratio direct simulation Monte Carlo calculations [BTN-95-EIX95182617457] p 267 A95-75728
 Instability of three-dimensional boundary layers due to streamline curvature [HTN-95-61070] p 430 A95-83654
 Boundary layer studies over an S-blade [HTN-95-92261] p 434 A95-85305
 Parameters of Nocilla gas/surface interaction model from measured accommodation coefficients [HTN-95-81639] p 541 A95-87687
 Multipoint inverse design of an infinite cascade of airfoils [HTN-95-81640] p 541 A95-87688
 An introduction to generalized functions with some applications in aerodynamics and aeroacoustics p 565 A95-88895
 Measurement in laminar and transitional boundary-layer flows on concave surface [BTN-95-EIX95282711333] p 632 A95-92408
 Experimental investigation of the flow in diffusers behind an axial flow compressor [BTN-95-EIX95282710057] p 632 A95-92472
 Correlation of unsteady pressure and inflow velocity fields of a pitching rotor blade [BTN-95-EIX0619952748169] p 589 A95-94463
 LDV measurements in separated flow on an elliptic wing mounted at an angle of attack on a wall [BTN-94-EIX94441380518] p 702 A95-96559

Simultaneous three-dimensional velocity and mixing measurements by use of laser Doppler velocimetry and fluorescence probes in a water tunnel [NASA-TP-3454] p 53 N95-13553
 Transport phenomena in stratified multi-fluid flow in the presence and absence of gravity p 95 N95-14563
 Single-pass method for the solution of inverse potential and rotational problems. Part 1: 2-D and quasi 3-D theory and application p 107 N95-16563
 Residual-correction type and related computational methods for aerodynamic design. Part 1: Airfoil and wing design p 128 N95-16566
 Residual-correction type and related computational methods for aerodynamic design. Part 2: Multi-point airfoil design p 128 N95-16567
 Measurement of gust response on a turbine cascade [NASA-TM-106776] p 117 N95-18457
 Aerodynamic investigation of the flow field in a 180 deg turn channel with sharp bend p 163 N95-19257
 A preliminary study of the airwake model used in an existing SH-60B/FFG-7 helicopter/ship simulation program [DSTO-TR-0015] p 224 N95-21659
 Studies in drag reduction p 478 N95-29094
 PIV investigation of compressibility effects on dynamic stall p 478 N95-29102
 A vorticity-velocity approach for three-dimensional unsteady viscous flow over wings p 478 N95-29108
 Effect of velocity and temperature distribution at the hole exit on film cooling of turbine blades [NASA-TM-106954] p 616 N95-30702
 Laser anemometer measurements of the three-dimensional rotor flow field in the NASA low-speed centrifugal compressor [NASA-TP-3527] p 618 N95-31985

VELOCITY MEASUREMENT
 Optimum full-scale subsonic wind tunnel [AIAA PAPER 86-0732] p 18 A95-60161
 LDV measurements in dynamically separated flows [ISBN 0-8194-1311-9] p 5 A95-60191
 Laser device for measuring a vessel's speed [HTN-95-60992] p 361 A95-80633
 Constant flux, turbulent convection data using infrared imaging [HTN-95-20731] p 435 A95-86621
 Flow alteration and drag reduction by riblets in a turbulent boundary layer [HTN-95-61199] p 461 A95-87572
 Laser velocimetry and blade pressure measurements of a blade-vortex interaction [HTN-95-01081] p 547 A95-90267
 Rotor-wake-induced flow separation on a lifting surface [HTN-95-01082] p 468 A95-90268
 Novel implementations of optical diagnostic techniques for aerospace applications [CONGRESS PAPER C428-21-081] p 550 A95-91726
 Measurement in laminar and transitional boundary-layer flows on concave surface [BTN-95-EIX95282711333] p 632 A95-92408
 Multivariable adaptive control using only input and output measurements for turbojet engines [BTN-95-EIX95292721165] p 677 A95-92597
 Laser velocimetry in the supersonic regime: Advancements, limitations, and outlook [SAE PAPER 931365] p 634 A95-93646
 LDV measurements in separated flow on an elliptic wing mounted at an angle of attack on a wall [BTN-94-EIX94441380518] p 702 A95-96559
 A new algorithm for five-hole probe calibration, data reduction, and uncertainty analysis [NASA-TM-106458] p 38 N95-12378
 Hypersonic Gas-Surface Energy Accommodation Test Facility [DE94-014468] p 39 N95-12652
 Simultaneous three-dimensional velocity and mixing measurements by use of laser Doppler velocimetry and fluorescence probes in a water tunnel [NASA-TP-3454] p 53 N95-13553
 Groundspeed filtering for CTAS [NASA-CR-197223] p 97 N95-15785
 Aerodynamic investigation of the flow field in a 180 deg turn channel with sharp bend p 163 N95-19257
 Experimental techniques for measuring transonic flow with a three dimensional laser velocimetry system. Application to determining the drag of a fuselage p 163 N95-19258
 Velocity measurements with hot-wires in a vortex-dominated flowfield p 121 N95-19261
 A three-dimensional orthogonal laser velocimeter for the NASA Ames 7- by 10-foot wind tunnel [NASA-TM-108864] p 249 N95-21323
 MHD-flow in slotted channels with conducting walls [DE94-018370] p 258 N95-21388

A preliminary study of the airwake model used in an existing SH-60B/FFG-7 helicopter/ship simulation program [DSTO-TR-0015] p 224 N95-21659

Impeller flow field characterization with a laser two-focus velocimeter p 313 N95-23440

Flutter clearance flight tests of an OV-10A airplane modified for wake vortex flight experiments [NASA-TM-109168] p 366 N95-26381

Calculation of three-dimensional (3-D) internal flow by means of the velocity-vorticity formulation on a staggered grid [NASA-TM-110352] p 376 N95-27258

Unsteady pressure and inflow velocity on a pitching rotor blade in hover p 480 N95-29771

Fabry-Perot interferometer measurement of static temperature and velocity for ASTOVL model tests [NASA-TM-107014] p 645 N95-30587

Laser anemometer measurements of the three-dimensional rotor flow field in the NASA low-speed centrifugal compressor [NASA-TP-3527] p 618 N95-31985

Spatially-resolved velocity measurements in steady, high-speed, reacting flows using laser-induced OH fluorescence p 650 N95-32109

VENTILATION

Cabin fuselage structural design with engine installation and control system [NASA-CR-197173] p 47 N95-12639

Computational simulations for some tests in transonic wind tunnels p 164 N95-19264

VENTING

Effect of passive venting on static pressure distributions in cavities at subsonic and transonic speeds [NASA-TM-4549] p 6 N95-10029

VENTS

Effect of passive venting on static pressure distributions in cavities at subsonic and transonic speeds [NASA-TM-4549] p 6 N95-10029

VERBAL COMMUNICATION

An analysis of tower (local) controller-pilot voice communications [AD-A283718] p 160 N95-18436

VERMICULITE

Laboratory evaluation of a reactive baffle approach to NOx control [AD-A283802] p 255 N95-19921

VERTICAL AIR CURRENTS

The ITWS microburst prediction algorithm p 655 A95-93456

Vertical wind estimation from horizontal wind measurements p 26 N95-10567

Airborne Windshear Detection and Warning Systems. Fifth and Final Combined Manufacturers' and Technologists' Conference, part 2 [NASA-CP-10139-PT-2] p 41 N95-13203

Microburst vertical wind estimation from horizontal wind measurements [NASA-TP-3460] p 131 N95-18198

Simulation of rotor blade element turbulence [NASA-TM-108862] p 232 N95-21186

VERTICAL DISTRIBUTION

Nonhydrostatic simulation of frontogenesis in a moist atmosphere. Part 3: Thermal wind imbalance and rainbands [HTN-95-90356] p 212 A95-66429

Possible near-IR channels for remote sensing precipitable water vapor from geostationary satellite platforms [HTN-95-70139] p 214 A95-69431

Ascent wind model for launch vehicle design [BTN-95-EIX95041503799] p 239 A95-70124

Sensitivity of two-dimensional model predictions of ozone response to stratospheric aircraft: An update [HTN-95-A0863] p 318 A95-76267

Vertical transport rates in the stratosphere in 1993 from observations of CO₂, N₂O, and CH₄ [HTN-95-70941] p 351 A95-78006

An analysis of aircraft exhaust plumes form accidental encounters [HTN-95-70943] p 351 A95-78008

Latitude variations of stratospheric trace gases [HTN-95-70948] p 352 A95-78013

Aircraft measurements of CLO and HCL during EASOE 1991/92 [HTN-95-00721] p 444 A95-86291

An overview of millimeter-wave spectroscopic measurements of chlorine monoxide at Thule, Greenland, February-March, 1992: Vertical profiles, diurnal variation, and longer-term trends [HTN-95-00722] p 444 A95-86292

Airborne lidar observation of mountain-wave-induced polar stratospheric clouds during EASOE [HTN-95-00738] p 444 A95-86308

Airborne measurements during the European Arctic Stratospheric Ozone Experiment column amounts of HNO₃ and O₃ derived from FTIR emission sounding [HTN-95-00742] p 445 A95-86312

Stratus' tephigram as a training/forecasting tool p 657 A95-93465

Jet stream winds: Comparisons of operational analyses with independent aircraft data at multiple longitudes p 665 A95-93506

VERTICAL FLIGHT

Comments on effect of wet snow on the null-reference ILS system [BTN-95-EIX95142555488] p 227 A95-72885

FAA vertical flight bibliography [DOT/FAA/RD-94/17] p 14 N95-11684

Vertical flight terminal operational procedures. A summary of FAA research and development [AD-A283550] p 85 N95-15328

VERTICAL LANDING

Simulation and flight test evaluation of head-up-display guidance for harrier approach transitions [BTN-95-EIX95062487533] p 194 A95-69241

NASA-Lewis tests Allison ASTOVL nozzle [HTN-95-20603] p 404 A95-84784

Noise levels of helicopters performing elevated pad take-off and landing procedures [HTN-95-92544] p 559 A95-87364

Moisture induced pressures in concrete airfield pavements [AD-A281974] p 52 N95-11789

Vertical flight terminal operational procedures. A summary of FAA research and development [AD-A283550] p 85 N95-15328

STOVL CFD model test case p 115 N95-17881

Heliprot/vertiprot MLS precision approaches [AD-A283505] p 126 N95-18059

VSTOL Systems Research Aircraft (VSRA) Harrier [NASA-TM-110117] p 126 N95-18347

Flow visualization studies of VTOL aircraft models during Hover in ground effect [NASA-TM-108860] p 272 N95-22666

Automatic flight control system for an unmanned helicopter system design and flight test results p 622 N95-32004

VERTICAL MOTION

Observations of fluxes and inland breezes over a heterogeneous surface [HTN-95-80258] p 212 A95-66315

VERTICAL MOTION SIMULATORS

Moving base simulation of an integrated flight and propulsion control system for an ejector-augmentor STOVL aircraft in hover [NASA-TM-108867] p 606 N95-30646

VERTICAL PERCEPTION

Evaluation of simulation motion fidelity criteria in the vertical and directional axes [HTN-94-00666] p 18 A95-60156

VERTICAL TAKEOFF

Noise levels of helicopters performing elevated pad take-off and landing procedures [HTN-95-92544] p 559 A95-87364

Moisture induced pressures in concrete airfield pavements [AD-A281974] p 52 N95-11789

VSTOL Systems Research Aircraft (VSRA) Harrier [NASA-TM-110117] p 126 N95-18347

Flow visualization studies of VTOL aircraft models during Hover in ground effect [NASA-TM-108860] p 272 N95-22666

VERTICAL TAKEOFF AIRCRAFT

Cypher moves toward autonomous flight [HTN-95-41394] p 283 A95-76390

Flying qualities development and flight simulation evaluation of the TW-68 tilt-wing VTOL aircraft [SAE PAPER 932517] p 386 A95-84555

Assessment of Russian VSTOL technology evaluating the YAK-38 'FORGER' and YAK-141 'FREESTYLE' Aircraft Symposium, 30th, Tsukuba, Japan, Sep. 30 - Oct. 2, 1992 [HTN-95-A1609] p 498 A95-91491

Some comments on current research and development of civil VTOL aircrafts p 499 A95-91572

Ducted fan VTOL and its flight control system p 500 A95-91573

The personal aircraft: Status and issues [NASA-TM-109174] p 223 N95-20688

Flow visualization studies of VTOL aircraft models during Hover in ground effect [NASA-TM-108860] p 272 N95-22666

Design and synthesis of a real-time controller for an unmanned air vehicle [AD-A289134] p 408 N95-26555

VERY HIGH FREQUENCIES

A VHF/UHF antenna for the Precision Antenna Measurement System (PAMS) [AD-A285673] p 156 N95-16621

VERY LARGE SCALE INTEGRATION

Fault detection in multiprocessor systems and array processors [BTN-95-EIX95242679097] p 359 A95-81253

VIBRATION

Measurement and analysis of nitric oxide radiation in an arcjet flow [BTN-95-EIX95082502727] p 243 A95-71040

Buckling and vibration analysis of laminated panels using VICONOPT [PAPER-1746] p 230 A95-72580

Control-nonlinear-nonstationary structural response and radiation near a supersonic jet [HTN-95-20929] p 463 A95-88968

Variations observed in the AC generator signal period of a Sea King helicopter [AD-A284280] p 230 N95-19963

Exploratory flow visualization investigation of mast-mounted sights in presence of a rotor [NASA-TM-4634] p 330 N95-24566

Modeling helicopter blade dynamics using a modified Myklestad-Prohl transfer matrix method [AD-A289891] p 400 N95-28626

VIBRATION DAMPING

H(sup 2)/H(sup INF) controller design for a two-dimensional thin airfoil flutter suppression [BTN-94-EIX94511433918] p 141 A95-64584

Design optimization of aircraft engine-mount systems. [BTN-94-EIX94351143325] p 195 A95-67298

Noise and vibration control [BTN-95-EIX95042477108] p 179 A95-68351

Using adaptive structures to attenuate rotary wing aeroelastic response [BTN-95-EIX95062487547] p 192 A95-68361

Multirate flutter suppression system design for a model wing [BTN-95-EIX95182619132] p 292 A95-76609

Summary of an active flexible wing program [BTN-95-EIX95182619209] p 283 A95-76635

Multiple-function digital controller system for active flexible wing wind-tunnel model [BTN-95-EIX95182619212] p 322 A95-76638

Flutter suppression control law design and testing for the active flexible wing [BTN-95-EIX95182619214] p 292 A95-76640

Design and multifunction tests of a frequency domain-based active flutter suppression system [BTN-95-EIX95182619215] p 292 A95-76641

Flutter suppression for the active flexible wing: A classical design [BTN-95-EIX95182619216] p 292 A95-76642

Effect of squeeze film damper land geometry on damper performance [HTN-95-92247] p 434 A95-85291

Transonic flutter suppression using active acoustic excitations [BTN-95-EIX95262694310] p 408 A95-85481

Torsional actuation with extension-torsion composite coupling and a magnetostrictive actuator [BTN-95-EIX95262694314] p 435 A95-85485

Aeroelastic response of composite rotor blades considering transverse shear and structural damping [HTN-95-81647] p 542 A95-87695

Noise and vibration control in aircraft: A global approach p 576 A95-90128

Effects of structural damping on aeroelastic stability of various shaped composite plate wing p 530 A95-91530

Theory and evaluation of active control as a means of reducing helicopter vibration [CONGRESS PAPER C428-19-124] p 517 A95-91721

Passive and active vibration control activities in the German helicopter industry [CONGRESS PAPER C428-19-126] p 517 A95-91722

Panel flutter limit-cycle suppression with piezoelectric actuation [BTN-95-EIX95302731089] p 618 A95-94208

Van der pol absorber for rotor vibrations [BTN-94-EIX94441385106] p 702 A95-96579

Noise Con 1994: Proceedings of the 1994 National Conference on Noise Control Engineering. Progress in Noise Control for Industry [LC-75-24750] p 28 N95-11259

Achievements and tasks for active noise control p 29 N95-11270

Active control of complex noise problems using a broadband, multichannel controller p 29 N95-11271

Active control of interior noise in a business jet using piezoceramic actuators p 29 N95-11276

Adaptive tuned vibration absorbers: Tuning laws, tracking agility, sizing, and physical implementations p 25 N95-11280

Comments on the use of structureborne noise analysis for large commercial airplanes p 30 N95-11287

Exact dynamic responses of periodic multi-span beams under convected pressure fields p 25 N95-11288

Effect of constraining layer stiffness on performance of damping tile materials using finite element modelling with Rayleigh integral p 30 N95-11306

Aeroelastic simulation of higher harmonic control [NASA-CR-4623] p 37 N95-11911

Higher harmonic control analysis for vibration reduction of helicopter rotor systems [NASA-TM-103855] p 66 N95-14419

Tuned mass damper for integrally bladed turbine rotor [NASA-CASE-MFS-28697-1] p 159 N95-18325

Acoustic radiation damping of flat rectangular plates subjected to subsonic flows p 172 N95-18542

Active control of panel vibrations induced by a boundary layer flow [NASA-CR-197867] p 273 N95-23182

Vibration reduction in helicopter rotors using an actively controlled partial span trailing edge flap located on the blade p 624 N95-32111

VIBRATION EFFECTS

Effects of vibration on inertial wind-tunnel model attitude measurement devices [NASA-TM-109083] p 21 N95-11466

Analytical and experimental vibration analysis of a faulty gear system [NASA-TM-106689] p 58 N95-12843

Vibrational behavior of adaptive aircraft wing structures modelled as composite thin-walled beams p 423 N95-28435

VIBRATION ISOLATORS

Effect of squeeze film damper land geometry on damper performance [HTN-95-92247] p 434 A95-85291

Van der pol absorber for rotor vibrations [BTN-94-EIX94441385106] p 702 A95-96579

Adaptive tuned vibration absorbers: Tuning laws, tracking agility, sizing, and physical implementations p 25 N95-11280

Microgravity isolation system design: A case study [NASA-TM-106804] p 104 N95-17657

Microgravity isolation system design: A modern control synthesis framework [NASA-TM-106805] p 105 N95-18197

Tuned mass damper for integrally bladed turbine rotor [NASA-CASE-MFS-28697-1] p 159 N95-18325

Microgravity isolation system design: A modern control analysis framework [NASA-TM-106803] p 105 N95-18486

VIBRATION MEASUREMENT

Vibration measurements on rotating machinery using laser Doppler velocimetry [BTN-94-EIX95011440597] p 429 A95-82986

Aircraft gear train diagnostics using the irregular rotation of the external shafts [CONGRESS PAPER C428-15-097] p 508 A95-91712

The use of math-dynamic models to aid the development of integrated health and usage monitoring systems [CONGRESS PAPER C428-19-079] p 457 A95-91720

Novel implements of optical diagnostic techniques for aerospace applications [CONGRESS PAPER C428-21-081] p 550 A95-91726

An example of airborne vibration monitoring improving flight safety in the Soloviev D-30-KU engine [CONGRESS PAPER C428-21-141] p 508 A95-91728

Condition monitoring for helicopters: 3303 Airborne vibration monitoring system [SAE PAPER 931360] p 610 A95-93642

Test Operation Procedure (TOP): Vibration testing of helicopter equipment [AD-A284433] p 81 N95-15815

A portable transmission vibration analysis system for the S-70A-9 Black Hawk helicopter [DSTO-TR-0072] p 348 N95-24203

VIBRATION METERS

Vibration measurements on rotating machinery using laser Doppler velocimetry [BTN-94-EIX95011440597] p 429 A95-82986

Condition monitoring for helicopters: 3303 Airborne vibration monitoring system [SAE PAPER 931360] p 610 A95-93642

Micro-time stress measurement device development [AD-A289511] p 448 N95-26845

VIBRATION MODE

Effect of wind tunnel acoustic modes on linear oscillating cascade aerodynamics [HTN-94-00760] p 14 A95-60199

Unbalance response of a dual rotor system: Theory and experiment [BTN-94-EIX94351143320] p 195 A95-65854

Application of Navier-Stokes aeroelastic methods to improve fighter wing maneuver performance [BTN-95-EIX95182619218] p 284 A95-76644

Stress considerations in reduced-size aeroelastic optimization [BTN-95-EIX95262694313] p 366 A95-85484

Exact dynamic responses of periodic multi-span beams under convected pressure fields p 25 N95-11288

Aeroelastic stability of wind turbine blade/aileron systems p 377 N95-27981

VIBRATION SIMULATORS

A portable transmission vibration analysis system for the S-70A-9 Black Hawk helicopter [DSTO-TR-0072] p 348 N95-24203

VIBRATION TESTS

Dynamics of the McDonnell-Douglas Large Scale Dynamic Rig and dynamic calibration of the rotor balance [NASA-TM-108855] p 65 N95-13891

Advanced Turbine Technology Applications Project (ATTAP) [NASA-CR-195393] p 101 N95-15743

Test Operation Procedure (TOP): Vibration testing of helicopter equipment [AD-A284433] p 81 N95-15815

High-temperature acoustic test facilities and methods p 174 N95-19149

Nonlinear dynamic response of aircraft structures to acoustic excitation p 135 N95-19151

An Echelle Grating Spectrometer (EGS) for mid-IR remote chemical detection [DE94-019310] p 249 N95-21478

VIBRATIONAL STATES

Flow models for the design of a hypersonic iodine vapor wind tunnel nozzle with chemical and vibrational nonequilibrium effects p 592 N95-30448

VIBRATORY LOADS

Analytical description of and forecast for stress relaxation of aviation materials under the vibration conditions [BTN-94-EIX94461408751] p 126 A95-63634

Higher harmonic control analysis for vibration reduction of helicopter rotor systems [NASA-TM-103855] p 66 N95-14419

Vibration reduction in helicopter rotors using an actively controlled partial span trailing edge flap located on the blade p 624 N95-32111

VIDEO EQUIPMENT

Color control in a multichannel simulator display: The display for advanced research and training [AD-A279717] p 239 N95-20992

Evaluation of the Haworth-Newman avionics Display Readability Scale [AD-A286127] p 235 N95-22232

Apparent size passive range method [AD-DO17360] p 611 N95-31180

VIDEO SIGNALS

Passive range measurement system [AD-DO16222] p 258 N95-21100

VIDEO TAPES

NASA video catalog [NASA-SP-7109(01)] p 363 N95-24238

VIEWING

Advanced interactive display formats for terminal area traffic control [NASA-CR-198576] p 384 N95-28188

VIKING LANDER SPACECRAFT

Fourth-generation Mars vehicle concepts [BTN-95-EIX95152583267] p 298 A95-73568

VIRIAL COEFFICIENTS

Empirical corrections of the rigid rotor interaction potential of H₂-H₂ in the attractive region: Dimer features in the FIR absorption spectra [HTN-95-41943] p 361 A95-81690

VIRTUAL REALITY

Virtual environment application with partial gravity simulation p 169 N95-15988

Virtual reality flight control display with six-degree-of-freedom controller and spherical orientation overlay [NASA-CASE-NPO-18733-1-CU] p 288 N95-22578

The photo-realistic AFIT virtual cockpit [AD-A289376] p 390 N95-26876

Telepresence media resource tape [NASA-TM-110648] p 569 N95-30248

VISCOELASTICITY

Non-linear viscoelastic-plastic constitutive relations for an aeronautical PMMA [HTN-95-71132] p 385 A95-83493

An analytical model for a nonlinear elastomeric lag damper and its effect on aeromechanical stability in Hover [HTN-95-61076] p 369 A95-83660

Stability of viscoelastic plate in supersonic flow under random loading [BTN-95-EIX95262694312] p 435 A95-85483

Effect of constraining layer stiffness on performance of damping tile materials using finite element modelling with Rayleigh integral p 30 N95-11306

VISCOPLASTICITY

Viscoplastic response of structures for intense local heating [HTN-95-41540] p 346 A95-77921

VISCOUSITY

Large-scale computational fluid dynamics by the finite element method [BTN-94-EIX94381359154] p 243 A95-71744

A flow pattern map for two-phase liquid-gas flow under reduced gravity conditions p 539 A95-87280

Development and verification of a resin film infusion/resin transfer molding simulation model for fabrication of advanced textile composites [NASA-CR-197439] p 301 N95-23179

VISCOUS DAMPING

Viscous contribution to the high Mach number damping in pitch of blunt slender cones at small angles of attack [HTN-95-01096] p 469 A95-90282

VISCOUS DRAG

An analysis code for the Rapid Engineering Estimation of Momentum and Energy Losses (REMEL) [NASA-CR-191178] p 108 N95-16887

VISCOUS FLOW

Computation of nonequilibrium viscous flows in arc-jet wind tunnel nozzles [AIAA PAPER 94-0254] p 2 A95-60173

A stationary flow of a viscous liquid in radial clearances of rotor bearings in the turbocompressor of an internal combustion engine [BTN-94-EIX94461408765] p 153 A95-63648

Construction of nearly orthogonal multiblock grids for compressible flow simulation [BTN-94-EIX94361133526] p 207 A95-65981

Solution-adaptive structured-unstructured grid method for unsteady turbomachinery analysis. Part I: Methodology [BTN-94-EIX94441380983] p 208 A95-67329

Thermochemical nonequilibrium viscous shock-layer analysis for a Mars aerocapture vehicle [BTN-95-EIX95082502732] p 239 A95-70139

Adaptive remeshing for convective heat transfer with variable fluid properties [BTN-95-EIX95082502720] p 243 A95-71033

Laplace interaction law for the computation of viscous airflow flow in low- and high-speed aerodynamics [BTN-95-EIX95142553037] p 263 A95-73461

Aerodynamic characteristics of a hypersonic viscous optimized waverider at high altitudes [BTN-95-EIX95152583251] p 266 A95-73552

Higher-order viscous shock-layer solutions for high-altitude flows [BTN-95-EIX95152583255] p 306 A95-73556

Viscous-inviscid interaction method for unsteady low-speed airflow flows [BTN-95-EIX95182619093] p 269 A95-75778

CFD optimization of a theoretical minimum-drag body [BTN-95-EIX95182619234] p 308 A95-76660

Two-dimensional viscous flow past a flat plate [HTN-95-42210] p 430 A95-84026

Computational analysis of buffet alleviation in viscous transonic flow over a porous airfoil [BTN-95-EIX95262694321] p 366 A95-85492

Effect of Reynolds number and turbulence on airfoil aerodynamics at -90-degree incidence [HTN-95-42320] p 370 A95-86149

General solution procedure for flows in local chemical equilibrium [HTN-95-42329] p 404 A95-86158

Mesh generation and adaptivity for the solution of compressible viscous high speed flows [BTN-95-EIX95262697157] p 538 A95-86893

Low-dimensional description of the dynamics in separated flow past thick airfoils [HTN-95-20832] p 544 A95-88093

Computational fluid dynamics with icing effects [SAE PAPER 932532] p 466 A95-89192

Numerical design methods for transonic NLF configurations p 471 A95-91498

Algorithmic trends in computational fluid dynamics; The Institute for Computer Applications in Science and Engineering (ICASE)/LaRC Workshop, NASA Langley Research Center, Hampton, VA, US, Sep. 15-17, 1991 [ISBN 0-387-94014-6] p 550 A95-91915

A viewpoint on discretization schemes for applied aerodynamic algorithms for complex configurations p 550 A95-91916

Beyond the Riemann problem, part 1 p 550 A95-91925

Numerical calculations of the turbulent flow through a controlled diffusion compressor cascade
 [BTN-95-EIX95282710056] p 632 A95-92473

A three-dimensional Navier-Stokes/full-potential coupled analysis for rotor blades
 [ISBN 1-879921-01-4] p 587 A95-93748

Numerical solutions of three dimensional viscous flows
 [ISBN 1-879921-01-4] p 587 A95-93749

Evaluation of a multigrid-based Navier-Stokes solver for aerothermodynamic computations
 [BTN-95-EIX95302694459] p 583 A95-94056

3-D Navier-Stokes analysis of crossing glancing shocks/turbulent boundary layer interactions
 [BTN-95-EIX95302729768] p 636 A95-94130

Aerodynamic applications of underexpanded hypersonic viscous jets
 [BTN-95-EIX0619952748162] p 589 A95-94456

Comparison of the predictive capabilities of several turbulence models
 [BTN-95-EIX0619952748167] p 589 A95-94461

Viscous flow simulation using the discrete vortex diffusion velocity method
 p 639 A95-95421

Implicit-multidomain calculation of viscous transonic flows without artificial viscosity or upwinding
 p 640 A95-95443

Agglomeration multigrid for viscous turbulent flows
 [AD-A284064] p 8 N95-10848

Development of an upwind, finite-volume code with finite-rate chemistry
 [NASA-CR-196749] p 9 N95-11366

Studies on the flow induced by an oscillating airfoil in a uniform stream
 [PB94-204450] p 40 N95-13250

Aero design of turbomachinery components: CFD in complex systems
 p 90 N95-14136

Numerical study of the effects of icing on viscous flow over wings
 [NASA-CR-197102] p 75 N95-14803

Time accurate computation of unsteady inlet flows with a dynamic flow adaptive mesh
 [AD-A285498] p 157 N95-16736

Three dimensional compressible turbulent flow computations for a diffusing S-duct with/without vortex generators
 [NASA-CR-195390] p 138 N95-17402

Investigation of the flow over a series of 14 percent-thick supercritical aerofoils with significant rear camber
 p 109 N95-17849

Measurements of the flow over a low aspect-ratio wing in the Mach number range 0.6 to 0.87 for the purpose of validation of computational methods. Part 1: Wing design, model construction, surface flow. Part 2: Mean flow in the boundary layer and wake, 4 test cases
 p 112 N95-17860

Solution of Navier-Stokes equations using high accuracy monotone schemes
 p 161 N95-19019

Simulation of steady and unsteady viscous flows in turbomachinery
 p 140 N95-19023

Viscous flow past aerofoils axisymmetric bodies and wings
 p 123 N95-19457

Inviscid and viscous flow modelling of complex aircraft configurations using the CFD simulation system sauna
 [ARA-MEMO-403] p 211 N95-19777

Experiments on the flow field physics of confluent boundary layers for high-lift systems
 [NASA-CR-197318] p 224 N95-21343

An assessment of viscous effects in computational simulation of benign and burst vortex flows on generic fighter wind-tunnel models using TEAM code
 [NASA-CR-4650] p 273 N95-23185

Development of an upwind, finite-volume code with finite-rate chemistry
 [NASA-CR-197747] p 374 N95-26760

Global flowfield about the V-22 Tiltrotor Aircraft
 [NASA-CR-198603] p 375 N95-27248

Calculation of three-dimensional (3-D) internal flow by means of the velocity-vorticity formulation on a staggered grid
 [NASA-TM-110352] p 376 N95-27258

Numerical study to assess sulfur hexafluoride as a medium for testing multielement airfoils
 [NASA-TP-3496] p 378 N95-28674

Block-structured grids for complex aerodynamic configurations: Current status
 p 551 N95-28736

A vorticity-velocity approach for three-dimensional unsteady viscous flow over wings
 p 478 N95-29108

Leading edge film cooling effects on turbine blade heat transfer
 [NASA-TM-106955] p 513 N95-29115

Finite element vorticity-based methods for the solution of the incompressible and compressible Navier-Stokes equations
 p 553 N95-29119

Solution of the Navier-Stokes equations on locally refined Cartesian meshes using state-vector splitting
 p 553 N95-29197

A numerical study of the starting process in a hypersonic shock tunnel
 p 626 N95-30493

Numerical solutions of inviscid and viscous flows about airfoils by TVD method
 p 684 N95-34521

Numerical simulation of unsteady viscous flow around an airfoil with oscillating spoiler
 p 685 N95-34547

Nonlinear stability of unsteady viscous flow
 [AD-A294931] p 707 N95-34597

VISCOUS FLUIDS

A stationary flow of a viscous liquid in radial clearances of rotor bearings in the turbocompressor of an internal combustion engine
 [BTN-94-EIX94461408765] p 153 A95-63648

Direct numerical simulations of on-demand vortex generators: Mathematical formulation
 p 251 N95-22452

VISIBILITY

A simulator study about effects of visibility upon helicopter pilot performance
 p 522 A95-91556

ITWS ceiling and visibility products
 p 654 A95-93454

Flying with automated surface observations
 p 659 A95-93472

Representativeness and responsiveness of automated weather systems
 p 660 A95-93482

The performance of forward scatter visibility sensors for application in autostations and runway visual range in snow and freezing precipitation events
 p 662 A95-93489

The aviation gridded forecast system verification program - A description of aviation-impact-variable evaluation plans
 p 664 A95-93498

Comprehensive verification of terminal forecast ceiling and visibility
 p 664 A95-93500

Verification of terminal forecasts
 p 664 A95-93502

Analysis of rapidly developing fog at the Kennedy Space Center
 p 671 A95-93531

Airborne Windshear Detection and Warning Systems. Fifth and Final Combined Manufacturers' and Technologists' Conference, part 2
 [NASA-CP-10139-PT-2] p 41 N95-13203

Characteristics of civil aviation atmospheric hazards
 p 42 N95-13208

Evaluation of retro-reflective beads in airport pavement markings
 [AD-A291065] p 523 N95-29967

Initial evaluation of the Oregon State University planetary boundary layer column model for ITWS applications
 [AD-A293775] p 677 N95-31465

Evaluation of alternative pavement marking materials
 [AD-A292973] p 626 N95-31468

VISUAL AIDS

Inadequacy of visual alarms in helicopter air medical transport
 [HTN-95-01218] p 484 A95-91450

Research requirements for future visual guidance systems
 [AD-A279188] p 191 N95-19810

VISUAL CONTROL

Developments in airfield lighting
 [CONGRESS PAPER C428-7-147] p 488 A95-91688

The 4-D approach to visual control of autonomous systems
 [AIAA PAPER 94-1243-CP] p 27 N95-11513

VISUAL FIELDS

Factors affecting the visual fragmentation of the field-of-view in partial binocular overlap displays
 [AD-A283081] p 172 N95-17334

Factors affecting the perception of luring in monocular regions of partial binocular overlap displays
 [AD-A286287] p 259 N95-22044

VISUAL FLIGHT

Perceptual dimensions of simulated scenes relevant for visual low-altitude flight
 [AD-A294385] p 700 N95-34344

VISUAL FLIGHT RULES

Federal aviation regulations, part 91. General operating and flight rules. Change 5
 [PB94-194883] p 123 N95-17476

Federal aviation regulations, part 91. General operating and flight rules. Change 8
 [PB94-217445] p 188 N95-19720

VISUAL OBSERVATION

Representativeness and responsiveness of automated weather systems
 p 660 A95-93482

VISUAL PERCEPTION

Functions of NAL fixed base simulator for helicopter research
 p 522 A95-91555

A simulator study about effects of visibility upon helicopter pilot performance
 p 522 A95-91556

The selective use of functional optical variables in the control of forward speed
 [NASA-TM-108849] p 35 N95-12227

Factors affecting the visual fragmentation of the field-of-view in partial binocular overlap displays
 [AD-A283081] p 172 N95-17334

Factors affecting the perception of luring in monocular regions of partial binocular overlap displays
 [AD-A286287] p 259 N95-22044

Visual contrast detection thresholds for aircraft contrails
 [AD-A288618] p 328 N95-25607

Characterization of corrosion and development of a breadboard of a D sight aircraft inspection system, phase 1
 [AD-A288347] p 380 N95-26527

Perceptual dimensions of simulated scenes relevant for visual low-altitude flight
 [AD-A294385] p 700 N95-34344

VISUAL SIGNALS

Inadequacy of visual alarms in helicopter air medical transport
 [HTN-95-01218] p 484 A95-91450

Cueing light configuration for aircraft navigation
 [NASA-CASE-ARC-11982-1] p 280 N95-23393

VOICE COMMUNICATION

Integrated voice and data communications for air traffic service applications
 p 600 A95-95090

An analysis of tower (local) controller-pilot voice communications
 [AD-A283718] p 160 N95-18436

Speech analysis and synthesis based on pitch-synchronous segmentation of the speech waveform
 [AD-A288824] p 435 N95-26349

Development of a coding form for approach control/pilot voice communications
 [DOT/FAA/AM-95/15] p 384 N95-28540

Tactical low-level helicopter communications
 p 702 N95-32492

VOICE DATA PROCESSING

Speech analysis and synthesis based on pitch-synchronous segmentation of the speech waveform
 [AD-A288824] p 435 N95-26349

VOLCANOES

Volcanic ash forecast transport and dispersion (VAFTAD) model
 [HTN-95-80702] p 254 A95-72546

Two dimensional stratospheric aerosol distributions during EASOE
 [HTN-95-00726] p 444 A95-86296

Airborne measurements during the Arctic stratospheric experiment: Observation of O3 and NO2
 [HTN-95-00748] p 445 A95-86318

Role of the aviation weather system in providing a real-time ATC volcanic ash advisory system
 p 663 A95-93494

Alaska's volcanic ash warning system
 p 663 A95-93495

VORTEX ADVISORY SYSTEM

A technique for detecting a tropical cyclone center using a Doppler radar
 [HTN-95-20631] p 215 A95-69574

VORTEX ALLEVIATION

Cornet vortex suppressor
 [AD-D016423] p 116 N95-18337

VORTEX AVOIDANCE

Characterizing the wake vortex signature for an active line of sight remote sensor
 [NASA-CR-197697] p 333 N95-24391

VORTEX BREAKDOWN

Aspects of vortex breakdown
 [HTN-95-A0001] p 183 A95-67828

Adaptive computations of flow around a delta wing with vortex breakdown
 [BTN-94-EIX94441386631] p 184 A95-68180

Numerical simulation of incidence and sweep effects on delta wing vortex breakdown
 [BTN-95-EIX95062487526] p 186 A95-69234

Transient structure of vortex breakdown on a delta wing
 [BTN-95-EIX95182619073] p 268 A95-75758

Compressible inviscid vortex flow of a sharp edge delta wing
 [BTN-95-EIX95262694308] p 370 A95-85479

Simple numerical criterion for vortex breakdown
 [HTN-95-61210] p 541 A95-87583

Effects of periodic spanwise blowing on Delta-wing configuration characteristics
 [HTN-95-81631] p 461 A95-87679

Dynamic pitch-up of a delta wing
 [HTN-95-81633] p 462 A95-87681

Effects of trailing-edge jet entrainment on delta wing vortices
 [HTN-95-81644] p 542 A95-87692

Adaptive computations of flow around a delta wing with vortex breakdown
 [HTN-95-20948] p 465 A95-88987

Criteria for location of vortex breakdown over delta wings
 [HTN-95-01092] p 468 A95-90278

Unsteady aerodynamic effects of trailing edge controls on delta wings
[HTN-95-01099] p 469 A95-90285

Numerical investigation of high incidence flow over a double-delta wing
[BTN-95-EIX0619952748160] p 588 A95-94454

Computation of vortex breakdown on a rolling delta wing
[BTN-95-EIX0619952748195] p 591 A95-94484

Numerical simulation of transient vortex breakdown above a pitching delta wing
[AD-A281075] p 107 N95-16808

Navier-Stokes, flight, and wind tunnel flow analysis for the F/A-18 aircraft
[NASA-TP-3478] p 120 N95-19114

Computation of vortex breakdown
p 165 N95-19462

Effect of juncture fillets on double-delta wings undergoing sideslip at high angles of attack
[AD-A286165] p 232 N95-22039

Numerical investigation into vortical flow about a delta-wing configuration up to incidences at which vortex breakdown occurs in experiment
[PB95-198024] p 593 N95-30837

VORTEX FILAMENTS

Vortex cutting by a blade, part 1: General theory and a simple solution
[HTN-95-20822] p 543 A95-88083

Computation of vortex breakdown
p 165 N95-19462

A numerical method for modelling wings with sharp edges maneuvering at high angles of attack
p 503 N95-29122

VORTEX FLAPS

Wing download reduction using vortex trapping plates
[HTN-94-00710] p 4 A95-60188

Aerodynamic characteristics of strake vortex flaps on a strake-wing configuration
[BTN-95-EIX95062487537] p 187 A95-69245

Estimation of aerodynamic characteristics for the vortex flaps by the suction analogy
p 471 A95-91496

Low speed aerodynamic characteristics of delta wings with vortex flaps: 60 deg and 70 deg delta wings
[NAL-TR-1245] p 331 N95-25105

Pressure based high order TVD methodology for dynamic stall control
[AD-A290149] p 479 N95-29316

VORTEX GENERATORS

Experimental study of three-dimensional separation
[BTN-94-EIX94441385752] p 179 A95-68216

Entrainment and acoustic variations in a round jet from introduced streamwise vorticity
[BTN-95-EIX95042474409] p 209 A95-68291

Flow structure in the wake of a wishbone vortex generator
[BTN-95-EIX95142553044] p 304 A95-73454

Separation control on high-lift airfoils via micro-vortex generators
[BTN-95-EIX95152582326] p 265 A95-73529

Mixing enhancement by and noise characteristics of streamwise vortices in an air jet
[HTN-95-42322] p 371 A95-86151

Low Reynolds number laminar separation bubble control using a backward facing step
[SAE PAPER 932572] p 467 A95-90061

Vortex generation and mixing in three-dimensional supersonic combustors
[BTN-95-EIX0616952745783] p 614 A95-94503

Axis switching and spreading of an asymmetric jet: Role of vorticity dynamics
[NASA-TM-106385] p 73 N95-14418

Mach number, flow angle, and loss measurements downstream of a transonic fan-blade cascade
[AD-A280907] p 108 N95-16824

Three dimensional compressible turbulent flow computations for a diffusing S-duct with/without vortex generators
[NASA-CR-195390] p 138 N95-17402

Experimental investigations of on-demand vortex generators
p 250 N95-22451

Direct numerical simulations of on-demand vortex generators: Mathematical formulation
p 251 N95-22452

Performance characterization of a highly-offset diffuser with and without blowing vortex generator jets
[AD-A289334] p 375 N95-26901

Collected papers on wind turbine technology
[NASA-CR-195432] p 447 N95-27970

Comparative performance tests on the Mod-2, 2.5-mW wind turbine with and without vortex generators
p 377 N95-27978

Comparison of measured and calculated dynamic loads for the Mod-2 2.5 mW wind turbine system
p 440 N95-27983

The decay of longitudinal vortices shed from airfoil vortex generators
[NASA-CR-198356] p 480 N95-29402

A wind tunnel investigation of the effects of micro-vortex generators and Gurney flaps on the high-lift characteristics of a business jet wing
[NASA-TM-110626] p 607 N95-30827

VORTEX IN CELL TECHNIQUE

Central-difference and upwind-biased schemes for steady and unsteady Euler aerfoil computations
[HTN-95-01094] p 469 A95-90280

Numerical solution of Euler and Navier-Stokes equations for 2D transonic problems
p 638 A95-95366

VORTEX LATTICE METHOD

Numerical simulation of steady and unsteady, vorticity-dominated aerodynamic interference
[BTN-95-EIX95062487524] p 186 A95-69232

Sidewash on the vertical tail in subsonic and supersonic flows
[BTN-95-EIX95152582316] p 264 A95-73519

Static aeroelastic characteristics of a composite wing
[BTN-95-EIX95152582340] p 282 A95-73542

Estimation of aerodynamic characteristics for the vortex flaps by the suction analogy
p 471 A95-91496

Vortex lattice method simulation of unsteady flow due to wing/external store combination
p 471 A95-91499

An experimental investigation of forward-swept wings at low Reynolds numbers
[SAE PAPER 931370] p 604 A95-93650

An efficient discrete vortex method for low Reynolds number incompressible flows
p 639 A95-95407

Panel methods
p 165 N95-19448

A nonlinear vortex lattice method for unsteady flow with separated vortex
[DLR-FB-94-32] p 704 N95-32787

VORTEX RINGS

Active open-loop control of particle dispersion in round jets
[HTN-95-42334] p 372 A95-86163

Experiments on microbursts
p 562 N95-29110

VORTEX SHEDDING

Vortex shedding noise control in idling circular saws using air ejection at the teeth
[BTN-94-EIX94371347214] p 257 A95-69970

Flow past a symmetric wedge with forward splitter plate
p 427 A95-82406

Sphere wakes at moderate Reynolds numbers in a turbulent environment
[HTN-95-42331] p 372 A95-86160

Low-dimensional description of the dynamics in separated flow past thick airfoils
[HTN-95-20832] p 544 A95-88093

A numerical investigation of flow around a square-section cylinder mounted with a splitter plate
p 639 A95-95401

Effects of splitter plate on wake formation from a circular cylinder: A discrete vortex simulation
p 639 A95-95404

Numerical simulation of the flow about the F-18 HARV at high angle of attack
[NASA-CR-196396] p 9 N95-10940

High angle of attack aerodynamics
p 74 N95-14450

Interaction, bursting and control of vortices of a cropped double-delta wing at high angle of attack
[AD-A283656] p 119 N95-18669

Research on bluff body vortex wakes
[AD-A286319] p 223 N95-20177

High frequency flow-structural interaction in dense subsonic fluids
[NASA-CR-4652] p 330 N95-24217

The acoustic characteristics of turbomachinery cavities
[NASA-CR-4671] p 476 N95-28720

The effects of three dimensional imposed disturbances on bluff body near wake flows
[AD-A290824] p 555 N95-29654

Validation of the helicopter rotor code HERO
[PB95-198040] p 607 N95-30838

VORTEX SHEETS

Vortex cutting by a blade, Part II: Computations of vortex response
[BTN-94-EIX94441386611] p 208 A95-67342

Tip vortex on a swept wing. Mean flow and unsteady phenomena
[BTN-94-EIX94441385755] p 184 A95-68219

Vorticity concentration at the edge of the inboard vortex sheet
[HTN-95-31010] p 221 A95-71180

Computation of vortex formation over ELAC-1 configuration using vorticity confinement
[AIAA PAPER 95-6157] p 470 A95-90469

Effect of density gradients in confined supersonic shear layers. Part 2: 3-D modes
[NASA-CR-198030] p 349 N95-24413

A numerical method for modelling wings with sharp edges maneuvering at high angles of attack
p 503 N95-29122

A nonlinear vortex lattice method for unsteady flow with separated vortex
[DLR-FB-94-32] p 704 N95-32787

VORTICES

Vortex cutting by a blade. Part II: Computations of vortex response
[BTN-94-EIX94441386611] p 208 A95-67342

Elliptic tip effects on the vortex wake of an axisymmetric body at incidence
[BTN-94-EIX94441386612] p 208 A95-67343

Aspects of vortex breakdown
[HTN-95-A0001] p 183 A95-67828

Lift analysis of a variable camber foil using the discrete vortex-blob method
[BTN-94-EIX94441386623] p 179 A95-68172

Adaptive computations of flow around a delta wing with vortex breakdown
[BTN-94-EIX94441386631] p 184 A95-68180

Experimental study of three-dimensional separation
[BTN-94-EIX94441385752] p 179 A95-68216

Phenomenological description and simplified modelling of the vortex wake issuing from a jet in a crossflow
[BTN-94-EIX94441385754] p 184 A95-68218

Suppression of vortex asymmetry and side force on a circular cone
[BTN-95-EIX95042474413] p 209 A95-68287

Entrainment and acoustic variations in a round jet from introduced streamwise vorticity
[BTN-95-EIX95042474409] p 209 A95-68291

Vortical flow structure near the F/A-18 LEX at high incidence
[BTN-95-EIX95062487555] p 186 A95-68369

Research aircraft observations of a polar flow at the east Greenland ice edge
[HTN-95-A0175] p 215 A95-69766

Time-resolved surface heat flux measurements in the wing/body junction vortex
[BTN-95-EIX95082502716] p 220 A95-71029

Flow structure in the wake of a wishbone vortex generator
[BTN-95-EIX95142553044] p 304 A95-73454

Effects of spatial order of accuracy on the computation of vortical fields
[BTN-95-EIX95152577604] p 305 A95-73479

Experimental investigation of the flowfield about an upswept afterbody
[BTN-95-EIX95152582321] p 265 A95-73524

Navier-Stokes prediction of large-amplitude delta-wing roll oscillations
[BTN-95-EIX95152582329] p 281 A95-73531

Forebody flow control on a full-scale F/A-18 aircraft
[BTN-95-EIX95152582333] p 281 A95-73535

Pneumatic concept for tip-stall control of cranked-arrow wings
[BTN-95-EIX95152582335] p 281 A95-73537

Effect of leeward flow dividers on the wing rock of a delta wing
[BTN-95-EIX95152582347] p 282 A95-73549

Transient structure of vortex breakdown on a delta wing
[BTN-95-EIX95182619073] p 268 A95-75758

Numerical study of sound generation due to a spinning vortex pair
[BTN-95-EIX95182619075] p 307 A95-75760

Diurnal variation of lee vortices in Taiwan and the surrounding area
[HTN-95-91363] p 318 A95-76394

Influence of streamwise curvature on longitudinal vortices imbedded in turbulent boundary layers
[BTN-94-EIX94401378820] p 307 A95-76489

On the role of the outer region in the turbulent-boundary-layer bursting process
[BTN-94-EIX95011441078] p 348 A95-81056

Measurements of vortex pair interaction with a clean or contaminated free surface
[BTN-94-EIX95011441063] p 429 A95-82798

Vortex methods for the computational analysis of rotor/body interaction
[HTN-95-61072] p 369 A95-83656

Structure of supersonic jet flow and its radiated sound
[HTN-95-51645] p 431 A95-85027

Crossflow topology of vortical flows
[HTN-95-51664] p 432 A95-85046

Force and moment on a Joukowski profile in the presence of point vortices
[BTN-95-EIX95262694298] p 434 A95-85469

Compressible inviscid vortex flow of a sharp edge delta wing
[BTN-95-EIX95262694308] p 370 A95-85479

Mixing enhancement by and noise characteristics of streamwise vortices in an air jet
[HTN-95-42322] p 371 A95-86151

- Quantitative investigation of compressible mixing: Staged transverse injection into Mach 2 flow [HTN-95-42330] p 404 A95-86159
- Near field of a coaxial jet with and without axial excitation [HTN-95-42332] p 372 A95-86161
- Interferometric investigations of compressible dynamic stall over a transiently pitching airfoil [HTN-95-42338] p 372 A95-86167
- Airborne measurements during the European Arctic Stratospheric Ozone Experiment: Observation of OClO [HTN-95-00745] p 445 A95-86315
- Pulsed jet ignition modeling with a full chemistry p 538 A95-87184
- Numerical model of boundary-layer control using air-jet generated vortices [HTN-95-42581] p 459 A95-87211
- Effects of spatial order of accuracy on the computation of vortical flowfields [HTN-95-42589] p 459 A95-87219
- Vorticity in an inviscid fluid at hypersonic speeds [HTN-95-42590] p 539 A95-87220
- Aerodynamics of delta wings with application to high-alpha flight mechanics p 460 A95-87395
- Head-on parallel blade-vortex interaction [HTN-95-61197] p 491 A95-87570
- Airfoil pressure measurements during oblique shock-wave/vortex interaction in a Mach 3 stream [HTN-95-81641] p 542 A95-87689
- Effects of time scales on lift of airfoils in an unsteady stream [HTN-95-81643] p 542 A95-87691
- Effects of trailing-edge jet entrainment on delta wing vortices [HTN-95-81644] p 542 A95-87692
- Doppler lidar investigation of wake vortex transport between closely spaced parallel runways [HTN-95-81645] p 462 A95-87693
- Some aspects of the aerodynamics of extreme-speed jets p 572 A95-88893
- Unsteady aerodynamics of vortical flows: Early and recent developments p 462 A95-88896
- Vortex cutting by a blade, Part 2: Computations of vortex response [HTN-95-20937] p 464 A95-88976
- Elliptic tip effects on the vortex wake of an axisymmetric body at incidence [HTN-95-20938] p 464 A95-88977
- Lift analysis of a variable camber foil using the discrete vortex-blob method [HTN-95-20940] p 545 A95-88979
- Nonlinear analysis of swept wing transitional boundary layers [SAE PAPER 932515] p 466 A95-89188
- Computation of vortex formation over ELAC-1 configuration using vorticity confinement [AIAA PAPER 95-6157] p 470 A95-90469
- High angle of attack missile aerodynamics [CONGRESS PAPER C428-3-060] p 475 A95-91673
- Recent research in ASTOVL aircraft ground environment [CONGRESS PAPER C428-9-040] p 475 A95-91694
- Estimation of atmospheric turbulence severity from in-situ aircraft measurements p 659 A95-93479
- Turbulence near thunderstorm tops p 675 A95-93553
- Primary and secondary vortex structures over accelerated-decelerated airfoils at high angles of attack [SAE PAPER 931368] p 586 A95-93649
- A three-dimensional Navier-Stokes/full-potential coupled analysis for rotor blades [ISBN 1-879921-01-4] p 587 A95-93748
- Numerical solutions of three dimensional viscous flows [ISBN 1-879921-01-4] p 587 A95-93749
- Quantifiable vortex features of F-106B aircraft at subsonic speeds [BTN-95-EIX0619952748161] p 588 A95-94455
- Jet transport response to a horizontal wind vortex [BTN-95-EIX0619952748163] p 619 A95-94457
- Computation of delta-wing roll maneuvers [BTN-95-EIX0619952748164] p 605 A95-94458
- Spectral mapping of quasiperiodic structures in a vortex flow [BTN-95-EIX0619952748165] p 589 A95-94459
- Flow physics of critical states for rolling delta wings [BTN-95-EIX0619952748180] p 590 A95-94473
- Effect of leading-edge extension fences on the vortex wake of an F/A-18 model [BTN-95-EIX0619952748192] p 591 A95-94481
- Computation of vortex breakdown on a rolling delta wing [BTN-95-EIX0619952748195] p 591 A95-94484
- Vortex generation and mixing in three-dimensional supersonic combustors [BTN-95-EIX0616952745783] p 614 A95-94503
- Computational fluid dynamics '92; Proceedings of the European Computational Fluid Dynamics Conference, 1st, Brussels, Belgium, Sep. 7-11, 1992. Vols. 1 & 2 [ISBN 0-444-89793-3] p 638 A95-95357
- Transonic vortical flow predicted with a structured multiblock Euler solver p 642 A95-95462
- Navier-Stokes simulation of turbulent vortex high-Re-number flows over a delta wing p 644 A95-95507
- Instabilities originating from suction holes used for Laminar Flow Control (LFC) [NASA-CR-196395] p 6 N95-10131
- Numerical study of Gortler instability: Application to the design of a quiet supersonic wind tunnel [PB94-184801] p 21 N95-10844
- Flow-visualization study of the X-29A aircraft at high angles of attack using a 1/48-scale model [NASA-TM-104268] p 8 N95-10858
- Effect of weak periodic pressure gradient on streamwise vortices near a wall p 29 N95-11263
- Potential impacts of advanced aerodynamic technology on air transportation system productivity [NASA-TM-109154] p 10 N95-11489
- Water-tunnel-flow-visualization-study-of-a 4.4-percent scale X-31 forebody [NASA-TM-104276] p 36 N95-11898
- Ground-based wake vortex monitoring, prediction, and ATC interface p 42 N95-13209
- Wake vortex detection at Denver Stapleton Airport with a pulsed 2-micron coherent lidar p 42 N95-13211
- Doppler radar detection of vortex hazard indicators p 42 N95-13212
- Simultaneous three-dimensional velocity and mixing measurements by use of laser Doppler velocimetry and fluorescence probes in a water tunnel [NASA-TP-3454] p 53 N95-13553
- Hybrid structured/unstructured grid computations for the F/A-18 at high angle of attack p 68 N95-14233
- F/A-18 and F-16 forebody vortex control, static and rotary-balance results p 72 N95-14254
- Low-energy pneumatic control of forebody vortices p 72 N95-14256
- Integration of a mechanical forebody vortex control system into the F-15 p 72 N95-14258
- Flight evaluation of pneumatic forebody vortex control in post-stall flight p 72 N95-14259
- Computational aerodynamics based on the Euler equations [AGARD-AG-325] p 72 N95-14264
- Axis switching and spreading of an asymmetric jet: Role of vorticity dynamics [NASA-TM-106385] p 73 N95-14418
- High angle of attack aerodynamics p 74 N95-14450
- Spectral analysis of vortex/free-surface interaction [AD-A283210] p 96 N95-14658
- Wake turbulence p 75 N95-14894
- Numerical simulation of transient vortex breakdown above a pitching delta wing [AD-A281075] p 107 N95-16808
- Transonic Navier-Stokes calculations about a 65 deg delta wing [NASA-CR-4635] p 108 N95-17273
- Three dimensional compressible turbulent flow computations for a diffusing S-duct with/without vortex generators [NASA-CR-195390] p 138 N95-17402
- Ellipsoid-cylinder model p 158 N95-17869
- Supersonic vortex flow around a missile body p 114 N95-17870
- Test data on a non-circular body for subsonic, transonic and supersonic Mach numbers p 158 N95-17871
- Wind tunnel test on a 65 deg delta wing with a sharp or rounded leading edge: The international vortex flow experiment p 114 N95-17872
- Delta-wing model p 114 N95-17873
- Experimental investigation of the vortex flow over a 76/60-deg double delta wing p 114 N95-17874
- Wind tunnel test on a 65 deg delta wing with rounded leading edges: The International Vortex Flow Experiment p 114 N95-17875
- Investigation of the flow development on a highly swept canard/wing research model with segmented leading- and trailing-edge flaps p 114 N95-17876
- Subsonic flow around US-orbiter model FALKE in the DNW p 115 N95-17877
- Corner vortex suppressor [AD-D016423] p 116 N95-18337
- Aircraft wake vortex takeoff tests at O'Hara International Airport [AD-A283828] p 118 N95-18624
- Interaction, bursting and control of vortices of a cropped double-delta wing at high angle of attack [AD-A283656] p 119 N95-18669
- Development of a multicomponent force and moment balance for water tunnel applications, volume 1 [NASA-CR-4642-VOL-1] p 161 N95-18955
- Navier-Stokes, flight, and wind tunnel flow analysis for the F/A-18 aircraft [NASA-TP-3478] p 120 N95-19114
- Velocity measurements with hot-wires in a vortex-dominated flowfield p 121 N95-19261
- Computation of vortex breakdown p 165 N95-19462
- Research on bluff body vortex wakes [AD-A286319] p 223 N95-20177
- Application of Direct and Large Eddy Simulation to Transition and Turbulence [AGARD-CP-551] p 248 N95-21061
- Computational studies of laminar to turbulence transition [AD-A285622] p 248 N95-21146
- Effect of juncture fillets on double-delta wings undergoing sideslip at high angles of attack [AD-A286165] p 232 N95-22039
- Unstructured-grid large-eddy simulation of flow over an airfoil p 225 N95-22448
- Large-eddy simulation of flow through a plane, asymmetric diffuser p 250 N95-22449
- Euler technology assessment for preliminary aircraft design: employing OVERFLOW code with multiblock structured-grid method [NASA-CR-4651] p 273 N95-23095
- An assessment of viscous effects in computational simulation of benign and burst vortex flows on generic fighter wind-tunnel models using TEAM code [NASA-CR-4650] p 273 N95-23185
- Crossflow instability control on a swept-wing: Preliminary studies p 274 N95-23283
- Preliminary identification of buffet problems in high speed civil transport p 294 N95-23319
- Aerodynamic surface distension system for high angle of attack forebody vortex control [NASA-CASE-ARC-11979-1] p 286 N95-23390
- Three-dimensional Navier-Stokes analysis and redesign of an imbedded bellmouth nozzle in a turbine cascade inlet section p 311 N95-23423
- A study of the vortex flow over 76/40-deg double-delta wing [NASA-CR-195032] p 314 N95-23466
- Three-dimensional interaction of wake/boundary-layer and vortex/boundary-layer data report [CUED/A-AEREO/TR-23] p 329 N95-24210
- The atmospheric effects of stratospheric aircraft: A fourth program report [NASA-RP-1359] p 357 N95-24274
- Characterizing the wake vortex signature for an active line of sight remote sensor [NASA-CR-197697] p 333 N95-24391
- Flutter clearance flight tests of an OV-10A airplane modified for vortex vortex flight experiments [NASA-TM-109168] p 366 N95-26381
- Suppressor of oscillations in airframe cavities [AD-D017265] p 388 N95-26507
- Numerical simulation of the flow about the F-18 HARV at high angle of attack [NASA-CR-197755] p 374 N95-26735
- Effects of three-dimensional imposed 3-D disturbances on bluff-body near wake flows [AD-A289553] p 374 N95-26757
- Performance characterization of a highly-offset diffuser with and without blowing vortex generator jets [AD-A289334] p 375 N95-26901
- The near-wake flow behavior of an oscillating airfoil with modified trailing edge p 375 N95-26953
- A general theory of two- and three-dimensional rotational flow in subsonic and transonic turbomachines [NASA-CR-4496] p 377 N95-28003
- The effects of three-dimensional imposed disturbances on bluff body near wake flows: Effects of taper and splitter plates on the near wake characteristics of a circular cylinder in uniform and shear flow [AD-A292113] p 477 N95-28921
- A noninvasive method of quantifying flow visualization data in vortex flow fields [AD-A289802] p 552 N95-28948
- PIV investigation of compressibility effects on dynamic stall p 478 N95-29102
- Navier-Stokes solution of wing wake structure and its perturbation p 479 N95-29121
- A numerical method for modelling wings with sharp edges maneuvering at high angles of attack p 503 N95-29122
- Dynamic stall of a NACA 0012 airfoil in laminar flow p 479 N95-29243
- The decay of longitudinal vortices shed from airfoil vortex generators [NASA-CR-198356] p 480 N95-29402
- The effects of three dimensional imposed disturbances on bluff body near wake flows [AD-A290824] p 555 N95-29654
- Growth and development of roughness-induced stationary crossflow vortices p 482 N95-30294

- A wind tunnel investigation of the effects of micro-vortex generators and Gurney flaps on the high-lift characteristics of a business jet wing
[NASA-TM-110626] p 607 N95-30827
- Unsteady transonic wind tunnel test on a semispan straked delta wing, oscillating in pitch. Part 1: Description of the model, test setup, data acquisition, and data processing
[AD-A293113] p 593 N95-30885
- A pulsed liquid fuel ramjet p 617 N95-31201
- Initial evaluation of the Oregon State University planetary boundary layer column model for ITWS applications
[AD-A293775] p 677 N95-31465
- Application of multigrid computational fluid dynamics (CFD) methods to rotor analysis
[AD-A293012] p 648 N95-31475
- Experimental and computational investigation of the tip clearance flow in a transonic axial compressor rotor
[NASA-TM-106711] p 649 N95-31738
- Flight evaluation of forebody vortex control in post-stall flight p 609 N95-32003
- Calculation for aerodynamic characteristics on delta wing with leading-edge separated vortex effect using boundary element method p 684 N95-34524
- Sidewall-effect of the wind tunnel on the estimation of the aerodynamic characteristics of a delta wing p 685 N95-34525
- Subscale study of engine bellmouth inlet vortices in test cell R1D
[AD-A294993] p 707 N95-34818
- VORTICITY**
- Nonhydrostatic simulation of frontogenesis in a moist atmosphere. Part 3: Thermal wind imbalance and rainbands
[HTN-95-90356] p 212 A95-66429
- Entrainment and acoustic variations in a round jet from introduced streamwise vorticity
[BTN-95-EIX95042474409] p 209 A95-68291
- Interaction of a streamwise vortex with a thin plate: A source of turbulent buffeting
[BTN-95-EIX95042474398] p 209 A95-68302
- Numerical simulation of steady and unsteady, vorticity-dominated aerodynamic interference
[BTN-95-EIX95062487524] p 186 A95-69232
- Measurement around a rotor blade excited in pitch. Part 1: Dynamic inflow
[HTN-95-31007] p 220 A95-71177
- Measurement around a rotor blade excited in pitch. Part 2: Unsteady surface pressure
[HTN-95-31008] p 220 A95-71178
- Aerodynamic and wake methodology evaluation using Model UH-60A experimental data
[HTN-95-31009] p 220 A95-71179
- Measurements of vortex pair interaction with a clean or contaminated free surface
[BTN-94-EIX95011441063] p 429 A95-82798
- Vortex methods for the computational analysis of rotor/body interaction
[HTN-95-61072] p 369 A95-83656
- Two-dimensional viscous flow past a flat plate
[HTN-95-42210] p 430 A95-84026
- Development of a large-aspect-ratio rectangular turbulent free jet
[HTN-95-42333] p 372 A95-86162
- Two dimensional stratospheric aerosol distributions during EASOE
[HTN-95-00726] p 444 A95-86296
- Vortex drift: A historical survey p 455 A95-88897
- Response of a thin airfoil encountering a strong density discontinuity p 462 A95-88900
- Axis switching and spreading of an asymmetric jet: Role of vorticity dynamics
[NASA-TM-106385] p 73 N95-14418
- Transverse vorticity measurements in the NASA Ames 80 x 120 wind tunnel boundary layer p 251 N95-22457
- Basic studies in turbulent shear flows
[AD-A289145] p 437 N95-26998
- Calculation of three-dimensional (3-D) internal flow by means of the velocity-vorticity formulation on a staggered grid
[NASA-TM-110352] p 376 N95-27258
- Interactions of spanwise and chordwise vorticity associated with three-dimensional dynamic stall over an oscillating wing
[AD-A290546] p 477 N95-29091
- PIV investigation of compressibility effects on dynamic stall p 478 N95-29102
- A vorticity-velocity approach for three-dimensional unsteady viscous flow over wings p 478 N95-29108
- Finite element vorticity-based methods for the solution of the incompressible and compressible Navier-Stokes equations p 553 N95-29119
- Vorticity dynamics and control of dynamic stall
[AD-A286658] p 620 N95-31400

VULNERABILITY

- Rationale for the Modular Air-system Vulnerability Estimation Network (MAVEN) methodology
[AD-A285797] p 284 N95-22510

W**WAFERS**

- Assuring Known Good Die (KGD) for reliable, cost effective MCMs p 246 N95-20644

WAKES

- Elliptic tip effects on the vortex wake of an axisymmetric body at incidence
[BTN-94-EIX94441386612] p 208 A95-67343
- Active control of wake/blade-row interaction noise
[BTN-95-EIX95042474389] p 196 A95-68311
- Effect of ground and ceiling planes on shape of energized wakes
[BTN-95-EIX95062487558] p 186 A95-68372
- Experimental investigation of the flowfield about an upswept afterbody
[BTN-95-EIX95152582321] p 265 A95-73524
- Separation control on high-lift airfoils via micro-vortex generators
[BTN-95-EIX95152582326] p 265 A95-73529
- Hypersonic rarefied flow past spheres including wake structure
[BTN-95-EIX95152583250] p 305 A95-73551
- Flow structure in the lee of an inclined 6:1 prolate spheroid
[BTN-94-EIX95011441127] p 348 A95-81027
- Numerical investigation of cylinder wake flow with a rear stagnation jet
[HTN-95-51669] p 433 A95-85051
- Prediction of two-dimensional momentumless wake by k-epsilon-gamma model
[BTN-95-EIX95262694299] p 434 A95-85470
- Elliptic tip effects on the vortex wake of an axisymmetric body at incidence
[HTN-95-20938] p 464 A95-88977
- The application of potential CFD methods to helicopter hover flows
[ISBN 1-879921-01-4] p 587 A95-93747
- Effect of leading-edge extension fences on the vortex wake of an F/A-18 model
[BTN-95-EIX0619952748192] p 591 A95-94481
- Effects of splitter plate on wake formation from a circular cylinder: A discrete vortex simulation p 639 A95-95404
- Control of wind tunnel operations using neural net interpretation of flow visualization records
[NASA-TM-106683] p 24 N95-10854
- Measurements of atmospheric turbulence effects on tail rotor acoustics
[NASA-TM-108843] p 38 N95-12360
- Ground-based wake vortex monitoring, prediction, and ATC interface p 42 N95-13209
- Surface pressure and wake drag measurements on the Boeing A4 airfoil in the IAR 1.5X1.5m Wind Tunnel Facility p 110 N95-17850
- Aircraft wake vortex takeoff tests at O'Hara International Airport
[AD-A283828] p 118 N95-18624
- Experimental study of vane heat transfer and aerodynamics at elevated levels of turbulence
[NASA-CR-4633] p 244 N95-19912
- Wake measurements in a strong adverse pressure gradient
[NASA-CR-197272] p 224 N95-21031
- Direct numerical simulations of on-demand vortex generators: Mathematical formulation p 251 N95-22452
- Flutter clearance flight tests of an OV-10A airplane modified for wake vortex flight experiments
[NASA-TM-109168] p 366 N95-26381
- Rarefied gas effects on aerobreaking/reentry vehicles with wakes
[NASA-CR-196586] p 415 N95-27093
- Interactions of spanwise and chordwise vorticity associated with three-dimensional dynamic stall over an oscillating wing
[AD-A290546] p 477 N95-29091
- The effects of three dimensional imposed disturbances on bluff body near wake flows
[AD-A290824] p 555 N95-29654
- Initial evaluation of the Oregon State University planetary boundary layer column model for ITWS applications
[AD-A293775] p 677 N95-31465
- WALL FLOW**
- Design and operation of a supersonic annular flow facility
[BTN-94-EIX94441386624] p 183 A95-68173
- Model for compressible turbulence in hypersonic wall boundary and high-speed mixing layers
[BTN-94-EIX94441386625] p 184 A95-68174
- Preliminary assessment of tunnel wall interference in the NDA cryogenic wind tunnel
[BTN-95-EIX95062487531] p 187 A95-69239
- Two-variable method for blockage wall interference in a circular tunnel
[BTN-95-EIX95062487540] p 187 A95-69248
- Main features of overexpanded triple jets
[BTN-95-EIX95142553040] p 304 A95-73458
- Effects of expansions on a supersonic boundary layer: Surface pressure measurements
[BTN-95-EIX95142553036] p 263 A95-73462
- Flow visualization studies on sidewall effects in two-dimensional transonic airfoil testing
[BTN-95-EIX95152582313] p 264 A95-73516
- Moving wall effect in relation to other dynamic stall flow mechanisms
[BTN-95-EIX95152582324] p 265 A95-73527
- Application of wall functions to generalized nonorthogonal curvilinear coordinate systems
[BTN-95-EIX95182619077] p 307 A95-75762
- Observations on using experimental data as boundary conditions for computations
[BTN-95-EIX95182619103] p 321 A95-76588
- Multiple instabilities of three-dimensional boundary layers along a concave wall
[HTN-95-71126] p 429 A95-83487
- The effects of wall perturbations on thermo-turbulent Couette flow
[HTN-95-92255] p 434 A95-85299
- Flow alteration and drag reduction by riblets in a turbulent boundary layer
[HTN-95-61199] p 461 A95-87572
- Adaptive wall technology for minimization of wind tunnel boundary interferences - where are we now?
p 519 A95-88903
- Corrective term in wall slip equations for Knudsen layer
[BTN-95-EIX95282705070] p 455 A95-89667
- Analysis of some interference effects in a transonic wind tunnel
[BTN-95-EIX0619952748166] p 589 A95-94460
- Permeable wall boundary conditions for transonic airfoil design p 641 A95-95445
- LDV measurements in separated flow on an elliptic wing mounted at an angle of attack on a wall
[BTN-94-EIX94441380518] p 702 A95-96559
- Effect of weak periodic pressure gradient on streamwise vortices near a wall p 29 N95-11263
- A wall interference assessment and correction system
[NASA-CR-196940] p 58 N95-12228
- Wall-signature methods for high speed wind tunnel wall interference corrections p 107 N95-16257
- 2-D airfoil tests including side wall boundary layer measurements p 158 N95-17847
- Data from the GARTEur (AD) Action Group 02 airfoil CAST 7/DOA1 experiments p 111 N95-17856
- A supercritical airfoil experiment p 111 N95-17858
- Boundary-flow measurement methods for wall interference assessment and correction: Classification and review p 163 N95-19262
- Adaptive wind tunnel walls versus wall interference correction methods in 2D flows at high blockage ratios p 147 N95-19267
- Interference determination for wind tunnels with slotted walls p 147 N95-19269
- Calculation of low speed wind tunnel wall interference from static pressure pipe measurements p 164 N95-19273
- Analysis of test section sidewall effects on a two dimensional airfoil: Experimental and numerical investigations p 165 N95-19276
- Calculation of wall effects of flow on a perforated wall with a code of surface singularities p 165 N95-19277
- A wall interference assessment/correction system
[NASA-CR-197421] p 309 N95-23183
- Supersonic quiet-tunnel development for laminar-turbulent transition research
[NASA-CR-198040] p 340 N95-24302
- Finite element vorticity-based methods for the solution of the incompressible and compressible Navier-Stokes equations p 553 N95-29119
- A method for the modelling of porous and solid wind tunnel walls in computational fluid dynamics codes p 523 N95-29795
- Experimental and computational investigation of the tip clearance flow in a transonic axial compressor rotor
[NASA-TM-106711] p 649 N95-31738
- WALL JETS**
- Active boundary-layer control in diffusers
[HTN-95-42580] p 458 A95-87210
- Investigation of scramjet injection strategies for high mach number flows
[BTN-95-EIX0616952745782] p 614 A95-94504

- Effects of cavity dimensions, boundary layer, and temperature on cavity noise with emphasis on benchmark data to validate computational aeroacoustic codes [NASA-CR-4653] p 361 N95-24879
- WALL PRESSURE**
 Experimental study of flow separation on an oscillating flap at Mach 2.4 [BTN-95-EIX95222650792] p 329 A95-79248
 Evaluation of scramjet nozzle performance p 402 A95-82321
 Fluctuating wall pressures near separation in highly swept turbulent interactions [HTN-95-20823] p 543 A95-88084
 Wall correction method with measured boundary conditions for low speed wind tunnels p 164 N95-19263
 Estimating wind tunnel interference due to vectored jet flows p 164 N95-19265
 Wall interaction effects for a full-scale helicopter rotor in the NASA Ames 80- by 120-foot wind tunnel p 121 N95-19270
 Application of wavelet-filtering techniques to intermittent turbulent and wall pressure events. Part 1: Exploratory results [AD-A286077] p 247 N95-20849
 A wall interference assessment/correction system [NASA-CR-197421] p 309 N95-23183
- WALL TEMPERATURE**
 Regenerative cooling for liquid propellant rocket thrust chambers [INPE-5565-TDI/540] p 150 N95-18720
 Viscous shock-layer analysis on hypersonic flow over reentry capsule with nonequilibrium chemistry [ISAS-656] p 436 N95-26739
- WALLS**
 Wall correction method with measured boundary conditions for low speed wind tunnels p 164 N95-19263
 Computational simulations for some tests in transonic wind tunnels p 164 N95-19264
 Wall interaction effects for a full-scale helicopter rotor in the NASA Ames 80- by 120-foot wind tunnel p 121 N95-19270
 Sidewall-effect of the wind tunnel on the estimation of the aerodynamic characteristics of a delta wing p 685 N95-34525
- WAR GAMES**
 ADST system test report for the rotary wing aircraft airmet aeromodel and weapon model merge with the ATAC 2 baseline [AD-A281580] p 127 N95-16171
 Integrated mission precision attack cockpit technology (IMPACT). Phase 1: Identifying technologies for air-to-ground fighter integration [AD-A289562] p 389 N95-26684
 A mathematical analysis of the Janus combat simulation weather effects models and sensitivity analysis of sky-to-ground brightness ratio on target detection [AD-A289629] p 446 N95-26858
- WARFARE**
 Bomber force 2000: Operational concepts for long-range combat aircraft [AD-A279378] p 230 N95-20181
 Low-Level and Nap-of-the-Earth (NOE) night operations [AGARD-CP-563] p 686 N95-32486
- WARNING SYSTEMS**
 Real-time decision aiding: Aircraft guidance for wind shear avoidance [BTN-95-EIX95202637575] p 332 A95-78583
 Part-task simulator evaluations of advanced terrain displays [SAE PAPER 932570] p 401 A95-84567
 The detection and measurement of microburst wind shear by an airborne lidar system p 543 A95-87798
 Inadequacy of visual alarms in helicopter air medical transport [HTN-95-01218] p 484 A95-91450
 Improving aircraft impact assessment with the integrated terminal weather system microburst detection algorithm p 654 A95-93453
 The ITWS microburst prediction algorithm p 655 A95-93456
 A comparative performance study of TDWR/LLWAS 3 integration algorithms for wind shear detection p 658 A95-93468
 An in-situ system for warning of icing conditions p 660 A95-93481
 The use of radar wind profiles to remove TDWR gust front algorithm false alarms caused by vertical wind shear p 661 A95-93488
 LLWAS 2 and LLWAS 3 performance evaluation p 662 A95-93491
 Test results of a low cost airport weather radar p 662 A95-93492
- Role of the aviation weather system in providing a real-time ATC volcanic ash advisory system p 663 A95-93494
- Alaska's volcanic ash warning system p 663 A95-93495
- MEMFOG - The Memphis fog algorithm p 668 A95-93516
- Windshear detection: TDWR and LLWAS operational experience in Denver 1988-1992 p 670 A95-93528
 Northwest Airlines atmospheric hazards advisory & avoidance system p 672 A95-93539
 Airborne Windshear Detection and Warning Systems. Fifth and Final Combined Manufacturers' and Technologists' Conference, part 1 [NASA-CP-10139-PT-1] p 10 N95-10566
 Thunderstorm hypothesis reasoner [AD-A282664] p 60 N95-12805
 Terminal Doppler Weather Radar Build 5A Operational Test and Evaluation (OT/E) integration and OT/E operational test plan p 61 N95-12996
 [AD-A283052] p 61 N95-12996
 Airborne Windshear Detection and Warning Systems. Fifth and Final Combined Manufacturers' and Technologists' Conference, part 2 [NASA-CP-10139-PT-2] p 41 N95-13203
 Aircraft maneuver envelope warning system [NASA-CASE-ARC-11953-1] p 82 N95-14518
 Control system design for the MOD-5A 7.3 mW wind turbine generator p 440 N95-27985
 Laser based obstacle warning sensors for helicopters p 686 N95-32499
- WARPAGE**
 Analysis of warping effects on the static and dynamic response of a seat-type structure [NIAR-94-12] p 348 N95-24211
- WASPALLOY**
 Fatigue crack growth in nickel-based superalloys at 500-700 C. 1: Waspaloy [BTN-94-EIX94371347843] p 206 A95-69136
- WASTE ENERGY UTILIZATION**
 Gas-turbine engines with increased efficiency of two circuits, due to the use of the utilizing steam-turbine circuit [BTN-94-EIX94461408755] p 153 A95-63638
- WATER**
 Study of the droplet spray characteristics of a subsonic wind tunnel [BTN-95-EIX95182619235] p 271 A95-76661
 Analysis of the physical state of one Arctic polar stratospheric cloud based on observations [HTN-95-70917] p 351 A95-77982
 Pressure measurements on a pitching airfoil in a water channel [HTN-95-61209] p 541 A95-87582
 Development of techniques for the in situ observation of OH and HO2 for studies of the impact of high-altitude supersonic aircraft on the stratosphere [NASA-CR-196759] p 61 N95-12832
 Simultaneous three-dimensional velocity and mixing measurements by use of laser Doppler velocimetry and fluorescence probes in a water tunnel [NASA-TP-3454] p 53 N95-13553
 A review of water mist technology for fire suppression [AD-A285738] p 225 N95-20071
 Airborne rotary air separator study [NASA-CR-189099] p 290 N95-24053
 Evaluation of commercial water-in-fuel test kits [AD-A292135] p 537 N95-29572
 Water blasting paint removal methods p 650 N95-32170
- WATER CURRENTS**
 Orbital velocities induced by surface waves [HTN-95-90902] p 253 A95-72411
- WATER FLOW**
 The stability of two-phase flow over a swept-wing [NASA-CR-194994] p 159 N95-18190
- WATER TABLES**
 Simple method of supersonic flow visualization using water table [BTN-95-EIX95182619105] p 269 A95-76590
- WATER TREATMENT**
 Water blasting paint removal methods p 650 N95-32170
- WATER TUNNEL TESTS**
 Flow-visualization study of the X-29A aircraft at high angles of attack using a 1/48-scale model [NASA-TM-104268] p 8 N95-10858
 Water tunnel flow visualization study of a 4.4 percent scale X-31 forebody [NASA-TM-104276] p 36 N95-11898
 Simultaneous three-dimensional velocity and mixing measurements by use of laser Doppler velocimetry and fluorescence probes in a water tunnel [NASA-TP-3454] p 53 N95-13553
- Comparison of X-31 flight, wind-tunnel, and water-tunnel yawing moment asymmetries at high angles of attack p 68 N95-14234
- Static and dynamic force/moment measurements in the Eidetics water tunnel p 69 N95-14238
 Spectral analysis of vortex/free-surface interaction [AD-A283210] p 96 N95-14658
 Interaction, bursting and control of vortices of a cropped double-delta wing at high angle of attack [AD-A283656] p 119 N95-18669
 Development of a multicomponent force and moment balance for water tunnel applications, volume 1 [NASA-CR-4642-VOL-1] p 161 N95-18955
 Development of a multicomponent force and moment balance for water tunnel applications, volume 2 [NASA-CR-4642-VOL-2] p 161 N95-18956
 Effect of juncture fillets on double-delta wings undergoing sideslip at high angles of attack [AD-A286165] p 232 N95-22039
 NASA Dryden flow visualization facility [NASA-TM-4631] p 449 N95-27914
 Experimental and theoretical studies of wakes in stratified flows [AD-A290203] p 553 N95-29060
 An investigation of the side-dump dual in-line ramjet combustor p 617 N95-31199
 Water model tests on the Allison T56 series 3 combustion system [DSTO-TR-0139] p 697 N95-33250
- WATER VAPOR**
 Possible near-IR channels for remote sensing precipitable water vapor from geostationary satellite platforms [HTN-95-70139] p 214 A95-69431
 Water vapor continuum absorption in mid-latitudes: Aircraft measurements and model comparisons [HTN-95-40756] p 252 A95-71186
 Aircraft measurements of water vapour continuum absorption at millimetre wavelengths [HTN-95-90884] p 253 A95-72393
 Gas turbine prediffuser-combustor performance during operation with air-water mixture [DOT/FAA/CT-93/52] p 83 N95-15683
 Correction of thin cirrus effects in AVIRIS images using the sensitive 1.375-micron cirrus detecting channel p 708 N95-33748
- WATER VEHICLES**
 Air cushioned landing craft (LCAC) based ship to shore movement simulation: A decision aid for the amphibious commander. A (SMMAT) application [AD-A289635] p 436 N95-26722
- WATER WAVES**
 Orbital velocities induced by surface waves [HTN-95-90902] p 253 A95-72411
 Fractal properties of whitecaps p 443 A95-83827
 [HTN-95-92121] p 443 A95-83827
 Airborne passive polarimetric measurements of sea surface anisotropy at 92 GHz [NASA-CR-197288] p 707 N95-32823
 Sea wave parameters, small altitudes and distances measurers design for movement control systems of ships, wing-in-surface effect crafts and seaplanes p 708 N95-33141
- WAVE DRAG**
 Application of two procedures for dual-point design of transonic airfoils [NASA-TP-3466] p 38 N95-12176
 In-flight lift-drag characteristics for a forward-swept wing aircraft and comparisons with contemporary aircraft [NASA-TP-3414] p 117 N95-18565
 Computational fluid dynamics and transonic flow [AD-A288962] p 436 N95-26405
 Wave drag coefficient for axisymmetric forecows at zero incidence (M sub infinity less than or equal to 1.5) [ESDU-94014] p 552 N95-28903
 Surface pressure coefficient distributions for axisymmetric forecows at zero incidence (M sub infinity less than or equal to 1.5) [ESDU-94015] p 477 N95-28904
- WAVE EQUATIONS**
 An extension of the Lighthill theory of jet noise to encompass refraction and shielding [NASA-TM-110163] p 580 N95-29452
- WAVE FRONTS**
 On wave-front curvature in linear stability theory [BTN-94-EIX94441385756] p 184 A95-68220
- WAVE INTERACTION**
 Computational studies of laminar to turbulence transition [AD-A285622] p 248 N95-21146
- WAVE PROPAGATION**
 Vortex cutting by a blade, part 1: General theory and a simple solution [HTN-95-20822] p 543 A95-88083

- Interaction of a weak shock with freestream disturbances
[BTN-95-EIX95332750473] p 638 A95-94687
- WAVE REFLECTION**
Comments on effect of wet snow on the null-reference ILS system
[BTN-95-EIX95142555488] p 227 A95-72885
- WAVE SCATTERING**
SEM representation of the early and late time fields scattered from wire targets
[BTN-94-EIX94381353142] p 306 A95-74496
- WAVEFORMS**
Composite waveform generation for EMP and lightning direct-drive testing
[AD-A284159] p 92 N95-14405
Effect of stratification and geometrical spreading on sonic boom rise time p 75 N95-14880
Atmospheric effects on the risetime and waveshape of sonic booms p 100 N95-14886
Waveform bounding and combination techniques for direct drive testing
[AD-A284075] p 161 N95-19035
Speech analysis and synthesis based on pitch-synchronous segmentation of the speech waveform
[AD-A288824] p 435 N95-26349
- WAVEGUIDE ANTENNAS**
Field verification of the wind tunnel coefficients
p 109 N95-17291
- WAVEGUIDES**
Modeling resonance in waveguide-to-microstrip junctions by unilateral fin line resonators
[BTN-94-EIX94381323445] p 242 A95-70844
Electro-optic characterization of ultrafast photodetectors using adiabatically compressed soliton pulses
[BTN-94-EIX94381359637] p 257 A95-72675
- WAVELENGTH DIVISION MULTIPLEXING**
Fiber Optic Control System integration for advanced aircraft. Electro-optic and sensor fabrication, integration, and environmental testing for flight control systems
[NASA-CR-191194] p 162 N95-19236
- WAVELENGTHS**
Geoid lineations of 1000 km wavelength over the central Pacific
[HTN-95-11304] p 319 A95-77009
- WAVELET ANALYSIS**
Wavelet transformations for helicopter identification via acoustic signatures
[AD-A279980] p 257 N95-20963
- WAVERIDERS**
Waveriders with finlets
[BTN-95-EIX95062487541] p 184 A95-68355
Navier-Stokes computation of a viscous optimized waverider
[BTN-95-EIX95041503782] p 193 A95-69213
Hypersonic waverider test vehicle: A logical next step
[BTN-95-EIX95041503783] p 193 A95-69214
Interpretation of waverider performance data using computational fluid dynamics
[BTN-95-EIX95062487534] p 193 A95-69242
Aerodynamic characteristics of a hypersonic viscous optimized waverider at high altitudes
[BTN-95-EIX95152583251] p 266 A95-73552
Integrated design of hypersonic waveriders including inlets and tailfins
[BTN-95-EIX95212645692] p 271 A95-76744
Optimization of waverider configurations generated from inclined circular and elliptic cones
[AIAA PAPER 95-6089] p 492 A95-89198
Aerodynamic off-design behavior of integrated waveriders from take-off up to hypersonic flight
[AIAA PAPER 95-6091] p 466 A95-89200
Low-speed wind tunnel tests of two waverider configuration models
[AIAA PAPER 95-6093] p 493 A95-89251
Sensitivity of engine-integrated waverider performance to static margin constraint
[AIAA PAPER 95-6142] p 496 A95-90458
Hypersonic waveriders generated from power-law shocks
[AIAA PAPER 95-6160] p 470 A95-90472
A waverider derived hypersonic X-vehicle
[AIAA PAPER 95-6162] p 496 A95-90473
Low-speed wind tunnel testing of the NPS and NASA Ames Mach 6 optimized waverider
[AD-A283585] p 75 N95-15319
Theoretical investigations of shock/boundary layer interactions on a Ma(infinity) = 8 waverider
[DLR-FB-94-12] p 119 N95-18910
- WAVES**
Noise radiation by instability waves in coaxial jets
[NASA-TM-106738] p 100 N95-14618
- WEAPON SYSTEM MANAGEMENT**
Case study of risk management in the USAF B-1B bomber program
[AD-A282371] p 62 N95-11944
- The development of the F100-PW-220 and F110-GE-100 engines: A case study of risk assessment and risk management
[AD-A282467] p 51 N95-13289
- WEAPON SYSTEMS**
Improved version of the Naval Surface Warfare Center aeroprojection code (AP93)
[BTN-95-EIX95152583260] p 267 A95-73561
ADST system test report for the rotary wing aircraft aimed aeromodel and weapon model merge with the ATAC 2 baseline
[AD-A281580] p 127 N95-16171
Low rate initial production in Army Aviation systems development
[AD-A281871] p 127 N95-16356
Design of a controller for a flexible pointing system using H(infinity) synthesis
[AD-A286572] p 256 N95-20828
- WEAPONS**
Scale effects on aircraft and weapon aerodynamics
[AGARD-AG-323] p 67 N95-14103
- WEAPONS DELIVERY**
A PC-based interactive simulation of the F-111C Paveway system and related sensor, avionics and aircraft aspects
[AD-A285500] p 129 N95-16969
- WEAPONS DEVELOPMENT**
Case study of risk management in the USAF B-1B bomber program
[AD-A282371] p 62 N95-11944
The development of the F100-PW-220 and F110-GE-100 engines: A case study of risk assessment and risk management
[AD-A282467] p 51 N95-13289
Low rate initial production in Army Aviation systems development
[AD-A281871] p 127 N95-16356
Report to Congressional Committees. Tactical Aircraft: Concurrence in development and production of F-22 aircraft should be reduced
[GAO/NSIAD-95-59] p 336 N95-26338
Report to Congressional Committees. Comanche Helicopter: Testing needs to be completed prior to production decisions
[GAO/NSIAD-95-112] p 397 N95-27910
A case study of the teaming concept in the procurement of the V-22 aircraft
[AD-A293770] p 608 N95-31578
Report to the Chairman, Legislation and National Security Subcommittee, Committee on Government Operations, House of Representatives. Unmanned aerial vehicles: Performance of short-range system still in question
[GAO/NSIAD-94-65] p 609 N95-32196
- WEAR**
Surface morphology and structure of carbon-carbon composites in high-energy sliding contact
[BTN-94-EIX94371347996] p 206 A95-69164
Gas path debris monitoring
[CONGRESS PAPER C428-15-031] p 508 A95-91710
Rolling bearing failure and wear debris detection
[CONGRESS PAPER C428-15-094] p 457 A95-91711
Developments in wear particle analysis using computerised procedures
[CONGRESS PAPER C428-15-216] p 457 A95-91713
Modelling wear at intermittently slipping high speed interfaces
[BTN-94-EIX94511433698] p 701 A95-96655
Static and dynamic friction behavior of candidate high temperature airframe seal materials
[NASA-TM-106571] p 152 N95-16905
The effect of wear on fire-blocking layer material effectiveness
[AD-A291520] p 485 N95-29855
Composite structure forming a wear surface
[AD-D017462] p 629 N95-30749
- WEAR RESISTANCE**
Corrosion prevention and control
[BTN-95-EIX95031502753] p 188 A95-68260
Impact, friction, and wear testing of microspheres of polycrystalline silicon
p 361 A95-79988
A CMC database for use in the next generation launch vehicles (rockets)
p 150 N95-18993
High velocity oxygen fuel spraying of erosion and wear resistant coatings on jet engine parts
p 202 N95-19680
- WEAR TESTS**
Brush seal performance and durability issues based on T-700 engine test results
[NASA-TM-106502] p 22 N95-11483
Evaluation of alternate F-14 wing lug coating
[AD-A283207] p 129 N95-17631
- Lubricant evaluation and performance, 2
[AD-A279144] p 242 N95-21969
Evaluation of thermal barrier and PS-200 self-lubricating coatings in an air-cooled rotary engine
[NASA-CR-195445] p 289 N95-23222
- WEATHER**
Towards improving the NMC aircraft data base
p 660 A95-93480
Field verification of the wind tunnel coefficients
p 109 N95-17291
Radar studies of aviation hazards
[AD-A285845] p 226 N95-21831
WINCLR: A computer code for heat transfer and clearance calculation in a compressor
[NASA-CR-195436] p 366 N95-26363
A mathematical analysis of the Janus combat simulation weather effects models and sensitivity analysis of sky-to-ground brightness ratio on target detection
[AD-A289629] p 446 N95-26858
Three-D weather displays for aircraft cockpits
[AD-A289759] p 508 N95-28691
Initial evaluation of the Oregon State University planetary boundary layer column model for ITWS applications
[AD-A293775] p 677 N95-31465
- WEATHER FORECASTING**
A technique for detecting a tropical cyclone center using a Doppler radar
[HTN-95-20631] p 215 A95-69574
Snow-band formation and evolution during the 15 November 1987 aircraft accident at Denver airport
[HTN-95-80699] p 254 A95-72543
Tropical cyclone observation and forecasting with and without aircraft reconnaissance
[HTN-95-80701] p 254 A95-72545
Volcanic ash forecast transport and dispersion (VAFTAD) model
[HTN-95-80702] p 254 A95-72546
Pilot Weather Advisor system
[BTN-95-EIX95152582314] p 316 A95-73517
International Conference on Aviation Weather Systems, 5th, Vienna, VA, Aug. 2-6, 1993. Preprint Volume
[HTN-95-92940] p 652 A95-93441
Knowing our users -- A challenge for meteorologists at the National Aviation Weather Advisory Unit
p 655 A95-93459
Transitioning to the aviation routine weather report (METAR) and the International Aerodrome Forecast (TAF) within the Federal Aviation Administration
p 656 A95-93461
Automation of observations in the Netherlands
p 661 A95-93485
Criteria of forecasting low level wind shear over Qatar
p 663 A95-93493
Development of a climatology for possible microburst occurrence in Canada
p 664 A95-93497
The aviation gridded forecast system verification program - A description of aviation-impact-variable evaluation plans
p 664 A95-93498
Comprehensive verification of terminal forecast ceiling and visibility
p 664 A95-93500
Objective verification of an enhanced terminal forecast experiment at Denver, Colorado
p 664 A95-93501
Verification of terminal forecasts
p 664 A95-93502
A new look at aviation meteorology: Integrating aircraft situation display (ASD) with conventional weather displays
p 665 A95-93505
Use of pilot reports for verification of aircraft icing diagnoses and forecasts
p 666 A95-93508
Examination of conditions in the proximity of pilot reports of aircraft icing during storm-fest
p 666 A95-93509
A short-term, high-resolution automated snowfall forecasting system
p 666 A95-93510
MEMFOG - The Memphis fog algorithm
p 668 A95-93516
MDCRS: Aircraft observations collection and uses
p 668 A95-93517
The improvement of meteorological data for air traffic management purposes
p 668 A95-93518
Aviation terminal forecasts based on automated observations (FTAUTO)
p 668 A95-93520
Dissemination of weather products
p 670 A95-93526
Development of a climatological data base to help forecast cloud cover conditions for shuttle landings at the Kennedy Space Center
p 670 A95-93529
Analysis of rapidly developing fog at the Kennedy Space Center
p 671 A95-93531
Developing the Aviation Gridded Forecast System
p 671 A95-93532
Developing and testing decision-making products for center weather service unit meteorologists
p 671 A95-93533
Using ATMS weather products for air traffic strategic planning
p 672 A95-93536
A study of the savings in time and fuel to aviation through the use of upper-air wind forecasts
p 672 A95-93538

- Northwest Airlines atmospheric hazards advisory & avoidance system p 672 A95-93539
- Airplane icing research at the Boeing Company: Participation in the second Canadian Atlantic Storms Program p 674 A95-93544
- An evaluation of clear-air turbulence indices p 674 A95-93548
- Offshore next generation weather radar (NEXRAD) OT&E integration and OT&E operational test [AD-A293223] p 646 N95-30902
- Integrated terminal weather system (ITWS) demonstration and validation operational test and evaluation [AD-A293932] p 602 N95-31521
- WEATHER RECONNAISSANCE AIRCRAFT**
- Application of airborne field mill data for use in launch support [HTN-95-50054] p 98 A95-62279
- WEATHER STATIONS**
- On designing and engineering the integrated terminal weather system p 653 A95-93449
- The Integrated Terminal Weather System (ITWS) storm cell information and weather impacted airspace detection algorithm p 654 A95-93452
- Improving aircraft impact assessment with the integrated terminal weather system microburst detection algorithm p 654 A95-93453
- ITWS gridded analysis p 654 A95-93455
- A comparative performance study of TDWR/LLWAS 3 integration algorithms for wind shear detection p 658 A95-93468
- Final results of the weather testing component of the Terminal Doppler Weather Radar operational test and evaluation p 658 A95-93471
- Terminal Doppler Weather Radar point target filter threshold selection p 662 A95-93490
- Test results of a low cost airport weather radar p 662 A95-93492
- Development of a climatology for possible microburst occurrence in Canada p 664 A95-93497
- Comprehensive verification of terminal forecast ceiling and visibility p 664 A95-93500
- Windshear detection: TDWR and LLWAS operational experience in Denver 1988-1992 p 670 A95-93528
- Developing the Aviation Gridded Forecast System p 671 A95-93532
- Developing and testing decision-making products for center weather service unit meteorologists p 671 A95-93533
- Assessment of the benefits for improved terminal weather information p 673 A95-93540
- The ATC operational evaluation of the prototype integrated terminal weather system (ITWS) at Dallas/Fort Worth and Orlando airports (May-September 1993) [AD-A293808] p 677 N95-31587
- WEATHERING**
- The rain erosion of PEEK (polyetheretherketone) [CONGRESS PAPER C428-4-039] p 531 A95-91676
- Ten-year ground exposure of composite materials used on the Bell Model 206L helicopter flight service program [NASA-TP-3468] p 55 N95-12357
- The use of electrochemistry and ellipsometry for identifying and evaluating corrosion on aircraft [AD-A288536] p 381 N95-27186
- WEATHERPROOFING**
- Mobile domes for TACTIC telescope p 453 A95-86113
- WEAVING**
- Characterization and manufacture of braided composites for large commercial aircraft structures p 426 N95-28478
- Weavability of dry polymer powder towpreg p 535 N95-29036
- WEDGE FLOW**
- Flow past a symmetric wedge with forward splitter plate p 427 A95-82406
- WEDGES**
- Flow past a symmetric wedge with forward splitter plate p 427 A95-82406
- Validation of the RPLUS3D code for supersonic inlet applications involving three-dimensional shock wave-boundary layer interactions [NASA-TM-106579] p 39 N95-13058
- WEIBULL DENSITY FUNCTIONS**
- Proof test methodology for composites p 424 N95-28445
- WEIGHT (MASS)**
- Lightweight high-temperature fuel metering valves [SAE PAPER 931444] p 635 A95-93693
- WEIGHT ANALYSIS**
- The analysis of the processing increased weight for pilot production of F-X aircraft [HTN-95-71133] p 385 A95-83494
- WEIGHT INDICATORS**
- An investigation of polynomial calibrations methods for wind tunnel balances p 144 N95-16258
- WEIGHT REDUCTION**
- Minimum-mass design of sandwich aerobreaks for a lunar transfer vehicle [BTN-95-EIX95212645707] p 299 A95-76759
- Materials and structures for the HSCAT [BTN-95-EIX95282711241] p 455 A95-89634
- Integrated aircraft thermal management and power generation [SAE PAPER 932055] p 500 A95-91636
- Global cost and weight evaluation of fuselage keel design concepts p 501 N95-28840
- A weight-efficient design strategy for cutouts in composite transport structures p 533 N95-28843
- Bell Helicopter Advanced Rotocraft Transmission (ART) program [NASA-CR-195479] p 555 N95-29538
- WEIGHTING FUNCTIONS**
- Plant and controller optimization by convex methods [AD-A283700] p 133 N95-18621
- On-line, adaptive state estimator for active noise control p 322 N95-23308
- Aerodynamic parameter estimation via Fourier modulating function techniques [NASA-CR-4654] p 335 N95-24630
- F/A-18 IFOSTP Fatigue test airbag load determination on the vertical and horizontal tails [DSTO-TR-0135] p 388 N95-26389
- Finite element vorticity-based methods for the solution of the incompressible and compressible Navier-Stokes equations p 553 N95-29119
- WEIGHTLESSNESS**
- Experimental investigation of composite channel heat pipe operation in micro-gravity environment p 428 A95-82645
- Virtual environment application with partial gravity simulation p 169 N95-15988
- WEIGHTLESSNESS SIMULATION**
- Users guide for NASA Lewis Research Center DC-9 Reduced-Gravity Aircraft Program [NASA-TM-106755] p 146 N95-18586
- WELDED STRUCTURES**
- JPRS report: Science and technology, Central Eurasia [JPRS-UST-95-011] p 335 N95-24541
- WELDING**
- Forming and bonding techniques for high-strength aluminum alloys [HTN-95-20605] p 418 A95-84786
- WENTZEL-KRAMER-BRILLOUIN METHOD**
- Analytical study of the neutral stability of a model hypersonic boundary layer [BTN-95-EIX9515257589] p 263 A95-73493
- WHEAT**
- Use of starch based blast media for dry paint stripping [SAE PAPER 932616] p 456 A95-90081
- WHEELS**
- Bicarbonate of soda blasting technology for aircraft wheel depainting [PB94-193323] p 104 N95-17466
- WIND (METEOROLOGY)**
- Comprehensive verification of terminal forecast ceiling and visibility p 664 A95-93500
- Jet transport response to a horizontal wind vortex [BTN-95-EIX0619952748163] p 619 A95-94457
- Atmospheric and wind modeling for ATC [NASA-CR-196786] p 98 N95-13725
- WIND DIRECTION**
- Ascent wind model for launch vehicle design [BTN-95-EIX95041503799] p 239 A95-70124
- Verification of terminal forecasts p 664 A95-93502
- Dissemination of terminal weather products to the flight deck via data link p 669 A95-93525
- Jet transport response to a horizontal wind vortex [BTN-95-EIX0619952748163] p 619 A95-94457
- Structural effects of unsteady aerodynamic forces on horizontal-axis wind turbines [DE94-011863] p 157 N95-16939
- Field verification of the wind tunnel coefficients p 109 N95-17291
- WIND EFFECTS**
- H^(sup 2)/H^(sup INF) controller design for a two-dimensional thin airfoil flutter suppression [BTN-94-EIX94511433918] p 141 A95-64584
- Real-time decision aiding: Aircraft guidance for wind shear avoidance [BTN-95-EIX95202637575] p 332 A95-78583
- Characteristics of a dry, pulsating microburst at Denver Stapleton Airport p 26 N95-10568
- WIND MEASUREMENT**
- Vertical wind estimation from horizontal wind measurements p 26 N95-10567
- Terminal Doppler Weather Radar Build 5A Operational Test and Evaluation (OT/E) integration and OT/E operational test plan [AD-A283052] p 61 N95-12996
- WIND PRESSURE**
- Load alleviation maneuvers for a launch vehicle p 342 A95-81360
- WIND PROFILES**
- Ascent wind model for launch vehicle design [BTN-95-EIX95041503799] p 239 A95-70124
- Comparison of wind profiler and aircraft wind measurements at Chebogue Point, Nova Scotia [HTN-95-41833] p 353 A95-80559
- ITWS gridded analysis p 654 A95-93455
- MDCRS: Aircraft observations collection and uses p 668 A95-93517
- The improvement of meteorological data for air traffic management purposes p 668 A95-93518
- FTGEN - An automated FT production system p 668 A95-93519
- A northern hemisphere clear air turbulence climatology p 674 A95-93547
- Atmospheric and wind modeling for ATC [NASA-CR-196786] p 98 N95-13725
- Comparison of meteorological data with fitted values extracted from projectile trajectory [AD-A285921] p 255 N95-19989
- WIND SHEAR**
- Conditions associated with large-drop regions [HTN-95-10686] p 214 A95-68845
- Optimal lateral-escape maneuvers for microburst encounters during final approach [BTN-95-EIX95182619127] p 276 A95-76604
- Real-time decision aiding: Aircraft guidance for wind shear avoidance [BTN-95-EIX95202637575] p 332 A95-78583
- The detection and measurement of microburst wind shear by an airborne lidar system p 543 A95-87798
- International Conference on Aviation Weather Systems, 5th, Vienna, VA, Aug. 2-6, 1993. Preprint Volume [HTN-95-92940] p 652 A95-93441
- Status of the terminal Doppler weather radar with deployment underway p 653 A95-93450
- Improving aircraft impact assessment with the integrated terminal weather system microburst detection algorithm p 654 A95-93453
- The ITWS microburst prediction algorithm p 655 A95-93456
- A comparative performance study of TDWR/LLWAS 3 integration algorithms for wind shear detection p 658 A95-93468
- The use of radar wind profiles to remove TDWR gust front algorithm false alarms caused by vertical wind shear p 661 A95-93488
- LLWAS 2 and LLWAS 3 performance evaluation p 662 A95-93491
- Test results of a low cost airport weather radar p 662 A95-93492
- Criteria of forecasting low level wind shear over Qatar p 663 A95-93493
- Development of a climatology for possible microburst occurrence in Canada p 664 A95-93497
- Dissemination of terminal weather products to the flight deck via data link p 669 A95-93525
- Windshear detection: TDWR and LLWAS operational experience in Denver 1988-1992 p 670 A95-93528
- Northwest Airlines atmospheric hazards advisory & avoidance system p 672 A95-93539
- Airborne Windshear Detection and Warning Systems. Fifth and Final Combined Manufacturers' and Technologists' Conference, part 1 [NASA-CP-10139-PT-1] p 10 N95-10566
- Vertical wind estimation from horizontal wind measurements p 26 N95-10567
- Characteristics of a dry, pulsating microburst at Denver Stapleton Airport p 26 N95-10568
- Future enhancements to ground-based microburst detection p 11 N95-10570
- Determining F-factor using ground-based Doppler radar: Validation and results p 11 N95-10571
- Terminal Doppler Weather Radar Build 5A Operational Test and Evaluation (OT/E) integration and OT/E operational test plan [AD-A283052] p 61 N95-12996
- Airborne Windshear Detection and Warning Systems. Fifth and Final Combined Manufacturers' and Technologists' Conference, part 2 [NASA-CP-10139-PT-2] p 41 N95-13203
- Windshear certification data base for forward-look detection systems p 41 N95-13204
- Certification methodology applied to the NASA experimental radar system p 41 N95-13205
- Certification of windshear performance with RTCA class D radomes p 41 N95-13206
- Airport surveillance using a solid state coherent lidar p 41 N95-13207
- Ground-based wake vortex monitoring, prediction, and ATC interface p 42 N95-13209
- Wind shear and its effects on aircraft p 77 N95-14898

- Heavy rain effects p 78 N95-14899
TDWR scan strategy implementation [AD-A284877] p 98 N95-15749
Microburst vertical wind estimation from horizontal wind measurements [NASA-TP-3460] p 131 N95-18198
Maximum-likelihood spectral estimation and adaptive filtering techniques with application to airborne Doppler weather radar [NASA-CR-197699] p 316 N95-23670
- WIND TUNNEL APPARATUS**
Time-of-flight mass spectrometer for impulse facilities [BTN-95-EIX95142553057] p 262 A95-73441
Boundary-layer transition and global skin friction measurement with an oil-fringe imaging technique [SAE PAPER 932550] p 547 A95-90054
Development of a pilot tube with multi-hole pyramidal head. 2: A five-hole yew probe of engineering model p 522 A95-91577
Test model designs for advanced refractory ceramic materials p 55 N95-11968
An investigation of polynomial calibrations methods for wind tunnel balances p 144 N95-16258
Dynamic Stability Instrumentation System (DSIS). Volume 1: Hardware description [NASA-TM-109160-VOL-1] p 171 N95-18899
The dynamic approach to rotor blade research: ARA's oscillatory test facility [ARA-MEMO-405] p 223 N95-20758
Testing in the ARA Transonic Wind Tunnel [ARA-MEMO-395] p 239 N95-20799
A hybrid electronically scanned pressure module for cryogenic environments [NASA-TM-110146] p 554 N95-29453
Flow quality improvements in the NASA Lewis Research Center 9- by 15-foot Low Speed Wind Tunnel [NASA-CR-195439] p 627 N95-31653
- WIND TUNNEL CALIBRATION**
Operating capability and current status of the reactivated NASA Lewis Research Center hypersonic tunnel facility [AIAA PAPER 95-6146] p 521 A95-90461
The NASA Langley 8-foot Transonic Pressure Tunnel calibration [NASA-TP-3437] p 8 N95-10739
Free-jet testing at Mach 3.44 in GASL's aero/thermo test facility p 145 N95-16320
Error propagation equations for estimating the uncertainty in high-speed wind tunnel test results [DE94-014136] p 145 N95-16509
The traditional and new methods of accounting for the factors distorting the flow over a model in large transonic wind tunnels p 165 N95-19275
Analysis of test section sidewall effects on a two dimensional airfoil: Experimental and numerical investigations p 165 N95-19276
Calculation of wall effects of flow on a perforated wall with a code of surface singularities p 165 N95-19277
Interference corrections for a centre-line plate mount in a porous-walled transonic wind tunnel p 122 N95-19280
Correction of support influences on measurements with sting mounted wind tunnel models p 122 N95-19281
The dynamic approach to rotor blade research: ARA's oscillatory test facility [ARA-MEMO-405] p 223 N95-20758
Flow quality improvements in the NASA Lewis Research Center 9- by 15-foot Low Speed Wind Tunnel [NASA-CR-195439] p 627 N95-31653
- WIND TUNNEL DRIVES**
Operating capability and current status of the reactivated NASA Lewis Research Center hypersonic tunnel facility [AIAA PAPER 95-6146] p 521 A95-90461
Improved speed control system for the 87,000 HP wind tunnel drive [NASA-TM-106840] p 211 N95-19794
- WIND TUNNEL MODELS**
Preliminary assessment of tunnel wall interference in the NDA cryogenic wind tunnel [BTN-95-EIX95062487531] p 187 A95-69239
Application of transonic small disturbance theory to the active flexible wing model [BTN-95-EIX95182619210] p 270 A95-76636
Multiple-function digital controller system for active flexible wing wind-tunnel model [BTN-95-EIX95182619212] p 322 A95-76638
Flutter suppression control law design and testing for the active flexible wing [BTN-95-EIX95182619214] p 292 A95-76640
Design and multifunction tests of a frequency domain-based active flutter suppression system [BTN-95-EIX95182619215] p 292 A95-76641
Flutter suppression for the active flexible wing: A classical design [BTN-95-EIX95182619216] p 292 A95-76642
- Low-speed wind tunnel tests of two waverider configuration models [AIAA PAPER 95-6093] p 493 A95-89251
Boundary-layer transition and global skin friction measurement with an oil-fringe imaging technique [SAE PAPER 932550] p 547 A95-90054
Effects of vibration on inertial wind-tunnel model attitude measurement devices [NASA-TM-109083] p 21 N95-11466
Test model designs for advanced refractory ceramic materials p 55 N95-11968
Experimental Aerodynamics Division [NAL-SP-9404] p 35 N95-12166
A wall interference assessment and correction system [NASA-CR-196940] p 58 N95-12228
Design and testing of an oblique all-wing supersonic transport [NASA-CR-196394] p 48 N95-12785
Mach number control in the High Speed Wind Tunnel of NLR [PB94-201670] p 53 N95-13243
Comparison of computational and experimental results for a supercritical airfoil [NASA-TM-4601] p 108 N95-16908
Evaluation of combined wall- and support-interference on wind tunnel models p 122 N95-19278
Interaction of a three strut support on the aerodynamic characteristics of a civil aviation model p 122 N95-19279
Interference corrections for a centre-line plate mount in a porous-walled transonic wind tunnel p 122 N95-19280
Correction of support influences on measurements with sting mounted wind tunnel models p 122 N95-19281
Calculation of support interference in dynamic wind-tunnel tests p 122 N95-19282
Multiport pressure measurements on continuously moving wind tunnel models [ARA-MEMO-391] p 188 N95-19772
The dynamic approach to rotor blade research: ARA's oscillatory test facility [ARA-MEMO-405] p 223 N95-20758
Testing in the ARA Transonic Wind Tunnel [ARA-MEMO-395] p 239 N95-20799
Dynamic response tests of inertial and optical wind-tunnel model attitude measurement devices [NASA-TM-109182] p 296 N95-23011
Development of a model protection and dynamic response monitoring system for the national transonic facility [NASA-CR-195041] p 340 N95-24388
Angular displacement measuring device [NASA-CASE-ARC-11937-1] p 362 N95-26015
Experimental investigation of static and dynamic ground effect on HOPE ALFLEX vehicle [NAL-TR-1236] p 388 N95-26525
Experimental investigation of aerodynamic devices for wind turbine rotational speed control, phase 1 [DE95-004034] p 564 N95-30016
Boundary-layer transition and global skin friction measurement with an oil-fringe imaging technique [NASA-CR-198814] p 557 N95-30224
A laser-based ice shape profilometer for use in icing wind tunnels [NASA-TM-106936] p 646 N95-30851
SOFIA 2 model telescope wind tunnel test report [NASA-TM-110668] p 683 N95-32764
- WIND TUNNEL NOZZLES**
Computation of nonequilibrium viscous flows in arc-jet wind tunnel nozzles [AIAA PAPER 94-0254] p 2 A95-60173
Operating capability and current status of the reactivated NASA Lewis Research Center hypersonic tunnel facility [AIAA PAPER 95-6146] p 521 A95-90461
Optimized design of a hypersonic nozzle p 297 N95-23304
Three-dimensional Navier-Stokes analysis and redesign of an imbedded bellmouth nozzle in a turbine cascade inlet section p 311 N95-23423
Supersonic quiet-tunnel development for laminar-turbulent transition research [NASA-CR-198040] p 340 N95-24302
Flow models for the design of a hypersonic iodine vapor wind tunnel nozzle with chemical and vibrational nonequilibrium effects p 592 N95-30448
- WIND TUNNEL STABILITY TESTS**
Full-scale hingeless rotor performance and loads [NASA-TM-110356] p 691 N95-32699
- WIND TUNNEL TESTS**
An experimental investigation of wing tip turbulence with applications to aerosound p 1 A95-60164
Wing download reduction using vortex trapping plates [HTN-94-00710] p 4 A95-60188
- Effect of wind tunnel acoustic modes on linear oscillating cascade aerodynamics [HTN-94-00760] p 14 A95-60199
Comparison of theory and experiment for non-linear flutter and stall response of a helicopter blade [BTN-94-EIX94351108100] p 191 A95-66500
Experimental study of three-dimensional separation [BTN-94-EIX94441385752] p 179 A95-68216
Tip vortex on a swept wing. Mean flow and unsteady phenomena [BTN-94-EIX94441385755] p 184 A95-68219
Suppression of vortex asymmetry and side force on a circular cone [BTN-95-EIX95042474413] p 209 A95-68287
Vortical flow structure near the F/A-18 LEX at high incidence [BTN-95-EIX95062487555] p 186 A95-68369
Effect of ground and ceiling planes on shape of energized wakes [BTN-95-EIX95062487558] p 186 A95-68372
Recent studies of rotorcraft blade-vortex interaction noise [BTN-95-EIX95062487521] p 218 A95-69229
Repeatability of ice shapes in the NASA Lewis icing research tunnel [BTN-95-EIX95062487528] p 204 A95-69236
Preliminary assessment of tunnel wall interference in the NDA cryogenic wind tunnel [BTN-95-EIX95062487531] p 187 A95-69239
Comparison of electrostatic and aerodynamic forces during parachute opening [BTN-95-EIX95062487532] p 187 A95-69240
Aerodynamic mechanism of galloping [BTN-94-EIX94371347709] p 219 A95-69968
Main features of overexpanded triple jets [BTN-95-EIX95142553040] p 304 A95-73458
Separation control on high-lift airfoils via micro-vortex generators [BTN-95-EIX95152582326] p 265 A95-73529
Analysis of a higher harmonic control test to reduce blade vortex interaction noise [BTN-95-EIX95152582330] p 265 A95-73532
Forebody flow control on a full-scale F/A-18 aircraft [BTN-95-EIX95152582333] p 281 A95-73535
Effect of underwing frost on a transport aircraft airfoil at flight Reynolds number [BTN-95-EIX95152582334] p 276 A95-73536
Pneumatic concept for tip-stall control of cranked-arrow wings [BTN-95-EIX95152582335] p 281 A95-73537
Flow study of supersonic wing-nacelle configuration [BTN-95-EIX95152582344] p 266 A95-73546
Computational study of plume-induced separation on a hypersonic powered model [BTN-95-EIX95152582346] p 266 A95-73548
Base drag prediction on missile configurations [BTN-95-EIX95152583256] p 266 A95-73557
Aerodynamic characteristics of a canard-controlled missile at high angles of attack [BTN-95-EIX95152583257] p 267 A95-73558
Some aspects of the aerodynamics of separating strap-ons [BTN-95-EIX95182617464] p 298 A95-75735
Comparison of linear stability results with flight transition data [BTN-95-EIX95182619097] p 283 A95-76582
Effect of ambient turbulence intensity on sphere wakes at intermediate Reynolds numbers [BTN-95-EIX95182619101] p 308 A95-76586
Observations on using experimental data as boundary conditions for computations [BTN-95-EIX95182619103] p 321 A95-76588
Simulation and model reduction for the active flexible wing program [BTN-95-EIX95182619211] p 295 A95-76637
On-line analysis capabilities developed to support the active flexible wing wind-tunnel tests [BTN-95-EIX95182619213] p 296 A95-76639
Flutter suppression control law design and testing for the active flexible wing [BTN-95-EIX95182619214] p 292 A95-76640
Design and multifunction tests of a frequency domain-based active flutter suppression system [BTN-95-EIX95182619215] p 292 A95-76641
Flutter suppression for the active flexible wing: A classical design [BTN-95-EIX95182619216] p 292 A95-76642
Rolling maneuver load alleviation using active controls [BTN-95-EIX95182619217] p 270 A95-76643
Dynamic investigation of the angular motion of a rotating body-parachute system [BTN-95-EIX95182619220] p 270 A95-76646
Natural laminar flow wing concept for supersonic transports [BTN-95-EIX95182619226] p 308 A95-76652

- Aerodynamic characteristics of external store configurations at low speeds
[BTN-95-EIX95182619230] p 271 A95-76656
- Study of the droplet spray characteristics of a subsonic wind tunnel
[BTN-95-EIX95182619235] p 271 A95-76661
- Laser velocimetry seed-particle behavior in shear layers at Mach 12
[BTN-95-EIX95212645712] p 272 A95-76764
- Hypersonic model testing in a shock tunnel
[BTN-95-EIX95222650789] p 329 A95-79245
- Similarity rule for jet-temperature effects on transonic base pressure
[BTN-95-EIX95222650791] p 329 A95-79247
- Design features of the NAL ramjet engine test facility
p 410 A95-82319
- Hypersonic wind tunnel test of sidewall compression type scramjet inlet
p 410 A95-82320
- An experimental investigation of scramjet nozzle flow
p 402 A95-82322
- Computational/experimental investigation of staged injection into a Mach 2 flow
[HTN-95-51646] p 432 A95-85028
- Surface interference in Rayleigh scattering measurements near forebodies
[HTN-95-51670] p 433 A95-85052
- Wind-tunnel tests of an inclined cylinder having helical grooves
[BTN-95-EIX95262694306] p 411 A95-85477
- Techniques for tailoring aircraft stall and post-stall behavior
[SAE PAPER 931226] p 458 A95-87199
- Aerodynamic characteristics of truncated airfoils at high angle of attack
[SAE PAPER 931227] p 460 A95-87365
- Measurement of free-flight dynamic stability derivatives of cones in a hypersonic gun tunnel
[AIAA PAPER 95-6082] p 519 A95-87411
- Effects of periodic spanwise blowing on Delta-wing configuration characteristics
[HTN-95-81631] p 461 A95-87679
- Dynamic pitch-up of a delta wing
[HTN-95-81633] p 462 A95-87681
- Separation of winged vehicles in supersonics
[AIAA PAPER 95-6092] p 526 A95-88601
- Operation of the adaptive-wall wind tunnel of TsAGI, Moscow
p 519 A95-88901
- Adaptive-wall wind-tunnel research at Ames Research Center: A retrospective
p 519 A95-88902
- Adaptive wall technology for minimization of wind tunnel boundary interferences - where are we now?
p 519 A95-88903
- Aerodynamic tailoring of the Learjet Model 60 wing
[SAE PAPER 932534] p 492 A95-89194
- Low-speed wind tunnel tests of two waverider configuration models
[AIAA PAPER 95-6093] p 493 A95-89251
- Air data prediction from surface pressure measurements on guided munitions
[BTN-95-EIX95282706664] p 466 A95-89641
- Preliminary study on the fixed transition technique for a shock tube transonic airfoil flow
[BTN-95-EIX95282705928] p 455 A95-89663
- Boundary-layer transition and global skin friction measurement with an oil-fringe imaging technique
[SAE PAPER 932550] p 547 A95-90054
- A note on the interpretation of mini-tuft photographs
[HTN-95-01089] p 468 A95-90275
- Measurement of drag using a momentum balance
[HTN-95-01090] p 468 A95-90276
- The verification of a theoretical helicopter rotor blade sailing method by means of windtunnel testing
[HTN-95-01093] p 468 A95-90279
- Characterization of a hot-film probe for hypersonic flow
[AIAA PAPER 95-6110] p 511 A95-90440
- The use of thermochromic liquid crystals for heat transfer measurements in short duration hypersonic wind tunnel facilities
[AIAA PAPER 95-6115] p 520 A95-90443
- Operating capability and current status of the reactivated NASA Lewis Research Center hypersonic tunnel facility
[AIAA PAPER 95-6146] p 521 A95-90461
- Buffeting tests in a cryogenic windtunnel
[HTN-95-92833] p 470 A95-90751
- High subsonic and high Reynolds number wind tunnel tests of two-dimensional natural-laminar-flow airfoils with suction boundary layer control
p 472 A95-91508
- Aerodynamic characteristics of supersonic air-intake/aircraft integrated models
p 472 A95-91512
- An experimental study on supersonic laminar flow control
p 473 A95-91523
- Experimental study for improving the lift to drag ratio of next generation SST
p 473 A95-91524
- Experimental investigation on aerothermodynamic characteristics of hypersonic transport
p 473 A95-91525
- A shock tunnel test of a winged hypersonic research vehicle
p 474 A95-91538
- Experimental study of the aerodynamic characteristics of the counter-rotation propellers
p 474 A95-91562
- Wake velocity measurement of counter-rotation propellers
p 474 A95-91563
- Preliminary tests of a transonic flutter control wing model
p 499 A95-91566
- An experimental investigation of forward-swept wings at low Reynolds numbers
[SAE PAPER 931370] p 604 A95-93650
- Quantifiable vortex features of F-106B aircraft at subsonic speeds
[BTN-95-EIX0619952748161] p 588 A95-94455
- Analysis of some interference effects in a transonic wind tunnel
[BTN-95-EIX0619952748166] p 589 A95-94460
- Actuated forebody strike controls for the F-16 High-Alpha Research Vehicle
[BTN-95-EIX0619952748173] p 619 A95-94467
- Operational and research aspects of a radio-controlled model flight test program
[BTN-95-EIX0619952748177] p 606 A95-94471
- Navier-Stokes applications to high-lift airfoil analysis
[BTN-95-EIX0619952748182] p 590 A95-94475
- Effect of leading- and trailing-edge flaps on clipped delta wings with and without wing camber at supersonic speeds
[NASA-TM-4542] p 5 N95-10028
- Two-dimensional converging-diverging rippled nozzles at transonic speeds - performed in the Langley 16-Foot Transonic Tunnel
[NASA-TP-3440] p 6 N95-10129
- Instabilities originating from suction holes used for Laminar Flow Control (LFC)
[NASA-CR-196395] p 6 N95-10131
- Numerical study of mixing in a high and low enthalpy supersonic test facility
p 7 N95-10467
- Control of wind tunnel operations using neural net interpretation of flow visualization records
[NASA-TM-106683] p 24 N95-10854
- Dynamic response of NASA Rotor Test Apparatus and Sikorsky S-76 hub mounted in the 80- by 120-Foot Wind Tunnel
[NASA-TM-108847] p 25 N95-11389
- A shadowgraph study of the National Launch System's 1 1/2 stage vehicle configuration and Heavy Lift Launch Vehicle configuration - Using the Marshall Space Flight Center's 14-Inch Trisonic Wind Tunnel
[NASA-RP-1347] p 35 N95-11710
- Shock-tunnel combustor testing for hypersonic vehicles
[NASA-CR-196836] p 52 N95-11938
- Measurements of pressure and thermal wakes in a transonic turbine cascade
[AD-A283464] p 38 N95-12548
- Supersonic base flow investigation over axisymmetric afterbodies
[PB94-180957] p 39 N95-12578
- Experimental aerodynamic characteristics of a generic hypersonic accelerator configuration at Mach numbers 1.5 and 2.0 - conducted in the Langley Unitary Plan Wind Tunnel
[NASA-TM-4413] p 39 N95-12770
- Design and testing of an oblique all-wing supersonic transport
[NASA-CR-196394] p 48 N95-12785
- NASA's Hypersonic Research Engine Project: A review
[NASA-TM-107759] p 50 N95-12860
- Role of wind tunnels and computer codes in the certification and qualification of rotorcraft for flight in forecast icing
[NASA-TM-106747] p 39 N95-13197
- VUV shock layer radiation in an arc-jet wind tunnel experiment
p 67 N95-13719
- Measured and calculated spectral radiation from a blunt body shock layer in an arc-jet wind tunnel
[AIAA PAPER 94-0086] p 67 N95-13720
- Dynamics of the McDonnell-Douglas Large Scale Dynamic Rig and dynamic calibration of the rotor balance
[NASA-TM-108855] p 65 N95-13891
- Scale effects on aircraft and weapon aerodynamics
[AGARD-AG-323] p 67 N95-14103
- Quality assessment for wind tunnel testing
[AGARD-AR-304] p 67 N95-14197
- A selection of experimental test cases for the validation of CFD codes, volume 1
[AGARD-AR-303-VOL-1] p 91 N95-14201
- High Alpha Technology Program (HATP) ground test to flight comparisons
p 68 N95-14230
- Flight and full-scale wind-tunnel comparison of pressure distributions from an F-18 aircraft at high angles of attack - Conducted in NASA Ames Research Center's 80 by 120 ft wind tunnel
p 68 N95-14231
- Comparison of X-31 flight, wind-tunnel, and water-tunnel yawing moment asymmetries at high angles of attack
p 68 N95-14234
- Free-to-roll tests of X-31 and F-18 subscale models with correlation to flight test results
p 69 N95-14237
- Computational analysis of forebody tangential slot blowing
p 71 N95-14253
- F/A-18 and F-16 forebody vortex control, static and rotary-balance results
p 72 N95-14254
- Ultra-high bypass ratio jet noise
[NASA-CR-195394] p 100 N95-14610
- Control of unsteady separated flow associated with the dynamic stall of airfoils
[NASA-CR-197024] p 74 N95-14613
- Low-speed wind tunnel testing of the NPS and NASA Ames Mach 6 optimized waverider
[AD-A283585] p 75 N95-15319
- Pressure measurements on an F/A-18 twin vertical tail in buffeting flow - Volume 2 - Steady and unsteady RMS pressure data
[AD-A281581] p 76 N95-15465
- Wind-tunnel blockage and actuation systems test of a two-dimensional scramjet inlet unstart model at Mach 6
[NASA-TM-109152] p 97 N95-15898
- Two-dimensional scramjet inlet unstart model: Wind-tunnel blockage and actuation systems test
[NASA-TM-109984] p 97 N95-15899
- Experimental study at low supersonic speeds of a missile concept having opposing wraparound tails
[NASA-TM-4582] p 106 N95-16069
- An approach to aerodynamic characteristics of low radar cross-section fuselages
p 106 N95-16251
- Wall-signature methods for high speed wind tunnel wall interference corrections
p 107 N95-16257
- Hypersonic air-breathing aeropropulsion facility test support requirements
p 144 N95-16319
- Free-jet testing at Mach 3.44 in GASL's aero/thermo test facility
p 145 N95-16320
- Error propagation equations for estimating the uncertainty in high-speed wind tunnel test results
[DE94-014136] p 145 N95-16509
- Measurements of unsteady pressure and structural response for an elastic supercritical wing
[NASA-TP-3443] p 104 N95-16560
- Structural effects of unsteady aerodynamic forces on horizontal-axis wind turbines
[DE94-011863] p 157 N95-16939
- Data acquisition and processing software for the Low Speed Wind Tunnel tests of the Jindivik auxiliary air intake
[AD-A285455] p 108 N95-17178
- Field verification of the wind tunnel coefficients
p 109 N95-17291
- Active load control during rolling maneuvers - performed in the Langley Transonic Dynamics Tunnel
[NASA-TP-3455] p 129 N95-17397
- A selection of experimental test cases for the validation of CFD codes, volume 2
[AGARD-AR-303-VOL-2] p 109 N95-17846
- 2-D airfoil tests including side wall boundary layer measurements
p 158 N95-17847
- Measurements on a two-dimensional airfoil with high-lift devices
p 109 N95-17848
- Investigation of the flow over a series of 14 percent-thick supercritical airfoils with significant rear camber
p 109 N95-17849
- Surface pressure and wake drag measurements on the Boeing A4 airfoil in the IAR 1.5X1.5m Wind Tunnel Facility
p 110 N95-17850
- 2-D airfoil effectiveness study
p 110 N95-17851
- Investigation of an NLF(1)-0416 airfoil in compressible subsonic flow
p 110 N95-17852
- Experiments in the trailing edge flow of an NLR 7702 airfoil
p 110 N95-17853
- Two-dimensional 16.5 percent thick supercritical airfoil NLR 7301
p 110 N95-17854
- Low-speed surface pressure and boundary layer measurement data for the NLR 7301 airfoil section with trailing edge flap
p 111 N95-17855
- Data from the GARTEur (AD) Action Group 02 airfoil CAST 7/DOA1 experiments
p 111 N95-17856
- OAT15A airfoil data
p 111 N95-17857
- A supercritical airfoil experiment
p 111 N95-17858
- Two-dimensional high-lift airfoil data for CFD code validation
p 112 N95-17859
- Measurements of the flow over a low aspect-ratio wing in the Mach number range 0.6 to 0.87 for the purpose of validation of computational methods. Part 1: Wing design, model construction, surface flow. Part 2: Mean flow in the boundary layer and wake, 4 test cases
p 112 N95-17860

- Detailed study at supersonic speeds of the flow around delta wings p 112 N95-17861
 Pressure distributions on research wing W4 mounted on an axisymmetric body p 112 N95-17862
 DLR-F4 wing body configuration p 130 N95-17863
 DLR-F5: Test wing for CFD and applied aerodynamics p 113 N95-17864
- Low aspect ratio wing experiment p 113 N95-17865
- Wind tunnel investigations of the appearance of shocks in the windward region of bodies with circular cross section at angle of attack p 113 N95-17866
 Three-dimensional boundary layer and flow field data of an inclined prolate spheroid p 158 N95-17867
 Force and pressure data of an ogive-nosed slender body at high angles of attack and different Reynolds numbers p 113 N95-17868
 Ellipsoid-cylinder model p 158 N95-17869
 Supersonic vortex flow around a missile body p 114 N95-17870
- Test data on a non-circular body for subsonic, transonic and supersonic Mach numbers p 158 N95-17871
 Wind tunnel test on a 65 deg delta wing with a sharp or rounded leading edge: The international vortex flow experiment p 114 N95-17872
 Delta-wing model p 114 N95-17873
 Experimental investigation of the vortex flow over a 76/60-deg double delta wing p 114 N95-17874
 Wind tunnel test on a 65 deg delta wing with rounded leading edges: The International Vortex Flow Experiment p 114 N95-17875
- Investigation of the flow development on a highly swept canard/wing research model with segmented leading- and trailing-edge flaps p 114 N95-17876
 Subsonic flow around US-orbiter model FALKE in the DNW p 115 N95-17877
 Low speed propeller slipstream aerodynamic effects p 116 N95-17882
- Wind tunnel performance comparative test results of a circular cylinder and 50 percent ellipse tailboom for circulation control antitorque applications
 [AD-A283335] p 130 N95-18008
 Overview of unsteady transonic wind tunnel test on a semispan straked delta wing oscillating in pitch
 [AD-A284097] p 117 N95-18380
 A selection of experimental test cases for the validation of CFD codes. Supplement: Datasets A-E
 [AGARD-AR-303-SUPPL] p 117 N95-18539
 Pressure measurements on an F/A-18 twin vertical tail in buffeting flow. Volume 4, part 2: Buffet cross spectral densities
 [AD-A285555] p 143 N95-18641
 Hypersonic wind tunnel test techniques
 [AD-A284057] p 118 N95-18663
 Static investigation of two fluidic thrust-vectoring concepts on a two-dimensional convergent-divergent nozzle
 [NASA-TM-4574] p 120 N95-19042
 Navier-Stokes, flight, and wind tunnel flow analysis for the F/A-18 aircraft
 [NASA-TP-3478] p 120 N95-19114
 2-D and 3-D oscillating wing aerodynamics for a range of angles of attack including stall
 [NASA-TM-4632] p 120 N95-19119
 Documentation and archiving of the Space Shuttle wind tunnel test data base. Volume 1: Background and description
 [NASA-TM-104806-VOL-1] p 151 N95-19237
 Wall Interference, Support Interference and Flow Field Measurements
 [AGARD-CP-535] p 162 N95-19251
 The crucial role of wall interference, support interference and flow field measurements in the development of advanced aircraft configurations p 162 N95-19252
 The utilization of a high speed reflective visualization system in the study of transonic flow over a delta wing p 121 N95-19259
 Transonic and supersonic flowfield measurements about axisymmetric afterbodies for validation of advanced CFD codes p 121 N95-19260
 Determination of solid/porous wall boundary conditions from wind tunnel data for computational fluid dynamics codes p 164 N95-19266
 Adaptive wind tunnel walls versus wall interference correction methods in 2D flows at high blockage ratios p 147 N95-19267
 Development of pneumatic test techniques for subsonic high-lift and in-ground-effect wind tunnel investigations p 121 N95-19268
 Interference determination for wind tunnels with slotted walls p 147 N95-19269
 Wall interaction effects for a full-scale helicopter rotor in the NASA Ames 80- by 120-foot wind tunnel p 121 N95-19270
 Unsteady flow testing in a passive low-correction wind tunnel p 147 N95-19272
- Calculation of low speed wind tunnel wall interference from static pressure pipe measurements p 164 N95-19273
 The traditional and new methods of accounting for the factors distorting the flow over a model in large transonic wind tunnels p 165 N95-19275
 Analysis of test section sidewall effects on a two dimensional airfoil: Experimental and numerical investigations p 165 N95-19276
 Calculation of wall effects of flow on a perforated wall with a code of surface singularities p 165 N95-19277
 Evaluation of combined wall- and support-interference on wind tunnel models p 122 N95-19278
 Interaction of a three strut support on the aerodynamic characteristics of a civil aviation model p 122 N95-19279
 Interference corrections for a centre-line plate mount in a porous-walled transonic wind tunnel p 122 N95-19280
 Correction of support influences on measurements with sting mounted wind tunnel models p 122 N95-19281
 Calculation of support interference in dynamic wind-tunnel tests p 122 N95-19282
 Methods for scaling icing test conditions
 [NASA-TM-106827] p 124 N95-19284
 An investigation of drag repeatability in half model testing in the ARA Transonic Wind Tunnel
 [ARA-MEMO-392] p 188 N95-19546
 Documentation and archiving of the Space Shuttle wind tunnel test data base. Volume 2: User's Guide to the Archived Data Base
 [NASA-TM-104806-VOL-2] p 205 N95-19624
 Prediction of wind tunnel effects on the installed F/A-18A inlet flow field at high angles-of-attack
 [NASA-CR-195429] p 197 N95-19651
 Multipoint pressure measurements on continuously moving wind tunnel models
 [ARA-MEMO-391] p 188 N95-19772
 Wind tunnel tests of a 42 inch diameter self-starting autogyro rotor
 [AD-A279922] p 188 N95-19863
 Static investigation of two fluidic thrust-vectoring concepts on a two-dimensional convergent-divergent nozzle
 [NASA-TM-4574] p 222 N95-19913
 Investigation of a thermal buoyancy effect on the drag of half models tested in the ARA Transonic Wind Tunnel
 [ARA-MEMO-407] p 222 N95-19946
 Flow coefficient behavior for boundary layer bleed holes and slots
 [NASA-TM-106846] p 244 N95-19953
 16-foot transonic tunnel test section flowfield survey
 [NASA-TM-109157] p 238 N95-20669
 The dynamic approach to rotor blade research: ARA's oscillatory test facility
 [ARA-MEMO-405] p 223 N95-20758
 Application of pressure sensitive paint in hypersonic flows
 [NASA-TM-106824] p 223 N95-20794
 Testing in the ARA Transonic Wind Tunnel
 [ARA-MEMO-395] p 239 N95-20799
 Wake measurements in a strong adverse pressure gradient
 [NASA-CR-197272] p 224 N95-21031
 Pressure measurements on an F/A-18 twin vertical tail in buffeting flow. Volume 4, part 1: Buffet cross spectral densities
 [AD-A285593] p 237 N95-21214
 Experiments on the flow field physics of confluent boundary layers for high-lift systems
 [NASA-CR-197318] p 224 N95-21343
 Pressure measurements on an F/A-18 twin vertical tail in buffeting flow. Volume 1: Wind tunnel test summary
 [AD-A279126] p 225 N95-21877
 Effects of yaw and pitch motion on model attitude measurements
 [NASA-TM-4641] p 250 N95-22109
 Large-eddy simulation of flow through a plane, asymmetric diffuser p 250 N95-22449
 Experimental investigations of on-demand vortex generators p 250 N95-22451
 Transverse vorticity measurements in the NASA Ames 80 x 120 wind tunnel boundary layer p 251 N95-22457
 Wing pressure distributions from subsonic tests of a high-wing transport model — in the Langley 14- by 22-Foot Subsonic Wind Tunnel
 [NASA-TM-4583] p 272 N95-22802
 Dynamic response tests of inertial and optical wind-tunnel model attitude measurement devices
 [NASA-TM-109182] p 296 N95-23011
 Experimental results for a hypersonic nozzle/afterbody flow field
 [NASA-TM-4638] p 274 N95-23250
- Performance of the 0.3-meter transonic cryogenic tunnel with air, nitrogen, and sulfur hexafluoride media under closed loop automatic control p 310 N95-23257
 [NASA-CR-195052]
 Crossflow instability control on a swept-wing: Preliminary studies p 274 N95-23283
 Preliminary identification of buffet problems in high speed civil transport p 294 N95-23319
 A study of the vortex flow over 76/40-deg double-delta wing
 [NASA-CR-195032] p 314 N95-23466
 Three-dimensional interaction of wake/boundary-layer and vortex/boundary-layer data report
 [CUED/A-AEREO/TR-23] p 329 N95-24210
 Supersonic quiet-tunnel development for laminar-turbulent transition research
 [NASA-CR-198040] p 340 N95-24302
 Study of compressible flow through a rectangular-to-semiannular transition duct
 [NASA-CR-4660] p 338 N95-24392
 DSMC calculations for 70-deg blunted cone at 3.2 km/s in nitrogen p 348 N95-24396
 [NASA-TM-109181]
 Performance of an aerodynamic yaw controller mounted on the space shuttle orbiter body flap at Mach 10
 [NASA-TM-109179] p 330 N95-24397
 Experimental study of the effects of Reynolds number on high angle of attack aerodynamic characteristics of forebodies during rotary motion
 [NASA-CR-195033] p 330 N95-24443
 Exploratory flow visualization investigation of mast-mounted sights in presence of a rotor
 [NASA-TM-4634] p 330 N95-24566
 Using digital filtering techniques as an aid in wind turbine data analysis p 357 N95-24853
 [DE94-011862]
 Effects of cavity dimensions, boundary layer, and temperature on cavity noise with emphasis on benchmark data to validate computational aeroacoustic codes
 [NASA-CR-4653] p 361 N95-24879
 Numerical and experimental study of drag characteristics of two-dimensional HLFC airfoils in high subsonic, high Reynolds number flow p 331 N95-24998
 [NAL-TR-1244T]
 Low speed aerodynamic characteristics of delta wings with vortex flaps: 60 deg and 70 deg delta wings
 [NAL-TR-1245] p 331 N95-25105
 Thrust measurements of a complete axisymmetric scramjet in an impulse facility p 339 N95-25395
 Scramjet thrust measurement in a shock tunnel p 339 N95-25396
 Balances for the measurement of multiple components of force in flows of a millisecond duration p 350 N95-25400
 Aerodynamic characteristics of the orbital reentry vehicle experimental probe fins in a supersonic flow
 [NAL-TR-1232] p 342 N95-25664
 Measurements of longitudinal static aerodynamic coefficients by the cable mount system
 [NAL-TR-1226] p 331 N95-25761
 Fundamental wind tunnel experiments on low-speed flutter of a tip-fin configuration wing p 332 N95-25762
 [NAL-TR-1228]
 Heat transfer measurements in small scale wind tunnels p 341 N95-26053
 [AD-A288689]
 Airfoil modification effects on subsonic and transonic pressure distributions and performance for the EA-6B airplane
 [NASA-TP-3516] p 373 N95-26382
 Experimental investigation of static and dynamic ground effect on HOPE ALFLEX vehicle
 [NAL-TR-1236] p 388 N95-26525
 Wind tunnel experiments on wake flow field behind a reentry capsule from a viewpoint of parachute deployment at supersonic speeds p 374 N95-26740
 [ISAS-655]
 Effects of three-dimensional imposed 3-D disturbances on bluff-body near wake flows
 [AD-A289553] p 374 N95-26757
 An experimental investigation of helicopter downwash and tailboom interaction at the Wichita State University 7x10 foot wind tunnel p 375 N95-26955
 Incorporating biplane wing theory into a large, subsonic, all-cargo transport p 391 N95-26956
 The lift-fan aircraft: Lessons learned
 [NASA-CR-196694] p 392 N95-27143
 Sailplane glide performance and control using fixed and articulating winglets
 [NASA-CR-198579] p 392 N95-27180
 Wind-tunnel test of the S814 thick root airfoil
 [DE95-000268] p 376 N95-27541
 Further investigations of icing effects on an advanced high-lift multi-element airfoil
 [NASA-TM-106947] p 381 N95-27762

Modeling of aircraft unsteady aerodynamic characteristics. Part 2: Parameters estimated from wind tunnel data
 [NASA-TM-110161] p 410 N95-27839

Collected papers on wind turbine technology
 [NASA-CR-195432] p 447 N95-27970

Horizontal axis wind turbine post stall airfoil characteristics synthesis
 p 376 N95-27974

Comparative wind tunnel tests of NACA 23024 airfoils with several aileron and spoiler configurations
 p 376 N95-27976

Comparative wind tunnel test at high Reynolds numbers of NACA 64 621 airfoils with two aileron configurations
 p 377 N95-27977

Flow structure generated by perpendicular blade vortex interaction and implications for helicopter noise predictions
 [NASA-CR-198590] p 377 N95-28193

Performance study for inlet installations
 [NASA-CR-189714] p 406 N95-28227

Measurements of store forces and moments and cavity pressures for a generic store in and near a box cavity at subsonic and transonic speeds
 [NASA-TM-4611] p 378 N95-28241

Construction and wind tunnel test of a 1/12th scale helicopter model
 [AD-A288487] p 378 N95-28331

Experimental investigation of inlet-combustor isolators for a dual-mode scramjet at a Mach number of 4
 [NASA-TP-3502] p 407 N95-28343

Study of potential aerodynamic benefits from spanwise blowing at wingtip
 [NASA-TP-3515] p 378 N95-28669

Numerical study to assess sulfur hexafluoride as a medium for testing multielement airfoils
 [NASA-TP-3496] p 378 N95-28674

Influence of turbulence parameters, Reynolds number, and body shape on stagnation-region heat transfer
 [NASA-TP-3487] p 550 N95-28719

The effects of three-dimensional imposed disturbances on bluff body near wake flows: Effects of taper and splitter plates on the near wake characteristics of a circular cylinder in uniform and shear flow
 [AD-A292113] p 477 N95-28921

A noninvasive method of quantifying flow visualization data in vortex flow fields
 [AD-A289802] p 552 N95-28948

Interactions of spanwise and chordwise vorticity associated with three-dimensional dynamic stall over an oscillating wing
 [AD-A290546] p 477 N95-29091

Computational Fluid Dynamics (CFD) analysis of a C-135 aircraft with a side-mounted splitter plate (with comparison to wind tunnel data)
 [AD-A292029] p 553 N95-29187

A two element laminar flow airfoil optimized for cruise
 [NASA-CR-198580] p 479 N95-29338

An experimental investigation of the time-dependent separation of tangent bodies in supersonic flow
 [AD-A290720] p 480 N95-29500

Transonic, supersonic and hypersonic wind-tunnel tests on aerodynamic characteristics of reentry body with blunted cone configuration
 [ISAS-658] p 480 N95-29640

The effects of three dimensional imposed disturbances on bluff body near wake flows
 [AD-A290824] p 555 N95-29654

Experimental studies on boundary-layer transition on a reentry vehicle at transonic and supersonic speeds
 [ISAS-659] p 555 N95-29712

Effects of elevated free-stream turbulence and streamwise acceleration on flow and thermal structures in transitional boundary layers
 p 556 N95-29729

Hailstone heat and mass transfer measurements
 [ISBN-0-315-86304-8] p 563 N95-29797

Experimental investigation of aerodynamic devices for wind turbine rotational speed control, phase 1
 [DE95-004034] p 564 N95-30016

Boundary-layer transition and global skin friction measurement with an oil-fringe imaging technique
 [NASA-CR-198814] p 557 N95-30224

Low-speed wind-tunnel investigation of the stability and control characteristics of a series of flying wings with sweep angles of 50 deg
 [NASA-TM-4640] p 505 N95-30226

Growth and development of roughness-induced stationary crossflow vortices
 p 482 N95-30294

Fabry-Perot interferometer measurement of static temperature and velocity for ASTOVL model tests
 [NASA-TM-107014] p 645 N95-30587

Axial loads on yawed rotors
 [PB95-214193] p 592 N95-30638

Transonic aerodynamic characteristics of a proposed wing-body reusable launch vehicle concept
 [NASA-TM-108489] p 592 N95-30712

A wind tunnel investigation of the effects of micro-vortex generators and Gurney flaps on the high-lift characteristics of a business jet wing
 [NASA-TM-110626] p 607 N95-30827

A laser-based ice shape profilometer for use in icing wind tunnels
 [NASA-TM-106936] p 646 N95-30851

Unsteady transonic wind tunnel test on a semispan straked delta wing, oscillating in pitch. Part 1: Description of the model, test setup, data acquisition, and data processing
 [AD-A293113] p 593 N95-30885

Hypervelocity wind tunnel number 9, high Mach number development program
 [AD-A289934] p 594 N95-30929

Hot jet/wake turbulent structure and laser propagation. Part 3: Laser propagation measurements and modeling
 p 647 N95-30992

Afterbody/nozzle pressure distributions of a twin-tail twin-engine fighter with axisymmetric nozzles at Mach numbers from 0.6 to 1.2
 [NASA-TP-3509] p 594 N95-31984

Control of unsteady separated flow associated with the dynamic stall of airfoils
 [NASA-CR-198972] p 594 N95-32193

Computer model to simulate testing at the National Transonic Facility
 [NASA-TM-4664] p 627 N95-32217

SOFIA: Aft cavities wind tunnel test
 [NASA-TM-110673] p 683 N95-32682

SOFIA 2 model telescope wind tunnel test report
 [NASA-TM-110668] p 683 N95-32764

Drag measurements of an axisymmetric nacelle mounted on a flat plate at supersonic speeds
 [NASA-TM-4660] p 684 N95-32821

Numerical simulation of high enthalpy shock tunnel
 p 700 N95-34514

Sidewall-effect of the wind tunnel on the estimation of the aerodynamic characteristics of a delta wing
 p 685 N95-34525

WIND TUNNEL WALLS

Preliminary assessment of tunnel wall interference in the NDA cryogenic wind tunnel
 [BTN-95-EIX95062487531] p 187 A95-69239

Two-variable method for blockage wall interference in a circular tunnel
 [BTN-95-EIX95062487540] p 187 A95-69248

Symposium on Aerodynamics & Aeroacoustics, Tucson, AZ, Mar. 1-2, 1993
 [ISBN 981-02-1732-3] p 462 A95-88892

Operation of the adaptive-wall wind tunnel of TsAGI, Moscow
 p 519 A95-88901

Adaptive-wall wind-tunnel research at Ames Research Center: A retrospective
 p 519 A95-88902

Adaptive wall technology for minimization of wind tunnel boundary interferences - where are we now?
 p 519 A95-88903

Use of partially open wind tunnel walls for blockage-free separated flows on bodies
 p 474 A95-91558

Wall-signature methods for high speed wind tunnel wall interference corrections
 p 107 N95-16257

Surface pressure and wake drag measurements on the Boeing A4 airfoil in the IAR 1.5X1.5m Wind Tunnel Facility
 p 110 N95-17850

2-D aileron effectiveness study
 p 110 N95-17851

Data from the GARTEur (AD) Action Group 02 airfoil CAST 7/DOA1 experiments
 p 111 N95-17856

OAT15A airfoil data
 p 111 N95-17857

A supercritical airfoil experiment
 p 111 N95-17858

Two-dimensional high-lift airfoil data for CFD code validation
 p 112 N95-17859

Wall Interference, Support Interference and Flow Field Measurements
 [AGARD-CP-535] p 162 N95-19251

The crucial role of wall interference, support interference and flow field measurements in the development of advanced aircraft configurations
 p 162 N95-19252

Boundary-flow measurement methods for wall interference assessment and correction: Classification and review
 p 163 N95-19262

Estimating wind tunnel interference due to vectored jet flows
 p 164 N95-19265

Determination of solid/porous wall boundary conditions from wind tunnel data for computational fluid dynamics codes
 p 164 N95-19266

Adaptive wind tunnel walls versus wall interference correction methods in 2D flows at high blockage ratios
 p 147 N95-19267

Interference determination for wind tunnels with slotted walls
 p 147 N95-19269

Unsteady flow testing in a passive low-correction wind tunnel
 p 147 N95-19272

Analysis of test section sidewall effects on a two dimensional airfoil: Experimental and numerical investigations
 p 165 N95-19276

Calculation of wall effects of flow on a perforated wall with a code of surface singularities
 p 165 N95-19277

Evaluation of combined wall- and support-interference on wind tunnel models
 p 122 N95-19278

Prediction of wind tunnel effects on the installed F/A-18A inlet flow field at high angles-of-attack
 [NASA-CR-195429] p 197 N95-19651

Investigation of a thermal buoyancy effect on the drag of half models tested in the ARA Transonic Wind Tunnel [ARA-MEMO-407] p 222 N95-19946

A wall interference assessment/correction system
 [NASA-CR-197421] p 309 N95-23183

A method for the modelling of porous and solid wind tunnel walls in computational fluid dynamics codes
 p 523 N95-29795

Investigation of water droplet trajectories within the NASA icing research tunnel
 [NASA-TM-107023] p 684 N95-32769

WIND TUNNELS

Aeroacoustic probe design for microphone to reduce flow-induced self-noise
 [AIAA PAPER 93-4343] p 19 A95-60163

Oblique incidence sound absorption of porous materials covered by perforated metal and exposed to tangential airflow
 [HTN-94-00681] p 19 A95-60165

Planar air density measurements near model surfaces by ultraviolet Rayleigh/Raman scattering
 [BTN-94-EIX94441386614] p 213 A95-67345

Measurement and analysis of nitric oxide radiation in an arcjet flow
 [BTN-95-EIX95082502727] p 243 A95-71040

Rarefied gas numerical wind tunnel: OREX and HOPE
 p 427 A95-82391

Experimental investigation of the sources of propeller noise due to the ingestion of turbulence at low speeds
 [BTN-95-EIX95262697042] p 569 A95-86859

Operation of the adaptive-wall wind tunnel of TsAGI, Moscow
 p 519 A95-88901

Review of new French facilities for PREPHA program [AIAA PAPER 95-6128] p 520 A95-90449

Effect of leading-edge extension fences on the vortex wake of an F/A-18 model
 [BTN-95-EIX0619952748192] p 591 A95-94481

Control of wind tunnel operations using neural net interpretation of flow visualization records
 [NASA-TM-106683] p 24 N95-10854

Test model designs for advanced refractory ceramic materials
 p 55 N95-11968

Developments in laser-based diagnostics for wind tunnels in the Aeromechanics Division: 1987-1992
 [AD-A283011] p 84 N95-13687

Quality assessment for wind tunnel testing
 [AGARD-AR-304] p 67 N95-14197

Computational analysis of forebody tangential slot blowing
 p 71 N95-14253

F/A-18 and F-16 forebody vortex control, static and rotary-balance results
 p 72 N95-14254

Flight evaluation of pneumatic forebody vortex control in post-stall flight
 p 72 N95-14259

Research and technology highlights, 1993
 [NASA-TM-4575] p 102 N95-15065

Low-speed wind tunnel testing of the NPS and NASA Ames Mach 6 optimized waverider
 [AD-A283585] p 75 N95-15319

STOVL CFD model test case
 p 115 N95-17881

Universal wind tunnel data acquisition and reduction software
 [AD-A283897] p 171 N95-18365

Hypersonic flight testing
 [AD-A283981] p 134 N95-18891

Wall correction method with measured boundary conditions for low speed wind tunnels
 p 164 N95-19263

Estimating wind tunnel interference due to vectored jet flows
 p 164 N95-19265

Development of pneumatic test techniques for subsonic high-lift and in-ground-effect wind tunnel investigations
 p 121 N95-19268

Wall interaction effects for a full-scale helicopter rotor in the NASA Ames 80- by 120-foot wind tunnel
 p 121 N95-19270

Prediction of wind tunnel effects on the installed F/A-18A inlet flow field at high angles-of-attack
 [NASA-CR-195429] p 197 N95-19651

Application of wavelet-filtering techniques to intermittent turbulent and wall pressure events. Part 1: Exploratory results
 [AD-A286077] p 247 N95-20849

A three-dimensional orthogonal laser velocimeter for the NASA Ames 7- by 10-foot wind tunnel
 [NASA-TM-108864] p 249 N95-21323

NTS-spill test facility wind tunnel exhaust plume characterization
 [DE95-003630] p 297 N95-24019

- Anechoic wind tunnel study of turbulence effects on wind turbine broadband noise p 451 N95-27992
 Unsteadiness of shock-induced turbulent boundary layer separation. An inherent feature of turbulent flow or solely a wind tunnel phenomenon
 [AD-A290367] p 554 N95-29228
 Telepresence media resource tape
 [NASA-TM-110648] p 569 N95-30248
 Patterns in the sky: Natural visualization of aircraft flow fields
 [NASA-SP-514] p 584 N95-31000
 Investigation of water droplet trajectories within the NASA icing research tunnel
 [NASA-TM-107023] p 684 N95-32769
 Sidewall-effect of the wind tunnel on the estimation of the aerodynamic characteristics of a delta wing
 p 685 N95-34525
 Direct numerical simulation of incompressible homogeneous isotropic turbulence using NWT
 p 706 N95-34530
 Performance evaluation of the NWT with incompressible NS code p 707 N95-34533
- WIND TURBINES**
 Aerodynamic characteristics of truncated airfoils at high angle of attack
 [SAE PAPER 931227] p 460 A95-87365
 TKKMOD: A computer simulation program for an integrated wind diesel system. Version 1.0: Document and user guide
 [PB94-179090] p 60 N95-11798
 Structural effects of unsteady aerodynamic forces on horizontal-axis wind turbines
 [DE94-011863] p 157 N95-16939
 Wind turbine blade aerodynamics: The combined experiment
 [DE94-011866] p 118 N95-18645
 Wind turbine blade aerodynamics: The analysis of field test data
 [DE94-011867] p 118 N95-18646
 Evidence that aerodynamic effects, including dynamic stall, dictate HAWT structural loads and power generation in highly transient time frames
 [DE94-011865] p 216 N95-19855
 Advanced wind turbine design studies: Advanced conceptual study
 [DE93-000031] p 256 N95-20985
 Using digital filtering techniques as an aid in wind turbine data analysis
 [DE94-011862] p 357 N95-24853
 NREL airfoil families for HAWTs
 [DE95-000267] p 357 N95-24882
 Wind technology development: Large and small turbines
 [DE95-000286] p 358 N95-26090
 A comparison of measured wind park load histories with the WISPER and WISPERX load spectra
 [DE95-000295] p 446 N95-27459
 Collected papers on wind turbine technology
 [NASA-CR-195432] p 447 N95-27970
 Horizontal axis wind turbine post stall airfoil characteristics synthesisization p 376 N95-27974
 Preliminary analysis of dynamic stall effects on a 91-meter wind turbine rotor p 376 N95-27975
 Comparative wind tunnel test at high Reynolds numbers of NACA 64 621 airfoils with two aileron configurations p 377 N95-27977
 Comparative performance tests on the Mod-2, 2.5-mW wind turbine with and without vortex generators p 377 N95-27978
 Design of a real-time wind turbine simulator using a custom parallel architecture p 449 N95-27979
 A NASTRAN-based computer program for structural dynamic analysis of Horizontal Axis Wind Turbines p 439 N95-27980
 Aeroelastic stability of wind turbine blade/aileron systems p 377 N95-27981
 Calculation of design load for the MOD-5A 7.3 mW wind turbine system p 440 N95-27982
 Comparison of measured and calculated dynamic loads for the Mod-2 2.5 mW wind turbine system p 440 N95-27983
 Control system design for the MOD-5A 7.3 mW wind turbine generator p 440 N95-27985
 Use of blade pitch control to provide power train damping for the Mod-2, 2.5-mW wind turbine p 440 N95-27986
 Variable speed generator application on the MOD-5A 7.3 mW wind turbine generator p 440 N95-27989
 Measurement and prediction of broadband noise from large horizontal axis wind turbine generators p 451 N95-27990
 Observed acoustic and aeroelastic spectral responses of a MOD-2 turbine blade to turbulence excitation p 451 N95-27991
 Anechoic wind tunnel study of turbulence effects on wind turbine broadband noise p 451 N95-27992
- Experimental investigation of aerodynamic devices for wind turbine rotational speed control, phase 1
 [DE95-004034] p 564 N95-30016
 PREDICHTAT: First order performance calculations of windturbine rotors using the method of the acceleration potential
 [PB95-206454] p 564 N95-30200
 Axial loads on yawed rotors
 [PB95-214193] p 592 N95-30638
 Acceleration potential models
 PREDICHTAT/PREDICDYN applied for calculation of axisymmetric dynamic inflow cases p 647 N95-30957
 Digital simulation of wind velocities for wind turbine rotors: General considerations
 [PB95-206447] p 677 N95-31157
 Wind turbine trailing edge aerodynamic brakes
 [DE95-004061] p 683 N95-32548
 Techniques for the determination of local dynamic pressure and angle of attack on a horizontal axis wind turbine
 [DE95-009204] p 707 N95-32685
- WIND VELOCITY**
 A technique for detecting a tropical cyclone center using a Doppler radar
 [HTN-95-20631] p 215 A95-69574
 Ascent wind model for launch vehicle design
 [BTN-95-EIX95041503799] p 239 A95-70124
 Verification of terminal forecasts p 664 A95-93502
 Jet stream winds: Comparisons of operational analyses with independent aircraft data at multiple longitudes p 665 A95-93506
 MEMFOG - The Memphis fog algorithm p 668 A95-93516
 Certification methodology applied to the NASA experimental radar system p 41 N95-13205
 Groundspeed filtering for CTAS
 [NASA-CR-197223] p 97 N95-15785
 Evaluation of an unlighted swinging airport sign
 [AD-A284763] p 146 N95-18087
 NTS-spill test facility wind tunnel exhaust plume characterization p 297 N95-24019
 Preliminary analysis of dynamic stall effects on a 91-meter wind turbine rotor p 376 N95-27975
 Comparative wind tunnel tests of NACA 23024 airfoils with several aileron and spoiler configurations p 376 N95-27976
 Comparative wind tunnel test at high Reynolds numbers of NACA 64 621 airfoils with two aileron configurations p 377 N95-27977
 Comparative performance tests on the Mod-2, 2.5-mW wind turbine with and without vortex generators p 377 N95-27978
 Comparison of measured and calculated dynamic loads for the Mod-2 2.5 mW wind turbine system p 440 N95-27983
 The performance of cargo airdrop systems using g-12E parachutes: Statistical determination of minimum altitude
 [AD-A291666] p 381 N95-28454
 Digital simulation of wind velocities for wind turbine rotors: General considerations
 [PB95-206447] p 677 N95-31157
- WIND VELOCITY MEASUREMENT**
 Comparison of wind profiler and aircraft wind measurements at Chebogue Point, Nova Scotia
 [HTN-95-41833] p 353 A95-80559
 The detection and measurement of microburst wind shear by an airborne lidar system p 543 A95-87798
 ITWS gridded analysis p 654 A95-93455
 Test results of a low cost airport weather radar p 662 A95-93492
 Microburst vertical wind estimation from horizontal wind measurements
 [NASA-TP-3460] p 131 N95-18198
 Comparative performance tests on the Mod-2, 2.5-mW wind turbine with and without vortex generators p 377 N95-27978
- WINDING**
 A time stepping coupled finite element-state space modeling environment for synchronous machine performance and design analysis in the ABC frame of reference p 649 N95-31948
- WINDOWS (APERTURES)**
 Science objectives and performance of a radiometer and window design for atmospheric entry experiments
 [NASA-TM-4637] p 63 N95-12190
 Science objectives and performance of a radiometer and window design for atmospheric entry experiments p 85 N95-13718
 Development of repair processes and sources for C/KC-135 aircraft windows/windshields
 [AD-A288348] p 367 N95-26629
- WINDOWS (INTERVALS)**
 Terminal Doppler Weather Radar point target filter threshold selection p 662 A95-93490
- WINDPOWER UTILIZATION**
 TKKMOD: A computer simulation program for an integrated wind diesel system. Version 1.0: Document and user guide
 [PB94-179090] p 60 N95-11798
 Structural effects of unsteady aerodynamic forces on horizontal-axis wind turbines
 [DE94-011863] p 157 N95-16939
 Advanced wind turbine design studies: Advanced conceptual study
 [DE93-000031] p 256 N95-20985
 Wind technology development: Large and small turbines
 [DE95-000286] p 358 N95-26090
 Collected papers on wind turbine technology
 [NASA-CR-195432] p 447 N95-27970
 Comparative performance tests on the Mod-2, 2.5-mW wind turbine with and without vortex generators p 377 N95-27978
 Design of a real-time wind turbine simulator using a custom parallel architecture p 449 N95-27979
- WINDPOWERED GENERATORS**
 TKKMOD: A computer simulation program for an integrated wind diesel system. Version 1.0: Document and user guide
 [PB94-179090] p 60 N95-11798
 Collected papers on wind turbine technology
 [NASA-CR-195432] p 447 N95-27970
 Control system design for the MOD-5A 7.3 mW wind turbine generator p 440 N95-27985
 Variable speed generator application on the MOD-5A 7.3 mW wind turbine generator p 440 N95-27989
 Measurement and prediction of broadband noise from large horizontal axis wind turbine generators p 451 N95-27990
- WINDS ALOFT**
 Real time for the calculation of the aerodynamic of aircrafts with delta wings p 460 A95-87399
 A study of the savings in time and fuel to aviation through the use of upper-air wind forecasts p 672 A95-93538
- WINDSHIELDS**
 Impact finite element analysis, as an alternative to the testing of windcreens for bird impact
 [CONGRESS PAPER C428-23-196] p 500 A95-91732
 Development of repair processes and sources for C/KC-135 aircraft windows/windshields
 [AD-A288348] p 367 N95-26629
 An analysis of B-1B exterior jet blast windshield anti-icing performance using pre-cooled compressor bleed air
 [AD-A292522] p 485 N95-28811
 Transmittance characteristics of US Army rotary-wing aircraft transparencies
 [AD-A295035] p 693 N95-34793
- WING CAMBER**
 Lift analysis of a variable camber foil using the discrete vortex-blob method
 [BTN-94-EIX94441386623] p 179 A95-68172
 Variable camber geometry for transport aircraft wings
 [CONGRESS PAPER C428-35-061] p 603 A95-93626
 Effect of leading- and trailing-edge flaps on clipped delta wings with and without wing camber at supersonic speeds
 [NASA-TM-4542] p 5 N95-10028
 Unique considerations in the design and experimental evaluation of tailored wings with elastically produced chordwise camber p 423 N95-28436
 Analysis and design methodology for chordwise deformable wings p 692 N95-33311
- WING FLAPS**
 Stability derivatives of a flapped plate in unsteady ground effect
 [BTN-95-EIX95182619225] p 270 A95-76651
 Numerical design of advanced multi-element airfoils
 [NASA-CR-197135] p 76 N95-15762
 Low-speed surface pressure and boundary layer measurement data for the NLR 7301 airfoil section with trailing edge flap p 111 N95-17855
 A wind tunnel investigation of the effects of micro-vortex generators and Gurney flaps on the high-lift characteristics of a business jet wing
 [NASA-TM-110626] p 607 N95-30827
- WING FLOW METHOD TESTS**
 Spectral mapping of quasiperiodic structures in a vortex flow
 [BTN-95-EIX0619952748165] p 589 A95-94459
- WING LOADING**
 Experimental investigations on limit cycle wing rock of slender wings
 [BTN-95-EIX95062487543] p 185 A95-68357
 Summary of an active flexible wing program
 [BTN-95-EIX95182619209] p 283 A95-76635
 Multiple-function digital controller system for active flexible wing wind-tunnel model
 [BTN-95-EIX95182619212] p 322 A95-76638

- Rolling maneuver load alleviation using active controls [BTN-95-EIX95182619217] p 270 A95-76643
- Aerodynamics of a finite wing with simulated ice [AD-A294126] p 270 A95-76653
- Hubload responses of a rotor in forward flight due to multiple frequency blade pitch variations p 515 A95-91504
- Experiment of the large elastic deformation of biconvex wing sections in an air-flow p 475 A95-91564
- Neural network approach to identification of aerodynamic loads on a wing. 1: Application to cantilevered beam models p 475 A95-91568
- Load alleviation for civil transport aircraft [CONGRESS PAPER C428-35-057] p 604 A95-93627
- Aeroelastic tailoring research [PB94-180031] p 6 N95-10135
- Computations of unsteady aerodynamic loads around oscillating wings. Part 1: Formulation [PB94-180049] p 7 N95-10136
- Computations of unsteady aerodynamic loads around oscillating wings. Part 2: Computed results and discussions [PB94-180056] p 7 N95-10137
- Active load control during rolling maneuvers — performed in the Langley Transonic Dynamics Tunnel [NASA-TP-3455] p 129 N95-17397
- 2-D aileron effectiveness study p 110 N95-17851
- Flight testing high lateral asymmetries on highly augmented Fighter/Attack aircraft [AD-A284206] p 130 N95-17953
- Determination of stores pointing error due to wing flexibility under flight load [NASA-TM-4646] p 134 N95-19044
- Development of load spectra for Airbus A330/A340 full scale fatigue tests p 135 N95-19479
- Derived gust spectra for the Macchi MB326H [ARL-TN-3] p 225 N95-21892
- Unsteady transonic wind tunnel test on a semispan straked delta wing, oscillating in pitch. Part 1: Description of the model, test setup, data acquisition, and data processing [AD-A293113] p 593 N95-30885
- WING NACELLE CONFIGURATIONS**
- Flow study of supersonic wing-nacelle configuration [BTN-95-EIX95152582344] p 266 A95-73546
- Civil aircraft propulsion integration: Current & future [SAE PAPER 932624] p 495 A95-90085
- Multigrid/multiblock method for transonic potential flow around wing/body/nacelle configurations including a slipstream p 591 A95-95451
- Transonic vortical flow predicted with a structured multiblock Euler solver p 642 A95-95462
- Cabin fuselage structural design with engine installation and control system [NASA-CR-197173] p 47 N95-12639
- Numerical analysis around the whole SST configuration p 693 N95-34541
- WING OSCILLATIONS**
- Dynamic stall of an oscillating wing. Part 1: Evaluation of turbulence models [AIAA PAPER 93-3403] p 3 A95-60184
- Experimental investigations on limit cycle wing rock of slender wings [BTN-95-EIX95062487543] p 185 A95-68357
- Direct adaptive and neural control of wing-rock motion of slender delta wings [BTN-95-EIX95242670748] p 327 A95-81099
- Transonic flutter suppression using active acoustic excitations [BTN-95-EIX95262694310] p 408 A95-85481
- Unsteady aerodynamic effects of trailing edge controls on delta wings [HTN-95-01099] p 469 A95-90285
- Computations of unsteady aerodynamic loads around oscillating wings. Part 1: Formulation [PB94-180049] p 7 N95-10136
- Computations of unsteady aerodynamic loads around oscillating wings. Part 2: Computed results and discussions [PB94-180056] p 7 N95-10137
- A computational investigation of wake-induced airfoil flutter in incompressible flow and active flutter control [AD-A281534] p 142 N95-16109
- 2-D and 3-D oscillating wing aerodynamics for a range of angles of attack including stall [NASA-TM-4632] p 120 N95-19119
- Fundamental wind tunnel experiments on low-speed flutter of a tip-fin configuration wing [NAL-TR-1228] p 332 N95-25762
- Navier-Stokes solution of wing wake structure and its perturbation p 479 N95-29121
- An interacting boundary layer method for unsteady compressible flows p 557 N95-30290
- Unsteady transonic wind tunnel test on a semispan straked delta wing, oscillating in pitch. Part 1: Description of the model, test setup, data acquisition, and data processing [AD-A293113] p 593 N95-30885
- WING PANELS**
- Optimum design of composite stiffened wing panels - a parametric study [HTN-95-01088] p 496 A95-90274
- Crack growth characteristics of integrally machined stringer-skin panels p 496 A95-90281
- Experiment of the large elastic deformation of biconvex wing sections in an air-flow p 475 A95-91564
- Non-contact calibration of a CNC riveting machine [CONGRESS PAPER C428-32-075] p 583 A95-93618
- Steady and unsteady three-dimensional transonic flow computations by integral equation method [NASA-CR-196777] p 10 N95-11582
- Fatigue and residual strength investigation of ARALL(R) -3 and GLARE(R) -2 panels with bonded stringers p 137 N95-19495
- Structural modification and repair of C-130 wing structure using bonded composites p 394 N95-27512
- Composite or metallic bolted repairs on self-stiffened carbon wing panel of the commuter ATR72 design criteria, analysis, verification by test p 396 N95-27525
- Test results from large wing and fuselage panels p 537 N95-29051
- WING PLANFORMS**
- Aeroservoelastic aspects of wing/control surface planform shape optimization [BTN-95-EIX95222650795] p 340 A95-79251
- WING PROFILES**
- Influence of wing shapes on surface pressure fluctuations at wing-body junctions [HTN-95-61196] p 491 A95-87569
- A theoretical and experimental investigation of the flow over supersonic leading edge wing/body configurations [DRA-TM-AERO-PROP-41] p 331 N95-25649
- Automatic multi-block grid generation for high-lift configuration wings p 567 N95-28764
- Low-speed wind-tunnel investigation of the stability and control characteristics of a series of flying wings with sweep angles of 50 deg [NASA-TM-4640] p 505 N95-30226
- WING ROOTS**
- Gemini: A long-range cargo transport [NASA-CR-197149] p 45 N95-12626
- The Aluminum Falcon: A low cost modern commercial transport [NASA-CR-197180] p 81 N95-15742
- WING SLOTS**
- Impingement cooling of an isothermally heated surface with a confined slot jet [BTN-94-EIX94421348950] p 347 A95-78494
- Computational study of a two-slot circulation control airfoil [SAE PAPER 932531] p 466 A95-89191
- Transonic flight test of a laminar flow leading edge with surface excrescences [NASA-TM-4597] p 9 N95-11158
- Numerical simulation of dynamic-stall suppression by tangential blowing [AD-A284887] p 120 N95-19110
- WING TANKS**
- Determination of stores pointing error due to wing flexibility under flight load [NASA-TM-4646] p 134 N95-19044
- WING TIP VORTICES**
- An experimental investigation of wing tip turbulence with applications to aerosound [AIAA PAPER 86-1918] p 1 A95-60164
- Tip vortex on a swept wing. Mean flow and unsteady phenomena [BTN-94-EIX94441385755] p 184 A95-68219
- A brief survey of wing tip devices for drag reduction [SAE PAPER 932574] p 467 A95-90063
- Collectively variable incidence wingtips for lift control and reduced gust sensitivity [HTN-95-92836] p 471 A95-90754
- On controlling the tip vortex flow of a lifting wing [ISBN 1-879921-01-4] p 587 A95-93736
- 3D visualization of unsteady 2D airplane wake vortices [AD-A284745] p 27 N95-11593
- WING TIPS**
- A brief survey of wing tip devices for drag reduction [SAE PAPER 932574] p 467 A95-90063
- Collectively variable incidence wingtips for lift control and reduced gust sensitivity [HTN-95-92836] p 471 A95-90754
- Fundamental wind tunnel experiments on low-speed flutter of a tip-fin configuration wing [NAL-TR-1228] p 332 N95-25762
- An LDV investigation of support structure influence on the flow field near the wingtip of a STOVL configuration in hover [AD-A294126] p 686 N95-34750
- WING-FUSELAGE STORES**
- Vortex lattice method simulation of unsteady flow due to wing/external store combination p 471 A95-91499
- Computer aided static aeroelastic analysis of wing/pylon/store combination p 499 A95-91531
- The aerodynamic design of an integrated wing lower surface and pylons for reduced drag [ARA-MEMO-406] p 194 N95-19789
- Airfoil modification effects on subsonic and transonic pressure distributions and performance for the EA-6B airplane [NASA-TP-3516] p 373 N95-26382
- WINGLETS**
- Aerodynamic effects of delta platform tip sails on wing performance [BTN-95-EIX95062487544] p 185 A95-68358
- Design and construction of a remote piloted flying wing [NASA-CR-197195] p 47 N95-12695
- Fatigue evaluation of empennage, forward wing, and winglets/tip fins on part 23 airplanes [PB94-196813] p 79 N95-13981
- Fundamental wind tunnel experiments on low-speed flutter of a tip-fin configuration wing [NAL-TR-1228] p 332 N95-25762
- Sailplane glide performance and control using fixed and articulating winglets [NASA-CR-198579] p 392 N95-27180
- WINGS**
- Dynamic stall of an oscillating wing. Part 1: Evaluation of turbulence models [AIAA PAPER 93-3403] p 3 A95-60184
- Wing download reduction using vortex trapping plates [HTN-94-00710] p 4 A95-60188
- An assessment of upper surface blowing for the reduction of tilt rotor download [HTN-94-00711] p 5 A95-60189
- Aerodynamic interactions between a rotor and wing in hover [HTN-94-00714] p 5 A95-60192
- Advancements in automatic fastening technology [BTN-94-EIX94461290277] p 65 A95-61734
- Planar air density measurements near model surfaces by ultraviolet Rayleigh/Raman scattering [BTN-94-EIX94441386614] p 213 A95-67345
- Launcher wing-leading-edge design [BTN-95-EIX95042477110] p 192 A95-68349
- Twisting smartly in the wind [BTN-95-EIX95041503093] p 184 A95-68353
- Application of circulation control to advanced subsonic transport aircraft. Part 1: Airfoil development [BTN-95-EIX95062487545] p 185 A95-68359
- Application of circulation control to advanced subsonic transport aircraft. Part 2: Transport application [BTN-95-EIX95062487546] p 185 A95-68360
- Influence of structural and aerodynamic modeling on flutter analysis [BTN-95-EIX95062487550] p 203 A95-68364
- Interference between tanker wing wake with roll-up and receiver aircraft [BTN-95-EIX95062487552] p 185 A95-68366
- Numerical simulation of steady and unsteady, vorticity-dominated aerodynamic interference [BTN-95-EIX95062487524] p 186 A95-69232
- Analysis of an oscillating Joukowski airfoil with surface suction and moving vortices [BTN-95-EIX95062487527] p 186 A95-69235
- Aerodynamic sensitivity coefficients using the three-dimensional full potential equation [BTN-95-EIX95062487530] p 186 A95-69238
- Aerodynamic characteristics of strake vortex flaps on a strake-wing configuration [BTN-95-EIX95062487537] p 187 A95-69245
- Ice accretion on aircraft wings [BTN-95-EIX95082502224] p 225 A95-71021
- Time-resolved surface heat flux measurements in the wing/body junction vortex [BTN-95-EIX95082502716] p 220 A95-71029
- Electro-optic characterization of ultrafast photodetectors using adiabatically compressed soliton pulses [BTN-94-EIX94381359637] p 257 A95-72675
- Eigenanalysis of unsteady flows about airfoils, cascades, and wings [BTN-95-EIX95152577597] p 305 A95-73486
- Sidewash on the vertical tail in subsonic and supersonic flows [BTN-95-EIX95152582316] p 264 A95-73519
- Nonlinear angle of twist of advanced composite wing boxes under pure torsion [BTN-95-EIX95152582323] p 281 A95-73526

- Moving wall effect in relation to other dynamic stall flow mechanisms
 [BTN-95-EIX95152582324] p 265 A95-73527
 Study of an airfoil with a flap and spoiler
 [BTN-95-EIX95152582327] p 265 A95-73530
 Effect of underwing frost on a transport aircraft airfoil at flight Reynolds number
 [BTN-95-EIX95152582334] p 276 A95-73536
 Pneumatic concept for tip-stall control of cranked-arrow wings
 [BTN-95-EIX95152582335] p 281 A95-73537
 Method for the prediction of the onset of wing rock
 [BTN-95-EIX95152582342] p 282 A95-73544
 Multirate flutter suppression system design for a model wing
 [BTN-95-EIX95182619132] p 292 A95-76609
 Application of Navier-Stokes aeroelastic methods to improve fighter wing maneuver performance
 [BTN-95-EIX95182619218] p 284 A95-76644
 Calculation of wing-alone aerodynamics to high angles of attack
 [BTN-95-EIX95212645713] p 261 A95-76765
 Aeroelastic aspects of wing/control surface platform shape optimization
 [BTN-95-EIX95222650795] p 340 A95-79251
 A concept of a hypersonic flight experiment of a winged vehicle
 [HTN-95-42340] p 414 A95-82477
 Atmospheric reentry flight test of winged space vehicle
 [HTN-95-71128] p 385 A95-83489
 An inverse design method of transonic airfoil and wing
 [HTN-95-71128] p 385 A95-83489
 Analysis of backscattering from wing and fuselage joints
 [HTN-95-71134] p 430 A95-83495
 Active plate and missile wing development using directionally attached piezoelectric elements
 [HTN-95-42340] p 408 A95-86169
 Eigenanalysis of unsteady flows about airfoils, cascades, and wings
 [HTN-95-42582] p 459 A95-87212
 An investigation of the accuracy of FEM analysis of a graphite epoxy box beam
 [SAE PAPER 931221] p 543 A95-88011
 Equivalent plate structural modeling for wing shape optimization including transverse shear
 [HTN-95-20839] p 492 A95-88100
 Aerodynamic tailoring of the Learjet Model 60 wing
 [SAE PAPER 932534] p 492 A95-89194
 Materials and structures for the HSCT
 [BTN-95-EIX95282711241] p 455 A95-89634
 Boundary-layer transition and global skin friction measurement with an oil-fringe imaging technique
 [SAE PAPER 932550] p 547 A95-90054
 Accurate drag prediction: A prerequisite for drag reduction research
 [SAE PAPER 932571] p 467 A95-90060
 Design and analysis of a telescopic wing
 [SAE PAPER 932605] p 495 A95-90075
 Effects of structural damping on aeroelastic stability of various shaped composite plate wing
 p 530 A95-91530
 Preliminary tests of a transonic flutter control wing model
 p 499 A95-91566
 The use of hot film for the investigation of boundary-layer transition
 [CONGRESS PAPER C428-9-199] p 475 A95-91697
 Static shape control for adaptive wings
 [HTN-95-A1767] p 627 A95-93330
 The mini-business approach at Chadderton
 [CONGRESS PAPER C428-26-037] p 681 A95-93602
 Hybrid laminar flow over wings enhanced by continuous boundary layer suction
 [SAE PAPER 931386] p 587 A95-93662
 Analytic solution of the thickness problem of a rectangular wing in steady subsonic flow
 [ISBN 1-879921-01-4] p 588 A95-93758
 Quantifiable vortex features of F-106B aircraft at subsonic speeds
 [BTN-95-EIX0619952748161] p 588 A95-94455
 Computation of delta-wing roll maneuvers
 [BTN-95-EIX0619952748164] p 605 A95-94458
 Spectral mapping of quasiperiodic structures in a vortex flow
 [BTN-95-EIX0619952748165] p 589 A95-94459
 In-flight pressure measurements on a subsonic transport high-lift wing section
 [BTN-95-EIX0619952748170] p 589 A95-94464
 High-lift calculations using Navier-Stokes methods
 p 641 A95-95444
 LDV measurements in separated flow on an elliptic wing mounted at an angle of attack on a wall
 [BTN-94-EIX94441380518] p 702 A95-96559
- Advanced composites structural concepts and materials technologies for primary aircraft structures: Design/manufacturing concept assessment
 [NASA-CR-4447] p 12 N95-10316
 The use of the Regier number in the structural design with flutter constraints
 [NASA-TM-109128] p 13 N95-11465
 Parallel aeroelastic computations for wing and wing-body configurations
 [NASA-CR-196835] p 36 N95-11766
 The development of a highly reliable power management and distribution system for civil transport aircraft
 [NASA-TM-106697] p 50 N95-11867
 Optimum aerodynamic design via boundary control
 [NASA-CR-195882] p 36 N95-11877
 Viper cabin-fuselage structural design concept with engine installation and wing structural design
 [NASA-CR-197162] p 45 N95-12305
 The FC-1D: The profitable alternative Flying Circus Commercial Aviation Group
 [NASA-CR-197152] p 46 N95-12628
 Cabin-fuselage-wing structural design concept with engine installation
 [NASA-CR-197172] p 49 N95-12993
 Numerical time dependent sheet cavitation simulations using a higher order panel method
 [PB94-204435] p 59 N95-13249
 Computational aerodynamics based on the Euler equations
 [AGARD-AG-325] p 72 N95-14264
 Development of a composite repair and the associated inspection intervals for the F-111C stiffener runout region
 p 66 N95-14477
 Numerical study of the effects of icing on viscous flow over wings
 [NASA-CR-197102] p 75 N95-14803
 Aerodynamic shape optimization
 p 128 N95-16572
 Investigation of the influence of pylons and stores on the wing lower surface flow
 p 116 N95-17885
 Wing design for a civil tiltrotor transport aircraft
 [NASA-CR-197523] p 130 N95-18090
 Parametric study on laminar flow for finite wings at supersonic speeds
 [NASA-TM-108852] p 116 N95-18101
 Course module for AA201: Wing structural design project
 [AD-A283618] p 133 N95-18616
 The accuracy of parameter estimation in system identification of noisy aircraft load measurement
 [NASA-CR-197516] p 134 N95-19130
 Development of load spectra for Airbus A330/A340 full scale fatigue tests
 p 135 N95-19479
 Wing pressure distributions from subsonic tests of a high-wing transport model — in the Langley 14-by 22-Foot Subsonic Wind Tunnel
 [NASA-TM-4583] p 272 N95-22802
 Control of flow separation in airfoil/wing design applications
 p 274 N95-23294
 High-lift flow-physics flight experiments on a subsonic civil transport aircraft (B737-100)
 p 275 N95-23333
 Lift enhancing tabs for airfoils
 [NASA-CASE-ARC-11990-1] p 286 N95-23395
 Geometric analysis of wing sections
 [NASA-TM-110346] p 335 N95-24629
 Fundamental wind tunnel experiments on low-speed flutter of a tip-fin configuration wing
 [NAL-TR-1228] p 332 N95-25762
 Demonstration study of hierarchical control of fluid-dynamic phenomena
 [AD-A289341] p 437 N95-26751
 A numerical method for unsteady transonic flow about wings with control surfaces
 [AD-A289631] p 375 N95-26859
 Advanced formation flight control
 [AD-A289271] p 409 N95-26981
 Design and structural validation of CF116 upper wing skin boron doubler
 p 393 N95-27510
 Vibrational behavior of adaptive aircraft wing structures modelled as composite thin-walled beams
 p 423 N95-28435
 Unique considerations in the design and experimental evaluation of tailored wings with elastically produced chordwise camber
 p 423 N95-28436
 C-130 Advanced Technology Center wing box conceptual design/cost study
 p 423 N95-28437
 Structural testing of the technology integration box beam
 p 441 N95-28467
 Test and analysis results for composite transport fuselage and wing structures
 p 398 N95-28470
 Application of damage tolerance methodology in certification of the Piaggio P-180 Avanti
 p 399 N95-28480
 Advanced wing design survivability testing and results
 p 400 N95-28488
- Investigation of wing upper surface flow-field disturbance due to NASA DC-8-72 in-flight inboard thrust-reverser deployment
 [NASA-TM-110351] p 457 N95-28816
 Shear force, bending moment and torque of rigid aircraft in symmetric steady maneuvering flight
 [ESDU-94045] p 502 N95-28896
 Advanced composites technology program
 p 534 N95-29032
 Interactions of spanwise and chordwise vorticity associated with three-dimensional dynamic stall over an oscillating wing
 [AD-A290546] p 477 N95-29091
 A vorticity-velocity approach for three-dimensional unsteady viscous flow over wings
 p 478 N95-29108
 Computational Fluid Dynamics (CFD) analysis of a C-135 aircraft with a side-mounted splitter plate (with comparison to wind tunnel data)
 [AD-A292029] p 553 N95-29187
 A two element laminar flow airfoil optimized for cruise
 [NASA-CR-198580] p 479 N95-29338
 Boundary-layer transition and global skin friction measurement with an oil-fringe imaging technique
 [NASA-CR-198814] p 557 N95-30224
 A numerical study of the small scale wing-body junction problem
 p 482 N95-30235
 Development of stitched/RTM primary structures for transport aircraft
 [NASA-CR-191441] p 630 N95-31421
 Performance improvement of composite wings through aeroelastic tailoring and modern control
 [AD-A293689] p 608 N95-31602
 A probabilistic design method applied to smart composite structures
 [NASA-TM-106715] p 651 N95-32206
 Development of a composite tailoring procedure for airplane wing
 [NASA-CR-199081] p 691 N95-32928
 Numerical simulation of two-dimensional PAR-WIG
 p 685 N95-34548
- WINTER**
 Aircraft icing measurements in East Coast winter storms
 [HTN-95-60505] p 214 A95-68756
 Mesoscale structure of precipitation bands in a North Atlantic winter storm
 [HTN-95-40659] p 215 A95-69803
 An overview of the EASOE campaign
 [HTN-95-00702] p 443 A95-86272
 Aircraft measurements of CLO and HCL during EASOE 1991/92
 [HTN-95-00721] p 444 A95-86291
 An overview of millimeter-wave spectroscopic measurements of chlorine monoxide at Thule, Greenland, February-March, 1992: Vertical profiles, diurnal variation, and longer-term trends
 [HTN-95-00722] p 444 A95-86292
 Two dimensional stratospheric aerosol distributions during EASOE
 [HTN-95-00726] p 444 A95-86296
 Airborne measurements during the European Arctic Stratospheric Ozone Experiment column amounts of HNO3 and O3 derived from FTIR emission sounding
 [HTN-95-00742] p 445 A95-86312
 Airborne measurements during the European Arctic Stratospheric Ozone Experiment: Observation of OClO
 [HTN-95-00745] p 445 A95-86315
 Airborne measurements during the Arctic stratospheric experiment: Observation of O3 and NO2
 [HTN-95-00748] p 445 A95-86318
 Airplane icing research at the Boeing Company: Participation in the second Canadian Atlantic Storms Program
 p 674 A95-93544
 The 1992-3 operational winter forecasting experiment for Stapleton airport
 p 677 A95-93561
- WIRE**
 SEM representation of the early and late time fields scattered from wire targets
 [BTN-94-EIX94381353142] p 306 A95-74496
 Reliability assessment of Multichip Module technologies via the Triservice/NASA RELTECH program
 p 245 N95-20643
- WIRELESS COMMUNICATION**
 Use of MOBITEK wireless wide area networks as a solution to land-based positioning and navigation
 [BTN-94-EIX94441386132] p 189 A95-68188
- WIRING**
 Aircraft wiring maintenance: Development of a computerized maintenance aid
 [SAE PAPER 932615] p 456 A95-90080
 Problems with aging wiring in Naval aircraft
 p 154 N95-16048
 Partial discharge testing of high voltage wiring harness for airborne displays
 [AD-A289150] p 401 N95-27003

AH-1F COBRA rewire program MANPRINT analysis
[AD-A289190] p 391 N95-27018
Development of LaRC (TM): IA thermoplastic polyimide
coated aerospace wiring
[NASA-CR-195048] p 537 N95-30252

WOOD

Development of processes, means, and theoretical
principles of thin-walled detail plastic forming at Kazan
Aviation Institute p 155 N95-16281

WORDS (LANGUAGE)

Conversion of the TRACON operations concepts
database into a formal sentence outline job task
taxonomy
[DOT/FAA/AM-95/16] p 488 N95-28819

WORKING FLUIDS

Dissolved gas - the hidden saboteur
[SAE PAPER 931404] p 628 A95-93674
Malone-brayton cycle engine/heat pump
[AD-D016573] p 244 N95-20295

WORKLOADS (PSYCHOPHYSIOLOGY)

Programmable cockpit research simulator
[AD-A279219] p 204 N95-19848
Integrated mission precision attack cockpit technology
(IMPACT). Phase - 1. Identifying technologies for
air-to-ground fighter integration
[AD-A289562] p 389 N95-26684
Full span flaperons for a biplane p 391 N95-26954

WORKSTATIONS

Parallel CFD design on network-based computer
[AIAA PAPER 95-0984] p 565 A95-90656
Developing and testing decision-making products for
center weather service unit meteorologists
p 671 A95-93533

A workstation based simulator for teaching compressible
aerodynamics
[NASA-TM-106799] p 170 N95-16906

Operational And Supportability Implementation System
(OASIS) test and evaluation master plan
[AD-A284765] p 126 N95-18088

An evaluation of Automatic Terminal Information Service
(ATIS) flight deck display presentation options
[AD-A280100] p 228 N95-21020

A study of workstation computational performance for
real-time flight simulation
[NASA-TM-109184] p 449 N95-27241

Developing a workstation-based, real-time simulation for
rapid handling qualities evaluations during design
[NASA-CR-198831] p 505 N95-30335

Synthetic Terrain Imagery for Helmet-Mounted Display.
Volume 2: Software design document
[AD-A293611] p 612 N95-31655

WOVEN COMPOSITES

Idealized textile composites for experimental/analytical
correlation p 301 N95-23277

Development of stitched/RTM composite primary
structures p 425 N95-28469

Novel cost controlled materials and processing for
primary structures p 532 N95-28830

Cross-stiffened continuous fiber structures p 536 N95-29041

X**X RAY ASTRONOMY**

Integrated X-ray testing of the electro-optical breadboard
model for the XMM reflection grating spectrometer
[DE95-008829] p 644 N95-30507

X RAY INSPECTION

POD assessment of NDI procedures using a round robin
test
[AGARD-R-809] p 315 N95-23602

Emerging nondestructive inspection for aging aircraft
[PB95-143053] p 328 N95-25401

X RAY SPECTROSCOPY

Integrated X-ray testing of the electro-optical breadboard
model for the XMM reflection grating spectrometer
[DE95-008829] p 644 N95-30507

X RAYS

Test and Evaluation Plan (TEP) for Improvised Explosive
Device Screening Systems (IEDSS)
[AD-A286382] p 227 N95-22319

Integrated X-ray testing of the electro-optical breadboard
model for the XMM reflection grating spectrometer
[DE95-008829] p 644 N95-30507

X WING ROTORS

Wall interaction effects for a full-scale helicopter rotor
in the NASA Ames 80- by 120-foot wind tunnel
p 121 N95-19270

Vibration reduction in helicopter rotors using an actively
controlled partial span trailing edge flap located on the
blade p 624 N95-32111

X-14 AIRCRAFT

Design of a model following, state variable feedback
controller for the X-14 VTOL aircraft
[HTN-94-00685] p 16 A95-60168

X-29 AIRCRAFT

X-29 high-angle-of-attack
[BTN-94-EIX94511309383] p 127 A95-64609

Numerical simulation of steady and unsteady,
vorticity-dominated aerodynamic interference
[BTN-95-EIX95062487524] p 186 A95-69232

X-29 high AOA flight test results: An overview
[SAE PAPER 931367] p 586 A95-93648

Flow-visualization study of the X-29A aircraft at high
angles of attack using a 1/48-scale model
[NASA-TM-104268] p 8 N95-10858

Integration of a mechanical forebody vortex control
system into the F-15 p 72 N95-14258

Flight evaluation of pneumatic forebody vortex control
in post-stall flight p 72 N95-14259

In-flight lift-drag characteristics for a forward-swept wing
aircraft and comparisons with contemporary aircraft
[NASA-TP-3414] p 117 N95-18565

Flight test of the X-29A at high angle of attack: Flight
dynamics and controls
[NASA-TP-3537] p 284 N95-22806

X-29 flight control system: Lessons learned
p 622 N95-32001

Flight evaluation of forebody vortex control in post-stall
flight p 609 N95-32003

X-31 AIRCRAFT

Aero-Space Plane: Flexible access to space
[NASA-TM-109904] p 22 N95-10553

X-31 resource tape
[NASA-TM-104300] p 13 N95-10745

X-31 tailless testing
[NASA-TM-104306] p 13 N95-10751

High-angle-of-attack yawing moment asymmetry of the
X-31 aircraft from flight test
[NASA-CR-186030] p 13 N95-11410

Water tunnel flow visualization study of a 4.4 percent
scale X-31 forebody
[NASA-TM-104276] p 36 N95-11898

Comparison of X-31 flight, wind-tunnel, and water-tunnel
yawing moment asymmetries at high angles of attack
p 68 N95-14234

Parameter identification for X-31A at high angles of
attack p 69 N95-14235

Validation of the NASA Dryden X-31 simulation and
evaluation of mechanization techniques
p 69 N95-14236

Free-to-roll tests of X-31 and F-18 subscale models with
correlation to flight test results p 69 N95-14237

X-31 post-stall envelope expansion and tactical utility
testing p 70 N95-14242

X-31 quasi-tailless flight demonstration
p 70 N95-14243

X-31 high angle of attack control system performance
p 70 N95-14244

Evaluation of proposed agility metrics using X-31 vs.
F/A-18 flight data
[AD-A292573] p 502 N95-28977

X-31: A program overview and flight test status
p 609 N95-32013

Y**YAG LASERS**

Research instrumentation for polytechnic university's
supersonic wind tunnel facility
[AD-A290232] p 523 N95-29468

YAKOVLEV AIRCRAFT

Assessment of Russian VSTOL technology evaluating
the YAK-38 'FORGER' and YAK-141 'FREESTYLE'
p 497 A95-90868

YAW

Forebody flow control on a full-scale F/A-18 aircraft
[BTN-95-EIX95152582333] p 281 A95-73535

Method for the prediction of the onset of wing rock
[BTN-95-EIX95152582342] p 282 A95-73544

Experimental performance of a ventral nozzle with pitch
and yaw vectoring capability for SSTOVL aircraft
[SAE PAPER 931412] p 614 A95-93678

Comparison of full-scale, small-scale, and CFD results
for F/A-18 forebody slot blowing p 72 N95-14255

Preparations for flight research to evaluate actuated
forebody strakes on the F-18 high-alpha research
vehicle p 72 N95-14257

Development of a multicomponent force and moment
balance for water tunnel applications, volume 2
[NASA-CR-4642-VOL-2] p 161 N95-18956

Effects of yaw and pitch motion on model attitude
measurements
[NASA-TM-4641] p 250 N95-22109

Feedback control laws for highly maneuverable
aircraft
[NASA-CR-197944] p 295 N95-23410

Axial loads on yawed rotors
[PB95-214193] p 592 N95-30638

YAWING MOMENTS

Forebody flow control on a full-scale F/A-18 aircraft
[BTN-95-EIX95152582333] p 281 A95-73535

Computational analysis of forebody tangential slot
blowing on the high alpha research vehicle
[NASA-CR-196750] p 10 N95-11367

High-angle-of-attack yawing moment asymmetry of the
X-31 aircraft from flight test
[NASA-CR-186030] p 13 N95-11410

Numerical analysis of tangential slot blowing on a generic
chined forebody
[NASA-TM-108845] p 37 N95-11927

Comparison of X-31 flight, wind-tunnel, and water-tunnel
yawing moment asymmetries at high angles of attack
p 68 N95-14234

Validation of the NASA Dryden X-31 simulation and
evaluation of mechanization techniques
p 69 N95-14236

Static and dynamic force/moment measurements in the
Eidetics water tunnel p 69 N95-14238

Computational analysis of forebody tangential slot
blowing p 71 N95-14253

Comparison of full-scale, small-scale, and CFD results
for F/A-18 forebody slot blowing p 72 N95-14255

Flight evaluation of pneumatic forebody vortex control
in post-stall flight p 72 N95-14259

Static aerodynamics CFD analysis for 120-mm
hypersonic KE projectile design
[ARL-MR-184] p 118 N95-18611

Development of a multicomponent force and moment
balance for water tunnel applications, volume 1
[NASA-CR-4642-VOL-1] p 161 N95-18955

Sailplane glide performance and control using fixed and
articulating winglets
[NASA-CR-198579] p 392 N95-27180

YIELD POINT

Fatigue life until small cracks in aircraft structures:
Durability and damage tolerance p 135 N95-19478

YTTRIA-STABILIZED ZIRCONIA

The effect of interface properties on nickel base alloy
composites
[NASA-CR-198363] p 629 N95-30787

YTTRIUM

Evolution of oxidation and creep damage mechanisms
in HIPed silicon nitride materials
[DE95-001360] p 300 N95-22689

YTTRIUM OXIDES

Thermal testing of high performance thermal barrier
coatings for turbine blades p 202 N95-19681

Z**ZERO ANGLE OF ATTACK**

Effects of a forward-swept front rotor on the flowfield
of a counterrotation propeller
[NASA-TM-106671] p 7 N95-10148

Increments in aerofoil lift coefficient at zero angle of
attack and in maximum lift coefficient due to deployment
of a plain trailing-edge flap, with or without a leading-edge
high-lift device, at low speeds
[ESDU-94028] p 477 N95-28885

Increments in aerofoil lift coefficient at zero angle of
attack and in maximum lift coefficient due to deployment
of a trailing-edge split flap, with or without a leading-edge
high-lift device, at low speeds
[ESDU-94029] p 479 N95-29129

Increments in aerofoil lift coefficient at zero angle of
attack and in maximum lift coefficient due to deployment
of various leading-edge high-lift devices at low speeds
[ESDU-94027] p 481 N95-29898

Introduction to the estimation of the lift coefficients at
zero angle of attack and at maximum lift for aerofoils with
high-lift devices at low speeds
[ESDU-94026] p 481 N95-29899

Introduction to the estimation of the lift coefficients at
zero angle of attack and at maximum lift for aerofoils with
high-lift devices at low speeds
[ESDU-94026] p 481 N95-29899

Introduction to the estimation of the lift coefficients at
zero angle of attack and at maximum lift for aerofoils with
high-lift devices at low speeds
[ESDU-94026] p 481 N95-29899

ZINC ALLOYS

Cadmium plating replacements p 631 N95-31773

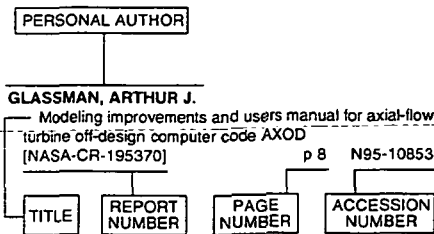
ZIRCONIUM OXIDES

Quality optimization of thermally sprayed coatings
produced by the JP-5000 (HVOF) gun using mathematical
modeling p 152 N95-19008

Thermal testing of high performance thermal barrier
coatings for turbine blades p 202 N95-19681

Thermal conductivity of zirconia thermal barrier
coatings p 345 N95-26133

Typical Personal Author Index Listing



Listings in this index are arranged alphabetically by personal author. The title of the document is used to provide a brief description of the subject matter. The report number helps to indicate the type of document (e.g., NASA report, translation, NASA contractor report). The page and accession numbers are located beneath and to the right of the title. Under any one author's name the accession numbers are arranged in sequence.

A

AARONSON, PHILIP
CFD optimization of a theoretical minimum-drag body [BTN-95-EIX95182619234] p 308 A95-76660

AARONSON, PHILIP G.
Supersonic transport grid generation, validation, and optimization [NASA-CR-197752] p 448 N95-26648

AARTS, H.
Integrated X-ray testing of the electro-optical breadboard model for the XMM reflection grating spectrometer [DE95-008829] p 644 N95-30507

ABACOUKIN, K.
Meteorological impacts on airport noise prediction by the 'Integrated Noise Model' application based on Hamiltonian Ray-Tracing program and measurements p 571 A95-88467

ABBAS, H.
Reaction-time response of aircraft crash [BTN-95-EIX95292721296] p 595 A95-92626

ABBASCHIAN, REZA
Innovative processing of composites for ultra-high temperature applications, book 1 [AD-A290889] p 537 N95-29842

ABBOTT, DAVID W.
User type certification for advanced flight control systems p 699 N95-34772

ABBOTT, TERENCE S.
A crew-centered flight deck design philosophy for High-Speed Civil Transport (HSCT) aircraft [NASA-TM-109171] p 335 N95-24582

ABBOTT, TROY D.
Flight validation of ground-based assessment for control power requirements at high angles of attack p 70 N95-14246

ABBUD-MADRID, A.
Stationary premixed flames in spherical and cylindrical geometries [HTN-95-42336] p 418 A95-86165

ABDOL-HAMID, KHALED S.
Application of Navier-Stokes code PAB3D with kappa-epsilon turbulence model to attached and separated flows [NASA-TP-3480] p 224 N95-21338

ABDUL NOUR, BASHAR S.
Hybrid laminar flow over wings enhanced by continuous boundary layer suction [SAE PAPER 931386] p 587 A95-93662

ABE, TAKASHI
Thermochemical nonequilibrium viscous shock-layer analysis for a Mars aerocapture vehicle [BTN-95-EIX95082502732] p 239 A95-70139
Reentry technology experiment on the first mission of reentry capsule 'EXPRESS' p 414 A95-82499
How 'HITEN's' aerobraking experiments were carried out p 415 A95-82553
Aero-thermodynamic flight environment at HITEN aerobrake experiment p 415 A95-82554
Viscous shock-layer analysis on hypersonic flow over reentry capsule with nonequilibrium chemistry [ISAS-656] p 436 N95-26739
Wind tunnel experiments on wake flow field behind a reentry capsule from a viewpoint of parachute deployment at supersonic speeds [ISAS-655] p 374 N95-26740
Transonic, supersonic and hypersonic wind-tunnel tests on aerodynamic characteristics of reentry body with blunted cone configuration [ISAS-658] p 480 N95-29640
Experimental studies on boundary-layer transition on a reentry vehicle at transonic and supersonic speeds [ISAS-659] p 555 N95-29712

ABEL, JONATHAN
On the exact solutions of pseudorange equations [BTN-95-EIX95142555477] p 278 A95-73433

ABELOFF, PATRICIA A.
Numerical simulation of powered-lift flows [HTN-94-00700] p 3 A95-60179

ABEYOUNIS, W. K.
16-foot transonic tunnel test section flowfield survey [NASA-TM-109157] p 238 N95-20669

ABLETT, R.
An investigation of piloting strategies for engine failures during takeoff from offshore platforms [HTN-95-92834] p 497 A95-90752

ABLETT, R. M.
Airborne collision avoidance systems - The UK experience [CONGRESS PAPER C428-7-146] p 488 A95-91687

ABRAHAM, JACOB
The Advanced Avionics Subsystem Technology Demonstration Program p 234 N95-20636

ABRAHAMSSON, S.
Scattering of short em-pulses by simple and complex targets using impulse radar p 486 A95-90953

ABSIL, L. H. J.
Experiments in the trailing edge flow of an NLR 7702 airfoil p 110 N95-17853

ABUMERI, G. H.
Analysis of aircraft engine blade subject to ice impact p 407 N95-28277

ABUMERI, GALIB
Technology Benefit Estimator (T/BEST): User's manual [NASA-TM-106785] p 167 N95-19501

ABUSALI, P. A. M.
Thermal force modeling for global positioning system satellites using the finite element method [BTN-95-EIX95152583270] p 278 A95-73571

ACEVES, S. M.
A hybrid vehicle evaluation code and its application to vehicle design. Revision 1 [DE95-008053] p 441 N95-28029
A hybrid vehicle evaluation code and its application to vehicle design, revision 2 [DE95-008060] p 441 N95-28139

ACHARYA, A.
Airborne rotary air separator study [NASA-CR-189099] p 290 N95-24053

ACKERS, DEANE E.
Design, analysis and control of large transports so that control of engine thrust can be used as a back-up of the primary flight controls [NASA-CR-198958] p 518 N95-30254

ACTIS, RICARDO L.
Elastic-plastic models for multi-site damage p 92 N95-14454

ADAMOV, N. P.
Separation of winged vehicles in supersonics [AIAA PAPER 95-6092] p 526 A95-88601

ADAMOVSKY, GRIGORY
The 1994 Fiber Optic Sensors for Aerospace Technology (FOSAT) Workshop [NASA-CP-10166] p 337 N95-24207

ADAMS, DANIEL O.
Idealized textile composites for experimental/analytical correlation p 301 N95-23277

ADAMS, RICHARD J.
Design of nonlinear control laws for high-angle-of-attack flight [BTN-94-EIX94511433920] p 141 A95-64586
Psycho-social safety perceptions: Helicopters as a case study p 596 A95-95192

ADAMS, WILLIAM M., JR.
Design and multifunction tests of a frequency domain-based active flutter suppression system [BTN-95-EIX95182619215] p 292 A95-76641

ADELFGANG, S. I.
Ascent wind model for launch vehicle design [BTN-95-EIX95041503799] p 239 A95-70124

ADELMAN, HENRY G.
Experimental and analytical investigations of wave enhanced supersonic combustors [AIAA PAPER 89-2787] p 14 A95-60172

ADELMAN, HOWARD M.
Integrated aerodynamic/dynamic/structural optimization of helicopter rotor blades using multilevel decomposition [NASA-TP-3465] p 285 N95-22953

ADKISSON, LORI
Identification of Artificial Intelligence (AI) applications for maintenance, monitoring, and control of airway facilities [AD-A282479] p 125 N95-17373

ADLER, ROBERT F.
Microwave and infrared simulations of an intense convective system and comparison with aircraft observations [HTN-95-60511] p 214 A95-68762

AFANAS'EV, I. V.
New approach to geometric profiling of the design elements of the passage part in turbo-machines [BTN-94-EIX94461408769] p 153 A95-63652

AGANOVIC, Z.
New filtering method for linear weakly coupled stochastic systems [BTN-95-EIX0608952736485] p 678 A95-92708

AGARWAL, R. K.
Aeromechanics technology, volume 1. Task 1: Three-dimensional Euler/Navier-Stokes Aerodynamic Method (TEAM) enhancements [AD-A285713] p 132 N95-18483
Transonic wind tunnel boundary interference correction p 147 N95-19271

AGARWALA, V. S.
Corrosion detection and monitoring of aircraft structures: An overview p 303 N95-23515

AGOSTA-GREENMAN, ROXANA M.
Computational analysis of forebody tangential slot blowing p 71 N95-14253

AGOSTA, ROXANA M.
Numerical analysis of tangential slot blowing on a generic chined forebody [NASA-TM-108845] p 37 N95-11927

AGRAWAL, S.
Simple numerical criterion for vortex breakdown [HTN-95-61210] p 541 A95-87583

AGRELL, JOHAN
Transonic and supersonic flowfield measurements about axisymmetric afterbodies for validation of advanced CFD codes p 121 N95-19260

AGRELL, NADA
Computational simulations for some tests in transonic wind tunnels p 164 N95-19264

AHARRAH, RALPH
The process for addressing the challenges of aircraft pilot coupling p 597 N95-31063

A 907

AHLRICH, RANDY C.

Marginal aggregates in flexible pavements: Background survey and experimental plan [DOT/FAA/CT-94/58] p 53 N95-12216

AHMAD, J. U.

Navier-Stokes simulation of rotor-body flowfield in hover using overset grids [PAPER C15] p 1 A95-60160

AHMED, M.

A study of the savings in time and fuel to aviation through the use of upper-air wind forecasts p 672 A95-93538
Creating a global climatology of freezing rain using numerical model output p 673 A95-93541

AHMED, N. A.

Novel implements of optical diagnostic techniques for aerospace applications [CONGRESS PAPER C428-21-081] p 550 A95-91726

AHMED, S.

Reattachment studies of an oscillating airfoil dynamic stall flowfield [HTN-95-51660] p 432 A95-85042

AHMED, SAAD A.

Cooling of aerospace plane using liquid hydrogen and methane [BTN-95-EIX0619952748171] p 590 A95-94465

AHN, JONG WOO

Prediction of two-dimensional momentumless wake by k-epsilon-gamma model [BTN-95-EIX95262694299] p 434 A95-85470

AHUJA, K. K.

Screach tones from free and ducted supersonic jets [HTN-95-51647] p 432 A95-85029

Temperature effects on acoustic interactions between altitude test facilities and jet engine plumes [NASA-CR-197638] p 258 N95-21170

Effects of cavity dimensions, boundary layer, and temperature on cavity noise with emphasis on benchmark data to validate computational aeroacoustic codes [NASA-CR-4653] p 361 N95-24879

AIBEL, DAVID W.

New technologies for space avionics [NASA-CR-197574] p 150 N95-18196

AIHARA, YASUHIKO

Experimental investigation on aerothermodynamic characteristics of hypersonic transport p 473 A95-91525

AITCHISON, D. R.

Development of an intelligent tool-condition monitoring system for FMS [CONGRESS PAPER C428-32-012] p 583 A95-93617

AIZAWA, YASUTAKA

A design of a robust scheduled autopilot p 516 A95-91532

A design of a self-learning robust scheduled autopilot p 516 A95-91533

AKIBA, RYOJIRO

Atmospheric reentry flight test of winged space vehicle p 414 A95-82483

Development and flight results of fiber reinforced balloon p 384 A95-82511

AKIMOTO, TOSHIO

NAL aerothermodynamic probing and CFD verification mission in OREX experiment p 368 A95-82413

AKIYAMA, HIROMITSU

Polar Patrol Balloon [BTN-95-EIX95152582318] p 316 A95-73521

AKIYAMA, M.

Polar Patrol Balloon system and preliminary experimental results p 368 A95-82513

AL-GARNI, AHMED Z.

Analytical solution for controls, heats, and states of flight trajectories [BTN-95-EIX95152583286] p 282 A95-73587

Cooling of aerospace plane using liquid hydrogen and methane [BTN-95-EIX0619952748171] p 590 A95-94465

ALAKSIN, P.

Flame-spreading phenomena in the fin-slot region of a solid rocket motor p 23 N95-10296

ALAVILLI, P.

Hypersonic Navier-Stokes computations about complex configurations p 644 A95-95497

ALBERS, STEVEN C.

ITWS gridded analysis p 654 A95-93455

ALBERSHEIM, STEVEN R.

Transitioning to the aviation routine weather report (METAR) and the International Aerodrome Forecast (TAF) within the Federal Aviation Administration p 656 A95-93461

ALBERTS, C. J.

Development of an Automated Nondestructive Inspection (ANDI) system for commercial aircraft, phase 1 [AD-A283500] p 40 N95-12623

ALBO, E. D.

Determining F-factor using ground-based Doppler radar: Validation and results p 11 N95-10571

ALBUS, J. S.

Overview of NASREM: The NASA/NBS standard reference model for telerobot control system architecture re [PB94-194560] p 58 N95-12854

ALDANA, JOSE F.

SUIT: The integration of aircraft subsystems [SAE PAPER 931381] p 604 A95-93657

ALEM, NABIH M.

A correlative investigation of simulated occupant motion and accident report in a helicopter crash [AD-A285190] p 123 N95-16404

Biodynamic simulation of pilot interaction with a helicopter multi-airbag restraint system [AD-A290196] p 485 N95-29057

ALEXANDER, KELLY

The OFF-6M transport jet [NASA-CR-197159] p 46 N95-12637

ALEXANDROV, NATALIA

Algorithms for bilevel optimization [NASA-CR-194980] p 170 N95-16897

ALEXOPOULOS, G. A.

Modeling of supersonic turbulent combustion using assumed probability density functions [BTN-95-EIX95112524190] p 206 A95-69318

ALGE, T. L.

Modern transport engine experience with environmental ingestion effects p 199 N95-19660

ALGER, T.

An Echelle Grating Spectrometer (EGS) for mid-IR remote chemical detection [DE94-019310] p 249 N95-21478

ALIAGA, D. A.

Convection heat transfer distributions over plates with square ribs from infrared thermography measurements [HTN-95-20713] p 435 A95-86603

ALIGHANBARI, H.

Postinstability behavior of a two-dimensional airfoil with a structural nonlinearity [BTN-95-EIX95152582337] p 266 A95-73539

ALKHOZAM, ABDULLAH M.

Interaction, bursting and control of vortices of a cropped double-delta wing at high angle of attack [AD-A283656] p 119 N95-18669

ALLAIRE, P. E.

Microgravity isolation system design: A case study [NASA-TM-106804] p 104 N95-17657

Microgravity isolation system design: A modern control synthesis framework [NASA-TM-106805] p 105 N95-18197

Microgravity isolation system design: A modern control analysis framework [NASA-TM-106803] p 105 N95-18486

ALLEN, C. B.

Central-difference and upwind-biased schemes for steady and unsteady Euler aerfoil computations [HTN-95-01094] p 469 A95-90280

ALLEN, CHRISTOPHER S.

On the scaling of small-scale jet noise to large scale [AIAA PAPER 92-02109] p 27 A95-60166

ALLEN, JERRY M.

Experimental study at low supersonic speeds of a missile concept having opposing wraparound tails [NASA-TM-4582] p 106 N95-16069

ALLEN, N. T.

Aircraft-borne, laser-induced fluorescence instrument for the in situ detection of hydroxyl and hydroperoxyl radicals [BTN-95-EIX95072499029] p 253 A95-71908

ALLES, W.

Automatic flight control system for an unmanned helicopter system design and flight test results p 622 N95-32004

ALLEW, CRISTOPHER S.

Aeracoustic probe design for microphone to reduce flow-induced self-noise [AIAA PAPER 93-4343] p 19 A95-60163

ALLGER, L.

Aerospace applications of new materials [CONGRESS PAPER C428-17-135] p 531 A95-91716

ALLISON, DENNIS O.

Application of two procedures for dual-point design of transonic airfoils [NASA-TP-3466] p 38 N95-12176

Airfoil modification effects on subsonic and transonic pressure distributions and performance for the EA-6B airplane [NASA-TP-3516] p 373 N95-26382

ALLISON, STEPHEN W.

Turbine-engine applications of thermographic-phosphor temperature measurements [DE95-003625] p 358 N95-25110

ALLMEN, J. R.

Modification of the Ames 40- by 80-foot wind tunnel for component acoustic testing for the second generation supersonic transport [NASA-TM-108850] p 65 N95-13642

ALM, NATHAN P.

Aviation weather education and the University of North Dakota aviation weather survey p 656 A95-93462

ALMAN, A. I.

Profiling of the working surface of electrodes-tools for circle electrochemical dimensional treatment of compressor blades [AD-A281580] p 127 N95-16171

ALMANZA, JOE

ADST system test report for the rotary wing aircraft aimed aeromodel and weapon model merge with the ATAC 2 baseline [AD-A281580] p 127 N95-16171

ALMOSINO, D.

Calculation of support interference in dynamic wind-tunnel tests p 122 N95-19282

ALMSTED, LARRY D.

Flight test evaluation of a 35 GHz forward looking altimeter for terrain avoidance [BTN-95-EIX95212641071] p 287 A95-76736

ALPERINE, S.

New Trends in coatings developments for turbine blades: Materials processing and repair p 201 N95-19676

ALTER, STEPHEN J.

Multiblock analysis for Shuttle Orbiter reentry heating from Mach 24 to Mach 12 [BTN-95-EIX95041503780] p 205 A95-69211

ALTMOM, ABDELAATI MUSTAFA

Criteria of forecasting low level wind shear over Qatar p 663 A95-93493

ALVAREZ, JAIME

The FC-1D: The profitable alternative Flying Circus Commercial Aviation Group [NASA-CR-197152] p 46 N95-12628

AMAGASA, S.

Study on the turbine vane and blade for a 1500 C class industrial gas turbine [BTN-94-EIX95011441254] p 431 A95-84211

AMANO, KANICH

Experimental study of the aerodynamic characteristics of the counter-rotation propellers p 474 A95-91562

AMANO, KANICHI

Wake velocity measurement of counter-rotation propellers p 474 A95-91563

AMATRUDO, GARY

Design and flight evaluation of an integrated navigation and near-terrain helicopter guidance system for night-time and adverse weather operations [NASA-TM-108837] p 11 N95-10846

AMBERKAR, S. S.

Design of a controller for a flexible pointing system using H(infinity) synthesis [AD-A286572] p 256 N95-20828

AMBUR, DAMODAR R.

Experimental evaluation of a box beam specifically tailored for chordwise deformation [BTN-95-EIX95182619088] p 283 A95-75773

Design and evaluation of a foam-filled hat-stiffened panel concept for aircraft primary structural applications [NASA-TM-109175] p 346 N95-26251

AMBERKAR, S. S.

Technology integration box beam failure study p 441 N95-28468

AMBERKAR, S. S.

Damage tolerance of a geodesically stiffened advanced composite structural concept for aircraft structural applications p 399 N95-28487

AMBERKAR, S. S.

Design and evaluation of a foam-filled hat-stiffened panel concept for aircraft primary structural applications p 502 N95-28841

AMBERKAR, S. S.

Technology integration box beam failure study p 552 N95-28847

AMDAHL, DAVID J.

Modeling aerodynamic problems using Smoothed Particle Hydrodynamics (SPH) [SAE PAPER 932512] p 465 A95-89185

AMEMIYA, TARO

Preliminary study on the fixed transition technique for a shock tube transonic airfoil flow [BTN-95-EIX95282705928] p 455 A95-89663

AMEMIYA, TARO

Fixed transition for shock tube transonic flow p 472 A95-91509

AMERI, A. A.

Grid orthogonality effects on predicted turbine midspan heat transfer and performance [NASA-TM-106931] p 554 N95-29371

AMES, FORREST E.

Experimental study of vane heat transfer and aerodynamics at elevated levels of turbulence [NASA-CR-4633] p 244 N95-19912

AMES, FORREST E.

Advanced k-epsilon modeling of heat transfer [NASA-CR-4679] p 648 N95-31423

- AMES, GREGORY H.**
Fiber-optic rotary joint with bundle collimator assemblies
[AD-D016504] p 258 N95-21673
- AMIDI, OMEAD**
Research on an autonomous vision-guided helicopter [AIAA PAPER 94-1240-CP] p 18 N95-11510
- AMIET, R. K.**
Airfoil leading-edge suction and energy conservation for compressible flow
[BTN-95-EIX95302730589] p 637 A95-94197
- AMINPOUR, MOHAMMAD A.**
A global/local analysis method for treating details in structural design p 552 N95-28848
- AMRANE, K.**
Second-law analysis of vapor compression heat pumps with solution circuit
[BTN-94-EIX95011441236] p 431 A95-84193
- AMSTUTZ, B. E.**
Influence of crack history on the stable tearing behavior of a thin-sheet material with multiple cracks p 93 N95-14467
- AN, MENG LIN**
Integrated design and manufacturing for the high speed civil transport
[NASA-CR-197183] p 48 N95-12700
- ANASTASSIU, HRISTOS T.**
Hybrid finite element-modal analysis of jet engine inlet scattering
[BTN-95-EIX95242673665] p 427 A95-82259
- ANDELMAN, RICH M.**
Cost model relationships between textile manufacturing processes and design details for transport fuselage elements p 536 N95-29043
- ANDERS, SCOTT G.**
The personal aircraft: Status and issues
[NASA-TM-109174] p 223 N95-20688
- ANDERSEN, T. T.**
Pressure and temperature distortion testing of a two-stage centrifugal compressor
[BTN-94-EIX95011441250] p 431 A95-84207
- ANDERSON, A.**
Description and flow characterization of hypersonic facilities
[AD-A284291] p 223 N95-20248
- ANDERSON, B. E.**
An analysis of aircraft exhaust plumes from accidental encounters
[HTN-95-70943] p 351 A95-78008
Meridional distributions of NO(X), NO(Y), and other species in the lower stratosphere and upper troposphere during AASE 2
[HTN-95-70944] p 352 A95-78009
- ANDERSON, BERNHARD H.**
A full Navier-Stokes analysis of subsonic diffuser of a bifurcated 70/30 supersonic inlet for high speed civil transport application
[NASA-TM-106637] p 8 N95-10820
Validation of the RPLUS3D code for supersonic inlet applications involving three-dimensional shock wave-boundary layer interactions
[NASA-TM-106579] p 39 N95-13058
Numerical simulation of supersonic compression corners and hypersonic inlet flows using the RPLUS2D code
[NASA-TM-106580] p 105 N95-16038
- ANDERSON, CHARLES R.**
The use of electrochemistry and ellipsometry for identifying and evaluating corrosion on aircraft
[AD-A290249] p 504 N95-29426
- ANDERSON, D.**
The NASA/UTA Center for hypersonic research
[AIAA PAPER 95-6106] p 520 A95-90438
- ANDERSON, DAVID N.**
Methods for scaling icing test conditions
[NASA-TM-106827] p 124 N95-19284
Ice accretion with varying surface tension
[NASA-TM-106826] p 124 N95-19285
- ANDERSON, DAVID T.**
Matrix isolated HF: the high-resolution infrared spectrum of a cryogenically solvated hindered rotor
[GTM-95-0301010494002231-16] p 578 A95-92210
- ANDERSON, ELGIN A.**
The effects of three-dimensional imposed disturbances on bluff body near wake flows: Effects of taper and splitter plates on the near wake characteristics of a circular cylinder in uniform and shear flow
[AD-A292113] p 477 N95-28921
- ANDERSON, FREDERICK**
Developing a workstation-based, real-time simulation for rapid handling qualities evaluations during design
[NASA-CR-198831] p 505 N95-30335
- ANDERSON, J. G.**
Aircraft-borne, laser-induced fluorescence instrument for the in situ detection of hydroxyl and hydroperoxyl radicals
[BTN-95-EIX95072499029] p 253 A95-71908
- The distribution of hydrogen, nitrogen, and chlorine radicals in the lower stratosphere: Implications for changes in O3 due to emission of NO(y) from supersonic aircraft
[HTN-95-70935] p 351 A95-78000
- ANDERSON, JAMES G.**
Development of techniques for the in situ observation of OH and HO2 for studies of the impact of high-altitude supersonic aircraft on the stratosphere
[NASA-CR-196759] p 61 N95-12832
- ANDERSON, JAY**
Aviation terminal forecasts based on automated observations (FTAUTO) p 668 A95-93520
- ANDERSON, M. B.**
Air data prediction from surface pressure measurements on guided munitions
[BTN-95-EIX95282706664] p 466 A95-89641
- ANDERSON, M. W.**
Flight test certification of primary category aircraft using TP101-41E sportplane design standard
[BTN-95-EIX0619952748184] p 606 A95-94477
- ANDERSON, MARK R.**
Drag function modeling for air traffic simulation
[BTN-95-EIX95182619154] p 279 A95-76631
- ANDERSON, MELVIN S.**
Buckling and vibration analysis of laminated panels using VICONOPT
[PAPER-1746] p 230 A95-72580
- ANDERSON, R. C.**
Two-dimensional imaging of OH in a lean burning high pressure combustor
[NASA-TM-106854] p 236 N95-21383
- ANDERSON, ROBERT L.**
Advanced tow placement of composite fuselage structure p 420 N95-28271
- ANDERSON, S.D.**
High heat sink fuels for improved aircraft thermal management
[SAE PAPER 932084] p 530 A95-91659
- ANDERSON, W. KYLE**
A grid generation and flow solution method for the Euler equations on unstructured grids
[HTN-95-20003] p 153 A95-63201
Numerical study to assess sulfur hexafluoride as a medium for testing multielement airfoils
[NASA-TP-3496] p 378 N95-28674
- ANDERSSON, BRODD LEIF**
Computation of transonic flow on composite overlapping grids in 2 D
[PB95-131348] p 248 N95-21132
- ANDERTON, GARY L.**
Additives in bituminous materials and fuel-resistant sealers
[DOT/FAA/CT-94/78] p 55 N95-12131
- ANDERTON, JAMES F.**
Stall precursor study of high frequency data for three high speed, swept compressor rotors
[AD-A289379] p 406 N95-26878
- ANDO, SHIGENORI**
Note on prediction of aerodynamic lift/drag ratio of WIG (Wing-In-Ground) at cruise
[BTN-95-EIX95282705925] p 467 A95-89665
- ANDO, YASUKATSU**
Preliminary tests of a transonic flutter control wing model p 499 A95-91566
- ANDO, YASUNORI**
An experimental study on interacting flow between supersonic flow and secondary flow injected normally through circular nozzle p 472 A95-91511
A study of supersonic mixing flow field with ramp injector p 706 N95-34512
- ANDRASTEK, DONALD A.**
Advanced subsonic airplane design and economic studies
[NASA-CR-195443] p 338 N95-24304
- ANDREA, MEINRAT O.**
An intercomparison of aircraft instrumentation for tropospheric measurements of carbonyl sulfide, hydrogen sulfide, and carbon disulfide
[HTN-95-91856] p 355 A95-80844
An intercomparison of instrumentation for tropospheric measurements of dimethyl sulfide: Aircraft results for concentrations at the parts-per-trillion level
[HTN-95-91857] p 355 A95-80845
- ANDRESEN, P.**
Planar air density measurements near model surfaces by ultraviolet Rayleigh/Raman scattering
[BTN-94-EIX94441386614] p 213 A95-67345
- ANDREW, M. J.**
The use of math-dynamic models to aid the development of integrated health and usage monitoring systems
[CONGRESS PAPER C428-19-079] p 457 A95-91720
- ANDREWS, C.**
Corrosion of aircraft materials: Correlation between nanometer scale and macroscopic structural damage parameters
[AD-A285930] p 241 N95-20299
- ANDREWS, EARL H.**
NASA's Hypersonic Research Engine Project: A review
[NASA-TM-107759] p 50 N95-12860
- ANDREWS, R. G.**
The effects of surface modification on fretting fatigue in Ti alloy turbine components p 404 A95-84909
- ANEMAAT, WILLIAM**
An easy way to analyze longitudinal and lateral-directional trim problems with AEO or OEI p 409 N95-26949
- ANGEVINE, WAYNE M.**
Comparison of wind profiler and aircraft wind measurements at Chebogue Point, Nova Scotia
[HTN-95-41833] p 353 A95-80559
- ANGRESEN, P.**
Planar air density measurements near model surfaces by ultraviolet Rayleigh/Raman scattering
[HTN-95-20950] p 546 A95-88989
- ANKENY, ALAN E.**
Evaluation of alternate F-14 wing lug coating
[AD-A283207] p 129 N95-17631
- ANNA, PAUL D.**
Flight test results of the F-16 aircraft modified with the axisymmetric vectored exhaust nozzle p 70 N95-14245
- ANNIGERI, BAL**
Small crack test program for helicopter materials p 92 N95-14455
- ANNIS, CHARLES**
Fatigue in single crystal nickel superalloys
[AD-A283459] p 56 N95-12546
Fatigue in single crystal nickel superalloys
[AD-A282917] p 88 N95-15415
Fatigue in single crystal nickel superalloys
[AD-A285727] p 152 N95-18068
- ANON**
Aircraft safety evaluation
[BTN-94-EIX94511309382] p 103 A95-64608
X-29 high-angle-of-attack
[BTN-94-EIX94511309383] p 127 A95-64609
Fiber-optic technology for transport aircraft
[BTN-94-EIX94511309384] p 103 A95-64610
Starter/generator testing
[BTN-95-EIX95072498877] p 210 A95-68393
National AeroSpace Plane: Technology transfer
[BTN-95-EIX95072498879] p 180 A95-68395
- ANSCHUETZ, ROBERT**
Advanced distributed simulation technology advanced rotary wing aircraft. System/segment specification. Volume 1: Simulation system module
[AD-A280238] p 20 N95-10350
Advanced distributed simulation technology advanced rotary wing aircraft. System/segment specification. Volume 2: Flight station module
[AD-A280432] p 20 N95-10352
Advanced distributed simulation technology advanced rotary wing aircraft. System/segment specification. Volume 5: Simulation system module AH-64D kit
[AD-A280433] p 20 N95-10353
Advanced distributed simulation technology advanced rotary wing aircraft. Software reusability report
[AD-A280434] p 20 N95-10354
ADST ARWA visual system module software design document
[AD-A283874] p 99 N95-14357
- ANSCHUETZ, ROBERT R., II**
Advanced distributed simulation technology advanced rotary wing aircraft. System/segment specification. Volume 3: Visual system module
[AD-A280239] p 20 N95-10351
- ANTAR, B. N.**
Study of heat transfer rates during quenching of a hot tube under microgravity p 428 A95-82641
- ANTAR, BASIL N.**
Low gravity quenching of hot tubes with cryogenics
[ISBN 1-879921-01-4] p 635 A95-93728
- ANTLEY, MICHAEL**
Assessing aircraft survivability to high frequency transient threats
[AD-A283999] p 134 N95-18726
- ANTON, D. J.**
RAF ejections - historical perspectives and future requirements
[CONGRESS PAPER C428-18-168] p 484 A95-91717
- ANTONIEWICZ, BOB**
Multi-application controls: Robust nonlinear multivariable aerospace controls applications p 71 N95-14249

- ANTONIK, PAUL**
Polarization diverse ultra-wideband antenna technology p 548 A95-90924
- AOKI, S.**
Study on the turbine vane and blade for a 1500 C class industrial gas turbine [BTN-94-EIX95011441254] p 431 A95-84211
- AOSHIMA, M.**
Dynamic behavior of valves with pneumatic chamber for reciprocating compressors [BTN-94-EIX94351143311] p 207 A95-65845
- AOYAMA, K.**
Study on the turbine vane and blade for a 1500 C class industrial gas turbine [BTN-94-EIX95011441254] p 431 A95-84211
- AOYAMA, TAKASHI**
Direct analysis of transonic rotor noise with CFD technique p 711 N95-34549
- APONSO, BIMAL L.**
Identification of higher order helicopter dynamics using linear modeling methods [HTN-95-80851] p 290 A95-75093
Proposed incorporation of mission-oriented flying qualities into MIL-STD-1797A [AD-A294211] p 698 N95-34306
- APOSTOLAKIS, G.**
Demonstration of the Dynamic Flowgraph Methodology using the Titan 2 Space Launch Vehicle Digital Flight Control System [NASA-CR-197517] p 150 N95-17493
- APPLEBY, J. W., JR.**
Jet engine applications for materials with nanometer-scale dimensions p 345 N95-26131
- APPLIN, ZACHARY T.**
Wing pressure distributions from subsonic tests of a high-wing transport model [NASA-TM-4583] p 272 N95-22802
- ARABSHAHI, ABDOLLAH**
Propulsion/airframe interference for ducted propfan engines with ground effect [NASA-CR-197110] p 81 N95-14909
- ARAI, K.**
Development of 70MW class superconducting generators [BTN-94-EIX95011440854] p 429 A95-82905
- ARAI, NORIO**
Heat transfer on bent-noise biconic in hypersonic flow p 639 A95-95394
A numerical investigation of flow around a square-section cylinder mounted with a splitter plate p 639 A95-95401
- ARAI, T.**
Turbulence characteristics of supersonic boundary layer past a backward facing step [AIAA PAPER 95-6126] p 470 A95-90447
- ARAI, TATSUO**
Design features of the NAL ramjet engine test facility p 410 A95-82319
- ARAKAWA, CHUICHI**
2-D and 3-D numerical simulation of a supersonic inlet flowfield p 641 A95-95457
- ARBOGAST, E.**
Nonhydrostatic simulation of frontogenesis in a moist atmosphere. Part 3: Thermal wind imbalance and rainbands [HTN-95-90356] p 212 A95-66429
- ARCHAMBAUD, J. P.**
Data from the GARTEur (AD) Action Group 02 airfoil CAST 7/DOA1 experiments p 111 N95-17856
OAT15A airfoil data p 111 N95-17857
Analysis of test section sidewall effects on a two dimensional airfoil: Experimental and numerical investigations p 165 N95-19276
- ARDEMA, MARK D.**
Optimal trajectories for hypersonic launch vehicles [HTN-95-61120] p 415 A95-84884
- ARENA, A. S., JR.**
Directional control at high angles of attack using blowing through a chined forebody [BTN-95-EIX0619952748179] p 619 A95-94472
- ARENA, ANDREW S., JR.**
Experimental investigations on limit cycle wing rock of slender wings [BTN-95-EIX95062487543] p 185 A95-68357
- ARENDRY, CORY**
Bending effects of unsymmetric adhesively bonded composite repairs on cracked aluminum panels p 92 N95-14456
- ARIARATHNAM, S. T.**
Lyapunov exponents and stochastic stability of two-dimensional parametrically excited random systems [BTN-94-EIX94361122401] p 207 A95-65897
- ARIOTTI, SCOTT**
Cabin-fuselage-wing structural design concept with engine installation [NASA-CR-197172] p 49 N95-12993
- ARKLEY, LARRY E.**
Modeling F/A-18 flight hour program costs using regression analysis [AD-A293771] p 608 N95-31579
- ARNAL, D.**
Shock layers and boundary layers in hypersonic flows [HTN-95-A0003] p 183 A95-67830
- ARNETTE, STEPHEN A.**
Effects of expansions on a supersonic boundary layer: Surface pressure measurements [BTN-95-EIX95142553036] p 263 A95-73462
- ARNOLD, F.**
Laplace interaction law for the computation of viscous airfoil flow in low- and high-speed aerodynamics [BTN-95-EIX95142553037] p 263 A95-73461
An overview of the EASOE campaign [HTN-95-00702] p 443 A95-86272
- ARNOLD, JACK H.**
Photovoltaic electric power applied to Unmanned Aerial Vehicles (UAV) p 245 N95-20530
- ARONE, R.**
Prediction of fatigue crack growth under constant amplitude and random loading using specimens with multiple cracks [AD-A291614] p 397 N95-28409
- ARRIETA, RODOLFO T.**
MOAMAP: A model that combines several different kinds of aircraft operations p 32 N95-11323
- ARRINGTON, E. ALLEN**
Flow quality improvements in the NASA Lewis Research Center 9- by 15-foot Low Speed Wind Tunnel [NASA-CR-195439] p 627 N95-31653
- ARTS, TONY**
Aerodynamic investigation of the flow field in a 180 deg turn channel with sharp bend p 163 N95-19257
- ASAI, KEISUKE**
Similarity rule for jet-temperature effects on transonic base pressure [BTN-95-EIX95222650791] p 329 A95-79247
- ASAI, SHIGERU**
On the flight control system for UF-104 p 507 A95-91560
- ASBURY, SCOTT C.**
Two-dimensional converging-diverging rippled nozzles at transonic speeds [NASA-TP-3440] p 6 N95-10129
The personal aircraft: Status and issues [NASA-TM-109174] p 223 N95-20688
- ASCOLI, EDWARD P.**
CFD analysis of turbopump volutes p 312 N95-23436
- ASGHAR, A.**
Suppression of vortex asymmetry and side force on a circular cone [BTN-95-EIX95042474413] p 209 A95-68287
- ASHBY, DALE L.**
Unsteady panel method for flows with multiple bodies moving along various paths [HTN-95-61203] p 540 A95-87576
- ASHDOWN, A. M.**
The application of Ada and formal methods to a safety critical engine control system p 710 N95-33142
- ASHILL, P. R.**
The use of hot film for the investigation of boundary-layer transition [CONGRESS PAPER C428-9-199] p 475 A95-91697
Investigation of the flow over a series of 14 percent-thick supercritical aerofoils with significant rear camber p 109 N95-17849
Boundary-flow measurement methods for wall interference assessment and correction: Classification and review p 163 N95-19262
A theoretical and experimental investigation of the flow over supersonic leading edge wing/body configurations [DRA-TM-AERO-PROP-41] p 331 N95-25649
- ASHRAFIJON, H.**
Design optimization of aircraft engine-mount systems. [BTN-94-EIX94351143325] p 195 A95-67298
- ASLAN, A. R.**
Aerodynamic characteristics of external store configurations at low speeds [BTN-95-EIX95182619230] p 271 A95-76656
- ASO, SHIGERU**
Numerical simulation of unsteady aerodynamic heating induced by shock reflections p 428 A95-82418
A study on aerodynamic heating phenomena in three-dimensional shock wave/turbulent boundary layer interaction induced by sweptback sharp fins at supersonic flow p 428 A95-82419
Numerical experiments on aerodynamic heating mechanism in shock reflection processes p 471 A95-91497
An experimental study on interacting flow between supersonic flow and secondary flow injected normally through circular nozzle p 472 A95-91511
- A study of supersonic mixing flow field with ramp injector p 706 N95-34512
Numerical simulations of dynamic stall phenomena in low speed flows p 685 N95-34546
- ASOK, RAY**
Output feedback control under randomly varying distributed delays [BTN-94-EIX94511433916] p 168 A95-64582
- ASWATHA NARAYANA, P. A.**
Boundary layer studies over an S-blade [HTN-95-92261] p 434 A95-85305
- ATALLA, N.**
Geometrical acoustics approach for calculating the effects of flow on acoustics scattering [BTN-94-EIX94321331207] p 61 A95-60790
- ATALLA, NOUREDDINE**
Coupled FEM-BEM approach for mean flow effects on vibro-acoustic behavior of planar structures [BTN-95-EIX95152577587] p 263 A95-73495
- ATASSI, H. M.**
Unsteady aerodynamics of vortical flows: Early and recent developments p 462 A95-88896
- ATASSI, HAFIZ M.**
The pressure field of a gust interacting with a flat plate p 557 N95-30161
- ATCHA, H.**
Novel implements of optical diagnostic techniques for aerospace applications [CONGRESS PAPER C428-21-081] p 550 A95-91726
- ATCHISON, M. KEVIN**
Development of a climatological data base to help forecast cloud cover conditions for shuttle landings at the Kennedy Space Center p 670 A95-93529
- ATHAVALE, M. M.**
Numerical analysis of intra-cavity and power-stream flow interaction in multiple gas-turbine disk-cavities [NASA-TM-106886] p 407 N95-28344
- ATHAVALE, MAHESH**
Comparison of numerical results and multicavity purge and rim seal data with extensions to dynamics [NASA-TM-106685] p 416 N95-27434
- ATHRE, K.**
Unbalance response of a dual rotor system: Theory and experiment [BTN-94-EIX94351143320] p 195 A95-65854
- ATKINS, H.**
Nonreflective boundary conditions for high-order methods [HTN-95-42328] p 371 A95-86157
- ATKINSON, R. M.**
Fault Diagnosis for condition monitoring applied to hydraulic circuits [CONGRESS PAPER C428-12-165] p 456 A95-91703
- ATLAS, E. L.**
Estimates of total organic and inorganic chlorine in the lower stratosphere from in situ and flask measurements during AASE 2 [HTN-95-A0861] p 317 A95-76265
- ATLURI, S. N.**
A FEAM based methodology for analyzing composite patch repairs of metallic structures p 394 N95-27511
- ATLURI, SATYA N.**
Growth of multiple cracks and their linkup in a fuselage lap joint [BTN-95-EIX95142553047] p 286 A95-73451
Residual life and strength estimates of aircraft structural components with MSD/MED p 136 N95-19485
- ATLURIS, SATYA N.**
Structural integrity of fuselage panels with multisite damage [BTN-95-EIX0619952748188] p 637 A95-94250
- ATTAR, MOSHE**
Lavi flight control system: Design requirements, development and flight test results p 621 N95-31994
- ATTENBOROUGH, KEITH**
Proceedings of the Sixth International Symposium on Long-Range Sound Propagation [AD-A290920] p 580 N95-30084
- ATTIA, M.**
Nonlinear dynamic simulation of single- and multipool core engines, part 1: Computational method [BTN-95-EIX95112524200] p 210 A95-69308
GETRAN: A generic, modularly structured computer code for simulation of dynamic behavior of aero- and power generation gas turbine engines [BTN-94-EIX95011441241] p 431 A95-84198
- ATWOOD, CHRISTOPHER**
The coupling of fluids, dynamics, and controls on advanced architecture computers [NASA-CR-197727] p 360 N95-25797
- ATWOOD, DAVID H.**
Vapor lock studies for gasolines with ethers [SAE PAPER 931233] p 529 A95-88962

B

- Ongoing research into high octane unleaded avgas
[SAE PAPER 931234] p 529 A95-88963
- AUBERT, S.**
Numerical simulation of the 3D turbulent flow around the combustor dome of an aircraft engine p 640 A95-95423
- AUBIN, BRUCE**
Maintenance programs [HTN-95-92310] p 365 A95-85354
- AUDEBERT, M.**
Balloon flights in France and in Europe p 204 A95-66301
- AUDONE, B.**
Electromagnetic compatibility effects of advanced packaging configurations p 247 N95-20658
- AUGUST, GERALD**
Tactical low-level helicopter communications p 702 N95-32492
- AULT, D. A.**
Experimental and computational results for the external flowfield of a scramjet inlet [BTN-94-EIX94441380977] p 195 A95-68161
Hypersonic shock wave/turbulent boundary layer interactions in the vicinity of an expansion corner [AIAA PAPER 95-6125] p 469 A95-90446
- AUPOIX, B.**
Shock layers and boundary layers in hypersonic flows [HTN-95-A0003] p 183 A95-67830
- AUSLENDER, A. H.**
Optimization of contoured hypersonic scramjet inlets with a least-squares parabolized Navier-Stokes procedure [HTN-95-20976] p 261 A95-74042
- AUSLENDER, AARON H.**
Numerical study of the performance of swept, curved compression surface scramjet inlets [BTN-95-EIX95112524198] p 197 A95-69310
Experimental investigation of inlet-combustor isolators for a dual-mode scramjet at a Mach number of 4 [NASA-TP-3502] p 407 N95-28343
- AUSTIN, FRED**
Static shape control for adaptive wings [HTN-95-A1767] p 627 A95-93330
- AUSTIN, JEFFREY G.**
Mach number, flow angle, and loss measurements downstream of a transonic fan-blade cascade [AD-A280907] p 108 N95-16824
- AVALLONE, LINNEA MARIE**
In situ measurements of ClO and implications for the chemistry of inorganic chlorine in the lower stratosphere p 563 N95-29830
- AVERY, W. B.**
Tension fracture of laminates for transport fuselage. Part 1: Material screening p 398 N95-28471
Impact damage resistance of composite fuselage structure, part 1 p 399 N95-28482
- AVIS, DANIEL**
The Elite: A high speed, low-cost general aviation aircraft for Aeroworld [NASA-CR-197161] p 45 N95-12530
- AWE, CYNTHIA A.**
The selective use of functional optical variables in the control of forward speed [NASA-TM-108849] p 35 N95-12227
- AXMANN, J. K.**
Reentry trajectories and their optimization by an evolution algorithm p 525 A95-87394
- AYDIN, N. H.**
Aerodynamic characteristics of external store configurations at low speeds [BTN-95-EIX95182619230] p 271 A95-76656
- AYER, T. C.**
Unsteady aerodynamic analyses for turbomachinery aeroelastic predictions p 141 N95-19381
- AYERS, BERT F.**
Development of a multicomponent force and moment balance for water tunnel applications, volume 1 [NASA-CR-4642-VOL-1] p 161 N95-18955
Development of a multicomponent force and moment balance for water tunnel applications, volume 2 [NASA-CR-4642-VOL-2] p 161 N95-18956
- AYERS, TRICIA K.**
Accurate drag prediction: A prerequisite for drag reduction research [SAE PAPER 932571] p 467 A95-90060
- AZZAM, H.**
The use of math-dynamic models to aid the development of integrated health and usage monitoring systems [CONGRESS PAPER C428-19-079] p 457 A95-91720
- BAART, DOUGLAS**
The 1994 updated National Aerospace System performance assessment for year 2005 [AD-A288652] p 380 N95-26485
A NASPAC-Based analysis of the delay and cost effects of the western-pacific region preliminary resectorization effort of 1993 [AD-A288696] p 601 N95-31013
- BABBITT, B. A.**
Assessment of cost and training effectiveness for a candidate training system using the Comparison-Based Prediction model [SAE PAPER 932598] p 379 A95-84570
- BABBITT, BETTINA A.**
Intelligent tutoring system: F-16 flight simulation p 521 A95-90649
- BABBITT, BOB**
High bypass separate flow exhaust system improved thrust efficiency by modifying the aft centerbody [SAE PAPER 932622] p 511 A95-90083
- BABIKIAN, DIKRAN S.**
Measurement and analysis of nitric oxide radiation in an arcjet flow [BTN-95-EIX95082502727] p 243 A95-71040
Measured and calculated spectral radiation from a blunt body shock layer in an arc-jet wind tunnel [AIAA PAPER 94-0086] p 67 N95-13720
- BACHMANN, GLEN R.**
H₂sup 2/H₂(sup INF) controller design for a two-dimensional thin airfoil flutter suppression [BTN-94-EIX94511433918] p 141 A95-64584
- BACK, G. G.**
A review of water mist technology for fire suppression [AD-A285738] p 225 N95-20071
- BACKES, PAUL G.**
A generic telerobotics architecture for C-5 industrial processes [AIAA PAPER 94-1264-CP] p 27 N95-11529
- BACMEISTER, JULIO T.**
An algorithm for forecasting mountain wave-related turbulence in the stratosphere [HTN-95-80656] p 254 A95-72500
- BACON, BARTON**
Simulation and model reduction for the active flexible wing program [BTN-95-EIX95182619211] p 295 A95-76637
- BACON, BARTON J.**
High-Alpha Research Vehicle (HARV) longitudinal controller: Design, analyses, and simulation results [NASA-TP-3446] p 17 N95-10860
- BACON, D. P.**
Operational multi-scale environment model with grid adaptivity (OMEGA) application to aviation weather p 676 A95-93556
- BADCOCK, K. J.**
Partially implicit method for simulating viscous aerofoil flows [BTN-94-EIX94522406680] p 709 A95-96299
- BADE, A.**
Reentry trajectories and their optimization by an evolution algorithm p 525 A95-87394
- BADIE, J.**
Temperature diagnostics in the hypersonic flow regime: An application to develop a stagnation temperature probe [AIAA PAPER 95-6114] p 511 A95-90442
- BAECKLUND, K.**
Military aviation maintenance industry in Western Europe: Concentration and internationalization [PB94-189180] p 104 N95-17451
- BAEDER, J. D.**
Recent advances in Euler and Navier-Stokes methods for calculating helicopter rotor aerodynamics and acoustics [HTN-94-00686] p 2 A95-60169
- BAEV, V. K.**
Integration of an hypersonic airbreathing vehicle: Assessment of overall aerodynamic performances and of uncertainties [AIAA PAPER 95-6100] p 492 A95-88007
- BAGANOFF, DONALD**
A study of fluid problems requiring a direct particle simulation [AD-A290212] p 567 N95-29074
- BAGINSKI, FRANK**
Variational principles for ascent shapes of large scientific balloons [BTN-95-EIX95262694320] p 387 A95-85491
- BAGOT, KEITH W.**
Evaluation of retro-reflective beads in airport pavement markings [AD-A291065] p 523 N95-29967
Evaluation of alternative pavement marking materials [AD-A292973] p 626 N95-31468
- BAHETI, S. K.**
Thermo-hydrodynamic solution of floating ring seals for high pressure compressors using the finite-element method [HTN-95-92246] p 433 A95-85290
- BAHM, CATHERINE M.**
Determination of stores pointing error due to wing flexibility under flight load [NASA-TM-4646] p 134 N95-19044
- BAILES, M.**
Period evolution of PSR B1259-63: Evidence for propeller-torque spindown [HTN-95-B0194] p 581 A95-87903
- BAILEY, DON**
Adaptive tuned vibration absorbers: Tuning laws, tracking agility, sizing, and physical implementations p 25 N95-11280
- BAILEY, JEFF**
Aircraft electric field measurements: Calibration and ambient field retrieval [HTN-95-90508] p 213 A95-67780
Field and data analysis studies related to the atmospheric environment [NASA-CR-196543] p 168 N95-18093
- BAILEY, JIM**
The controller memory guide. Concepts from the field [AD-A289263] p 383 N95-26978
- BAILEY, JOHN**
Impact of Ada and object-oriented design in the flight dynamics division at Goddard Space Flight Center [NASA-CR-189412] p 567 N95-28807
- BAILEY, P.**
Cost effective small-scale experiments to aid the design of ASTOVL aircraft [CONGRESS PAPER C428-9-098] p 475 A95-91695
- BAILEY, THOMAS E.**
Psycho-social safety perceptions: Helicopters as a case study p 596 A95-95192
- BAILLIE, STEWART**
Improving prediction: The incorporation of simplified rotor dynamics in a mathematical model of the bell 412HP [BTN-95-EIX95152584679] p 282 A95-73591
- BAILLIE, STEWART W.**
Practical experiences in control systems design using the NCR Bell 205 Airborne Simulator p 624 N95-32015
- BAILLY, CHRISTOPHE**
Stochastic approach to noise modeling for free turbulent flows [HTN-95-42321] p 371 A95-86150
- BAIN, D. B.**
Jet mixing and emission characteristics of transverse jets in annular and cylindrical confined crossflow [NASA-TM-106976] p 616 N95-30698
- BAINS, JANE C.**
Nonlinear analysis of damaged stiffened fuselage shells subjected to combined loads p 137 N95-19499
- BAKER, A. A.**
Bonded composite repair of metallic aircraft components: Overview of Australian activities p 392 N95-27505
Bonded composite repair of thin metallic materials: Variable load amplitude and temperature cycling effects p 393 N95-27509
Scarf repairs to graphite/epoxy components p 396 N95-27523
- BAKER, A. J.**
Accuracy and efficiency assessments for a weak statement CFD algorithm for high-speed aerodynamics [BTN-94-EIX95011441238] p 370 A95-84195
- BAKER, A. M.**
A fixed time performance evaluation of parallel CFD applications [DE94-014240] p 436 N95-26445
- BAKER, DONALD J.**
Ten-year ground exposure of composite materials used on the Bell Model 206L helicopter flight service program [NASA-TP-3468] p 55 N95-12357
- BAKER, IAN**
Preliminary studies of ice formation in upslope clouds p 674 A95-93546
- BAKER, ROBERT L.**
Fly-By-Light/Power-By-Wire Requirements and Technology Workshop [NASA-CP-10108] p 12 N95-10245
- BAKHLE, MILIND A.**
Flutter analysis of supersonic axial flow cascades using a high resolution Euler solver. Part 1: Formulation and validation [NASA-TM-105798] p 23 N95-10244
FPCAS2D user's guide, version 1.0 [NASA-CR-195413] p 156 N95-16588
FPCAS3D User's guide: A three dimensional full potential aeroelastic program, version 1 [NASA-CR-198367] p 651 N95-32205

BAKKER, P. G.

Quantitative comparison between interferometric measurements and Euler computations for supersonic cone flows
[BTN-95-EIX95222650782] p 358 A95-79238

BAKOS, R.

An assessment of ground-test facility capabilities for measurement of hypervelocity scramjet performance
[AIAA PAPER 95-6148] p 512 A95-90462

BAKOS, R. J.

Shock tunnel studies of scramjet phenomena 1993
[NASA-CR-195038] p 350 N95-25394

BAKOS, ROBERT J.

Chemical recombination in an expansion tube
[HTN-95-20844] p 544 A95-88105
Numerical simulations of the flow in the HYPULSE expansion tube
[NASA-TM-110357] p 523 N95-30228

BALABASKARAN, V.

Boundary layer studies over an S-blade
[HTN-95-92261] p 434 A95-85305

BALAKRISHNA, S.

Effects of vibration on inertial wind-tunnel model attitude measurement devices
[NASA-TM-109083] p 21 N95-11466

Performance of the 0.3-meter transonic cryogenic tunnel with air, nitrogen, and sulfur hexafluoride media under closed loop automatic control
[NASA-CR-195052] p 310 N95-23257

Development of a model protection and dynamic response monitoring system for the national transonic facility
[NASA-CR-195041] p 340 N95-24388

BALAKRISHNAN, TANAPAAL

Cabin fuselage structural design with engine installation and control system
[NASA-CR-197173] p 47 N95-12639

BALAN, CHELLAPPA

Propulsion simulator for high bypass turbofan performance evaluation
[SAE PAPER 931410] p 625 A95-93676

BALANIS, CONSTANTINE A.

RCS measurements, transformations, and comparisons under cylindrical and plane wave illumination
[BTN-94-EIX94371347126] p 242 A95-69976

BALAS, GARY J.

Robust dynamic inversion for control of highly maneuverable aircraft
[BTN-95-EIX95242670747] p 359 A95-81100

Feedback control laws for highly maneuverable aircraft
[NASA-CR-197944] p 295 N95-23410

BALASHOV, I. N.

On a program-information system Tsoft
[BTN-94-EIX94461408773] p 175 A95-63656

BALDERSON, KEITH A.

Comparison of frequency response and perturbation methods to extract linear models from a nonlinear simulation
[AD-A284115] p 146 N95-18405

BALDUS, M.

Broadband polarization-transfer experiments for rotating solids
[GTN-95-0009261494012091-58] p 579 A95-92319

BALDWIN, EDWARD M., III

The evolution of airport noise monitoring systems: Recent achievements and further needs
p 562 A95-90125

BALDWIN, JAMES DANIEL

An investigation of the accuracy of FEM analysis of a graphite epoxy box beam
[SAE PAPER 931221] p 543 A95-88011

BALL, A. S.

Adhesively bonded composite patch repair of cracked aluminum alloy structures
p 393 N95-27507

BALL, D. N.

Development of an aircraft cabin water spray system
[CONGRESS PAPER C428-25-030] p 595 A95-93599

BALLA, R. JEFFREY

Planar Rayleigh scattering and laser-induced fluorescence for visualization of a hot, Mach 2 annular air jet
[NASA-TM-4576] p 54 N95-13196

BALLARD, DAN

PalymSys (TM): An extended version of CLIPS for construction and reasoning using blackboards
p 217 N95-19767

BALLIN, MARK G.

Validation of the dynamic response of a blade-element UH-60 simulation model in hovering flight
[HTN-94-00663] p 18 A95-60155

BALLISH, BRADLEY A.

Towards improving the NMC aircraft data base
p 660 A95-93480

BALLMANN, J.

Prediction of rotor-blade deformations due to unsteady airloads
[AD-A284467] p 81 N95-15821

BALLMANN, JOSEF

Prediction of rotor-blade deformations due to unsteady airloads
[AD-A286593] p 231 N95-20860

BALZAROTTI, G.

An approach to sensor data fusion for flying and landing aid purpose
p 686 N95-32488

BANDA, SIVA S.

Design of nonlinear control laws for high-angle-of-attack flight
[BTN-94-EIX94511433920] p 141 A95-64586

Robust longitudinal axis flight control for an aircraft with thrust vectoring
[BTN-95-EIX95122538875] p 408 A95-83000

BANDY, ALAN R.

An intercomparison of aircraft instrumentation for tropospheric measurements of sulfur dioxide
[HTN-95-91855] p 354 A95-80843

An intercomparison of aircraft instrumentation for tropospheric measurements of carbonyl sulfide, hydrogen sulfide, and carbon disulfide
[HTN-95-91856] p 355 A95-80844

An intercomparison of instrumentation for tropospheric measurements of dimethyl sulfide: Aircraft results for concentrations at the parts-per-trillion level
[HTN-95-91857] p 355 A95-80845

BANDYOPADHYAY, PROMODE R.

Cornet vortex suppressor
[AD-D016423] p 116 N95-18337

BANFORD, MICHAEL

Pressure measurements on an F/A-18 twin vertical tail in buffeting flow. Volume 3: Buffet power spectral densities
[AD-A281444] p 36 N95-11829

Pressure measurements on an F/A-18 twin vertical tail in buffeting flow. Volume 2: Steady and unsteady RMS pressure data
[AD-A281581] p 76 N95-15465

Pressure measurements on an F/A-18 twin vertical tail in buffeting flow. Volume 4, part 2: Buffet cross spectral densities
[AD-A285555] p 143 N95-18641

Pressure measurements on an F/A-18 twin vertical tail in buffeting flow. Volume 4, part 1: Buffet cross spectral densities
[AD-A285593] p 237 N95-21214

Pressure measurements on an F/A-18 twin vertical tail in buffeting flow. Volume 1: Wind tunnel test summary
[AD-A279126] p 225 N95-21877

BANG, ERIC S.

Flight-deck displays on the Boeing 777
[BTN-95-EIX95142562402] p 286 A95-73438

BANILOWER, HOWARD

Bird ingestion into large turbofan engines
[DOT/FAA/CT-93/14] p 333 N95-24631

BANKS, D. W.

High Alpha Technology Program (HATP) ground test to flight comparisons
p 68 N95-14230

BANKS, DANIEL W.

Passive porosity with free and fixed separation on a tangent-ogive forebody
[BTN-95-EIX95062487554] p 185 A95-68368

BANNINK, W. J.

The utilization of a high speed reflective visualization system in the study of transonic flow over a delta wing
p 121 N95-19259

BANOWETZ, VIRGIL

An evaluation of the Software Through Pictures/T Tool (STP/T) for the Software Support Activity (SSA)
[AD-A288822] p 447 N95-26348

BAO, JINSONG

Investigation of dynamic inflow's influence on rotor control derivatives
p 155 N95-16250

BAR-SHALOM, YAAKOV

MATSurv multisensor air traffic surveillance
[AD-A292253] p 489 N95-28887

BARBAGALETA, S.

FASTPACK: Optimized solutions for modular avionics derived from a parametric study. Part 1: Platform features
p 233 N95-20634

BARBATO, GREGORY J.

Integrated mission precision attack cockpit technology (IMPACT). Phase 1: Identifying technologies for air-to-ground fighter integration
[AD-A289562] p 389 N95-26684

BARBERIS, D.

Experimental study of three-dimensional separation
[BTN-94-EIX94441385752] p 179 A95-68216

Ellipsoid-cylinder model
p 158 N95-17869

Supersonic vortex flow around a missile body
p 114 N95-17870

Delta-wing model
p 114 N95-17873

BARDES, BRUCE P.

Trends in aerospace forgings in the 1990s
[HTN-95-B0408] p 456 A95-90756

BARDES, MATT

Icarus Rewaxed: A high speed, low-cost general aviation aircraft for Aeroworld
[NASA-CR-197155] p 45 N95-12609

BARING, T. J.

Estimates of total organic and inorganic chlorine in the lower stratosphere from in situ and flask measurements during AAEE 2
[HTN-95-A0861] p 317 A95-76265

BARKER, WALTER R.

Super-heavy aircraft study
[AD-A279602] p 238 N95-19955

BARKER, WILLIAM P.

Hydrofoil force balance
[AD-D016475] p 160 N95-18461

BARKHIMER, R. L.

Advanced diesel electronic fuel injection and turbocharging
[AD-A279176] p 211 N95-19809

BARLOW, DOUGLAS N.

Effect of surface roughness on local film cooling effectiveness and heat transfer coefficients
[AD-A283802] p 91 N95-14351

BARLOW, TODD

Resource document for the design of electronic instrument approach procedure displays
[AD-A295108] p 691 N95-34797

BARNARD, R. H.

Collectively variable incidence wingtips for lift control and reduced gust sensitivity
[HTN-95-92836] p 471 A95-90754

BARNES, A. G.

Modeling requirements in flight simulation
[HTN-95-C0004] p 585 A95-93392

BARNES, TERENCE

The FAA regional/computer aircraft flight loads data collection program
[SAE PAPER 931258] p 493 A95-89224

BARNETT, LEE

Certification of windshear performance with RTCA class D radomes
p 41 N95-13206

BARNETT, M.

Unsteady aerodynamic analyses for turbomachinery aeroelastic predictions
p 141 N95-19381

BARNETT, R. M.

Simple numerical criterion for vortex breakdown
[HTN-95-61210] p 541 A95-87583

BARNHARDT, MICHAEL B.

Standardization of aircraft noise insulation measures without compromising results
p 561 A95-90115

BARONTI, S.

MAX-91: Polarimetric SAR results on Montespertoli site
p 320 N95-23940

BARRETT, RON

Active plate and missile wing development using directionally attached piezoelectric elements
[HTN-95-42340] p 408 A95-86169

BARRICK, JOHN D.

An intercomparison of aircraft instrumentation for tropospheric measurements of carbonyl sulfide, hydrogen sulfide, and carbon disulfide
[HTN-95-91856] p 355 A95-80844

BARRIE, RONALD E.

Advanced textile applications for primary aircraft structures
p 399 N95-28476

Textile composite fuselage structures development
p 534 N95-29033

BARRIENTOS, J. M.

The effect of wear on fire-blocking layer material effectiveness
[AD-A291520] p 485 N95-29855

BARRIOCARDABA, A.

Repairs of CFC primary structures
p 396 N95-27527

BARRY, B. C.

Erosion of T56 5th stage rotor blades due to bleed hole overtip flow
p 200 N95-19666

BARTELHEIMER, W.

2-D airfoil tests including side wall boundary layer measurements
p 158 N95-17847

BARTELS, ROBERT EDWIN

An interacting boundary layer method for unsteady compressible flows
p 557 N95-30290

BARTHOLOMEUSZ, R. A.

Bonded composite repair of cracked load-bearing holes
[BTN-94-EIX94401360553] p 243 A95-71867

BARTLETT, C. S.

Icing simulation in the aeropropulsion systems test facility propulsion development test cell C-2
[AD-A293039] p 599 N95-31667

- BARTLETT, D. L.**
The corrosion and protection of advanced aluminium - lithium airframe alloys p 302 N95-23497
- BARTON, ROBERT S.**
Control system design for the MOD-5A 7.3 mW wind turbine generator p 440 N95-27985
Variable speed generator application on the MOD-5A 7.3 mW wind turbine generator p 440 N95-27989
- BARTZ, A.**
PVD TBC experience on GE aircraft engines p 345 N95-26126
- BARUZZI, G. S.**
An improved finite element method for the solution of the compressible Euler and Navier-Stokes equations p 640 A95-95439
- BARWEY, D.**
Dynamic-stall and structural-modeling effects on helicopter blade stability with experimental correlation [HTN-95-81646] p 542 A95-87694
- BASCIANI, M.**
Adaptive wind tunnel walls versus wall interference correction methods in 2D flows at high blockage ratios p 147 N95-19267
- BASHFORD, P. J.**
Ageing aircraft after ALOHA [CONGRESS PAPER C428-11-188] p 484 A95-91701
- BASHKIRTSEV, A. V.**
Modelling for optimal operations of line milling of aerodynamic surfaces [BTN-94-EIX94461408774] p 138 A95-63657
- BASIL, VICTOR**
Software process improvement in the NASA software engineering laboratory [AD-A289912] p 450 N95-28627
- BASS, HENRY E.**
Atmospheric effects on the risetime and waveshape of sonic booms p 100 N95-14886
- BASSO, GORDON L.**
Noise transmission and reduction in turboprop aircraft p 175 N95-19164
- BAST, CALLIE C.**
Probabilistic material strength degradation model for Inconel 718 components subjected to high temperature, high-cycle and low-cycle mechanical fatigue, creep and thermal fatigue effects [NASA-CR-197832] p 419 N95-27167
- BASURAH, H. M.**
Variations of perturbations in perigee height with eccentricity for artificial Earth's satellites due to air drag [HTN-95-40013] p 85 A95-62657
- BATINA, JOHN T.**
Implicit upwind-Euler solution algorithms for unstructured-grid applications p 641 A95-95454
- BATORY, DON**
The ADAGE avionics reference architecture [AIAA PAPER 95-1021] p 566 A95-90693
- BATTIS, J. C.**
The effects of aircraft (B-52) overflights on ancient structures [BTN-94-EIX94341340070] p 171 A95-63522
- BATTLE, CATHERINE M.**
Analysis of en route controller hazardous weather-related tasks p 665 A95-93503
- BATTS, G. W.**
Ascent wind model for launch vehicle design [BTN-95-EIX95041503799] p 239 A95-70124
- BATY, ROY S.**
Functional dependence of trajectory dispersion on initial condition errors [BTN-95-EIX95152583263] p 298 A95-73564
- BAUCHAU, O. A.**
On the choice of appropriate bases for nonlinear dynamic modal analysis [HTN-95-A0495] p 221 A95-72566
- BAUCHAU, OLIVIER A.**
Dynamic analysis of bearingless tail rotor blades based on nonlinear shell modes [BTN-95-EIX95152582338] p 281 A95-73540
- BAUER, F.**
Acoustic field in unsteady moving media [NASA-CR-198162] p 438 N95-27179
- BAUER, J.**
On aircraft repair verification of a fighter A/C integrally stiffened fuselage skin p 394 N95-27515
- BAUER, JEFFREY E.**
Flight test of the X-29A at high angle of attack: Flight dynamics and controls [NASA-TP-3537] p 284 N95-22806
X-29 flight control system: Lessons learned p 622 N95-32001
- BAUER, STEVEN X. S.**
Passive porosity with free and fixed separation on a tangent-ogive forebody [BTN-95-EIX95062487554] p 185 A95-68368
- Base passive porosity for drag reduction [NASA-CASE-LAR-15246-1] p 91 N95-14183
- BAUHOF, CHRISTINA R.**
The data link flight information service application p 665 A95-93504
- BAUM, CARL E.**
Impulse radiating antennas p 548 A95-90920
- BAUMBICK, ROBERT**
The 1994 Fiber Optic Sensors for Aerospace Technology (FOSAT) Workshop [NASA-CP-10166] p 337 N95-24207
Assessment of avionics technology in European aerospace organizations [NASA-CR-189201] p 337 N95-24624
- BAUMEISTER, JOSEPH F.**
Radiant energy measurements from a scaled jet engine axisymmetric exhaust nozzle for a baseline code validation case [NASA-TM-106686] p 25 N95-11409
- BAUMEISTER, KENNETH J.**
Acoustic scattering from ellipses by the modal element method [NASA-TM-106935] p 579 N95-29401
- BAUMERT, W.**
Pressure distribution measurements on an isolated TPS 441 nacelle p 115 N95-17878
- BAUMGARDNER, D.**
Performance of a focused cavity aerosol spectrometer for measurements in the stratosphere of particle size in the 0.06-2.0-micrometer-diameter range [HTN-95-90914] p 253 A95-72423
Analysis of the physical state of one Arctic polar stratospheric cloud based on observations [HTN-95-70917] p 351 A95-77982
- BAURLE, R. A.**
Modeling of supersonic turbulent combustion using assumed probability density functions [BTN-95-EIX95112524190] p 206 A95-69318
- BAYAR, CAN**
Vortex lattice method simulation of unsteady flow due to wing/external store combination p 471 A95-91499
- BAYAR, K. CAN**
Computer aided static aeroelastic analysis of wing/pylon/store combination p 499 A95-91531
- BAYERDOERFER, G.**
Design and operation of a thermoacoustic test facility p 147 N95-19150
- BAYERDOERFER, GERHARD**
Thermoacoustic environments to simulate reentry conditions p 86 N95-14096
- BAYHA, T. D.**
Advanced resin systems and 3D textile preforms for low cost composite structures p 535 N95-29035
- BAYHA, TOM D.**
Advanced composites structural concepts and materials technologies for primary aircraft structures: Design/manufacturing concept assessment [NASA-CR-4447] p 12 N95-10316
- BAYLISS, A.**
Interaction of jet noise with a nearby panel assembly [BTN-95-EIX95262694295] p 434 A95-85466
On the interaction of jet noise with a nearby flexible structure [NASA-CR-194934] p 57 N95-11812
Response of multi-panel assembly to noise from a jet in forward motion [NASA-CR-198164] p 442 N95-28673
- BAYSAL, OKTAY**
Aerodynamic shape optimization using preconditioned conjugate gradient methods [BTN-95-EIX95142553033] p 263 A95-73465
Preconditioned domain decomposition scheme for three-dimensional aerodynamic sensitivity analysis [BTN-95-EIX95152577612] p 321 A95-73471
Dynamic unstructured method for flows past multiple objects in relative motion [BTN-95-EIX95262694303] p 435 A95-85474
Preconditioned domain decomposition scheme for three-dimensional aerodynamic sensitivity analysis [HTN-95-42597] p 459 A95-87227
Improving the efficiency of aerodynamic shape optimization [HTN-95-61204] p 540 A95-87577
A CFD study of complex missile and store configurations in relative motion [NASA-CR-197912] p 285 N95-22949
Aerodynamic design optimization with sensitivity analysis and computational fluid dynamics [NASA-CR-197419] p 274 N95-23218
- BEACH, R.**
Overview of remote sensing laser development and semiconductor laser technology [DE94-019103] p 256 N95-21552
- BEALE, DAVID G.**
A correlative investigation of simulated occupant motion and accident report in a helicopter crash [AD-A285190] p 123 N95-16404
- BEARD, ANDREW**
Adaptive tuned vibration absorbers: Tuning laws, tracking agility, sizing, and physical implementations p 25 N95-11280
- BEARMAN, PETER**
The effects of three dimensional imposed disturbances on bluff body near wake flows [AD-A290824] p 555 N95-29654
- BEARMAN, PETER W.**
Effects of three-dimensional imposed 3-D disturbances on bluff-body near wake flows [AD-A289553] p 374 N95-26757
- BEASLEY, HOWARD H.**
Factors affecting the visual fragmentation of the field-of-view in partial binocular overlap displays [AD-A283081] p 172 N95-17334
Factors affecting the perception of luring in monocular regions of partial binocular overlap displays [AD-A286287] p 259 N95-22044
- BEATTIE, ALLAN**
Emerging nondestructive inspection for aging aircraft [PB95-143053] p 328 N95-25401
- BEATTY, DAVID A.**
Energy absorption device for shock loading [AD-D017476] p 706 N95-34449
- BEATTY, ROGER**
Cooperative problem solving between airline operations control and ATC traffic flow management p 681 A95-95066
- BECHARA, WALID**
Stochastic approach to noise modeling for free turbulent flows [HTN-95-42321] p 371 A95-86150
- BECK, N. J.**
Advanced diesel electronic fuel injection and turbocharging [AD-A279176] p 211 N95-19809
- BECK, W. H.**
The high enthalpy shock tunnel in Goettingen (HEG) p 518 A95-87391
- BECKER, J.**
Structural aspects of active control technology p 623 N95-32006
- BECKER, K. H.**
Nitrous oxide and methane emissions from aero engines [HTN-95-21363] p 353 A95-78678
- BECKER, ROBERT C.**
Flight test evaluation of a 35 GHz forward looking altimeter for terrain avoidance [BTN-95-EIX95212641071] p 287 A95-76736
- BECKLEY, B.**
Using IRI for the computation of ionospheric corrections for altimeter data analysis p 212 A95-66949
- BECKMAN, BRIAN C.**
Virtual reality flight control display with six-degree-of-freedom controller and spherical orientation overlay [NASA-CASE-NPO-18733-1-CU] p 288 N95-22578
- BECKS, EDWARD A.**
Improved speed control system for the 87,000 HP wind tunnel drive [NASA-TM-106840] p 211 N95-19794
- BEDOYA, CARLOS A.**
An advanced vehicle management system [SAE PAPER 931376] p 618 A95-93655
Fiber Optic Control System integration for advanced aircraft. Electro-optic and sensor fabrication, integration, and environmental testing for flight control systems [NASA-CR-191194] p 162 N95-19236
- BEECHER, S. C.**
Thermal conductivity of zirconia thermal barrier coatings p 345 N95-26133
- BEENE, JEFFREY K.**
Bomber force 2000: Operational concepts for long-range combat aircraft [AD-A279378] p 230 N95-20181
- BEHEIM, GLENN**
The 1994 Fiber Optic Sensors for Aerospace Technology (FOSAT) Workshop [NASA-CP-10166] p 337 N95-24207
- BEIER, K.**
Modeling of aircraft exhaust emissions and infrared spectra for remote measurement of nitrogen oxides [HTN-95-51276] p 355 A95-80861
- BEISSNER, ROBERT E.**
Eddy current for detecting second-layer cracks under installed fasteners [AD-A279871] p 244 N95-20414

- BEKKI, S.**
Sensitivity of supersonic aircraft modelling studies to HNO₃ photolysis rate [HTN-95-11475] p 353 A95-79453
- BELALA, Y.**
Transport aircraft loading and balancing system: Using a CLIPS expert system for military aircraft load planning p 217 N95-19751
- BELASON, BRUCE**
Evaluation of bonded boron/epoxy doublers for commercial aircraft aluminum structures p 92 N95-14457
- BELASON, E. B.**
Status of bonded boron/epoxy doublers for military and commercial aircraft structures p 393 N95-27506
- BELL, DAVID K.**
Proof test methodology for composites p 424 N95-28445
- BELL, DOUGLAS P.**
A comparative study of internally and externally capped balloons using small scale test balloons p 181 A95-66285
- BELL, HERBERT H.**
Intelligent tutoring system: F-16 flight simulation p 521 A95-90649
- BELLINGER, N. C.**
Modelling of pillowing due to corrosion in fuselage lap joints [BTN-95-EIX95082502227] p 240 A95-71024
Double pass retroreflection for corrosion detection in aircraft structures p 323 N95-23503
- BELMORE, MICHAEL**
Application of airborne field mill data for use in launch support [HTN-95-50054] p 98 A95-62279
- BELLUATI, PIER LUIGI**
Digital autopilot design for combat aircraft in ALENIA p 623 N95-32009
- BELOUS, YU. P.**
Navigational technology of dual usage p 688 N95-33131
- BELTZ, NOBERT**
An intercomparison of aircraft instrumentation for tropospheric measurements of sulfur dioxide [HTN-95-91855] p 354 A95-80843
- BELUE, LISA M.**
Selecting optimal experiments for feedforward multilayer perceptrons [AD-A290856] p 678 N95-30406
- BELYTSCHKO, T.**
Fatigue reliability method with in-service inspections p 94 N95-14475
- BEN-ASHER, JOSEPH Z.**
Optimal trajectories for an unmanned air-vehicle in the horizontal plane [BTN-95-EIX0619952748191] p 606 A95-94480
- BENAK, T. J.**
Bonded composite repair of thin metallic materials: Variable load amplitude and temperature cycling effects p 393 N95-27509
- BENCIC, TIMOTHY J.**
Improved speed control system for the 87,000 HP wind tunnel drive [NASA-TM-106840] p 211 N95-19794
- BENDIKSEN, ODDVAR O.**
Limit cycle phenomena in computational transonic aeroelasticity [BTN-95-EIX95152582317] p 264 A95-73520
- BENELL, RUSSELL A.**
Future ATC system integration: Tools for developing a shared vision p 600 A95-95085
- BENGTTSSON, M.**
Orientation determination of aircraft using visual 3D matching and radar. Case study 2 [PB95-165791] p 350 N95-25749
- BENNANI, S.**
Robust control: A structured approach to solve aircraft flight control problems p 621 N95-31995
- BENNER, WILLIAM**
Weather And Radar Processor (WARP) Test and Evaluation Master Plan (TEMP) [AD-A288280] p 445 N95-26453
- BENNER, WILLIAM E.**
Operational And Supportability Implementation System (OASIS) test and evaluation master plan [AD-A284765] p 126 N95-18088
- BENNETT, GEORGE**
Rapid prototyping of composite aircraft structures [SAE PAPER 931219] p 539 A95-87530
- BENNETT, J.**
Enhancement of F/A-18 operational flight measurements: Data report for phase 1 [DSTO-TR-0049] p 286 N95-23666
- BENNETT, JOE**
Lightweight high-temperature fuel metering valves [SAE PAPER 931444] p 635 A95-93693
- BENNETT, P. A.**
Evolving standards for safety critical software [CONGRESS PAPER C428-24-142] p 678 A95-93595
- BENNETT, ROBERT M.**
Application of transonic small disturbance theory to the active flexible wing model [BTN-95-EIX95182619210] p 270 A95-76636
- BENNEY, RICHARD J.**
Parachute inflation: A problem in aeroelasticity [AD-A284375] p 117 N95-18340
- BENOIT, ANDRE**
On-line handling of air traffic: Management, guidance and control [AGARD-AG-321] p 126 N95-18927
- BENSON, RUSTY A.**
Time accurate computation of unsteady inlet flows with a dynamic flow adaptive mesh [AD-A285498] p 157 N95-16736
- BENSON, THOMAS J.**
A workstation based simulator for teaching compressible aerodynamics [NASA-TM-106799] p 170 N95-16906
Interactive computer graphics applications for compressible aerodynamics [NASA-TM-106802] p 170 N95-17264
- BENSON, VERNON M.**
Automated fiber placement: Evolution and current demonstrations p 532 N95-28832
- BENT, PAUL H.**
Fan noise prediction assessment [NASA-CR-195051] p 711 N95-33831
- BENTS, DAVID J.**
Design of a GaAs/Ge solar array for unmanned aerial vehicles [NASA-TM-106870] p 320 N95-23259
- BENZARIA, E.**
Secondary source locations in active noise control: Selection or optimization? [BTN-94-EIX94381352222] p 257 A95-71738
- BEPPU, GORO**
A detailed Euler flow analysis of TPS and fanjet engine p 473 A95-91515
A study of computational difficulty of numerical method in optimal control p 507 A95-91585
Numerical solutions of inviscid and viscous flows about airfoils by TVD method p 684 A95-34521
- BERENS, THOMAS M.**
Experimental and numerical analysis of a two-duct nozzle/afterbody model at supersonic Mach numbers [AIAA PAPER 95-6085] p 490 A95-87414
- BERCZIN, CHARLES R.**
Aerodynamic and wake methodology evaluation using Model UH-60A experimental data [HTN-95-31009] p 220 A95-71179
- BERG, MARTIN C.**
Multirate flutter suppression system design for a model wing [BTN-95-EIX95182619132] p 292 A95-76609
- BERGAMINI, LORENZO**
Using the Liou-Steffen algorithm for the Euler and Navier-Stokes equations [HTN-95-42348] p 373 A95-86177
- BERGLIND, TORSTEN**
Navier-Stokes computations around a realistic fighter configuration p 591 A95-95440
- BERGSTROM, SHERRY**
Maintenance programs [HTN-95-92310] p 365 A95-85354
- BERHAULT, J.-P.**
Noise and vibration control in aircraft: A global approach [AD-A286382] p 576 A95-90128
ASTRYD: A new numerical tool for aircraft cabin and environmental noise prediction p 576 A95-90129
- BERKOWITZ, J. P.**
Test and evaluation report for the Manual Domestic Passive Profiling System (MDPPS) [AD-A286312] p 225 N95-20093
- BERKOWITZ, JACK**
Test and Evaluation Plan (TEP) for Improvised Explosive Device Screening Systems (IEDSS) [AD-A286382] p 227 N95-22319
- BERNARD, DOUGLAS E.**
The Cassini spacecraft: Object oriented flight control software p 359 A95-80405
- BERNELLA, DAVID M.**
Status of the terminal Doppler weather radar with deployment underway p 653 A95-93450
- BERNER, C.**
Supersonic base flow investigation over axisymmetric afterbodies [PB94-180957] p 39 N95-12578
- BERNSTEIN, BEN C.**
Use of pilot reports for verification of aircraft icing diagnoses and forecasts p 666 A95-93508
- Examination of conditions in the proximity of pilot reports of aircraft icing during storm-fest p 666 A95-93509
The production of supercooled liquid water by a secondary cold front p 673 A95-93542
- BERNSTEIN, DENNIS S.**
Robust fixed-structure control [AD-A286515] p 257 N95-22216
Robust fixed-structure control [AD-A292883] p 679 N95-30961
- BERRICHE, R.**
Evaluation of advanced aerospace materials by depth sensing indentation and scratch methods [BTN-95-EIX95152584678] p 282 A95-73590
- BERRIER, BOBBY L.**
Single-engine tail interference model p 115 N95-17879
- BERRY, B. F.**
Modeling lateral attenuation of aircraft flight noise p 570 A95-88464
A prediction model for noise from low-altitude military aircraft p 571 A95-88466
- BERRY, CASSIE**
Viper [NASA-CR-197191] p 79 N95-13703
- BERRY, DENNIS L.**
Civil aircraft propulsion integration: Current & future [SAE PAPER 932624] p 495 A95-90085
- BERRY, L. A.**
Cu deposition using a permanent magnet electron cyclotron resonance microwave plasma source [DE94-017768] p 304 N95-23981
- BERRY, LEE A.**
Permanent magnet electron cyclotron resonance plasma source with remote window [BTN-95-EIX95242674338] p 450 A95-82176
- BERSHADER, DANIEL**
Head-on parallel blade-vortex interaction [HTN-95-61197] p 491 A95-87570
- BERT, C. W.**
Experimental investigation of thermoelastic deformation in turbojet-engine bearings under maintenance inspection [BTN-95-EIX95292721173] p 546 A95-89904
- BERTAMINI, L.**
Thermal testing of high performance thermal barrier coatings for turbine blades p 202 N95-19681
- BERTON, B.**
Intermetallic and titanium matrix composite materials for hypersonic applications [AIAA PAPER 95-6132] p 530 A95-90451
- BERTRAM, JAMES L.**
Development of RTM and powder prepreg resins for subsonic aircraft primary structures p 536 N95-29044
- BESMANN, T. M.**
Scale-up and modeling of forced chemical vapor infiltration [DE94-017769] p 247 N95-20781
- BESS, PHILIP K.**
Spread spectrum applications in unmanned aerial vehicles [AD-A281035] p 156 N95-16448
- BEST, S.**
Hypervelocity Impact Test Facility: A gun for hire [TABES PAPER 94-605] p 86 N95-14639
- BETTAMY-KNIGHTS, P. G.**
An efficient discrete vortex method for low Reynolds number incompressible flows p 639 A95-95407
- BETTNER, JAMES L.**
Propulsion system assessment for very high UAV under ERAST [NASA-CR-195469] p 406 N95-27866
- BETTS, C. J.**
The use of hot film for the investigation of boundary-layer transition [CONGRESS PAPER C428-9-199] p 475 A95-91697
- BETTS, JOHN T.**
Application of direct transcription to commercial aircraft trajectory optimization [BTN-95-EIX95242670766] p 359 A95-81081
- BEUSHAUSEN, V.**
Planar air density measurements near model surfaces by ultraviolet Rayleigh/Raman scattering [BTN-94-EIX94441386614] p 213 A95-67345
Planar air density measurements near model surfaces by ultraviolet Rayleigh/Raman scattering [HTN-95-20950] p 546 A95-88989
- BEUTNER, THOMAS J.**
Determination of solid/porous wall boundary conditions from wind tunnel data for computational fluid dynamics codes p 164 N95-19266
- BEUTNER, THOMAS JOHN**
A method for the modelling of porous and solid wind tunnel walls in computational fluid dynamics codes p 523 N95-29795

- BEYLER, C. L.**
A review of water mist technology for fire suppression
[AD-A285738] p 225 N95-20071
- BHAGAT, P. K.**
Corrosion detection and monitoring of aircraft structures:
An overview p 303 N95-23515
- BHAT, C. L.**
Mobile domes for TACTIC telescope p 453 A95-86113
- BHAT, THONSE R. S.**
Mach wave emission from a high-temperature
supersonic jet [BTN-95-EIX95152577586] p 264 A95-73496
Mach wave emission from a high-temperature
supersonic jet [HTN-95-42571] p 458 A95-87201
- BHATTACHARYA, A.**
Dynamics of phase ordering of nematics in a pore
[DE95-607662] p 362 N95-25978
- BHOL, D. G.**
Transverse vorticity measurements in the NASA Ames
80 x 120 wind tunnel boundary layer p 251 N95-22457
- BI, NAI-PEI**
Experimental data on the aerodynamic interactions
between a helicopter rotor and an airframe p 116 N95-17883
- BIANCO, JEAN**
NASA Lewis Research Center's combustor test facilities
and capabilities [NASA-TM-106903] p 412 N95-27176
- BIBER, KASIM**
Flow study of supersonic wing-nacelle configuration
[BTN-95-EIX95152582344] p 266 A95-73546
An overview of static and dynamic airfoil performance
[SAE PAPER 931228] p 463 A95-88960
- BICKLEY, GEORGE**
Guidance and control, 1993; Annual Rocky Mountain
Guidance and Control Conference, 16th, Keystone, CO,
Feb. 6-10, 1993 [ISBN-0-87703-365-X] p 341 A95-80389
- BIDWELL, COLIN S.**
Collection efficiency and ice accretion calculations for
a sphere, a swept MS(1)-317 wing, a swept NACA-0012
wing tip, an axisymmetric inlet, and a Boeing 737-300
[NASA-TM-106831] p 123 N95-18582
Additional improvements to the NASA Lewis ice
accretion code LEWICE [NASA-TM-106849] p 309 N95-22669
- BIEDRON, ROBERT T.**
Hybrid structured/unstructured grid computations for the
F/A-18 at high angle of attack p 68 N95-14233
- BIETERMAN, M. B.**
TranAir: A full-potential, solution-adaptive, rectangular
grid code for predicting subsonic, transonic, and
supersonic flows about arbitrary configurations. User's
manual [NASA-CR-4349] p 377 N95-28230
TranAir: A full-potential, solution-adaptive, rectangular
grid code for predicting subsonic, transonic, and
supersonic flows about arbitrary configurations. Theory
document [NASA-CR-4348] p 378 N95-28265
- BIEZAD, DANIEL J.**
Direct-lift design strategy for longitudinal control of
hypersonic aircraft [BTN-95-EIX95182619131] p 291 A95-76608
Developing a workstation-based, real-time simulation for
rapid handling qualities evaluations during design
[NASA-CR-198831] p 505 N95-30335
- BIGGERS, SHERRILL B.**
Shear buckling response of tailored composite plates
[HTN-95-51680] p 418 A95-85062
- BIHRLE, WILLIAM, JR.**
Techniques for tailoring aircraft stall and post-stall
behavior [SAE PAPER 931226] p 458 A95-87199
- BILANIN, ALAN J.**
Wing download reduction using vortex trapping plates
[HTN-94-00710] p 4 A95-60188
Ice accretion with varying surface tension
[NASA-TM-106826] p 124 N95-19285
- BILIMORIA, KARL D.**
Integrated development of the equations of motion for
elastic hypersonic flight vehicles [BTN-95-EIX95242670755] p 327 A95-81092
- BILITZA, D.**
Using IRI for the computation of ionospheric corrections
for altimeter data analysis p 212 A95-66949
- BILLICA, R. D.**
A surgical support system for Space Station Freedom
p 149 N95-16776
- BILLMANN, BARRY**
Minima reduction simulation test results
[AD-A285626] p 228 N95-21148
- BINGAMAN, DONALD C.**
Performance study for inlet installations
[NASA-CR-189714] p 406 N95-28227
- BINNS, K. E.**
High heat sink fuels for improved aircraft thermal
management [SAE PAPER 932084] p 530 A95-91659
- BINTANJA, RICHARD**
Momentum and scalar transfer coefficients over
aerodynamically smooth Antarctic surfaces
[HTN-95-92932] p 562 A95-91870
- BIRCH, STUART**
Trent engine development [BTN-94-EIX94461290507] p 82 A95-61727
Aircraft engine emission reduction
[BTN-95-EIX95031502750] p 196 A95-68257
Maintenance requirements for a supersonic transport
[BTN-95-EIX95031502751] p 179 A95-68258
Aircraft stripping and painting
[BTN-95-EIX95182617810] p 300 A95-75755
Aircraft stripping and painting
[HTN-95-92311] p 365 A95-85355
- BIRKELBAW, LOURDES G.**
Aerodynamics-model-for-a-generic-ASTOVL-lift-fan
aircraft [NASA-TM-110347] p 332 N95-26302
- BIRKAN, M. A.**
AFOSR Contractors Meeting in Propulsion
[AD-A282729] p 54 N95-12507
- BIRKETT, P. R.**
The application of helicopter mission simulation to
Nap-of-the-Earth operations p 710 N95-32496
- BIRTCHEK, CRAIG R.**
RCS measurements, transformations, and comparisons
under cylindrical and plane wave illumination
[BTN-94-EIX94371347126] p 242 A95-69976
- BISCHOF, C.**
Applications of automatic differentiation in computational
fluid dynamics p 156 N95-16461
- BISCHOF, C. H.**
Applications of automatic differentiation in CFD
[NASA-TM-109948] p 157 N95-16828
Parallel calculation of sensitivity derivatives for aircraft
design using automatic differentiation
[NASA-TM-110103] p 231 N95-20370
- BISHOP, FRANK E.**
New sensor technology for aircraft hydraulic system
diagnostics [SAE PAPER 932586] p 494 A95-90070
- BISHOP, M. T.**
Novel matrix resins for composites for aircraft primary
structures, phase 1 [NASA-CR-189657] p 23 N95-10318
- BISHOP, MIKE**
Cabin fuselage structural design with engine installation
and control system [NASA-CR-197173] p 47 N95-12639
- BISSON, A. C.**
Health monitoring and cost implications for an airline
operator [CONGRESS PAPER C428-12-166] p 457 A95-91704
- BISWAS, K. K.**
Some aspects of the aerodynamics of separating
strap-ons [BTN-95-EIX95182617464] p 298 A95-75735
- BISWAS, RUPAK**
Mesh quality control for multiply-refined tetrahedral
grids [NASA-CR-197595] p 160 N95-18737
- BITER, CLEON**
Windshear detection: TDWR and LLWAS operational
experience in Denver 1988-1992 p 670 A95-93528
The prototype aviation weather products generator a
vehicle to assess user needs p 671 A95-93534
- BITER, CLEON J.**
User involvement in the development of an advanced
icing product for use in aviation p 672 A95-93537
- BITTNER, R. D.**
Investigation of scramjet injection strategies for high
mach number flows [BTN-95-EIX0616952745782] p 614 A95-94504
- BITZER, M.**
Verification of engineering methods of aerodynamics for
reentry vehicles by DSMC p 525 A95-87386
- BITZER, MICHAEL**
Reentry technology experiment on the first mission of
reentry capsule 'EXPRESS' p 414 A95-82499
- BIVENS, COURTLAND C.**
Aircraft maneuver envelope warning system
[NASA-CASE-ARC-11953-1] p 82 N95-14518
- BIXLER, J. V.**
Integrated X-ray testing of the electro-optical breadboard
model for the XMM reflection grating spectrometer
[DE95-008829] p 644 N95-30507
- BJARKE, LISA J.**
Flow-visualization study of the X-29A aircraft at high
angles of attack using a 1/48-scale model
[NASA-TM-104268] p 8 N95-10858
- BLACK, THOMAS L.**
Preliminary results of turbulence predictions for use in
aviation weather forecasting p 675 A95-93551
- BLACKBURN, GARY**
The prototype aviation weather products generator a
vehicle to assess user needs p 671 A95-93534
- BLACKBURN, R. R.**
Development of anti-icing technology
[PB94-195369] p 78 N95-15439
- BLACKSTOCK, DAVID T.**
Effect of stratification and geometrical spreading on
sonic boom rise time p 75 N95-14880
- BLACKWELDER, RON F.**
On the role of the outer region in the
turbulent-boundary-layer bursting process
[BTN-94-EIX95011441078] p 348 A95-81056
- BLACKWELL, JEREMY**
Tie-down trials involving a Sikorsky S-70B-2 helicopter
[DSTO-TR-0132] p 400 N95-28567
- BLAKE, D. R.**
Meridional distributions of NO(X), NO(Y), and other
species in the lower stratosphere and upper troposphere
during AASE 2 [HTN-95-70944] p 352 A95-78009
- BLAKE, N. J.**
Meridional distributions of NO(X), NO(Y), and other
species in the lower stratosphere and upper troposphere
during AASE 2 [HTN-95-70944] p 352 A95-78009
- BLANCHARD, R. C.**
Orbiter rarefied-flow reentry measurements from the
OARE on STS-62 [NASA-TM-110182] p 646 N95-30783
- BLANCHARD, ROBERT E.**
Development of qualification guidelines for personal
computer-based aviation training devices
[DOT/FAA/AM-95/6] p 323 N95-23603
- BLANCHETIERE-CIARLETTI, V.**
Experimental study of the helicopter-mobile
radioelectrical channel and possible extension to the
satellite-mobile channel p 247 N95-20945
- BLAND, T. J.**
Advanced passive cooling for high power
electromechanical actuators [SAE PAPER 931397] p 634 A95-93669
- BLANDFORD, CRAIG S.**
Propulsion system assessment for very high UAV under
ERAST [NASA-CR-195469] p 406 N95-27866
- BLANDING, DAVID E.**
SUIT: The integration of aircraft subsystems
[SAE PAPER 931381] p 604 A95-93657
- BLANKEN, C. L.**
An investigation of the effects of pitch-roll (de)coupling
on helicopter handling qualities [NASA-TM-110349] p 409 N95-26773
- BLANKEN, CHRIS L.**
Investigation of the effects of bandwidth and time delay
on helicopter roll-axis handling qualities
[HTN-95-80853] p 290 A95-75095
- BLAVIER, J.-F.**
Latitude variations of stratospheric trace gases
[HTN-95-70948] p 352 A95-78013
- BLAYLOCK, JAMES**
Application of advanced safety technique to ring laser
gyro inertial navigation system integration p 689 N95-33140
- BLEICHER, P.**
FASTPACK: Optimized solutions for modular avionics
derived from a parametric study. Part 2: Avionics
p 233 N95-20635
- BLERMAN, GREGORY S.**
Error modeling for differential GPS
[NASA-CR-188367] p 488 N95-28716
- BLESS, ROBERT R.**
Load alleviation maneuvers for a launch vehicle
p 342 A95-81360
- BLEVINS, ROBERT D.**
Thermo-acoustic fatigue design for hypersonic vehicle
skin panels p 162 N95-19161
- BLISS, D. B.**
Vortex methods for the computational analysis of
rotor/body interaction [HTN-95-61072] p 369 A95-83656
- BLISSELL, W. A., JR.**
Use of blade pitch control to provide power train damping
for the Mod-2, 2.5-mW wind turbine p 440 N95-27986
- BLOM, C. E.**
Airborne measurements during the European Arctic
Stratospheric Ozone Experiment column amounts of
HNO3 and O3 derived from FTIR emission sounding
[HTN-95-00742] p 445 A95-86312

- BLOMENHOFER, HELMUT**
On-the-fly carrier phase ambiguity resolution for precise aircraft landing
[BTN-95-EIX95112522535] p 190 A95-69328
- BLOOMFIELD, A. P.**
Possible guidelines for helicopter noise assessment
[HTN-95-92535] p 558 A95-87355
- BLOOMFIELD, DAVID P.**
Linear Motor Free Piston Compressor
[AD-A293452] p 647 N95-31374
- BLOY, A. W.**
Interference between tanker wing wake with roll-up and receiver aircraft
[BTN-95-EIX95062487552] p 185 A95-68366
- BLUMENTHAL, PHILIP Z.**
Improved speed control system for the 87,000 HP wind tunnel drive
[NASA-TM-106840] p 211 N95-19794
A PC program for estimating measurement uncertainty for aeronautics test instrumentation
[NASA-CR-198361] p 523 N95-30067
- BLUNT, D. M.**
Variations observed in the AC generator signal period of a Sea King helicopter
[AD-A284280] p 230 N95-19963
A portable transmission vibration analysis system for the S-70A-9 Black Hawk helicopter
[DSTO-TR-0072] p 348 N95-24203
- BOALBEY, RICHARD E.**
Integration of a mechanical forebody vortex control system into the F-15 p 72 N95-14258
- BOBISH, KIMBERLY**
CAE for thermal management of aerospace electronic boards using the BETAsoft program p 438 N95-27354
- BOBULA, G. A.**
Pressure and temperature distortion testing of a two-stage centrifugal compressor
[BTN-94-EIX95011441250] p 431 A95-84207
- BODDY, MARK S.**
Empirical results on scheduling and dynamic backtracking p 299 N95-23761
- BODILLY, SUSAN J.**
Case study of risk management in the USAF B-1B bomber program
[AD-A282371] p 62 N95-11944
- BODINE, J. B.**
Design, analysis, and fabrication of a pressure box test fixture for tension damage tolerance testing of curved fuselage panels p 533 N95-28839
- BODONYI, RICHARD J.**
Wing-body juncture flows
[AD-A281526] p 106 N95-16099
- BODSON, MARC**
New adaptive methods for reconfigurable flight control systems, appendix 1
[AD-A292711] p 619 N95-30937
- BOER, RUUD G. DEN**
Overview of unsteady transonic wind tunnel test on a semispan straked delta wing oscillating in pitch
[AD-A284097] p 117 N95-18380
- BOERING, K. A.**
In situ observations in aircraft exhaust plumes in the lower stratosphere at midlatitudes
[HTN-95-A0862] p 318 A95-76266
- BOERING, KRISTIE A.**
Vertical transport rates in the stratosphere in 1993 from observations of CO₂, N₂O, and CH₄
[HTN-95-70941] p 351 A95-78006
- BOERSTOEL, J. W.**
Surface grid generation for multi-block structured grids p 643 A95-95478
- BOETTCHER, JAN**
Broadband noise characteristics of a model counter-rotating shrouded propfan p 572 A95-88470
- BOGDANOFF, DAVID W.**
New end tube closure system for the ram accelerator
[BTN-94-EIX94411380974] p 195 A95-68158
- BOGENBERGER, R.**
Optical backplane for modular avionics p 257 N95-20652
- BOGGS, S. L.**
Independent review of Aviation Technology and Research Information Analysis System (ATRIAS) database
[AD-A284049] p 226 N95-21518
- BOGUCZ, E.**
Research and educational initiatives at the Syracuse University Center for Hypersonics
[AIAA PAPER 95-6107] p 520 A95-90439
- BOHLE, M.**
Numerical modeling and simulation of chemically reacting reentry flows p 525 A95-87387
- BOHON, HERMAN L.**
Ninth DOD/NASA/FAA Conference on Fibrous Composites in Structural Design, volume 3
[NASA-CR-198718] p 420 N95-28266
Ninth DOD/NASA/FAA Conference on Fibrous Composites in Structural Design, volume 1
[NASA-CR-198723] p 421 N95-28420
Ninth DOD/NASA/FAA Conference on Fibrous Composites in Structural Design, volume 2
[NASA-CR-198722] p 424 N95-28462
Third NASA Advanced Composites Technology Conference, volume 1, part 2
[NASA-CP-3178-VOL-1-PT-2] p 531 N95-28823
Third NASA Advanced Composites Technology Conference, volume 1, part 1
[NASA-CP-3178-VOL-1-PT-1] p 534 N95-29029
- BOITNOTT, RICHARD L.**
An analytical and experimental investigation of the response of the curved, composite frame/skin specimens
[HTN-95-80857] p 283 A95-75099
- BOLDI, ROBERT**
Use of high resolution lightning detection and localization sensors for hazardous aviation weather nowcasting p 661 A95-93486
- BOLENDER, MICHAEL A.**
Assessment of CTAS ETA prediction capabilities
[NASA-CR-197224] p 97 N95-15728
- BOLLA, L.**
Electromagnetic compatibility effects of advanced packaging configurations p 247 N95-20658
- BOLTON, D.**
Cabin-fuselage-wing structural design concept with engine installation
[NASA-CR-197172] p 49 N95-12993
- BOLTON, J. S.**
Sound propagation from an arbitrarily oriented multipole placed near a plane, finite impedance surface
[BTN-94-EIX94371338964] p 257 A95-70797
The propagation of sound from an arbitrarily oriented dipole over a finite impedance plane p 570 A95-88459
- BOLTRALIK, WILLIAM J.**
AH-1F COBRA rewire program MANPRINT analysis
[AD-A289190] p 391 N95-27018
- BOLUKBASI, AKIF O.**
Prediction of energy absorption capability of composite stiffeners
[HTN-95-A0500] p 230 A95-72571
- BOMAR, JOHN B., JR.**
The large radius track centrifuge concept as an acceleration research and simulation device p 379 A95-84560
- BOND, THOMAS H.**
Repeatability of ice shapes in the NASA Lewis icing research tunnel
[BTN-95-EIX95062487528] p 204 A95-69236
Role of wind tunnels and computer codes in the certification and qualification of rotorcraft for flight in forecast icing
[NASA-TM-106747] p 39 N95-13197
- BONEV, B.**
A program for scientific and applied investigations using aerostat complexes p 182 A95-66304
- BONHAUS, DARYL L.**
Numerical study to assess sulfur hexafluoride as a medium for testing multielement airfoils
[NASA-TP-3496] p 378 N95-28674
- BONNEFOND, P.**
Precise orbit determination with a short-arc technique p 240 A95-70543
- BONNEFOND, T.**
Separation of winged vehicles in supersonics
[AIAA PAPER 95-6092] p 526 A95-88601
- BONNET, A.**
Interaction of a three strut support on the aerodynamic characteristics of a civil aviation model p 122 N95-19279
- BOODEY, J. B.**
Corrosion of landing gear steels p 302 N95-23500
- BOOTH, EARL R., JR.**
Analysis of a higher harmonic control test to reduce blade vortex interaction noise
[BTN-95-EIX95152582330] p 265 A95-73532
A higher harmonic control test in the DNW to reduce impulsive BVI noise
[HTN-95-61071] p 385 A95-83655
- BOOTHE, RICHARD E.**
Standardization of surface contamination analysis systems p 631 N95-31798
- BOOZ, JULIETA E.**
Evaluation of proposed agility metrics using X-31 vs. F/A-18 flight data
[AD-A292573] p 502 N95-28977
- BORCHERS, MARY F.**
Lubricant evaluation and performance, 2
[AD-A279144] p 242 N95-21969
- BORCHERS, PAUL F.**
Simulation model of the integrated flight/propulsion control system, displays, and propulsion system for ASTOVL lift-fan aircraft
[NASA-TM-108866] p 405 N95-26412
- BORE, C. L.**
Evaluation and management of research and development in aeronautics
[CONGRESS PAPER C428-8-102] p 581 A95-91691
- BOREL, C.**
Implicit multi-domain method for unsteady compressible inviscid fluid flows around 3D projectiles p 548 A95-91482
High performance parallelized implicit Euler solver for the analysis of unsteady aerodynamic flows p 644 A95-95495
- BOROVSKIJ, S. M.**
Mechanism and technological particular features of thermomagnetic hardening
[BTN-94-EIX94461407953] p 89 A95-62627
- BORRMANN, S.**
Performance of a focused cavity aerosol spectrometer for measurements in the stratosphere of particle size in the 0.06-2.0-micrometer-diameter range
[HTN-95-90914] p 253 A95-72423
- BORSI, M.**
Aerodynamic design and optimization at Alenia D.V.D. p 491 A95-87564
- BORTINS, RICHARD**
ACSYNT inner loop flight control design study
[NASA-CR-196316] p 17 N95-11223
- BORUE, VADIM**
Numerical studies of turbulent free surface flows and unsteady propeller flows
[AD-A294377] p 706 N95-34343
- BOS, J. F. T.**
Mach number control in the High Speed Wind Tunnel of NLR
[PB94-201670] p 53 N95-13243
- BOSCHAN, R. H.**
Thermally stable organic polymers
[AD-A281380] p 87 N95-14363
- BOSCHAN, R. S.**
Thermally stable organic polymers
[AD-A290755] p 537 N95-29482
- BOSE, B.**
Simple method of supersonic flow visualization using watertable
[BTN-95-EIX95182619105] p 269 A95-76590
- BOSE, NEIL**
Explicit Kutta condition for an unsteady two-dimensional constant potential panel method
[HTN-95-51679] p 433 A95-85061
- BOSE, S.**
Thermal barrier coating experience in the gas turbine engine p 345 N95-26125
- BOSE, T. K.**
WINCLR: A computer code for heat transfer and clearance calculation in a compressor
[NASA-CR-195436] p 366 N95-26363
- BOSGRA, O. H.**
Robust control: A structured approach to solve aircraft flight control problems p 621 N95-31995
- BOSNYAK, C. P.**
Failure analysis for polycarbonate transparencies
[AD-A292992] p 630 N95-31471
- BOSSCHERS, J.**
Validation of the helicopter rotor code HERO
[PB95-198040] p 607 N95-30838
- BOSSI, BRENT W.**
Aerodynamic interference for supersonic low-aspect-ratio missiles
[BTN-95-EIX95302694469] p 588 A95-94065
- BOSWORTH, JOHN T.**
X-29 flight control system: Lessons learned p 622 N95-32001
- BOTHWELL, CHRISTOPHER M.**
Torsional actuation with extension-torsion composite coupling and a magnetostrictive actuator
[BTN-95-EIX95262694314] p 435 A95-85485
- BOTROS, SHERIF M.**
A neural expert approach to self designing flight control systems
[AD-A279965] p 237 N95-21122
- BOTT, RICHARD**
Composite flight-control actuator development p 410 N95-28281
- BOTTS, MICHAEL**
Field and data analysis studies related to the atmospheric environment
[NASA-CR-196543] p 168 N95-18093

- BOUCHARD, M. P.**
An analysis of B-1B exterior jet blast windshield anti-icing performance using pre-cooled compressor bleed air [AD-A292522] p 485 N95-28811
- BOUCHARDY, P.**
Measurement by coherent anti-Stokes Raman scattering in the R5Ch hypersonic wind tunnel [BTN-95-EIX95112523811] p 188 A95-69322
- BOUCHEZ, MARC**
Scramjet combustor design in France [AIAA PAPER 95-6094] p 510 A95-88002
- BOULANGER, PATRICE**
Atmospheric effects on the risetime and waveshape of sonic booms p 100 N95-14886
- BOURGOIS, KAREN**
Advanced distributed simulation technology advanced rotary wing aircraft. Software reusability report [AD-A280434] p 20 N95-10354
- BOUSLOG, STANLEY A.**
Reentry analysis for low Earth orbiting spacecraft p 415 A95-85774
- BOUSMAN, W. SCOTT**
Characterization of annular two-phase gas-liquid flows in microgravity p.95 N95-14856
- BOUWER, G.**
Autonomous helicopter hover positioning by optical tracking [HTN-95-C0006] p 585 A95-93394
- BOUWER, GERD**
Model following control for tailoring handling qualities: ACT experience with ATThES p 622 N95-32000
- BOWDEN, FRED D.**
A PC-based interactive simulation of the F-111C Tack system and related sensor, avionics and aircraft aspects [AD-A285500] p 129 N95-16969
- BOWEN, BRENT D.**
The airline quality report, 1994 [NIAR-94-11] p 277 N95-24012
- BOWER, DANIEL R.**
Analytical study of the neutral stability of a model hypersonic boundary layer [BTN-95-EIX95152577589] p 263 A95-73493
- BOWER, W. W.**
Comparison of spatial numerical operators for duct-nozzle acoustics p 580 N95-30158
- BOWERS, ALBION H.**
F-18 high alpha research vehicle: Lessons learned p 69 N95-14240
- BOWERS, J. S.**
Electrochemical impedance pattern recognition for detection of hidden chemical corrosion on aircraft components, phase 1 [AD-A291345] p 556 N95-29946
- BOWERS, JAMES S.**
Electrochemical impedance pattern recognition for detection of hidden chemical corrosion on aircraft components [AD-A284998] p 241 N95-20481
Electrochemical impedance pattern recognition for detection of hidden chemical corrosion on aircraft components [AD-A285998] p 241 N95-20716
- BOWERSOX, RODNEY D. W.**
Model for compressible turbulence in hypersonic wall boundary and high-speed mixing layers [BTN-95-EIX94441386625] p 184 A95-68174
- BOWLES, JEFFREY V.**
Optimal trajectories for hypersonic launch vehicles [HTN-95-61120] p 415 A95-84884
- BOWLES, ROLAND L.**
The detection and measurement of microburst wind shear by an airborne lidar system p 543 A95-87798
- BOYCE, LOLA**
Probabilistic material strength degradation model for Inconel 718 components subjected to high temperature, high-cycle and low-cycle mechanical fatigue, creep and thermal fatigue effects [NASA-CR-197832] p 419 N95-27167
- BOYD, D. DOUGLAS, JR.**
Analysis of a higher harmonic control test to reduce blade vortex interaction noise [BTN-95-EIX95152582330] p 265 A95-73532
- BOYD, IAIN**
Particle kinetic simulation of high altitude hypervelocity flight [NASA-CR-197383] p 309 N95-22481
- BOYD, JANICE D.**
Evaluation of the Spartan tight-tolerance AXBT [HTN-95-40728] p 251 A95-70473
- BOYDEN, R. P.**
Buffeting tests in a cryogenic windtunnel [HTN-95-92833] p 470 A95-90751
Dynamic Stability Instrumentation System (DSIS). Volume 1: Hardware description [NASA-TM-109160-VOL-1] p 171 N95-18899
- BOYER, BRADLEY S.**
Three-D weather displays for aircraft cockpits [AD-A289759] p 508 N95-28691
- BOYER, DON L.**
Experimental and theoretical studies of wakes in stratified flows [AD-A290203] p 553 N95-29060
- BOYER, KEITH**
Characterization of stall inception in high-speed single-stage compressors [AD-A291275] p 514 N95-29934
- BOYLE, R. J.**
Grid orthogonality effects on predicted turbine midspan heat transfer and performance [NASA-TM-106931] p 554 N95-29371
- BOZKURT, SALIH**
Vortex lattice method simulation of unsteady flow due to wing/external store combination p 471 A95-91499
- BOZKURT, Y.**
Aerodynamic characteristics of external store configurations at low speeds [BTN-95-EIX95182619230] p 271 A95-76656
- BRAATEN, M.**
Combustion system CFD modeling at GE Aircraft Engines p 439 N95-27889
- BRAATHEN, G.**
An overview of the EASOE campaign [HTN-95-00702] p 443 A95-86272
- BRACALENTE, EMEDIO M.**
Certification methodology applied to the NASA experimental radar system p 41 N95-13205
- BRADLEY, JAMES T.**
Representativeness and responsiveness of automated weather systems p 660 A95-93482
- BRADLEY, KEVIN A.**
The effect of onset rate on annoyance to military aircraft noise p 561 A95-90119
- BRADLEY, MARTY KEITH**
Flow models for the design of a hypersonic iodine vapor wind tunnel nozzle with chemical and vibrational nonequilibrium effects p 592 N95-30448
- BRADLEY, R.**
An investigation of piloting strategies for engine failures during takeoff from offshore platforms [HTN-95-92834] p 497 A95-90752
- BRADSHAW, PETER**
Compressible Navier-Stokes calculations of the flow over airfoil sections. Comparisons of 1st and 2nd order turbulence models [SAE PAPER 932510] p 546 A95-89183
- BRADY, RAYMOND H., III**
Identification of aviation weather hazards based on the integration of radar and lightning data [HTN-95-51323] p 356 A95-80908
The inference of aviation weather hazards based on the integration of radar and lightning data p 660 A95-93483
- BRAGG, M. B.**
Effect of underwing frost on a transport aircraft airfoil at flight Reynolds number [BTN-95-EIX95152582334] p 276 A95-73536
Aerodynamics of a finite wing with simulated ice [BTN-95-EIX95182619227] p 270 A95-76653
- BRAGG, MICHAEL B.**
Study of the droplet spray characteristics of a subsonic wind tunnel [BTN-95-EIX95182619235] p 271 A95-76661
- BRAHIMI, M. T.**
Ice accretion on aircraft wings [BTN-95-EIX95082502224] p 225 A95-71021
- BRAININ, L.**
Stress considerations in reduced-size aeroelastic optimization [BTN-95-EIX95262694313] p 366 A95-85484
- BRAMKAMP, F. D.**
Transverse vorticity measurements in the NASA Ames 80 x 120 wind tunnel boundary layer p 251 N95-22457
- BRAND, SAM**
Environmental support of naval aviation [AD-A292873] p 598 N95-31454
- BRANDES, E. A.**
Sensing thunderstorm microphysics with multiparameter radar: Application for aviation p 657 A95-93467
- BRANDES, EDWARD A.**
The real-time analysis and prediction of storms program p 655 A95-93457
- BRANDON, JAY**
Quantifiable vortex features of F-106B aircraft at subsonic speeds [BTN-95-EIX0619952748161] p 588 A95-94455
- BRANDSMA, F. J.**
Numerical investigation into vortical flow about a delta-wing configuration up to incidences at which vortex breakdown occurs in experiment [PB95-198024] p 593 N95-30837
- BRANDSTATTER, W.**
Multidimensional calculation of spark flame initiation by adopting a generic hydrocarbon kinetic scheme p 528 A95-87566
- BRANDTJEN, RONALD**
Airborne measurements during the European Arctic Stratospheric Ozone Experiment: Observation of OClO [HTN-95-00745] p 445 A95-86315
- BRANIGAN, ROBERT G.**
Flight test of a low-altitude helicopter guidance system with obstacle avoidance capability p 688 N95-32490
Development and flight testing of an Obstacle Avoidance System for US Army helicopters p 687 N95-32500
- BRANSON, ROGER**
Advanced distributed simulation technology advanced rotary wing aircraft. Strawman verification and validation plan for the ARWA simulator system [AD-A280237] p 19 N95-10349
Advanced distributed simulation technology advanced rotary wing aircraft. System/segment specification. Volume 1: Simulation system module [AD-A280238] p 20 N95-10350
Advanced distributed simulation technology advanced rotary wing aircraft. System/segment specification. Volume 3: Visual system module [AD-A280239] p 20 N95-10351
Advanced distributed simulation technology advanced rotary wing aircraft. System/segment specification. Volume 2: Flight station module [AD-A280432] p 20 N95-10352
Advanced distributed simulation technology advanced rotary wing aircraft. System/segment specification. Volume 5: Simulation system module AH-64D kit [AD-A280433] p 20 N95-10353
Advanced distributed simulation technology advanced rotary wing aircraft. Software reusability report [AD-A280434] p 20 N95-10354
Advanced distributed simulation technology advanced rotary wing aircraft. Study comparing approaches to modeling the ARWA main rotor [AD-A280824] p 79 N95-14306
- BRANSTETTER, REAGAN**
Ultra-Reliable Digital Avionics (URDA) processor p 245 N95-20638
- BRASSEUR, G. P.**
Impact of present aircraft emissions of nitrogen oxides on tropospheric ozone and climate forcing [HTN-95-21364] p 353 A95-78679
- BRASSEUR, GUY**
Three-dimensional model interpretation of NO(x) measurements from the lower stratosphere [HTN-95-90534] p 213 A95-67806
- BRAUN, M. J.**
Analytical and experimental vibration analysis of a faulty gear system [NASA-TM-106689] p 58 N95-12843
- BRAUNINGER, H.**
Integrated X-ray testing of the electro-optical breadboard model for the XMM reflection grating spectrometer [DE95-008829] p 644 N95-30507
- BRAY, G. H.**
Prediction of R-curves from small coupon tests p 167 N95-19496
- BRAZA, M.**
Two-equation turbulence model for unsteady separated flows around airfoils [BTN-95-EIX95142553054] p 262 A95-73444
- BRAZIER, J. PH.**
Shock layers and boundary layers in hypersonic flows [HTN-95-A0003] p 183 A95-67830
- BREDIF, M.**
High performance parallelized implicit Euler solver for the analysis of unsteady aerodynamic flows p 644 A95-95495
- BREEMAN, J. H.**
Identification of dynamic systems. Volume 3: Applications to aircraft. Part 2: Nonlinear analysis and manoeuvre design [AGARD-AG-300-VOL-3-PT-2] p 79 N95-14102
- BREHM, ERIC W.**
Integrated performance and reliability specification for digital avionics systems [AIAA PAPER 95-0953] p 506 A95-90632
- BREININGER, DAVID R.**
A review of falconry as a bird control technique with recommendations for use at the Shuttle Landing Facility, John F. Kennedy Space Center, Florida, USA [NASA-TM-110142] p 381 N95-27859
- BREIT, G. A.**
Simulation of Shuttle launch G forces and acoustic loads using the NASA Ames Research Center 20G centrifuge p 86 N95-14089
- BREITBACH, ELMAR J.**
Using adaptive structures to attenuate rotary wing aeroelastic response [BTN-95-EIX95062487547] p 192 A95-68361

- BREITSAMTER, CHRISTIAN**
Velocity measurements with hot-wires in a vortex-dominated flowfield p 121 N95-19261
- BRENNAN, SEAN**
Airship applications of modern flight test techniques [AD-A284253] p 194 N95-19731
- BRENNINKMEIJER, C. A. M.**
An air-driven pressure booster pump for aircraft-based air sampling [HTN-95-40689] p 216 A95-69833
- BRENTNALL, W. D.**
Perspective on thermal barrier coatings for industrial gas turbine applications p 345 N95-26128
- BRENTNER, KENNETH S.**
Sensitivity of acoustic predictions to variation of input parameters [HTN-95-80855] p 267 A95-75097
The personal aircraft: Status and issues [NASA-TM-109174] p 223 N95-20688
- BREWER, J. C.**
Estimate of probability of crack detection from service difficulty report data [PB95-149381] p 328 N95-24295
- BREWER, JASON**
Integrated design and manufacturing for the high speed civil transport [NASA-CR-197183] p 48 N95-12700
- BREWER, JOHN**
Inspecting for widespread fatigue damage: Is partial debonding the key? p 93 N95-14458
- BREZINSKI, KENNETH**
MIL-STD-461/MIL-STD-704 investigation [SAE PAPER 932561] p 505 A95-90058
- BRIANT, C. L.**
Effect of annealing and desulfurization on oxide spallation of turbine airfoil material [BTN-95-EIX9528270724] p 528 A95-88264
- BRIDGES, DAVID H.**
Elliptic tip effects on the vortex wake of an axisymmetric body at incidence [BTN-94-EIX94441386612] p 208 A95-67343
Elliptic tip effects on the vortex wake of an axisymmetric body at incidence [HTN-95-20938] p 464 A95-88977
Crossflow instability control on a swept-wing: Preliminary studies p 274 N95-23283
- BRIDGES, JAMES E.**
Laser doppler velocimeter system for subsonic jet mixer nozzle testing at the NASA Lewis Aeroacoustic Propulsion Lab [NASA-TM-106984] p 457 N95-30229
- BRIGHT, MICHELLE M.**
Piloted evaluation of an integrated methodology for propulsion and airframe control design [AD-A290207] p 51 N95-12763
- BRINDLEY, W. J.**
Thermal Barrier Coating Workshop [NASA-CP-10170] p 344 N95-26119
- BRINK-SPALINK, J.**
Treatment of non-linear systems by timeplane-transformed CT methods: The spectral gust method p 143 N95-18600
- BRINKER, DAVID J.**
Design of a GaAs/Ge solar array for unmanned aerial vehicles [NASA-TM-106870] p 320 N95-23259
- BRINKMAN, A. C.**
Integrated X-ray testing of the electro-optical breadboard model for the XMM reflection grating spectrometer [DE95-008829] p 644 N95-30507
- BRINSON, HAL F.**
Micro-measurements of mechanical properties for adhesives and composites using digital imaging technology [NASA-CR-196111] p 22 N95-10231
- BRIOTTET, XAVIER**
Low-level data fusion for landing runways detection p 689 N95-33136
- BRISTOW, J. W.**
The basis of civil certification and continued airworthiness for composite aircraft structures [CONGRESS PAPER C428-37-173] p 628 A95-93632
- BRITCHER, COLIN P.**
Extension to the dynamic modeling of the large angle magnetic suspension test fixture [NASA-CR-197801] p 411 N95-26768
- BRITT, CHARLES L.**
Certification methodology applied to the NASA experimental radar system p 41 N95-13205
- BRITT, VICKI O.**
Nonlinear analysis of damaged stiffened fuselage shells subjected to combined loads p 137 N95-19499
- BRITTON, RANDALL K.**
Role of wind tunnels and computer codes in the certification and qualification of rotorcraft for flight in forecast icing [NASA-TM-106747] p 39 N95-13197
- BRITTON, T. W.**
Development of a coding form for approach control/pilot voice communications [DOT/FAA/AM-95/15] p 384 N95-28540
- BROATCH, S. A.**
A tactical navigation and routing system for low-level flight p 709 N95-32494
- BROCK, C. A.**
Performance of a focused cavity aerosol spectrometer for measurements in the stratosphere of particle size in the 0.06-2.0-micrometer-diameter range [HTN-95-90914] p 253 A95-72423
- BROCKHAUS, R.**
Handling qualities of hypersonic aircraft and related control requirements p 515 A95-87398
- BROCKMEYER, J. W.**
Ceramic composite attachments for transmission of high-torque loads [BTN-94-EIX95011441256] p 417 A95-84213
- BRODETSKY, M. D.**
Separation of winged vehicles in supersonics [AIAA PAPER 95-6092] p 526 A95-88601
- BROEK, DAVID**
Testing and analysis of flat and curved panels with multiple cracks p 93 N95-14460
- BROICHHAUSEN, KLAUS**
Aero design of turbomachinery components: CFD in complex systems p 90 N95-14136
- BROOKS, CUYLER W., JR.**
The NASA Langley 8-foot Transonic Pressure Tunnel calibration [NASA-TP-3437] p 8 N95-10739
- BROOKS, CYNTHIA L.**
Automation technology using Geographic Information System (GIS) p 324 N95-23284
- BROOKS, T. F.**
Recent studies of rotorcraft blade-vortex interaction noise [BTN-95-EIX95062487521] p 218 A95-69229
- BROOKS, THOMAS F.**
Analysis of a higher harmonic control test to reduce blade vortex interaction noise [BTN-95-EIX95152582330] p 265 A95-73532
A higher harmonic control test in the DNW to reduce impulsive BVI noise [HTN-95-61071] p 385 A95-83655
Studies of blade-vortex interaction noise reduction by rotor blade modification p 573 A95-90093
- BROT, ABRAHAM**
Probabilistic inspection strategies for minimizing service failures p 93 N95-14461
- BROUGHTON, T.**
Simultaneous engineering in aero gas turbine design and manufacture [CONGRESS PAPER C428-20-204] p 581 A95-91723
- BROWN, ART**
Labs behind Boeing's new 777 [BTN-95-EIX95142562403] p 280 A95-73437
- BROWN, BARBARA G.**
Use of pilot reports for verification of aircraft icing diagnoses and forecasts p 666 A95-93508
Examination of conditions in the proximity of pilot reports of aircraft icing during storm-fest p 666 A95-93509
- BROWN, DANSEN**
Pressure measurements on an F/A-18 twin vertical tail in buffeting flow. Volume 3: Buffet power spectral densities [AD-A281444] p 36 N95-11829
Pressure measurements on an F/A-18 twin vertical tail in buffeting flow. Volume 2: Steady and unsteady RMS pressure data [AD-A281581] p 76 N95-15465
Pressure measurements on an F/A-18 twin vertical tail in buffeting flow. Volume 4, part 2: Buffet cross spectral densities [AD-A285555] p 143 N95-18641
Pressure measurements on an F/A-18 twin vertical tail in buffeting flow. Volume 4, part 1: Buffet cross spectral densities [AD-A285593] p 237 N95-21214
Pressure measurements on an F/A-18 twin vertical tail in buffeting flow. Volume 1: Wind tunnel test summary [AD-A279126] p 225 N95-21877
- BROWN, DAVE**
Integrated Thermal Energy Management (I-TEM): An evaluation tool for aircraft [SAE PAPER 932577] p 493 A95-90065
- BROWN, JOHN M.**
Forecasting for a large field program: STORM-FEST [HTN-95-90694] p 215 A95-69721
- BROWN, PHILIP W.**
High-Alpha Research Vehicle (HARV) longitudinal controller: Design, analyses, and simulation results [NASA-TP-3446] p 17 N95-10860
- BROWN, RICHARD T.**
Through-the Thickness(R) braided composites for aircraft applications p 421 N95-28273
- BROWN, ROBERT E.**
INM contour validation: A case study p 31 N95-11321
- BROWN, SCOTT**
Rapid prototyping of composite aircraft structures [SAE PAPER 931219] p 539 A95-87530
- BROWN, STEVE WESLEY**
Documentation and archiving of the Space Shuttle wind tunnel test data base. Volume 1: Background and description [NASA-TM-104806-VOL-1] p 151 N95-19237
Documentation and archiving of the Space Shuttle wind tunnel test data base. Volume 2: User's Guide to the Archived Data Base [NASA-TM-104806-VOL-2] p 205 N95-19624
- BROWN, T.**
Composite fuselage crown panel manufacturing technology p 399 N95-28474
Manufacturing scale-up of composite fuselage crown panels p 532 N95-28835
- BROWNE, G. T.**
US Navy operating experience with new aircraft construction materials p 303 N95-23517
- BROZOWSKI, L. A.**
Impeller flow field characterization with a laser two-focus velocimeter p 313 N95-23440
- BRUBAKER, J.**
Reducing process noise in superconducting helium liquid level probes [DE95-008956] p 629 N95-30765
- BRUCATO, ROBERT**
Unmanned aerial vehicle heavy fuel engine test [AD-A284332] p 139 N95-18383
- BRUCE, DAVID A.**
Non-destructive detection of corrosion for life management p 314 N95-23505
- BRUCKART, J. E.**
First medical test of the UH-60Q and equipment for use in US Army medevac helicopters p 568 N95-29620
- BRUEMMER, A.**
Low-speed aerodynamic characteristics of a slender wing with vertical fins p 460 A95-87400
- BRUINJES, R. T.**
Preliminary comparisons between MM5 NCAR/Penn State model generated icing forecasts and observations p 655 A95-93458
- BRUMBAUGH, RANDAL W.**
Aircraft model for the AIAA controls design challenge [BTN-94-EIX94511433921] p 142 A95-64587
- BRUN, G.**
Numerical simulation of the 3D turbulent flow around the combustor dome of an aircraft engine p 640 A95-95423
- BRUN, M. K.**
Toughened Silcomp composites for gas turbine engine applications [DE95-002851] p 235 N95-21243
- BRUNE, G. W.**
Two-dimensional high-lift airfoil data for CFD code validation p 112 N95-17859
- BRUNEAU, STEPHEN D.**
A Lifting Ball Valve for cryogenic fluid applications p 156 N95-16349
- BRUNGER, CLIFFORD A.**
Artificial neural network modeling of damaged aircraft [AD-A283227] p 80 N95-14849
- BRUNO, J.**
Advanced wing design survivability testing and results p 400 N95-28488
- BRUSMARK, B.**
Scattering of short em-pulses by simple and complex targets using impulse radar p 486 A95-90953
- BRUZA, K. J.**
Novel matrix resins for composites for aircraft primary structures, phase 1 [NASA-CR-189657] p 23 N95-10318
- BRUZZINI, MICHAEL A.**
Development of a TECS control-law for the lateral directional axis of the McDonnell Douglas F-15 Eagle [AD-A289771] p 410 N95-28598
- BRYANT, BOBBY**
A computer-based multimedia prototype for night vision goggles [AD-A286208] p 258 N95-21882
- BRYANT, MARK**
The Aluminum Falcon: A low cost modern commercial transport [NASA-CR-197180] p 81 N95-15742

- BRYSON, TRAVIS**
 PolymSys (TM): An extended version of CLIPS for construction and reasoning using blackboards
 p 217 N95-19767
- BUCCI, R. J.**
 Prediction of R-curves from small coupon tests
 p 167 N95-19496
- BUCH, A.**
 Review of some results of the author's fatigue investigations with applications in engineering and material science
 [TAE-698] p 316 N95-23662
- BUCHHOLZ, JOERG J.**
 SCARLET: DLR rate saturation flight experiment
 p 598 N95-31068
- BUCKHARDT, GARY L.**
 Eddy current for detecting second-layer cracks under installed fasteners
 [AD-A279871] p 244 N95-20414
- BUDD, GERALD D.**
 Operational and research aspects of a radio-controlled model flight test program
 [BTN-95-EIX0619952748177] p 606 A95-94471
- BUDNICK, E. K.**
 A review of water mist technology for fire suppression
 [AD-A285738] p 225 N95-20071
- BUECHLER, DENNIS**
 Field and data analysis studies related to the atmospheric environment
 [NASA-CR-196543] p 168 N95-18093
- BUECHTEMANN, W.**
 Laser based obstacle warning sensors for helicopters
 p 686 N95-32499
- BUEHRLE, R. D.**
 Dynamic response tests of inertial and optical wind-tunnel model attitude measurement devices
 [NASA-TM-109182] p 296 N95-23011
- BUEHRLE, RALPH D.**
 Effects of vibration on inertial wind-tunnel model attitude measurement devices
 [NASA-TM-109083] p 21 N95-11466
- BUELOW, B. E. O.**
 Convergence acceleration of implicit schemes in the presence of high aspect ratio grid cells
 p 313 N95-23446
- BUETEFISCH, K. A.**
 Wind tunnel test on a 65 deg delta wing with rounded leading edges: The International Vortex Flow Experiment
 p 114 N95-17875
- BUFFAT, M.**
 Numerical simulation of the 3D turbulent flow around the combustor dome of an aircraft engine
 p 640 A95-95423
- BUFFINGTON, JAMES M.**
 Design of nonlinear control laws for high-angle-of-attack flight
 [BTN-94-EIX94511433920] p 141 A95-64586
 Robust longitudinal axis flight control for an aircraft with thrust vectoring
 [BTN-95-EIX95122538875] p 408 A95-83000
- BUFFUM, D. H.**
 Effect of wind tunnel acoustic modes on linear oscillating cascade aerodynamics
 [HTN-94-00760] p 14 A95-60199
- BUGAJSKI, DAN**
 Dynamic inversion: An evolving methodology for flight control design
 p 621 N95-31996
- BUGAJSKI, DANIEL J.**
 Multi-application controls: Robust nonlinear multivariable aerospace controls applications
 p 71 N95-14249
- BUGELE, ALVIN E.**
 Control of wind tunnel operations using neural net interpretation of flow visualization records
 [NASA-TM-106683] p 24 N95-10854
- BUISSON, JAMES A.**
 Effect of broadcast and precise ephemerides on estimates of the frequency stability of GPS Navstar clocks
 [BTN-95-EIX95112522530] p 190 A95-69333
- BUIVUN, N. A.**
 The joint Russian-Brasil research on balloons
 p 182 A95-66303
- BUKLEY, JERRY**
 Application of fuzzy logic to optimize placement of an acquisition, tracking, and pointing experiment
 p 341 A95-80390
- BUKOV, A.**
 Optical surface pressure measurements: Accuracy and application field evaluation
 p 175 N95-19274
- BULZAN, DANIEL L.**
 Structure of a swirl-stabilized, combusting spray
 [NASA-TM-106724] p 50 N95-11890
- BUNSHAH, ROINTAN F.**
 Effects of activated reactive evaporation process parameters on the microhardness of polycrystalline silicon carbide thin films
 [GTN-95-00406090-4621] p 680 A95-93965
- BURCHAM, FRANK W.**
 Dynamic ground effects flight test of an F-15 aircraft
 [NASA-TM-4604] p 38 N95-12191
 Engines-only flight control system
 [NASA-CASE-ARC-11944-1] p 294 N95-23389
- BURCHAM, FRANK W., JR.**
 An overview of integrated flight-propulsion controls flight research on the NASA F-15 research airplane
 p 694 N95-33010
 Background and principles of throttles-only flight control
 p 697 N95-33021
 Flight test of a propulsion controlled aircraft system on the NASA F-15 airplane
 p 691 N95-33023
 Design challenges encountered in the F-15 PCA flight test program
 p 692 N95-33025
- BURDETTE, GEORGE W.**
 Solid fuel ramjet composition
 [AD-D016458] p 152 N95-19090
- BURDISO, RICARDO A.**
 Active control of fan noise from a turbofan engine
 [HTN-95-61198] p 570 A95-85751
 Analytical investigation of adaptive control of radiated inlet noise from turbofan engines
 p 30 N95-11277
- BURGETT, S.**
 SAR image registration in absolute coordinates using GPS carrier phase position and velocity information
 [DE94-018738] p 228 N95-20195
- BURGREEN, GREG W.**
 Aerodynamic shape optimization using preconditioned conjugate gradient methods
 [BTN-95-EIX95142553033] p 263 A95-73465
 Improving the efficiency of aerodynamic shape optimization
 [HTN-95-61204] p 540 A95-87577
- BURGREEN, GREGORY WAYNE**
 Three-dimensional aerodynamic shape optimization using discrete sensitivity analysis
 p 691 N95-32904
- BURKEN, JOHN**
 Design challenges encountered in the F-15 PCA flight test program
 p 692 N95-33025
- BURKEN, JOHN J.**
 Flight test of the X-29A at high angle of attack: Flight dynamics and controls
 [NASA-TP-3537] p 284 N95-22806
 X-29 flight control system: Lessons learned
 p 622 N95-32001
- BURKERT, W.**
 Integrated X-ray testing of the electro-optical breadboard model for the XMM reflection grating spectrometer
 [DE95-008829] p 644 N95-30507
- BURKHALTER, JOHN E.**
 Nonlinear aerodynamic analysis of grid fin configurations
 [BTN-95-EIX0619952748172] p 590 A95-94466
- BURKHARD, ALAN H.**
 Concepts for aircraft subsystem integration
 [SAE PAPER 931377] p 604 A95-93656
- BURKHOLDER, P. S.**
 Allison engine testing CMSX-4 (reg sign) single crystal turbine blades and vanes
 [DE95-010308] p 694 N95-32636
- BURLEY, CASEY L.**
 Sensitivity of acoustic predictions to variation of input parameters
 [HTN-95-80855] p 267 A95-75097
 Aircraft noise prediction program theoretical manual: Rotorcraft System Noise Prediction System (ROTONET), part 4
 [NASA-TM-83199-PT-4] p 451 N95-26392
- BURLEY, RICHARD R.**
 Design and development of an F/A-18 inlet distortion rake: A cost and time saving solution
 p 69 N95-14241
- BURNER, A. W.**
 Dynamic response tests of inertial and optical wind-tunnel model attitude measurement devices
 [NASA-TM-109182] p 296 N95-23011
- BURNETT, DAVID W.**
 Hypersonic waverider test vehicle: A logical next step
 [BTN-95-EIX95041503783] p 193 A95-69214
- BURNETTE, KEITH T.**
 An evaluation of aircraft CRT and dot-matrix display legibility requirements
 [AD-A283933] p 138 N95-18164
- BURNHAM, D.**
 Aircraft wake vortex takeoff tests at O'Hara International Airport
 [AD-A283828] p 118 N95-18624
- BURNHAM, EDWARD ALONZA, JR.**
 Investigation of starting and ignition transients in the thermally choked ram accelerator
 p 698 N95-34805
- BURNS, I. F.**
 An investigation of drag repeatability in half model testing in the ARA Transonic Wind Tunnel
 [ARA-MEMO-392] p 188 N95-19546
- BURNS, IAN F.**
 Investigation of a thermal buoyancy effect on the drag of half models tested in the ARA Transonic Wind Tunnel
 [ARA-MEMO-407] p 222 N95-19946
- BURNS, J. A.**
 Computational methods for control and optimal design of aerospace systems
 [AD-A292861] p 608 N95-31451
- BURPO, S. J.**
 ACT/ICAPS: Thermoplastic composite activities
 p 421 N95-28274
- BURRIS, STEPHEN A.**
 Course module for AA201: Wing structural design project
 [AD-A283618] p 133 N95-18616
- BURROUGHS, COURTNEY B.**
 A theoretical analysis of airborne sound transfer for a resiliently mounted machine to its foundation
 p 30 N95-11304
- BURROWS, A. P.**
 An efficient discrete vortex method for low Reynolds number incompressible flows
 p 639 A95-95407
- BURROWS, C. R.**
 Fault Diagnosis for condition monitoring applied to hydraulic circuits
 [CONGRESS PAPER C428-12-165] p 456 A95-91703
- BURRUS, D.**
 Combustion system CFD modeling at GE Aircraft Engines
 p 439 N95-27889
- BURT, MARTIN**
 Transonic and supersonic flowfield measurements about axisymmetric afterbodies for validation of advanced CFD codes
 p 121 N95-19260
- BURTON, RALPH A.**
 The effects of wall perturbations on thermo-turbulent Couette flow
 [HTN-95-92255] p 434 A95-85299
- BURWARD-HOY, TREVOR**
 Concepts for the control of rotor noise
 p 573 A95-90092
- BUSHMAN, MARK**
 F-15 propulsion system
 p 695 N95-33012
- BUSHNELL, DENNIS M.**
 Potential impacts of advanced aerodynamic technology on air transportation system productivity
 [NASA-TM-109154] p 10 N95-11489
 The personal aircraft: Status and issues
 [NASA-TM-109174] p 223 N95-20688
- BUSKA, STEVEN**
 Micro-time stress measurement device development
 [AD-A289511] p 448 N95-26845
- BUSQUETS, ANTHONY M.**
 Spatial awareness comparisons between large-screen, integrated pictorial displays and conventional EFIS displays during simulated landing approaches
 [NASA-TP-3467] p 80 N95-14852
- BUSSMANN, J.**
 Chemically reacting non-equilibrium boundary layers in air breathing propulsion systems
 [AIAA PAPER 95-6139] p 512 A95-90456
- BUSSOLETTI, J. E.**
 TranAir: A full-potential, solution-adaptive, rectangular grid code for predicting subsonic, transonic, and supersonic flows about arbitrary configurations. User's manual
 [NASA-CR-4349] p 377 N95-28230
 TranAir: A full-potential, solution-adaptive, rectangular grid code for predicting subsonic, transonic, and supersonic flows about arbitrary configurations. Theory document
 [NASA-CR-4348] p 378 N95-28265
- BUSSONNET, P. X.**
 Design of fan blades subjected to bird impact
 p 200 N95-19669
- BUSTO, MARIO**
 Nonlinear angle of twist of advanced composite wing boxes under pure torsion
 [BTN-95-EIX95152582323] p 281 A95-73526
- BUTLER, BARCLAY P.**
 A correlative investigation of simulated occupant motion and accident report in a helicopter crash
 [AD-A285190] p 123 N95-16404
- BUTLER, R.**
 Optimum design of composite stiffened wing panels - a parametric study
 [HTN-95-01088] p 496 A95-90274
- BUTLER, RICKY W.**
 Formal design and verification of a reliable computing platform for real-time control (phase 3 results)
 [NASA-TM-109140] p 33 N95-10873

BUTTRILL, CAREY

Simulation and model reduction for the active flexible wing program
[BTN-95-EIX95182619211] p 295 A95-76637

BUTTS, D. G.

Aircraft stress sequence development: A complex engineering process made simple p 136 N95-19480

BUTZEL, LEO M.

Comments on the use of structureborne noise analysis for large commercial airplanes p 30 N95-11287

BYBEE, J. L.

Computer aided diagnostic testing of installed flight control servo-actuators
[SAE PAPER 932584] p 494 A95-90068

BYRNES, R. T.

Fatigue crack growth in nickel-based superalloys at 500-700 C. 1: Waspaloy
[BTN-94-EIX94371347843] p 206 A95-69136

BYUN, CHANSUP

Parallel aeroelastic computations for wing and wing-body configurations
[NASA-CR-196835] p 36 N95-11766
Aeroelasticity of wing and wing-body configurations on parallel computers
[NASA-CR-197756] p 389 N95-26590

C

CABELL, R. H.

Artificial neural networks for predicting nonlinear dynamic helicopter loads
[HTN-95-51678] p 404 A95-85060

CADOUX, ROY E.

The use of the Equivalent Continuous Sound Level (L(sub eq)) as an aircraft noise index
[HTN-95-92542] p 558 A95-87362

CAGLAYAN, ALPER K.

A neural expert approach to self designing flight control systems
[AD-A279965] p 237 N95-21122

CAHILL, PATRICIA

Electrical short circuit and current overload tests on aircraft wiring
[AD-A293308] p 646 N95-30922

CAI, TIMIN

Simulation on the 3-D turbulent flow in the passages of finocyl grain
[BTN-95-EIX95202638962] p 279 A95-76674

CAI, ZHONG

Development of hypersonic engine seals: Flow effects of preload and engine pressures
[BTN-95-EIX95112524204] p 196 A95-69304

CAILLY, C.

Nonhydrostatic simulation of frontogenesis in a moist atmosphere. Part 3: Thermal wind imbalance and rainbands
[HTN-95-90356] p 212 A95-66429

CAIN, A. B.

Comparison of spatial numerical operators for duct-nozzle acoustics p 580 N95-30158

CAIN, ALAN B.

Modelling structurally damaging twin-jet screech p 135 N95-19154

CAIPEN, T. L.

The coplanar projectile motion problem including the effects of lift and drag
[ISBN 1-879921-01-4] p 635 A95-93723

CAIRNS, MARY

Developing and testing decision-making products for center weather service unit meteorologists p 671 A95-93533

CAIRNS, MARY M.

The aviation gridded forecast system verification program - A description of aviation-impact-variable evaluation plans p 664 A95-93498

CALCAGNO, P.

Geoid lineations of 1000 km wavelength over the central Pacific
[HTN-95-11304] p 319 A95-77009

CALDWELL, B.

Flight control systems/structural coupling BAe Warton experience in aero-servo elasticity
[CONGRESS PAPER C428-35-059] p 610 A95-93628

CALDWELL, B. D.

The FCS-structural coupling problem and its solution p 623 N95-32005

CALDWELL, D. J.

Modeling aerosol emissions from the combustion of composite materials p 301 N95-23038

CALDWELL, JOHN A. JR.

The effects of UH-1 experience on UH-60 simulator performance: A preliminary study
[AD-A289457] p 391 N95-26993

CALEDONIA, GEORGE E.

Ultraviolet emissions occurring about hypersonic vehicles in rarefied flows
[AD-A281452] p 106 N95-16076

CALISE, ANTHONY J.

Analytical investigations in aircraft and spacecraft trajectory optimization and optimal guidance
[NASA-CR-4672] p 526 N95-29339

CALLAHAN, CYNTHIA B.

Design optimization of rotor blades for improved performance and vibration
[HTN-95-A0498] p 229 A95-72569

CALVERT, JEFFREY M.

High aspect ratio metal microstructures and method for preparing the same
[AD-D017463] p 629 N95-30750

CALZETTA, ROBERT K.

An approach to weather requirements management p 653 A95-93448

CALZONE, R. F.

Integral rocket ramjets
[AD-A285135] p 240 N95-20906

CAMACHO, Y.

A study of the effect of store unsteady aerodynamics on gust and turbulence loads p 133 N95-18601

CAMBIER, JEAN-LUC

Experimental and analytical investigations of wave enhanced supersonic combustors
[AIAA PAPER 89-2787] p 14 A95-60172

CAMELL, D. G.

Measurements of shielding effectiveness and cavity characteristics of airplanes
[PB94-210051] p 244 N95-20191

CAMERON, KEITH

Unmanned Aerial Vehicle technology
[DSTO-GD-0044] p 503 N95-29362

CAMM, FRANK

The development of the F100-PW-220 and F110-GE-100 engines: A case study of risk assessment and risk management
[AD-A282467] p 51 N95-13289

The F-16 multinational staged improvement program: A case study of risk assessment and risk management
[AD-A281706] p 81 N95-15451

CAMPBELL, EDWINA

Inadequacy of visual alarms in helicopter air medical transport
[HTN-95-01218] p 484 A95-91450

CAMPBELL, FRANK J.

Problems with aging wiring in Naval aircraft p 154 N95-16048

CAMPBELL, JAMES F.

Patterns in the sky: Natural visualization of aircraft flow fields
[NASA-SP-514] p 584 N95-31000

CAMPBELL, M. R.

A surgical support system for Space Station Freedom p 149 N95-16776

CAMPBELL, RICHARD L.

Application of two procedures for dual-point design of transonic airfoils
[NASA-TP-3466] p 38 N95-12176

CAMPBELL, STEVEN D.

Dissemination of terminal weather products to the flight deck via data link p 669 A95-93525

Future enhancements to ground-based microburst detection p 11 N95-10570

Ground-based wake vortex monitoring, prediction, and ATC interface p 42 N95-13209

CAMPOS, S.

Computing quantitative characteristics of finite-state real-time systems
[AD-A282839] p 83 N95-14343

CANDEL, SEBASTIEN M.

Stochastic approach to noise modeling for free turbulent flows
[HTN-95-42321] p 371 A95-86150

CANNELL, MICHAEL J.

175Hp contrarotating homopolar motor design report
[AD-A291138] p 557 N95-30122

CANNON, M. E.

Attitude determination using dedicated and nondedicated multi-antenna GPS sensors
[BTN-95-EIX95142555482] p 228 A95-72891

Assessment of a non-dedicated GPS receiver system for precise airborne attitude determination
[DE94-019309] p 229 N95-21520

CANNON, M. R.

Object-oriented technology for compressor simulation
[NASA-TM-106723] p 49 N95-11864

CANTER, DAVE

X-31 post-stall envelope expansion and tactical utility testing p 70 N95-14242

CAO, XI

A method for calculating mean aerodynamic center and zero-lift moment coefficient of aircraft without tail by using measured flight loads p 474 A95-91552

Neural network approach to identification of aerodynamic loads on a wing. 1: Application to cantilevered beam models p 475 A95-91568

CAPASSO, MICHAEL A.

Construction and wind tunnel test of a 1/12th scale helicopter model
[AD-A288487] p 378 N95-28331

CAPLOT, M.

FASTPACK: Optimized solutions for modular avionics derived from a parametric study. Part 2: Avionics p 233 N95-20635

Composite cases for airborne electronic equipment: A technology study and EMC p 241 N95-20655

Modular supplies for a distributed architecture p 234 N95-20657

CAPOGNA, C.

FASTPACK: Optimized solutions for modular avionics derived from a parametric study. Part 2: Avionics p 233 N95-20635

CAPOTONDI, ANTONIETTA

Assimilation of altimeter data in a quasi-geostrophic model of the Gulf Stream system: A dynamical perspective
[NASA-CR-196313] p 320 N95-23766

CAPOZZI, BRIAN

Icarus Rewaxed: A high speed, low-cost general aviation aircraft for Aeroworld
[NASA-CR-197155] p 45 N95-12609

CARABELL, KEVIN DAVID

Air/fuel ratio visualization in a diesel spray p 556 N95-29807

CARADONNA, F. X.

The application of potential CFD methods to helicopter hover flows
[ISBN 1-879921-01-4] p 587 A95-93747

CARBONARO, MARIO

Application of pressure sensitive paint in hypersonic flows
[NASA-TM-106824] p 223 N95-20794

CARBONARO, MARIO C.

Experimental investigation of the flowfield about an upswept afterbody
[BTN-95-EIX95152582321] p 265 A95-73524

CARBONELL, J. M.

Liquid flow-through cooling of electronic modules p 246 N95-20647

CARDEN, HUEY D.

Effects of floor location on response of composite fuselage frames p 423 N95-28439

CARDICK, ARTHUR W.

A method of calculating the safe fatigue life of compact, highly-stressed components p 93 N95-14464

CARDIN, JOSEPH M.

A Lifting Ball Valve for cryogenic fluid applications p 156 N95-16349

CARDOSI, KIM M.

An analysis of tower (local) controller-pilot voice communications
[AD-A283718] p 160 N95-18436

CARDRICK, A. W.

The certification of composite structures for military aircraft
[CONGRESS PAPER C428-37-198] p 628 A95-93633

CARLE, A.

Applications of automatic differentiation in computational fluid dynamics p 156 N95-16461

Applications of automatic differentiation in CFD
[NASA-TM-109948] p 157 N95-16828

CARLSON, JOHN R.

Two-dimensional converging-diverging rippled nozzles at transonic speeds
[NASA-TP-3440] p 6 N95-10129

Application of Navier-Stokes code PAB3D with kappa-epsilon turbulence model to attached and separated flows
[NASA-TP-3480] p 224 N95-21338

CARLSON, LELAND A.

Aerodynamic sensitivity coefficients using the three-dimensional full potential equation
[BTN-95-EIX95062487530] p 186 A95-69238

CARLSON, N. W.

Overview of remote sensing laser development and semiconductor laser technology
[DE94-019103] p 256 N95-21552

CARON, JOHN

The prototype aviation weather products generator a vehicle to assess user needs p 671 A95-93534

CARPINILOGLU, M. O.

Effect of spherical roughness elements upon transition of a 3-D boundary layer
[HTN-95-92835] p 471 A95-90753

- CARR, D.**
Viper cabin-fuselage structural design concept with engine installation and wing structural design [NASA-CR-197162] p 45 N95-12305
- CARR, L. W.**
Interferometry and computational studies of an oscillating airfoil compressible dynamic stall flow field [HTN-94-00703] p 3 A95-60182
Interferometric investigations of compressible dynamic stall over a transiently pitching airfoil [HTN-95-42338] p 372 A95-86167
- CARR, LAWRENCE W.**
A study of compressibility effects on dynamic stall of rapidly pitching airfoils [HTN-94-00715] p 5 A95-60193
- CARRANNANTO, PAUL G.**
Lift-enhancing tabs on multielement airfoils [BTN-95-EIX0619952748187] p 591 A95-94479
- CARRASCO, ARMANDO**
VUV shock layer radiation in an arc-jet wind tunnel experiment [HTN-95-42338] p 372 A95-86167
- CARRERE, F.**
Optimal shape design in hypersonic aerodynamics and electromagnetics p 639 A95-95397
- CARRINGTON, C. K.**
Building complex simulations rapidly using MATRIX(x): The Space Station redesign [TABES PAPER 94-632] p 87 N95-14653
- CARROLL, FRANK T.**
Testing considerations for military aircraft engines in corrosive environments (a Navy perspective) p 202 N95-19684
- CARSON, LAURIE PASCHAL**
A short-term, high-resolution automated snowfall forecasting system p 666 A95-93510
- CARTER, DALE**
Flow visualization studies of VTOL aircraft models during Hover in ground effect [NASA-TM-108860] p 272 N95-22666
- CARTER, DOUGLAS W.**
Rapid repair of large area damage to contoured aircraft structures p 394 N95-27516
- CARTER, GARY M.**
Identification of aviation weather hazards based on the integration of radar and lightning data [HTN-95-51323] p 356 A95-80908
The inference of aviation weather hazards based on the integration of radar and lightning data p 660 A95-93483
- CARTER, H. (NICK), III**
A subsystem integration technology concept [SAE PAPER 931382] p 604 A95-93658
- CARTER, JOHN**
Multi-application controls: Robust nonlinear multivariable aerospace controls applications p 71 N95-14249
- CARUSO, STEVEN C.**
Aerodynamic design of pegasus: Concept to flight with computational fluid dynamics [BTN-95-EIX95182617463] p 298 A95-75734
- CARUTHERS, JOHN**
A note on the Kutta-Joukowski formula [ISBN 1-879921-01-4] p 635 A95-93735
- CARZOO, SUSAN W.**
High-Alpha Research Vehicle (HARV) longitudinal controller: Design, analyses, and simulation results [NASA-TP-3446] p 17 N95-10860
- CASALENGUA, J.**
A study of the effect of store unsteady aerodynamics on gust and turbulence loads p 133 N95-18601
- CASARELLA, MARIO J.**
Application of wavelet-filtering techniques to intermittent turbulent and wall pressure events. Part 1: Exploratory results [AD-A286077] p 247 N95-20849
- CASDORPH, VAN**
On-line learning nonlinear direct neurocontrollers for restructurable control systems [BTN-95-EIX95242670768] p 359 A95-81079
- CASEY, M. V.**
Computational methods for preliminary design and geometry definition in turbomachinery p 89 N95-14128
The industrial use of CFD in the design of turbomachinery p 90 N95-14133
- CASPER, ANN M.**
Dynamically timed electric motor [NASA-CASE-MFS-28958-1] p 437 N95-26890
- CASPER, JAY**
Nonreflective boundary conditions for high-order methods [HTN-95-42328] p 371 A95-86157
Computing unsteady shock waves for aeroacoustic applications [HTN-95-20928] p 463 A95-88967
- CASTELLANI, A.**
Selecting and management of fire fighter aircraft [BTN-95-EIX95062487538] p 193 A95-69246
- CATALI FAUD, J.**
Aircraft interior sound field analysis in view of active control: Results from the ASANCA project p 575 A95-90109
- CAUDRON, F.**
Experimental investigation of the flowfield about an upswept afterbody [BTN-95-EIX95152582321] p 265 A95-73524
- CAUGHEY, DAVID A.**
Computing unsteady shock waves for aeroacoustic applications [HTN-95-20928] p 463 A95-88967
- CAULKINS, RONALD W.**
Condition monitoring and diagnostics [HTN-95-92312] p 387 A95-85356
Condition monitoring for helicopters: 3303 Airborne vibration monitoring system [SAE PAPER 931360] p 610 A95-93642
- CAZENAIVE, A.**
Geoid lineations of 1000 km wavelength over the central Pacific [HTN-95-11304] p 319 A95-77009
- CEBECI, TUNCER**
Predicting stall and post-stall behavior of airfoils at low mach numbers [BTN-95-EIX95262694297] p 365 A95-85468
- CEDAR, RICHARD D.**
Engine/airframe installation CFD for commercial transports: An engine manufacturer's perspective [SAE PAPER 932623] p 495 A95-90084
- CEDRUN, MARK E.**
Low-speed wind tunnel testing of the NPS and NASA Ames Mach 6 optimized waverider [AD-A283585] p 75 N95-15319
- CELESTINA, MARK L.**
Experimental and computational investigation of the tip clearance flow in a transonic axial compressor rotor [NASA-TM-106711] p 649 N95-31738
- CELLI, ROBERTO**
High-order state space simulation models of helicopter flight mechanics [HTN-95-A0494] p 237 A95-72565
Efficient sensitivity analysis for rotary-wing aeromechanical problems [BTN-95-EIX95152577585] p 264 A95-73497
Effects of high order dynamics on helicopter flight control law design [HTN-95-80852] p 290 A95-75094
Efficient sensitivity analysis for rotary-wing aeromechanical problems [HTN-95-42570] p 458 A95-87200
- CELIK, ZEKI Z.**
Determination of solid/porous wall boundary conditions from wind tunnel data for computational fluid dynamics codes p 164 N95-19266
- CENEDESE, F.**
Experimental results of the European HELINOISE aeroacoustic rotor test [HTN-95-01080] p 578 A95-90266
- CEPEDA, A.**
Cabin-fuselage-wing structural design concept with engine installation [NASA-CR-197172] p 49 N95-12993
- CERVENKA, PETER O.**
Laws of infrared similitude [AD-A282209] p 62 N95-12426
Nonlinear calibration of an infrared radiometer [AD-A292436] p 579 N95-28996
- CETE, A. R.**
Effects of splitter plate on wake formation from a circular cylinder: A discrete vortex simulation p 639 A95-95404
- CHA, SOYOUNG S.**
Holographic interferometric tomography for reconstructing flow fields p 310 N95-23287
- CHA, YONGHWA CHRIS**
Effects of activated reactive evaporation process parameters on the microhardness of polycrystalline silicon carbide thin films [GTN-95-00406090-4621] p 680 A95-93965
- CHADERJIAN, NEAL M.**
Navier-Stokes prediction of large-amplitude delta-wing roll oscillations [BTN-95-EIX95152582329] p 281 A95-73531
- CHAFFEE, JAMES**
On the exact solutions of pseudorange equations [BTN-95-EIX95142555477] p 278 A95-73433
- CHAIT, RICHARD**
Utilization of composite materials by the US Army: A look ahead p 421 N95-28421
- CHAKRABARTI, A.**
Dynamics of phase ordering of nematics in a pore [DE95-607662] p 362 N95-25978
- CHAKRAVARTHY, S. R.**
High-speed reacting flow simulation using USA-series codes p 540 A95-87559
- CHAKRAVARTY, S.**
The effects of surface modification on fretting fatigue in Ti alloy turbine components [HTN-95-61145] p 404 A95-84909
- CHALK, CHARLES R.**
Calspan experience of PIO and the effects of rate limiting p 598 N95-31072
- CHALOUPEK, T.**
Hypervelocity Impact Test Facility: A gun for hire [TABES PAPER 94-605] p 86 N95-14639
- CHAMBERS, JOSEPH R.**
Patterns in the sky: Natural visualization of aircraft flow fields [NASA-SP-514] p 584 N95-31000
- CHAMIS, C. C.**
Ice-impact analysis of blades p 200 N95-19672
Analysis of aircraft engine blade subject to ice impact p 407 N95-28277
IPACS (Integrated Probabilistic Assessment of Composite Structures): Code development and applications p 534 N95-28849
- CHAMIS, CHRISTOS C.**
Optimization of adaptive intraply hybrid fiber composites with reliability considerations [NASA-TM-106632] p 157 N95-16911
Technology Benefit Estimator (T/BEST): User's manual [NASA-TM-106785] p 167 N95-19501
Probabilistic evaluation of fuselage-type composite structures p 398 N95-28444
A probabilistic design method applied to smart composite structures [NASA-TM-106715] p 651 N95-32206
- CHAMPIGNY, P.**
Side forces at high angles of attack. Why, when, how? [BTN-95-EIX95112523809] p 194 A95-69324
Lateral jet control for tactical missiles p 84 N95-14448
High angle of attack aerodynamics p 74 N95-14450
Test data on a non-circular body for subsonic, transonic and supersonic Mach numbers p 158 N95-17871
- CHAN, DANIEL C.**
CFD analysis of turbopump volutes p 312 N95-23436
- CHAN, K. R.**
Fine-scale, poleward transport of tropical air during AASE 2 [HTN-95-70949] p 352 A95-78014
- CHAN, K. ROLAND**
An algorithm for forecasting mountain wave-related turbulence in the stratosphere [HTN-95-80656] p 254 A95-72500
- CHAN, K. S.**
Analysis of small crack behavior for airframe applications p 95 N95-14484
- CHAN, W.**
The NASA/UTA Center for hypersonic research [AIAA PAPER 95-6106] p 520 A95-90438
- CHANCE, JOHN E.**
Real-time testing and demonstration of the US Army Corps of Engineers' Real-Time On-The-Fly positioning system [AD-A288624] p 334 N95-25609
- CHANCE, KELLY V.**
Chemical change in the arctic vortex during AASE 2 [HTN-95-70947] p 352 A95-78012
- CHANDLER, N.**
MCMs for avionics: Technology selection and intermodule interconnection p 234 N95-20641
- CHANDRA, DIVYA**
Design of head-up display symbology for recovery from unusual attitudes p 611 A95-95044
- CHANDRA, RAMESH**
Torsional actuation with extension-torsion composite coupling and a magnetostrictive actuator [BTN-95-EIX95262694314] p 435 A95-85485
- CHANDRASEKHARA, M. S.**
Interferometry and computational studies of an oscillating airfoil compressible dynamic stall flow field [HTN-94-00703] p 3 A95-60182
Oscillating airfoil compressible dynamic stall studies [HTN-94-00704] p 3 A95-60183
LDV measurements in dynamically separated flows [ISBN 0-8194-1311-9] p 5 A95-60191
A study of compressibility effects on dynamic stall of rapidly pitching airfoils [HTN-95-42338] p 372 A95-86167

- Analysis of low Reynolds number airfoil flows
[BTN-95-EIX0619952748183] p 590 A95-94476
- Compressibility effects on and control of dynamic stall of oscillating airfoil
[AD-A291804] p 480 N95-29428
- CHANDRASEKHARAN, REUBEN M.**
Aerodynamic tailoring of the Learjet Model 60 wing
[SAE PAPER 932534] p 492 A95-89194
- CHANETZ, B.**
Measurement by coherent anti-Stokes Raman scattering in the R5Ch hypersonic wind tunnel
[BTN-95-EIX95112523811] p 188 A95-69322
- CHANG, A. T.**
Computational predictive methods for fracture and fatigue
p 93 N95-14466
- CHANG, BOR-CHIN**
Design of robust optimal control systems and stability analysis of real structured uncertainties
[AD-A279089] p 256 N95-21913
- CHANG, C. I.**
Proceedings of the 2d USAF Aging Aircraft Conference
[AD-A288217] p 336 N95-25578
- CHANG, I.-CHUNG**
Geometric analysis of wing sections
[NASA-TM-110346] p 335 N95-24629
- CHANG, KEUN-SHIK**
Three-dimensional structure of a supersonic jet impinging on an inclined plate
[BTN-95-EIX95152583259] p 267 A95-73560
- CHANG, RAY C.**
High angle-of-attack airfoil performance improvement by internal acoustic excitation
[HTN-95-42347] p 372 A95-86176
- CHANG, STEPHEN**
Experimental evaluation of a box beam specifically tailored for chordwise deformation
[BTN-95-EIX95182619088] p 283 A95-75773
- Unique considerations in the design and experimental evaluation of tailored wings with elastically produced chordwise camber
p 423 N95-28436
- CHANG, WEN-HUAN**
Effect of juncture fillets on double-delta wings undergoing sideslip at high angles of attack
[AD-A286165] p 232 N95-22039
- CHANG, XIN-YU**
An experimental study on radiation from strong shock layer
p 368 A95-82421
- CHANG, YAU-SHEUN**
Analysis and design methodology for chordwise deformable wings
p 692 N95-33311
- CHAO, KENNETH K.**
Lubricant evaluation and performance, 2
[AD-A279144] p 242 N95-21969
- CHAPMAN, DEAN R.**
High altitude hypersonic flowfield radiation
[AD-A281386] p 106 N95-16160
- CHAPMAN, GARY T.**
Experimental study of flow separation on an oscillating flap at Mach 2.4
[BTN-95-EIX95222650792] p 329 A95-79248
- CHAPMAN, J. J.**
A hybrid electronically scanned pressure module for cryogenic environments
[NASA-TM-110146] p 554 N95-29453
- CHAPPELOW, C. C.**
Development of anti-icing technology
[PB94-195369] p 78 N95-15439
- CHARGIN, MLADEN K.**
Experimental/analytical approach to understanding mistuning in a transonic wind tunnel compressor
[NASA-TM-108833] p 95 N95-14617
- CHATRENET, D.**
Flying qualities of civil transport aircraft with electrical flight control
p 624 N95-32016
- CHATTOPADHYAY, ADITI**
Multilevel decomposition procedure for efficient design optimization of helicopter rotor blades
[BTN-95-EIX95222650784] p 334 A95-79240
- Development of a composite tailoring procedure for airplane wing
[NASA-CR-199081] p 691 N95-32928
- CHATURVEDI, ARVIND K.**
Aircraft fires, smoke toxicity, and survival: An overview
[DOT/FAA/AM-95/8] p 277 N95-24024
- CHAU, JOHNNY**
Advanced subsonic airplane design and economic studies
[NASA-CR-195443] p 338 N95-24304
- CHAUVEAU, C.**
High pressure vaporization and burning of methanol droplets in reduced gravity
p 527 A95-87285
- CHAVEZ, FRANK R.**
Analytical aeropropulsive/aeroelastic hypersonic-vehicle model with dynamic analysis
[BTN-95-EIX95182619138] p 269 A95-76615
- CHAVIAROPOULOS, P.**
A robust inverse inviscid method for airfoil design
p 640 A95-95431
- Single-pass method for the solution of inverse potential and rotational problems. Part 1: 2-D and quasi 3-D theory and application
p 107 N95-16563
- Single-pass method for the solution of inverse potential and rotational problems. Part 2: Fully 3-D potential theory and applications
p 107 N95-16564
- CHAWLA, KALPANA**
Numerical simulation of powered-lift flows
[HTN-94-00700] p 3 A95-60179
- Numerical simulation of a complete STOVL aircraft in ground effect
[AIAA PAPER 93-4880] p 4 A95-60187
- Aerodynamic optimization studies on advanced architecture computers
[NASA-CR-198045] p 330 N95-24379
- CHEN, A. S. C.**
Bicarbonate of soda blasting technology for aircraft wheel repainting
[PB94-193323] p 104 N95-17466
- CHEN, CHANG-REN**
Computational study of boundary layer control for improving airfoil performance
[SAE PAPER 932513] p 466 A95-89186
- CHEN, CHARLES C.**
Rotorcraft ditchings and water-related impacts that occurred from 1982 to 1989, phase 1
[AD-A279164] p 189 N95-19805
- Commuter/air taxi ditchings and water-related impacts that occurred from 1979 to 1989
[AD-A285691] p 226 N95-20275
- CHEN, CHIN-TU**
Advanced data visualization and sensor fusion: Conversion of techniques from medical imaging to Earth science
p 711 N95-34236
- CHEN, DEYUAN**
Nonlinear observer and its application in flight control
p 447 A95-82449
- CHEN, FUJIAN**
Direct splitting of coefficient matrix for numerical calculation of transonic nozzle flow
[BTN-94-EIX94481415356] p 103 A95-65346
- CHEN, G.**
Linear instability waves in supersonic jets confined in circular and non-circular ducts
[BTN-94-EIX94341340068] p 103 A95-63520
- CHEN, G. S.**
Corrosion and corrosion fatigue of airframe aluminum alloys
p 87 N95-14465
- CHEN, GUANGREN**
Development of aeronautical mobile satellite services over the past thirty years
[BTN-95-EIX95152569458] p 305 A95-73498
- CHEN, JONG-SHENG**
Damage tolerance certification of a fighter horizontal stabilizer
[BTN-95-EIX0619952748186] p 637 A95-94478
- CHEN, K. M.**
Time-domain imaging of airborne targets using ultra-wideband or short-pulse radar
[BTN-95-EIX95242673673] p 450 A95-82251
- CHEN, P.-S.**
High-performance parallel analysis of coupled problems for aircraft propulsion
[NASA-CR-197440] p 289 N95-23088
- CHEN, PING**
The spectrum and directivity of turbulent mixing noise from supersonic jets
p 579 N95-29415
- CHEN, ROBERT P.**
Statistical discrete gust-power spectral density methods overlap-holistic proof and beyond
[BTN-95-EIX0619952748175] p 584 A95-94469
- CHEN, T. J.**
Failure analysis for polycarbonate transparencies
[AD-A292992] p 630 N95-31471
- CHEN, VICTOR L.**
Test and analysis results for composite transport fuselage and wing structures
p 398 N95-28470
- CHEN, Y. K.**
Hypersonic convective heat transfer over 140-deg blunt cones in different gases
[BTN-95-EIX95152583253] p 306 A95-73554
- CHEN, Y.-K.**
Hypersonic nonequilibrium Navier-Stokes solutions over an ablating graphite nosetip
[BTN-95-EIX95152583252] p 305 A95-73553
- CHENG, VICTOR H. L.**
Automatic guidance and control for helicopter obstacle avoidance
[BTN-95-EIX95182619130] p 291 A95-76607
- CHERINGTON, MICHAEL**
Deaths and injuries as a result of lightning strikes to aircraft
[HTN-95-12213] p 485 A95-91913
- CHERN, JENG-SHING**
Ideal proportional navigation
p 342 A95-81374
- CHERN, JUUN-DAR**
Diurnal variation of lee vortices in Taiwan and the surrounding area
[HTN-95-91363] p 318 A95-76394
- CHERNIKOV, S. K.**
On calculated models for impellers of centrifugal compressors
[BTN-94-EIX94461407947] p 88 A95-62265
- CHERNYAVETS, V. V.**
Sea wave parameters, small altitudes and distances measurers design for movement control systems of ships, wing-in-surface effect crafts and seaplanes
p 708 N95-33141
- CHESNEAU, X.**
High pressure vaporization and burning of methanol droplets in reduced gravity
p 527 A95-87285
- CHESTER, R. J.**
Scarf repairs to graphite/epoxy components
p 396 N95-27523
- CHEUNG, ANNY**
The 1994 updated National Airspace System performance assessment for year 2005
[AD-A288652] p 380 N95-26485
- CHEUNG, BENNY K.**
System for determining aerodynamic imbalance
[NASA-CASE-ARC-11913-1] p 311 N95-23377
- CHEUNG, SAMSON**
CFD optimization of a theoretical minimum-drag body
[BTN-95-EIX95182619234] p 308 A95-76660
- Parallel CFD design on network-based computer
[AIAA PAPER 95-0984] p 565 A95-90656
- High speed civil transport: Sonic boom softening and aerodynamic optimization
[NASA-CR-196397] p 28 N95-11192
- Supersonic civil airplane study and design: Performance and sonic boom
[NASA-CR-197745] p 390 N95-26813
- CHEVALIER, A.**
Review of new French facilities for PREPHA program
[AIAA PAPER 95-6128] p 520 A95-90449
- CHEW, Y. T.**
Measurement in laminar and transitional boundary-layer flows on concave surface
[BTN-95-EIX95282711333] p 632 A95-92408
- CHIANG, WUYING**
Dynamic analysis of bearingless tail rotor blades based on nonlinear shell modes
[BTN-95-EIX95152582338] p 281 A95-73540
- CHIAPPETTI, CHARLES F.**
Evaluation of the Haworth-Newman avionics Display Readability Scale
[AD-A286127] p 235 N95-22232
- CHIGIER, NORMAN**
Transport phenomena in stratified multi-fluid flow in the presence and absence of gravity
p 95 N95-14563
- CHILDERS, BROOKS A.**
Computer-aided light sheet flow visualization using photogrammetry
[NASA-TP-3416] p 26 N95-10859
- CHILDS, P. N.**
SAUNA: A system for grid generation and flow simulation using hybrid structured/unstructured grids
p 642 A95-95470
- Validation and evaluation of the advanced aeronautical CFD system SAUNA: A method developer's view
[ARA-MEMO-390] p 210 N95-19774
- CHIMA, RODRICK V.**
The effect of adding roughness and thickness to a transonic axial compressor rotor
[NASA-TM-106958] p 645 N95-30524
- CHIN, V. D.**
2-D aileron effectiveness study
p 110 N95-17851
- CHING, CHAN Y.**
Influence of turbulence parameters, Reynolds number, and body shape on stagnation-region heat transfer
[NASA-TP-3487] p 550 N95-28719
- CHING, FRED**
Composite flight-control actuator development
p 410 N95-28281
- CHINITZ, W.**
An assessment of ground-test facility capabilities for measurement of hypervelocity scramjet performance
[AIAA PAPER 95-6148] p 512 A95-90462
- CHINZEI, NOBUO**
Prediction of pre-combustion shock in scramjet combustors: A new method
p 402 A95-82323
- CHITSOMBOON, TAWIT**
Modification of the two-equation turbulence model in NPARC to a Chien low Reynolds number k-epsilon formulation
[NASA-TM-106710] p 37 N95-11917

- CHITNUM, C. B.**
Aircraft evacuations through Type-3 exits I: Effects of seat placement at the exit
[DOT/FAA/AM-95/22] p 599 N95-31845
- CHIU, CHYN-SHAN**
Analysis of an oscillating Joukowski airfoil with surface suction and moving vortices
[BTN-95-EIX95062487527] p 186 A95-69235
Sidewash on the vertical tail in subsonic and supersonic flows
[BTN-95-EIX95152582316] p 264 A95-73519
- CHIU, W. K.**
Development of a composite repair and the associated inspection intervals for the F-111C stiffener runout region p 66 N95-14477
- CHO, MAENG HYO**
Aeroelastic stability of hingeless rotor blade in hover using large deflection theory
[BTN-94-EIX94441386616] p 183 A95-67347
Aeroelastic stability of hingeless rotor blade in hover using large deflection theory
[HTN-95-20952] p 546 A95-88991
- CHO, SOO-YONG**
Three dimensional compressible turbulent flow computations for a diffusing S-duct with/without vortex generators
[NASA-CR-195390] p 138 N95-17402
- CHO, SUL**
Nonlinear adaptive control of highly maneuverable high performance aircraft p 710 N95-33712
- CHOBOTOV, V. A.**
Effects of satellite bunching on the probability of collision in geosynchronous orbit
[BTN-95-EIX95152583276] p 298 A95-73577
- CHOCOL, C. J.**
CALIPE and TAISIR airborne experiment platform
[DE94-018328] p 250 N95-22299
- CHOI, D. H.**
Two-dimensional viscous flow past a flat plate
[HTN-95-42210] p 430 A95-84026
- CHOI, JAE WEON**
Design of an effective controller via disturbance accommodating left eigenstructure assignment
[BTN-95-EIX95282706663] p 565 A95-88178
Design of a modern pitch pointing control system
[BTN-95-EIX95302731226] p 618 A95-94045
- CHOI, MYUNG-RYUL**
Numerical calculations of the turbulent flow through a controlled diffusion compressor cascade
[BTN-95-EIX95282710056] p 632 A95-92473
- CHOKANI, NDAONA**
Hypersonic flow past open cavities
[HTN-95-42577] p 458 A95-87207
- CHOO, YUNG K.**
Surface Modeling, Grid Generation, and Related Issues in Computational Fluid Dynamic (CFD) Solutions
[NASA-CP-3291] p 476 N95-28723
Surface modeling and grid generation for aeropropulsion CFD p 551 N95-28732
- CHOPRA, INDERJIT**
Air and ground resonance of helicopters with elastically tailored composite rotor blades
[HTN-95-A0497] p 222 A95-72568
Air resonance of hingeless rotor helicopters in trimmed forward flight
[HTN-95-61075] p 369 A95-83659
An analytical model for a nonlinear elastomeric lag damper and its effect on aeromechanical stability in Hover
[HTN-95-61076] p 369 A95-83660
Torsional actuation with extension-torsion composite coupling and a magnetostrictive actuator
[BTN-95-EIX95262694314] p 435 A95-85485
- CHOU, JACK C.**
Static and fatigue testing of full-scale fuselage panels fabricated using a Therm-X(R) process p 420 N95-28270
- CHOU, Y. J.**
Impingement cooling of an isothermally heated surface with a confined slot jet
[BTN-94-EIX94421348950] p 347 A95-78494
- CHOU, YUNG-TAI**
Nonlinear asymptotic theory of hypersonic flow past a circular cone
[HTN-95-92599] p 461 A95-87415
- CHOUDHARI, MEELAN**
Acoustic receptivity due to weak surface inhomogeneities in adverse pressure gradient boundary layers
[NASA-TM-4577] p 249 N95-21258
- CHOUDHURI, P. G.**
Two-dimensional unsteady leading-edge separation on a pitching airfoil
[HTN-95-81628] p 461 A95-87676
- CHOUDHURY, P. ROY**
Programmed ignition of metal compounds in a scramjet p 16 N95-10466
- CHOULES, B. D.**
Thermal fracture mechanisms in ceramic thermal barrier coatings p 346 N95-26138
- CHOW, ANDREA W.**
Advanced composite structural concepts and materials technologies for primary aircraft structures: Advanced material concepts
[NASA-CR-4485] p 503 N95-29027
- CHOW, PAO-LIU**
Active control of panel vibrations induced by a boundary layer flow
[NASA-CR-197867] p 273 N95-23182
- CHOY, F. K.**
Analytical and experimental vibration analysis of a faulty gear system
[NASA-TM-106689] p 58 N95-12843
- CHRISS, RANDALL M.**
Laser anemometer measurements of the three-dimensional rotor flow field in the NASA low-speed centrifugal compressor
[NASA-TP-3527] p 618 N95-31985
- CHRISTENSEN, DIANE G.**
Development of an intervention program to encourage shoulder harness use and aircraft retrofit in general aviation aircraft, phases 1 and 2
[DOT/FAA/AM-95/2] p 333 N95-24384
Development of an intervention program to encourage shoulder harness use and aircraft retrofit in general aviation aircraft: Phases 1 and 2
[AD-A290966] p 485 N95-29873
- CHRISTENSEN, PAUL E.**
Recent advances in graphite/epoxy motor cases p 149 N95-16333
- CHRISTHILF, DAVID M.**
Design and multifunction tests of a frequency domain-based active flutter suppression system
[BTN-95-EIX95182619215] p 292 A95-76641
- CHRISTIAN, HUGH J.**
Aircraft electric field measurements: Calibration and ambient field retrieval
[HTN-95-90508] p 213 A95-67780
- CHRISTODOULOU, CHRISTODOULOS**
Studies in drag reduction p 478 N95-29094
- CHU, CHING-MEI**
Efficient and effective handling of cycle slips in global positioning system data p 43 N95-12230
- CHU, D. C.**
Laminar and turbulent flow over optimal riblets p 639 A95-95383
- CHU, H. C.**
Experiments on the flow field physics of confluent boundary layers for high-lift systems
[NASA-CR-197318] p 224 N95-21343
- CHU, ROBERT L.**
Advanced composites structural concepts and materials technologies for primary aircraft structures: Design/manufacturing concept assessment
[NASA-CR-4447] p 12 N95-10316
Textile composite fuselage structures development p 534 N95-29033
- CHUDNOVSKY, A.**
Failure analysis for polycarbonate transparencies
[AD-A292992] p 630 N95-31471
- CHUNG, CHAN H.**
Numerical analysis of hypersonic low-density scramjet inlet flow
[BTN-95-EIX95212645694] p 272 A95-76746
- CHUNG, VICTORIA I.**
Transport delays associated with NASA Langley Flight Simulation Facility
[NASA-TM-110150] p 568 N95-29454
- CHUNG, W. Y. WILLIAM**
Simulation model of the integrated flight/propulsion control system, displays, and propulsion system for ASTOVL lift-fan aircraft
[NASA-TM-108866] p 405 N95-26412
- CHUNG, WILLIAM W.**
Moving base simulation of an integrated flight and propulsion control system for an ejector-augmentor STOVL aircraft in hover
[NASA-TM-108867] p 606 N95-30646
- CHURCHILL, GARY B.**
System for determining aerodynamic imbalance
[NASA-CASE-ARC-11913-1] p 311 N95-23377
- CHURNSIDE, J. H.**
Hot jet/wake turbulent structure and laser propagation. Part 3: Laser propagation measurements and modeling p 647 N95-30992
- CHYU, WEI J.**
A procedure for automating CFD simulations of an inlet-bleed problem p 552 N95-28768
- CICON, D. E.**
Method for extracting forward acoustic wave components from rotating microphone measurements in the inlets of turbofan engines
[NASA-CR-195457] p 616 N95-30779
- CINNELLA, PASQUALE**
General solution procedure for flows in local chemical equilibrium
[HTN-95-42329] p 404 A95-86158
Using the Liou-Steffen algorithm for the Euler and Navier-Stokes equations
[HTN-95-42348] p 373 A95-86177
- CITURS, KEVIN D.**
High angle of attack flying qualities criteria for longitudinal rate command systems p 70 N95-14247
Integration of a mechanical forebody vortex control system into the F-15 p 72 N95-14258
The control system design methodology of the STOL and maneuver technology demonstrator p 621 N95-31998
- CIVINSKAS, KESTUTIS C.**
An aerodynamic analysis of a mixed flow turbine
[NASA-TM-106674] p 15 N95-10153
- CLAEYS, H. M.**
Integrated aircraft thermal management and power generation
[SAE PAPER 932055] p 500 A95-91636
- CLARK, C. M.**
Flight testing high lateral asymmetries on highly augmented Fighter/Attack aircraft
[AD-A284206] p 130 N95-17953
- CLARK, DAVID A.**
Assessment of the benefits for improved terminal weather information p 673 A95-93540
- CLARK, E. L.**
Error propagation equations for estimating the uncertainty in high-speed wind tunnel test results
[DE94-014136] p 145 N95-16509
- CLARK, G.**
Fatigue resistance of peened 7050-T7451 aluminum alloy: Repair and re-treatment of a component surface
[BTN-94-EIX94371347838] p 206 A95-69131
- CLARK, JAMES R.**
Potential applications of the SSM/I cloud liquid water parameter to the estimation of marine aircraft icing
[HTN-95-80651] p 254 A95-72495
- CLARK, JOEL P.**
The potential for CMCs to replace superalloys in engine exhaust ducts
[HTN-95-42298] p 418 A95-84992
- CLARK, MICHELLE L.**
Triton 2 (1B)
[NASA-CR-197188] p 46 N95-12636
- CLARK, P.**
Flying with automated surface observations p 659 A95-93472
- CLARK, RAYMOND**
Design and flight evaluation of an integrated navigation and near-terrain helicopter guidance system for night-time and adverse weather operations
[NASA-TM-108837] p 11 N95-10846
- CLARK, RAYMOND F.**
Flight test of a low-altitude helicopter guidance system with obstacle avoidance capability p 688 N95-32490
- CLARKE, E.**
Computing quantitative characteristics of finite-state real-time systems
[AD-A282839] p 83 N95-14343
- CLARKE, ROBERT**
Flight test of the X-29A at high angle of attack: Flight dynamics and controls
[NASA-TP-3537] p 284 N95-22806
X-29 flight control system: Lessons learned p 622 N95-32001
- CLARKE, ROBERT A.**
AH-1F COBRA rewire program MANPRINT analysis
[AD-A289190] p 391 N95-27018
- CLAYTON, A. C.**
Measurement of particle emissions from clean room gas-handling components
[BTN-94-EIX94381359040] p 295 A95-74554
- CLAYTON, J. Q.**
Fatigue resistance of peened 7050-T7451 aluminum alloy: Repair and re-treatment of a component surface
[BTN-94-EIX94371347838] p 206 A95-69131
- CLECKNER, CRAIG S.**
Design and evaluation of candidate pressure ports for the HYFLITE experiment
[NASA-TM-109146] p 22 N95-11003
- CLEMENT, M.**
Temperature diagnostics in the hypersonic flow regime: An application to develop a stagnation temperature probe
[AIAA PAPER 95-6114] p 511 A95-90442

CLERC, C.

- ASTRYD: A new numerical tool for aircraft cabin and environmental noise prediction p 576 A95-90129
- CLEVELAND, JEFF I, II**
A study of workstation computational performance for real-time flight simulation [NASA-TM-109184] p 449 N95-27241
- CLEVELAND, ROBIN O.**
Effect of stratification and geometrical spreading on sonic boom rise time p 75 N95-14880
- CLIFF, E. M.**
Computational methods for control and optimal design of aerospace systems [AD-A292861] p 608 N95-31451
- CLIFTON, JAMES M.**
Wind-tunnel tests of an inclined cylinder having helical grooves [BTN-95-EIX95262694306] p 411 A95-85477
- CLIMMENT, H.**
A study of the effect of store unsteady aerodynamics on gust and turbulence loads p 133 N95-18601
- CLINE, M. C.**
Efficient mapping topology for turbine combustors with inclined slots/staggered holes [BTN-95-EIX0616952745805] p 614 A95-94485
- CLOUD, HARLEY A.**
The opportunities for and challenges of common integrated electronics [AD-A279991] p 248 N95-20966
- CLOUTIER, JAMES R.**
High-performance, robust, bank-to-turn missile autopilot design [BTN-95-EIX95242670751] p 336 A95-81096
- COATS, T. J.**
Numerical investigation of sound transmission through double wall cylinders with respect to active noise control p 577 A95-90134
- COBER, STEWART G.**
Aircraft icing measurements in East Coast winter storms [HTN-95-60505] p 214 A95-68756
Airplane icing research at the Boeing Company: Participation in the second Canadian Atlantic Storms Program p 674 A95-93544
- COBLEIGH, BRENT R.**
High-angle-of-attack yawing moment asymmetry of the X-31 aircraft from flight test [NASA-CR-186030] p 13 N95-11410
Water tunnel flow visualization study of a 4.4 percent scale X-31 forebody [NASA-TM-104276] p 36 N95-11898
Comparison of X-31 flight, wind-tunnel, and water-tunnel yawing moment asymmetries at high angles of attack p 68 N95-14234
- COCHRAN, J. E., JR.**
Dynamics and control of a tethered flight vehicle [BTN-95-EIX95242670754] p 342 A95-81093
- COCHRAN, JOHN E., JR.**
Aerodynamic flight control to increase payload capability of future launch vehicles [NAS-CR-196560] p 300 N95-24032
- COCHRAN, R.**
Field repair materials for naval aircraft p 394 N95-27514
- COCHRAN, R. C.**
Navy composite maintenance and repair experience p 424 N95-28446
- COCKRELL, CHARLES E., JR.**
Interpretation of waverider performance data using computational fluid dynamics [BTN-95-EIX95062487534] p 193 A95-69242
Low-speed wind tunnel tests of two waverider configuration models [AIAA PAPER 95-6093] p 493 A95-89251
- COFFEY, M. T.**
Comparison of column abundances from three infrared spectrometers during AASE 2 [HTN-95-70946] p 352 A95-78011
- COGLIANESE, LOU**
The ADAGE avionics reference architecture [AIAA PAPER 95-1021] p 566 A95-90693
- COHEN, CLARK E.**
Space flight tests of attitude determination using GPS [BTN-95-EIX95112522529] p 190 A95-69334
- COHEN, EDWARD I.**
Composite structure forming a wear surface [AD-D017462] p 629 N95-30749
- COHEN, JEFFREY M.**
Evaluation of the transient operation of advanced gas turbine combustors [BTN-95-EIX0616952745793] p 614 A95-94495
- COHEN, R. C.**
Aircraft-borne, laser-induced fluorescence instrument for the in situ detection of hydroxyl and hydroperoxyl radicals [BTN-95-EIX95072499029] p 253 A95-71908

The distribution of hydrogen, nitrogen, and chlorine radicals in the lower stratosphere: Implications for changes in O₃ due to emission of NO(y) from supersonic aircraft [HTN-95-70935] p 351 A95-78000

COIRIER, WILLIAM J.

A Cartesian, cell-based approach for adaptively-refined solutions of the Euler and Navier-Stokes equations [NASA-TM-106786] p 73 N95-14297

COLE, J. A.

Preliminary results of high resolution measurements of snowfall at Stapleton International Airport during the winter of 1992-93 p 661 A95-93484

COLE, J., III

The acoustic characteristics of turbomachinery cavities [NASA-CR-4671] p 476 N95-28720

COLE, JULIAN D.

Interaction of a weak shock with freestream disturbances [BTN-95-EIX95332750473] p 638 A95-94687

COLE, RODNEY E.

ITWS gridded analysis p 654 A95-93455
A comparative performance study of TDWR/LLWAS 3 integration algorithms for wind shear detection p 658 A95-93468
LLWAS 2 and LLWAS 3 performance evaluation p 662 A95-93491

COLE, STANLEY R.

Summary of an active flexible wing program [BTN-95-EIX95182619209] p 283 A95-76635

COLLELLA, NICHOLAS J.

Unitized Regenerative Fuel Cells for solar rechargeable aircraft and zero emission vehicles [DE95-010684] p 708 N95-33642

COLEMAN, ANTHONY S.

The development of a highly reliable power management and distribution system for civil transport aircraft [NASA-TM-106697] p 50 N95-11867

COLIN, C.

Intermetallic and titanium matrix composite materials for hypersonic applications [AIAA PAPER 95-6132] p 530 A95-90451

COLIN, LESLIE R.

Comprehensive verification of terminal forecast ceiling and visibility p 664 A95-93500

COLLICOTT, STEVEN H.

Surface interference in Rayleigh scattering measurements near forebodies [HTN-95-51670] p 433 A95-85052

COLLING, JAMES DAVID

Sailplane glide performance and control using fixed and articulating winglets [NASA-CR-198579] p 392 N95-27180

COLLINGS, DAVID A.

Reducing low frequency noise emissions from a Langley Air Force Base Hush-House p 561 A95-90112

COLLINS, FRANK G.

Determination of wall boundary conditions for high-speed-ratio direct simulation Monte Carlo calculations [BTN-95-EIX95182617457] p 267 A95-75728

Parameters of Nocilla gas/surface interaction model from measured accommodation coefficients [HTN-95-81639] p 541 A95-87687

Unanswered questions concerning the Nocilla gas-surface interaction model [ISBN 1-879921-01-4] p 628 A95-93716

Low gravity quenching of hot tubes with cryogens [ISBN 1-879921-01-4] p 635 A95-93728

COLLINS, J. E.

Meridional distributions of NO(x), NO(y), and other species in the lower stratosphere and upper troposphere during AASE 2 [HTN-95-70944] p 352 A95-78009

COLLINS, J. E., JR.

An analysis of aircraft exhaust plumes from accidental encounters [HTN-95-70943] p 351 A95-78008

COLLINS, JAMES E.

Three-dimensional model interpretation of NO(x) measurements from the lower stratosphere [HTN-95-90534] p 213 A95-67806

COLLINS, LAURIE

Field and data analysis studies related to the atmospheric environment [NASA-CR-196543] p 168 N95-18093

COLLINS, WILLIAM E.

A review of civil aviation fatal accidents in which lost/disoriented was a cause/factor: 1981-1990 [DOT/FAA/AM-95/1] p 278 N95-24071

COLOZZA, ANTHONY J.

Design of a GaAs/Ge solar array for unmanned aerial vehicles [NASA-TM-106870] p 320 N95-23259

COLTMAN, JOSEPH W.

Rotorcraft crashworthy airframe and fuel system technology development program [AD-A289986] p 382 N95-28630

COLVARD, RICHARD D.

A case study of the teaming concept in the procurement of the V-22 aircraft [AD-A293770] p 608 N95-31578

COMASKEY, B.

Overview of remote sensing laser development and semiconductor laser technology [DE94-019103] p 256 N95-21552

CONEL, J. E.

Possible near-IR channels for remote sensing precipitable water vapor from geostationary satellite platforms [HTN-95-70139] p 214 A95-69431

CONEL, JAMES E.

In-flight radiometric calibration of AVIRIS in 1994 p 705 N95-33754

CONGER, RAND N.

Pressure measurements on a pitching airfoil in a water channel [HTN-95-61209] p 541 A95-87582

CONLEY, JOSEPH L.

Engines-only flight control system [NASA-CASE-ARC-11944-1] p 294 N95-23389

CONNELL, LINDA J.

EMS helicopter incidents reported to the NASA Aviation Safety Reporting System p 596 A95-95201

CONNELL, STUART D.

Grid generation and surface modeling for CFD p 551 N95-28726

CONNERS, TIMOTHY R.

Rapid deceleration mode evaluation p 696 N95-33018

CONNOLLY, JEROME J.

Repair of high temperature composite aircraft structure p 395 N95-27520

CONNOLLY, KELLY

National aviation weather program plan p 652 A95-93445

CONNOR, THOMAS L.

Factors affecting measured aircraft sound levels in the vicinity of start-of-takeoff roll p 571 A95-88465

CONSIDINE, DAVID B.

Sensitivity of two-dimensional model predictions of ozone response to stratospheric aircraft: An update [HTN-95-A0863] p 318 A95-76267

Effects of a polar stratosphere cloud parameterization on ozone depletion due to stratospheric aircraft in a two-dimensional model [HTN-95-A1038] p 443 A95-84543

CONSTANTINE, BETSY

Optimizing cockpit display configurations with a genetic algorithm system [AD-A289799] p 508 N95-29123

CONSTANTINESCU, CRISTIAN

Impact of near-coincident faults on digital flight control systems [BTN-95-EIX95242670759] p 359 A95-81088

COO, DENNIS

Advanced flight computer. Special study [NASA-CR-198165] p 449 N95-27246

COOK, A. B.

Artificial neural networks for predicting nonlinear dynamic helicopter loads [HTN-95-51678] p 404 A95-85060

COOK, BRENDA

Assessing effects of military aircraft noise on residential property values near airbases p 31 N95-11310

COOK, BRENDA W.

A review of Air Force policy and noise models pertaining to the noise environment under low-altitude, high-speed training areas p 561 A95-90118

COOK, S. R.

Hypersonic Gas-Surface Energy Accommodation Test Facility [DE94-014468] p 39 N95-12652

COON, MICHAEL D.

Experimental study of flow separation on an oscillating flap at Mach 2.4 [BTN-95-EIX95222650792] p 329 A95-79248

COONROD, KURT H.

Fault detection techniques for complex cable shield topologies [AD-A286632] p 247 N95-20771

TIM-SCT cable testing protocol [AD-A286633] p 231 N95-20772

COOPER, BETH A.

A large hemi-anechoic enclosure for community-compatible aeroacoustic testing of aircraft propulsion systems p 577 A95-90132

- COOPER, DAVID J.**
An intercomparison of instrumentation for tropospheric measurements of dimethyl sulfide: Aircraft results for concentrations at the parts-per-trillion level
[HTN-95-91857] p 355 A95-80845
- COOPER, DONALD L.**
A three-dimensional orthogonal laser velocimeter for the NASA Ames 7- by 10-foot wind tunnel
[NASA-TM-108864] p 249 N95-21323
- COOPER, GENE R.**
Comparison of meteorological data with fitted values extracted from projectile trajectory
[AD-A285921] p 255 N95-19989
- COOPER, P. D.**
Rolling bearing failure and wear debris detection
[CONGRESS PAPER C428-15-094] p 457 A95-91711
- COOPER, THOMAS D.**
Proceedings of the USAF Structural Integrity Program Conference
[AD-A285684] p 194 N95-19517
- CORBETT, N. C.**
Control requirements for the RB 211 low-emission combustion system
[BTN-94-EIX95011441244] p 416 A95-84201
- CORDA, STEPHEN**
Dynamic ground effects flight test of an F-15 aircraft
[NASA-TM-4604] p 38 N95-12191
Dynamic ground effects flight test of the NASA F-15 aircraft
p 692 N95-33024
- CORDES, J.**
Computational predictive methods for fracture and fatigue
p 93 N95-14466
- CORLISS, J. M.**
Simulation of Shuttle launch G forces and acoustic loads using the NASA Ames Research Center 20G centrifuge
p 86 N95-14089
- CORLISS, L. D.**
Design of a model following, state variable feedback controller for the X-14 VTOL aircraft
[HTN-94-00685] p 16 A95-60168
- CORMAN, G. S.**
Toughened Silcomp composites for gas turbine engine applications
[DE95-002851] p 235 N95-21243
- CORNMAN, LARRY B.**
Real-time estimation of atmospheric turbulence severity from in-situ aircraft measurements
[BTN-95-EIX95182619231] p 319 A95-76657
Estimation of atmospheric turbulence severity from in-situ aircraft measurements
p 659 A95-93479
- CORNWELL, MICHAEL D.**
Thermal chemical energy of ablating silica surfaces in air breathing solid rocket engines
p 148 N95-16316
- CORREA, S.**
Combustion system CFD modeling at GE Aircraft Engines
p 439 N95-27889
- CORWIN, BILL**
Synthetic Terrain Imagery for Helmet-Mounted Display. Volume 2: Software design document
[AD-A293611] p 612 N95-31655
Synthetic Terrain Imagery for Helmet-Mounted Display, volume 1
[AD-A293612] p 612 N95-31656
- COSTA, ALFRED J.**
Design and construction of a remote piloted flying wing
[NASA-CR-197195] p 47 N95-12695
- COTON, F. N.**
Preliminary results from a particle image velocimetry study of blade-vortex interaction
[HTN-95-01098] p 547 A95-90284
- COTTON, STACEY J.**
Flow-visualization study of the X-29A aircraft at high angles of attack using a 1/48-scale model
[NASA-TM-104268] p 8 N95-10858
- COULLAUD, STEPHANE**
Flow visualization studies of VTOL aircraft models during Hover in ground effect
[NASA-TM-108860] p 272 N95-22666
- COULTER, S.**
A review of free-stream flow fluctuation and steady-state flow quality measurements in the AEDC/VKF Supersonic Tunnel A and Hypersonic Tunnel B
[AIAA PAPER 95-6137] p 520 A95-90454
- COULTON, DAVID G.**
Multiport pressure measurements on continuously moving wind tunnel models
[ARA-MEMO-391] p 188 N95-19772
- COUSINS, W. T.**
Pressure and temperature distortion testing of a two-stage centrifugal compressor
[BTN-94-EIX95011441250] p 431 A95-84207
- COUSTEIX, J.**
Shock layers and boundary layers in hypersonic flows
[HTN-95-A0003] p 183 A95-67830
- COUTERMARSH, BARRY**
Analyzing the stability of floating ice floes
[AD-A292149] p 563 N95-29160
- COUTLEY, R. L.**
Numerical investigation of high incidence flow over a double-delta wing
[BTN-95-EIX0619952748160] p 588 A95-94454
- COVELL, PETER F.**
Effect of leading- and trailing-edge flaps on clipped delta wings with and without wing camber at supersonic speeds
[NASA-TM-4542] p 5 N95-10028
Experimental aerodynamic characteristics of a generic hypersonic accelerator configuration at Mach numbers 1.5 and 2.0
[NASA-TM-4413] p 39 N95-12770
- COWAN, ELIZABETH**
Combustion-acoustic stability analysis for premixed gas turbine combustors
[NASA-TM-107024] p 694 N95-32931
- COWARD, ADRIAN**
The stability of two-phase flow over a swept-wing
[NASA-CR-194994] p 159 N95-18190
- COX, B. N.**
Fundamental concepts in the suppression of delamination buckling by stitching
p 426 N95-28486
- COX, CAREY F.**
General solution procedure for flows in local chemical equilibrium
[HTN-95-42329] p 404 A95-86158
- COX, G. B., JR.**
Phase 2: HGM air flow tests in support of HEX vane investigation
p 312 N95-23438
- COX, R. A.**
Waveriders with finlets
[BTN-95-EIX95062487541] p 184 A95-68355
An overview of the EASOE campaign
[HTN-95-00702] p 443 A95-86272
- COX, T.**
A flying qualities study of longitudinal long-term dynamics of hypersonic planes
[AIAA PAPER 95-6150] p 521 A95-90464
- COXON, B. R.**
Impact damage resistance of composite fuselage structure, part 1
p 399 N95-28482
- CRABILL, NORMAN L.**
Pilot Weather Advisor system
[BTN-95-EIX95152582314] p 316 A95-73517
- CRABTREE, RONALD**
What's next in commercial aircraft environmental control systems?
[SAE PAPER 932057] p 513 A95-91638
- CRAGGS, A.**
Finite element model for a flexible non-symmetric rotor on distributed bearing: A stability study
[BTN-94-EIX94381352212] p 306 A95-74612
- CRAIG, ROGER A.**
Science objectives and performance of a radiometer and window design for atmospheric entry experiments
[NASA-TM-4637] p 63 N95-12190
Planetary entry experiments
[NASA-CR-194215] p 101 N95-13717
Science objectives and performance of a radiometer and window design for atmospheric entry experiments
p 85 N95-13718
VUV shock layer radiation in an arc-jet wind tunnel experiment
p 67 N95-13719
Measured and calculated spectral radiation from a blunt body shock layer in an arc-jet wind tunnel
[AIAA PAPER 94-0086] p 67 N95-13720
- CRAIG, W.**
Integrated X-ray testing of the electro-optical breadboard model for the XMM reflection grating spectrometer
[DE95-008829] p 644 N95-30507
- CRAMER, EVIN J.**
Application of direct transcription to commercial aircraft trajectory optimization
[BTN-95-EIX95242670766] p 359 A95-81081
- CRAMER, K. E.**
New nondestructive techniques for the detection and quantification of corrosion in aircraft structures
p 315 N95-23512
- CRANE, JEAN M.**
Flight-deck displays on the Boeing 777
[BTN-95-EIX95142562402] p 286 A95-73438
- CRANS, BEREND J. H.**
EC Aviation Scene
[HTN-95-50223] p 176 A95-64860
- CRANSTON, ROBERT**
Offshore next generation weather radar (NEXRAD) test and evaluation master plan (TEMP)
[AD-A291435] p 556 N95-30072
- CRAS, STEVEN P.**
EC Aviation Scene
[HTN-95-50223] p 176 A95-64860
- CRAVEN, D. A.**
Programmable cockpit research simulator
[AD-A279219] p 204 N95-19848
- CRAWFORD, C. H.**
Laminar and turbulent flow over optimal riblets
p 639 A95-95383
- CRAWFORD, G.**
Hypervelocity Impact Test Facility: A gun for hire
[TABES PAPER 94-605] p 86 N95-14639
- CRAWFORD, M. L.**
Measurements of shielding effectiveness and cavity characteristics of airplanes
[PB94-210051] p 244 N95-20191
- CRAWFORD, R. A.**
Description and flow characterization of hypersonic facilities
[AD-A284291] p 223 N95-20248
- CRAWLEY, EDWARD F.**
Fundamental mechanisms of aeroelastic control with control surface and strain actuation
[BTN-95-EIX95242670746] p 327 A95-81101
- CREASMAN, F.**
Transonic--wind--tunnel--boundary--interference correction
p 147 N95-19271
- CREEK, EDITH A.**
Eddy current for detecting second-layer cracks under installed fasteners
[AD-A279871] p 244 N95-20414
- CREMA, L. BALIS**
Selecting and management of fire fighter aircraft
[BTN-95-EIX95062487538] p 193 A95-69246
- CREONTE, JOSEPH**
Optimal design of composite helicopter power transmission shafts with axially varying fiber layout
[HTN-95-01086] p 529 A95-90272
- CRESCI, D.**
Free-jet testing at Mach 3.44 in GASL's aero/thermo test facility
p 145 N95-16320
- CRESCO, ANTONIO**
Optical processing and control
[AD-A279157] p 259 N95-21975
- CREWELL, S.**
Aircraft measurements of CLO and HCL during EASOE 1991/92
[HTN-95-00721] p 444 A95-86291
- CRISLER, WILLIAM PAUL**
PIV investigation of compressibility effects on dynamic stall
p 478 N95-29102
- CRITES, R. C.**
The crucial role of wall interference, support interference and flow field measurements in the development of advanced aircraft configurations
p 162 N95-19252
Transonic wind tunnel boundary interference correction
p 147 N95-19271
- CROOK, ANDREW**
Snow-band formation and evolution during the 15 November 1987 aircraft accident at Denver airport
[HTN-95-80699] p 254 A95-72543
- CROOK, N. ANDREW**
The real-time analysis and prediction of storms program
p 655 A95-93457
- CROOM, MARK A.**
Comparison of X-31 flight, wind-tunnel, and water-tunnel yawing moment asymmetries at high angles of attack
p 68 N95-14234
- CROSS, J. B.**
Hypersonic Gas-Surface Energy Accommodation Test Facility
[DE94-014468] p 39 N95-12652
- CROSSLEY, T. R.**
Non-contact calibration of a CNC riveting machine
[CONGRESS PAPER C428-32-075] p 583 A95-93618
- CROSSLEY, WILLIAM A.**
The potential of genetic algorithms for conceptual design of rotor systems
[NASA-CR-196813] p 43 N95-11699
- CROSTON, I. R.**
MCMs for avionics: Technology selection and intermodule interconnection
p 234 N95-20641
- CROUCH, KEITH E.**
Aircraft fuel system lightning protection design and qualification test procedures development
[AD-A288401] p 380 N95-26497
- CROUSE, PATRICK**
The effect of high lift to drag ratio on aerobraking
p 415 A95-85807
- CROW, STEVEN C.**
Engineering design of Starcar 3
[SAE PAPER 932602] p 494 A95-90072
- CROWLEY, JOHN S.**
The effects of UH-1 experience on UH-60 simulator performance: A preliminary study
[AD-A289457] p 391 N95-26993

- CRUMPLER, M.**
Hypervelocity Impact Test Facility: A gun for hire
[TABES PAPER 94-605] p 86 N95-14639
- CRUSE, T. A.**
Mechanical system reliability and risk assessment
[BTN-95-EIX95142553046] p 304 A95-73452
- CRUZ, JUAN R.**
Buckling analysis of curved composite sandwich panels subjected to inplane loadings p 533 N95-28845
- CUCINOTTA, FRANCIS A.**
Radiation safety aspects of commercial high-speed flight transportation
[NASA-TP-3524] p 453 N95-26427
- CUERNO, CRISTINA**
Design constraints in the payload-range diagram of ultrahigh capacity transport airplanes
[BTN-95-EIX95152582319] p 276 A95-73522
- CUESTA, JUAN D.**
Modeling helicopter blade dynamics using a modified Myklestad-Prohl transfer matrix method
[AD-A289891] p 400 N95-28626
- CUI, JIYA**
Improved analytical solution for varying specific heat parallel stream mixing
[BTN-94-EIX94481415349] p 103 A95-65339
- CULP, ROBERT D.**
Guidance and control, 1993; Annual Rocky Mountain Guidance and Control Conference, 16th, Keystone, CO, Feb. 6-10, 1993
[ISBN-0-87703-365-X] p 341 A95-80389
- CULSHAW, BRIAN**
SMART materials: Surfaces, transforms and interfaces. The commensurate engineering dimension
[AD-A289598] p 442 N95-28649
- CUMMINGS, MARY L.**
A computer code (SKINTEMP) for predicting transient missile and aircraft heat transfer characteristics
[AD-A286044] p 248 N95-21001
- CUMMINGS, R. M.**
Supersonic, turbulent flow computation and drag optimization for axisymmetric afterbodies
[BTN-95-EIX95302729772] p 637 A95-94134
- CUMMINGS, RUSSELL M.**
Computational analysis of forebody tangential slot blowing p 71 N95-14253
Numerical design of advanced multi-element airfoils
[NASA-CR-197135] p 76 N95-15762
- CUMMINS, R. J.**
Application of superplastically formed and diffusion bonded structures in high intensity noise environments p 174 N95-19162
- CUNNING, GARY**
Real-time estimation of atmospheric turbulence severity from in-situ aircraft measurements
[BTN-95-EIX95182619231] p 319 A95-76657
Estimation of atmospheric turbulence severity from in-situ aircraft measurements p 659 A95-93479
- CUNNINGHAM, A. M., JR.**
Unsteady transonic wind tunnel test on a semispan straked delta wing, oscillating in pitch. Part 1: Description of the model, test setup, data acquisition, and data processing
[AD-A293113] p 593 N95-30885
- CUNNINGHAM, ATLEE M., JR.**
Overview of unsteady transonic wind tunnel test on a semispan straked delta wing oscillating in pitch
[AD-A284097] p 117 N95-18380
- CURETON, K. L.**
Strategic avionics technology definition studies. Subtask 3-1A3: Electrical Actuation (ELA) Systems Test Facility
[NASA-CR-188360] p 143 N95-18567
- CURLETT, BRIAN P.**
Graphical user interface for the NASA FLOPS aircraft performance and sizing code
[NASA-TM-106649] p 80 N95-14804
Object-oriented approach for gas turbine engine simulation
[NASA-TM-106970] p 615 N95-30594
- CURLEY, J. A.**
Pitot/static leak testing
[CONGRESS PAPER C428-9-035] p 508 A95-91696
- CURRAN, LAWRENCE J., JR.**
Investigation of flight data recorder fire test requirements
[AD-A285832] p 232 N95-20032
- CURRIE, T. C.**
Erosion of T56 5th stage rotor blades due to bleed hole overtip flow p 200 N95-19666
- CURRY, JUDITH A.**
An integrated system to improve aviation weather forecasts for the Alaska Range p 656 A95-93460
- CURRY, ROBERT E.**
Dynamic ground effects flight test of an F-15 aircraft
[NASA-TM-4604] p 38 N95-12191
- CURSOLLE, JEAN-PIERRE**
A helmet mounted display for night missions at low altitude p 693 N95-32503
- CURTIS, JOEL C.**
Alaska's volcanic ash warning system p 663 A95-93495
- CURTIS, P. T.**
The certification of composite structures for military aircraft
[CONGRESS PAPER C428-37-198] p 628 A95-93633
- CUSCHIERI, JOSEPH M.**
Noise Con 1994: Proceedings of the 1994 National Conference on Noise Control Engineering. Progress in Noise Control for Industry
[LC-75-24750] p 28 N95-11259
- CUSUMANO, J. P.**
Critical speed analysis of a non-linear strain ring dynamical model for aircraft tires
[SAE PAPER 932580] p 494 A95-90067
- CVETICANIN, L.**
Van der pol absorber for rotor vibrations
[BTN-94-EIX94441385106] p 702 A95-96579
- CZAJKOWSKI, MIKE**
Design and analysis of a telescopic wing
[SAE PAPER 932605] p 495 A95-90075

D

- D'AMATO, C. A.**
Numerical and flight measured interior noise characteristics of a twin-engine turboprop general aviation aircraft p 573 A95-90094
- D'AMICO, N.**
Period evolution of PSR B1259-63: Evidence for propeller-torque spindown
[HTN-95-B0194] p 581 A95-87903
- D'AZZO, J. J.**
Automatic formation flight control
[BTN-95-EIX95182619153] p 292 A95-76630
- DA, REN**
New failure detection approach and its application to GPS autonomous integrity monitoring
[BTN-95-EIX95202637613] p 279 A95-76676
Failure detection and isolation structure for global positioning system autonomous integrity monitoring
[BTN-95-EIX95282706656] p 486 A95-89648
- DABUNDO, CHARLES**
Advanced flight control technology achievements at Boeing Helicopters p 624 N95-32014
- DACRES, CHESTER M.**
The use of electrochemistry and ellipsometry for identifying and evaluating corrosion on aircraft
[AD-A285323] p 151 N95-16371
The use of electrochemistry and ellipsometry for identifying and evaluating corrosion on aircraft
[AD-A288536] p 381 N95-27186
The use of electrochemistry and ellipsometry for identifying and evaluating corrosion on aircraft
[AD-A290249] p 504 N95-29426
- DADD, G. D.**
Surge recovery and compressor working line control using compressor exit mach number measurement
[CONGRESS PAPER C428-33-210] p 610 A95-93622
- DADONE, LEO**
Laser velocimetry and blade pressure measurements of a blade-vortex interaction
[HTN-95-01081] p 547 A95-90267
- DAHER, JOHN K.**
Evaluation of the radio frequency susceptibility of commercial GPS receivers
[BTN-95-EIX95042474624] p 189 A95-68278
- DAHL, MILO D.**
Noise radiation by instability waves in coaxial jets
[NASA-TM-106738] p 100 N95-14618
The aeroacoustics of supersonic coaxial jets
[NASA-TM-106782] p 101 N95-15059
Supersonic jet noise reductions predicted with increased jet spreading rate
[NASA-TM-106872] p 323 N95-23178
Supersonic coaxial jet noise predictions
[NASA-TM-106917] p 451 N95-26801
- DAHLKE, LUTZ**
Emerging nondestructive inspection for aging aircraft
[PB95-143053] p 328 N95-25401
- DAHLMAN, CARL J.**
The value of simulation for training
[AD-A289174] p 411 N95-26556
- DAI, YI**
Thermal-mechanical fatigue crack growth in aircraft engine materials
[ISBN-0-315-86543-1] p 647 N95-31098
- DAIGLE, GILLES A.**
Inter-Noise 92: Noise control and the public; International Congress on Noise Control Engineering, Toronto, Ontario, Canada, July 20 - 22, 1992. Vols. 1 & 2
[ISBN 0-931784-25-5] p 559 A95-88457
Proceedings of the Sixth International Symposium on Long-Range Sound Propagation
[AD-A290920] p 580 N95-30084
- DALANG-SECRETAN, MAIRE-ALIX**
Validation of the dynamic response of a blade-element UH-60 simulation model in hovering flight
[HTN-94-00663] p 18 A95-60155
- DALLE-MURA, E.**
Impact of noise environment on engine nacelle design p 173 N95-19147
- DALTON, FRANK**
Dissemination of weather products p 670 A95-93526
- DALTON, K. K.**
Pressure and temperature distortion testing of a two-stage centrifugal compressor
[BTN-94-EIX95011441250] p 431 A95-84207
- DALY, PETER**
Integrated GPS/Glonass navigation: Algorithms and results
[BTN-95-EIX9511252531] p 190 A95-69332
- DAMLE, S. V.**
Recent trends in balloon flights from TIFR's National Balloon Facility, Hyderabad p 191 A95-66300
- DAMODARAN, M.**
Multi-block finite volume calculation of compressible flow past aerodynamic configurations p 643 A95-95473
- DANCEY, C. L.**
Computational/experimental investigation of staged injection into a Mach 2 flow
[HTN-95-51646] p 432 A95-85028
- DANG, T.**
Research and educational initiatives at the Syracuse University Center for Hypersonics
[AIAA PAPER 95-6107] p 520 A95-90439
- DANIEL, D. W.**
The air systems controllerate initiatives and policies for the procurement of reliable and maintainable equipment
[CONGRESS PAPER C428-6-113] p 549 A95-91682
- DANIEL, W. J.**
Balances for the measurement of multiple components of force in flows of a millisecond duration p 350 N95-25400
- DANIELS, CHARLES L., II**
Comparison of fixed wing aircraft algorithms for JANUS
[AD-A288503] p 389 N95-26652
- DANIELS, T. S.**
Dynamic Stability Instrumentation System (DSIS). Volume 1: Hardware description
[NASA-TM-109160-VOL-1] p 171 N95-18899
- DANIELSON, ARNOLD O.**
Integrated aerodynamic fin and stowable TVC vane system
[AD-D016457] p 151 N95-19073
- DANILIN, MICHAEL Y.**
Evolution of the concentrations of trace species in an aircraft plume: Trajectory study
[HTN-95-A1044] p 443 A95-84549
- DANNENHOFFER, JOHN F., III**
Three-dimensional adaptive grid-embedding Euler technique
[HTN-95-20825] p 543 A95-88086
Automatic blocking for complex three-dimensional configurations p 566 N95-28734
- DAPKUNAS, S. J.**
Thermal Barrier Coating Workshop
[NASA-CP-10170] p 344 N95-26119
Measurement methods and standards for processing and application of thermal barrier coatings p 344 N95-26123
- DARGAN, J. L.**
Automatic formation flight control
[BTN-95-EIX95182619153] p 292 A95-76630
- DARIAN, ARMEN**
CFD analysis of turbopump volutes p 312 N95-23436
- DARLING, DOUGLAS**
Sensitivity of combustion-acoustic instabilities to boundary conditions for premixed gas turbine combustors
[NASA-TM-106890] p 289 N95-23550
Review of combustion-acoustic instabilities
[NASA-TM-107020] p 705 N95-32930
Combustion-acoustic stability analysis for premixed gas turbine combustors
[NASA-TM-107024] p 694 N95-32931
- DARLOW, MARK S.**
Optimal design of composite helicopter power transmission shafts with axially varying fiber layup
[HTN-95-01086] p 529 A95-90272

- DASEY, TIMOTHY J.**
Improving aircraft impact assessment with the integrated terminal weather system microburst detection algorithm p 654 A95-93453
Future enhancements to ground-based microburst detection p 11 N95-10570
- DASKIEWICH, DANIEL E.**
Assuring Known Good Die (KGD) for reliable, cost effective MCMs p 246 N95-20644
- DASTIN, S.**
Comparison of resin film infusion, resin transfer molding, and consolidation of textile preforms for primary aircraft structure p 425 N95-28477
- DASTIN, S. J.**
Novel cost controlled materials and processing for primary structures p 532 N95-28830
- DATTA, ANINDITA**
Lee waves benign and malignant p 595 A95-93554
- DAUBE, B. C.**
In situ observations in aircraft exhaust plumes in the lower stratosphere at midlatitudes [HTN-95-A0862] p 318 A95-76266
- DAUBE, BRUCE C., JR.**
Vertical transport rates in the stratosphere in 1993 from observations of CO₂, N₂O, and CH₄ [HTN-95-70941] p 351 A95-78006
- DAVID, C.**
Airborne lidar observation of mountain-wave-induced polar stratospheric clouds during EASOE [HTN-95-00738] p 444 A95-86308
- DAVIDHAZY, ANDREW**
Scientific and technical photography at NASA Langley Research Center p 310 N95-23290
- DAVIDHEISER, ROGER**
Passive millimeter wave camera for aircraft landing in low visibility conditions [BTN-95-EIX95292721321] p 609 A95-92513
- DAVIDSON, B.**
Research and educational initiatives at the Syracuse University Center for Hypersonics [AIAA PAPER 95-6107] p 520 A95-90439
- DAVIDSON, D. L.**
Analysis of small crack behavior for airframe applications p 95 N95-14484
- DAVIDSON, J. A.**
SOFIA: Stratospheric Observatory for Infrared Astronomy p 363 A95-81583
- DAVIDSON, JOHN B.**
Extended cooperative control synthesis [NASA-TM-4561] p 17 N95-10220
High angle of attack flying qualities criteria for longitudinal rate command systems p 70 N95-14247
- DAVIDSON, LARS**
Turbulent transonic airfoil flow simulation using a pressure-based algorithm [BTN-95-EIX95182619078] p 269 A95-75763
- DAVIES, ELIZABETH**
The use of genetic algorithms for flight test and evaluation of artificial intelligence and complex software systems [AD-A284824] p 217 N95-19688
- DAVIES, G. A. O.**
Buckling and postbuckling of composite structures [HTN-95-71387] p 528 A95-87605
- DAVIES, MIKE**
A PC-based interactive simulation of the F-111C Tack system and related sensor, avionics and aircraft aspects [AD-A285500] p 129 N95-16969
- DAVIS, D. D., JR.**
Technology integration box beam failure study p 441 N95-28468
Technology integration box beam failure study p 552 N95-28847
- DAVIS, D. O.**
Flow coefficient behavior for boundary layer bleed holes and slots [NASA-TM-106846] p 244 N95-19953
- DAVIS, DOUGLAS D.**
An intercomparison of aircraft instrumentation for tropospheric measurements of sulfur dioxide [HTN-95-91855] p 354 A95-80843
An intercomparison of aircraft instrumentation for tropospheric measurements of carbonyl sulfide, hydrogen sulfide, and carbon disulfide [HTN-95-91856] p 355 A95-80844
An intercomparison of instrumentation for tropospheric measurements of dimethyl sulfide: Aircraft results for concentrations at the parts-per-trillion level [HTN-95-91857] p 355 A95-80845
- DAVIS, HU**
Advanced composites structural concepts and materials technologies for primary aircraft structures: Design/manufacturing concept assessment [NASA-CR-4447] p 12 N95-10316
- DAVIS, JAMES M.**
Advanced flight control technology achievements at Boeing Helicopters p 624 N95-32014
- DAVIS, JOHN G., JR.**
Overview of the ACT program p 424 N95-28463
Third NASA Advanced Composites Technology Conference, volume 1, part 2 [NASA-CP-3178-VOL-1-PT-2] p 531 N95-28823
Third NASA Advanced Composites Technology Conference, volume 1, part 1 [NASA-CP-3178-VOL-1-PT-1] p 534 N95-29029
Advanced composites technology program p 534 N95-29032
- DAVIS, LAWRENCE**
Optimizing cockpit display configurations with a genetic algorithm system [AD-A289799] p 508 N95-29123
- DAVIS, M. J.**
The development of an engineering standard for composite repairs p 396 N95-27528
- DAVIS, R. C.**
Technology integration box beam failure study p 441 N95-28468
Technology integration box beam failure study p 552 N95-28847
- DAVIS, R. L.**
Computational fluid dynamics study of the variable-pitch split-blade fan concept [NASA-CR-189206] p 15 N95-10247
- DAVIS, ROGER L.**
Three-dimensional adaptive grid-embedding Euler technique [HTN-95-20825] p 543 A95-88086
- DAVIS, RYAN EDWIN**
Central coast designs: The Eightball Express. Taking off with convention, cruising with improvements and landing with absolute success [NASA-CR-197181] p 47 N95-12643
- DAVIS, SANFORD S.**
Aeroacoustic model for weak shock waves based on Burgers equation [BTN-95-EIX95182619076] p 269 A95-75761
- DAVIS, STUART L.**
Fault detection techniques for complex cable shield topologies [AD-A286632] p 247 N95-20771
- DAVIS, TOM**
Design and flight evaluation of an integrated navigation and near-terrain helicopter guidance system for night-time and adverse weather operations [NASA-TM-108837] p 11 N95-10846
- DAVY, WILLIAM C.**
Science objectives and performance of a radiometer and window design for atmospheric entry experiments [NASA-TM-4637] p 63 N95-12190
Science objectives and performance of a radiometer and window design for atmospheric entry experiments p 85 N95-13718
- DAWES, W. N.**
Simulation of the unsteady interaction of a centrifugal impeller with its vaned diffuser: flow analysis [BTN-95-EIX95282710055] p 633 A95-92474
- DAWICKE, D. S.**
Influence of crack history on the stable tearing behavior of a thin-sheet material with multiple cracks p 93 N95-14467
- DAWICKE, DAVE**
Analytical developments in support of the NASA aging aircraft program with an application to crack growth from rivets [SAE PAPER 931223] p 545 A95-88789
- DAWSON, ANNE MARIE**
Central coast designs: The Eightball Express. Taking off with convention, cruising with improvements and landing with absolute success [NASA-CR-197181] p 47 N95-12643
- DAWSON, JONATHAN A.**
Effects of expansions on a supersonic boundary layer: Surface pressure measurements [BTN-95-EIX95142553036] p 263 A95-73462
- DAY, GLENROY E., JR.**
A computer-based multimedia prototype for night vision goggles [AD-A286208] p 258 N95-21882
- DAYTON, RON**
Dynamic stiffness and damping of foil bearings for gas turbine engines [SAE PAPER 931449] p 635 A95-93698
- DE COCK, K. M. J.**
Grid adaptation for problems in computational fluid dynamics p 643 A95-95472
- DE FRANCESCO, GREGORY L.**
Condensing cycle air conditioning system [SAE PAPER 932056] p 513 A95-91637
- DE NICOLA, C.**
Estimation of supersonic leading-edge thrust by a Euler flow model [BTN-95-EIX0619952748194] p 591 A95-94483
- DE ROSA, S.**
Numerical and flight measured interior noise characteristics of a twin-engine turboprop general aviation aircraft p 573 A95-90094
- DE TROIA, R.**
Matrix fraction approach for finite-state aerodynamic modeling [BTN-95-EIX95262694311] p 365 A95-85482
- DE VERTEUIL, FRANCES**
Stratus' tephigram as a training/forecasting tool p 657 A95-93465
- DE ZAFFRA, R. L.**
An overview of millimeter-wave spectroscopic measurements of chlorine monoxide at Thule, Greenland, February-March, 1992: Vertical profiles, diurnal variation, and longer-term trends [HTN-95-00722] p 444 A95-86292
- DEAN, JEFFREY S.**
ATE enabling technologies [BTN-95-EIX95172595294] p 287 A95-75718
- DEANE, ANIL E.**
Low-dimensional description of the dynamics in separated flow past thick airfoils [HTN-95-20832] p 544 A95-88093
- DEARING, MUNRO G.**
Simulation development of a forward sensor-enhanced low-altitude guidance system [HTN-94-00688] p 17 A95-60170
Design and flight evaluation of an integrated navigation and near-terrain helicopter guidance system for night-time and adverse weather operations [NASA-TM-108837] p 11 N95-10846
- DEATON, JERRY W.**
Development and verification of a resin film infusion/resin transfer molding simulation model for fabrication of advanced textile composites [NASA-CR-197439] p 301 N95-23179
Test and analysis results for composite transport fuselage and wing structures p 398 N95-28470
Mechanical characterization of 2D, 2D stitched, and 3D braided/RTM materials p 535 N95-29038
- DEB, SOMNATH**
MATSurv multisensor air traffic surveillance [AD-A292253] p 489 N95-28887
- DEBONIS, JAMES R.**
Validation of the NPARC code for nozzle afterbody flows at transonic speeds [NASA-TM-106971] p 592 N95-30704
- DEC, JOHN**
Integrated design and manufacturing for the high speed civil transport [NASA-CR-197183] p 48 N95-12700
- DECHANT, LAWRENCE J.**
An analysis code for the Rapid Engineering Estimation of Momentum and Energy Losses (REMEL) [NASA-CR-191178] p 108 N95-16887
- DECKER, ARTHUR J.**
Control of wind tunnel operations using neural net interpretation of flow visualization records [NASA-TM-106683] p 24 N95-10854
- DECKER, DOUGLAS D.**
Flight control design using mixed H₂/micron optimization [AD-A289288] p 410 N95-27036
- DECKER, HARRY J.**
Detecting gear tooth fracture in a high contact ratio face gear mesh [NASA-TM-106822] p 162 N95-19125
- DECKER, R. A.**
Lift analysis of a variable camber foil using the discrete vortex-blob method [BTN-94-EIX94441386623] p 179 A95-68172
Lift analysis of a variable camber foil using the discrete vortex-blob method [HTN-95-20940] p 545 A95-88979
- DECKER, RAND A.**
Tracking of raindrops in flow over an airfoil [BTN-95-EIX95182619221] p 308 A95-76647
- DECKER, T.**
Integrated X-ray testing of the electro-optical breadboard model for the XMM reflection grating spectrometer [DE95-008829] p 644 N95-30507
- DECKERT, WALLACE H.**
The lift-fan aircraft: Lessons learned [NASA-CR-196694] p 392 N95-27143
- DECOCK, K. M. J.**
Demonstration of an automated CFD system for three-dimensional flow simulations p 551 N95-28767
Multigrid convergence acceleration for the 2D Euler equations applied to high-lift systems [PB95-198081] p 593 N95-30814

DECONINCK, H.

A 2D parallel multiblock Navier-Stokes solver with applications on shared- and disturbed memory machines p 643 A95-95475

DEDOUSSIS, V.

A robust inverse inviscid method for airfoil design p 640 A95-95431
Single-pass method for the solution of inverse potential and rotational problems. Part 1: 2-D and quasi 3-D theory and application p 107 N95-16563
Single-pass method for the solution of inverse potential and rotational problems. Part 2: Fully 3-D potential theory and applications p 107 N95-16564

DEESE, J. E.

Transonic wind tunnel boundary interference correction p 147 N95-19271

DEETER, THOMAS E.

Survey and implementation of commercial manual controllers for a generic telerobotics architecture [AD-A289215] p 449 N95-26990

DEFIORE, TOM

The FAA regional/commuter aircraft flight loads data collection program [SAE PAPER 931258] p 493 A95-89224

DEGTAREV, G. L.

Joint Proceedings on Aeronautics and Astronautics (JPAA) [ISBN-7-80-046602-7] p 104 N95-16249

DEIVERT, ROBERT A.

An analysis of the KC-135 three-person cockpit [AD-A289540] p 390 N95-26873

DEJARNETTE, F. R.

Approximate method for calculating heating rates on three-dimensional vehicles [BTN-95-EIX95041503778] p 210 A95-69209

DEJONGE, J. B.

Reanalysis of European flight loads data [AD-A282052] p 9 N95-11179
Review of aeronautical fatigue investigation in the Netherlands during the period March 1991-March 1993 [PB95-139184] p 285 N95-23161

DEKONINGGANS, H. J.

Numerical time dependent sheet cavitation simulations using a higher order panel method [PB94-204435] p 59 N95-13249

DELANEY, ROBERT A.

Investigation of advanced counterrotation blade configuration concepts for high speed turboprop systems. Task 8: Cooling flow/heat transfer analysis [NASA-CR-195359] p 50 N95-11901
Investigation of advanced counterrotation blade configuration concepts for high speed turboprop systems. Task 8: Cooling flow/heat transfer analysis user's manual [NASA-CR-195360] p 50 N95-11951

DELANOY, RICHARD L.

The ITWS microburst prediction algorithm p 655 A95-93456

DELANY, A.

A comparison of some aerodynamic resistance methods using measurements over cotton and grass from the 1991 California ozone deposition experiment [HTN-95-11295] p 319 A95-77000

DELERY, JEAN M.

Aspects of vortex breakdown [HTN-95-A0001] p 183 A95-67828

DELFRATE, JOHN

Water tunnel flow visualization study of a 4.4 percent scale X-31 forebody [NASA-TM-104276] p 36 N95-11898

DELFRATE, JOHN H.

Development of a low-aspect ratio fin for flight research experiments [NASA-TM-4596] p 108 N95-16858
NASA Dryden flow visualization facility [NASA-TM-4631] p 449 N95-27914

DELGRANDE, NANCY K.

Mapping hidden aircraft defects with dual-band infrared computed tomography [DE95-011531] p 584 N95-32164

DELLACORTE, C.

Static and dynamic friction behavior of candidate high temperature airframe seal materials [NASA-TM-106571] p 152 N95-16905

DELLER, R. W.

Second generation smart actuator [SAE PAPER 932585] p 505 A95-90069

DELORE, VICTOR E.

Airborne Windshear Detection and Warning Systems. Fifth and Final Combined Manufacturers' and Technologists' Conference, part 1 [NASA-CP-10139-PT-1] p 10 N95-10566
Airborne Windshear Detection and Warning Systems. Fifth and Final Combined Manufacturers' and Technologists' Conference, part 2 [NASA-CP-10139-PT-2] p 41 N95-13203

DELP, STEVE

The prototype aviation weather products generator a vehicle to assess user needs p 671 A95-93534

DELUCA, D. P.

Fatigue in single crystal nickel superalloys [AD-A282917] p 88 N95-15415

DELUCA, DANIEL P.

Fatigue in single crystal nickel superalloys [AD-A283459] p 56 N95-12546
Fatigue in single crystal nickel superalloys [AD-A285727] p 152 N95-18068

DELVINQUIER, J. P.

Modular supplies for a distributed architecture p 234 N95-20657

DEMASI-MARCIN, J.

Thermal barrier coating experience in the gas turbine engine p 345 N95-26125

DEMIRKALE, SEYTAK YILMAZ

At Istanbul-Ataturk Airport measurement and analysis of noise in due of take-off time p 31 N95-11319

DEMMA, NICK

2 micron LIDAR for laser-based remote sensing: Flight demonstration and application survey [BTN-95-EIX95212641072] p 319 A95-76737

DEMUSZ, J. N.

Aircraft-borne, laser-induced fluorescence instrument for the in situ detection of hydroxyl and hydroperoxyl radicals [BTN-95-EIX95072499029] p 253 A95-71908

DENBOER, R. G.

Unsteady transonic wind tunnel test on a semispan straked delta wing, oscillating in pitch. Part 1: Description of the model, test setup, data acquisition, and data processing [AD-A293113] p 593 N95-30885

DENBOGGEND, T.

Integrated X-ray testing of the electro-optical breadboard model for the XMM reflection grating spectrometer [DE95-008829] p 644 N95-30507

DENDA, MITSUNORI

Study of multiple cracks in airplane fuselage by micromechanics and complex variables p 94 N95-14468

DENG, FANG

A time stepping coupled finite element-state space modeling environment for synchronous machine performance and design analysis in the ABC frame of reference p 649 N95-31948

DENNENO, ANDREW

The Integrated Terminal Weather System (ITWS) storm cell information and weather impacted airspace detection algorithm p 654 A95-93452

DENNIS, J. E., JR.

Algorithms for bilevel optimization [NASA-CR-194980] p 170 N95-16897

DENTON, J. D.

Designing in three dimensions p 90 N95-14130

DENYER, ANTHONY G.

Extracting a representative loading spectrum from recorded flight data p 80 N95-14469

DEPASQUALE, WILLIAM

E-6A hardness assurance, maintenance and surveillance program [AD-A283994] p 134 N95-19067

DEPLACHETT, CHARLES P.

A graphical user interface for design and analysis of air breathing propulsion systems [TABES PAPER 94-616] p 83 N95-14645

DEPPE, M. W.

An investigation of the side-dump dual in-line ramjet combustor p 617 N95-31199

DEPPE, MARTIN W.

Combustion efficiency in a dual-inlet side-dump ramjet combustor [AD-A283564] p 83 N95-15329

DEROSA, S.

Structural acoustic calculations in the low-frequency range [BTN-95-EIX95152582336] p 323 A95-73538

DERUNOV, E. K.

Separation of winged vehicles in supersonics [AIAA PAPER 95-6092] p 526 A95-88601

DESAI, S. S.

Viscous flow past aerofoils axisymmetric bodies and wings p 123 N95-19457

DESHPANDE, MANISH

Cavitation modeling in Euler and Navier-Stokes codes p 315 N95-23630

DESJARDINS, R. L.

Observations of fluxes and inland breezes over a heterogeneous surface [HTN-95-80258] p 212 A95-66315

DESSLER, A. E.

In situ observations in aircraft exhaust plumes in the lower stratosphere at midlatitudes [HTN-95-A0862] p 318 A95-76266

DESSORNES, O.

Injection studies in the French hypersonic technology program [AIAA PAPER 95-6096] p 510 A95-88004

DETURK, ROBIN

Impact of agility requirements on configuration synthesis [NASA-CR-4627] p 44 N95-11952

DEVENPORT, WILLIAM J.

Flow structure generated by perpendicular blade vortex interaction and implications for helicopter noise predictions [NASA-CR-198590] p 377 N95-28193

DEWESE, RICHARD

The performance of child restraint devices in transport airplane passenger seats [DOT/FAA/AM-94/19] p 40 N95-12146

DEWITT, KENNETH J.

Effect of curvature in the numerical simulation of an electrothermal de-icer pad [BTN-95-EIX95182619219] p 276 A95-76645

DEWITT, KENNETH J.

Numerical analysis of hypersonic low-density scramjet inlet flow [BTN-95-EIX95212645694] p 272 A95-76746

DEXTER, H. BENSON

Development and verification of a resin film infusion/resin transfer molding simulation model for fabrication of advanced textile composites [NASA-CR-197439] p 301 N95-23179

DEXTER, H. BENSON

Resin transfer molding of textile preforms for aircraft structural applications p 421 N95-28276
Recent progress in NASA Langley textile reinforced composites program p 425 N95-28475

DEXTER, H. BENSON

Performance of resin transfer molded multifaxial warp knit composites p 535 N95-29039

DEXTER, P. C.

High angle of attack missile aerodynamics [CONGRESS PAPER C428-3-060] p 475 A95-91673

DHANAK, MANHAR R.

Effect of weak periodic pressure gradient on streamwise vortices near a wall p 29 N95-11263

DHAUSSY, J. C.

FASTPACK: Optimized solutions for modular avionics derived from a parametric study. Part 2: Avionics p 233 N95-20635

DHEENADAYALAN, J.

Use of partially open wind tunnel walls for blockage-free separated flows on bodies p 474 A95-91558

DHUYVETTER, H.

A new guidance and flight control system for the DELTA 2 launch vehicle p 342 A95-80427

DIAZ, MILTON E.

The photo-realistic AFIT virtual cockpit [AD-A289376] p 390 N95-26876

DIBERARDINO, M.

Field repair materials for naval aircraft p 394 N95-27514

DICARLO, DANIEL J.

Actuated forebody strake controls for the F-18 High-Alpha Research Vehicle [BTN-95-EIX0619952748173] p 619 A95-94467

DICARLO, DANIEL J.

Preparations for flight research to evaluate actuated forebody strakes on the F-18 high-alpha research vehicle p 72 N95-14257

DICKES, E.

Experimental study of the effects of Reynolds number on high angle of attack aerodynamic characteristics of forebodies during rotary motion [NASA-CR-195033] p 330 N95-24443

DICKES, EDWARD

Validation of the NASA Dryden X-31 simulation and evaluation of mechanization techniques p 69 N95-14236

DICKMANN, ERNST D.

The 4-D approach to visual control of autonomous systems [AIAA PAPER 94-1243-CP] p 27 N95-11513

DIEHL, ALAN E.

Organizational ergonomics and aviation safety p 596 A95-95083

DIETRICH, DONALD A.

Engine/airframe installation CFD for commercial transports: An engine manufacturer's perspective [SAE PAPER 932623] p 495 A95-90084

DIETZ, G.

Investigation of an NLF(1)-0416 airfoil in compressible subsonic flow p 110 N95-17852

DIGAVALLI, SASI K.

Dynamic stall of a NACA 0012 airfoil in laminar flow p 479 N95-29243

DIGGLE, DAVID WILLIAM

An investigation into the use of satellite-based positioning systems for flight reference/autoland operations p 489 N95-29542

- DIGIANFRANCESCO, A.**
Thermal testing of high performance thermal barrier coatings for turbine blades p 202 N95-19681
- DIGNAN, MICHAEL**
An active liner system for jet engine exhaust silencers, phase 1 [AD-A293277] p 617 N95-31191
- DILLENIUS, MARNIX F. E.**
Aerodynamic design of pegasus: Concept to flight with computational fluid dynamics [BTN-95-EIX95182617463] p 298 A95-75734
- DILLER, T. E.**
Time-resolved surface heat flux measurements in the wing/body junction vortex [BTN-95-EIX95082502716] p 220 A95-71029
- DIMANLIG, ARSENIO C. B.**
Numerical simulation of helicopter engine plume in forward flight [NASA-CR-197488] p 107 N95-16589
- DIMARCO, PETER CHARLES**
Navy foreign object damage and its impact on future gas turbine engine low pressure compression systems p 198 N95-19658
- DIMICHELE, ROBERTO**
Proceedings of the AIAA/FAA joint symposium on general aviation systems [AD-A289830] p 368 N95-28610
- DIMSDALE, BERNARD**
Multidimensional lines 2: Proximity and applications [BTN-94-EIX94341340329] p 61 A95-60865
- DINENNO, P. J.**
A review of water mist technology for fire suppression [AD-A285738] p 225 N95-20071
- DINGUS, PETER**
New technologies for space avionics [NASA-CR-197574] p 150 N95-18196
- DINH, Q. V.**
A cartesian grid finite element method for aerodynamics of moving rigid bodies p 642 A95-95471
- DINICOLA, ALBERT J.**
Static and fatigue testing of full-scale fuselage panels fabricated using a Therm-X(R) process p 420 N95-28270
- DINU, ADRIAN**
Direct boundary integral equations method to subsonic flow with circulation past thin airfoils in ground effect [BTN-95-EIX95242673940] p 365 A95-82224
- DINWIDDIE, R. B.**
Thermal conductivity of zirconia thermal barrier coatings p 345 N95-26133
- DISIMILE, PETER J.**
Observations on using experimental data as boundary conditions for computations [BTN-95-EIX95182619103] p 321 A95-76588
- DITTMAR, JAMES H.**
Background noise levels measured in the NASA Lewis 9- by 15-foot low-speed wind tunnel [NASA-TM-106817] p 145 N95-18054
- DIVINEY, WILLIAM**
Offshore next generation weather radar (NEXRAD) OTE&E integration and OT&E operational test [AD-A293223] p 646 N95-30902
- DIVITO, BEN L.**
Formal design and verification of a reliable computing platform for real-time control (phase 3 results) [NASA-TM-109140] p 33 N95-10873
- DIXON, MICHAEL**
The real-time analysis and prediction of storms program p 655 A95-93457
Automated aircraft routing through weather-impacted airspace p 666 A95-93512
- DJEPA-PETROVA, V. S.**
A program for scientific and applied investigations using aerostal complexes p 182 A95-66304
- DJOMEHRI, M. JAHED**
An assessment of the adaptive unstructured tetrahedral grid, Euler Flow Solver Code FELISA [NASA-TP-3526] p 119 N95-19041
- DOANE, WILLIAM J.**
Development of a low-cost, modified resin transfer molding process using elastomeric tooling and automated preform fabrication p 420 N95-28268
- DOBRYNSKI, WERNER**
Broadband noise characteristics of a model counter-rotating shrouded propfan p 572 A95-88470
- DOCKUS, D. A.**
MEMFOG - The Memphis fog algorithm p 668 A95-93516
- DODSON, LORI J.**
Supersonic and hypersonic shock/boundary-layer interaction database [BTN-94-EIX94441386604] p 182 A95-67335
Supersonic and hypersonic shock/boundary-layer interaction database [HTN-95-20930] p 463 A95-88969
- DOERR, HANS J.**
Effects of activated reactive evaporation process parameters on the microhardness of polycrystalline silicon carbide thin films [GTN-95-00406090-4621] p 680 A95-93965
- DOGGER, C. S.**
Unsteady transonic wind tunnel test on a semispan straked delta wing, oscillating in pitch. Part 1: Description of the model, test setup, data acquisition, and data processing [AD-A293113] p 593 N95-30885
- DOGGETT, ROBERT V., JR.**
The use of the Regier number in the structural design with flutter constraints [NASA-TM-109128] p 13 N95-11465
Flutter clearance flight tests of an OV-10A airplane modified for wake vortex flight experiments [NASA-TM-109168] p 366 N95-26381
- DOGRA, V. K.**
DSMC calculations for 70-deg blunted cone at 3.2 km/s in nitrogen [NASA-TM-109181] p 348 N95-24396
- DOGRA, VIRENDRA K.**
Hypersonic rarefied flow past spheres including wake structure [BTN-95-EIX95152583250] p 305 A95-73551
Zonally decoupled direct simulation Monte Carlo solutions of hypersonic blunt-body wake flows [BTN-95-EIX95182617458] p 268 A95-75729
- DOHERR, KARL-FRIEDRICH**
Analytical solution and parameter estimation of projectile dynamics [BTN-95-EIX95212645695] p 272 A95-76747
- DOHME, JACK A.**
Intelligent flight trainer for initial rotary wing training [SAE PAPER 932536] p 386 A95-84558
Automated hover training: An empirical evaluation [SAE PAPER 932536] p 379 A95-84559
- DOHRMANN, ULRICH**
Drag and lift in nonadiabatic transonic flow [HTN-95-61208] p 540 A95-87581
- DOIRON, M. D.**
Turbulent flow measurements with a triple-split hot-film probe [HTN-95-A1774] p 634 A95-93337
- DOLAN, N. J.**
Test and evaluation report for the Manual Domestic Passive Profiling System (MDPPS) [AD-A286312] p 225 N95-20093
- DOLEZAL, WILLIAM K.**
Draft standard for color active matrix liquid crystal displays (AMLCDs) in US Military aircraft. Recommended best practices [AD-A282950] p 49 N95-12591
- DOLLING, D. S.**
Fluctuating wall pressures near separation in highly swept turbulent interactions [HTN-95-20823] p 543 A95-88084
Leading-edge sweepback and shape effects on fin-induced fluctuating pressures [BTN-95-EIX95302694471] p 636 A95-94067
Unsteadiness of shock-induced turbulent boundary layer separation. An inherent feature of turbulent flow or solely a wind tunnel phenomenon [AD-A290367] p 554 N95-29228
- DOLMAN, W. C.**
The application of Ada and formal methods to a safety critical engine control system p 710 N95-33142
- DOLVIN, DOUGLAS J.**
Structural design optimization with survivability dependent constraints application: Primary wing box of a multi-role fighter p 398 N95-28440
- DOMINIK, C. J.**
2-D aileron effectiveness study p 110 N95-17851
- DOMINO, DAVID A.**
Future ATC system integration: Tools for developing a shared vision p 600 A95-95085
- DOMINY, JOHN**
Structural composites in civil gas turbine aero engines [HTN-95-B0258] p 529 A95-89202
- DON, W. S.**
High order accuracy computational methods in aerodynamics using parallel architectures [AD-A294167] p 686 N95-34763
- DONALDSON, J.**
A review of free-stream flow fluctuation and steady-state flow quality measurements in the AEDC/VKF Supersonic Tunnel A and Hypersonic Tunnel B [AIAA PAPER 95-6137] p 520 A95-90454
- DONALDSON, RALPH S., JR.**
Radar studies of aviation hazards [AD-A285845] p 226 N95-21831
- DONBAR, J. M.**
Numerical study of mixing in a high and low enthalpy supersonic test facility p 7 N95-10467
- DONELSON, MICHAEL J.**
Long distance propagation model and its application to aircraft en route noise prediction [HTN-95-61221] p 491 A95-87594
- DONG, Y. F.**
Study of multiple cracks in airplane fuselage by micromechanics and complex variables p 94 N95-14468
- DONNELLAN, T. M.**
Navy composite maintenance and repair experience p 424 N95-28446
- DONOFRIO, KEVIN**
Integrated design and manufacturing for the high speed civil transport [NASA-CR-197183] p 48 N95-12700
- DONOHUE, S. R.**
The utilization of a high speed reflective visualization system in the study of transonic flow over a delta wing p 121 N95-19259
- DONOVAN, R. P.**
Measurement of particle emissions from clean room gas-handling components [BTN-94-EIX94381359040] p 295 A95-74554
Measurement of moisture and total hydrocarbon contributions by valves used in clean room gas-delivery systems [BTN-94-EIX94381359041] p 295 A95-74629
- DONTAS, KEJITAN**
Identification of Artificial Intelligence (AI) applications for maintenance, monitoring, and control of airway facilities [AD-A282479] p 125 N95-17373
- DOR, J. B.**
Experimental techniques for measuring transonic flow with a three dimensional laser velocimetry system. Application to determining the drag of a fuselage p 163 N95-19258
- DORENBERG, FRANK M. G.**
Overview of AlliedSignal's avionics development in the CIS [BTN-95-EIX95212641069] p 287 A95-76734
- DORR, D. W.**
Simulation and flight test evaluation of head-up-display guidance for barrier approach transitions [BTN-95-EIX95062487533] p 194 A95-69241
- DORRIS, WILLIAM J.**
Advanced composites structural concepts and materials technologies for primary aircraft structures: Structural response and failure analysis [NASA-CR-4448] p 11 N95-10240
ISPAN (Interactive Stiffened Panel Analysis): A tool for quick concept evaluation and design trade studies p 533 N95-28846
- DOSANJH, DARSHAN**
The noise reduction potential of dual-stream coaxial rectangular improperly expanded jet flows [NASA-CR-197820] p 437 N95-26995
- DOST, E. F.**
Impact damage resistance of composite fuselage structure, part 1 p 399 N95-28482
- DOST, ERNEST**
In situ processing methods for composite fuselage sandwich structures p 531 N95-28826
- DOST, ERNEST F.**
Impact damage resistance of composite fuselage structure, part 2 p 533 N95-28838
- DOUGHERTY, JOHN J.**
GPS modeling for designing aerospace vehicle navigation systems [BTN-95-EIX95302731223] p 600 A95-94044
- DOUGLAS, MICHAEL W.**
Research aircraft observations of a polar low at the east Greenland ice edge [HTN-95-A0175] p 215 A95-69766
- DOUGLASS, ANNE R.**
Trajectory modeling of emissions from lower stratospheric aircraft [HTN-95-41219] p 317 A95-75031
Sensitivity of two-dimensional model predictions of ozone response to stratospheric aircraft: An update [HTN-95-A0863] p 318 A95-76267
Tracer transport for realistic aircraft emission scenarios calculated using a three-dimensional model [HTN-95-41799] p 353 A95-80525
Effects of a polar stratosphere cloud parameterization on ozone depletion due to stratospheric aircraft in a two-dimensional model [HTN-95-A1038] p 443 A95-84543
Three dimensional model calculations of the global dispersion of high speed aircraft exhaust and implications for stratospheric ozone loss p 26 N95-10657
- DOW, MARVIN B.**
Development of stitched/RTM composite primary structures p 425 N95-28469
The effects of aircraft fuel and fluids on the strength properties of Resin Transfer Molded (RTM) composites p 536 N95-29047

DOWELL, E. H.

DOWELL, E. H.

Comparison of theory and experiment for non-linear flutter and stall response of a helicopter blade

[BTN-94-EIX94351108100] p 191 A95-66500

Response of a nonrotating rotor blade to lateral turbulence. Part 1: Theory

[BTN-95-EIX95182619228] p 284 A95-76654

Response of a nonrotating rotor blade to lateral turbulence. Part 2: Experiment

[BTN-95-EIX95182619229] p 284 A95-76655

DOWELL, EARL H.

Flutter of an infinitely long panel in a duct

[BTN-95-EIX95182619087] p 291 A95-75772

Nonlinear dynamics and aeroelasticity of rotorcraft in forward flight

[AD-A291714] p 400 N95-28504

DOWLING, ANN P.

Active boundary-layer control in diffusers

[HTN-95-42580] p 458 A95-87210

DOWN, M. G.

Out of area experiences with the RB199 in Toronto

p 198 N95-19654

DOWNEN, TROY

Preliminary design problems and solutions for a supersonic oblique all-wing transport aircraft

p 390 N95-26942

Design of a high altitude long endurance aircraft with manufacturing considerations

p 391 N95-26947

Prevention and control of inlet unstart using an SR-71 simulation

p 367 N95-26948

DOWNING, DAVID R.

Functional agility metrics and optimal trajectory analysis

[BTN-95-EIX95182619121] p 321 A95-76598

DOWNING, MICAH

USAF single-event sonic boom prediction model: PCBoom3

p 101 N95-14889

DOWNS, JOSHUA LEE

Airborne air traffic control: An application of distributed processing in the air traffic control environment

[HTN-95-12417] p 611 A95-95210

DOWNS, P. R.

Computer simulation of ejection seat motion

[CONGRESS PAPER C428-18-169] p 484 A95-91718

DOYAL, JEFFREY A.

Visual contrast detection thresholds for aircraft contrails

[AD-A288618] p 328 N95-25607

DOYLE, STACY A.

Analyzing fault tolerance using DREDD

[AIAA PAPER 95-0952] p 565 A95-90631

DRABCCZUK, R. P.

Eglin Air Force Base Ram Accelerator Research Facility

p 19 N95-10284

DRAGOS, LAZAR

Direct boundary integral equations method to subsonic flow with circulation past thin airfoils in ground effect

[BTN-95-EIX95242673940] p 365 A95-82224

DRAGT, J. B.

Digital simulation of wind velocities for wind turbine rotors: General considerations

[PB95-206447] p 677 N95-31157

DRAKE, AARON

Transonic flight test of a laminar flow leading edge with surface excrescences

[NASA-TM-4597] p 9 N95-11158

DRAKE, JOHN L.

175Hp contrarotating homopolar motor design report

[AD-A291138] p 557 N95-30122

DRDA, B.

Cost effective, dual-purpose machine vision-based detectors for (1) smoke and flame detection, and (2) engine overhead/burn-through and flame detection

[AD-A292284] p 579 N95-28870

DRDLA, K.

Analysis of the physical state of one Arctic polar stratospheric cloud based on observations

[HTN-95-70917] p 351 A95-77982

DRECHSLER, GENA K.

Conversion of the TRACON operations concepts database into a formal sentence outline job task taxonomy

[DOT/FAA/AM-95/16] p 488 N95-28819

DREGALIN, A. F.

On introduction of artificial intelligence elements to heat power engineering

[BTN-94-EIX94461407961] p 100 A95-62635

On a program-information system TDsoft

[BTN-94-EIX94461408773] p 175 A95-63656

Service and physical properties of liquid-jet fuels

p 151 N95-16256

DREKSLER, STEVEN B.

Environmental support of naval aviation

[AD-A292873] p 598 N95-31454

DRESS, D. A.

Dynamic Stability Instrumentation System (DSIS).

Volume 1: Hardware description

[NASA-TM-109160-VOL-1] p 171 N95-18899

DREXLER, J.

Optimal separation and ascent of lifting upper stages

p 525 A95-87396

DRIVER, MARK A.

Improved modeling of unsteady heat transfer (The first step)

[AD-A292777] p 648 N95-31432

DRNEVICH, R. F.

Airborne rotary separator study

[NASA-CR-191045] p 150 N95-18743

DROEGEMEIER, KELVIN K.

Investigation of outflow strength variability in Florida downburst-producing storms

p 659 A95-93476

DRUET, MICHELE

Comet repair of metallic airframe: Twenty years of experience

p 393 N95-27508

DRUMMOND, C. K.

Object-oriented technology for compressor simulation

[NASA-TM-106723] p 49 N95-11864

DUCOT, ELIZABETH R.

On designing and engineering the integrated terminal weather system

p 653 A95-93449

DUDEK, JULIANNE C.

Grid resolution and turbulent inflow boundary condition recommendations for NPARC calculations

[NASA-TM-106959] p 482 N95-30253

DUDLEY, D. G.

Ultra-wideband electromagnetic target identification

p 486 A95-90955

DUFFA, GEORGES

Corrective term in wall slip equations for Knudsen layer

[BTN-95-EIX95282705070] p 455 A95-89667

DUFFELL, H. R. F.

Aircraft cabin water spray systems - research and regulatory issues

[CONGRESS PAPER C428-25-150] p 595 A95-93600

DUFFY, C. J.

Novel implements of optical diagnostic techniques for aerospace applications

[CONGRESS PAPER C428-21-081] p 550 A95-91726

DUGAN, JOANNE BECHTA

Analyzing fault tolerance using DREDD

[AIAA PAPER 95-0952] p 565 A95-90631

DUH, J. C.

Marangoni-Benard convection in a low-aspect-ratio liquid layer

p 56 A95-61544

DUISENBERG, KEN

Simulation of rotor blade element turbulence

[NASA-TM-108862] p 232 N95-21186

DUKE, M. R., JR.

Numerical investigation of cylinder wake flow with a rear stagnation jet

[HTN-95-51669] p 433 A95-85051

DUMONT, B.

Composite cases for airborne electronic equipment: A technology study and EMC

p 241 N95-20655

DUNAGAN, STEPHEN E.

A three-dimensional orthogonal laser velocimeter for the NASA Ames 7- by 10-foot wind tunnel

[NASA-TM-108864] p 249 N95-21323

DUNBAR, BRIAN

NEXRAD/ARSR operational comparison

p 658 A95-93470

DUNCAN, B.

Hypersonic waveriders generated from power-law shocks

[AIAA PAPER 95-6160] p 470 A95-90472

DUNCAN, BEVERLY S.

Computational analysis in support of the SSTO flowpath test

[NASA-TM-106757] p 89 N95-13665

DUNGAN, G. D.

Fight testing high lateral asymmetries on highly augmented Fighter/Attack aircraft

[AD-A284206] p 130 N95-17953

DUNHAM, R. EARL, JR.

Heavy rain effects

p 78 N95-14899

DUNN, H. J.

The use of the Regier number in the structural design with flutter constraints

[NASA-TM-109128] p 13 N95-11465

DUNN, T. J.

Operational multi-scale environment model with grid adaptivity (OMEGA) application to aviation weather

p 676 A95-93556

DUNN, W. N.

A user's guide to LUGSAN 1.1: A computer program to calculate and archive lug and sway brace loads for aircraft-carried stores

[DE95-001919] p 232 N95-21730

DUQUE, EARL P. N.

Numerical simulation of helicopter engine plume in forward flight

[NASA-CR-197488] p 107 N95-16589

DUQUETTE, JAIME

Design and construction of a remote piloted flying wing

[NASA-PAPER-197195] p 47 N95-12695

DURAKO, BILL

In situ processing methods for composite fuselage sandwich structures

p 531 N95-28826

DURAND, JEAN-CLAUDE

A processing centre for the CNES CE-GPS experimentation

p 125 N95-17196

DURBIN, PAUL A.

A comparison of turbulence models in computing multi-element airfoil flows

[AIAA PAPER 94-0291] p 4 A95-60185

DURBIN, PHILIP F.

Mapping hidden aircraft defects with dual-band infrared computed tomography

[DE95-011531] p 584 N95-32164

DURHAM, WAYNE C.

Kinematics and aerodynamics of velocity-vector roll

[BTN-95-EIX95182619126] p 291 A95-76603

Attainable moments for the constrained control allocation problem

[BTN-95-EIX95182619149] p 322 A95-76626

DURKIN, E.

Flex cycle combustor development and demonstration

[BTN-94-EIX95011441245] p 417 A95-84202

DURKIN, ED

Dynamic stiffness and damping of foil bearings for gas turbine engines

[SAE PAPER 931449] p 635 A95-93698

DUTTON, CRAIG J.

Study of subsonic base cavity flowfield structure using particle image velocimetry

[BTN-95-EIX9522650781] p 327 A95-79237

DUTTON, GEOFFREY S.

Vertical transport rates in the stratosphere in 1993 from observations of CO₂, N₂O, and CH₄

[HTN-95-70941] p 351 A95-78006

DUTTON, J. C.

Supersonic near-wake afterbody boattailing effects on axisymmetric bodies

[BTN-95-EIX95182617465] p 268 A95-75736

DUTTON, JAMES P., JR.

Development of a nonlinear simulation for the McDonnell Douglas F-15 Eagle with a longitudinal TECS control-law

[AD-A288610] p 388 N95-26481

DUTTON, S. A.

Preparation of S-70A-9 Black Hawk helicopter for flight tests to investigate cause of cracking of inner fuselage panel

[AD-A293891] p 608 N95-31544

DUYAR, AHMET

Sensor fault detection and diagnosis simulation of a helicopter engine in an intelligent control framework

[AD-A290223] p 137 N95-15970

DWEYER, JOHN P.

Crew aided and automation: A system concept for terminal area operations, and guidelines for automation design

[NASA-CR-4631] p 228 N95-19950

DYE, J. E.

Performance of a focused cavity aerosol spectrometer for measurements in the stratosphere of particle size in the 0.06-2.0-micrometer-diameter range

[HTN-95-90914] p 253 A95-72423

Analysis of the physical state of one Arctic polar stratospheric cloud based on observations

[HTN-95-70917] p 351 A95-77982

DZIEGIEL, R. J., JR.

A reuse framework for software fault tolerance

[AIAA PAPER 95-1012] p 566 A95-90683

E

EARHART, E.

Bearing defect signature analysis using advanced nonlinear signal analysis in a controlled environment

[NASA-TM-108491] p 441 N95-28364

EAST, R.

The use of thermochromic liquid crystals for heat transfer measurements in short duration hypersonic wind tunnel facilities

[AIAA PAPER 95-6115] p 520 A95-90443

- EAST, R. A.**
Measurement of free-flight dynamic stability derivatives of cones in a hypersonic gun tunnel
[AIAA PAPER 95-6082] p 519 A95-87411
- EASTAUGH, GRAEME F.**
Multiple site fatigue damage in fuselage skin splices: Experimental simulation and theoretical prediction
[BTN-95-EIX95152584676] p 276 A95-73588
- EASTLAND, KEVIN**
The Balsa bullet: A high speed, low-cost general aviation aircraft for Aeroworld
[NASA-CR-197165] p 46 N95-12638
- EATON, JOHN K.**
Near field of a coaxial jet with and without axial excitation
[HTN-95-42332] p 372 A95-86161
Active open-loop control of particle dispersion in round jets
[HTN-95-42334] p 372 A95-86163
- EBEL, ADOLF**
Evolution of the concentrations of trace species in an aircraft plume: Trajectory study
[HTN-95-A1044] p 443 A95-84549
- EBERHARDT, SCOTT**
Automatic multi-block grid generation for high-lift configuration wings
p 567 N95-28764
- EBINA, IWAO**
Introduction of the GPS to civil aviation field
p 487 A95-91536
- EBY, STEVEN C.**
Design of a vehicle based system to prevent ozone loss
[NASA-CR-197199] p 48 N95-12702
- ECA, L. R. C.**
Discretization of the parabolised Navier-Stokes equations
p 638 A95-95362
- ECER, A.**
Parallel computational fluid dynamics '91; Conference Proceedings, Stuttgart, Germany, Jun. 10-12, 1991
[ISBN 0-444-89363-6] p 548 A95-91479
- ECKERT, D.**
Correction of support influences on measurements with sting mounted wind tunnel models
p 122 N95-19281
- ECKLUND, ROWENA H.**
Composite intermediate case manufacturing scale-up for advanced engines
p 406 N95-28275
- ECKSTROM, CLINTON V.**
Measurements of unsteady pressure and structural response for an elastic supercritical wing
[NASA-TP-3443] p 104 N95-16560
- ECONOMIDES, GREGORY**
Knowledge-based processing for aircraft flight control
[NASA-CR-194976] p 99 N95-13727
- EDAMOTO, K.**
Arbitrary Lagrangian-Eulerian finite element analysis for flow-induced vibration of rigid body
p 643 A95-95485
- EDGE, K. A.**
Fault Diagnosis for condition monitoring applied to hydraulic circuits
[CONGRESS PAPER C428-12-165] p 456 A95-91703
- EDLOW, RALPH**
COINS: A composites information database system
p 453 N95-28465
- EDWARDS, MARK B.**
The role of flight progress strips in en route air traffic control: A time-series analysis
[DOT/FAA/AM-95/4] p 280 N95-23565
Automation and cognition in air traffic control: An empirical investigation
[AD-A291932] p 488 N95-28790
- EDWARDS, THOMAS**
CFD optimization of a theoretical minimum-drag body
[BTN-95-EIX95182619234] p 308 A95-76660
- EDWARDS, VERNON R.**
US Army rotorcraft turboshaft engines sand and dust erosion considerations
p 198 N95-19656
- EGGERS, T.**
Estimation of aerodynamic derivatives: Euler scheme validation and approximate methods for hypersonic configurations
p 460 A95-87385
Aerodynamic off-design behavior of integrated waveriders from take-off up to hypersonic flight
[AIAA PAPER 95-6091] p 466 A95-89200
- EGGLESTON, DEBRA S.**
The 1993 JANNAF Propulsion Meeting, volume 1
[CPIA-PUBL-602-VOL-1] p 148 N95-16312
- EGOLF, T. ALAN**
Evaluation of a doubly-swept blade tip for rotorcraft noise reduction
[NASA-CR-189677] p 452 N95-28264
- EGOLFOPOULOS, F. N.**
Intrinsic transport and chemistry coupling in combustion phenomena
p 538 A95-87191
- EGUCHI, HIROFUMI**
A design of a robust scheduled autopilot
p 516 A95-91532
A design of a self-learning robust scheduled autopilot
p 516 A95-91533
Missile autopilot designs using full state feedback
p 507 A95-91587
- EGUCHI, KUNIHISA**
An advanced scramjet propulsion concept for A 350 MG SSTO space plane
p 402 A95-82325
- EHLER, R. J.**
Development of composite carrythrough bulkhead
p 423 N95-28438
- EHLERS, ROBERT C.**
NASA Lewis Research Center's preheated combustor and materials test facility
[NASA-TM-106676] p 626 N95-30592
- EHRET, G.**
Two dimensional stratospheric aerosol distributions during EASOE
[HTN-95-00726] p 444 A95-86296
- EHRHART, JOHN E., JR.**
KC-135 cockpit modernization study. Phase 1: Equipment evaluation
[AD-A284099] p 131 N95-18398
- EHRICH, F.**
Rotor whirl forces induced by the tip clearance effect in axial flow compressors
[BTN-94-EIX94351143331] p 207 A95-67304
- EIBERT, M.**
Laser based obstacle warning sensors for helicopters
p 686 N95-32499
- EICHSTEDT, DAVID**
Operational and research aspects of a radio-controlled model flight test program
[BTN-95-EIX0619952748177] p 606 A95-94471
- EIDE, PETER K.**
Implementation and demonstration of a multiple model adaptive estimation failure detection system for the F-16
[AD-A289301] p 391 N95-27042
- EILTS, MICHAEL D.**
Use of WSR-88D data in the FAA's weather impacted aerospace product
p 658 A95-93469
Final results of the weather testing component of the Terminal Doppler Weather Radar operational test and evaluation
p 658 A95-93471
Investigation of outflow strength variability in Florida downburst-producing storms
p 659 A95-93476
- EISELE, F. L.**
Measurements of ions formed in jet engine exhaust plumes
[AD-A290940] p 514 N95-29764
- EISENBIES, CHRISTOPHER L.**
Classification of ultra high range resolution radar using decision boundary analysis
[AD-A289378] p 437 N95-26877
- EISENHART, D. W.**
Phase 2: HGM air flow tests in support of HEX vane investigation
p 312 N95-23438
- EITELBERG, G.**
The high enthalpy shock tunnel in Goettingen (HEG)
p 518 A95-87391
- EJIRI, H.**
Aeroelastic tailoring research
[PB94-180031] p 6 N95-10135
- EJIRI, M.**
Polar Patrol Balloon system and preliminary experimental results
p 368 A95-82513
- EKATERINARIS, J. A.**
Interferometry and computational studies of an oscillating airfoil compressible dynamic stall flow field
[HTN-94-00703] p 3 A95-60182
Dynamic stall of an oscillating wing. Part 1: Evaluation of turbulence models
[AIAA PAPER 93-3403] p 3 A95-60184
Numerical simulation of incidence and sweep effects on delta wing vortex breakdown
[BTN-95-EIX95062487526] p 186 A95-69234
Effects of spatial order of accuracy on the computation of vertical flowfields
[BTN-95-EIX95152577604] p 305 A95-73479
Computation of oscillating airfoil flows with one- and two-equation turbulence models
[BTN-95-EIX95152577588] p 263 A95-73494
Effects of spatial order of accuracy on the computation of vertical flowfields
[HTN-95-42589] p 459 A95-87219
Numerical investigation of high incidence flow over a double-delta wing
[BTN-95-EIX0619952748160] p 588 A95-94454
Analysis of low Reynolds number airfoil flows
[BTN-95-EIX0619952748183] p 590 A95-94476
- EKATERINARIS, JOHN A.**
Viscous-inviscid interaction method for unsteady low-speed airfoil flows
[BTN-95-EIX95182619093] p 269 A95-75778
- EKLUND, D. R.**
Computational/experimental investigation of staged injection into a Mach 2 flow
[HTN-95-51646] p 432 A95-85028
- EKSTROM, C.**
Interfacing a digital compass to a remote-controlled helicopter
[PB95-164927] p 340 N95-24260
- EKSTROM, M.**
Bonded composite repair of cracked load-bearing holes
[BTN-94-EIX94401360553] p 243 A95-71867
- EKSUZIAN, D. J.**
TRISTAR 1: Evaluation methods for testing head-up display (HUD) flight symbology
[NASA-TM-4665] p 288 N95-24030
- EL-BANNA, HESHAM M.**
Aerodynamic sensitivity coefficients using the three-dimensional full potential equation
[BTN-95-EIX95062487530] p 186 A95-69238
- EL-SHERIEF, HOSSNY**
Real-time navigation using the global positioning system
[BTN-95-EIX95172595298] p 279 A95-75714
GPS modeling for designing aerospace vehicle navigation systems
[BTN-95-EIX95302731223] p 600 A95-94044
- ELALDI, F.**
Scar joint technique with cocured and precured patches for composite repair
p 396 N95-27524
- ELBERN, HENDRIK**
Evolution of the concentrations of trace species in an aircraft plume: Trajectory study
[HTN-95-A1044] p 443 A95-84549
- ELBULUK, MALIK E.**
Motor drive technologies for the power-by-wire (PBW) program: Options, trends and tradeoffs
[NASA-TM-106885] p 295 N95-23671
- ELDEM, CUNEYT**
Navier-Stokes simulation of turbulent vortex high-Re-number flows over a delta wing
p 644 A95-95507
- ELDER, R. L.**
Novel implements of optical diagnostic techniques for aerospace applications
[CONGRESS PAPER C428-21-081] p 550 A95-91726
Particle trajectories in gas turbine engines
p 199 N95-19663
- ELDRED, KENNETH MCK.**
Monitoring noise from aircraft operations in the vicinity of airports
p 570 A95-88462
- ELESCHAKY, MOHAMED E.**
Preconditioned domain decomposition scheme for three-dimensional aerodynamic sensitivity analysis
[BTN-95-EIX95152577612] p 321 A95-73471
Preconditioned domain decomposition scheme for three-dimensional aerodynamic sensitivity analysis
[HTN-95-42597] p 459 A95-87227
Improving the efficiency of aerodynamic shape optimization
[HTN-95-61204] p 540 A95-87577
- ELGERONA, PER-OLOV**
SAAB experience with PIO
p 598 N95-31069
- ELIASSON, P.**
Hypersonic Navier-Stokes computations about complex configurations
p 644 A95-95497
- ELIASSON, PETER**
Navier-Stokes computations around a realistic fighter configuration
p 591 A95-95440
- ELKINS, J. W.**
Estimates of total organic and inorganic chlorine in the lower stratosphere from in situ and flask measurements during AASE 2
[HTN-95-A0861] p 317 A95-76265
Fine-scale, poleward transport of tropical air during AASE 2
[HTN-95-70949] p 352 A95-78014
- ELKINS, JAMES W.**
Vertical transport rates in the stratosphere in 1993 from observations of CO₂, N₂O, and CH₄
[HTN-95-70941] p 351 A95-78006
- ELKS, CARL**
A highly reliable, high performance open avionics architecture for real time Nap-of-the-Earth operations
p 693 N95-32497
- ELLER, B. G.**
Vista/F-16 Multi-Axis Thrust Vectoring (MATV) control law design and evaluation
p 71 N95-14248
- ELLIOTT, CHARLES B., III**
The role of fretting corrosion and fretting fatigue in aircraft rivet hole cracking
p 94 N95-14470
- ELLIOTT, WILLIAM R.**
USAF aging aircraft program
[BTN-95-EIX95072498878] p 180 A95-68394

ELLROD, GARY P.

A northern hemisphere clear air turbulence climatology p 674 A95-93547

ELMER, KEVIN R.

Noise impact of advanced high lift systems [NASA-CR-195028] p 362 N95-26160

ELMORE, K. L.

Determining F-factor using ground-based Doppler radar. Validation and results p 11 N95-10571

ELMQUIST, A. R.

Computational fluid dynamics study of the variable-pitch split-blade fan concept [NASA-CR-189206] p 15 N95-10247

ELSENAAR, A.

Wind tunnel test on a 65 deg delta wing with a sharp or rounded leading edge: The international vortex flow experiment p 114 N95-17872

ELY, WAYNE L.

Integration of a mechanical forebody vortex control system into the F-15 p 72 N95-14258

ELZEBDA, JAMAL M.

Numerical simulation of steady and unsteady, vorticity-dominated aerodynamic interference [BTN-95-EIX95062487524] p 186 A95-69232

EMAMI, SAIED

Experimental investigation of inlet-combustor isolators for a dual-mode scramjet at a Mach number of 4 [NASA-TP-3502] p 407 N95-28343

EMANUEL, M.

Overview of remote sensing laser development and semiconductor laser technology [DE94-019103] p 256 N95-21552

EMERSON, D. R.

An efficient discrete vortex method for low Reynolds number incompressible flows p 639 A95-95407

EMERY, Y.

Airborne lidar observation of mountain-wave-induced polar stratospheric clouds during EASOE [HTN-95-00738] p 444 A95-86308

EMIN, O. N.

Gas-turbine engines with increased efficiency of two circuits, due to the use of the utilizing steam-turbine circuit [BTN-94-EIX94461408755] p 153 A95-63638

EMMER, D. S.

An analysis of B-1B exterior jet blast windshield anti-icing performance using pre-cooled compressor bleed air [AD-A292522] p 485 N95-28811

EMMONS, L. K.

An overview of millimeter-wave spectroscopic measurements of chlorine monoxide at Thule, Greenland, February-March, 1992: Vertical profiles, diurnal variation, and longer-term trends [HTN-95-00722] p 444 A95-86292

EMSLEY, HOWARD T.

Computational Fluid Dynamics (CFD) analysis of a C-135 aircraft with a side-mounted splitter plate (with comparison to wind tunnel data) [AD-A292029] p 553 N95-29187

ENDOH, MASANORI

Some comments on current research and development of civil VTOL aircrafts p 499 A95-91572

ENG, ANTHONY T.

Organic coating technology for the protection of aircraft against corrosion p 303 N95-23513

ENGELSTAD, S. P.

Application of FEM/SEA for prediction of aircraft cockpit noise p 576 A95-90130

ENGEN, DONALD D.

Earthwinds Hilton III: Balloon project p 497 A95-90871

ENGERS, R.

The panel oxidation and erosion test (POET) facility [AIAA PAPER 95-6151] p 521 A95-90465

ENGLAR, ROBERT J.

Application of circulation control to advanced subsonic transport aircraft. Part 1: Airfoil development [BTN-95-EIX95062487545] p 185 A95-68359

Application of circulation control to advanced subsonic transport aircraft. Part 2: Transport application [BTN-95-EIX95062487546] p 185 A95-68360

Development of pneumatic test techniques for subsonic high-lift and in-ground-effect wind tunnel investigations p 121 N95-19268

ENGLISH, S. J.

Aircraft measurements of water vapour continuum absorption at millimetre wavelengths [HTN-95-90884] p 253 A95-72393

ENNS, DALE

Dynamic inversion: An evolving methodology for flight control design p 621 N95-31996

ENNS, DALE F.

Multi-application controls: Robust nonlinear multivariable aerospace controls applications p 71 N95-14249

ENOCHS, EDGAR R.

An LDV investigation of support structure influence on the flow field near the wingtip of a STOVL configuration in hover [AD-A294126] p 686 N95-34750

ENOMOTO, SHUNJI

2-D and 3-D numerical simulation of a supersonic inlet flowfield p 641 A95-95457

ENSOR, D. S.

Measurement of particle emissions from clean room gas-handling components [BTN-94-EIX94381359040] p 295 A95-74554

Measurement of moisture and total hydrocarbon contributions by valves used in clean room gas-delivery systems [BTN-94-EIX94381359041] p 295 A95-74629

EPPEL, JOSEPH C.

Flight investigation of the use of a nose gear jump strut to reduce takeoff ground roll distance of STOL aircraft [NASA-TM-108819] p 44 N95-12225

EPSTEIN, ALAN H.

Intelligent turbine engines for Army applications [AD-A290532] p 514 N95-29496

EPSTEIN, RONALD J.

Experimental investigation of the flowfield about an upswept afterbody [BTN-95-EIX95152582321] p 265 A95-73524

Flutter of an infinitely long panel in a duct [BTN-95-EIX95182619087] p 291 A95-75772

ERCOLINE, W. R.

TRISTRAR 1: Evaluation methods for testing head-up display (HUD) flight symbology [NASA-TM-4665] p 288 N95-24030

ERDOS, J.

An assessment of ground-test facility capabilities for measurement of hypervelocity scramjet performance [AIAA PAPER 95-6148] p 512 A95-90462

ERENGIL, M. E.

Unsteadiness of shock-induced turbulent boundary layer separation. An inherent feature of turbulent flow or solely a wind tunnel phenomenon [AD-A290367] p 554 N95-29228

ERENTHAL, ELI

Lavi flight control system: Design requirements, development and flight test results p 621 N95-31994

ERICKSON, E. F.

SOFIA: Stratospheric Observatory for Infrared Astronomy p 363 A95-81583

ERICKSON, G. L.

Allison engine testing CMSX-4(reg sign) single crystal turbine blades and vanes [DE95-010308] p 694 N95-32636

ERICKSON, LARRY L.

An assessment of the adaptive unstructured tetrahedral grid, Euler Flow Solver Code FELISA [NASA-TP-3526] p 119 N95-19041

ERICSSON, LARS E.

Moving wall effect in relation to other dynamic stall flow mechanisms [BTN-95-EIX95152582324] p 265 A95-73527

Further analysis of high-rate rolling experiments of a 65-deg delta wing [BTN-95-EIX95152582331] p 281 A95-73533

Flow physics of critical states for rolling delta wings [BTN-95-EIX0619952748180] p 590 A95-94473

ERIDON, J. M.

Allison engine testing CMSX-4(reg sign) single crystal turbine blades and vanes [DE95-010308] p 694 N95-32636

ERKELENS, L. J. J.

Development of advanced approach and departure procedures. Failure scenarios [PB95-198123] p 601 N95-30815

ERM, LINCOLN P.

A preliminary study of the airwake model used in an existing SH-60B/FFG-7 helicopter/ship simulation program [DSTO-TR-0015] p 224 N95-21659

ERNST, HUGO A.

Fracture mechanics validity limits p 95 N95-14480

ERNST, R. R.

Broadband polarization-transfer experiments for rotating solids [GTN-95-0009261494012091-58] p 579 A95-92319

ERVIN, ROBERT D.

Electrorheologically controlled landing gear [BTN-94-EIX94461047055] p 78 A95-61740

An electrorheologically controlled semi-active landing gear [SAE PAPER 931403] p 605 A95-93673

ESCH, H.

Wind tunnel investigations of the appearance of shocks in the windward region of bodies with circular cross section at angle of attack p 113 N95-17866

ESHOW, MICHELLE M.

Identification and simulation evaluation of a combat helicopter in hover [BTN-95-EIX95242670749] p 335 A95-81098

ESKER, BARBARA S.

Experimental performance of a ventral nozzle with pitch and yaw vectoring capability for SSTOVL aircraft [SAE PAPER 931412] p 614 A95-93678

ESPANA, MARTIN

On the use of controls for subsonic transport performance improvement: Overview and future directions [NASA-TM-4605] p 10 N95-11408

ESPANA, MARTIN D.

Direct adaptive performance optimization of subsonic transports: A periodic perturbation technique [NASA-TM-4676] p 284 N95-22829

EST, BRIAN E.

Wing vertical position effects on wing-body carryover for noncircular missiles [BTN-95-EIX95182617462] p 268 A95-75733

ETEM, KAMIL

General aviation landing incidents and accidents: A review of ASRS and AOPA research findings p 596 A95-95198

EUBANKS, A. DALE

Alaska's volcanic ash warning system p 663 A95-93495

EVANS, ALYSON E.

Human factors certification in the development of future air traffic control systems p 690 N95-34770

EVANS, JAMES E.

Status of the terminal Doppler weather radar with deployment underway p 653 A95-93450

Role of the aviation weather system in providing a real-time ATC volcanic ash advisory system p 663 A95-93494

Assessment of the benefits for improved terminal weather information p 673 A95-93540

Ground-based wake vortex monitoring, prediction, and ATC interface p 42 N95-13209

EVANS, R. H.

TRISTRAR 1: Evaluation methods for testing head-up display (HUD) flight symbology [NASA-TM-4665] p 288 N95-24030

EVEKER, KEVIN MICHAEL

Model development for active control of stall phenomena in aircraft gas turbine engines p 514 N95-29679

EVERBERG, CARL

Minima reduction simulation test results [AD-A285626] p 228 N95-21148

EVERETT, WIN

Preliminary evaluation of the F/A-18 quantity/multiple envelope expansion [AD-A284119] p 132 N95-18407

EVERS, JOHNNY H.

High-performance, robust, bank-to-turn missile autopilot design [BTN-95-EIX95242670751] p 336 A95-81096

EVERSMAN, WALTER

Ducted fan acoustic radiation including the effects of nonuniform mean flow and acoustic treatment [NASA-CR-197449] p 172 N95-16401

EVTUSHENKO, I. A.

MHD-flow in slotted channels with conducting walls [DE94-018370] p 258 N95-21388

EWEN, JOHN R.

Cross-stiffened continuous fiber structures p 536 N95-29041

EXERTIER, P.

Precise orbit determination with a short-arc technique p 240 A95-70543

EYI, S.

Two-point transonic airfoil design using optimization for improved off-design performance [BTN-95-EIX95062487542] p 192 A95-68356

F

FAASSE, P. R.

Mach number control in the High Speed Wind Tunnel of NLR [PB94-201670] p 53 N95-13243

FABIAN, P.

Dynamics of aircraft exhaust plumes in the jet-regime [HTN-95-51275] p 355 A95-80860

FAETH, G. M.

Effect of ambient turbulence intensity on sphere wakes at intermediate Reynolds numbers [BTN-95-EIX95182619101] p 308 A95-76586

Sphere wakes at moderate Reynolds numbers in a turbulent environment [HTN-95-42331] p 372 A95-86160

- FAHEY, D. W.**
Estimates of total organic and inorganic chlorine in the lower stratosphere from in situ and flask measurements during AASE 2 [HTN-95-A0861] p 317 A95-76265
In situ observations in aircraft exhaust plumes in the lower stratosphere at midlatitudes [HTN-95-A0862] p 318 A95-76266
The distribution of hydrogen, nitrogen, and chlorine radicals in the lower stratosphere: Implications for changes in O₃ due to emission of NO(y) from supersonic aircraft [HTN-95-70935] p 351 A95-78000
- FAHEY, DAVID W.**
Vertical transport rates in the stratosphere in 1993 from observations of CO₂, N₂O, and CH₄ [HTN-95-70941] p 351 A95-78006
- FAHEY, THOMAS H., III**
Northwest Airlines atmospheric hazards advisory & avoidance system p 672 A95-93539
- FAIRBANKS, J. W.**
Thermal barrier coatings application in diesel engines p 345 A95-26124
- FALASCO, THOMAS**
H-76B fantail demonstrator composite fan blade fabrication [HTN-95-80856] p 283 A95-75098
- FALCONE, ANTHONY**
The effects of aircraft fuel and fluids on the strength properties of Resin Transfer Molded (RTM) composites p 536 A95-29047
- FALEMPIN, F.**
Review of new French facilities for PREPHA program [AIAA PAPER 95-6128] p 520 A95-90449
- FALEN, GERALD L.**
Analysis and simulation of narrowband GPS jamming using digital excision temporal filtering [AD-A289328] p 383 A95-26898
- FALLAVOLITA, MICHAEL A.**
Flow resolution and domain influence in rarefied hypersonic blunt-body flows [BTN-95-EIX95082502729] p 220 A95-70136
- FALLER, WILLIAM E.**
Neural network prediction of three-dimensional unsteady separated flowfields [BTN-95-EIX95182619232] p 308 A95-76658
Application of neural networks to unsteady aerodynamic control p 360 A95-25264
- FANSLER, KEVIN S.**
Comparison of meteorological data with fitted values extracted from projectile trajectory [AD-A285921] p 255 A95-19989
- FARASSAT, F.**
An introduction to generalized functions with some applications in aerodynamics and aeroacoustics p 565 A95-88895
- FARGES, C.**
Multilayer anti-erosion coatings p 201 A95-19679
- FARHAT, C.**
Matching fluid and structure meshes for aeroelastic computations: a parallel approach [BTN-95-EIX95302679864] p 636 A95-94102
High performance parallel analysis of coupled problems for aircraft propulsion [NASA-CR-195355] p 23 A95-10132
High-performance parallel analysis of coupled problems for aircraft propulsion [NASA-CR-197440] p 289 A95-23088
- FARLEY, G. L.**
Technology integration box beam failure study p 441 A95-28468
Technology integration box beam failure study p 552 A95-28847
- FARMAN, J. C.**
An overview of the EASOE campaign [HTN-95-00702] p 443 A95-86272
- FARR, EVERETT G.**
Impulse radiating antennas p 548 A95-90920
- FARRENS, BRYAN**
Icarus Rewaxed: A high speed, low-cost general aviation aircraft for Aeroworld [NASA-CR-197155] p 45 A95-12609
- FARTHING, CHARLES L.**
Electromagnetic reverberation characteristics of a large transport aircraft [AD-A282923] p 82 A95-15392
- FASANELLA, EDWIN L.**
Effects of floor location on response of composite fuselage frames p 423 A95-28439
- FAUCON, P.**
An overview of the EASOE campaign [HTN-95-00702] p 443 A95-86272
- FAWCETT, P. A.**
Rotor-wake-induced flow separation on a lifting surface [HTN-95-01082] p 468 A95-90268
- FAY, JONATHAN**
The Elite: A high speed, low-cost general aviation aircraft for Aeroworld [NASA-CR-197161] p 45 A95-12530
- FAY, RUSSELL**
Application of advanced material systems to composite frame elements p 422 A95-28432
- FAYE, ROBERT E.**
An assessment of upper surface blowing for the reduction of tilt rotor download [HTN-94-00711] p 5 A95-60189
- FAYETTE, DANIEL F.**
Reliability assessment of Multichip Module technologies via the Triservice/NASA RELTECH program p 245 A95-20643
- FEARS, SCOTT P.**
Low-speed wind-tunnel investigation of the stability and control characteristics of a series of flying wings with sweep angles of 50 deg [NASA-TM-4640] p 505 A95-30226
- FECHT, PAUL HANS**
Central coast designs: The Eightball Express. Taking off with convention, cruising with improvements and landing with absolute success [NASA-CR-197181] p 47 A95-12643
- FEDOR, L. S.**
Research aircraft observations of a polar low at the east Greenland ice edge [HTN-95-A0175] p 215 A95-69766
- FEDRO, MARK J.**
Characterization and manufacture of braided composites for large commercial aircraft structures p 426 A95-28478
- FEES, WILLIAM A.**
Space flight tests of attitude determination using GPS [BTN-95-EIX95112522529] p 190 A95-69334
- FEGEL, E.**
Real time for the calculation of the aerodynamic of aircrafts with delta wings p 460 A95-87399
- FEHRENBACHER, LARRY L.**
Ceramic composite combustor cans for expendable turbine engines [AD-A289551] p 407 A95-28646
- FEINER, L. J.**
Evaluation of all-electric secondary power for transport aircraft [NASA-CR-189077] p 441 A95-27999
- FELDER, JAMES L.**
Object-oriented approach for gas turbine engine simulation [NASA-TM-106970] p 615 A95-30594
- FELIPPA, C. A.**
High performance parallel analysis of coupled problems for aircraft propulsion [NASA-CR-195355] p 23 A95-10132
High-performance parallel analysis of coupled problems for aircraft propulsion [NASA-CR-197440] p 289 A95-23088
- FELKER, FORT F.**
An assessment of upper surface blowing for the reduction of tilt rotor download [HTN-94-00711] p 5 A95-60189
Aerodynamic interactions between a rotor and wing in hover [HTN-94-00714] p 5 A95-60192
- FENG, CHAO-KANG**
Nonlinear asymptotic theory of hypersonic flow past a circular cone [HTN-95-92599] p 461 A95-87415
- FENG, JINZHANG**
Cavitation modeling in Euler and Navier-Stokes codes p 315 A95-23630
- FENNO, C. C., JR.**
Response of multi-panel assembly to noise from a jet in forward motion [NASA-CR-198164] p 442 A95-28673
- FENTRESS, MICHAEL L.**
Experimental evaluation of a box beam specifically tailored for chordwise deformation [BTN-95-EIX95182619088] p 283 A95-75773
Unique considerations in the design and experimental evaluation of tailored wings with elastically produced chordwise camber p 423 A95-28436
- FERBER, M. K.**
Evolution of oxidation and creep damage mechanisms in HIPed silicon nitride materials [DE95-001350] p 300 A95-22689
- FEREBEE, I. C.**
The use of satellites for aeronautical communications, navigation and surveillance [CONGRESS PAPER C428-30-159] p 600 A95-93613
- FEREK, RONALD J.**
An intercomparison of aircraft instrumentation for tropospheric measurements of sulfur dioxide [HTN-95-91855] p 354 A95-80843
- An intercomparison of instrumentation for tropospheric measurements of dimethyl sulfide: Aircraft results for concentrations at the parts-per-trillion level [HTN-95-91857] p 355 A95-80845
- FERGIONE, J. A.**
T-45A high angle attack testing [HTN-95-81499] p 386 A95-85213
- FERGUSON, CHRIS J.**
Application of photogrammetry of F-14D store separation [AD-A284154] p 132 A95-18417
- FERGUSON, D. J.**
Computational study of a two-slot circulation control airfoil [SAE PAPER 932531] p 466 A95-89191
- FERGUSON, J. S.**
Composite repair issues on the CF-18 aircraft p 395 A95-27518
- FERGUSON, T. V.**
Impeller flow field characterization with a laser two-focus velocimeter p 313 A95-23440
- FERMAN, M. A.**
Acoustic fatigue characteristics of advanced materials and structures p 174 A95-19157
- FERNANDO, H. J.**
Experimental and theoretical studies of wakes in stratified flows [AD-A290203] p 553 A95-29060
- FERNKRANS, LARS**
Calculation of low speed wind tunnel wall interference from static pressure pipe measurements p 164 A95-19273
- FERON, ERIC MARIE**
Linear matrix inequalities for the problem of absolute stability of control systems p 518 A95-29680
- FERRANDON, O.**
Injection studies in the French hypersonic technology program [AIAA PAPER 95-6096] p 510 A95-88004
- FERRANTI, RICHARD L.**
Solid state radar demonstration test results at the FAA Technical Center [AD-A281520] p 154 A95-16097
- FERRARA, AUGUSTO**
Ongoing research into high octane unleaded avgas [SAE PAPER 931234] p 529 A95-88963
- FERRARA, GUS**
Vapor lock studies for gasolines with ethers [SAE PAPER 931233] p 529 A95-88962
Proceedings of the AIAA/FAA joint symposium on general aviation systems [AD-A289830] p 368 A95-28610
- FERRAROTTO, P.**
Preparation of S-70A-9 Black Hawk helicopter for flight tests to investigate cause of cracking of inner fuselage panel [AD-A293891] p 608 A95-31544
- FERREIRA, C. A.**
Detailed design of a 250-kW switched reluctance starter/generator for an aircraft engine [SAE PAPER 931389] p 613 A95-93665
- FERRI, P.**
EURECA mission control experience and messages for the future p 149 A95-17252
- FERRY, G. V.**
Performance of a focused cavity aerosol spectrometer for measurements in the stratosphere of particle size in the 0.06-2.0-micrometer-diameter range [HTN-95-90914] p 253 A95-72423
- FERTIG, TIMOTHY**
High density monolithic packaging technology for digital/microwave avionics p 240 A95-20646
- FERTIS, DEMETER G.**
New airfoil-design concept with improved aerodynamic characteristics [PAPER-4384] p 230 A95-72585
- FEULNER, MATTHEW ROGER**
Modeling and control of rotating stall in high speed multi-stage axial compressors p 511 A95-29244
- FICHEL, EDWARD J.**
High temperature strain gage technology for gas turbine engines [NASA-CR-191177] p 57 A95-11996
- FIDDES, S. P.**
A three-dimensional moving mesh method for the calculation of unsteady transonic flows [HTN-95-C0007] p 585 A95-93395
- FIDELL, SANFORD**
Assessing effects of military aircraft noise on residential property values near airbases p 31 A95-11310
- FIELD, FRANK R., III**
The potential for CMCs to replace superalloys in engine exhaust ducts [HTN-95-42298] p 418 A95-84992

FIELDING, C.

Flight demonstration of an advanced pitch control law in the VAAC Harrier aircraft p 623 N95-32012

FIELDS, JAMES M.

Criticism of the Leq as an Index for aircraft noise and other discontinuous noise sources p 559 A95-88478

FILIPENCO, V.

Unsteady flow phenomena in discrete passage diffusers for centrifugal compressors [AD-A281412] p 155 N95-16163

FILISKO, FRANK E.

Electrorheologically controlled landing gear [BTN-94-EIX94461047055] p 78 A95-61740

An electrorheologically controlled semi-active landing gear [SAE PAPER 931403] p 605 A95-93673

FINAISH, FATHI

Primary and secondary vortex structures over accelerated-decelerated airfoils at high angles of attack [SAE PAPER 931368] p 586 A95-93649

FINCH, STEVE

Systems engineering design and technical analyses for Strategic Avionics Crew-station Design Evaluation Facility (SACDEF) [AD-A286239] p 235 N95-22024

FINCO, JOE

The role of simulations in 777 FSEU development [AIAA PAPER 95-0995] p 506 A95-90665

FINEGOLD, LAWRENCE S.

Development and field test of the Beta version of the USAF Assessment System for Aircraft Noise (ASAN) p 561 A95-90121

Environmental noise research using the Human Response Monitor (HRM). Phase 1: System development p 562 A95-90122

FINK, C. L.

Evaluation of neutron techniques for illicit substance detection [DE95-002988] p 300 N95-22764

FINLEY, DENNIS B.

Euler Technology Assessment program for preliminary aircraft design employing SPLITFLOW code with Cartesian unstructured grid method [NASA-CR-4649] p 273 N95-22917

FINLEY, T. D.

Dynamic response tests of inertial and optical wind-tunnel model attitude measurement devices [NASA-TM-109182] p 296 N95-23011

FINLEY, TOM D.

Effects of yaw and pitch motion on model attitude measurements [NASA-TM-4641] p 250 N95-22109

FINN, SCOTT R.

Compressive strength of damaged and repaired composite plates p 442 N95-28484

Impact damage resistance of composite fuselage structure, part 2 p 533 N95-28838

FIORE, ERIC E.

Pilot rating scale for aircraft handling qualities [HTN-95-42269] p 380 A95-84963

FIORI, L.

An approach to sensor data fusion for flying and landing aid purpose p 686 N95-32488

FIORUCCI, T.

Bearing defect signature analysis using advanced nonlinear signal analysis in a controlled environment [NASA-TM-108491] p 441 N95-28364

FIRMIN, M. C. P.

Measurements of the flow over a low aspect-ratio wing in the Mach number range 0.6 to 0.87 for the purpose of validation of computational methods. Part 1: Wing design, model construction, surface flow. Part 2: Mean flow in the boundary layer and wake, 4 test cases p 112 N95-17860

FISCHER, D. S.

Test and evaluation report for the Manual Domestic Passive Profiling System (MDPPS) [AD-A286312] p 225 N95-20093

FISCHER, DOUGLAS S.

Test and Evaluation Plan (TEP) for Improvised Explosive Device Screening Systems (IEDSS) [AD-A286382] p 227 N95-22319

FISCHER, H.

Airborne measurements during the European Arctic Stratospheric Ozone Experiment column amounts of HNO₃ and O₃ derived from FTIR emission sounding [HTN-95-00742] p 445 A95-86312

FISCHER, P.

High order accuracy computational methods in aerodynamics using parallel architectures [AD-A294167] p 686 N95-34763

FISHER, C. E.

Gas path debris monitoring [CONGRESS PAPER C428-15-031] p 508 A95-91710

FISHER, DAVID F.

High Alpha Technology Program (HATP) ground test to flight comparisons p 68 N95-14230

Flight and full-scale wind-tunnel comparison of pressure distributions from an F-18 aircraft at high angles of attack p 68 N95-14231

Free-to-roll tests of X-31 and F-18 subscale models with correlation to flight test results p 69 N95-14237

FISHER, DAVID T.

Wind tunnel performance comparative test results of a circular cylinder and 50 percent ellipse tailboom for circulation control antitorque applications [AD-A283335] p 130 N95-18008

FISHER, JAY L.

Eddy current for detecting second-layer cracks under installed fasteners [AD-A279871] p 244 N95-20414

FISHER, M. J.

Near field noise prediction requirements [ISVR-TR-234] p 27 N95-11166

FITZGERMAN, A.

Pressure updating methods for the steady-state fluid equations [NASA-CR-198163] p 569 N95-30353

FITZPATRICK, C.

Cost effective, dual-purpose machine vision-based detectors for (1) smoke and flame detection, and (2) engine overhead/burn-through and flame detection [AD-A292284] p 579 N95-28870

FIX, BRADLEY L.

Machinability study of Aermet 100 [DE95-011532] p 701 N95-33408

FLAHERTY, J. E.

Automated adaptive time-discontinuous finite element method for unsteady compressible airfoil aerodynamics [HTN-95-81637] p 541 A95-87685

FLAMM, JEFFREY D.

Drag measurements of an axisymmetric nacelle mounted on a flat plate at supersonic speeds [NASA-TM-4660] p 684 N95-32821

FLEECE, E. J.

Development of anti-icing technology [PB94-195369] p 78 N95-15439

FLEETER, S.

Effect of wind tunnel acoustic modes on linear oscillating cascade aerodynamics [HTN-94-00760] p 14 A95-60199

FLEETER, SANFORD

Active control of turbomachine discrete tones p 29 N95-11275

Aero-thermodynamic distortion induced structured dynamic response [AD-A279931] p 203 N95-19864

FLEMING, GREGG G.

Factors affecting measured aircraft sound levels in the vicinity of start-of-takeoff roll p 571 A95-88465

FLEMING, M.

Fatigue reliability method with in-service inspections p 94 N95-14475

FLEMING, ROBERT J.

Role of wind tunnels and computer codes in the certification and qualification of rotorcraft for flight in forecast icing [NASA-TM-106747] p 39 N95-13197

FLESIA, C.

Airborne lidar observation of mountain-wave-induced polar stratospheric clouds during EASOE [HTN-95-00738] p 444 A95-86308

FLETCHER, D. G.

Computational/experimental investigation of staged injection into a Mach 2 flow [HTN-95-51646] p 432 A95-85028

FLEYGNAC, D.

Catapult-launching of the RAFALE design and experimentation p 609 N95-32008

FLICK, BRADLEY C.

F-18 high alpha research vehicle: Lessons learned p 69 N95-14240

FLINDELL, I. H.

Environmental noise monitoring - source identification [HTN-95-92537] p 558 A95-87357

FLINT, JOHN H.

Remote sensing of turbulence in the clear atmosphere with 2-micron lidars p 59 N95-13213

FLOKAS, VASSILIOS

Inband radar cross section of phased arrays with parallel feeds [AD-A284249] p 210 N95-19730

FLOMENHOFT, HUBERT I.

Brief history of gust models for aircraft design [BTN-95-EIX95062487557] p 203 A95-68371

FLORES, R. R.

Evaluation of all-electric secondary power for transport aircraft [NASA-CR-189077] p 441 N95-27999

FLOWERS, G. T.

Dynamic behavior of a magnetic bearing supported jet engine rotor with auxiliary bearings [NASA-CR-197860] p 338 N95-24213

FLOWERS, GEORGE T.

Influence of backup bearings and support structure dynamics on the behavior of rotors with active supports [NASA-CR-197438] p 310 N95-23190

Influence of backup bearings and support structure dynamics on the behavior of rotors with active supports [NASA-CR-199080] p 703 N95-32689

Steady-state dynamic behavior of an auxiliary bearing supported rotor system p 703 N95-32690

Dynamic behavior of a magnetic bearing supported jet engine rotor with auxiliary bearings p 703 N95-32691

Dynamic modelling and response characteristics of a magnetic bearing rotor system with auxiliary bearings p 703 N95-32692

Synchronous dynamics of a coupled shaft/bearing/housing system with auxiliary support from a clearance bearing: Analysis and experiment p 703 N95-32693

FLYNN, B. W.

Dimensional stability of curved panels with coured stiffeners and cobonded frames p 532 N95-28836

Global cost and weight evaluation of fuselage keel design concepts p 501 N95-28840

FLYNN, WILLIAM A.

An investigation of pilot induced oscillation phenomena in digital-flight control systems p 623 N95-32011

FOBES, J. L.

Test and evaluation report for the Manual Domestic Passive Profiling System (MDPPS) [AD-A286312] p 225 N95-20093

FOBES, JAMES L.

Test and Evaluation Plan (TEP) for Improvised Explosive Device Screening Systems (IEDSS) [AD-A286382] p 227 N95-22319

FOERSCHING, H.

Aeroelastic stability of cascades in turbomachinery [HTN-95-61156] p 405 A95-86255

FOGARTY, K. M.

Rotorcraft ditchings and water-related impacts that occurred from 1982 to 1989, phase 1 [AD-A279164] p 189 N95-19805

FOGG, DAVID A.

A PC-based interactive simulation of the F-111C Pave Tack system and related sensor, avionics and aircraft aspects [AD-A285500] p 129 N95-16969

FOLEY, BRIAN T.

Design and evaluation of a LQR controller for the bluebird unmanned air vehicle [AD-A289769] p 504 N95-29457

FOLEY, S. M.

Rotor-wake-induced flow separation on a lifting surface [HTN-95-01082] p 468 A95-90268

FOLKINS, IAN

Three-dimensional model interpretation of NO(x) measurements from the lower stratosphere [HTN-95-90534] p 213 A95-67806

FOLLEN, G. J.

Object-oriented technology for compressor simulation [NASA-TM-106723] p 49 N95-11864

FOLTA, DAVID C.

Reentry analysis for low Earth orbiting spacecraft p 415 A95-85774

FONTENOT, J.

Noise and vibration control in aircraft: A global approach p 576 A95-90128

FORBES, GREGORY S.

Use of pilot reports for verification of aircraft icing diagnoses and forecasts p 666 A95-93508

Examination of conditions in the proximity of pilot reports of aircraft icing during storm-fest p 666 A95-93509

FOREMAN, C. R.

C-130 Advanced Technology Center wing box conceptual design/cost study p 423 N95-28437

FORMAGGIA, L.

An unstructured node centered scheme for the simulation of 3-D inviscid flows p 642 A95-95463

FORMAN, BARBARA E.

The ITWS microburst prediction algorithm p 655 A95-93456

FORMAN, R. G.

Development of the NASA/FLAGRO computer program for analysis of airframe structures p 94 N95-14473

FORREST, DANA K.

Experimental aerodynamic characteristics of a generic hypersonic accelerator configuration at Mach numbers 1.5 and 2.0 [NASA-TM-4413] p 39 N95-12770

FORREST, WILLIAM C.

Creating an alternative parameter optimization method (APO) p 375 N95-26946

- FORRESTER, B. D.**
A portable transmission vibration analysis system for the S-70A-9 Black Hawk helicopter [DSTO-TR-0072] p 348 N95-24203
- FORRESTER, DAVID A.**
The improvement of meteorological data for air traffic management purposes p 668 A95-93518
- FORTIN, M.**
Large-scale computational fluid dynamics by the finite element method [BTN-94-EIX94381359154] p 243 A95-71744
- FOSS, JOHN F.**
Transverse vorticity measurements in the NASA Ames 80 x 120 wind tunnel boundary layer p 251 N95-22457
- FOSTER, JEFFRY**
Study of compressible flow through a rectangular-to-semiannular transition duct [NASA-CR-4660] p 338 N95-24392
- FOSTER, JEFFRY D.**
The decay of longitudinal vortices shed from airfoil vortex generators [NASA-CR-198356] p 480 N95-29402
- FOSTER, JOHN F.**
High-Alpha Research Vehicle (HARV) longitudinal controller: Design, analyses, and simulation results [NASA-TP-3446] p 17 N95-10860
- FOSTER, JOHN V.**
Flight validation of ground-based assessment for control power requirements at high angles of attack p 70 N95-14246
- FOSTER, LUCAS E.**
Extension to the dynamic modeling of the large angle magnetic suspension test fixture [NASA-CR-197801] p 411 N95-26768
- FOSTER, TERRY**
Water blasting paint removal methods p 650 N95-32170
Facilities used for plastic media blasting p 627 N95-32176
Operational parameters and material effects p 651 N95-32179
- FOURNIER, GILLES**
Transport Canada proposed R&D program for the development of a multi-parameter dual X-Ka band Doppler radar for aviation meteorology applications p 659 A95-93477
- FOUTCH, D. W.**
A modular system for computational fluid dynamics p 641 A95-95446
- FOWLER, T. K.**
Whirl plus tilt [DE95-007948] p 452 N95-28108
- FOWLER, TRESSA L.**
Use of pilot reports for verification of aircraft icing diagnoses and forecasts p 666 A95-93508
- FOX, DENNIS S.**
Resistance of silicon nitride turbine components to erosion and hot corrosion/oxidation attack p 202 N95-19683
- FOX, J. H.**
A one-dimensional inviscid nonequilibrium flow solver [ISBN 1-879921-01-4] p 588 A95-93752
- FRADKIN, M. I.**
The joint Russian-Brazil research on balloons p 182 A95-66303
- FRAILEY, JAMES A.**
Rapid repair of large area damage to contoured aircraft structures p 394 N95-27516
- FRAME, C. S.**
Composite repair of composite structures p 395 N95-27521
- FRANCINI, R. B.**
Ultrasonic techniques for repair of aircraft structures with bonded composite patches p 136 N95-19486
- FRANGANILLO, A.**
Repairs of CFC primary structures p 396 N95-27527
- FRANK, JASON**
Preliminary results and research capabilities of a new jet facility at the University of Kansas p 412 N95-26951
- FRANKE, M. E.**
Computational study of a two-slot circulation control airfoil [SAE PAPER 932531] p 466 A95-89191
- FRANKLIN, JAMES A.**
Simulation model of the integrated flight/propulsion control system, displays, and propulsion system for ASTOVL lift-fan aircraft [NASA-TM-108866] p 405 N95-26412
- FRANSEN, LAWRENCE J.**
Speech analysis and synthesis based on pitch-synchronous segmentation of the speech waveform [AD-A288824] p 435 N95-26349
- FRANSEN, WIEGER**
Atmospheric effects of high-flying subsonic aircraft: A catalogue of perturbing influences [KNMI-SR-94-03] p 168 N95-18722
- FRASER, K. F.**
Characteristics of the turbine inlet temperature sensing circuit for the T56 turbo-prop engine [DSTO-TR-0095] p 405 N95-26424
- FRASER, KEN F.**
An overview of Health and Usage Monitoring Systems (HUMS) for military helicopters [DSTO-TR-0061] p 327 N95-24200
Helicopter life substantiation: Review of some USA and UK initiatives [DSTO-TR-0062] p 328 N95-24201
Helicopter life substantiation: Review of some USA and UK initiatives [AD-A290045] p 502 N95-28851
- FRASER, STEPHANIE B.**
Effects of civil titrotor service in the northeast corridor on en route airspace loads [AD-A293586] p 599 N95-31687
- FRASIER, D. J.**
Allison engine testing CMSX-4(reg. sign) single crystal turbine blades and vanes [DE95-010308] p 694 N95-32636
- FRAZIER, S. J.**
Composite waveform generation for EMP and lightning direct-drive testing [AD-A284159] p 92 N95-14405
- FRAZIER, SAMUEL**
Waveform bounding and combination techniques for direct drive testing [AD-A284075] p 161 N95-19035
- FRAZIER, SAMUEL J.**
Assessing aircraft survivability to high frequency transient threats [AD-A283999] p 134 N95-18726
- FREDELL, ROBERT S.**
Damage tolerant repair techniques for pressurized aircraft fuselages [AD-A281982] p 65 N95-14144
Damage tolerant repair techniques for pressurized aircraft fuselages p 219 N95-22046
- FREDERICK, RAMON L.**
Natural convection in central microcavities of vertical, finned enclosures of very high aspect ratios [BTN-95-EIX95282711336] p 632 A95-92405
- FREE, APRIL M.**
Dynamic modelling and response characteristics of a magnetic bearing rotor system with auxiliary bearings p 703 N95-32692
- FREEDMAN, JEROME E.**
Doppler radar detection of vortex hazard indicators p 42 N95-13212
- FREEMAN, L. MICHAEL**
Predicting exhaust plume boundaries with supersonic external flows [BTN-95-EIX95152583258] p 297 A95-73559
- FREEMAN, W.**
Designers' unified cost model p 424 N95-28464
- FREESTONE, M. M.**
Interference determination for wind tunnels with slotted walls p 147 N95-19269
- FREYBERG, L.**
Design and operation of a thermoacoustic test facility p 147 N95-19150
- FREYER, GUSTAV J.**
Electromagnetic reverberation characteristics of a large transport aircraft [AD-A282923] p 82 N95-15392
- FRIEDMAN, AVNER**
Emerging applications in probability (Sensor management) [AD-A292781] p 601 N95-31433
- FRIEDMANN, P. P.**
Aeroelasticity and structural optimization of composite helicopter rotor blades with swept tips [NASA-CR-4665] p 397 N95-28262
- FRIEDMANN, PERETZ P.**
Aeroelastic simulation of higher harmonic control [NASA-CR-4623] p 37 N95-11911
- FRIEDRICH, HORST E.**
Forming and bonding techniques for high-strength aluminum alloys [HTN-95-20605] p 418 A95-84786
- FRIGERIO, JACOPO**
Primary and secondary vortex structures over accelerated-decelerated airfoils at high angles of attack [SAE PAPER 931368] p 586 A95-93649
- FRINK, NEAL T.**
Unstructured grid solutions to a wing/pylon/store configuration [BTN-95-EIX95152582322] p 265 A95-73525
- An unstructured-grid software system for solving complex aerodynamic problems p 476 N95-28743
- FRINK, WILLIAM D., JR.**
Effect of leading-edge extension fences on the vortex wake of an F/A-18 model [BTN-95-EIX0619952748192] p 591 A95-94481
- FRISCHBIER, J.**
Impact loading of compressor stator vanes by hailstone ingestion p 200 N95-19670
- FRITH, P. C. W.**
Assessment of overhaul surge margin tests applied to the T53 engines in ADF Iroquois helicopters [AR-008-389] p 339 N95-25936
- FRITSCHKE, BENT**
Flow field investigation in a free jet - free jet core system for the generation of high intensity molecular beams [DLR-FB-94-11] p 172 N95-18912
- FRODGE, SALLY L.**
Real-time testing and demonstration of the US Army Corps of Engineers' Real-Time On-The-Fly positioning system [AD-A288624] p 334 N95-25609
- FROMM, ROBERT E., JR.**
Inadequacy of visual alarms in helicopter air medical transport [HTN-95-01218] p 484 A95-91450
- FRULLA, GIACOMO**
Nonlinear angle of twist of advanced composite wing boxes under pure torsion [BTN-95-EIX95152582323] p 281 A95-73526
- FRUSTIE, M. J.**
Corrosion in service experience with aircraft in France p 303 N95-23518
- FRY, H. A.**
A laboratory scale supersonic combustive flow system [DE95-006347] p 420 N95-27851
- FRY, HOWARD**
Advanced distributed simulation technology advanced rotary wing aircraft. Strawman verification and validation plan for the ARWA simulator system [AD-A280237] p 19 N95-10349
- FRY, ROMAN ZYBASH**
Central coast designs: The Eightball Express. Taking off with convention, cruising with improvements and landing with absolute success [NASA-CR-197181] p 47 N95-12643
- FU, T. C.**
Flow structure in the lee of an inclined 6:1 prolate spheroid [BTN-95-EIX95011441127] p 348 A95-81027
- FUJIEDA, HIROTOSHI**
Low speed aerodynamic characteristics of delta wings with vortex flaps: 60 deg and 70 deg delta wings [NAL-TR-1245] p 331 N95-25105
- FUJII, KENJI**
Preliminary tests of a transonic flutter control wing model p 499 A95-91566
- FUJII, KOZO**
Numerical investigation of supersonic flows around a spiked blunt body [BTN-95-EIX95212645690] p 271 A95-76742
Sidewall-effect of the wind tunnel on the estimation of the aerodynamic characteristics of a delta wing p 685 N95-34525
- FUJII, MASAMI**
Development and flight results of fiber reinforced balloon p 384 A95-82511
- FUJII, R.**
Polar Patrol Balloon system and preliminary experimental results p 368 A95-82513
- FUJIMORI, TOSHIRO**
An experimental study on interacting flow between supersonic flow and secondary flow injected normally through circular nozzle p 472 A95-91511
- FUJITA, TOSHIMI**
Low speed aerodynamic characteristics of delta wings with vortex flaps: 60 deg and 70 deg delta wings [NAL-TR-1245] p 331 N95-25105
Experimental investigation of static and dynamic ground effect on HOPE ALFLEX vehicle [NAL-TR-1236] p 388 N95-26525
- FUJIWARA, TOSHI**
An experimental study on radiation from strong shock layer p 368 A95-82421
- FUJIWARA, TSUTOMU**
An advanced scramjet propulsion concept for A 350 MG SSTO space plane p 402 A95-82325
- FUKUDA, MASAHIRO**
A study of supersonic mixing flow field with ramp injector p 706 N95-34512
- FUKUSHIMA, SOUNOSUKE**
CCLA operation on MLS p 487 A95-91540
- FULKER, J. L.**
Pressure distributions on research wing W4 mounted on an axisymmetric body p 112 N95-17862

- A theoretical and experimental investigation of the flow over supersonic leading edge wing/body configurations [DRA-TM-AERO-PROCP-41] p 331 N95-25649
- FULLERSON, DAN**
Icarus Rewaxed: A high speed, low-cost general aviation aircraft for Aeroworld [NASA-CR-197155] p 45 N95-12609
- FULLER, C. R.**
Artificial neural networks for predicting nonlinear dynamic helicopter loads [HTN-95-51678] p 404 A95-85060
- FULLER, CHRIS R.**
Active control of interior noise in a business jet using piezoceramic actuators p 29 N95-11276
- FULLER, CHRISTOPHER R.**
Active control of fan noise from a turbofan engine [HTN-95-61198] p 570 A95-87571
- FULLER, DANA**
The role of flight progress strips in en route air traffic control: A time-series analysis [DOT/FAA/AM-95/4] p 280 N95-23565
- FULLER, DANA K.**
Automation and cognition in air traffic control: An empirical investigation [AD-A291932] p 488 N95-28790
- FULLER, RAY**
Safety in airport ground handling p 626 A95-95193
- FULLERTON, C. GORDON**
Propulsion controlled aircraft research p 497 A95-90869
- FULLERTON, CHARLES G.**
Engines-only flight control system [NASA-CASE-ARC-11944-1] p 294 N95-23389
- FULTON, MARK V.**
Stability analysis for elastically tailored rotor blades [ISBN 1-879921-01-4] p 635 A95-93703
- FUNABIKI, KOHEI**
Functions of NAL fixed base simulator for helicopter research p 522 A95-91555
A simulator study about effects of visibility upon helicopter pilot performance p 522 A95-91556
Flight reference display for powered-lift STOL aircraft [NAL-TR-1251] p 337 N95-25005
- FUNG, K.-Y.**
Symposium on Aerodynamics & Aeroacoustics, Tucson, AZ, Mar. 1-2, 1993 [ISBN 981-02-1732-3] p 462 A95-88892
- FUNK, R. B.**
Rotor-wake-induced flow separation on a lifting surface [HTN-95-01082] p 468 A95-90268
- FUNKHOUSER, G. E.**
Aircraft evacuations through Type-3 exits I: Effects of seat placement at the exit [DOT/FAA/AM-95/22] p 599 N95-31845
- FURRER, R.**
Mapping of forest fire damages using imaging spectroscopy p 442 A95-83627
- FURUYA, TAKAO**
Heat transfer on bent-noise biconic in hypersonic flow p 639 A95-95394
- FUTATSUDERA, NAOKI**
Overview of feasibility study on propulsion concepts for high speed civil transport p 498 A95-91518
Conceptual study of next generation high-speed civil transport: A candidate with horizontal tail p 499 A95-91521
- G**
- GAIBLE, F.**
Computation of supersonic air-intakes p 74 N95-14452
- GAITONDE, A. L.**
A three-dimensional moving mesh method for the calculation of unsteady transonic flows [HTN-95-C0007] p 585 A95-93395
- GAITONDE, DATTA**
Structure of a double-fin turbulent interaction at high speed [BTN-95-EIX95222650780] p 347 A95-79236
- GAJIC, Z.**
New filtering method for linear weakly coupled stochastic systems [BTN-95-EIX0608952736485] p 678 A95-92708
- GAL-OR, B.**
Fundamentals of catastrophic failure prevention by thrust vectoring [BTN-95-EIX0619952748176] p 606 A95-94470
- GALBRAITH, R. A. MCD.**
Preliminary results from a particle image velocimetry study of blade-vortex interaction [HTN-95-01098] p 547 A95-90284
- GALE, S. L.**
Flight demonstration of an advanced pitch control law in the VAAC Harrier aircraft p 623 N95-32012
- GALEA, S. C.**
Residual strength of composites with multiple impact damage [AD-A284230] p 87 N95-14409
- GALLIANO, J.**
Characteristics of civil aviation atmospheric hazards p 42 N95-13208
- GALLIANO, JOE**
High-resolution imaging of rain systems with the advanced microwave precipitation radiometer [HTN-95-70133] p 252 A95-70655
- GALLY, THOMAS A.**
Control of flow separation in airfoil/wing design applications p 274 N95-23294
- GALWAY, ROBIN D.**
Interference corrections for a centre-line plate mount in a porous-walled transonic wind tunnel p 122 N95-19280
- GAMBILL, J. M.**
Integrated aircraft thermal management and power generation [SAE PAPER 932055] p 500 A95-91636
- GAMMAL, YOUSSEF EL**
International cooperation in standardization p 452 A95-82665
- GANAPATHI, M.**
Field-consistent element applied to flutter analysis of circular cylindrical shells [BTN-94-EIX94341341971] p 56 A95-60871
- GANDHI, FARHAN**
An analytical model for a nonlinear elastomeric lag damper and its effect on aeromechanical stability in Hover [HTN-95-61076] p 369 A95-83660
- GANGLOFF, RICHARD P.**
NASA-UVA light aerospace alloy and structures technology program (LA2ST) [NASA-CR-198041] p 343 N95-24220
- GANN, R. G.**
Evaluation of alternative in-flight fire suppressants for full-scale testing in simulated aircraft engine nacelles and dry bays [PB94-203403] p 42 N95-13247
- GAO, B.-C.**
Possible near-IR channels for remote sensing precipitable water vapor from geostationary satellite platforms [HTN-95-70139] p 214 A95-69431
- GAO, BO-CAI**
Correction of thin cirrus effects in AVIRIS images using the sensitive 1.375-micron cirrus detecting channel p 708 N95-33748
Remote sensing of smoke, clouds, and radiation using AVIRIS during SCAR experiments p 708 N95-33749
- GAO, C.**
A generalized algorithm for inverse simulation applied to helicopter maneuvering flight [HTN-95-A0493] p 236 A95-72564
- GAO, M.**
Corrosion and corrosion fatigue of airframe aluminum alloys p 87 N95-14465
- GAO, R. S.**
In situ observations in aircraft exhaust plumes in the lower stratosphere at midlatitudes [HTN-95-A0862] p 318 A95-76266
The distribution of hydrogen, nitrogen, and chlorine radicals in the lower stratosphere: Implications for changes in O₃ due to emission of NO(y) from supersonic aircraft [HTN-95-70935] p 351 A95-78000
- GAONKAR, G. H.**
Automatic identification of modal damping from Floquet analysis [HTN-95-01084] p 506 A95-90270
- GAONKAR, GOPAL H.**
Flap-lag damping in hover and forward flight with a three-dimensional wake [HTN-95-A0496] p 221 A95-72567
Dynamic-stall and structural-modeling effects on helicopter blade stability with experimental correlation [HTN-95-81646] p 542 A95-87694
High- and low-frequency dynamics of isolated blades and rotors with dynamic stall and wake [AD-A290358] p 503 N95-29322
- GAPOCHKIN, EDWARD M.**
Calculation of satellite drag coefficients [AD-A285118] p 300 N95-23781
- GARABEDIAN, PAUL R.**
Computational fluid dynamics and transonic flow [AD-A28962] p 436 N95-26405
- GARBER, DONALD P.**
En route noise levels from propfan test assessment airplane [NASA-TP-3451] p 62 N95-12341
- GARCEA, RALPH**
Development and validation of a numerical acoustic analysis program for aircraft interior noise prediction p 572 A95-88471
- GARCIA-AVELLO, C.**
On-line handling of air traffic: Management, guidance and control [AGARD-AG-321] p 126 N95-18927
- GARCIA, JOSEPH AVILA**
Parametric study on laminar flow for finite wings at supersonic speeds [NASA-TM-108852] p 116 N95-18101
- GARCIANUNEZ, H.C.**
Repairs of CFC primary structures p 396 N95-27527
- GARDINER, PETER T.**
SMART materials: Surfaces, transforms and interfaces. The commensurate engineering dimension [AD-A289598] p 442 N95-28649
- GARDNER, CHARLES K.**
Flight-testing and frequency-domain analysis for rotorcraft handling qualities [HTN-95-01083] p 515 A95-90269
- GARFINKLE, MOISHE**
Twisting smartly in the wind [BTN-95-EIX95041503093] p 184 A95-68353
- GARG, SANJAY**
Application of an integrated methodology for propulsion and airframe control design to a STOVL aircraft [NASA-TM-106729] p 16 N95-11159
Pilot evaluation of an integrated methodology for propulsion and airframe control design [AD-A290207] p 51 N95-12763
Stable H(infinity) controller design for the longitudinal dynamics of an aircraft [NASA-TM-106847] p 293 N95-22954
- GARG, VIJAY K.**
Leading edge film cooling effects on turbine blade heat transfer [NASA-TM-106955] p 513 N95-29115
Effect of velocity and temperature distribution at the hole exit on film cooling of turbine blades [NASA-TM-106954] p 616 N95-30702
- GARNER, M.**
Cabin-fuselage-wing structural design concept with engine installation [NASA-CR-197172] p 49 N95-12993
- GARNERO, P.**
Computation of supersonic air-intakes p 74 N95-14452
- GARRARD, WILLIAM L.**
Robust dynamic inversion for control of highly maneuverable aircraft [BTN-95-EIX95242670747] p 359 A95-81100
Feedback control laws for highly maneuverable aircraft [NASA-CR-197944] p 295 N95-23410
- GARRISON, T. J.**
Laser interferometer skin-friction measurements of crossing-shock-wave/turbulent-boundary-layer ns [HTN-95-20834] p 544 A95-88095
- GARTENBERG, EHUD**
Aerodynamic Investigation with focusing schlieren in a cryogenic wind tunnel [HTN-95-20835] p 544 A95-88096
- GARY, B. L.**
Meridional distributions of NO(X), NO(Y), and other species in the lower stratosphere and upper troposphere during AASE 2 [HTN-95-70944] p 352 A95-78009
- GARY, BRUCE L.**
An algorithm for forecasting mountain wave-related turbulence in the stratosphere [HTN-95-80656] p 254 A95-72500
- GASICK, MICHAEL F.**
Analysis techniques for the prediction of springback in formed and bonded composite components p 421 N95-28289
- GASIEWSKI, A. J.**
Airborne passive polarimetric measurements of sea surface anisotropy at 92 GHz [NASA-CR-197288] p 707 N95-32823
- GATLIN, DONALD H.**
An overview of integrated flight-propulsion controls flight research on the NASA F-15 research airplane p 694 N95-33010
- GATTO, J. L.**
Stationary premixed flames in spherical and cylindrical geometries [HTN-95-42336] p 418 A95-86165
- GAUDET, L.**
The use of hot film for the investigation of boundary-layer transition [CONGRESS PAPER C428-9-199] p 475 A95-91697

- GAUGLER, RAYMOND E.**
Leading edge film cooling effects on turbine blade heat transfer
[NASA-TM-106955] p 513 N95-29115
Effect of velocity and temperature distribution at the hole exit on film cooling of turbine blades
[NASA-TM-106954] p 616 N95-30702
- GAUNAURD, G. C.**
Scattering of short em-pulses by simple and complex targets using impulse radar p 486 A95-90953
- GAUNTNER, JIM W.**
NASA Lewis Research Center Workshop on Forced Response in Turbomachinery
[NASA-CP-10147] p 141 N95-19380
- GAUTHIER, P.**
Corrosion in service experience with aircraft in France p 303 N95-23518
- GAVER, ERIC**
High density monolithic packaging technology for digital/microwave avionics p 240 N95-20646
- GAWRONSKI, W. K.**
Field verification of the wind tunnel coefficients p 109 N95-17291
- GAYNOR, T. L.**
Program test objectives milestone 3
[NASA-CR-197030] p 127 N95-15971
- GDOUTOS, E. E.**
Evaluation of patch effectiveness in repairing aircraft components p 394 N95-27513
- GE, FUYING**
Application of optimization technique to control system design for departure prevention and aircraft model estimation through dynamic inversion p 517 N95-29156
- GEDEON, D. R.**
Oscillating-flow regenerator test rig
[NASA-CR-196982] p 53 N95-13200
- GEE, KEN**
Computational analysis of forebody tangential slot blowing on the high alpha research vehicle
[NASA-CR-196750] p 10 N95-11367
Computational analysis of forebody tangential slot blowing p 71 N95-14253
Computational analysis of forebody tangential slot blowing on the high alpha research vehicle
[NASA-CR-197754] p 389 N95-26591
- GEERING, HANS P.**
Test bench for rotorcraft hover control
[BTN-94-EIX94511433919] p 169 A95-64585
- GEHAUSEN, PAUL**
Putting the ACSYNT on aircraft design
[BTN-95-EIX95072419881] p 180 A95-68398
- GEHLHAR, BURKHARD**
Broadband noise characteristics of a model counter-rotating shrouded propfan p 572 A95-88470
- GEIS, JACK**
Photovoltaic electric power applied to Unmanned Aerial Vehicles (UAV) p 245 N95-20530
- GELL, MAURICE**
Applying nanostructured materials to future gas turbine engines
[HTN-95-11909] p 404 A95-85990
- GELSEY, ANDREW**
A computational environment for exhaust nozzle design
[AIAA PAPER 95-1016] p 566 A95-90688
- GENERAZIO, EDWARD R.**
Technology Benefit Estimator (T/BEST): User's manual
[NASA-TM-106785] p 167 N95-19501
- GENEROLI, ROBERT M.**
Preload release mechanism
[NASA-CASE-MSC-22327-1] p 350 N95-25592
- GENTRY, GARL L, JR.**
Wing pressure distributions from subsonic tests of a high-wing transport model
[NASA-TM-4583] p 272 N95-22802
- GEORGALA, J. M.**
SAUNA: A system for grid generation and flow simulation using hybrid structured/unstructured grids p 642 A95-95470
Validation and evaluation of the advanced aeronautical CFD system SAUNA: A method developer's view
[ARA-MEMO-390] p 210 N95-19774
- GEORGALA, JEANETTE M.**
Application of three-dimensional hybrid structured/unstructured grids to land, sea and air vehicles
[ARA-MEMO-399] p 210 N95-19775
- GEORGANTOPOULOS, G. A.**
Investigation of shear layer transition using various turbulence models p 248 N95-21096
- GEORGE, M. H.**
Aircraft evacuations through Type-3 exits I: Effects of seat placement at the exit
[DOT/FAA/AM-95/22] p 599 N95-31845
- GEORGER, JACQUE H., JR.**
High aspect ratio metal microstructures and method for preparing the same
[AD-D017463] p 629 N95-30750
- GEORGIADIS, NICHOLAS J.**
Modification of the two-equation turbulence model in NPARC to a Chien low Reynolds number k-epsilon formulation
[NASA-TM-106710] p 37 N95-11917
Grid resolution and turbulent inflow boundary condition recommendations for NPARC calculations
[NASA-TM-106959] p 482 N95-30253
Validation of the NPARC code for nozzle afterbody flows at transonic speeds
[NASA-TM-106971] p 592 N95-30704
- GERASIMOV, V. F.**
Profiling of the working surface of electrodes-tools for circle electrochemical dimensional treatment of compressor blades
[BTN-94-EIX94461407964] p 83 A95-62638
- GERHARDT, HEINZ A.**
Natural laminar flow wing concept for supersonic transports
[BTN-95-EIX95182619226] p 308 A95-76652
- GERHOLD, THOMAS**
Numerical simulation and analysis of the hypersonic turbulent flow past a blunt-fin/ramp configuration
[DLR-FB-94-19] p 483 N95-30349
- GERI, GEORGE A.**
Image representation using fast algorithms based on the Zak transform
[AD-A293416] p 679 N95-31684
- GERKEN, M.**
Trim conditions for optimal flight performance of hypersonic aircraft p 514 A95-87397
- GERREM, DONNA S.**
Design, analysis and control of large transports so that control of engine thrust can be used as a back-up of the primary flight controls
[NASA-CR-198958] p 518 N95-30254
- GERSTEIN, M.**
Programmed ignition of metal compounds in a scramjet p 16 N95-10466
- GERTNER, IZIDOR C.**
Image representation using fast algorithms based on the Zak transform
[AD-A293416] p 679 N95-31684
- GESSEL, M.**
Manufacturing scale-up of composite fuselage crown panels p 532 N95-28835
- GESSNER, F. B.**
Design and operation of a supersonic annular flow facility
[BTN-94-EIX94441386624] p 183 A95-68173
Design and operation of a supersonic annular flow facility
[HTN-95-20941] p 465 A95-88980
- GETSON, E. S.**
Application of photogrammetry of F-14D store separation
[AD-A284154] p 132 N95-18417
- GEURTS, E. G.**
Unsteady transonic wind tunnel test on a semispan straked delta wing, oscillating in pitch. Part 1: Description of the model, test setup, data acquisition, and data processing
[AD-A293113] p 593 N95-30885
- GHAFFARI, F.**
High Alpha Technology Program (HATP) ground test to flight comparisons p 68 N95-14230
- GHAFFARI, FARHAD**
Navier-Stokes, flight, and wind tunnel flow analysis for the F/A-18 aircraft
[NASA-TP-3478] p 120 N95-19114
- GHALY, W. S.**
Large-scale computational fluid dynamics by the finite element method
[BTN-94-EIX94381359154] p 243 A95-71744
- GHARIB, MORTEZA**
Research on bluff body vortex wakes
[AD-A286319] p 223 N95-20177
- GHEE, TERENCE A.**
Exploratory flow visualization investigation of mast-mounted sights in presence of a rotor
[NASA-TM-4634] p 330 N95-24566
- GHIRINGHELLI, G. L.**
Matrix fraction approach for finite-state aerodynamic modeling
[BTN-95-EIX95262694311] p 365 A95-85482
- GIBBONS, ANDREW S.**
New tools for creating instruction and simulations
[SAE PAPER 932600] p 380 A95-84572
- GIBBS, GARY P.**
Active control of interior noise in a business jet using piezoceramic actuators p 29 N95-11276
- GIBERT, JACEK**
Expert systems and artificial intelligence applications in engineering design and inspection p 710 N95-33008
- GIBSON, BERRY T.**
Natural laminar flow wing concept for supersonic transports
[BTN-95-EIX95182619226] p 308 A95-76652
- GIBSON, J. C.**
The prevention of PIO by design p 620 N95-31991
- GIBSON, JOHN C.**
Looking for the simple PIO model p 597 N95-31066
- GIDDINGS, THOMAS E.**
Interaction of a weak shock with freestream disturbances
[BTN-95-EIX95332750473] p 638 A95-94687
- GIEL, P. W.**
Three-dimensional Navier-Stokes analysis and redesign of an imbedded bellmouth nozzle in a turbine cascade inlet section p 311 N95-23423
- GIELDA, T. P.**
Aeromechanics technology, volume 1. Task 1: Three-dimensional Euler/Navier-Stokes Aerodynamic Method (TEAM) enhancements
[AD-A285713] p 132 N95-18483
- GIELEN, L.**
In-flight interior sound field mapping in propeller aircraft p 572 A95-88472
- GIESKE, J. H.**
Evaluation of scanners for C-scan imaging in nondestructive inspection of aircraft
[DE94-012473] p 152 N95-19100
- GIESKE, JOHN**
Emerging nondestructive inspection for aging aircraft
[P95-143053] p 328 N95-25401
- GIFFORD, LISA A.**
Environmental Compliance Assessment and Management Program
[AD-A279605] p 255 N95-20441
- GILBERT, L. E. PAUL**
Viper
[NASA-CR-197191] p 79 N95-13703
- GILES, GARY L.**
Coupling equivalent plate and finite element formulations in multiple-method structural analyses
[BTN-95-EIX95062487548] p 192 A95-68362
- GILLAN, MARK A.**
Computational analysis of buffet alleviation in viscous transonic flow over a porous airfoil
[BTN-95-EIX95262694321] p 366 A95-85492
- GILLET, DAVE**
Strategy in the commercial aircraft industry in the United States: A comparison of decisionmaking by McDonnell-Douglas and Boeing aircraft companies from 1977-1983
[AD-A288289] p 366 N95-26409
- GILMAN, RONALD L.**
Operational and research aspects of a radio-controlled model flight test program
[BTN-95-EIX0619952748177] p 606 A95-94471
- GILMOUR, THOMAS A.**
Malone-brayton cycle engine/heat pump
[AD-DO16573] p 244 N95-20295
- GILPIN, T. M.**
Estimates of total organic and inorganic chlorine in the lower stratosphere from in situ and flask measurements during AASE 2
[HTN-95-A0861] p 317 A95-76265
- GILSON, RICHARD D.**
User type certification for advanced flight control systems p 699 N95-34772
- GILSON, WILLIAM H.**
Aircraft wake RCS measurement p 59 N95-13210
- GILYARD, GLENN**
On the use of controls for subsonic transport performance improvement: Overview and future directions
[NASA-TM-4605] p 10 N95-11408
Direct adaptive performance optimization of subsonic transports: A periodic perturbation technique
[NASA-TM-4676] p 284 N95-22829
- GILYARD, GLENN B.**
Engines-only flight control system
[NASA-CASE-ARC-11944-1] p 294 N95-23389
- GIORI, KATHY**
Application of airborne field mill data for use in launch support
[HTN-95-50054] p 98 A95-62279
- GIRVIN, RAQUEL**
Advanced subsonic airplane design and economic studies
[NASA-CR-195443] p 338 N95-24304
- GIUFFRE, G.**
Impact of noise environment on engine nacelle design p 173 N95-19147

GIUZIO, R.

- Impact of noise environment on engine nacelle design p 173 N95-19147
- An overall approach of cockpit noise verification in a military aircraft p 175 N95-19163
- GJESTLAND, T.**
Assessment of helicopter noise annoyance: A comparison between noise from helicopters and from jet aircraft [BTN-94-EIX94341341967] p 62 A95-60867
- Response to noise around Vaernes and Bodoe airports [PB94-207065] p 62 N95-13575
- GJESTLAND, TRULS**
Assessment of helicopter noise annoyance: A comparison between helicopters and jet aircraft p 560 A95-88480
- GLADDEN, HERBERT J.**
Hypersonic engine leading edge experiments in a high heat flux, supersonic flow environment [NASA-TM-106742] p 91 N95-14299
- GLADFELDER, JAMES A.**
Electrical power system upgrade methodology for in-service aircraft [SAE PAPER 932562] p 511 A95-90059
- GLASER, JOHN**
A review of gust load calculation methods at de Havilland p 118 N95-18604
- GLASS, CHRISTOPHER E.**
The personal aircraft: Status and issues [NASA-TM-109174] p 223 N95-20688
- GLASS, EMILY**
Knowledge-based processing for aircraft flight control [NASA-CR-194976] p 99 N95-13727
- GLASSMAN, ARTHUR J.**
Modeling improvements and users manual for axial-flow turbine off-design computer code AXOD [NASA-CR-195370] p 8 N95-10853
- Enhanced capabilities and updated users manual for axial-flow turbine preliminary sizing code TURBAN [NASA-CR-195405] p 76 N95-15912
- Enhanced capabilities and modified users manual for axial-flow compressor conceptual design code CSPAN [NASA-TM-106833] p 119 N95-18933
- Turbine design and application volumes 1, 2, and 3 [E-5666-Vol-1-3] p 236 N95-22341
- Enhanced analysis and users manual for radial-inflow turbine conceptual design code RTD [NASA-CR-195454] p 275 N95-23462
- GLATTHOR, N.**
Airborne measurements during the European Arctic Stratospheric Ozone Experiment column amounts of HNO₃ and O₃ derived from FTIR emission sounding [HTN-95-00742] p 445 A95-86312
- GLEGG, S.**
Geometrical acoustics approach for calculating the effects of flow on acoustics scattering [BTN-94-EIX94321331207] p 61 A95-60790
- GLEGG, STEWART A. L.**
Noise Con 1994: Proceedings of the 1994 National Conference on Noise Control Engineering. Progress in Noise Control for Industry [LC-75-24750] p 28 N95-11259
- Flow structure generated by perpendicular blade vortex interaction and implications for helicopter noise predictions [NASA-CR-198590] p 377 N95-28193
- GLENNLIGHTSEY, E.**
Space flight tests of attitude determination using GPS [BTN-95-EIX95112522529] p 190 A95-69334
- GLICKMAN, TODD S.**
Aviation value-added products and services from the NEXRAD Information Dissemination Service (NIDS) p 671 A95-93535
- GLIEBE, P. R.**
Active control of fan noise-feasibility study. Volume 1: Flyover system noise studies [NASA-CR-195392-VOL-1] p 258 N95-21888
- GLIEBE, PHILIP R.**
UHB engine fan broadband noise reduction study [NASA-CR-198357] p 580 N95-29641
- GLOVER, BILLY M.**
Transmission loss characteristics of aircraft sidewall systems to control cabin interior noise p 28 N95-11261
- GLOVER, GRAHAM**
National aviation weather program plan p 652 A95-93445
- GLOVER, GRAHAM K.**
Operational aviation weather regulations p 652 A95-93446
- GLUCK, R.**
Design of a real-time wind turbine simulator using a custom parallel architecture p 449 N95-27979

GLYNN, G.

- High performance backplane components for modular avionics p 247 N95-20653
- GNOFFO, PETER A.**
Navier-Stokes simulations of Orbiter aerodynamic characteristics including pitch trim and bodyflap [BTN-95-EIX95041503779] p 204 A95-69210
- Multiblock analysis for Shuttle Orbiter reentry heating from Mach 24 to Mach 12 [BTN-95-EIX95041503780] p 205 A95-69211
- GOCHBERG, LAWRENCE A.**
Bibliography of Doctor Chul Park [NASA-TM-110353] p 527 N95-29351
- GODBOLE, P. N.**
Reaction-time response of aircraft crash [BTN-95-EIX95292721296] p 595 A95-92626
- GODIN, S.**
Airborne lidar observation of mountain-wave-induced polar stratospheric clouds during EASOE [HTN-95-00738] p 444 A95-86308
- GODSCHALX, J. P.**
Novel matrix resins for composites for aircraft primary structures, phase 1 [NASA-CR-189657] p 23 N95-10318
- GOEDEKE, A. D.**
Cost effective, dual-purpose machine vision-based detectors for (1) smoke and flame detection, and (2) engine overhead/burn-through and flame detection [AD-A292284] p 579 N95-28870
- GOEDJEN, J. G.**
Thermal Barrier Coating Workshop [NASA-CR-10170] p 344 N95-26119
- GOEKSEL, O. T.**
Effect of spherical roughness elements upon transition of a 3-D boundary layer [HTN-95-92835] p 471 A95-90753
- GOETTGE, ROBERT T.**
Integrated performance and reliability specification for digital avionics systems [AIAA PAPER 95-0953] p 506 A95-90632
- GOETZ, A. F. H.**
Possible near-IR channels for remote sensing precipitable water vapor from geostationary satellite platforms [HTN-95-70139] p 214 A95-69431
- GOGGIN, PATRICK J.**
Comparison of stochastic and deterministic nonlinear gust analysis methods to meet continuous turbulence criteria p 133 N95-18602
- GOHEEN, KEVIN R.**
Practical experiences in control systems design using the NCR Bell 205 Airborne Simulator p 624 N95-32015
- GOKALP, I.**
High pressure vaporization and burning of methanol droplets in reduced gravity p 527 A95-87285
- GOKCEN, TAHIR**
Computation of nonequilibrium viscous flows in arc-jet wind tunnel nozzles [AIAA PAPER 94-0254] p 2 A95-60173
- GOLDHAGEN, PAUL**
Radiation safety aspects of commercial high-speed flight transportation [NASA-TP-3524] p 453 N95-26427
- GOLDMAN, P.**
Wind technology development: Large and small turbines [DE95-000286] p 358 N95-26090
- GOLDMAN, ROBERT P.**
Empirical results on scheduling and dynamic backtracking p 299 N95-23761
- GOLDSMITH, BARRY S.**
Objective verification of an enhanced terminal forecast experiment at Denver, Colorado p 664 A95-93501
- GOLDTHORPE, STEVE H.**
Guidance and control requirements for high-speed Rollout and Turnoff (ROTO) [NASA-CR-195026] p 292 N95-22674
- GOLDWIRE, H.**
NTS-spill test facility wind tunnel exhaust plume characterization [DE95-003630] p 297 N95-24019
- GOLLVIK, STEFAN**
Nortaf: Computer generated aerodome forecasts p 668 A95-93521
- GOLOVANOV, V. V.**
Aircraft gear train diagnostics using the irregular rotation of the external shafts [CONGRESS PAPER C428-15-097] p 508 A95-91712
- GOLUB, ROBERT A.**
Aircraft noise prediction program theoretical manual: Rotorcraft System Noise Prediction System (ROTONET), part 4 [NASA-TM-83199-PT-4] p 451 N95-26392

GOMAN, M.

- State-space representation of aerodynamic characteristics of an aircraft at high angles of attack [BTN-95-EIX95062487536] p 187 A95-69244
- GONDHALEKAR, SUDHIR**
Analytical developments in support of the NASA aging aircraft program with an application to crack growth from rivets [SAE PAPER 931223] p 545 A95-88789
- GONG, J.**
Simulation of patch and slot antennas using FEM with prismatic elements and investigations of artificial absorber mesh termination schemes [NASA-CR-198974] p 704 N95-32822
- GONIAK, REMY**
Corrective term in wall slip equations for Knudsen layer [BTN-95-EIX95282705070] p 455 A95-89667
- GONSALEZ, JOSE C.**
Flow quality improvements in the NASA Lewis Research Center 9- by 15-foot Low Speed Wind Tunnel [NASA-CR-195439] p 627 N95-31653
- GONSALVES, PAUL G.**
Intelligent flight trainer for initial rotary wing training [SAE PAPER 932536] p 386 A95-84558
- GONZALES-MARTIN, A.**
Corrosion of aircraft materials: Correlation between nanometer scale and macroscopic structural damage parameters [AD-A285930] p 241 N95-20299
- GONZALEZ, CARLOS R.**
Super-heavy aircraft study [AD-A279602] p 238 N95-19955
- GOOCH, CARL FREDERICK**
Solution of the Navier-Stokes equations on locally refined Cartesian meshes using state-vector splitting p 553 N95-29197
- GOODALL, COLIN**
Bird ingestion into large turbofan engines [DOT/FAA/CT-93/14] p 333 N95-24631
- GOODEN, J. H. M.**
Low-speed surface pressure and boundary layer measurement data for the NLR 7301 airfoil section with trailing edge flap p 111 N95-17855
- GOODFELLOW, R. C.**
High performance backplane components for modular avionics p 247 N95-20653
- GOODRICH, R. K.**
Determining F-factor using ground-based Doppler radar: Validation and results p 11 N95-10571
- GOODWIN, M. J.**
High performance backplane components for modular avionics p 247 N95-20653
- GOPAUL, NIGEL K. J. M.**
Measurement and analysis of nitric oxide radiation in an arcjet flow [BTN-95-EIX95082502727] p 243 A95-71040
- GORA, YU. V.**
JPRS report: Science and technology. Central Eurasia: Engineering and equipment. Gas dynamics of supersonic shortened nozzles [JPRS-UST-94-003-L] p 22 N95-10931
- GORANSON, ULF G.**
Elements of structural integrity assurance p 387 A95-85896
- GORBATKIN, S. M.**
Permanent magnet electron cyclotron resonance plasma source with remote window [BTN-95-EIX95242674338] p 450 A95-82176
- Cu deposition using a permanent magnet electron cyclotron resonance microwave plasma source [DE94-017768] p 304 N95-23981
- GORDNER, RAYMOND E.**
Crossflow topology of vortical flows [HTN-95-51664] p 432 A95-85046
- Computation of delta-wing roll maneuvers [BTN-95-EIX0619952748164] p 605 A95-94458
- Computation of vortex breakdown on a rolling delta wing [BTN-95-EIX0619952748195] p 591 A95-94484
- GORDON, A. C.**
Progress and experience with helicopter health and usage monitoring [CONGRESS PAPER C428-31-151] p 603 A95-93615
- GORDON, B. E. A.**
Repairs to composite structure on military aircraft [CONGRESS PAPER C428-4-067] p 531 A95-91677
- GORDON, ELMAREE**
The assessment of the AH-64D, longbow, mast-mounted assembly noise hazard for maintenance personnel [AD-A284971] p 171 N95-16226
- GORDON, NEIL**
Verification of terminal forecasts p 664 A95-93502

- GORDON, SALLIE E.**
Intelligent tutoring system: F-16 flight simulation
p 521 A95-90649
- GORTON, SUSAN ALTHOFF**
Laser velocimetry and blade pressure measurements of a blade-vortex interaction
[HTN-95-01081] p 547 A95-90267
- GOSSETT, T. D.**
Design of a model following, state variable feedback controller for the X-14 VTOL aircraft
[HTN-94-00685] p 16 A95-60168
- GOTO, NORIHIRO**
Determination of piloting feedback structures for an altitude tracking task
[BTN-95-EIX95242670770] p 327 A95-81077
- GOTTLIEB, DAVID**
High order accuracy computational methods in aerodynamics using parallel architectures
[AD-A294167] p 686 N95-34763
- GOTTSMANN, C. F.**
Airborne rotary air separator study
[NASA-CR-189099] p 290 N95-24053
- GOULD, R. W.**
Double pass retroreflection for corrosion detection in aircraft structures
p 323 N95-23503
- GOVINDARAJ, T.**
Operator modeling in commercial aviation: Cognitive models, intelligent displays, and pilot's assistants
[NASA-CR-198609] p 401 N95-28203
- GOWDY, VAN**
The performance of child restraint devices in transport airplane passenger seats
[DOT/FAA/AM-94/19] p 40 N95-12146
- GRABL, H.**
Environmental aspects of Orbital transport:
p 559 A95-87377
- GRAESSER, D.**
Local design optimization for composite transport fuselage crown panels
p 398 N95-28473
- GRAFT, WOLF O.**
Flight control system mode transitions influence on handling qualities and task performance
[BTN-95-EIX95062487525] p 203 A95-69233
- GRAHAM, KENNETH**
Prediction of airplane states
[BTN-95-EIX0619952748174] p 584 A95-94468
- GRAHAM, R. J.**
Creating a global climatology of freezing rain using numerical model output
p 673 A95-93541
- GRAHAM, W. R.**
Evaluation of a model for boundary-layer induced noise in aircraft
p 574 A95-90102
- GRANDAGE, J. M.**
A review of Australian and New Zealand investigations on aeronautical fatigue during the period Apr. 1993 - Mar. 1995
[AR-009-202] p 397 N95-27918
- GRANDE, D. H.**
Impact damage resistance of composite fuselage structure, part 1
p 399 N95-28482
- GRANIER, C.**
Impact of present aircraft emissions of nitrogen oxides on tropospheric ozone and climate forcing
[HTN-95-21364] p 353 A95-78679
- GRANOIEN, L. L. N.**
Response to noise around Vaernes and Bodo airports
[PB94-207065] p 62 N95-13575
- GRANOIEN, IDAR L. N.**
Aircraft noise zoning in Norway
p 581 A95-88476
Assessment of helicopter noise annoyance: A comparison between helicopters and jet aircraft
p 560 A95-88480
- GRANOVSKII, A. V.**
Application of multidisciplinary models to the cooled turbine rotor design
p 140 N95-19024
- GRANT, C.**
Composite fuselage crown panel manufacturing technology
p 399 N95-28474
- GRANT, CARROLL G.**
Advanced tow placement of composite fuselage structure
p 420 N95-28271
Automated fiber placement: Evolution and current demonstrations
p 532 N95-28832
Manufacturing scale-up of composite fuselage crown panels
p 532 N95-28835
- GRANT, CATHERINE**
Design of a high altitude long endurance aircraft with manufacturing considerations
p 391 N95-26947
- GRANT, DOUGLAS M.**
Maintenance training to cope with high-tech innovations
[SAE PAPER 932619] p 456 A95-90082
- GRANT, I.**
Preliminary results from a particle image velocimetry study of blade-vortex interaction
[HTN-95-01098] p 547 A95-90284
- GRASSO, F.**
Simulation of transverse gas injection in turbulent supersonic air flows
[BTN-95-EIX95182619080] p 269 A95-75765
- GRAVES, C. M., JR.**
Composite waveform generation for EMP and lightning direct-drive testing
[AD-A284159] p 92 N95-14405
- GRAY, J. A.**
The corrosion and protection of advanced aluminium - lithium airframe alloys
p 302 N95-23497
- GRAY, P. M.**
Probabilistic design of advanced composite structure
p 424 N95-28443
- GRAY, ROBERT A.**
An integrated GPS/INS/BARO and radar altimeter system for aircraft precision approach landings
[AD-A289280] p 383 N95-26985
- GRAY, WILLIAM M.**
Tropical cyclone observation and forecasting with and without aircraft reconnaissance
[HTN-95-80701] p 254 A95-72545
- GREAVES, R. W.**
An example of airborne vibration monitoring improving flight safety in the Soloviev D-30-KU engine
[CONGRESS PAPER C428-21-141] p 508 A95-91728
- GREBENYUK, L. Z.**
JPRS report: Science and technology. Central Eurasia: Engineering and equipment. Gas dynamics of supersonic shortened nozzles
[JPRS-UST-94-003-L] p 22 N95-10931
- GREBER, ISAAC**
Three dimensional compressible turbulent flow computations for a diffusing S-duct with/without vortex generators
[NASA-CR-195390] p 138 N95-17402
- GREEN, HARRY E.**
Electromagnetic backscattering from a helicopter rotor in the decametric wave band regime
[BTN-94-EIX94381353130] p 243 A95-72648
- GREEN, J. E.**
An investigation of drag repeatability in half model testing in the ARA Transonic Wind Tunnel
[ARA-MEMO-392] p 188 N95-19546
- GREEN, JOHN E.**
Investigation of a thermal buoyancy effect on the drag of half models tested in the ARA Transonic Wind Tunnel
[ARA-MEMO-407] p 222 N95-19946
- GREEN, K. A. H.**
Regulatory impact analysis and regulatory support document: Control of air pollution; determination of significance for nonroad sources and emission standards for new nonroad compression-ignition engines at or above 37 kilowatts (50 horsepower)
[PB94-194594] p 61 N95-12855
- GREEN, L. L.**
Applications of automatic differentiation in CFD
[NASA-TM-109948] p 157 N95-16828
Parallel calculation of sensitivity derivatives for aircraft design using automatic differentiation
[NASA-TM-110103] p 231 N95-20370
- GREEN, LAWRENCE L.**
Applications of automatic differentiation in computational fluid dynamics
p 156 N95-16461
- GREEN, P. D.**
Current and future problems in structural acoustic fatigue
p 173 N95-19143
- GREEN, R. O.**
Possible near-IR channels for remote sensing precipitable water vapor from geostationary satellite platforms
[HTN-95-70139] p 214 A95-69431
- GREEN, ROBERT O.**
In-flight radiometric calibration of AVIRIS in 1994
p 705 N95-33754
- GREENAN, BLAIR JOHN WILLIAM**
Hailstone heat and mass transfer measurements
[ISBN-0-315-86304-8] p 563 N95-29797
- GREENBERG, H. S.**
Requirements report for SSTO vertical take-off and horizontal landing vehicle
[NASA-CR-197029] p 80 N95-14794
- GREENDYKE, ROBERT B.**
Convective and radiative heat transfer analysis for the fire 2 forebody
[BTN-95-EIX95182617460] p 268 A95-75731
- GREENE, FRANCIS A.**
Approximate method for calculating heating rates on three-dimensional vehicles
[BTN-95-EIX95041503778] p 210 A95-69209
- Navier-Stokes simulations of Orbiter aerodynamic characteristics including pitch trim and bodyflap
[BTN-95-EIX95041503779] p 204 A95-69210
Application of the multigrid solution technique to hypersonic entry vehicles
[BTN-95-EIX95152583254] p 306 A95-73555
- GREENHALGH, SAMUEL**
Lift enhancement device
[AD-D016522] p 224 N95-21864
- GREENMAN, MATTHEW**
Flutter analysis of composite box beams
[NASA-CR-197931] p 294 N95-23392
- GREENWOOD, SEAN**
The Balsa bullet: A high speed, low-cost general aviation aircraft for Aeroworld
[NASA-CR-197165] p 46 N95-12638
- GREER, DONALD S.**
Numerical modeling of a cryogenic fluid within a fuel tank
[NASA-TM-4651] p 89 N95-13892
- GREGOREK, G. M.**
Comparative wind tunnel test at high Reynolds numbers of NACA 64 621 airfoils with two aileron configurations
p 377 N95-27977
- GREGORY, G. L.**
Compendium of NASA data base for the Global Tropospheric Experiment's Pacific Exploratory Mission West-A (PEM West-A)
[NASA-TM-109177] p 320 N95-23009
- GREGORY, GERALD L.**
An intercomparison of aircraft instrumentation for tropospheric measurements of sulfur dioxide
[HTN-95-91855] p 354 A95-80843
An intercomparison of aircraft instrumentation for tropospheric measurements of carbonyl sulfide, hydrogen sulfide, and carbon disulfide
[HTN-95-91856] p 355 A95-80844
An intercomparison of instrumentation for tropospheric measurements of dimethyl sulfide: Aircraft results for concentrations at the parts-per-trillion level
[HTN-95-91857] p 355 A95-80845
- GREGORY, IRENE M.**
Matlab as a robust control design tool
p 169 N95-16474
- GREGORY, J. D. L.**
The principles of flight test assessment of flight safety-critical systems in helicopters
[AGARD-AG-300-VOL-12] p 77 N95-14199
- GREITZER, E. M.**
Unsteady flow phenomena in discrete passage diffusers for centrifugal compressors
[AD-A281412] p 155 N95-16163
- GREITZER, F. L.**
An artificial neural network system for diagnosing gas turbine engine fuel faults
[DE94-013960] p 138 N95-17371
- GRETHLEIN, CHRISTIAN E.**
Impact of agility requirements on configuration synthesis
[NASA-CR-4627] p 44 N95-11952
- GREYVENSTEIN, G. P.**
Differentencing of density in compressible flow for a pressure-based approach
[HTN-95-42349] p 373 A95-86178
- GRIESS, K. H.**
Global cost and weight evaluation of fuselage keel design concepts
p 501 N95-28840
- GRIFFIN, C. F.**
Structural testing of the technology integration box beam
p 441 N95-28467
- GRIFFIN, O. HAYDEN, JR.**
An analytical and experimental investigation of the response of the curved, composite frame/skin specimens
[HTN-95-80857] p 283 A95-75099
- GRIFFIN, VANESSA L.**
High-resolution imaging of rain systems with the advanced microwave precipitation radiometer
[HTN-95-70133] p 252 A95-70655
- GRIFFITH, D. V.**
Flight demonstration of an advanced pitch control law in the VAAC Harrier aircraft
p 623 N95-32012
- GRIFFITH, J. B.**
Simulation of Shuttle launch G forces and acoustic loads using the NASA Ames Research Center 20G centrifuge
p 86 N95-14089
- GRIFFITH, WAYLAND C.**
Supercooling in hypersonic nitrogen wind tunnels
[BTN-94-EIX95011441134] p 340 A95-81020
- GRILLO, C.**
A Kutta condition conscious perturbation stream function boundary element algorithm for 2-D potential aerodynamics
[ISBN 1-879921-01-4] p 587 A95-93751

- GROAT, JEFF**
Synthetic Terrain Imagery for Helmet-Mounted Display. Volume 2: Software design document [AD-A293611] p 612 N95-31655
Synthetic Terrain Imagery for Helmet-Mounted Display, volume 1 [AD-A293612] p 612 N95-31656
- GRODSINSKY, C. M.**
Microgravity isolation system design: A case study [NASA-TM-106804] p 104 N95-17657
Microgravity isolation system design: A modern control synthesis framework [NASA-TM-106805] p 105 N95-18197
Microgravity isolation system design: A modern control analysis framework [NASA-TM-106803] p 105 N95-18486
- GROENEWEG, JOHN F.**
Fan noise research at NASA p 28 N95-11260
- GROLEAU, MICHAEL R.**
Development of RTM and powder prepreg resins for subsonic aircraft primary structures p 536 N95-29044
- GRONIG, H.**
Hypersonic model testing in a shock tunnel [BTN-95-EIX95222650789] p 329 A95-79245
- GROSE, WILLIAM L.**
The atmospheric effects of stratospheric aircraft: A fourth program report [NASA-RP-1359] p 357 N95-24274
- GROSHART, EARL C.**
Cadmium plating replacements p 631 N95-31773
- GROSKO, J.**
Structural modification and repair of C-130 wing structure using bonded composites p 394 N95-27512
- GROSSE, IAN R.**
Intelligent finite element submodeling of multichip modules for reliability analysis [AD-A292911] p 679 N95-31455
- GROSSHANDLER, W. L.**
Evaluation of alternative in-flight fire suppressants for full-scale testing in simulated aircraft engine nacelles and dry bays [PB94-203403] p 42 N95-13247
- GROSSMAN, JON**
Commercial applications for military laser radars p 543 A95-87794
- GROSSMAN, T.**
The effect of interface properties on nickel base alloy composites [NASA-CR-198363] p 629 N95-30787
- GROVELD, F. W.**
Measurement and prediction of broadband noise from large horizontal axis wind turbine generators p 451 N95-27990
- GROTE, JAMES**
Optical processing and control [AD-A279157] p 259 N95-21975
- GROVES-KIRKBY, C. J.**
High performance backplane components for modular avionics p 247 N95-20653
- GROVES, M.**
The effect of interface properties on nickel base alloy composites [NASA-CR-198363] p 629 N95-30787
- GRUBER, M. L.**
Full-scale testing and analysis of fuselage structure p 95 N95-14485
- GRUENEFELD, G.**
Planar air density measurements near model surfaces by ultraviolet Rayleigh/Raman scattering [BTN-94-EIX94441386614] p 213 A95-67345
Planar air density measurements near model surfaces by ultraviolet Rayleigh/Raman scattering [HTN-95-20950] p 546 A95-88989
- GRUNWALD, ARTHUR J.**
Advanced interactive display formats for terminal area traffic control [NASA-CR-198576] p 384 N95-28188
- GRYAZNOV, B. A.**
Fatigue strength of high-temperature alloys under conditions of cyclic temperature variation. Communication 1: Experimental procedure and results [BTN-94-EIX94401363884] p 307 A95-75516
- GUARNIERA, S.**
Selecting and management of fire fighter aircraft [BTN-95-EIX95062487538] p 193 A95-69246
- GUARRO, S.**
Demonstration of the Dynamic Flowgraph Methodology using the Titan 2 Space Launch Vehicle Digital Flight Control System [NASA-CR-197517] p 150 N95-17493
- GUENTHER, G.**
Composite repair of a CF18: Vertical stabilizer leading edge p 395 N95-27517
- GUERNSEY, D.**
On the choice of appropriate bases for nonlinear dynamic modal analysis [HTN-95-A0495] p 221 A95-72566
- GUERRIERI, D. A.**
Regulatory impact analysis and regulatory support document: Control of air pollution; determination of significance for nonroad sources and emission standards for new nonroad compression-ignition engines at or above 37 kilowatts (50 horsepower) [PB94-194594] p 61 N95-12855
- GUEVREMONT, GRANT**
Finite element vorticity-based methods for the solution of the incompressible and compressible Navier-Stokes equations p 553 N95-29119
- GUFFOND, D.**
Prediction of ice accretion: Comparison between the 2D and 3D codes [BTN-94-EIX94441385753] p 213 A95-68217
- GUIDOS, BERNARD J.**
Static aerodynamics CFD analysis for 120-mm hypersonic KE projectile design [ARL-MR-184] p 118 N95-18611
- GUILLOU, C.**
Aircraft measurements of water vapour continuum absorption at millimetre wavelengths [HTN-95-90884] p 253 A95-72393
- GUIST, ROY**
Experimental/analytical approach to understanding mistuning in a transonic wind tunnel compressor [NASA-TM-108833] p 95 N95-14617
- GULDE, T.**
Airborne measurements during the European Arctic Stratospheric Ozone Experiment column amounts of HNO₃ and O₃ derived from FTIR emission sounding [HTN-95-00742] p 445 A95-86312
- GUMASTE, U.**
High performance parallel analysis of coupled problems for aircraft propulsion [NASA-CR-195355] p 23 N95-10132
High-performance parallel analysis of coupled problems for aircraft propulsion [NASA-CR-197440] p 289 N95-23088
- GUMUS, ILKER**
Cabin fuselage structural design with engine installation and control system [NASA-CR-197173] p 47 N95-12639
- GUNDO, D. P.**
Simulation of Shuttle launch G forces and acoustic loads using the NASA Ames Research Center 20G centrifuge p 86 N95-14089
- GUNN, WALTER J.**
Development of an intervention program to encourage shoulder harness use and aircraft retrofit in general aviation aircraft, phases 1 and 2 [DOT/FAA/AM-95/2] p 333 N95-24384
Development of an intervention program to encourage shoulder harness use and aircraft retrofit in general aviation aircraft: Phases 1 and 2 [AD-A290966] p 485 N95-29873
- GUNTERMANN, P.**
Investigation of an NLF(1)-0416 airfoil in compressible subsonic flow p 110 N95-17852
- GUO, R. W.**
Swirl control in an S-duct at high angle of attack [HTN-95-20846] p 545 A95-88107
- GUPTA, A.**
Hypersonic aerodynamics test facility using the external propulsion accelerator [AIAA PAPER 95-6138] p 470 A95-90455
- GUPTA, ANURAG**
Integrated design and manufacturing for the high speed civil transport [NASA-CR-197183] p 48 N95-12700
- GUPTA, ASHWANI K.**
The NASA-sponsored Maryland center for hypersonic education and research [AIAA PAPER 95-6105] p 519 A95-88010
- GUPTA, K.**
Unbalance response of a dual rotor system: Theory and experiment [BTN-94-EIX94351143320] p 195 A95-65854
- GUPTA, K. D.**
Unbalance response of a dual rotor system: Theory and experiment [BTN-94-EIX94351143320] p 195 A95-65854
- GUPTA, ROOP N.**
Higher-order viscous shock-layer solutions for high-altitude flows [BTN-95-EIX95152583255] p 306 A95-73556
- GUREVICH, INNA**
New technologies for space avionics [NASA-CR-197574] p 150 N95-18196
- GURSUL, I.**
Effects of time scales on lift of airfoils in an unsteady stream [HTN-95-81643] p 542 A95-87691
Criteria for location of vortex breakdown over delta wings [HTN-95-01092] p 468 A95-90278
- GURUSWAMY, GURU P.**
User's guide for ENSAERO: A multidisciplinary program for fluid/structural/control interaction studies of aircraft (release 1) [NASA-TM-108853] p 65 N95-13662
- GUSSY, JOEL**
Cabin fuselage structural design with engine installation and control system [NASA-CR-197173] p 47 N95-12639
- GUTHLEIN, PETER**
Terminal Doppler Weather Radar Flight 5A Operational Test and Evaluation (OT/E) integration and OT/E operational test plan [AD-A283052] p 61 N95-12996
Offshore next generation weather radar (NEXRAD) OT&E integration and OT&E operational test [AD-A293223] p 646 N95-30902
- GUTMARK, E. J.**
A pulsed liquid fuel ramjet p 617 N95-31201
- GUTMARK, EPHRAIM**
Suppressor of oscillations in airframe cavities [AD-D017265] p 388 N95-26507
- GUTOWSKI, T.**
Designers' unified cost model p 424 N95-28464
- GWINN, KENNETH W.**
High strain-rate testing of parachute materials [DE95-009577] p 648 N95-31614

H

- HAAKER, T. I.**
On the dynamics of aeroelastic oscillators with one degree of freedom [BTN-94-EIX94501431527] p 153 A95-64524
- HAAS, BRIAN L.**
Flow resolution and domain influence in rarefied hypersonic blunt-body flows [BTN-95-EIX95082502729] p 220 A95-70136
Particle kinetic simulation of high altitude hypervelocity flight [NASA-CR-197383] p 309 N95-22481
- HAAS, MICHAEL N.**
Bicarbonate of soda paint stripping process validation and material characterization p 631 N95-31778
- HABASHI, W. G.**
Large-scale computational fluid dynamics by the finite element method [BTN-94-EIX94381359154] p 243 A95-71744
An improved finite element method for the solution of the compressible Euler and Navier-Stokes equations p 640 A95-95439
- HABOLY, EDWARD F.**
Aircraft noise at a West Coast airport in the next century p 560 A95-90095
- HACKNEY, JOHN C.**
The Cassini spacecraft: Object oriented flight control software p 359 A95-80405
- HADCOCK, RICHARD N.**
Composite chronicles: A study of the lessons learned in the development, production, and service of composite structures [NASA-CR-4620] p 151 N95-16859
- HAENEL, D.**
Solution of the Navier-Stokes equations on a massively parallel transporter system p 549 A95-91490
- HAERTEL, CHARMINE**
Controller resource management: What can we learn from aircrews? [DOT/FAA/AM-95/21] p 602 N95-32186
- HAERTEL, GUENTHER F.**
Controller resource management: What can we learn from aircrews? [DOT/FAA/AM-95/21] p 602 N95-32186
- HAUSER, JOCHEM**
Parallel computational fluid dynamics '91; Conference Proceedings, Stuttgart, Germany, Jun. 10-12, 1991 [ISBN 0-444-89363-6] p 548 A95-91479
Aerodynamic simulation on massively parallel systems p 549 A95-91487
- HAUFERMANN, D.**
Verification of engineering methods of aerodynamics for reentry vehicles by DSMC p 525 A95-87386
- HAFEZ, M. M.**
An improved finite element method for the solution of the compressible Euler and Navier-Stokes equations p 640 A95-95439

- HAFFNER, STEPHEN W.**
Noise exposure reduction of advanced high-lift systems
[NASA-CR-195077] p 452 N95-28670
- HAGE, FRANK**
The prototype aviation weather products generator a vehicle to assess user needs p 671 A95-93534
- HAGEN, MARTIN J.**
Measurements of atmospheric turbulence effects on tail rotor acoustics
[NASA-TM-108843] p 38 N95-12360
- HAGENIERS, O. L.**
Double pass retroreflection for corrosion detection in aircraft structures p 323 N95-23503
Characterization of corrosion and development of a breadboard of a D sight aircraft inspection system, phase 1
[AD-A288347] p 380 N95-26527
- HAGER, J. O.**
Two-point transonic airfoil design using optimization for improved off-design performance
[BTN-95-EIX95062487542] p 192 A95-68356
- HAGMEIJER, R.**
Grid adaptation-for-problems in computational-fluid dynamics p 643 A95-95472
Demonstration of an automated CFD system for three-dimensional flow simulations p 551 N95-28767
- HAGN, GEORGE H.**
Tactical low-level helicopter communications p 702 N95-32492
- HAHN, E. J.**
Effect of squeeze film damper land geometry on damper performance
[HTN-95-92247] p 434 A95-85291
- HAHN, K.-J.**
Advanced gust management systems: Lessons learned and perspectives p 622 N95-32002
- HAHNE, DAVID E.**
Low-speed wind tunnel tests of two waverider configuration models
[AIAA PAPER 95-6093] p 493 A95-89251
- HAIGH, S. J.**
Damage to composite aircraft structures from lightning strike attachment to unprotected CFC and internal sparking causing fuel injection
[CONGRESS PAPER C428-4-026] p 531 A95-91675
- HAIGLER, K. J.**
Parallel calculation of sensitivity derivatives for aircraft design using automatic differentiation
[NASA-TM-110103] p 231 N95-20370
- HAIGLER, KARA J.**
Applications of automatic differentiation in computational fluid dynamics p 156 N95-16461
- HAILES, CHRIS**
Conceptual design of the AE481 Demon Remotely Piloted Vehicle (RPV)
[NASA-CR-197164] p 44 N95-12294
- HAILYE, MICHAEL**
Preliminary design of a single engine business jet
[SAE PAPER 931253] p 493 A95-89222
- HAINES, A. BARRY**
Scale effects on aircraft and weapon aerodynamics
[AGARD-AG-323] p 67 N95-14103
- HAINES, G. H.**
Polymer composite applications to aerospace equipment
[HTN-95-B0257] p 529 A95-89201
- HAINES, JOEL**
E-GA hardness assurance, maintenance and surveillance program
[AD-A283994] p 134 N95-19067
- HAIRR, JOHN W.**
Advanced composites structural concepts and materials technologies for primary aircraft structures: Structural response and failure analysis
[NASA-CR-4448] p 11 N95-10240
Advanced composites structural concepts and materials technologies for primary aircraft structures. Structural response and failure analysis: ISPAN modules users manual
[NASA-CR-4449] p 12 N95-10242
ISpan (Interactive Stiffened Panel Analysis): A tool for quick concept evaluation and design trade studies p 533 N95-28846
- HAJ-HARIRI, HOSSEIN**
Effects of the chemical reaction model on calculations of supersonic combustion flows
[BTN-95-EIX0616952745802] p 638 A95-94487
- HAJEK, PAVEL**
In-flight radiometric calibration of AVIRIS in 1994 p 705 N95-33754
- HAJNAL, FERENC**
Radiation safety aspects of commercial high-speed flight transportation
[NASA-TP-3524] p 453 N95-26427
- HALE, JACQUELINE**
International access to aeromedical evacuation medical equipment assessment data p 569 N95-29622
- HALL, DAVID G.**
Background noise levels measured in the NASA Lewis 9- by 15-foot low-speed wind tunnel
[NASA-TM-106817] p 145 N95-18054
- HALL, EDWARD J.**
Investigation of advanced counterrotation blade configuration concepts for high speed turboprop systems. Task 8: Cooling flow/heat transfer analysis
[NASA-CR-195359] p 50 N95-11901
Investigation of advanced counterrotation blade configuration concepts for high speed turboprop systems. Task 8: Cooling flow/heat transfer analysis user's manual
[NASA-CR-195360] p 50 N95-11951
- HALL, J. P.**
High performance backplane components for modular avionics p 247 N95-20653
- HALL, KEITH A.**
The development of computer-based instructional simulations for the airline industry p 625 A95-95159
- HALL, KENNETH**
Rapid prototyping of composite aircraft structures
[SAE PAPER 931219] p 539 A95-87530
- HALL, KENNETH C.**
Eigenanalysis of unsteady flows about airfoils, cascades, and wings
[BTN-95-EIX95152577597] p 305 A95-73486
Eigenanalysis of unsteady flows about airfoils, cascades, and wings
[HTN-95-42582] p 459 A95-87212
- HALL, PHILIP**
The stability of two-phase flow over a swept-wing
[NASA-CR-194994] p 159 N95-18190
- HALL, R. M.**
High Alpha Technology Program (HATP) ground test to flight comparisons p 68 N95-14230
- HALL, RICHARD L.**
Alternatives to ozone depleting refrigerants in test equipment p 630 N95-31767
- HALL, RONALD G.**
Development of a low-cost, modified resin transfer molding process using elastomeric tooling and automated preform fabrication p 420 N95-28268
- HALL, RONALD O.**
Automated test environment for a real-time control system
[TABES PAPER 94-631] p 99 N95-14652
- HALL, WILLIAM**
Weather And Radar Processor (WARP) Test and Evaluation Master Plan (TEMP)
[AD-A288280] p 445 N95-26453
- HALLETT, JOHN**
Replicator for characterization of cirrus and polar stratospheric cloud particles
[NASA-CR-197785] p 445 N95-26669
- HALLIWELL, N. A.**
Vibration measurements on rotating machinery using laser Doppler velocimetry
[BTN-94-EIX95011440597] p 429 A95-82986
- HALLOWELL, ROBERT G.**
The ITWS microburst prediction algorithm p 655 A95-93456
MDCRS: Aircraft observations collection and uses p 668 A95-93517
- HALTURIN, V. A.**
Simulation of multidisciplinary problems for the thermostress state of cooled high temperature turbines p 140 N95-19021
- HAM, JOHNNIE A.**
Flight-testing and frequency-domain analysis for rotorcraft handling qualities
[HTN-95-01083] p 515 A95-90269
- HAMADA, YOSHIHIRO**
Experimental study of shock/shock interference heating on a swept cylinder p 472 A95-91510
- HAMED, A.**
Experimental and numerical simulations of the effects of ingested particles in gas turbine engines p 199 N95-19662
- HAMID, HEDAYAT U.**
Investigation of wing upper surface flow-field disturbance due to NASA DC-8-72 in-flight inboard thrust-reverser deployment
[NASA-TM-110351] p 457 N95-28816
- HAMIDI, L.**
Modal parameters for cracked rotors: models and comparisons
[BTN-94-EIX94522410226] p 702 A95-96378
- HAMILL, T. G.**
MCMs for avionics: Technology selection and intermodule interconnection p 234 N95-20641
- HAMILTON, H. HARRIS**
Approximate method for calculating heating rates on three-dimensional vehicles
[BTN-95-EIX95041503778] p 210 A95-69209
- HAMILTON, MARK F.**
Effect of stratification and geometrical spreading on sonic boom rise time p 75 N95-14880
- HAMLIN, RICHARD D.**
Advanced composite structural concepts and materials technologies for primary aircraft structures: Advanced material concepts
[NASA-CR-4485] p 503 N95-29027
- HAMM, CLAUD D.**
Corrosion protection measures for CFC/metal joints of fuel integral tank structures of advanced military aircraft p 303 N95-23510
- HAMM, KEN**
Experimental/analytical approach to understanding mistuning in a transonic wind tunnel compressor
[NASA-TM-108833] p 95 N95-14617
- HAMMADI, MUNIR AL**
Study of an airfoil with a flap and spoiler
[BTN-95-EIX95152582327] p 265 A95-73530
- HAMMON, COLIN P.**
The value of simulation for training
[AD-A289174] p 411 N95-26556
- HAMORY, PHILIP J.**
Flight experience with lightweight, low-power miniaturized instrumentation systems
[BTN-95-EIX95062487522] p 180 A95-69230
- HAMPSON, C. D.**
Evaluation of prediction methods for fluctuating pressures under attached turbulent boundary layers using flight test data p 574 A95-90103
- HAMPTON, R. D.**
Microgravity isolation system design: A case study
[NASA-TM-106804] p 104 N95-17657
Microgravity isolation system design: A modern control synthesis framework
[NASA-TM-106805] p 105 N95-18197
Microgravity isolation system design: A modern control analysis framework
[NASA-TM-106803] p 105 N95-18486
- HAMPTON, ROY W.**
Experimental/analytical approach to understanding mistuning in a transonic wind tunnel compressor
[NASA-TM-108833] p 95 N95-14617
- HAN, BUZHANG**
An investigation of polynomial calibrations methods for wind tunnel balances p 144 N95-16258
- HAN, S. O. T. H.**
Two-dimensional 16.5 percent thick supercritical airfoil NLR 7301 p 110 N95-17854
- HANAGUD, S.**
Smart structures in the control of airframe vibrations
[HTN-95-31014] p 236 A95-71184
Adaptive airfoils
[ISBN 1-879921-01-4] p 625 A95-93744
- HANAMITSU, A.**
Numerical studies of Mach reflection with air chemistry p 548 A95-90575
- HAND, LAWRENCE A.**
A supercritical airfoil experiment p 111 N95-17858
- HANDSCHUH, R. F.**
Analytical and experimental vibration analysis of a faulty gear system
[NASA-TM-106689] p 58 N95-12843
- HANDSCHUH, ROBERT F.**
Detecting gear tooth fracture in a high contact ratio face gear mesh
[NASA-TM-106822] p 162 N95-19125
- HANER, D.**
Airborne lidar observation of mountain-wave-induced polar stratospheric clouds during EASOE
[HTN-95-00738] p 444 A95-86308
- HANEY, J. W.**
A waverider derived hypersonic X-vehicle
[AIAA PAPER 95-6162] p 496 A95-90473
- HANFF, ERNEST S.**
Further analysis of high-rate rolling experiments of a 65-deg delta wing
[BTN-95-EIX95152582331] p 281 A95-73533
- HANGE, CRAIG**
Flow visualization studies of VTOL aircraft models during Hover in ground effect
[NASA-TM-108860] p 272 N95-22666
- HANGEN, J.**
A weight-efficient design strategy for cutouts in composite transport structures p 533 N95-28843
- HANIGOFSKY, JOHN A.**
Ceramic composite combustor cans for expendable turbine engines
[AD-A289551] p 407 N95-28646

- HANISCO, T. F.**
Aircraft-borne, laser-induced fluorescence instrument for the in situ detection of hydroxyl and hydroperoxy radicals
[BTN-95-EIX95072499029] p 253 A95-71908
- HANKE, DIETRICH**
Handling qualities analysis on rate limiting elements in flight control systems p 619 N95-31071
- HANKEY, J.**
High performance backplane components for modular avionics p 247 N95-20653
- HANNON, JUDITH A.**
Computer model to simulate testing at the National Transonic Facility
[NASA-TM-4664] p 627 N95-32217
- HANNON, STEPHEN M.**
Airport surveillance using a solid state coherent lidar
p 41 N95-13207
Wake vortex detection at Denver Stapleton Airport with a pulsed 2-micron coherent lidar p 42 N95-13211
- HANSCHKE, BRUCE**
Emerging nondestructive inspection for aging aircraft
[PB95-143053] p 328 N95-25401
- HANSEN, CHRISTOPHER P.**
Landing gear energy absorption system
[NASA-CASE-MSC-22277-1] p 96 N95-15306
- HANSEN, IRVING G.**
Power system characteristics for more electric aircraft
[SAE PAPER 931406] p 613 A95-93675
The development of a highly reliable power management and distribution system for civil transport aircraft
[NASA-TM-106697] p 50 N95-11867
- HANSEN, REED S.**
Experimental/analytical approach to understanding mistuning in a transonic wind tunnel compressor
[NASA-TM-108833] p 95 N95-14617
- HANSFORD, ROBERT E.**
Considerations in the development of the coupled rotor fuselage model
[HTN-95-61077] p 370 A95-83661
- HANSMAN, R. J., JR.**
An exploratory survey of information requirements for instrument approach charts
[AD-A293882] p 601 N95-31520
Current issues in the design and information content of instrument approach charts
[AD-A294752] p 690 N95-34562
- HANSMAN, R. JOHN**
Part-task simulator evaluations of advanced terrain displays
[SAE PAPER 932570] p 401 A95-84567
- HANSON, R. K.**
Comparison of NO and OH planar fluorescence temperature measurements in scramjet model flowfields
[BTN-95-EIX95042474388] p 209 A95-68312
- HANUS, GARY J.**
Design features of the NAL ramjet engine test facility
p 410 A95-82319
- HANZAWA, A.**
Development of a pilot tube with multi-hole pyramidal head. 2: A five-hole yew probe of engineering model
p 522 A95-91577
- HARADA, MASANORI**
A study of computational difficulty of numerical method in optimal control p 507 A95-91585
- HARBAUGH, STEPHEN P.**
Integration of a mechanical forebody vortex control system into the F-15 p 72 N95-14258
- HARDEN, JOHN H., JR.**
Naval Aviation System TEAM mapping, charting, and geodesy handbook
[AD-A288590] p 446 N95-26841
- HARDIN, JAY D.**
In-flight pressure measurements on a subsonic transport high-lift wing section
[BTN-95-EIX0619952748170] p 589 A95-94464
- HARDY, G. L.**
Corrosion detection and monitoring of aircraft structures: An overview p 303 N95-23515
- HARDY, GORDON**
Flight investigation of the use of a nose gear jump strut to reduce takeoff ground roll distance of STOL aircraft
[NASA-TM-108819] p 44 N95-12225
Investigation of wing upper surface flow-field disturbance due to NASA DC-8-72 in-flight inboard thrust-reverser deployment
[NASA-TM-110351] p 457 N95-28816
- HARDY, GORDON H.**
Simulation development of a forward sensor-enhanced low-altitude guidance system
[HTN-94-00688] p 17 A95-60170
Design and flight evaluation of an integrated navigation and near-terrain helicopter guidance system for night-time and adverse weather operations
[NASA-TM-108837] p 11 N95-10846
- HARE, D. A.**
Dynamic Stability Instrumentation System (DSIS). Volume 1: Hardware description
[NASA-TM-109160-VOL-1] p 171 N95-18899
- HARGREAVES, J.**
Tooling - a source of productivity
[CONGRESS PAPER C428-32-017] p 583 A95-93619
- HARKNESS, H. H.**
Fatigue reliability method with in-service inspections p 94 N95-14475
- HARLOFF, G. J.**
Design and operation of a supersonic annular flow facility
[BTN-94-EIX94441386624] p 183 A95-68173
Design and operation of a supersonic annular flow facility
[HTN-95-20941] p 465 A95-88980
Numerical simulation of supersonic flow using a new analytical bleed boundary condition
[NASA-CR-198368] p 697 N95-33208
- HARLOFF, GARY J.**
On supersonic-inlet boundary-layer bleed flow
[NASA-CR-195426] p 202 N95-19769
- HARLOW, D. G.**
Corrosion and corrosion fatigue of airframe aluminum alloys p 87 N95-14465
- HARMAN, WILLIAM H.**
GPS-Squitter capacity analysis
[AD-A280037] p 245 N95-20599
- HARMAN, WILLIAM H., III**
GPS-Squitter interference analysis
[AD-A293690] p 689 N95-33480
- HARP, STEVEN A.**
Modeling student knowledge with self-organizing feature maps
[BTN-95-EIX95262697073] p 564 A95-86862
- HARPER, RICHARD E.**
A highly reliable, high performance open avionics architecture for real time Nap-of-the-Earth operations p 693 N95-32497
- HARRAND, V. J.**
Pressure based high order TVD methodology for dynamic stall control
[AD-A290149] p 479 N95-29316
- HARRIMAN, WALTER L.**
Passive range measurement system
[AD-D016222] p 258 N95-21100
Apparent size passive range method
[AD-D017360] p 611 N95-31180
- HARRINGTON, BROOK**
The FC-1D: The profitable alternative Flying Circus Commercial Aviation Group
[NASA-CR-197152] p 46 N95-12628
- HARRIS-HOBBS, RAY**
Application of airborne field mill data for use in launch support
[HTN-95-50054] p 98 A95-62279
- HARRIS, BRENDA W.**
An assessment of viscous effects in computational simulation of benign and burst vortex flows on generic fighter wind-tunnel models using TEAM code
[NASA-CR-4650] p 273 N95-23185
- HARRIS, C. E.**
Tension fracture of laminates for transport fuselage. Part 1: Material screening p 398 N95-28471
- HARRIS, CHARLES D.**
The NASA Langley 8-foot Transonic Pressure Tunnel calibration
[NASA-TP-3437] p 8 N95-10739
- HARRIS, CHARLES E.**
FAA/NASA International Symposium on Advanced Structural Integrity Methods for Airframe Durability and Damage Tolerance
[NASA-CP-3274-PT-1] p 92 N95-14453
FAA/NASA International Symposium on Advanced Structural Integrity Methods for Airframe Durability and Damage Tolerance, part 2
[NASA-CP-3274-PT-2] p 124 N95-19468
Recent progress in NASA Langley textile reinforced composites program p 425 N95-28475
- HARRIS, F. I.**
Radar studies of aviation hazards
[AD-A285845] p 226 N95-21831
- HARRIS, JOSEPH M.**
Evaluation of the radio frequency susceptibility of commercial GPS receivers
[BTN-95-EIX95042474624] p 189 A95-68278
- HARRIS, K.**
Allison engine testing CMSX-4 (reg sign) single crystal turbine blades and vanes
[DE95-010308] p 694 N95-32636
- HARRIS, M. J.**
Development of software for safety critical applications for the EH101 Helicopter
[CONGRESS PAPER C428-24-160] p 678 A95-93597
- HARRIS, M. M.**
Flex cycle combustor development and demonstration
[BTN-94-EIX95011441245] p 417 A95-84202
- HARRIS, N. R. P.**
An overview of the EASOE campaign
[HTN-95-00702] p 443 A95-86272
- HARRIS, P. K.**
Particle trajectories in gas turbine engines p 199 N95-19663
- HARRIS, W. L.**
Anechoic wind tunnel study of turbulence effects on wind turbine broadband noise p 451 N95-27992
- HARRISON, G. F.**
The role of material behaviour modelling in stressing and life assessment of modern Aero-engine components
[CONGRESS PAPER C428-27-127] p 612 A95-93606
- HARRISON, K.**
The Anglo-French Compact Laser Radar demonstrator programme p 703 N95-32501
- HARRISON, L.**
Artificial intelligence with applications for aircraft
[DOT/FAA/CT-94/41] p 99 N95-13895
Digital systems validation. Chapter 20 Artificial Intelligence with applications for aircraft. Handbook, volume 2
[AD-A288492] p 448 N95-26638
- HARRISON, W. E., III**
High heat sink fuels for improved aircraft thermal management
[SAE PAPER 932084] p 530 A95-91659
- HARRY, N. A.**
The development of a model specification for ground support equipment
[CONGRESS PAPER C428-38-095] p 625 A95-93636
- HART-SMITH, L. J.**
The key to designing durable adhesively bonded joints
[HTN-95-12033] p 528 A95-88496
- HARTEL, MARTIN C.**
Flight-deck displays on the Boeing 777
[BTN-95-EIX95142562402] p 286 A95-73438
- HARTFIELD, R. J., JR.**
Computational/experimental investigation of staged injection into a Mach 2 flow
[HTN-95-51646] p 432 A95-85028
- HARTFIELD, ROY J.**
Nonlinear aerodynamic analysis of grid fin configurations
[BTN-95-EIX0619952748172] p 590 A95-94466
- HARTFIELD, ROY J., JR.**
Quantitative investigation of compressible mixing: Staged transverse injection into Mach 2 flow
[HTN-95-42330] p 404 A95-86159
- HARTLE, MICHAEL S.**
Ply layout optimization and micromechanics tailoring of composite aircraft engine structures
[BTN-95-EIX95112524206] p 196 A95-69302
- HARTMAN, KATHY R.**
Flight Mechanics/Estimation Theory Symposium 1995
[NASA-CP-3299] p 416 N95-27763
- HARTMAN, TROY**
LCX: Proposal for a low-cost commercial transport
[NASA-CR-197186] p 47 N95-12645
- HARTMANN, K.**
Force and pressure data of an ogive-nosed slender body at high angles of attack and different Reynolds numbers p 113 N95-17868
Wind tunnel test on a 65 deg delta wing with rounded leading edges: The International Vortex Flow Experiment p 114 N95-17875
- HARTOGH, P.**
Aircraft measurements of CLO and HCL during EASOE 1991/92
[HTN-95-00721] p 444 A95-86291
- HARTUNG, LIN C.**
Convective and radiative heat transfer analysis for the fire 2 forebody
[BTN-95-EIX95182617460] p 268 A95-75731
- HARTWICH, PETER M.**
Comparison of coordinate-invariant and coordinate-aligned upwinding for the Euler equations
[HTN-95-A1753] p 633 A95-93316
- HARVEY, GALE A.**
Hardware cleanliness methodology and certification p 419 N95-27656
- HARVEY, GARY**
Micro-time stress measurement device development
[AD-A289511] p 448 N95-26845

- HARVEY, W. DON**
Aviation system capacity improvements through technology
[NASA-TM-109165] p 333 N95-24633
- HARWOOD, D. W.**
Development of anti-icing technology
[PB94-195369] p 78 N95-15439
- HASDORFF, L.**
Design of a model following, state variable feedback controller for the X-14 VTOL aircraft
[HTN-94-00685] p 16 A95-60168
- HASEGAWA, GIZO**
Hubload responses of a rotor in forward flight due to multiple frequency blade pitch variations
p 515 A95-91504
- HASEGAWA, HIDEO**
CCLA operation on MLS
p 487 A95-91540
- HASHIDATE, MASATAKA**
Experimental study of the aerodynamic characteristics of the counter-rotation propellers
p 474 A95-91562
Wake velocity measurement of counter-rotation propellers
p 474 A95-91563
Preliminary tests of a transonic flutter control wing model
p 499 A95-91566
Analysis and scale-model experiment of propeller driving motor for microwave-powered airplane
p 487 A95-91576
- HASKINS, WILLIAM L.**
Concepts for aircraft subsystem integration
[SAE PAPER 931377] p 604 A95-93656
- HASKO, GREGORY H.**
Resin transfer molding of textile preforms for aircraft structural applications
p 421 N95-28276
Performance of resin transfer molded multifaxial warp knit composites
p 535 N95-29039
- HASKO, GREGORY H.**
Development and verification of a resin film infusion/resin transfer molding simulation model for fabrication of advanced textile composites
[NASA-CR-197439] p 301 N95-23179
- HASSA, CHRISTOPH**
Experimental investigation of turbulent particle dispersion in swirling flows
[DLR-FB-94-20] p 647 N95-31355
- HASSAN, A. A.**
Numerical model for circulation-control flows
[HTN-95-81632] p 461 A95-87680
- HASSAN, AHMED A.**
Effects of leading and trailing edge flaps on the aerodynamics of airfoil/vortex interactions
[HTN-95-31011] p 221 A95-71181
- HASSAN, H. A.**
Modeling of supersonic turbulent combustion using assumed probability density functions
[BTN-95-EIX95112524190] p 206 A95-69318
- HASSAN, O.**
Mesh generation and adaptivity for the solution of compressible viscous high speed flows
[BTN-95-EIX95262697157] p 538 A95-86893
- HATFIELD, MICHAEL O.**
Electromagnetic reverberation characteristics of a large transport aircraft
[AD-A282923] p 82 N95-15392
- HATHAWAY, MICHAEL D.**
Laser anemometer measurements of the three-dimensional rotor flow field in the NASA low-speed centrifugal compressor
[NASA-TP-3527] p 618 N95-31985
- HAUF, THOMAS**
An in-situ system for warning of icing conditions
p 660 A95-93481
- HAUGLUSTAIN, D. A.**
Impact of present aircraft emissions of nitrogen oxides on tropospheric ozone and climate forcing
[HTN-95-21364] p 353 A95-78679
- HAUPT, M.**
Integrated thermal and mechanical analysis of hypersonic vehicles by using adaptive finite element methods
p 524 A95-87383
- HAUSS, BRUCE**
Passive millimeter wave camera for aircraft landing in low visibility conditions
[BTN-95-EIX95292721321] p 609 A95-92513
- HAVELOCK, DAVID H.**
Proceedings of the Sixth International Symposium on Long-Range Sound Propagation
[AD-A290920] p 580 N95-30084
- HAVEN, CHRISTINE E.**
Quiet-flow Ludweig tube for high-speed transition research
[BTN-95-EIX95262694309] p 370 A95-85480
- HAVERLAND, M.**
Integrated special mission flight management for a flight inspection aircraft
p 692 N95-33145
- HAWKE, VERONICA M.**
Aerodynamic tailoring of the Learjet Model 60 wing
[SAE PAPER 932534] p 492 A95-89194
- HAWKINS, ANTHONY**
Standard Hardware Acquisition and Reliability Program (SHARP) advanced SEM-E packaging
p 233 N95-20633
- HAWLEY, ARTHUR V.**
Development of stitched/RTM primary structures for transport aircraft
[NASA-CR-191441] p 630 N95-31421
- HAWORTH, L. A.**
TRISTAR 1: Evaluation methods for testing head-up display (HUD) flight symbology
[NASA-TM-4665] p 288 N95-24030
- HAYASAKA, TADAHIRO**
Air truth validation of cloud albedo estimated from NOAA advanced very high resolution radiometer data
[HTN-95-A1021] p 443 A95-84526
- HAYASHI, A. K.**
Pulsed jet ignition modeling with a full chemistry
p 538 A95-87184
- HAYASHI, MASANORI**
Numerical experiments on aerodynamic heating mechanism in shock reflection processes
p 471 A95-91497
- HAYATDAVOUDI, MAZIAR**
LCX: Proposal for a low-cost commercial transport
[NASA-CR-197186] p 47 N95-12645
- HAYER, M. EHTESHAM**
Structure of supersonic jet flow and its radiated sound
[HTN-95-51645] p 431 A95-85027
- HAYES, HALFORD I.**
Wavelet transformations for helicopter identification via acoustic signatures
[AD-A279980] p 257 N95-20963
- HAYES, JAMES R.**
Heat transfer measurements in small scale wind tunnels
[AD-A288689] p 341 N95-26053
- HAYHURST, KELLY J.**
A study of software standards used in the avionics industry
p 137 N95-16456
- HAYNE, CAMERON**
Stratus' tephigram as a training/forecasting tool
p 657 A95-93465
- HAYNES, TIMOTHY S.**
Transition correlations in three-dimensional boundary layers
[HTN-95-51648] p 432 A95-85030
- HAZEN, N. L.**
Aircraft-borne, laser-induced fluorescence instrument for the in situ detection of hydroxyl and hydroperoxyl radicals
[BTN-95-EIX95072499029] p 253 A95-71908
- HAZLEWOOD, RICHARD**
Design of a high altitude long endurance aircraft with manufacturing considerations
p 391 N95-26947
- HE, HONGQING**
Simulation on the 3-D turbulent flow in the passages of finocyl grain
[BTN-95-EIX95202638962] p 279 A95-76674
Numerical analysis of flow field around gas rudder
p 407 A95-82333
- HE, J. W.**
A cartesian grid finite element method for aerodynamics of moving rigid bodies
p 642 A95-95471
- HE, X.**
Waveriders with finlets
[BTN-95-EIX95062487541] p 184 A95-68355
- HEADLEY, DEAN E.**
The airline quality report, 1994
[NIAR-94-11] p 277 N95-24012
- HEALEY, G.**
Cost effective, dual-purpose machine vision-based detectors for (1) smoke and flame detection, and (2) engine overhead/burn-through and flame detection
[AD-A292284] p 579 N95-28870
- HEATH, J. B. R.**
Bonded composite repair of thin metallic materials: Variable load amplitude and temperature cycling effects
p 393 N95-27509
- HEATON, HARRY**
Systems engineering design and technical analyses for Strategic Avionics Crew-station Design Evaluation Facility (SACDEF)
[AD-A286239] p 235 N95-22024
- HEBBAR, SHESHAGIRI**
Aerodynamic characteristics of a canard-controlled missile at high angles of attack
[BTN-95-EIX95152583257] p 267 A95-73558
- HEBBAR, SHESHAGIRI K.**
Effect of leading-edge extension fences on the vortex wake of an F/A-18 model
[BTN-95-EIX0619952748192] p 591 A95-94481
- HEBERT, JOSEPH E.**
Analysis and modeling of an airport departure process
[AD-A293782] p 602 N95-31581
- HECKMAN, SCOT T.**
An application of some cloud modeling techniques to a regional model simulation of an icing event
p 673 A95-93543
- HEDDE, T.**
Prediction of ice accretion: Comparison between the 2D and 3D codes
[BTN-94-EIX94441385753] p 213 A95-68217
- HEDMAN, SVEN G.**
Multigrid/multiblock method for transonic potential flow around wing/body/nacelle configurations including a slipstream
p 591 A95-95451
- HEEG, JENNIFER**
Simulation and model reduction for the active flexible wing program
[BTN-95-EIX95182619211] p 295 A95-76637
- HEFAZI, HAMID**
Predicting stall and post-stall behavior of airfoils at low mach numbers
[BTN-95-EIX262694297] p 365 A95-85468
- HEFFTER, JEROME L.**
Volcanic ash forecast transport and dispersion (VAFTAD) model
[HTN-95-80702] p 254 A95-72546
- HEGEDUS, CHARLES R.**
Organic coating technology for the protection of aircraft against corrosion
p 303 N95-23513
- HEIDA, J. H.**
Eddy current detection of pitting corrosion around fastener holes
p 315 N95-23507
- HEIDBREDER, GLEN R.**
Apparatus and method for producing three-dimensional images
[AD-DO17455] p 646 N95-30727
- HEIDEGGER, NATHAN J.**
Investigation of advanced counterrotation blade configuration concepts for high speed turboprop systems. Task 8: Cooling flow/heat transfer analysis
[NASA-CR-195359] p 50 N95-11901
Investigation of advanced counterrotation blade configuration concepts for high speed turboprop systems. Task 8: Cooling flow/heat transfer analysis user's manual
[NASA-CR-195360] p 50 N95-11951
- HEIDT, L. E.**
Estimates of total organic and inorganic chlorine in the lower stratosphere from in situ and flask measurements during AA5E 2
[HTN-95-A0861] p 317 A95-76265
- HEIL, ROBERT MILTON**
Characterizing the wake vortex signature for an active line of sight remote sensor
[NASA-CR-197697] p 333 N95-24391
- HEIMERDINGER, M. W.**
Repair technology for thermoplastic aircraft structures
p 395 N95-27519
- HEIN, GUENTER W.**
On-the-fly carrier phase ambiguity resolution for precise aircraft landing
[BTN-95-EIX95112522535] p 190 A95-69328
- HEINEMANN, KLAUS W.**
Development and application of structural dynamics analysis capabilities
[NASA-CR-197229] p 96 N95-14922
- HEINLE, ROBERT A.**
Determination of stores pointing error due to wing flexibility under flight load
[NASA-TM-4646] p 134 N95-19044
- HEINRICH, D. C.**
Effect of underwing frost on a transport aircraft airfoil at flight Reynolds number
[BTN-95-EIX95152582334] p 276 A95-73536
- HEINZE, BILL**
Maintenance programs
[HTN-95-92310] p 365 A95-85354
- HEISER, W. H.**
Simulating heat addition via mass addition in constant area compressible flows
[BTN-95-EIX95182619100] p 307 A95-76585
Visualization of one-dimensional flow processes in a dual-mode scramjet engine
p 15 N95-10465
- HEISEY, C. W.**
Subsidence of aircraft engine exhaust in the stratosphere: Implications for calculated ozone depletions
[PAPER-93GL03426] p 251 A95-70297
- HELALI, Y. E.**
Variations of perturbations in perigee height with eccentricity of artificial Earth's satellites due to air drag
[HTN-95-40013] p 85 A95-62657

- HELIE, P.**
FASTPACK: Optimized solutions for modular avionics derived from a parametric study. Part 1: Platform features p 233 N95-20634
- HELIN, H. E.**
Effects of trailing-edge jet entrainment on delta wing vortices [HTN-95-81644] p 542 A95-87692
- HELMINGER, MARK**
In-flight radiometric calibration of AVIRIS in 1994 p 705 N95-33754
- HELTSLEY, F. L.**
Analysis of planar laser-induced fluorescence images obtained during shakedown testing of the AEDC impulse facility [AD-A293237] p 646 N95-30906
- HEMDAN, HAMD I.**
Similarity solutions for hypersonic flow past slender bodies of revolution at small incidence [HTN-95-12195] p 475 A95-91895
- HEMMI, MAKOTO**
An experimental study on radiation from strong shock layer p 368 A95-82421
- HEMSCH, MICHAEL J.**
Effect of passive venting on static pressure distributions in cavities at subsonic and transonic speeds [NASA-TM-4549] p 6 N95-10029
Measurements of store forces and moments and cavity pressures for a generic store in and near a box cavity at subsonic and transonic speeds [NASA-TM-4611] p 378 N95-28241
- HENAKU, B. D. K.**
The ICAO CNS/ATM system: New king, new law? [HTN-95-50218] p 175 A95-64855
- HENDERSON, ULESES C., JR.**
Simultaneous three-dimensional velocity and mixing measurements by use of laser Doppler velocimetry and fluorescence probes in a water tunnel [NASA-TP-3454] p 53 N95-13553
- HENDRICK, RUSS**
Dynamic inversion: An evolving methodology for flight control design p 621 N95-31996
- HENDRICKS, R. C.**
Brush seal performance and durability issues based on T-700 engine test results [NASA-TM-106502] p 22 N95-11483
Numerical analysis of intra-cavity and power-stream flow interaction in multiple gas-turbine disk-cavities [NASA-TM-106886] p 407 N95-28344
- HENDRICKS, ROBERT C.**
Comparison of numerical results and multicavity purge and rim seal data with extensions to dynamics [NASA-TM-106685] p 416 N95-27434
- HENDRICKSON, J. T.**
TIM-SCT cable testing protocol [AD-A286633] p 231 N95-20772
- HENDRIX, A. M.**
Development of a coding form for approach control/pilot voice communications [DOT/FAA/AM-95/15] p 384 N95-28540
- HENEGHAN, BRIAN**
The OFP-6M transport jet [NASA-CR-197159] p 46 N95-12637
- HENLINE, W. D.**
Hypersonic nonequilibrium Navier-Stokes solutions over an ablating graphite nosetip [BTN-95-EIX95152583252] p 305 A95-73553
- HENLINE, WILLIAM D.**
Trajectory-based heating analysis for the European Space Agency/Rosetta Earth Return Vehicle [BTN-95-EIX95041503787] p 205 A95-69218
- HENNEQUIN, Y.**
Numerical study of Gortler instability: Application to the design of a quiet supersonic wind tunnel [PB94-184801] p 21 N95-10844
- HENNIG, P.**
Aeromechanical design of modern missiles p 73 N95-14446
- HENRY, F. S.**
Numerical model of boundary-layer control using air-jet generated vortices [HTN-95-42581] p 459 A95-87211
- HENRY, SANDRA G.**
Developing thunderstorm forecast rules utilizing first detectable cloud radar-echoes p 667 A95-93514
- HENRY, ZACHARY S.**
Bell Helicopter Advanced Rotocraft Transmission (ART) program [NASA-CR-195479] p 555 N95-29538
- HENSEL, EDWARD**
Demonstration study of hierarchical control of fluid-dynamic phenomena [AD-A289341] p 437 N95-26751
- HEPPNER, P. O. G.**
A new look at aviation meteorology: Integrating aircraft situation display (ASD) with conventional weather displays p 665 A95-93505
- HERAKOVICH, CARL T.**
NASA-UVA light aerospace alloy and structures technology program (LA2ST) [NASA-CR-198041] p 343 N95-24220
- HERBERT, THORWALD**
Nonlinear analysis of swept wing transitional boundary layers [SAE PAPER 932515] p 466 A95-89188
- HERMANN, ROBERT**
A brief survey of constrained mechanics and variational problems in terms of differential forms p 360 N95-25803
- HERNANDEZ, ESTELA**
The Aluminum Falcon: A low cost modern commercial transport [NASA-CR-197180] p 81 N95-15742
- HERNANDEZ, GLORIA**
Effect of leading- and trailing-edge flaps on clipped delta wings with and without wing camber at supersonic speeds [NASA-TM-4542] p 5 N95-10028
- HEROLD, K. E.**
Liquid flow-through cooling of electronic modules p 246 N95-20647
- HERREWYN, J.**
FASTPACK: Optimized solutions for modular avionics derived from a parametric study. Part 2: Avionics p 233 N95-20635
- HERRIN, J. L.**
Supersonic near-wake afterbody boattailing effects on axisymmetric bodies [BTN-95-EIX95182617465] p 268 A95-75736
- HERRMANN, U.**
Estimation of aerodynamic derivatives: Euler scheme validation and approximate methods for hypersonic configurations p 460 A95-87385
- HESS, R. A.**
Rotorcraft control system design for uncertain vehicle dynamics using quantitative feedback theory [HTN-95-31012] p 236 A95-71182
A generalized algorithm for inverse simulation applied to helicopter maneuvering flight [HTN-95-A0493] p 236 A95-72564
Rotorcraft handling qualities in turbulence [BTN-95-EIX95242670750] p 334 A95-81097
- HESS, RONALD A.**
Analysis of the longitudinal handling qualities and pilot-induced-oscillation tendencies of the High-Angle-of-Attack Research Vehicle (HARV) p 293 N95-23297
- HESSHEIMER, MICHAEL**
The large radius track centrifuge concept as an acceleration research and simulation device p 379 A95-84560
- HETTENA, E.**
An unstructured node centered scheme for the simulation of 3-D inviscid flows p 642 A95-95463
- HETTINGA, JOEL**
LCX: Proposal for a low-cost commercial transport [NASA-CR-197186] p 47 N95-12645
- HETU, JEAN-FRANCOIS**
Adaptive remeshing for convective heat transfer with variable fluid properties [BTN-95-EIX95082502720] p 243 A95-71033
Adaptive finite element method for turbulent flow near a propeller [BTN-95-EIX95142553038] p 305 A95-73460
- HEUWINKEL, RICHARD**
National aviation weather program plan p 652 A95-93445
Pilot training initiatives for the '90s p 657 A95-93463
- HEUWINKEL, RICHARD J.**
A status report on the development of the Federal Aviation Administration/National Oceanic and Atmospheric Administration Memorandum of Agreement p 652 A95-93447
Transitioning to the aviation routine weather report (METAR) and the International Aerodrome Forecast (TAF) within the Federal Aviation Administration p 656 A95-93461
- HEWITT, C.**
A tactical navigation and routeing system for low-level flight p 709 N95-32494
- HICKMAN, JAMES J.**
High aspect ratio metal microstructures and method for preparing the same [AD-DO17463] p 629 N95-30750
- HICKS, BETTY**
General aviation landing incidents and accidents: A review of ASRS and AOPA research findings p 596 A95-95198
- HICKS, JOHN W.**
In-flight lift-drag characteristics for a forward-swept wing aircraft and comparisons with contemporary aircraft [NASA-TP-3414] p 117 N95-18565
- HICKS, Y. R.**
Two-dimensional imaging of OH in a lean burning high pressure combustor [NASA-TM-106854] p 236 N95-21383
- HIERS, ROBERT S., JR.**
Subscale study of engine bellmouth inlet vortices in test cell R1D [AD-A294993] p 707 N95-34818
- HIGASHINO, FUMIO**
Numerical investigation of supersonic flows around a spiked blunt body [BTN-95-EIX95212645690] p 271 A95-76742
- HIGASHINO, SHINICHIRO**
A systems for flight data acquisition and analysis for a remotely-piloted research vehicle p 517 A95-91554
- HILL, D. A.**
Measurements of shielding effectiveness and cavity characteristics of airplanes [PB94-210051] p 244 N95-20191
- HILL, D. C.**
Hypervelocity Impact Test Facility: A gun for hire [TABES PAPER 94-605] p 86 N95-14639
- HILL, PHILIP G.**
An educational introduction to transonic compressor stage design principles [SAE PAPER 931393] p 613 A95-93668
- HILL, S. D.**
Enhancement of F/A-18 operational flight measurements: Data report for phase 1 [DSTO-TR-0049] p 286 N95-23666
- HILLGER, WOLFGANG**
Ultrasonic imaging of damages in CRFT-laminates p 578 A95-90828
- HILLIER, R.**
Kinetic heating in hypersonic flight [CONGRESS PAPER C428-3-056] p 475 A95-91674
- HILMES, C. L.**
TranAir: A full-potential, solution-adaptive, rectangular grid code for predicting subsonic, transonic, and supersonic flows about arbitrary configurations. User's manual [NASA-CR-4349] p 377 N95-28230
TranAir: A full-potential, solution-adaptive, rectangular grid code for predicting subsonic, transonic, and supersonic flows about arbitrary configurations. Theory document [NASA-CR-4348] p 378 N95-28265
- HINADA, MOTOKI**
The aerodynamic characteristics of cup-like body in supersonic flow p 427 A95-82407
Atmospheric reentry flight test of winged space vehicle p 414 A95-82483
Reentry technology experiment on the first mission of reentry capsule 'EXPRESS' p 414 A95-82499
Development and flight results of fiber reinforced balloon p 384 A95-82511
- HINDMAN, RICHARD G.**
An approach for dynamic grids [NASA-TM-106774] p 76 N95-15853
- HINGST, W. R.**
Flow structure in the wake of a wishbone vortex generator [BTN-95-EIX95142553044] p 304 A95-73454
Flow coefficient behavior for boundary layer bleed holes and slots [NASA-TM-106846] p 244 N95-19953
- HINGU, TATSURO**
Determination of flight simulator time delay p 522 A95-91553
- HINSON, MICHAEL L.**
Aerodynamic tailoring of the Learjet Model 60 wing [SAE PAPER 932534] p 492 A95-89194
- HINTON, DAVID A.**
Windshear certification data base for forward-look detection systems p 41 N95-13204
- HINTSA, E. J.**
In situ observations in aircraft exhaust plumes in the lower stratosphere at midlatitudes [HTN-95-A0862] p 318 A95-76266
- HIRAIWA, TETSUO**
Three-dimensional analysis of scramjet nozzle flows [BTN-94-EIX94441380978] p 196 A95-68162
Performance variation of scramjet nozzle at various nozzle pressure ratios [BTN-95-EIX0616952745781] p 615 A95-94505
- HIRAKI, KOJU**
The aerodynamic characteristics of cup-like body in supersonic flow p 427 A95-82407
- HIRAMOTO, TAKASHI**
The concept of high speed commercial transporter structure p 498 A95-91517

- HIRANO, KIMITAKA**
A singularity method for a two dimensional stratified shear flow p 473 A95-91513
- HIRASAWA, T.**
Polar Patrol Balloon system and preliminary experimental results p 368 A95-82513
- HIRATA, KATSUYA**
Aerodynamic mechanism of galloping [BTN-94-EIX94371347709] p 219 A95-69968
- HIRATA, NOBUYUKI**
Numerical simulation of two-dimensional PAR-WIG p 685 N95-34548
- HIROKAWA, JUNICHI**
Overview of feasibility study on propulsion concepts for high speed civil transport p 498 A95-91518
- HIROSE, NAOKI**
A detailed Euler flow analysis of TPS and fanjet engine p 473 A95-91515
- HIRSA, A.**
Measurements of vortex pair interaction with a clean or contaminated free surface [BTN-94-EIX95011441063] p 429 A95-82798
- HIRSCH, CH.**
Computational methods in applied sciences; European Computational Fluid Dynamics Conference, 1st, Brussels, Belgium, Sept. 7-11, 1992 [ISBN 0-444-89795-X] p 539 A95-87552
- HIRSCH, CHARLES**
Computational fluid dynamics '92; Proceedings of the European Computational Fluid Dynamics Conference, 1st, Brussels, Belgium, Sep. 7-11, 1992. Vols. 1 & 2 [ISBN 0-444-89793-3] p 638 A95-95357
Hypersonic Navier-Stokes computations about complex configurations p 644 A95-95497
- HIRSCHORN, MARTIN**
Reducing low frequency noise emissions from a Langley Air Force Base Hush-House p 561 A95-90112
- HIRST, DONALD J.**
A comparison of coating alternatives for US Coast Guard aircraft [AD-A293270] p 629 N95-31124
- HISHIDA, M.**
Pulsed jet ignition modeling with a full chemistry p 538 A95-87184
- HITCHCOCK, L.**
Independent review of Aviation Technology and Research Information Analysis System (ATRIAS) database [AD-A284049] p 226 N95-21518
- HITOMI, ATUSHI**
Flight test of STS radio controlled scale model p 499 A95-91539
- HITT, ELLIS**
Assessment of avionics technology in European aerospace organizations [NASA-CR-189201] p 337 N95-24624
- HO, C.-M.**
Effects of time scales on lift of airfoils in an unsteady stream [HTN-95-81643] p 542 A95-87691
- HO, PATRICK Y.**
UHB engine fan broadband noise reduction study [NASA-CR-198357] p 580 N95-29641
- HO, Y.-L.**
Operational multi-scale environment model with grid adaptivity (OMEGA) application to aviation weather p 676 A95-93556
- HOADLEY, SHERWOOD T.**
Multiple-function digital controller system for active flexible wing wind-tunnel model [BTN-95-EIX95182619212] p 322 A95-76638
On-line analysis capabilities developed to support the active flexible wing wind-tunnel tests [BTN-95-EIX95182619213] p 296 A95-76639
Rolling maneuver load alleviation using active controls [BTN-95-EIX95182619217] p 270 A95-76643
Active load control during rolling maneuvers [NASA-TP-3455] p 129 N95-17397
- HOANG, N. T.**
Dynamic pitch-up of a delta wing [HTN-95-81633] p 462 A95-87681
- HOANG, TY**
A real-time algorithm for integrating differential satellite and inertial navigation information during helicopter approach [NASA-CR-197409] p 229 N95-21891
- HOCK, S. M.**
Wind technology development: Large and small turbines [DE95-000286] p 358 N95-26090
- HODGE, B. K.**
Supersonic axisymmetric conical flow solutions for different ratios of specific heats [BTN-95-EIX95152583263] p 306 A95-73584
- HODGES, DEWEY H.**
Stability analysis for elastically tailored rotor blades [ISBN 1-879921-01-4] p 635 A95-93703
Flutter analysis of composite box beams [NASA-CR-197931] p 294 N95-23392
- HODGES, WILLIAM T.**
The personal aircraft: Status and issues [NASA-TM-109174] p 223 N95-20688
- HODGKINSON, J.**
The importance of flying qualities design specifications for active control systems p 621 N95-31992
- HODGKINSON, JOHN**
The relation of handling qualities ratings to aircraft safety p 597 N95-31067
- HODKO, D.**
Corrosion of aircraft materials: Correlation between nanometer scale and macroscopic structural damage parameters [AD-A285930] p 241 N95-20299
- HOEIJMAKERS, H. W. M.**
Numerical investigation into vortical flow about a delta-wing configuration up to incidences at which vortex breakdown occurs in experiment [PB95-198024] p 593 N95-30837
- HOEKSTRA, M.**
Discretization of the parabolised Navier-Stokes equations p 638 A95-95362
- HOENLINGER, H.**
Structural aspects of active control technology p 623 N95-32006
- HOEPPNER, DAVID W.**
The role of fretting corrosion and fretting fatigue in aircraft rivet hole cracking p 94 N95-14470
The effects of pitting on fatigue crack nucleation in 7075-T6 aluminum alloy p 88 N95-14482
- HOFBECK, ERIC V.**
Transmission loss characteristics of aircraft sidewall systems to control cabin interior noise p 28 N95-11261
- HOFERT, GLENN D.**
Spectral analysis of vortex/free-surface interaction [AD-A283210] p 96 N95-14658
- HOFF, GREGORY E.**
Propulsion simulator for high bypass turbofan performance evaluation [SAE PAPER 931410] p 625 A95-93676
- HOFFBAUER, M. A.**
Hypersonic Gas-Surface Energy Accommodation Test Facility [DE94-014468] p 39 N95-12652
- HOFFENBERG, R.**
Wake measurements in a strong adverse pressure gradient [NASA-CR-197272] p 224 N95-21031
- HOFFLER, KEITH D.**
High-Alpha Research Vehicle (HARV) longitudinal controller: Design, analyses, and simulation results [NASA-TP-3446] p 17 N95-10860
- HOFFMAN, JOHN A.**
Design of a real-time wind turbine simulator using a custom parallel architecture p 449 N95-27979
- HOFFMAN, PETER M.**
Design and synthesis of a real-time controller for an unmanned air vehicle [AD-A289134] p 408 N95-26555
- HOGAN, P. A.**
Fault Diagnosis for condition monitoring applied to hydraulic circuits [CONGRESS PAPER C428-12-165] p 456 A95-91703
- HOGG, G. M.**
The Anglo-French Compact Laser Radar demonstrator programme p 703 N95-32501
- HOH, ROGER H.**
Unified criteria for ACT aircraft longitudinal dynamics p 607 N95-31065
The role of handling qualities specifications in flight control system design p 620 N95-31990
Proposed incorporation of mission-oriented flying qualities into MIL-STD-1797A [AD-A294211] p 698 N95-34306
- HOINKA, KLAUS P.**
North Atlantic air traffic within the lower stratosphere: Cruising times and corresponding emissions [HTN-95-91841] p 354 A95-80829
- HOL, P. A.**
Reanalysis of European flight loads data [AD-A282052] p 9 N95-11179
- HOLBOURN, P. E.**
MCMs for avionics: Technology selection and intermodule interconnection p 234 N95-20641
- HOLCOMB, LEE**
NASA High Performance Computing and Communications program [NASA-TM-4653] p 176 N95-18573
- HOLDEMAN, J. D.**
Numerical mixing calculations of confined reacting jet flows in a cylindrical duct [NASA-TM-106736] p 139 N95-18133
Crossflow mixing of noncircular jets [NASA-TM-106865] p 338 N95-24390
Effects of initial conditions on a single jet in crossflow [NASA-TM-107002] p 615 N95-30589
Jet mixing and emission characteristics of transverse jets in annular and cylindrical confined crossflow [NASA-TM-106976] p 616 N95-30698
Jet mixing in a reacting cylindrical crossflow [NASA-TM-106975] p 616 N95-30853
- HOLDER, SANDRA L.**
Development and flight testing of an Obstacle Avoidance System for US Army helicopters p 687 N95-32500
- HOLDREN, M. W.**
Chemical composition and photochemical reactivity of exhaust from aircraft turbine engines [HTN-95-51277] p 356 A95-80862
- HOLDRIDGE, GEOFFREY M.**
JTEC/WTEC annual report and program summary: 1993/94 [NASA-CR-198563] p 454 N95-28038
- HOLEHOUSE, IAN**
Thermo-acoustic fatigue design for hypersonic vehicle skin panels p 162 N95-19161
- HOLIFIELD, WALT**
Rapid prototyping of composite aircraft structures [SAE PAPER 931219] p 539 A95-87530
- HOLLAND, K. R.**
Near field noise prediction requirements [ISVR-TR-234] p 27 N95-11166
- HOLLAND, SCOTT D.**
Wind-tunnel blockage and actuation systems test of a two-dimensional scramjet inlet unstart model at Mach 6 [NASA-TM-109152] p 97 N95-15898
Two-dimensional scramjet inlet unstart model: Wind-tunnel blockage and actuation systems test [NASA-TM-109984] p 97 N95-15899
Mach 10 computational study of a three-dimensional scramjet inlet flow field [NASA-TM-4602] p 309 N95-23015
Mach 10 computational study of a three-dimensional scramjet inlet flow field [NASA-TM-4602] p 310 N95-23210
- HOLLINGSWORTH, WILLIAM B.**
Integration of a mechanical forebody vortex control system into the F-15 p 72 N95-14258
- HOLLO, STEVEN D.**
Quantitative investigation of compressible mixing: Staged transverse injection into Mach 2 flow [HTN-95-42330] p 404 A95-86159
- HOLLOWAY, C. MICHAEL**
Formal design and verification of a reliable computing platform for real-time control (phase 3 results) [NASA-TM-109140] p 33 N95-10873
- HOLMES, JOULES**
The OFP-6M transport jet [NASA-CR-197159] p 46 N95-12637
- HOLST, TERRY L.**
Computational fluid dynamics uses in fluid dynamics/aerodynamics education [NASA-TM-108834] p 8 N95-10847
Numerical solution of the full potential equation using a chimera grid approach [NASA-TM-110360] p 594 N95-32188
- HOLTHOFF, H.**
Numerical modeling and simulation of chemically reacting reentry flows p 525 A95-87387
- HOLZ, R. G.**
Numerical model for circulation-control flows [HTN-95-81632] p 461 A95-87680
- HOMAFAR, ABDOLLAH**
Dynamic behavior of a magnetic bearing supported jet engine rotor with auxiliary bearings [NASA-CR-197860] p 338 N95-24213
- HOMAREDA, M.**
Turbulence characteristics of supersonic boundary layer past a backward facing step [AIAA PAPER 95-6126] p 470 A95-90447
- HOMICZ, G. F.**
Navier-Stokes simulations of WECS airfoil flowfields [DE94-013341] p 7 N95-10226
- HONAMI, SHINJI**
Some considerations on system design of the hypersonic transport and supersonic air-intakes p 473 A95-91522
- HONDL, KURT D.**
The use of radar wind profiles to remove TDWR gust front algorithm false alarms caused by vertical wind shear p 661 A95-93488
- HONG, STEVEN W.**
An analytic modeling and system identification study of helicopter dynamics p 505 N95-29787

HOOD, R. E.

Behavior of an inversion-based precipitation retrieval algorithm with high-resolution AMPR measurements including a low-frequency 10.7-GHz channel
[HTN-95-70134] p 252 A95-70656

HOOD, ROBBIE E.

High-resolution imaging of rain systems with the advanced microwave precipitation radiometer
[HTN-95-70133] p 252 A95-70655

HOOK, SIMON

TIMS observations of surface emissivity in HAPEX-Sahel p 709 N95-33799

HOOPER, MATT

LCX: Proposal for a low-cost commercial transport [NASA-CR-197186] p 47 N95-12645

HOOPER, STEVEN J.

Analysis of warping effects on the static and dynamic response of a seat-type structure [NIAR-94-12] p 348 N95-24211

HOOSE, K. V.

Combustor kinetic energy efficiency analysis of the hypersonic research engine data p 148 N95-16321

HOPFNER, M.

Airborne measurements during the European Arctic Stratospheric Ozone Experiment column amounts of HNO₃ and O₃ derived from FTIR emission sounding [HTN-95-00742] p 445 A95-86312

HOPPEL, K. W.

Statistics of multi-look AIRSAR imagery: A comparison of theory with measurements p 320 N95-23947

HOPPER, DARREL G.

Draft standard for color active matrix liquid crystal displays (AMLCDs) in US Military aircraft. Recommended best practices [AD-A282950] p 49 N95-12591

HOPPER, JAMES

Systems engineering design and technical analyses for Strategic Avionics Crew-station Design Evaluation Facility (SACDEF) [AD-A286239] p 235 N95-22024

HOPSON, P., JR.

A hybrid electronically scanned pressure module for cryogenic environments [NASA-TM-110146] p 554 N95-29453

HOQUE, MUHAMMED S.

Dynamic response of NASA Rotor Test Apparatus and Sikorsky S-76 hub mounted in the 80- by 120-Foot Wind Tunnel [NASA-TM-108847] p 25 N95-11389

HORAK, K.

Solid-state data recorder, next development and use p 705 N95-33143

HORENSTEIN, M.

Comparison of electrostatic and aerodynamic forces during parachute opening [BTN-95-EIX95062487532] p 187 A95-69240

HORGAN, C. O.

Severe edge effects and simple complimentary interior solutions for thin-walled anisotropic and composite structures [AD-A290645] p 555 N95-29562

HORISAWA, HIDEYUKI

Studies on plasma jet igniters p 403 A95-82680

HORNER, M. B.

Preliminary results from a particle image velocimetry study of blade-vortex interaction [HTN-95-01098] p 547 A95-90284

HORNUNG, HANS G.

Elliptic tip effects on the vortex wake of an axisymmetric body at incidence [BTN-94-EIX94441386612] p 208 A95-67343

Elliptic tip effects on the vortex wake of an axisymmetric body at incidence [HTN-95-20938] p 464 A95-88977

HORSTMAN, C. C.

Heat-transfer measurements and computations of swept-shock-wave boundary-layer interactions [HTN-95-81634] p 541 A95-87682

HORSTMANN, K. H.

2-D airfoil tests including side wall boundary layer measurements p 158 N95-17847

HORTON, G. C.

The calculation of erosion in a gas turbine compressor rotor p 199 N95-19664

HORTON, RAY E.

Advanced composite fuselage technology p 535 N95-29034

HORWATH, JOHN

Partial discharge testing of high voltage wiring harness for airborne displays [AD-A289150] p 401 N95-27003

HOSHINO, HIDEO

Experimental study of the aerodynamic characteristics of the counter-rotation propellers p 474 A95-91562

HOSOKAWA, IWAO

Direct numerical simulation of incompressible homogeneous isotropic turbulence using NWT p 706 N95-34530

HOSP, THEODORE J.

Control system design for the MOD-5A 7.3 mW wind turbine generator p 440 N95-27985

HOTIMSKII, S.

A program for scientific and applied investigations using aerostat complexes p 182 A95-66304

HOU, GENE J. W.

Discrete shape sensitivity equations for aerodynamic problems [BTN-94-EIX94451393721] p 88 A95-61720

HOU, GENE W.

Methodology for sensitivity analysis, approximate analysis, and design optimization in CFD for multidisciplinary applications [NASA-CR-196981] p 58 N95-13201

HOUBOLT, JOHN C.

Special effects of gust loads on military aircraft p 133 N95-18605

HOUCK, JACOB

Simulation and model reduction for the active flexible wing program [BTN-95-EIX95182619211] p 295 A95-76637

HOUGHLAND, DANA S.

Standardization of aircraft noise insulation measures without compromising results p 561 A95-90115

HOUSH, CLINTON

A design trade study using CFD modeling of reaction jets for aerodynamic control [SAE PAPER 931384] p 586 A95-93660

HOUTMAN, E. M.

Quantitative comparison between interferometric measurements and Euler computations for supersonic cone flows [BTN-95-EIX95222650782] p 358 A95-79238

HOUWINK, R.

Sectional prediction of 3D effects for separated flow on rotating blades [PB94-201696] p 117 N95-18503

HOVENAC, EDWARD A.

A laser-based ice shape profilometer for use in icing wind tunnels [NASA-TM-106936] p 646 N95-30851

HOWARD, C. D.

Energy absorption device for shock loading [AD-D017476] p 706 N95-34449

HOWARD, CELESTE M.

Color control in a multichannel simulator display: The display for advanced research and training [AD-A279717] p 239 N95-20992

HOWARD, THOMAS J.

Reliability and maintainability [BTN-95-EIX95042477109] p 179 A95-68350

HOWELL, JAN M.

AGARD flight test techniques series. Volume 13: Reliability and maintainability [AGARD-AG-300-VOL-13] p 504 N95-29503

HOWELL, W. EDWARD

NASA evaluation of Type 2 chemical depositions [SAE PAPER 932582] p 495 A95-90086

HOYNIK, DAN

NASA Lewis Research Center Workshop on Forced Response in Turbomachinery [NASA-CP-10147] p 141 N95-19380

Steady potential solver for unsteady aerodynamic analyses p 141 N95-19382

HOZAKI, SHIG

Development and application of structural dynamics analysis capabilities [NASA-CR-197229] p 96 N95-14922

HOZUMI, KOICHI

Experimental investigation on aerothermodynamic characteristics of hypersonic transport p 473 A95-91525

HOZUMI, KOKI

Analysis of an MLS automatic landing control law for the NAL experimental research aircraft DO-228. 2: Curved approach and landing p 508 A95-91588

HOZUMI, KOICHI

Hypersonic wind tunnel test of sidewall compression type scramjet inlet p 410 A95-82320

HREHA, MARK A.

Flight test validation of a frequency-based system identification method on an F-15 aircraft [NASA-TM-4704] p 620 N95-31846

HSIANG, LIEN-PENG

Near-limit drop deformation and secondary breakup p 704 N95-32902

HSIAO, FEI-BIN

High angle-of-attack airfoil performance improvement by internal acoustic excitation [HTN-95-42347] p 372 A95-86176

HSU, L. L.

Perspective on thermal barrier coatings for industrial gas turbine applications p 345 N95-26128

HSU, SHIH-CHE

Solutions of generalized proportional navigation with maneuvering and nonmaneuvering targets [BTN-95-EIX95202637606] p 279 A95-76683

HSU, WAYNE W.

CFD analysis of turbopump volutes p 312 N95-23436

HU, HONG

Steady and unsteady three-dimensional transonic flow computations by integral equation method [NASA-CR-196777] p 10 N95-11582

Development of a rotary wing Navier-Stokes CFD code based on TLNS3D code [AD-A290421] p 554 N95-29387

Application of multigrid computational fluid dynamics (CFD) methods to rotor analysis [AD-A293012] p 648 N95-31475

HU, YONGYUN

Examination of conditions in the proximity of pilot reports of aircraft icing during storm-fest p 666 A95-93509

HU, Z.

Sound propagation from an arbitrarily oriented multipole placed near a plane, finite impedance surface [BTN-94-EIX94371338964] p 257 A95-70797

The propagation of sound from an arbitrarily oriented dipole over a finite impedance plane p 570 A95-88459

HU, ZHAO-FENG

Nonlinear decoupling control study for aircraft maneuvering flight [HTN-95-71130] p 408 A95-83491

HUA, J.

Numerical design methods for transonic NLF configurations p 471 A95-91498

HUANG, GEORGE

Compressible Navier-Stokes calculations of the flow over airfoil sections. Comparisons of 1st and 2nd order turbulence models [SAE PAPER 932510] p 546 A95-89183

HUANG, J. R.

Effect of curvature in the numerical simulation of an electrothermal de-icer pad [BTN-95-EIX95182619219] p 276 A95-76645

HUANG, JEN-KUANG

Panel flutter limit-cycle suppression with piezoelectric actuation [BTN-95-EIX95302731089] p 618 A95-94208

System identification of the Large-Angle Magnetic Suspension Test Fixture (LAMSTF) p 296 N95-23299

HUANG, JIA-YEN

Damage tolerance certification of a fighter horizontal stabilizer [BTN-95-EIX0619952748186] p 637 A95-94478

HUANG, JIN-KUANG

Multivariable adaptive control using only input and output measurements for turbojet engines [BTN-95-EIX95292721165] p 677 A95-92597

HUANG, JUI-TEN

Advanced composites structural concepts and materials technologies for primary aircraft structures. Structural response and failure analysis: ISPAN modules users manual [NASA-CR-4449] p 12 N95-10242

HUANG, JUI-TIEN

Advanced composites structural concepts and materials technologies for primary aircraft structures: Structural response and failure analysis [NASA-CR-4448] p 11 N95-10240

HUANG, Q.

Mechanical system reliability and risk assessment [BTN-95-EIX95142553046] p 304 A95-73452

HUANG, STEVE

An exploratory application of neural networks for airfoil design p 448 N95-26943

HUANG, T. T.

Flow structure in the lee of an inclined 6:1 prolate spheroid [BTN-94-EIX95011441127] p 348 A95-81027

HUANG, XU-SHENG

Non-linear viscoelastic-plastic constitutive relations for an aeronautical PMMA [HTN-95-71132] p 385 A95-83493

HUBBARD, DAVID C.

Altitude quing effectiveness of terrain texture characteristics in simulated low-altitude flight [AD-A294369] p 700 N95-34362

HUBBARD, H. H.

Measurement and prediction of broadband noise from large horizontal axis wind turbine generators p 451 N95-27990

- HUBBARD, HARVEY H.**
Noise control in aeroacoustics; Proceedings of the 1993 National Conference on Noise Control Engineering, NOISE-CON 93, Williamsburg, VA, May 2-5, 1993 [ISBN 0-931784-26-3] p 573 A95-90088
- HUBER, F. W.**
Aerodynamic design and analysis of a highly loaded turbine exhaust p 312 N95-23435
- HUBER, PETER**
X-31 quasi-tailless flight demonstration p 70 N95-14243
X-31 high angle of attack control system performance p 70 N95-14244
- HUBNER, JAMES P.**
Spectral mapping of quasiperiodic structures in a vortex flow [BTN-95-EIX0619952748165] p 589 A95-94459
- HUCHIN, J. P.**
New Trends in coatings developments for turbine blades: Materials processing and repair p 201 N95-19676
- HUDAK, S. J., JR.**
Analysis of small crack behavior for airframe applications p 95 N95-14484
- HUDSON, B.**
Doppler radar detection of vortex hazard indicators p 42 N95-13212
- HUDSON, R. D.**
Eglin Air Force Base Ram Accelerator Research Facility p 19 N95-10284
- HUEBNER, H.**
EURECA mission control experience and messages for the future p 149 N95-17252
- HUEBNER, L. D.**
Computational study of plume-induced separation on a hypersonic powered model [BTN-95-EIX95152582346] p 266 A95-73548
- HUECKEL, MACY**
Icarus Rewaxed: A high speed, low-cost general aviation aircraft for Aeroworld [NASA-CR-197155] p 45 N95-12609
- HUESCHER, RICHARD M.**
Modeling of Instrument Landing System (ILS) localizer signal on runway 25L at Los Angeles International Airport [NASA-TM-4588] p 125 N95-17384
- HUETE, RODRIGO J.**
Test and evaluation crew resource management p 483 A95-90867
- HUFF, DENNIS L.**
Flutter analysis of supersonic axial flow cascades using a high resolution Euler solver. Part 1: Formulation and validation [NASA-TM-105798] p 23 N95-10244
- HUFFAKER, R. MILTON**
Airport surveillance using a solid state coherent lidar p 41 N95-13207
- HUFFORD, GARY L.**
Alaska's volcanic ash warning system p 663 A95-93495
- HUGGE, PAUL B.**
Lean manufacturing for lean times [BTN-95-EIX95302730538] p 583 A95-94036
- HUGH, MAYLENE K.**
Weavability of dry polymer powder towpreg p 535 N95-29036
- HUGHES, BRET**
The OFP-6M transport jet [NASA-CR-197159] p 46 N95-12637
- HUGHES, D. A.**
Soft body impact on titanium fan blades p 200 N95-19671
- HUGHES, P.**
Advanced wind turbine design studies: Advanced conceptual study [DE93-000031] p 256 N95-20985
- HUGHES, T. C.**
TRISTAR 1: Evaluation methods for testing head-up display (HUD) flight symbology [NASA-TM-4665] p 288 N95-24030
- HUGHES, THOMAS C.**
KC-135 cockpit modernization study. Phase 1: Equipment evaluation [AD-A284099] p 131 N95-18398
- HUGO, G. R.**
Scar repairs to graphite/epoxy components p 396 N95-27523
- HUI, FRANK C. L.**
Experimental results for a hypersonic nozzle/afterbody flow field [NASA-TM-4638] p 274 N95-23250
- HUI, KENNETH**
Improving prediction: The incorporation of simplified rotor dynamics in a mathematical model of the bell 412HP [BTN-95-EIX95152584679] p 282 A95-73591
- HUISKEN, AMY B.**
Impact damage resistance of composite fuselage structure, part 2 p 533 N95-28838
- HULEK, T.**
Numerical solution of Euler and Navier-Stokes equations for 2D transonic problems p 638 A95-95366
- HULL, D. L.**
Design limit loads based upon statistical discrete gust methodology p 133 N95-18603
- HUMI, MAYER**
Turbulent effects on parachute drag [BTN-95-EIX0619952748193] p 591 A95-94482
- HUMM, P.**
Evaluation of neutron techniques for illicit substance detection [DE95-002988] p 300 N95-22764
- HUMMEL, D.**
Low-speed aerodynamic characteristics of a slender wing with vertical fins p 460 A95-87400
- HUMPHREY, R. J.**
Global cost and weight evaluation of fuselage keel design concepts p 501 N95-28840
- HUMPHREYS, CAROLINE M.**
The dynamic approach to rotor blade research: ARA's oscillatory test facility [ARA-MEMO-405] p 223 N95-20758
- HUNEK, M.**
Numerical solution of Euler and Navier-Stokes equations for 2D transonic problems p 638 A95-95366
- HUNG, Y. H.**
Impingement cooling of an isothermally heated surface with a confined slot jet [BTN-94-EIX94421348950] p 347 A95-78494
- HUNT, L. R.**
Nonlinear system guidance in the presence of transmission zero dynamics [NASA-TM-4661] p 309 N95-22804
- HUNT, M. L.**
Influence of injectant Mach number and temperature on supersonic film cooling [BTN-94-EIX94441386686] p 184 A95-68195
Flowfield measurements in supersonic film cooling including the effect of shock-wave interaction [HTN-95-42337] p 405 A95-86166
- HUNTER, CRAIG A.**
An approximate theoretical method for modeling the static thrust performance of non-axisymmetric two-dimensional convergent-divergent nozzles [NASA-CR-195050] p 273 N95-23193
- HUNTER, PAUL**
NASA High Performance Computing and Communications program [NASA-TM-4653] p 176 N95-18573
- HUNTLEY, M. S., JR.**
Guidelines for the design of GPS and LORAN receiver controls and displays [AD-A293753] p 602 N95-31572
- HURDLEBRINK, DEBRA**
New technologies for space avionics [NASA-CR-197574] p 150 N95-18196
- HUSSAIN, FAZLE**
Basic studies in turbulent shear flows [AD-A289145] p 437 N95-26998
- HUSSAINI, M. Y.**
Algorithmic trends in computational fluid dynamics; The Institute for Computer Applications in Science and Engineering (ICASE)/LaRC Workshop, NASA Langley Research Center, Hampton, VA, US, Sep. 15-17, 1991 [ISBN 0-387-94014-6] p 550 A95-91915
- HUTATSUDERA, NAOKI**
A conceptual design of the SST without horizontal tail p 498 A95-91520
- HUTCHEON, RICHARD J.**
Alaska's volcanic ash warning system p 663 A95-93495
- HWA, REBECCA**
Optimizing cockpit display configurations with a genetic algorithm system [AD-A289799] p 508 N95-29123
- HWOSCHINSKY, PETER V.**
Psycho-social safety perceptions: Helicopters as a case study p 596 A95-95192
- HYLANDER, KEN**
Maintenance programs [HTN-95-92310] p 365 A95-85354
- HYMER, T.**
Base drag prediction on missile configurations [BTN-95-EIX95152583256] p 266 A95-73557
Improved version of the Naval Surface Warfare Center aeroprediction code (AP93) [BTN-95-EIX95152583260] p 267 A95-73561
- HYMER, TOM**
The 1995 version of the NSWC aeroprediction code. Part 1: Summary of new theoretical methodology [AD-A291518] p 481 N95-29853
- HYNEK, DANIEL P.**
TDWR scan strategy implementation [AD-A284877] p 98 N95-15749
- IANNELLI, G. S.**
Accuracy and efficiency assessments for a weak statement CFD algorithm for high-speed aerodynamics [BTN-94-EIX95011441238] p 370 A95-84195
A Kutta condition conscious perturbation stream function boundary element algorithm for 2-D potential aerodynamics [ISBN 1-879921-01-4] p 587 A95-93751
- IBRAHIM, MOUNIR**
Investigation of water droplet trajectories within the NASA icing research tunnel [NASA-TM-107023] p 684 N95-32769
- ICHIKAWA, AKIO**
A singularity method for a two dimensional stratified shear flow p 473 A95-91513
- ICHIKAWA, T.**
Development of 70MW class superconducting generators [BTN-94-EIX95011440854] p 429 A95-82905
- ICHIMIYA, R.**
Vortex shedding noise control in idling circular saws using air ejection at the teeth [BTN-94-EIX94371347214] p 257 A95-69970
- IFJU, PETER G.**
Interlaminar shear test method development for long term durability testing of composites p 301 N95-23300
- ILCEWICZ, L.**
Designers' unified cost model p 424 N95-28464
- ILCEWICZ, L. B.**
Tension fracture of laminates for transport fuselage. Part 1: Material screening p 398 N95-28471
Local design optimization for composite transport fuselage crown panels p 398 N95-28473
Impact damage resistance of composite fuselage structure, part 1 p 399 N95-28482
- ILCEWICZ, LARRY B.**
Tension fracture of laminates for transport fuselage. Part 2: Large notches p 532 N95-28837
Advanced composite fuselage technology p 535 N95-29034
- ILIAKOPOULOU, ENNY**
Maintenance programs [HTN-95-92310] p 365 A95-85354
- ILINCA, FLORIN**
Adaptive remeshing for convective heat transfer with variable fluid properties [BTN-95-EIX95082502720] p 243 A95-71033
Adaptive finite element method for turbulent flow near a propeller [BTN-95-EIX95142553038] p 305 A95-73460
- ILLI, O. J., JR.**
An artificial neural network system for diagnosing gas turbine engine fuel faults [DE94-013960] p 138 N95-17371
- IMAL, KIWAMU**
Experiment and analysis on heat transfer of a scramjet leading edge model p 403 A95-82420
- IMBERT, N.**
Evaluation of the techniques of fuzzy control for the piloting an aircraft p 621 N95-31997
- IMMARIGEON, J. P.**
Protective coatings for compressor gas path components p 201 N95-19675
- IN, K. M.**
Two-dimensional viscous flow past a flat plate [HTN-95-42210] p 430 A95-84026
- INABA, KENJI**
The concept of high speed commercial transporter structure p 498 A95-91517
- INAGAKI, TOSHIHARU**
Flight evaluation of DGPS and DGPS-INS navigation systems p 382 A95-82462
Analysis of an MLS automatic landing control law for the NAL experimental research aircraft DO-228. 2: Curved approach and landing p 508 A95-91588
Flight reference display for powered-lift STOL aircraft [NAL-TR-1251] p 337 N95-25005
- INASHI, SADAMU**
Missile autopilot designs using full state feedback p 507 A95-91587
- INATANI, YOSHIFUMI**
The aerodynamic characteristics of cup-like body in supersonic flow p 427 A95-82407
Air data sensors for atmospheric reentry flight test of winged space vehicle p 413 A95-82412
Atmospheric reentry flight test of winged space vehicle p 414 A95-82483

- Reentry technology experiment on the first mission of reentry capsule 'EXPRESS' p 414 A95-82499
Development and flight results of fiber reinforced balloon p 384 A95-82511
- ING, D. N.**
Cost effective small-scale experiments to aid the design of ASTOVL aircraft [CONGRESS PAPER C428-9-098] p 475 A95-91695
- INGER, GEORGE R.**
Scaling of incipient separation in supersonic/transonic speed laminar flows [BTN-95-EIX95182619104] p 269 A95-76589
- INGLE, STEVEN J.**
Effects of high order dynamics on helicopter flight control law design [HTN-95-80852] p 290 A95-75094
- INGRAFFEA, ANTHONY R.**
Discrete crack growth analysis methodology for through cracks in pressurized fuselage structures [BTN-95-EIX0608952737538] p 633 A95-92751
Discrete crack growth analysis methodology for through cracks in pressurized fuselage structures p 166 N95-19473
- INGRAM, J. ED**
Advanced composites structural concepts and materials technologies for primary aircraft structures: Design/manufacturing concept assessment [NASA-CR-4447] p 12 N95-10316
- INGRAM, J. EDWARD**
Advanced composites structural concepts and materials technologies for primary aircraft structures: Structural response and failure analysis [NASA-CR-4448] p 11 N95-10240
Advanced composites structural concepts and materials technologies for primary aircraft structures: Structural response and failure analysis: ISPAN modules users manual [NASA-CR-4449] p 12 N95-10242
ISPAN (Interactive Stiffened Panel Analysis): A tool for quick concept evaluation and design trade studies p 533 N95-28846
- INGRAM, ROBERT B.**
Determination of minimum fuel octane number piston aircraft engines [SAE PAPER 931230] p 528 A95-88961
- INOKUCHI, HAMAKI**
Flight Test Monitoring System using X-window p 500 A95-91574
- INOUE, TAKASHI**
A conceptual design of the SST without horizontal tail p 498 A95-91520
- INOUE, YASUTOSHI**
NAL aerothermodynamic probing and CFD verification mission in OREX experiment p 368 A95-82413
- INSELBERG, ALFRED**
Multidimensional lines 2: Proximity and applications [BTN-94-EIX94341340329] p 61 A95-60865
- INWOOD, SIMON**
Stratus' tephigram as a training/forecasting tool p 657 A95-93465
- IOB, M.**
Programmable cockpit research simulator [AD-A279219] p 204 N95-19848
- IRELAND, GLEN J.**
Design of a vehicle based system to prevent ozone loss [NASA-CR-197199] p 48 N95-12702
- IRELAND, P. T.**
Particle deposition in gas turbine blade film cooling holes p 199 N95-19661
- ISAAC, GEORGE A.**
Aircraft icing measurements in East Coast winter storms [HTN-95-60505] p 214 A95-68756
Airplane icing research at the Boeing Company: Participation in the second Canadian Atlantic Storms Program p 674 A95-93544
- ISAKETT, D.**
High temperature aspects of the European Hermes programs p 524 A95-87379
- ISHIDA, YOJI**
High subsonic and high Reynolds number wind tunnel tests of two-dimensional natural-laminar-flow airfoils with suction boundary layer control p 472 A95-91508
Numerical and experimental study of drag characteristics of two-dimensional HLFC airfoils in high subsonic, high Reynolds number flow [NAL-TR-1244T] p 331 N95-24998
- ISHIGURO, MITSUO**
Application of CFD technique for HYFLEX aerodynamic design p 693 N95-34542
- ISHIGURO, TOMIKO**
Three-dimensional analysis of scramjet nozzle flows [BTN-94-EIX94441380978] p 196 A95-68162
- ISHIHARA, TADASHI**
Surface morphology and structure of carbon-carbon composites in high-energy sliding contact [BTN-94-EIX94371347996] p 206 A95-69164
- ISHII, MASAHIRO**
Life evaluation of a low power arcjet thruster p 403 A95-82337
- ISHII, NOBUAKI**
Development and flight results of fiber reinforced balloon p 384 A95-82511
- ISHIKAWA, KAZUTOSHI**
Flight evaluation of DGPS and DGPS-INS navigation systems p 382 A95-82462
Performance evaluation test of GPS/DGPS navigation system installed in the NAL Dornier 228: Preliminary ground test results p 487 A95-91575
Analysis of an MLS automatic landing control law for the NAL experimental research aircraft DO-228. 2: Curved approach and landing p 508 A95-91588
Flight evaluation of GPS/DGPS sensor systems installed in NAL Do228 [NAL-TR-1230] p 382 N95-26585
- ISHIKAWA, MUNENORI**
Development of Fly-By-Wire system for BK117 p 516 A95-91506
- ISHIMOTO, SHINJI**
A guidance concept for hypersonic aerospacecrafts p 526 A95-91549
- ISIDA, R.**
Neural network approach to identification of aerodynamic loads on a wing. 1: Application to cantilevered beam models p 475 A95-91568
- ISOGAI, KOJI**
Numerical simulation of unsteady viscous flow around an airfoil with oscillating spoiler p 685 N95-34547
- ITO, RYOZO**
Parallel computation of transonic flows about an aircraft configuration using multi-block structured grids p 685 N95-34537
- ITO, T.**
Aerodynamic characteristics of supersonic air-intake/aircraft integrated models p 472 A95-91512
- ITO, TAKESHI**
Hypersonic wind tunnel test of sidewall compression type scramjet inlet p 410 A95-82320
A shock tunnel test of a winged hypersonic research vehicle p 474 A95-91538
- ITOH, KATSUHIRO**
Experiment and analysis on heat transfer of a scramjet leading edge model p 403 A95-82420
Numerical simulation of high enthalpy shock tunnel p 700 N95-34514
- ITOH, NOBU TAKE**
Multiple instabilities of three-dimensional boundary layers along a concave wall [HTN-95-71126] p 429 A95-83487
Observation of traveling waves in the three-dimensional boundary layer along a yawed cylinder [HTN-95-61064] p 430 A95-83648
Instability of three-dimensional boundary layers due to streamline curvature [HTN-95-61070] p 430 A95-83654
Nonlinear analysis of the Gortler instability [BTN-95-EIX95282705926] p 455 A95-89664
- ITOH, YASUHIRO**
Mechanical properties of advanced toughened bismaleimide matrix composite p 530 A95-91570
- IVANOV, M. S.**
Verification of engineering methods of aerodynamics for reentry vehicles by DSMC p 525 A95-87386
- IVANOV, MIKHAIL J.**
Solution of Navier-Stokes equations using high accuracy monotone schemes p 161 N95-19019
The mathematical models of flow passage for gas turbine engines and their components p 140 N95-19020
Perspective problems of gas turbine engines simulation p 140 N95-19026
- IVANOVA, A. R.**
Aviation weather forecasting automated methods in the RAFC Moscow and the Airport Vnukovo p 669 A95-93523
- IVEY, REBECCA H.**
Transmittance characteristics of US Army rotary-wing aircraft transparencies [AD-A295035] p 693 N95-34793
- IWASA, MASAMICHI**
Grid generation around airfoil with a flap using boundary element method p 686 N95-34552
- IWASAKI, AKIHITO**
Low speed aerodynamic characteristics of delta wings with vortex flaps: 60 deg and 70 deg delta wings [NAL-TR-1245] p 331 N95-25105
Experimental investigation of static and dynamic ground effect on HOPE ALFLEX vehicle [NAL-TR-1236] p 388 N95-26525
- IWASAKI, KAZUO**
Fundamental wind tunnel experiments on low-speed flutter of a tip-fin configuration wing [NAL-TR-1228] p 332 N95-25762
- IWATA, JIRO**
The near-wake flow behavior of an oscillating airfoil with modified trailing edge p 375 N95-26953
- IWATA, T.**
Development of a pilot tube with multi-hole pyramidal head. 2: A five-hole yaw probe of engineering model p 522 A95-91577
- IWATSUKI, K.**
Electro-optic characterization of ultrafast photodetectors using adiabatically compressed soliton pulses [BTN-94-EIX94381359637] p 257 A95-72675
- IVYER, RAVI**
The Advanced Avionics Subsystem Technology Demonstration Program p 234 N95-20636

J

- JACKMAN, CHARLES H.**
Sensitivity of two-dimensional model predictions of ozone response to stratospheric aircraft: An update [HTN-95-A0863] p 318 A95-76267
Effects of a polar stratosphere cloud parameterization on ozone depletion due to stratospheric aircraft in a two-dimensional model [HTN-95-A1038] p 443 A95-84543
Three dimensional model calculations of the global dispersion of high speed aircraft exhaust and implications for stratospheric ozone loss p 26 N95-10657
- JACKSON, ANTHONY C.**
Advanced textile applications for primary aircraft structures p 399 N95-28476
Textile composite fuselage structures development p 534 N95-29033
- JACKSON, E. BRUCE**
Manual for a workstation-based generic flight simulation program (LaRCsim), version 1.4 [NASA-TM-110164] p 518 N95-30327
- JACKSON, KATHERINE**
Industry review of a crew-centered cockpit design process and toolset [AD-A282966] p 130 N95-17661
- JACKSON, MARK E.**
An echo motion algorithm for air traffic management using a national radar mosaic p 667 A95-93513
- JACKSON, R. W.**
Configuration and other differences between Black Hawk and Seahawk helicopters in military service in the USA and Australia [AR-008-386] p 336 N95-25935
- JACKSON, RYMOND H.**
Shear buckling analysis of a hat-stiffened panel [NASA-TM-4644] p 158 N95-17490
- JACOB, DENIS**
Stratus' tephigram as a training/forecasting tool p 657 A95-93465
- JACOB, THOMAS**
High accuracy navigation and landing system using GPS/IMU system integration [BTN-94-EIX94441386129] p 189 A95-68185
- JACOBS, E. W.**
Observed acoustic and aeroelastic spectral responses of a MOD-2 turbine blade to turbulence excitation p 451 N95-27991
- JACOBS, J. H.**
Acoustic fatigue characteristics of advanced materials and structures p 174 N95-19157
- JACOBSON, M. Z.**
Analysis of the physical state of one Arctic polar stratospheric cloud based on observations [HTN-95-70917] p 351 A95-77982
- JACQUIN, L.**
Phenomenological description and simplified modelling of the vortex wake issuing from a jet in a crossflow [BTN-94-EIX94441385754] p 184 A95-68218
- JAIN, AMOLAK C.**
Rarefied gas effects on aerobraking/reentry vehicles with wakes [NASA-CR-196586] p 415 N95-27093
- JAIN, ATUL**
Dynamic imaging and RCS measurements of aircraft [BTN-95-EIX95202637582] p 347 A95-78576
- JAIN, SULEKH C.**
Trends in aerospace forgings in the 1990s [HTN-95-B0408] p 456 A95-90756
- JALVING, B.**
Results from tests of the Kearsott T16-B Inertial Measurement Unit [PB95-212031] p 644 N95-30502
Results from tests of the Honeywell integrated flight management unit [PB95-211355] p 601 N95-30597

- JAMES, KEVIN D.**
Comparison of full-scale, small-scale, and CFD results for F/A-18 forebody slot blowing p 72 N95-14255
- JAMES, R. D.**
Development of an intelligent tool-condition monitoring system for FMS [CONGRESS PAPER C428-32-012] p 583 A95-93617
- JAMESON, ANTONY**
Static shape control for adaptive wings [HTN-95-A1767] p 627 A95-93330
Optimum aerodynamic design via boundary control [NASA-CR-195882] p 36 N95-11877
Control theory based airfoil design using the Euler equations [NASA-CR-196360] p 36 N95-11884
Optimum aerodynamic design via boundary control p 127 N95-16565
Aerodynamic shape optimization of wing and wing-body configurations using control theory [NASA-CR-198024] p 335 N95-25334
Computational algorithms for aerodynamic analysis and design [AD-A291084] p 482 N95-29972
Requirements and trends of computational aerodynamics as a tool for aircraft design p 692 N95-34506
- JAMISON, BRIAN D.**
A prototype for displaying aviation forecast variables using Eta numerical model output p 676 A95-93555
- JANARDAN, B. A.**
Active control of fan noise-feasibility study. Volume 1: Flyover system noise studies [NASA-CR-195392-VOL-1] p 258 N95-21888
- JANDOLFINI, P.**
The DCAF: A high-enthalpy long-duration, direct-connect scramjet test facility [AIAA PAPER 95-6130] p 512 A95-90450
- JANECKI, DARIUSZ**
Actuating signals in adaptive control systems [IFTR-13/1994] p 361 N95-26330
- JANIK, TADEUSZ**
Effect of initial conditions on the response of nonlinear dynamical systems with the application to helicopter rotor dynamics [ISBN 1-879921-01-4] p 605 A95-93731
- JANOVSKY, R.**
Design optimization of an airbreathing aerospaceplane p 524 A95-87382
- JANOWITZ, J.**
Artificial intelligence with applications for aircraft [DOT/FAA/CT-94/41] p 99 N95-13895
Digital systems validation. Chapter 20 Artificial Intelligence with applications for aircraft. Handbook, volume 2 [AD-A288492] p 448 N95-26638
- JANSEN, KENNETH**
Unstructured-grid large-eddy simulation of flow over an airfoil p 225 N95-22448
- JANUS, RAY**
A PC-based interactive simulation of the F-111C Pavé Tack system and related sensor, avionics and aircraft aspects [AD-A285500] p 129 N95-16969
- JARFALL, L.**
Verification of the damage tolerance of a fighter aircraft p 388 A95-85897
- JARRABET, G. P.**
Compliant interlayer [BTN-95-EIX95142562401] p 304 A95-73439
- JARVIS, M. S.**
Applicability of electrically driven accessories for turboshaft engines [BTN-95-EIX95292721153] p 612 A95-92589
- JAWORSKI, WITOLD**
A tool for airframe shaping - idea and application [SAE PAPER 931224] p 491 A95-87568
- JEGLEY, DAWN**
Effect of low-speed impact damage and damage location on behavior of composite panels p 426 N95-28481
- JENG, YAUG-FAA**
Multiaxis pilot ratings for damaged aircraft [BTN-95-EIX95182619128] p 269 A95-76605
- JENKINS, L. N.**
A study of the vortex flow over 76/40-deg double-delta wing [NASA-CR-195032] p 314 N95-23466
- JENKINS, MICHAEL D.**
Integrated voice and data communications for air traffic service applications p 600 A95-95090
- JENNIONS, IAN K.**
Elements of a modern turbomachinery design system p 90 N95-14129
The role of CFD in the design process p 90 N95-14135
- JENSSEN, CARL B.**
Implicit multiblock Euler and Navier-Stokes calculations [HTN-95-A1755] p 634 A95-93318
- JEONG, DAVID Y.**
Testing and analysis of flat and curved panels with multiple cracks p 93 N95-14460
Nonlinear bulging factor based on R-curve data p 94 N95-14476
Evaluation of the fuselage lap joint fatigue and terminating action repair p 166 N95-19477
- JESKE, JAMES A.**
Flightpath synthesis and HUD scaling for V/STOL terminal area operations [NASA-TM-110348] p 383 N95-26587
- JESUROGA, RICHARD T.**
Using ATMS weather products for air traffic strategic planning p 672 A95-93536
- JHA, R. M.**
Geodesic constant method: A novel approach to analytical surface-ray tracing on convex conducting bodies [BTN-95-EIX95302731054] p 637 A95-94205
- JIANG, H.**
Role of Kutta waves on oscillatory shock motion on an airfoil [HTN-95-81642] p 542 A95-87690
- JIANG, XINGHONG**
Direct splitting of coefficient matrix for numerical calculation of transonic nozzle flow [BTN-94-EIX94481415356] p 103 A95-65346
- JIBB, D. J.**
High performance backplane components for modular avionics p 247 N95-20653
- JIJEN, J.**
Field-consistent element applied to flutter analysis of circular cylindrical shells [BTN-94-EIX94341341971] p 56 A95-60871
- JIN, G.**
Two-equation turbulence model for unsteady separated flows around airfoils [BTN-95-EIX95142553054] p 262 A95-73444
- JIWAN, XU**
Thermal design of returnable satellites [AD-A294113] p 701 N95-34500
- JOBY, M. J.**
Design trends in propulsion control systems [CONGRESS PAPER C428-33-123] p 610 A95-93620
- JOHNK, R. T.**
Measurements of shielding effectiveness and cavity characteristics of airplanes [PB94-210051] p 244 N95-20191
- JOHNSON, BONNIE L.**
Full span flapersons for a biplane p 391 N95-26954
- JOHNSON, C. G.**
Effects of satellite bunching on the probability of collision in geosynchronous orbit [BTN-95-EIX95152583276] p 298 A95-73577
- JOHNSON, CALVIN R.**
Hypervelocity Impact Test Facility: A gun for hire [TABES PAPER 94-605] p 86 N95-14639
- JOHNSON, D. G.**
Comparison of column abundances from three infrared spectrometers during AASE 2 [HTN-95-70946] p 352 A95-78011
- JOHNSON, D. M.**
Load alleviation for civil transport aircraft [CONGRESS PAPER C428-35-057] p 604 A95-93627
Electromagnetic reverberation characteristics of a large transport aircraft [AD-A282923] p 82 N95-15392
- JOHNSON, DAVID G.**
Chemical change in the arctic vortex during AASE 2 [HTN-95-70947] p 352 A95-78012
- JOHNSON, ERIC R.**
Compression strength of composite primary structural components [NASA-CR-197554] p 160 N95-18388
Load transfer in the stiffener-to-skin joints of a pressurized fuselage [NASA-CR-198610] p 439 N95-27865
- JOHNSON, F. T.**
TranAir: A full-potential, solution-adaptive, rectangular grid code for predicting subsonic, transonic, and supersonic flows about arbitrary configurations. User's manual [NASA-CR-4349] p 377 N95-28230
TranAir: A full-potential, solution-adaptive, rectangular grid code for predicting subsonic, transonic, and supersonic flows about arbitrary configurations. Theory document [NASA-CR-4348] p 378 N95-28265
- JOHNSON, INGMAR**
An investigation of polynomial calibrations methods for wind tunnel balances p 144 N95-16258
- JOHNSON, J. T.**
Use of WSR-88D data in the FAA's weather impacted aerospace product p 658 A95-93469
Investigation of outflow strength variability in Florida downburst-producing storms p 659 A95-93476
- JOHNSON, JAMES E.**
An intercomparison of aircraft instrumentation for tropospheric measurements of carbonyl sulfide, hydrogen sulfide, and carbon disulfide [HTN-95-91856] p 355 A95-80844
An intercomparison of instrumentation for tropospheric measurements of dimethyl sulfide: Aircraft results for concentrations at the parts-per-trillion level [HTN-95-91857] p 355 A95-80845
- JOHNSON, JERRY**
Application of damage tolerance methodology in certification of the Piaggio P-180 Avanti p 399 N95-28480
- JOHNSON, MADELEINE R.**
Alternatives to ozone depleting refrigerants in test equipment p 630 N95-31767
- JOHNSON, MATT**
Design of a vehicle based system to prevent ozone loss [NASA-CR-197199] p 48 N95-12702
- JOHNSON, THOMAS D., JR.**
Quantifiable vortex features of F-106B aircraft at subsonic speeds [BTN-95-EIX0619952748161] p 588 A95-94455
- JOHNSON, W. G.**
Buffeting tests in a cryogenic windtunnel [HTN-95-92833] p 470 A95-90751
- JOHNSON, W. L.**
Collected papers of the Soar/IFOR project, Spring 1994 [AD-A280063] p 238 N95-20624
- JOHNSON, W. S.**
Modeling and life prediction methodology for Titanium Matrix Composites subjected to mission profiles [NASA-TM-109148] p 55 N95-11915
- JOHNSON, WALTER A.**
Identification of higher order helicopter dynamics using linear modeling methods [HTN-95-80851] p 290 A95-75093
- JOHNSON, WALTER J.**
Cueing light configuration for aircraft navigation [NASA-CASE-ARC-11982-1] p 280 N95-23393
- JOHNSON, WALTER W.**
The selective use of functional optical variables in the control of forward speed [NASA-TM-108849] p 35 N95-12227
- JOHNSON, WILLIAM R.**
Maintenance-free lead acid battery for inertial navigation systems aircraft [BTN-95-EIX95292721316] p 633 A95-92511
- JOHNSTON, DONALD E.**
Identification of higher order helicopter dynamics using linear modeling methods [HTN-95-80851] p 290 A95-75093
- JOHNSTON, G. W.**
Compressible Navier-Stokes computations of multielement airfoil flows using multiblock grids [HTN-95-42327] p 371 A95-86156
- JOHNSTON, GORDON T.**
Results and performance of multi-site reference station differential GPS [BTN-95-EIX95112522534] p 190 A95-69329
- JOHNSTON, J. M.**
Unsteady flow phenomena in discrete passage diffusers for centrifugal compressors [AD-A281412] p 155 N95-16163
- JOHNSTON, NORMAN J.**
Recent progress in NASA Langley textile reinforced composites program p 425 N95-28475
Weavability of dry polymer powder towpreg p 535 N95-29036
- JOHNSTON, P. H.**
New nondestructive techniques for the detection and quantification of corrosion in aircraft structures p 315 N95-23512
- JOHNSTON, S.**
Period evolution of PSR B1259-63: Evidence for propeller-torque spindown [HTN-95-B0194] p 581 A95-87903
- JOHNSTON, S. L.**
A surgical support system for Space Station Freedom p 149 N95-16776
- JOLLY, G. W.**
Validation of empirical orbit error corrections using crossover difference differences [HTN-94-00912] p 25 A95-60227

JOLLY, STEVEN

An integrated system to improve aviation weather forecasts for the Alaska Range p 656 A95-93460

JONAS, P. R.

Microphysical and radiative properties of small cumulus clouds over the sea [HTN-95-A0526] p 255 A95-73180

On the link between cloud-top radiative properties and sub-cloud aerosol concentrations [HTN-95-A0527] p 255 A95-73181

JONES, A. E.

Sensitivity of supersonic aircraft modelling studies to HNO₃ photolysis rate [HTN-95-11475] p 353 A95-79453

JONES, C. J.

Aircraft noise and sleep disturbance: A field study [HTN-95-92543] p 558 A95-87363

JONES, D. C.

Aircraft measurements of water vapour continuum absorption at millimetre wavelengths [HTN-95-90884] p 253 A95-72393

JONES, D. J.

Surface pressure and wake drag measurements on the Boeing A4 airfoil in the IAR 1.5X1.5m Wind Tunnel Facility p 110 N95-17850

JONES, HENRY E.

Sensitivity derivatives for three dimensional supersonic Euler code using incremental iterative strategy [HTN-95-20845] p 545 A95-88106

JONES, JACK

Immersion/two phase cooling p 246 N95-20648

JONES, JESSE

Precision landing system mathematical modeling study report for Andrews Air Force Base, runway 19L, Camp Springs, MD [AD-A289015] p 384 N95-27903

JONES, L. A.

Improving the fire resistance of aircraft structures [CONGRESS PAPER C428-31-152] p 603 A95-93616

JONES, LISA E.

Effects of floor location on response of composite fuselage frames p 423 N95-28439

JONES, R.

Bonded composite repair of cracked load-bearing holes [BTN-94-EIX94401360553] p 243 A95-71867

Residual strength of composites with multiple impact damage [BTN-94-EIX94511433967] p 701 A95-96664

Residual strength of composites with multiple impact damage [AD-A284230] p 87 N95-14409

Development of a composite repair and the associated inspection intervals for the F-111C stiffener runout region p 66 N95-14477

JONES, R. L.

An overview of the EASOE campaign [HTN-95-00702] p 443 A95-86272

JONES, R. R.

Temperature effects on acoustic interactions between altitude test facilities and jet engine plumes [NASA-CR-197638] p 258 N95-21170

JONES, R. R., III

Screach tones from free and ducted supersonic jets [HTN-95-51647] p 432 A95-85029

JONES, RANDOLPH M.

Collected papers of the Soar/IFOR project, Spring 1994 [AD-A280063] p 238 N95-20624

JONES, S. E.

The coplanar projectile motion problem including the effects of lift and drag [ISBN 1-879921-01-4] p 635 A95-93723

JONES, T. V.

Particle deposition in gas turbine blade film cooling holes p 199 N95-19661

JONES, WILLIAM T.

A grid generation system for multi-disciplinary design optimization p 567 N95-28763

JONSSON, H. H.

Performance of a focused cavity aerosol spectrometer for measurements in the stratosphere of particle size in the 0.06-2.0-micrometer-diameter range [HTN-95-90914] p 253 A95-72423

JORDAN, DICK

Testing in the ARA Transonic Wind Tunnel [ARA-MEMO-395] p 239 N95-20799

JORDAN, T. L.

Dynamic Stability Instrumentation System (DSIS). Volume 1: Hardware description [NASA-TM-109160-VOL-1] p 171 N95-18899

JOSHI, M. N.

Recent trends in balloon flights from TIFR's National Balloon Facility, Hyderabad p 191 A95-66300

JOSHI, MAHENDRA C.

Noise impact of advanced high lift systems [NASA-CR-195028] p 362 N95-26160

JOST, G. S.

A review of Australian and New Zealand investigations on aeronautical fatigue during the period Apr. 1993 - Mar. 1995 [AR-009-202] p 397 N95-27918

JOUNOUCHI, TADAMASA

Role of computational fluid dynamics in aeronautical engineering. Number 12: Formulation and verification of uni-particle upwind schemes for the Euler equations p 707 N95-34540

JU, YIGUANG

Ignition analysis of hydrogen/air mixture in supersonic mixing layer p 416 A95-82301

JUCKS, K. W.

Comparison of column abundances from three infrared spectrometers during AASE 2 [HTN-95-70946] p 352 A95-78011

JUCKS, KENNETH W.

Chemical change in the arctic vortex during AASE 2 [HTN-95-70947] p 352 A95-78012

JUHANY, K. A.

Influence of injectant Mach number and temperature on supersonic film cooling [BTN-94-EIX94441386686] p 184 A95-68195

Flowfield measurements in supersonic film cooling including the effect of shock-wave interaction [HTN-95-42337] p 405 A95-86166

JULES, KENOL

Application of pressure sensitive paint in hypersonic flows [NASA-TM-106824] p 223 N95-20794

JULL, EDWARD V.

Depolarizing trihedral corner reflectors for radar navigation and remote sensing [BTN-95-EIX95302727634] p 636 A95-94108

JUMPER, STEPHEN J.

Aircraft noise prediction program theoretical manual: Rotorcraft System Noise Prediction System (ROTONET), part 4 [NASA-TM-83199-PT-4] p 451 N95-26392

JUNG, SUNG NAM

Aeroelastic response of composite rotor blades considering transverse shear and structural damping [HTN-95-81647] p 542 A95-87695

JUNG, YOON

Comprehensive aeromechanics analysis of complex rotorcraft using 2GCHAS [HTN-94-00695] p 2 A95-60174

JUNGER, M.

The acoustic characteristics of turbomachinery cavities [NASA-CR-4671] p 476 N95-28720

JURISSON, KARL R.

TIM-SCT cable testing protocol [AD-A286633] p 231 N95-20772

JURKOVICH, MARK S.

Computational aerodynamic analysis on the Open Skies aircraft [SAE PAPER 932514] p 466 A95-89187

Open Skies project computational fluid dynamic analysis [AD-A285928] p 223 N95-19991

K

KACHURIN, V. K.

Laser device for measuring a vessel's speed [HTN-95-60992] p 361 A95-80633

KADOKURA, A.

Polar Patrol Balloon system and preliminary experimental results p 368 A95-82513

KADOWAKI, M.

Study on the turbine vane and blade for a 1500 C class industrial gas turbine [BTN-94-EIX95011441254] p 431 A95-84211

KAERCHER, B.

Dynamics of aircraft exhaust plumes in the jet-regime [HTN-95-51275] p 355 A95-80860

KAHLA, N. BEN

Equivalent beam-column analysis of guyed towers [BTN-95-EIX95262696644] p 435 A95-85519

KAHLE, ANNE

TIMS observations of surface emissivity in HAPEX-Sahel p 709 N95-33799

KAI, YAN YIP

Use of MOBITEK wireless wide area networks as a solution to land-based positioning and navigation [BTN-94-EIX94441386132] p 189 A95-68188

KAISER, MARY K.

Cueing light configuration for aircraft navigation [NASA-CASE-ARC-11982-1] p 280 N95-23393

KAISER, TERI

Experimental/analytical approach to understanding mistuning in a transonic wind tunnel compressor [NASA-TM-108833] p 95 N95-14617

KAJI, SHOJIRO

A study on the convergence of a 3-D Euler code for cascade flow calculations p 706 N95-34508

Static pressure drop by swirling flow of an internal cooling air system through a turbine shaft p 698 N95-34560

KALDELLIS, J. K.

Investigation of shear layer transition using various turbulence models p 248 N95-21096

KALKHORAN, I. M.

Airfoil pressure measurements during oblique shock-wave/vortex interaction in a Mach 3 stream [HTN-95-81641] p 542 A95-87689

KALKHORAN, IRAJ M.

Research instrumentation for polytechnic university's supersonic wind tunnel facility [AD-A290232] p 523 N95-29468

KALLERGIS, KONSTANTIN M.

Flyover noise reduction of piston-engine propeller aeroplanes using an active noise control technique [SAE PAPER 931218] p 509 A95-87466

KALLERGIS, MICHAEL K.

Flyover noise reduction of piston-engine propeller aeroplanes using an active noise control technique [SAE PAPER 931218] p 509 A95-87466

KALTENBACH, HANS-JAKOB

Large-eddy simulation of flow through a plane, asymmetric diffuser p 250 N95-22449

KALUGINA, G. YU.

Aviation weather forecasting automated methods in the RAFC Moscow and the Airport Vnukovo p 669 A95-93523

KAMBLE, S. H.

Mobile domes for TACTIC telescope p 453 A95-86113

KAMMEYER, MARK

Application of wavelet-filtering techniques to intermittent turbulent and wall pressure events. Part 1: Exploratory results [AD-A286077] p 247 N95-20849

KAN, HAN-PIN

Analysis of composite structures with delaminations under combined bending and compression p 422 N95-28429

Reliability analysis of composite structures p 423 N95-28441

KAN, S. H.-T.

Electromagnetic on-aircraft antenna radiation in the presence of composite plates [NASA-CR-196126] p 58 N95-12856

KANADE, TAKEO

Research on an autonomous vision-guided helicopter [AIAA PAPER 94-1240-CP] p 18 N95-11510

KANAI, K.

Application of restructurable flight control system to large transport aircraft [BTN-95-EIX95282706666] p 515 A95-89639

KANARACHOS, A.

Multigrid solution for the compressible Euler equations by an implicit characteristic-flux-averaging p 642 A95-95459

KANAWATI, GHANI

The Advanced Avionics Subsystem Technology Demonstration Program p 234 N95-20636

KANDA, HIROSHI

Flow visualization studies on sidewall effects in two-dimensional transonic airfoil testing [BTN-95-EIX95152582313] p 264 A95-73516

High subsonic and high Reynolds number wind tunnel tests of two-dimensional natural-laminar-flow airfoils with suction boundary layer control p 472 A95-91508

Numerical and experimental study of drag characteristics of two-dimensional HLFC airfoils in high subsonic, high Reynolds number flow [NAL-TR-12447] p 331 N95-24998

KANDA, TAKESHI

Effect of film cooling/regenerative cooling on scramjet engine performances [NAL-TR-1242] p 339 N95-24990

KANDBO, STANLEY W.

NASA-Lewis tests Allison ASTOVL nozzle [HTN-95-20603] p 404 A95-84784

KANDBO, STANLEY W.

Lycoming to test new engine core [HTN-95-41393] p 288 A95-76389

Cypher moves toward autonomous flight [HTN-95-41394] p 283 A95-76390

KANE, RUSSELL

The legal status and liability of the copilot, part 2 [HTN-95-A0578] p 452 A95-83158

KANEKO, ATSUSHI

Experimental study of shock/shock interference heating on a swept cylinder p 472 A95-91510

- Experimental study of the aerodynamic characteristics of the counter-rotation propellers p 474 A95-91562
- KANEKO, SHINICHI**
Experimental study of the aerodynamic characteristics of the counter-rotation propellers p 474 A95-91562
Wake velocity measurement of counter-rotation propellers p 474 A95-91563
- KANG, GEORGE S.**
Speech analysis and synthesis based on pitch-synchronous segmentation of the speech waveform [AD-A288824] p 435 N95-26349
- KANG, JIAREN**
Nonlinear observer and its application in flight control p 447 A95-82449
- KANG, KI HO**
Electro-hydrostatic actuator controller design using quantitative feedback theory [AD-A289220] p 409 N95-26957
- KANG, SHIN-HYOUNG**
Numerical calculations of the turbulent flow through a controlled diffusion compressor cascade [BTN-95-EIX95282710056] p 632 A95-92473
- KANG, TAESAM**
Design of an effective controller via disturbance accommodating left eigenstructure assignment [BTN-95-EIX95282706663] p 565 A95-88178
- KANGAS, L. J.**
An artificial neural network system for diagnosing gas turbine engine fuel faults [DE94-013960] p 138 N95-17371
- KANKAM, M. DAVID**
Motor drive technologies for the power-by-wire (PBW) program: Options, trends and tradeoffs [NASA-TM-106885] p 295 N95-23671
- KANNAN, S. M.**
Evaluation of the dynamic stability characteristics of the NAL Light Transport Aircraft [NAL-PD-CA-9217] p 142 N95-16392
- KANNO, YOSHITSUGU**
A conceptual design of hypersonic research vehicle with subscale scramjet engine p 384 A95-82482
- KAPOOR, KAMLESH**
A full Navier-Stokes analysis of subsonic diffuser of a bifurcated 70/30 supersonic inlet for high speed civil transport application [NASA-TM-106637] p 8 N95-10820
Validation of the RPLUS3D code for supersonic inlet applications involving three-dimensional shock wave-boundary layer interactions [NASA-TM-106579] p 39 N95-13058
Numerical simulation of supersonic compression corners and hypersonic inlet flows using the RPLUS2D code [NASA-TM-106580] p 105 N95-16038
- KARABALIS, DIMITRIS L.**
Simplified analysis of general instability of stiffened shells with cutouts in pure bending [BTN-95-EIX9504274418] p 209 A95-68282
- KARASHIMA, KEIICHI**
Sidewall-effect of the wind tunnel on the estimation of the aerodynamic characteristics of a delta wing p 685 N95-34525
- KARATSINIDES, SPIRO P.**
Enhancing filter robustness in cascaded GPS-INS integrations [BTN-95-EIX95142555475] p 278 A95-73435
- KARCHER, B.**
Transport of exhaust products in the near trail of a jet engine under atmospheric conditions [HTN-95-91421] p 319 A95-77334
- KARIM, MICHAEL**
The development of computer-based instructional simulations for the airline industry p 625 A95-95159
- KARIMIAN, S. M. H.**
Application of a control-volume-based finite-element formulation to the shock tube problem [BTN-95-EIX95182619099] p 295 A95-76584
- KARIMOV, A. KH.**
Profiling of the working surface of electrodes-tools for circle electrochemical dimensional treatment of compressor blades [BTN-94-EIX94461407964] p 83 A95-62638
- KARIMOVA, A. G.**
Heat transfer in the flow-through part of axial compressors [BTN-94-EIX94461407949] p 89 A95-62267
- KARKERA, B. N.**
Mobile domes for TACTIC telescope p 453 A95-86113
- KARLSSON, ANDERS**
How to fly an aircraft with control theory and splines p 360 N95-25805
- KARNA, ANITA**
Identification of Artificial Intelligence (AI) applications for maintenance, monitoring, and control of airway facilities [AD-A282479] p 125 N95-17373
- KARNA, KAMAL**
Identification of Artificial Intelligence (AI) applications for maintenance, monitoring, and control of airway facilities [AD-A282479] p 125 N95-17373
- KARNIADAKIS, G. E.**
Laminar and turbulent flow over optimal riblets p 639 A95-95383
- KARPALA, F.**
Double pass retroreflection for corrosion detection in aircraft structures p 323 N95-23503
Characterization of corrosion and development of a breadboard of a D sight aircraft inspection system, phase 1 [AD-A288347] p 380 N95-26527
- KARPEL, M.**
Stress considerations in reduced-size aeroelastic optimization [BTN-95-EIX95262694313] p 366 A95-85484
- KARPEL, MORDECHAY**
Continuous gust response and sensitivity derivatives using state-space models [BTN-95-EIX95062487551] p 203 A95-68365
- KARPOVSKY, MARK G.**
Fault detection in multiprocessor systems and array processors [BTN-95-EIX95242679097] p 359 A95-81253
- KARTASHOV, E. M.**
On the particular features of dynamic processes in solids with varying boundary during interaction with intensive heat flows [BTN-94-EIX94461408756] p 171 A95-63639
- KASSAPAKIS, E. G.**
Predictive algorithms for the roll control autopilot of a jet fighter aircraft [HTN-95-21047] p 515 A95-90424
- KASSAPOGLOU, C.**
The effects of design details on cost and weight of fuselage structures p 501 N95-28831
- KASSAPOGLOU, CHRISTOS**
Static and fatigue testing of full-scale fuselage panels fabricated using a Therm-X(R) process p 420 N95-28270
- KASTELLA, KEITH**
Emerging applications in probability (Sensor management) [AD-A292781] p 601 N95-31433
- KASUMOV, E. V.**
On calculated models for impellers of centrifugal compressors [BTN-94-EIX94461407947] p 88 A95-62265
- KATAEV, YU. P.**
Analytical description of and forecast for stress relaxation of aviation materials under the vibration conditions [BTN-94-EIX94461408751] p 126 A95-63634
- KATAYAMA, T.**
Neural network approach to identification of aerodynamic loads on a wing. 1: Application to cantilevered beam models p 475 A95-91568
- KATAYANAGI, RYOJI**
Effect of coupling term on stability for the two input control system p 507 A95-91583
Comparison of the method of analyzing stability margin by using Minus Inverse Vector Locus with classical method p 507 A95-91584
- KATAYANGI, RYOJI**
Exact solution of stability margin for the MIMO control system p 507 A95-91582
- KATO, K.**
Electro-optic characterization of ultrafast photodetectors using adiabatically compressed soliton pulses [BTN-94-EIX94381359637] p 257 A95-72675
- KATO, M.**
Dynamic behavior of valves with pneumatic chamber for reciprocating compressors [BTN-94-EIX94351143311] p 207 A95-65845
- KATRAGADDA, PRASANNA**
Intelligent finite element submodeling of multichip modules for reliability analysis [AD-A292911] p 679 N95-31455
- KATZ, AMNON**
Event correlation for networked simulators [BTN-95-EIX0619952748168] p 625 A95-94462
Prediction of airplane states [BTN-95-EIX0619952748174] p 584 A95-94468
- KATZ, DONALD**
Identification of Artificial Intelligence (AI) applications for maintenance, monitoring, and control of airway facilities [AD-A282479] p 125 N95-17373
- KATZ, ERIC**
Prototype stop bar system evaluation at Seattle-Tacoma International Airport [AD-A290136] p 490 N95-30031
- KATZ, ERIC S.**
Evaluation of an unlighted swinging airport sign [AD-A284763] p 146 N95-18087
- KATZ, J.**
Flow structure in the lee of an inclined 6:1 prolate spheroid [BTN-94-EIX95011441127] p 348 A95-81027
- KATZ, JOSEPH**
Unsteady panel method for flows with multiple bodies moving along various paths [HTN-95-61203] p 540 A95-87576
- KATZ, KENNETH**
Conceptual design of the AE481 Demon Remotely Piloted Vehicle (RPV) [NASA-CR-197164] p 44 N95-12294
- KAUFMAN, W. M.**
Development of an Automated Nondestructive Inspection (ANDI) system for commercial aircraft, phase 1 [AD-A283500] p 40 N95-12623
- KAUFMAN, YORMAN J.**
Correction of thin cirrus effects in AVIRIS images using the sensitive 1.375-micron cirrus detecting channel p 708 N95-33748
Remote sensing of smoke, clouds, and radiation using AVIRIS during SCAR experiments p 708 N95-33749
- KAUFMANN, DAVID N.**
Flight test evaluation of the Stanford University/United Airlines differential GPS Category 3 automatic landing system [NASA-TM-110354] p 593 N95-30788
- KAUL, SURINDER K.**
Fatigue life estimation program for Part 23 airplanes, 'AFS.FOR' [SAE PAPER 931249] p 565 A95-89221
- KAUTZ, EDWARD**
Analysis of composite structures with delaminations under combined bending and compression p 422 N95-28429
- KAWACHI, KEIJI**
Aerofoil characteristics at low Reynolds number p 472 A95-91507
- KAWAGUCHI, JUN-ICHIRO**
Aero-thermodynamic flight environment at HITEN aerobrace experiment p 415 A95-82554
- KAWAGUCHI, JUN'ICHIRO**
How 'HITEN's' aerobraking experiments were carried out p 415 A95-82553
- KAWAHARA, HIROYASU**
Functions of NAL fixed base simulator for helicopter research p 522 A95-91555
A simulator study about effects of visibility upon helicopter pilot performance p 522 A95-91556
Preliminary experiments of an optical fiber display [NAL-TR-1257] p 362 N95-25004
Flight reference display for powered-lift STOL aircraft [NAL-TR-1251] p 337 N95-25005
- KAWAHARA, M.**
Arbitrary Lagrangian-Eulerian finite element analysis for flow-induced vibration of rigid body p 643 A95-95485
- KAWAI, H.**
Study on the turbine vane and blade for a 1500 C class industrial gas turbine [BTN-94-EIX95011441254] p 431 A95-84211
- KAWAJI, M.**
Study of heat transfer rates during quenching of a hot tube under microgravity p 428 A95-82641
Experimental investigation of flow-boiling heat transfer under microgravity p 428 A95-82642
Low gravity quenching of hot tubes with cryogenics [ISBN 1-879921-01-4] p 635 A95-93728
- KAWAJI, MASAHIRO**
Experimental investigation of composite channel heat pipe operation in micro-gravity environment p 428 A95-82645
- KAWAMATA, YOSHIHIRO**
Calculation of supersonic combustion in SCRAMJET engines p 698 N95-34513
- KAWASHIMA, ENJI**
Conceptual study of next generation high-speed civil transport: A candidate with horizontal tail p 499 A95-91521
- KAWIECKI, GRZEGORZ**
Bilinear formulation applied to the response and stability of helicopter rotor blade [BTN-95-EIX95042744000] p 192 A95-68300
Effect of initial conditions on the response of nonlinear dynamical systems with the application to helicopter rotor dynamics [ISBN 1-879921-01-4] p 605 A95-93731
- KAY, IRA W.**
Hydrocarbon-fueled ramjet/scramjet technology program, phase 2 extension [NASA-CR-189659] p 15 N95-10319
- KAY, JACOB**
Validation of the NASA Dryden X-31 simulation and evaluation of mechanization techniques p 69 N95-14236

KAYABA, SHIGEO

Wake velocity measurement of counter-rotation propellers p 474 A95-91563

KAYKAYOGLU, C. RUHI

Vortex lattice method simulation of unsteady flow due to wing/external store combination p 471 A95-91499
Computer aided static aeroelastic analysis of wing/pylon/store combination p 499 A95-91531

KAYLOE, JORDAN R.

EASY-SIM: A visual simulation system software architecture with an Ada 9X application framework [AD-A289325] p 448 N95-26895

KAYSER, DETLEF

Effects of the specific military aspects of satellite navigation on the civil use of GPS/GLONASS p 688 N95-33134

KAZUMORI, M.

Development of 70MW class superconducting generators [BTN-94-EIX95011440854] p 429 A95-82905

KEARNS, EDWARD P., III

Air cushioned landing craft (LCAC) based ship to shore movement simulation: A decision aid for the amphibious commander. A (SMMAT) application [AD-A289635] p 436 N95-26722

KEAS, PAUL

SOFIA 2 model telescope wind tunnel test report [NASA-TM-110668] p 683 N95-32764

KEATING, JACK

Development of LaRC (TM): IA thermoplastic polyimide coated aerospace wiring [NASA-CR-195048] p 537 N95-30252

KEE-BOWLING, BONNIE

Background noise levels measured in the NASA Lewis 9- by 15-foot low-speed wind tunnel [NASA-TM-106817] p 145 N95-18054

KEE, CHANGDON

Wide Area Differential GPS (WADGPS) p 489 N95-29107

KEEHAN, CHRIS

Evaluation of commercial water-in-fuel test kits [AD-A292135] p 537 N95-29572

KEEL, JONICA

GateLink highspeed communications with parked aircraft [SAE PAPER 932610] p 486 A95-90079

KEELING, S. L.

A one-dimensional inviscid nonequilibrium flow solver [ISBN 1-879921-01-4] p 588 A95-93752

KEENER, EARL R.

Experimental results for a hypersonic nozzle/afterbody flow field [NASA-TM-4638] p 274 N95-23250

KEIM, E. R.

In situ observations in aircraft exhaust plumes in the lower stratosphere at midlatitudes [HTN-95-A0862] p 318 A95-76266

The distribution of hydrogen, nitrogen, and chlorine radicals in the lower stratosphere: Implications for changes in O₃ due to emission of NO(y) from supersonic aircraft [HTN-95-70935] p 351 A95-78000

KEIRL, J. M.

The advanced flight simulator complex [CONGRESS PAPER C428-5-025] p 522 A95-91679

KEIRSEY, DAVID

Collected papers of the Soar/IFOR project, Spring 1994 [AD-A280063] p 238 N95-20624

KEITH, THEO G., JR.

Effect of curvature in the numerical simulation of an electrothermal de-icer pad [BTN-95-EIX95182619219] p 276 A95-76645

Optimization of aerospace structures [NASA-CR-196763] p 48 N95-12787

KELLER, J. L.

Initial evaluation of the Oregon State University planetary boundary layer column model for ITWS applications [AD-A293775] p 677 N95-31465

KELLER, JAMES F.

Advanced flight control technology achievements at Boeing Helicopters p 624 N95-32014

KELLER, JEFFREY D.

An investigation of helicopter dynamic coupling using an analytical model [NASA-CR-197420] p 285 N95-23217

KELLER, JOHN

ITWS ceiling and visibility products p 654 A95-93454

KELLER, K.

Launcher wing-leading-edge design [BTN-95-EIX95042477110] p 192 A95-68349

KELLER, MICHAEL A.

Lubricant evaluation and performance, 2 [AD-A279144] p 242 N95-21969

KELLER, TEDDIE L.

Amplification and breaking of atmospheric gravity waves p 675 A95-93552

KELLEY, H. LEE

Alaska's volcanic ash warning system p 663 A95-93495

KELLEY, HENRY L.

Exploratory flow visualization investigation of mast-mounted sights in presence of a rotor [NASA-TM-4634] p 330 N95-24566

KELLEY, N. D.

A comparison of measured wind park load histories with the WISPER and WISPERX load spectra [DE95-000295] p 446 N95-27459

Observed acoustic and aeroelastic spectral responses of a MOD-2 turbine blade to turbulence excitation p 451 N95-27991

KELLEY, SEAN M.

Application of circulation control to advanced subsonic transport aircraft. Part 1: Airfoil development [BTN-95-EIX95062487545] p 185 A95-68359

Application of circulation control to advanced subsonic transport aircraft. Part 2: Transport application [BTN-95-EIX95062487546] p 185 A95-68360

KELLY, ALONZO

A feedforward control approach to the local navigation problem for autonomous vehicles [AD-A282787] p 126 N95-17706

KELLY, DAN

The Balsa bullet: A high speed, low-cost general aviation aircraft for Aeroworld [NASA-CR-197165] p 46 N95-12638

KELLY, J. E.

Advanced diesel electronic fuel injection and turbocharging [AD-A279176] p 211 N95-19809

KELLY, JEFFREY J.

The influence of source acceleration on acoustic signals p 577 A95-90136

Effects of signal analysis parameters and noise removal on measured aircraft spectra p 578 A95-90137

Signal processing of noise data from high-speed flyovers [BTN-95-EIX0619952748178] p 680 A95-94248

KELLY, JOHN C., JR.

Dynamic behavior of a magnetic bearing supported jet engine rotor with auxiliary bearings [NASA-CR-197860] p 338 N95-24213

KELLY, PAUL

Advanced distributed simulation technology advanced rotary wing aircraft. Software reusability report [AD-A280434] p 20 N95-10354

KELLY, R. E.

Effect of density gradients in confined supersonic shear layers, part 1 [NASA-CR-198029] p 348 N95-24412

Effect of density gradients in confined supersonic shear layers. Part 2: 3-D modes [NASA-CR-198030] p 349 N95-24413

KEMPEL, LEO CHARLES

Scattering and radiation from cylindrically conformal antennas p 645 N95-30669

KEMPEL, ROBERT W.

Development and flight testing of the HL-10 lifting body p 498 A95-90872

KEMPER, JAMES E.

Alaska's volcanic ash warning system p 663 A95-93495

KEMPPINEN, MARTTI

Airborne imaging radiometer scan simulation [BTN-95-EIX95332753018] p 638 A95-94793

KENNEDY, DAVID

Buckling and vibration analysis of laminated panels using VICONOPT [PAPER-1746] p 230 A95-72580

KENNELLY, ROBERT A., JR.

Aerodynamic tailoring of the Learjet Model 60 wing [SAE PAPER 932534] p 492 A95-89194

Transonic flight test of a laminar flow leading edge with surface excrescences [NASA-TM-4597] p 9 N95-11158

KENT, J. A.

NASA-ACEE/Boeing 737 graphite-epoxy horizontal stabilizer service p 400 N95-28489

KEOGH, P. S.

The dynamic nature of rotor thermal bending due to unsteady lubricant shearing within a bearing [HTN-95-42091] p 430 A95-83857

KEPLER, C. E.

Computational fluid dynamics study of the variable-pitch split-blade fan concept [NASA-CR-189206] p 15 N95-10247

KERMAN, B. R.

Fractal properties of whitecaps p 443 A95-83827

KERN, S. B.

A study of the vortex flow over 76/40-deg double-delta wing [NASA-CR-195032] p 314 N95-23466

KERNEY, PAUL T.

Recirculating cavity casing treatment failure [AD-A289330] p 513 N95-28908

KERNIK, ALAN C.

Guidance and control requirements for high-speed Rollout and Turnoff (ROTO) [NASA-CR-195026] p 292 N95-22674

KERR, R.

NTS-spill test facility wind tunnel exhaust plume characterization [DE95-003630] p 297 N95-24019

KERR, S. A.

Moving mass trim control for aerospace vehicles [DE95-002602] p 299 N95-23532

KERREBROCK, JACK L.

Assessment of the Space Station program p 149 N95-16352

KESSELI, J. B.

Small gas turbine component evaluation study [PB95-147542] p 338 N95-24293

KESSINGER, C. J.

Sensing thunderstorm microphysics with multiparameter radar: Application for aviation p 657 A95-93467

KESSINGER, CATHY

Snow-band formation and evolution during the 15 November 1987 aircraft accident at Denver airport [HTN-95-80699] p 254 A95-72543

The real-time analysis and prediction of storms program p 655 A95-93457

KESSLER, BRADLEY L.

Fiber Optic Control System integration for advanced aircraft. Electro-optic and sensor fabrication, integration, and environmental testing for flight control systems: Laboratory test results [NASA-CR-195408] p 161 N95-18938

Fiber Optic Control System integration for advanced aircraft. Electro-optic and sensor fabrication, integration, and environmental testing for flight control systems [NASA-CR-191194] p 162 N95-19236

KESSLER, G. K.

TRISTAR 1: Evaluation methods for testing head-up display (HUD) flight symbology [NASA-TM-4665] p 288 N95-24030

KESTORAS, M. D.

Effects of free-stream turbulence intensity on a boundary layer recovering from concave curvature effects [BTN-95-EIX95282710058] p 632 A95-92471

KETTERING, MARK

The OFP-6M transport jet [NASA-CR-197159] p 46 N95-12637

KEZAI, TAHAR

Modeling resonance in waveguide-to-microstrip junctions by unilateral fin line resonators [BTN-94-EIX94381323445] p 242 A95-70844

KHALFALLAH, K.

Implicit multidomain calculation of viscous transonic flows without artificial viscosity or upwinding p 640 A95-95443

KHALID, M.

Viscous contribution to the high Mach number damping in pitch of blunt slender cones at small angles of attack [HTN-95-01096] p 469 A95-90282

KHAN, M. ASIF

Nonsmooth trajectory optimization: An approach using continuous simulated annealing [BTN-94-EIX94511433914] p 168 A95-64580

KHARGONEKAR, P. P.

Design of a controller for a flexible pointing system using H(infinity) synthesis [AD-A286572] p 256 N95-20828

KHARITONOV, A. M.

Separation of winged vehicles in supersonics [AIAA PAPER 95-6092] p 526 A95-88601

KHEIRANDISH, HAMID REZA

Numerical solutions of inviscid and viscous flows about airfoils by TVD method p 684 N95-34521

KHINOO, L. A.

Helicopter in-flight simulation development and use in test pilot training [AD-A283998] p 146 N95-18725

KHODADOUST, A.

Aerodynamics of a finite wing with simulated ice [BTN-95-EIX95182619235] p 270 A95-76653

KHODADOUST, ABDOLLAH

Study of the droplet spray characteristics of a subsonic wind tunnel [BTN-95-EIX95182619235] p 271 A95-76661

Further investigations of icing effects on an advanced high-lift multi-element airfoil [NASA-TM-106947] p 381 N95-27762

- KHRABROV, A.**
State-space representation of aerodynamic characteristics of an aircraft at high angles of attack [BTN-95-EIX95062487536] p 187 A95-69244
- KHULIEF, Y. A.**
Modal characteristics of rotors using a conical shaft finite element [BTN-94-EIX94401359745] p 346 A95-77379
- KIDDER, STANLEY**
Field and data analysis studies related to the atmospheric environment [NASA-CR-196543] p 168 N95-18093
- KIDMAN, D.**
Flight test results of the F-16 aircraft modified with axisymmetric vectoring exhaust nozzle p 609 N95-32007
- KIDMAN, DAVID S.**
Flight test results of the F-16 aircraft modified with the axisymmetric vectoring exhaust nozzle p 70 N95-14245
- KIELLAND, P.**
Attitude determination using dedicated and nondedicated multiantenna GPS sensors [BTN-95-EIX95142555482] p 228 A95-72891
- KIEREIN-YOUNG, KATHRYN S.**
Integration of AIRSAR and AVIRIS data for Trail Canyon alluvial fan, Death Valley, California p 709 N95-33760
- KIKUCHI, AKIHIRO**
Calculation for aerodynamic characteristics on delta wing with leading-edge separated vortex effect using boundary element method p 684 N95-34524
- KIKUCHI, K.**
Design of secondary flow control cascade using numerical simulation p 698 N95-34507
- KIKUCHI, KATSUHIRO**
Calculation for aerodynamic characteristics on delta wing with leading-edge separated vortex effect using boundary element method p 684 N95-34524
- KIKUCHI, KAZUO**
Verification of turbine cascade flow with tip clearance p 698 N95-34511
- KIKUCHI, T.**
Aeroelastic tailoring research [PB94-180031] p 6 N95-10135
- KILGORE, W. ALLEN**
Effects of vibration on inertial wind-tunnel model attitude measurement devices [NASA-TM-109083] p 21 N95-11466
- Performance of the 0.3-meter transonic cryogenic tunnel with air, nitrogen, and sulfur hexafluoride media under closed loop automatic control [NASA-CR-195052] p 310 N95-23257
- Development of a model protection and dynamic response monitoring system for the national transonic facility [NASA-CR-195041] p 340 N95-24388
- KILLEEN, B.**
Blade-by-blade tip clearance measurement system for gas turbine applications [BTN-95-EIX95292721167] p 546 A95-89899
- KILPATRICK, WILLIAM T.**
More supportable T-38A enhancement study [AD-A283671] p 66 N95-15331
- KILPINEN, JUHA**
The combination of forecasts in an automated aviation weather forecasting system p 669 A95-93522
- KILSBY, C. G.**
Water vapor continuum absorption in mid-latitudes: Aircraft measurements and model comparisons [HTN-95-40756] p 252 A95-71186
- KIM, BYOUNGSOO**
Automatic multi-block grid generation for high-lift configuration wings p 567 N95-28764
- KIM, CHAN M.**
An aerodynamic analysis of a mixed flow turbine [NASA-TM-106674] p 15 N95-10153
- KIM, FREDERICK D.**
High-order state space simulation models of helicopter flight mechanics [HTN-95-A0494] p 237 A95-72565
- KIM, GOO**
A vorticity-velocity approach for three-dimensional unsteady viscous flow over wings p 478 N95-29108
- KIM, GUHO**
Effects of activated reactive evaporation process parameters on the microhardness of polycrystalline silicon carbide thin films [GTN-95-00406090-4621] p 680 A95-93965
- KIM, J. M.**
Vorticity concentration at the edge of the inboard vortex sheet [HTN-95-31010] p 221 A95-71180
- KIM, KYOUNG-HO**
Three-dimensional structure of a supersonic jet impinging on an inclined plate [BTN-95-EIX95152583259] p 267 A95-73560
- KIM, KYUNG-YUP**
Numerical calculations of the turbulent flow through a controlled diffusion compressor cascade [BTN-95-EIX95282710056] p 632 A95-92473
- KIM, M.-U.**
Two-dimensional viscous flow past a flat plate [HTN-95-42210] p 430 A95-84026
- KIM, S.-W.**
Time-accurate finite volume method valid at all flow velocities p 314 N95-23447
- KIM, SEUNG JO**
Aerelastic response of composite rotor blades considering transverse shear and structural damping [HTN-95-81647] p 542 A95-87695
- KIM, SEUNG-HO**
Static aeroelastic characteristics of a composite wing [BTN-95-EIX95152582340] p 282 A95-73542
- KIM, SUK C.**
Numerical analysis of hypersonic low-density scramjet inlet flow [BTN-95-EIX95212645694] p 272 A95-76746
- KIM, W. J.**
Influence of streamwise curvature on longitudinal vortices imbedded in turbulent boundary layers [BTN-94-EIX94401378820] p 307 A95-76489
- KIM, Y.**
Computational predictive methods for fracture and fatigue p 93 N95-14466
- KIM, YOUNG DAN**
Design of an effective controller via disturbance accommodating left eigenstructure assignment [BTN-95-EIX95282706663] p 565 A95-88178
- KIM, YOUNG-WON**
Ordered intermetallic alloys, part 3: Gamma titanium aluminides [HTN-95-B0396] p 530 A95-90477
- KIMBALL, DWAYNE F.**
Flying qualities development and flight simulation evaluation of the TW-68 tilt-wing VTOL aircraft [SAE PAPER 932517] p 386 A95-94555
- KIMMINAU, DONALD F.**
Patient/aircraft forecasting for the strategic aeromedical evacuation lift-bed process [AD-A293902] p 599 N95-31512
- KIMOTO, MASAYUKI**
Wake velocity measurement of counter-rotation propellers p 474 A95-91563
- KIMURA, T.**
MIMO H infinity control design method combined with exact model matching p 506 A95-91492
- KINARD, TIM A.**
An assessment of viscous effects in computational simulation of benign and burst vortex flows on generic fighter wind-tunnel models using TEAM code [NASA-CR-4650] p 273 N95-23185
- KINDER, ROBERT H.**
Impact of composites on future transport aircraft p 534 N95-29030
- KING, GREGORY**
The Aluminum Falcon: A low cost modern commercial transport [NASA-CR-197180] p 81 N95-15742
- KIOCK, R.**
Pressure distribution measurements on an isolated TPS 441 nacelle p 115 N95-17878
- KIRILLOV, I. R.**
MHD-flow in slotted channels with conducting walls [DE94-018370] p 258 N95-21388
- KIRIU, NOBUAKI**
Studies on gain performance of a combustion driven CO2 gas dynamic laser p 428 A95-82679
- KIRK, R. G.**
Thermo-hydrodynamic solution of floating ring seals for high pressure compressors using the finite-element method [HTN-95-92246] p 433 A95-85290
- KIRKHOPE, J.**
New eigensolutions and modal analysis for gyroscopic/rotor systems, part 1: undamped systems [BTN-94-EIX94522410219] p 702 A95-96373
- New eigensolutions and modal analysis for gyroscopic/rotor systems, part 2: perturbation analysis for damped systems [BTN-94-EIX94522410220] p 702 A95-96374
- KIRKLAND, LARRY V.**
ATE enabling technologies [BTN-95-EIX95172595294] p 287 A95-75718
- KIRKLAND, T. P.**
Evolution of oxidation and creep damage mechanisms in HIPed silicon nitride materials [DE95-001360] p 300 N95-22689
- KIRUBARAJAN, T.**
MATSurv multisensor air traffic surveillance [AD-A292253] p 489 N95-28887
- KISH, BRIAN A.**
A comparison of the Neal-Smith and omega Tau function, zeta function and tau function flying qualities criteria [AD-A289503] p 390 N95-26844
- KISHIBE, TADAHARU**
Static pressure drop by swirling flow of an internal cooling air system through a turbine shaft p 698 N95-34560
- KISHIMOTO, TAKUJI**
A large scale 3D Navier-Stokes analysis using NAL-NWT p 707 N95-34539
- KISHORE**
Failure behaviour of carbon fiber/epoxy composites in pin-ended buckling and bending tests [HTN-95-71388] p 528 A95-87606
- KITADA, MAKOTO**
Experimental investigation of composite channel heat pipe operation in micro-gravity environment p 428 A95-82645
- KITAJIMA, T.**
Development of 70MW class superconducting generators [BTN-94-EIX95011440854] p 429 A95-82905
- KITAMURA, ATSUSHI**
Simultaneous structure/aerodynamic design optimization for a flexible wing structure p 499 A95-91565
- KIWAN, ABDUL R.**
Helicopter Performance Evaluation (HELPE) computer model [AD-A284319] p 131 N95-18381
- KLAASS, R. M. FRED**
Dynamic stiffness and damping of foil bearings for gas turbine engines [SAE PAPER 931449] p 635 A95-93698
- KLAVUHN, KURT G.**
Spatially-resolved velocity measurements in steady, high-speed, reacting flows using laser-induced OH fluorescence p 650 N95-32109
- KLEFFMANN, J.**
Nitrous oxide and methane emissions from aero engines [HTN-95-21363] p 353 A95-78678
- KLEIFGES, K.**
Leading-edge sweepback and shape effects on fin-induced fluctuating pressures [BTN-95-EIX95302694471] p 636 A95-94067
- KLEIN, D. E.**
Convection heat transfer distributions over plates with square ribs from infrared thermography measurements [HTN-95-20713] p 435 A95-86603
- Constant flux, turbulent convection data using infrared imaging [HTN-95-20731] p 435 A95-86621
- KLEIN, KURT**
The DLR research programme on an integrated multi sensor system for surface movement guidance and control p 689 N95-33135
- KLEIN, VLADISLAV**
Determining the accuracy of maximum likelihood parameter estimates with colored residuals [NASA-CR-194893] p 51 N95-11869
- Modeling of aircraft unsteady aerodynamic characteristics. Part 2: Parameters estimated from wind tunnel data [NASA-TM-110161] p 410 N95-27839
- KLEISS, JAMES A.**
Perceptual dimensions of simulated scenes relevant for visual low-altitude flight [AD-A294385] p 700 N95-34344
- KLETZLI, D. W., JR.**
Foliage transmission measurements using a ground-based ultrawide band (300-1300 MHz) SAR system [BTN-94-EIX94381351617] p 252 A95-70950
- KLEWICKI, J. G.**
Transverse vorticity measurements in the NASA Ames 80 x 120 wind tunnel boundary layer p 251 N95-22457
- KLIMOV, A. V.**
Aircraft gear train diagnostics using the irregular rotation of the external shafts [CONGRESS PAPER C428-15-097] p 508 A95-91712
- KLINGELE, EMILE E.**
Data processing and mapping in airborne radiometric surveys [HTN-95-51587] p 442 A95-83591
- KLINGLE-WILSON, DIANA**
The Integrated Terminal Weather System (ITWS) storm cell information and weather impacted airspace detection algorithm p 654 A95-93452

- KLINGLE-WILSON, DIANA L.**
Integrated terminal weather system (ITWS) demonstration and validation operational test and evaluation
[AD-A293932] p 602 N95-31521
- KLOPFER, GOETZ H.**
Computational support of the laminar flow supersonic wind tunnel, CNSFV code development, Maglev, and grid generation
[NASA-CR-197750] p 411 N95-26775
- KLOTZ, STEPHEN P.**
Numerical simulation of the SOFIA flowfield
[NASA-CR-197025] p 74 N95-14612
Numerical simulation of the SOFIA flow field
[NASA-CR-197757] p 436 N95-26589
- KLUPFEL, T.**
Airborne measurements during the European Arctic Stratospheric Ozone Experiment : Observation of OCIO
[HTN-95-00745] p 445 A95-86315
- KLUTE, S. M.**
Dynamic pitch-up of a delta wing
[HTN-95-81633] p 462 A95-87681
- KLZYDE, DAVID H.**
Proposed incorporation of mission-oriented flying qualities into MIL-STD-1797A
[AD-A294211] p 698 N95-34306
- KLYMENKO, VICTOR**
Factors affecting the visual fragmentation of the field-of-view in partial binocular overlap displays
[AD-A283081] p 172 N95-17334
Factors affecting the perception of tuning in monocular regions of partial binocular overlap displays
[AD-A286287] p 259 N95-22044
- KMETEC, JEFFREY D.**
2 micron LIDAR for laser-based remote sensing: Flight demonstration and application survey
[BTN-95-EIX95212641072] p 319 A95-76737
- KNAELL, KENNETH K.**
Apparatus and method for producing three-dimensional images
[AD-D017455] p 646 N95-30727
- KNAUFF, T. L., JR.**
Parallel calculation of sensitivity derivatives for aircraft design using automatic differentiation
[NASA-TM-110103] p 231 N95-20370
- KNEPP, JOHN E.**
Conversion of production automotive engines for aviation use
[SAE PAPER 932606] p 495 A95-90076
- KNIGHT, D. D.**
Two-dimensional unsteady leading-edge separation on a pitching airfoil
[HTN-95-81628] p 461 A95-87676
Laser interferometer skin-friction measurements of crossing-shock-wave/turbulent-boundary-layer
[HTN-95-20834] p 544 A95-88095
- KNOFF, R. E.**
Containing military autotest cost growth through the use of commercial standard equipment architectures
[BTN-95-EIX95172595295] p 287 A95-75717
- KNOLL, A.**
A flying qualities study of longitudinal long-term dynamics of hypersonic planes
[AIAA PAPER 95-6150] p 521 A95-90464
- KNOLLENBERG, R. G.**
Performance of a focused cavity aerosol spectrometer for measurements in the stratosphere of particle size in the 0.06-2.0-micrometer-diameter range
[HTN-95-90914] p 253 A95-72423
- KNOPS, H. A. J.**
Numerical simulation of crack growth in pressurized fuselages
[PB95-192415] p 400 N95-28636
- KNOSPE, C. R.**
Microgravity isolation system design: A case study
[NASA-TM-106804] p 104 N95-17657
Microgravity isolation system design: A modern control synthesis framework
[NASA-TM-106805] p 105 N95-18197
Microgravity isolation system design: A modern control analysis framework
[NASA-TM-106803] p 105 N95-18486
- KNOWLES, D. I.**
The air systems controllerate initiatives and policies for the procurement of reliable and maintainable equipment
[CONGRESS PAPER C428-6-113] p 549 A95-91682
- KNOWLES, GARETH**
Static shape control for adaptive wings
[HTN-95-A1767] p 627 A95-93330
- KNOWLES, K.**
Reduction of supersonic jet noise using swirl: A concept revisited
p 574 A95-90101
Recent research in ASTOVL aircraft ground environment
[CONGRESS PAPER C428-9-040] p 475 A95-91694
- KNOX, CHARLES E.**
Modeling of Instrument Landing System (ILS) localizer signal on runway 25L at Los Angeles International Airport
[NASA-TM-4588] p 125 N95-17384
- KNOX, E. C.**
Determination of wall boundary conditions for high-speed-ratio direct simulation Monte Carlo calculations
[BTN-95-EIX95182617457] p 267 A95-75728
Parameters of Nocilla gas/surface interaction model from measured accommodation coefficients
[HTN-95-81639] p 541 A95-87687
- KNUDSEN, B. M.**
Airborne measurements during the European Arctic Stratospheric Ozone Experiment : Observation of OCIO
[HTN-95-00745] p 445 A95-86315
- KO, FRANK K.**
Development of hypersonic engine seals: Flow effects of preload and engine pressures
[BTN-95-EIX95112524204] p 196 A95-69304
- KO, M. K. W.**
Subsidence of aircraft engine exhaust in the stratosphere: Implications for calculated ozone depletions
[PAPER-93GL03426] p 251 A95-70297
- KO, MALCOLM K. W.**
Effects on stratospheric ozone from high-speed civil transport: Sensitivity to stratospheric aerosol loading
[HTN-95-91842] p 354 A95-80830
- KO, WILLIAM L.**
Shear buckling analysis of a hat-stiffened panel
[NASA-TM-4644] p 158 N95-17490
- KOBAYAKAWA, MAKOTO**
An intelligent tutoring system for civil aviation flight training
p 521 A95-91535
- KOBAYASHI, A. S.**
Axial crack propagation and arrest in pressurized fuselage
p 94 N95-14479
- KOBAYASHI, TOMOYUKI**
Research and development of thermal protection system of HOPE re-entry vehicle
p 413 A95-82358
- KOBLINSKY, C.**
Using IRI for the computation of ionospheric corrections for altimeter data analysis
p 212 A95-66949
- KOCH, W. J.**
Design, analysis, and fabrication of a pressure box test fixture for tension damage tolerance testing of curved fuselage panels
p 533 N95-28839
- KOCHEVAR, A. J.**
Experimental investigation of thermoelastic deformation in turbojet-engine bearings under maintenance inspection
[BTN-95-EIX95292721173] p 546 A95-89904
- KODAMA, H.**
Design of secondary flow control cascade using numerical simulation
p 698 N95-34507
- KODIYALAM, SRINIVAS**
Ply layup optimization and micromechanics tailoring of composite aircraft engine structures
[BTN-95-EIX95112524206] p 196 A95-69302
- KODRES, C. A.**
Moisture induced pressures in concrete airfield pavements
[AD-A281974] p 52 N95-11789
- KOENIG, KEITH**
Supersonic axisymmetric conical flow solutions for different ratios of specific heats
[BTN-95-EIX95152583283] p 306 A95-73584
- KOENIG, KLAUS**
Acoustic fatigue testing on different materials and skin-stringer elements
p 174 N95-19156
- KOENIG, P.**
Damage of high temperature components by dust-laden air
p 201 N95-19673
- KOENIG, R.**
Advanced gust management systems: Lessons learned and perspectives
p 622 N95-32002
- KOFF, B. L.**
Aircraft gas turbine emissions challenge
[BTN-94-EIX95011441239] p 403 A95-84196
- KOGA, DENNIS J.**
Transonic flight test of a laminar flow leading edge with surface excrescences
[NASA-TM-4597] p 9 N95-11158
- KOGAN, M. N.**
Kinetic theory in aerothermodynamics
[HTN-95-A0002] p 183 A95-67829
- KOIKE, AKIRA**
Preliminary tests of a transonic flutter control wing model
p 499 A95-91566
- KOJIMA, FUMIO**
A method for disbond detection in thermal tomography by domain decomposition method
p 545 A95-88955
- KOKAL, R. A.**
Flame-spreading phenomena in the fin-slot region of a solid rocket motor
p 23 N95-10296
- KOKINI, K.**
Thermal fracture mechanisms in ceramic thermal barrier coatings
p 346 N95-26138
- KOKUBUN, S.**
Polar Patrol Balloon
[BTN-95-EIX95152582318] p 316 A95-73521
Polar Patrol Balloon system and preliminary experimental results
p 368 A95-82513
- KOLB, C. E.**
Subsidence of aircraft engine exhaust in the stratosphere: Implications for calculated ozone depletions
[PAPER-93GL03426] p 251 A95-70297
- KOLENSKI, J. D.**
Viscoplastic response of structures for intense local heating
[HTN-95-41540] p 346 A95-77921
- KOLKMAN, H. J.**
Gas turbine compressor corrosion and erosion in Western Europe
[AD-B1961781] p 201 N95-19678
- KOLLECK, MATHIAS L.**
Aircraft wiring maintenance: Development of a computerized maintenance aid
[SAE PAPER 932615] p 456 A95-90080
- KOLVE, D. I.**
Describing an attitude
p 342 A95-80409
- KOLVER, JILL**
Conceptual design of the AE481 Demon Remotely Piloted Vehicle (RPV)
[NASA-CR-197164] p 44 N95-12294
- KOLWEY, HERMAN**
Add a dimension to your analysis of the helicopter low airspeed environment
[AD-A283982] p 79 N95-14205
- KOMAROV, S. S.**
Soft landing on the slope surface of a landing vehicle with an air shock-absorber of forced pressurization
[BTN-94-EIX94461407941] p 85 A95-62259
- KOMATSU, TATSUAKI**
On the flight control system for UF-104
p 507 A95-91560
- KOMATSU, YUKIO**
Preliminary tests of a transonic flutter control wing model
p 499 A95-91566
- KOMEL, S. V.**
Ultimate characteristics of a rocket engine with a turbo-pump supply system
[BTN-94-EIX94461408757] p 148 A95-63640
- KOMERATH, N. M.**
Measurement around a rotor blade excited in pitch. Part 1: Dynamic inflow
[HTN-95-31007] p 220 A95-71177
Measurement around a rotor blade excited in pitch. Part 2: Unsteady surface pressure
[HTN-95-31008] p 220 A95-71178
Vorticity concentration at the edge of the inboard vortex sheet
[HTN-95-31010] p 221 A95-71180
Rotor-wake-induced flow separation on a lifting surface
[HTN-95-01082] p 468 A95-90268
Correlation of unsteady pressure and inflow velocity fields of a pitching rotor blade
[BTN-95-EIX0619952748169] p 589 A95-94463
- KOMERATH, NARAYANAN M.**
Spectral mapping of quasiperiodic structures in a vortex flow
[BTN-95-EIX0619952748165] p 589 A95-94459
- KOMIYAMA, FUMIO**
Effects of cavity bleed and its configuration on aerodynamic characteristics of supersonic internal flow
[NAL-TR-1247] p 594 N95-31715
- KOMOROWSKI, J. P.**
Modelling of pillowwing due to corrosion in fuselage lap joints
[BTN-95-EIX95082502227] p 240 A95-71024
Double pass retroreflection for corrosion detection in aircraft structures
p 323 N95-23503
- KOMURO, TOMOYUKI**
Experiment on a rectangular cross section scramjet combustor. 2: Effects of fuel injector geometry
[NAL-TR-1220] p 405 N95-26600
- KONDO, HIROFUMI**
Wake velocity measurement of counter-rotation propellers
p 474 A95-91563
- KONG, JEFFREY**
The accuracy of parameter estimation in system identification of noisy aircraft load measurement
[NASA-CR-197516] p 134 N95-19130
- KONG, L.**
Unsteady flow testing in a passive low-correction wind tunnel
p 147 N95-19272

- KONTOS, G. C.**
Active control of fan noise-feasibility study. Volume 1: Flyover system noise studies [NASA-CR-195392-VOL-1] p 258 N95-21888
- KOO, KYO-NAM**
Effects of structural damping on aeroelastic stability of various shaped composite plate wing p 530 A95-91530
- KOO, SAM OK**
Numerical study of sound generation due to a spinning vortex pair [BTN-95-EIX95182619075] p 307 A95-75760
- KOONTZ, S.**
Free-jet testing at Mach 3.44 in GASL's aero/thermo test facility p 145 N95-16320
- KOOPMAN, FRITZ**
Design and construction of a remote piloted flying wing [NASA-CR-197195] p 47 N95-12695
- KOPP, F.**
Doppler lidar investigation of wake vortex transport between closely spaced parallel runways [HTN-95-81645] p 462 A95-87693
- KORDULLA, W.**
Computational fluid dynamics '92; Proceedings of the European Computational Fluid Dynamics Conference, 1st, Brussels, Belgium, Sep. 7-11, 1992. Vols. 1 & 2 [ISBN 0-444-89793-3] p 638 A95-95357
- KORIVI, VAMSHI M.**
Discrete shape sensitivity equations for aerodynamic problems [BTN-94-EIX94451393721] p 88 A95-61720
- KORIVI, VAMSHI MOHAN**
Sensitivity derivatives for three dimensional supersonic Euler code using incremental iterative strategy [HTN-95-20845] p 545 A95-88106
- KORLEVIC, K.**
Powerful bolide explosion over North Italy [HTN-95-80564] p 218 A95-69658
- KORNER, H.**
Orbital transport: Technical, meteorological and chemical aspects; Aerospace Symposium, 3rd, Braunschweig, Germany, Aug. 26-28, 1991 [ISBN 3-540-563180] p 524 A95-87373
- KOROVIN, E. M.**
Modelling for optimal operations of line milling of aerodynamic surfaces [BTN-94-EIX94461408774] p 138 A95-63657
- KORTE, J. J.**
Optimization of contoured hypersonic scramjet inlets with a least-squares parabolized Navier-Stokes procedure [HTN-95-20976] p 261 A95-74042
- KORTE, JOHN J.**
Numerical study of the performance of swept, curved compression surface scramjet inlets [BTN-95-EIX95112524198] p 197 A95-69310
- KORTELING, J. E.**
Partial camera automation in a simulated Unmanned Air Vehicle [AD-A288786] p 337 N95-26190
- KORYAKIN, L. M.**
Universal electrohydraulic system for the steering gear loading [CONGRESS PAPER C428-10-106] p 517 A95-91700
- KOSAI, M.**
Axial crack propagation and arrest in pressurized fuselage p 94 N95-14479
- KOSAL, HALUK**
Control mechanism to prevent correlated message arrivals from degrading signaling no. 7 network performance [BTN-94-EIX94341342286] p 56 A95-60842
- KOSCHEL, W.**
Chemically reacting non-equilibrium boundary layers in air breathing propulsion systems [AIAA PAPER 95-6139] p 512 A95-90456
- KOSHAK, WILLIAM J.**
Aircraft electric field measurements: Calibration and ambient field retrieval [HTN-95-90508] p 213 A95-67780
- KOSS, FRANK V.**
Collected papers of the Soar/IFOR project, Spring 1994 [AD-A280063] p 238 N95-20624
- KOSSEL, HORST**
Activated buoyancy propulsion = Paradox Power (tm) [TABES PAPER 94-619] p 74 N95-14646
- KOSSIRA, H.**
Integrated thermal and mechanical analysis of hypersonic vehicles by using adaptive finite element methods p 524 A95-87383
- KOSTEGE, VALEREY K.**
Simulation of multidisciplinary problems for the thermostress state of cooled high temperature turbines p 140 N95-19021
Verification of multidisciplinary models for turbomachines p 140 N95-19025
- KOSTEGE, VALERY K.**
Application of multidisciplinary models to the cooled turbine rotor design p 140 N95-19024
- KOUL, A. K.**
The effects of surface modification on fretting fatigue in Ti alloy turbine components [HTN-95-61145] p 404 A95-84909
- KOUL, R.**
Mobile domes for TACTIC telescope p 453 A95-86113
- KOUMOUTSAKOS, PETROS**
Direct numerical simulations of on-demand vortex generators: Mathematical formulation p 251 N95-22452
- KOUNTZ, JOHN**
Effect of leeward flow dividers on the wing rock of a delta wing [BTN-95-EIX95152582347] p 282 A95-73549
- KOURA, KATSUHISA**
Rarefied gas numerical wind tunnel: OREX and HOPE p 427 A95-82391
- KOUROUS, HELEN E.**
Fabry-Perot interferometer measurement of static temperature and velocity for ASTOVL model tests [NASA-TM-107014] p 645 N95-30587
- KOUSEN, KENNETH A.**
Active control of wake/blade-row interaction noise [BTN-95-EIX95042474389] p 196 A95-68311
Limit cycle phenomena in computational transonic aeroelasticity [BTN-95-EIX95152582317] p 264 A95-73520
Development of a linearized unsteady Euler analysis for turbomachinery blade rows [NASA-CR-4677] p 592 N95-30611
- KOVALENKO, N. D.**
JPRS report: Science and technology. Central Eurasia: Engineering and equipment. Gas dynamics of supersonic shortened nozzles [JPRS-UST-94-003-L] p 22 N95-10931
- KOZAK, J.**
Solid-state data recorder, next development and use p 705 N95-33143
- KOZEL, K.**
Numerical solution of Euler and Navier-Stokes equations for 2D transonic problems p 638 A95-95366
- KOZEN, A.**
Electro-optic characterization of ultrafast photodetectors using adiabatically compressed soliton pulses [BTN-94-EIX94381359637] p 257 A95-72675
- KOZHEVNIKOV, YU. V.**
Theoretical fundamentals of the aircraft GTE tests p 138 N95-16265
- KOZOL, J.**
Corrosion of landing gear steels p 302 N95-23500
- KRABACHER, WILLIAM E.**
Aircraft landing gear dynamics present and future [SAE PAPER 931400] p 604 A95-93670
- KRAEMER, E.**
An innovative algorithm to accurately solve the Euler equations for rotary wing flow p 642 A95-95467
- KRAFT, RICHARD**
Initial exploration of the ASRS database p 681 A95-95204
- KRAFT, ROBERT E.**
Active control of fan noise-feasibility study. Volume 1: Flyover system noise studies [NASA-CR-195392-VOL-1] p 258 N95-21888
Aircraft IR/acoustic detection evaluation. Volume 2: Development of a ground-based acoustic sensor system for the detection of subsonic jet-powered aircraft [NASA-CR-189705-VOL-2] p 452 N95-28073
- KRAL, LINDA D.**
The applicability of turbulence models to aerodynamic and propulsion flowfields at McDonnell-Douglas Aerospace p 439 N95-27886
- KRAMER, BRIAN**
F/A-18 and F-16 forebody vortex control, static and rotary-balance results p 72 N95-14254
- KRAMER, BRIAN R.**
Development of a multicomponent force and moment balance for water tunnel applications, volume 1 [NASA-CR-4642-VOL-1] p 161 N95-18955
Development of a multicomponent force and moment balance for water tunnel applications, volume 2 [NASA-CR-4642-VOL-2] p 161 N95-18956
- KRANTZ, TIMOTHY L.**
Vibration analysis of a split path gearbox [NASA-TM-106875] p 438 N95-27855
- KRAUS, MICHAEL J.**
The forecast systems laboratory's role in the FAA's aviation weather development program p 652 A95-93443
- KRAUSE, SCOTT**
Design and construction of a remote piloted flying wing [NASA-CR-197195] p 47 N95-12695
- KRECH, ROBERT H.**
Ultraviolet emissions occurring about hypersonic vehicles in rarefied flows [AD-A281452] p 106 N95-16076
- KREHBIEL, PAUL**
Use of high resolution lightning detection and localization sensors for hazardous aviation weather nowcasting p 661 A95-93486
- KREIDER, KEVIN L.**
Acoustic scattering from ellipses by the modal element method [NASA-TM-106935] p 579 N95-29401
- KREITMAIR-STECK, W.**
HeliRadar: A rotating antenna synthetic aperture radar for helicopter allweather operations p 705 N95-33137
- KREMER, F.**
Influence of the flight trajectory on the exhaust gas composition of a H2-fueled air-breathing ramjet engine p 509 A95-87404
- KREMER, JEAN-PAUL**
Shuttle entry guidance revisited using nonlinear geometric methods [BTN-95-EIX95182619144] p 299 A95-76621
- KREPLIN, H.-P.**
Three-dimensional boundary layer and flow field data of an inclined prolate spheroid p 158 N95-17867
- KRETSCHMER, J.**
Secondary power system study for the hytex RA3 flight test vehicle [AIAA PAPER 95-6158] p 512 A95-90470
- KREUTZ, T. G.**
Intrinsic transport and chemistry coupling in combustion phenomena p 538 A95-87191
- KRIEG, E. J.**
Ceramic composite attachments for transmission of high-torque loads [BTN-94-EIX95011441256] p 417 A95-84213
- KRISHNAKUMAR, K.**
Neuro-controllers for adaptive helicopter training [SAE PAPER 932535] p 379 A95-84557
Neuro-controllers for adaptive helicopter hover training [BTN-94-EIX94522407592] p 709 A95-96241
- KRISHNAKUMAR, S.**
Modelling of pilling due to corrosion in fuselage lap joints [BTN-95-EIX95082502227] p 240 A95-71024
Double pass retroreflection for corrosion detection in aircraft structures p 323 N95-23503
- KRISHNAMURTHY, RAMESH**
Optimized design of a hypersonic nozzle p 297 N95-23304
- KRISHNAN, C. G.**
Some aspects of the aerodynamics of separating strap-ons [BTN-95-EIX95182617464] p 298 A95-75735
- KROO, ILAN**
Tailless aircraft design-recent experiences p 492 A95-88899
- KRUCK, MARY**
ADST system test report for the rotary wing aircraft airmet aeromodel and weapon model merge with the ATAC 2 baseline [AD-A281580] p 127 N95-16171
- KRUCZYNSKI, DAVID L.**
Proceeding towards hypervelocities in ram accelerators p 19 N95-10285
- KRUEGER, W.**
Testing the hypersonic technology demonstration nozzle: Results from the test campaign 1993/94 [AIAA PAPER 95-6084] p 509 A95-87413
- KRUMPHOLZ, O.**
Optical backplane for modular avionics p 257 N95-20652
- KRUPA, VLADISLAV G.**
Solution of Navier-Stokes equations using high accuracy monotone schemes p 161 N95-19019
Simulation of steady and unsteady viscous flows in turbomachinery p 140 N95-19023
- KRUPAR, MARTIN J.**
Laser doppler velocimeter system for subsonic jet mixer nozzle testing at the NASA Lewis Aeroacoustic Propulsion Lab [NASA-TM-106984] p 457 N95-30229
- KRUPKE, B.**
Overview of remote sensing laser development and semiconductor laser technology [DE94-019103] p 256 N95-21552

KRUSE, N.

A hybrid electronically scanned pressure module for cryogenic environments
[NASA-TM-110146] p 554 N95-29453

KRUSE, SCOT

An experimental investigation of helicopter downwash and tailboom interaction at the Wichita State University 7x10 foot wind tunnel p 375 N95-26955

KUBE, ROLAND

Analysis of a higher harmonic control test to reduce blade vortex interaction noise
[BTN-95-EIX95152582330] p 265 A95-73532

A higher harmonic control test in the DNW to reduce impulsive BVI noise
[HTN-95-61071] p 385 A95-83655

KUBO, TRACY S.

2 micron LIDAR for laser-based remote sensing: Flight demonstration and application survey
[BTN-95-EIX95212641072] p 319 A95-76737

KUBOTA, HIROTOshi

Hypersonic thermal protection with mass injection at angle of attack p 414 A95-82414

KUCHAR, JAMES K.

Part-task simulator evaluations of advanced terrain displays
[SAE PAPER 932570] p 401 A95-84567

KUDO, NATSUKO

A systems for flight data acquisition and analysis for a remotely-piloted research vehicle p 517 A95-91554

KUDOU, KENJI

Experiment on a rectangular cross section scramjet combustor. 2: Effects of fuel injector geometry
[NAL-TR-1220] p 405 N95-26600

KUEPPER, A.

Wall correction method with measured boundary conditions for low speed wind tunnels p 164 N95-19263

KUEPPER, T.

Trim conditions for optimal flight performance of hypersonic aircraft p 514 A95-87397

KUGLER, B. ANDREW

Development and field test of the Beta version of the USAF Assessment System for Aircraft Noise (ASAN)
p 561 A95-90121

KUHLMANN, K. J.

Modeling aerosol emissions from the combustion of composite materials p 301 N95-23038

KUH, GARY D.

Aerodynamic design of pegasus: Concept to flight with computational fluid dynamics
[BTN-95-EIX95182617463] p 298 A95-75734

KUJI, MAKOTO

Air truth validation of cloud albedo estimated from NOAA advanced very high resolution radiometer data
[HTN-95-A1021] p 443 A95-84526

KUK, V. H. M.

Particle deposition in gas turbine blade film cooling holes p 199 N95-19661

KULAGIN, S. V.

On calculated models for impellers of centrifugal compressors
[BTN-94-EIX94461407947] p 88 A95-62265

KULLBERG, E.

SAAB experience with PIO p 598 N95-31069

KULLERD, SUSAN M.

Development of stitched/RTM composite primary structures p 425 N95-28469

Test and analysis results for composite transport fuselage and wing structures p 398 N95-28470

Mechanical characterization of 2D, 2D stitched, and 3D braided/RTM materials p 535 N95-29038

KULWICKI, PHILIP

Industry review of a crew-centered cockpit design process and toolset
[AD-A282966] p 130 N95-17661

KUMAMOTO, YUICHI

Numerical simulations of dynamic stall phenomena in low speed flows p 685 N95-34546

KUMAR, A.

Algorithmic trends in computational fluid dynamics; The Institute for Computer Applications in Science and Engineering (ICASE)/LaRC Workshop, NASA Langley Research Center, Hampton, VA, US, Sep. 15-17, 1991
[ISBN 0-387-94014-6] p 550 A95-91915

KUMAR, AJAY

Numerical study of the performance of swept, curved compression surface scramjet inlets
[BTN-95-EIX95112524198] p 197 A95-69310

KUMAR, DHARMENDRA

Application of parallel processing technology in complex helicopter analysis. Phase 1
[NASA-CR-197850] p 502 N95-28928

KUMARI, M.

Free convection past a uniform flux surface inclined at a small angle to the horizontal
[HTN-95-42213] p 430 A95-84029

KUNKEE, D. B.

Airborne passive polarimetric measurements of sea surface anisotropy at 92 GHz
[NASA-CR-197288] p 707 N95-32823

KUNZ, STEVEN E.

The performance of cargo airdrop systems using g-12E parachutes: Statistical determination of minimum altitude
[AD-A291666] p 381 N95-28454

KUNZI, K.

Aircraft measurements of CLO and HCL during EASOE 1991/92
[HTN-95-00721] p 444 A95-86291

KUO, KENNETH K.

Flame-spreading phenomena in the fin-slot region of a solid rocket motor p 23 N95-10296

KURKOV, A. P.

Measurement of gust response on a turbine cascade
[NASA-TM-106776] p 117 N95-18457

KUROHASHI, M.

Dynamic behavior of valves with pneumatic chamber for reciprocating compressors
[BTN-94-EIX94351143311] p 207 A95-65845

KURTENBACH, R.

Nitrous oxide and methane emissions from aero engines
[HTN-95-21363] p 353 A95-78678

KURTKAYA, MEHMET

Sensor fault detection and diagnosis simulation of a helicopter engine in an intelligent control framework
[AD-A290223] p 137 N95-15970

KURUVILA, G.

Airfoil optimization by the one-shot method p 128 N95-16569

KUTSCHENREUTER, P.

Scramjet testing guidelines p 138 N95-16317

KUWANO, N.

Development of a pilot tube with multi-hole pyramidal head. 2: A five-hole yew probe of engineering model p 522 A95-91577

KUYVENHOVEN, J. L.

Surface grid generation for multi-block structured grids p 643 A95-95478

KUZMENKO, P.

An Echelle Grating Spectrometer (EGS) for mid-IR remote chemical detection
[DE94-019310] p 249 N95-21478

KUZMIN, M.

Optical surface pressure measurements: Accuracy and application field evaluation p 175 N95-19274

KUZNETSOV, V. I.

Gas-turbine engines with increased efficiency of two circuits, due to the use of the utilizing steam-turbine circuit
[BTN-94-EIX94461408755] p 153 A95-63638

KWA, TECK-SENG

COINS: A composites information database system p 453 N95-28465

KWAN, JIMMY S. W.

Auxiliary power unit noise of Boeing B737 and B747 aircraft p 571 A95-88468

KWEI, G. H.

Phonon characteristics of high (T sub c) superconductors from neutron Doppler broadening measurements
[DE95-003703] p 324 N95-24076

KWON, OKEY

Advanced k-epsilon modeling of heat transfer
[NASA-CR-4679] p 648 N95-31423

KWONG, ANTHONY H. M.

Active boundary-layer control in diffusers
[HTN-95-42580] p 458 A95-87210

LAANANEN, DAVID H.

Prediction of energy absorption capability of composite stiffeners
[HTN-95-A0500] p 230 A95-72571

The potential of genetic algorithms for conceptual design of rotor systems
[NASA-CR-196813] p 43 N95-11699

LABAUNE, G.

FASTPACK: Optimized solutions for modular avionics derived from a parametric study. Part 2: Avionics p 233 N95-20635

Composite cases for airborne electronic equipment: A technology study and EMC p 241 N95-20655

LABBE, M.

Transport aircraft loading and balancing system: Using a CLIPS expert system for military aircraft load planning p 217 N95-19751

LABONTE, S.

Validation of an effective flat cruciform-shaped specimen to study CFRP composite laminates under biaxial loading
[BTN-95-EIX95152584677] p 282 A95-73589

LABRUJERE, TH. E.

Residual-correction type and related computational methods for aerodynamic design. Part 1: Airfoil and wing design p 128 N95-16566

Residual-correction type and related computational methods for aerodynamic design. Part 2: Multi-point airfoil design p 128 N95-16567

LACAU, P. G.

Aeromechanical design of modern missiles p 73 N95-14446

LACAU, R. G.

Lateral jet control for tactical missiles p 84 N95-14448

Computation of supersonic air-intakes p 74 N95-14452

LACHAPPELLE, G.

Attitude determination using dedicated and nondedicated multi-antenna GPS sensors
[BTN-95-EIX95142555482] p 228 A95-72891

LACHENMAIER, RALPH

The IEEE scalable coherent interface: An approach for a unified avionics network p 234 N95-20650

LACKEY, JAMES B.

Flight validation of ground-based assessment for control power requirements at high angles of attack p 70 N95-14246

Navy and the HARV: High angle of attack tactical utility issues p 71 N95-14252

LACOMBE, G.

Implicit multidomain calculation of viscous transonic flows without artificial viscosity or upwinding p 640 A95-95443

LACOR, C.

Hypersonic Navier-Stokes computations about complex configurations p 644 A95-95497

LADD, JOHN A.

The applicability of turbulence models to aerodynamic and propulsion flowfields at McDonnell-Douglas Aerospace p 439 N95-27886

LAFARGE, ROBERT A.

Functional dependence of trajectory dispersion on initial condition errors
[BTN-95-EIX95152583263] p 298 A95-73564

LAFON, A.

Shock layers and boundary layers in hypersonic flows
[HTN-95-A0003] p 183 A95-67830

LAFON, PHILIPPE

Stochastic approach to noise modeling for free turbulent flows
[HTN-95-42321] p 371 A95-86150

LAFONTAINE, FRANK J.

High-resolution imaging of rain systems with the advanced microwave precipitation radiometer
[HTN-95-70133] p 252 A95-70655

LAFORE, J.-P.

Nonhydrostatic simulation of frontogenesis in a moist atmosphere. Part 3: Thermal wind imbalance and rainbands
[HTN-95-90356] p 212 A95-66429

LAFORET, S.

Composite cases for airborne electronic equipment: A technology study and EMC p 241 N95-20655

LAFORGE, LEO G.

Overview of AlliedSignal's avionics development in the CIS
[BTN-95-EIX95212641069] p 287 A95-76734

LAGANELLI, ANTHONY L.

Enhancements to integral solutions to ablation and charring
[BTN-95-EIX95302694461] p 636 A95-94058

LAGIER, MARK T.

An application of virtual prototyping to the flight test and evaluation of an unmanned air vehicle
[AD-A281749] p 14 N95-11595

LAGRAFF, J.

Research and educational initiatives at the Syracuse University Center for Hypersonics
[AIAA PAPER 95-6107] p 520 A95-90439

LAGRANGE, DONALD E.

Energy absorption device for shock loading
[AD-D017476] p 706 N95-34449

LAI, H. T.

Numerical study of contaminant effects on combustion of hydrogen, ethane, and methane in air
[AIAA PAPER 95-6097] p 510 A95-88005

LAI, JONATHAN Y.

Maximum-likelihood spectral estimation and adaptive filtering techniques with application to airborne Doppler weather radar
[NASA-CR-197699] p 316 N95-23670

LAI, ZHIHONG

Panel flutter limit-cycle suppression with piezoelectric actuation
[BTN-95-EIX95302731089] p 618 A95-94208

- LAING, P.**
Gas turbine prediffuser-combustor performance during operation with air-water mixture
[DOT/FAA/CT-93/52] p 83 N95-15683
- LAIRD, JOHN E.**
Collected papers of the Soar/IFOR project, Spring 1994
[AD-A280063] p 238 N95-20624
- LAIT, L. R.**
Fine-scale, poleward transport of tropical air during AASE 2
[HTN-95-70949] p 352 A95-78014
- LAIT, LESLIE R.**
Trajectory modeling of emissions from lower stratospheric aircraft
[HTN-95-41219] p 317 A95-75031
- LAITONE, EDMUND V.**
Minimum sink-speed in power-off glide
[BTN-95-EIX95062487556] p 193 A95-68370
- LAKE, R. C.**
Demonstration of an elastically coupled twist control concept for tilt rotor blade application
[BTN-94-EIX94441386633] p 196 A95-68182
Demonstration of an elastically coupled twist control concept for tilt rotor blade application
[HTN-95-20959] p 465 A95-88998
- LAKSHMANAN, B.**
Application of Navier-Stokes code PAB3D with kappa-epsilon turbulence model to attached and separated flows
[NASA-TP-3480] p 224 N95-21338
- LAKSHMINARAYANA, B.**
Numerical computation of aerodynamics and heat transfer in a turbine cascade and a turn-around duct using advanced turbulence models p 313 N95-23444
- LAL, MIHIR K.**
Correlation of unsteady pressure and inflow velocity fields of a pitching rotor blade
[BTN-95-EIX0619952748169] p 589 A95-94463
- LAL, MIHIR KUMAR**
Measurement around a rotor blade excited in pitch. Part 1: Dynamic inflow
[HTN-95-31007] p 220 A95-71177
Measurement around a rotor blade excited in pitch. Part 2: Unsteady surface pressure
[HTN-95-31008] p 220 A95-71178
Unsteady pressure and inflow velocity on a pitching rotor blade in hover p 480 N95-29771
- LALLO, ART**
H-76B fantail demonstrator composite fan blade fabrication
[HTN-95-80856] p 283 A95-75098
- LAM, C.-M. G.**
Vortex methods for the computational analysis of rotor/body interaction
[HTN-95-61072] p 369 A95-83656
- LAM, DAVID W.**
Use of the PARC code to estimate the off-design transonic performance of an over/under turbojet nozzle
[NASA-TM-106924] p 482 N95-30091
- LAM, S. S.**
Data acquisition and processing software for the Low Speed Wind Tunnel tests of the Jindivik auxiliary air intake
[AD-A285455] p 108 N95-17178
- LAM, T.**
Automatic guidance and control for helicopter obstacle avoidance
[BTN-95-EIX95182619130] p 291 A95-76607
- LAMAR, JOHN E.**
Quantifiable vortex features of F-106B aircraft at subsonic speeds
[BTN-95-EIX0619952748161] p 588 A95-94455
- LAMB, J. P.**
Convection heat transfer distributions over plates with square ribs from infrared thermography measurements
[HTN-95-20713] p 435 A95-86603
Constant flux, turbulent convection data using infrared imaging
[HTN-95-20731] p 435 A95-86621
- LAMB, J. PARKER**
Review and development of base pressure and base heating correlations in supersonic flow
[BTN-95-EIX95212645688] p 271 A95-76740
- LAMB, MILTON**
Internal performance characteristics of thrust-vectoring axisymmetric ejector nozzles
[NASA-TM-4610] p 331 N95-25338
- LAMBERT, DENNIS M.**
Fracture mechanics validity limits p 95 N95-14480
- LAMBIRIS, B.**
Adaptive modeling of jet engine performance with application to condition monitoring
[BTN-95-EIX95112524205] p 196 A95-69303
- LAMBORN, DANA**
Viper
[NASA-CR-197191] p 79 N95-13703
- LAMSON, SCOTT H.**
Grid generation and surface modeling for CFD
p 551 N95-28726
- LAN, C. EDWARD**
Computational fluid dynamics with icing effects
[SAE PAPER 932532] p 466 A95-89192
- LANCIAULT, MARK**
New technologies for space avionics
[NASA-CR-197574] p 150 N95-18196
- LANDIS, ABRAHAM L.**
Advanced composite structural concepts and materials technologies for primary aircraft structures: Advanced material concepts
[NASA-CR-4485] p 503 N95-29027
- LANDIS, KENNETH H.**
Advanced flight control technology achievements at Boeing Helicopters p 624 N95-32014
- LANDMANN, ALAN E.**
Effect of constraining layer stiffness on performance of damping tile materials using finite element modelling with Rayleigh integral p 30 N95-11306
- LANEN, T. A. W. M.**
Quantitative comparison between interferometric measurements and Euler computations for supersonic cone flows
[BTN-95-EIX95222650782] p 358 A95-79238
- LANG, JAMES D.**
Lean manufacturing for lean times
[BTN-95-EIX95302730538] p 583 A95-94036
- LANGHALS, TAMMY**
Further investigations of icing effects on an advanced high-lift multi-element airfoil
[NASA-TM-106947] p 381 N95-27762
- LANHAM, N. W.**
Aircraft-borne, laser-induced fluorescence instrument for the in situ detection of hydroxyl and hydroperoxyl radicals
[BTN-95-EIX95072499029] p 253 A95-71908
- LANSER, WENDY R.**
Forebody flow control on a full-scale F/A-18 aircraft
[BTN-95-EIX95152582333] p 281 A95-73535
High Alpha Technology Program (HATP) ground test to flight comparisons p 68 N95-14230
Flight and full-scale wind-tunnel comparison of pressure distributions from an F-18 aircraft at high angles of attack p 68 N95-14231
Comparison of full-scale, small-scale, and CFD results for F/A-18 forebody slot blowing p 72 N95-14255
- LANTERI, S.**
High performance parallel analysis of coupled problems for aircraft propulsion
[NASA-CR-195355] p 23 N95-10132
- LAPIN, MARK**
Labs behind Boeing's new 777
[BTN-95-EIX95142562403] p 280 A95-73437
- LAPSHIN, V.**
A program for scientific and applied investigations using aerostat complexes p 182 A95-66304
- LAPSHIN, V. I.**
The scientific ballooning in Russia
p 191 A95-66302
The joint Russian-Brasil research on balloons p 182 A95-66303
- LAPSON, L. B.**
Aircraft-borne, laser-induced fluorescence instrument for the in situ detection of hydroxyl and hydroperoxyl radicals
[BTN-95-EIX95072499029] p 253 A95-71908
- LAPUCHA, DARIUSZ**
Real-time testing and demonstration of the US Army Corps of Engineers' Real-Time On-The-Fly positioning system
[AD-A288624] p 334 N95-25609
- LAROCHE, PIERRE**
Use of high resolution lightning detection and localization sensors for hazardous aviation weather nowcasting p 661 A95-93486
- LARSEN, F. K.**
Flying ambulances: The approach of a small air force to long distance aeromedical evacuation of critically injured patients p 568 N95-29618
- LARSON, KATE M. S.**
The present and future of aircraft noise models: A user's perspective p 32 N95-11324
- LARSON, VICKIE L.**
A review of falconry as a bird control technique with recommendations for use at the Shuttle Landing Facility, John F. Kennedy Space Center, Florida, USA
[NASA-TM-110142] p 381 N95-27859
- LARSSON, TORBJOERN**
High-lift calculations using Navier-Stokes methods p 641 A95-95444
- LASCHKA, BORIS**
Velocity measurements with hot-wires in a vortex-dominated flowfield p 121 N95-19261
- LASH, THOMAS J.**
Hardware cleanliness methodology and certification p 419 N95-27656
- LASSWELL, JAMES W.**
The effects of display location and dimensionality on taxiway navigation
[AD-A294878] p 690 N95-34570
- LATORELLA, KARA A.**
A crew-centered flight deck design philosophy for High-Speed Civil Transport (HSCT) aircraft
[NASA-TM-109171] p 335 N95-24582
- LATOS, THOMAS S.**
System design considerations for an APU starter-generator
[SAE PAPER 932559] p 511 A95-90056
- LATYPOV, A. F.**
Integration of an hypersonic airbreathing vehicle: Assessment of overall aerodynamic performances and of uncertainties
[AIAA PAPER 95-6100] p 492 A95-88007
- LAU, BENTON**
Dynamics of the McDonnell-Douglas Large Scale Dynamic Rig and dynamic calibration of the rotor balance
[NASA-TM-108855] p 65 N95-13891
- LAU, KREISLER S. Y.**
Advanced composite structural concepts and materials technologies for primary aircraft structures: Advanced material concepts
[NASA-CR-4485] p 503 N95-29027
- LAUBERTS, A.**
Aspect estimation of an aircraft using library model silhouettes
[PB95-141834] p 360 N95-25894
- LAUCLIE, GERALD C.**
Empirical refinements to boundary layer transition noise models p 28 N95-11262
- LAUDIEN, E.**
Helicopter internal noise p 173 N95-19144
- LARRIER, E.**
Numerical modeling and simulation of chemically reacting reentry flows p 525 A95-87387
- LAVELLE, THOMAS M.**
Graphical user interface for the NASA FLOPS aircraft performance and sizing code
[NASA-TM-106649] p 80 N95-14604
Enhanced capabilities and modified users manual for axial-flow compressor conceptual design code CSPAN
[NASA-TM-106833] p 119 N95-18933
- LAVERDURE, JOHN P.**
Reliability and maintainability
[BTN-95-EIX95042477109] p 179 A95-68350
- LAW, C. K.**
Intrinsic transport and chemistry coupling in combustion phenomena p 538 A95-87191
Studies on high pressure and unsteady flame phenomena
[AD-A284126] p 152 N95-18410
- LAW, G. E.**
Applications of a damage tolerance analysis methodology in aircraft design and production p 426 N95-28483
- LAWEN, JAMES L., JR.**
Synchronous dynamics of a coupled shaft/bearing/housing system with auxiliary support from a clearance bearing: Analysis and experiment p 703 N95-32693
- LAWRENCE, CHARLES**
Steady-state dynamic behavior of an auxiliary bearing supported rotor system p 703 N95-32690
- LAWRENCE, W. R.**
Air data prediction from surface pressure measurements on guided munitions
[BTN-95-EIX95282706664] p 466 A95-89641
- LAWTON, JOSEPH**
Unmanned aerial vehicle heavy fuel engine test
[AD-A284332] p 139 N95-18383
- LAY, RICHARD J.**
Recommendation on transition from primary/secondary radar to secondary-only radar capability
[AD-A286279] p 249 N95-22005
- LAZARUS, KENNETH B.**
Fundamental mechanisms of aeroelastic control with control surface and strain actuation
[BTN-95-EIX95242670746] p 327 A95-81101
- LAZUTIN, L. L.**
The scientific ballooning in Russia
p 191 A95-66302
The joint Russian-Brasil research on balloons p 182 A95-66303
- LE TALLEC, P.**
Optimal shape design in hypersonic aerodynamics and electromagnetics p 639 A95-95397

LE, TUAN

- The Elite: A high speed, low-cost general aviation aircraft for Aeroworld
[NASA-CR-197161] p 45 N95-12530
- LEACH, BARRIE W.**
Comments on 'correction of inertial navigation with Loran C on NOAA's P-3 aircraft'
[HTN-95-70149] p 227 A95-70671
- LEAHY, KEVIN**
High density monolithic packaging technology for digital/microwave avionics p 240 N95-20646
- LEAHY, MICHAEL B., JR.**
A generic telerobotics architecture for C-5 industrial processes
[AIAA PAPER 94-1264-CP] p 27 N95-11529
- LEATHERWOOD, JACK D.**
Recent laboratory studies of loudness and annoyance to sonic booms p 575 A95-90117
- LEBOUCHER, CHRISTOPHE**
Scramjet combustor design in France
[AIAA PAPER 95-6094] p 510 A95-88002
- LEBOZEC, A.**
Hypersonic model testing in a shock tunnel
[BTN-95-EIX95222650789] p 329 A95-79245
- LECCE, L.**
Structural acoustic calculations in the low-frequency range
[BTN-95-EIX95152582336] p 323 A95-73538
Numerical and flight measured interior noise characteristics of a twin-engine turboprop general aviation aircraft p 573 A95-90094
- LECHNER, WOLFGANG**
GPS/GLONASS/INS test program
[BTN-94-EIX94441386131] p 189 A95-68187
- LECHTENBERG, LEON**
Design and development of an F/A-18 inlet distortion rake: A cost and time saving solution p 69 N95-14241
- LECUELLET, J.**
Composite cases for airborne electronic equipment: A technology study and EMC p 241 N95-20655
- LEDERER, MELISSA A.**
Hypervelocity wind tunnel number 9, high Mach number development program
[AD-A289934] p 594 N95-30929
- LEDERER, R.**
Testing the hypersonic technology demonstration nozzle: Results from the test campaign 1993/94
[AIAA PAPER 95-6084] p 509 A95-87413
- LEDUC, VINCENT**
Transport aircraft loading and balancing system: Using a CLIPS expert system for military aircraft load planning p 217 N95-19751
- LEE EDWIN E., JR.**
Aerodynamic investigation with focusing schlieren in a cryogenic wind tunnel
[HTN-95-20835] p 544 A95-88096
- LEE, A. H. W.**
Constant flux, turbulent convection data using infrared imaging
[HTN-95-20731] p 435 A95-86621
- LEE, ABRAHAM P.**
Impact, friction, and wear testing of microsamples of polycrystalline silicon p 361 A95-79988
- LEE, ALEX K. H.**
Multi-block finite volume calculation of compressible flow past aerodynamic configurations p 643 A95-95473
- LEE, B. H. K.**
Vortical flow structure near the F/A-18 LEX at high incidence
[BTN-95-EIX95062487555] p 186 A95-68369
Postinstability behavior of a two-dimensional airfoil with a structural nonlinearity
[BTN-95-EIX95152582337] p 266 A95-73539
Role of Kutta waves on oscillatory shock motion on an airfoil
[HTN-95-81642] p 542 A95-87690
- LEE, BURNETT**
Aircraft maneuver envelope warning system
[NASA-CASE-ARC-11953-1] p 82 N95-14518
- LEE, CALVIN K.**
Radial reefing method for accelerated and controlled parachute opening
[BTN-95-EIX95062487539] p 187 A95-69247
- LEE, CHRISTOPHER A.**
Design and testing of an oblique all-wing supersonic transport
[NASA-CR-196394] p 48 N95-12785
Design and testing of low sonic boom configurations and an oblique all-wing supersonic transport
[NASA-CR-197744] p 389 N95-26651
- LEE, DAL HO**
Comparison of parameter identification algorithms for flight vehicles
[BTN-94-EIX94371347708] p 219 A95-69967

LEE, DUCK JOO

- Numerical study of sound generation due to a spinning vortex pair
[BTN-95-EIX95182619075] p 307 A95-75760
- LEE, E. U.**
Corrosion of landing gear steels p 302 N95-23500
- LEE, EUN U.**
Corrosion behavior of landing gear steels
[AD-A285862] p 242 N95-22132
- LEE, EUN YOUNG**
A numerical study of the small scale wing-body junction problem p 482 N95-30235
- LEE, IN**
Aeroelastic stability of hingeless rotor blade in hover using large deflection theory
[BTN-94-EIX94441386616] p 183 A95-67347
Static aeroelastic characteristics of a composite wing
[BTN-95-EIX95152582340] p 282 A95-73542
Aeroelastic stability of hingeless rotor blade in hover using large deflection theory p 546 A95-88991
Effects of structural damping on aeroelastic stability of various shaped composite plate wing p 530 A95-91530
- LEE, J.**
Log structural for turbulent boundary layers over rough bleed surfaces
[BTN-94-EIX94441380981] p 208 A95-68165
- LEE, J. S.**
Statistics of multi-look AIRSAR imagery: A comparison of theory with measurements p 320 N95-23947
- LEE, JAE MOON**
Integrated design and manufacturing for the high speed civil transport
[NASA-CR-197183] p 48 N95-12700
- LEE, JAEWOOL**
Aerodynamically blunt and sharp bodies
[BTN-95-EIX95041503781] p 205 A95-69212
Development of an efficient inverse method for supersonic and hypersonic body design
[BTN-95-EIX95041503784] p 180 A95-69215
Minimum-drag axisymmetric bodies in the supersonic/hypersonic flow regimes
[BTN-95-EIX95041503785] p 180 A95-69216
- LEE, JANG GYU**
Comparison of parameter identification algorithms for flight vehicles
[BTN-94-EIX94371347708] p 219 A95-69967
Covariance analysis of strapdown INS considering gyrocompass characteristics
[BTN-95-EIX95202637592] p 279 A95-76697
Design of an effective controller via disturbance accommodating left eigenstructure assignment
[BTN-95-EIX95282706663] p 565 A95-88178
Design of a modern pitch pointing control system
[BTN-95-EIX95302731226] p 618 A95-94045
- LEE, JANG-YEON**
A numerical study of the starting process in a hypersonic shock tunnel p 626 N95-30493
- LEE, JINHO**
Surface modeling and grid generation for aeropropulsion CFD p 551 N95-28732
- LEE, JOON SIK**
Numerical calculations of the turbulent flow through a controlled diffusion compressor cascade
[BTN-95-EIX95282710056] p 632 A95-92473
- LEE, K. D.**
Two-point transonic airfoil design using optimization for improved off-design performance
[BTN-95-EIX95062487542] p 192 A95-68356
- LEE, K. M.**
Multi-block finite volume calculation of compressible flow past aerodynamic configurations p 643 A95-95473
- LEE, KAM-PUJ**
Higher-order viscous shock-layer solutions for high-altitude flows
[BTN-95-EIX95152583255] p 306 A95-73556
- LEE, LEE S.**
Flame-spreading phenomena in the fin-slot region of a solid rocket motor p 23 N95-10296
- LEE, M. F.**
F/A-18 IFOSTP Fatigue test airbag load determination on the vertical and horizontal tails
[DSTO-TR-0135] p 388 N95-26389
- LEE, PAUL**
Passive millimeter wave camera for aircraft landing in low visibility conditions
[BTN-95-EIX95292721321] p 609 A95-92513
- LEE, ROBERT A.**
Incorporation of topography effects in aircraft noise modeling p 578 A95-90140
Noise modeling for MOAs and ranges p 32 N95-11322
- LEE, ROBERT E.**
An investigation of pilot induced oscillation phenomena in digital-flight control systems p 623 N95-32011

LEE, S.

- Scarf joint technique with cocured and precured patches for composite repair p 396 N95-27524
- LEE, SHEN C.**
Computational study of boundary layer control for improving airfoil performance
[SAE PAPER 932513] p 466 A95-89186
- LEE, SOOGAB**
Dynamic stall control for advanced rotorcraft application
[BTN-95-EIX95222650793] p 334 A95-79249
Reduction of blade-vortex interaction noise through porous leading edge
[HTN-95-42324] p 371 A95-86153
Head-on parallel blade-vortex interaction
[HTN-95-61197] p 491 A95-87570
- LEE, TA-CHENG**
Navier-Stokes solution of wing wake structure and its perturbation p 479 N95-29121
- LEE, THOMAS F.**
Potential applications of the SSM/I cloud liquid water parameter to the estimation of marine aircraft icing
[HTN-95-80651] p 254 A95-72495
- LEE, W. Y.**
Thermal Barrier Coating Workshop
[NASA-CP-10170] p 344 N95-26119
Thermal barrier coatings issues in advanced land-based gas turbines p 344 N95-26122
- LEE, Y.**
Heat-transfer measurements and computations of swept-shock-wave boundary-layer interactions
[HTN-95-81634] p 541 A95-87682
- LEFEBVRE, D.**
Validation of an effective flat cruciform-shaped specimen to study CFRP composite laminates under biaxial loading
[BTN-95-EIX95152584677] p 282 A95-73589
- LEFEBVRE, M.**
Measurement by coherent anti-Stokes Raman scattering in the R5Ch hypersonic wind tunnel
[BTN-95-EIX95112523811] p 188 A95-69322
- LEFEBVRE, PAUL J.**
Hydrofoil force balance
[AD-D016475] p 160 N95-18461
- LEFEVRE, FRANCK**
Three-dimensional model interpretation of NO(x) measurements from the lower stratosphere
[HTN-95-90534] p 213 A95-67806
- LEGER, ALAIN**
A helmet mounted display for night missions at low altitude p 693 N95-32503
- LEGGETT, DAVID B.**
Summary of a joint program of research into aircraft flight control concepts
[AD-A280012] p 237 N95-20004
- LEGIDAKES, LEO J.**
An analysis of the impact of ASPA on organizational and depot level maintenance
[AD-A292670] p 457 N95-29414
- LEHMAN, EDWARD**
Industry review of a crew-centered cockpit design process and toolset
[AD-A282966] p 130 N95-17661
- LEIGH, BARRY**
Development and validation of a numerical acoustic analysis program for aircraft interior noise prediction p 572 A95-88471
Noise transmission and reduction in turboprop aircraft p 175 N95-19164
- LEIGH, JAMES E.**
An experimental investigation of helicopter downwash and tailboom interaction at the Wichita State University 7x10 foot wind tunnel p 375 N95-26955
- LEISHMAN, J. G.**
On the influence of time-varying flow velocity on unsteady aerodynamics
[HTN-95-61073] p 369 A95-83657
Experimental data on the aerodynamic interactions between a helicopter rotor and an airframe p 116 N95-17883
- LELEUX, TODD M.**
Nonlinear aerodynamic analysis of grid fin configurations
[BTN-95-EIX0619952748172] p 590 A95-94466
- LEMAITRE, J.**
On-line handling of air traffic: Management, guidance and control
[AGARD-AG-321] p 126 N95-18927
- LEMASURIER, PHILLIP**
Improvement of the predicted aural detection code ICHIN (I Can Hear It Now) p 576 A95-90123
- LEMENN, P.**
Experimental study of the helicopter-mobile radioelectrical channel and possible extension to the satellite-mobile channel p 247 N95-20945

- LEMONT, HAROLD E.**
Concepts for the control of rotor noise
p 573 A95-90092
- LENG, GERARD**
Reduced-order nonlinear analysis of aircraft dynamics
[BTN-95-EIX95282706665] p 455 A95-89640
- LEONNE, M.**
High-performance parallel analysis of coupled problems for aircraft propulsion
[NASA-CR-197440] p 289 N95-23088
- LEONARD, ANTHONY**
Research on bluff body vortex wakes
[AD-A286319] p 223 N95-20177
- LEONARD, CHUCK**
The Balsa bullet: A high speed, low-cost general aviation aircraft for Aeroworld
[NASA-CR-197165] p 46 N95-12638
- LEONARD, G.**
Development of an aeroderivative gas turbine dry low emissions combustion system
[BTN-94-EIX95011441246] p 417 A95-84203
- LEONARD, O.**
Permeable wall boundary conditions for transonic airfoil design
p 641 A95-95445
- LEONARD, THOMAS L.**
Integrated flight crew transition training for the advanced flight deck aircraft
[SAE PAPER 932599] p 380 A95-84571
- LEONDES, CORNELIUS**
Assessment of avionics technology in European aerospace organizations
[NASA-CR-189201] p 337 N95-24624
- LEONE, SCOTT A.**
Enhancements to integral solutions to ablation and charring
[BTN-95-EIX95302694461] p 636 A95-94058
- LEONG, M. Y.**
Jet mixing in a reacting cylindrical crossflow
[NASA-TM-106975] p 616 N95-30853
- LEPPERT, FRANCK**
A helmet mounted display for night missions at low altitude
p 693 N95-32503
- LEQUEUX, L.**
Catapult-launching of the RAFALE design and experimentation
p 609 N95-32008
- LERAT, A.**
Implicit multidomain calculation of viscous transonic flows without artificial viscosity or upwinding
p 640 A95-95443
- LEROY, G.**
The calculation of erosion in a gas turbine compressor rotor
p 199 N95-19664
- LESCHZNER, M. A.**
Modelling 2D separation from a high lift aerofoil with a non-linear eddy-viscosity model and second-moment closure
[HTN-95-C0005] p 585 A95-93393
- LESHCHYSHYN, ANDREW**
Anechoic chamber upgrade
[AD-A294375] p 700 N95-34342
- LESIEUTRE, DANIEL J.**
Aerodynamic design of pegasus: Concept to flight with computational fluid dynamics
[BTN-95-EIX95182617463] p 298 A95-75734
- LESTER, H. C.**
Numerical investigation of sound transmission through double wall cylinders with respect to active noise control
p 577 A95-90134
- LESTER, MICHAEL T.**
A platform independent application of Lux illumination prediction algorithms
[AD-A283669] p 170 N95-18018
- LESTER, PETER F.**
Turbulence near thunderstorm tops
p 675 A95-93553
- LEVIN, D.**
Dynamic investigation of the angular motion of a rotating body-parachute system
[BTN-95-EIX95182619220] p 270 A95-76646
- LEVINE, WILLIAM S.**
Techniques for designing rotorcraft control systems
[NASA-CR-196192] p 52 N95-12791
- LEVSHUK, B.**
A program for scientific and applied investigations using aerostat complexes
p 182 A95-66304
- LEVY, DAVID W.**
Preliminary design of a single engine business jet
[SAE PAPER 931253] p 493 A95-89222
- LEW, T.**
Theoretical and actual performance of a long duration superpressure balloon made from a biaxially oriented nylon-6 film
p 181 A95-66282
- LEW, THOMAS M.**
Recent developments in nylon superpressure balloons
p 385 A95-82512
- LEWANDOWSKI, LAURAND H.**
Additives in bituminous materials and fuel-resistant sealers
[DOT/FAA/CT-94/78] p 55 N95-12131
- LEWICKI, DAVID G.**
Detecting gear tooth fracture in a high contact ratio face gear mesh
[NASA-TM-106822] p 162 N95-19125
- LEWIS, D. J.**
Time-resolved surface heat flux measurements in the wing/body junction vortex
[BTN-95-EIX95082502716] p 220 A95-71029
- LEWIS, H. O.**
Measurement of free-flight dynamic stability derivatives of cones in a hypersonic gun tunnel
[AIAA PAPER 95-6082] p 519 A95-87411
- LEWIS, M.**
Hypersonic aerodynamics test facility using the external propulsion accelerator
[AIAA PAPER 95-6138] p 470 A95-90455
- Sensitivity of engine-integrated waverider performance to static margin constraint
[AIAA PAPER 95-6142] p 496 A95-90458
- LEWIS, MARK**
The effect of high lift to drag ratio on aerobraking
p 415 A95-85807
- LEWIS, MARK J.**
Navier-Stokes computation of a viscous optimized waverider
[BTN-95-EIX95041503782] p 193 A95-69213
- The NASA-sponsored Maryland center for hypersonic education and research
[AIAA PAPER 95-6105] p 519 A95-88010
- LEWIS, RICHARD**
Representativeness and responsiveness of automated weather systems
p 660 A95-93482
- LEWIS, T. B.**
Foliage transmission measurements using a ground-based ultrawide band (300-1300 MHz) SAR system
[BTN-94-EIX94381351617] p 252 A95-70950
- LEWTER, W. J.**
A programmable heater control circuit for spacecraft
[NASA-TM-108459] p 9 N95-11157
- LEWY, S.**
High-frequency acoustic radiation from a curved duct of circular cross section
p 573 A95-90098
- LEYH, CARL H.**
Test results of a low cost airport weather radar
p 662 A95-93492
- LI-YI, WU**
An inverse design method of transonic airfoil and wing
[HTN-95-71128] p 385 A95-83489
- LI, FEI**
Computational studies of laminar to turbulence transition
[AD-A285622] p 248 N95-21146
- LI, G. X.**
Modelling and analysis of a dual-wheel nosegear: Shimmy instability and impact motions
[SAE PAPER 931402] p 605 A95-93672
- LI, W.**
Automation of reverse engineering process in aircraft modeling and related optimization problems
[NASA-CR-197109] p 129 N95-16899
- LI, WEI-LIN**
Aeroservoelastic aspects of wing/control surface platform shape optimization
[BTN-95-EIX95222650795] p 340 A95-79251
- LIASJO, KARE H.**
Aircraft noise zoning in Norway
p 581 A95-88476
- Assessment of helicopter noise annoyance: A comparison between helicopters and jet aircraft
p 560 A95-88480
- LIASJOE, K. H.**
Response to noise around Vaernes and Bodoe airports
[PB94-207065] p 62 N95-13575
- LIBBY, P. A.**
Theories of turbulent combustion in high speed flows
[AD-A280933] p 23 N95-10535
- LIBERIO, PATRICIA D.**
Environmentally safe aviation fuels
p 631 N95-31768
- LIBESKIND, M.**
Development of composite carrythrough bulkhead
p 423 N95-28438
- LIBRESCU, L.**
Vibrational behavior of adaptive aircraft wing structures modelled as composite thin-walled beams
p 423 N95-28435
- LICCIONE, JOHN W.**
Draft standard for color active matrix liquid crystal displays (AMLCDs) in US Military aircraft. Recommended best practices
[AD-A282950] p 49 N95-12591
- LICHTSINDER, M.**
Fundamentals of catastrophic failure prevention by thrust vectoring
[BTN-95-EIX0619952748176] p 606 A95-94470
- LICINA, J. R.**
First medical test of the UH-600 and equipment for use in US Army medevac helicopters
p 568 N95-29620
- LIEBECK, ROBERT H.**
Advanced subsonic airplane design and economic studies
[NASA-CR-195443] p 338 N95-24304
- LIEBST, BRAD S.**
Method for the prediction of the onset of wing rock
[BTN-95-EIX95152582342] p 282 A95-73544
- LIEN, F. S.**
Modelling 2D separation from a high lift aerofoil with a non-linear eddy-viscosity model and second-moment closure
[HTN-95-C0005] p 585 A95-93393
- LIEPINS, MARGITA C.**
The ITWS microburst prediction algorithm
p 655 A95-93456
- LIGHT, JEFFREY S.**
Wing download reduction using vortex trapping plates
[HTN-94-00710] p 4 A95-60188
- An assessment of upper surface blowing for the reduction of tilt rotor download
[HTN-94-00711] p 5 A95-60189
- Study of noise on a small-scale hovering tilt rotor
[HTN-94-00712] p 5 A95-60190
- Aerodynamic interactions between a rotor and wing in hover
[HTN-94-00714] p 5 A95-60192
- LIGHTHILL, JAMES**
Some aspects of the aeroacoustics of extreme-speed jets
p 572 A95-88893
- LIM, MARTIN G.**
Impact, friction, and wear testing of microsamples of polycrystalline silicon
p 361 A95-79988
- LIM, TAE W.**
On-line, adaptive state estimator for active noise control
p 322 N95-23308
- LIN, C. A.**
Modelling three-dimensional gas-turbine combustor model flow using second-moment closure
[HTN-95-20935] p 464 A95-88974
- LIN, CHARRISSA Y.**
Fundamental mechanisms of aeroelastic control with control surface and strain actuation
[BTN-95-EIX95242670746] p 327 A95-81101
- LIN, CHING-FANG**
New failure detection approach and its application to GPS autonomous integrity monitoring
[BTN-95-EIX95202637613] p 279 A95-76676
- High-performance, robust, bank-to-turn missile autopilot design
[BTN-95-EIX95242670751] p 336 A95-81096
- Failure detection and isolation structure for global positioning system autonomous integrity monitoring
[BTN-95-EIX95282706656] p 486 A95-89648
- LIN, H.**
Effects of time scales on lift of airfoils in an unsteady stream
[HTN-95-81643] p 542 A95-87691
- LIN, I. J.**
Sidewash on the vertical tail in subsonic and supersonic flows
[BTN-95-EIX95152582316] p 264 A95-73519
- LIN, J. -C.**
Transient structure of vortex breakdown on a delta wing
[BTN-95-EIX95182619073] p 268 A95-75758
- LIN, JOHN C.**
Separation control on high-lift airfoils via micro-vortex generators
[BTN-95-EIX95152582326] p 265 A95-73529
- LIN, S.**
Optimization of waverider configurations generated from inclined circular and elliptic cones
[AIAA PAPER 95-6089] p 492 A95-89198
- LIN, SHEAM-CHYUN**
Integrated design of hypersonic waveriders including inlets and tailfins
[BTN-95-EIX95212645692] p 271 A95-76744
- Nonlinear asymptotic theory of hypersonic flow past a circular cone
[HTN-95-92599] p 461 A95-87415
- LINCOLN, JOHN W.**
USAF aging aircraft program
[BTN-95-EIX95072498878] p 180 A95-68394
- Challenges for the aircraft structural integrity program
p 80 N95-14481
- Proceedings of the USAF Structural Integrity Program Conference
[AD-A285684] p 194 N95-19517

- LINDBLAD, I.**
Hypersonic Navier-Stokes computations about complex configurations p 644 A95-95497
- LINDGREN, G.**
The Saab-Scania approach to development simulators [CONGRESS PAPER C428-10-137] p 522 A95-91698
- LINDSLEY, NED J.**
Critical speed analysis of a non-linear strain ring dynamical model for aircraft tires [SAE PAPER 932580] p 494 A95-90067
- LINES, N. P.**
Control requirements for the RB 211 low-emission combustion system [BTN-94-EIX95011441244] p 416 A95-84201
- LINHUA, WANG**
Study on a scheme for the prolongation of microgravity time of balloon-borne drop capsule p 414 A95-82515
- LINNETT, I. W.**
Subharmonic and quasi-periodic motions of an eccentric squeeze film damper-mounted rigid rotor [BTN-94-EIX95011440601] p 429 A95-82982
- LINNETT, KIM**
What's next in commercial aircraft environmental control systems? [SAE PAPER 932057] p 513 A95-91638
- LINTON, SAMUEL W.**
Computation of the poststall behavior of a circulation controlled airfoil [BTN-95-EIX95152582320] p 264 A95-73523
- LINZELL, ROBERT S.**
Evaluation of the Sparton tight-tolerance AXBT [HTN-95-40728] p 251 A95-70473
- LIOTTI, G.**
Calculation of control laws for the digital fuel control unit of a small thrust turbojet [SAE PAPER 931411] p 614 A95-93677
- LIU, MENG-SING**
An approach for dynamic grids [NASA-TM-106774] p 76 N95-15853
- LIU, S. G.**
Vorticity concentration at the edge of the inboard vortex sheet [HTN-95-31010] p 221 A95-71180
Correlation of unsteady pressure and inflow velocity fields of a pitching rotor blade [BTN-95-EIX0619952748169] p 589 A95-94463
- LIU, SHIUH-GUANG**
Measurement around a rotor blade excited in pitch. Part 1: Dynamic inflow [HTN-95-31007] p 220 A95-71177
Measurement around a rotor blade excited in pitch. Part 2: Unsteady surface pressure [HTN-95-31008] p 220 A95-71178
- LIPPKÉ, C.**
Nonlinear dynamic simulation of single- and multispool core engines, part 1: Computational method [BTN-95-EIX95112524200] p 210 A95-69308
GETRAN: A generic, modularly structured computer code for simulation of dynamic behavior of aero- and power generation gas turbine engines [BTN-94-EIX95011441241] p 431 A95-84198
- LISCINSKY, D. S.**
Crossflow mixing of noncircular jets [NASA-TM-106865] p 338 N95-24390
Effects of initial conditions on a single jet in crossflow [NASA-TM-107002] p 615 N95-30589
- LITNETSKIJ, A. V.**
A new generation of instruments for flying laboratories [BTN-94-EIX94401363947] p 317 A95-75532
- LITT, JONATHAN**
Sensor fault detection and diagnosis simulation of a helicopter engine in an intelligent control framework [AD-A290223] p 137 N95-15970
- LITTKÉ, B.**
The Saab-Scania approach to development simulators [CONGRESS PAPER C428-10-137] p 522 A95-91698
- LITTLE, R. C.**
Laboratory evaluation of a reactive baffle approach to NOx control [AD-A283802] p 255 N95-19921
- LITTMAN, DAVID C.**
Energy absorption device for shock loading [AD-D017476] p 706 N95-34449
- LITRELL, D. M.**
Eglin Air Force Base Ram Accelerator Research Facility p 19 N95-10284
- LIU, BAW-LIN**
High frequency flow-structural interaction in dense subsonic fluids [NASA-CR-4652] p 330 N95-24217
- LIU, CHING SHI**
Analytical study of the neutral stability of a model hypersonic boundary layer [BTN-95-EIX9515257589] p 263 A95-73493
- LIU, J. W. H.**
Large-scale computational fluid dynamics by the finite element method [BTN-94-EIX94381359154] p 243 A95-71744
- LIU, JIANYE**
Application of GPS/SINS/RA integrated system to aircraft approach landing p 125 N95-16277
- LIU, MENG-ZHAO**
The analysis of the processing increased weight for pilot production of F-X aircraft [HTN-95-71133] p 385 A95-83494
- LIU, S. C.**
An analysis of aircraft exhaust plumes form accidental encounters [HTN-95-70943] p 351 A95-78008
- LIU, YU**
Simulation on the 3-D turbulent flow in the passages of finocyl grain [BTN-95-EIX95202638962] p 279 A95-76674
- LIVNE, ELI**
Aerosevovlastic aspects of wing/control surface planform shape optimization [BTN-95-EIX95222650795] p 340 A95-79251
Equivalent plate structural modeling for wing shape optimization including transverse shear [HTN-95-20839] p 492 A95-88100
- LORENTE, STEVEN**
Application of advanced material systems to composite frame elements p 422 N95-28432
- LO, C. F.**
Two-variable method for blockage wall interference in a circular tunnel [BTN-95-EIX95062487540] p 187 A95-69248
A wall interference assessment and correction system [NASA-CR-196940] p 58 N95-12228
A wall interference assessment/correction system [NASA-CR-197421] p 309 N95-23183
- LO, CHING F.**
Supersonic laminar flow control research [NASA-CR-196049] p 249 N95-21340
- LOBITZ, DON W.**
A NASTRAN-based computer program for structural dynamic analysis of Horizontal Axis Wind Turbines p 439 N95-27980
- LOBL, ELENA**
High-resolution imaging of rain systems with the advanced microwave precipitation radiometer [HTN-95-70133] p 252 A95-70655
- LOCKE, R. J.**
Two-dimensional imaging of OH in a lean burning high pressure combustor [NASA-TM-106854] p 236 N95-21383
- LOCKHART, RONALD**
Precision landing system mathematical modeling study report for Andrews Air Force Base, runway 19L, Camp Springs, MD [AD-A289015] p 384 N95-27903
- LOCKWOOD, MARY KAE**
Modelling structurally damaging twin-jet screech p 135 N95-19154
- LOELLBACH, JAMES**
Surface modeling and grid generation for aeropropulsion CFD p 551 N95-28732
- LOEWENSTEIN, M.**
Fine-scale, poleward transport of tropical air during AASE 2 [HTN-95-70949] p 352 A95-78014
- LOEWENSTEIN, MAX**
Vertical transport rates in the stratosphere in 1993 from observations of CO₂, N₂O, and CH₄ [HTN-95-70941] p 351 A95-78006
- LOFARO, RONALD J.**
Test and evaluation report for the Manual Domestic Passive Profiling System (MDPPS) [AD-A286312] p 225 N95-20093
Independent review of Aviation Technology and Research Information Analysis System (ATRIAS) database [AD-A284049] p 226 N95-21518
Test and Evaluation Plan (TEP) for Improvised Explosive Device Screening Systems (IEDSS) [AD-A286382] p 227 N95-22319
- LOHMANN, R. P.**
In situ observations in aircraft exhaust plumes in the lower stratosphere at midlatitudes [HTN-95-A0862] p 318 A95-76266
- LOKAJ, V. I.**
Heat transfer in the flow-through part of axial compressors [BTN-94-EIX94461407949] p 89 A95-62267
- LOKOS, WILLIAM A.**
Determination of stores pointing error due to wing flexibility under flight load [NASA-TM-4646] p 134 N95-19044
- LOMBARDI, GIOVANNI**
Analysis of some interference effects in a transonic wind tunnel [BTN-95-EIX0619952748166] p 589 A95-94460
- LOMBARDO, D. C.**
Preparation of S-70A-9 Black Hawk helicopter for flight tests to investigate cause of cracking of inner fuselage panel [AD-A293891] p 608 N95-31544
- LOMBARDO, G.**
Artificial intelligence for turboprop engine maintenance [HTN-95-92313] p 404 A95-85357
- LOMBARDO, GIUSEPPE**
An airborne monitoring system for FOD and erosion faults p 200 N95-19668
- LONDENBERG, W. KELLY**
Transonic Navier-Stokes calculations about a 65 deg delta wing [NASA-CR-4635] p 108 N95-17273
- LONEY, NORMAN W.**
Design of a variable area diffuser for a 15-inch Mach 6 open-jet tunnel p 297 N95-23309
- LONGMIRE, ELLEN K.**
Active open-loop control of particle dispersion in round jets [HTN-95-42334] p 372 A95-86163
- LONGO, J. M. A.**
Compressible inviscid vortex flow of a sharp edge delta wing [BTN-95-EIX95262694308] p 370 A95-85479
- LOOMIS, MARK P.**
Shock-tunnel combustor testing for hypersonic vehicles [NASA-CR-196836] p 52 N95-11938
- LOOS, ALFRED C.**
Development and verification of a resin film infusion/resin transfer molding simulation model for fabrication of advanced textile composites [NASA-CR-197439] p 301 N95-23179
- LOOSE, R. R.**
Wind technology development: Large and small turbines [DE95-000286] p 358 N95-26090
- LOOTEN, A.**
Criticism of the Leq as an index for aircraft noise and other discontinuous noise sources p 559 A95-88477
- LOPEZ, ALFRED R.**
Comments on effect of wet snow on the null-reference ILS system [BTN-95-EIX95142555488] p 227 A95-72885
- LOPEZ, J. L.**
Air data prediction from surface pressure measurements on guided munitions [BTN-95-EIX95282706664] p 466 A95-89641
- LOPEZ, VIRGINIA C.**
Powered lift for land and sea [BTN-95-EIX95041503010] p 192 A95-68313
- LOR, ALEX CHOUA**
The Aluminum Falcon: A low cost modern commercial transport [NASA-CR-197180] p 81 N95-15742
- LOTTATI, I.**
Operational multi-scale environment model with grid adaptivity (OMEGA) application to aviation weather p 676 A95-93556
- LOTTS, C. G.**
Technology integration box beam failure study p 441 N95-28468
Technology integration box beam failure study p 552 N95-28847
- LOU, ZHENG**
Electrorheologically controlled landing gear [BTN-94-EIX94461047055] p 78 A95-61740
An electrorheologically controlled semi-active landing gear [SAE PAPER 931403] p 605 A95-93673
- LOUIS, STEVEN**
Micro-time stress measurement device development [AD-A289511] p 448 N95-26845
- LOUISNARD, N.**
Potential effects on ozone of future supersonic aircraft/2D simulation [HTN-95-51282] p 356 A95-80867
- LOW, JOHN K. C.**
Ultra-high bypass ratio jet noise [NASA-CR-195394] p 100 N95-14610
- LOW, T. B.**
Development of a climatology for possible microburst occurrence in Canada p 664 A95-93497
- LOWSON, M. V.**
Drag reduction in a rectangular duct using riblets [HTN-95-01091] p 468 A95-90277
- LOYD, B.**
Anechoic wind tunnel study of turbulence effects on wind turbine broadband noise p 451 N95-27992

- LU, C. M.**
Modeling three-dimensional gas-turbine combustor modal flow using second-moment closure [HTN-95-20935] p 464 A95-88974
- LU, G.**
Attitude determination using dedicated and nondedicated multiantenna GPS sensors [BTN-95-EIX95142555482] p 228 A95-72891
- LU, PING**
Nonsmooth trajectory optimization: An approach using continuous simulated annealing [BTN-94-EIX94511433914] p 168 A95-64580
- LU, PONG-JEU**
Transonic flutter suppression using active acoustic excitations [BTN-95-EIX95262694310] p 408 A95-85481
- LUBOSCH, BERND**
E-6A hardness assurance, maintenance and surveillance program [AD-A283994] p 134 N95-19067
- LUCAS, M. J.**
The acoustic characteristics of turbomachinery cavities [NASA-CR-4671] p 476 N95-28720
- LUCAS, MICHAEL J.**
A review of Air Force policy and noise models pertaining to the noise environment under low-altitude, high-speed training areas p 561 A95-90118
Selecting optimum sonic boom monitoring sites in a special-use airspace p 576 A95-90124
Noise modeling for MOAs and ranges p 32 N95-11322
- LUCCI, B. L.**
Measurement of gust response on a turbine cascade [NASA-TM-106776] p 117 N95-18457
- LUCIANI, S.**
MAX-91: Polarimetric SAR results on Montesperolo site p 320 N95-23940
- LUCKHAM, DAVID C.**
Foundations of technology for constructing highly reliable distributed realtime systems [AD-A293254] p 678 N95-30892
- LUI, R. K.**
Experimental investigation of flow-boiling heat transfer under microgravity p 428 A95-82642
- LUJAN, MICHAEL A.**
The FC-1D: The profitable alternative Flying Circus Commercial Aviation Group [NASA-CR-197152] p 46 N95-12628
- LUKASZEWICZ, V.**
Static and dynamic friction behavior of candidate high temperature airframe seal materials [NASA-TM-106571] p 152 N95-16905
- LUKE, SUE**
In-flight lift-drag characteristics for a forward-swept wing aircraft and comparisons with contemporary aircraft [NASA-TP-3414] p 117 N95-18565
- LUMIA, R.**
Overview of NASREM: The NASA/NBS standard reference model for telerobot control system architecture re [PB94-194560] p 58 N95-12854
- LUNDQUIST, R. C.**
Dimensional stability of curved panels with cocured stiffeners and cobonded frames p 532 N95-28836
- LUNEV, A. N.**
Calculation of geometry of stamps with small allowances for pieces of the aerodynamic profile [BTN-94-EIX94461408772] p 103 A95-63655
- LUNNON, R. W.**
A study of the savings in time and fuel to aviation through the use of upper-air wind forecasts p 672 A95-93538
Creating a global climatology of freezing rain using numerical model output p 673 A95-93541
- LUNSFORD, ARLEEN**
Application of airborne field mill data for use in launch support [HTN-95-50054] p 98 A95-62279
- LUO, J.**
Numerical computation of aerodynamics and heat transfer in a turbine cascade and a turn-around duct using advanced turbulence models p 313 N95-23444
- LUO, Y.**
Optimization of waverider configurations generated from inclined circular and elliptic cones [AIAA PAPER 95-6089] p 492 A95-89198
- LUO, YU-SHAN**
Integrated design of hypersonic waveriders including inlets and tailfins [BTN-95-EIX95212645692] p 271 A95-76744
- LUSEBRINK, H.**
Treatment of non-linear systems by timeplane-transformed CT methods: The spectral gust method p 143 N95-18600
- LUTHRA, K. L.**
Toughened Silcomp composites for gas turbine engine applications [DE95-002851] p 235 N95-21243
- LUTTGES, M. W.**
Wind turbine blade aerodynamics: The combined experiment [DE94-011866] p 118 N95-18645
Wind turbine blade aerodynamics: The analysis of field test data [DE94-011867] p 118 N95-18646
Evidence that aerodynamic effects, including dynamic stall, dictate HAWT structural loads and power generation in highly transient time frames [DE94-011865] p 216 N95-19855
Techniques for the determination of local dynamic pressure and angle of attack on a horizontal axis wind turbine [DE95-009204] p 707 N95-32685
- LUTTGES, MARVIN W.**
Neural network prediction of three-dimensional unsteady separated flowfields [BTN-95-EIX95182619232] p 308 A95-76658
Application of neural networks to unsteady aerodynamic control p 360 N95-25264
- LUTZE, FREDERICK H.**
Kinematics and aerodynamics of velocity-vector roll [BTN-95-EIX95182619126] p 291 A95-76603
- LYDUCH, S.**
Flying ambulances: The approach of a small air force to long distance aeromedical evacuation of critically injured patients p 568 N95-29618
- LYLE, KAREN HEITMAN**
Acoustic radiation damping of flat rectangular plates subjected to subsonic flows p 172 N95-18542
- LYNCH, AMANDA**
An integrated system to improve aviation weather forecasts for the Alaska Range p 656 A95-93460
- LYNCH, F. T.**
2-D aileron effectiveness study p 110 N95-17851
The crucial role of wall interference, support interference and flow field measurements in the development of advanced aircraft configurations p 162 N95-19252
- LYNCH, S. P.**
Fatigue crack growth in nickel-based superalloys at 500-700 C. 1: Waspaloy [BTN-94-EIX94371347843] p 206 A95-69136
- LYNE, A. G.**
Period evolution of PSR B1259-63: Evidence for propeller-torque spindown [HTN-95-B0194] p 581 A95-87903
- LYNN, J. E.**
Phonon characteristics of high (T sub c) superconductors from neutron Doppler broadening measurements [DE95-003703] p 324 N95-24076
- LYON, ROGER**
Advanced subsonic airplane design and economic studies [NASA-CR-195443] p 338 N95-24304
- LYON, T. F.**
Chemical composition and photochemical reactivity of exhaust from aircraft turbine engines [HTN-95-51277] p 356 A95-80862
Nitrogen oxide emissions characteristics of augmented turbofan engines [HTN-94-EIX95011441240] p 403 A95-84197
- LYRINTZIS, A. S.**
Rotating Kirchhoff method for three-dimensional transonic blade-vortex interaction hover noise [BTN-94-EIX94441386601] p 182 A95-67332
Rotating Kirchhoff method for three-dimensional transonic blade-vortex interaction hover noise [HTN-95-20927] p 463 A95-88966

M

- MA, DEREN**
A multibody/finite element analysis approach for modeling of crash dynamic responses [NIAR-94-3] p 277 N95-24050
- MA, HUI-YANG**
A note on the Kutta-Joukowski formula [ISBN 1-879921-01-4] p 635 A95-93735
- MA, JIAJU**
A new type of simulator for simulating the flow-field distortion of engine inlet [BTN-95-EIX95202638963] p 289 A95-76673
- MA, KWAN-LIU**
3D visualization of unsteady 2D airplane wake vortices [AD-A284745] p 27 N95-11593
- MA, LI**
The effects of pitting on fatigue crack nucleation in 7075-T6 aluminum alloy p 88 N95-14482
- MA, LIBIN**
Numerical analysis of flow field around gas rudder p 407 A95-82333
- MABEY, D. G.**
A note on the interpretation of mini-tuft photographs [HTN-95-01089] p 468 A95-90275
Buffeting tests in a cryogenic windtunnel [HTN-95-92833] p 470 A95-90751
- MABSON, G. E.**
Dimensional stability of curved panels with cocured stiffeners and cobonded frames p 532 N95-28836
- MACABANTAD, DOMINIQUE DUJALE**
Central coast designs: The Eightball Express. Taking off with convention, cruising with improvements and landing with absolute success [NASA-CR-197181] p 47 N95-12643
- MACCORMACK, ROBERT W.**
Algorithmic trends in CFD in the 1990's for aerospace flow field calculations p 550 A95-91917
High altitude hypersonic flowfield radiation [AD-A281386] p 106 N95-16160
- MACDONALD-SMITH, DIAN F. M.**
The aerodynamic design of an integrated wing lower surface and pylons for reduced drag [ARA-MEMO-406] p 194 N95-19789
- MACH, DOUGLAS**
Field and data analysis studies related to the atmospheric environment [NASA-CR-196543] p 168 N95-18093
- MACH, DOUGLAS M.**
Aircraft electric field measurements: Calibration and ambient field retrieval [HTN-95-90508] p 213 A95-67780
- MACH, K. D.**
A perspective of rarefied gas flow problems relevant to high altitude flight [SAE PAPER 931366] p 586 A95-93647
- MACHERET, Y.**
Prediction of R-curves from small coupon tests p 167 N95-19496
- MACKLEY, ERNEST A.**
NASA's Hypersonic Research Engine Project: A review [NASA-TM-107759] p 50 N95-12860
- MACLEAN, B. J.**
Lift analysis of a variable camber foil using the discrete vortex-blob method [BTN-94-EIX94441386623] p 179 A95-68172
Lift analysis of a variable camber foil using the discrete vortex-blob method [HTN-95-20940] p 545 A95-88979
- MACLEOD, IAIN S.**
Quality assurance and risk management: Perspectives on Human Factors Certification of Advanced Aviation Systems p 690 N95-34771
- MACLEOD, J. D.**
Protective coatings for compressor gas path components p 201 N95-19675
- MACLEOD, KENNETH J.**
Aviation and the environment p 657 A95-93464
- MACMARTIN, DOUGLAS G.**
Noise transmission and reduction in turboprop aircraft p 175 N95-19164
- MACPHERSON, J. I.**
Observations of fluxes and inland breezes over a heterogeneous surface [HTN-95-80258] p 212 A95-66315
- MACPHERSON, J. IAN**
Comments on 'correction of inertial navigation with Loran C on NOAA's P-3 aircraft' [HTN-95-70149] p 227 A95-70671
Comparison of wind profiler and aircraft wind measurements at Chebogue Point, Nova Scotia [HTN-95-41833] p 353 A95-80559
- MACRAE, JOHN DOUGLAS**
Development and verification of a resin film infusion/resin transfer molding simulation model for fabrication of advanced textile composites [NASA-CR-197439] p 301 N95-23179
- MADAN, RAM C.**
Test and analysis results for composite transport fuselage and wing structures p 398 N95-28470
Test results from large wing and fuselage panels p 537 N95-29051
- MADAVAN, NATERI K.**
Solution-adaptive structured-unstructured grid method for unsteady turbomachinery analysis. Part I: Methodology [BTN-94-EIX94441380983] p 208 A95-67329
- MADDALON, JEFFREY M.**
A study of workstation computational performance for real-time flight simulation [NASA-TM-109184] p 449 N95-27241
- MADENCI, ERDOGAN**
Residual strength of thin panels with cracks p 311 N95-23311

MADERUELO, C.

A study of the effect of store unsteady aerodynamics on gust and turbulence loads p 133 N95-18601

MADHUSUDAN, R. S.

Boundary layer studies over an S-blade [HTN-95-92261] p 434 A95-85305

MADSON, MICHAEL D.

Aerodynamic tailoring of the Learjet Model 60 wing [SAE PAPER 932534] p 492 A95-89194

MAEKAWA, SHOZO

An experimental study on interacting flow between supersonic flow and secondary flow injected normally through circular nozzle p 472 A95-91511

MAEKAWA, SYOZO

A study on aerodynamic heating phenomena in three-dimensional shock wave/turbulent boundary layer interaction induced by sweptback sharp fins at supersonic flow p 428 A95-82419

MAESTRELLO, L.

Interaction of jet noise with a nearby panel assembly [BTN-95-EIX95262694295] p 434 A95-85466

On the interaction of jet noise with a nearby flexible structure [NASA-CR-194934] p 57 N95-11812

Acoustic field in unsteady moving media [NASA-CR-198162] p 438 N95-27179

Response of multi-panel assembly to noise from a jet in forward motion [NASA-CR-198164] p 442 N95-28673

MAESTRELLO, LUCIO

Control-nonlinear-nonstationary structural response and radiation near a supersonic jet [HTN-95-20929] p 463 A95-88968

MAFFEO, R. J.

Engine structures analysis software: Component Specific Modeling (COSMO) [NASA-CR-195378] p 57 N95-11711

MAGDELANEO, RAYMOND E.

Identification of higher order helicopter dynamics using linear modeling methods [HTN-95-80851] p 290 A95-75093

MAGGIO, ANTHONY

Unmanned aerial vehicle heavy fuel engine test [AD-A284332] p 139 N95-18383

MAGI, V.

Simulation of transverse gas injection in turbulent supersonic air flows [BTN-95-EIX95182619080] p 269 A95-75765

MAGORIEN, VINCENT G.

Dissolved gas - the hidden saboteur [SAE PAPER 931404] p 628 A95-93674

MAH, G. R.

AVIRIS and TIMS data processing and distribution at the land processes distributed active archive center [HTN-95-80851] p 290 A95-75093

MAHADEVAN, S.

Mechanical system reliability and risk assessment [BTN-95-EIX95142553046] p 304 A95-73452

MAHANTA, KAMALA

A CMC database for use in the next generation launch vehicles (rockets) p 150 N95-18993

MAHMOOD, M.

Suppression of vortex asymmetry and side force on a circular cone [BTN-95-EIX95042474413] p 209 A95-68287

MAHONEY, WILLIAM P., III

Windshear detection: TDWR and LLWAS operational experience in Denver 1988-1992 p 670 A95-93528

The prototype aviation weather products generator a vehicle to assess user needs p 671 A95-93534

MAHRT, L.

Observations of fluxes and inland breezes over a heterogeneous surface [HTN-95-80258] p 212 A95-66315

MAIDEN, JANICE R.

Weavability of dry polymer powder towpreg p 535 N95-29036

MAIER, A.

On aircraft repair verification of a fighter A/C integrally stiffened fuselage skin p 394 N95-27515

MAIER, A. E.

Composite repair of a CF18: Vertical stabilizer leading edge p 395 N95-27517

MAIN, PERRY S.

The CBT alternative for aviation training: Is it meeting the need? [SAE PAPER 932596] p 379 A95-84568

MAINE, TRINDEL A.

Flight test of a propulsion controlled aircraft system on the NASA F-15 airplane p 691 N95-33023

Design challenges encountered in the F-15 PCA flight test program p 692 N95-33025

MAJEED, O.

Numerical modelling of transverse impact on composite coupons [BTN-95-EIX95082502225] p 240 A95-71022

MAKINO, MITUO

Experiment of the large elastic deformation of biconvex wing sections in an air-flow p 475 A95-91564

MALACANE, CHRISTINE A.

A status report on the development of the Federal Aviation Administration/National Oceanic and Atmospheric Administration Memorandum of Agreement p 652 A95-93447

MALAVALLON, OLIVIER

Selective chemical stripping p 650 N95-32175

Process evaluation p 651 N95-32180

Standardization work p 651 N95-32181

MALCOLM, GERALD N.

Static and dynamic force/moment measurements in the Eidetics water tunnel p 69 N95-14238

Development of a multicomponent force and moment balance for water tunnel applications, volume 1 [NASA-CR-4642-VOL-1] p 161 N95-18955

Development of a multicomponent force and moment balance for water tunnel applications, volume 2 [NASA-CR-4642-VOL-2] p 161 N95-18956

MALIK, M. R.

Comparison of linear stability results with flight transition data [BTN-95-EIX95182619097] p 283 A95-76582

Effect of crossflow on Goertler instability in incompressible boundary layers [NASA-CR-195007] p 159 N95-18193

MALIK, MUJEEB R.

Computational studies of laminar to turbulence transition [AD-A285622] p 248 N95-21146

MALINAS, N. P.

Foliage transmission measurements using a ground-based ultrawide band (300-1300 MHz) SAR system [BTN-94-EIX94381351617] p 252 A95-70950

MALITSKY, CHRISTOPHER

Weather And Radar Processor (WARP) Test and Evaluation Master Plan (TEMP) [AD-A288280] p 445 N95-26453

MALLORY, MARK

E-6A hardness assurance, maintenance and surveillance program [AD-A283994] p 134 N95-19067

MALONE, ROBERT L.

Test and Evaluation Plan (TEP) for Improvised Explosive Device Screening Systems (IEDSS) [AD-A286382] p 227 N95-22319

MALPICA, F.

Contribution of thermal radiation to the temperature profile of ceramic composite materials [BTN-94-EIX95011441252] p 417 A95-84209

MAMAN, N.

Matching fluid and structure meshes for aeroelastic computations: a parallel approach [BTN-95-EIX95302679864] p 636 A95-94102

High performance parallel analysis of coupled problems for aircraft propulsion [NASA-CR-195355] p 23 N95-10132

MANCHESTER, R. N.

Period evolution of PSR B1259-63: Evidence for propeller-torque spindown [HTN-95-B0194] p 581 A95-87903

MANGIACASALE, L.

Control law design using H-infinity and mu-synthesis short-period controller for a tail-airplane p 622 N95-31999

MANGO, S. A.

Statistics of multi-look AIRSAR imagery: A comparison of theory with measurements p 320 N95-23947

MANI, MORI

The applicability of turbulence models to aerodynamic and propulsion flowfields at McDonnell-Douglas Aerospace p 439 N95-27886

MANI, RAMANI

UHB engine fan broadband noise reduction study [NASA-CR-198357] p 580 N95-29641

MANJUNATH, A. R.

Flap-lag damping in hover and forward flight with a three-dimensional wake [HTN-95-A0496] p 221 A95-72567

MANKBADI, REDA R.

Structure of supersonic jet flow and its radiated sound [HTN-95-51645] p 431 A95-85027

MANKIN, W. G.

Comparison of column abundances from three infrared spectrometers during AASE 2 [HTN-95-70946] p 352 A95-78011

MANN, DARRELL L.

Future directions in helicopter protection system configuration p 198 N95-19657

MANN, EVELYN

The Integrated Terminal Weather System (ITWS) storm cell information and weather impacted airspace detection algorithm p 654 A95-93452

MANNINEN, L. M.

TKKMOD: A computer simulation program for an integrated wind diesel system. Version 1.0: Document and user guide [PB94-179090] p 60 N95-11798

MANNING, CAROL A.

Evaluating the effects of air traffic control automation p 601 A95-95091

The role of flight progress strips in en route air traffic control: A time-series analysis [DOT/FAA/AM-95/4] p 280 N95-23565

Automation and cognition in air traffic control: An empirical investigation [AD-A291932] p 488 N95-28790

MANSOUR, NAGI N.

A comparison of turbulence models in computing multi-element airfoil flows [AIAA PAPER 94-0291] p 4 A95-60185

MANSOUR, W. M.

Modal parameters for cracked rotors: models and comparisons [BTN-94-EIX94522410226] p 702 A95-96378

MANSUR, M. HOSSEIN

Development and validation of a blade-element mathematical model for the AH-64A Apache helicopter [NASA-TM-108863] p 367 N95-26710

MANTAY, WAYNE R.

Integrated aerodynamic/dynamic/structural optimization of helicopter rotor blades using multilevel decomposition [NASA-TP-3465] p 285 N95-22953

MANTEGAZZA, P.

Matrix fraction approach for finite-state aerodynamic modeling [BTN-95-EIX95262694311] p 365 A95-85482

MANTEL, B.

A cartesian grid finite element method for aerodynamics of moving rigid bodies p 642 A95-95471

Review of the EUROPT Project AERO-0026 p 129 N95-16573

MANUKYAN, B. S.

Universal electrohydraulic system for the steering gear loading [CONGRESS PAPER C428-10-106] p 517 A95-91700

MARBLE, FRANK E.

Response of a thin airfoil encountering a strong density discontinuity p 462 A95-88900

MARBOE, RICHARD C.

Empirical refinements to boundary layer transition noise models p 28 N95-11262

MARCHANT, M. J.

Construction of nearly orthogonal multiblock grids for compressible flow simulation [BTN-94-EIX94361133526] p 207 A95-65981

MARCHANT, W.

Design decisions from the history of the EUVE science payload [HTN-95-60545] p 205 A95-69854

MARCHELLO, JOSEPH M.

Weavability of dry polymer powder towpreg p 535 N95-29036

MARCHESSEAU, B.

Viper cabin-fuselage structural design concept with engine installation and wing structural design [NASA-CR-197162] p 45 N95-12305

MARCOLINI, MICHAEL A.

Sensitivity of acoustic predictions to variation of input parameters [HTN-95-80855] p 267 A95-75097

MARETIC, R.

Van der pol absorber for rotor vibrations [BTN-94-EIX94441385106] p 702 A95-96579

MARGASON, RICHARD J.

Jet to freestream velocity ratio computations for a jet in a crossflow [AIAA PAPER 93-4860] p 2 A95-60178

Flow visualization studies of VTOL aircraft models during Hover in ground effect [NASA-TM-108860] p 272 N95-22666

Investigation of wing upper surface flow-field disturbance due to NASA DC-8-72 in-flight inboard thrust-reverser deployment [NASA-TM-110351] p 457 N95-28816

MARIJNISSEN, G.

Braze repair possibilities for hot section gas turbine parts p 201 N95-19677

MARIOCCHI, A.

PVD TBC experience on GE aircraft engines p 345 N95-26126

MARKOPOULOS, NIKOS

Analytical investigations in aircraft and spacecraft trajectory optimization and optimal guidance [NASA-CR-4672] p 526 N95-29339

- MARKS, JOE**
Optimizing cockpit display configurations with a genetic algorithm system
[AD-A289799] p 508 N95-29123
- MARKUS, ALAN**
Progress in manufacturing large primary aircraft structures using the stitching/RTM process
p 537 N95-29050
- MAROLO, SAMUEL A.**
Conference on Aerospace Transparent Materials and Enclosures. Volume 2: Sessions 5-9
[AD-A283926] p 131 N95-18162
Conference on Aerospace Transparent Materials and Enclosures, volume 1
[AD-A283925] p 133 N95-18677
- MARRA, JOHN J.**
Tuned mass damper for integrally bladed turbine rotor
[NASA-CASE-MFS-28697-1] p 159 N95-18325
- MARRERO, W.**
Computing quantitative characteristics of finite-state real-time systems
[AD-A282839] p 83 N95-14343
- MARRIOT, J. F.**
Chinook goes FADEC
[CONGRESS PAPER C428-33-078] p 610 A95-93621
- MARROCCO, MATTHEW**
Thermally stable organic polymers
[AD-A281380] p 87 N95-14363
Thermally stable organic polymers
[AD-A290755] p 537 N95-29482
- MARROQUIN, ADRIAN**
Testing of TKE parameterizations in numerical models for clear-air turbulence forecasting p 667 A95-93515
Preliminary results of turbulence predictions for use in aviation weather forecasting p 675 A95-93551
A prototype for displaying aviation forecast variables using Eta numerical model output p 676 A95-93555
- MARSDEN, PAUL**
Gas chromatography/ion mobility spectrometry as a hyphenated technique for improved explosives detection and analysis p 701 N95-33278
- MARSH, D. N.**
Flex cycle combustor development and demonstration
[BTN-94-EIX95011441245] p 417 A95-84202
- MARSHALL, D. F.**
Ultra-wideband electromagnetic target identification
p 486 A95-90955
- MARSHALL, J. S.**
Vortex cutting by a blade. Part II: Computations of vortex response
[BTN-94-EIX94441386611] p 208 A95-67342
Vortex cutting by a blade, part 1: General theory and a simple solution
[HTN-95-20822] p 543 A95-88083
Vortex cutting by a blade, Part 2: Computations of vortex response
[HTN-95-20937] p 464 A95-88976
- MARSHALL, ROBERT E.**
Characteristics of civil aviation atmospheric hazards
p 42 N95-13208
- MARSHALL, STEVEN E.**
Prediction of airplane cabin noise due to engine shock cell excitation using statistical energy analysis
p 577 A95-90131
Comments on the use of structureborne noise analysis for large commercial airplanes p 30 N95-11287
- MARTENS, J.**
The mm-wave resonant methods for the detection of corrosion, phase 1
[AD-A291315] p 556 N95-29941
- MARTIN, I. M.**
The joint Russian-Brazil research on balloons
p 182 A95-66303
- MARTIN, JAMES L.**
Flight investigation of the use of a nose gear jump strut to reduce takeoff ground roll distance of STOL aircraft
[NASA-TM-108819] p 44 N95-12225
- MARTIN, JENNIFER R.**
SCARLET: DLR rate saturation flight experiment
p 598 N95-31068
- MARTIN, JOEL D.**
Tropical cyclone observation and forecasting with and without aircraft reconnaissance
[HTN-95-80701] p 254 A95-72545
- MARTIN, JOHN S.**
Factors affecting the visual fragmentation of the field-of-view in partial binocular overlap displays
[AD-A283081] p 172 N95-17334
Factors affecting the perception of fusing in monocular regions of partial binocular overlap displays
[AD-A286287] p 259 N95-22044
- MARTIN, M. M.**
Evaluation of neutron techniques for illicit substance detection
[DE95-002988] p 300 N95-22764
- MARTIN, PETER**
Aircraft accident investigation and airworthiness -- A practical example of the interaction of two disciplines with some reflections on possible legal consequences
[HTN-95-50219] p 176 A95-64856
- MARTIN, R. M.**
Recent studies of rotorcraft blade-vortex interaction noise
[BTN-95-EIX95062487521] p 218 A95-69229
- MARTIN, ROBERT C., IV**
A gain scheduling optimization method using genetic algorithms
[AD-A289306] p 448 N95-26920
- MARTIN, RONALD C.**
MDCRS: Aircraft observations collection and uses
p 668 A95-93517
Dissemination of terminal weather products to the flight deck via data link p 669 A95-93525
- MARTIN, STEPHEN ALLEN**
Turbulent airflow noise production and propagation patterns of a subsonic jet impinging on a flat plate
p 580 N95-29502
- MARTIN, V.**
Secondary source locations in active noise control: Selection or optimization?
[BTN-94-EIX94381352222] p 257 A95-71738
- MARTINDALE, I.**
Soft body impact on titanium fan blades
p 200 N95-19671
- MARTINEC, D. A.**
Assessment of avionics technology in European aerospace organizations
[NASA-CR-189201] p 337 N95-24624
- MARTINELLI, LUIGI**
Computational algorithms for aerodynamic analysis and design
[AD-A291084] p 482 N95-29972
- MARTINEZ-VAL, RODRIGO**
Design constraints in the payload-range diagram of ultrahigh capacity transport airplanes
[BTN-95-EIX95152582319] p 276 A95-73522
- MARTINEZ, DEBBIE**
Transport delays associated with NASA Langley Flight Simulation Facility
[NASA-TM-110150] p 568 N95-29454
- MARTINEZ, R.**
The use of cowl camber and taper to reduce rotor/stator interaction noise
[NASA-CR-195421] p 323 N95-22675
- MARTINEZ, RADAME**
Terminal Doppler Weather Radar Build 5A Operational Test and Evaluation (OT/E) integration and OT/E operational test plan
[AD-A283052] p 61 N95-12996
Offshore next generation weather radar (NEXRAD) test and evaluation master plan (TEMP)
[AD-A291435] p 556 N95-30072
Offshore next generation weather radar (NEXRAD) OT&E integration and OT&E operational test
[AD-A293223] p 646 N95-30902
- MARTINO, WILLIAM R.**
175Hp contrarotating homopolar motor design report
[AD-A291138] p 557 N95-30122
- MARTINOU, R.**
New Trends in coatings developments for turbine blades: Materials processing and repair p 201 N95-19676
- MARTINSON, ROBERT J.**
Remote sensing of turbulence in the clear atmosphere with 2-micron lidars p 59 N95-13213
- MARTUCCIO, MICHELLE THERESE**
A wind tunnel investigation of the effects of micro-vortex generators and Gurney flaps on the high-lift characteristics of a business jet wing
[NASA-TM-110626] p 607 N95-30827
- MARULO, F.**
Structural acoustic calculations in the low-frequency range
[BTN-95-EIX95152582336] p 323 A95-73538
Numerical and flight measured interior noise characteristics of a twin-engine turboprop general aviation aircraft p 573 A95-90094
- MARUTHAYAPPAN, RAMAKRISHNAN**
Plastic hinge modeling of structures
[NIAR-94-14] p 24 N95-11168
- MARVIN, JOSEPH G.**
Dryden lectureship in research, a perspective on CFD validation
[AIAA PAPER 93-0002] p 3 A95-60180
- MARWITZ, JOHN D.**
Conditions associated with large-drop regions
[HTN-95-10686] p 214 A95-68845
- MASAD, J. A.**
Comparison of linear stability results with flight transition data
[BTN-95-EIX95182619097] p 283 A95-76582
- MASAKI, DAISAKU**
A study on the convergence of a 3-D Euler code for cascade flow calculations p 706 N95-34508
- MASELAND, J. E. J.**
Experimental investigation of the vortex flow over a 76/60-deg double delta wing p 114 N95-17874
Demonstration of an automated CFD system for three-dimensional flow simulations p 551 N95-28767
- MASIULANIEC, KONSTANTY C.**
User's manual for the NASA Lewis ice accretion/heat transfer prediction code with electrothermal deicer input
[NASA-CR-4530] p 57 N95-11888
- MASON, GREGORY S.**
Multirate flutter suppression system design for a model wing
[BTN-95-EIX95182619132] p 292 A95-76609
- MASON, RALPH**
Precise navigation using adaptive FIR filtering and time domain spectral estimation
[BTN-95-EIX95142555485] p 227 A95-72888
- MASON, V. BRADFORD**
Broadband, wide-area active control of sound radiated from vibrating structures using local surface-mounted radiation suppression devices p 30 N95-11283
- MASON, W. H.**
Aerodynamically blunt and sharp bodies
[BTN-95-EIX95041503781] p 205 A95-69212
Development of an efficient inverse method for supersonic and hypersonic body design
[BTN-95-EIX95041503784] p 180 A95-69215
Minimum-drag axisymmetric bodies in the supersonic/hypersonic flow regimes
[BTN-95-EIX95041503785] p 180 A95-69216
- MASON, WILLIAM**
Kinematics and aerodynamics of velocity-vector roll
[BTN-95-EIX95182619126] p 291 A95-76603
- MASSA, LOU**
Laws of infrared similitude
[AD-A282209] p 62 N95-12426
Nonlinear calibration of an infrared radiometer
[AD-A292436] p 579 N95-28996
- MASSEY, K. C.**
Temperature effects on acoustic interactions between altitude test facilities and jet engine plumes
[NASA-CR-197638] p 258 N95-21170
- MASSMAN, W. J.**
A comparison of some aerodynamic resistance methods using measurements over cotton and grass from the 1991 California ozone deposition experiment
[HTN-95-11295] p 319 A95-77000
- MASSON, BERTRAND**
Compressible Navier-Stokes calculations of the flow over airfoil sections. Comparisons of 1st and 2nd order turbulence models
[SAE PAPER 932510] p 546 A95-89183
- MASSOUD, M.**
Modal parameters for cracked rotors: models and comparisons
[BTN-94-EIX94522410226] p 702 A95-96378
- MASTRODDI, F.**
Matrix fraction approach for finite-state aerodynamic modeling
[BTN-95-EIX95262694311] p 365 A95-85482
- MASUI, KAZUYA**
An application of TLS (Total Least Squares) method to estimation of aircraft aerodynamic derivatives
p 517 A95-91551
Analysis of an MLS automatic landing control law for the NAL experimental research aircraft D0-228. 2: Curved approach and landing p 508 A95-91588
- MASUYA, GORO**
Effect of film cooling/regenerative cooling on scramjet engine performances
[NAL-TR-1242] p 339 N95-24990
- MATEER, GEORGE G.**
Boundary-layer transition and global skin friction measurement with an oil-fringe imaging technique
[SAE PAPER 932550] p 547 A95-90054
A supercritical airfoil experiment p 111 N95-17858
Boundary-layer transition and global skin friction measurement with an oil-fringe imaging technique
[NASA-CR-198814] p 557 N95-30224
- MATESKI, J. E.**
Independent review of Aviation Technology and Research Information Analysis System (ATRIAS) database
[AD-A284049] p 226 N95-21518
- MATHEW, JOSEPH**
Study of an airfoil with a flap and spoiler
[BTN-95-EIX95152582327] p 265 A95-73530
- MATHEWS, BRUCE D.**
Certification of windshear performance with RTCA class D radomes p 41 N95-13206
- MATHIAS, DONOVAN L.**
Numerical design of advanced multi-element airfoils
[NASA-CR-197135] p 76 N95-15762

MATHIOUDAKIS, K.

Adaptive modeling of jet engine performance with application to condition monitoring
[BTN-95-EIX95112524205] p 196 A95-69303

MATHUR, SANJAY R.

Solution-adaptive structured-unstructured grid method for unsteady turbomachinery analysis. Part I: Methodology
[BTN-94-EIX94441380983] p 208 A95-67329

MATHYS, KARLA

Deaths and injuries as a result of lightning strikes to aircraft
[HTN-95-12213] p 485 A95-91913

MATINELLI, L.

Multigrid solution of compressible turbulent flow on unstructured meshes using a two-equation model
[BTN-94-EIX94401378794] p 307 A95-76484

MATSUBARA, MANABU

A systems for flight data acquisition and analysis for a remotely-piloted research vehicle p 517 A95-91554

MATSUMOTO, HIROAKI

Rarefied gas numerical wind tunnel: OREX and HOPE p 427 A95-82391

MATSUMOTO, MASASHI

Evaluation of scramjet nozzle performance p 402 A95-82321
Performance variation of scramjet nozzle at various nozzle pressure ratios
[BTN-95-EIX0616952745781] p 615 A95-94505

MATSUMOTO, SHIGEO

Optimum aerodynamic design of aircraft fuselage using boundary element method p 473 A95-91514

MATSUMOTO, SHINICHI

Hypersonic thermal protection with mass injection at angle of attack p 414 A95-82414

MATSUMOTO, SHUICHI

Flight evaluation of GPS/DGPS sensor systems installed in NAL Do228
[NAL-TR-1230] p 382 N95-26585

MATSUNO, KENICHI

Flow visualization studies on sidewall effects in two-dimensional transonic airfoil testing
[BTN-95-EIX95152582313] p 264 A95-73516

MATSUNOBU, Y.

Development of 70MW class superconducting generators
[BTN-94-EIX95011440854] p 429 A95-82905

MATSUSHIMA, KISA

Computations of low speed flow about space-plane p 685 N95-34544

MATSUSHIMA, KOICHI

Flight evaluation of DGPS and DGPS-INS navigation systems p 382 A95-82462

MATSUURA, TSUKASA

Arrival traffic handling for a parallel runway airport p 487 A95-91537

MATSUZAKI, YUJI

Supersonic flutter analysis of cantilevered composite plate-wings p 499 A95-91567

MATTERN, DUANE

Application of an integrated methodology for propulsion and airframe control design to a STOVL aircraft
[NASA-TM-106729] p 16 N95-11159

MATTERN, DUANE L.

Piloted evaluation of an integrated methodology for propulsion and airframe control design
[AD-A290207] p 51 N95-12763

MATTES, ROBERT E.

Fiber Optic Control System integration for advanced aircraft. Electro-optic and sensor fabrication, integration, and environmental testing for flight control systems
[NASA-CR-191194] p 162 N95-19236

MATTHEWS, MICHAEL P.

Improving aircraft impact assessment with the integrated terminal weather system microburst detection algorithm p 654 A95-93453

MATTHEWS, MICHAEL P.

Future enhancements to ground-based microburst detection p 11 N95-10570

MATTHEWS, R. K.

Hypersonic wind tunnel test techniques
[AD-A284057] p 118 N95-18663

Hypersonic flow-field measurements: Intrusive and nonintrusive
[AD-A283867] p 119 N95-18674

MATTHEWS, R. K.

Hypersonic flight testing
[AD-A283981] p 134 N95-18891

Description and flow characterization of hypersonic facilities
[AD-A284291] p 223 N95-20248

MATTHEWS, RAYMOND H.

Vertical flight terminal operational procedures. A summary of FAA research and development
[AD-A283550] p 85 N95-15328

MATTICE, MICHAEL S.

Design of a controller for a flexible pointing system using H(infinity) synthesis
[AD-A286572] p 256 N95-20828

MATTOON, JOSEPH S.

Instructional control and part/whole-task training: A review of the literature and an experimental comparison of strategies applied to instructional simulation
[AD-A280860] p 21 N95-10919

MATULICH, D. S.

Integrated aircraft thermal management and power generation
[SAE PAPER 932055] p 500 A95-91636

MATULICH, DAN S.

A subsystem integration technology concept
[SAE PAPER 931382] p 604 A95-93658

MATYASH, S.

Optical surface pressure measurements: Accuracy and application field evaluation p 175 N95-19274

MAURICE, M. S.

Laser velocimetry seed-particle behavior in shear layers at Mach 12
[BTN-95-EIX95212645712] p 272 A95-76764

MAURICE, MARK S.

Laser velocimetry in the supersonic regime: Advancements, limitations, and outlook
[SAE PAPER 931365] p 634 A95-93646

Developments in laser-based diagnostics for wind tunnels in the Aeromechanics Division: 1987-1992
[AD-A283011] p 84 N95-13687

MAUS, J. R.

Hypersonic flight testing
[AD-A283981] p 134 N95-18891

Description and flow characterization of hypersonic facilities
[AD-A284291] p 223 N95-20248

MAVRIPLIS, CATHERINE

Low-dimensional description of the dynamics in separated flow past thick airfoils
[HTN-95-20832] p 544 A95-88093

MAVRIPLIS, D. J.

Multigrid solution of compressible turbulent flow on unstructured meshes using a two-equation model
[BTN-94-EIX94401378794] p 307 A95-76484
Agglomeration multigrid for viscous turbulent flows
[AD-A284064] p 8 N95-10848

MAVRIPLIS, DIMITRI J.

Navier-Stokes applications to high-lift airfoil analysis
[BTN-95-EIX0619952748182] p 590 A95-94475
Numerical study to assess sulfur hexafluoride as a medium for testing multielement airfoils
[NASA-TP-3496] p 378 N95-28674

MAY, NICHOLAS E.

Application of three-dimensional hybrid structured/unstructured grids to land, sea and air vehicles
[ARA-MEMO-399] p 210 N95-19775

Verification of the CFD simulation system SAUNA for complex aircraft configurations
[ARA-MEMO-401] p 211 N95-19776

Inviscid and viscous flow modelling of complex aircraft configurations using the CFD simulation system sauna
[ARA-MEMO-403] p 211 N95-19777

MAYER, DAVID W.

Prediction of supersonic inlet unstart caused by freestream disturbances
[BTN-95-EIX95222650790] p 329 A95-79246

Boundary conditions for unsteady supersonic inlet analyses
[HTN-95-20829] p 544 A95-88090

MAYHEW, ELLEN R.

Air Force seal activities p 60 N95-13600

MAYNARD, JULIAN D.

Anisotropic heat exchangers/stack configurations for thermoacoustic heat engines
[AD-A280974] p 168 N95-16506

MAYNARD, S.

Novel matrix resins for composites for aircraft primary structures, phase 1
[NASA-CR-189657] p 23 N95-10318

MAYNARD, SHAWN J.

Development of RTM and powder prepreg resins for subsonic aircraft primary structures p 536 N95-29044

MAYORI, ALEJANDRO

Interaction of a streamwise vortex with a thin plate: A source of turbulent buffeting
[BTN-95-EIX95042474398] p 209 A95-68302

MAYTON, MONICA

Assessment of avionics technology in European aerospace organizations
[NASA-CR-189201] p 337 N95-24624

MALISTER, KENNETH W.

Dynamic stall control for advanced rotorcraft application
[BTN-95-EIX95222650793] p 334 A95-79249

MCARDLE, JACK G.

Experimental performance of a ventral nozzle with pitch and yaw vectoring capability for SSTOVL aircraft
[SAE PAPER 931412] p 614 A95-93678

MCCARTHUR, MALCOLM J.

System design considerations for an APU starter-generator
[SAE PAPER 932559] p 511 A95-90056

MCBEE, LARRY S.

Guidance and control requirements for high-speed Rollout and Turnoff (ROTO)
[NASA-CR-195026] p 292 N95-22674

MCCABE, GRANT T.

Water model tests on the Allison T56 series 3 combustion system
[DSTO-TR-0139] p 697 N95-33250

MCCALLION, K. J.

The application of Ada and formal methods to a safety critical engine control system p 710 N95-33142

MCCANN, DONALD W.

WINDEX - A new index for forecasting microburst potential
[HTN-95-90690] p 215 A95-69717
An evaluation of clear-air turbulence indices p 674 A95-93548

MCCARTHY, D. R.

A modular system for computational fluid dynamics p 641 A95-95446

MCCARTHY, R. F. J.

Polymer composite applications to aerospace equipment
[HTN-95-B0257] p 529 A95-89201

MCCARTHY, THOMAS R.

Multilevel decomposition procedure for efficient design optimization of helicopter rotor blades
[BTN-95-EIX95222650784] p 334 A95-79240

MCCASKILL, THOMAS B.

Effect of broadcast and precise ephemerides on estimates of the frequency stability of GPS Navstar clocks
[BTN-95-EIX95112522530] p 190 A95-69333

MCCASLIN, PAULA T.

The development of an aircraft icing forecast technique using data from maps p 675 A95-93549

MCCLEARY, SUSAN L.

A global/local analysis method for treating details in structural design p 552 N95-28848

MCCLEINTON, C. R.

Thrust modeling for hypersonic engines
[AIAA PAPER 95-6081] p 509 A95-87410
Investigation of scramjet injection strategies for high mach number flows
[BTN-95-EIX0616952745782] p 614 A95-94504

MCCLLUNG, R. C.

Analysis of small crack behavior for airframe applications p 95 N95-14484

MCCLLURE, W. B.

Simulating heat addition via mass addition in constant area compressible flows
[BTN-95-EIX95182619100] p 307 A95-76585

MCCONNELL, RICHARD A.

175Hp contrarotating homopolar motor design report
[AD-A291138] p 557 N95-30122

MCCORCLE, M. D.

Operational multi-scale environment model with grid adaptivity (OMEGA) application to aviation weather p 676 A95-93556

MCCORKLE, T.

Viper cabin-fuselage structural design concept with engine installation and wing structural design
[NASA-CR-197162] p 45 N95-12305

MCCORMICK, B. W.

Aerodynamics of delta wings with application to high-alpha flight mechanics p 460 A95-87395

MCCORMICK, BARNES W.

Wake turbulence p 75 N95-14894

MCCOY, C. ELAINE

User involvement in the development of an advanced icing product for use in aviation p 672 A95-93537

MCCROSKY, W. J.

Dynamic stall of an oscillating wing. Part 1: Evaluation of turbulence models
[AIAA PAPER 93-3403] p 3 A95-60184

MCCUISSH, A.

Experimental Aircraft Programme (EAP): Flight control system design and test p 623 N95-32010

MCCULLOUGH, JAMES A.

Operational And Supportability Implementation System (OASIS) test and evaluation master plan
[AD-A284765] p 126 N95-18088

MCCURDY, DAVID A.

High-Speed Research: 1994 Sonic Boom Workshop: Atmospheric Propagation and Acceptability Studies
[NASA-CP-3279] p 75 N95-14878

- MCDANIEL, AMOS D.**
High temperature strain gage technology for gas turbine engines
[NASA-CR-191177] p 57 N95-11996
- MCDANIEL, J. C.**
Computational/experimental investigation of staged injection into a Mach 2 flow
[HTN-95-51646] p 432 A95-85028
- MCDANIEL, JAMES C.**
Quantitative investigation of compressible mixing: Staged transverse injection into Mach 2 flow
[HTN-95-42330] p 404 A95-86159
Effects of the chemical reaction model on calculations of supersonic combustion flows
[BTN-95-EIX0616952745802] p 638 A95-94487
- MCDANIEL, MICHAEL**
Airship applications of modern flight test techniques
[AD-A284253] p 194 N95-19731
- MCDERMID, J. A.**
Dependable software - the state of the art
[CONGRESS PAPER C428-24-212] p 678 A95-93596
- MCDONACH, ALASTER**
SMART materials: Surfaces, transforms and interfaces. The commensurate engineering dimension
[AD-A289598] p 442 N95-28649
- MCDONALD, M. A.**
Measurements of the flow over a low aspect-ratio wing in the Mach number range 0.6 to 0.87 for the purpose of validation of computational methods. Part 1: Wing design, model construction, surface flow. Part 2: Mean flow in the boundary layer and wake, 4 test cases
p 112 N95-17860
- MCDONALD, NICK**
Safety in airport ground handling p 626 A95-95193
- MCDONALD, PHILIP A.**
A prototype for displaying aviation forecast variables using Eta numerical model output p 676 A95-93555
- MCDOWELL, P.**
STOVL Control Integration Program
[NASA-CR-195358] p 18 N95-11487
- MCELROY, MICHAEL B.**
Vertical transport rates in the stratosphere in 1993 from observations of CO₂, N₂O, and CH₄
[HTN-95-70941] p 351 A95-78006
- MCKERLEAN, DONALD P.**
Benefits and limitations of composites in carrier-based aircraft p 422 N95-28422
- MCEWEN, RON S.**
SMART materials: Surfaces, transforms and interfaces. The commensurate engineering dimension
[AD-A289598] p 442 N95-28649
- MCFARLAND, R. E.**
Simulation of rotor blade element turbulence
[NASA-TM-108862] p 232 N95-21186
- MCFARLAND, RICHARD H.**
Commentary on Walton correspondence relating to the ILS glide slope
[BTN-94-EIX94441380856] p 125 A95-64288
- MCFARLANE, I.**
The auxiliary and emergency power supply on the Saab JAS39 Gripen aircraft
[CONGRESS PAPER C428-36-192] p 612 A95-93631
- MCFIGGANS, I. R.**
Changing MRP Systems within the aerospace industry
[CONGRESS PAPER C428-26-051] p 681 A95-93603
- MCGARRY, FRANK**
Software process improvement in the NASA software engineering laboratory
[AD-A28912] p 450 N95-28627
- MCGHEE, R. J.**
Effect of underwing frost on a transport aircraft airfoil at flight Reynolds number
[BTN-95-EIX95152582334] p 276 A95-73536
- MCGHEE, ROBERT J.**
Separation control on high-lift airfoils via micro-vortex generators
[BTN-95-EIX95152582326] p 265 A95-73529
- MCGILVARY, RANDY**
Analyzing the stability of floating ice floes
[AD-A292149] p 563 N95-29160
- MCGINLEY, C.**
Characterization of a hot-film probe for hypersonic flow
[AIAA PAPER 95-6110] p 511 A95-90440
- MCGINLEY, JOHN A.**
Forecasting for a large field program: STORM-FEST
[HTN-95-90694] p 215 A95-69721
ITWS gridded analysis p 654 A95-93455
The development of an aircraft icing forecast technique using data from maps p 675 A95-93549
- MCGLOTHLIN, LARRY**
MOAMAP: A model that combines several different kinds of aircraft operations p 32 N95-11323
- MCGOVERN, JANET L.**
Evaluation of alternate F-14 wing lug coating
[AD-A283207] p 129 N95-17631
- MCGOWIN, EVERETTE, III**
Transmittance characteristics of US Army rotary-wing aircraft transparencies
[AD-A295035] p 693 N95-34793
- MCGRANE, E. J.**
Development of anti-icing technology
[PB94-195369] p 78 N95-15439
- MCGRATH, JAMES**
Thermally stable organic polymers
[AD-A281380] p 87 N95-14363
Thermally stable organic polymers
[AD-A290755] p 537 N95-29482
- MCGRAW, SANDRA M.**
Multiple-function digital controller system for active flexible wing wind-tunnel model
[BTN-95-EIX95182619212] p 322 A95-76638
On-line analysis capabilities developed to support the active flexible wing wind-tunnel tests
[BTN-95-EIX95182619213] p 296 A95-76639
- MCGREEVY, J. L.**
Interaction of jet noise with a nearby panel assembly
[BTN-95-EIX95262694295] p 434 A95-85466
On the interaction of jet noise with a nearby flexible structure
[NASA-CR-194934] p 57 N95-11812
Response of multi-panel assembly to noise from a jet in forward motion
[NASA-CR-198164] p 442 N95-28673
- MCLIVEN, J. S.**
External viewing airborne CCTV system
[CONGRESS PAPER C428-25-172] p 595 A95-93598
- MCINERNEY, S. A.**
An experimental investigation of wing tip turbulence with applications to aeround
[AIAA PAPER 86-1918] p 1 A95-60164
- MCINNER, COLIN R.**
Dynamical instability of the aerogravity assist maneuver
[BTN-95-EIX95152583282] p 298 A95-73583
- MCINNIS, LONA A.**
Mechanism of deposit formation on fuel-wetted hot metal surfaces
[AD-A289847] p 426 N95-28621
- MCINTYRE, T. J.**
The high enthalpy shock tunnel in Goettingen (HEG)
p 518 A95-87391
- MCINVILLE, R.**
Improved version of the Naval Surface Warfare Center aeroprediction code (AP93)
[BTN-95-EIX95152583260] p 267 A95-73561
- MCINVILLE, R. M.**
Calculation of wing-alone aerodynamics to high angles of attack
[BTN-95-EIX95212645713] p 261 A95-76765
- MCINVILLE, ROY M.**
The 1995 version of the NSWC aeroprediction code. Part 1: Summary of new theoretical methodology
[AD-A291518] p 481 N95-29853
- MCKAY, K.**
Pilot Induced Oscillation: A report on the AGARD Workshop on PIO p 624 N95-32017
- MCKELVEY, TERESA**
Systems engineering design and technical analyses for Strategic Avionics Crew-station Design Evaluation Facility (SACDEF)
[AD-A286239] p 235 N95-22024
- MCKENNA, H. E.**
Observed acoustic and aeroelastic spectral responses of a MOD-2 turbine blade to turbulence excitation p 451 N95-27991
- MCKILLIP, ROBERT, JR.**
A novel instrumentation system for measurement of helicopter rotor motions and loads data, phase 1
[AD-A293309] p 607 N95-30923
- MCKNIGHT, R. L.**
Engine structures analysis software: Component Specific Modeling (COSMO)
[NASA-CR-195378] p 57 N95-11711
- MCKNIGHT, RICHARD L.**
Ply layout optimization and micromechanics tailoring of composite aircraft engine structures
[BTN-95-EIX95112524206] p 196 A95-69302
- MCLAUGHLIN, J. C.**
Scale-up and modeling of forced chemical vapor infiltration
[DE94-017769] p 247 N95-20781
- MCLEAN, G. A.**
Aircraft evacuations through Type-3 exits I: Effects of seat placement at the exit
[DOT/FAA/AM-95/22] p 599 N95-31845
- MCLEAN, L. J.**
Subharmonic and quasi-periodic motions of an eccentric squeeze film damper-mounted rigid rotor
[BTN-94-EIX95011440601] p 429 A95-82982
- MCLEAN, WILLIAM E.**
Factors affecting the visual fragmentation of the field-of-view in partial binocular overlap displays
[AD-A283081] p 172 N95-17334
Factors affecting the perception of furling in monocular regions of partial binocular overlap displays
[AD-A286287] p 259 N95-22044
Transmittance characteristics of US Army rotary-wing aircraft transparencies
[AD-A295035] p 693 N95-34793
- MCLEMORE, DONALD**
Assessing aircraft survivability to high frequency transient threats
[AD-A283999] p 134 N95-18726
- MCLEMORE, DONALD P.**
Fault detection techniques for complex cable shield topologies
[AD-A286632] p 247 N95-20771
TIM-SCT cable testing protocol
[AD-A286633] p 231 N95-20772
- MCMASTER, JOHN**
The use of genetic algorithms for flight test and evaluation of artificial intelligence and complex software systems
[AD-A284824] p 217 N95-19688
- MC MILLIN, B. K.**
Comparison of NO and OH planar fluorescence temperature measurements in scramjet model flowfields
[BTN-95-EIX95042474388] p 209 A95-68312
- MCNEIL, WALTER E.**
Aerodynamics model for a generic ASTOVL lift-fan aircraft
[NASA-TM-110347] p 332 N95-26302
- MCNEILL, WALTER, E.**
Moving base simulation of an integrated flight and propulsion control system for an ejector-augmented STOVL aircraft in hover
[NASA-TM-108867] p 606 N95-30646
- MCQUILLEN, JOHN B.**
Characterization of annular two-phase gas-liquid flows in microgravity p 95 N95-14556
Two-phase flow research using the learjet apparatus
[NASA-TM-106814] p 438 N95-27854
- MCQUINN, NOREEN**
Human factors issues in aircraft cabin design
[SAE PAPER 932527] p 386 A95-84556
- MCRAE, D. S.**
Time accurate computation of unsteady inlet flows with a dynamic flow adaptive mesh
[AD-A285498] p 157 N95-16736
- MCRBERTS, BRADLEY J.**
Lightweight, opto-electronic engine control system for aerospace turbine engines
[SAE PAPER 931442] p 614 A95-93692
- MCRUER, DUANE T.**
PIO: A historical perspective p 597 N95-31062
- MCWHORTER, JOHN C., III**
An investigation of the accuracy of FEM analysis of a graphite epoxy box beam
[SAE PAPER 931221] p 543 A95-88011
Analysis and testing of a graphite-epoxy sandwich shell fuselage test structure
[ISBN 1-879921-01-4] p 605 A95-93746
- MCWITHEY, MICHAEL C.**
Design of a vehicle based system to prevent ozone loss
[NASA-CR-197199] p 48 N95-12702
- MEACHAM, WALTER L.**
Dynamic stiffness and damping of foil bearings for gas turbine engines
[SAE PAPER 931449] p 635 A95-93698
- MEADOWS, KRISTINE R.**
A numerical study of fundamental shock noise mechanisms
[NASA-TM-110608] p 451 N95-27908
- MEADOWS, KRISTINE R.**
Computing unsteady shock waves for aeroacoustic applications
[HTN-95-20928] p 463 A95-88967
- MEAKIN, ROBERT L.**
Global flowfield about the V-22 Tiltrotor Aircraft
[NASA-CR-198603] p 375 N95-27248
- MEASE, KENNETH D.**
Shuttle entry guidance revisited using nonlinear geometric methods
[BTN-95-EIX95182619144] p 299 A95-76621
- MEDLER, LAWRENCE P.**
Low rate initial production in Army Aviation systems development
[AD-A281871] p 127 N95-16356

MEDWIN, STEVEN

Application of advanced material systems to composite frame elements p 422 N95-28432

MEE, D.

Shock tunnel studies of scramjet phenomena 1993 [NASA-CR-195038] p 350 N95-25394

Thrust measurements of a complete axisymmetric scramjet in an impulse facility p 339 N95-25395

MEE, D. J.

Shock tunnel measurements of hypervelocity blunted cone drag [BTN-95-EIX95152577606] p 305 A95-73477

Shock tunnel measurements of hypervelocity blunted cone drag [HTN-95-42591] p 459 A95-87221

Scramjet thrust measurement in a shock tunnel [HTN-95-C0008] p 586 A95-93396

Scramjet thrust measurement in a shock tunnel p 339 N95-25396

Balances for the measurement of multiple components of force in flows of a millisecond duration p 350 N95-25400

MEECHAM, W. C.

An experimental investigation of wing tip turbulence with applications to aerosound [AIAA PAPER 86-1918] p 1 A95-60164

MEGGERS, K.

Phonon characteristics of high (T sub c) superconductors from neutron Doppler broadening measurements [DE95-003703] p 324 N95-24076

MEGIE, G.

Impact of present aircraft emissions of nitrogen oxides on tropospheric ozone and climate forcing [HTN-95-21364] p 353 A95-78679

An overview of the EASOE campaign [HTN-95-00702] p 443 A95-86272

Airborne lidar observation of mountain-wave-induced polar stratospheric clouds during EASOE [HTN-95-00738] p 444 A95-86308

MEGUID, S. A.

Theoretical and experimental studies of fretting-initiated fatigue failure of aeroengine compressor discs [BTN-94-EIX94421372285] p 343 A95-78467

MEHRKAM, P.

Field repair materials for naval aircraft p 394 N95-27514

MEHTA, S.

Mechanical system reliability and risk assessment [BTN-95-EIX95142553046] p 304 A95-73452

MEHTA, UNMEEL B.

Air-breathing aerospace plane development essential: Hypersonic propulsion flight tests [NASA-TM-108857] p 66 N95-14921

MEI, CHUH

Finite element time domain - modal formulation for nonlinear flutter of composite panels [BTN-95-EIX95042474401] p 203 A95-68299

Panel flutter limit-cycle suppression with piezoelectric actuation [BTN-95-EIX95302731089] p 618 A95-94208

MEI, RENWEI

Flow due to an oscillating sphere and an expression for unsteady drag on the sphere at finite Reynolds number [BTN-94-EIX95011441142] p 347 A95-81012

MEIER, B. H.

Broadband polarization-transfer experiments for rotating solids [GTN-95-0009261194012091-58] p 579 A95-92319

MEINDL, M.

SAR image registration in absolute coordinates using GPS carrier phase position and velocity information [DE94-018738] p 228 N95-20195

MEINDL, M. A.

Assessment of a non-dedicated GPS receiver system for precise airborne attitude determination [DE94-019309] p 229 N95-21520

MEIROVITCH, LEONARD

Performance improvement of composite wings through aeroelastic tailoring and modern control [AD-A293689] p 608 N95-31602

MEISS, A. G.

Triton 2 (1B) [NASA-CR-197188] p 46 N95-12636

MELIS, MATTHEW E.

Hypersonic engine leading edge experiments in a high heat flux, supersonic flow environment [NASA-TM-106742] p 91 N95-14299

MELLSTROM, J. A.

Field verification of the wind tunnel coefficients p 109 N95-17291

MELVIN, R. G.

TranAir: A full-potential, solution-adaptive, rectangular grid code for predicting subsonic, transonic, and supersonic flows about arbitrary configurations. User's manual [NASA-CR-4349] p 377 N95-28230

TranAir: A full-potential, solution-adaptive, rectangular grid code for predicting subsonic, transonic, and supersonic flows about arbitrary configurations. Theory document [NASA-CR-4348] p 378 N95-28265

MENA, ANDREW C.

CASS: Design for supportability [BTN-95-EIX95172595296] p 287 A95-75716

MENDENHALL, MICHAEL R.

Aerodynamic design of pegasus: Concept to flight with computational fluid dynamics [BTN-95-EIX95182617463] p 298 A95-75734

MENDOZA, J.

Effects of cavity dimensions, boundary layer, and temperature on cavity noise with emphasis on benchmark data to validate computational aeroacoustic codes [NASA-CR-4653] p 361 N95-24879

MENDOZA, JOEL

Flow study of supersonic wing-nacelle configuration [BTN-95-EIX95152582344] p 266 A95-73546

MENEES, GENE P.

Experimental and analytical investigations of wave enhanced supersonic combustors [AIAA PAPER 89-2787] p 14 A95-60172

MENGALI, GIOVANNI

Simulation of turbulent fluctuations [BTN-95-EIX95142553041] p 304 A95-73457

MENSINK, C.

A 2D parallel multiblock Navier-Stokes solver with applications on shared- and disturbed memory machines p 643 A95-95475

MENTER, F. R.

Computation of oscillating airfoil flows with one- and two-equation turbulence models [BTN-95-EIX95152577588] p 263 A95-73494

MENTER, FLORIAN

A comparison of turbulence models in computing multi-element airfoil flows [AIAA PAPER 94-0291] p 4 A95-60185

MENTER, FLORIAN R.

Boundary-layer transition and global skin friction measurement with an oil-fringe imaging technique [SAE PAPER 932550] p 547 A95-90054

Boundary-layer transition and global skin friction measurement with an oil-fringe imaging technique [NASA-CR-198814] p 557 N95-30224

MERCADO, AL

Gas chromatography/ion mobility spectrometry as a hyphenated technique for improved explosives detection and analysis p 701 N95-33278

MERCER, D. H.

Health monitoring and cost implications for an airline operator [CONGRESS PAPER C428-12-166] p 457 A95-91704

MERKLE, C. L.

Convergence acceleration of implicit schemes in the presence of high aspect ratio grid cells p 313 N95-23446

MERKLE, CHARLES L.

Cavitation modeling in Euler and Navier-Stokes codes p 315 N95-23630

MERRICK, V. K.

Simulation and flight test evaluation of head-up-display guidance for harrier approach transitions [BTN-95-EIX95062487533] p 194 A95-69241

MERRICK, VERNON K.

Flightpath synthesis and HUD scaling for V/STOL terminal area operations [NASA-TM-110348] p 383 N95-26587

MERSCH, T.

Computation of vortex formation over ELAC-1 configuration using vorticity confinement [AIAA PAPER 95-6157] p 470 A95-90469

MESAKI, YUJI

Research on an autonomous vision-guided helicopter [AIAA PAPER 94-1240-CP] p 18 N95-11510

MESCHTER, P. J.

Toughened Silcomp composites for gas turbine engine applications [DE95-002851] p 235 N95-21243

MESSINA, MICHAEL D.

High-Alpha Research Vehicle (HARV) longitudinal controller: Design, analyses, and simulation results [NASA-TP-3446] p 17 N95-10860

MESTRE, VINCENT

Determining the effects of alternative departure cutback altitudes and power settings: A case study, John Wayne Airport p 31 N95-11320

METSCHAN, S.

Composite fuselage crown panel manufacturing technology p 399 N95-28474

METSCHAN, S. L.

The effects of design details on cost and weight of fuselage structures p 501 N95-28831

Global cost and weight evaluation of fuselage keel design concepts p 501 N95-28840

METSCHAN, STEPHEN L.

Cost model relationships between textile manufacturing processes and design details for transport fuselage elements p 536 N95-29043

METZ, WERNER

North Atlantic air traffic within the lower stratosphere: Cruising times and corresponding emissions [HTN-95-91841] p 354 A95-80829

METZKO, JOHN

The value of simulation for training [AD-A289174] p 411 N95-26556

MEVREL, R.

New Trends in coatings developments for turbine blades: Materials processing and repair p 201 N95-19676

MEWHINNEY, MICHAEL

NASA develops new digital flight control system [NASA-NEWS-RELEASE-94-47] p 144 N95-19029

MEY, G.

Modular CNI avionics system p 234 N95-20659

MEYER-HILBERG, JOCHEN

High accuracy navigation and landing system using GPS/IMU system integration [BTN-94-EIX94441386129] p 189 A95-68185

MEYER, G.

Nonlinear system guidance in the presence of transmission zero dynamics [NASA-TM-4661] p 309 N95-22804

MEYER, J.

Effects of periodic spanwise blowing on Delta-wing configuration characteristics [HTN-95-81631] p 461 A95-87679

MEYER, J. L.

Fuel-optimal bank-angle control for lunar-return aerocapture [BTN-95-EIX95212645706] p 299 A95-76758

MEYER, J. P.

Differencing of density in compressible flow for a pressure-based approach [HTN-95-42349] p 373 A95-86178

MEYERS, GARY W.

Solid fuel ramjet composition [AD-D016458] p 152 N95-19090

MEYERS, MICHAEL J.

Tilt Rotor Unmanned Air Vehicle System (TRUS) demonstrator flight test program [AD-A284151] p 132 N95-18415

MEYN, LARRY A.

Optimum full-scale subsonic wind tunnel [AIAA PAPER 86-0732] p 18 A95-60161

Forebody flow control on a full-scale F/A-18 aircraft [BTN-95-EIX95152582333] p 281 A95-73535

Comparison of full-scale, small-scale, and CFD results for F/A-18 forebody slot blowing p 72 N95-14255

MEZA, VICTOR J.

The FC-1D: The profitable alternative Flying Circus Commercial Aviation Group [NASA-CR-197152] p 46 N95-12628

MEZYNSKI, ALEXIS

Measurements of pressure and thermal wakes in a transonic turbine cascade [AD-A283464] p 38 N95-12548

MIAKE-LYE, R. C.

Subsidence of aircraft engine exhaust in the stratosphere: Implications for calculated ozone depletions [PAPER-93GL03426] p 251 A95-70297

MICHELL, MARCO

Simulation of turbulent fluctuations [BTN-95-EIX95142553041] p 304 A95-73457

MICHELSON, DAVID G.

Depolarizing trihedral corner reflectors for radar navigation and remote sensing [BTN-95-EIX9530272634] p 636 A95-94108

MICHONNEAU, J. F.

Analysis of test section sidewall effects on a two dimensional airfoil: Experimental and numerical investigations p 165 N95-19276

MICKLICH, B. J.

Evaluation of neutron techniques for illicit substance detection [DE95-002988] p 300 N95-22764

MIDDLETON, DAVID B.

Flight test of takeoff performance monitoring system [NASA-TP-3403] p 51 N95-12664

Airplane takeoff and landing performance monitoring system [NASA-CASE-LAR-14745-2-SB] p 85 N95-14415

- MIOLLINI, B.**
An approach to sensor data fusion for flying and landing aid purpose p 686 N95-32488
- MIGLIORE, P. G.**
Wind turbine trailing edge aerodynamic brakes [DE95-004061] p 683 N95-32548
- MIGNERY, L. A.**
Applications of a damage tolerance analysis methodology in aircraft design and production p 426 N95-28483
- MIGNOSI, A.**
Data from the GARTEur (AD) Action Group 02 airfoil CAST 7/DOA1 experiments p 111 N95-17856
Experimental techniques for measuring transonic flow with a three dimensional laser velocimetry system. Application to determining the drag of a fuselage p 163 N95-19258
Analysis of test section sidewall effects on a two dimensional airfoil: Experimental and numerical investigations p 165 N95-19276
- MIKI, YOICHIRO**
An advanced scramjet propulsion concept for A 350 MG SSTO space plane p 402 A95-82325
- MILATOVIĆ, BORISLAV**
Portable static test facility for small, expendable, turbojet engines, phase 1 [AD-A286337] p 239 N95-21719
- MILGRAM, JUDAH H.**
Air resonance of hingeless rotor helicopters in trimmed forward flight [HTN-95-61075] p 369 A95-83659
- MILLER, ALBERT B.**
Mode of human image representation and error checking strategies in complex visual displays [AD-A290107] p 485 N95-29210
- MILLER, C. DEAN**
Laser velocimetry in the supersonic regime: Advancements, limitations, and outlook [SAE PAPER 931365] p 634 A95-93646
- MILLER, D. P.**
Inlet flow test calibration for a small axial compressor facility. Part 1: Design and experimental results [NASA-TM-106719] p 16 N95-11005
Inlet flow test calibration for a small axial compressor rig. Part 2: CFD compared with experimental results [NASA-TM-106999] p 514 N95-30007
- MILLER, DEAN**
Further investigations of icing effects on an advanced high-lift multi-element airfoil [NASA-TM-106947] p 381 N95-27762
- MILLER, ERIK M.**
Gatelink highspeed communications with parked aircraft [SAE PAPER 932610] p 486 A95-90079
- MILLER, FRAN**
Certification of windshear performance with RTCA class D radomes p 41 N95-13206
- MILLER, G. E.**
Comparative performance tests on the Mod-2, 2.5-mW wind turbine with and without vortex generators p 377 N95-27978
- MILLER, GERALD D.**
Summary of an active flexible wing program [BTN-95-EIX95182619209] p 283 A95-76635
- MILLER, L. S.**
An exploratory application of neural networks for airfoil design p 448 N95-26943
Experimental investigation of aerodynamic devices for wind turbine rotational speed control, phase 1 [DE95-004034] p 564 N95-30016
- MILLER, L. SCOTT**
An experimental investigation of forward-swept wings at low Reynolds numbers [SAE PAPER 931370] p 604 A95-93650
Wind turbine trailing edge aerodynamic brakes [DE95-004061] p 683 N95-32548
- MILLER, M.**
Full-scale testing and analysis of fuselage structure p 95 N95-14485
- MILLER, M. S.**
Structural effects of unsteady aerodynamic forces on horizontal-axis wind turbines [DE94-011863] p 157 N95-16939
Wind turbine blade aerodynamics: The combined experiment [DE94-011866] p 118 N95-18645
Wind turbine blade aerodynamics: The analysis of field test data [DE94-011867] p 118 N95-18646
Evidence that aerodynamic effects, including dynamic stall, dictate HAWT structural loads and power generation in highly transient time frames [DE94-011865] p 216 N95-19855
- Techniques for the determination of local dynamic pressure and angle of attack on a horizontal axis wind turbine [DE95-009204] p 707 N95-32685
- MILLER, MATT**
Labs behind Boeing's new 777 [BTN-95-EIX95142562403] p 280 A95-73437
- MILLER, MATTHEW**
Evaluation of bonded boron/epoxy doublers for commercial aircraft aluminum structures p 92 N95-14457
The characterization of widespread fatigue damage in fuselage structure [NASA-TM-109142] p 88 N95-14920
The characterization of widespread fatigue damage in fuselage structure p 166 N95-19472
- MILLER, PHILIP**
Transonic and supersonic flowfield measurements about axisymmetric afterbodies for validation of advanced CFD codes p 121 N95-19260
- MILLER, R. A.**
Thermal barrier coatings for aircraft engines: History and directions p 344 N95-26121
- MILLER, R. D.**
Comparison of measured and calculated dynamic loads for the Mod-2 2.5 mW wind turbine system p 440 N95-27983
- MILLER, R. F.**
Residual Stress Measurements with Laser Speckle Correlation Interferometry and Local Heat Treating [DE95-060082] p 349 N95-24598
- MILLER, R. V.**
Helicopter in-flight simulation development and use in test pilot training [AD-A283998] p 146 N95-18725
- MILLER, ROBERT GLENN**
Central coast designs: The Eightball Express. Taking off with convention, cruising with improvements and landing with absolute success [NASA-CR-197181] p 47 N95-12643
- MILLER, RON**
Developing and testing decision-making products for center weather service unit meteorologists p 671 A95-93533
- MILLER, RONALD J.**
The aviation gridded forecast system verification program - A description of aviation-impact-variable evaluation plans p 664 A95-93498
- MILLER, STEVEN P.**
Formal verification of an avionics microprocessor [NASA-CR-4682] p 710 N95-33396
- MILLER, T.**
Damage of high temperature components by dust-laden air p 201 N95-19673
- MILLOTT, THOMAS ALEXANDER**
Vibration reduction in helicopter rotors using an actively controlled partial span trailing edge flap located on the blade p 624 N95-32111
- MILNE, A. K.**
AIRSAR deployment in Australia, September 1993: Management and objectives p 321 N95-23948
- MILOS, FRANK S.**
Review of numerical procedures for computational surface thermochemistry [BTN-94-EIX94441386682] p 205 A95-68191
- MINEA, M.**
Computing quantitative characteristics of finite-state real-time systems [AD-A282839] p 83 N95-14343
- MINECK, RAYMOND E.**
Application of two procedures for dual-point design of transonic airfoils [NASA-TP-3466] p 38 N95-12176
Study of potential aerodynamic benefits from spanwise blowing at wingtip [NASA-TP-3515] p 378 N95-28669
Computer model to simulate testing at the National Transonic Facility [NASA-TM-4664] p 627 N95-32217
- MINEGISHI, M.**
Aeroelastic tailoring research [PB94-180031] p 6 N95-10135
- MINENO, HITOSHI**
Flight evaluation of GPS/DGPS sensor systems installed in NAL Do228 [NAL-TR-1230] p 382 N95-26585
- MINEO, AKIYOSHI**
Experiment of the large elastic deformation of biconvex wing sections in an air-flow p 475 A95-91564
- MINGDE, ZHOU**
Plate manipulators [AD-A289601] p 374 N95-26719
- MINGUET, PIERRE**
Application of advanced material systems to composite frame elements p 422 N95-28432
- MINISCLOU, S.**
The Anglo-French Compact Laser Radar demonstrator programme p 703 N95-32501
- MINNETT, P. J.**
Water vapor continuum absorption in mid-latitudes: Aircraft measurements and model comparisons [HTN-95-40756] p 252 A95-71186
- MINUS, DONALD K.**
Fuel-type classification and parameters prediction by Gas Liquid Chromatography analysis [AD-A293442] p 630 N95-31368
- MIODUSHEVSKY, P. V.**
Advanced method and processing technology for complicated shape airframe part forming p 80 N95-14486
- MIRANDY, L.**
Aeroelastic stability of wind turbine blade/aileron systems p 377 N95-27981
Calculation of design load for the MOD-5A 7.3 mW wind turbine system p 440 N95-27982
- MIRDAMADI, M.**
Modeling and life prediction methodology for Titanium Matrix Composites subjected-to-mission profiles [NASA-TM-109148] p 55 N95-11915
- MIRICK, P. H.**
Demonstration of an elastically coupled twist control concept for tilt rotor blade application [BTN-94-EIX94441386633] p 196 A95-68182
Demonstration of an elastically coupled twist control concept for tilt rotor blade application [HTN-95-20959] p 465 A95-88998
- MISKAKTIN, N. I.**
Soft landing on the slope surface of a landing vehicle with an air shock-absorber of forced pressurization [BTN-94-EIX94461407941] p 85 A95-62259
- MITANI, TOHRU**
Three-dimensional analysis of scramjet nozzle flows [BTN-94-EIX94441380978] p 196 A95-68162
Evaluation of scramjet nozzle performance p 402 A95-82321
Performance variation of scramjet nozzle at various nozzle pressure ratios [BTN-95-EIX0616952745781] p 615 A95-94505
- MITCHELL, C. M.**
Operator modeling in commerial aviation: Cognitive models, intelligent displays, and pilot's assistants [NASA-CR-198609] p 401 N95-28203
- MITCHELL, DAVID G.**
The role of handling qualities specifications in flight control system design p 620 N95-31990
Proposed incorporation of mission-oriented flying qualities into MIL-STD-1797A [AD-A294211] p 698 N95-34306
- MITCHEL TREE, ROBERT A.**
Zonally decoupled direct simulation Monte Carlo solutions of hypersonic blunt-body wake flows [BTN-95-EIX95182617458] p 268 A95-75729
- MITLITSKY, FRED**
Unitized Regenerative Fuel Cells for solar rechargeable aircraft and zero emission vehicles [DE95-010684] p 708 N95-33642
- MITLYNG, DAVID**
The FC-1D: The profitable alternative Flying Circus Commercial Aviation Group [NASA-CR-197152] p 46 N95-12628
- MITTELMAN, JEFF**
NEXRAD/ARSR operational comparison p 658 A95-93470
- MITTER, SANJOY K.**
Workshop on Formal Models for Intelligent Control [AD-A281399] p 169 N95-16864
- MIURA, HIROKAZU**
Static aeroelastic characteristics of a composite wing [BTN-95-EIX95152582340] p 282 A95-73542
- MIVILLE, FRANK**
Ultra-Reliable Digital Avionics (URDA) processor p 245 N95-20638
- MIYAJI, KOJI**
Sidewall-effect of the wind tunnel on the estimation of the aerodynamic characteristics of a delta wing p 685 N95-34525
- MIYAJIMA, HIROSHI**
Design features of the NAL ramjet engine test facility p 410 A95-82319
- MIYAKE, YOSHIKI**
Verification of turbine cascade flow with tip clearance p 698 N95-34511
- MIYAMOTO, SHINICHI**
Mechanical properties of advanced toughened bismaleimide matrix composite p 530 A95-91570
- MIYANO, TOMOYUKI**
Flight evaluation of DGPS and DGPS-INS navigation systems p 382 A95-82462

MIYAZAWA, YOSHIKAZU

Flight control system design with Multiple Delay Model/ Multiple Design Point Approach p 507 A95-91586

MIZOBUCHI, YASUHIRO

Studies on gain performance of a combustion driven CO₂ gas dynamic laser p 428 A95-82679

MIZOGUCHI, SEICHI

Experience of aircraft manufacturer for paint removal using dry stripping method p 456 A95-91501

MIZUKAMI, M.

Parametrics on 2D Navier-Stokes analysis of a Mach 2.68 bifurcated rectangular mixed-compression inlet [NASA-TM-107003] p 617 N95-30861

MIZUNO, HIROSHI

Requirements for next generation supersonic transports p 498 A95-91516

MO, J. D.

Numerical investigation of cylinder wake flow with a rear stagnation jet [HTN-95-51669] p 433 A95-85051

MOAS, EDUARDO

An analytical and experimental investigation of the response of the curved, composite frame/skin specimens [HTN-95-80857] p 283 A95-75099

MOATS, MICHAEL L.

Automation of hardware-in-the-loop testing of control systems for unmanned air vehicles [AD-A284833] p 194 N95-19693

MODIANO, DAVID L.

Adaptive computations of flow around a delta wing with vortex breakdown [BTN-94-EIX94441386631] p 184 A95-68180

Adaptive computations of flow around a delta wing with vortex breakdown [HTN-95-20948] p 465 A95-88987

MODICA, GEORGE D.

An application of some cloud modeling techniques to a regional model simulation of an icing event p 673 A95-93543

MOEHRING, J. T.

Modern transport engine experience with environmental ingestion effects p 199 N95-19660

MOESSER, MARK

The role of fretting corrosion, and fretting fatigue in aircraft rivet hole cracking p 94 N95-14470

MOHAMMADI, JAMSHID

Flight parameters monitoring system for tracking structural integrity of rotary-wing aircraft p 135 N95-19469

MOHAN, S. R.

Interference determination for wind tunnels with slotted walls p 147 N95-19269

MOHIUDDIN, M. A.

Modal characteristics of rotors using a conical shaft finite element [BTN-94-EIX94401359745] p 346 A95-77379

MOHLENKAMP, K.

Real time for the calculation of the aerodynamic of aircrafts with delta wings p 460 A95-87399

MOHLER, STANLEY R., JR.

Collection efficiency and ice accretion calculations for a sphere, a swept MS(1)-317 wing, a swept NACA-0012 wing tip, an axisymmetric inlet, and a Boeing 737-300 [NASA-TM-106831] p 123 N95-18582

MOHR, JOHN L.

An advanced vehicle management system [SAE PAPER 931376] p 618 A95-93655

MOIR, I. R. M.

Measurements on a two-dimensional aerofoil with high-lift devices p 109 N95-17848

MOISEEVA, L. T.

Calculation of geometry of stamps with small allowances for pieces of the aerodynamic profile [BTN-94-EIX94461408772] p 103 A95-63655

MOKRY, M.

Evaluation of combined wall- and support-interference on wind tunnel models p 122 N95-19278

MOLENT, L.

Development of a composite repair and the associated inspection intervals for the F-111C stiffener runout region p 66 N95-14477

MOLEZZI, MICHAEL J.

Study of subsonic base cavity flowfield structure using particle image velocimetry [BTN-95-EIX95222650781] p 327 A95-79237

MOLINO, JOHN A.

The effect of onset rate on annoyance to military aircraft noise p 561 A95-90119

MOLLER, PAUL S.

Evaluation of thermal barrier and PS-200 self-lubricating coatings in an air-cooled rotary engine [NASA-CR-195445] p 289 N95-23222

MOLVIK, GREGORY A.

Development of an upwind, finite-volume code with finite-rate chemistry [NASA-CR-196749] p 9 N95-11366

Development of an upwind, finite-volume code with finite-rate chemistry [NASA-CR-197747] p 374 N95-26760

MONAGHAN, PHILIP

A new paradigm: The investment casting cooperative arrangement [HTN-95-92510] p 539 A95-87330

MONAGHAN, T.

Dependability issues in the reuse of standard components in open architectures [AIAA PAPER 95-1006] p 566 A95-90678

MONAGHAN, TIM

The Advanced Avionics Subsystem Technology Demonstration Program p 234 N95-20636

MONDOLINI, STEPHANE LUCIEN

A numerical method for modelling wings with sharp edges maneuvering at high angles of attack p 503 N95-29122

MONGE-CADET, P.

Multilayer anti-erosion coatings p 201 N95-19679

MONGIA, H.

Combustion system CFD modeling at GE Aircraft Engines p 439 N95-27889

MONSON, DARYL J.

Boundary-layer transition and global skin friction measurement with an oil-fringe imaging technique [SAE PAPER 932550] p 547 A95-90054

Boundary-layer transition and global skin friction measurement with an oil-fringe imaging technique [NASA-CR-198814] p 557 N95-30224

MONTECALVO, ANTHONY J.

Integrated mission precision attack cockpit technology (IMPACT). Phase 1: Identifying technologies for air-to-ground fighter integration [AD-A289562] p 389 N95-26684

MONTESEDECCA, X. A.

Aerodynamic design and analysis of a highly loaded turbine exhaust p 312 N95-23435

MONTGOMERY, BRAD

Parts washing alternatives study: United States Coast Guard. Project summary and report [PB95-166146] p 343 N95-26004

MONTGOMERY, KENT R.

Life cycle costs of alternatives for F-16 printed circuit board diagnosis equipment [AD-A288744] p 401 N95-28586

MONTGOMERY, MATTHEW D.

Development of a linearized unsteady Euler analysis for turbomachinery blade rows [NASA-CR-4677] p 592 N95-30611

MONTMAYEUR, N.

Injection studies in the French hypersonic technology program [AIAA PAPER 95-6096] p 510 A95-88004

MONTMAYEUR, NICOLE

Scramjet combustor design in France [AIAA PAPER 95-6094] p 510 A95-88002

MONTTOYA, J.

Characteristics of civil aviation atmospheric hazards p 42 N95-13208

MONYAK, JOHN T.

Statistical analysis of Turbine Engine Diagnostic (TED) field test data [AD-A286032] p 248 N95-20998

MOOK, DEAN T.

Numerical simulation of steady and unsteady, vorticity-dominated aerodynamic interference [BTN-95-EIX95062487524] p 186 A95-69232

MOORE, A. R.

Drag reduction in a rectangular duct using riblets [HTN-95-01091] p 468 A95-90277

MOORE, C. S.

Thermal conductivity of zirconia thermal barrier coatings p 345 N95-26133

MOORE, F. G.

Base drag prediction on missile configurations [BTN-95-EIX95152583256] p 266 A95-73557

Improved version of the Naval Surface Warfare Center aeroprediction code (AP93) [BTN-95-EIX95152583260] p 267 A95-73561

Calculation of wing-alone aerodynamics to high angles of attack [BTN-95-EIX95212645713] p 261 A95-76765

MOORE, FRANK G.

Engineering Codes for aeroprediction: State-of-the-art and new methods p 73 N95-14447

MOORE, G. V.

Determining GPS average performance metrics p 383 N95-27791

MOORE, JOHN

Supersonic flow and shock formation in turbine tip gaps p 312 N95-23429

MOORE, KEVIN A.

An experimental investigation of helicopter downwash and tailboom interaction at the Wichita State University 7x10 foot wind tunnel p 375 N95-26955

MOORE, M.

The short range attack missile/light weight exo-atmospheric projectile (SRAM/LEAP) missile tests program [HTN-95-81498] p 386 A95-85212

MOORE, P.

Validation of empirical orbit error corrections using crossover difference differences [HTN-94-00912] p 25 A95-60227

MOORE, PATRICK D.

Identification of aviation weather hazards based on the integration of radar and lightning data [HTN-95-51323] p 356 A95-80908

The inference of aviation weather hazards based on the integration of radar and lightning data p 660 A95-93483

MOORE, SALLY

Human factors issues in aircraft cabin design [SAE PAPER 932527] p 386 A95-84556

MOORE, TOM

Labs behind Boeing's new 777 [BTN-95-EIX95142562403] p 280 A95-73437

MOORHOUSE, DAVID J.

The control system design methodology of the STOL and maneuver technology demonstrator p 621 N95-31998

MORAGA, CLAUDIO

Fault detection in multiprocessor systems and array processors [BTN-95-EIX95242679097] p 359 A95-81253

MORALEZ, E., III

Simulation and flight test evaluation of head-up-display guidance for harrier approach transitions [BTN-95-EIX95062487533] p 194 A95-69241

MORAN, B.

Fatigue reliability method with in-service inspections p 94 N95-14475

MORAN, KENNETH JOHN

An aerodynamic and static-stability analysis of the Hypersonic Applied Research Technology (HART) missile [DA9426923] p 481 N95-29965

MORAN, TOM

Maintenance programs [HTN-95-92310] p 365 A95-85354

MORE, K. L.

Evolution of oxidation and creep damage mechanisms in HiPep silicon nitride materials [DE95-001360] p 300 N95-22689

MOREAU, A.

Modular supplies for a distributed architecture p 234 N95-20657

MOREAU, STEPHANE

Computation of high-altitude hypersonic flow-field radiation p 593 N95-30843

MOREL, MICHAEL

NASA Lewis Research Center Workshop on Forced Response in Turbomachinery [NASA-CP-10147] p 141 N95-19380

MORELLI, EUGENE A.

Determining the accuracy of maximum likelihood parameter estimates with colored residuals [NASA-CR-194893] p 51 N95-11869

MORELLI, MAURO

Analysis of some interference effects in a transonic wind tunnel [BTN-95-EIX0619952748166] p 589 A95-94460

MORETTI, S.

MAX-91: Polarimetric SAR results on Montespertoli site p 320 N95-23940

MORGAN, J. MURRAY

Practical experiences in control systems design using the NCR Bell 205 Airborne Simulator p 624 N95-32015

MORGAN, K.

Mesh generation and adaptivity for the solution of compressible viscous high speed flows [BTN-95-EIX95262697157] p 538 A95-86893

MORGAN, R. G.

Shock tunnel studies of scramjet phenomena 1993 [NASA-CR-195038] p 350 N95-25394

The Superorbital Expansion Tube concept, experiment and analysis p 341 N95-25399

MORGAN, REED

The impact of advanced packaging technology on modular avionics architectures p 233 N95-20632

MORGAN, RICHARD G.

Chemical recombination in an expansion tube [HTN-95-20844] p 544 A95-88105

MORGENSTERN, ALGACYR, JR.

Hypersonic flow past open cavities [HTN-95-42577] p 458 A95-87207

- MORINO, L.**
Matrix fraction approach for finite-state aerodynamic modeling
[BTN-95-EIX95262694311] p 365 A95-85482
- MORINO, YOSHIKI**
R & D on HOPE structure p 413 A95-82355
Research and development of thermal protection system of HOPE re-entry vehicle p 413 A95-82358
- MORISHITA, ETSUO**
Ground effect calculation of two-dimensional airfoil [BTN-94-EIX94371347710] p 219 A95-69969
Experimental investigation on aerothermodynamic characteristics of hypersonic transport p 473 A95-91525
- MORL, P.**
Two dimensional stratospheric aerosol distributions during EASOE [HTN-95-00726] p 444 A95-86296
- MORRE, FRANK G.**
The 1995 version of the NSWC aeroprediction code. Part 1: Summary of new theoretical methodology [AD-A291518] p 481 N95-29853
- MORRIS, D. E.**
Static and dynamic friction behavior of candidate high temperature airframe seal materials [NASA-TM-106571] p 152 N95-16905
- MORRIS, M. R.**
The effects of design details on cost and weight of fuselage structures p 501 N95-28831
Global cost and weight evaluation of fuselage keel design concepts p 501 N95-28840
- MORRIS, P. J.**
Linear instability waves in supersonic jets confined in circular and non-circular ducts [BTN-94-EIX94341340068] p 103 A95-63520
- MORRIS, PHILIP J.**
Noise radiation by instability waves in coaxial jets [NASA-TM-106738] p 100 N95-14618
Supersonic jet noise reductions predicted with increased jet spreading rate [NASA-TM-106872] p 323 N95-23178
Supersonic coaxial jet noise predictions [NASA-TM-106917] p 451 N95-26801
- MORRIS, R. W.**
High heat sink fuels for improved aircraft thermal management [SAE PAPER 932084] p 530 A95-91659
- MORRIS, SHELBY J., JR.**
The personal aircraft: Status and issues [NASA-TM-109174] p 223 N95-20688
- MORRIS, VIRGINIA L.**
Environmentally regulated aerospace coatings p 631 N95-31775
- MORRISSETTE, MONICA**
Integrated design and manufacturing for the high speed civil transport [NASA-CR-197183] p 48 N95-12700
- MORRISON, ROWENA**
General aviation landing incidents and accidents: A review of ASRS and AOPA research findings p 596 A95-95198
- MORRISON, T.**
Chinook goes FADEC [CONGRESS PAPER C428-33-078] p 610 A95-93621
- MORSE, CORINNE S.**
Real-time estimation of atmospheric turbulence severity from in-situ aircraft measurements [BTN-95-EIX95182619231] p 319 A95-76657
Estimation of atmospheric turbulence severity from in-situ aircraft measurements p 659 A95-93479
- MORT, K. W.**
Optimum full-scale subsonic wind tunnel [AIAA PAPER 86-0732] p 18 A95-60161
- MORTLOCK, ALAN K.**
The high speed civil transport: A technology challenge p 496 A95-90089
- MORTON, P. G.**
The dynamic nature of rotor thermal bending due to unsteady lubricant shearing within a bearing [HTN-95-42091] p 430 A95-83857
- MOSBARGER, NEAL ANTHONY**
An experimental investigation of the time-dependent separation of tangent bodies in supersonic flow [AD-A290720] p 480 N95-29500
- MOSER, G.**
Secondary power system study for the hixtel RA3 flight test vehicle [AIAA PAPER 95-6158] p 512 A95-90470
Microchannel heat pipe cooling of modules p 246 N95-20649
- MOSHAROV, V.**
Optical surface pressure measurements: Accuracy and application field evaluation p 175 N95-19274
- MOSHER, MARIANNE**
Study of noise on a small-scale hovering tilt rotor [HTN-94-00712] p 5 A95-60190
Measurements of atmospheric turbulence effects on tail rotor acoustics [NASA-TM-108843] p 38 N95-12360
- MOSIER, MARY H.**
Standard Hardware Acquisition and Reliability Program (SHARP) advanced SEM-E packaging p 233 N95-20633
- MOSS, J. N.**
DSMC calculations for 70-deg blunted cone at 3.2 km/s in nitrogen [NASA-TM-109181] p 348 N95-24396
- MOSS, JAMES N.**
Hypersonic rarefied flow past spheres including wake structure [BTN-95-EIX95152583250] p 305 A95-73551
Zonally decoupled direct simulation Monte Carlo solutions of hypersonic blunt-body wake flows [BTN-95-EIX95182617458] p 268 A95-75729
- MOTALLEBI, F.**
A review of the hot-wire technique in 2-D compressible flow [HTN-95-61157] p 373 A95-86256
- MOTE, C. D.**
Vortex shedding noise control in idling circular saws using air ejection at the teeth [BTN-94-EIX94371347214] p 257 A95-69970
- MOTYLEWSKI, JERZY**
Photoacoustic chambers for studying solids and gases: Theory and practical examples [IFTR-39/1994] p 412 N95-26837
- MOUCH, THOMAS N.**
Computational fluid dynamics with icing effects [SAE PAPER 932532] p 466 A95-89192
- MOUL, THOMAS M.**
Low-speed wind-tunnel investigation of the stability and control characteristics of a series of flying wings with sweep angles of 50 deg [NASA-TM-4640] p 505 N95-30226
- MOULTON, CAREY L.**
Incorporation of topography effects in aircraft noise modeling p 578 A95-90140
- MOURTOS, NIKOS J.**
Flow visualization studies of VTOL aircraft models during Hover in ground effect [NASA-TM-108860] p 272 N95-22666
- MOUSTAFA, GAMAL H.**
Main features of overexpanded triple jets [BTN-95-EIX95142553040] p 304 A95-73458
- MOZO, BEN T.**
The assessment of the AH-64D, longbow, mast-mounted assembly noise hazard for maintenance personnel [AD-A284971] p 171 N95-16226
- MU, XINHUA**
The computer analysis of the prediction of aircraft electrical power supply system reliability p 155 N95-16278
- MUDKAVI, VIDYADHAR Y.**
Computation of vortex breakdown p 165 N95-19462
- MUEHLECK, P.**
Influence of the flight trajectory on the exhaust gas composition of a H2-fueled air-breathing ramjet engine p 509 A95-87404
- MUELLER, ARNOLD W.**
Improvement of the predicted aural detection code ICHIN (I Can Hear It Now) p 576 A95-90123
- MUELLER, BOYD A.**
A new paradigm: The investment casting cooperative arrangement [HTN-95-92510] p 539 A95-87330
- MUELLER, CINDY**
The real-time analysis and prediction of storms program p 655 A95-93457
- MUELLER, CRAIG**
Integrated design and manufacturing for the high speed civil transport [NASA-CR-197183] p 48 N95-12700
- MUELLER, JENS-DOMINIK**
Quality estimates and stretched meshes based on Delaunay triangulations [HTN-95-42575] p 564 A95-87205
- MUELLER, MARC K.**
Hybrid laminar flow over wings enhanced by continuous boundary layer suction [SAE PAPER 931386] p 587 A95-93662
- MUELLER, T. J.**
Experimental investigation of the sources of propeller noise due to the ingestion of turbulence at low speeds [BTN-95-EIX95262697042] p 569 A95-86859
- MUGNAI, A.**
Behavior of an inversion-based precipitation retrieval algorithm with high-resolution AMPR measurements including a low-frequency 10.7-GHz channel [HTN-95-70134] p 252 A95-70656
- MUILENBURG, DENNIS A.**
Euler technology assessment for preliminary aircraft design employing OVERFLOW code with multiblock structured-grid method [NASA-CR-4651] p 273 N95-23095
- MUKHIN, V. S.**
Mechanism and technological particular features of thermomagnetic hardening [BTN-94-EIX94461407953] p 89 A95-62627
- MUKHOPADHYAY, VIVEK**
Flutter suppression control law design and testing for the active flexible wing [BTN-95-EIX95182619214] p 292 A95-76640
- MULDER, J. A.**
Identification of dynamic systems. Volume 3: Applications to aircraft. Part 2: Nonlinear analysis and manoeuvre design [AGARD-AG-300-VOL-3-PT-2] p 79 N95-14102
Robust control: A structured approach to solve aircraft flight control problems p 621 N95-31995
- MULENBURG, G. M.**
Simulation of Shuttle launch G forces and acoustic loads using the NASA Ames Research Center 20G centrifuge p 86 N95-14089
- MULLEN, ROBERT L.**
Conversion of production automotive engines for aviation use [SAE PAPER 932606] p 495 A95-90076
- MULLER, M.**
Rotorcraft ditchings and water-related impacts that occurred from 1982 to 1989, phase 1 [AD-A279164] p 189 N95-19805
- MULLER, MARK**
Commuter/air taxi ditchings and water-related impacts that occurred from 1979 to 1989 [AD-A285691] p 226 N95-20275
- MULLINS, M. J.**
Novel matrix resins for composites for aircraft primary structures, phase 1 [NASA-CR-189657] p 23 N95-10318
- MULVEHILL, ALICE M.**
Thunderstorm hypothesis reasoner [AD-A282664] p 60 N95-12805
- MUNOZ, TOMAS**
Design constraints in the payload-range diagram of ultrahigh capacity transport airplanes [BTN-95-EIX95152582319] p 276 A95-73522
- MUNSON, JOHN**
Compressor discharge film riding face seals p 60 N95-13599
- MURAKAMI, A.**
Aerodynamic characteristics of supersonic air-intake/aircraft integrated models p 472 A95-91512
- MURAKAMI, AKIRA**
A shock tunnel test of a winged hypersonic research vehicle p 474 A95-91538
Effects of cavity bleed and its configuration on aerodynamic characteristics of supersonic internal flow [NAL-TR-1247] p 594 N95-31715
- MURAKAMI, ATSUO**
Experiment on a rectangular cross section scramjet combustor. 2: Effects of fuel injector geometry [NAL-TR-1220] p 405 N95-26600
- MURAKAMI, ATSUSHI**
R & D on HOPE structure p 413 A95-82355
- MURAKAMI, MASAOKI**
Experimental investigation of composite channel heat pipe operation in micro-gravity environment p 428 A95-82645
- MURATA, MASAOKI**
Flight evaluation of GPS/DGPS sensor systems installed in NAL Do228 [NAL-TR-1230] p 382 N95-26585
- MURMAN, EARLL M.**
Adaptive computations of flow around a delta wing with vortex breakdown [BTN-94-EIX94441386631] p 184 A95-68180
Adaptive computations of flow around a delta wing with vortex breakdown [HTN-95-20948] p 465 A95-88987
- MURMAN, SCOTT M.**
Numerical simulation of the flow about the F-18 HARV at high angle of attack p 9 N95-10940 [NASA-CR-196396]
Numerical simulation of the flow about an F-18 aircraft in the high-alpha regime p 68 N95-14232
Numerical simulation of the flow about the F-18 HARV at high angle of attack p 74 N95-14614

- Numerical simulation of the flow about the F-18 HARV at high angle of attack [NASA-CR-197755] p 374 N95-26735
- MUROTA, KATSUICHI**
Experimental study of the aerodynamic characteristics of the counter-rotation propellers p 474 A95-91562
Measurements of longitudinal static aerodynamic coefficients by the cable mount system [NAL-TR-1226] p 331 N95-25761
- MURPHY, D.**
Non-linear analysis provides new insights into impact damage of composite structures [HTN-95-42368] p 418 A95-86197
- MURPHY, DANIEL P.**
Impact damage resistance of composite fuselage structure, part 2 p 533 N95-28838
- MURPHY, JACK**
Viper [NASA-CR-197191] p 79 N95-13703
- MURPHY, JAMES H.**
Study of strapdown navigation attitude algorithms [BTN-95-EIX95282706655] p 486 A95-89649
- MURPHY, O. J.**
Corrosion of aircraft materials: Correlation between nanometer scale and macroscopic structural damage parameters [AD-A285930] p 241 N95-20299
- MURPHY, W. H.**
Effect of annealing and desulfurization on oxide spallation of turbine airfoil material [BTN-95-EIX95282707024] p 528 A95-88264
- MURRAY, JAMES E.**
Flight experience with lightweight, low-power miniaturized instrumentation systems [BTN-95-EIX95062487522] p 180 A95-69230
Development and flight test of a deployable precision landing system [BTN-95-EIX95062487535] p 190 A95-69243
- MURRAY, W. E.**
Evaluation of all-electric secondary power for transport aircraft [NASA-CR-189077] p 441 N95-27999
- MURRI, D. G.**
High Alpha Technology Program (HATP) ground test to flight comparisons p 68 N95-14230
- MURRI, DANIEL G.**
Actuated forebody strake controls for the F-18 High-Alpha Research Vehicle [BTN-95-EIX0619952748173] p 619 A95-94467
Preparations for flight research to evaluate actuated forebody strakes on the F-18 high-alpha research vehicle p 72 N95-14257
- MURTHY, DURBHA V.**
NASA Lewis Research Center Workshop on Forced Response in Turbomachinery [NASA-CP-10147] p 141 N95-19380
- MURTHY, G. S. K.**
Mobile domes for TACTIC telescope p 453 A95-86113
- MURTHY, P. L. N.**
Ice-impact analysis of blades p 200 N95-19672
Analysis of aircraft engine blade subject to ice impact p 407 N95-28277
- MURTHY, S.**
International collaboration in hypersonic technologies - A specific and worthwhile initiative [AIAA PAPER 95-6140] p 581 A95-90457
- MURTHY, S. N. B.**
Gas turbine prediffuser-combustor performance during operation with air-water mixture [DOT/FAA/CT-93/52] p 83 N95-15683
WINCLR: A computer code for heat transfer and clearance calculation in a compressor [NASA-CR-195436] p 366 N95-26363
- MURTY, H.**
Role of Kutta waves on oscillatory shock motion on an airfoil [HTN-95-81642] p 542 A95-87690
- MUSOFF, HOWARD**
Study of strapdown navigation attitude algorithms [BTN-95-EIX95282706655] p 486 A95-89649
- MUSSER, JANA**
The Aluminum Falcon: A low cost modern commercial transport [NASA-CR-197180] p 81 N95-15742
- MUSSETTO, MICHAEL**
Passive millimeter wave camera for aircraft landing in low visibility conditions [BTN-95-EIX95292721321] p 609 A95-92513
- MUSTER, DOUGLAS**
Condition monitoring and diagnostics [HTN-95-92312] p 387 A95-85356
- MUTASIM, Z. Z.**
Perspective on thermal barrier coatings for industrial gas turbine applications p 345 N95-26128
- MUTHARASAN, RAJAKANNU**
Development of hypersonic engine seals: Flow effects of preload and engine pressures [BTN-95-EIX95112524204] p 196 A95-69304
- MUZZO, DOUG**
Experimental/analytical approach to understanding mistuning in a transonic wind tunnel compressor [NASA-TM-108833] p 95 N95-14617
- MYERS, BLAKE**
Unitized Regenerative Fuel Cells for solar rechargeable aircraft and zero emission vehicles [DE95-010684] p 708 N95-33642
- MYERS, J.**
AVIRIS and TIMS data processing and distribution at the land processes distributed active archive center p 325 N95-23872
- MYERS, STEVE**
Integrated test system single point control of aircraft checkout [SAE PAPER 931417] p 583 A95-93682
- MYKITSHYN, MARK**
An exploratory survey of information requirements for instrument approach charts [AD-A293882] p 601 N95-31520
Current issues in the design and information content of instrument approach charts [AD-A294752] p 690 N95-34562
- MYKLEBUST, ARVID**
Putting the ACSYNT on aircraft design [BTN-95-EIX95072419881] p 180 A95-68398
- MYOSE, ROY Y.**
On the role of the outer region in the turbulent-boundary-layer bursting process [BTN-94-EIX95011441078] p 348 A95-81056
The near-wake flow behavior of an oscillating airfoil with modified trailing edge p 375 N95-26953
- N**
- NAEGELI, D. W.**
A study of aircraft post-crash fuel fire mitigation [AD-A282208] p 40 N95-12499
- NAGABHUSHANAM, J.**
Flap-lag damping in hover and forward flight with a three-dimensional wake [HTN-95-AD0496] p 221 A95-72567
Automatic identification of modal damping from Floquet analysis [HTN-95-01084] p 506 A95-90270
- NAGAI, SHINJI**
A shock tunnel test of a winged hypersonic research vehicle p 474 A95-91538
- NAGAMATSU, HENRY T.**
Numerical analysis of hypersonic low-density scramjet inlet flow [BTN-95-EIX95212645694] p 272 A95-76746
- NAGAO, YOSUKE**
Flight test of STS radio controlled scale model p 499 A95-91539
- NAGARAJ, B. A.**
Thermal conductivity of zirconia thermal barrier coatings p 345 N95-26133
- NAGARAJA, K. S.**
A perspective of rarefied gas flow problems relevant to high altitude flight [SAE PAPER 931366] p 586 A95-93647
- NAGASHIMA, TOMOARI**
Hubload responses of a rotor in forward flight due to multiple frequency blade pitch variations p 515 A95-91504
- NAGATOMO, MAKOTO**
Atmospheric reentry flight test of winged space vehicle p 414 A95-82483
- NAGATSUMA, T.**
Electro-optic characterization of ultrafast photodetectors using adiabatically compressed soliton pulses [BTN-94-EIX94381359637] p 257 A95-72675
- NAGESH BABU, G. L.**
Smart structures in the control of airframe vibrations [HTN-95-31014] p 236 A95-71184
- NAGHSHINEH, KOOROSH**
Broadband, wide-area active control of sound radiated from vibrating structures using local surface-mounted radiation suppression devices p 30 N95-11283
- NAGY, D. R.**
Protective coatings for compressor gas path components p 201 N95-19675
- NAIRUS, JOHN G.**
Solid state power controller technology [SAE PAPER 931422] p 495 A95-90087
- NAKABAYASHI, Y.**
Development of 70MW class superconducting generators [BTN-94-EIX95011440854] p 429 A95-82905
- NAKAJIMA, TAKASHI**
The aerodynamic characteristics of cup-like body in supersonic flow p 427 A95-82407
- NAKAMICHI, J.**
Aeroelastic tailoring research [PB94-180031] p 6 N95-10135
Computations of unsteady aerodynamic loads around oscillating wings. Part 1: Formulation [PB94-180049] p 7 N95-10136
Computations of unsteady aerodynamic loads around oscillating wings. Part 2: Computed results and discussions [PB94-180056] p 7 N95-10137
- NAKAMICHI, JIRO**
Numerical solutions of inviscid and viscous flows about airfoils by TVD method p 684 N95-34521
- NAKAMURA, CASMARA**
A simulation of damping process of pendulum motion due to aerodynamic forces p 711 N95-34551
- NAKAMURA, KATUHIKO**
Analysis and scale-model experiment of propeller driving motor for microwave-powered airplane p 487 A95-91576
- NAKAMURA, MASARU**
Flight reference display for powered-lift STOL aircraft [NAL-TR-1251] p 337 N95-25005
- NAKAMURA, SHIN'ITI**
Prediction level of noise by a helicopter p 571 A95-88469
- NAKAMURA, SHINGO**
Experimental study of the aerodynamic characteristics of the counter-rotation propellers p 474 A95-91562
Wake velocity measurement of counter-rotation propellers p 474 A95-91563
- NAKAMURA, SYUJI**
Development of Fly-By-Wire system for BK117 p 516 A95-91506
- NAKAMURA, TAKASHI**
Performance evaluation of the NWT with incompressible NS code p 707 N95-34533
- NAKAMURA, YASU HARU**
Aerodynamic mechanism of galloping [BTN-94-EIX94371347709] p 219 A95-69968
- NAKAMURA, YOSHIKI**
A simulation of damping process of pendulum motion due to aerodynamic forces p 711 N95-34551
- NAKAO, SHIGEHIDE**
A study on aerodynamic heating phenomena in three-dimensional shock wave/turbulent boundary layer interaction induced by sweptback sharp fins at supersonic flow p 428 A95-82419
- NAKAYA, T.**
Development of a pilot tube with multi-hole pyramidal head. 2: A five-hole yaw probe of engineering model p 522 A95-91577
- NAKAYASU, HIDEHIKO**
Experimental investigation of static and dynamic ground effect on HOPE ALFLEX vehicle [NAL-TR-1236] p 388 N95-26525
- NALIM, M. RAZI**
Preliminary assessment of combustion modes for internal combustion wave rotors [NASA-TM-107000] p 616 N95-30632
- NALIM, MOHAMED RAZI**
Wave cycle design for wave rotor engines with limited nitrogen oxide emissions p 161 N95-18901
- NALLASAMY, M.**
Effects of a forward-swept front rotor on the flowfield of a counterrotation propeller [NASA-TM-106671] p 7 N95-10148
Computation of noise radiation from turbofans: A parametric study [NASA-CR-198359] p 710 N95-32836
- NALLS, ART**
Assessment of Russian VSTOL technology evaluating the YAK-38 'FORGER' and YAK-141 'FREESTYLE' p 497 A95-90868
- NAMKUNG, M.**
New nondestructive techniques for the detection and quantification of corrosion in aircraft structures p 315 N95-23512
- NANCE, JOHN J.**
Test and evaluation crew resource management p 483 A95-90867
- NANGIA, R. K.**
Estimating wind tunnel interference due to vectored jet flows p 164 N95-19265
- NAPOLITANO, MARCELLO R.**
On-line learning nonlinear direct neurocontrollers for restructurable control systems [BTN-95-EIX95242670768] p 359 A95-81079
Determination of stability and control derivatives from the NASA F/A-18 HARV from flight data using the maximum likelihood method [NASA-CR-197320] p 204 N95-19576

- NARAYANSWAMI, N.**
Laser interferometer skin-friction measurements of crossing-shock-wave/turbulent-boundary-layer
[HTN-95-20834] p 544 A95-88095
- NARUO, YOSHIHIRO**
Test results on air turbo ramjet engine for a future space plane p 402 A95-82327
- NASH, KYLE L.**
Predicting exhaust plume boundaries with supersonic external flows
[BTN-95-EIX95152583258] p 297 A95-73559
- NASH, TREVOR**
Flight Simulators: Better than the real thing?
[HTN-95-42619] p 518 A95-87249
- NATH, G.**
Free convection past a uniform flux surface inclined at a small angle to the horizontal
[HTN-95-42213] p 430 A95-84029
- NATHMAN, JAMES K.**
Precision requirement for potential-based panel methods
[HTN-95-51666] p 433 A95-85048
- NAYAK, G. C.**
Reaction-time response of aircraft crash
[BTN-95-EIX95292721296] p 595 A95-92626
- NAYANI, SUDHEER N.**
Higher-order viscous shock-layer solutions for high-altitude flows
[BTN-95-EIX95152583255] p 306 A95-73556
- NAYFEH, ALI H.**
Numerical simulation of steady and unsteady, vorticity-dominated aerodynamic interference
[BTN-95-EIX95062487524] p 186 A95-69232
- NAYLOR, STEVE**
On-line learning nonlinear direct neurocontrollers for restructurable control systems
[BTN-95-EIX95242670768] p 359 A95-81079
- NAZYROVA, R. R.**
On introduction of artificial intelligence elements to heat power engineering
[BTN-94-EIX94461407961] p 100 A95-62635
On a program-information system Tdsoft
[BTN-94-EIX94461408773] p 175 A95-63656
- NCNALLY, B. DAVID**
Flight test evaluation of the Stanford University/United Airlines differential GPS Category 3 automatic landing system
[NASA-TM-110354] p 593 N95-30788
- NEALY, JOHN E.**
Radiation safety aspects of commercial high-speed flight transportation
[NASA-TP-3524] p 453 N95-26427
- NEBYLOV, A. V.**
Sea wave parameters, small altitudes and distances measurers design for movement control systems of ships, wing-in-surface effect crafts and seaplanes p 708 N95-33141
- NEEDLEMAN, H. C.**
Status of the NASA balloon program p 181 A95-66296
- NEELY, A. J.**
The Superorbital Expansion Tube concept, experiment and analysis p 341 N95-25399
- NEHER, JASON R.**
Triton 2 (1B)
[NASA-CR-197188] p 46 N95-12636
- NEIGHBORS, KEN**
Integrated flight/propulsion control for helicopters
[HTN-95-80854] p 290 A95-75096
- NEILLEY, PETER P.**
The real-time analysis and prediction of storms program p 655 A95-93457
A short-term, high-resolution automated snowfall forecasting system p 666 A95-93510
- NEJAD, A. S.**
Numerical study of mixing in a high and low enthalpy supersonic test facility p 7 N95-10467
- NELSON, H. F.**
Wing vertical position effects on wing-body carryover for noncircular missiles
[BTN-95-EIX95182617462] p 268 A95-75733
Aerodynamic interference for supersonic low-aspect-ratio missiles
[BTN-95-EIX95302694469] p 588 A95-94065
- NELSON, J. R.**
The opportunities for and challenges of common integrated electronics
[AD-A279991] p 248 N95-20966
- NELSON, MARY J.**
Cadmium plating replacements p 631 N95-31773
- NELSON, N.**
Computational predictive methods for fracture and fatigue p 93 N95-14466
- NELSON, R. C.**
Directional control at high angles of attack using blowing through a chined forebody
[BTN-95-EIX0619952748179] p 619 A95-94472
- NELSON, ROBERT C.**
Experimental investigations on limit cycle wing rock of slender wings
[BTN-95-EIX95062487543] p 185 A95-68357
Free-to-roll tests of X-31 and F-18 subscale models with correlation to flight test results p 69 N95-14237
Experiments on the flow field physics of confluent boundary layers for high-lift systems
[NASA-CR-197318] p 224 N95-21343
- NELSON, S. G.**
Laboratory evaluation of a reactive baffle approach to NOx control
[AD-A283802] p 255 N95-19921
- NELSON, T. E.**
Compressible Navier-Stokes computations of multielement airfoil flows using multiblock grids
[HTN-95-42327] p 371 A95-86156
- NEMETS, STEVE A.**
NASA Lewis Research Center's preheated combustor and materials test facility
[NASA-TM-106676] p 626 N95-30592
- NEPPACH, CHARLES**
On-line learning nonlinear direct neurocontrollers for restructurable control systems
[BTN-95-EIX95242670768] p 359 A95-81079
- NERAVETLA, B. R.**
Effect of weak periodic pressure gradient on streamwise vortices near a wall p 29 N95-11263
- NERI, LARRY**
Analysis of composite structures with delaminations under combined bending and compression p 422 N95-28429
- NERI, LAWRENCE M.**
Ninth DOD/NASA/FAA Conference on Fibrous Composites in Structural Design, volume 3
[NASA-CR-198718] p 420 N95-28266
Ninth DOD/NASA/FAA Conference on Fibrous Composites in Structural Design, volume 1
[NASA-CR-198723] p 421 N95-28420
Ninth DOD/NASA/FAA Conference on Fibrous Composites in Structural Design, volume 2
[NASA-CR-198722] p 424 N95-28462
- NESBITT, DAVID J.**
State-to-state collisional dynamics of atmospheric species
[AD-A285053] p 245 N95-20484
- NESENYUK, L. P.**
Navigational technology of dual usage p 688 N95-33131
- NESPOR, JERALD D.**
Doppler radar detection of vortex hazard indicators p 42 N95-13212
- NESTOR, JULIE**
Conceptual design of the AE481 Demon Remotely Piloted Vehicle (RPV)
[NASA-CR-197164] p 44 N95-12294
- NESVISZSKY, G.**
Prediction of fatigue crack growth under constant amplitude and random loading using specimens with multiple cracks
[AD-A291614] p 397 N95-28409
- NETT, H.**
Aircraft measurements of CLO and HCL during EASOE 1991/92
[HTN-95-00721] p 444 A95-86291
- NETZER, D. W.**
An investigation of the side-dump dual in-line ramjet combustor p 617 N95-31199
- NEUBERGER, U.**
X-31: A program overview and flight test status p 609 N95-32013
- NEUFELD, DAVID C.**
Development and flight test of a deployable precision landing system
[BTN-95-EIX95062487535] p 190 A95-69243
- NEUHART, DAN H.**
Simultaneous three-dimensional velocity and mixing measurements by use of laser Doppler velocimetry and fluorescence probes in a water tunnel
[NASA-TP-3454] p 53 N95-13553
- NEUMANN, ERIC S.**
Two-phase flow research using the leerjet apparatus
[NASA-TM-106814] p 438 N95-27854
- NEWLEY, R. A.**
Polymer composite applications to aerospace equipment
[HTN-95-80257] p 529 A95-89201
- NEWMAN, BRETT**
Aerelastic vehicle multivariable control synthesis with analytical robustness evaluation
[BTN-95-EIX95182619115] p 321 A95-76592
- Multivariable stability and robustness of sequentially designed feedback systems
[BTN-95-EIX95182619125] p 322 A95-76602
- NEWMAN, BRETT A.**
Inner loop flight control for the High-Speed Civil Transport p 293 N95-23314
- NEWMAN, D. M.**
Six degree of freedom flight dynamic and performance simulation of a remotely-piloted vehicle
[AERO-TN-9301] p 131 N95-18097
- NEWMAN, E. H.**
A users manual for the method of moments Aircraft Modeling Code (AMC), version 2
[NASA-CR-196445] p 24 N95-11252
- NEWMAN, J. C. JR.**
Influence of crack history on the stable tearing behavior of a thin-sheet material with multiple cracks p 93 N95-14467
Development of the NASA/FLAGRO computer program for analysis of airframe structures p 94 N95-14473
- NEWMAN, JAMES C.**
Dynamic unstructured method for flows past multiple objects in relative motion
[BTN-95-EIX95262694303] p 435 A95-85474
- NEWMAN, LAURI KRAFT**
Reentry analysis for low Earth orbiting spacecraft p 415 A95-85774
- NEWMAN, P. A.**
Fine-scale, poleward transport of tropical air during AASE 2
[HTN-95-70949] p 352 A95-78014
Applications of automatic differentiation in CFD
[NASA-TM-109948] p 157 N95-16828
- NEWMAN, PAUL A.**
An algorithm for forecasting mountain wave-related turbulence in the stratosphere
[HTN-95-80656] p 254 A95-72500
Trajectory modeling of emissions from lower stratospheric aircraft
[HTN-95-41219] p 317 A95-75031
- NEWMAN, PERRY A.**
Sensitivity derivatives for three dimensional supersonic Euler code using incremental iterative strategy
[HTN-95-20845] p 545 A95-88106
Applications of automatic differentiation in computational fluid dynamics p 156 N95-16461
- NEWMAN, R. L.**
TRISTAR 1: Evaluation methods for testing head-up display (HUD) flight symbology
[NASA-TM-46665] p 288 N95-24030
- NEWMAN, S. J.**
The verification of a theoretical helicopter rotor blade sailing method by means of windtunnel testing
[HTN-95-01093] p 468 A95-90279
- NEWSOME, J. R.**
Measurement of moisture and total hydrocarbon contributions by valves used in clean room gas-delivery systems
[BTN-94-EIX94381359041] p 295 A95-74629
- NEWTON, R.**
Performance of a focused cavity aerosol spectrometer for measurements in the stratosphere of particle size in the 0.06-2.0-micrometer-diameter range
[HTN-95-90914] p 253 A95-72423
- NEYLAND, V. M.**
Operation of the adaptive-wall wind tunnel of TsAGI, Moscow p 519 A95-88901
The traditional and new methods of accounting for the factors distorting the flow over a model in large transonic wind tunnels p 165 N95-19275
- NG, LIAN**
Acoustic receptivity due to weak surface inhomogeneities in adverse pressure gradient boundary layers
[NASA-TM-4577] p 249 N95-21258
- NG, T. TERRY**
Effect of leeward flow dividers on the wing rock of a delta wing
[BTN-95-EIX95152582347] p 282 A95-73549
- NG, W. F.**
Fan noise reduction from a supersonic inlet during simulated aircraft approach
[BTN-95-EIX95292721155] p 572 A95-89894
- NGUYEN, D. D.**
A programmable heater control circuit for spacecraft
[NASA-TM-108459] p 9 N95-11157
- NGUYEN, KHANH**
Dynamics of the McDonnell-Douglas Large Scale Dynamic Rig and dynamic calibration of the rotor balance p 65 N95-13891
[NASA-TM-108855] p 65 N95-13891
- NGUYEN, KHANH Q.**
Higher harmonic control analysis for vibration reduction of helicopter rotor systems
[NASA-TM-103855] p 66 N95-14419

NGUYEN, NHAN

Experimental/analytical approach to understanding mistuning in a transonic wind tunnel compressor [NASA-TM-108833] p 95 N95-14617

NGUYEN, PHONG

LCX: Proposal for a low-cost commercial transport [NASA-CR-197186] p 47 N95-12645

NGUYEN, V. D.

Applications of the five-hole probe technique for flow field surveys at the Institute for Aerospace Research p 163 N95-19255

NGUYEN, V.-N.

Large-scale computational fluid dynamics by the finite element method [HTN-94-EIX94381359154] p 243 A95-71744

NI, R. H.

Unsteady flows in turbines: Impact on design procedure p 90 N95-14132

NI, YONGXI

Application of GPS/SINS/RA integrated system to aircraft approach landing p 125 N95-16277

NICASTRO, L.

Period evolution of PSR B1259-63: Evidence for propeller-torque spindown [HTN-95-B0194] p 581 A95-87903

NICHOLS, JAMES

The generic simulation executive at Manned Flight Simulator [AD-A283997] p 146 N95-18724

NICHOLSON, J. Y.

Orbiter rarefied-flow reentry measurements from the OARE on STS-62 [NASA-TM-110182] p 646 N95-30783

NICHOLSON, JOHN C.

Numerical optimization of synergetic maneuvers [AD-A283398] p 109 N95-17435

NICKEL, H.

Aerodynamic off-design behavior of integrated waveriders from take-off up to hypersonic flight [AIAA PAPER 95-6091] p 466 A95-89200

NICKERSON, EVERETT

Testing of TKE parameterizations in numerical models for clear-air turbulence forecasting p 667 A95-93515

NICOLAS, JEAN

Coupled FEM-BEM approach for mean flow effects on vibro-acoustic behavior of planar structures [BTN-95-EIX9515257587] p 263 A95-73495

NIELSEN, J. NYBO

Flying ambulances: The approach of a small air force to long distance aeromedical evacuation of critically injured patients p 568 N95-29618

NIELSEN, P. A.

Ultra-wideband electromagnetic target identification p 486 A95-90955

NIELSEN, THOMAS

Development of load spectra for Airbus A330/A340 full scale fatigue tests p 135 N95-19479

NIESER, DONALD E.

Oklahoma City air logistics center (USAF) aging aircraft cockack program p 262 N95-23519

NIESL, G.

Experimental results of the European HELINOISE aeroacoustic rotor test [HTN-95-01080] p 578 A95-90266
Helicopter internal noise p 173 N95-19144

NIESL, GEORG

A higher harmonic control test in the DNW to reduce impulsive BVI noise [HTN-95-61071] p 385 A95-83655

NIESL, GEORG H.

Analysis of a higher harmonic control test to reduce blade vortex interaction noise [BTN-95-EIX95152582330] p 265 A95-73532

NIEWOEHNER, ROBERT J., JR.

Plant and controller optimization by convex methods [AD-A283700] p 133 N95-18621

NIGMATULLIN, RAVIL Z.

The mathematical models of flow passage for gas turbine engines and their components p 140 N95-19020
Application of multicomponent models to flow passage simulation in multistage turbomachines and whole gas turbine engines p 140 N95-19022

NIINO, MASAYUKI

A conceptual design of hypersonic research vehicle with subscale scramjet engine p 384 A95-82482

NIIOKA, TAKASHI

Ignition analysis of hydrogen/air mixture in supersonic mixing layer p 416 A95-82301

NIKOLOV, N.

A program for scientific and applied investigations using aerostat complexes p 182 A95-66304

NIKOLSKY, S. I.

The scientific ballooning in Russia p 191 A95-66302
The joint Russian-Brazil research on balloons p 182 A95-66303

NISHIDA, M.

Numerical studies of Mach reflection with air chemistry p 548 A95-90575

NISHIDA, MICHIO

VSL analysis of hypersonic flows around a reentry vehicle with equilibrium air chemistry p 413 A95-82400

NISHIMURA, J.

Polar Patrol Balloon system and preliminary experimental results p 368 A95-82513

NISHIMURA, JUN

Polar Patrol Balloon [BTN-95-EIX95152582318] p 316 A95-73521

NISHIMURA, Y.

Surface pressure and wake drag measurements on the Boeing A4 airfoil in the IAR 1.5X1.5m Wind Tunnel Facility p 110 N95-17850

NISHIOKA, MAKIHIITO

Prediction of NO(x) emission index of turbulent diffusion flame p 538 A95-87195

NISSLEY, D. M.

Thermal barrier coating life modeling in aircraft gas turbine engines p 346 N95-26140

NISTLER, CANDY JEAN

Civil Reserve Air Fleet-Aeromedical Evacuation Shipset (CRAF-AESS) p 568 N95-29619

NITTA, KYOKO

Application of ACT to unstable motions of an airfoil in ground effect p 471 A95-91500

NISSI, F.

Experimental results of the European HELINOISE aeroacoustic rotor test [HTN-95-01080] p 578 A95-90266

NITZSCHE, FRED

Using adaptive structures to attenuate rotary wing aeroelastic response [BTN-95-EIX95062487547] p 192 A95-68361

NIWA, SHOHEI

Ducted fan VTOL and its flight control system p 500 A95-91573

NIXON, DAVID

Vorticity in an inviscid fluid at hypersonic speeds [HTN-95-42590] p 539 A95-87220

NIXON, M. W.

Demonstration of an elastically coupled twist control concept for tilt rotor blade application [BTN-94-EIX94441386633] p 196 A95-68182

Demonstration of an elastically coupled twist control concept for tilt rotor blade application [HTN-95-20959] p 465 A95-88998

NIXON, MARK W.

Parametric studies for tiltrotor aeroelastic stability in highspeed flight [HTN-95-A0499] p 222 A95-72570

NO, T. S.

Dynamics and control of a tethered flight vehicle [BTN-95-EIX95242670754] p 342 A95-81093

NOACK, RALPH W.

Three-dimensional hybrid grid generation using advancing front techniques p 567 N95-28745

NOBBS, STEVEN

PSC implementation and integration p 695 N95-33014

NOBBS, STEVEN G.

F-15 propulsion system p 695 N95-33012
PSC algorithm description p 695 N95-33013
Minimum fuel mode evaluation p 695 N95-33015
Minimum fan turbine inlet temperature mode evaluation p 696 N95-33016
Maximum thrust mode evaluation p 696 N95-33017
Rapid deceleration mode evaluation p 696 N95-33018

NODA, FUMIO

Status of Enhanced Vision System p 506 A95-91542

NODA, J.

Aerodynamic characteristics of supersonic air-intake/aircraft integrated models p 472 A95-91512

NODA, JUNICHI

Aerodynamic characteristics of the orbital reentry vehicle experimental probe fins in a supersonic flow [NAL-TR-1232] p 342 N95-25664

NODA, MINORU

Mechanical properties of advanced toughened bismaleimide matrix composite p 530 A95-91570

NODERER, KEITH D.

Modeling of aircraft unsteady aerodynamic characteristics. Part 2: Parameters estimated from wind tunnel data [NASA-TM-110161] p 410 N95-27839

NOEL, BRUCE W.

Turbine-engine applications of thermographic-phosphor temperature measurements [DE95-003625] p 358 N95-25110

NOGUCHI, MASAYOSHI

High subsonic and high Reynolds number wind tunnel tests of two-dimensional natural-laminar-flow airfoils with suction boundary layer control p 472 A95-91508
Numerical and experimental study of drag characteristics of two-dimensional HLFC airfoils in high subsonic, high Reynolds number flow [NAL-TR-1244T] p 331 N95-24998

NOGUCHI, R. A.

Environmental effects on composite airframes: A study conducted for the ARM UAV Program (Atmospheric Radiation Measurement Unmanned Aerospace Vehicle) [DE94-015351] p 206 N95-19579

NOGUCHI, YAAUO

Behavior of the Johnson-King turbulence model in Axisymmetric supersonic flows [HTN-95-20932] p 464 A95-88971

NOGUCHI, YASUO

Behavior of the Johnson-King turbulence model in axisymmetric supersonic flows [BTN-94-EIX94441386606] p 183 A95-67337

NOGUCHI, YOSHIO

Study on tensile fatigue testing method of unidirectional fiber-resin matrix composites [NAL-TR-1241] p 343 N95-24989

NOLAN, ROBERT C.

Method for the prediction of the onset of wing rock [BTN-95-EIX95152582342] p 282 A95-73544

NOLD, DEAN E.

Spatial awareness comparisons between large-screen, integrated pictorial displays and conventional EFIS displays during simulated landing approaches [NASA-TP-3467] p 80 N95-14852

NOMURA, SIGEAKI

Experimental investigation on aerothermodynamic characteristics of hypersonic transport p 473 A95-91525

NONAKA, OSAMU

Wake velocity measurement of counter-rotation propellers p 474 A95-91563

NORBERG, C.

Experimental investigation of the flow around a circular cylinder: Influence of aspect ratio [BTN-94-EIX95011441120] p 347 A95-80044

NOREEN, R.

The acoustic characteristics of turbomachinery cavities [NASA-CR-4671] p 476 N95-28720

NORESE, M.

An overall approach of cockpit noise verification in a military aircraft p 175 N95-19163

NORMAN, R. MICHAEL

Education, training, and human engineering in aerospace; SAE Aerotech '93, Costa Mesa, CA, Sep. 27-30, 1993 [SAE SP-992] p 417 A95-84553

NORMAND, EUGENE

Investigation and characterization of SEU effects and hardening strategies in avionics [AD-A291058] p 509 N95-29950

NORTH, D. R.

Regulatory impact analysis and regulatory support document: Control of air pollution; determination of significance for nonroad sources and emission standards for new nonroad compression-ignition engines at or above 37 kilowatts (50 horsepower) [PB94-194594] p 61 N95-12855

NORTH, G. L.

Two-dimensional imaging of OH in a lean burning high pressure combustor [NASA-TM-106854] p 236 N95-21383

NORTHAM, G. B.

Computational/experimental investigation of staged injection into a Mach 2 flow [HTN-95-51646] p 432 A95-85028

NORTON, W. J.

Aeroelastic pilot-in-the-loop oscillations p 598 N95-31070

NORWOOD, KEITH

Coupling equivalent plate and finite element formulations in multiple-method structural analyses [BTN-95-EIX95062487548] p 192 A95-68362

NOVOZHILOV, K. A.

The effect of rotating loads suspended under a helicopter on their amplitude-frequency characteristics [BTN-94-EIX94461407959] p 78 A95-62633

NOWLIN, WILLIAM C.

Active control of complex noise problems using a broadband, multichannel controller p 29 N95-11271

NOWOBILSKI, J. J.

Airborne rotary separator study [NASA-CR-191045] p 150 N95-18743

Airborne rotary air separator study [NASA-CR-189099] p 290 N95-24053

- NOZAKI, O.**
Design of secondary flow control cascade using numerical simulation p 698 N95-34507
- NOZAKI, OSAMU**
Verification of turbine cascade flow with tip clearance p 698 N95-34511
- NUCKOLLS, W. E.**
Fan noise reduction from a supersonic inlet during simulated aircraft approach [BTN-95-EIX95292721155] p 572 A95-89894
- NUHAIT, A. O.**
Stability derivatives of a flapped plate in unsteady ground effect [BTN-95-EIX95182619225] p 270 A95-76651
Unsteady ground effects on aerodynamic coefficients of finite wings with camber [BTN-95-EIX95182619233] p 271 A95-76659
- NUMBERS, KEITH E.**
Survey of CFD applications for high speed inlets [AD-A291365] p 557 N95-30087
- NURICK, ALAN**
Static pressure distribution in the inlet of a helicopter turbine compressor [BTN-95-EIX95152582339] p 266 A95-73541
Erosion of dust-filtered helicopter turbine engines. Part 1: Basic theoretical considerations [BTN-95-EIX95182619222] p 288 A95-76648
Erosion of dust-filtered helicopter turbine engines. Part 2: Erosion reduction [BTN-95-EIX95182619223] p 289 A95-76649
Life prediction of helicopter engines fitted with dust filters [BTN-95-EIX95182619224] p 289 A95-76650
- NURNBERGER, M.**
Simulation of patch and slot antennas using FEM with prismatic elements and investigations of artificial absorber mesh termination schemes [NASA-CR-198974] p 704 N95-32822
- NURNBERGER, MICHAEL W.**
Design considerations for an archimedean slot spiral antenna p 211 N95-19798
- NUSCA, MICHAEL J.**
Numerical simulation of ram accelerator performance including transient effects during initiation of combustion and sensitivity studies p 629 N95-31203
- NYBERG, GREGORY**
Impact of agility requirements on configuration synthesis [NASA-CR-4627] p 44 N95-11952
- NYBLOM, K.**
Military aviation maintenance industry in Western Europe: Concentration and internationalization [PB94-189180] p 104 N95-17451
- NYE, H. R.**
Packet utilisation definitions for the ESA XMM mission p 150 N95-17596
- NYQUIST, D. P.**
Time-domain imaging of airborne targets using ultra-wideband or short-pulse radar [BTN-95-EIX95242673673] p 450 A95-82251
- O**
- O'BRIEN, E. W.**
A better than average stress model-photoelastic analysis for airbus design [CONGRESS PAPER C428-23-005] p 500 A95-91730
- O'BRIEN, W. F.**
Artificial neural networks for predicting nonlinear dynamic helicopter loads [HTN-95-51678] p 404 A95-85060
- O'BRIEN, WALTER F.**
Active control of fan noise from a turbofan engine [HTN-95-61198] p 570 A95-87571
- O'NEILL, A.**
An overview of the EASOE campaign [HTN-95-7002] p 443 A95-86272
- OAKES, STEPHEN**
Expert systems and artificial intelligence applications in engineering design and inspection p 710 N95-33008
- OBAYASHI, HIDEHIKO**
Application of GPS and Fuzzy Theory to a helicopter p 516 A95-91505
- OBAYASHI, SHIGERU**
Practical formulation of a positively conservative scheme [HTN-95-51668] p 433 A95-85050
- OBBERKAMPF, WILLIAM L.**
Review and development of base pressure and base heating correlations in supersonic flow [BTN-95-EIX95212645688] p 271 A95-76740
- OCHI, Y.**
Application of restructurable flight control system to large transport aircraft [BTN-95-EIX95282706666] p 515 A95-89639
- OCHI, YOSHIMASA**
Design of a flight control system by a new way of pole placement in LQR p 516 A95-91534
- OCKIER, C. J.**
An investigation of the effects of pitch-roll (de)coupling on helicopter handling qualities [NASA-TM-110349] p 409 N95-26773
Experiences with ADS-33 helicopter specification testing and contributions to refinement research p 621 N95-31993
- OCKUNZZI, K. A.**
Two-dimensional imaging of OH in a lean burning high pressure combustor [NASA-TM-106854] p 236 N95-21383
- OCANNOR, JOHN C.**
Probabilistic reliability modeling of fatigue on the H-46 tie bar [AD-A289926] p 607 N95-30927
- ODA, KENSHI**
Development and flight results of fiber reinforced balloon p 384 A95-82511
- ODONOGHUE, DENNIS P.**
Piloted evaluation of an integrated methodology for propulsion and airframe control design [AD-A290207] p 51 N95-12763
- OECHSLE, VICTOR L.**
Numerical mixing calculations of confined reacting jet flows in a cylindrical duct [NASA-TM-106736] p 139 N95-18133
- ODING, ROBERT G.**
Response of the B-1B air data sensor to simulated dust cloud environments [AD-A286134] p 235 N95-22036
- OERTEL, C.-H.**
Autonomous helicopter hover positioning by optical tracking [HTN-95-C0006] p 585 A95-93394
- OERTEL, H., JR.**
Orbital transport: Technical, meteorological and chemical aspects; Aerospace Symposium, 3rd, Braunschweig, Germany, Aug. 26-28, 1991 [ISBN 3-540-563180] p 524 A95-87373
The aerothermodynamic validation reentry experiment HYPERBA p 524 A95-87380
- OERTEL, HERBERT**
Reentry technology experiment on the first mission of reentry capsule 'EXPRESS' p 414 A95-82499
- OEZBAY, HITAY**
H(sup 2)/H(sup INF) controller design for a two-dimensional thin airfoil flutter suppression [BTN-94-EIX94511433918] p 141 A95-64584
Stable H(infinity) controller design for the longitudinal dynamics of an aircraft [NASA-TM-106847] p 293 N95-22954
- OFARRELL, J. M.**
High frequency flow-structural interaction in dense subsonic fluids [NASA-CR-4652] p 330 N95-24217
- OGASAWARA, KOU**
Application of CFD technique for HYFLEX aerodynamic design p 693 N95-34542
- OGAWA, SATORU**
Vector-parallel simulations of transonic wind tunnel flows about a fully configured model of aircraft p 685 N95-34538
- OGBURN, MARILYN E.**
Flight validation of ground-based assessment for control power requirements at high angles of attack p 70 N95-14246
- OGURA, ELJI**
Studies on gain performance of a combustion driven CO2 gas dynamic laser p 428 A95-82679
- OGUSHI, T.**
Experimental investigation of flow-boiling heat transfer under microgravity p 428 A95-82642
- OGUSHI, TETSUROU**
Experimental investigation of composite channel heat pipe operation in micro-gravity environment p 428 A95-82645
- OH, Y. H.**
Supersonic, turbulent flow computation and drag optimization for axisymmetric afterbodies [BTN-95-EIX95302729772] p 637 A95-94134
- OHKITA, Y.**
Design of secondary flow control cascade using numerical simulation p 698 N95-34507
- OHMAN, L. H.**
Applications of the five-hole probe technique for flow field surveys at the Institute for Aerospace Research p 163 N95-19255
- OHNO, M.**
MIMO H infinity control design method combined with exact model matching p 506 A95-91492
- OHNUKI, TAKESHI**
Experimental investigation of static and dynamic ground effect on HOPE ALFLEX vehicle [NAL-TR-1236] p 388 N95-26525
- OHOTA, S.**
Polar Patrol Balloon system and preliminary experimental results p 368 A95-82513
- OHSHIMA, S.**
Development of 70MW class superconducting generators [BTN-94-EIX95011440854] p 429 A95-82905
- OHYAMA, KENICHI**
Numerical simulation of unsteady aerodynamic heating induced by shock reflections p 428 A95-82418
Numerical experiments on aerodynamic heating mechanism in shock reflection processes p 471 A95-91497
- OIDE, SHIN-ICHI**
Direct numerical simulation of incompressible homogeneous isotropic turbulence using NWT p 706 N95-34530
- OKELLY, CHRIS**
Viper [NASA-CR-197191] p 79 N95-13703
- OKIISHI, THEODORE H.**
Study of compressible flow through a rectangular-to-semiannular transition duct [NASA-CR-4660] p 338 N95-24392
- OKON, I. M.**
Navigational technology of dual usage p 688 N95-33131
- OKUNUKI, TAKEO**
Experimental investigation on aerothermodynamic characteristics of hypersonic transport p 473 A95-91525
- OKUYAMA, SATOSHI**
An experimental study on interacting flow between supersonic flow and secondary flow injected normally through circular nozzle p 472 A95-91511
- OLALDE, G.**
Temperature diagnostics in the hypersonic flow regime: An application to develop a stagnation temperature probe [AIAA PAPER 95-6114] p 511 A95-90442
- OLARIU, STEPHEN**
Geometric modeling for computer aided design [NASA-CR-198828] p 679 N95-31982
- OLBERT, C.**
Mapping of forest fire damages using imaging spectroscopy p 442 A95-83627
- OLCMEN, SEMIH M.**
Influence of wing shapes on surface pressure fluctuations at wing-body junctions [HTN-95-61196] p 491 A95-87569
- OLFENBUTTEL, R. F.**
Bicarbonate of soda blasting technology for aircraft wheel depainting [PB94-193323] p 104 N95-17466
- OLIGER, JOSEPH**
Computing methods for the approximate solution of time dependent problems [AD-A286007] p 256 N95-20719
- OLIVER, J. F.**
Aircraft-borne, laser-induced fluorescence instrument for the in situ detection of hydroxyl and hydroperoxyl radicals [BTN-95-EIX95072499029] p 253 A95-71908
- OLIVER, M.**
A study of the effect of store unsteady aerodynamics on gust and turbulence loads p 133 N95-18601
- OLVIER, H.**
Hypersonic model testing in a shock tunnel [BTN-95-EIX95222650789] p 329 A95-79245
- OLKIEWICZ, CRAIG**
Flight parameters monitoring system for tracking structural integrity of rotary-wing aircraft p 135 N95-19469
- OLLERHEAD, J. B.**
Aircraft noise and sleep disturbance: A field study [HTN-95-92543] p 558 A95-87363
Past and present UK research on aircraft noise effects p 560 A95-90090
- OLSEN, HEROLD**
Assessment of helicopter noise annoyance: A comparison between helicopters and jet aircraft p 560 A95-88480
- OLSEN, J. R.**
Strategic avionics technology definition studies. Subtask 3-1A3: Electrical Actuation (ELA) Systems Test Facility [NASA-CR-188360] p 143 N95-18567
- OLSEN, MIKE**
Low aspect ratio wing experiment p 113 N95-17865

OLSON, DANIEL

The Advanced Avionics Subsystem Technology Demonstration Program p 234 N95-20636

OLSON, HAROLD W.

Research requirements for future visual guidance systems [AD-A279188] p 191 N95-19810

OLSON, JOHN M.

Mishap risk control for advanced aerospace/composite materials p 301 N95-23031

OLSON, RICHARD J.

Development of repair processes and sources for C/KC-135 aircraft windows/windshields [AD-A288348] p 367 N95-26629

OLSSON, ERIK

Turbulent transonic airfoil flow simulation using a pressure-based algorithm [BTN-95-EIX95182619078] p 269 A95-75763

OLSSON, ESBJORN

Nortaf: Computer generated aerodome forecasts p 668 A95-93521

OLSSON, H. A.

Orientation determination of aircraft using visual 3D matching and radar. Case study 2 [PB95-165791] p 350 N95-25749

OMAN, HENRY

New commercial off-the-shelf testers are automatic and intelligent [BTN-95-EIX95172595292] p 287 A95-75720
 'Global avionics in the future' report from the 10th annual battery conference [BTN-95-EIX95282706404] p 545 A95-88184

ONATE, E.

Computational methods in applied sciences; European Computational Fluid Dynamics Conference, 1st, Brussels, Belgium, Sept. 7-11, 1992 [ISBN 0-444-89795-X] p 539 A95-87552

ONCLEY, S. P.

A comparison of some aerodynamic resistance methods using measurements over cotton and grass from the 1991 California ozone deposition experiment [HTN-95-11295] p 319 A95-77000

ONCLEY, STEVEN

On the Lighthill relationship and sound generation from isotropic turbulence [NASA-CR-195005] p 159 N95-18191

ONDREJKA, A. R.

Measurements of shielding effectiveness and cavity characteristics of airplanes [PB94-210051] p 244 N95-20191

ONEIL, PATRICK J.

Impact of agility requirements on configuration synthesis [NASA-CR-4627] p 44 N95-11952

ONG, CHING-LONG

Damage tolerance certification of a fighter horizontal stabilizer [BTN-95-EIX0619952748186] p 637 A95-94478

ONO, F.

Experiment of rocket-ram annular combustor p 412 A95-82324

ONO, FUMIEI

Effect of film cooling/regenerative cooling on scramjet engine performances [NAL-TR-1242] p 339 N95-24990

ONO, TAKATSUGU

Flight evaluation of DGPS and DGPS-INS navigation systems p 382 A95-82462
 Performance evaluation test of GPS/DGPS navigation system installed in the NAL Domier 228: Preliminary ground test results p 487 A95-91575

Flight reference display for powered-lift STOL aircraft [NAL-TR-1251] p 337 N95-25005

Flight evaluation of GPS/DGPS sensor systems installed in NAL Do228 [NAL-TR-1230] p 382 N95-26585

ONOE, KEN-ICHI

Life evaluation of a low power arcjet thruster p 403 A95-82337

ONOZUKA, SACHIKO

Arrival traffic handling for a parallel runway airport p 487 A95-91537

ORKWIS, PAUL D.

Observations on using experimental data as boundary conditions for computations [BTN-95-EIX95182619103] p 321 A95-76588

ORLANDO, VINCENT A.

GPS-Squitter capacity analysis [AD-A280037] p 245 N95-20599

GPS-Squitter interference analysis [AD-A293690] p 689 N95-33480

ORLANSKY, JESSE

The value of simulation for training [AD-A289174] p 411 N95-26556

ORLOV, A.

Optical surface pressure measurements: Accuracy and application field evaluation p 175 N95-19274

ORME, JOHN S.

Flight assessment of the onboard propulsion system model for the Performance Seeking Control algorithm on an F-15 aircraft [NASA-TM-4705] p 617 N95-31425

Flight test validation of a frequency-based system identification method on an F-15 aircraft [NASA-TM-4704] p 620 N95-31846

Performance seeking control program overview p 695 N95-33011

Minimum fuel mode evaluation p 695 N95-33015

Minimum fan turbine inlet temperature mode evaluation p 696 N95-33016

Maximum thrust mode evaluation p 696 N95-33017

Rapid deceleration mode evaluation p 696 N95-33018

Performance seeking control (PSC) for the F-15 highly integrated digital electronic control (HIDEC) aircraft p 697 N95-33020

ORMISTON, ROBERT A.

Comprehensive aeromechanics analysis of complex rotorcraft using 2GCHAS [HTN-94-00695] p 2 A95-60174

First level release of 2GCHAS for comprehensive helicopter analysis - a status report [HTN-94-00697] p 2 A95-60176

OROURKE, CAROLYN

Environmental Compliance Assessment and Management Program [AD-A279605] p 255 N95-20441

ORR, HORACE A.

Integrated mission precision attack cockpit technology (IMPACT). Phase 1: Identifying technologies for air-to-ground fighter integration [AD-A289562] p 389 N95-26684

ORSZAG, STEVEN A.

Numerical studies of turbulent free surface flows and unsteady propeller flows [AD-A294377] p 706 N95-34343

ORTASSE, RAPHAEL

Fatigue loads spectra derivation for the Space Shuttle: Second cycle p 166 N95-19470

ORTIZ, VINCENT M.

Evaluation of energy-sink stability criteria for dual-spin spacecraft [AD-A283228] p 87 N95-14850

ORTNER, E.

Solution of the Navier-Stokes equations on a massively parallel sputer system p 549 A95-91490

ORZECHOWSKI, JEFFREY M.

Effect of constraining layer stiffness on performance of damping tile materials using finite element modelling with Rayleigh integral p 30 N95-11306

OSBORNE, LEON F.

Aviation weather education and the University of North Dakota aviation weather survey p 656 A95-93462

Aviation meteorology education in an AB initio setting p 657 A95-93466

OSHRAT, J.

Prediction of fatigue crack growth under constant amplitude and random loading using specimens with multiple cracks [AD-A291614] p 397 N95-28409

OSIPOV, I. L.

New approach to geometric profiling of the design elements of the passage part in turbo-machines [BTN-94-EIX94461408769] p 153 A95-63652

OSTER, JOHN

Preliminary evaluation of the F/A-18 quantity/multiple envelope expansion [AD-A284119] p 132 N95-18407

OSTERGREN, W. J.

Applicability of electrically driven accessories for turboshaft engines [BTN-95-EIX95292721153] p 612 A95-92589

OSTERMAN, M. D.

Liquid flow-through cooling of electronic modules p 246 N95-20647

OSTGAARD, JOHN

The impact of advanced packaging technology on modular avionics architectures p 233 N95-20632

OSTOWARI, CYRUS

Horizontal axis wind turbine post stall airfoil characteristics synthesis p 376 N95-27974

OSTRANDER, MARK J.

Engine/airframe installation CFD for commercial transports: An engine manufacturer's perspective [SAE PAPER 932623] p 495 A95-90084

OSTROFF, AARON J.

High-Alpha Research Vehicle (HARV) longitudinal controller: Design, analyses, and simulation results [NASA-TP-3446] p 17 N95-10860

OSWALD, FRED B.

Influence of tooth profile modification on spur gear dynamic tooth strain [AD-A281069] p 553 N95-29112

OTOOLE, BRENDAN J.

The effect of material heterogeneity in curved composite beams for use in aircraft structures p 422 N95-28426

OTTE, D.

In-flight interior sound field mapping in propeller aircraft p 572 A95-88472

OTTE, DIRK

Aircraft interior sound field analysis in view of active control: Results from the ASANCA project p 575 A95-90109

OTUGEN, M. V.

Research instrumentation for polytechnic university's supersonic wind tunnel facility [AD-A290232] p 523 N95-29468

OWEN, J. W.

A programmable heater control circuit for spacecraft [NASA-TM-108459] p 9 N95-11157

OWEN, T. E.

Assessment of a non-dedicated GPS receiver system for precise airborne attitude determination [DE94-019309] p 229 N95-21520

OWENBURG, JEFFREY

Test results of a low cost airport weather radar p 662 A95-93492

OWENS, LEWIS R., JR.

Computer model to simulate testing at the National Transonic Facility [NASA-TM-4664] p 627 N95-32217

OWENS, S. D.

Applications of a damage tolerance analysis methodology in aircraft design and production p 426 N95-28483

OYEDIRAN, AYO

Sensitivity of combustion-acoustic instabilities to boundary conditions for premixed gas turbine combustors [NASA-TM-106890] p 289 N95-23550

Review of combustion-acoustic instabilities [NASA-TM-107020] p 705 N95-32930

Combustion-acoustic stability analysis for premixed gas turbine combustors [NASA-TM-107024] p 694 N95-32931

OZCAN, O.

Aerodynamic characteristics of external store configurations at low speeds [BTN-95-EIX95182619230] p 271 A95-76656

OZDEMIR, T.

Simulation of patch and slot antennas using FEM with prismatic elements and investigations of artificial absorber mesh termination schemes [NASA-CR-198974] p 704 N95-32822

P

PACHTER, M.

Automatic formation flight control [BTN-95-EIX95182619153] p 292 A95-76630

PACK, W.

Operating capability and current status of the reactivated NASA Lewis Research Center hypersonic tunnel facility [AIAA PAPER 95-6146] p 521 A95-90461

PACK, WILLIAM D.

Operating capability and current status of the reactivated NASA Lewis Research Center Hypersonic Tunnel Facility [NASA-TM-106808] p 148 N95-19286

PADMADINATA, U. H.

Prediction of fatigue crack growth under flight-simulation loading with the modified CORPUS model p 166 N95-19471

PADMANABHAN, K.

Failure behaviour of carbon fiber/epoxy composites in pin-ended buckling and bending tests [HTN-95-71388] p 528 A95-87606

PADOVAN, J.

Modelling wear at intermittently slipping high speed interfaces [BTN-94-EIX94511433698] p 701 A95-96655

PADOVAN, P.

Modelling wear at intermittently slipping high speed interfaces [BTN-94-EIX94511433698] p 701 A95-96655

PADRO, J.

A comparison of some aerodynamic resistance methods using measurements over cotton and grass from the 1991 California ozone deposition experiment [HTN-95-11295] p 319 A95-77000

PAGALDIPTI, NARAYANAN

Multilevel decomposition procedure for efficient design optimization of helicopter rotor blades [BTN-95-EIX95222650784] p 334 A95-79240

- PAGE, A. G.**
Programmable cockpit research simulator
[AD-A279219] p 204 N95-19848
- PAGE, GERALD**
Software process improvement in the NASA software engineering laboratory
[AD-A289912] p 450 N95-28627
- PAGE, JULIET A.**
USAF single-event sonic boom prediction model: PCBoom3
p 101 N95-14889
- PAGEAU, STEPHANE S.**
Shear buckling response of tailored composite plates
[HTN-95-51680] p 418 A95-85062
- PAHLE, JOSEPH W.**
Flight validation of ground-based assessment for control power requirements at high angles of attack
p 70 N95-14246
- PAINTER, JOHN H.**
Knowledge-based processing for aircraft flight control
[NASA-CR-194976] p 99 N95-13727
- PAINTER, WENETH D.**
Development and flight testing of the HL-10 lifting body
p 498 A95-90872
- PAJERSKI, ROSE**
Software process improvement in the NASA software engineering laboratory
[AD-A289912] p 450 N95-28627
- PAL, A. K.**
Simple method of supersonic flow visualization using watertable
[BTN-95-EIX95182619105] p 269 A95-76590
- PAL, DIPANKAR**
On the differences between the effect of acoustic perturbation and unsteady bleed in controlling flow separation over a cylinder
[SAE PAPER 932573] p 467 A95-90062
- PALANISWAMY, S.**
High-speed reacting flow simulation using USA-series codes
p 540 A95-87559
- PALERMI, S.**
Impact on ozone of high-speed stratospheric aircraft: Effects of the emission scenario
[HTN-95-51283] p 356 A95-80868
- PALM, T. E.**
A weight-efficient design strategy for cutouts in composite transport structures
p 533 N95-28843
- PALMER, D. L.**
Design and development of an advanced two-stage centrifugal compressor
[BTN-95-EIX95282710054] p 633 A95-92475
- PALMER, GRANT**
A comparison of three-dimensional nonequilibrium solution algorithms applied to hypersonic flows with stiff chemical source terms
[AIAA PAPER 93-2861] p 4 A95-60186
Measured and calculated spectral radiation from a blunt body shock layer in an arc-jet wind tunnel
[AIAA PAPER 94-0086] p 67 N95-13720
- PALMER, MICHAEL T.**
A crew-centered flight deck design philosophy for High-Speed Civil Transport (HSCT) aircraft
[NASA-TM-109171] p 335 N95-24582
- PALOSCIA, S.**
MAX-91: Polarimetric SAR results on Montespetoli site
p 320 N95-23940
- PALUMBO, GIUSEPPE**
VUV shock layer radiation in an arc-jet wind tunnel experiment
p 67 N95-13719
Measured and calculated spectral radiation from a blunt body shock layer in an arc-jet wind tunnel
[AIAA PAPER 94-0086] p 67 N95-13720
- PAMADI, BANDU N.**
A simple analytical aerodynamic model of Langley Winged-Cone Aerospace Plane concept
[NASA-CR-194987] p 54 N95-12175
- PAN, DARTZI**
Transonic flutter suppression using active acoustic excitations
[BTN-95-EIX95262694310] p 408 A95-85481
- PAN, JIAZHENG**
An approach to aerodynamic characteristics of low radar cross-section fuselages
p 106 N95-16251
- PAN, RUO-GANG**
The analysis of the processing increased weight for pilot production of F-X aircraft
[HTN-95-71133] p 385 A95-83494
- PANCRATZ, DAVID J.**
The large radius track centrifuge concept as an acceleration research and simulation device
p 379 A95-84560
- PANDA, B.**
Advance finite element modeling of rotor blade aeroelasticity
[HTN-95-31013] p 221 A95-71183
- PANKAJAKSHAN, RAMESH**
Propulsion/airframe interference for ducted propfan engines with ground effect
[NASA-CR-197110] p 81 N95-14909
- PANOS, JEAN B.**
High-speed seal and bearing test facility
p 53 N95-13601
- PAONESSA, A.**
Experimental active control of sound in the ATR 42
p 575 A95-90110
- PAPAILIOU, K.**
Adaptive modeling of jet engine performance with application to condition monitoring
[BTN-95-EIX95112524205] p 196 A95-69303
- PAPAILIOU, K. D.**
A robust inverse inviscid method for airfoil design
p 640 A95-95431
Single-pass method for the solution of inverse potential and rotational problems. Part 1: 2-D and quasi 3-D theory and application
p 107 N95-16563
Single-pass method for the solution of inverse potential and rotational problems. Part 2: Fully 3-D potential theory and applications
p 107 N95-16564
- PAPANIKAS, D. G.**
Experimental results of the European HELINOISE aeroacoustic rotor test
[HTN-95-01080] p 578 A95-90266
- PAPANIKOS, P.**
Theoretical and experimental studies of fretting-initiated fatigue failure of aeroengine compressor discs
[BTN-94-EIX94421372285] p 343 A95-78467
- PAPARONE, L.**
Estimation of supersonic leading-edge thrust by a Euler flow model
[BTN-95-EIX0619952748194] p 591 A95-94483
- PAPAY, MICHAEL LAWRENCE**
A general inverse design procedure for aerodynamic bodies
p 606 N95-30497
- PAPROCKI, THOMAS H.**
Research requirements for future visual guidance systems
[AD-A279188] p 191 N95-19810
- PARAMESWARAN, V. R.**
Protective coatings for compressor gas path components
p 201 N95-19675
- PARASCHIOIU, I.**
Ice accretion on aircraft wings
[BTN-95-EIX95082502224] p 225 A95-71021
- PAREKH, D. E.**
Entrainment and acoustic variations in a round jet from introduced streamwise vorticity
[BTN-95-EIX95042474409] p 209 A95-68291
Mixing enhancement by and noise characteristics of streamwise vortices in an air jet
[HTN-95-42322] p 371 A95-86151
- PARET, A.**
Aeroacoustic qualification of HERMES shingles
p 173 N95-19145
- PARIKH, PARESH**
Unstructured grid solutions to a wing/pylon/store configuration
[BTN-95-EIX95152582322] p 265 A95-73525
An unstructured-grid software system for solving complex aerodynamic problems
p 476 N95-28743
- PARIMUHA, EDWARD**
Waveform bounding and combination techniques for direct drive testing
[AD-A284075] p 161 N95-19035
- PARIMUHA, EDWARD M.**
Assessing aircraft survivability to high frequency transient threats
[AD-A283999] p 134 N95-18726
- PARISH, DEBORAH R.**
Testing considerations for military aircraft engines in corrosive environments (a Navy perspective)
p 202 N95-19684
- PARK, CHAN GOOK**
Covariance analysis of strapdown INS considering gyrocompass characteristics
[BTN-95-EIX95202637592] p 279 A95-76697
- PARK, CHUL**
Measurement and analysis of nitric oxide radiation in an arcjet flow
[BTN-95-EIX95082502727] p 243 A95-71040
Measured and calculated spectral radiation from a blunt body shock layer in an arc-jet wind tunnel
[AIAA PAPER 94-0086] p 67 N95-13720
Bibliography of Doctor Chul Park
[NASA-TM-110353] p 527 N95-29351
- PARK, HEUNG WON**
Covariance analysis of strapdown INS considering gyrocompass characteristics
[BTN-95-EIX95202637592] p 279 A95-76697
- PARK, IL-PYUNG**
Qualitative environmental navigation: Theory and practice
p 601 N95-30486
- PARK, JAI H.**
Growth of multiple cracks and their linkup in a fuselage lap joint
[BTN-95-EIX95142553047] p 286 A95-73451
Structural integrity of fuselage panels with multisite damage
[BTN-95-EIX0619952748188] p 637 A95-94250
Residual life and strength estimates of aircraft structural components with MSD/MED
p 136 N95-19485
- PARK, S.-Y.**
Trajectory optimization using parallel shooting method on parallel computer
[BTN-95-EIX95282706670] p 564 A95-88175
- PARK, SEONG-RYONG**
Flow alteration and drag reduction by riblets in a turbulent boundary layer
[HTN-95-61199] p 461 A95-87572
- PARKER, JAMES F., JR.**
Development of an intervention program to encourage shoulder harness use and aircraft retrofit in general aviation aircraft, phases 1 and 2
[DOT/FAA/AM-95/2] p 333 N95-24384
Development of an intervention program to encourage shoulder harness use and aircraft retrofit in general aviation aircraft: Phases 1 and 2
[AD-A290966] p 485 N95-29873
- PARKHOMOV, D. A.**
Universal electrohydraulic system for the steering gear loading
[CONGRESS PAPER C428-10-106] p 517 A95-91700
- PARKINSON, BRADFORD W.**
Space flight tests of attitude determination using GPS
[BTN-95-EIX95112522529] p 190 A95-69334
- PARKINSON, G. V.**
Unsteady flow testing in a passive low-correction wind tunnel
p 147 N95-19272
- PARKS, W. P.**
Thermal barrier coatings issues in advanced land-based gas turbines
p 344 N95-26122
- PARLETTE, EDWARD B.**
Block-structured grids for complex aerodynamic configurations: Current status
p 551 N95-28736
- PARRISH, RUSSELL V.**
Spatial awareness comparisons between large-screen, integrated pictorial displays and conventional EFIS displays during simulated landing approaches
[NASA-TP-3467] p 80 N95-14852
- PARROTT, EDITH**
NASA Lewis Research Center's preheated combustor and materials test facility
[NASA-TM-106676] p 626 N95-30592
- PARRY, P. L.**
The mini-business approach at Chadderton
[CONGRESS PAPER C428-26-037] p 681 A95-93602
- PARSONS, B.**
Geoid lineations of 1000 km wavelength over the central Pacific
[HTN-95-11304] p 319 A95-77009
- PARTHASARATHY, R. N.**
LDV measurements in separated flow on an elliptic wing mounted at an angle of attack on a wall
[BTN-94-EIX94441380518] p 702 A95-96559
- PARTHASARATHY, V. N.**
Ply layup optimization and micromechanics tailoring of composite aircraft engine structures
[BTN-95-EIX95112524206] p 196 A95-69302
- PASSCHIER, D. M.**
Experiments in the trailing edge flow of an NLR 7702 airfoil
p 110 N95-17853
- PASTOREL, H.**
Modal parameters for cracked rotors: models and comparisons
[BTN-94-EIX94522410226] p 702 A95-96378
- PATEL, BHAVESH B.**
Supersonic axisymmetric conical flow solutions for different ratios of specific heats
[BTN-95-EIX95152583283] p 306 A95-73584
- PATEL, INDU**
Dynamic imaging and RCS measurements of aircraft
[BTN-95-EIX95202637582] p 347 A95-78576
- PATEL, V. C.**
Influence of streamwise curvature on longitudinal vortices imbedded in turbulent boundary layers
[BTN-94-EIX94401378820] p 307 A95-76489
LDV measurements in separated flow on an elliptic wing mounted at an angle of attack on a wall
[BTN-94-EIX94441380518] p 702 A95-96559
- PATER, LARRY**
Hangars as noise barriers for helicopter noise
p 560 A95-90111
- PATES, CARL S., III**
Boundary element analysis of the acoustic field inside three-dimensional regular and irregular ducts
p 573 A95-90097

- PATNAIK, P. C.**
The effects of surface modification on fretting fatigue in Ti alloy turbine components
[HTN-95-61145] p 404 A95-84909
- PATNAIK, SURYA N.**
Optimization of aerospace structures
[NASA-CR-196763] p 48 N95-12787
- PATNOE, MICHAEL W.**
Airplane icing research at the Boeing Company: Participation in the second Canadian Atlantic Storms Program p 674 A95-93544
- PATRICK, SHERYL M.**
The pressure field of a gust interacting with a flat plate p 557 N95-30161
- PATTERSON, A. K.**
Preparation of S-70A-9 Black Hawk helicopter for flight tests to investigate cause of cracking of inner fuselage panel
[AD-A293891] p 608 N95-31544
- PATTERSON, MIKE**
Conceptual design of the AE481 Demon Remotely Piloted Vehicle (RPV)
[NASA-CR-197164] p 44 N95-12294
- PATTIPATI, KRISHNA R.**
MATSurv multisensor air traffic surveillance
[AD-A292253] p 489 N95-28887
- PATTON, T.**
Low frequency ultrasonic nondestructive inspection of aluminum/adhesive fuselage lap splices
[DE94-014242] p 24 N95-11135
- PAUL, D. K.**
Reaction-time response of aircraft crash
[BTN-95-EIX95292721296] p 595 A95-92626
- PAUL, J.**
Bonded composite repair of cracked load-bearing holes
[BTN-94-EIX94401360553] p 243 A95-71867
Development of a composite repair and the associated inspection intervals for the F-111C stiffener runout region p 66 N95-14477
- PAUL, J. J.**
Residual strength of composites with multiple impact damage
[AD-A284230] p 87 N95-14409
- PAUL, P. H.**
A model for temperature-dependent collisional quenching of OH A(sup 2) Sigma(sup +)
[HTN-95-42308] p 450 A95-85002
- PAULAUSKAS, M.**
Flame-spreading phenomena in the fin-stol region of a solid rocket motor p 23 N95-10296
- PAULEY, H.**
Experimental study of the effects of Reynolds number on high angle of attack aerodynamic characteristics of forebodies during rotary motion
[NASA-CR-195033] p 330 N95-24443
- PAULL, ROBERT A.**
Use of starch based blast media for dry paint stripping
[SAE PAPER 932616] p 456 A95-90081
- PAULL, A.**
Shock tunnel measurements of hypervelocity blunted cone drag
[BTN-95-EIX95152577606] p 305 A95-73477
Shock tunnel measurements of hypervelocity blunted cone drag
[HTN-95-42591] p 459 A95-87221
Scramjet thrust measurement in a shock tunnel
[HTN-95-C0008] p 586 A95-93396
Shock tunnel studies of scramjet phenomena 1993
[NASA-CR-195038] p 350 N95-25394
Thrust measurements of a complete axisymmetric scramjet in an impulse facility p 339 N95-25395
Scramjet thrust measurement in a shock tunnel p 339 N95-25396
- PAULSON, G. A.**
Air traffic management: The future challenge
[CONGRESS PAPER C428-7-145] p 486 A95-91686
- PAUSDER, H. J.**
An investigation of the effects of pitch-roll (de)coupling on helicopter handling qualities
[NASA-TM-110349] p 409 N95-26773
- PAUSDER, H.-J.**
Experiences with ADS-33 helicopter specification testing and contributions to refinement research p 621 N95-31993
- PAUSDER, HEINZ-JUERGEN**
Model following control for tailoring handling qualities: ACT experience with ATHeS p 622 N95-32000
- PAUSDER, HEINZ-JURGEN**
Investigation of the effects of bandwidth and time delay on helicopter roll-axis handling qualities
[HTN-95-80853] p 290 A95-75095
- PAVARANI, ALBERTO**
A low fin height heat exchanger technology demonstrator for Hermes
[SAE PAPER 932119] p 526 A95-90360
- PAWLKOWSKI, ELLEN M.**
Surviving the peace. Lessons learned from the aircraft industry in the 1920s and 1930s
[AD-A288284] p 366 N95-26455
- PAXSON, D. E.**
A numerical model for dynamic wave rotor analysis
[NASA-TM-106997] p 615 N95-30617
- PAXSON, DANIEL E.**
Recent improvements to and validation of the one dimensional NASA wave rotor model
[NASA-TM-106913] p 332 N95-25962
Optimization of wave rotors for use as gas turbine engine topping cycles
[NASA-TM-106951] p 406 N95-27860
Wave rotor-enhanced gas turbine engines
[NASA-TM-106998] p 615 N95-30517
- PAXTON, M.**
Experimental active control of sound in the ATR 42 p 575 A95-90110
- PAYNE, J. L.**
Verification of computational aerodynamic predictions for complex hypersonic vehicles using the INCA(trademark) code
[DE95-004757] p 330 N95-24308
- PAYNE, R. C.**
Effect of atmospheric pressure on measured aircraft noise levels
[PB95-130423] p 232 N95-21425
- PAYNTER, G. C.**
Lag model for turbulent boundary layers over rough bleed surfaces
[BTN-94-EIX94441380981] p 208 A95-68165
- PAYNTER, GERALD C.**
Prediction of supersonic inlet unstart caused by freestream disturbances
[BTN-95-EIX9522650790] p 329 A95-79246
Boundary conditions for unsteady supersonic inlet analyses
[HTN-95-20829] p 544 A95-88090
- PEACE, A. J.**
SAUNA: A system for grid generation and flow simulation using hybrid structured/unstructured grids p 642 A95-95470
Validation and evaluation of the advanced aeronautical CFD system SAUNA: A method developer's view
[ARA-MEMO-390] p 210 N95-19774
- PEACE, ANDREW J.**
Verification of the CFD simulation system SAUNA for complex aircraft configurations
[ARA-MEMO-401] p 211 N95-19776
Inviscid and viscous flow modelling of complex aircraft configurations using the CFD simulation system sauna
[ARA-MEMO-403] p 211 N95-19777
- PEAKE, N.**
Unsteady lift on a swept blade tip
[BTN-94-EIX95011441154] p 329 A95-80030
- PEARCE, HOWARD**
The role of simulations in 777 FSEU development
[AIAA PAPER 95-0995] p 506 A95-90665
- PEARCEY, H. H.**
Numerical model of boundary-layer control using air-jet generated vortices
[HTN-95-42581] p 459 A95-87211
- PEARSON, A. E.**
Aerodynamic parameter estimation via Fourier modulating function techniques
[NASA-CR-4654] p 335 N95-24630
- PEARSON, JEROME**
High-temperature acoustic test facilities and methods p 174 N95-19149
- PECCIA, N.**
Safety aspects of spacecraft commanding p 149 N95-17248
- PECHERSKY, M. J.**
Residual Stress Measurements with Laser Speckle Correlation Interferometry and Local Heat Treating
[DE95-060082] p 349 N95-24598
- PECKERAR, MARTIN C.**
High aspect ratio metal microstructures and method for preparing the same
[AD-D017463] p 629 N95-30750
- PECKHAM, S. E.**
Operational multi-scale environment model with grid adaptivity (OMEGA) application to aviation weather p 676 A95-93556
- PEDERSON, J. R.**
Observations of fluxes and inland breezes over a heterogeneous surface
[HTN-95-80258] p 212 A95-66315
- PEGG, ROBERT J.**
Low-speed wind tunnel tests of two waverider configuration models
[AIAA PAPER 95-6093] p 493 A95-89251
- PEIGIN, S. V.**
Numerical simulation of three-dimensional hypersonic reacting flows over blunt bodies with catalytic surface
[HTN-95-61184] p 539 A95-87557
- PEISEN, DEBORAH**
Heliport/vertiport MLS precision approaches
[AD-A283505] p 126 N95-18059
- PELEGRIN, M.**
On-line handling of air traffic: Management, guidance and control
[AGARD-AG-321] p 126 N95-18927
- PELIZZARI, CHARLES**
Advanced data visualization and sensor fusion: Conversion of techniques from medical imaging to Earth science p 711 N95-34236
- PELLERIN, F.**
Multilayer anti-erosion coatings p 201 N95-19679
- PELLETIER, DOMINIQUE**
Adaptive remeshing for convective heat transfer with variable fluid properties
[BTN-95-EIX95082502720] p 243 A95-71033
Adaptive finite element method for turbulent flow near a propeller
[BTN-95-EIX95142553038] p 305 A95-73460
- PEN, JIBING**
The computer analysis of the prediction of aircraft electrical power supply system reliability p 155 N95-16278
- PENAFIEL, PABLO B.**
Application of wavelet-filtering techniques to intermittent turbulent and wall pressure events. Part 1: Exploratory results
[AD-A286077] p 247 N95-20849
- PENDLETON, ED**
Pressure measurements on an F/A-18 twin vertical tail in buffeting flow. Volume 3: Buffet power spectral densities
[AD-A281444] p 36 N95-11829
Pressure measurements on an F/A-18 twin vertical tail in buffeting flow. Volume 2: Steady and unsteady RMS pressure data
[AD-A281581] p 76 N95-15465
Pressure measurements on an F/A-18 twin vertical tail in buffeting flow. Volume 4, part 2: Buffet cross spectral densities
[AD-A285555] p 143 N95-18641
Pressure measurements on an F/A-18 twin vertical tail in buffeting flow. Volume 4, part 1: Buffet cross spectral densities
[AD-A285593] p 237 N95-21214
Pressure measurements on an F/A-18 twin vertical tail in buffeting flow. Volume 1: Wind tunnel test summary
[AD-A279126] p 225 N95-21877
- PENG, CHENGYI**
A new type of simulator for simulating the flow-field distortion of engine inlet
[BTN-95-EIX95202638963] p 289 A95-76673
- PERAIRE, J.**
Mesh generation and adaptivity for the solution of compressible viscous high speed flows
[BTN-95-EIX95262697157] p 538 A95-86893
- PEREZ, EMILJO**
Design constraints in the payload-range diagram of ultrahigh capacity transport airplanes
[BTN-95-EIX95152582319] p 276 A95-73522
- PEREZ, GUSTAVO, JR.**
Central coast designs: The Eightball Express. Taking off with convention, cruising with improvements and landing with absolute success
[NASA-CR-197181] p 47 N95-12643
- PERIASAMY, R.**
Measurement of particle emissions from clean room gas-handling components
[BTN-94-EIX94381359040] p 295 A95-74554
Measurement of moisture and total hydrocarbon contributions by valves used in clean room gas-delivery systems
[BTN-94-EIX94381359041] p 295 A95-74629
- PERIAUX, J.**
Computational methods in applied sciences; European Computational Fluid Dynamics Conference, 1st, Brussels, Belgium, Sept. 7-11, 1992
[ISBN 0-444-89795-X] p 539 A95-87552
Parallel computational fluid dynamics '91; Conference Proceedings, Stuttgart, Germany, Jun. 10-12, 1991
[ISBN 0-444-89363-6] p 548 A95-91479
Computational fluid dynamics '92; Proceedings of the European Computational Fluid Dynamics Conference, 1st, Brussels, Belgium, Sep. 7-11, 1992. Vols. 1 & 2
[ISBN 0-444-89793-3] p 638 A95-95357
Review of the EUROPT Project AERO-0026 p 129 N95-16573
- PERKOSKI, EMMETT**
Immersion/two phase cooling p 246 N95-20648

- PERNER, D.**
Airborne measurements during the European Arctic Stratospheric Ozone Experiment : Observation of OClO [HTN-95-00745] p 445 A95-86315
- PEROUMIAN, OSHIN**
Effect of density gradients in confined supersonic shear layers, part 1 [NASA-CR-198029] p 348 N95-24412
Effect of density gradients in confined supersonic shear layers. Part 2: 3-D modes [NASA-CR-198030] p 349 N95-24413
- PEROS, VASILIOS**
Application of fiber-reinforced bismaleimide materials to aircraft nacelle structures p 397 N95-28278
- PERRIER, P.**
Integration of an hypersonic airbreathing vehicle: Assessment of overall aerodynamic performances and of uncertainties [AIAA PAPER 95-6100] p 492 A95-88007
- PERRY, BOYD, III**
Summary of an active flexible wing program [BTN-95-EIX95182619209] p 283 A95-76635
- PERSON, LEE H., JR.**
Flight test of takeoff performance monitoring system [NASA-TP-3403] p 51 N95-12664
Airplane takeoff and landing performance monitoring system [NASA-CASE-LAR-14745-2-SB] p 85 N95-14415
- PERUSSE, PATRICK**
T-45A High Angle of Attack Testing: US Naval Test Pilot School 46th Annual Reunion and Symposium [AD-A284000] p 231 N95-20466
- PESETSKY, V.**
Optical surface pressure measurements: Accuracy and application field evaluation p 175 N95-19274
- PESHKHOV, V. G.**
Navigational technology of dual usage p 688 N95-33131
- PETERS, DAVID A.**
Flap-lag damping in hover and forward flight with a three-dimensional wake [HTN-95-A0496] p 221 A95-72567
Fast Floquet theory and trim for multi-bladed rotorcraft [HTN-95-61078] p 370 A95-83662
- PETERS, M. E.**
A users manual for the method of moments Aircraft Modeling Code (AMC), version 2 [NASA-CR-196445] p 24 N95-11252
- PETERSON, D. KENT**
Active control of complex noise problems using a broadband, multichannel controller p 29 N95-11271
- PETERSON, R. A.**
Laboratory evaluation of a reactive baffle approach to NOx control [AD-A283802] p 255 N95-19921
- PETERSON, RANDALL L.**
Dynamic response of NASA Rotor Test Apparatus and Sikorsky S-76 hub mounted in the 80- by 120-Foot Wind Tunnel [NASA-TM-108847] p 25 N95-11389
Full-scale hingeless rotor performance and loads [NASA-TM-110356] p 691 N95-32699
- PETIAU, C.**
Aeroacoustic qualification of HERMES shingles p 173 N95-19145
- PETOT, BERTRAND**
New methods, new methodology: Advanced CFD in the Snecma turbomachinery design process p 90 N95-14134
- PETRAKOV, V. M.**
Two projects of V. M. Myasishchev [HTN-95-50269] p 176 A95-65764
- PETRE, E.**
On-line handling of air traffic: Management, guidance and control [AGARD-AG-321] p 126 N95-18927
- PETROV, P.**
A program for scientific and applied investigations using aerostal complexes p 182 A95-66304
- PETRUZZIELLO, MAURIZIO**
A low fin height heat exchanger technology demonstrator for Hermes [SAE PAPER 932119] p 526 A95-90360
- PETRY, HERIBERT**
Evolution of the concentrations of trace species in an aircraft plume: Trajectory study [HTN-95-A1044] p 443 A95-84549
- PETTIT, CHRIS**
Pressure measurements on an F/A-18 twin vertical tail in buffeting flow. Volume 3: Buffet power spectral densities [AD-A281444] p 36 N95-11829
Pressure measurements on an F/A-18 twin vertical tail in buffeting flow. Volume 2: Steady and unsteady RMS pressure data [AD-A281581] p 76 N95-15465
- Pressure measurements on an F/A-18 twin vertical tail in buffeting flow. Volume 4, part 2: Buffet cross spectral densities [AD-A285555] p 143 N95-18641
Pressure measurements on an F/A-18 twin vertical tail in buffeting flow. Volume 4, part 1: Buffet cross spectral densities [AD-A285593] p 237 N95-21214
Pressure measurements on an F/A-18 twin vertical tail in buffeting flow. Volume 1: Wind tunnel test summary [AD-A279126] p 225 N95-21877
- PEZZULLO, G.**
Structural acoustic calculations in the low-frequency range [BTN-95-EIX95152582336] p 323 A95-73538
- PFEIFFER, KARL DURANT**
A numerical model to predict the fate of jettisoned aviation fuel [AD-A289336] p 419 N95-26842
- PFEILSTICKER, K.**
Airborne measurements during the Arctic stratospheric experiment: Observation of O3 and NO2 [HTN-95-00748] p 445 A95-86318
- PHILIPPART, A.**
Data link terminal DLT document [PB95-110805] p 229 N95-21369
- PHILLIPS, CHARLES T.**
Integration of air traffic databases: A case study [AD-A293691] p 602 N95-32022
- PHILLIPS, MICHAEL R.**
High-Alpha Research Vehicle (HARV) longitudinal controller: Design, analyses, and simulation results [NASA-TP-3446] p 17 N95-10860
- PHILLIPS, RONALD L.**
Integration of a mechanical forebody vortex control system into the F-15 p 72 N95-14258
- PHILLIPS, SCOTT N.**
A quantitative feedback theory FCS design for the subsonic envelope of the VISTA F-16 including configuration variation [AD-A289221] p 409 N95-26958
- PHIPPES, GARY**
Emerging nondestructive inspection for aging aircraft [PB95-143053] p 328 N95-25401
- PHONOV, S.**
Optical surface pressure measurements: Accuracy and application field evaluation p 175 N95-19274
- PIASCIK, ROBERT S.**
The characterization of widespread fatigue damage in fuselage structure [NASA-TM-109142] p 88 N95-14920
The characterization of widespread fatigue damage in fuselage structure p 166 N95-19472
- PIAT, J. F.**
Calculation of wall effects of flow on a perforated wall with a code of surface singularities p 165 N95-19277
- PIAUD, J. B.**
Modal parameters for cracked rotors: models and comparisons [BTN-94-EIX94522410226] p 702 A95-96378
- PIERCE, ALLAN D.**
Progressive wave equations and algorithms for sonic boom propagation p 575 A95-90104
- PIERCE, DOUGLAS C.**
Development of a bipolar lead/acid battery for the more electric aircraft [AD-A284050] p 160 N95-18660
- PIERCE, G. A.**
Measurement around a rotor blade excited in pitch. Part 2: Unsteady surface pressure [HTN-95-31008] p 220 A95-71178
Correlation of unsteady pressure and inflow velocity fields of a pitching rotor blade [BTN-95-EIX0619952748169] p 589 A95-94463
- PIERRE, CHRISTOPHE**
Forced response of mistuned bladed disks p 141 N95-19383
- PIERS, W. J.**
Sectional prediction of 3D effects for separated flow on rotating blades [PB94-201696] p 117 N95-18503
- PIKE, VERA J.**
A method of calculating the safe fatigue life of compact, highly-stressed components p 93 N95-14464
- PILIPENKO, V. V.**
JPRS report: Science and technology. Central Eurasia: Engineering and equipment. Gas dynamics of supersonic shortened nozzles [JPRS-UST-94-003-L] p 22 N95-10931
- PILKINGTON, D. J.**
Unsteady aerodynamic effects of trailing edge controls on delta wings [HTN-95-01099] p 469 A95-90285
- PILLAY, K. D. A.**
Fault Diagnosis for condition monitoring applied to hydraulic circuits [CONGRESS PAPER C428-12-165] p 456 A95-91703
- PIMSHEIN, V. G.**
Disturbance generation in supersonic jets under acoustic excitation [HTN-95-20926] p 463 A95-88965
- PIN, O.**
Temperature diagnostics in the hypersonic flow regime: An application to develop a stagnation temperature probe [AIAA PAPER 95-6114] p 511 A95-90442
- PIPERIAS, P.**
Derived gust spectra for the Macchi MB326H [ARL-TN-3] p 225 N95-21892
- PIPERNO, S.**
High performance parallel analysis of coupled problems for aircraft propulsion [NASA-CR-195355] p 23 N95-10132
- PIPKINS, D. S.**
A FEAM based methodology for analyzing composite patch repairs of metallic structures p 394 N95-27511
- PIQUEREAU, A.**
Evaluation of the techniques of fuzzy control for the piloting an aircraft p 621 N95-31997
- PIRONNEAU, O.**
Optimal shape design for aerodynamics p 128 N95-16568
- PIRZADEH, SHAHYAR**
Unstructured grid solutions to a wing/pylon/store configuration [BTN-95-EIX95152582322] p 265 A95-73525
An unstructured-grid software system for solving complex aerodynamic problems p 476 N95-28743
- PISANO, ALBERT P.**
Impact, friction, and wear testing of microsamples of polycrystalline silicon p 361 A95-79988
- PISOWISZCZ, V. L.**
Stationary premixed flames in spherical and cylindrical geometries [HTN-95-42336] p 418 A95-86165
- PITARI, G.**
Possible effects of CO2 increase on the high-speed civil transport impact on ozone [HTN-95-60779] p 317 A95-75976
High-speed civil transport impact: Role of sulfate, nitric acid trihydrate, and ice aerosols studied with a two-dimensional model including aerosol physics [HTN-95-91843] p 354 A95-80831
Impact on ozone of high-speed stratospheric aircraft: Effects of the emission scenario [HTN-95-51283] p 356 A95-80868
- PITTS, FELIX L.**
Fly-By-Light/Power-By-Wire Requirements and Technology Workshop [NASA-CP-10108] p 12 N95-10245
- PITTS, W. M.**
Evaluation of alternative in-flight fire suppressants for full-scale testing in simulated aircraft engine nacelles and dry bays [PB94-203403] p 42 N95-13247
- PIZIALI, R. A.**
2-D and 3-D oscillating wing aerodynamics for a range of angles of attack including stall [NASA-TM-4632] p 120 N95-19119
- PLAETSCHKE, ERMIN**
Parameter identification for X-31A at high angles of attack p 69 N95-14235
- PLATT, ROBERT**
High-resolution imaging of rain systems with the advanced microwave precipitation radiometer [HTN-95-70133] p 252 A95-70655
- PLATT, U.**
Airborne measurements during the Arctic stratospheric experiment: Observation of O3 and NO2 [HTN-95-00748] p 445 A95-86318
- PLATZER, M. F.**
Numerical investigation of high incidence flow over a double-delta wing [BTN-95-EIX0619952748160] p 588 A95-94454
Analysis of low Reynolds number airflow flows [BTN-95-EIX0619952748183] p 590 A95-94476
- PLATZER, MAX F.**
Aerodynamic characteristics of a canard-controlled missile at high angles of attack [BTN-95-EIX95152583257] p 267 A95-73558
Viscous-inviscid interaction method for unsteady low-speed airflow flows [BTN-95-EIX95182619093] p 269 A95-75778
Effect of leading-edge extension fences on the vortex wake of an F/A-18 model [BTN-95-EIX0619952748192] p 591 A95-94481

PLEITNER, J.

Integrated thermal and mechanical analysis of hypersonic vehicles by using adaptive finite element methods p 524 A95-87383

PLENTOVICH, E. B.

Measurements of store forces and moments and cavity pressures for a generic store in and near a box cavity at subsonic and transonic speeds [NASA-TM-4611] p 378 N95-28241

PLENTOVICH, ELIZABETH B.

Effect of passive venting on static pressure distributions in cavities at subsonic and transonic speeds [NASA-TM-4549] p 6 N95-10029

PLETCHER, RICHARD H.

Application of wall functions to generalized nonorthogonal curvilinear coordinate systems [BTN-95-EIX95182619077] p 307 A95-75762

PLOTKIN, KENNETH J.

The effect of onset rate on annoyance to military aircraft noise p 561 A95-90119
Incorporation of topography effects in aircraft noise modeling p 578 A95-90140
USAF single-event sonic boom prediction model: PCBooms3 p 101 N95-14889

PLOVSING, BIRGER

Nordic Standards for measurement of aircraft noise immersion in residential areas and noise reduction of dwellings p 570 A95-88463

PLUMB, R. A.

Fine-scale, poleward transport of tropical air during AASE 2 [HTN-95-70949] p 352 A95-78014

PLUMER, J. A.

Lightning protection technology for small general aviation composite material aircraft [SAE PAPER 931241] p 483 A95-88964

POBANZ, BRENDA M.

Conditions associated with large-drop regions [HTN-95-10686] p 214 A95-68845

POCOCK, MARK F.

Application of three-dimensional hybrid structured/unstructured grids to land, sea and air vehicles [ARA-MEMO-399] p 210 N95-19775

Verification of the CFD simulation system SAUNA for complex aircraft configurations [ARA-MEMO-401] p 211 N95-19776
Inviscid and viscous flow modelling of complex aircraft configurations using the CFD simulation system sauna [ARA-MEMO-403] p 211 N95-19777

PODBOY, GARY G.

Effects of a forward-swept front rotor on the flowfield of a counterrotation propeller [NASA-TM-106671] p 7 N95-10148
Laser doppler velocimeter system for subsonic jet mixer nozzle testing at the NASA Lewis Aeroacoustic Propulsion Lab [NASA-TM-106984] p 457 N95-30229

PODLESKI, S. D.

F/A-18 inlet calculations at 60-deg angle of attack and 10-deg sideslip [BTN-95-EIX95112524199] p 195 A95-69309

PODOLSKJE, J. R.

Fine-scale, poleward transport of tropical air during AASE 2 [HTN-95-70949] p 352 A95-78014

PODOLSKJE, JAMES R.

Vertical transport rates in the stratosphere in 1993 from observations of CO₂, N₂O, and CH₄ [HTN-95-70941] p 351 A95-78006

POE, C. C., JR.

Tension fracture of laminates for transport fuselage. Part 1: Material screening p 398 N95-28471
Tension fracture of laminates for transport fuselage. Part 2: Large notches p 532 N95-28837

POELLOT, MICHAEL R.

Aviation weather education and the University of North Dakota aviation weather survey p 656 A95-93462
Aviation meteorology education in an AB initio setting p 657 A95-93466

Preliminary analysis of University of North Dakota aircraft data from the FIRE Cirrus IFO-2 [NASA-CR-198038] p 357 N95-24219

POISSON-QUINTON, PHILIPPE

Future SSTs a European approach [BTN-95-EIX95072419883] p 180 A95-68396

POKORA, DARLENE C.

A shadowgraph study of the National Launch System's 1 1/2 stage vehicle configuration and Heavy Lift Launch Vehicle configuration [NASA-RP-1347] p 35 N95-11710

POLING, DAVID R.

Laser velocimetry and blade pressure measurements of a blade-vortex interaction [HTN-95-01081] p 547 A95-90267

POLITOVICH, MARCIA K.

Conditions associated with large-drop regions [HTN-95-10686] p 214 A95-68845

Examination of conditions in the proximity of pilot reports of aircraft icing during storm-fest p 666 A95-93509
The production of supercooled liquid water by a secondary cold front p 673 A95-93542
Aircraft icing: Meteorological effects on aircraft performance p 674 A95-93545

POLL, D. I. A.

The effect of wing sweep back upon transition in hypersonic flow [AIAA PAPER 95-6090] p 466 A95-89199

POLLACK, W. H.

Estimates of total organic and inorganic chlorine in the lower stratosphere from in situ and flask measurements during AASE 2 [HTN-95-A0861] p 317 A95-76265

POLLAND, D. R.

Tension fracture of laminates for transport fuselage. Part 2: Large notches p 532 N95-28837

POLYSHCHUK, V.

Analytical and experimental vibration analysis of a faulty gear system [NASA-TM-106689] p 58 N95-12843

POMFRET, CHRIS J.

Engine life measurement and diagnostics [BTN-95-EIX95041505024] p 235 A95-70133

PONTON, MICHAEL K.

Mach wave emission from a high-temperature supersonic jet [BTN-95-EIX95152577586] p 264 A95-73496

Mach wave emission from a high-temperature supersonic jet [HTN-95-42571] p 458 A95-87201

POOLE, P.

Adhesively bonded composite patch repair of cracked aluminum alloy structures p 393 N95-27507

POOLE, RICHARD J. D.

Interference corrections for a centre-line plate mount in a porous-walled transonic wind tunnel p 122 N95-19280

POON, C.

Numerical modelling of transverse impact on composite coupons [BTN-95-EIX95082502225] p 240 A95-71022

POOR, WALTER A.

Description of a GNSS availability model and its use in developing requirements [BTN-95-EIX95202637603] p 308 A95-76686

POP, I.

Free convection past a uniform flux surface inclined at a small angle to the horizontal [HTN-95-42213] p 430 A95-84029

POPE, G. G.

Aeronautical technology - recent advances and future prospects [HTN-95-01097] p 496 A95-90283

POPERNACK, T. G., JR.

Dynamic response tests of inertial and optical wind-tunnel model attitude measurement devices [NASA-TM-109182] p 296 N95-23011

PORCELLO, JOHN

Offshore next generation weather radar (NEXRAD) test and evaluation master plan (TEMP) [AD-A291435] p 556 N95-30072

Offshore next generation weather radar (NEXRAD) OT&E integration and OT&E operational test [AD-A293223] p 646 N95-30902

PORDON, R.

A new guidance and flight control system for the DELTA 2 launch vehicle p 342 A95-80427

PORTANOVA, MARC A.

Mechanical characterization of 2D, 2D stitched, and 3D braided/RTM materials p 535 N95-29038

PORTER, L.

Shock tunnel studies of scramjet phenomena 1993 [NASA-CR-195038] p 350 N95-25394

PORTER, L. M.

Shock tunnel measurements of hypervelocity blunted cone drag [BTN-95-EIX95152577606] p 305 A95-73477

Shock tunnel measurements of hypervelocity blunted cone drag [HTN-95-42591] p 459 A95-87221

PORTER, M. J.

Surge recovery and compressor working line control using compressor exit mach number measurement [CONGRESS PAPER C428-33-210] p 610 A95-93622

POSENAU, MARY-ANNE K.

Algorithms for high aspect ratio oriented triangulations p 476 N95-28731

POSTLETHWAITE, B. C.

Noise levels of helicopters performing elevated pad take-off and landing procedures [HTN-95-92544] p 559 A95-87364

POT, T.

Measurement by coherent anti-Stokes Raman scattering in the R5Ch hypersonic wind tunnel [BTN-95-EIX95112523811] p 188 A95-69322

POTAPOV, VADIM D.

Stability of viscoelastic plate in supersonic flow under random loading [BTN-95-EIX95262694312] p 435 A95-85483

POTOTZKY, ANTHONY S.

Rolling maneuver load alleviation using active controls [BTN-95-EIX95182619217] p 270 A95-76643

Active load control during rolling maneuvers [NASA-TP-3455] p 129 N95-17397

POTTS, ROBERT L.

Application of integral methods to ablation charring erosion, a review [BTN-95-EIX95302694460] p 636 A95-94057

Enhancements to integral solutions to ablation and charring [BTN-95-EIX95302694461] p 636 A95-94058

POTYONDY, DAVID O.

Discrete crack growth analysis methodology for through cracks in pressurized fuselage structures [BTN-95-EIX0608952737538] p 633 A95-92751

Discrete crack growth analysis methodology for through cracks in pressurized fuselage structures p 166 N95-19473

POURBAIX, A.

In-situ detection of surface passivation or activation and of localized corrosion: Experiences and prospectives in aircraft p 302 N95-23508

Test method and test results for environmental assessment of aircraft materials p 302 N95-23509

POVINELLI, LOUIS A.

Structure of supersonic jet flow and its radiated sound [HTN-95-51645] p 431 A95-85027

POWELL, E. A.

Evaluation of prediction methods for fluctuating pressures under attached turbulent boundary layers using flight test data p 574 A95-90103

POWELL, E. S.

A model for preliminary facility design including simulation issues p 144 N95-16318

POWELL, KENNETH G.

A Cartesian, cell-based approach for adaptively-refined solutions of the Euler and Navier-Stokes equations [NASA-TM-106786] p 73 N95-14297

POWERS, SHERYLL GOECKE

An Electronic Workshop on the Performance Seeking Control and Propulsion Controlled Aircraft Results of the F-15 Highly Integrated Digital Electronic Control Flight Research Program [NASA-TM-104278] p 694 N95-33009

POWLESLAND, I. G.

Preparation of S-70A-9 Black Hawk helicopter for flight tests to investigate cause of cracking of inner fuselage panel [AD-A293891] p 608 N95-31544

PRABHU, B. S.

Transient analysis of a cracked rotor passing through critical speed [BTN-94-EIX94401360022] p 306 A95-74702

PRABHU, DINESH K.

Parabolized Navier-Stokes solution of supersonic/hypersonic flows p 123 N95-19464

PRABHU, RAMADAS K.

An approximate Riemann solver for thermal and chemical nonequilibrium flows [NASA-CR-195003] p 96 N95-14912

PRAHST, P. S.

Inlet flow test calibration for a small axial compressor facility. Part 1: Design and experimental results [NASA-TM-106719] p 16 N95-11005

Inlet flow test calibration for a small axial compressor rig. Part 2: CFD compared with experimental results [NASA-TM-106999] p 514 N95-30007

PRAIRIE, MIKE

Optical processing and control [AD-A279157] p 259 N95-21975

PRAKASH, CHANDER

A summary of computational experience at GE Aircraft Engines for complex turbulent flows in gas turbines p 439 N95-27885

PRASAD, N.

Microwave and infrared simulations of an intense convective system and comparison with aircraft observations [HTN-95-60511] p 214 A95-68762

PRASKOVSKY, ALEXANDER

On the Lighthill relationship and sound generation from isotropic turbulence [NASA-CR-195005] p 159 N95-18191

- PRATHER, WILLIAM**
Assessing aircraft survivability to high frequency transient threats
[AD-A283999] p 134 N95-18726
- PRATT, A. J. S.**
Manufacture technology
[CONGRESS PAPER C428-27-088] p 612 A95-93605
- PRATT, DAVID T.**
Visualization of one-dimensional flow processes in a dual-mode scramjet engine p 15 N95-10465
- PRATT, DON**
The role of simulations in 777 FSEU development
[AIAA PAPER 95-0995] p 506 A95-90665
- PRATT, R. W.**
ASTOVL Aircraft: Some thoughts on new control strategies
[CONGRESS PAPER C428-5-011] p 517 A95-91680
- PREDTECHENSKY, A. N.**
General requirements for the electrohydraulic systems of the aircraft controls loading force on the simulators
[CONGRESS PAPER C428-5-138] p 522 A95-91681
- PREISSER, J. S.**
Recent studies of rotorcraft blade-vortex interaction noise
[BTN-95-EIX95062487521] p 218 A95-69229
- PRESS, HAYES N.**
A crew-centered flight deck design philosophy for High-Speed Civil Transport (HSCT) aircraft
[NASA-TM-109171] p 335 N95-24582
- PRESTON, ORV W.**
Guidance and control requirements for high-speed Rollout and Turnoff (ROTO)
[NASA-CR-195026] p 292 N95-22674
- PREUSS, C. H.**
Design, analysis, and fabrication of a pressure box test fixture for tension damage tolerance testing of curved fuselage panels p 533 N95-28839
- PRICE, J. M.**
DSMC calculations for 70-deg blunted cone at 3.2 km/s in nitrogen
[NASA-TM-109181] p 348 N95-24396
- PRICE, JOSEPH M.**
Hypersonic rarefied flow past spheres including wake structure
[BTN-95-EIX95152583250] p 305 A95-73551
- PRICE, S. J.**
Postinstability behavior of a two-dimensional airfoil with a structural nonlinearity
[BTN-95-EIX95152582337] p 266 A95-73539
- PRIEBE, CAREY E.**
Wavelet transformations for helicopter identification via acoustic signatures
[AD-A279980] p 257 N95-20963
- PRIGENT, C.**
Aircraft measurements of water vapour continuum absorption at millimetre wavelengths
[HTN-95-90884] p 253 A95-72393
- PRINTY, MATTHEW**
Weather And Radar Processor (WARP) Test and Evaluation Master Plan (TEMP)
[AD-A288280] p 445 N95-26453
- PRINZO, O. V.**
Development of a coding form for approach control/pilot voice communications
[DOT/FAA/AM-95/15] p 384 N95-28540
- PRITCHARD, JOCELYN I.**
Integrated aerodynamic/dynamic/structural optimization of helicopter rotor blades using multilevel decomposition
[NASA-TP-3465] p 285 N95-22953
- PRİYONO, EDDY**
An investigation of the transonic pressure drag coefficient for axi-symmetric bodies
[AD-A280990] p 105 N95-15994
- PROBERT, E. J.**
Mesh generation and adaptivity for the solution of compressible viscous high speed flows
[BTN-95-EIX95262697157] p 538 A95-86893
- PROCTOR, FRED H.**
Characteristics of a dry, pulsating microburst at Denver Stapleton Airport p 26 N95-10568
Windshear certification data base for forward-look detection systems p 41 N95-13204
- PROFFITT, MELISSA S.**
High-Alpha Research Vehicle (HARV) longitudinal controller: Design, analyses, and simulation results
[NASA-TP-3446] p 17 N95-10860
- PROTHEROE, C.**
Explosive sabotage: The potential effects of explosive charges on aircraft
[CONGRESS PAPER C428-11-034] p 484 A95-91702
- PRUDHOMME, S.**
Experimental techniques for measuring transonic flow with a three dimensional laser velocimetry system. Application to determining the drag of a fuselage p 163 N95-19258
- PRUETT, C. DAVID**
A spectrally accurate boundary-layer code for infinite swept wings
[NASA-CR-195014] p 159 N95-18042
- PRZEKWAŚ, A. J.**
Numerical analysis of intra-cavity and power-stream flow interaction in multiple gas-turbine disk-cavities
[NASA-TM-106886] p 407 N95-28344
Pressure based high order TVD methodology for dynamic stall control
[AD-A290149] p 479 N95-29316
- PRZEKWAŚ, ANDRZEJ J.**
Comparison of numerical results and multicavity purge and rim seal data with extensions to dynamics
[NASA-TM-106685] p 416 N95-27434
- PSZOLLA, H.**
Wind tunnel test on a 65 deg delta wing with rounded leading edges: The International Vortex Flow Experiment p 114 N95-17875
- PUCKETT, P. M.**
Novel matrix resins for composites for aircraft primary structures, phase 1
[NASA-CR-189657] p 23 N95-10318
- PUCKETT, PAUL M.**
Development of RTM and powder prepreg resins for subsonic aircraft primary structures p 536 N95-29044
- PUESCHEL, R.**
Performance of a focused cavity aerosol spectrometer for measurements in the stratosphere of particle size in the 0.06-2.0-micrometer-diameter range
[HTN-95-90914] p 253 A95-72423
- PUESCHEL, R. F.**
Three-dimensional model interpretation of NO(x) measurements from the lower stratosphere
[HTN-95-90534] p 213 A95-67806
- PUFFERT-MEISSNER, W.**
2-D airfoil tests including side wall boundary layer measurements p 158 N95-17847
- PUFFETT, A. W.**
Developments in airfield lighting
[CONGRESS PAPER C428-7-147] p 488 A95-91688
- PUGACZ, EDWARD**
Minima reduction simulation test results
[AD-A285626] p 228 N95-21148
- PULLIAM, THOMAS H.**
Accuracy enhancements for overset grids using a defect correction approach
[AIAA PAPER 94-0523] p 3 A95-60181
- PUMPPEL, HERBERT**
A poor man's expert system for aviation VSRF in complex terrain p 669 A95-93524
- PURCELL, RICHARD G.**
Replicator for characterization of cirrus and polar stratospheric cloud particles
[NASA-CR-197785] p 445 N95-26669
- PURI, I. K.**
Mobile domes for TACTIC telescope p 453 A95-86113
- PURVER, M.**
Experimental active control of sound in the ATR 42 p 575 A95-90110
- PURVIS, BRADLEY D.**
Visual contrast detection thresholds for aircraft contrails
[AD-A288618] p 328 N95-25607
- PURVIS, CHRISTOPHER REECE**
Design and flight test of a simplified control system for a transport helicopter p 144 N95-18902
- PYLE, J. A.**
Sensitivity of supersonic aircraft modelling studies to HNO3 photolysis rate
[HTN-95-11475] p 353 A95-79453
An overview of the EASOE campaign
[HTN-95-00702] p 443 A95-86272
- PYNE, C. R.**
A note on the interpretation of mini-tuft photographs
[HTN-95-01089] p 468 A95-90275
- PYNE, TONY**
The legal status and liability of the copilot, part 2
[HTN-95-A0578] p 452 A95-83158
- PYO, CHANG R.**
Structural integrity of fuselage panels with multisite damage
[BTN-95-EIX0619952748188] p 637 A95-94250
- Q**
- QIAN, X.**
Two-variable method for blockage wall interference in a circular tunnel
[BTN-95-EIX95062487540] p 187 A95-69248
- QUACKENBUSH, T. R.**
Vortex methods for the computational analysis of rotor/body interaction
[HTN-95-61072] p 369 A95-83656
- QUANDT, GENE A.**
Wind turbine trailing edge aerodynamic brakes
[DE95-004061] p 683 N95-32548
- QUAST, A.**
Subsonic flow around US-orbiter model FALKE in the DNW p 115 N95-17877
- QUATTLEBAUM, M. D.**
First medical test of the UH-60Q and equipment for use in US Army medevac helicopters p 568 N95-29620
- QUEMARD, C.**
Interaction of a three strut support on the aerodynamic characteristics of a civil aviation model p 122 N95-19279
- QUESNEL, E.**
Multilayer anti-erosion coatings p 201 N95-19679
- QUICK, HOWARD A.**
Estimation of aerodynamic load distributions on the F/A-18 aircraft using a CFD panel code
[DSTO-TR-0147] p 504 N95-29445
- QUINLIAN, J. T.**
NASA-ACEE/Boeing 737 graphite-epoxy horizontal stabilizer service p 400 N95-28489
- QUINLIAN, JOHN**
Challenges and payoff of composites in transport aircraft: 777 empennage and future applications p 534 N95-29031
- QUINN, W. R.**
Development of a large-aspect-ratio rectangular turbulent free jet
[HTN-95-42333] p 372 A95-86162
- QUINTERO, R.**
Overview of NASREM: The NASA/NBS standard reference model for teleoperator control system architecture re
[PB94-194560] p 58 N95-12854
- R**
- RABY, PETER**
Integrated GPS/Glonass navigation: Algorithms and results
[BTN-95-EIX95112522531] p 190 A95-69332
- RADCHENKO, V.**
Optical surface pressure measurements: Accuracy and application field evaluation p 175 N95-19274
- RADDIN, JAMES H., JR.**
The large radius track centrifuge concept as an acceleration research and simulation device p 379 A95-84560
- RADERMACHER, R.**
Second-law analysis of vapor compression heat pumps with solution circuit
[BTN-94-EIX95011441236] p 431 A95-84193
- RADESPIEL, R.**
Aerodynamic off-design behavior of integrated waveriders from take-off up to hypersonic flight
[AIAA PAPER 95-6091] p 466 A95-89200
Subsonic flow around US-orbiter model FALKE in the DNW p 115 N95-17877
- RADEZTSKY, RONALD HENRY, JR.**
Growth and development of roughness-induced stationary crossflow vortices p 482 N95-30294
- RADHAKRISHNAN, KRISHNAN**
Sensitivity of combustion-acoustic instabilities to boundary conditions for premixed gas turbine combustors
[NASA-TM-106890] p 289 N95-23550
Review of combustion-acoustic instabilities
[NASA-TM-107020] p 705 N95-32930
Combustion-acoustic stability analysis for premixed gas turbine combustors
[NASA-TM-107024] p 694 N95-32931
- RADTKE, T. C.**
Fatigue crack growth in nickel-based superalloys at 500-700 C. 1: Waspaloy
[BTN-94-EIX94371347843] p 206 A95-69136
Scarf repairs to graphite/epoxy components p 396 N95-27523
- RADUN, ARTHUR**
A detailed power inverter design for a 250 kW switched reluctance aircraft engine starter/generator
[SAE PAPER 931388] p 613 A95-93664

- RAGA, G. B.**
Mesoscale structure of precipitation bands in a North Atlantic winter storm
[HTN-95-40659] p 215 A95-69803
Microphysical and radiative properties of small cumulus clouds over the sea
[HTN-95-A0526] p 255 A95-73180
On the link between cloud-top radiative properties and sub-cloud aerosol concentrations
[HTN-95-A0527] p 255 A95-73181
- RAGSDALE, WILLIAM C.**
Supercooling in hypersonic nitrogen wind tunnels
[BTN-94-EIX95011441134] p 340 A95-81020
- RAHEMATPURA, MANOJ**
Analysis of warping effects on the static and dynamic response of a seat-type structure
[NIAR-94-12] p 348 N95-24211
- RAI, R.**
Theoretical and actual performance of a long duration superpressure balloon made from a biaxially oriented nylon-6 film
p 181 A95-66282
- RAINWATER, B. A.**
Moving mass trim control for aerospace vehicles
[DE95-002602] p 299 N95-23532
- RAIS-ROHANI, MASOUD**
Rapid prototyping of composite aircraft structures
[SAE PAPER 931219] p 539 A95-87530
Wing design for a civil tiltrotor transport aircraft
[NASA-CR-197523] p 130 N95-18090
Thin tailored composite wing for civil tiltrotor
p 285 N95-23317
- RAIZENNE, M. D.**
Bonded composite repair of thin metallic materials: Variable load amplitude and temperature cycling effects
p 393 N95-27509
- RAJ, PRADEEP**
An assessment of viscous effects in computational simulation of benign and burst vortex flows on generic fighter wind-tunnel models using TEAM code
[NASA-CR-4650] p 273 N95-23185
Requirements for effective use of CFD in aerospace design
p 551 N95-28725
- RAJ, SHREERAM**
Evaluation of bonded boron/epoxy doublers for commercial aircraft aluminum structures
p 92 N95-14457
- RAJAGOPAL, PAVAN**
Flight control system mode transitions influence on handling qualities and task performance
[BTN-95-EIX95062487525] p 203 A95-69233
- RAJAGOPALAN, R. GANESH**
Solution-adaptive structured-unstructured grid method for unsteady turbomachinery analysis. Part I: Methodology
[BTN-94-EIX94441380983] p 208 A95-67329
Navier-Stokes calculations of rotor-airframe interaction in forward flight
[HTN-95-01087] p 468 A95-90273
- RAJEVSKAYA, G. A.**
Advanced method and processing technology for complicated shape airframe part forming
p 80 N95-14486
- RALPH, HARRY C.**
Special purpose landing gear: A survey of historical designs
[SAE PAPER 932579] p 494 A95-90066
- RALSTON, J.**
Experimental study of the effects of Reynolds number on high angle of attack aerodynamic characteristics of forebodies during rotary motion
[NASA-CR-195033] p 330 N95-24443
- RALSTON, JOHN**
Validation of the NASA Dryden X-31 simulation and evaluation of mechanization techniques
p 69 N95-14236
- RAMACHANDRAN, K.**
The application of potential CFD methods to helicopter hover flows
[ISBN 1-879921-01-4] p 587 A95-93747
- RAMAMURTI, SITA**
Variational principles for ascent shapes of large scientific balloons
[BTN-95-EIX95262694320] p 387 A95-85491
- RAMAN, G.**
Enhanced mixing of multiple supersonic rectangular jets by synchronized screech
[HTN-95-42592] p 459 A95-87222
- RAMAN, GANESH**
Resonant interaction of a linear array of supersonic rectangular jets: An experimental study
[NASA-CR-195398] p 76 N95-15852
Visualization of the multiple supersonic jet oscillations by swept focused strobed schlieren technique
p 367 N95-26952
- RAMAN, SHANKAR**
Intelligent finite element submodeling of multichip modules for reliability analysis
[AD-A292911] p 679 N95-31455
- RAMANATHAN, VEERABHADRAN**
Advanced data visualization and sensor fusion: Conversion of techniques from medical imaging to Earth science
p 711 N95-34236
- RAMAPRIAN, B. R.**
Pressure measurements on a pitching airfoil in a water channel
[HTN-95-61209] p 541 A95-87582
Interactions of spanwise and chordwise vorticity associated with three-dimensional dynamic stall over an oscillating wing
[AD-A290546] p 477 N95-29091
- RAMAROSON, R.**
Potential effects on ozone of future supersonic aircraft/2D simulation
[HTN-95-51282] p 356 A95-80867
- RAMER, DAVID P.**
Visual contrast detection thresholds for aircraft contrails
[AD-A288618] p 328 N95-25607
- RAMSEY, KERI**
Icarus Rewaxed: A high speed, low-cost general aviation aircraft for Aeroworld
[NASA-CR-197155] p 45 N95-12609
- RAMSEY, ROBERT G.**
An analysis of the impact of ASPA on organizational and depot level maintenance
[AD-A292670] p 457 N95-29414
- RANAUDO, RICHARD J.**
Piloted evaluation of an integrated methodology for propulsion and airframe control design
[AD-A290207] p 51 N95-12763
- RAND, JAMES L.**
Long duration balloons
p 191 A95-66305
Recent developments in nylon superpressure balloons
p 385 A95-82512
- RANDLE, SCOTT**
An experimental investigation of helicopter downwash and tailboom interaction at the Wichita State University 7x10 foot wind tunnel
p 375 N95-26955
- RANDLE, SCOTT A.**
An experimental investigation of forward-swept wings at low Reynolds numbers
[SAE PAPER 931370] p 604 A95-93650
- RANGARAJAN, R.**
Computation of inviscid flows: Full potential method
p 165 N95-19447
- RANGWALLA, AKIL A.**
Three-dimensional unsteady flow calculations in an advanced gas generator turbine
p 312 N95-23425
Turbomachinery design and tonal acoustics computations
[NASA-CR-197749] p 406 N95-26777
- RANKIN, CHARLES C.**
Nonlinear analysis of damaged stiffened fuselage shells subjected to combined loads
p 137 N95-19499
- RANKIN, JAMES M.**
Differential GPS and system integration of the Low Visibility Landing and Surface Operations (LVLASO) demonstration
p 280 N95-23318
- RANSOM, JONATHAN B.**
A global/local analysis method for treating details in structural design
p 552 N95-28848
- RAO, DHANVADA M.**
Pneumatic concept for tip-stall control of cranked-arrow wings
[BTN-95-EIX95152582335] p 281 A95-73537
- RAO, G. N. V.**
Low speed wind tunnel blockage corrections for airfoils at medium to large angles of attack
p 474 A95-91557
Use of partially open wind tunnel walls for blockage-free separated flows on bodies
p 474 A95-91558
- RAO, M.**
Dynamics of phase ordering of nematics in a pore
[DE95-607662] p 362 N95-25978
- RASH, CLARENCE E.**
Transmittance characteristics of US Army rotary-wing aircraft transparencies
[AD-A295035] p 693 N95-34793
- RASHIDI, MAJID**
Vibration analysis of a split path gearbox
[NASA-TM-106875] p 438 N95-27855
- RASHIDNIA, NASSER**
Transport phenomena in stratified multi-fluid flow in the presence and absence of gravity
p 95 N95-14563
- RASKY, DANIEL J.**
Review of numerical procedures for computational surface thermochemistry
[BTN-94-EIX94441386682] p 205 A95-68191
- RASMUSSEN, M.**
Hypersonic waveriders generated from power-law shocks
[AIAA PAPER 95-6160] p 470 A95-90472
- RASMUSSEN, M. L.**
Waveriders with finlets
[BTN-95-EIX95062487541] p 184 A95-68355
- RASMUSSEN, R. GARY**
ITWS ceiling and visibility products
p 654 A95-93454
- RASMUSSEN, R. M.**
Preliminary comparisons between MMS NCAR/Penn State model generated icing forecasts and observations
p 655 A95-93458
Preliminary results of high resolution measurements of snowfall at Stapleton International Airport during the winter of 1992-93
p 661 A95-93484
- RASMUSSEN, ROBERT D.**
The Cassini spacecraft: Object oriented flight control software
p 359 A95-80405
- RASMUSSEN, ROY**
The 1992-3 operational winter forecasting experiment for Stapleton airport
p 677 A95-93561
- RASMUSSEN, ROY M.**
Snow-band formation and evolution during the 15 November 1987 aircraft accident at Denver airport
[HTN-95-80699] p 254 A95-72543
Preliminary studies of ice formation in upslope clouds
p 674 A95-93546
- RASPET, RICHARD**
Atmospheric effects on the risetime and waveshape of sonic booms
p 100 N95-14886
- RASTOGI, NAVEEN**
Load transfer in the stiffener-to-skin joints of a pressurized fuselage
[NASA-CR-198610] p 439 N95-27865
- RATAN, SANTOSH**
Modal identification and its applications to damage detection in vibrating structures
p 704 N95-32920
- RATHAKRISHNAN, E.**
Flow past a symmetric wedge with forward splitter plate
p 427 A95-82406
- RAU, GUIDO**
Aerodynamic investigation of the flow field in a 180 deg turn channel with sharp bend
p 163 N95-19257
- RAULOT, A.**
Implicit multidomain calculation of viscous transonic flows without artificial viscosity or upwinding
p 640 A95-95443
- RAULT, D. F. G.**
Cercignani-Lampis-Lord gas-surface interaction model: Comparisons between theory and simulation
[BTN-95-EIX95041503806] p 242 A95-70131
- RAULT, DIDIER F. G.**
Aerodynamic characteristics of a hypersonic viscous optimized waverider at high altitudes
[BTN-95-EIX95152583251] p 266 A95-73552
Aerodynamics of the Shuttle Orbiter at high altitudes
[BTN-95-EIX95182617454] p 298 A95-75725
- RAUW, MARC O.**
A SIMULINK environment for flight dynamics and control analysis: Application to the DHC-2 Beaver. Part 1: Implementation of a model library in SIMULINK. Part 2: Nonlinear analysis of the Beaver autopilot
[NONP-NASA-SUPPL-DK-94-2802] p 84 N95-14815
- RAVINDRA, KRISHNASWAMY**
Preliminary identification of buffet problems in high speed civil transport
p 294 N95-23319
- RAVINDRABABU, K.**
Switched bias proportional navigation for homing guidance against highly maneuvering targets
[BTN-95-EIX95182619145] p 279 A95-76622
- RAVISHANKARA, A. R.**
The atmospheric effects of stratospheric aircraft: A fourth program report
[NASA-RP-1359] p 357 N95-24274
- RAWDON, BLAINE K.**
Advanced subsonic airplane design and economic studies
[NASA-CR-195443] p 338 N95-24304
- RAWLINGS, J.**
NTS-spill test facility wind tunnel exhaust plume characterization
[DE95-003630] p 297 N95-24019
- RAWLS, J. RICHARD**
Hardware cleanliness methodology and certification
p 419 N95-27656
- RAY, DAVID M.**
Virtual environment application with partial gravity simulation
p 169 N95-15988
- RAY, RONALD J.**
Design and development of an F/A-18 inlet distortion rake: A cost and time saving solution
p 69 N95-14241

- RAYMER, DANIEL P.**
Aircraft aerodynamic analysis on a personal computer (using the RDS aircraft design software)
[SAE PAPER 932530] p 492 A95-89190
- READER, KENNETH R.**
An unmanned air vehicle concept with tipjet drive
[HTN-95-80858] p 283 A95-75100
- READEY, M. J.**
Ceramic manufacturing: Optimizing a multivariable system
[DE94-015016] p 56 N95-13184
- REAGON, PATRICIA G.**
The NASA Langley 8-foot Transonic Pressure Tunnel calibration
[NASA-TP-3437] p 8 N95-10739
- REBBECCHI, B.**
A portable transmission vibration analysis system for the S-70A-9 Black Hawk helicopter
[DSTO-TR-0072] p 348 N95-24203
- REBBERT, MILTON L.**
High aspect ratio metal microstructures and method for preparing the same
[AD-D017463] p 629 N95-30750
- REDDEN, MARK C.**
Integrated mission precision attack cockpit technology (IMPACT). Phase 1: Identifying technologies for air-to-ground fighter integration
[AD-A289562] p 389 N95-26684
- REDDY, D. R.**
3-D Navier-Stokes analysis of crossing glancing shocks/turbulent boundary layer interactions
[BTN-95-EIX95302729768] p 636 A95-94130
- REDDY, E. S.**
Ice-impact analysis of blades p 200 N95-19672
Analysis of aircraft engine blade subject to ice impact p 407 N95-28277
- REDDY, K. R.**
Low speed wind tunnel blockage corrections for airfoils at medium to large angles of attack p 474 A95-91557
- REDDY, N. N.**
A prediction method for broadband shock associated noise from supersonic rectangular jets p 574 A95-90100
Evaluation of prediction methods for fluctuating pressures under attached turbulent boundary layers using flight test data p 574 A95-90103
- REDDY, S. V.**
Fatigue and residual strength investigation of ARALL(R) -3 and GLARE(R) -2 panels with bonded stringers p 137 N95-19495
- REDDY, T. S. R.**
Flutter analysis of supersonic axial flow cascades using a high resolution Euler solver. Part 1: Formulation and validation
[NASA-TM-105798] p 23 N95-10244
User's guide for ECAP2D: An Euler unsteady aerodynamic and aeroelastic analysis program for two dimensional oscillating cascades, version 1.0
[NASA-CR-189146] p 316 N95-24189
- REDEKER, A.**
Integrated special mission flight management for a flight inspection aircraft p 692 N95-33145
- REDEKER, G.**
DLR-F4 wing body configuration p 130 N95-17863
- REDELSPERGER, J.-L.**
Nonhydrostatic simulation of frontogenesis in a moist atmosphere. Part 3: Thermal wind imbalance and rainbands
[HTN-95-90356] p 212 A95-66429
- REDINIOTIS, O. K.**
Dynamic pitch-up of a delta wing
[HTN-95-81633] p 462 A95-87681
- REED, C. B.**
MHD-flow in slotted channels with conducting walls
[DE94-018370] p 258 N95-21388
- REED, HELEN L.**
Linear disturbances in hypersonic, chemically reacting shock layers
[BTN-94-EIX94441386605] p 182 A95-67336
Transition correlations in three-dimensional boundary layers
[HTN-95-51648] p 432 A95-85030
Numerical model for circulation-control flows
[HTN-95-81632] p 461 A95-87680
Linear disturbances in hypersonic, chemically reacting shock layers
[HTN-95-20931] p 464 A95-88970
- REED, JAMES A.**
Subscale study of engine bellmouth inlet vortices in test cell R1D
[AD-A294993] p 707 N95-34818
- REED, R. DALE**
Development and flight test of a deployable precision landing system
[BTN-95-EIX95062487535] p 190 A95-69243
- REEHORST, ANDREW**
Investigation of water droplet trajectories within the NASA icing research tunnel
[NASA-TM-107023] p 684 N95-32769
- REEVE, T.**
An artificial neural network system for diagnosing gas turbine engine fuel faults
[DE94-013960] p 138 N95-17371
- REEVES, J. M.**
An overview of millimeter-wave spectroscopic measurements of chlorine monoxide at Thule, Greenland, February-March, 1992: Vertical profiles, diurnal variation, and longer-term trends
[HTN-95-00722] p 444 A95-86292
- REEVES, JOHN**
Balanced on air aircraft
[AD-D017251] p 389 N95-26537
- REGENIE, VICTORIA A.**
F-18 high alpha research vehicle: Lessons learned
p 69 N95-14240
- REGINATTO, MARCEL**
Radiation safety aspects of commercial high-speed flight transportation
[NASA-TP-3524] p 453 N95-26427
- REHFELD, LAWRENCE W.**
Experimental evaluation of a box beam specifically tailored for chordwise deformation
[BTN-95-EIX95182619088] p 263 A95-75773
Unique considerations in the design and experimental evaluation of tailored wings with elastically produced chordwise camber p 423 N95-28436
- REHMANN, SYED M.**
A study of mesh adaption techniques in structured and unstructured meshes
[ISBN 1-879921-01-4] p 678 A95-93757
- REHMANN, ALBERT**
An evaluation of Automatic Terminal Information Service (ATIS) flight deck display presentation options
[AD-A280100] p 228 N95-21020
- REICH, G.**
Launcher wing-leading-edge design
[BTN-95-EIX95042477110] p 192 A95-68349
- REICHERT, BRUCE A.**
A new algorithm for five-hole probe calibration, data reduction, and uncertainty analysis
[NASA-TM-106458] p 38 N95-12378
Study of compressible flow through a rectangular-to-semiannular transition duct
[NASA-CR-4660] p 338 N95-24392
The decay of longitudinal vortices shed from airfoil vortex generators
[NASA-CR-198356] p 480 N95-29402
- REICHERT, G.**
Trim conditions for optimal flight performance of hypersonic aircraft p 514 A95-87397
- REID, G. W.**
Damage to composite aircraft structures from lightning strike attachment to unprotected CFC and internal sparking causing fuel injection
[CONGRESS PAPER C428-4-026] p 531 A95-91675
- REID, LLOYD D.**
Flight control system mode transitions influence on handling qualities and task performance
[BTN-95-EIX95062487525] p 203 A95-69233
- REID, WILSON G.**
Effect of broadcast and precise ephemerides on estimates of the frequency stability of GPS Navstar clocks
[BTN-95-EIX95112522530] p 190 A95-69333
- REINER, JACOB**
Robust dynamic inversion for control of highly maneuverable aircraft
[BTN-95-EIX95242670747] p 359 A95-81100
- REINHARDT, MANFRED E.**
North Atlantic air traffic within the lower stratosphere: Cruising times and corresponding emissions
[HTN-95-91841] p 354 A95-80829
- REINICKE, ROBERT H.**
A Lifting Ball Valve for cryogenic fluid applications p 156 N95-16349
- REINMANN, JOHN J.**
Icing: Accretion, detection, protection p 77 N95-14897
- REINSCH, K. G.**
Parallel computational fluid dynamics '91; Conference Proceedings, Stuttgart, Germany, Jun. 10-12, 1991
[ISBN 0-444-89363-6] p 548 A95-91479
- REISENTHAL, PATRICK H.**
Vorticity dynamics and control of dynamic stall
[AD-A288658] p 620 N95-31400
- REISNER, J.**
Preliminary comparisons between MM5 NCAR/Penn State model generated icing forecasts and observations p 655 A95-93458
- REITBERGER, P. H.**
Modular CNI avionics system p 234 N95-20659
- RELMAN, PAUL**
Concorde: Silver jubilee Mach 2 marks 25 years
[HTN-95-42618] p 483 A95-87248
- REMER, FRED M.**
Aviation meteorology education in an AB initio setting p 657 A95-93466
- REMER, LORRAINE**
Remote sensing of smoke, clouds, and radiation using AVIRIS during SCAR experiments p 708 N95-33749
- REMONDI, BENJAMIN W.**
Real-time testing and demonstration of the US Army Corps of Engineers' Real-Time On-The-Fly positioning system
[AD-A288624] p 334 N95-25609
- RENGER, W.**
Two dimensional stratospheric aerosol distributions during EASOE
[HTN-95-00726] p 444 A95-86296
- RENIERI, GARY D.**
Analysis techniques for the prediction of springback in formed and bonded composite components p 421 N95-28289
- RENIERI, M. P.**
ACT/ICAPS: Thermoplastic composite activities p 421 N95-28274
- RENKSIZBULUT, M.**
Drag coefficients of spherical liquid droplets. Part 1: Quiescent gaseous fields
[BTN-95-EIX95262697040] p 538 A95-86857
Drag coefficients of spherical liquid droplets. Part 2: Turbulent gaseous fields
[BTN-95-EIX95262697041] p 538 A95-86858
- RETEL, A. P.**
Unsteady transonic wind tunnel test on a semispan straked delta wing, oscillating in pitch. Part 1: Description of the model, test setup, data acquisition, and data processing
[AD-A293113] p 593 N95-30885
- RETTNER, BERNARD L.**
The opportunities for and challenges of common integrated electronics
[AD-A279991] p 248 N95-20966
- REUTHER, JAMES**
Control theory based airfoil design using the Euler equations
[NASA-CR-196360] p 36 N95-11884
Aerodynamic shape optimization of wing and wing-body configurations using control theory
[NASA-CR-198024] p 335 N95-25334
Computational algorithms for aerodynamic analysis and design
[AD-A291084] p 482 N95-29972
- REX, D.**
Reentry trajectories and their optimization by an evolution algorithm p 525 A95-87394
- REY, J. M.**
Modular supplies for a distributed architecture p 234 N95-20657
- REYNARD, WILLIAM D.**
EMS helicopter incidents reported to the NASA Aviation Safety Reporting System p 596 A95-95201
- REYNOLDS, ANTHONY P.**
Multi-lab comparison on R-curve methodologies: Alloy 2024-T3
[NASA-CR-195004] p 151 N95-16860
- REYNOLDS, DICK**
In situ processing methods for composite fuselage sandwich structures p 531 N95-28826
- REYNOLDS, GREGORY A.**
Demonstration study of hierarchical control of fluid-dynamic phenomena
[AD-A289341] p 437 N95-26751
- REZKALLAH, K. S.**
A flow pattern map for two-phase liquid-gas flow under reduced gravity conditions p 539 A95-87280
- REZY, BERNIE J.**
Propulsion system assessment for very high UAV under ERAST
[NASA-CR-195469] p 406 N95-27866
- RHOADES, R. L.**
Cu deposition using a permanent magnet electron cyclotron resonance microwave plasma source
[DE94-017768] p 304 N95-23981
- RHOADS, GREGORY L.**
Partial discharge testing of high voltage wiring harness for airborne displays
[AD-A289150] p 401 N95-27003
- RHODES, G. S.**
Portable parallel stochastic optimization for the design of aeropropulsion components
[NASA-CR-195312] p 154 N95-16072
- RHUDY, R. W.**
Hypersonic wind tunnel test techniques
[AD-A284057] p 118 N95-18663

RIABOV, V. V.
Aerodynamic applications of underexpanded hypersonic viscous jets
[BTN-95-EIX0619952748162] p 589 A95-94456

RIBNER, HERBERT S.
An extension of the Lighthill theory of jet noise to encompass refraction and shielding
[NASA-TM-110163] p 580 N95-29452

RICCI, R.
Buckling and postbuckling of composite structures
[HTN-95-71387] p 528 A95-87605

RICCIARDI, BERNARD V.
Tactical low-level helicopter communications
p 702 N95-32492

RICCIARDULLI, L.
High-speed civil transport impact: Role of sulfate, nitric acid trihydrate, and ice aerosols studied with a two-dimensional model including aerosol physics
[HTN-95-91843] p 354 A95-80831

RICE, EDWARD J.
Jet mixer noise suppressor using acoustic feedback
[NASA-CASE-LEW-15170-2] p 362 N95-26187

RICH, WILLIAM F.
The navigation toolkit
[NASA-CR-197290] p 229 N95-22161

RICHARD, HORONJEFF
Factors affecting measured aircraft sound levels in the vicinity of start-of-takeoff roll
p 571 A95-88465

RICHARD, JACQUES C.
Low-order nonlinear dynamic model of IC engine-variable pitch propeller system for general aviation aircraft
[NASA-TM-107006] p 694 N95-32916

RICHARDS, MARK A.
Characteristics of civil aviation atmospheric hazards
p 42 N95-13208

RICHARDS, MICHAEL A.
SEM representation of the early and late time fields scattered from wire targets
[BTN-94-EIX94381353142] p 306 A95-74496

RICHARDSON, I. G.
A survey of bidirectional greater than or equal to MeV ion flows during the Helios 1 and Helios 2 mission: Observations from the Goddard Space Flight Center instruments
[HTN-95-70542] p 237 A95-71656

RICHARDSON, J.
Transport aircraft loading and balancing system: Using a CLIPS expert system for military aircraft load planning
p 217 N95-19751

RICHARDSON, THOMAS F.
Unsteady panel method for flows with multiple bodies moving along various paths
[HTN-95-61203] p 540 A95-87576

RICHIE, JOSEPH M.
A NASPAC-Based analysis of the delay and cost effects of the western-pacific region preliminary resectorization effort of 1993
[AD-A288696] p 601 N95-31013

RICHTER, EIKE
A detailed power inverter design for a 250 kW switched reluctance aircraft engine starter/generator
[SAE PAPER 931388] p 613 A95-93664
Detailed design of a 250-kW switched reluctance starter/generator for an aircraft engine
[SAE PAPER 931389] p 613 A95-93665

RICHWINE, DAVID M.
Development of a low-aspect ratio fin for flight research experiments
[NASA-TM-4596] p 108 N95-16858

RICKERBY, D.
Multilayer anti-erosion coatings
p 201 N95-19679

RICKEY, JUNE ELIZABETH
The effect of altitude conditions on the particle emissions of a J85-GE-5L turbojet engine
[NASA-TM-106669] p 339 N95-24561

RICKLEY, EDWARD J.
Factors affecting measured aircraft sound levels in the vicinity of start-of-takeoff roll
p 571 A95-88465

RIDDICK, J. C.
Minimum-mass design of sandwich aerobrakes for a lunar transfer vehicle
[BTN-95-EIX95212645707] p 299 A95-76759

RIDDLE, J.
Measurement of particle emissions from clean room gas-handling components
[BTN-94-EIX94381359040] p 295 A95-74554
Measurement of moisture and total hydrocarbon contributions by valves used in clean room gas-delivery systems
[BTN-94-EIX94381359041] p 295 A95-74629

RIDLEY, B. A.
An analysis of aircraft exhaust plumes form accidental encounters
[HTN-95-70943] p 351 A95-78008

Mentional distributions of NO(X), NO(Y), and other species in the lower stratosphere and upper troposphere during AASE 2
[HTN-95-70944] p 352 A95-78009

RIDLEY, BRIAN A.
Three-dimensional model interpretation of NO(x) measurements from the lower stratosphere
[HTN-95-90534] p 213 A95-67806

RIEDLER, W.
Balloon technology and observations; Symposium P3 of the COSPAR Plenary Meeting, 29th, Washington, DC, Aug. 28-Sept. 5, 1992
[HTN-95-70250] p 181 A95-66276

RIES, JOHN C.
Precision orbit determination of altimetric satellites
p 86 N95-14282

RIGGALL, B.
The avionics integrity programme (AVIP)
[CONGRESS PAPER C428-6-115] p 549 A95-91684

ROBINSON, R. M.
Chemical composition and photochemical reactivity of exhaust from aircraft turbine engines
[HTN-95-51277] p 356 A95-80862

RIGGINS, D. W.
Thrust modeling for hypersonic engines
[AIAA PAPER 95-6081] p 509 A95-87410
Vortex generation and mixing in three-dimensional supersonic combustors
[BTN-95-EIX0616952745783] p 614 A95-94503
Investigation of scramjet injection strategies for high mach number flows
[BTN-95-EIX0616952745782] p 614 A95-94504

RIGGS, H. RONALD
Accurate interlaminar stress recovery from finite element analysis
[NASA-TM-109149] p 57 N95-11815

RILEY, EDWARD W.
Intelligent flight trainer for initial rotary wing training
[SAE PAPER 932536] p 386 A95-84558

RIMBEY, P. R.
Consistent approach to describing aircraft HIRF protection
[NASA-CR-195067] p 334 N95-25341

RIMLINGER, MARK J.
A procedure for automating CFD simulations of an inlet-bleed problem
p 552 N95-28768

RINEK, LARRY M.
Charles Norvin Rinek; an early American pioneer in advanced aviation engines
[SAE PAPER 930485] p 386 A95-84554

RINOIE, KENICHI
Estimation of aerodynamic characteristics for the vortex flaps by the suction analogy
p 471 A95-91496
Low speed aerodynamic characteristics of delta wings with vortex flaps: 60 deg and 70 deg delta wings
[NAL-TR-1245] p 331 N95-25105
Experimental investigation of static and dynamic ground effect on HOPE ALFLEX vehicle
[NAL-TR-1236] p 388 N95-26525

RISI, JOHN D.
Analytical investigation of adaptive control of radiated inlet noise from turbofan engines
p 30 N95-11277

RISKALLA, M. G.
Probabilistic design of advanced composite structure
p 424 N95-28443

RITTENHOUSE, KIRK
Certification of windshear performance with RTCA class D radomes
p 41 N95-13206

RIVERA, JOSE A., JR.
Flutter clearance flight tests of an OV-10A airplane modified for wake vortex flight experiments
[NASA-TM-109168] p 366 N95-26381

RIVERS, MELISSA B.
Comparison of computational and experimental results for a supercritical airfoil
[NASA-TM-4601] p 108 N95-16908

RIVERS, ROBERT A.
High-Alpha Research Vehicle (HARV) longitudinal controller: Design, analyses, and simulation results
[NASA-TP-3446] p 17 N95-10860

RIZI, V.
High-speed civil transport impact: Role of sulfate, nitric acid trihydrate, and ice aerosols studied with a two-dimensional model including aerosol physics
[HTN-95-91843] p 354 A95-80831

RIZK, YEHIA M.
Numerical simulation of the flow about an F-18 aircraft in the high-alpha regime
p 68 N95-14232
Computational analysis of forebody tangential slot blowing
p 71 N95-14253

RIZZI, A.
Hypersonic Navier-Stokes computations about complex configurations
p 644 A95-95497

RIZZI, ARTHUR
Navier-Stokes simulation of turbulent vortex high-Re-number flows over a delta wing
p 644 A95-95507

RKHIMA, A. A.
On the particular features of dynamic processes in solids with varying boundary during interaction with intensive heat flows
[BTN-94-EIX94461408756] p 171 A95-63639

ROACH, DEIRDRE
The prototype aviation weather products generator a vehicle to assess user needs
p 671 A95-93534

ROACH, DENNIS
Emerging nondestructive inspection for aging aircraft
[PB95-143053] p 328 N95-25401

ROACH, LISA K.
Rationale for the Modular Air-system Vulnerability Estimation Network (MAVEN) methodology
[AD-A285797] p 284 N95-22510

ROBELEN, DAVID B.
Vapor generator wand
[NASA-CASE-LAR-15058-1] p 238 N95-20080

ROBERTS, G.
The use of thermochromic liquid crystals for heat transfer measurements in short duration hypersonic wind tunnel facilities
[AIAA PAPER 95-6115] p 520 A95-90443

ROBERTS, LEONARD
Determination of solid/porous wall boundary conditions from wind tunnel data for computational fluid dynamics codes
p 164 N95-19266

ROBERTS, N.
Comparison of electrostatic and aerodynamic forces during parachute opening
[BTN-95-EIX95062487532] p 187 A95-69240

ROBERTS, P. A.
An air-driven pressure booster pump for aircraft-based air sampling
[HTN-95-40689] p 216 A95-69833

ROBERTS, RITA
The real-time analysis and prediction of storms program
p 655 A95-93457

ROBERTS, WILLIAM B.
The effect of adding roughness and thickness to a transonic axial compressor rotor
[NASA-TM-106958] p 645 N95-30524

ROBICHAUD, M.
Large-scale computational fluid dynamics by the finite element method
[BTN-94-EIX94381359154] p 243 A95-71744

ROBINETT, R. D.
Moving mass trim control for aerospace vehicles
[DE95-002602] p 299 N95-23532

ROBINSON, B. A.
Simple numerical criterion for vortex breakdown
[HTN-95-61210] p 541 A95-87583

ROBINSON, LAWSON H.
Aeroelastic simulation of higher harmonic control
[NASA-CR-4623] p 37 N95-11911

ROBINSON, M. C.
Wind turbine blade aerodynamics: The combined experiment
[DE94-011866] p 118 N95-18645
Wind turbine blade aerodynamics: The analysis of field test data
[DE94-011867] p 118 N95-18646
Evidence that aerodynamic effects, including dynamic stall, dictate HAWT structural loads and power generation in highly transient time frames
[DE94-011865] p 216 N95-19855
Techniques for the determination of local dynamic pressure and angle of attack on a horizontal axis wind turbine
[DE95-009204] p 707 N95-32685

ROBINSON, PAUL A.
The detection and measurement of microburst wind shear by an airborne lidar system
p 543 A95-87798

ROBINSON, STEPHEN K.
Separation control on high-lift airfoils via micro-vortex generators
[BTN-95-EIX95152582326] p 265 A95-73529

ROBSON, J.
NTS-spill test facility wind tunnel exhaust plume characterization
[DE95-003630] p 297 N95-24019

ROCHE, NIGEL R.
Automatic riveting cell for commercial aircraft floor grid assembly
[BTN-95-EIX95182617807] p 261 A95-75752
Automatic riveting cell for commercial aircraft floor grid assembly
[HTN-95-92309] p 365 A95-85353

ROCK, STEPHEN M.
Integrated flight/propulsion control for helicopters
[HTN-95-80854] p 290 A95-75096

- ROCKWELL, D.**
Transient structure of vortex breakdown on a delta wing
[BTN-95-EIX95182619073] p 268 A95-75758
- ROCKWELL, DONALD**
Interaction of a streamwise vortex with a thin plate: A source of turbulent buffeting
[BTN-95-EIX95042474398] p 209 A95-68302
- RODCHENKO, V. V.**
General requirements for the electrohydraulic systems of the aircraft controls loading force on the simulators
[CONGRESS PAPER C428-5-138] p 522 A95-91681
- RODDE, A. M.**
OAT15A airfoil data p 111 N95-17857
- RODEN, D. W.**
The application of helicopter mission simulation to Nap-of-the-Earth operations p 710 N95-32496
- RODGERS, C.**
Small turbojets: Designs and installations p 138 N95-16323
- RODGERS, DENNIS**
Forecasting for a large field program: STORM-FEST
[HTN-95-90694] p 215 A95-69721
- RODGERS, MARK D.**
Conversion of the TRACON operations concepts database into a formal sentence outline job task taxonomy
[DOT/FAA/AM-95/16] p 488 N95-28819
- RODRIGUES, EDUARDO ALVES**
Linear and nonlinear discrete-time state-space modeling of dynamic systems for control applications p 567 N95-29251
- RODRIGUEZ, D. L.**
2-D aileron effectiveness study p 110 N95-17851
- RODRIGUEZ, J. M.**
Subsidence of aircraft engine exhaust in the stratosphere: Implications for calculated ozone depletions
[PAPER-93GL03426] p 251 A95-70297
- RODRIGUEZ, JOSE**
Low Reynolds number laminar separation bubble control using a backward facing step
[SAE PAPER 932572] p 467 A95-90061
- RODRIGUEZ, JOSE M.**
Effects on stratospheric ozone from high-speed civil transport: Sensitivity to stratospheric aerosol loading
[HTN-95-91842] p 354 A95-80830
The atmospheric effects of stratospheric aircraft: A fourth program report
[NASA-RP-1359] p 357 N95-24274
- ROE, PHILIP L.**
Beyond the Riemann problem, part 1 p 550 A95-91925
- ROEBROEKS, G. H. J. J.**
Fibre-Metal laminates p 387 A95-85895
- ROGALEWICZ, R. A.**
An example of airborne vibration monitoring improving flight safety in the Soloviev D-30-KU engine
[CONGRESS PAPER C428-21-141] p 508 A95-91728
- ROGERS, C. A.**
Vibrational behavior of adaptive aircraft wing structures modelled as composite thin-walled beams p 423 N95-28435
- ROGERS, C. B.**
Entrainment and acoustic variations in a round jet from introduced streamwise vorticity
[BTN-95-EIX95042474409] p 209 A95-68291
Mixing enhancement by and noise characteristics of streamwise vortices in an air jet
[HTN-95-42322] p 371 A95-86151
- ROGERS, ERNEST O.**
An unmanned air vehicle concept with tipjet drive
[HTN-95-80858] p 283 A95-75100
- ROGERS, GEORGE W.**
Wavelet transformations for helicopter identification via acoustic signatures
[AD-A279980] p 257 N95-20963
- ROGERS, J. P.**
Strategic avionics technology definition studies. Subtask 3-1A3: Electrical Actuation (ELA) Systems Test Facility
[NASA-CR-188360] p 143 N95-18567
- ROGERS, MAX**
T-45A High Angle of Attack Testing: US Naval Test Pilot School 46th Annual Reunion and Symposium
[AD-A284000] p 231 N95-20466
- ROGERS, R. C.**
Investigation of scramjet injection strategies for high mach number flows
[BTN-95-EIX0616952745782] p 614 A95-94504
- ROGERS, STUART E.**
Accuracy enhancements for overset grids using a defect correction approach
[AIAA PAPER 94-0523] p 3 A95-60181
- A comparison of turbulence models in computing multi-element airfoil flows
[AIAA PAPER 94-0291] p 4 A95-60185
Progress in high-lift aerodynamic calculations
[BTN-95-EIX95152582315] p 264 A95-73518
- ROGERS, WILLIAM H.**
A crew-centered flight deck design philosophy for High-Speed Civil Transport (HSCT) aircraft
[NASA-TM-109171] p 335 N95-24582
- ROGLIN, R. L.**
Adaptive airfoils
[ISBN 1-879921-01-4] p 625 A95-93744
- ROHLF, D.**
Parameter identification for X-31A at high angles of attack p 69 N95-14235
- ROHRER, RANDI**
Human factors issues in aircraft cabin design
[SAE PAPER 932527] p 386 A95-84556
- ROHWER, KIM**
Progress in manufacturing large primary aircraft structures using the stitching/RTM process p 537 N95-29050
- ROIIVAINEN, P.**
Orientation determination of aircraft using visual 3D matching and radar. Case study 2
[PB95-165791] p 350 N95-25749
- ROJAS, L.**
Impeller flow field characterization with a laser two-focus velocimeter p 313 N95-23440
- ROJAS, R. G.**
Electromagnetic on-aircraft antenna radiation in the presence of composite plates
[NASA-CR-196126] p 58 N95-12856
- ROKHSAZ, KAMRAN**
Application of artificial neural networks in nonlinear aerodynamics and aircraft design
[SAE PAPER 932533] p 492 A95-89193
A brief survey of wing tip devices for drag reduction
[SAE PAPER 932574] p 467 A95-90063
- ROKNALDIN, FARZAM**
Predicting stall and post-stall behavior of airfoils at low mach numbers
[BTN-95-EIX95262694297] p 365 A95-85468
- ROKUTANDA, ITARU**
Test results on air turbo ramjet engine for a future space plane p 402 A95-82327
- ROLADER, G. E.**
Eglin Air Force Base Ram Accelerator Research Facility p 19 N95-10284
- ROLEK, EVAN P.**
Integrated mission precision attack cockpit technology (IMPACT). Phase 1: Identifying technologies for air-to-ground fighter integration
[AD-A289562] p 389 N95-26684
- ROLLINGS, RAYMOND S.**
Marginal aggregates in flexible pavements: Background survey and experimental plan
[DOT/FAA/CT-94/58] p 53 N95-12216
- ROM, J.**
Hypersonic aerodynamics test facility using the external propulsion accelerator
[AIAA PAPER 95-6138] p 470 A95-90455
- ROMAN, JUAN F.**
Foliage transmission measurements using a ground-based ultrawide band (300-1300 MHz) SAR system
[BTN-94-EIX94381351617] p 252 A95-70950
- ROMANENKO, L. G.**
Selection of optimal parameters for a system, controlling the flight height, when information about the state vector is incomplete
[BTN-94-EIX94461408753] p 168 A95-63636
- ROMEIO, GIULIO**
Nonlinear angle of twist of advanced composite wing boxes under pure torsion
[BTN-95-EIX95152582323] p 281 A95-73526
- ROMERE, PAUL O.**
Documentation and archiving of the Space Shuttle wind tunnel test data base. Volume 1: Background and description
[NASA-TM-104806-VOL-1] p 151 N95-19237
Documentation and archiving of the Space Shuttle wind tunnel test data base. Volume 2: User's Guide to the Archived Data Base
[NASA-TM-104806-VOL-2] p 205 N95-19624
- RONNEY, P. D.**
Stationary premixed flames in spherical and cylindrical geometries
[HTN-95-42336] p 418 A95-86165
- ROOD, RICHARD B.**
Tracer transport for realistic aircraft emission scenarios calculated using a three-dimensional model
[HTN-95-41799] p 353 A95-80525
Three dimensional model calculations of the global dispersion of high speed aircraft exhaust and implications for stratospheric ozone loss p 26 N95-10657
- ROOFF, JOHN**
The Balsa bullet: A high speed, low-cost general aviation aircraft for Aeroworld
[NASA-CR-197165] p 46 N95-12638
- ROOP, J. A.**
Modeling aerosol emissions from the combustion of composite materials p 301 N95-23038
- ROOS, FREDERICK W.**
Low-energy pneumatic control of forebody vortices p 72 N95-14256
- ROSADO, JOEL M.**
Aircraft maneuver envelope warning system
[NASA-CASE-ARC-11953-1] p 82 N95-14518
- ROSE, M. F.**
Hypervelocity Impact Test Facility: A gun for hire
[TABES PAPER 94-605] p 86 N95-14639
- ROSE, M. G.**
Particle deposition in gas turbine blade film cooling holes p 199 N95-19661
- ROSE, WILLIAM C.**
Application of CFD to the analysis and design of high-speed inlets
[NASA-CR-198574] p 438 N95-27240
- ROSELLO, ANTHONY DAVID**
A vehicle health monitoring system for the Space Shuttle Reaction Control System during reentry
[NASA-CR-188370] p 527 N95-29447
- ROSEN, A.**
The influence of alternate inter-blade connections on ground resonance
[HTN-95-80859] p 267 A95-75101
- ROSENBERGER, TODD E.**
Workshop report: Measurement techniques in highly transient, spectrally rich combustion environments
[AD-A288395] p 350 N95-25606
Workshop report: Measurement techniques in highly transient, spectrally rich combustion environments p 629 N95-31208
- ROSENFELD, MOSHE**
Grid refinement test of time-periodic flows over bluff bodies
[BTN-94-EIX94401378822] p 307 A95-76491
- ROSENZWEIG, E. L.**
Navy composite maintenance and repair experience p 424 N95-28446
- ROSFJORD, THOMAS J.**
Evaluation of the transient operation of advanced gas turbine combustors
[BTN-95-EIX0616952745793] p 614 A95-94495
- ROSHKO, ANATOL**
Research on bluff body vortex wakes
[AD-A286319] p 223 N95-20177
- ROSKAM, JAN**
Should large business jets have four under the wing?
[SAE 931256] p 493 A95-89223
An easy way to analyze longitudinal and lateral-directional trim problems with AEO or OEI
p 409 N95-26949
Design, analysis and control of large transports so that control of engine thrust can be used as a back-up of the primary flight controls
[NASA-CR-198958] p 518 N95-30254
- ROSNER, DANIEL E.**
Transport phenomena and interfacial kinetics in multiphase combustion systems
[AD-A289297] p 418 N95-26417
- ROSNES, R.**
Metascientific problems in safety science
[PB95-196408] p 645 N95-30521
- ROSS, BRIAN P.**
Reentry analysis for low Earth orbiting spacecraft p 415 A95-85774
- ROSS, C. F.**
Experimental active control of sound in the ATR 42 p 575 A95-90110
- ROSS, DANIEL C.**
Hybrid finite element-modal analysis of jet engine inlet scattering
[BTN-95-EIX95242673665] p 427 A95-82259
- ROSS, GIL H.**
Weather products for aviation from WAFC Bracknell p 670 A95-93527
- ROSS, H.**
X-31: A program overview and flight test status p 609 N95-32013
- ROSS, HOLLY M.**
Flight validation of ground-based assessment for control power requirements at high angles of attack p 70 N95-14246
Low-speed wind-tunnel investigation of the stability and control characteristics of a series of flying wings with sweep angles of 50 deg
[NASA-TM-4640] p 505 N95-30226
- ROSS, J. C.**
High Alpha Technology Program (HATP) ground test to flight comparisons p 68 N95-14230

- ROSS, J. E.**
Time-domain imaging of airborne targets using ultra-wideband or short-pulse radar [BTN-95-EIX95242673673] p 450 A95-82251
- ROSS, JAMES C.**
Lift-enhancing tabs on multielement airfoils [BTN-95-EIX0619952748187] p 591 A95-94479
Lift enhancing tabs for airfoils [NASA-CASE-ARC-11990-1] p 286 N95-23395
- ROSSI, MICHAEL J.**
Static shape control for adaptive wings [HTN-95-A1767] p 627 A95-93330
- ROSSITTO, K. F.**
The importance of flying qualities design specifications for active control systems p 621 N95-31992
- ROSSMANN, A.**
Damage of high temperature components by dust-laden air p 201 N95-19673
- ROSSOW, VERNON J.**
Effect of ground and ceiling planes on shape of energized wakes [BTN-95-EIX95062487558] p 186 A95-68372
- ROSTAND, P.**
Integration of an hypersonic airbreathing vehicle: Assessment of overall aerodynamic performances and of uncertainties [AIAA PAPER 95-6100] p 492 A95-88007
- ROTH, KARLIN R.**
STOVL CFD model test case p 115 N95-17881
- ROTH, RICHARD**
The potential for CMCs to replace superalloys in engine exhaust ducts [HTN-95-42298] p 418 A95-84992
- ROTHAM, DOMINIQUE**
Low Reynolds number laminar separation bubble control using a backward facing step [SAE PAPER 932572] p 467 A95-90061
- ROTHBERG, S. J.**
Vibration measurements on rotating machinery using laser Doppler velocimetry [BTN-94-EIX95011440597] p 429 A95-82986
- ROTHER, S. L.**
Air traffic operational inventory CY 1994 [AD-A288281] p 382 N95-26454
- ROTHMAYER, A. P.**
Nonlinear stability of unsteady viscous flow [AD-A294931] p 707 N95-34597
- ROTHWELL, E. J.**
Time-domain imaging of airborne targets using ultra-wideband or short-pulse radar [BTN-95-EIX95242673673] p 450 A95-82251
- ROTT, NICHOLAS**
Vortex drift: A historical survey p 455 A95-88897
- ROUCH, K. W.**
Modeling rotating shafts using axisymmetric solid finite elements with matrix reduction [BTN-94-EIX94351143328] p 207 A95-67301
- ROULSTON, J. F.**
The impact of new technology on reliability of avionic equipment [CONGRESS PAPER C428-6-114] p 549 A95-91683
- ROUNDY, L. M.**
ACT/ICAPS: Thermoplastic composite activities p 421 N95-28274
- ROUNTREE, MICHAEL**
Industry review of a crew-centered cockpit design process and toolset [AD-A282966] p 130 N95-17661
- ROUSE, MARSHALL**
Damage tolerance of a geodesically stiffened advanced composite structural concept for aircraft structural applications p 399 N95-28487
- ROUSE, PETER L.**
US Army rotorcraft turboshaft engines sand and dust erosion considerations p 198 N95-19656
- ROUX, F. X.**
Implicit multi-domain method for unsteady compressible inviscid fluid flows around 3D projectiles p 548 A95-91482
- ROVER, RICHARD C., III**
Application of circulation control to advanced subsonic transport aircraft. Part 1: Airfoil development [BTN-95-EIX95062487545] p 185 A95-68359
Application of circulation control to advanced subsonic transport aircraft. Part 2: Transport application [BTN-95-EIX95062487546] p 185 A95-68360
- ROWE, SEAN P.**
A review of falconry as a bird control technique with recommendations for use at the Shuttle Landing Facility, John F. Kennedy Space Center, Florida, USA [NASA-TM-110142] p 381 N95-27859
- ROWE, WILLIAM**
Certification of windshear performance with RTCA class D radomes p 41 N95-13206
- ROWEY, R. J.**
Aerodynamic design and analysis of a highly loaded turbine exhaust p 312 N95-23435
- ROWLAND, F. S.**
Meridional distributions of NO(X), NO(Y), and other species in the lower stratosphere and upper troposphere during AASE 2 [HTN-95-70944] p 352 A95-78009
- ROY, C.**
Validation of an effective flat cruciform-shaped specimen to study CFRP composite laminates under biaxial loading [BTN-95-EIX95152584677] p 282 A95-73589
- ROY, INDRANIL DANDA**
Ducted fan acoustic radiation including the effects of nonuniform mean flow and acoustic treatment [NASA-CR-197449] p 172 N95-16401
- ROYER, RODNEY B.**
Aerospace applications of beta titanium alloys [HTN-95-B0394] p 530 A95-90475
- ROYLANCE, B. J.**
Developments in wear particle analysis using computerised procedures [CONGRESS PAPER C428-15-216] p 457 A95-91713
- ROZINER, TATYANA D.**
Fault detection in multiprocessor systems and array processors [BTN-95-EIX95242679097] p 359 A95-81253
- RUAN, YING-ZHENG**
Analysis of backscattering from wing and fuselage joints [HTN-95-71134] p 430 A95-83495
- RUALT, P.**
Data link terminal DLT document [PB95-110805] p 229 N95-21369
- RUBIN, A. G.**
On the particular features of dynamic processes in solids with varying boundary during interaction with intensive heat flows [BTN-94-EIX94461408756] p 171 A95-63639
- RUBIN, D.**
The panel oxidation and erosion test (POET) facility [AIAA PAPER 95-6151] p 521 A95-90465
- RUBIN, RAFAEL LEVY**
Regenerative cooling for liquid propellant rocket thrust chambers [INPE-5565-TDI/540] p 150 N95-18720
- RUBIN, WILLIAM L.**
Test results of a low cost airport weather radar p 662 A95-93492
- RUBLEIN, GEORGE T.**
Preparation of course materials: Elementary mathematics of powered flight p 324 N95-23320
- RUDD, JAMES L.**
Proceedings of the USAF Structural Integrity Program Conference [AD-A285684] p 194 N95-19517
- RUDMAN, S. D.**
Water vapor continuum absorption in mid-latitudes: Aircraft measurements and model comparisons [HTN-95-40756] p 252 A95-71186
- RUDOLPH, RICHARD H.**
Triton 2 (1B) [NASA-CR-197188] p 46 N95-12636
- RUEGER, M. L.**
Transonic wind tunnel boundary interference correction p 147 N95-19271
- RUETER, AMY**
The Elite: A high speed, low-cost general aviation aircraft for Aeroworld [NASA-CR-197161] p 45 N95-12530
- RUFFY, ALAN E.**
Parallel block implicit integration technique for trajectory parallelism [AD-A288961] p 450 N95-28335
- RUIZ, C.**
Soft body impact on titanium fan blades p 200 N95-19671
- RUMSEY, CHRISTOPHER L.**
Comparison of the predictive capabilities of several turbulence models [BTN-95-EIX0619952748167] p 589 A95-94461
- RUNTZ, KEN J.**
Precise navigation using adaptive FIR filtering and time domain spectral estimation [BTN-95-EIX95142555485] p 227 A95-72888
- RUPP, P. L.**
Dimensional stability of curved panels with coaxed stiffeners and cobanded frames p 532 N95-28836
- RUSAK, Z.**
Novel similarity solutions of the sonic small-disturbance equation with applications to airfoil transonic aerodynamics [BTN-94-EIX94341340316] p 35 A95-60852
- Automated adaptive time-discontinuous finite element method for unsteady compressible airfoil aerodynamics [HTN-95-81637] p 541 A95-87685
- RUSAK, ZVI**
Interaction of a weak shock with freestream disturbances [BTN-95-EIX95332750473] p 638 A95-94687
- RUSHTON, ELLIOTT**
Precision landing system mathematical modeling study report for Andrews Air Force Base, runway 19L, Camp Springs, MD [AD-A289015] p 384 N95-27903
- RUSSELL, A. J.**
Composite repair issues on the CF-18 aircraft p 395 N95-27518
- RUSSELL, PAUL**
Knowledge-based processing for aircraft flight control [NASA-CR-194976] p 99 N95-13727
- RUSSELL, S. G.**
A weight-efficient design strategy for cutouts in composite transport structures p 533 N95-28843
- RUSSO, G. P.**
Adaptive wind tunnel walls versus wall interference correction methods in 2D flows at high blockage ratios p 147 N95-19267
- RUSZCZYK, WILLIAM**
Ultra-Reliable Digital Avionics (URDA) processor p 245 N95-20638
- RUTH, JOHN**
Application of fiber-reinforced bismaleimide materials to aircraft nacelle structures p 397 N95-28278
- RUTHERFORD, PAUL**
Evaluation of bonded boron/epoxy doublers for commercial aircraft aluminum structures p 92 N95-14457
- RUTKOWSKI, MICHAEL J.**
Comprehensive aeromechanics analysis of complex rotorcraft using 2GCHAS [HTN-94-00695] p 2 A95-60174
First level release of 2GCHAS for comprehensive helicopter analysis - a status report [HTN-94-00697] p 2 A95-60176
- RUYTEN, W. M.**
Analysis of planar laser-induced fluorescence images obtained during shakedown testing of the AEDC impulse facility [AD-A293237] p 646 N95-30906
- RUZICKA, GENE C.**
Comprehensive aeromechanics analysis of complex rotorcraft using 2GCHAS [HTN-94-00695] p 2 A95-60174
First level release of 2GCHAS for comprehensive helicopter analysis - a status report [HTN-94-00697] p 2 A95-60176
- RYAN, FIONA**
Safety in airport ground handling p 626 A95-95193
- RYAN, GEORGE W., III**
Functional agility metrics and optimal trajectory analysis [BTN-95-EIX95182619121] p 321 A95-76598
- RYAN, JAMES S.**
High speed civil transport aerodynamic optimization [NASA-CR-196960] p 38 N95-12389
CFD research, parallel computation and aerodynamic optimization [NASA-CR-197748] p 373 N95-26649
- RYBACH, LADISLAUS**
Data processing and mapping in airborne radiometric surveys [HTN-95-51587] p 442 A95-83591
- RYZHOV, A. A.**
On profiling a cam of an axial aviation diesel engine by periodic splines [BTN-94-EIX94461407946] p 82 A95-62264

S

- SABOURIN, M. A.**
Regulatory impact analysis and regulatory support document: Control of air pollution; determination of significance for nonroad sources and emission standards for new nonroad compression-ignition engines at or above 37 kilowatts (50 horsepower)
[PB94-194594] p 61 N95-12855
- SACHER, P. W.**
Hypersonic technology experimental vehicles (The need for flight testing at hypersonic speed)
p 490 A95-87378
- SACHS, G.**
Optimal separation and ascent of lifting upper stages
p 525 A95-87396
A flying qualities study of longitudinal long-term dynamics of hypersonic planes
[AIAA PAPER 95-6150] p 521. A95-90464
- SACHSE, G. W.**
An analysis of aircraft exhaust plumes from accidental encounters
[HTN-95-70943] p 351 A95-78008
Meridional distributions of NO(X), NO(Y), and other species in the lower stratosphere and upper troposphere during AASE 2
[HTN-95-70944] p 352 A95-78009
- SACHTJEN, S.**
The mm-wave resonant methods for the detection of corrosion, phase 1
[AD-A291315] p 556 N95-29941
- SACKS, HOWARD**
Design of a high altitude long endurance aircraft with manufacturing considerations p 391 N95-26947
- SADDOUGHI, SEYED G.**
Experimental investigations of on-demand vortex generators p 250 N95-22451
- SADOVSKII, N.**
Optical surface pressure measurements: Accuracy and application field evaluation p 175 N95-19274
- SAFRONOV, A. V.**
Engineering methods for the evaluation of transonic flutter characteristics for aerodynamic control surfaces
[BTN-94-EIX94461408589] p 141 A95-63064
- SAFRONOV, V. A.**
Engineering methods for the evaluation of transonic flutter characteristics for aerodynamic control surfaces
[BTN-94-EIX94461408589] p 141 A95-63064
- SAGALOVSKY, L.**
Evaluation of neutron techniques for illicit substance detection
[DE95-002988] p 300 N95-22764
- SAGDEO, PRADIP**
Conceptual design of the AE481 Demon Remotely Piloted Vehicle (RPV)
[NASA-CR-197164] p 44 N95-12294
- SAGISAKA, MASAKAZU**
Experimental investigation of static and dynamic ground effect on HOPE ALFLEX vehicle
[NAL-TR-1236] p 388 N95-26525
- SAHIN, AHMET Z.**
Cooling of aerospace plane using liquid hydrogen and methane
[BTN-95-EIX0619952748171] p 590 A95-94465
- SAHU, JUBARAJ**
Numerical computations of supersonic base flow with special emphasis on turbulence modeling
[BTN-94-EIX94441386632] p 179 A95-68181
Numerical computations of supersonic base flow with special emphasis on turbulence modeling
[HTN-95-20949] p 546 A95-88988
Navier-Stokes predictions of missile aerodynamics
p 74 N95-14451
Numerical computations of supersonic base flow with special emphasis on turbulence modeling
[AD-A283688] p 119 N95-18670
- SAITO, KATSUYA**
Experimental study of the aerodynamic characteristics of the counter-rotation propellers p 474 A95-91562
- SAITO, SHIGERU**
Direct analysis of transonic rotor noise with CFD technique p 711 N95-34549
- SAITO, T.**
Development of a pilot tube with multi-hole pyramidal head. 2: A five-hole yew probe of engineering model
p 522 A95-91577
- SAITO, TERUO**
Preliminary assessment of tunnel wall interference in the NDA cryogenic wind tunnel
[BTN-95-EIX95062487531] p 187 A95-69239
- SAITO, TOSHIHITO**
Experiment and analysis on heat transfer of a scramjet leading edge model p 403 A95-82420
Effect of film cooling/regenerative coating on scramjet engine performances
[NAL-TR-1242] p 339 N95-24990
- SAITOH, SATOSHI**
A numerical investigation of flow around a square-section cylinder mounted with a splitter plate
p 639 A95-95401
- SAIYED, NASEEM H.**
Laser doppler velocimeter system for supersonic jet mixer nozzle testing at the NASA Lewis Aeroacoustic Propulsion Lab
[NASA-TM-106984] p 457 N95-30229
- SAKAI, TOSHIHO**
Analysis of an MLS automatic landing control law for the NAL experimental research aircraft DO-228. 2: Curved approach and landing p 508 A95-91588
- SAKAMOTO, H.**
Experiment of rocket-ram annular combustor
p 412 A95-82324
- SAKAMURA, YOSHITAKA**
VSL analysis of hypersonic flows around a reentry vehicle with equilibrium air chemistry p 413 A95-82400
- SAKATA, K.**
Aerodynamic characteristics of supersonic air-intake/aircraft integrated models p 472 A95-91512
- SAKATA, KIMIO.**
Some considerations on system design of the hypersonic transport and supersonic air-intakes p 473 A95-91522
Effects of cavity bleed and its configuration on aerodynamic characteristics of supersonic internal flow
[NAL-TR-1247] p 594 N95-31715
- SAKAUE, TADASHI**
Preliminary assessment of tunnel wall interference in the NDA cryogenic wind tunnel
[BTN-95-EIX95062487531] p 187 A95-69239
- SAKURA, KIYOSHI**
Aerosevostic coupling on the UF-104 aircraft
p 517 A95-91561
- SAKURAI, AKIRA**
A systems for flight data acquisition and analysis for a remotely-piloted research vehicle p 517 A95-91554
- SAKURANAKA, NOBORU**
Experiment and analysis on heat transfer of a scramjet leading edge model p 403 A95-82420
- SALAS, M. D.**
Algorithmic trends in computational fluid dynamics; The Institute for Computer Applications in Science and Engineering (ICASE)/LaRC Workshop, NASA Langley Research Center, Hampton, VA, US, Sep. 15-17, 1991
[ISBN 0-387-94014-6] p 550 A95-91915
Airfoil optimization by the one-shot method
p 128 N95-16569
- SALAWITCH, R. J.**
The distribution of hydrogen, nitrogen, and chlorine radicals in the lower stratosphere: Implications for changes in O3 due to emission of NO(y) from supersonic aircraft
[HTN-95-70935] p 351 A95-78000
- SALIK, M. D.**
High performance backplane components for modular avionics p 247 N95-20653
- SALVO, N. N.**
Investigation of heat transfer in a rotating ring gap with the axial flow of a coolant during the rotation of the central shaft
[BTN-94-EIX94461407951] p 89 A95-62625
Investigation of heat transfer between rotating shafts of transmissions of turbojet engines
[BTN-94-EIX94461408760] p 138 A95-63643
- SALTER, CHARLES A.**
The effects of UH-1 experience on UH-60 simulator performance: A preliminary study
[AD-A289457] p 391 N95-26993
- SALTZMAN, EDWIN J.**
In-flight lift-drag characteristics for a forward-swept wing aircraft and comparisons with contemporary aircraft
[NASA-TP-3414] p 117 N95-18565
- SALTZMAN, ERIC S.**
An intercomparison of aircraft instrumentation for tropospheric measurements of carbonyl sulfide, hydrogen sulfide, and carbon disulfide
[HTN-95-91856] p 355 A95-80844
An intercomparison of instrumentation for tropospheric measurements of dimethyl sulfide: Aircraft results for concentrations at the parts-per-trillion level
[HTN-95-91857] p 355 A95-80845
- SALYER, R. F.**
An investigation of the side-dump dual in-line ramjet combustor p 617 N95-31199
- SAMAD, TARIQ**
Modeling student knowledge with self-organizing feature maps
[BTN-95-EIX95262697073] p 564 A95-86862
- SAMANT, S. S.**
TranAir: A full-potential, solution-adaptive, rectangular grid code for predicting subsonic, transonic, and supersonic flows about arbitrary configurations. User's manual
[NASA-CR-4349] p 377 N95-28230
- TranAir: A full-potential, solution-adaptive, rectangular grid code for predicting subsonic, transonic, and supersonic flows about arbitrary configurations. Theory document
[NASA-CR-4348] p 378 N95-28265
- SAMAREH-ABOLHASSANI, JAMSHID**
A grid generation system for multi-disciplinary design optimization p 567 N95-28763
- SAMAVEDAM, GOPAL**
Evaluation of the fuselage lap joint fatigue and terminating action repair p 166 N95-19477
- SAMIMY, MO**
Effects of expansions on a supersonic boundary layer: Surface pressure measurements
[BTN-95-EIX95142553036] p 263 A95-73462
- SAMMELLS, A. F.**
Electrochemical impedance pattern recognition for detection of hidden chemical corrosion on aircraft components, phase 1
[AD-A291345] p 556 N95-29946
- SAMMELLS, ANTHONY F.**
Electrochemical impedance pattern recognition for detection of hidden chemical corrosion on aircraft components
[AD-A284998] p 241 N95-20481
Electrochemical impedance pattern recognition for detection of hidden chemical corrosion on aircraft components
[AD-A285998] p 241 N95-20716
- SAMS, E. C.**
A laboratory scale supersonic combustive flow system
[DE95-006347] p 420 N95-27851
- SAMUELSEN, G. S.**
Jet mixing in a reacting cylindrical crossflow
[NASA-TM-106975] p 616 N95-30853
- SAMUELSSON, I.**
Low speed propeller slipstream aerodynamic effects
p 116 N95-17882
- SANANDRES, LUIS**
Thermohydrodynamic analysis of cryogenic liquid turbulent flow fluid film bearings, phase 2
[NASA-CR-197412] p 349 N95-24461
- SAND, WAYNE R.**
User involvement in the development of an advanced icing product for use in aviation p 672 A95-93537
- SANDERS, DONALD C.**
Aircraft fires, smoke toxicity, and survival: An overview
[DOT/FAA/AM-95/8] p 277 N95-24024
- SANDERSON, S. R.**
Shock wave interactions in hypervelocity flow
[AD-A286507] p 250 N95-22212
- SANDFORD, MAYNARD C.**
Measurements of unsteady pressure and structural response for an elastic supercritical wing
[NASA-TP-3443] p 104 N95-16560
- SANETRIK, MARK D.**
Block-structured grids for complex aerodynamic configurations: Current status p 551 N95-28736
- SANGHA, K. B.**
Advance finite element modeling of rotor blade aeroelasticity
[HTN-95-31013] p 221 A95-71183
- SANKAR, L. N.**
Effects of leading and trailing edge flaps on the aerodynamics of airfoil/vortex interactions
[HTN-95-31011] p 221 A95-71181
A three-dimensional Navier-Stokes/full-potential coupled analysis for rotor blades
[ISBN 1-879921-01-4] p 587 A95-93748
Numerical study of the effects of icing on viscous flow over wings
[NASA-CR-197102] p 75 N95-14803
- SANKEY, DAVID A.**
An overview of FAA-sponsored aviation weather research and development p 652 A95-93442
- SANTARE, MICHAEL H.**
The effect of material heterogeneity in curved composite beams for use in aircraft structures p 422 N95-28426
- SANTILLAN, S.**
Transonic vortical flow predicted with a structured multiblock Euler solver p 642 A95-95462
- SARAVANAMUTTOO, H. I. H.**
Propulsion education at Carlton University
[SAE PAPER 931391] p 613 A95-93667
- SARH, BRANKO**
Design methodology and infrastructures for flying automobiles
[SAE PAPER 932604] p 495 A95-90074
- SARMA, I. G.**
Switched bias proportional navigation for homing guidance against highly maneuvering targets
[BTN-95-EIX95182619145] p 279 A95-76622
- SARMA, R. A.**
Operational multi-scale environment model with grid adaptivity (OMEGA) application to aviation weather
p 676 A95-93556

SARNO, C.

FASTPACK: Optimized solutions for modular avionics derived from a parametric study. Part 2: Avionics p 233 N95-20635
Lightweight electronic enclosures using composite materials p 241 N95-20656

SAROUGHIAN, ANDY

The FC-1D: The profitable alternative Flying Circus Commercial Aviation Group [NASA-CR-197152] p 46 N95-12628

SASAKI, M.

Experiment of rocket-ram annular combustor p 412 A95-82324

SASOH, AKIHIRO

An experimental study on radiation from strong shock layer p 368 A95-82421

SATMARK, T.

Secondary power system study for the hytex RA3 flight test vehicle [AIAA PAPER 95-6158] p 512 A95-90470

SATO, JUNZO

Optimum aerodynamic design of aircraft fuselage using boundary element method p 473 A95-91514

SATO, K.

Experiment of rocket-ram annular combustor p 412 A95-82324

SATO, MAMORU

Flow visualization studies on sidewall effects in two-dimensional transonic airfoil testing [BTN-95-EIX95152582313] p 264 A95-73516

High subsonic and high Reynolds number wind tunnel tests of two-dimensional natural-laminar-flow airfoils with suction boundary layer control p 472 A95-91508

Numerical and experimental study of drag characteristics of two-dimensional HLFC airfoils in high subsonic, high Reynolds number flow [NAL-TR-1244T] p 331 N95-24998

SATO, MITSUMASA

Determination of flight simulator time delay p 522 A95-91553

SATO, SHIGERU

Evaluation of scramjet nozzle performance p 402 A95-82321

SATO, YOICHI

Research and development of thermal protection system of HOPE re-entry vehicle p 413 A95-82358

SAUCRAY, J. M.

Cycroscopic and propeller aerodynamic effects on engine mounts dynamic loads in turbulence conditions p 132 N95-18599

SAUKKONEN, LEA

Research aircraft observations of a polar low at the east Greenland ice edge [HTN-95-A0175] p 215 A95-69766

SAUNDERS, C. P.

Collaborative research on aircraft icing and charging processes in ice [AD-A285102] p 276 N95-23201

SAUNDERS, J. D.

Parametrics on 2D Navier-Stokes analysis of a Mach 2.68 bifurcated rectangular mixed-compression inlet [NASA-TM-107003] p 617 N95-30861

SAUNDERS, P.

Artificial intelligence with applications for aircraft [DOT/FAA/CT-94/41] p 99 N95-13895

Digital systems validation. Chapter 20 Artificial Intelligence with applications for aircraft. Handbook, volume 2 [AD-A288492] p 448 N95-26638

SAUNDERS, R. W.

Water vapor continuum absorption in mid-latitudes: Aircraft measurements and model comparisons [HTN-95-40756] p 252 A95-71186

SAUNDERS, T.

Development of a composite repair and the associated inspection intervals for the F-111C stiffener runout region p 66 N95-14477

SAVAGE, RICHARD C.

Advanced data visualization and sensor fusion: Conversion of techniques from medical imaging to Earth science p 711 N95-34236

SAWAGUCHI, SEIICHI

A study of supersonic mixing flow field with ramp injector p 706 N95-34512

SAWAZAKI, H.

Development of 70MW class superconducting generators [BTN-94-EIX95011440854] p 429 A95-82905

SAWHNEY, S.

Neuro-controllers for adaptive helicopter training [SAE PAPER 932535] p 379 A95-84557

Neuro-controllers for adaptive helicopter hover training [BTN-94-EIX94522407592] p 709 A95-96241

SAWYER, BRIAN

Heliport/vertiport MLS precision approaches [AD-A283505] p 126 N95-18059

SCALEA, ANN MARIE

Transitioning to the aviation routine weather report (METAR) and the International Aerodrome Forecast (TAF) within the Federal Aviation Administration p 656 A95-93461

Pilot training initiatives for the '90s p 657 A95-93463

SCALLION, W. I.

Performance of an aerodynamic yaw controller mounted on the space shuttle orbiter body flap at Mach 10 [NASA-TM-109179] p 330 N95-24397

SCHAALE, M.

Mapping of forest fire damages using imaging spectroscopy p 442 A95-83627

SCHAB, DANIEL E.

Drag function modeling for air traffic simulation [BTN-95-EIX95182619154] p 279 A95-76631

SCHADLOW, K. C.

A pulsed liquid fuel ramjet p 617 N95-31201

SCHADOW, KLAUS C.

Suppressor of oscillations in airframe cavities [AD-D017265] p 388 N95-26507

SCHAEFER, J.

Empirical corrections of the rigid rotor interaction potential of H₂-H₂ in the attractive region: Dimer features in the FIR absorption spectra [HTN-95-41943] p 361 A95-81690

SCHAEFER, PETER

Design challenges encountered in the F-15 PCA flight test program p 692 N95-33025

SCHAEFFER, J. C.

Effect of annealing and desulfurization on oxide spallation of turbine airfoil material [BTN-95-EIX95282707024] p 528 A95-88264

SCHAEFFLER, A.

Performance deterioration of axial compressors due to blade defects p 199 N95-19665

SCHAEZNER, GUNTHER

Effects of the specific military aspects of satellite navigation on the civil use of GPS/GLONASS p 688 N95-33134

SCHAEFFER, T.

NTS-spill test facility wind tunnel exhaust plume characterization [DE95-003630] p 297 N95-24019

SCHAIERER, EDWARD T.

Adaptive-wall wind-tunnel research at Ames Research Center: A retrospective p 519 A95-88902

SCHANZENBACH, GEORGE P.

Control system design for the MOD-5A 7.3 mW wind turbine generator p 440 N95-27985

SCHARLEMANN, T.

Overview of remote sensing laser development and semiconductor laser technology [DE94-019103] p 256 N95-21552

SCHARPF, D. F.

Experimental investigation of the sources of propeller noise due to the ingestion of turbulence at low speeds [BTN-95-EIX95262697042] p 569 A95-86859

SCHAUFFLER, S. M.

Estimates of total organic and inorganic chlorine in the lower stratosphere from in situ and flask measurements during AASE 2 [HTN-95-A0861] p 317 A95-76265

SCHEFFEY, JOSEPH L.

Analysis of test criteria for specifying foam firefighting agents for aircraft rescue and firefighting [AD-A286381] p 227 N95-22352

SCHEIMAN, DAVID A.

Design of a GaAs/Ge solar array for unmanned aerial vehicles [NASA-TM-106870] p 320 N95-23259

SCHELLENGER, HARVEY G.

X-31 quasi-tailless flight demonstration p 70 N95-14243

SCHEROCK, JEFF

The Balsa bullet: A high speed, low-cost general aviation aircraft for Aeroworld [NASA-CR-197165] p 46 N95-12638

SCHERRER, D.

Injection studies in the French hypersonic technology program [AIAA PAPER 95-6096] p 510 A95-88004

SCHETZ, JOSEPH A.

Model for compressible turbulence in hypersonic wall boundary and high-speed mixing layers [BTN-94-EIX94441386625] p 184 A95-68174

SCHIAVON, G.

MAX-91: Polarimetric SAR results on Montespertoli site p 320 N95-23940

SCHIERMAN, JOHN D.

Cooperative control theory and integrated flight and propulsion control [NASA-CR-197493] p 142 N95-17404

SCHIFF, L. B.

Directional control at high angles of attack using blowing through a chined forebody [BTN-95-EIX0619952748179] p 619 A95-94472

SCHIFF, LEWIS B.

Numerical simulation of incidence and sweep effects on delta wing vortex breakdown [BTN-95-EIX95062487526] p 186 A95-69234

Numerical investigation of high incidence flow over a double-delta wing [BTN-95-EIX0619952748160] p 588 A95-94454

Computational analysis of forebody tangential slot blowing p 71 N95-14253

SCHIFF, MORTON I.

Reducing low frequency noise emissions from a Langley Air Force Base Hush-House p 561 A95-90112

SCHIJVE, J.

Fatigue of aircraft materials and structures p 387 A95-85894

Prediction of fatigue crack growth under flight-simulation loading with the modified CORPUS model p 166 N95-19471

Fatigue life until small cracks in aircraft structures: Durability and damage tolerance p 135 N95-19478

SCHILLING, HARTMUT

Analytical solution and parameter estimation of projectile dynamics [BTN-95-EIX95212645695] p 272 A95-76747

SCHINDLER, R.

External patch repair of CFRP/honeycomb sandwich p 395 N95-27522

SCHKOLNIK, GERARD

Performance seeking control excitation mode p 696 N95-33019

SCHKOLNIK, GERARD S.

Flight assessment of the onboard propulsion system model for the Performance Seeking Control algorithm on an F-15 aircraft [NASA-TM-4705] p 617 N95-31425

Flight test validation of a frequency-based system identification method on an F-15 aircraft [NASA-TM-4704] p 620 N95-31846

SCHLECHTRIEM, S.

Prediction of rotor-blade deformations due to unsteady airloads [AD-A284467] p 81 N95-15821

SCHLECHTRIEM, STEFAN

Prediction of rotor-blade deformations due to unsteady airloads [AD-A286593] p 231 N95-20860

SCHLIETER, PATRICIA

Inadequacy of visual alarms in helicopter air medical transport [HTN-95-01218] p 484 A95-91450

SCHLUNDT, DONALD W.

SUIT: The integration of aircraft subsystems [SAE PAPER 931381] p 604 A95-93657

SCHMIDT, DAVID K.

Aeroelastic vehicle multivariable control synthesis with analytical robustness evaluation [BTN-95-EIX95182619115] p 321 A95-76592

Multivariable stability and robustness of sequentially designed feedback systems [BTN-95-EIX95182619125] p 322 A95-76602

Analytical aeropropulsive/aeroelastic hypersonic-vehicle model with dynamic analysis [BTN-95-EIX95182619138] p 269 A95-76615

Integrated development of the equations of motion for elastic hypersonic flight vehicles [BTN-95-EIX95242670755] p 327 A95-81092

Extended cooperative control synthesis [NASA-TM-4561] p 17 N95-10220

Cooperative control theory and integrated flight and propulsion control [NASA-CR-197493] p 142 N95-17404

SCHMIDT, H.-J.

Development of load spectra for Airbus A330/A340 full scale fatigue tests p 135 N95-19479

SCHMIDT, LOUIS V.

Wind-tunnel tests of an inclined cylinder having helical grooves [BTN-95-EIX95262694306] p 411 A95-85477

SCHMIDT, W.

Parallel computational fluid dynamics '91; Conference Proceedings, Stuttgart, Germany, Jun. 10-12, 1991 [ISBN 0-444-89363-6] p 548 A95-91479

Computational aerodynamics based on the Euler equations [AGARD-AG-325] p 72 N95-14264

SCHMISSEUR, J. D.

Laser velocimetry seed-particle behavior in shear layers at Mach 12 [BTN-95-EIX95212645712] p 272 A95-76764

Fluctuating wall pressures near separation in highly swept turbulent interactions [HTN-95-20823] p 543 A95-88084

- SCHMISSEUR, JOHN D.**
Developments in laser-based diagnostics for wind tunnels in the Aeromechanics Division: 1987-1992 [AD-A283011] p 84 N95-13687
- SCHMITZ, F. H.**
Modification of the Ames 40- by 80-foot wind tunnel for component acoustic testing for the second generation supersonic transport [NASA-TM-108850] p 65 N95-13642
- SCHMUECKER, J.**
Performance deterioration of axial compressors due to blade defects p 199 N95-19665
- SCHMUGGE, THOMAS**
TIMS observations of surface emissivity in HAPEX-Sahel p 709 N95-33799
- SCHNEIDER, G. E.**
Application of a control-volume-based finite-element formulation to the shock tube problem [BTN-95-EIX95182619099] p 295 A95-76584
- SCHNEIDER, GEORGE**
Small crack test program for helicopter materials p 92 N95-14455
- SCHNEIDER, JOHN R.**
Evolutionary Telemetry and Command Processor (TCP) architecture p 86 N95-14162
- SCHNEIDER, M. G.**
Advanced passive cooling for high power electromechanical actuators [SAE PAPER 931397] p 634 A95-93669
- SCHNEIDER, MARK S.**
Design of a vehicle based system to prevent ozone loss [NASA-CR-197199] p 48 N95-12702
- SCHNEIDER, S. P.**
Wake measurements in a strong adverse pressure gradient [NASA-CR-197272] p 224 N95-21031
- SCHNEIDER, STEVEN P.**
Quiet-flow Ludwieg tube for high-speed transition research [BTN-95-EIX95262694309] p 370 A95-85480
Development of quiet-flow supersonic wind tunnels for laminar-turbulent transition research [NASA-CR-197286] p 239 N95-21436
Supersonic quiet-tunnel development for laminar-turbulent transition research [NASA-CR-198040] p 340 N95-24302
- SCHNERR, GUENTER H.**
Drag and lift in nonadiabatic transonic flow [HTN-95-61208] p 540 A95-87581
- SCHOBEIRI, M. T.**
Nonlinear dynamic simulation of single- and multispool core engines, part 1: Computational method [BTN-95-EIX95112524200] p 210 A95-69308
GETRAN: A generic, modularly structured computer code for simulation of dynamic behavior of aero- and power generation gas turbine engines [BTN-94-EIX95011441241] p 431 A95-84198
- SCHODER, W.**
Optimal separation and ascent of lifting upper stages p 525 A95-87396
- SCHOEBERL, M. R.**
Fine-scale, poleward transport of tropical air during AASE 2 [HTN-95-70949] p 352 A95-78014
- SCHOEBERL, MARK R.**
Trajectory modeling of emissions from lower stratospheric aircraft [HTN-95-41219] p 317 A95-75031
- SCHOMER, PAUL D.**
Time-average aircraft noise descriptors: Confusion with no benefit p 559 A95-88474
- SCHONE, J.**
Estimation of aerodynamic derivatives: Euler scheme validation and approximate methods for hypersonic configurations p 460 A95-87385
- SCHRADER, K. H.**
Aircraft stress sequence development: A complex engineering process made simple p 136 N95-19480
- SCHRAMM, M. R.**
Global cost and weight evaluation of fuselage keel design concepts p 501 N95-28840
- SCHRAUF, G.**
On wave-front curvature in linear stability theory [BTN-94-EIX94441385756] p 184 A95-68220
- SCHRECK, SCOTT J.**
Neural network prediction of three-dimensional unsteady separated flowfields [BTN-95-EIX95182619232] p 308 A95-76658
Application of neural networks to unsteady aerodynamic control p 360 N95-25264
- SCHREIER, F.**
Modeling of aircraft exhaust emissions and infrared spectra for remote measurement of nitrogen oxides [HTN-95-51276] p 355 A95-80861
- SCHROEDER, JEFFERY A.**
Evaluation of simulation motion fidelity criteria in the vertical and directional axes [HTN-94-00666] p 18 A95-60156
Identification and simulation evaluation of a combat helicopter in hover [BTN-95-EIX95242670749] p 335 A95-81098
- SCHUETZ, H.**
Influence of the flight trajectory on the exhaust gas composition of a H2-fueled air-breathing ramjet engine p 509 A95-87404
- SCHULTZ, J. L.**
Numerical simulation of the 3D turbulent flow around the combustor dome of an aircraft engine p 640 A95-95423
- SCHULTZ, KLAUS-J.**
Analysis of a higher harmonic control test to reduce blade vortex interaction noise [BTN-95-EIX95152582330] p 265 A95-73532
A higher harmonic control test in the DNW to reduce impulsive BVI noise [HTN-95-61071] p 385 A95-83655
- SCHULTZ, VINCENT P.**
An approach to weather requirements management p 653 A95-93448
- SCHUR, KEITH**
Draft standard for color active matrix liquid crystal displays (AMLCDs) in US Military aircraft. Recommended best practices [AD-A282950] p 49 N95-12591
- SCHUSTER, DAVID M.**
Application of Navier-Stokes aeroelastic methods to improve fighter wing maneuver performance [BTN-95-EIX95182619218] p 284 A95-76644
- SCHUTZ, BOB E.**
Thermal force modeling for global positioning system satellites using the finite element method [BTN-95-EIX95152583270] p 278 A95-73571
- SCHWANTJE, ROBERT**
Earth Observing System (EOS)/Advanced Microwave Sounding Unit-A (AMSU-A) software assurance plan [NASA-CR-196059] p 98 N95-13885
- SCHWARTEN, H.**
Pressure controlled surfaces - a 3D inverse panel method as a design tool p 491 A95-87565
- SCHWARTZ, ALAN W.**
An unmanned air vehicle concept with tipjet drive [HTN-95-80859] p 283 A95-75100
- SCHWARTZ, S.**
Engine structures analysis software: Component Specific Modeling (COSMO) [NASA-CR-195378] p 57 N95-11711
- SCHWARZ, GEORG F.**
Data processing and mapping in airborne radiometric surveys [HTN-95-51587] p 442 A95-83591
- SCHWEICKART, DANIEL**
Partial discharge testing of high voltage wiring harness for airborne displays [AD-A289150] p 401 N95-27003
- SCHWIND, JOSEPH**
Assessment of avionics technology in European aerospace organizations [NASA-CR-189201] p 337 N95-24624
- SCHWING, JAMES L.**
Geometric modeling for computer aided design [NASA-CR-198828] p 679 N95-31982
- SCORER, A. G.**
Automatic vehicle location and airfield ground movement [CONGRESS PAPER C428-7-148] p 488 A95-91689
- SCOTT, A. D., JR.**
Compendium of NASA data base for the Global Tropospheric Experiment's Pacific Exploratory Mission West-A (PEM West-A) [NASA-TM-109177] p 320 N95-23009
- SCOTT, JONES M.**
Wave rotor-enhanced gas turbine engines [NASA-TM-106998] p 615 N95-30517
- SCOTT, MICHAEL A.**
The personal aircraft: Status and issues [NASA-TM-109174] p 223 N95-20688
- SCOTT, PAUL W.**
Advanced subsonic airplane design and economic studies [NASA-CR-195443] p 338 N95-24304
- SCOTT, R. F.**
Scarf joint technique with cocured and precured patches for composite repair p 396 N95-27524
- SCOTT, WILLIAM B.**
SR-71 may launch targets for missile defense tests [HTN-95-91872] p 335 A95-81974
Cuts endanger airborne research [HTN-95-20602] p 443 A95-84783
- SCOTTI, STEPHEN J.**
Structural design using equilibrium programming formulations [NASA-TM-110175] p 645 N95-30682
- SCULLY, JOHN R.**
NASA-UVA light aerospace alloy and structures technology program (LA2ST) [NASA-CR-198041] p 343 N95-24220
- SEACHOLTZ, RICHARD G.**
Fabry-Perot interferometer measurement of static temperature and velocity for ASTOVL model tests [NASA-TM-107014] p 645 N95-30587
- SEAL, DANIEL W.**
Impact of agility requirements on configuration synthesis [NASA-CR-4627] p 44 N95-11952
Fiber Optic Control System integration for advanced aircraft. Electro-optic and sensor fabrication, integration, and environmental testing for flight control systems [NASA-CR-191194] p 162 N95-19236
- SEAMOUNT, PATRICIA**
X-31 high angle of attack control system performance p 70 N95-14244
- SEEGMILLER, H. LEE**
A supercritical airfoil experiment p 111 N95-17858
Low aspect ratio wing experiment p 113 N95-17865
- SEEGMILLER, H. LEE B.**
Angular displacement measuring device [NASA-CASE-ARC-11937-1] p 362 N95-26015
- SEELY, L.**
Theoretical and actual performance of a long duration superpressure balloon made from a biaxially oriented nylon-6 film p 181 A95-66282
- SEELY, LOREN G.**
Recent developments in nylon superpressure balloons p 385 A95-82512
- SEGAL, CORIN**
Effects of the chemical reaction model on calculations of supersonic combustion flows [BTN-95-EIX0616952745802] p 638 A95-94487
- SEGAWA, SHINYA**
Development and flight results of fiber reinforced balloon p 384 A95-82511
- SEGNER, A.**
Effects of periodic spanwise blowing on Delta-wing configuration characteristics [HTN-95-81631] p 461 A95-87679
- SEHANOBIKH, K.**
Failure analysis for polycarbonate transparencies [AD-A292992] p 630 N95-31471
- SEI, VINCENT J.**
A nonintrusive method of quantifying flow visualization data in vortex flow fields [AD-A289802] p 552 N95-28948
- SEIBERT, GEORGE L.**
Laser velocimetry in the supersonic regime: Advancements, limitations, and outlook [SAE PAPER 931365] p 634 A95-93646
Developments in laser-based diagnostics for wind tunnels in the Aeromechanics Division: 1987-1992 [AD-A283011] p 84 N95-13687
- SEIDEL, DAVID A.**
Measurements of unsteady pressure and structural response for an elastic supercritical wing [NASA-TP-3443] p 104 N95-16560
- SEIDER, G.**
Solution of the Navier-Stokes equations on a massively parallel transporter system p 549 A95-91490
- SEINER, J. M.**
Impact of dynamic loads on propulsion integration p 174 N95-19148
- SEINER, JOHN M.**
Mach wave emission from a high-temperature supersonic jet [BTN-95-EIX95152577586] p 264 A95-73496
Mach wave emission from a high-temperature supersonic jet [HTN-95-42571] p 458 A95-87201
- SEITZMAN, J. M.**
Comparison of NO and OH planar fluorescence temperature measurements in scramjet model flowfields [BTN-95-EIX95042474388] p 209 A95-68312
- SEKAR, BALU**
Conceptual studies of high speed combustors for mixing enhancement mechanisms [AIAA PAPER 95-6095] p 510 A95-88003
Numerical study of mixing in a high and low enthalpy supersonic test facility p 7 N95-10467
- SEKHAR, A. S.**
Transient analysis of a cracked rotor passing through critical speed [BTN-94-EIX94401360022] p 306 A95-74702
- SEKIDO, TOSHINORI**
Overview of feasibility study on propulsion concepts for high speed civil transport p 498 A95-91518

- SEKIMOTO, KIYOHIDE**
Fixed transition for shock tube transonic flow
p 472 A95-91509
- SEKINE, H.**
Aerodynamic characteristics of supersonic air-intake/aircraft integrated models p 472 A95-91512
- SEKINE, HIDEO**
Aerodynamic characteristics of the orbital reentry vehicle experimental probe fins in a supersonic flow [NAL-TR-1232] p 342 N95-25664
- SELA, N. M.**
The influence of alternate inter-blade connections on ground resonance [HTN-95-80859] p 267 A95-75101
- SELBERG, BRUCE P.**
Some additional stability and performance characteristics of the scissor/pivot wing configurations [SAE PAPER 931383] p 618 A95-93659
- SELIG, M. S.**
Multipoint inverse design of an infinite cascade of airfoils [HTN-95-81640] p 541 A95-87688
- SELMIN, V.**
Transonic vortical flow predicted with a structured multiblock Euler solver p 642 A95-95462
An unstructured node centered scheme for the simulation of 3-D inviscid flows p 642 A95-95463
- SELOW, JAN**
Conceptual design of the AE481 Demon Remotely Piloted Vehicle (RPV) [NASA-CR-197164] p 44 N95-12294
- SELVES, G.**
External viewing airborne CCTV system [CONGRESS PAPER C428-25-172] p 595 A95-93598
- SEMENOV, A. V.**
Operation of the adaptive-wall wind tunnel of TsAGI, Moscow p 519 A95-88901
- SEMEKOVA, O. K.**
Operation of the adaptive-wall wind tunnel of TsAGI, Moscow p 519 A95-88901
- SEMPLE, C. A.**
Assessment of cost and training effectiveness for a candidate training system using the Comparison-Based Prediction model [SAE PAPER 932598] p 379 A95-84570
- SENAPATI, N.**
Ultrasonic techniques for repair of aircraft structures with bonded composite patches p 136 N95-19486
- SENEMEIER, M.**
The effect of interface properties on nickel base alloy composites [NASA-CR-198363] p 629 N95-30787
- SENSBURG, O.**
Structural aspects of active control technology p 623 N95-32006
- SENSENEY, MICHAEL B.**
Performance characterization of a highly-offset diffuser with and without blowing vortex generator jets [AD-A289334] p 375 N95-26901
- SENYTKO, RICHARD G.**
NASA low-speed axial compressor for fundamental research [NASA-TM-4635] p 296 N95-23192
- SERATI, PAUL M.**
Transmission loss characteristics of aircraft sidewall systems to control cabin interior noise p 28 N95-11261
- SERAUDIE, A.**
Experimental techniques for measuring transonic flow with a three dimensional laser velocimetry system. Application to determining the drag of a fuselage p 163 N95-19258
- SEREGIN, YU. A.**
A new generation of instruments for flying laboratories [BTN-94-EIX94401363947] p 317 A95-75532
- SERFOSS, GARY L.**
Altitude cuing effectiveness of terrain texture characteristics in simulated low-altitude flight [AD-A294369] p 700 N95-34362
- SERGIENKO, A. A.**
Ultimate characteristics of a rocket engine with a turbo-pump supply system [BTN-94-EIX94461408757] p 148 A95-63640
- SETHI, SHASHI**
Pilot Weather Advisor system [BTN-95-EIX95152582314] p 316 A95-73517
- SETO, S. P.**
Nitrogen oxide emissions characteristics of augmented turbofan engines [BTN-94-EIX95011441240] p 403 A95-84197
- SETTLES, G. S.**
Heat-transfer measurements and computations of swept-shock-wave boundary-layer interactions [HTN-95-81634] p 541 A95-87682
- Laser interferometer skin-friction measurements of crossing-shock-wave/turbulent-boundary-layer ns [HTN-95-20834] p 544 A95-88095
- SETTLES, GARY S.**
Supersonic and hypersonic shock/boundary-layer interaction database [BTN-94-EIX94441386604] p 182 A95-67335
- Supersonic and hypersonic shock/boundary-layer interaction database [HTN-95-20930] p 463 A95-88969
- SETZER, T. E.**
Lightning protection technology for small general aviation composite material aircraft [SAE PAPER 931241] p 483 A95-88964
- SEVERANCE, KURT**
Computer-aided light sheet flow visualization using photogrammetry [NASA-TP-3416] p 26 N95-10859
- SEWALL, WILLIAM G.**
Airfoil modification effects on subsonic and transonic pressure distributions and performance for the EA-6B airplane [NASA-TP-3516] p 373 N95-26382
- SEXTON, BOBBY W.**
FAA's Aging Commuter Airplane Program [SAE PAPER 931248] p 483 A95-89220
- SEYWALD, HANS**
Load alleviation maneuvers for a launch vehicle p 342 A95-81360
- SFORZA, P. M.**
Airfoil pressure measurements during oblique shock-wave/vortex interaction in a Mach 3 stream [HTN-95-81641] p 542 A95-87689
- SGARD, FRANCK**
Coupled FEM-BEM approach for mean flow effects on vibro-acoustic behavior of planar structures [BTN-95-EIX95152577587] p 263 A95-73495
- SHABBI, AAMIR**
Industry-Wide Workshop on Computational Turbulence Modeling [NASA-CP-10165] p 439 N95-27882
- SHABIBI, ABDULLAH AL**
Study of an airfoil with a flap and spoiler [BTN-95-EIX95152582327] p 265 A95-73530
- SHAFER, STEVE**
The ADAGE avionics reference architecture [AIAA PAPER 95-1021] p 566 A95-90693
- SHAGAM, RICH**
Emerging nondestructive inspection for aging aircraft [PB95-143053] p 328 N95-25401
- SHAH, BHARAT M.**
Advanced composites structural concepts and materials technologies for primary aircraft structures: Structural response and failure analysis [NASA-CR-4448] p 11 N95-10240
- Advanced composites structural concepts and materials technologies for primary aircraft structures. Structural response and failure analysis: ISPAN modules users manual [NASA-CR-4449] p 12 N95-10242
- Advanced textile applications for primary aircraft structures p 399 N95-28476
- ISPAN (Interactive Stiffened Panel Analysis): A tool for quick concept evaluation and design trade studies p 533 N95-28846
- SHAH, GAUTAM H.**
Actuated forebody strake controls for the F-18 High-Alpha Research Vehicle [BTN-95-EIX0619952748173] p 619 A95-94467
- Preparations for flight research to evaluate actuated forebody strakes on the F-18 high-alpha research vehicle p 72 N95-14257
- SHAKINA, N. P.**
Aviation weather forecasting automated methods in the RAFC Moscow and the Airport Vnukovo p 669 A95-93523
- SHANG, J. S.**
Structure of a double-fin turbulent interaction at high speed [BTN-95-EIX95222650780] p 347 A95-79236
- Assessment of technology for aircraft development [BTN-95-EIX0619952748181] p 606 A95-94474
- SHANKS, R. W.**
Tooling - a source of productivity [CONGRESS PAPER C428-32-017] p 583 A95-93619
- SHANNON, BRAD**
Aviation terminal forecasts based on automated observations (FTAUTO) p 668 A95-93520
- SHANNON, JENIFER M.**
A switched reluctance machine rotor position estimator: A neural network application [SAE PAPER 932560] p 511 A95-90057
- SHAO, XUAN-MINH**
Use of high resolution lightning detection and localization sensors for hazardous aviation weather nowcasting p 661 A95-93486
- SHAPIRO, ALAN R.**
Hot jet/wake turbulent structure and laser propagation. Part 3: Laser propagation measurements and modeling p 647 N95-30992
- SHAPIRO, DIANE C.**
Education, training, and human engineering in aerospace; SAE Aerotech '93, Costa Mesa, CA, Sep. 27-30, 1993 [SAE SP-992] p 417 A95-84553
- SHAPIRO, M. A.**
Research aircraft observations of a polar low at the east Greenland ice edge [HTN-95-A0175] p 215 A95-69766
- SHARMA, NARESH**
Functional requirements of an aerospace Design Representation Programming Interface [AIAA PAPER 95-0967] p 497 A95-90643
- SHARMA, O. P.**
Unsteady flows in turbines: Impact on design procedure p 90 N95-14132
- SHARMA, SURENDRA P.**
Research activity at the shock tube facility at NASA Ames p 547 A95-90559
- Measured and calculated spectral radiation from a blunt body shock layer in an arc-jet wind tunnel [AIAA PAPER 94-0086] p 67 N95-13720
- SHARMAN, ROBERT D.**
Lee waves benign and malignant p 595 A95-93554
- SHARP, BEN H.**
25 years of airport sound insulation programs p 31 N95-11307
- SHARP, P. K.**
Fatigue resistance of peened 7050-T7451 aluminium alloy: Repair and re-treatment of a component surface [BTN-94-EIX94371347838] p 206 A95-69131
- SHARP, PAUL A.**
Development and field test of the Beta version of the USAF Assessment System for Aircraft Noise (ASAN) p 561 A95-90121
- SHARPE, RON**
Expert systems and artificial intelligence applications in engineering design and inspection p 710 N95-33008
- SHARPLESS, GARRETT C.**
Cost model relationships between textile manufacturing processes and design details for transport fuselage elements p 536 N95-29043
- SHATALOV, YU. S.**
On profiling a cam of an axial aviation diesel engine by periodic splines [BTN-94-EIX94461407946] p 82 A95-62264
- SHAW, BEVIL J.**
An artificial corrosion protocol for lap-splices in aircraft skin p 152 N95-19482
- SHAW, J. A.**
SAUNA: A system for grid generation and flow simulation using hybrid structured/unstructured grids p 642 A95-95470
- Validation and evaluation of the advanced aeronautical CFD system SAUNA: A method developer's view [ARA-MEMO-390] p 210 N95-19774
- SHAW, JONATHAN A.**
Application of three-dimensional hybrid structured/unstructured grids to land, sea and air vehicles [ARA-MEMO-399] p 210 N95-19775
- Verification of the CFD simulation system SAUNA for complex aircraft configurations [ARA-MEMO-401] p 211 N95-19776
- Inviscid and viscous flow modelling of complex aircraft configurations using the CFD simulation system sauna [ARA-MEMO-403] p 211 N95-19777
- SHAW, L. L.**
Weapons bay acoustic environment p 173 N95-19146
- SHAW, MICHAEL F.**
A theoretical analysis of airborne sound transfer for a resiliently mounted machine to its foundation p 30 N95-11304
- SHAW, R. H.**
A comparison of some aerodynamic resistance methods using measurements over cotton and grass from the 1991 California ozone deposition experiment [HTN-95-11295] p 319 A95-77000
- SHAW, ROBERT J.**
A full Navier-Stokes analysis of subsonic diffuser of a bifurcated 70/30 supersonic inlet for high speed civil transport application [NASA-TM-106637] p 8 N95-10820
- Validation of the RPLUS3D code for supersonic inlet applications involving three-dimensional shock wave-boundary layer interactions [NASA-TM-106579] p 39 N95-13058

- Numerical simulation of supersonic compression corners and hypersonic inlet flows using the RPLUS2D code [NASA-TM-106580] p 105 N95-16038
The high speed civil transport and NASA's High Speed Research (HSR) program p 390 N95-26945
- SHAW, T. L.**
Simulation of Shuttle launch G forces and acoustic loads using the NASA Ames Research Center 20G centrifuge p 86 N95-14089
- SHAY, LYNN K.**
Orbital velocities induced by surface waves [HTN-95-90902] p 253 A95-72411
- SHEARD, A. G.**
Blade-by-blade tip clearance measurement system for gas turbine applications [BTN-95-EIX95292721167] p 546 A95-89899
- SHEEHY, MICHAEL**
Intelligent finite element submodeling of multichip modules for reliability analysis [AD-A292911] p 679 N95-31455
- SHEEN, D. R.**
Foliage transmission measurements using a ground-based ultrawide band (300-1300 MHz) SAR system [BTN-94-EIX94381351617] p 252 A95-70950
- SHEIKH, M. ASHFAQ**
Crack growth characteristics of integrally machined stringer-skin panels [HTN-95-01095] p 496 A95-90281
- SHEKARRIZ, A.**
Flow structure in the lee of an inclined 6:1 prolate spheroid [BTN-94-EIX95011441127] p 348 A95-81027
- SHELDON, DAVID**
Further investigations of icing effects on an advanced high-lift multi-element airfoil [NASA-TM-106947] p 381 N95-27762
- SHENGXI, SHI**
Plate manipulators [AD-A289601] p 374 N95-26719
- SHEPARD, WILLIAM T.**
Development of an intervention program to encourage shoulder harness use and aircraft retrofit in general aviation aircraft, phases 1 and 2 [DOT/FAA/AM-95/2] p 333 N95-24384
- SHEPARDSON, KENNETH**
Integrating NOISEMAP with the Geographic Resource Analysis Support System (GRASS) to enhance environmental impact assessments and land use compatibility studies p 31 N95-11311
- SHEPHERD, M. S.**
Automated adaptive time-discontinuous finite element method for unsteady compressible airfoil aerodynamics [HTN-95-81637] p 541 A95-87685
- SHEPHERD, K. P.**
Measurement and prediction of broadband noise from large horizontal axis wind turbine generators p 451 N95-27990
- SHEPHERD, WILLIAM T.**
Development of an intervention program to encourage shoulder harness use and aircraft retrofit in general aviation aircraft: Phases 1 and 2 [AD-A290966] p 485 N95-29873
- SHEPLAK, M.**
Characterization of a hot-film probe for hypersonic flow [AIAA PAPER 95-6110] p 511 A95-90440
- SHEPPARD, WILLIAM R.**
Eddy current for detecting second layer cracks under installed fasteners [AD-A282412] p 158 N95-17507
- SHERBAUM, V.**
Fundamentals of catastrophic failure prevention by thrust vectoring [BTN-95-EIX0619952748176] p 606 A95-94470
- SHERRETZ, LYNN**
Developing the Aviation Gridded Forecast System p 671 A95-93532
Developing and testing decision-making products for center weather service unit meteorologists p 671 A95-93533
- SHERWIN, R.**
Advanced wind turbine design studies: Advanced conceptual study [DE93-000031] p 256 N95-20985
- SHERWOOD, BRENT**
Fourth-generation Mars vehicle concepts [BTN-95-EIX95152583267] p 298 A95-73568
- SHERWOOD, TOM**
Preliminary results and research capabilities of a new jet facility at the University of Kansas p 412 N95-26951
- SHEVELEVA, O. V.**
Aviation weather forecasting automated methods in the RAFC Moscow and the Airport Vnukovo p 669 A95-93523
- SHIA, R.-L.**
Subsidence of aircraft engine exhaust in the stratosphere: Implications for calculated ozone depletions [PAPER-93GL03426] p 251 A95-70297
- SHIAO, MICHAEL C.**
Optimization of adaptive intraply hybrid fiber composites with reliability considerations [NASA-TM-106632] p 157 N95-16911
Probabilistic evaluation of fuselage-type composite structures p 398 N95-28444
IPACS (Integrated Probabilistic Assessment of Composite Structures): Code development and applications p 534 N95-28849
A probabilistic design method applied to smart composite structures [NASA-TM-106715] p 651 N95-32206
- SHIBAYAMA, HIDEO**
Prediction level of noise by a helicopter p 571 A95-88469
- SHIEBER, STUART**
Optimizing cockpit display configurations with a genetic algorithm system [AD-A289799] p 508 N95-29123
- SHIELD, B. M.**
Possible guidelines for helicopter noise assessment [HTN-95-92535] p 558 A95-87355
- SHIFLET, GARY J.**
NASA-UVA light aerospace alloy and structures technology program (LA2ST) [NASA-CR-198041] p 343 N95-24220
- SHIFRIN, CAROLE A.**
European firms team on supersonic studies [HTN-95-42215] p 386 A95-84031
- SHIGEMI, MASASHI**
Experimental investigation of static and dynamic ground effect on HOPE ALFLEX vehicle [NAL-TR-1236] p 388 N95-26525
- SHIGIN, L. B.**
Heat transfer in the flow-through part of axial compressors [BTN-94-EIX94461407949] p 89 A95-62267
- SHIH, MING H.**
TIGER: A user-friendly interactive grid generation system for complicated turbomachinery and axis-symmetric configurations p 322 N95-23419
- SHIH, TOM I.-P.**
A procedure for automating CFD simulations of an inlet-bleed problem p 552 N95-28768
- SHIMA, EIJI**
Role of computational fluid dynamics in aeronautical engineering. Number 12: Formulation and verification of uni-particle upwind schemes for the Euler equations p 707 N95-34540
- SHIMAMOTO, A.**
Axial crack propagation and arrest in pressurized fuselage p 94 N95-14479
- SHIMIZU, KUNIHIRO**
Verification of turbine cascade flow with tip clearance p 698 N95-34511
- SHIMOMURA, K.**
Study on the turbine vane and blade for a 1500 C class industrial gas turbine [BTN-94-EIX95011441254] p 431 A95-84211
- SHIMOMURA, YUTAKA**
The concept of high speed commercial transporter structure p 498 A95-91517
- SHIMOVETZ, R. M.**
Weapons bay acoustic environment p 173 N95-19146
- SHIN, JAIWON**
Repeatability of ice shapes in the NASA Lewis icing research tunnel [BTN-95-EIX95062487528] p 204 A95-69236
Further investigations of icing effects on an advanced high-lift multi-element airfoil [NASA-TM-106947] p 381 N95-27762
- SHINAGAWA, M.**
Electro-optic characterization of ultrafast photodetectors using adiabatically compressed soliton pulses [BTN-94-EIX94381359637] p 257 A95-72675
- SHINDELL, D. T.**
An overview of millimeter-wave spectroscopic measurements of chlorine monoxide at Thule, Greenland, February-March, 1992: Vertical profiles, diurnal variation, and longer-term trends [HTN-95-00722] p 444 A95-86292
- SHINDO, S.**
Aerodynamic characteristics of supersonic air-intake/aircraft integrated models p 472 A95-91512
- SHINDO, SIGEMI**
Effects of cavity bleed and its configuration on aerodynamic characteristics of supersonic internal flow [NAL-TR-1247] p 594 N95-31715
- SHINGU, HIROKIMI**
Flight evaluation of DGPS and DGPS-INS navigation systems p 382 A95-82462
- SHINN, JUDY L.**
Radiation safety aspects of commercial high-speed flight transportation [NASA-TP-3524] p 453 N95-26427
- SHINODA, PATRICK M.**
Wall interaction effects for a full-scale helicopter rotor in the NASA Ames 80-by-120-foot wind tunnel p 121 N95-19270
- SHIPLEY, D. E.**
Structural effects of unsteady aerodynamic forces on horizontal-axis wind turbines [DE94-011863] p 157 N95-16939
Wind turbine blade aerodynamics: The combined experiment [DE94-011866] p 118 N95-18645
Wind turbine blade aerodynamics: The analysis of field test data [DE94-011867] p 118 N95-18646
Evidence that aerodynamic effects, including dynamic stall, dictate HAWT structural loads and power generation in highly transient time frames p 216 N95-19855
Techniques for the determination of local dynamic pressure and angle of attack on a horizontal axis wind turbine [DE95-009204] p 707 N95-32685
- SHIPLEY, S. A.**
Comparison of measured and calculated dynamic loads for the Mod-2 2.5 mW wind turbine system p 440 N95-27983
- SHIRAHATTI, UDAY**
Boundary element analysis of the acoustic field inside three-dimensional regular and irregular ducts p 573 A95-90097
- SHIRAI, MASATAKA**
Flight Test Monitoring System using X-window p 500 A95-91574
- SHIRAI, K.**
Aerodynamic characteristics of supersonic air-intake/aircraft integrated models p 472 A95-91512
- SHIRATORU, TOSHIMASA**
Behavior of the Johnson-King turbulence model in axisymmetric supersonic flows [BTN-94-EIX94441386606] p 183 A95-67337
Behavior of the Johnson-King turbulence model in Axisymmetric supersonic flows [HTN-95-20932] p 464 A95-88971
- SHIRES, A.**
A theoretical and experimental investigation of the flow over supersonic leading edge wing/body configurations [DRA-TM-AERO-PROP-41] p 331 N95-25649
- SHIROUZO, MASAO**
A shock tunnel test of a winged hypersonic research vehicle p 474 A95-91538
- SHIROUZO, MASAO**
A concept of a hypersonic flight experiment of a winged vehicle p 414 A95-82477
- SHIVAKUMAR, K. N.**
Minimum-mass design of sandwich aerobrakes for a lunar transfer vehicle [BTN-95-EIX95212645707] p 299 A95-76759
- SHIVAKUMAR, V.**
Development of the NASA/FLAGRO computer program for analysis of airframe structures p 94 N95-14473
- SHIVELY, DAVID G.**
Spiral microstrip antenna with resistance [NASA-CASE-LAR-15088-1] p 91 N95-14139
- SHIVELY, R. JAY**
Emergency medical service (EMS): A unique flight environment p 596 A95-95203
- SHMUL, MENAHEM**
Lavi flight control system: Design requirements, development and flight test results p 621 N95-31994
- SHNITKIN, HAROLD**
Joint stars phased array radar antenna [BTN-95-EIX95042474626] p 209 A95-68280
- SHOKRI, E. H.**
A reuse framework for software fault tolerance [AIAA PAPER 95-1012] p 566 A95-90683
- SHORE, CHARLES P.**
Nonlinear analysis of damaged stiffened fuselage shells subjected to combined loads p 137 N95-19499
- SHORTLAND, H.**
Ablative thermal management structural material on the hypersonic vehicles [AIAA PAPER 95-6133] p 547 A95-90452
- SHORTS, VINCIENT F.**
A mathematical analysis of the Janus combat simulation weather effects models and sensitivity analysis of sky-to-ground brightness ratio on target detection [AD-A289629] p 446 N95-26858

- SHOUCRI, MERIT**
Passive millimeter wave camera for aircraft landing in low visibility conditions
[BTN-95-EIX95292721321] p 609 A95-92513
Passive MMW camera for low visibility landings
p 59 N95-13215
- SHPUND, Z.**
Dynamic investigation of the angular motion of a rotating body-parachute system
[BTN-95-EIX95182619220] p 270 A95-76646
- SHROYER, CYNTHIA A.**
Large amplitude nonlinear response of flat aluminum, and carbon fiber plastic beams and plates
[AD-A282440] p 96 N95-15547
- SHU, C. W.**
High order accuracy computational methods in aerodynamics using parallel architectures
[AD-A294167] p 686 N95-34763
- SHUART, M. J.**
Technology integration box beam failure study
p 552 N95-28847
- SHUART, MARK J.**
Composite fuselage shell structures research at NASA Langley Research Center
p 425 N95-28466
Technology integration box beam failure study
p 441 N95-28468
- SHUCHENG, ZHANG**
Numerical investigation to S-inlet flows (Numerical simulation study of S-inlet flows)
[AD-A289590] p 374 N95-26713
- SHUKLA, J. G.**
Advanced resin systems and 3D textile preforms for low cost composite structures
p 535 N95-29035
- SHUKLA, JAY G.**
Advanced composites structural concepts and materials technologies for primary aircraft structures: Design/manufacturing concept assessment
[NASA-CR-4447] p 12 N95-10316
Advanced textile applications for primary aircraft structures
p 399 N95-28476
- SHUM, C. K.**
Precision orbit determination of altimetric satellites
p 86 N95-14282
- SHUMSKY, V. V.**
Integration of an hypersonic airbreathing vehicle: Assessment of overall aerodynamic performances and of uncertainties
[AIAA PAPER 95-6100] p 492 A95-88007
- SHURTLEFF, G. E.**
A modular system for computational fluid dynamics
p 641 A95-95446
- SHYPRYKEVICH, PETER**
Aircraft advanced materials research and development program plan
[AD-A290542] p 505 N95-29565
- SHYU, RONG-NAN**
High angle-of-attack airfoil performance improvement by internal acoustic excitation
[HTN-95-42347] p 372 A95-86176
- SI, ERJIAN**
The application of Newman crack-closure model to predicting fatigue crack growth
p 167 N95-19483
- SIDDIQI, S.**
Lightning protection technology for small general aviation composite material aircraft
[SAE PAPER 931241] p 483 A95-88964
- SIDDIQI, SHAHID**
COINS: A composites information database system
p 453 N95-28465
- SIEGEL, M. W.**
Development of an Automated Nondestructive Inspection (ANDI) system for commercial aircraft, phase 1
[AD-A283500] p 40 N95-12623
- SIGIMONDI, S.**
MAX-91: Polarimetric SAR results on Montespertoli site
p 320 N95-23940
- SIGNOR, DAVID B.**
Measurements of atmospheric turbulence effects on tail rotor acoustics
[NASA-TM-108843] p 38 N95-12360
- SIH, G. C.**
Evaluation of patch effectiveness in repairing aircraft components
p 394 N95-27513
- SIKKENGA, S. L.**
Allison engine testing CMSX-4 (reg sign) single crystal turbine blades and vanes
[DE95-010308] p 694 N95-32636
- SILCOX, R. J.**
Numerical investigation of sound transmission through double wall cylinders with respect to active noise control
p 577 A95-90134
- SILVA, ALEX**
The FC-1D: The profitable alternative Flying Circus Commercial Aviation Group
[NASA-CR-197152] p 46 N95-12628
- SILVA, K.**
C-130 Advanced Technology Center wing box conceptual design/cost study
p 423 N95-28437
- SILVA, WALTER A.**
Application of transonic small disturbance theory to the active flexible wing model
[BTN-95-EIX95182619210] p 270 A95-76636
- SILVATI, LAURA**
Assessing effects of military aircraft noise on residential property values near airbases
p 31 N95-11310
- SILVERBERG, L.**
Fuel-optimal bank-angle control for lunar-return aerocapture
[BTN-95-EIX95212645706] p 299 A95-76758
- SIM, ALEX G.**
Development and flight test of a deployable precision landing system
[BTN-95-EIX95062487535] p 190 A95-69243
- SIM, MATTIE**
Functional requirements of an aerospace Design Representation Programming Interface
[AIAA PAPER 95-0967] p 497 A95-90643
- SIMEI, FRANK A., JR.**
Development of an experimental facility for analysis of rotordynamic phenomena
[AD-A281897] p 25 N95-11330
- SIMMONDS, J. G.**
Severe edge effects and simple complimentary interior solutions for thin-walled anisotropic and composite structures
[AD-A290645] p 555 N95-29562
- SIMMONS, J. M.**
Shock tunnel measurements of hypervelocity blunted cone drag
[BTN-95-EIX95152577606] p 305 A95-73477
Shock tunnel measurements of hypervelocity blunted cone drag
[HTN-95-42591] p 459 A95-87221
Shock tunnel studies of scramjet phenomena 1993
[NASA-CR-195038] p 350 N95-25394
Balances for the measurement of multiple components of force in flows of a millisecond duration
p 350 N95-25400
- SIMMONS, M. J.**
Detailed study at supersonic speeds of the flow around delta wings
p 112 N95-17861
- SIMMS, D. A.**
Evidence that aerodynamic effects, including dynamic stall, dictate HAWT structural loads and power generation in highly transient time frames
[DE94-011865] p 216 N95-19855
Techniques for the determination of local dynamic pressure and angle of attack on a horizontal axis wind turbine
[DE95-009204] p 707 N95-32685
- SIMON, DAN**
Real-time navigation using the global positioning system
[BTN-95-EIX95172595298] p 279 A95-75714
- SIMON, DANIEL J.**
GPS modeling for designing aerospace vehicle navigation systems
[BTN-95-EIX95302731223] p 600 A95-94044
- SIMON, DONALD L.**
Piloted evaluation of an integrated methodology for propulsion and airframe control design
[AD-A290207] p 51 N95-12763
- SIMON, HORST D.**
Aerodynamic simulation on massively parallel systems
p 549 A95-91487
- SIMON, T. W.**
Effects of free-stream turbulence intensity on a boundary layer recovering from concave curvature effects
[BTN-95-EIX95282710058] p 632 A95-92471
- SIMONEAU, ROBERT J.**
Influence of turbulence parameters, Reynolds number, and body shape on stagnation-region heat transfer
[NASA-TP-3487] p 550 N95-28719
- SIMPSON, D. L.**
Bonded composite repair of thin metallic materials: Variable load amplitude and temperature cycling effects
p 393 N95-27509
- SIMPSON, DAVID L.**
Multiple site fatigue damage in fuselage skin splices: Experimental simulation and theoretical prediction
[BTN-95-EIX95152584676] p 276 A95-73588
- SIMPSON, R. L.**
Time-resolved surface heat flux measurements in the wing/body junction vortex
[BTN-95-EIX95082502716] p 220 A95-71029
- SIMPSON, ROGER L.**
Influence of wing shapes on surface pressure fluctuations at wing-body junctions
[HTN-95-61196] p 491 A95-87569
- SINCELL, MARK WILLIAM**
Induced Compton scattering by relativistic electrons in magnetized astrophysical plasmas
p 563 N95-29885
- SINGER, S. FRED**
Ozone, skin cancer, and the SST
[BTN-95-EIX95041503011] p 213 A95-68314
- SINGH, AMARJIT**
Experimental investigation of hypersonic flow over a wing-body combination
[AIAA PAPER 95-6083] p 460 A95-87412
- SINGH, D. J.**
Numerical study of the performance of swept, curved compression surface scramjet inlets
[BTN-95-EIX95112524198] p 197 A95-69310
- SINGH, KAMAKHYA P.**
Dynamic unstructured method for flows past multiple objects in relative motion
[BTN-95-EIX952626943003] p 435 A95-85474
- SINGH, RIPUDAMAN**
Growth of multiple cracks and their linkup in a fuselage lap joint
[BTN-95-EIX95142553047] p 286 A95-73451
Structural integrity of fuselage panels with multisite damage
[BTN-95-EIX0619952748188] p 637 A95-94250
Residual life and strength estimates of aircraft structural components with MSD/MED
p 136 N95-19485
- SINGH, SAHJENDRA N.**
Direct adaptive and neural control of wing-rock motion of slender delta wings
[BTN-95-EIX95242670748] p 327 A95-81099
- SINGHAL, S. N.**
Ice-impact analysis of blades
p 200 N95-19672
- SINGLETON, J. D.**
Demonstration of an elastically coupled twist control concept for tilt rotor blade application
[BTN-94-EIX94441386633] p 196 A95-68182
Demonstration of an elastically coupled twist control concept for tilt rotor blade application
[HTN-95-20959] p 465 A95-88998
- SINHA, S. C.**
Dynamic behavior of a magnetic bearing supported jet engine rotor with auxiliary bearings
[NASA-CR-197860] p 338 N95-24213
Dynamic behavior of a magnetic bearing supported jet engine rotor with auxiliary bearings
p 703 N95-32691
- SINHA, SUMON K.**
On the differences between the effect of acoustic perturbation and unsteady bleed in controlling flow separation over a cylinder
[SAE PAPER 932573] p 467 A95-90062
Investigating the use of smart acoustically active surfaces for flow separation control in turbomachinery
[AD-A292819] p 648 N95-31443
- SIOURIS, GEORGE M.**
Design of a modern pitch pointing control system
[BTN-95-EIX95302731226] p 618 A95-94045
- SIPAROV, S. V.**
The effect of rotating loads suspended under a helicopter on their amplitude-frequency characteristics
[BTN-94-EIX94461407959] p 78 A95-62633
- SIRAZETDINOV, R. T.**
Mathematical modelling concerning the development of a system of similar installations, taking into account their operational intensity (an aircraft-helicopter fleet taken as an example)
[BTN-94-EIX94461408763] p 103 A95-63646
- SIRBAUGH, J. R.**
Three-dimensional Navier-Stokes analysis and redesign of an imbedded bellmouth nozzle in a turbine cascade inlet section
p 311 N95-23423
- SIRS, R. C.**
The operation of gas turbine engines in hot and sandy conditions: Royal Air Force experiences in the Gulf conflict
p 198 N95-19655
- SIRVIENTE, A. I.**
LDV measurements in separated flow on an elliptic wing mounted at an angle of attack on a wall
[BTN-94-EIX94441380518] p 702 A95-96559
- SITDIKOV, T. R.**
On a program-information system TDsoft
[BTN-94-EIX94461408773] p 175 A95-63656
- SIVANERI, NITHIAM TI**
Bilinear formulation applied to the response and stability of helicopter rotor blade
[BTN-95-EIX95042474400] p 192 A95-68300
Effect of initial conditions on the response of nonlinear dynamical systems with the application to helicopter rotor dynamics
[ISBN 1-879921-01-4] p 605 A95-93731
- SIVASHANKAR, N.**
Design of a controller for a flexible pointing system using H(infinity) synthesis
[AD-A286572] p 256 N95-20828

- SIVO, J. M.**
Influence of injectant Mach number and temperature on supersonic film cooling
[BTN-94-EIX94441386686] p 184 A95-68195
- SJOLANDER, S. A.**
Propulsion education at Carlton University
[SAE PAPER 931391] p 613 A95-93667
- SKAFF, TONY**
Effect of leeward flow dividers on the wing rock of a delta wing
[BTN-95-EIX95152582347] p 282 A95-73549
- SKIDMORE, J.**
Overview of remote sensing laser development and semiconductor laser technology
[DE94-019103] p 256 N95-21552
- SKINNER, K.**
Shock tunnel studies of scramjet phenomena 1993
[NASA-CR-195038] p 350 N95-25394
- SKINNER, K. A.**
Time-of-flight mass spectrometer for impulse facilities
[BTN-95-EIX95142553057] p 262 A95-73441
- SKINNER, ROGER**
Maintenance programs
[HTN-95-92310] p 365 A95-85354
- SKOMOROKHOV, V. I.**
Service and physical properties of liquid-jet fuels
p 151 N95-16256
- SKOOG, RONALD A.**
Control mechanism to prevent correlated message arrivals from degrading signaling no. 7 network performance
[BTN-94-EIX94341342286] p 56 A95-60842
- SLATER, GARY L.**
Atmospheric and wind modeling for ATC
[NASA-CR-196786] p 98 N95-13725
Groundspeed filtering for CTAS
[NASA-CR-197223] p 97 N95-15785
- SLATER, JOHN W.**
An approach for dynamic grids
[NASA-TM-106774] p 76 N95-15853
A combined geometric approach for solving the Navier-Stokes equations on dynamic grids
[NASA-TM-106919] p 332 N95-26075
Surface modeling and grid generation for aeropropulsion CFD
p 551 N95-28732
- SLATON, DAVE**
Field and data analysis studies related to the atmospheric environment
[NASA-CR-196543] p 168 N95-18093
- SLAVEY, JAMES C.**
Computational aerodynamic analysis on the Open Skies aircraft
[SAE PAPER 932514] p 466 A95-89187
Open Skies project computational fluid dynamic analysis
[AD-A285928] p 223 N95-19991
- SLINGERLAND, F. W.**
Spectrogram diagnosis of aircraft disasters
p 124 N95-19167
- SLIWA, LAURE**
Low-level data fusion for landing runways detection
p 689 N95-93136
- SLOAN, M. L.**
Lag model for turbulent boundary layers over rough bleed surfaces
[BTN-94-EIX94441380981] p 208 A95-68165
- SLOOFF, J. W.**
Computational aerodynamics based on the Euler equations
[AGARD-AG-325] p 72 N95-14264
- SMAGIN, V. I.**
Local-optimal control of a flying vehicle, with final state optimized
[BTN-94-EIX94461407957] p 83 A95-62631
- SMALLEY, DAVID J.**
Radar studies of aviation hazards
[AD-A285845] p 226 N95-21831
- SMART, J. D.**
Health and usage monitoring systems: Corrosion surveillance
p 262 N95-23506
- SMART, JOHN R.**
The development of an aircraft icing forecast technique using data from maps
p 675 A95-93549
- SMEETS, G.**
Shock tube investigations of combustion phenomena in supersonic flows
[PB94-175262] p 55 N95-11796
- SMICK, DOUG**
Integrated design and manufacturing for the high speed civil transport
[NASA-CR-197183] p 48 N95-12700
- SMITH, B.**
Applicability of electrically driven accessories for turbohaft engines
[BTN-95-EIX95292721153] p 612 A95-92589
- SMITH, BROOKE**
F/A-18 and F-16 forebody vortex control, static and rotary-balance results
p 72 N95-14254
- SMITH, BROOKE C.**
Development of a multicomponent force and moment balance for water tunnel applications, volume 1
[NASA-CR-4642-VOL-1] p 161 N95-18955
Development of a multicomponent force and moment balance for water tunnel applications, volume 2
[NASA-CR-4642-VOL-2] p 161 N95-18956
- SMITH, C. B.**
Initial evaluation of the Oregon State University planetary boundary layer column model for ITWS applications
[AD-A293775] p 677 N95-31465
- SMITH, C. E.**
Jet mixing and emission characteristics of transverse jets in annular and cylindrical confined crossflow
[NASA-TM-106976] p 616 N95-30698
- SMITH, C. J. E.**
The corrosion and protection of advanced aluminium - lithium airframe alloys
p 302 N95-23497
- SMITH, C. S.**
New computer delivered training systems to support technical crew training programmes
[CONGRESS PAPER C428-5-036] p 522 A95-91678
- SMITH, CHARLES A.**
Evolution of a nose-wheel steering system
[BTN-94-EIX94461047056] p 78 A95-61739
- SMITH, CHARLES D.**
Improvement of the predicted aural detection code ICHIN (I Can Hear It Now)
p 576 A95-90123
- SMITH, CHRISTOPHER**
Proceedings of the FAA Inspection Program Area Review
[AD-A283849] p 77 N95-14350
- SMITH, CLAUDE**
Earth Observing System (EOS)/Advanced Microwave Sounding Unit-A (AMSU-A) software assurance plan
[NASA-CR-196059] p 98 N95-13885
- SMITH, CRAWFORD F.**
Prediction of wind tunnel effects on the installed F/A-18A inlet flow field at high angles-of-attack
[NASA-CR-195429] p 197 N95-19651
Validation of the NPARC code for nozzle afterbody flows at transonic speeds
[NASA-TM-106971] p 592 N95-30704
- SMITH, D.**
NTS-spill test facility wind tunnel exhaust plume characterization
[DE95-003630] p 297 N95-24019
- SMITH, D. A.**
A programmable heater control circuit for spacecraft
[NASA-TM-108459] p 9 N95-11157
- SMITH, D. P.**
Development of an aircraft cabin water spray system
[CONGRESS PAPER C428-25-030] p 595 A95-93599
- SMITH, DON**
A computational environment for exhaust nozzle design
[AIAA PAPER 95-1016] p 566 A95-90688
- SMITH, E. A.**
Behavior of an inversion-based precipitation retrieval algorithm with high-resolution AMPR measurements including a low-frequency 10.7-GHz channel
[HTN-95-70134] p 252 A95-70656
- SMITH, EDMUND H.**
Aerodynamic characteristics of a canard-controlled missile at high angles of attack
[BTN-95-EIX95152583257] p 267 A95-73558
- SMITH, EDWARD C.**
Air and ground resonance of helicopters with elastically tailored composite rotor blades
[HTN-95-A0497] p 222 A95-72568
- SMITH, ERIC A.**
High-resolution imaging of rain systems with the advanced microwave precipitation radiometer
[HTN-95-70133] p 252 A95-70655
- SMITH, G. E.**
Numerical simulation of supersonic flow using a new analytical bleed boundary condition
[NASA-CR-198368] p 697 N95-33208
- SMITH, G. H.**
Preliminary results from a particle image velocimetry study of blade-vortex interaction
[HTN-95-01098] p 547 A95-90284
- SMITH, GLEN**
Integrated Thermal Energy Management (I-TEM): An evaluation tool for aircraft
[SAE PAPER 932777] p 493 A95-90065
- SMITH, GREGORY E.**
On supersonic-inlet boundary-layer bleed flow
[NASA-CR-195426] p 202 N95-19769
- SMITH, HOOVER A.**
Lubricant evaluation and performance, 2
[AD-A279144] p 242 N95-21969
- SMITH, I. STEVE, JR.**
Overview of the NASA balloon R&D program
p 181 A95-66297
- SMITH, J.**
Design and structural validation of CF116 upper wing skin boron doubler
p 393 N95-27510
- SMITH, J. R.**
A hybrid vehicle evaluation code and its application to vehicle design. Revision 1
[DE95-008053] p 441 N95-28029
A hybrid vehicle evaluation code and its application to vehicle design, revision 2
[DE95-008060] p 441 N95-28139
- SMITH, L. A.**
Bicarbonate of soda blasting technology for aircraft wheel deapainting
[PB94-193323] p 104 N95-17466
- SMITH, LINDA G.**
Laser velocimetry in the supersonic regime: Advancements, limitations, and outlook
[SAE PAPER 931365] p 634 A95-93646
Developments in laser-based diagnostics for wind tunnels in the Aeromechanics Division: 1987-1992
[AD-A283011] p 84-N95-13687
- SMITH, MARILYN J.**
Application of circulation control to advanced subsonic transport aircraft. Part 1: Airfoil development
[BTN-95-EIX95062487545] p 185 A95-68359
Application of circulation control to advanced subsonic transport aircraft. Part 2: Transport application
[BTN-95-EIX95062487546] p 185 A95-68360
- SMITH, MARILYN JONES**
A fourth order Euler/Navier-Stokes prediction method for the aerodynamics and aeroelasticity of hovering rotor blades
p 554 N95-29242
- SMITH, MERRITT H.**
Numerical simulation of powered-lift flows
[HTN-94-00700] p 3 A95-60179
Numerical simulation of a complete STOVL aircraft in ground effect
[AIAA PAPER 93-4880] p 4 A95-60187
- SMITH, O. E.**
Ascent wind model for launch vehicle design
[BTN-95-EIX95041503799] p 239 A95-70124
- SMITH, P. J.**
Design, analysis, and fabrication of a pressure box test fixture for tension damage tolerance testing of curved fuselage panels
p 533 N95-28839
Global cost and weight evaluation of fuselage keel design concepts
p 501 N95-28840
- SMITH, PAUL**
NASA High Performance Computing and Communications program
[NASA-TM-4653] p 176 N95-18573
- SMITH, PETER J.**
Advanced composite fuselage technology
p 535 N95-29034
- SMITH, R. A.**
A pulsed liquid fuel ramjet
p 617 N95-31201
- SMITH, R. D.**
Aircraft corrosion study
[AD-A279527] p 241 N95-21687
- SMITH, R. E.**
PIO: A historical perspective
p 597 N95-31062
- SMITH, R. L.**
Risk analysis for the fire safety of airline passengers
[PB94-194065] p 77 N95-14179
- SMITH, R. MARSHALL**
Transport delays associated with NASA Langley Flight Simulation Facility
[NASA-TM-110150] p 568 N95-29454
- SMITH, RALPH H.**
Observations on PIO
p 597 N95-31064
- SMITH, ROBERT A.**
Suppressor of oscillations in airframe cavities
[AD-DO17265] p 388 N95-26507
- SMITH, ROBERT D.**
FAA vertical flight bibliography
[DOT/FAA/RD-94/17] p 14 N95-11684
- SMITH, ROBERT E.**
Rapid Airplane Parametric Input Design (RAPID)
p 501 N95-28730
- SMITH, ROGERS E.**
Evaluation of F-18A approach and landing flying qualities using an in-flight simulator
[CALSPAN-6241-F-1] p 12 N95-10442
- SMITH, RONALD L.**
The effects of UH-1 experience on UH-60 simulator performance: A preliminary study
[AD-A289457] p 391 N95-26993
- SMITH, S. H.**
Ultrasonic techniques for repair of aircraft structures with bonded composite patches
p 136 N95-19486
- SMITH, V. K.**
Hypersonic flight testing
[AD-A283981] p 134 N95-18891

- SMITH, W.**
X-29 high AOA flight test results: An overview
[SAE PAPER 931367] p 586 A95-93648
- SMOLARKIEWICZ, PIOTR K.**
Amplification and breaking of atmospheric gravity waves p 675 A95-93552
- SNEEDON, MATTHEW D.**
Plaster damage experiments at the BBN Sonic Boom Test Facility p 529 A95-90120
Environmental noise research using the Human Response Monitor (HRM). Phase 1: System development p 562 A95-90122
- SNEL, H.**
Sectional prediction of 3D effects for separated flow on rotating blades
[PB94-201696] p 117 N95-18503
- SNYDER, M. H.**
Comparative wind tunnel tests of NACA 23024 airfoils with several aileron and spoiler configurations p 376 N95-27976
- SOBANIK, JOHN BERTRAM**
The fluid mechanics of a high aspect ratio slot with an impressed pressure gradient and secondary injection p 557 N95-30304
- SOBER, JANET S.**
Grid generation and surface modeling for CFD p 551 N95-28726
- SOBIECZKY, H.**
DLR-F5: Test wing for CFD and applied aerodynamics p 113 N95-17864
- SOBIESKI, JAROSLAW**
An efficiency study of the simultaneous analysis and design of structures
[NASA-TM-110168] p 501 N95-28820
- SOBOLESKI, CRAIG**
Design and construction of a remote piloted flying wing
[NASA-CR-197195] p 47 N95-12695
- SODERMAN, P. T.**
Optimum full-scale subsonic wind tunnel
[AIAA PAPER 86-0732] p 18 A95-60161
An experimental investigation of wing tip turbulence with applications to aerosound
[AIAA PAPER 86-1918] p 1 A95-60164
Modification of the Ames 40- by 80-foot wind tunnel for component acoustic testing for the second generation supersonic transport
[NASA-TM-108850] p 65 N95-13642
- SODERMAN, PAUL T.**
Aeroacoustic probe design for microphone to reduce flow-induced self-noise
[AIAA PAPER 93-4343] p 19 A95-60163
Oblique incidence sound absorption of porous materials covered by perforated metal and exposed to tangential airflow
[HTN-94-00681] p 19 A95-60165
On the scaling of small-scale jet noise to large scale
[AIAA PAPER 92-02109] p 27 A95-60166
- SODERQUIST, JOE**
Aircraft advanced materials research and development program plan
[AD-A290542] p 505 N95-29565
- SODERQUIST, JOSEPH R.**
Ninth DOD/NASA/FAA Conference on Fibrous Composites in Structural Design, volume 3
[NASA-CR-198718] p 420 N95-28266
Ninth DOD/NASA/FAA Conference on Fibrous Composites in Structural Design, volume 1
[NASA-CR-198723] p 421 N95-28420
Ninth DOD/NASA/FAA Conference on Fibrous Composites in Structural Design, volume 2
[NASA-CR-198722] p 424 N95-28462
- SOECHTING, F. O.**
A design perspective on thermal barrier coatings p 344 N95-26120
- SOEDER, RONALD H.**
NASA Lewis Propulsion Systems Laboratory test article systems criteria
[NASA-TM-106589] p 20 N95-10446
NASA Lewis Propulsion Systems Laboratory customer guide manual
[NASA-TM-106569] p 21 N95-10822
- SOPFRIN, T. G.**
Method for extracting forward acoustic wave components from rotating microphone measurements in the inlets of turbofan engines
[NASA-CR-195457] p 616 N95-30779
- SOGA, KUNIO**
Experimental study of shock/shock interference heating on a swept cylinder p 472 A95-91510
- SOLARZ, R.**
Overview of remote sensing laser development and semiconductor laser technology
[DE94-019103] p 256 N95-21552
- SOLIES, U. P.**
Offset thrust axes and pitch stability
[BTN-95-EIX95062487553] p 203 A95-68367
- SOLIES, U. PETER**
Handling qualities of the High Speed Civil Transport p 294 N95-23325
- SOLKA, JEFFREY L.**
Wavelet transformations for helicopter identification via acoustic signatures
[AD-A279980] p 257 N95-20963
- SOLLO, A.**
Experimental active control of sound in the ATR 42 p 575 A95-90110
- SOLOMON, S.**
Estimates of total organic and inorganic chlorine in the lower stratosphere from in situ and flask measurements during AASE 2
[HTN-95-A0861] p 317 A95-76265
- SOMERS, D. M.**
NREL airfoil families for HAWTs
[DE95-000267] p 357 N95-24882
Wind-tunnel test of the S814 thick root airfoil
[DE95-000268] p 376 N95-27541
- SOMMERFELDT, SCOTT D.**
Active minimization of energy density in three-dimensional enclosures
[NASA-CR-197213] p 172 N95-16848
- SOMMERHAEUSER, J.**
Chemically reacting non-equilibrium boundary layers in air breathing propulsion systems
[AIAA PAPER 95-6139] p 512 A95-90456
- SONDAK, DOUGLAS L.**
Application of wall functions to generalized nonorthogonal curvilinear coordinate systems
[BTN-95-EIX95182619077] p 307 A95-75762
- SONG, O.**
Vibrational behavior of adaptive aircraft wing structures modelled as composite thin-walled beams p 423 N95-28435
- SONI, BHARAT K.**
Grid generation: Algebraic and partial differential equations techniques revisited p 643 A95-95477
TIGER: A user-friendly interactive grid generation system for complicated turbomachinery and axis-symmetric configurations p 322 N95-23419
- SORENSEN, H. BARBARA**
Intelligent tutoring system: F-16 flight simulation p 521 A95-90649
- SORENSEN, JOHN A.**
ACSINT inner loop flight control design study
[NASA-CR-196316] p 17 N95-11223
- SORNEK, RAFAL**
A tool for airframe shaping - idea and application
[SAE PAPER 931224] p 491 A95-87568
- SOTOMAYOR, JORGE**
The 1994 Fiber Optic Sensors for Aerospace Technology (FOSAT) Workshop
[NASA-CP-10166] p 337 N95-24207
- SOTOZAKI, T.**
Aeroelastic tailoring research
[PB94-180031] p 6 N95-10135
- SOTOZAKI, TOKUO**
Fundamental wind tunnel experiments on low-speed flutter of a tip-fin configuration wing
[NAL-TR-1228] p 332 N95-25762
- SOUBRIER, A.**
French contribution to new balloon designs and materials p 181 A95-66277
Balloon flights in France and in Europe p 204 A95-66301
- SOUCHET, MICHEL**
Scramjet combustor design in France
[AIAA PAPER 95-6094] p 510 A95-88002
- SOUSA, MIKE**
Brush seals for turbine engine fuel conservation p 59 N95-13595
- SOUTHERLAND, L. D.**
The acoustic characteristics of turbomachinery cavities
[NASA-CR-4671] p 476 N95-28720
- SPADAFORA, STEPHEN J.**
Organic coating technology for the protection of aircraft against corrosion p 303 N95-23513
A comparison of coating alternatives for US Coast Guard aircraft
[AD-A293270] p 629 N95-31124
- SPAUD, F. W.**
The crucial role of wall interference, support interference and flow field measurements in the development of advanced aircraft configurations p 162 N95-19252
- SPAUD, FRANK W.**
Experimental results for a hypersonic nozzle/afterbody flow field
[NASA-TM-4638] p 274 N95-23250
- SPARACO, PIERRE**
European firms team on supersonic studies
[HTN-95-42215] p 386 A95-84031
- SPARKS, ANDREW G.**
Robust longitudinal axis flight control for an aircraft with thrust vectoring
[BTN-95-EIX95122538875] p 408 A95-83000
- SPARKS, R. J.**
Assessment of cost and training effectiveness for a candidate training system using the Comparison-Based Prediction model
[SAE PAPER 932598] p 379 A95-84570
- SPARKS, W. A.**
Aircraft stress sequence development: A complex engineering process made simple p 136 N95-19480
- SPARLING, LYNN C.**
Trajectory modeling of emissions from lower stratospheric aircraft
[HTN-95-41219] p 317 A95-75031
- SPARROW, VICTOR W.**
A total variation diminishing finite difference algorithm for sonic boom propagation models p 575 A95-90105
The effect of aircraft speed on the penetration of sonic boom noise into a flat ocean p 100 N95-14887
- SPEAKMAN, J. D.**
Modeling lateral attenuation of aircraft flight noise p 570 A95-88464
A prediction model for noise from low-altitude military aircraft p 571 A95-88466
- SPEARMAN, M. LEROY**
A review of 50 years of aerodynamic research with NACA/NASA
[NASA-TM-109163] p 102 N95-13663
- SPEKREIJSE, S. P.**
Surface grid generation for multi-block structured grids p 643 A95-95478
- SPENCE, ANNE MARIE**
Efficient sensitivity analysis for rotary-wing aeromechanical problems
[BTN-95-EIX95152577585] p 264 A95-73497
Efficient sensitivity analysis for rotary-wing aeromechanical problems
[HTN-95-42570] p 458 A95-87200
- SPENCER, JOHN H.**
1994 NASA-HU American Society for Engineering Education (ASEE) Summer Faculty Fellowship Program
[NASA-CR-194972] p 325 N95-23276
- SPENCER, R. W.**
Behavior of an inversion-based precipitation retrieval algorithm with high-resolution AMPR measurements including a low-frequency 10.7-GHz channel
[HTN-95-70134] p 252 A95-70656
- SPENCER, ROY W.**
High-resolution imaging of rain systems with the advanced microwave precipitation radiometer
[HTN-95-70133] p 252 A95-70655
- SPERA, DAVID A.**
Collected papers on wind turbine technology
[NASA-CR-195432] p 447 N95-27970
- SPICER, C. W.**
Chemical composition and photochemical reactivity of exhaust from aircraft turbine engines
[HTN-95-51277] p 356 A95-80862
- SPILLMAN, J. J.**
Variable camber geometry for transport aircraft wings
[CONGRESS PAPER C428-35-061] p 603 A95-93626
- SPILMAN, DARIN R.**
Jet transport response to a horizontal wind vortex
[BTN-95-EIX0619952748163] p 619 A95-94457
- SPINA, E.**
Research and educational initiatives at the Syracuse University Center for Hypersonics
[AIAA PAPER 95-6107] p 520 A95-90439
Characterization of a hot-film probe for hypersonic flow
[AIAA PAPER 95-6110] p 511 A95-90440
- SPINA, ERIC F.**
The noise reduction potential of dual-stream coaxial rectangular impromperly expanded jet flows
[NASA-CR-197820] p 437 N95-26995
- SPIVEY, KATHY H.**
Quantity-distance requirements for earth-bermed aircraft shelters
[AD-A279692] p 341 N95-24424
- SPLETTSTOESSER, W. R.**
Experimental results of the European HELINOISE aeroacoustic rotor test
[HTN-95-01080] p 578 A95-90266
- SPLETTSTOESSER, WOLF R.**
Analysis of a higher harmonic control test to reduce blade vortex interaction noise
[BTN-95-EIX95152582330] p 265 A95-73532
A higher harmonic control test in the DNW to reduce impulsive BVI noise
[HTN-95-61071] p 385 A95-83655

- SPRING, D. J.**
Development of an aircraft cabin water spray system
[CONGRESS PAPER C428-25-030] p 595 A95-93599
- SPRINGER, A. M.**
Transonic aerodynamic characteristics of a proposed wing-body reusable launch vehicle concept
[NASA-TM-108489] p 592 N95-30712
- SPRINGER, ANTHONY M.**
A shadowgraph study of the National Launch System's 1 1/2 stage vehicle configuration and Heavy Lift Launch Vehicle configuration
[NASA-RP-1347] p 35 N95-11710
- SPRINGER, GEORGE S.**
Compressive strength of damaged and repaired composite plates p 442 N95-28484
- SPRINKLE, CHARLES H.**
Aviation and the environment p 657 A95-93464
- SQUARER, DAVID**
Transport phenomena in stratified multi-fluid flow in the presence and absence of gravity p 95 N95-14563
- SQUIER, STEVE**
Integrated Thermal Energy Management (I-TEM): An evaluation tool for aircraft
[SAE PAPER 932577] p 493 A95-90065
- SQUIRE, DWIGHT V.**
Machinability study of Aermet 100
[DE95-011532] p 701 N95-33408
- SQUIRE, L. C.**
Measurement of drag using a momentum balance
[HTN-95-01090] p 468 A95-90276
Three-dimensional interaction of wake/boundary-layer and vortex/boundary-layer data report
[CJED/A-AEREO/TR-23] p 329 N95-24210
- SRICHANDER, R.**
Aircraft controller synthesis by solving a nonconvex optimization problem
[BTN-95-EIX95282706672] p 515 A95-89636
- SRIDHAR, J. K.**
Identification of dynamic systems. Volume 3: Applications to aircraft. Part 2: Nonlinear analysis and manoeuvre design
[AGARD-AG-300-VOL-3-PT-2] p 79 N95-14102
- SRIDHAR, S.**
Liquid flow-through cooling of electronic modules p 246 N95-20647
Design of a real-time wind turbine simulator using a custom parallel architecture p 449 N95-27979
- SRINATHKUMAR, S.**
Flutter suppression for the active flexible wing: A classical design
[BTN-95-EIX95182619216] p 292 A95-76642
- SRINIVASA, C.**
Solution of full potential equation on an airfoil by multigrad technique
[NAL-TM-CSS-9303] p 119 N95-18904
- SRINIVASAN, G. R.**
Navier-Stokes simulation of rotor-body flowfield in hover using overset grids
[PAPER C15] p 1 A95-60160
Recent advances in Euler and Navier-Stokes methods for calculating helicopter rotor aerodynamics and acoustics
[HTN-94-00686] p 2 A95-60169
Dynamic stall of an oscillating wing. Part 1: Evaluation of turbulence models
[AIAA PAPER 93-3403] p 3 A95-60184
- SRINIVASAN, RAMAKRISHNA**
Flutter of an infinitely long panel in a duct
[BTN-95-EIX95182619087] p 291 A95-75772
- SRIVAS, MANDAYAM, K.**
Formal verification of an avionics microprocessor
[NASA-CR-4682] p 710 N95-33396
- SRIVASTAVA, ASHOK**
Panel methods p 165 N95-19448
- SRIVATSAN, RAGHAVACHARI**
Flight test of takeoff performance monitoring system
[NASA-TP-3403] p 51 N95-12664
Airplane takeoff and landing performance monitoring system
[NASA-CASE-LAR-14745-2-SB] p 85 N95-14415
- STACY, KATHRYN**
Computer-aided light sheet flow visualization using photogrammetry
[NASA-TP-3416] p 26 N95-10859
- STAHL, W. H.**
Suppression of vortex asymmetry and side force on a circular cone
[BTN-95-EIX95042474413] p 209 A95-68287
- STALKER, R. J.**
Time-of-flight mass spectrometer for impulse facilities
[BTN-95-EIX95142553057] p 262 A95-73441
Scramjet thrust measurement in a shock tunnel
[HTN-95-C0008] p 586 A95-93396
Shock tunnel studies of scramjet phenomena 1993
[NASA-CR-195038] p 350 N95-25394
- Thrust measurements of a complete axisymmetric scramjet in an impulse facility p 339 N95-25395
Scramjet thrust measurement in a shock tunnel p 339 N95-25396
- STALLINGS, ROBERT L, JR.**
Effect of passive venting on static pressure distributions in cavities at subsonic and transonic speeds
[NASA-TM-4549] p 6 N95-10029
Measurements of store forces and moments and cavity pressures for a generic store in and near a box cavity at subsonic and transonic speeds
[NASA-TM-4611] p 378 N95-28241
- STAMATIS, A.**
Adaptive modeling of jet engine performance with application to condition monitoring
[BTN-95-EIX95112524205] p 196 A95-69303
- STANEWSKY, E.**
Data from the GARTeur (AD) Action Group 02 airfoil CAST 7/DOA1 experiments p 111 N95-17856
- STANNILAND, D.**
Investigation of the flow development on a highly swept canard/wing research model with segmented leading- and trailing-edge flaps p 114 N95-17876
Investigation into the aerodynamic characteristics of a combat aircraft research model fitted with a forward swept wing p 116 N95-17884
Investigation of the influence of pylons and stores on the wing lower surface flow p 116 N95-17885
- STANNILAND, D. R.**
An investigation of drag repeatability in half model testing in the ARA Transonic Wind Tunnel
[ARA-MEMO-392] p 188 N95-19546
- STANNILAND, DENNIS R.**
The aerodynamic design of an integrated wing lower surface and pylons for reduced drag
[ARA-MEMO-406] p 194 N95-19789
Investigation of a thermal buoyancy effect on the drag of half models tested in the ARA Transonic Wind Tunnel
[ARA-MEMO-407] p 222 N95-19946
- STAPLE, A. E.**
Theory and evaluation of active control as a means of reducing helicopter vibration
[CONGRESS PAPER C428-19-124] p 517 A95-91721
- STARK, MARY**
The use of genetic algorithms for flight test and evaluation of artificial intelligence and complex software systems
[AD-A284824] p 217 N95-19688
- STARKE, MIKE**
Impact of Ada and object-oriented design in the flight dynamics division at Goddard Space Flight Center
[NASA-CR-189412] p 567 N95-28807
- STARKE, E. A., JR.**
NASA-UVA light aerospace alloy and structures technology program supplement: Aluminum-based materials for high speed aircraft
[NASA-CR-4645] p 343 N95-24878
- STARKE, EDGAR A., JR.**
NASA-UVA light aerospace alloy and structures technology program (LA2ST)
[NASA-CR-198041] p 343 N95-24220
- STARINES, JAMES H., JR.**
Nonlinear analysis of damaged stiffened fuselage shells subjected to combined loads p 137 N95-19499
Composite fuselage shell structures research at NASA Langley Research Center p 425 N95-28466
- STAROSELSKY, ILYA**
Numerical studies of turbulent free surface flows and unsteady propeller flows
[AD-A294377] p 706 N95-34343
- STARR, T. L.**
Scale-up and modeling of forced chemical vapor infiltration
[DE94-017769] p 247 N95-20781
- STAUDMEISTER, DOUGLAS**
The Elite: A high speed, low-cost general aviation aircraft for Aeroworld
[NASA-CR-197161] p 45 N95-12530
- STAUFENBIEL, R.**
Design optimization of an airbreathing aerospaceplane p 524 A95-87382
- STAVINOH, LEO L.**
Mechanism of deposit formation on fuel-wetted hot metal surfaces
[AD-A289847] p 426 N95-28621
- STECK, J. E.**
An exploratory application of neural networks for airfoil design p 448 N95-26943
- STECK, JAMES E.**
Application of artificial neural networks in nonlinear aerodynamics and aircraft design
[SAE PAPER 932533] p 492 A95-89193
- STEELE, L. L.**
Phase 2: HGM air flow tests in support of HEX vane investigation p 312 N95-23438
- STEEN, GREGORY GLEN**
A two element laminar flow airfoil optimized for cruise
[NASA-CR-198580] p 479 N95-29338
- STEENKEN, WILLIAM G.**
Design and development of an F/A-18 inlet distortion rake: A cost and time saving solution p 69 N95-14241
- STEFKO, GEORGE L.**
NASA Lewis Research Center Workshop on Forced Response in Turbomachinery
[NASA-CP-10147] p 141 N95-19380
- STEGALL, R. L.**
Doppler radar detection of vortex hazard indicators p 42 N95-13212
- STEGER, JOSEPH L.**
A viewpoint on discretization schemes for applied aerodynamic algorithms for complex configurations p 550 A95-91916
- STEGMAIER, J.**
Development of an aeroderivative gas turbine dry low emissions combustion system
[BTN-94-EIX95011441246] p 417 A95-84203
- STEIN, EARL S.**
The controller-memory guide... Concepts from the field
[AD-A289263] p 383 N95-26978
- STEIN, GUNTER**
Dynamic inversion: An evolving methodology for flight control design p 621 N95-31996
- STEIN, KEITH R.**
Parachute inflation: A problem in aeroelasticity
[AD-A284375] p 117 N95-18340
- STEINBERG, RICHARD K.**
A graphical user interface for design and analysis of air breathing propulsion systems
[TABES PAPER 94-616] p 83 N95-14645
- STEINBRENNER, JOHN P.**
Three-dimensional hybrid grid generation using advancing front techniques p 567 N95-28745
- STEINETZ, B. M.**
Static and dynamic friction behavior of candidate high temperature airframe seal materials
[NASA-TM-106571] p 152 N95-16905
Numerical analysis of intra-cavity and power-stream flow interaction in multiple gas-turbine disk-cavities
[NASA-TM-106886] p 407 N95-28344
- STEINETZ, BRUCE M.**
Development of hypersonic engine seals: Flow effects of preload and engine pressures
[BTN-95-EIX95112524204] p 196 A95-69304
Hypersonic engine seal development at NASA Lewis Research Center p 60 N95-13602
Comparison of numerical results and multicavity purge and rim seal data with extensions to dynamics
[NASA-TM-106685] p 416 N95-27434
- STEINMEYER, D. C.**
Advanced diesel electronic fuel injection and turbocharging
[AD-A279176] p 211 N95-19809
- STEINOFF, J.**
Computation of vortex formation over ELAC-1 configuration using vorticity confinement
[AIAA PAPER 95-6157] p 470 A95-90469
- STELMAKOV, E. S.**
The effect of rotating loads suspended under a helicopter on their amplitude-frequency characteristics
[BTN-94-EIX94461407959] p 78 A95-62633
- STEM, STEVEN**
The Elite: A high speed, low-cost general aviation aircraft for Aeroworld
[NASA-CR-197161] p 45 N95-12530
- STEMMER, G.**
Damage occurrence on composites during testing and fleet service: Repair of Airbus aircraft p 396 N95-27526
- STENGEL, JOHN D.**
Systems engineering design and technical analyses for Strategic Avionics Crew-station Design Evaluation Facility (SACDEF)
[AD-A286239] p 235 N95-22024
- STENGEL, ROBERT F.**
Jet transport response to a horizontal wind vortex
[BTN-95-EIX0619952748163] p 619 A95-94457
- STENGEL, ROBERTS**
Real-time decision aiding: Aircraft guidance for wind shear avoidance
[BTN-95-EIX95202637575] p 332 A95-78583
- STEPHENS, B.**
Hypervelocity Impact Test Facility: A gun for hire
[TABES PAPER 94-605] p 86 N95-14639
- STEPHENS, WENDELL B.**
First level release of 2GCHAS for comprehensive helicopter analysis - a status report
[HTN-94-00697] p 2 A95-60176
- STEPHENSON, MARK T.**
Dynamic ground effects flight test of an F-15 aircraft
[NASA-TM-4604] p 38 N95-12191

- STEPHENSON, R. W.**
Modeling rotating shafts using axisymmetric solid finite elements with matrix reduction
[BTN-94-EIX94351143328] p 207 A95-67301
- STERIN, E.**
Prediction of fatigue crack growth under constant amplitude and random loading using specimens with multiple cracks
[AD-A291614] p 397 N95-28409
- STERN, ANDREW D.**
Identification of aviation weather hazards based on the integration of radar and lightning data
[HTN-95-51323] p 356 A95-80908
The inference of aviation weather hazards based on the integration of radar and lightning data
p 660 A95-93483
- STERN, P.**
High-performance parallel analysis of coupled problems for aircraft propulsion
[NASA-CR-197440] p 289 N95-23088
- STERNBERG, CHARLES A.**
Flight validation of ground-based assessment for control power requirements at high angles of attack
p 70 N95-14246
Navy and the HARV: High angle of attack tactical utility issues
p 71 N95-14252
- STEVENS, C.**
Viper cabin-fuselage structural design concept with engine installation and wing structural design
[NASA-CR-197162] p 45 N95-12305
- STEVENS, C. G.**
An Echelle Grating Spectrometer (EGS) for mid-IR remote chemical detection
[DE94-019310] p 249 N95-21478
- STEVENS, DALE**
Optical processing and control
[AD-A279157] p 259 N95-21975
- STEVENS, K. A.**
Buckling and postbuckling of composite structures
[HTN-95-71387] p 528 A95-87605
- STEWART, D. A.**
Hypersonic convective heat transfer over 140-deg blunt cones in different gases
[BTN-95-EIX95152583253] p 306 A95-73554
- STEWART, ERIC C.**
Flutter clearance flight tests of an OV-10A airplane modified for wake vortex flight experiments
[NASA-TM-109168] p 366 N95-26381
- STEWART, J. N.**
Preliminary results from a particle image velocimetry study of blade-vortex interaction
[HTN-95-01098] p 547 A95-90284
- STEWART, JAMES F.**
Engines-only flight control system
[NASA-CASE-ARC-11944-1] p 294 N95-23389
An overview of integrated flight-propulsion controls flight research on the NASA F-15 research airplane
p 694 N95-33010
- STEWART, JOHN E.**
The simulator training research advance testbed for aviation (STRATA): A simulation research facility for army aviation
p 626 A95-95161
- STEWART, JOHN E., II**
Using the backward transfer paradigm to validate the AH-64 Simulator Training Research Advanced Testbed for Aviation
[AD-A285758] p 238 N95-19931
- STEWART, MICHAEL**
Field and data analysis studies related to the atmospheric environment
[NASA-CR-196543] p 168 N95-18093
- STEWART, R. E.**
Mesoscale structure of precipitation bands in a North Atlantic winter storm
[HTN-95-40659] p 215 A95-69803
- STICH, R.**
A flying qualities study of longitudinal long-term dynamics of hypersonic planes
[AIAA PAPER 95-6150] p 521 A95-90464
- STILES, PALMER**
CaRnard: A new roadable aircraft concept
[SAE PAPER 932601] p 494 A95-90071
- STIMPFFLE, R. M.**
The distribution of hydrogen, nitrogen, and chlorine radicals in the lower stratosphere: Implications for changes in O₃ due to emission of NO_y from supersonic aircraft
[HTN-95-70935] p 351 A95-78900
- STINSON, MICHAEL R.**
Inter-Noise 92: Noise control and the public; International Congress on Noise Control Engineering, Toronto, Ontario, Canada, July 20 - 22, 1992. Vols. 1 & 2
[ISBN 0-931784-25-5] p 559 A95-88457
Proceedings of the Sixth International Symposium on Long-Range Sound Propagation
[AD-A290920] p 580 N95-30084
- STOCKWELL, ALAN E.**
A verification procedure for MSC/NASTRAN Finite Element Models
[NASA-CR-4675] p 392 N95-27371
- STOKKE, P.**
Scandinavian Airlines Systems experience on erosion, corrosion and foreign object damage effects on gas turbines
p 198 N95-19659
- STOLARSKI, RICHARD S.**
The atmospheric effects of stratospheric aircraft: A fourth program report
[NASA-RP-1359] p 357 N95-24274
- STOLLERY, J. L.**
Experimental investigation of hypersonic flow over a wing-body combination
[AIAA PAPER 95-6083] p 460 A95-87412
- STONE, MELVIN L.**
Role of the aviation weather system in providing a real-time ATC volcanic ash advisory system
p 663 A95-93494
- STONER, GLENN E.**
NASA-UVA light aerospace alloy and structures technology program (LA2ST)
[NASA-CR-198041] p 343 N95-24220
- STORAASLI, OLAF O.**
Rapid solution of large-scale systems of equations
p 169 N95-16458
- STOREY, BRETT**
Industry review of a crew-centered cockpit design process and toolset
[AD-A282966] p 130 N95-17661
- STORMS, BRUCE L.**
Lift-enhancing tabs on multielement airfoils
[BTN-95-EIX0619952748187] p 591 A95-94479
- STORTZ, MICHAEL**
Assessment of Russian VSTOL technology evaluating the YAK-38 'FORGER' and YAK-141 'FREESTYLE'
p 497 A95-90868
- STORTZ, MICHAEL W.**
Moving base simulation of an integrated flight and propulsion control system for an ejector-augmentor STOVL aircraft in hover
[NASA-TM-108867] p 606 N95-30646
- STOSSMEISTER, GREG**
The 1992-3 operational winter forecasting experiment for Stapleton airport
p 677 A95-93561
- STOTTIER, RICHARD H.**
Artificial intelligence techniques for flight test planning, phase 1
[AD-A293962] p 608 N95-31525
- STOUFFLET, B.**
Integration of an hypersonic airbreathing vehicle: Assessment of overall aerodynamic performances and of uncertainties
[AIAA PAPER 95-6100] p 492 A95-88007
Review of the EUROPT Project AERO-0026
p 129 N95-16573
- STOUT, WAYNE**
Aircraft nosewheel steering simulation
p 412 N95-26944
- STOVALL, JOHN R.**
An avionics scenario and command model description for Space Generic Open Avionics Architecture (SGOAA)
[NASA-CR-188330] p 49 N95-11913
Space Generic Open Avionics Architecture (SGOAA): Overview
p 99 N95-14161
- STOZHKOV, YU. I.**
The scientific ballooning in Russia
p 191 A95-66302
The joint Russian-Brasil research on balloons
p 182 A95-66303
- STRAIN, J. C.**
Aeroelastic stability of wind turbine blade/aileron systems
p 377 N95-27981
Calculation of design load for the MOD-5A 7.3 mW wind turbine system
p 440 N95-27982
- STRANGMEN, THOMAS E.**
Resistance of silicon nitride turbine components to erosion and hot corrosion/oxidation attack
p 202 N95-19683
- STRAPP, J. W.**
Aircraft icing measurements in East Coast winter storms
[HTN-95-60505] p 214 A95-68756
Mesoscale structure of precipitation bands in a North Atlantic winter storm
[HTN-95-40659] p 215 A95-69803
Airplane icing research at the Boeing Company: Participation in the second Canadian Atlantic Storms Program
p 674 A95-93544
- STRATTON, D. ALEXANDER**
Real-time decision aiding: Aircraft guidance for wind shear avoidance
[BTN-95-EIX95202637575] p 332 A95-78583
- STRATTON, MICHAEL D.**
Visual contrast detection thresholds for aircraft contrails
[AD-A288618] p 328 N95-25607
- STRAUB, A. C.**
Ceramic composite attachments for transmission of high-torque loads
[BTN-94-EIX95011441256] p 417 A95-84213
- STRAUB, F. K.**
Advance finite element modeling of rotor blade aeroelasticity
[HTN-95-31013] p 221 A95-71183
- STRAUB, FREDRICH K.**
Design optimization of rotor blades for improved performance and vibration
[HTN-95-A0498] p 229 A95-72569
- STRAWN, GREGORY**
Biodynamic simulation of pilot interaction with a helicopter multi-airbag restraint system
[AD-A290196] p 485 N95-29057
- STRAWN, ROGER**
Mesh quality control for multiply-refined tetrahedral grids
[NASA-CR-197595] p 160 N95-18737
- STRAZISAR, ANTHONY J.**
The effect of adding roughness and thickness to a transonic axial compressor rotor
[NASA-TM-106958] p 645 N95-30524
Laser anemometer measurements of the three-dimensional rotor flow field in the NASA low-speed centrifugal compressor
[NASA-TP-3527] p 618 N95-31985
- STRAZNICKY, P. V.**
Numerical modelling of transverse impact on composite coupons
[BTN-95-EIX95082502225] p 240 A95-71022
- STRAZNICKY, PAUL V.**
Multiple site fatigue damage in fuselage skin splices: Experimental simulation and theoretical prediction
[BTN-95-EIX95152584676] p 276 A95-73588
- STREBY, OLIVIER**
Analysis of a higher harmonic control test to reduce blade vortex interaction noise
[BTN-95-EIX95152582330] p 265 A95-73532
A higher harmonic control test in the DNW to reduce impulsive BVI noise
[HTN-95-61071] p 385 A95-83655
- STREET, TROY A.**
Aero-optics system integration
[TABES PAPER 94-604] p 100 N95-14638
- STREET, CRAIG**
Acoustic receptivity due to weak surface inhomogeneities in adverse pressure gradient boundary layers
[NASA-TM-4577] p 249 N95-21258
- STREHLOW, H.**
Passive and active vibration control activities in the German helicopter industry
[CONGRESS PAPER C428-19-126] p 517 A95-91722
- STREIFINGER, H.**
Secondary power system study for the hytex RA3 flight test vehicle
[AIAA PAPER 95-6158] p 512 A95-90470
- STREITLIEN, K.**
Force and moment on a Joukowski profile in the presence of point vortices
[BTN-95-EIX95262694298] p 434 A95-85469
- STRELNIKOV, G. A.**
JPRS report: Science and technology. Central Eurasia: Engineering and equipment. Gas dynamics of supersonic shortened nozzles
[JPRS-UST-94-003-L] p 22 N95-10931
- STREMEL, PAUL M.**
Wing download reduction using vortex trapping plates
[HTN-94-00710] p 4 A95-60188
Effect of Reynolds number and turbulence on airfoil aerodynamics at -90-degree incidence
[HTN-95-42320] p 370 A95-86149
Calculation of three-dimensional (3-D) internal flow by means of the velocity-vorticity formulation on a staggered grid
[NASA-TM-110352] p 376 N95-27258
- STRETCH, THOMAS**
The IEEE scalable coherent interface: An approach for a unified avionics network
p 234 N95-20650
- STRETCHER, BAXTER**
Offshore next generation weather radar (NEXRAD) OT&E integration and OT&E operational test
[AD-A293223] p 646 N95-30902
- STRIBULA, CHUCK**
Application of advanced safety technique to ring laser gyro inertial navigation system integration
p 689 N95-33140

- STRIFORS, H. C.**
Scattering of short em-pulses by simple and complex targets using impulse radar p 486 A95-90953
- STRIZ, ALFRED G.**
Influence of structural and aerodynamic modeling on flutter analysis [BTN-95-EIX95062487550] p 203 A95-68364
An efficiency study of the simultaneous analysis and design of structures [NASA-TM-110168] p 501 N95-28820
- STROHMEYER, D.**
Aerodynamic off-design behavior of integrated waveriders from take-off up to hypersonic flight [AIAA PAPER 95-6091] p 466 A95-89200
- STROM, STEPHEN W.**
The navigation toolkit [NASA-CR-197290] p 229 N95-22161
- STRONG, A. B.**
Drag coefficients of spherical liquid droplets. Part 1: Quiescent gaseous fields [BTN-95-EIX95262697040] p 538 A95-86857
Drag coefficients of spherical liquid droplets. Part 2: Turbulent gaseous fields [BTN-95-EIX95262697041] p 538 A95-86858
- STROPKI, J. T.**
Aircraft corrosion study [AD-A279527] p 241 N95-21687
- STRYKER, HOWARD Y.**
Twenty-first century commercial transport engines p 512 A95-91495
- STUART, THOMAS D.**
Wind-tunnel tests of an inclined cylinder having helical grooves [BTN-95-EIX95262694306] p 411 A95-85477
- STUBBS, SANDY M.**
NASA evaluation of Type 2 chemical depositions [SAE PAPER 932582] p 495 A95-90086
- STUCKERT, GREG**
Linear disturbances in hypersonic, chemically reacting shock layers [BTN-94-EIX94441386605] p 182 A95-67336
Linear disturbances in hypersonic, chemically reacting shock layers [HTN-95-20931] p 464 A95-88970
- STUCKERT, GREGORY K.**
Nonlinear analysis of swept wing transitional boundary layers [SAE PAPER 932515] p 466 A95-89188
- STUKE, H.**
Pressure controlled surfaces - a 3D inverse panel method as a design tool p 491 A95-87565
- STUMPF, GREGORY J.**
The use of radar wind profiles to remove TDWR gust front algorithm false alarms caused by vertical wind shear p 661 A95-93488
- STUNDER, BARBARA J. B.**
Volcanic ash forecast transport and dispersion (VAFTAD) model [HTN-95-80702] p 254 A95-72546
- STURISKY, HILTON**
Integrated design and manufacturing for the high speed civil transport [NASA-CR-197183] p 48 N95-12700
- STURISKY, SELWYN HOWARD**
A linear system identification and validation of an AH-64 Apache aeroelastic simulation model p 146 N95-18903
- STURTEVANT, B.**
Shock wave interactions in hypervelocity flow [AD-A286507] p 250 N95-22212
- STUSNICK, ERIC**
The effect of onset rate on annoyance to military aircraft noise p 561 A95-90119
- SU, AY**
Flap-lag damping in hover and forward flight with a three-dimensional wake [HTN-95-A0496] p 221 A95-72567
- SU, M.**
Simulation investigation on system identification of gas turbine [PB95-104238] p 139 N95-17749
- SU, R.**
Nonlinear system guidance in the presence of transmission zero dynamics [NASA-TM-4661] p 309 N95-22804
- SUARD, NORBERT**
A processing centre for the CNES CE-GPS experimentation p 125 N95-17196
- SUAREZ, CARLOS J.**
Static and dynamic force/moment measurements in the Eidetics water tunnel p 69 N95-14238
Development of a multicomponent force and moment balance for water tunnel applications, volume 1 [NASA-CR-4642-VOL-1] p 161 N95-18955
- Development of a multicomponent force and moment balance for water tunnel applications, volume 2 [NASA-CR-4642-VOL-2] p 161 N95-18956
- SUAREZ, J.**
Comparison of resin film infusion, resin transfer molding, and consolidation of textile preforms for primary aircraft structure p 425 N95-28477
- SUAREZ, JIM A.**
Cross-stiffened continuous fiber structures p 536 N95-29041
- SUDANI, NORIKAZU**
Flow visualization studies on sidewall effects in two-dimensional transonic airfoil testing [BTN-95-EIX95152582313] p 264 A95-73516
- SUDER, KENNETH L.**
The effect of adding roughness and thickness to a transonic axial compressor rotor [NASA-TM-106958] p 645 N95-30524
Experimental and computational investigation of the tip clearance flow in a transonic axial compressor rotor [NASA-TM-106711] p 649 N95-31738
- SUES, ROBERT H.**
Portable, parallel stochastic optimization for the design of aeropropulsion components [NASA-CR-195312] p 154 N95-16072
- SUGIMOTO, KEI**
Analysis of approach paths of two aircraft p 487 A95-91494
- SUGIYAMA, H.**
Turbulence characteristics of supersonic boundary layer past a backward facing step [AIAA PAPER 95-6126] p 470 A95-90447
- SUGIYAMA, N.**
Derivation of system matrices from nonlinear dynamic simulation of jet engines [BTN-95-EIX95182619139] p 288 A95-76616
- SUGIYAMA, Y.**
Neural network approach to identification of aerodynamic loads on a wing. 1: Application to cantilevered beam models p 475 A95-91568
- SUGIYAMA, YOSHIHIKO**
A method for calculating mean aerodynamic center and zero-lift moment coefficient of aircraft without tail by using measured flight loads p 474 A95-91552
- SUI, JUNYOU**
Aerodynamic design and calculation of flow around the plane cascade of turbine [BTN-94-EIX94481415357] p 104 A95-65347
- SULLIVAN, BRENDA M.**
Recent laboratory studies of loudness and annoyance to sonic booms p 575 A95-90117
- SULLIVAN, JOHN P.**
Wake measurements in a strong adverse pressure gradient [NASA-CR-197272] p 224 N95-21031
- SULLIVAN, RANI**
Rapid prototyping of composite aircraft structures [SAE PAPER 931219] p 539 A95-87530
- SUMITA, JUNICHIRO**
On the UF-104 system p 507 A95-91559
Aeroseoelastic coupling on the UF-104 aircraft p 517 A95-91561
- SUMITA, JUNICHIROU**
On the flight control system for UF-104 p 507 A95-91560
- SUMMERFIELD, P. H.**
The world of regional aircraft - challenges and opportunities [HTN-95-C0002] p 595 A95-93390
- SUMWALT, ROBERT L., III**
ASRS problems involving air carrier ground deicing/anti-icing p 611 A95-95194
- SUN, C. T.**
Bending effects of unsymmetric adhesively bonded composite repairs on cracked aluminum panels p 92 N95-14456
- SUN, D. C.**
Wormgear geometry adopted for implementing hydrostatic lubrication and formulation of the lubrication problem [AD-A290331] p 210 N95-19567
- SUN, H.**
Assessment of a non-dedicated GPS receiver system for precise airborne attitude determination [DE94-019309] p 229 N95-21520
- SUN, JIAN-GUO**
Multivariable adaptive control using only input and output measurements for turbojet engines [BTN-95-EIX95292721165] p 677 A95-92597
- SUN, JIELUN**
Observations of fluxes and inland breezes over a heterogeneous surface [HTN-95-80258] p 212 A95-66315
- SUN, WEN-YIH**
Diurnal variation of lee vortices in Taiwan and the surrounding area [HTN-95-91363] p 318 A95-76394
- SUNADA, SHIGERU**
Aerofoil characteristics at low Reynolds number p 472 A95-91507
- SUNDER, R.**
Ageing nuclear power plant management: An aeronautical viewpoint [NAL-PD-SN-9306] p 105 N95-18606
- SUNDURIN, V. G.**
Simulation of multidisciplinary problems for the thermostress state of cooled high temperature turbines p 140 N95-19021
- SUNG, HYUNG JIN**
Prediction of two-dimensional momentumless wake by k - ϵ - γ model [BTN-95-EIX95262694299] p 434 A95-85470
- SURDON, G.**
Intermetallic and titanium matrix composite materials for hypersonic applications [AIAA PAPER 95-6132] p 530 A95-90451
- SURI, N.**
Dependability issues in the reuse of standard components in open architectures [AIAA PAPER 95-1006] p 566 A95-90678
- SURKS, P.**
Entrainment and acoustic variations in a round jet from introduced streamwise vorticity [BTN-95-EIX95042474409] p 209 A95-68291
- SUSKO, DAVID**
Design and construction of a remote piloted flying wing [NASA-CR-197195] p 47 N95-12695
- SUSSMAN, MYLES A.**
Numerical simulations of the flow in the HYPULSE expansion tube [NASA-TM-110357] p 523 N95-30228
- SUTHAR, R. L.**
Mobile domes for TACTIC telescope p 453 A95-86113
- SUTTIE, EDWARD D.**
Antarctic snow record of southern hemisphere lead pollution [HTN-95-40359] p 212 A95-66869
- SUTTON, M. A.**
Influence of crack history on the stable tearing behavior of a thin-sheet material with multiple cracks p 93 N95-14467
- SUZUKI, ANDREW**
Optical processing and control [AD-A279157] p 259 N95-21975
- SUZUKI, HIDETO**
Guidance and control of HOPE and its future technologies p 506 A95-91543
- SUZUKI, HIROKAZU**
Reentry guidance for hypersonic Flight Experiment (HYFLEX) vehicle [NAL-TR-1235] p 334 N95-25764
- SUZUKI, K.**
Electro-optic characterization of ultrafast photodetectors using adiabatically compressed soliton pulses [BTN-94-EIX94381359637] p 257 A95-72675
- SUZUKI, KOICHI**
Preliminary tests of a transonic flutter control wing model p 499 A95-91566
- SUZUKI, KOJIRO**
Thermochemical nonequilibrium viscous shock-layer analysis for a Mars aerocapture vehicle [BTN-95-EIX95082502732] p 239 A95-70139
Reentry technology experiment on the first mission of reentry capsule 'EXPRESS' p 414 A95-82499
Viscous shock-layer analysis on hypersonic flow over reentry capsule with nonequilibrium chemistry [ISAS-656] p 436 N95-26739
Wind tunnel experiments on wake flow field behind a reentry capsule from a viewpoint of parachute deployment at supersonic speeds [ISAS-655] p 374 N95-26740
Transonic, supersonic and hypersonic wind-tunnel tests on aerodynamic characteristics of reentry body with blunted cone configuration [ISAS-658] p 480 N95-29640
Experimental studies on boundary-layer transition on a reentry vehicle at transonic and supersonic speeds [ISAS-659] p 555 N95-29712
- SUZUKI, MASAMITSU**
Preliminary tests of a transonic flutter control wing model p 499 A95-91566
- SUZUKI, MASAYUKI**
Ducted fan VTOL and its flight control system p 500 A95-91573
- SUZUKI, NORIO**
Flight test of STS radio controlled scale model p 499 A95-91539

SUZUKI, S.

- SUZUKI, S.**
Development of a pilot tube with multi-hole pyramidal head. 2: A five-hole yaw probe of engineering model p 522 A95-91577
- SUZUKI, SEIZO**
Preliminary tests of a transonic flutter control wing model p 499 A95-91566
- SUZUKI, SHINJI**
Multiobjective trajectory optimization by goal programming with fuzzy decision p 526 A95-91544
Simultaneous structure/aerodynamic design optimization for a flexible wing structure p 499 A95-91565
- SVANE, CHRISTIAN**
Nordic Standards for measurement of aircraft noise immersion in residential areas and noise reduction of dwellings p 570 A95-88463
- SVOBODA, J.**
Solid-state data recorder, next development and use p 705 N95-33143
- SWADLEY, STEVEN D.**
Potential applications of the SSM/I cloud liquid water parameter to the estimation of marine aircraft icing [HTN-95-80651] p 254 A95-72495
- SWAFFORD, TIMOTHY W.**
Flutter analysis of supersonic axial flow cascades using a high resolution Euler solver. Part 1: Formulation and validation [NASA-TM-105798] p 23 N95-10244
- SWAIM, ROBERT L.**
Multiaxis pilot ratings for damaged aircraft [BTN-95-EIX95182619128] p 269 A95-76605
- SWAMY, K. N.**
Switched bias proportional navigation for homing guidance against highly maneuvering targets [BTN-95-EIX95182619145] p 279 A95-76622
- SWANSON, G.**
Designers' unified cost model p 424 N95-28464
- SWANSON, G. D.**
Local design optimization for composite transport fuselage crown panels p 398 N95-28473
The effects of design details on cost and weight of fuselage structures p 501 N95-28831
Dimensional stability of curved panels with cocured stiffeners and cobonded frames p 532 N95-28836
Global cost and weight evaluation of fuselage keel design concepts p 501 N95-28840
- SWANTON, G.**
Design and development of a test rig for the high frequency testing of rolling sleeve airsprings [DSTO-TN-0001] p 411 N95-26378
- SWARTWOUT, W.**
The panel oxidation and erosion test (POET) facility [AIAA PAPER 95-6151] p 521 A95-90465
- SWENSON, DANIEL**
Analytical developments in support of the NASA aging aircraft program with an application to crack growth from rivets [SAE PAPER 931223] p 545 A95-88789
- SWENSON, HARRY N.**
Simulation development of a forward sensor-enhanced low-altitude guidance system [HTN-94-00688] p 17 A95-60170
Design and flight evaluation of an integrated navigation and near-terrain helicopter guidance system for night-time and adverse weather operations [NASA-TM-108837] p 11 N95-10846
- SWETTIS, J.**
Automation of reverse engineering process in aircraft modeling and related optimization problems [NASA-CR-197109] p 129 N95-16899
- SWIERTRA, S.**
On-line handling of air traffic: Management, guidance and control [AGARD-AG-321] p 126 N95-18927
- SWIETLIK, C.**
Parallel methods for the flight simulation model [DE94-013330] p 52 N95-11752
- SWIFT, T.**
Damage tolerance capability p 388 A95-85898
Widespread fatigue damage monitoring: Issues and concerns p 136 N95-19488
- SWIHART, DONALD**
Application of advanced safety technique to ring laser gyro inertial navigation system integration p 689 N95-33140
- SWITZER, GEORGE F.**
Windshear certification data base for forward-look detection systems p 41 N95-13204
Certification methodology applied to the NASA experimental radar system p 41 N95-13205
- SWOLINSKY, MANFRED**
Turbulence: Engineering models, aircraft response p 84 N95-14900

- SYLVAIN, M.**
Experimental study of the helicopter-mobile radioelectrical channel and possible extension to the satellite-mobile channel p 247 N95-20945
- SYN, CHOL K.**
Machinability study of Aermot 100 [DE95-011532] p 701 N95-33408
- SYNDER, RICHARD D.**
A non-iterative grid deformation algorithm for computational fluid dynamics for aeroelasticity [AD-A288298] p 436 N95-26418
- SZABO, BARN A.**
Elastic-plastic models for multi-site damage p 92 N95-14454
- SZE, NIEN-DAK**
Effects on stratospheric ozone from high-speed civil transport: Sensitivity to stratospheric aerosol loading [HTN-95-91842] p 354 A95-80830
- SZEBRAT, XAVIER P.**
Effects of civil tiltrotor service in the northeast corridor on en route airspace loads [AD-A293586] p 599 N95-31687
- SZETO, J. T.**
Latitude variations of stratospheric trace gases [HTN-95-70948] p 352 A95-78013
- SZETO, K.**
Fractal properties of whitecaps [HTN-95-92121] p 443 A95-83827
- SZEWCZYK, ALBIN A.**
Effects of three-dimensional imposed 3-D disturbances on bluff-body near wake flows [AD-A289553] p 374 N95-26757
The effects of three-dimensional imposed disturbances on bluff body near wake flows: Effects of taper and splitter plates on the near wake characteristics of a circular cylinder in uniform and shear flow [AD-A292113] p 477 N95-28921
- SZODRUCH, JOACHIM**
A supercritical airfoil experiment p 111 N95-17858
- SZOKO, ED**
The 1992-3 operational winter forecasting experiment for Stapleton airport p 677 A95-93561
- SZOKO, EDWARD J.**
Forecasting for a large field program: STORM-FEST [HTN-95-90694] p 215 A95-69721

T

- TAASAN, SHLOMO**
Airfoil optimization by the one-shot method p 128 N95-16569
- TABACHNICK, BARBARA**
Assessing effects of military aircraft noise on residential property values near airbases p 31 N95-11310
- TABAKOFF, W.**
Experimental and numerical simulations of the effects of ingested particles in gas turbine engines p 199 N95-19662
- TABAZADEH, A.**
Analysis of the physical state of one Arctic polar stratospheric cloud based on observations [HTN-95-70917] p 351 A95-77982
- TABER, ALLEN H.**
Investigation and characterization of SEU effects and hardening strategies in avionics [AD-A291058] p 509 N95-29950
- TADGHIGHI, H.**
Effects of leading and trailing edge flaps on the aerodynamics of airfoil/vortex interactions [HTN-95-31011] p 221 A95-71181
- TAGGART, BRIAN C.**
The use of electrochemistry and ellipsometry for identifying and evaluating corrosion on aircraft [AD-A290249] p 504 N95-29426
- TAGHAVI, R.**
Enhanced mixing of multiple supersonic rectangular jets by synchronized screech [HTN-95-42592] p 459 A95-87222
- TAGHAVI, RAY**
Resonant interaction of a linear array of supersonic rectangular jets: An experimental study [NASA-CR-195398] p 76 N95-15852
Preliminary results and research capabilities of a new jet facility at the University of Kansas p 412 N95-26951
Visualization of the multiple supersonic jet oscillations by swept focused strobed schlieren technique p 367 N95-26952
- TAGUCHI, HIDEYUKI**
Calculation of supersonic combustion in SCRAMJET engines p 698 N95-34513
- TAI, A. T.**
A reuse framework for software fault tolerance [AIAA PAPER 95-1012] p 566 A95-90683
- TAJIMA, HIROHISA**
CCLA operation on MLS p 487 A95-91540
- TAKAGI, SHOHEI**
Observation of traveling waves in the three-dimensional boundary layer along a yawed cylinder [HTN-95-61064] p 430 A95-83648
- TAKAHAMA, M.**
MIMO H infinity control design method combined with exact model matching p 506 A95-91492
- TAKAHASHI, KOUSAKU**
Supersonic flutter analysis of cantilevered composite plate-wings p 499 A95-91567
- TAKAHASHI, M.**
Experiment of rocket-ram annular combustor p 412 A95-82324
- TAKAHASHI, MARC D.**
H-infinity helicopter flight control law design with and without rotor state feedback [BTN-95-EIX95182619129] p 291 A95-76606
- TAKAHASHI, MASAHIRO**
Numerical simulation of high enthalpy shock tunnel p 700 N95-34514
- TAKAHIRA, MIKINARI**
Rarefied gas numerical wind tunnel: OREX and HOPE p 427 A95-82391
- TAKAKI, RYUJI**
Three-dimensional analysis of scramjet nozzle flows [BTN-94-EIX94441380978] p 196 A95-68162
- TAKAKURA, YOKO**
Vector-parallel simulations of transonic wind tunnel flows about a fully configured model of aircraft p 685 N95-34538
- TAKALLU, M. A.**
Wing pressure distributions from subsonic tests of a high-wing transport model [NASA-TM-4583] p 272 N95-22802
- TAKAMI, HIKARU**
Conceptual study of next generation high-speed civil transport: A candidate with horizontal tail p 499 A95-91521
- TAKANASHI, SUSUMU**
Automatic grid generation procedure for complex aircraft configurations [BTN-95-EIX95302729765] p 605 A95-94127
Parallel computation of transonic flows about an aircraft configuration using multi-block structured grids p 685 N95-34537
Computations of low speed flow about space-plane p 685 N95-34544
- TAKASAWA, KINGO**
Analysis and scale-model experiment of propeller driving motor for microwave-powered airplane p 487 A95-91576
- TAKASHIMA, NARUHISA**
Navier-Stokes computation of a viscous optimized waverider [BTN-95-EIX95041503782] p 193 A95-69213
- TAKAYAMA, TAKASHI**
Prediction level of noise by a helicopter p 571 A95-88469
- TAKEISHI, K.**
Study on the turbine vane and blade for a 1500 C class industrial gas turbine [BTN-94-EIX95011441254] p 431 A95-84211
- TAKEMOTO, MASAMI**
Automatic grid generation procedure for complex aircraft configurations [BTN-95-EIX95302729765] p 605 A95-94127
- TAKENO, TADAO**
Prediction of NO(x) emission index of turbulent diffusion flame p 538 A95-87195
- TAKEUCHI, Y. R.**
Thermal fracture mechanisms in ceramic thermal barrier coatings p 346 N95-26138
- TALBOT, MATTHEW D.**
Design of a vehicle based system to prevent ozone loss [NASA-CR-197199] p 48 N95-12702
- TALBOT, N.**
An investigation of piloting strategies for engine failures during takeoff from offshore platforms [HTN-95-92834] p 497 A95-90752
- TALBOT, T.**
Aircraft wake vortex takeoff tests at O'Hara International Airport [AD-A283828] p 118 N95-18624
- TALBOTEC, J.**
Design of fan blades subjected to bird impact p 200 N95-19669
- TAM, C. K. W.**
Screech tones from free and ducted supersonic jets [HTN-95-51647] p 432 A95-85029
- TAM, CHRISTOPHER K. W.**
A prediction method for broadband shock associated noise from supersonic rectangular jets p 574 A95-90100

- TAM, CHUNG-JEN**
Observations on using experimental data as boundary conditions for computations
[BTN-95-EIX95182619103] p 321 A95-76588
- TAMAKI, TEIICHI**
Aero-engine R&D efforts for environmental protection
p 512 A95-91502
- TAMARU, TAKASHI**
Numerical simulation of combustion flow around a flame holder with hydrogen injection
[NAL-TR-1233] p 419 N95-26523
- TAMRAT, B. F.**
Comparison of X-31 flight, wind-tunnel, and water-tunnel yawing moment asymmetries at high angles of attack
p 68 N95-14234
- TAMURA, A.**
Design of secondary flow control cascade using numerical simulation p 698 N95-34507
- TAMURA, ATSUHIRO**
Verification of turbine cascade flow with tip clearance
p 698 N95-34511
- TAMURA, HIROBUMI**
R & D on HOPE structure p 413 A95-82355
- TAN, C. K.**
Temperature effects on acoustic interactions between altitude test facilities and jet engine plumes
[NASA-CR-197638] p 258 N95-21170
- TAN, J. L.**
Multi-block finite volume calculation of compressible flow past aerodynamic configurations p 643 A95-95473
- TAN, P.**
Axial crack propagation and arrest in pressurized fuselage p 94 N95-14479
- TAN, S. C.**
Particle trajectories in gas turbine engines
p 199 N95-19663
- TANAKA, A.**
Aerodynamic characteristics of supersonic air-intake/aircraft integrated models p 472 A95-91512
- TANAKA, HIROSHI**
Research of the method for evaluating noise caused by sonic boom p 562 A95-91519
- TANAKA, HIROYUKI**
Aeroservoelastic coupling on the UF-104 aircraft
p 517 A95-91561
- TANAKA, KEIJI**
Functions of NAL fixed base simulator for helicopter research p 522 A95-91555
A simulator study about effects of visibility upon helicopter pilot performance p 522 A95-91556
Flight reference display for powered-lift STOL aircraft [NAL-TR-1251] p 337 N95-25005
- TANAKA, MASAYUKI**
Air truth validation of cloud albedo estimated from NOAA advanced very high resolution radiometer data
[HTN-95-A1021] p 443 A95-84526
- TANAKA, TOSHIYUKI**
A design of a robust scheduled autopilot
p 516 A95-91532
A design of a self-learning robust scheduled autopilot
p 516 A95-91533
- TANASE, SYOUJI**
Development of Fly-By-Wire system for BK117
p 516 A95-91506
- TANATSUGU, NOBUHIRO**
Test results on air turbo ramjet engine for a future space plane p 402 A95-82327
- TANEDA, HIROSHI**
Hypersonic wind tunnel test of sidewall compression type scramjet inlet p 410 A95-82320
- TANG, D. M.**
Comparison of theory and experiment for non-linear flutter and stall response of a helicopter blade
[BTN-94-EIX94351108100] p 191 A95-66500
Response of a nonrotating rotor blade to lateral turbulence. Part 1: Theory
[BTN-95-EIX95182619228] p 284 A95-76654
Response of a nonrotating rotor blade to lateral turbulence. Part 2: Experiment
[BTN-95-EIX95182619229] p 284 A95-76655
- TANGLER, J. L.**
NREL airfoil families for HAWTs
[DE95-000267] p 357 N95-24882
Wind-tunnel test of the S814 thick root airfoil
[DE95-000268] p 376 N95-27541
- TANGLER, JAMES L.**
Horizontal axis wind turbine post stall airfoil characteristics synthesis p 376 N95-27974
- TANI, KOUICHIRO**
Evaluation of scramjet nozzle performance
p 402 A95-82321
- TANI, YASUHIRO**
An experimental study on supersonic laminar flow control p 473 A95-91523
- TANK, WILLIAM G.**
Airplane icing research at the Boeing Company: Participation in the second Canadian Atlantic Storms Program p 674 A95-93544
- TANRIKUT, S.**
Unsteady flows in turbines: Impact on design procedure p 90 N95-14132
- TAO, WEI-KUO**
Microwave and infrared simulations of an intense convective system and comparison with aircraft observations
[HTN-95-60511] p 214 A95-68762
- TAPLEY, BYRON D.**
Precision orbit determination of altimetric satellites
p 86 N95-14282
- TAPLEY, L. J.**
AIRSAR deployment in Australia, September 1993: Management and objectives p 321 N95-23948
- TAPSCOTT, ROBERT E.**
Chemical options to halons for aircraft use
[AD-A293741] p 599 N95-31569
- TARDUCCI, D.**
Electromagnetic compatibility effects of advanced packaging configurations p 247 N95-20658
- TARG, RUSSELL**
The detection and measurement of microburst wind shear by an airborne lidar system p 543 A95-87798
- TARPLEY, C.**
Sensitivity of engine-integrated waverider performance to static margin constraint
[AIAA PAPER 95-6142] p 496 A95-90458
- TARTAKOVSKY, ALEXANDER**
Minimal time detection algorithms and applications to flight systems
[TR-2-FSRC-93] p 171 N95-18564
- TATAM, R. P.**
Novel implements of optical diagnostic techniques for aerospace applications
[CONGRESS PAPER C428-21-081] p 550 A95-91726
- TATE, A.**
Aerodynamic characteristics of supersonic air-intake/aircraft integrated models p 472 A95-91512
- TATE, ATSUHI**
Aerodynamic characteristics of the orbital reentry vehicle experimental probe fins in a supersonic flow
[NAL-TR-1232] p 342 N95-25664
- TATSCHL, R.**
Multidimensional calculation of spark flame initiation by adopting a generic hydrocarbon kinetic scheme
p 528 A95-87566
- TATTERSHALL, P.**
The rain erosion of PEEK (polyetheretherketone)
[CONGRESS PAPER C428-4-039] p 531 A95-91676
- TATUM, KENNETH E.**
Computer code for determination of thermally perfect gas properties
[NASA-TP-3447] p 37 N95-11995
- TATUM, P. A.**
A review of water mist technology for fire suppression
[AD-A285738] p 225 N95-20071
- TATUTA, YUKIHIRO**
Determination of flight simulator time delay
p 522 A95-91553
- TAUBER, MICHAEL E.**
Trajectory-based heating analysis for the European Space Agency/Rosetta Earth Return Vehicle
[BTN-95-EIX95041503787] p 205 A95-69218
- TAWFIK, HAZEM**
Quality optimization of thermally sprayed coatings produced by the JP-5000 (HVOF) gun using mathematical modeling p 152 N95-19008
- TAYA, HIDEOTO**
Research of the method for evaluating noise caused by sonic boom p 562 A95-91519
- TAYLOR, A. G.**
Finite element model for a flexible non-symmetric rotor on distributed bearing: A stability study
[BTN-94-EIX94381352212] p 306 A95-74612
- TAYLOR, ARTHUR C.**
Discrete shape sensitivity equations for aerodynamic problems
[BTN-94-EIX94451393721] p 88 A95-61720
- TAYLOR, ARTHUR C., III**
Sensitivity derivatives for three dimensional supersonic Euler code using incremental iterative strategy
[HTN-95-20845] p 545 A95-88106
Methodology for sensitivity analysis, approximate analysis, and design optimization in CFD for multidisciplinary applications
[NASA-CR-196981] p 58 N95-13201
- TAYLOR, C. D.**
An investigation of piloting strategies for engine failures during takeoff from offshore platforms
[HTN-95-92834] p 497 A95-90752
- TAYLOR, CHRIS**
Design of a vehicle based system to prevent ozone loss
[NASA-CR-197199] p 48 N95-12702
- TAYLOR, D. W. A.**
Geophex airborne unmanned survey system
[DE95-007566] p 392 N95-27440
- TAYLOR, ED**
MIL-STD-461/MIL-STD-704 investigation
[SAE PAPER 932561] p 505 A95-90058
- TAYLOR, G.**
The avionics integrity programme (AVIF)
[CONGRESS PAPER C428-6-115] p 549 A95-91684
- TAYLOR, HENRY L.**
The value of simulation for training
[AD-A289174] p 411 N95-26556
- TAYLOR, MALCOLM S.**
Statistical analysis of Turbine Engine Diagnostic (TED) field test data
[AD-A286032] p 248 N95-20998
- TAYLOR, ROBERT M.**
Quality assurance and risk management: Perspectives on Human Factors Certification of Advanced Aviation Systems p 690 N95-34771
- TAYMAN, STEVEN K.**
Wind tunnel tests of a 42 inch diameter self-starting autogyro rotor
[AD-A279922] p 188 N95-19863
- TCHENG, P.**
Dynamic response tests of inertial and optical wind-tunnel model attitude measurement devices
[NASA-TM-109182] p 296 N95-23011
- TCHENG, PING**
Effects of yaw and pitch motion on model attitude measurements
[NASA-TM-4641] p 250 N95-22109
- TEALE, TIM**
The FC-1D: The profitable alternative Flying Circus Commercial Aviation Group
[NASA-CR-197152] p 46 N95-12628
- TELJONIS, D. P.**
Dynamic pitch-up of a delta wing
[HTN-95-81633] p 462 A95-87681
- TENEBBAUM, J.**
Jet stream winds: Comparisons of operational analyses with independent aircraft data at multiple longitudes
p 665 A95-93506
- TENSI, J.**
Tip vortex on a swept wing. Mean flow and unsteady phenomena
[BTN-94-EIX94441385755] p 184 A95-68219
- TERESHCHUK, V. S.**
Generalized method of solving topological optimization problems for electrical airplane equipment systems in computer-aided design p 169 N95-16272
- TERUI, YUSHI**
Flight reference display for powered-lift STOL aircraft
[NAL-TR-1251] p 337 N95-25005
- TESSLER, ALEXANDER**
Accurate interlaminar stress recovery from finite element analysis
[NASA-TM-109149] p 57 N95-11815
- TETER, JOHN E., JR.**
Design and evaluation of candidate pressure ports for the HYFLITE experiment
[NASA-TM-109146] p 22 N95-11003
- TEZUKA, KAORU**
Ground effect calculation of two-dimensional airfoil
[BTN-94-EIX94371347710] p 219 A95-69969
- THART, W. G. J.**
Eddy current detection of pitting corrosion around fastener holes p 315 N95-23507
- THEDENS, JOHN R.**
Modular avionics: Taking today's aircraft into tomorrow
[SAE PAPER 931416] p 610 A95-93681
- THIELE, F.**
Laplace interaction law for the computation of viscous airfoil flow in low- and high-speed aerodynamics
[BTN-95-EIX95142553037] p 263 A95-73461
- THOMADAKIS, M. P.**
On the prediction of transonic unsteady flows using second order time accuracy p 641 A95-95448
- THOMAS, ALMUTTIL M.**
Aerodynamic shape optimization of a HSCT type configuration with improved surface definition
[NASA-CR-197011] p 67 N95-13701
- THOMAS, F. O.**
Experiments on the flow field physics of confluent boundary layers for high-lift systems
[NASA-CR-197318] p 224 N95-21343
- THOMAS, M. C.**
Allison engine testing CMSX-4 (reg sign) single crystal turbine blades and vanes
[DE95-010308] p 694 N95-32636

- THOMAS, N.**
An Echelle Grating Spectrometer (EGS) for mid-IR remote chemical detection
[DE94-019310] p 249 N95-21478
- THOMAS, RUSSELL H.**
Active control of fan noise from a turbofan engine
[HTN-95-61198] p 570 A95-87571
- THOMAS, S.**
Operating capability and current status of the reactivated NASA Lewis Research Center hypersonic tunnel facility
[AIAA PAPER 95-6146] p 521 A95-90461
- THOMAS, S. R.**
Numerical study of contaminant effects on combustion of hydrogen, ethane, and methane in air
[AIAA PAPER 95-6097] p 510 A95-88005
- THOMAS, SCOTT R.**
Operating capability and current status of the reactivated NASA Lewis Research Center Hypersonic Tunnel Facility
[NASA-TM-106808] p 148 N95-19286
- THOMPSON, KYLE**
Emerging nondestructive inspection for aging aircraft
[PB95-143053] p 328 N95-25401
- THOMPSON, LYNN**
ADST system test report for the rotary wing aircraft airnet aeromodel and weapon model merge with the ATAC 2 baseline
[AD-A281580] p 127 N95-16171
- THOMPSON, M.**
The DCAF: A high-enthalpy long-duration, direct-connect scramjet test facility
[AIAA PAPER 95-6130] p 512 A95-90450
- THOMSON, D. G.**
An investigation of piloting strategies for engine failures during takeoff from offshore platforms
[HTN-95-92834] p 497 A95-90752
- THOMSON, DOUGLAS**
Testing and analysis of flat and curved panels with multiple cracks p 93 N95-14460
Evaluation of the fuselage lap joint fatigue and terminating action repair p 166 N95-19477
- THOMSON, J. ALEX**
Wake vortex detection at Denver Stapleton Airport with a pulsed 2-micron coherent lidar p 42 N95-13211
- THORNTON, DON**
Design and development of an F/A-18 inlet distortion rake: A cost and time saving solution p 69 N95-14241
- THORNTON, DONALD C.**
An intercomparison of aircraft instrumentation for tropospheric measurements of sulfur dioxide
[HTN-95-91855] p 354 A95-80843
An intercomparison of aircraft instrumentation for tropospheric measurements of carbonyl sulfide, hydrogen sulfide, and carbon disulfide
[HTN-95-91856] p 355 A95-80844
- THORNTON, EARL A.**
Viscoplastic response of structures for intense local heating
[HTN-95-41540] p 346 A95-77921
- THORSTENSON, CLIFFORD B.**
Life cycle costs of alternatives for F-16 printed circuit board diagnosis equipment
[AD-A288744] p 401 N95-28586
- THRASH, PATRICK**
Progress in manufacturing large primary aircraft structures using the stitching/RTM process p 537 N95-29050
- THRESHER, R. W.**
Wind technology development: Large and small turbines
[DE95-000286] p 358 N95-26090
- TIAN, JUN**
Analysis of backscattering from wing and fuselage joints
[HTN-95-71134] p 430 A95-83495
- TICHY, JIRI**
Achievements and tasks for active noise control p 29 N95-11270
- TIEN, C. L.**
Analysis of flow channeling near the wall in packed beds
[HTN-94-00698] p 2 A95-60177
- TIERNEY, THOMAS P.**
Grid resolution and turbulent inflow boundary condition recommendations for NPARC calculations
[NASA-TM-106959] p 482 N95-30253
- TILLEY, JEFFREY S.**
An integrated system to improve aviation weather forecasts for the Alaska Range p 656 A95-93460
- TIMMERMAN, NANCY S.**
Identification of noise events as aircraft p 576 A95-90126
Features of Massport's new noise monitoring system p 562 A95-90127
- TINCHER, DOUGLAS J.**
Hypersonic waverider test vehicle: A logical next step
[BTN-95-EIX95041503783] p 193 A95-69214
- TING, L.**
Acoustic field in unsteady moving media
[NASA-CR-198162] p 438 N95-27179
- TIPTON, FRANKLIN J.**
Applications of digital video and synthetic environments to unmanned aerial vehicles
[AD-A291875] p 504 N95-29437
- TISCHLER, MARK B.**
High-order state space simulation models of helicopter flight mechanics
[HTN-95-A0494] p 237 A95-72565
Identification and simulation evaluation of a combat helicopter in hover
[BTN-95-EIX95242670749] p 335 A95-81098
Flight-testing and frequency-domain analysis for rotorcraft handling qualities
[HTN-95-01083] p 515 A95-90269
- TISHKOFF, J. M.**
AFOSR Contractors Meeting in Propulsion
[AD-A282729] p 54 N95-12507
- TIWARI, SURENDRA N.**
Aerodynamic shape optimization of a HSC T type configuration with improved surface definition
[NASA-CR-197011] p 67 N95-13701
- TOBIAS, M.**
Advanced wing design survivability testing and results p 400 N95-28488
- TODA, NOBUO**
Aeroviscoelastic coupling on the UF-104 aircraft p 517 A95-91561
- TODD, RUSSELL F.**
A comparative performance study of TDWR/LLWAS 3 integration algorithms for wind shear detection p 658 A95-93468
- TODD, S. M.**
ACT/ICAPS: Thermoplastic composite activities p 421 N95-28274
- TOFUKUJI, NORIYASU**
Arrival traffic handling for a parallel runway airport p 487 A95-91537
- TOGAWA, MORITO**
An advanced scramjet propulsion concept for A 350 MG SSTO space plane p 402 A95-82325
- TOGNACCINI, R.**
Estimation of supersonic leading-edge thrust by a Euler flow model
[BTN-95-EIX0619952748194] p 591 A95-94483
- TOKARCIC, SUSAN A.**
Computational flow predictions for hypersonic drag devices p 37 N95-11967
- TOKUDA, E.**
MIMO H infinity control design method combined with exact model matching p 506 A95-91492
- TOKUNAGA, TATSURU**
An advanced scramjet propulsion concept for A 350 MG SSTO space plane p 402 A95-82325
- TOKUYAMA, AYANO**
Research of the method for evaluating noise caused by sonic boom p 562 A95-91519
- TOLPADI, ANIL K.**
Combustion system CFD modeling at GE Aircraft Engines p 439 N95-27889
- TOM, MICHAEL**
Integrated IR sensors
[BTN-95-EIX95041505023] p 242 A95-70132
- TOMASELLI, M.**
Broadband polarization-transfer experiments for rotating solids
[GTN-95-0009261494012091-58] p 579 A95-92319
- TOMBAZIS, NICHOLAS**
The effects of three dimensional imposed disturbances on bluff body near wake flows
[AD-A290824] p 555 N95-29654
- TOMIKE, JUNICHIRO**
A conceptual design of hypersonic research vehicle with subscale scramjet engine p 384 A95-82482
- TOMIO, TAKESHI**
Development of Fly-By-Wire system for BK117 p 516 A95-91506
- TOMIOKA, SADATAKE**
Performance variation of scramjet nozzle at various nozzle pressure ratios
[BTN-95-EIX0616952745781] p 615 A95-94505
- TOMITA, HIROSHI**
Flight evaluation of DGPS and DGPS-INS navigation systems p 382 A95-82462
- TOMPETRINI, K.**
A new guidance and flight control system for the DELTA 2 launch vehicle p 342 A95-80427
- TONEV, PETER T.**
Thundercloud electric field modeling for the ionosphere-Earth region. 1: Dependence on cloud charge distribution
[HTN-95-41223] p 317 A95-75035
- TONG, DONALD**
The role of simulations in 777 FSEU development
[AIAA PAPER 95-0995] p 506 A95-90665
- TONG, PIN**
Nonlinear bulging factor based on R-curve data p 94 N95-14476
- TONON, ALDO**
Digital autopilot design for combat aircraft in ALENIA p 623 N95-32009
- TOON, G. C.**
Comparison of column abundances from three infrared spectrometers during AASE 2 p 352 A95-78011
Latitude variations of stratospheric trace gases
[HTN-95-70948] p 352 A95-78013
- TOPP, DAVID A.**
Investigation of advanced counterrotation blade configuration concepts for high speed turboprop systems. Task 8: Cooling flow/heat transfer analysis
[NASA-CR-195359] p 50 N95-11901
Investigation of advanced counterrotation blade configuration concepts for high speed turboprop systems. Task 8: Cooling flow/heat transfer analysis user's manual
[NASA-CR-195360] p 50 N95-11951
- TORELLA, G.**
Artificial intelligence for turboprop engine maintenance
[HTN-95-92313] p 404 A95-85357
Calculation of control laws for the digital fuel control unit of a small thrust turbojet
[SAE PAPER 931411] p 614 A95-93677
- TORELLA, GIOVANNI**
An airborne monitoring system for FOD and erosion faults p 200 N95-19668
- TORKAR, K. M.**
Balloon technology and observations; Symposium P3 of the COSPAR Plenary Meeting, 29th, Washington, DC, Aug. 28-Sept. 5, 1992
[HTN-95-70250] p 181 A95-66276
- TOROK, MICHAEL S.**
Aerodynamic and wake methodology evaluation using Model UH-60A experimental data
[HTN-95-31009] p 220 A95-71179
- TORRES, FRANCISCO J.**
Geometric analysis of wing sections
[NASA-TM-110346] p 335 N95-24629
- TOTH, DOUGLAS K.**
Lubricant evaluation and performance, 2
[AD-A279144] p 242 N95-21969
- TOTH, G. K.**
Broadband, wide-area active control of sound radiated from vibrating structures using local surface-mounted radiation suppression devices p 30 N95-11283
- TOTH, JOE M.**
Precise navigation using adaptive FIR filtering and time domain spectral estimation
[BTN-95-EIX95142555485] p 227 A95-72888
- TOTTEN, JOHN J.**
High strain-rate testing of parachute materials
[DE95-009577] p 648 N95-31614
- TOUGARD, D.**
Brite-Euram programme: ACOUFAT acoustic fatigue and related damage tolerance of advanced composite and metallic structures p 174 N95-19159
- TOWER, FRANCIS G.**
An overview of issues encountered in parallelizing high-resolution weather prediction models p 676 A95-93560
- TOWNE, MATTHEW C.**
Numerical simulation of dynamic-stall suppression by tangential blowing
[AD-A284887] p 120 N95-19110
- TOWNSEND, D. P.**
Analytical and experimental vibration analysis of a faulty gear system
[NASA-TM-106689] p 58 N95-12843
- TOWNSEND, DENNIS P.**
Influence of tooth profile modification on spur gear dynamic tooth strain
[NASA-TM-106952] p 553 N95-29112
- TOWNSEND, M. A.**
Stability of magnetic bearing-rotor systems and the effects of gravity and damping
[BTN-94-EIX94441386619] p 208 A95-68168
Stability of magnetic bearing-rotor systems and the effects of gravity and damping
[HTN-95-20955] p 465 A95-88994
- TRABANDT, U.**
Launcher wing-leading-edge design
[BTN-95-EIX95042477110] p 192 A95-68349

- TRABOCCO, R.**
Field repair materials for naval aircraft
p 394 N95-27514
- TRABOCCO, R. E.**
Navy composite maintenance and repair experience
p 424 N95-28446
- TRACY, M. B.**
Measurements of store forces and moments and cavity pressures for a generic store in and near a box cavity at subsonic and transonic speeds
[NASA-TM-4611] p 378 N95-28241
- TRACY, MAUREEN B.**
Effect of passive venting on static pressure distributions in cavities at subsonic and transonic speeds
[NASA-TM-4549] p 6 N95-10029
- TRACZ, WILL.**
The ADAGE avionics reference architecture
[AIAA PAPER 95-1021] p 566 A95-90693
- TRAMEL, R. W.**
A one-dimensional inviscid nonequilibrium flow solver
[ISBN 1-879921-01-4] p 588 A95-93752
- TRAN, HUY KIM**
Test model designs for advanced refractory ceramic materials
p 55 N95-11968
- TRAN, KEN**
CFD analysis of turbopump volutes
p 312 N95-23436
- TRAN, P.**
Ice accretion on aircraft wings
[BTN-95-EIX95082502224] p 225 A95-71021
- TRANQUILLA, JAMES**
Modeling and analysis for the GPS pseudo-range observable
[BTN-95-EIX95302731227] p 600 A95-94046
- TRAUB, LANCE W.**
Aerodynamic effects of delta planform tip sails on wing performance
[BTN-95-EIX95062487544] p 185 A95-68358
Aerodynamic characteristics of strake vortex flaps on a strake-wing configuration
[BTN-95-EIX95062487537] p 187 A95-69245
Analytic prediction of lift for delta wings with partial leading-edge thrust
[BTN-95-EIX95152582345] p 266 A95-73547
- TRAUB, W. A.**
Comparison of column abundances from three infrared spectrometers during AASE 2
[HTN-95-70946] p 352 A95-78011
- TRAUB, WESLEY A.**
Chemical change in the arctic vortex during AASE 2
[HTN-95-70947] p 352 A95-78012
- TRAVEN, RICARDO**
Flight validation of ground-based assessment for control power requirements at high angles of attack
p 70 N95-14246
Navy and the HARV: High angle of attack tactical utility issues
p 71 N95-14252
- TRAWINSKI, DAVID**
Application of fiber-reinforced bismaleimide materials to aircraft nacelle structures
p 397 N95-28278
- TRAYBAR, JOSEPH**
Assessment of avionics technology in European aerospace organizations
[NASA-CR-189201] p 337 N95-24624
- TREFNY, C.**
Operating capability and current status of the reactivated NASA Lewis Research Center hypersonic tunnel facility
[AIAA PAPER 95-6146] p 521 A95-90461
- TREFNY, CHARLES J.**
Computational analysis in support of the SSTO flowpath test
[NASA-TM-106757] p 89 N95-13665
Operating capability and current status of the reactivated NASA Lewis Research Center Hypersonic Tunnel Facility
[NASA-TM-106808] p 148 N95-19286
- TREGO, LINDA E.**
Composite propeller system for Dornier 328
[BTN-94-EIX94461290506] p 66 A95-61728
Maintenance challenges and trends
[BTN-95-EIX95182617808] p 261 A95-75753
Maintenance programs
[BTN-95-EIX95182617809] p 261 A95-75754
Aircraft stripping and painting
[BTN-95-EIX95182617810] p 300 A95-75755
Maintenance programs
[HTN-95-92310] p 365 A95-85354
Aircraft stripping and painting
[HTN-95-92311] p 365 A95-85355
- TREGO, LINDA F.**
Noise and vibration control
[BTN-95-EIX95042477108] p 179 A95-68351
- TREIBER, DAVID A.**
Euler technology assessment for preliminary aircraft design employing OVERFLOW code with multiblock structured-grid method
[NASA-CR-4651] p 273 N95-23095
- TRELA, W. J.**
Phonon characteristics of high (T sub c) superconductors from neutron Doppler broadening measurements
[DE95-003703] p 324 N95-24076
- TREMANTE, A.**
Contribution of thermal radiation to the temperature profile of ceramic composite materials
[BTN-94-EIX95011441252] p 417 A95-84209
- TRENT, VICTOR S.**
Dynamic modelling and response characteristics of a magnetic bearing rotor system with auxiliary bearings
p 703 N95-32692
- TREXLER, CARL A.**
Experimental investigation of inlet-combustor isolators for a dual-mode scramjet at a Mach number of 4
[NASA-TP-3502] p 407 N95-28343
- TRIANTAFYLLOU, M. S.**
Force and moment on a Joukowski profile in the presence of point vortices
[BTN-95-EIX95262694298] p 434 A95-85469
- TRIEU, THAI-BA**
Design and construction of a remote piloted flying wing
[NASA-CR-197195] p 47 N95-12695
- TRIEU, THUYBA**
Design and construction of a remote piloted flying wing
[NASA-CR-197195] p 47 N95-12695
- TRIGEIRO, WILLIAM W.**
Effects of civil tiltrotor service in the northeast corridor on en route airspace loads
[AD-A293586] p 599 N95-31687
- TRIGGS, MIKE**
Cabin fuselage structural design with engine installation and control system
[NASA-CR-197173] p 47 N95-12639
- TRIGS, DEANNE**
The Aluminum Falcon: A low cost modern commercial transport
[NASA-CR-197180] p 81 N95-15742
- TRILLING, TODD W.**
Actuated forebody strake controls for the F-18 High-Alpha Research Vehicle
[BTN-95-EIX0619952748173] p 619 A95-94467
- TRIMBLE, T.**
Regulatory impact analysis and regulatory support document: Control of air pollution; determination of significance for nonroad sources and emission standards for new nonroad compression-ignition engines at or above 37 kilowatts (50 horsepower)
[PB94-194594] p 61 N95-12855
- TRIPP, J. S.**
Dynamic response tests of inertial and optical wind-tunnel model attitude measurement devices
[NASA-TM-109182] p 296 N95-23011
- TRIPP, JOHN S.**
Effects of yaw and pitch motion on model attitude measurements
[NASA-TM-4641] p 250 N95-22109
- TROPIS, A.**
Composite or metallic bolted repairs on self-stiffened carbon wing panel of the commuter ATR72 design criteria. Analysis, verification by test
p 396 N95-27525
- TROSHCHENKO, V. T.**
Fatigue strength of high-temperature alloys under conditions of cyclic temperature variation. Communication 1: Experimental procedure and results
[BTN-94-EIX94401363884] p 307 A95-75516
- TRUE, B.**
Crossflow mixing of noncircular jets
[NASA-TM-106865] p 338 N95-24390
Effects of initial conditions on a single jet in crossflow
[NASA-TM-107002] p 615 N95-30589
- TRUJILLO, EDWARD**
Integrated IR sensors
[BTN-95-EIX95041505023] p 242 A95-70132
- TSAI, C.**
Ablative thermal management structural material on the hypersonic vehicles
[AIAA PAPER 95-6133] p 547 A95-90452
- TSAI, C. Y.**
Free-jet testing at Mach 3.44 in GASL's aero/thermo test facility
p 145 N95-16320
- TSAI, MING-YANG**
Damage tolerance certification of a fighter horizontal stabilizer
[BTN-95-EIX0619952748186] p 637 A95-94478
- TSANG, S. K.**
Fatigue design of axially loaded semicircular lugs
[BTN-95-EIX0619952748190] p 637 A95-94252
- TSANGARIS, S.**
On the prediction of transonic unsteady flows using second order time accuracy
p 641 A95-95448
- TSIANG, T. H.**
Process and control systems for composites manufacturing
p 420 N95-28267
- TSO, JIN**
Jet to freestream velocity ratio computations for a jet in a crossflow
[AIAA PAPER 93-4860] p 2 A95-60178
- TSO, K. S.**
A reuse framework for software fault tolerance
[AIAA PAPER 95-1012] p 566 A95-90683
- TSOUKA, D. G.**
Meteorological impacts on airport noise prediction by the 'Integrated Noise Model' application based on Hamiltonian Ray-Tracing program and measurements
p 571 A95-88467
- TSOUKA, DESPINA G.**
Enroute NASA/FAA low-frequency propfan test in Alabama (October 1987): A versatile atmospheric aircraft long-range noise prediction system
p 573 A95-90099
- TSUJII, TOSHIKI**
Flight evaluation of DGPS and DGPS-INS navigation systems
p 382 A95-82462
Flight evaluation of GPS/DGPS sensor systems installed in NAL Do228
[NAL-TR-1230] p 382 N95-26585
- TSUKANO, YUKICH**
A gust alleviation method by the response feedback
p 506 A95-91493
- TSUKANO, YUKICHI**
Flight reference display for powered-lift STOL aircraft
[NAL-TR-1251] p 337 N95-25005
- TSUKIJI, TADASHI**
Flight testing of the composite material bearingless rotor system for the helicopter
p 498 A95-91503
- TSUNG, FU-LIN**
A three-dimensional Navier-Stokes/full-potential coupled analysis for rotor blades
[ISBN 1-879921-01-4] p 587 A95-93748
- TSURI, SHUICHI**
Life evaluation of a low power arcjet thruster
p 403 A95-82337
- TUCKER, P. KEVIN**
Validation of a Computational Fluid Dynamics (CFD) code for supersonic axisymmetric base flow
p 315 N95-23652
- TULAPURKARA, E. G.**
Boundary layer studies over an S-blade
[HTN-95-92261] p 434 A95-85305
- TULUMELLO, L.**
A Kutta condition conscious perturbation stream function boundary element algorithm for 2-D potential aerodynamics
[ISBN 1-879921-01-4] p 587 A95-93751
- TUMA, MEG**
The 1994 Fiber Optic Sensors for Aerospace Technology (FOSAT) Workshop
[NASA-CP-10166] p 337 N95-24207
- TUMMALA, MURALI**
Waveform bounding and combination techniques for direct drive testing
[AD-A284075] p 161 N95-19035
- TUNCER, ISMAIL H.**
Viscous-inviscid interaction method for unsteady low-speed airfoil flows
[BTN-95-EIX95182619093] p 269 A95-75778
- TUNG, C.**
The application of potential CFD methods to helicopter hover flows
[ISBN 1-879921-01-4] p 587 A95-93747
- TUNG, CHEE**
Dynamic stall control for advanced rotorcraft application
[BTN-95-EIX95222650793] p 334 A95-79249
Numerical study of multi-element airfoil aerodynamics
[ISBN 1-879921-01-4] p 587 A95-93750
Geometric analysis of wing sections
[NASA-TM-110346] p 335 N95-24629
- TUNG, SHU-LIN**
Radar studies of aviation hazards
[AD-A285845] p 226 N95-21831
- TURCICH, ELIZABETH**
Final results of the weather testing component of the Terminal Doppler Weather Radar operational test and evaluation
p 658 A95-93471
- TURCO, R. P.**
Analysis of the physical state of one Arctic polar stratospheric cloud based on observations
[HTN-95-70917] p 351 A95-77982
- TURKEL, E.**
Pressure updating methods for the steady-state fluid equations
[NASA-CR-198163] p 569 N95-30353

- TURLEY, W. DALE**
Turbine-engine applications of thermographic-phosphor temperature measurements [DE95-003625] p 358 N95-25110
- TURNBULL, DONALD**
Status of the terminal Doppler weather radar with deployment underway p 653 A95-93450
- TURNER, D.**
Viper cabin-fuselage structural design concept with engine installation and wing structural design [NASA-CR-197162] p 45 N95-12305
- TURNER, MARK A.**
A computational investigation of wake-induced airfoil flutter in incompressible flow and active flutter control [AD-A281534] p 142 N95-16109
- TURTELLY, A. JR.**
The joint Russian-Brasil research on balloons p 182 A95-66303
- TUTTLE, J. D.**
Sensing thunderstorm microphysics with multiparameter radar: Application for aviation p 657 A95-93467
- TUTTLE, JOHN**
The real-time analysis and prediction of storms program p 655 A95-93457
- TUTTLE, M.**
Local design optimization for composite transport fuselage crown panels p 398 N95-28473
- TUTTLE, M. M.**
Investigation of static and cyclic bearing failure mechanisms for GR/EP laminates p 422 N95-28427
- TUTTLE, S.**
Shock tunnel studies of scramjet phenomena 1993 [NASA-CR-195038] p 350 N95-25394
- TUTTLE, S. L.**
Balances for the measurement of multiple components of force in flows of a millisecond duration p 350 N95-25400
- TUTTLE, SEAN**
Thrust measurement in a 2-D scramjet nozzle p 339 N95-25397
- TWOHY, C.**
Analysis of the physical state of one Arctic polar stratospheric cloud based on observations [HTN-95-70917] p 351 A95-77982
- TYLER, CHARLES**
Laser velocimetry in the supersonic regime: Advancements, limitations, and outlook [SAE PAPER 931365] p 634 A95-93646
Developments in laser-based diagnostics for wind tunnels in the Aeromechanics Division: 1987-1992 [AD-A283011] p 84 N95-13687
- TYLER, S. G.**
MCMs for avionics: Technology selection and intermodule interconnection p 234 N95-20641
- TYURIN, B. F.**
The effect of rotating loads suspended under a helicopter on their amplitude-frequency characteristics [BTN-94-EIX94461407959] p 78 A95-62633
- U**
- UCHIDA, TADAO**
Analysis of an MLS automatic landing control law for the NAL experimental research aircraft D0-228. 2: Curved approach and landing p 508 A95-91588
- UCHIDA, TAKASHI**
Requirements for next generation supersonic transports p 498 A95-91516
The concept of high speed commercial transporter structure p 498 A95-91517
Numerical analysis around the whole SST configuration p 693 N95-34541
- UCHIDA, TATSURO**
A detailed Euler flow analysis of TPS and fanjet engine p 473 A95-91515
- UEDA, A.**
Development of 70MW class superconducting generators [BTN-94-EIX95011440854] p 429 A95-82905
- UEDA, SHUICHI**
Evaluation of scramjet nozzle performance p 402 A95-82321
Experiment and analysis on heat transfer of a scramjet leading edge model p 403 A95-82420
- UEDA, SHUICHI**
Performance variation of scramjet nozzle at various nozzle pressure ratios [BTN-95-EIX0616952745781] p 615 A95-94505
- UEDA, TETSUHIKO**
Fundamental wind tunnel experiments on low-speed flutter of a tip-fin configuration wing [NAL-TR-1228] p 332 N95-25762
- UEMATSU, KAZUO**
Life evaluation of a low power arcjet thruster p 403 A95-82337
- UENO, SEIYA**
Optimality of the steady-state flight for hypersonic aircraft p 526 A95-91550
- UESUGI, KUNINORI**
How "HITEN's" aerobraking experiments were carried out p 415 A95-82553
Aero-thermodynamic flight environment at HITEN aerobrake experiment p 415 A95-82554
- ULANOV, B. V.**
Stabilization of objects with unknown nonstationary parameters, using adaptive nonlinear continuous control systems [BTN-94-EIX94461407944] p 98 A95-62262
- ULBRICH, N.**
Analytic solution of the thickness problem of a rectangular wing in steady subsonic flow [ISBN 1-879921-01-4] p 588 A95-93758
- UNAL, M. F.**
Aerodynamic characteristics of external store configurations at low speeds [BTN-95-EIX95182619230] p 271 A95-76656
Effects of splitter plate on wake formation from a circular cylinder: A discrete vortex simulation p 639 A95-95404
- UNDERWOOD, F. M.**
Intelligent skins development for future military aircraft [CONGRESS PAPER C428-17-189] p 531 A95-91714
- UNGS, TIMOTHY J.**
Explanatory factors for the geographic distribution of U.S. Civil aviation mortality [HTN-95-92908] p 484 A95-91846
- UNO, N.**
Turbulence characteristics of supersonic boundary layer past a backward facing step [AIAA PAPER 95-6126] p 470 A95-90447
- URITA, AKIRA**
Hypersonic flow simulation with thermoelectric effect p 368 A95-82669
- URNES, JAMES M., SR.**
Propulsion Controlled Aircraft design and development p 697 N95-33022
- USAMI, M.**
Development of a pilot tube with multi-hole pyramidal head. 2: A five-hole yew probe of engineering model p 522 A95-91577
- USTILOVSKY, SH.**
Prediction of fatigue crack growth under constant amplitude and random loading using specimens with multiple cracks [AD-A291614] p 397 N95-28409
- UZUNALI, ALTUG**
Computer aided static aeroelastic analysis of wing/pylon/store combination p 499 A95-91531
- V**
- VADALI, S. R.**
Trajectory optimization using parallel shooting method on parallel computer [BTN-95-EIX95282706670] p 564 A95-88175
- VAKHITOV, M. V.**
Development of strength analysis methods and design model for aircraft constructions in Kazan Aviation Institute p 127 N95-16264
- VAKHITOV, YU. M.**
Profiling of the working surface of electrodes-tools for circle electrochemical dimensional treatment of compressor blades [BTN-94-EIX94461407964] p 83 A95-62638
- VALAREZO, W. O.**
Effect of underwing frost on a transport aircraft airfoil at flight Reynolds number [BTN-95-EIX95152582334] p 276 A95-73536
- VALAREZO, WALTER O.**
Separation control on high-lift airfoils via micro-vortex generators [BTN-95-EIX95152582326] p 265 A95-73529
Navier-Stokes applications to high-lift airfoil analysis [BTN-95-EIX0619952748182] p 590 A95-94475
- VALAVANI, LENA**
Design of high performance multivariable control systems for supermaneuverable aircraft at high angle of attack [NASA-CR-197661] p 293 N95-22908
- VALDRE, G.**
Powerful bolide explosion over North Italy [HTN-95-80564] p 218 A95-69658
- VALENCIA, ALVARO**
Natural convection in central microcavities of vertical, finned enclosures of very high aspect ratios [BTN-95-EIX95282711336] p 632 A95-92405
- VALENTINE, JAMES R.**
Tracking of raindrops in flow over an airfoil [BTN-95-EIX95182619221] p 308 A95-76647
- VALERIO, N. R.**
Vortical flow structure near the F/A-18 LEX at high incidence [BTN-95-EIX95062487555] p 186 A95-68369
- VALLURI, SIDDHARTHA**
Flow past a symmetric wedge with forward splitter plate p 427 A95-82406
- VAN CAUWENBERGHE, R.**
The performance of forward scatter visibility sensors for application in autostations and runway visual range in snow and freezing precipitation events p 662 A95-93489
- VAN DALSEM, WILLIAM R.**
Numerical simulation of powered-lift flows [HTN-94-00700] p 3 A95-60179
Numerical simulation of a complete STOVL aircraft in ground effect [AIAA PAPER 93-4880] p 4 A95-60187
- VAN DAM, C. P.**
Accurate drag prediction: A prerequisite for drag reduction research [SAE PAPER 932571] p 467 A95-90060
In-flight pressure measurements on a subsonic transport high-lift wing section [BTN-95-EIX0619952748170] p 589 A95-94464
- VAN DEN BRAEMBUSSCHE, R.**
Permeable wall boundary conditions for transonic airfoil design p 641 A95-95445
- VAN DEN BROEKE, MICHIEL R.**
Momentum and scalar transfer coefficients over aerodynamically smooth Antarctic surfaces [HTN-95-92932] p 562 A95-91870
- VAN DER AUWERAER, H.**
In-flight interior sound field mapping in propeller aircraft p 572 A95-88472
- VAN DER AUWERAER, HERMAN**
Aircraft interior sound field analysis in view of active control: Results from the ASANCA project p 575 A95-90109
- VAN DER MAREL, M. J.**
Surface grid generation for multi-block structured grids p 643 A95-95478
- VAN DER WALL, B. G.**
On the influence of time-varying flow velocity on unsteady aerodynamics [HTN-95-61073] p 369 A95-83657
- VAN DIJK, W. C. M.**
Automation of observations in the Netherlands p 661 A95-93485
- VAN DOMMELEN, LEON L.**
Determining unsteady 2D AND 3D boundary layer separation p 462 A95-88898
- VAN NOSTRAND, WILLIAM**
Static shape control for adaptive wings [HTN-95-A1767] p 627 A95-93330
- VANAYEV, A. P.**
Sea wave parameters, small altitudes and distances measurers design for movement control systems of ships, wing-in-surface effect crafts and seaplanes p 708 N95-33141
- VANBUSSEL, G. J. W.**
PREDICAT: First order performance calculations of windturbine rotors using the method of the acceleration potential [PB95-206454] p 564 N95-30200
Axial loads on yawed rotors [PB95-214193] p 592 N95-30638
Acceleration potential models
PREDICAT/PREDICDYN applied for calculation of axisymmetric dynamic inflow cases [PB95-207015] p 647 N95-30957
- VANCHAU, MICHAEL N.**
Virtual environment application with partial gravity simulation p 169 N95-15988
- VANDAM, CORNELIS P.**
Numerical simulation of helicopter engine plume in forward flight [NASA-CR-197488] p 107 N95-16589
High-lift flow-physics flight experiments on a subsonic civil transport aircraft (B737-100) p 275 N95-23333
- VANDENBERG, B.**
Low-speed surface pressure and boundary layer measurement data for the NLR 7301 airfoil section with trailing edge flap p 111 N95-17855
- VANDENBERG, J. I.**
Numerical investigation into vortical flow about a delta-wing configuration up to incidences at which vortex breakdown occurs in experiment [PB95-198024] p 593 N95-30837
- VANDENBOSCH, JEANNETTE**
In-flight radiometric calibration of AVIRIS in 1994 p 705 N95-33754
- VANDERBORG, W.**
Partial camera automation in a simulated Unmanned Air Vehicle [AD-A288786] p 337 N95-26190

- VANDERBURG, J. W.**
Demonstration of an automated CFD system for three-dimensional flow simulations p 551 N95-28767
- VANDERBURGH, A. H. P.**
On the dynamics of aeroelastic oscillators with one degree of freedom [BTN-94-EIX94501431527] p 153 A95-64524
Dynamical systems as models for flow-induced vibrations [PB95-206991] p 647 N95-30956
- VANDERMERWE, JUAN**
Aerodynamic characteristics of strake vortex flaps on a strake-wing configuration [BTN-95-EIX95062487537] p 187 A95-69245
- VANDERVELDEN, A.**
Tools for applied engineering optimization p 128 N95-16570
The global aircraft shape p 128 N95-16571
Aerodynamic shape optimization p 128 N95-16572
- VANDERVORST, ANDRE**
Modeling resonance in waveguide-to-microstrip junctions by unilateral fin line resonators [BTN-94-EIX94381323445] p 242 A95-70844
- VANDERWALT, JOHANNES P.**
Static pressure distribution in the inlet of a helicopter turbine compressor [BTN-95-EIX95152582339] p 266 A95-73541
Erosion of dust-filtered helicopter turbine engines. Part 1: Basic theoretical considerations [BTN-95-EIX95182619222] p 288 A95-76648
Erosion of dust-filtered helicopter turbine engines. Part 2: Erosion reduction [BTN-95-EIX95182619223] p 289 A95-76649
Life prediction of helicopter engines fitted with dust filters [BTN-95-EIX95182619224] p 289 A95-76650
- VANDERWERT, TERRY L.**
Advances in the application of laser cutting, drilling, and welding aerospace parts [SAE PAPER 932544] p 547 A95-90052
Laser processing aircraft and turbine engine parts [SAE PAPER 931356] p 634 A95-93640
- VANDEVOORT, GERALD C.**
A market perspective on FANS [SAE PAPER 932521] p 486 A95-89189
- VANDRONKELAAR, J. H.**
Development of advanced approach and departure procedures. Failure scenarios [PB95-198123] p 601 N95-30815
- VANDYKEN, R. D.**
LDV measurements in dynamically separated flows [ISBN 0-8194-1311-9] p 5 A95-60191
- VANFOSSEN, G. JAMES**
Influence of turbulence parameters, Reynolds number, and body shape on stagnation-region heat transfer [NASA-TP-3487] p 550 N95-28719
- VANGELDER, P. A.**
Reanalysis of European flight loads data [AD-A282052] p 9 N95-11179
- VANGESTEL, R.**
Braze repair possibilities for hot section gas turbine parts p 201 N95-19677
- VANGRIETHUYSEN, VALERIE J.**
An engineering code to analyze hypersonic thermal management systems p 155 N95-16322
- VANHOUTEN, JOHN S.**
Forecasting aircraft mishaps using monthly maintenance reports [AD-A286049] p 227 N95-22417
- VANHOV, D.**
Flight test results of the F-16 aircraft modified with axisymmetric vectoring exhaust nozzle p 609 N95-32007
- VANROSENDALE, JOHN**
Floating shock fitting via Lagrangian adaptive meshes [AD-A289758] p 170 N95-18110
- VANSCHAACK, DONALD J.**
Developing an emission factor for hazardous air pollutants for an F-16 using JP-8 fuel [AD-A284802] p 216 N95-19685
- VANSTONE, D. A.**
Laboratory evaluation of a reactive baffle approach to NOx control [AD-A283802] p 255 N95-19921
- VANTREUREN, KENNETH W.**
Impingement flow heat transfer measurements of turbine blades using a jet array [AD-A283450] p 62 N95-12512
- VANTRINET, ROBERT**
Central coast designs: The Eightball Express. Taking off with convention, cruising with improvements and landing with absolute success [NASA-CR-197181] p 47 N95-12643
- VANWIE, D. M.**
Experimental and computational results for the external flowfield of a scramjet inlet [BTN-94-EIX94441380877] p 195 A95-68161
- VANWIE, DAVID M.**
Application of scramjet engine technology to the design of ram accelerator projectiles p 19 N95-10282
- VARADAN, T. K.**
Field-consistent element applied to flutter analysis of circular cylindrical shells [BTN-94-EIX94341341971] p 56 A95-60871
- VARGAS, MARIO**
A laser-based ice shape profilometer for use in icing wind tunnels [NASA-TM-106936] p 646 N95-30851
- VARGHESE, PH.**
Measurement by coherent anti-Stokes Raman scattering in the R5Ch hypersonic wind tunnel [BTN-95-EIX95112523811] p 188 A95-69322
- VASENYOV, L. G.**
Separation of winged vehicles in supersonics [AIAA PAPER 95-6092] p 526 A95-88601
- VASIL'EV, G. V.**
Analytical description of and forecast for stress relaxation of aviation materials under the vibration conditions [BTN-94-EIX94461408751] p 126 A95-63634
- VASILOFF, STEVEN V.**
Final results of the weather testing component of the Terminal Doppler Weather Radar operational test and evaluation p 658 A95-93471
- VATSA, V.**
Pressure updating methods for the steady-state fluid equations [NASA-CR-198163] p 569 N95-30353
- VATSA, VEER N.**
Evaluation of a multigrid-based Navier-Stokes solver for aerothermodynamic computations [BTN-95-EIX95302694459] p 583 A95-94056
Comparison of the predictive capabilities of several turbulence models [BTN-95-EIX0619952748167] p 589 A95-94461
Block-structured grids for complex aerodynamic configurations: Current status p 551 N95-28736
- VAUGHAN, K. W.**
A portable transmission vibration analysis system for the S-70A-9 Black Hawk helicopter [DSTO-TR-0072] p 348 N95-24203
- VEBER, G.**
FASTPACK: Optimized solutions for modular avionics derived from a parametric study. Part 1: Platform features p 233 N95-20634
- VELICKI, ALEX**
Materials and structures for the HSCT [BTN-95-EIX95282711241] p 455 A95-89634
- VELINOV, PETER I. Y.**
Thundercloud electric field modeling for the ionosphere-Earth region. 1: Dependence on cloud charge distribution [HTN-95-41223] p 317 A95-75035
- VELSKO, S.**
Overview of remote sensing laser development and semiconductor laser technology [DE94-019103] p 256 N95-21552
- VEMAGANTI, GURURAJA R.**
Laminar and turbulent flow computations of Type 4 shock-shock interference aerothermal loads using unstructured grids [NASA-CR-195008] p 97 N95-15604
- VENEDIKTOV, V. D.**
Application of multidisciplinary models to the cooled turbine rotor design p 140 N95-19024
- VENET, G.**
Aircraft interior sound field analysis in view of active control: Results from the ASANCA project p 575 A95-90109
Noise and vibration control in aircraft: A global approach p 576 A95-90128
ASTRYD: A new numerical tool for aircraft cabin and environmental noise prediction p 576 A95-90129
- VENKATKRISHNAN, V.**
Parallel implicit unstructured grid Euler solvers [BTN-95-EIX95042474393] p 217 A95-68307
Agglomeration multigrid for viscous turbulent flows [AD-A284064] p 8 N95-10848
- VENKATAPATHY, ETHIRAJ**
A comparison of three-dimensional nonequilibrium solution algorithms applied to hypersonic flows with stiff chemical source terms [AIAA PAPER 93-2861] p 4 A95-60186
Computational flow predictions for hypersonic drag devices p 37 N95-11967
Bibliography of Doctor Chul Park [NASA-TM-110353] p 527 N95-29351
- VENKATESWARAN, S.**
Convergence acceleration of implicit schemes in the presence of high aspect ratio grid cells p 313 N95-23446
- VENKAYYA, VIPPERLA B.**
Influence of structural and aerodynamic modeling on flutter analysis [BTN-95-EIX95062487550] p 203 A95-68364
- VER, ISTVAN L.**
An active liner system for jet engine exhaust silencers, phase 1 [AD-A293277] p 617 N95-31191
- VERBEEK, A. T. J.**
High velocity oxygen fuel spraying of erosion and wear resistant coatings on jet engine parts p 202 N95-19680
- VERDE, G.**
Numerical and flight measured interior noise characteristics of a twin-engine turboprop general aviation aircraft p 573 A95-90094
- VERDERAIME, V.**
Illustrated structural application of universal first-order reliability method [NASA-TP-3501] p 54 N95-11870
- VERDON, JOSEPH M.**
Active control of wake/blade-row interaction noise [BTN-95-EIX95042474389] p 196 A95-68311
Unsteady aerodynamic analyses for turbomachinery aeroelastic predictions p 141 N95-19381
Development of a linearized unsteady Euler analysis for turbomachinery blade rows [NASA-CR-4677] p 592 N95-30611
- VERHAAGEN, N. G.**
Experimental investigation of the vortex flow over a 76/60-deg double delta wing p 114 N95-18784
A study of the vortex flow over 76/40-deg double-delta wing [NASA-CR-195032] p 314 N95-23466
- VERONA, ROBERT W.**
Factors affecting the visual fragmentation of the field-of-view in partial binocular overlap displays [AD-A283081] p 172 N95-17334
Factors affecting the perception of luning in monocular regions of partial binocular overlap displays [AD-A286287] p 259 N95-22044
- VETH, MICHAEL J.**
Advanced formation flight control [AD-A289271] p 409 N95-26981
- VEZZETTI, CATHY**
Accelerated application development for flight software [AIAA PAPER 95-1031] p 566 A95-90703
- VICKERS, DEAN**
Observations of fluxes and inland breezes over a heterogeneous surface [HTN-95-80258] p 212 A95-66315
- VICROY, DAN D.**
Vertical wind estimation from horizontal wind measurements p 26 N95-10567
Microburst vertical wind estimation from horizontal wind measurements [NASA-TP-3460] p 131 N95-18198
- VIDIECAN, J.**
Solid-state data recorder, next development and use p 705 N95-33143
- VIEIRA, J.**
Cabin-fuselage-wing structural design concept with engine installation [NASA-CR-197172] p 49 N95-12993
- VIEWEG, STEFAN**
GPS/GLONASS/INS test program [BTN-94-EIX94441386131] p 189 A95-68187
- VIGLIALORO, G.**
An approach to sensor data fusion for flying and landing aid purpose p 686 N95-32488
- VIGNAU, H.**
The calculation of erosion in a gas turbine compressor rotor p 199 N95-19664
- VIGNOLLES, P.**
Design of fan blades subjected to bird impact p 200 N95-19669
- VIGUE, YVONNE**
Thermal force modeling for global positioning system satellites using the finite element method [BTN-95-EIX95152583270] p 278 A95-73571
- VIJGEN, PAUL M. H. W.**
In-flight pressure measurements on a subsonic transport high-lift wing section [BTN-95-EIX0619952748170] p 589 A95-94464
- VIKRAM, C. S.**
Residual Stress Measurements with Laser Speckle Correlation Interferometry and Local Heat Treating [DE95-060082] p 349 N95-24598

VILCANS, JANIS

VILCANS, JANIS

Recommendation on transition from primary/secondary radar to secondary-only radar capability
[AD-A286279] p 249 N95-22005

VILLANO, MICHAEL

Modeling student knowledge with self-organizing feature maps
[BTN-95-EIX95262697073] p 564 A95-86862

VINSON, S. E.

The use of structural optimisation within aerospace
[CONGRESS PAPER C428-23-008] p 500 A95-91729

VISBAL, M. R.

Two-dimensional unsteady leading-edge separation on a pitching airfoil
[HTN-95-81628] p 461 A95-87676

VISBAL, MIGUEL

Structure of a double-fin turbulent interaction at high speed
[BTN-95-EIX95222650780] p 347 A95-79236

VISBAL, MIGUEL R.

Crossflow topology of vortical flows
[HTN-95-51664] p 432 A95-85046
Numerical simulation of transient vortex breakdown above a pitching delta wing
[AD-A281075] p 107 N95-16808

VISCANTI, G.

Possible effects of CO₂ increase on the high-speed civil transport impact on ozone
[HTN-95-60779] p 317 A95-75976

High-speed civil transport impact: Role of sulfate, nitric acid trihydrate, and ice aerosols studied with a two-dimensional model including aerosol physics
[HTN-95-91843] p 354 A95-80831

Impact on ozone of high-speed stratospheric aircraft: Effects of the emission scenario
[HTN-95-51283] p 356 A95-80868

VISINGARDI, P.

Estimation of supersonic leading-edge thrust by a Euler flow model
[BTN-95-EIX0619952748194] p 591 A95-94483

VISSER, BENTON E.

Determination of minimum fuel octane number piston aircraft engines
[SAE PAPER 931230] p 528 A95-88961

VISSER, H. G.

Optimal lateral-escape maneuvers for microburst encounters during final approach
[BTN-95-EIX95182619127] p 276 A95-76604

VISWANATHAN, K.

Linear instability waves in supersonic jets confined in circular and non-circular ducts
[BTN-94-EIX94341340068] p 103 A95-63520

VITT, P. H.

Vortex generation and mixing in three-dimensional supersonic combustors
[BTN-95-EIX0616952745783] p 614 A95-94503

VITT, PAUL

Some additional stability and performance characteristics of the scissor/pivot wing configurations
[SAE PAPER 931383] p 618 A95-93659

VIVEIROS, STEVEN

Terminal Doppler Weather Radar Build 5A Operational Test and Evaluation (OT/E) integration and OT/E operational test plan
[AD-A283052] p 61 N95-12996

VIVEKANANDAN, J.

Sensing thunderstorm microphysics with multiparameter radar: Application for aviation
p 657 A95-93467

VIZ, MARK J.

Fatigue crack growth in 2024-T3 aluminum under tensile and transverse shear stresses
p 153 N95-19490

VLCEK, KEVIN M.

An investigation of the AFIT 2-inch shock tube as a flow source for supersonic testing
[AD-A289246] p 412 N95-26966

VLEGER, H.

Results of uniaxial and biaxial tests on riveted fuselage lap joint specimens
p 136 N95-19491

VOEGT, S.

Reentry trajectories and their optimization by an evolution algorithm
p 525 A95-87394

VOKURA, V. J.

RCS measurements, transformations, and comparisons under cylindrical and plane wave illumination
[BTN-94-EIX94371347126] p 242 A95-69976

VOLAKIS, J.

Simulation of patch and slot antennas using FEM with prismatic elements and investigations of artificial absorber mesh termination schemes
[NASA-CR-198974] p 704 N95-32822

VOLAKIS, JOHN L.

Hybrid finite element-modal analysis of jet engine inlet scattering
[BTN-95-EIX95242673665] p 427 A95-82259

Design considerations for an archimedean slot spiral antenna
p 211 N95-19798

VOLDMAN, MIKE

Test results from large wing and fuselage panels
p 537 N95-29051

VOLKOV, V. V.

A new generation of instruments for flying laboratories
[BTN-94-EIX94401363947] p 317 A95-75532

VON GRUNHAGEN, W.

Autonomous helicopter hover positioning by optical tracking
[HTN-95-C0006] p 585 A95-93394

VONFLOTOW, ANDREAS H.

Adaptive tuned vibration absorbers: Tuning laws, tracking agility, sizing, and physical implementations
p 25 N95-11280

VONGAS, G.

Airborne integrated communications system
[CONGRESS PAPER C428-30-162] p 610 A95-93612

VONGRUENHAGEN, WOLFGANG

Model following control for tailoring handling qualities: ACT experience with ATTHes
p 622 N95-32000

VONTHUMER, ALFRED E.

Design and evaluation of candidate pressure ports for the HYFLITE experiment
[NASA-TM-109146] p 22 N95-11003

VORTAC, O. U.

The role of flight progress strips in en route air traffic control: A time-series analysis
[DOT/FAA/AM-95/4] p 280 N95-23565

Automation and cognition in air traffic control: An empirical investigation
[AD-A291932] p 488 N95-28790

VOS, E. A.

Flex cycle combustor development and demonstration
[BTN-94-EIX95011441245] p 417 A95-84202

VOS, JAN

Navier-Stokes simulation of turbulent vortex high-Re-number flows over a delta wing
p 644 A95-95507

VOSS, H. J.

Experience of in-service corrosion on military aircraft
p 303 N95-23516

VOSTEEN, LOUIS F.

Composite chronicles: A study of the lessons learned in the development, production, and service of composite structures
[NASA-CR-4620] p 151 N95-16859

COINS: A composites information database system
p 453 N95-28465

VOURNAS, I.

Multigrad solution for the compressible Euler equations by an implicit characteristic-flux-averaging
p 642 A95-95459

VU, PHUONG

Direct-lift design strategy for longitudinal control of hypersonic aircraft
[BTN-95-EIX95182619131] p 291 A95-76608

VUILLEZ, CHRISTOPHE

New methods, new methodology: Advanced CFD in the Snecma turbomachinery design process
p 90 N95-14134

VULGAKOV, E. B.

Aircraft gear train diagnostics using the irregular rotation of the external shafts
[CONGRESS PAPER C428-15-097] p 508 A95-91712

VUTETAKIS, DAVID G.

Maintenance-free lead acid battery for inertial navigation systems aircraft
[BTN-95-EIX95292721316] p 633 A95-92511

W

WADA, YASUHIRO

NAL aerothermodynamic probing and CFD verification mission in OREX experiment
p 368 A95-82413

Practical formulation of a positively conservative scheme
[HTN-95-51668] p 433 A95-85050

A shock tunnel test of a winged hypersonic research vehicle
p 474 A95-91538

Hypersonic CFD analysis for the aerothermodynamic design of HOPE
p 684 N95-34520

WADAWADIGI, GANESH

Computation of the integrated aerodynamic and propulsive flowfields of a generic hypersonic space plane
p 481 N95-29788

WAGENER, THOMAS J.

2 micron LIDAR for laser-based remote sensing: Flight demonstration and application survey
[BTN-95-EIX95212641072] p 319 A95-76737

WAGNER, CHARLES A.

Effects of mass on aircraft sidearm controller characteristics
[NASA-TM-104277] p 51 N95-11868

WAGNER, S.

An innovative algorithm to accurately solve the Euler equations for rotary wing flow
p 642 A95-95467

WAHLS, RICHARD A.

Comparison of computational and experimental results for a supercritical airfoil
[NASA-TM-4601] p 108 N95-16908

Computer model to simulate testing at the National Transonic Facility
[NASA-TM-4664] p 627 N95-32217

WAL, R.

Neuro-controllers for adaptive helicopter training
[SAE PAPER 932535] p 379 A95-84557

Neuro-controllers for adaptive helicopter hover training
[BTN-94-EIX94522407592] p 709 A95-96241

WAIBEL, MICHAEL

Theoretical investigations of shock/boundary layer interactions on a Ma(infinity) = 8 waverider
[DLR-FB-94-12] p 119 N95-18910

WAKAIRO, KAORU

Functions of NAL fixed base simulator for helicopter research
p 522 A95-91555

A simulator study about effects of visibility upon helicopter pilot performance
p 522 A95-91556

Preliminary experiments of an optical fiber display
[NAL-TR-1257] p 362 N95-25004

WAKAMATSU, YOSHIO

Experiment and analysis on heat transfer of a scramjet leading edge model
p 403 A95-82420

Effect of film cooling/regenerative cooling on scramjet engine performances
[NAL-TR-1242] p 339 N95-24990

WAKANA, HIROMITSU

Aeronautical satellite communications using the ETS-5 satellite
p 487 A95-91541

WAKE, BRIAN E.

Evaluation of a doubly-swept blade tip for rotorcraft noise reduction
[NASA-CR-189677] p 452 N95-28264

WALBERG, G. D.

Fuel-optimal bank-angle control for lunar-return aerocapture
[BTN-95-EIX95212645706] p 299 A95-76758

WALCHLI, LAWRENCE A.

Flight evaluation of pneumatic forebody vortex control in post-stall flight
p 72 N95-14259

Flight evaluation of forebody vortex control in post-stall flight
p 609 N95-32003

WALDEN, RAINER

Time-optimal turn to a heading: An analytic solution
[BTN-94-EIX94511433940] p 142 A95-64606

WALDMAN, J.

Corrosion of landing gear steels
p 302 N95-23500

WALEGA, J. G.

Mentional distributions of NO(X), NO(Y), and other species in the lower stratosphere and upper troposphere during AASE 2
[HTN-95-70944] p 352 A95-78009

WALEGA, JAMES G.

Three-dimensional model interpretation of NO(x) measurements from the lower stratosphere
[HTN-95-90534] p 213 A95-67806

WALEJEWSKI, CHARLES T.

Lightweight, opto-electronic engine control system for aerospace turbine engines
[SAE PAPER 931442] p 614 A95-93692

WALEN, D. B.

Consistent approach to describing aircraft HIRF protection
[NASA-CR-195067] p 334 N95-25341

WALIGORA, SHARON

Software process improvement in the NASA software engineering laboratory
[AD-A289912] p 450 N95-28627

Impact of Ada and object-oriented design in the flight dynamics division at Goddard Space Flight Center
[NASA-CR-189412] p 567 N95-28807

WALKER, DENISE

Developing and testing decision-making products for center weather service unit meteorologists
p 671 A95-93533

WALKER, IRA J.

Experimental aerodynamic characteristics of a generic hypersonic accelerator configuration at Mach numbers 1.5 and 2.0
[NASA-TM-4413] p 39 N95-12770

WALKER, LEN

Experimental/analytical approach to understanding mistuning in a transonic wind tunnel compressor
[NASA-TM-108833] p 95 N95-14617

- WALKER, M. A.**
Verification of computational aerodynamic predictions for complex hypersonic vehicles using the INCA(trademark) code [DE95-004757] p 330 N95-24308
- WALKER, S. L.**
Axial crack propagation and arrest in pressurized fuselage p 94 N95-14479
- WALKER, STEVEN H.**
Modelling structurally damaging twin-jet screech p 135 N95-19154
- WALKER, T. H.**
Tension fracture of laminates for transport fuselage. Part 1: Material screening p 398 N95-28471
Local design optimization for composite transport fuselage crown panels p 398 N95-28473
- WALKER, TOM H.**
Tension fracture of laminates for transport fuselage. Part 2: Large notches p 532 N95-28837
- WALLACE, CLARK E.**
An engineering code to analyze hypersonic thermal management systems p 155 N95-16322
- WALLACE, JAMES M.**
Flow alteration and drag reduction by riblets in a turbulent boundary layer [HTN-95-61199] p 461 A95-87572
- WALMSLEY, STANLEY**
A low fin height heat exchanger technology demonstrator for Hermes [SAE PAPER 932119] p 526 A95-90360
- WALSH, DAVID**
On-the-fly carrier ambiguity resolution for precise aircraft landing [BTN-95-EIX95112522535] p 190 A95-69328
- WALSH, EDWARD J.**
Orbital velocities induced by surface waves [HTN-95-90902] p 253 A95-72411
- WALSH, JOANNE L.**
Integrated aerodynamic/dynamic/structural optimization of helicopter rotor blades using multilevel decomposition [NASA-TP-3465] p 285 N95-22953
- WALSH, WILLIAM**
Safety in airport ground handling p 626 A95-95193
- WALTER, C.**
Dependability issues in the reuse of standard components in open architectures [AIAA PAPER 95-1006] p 566 A95-90678
- WALTER, DONALD ALAN**
An analysis of the costs and benefits in improving F402-RR-406A High Pressure Turbine, second stage blades under the aircraft engine Component Improvement Program (CIP) [AD-A285127] p 197 N95-19595
- WALTER, R. W.**
Investigation of static and cyclic bearing failure mechanisms for GR/EP laminates p 422 N95-28427
- WALTER, THERESA**
High density monolithic packaging technology for digital/microwave avionics p 240 N95-20646
- WALTHER, J. H.**
Viscous flow simulation using the discrete vortex diffusion velocity method p 639 A95-95421
- WANAMAKER, JOHN L.**
Process and control systems for composites manufacturing p 420 N95-28267
- WANG, CLIN M.**
Dynamic stall control for advanced rotorcraft application [BTN-95-EIX95222650793] p 334 A95-79249
Numerical solutions of three dimensional viscous flows [ISBN 1-879921-01-4] p 587 A95-93749
Numerical study of multi-element airfoil aerodynamics [ISBN 1-879921-01-4] p 587 A95-93750
- WANG, DIEQIAN**
Multigrid/multiblock method for transonic potential flow around wing/body/nacelle configurations including a slipstream p 591 A95-95451
- WANG, GUOHUA H.**
A stochastic adaptive control application to flight systems p 699 N95-34806
- WANG, HONGLI**
Effects of AMB parameters on the dynamic stability of the rotor [BTN-94-EIX94381353450] p 323 A95-75494
- WANG, J. A.**
Computational/experimental investigation of staged injection into a Mach 2 flow [HTN-95-51646] p 432 A95-85028
- WANG, J. T.**
Technology integration box beam failure study p 441 N95-28468
Technology integration box beam failure study p 552 N95-28847
- WANG, JIANLIANG**
Scheduling of local nonlinear control laws by exogenous signals - an application to flight control [BTN-95-EIX95262694059] p 447 A95-85675
- WANG, JIGEN**
Development and application of the double V type flame stabilizer [BTN-94-EIX94481415355] p 154 A95-65345
- WANG, K. C.**
An axisymmetric analog two-layer convective heating procedure with application to the evaluation of Space Shuttle Orbiter wing leading edge and windward surface heating [NASA-CR-188343] p 54 N95-11937
- WANG, KON-SHENG CHARLES**
In-flight imaging of transverse gas jets injected into transonic and supersonic crossflows: Design and development [NASA-CR-186031] p 157 N95-17418
- WANG, LI-XIN**
Nonlinear decoupling control study for aircraft maneuvering flight [HTN-95-71130] p 408 A95-83491
- WANG, MENG**
Acoustics of laminar boundary layers breakdown p 251 N95-22455
- WANG, SZU-CHUAN**
Determining unsteady 2D AND 3D boundary layer separation p 462 A95-88898
- WANG, W.**
New eigensolutions and modal analysis for gyroscopic/rotor systems, part 1: undamped systems [BTN-94-EIX94522410219] p 702 A95-96373
New eigensolutions and modal analysis for gyroscopic/rotor systems, part 2: perturbation analysis for damped systems [BTN-94-EIX94522410220] p 702 A95-96374
- WANG, Y. H.**
Effect of squeeze film damper land geometry on damper performance [HTN-95-92247] p 434 A95-85291
- WANG, YIFEI**
An approach to aerodynamic characteristics of low radar cross-section fuselages p 106 N95-16251
- WANG, Z.**
Studies on the flow induced by an oscillating airfoil in a uniform stream [PB94-204450] p 40 N95-13250
- WANG, Z. J.**
Pressure based high order TVD methodology for dynamic stall control [AD-A290149] p 479 N95-29316
- WANG, ZICAI**
Nonlinear observer and its application in flight control p 447 A95-82449
- WANHILL, R. J. H.**
Flight simulation fatigue crack growth testing of aluminum alloys [HTN-95-00652] p 418 A95-84731
Status and prospects for aluminum-lithium alloys in aircraft structures p 387 A95-85893
- WANTUCK, P. J.**
A laboratory scale supersonic combustive flow system [DE95-006347] p 420 N95-27851
- WARDWELL, DOUG**
Flow visualization studies of VTOL aircraft models during Hover in ground effect [NASA-TM-108860] p 272 N95-22666
- WARDWELL, DOUGLAS A.**
Aerodynamics model for a generic ASTOVL lift-fan aircraft [NASA-TM-110347] p 332 N95-26302
- WARMAN, R. M.**
The impact of non-linear flight control systems on the prediction of aircraft loads due to turbulence p 143 N95-18598
- WARNER, HAROLD D.**
Altitude cueing effectiveness of terrain texture characteristics in simulated low-altitude flight [AD-A294369] p 700 N95-34362
- WARNES, GORDON D.**
Future directions in helicopter protection system configuration p 198 N95-19657
- WARNICA, W. D.**
Drag coefficients of spherical liquid droplets. Part 1: Quiescent gaseous fields [BTN-95-EIX95262697040] p 538 A95-86857
Drag coefficients of spherical liquid droplets. Part 2: Turbulent gaseous fields [BTN-95-EIX95262697041] p 538 A95-86858
- WARREN, DANIEL E.**
A VHF/UHF antenna for the Precision Antenna Measurement System (PAMS) [AD-A285673] p 156 N95-16621
- WARREN, HUGH E.**
Effect of broadcast and precise ephemerides on estimates of the frequency stability of GPS Navstar clocks [BTN-95-EIX95112522530] p 190 A95-69333
- WARREN, LINDA S.**
An intercomparison of instrumentation for tropospheric measurements of dimethyl sulfide: Aircraft results for concentrations at the parts-per-trillion level [HTN-95-91857] p 355 A95-80845
- WARWICK, K.**
Predictive algorithms for the roll control autopilot of a jet fighter aircraft [HTN-95-21047] p 515 A95-90424
- WASHBURN, A. E.**
A study of the vortex flow over 76/40-deg double-delta wing [NASA-CR-195032] p 314 N95-23466
- WASSERBERGH, HENRI A.**
World trends in air transport policies. (Approaching the 21st century) [HTN-95-50220] p 176 A95-64857
- WASSERBAUER, CHARLES A.**
NASA low-speed axial compressor for fundamental research [NASA-TM-4635] p 296 N95-23192
- WASZAK, M. R.**
Flutter suppression for the active flexible wing: A classical design [BTN-95-EIX95182619216] p 292 A95-76642
- WATANABE, AKIRA**
Functions of NAL fixed base simulator for helicopter research p 522 A95-91555
A simulator study about effects of visibility upon helicopter pilot performance p 522 A95-91556
Preliminary experiments of an optical fiber display [NAL-TR-1257] p 362 N95-25004
- WATANABE, M.**
Aerodynamic characteristics of supersonic air-intake/aircraft integrated models p 472 A95-91512
- WATANABE, MITSUNORI**
Aerodynamic characteristics of the orbital reentry vehicle experimental probe fins in a supersonic flow [NAL-TR-1232] p 342 N95-25664
- WATANABE, NAUYUKI**
Development and flight results of fiber reinforced balloon p 384 A95-82511
- WATANABE, SHIGEYA**
An experimental investigation of scramjet nozzle flow p 402 A95-82322
A concept of a hypersonic flight experiment of a winged vehicle p 414 A95-82477
Application of CFD technique for HYFLEX aerodynamic design p 693 N95-34542
- WATANABE, YASUFUMI**
Flight Test Monitoring System using X-window p 500 A95-91574
- WATANABE, YASUO**
NAL aerothermodynamic probing and CFD verification mission in OREX experiment p 368 A95-82413
- WATANBE, SHIGEYA**
A shock tunnel test of a winged hypersonic research vehicle p 474 A95-91538
- WATANUKI, TADAHARU**
Hypersonic thermal protection with mass injection at angle of attack p 414 A95-82414
- WATERMAN, W. F.**
Design and development of an advanced two-stage centrifugal compressor [BTN-95-EIX95282710054] p 633 A95-92475
- WATKISS, ERIC J.**
Flight dynamics of an unmanned aerial vehicle [AD-A282259] p 45 N95-12410
- WATMUFF, JONATHAN H.**
Instabilities originating from suction holes used for Laminar Flow Control (LFC) [NASA-CR-196395] p 6 N95-10131
- WATRY, C. W.**
Effects of trailing-edge jet entrainment on delta wing vortices [HTN-95-81644] p 542 A95-87692
- WATSON, CAROLYN B.**
Experimental study at low supersonic speeds of a missile concept having opposing wraparound tails [NASA-TM-4582] p 106 N95-16069
- WATSON, DOUGLAS C.**
Identification and simulation evaluation of a combat helicopter in hover [BTN-95-EIX95242670749] p 335 A95-81098
- WATSUSHITA, HIROSHI**
Preliminary tests of a transonic flutter control wing model p 499 A95-91566
- WATTS, S.**
STOVL Control Integration Program [NASA-CR-195358] p 18 N95-11487

WAUGH, D. W.

Fine-scale, poleward transport of tropical air during AASE 2
[HTN-95-70949] p 352 A95-78014

WAWRZYNEK, PAUL A.

Discrete crack growth analysis methodology for through cracks in pressurized fuselage structures
[BTN-95-EIX0608952737538] p 633 A95-92751
Discrete crack growth analysis methodology for through cracks in pressurized fuselage structures
p 166 N95-19473

WAYE, DONALD E.

High strain-rate testing of parachute materials
[DE95-009577] p 648 N95-31614

WE-NBERG, P. O.

The distribution of hydrogen, nitrogen, and chlorine radicals in the lower stratosphere: Implications for changes in O₃ due to emission of NO(y) from supersonic aircraft
[HTN-95-70935] p 351 A95-78000

WEATHERILL, N. P.

Construction of nearly orthogonal multiblock grids for compressible flow simulation
[BTN-94-EIX94361133526] p 207 A95-65981

WEATERS, JEFFREY T.

Comparison of frequency response and perturbation methods to extract linear models from a nonlinear simulation
[AD-A284115] p 146 N95-18405

WEAVER, CLARK J.

Trajectory modeling of emissions from lower stratospheric aircraft
[HTN-95-41219] p 317 A95-75031
Tracer transport for realistic aircraft emission scenarios calculated using a three-dimensional model
[HTN-95-41799] p 353 A95-80525
Three dimensional model calculations of the global dispersion of high speed aircraft exhaust and implications for stratospheric ozone loss
p 26 N95-10657

WEAVER, HAROLD F.

NASA low-speed axial compressor for fundamental research
[NASA-TM-4635] p 296 N95-23192

WEAVER, THOMAS L.

Fiber Optic Control System integration for advanced aircraft. Electro-optic and sensor fabrication, integration, and environmental testing for flight control systems
[NASA-CR-191194] p 162 N95-19236

WEBB, GRANVILLE L.

NASA evaluation of Type 2 chemical depositions
[SAE PAPER 932582] p 495 A95-90086

WEBER, CARLOS

Turbulence models in the Navier-Stokes simulation of airfoil stall
[TRITA-NA-9312] p 705 N95-33059

WEBER, MARK

Use of high resolution lightning detection and localization sensors for hazardous aviation weather nowcasting
p 661 A95-93486

WEBSTER, B. E.

Automated adaptive time-discontinuous finite element method for unsteady compressible airfoil aerodynamics
[HTN-95-81637] p 541 A95-87685

WEBSTER, HARRY

Fuselage burnthrough from large exterior fuel fires
[AD-A266295] p 226 N95-22318

WEDGE, DONNE

Terminal Doppler Weather Radar Build 5A Operational Test and Evaluation (OT/E) integration and OT/E operational test plan
[AD-A283052] p 61 N95-12996

WEEKS, WILLIAM A.

Active control of complex noise problems using a broadband, multichannel controller
p 29 N95-11271

WEETMAN, D. C.

Health and usage monitoring systems: Corrosion surveillance
p 262 N95-23506

WEHR, T.

Aircraft measurements of ClO and HCL during EASOE 1991/92
[HTN-95-00721] p 444 A95-86291

WEI, R. P.

Corrosion and corrosion fatigue of airframe aluminum alloys
p 87 N95-14465

WEI, YING-JYI PAUL

Intelligent control law tuning for AIAA controls design challenge
[BTN-94-EIX94511433922] p 169 A95-64588

WEIBRING, G.

Modeling of plume chemistry of high flying aircraft with H₂ combustion engines
p 509 A95-87405

WEIDEL, M.

Automatic flight control system for an unmanned helicopter system design and flight test results
p 622 N95-32004

WEIDEMAN, MARK H.

Resin transfer molding of textile preforms for aircraft structural applications
p 421 N95-28276

WEIDNER, JOHN P.

Experimental investigation of inlet-combustor isolators for a dual-mode scramjet at a Mach number of 4
[NASA-TP-3502] p 407 N95-28343

WEILENMANN, MARTIN F.

Test bench for rotorcraft hover control
[BTN-94-EIX94511433919] p 169 A95-64585

WEILMUNSTER, K. JAMES

Navier-Stokes simulations of Orbiter aerodynamic characteristics including pitch trim and bodyflap
[BTN-95-EIX95041503779] p 204 A95-69210

Multiblock analysis for Shuttle Orbiter reentry heating from Mach 24 to Mach 12
[BTN-95-EIX95041503780] p 205 A95-69211

WEINACHT, PAUL

Navier-Stokes predictions of missile aerodynamics
p 74 N95-14451

WEINHEIMER, A. J.

Three-dimensional model interpretation of NO(x) measurements from the lower stratosphere
[HTN-95-90534] p 213 A95-67806

An analysis of aircraft exhaust plumes from accidental encounters
[HTN-95-70943] p 351 A95-78008

Meridional distributions of NO(X), NO(Y), and other species in the lower stratosphere and upper troposphere during AASE 2
[HTN-95-70944] p 352 A95-78009

WEINSTEIN, L. F.

TRISTAR 1: Evaluation methods for testing head-up display (HUD) flight symbology
[NASA-TM-4665] p 288 N95-24030

WEINSTEIN, LEONARD M.

Aerodynamic investigation with focusing schlieren in a cryogenic wind tunnel
[HTN-95-20835] p 544 A95-88096

An optical technique for examining aircraft shock wave structures in flight
p 96 N95-14879

WEINSTEIN, S.

A new guidance and flight control system for the DELTA 2 launch vehicle
p 342 A95-80427

WEINTRAUB, DANIEL J.

Design of head-up display symbology for recovery from unusual attitudes
p 611 A95-95044

WEINTRAUB, DAVID

Development of an Automated Airfield Dynamic Cone Penetrometer (AADCP) prototype and the evaluation of unsurfaced airfield seismic surveying using Spectral Analysis of Surface Waves (SASW) technology
[AD-A281985] p 145 N95-17444

WEIR, DONALD S.

Aircraft noise prediction program theoretical manual: Rotorcraft System Noise Prediction System (ROTONET), part 4
[NASA-TM-83199-PT-4] p 451 N95-26392

WEIRICH, R. F.

Transonic wind tunnel boundary interference correction
p 147 N95-19271

WEISE, TIMOTHY MICHAEL

Central coast designs: The Eightball Express. Taking off with convention, cruising with improvements and landing with absolute success
[NASA-CR-197181] p 47 N95-12643

WEISENSTEIN, DEBRA K.

Effects on stratospheric ozone from high-speed civil transport: Sensitivity to stratospheric aerosol loading
[HTN-95-91842] p 354 A95-80830

WEISS, C.

STOVL Control Integration Program
[NASA-CR-195358] p 18 N95-11487

WEISS, C. F.

Integrated aircraft thermal management and power generation
[SAE PAPER 932055] p 500 A95-91636

WEISS, CARL F.

A subsystem integration technology concept
[SAE PAPER 931382] p 604 A95-93658

WEISS, MERKEL F.

Design and styling of an advanced flying automobile
[SAE PAPER 932603] p 494 A95-90073

WEISS, S.

Parameter identification for X-31A at high angles of attack
p 69 N95-14235

WEISS, STEVEN

Anechoic chamber upgrade
[AD-A294375] p 700 N95-34342

WEISS, SUSANNE

Analytical solution and parameter estimation of projectile dynamics
[BTN-95-EIX95212645695] p 272 A95-76747

WEISS, THOMAS M.

The ATC operational evaluation of the prototype integrated terminal weather system (ITWS) at Dallas/Fort Worth and Orlando airports (May-September 1993)
[AD-A293808] p 677 N95-31587

WEISSHAAR, TERENCE A.

Design of a high capacity long range cargo aircraft
[NASA-CR-197176] p 45 N95-12363

WEISTENSTEIN, D. K.

Subsidence of aircraft engine exhaust in the stratosphere: Implications for calculated ozone depletions
[PAPER-93GL03426] p 251 A95-70297

WELCH, GERARD E.

Wave rotor-enhanced gas turbine engines
[NASA-TM-106998] p 615 N95-30517

WELLS, EDWARD A.

Propulsion Controlled Aircraft design and development
p 697 N95-33022

WELLS, JENNIFER

The OFP-6M transport jet
[NASA-CR-197159] p 46 N95-12637

WELLS, VALANA L.

The potential of genetic algorithms for conceptual design of rotor systems
[NASA-CR-196813] p 43 N95-11699

WELLS, WILLIAM R.

Direct adaptive and neural control of wing-rock motion of slender delta wings
[BTN-95-EIX95242670748] p 327 A95-81099

WELSH, B. L.

A note on the interpretation of mini-tuft photographs
[HTN-95-01089] p 468 A95-90275

WENDT, B. J.

Flow structure in the wake of a wishbone vortex generator
[BTN-95-EIX95142553044] p 304 A95-73454

WENDT, BRUCE J.

A new algorithm for five-hole probe calibration, data reduction, and uncertainty analysis
[NASA-TM-106458] p 38 N95-12378

Study of compressible flow through a rectangular-to-semiannular transition duct
[NASA-CR-4660] p 338 N95-24392

The decay of longitudinal vortices shed from airfoil vortex generators
[NASA-CR-198356] p 480 N95-29402

WENDT, M.

Shock tunnel studies of scramjet phenomena 1993
[NASA-CR-195038] p 350 N95-25394

WENG, P. F.

Swirl control in an S-duct at high angle of attack
[HTN-95-20846] p 545 A95-88107

WENGLAR, LYDIA

New technologies for space avionics
[NASA-CR-197574] p 150 N95-18196

WENHAN, QIN

Aerodynamic parameters of crop canopies estimated with a center-of-pressure technique
[HTN-95-41901] p 356 A95-81648

WENNERBERG, P. O.

Aircraft-borne, laser-induced fluorescence instrument for the in situ detection of hydroxyl and hydroperoxyl radicals
[BTN-95-EIX95072499029] p 253 A95-71908

WENTWORTH, SEAN L.

Transmittance characteristics of US Army rotary-wing aircraft transparencies
[AD-A295035] p 693 N95-34793

WENTZ, KENNETH R.

Thermo-acoustic fatigue design for hypersonic vehicle skin panels
p 162 N95-19161

WENTZ, W. H., JR.

Comparative wind tunnel tests of NACA 23024 airfoils with several aileron and spoiler configurations
p 376 N95-27976

WENTZ, WILLIAM H.

AIAA Techfest 20 Proceedings
[NIAAR-94-1] p 367 N95-26941

WENTZ, WILLIAM H., JR.

Aerodynamic characteristics of truncated airfoils at high angle of attack
[SAE PAPER 931227] p 460 A95-87365

WENZ, CRAIG J.

Conceptual design of a map interactive system for military aircraft cockpits
[AD-A289760] p 508 N95-28692

WERESZCZAK, A. A.

Evolution of oxidation and creep damage mechanisms in HIPed silicon nitride materials
[DE95-001360] p 300 N95-22689

WERT, JOHN A.

NASA-JVA light aerospace alloy and structures technology program (LA2ST)
[NASA-CR-198041] p 343 N95-24220

- WESLER, JOHN E.**
Noise metrics and aviation noise control: The case for DNL p 559 A95-88475
- WESLEY, D. A.**
Preliminary results of high resolution measurements of snowfall at Stapleton International Airport during the winter of 1992-93 p 661 A95-93484
- WESLEY, DOUGLAS A.**
The 1992-3 operational winter forecasting experiment for Stapleton airport p 677 A95-93561
- WESOKY, HOWARD L.**
The atmospheric effects of stratospheric aircraft: A fourth program report [NASA-RP-1359] p 357 N95-24274
- WEST, M. G.**
Interference between tanker wing wake with roll-up and receiver aircraft [BTN-95-EIX95062487552] p 185 A95-68366
- WESTBROOK, STEVEN R.**
Mechanism of deposit formation on fuel-wetted hot metal surfaces [AD-A289847] p 426 N95-28621
- WESTBYE, C. J.**
Study of heat transfer rates during quenching of a hot tube under microgravity p 428 A95-82641
- WESTFIELD, WILLIAM T.**
Corrosion of fire-damaged aircraft [AD-A294968] p 693 N95-34583
- WESTON, R. J.**
The effects and prediction of rotary wing aircraft noise on the community [HTN-95-92536] p 558 A95-87356
- WESTPHAL, RUSSELL V.**
Transonic flight test of a laminar flow leading edge with surface excrescences [NASA-TM-4597] p 9 N95-11158
- WESTWATER, ED R.**
Possible near-IR channels for remote sensing precipitable water vapor from geostationary satellite platforms [HTN-95-70139] p 214 A95-69431
- WETTLAUER, BRIAN**
Hypersonic air-breathing aeropropulsion facility test support requirements p 144 N95-16319
- WEYER, ROBERT M.**
Open Skies project computational fluid dynamic analysis [AD-A285928] p 223 N95-19991
- WEYER, ROBERT W.**
Computational aerodynamic analysis on the Open Skies aircraft [SAE PAPER 932514] p 466 A95-89187
- WHALING, K. N.**
Stationary premixed flames in spherical and cylindrical geometries [HTN-95-42336] p 418 A95-86165
- WHEELER, MARK L.**
Evaluation of the radio frequency susceptibility of commercial GPS receivers [BTN-95-EIX95042474624] p 189 A95-68278
- WHEELER, MARK M.**
Analysis of rapidly developing fog at the Kennedy Space Center p 671 A95-93531
- WHELAN, TODD**
The OFP-6M transport jet [NASA-CR-197159] p 46 N95-12637
- WHETSTONE, J. R.**
Allison engine testing CMSX-4(reg sign) single crystal turbine blades and vanes [DE95-010308] p 694 N95-32636
- WHIFFEN, BRUCE**
FTGEN - An automated FT production system p 668 A95-93519
- WHILLOCK, RAND**
Synthetic Terrain Imagery for Helmet-Mounted Display. Volume 2: Software design document [AD-A293611] p 612 N95-31655
Synthetic Terrain Imagery for Helmet-Mounted Display, volume 1 [AD-A293612] p 612 N95-31656
- WHISNANT, PAM**
The use of electrochemistry and ellipsometry for identifying and evaluating corrosion on aircraft [AD-A290249] p 504 N95-29426
- WHITAKER, DAVID L.**
Hybrid structured/unstructured grid computations for the F/A-18 at high angle of attack p 68 N95-14233
- WHITAKER, KEVIN W.**
Predicting exhaust plume boundaries with supersonic external flows [BTN-95-EIX95152583258] p 297 A95-73559
- WHITE, GEORGE**
Safety in airport ground handling p 626 A95-95193
- WHITE, JOHN A.**
Fiber optic hardware for transport aircraft [SAE PAPER 931439] p 680 A95-93691
- WHITE, M. E.**
Hypersonic shock wave/turbulent boundary layer interactions in the vicinity of an expansion corner [AIAA PAPER 95-6125] p 469 A95-90446
- WHITE, R. G.**
Nonlinear dynamic response of aircraft structures to acoustic excitation p 135 N95-19151
- WHITE, S. M.**
Analysis of flow channeling near the wall in packed beds [HTN-94-00698] p 2 A95-60177
- WHITEHEAD, R. S.**
C-130 Advanced Technology Center wing box conceptual design/cost study p 423 N95-28437
- WHITESIDE, J.**
Aerospace applications of new materials [CONGRESS PAPER C428-17-135] p 531 A95-91716
- WHITING, ELLIS E.**
Science objectives and performance of a radiometer and window design for atmospheric entry experiments [NASA-TM-4637] p 63 N95-12190
Science objectives and performance of a radiometer and window design for atmospheric entry experiments p 85-N95-13718
- WHITMER, GARY A.**
GPS modeling for designing aerospace vehicle navigation systems [BTN-95-EIX95302731223] p 600 A95-94044
- WHITNEY, MARK G.**
Quantity-distance requirements for earth-bermed aircraft shelters [AD-A279692] p 341 N95-24424
- WHITTAKER, THOMAS**
Optimal trajectories for hypersonic launch vehicles [HTN-95-61120] p 415 A95-84884
- WICKER, RYAN B.**
Near field of a coaxial jet with and without axial excitation [HTN-95-42332] p 372 A95-86161
- WICKS, B. J.**
Fatigue crack growth in nickel-based superalloys at 500-700 C. 1: Waspaloy [BTN-94-EIX94371347843] p 206 A95-69136
- WICKS, MICHAEL C.**
Polarization diverse ultra-wideband antenna technology p 488 A95-90924
- WIELER, J. G.**
Terminal Doppler Weather Radar point target filter threshold selection p 662 A95-93490
- WIELER, JIM**
Final results of the weather testing component of the Terminal Doppler Weather Radar operational test and evaluation p 658 A95-93471
- WIENER, GERRY**
Automated aircraft routing through weather-impacted airspace p 666 A95-93512
- WIESBAUM, J.**
Numerical modeling and simulation of chemically reacting reentry flows p 525 A95-87387
- WIESBECK, W.**
Geodesic constant method: A novel approach to analytical surface-ray tracing on convex conducting bodies [BTN-95-EIX95302731054] p 637 A95-94205
- WIESE, D. E.**
Integrated aircraft thermal management and power generation [SAE PAPER 932055] p 500 A95-91636
- WIESEMAN, CAROL D.**
On-line analysis capabilities developed to support the active flexible wing wind-tunnel tests [BTN-95-EIX95182619213] p 296 A95-76639
- WIESEN, P.**
Nitrous oxide and methane emissions from aero engines [HTN-95-21363] p 353 A95-78678
- WIGHTMAN, DENNIS C.**
The simulator training research advance testbed for aviation (STRATA): A simulation research facility for army aviation p 626 A95-95161
- WILBUR, M. L.**
Demonstration of an elastically coupled twist control concept for tilt rotor blade application [BTN-94-EIX94441386633] p 196 A95-68182
Demonstration of an elastically coupled twist control concept for tilt rotor blade application [HTN-95-20959] p 465 A95-88998
- WILCOX, F.**
Base drag prediction on missile configurations [BTN-95-EIX95152583256] p 266 A95-73557
- WILCOX, FLOYD J., JR.**
Drag measurements of an axisymmetric nacelle mounted on a flat plate at supersonic speeds [NASA-TM-4660] p 684 N95-32821
- WILCOX, PETER**
Further investigations of icing effects on an advanced high-lift multi-element airfoil [NASA-TM-106947] p 381 N95-27762
- WILDEN, KURTIS S.**
Cost model relationships between textile manufacturing processes and design details for transport fuselage elements p 536 N95-29043
- WILDER, GREG**
User documentation of the CTA program [AD-A289508] p 375 N95-26854
- WILDER, M. C.**
Interferometric investigations of compressible dynamic stall over a transiently pitching airfoil [HTN-95-42338] p 372 A95-86167
Control of unsteady separated flow associated with the dynamic stall of airfoils [NASA-CR-197024] p 74 N95-14613
Control of unsteady separated flow associated with the dynamic stall of airfoils [NASA-CR-198972] p 594 N95-32193
- WILES, J.**
Civil aircraft performance - developments for improved safety [CONGRESS PAPER C428-25-175] p 596 A95-93601
- WILHELM, KNUT**
Summary of a joint program of research into aircraft flight control concepts [AD-A280012] p 237 N95-20004
- WILKINS, K. E.**
Full-scale testing and analysis of fuselage structure p 95 N95-14485
- WILLARD, SCOTT A.**
The characterization of widespread fatigue damage in fuselage structure [NASA-TM-109142] p 88 N95-14920
The characterization of widespread fatigue damage in fuselage structure p 166 N95-19472
- WILLAUME, J.**
Interaction of a three strut support on the aerodynamic characteristics of a civil aviation model p 122 N95-19279
- WILLDEN, KURTIS**
Composite fuselage crown panel manufacturing technology p 399 N95-28474
Characterization and manufacture of braided composites for large commercial aircraft structures p 426 N95-28478
In situ processing methods for composite fuselage sandwich structures p 531 N95-28826
Manufacturing scale-up of composite fuselage crown panels p 532 N95-28835
- WILLIAMS, D. A.**
ASTRA - A safe, simplex, fly-by-wire aircraft control system [CONGRESS PAPER C428-37-218] p 610 A95-93634
- WILLIAMS, DAVID L., II**
Free-to-roll tests of X-31 and F-18 subscale models with correlation to flight test results p 69 N95-14237
- WILLIAMS, F. A.**
Theories of turbulent combustion in high speed flows [AD-A280933] p 23 N95-10535
- WILLIAMS, FRED W.**
Buckling and vibration analysis of laminated panels using VICONOPT [PAPER-1746] p 230 A95-72580
- WILLIAMS, GLENN W.**
Universal wind tunnel data acquisition and reduction software [AD-A283897] p 171 N95-18365
- WILLIAMS, K. E.**
Design and operation of a supersonic annular flow facility [BTN-94-EIX94441386624] p 183 A95-68173
Design and operation of a supersonic annular flow facility [HTN-95-20941] p 465 A95-88980
- WILLIAMS, KEVIN W.**
Development of qualification guidelines for personal computer-based aviation training devices [DOT/FAA/AM-95/6] p 323 N95-23603
- WILLIAMS, M. J.**
Out of area experiences with the RB199 in Toronto p 198 N95-19654
- WILLIAMS, RICHARD J.**
Knowing our users - A challenge for meteorologists at the National Aviation Weather Advisory Unit p 655 A95-93459
- WILLIAMS, S. L.**
Computational study of a two-slot circulation control airfoil [SAE PAPER 932531] p 466 A95-89191

- WILLIAMS, STEVEN P.**
Spatial awareness comparisons between large-screen, integrated pictorial displays and conventional EFIS displays during simulated landing approaches [NASA-TP-3467] p 80 N95-14852
- WILLIAMS, W. D.**
Hypersonic flow-field measurements: Intrusive and nonintrusive [AD-A283867] p 119 N95-18674
Analysis of planar laser-induced fluorescence images obtained during shakedown testing of the AEDC impulse facility [AD-A293237] p 646 N95-30906
- WILLIAMS, WILLIAM R.**
Evaluation of commercial water-in-fuel test kits [AD-A292135] p 537 N95-29572
- WILLIAMSON, R.**
Using IRI for the computation of ionospheric corrections for altimeter data analysis p 212 A95-66949
- WILLIS, B. P.**
Flow coefficient behavior for boundary layer bleed holes and slots [NASA-TM-106846] p 244 N95-19953
- WILLIS, ZDENKA S.**
Naval Aviation System TEAM mapping, charting, and geodesy handbook [AD-A288590] p 446 N95-26841
- WILLMARTH, W. W.**
Measurements of vortex pair interaction with a clean or contaminated free surface [BTN-94-EIX95011441063] p 429 A95-82798
- WILLSHIRE, WILLIAM L., JR.**
En route noise levels from propfan test assessment airplane [NASA-TP-3451] p 62 N95-12341
- WILMOTH, RICHARD G.**
Hypersonic rarefied flow past spheres including wake structure [BTN-95-EIX95152583250] p 305 A95-73551
Zonally decoupled direct simulation Monte Carlo solutions of hypersonic blunt-body wake flows [BTN-95-EIX95182617458] p 268 A95-75729
- WILSON, D.**
The NASA/UTA Center for hypersonic research [AIAA PAPER 95-6106] p 520 A95-90438
The mini-business approach at Chadderton [CONGRESS PAPER C428-26-037] p 681 A95-93602
- WILSON, D. R.**
NASA-ACEE/Boeing 737 graphite-epoxy horizontal stabilizer service p 400 N95-28489
- WILSON, DALE A.**
Fatigue and residual strength investigation of ARALL(R) -3 and GLARE(R) -2 panels with bonded stringers p 137 N95-19495
- WILSON, DAVID J.**
High angle of attack flying qualities criteria for longitudinal rate command systems p 70 N95-14247
- WILSON, EMILY**
A market perspective on FANS [SAE PAPER 932521] p 486 A95-89189
- WILSON, F. W.**
Initial evaluation of the Oregon State University planetary boundary layer column model for ITWS applications [AD-A293775] p 677 N95-31465
- WILSON, F. WESLEY, JR.**
ITWS ceiling and visibility products p 654 A95-93454
ITWS gridded analysis p 654 A95-93455
LLWAS 2 and LLWAS 3 performance evaluation p 662 A95-93491
- WILSON, GREGORY J.**
Numerical simulations of the flow in the HYPULSE expansion tube [NASA-TM-110357] p 523 N95-30228
- WILSON, J. C.**
Performance of a focused cavity aerosol spectrometer for measurements in the stratosphere of particle size in the 0.06-2.0-micrometer-diameter range [HTN-95-90914] p 253 A95-72423
- WILSON, JACK**
Recent improvements to and validation of the one dimensional NASA wave rotor model [NASA-TM-106913] p 332 N95-25962
Optimization of wave rotors for use as gas turbine engine topping cycles [NASA-TM-106951] p 406 N95-27860
- WILSON, JAMES W.**
The real-time analysis and prediction of storms program p 655 A95-93457
Developing thunderstorm forecast rules utilizing first detectable cloud radar-echoes p 667 A95-93514
- WILSON, JOHN R.**
A rose by any other name: Certification seen as process rather than content p 688 N95-34766
- WILSON, JOHN W.**
Radiation safety aspects of commercial high-speed flight transportation [NASA-TP-3524] p 453 N95-26427
- WILSON, K. J.**
A pulsed liquid fuel ramjet p 617 N95-31201
- WILSON, KENNETH J.**
Suppressor of oscillations in airframe cavities [AD-D017265] p 388 N95-26507
- WILSON, MARK R.**
The influence of source acceleration on acoustic signals p 577 A95-90136
Effects of signal analysis parameters and noise removal on measured aircraft spectra p 578 A95-90137
Signal processing of noise data from high-speed flyovers [BTN-95-EIX0619952748178] p 680 A95-94248
- WILSON, ROBERT E.**
Preliminary analysis of dynamic stall effects on a 91-meter wind turbine rotor p 376 N95-27975
- WILSON, WILLIAM G.**
Recent advances in graphite/epoxy motor cases p 149 N95-16333
- WIMMER, W.**
EURECA mission control experience and messages for the future p 149 N95-17252
- WIMMERSTROEM, P.**
Propulsion research concerning SFRJ-motors [PB94-179520] p 14 N95-10083
- WINFREE, W. P.**
New nondestructive techniques for the detection and quantification of corrosion in aircraft structures p 315 N95-23512
- WING, DAVID J.**
Simultaneous three-dimensional velocity and mixing measurements by use of laser Doppler velocimetry and fluorescence probes in a water tunnel [NASA-TP-3454] p 53 N95-13553
Twin engine afterbody model p 115 N95-17880
Static investigation of two fluidic thrust-vectoring concepts on a two-dimensional convergent-divergent nozzle [NASA-TM-4574] p 120 N95-19042
Static investigation of two fluidic thrust-vectoring concepts on a two-dimensional convergent-divergent nozzle [NASA-TM-4574] p 222 N95-19913
Afterbody/nozzle pressure distributions of a twin-tail twin-engine fighter with axisymmetric nozzles at Mach numbers from 0.6 to 1.2 [NASA-TP-3509] p 594 N95-31984
- WINKLER, CHRISTOPHER B.**
Electrorheologically controlled landing gear [BTN-94-EIX94461047055] p 78 A95-61740
An electrorheologically controlled semi-active landing gear [SAE PAPER 931403] p 605 A95-93673
- WINN, JOHN S.**
Matrix isolated HF: the high-resolution infrared spectrum of a cryogenically solvated hindered rotor [GTN-95-0301010494002231-16] p 578 A95-92210
- WINNENBERG, THOMAS F.**
Waveform bounding and combination techniques for direct drive testing [AD-A284075] p 161 N95-19035
- WINOTO, S. H.**
Measurement in laminar and transitional boundary-layer flows on concave surface [BTN-95-EIX95282711333] p 632 A95-92408
- WINTER, J.**
Advanced gust management systems: Lessons learned and perspectives p 622 N95-32002
- WIRKANDER, S. L.**
Evaluation of an autopilot based multimodelling [PB94-190725] p 142 N95-17454
- WIRTH, M.**
Two dimensional stratospheric aerosol distributions during EASOE [HTN-95-00726] p 444 A95-86296
- WIRTHMAN, D. J.**
Trajectory optimization using parallel shooting method on parallel computer [BTN-95-EIX95282706670] p 564 A95-88175
- WISELY, PAUL L.**
Design of wide angle head up displays for synthetic vision [BTN-95-EIX95212641070] p 287 A95-76735
- WITTE, DAVID W.**
Computer code for determination of thermally perfect gas properties [NASA-TP-3447] p 37 N95-11995
- WITTLIN, G.**
Commuter airplane accident data analysis [AD-A286315] p 226 N95-20174
- WOFSY, S. C.**
In situ observations in aircraft exhaust plumes in the lower stratosphere at midlatitudes [HTN-95-A0862] p 318 A95-76266
The distribution of hydrogen, nitrogen, and chlorine radicals in the lower stratosphere: Implications for changes in O3 due to emission of NO(y) from supersonic aircraft [HTN-95-70935] p 351 A95-78000
- WOFSY, STEVEN C.**
Vertical transport rates in the stratosphere in 1993 from observations of CO2, N2O, and CH4 [HTN-95-70941] p 351 A95-78006
The atmospheric effects of stratospheric aircraft: A fourth program report [NASA-RP-1359] p 357 N95-24274
- WOLF, K.**
External patch repair of CFRP/honeycomb sandwich p 395 N95-27522
- WOLF, STEPHEN W. D.**
Adaptive wall technology for minimization of wind tunnel boundary interferences - where are we now? p 519 A95-88903
- WOLFE, H. F.**
Nonlinear dynamic response of aircraft structures to acoustic excitation p 135 N95-19151
- WOLFE, HOWARD F.**
Large amplitude nonlinear response of flat aluminum, and carbon fiber plastic beams and plates [AD-A282440] p 96 N95-15547
- WOLFF, ERIC W.**
Antarctic snow record of southern hemisphere lead pollution [HTN-95-40359] p 212 A95-66869
- WOLFRAMM, A. P.**
HeliRadar: A rotating antenna synthetic aperture radar for helicopter allweather operations p 705 N95-33137
- WOLFSON, MARILYN M.**
The ITWS microburst prediction algorithm p 655 A95-93456
MDCRS: Aircraft observations collection and uses p 668 A95-93517
- WON, I. J.**
Geophex airborne unmanned survey system [DE95-007566] p 392 N95-27440
- WONG, ERIC Y.**
An extension of the continuum model by Grad's thirteen moment equations for hypersonic rarefied flows p 478 N95-29118
- WONG, J. P. C.**
Application of superplastically formed and diffusion bonded structures in high intensity noise environments p 174 N95-19162
- WONG, K. C.**
Six degree of freedom flight dynamic and performance simulation of a remotely-piloted vehicle [AERO-TN-9301] p 131 N95-18097
- WONG, KENT J.**
Accurate drag prediction: A prerequisite for drag reduction research [SAE PAPER 932571] p 467 A95-90060
- WONG, R. L. M.**
Development and validation of a numerical acoustic analysis program for aircraft interior noise prediction p 572 A95-88471
- WOOD, EDMUND P.**
Novel matrix resins for composites for aircraft primary structures, phase 1 [NASA-CR-189657] p 23 N95-10318
Development of RTM and powder prepreg resins for subsonic aircraft primary structures p 536 N95-29044
- WOOD, C. W.**
Simulating heat addition via mass addition in constant area compressible flows [BTN-95-EIX95182619100] p 307 A95-76585
- WOOD, DAVID**
Simulation and model reduction for the active flexible wing program [BTN-95-EIX95182619211] p 295 A95-76637
- WOOD, J. G.**
Oscillating-flow regenerator test rig [NASA-CR-196982] p 53 N95-13200
- WOOD, JERRY R.**
Laser anemometer measurements of the three-dimensional rotor flow field in the NASA low-speed centrifugal compressor [NASA-TP-3527] p 618 N95-31985
- WOOD, M. J.**
Electromagnetic compatibility - A general overview [CONGRESS PAPER C428-38-084] p 634 A95-93637
- WOOD, N. J.**
Unsteady aerodynamic effects of trailing edge controls on delta wings [HTN-95-01099] p 469 A95-90285

- WOOD, RICHARD J.**
Generic architectures for future flight systems
p 99 N95-14159
- WOOD, RICHARD M.**
Passive porosity with free and fixed separation on a tangent-ogive forebody
[BTN-95-EIX95062487554] p 185 A95-68368
Effect of leading- and trailing-edge flaps on clipped delta wings with and without wing camber at supersonic speeds
[NASA-TM-4542] p 5 N95-10028
Base passive porosity for drag reduction
[NASA-CASE-LAR-15246-1] p 91 N95-14183
- WOOD, VINCENT T.**
A technique for detecting a tropical cyclone center using a Doppler radar
[HTN-95-20631] p 215 A95-69574
- WOODBIDGE, E. L.**
Estimates of total organic and inorganic chlorine in the lower stratosphere from in situ and flask measurements during AASE 2
[HTN-95-A0861] p 317 A95-76265
In situ observations in aircraft exhaust plumes in the lower stratosphere at midlatitudes
[HTN-95-A0862] p 318 A95-76266
The distribution of hydrogen, nitrogen, and chlorine radicals in the lower stratosphere: Implications for changes in O3 due to emission of NO(y) from supersonic aircraft
[HTN-95-70935] p 351 A95-78000
- WOODBURN, P. A.**
External viewing airborne CCTV system
[CONGRESS PAPER C428-25-172] p 595 A95-93598
- WOODCOCK, ROBERT W.**
Summary of a joint program of research into aircraft flight control concepts
[AD-A280012] p 237 N95-20004
- WOODFIELD, ALAN A.**
Wind shear and its effects on aircraft
p 77 N95-14898
- WOODHOUSE, GEOFFREY D.**
Auxiliary Power Unit evolution: Meeting tomorrow's challenges
[SAE PAPER 932541] p 510 A95-89195
- WOODS-VEDELER, JESSICA A.**
Rolling maneuver load alleviation using active controls
[BTN-95-EIX95182619217] p 270 A95-76643
Active load control during rolling maneuvers
[NASA-TP-3455] p 129 N95-17397
- WOODWARD, M. R.**
Applications of a damage tolerance analysis methodology in aircraft design and production
p 426 N95-28483
- WOODWARD, RICHARD P.**
Background noise levels measured in the NASA Lewis 9- by 15-foot low-speed wind tunnel
[NASA-TM-106817] p 145 N95-18054
- WOODYATT, B. A.**
Enhancement of F/A-18 operational flight measurements: Data report for phase 1
[DSTO-TR-0049] p 286 N95-23666
- WOOLONS, D. J.**
Fault Diagnosis for condition monitoring applied to hydraulic circuits
[CONGRESS PAPER C428-12-165] p 456 A95-91703
- WORDEN, R. E.**
Full-scale testing and analysis of fuselage structure
p 95 N95-14485
- WORONOWICZ, M. S.**
Cercignani-Lampis-Lord gas-surface interaction model: Comparisons between theory and simulation
[BTN-95-EIX95041503806] p 242 A95-70131
- WORSWICK, M. J.**
Numerical modelling of transverse impact on composite coupons
[BTN-95-EIX95082502225] p 240 A95-71022
- WORTMAN, D. J.**
PVD TBC experience on GE aircraft engines
p 345 N95-26126
- WRAY, BUNTINE**
Initial exploration of the ASRS database
p 681 A95-95204
- WRAY, RICHARD B.**
An avionics scenario and command model description for Space Generic Open Avionics Architecture (SGOAA)
[NASA-CR-188330] p 49 N95-11913
Space Generic Open Avionics Architecture (SGOAA): Overview
p 99 N95-14161
- WRAY, S.**
Impact finite element analysis, as an alternative to the testing of windscreens for bird impact
[CONGRESS PAPER C428-23-196] p 500 A95-91732
- WRIGHT, A.**
Aircraft wake vortex takeoff tests at O'Hara International Airport
[AD-A283828] p 118 N95-18624
- WRIGHT, B. R.**
A study of aircraft post-crash fuel fire mitigation
[AD-A282208] p 40 N95-12499
- WRIGHT, I. G.**
Thermal barrier coatings issues in advanced land-based gas turbines
p 344 N95-26122
- WRIGHT, JOSEPH A.**
Analysis of test criteria for specifying foam firefighting agents for aircraft rescue and firefighting
[AD-A286381] p 227 N95-22352
- WRIGHT, K.**
The effect of interface properties on nickel base alloy composites
[NASA-CR-198363] p 629 N95-30787
- WRIGHT, MELANIE C.**
Resource document for the design of electronic instrument approach procedure displays
[AD-A295108] p 691 N95-34797
- WRIGHT, P.**
Environmental noise monitoring - source identification
[HTN-95-92537] p 558 A95-87357
- WRIGHT, ROBERT A.**
Advanced subsonic airplane design and economic studies
[NASA-CR-195443] p 338 N95-24304
- WRIGHT, WILLIAM B.**
User's manual for the NASA Lewis ice accretion/heat transfer prediction code with electrothermal deicer input
[NASA-CR-4530] p 57 N95-11888
Additional improvements to the NASA Lewis ice accretion code LEWICE
[NASA-TM-106849] p 309 N95-22669
Users manual for the improved NASA Lewis ice accretion code LEWICE 1.6
[NASA-CR-198355] p 485 N95-29132
- WU, CHANG-HUEI**
DC electrostatic gyro suspension system for the Gravity Probe B experiment
p 527 N95-29794
- WU, CHUNG-HUA**
A general theory of two- and three-dimensional rotational flow in subsonic and transonic turbomachines
[NASA-CR-4496] p 377 N95-28003
- WU, CLIFF Y. Y.**
Controlling mechanisms of ignition of solid fuel in a sudden-expansion combustor
[BTN-95-EIX0616952745791] p 628 A95-94255
- WU, EDWARD M.**
Proof test methodology for composites
p 424 N95-28445
- WU, H. F.**
MIL-HDBK-5 design allowables for fibre/metal laminates: ARALL 2 and ARALL 3
[BTN-94-EIX94371346933] p 300 A95-73345
- WU, J.-S.**
Effect of ambient turbulence intensity on sphere wakes at intermediate Reynolds numbers
[BTN-95-EIX95182619101] p 308 A95-76586
Sphere wakes at moderate Reynolds numbers in a turbulent environment
[HTN-95-42331] p 372 A95-86160
- WU, JAIN-MING JAMES**
On controlling the tip vortex flow of a lifting wing
[ISBN 1-879921-01-4] p 587 A95-93736
- WU, JAMES, C.**
Numerical solutions of three dimensional viscous flows
[ISBN 1-879921-01-4] p 587 A95-93749
- WU, JIE-ZHI**
A note on the Kutta-Joukowski formula
[ISBN 1-879921-01-4] p 635 A95-93735
- WU, L. L.**
MIL-HDBK-5 design allowables for fibre/metal laminates: ARALL 2 and ARALL 3
[BTN-94-EIX94371346933] p 300 A95-73345
- WU, MING**
Fatigue and residual strength investigation of ARALL(R) -3 and GLARE(R) -2 panels with bonded stringers
p 137 N95-19495
- WU, XIAOQING**
Linear prediction data extrapolation super-resolution radar imaging
p 155 N95-16268
- WU, XINGPING**
Direct splitting of coefficient matrix for numerical calculation of transonic nozzle flow
[BTN-94-EIX94481415356] p 103 A95-65346
- WU, XINPING**
Simulation on the 3-D turbulent flow in the passages of finocyl grain
[BTN-95-EIX95202638962] p 279 A95-76674
- WU, Z. N.**
Implicit multidomain calculation of viscous transonic flows without artificial viscosity or upwinding
p 640 A95-95443
- WU, ZHIQI**
An efficiency study of the simultaneous analysis and design of structures
[NASA-TM-110168] p 501 N95-28820
- WU, ZHIQIANG**
Effects of AMB parameters on the dynamic stability of the rotor
[BTN-94-EIX94381353450] p 323 A95-75494
- WURTELE, MORTON G.**
Lee waves benign and malignant
p 595 A95-93554

X

- XI, D. K.**
Numerical design methods for transonic NLF configurations
p 471 A95-91498
- XIANG, X.**
Behavior of an inversion-based precipitation retrieval algorithm with high-resolution AMPR measurements including a low-frequency 10.7-GHz channel
[HTN-95-70134] p 252 A95-70656
- XIE, H.**
Dynamic behavior of a magnetic-bearing supported jet engine rotor with auxiliary bearings
[NASA-CR-197860] p 338 N95-24213
- XIE, HUAJUN**
Steady-state dynamic behavior of an auxiliary bearing supported rotor system
p 703 N95-32690
Dynamic behavior of a magnetic bearing supported jet engine rotor with auxiliary bearings
p 703 N95-32691
- XIE, WEI-CHAU**
Lyapunov exponents and stochastic stability of two-dimensional parametrically excited random systems
[BTN-94-EIX94361122401] p 207 A95-65897
- XIE, YOU-BAI**
New strategy combining backward inference with forward inference in monitoring and diagnosing techniques for hydrodynamic bearing-rotor systems
[BTN-94-EIX94331336949] p 88 A95-61795
- XIJUN, HUANG**
Numerical investigation to S-inlet flows (Numerical simulation study of S-inlet flows)
[AD-A289590] p 374 N95-26713
- XIONG, FUQIN**
Development of aeronautical mobile satellite services over the past thirty years
[BTN-95-EIX95152569458] p 305 A95-73498
- XIONG, WEI-ZHONG**
Parallel methods for the flight simulation model
[DE94-013330] p 52 N95-11752
- XU, MIN**
Transport phenomena in stratified multi-fluid flow in the presence and absence of gravity
p 95 N95-14563
- XUE, DAVID Y.**
Finite element time domain - modal formulation for nonlinear flutter of composite panels
[BTN-95-EIX95042474401] p 203 A95-68299
Panel flutter limit-cycle suppression with piezoelectric actuation
[BTN-95-EIX95302731089] p 618 A95-94208
- XUE, YU**
Rotating Kirchhoff method for three-dimensional transonic blade-vortex interaction hover noise
[BTN-94-EIX94441386601] p 182 A95-67332
Rotating Kirchhoff method for three-dimensional transonic blade-vortex interaction hover noise
[HTN-95-20927] p 463 A95-88966

Y

- YAGER, THOMAS J.**
NASA evaluation of Type 2 chemical depositions
[SAE PAPER 932582] p 495 A95-90086
Aircraft nose gear shimmy studies
[SAE PAPER 931401] p 628 A95-93671
- YAGI, Y.**
Development of 70MW class superconducting generators
[BTN-94-EIX95011440854] p 429 A95-82905
- YAITA, M.**
Electro-optic characterization of ultrafast photodetectors using adiabatically compressed soliton pulses
[BTN-94-EIX94381359637] p 257 A95-72675
- YAJIMA, N.**
Polar Patrol Balloon system and preliminary experimental results
p 368 A95-82513
- YAJIMA, NOBUYUKI**
Polar Patrol Balloon
[BTN-95-EIX95152582318] p 316 A95-73521
Development and flight results of fiber reinforced balloon
p 384 A95-82511
- YAKOVLEV, V. A.**
Laser device for measuring a vessel's speed
[HTN-95-60992] p 361 A95-80633

- YALAMANCHILI, R.**
Vortex cutting by a blade. Part II: Computations of vortex response
[BTN-94-EIX94441386611] p 208 A95-67342
Vortex cutting by a blade, Part 2: Computations of vortex response
[HTN-95-20937] p 464 A95-88976
- YALIF, GUY U.**
The Computer Aided Aircraft-design Package (CAAP)
p 217 N95-19759
- YAMAGAMI, T.**
Polar Patrol Balloon system and preliminary experimental results
p 368 A95-82513
- YAMAGUCHI, SHIGERU**
Fixed transition for shock tube transonic flow
p 472 A95-91509
- YAMAGUCHI, YUTAKA**
Preliminary assessment of tunnel wall interference in the NDA cryogenic wind tunnel
[BTN-95-EIX95062487531] p 187 A95-69239
Preliminary study on the fixed transition technique for a shock tube transonic airfoil flow
[BTN-95-EIX95282705928] p 455 A95-89663
Fixed transition for shock tube transonic flow
p 472 A95-91509
- YAMAKAWA, EIICHI**
Application of GPS and Fuzzy Theory to a helicopter
p 516 A95-91505
- YAMAMOTO, KINGO J.**
Long distance propagation model and its application to aircraft en route noise prediction
[HTN-95-61221] p 491 A95-87594
- YAMAMOTO, KIYOSHI**
Direct numerical simulation of incompressible homogeneous isotropic turbulence using NWT
p 706 N95-34530
- YAMAMOTO, MASAHIKO**
Evaluation of scramjet nozzle performance
p 402 A95-82321
Performance variation of scramjet nozzle at various nozzle pressure ratios
[BTN-95-EIX0616952745781] p 615 A95-94505
- YAMAMOTO, NOBUO**
Analysis and scale-model experiment of propeller driving motor for microwave-powered airplane
p 487 A95-91576
- YAMAMOTO, SHIRO**
Hypersonic thermal protection with mass injection at angle of attack
p 414 A95-82414
- YAMAMOTO, TAKESHI**
Numerical simulation of combustion flow around a flame holder with hydrogen injection
[NAL-TR-1233] p 419 N95-26523
- YAMAMOTO, YUKIMITSU**
Numerical simulation of real gas effects and aerodynamic heating of hypersonic space transportation vehicles
p 540 A95-87558
Hypersonic CFD analysis for the aerothermodynamic design of HOPE
p 684 N95-34520
Application of CFD technique for HYFLEX aerodynamic design
p 693 N95-34542
- YAMANAKA, TATSUO**
An advanced scramjet propulsion concept for A 350 MG SSTO space plane
p 402 A95-82325
- YAMANE, TAKASHI**
An unsteady simulation of a centrifugal compressor stage using the NWT
p 707 N95-34536
- YAMANE, YOSHIYUKI**
A study of supersonic mixing flow field with ramp injector
p 706 N95-34512
- YAMASHITA, HIROSHI**
Prediction of NO(x) emission index of turbulent diffusion flame
p 538 A95-87195
- YAMASITA, TADASHI**
Missile autopilot designs using full state feedback
p 507 A95-91587
- YAMAUCHI, GLORIA K.**
Measurements of atmospheric turbulence effects on tail rotor acoustics
[NASA-TM-108843] p 38 N95-12360
- YAMAUCHI, MASAFUMI**
Numerical investigation of supersonic flows around a spiked blunt body
[BTN-95-EIX95212645690] p 271 A95-76742
- YAMAZAKI, TAKASHI**
Experimental study of shock/shock interference heating on a swept cylinder
p 472 A95-91510
A shock tunnel test of a winged hypersonic research vehicle
p 474 A95-91538
- YAMAZAKI, TETSUO**
Numerical analysis around the whole SST configuration
p 693 N95-34541
- YAMSHANOV, YU. B.**
Fatigue strength of high-temperature alloys under conditions of cyclic temperature variation. Communication 1: Experimental procedure and results
[BTN-94-EIX94401363884] p 307 A95-75516
- YAN, YANGGUANG**
The computer analysis of the prediction of aircraft electrical power supply system reliability
p 155 N95-16278
- YANAGI, RYOJI**
Some considerations on system design of the hypersonic transport and supersonic air-intakes
p 473 A95-91522
- YANAGIHARA, MASAOKI**
Measurements of longitudinal static aerodynamic coefficients by the cable mount system
[NAL-TR-1226] p 331 N95-25761
- YANAGIMOTO, K.**
Vortex shedding noise control in idling circular saws using air ejection at the teeth
[BTN-94-EIX94371347214] p 257 A95-69970
- YANAGIZAWA, MITSUNORI**
Calculation for aerodynamic characteristics on delta wing with leading-edge separated vortex effect using boundary element method
p 684 N95-34524
Grid generation around airfoil with a flap using boundary element method
p 686 N95-34552
- YANG, H.**
Using landmarks for the vehicle location measurement
[PB94-184512] p 43 N95-12582
- YANG, H. Q.**
Pressure based high order TVD methodology for dynamic stall control
[AD-A290149] p 479 N95-29316
- YANG, H. T.**
Supersonic, turbulent flow computation and drag optimization for axisymmetric afterbodies
[BTN-95-EIX95302729772] p 637 A95-94134
- YANG, JING-TANG**
Controlling mechanisms of ignition of solid fuel in a sudden-expansion combustor
[BTN-95-EIX0616952745791] p 628 A95-94255
- YANG, Q. Z.**
Numerical design methods for transonic NLF configurations
p 471 A95-91498
- YANG, S. J. ERIC**
Auxiliary power unit noise of Boeing B737 and B747 aircraft
p 571 A95-88468
- YANG, S. L.**
Efficient mapping topology for turbine combustors with inclined slots/staggered holes
[BTN-95-EIX0616952745805] p 614 A95-94485
- YANG, THOMAS T.**
Use of MOBITEC wireless wide area networks as a solution to land-based positioning and navigation
[BTN-94-EIX94441386132] p 189 A95-68188
- YANIEC, JOHN S.**
Users guide for NASA Lewis Research Center DC-9 Reduced-Gravity Aircraft Program
[NASA-TM-106755] p 146 N95-18586
- YANO, STEVE E.**
Arcjet thruster research and technology, phase 2
[NASA-CR-182276] p 105 N95-18044
- YANTA, WILLIAM J.**
Supercooling in hypersonic nitrogen wind tunnels
[BTN-94-EIX95011441134] p 340 A95-81020
- YAO, AKIRA**
Experimental investigation of composite channel heat pipe operation in micro-gravity environment
p 428 A95-82645
- YAO, JIE**
Experiments on microbursts
p 562 N95-29110
- YAO, YU**
Nonlinear observer and its application in flight control
p 447 A95-82449
- YARMUS, J.**
Aircraft wake vortex takeoff tests at O'Hara International Airport
[AD-A283828] p 118 N95-18624
- YAROSLAVTSEV, M. I.**
Integration of an hypersonic airbreathing vehicle: Assessment of overall aerodynamic performances and of uncertainties
[AIAA PAPER 95-6100] p 492 A95-88007
- YASHIN, YU. P.**
General requirements for the electrohydraulic systems of the aircraft controls loading force on the simulators
[CONGRESS PAPER C428-5-138] p 522 A95-91681
- YASUI, HIDEMI**
NAL aerothermodynamic probing and CFD verification mission in OREX experiment
p 368 A95-82413
- YASUI, HISAKO**
On the flight control system for UF-104
p 507 A95-91560
- YATSUYANAGI, N.**
Experiment of rocket-ram annular combustor
p 412 A95-82324
- YAU, M.**
Demonstration of the Dynamic Flowgraph Methodology using the Titan 2 Space Launch Vehicle Digital Flight Control System
[NASA-CR-197517] p 150 N95-17493
- YAZAWA, KENJI**
Flight Test Monitoring System using X-window
p 500 A95-91574
- YE, ZHENG-YIN**
A nonlinear vortex lattice method for unsteady flow with separated vortex
[DLR-FB-94-32] p 704 N95-32787
- YE, ZHENRU**
Linear prediction data extrapolation superresolution radar imaging
p 155 N95-16268
- YEAGER, DAVID M.**
Noise Con 1994: Proceedings of the 1994 National Conference on Noise Control Engineering. Progress in Noise Control for Industry
[LC-75-24750] p 28 N95-11259
- YEDDANAPUDI, MURALI**
MATSurv multisensor air traffic surveillance
[AD-A292253] p 489 N95-28887
- YEE, SUSAN**
The Aluminum Falcon: A low cost modern commercial transport
[NASA-CR-197180] p 81 N95-15742
- YEE, ZEE**
Flight test development and evaluation of a Kalman filter state estimator for low-altitude flight
[HTN-94-00684] p 16 A95-60167
- YEH, DUN-YANN**
Transonic flutter suppression using active acoustic excitations
[BTN-95-EIX95262694310] p 408 A95-85481
- YEH, HWA-YOUNG M.**
Microwave and infrared simulations of an intense convective system and comparison with aircraft observations
[HTN-95-60511] p 214 A95-68762
- YEH, J. R.**
Prediction of R-curves from small coupon tests
p 167 N95-19496
- YELVERTON, J. NED**
Technology-insertion life-cycle-cost model
[AIAA PAPER 95-0961] p 581 A95-90638
- YEN, BING K.**
Surface morphology and structure of carbon-carbon composites in high-energy sliding contact
[BTN-94-EIX94371347996] p 206 A95-69164
- YEN, GUAN-WEI**
Unsteady flow simulations about moving boundary configurations using dynamic domain decomposition techniques
p 649 N95-31837
- YEN, JING G.**
Effects of blade tip shape on dynamics, cost, weight, aerodynamic performance, and aeroelastic response
[HTN-95-61074] p 369 A95-83658
- YESIL, OKTAY**
Transmission loss characteristics of aircraft sidewall systems to control cabin interior noise
p 28 N95-11261
- YETTER, J. A.**
16-foot transonic tunnel test section flowfield survey
[NASA-TM-109157] p 238 N95-20669
- YETTER, JEFFREY A.**
Why do airlines want and use thrust reversers? A compilation of airline industry responses to a survey regarding the use of thrust reversers on commercial transport airplanes
[NASA-TM-109158] p 226 N95-20706
- YEUNG, C. P.**
Three-dimensional interaction of wake/boundary-layer and vortex/boundary-layer data report
[CUED/A-AEREO/TR-23] p 329 N95-24210
- YI, WEI ZHI**
New experimental approach to determine initial fatigue quality with fastener holes
[BTN-94-EIX94522406136] p 701 A95-96273
- YILBAS, BEKIR S.**
Cooling of aerospace plane using liquid hydrogen and methane
[BTN-95-EIX0619952748171] p 590 A95-94465
- YIM, WOOSOO**
Direct adaptive and neural control of wing-rock motion of slender delta wings
[BTN-95-EIX95242670748] p 327 A95-81099
- YING, JUFENFEI**
A new type of simulator for simulating the flow-field distortion of engine inlet
[BTN-95-EIX95202638963] p 289 A95-76673
- YING, S. X.**
A fixed time performance evaluation of parallel CFD applications
[DE94-014240] p 436 N95-26445

Z

- YIP, LONG P.**
In-flight pressure measurements on a subsonic transport high-lift wing section
[BTN-95-EIX0619952748170] p 589 A95-94464
- YOKOYAMA, HISASHI**
Flight evaluation of DGPS and DGPS-INS navigation systems p 382 A95-82462
CCLM operation on MLS p 487 A95-91540
- YONEMOTO, KOICHI**
Hypersonic trajectory control of aerospace plane with integrated SCRAMJET engine p 413 A95-82384
Air data sensors for atmospheric reentry flight test of winged space vehicle p 413 A95-82412
A conceptual design of hypersonic research vehicle with subscale scramjet engine p 384 A95-82482
- YORK, JAMES L.**
Recent advances in graphite/epoxy motor cases p 149 N95-16333
- YOROZU, MASAHIRO**
Preliminary assessment of tunnel wall interference in the NDA cryogenic wind tunnel
[BTN-95-EIX95062487531] p 187 A95-69239
- YOSEF, REUVEN**
A review of falconry as a bird control technique with recommendations for use at the Shuttle Landing Facility, John F. Kennedy Space Center, Florida, USA
[NASA-TM-110142] p 381 N95-27859
- YOSHIDA, KENJI**
Experimental study for improving the lift to drag ratio of next generation SST p 473 A95-91524
- YOSHIDA, MASAHIRO**
Performance evaluation of the NWT with incompressible NS code p 707 N95-34533
Numerical simulation of unsteady viscous flow around an airfoil with oscillating spoiler p 685 N95-34547
- YOSHIKAWA, TAKAO**
Life evaluation of a low power arcjet thruster p 403 A95-82337
- YOSHIOKA, MINAKO**
Hypersonic CFD analysis for the aerothermodynamic design of HOPE p 684 N95-34520
- YOSHIZAWA, AKIRA**
Hypersonic wind tunnel test of sidewall compression type scramjet inlet p 410 A95-82320
- YOSHIZAWA, TAKESHI**
Multiobjective trajectory optimization by goal programming with fuzzy decision p 526 A95-91544
- YOST, J. D.**
Aircraft fatigue and crack growth considering loads by structural component p 137 N95-19497
- YOUNG, A.**
Adhesively bonded composite patch repair of cracked aluminum alloy structures p 393 N95-27507
- YOUNG, A. D.**
Scale effects on aircraft and weapon aerodynamics [AGARD-AG-323] p 67 N95-14103
- YOUNG, C. P., JR.**
Dynamic response tests of inertial and optical wind-tunnel model attitude measurement devices
[NASA-TM-109182] p 296 N95-23011
- YOUNG, CLARENCE P., JR.**
Effects of vibration on inertial wind-tunnel model attitude measurement devices
[NASA-TM-109083] p 21 N95-11466
Development of a model protection and dynamic response monitoring system for the national transonic facility
[NASA-CR-195041] p 340 N95-24388
- YOUNG, D. P.**
TranAir: A full-potential, solution-adaptive, rectangular grid code for predicting subsonic, transonic, and supersonic flows about arbitrary configurations. User's manual
[NASA-CR-4349] p 377 N95-28230
TranAir: A full-potential, solution-adaptive, rectangular grid code for predicting subsonic, transonic, and supersonic flows about arbitrary configurations. Theory document
[NASA-CR-4348] p 378 N95-28265
- YOUNG, DEBORAH B.**
1994 NASA-HU American Society for Engineering Education (ASEE) Summer Faculty Fellowship Program
[NASA-CR-194972] p 325 N95-23276
- YOUNG, HARRY J.**
Preload release mechanism
[NASA-CASE-MSC-22327-1] p 350 N95-25592
- YOUNG, J. B.**
Crack growth characteristics of integrally machined stringer-skin panels
[HTN-95-01095] p 496 A95-90281
Condensation in jet engine intake ducts during stationary operation
[BTN-95-EIX95292721154] p 612 A95-92590
- YOUNG, KATHERINE C.**
Integrated aerodynamic/dynamic/structural optimization of helicopter rotor blades using multilevel decomposition
[NASA-TP-3465] p 285 N95-22953
- YOUNG, RICHARD D.**
Nonlinear analysis of damaged stiffened fuselage shells subjected to combined loads p 137 N95-19499
- YOUNG, S.**
Operational multi-scale environment model with grid adaptivity (OMEGA) application to aviation weather p 676 A95-93556
- YOUNG, STEVE**
Passive millimeter wave camera for aircraft landing in low visibility conditions
[BTN-95-EIX95292721321] p 609 A95-92513
- YOUNG, T. S.**
Wind turbine blade aerodynamics: The combined experiment
[DE94-011866] p 118 N95-18645
Wind turbine blade aerodynamics: The analysis of field test data
[DE94-011867] p 118 N95-18646
- YOUNG, TERESA**
Using digital filtering techniques as an aid in wind turbine data analysis
[DE94-011862] p 357 N95-24853
- YOUNGBLOOD, DANIEL L.**
Design of a vehicle based system to prevent ozone loss
[NASA-CR-197199] p 48 N95-12702
- YOUNGBLUT, CHRISTINE**
The value of simulation for training
[AD-A289174] p 411 N95-26556
- YOUSEFI, RAMAN**
Hangars as noise barriers for helicopter noise p 560 A95-90111
- YOUSSEF, Y.**
Validation of an effective flat cruciform-shaped specimen to study CFRP composite laminates under biaxial loading
[BTN-95-EIX95152584677] p 282 A95-73589
- YOUSUFF, AJMAL**
Design of robust optimal control systems and stability analysis of real structured uncertainties
[AD-A279089] p 256 N95-21913
- YU, C.-T.**
Axial crack propagation and arrest in pressurized fuselage p 94 N95-14479
- YU, TAO**
A numerical method for unsteady transonic flow about wings with control surfaces
[AD-A289631] p 375 N95-26859
- YU, YUNG H.**
Dynamic stall control for advanced rotorcraft application
[BTN-95-EIX95222650793] p 334 A95-79249
- YUAN, K. A.**
Aeroelasticity and structural optimization of composite helicopter rotor blades with swept tips
[NASA-CR-4665] p 397 N95-28262
- YUAN, PIN-JAR**
Solutions of generalized proportional navigation with maneuvering and nonmaneuvering targets
[BTN-95-EIX95202637606] p 279 A95-76683
Ideal proportional navigation p 342 A95-81374
- YUAN, QIN**
Wormgear geometry adopted for implementing hydrostatic lubrication and formulation of the lubrication problem
[AD-A290331] p 210 N95-19567
- YUAN, XIN**
Application of GPS/SINS/RA integrated system to aircraft approach landing p 125 N95-16277
- YUDILEVITCH, GIL**
Techniques for designing rotorcraft control systems
[NASA-CR-196192] p 52 N95-12791
- YUE, LOU**
Study on a scheme for the prolongation of microgravity time of balloon-borne drop capsule p 414 A95-82515
- YUNAS, ANDREW J.**
Design and development of an F/A-18 inlet distortion rake: A cost and time saving solution p 69 N95-14241
- YUJIRI, LARRY**
Passive millimeter wave camera for aircraft landing in low visibility conditions
[BTN-95-EIX95292721321] p 609 A95-92513
- YULE, T. J.**
Evaluation of neutron techniques for illicit substance detection
[DE95-002988] p 300 N95-22764
- ZABINSKY, Z.**
Local design optimization for composite transport fuselage crown panels p 398 N95-28473
- ZACHAR, EDWARD**
H-76B fantail demonstrator composite fan blade fabrication
[HTN-95-80856] p 283 A95-75098
- ZACHARIAS, GREG L.**
Intelligent flight trainer for initial rotary wing training
[SAE PAPER 932536] p 386 A95-84558
A neural expert approach to self designing flight control systems
[AD-A279965] p 237 N95-21122
- ZACK, J.**
Operational multi-scale environment model with grid adaptivity (OMEGA) application to aviation weather p 676 A95-93556
- ZAKARIA, ZAIDI B.**
Surface interference in Rayleigh scattering measurements near forebodies
[HTN-95-51670] p 433 A95-85052
- ZAKIROV, I. M.**
Development of processes, means, and theoretical principles of thin-walled detail plastic forming at Kazan Aviation Institute p 155 N95-16281
- ZAKOUT, WAEL MOHAMED**
Modeling spatio-temporal databases to measure the performance of the GPS satellite constellation p 489 N95-29596
- ZAKRAJSEK, J. J.**
Analytical and experimental vibration analysis of a faulty gear system
[NASA-TM-106689] p 58 N95-12843
- ZAKRAJSEK, JAMES J.**
Detecting gear tooth fracture in a high contact ratio face gear mesh
[NASA-TM-106822] p 162 N95-19125
- ZALLEN, D. M.**
A study of aircraft post-crash fuel fire mitigation
[AD-A282208] p 40 N95-12499
- ZAMAN, K. B. M. Q.**
Axis switching and spreading of an asymmetric jet: Role of vorticity dynamics
[NASA-TM-106385] p 73 N95-14418
- ZAYCHIK, L. E.**
General requirements for the electrohydraulic systems of the aircraft controls loading force on the simulators
[CONGRESS PAPER C428-5-138] p 522 A95-91681
- ZEDAN, M. F.**
Stability derivatives of a flapped plate in unsteady ground effect
[BTN-95-EIX95182619225] p 270 A95-76651
- ZEHDNER, ALAN T.**
Fatigue crack growth in 2024-T3 aluminum under tensile and transverse shear stresses p 153 N95-19490
- ZEIDAN, FAISAL**
An intelligent tutoring system for civil aviation flight training p 521 A95-91535
- ZELENKA, RICHARD E.**
Flight test development and evaluation of a Kalman filter state estimator for low-altitude flight
[HTN-94-00684] p 16 A95-60167
Simulation development of a forward sensor-enhanced low-altitude guidance system
[HTN-94-00688] p 17 A95-60170
Design and flight evaluation of an integrated navigation and near-terrain helicopter guidance system for night-time and adverse weather operations
[NASA-TM-108837] p 11 N95-10846
Flight test of a low-altitude helicopter guidance system with obstacle avoidance capability p 688 N95-32490
- ZELKOWITZ, MARVIN**
Software process improvement in the NASA software engineering laboratory
[AD-A289912] p 450 N95-28627
- ZELL, PETER T.**
Aerodynamic surface distension system for high angle of attack forebody vortex control
[NASA-CASE-ARC-11979-1] p 286 N95-23390
- ZELLNER, R.**
Modeling of plume chemistry of high flying aircraft with H2 combustion engines p 509 A95-87405
- ZEMSCH, STEPHAN**
Application of pressure sensitive paint in hypersonic flows
[NASA-TM-106824] p 223 N95-20794
- ZERKLE, D. K.**
A laboratory scale supersonic combustive flow system
[DE95-006347] p 420 N95-27851
- ZERKLE, RONALD D.**
A summary of computational experience at GE Aircraft Engines for complex turbulent flows in gas turbines p 439 N95-27885

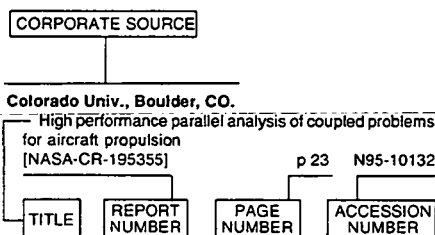
- ZHANG, CAIWEN**
An approach to aerodynamic characteristics of low radar cross-section fuselages p 106 N95-16251
An improved method of airfoil design p 106 N95-16252
- ZHANG, D. H.**
Measurement in laminar and transitional boundary-layer flows on concave surface [BTN-95-EIX95282711333] p 632 A95-92408
- ZHANG, HONGBIN**
Development and application of the double V type flame stabilizer [BTN-94-EIX94481415355] p 154 A95-65345
- ZHANG, JIANBAI**
A numerical method for unsteady transonic flow about wings with control surfaces [AD-A289631] p 375 N95-26859
- ZHANG, PEN CHEN**
Orbital velocities induced by surface waves [HTN-95-90902] p 253 A95-72411
- ZHANG, QIWEI**
Wall-signature methods for high speed wind tunnel wall interference corrections p 107 N95-16257
- ZHANG, SEN**
Development of a composite tailoring procedure for airplane wing [NASA-CR-199081] p 691 N95-32928
- ZHANG, XIAOGU**
Investigation of dynamic inflow's influence on rotor control derivatives p 155 N95-16250
- ZHANG, YANSI**
Numerical studies of turbulent free surface flows and unsteady propeller flows [AD-A294377] p 706 N95-34343
- ZHANG, YOU-YUN**
New strategy combining backward inference with forward inference in monitoring and diagnosing techniques for hydrodynamic bearing-rotor systems [BTN-94-EIX94331336949] p 88 A95-61795
- ZHANG, Z. Y.**
Numerical design methods for transonic NLF configurations p 471 A95-91498
- ZHAO, J. Y.**
Subharmonic and quasi-periodic motions of an eccentric squeeze film damper-mounted rigid rotor [BTN-94-EIX95011440601] p 429 A95-82982
- ZHAO, L.**
A flow pattern map for two-phase liquid-gas flow under reduced gravity conditions p 539 A95-87280
- ZHARINOV, V. G.**
A stationary flow of a viscous liquid in radial clearances of rotor bearings in the turbocompressor of an internal combustion engine [BTN-94-EIX94461408765] p 153 A95-63648
- ZHENG, J.**
An analysis of aircraft exhaust plumes form accidental encounters [HTN-95-70943] p 351 A95-78008
- ZHENG, Z. C.**
3D visualization of unsteady 2D airplane wake vortices [AD-A284745] p 27 N95-11593
- ZHI-XUM, XIA**
An inverse design method of transonic airfoil and wing [HTN-95-71128] p 385 A95-83489
- ZHONG, P.**
Stability of magnetic bearing-rotor systems and the effects of gravity and damping [BTN-94-EIX94441386619] p 208 A95-68168
Stability of magnetic bearing-rotor systems and the effects of gravity and damping [HTN-95-20955] p 465 A95-88994
- ZHOU, DADONG**
Effects of elevated free-stream turbulence and streamwise acceleration on flow and thermal structures in transitional boundary layers p 556 N95-29729
- ZHOU, GANG**
Turbulent transonic airfoil flow simulation using a pressure-based algorithm [BTN-95-EIX95182619078] p 269 A95-75763
- ZHOU, R. C.**
Finite element time domain - modal formulation for nonlinear flutter of composite panels [BTN-95-EIX95042474401] p 203 A95-68299
- ZHOU, YE**
On the Lighthill relationship and sound generation from isotropic turbulence [NASA-CR-195005] p 159 N95-18191
- ZHOU, Z.**
Failure analysis for polycarbonate transparencies [AD-A292992] p 630 N95-31471
- ZHU, GUO-RUI**
Non-linear viscoelastic-plastic constitutive relations for an aeronautical PMMA [HTN-95-71132] p 385 A95-83493
- ZHU, JIANG**
Modification of the two-equation turbulence model in NPARC to a Chien low Reynolds number k-epsilon formulation [NASA-TM-106710] p 37 N95-11917
- ZHU, JIANYING**
Joint Proceedings on Aeronautics and Astronautics (JPAA) [ISBN-7-80-046602-7] p 104 N95-16249
- ZHU, LI-PING**
Exact dynamic responses of periodic multi-span beams under convected pressure fields p 25 N95-11288
- ZHU, XI-XIONG**
Non-linear viscoelastic-plastic constitutive relations for an aeronautical PMMA [HTN-95-71132] p 385 A95-83493
- ZHU, ZHAODA**
Linear prediction data extrapolation superresolution radar imaging p 155 N95-16268
- ZHUANG, WEIHUA**
Modeling and analysis for the GPS pseudo-range observable [BTN-95-EIX95302731227] p 600 A95-94046
- ZI-QIANG, ZHU**
An inverse design method of transonic airfoil and wing [HTN-95-71128] p 385 A95-83489
- ZIA, S.**
Using IRI for the computation of ionospheric corrections for altimeter data analysis p 212 A95-66949
- ZIERER, T.**
Experimental investigation of the flow in diffusers behind an axial flow compressor [BTN-95-EIX95282710057] p 632 A95-92472
- ZIMMERMAN, D. K.**
Comparison of measured and calculated dynamic loads for the Mod-2 2.5 mW wind turbine system p 440 N95-27983
- ZIMMERMAN, WAYNE**
A generic telerobotics architecture for C-5 industrial processes [AIAA PAPER 94-1264-CP] p 27 N95-11529
- ZIMMERMANN, H.**
Structural aspects of active control technology p 623 N95-32006
- ZINGG, D. W.**
Compressible Navier-Stokes computations of multielement airfoil flows using multiblock grids [HTN-95-42327] p 371 A95-86156
Turbulent flow measurements with a triple-split hot-film probe [HTN-95-A1774] p 634 A95-93337
- ZIRKLER, ANDRE**
Flight test development and evaluation of a Kalman filter state estimator for low-altitude flight [HTN-94-00684] p 16 A95-60167
Design and flight evaluation of an integrated navigation and near-terrain helicopter guidance system for night-time and adverse weather operations [NASA-TM-108837] p 11 N95-10846
- ZISCHKA, PETER J.**
Experimental evaluation of a box beam specifically tailored for chordwise deformation [BTN-95-EIX95182619088] p 283 A95-75773
Unique considerations in the design and experimental evaluation of tailored wings with elastically produced chordwise camber p 423 N95-28436
- ZMIERCZAK, TOMASZ**
Photoacoustic chambers for studying solids and gases: Theory and practical examples [IFTR-39/1994] p 412 N95-26837
- ZOBY, ERNEST V.**
Higher-order viscous shock-layer solutions for high-altitude flows [BTN-95-EIX95152583255] p 306 A95-73556
- ZOLADZ, T.**
Bearing defect signature analysis using advanced nonlinear signal analysis in a controlled environment [NASA-TM-108491] p 441 N95-28364
- ZOLE, ARIE**
Continuous gust response and sensitivity derivatives using state-space models [BTN-95-EIX95062487551] p 203 A95-68365
- ZORI, LAITH A. J.**
Navier-Stokes calculations of rotor-airframe interaction in forward flight [HTN-95-01087] p 468 A95-90273
- ZUBRIN, ROBERT M.**
The Methane-Acetylene Cycle Aerospace Plane: A potential option for inexpensive Earth to orbit transportation [HTN-95-51845] p 525 A95-87483
- ZUNIGA, FANNY A.**
Transonic flight test of a laminar flow leading edge with surface excrescences [NASA-TM-4597] p 9 N95-11158
- ZUPPARDI, G.**
Adaptive wind tunnel walls versus wall interference correction methods in 2D flows at high blockage ratios p 147 N95-19267
- ZUPPARDO, JOSEPH C.**
Open Skies project computational fluid dynamic analysis [AD-A285928] p 223 N95-19991
- ZURABYAN, A. Z.**
Laser device for measuring a vessel's speed [HTN-95-60992] p 361 A95-80633
- ZURIGAT, Y. H.**
Effect of crossflow on Goertler instability in incompressible boundary layers [NASA-CR-195007] p 159 N95-18193
- ZWACK, PETER**
ITWS cetering and visibility products p 654 A95-93454
Stratus' tephigram as a training/forecasting tool p 657 A95-93465
- ZWERNEMAN, W. D.**
Vista/F-16 Multi-Axis Thrust Vectoring (MATV) control law design and evaluation p 71 N95-14248
- ZYSKOWSKI, MICHAEL K.**
Incorporating biplane wing theory into a large, subsonic, all-cargo transport p 391 N95-26956

CORPORATE SOURCE INDEX

AERONAUTICAL ENGINEERING / A Continuing Bibliography
1995 Cumulative Index

December 1995

Typical Corporate Source Index Listing



Listings in this index are arranged alphabetically by corporate source. The title of the document is used to provide a brief description of the subject matter. The page number and the accession number are included in each entry to assist the user in locating the abstract in the abstract section. If applicable, a report number is also included as an aid in identifying the document.

A

AC Engineering, Inc., Huntsville, AL.
Standardization of surface contamination analysis systems p 631 N95-31798

Academy of Sciences (USSR), Moscow (USSR).
Advanced method and processing technology for complicated shape airframe part forming p 80 N95-14486

Advanced Rotorcraft Technology, Inc., Mountain View, CA.
Application of parallel processing technology in complex helicopter analysis. Phase 1 [NASA-CR-197850] p 502 N95-28928

Advisory Group for Aeronautical Research and Development, Oxford (England).
POD assessment of NDI procedures using a round robin test [AGARD-R-809] p 315 N95-23602

Advisory Group for Aerospace Research and Development, Neuilly-Sur-Seine (France).
AGARD highlights 94/2 [AGARD-HIGHLIGHTS-94/2] p 102 N95-13640
Identification of dynamic systems. Volume 3: Applications to aircraft. Part 2: Nonlinear analysis and manoeuvre design [AGARD-AG-300-VOL-3-PT-2] p 79 N95-14102
Scale effects on aircraft and weapon aerodynamics [AGARD-AG-323] p 67 N95-14103
Turbomachinery Design Using CFD [AGARD-LS-195] p 89 N95-14127
Quality assessment for wind tunnel testing [AGARD-AR-304] p 67 N95-14197
The principles of flight test assessment of flight-safety-critical systems in helicopters [AGARD-AG-300-VOL-12] p 77 N95-14199
A selection of experimental test cases for the validation of CFD codes, volume 1 [AGARD-AR-303-VOL-1] p 91 N95-14201

Computational aerodynamics based on the Euler equations [AGARD-AG-325] p 72 N95-14264
Missile Aerodynamics [AGARD-R-804] p 73 N95-14445
Flight in an Adverse Environment [AGARD-LS-197] p 77 N95-14893
Optimum Design Methods for Aerodynamics [AGARD-R-803] p 127 N95-16562
Experimental and analytical methods for the determination of connected-pipe ramjet and ducted rocket internal performance [AGARD-AR-323] p 149 N95-17278
Aircraft and sub-system certification by piloted simulation [AGARD-AR-278] p 145 N95-17388
A selection of experimental test cases for the validation of CFD codes, volume 2 [AGARD-AR-303-VOL-2] p 109 N95-17846
A selection of experimental test cases for the validation of CFD codes. Supplement: Datasets A-E [AGARD-AR-303-SUPPL] p 117 N95-18539
Aircraft Loads due to Turbulence and their Impact on Design and Certification [AGARD-R-798] p 143 N95-18597
On-line handling of air traffic: Management, guidance and control [AGARD-AG-321] p 126 N95-18927
Mathematical Models of Gas Turbine Engines and their Components [AGARD-LS-198] p 139 N95-19017
Impact of Acoustic Loads on Aircraft Structures [AGARD-CP-549] p 173 N95-19142
Wall Interference, Support Interference and Flow Field Measurements [AGARD-CP-535] p 162 N95-19251
Erosion, Corrosion and Foreign Object Damage Effects in Gas Turbines [AGARD-CP-558] p 197 N95-19653
Advanced Packaging Concepts for Digital Avionics [AGARD-CP-562] p 233 N95-20631
Application of Direct and Large Eddy Simulation to Transition and Turbulence [AGARD-CP-551] p 248 N95-21061
Corrosion detection and management of advanced airframe materials [AGARD-CP-565] p 302 N95-23496
Composite Repair of Military Aircraft Structures [AGARD-CP-550] p 392 N95-27504
AGARD flight test techniques series. Volume 13: Reliability and maintainability [AGARD-AG-300-VOL-13] p 504 N95-29503
Flight Vehicle Integration Panel Workshop on Pilot Induced Oscillations [AGARD-AR-335] p 597 N95-31061
Active control technology: Applications and lessons learned [AGARD-CP-560] p 620 N95-31989
Environmentally Safe and Effective Processes for Paint Removal [AGARD-LS-201] p 650 N95-32165
Low-Level and Nap-of-the-Earth (NOE) night operations [AGARD-CP-563] p 686 N95-32486
AGARD index of publications: 1992-1994 [AGARD-INDEXT-92-94] p 711 N95-33198

AEPCO, Inc., Rockville, MD.
AH-1F COBRA rewire program MANPRINT analysis [AD-A289190] p 391 N95-27018

Aerodats Flugmesstechnik G.m.b.H., Brunswick (Germany).
Integrated special mission flight management for a flight inspection aircraft p 692 N95-33145

Aerojet-General Corp., Azusa, CA.
Earth Observing System (EOS)/Advanced Microwave Sounding Unit-A (AMSU-A) software assurance plan [NASA-CR-196059] p 98 N95-13885

Aeronautica Macchi S.p.A., Varese (Italy).
Control law design using H-infinity and mu-synthesis short-period controller for a tail-airplane p 622 N95-31999

Aeronautical Research Inst. of Sweden, Bromma.
Low speed propeller slipstream aerodynamic effects p 116 N95-17882
Computational simulations for some tests in transonic wind tunnels p 164 N95-19264
Calculation of low speed wind tunnel wall interference from static pressure pipe measurements p 164 N95-19273

Aeronautical Research Labs., Melbourne (Australia).
Residual strength of composites with multiple impact damage [AD-A284230] p 87 N95-14409
Programmable cockpit research simulator [AD-A279219] p 204 N95-19848
Derived gust spectra for the Macchi MB326H [ARL-TN-3] p 225 N95-21892
Configuration and other differences between Black Hawk and Seahawk helicopters in military service in the USA and Australia [AR-008-386] p 336 N95-25935
Assessment of overhaul surge margin tests applied to the T53 engines in ADF Iroquois helicopters [AR-008-389] p 339 N95-25936

Aeronautical Systems Div., Eglin AFB, FL.
User documentation of the CTA program [AD-A289508] p 375 N95-26854

Aeronautical Systems Div., Wright-Patterson AFB, OH.
Challenges for the aircraft structural integrity program p 80 N95-14481
KC-135 cockpit modernization study. Phase 1: Equipment evaluation [AD-A284099] p 131 N95-18398
Open Skies project computational fluid dynamic analysis [AD-A285928] p 223 N95-19991

Aerospatiale, Toulouse (France).
Gyroscopic and propeller aerodynamic effects on engine mounts dynamic loads in turbulence conditions p 132 N95-18599
Interaction of a three strut support on the aerodynamic characteristics of a civil aviation model p 122 N95-19279
Corrosion in service experience with aircraft in France p 303 N95-23518
Composite or metallic bolted repairs on self-stiffened carbon wing panel of the commuter ATR72 design criteria, analysis, verification by test p 396 N95-27525
Flying qualities of civil transport aircraft with electrical flight control p 624 N95-32016
Selective chemical stripping p 650 N95-32175
Process evaluation p 651 N95-32180
Standardization work p 651 N95-32181

Aerospatiale, Verrieres-le-Buisson (France).
Computation of supersonic air-intakes p 74 N95-14452

Air Force Academy, CO.
Application of neural networks to unsteady aerodynamic control p 360 N95-25264

Air Force Environmental Technical Applications Center, Scott AFB, IL.
Artificial intelligence techniques for flight test planning, phase 1 [AD-A293962] p 608 N95-31525

Air Force Flight Test Center, Edwards AFB, CA.
Flight test results of the F-16 aircraft modified with axisymmetric vectoring exhaust nozzle p 609 N95-32007
An investigation of pilot induced oscillation phenomena in digital-flight control systems p 623 N95-32011

Air Force Human Resources Lab., Brooks AFB, TX.
Instructional control and part/whole-task training: A review of the literature and an experimental comparison of strategies applied to instructional simulation [AD-A280860] p 21 N95-10919

Air Force Inst. of Tech., Wright-Patterson AFB, OH.
Impingement flow heat transfer measurements of turbine blades using a jet array [AD-A283450] p 62 N95-12512
Measurements of pressure and thermal wakes in a transonic turbine cascade [AD-A283464] p 38 N95-12548

SOURCE

Damage tolerant repair techniques for pressurized aircraft fuselages [AD-A281982] p 65 N95-14144

Effect of surface roughness on local film cooling effectiveness and heat transfer coefficients [AD-A283854] p 91 N95-14351

Development of an Automated Airfield Dynamic Cone Penetrometer (AADCP) prototype and the evaluation of unsurfaced airfield seismic surveying using Spectral Analysis of Surface Waves (SASW) technology [AD-A281985] p 145 N95-17444

Numerical simulation of dynamic-stall suppression by tangential blowing [AD-A284887] p 120 N95-19110

Developing an emission factor for hazardous air pollutants for an F-16 using JP-8 fuel [AD-A284802] p 216 N95-19685

Modeling aerosol emissions from the combustion of composite materials p 301 N95-23038

Development of a nonlinear simulation for the McDonnell Douglas F-15 Eagle with a longitudinal TECS control-law [AD-A288610] p 388 N95-26481

A numerical model to predict the fate of jettisoned aviation fuel [AD-A289336] p 419 N95-26842

A comparison of the Neal-Smith and omega Tau function, zeta function and tau function flying qualities criteria [AD-A289503] p 390 N95-26844

An analysis of the KC-135 three-person cockpit [AD-A289540] p 390 N95-26873

The photo-realistic AFIT virtual cockpit [AD-A289376] p 390 N95-26876

Classification of ultra high range resolution radar using decision boundary analysis [AD-A289378] p 437 N95-26877

Stall precursor study of high frequency data for three high speed, swept compressor rotors [AD-A289379] p 406 N95-26878

EASY-SIM: A visual simulation system software architecture with an Ada 9X application framework [AD-A289325] p 448 N95-26895

Analysis and simulation of narrowband GPS jamming using digital excision temporal filtering [AD-A289328] p 383 N95-26898

Performance characterization of a highly-offset diffuser with and without blowing vortex generator jets [AD-A289334] p 375 N95-26901

A gain scheduling optimization method using genetic algorithms [AD-A289306] p 448 N95-26920

Electro-hydrostatic actuator controller design using quantitative feedback theory [AD-A289220] p 409 N95-26957

A quantitative feedback theory FCS design for the subsonic envelope of the VISTA F-16 including configuration variation [AD-A289221] p 409 N95-26958

An investigation of the AFIT 2-inch shock tube as a flow source for supersonic testing [AD-A289246] p 412 N95-26966

Advanced formation flight control [AD-A289271] p 409 N95-26981

An integrated GPS/INS/BARO and radar altimeter system for aircraft precision approach landings [AD-A289280] p 383 N95-26985

Survey and implementation of commercial manual controllers for a generic telerobotics architecture [AD-A289215] p 449 N95-26990

Flight control design using mixed H2/micron optimization [AD-A289288] p 410 N95-27036

Implementation and demonstration of a multiple model adaptive estimation failure detection system for the F-16 [AD-A289301] p 391 N95-27042

Life cycle costs of alternatives for F-16 printed circuit board diagnosis equipment [AD-A288744] p 401 N95-28586

Development of a TECS control-law for the lateral directional axis of the McDonnell Douglas F-15 Eagle [AD-A289771] p 410 N95-28598

Three-D weather displays for aircraft cockpits [AD-A289759] p 508 N95-28691

Conceptual design of a map interactive system for military aircraft cockpits [AD-A289760] p 508 N95-28692

A noninvasive method of quantifying flow visualization data in vortex flow fields [AD-A289802] p 552 N95-28948

An experimental investigation of the time-dependent separation of tangent bodies in supersonic flow [AD-A290720] p 480 N95-29500

An aerodynamic and static-stability analysis of the Hypersonic Applied Research Technology (HART) missile [DA9426923] p 481 N95-29965

Selecting optimal experiments for feedforward multilayer perceptrons [AD-A290856] p 678 N95-30406

Patient/aircraft forecasting for the strategic aeromedical evacuation lift-bed process [AD-A293902] p 599 N95-31512

Analysis and modeling of an airport departure process [AD-A293782] p 602 N95-31581

Analysis of heads-up display quickening versus handling qualities [AD-A293797] p 611 N95-31584

The effects of display location and dimensionality on taxiway navigation [AD-A294878] p 690 N95-34570

Air Force Office of Scientific Research, Bolling AFB, Washington, DC.

AFOSR Contractors Meeting in Propulsion [AD-A282729] p 54 N95-12507

Air Force Systems Command, McChlellan AFB, CA.

Mishap risk control for advanced aerospace/composite materials p 301 N95-23031

Air Force Systems Command, Wright-Patterson AFB, OH.

Photovoltaic electric power applied to Unmanned Aerial Vehicles (UAV) p 245 N95-20530

Numerical investigation to S-inlet flows (Numerical simulation study of S-inlet flows) [AD-A289590] p 374 N95-26713

Plate manipulators [AD-A289601] p 374 N95-26719

A numerical method for unsteady transonic flow about wings with control surfaces [AD-A289631] p 375 N95-26859

Thermal design of returnable satellites [AD-A294113] p 701 N95-34500

Air Products and Chemicals, Inc., Allentown, PA.

Organic coating technology for the protection of aircraft against corrosion p 303 N95-23513

Aircraft Research Association Ltd., Bedford (England).

Investigation of the flow development on a highly swept canard/wing research model with segmented leading- and trailing-edge flaps p 114 N95-17876

Investigation into the aerodynamic characteristics of a combat aircraft research model fitted with a forward swept wing p 116 N95-17884

Investigation of the influence of pylons and stores on the wing lower surface flow p 116 N95-17885

An investigation of drag repeatability in half model testing in the ARA Transonic Wind Tunnel [ARA-MEMO-392] p 188 N95-19546

Multipoint pressure measurements on continuously moving wind tunnel models [ARA-MEMO-391] p 188 N95-19772

Validation and evaluation of the advanced aeronautical CFD system SAUNA: A method developer's view [ARA-MEMO-390] p 210 N95-19774

Application of three-dimensional hybrid structured/unstructured grids to land, sea and air vehicles [ARA-MEMO-399] p 210 N95-19775

Verification of the CFD simulation system SAUNA for complex aircraft configurations [ARA-MEMO-401] p 211 N95-19776

Inviscid and viscous flow modelling of complex aircraft configurations using the CFD simulation system sauna [ARA-MEMO-403] p 211 N95-19777

The aerodynamic design of an integrated wing lower surface and pylons for reduced drag [ARA-MEMO-406] p 194 N95-19789

Investigation of a thermal buoyancy effect on the drag of half models tested in the ARA Transonic Wind Tunnel [ARA-MEMO-407] p 222 N95-19946

The dynamic approach to rotor blade research: ARA's oscillatory test facility [ARA-MEMO-405] p 223 N95-20758

Testing in the ARA Transonic Wind Tunnel [ARA-MEMO-395] p 239 N95-20799

Alabama Univ., Huntsville, AL.

Field and data analysis studies related to the atmospheric environment [NASA-CR-196543] p 168 N95-18093

Alcoa Technical Center, Alcoa Center, PA.

An artificial corrosion protocol for lap-splices in aircraft skin p 152 N95-19482

Alenia, Turin (Italy).

Impact of noise environment on engine nacelle design p 173 N95-19147

Electromagnetic compatibility effects of advanced packaging configurations p 247 N95-20658

Alenia Aeronautica, Turin (Italy).

Digital autopilot design for combat aircraft in ALENIA p 623 N95-32009

Alenia Spazio S.p.A., Turin (Italy).

An overall approach of cockpit noise verification in a military aircraft p 175 N95-19163

Allied-Signal Aerospace Co., Phoenix, AZ.

Advanced Turbine Technology Applications Project (ATTAP) [NASA-CR-195393] p 101 N95-15743

Allison Engine Co., Indianapolis, IN.

Investigation of advanced counterrotation blade configuration concepts for high speed turboprop systems. Task 8: Cooling flow/heat transfer analysis [NASA-CR-195359] p 50 N95-11901

Investigation of advanced counterrotation blade configuration concepts for high speed turboprop systems. Task 8: Cooling flow/heat transfer analysis user's manual [NASA-CR-195360] p 50 N95-11951

Propulsion system assessment for very high UAV under ERAT [NASA-CR-195469] p 406 N95-27866

Advanced k-epsilon modeling of heat transfer [NASA-CR-4679] p 648 N95-31423

Advanced turbine systems program conceptual design and product development [DE95-000088] p 650 N95-32163

Allison engine testing CMSX-4 (reg sign) single crystal turbine blades and vanes [DE95-010308] p 694 N95-32636

Aluminum Co. of America, Alcoa Center, PA.

Prediction of R-curves from small coupon tests p 167 N95-19496

American Inst. of Aeronautics and Astronautics, Washington, DC.

Proceedings of the AIAA/FAA joint symposium on general aviation systems [AD-A289830] p 368 N95-28610

Ames Lab., IA.

Low frequency ultrasonic nondestructive inspection of aluminum/adhesive fuselage lap splices [DE94-014242] p 24 N95-11135

Analytic Power Corp., Boston, MA.

Linear Motor Free Piston Compressor [AD-A293452] p 647 N95-31374

Analytical Methods, Inc., Redmond, WA.

Calculation of support interference in dynamic wind-tunnel tests p 122 N95-19282

Analytical Services and Materials, Inc., Hampton, VA.

Hybrid structured/unstructured grid computations for the F/A-18 at high angle of attack p 68 N95-14233

Composite chronicles: A study of the lessons learned in the development, production, and service of composite structures [NASA-CR-4620] p 151 N95-16859

Multi-lab comparison on R-curve methodologies: Alloy 2024-T3 [NASA-CR-195004] p 151 N95-16860

COINS: A composites information database system p 453 N95-28465

Applied Research Associates, Inc., Raleigh, NC.

Portable parallel stochastic optimization for the design of aeropropeulsion components [NASA-CR-195312] p 154 N95-16072

Applied Thermal Sciences, Orono, ME.

Combustor kinetic energy efficiency analysis of the hypersonic research engine data p 148 N95-16321

Argonne National Lab., IL.

Parallel methods for the flight simulation model [DE94-013330] p 52 N95-11752

MHD-flow in slotted channels with conducting walls [DE94-018370] p 258 N95-21388

Evaluation of neutron techniques for illicit substance detection [DE95-002988] p 300 N95-22764

Arizona State Univ., Tempe, AZ.

The potential of genetic algorithms for conceptual design of rotor systems [NASA-CR-196813] p 43 N95-11699

Experimental and theoretical studies of wakes in stratified flows [AD-A290203] p 553 N95-29060

Growth and development of roughness-induced stationary crossflow vortices p 482 N95-30294

Development of a composite tailoring procedure for airplane wing [NASA-CR-199081] p 691 N95-32928

Arizona Univ., Tucson, AZ.

Residual strength of thin panels with cracks p 311 N95-23311

Arkansas Univ., Pine Bluff, AR.

Automation technology using Geographic Information System (GIS) p 324 N95-23284

Army Aeromedical Research Lab., Fort Rucker, AL.

The assessment of the AH-64D, longbow, mast-mounted assembly noise hazard for maintenance personnel [AD-A284971] p 171 N95-16226

A correlative investigation of simulated occupant motion and accident report in a helicopter crash [AD-A285190] p 123 N95-16404

Factors affecting the visual fragmentation of the field-of-view in partial binocular overlap displays [AD-A283081] p 172 N95-17334

Factors affecting the perception of luning in monocular regions of partial binocular overlap displays [AD-A286287] p 259 N95-22044

The effects of UH-1 experience on UH-60 simulator performance: A preliminary study [AD-A289457] p 391 N95-26993

Biodynamic simulation of pilot interaction with a helicopter multifairbag restraint system [AD-A290196] p 485 N95-29057

First medical test of the UH-60Q and equipment for use in US Army medevac helicopters p 568 N95-29620

Transmittance characteristics of US Army rotary-wing aircraft transparencies [AD-A295035] p 693 N95-34793

Army Armament Research, Development and Engineering Center, Picatinny Arsenal, NJ.
Anechoic chamber upgrade [AD-A294375] p 700 N95-34342

Army Aviation Research and Development Command, Moffett Field, CA.
Wall interaction effects for a full-scale helicopter rotor in the NASA Ames 80- by 120-foot wind tunnel p 121 N95-19270

Army Aviation Systems Command, Hampton, VA.
Exploratory flow visualization investigation of mast-mounted sights in presence of a rotor [NASA-TM-4634] p 330 N95-24566

Development and validation of a blade-element mathematical model for the AH-64A Apache helicopter [NASA-TM-108863] p 367 N95-26710

Army Aviation Systems Command, Moffett Field, CA.
2-D and 3-D oscillating wing aerodynamics for a range of angles of attack including stall [NASA-TM-4632] p 120 N95-19119

An investigation of the effects of pitch-roll (de)coupling on helicopter handling qualities [NASA-TM-110349] p 409 N95-26773

Army Aviation Systems Command, Saint Louis, MO.
US Army rotorcraft turboshaft engines sand and dust erosion considerations p 198 N95-19656

Army Aviation Technical Test Center, Fort Rucker, AL.
Test operations procedure (TOP) 7-3-534 airworthiness testing of fixed wing aircraft: Asymmetric power testing [AD-A289458] p 391 N95-26994

Army Cold Regions Research and Engineering Lab., Hanover, NH.
Analyzing the stability of floating ice floes [AD-A292149] p 563 N95-29160

Army Communications-Electronics Command, Fort Monmouth, NJ.
Spatial awareness comparisons between large-screen, integrated pictorial displays and conventional EFIS displays during simulated landing approaches [NASA-TP-3457] p 80 N95-14852

Tactical low-level helicopter communications p 702 N95-32492

Army Construction Engineering Research Lab., Champaign, IL.
Environmental Compliance Assessment and Management Program [AD-A279605] p 255 N95-20441

Army Engineer Waterways Experiment Station, Vicksburg, MS.
Additives in bituminous materials and fuel-resistant sealers [DOT/FAA/CT-94/78] p 55 N95-12131

Marginal aggregates in flexible pavements: Background survey and experimental plan [DOT/FAA/CT-94/58] p 53 N95-12216

Super-heavy aircraft study [AD-A279602] p 238 N95-19955

Real-time testing and demonstration of the US Army Corps of Engineers' Real-Time On-The-Fly positioning system [AD-A288624] p 334 N95-25609

Army Materiel Command, Aberdeen Proving Ground, MD.
Utilization of composite materials by the US Army: A look ahead p 421 N95-28421

Army Natick Research and Development Command, MA.
Parachute inflation: A problem in aeroelasticity [AD-A284375] p 117 N95-18340

The performance of cargo airdrop systems using g-12E parachutes: Statistical determination of minimum altitude [AD-A291666] p 381 N95-28454

Army Night Vision Lab., Fort Belvoir, VA.
Development and flight testing of an Obstacle Avoidance System for US Army helicopters p 687 N95-32500

Army Research Inst. for the Behavioral and Social Sciences, Alexandria, VA.
Using the backward transfer paradigm to validate the AH-64 Simulator Training Research Advanced Testbed for Aviation [AD-A285758] p 238 N95-19931

Army Research Lab., Aberdeen Proving Ground, MD.
Proceeding towards hypervelocities in ram accelerators p 19 N95-10285

Navier-Stokes predictions of missile aerodynamics p 74 N95-14451

Helicopter Performance Evaluation (HELPE) computer model [AD-A284319] p 131 N95-18381

Static aerodynamics CFD analysis for 120-mm hypersonic KE projectile design [ARL-MR-184] p 118 N95-18611

Numerical computations of supersonic base flow with special emphasis on turbulence modeling [AD-A283688] p 119 N95-18670

Comparison of meteorological data with fitted values extracted from projectile trajectory [AD-A285921] p 255 N95-19989

Statistical analysis of Turbine Engine Diagnostic (TED) field test data [AD-A286032] p 248 N95-20998

Workshop report: Measurement techniques in highly transient, spectrally rich combustion environments [AD-A288395] p 350 N95-25606

Numerical simulation of ram accelerator performance including transient effects during initiation of combustion and sensitivity studies p 629 N95-31203

Workshop report: Measurement techniques in highly transient, spectrally rich combustion environments p 629 N95-31208

Army Research Lab., Cleveland, OH.
Sensor fault detection and diagnosis simulation of a helicopter engine in an intelligent control framework [AD-A290223] p 137 N95-15970

Detecting gear tooth fracture in a high contact ratio face gear mesh [NASA-TM-106822] p 162 N95-19125

Vibration analysis of a split path gearbox [NASA-TM-106875] p 438 N95-27855

Army Research Lab., Watertown, MA.
Rationale for the Modular Air-system Vulnerability Estimation Network (MAVEN) methodology [AD-A285797] p 284 N95-22510

Army Strategic Defense Command, Huntsville, AL.
Aero-optics system integration [TABES PAPER 94-604] p 100 N95-14638

Army Tank-Automotive Command, Warren, MI.
Fuel-type classification and parameters prediction by Gas Liquid Chromatography analysis [AD-A283442] p 630 N95-31368

Army Tank-Automotive Systems Development Center, Warren, MI.
Evaluation of commercial water-in-fuel test kits [AD-A292135] p 537 N95-29572

Army Test and Evaluation Command, Aberdeen Proving Ground, MD.
Test Operation Procedure (TOP): Vibration testing of helicopter equipment [AD-A284433] p 81 N95-15815

Arnold Engineering Development Center, Arnold AFS, TN.
A model for preliminary facility design including simulation issues p 144 N95-16318

Hypersonic air-breathing aeropropulsion facility test support requirements p 144 N95-16319

Hypersonic wind tunnel test techniques [AD-A284057] p 118 N95-18663

Hypersonic flow-field measurements: Intrusive and nonintrusive [AD-A283867] p 119 N95-18674

Hypersonic flight testing [AD-A283981] p 134 N95-18891

Description and flow characterization of hypersonic facilities [AD-A284291] p 223 N95-20248

Analysis of planar laser-induced fluorescence images obtained during shakedown testing of the AEDC impulse facility [AD-A293237] p 646 N95-30906

Icing simulation in the aeropropulsion systems test facility propulsion development test cell C-2 [AD-A293039] p 599 N95-31667

Subscale study of engine bellmouth inlet vortices in test cell R1D [AD-A294993] p 707 N95-34818

Atlantic Orient Corp., Norwich, VT.
Advanced wind turbine design studies: Advanced conceptual study [DE93-000031] p 256 N95-20985

Atlantic Research Corp., Alexandria, VA.
Through-the Thickness(R) braided composites for aircraft applications p 421 N95-28273

Auburn Univ., AL.
Hypervelocity Impact Test Facility: A gun for hire [TABES PAPER 94-605] p 86 N95-14639

Influence of backup bearings and support structure dynamics on the behavior of rotors with active supports [NASA-CR-197438] p 310 N95-32190

Aerodynamic flight control to increase payload capability of future launch vehicles [NAS-CR-196560] p 300 N95-24032

Dynamic behavior of a magnetic bearing supported jet engine rotor with auxiliary bearings [NASA-CR-197860] p 338 N95-24213

Influence of backup bearings and support structure dynamics on the behavior of rotors with active supports [NASA-CR-199080] p 703 N95-32689

Dynamic behavior of a magnetic bearing supported jet engine rotor with auxiliary bearings p 703 N95-32691

Dynamic modelling and response characteristics of a magnetic bearing rotor system with auxiliary bearings p 703 N95-32692

Synchronous dynamics of a coupled shaft/bearing/housing system with auxiliary support from a clearance bearing: Analysis and experiment p 703 N95-32693

Avions Marcel Dassault-Breguet Aviation, Saint-Cloud (France).
Review of the EUROPT Project AERO-0026 p 129 N95-16573

AVRO International Aerospace, Woodford (England).
Health and usage monitoring systems: Corrosion surveillance p 262 N95-23506

B

Baker (Wilfred) Engineering, Inc., San Antonio, TX.
Quantity-distance requirements for earth-bermed aircraft shelters [AD-A279692] p 341 N95-24424

Battelle Columbus Labs., OH.
Bicarbonate of soda blasting technology for aircraft wheel depainting [PB94-193323] p 104 N95-17466

Ultrasonic techniques for repair of aircraft structures with bonded composite patches p 136 N95-19486

Aircraft corrosion study [AD-A279527] p 241 N95-21687

Battelle Memorial Inst., Columbus, OH.
Development of repair processes and sources for C/KC-135 aircraft windows/windshields [AD-A288348] p 367 N95-26629

Alternatives to ozone depleting refrigerants in test equipment p 630 N95-31767

Resource document for the design of electronic instrument approach procedure displays [AD-A295108] p 691 N95-34797

BBN Systems and Technologies Corp., Cambridge, MA.
An active liner system for jet engine exhaust silencers, phase 1 [AD-A293277] p 617 N95-31191

BBN Systems and Technologies Corp., Canoga Park, CA.
Assessing effects of military aircraft noise on residential property values near airbases p 31 N95-11310

Belgian Center for Corrosion Study, Brussels (Belgium).
In-situ detection of surface passivation or activation and of localized corrosion: Experiences and perspectives in aircraft p 302 N95-23508

Test method and test results for environmental assessment of aircraft materials p 302 N95-23509

Bihrie Applied Research, Inc., Hampton, VA.
Experimental study of the effects of Reynolds number on high angle of attack aerodynamic characteristics of forebodies during rotary motion [NASA-CR-195033] p 330 N95-24443

Bihrie Applied Research, Inc., Jericho, NY.
Validation of the NASA Dryden X-31 simulation and evaluation of mechanization techniques p 69 N95-14236

Bionetics Corp., Hampton, VA.
Measurement and prediction of broadband noise from large horizontal axis wind turbine generators p 451 N95-27990

BioTechnology, Inc., Falls Church, VA.
Development of an intervention program to encourage shoulder harness use and aircraft retrofit in general aviation aircraft: Phases 1 and 2 [AD-A290966] p 485 N95-29873

BKM, Inc., San Diego, CA.
Advanced diesel electronic fuel injection and turbocharging [AD-A279176] p 211 N95-19809

Boeing Aerospace Co., Seattle, WA.

Comparative performance tests on the Mod-2, 2.5-mW wind turbine with and without vortex generators
p 377 N95-27978

Comparison of measured and calculated dynamic loads for the Mod-2 2.5 mW wind turbine system
p 440 N95-27983

Use of blade pitch control to provide power train damping for the Mod-2, 2.5-mW wind turbine
p 440 N95-27986

Boeing Co., Seattle, WA.

Full-scale testing and analysis of fuselage structure
p 95 N95-14485

Impact damage resistance of composite fuselage structure, part 2
p 533 N95-28838

Challenges and payoff of composites in transport aircraft: 777 empennage and future applications
p 534 N95-29031

Boeing Commercial Airplane Co., Seattle, WA.

Transmission loss characteristics of aircraft sidewall systems to control cabin interior noise
p 28 N95-11261

Comments on the use of structureborne noise analysis for large commercial airplanes
p 30 N95-11287

Effect of constraining layer stiffness on performance of damping tile materials using finite element modelling with Rayleigh integral
p 30 N95-11306

Two-dimensional high-lift airfoil data for CFD code validation
p 112 N95-17859

The application of Newman crack-closure model to predicting fatigue crack growth
p 167 N95-19483

Consistent approach to describing aircraft HIRF protection
[NASA-CR-195067] p 334 N95-25341

Local design optimization for composite transport fuselage crown panels
p 398 N95-28473

Composite fuselage crown panel manufacturing technology
p 399 N95-28474

Impact damage resistance of composite fuselage structure, part 1
p 399 N95-28482

NASA-ACEE/Boeing 737 graphite-epoxy horizontal stabilizer service
p 400 N95-28489

Noise exposure reduction of advanced high-lift systems
[NASA-CR-195077] p 452 N95-28670

The effects of design details on cost and weight of fuselage structures
p 501 N95-28831

Manufacturing scale-up of composite fuselage crown panels
p 532 N95-28835

Dimensional stability of curved panels with cocured stiffeners and cobonded frames
p 532 N95-28836

Design, analysis, and fabrication of a pressure box test fixture for tension damage tolerance testing of curved fuselage panels
p 533 N95-28839

Global cost and weight evaluation of fuselage keel design concepts
p 501 N95-28840

Advanced composite fuselage technology
p 535 N95-29034

Cost model relationships between textile manufacturing processes and design details for transport fuselage elements
p 536 N95-29043

Boeing Defense and Space Group, Philadelphia, PA.

Application of advanced material systems to composite frame elements
p 422 N95-28432

Characterization and manufacture of braided composites for large commercial aircraft structures
p 426 N95-28478

Advanced flight control technology achievements at Boeing Helicopters
p 624 N95-32014

Boeing Defense and Space Group, Seattle, WA.

Euler technology assessment for preliminary aircraft design employing OVERFLOW code with multiblock structured-grid method
[NASA-CR-4651] p 273 N95-23095

Investigation of static and cyclic bearing failure mechanisms for GR/EP laminates
p 422 N95-28427

Investigation and characterization of SEU effects and hardening strategies in avionics
[AD-A291058] p 509 N95-29950

Cadmium plating replacements
p 631 N95-31773

Boeing Military Airplane Development, Seattle, WA.

TranAir: A full-potential, solution-adaptive, rectangular grid code for predicting subsonic, transonic, and supersonic flows about arbitrary configurations. User's manual
[NASA-CR-4349] p 377 N95-28230

TranAir: A full-potential, solution-adaptive, rectangular grid code for predicting subsonic, transonic, and supersonic flows about arbitrary configurations. Theory document
[NASA-CR-4348] p 378 N95-28265

Bombardier, Inc., Montreal (Quebec).

Design and structural validation of CF116 upper wing skin boron doubler
p 393 N95-27510

British Aerospace Airbus Ltd., Bristol (England).

The impact of non-linear flight control systems on the prediction of aircraft loads due to turbulence
p 143 N95-18598

British Aerospace Aircraft Group, Bristol (England). Application of superplastically formed and diffusion bonded structures in high intensity noise environments
p 174 N95-19162

British Aerospace Aircraft Group, Preston (England). Transonic and supersonic flowfield measurements about axisymmetric afterbodies for validation of advanced CFD codes
p 121 N95-19260

British Aerospace Aircraft Group, Warton (England). Current and future problems in structural acoustic fatigue
p 173 N95-19143

British Aerospace Defence Ltd., Preston (England). Composite repair of composite structures
p 395 N95-27521

The FCS-structural coupling problem and its solution
p 623 N95-32005

Pilot Induced Oscillation: A report on the AGARD Workshop on PIO
p 624 N95-32017

British Aerospace Defence Ltd., Warton (England). Experimental Aircraft Programme (EAP): Flight control system design and test
p 623 N95-32010

Flight demonstration of an advanced pitch control law in the VAAC Harrier aircraft
p 623 N95-32012

British Columbia Univ., Vancouver (British Columbia). Unsteady flow testing in a passive low-correction wind tunnel
p 147 N95-19272

Brown-Buntin Associates, Inc., Visalia, CA. INM contour validation: A case study
p 31 N95-11321

Brown Univ., Providence, RI. Aerodynamic parameter estimation via Fourier modulating function techniques
[NASA-CR-4654] p 335 N95-24630

High order accuracy computational methods in aerodynamics using parallel architectures
[AD-A294167] p 666 N95-34763

Burnette Engineering, Fairborn, OH. An evaluation of aircraft CRT and dot-matrix display legibility requirements
[AD-A283933] p 138 N95-18164

C**California Inst. of Tech., Pasadena, CA.**

Research on bluff body vortex wakes
[AD-A286319] p 223 N95-20177

Shock wave interactions in hypervelocity flow
[AD-A286507] p 250 N95-22212

California Polytechnic State Univ., San Luis Obispo, CA. The FC-1D: The profitable alternative Flying Circus Commercial Aviation Group
[NASA-CR-197152] p 46 N95-12628

The OFP-6M transport jet
[NASA-CR-197159] p 46 N95-12637

Central coast designs: The Eightball Express. Taking off with convention, cruising with improvements and landing with absolute success
[NASA-CR-197181] p 47 N95-12643

Numerical design of advanced multi-element airfoils
[NASA-CR-197195] p 76 N95-15762

A real-time algorithm for integrating differential satellite and inertial navigation information during helicopter approach
[NASA-CR-197409] p 229 N95-21891

Developing a workstation-based, real-time simulation for rapid handling qualities evaluations during design
[NASA-CR-198831] p 505 N95-30335

California Univ., Davis, CA. Numerical simulation of helicopter engine plume in forward flight
[NASA-CR-197488] p 107 N95-16589

Analysis of the longitudinal handling qualities and pilot-induced-oscillation tendencies of the High-Angle-of-Attack Research Vehicle (HARV)
p 293 N95-23297

High-lift flow-physics flight experiments on a subsonic civil transport aircraft (B737-100)
p 275 N95-23333

Unique considerations in the design and experimental evaluation of tailored wings with elastically produced chordwise camber
p 423 N95-28436

Analysis and design methodology for chordwise deformable wings
p 692 N95-33311

California Univ., Los Angeles, CA. Aeroelastic simulation of higher harmonic control
[NASA-CR-4623] p 37 N95-11911

In-flight imaging of transverse gas jets injected into transonic and supersonic crossflows: Design and development
[NASA-CR-186031] p 157 N95-17418

Demonstration of the Dynamic Flowgraph Methodology using the Titan 2 Space Launch Vehicle Digital Flight Control System
[NASA-CR-197517] p 150 N95-17493

Minimal time detection algorithms and applications to flight systems
[TR-2-FSRC-93] p 171 N95-18564

The accuracy of parameter estimation in system identification of noisy aircraft load measurement
[NASA-CR-197516] p 134 N95-19130

Effect of density gradients in confined supersonic shear layers, part 1
[NASA-CR-198029] p 348 N95-24412

Effect of density gradients in confined supersonic shear layers. Part 2: 3-D modes
[NASA-CR-198030] p 349 N95-24413

Aeroelasticity and structural optimization of composite helicopter rotor blades with swept tips
[NASA-CR-4665] p 397 N95-28262

Turbulent airflow noise production and propagation patterns of a subsonic jet impinging on a flat plate
p 580 N95-29502

Vibration reduction in helicopter rotors using an actively controlled partial span trailing edge flap located on the blade
p 624 N95-32111

A stochastic adaptive control application to flight systems
p 699 N95-34806

California Univ., San Diego, La Jolla, CA. Theories of turbulent combustion in high speed flows
[AD-A280933] p 23 N95-10535

Calspan Advanced Technology Center, Buffalo, NY. Evaluation of F-18A approach and landing flying qualities using an in-flight simulator
[CALSPAN-6241-F-1] p 12 N95-10442

Cambridge Acoustical Associates, Inc., Cambridge, MA. The use of cowl camber and taper to reduce rotor/stator interaction noise
[NASA-CR-195421] p 323 N95-22675

Cambridge Hydrodynamics, Inc., Princeton, NJ. Numerical studies of turbulent free surface flows and unsteady propeller flows
[AD-A294377] p 706 N95-34343

Cambridge Univ., Cambridge (England). Designing in three dimensions
p 90 N95-14130

Three-dimensional interaction of wake/boundary-layer and vortex/boundary-layer data report
[CUE/D/A-AEREO/TR-23] p 329 N95-24210

Carnegie-Mellon Inst. of Research, Pittsburgh, PA. Development of an Automated Nondestructive Inspection (ANDI) system for commercial aircraft, phase 1
[AD-A283500] p 40 N95-12623

Carnegie-Mellon Univ., Pittsburgh, PA. Research on an autonomous vision-guided helicopter
[AIAA PAPER 94-1240-CP] p 18 N95-11510

Computing quantitative characteristics of finite-state real-time systems
[AD-A282839] p 83 N95-14343

Transport phenomena in stratified multi-fluid flow in the presence and absence of gravity
p 95 N95-14563

A feedforward control approach to the local navigation problem for autonomous vehicles
[AD-A282787] p 126 N95-17706

Collected papers of the Soar/IFOR project, Spring 1994
[AD-A280063] p 238 N95-20624

Software process improvement in the NASA software engineering laboratory
[AD-A289912] p 450 N95-28627

New adaptive methods for reconfigurable flight control systems, appendix 1
[AD-A292711] p 619 N95-30937

Case Western Reserve Univ., Cleveland, OH. Three dimensional compressible turbulent flow computations for a diffusing S-duct with/without vortex generators
[NASA-CR-195390] p 138 N95-17402

Catholic Univ. of America, Washington, DC. Application of wavelet-filtering techniques to intermittent turbulent and wall pressure events. Part 1: Exploratory results
[AD-A286077] p 247 N95-20849

CCG Associates, Inc., Silver Spring, MD. Identification of Artificial Intelligence (AI) applications for maintenance, monitoring, and control of airway facilities
[AD-A282479] p 125 N95-17373

Central Aerohydrodynamics Inst., Zhukovskiy (Russia). Optical surface pressure measurements: Accuracy and application field evaluation
p 175 N95-19274

Central Inst. of Aviation Motors, Moscow (Russia). Solution of Navier-Stokes equations using high accuracy monotone schemes
p 161 N95-19019

The mathematical models of flow passage for gas turbine engines and their components
p 140 N95-19020

- Simulation of multidisciplinary problems for the thermostress state of cooled high temperature turbines p 140 N95-19021
- Application of multicomponent models to flow passage simulation in multistage turbomachines and whole gas turbine engines p 140 N95-19022
- Simulation of steady and unsteady viscous flows in turbomachinery p 140 N95-19023
- Application of multidisciplinary models to the cooled turbine rotor design p 140 N95-19024
- Verification of multidisciplinary models for turbomachines p 140 N95-19025
- Perspective problems of gas turbine engines simulation p 140 N95-19026
- Central Research and Development Inst. Elektropribor, Saint Petersburg (Russia).**
Navigational technology of dual usage p 688 N95-33131
- Centre d'Etudes et de Recherches, Toulouse (France).**
Experimental techniques for measuring transonic flow with a three dimensional laser velocimetry system. Application to determining the drag of a fuselage p 163 N95-19258
- Analysis of test section sidewall effects on a two dimensional airfoil: Experimental and numerical investigations p 165 N95-19276
- Low-level data fusion for landing runways detection p 689 N95-33136
- Centre de Recherches en Physique de l'Environnement, Velizy (France).**
Experimental study of the helicopter-mobile radioelectric channel and possible extension to the satellite-mobile channel p 247 N95-20945
- Centre National d'Etudes Spatiales, Toulouse (France).**
A processing centre for the CNES CE-GPS experimentation p 125 N95-17196
- Centro Sviluppo Materiali S.p.A., Trento (Italy).**
Thermal testing of high performance thermal barrier coatings for turbine blades p 202 N95-19681
- Ceramic Composites, Inc., Millersville, MD.**
Ceramic composite combustor cans for expendable turbine engines [AD-A289551] p 407 N95-28646
- Cessna Aircraft Co., Wichita, KS.**
Design limit loads based upon statistical discrete gust methodology p 133 N95-18603
- CFD Research Corp., Huntsville, AL.**
Pressure based high order TVD methodology for dynamic stall control [AD-A290149] p 479 N95-29316
- Chalk (Charles R.), Williamsville, NY.**
Calspan experience of PIO and the effects of rate limiting p 598 N95-31072
- Charles River Analytics, Inc., Cambridge, MA.**
A neural expert approach to self designing flight control systems [AD-A279965] p 237 N95-21122
- Civil Aviation Authority, Farnborough (England).**
Human factors certification in the development of future air traffic control systems p 690 N95-34770
- Christian Brothers Coll., Memphis, TN.**
Improved modeling of unsteady heat transfer (The first step) [AD-A292777] p 648 N95-31432
- Cincinnati Univ., OH.**
Atmospheric and wind modeling for ATC [NASA-CR-196786] p 98 N95-13725
- Assessment of CTAS ETA prediction capabilities [NASA-CR-197224] p 97 N95-15728
- Groundspeed filtering for CTAS [NASA-CR-197223] p 97 N95-15785
- Experimental and numerical simulations of the effects of ingested particles in gas turbine engines p 199 N95-19662
- City Coll. of the City Univ. of New York, NY.**
Image representation using fast algorithms based on the Zak transform [AD-A293416] p 679 N95-31684
- City Univ., London (England).**
Interference determination for wind tunnels with slotted walls p 147 N95-19269
- Civil Aeromedical Inst., Oklahoma City, OK.**
The performance of child restraint devices in transport airplane passenger seats [DOT/FAA/AM-94/19] p 40 N95-12146
- The role of flight progress strips in en route air traffic control: A time-series analysis [DOT/FAA/AM-95/4] p 280 N95-23565
- Development of qualification guidelines for personal computer-based aviation training devices [DOT/FAA/AM-95/6] p 323 N95-23603
- Aircraft fires, smoke toxicity, and survival: An overview [DOT/FAA/AM-95/8] p 277 N95-24024
- A review of civil aviation fatal accidents in which lost/disoriented was a cause/factor: 1981-1990 [DOT/FAA/AM-95/1] p 278 N95-24071
- Development of an intervention program to encourage shoulder harness use and aircraft retrofit in general aviation aircraft, phases 1 and 2 [DOT/FAA/AM-95/2] p 333 N95-24384
- Conversion of the TRACON operations concepts database into a formal sentence outline job task taxonomy [DOT/FAA/AM-95/16] p 488 N95-28819
- Clarkson Univ., Potsdam, NY.**
A time stepping coupled finite element-state space modeling environment for synchronous machine performance and design analysis in the ABC frame of reference p 649 N95-31948
- Clemson Univ., SC.**
Maximum-likelihood spectral estimation and adaptive filtering techniques with application to airborne Doppler weather radar [NASA-CR-197699] p 316 N95-23670
- Characterizing the wake vortex signature for an active line of sight remote sensor [NASA-CR-197697] p 333 N95-24391
- A general theory of two- and three-dimensional rotational flow in subsonic and transonic turbomachines [NASA-CR-4496] p 377 N95-28003
- Effects of elevated free-stream turbulence and streamwise acceleration on flow and thermal structures in transitional boundary layers p 556 N95-29729
- Coherent Technologies, Inc., Boulder, CO.**
Airport surveillance using a solid state coherent lidar p 41 N95-13207
- Wake vortex detection at Denver Stapleton Airport with a pulsed 2-micron coherent lidar p 42 N95-13211
- College of William and Mary, Williamsburg, VA.**
A spectrally accurate boundary-layer code for infinite swept wings [NASA-CR-195014] p 159 N95-18042
- Preparation of course materials: Elementary mathematics of powered flight p 324 N95-23320
- Colorado Univ., Boulder, CO.**
High performance parallel analysis of coupled problems for aircraft propulsion [NASA-CR-195355] p 23 N95-10132
- Structural effects of unsteady aerodynamic forces on horizontal-axis wind turbines [DE94-011863] p 157 N95-16939
- State-to-state collisional dynamics of atmospheric species [AD-A285053] p 245 N95-20484
- High-performance parallel analysis of coupled problems for aircraft propulsion [NASA-CR-197440] p 289 N95-23088
- Integration of AIRSAR and AVIRIS data for Trail Canyon alluvial fan, Death Valley, California p 709 N95-33760
- Columbia Univ., New York, NY.**
Qualitative environmental navigation: Theory and practice p 601 N95-30486
- Combustion Inst., Pittsburgh, PA.**
The 25th International Symposium on Combustion [AD-A286825] p 630 N95-31268
- Commonwealth Scientific and Industrial Research Organization, Highett, Victoria (Australia).**
Expert systems and artificial intelligence applications in engineering design and inspection p 710 N95-33008
- Computer Sciences Corp., Hampton, VA.**
A grid generation system for multi-disciplinary design optimization p 567 N95-28763
- Concordia Univ., Montreal (Quebec).**
Finite element vorticity-based methods for the solution of the incompressible and compressible Navier-Stokes equations p 553 N95-29119
- Conductus, Inc., Sunnysvale, CA.**
The mm-wave resonant methods for the detection of corrosion, phase 1 [AD-A291315] p 556 N95-29941
- Connecticut Univ., Storrs, CT.**
MATSurv multisensor air traffic surveillance [AD-A292253] p 489 N95-28887
- The fluid mechanics of a high aspect ratio slot with an impressed pressure gradient and secondary injection p 557 N95-30304
- Consiglio Nazionale delle Ricerche, Rome (Italy).**
MAX-91: Polarimetric SAR results on Montespertoli site p 320 N95-23940
- Construcciones Aeronauticas S.A., Madrid (Spain).**
A study of the effect of store unsteady aerodynamics on gust and turbulence loads p 133 N95-18601
- Repairs of CFC primary structures p 396 N95-27527
- Continuum Dynamics, Inc., Princeton, NJ.**
A novel instrumentation system for measurement of helicopter rotor motions and loads data, phase 1 [AD-A293309] p 607 N95-30923
- Coordinating Research Council, Inc., Atlanta, GA.**
The effect of aviation fuels containing low amounts of static dissipater additive on electrostatic charge generation [AD-A280075] p 420 N95-28152
- Cornell Univ., Ithaca, NY.**
Wave cycle design for wave rotor engines with limited nitrogen oxide emissions p 161 N95-18901
- Fatigue crack growth in 2024-T3 aluminum under tensile and transverse shear stresses p 153 N95-19490
- Cranfield Univ., Bedford (England).**
Particle trajectories in gas turbine engines p 199 N95-19663
- D**
- DACCO SCI, Inc., Columbia, MD.**
The use of electrochemistry and ellipsometry for identifying and evaluating corrosion on aircraft [AD-A285323] p 151 N95-16371
- The use of electrochemistry and ellipsometry for identifying and evaluating corrosion on aircraft [AD-A288536] p 381 N95-27186
- The use of electrochemistry and ellipsometry for identifying and evaluating corrosion on aircraft [AD-A290249] p 504 N95-29426
- Daiko Ltd. (Japan).**
Parallel computation of transonic flows about an aircraft configuration using multi-block structured grids p 685 N95-34537
- DASCON Engineering, Bay Village, OH.**
Collected papers on wind turbine technology [NASA-CR-195432] p 447 N95-27970
- Dassault Aviation, Saint-Cloud (France).**
Aeroacoustic qualification of HERMES shingles p 173 N95-19145
- Brite-Euram programme: ACOUFAT acoustic fatigue and related damage tolerance of advanced composite and metallic structures p 174 N95-19159
- FASTPACK: Optimized solutions for modular avionics derived from a parametric study. Part 1: Platform features p 233 N95-20634
- Composite repair of metallic airframe: Twenty years of experience p 393 N95-27508
- Catapult-launching of the RAFALE design and experimentation p 609 N95-32008
- Dayton Univ., OH.**
Conference on Aerospace Transparent Materials and Enclosures, volume 1 [AD-A283925] p 133 N95-18677
- Lubricant evaluation and performance, 2 [AD-A279144] p 242 N95-21969
- An analysis of B-1B exterior jet blast windshield anti-icing performance using pre-cooled compressor bleed air [AD-A292522] p 485 N95-28811
- Image representation using fast algorithms based on the Zak transform [AD-A293416] p 679 N95-31684
- Perceptual dimensions of simulated scenes relevant for visual low-altitude flight [AD-A294385] p 700 N95-34344
- Altitude cuing effectiveness of terrain texture characteristics in simulated low-altitude flight [AD-A294369] p 700 N95-34362
- Dayton Univ. Research Inst., OH.**
Conference on Aerospace Transparent Materials and Enclosures. Volume 2: Sessions 5-9 [AD-A283926] p 131 N95-18162
- Color control in a multichannel simulator display: The display for advanced research and training [AD-A279717] p 239 N95-20992
- De Havilland Aircraft Co. of Canada Ltd., Downsview (Ontario).**
A review of gust load calculation methods at de Havilland p 118 N95-18604
- Interference corrections for a centre-line plate mount in a porous-walled transonic wind tunnel p 122 N95-19280
- Defence Research Agency, Bedford (England).**
Investigation of the flow over a series of 14 percent-thick supercritical aerofoils with significant rear camber p 109 N95-17849
- Detailed study at supersonic speeds of the flow around delta wings p 112 N95-17861
- Pressure distributions on research wing W4 mounted on an axisymmetric body p 112 N95-17862
- Boundary-flow measurement methods for wall interference assessment and correction: Classification and review p 163 N95-19262
- The Anglo-French Compact Laser Radar demonstrator programme p 703 N95-32501
- Defence Research Agency, Farnborough, Hampshire (England).**
A method of calculating the safe fatigue life of compact, highly-stressed components p 93 N95-14664

- Measurements on a two-dimensional aerofoil with high-lift devices p 109 N95-17848
- Measurements of the flow over a low aspect-ratio wing in the Mach number range 0.6 to 0.87 for the purpose of validation of computational methods. Part 1: Wing design, model construction, surface flow. Part 2: Mean flow in the boundary layer and wake, 4 test cases p 112 N95-17860
- The operation of gas turbine engines in hot and sandy conditions: Royal Air Force experiences in the Gulf conflict p 198 N95-19655
- The calculation of erosion in a gas turbine compressor rotor p 199 N95-19664
- The corrosion and protection of advanced aluminium - lithium airframe alloys p 302 N95-23497
- Non-destructive detection of corrosion for life management p 314 N95-23505
- A theoretical and experimental investigation of the flow over supersonic leading edge wing/body configurations [DRA-TM-AERO-PROP-41] p 331 N95-25649
- Adhesively bonded composite patch repair of cracked aluminum alloy structures p 393 N95-27507
- The application of helicopter mission simulation to Nap-of-the-Earth operations p 710 N95-32496
- Defence Research Establishment Pacific, Victoria (British Columbia).**
- Composite repair issues on the CF-18 aircraft p 395 N95-27518
- Defence Science and Technology Organisation, Canberra (Australia).**
- Helicopter life substantiation: Review of some USA and UK initiatives [AD-A290045] p 502 N95-28851
- Preparation of S-70A-9 Black Hawk helicopter for flight tests to investigate cause of cracking of inner fuselage panel [AD-A293891] p 608 N95-31544
- Defence Science and Technology Organisation, Melbourne (Australia).**
- Data acquisition and processing software for the Low Speed Wind Tunnel tests of the Jindivik auxiliary air intake [AD-A285455] p 108 N95-17178
- Variations observed in the AC generator signal period of a Sea King helicopter [AD-A284280] p 230 N95-19963
- A preliminary study of the airwake model used in an existing SH-60B/FFG-7 helicopter/ship simulation program [DSTO-TR-0015] p 224 N95-21659
- Enhancement of F/A-18 operational flight measurements: Data report for phase 1 [DSTO-TR-0049] p 286 N95-23666
- An overview of Health and Usage Monitoring Systems (HUMS) for military helicopters [DSTO-TR-0061] p 327 N95-24200
- Helicopter life substantiation: Review of some USA and UK initiatives [DSTO-TR-0062] p 328 N95-24201
- A portable transmission vibration analysis system for the S-70A-9 Black Hawk helicopter [DSTO-TR-0072] p 348 N95-24203
- Design and development of a test rig for the high frequency testing of rolling sleeve airsprings [DSTO-TN-0001] p 411 N95-26378
- F/A-18 IFOSTP Fatigue test airbag load determination on the vertical and horizontal tails [DSTO-TR-0135] p 388 N95-26389
- Characteristics of the turbine inlet temperature sensing circuit for the T56 turbo-prop engine [DSTO-TR-0095] p 405 N95-26424
- Bonded composite repair of metallic aircraft components: Overview of Australian activities p 392 N95-27505
- Scarf repairs to graphite/epoxy components p 396 N95-27523
- A review of Australian and New Zealand investigations on aeronautical fatigue during the period Apr. 1993 - Mar. 1995 [AR-009-202] p 397 N95-27918
- Tie-down trials involving a Sikorsky S-70B-2 helicopter [DSTO-TR-0132] p 400 N95-28567
- Unmanned Aerial Vehicle technology [DSTO-GD-0044] p 503 N95-29362
- Estimation of aerodynamic load distributions on the F/A-18 aircraft using a CFD panel code [DSTO-TR-0147] p 504 N95-29445
- Water model tests on the Allison T56 series 3 combustion system [DSTO-TR-0139] p 697 N95-33250
- Defence Advanced Research Projects Agency, Arlington, VA.**
- Technology reinvestment project's focus area: Affordable polymer matrix composites for airframe structures [PB95-136032] p 324 N95-23168
- Delavan, Inc., West Des Moines, IA.**
- Thermal chemical energy of ablating silica surfaces in air breathing solid rocket engines p 148 N95-16316
- Delaware State Coll., Dover, DE.**
- Mode of human image representation and error checking strategies in complex visual displays [AD-A290107] p 485 N95-29210
- Delaware Univ., Newark, DE.**
- The effect of material heterogeneity in curved composite beams for use in aircraft structures p 422 N95-28426
- Department of Defense, Fort Meade, MD.**
- Unmanned aerial vehicles. 1994 master plan p 607 N95-31416
- Department of Defense, Washington, DC.**
- Unmanned aerial vehicles p 231 N95-20329
- Unmanned aerial vehicles, 1994 master plan [AD-A291628] p 398 N95-28411
- Department of Energy, Washington, DC.**
- Thermal barrier coatings issues in advanced land-based gas turbines p 344 N95-26122
- Thermal barrier coatings application in diesel engines p 345 N95-26124
- Department of the Air Force, Brooks AFB, TX.**
- Civil Reserve Air Fleet-Aeromedical Evacuation Shipset (CRAF-AESS) p 568 N95-29619
- International access to aeromedical evacuation medical equipment assessment data p 569 N95-29622
- Department of the Air Force, California City, CA.**
- Aeroelastic pilot-in-the-loop oscillations p 598 N95-31070
- Department of the Air Force, Tinker AFB, OK.**
- Oklahoma City air logistics center (USAF) aging aircraft corrosion program p 262 N95-23519
- Department of the Air Force, Wright-Patterson AFB, OH.**
- Environmentally safe aviation fuels p 631 N95-31768
- Department of the Navy, Washington, DC.**
- Corner vortex suppressor [AD-D016423] p 116 N95-18337
- Hydrofoil force balance [AD-D016475] p 160 N95-18461
- Integrated aerodynamic fin and stowable TVC vane system [AD-D016457] p 151 N95-19073
- Solid fuel ramjet composition [AD-D016458] p 152 N95-19090
- Malone-brayton cycle engine/heat pump [AD-D016573] p 244 N95-20295
- Passive range measurement system [AD-D016222] p 258 N95-21100
- Lift enhancement device [AD-D016522] p 224 N95-21864
- Suppressor of oscillations in airframe cavities [AD-D017265] p 388 N95-26507
- Balanced on air aircraft [AD-D017251] p 389 N95-26537
- Apparatus and method for producing three-dimensional images [AD-D017455] p 646 N95-30727
- Composite structure forming a wear surface [AD-D017462] p 629 N95-30749
- High aspect ratio metal microstructures and method for preparing the same [AD-D017463] p 629 N95-30750
- Apparent size passive range method [AD-D017360] p 611 N95-31180
- Energy absorption device for shock loading [AD-D017476] p 706 N95-34449
- Desert Research Inst., Reno, NV.**
- Replicator for characterization of cirrus and polar stratospheric cloud particles [NASA-CR-197785] p 445 N95-26669
- Detroit Diesel Allison, Indianapolis, IN.**
- Compressor discharge film riding face seals p 60 N95-13599
- Experimental study of vane heat transfer and aerodynamics at elevated levels of turbulence [NASA-CR-4633] p 244 N95-19912
- Deutsche Aerospace A.G., Bremen (Germany).**
- Acoustic fatigue testing on different materials and skin-stringer elements p 174 N95-19156
- Deutsche Aerospace A.G., Munich (Germany).**
- X-31 quasi-tailless flight demonstration p 70 N95-14243
- Aeromechanical design of modern missiles p 73 N95-14446
- Microchannel heat pipe cooling of modules p 246 N95-20649
- Optical backplane for modular avionics p 257 N95-20652
- Corrosion protection measures for CFC/metal joints of fuel integral tank structures of advanced military aircraft p 303 N95-23510
- Experience of in-service corrosion on military aircraft p 303 N95-23516
- On aircraft repair verification of a fighter A/C integrally stiffened fuselage skin p 394 N95-27515
- Composite repair of a CF18: Vertical stabilizer leading edge p 395 N95-27517
- X-31: A program overview and flight test status p 609 N95-32013
- Deutsche Airbus G.m.b.H., Bremen (Germany).**
- Tools for applied engineering optimization p 128 N95-16570
- The global aircraft shape p 128 N95-16571
- Aerodynamic shape optimization p 128 N95-16572
- Deutsche Airbus G.m.b.H., Hamburg (Germany).**
- Treatment of non-linear systems by timeplane-transformed CT methods: The spectral gust method p 143 N95-18600
- Development of load spectra for Airbus A330/A340 full scale fatigue tests p 135 N95-19479
- Damage occurrence on composites during testing and fleet service: Repair of Airbus aircraft p 396 N95-27526
- Deutsche Forschungs- und Versuchsanstalt fuer Luft- und Raumfahrt, Brunswick (Germany).**
- Parameter identification for X-31A at high angles of attack p 69 N95-14235
- Deutsche Forschungs- und Versuchsanstalt fuer Luft- und Raumfahrt, Goettingen (Germany).**
- Numerical simulation and analysis of the hypersonic turbulent flow past a blunt-fin/ramp configuration [DLR-FB-94-19] p 483 N95-30349
- Deutsche Forschungsanstalt fuer Luft- und Raumfahrt, Brunswick (Germany).**
- 2-D airfoil tests including side wall boundary layer measurements p 158 N95-17847
- DLR-F4 wing body configuration p 130 N95-17863
- Subsonic flow around US-orbiter model FALKE in the DNW p 115 N95-18777
- Pressure distribution measurements on an isolated TPS 441 nacelle p 115 N95-17878
- Theoretical investigations of shock/boundary layer interactions on a Ma(infinity) = 8 waverider [DLR-FB-94-12] p 119 N95-18910
- Wall correction method with measured boundary conditions for low speed wind tunnels p 164 N95-19263
- SCARLET: DLR rate saturation flight experiment p 598 N95-31068
- Handling qualities analysis on rate limiting elements in flight control systems p 619 N95-31071
- Experiences with ADS-33 helicopter specification testing and contributions to refinement research p 621 N95-31993
- Model following control for tailoring handling qualities: ACT experience with ATTHes p 622 N95-32000
- Advanced gust management systems: Lessons learned and perspectives p 622 N95-32002
- The DLR research programme on an integrated multi sensor system for surface movement guidance and control p 689 N95-33135
- Deutsche Forschungsanstalt fuer Luft- und Raumfahrt, Cologne (Germany).**
- Wind tunnel investigations of the appearance of shocks in the windward region of bodies with circular cross section at angle of attack p 113 N95-17866
- Experimental investigation of turbulent particle dispersion in swirling flows [DLR-FB-94-20] p 647 N95-31355
- Deutsche Forschungsanstalt fuer Luft- und Raumfahrt, Goettingen (Germany).**
- DLR-F5: Test wing for CFD and applied aerodynamics p 113 N95-17864
- Three-dimensional boundary layer and flow field data of an inclined prolate spheroid p 158 N95-17867
- Force and pressure data of an ogive-nosed slender body at high angles of attack and different Reynolds numbers p 113 N95-17868
- Wind tunnel test on a 65 deg delta wing with rounded leading edges: The International Vortex Flow Experiment p 114 N95-17875
- Flow field investigation in a free jet - free jet core system for the generation of high intensity molecular beams [DLR-FB-94-11] p 172 N95-18912
- Structural aspects of active control technology p 623 N95-32006
- A nonlinear vortex lattice method for unsteady flow with separated vortex [DLR-FB-94-32] p 704 N95-32787
- Diffracto Ltd., Windsor (Ontario).**
- Characterization of corrosion and development of a breadboard of a D sight aircraft inspection system, phase 1 [AD-A288347] p 380 N95-26527

Donmar Ltd., Newport Beach, CA.

Cost effective, dual-purpose machine vision-based detectors for (1) smoke and flame detection, and (2) engine overhead/burn-through and flame detection
[AD-A292284] p 579 N95-28870

Dornier Luftfahrt G.m.b.H., Friedrichshafen (Germany).
Automatic flight control system for an unmanned helicopter system design and flight test results
p 622 N95-32004

Douglas Aircraft Co., Inc., Long Beach, CA.

Evaluation of all-electric secondary power for transport aircraft
[NASA-CR-189077] p 441 N95-27999
Aircraft IR/acoustic detection evaluation. Volume 2: Development of a ground-based acoustic sensor system for the detection of subsonic jet-powered aircraft
[NASA-CR-189705-VOL-2] p 452 N95-28073
Impact of composites on future transport aircraft
p 534 N95-29030
Progress in manufacturing large primary aircraft structures using the stitching/RTM process
p 537 N95-29050
Test results from large wing and fuselage panels
p 537 N95-29051

Dow Chemical Co., Midland, MI.

Novel matrix resins for composites for aircraft primary structures, phase 1
[NASA-CR-189657] p 23 N95-10318
Development of RTM and powder prepreg resins for subsonic aircraft primary structures
p 536 N95-29044

Dow-United Technologies Composite Products, Inc., Wallingford, CT.

Application of damage tolerance methodology in certification of the Piaggio P-180 Avanti
p 399 N95-28480

Draper (Charles Stark) Lab., Inc., Cambridge, MA.

Error modeling for differential GPS
[NASA-CR-188367] p 488 N95-28716
A vehicle health monitoring system for the Space Shuttle Reaction Control System during reentry
[NASA-CR-188370] p 527 N95-29447

Drexel Univ., Philadelphia, PA.

Design of robust optimal control systems and stability analysis of real structured uncertainties
[AD-A279089] p 256 N95-21913

Duke Univ., Durham, NC.

Acoustic radiation damping of flat rectangular plates subjected to subsonic flows
p 172 N95-18542
Nonlinear dynamics and aeroelasticity of rotorcraft in forward flight
[AD-A291714] p 400 N95-28504

Dynamic Soft Analysis, Inc., Pittsburgh, PA.

CAE for thermal management of aerospace electronic boards using the BETAsoft program
p 438 N95-27354

E**Eagle Ventures, Rockville, MD.**

Independent review of Aviation Technology and Research Information Analysis System (ATRIAS) database
[AD-A284049] p 226 N95-21518

Ecole Nationale Supérieure de l'Aéronautique et de l'Espace, Toulouse (France).

Numerical study of Gortler instability: Application to the design of a quiet supersonic wind tunnel
[PB94-184801] p 21 N95-10844

Ecole Polytechnique, Montreal (Quebec).

Thermal-mechanical fatigue crack growth in aircraft engine materials
[ISBN-0-315-86543-1] p 647 N95-31098

EG and G Energy Measurements, Inc., Goleta, CA.

Turbine-engine applications of thermographic-phosphor temperature measurements
[DE95-003625] p 358 N95-25110

Eidetics Aircraft, Inc., Torrance, CA.

Static and dynamic force/moment measurements in the Eidetics water tunnel
p 69 N95-14238
F/A-18 and F-16 forebody vortex control, static and rotary-balance results
p 72 N95-14254

Eidetics International, Inc., Torrance, CA.

Development of a multicomponent force and moment balance for water tunnel applications, volume 1
[NASA-CR-4642-VOL-1] p 161 N95-18955
Development of a multicomponent force and moment balance for water tunnel applications, volume 2
[NASA-CR-4642-VOL-2] p 161 N95-18956

Electronics Research Lab., Salisbury (Australia).

A PC-based interactive simulation of the F-111C Pavé Tack system and related sensor, avionics and aircraft aspects
[AD-A285500] p 129 N95-16969

Eloret Corp., Palo Alto, CA.

Computational flow predictions for hypersonic drag devices
p 37 N95-11967

Development and application of structural dynamics analysis capabilities
[NASA-CR-197229] p 96 N95-14922

Particle kinetic simulation of high altitude hypervelocity flight
[NASA-CR-197383] p 309 N95-22481

Eltro G.m.b.H., Heidelberg (Germany).

Laser based obstacle warning sensors for helicopters
p 686 N95-32499

Eltron Research, Inc., Boulder, CO.

Electrochemical impedance pattern recognition for detection of hidden chemical corrosion on aircraft components
[AD-A284998] p 241 N95-20481

Electrochemical impedance pattern recognition for detection of hidden chemical corrosion on aircraft components
[AD-A285998] p 241 N95-20716

Electrochemical impedance pattern recognition for detection of hidden chemical corrosion on aircraft components, phase 1
[AD-A291345] p 556 N95-29946

Embry-Riddle Aeronautical Univ., Daytona Beach, FL.

Viper cabin-fuselage structural design concept with engine installation and wing structural design
[NASA-CR-197162] p 45 N95-12305

Triton 2 (1B)

[NASA-CR-197188] p 46 N95-12636
Cabin fuselage structural design with engine installation and control system
[NASA-CR-197173] p 47 N95-12639

Energy and Environmental Analysis, Inc., Arlington, VA.

Air pollution mitigation measures for airports and associated activity
[PB94-207610] p 216 N95-19582

Energy and Environmental Research Corp., Durham, NC.

Nitrogen oxide emissions and their control from uninstalled aircraft engines in enclosed test cells: Joint report to Congress on the Environmental Protection Agency - Department of Transportation study
[PB95-166237] p 358 N95-26005

Engineering Software Research and Development, Inc., Saint Louis, MO.

Elastic-plastic models for multi-site damage
p 92 N95-14454

Environmental Protection Agency, Ann Arbor, MI.

Regulatory impact analysis and regulatory support document: Control of air pollution; determination of significance for nonroad sources and emission standards for new nonroad compression-ignition engines at or above 37 kilowatts (50 horsepower)
[PB94-194594] p 61 N95-12855

Environmental Protection Agency, Cincinnati, OH.

Bicarbonate of soda blasting technology for aircraft wheel repainting
[PB94-193323] p 104 N95-17466

ESDU International Ltd., London (England).

Symmetric steady manoeuvre loads on rigid aircraft of classical configuration at subsonic speeds
[ESDU-94009] p 43 N95-11774

Application of multivariate optimisation techniques to determination of optimum flight path trajectories
[ESDU-94012] p 44 N95-11793

Examples of flight path optimisation using a multivariate gradient-search method. Addendum A: Variation of optimum flight profile parameters with range
[ESDU-94016-ADD-A] p 44 N95-11794

Ejectors and jet pumps: Computer program for design and performance for steam/gas flow
[ESDU-94046] p 500 N95-28704

Effects of small changes on rate of climb
[ESDU-94039] p 501 N95-28707

Computer program for estimation of leading-edge suction distribution for plane thin wings at subsonic speeds
[ESDU-94038] p 476 N95-28708

Leading-edge suction distribution for plane thin wings at subsonic speeds
[ESDU-94037] p 477 N95-28800

Increments in aerofoil lift coefficient at zero angle of attack and in maximum lift coefficient due to deployment of a plain trailing-edge flap, with or without a leading-edge high-lift device, at low speeds
[ESDU-94028] p 477 N95-28885

Shear force, bending moment and torque of rigid aircraft in symmetric steady maneuvering flight
[ESDU-94045] p 502 N95-28896

Excrescence drag levels on aircraft
[ESDU-94044] p 477 N95-28897

Wave drag coefficient for axisymmetric forecows at zero incidence (M sub infinity less than or equal to 1.5)
[ESDU-94014] p 552 N95-28903

Surface pressure coefficient distributions for axisymmetric forecows at zero incidence (M sub infinity less than or equal to 1.5)
[ESDU-94015] p 477 N95-28904

Effects of cabin pressure on climb and descent rates
[ESDU-94040] p 503 N95-29016

Increments in aerofoil lift coefficient at zero angle of attack and in maximum lift coefficient due to deployment of a trailing-edge split flap, with or without a leading-edge high-lift device, at low speeds
[ESDU-94029] p 479 N95-29129

Increments in aerofoil lift coefficient at zero angle of attack and in maximum lift coefficient due to deployment of various leading-edge high-lift devices at low speeds
[ESDU-94027] p 481 N95-29898

Introduction to the estimation of the lift coefficients at zero angle of attack and at maximum lift for aerofoils with high-lift devices at low speeds
[ESDU-94026] p 481 N95-29899

Esquimat Defence Research Detachment, Victoria (British Columbia).

Water blasting paint removal methods
p 650 N95-32170

Facilities used for plastic media blasting
p 627 N95-32176

Operational parameters and material effects
p 651 N95-32179

Eurocontrol Experimental Centre, Bretigny (France).

Data link terminal DLT document
[PB95-110805] p 229 N95-21369

Eurocopter Deutschland G.m.b.H., Munich (Germany).
Helicopter internal noise
p 173 N95-19144

External patch repair of CFRP/honeycomb sandwich
p 395 N95-27522

HeliRadar: A rotating antenna synthetic aperture radar for helicopter allweather operations
p 705 N95-33137

European Space Agency, European Space Operations Center, Darmstadt (Germany).
Safety aspects of spacecraft commanding
p 149 N95-17248

EURECA mission control experience and messages for the future
p 149 N95-17252

Packet utilisation definitions for the ESA XMM mission
p 150 N95-17596

F**Fabrica Italiana Apparecchiature Radioelettriche S.p.A., Milan (Italy).**

An approach to sensor data fusion for flying and landing aid purpose
p 686 N95-32488

Fairchild Space Co., Germantown, MD.

Evolutionary Telemetry and Command Processor (TCP) architecture
p 86 N95-14162

Federal Aviation Administration, Atlanta, GA.

Evaluation of an unlighted swinging airport sign
[AD-A284763] p 146 N95-18087

Operational And Supportability Implementation System (OASIS) test and evaluation master plan
[AD-A284765] p 126 N95-18088

Fuselage burnthrough from large exterior fuel fires
[AD-A286295] p 226 N95-22318

Weather And Radar Processor (WARP) Test and Evaluation Master Plan (TEMP)
[AD-A288280] p 445 N95-26453

The 1994 updated National Airspace System performance assessment for year 2005
[AD-A288652] p 380 N95-26485

Precision landing system mathematical modeling study report for Andrews Air Force Base, runway 19L, Camp Springs, MD
[AD-A289015] p 384 N95-27903

Federal Aviation Administration, Atlantic City, NJ.

Terminal Doppler Weather Radar Build 5A Operational Test and Evaluation (OT/E) integration and OT/E operational test plan
[AD-A283052] p 61 N95-12996

Proceedings of the FAA Inspection Program Area Review
[AD-A283849] p 77 N95-14350

Investigation of flight data recorder fire test requirements
[AD-A285832] p 232 N95-20032

An evaluation of Automatic Terminal Information Service (ATIS) flight deck display presentation options
[AD-A280100] p 228 N95-21020

Minima reduction simulation test results
[AD-A285626] p 228 N95-21148

Bird ingestion into large turbofan engines
[DOT/FAA/CT-93/14] p 333 N95-24631

The controller memory guide. Concepts from the field
[AD-A289263] p 383 N95-26978

- Aircraft advanced materials research and development program plan [AD-A290542] p 505 N95-29565
- The effect of wear on fire-blocking layer material effectiveness [AD-A291520] p 485 N95-29855
- Evaluation of retro-reflective beads in airport pavement markings [AD-A291065] p 523 N95-29967
- Prototype stop bar system evaluation at Seattle-Tacoma International Airport [AD-A290136] p 490 N95-30031
- Offshore next generation weather radar (NEXRAD) test and evaluation master plan (TEMP) [AD-A291435] p 556 N95-30072
- Offshore next generation weather radar (NEXRAD) OT&E integration and OT&E operational test [AD-A293223] p 646 N95-30902
- Electrical short circuit and current overload tests on aircraft wiring [AD-A293308] p 646 N95-30922
- A NASPAC-Based analysis of the delay and cost effects of the western-pacific region preliminary resectorization effort of 1993 [AD-A288696] p 601 N95-31013
- Evaluation of alternative pavement marking materials [AD-A292973] p 626 N95-31468
- Chemical options to halons for aircraft use [AD-A293741] p 599 N95-31569
- The ATC operational evaluation of the prototype integrated terminal weather system (ITWS) at Dallas/Fort Worth and Orlando airports (May-September 1993) [AD-A293808] p 677 N95-31587
- Gas chromatography/ion mobility spectrometry as a hyphenated technique for improved explosives detection and analysis p 701 N95-33278
- Federal Aviation Administration, Cambridge, MA.**
- Inspecting for widespread fatigue damage: Is partial debonding the key? p 93 N95-14458
- Nonlinear bulging factor based on R-curve data p 94 N95-14476
- An analysis of tower (local) controller-pilot voice communications [AD-A283718] p 160 N95-18436
- Aircraft wake vortex takeoff tests at O'Hare International Airport [AD-A283828] p 118 N95-18624
- Recommendation on transition from primary/secondary radar to secondary-only radar capability [AD-A286279] p 249 N95-22005
- Estimate of probability of crack detection from service difficulty report data [PB95-149381] p 328 N95-24295
- Aviation capacity enhancement plan 1994 [AD-A292758] p 598 N95-31428
- Guidelines for the design of GPS and LORAN receiver controls and displays [AD-A293753] p 602 N95-31572
- Integration of air traffic databases: A case study [AD-A293691] p 602 N95-32022
- Federal Aviation Administration, Kansas City, MO.**
- Fatigue evaluation of empennage, forward wing, and winglets/tip fins on part 23 airplanes [PB94-196813] p 79 N95-13981
- Federal Aviation Administration, Long Beach, CA.**
- Widespread fatigue damage monitoring: Issues and concerns p 136 N95-19488
- Federal Aviation Administration, Oklahoma City, OK.**
- Automation and cognition in air traffic control: An empirical investigation [AD-A291932] p 488 N95-28790
- Aircraft evacuations through Type-3 exits I: Effects of seat placement at the exit [DOT/FAA/AM-95/22] p 599 N95-31845
- Federal Aviation Administration, Washington, DC.**
- Airborne Windshear Detection and Warning Systems. Fifth and Final Combined Manufacturers' and Technologists' Conference, part 1 [NASA-CP-10139-PT-1] p 10 N95-10566
- FAA vertical flight bibliography [DOT/FAA/RD-94/17] p 14 N95-11684
- Airborne Windshear Detection and Warning Systems. Fifth and Final Combined Manufacturers' and Technologists' Conference, part 2 [NASA-CP-10139-PT-2] p 41 N95-13203
- Federal aviation regulations, part 91. General operating and flight rules. Change 5 [PB94-194883] p 123 N95-17476
- Federal aviation regulations, part 91. General operating and flight rules. Change 8 [PB94-217445] p 188 N95-19720
- Census US civil aircraft calendar year 1993 [AD-A286309] p 219 N95-20091
- Oceanic operations: An authoritative guide to oceanic operations [FAA-AFS-550] p 277 N95-24065
- Federal Aviation Administration plan for research, engineering and development, 1995 p 363 N95-24202
- Enplanement and all cargo activity [AD-A280074] p 412 N95-28151
- Ninth DOD/NASA/FAA Conference on Fibrous Composites in Structural Design, volume 3 [NASA-CR-198718] p 420 N95-28266
- Ninth DOD/NASA/FAA Conference on Fibrous Composites in Structural Design, volume 2 [NASA-CR-198722] p 424 N95-28462
- Development of a coding form for approach control/pilot voice communications [DOT/FAA/AM-95/15] p 384 N95-28540
- Federal aviation administration plan for research, engineering and development [AD-A290952] p 490 N95-29733
- Terminal area forecasts-fiscal years 1993-2010 [AD-A290835] p 490 N95-29880
- FAA aviation forecasts: Fiscal year 1995-2006 [AD-A293682] p 584 N95-31598
- Fermi National Accelerator Lab., Batavia, IL.**
- Reducing process noise in superconducting helium liquid level probes [DE95-008956] p 629 N95-30765
- Florida Atlantic Univ., Boca Raton, FL.**
- Effect of weak periodic pressure gradient on streamwise vortices near a wall p 29 N95-11263
- Exact dynamic responses of periodic multi-span beams under convected pressure fields p 25 N95-11288
- High-and low-frequency dynamics of isolated blades and rotors with dynamic stall and wake [AD-A290358] p 503 N95-29322
- Florida State Univ., Gainesville, FL.**
- PIV investigation of compressibility effects on dynamic stall p 478 N95-29102
- Florida State Univ., Tallahassee, FL.**
- The spectrum and directivity of turbulent mixing noise from supersonic jets p 579 N95-29415
- Florida Univ., Gainesville, FL.**
- Interlaminar shear test method development for long term durability testing of composites p 301 N95-23300
- Innovative processing of composites for ultra-high temperature applications, book 1 [AD-A290889] p 537 N95-29842
- Foreign Broadcasting Information Service, Washington, DC.**
- FBI report: Science and technology. Central Eurasia [FBIS-UST-95-029] p 649 N95-31728
- Foster-Miller Associates, Inc., Waltham, MA.**
- Evaluation of the fuselage lap joint fatigue and terminating action repair p 166 N95-19477
- Foundation for Scientific and Industrial Research, Trondheim (Norway).**
- Response to noise around Vaernes and Bodo airports [PB94-207065] p 62 N95-13575
- Fracture Research, Inc., Galena, OH.**
- Testing and analysis of flat and curved panels with multiple cracks p 93 N95-14460
- Fujitsu Ltd., Tokyo (Japan).**
- Numerical analysis around the whole SST configuration p 693 N95-34541
- Computations of low speed flow about space-plane p 685 N95-34544
- G**
- Galaxy Scientific Corp., Hampton, VA.**
- Ninth DOD/NASA/FAA Conference on Fibrous Composites in Structural Design, volume 1 [NASA-CR-198723] p 421 N95-28420
- Galaxy Scientific Corp., Pleasantville, NJ.**
- Artificial intelligence with applications for aircraft [DOT/FAA/CT-94/41] p 99 N95-13895
- Rotorcraft ditchings and water-related impacts that occurred from 1982 to 1989, phase 1 [AD-A279164] p 189 N95-19805
- Test and evaluation report for the Manual Domestic Passive Profiling System (MDPPS) [AD-A286312] p 225 N95-20093
- Commuter airplane accident data analysis [AD-A286315] p 226 N95-20174
- Commuter/air taxi ditchings and water-related impacts that occurred from 1979 to 1989 [AD-A285691] p 226 N95-20275
- Test and Evaluation Plan (TEP) for Improvised Explosive Device Screening Systems (IEDSS) [AD-A286382] p 227 N95-22319
- Digital systems validation. Chapter 20 Artificial Intelligence with applications for aircraft. Handbook, volume 2 [AD-A288492] p 448 N95-26638
- Corrosion of fire-damaged aircraft [AD-A294968] p 693 N95-34583
- GEC-Marconi Avionics Ltd., Rochester (England).**
- A tactical navigation and routing system for low-level flight p 709 N95-32494
- GEC-Marconi Materials Technology, Towcester (England).**
- High performance backplane components for modular avionics p 247 N95-20653
- GEC-Marconi Research Centre, Great Baddow (England).**
- MCMs for avionics: Technology selection and intermodule interconnection p 234 N95-20641
- General Accounting Office, Washington, DC.**
- European aeronautics: Strong government presence in industry structure and research and development support. Report to Congressional Requesters [GAO/NSIAD-94-71] p 176 N95-18578
- Naval aviation: F-14 upgrades are not adequately justified. Report to Congressional Committees [AD-A286338] p 231 N95-20212
- Report to the Secretary of Defense. Unmanned aerial vehicles: No more Hunter systems should be bought until problems are fixed [GAO/NSIAD-95-52] p 286 N95-24091
- Report to Congressional Committees. Tactical Aircraft: Concurrency in development and production of F-22 aircraft should be reduced [GAO/NSIAD-95-59] p 336 N95-26338
- Asian Aeronautics: Technology acquisition drives industry development. Report to Congressional requesters [GAO/NSIAD-94-140] p 367 N95-26817
- Report to Congressional Committees. Comanche Helicopter: Testing needs to be completed prior to production decisions [GAO/NSIAD-95-112] p 397 N95-27910
- Report to the Chairman, Legislation and National Security Subcommittee, Committee on Government Operations, House of Representatives. Tactical aircraft: F-15 replacement is premature as currently planned [GAO/NSIAD-94-118] p 679 N95-31987
- Report to the Chairman, Legislation and National Security Subcommittee, Committee on Government Operations, House of Representatives. C-17 Aircraft program: Improvements in initial provisioning process [GAO/NSIAD-94-63] p 584 N95-32194
- Report to the Chairman, Legislation and National Security Subcommittee, Committee on Government Operations, House of Representatives. Unmanned aerial vehicles: Performance of short-range system still in question [GAO/NSIAD-94-65] p 609 N95-32196
- Fact sheet for Congressional Committees. Air traffic control: Status of FAA's modernization program [GAO/RCED-94-167FS] p 603 N95-32197
- Report to Congressional Committees. Military airlift: C-17 settlement is not a good deal [GAO/NSIAD-94-141] p 585 N95-32198
- Report to the Chairman, Subcommittee on Aviation, Transportation and Related Agencies, Committee on Appropriations, House of Representatives. Air traffic control: Status of FAA's plans to close and contract out low-activity towers [GAO/RCED-94-265] p 603 N95-32199
- Report to the Chairman, Subcommittee on Aviation, Committee on Commerce, Science, and Transportation, US Senate. Aviation safety: Data problems threaten FAA strides on safety analysis system [GAO/AIMD-95-27] p 687 N95-32705
- Fact sheet for Congressional requesters. Airport competition: Essential air service slots at O'Hare International Airport [GAO/RCED-94-118FS] p 699 N95-32759
- Army aviation: Modernization strategy needs to be reassessed. Report to Congressional requesters [GAO/NSIAD-95-9] p 683 N95-32783
- Report to the Chairman, Subcommittee on Aviation, Committee on Commerce, Science, and Transportation, US Senate. Aviation Safety: FAA can better prepare general aviation pilots for mountain flying risks [GAO/RCED-94-15] p 687 N95-32784
- Report to the Chairman, Subcommittee on Aviation, Transportation and Related Agencies, Committee on Appropriations, US Senate. Airport Improvement Program: Reliever airport set-aside funds could be redirected [GAO/RCED-94-226] p 699 N95-32786
- Aviation security: Development of new security technology has not met expectations. Report to Congressional requesters [GAO/RCED-94-142] p 687 N95-32885

- Report to the Chairman, Subcommittee on Transportation and Related Agencies, Committee on Appropriations, US Senate. Airport Improvement Program: The Military Airport Program has not achieved intended impact
[GAO/RCED-94-209] p 700 N95-32888
- General Applied Science Labs., Inc., Ronkonkoma, NY.**
Free-jet testing at Mach 3.44 in GASL's aero/thermo test facility p 145 N95-16320
- General Dynamics/Convair, San Diego, CA.**
Development of a low-cost, modified resin transfer molding process using elastomeric tooling and automated preform fabrication p 200 N95-28268
- General Dynamics Corp., Fort Worth, TX.**
Applications of a damage tolerance analysis methodology in aircraft design and production p 426 N95-28483
- General Electric Co., Cincinnati, OH.**
Engine structures analysis software: Component Specific Modeling (COSMO)
[NASA-CR-195378] p 57 N95-11711
Elements of a modern turbomachinery design system p 90 N95-14129
The role of CFD in the design process p 90 N95-14135
Scramjet testing guidelines p 138 N95-16317
Modern transport engine experience with environmental ingestion effects p 199 N95-19660
Active control of fan noise-feasibility study. Volume 1: Flyover system noise studies
[NASA-CR-195392-VOL-1] p 258 N95-21888
PVD TBC experience on GE aircraft engines p 345 N95-26126
A summary of computational experience at GE Aircraft Engines for complex turbulent flows in gas turbines p 439 N95-27885
Combustion system CFD modeling at GE Aircraft Engines p 439 N95-27889
UHB engine fan broadband noise reduction study
[NASA-CR-198357] p 580 N95-29641
The effect of interface properties on nickel base alloy composites
[NASA-CR-198363] p 629 N95-30787
- General Electric Co., Lynn, MA.**
Brush seals for turbine engine fuel conservation p 59 N95-13595
- General Electric Co., Philadelphia, PA.**
Aeroelastic stability of wind turbine blade/aileron systems p 377 N95-27981
Control system design for the MOD-5A 7.3 mW wind turbine generator p 440 N95-27985
Variable speed generator application on the MOD-5A 7.3 mW wind turbine generator p 440 N95-27989
- General Electric Co., Schenectady, NY.**
Toughened Silcomp composites for gas turbine engine applications
[DE95-002851] p 235 N95-21243
Calculation of design load for the MOD-5A 7.3 mW wind turbine system p 440 N95-27982
Grid generation and surface modeling for CFD p 551 N95-28726
- General Motors Corp., Lagrange, IL.**
High-speed seal and bearing test facility p 53 N95-13601
- Geophex Ltd., Raleigh, NC.**
Geophex airborne unmanned survey system
[DE95-007566] p 392 N95-27440
- Georgia Inst. of Tech., Atlanta, GA.**
Integrated design and manufacturing for the high speed civil transport
[NASA-CR-197183] p 48 N95-12700
Fracture mechanics validity limits p 95 N95-14480
Numerical study of the effects of icing on viscous flow over wings
[NASA-CR-197102] p 75 N95-14803
A linear system identification and validation of an AH-64 Apache aeroelastic simulation model p 146 N95-18903
Development of pneumatic test techniques for subsonic high-lift and in-ground-effect wind tunnel investigations p 121 N95-19268
Discrete crack growth analysis methodology for through cracks in pressurized fuselage structures p 166 N95-19473
Residual life and strength estimates of aircraft structural components with MSD/MED p 136 N95-19485
A FEAM based methodology for analyzing composite patch repairs of metallic structures p 394 N95-27511
Operator modeling in commerial aviation: Cognitive models, intelligent displays, and pilot's assistants
[NASA-CR-198609] p 401 N95-28203
A vorticity-velocity approach for three-dimensional unsteady viscous flow over wings p 478 N95-29108
A fourth order Euler/Navier-Stokes prediction method for the aerodynamics and aeroelasticity of hovering rotor blades p 554 N95-29242
- Analytical investigations in aircraft and spacecraft trajectory optimization and optimal guidance
[NASA-CR-4672] p 526 N95-29339
Model development for active control of stall phenomena in aircraft gas turbine engines p 514 N95-29679
Unsteady pressure and inflow velocity on a pitching rotor blade in hover p 480 N95-29771
Airborne passive polarimetric measurements of sea surface anisotropy at 92 GHz
[NASA-CR-197288] p 707 N95-32823
- Georgia Tech Research Inst., Atlanta, GA.**
Temperature effects on acoustic interactions between altitude test facilities and jet engine plumes
[NASA-CR-197638] p 258 N95-21170
Flutter analysis of composite box beams
[NASA-CR-197931] p 294 N95-23392
Effects of cavity dimensions, boundary layer, and temperature on cavity noise with emphasis on benchmark data to validate computational aeroacoustic codes
[NASA-CR-4653] p 361 N95-24879
Measurements of ions formed in jet engine exhaust plumes
[AD-A290940] p 514 N95-29764
- German-Dutch Wind Tunnel, North East Polder (Netherlands).**
Correction of support influences on measurements with sting mounted wind tunnel models p 122 N95-19281
- Gibson (J. C.), Saint Annes (England).**
Looking for the simple PIO model p 597 N95-31066
The prevention of PIO by design p 620 N95-31991
- Grumman Aerospace Corp., Bethpage, NY.**
Comparison of resin film infusion, resin transfer molding, and consolidation of textile preforms for primary aircraft structure p 425 N95-28477
Advanced wing design survivability testing and results p 400 N95-28488
- Grumman Aircraft Engineering Corp., Bethpage, NY.**
Novel cost controlled materials and processing for primary structures p 532 N95-28830
Cross-stiffened continuous fiber structures p 536 N95-29041
- H**
- Hampton Univ., VA.**
Steady and unsteady three-dimensional transonic flow computations by integral equation method
[NASA-CR-196777] p 10 N95-11582
1994 NASA-HU American Society for Engineering Education (ASEE) Summer Faculty Fellowship Program
[NASA-CR-194972] p 325 N95-23276
Development of a rotary wing Navier-Stokes CFD code based on TLNS3D code
[AD-A290421] p 554 N95-29387
Application of multigrid computational fluid dynamics (CFD) methods to rotor analysis
[AD-A293012] p 648 N95-31475
- Harris, Miller, Miller and Hanson, Inc., Lexington, MA.**
The present and future of aircraft noise models: A user's perspective p 32 N95-11324
- Harvard Univ., Cambridge, MA.**
Development of techniques for the in situ observation of OH and HO2 for studies of the impact of high-altitude supersonic aircraft on the stratosphere
[NASA-CR-196759] p 61 N95-12832
In situ measurements of ClO and implications for the chemistry of inorganic chlorine in the lower stratosphere p 563 N95-29830
- Hellenic Air Force Academy, Athens (Greece).**
Investigation of shear layer transition using various turbulence models p 248 N95-21096
- Helsinki Univ. of Technology, Espoo (Finland).**
TKKMOD: A computer simulation program for an integrated wind diesel system. Version 1.0: Document and user guide
[PB94-179090] p 60 N95-11798
Using landmarks for the vehicle location measurement
[PB94-184512] p 43 N95-12582
- Hercules Aerospace Co., Magna, UT.**
Recent advances in graphite/epoxy motor cases p 149 N95-16333
Advanced tow placement of composite fuselage structure p 420 N95-28271
Automated fiber placement: Evolution and current demonstrations p 532 N95-28832
- High Plains Engineering, Tehachapi, CA.**
Observations on PIO p 597 N95-31064
- High Technology Corp., Hampton, VA.**
Computational studies of laminar to turbulence transition
[AD-A285622] p 248 N95-21146
- Hoh Aeronautics, Inc., Lomita, CA.**
Unified criteria for ACT aircraft longitudinal dynamics p 607 N95-31065
- The role of handling qualities specifications in flight control system design p 620 N95-31990
- Honeywell, Inc., Minneapolis, MN.**
Micro-time stress measurement device development
[AD-A289511] p 448 N95-26845
Dynamic inversion: An evolving methodology for flight control design p 621 N95-31996
- Honeywell Technology Center, Minneapolis, MN.**
Empirical results on scheduling and dynamic backtracking p 299 N95-23761
Synthetic Terrain Imagery for Helmet-Mounted Display. Volume 2: Software design document
[AD-A293611] p 612 N95-31655
Synthetic Terrain Imagery for Helmet-Mounted Display, volume 1 p 612 N95-31656
[AD-A293612] p 612 N95-31656
- Hood Technology Corp., Hood River, OR.**
Adaptive tuned vibration absorbers: Tuning laws, tracking agility, sizing, and physical implementations p 25 N95-11280
- Houston Univ., TX.**
Basic studies in turbulent shear flows
[AD-A289145] p 437 N95-26998
- Hughes Aircraft Co., Culver City, CA.**
Advanced data visualization and sensor fusion: Conversion of techniques from medical imaging to Earth science p 711 N95-34236
- Hughes Associates, Inc., Columbia, MD.**
Analysis of test criteria for specifying foam firefighting agents for aircraft rescue and firefighting
[AD-A286381] p 227 N95-22352
- Hughes STX, Inc., Lexington, MA.**
Radar studies of aviation hazards
[AD-A285845] p 226 N95-21831
- I**
- Illinois Univ., Chicago, IL.**
Holographic interferometric tomography for reconstructing flow fields p 310 N95-23287
Failure analysis for polycarbonate transparencies
[AD-A292992] p 630 N95-31471
- IMITECH, Inc., Schenectady, NY.**
Development of LaRC (TM): IA thermoplastic polyimide coated aerospace wiring
[NASA-CR-195048] p 537 N95-30252
- Imperial Coll. of Science and Technology, London (England).**
The effects of three dimensional imposed disturbances on bluff body near wake flows
[AD-A290824] p 555 N95-29654
- Industrial Coll. of the Armed Forces, Washington, DC.**
Strategy in the commercial aircraft industry in the United States: A comparison of decisionmaking by McDonnell-Douglas and Boeing aircraft companies from 1977-1983
[AD-A288289] p 366 N95-26409
Surviving the peace. Lessons learned from the aircraft industry in the 1920s and 1930s p 366 N95-26455
- Industrieanlagen-Betriebsgesellschaft m.B.H., Ottobrunn (Germany).**
Thermoacoustic environments to simulate reentry conditions p 86 N95-14096
Design and operation of a thermoacoustic test facility p 147 N95-19150
- Institut Franco-Allemand de Recherches, Saint-Louis (France).**
Shock tube investigations of combustion phenomena in supersonic flows
[PB94-175262] p 55 N95-11796
Supersonic base flow investigation over axisymmetric afterbodies
[PB94-180957] p 39 N95-12578
- Institute for Aerospace Research, Ottawa (Ontario).**
Applications of the five-hole probe technique for flow field surveys at the Institute for Aerospace Research p 163 N95-19255
Evaluation of combined wall- and support-interference on wind tunnel models p 122 N95-19278
Double pass retroreflection for corrosion detection in aircraft structures p 323 N95-23503
- Institute for Computer Applications in Science and Engineering, Hampton, VA.**
Agglomeration multigrid for viscous turbulent flows
[AD-A284064] p 8 N95-10848
3D visualization of unsteady 2D airplane wake vortices
[AD-A284745] p 27 N95-11593
On the interaction of jet noise with a nearby flexible structure
[NASA-CR-194934] p 57 N95-11812
Research in progress in applied mathematics, numerical analysis, fluid mechanics, and computer science
[AD-A284982] p 61 N95-11932

J

- Algorithms for bilevel optimization
[NASA-CR-194980] p 170 N95-16897
- ICASE
[NASA-CR-195001] p 170 N95-16898
- Floating shock fitting via Lagrangian adaptive meshes
[AD-A289758] p 170 N95-18110
- The stability of two-phase flow over a swept-wing
[NASA-CR-194994] p 159 N95-18190
- On the Lighthill relationship and sound generation from isotropic turbulence
[NASA-CR-195005] p 159 N95-18191
- Effect of crossflow on Goertler instability in incompressible boundary layers
[NASA-CR-195007] p 159 N95-18193
- A study of the vortex flow over 76/40-deg double-delta wing
[NASA-CR-195032] p 314 N95-23466
- Cumulative reports and publications through December 31, 1994
[NASA-CR-195043] p 361 N95-26085
- Acoustic field in unsteady moving media
[NASA-CR-198162] p 438 N95-27179
- Response of multi-panel assembly to noise from a jet in forward motion
[NASA-CR-198164] p 442 N95-28673
- Pressure updating methods for the steady-state fluid equations
[NASA-CR-198163] p 569 N95-30353
- Institute for Defense Analyses, Alexandria, VA.**
The opportunities for and challenges of common integrated electronics
[AD-A279991] p 248 N95-20966
- The value of simulation for training
[AD-A289174] p 411 N95-26556
- Institute of Noise Control Engineering, Poughkeepsie, NY.**
Noise Con 1994: Proceedings of the 1994 National Conference on Noise Control Engineering. Progress in Noise Control for Industry
[LC-75-24750] p 28 N95-11259
- Instituto de Pesquisas Espaciais, Sao Paulo (Brazil).**
Regenerative cooling for liquid propellant rocket thrust chambers
[INPE-5565-TD/540] p 150 N95-18720
- International Centre for Theoretical Physics, Trieste (Italy).**
Dynamics of phase ordering of nematics in a pore
[DE95-607662] p 362 N95-25978
- Interturbine Holding B.V., Lomm (Netherlands).**
Braze repair possibilities for hot section gas turbine parts
p 201 N95-19677
- Iowa State Univ. of Science and Technology, Ames, IA.**
Idealized textile composites for experimental/analytical correlation
p 301 N95-23277
- Study of compressible flow through a rectangular-to-semiannular transition duct
[NASA-CR-4660] p 338 N95-24392
- A fixed time performance evaluation of parallel CFD applications
[DE94-014240] p 436 N95-26445
- Computation of the integrated aerodynamic and propulsive flowfields of a generic hypersonic space plane
p 481 N95-29788
- An interacting boundary layer method for unsteady compressible flows
p 557 N95-30290
- Nonlinear stability of unsteady viscous flow
[AD-A294931] p 707 N95-34597
- Ishikawajima-Harima Heavy Industries Co. Ltd., Tokyo (Japan).**
Design of secondary flow control cascade using numerical simulation
p 698 N95-34507
- A study of supersonic mixing flow field with ramp injector
p 706 N95-34512
- Israel Aircraft Industries Ltd., Ben-Gurion Airport (Israel).**
Lavi flight control system: Design requirements, development and flight test results
p 621 N95-31994
- Israel Aircraft Industries Ltd., Tashan (Israel).**
Probabilistic inspection strategies for minimizing service failures
p 93 N95-14461
- Israel Inst. of Metals, Haifa (Israel).**
Prediction of fatigue crack growth under constant amplitude and random loading using specimens with multiple cracks
[AD-A291614] p 397 N95-28409
- Istanbul Univ. (Turkey).**
At Istanbul-Ataturk Airport measurement and analysis of noise in due of take-off time
p 31 N95-11319

Jet Propulsion Lab., California Inst. of Tech., Pasadena, CA.

- Possible near-IR channels for remote sensing precipitable water vapor from geostationary satellite platforms
[HTN-95-70139] p 214 A95-69431
- Estimates of total organic and inorganic chlorine in the lower stratosphere from in situ and flask measurements during AASE 2
[HTN-95-A0861] p 317 A95-76265
- In situ observations in aircraft exhaust plumes in the lower stratosphere at midlatitudes
[HTN-95-A0862] p 318 A95-76266
- Meridional distributions of NO(X), NO(Y), and other species in the lower stratosphere and upper troposphere during AASE 2
[HTN-95-70944] p 352 A95-78009
- Comparison of column abundances from three infrared spectrometers during AASE 2
[HTN-95-70946] p 352 A95-78011
- Latitude variations of stratospheric trace gases
[HTN-95-70948] p 352 A95-78013
- Guidance and control, 1993; Annual Rocky Mountain Guidance and Control Conference, 16th, Keystone, CO, Feb. 6-10, 1993
[ISBN-0-87703-365-X] p 341 A95-80389
- The Cassini spacecraft: Object oriented flight control software
p 359 A95-80405
- A generic telerobotics architecture for C-5 industrial processes
[AIAA PAPER 94-1264-CP] p 27 N95-11529
- Field verification of the wind tunnel coefficients
p 109 N95-17291
- Virtual reality flight control display with six-degree-of-freedom controller and spherical orientation overlay
[NASA-CASE-NPO-18733-1-CU] p 288 N95-22578
- In-flight radiometric calibration of AVIRIS in 1994
p 705 N95-33754
- TIMS observations of surface emissivity in HAPEX-Sahel
p 709 N95-33799
- Jiaotong Univ., Shanghai (China).**
Simulation investigation on system identification of gas turbine
[PB95-104238] p 139 N95-17749
- Johns Hopkins Univ., Baltimore, MD.**
Induced Compton scattering by relativistic electrons in magnetized astrophysical plasmas
p 563 N95-29885
- Johns Hopkins Univ., Columbia, MD.**
The 1993 JANNAF Propulsion Meeting, volume 1
[CPA-PUBL-602-VOL-1] p 148 N95-16312
- Johns Hopkins Univ., Laurel, MD.**
Application of scramjet engine technology to the design of ram accelerator projectiles
p 19 N95-10282
- Johnson Controls, Inc., Milwaukee, WI.**
Development of a bipolar lead/acid battery for the more electric aircraft
[AD-A284050] p 160 N95-18660
- Joint Inst. for Advancement of Flight Sciences, Hampton, VA.**
An approximate theoretical method for modeling the static thrust performance of non-axisymmetric two-dimensional convergent-divergent nozzles
[NASA-CR-195050] p 273 N95-23193
- Joint Publications Research Service, Arlington, VA.**
JPRS report: Science and technology. Central Eurasia: Engineering and equipment. Gas dynamics of supersonic shortened nozzles
[JPRS-UST-94-003-L] p 22 N95-10931
- JPRS report: Science and technology. Central Eurasia
[JPRS-UST-95-011] p 335 N95-24541
- JPRS report: Science and technology. Central Eurasia
[JPRS-UST-94-022] p 438 N95-27699
- Joint Publications Research Service, Washington, DC.**
JPRS report: Science and technology. Central Eurasia
[JPRS-UST-94-027] p 349 N95-24470
- JPRS report: Science and technology. Central Eurasia
[JPRS-UST-94-018] p 349 N95-24472
- JPRS Report: Science and technology. Central Eurasia
[JPRS-UST-94-032] p 350 N95-24759
- K. T. Analytics, Inc. Frederick, MD.**
Air pollution mitigation measures for airports and associated activity
[PB94-207610] p 216 N95-19582
- Kaman Sciences Corp., Albuquerque, NM.**
Fault detection techniques for complex cable shield topologies
[AD-A286632] p 247 N95-20771

K

- TIM-SCT cable testing protocol
[AD-A286633] p 231 N95-20772
- Kansas Univ., Lawrence, KS.**
Gemini: A long-range cargo transport
[NASA-CR-197149] p 45 N95-12626
- A preliminary design proposal for a maritime patrol strike aircraft: MPS-2000 Condor
[NASA-CR-197182] p 47 N95-12689
- On-line, adaptive state estimator for active noise control
p 322 N95-23308
- Preliminary design problems and solutions for a supersonic oblique all-wing transport aircraft
p 390 N95-26942
- Design of a high altitude long endurance aircraft with manufacturing considerations
p 391 N95-26947
- Prevention and control of inlet unstart using an SR-71 simulation
p 367 N95-26948
- An easy way to analyze longitudinal and lateral-directional trim problems with AEO or OEI
p 409 N95-26949
- Preliminary results and research capabilities of a new jet facility at the University of Kansas
p 412 N95-26951
- Navier-Stokes solution of wing wake structure and its perturbation
p 479 N95-29121
- Kansas Univ. Center for Research, Inc., Lawrence, KS.**
Application of optimization technique to control system design for departure prevention and aircraft model estimation through dynamic inversion
p 517 N95-29156
- Design, analysis and control of large transports so that control of engine thrust can be used as a back-up of the primary flight controls
[NASA-CR-198958] p 518 N95-30254
- Kawasaki Heavy Industries Ltd., Tokyo (Japan).**
A large scale 3D Navier-Stokes analysis using NAL-NWT
p 707 N95-34539
- Role of computational fluid dynamics in aeronautical engineering. Number 12: Formulation and verification of uni-particle upwind schemes for the Euler equations
p 707 N95-34540
- Kazan Aviation Inst. (USSR).**
Joint Proceedings on Aeronautics and Astronautics (JPA)A
[ISBN-7-80-046602-7] p 104 N95-16249
- Service and physical properties of liquid-jet fuels
p 151 N95-16256
- Development of strength analysis methods and design model for aircraft constructions in Kazan Aviation Institute
p 127 N95-16264
- Theoretical fundamentals of the aircraft GTE tests
p 138 N95-16265
- Generalized method of solving topological optimization problems for electrical airplane equipment systems in computer-aided design
p 169 N95-16272
- Development of processes, means, and theoretical principles of thin-walled detail plastic forming at Kazan Aviation Institute
p 155 N95-16281
- Kossel (Horst), Shrewsbury, MA.**
Activated buoyancy propulsion = Paradox Power (tm)
[TABES PAPER 94-619] p 74 N95-14646
- Krug Life Sciences, Inc., Houston, TX.**
A surgical support system for Space Station Freedom
p 149 N95-16776
- Kyushu Univ., Kasuga (Japan)**
Numerical simulations of dynamic stall phenomena in low speed flows
p 685 N95-34546
- Numerical simulation of unsteady viscous flow around an airfoil with oscillating spoiler
p 685 N95-34547
- Laboratory for Strength of Materials Components and Structures, Puspiptek (Indonesia).**
Prediction of fatigue crack growth under flight-simulation loading with the modified CORPUS model
p 166 N95-19471
- Lamont-Doherty Geological Observatory, Palisades, NY.**
An in situ evaluation of TOPEX/Poseidon altimetric measurements versus measurements made by moorings and inverted echo sounders for sea surface height
[NASA-CR-198621] p 447 N95-27805
- Lawrence Livermore National Lab., Livermore, CA.**
An Echelle Grating Spectrometer (EGS) for mid-IR remote chemical detection
[DE94-019310] p 249 N95-21478
- Overview of remote sensing laser development and semiconductor laser technology
[DE94-019103] p 256 N95-21552
- CALOPE and TAISIR airborne experiment platform
[DE94-018328] p 250 N95-22299
- A hybrid vehicle evaluation code and its application to vehicle design. Revision 1
[DE95-008053] p 441 N95-28029

L

- Whirl plus tilt
[DE95-007948] p 452 N95-28108
A hybrid vehicle evaluation code and its application to vehicle design, revision 2
[DE95-008060] p 441 N95-28139
Integrated X-ray testing of the electro-optical breadboard model for the XMM reflection grating spectrometer
[DE95-008829] p 644 N95-30507
Mapping hidden aircraft defects with dual-band infrared computed tomography
[DE95-011531] p 584 N95-32164
Machinability study of Aermet 100
[DE95-011532] p 701 N95-33408
Unitized Regenerative Fuel Cells for solar rechargeable aircraft and zero emission vehicles
[DE95-010684] p 708 N95-33642
- Lear Jet Industries, Inc., Wichita, KS.**
Aircraft nosewheel steering simulation
p 412 N95-26944
- Lehigh Univ., Bethlehem, PA.**
Corrosion and corrosion fatigue of airframe aluminum alloys
p 87 N95-14465
Evaluation of patch effectiveness in repairing aircraft components
p 394 N95-27513
- Liburd Engineering Ltd., Hamilton (Ontario).**
Protective coatings for compressor gas path components
p 201 N95-19675
- Lightning Technologies, Inc., Pittsfield, MA.**
Aircraft fuel system lightning protection design and qualification test procedures development
[AD-A288401] p 380 N95-26497
- Lightwave Atmospherics, Inc., Marblehead, MA.**
Remote sensing of turbulence in the clear atmosphere with 2-micron lidars
p 59 N95-13213
- Linköping Univ. (Sweden).**
Aspect estimation of an aircraft using library model silhouettes
[PB95-141834] p 360 N95-25894
- Lockheed Aeronautical Systems Co., Burbank, CA.**
Process and control systems for composites manufacturing
p 420 N95-28267
- Lockheed Aeronautical Systems Co., Marietta, GA.**
Advanced composites structural concepts and materials technologies for primary aircraft structures: Structural response and failure analysis
[NASA-CR-4448] p 11 N95-10240
Advanced composites structural concepts and materials technologies for primary aircraft structures: Structural response and failure analysis: ISPAN modules users manual
[NASA-CR-4449] p 12 N95-10242
Advanced composites structural concepts and materials technologies for primary aircraft structures: Design/manufacturing concept assessment
[NASA-CR-4447] p 12 N95-10316
Thermally stable organic polymers
[AD-A281380] p 87 N95-14363
An assessment of viscous effects in computational simulation of benign and burst vortex flows on generic fighter wind-tunnel models using TEAM code
[NASA-CR-4650] p 273 N95-23185
Structural modification and repair of C-130 wing structure using bonded composites
p 394 N95-27512
Structural testing of the technology integration box beam
p 441 N95-28467
Advanced textile applications for primary aircraft structures
p 399 N95-28476
Requirements for effective use of CFD in aerospace design
p 551 N95-28725
[SPAN (Interactive Stiffened Panel Analysis): A tool for quick concept evaluation and design trade studies
p 533 N95-28846
Advanced composite structural concepts and materials technologies for primary aircraft structures: Advanced material concepts
[NASA-CR-4485] p 503 N95-29027
Textile composite fuselage structures development
p 534 N95-29033
Advanced resin systems and 3D textile preforms for low cost composite structures
p 535 N95-29035
Thermally stable organic polymers
[AD-A290755] p 537 N95-29482
- Lockheed Corp., Fort Worth, TX.**
Flight test results of the F-16 aircraft modified with the axisymmetric vectoring exhaust nozzle
p 70 N95-14245
Vista/F-16 Multi-Axis Thrust Vectoring (MATV) control law design and evaluation
p 117 N95-14248
Overview of unsteady transonic wind tunnel test on a semispan straked delta wing oscillating in pitch
[AD-A284097] p 117 N95-18380
Unsteady transonic wind tunnel test on a semispan straked delta wing, oscillating in pitch. Part 1: Description of the model, test setup, data acquisition, and data processing
[AD-A293113] p 593 N95-30885
- Lockheed Engineering and Sciences Co., Hampton, VA.**
Determining the accuracy of maximum likelihood parameter estimates with colored residuals
[NASA-CR-194893] p 51 N95-11869
An approximate Riemann solver for thermal and chemical nonequilibrium flows
[NASA-CR-195003] p 96 N95-14912
Laminar and turbulent flow computations of Type 4 shock-shock interference aerothermal loads using unstructured grids
[NASA-CR-195008] p 97 N95-15604
A verification procedure for MSC/NASTRAN Finite Element Models
[NASA-CR-4675] p 392 N95-27371
- Lockheed Engineering and Sciences Co., Houston, TX.**
An avionics scenario and command model description for Space Generic Open Avionics Architecture (SGOAA)
[NASA-CR-188330] p 49 N95-11913
An axisymmetric analog two-layer convective heating procedure with application to the evaluation of Space Shuttle Orbiter wing leading edge and windward surface heating
[NASA-CR-188343] p 54 N95-11937
Space Generic Open Avionics Architecture (SGOAA): Overview
p 99 N95-14161
- Lockheed Environmental Systems and Technologies Co., Las Vegas, NV.**
Parts washing alternatives study: United States Coast Guard. Project summary and report
[PB95-166146] p 343 N95-26004
- Lockheed-Fort Worth Co., Fort Worth, TX.**
Euler Technology Assessment program for preliminary aircraft design employing SPLITFLOW code with Cartesian unstructured grid method
[NASA-CR-4649] p 273 N95-22917
Rapid repair of large area damage to contoured aircraft structures
p 394 N95-27516
Application of advanced safety technique to ring laser gyro inertial navigation system integration
p 689 N95-33140
- Lockheed Martin Corp., Denver, CO.**
Determining GPS average performance metrics
p 383 N95-27791
- Lockheed Sanders, Inc., Nashua, NH.**
New technologies for space avionics
[NASA-CR-197574] p 150 N95-18196
- Loral Federal Systems, Manassas, VA.**
Advanced flight computer. Special study
[NASA-CR-198165] p 449 N95-27246
- Loral Systems, Inc., Orlando, FL.**
Advanced distributed simulation technology advanced rotary wing aircraft. Strawman verification and validation plan for the ARWA simulator system
[AD-A280237] p 19 N95-10349
Advanced distributed simulation technology advanced rotary wing aircraft. System/segment specification. Volume 1: Simulation system module
[AD-A280238] p 20 N95-10350
Advanced distributed simulation technology advanced rotary wing aircraft. System/segment specification. Volume 3: Visual system module
[AD-A280239] p 20 N95-10351
Advanced distributed simulation technology advanced rotary wing aircraft. System/segment specification. Volume 2: Flight station module
[AD-A280432] p 20 N95-10352
Advanced distributed simulation technology advanced rotary wing aircraft. System/segment specification. Volume 5: Simulation system module AH-64D kit
[AD-A280433] p 20 N95-10353
Advanced distributed simulation technology advanced rotary wing aircraft. Software reusability report
[AD-A280434] p 20 N95-10354
Advanced distributed simulation technology advanced rotary wing aircraft. Study comparing approaches to modeling the ARWA main rotor
[AD-A280824] p 79 N95-14306
ADST ARWA visual system module software design document
[AD-A283874] p 99 N95-14357
ADST system test report for the rotary wing aircraft airmet aeromodel and weapon model merge with the ATAC 2 baseline
[AD-A281580] p 127 N95-16171
- Los Alamos National Lab., NM.**
Hypersonic Gas-Surface Energy Accommodation Test Facility
[DE94-014468] p 39 N95-12652
NTS-spill test facility wind tunnel exhaust plume characterization
[DE95-003630] p 297 N95-24019
Phonon characteristics of high (T sub c) superconductors from neutron Doppler broadening measurements
[DE95-003703] p 324 N95-24076
- A laboratory scale supersonic combustive flow system
[DE95-006347] p 420 N95-27851
- Loyola Coll., Baltimore, MD.**
JTEC/WTEC annual report and program summary: 1993/94
[NASA-CR-198563] p 454 N95-28038
- LTV Aerospace and Defense Co., Dallas, TX.**
Probabilistic design of advanced composite structure
p 424 N95-28443
- Lucas Electronics, Birmingham (England).**
The application of Ada and formal methods to a safety critical engine control system
p 710 N95-33142
- Lynntech, Inc., College Station, TX.**
Corrosion of aircraft materials: Correlation between nanometer scale and macroscopic structural damage parameters
[AD-A285930] p 241 N95-20299

M

- Manchester Univ. (England).**
Collaborative research on aircraft icing and charging processes in ice
[AD-A285102] p 276 N95-23201
- Marotta Scientific Controls, Inc., Montville, NJ.**
A Lifting Ball Valve for cryogenic fluid applications
p 156 N95-16349
- Martin Marietta Corp., Baltimore, MD.**
Application of fiber-reinforced bismaleimide materials to aircraft nacelle structures
p 397 N95-28278
- Martin Marietta Corp., Moorestown, NJ.**
Doppler radar detection of vortex hazard indicators
p 42 N95-13212
- Maryland Univ., College Park, MD.**
Techniques for designing rotorcraft control systems
[NASA-CR-196192] p 52 N95-12791
Cooperative control theory and integrated flight and propulsion control
[NASA-CR-197493] p 142 N95-17404
Experimental data on the aerodynamic interactions between a helicopter rotor and an airframe
p 116 N95-17883
Liquid flow-through cooling of electronic modules
p 246 N95-20647
A numerical study of the starting process in a hypersonic shock tunnel
p 626 N95-30493
- Massachusetts Inst. of Tech., Cambridge, MA.**
TDWR scan strategy implementation
[AD-A284877] p 98 N95-15749
Unsteady flow phenomena in discrete passage diffusers for centrifugal compressors
[AD-A281412] p 155 N95-16163
Workshop on Formal Models for Intelligent Control
[AD-A281399] p 169 N95-16864
Design of high performance multivariable control systems for supermaneuverable aircraft at high angle of attack
[NASA-CR-197661] p 293 N95-22908
Anechoic wind tunnel study of turbulence effects on wind turbine broadband noise
p 451 N95-27992
A numerical method for modelling wings with sharp edges maneuvering at high angles of attack
p 503 N95-29122
Dynamic stall of a NACA 0012 airfoil in laminar flow
p 479 N95-29243
Modeling and control of rotating stall in high speed multi-stage axial compressors
p 513 N95-29244
Intelligent turbine engines for Army applications
[AD-A290532] p 514 N95-29496
An exploratory survey of information requirements for instrument approach charts
[AD-A293882] p 601 N95-31520
Current issues in the design and information content of instrument approach charts
[AD-A294752] p 690 N95-34562
- Massachusetts Inst. of Tech., Lexington, MA.**
Future enhancements to ground-based microburst detection
p 11 N95-10570
Ground-based wake vortex monitoring, prediction, and ATC interface
p 42 N95-13209
Aircraft wake RCS measurement
p 59 N95-13210
Solid state radar demonstration test results at the FAA Technical Center
[AD-A281520] p 154 N95-16097
GPS-Squitter capacity analysis
[AD-A280037] p 245 N95-20599
Calculation of satellite drag coefficients
[AD-A285118] p 300 N95-23781
Initial evaluation of the Oregon State University planetary boundary layer column model for ITWS applications
[AD-A293775] p 677 N95-31465
Integrated terminal weather system (ITWS) demonstration and validation operational test and evaluation
[AD-A293932] p 602 N95-31521

- GPS-Squitter interference analysis
[AD-A293690] p 689 N95-33480
- Massachusetts Univ., Amherst, MA.**
Intelligent finite element submodeling of multichip modules for reliability analysis
[AD-A292911] p 679 N95-31455
- MCAT Inst., Moffett Field, CA.**
Parallel aeroelastic computations for wing and wing-body configurations
[NASA-CR-196835] p 36 N95-11766
Planetary entry experiments
[NASA-CR-194215] p 101 N95-13717
Science objectives and performance of a radiometer and window design for atmospheric entry experiments
p 85 N95-13718
Three-dimensional unsteady flow calculations in an advanced gas generator turbine
p 312 N95-23425
- MCAT Inst., San Jose, CA.**
Instabilities originating from suction holes used for Laminar Flow Control (LFC)
[NASA-CR-196395] p 6 N95-10131
Numerical simulation of the flow about the F-18 HARV at high angle of attack
[NASA-CR-196396] p 9 N95-10940
High speed civil transport: Sonic boom softening and aerodynamic optimization
[NASA-CR-196397] p 28 N95-11192
Development of an upwind, finite-volume code with finite-rate chemistry
[NASA-CR-196749] p 9 N95-11366
Computational analysis of forebody tangential slot blowing on the high alpha research vehicle
[NASA-CR-196750] p 10 N95-11367
Shock-tunnel combustor testing for hypersonic vehicles
[NASA-CR-196836] p 52 N95-11938
High speed civil transport aerodynamic optimization
[NASA-CR-196960] p 38 N95-12389
Design and testing of an oblique all-wing supersonic transport
[NASA-CR-196394] p 48 N95-12785
Numerical simulation of the SOFIA flowfield
[NASA-CR-197025] p 74 N95-14612
Control of unsteady separated flow associated with the dynamic stall of airfoils
[NASA-CR-197024] p 74 N95-14613
Numerical simulation of the flow about the F-18 HARV at high angle of attack
[NASA-CR-197023] p 74 N95-14614
Numerical simulation of the SOFIA flow field
[NASA-CR-197757] p 436 N95-26589
Aeroelasticity of wing and wing-body configurations on parallel computers
[NASA-CR-197756] p 389 N95-26590
Computational analysis of forebody tangential slot blowing on the high alpha research vehicle
[NASA-CR-197754] p 389 N95-26591
Supersonic transport grid generation, validation, and optimization
[NASA-CR-197752] p 448 N95-26648
CFD research, parallel computation and aerodynamic optimization
[NASA-CR-197748] p 373 N95-26649
Design and testing of low sonic boom configurations and an oblique all-wing supersonic transport
[NASA-CR-197744] p 389 N95-26651
Numerical simulation of the flow about the F-18 HARV at high angle of attack
[NASA-CR-197755] p 374 N95-26735
Development of an upwind, finite-volume code with finite-rate chemistry
[NASA-CR-197747] p 374 N95-26760
Computational support of the laminar flow supersonic wind tunnel, CNSFV code development, Maglev, and grid generation
[NASA-CR-197750] p 411 N95-26775
Turbomachinery design and tonal acoustics computations
[NASA-CR-197749] p 406 N95-26777
Supersonic civil airplane study and design: Performance and sonic boom
[NASA-CR-197745] p 390 N95-26813
Control of unsteady separated flow associated with the dynamic stall of airfoils
[NASA-CR-198972] p 594 N95-32193
- McDonnell Aircraft Co., Saint Louis, MO.**
ACT/ICAPS: Thermoplastic composite activities
p 421 N95-28274
Analysis techniques for the prediction of springback in formed and bonded composite components
p 421 N95-28289
Development of composite carrythrough bulkhead
p 423 N95-28438
- McDonnell-Douglas Aerospace, Long Beach, CA.**
Comparison of stochastic and deterministic nonlinear gust analysis methods to meet continuous turbulence criteria
p 133 N95-18602
The crucial role of wall interference, support interference and flow field measurements in the development of advanced aircraft configurations
p 162 N95-19252
Crew aiding and automation: A system concept for terminal area operations, and guidelines for automation design
[NASA-CR-4631] p 228 N95-19950
Guidance and control requirements for high-speed Rollout and Turnoff (ROTO)
[NASA-CR-195026] p 292 N95-22674
Advanced subsonic airplane design and economic studies
[NASA-CR-195443] p 338 N95-24304
Noise impact of advanced high lift systems
[NASA-CR-195028] p 362 N95-26160
The relation of handling qualities ratings to aircraft safety
p 597 N95-31067
Development of stitched/RTM primary structures for transport aircraft
[NASA-CR-191441] p 630 N95-31421
The importance of flying qualities design specifications for active control systems
p 621 N95-31992
Fan noise prediction assessment
[NASA-CR-195051] p 711 N95-33831
- McDonnell-Douglas Aerospace, Saint Louis, MO.**
Impact of agility requirements on configuration synthesis
[NASA-CR-4627] p 44 N95-11952
Fiber Optic Control System integration for advanced aircraft. Electro-optic and sensor fabrication, integration, and environmental testing for flight control systems: Laboratory test results
[NASA-CR-195408] p 161 N95-18938
Fiber Optic Control System integration for advanced aircraft. Electro-optic and sensor fabrication, integration, and environmental testing for flight control systems
[NASA-CR-191194] p 162 N95-19236
Transonic wind tunnel boundary interference correction
p 147 N95-19271
Transverse vorticity measurements in the NASA Ames 80 x 120 wind tunnel boundary layer
p 251 N95-22457
The applicability of turbulence models to aerodynamic and propulsion flowfields at McDonnell-Douglas Aerospace
p 439 N95-27886
- McDonnell-Douglas Corp., Long Beach, CA.**
2-D aileron effectiveness study
p 110 N95-17851
- McDonnell-Douglas Corp., Saint Louis, MO.**
Integration of a mechanical forebody vortex control system into the F-15
p 72 N95-14258
Aeromechanics technology, volume 1. Task 1: Three-dimensional Euler/Navier-Stokes Aerodynamic Method (TEAM) enhancements
[AD-A285713] p 132 N95-18483
Acoustic fatigue characteristics of advanced materials and structures
p 174 N95-19157
Performance study for inlet installations
[NASA-CR-189714] p 406 N95-28227
Comparison of spatial numerical operators for duct-nozzle acoustics
p 580 N95-30158
PSC algorithm description
p 695 N95-33013
PSC implementation and integration
p 695 N95-33014
Propulsion Controlled Aircraft design and development
p 697 N95-33022
- McDonnell-Douglas Research Labs., Saint Louis, MO.**
Low-energy pneumatic control of forebody vortices
p 72 N95-14256
- MDA Engineering, Inc., Arlington, TX.**
Three-dimensional hybrid grid generation using advancing front techniques
p 567 N95-28745
- Mechanical Engineering Lab., Sakura (Japan).**
Long endurance stratospheric solar powered airship
[PB95-17872] p 336 N95-26009
- Mestre Greve Associates, Newport Beach, CA.**
Determining the effects of alternative departure cutback altitudes and power settings: A case study, John Wayne Airport
p 31 N95-11320
- Michigan Univ., Ann Arbor, MI.**
Conceptual design of the AE481 Demon Remotely Piloted Vehicle (RPV)
[NASA-CR-197164] p 44 N95-12294
Forced response of mistuned bladed disks
p 141 N95-19383
Design considerations for an archimedean slot spiral antenna
p 211 N95-19798
Design of a controller for a flexible pointing system using H(infinity) synthesis
[AD-A286572] p 256 N95-20828
Robust fixed-structure control
[AD-A286515] p 257 N95-22216
- Scattering and radiation from cylindrically conformal antennas
p 645 N95-30669
Robust fixed-structure control
[AD-A292883] p 679 N95-30961
Simulation of patch and slot antennas using FEM with prismatic elements and investigations of artificial absorber mesh termination schemes
[NASA-CR-198974] p 704 N95-32822
Near-limit drop deformation and secondary breakup
p 704 N95-32902
- Midwest Research Inst., Golden, CO.**
Observed acoustic and aeroelastic spectral responses of a MOD-2 turbine blade to turbulence excitation
p 451 N95-27991
- Midwest Research Inst., Kansas City, MO.**
Development of anti-icing technology
[PB94-195369] p 78 N95-15439
- Minnesota Dept. of Transportation, Duluth, MN.**
Development of anti-icing technology
[PB94-195369] p 78 N95-15439
- Minnesota Univ., Minneapolis, MN.**
Feedback control laws for highly maneuverable aircraft
[NASA-CR-197944] p 295 N95-23410
Studies in drag reduction
p 478 N95-29094
Experiments on microbursts
p 562 N95-29110
Emerging applications in probability (Sensor management)
[AD-A292781] p 601 N95-31433
- Mississippi State Univ., Mississippi State, MS.**
Wing design for a civil tiltrotor transport aircraft
[NASA-CR-197523] p 130 N95-18090
Crossflow instability control on a swept-wing: Preliminary studies
p 274 N95-23283
Thin tailored composite wing for civil tiltrotor
p 285 N95-23317
TIGER: A user-friendly interactive grid generation system for complicated turbomachinery and axis-symmetric configurations
p 322 N95-23419
- Mississippi State Univ., State College, MS.**
Propulsion/airframe interference for ducted propfan engines with ground effect
[NASA-CR-197110] p 81 N95-14909
- Mississippi Univ., University, MS.**
Atmospheric effects on the risetime and waveshape of sonic booms
p 100 N95-14886
Proceedings of the Sixth International Symposium on Long-Range Sound Propagation
[AD-A290920] p 580 N95-30084
Investigating the use of smart acoustically active surfaces for flow separation control in turbomachinery
[AD-A292819] p 648 N95-31443
- Missouri Univ., Rolla, MO.**
Ducted fan acoustic radiation including the effects of nonuniform mean flow and acoustic treatment
[NASA-CR-197449] p 172 N95-16401
- MITech, Inc., Pleasantville, NJ.**
Research requirements for future visual guidance systems
[AD-A279188] p 191 N95-19810
- Mitre Corp., Bedford, MA.**
Thunderstorm hypothesis reasoner
[AD-A282664] p 60 N95-12805
- Mitre Corp., McLean, VA.**
Air traffic operational inventory CY 1994
[AD-A288281] p 382 N95-26454
Effects of civil tiltrotor service in the northeast corridor on en route airspace loads
[AD-A293586] p 599 N95-31687
- Mitsubishi Heavy Industries Ltd., Tokyo (Japan).**
Activities of Mitsubishi Heavy Industries Ltd.
[PB94-179694] p 22 N95-10085
Verification of turbine cascade flow with tip clearance
p 698 N95-34511
Calculation of supersonic combustion in SCRAMJET engines
p 698 N95-34513
- Modern Technologies Corp., Middleburg Heights, OH.**
The decay of longitudinal vortices shed from airfoil vortex generators
[NASA-CR-198356] p 480 N95-29402
- Moller International, Inc., Davis, CA.**
Evaluation of thermal barrier and PS-200 self-lubricating coatings in an air-cooled rotary engine
[NASA-CR-195445] p 289 N95-23222
- Monash Univ., Clayton (Australia).**
Development of a composite repair and the associated inspection intervals for the F-111C stiffener runout region
p 66 N95-14477
- Motoren- und Turbinen-Union Muenchen G.m.b.H., Munich (Germany).**
Performance deterioration of axial compressors due to blade defects
p 199 N95-19665
Impact loading of compressor stator vanes by hailstone ingestion
p 200 N95-19670
Damage of high temperature components by dust-laden air
p 201 N95-19673

N

- Nagoya Univ., Nagoya (Japan).**
A simulation of damping process of pendulum motion due to aerodynamic forces p 711 N95-34551
- Nangia Associates, Bristol (England).**
Estimating wind tunnel interference due to vectored jet flows p 164 N95-19265
- Nanjing Univ. of Aeronautics and Astronautics, Nanjing, Jiangsu (China).**
Joint Proceedings on Aeronautics and Astronautics (JPA) p 104 N95-16249
Investigation of dynamic inflow's influence on rotor control derivatives p 155 N95-16250
An approach to aerodynamic characteristics of low radar cross-section fuselages p 106 N95-16251
An improved method of airfoil design p 106 N95-16252
Wall-signature methods for high speed wind tunnel wall interference corrections p 107 N95-16257
An investigation of polynomial calibrations methods for wind tunnel balances p 144 N95-16258
Linear prediction data extrapolation superresolution radar imaging p 155 N95-16268
Application of GPS/SINS/RA integrated system to aircraft approach landing p 125 N95-16277
The computer analysis of the prediction of aircraft electrical power supply system reliability p 155 N95-16278
- Naples Univ. (Italy).**
Adaptive wind tunnel walls versus wall interference correction methods in 2D flows at high blockage ratios p 147 N95-19267
- National Academy of Sciences - National Research Council, Washington, DC.**
Aeronautics and space technology, past, present, and future p 35 N95-11892
Assessment of the Space Station program p 149 N95-16352
Airborne geophysics and precise positioning: Scientific issues and future directions [LC-94-68678] p 446 N95-27156
High-stakes aviation: US-Japan technology linkages in transport aircraft [LC-94-65759] p 381 N95-27907
- National Aeronautical Lab., Bangalore (India).**
Evaluation of the dynamic stability characteristics of the NAL Light Transport Aircraft [NAL-PD-CA-9217] p 142 N95-16392
- National Aeronautics and Space Administration, Washington, DC.**
Microwave and infrared simulations of an intense convective system and comparison with aircraft observations [HTN-95-60511] p 214 N95-68762
Orbital velocities induced by surface waves [HTN-95-90902] p 253 N95-72411
Buckling and vibration analysis of laminated panels using VICONOPT [PAPER-1746] p 230 N95-72580
Analysis of the physical state of one Arctic polar stratospheric cloud based on observations [HTN-95-70917] p 351 N95-77982
The distribution of hydrogen, nitrogen, and chlorine radicals in the lower stratosphere: Implications for changes in O₃ due to emission of NO(y) from supersonic aircraft [HTN-95-70935] p 351 N95-78000
An analysis of aircraft exhaust plumes from accidental encounters [HTN-95-70943] p 351 N95-78008
Fine-scale, poleward transport of tropical air during AASE 2 [HTN-95-70949] p 352 N95-78014
Guidance and control, 1993; Annual Rocky Mountain Guidance and Control Conference, 16th, Keystone, CO, Feb. 6-10, 1993 [ISBN-0-87703-365-X] p 341 N95-80389
Education, training, and human engineering in aerospace; SAE Aerotech '93, Costa Mesa, CA, Sep. 27-30, 1993 [SAE SP-992] p 417 N95-84553
An overview of millimeter-wave spectroscopic measurements of chlorine monoxide at Thule, Greenland, February-March, 1992: Vertical profiles, diurnal variation, and longer-term trends [HTN-95-00722] p 444 N95-86292
Hypersonic flow past open cavities [HTN-95-42577] p 458 N95-87207
The NASA-sponsored Maryland center for hypersonic education and research [AIAA PAPER 95-6105] p 519 N95-88010
Research and educational initiatives at the Syracuse University Center for Hypersonics [AIAA PAPER 95-6107] p 520 N95-90439
- Characterization of a hot-film probe for hypersonic flow [AIAA PAPER 95-6110] p 511 N95-90440
Hypersonic aerodynamics test facility using the external propulsion accelerator [AIAA PAPER 95-6138] p 470 N95-90455
Sensitivity of engine-integrated waverider performance to static margin constraint [AIAA PAPER 95-6142] p 496 N95-90458
Scramjet thrust measurement in a shock tunnel [HTN-95-C0008] p 586 N95-93396
Low gravity quenching of hot tubes with cryogenics [ISBN 1-879921-01-4] p 635 N95-93728
Numerical study of multi-element airfoil aerodynamics [ISBN 1-879921-01-4] p 587 N95-93750
The High Speed Research Program [NASA-TM-109869] p 10 N95-10548
The model builders [NASA-TM-109902] p 20 N95-10552
Aero-Space Plane: Flexible access to space [NASA-TM-109904] p 22 N95-10553
Scientific balloons [NASA-TM-109907] p 7 N95-10556
General Aviation Task Force report [NASA-TM-109950] p 1 N95-11463
Revitalizing general aviation [NASA-TM-110113] p 129 N95-16982
NASA High Performance Computing and Communications program [NASA-TM-4653] p 176 N95-18573
Aeronautical engineering: A continuing bibliography with indexes (supplement 315) [NASA-SP-7037(315)] p 219 N95-21640
Turbine design and application volumes 1, 2, and 3 [E-5666-Vol-1-3] p 236 N95-22341
NASA video catalog [NASA-SP-7109(01)] p 363 N95-24238
The atmospheric effects of stratospheric aircraft: A fourth program report [NASA-PP-1359] p 357 N95-24274
Aeronautical engineering: A continuing bibliography with indexes (supplement 316) [NASA-SP-7037(316)] p 328 N95-24465
Aeronautical engineering: A continuing bibliography with indexes (supplement 317) [NASA-SP-7037(317)] p 328 N95-25798
Aeronautical engineering: A continuing bibliography with indexes (supplement 318) [NASA-SP-7037(318)] p 367 N95-27543
Research and Technology Objectives and Plans Summary (RTOPS) [NASA-TM-108574] p 453 N95-28002
The process for addressing the challenges of aircraft pilot coupling p 597 N95-31063
Aeronautics and space report of the President [NASA-TM-110743] p 681 N95-31979
- National Aeronautics and Space Administration, Ames Research Center, Moffett Field, CA.**
Validation of the dynamic response of a blade-element UH-60 simulation model in hovering flight [HTN-94-00663] p 18 N95-60155
Evaluation of simulation motion fidelity criteria in the vertical and directional axes [HTN-94-00666] p 18 N95-60156
Navier-Stokes simulation of rotor-body flowfield in hover using overset grids [PAPER C15] p 1 N95-60160
Optimum full-scale subsonic wind tunnel [AIAA PAPER 86-0732] p 18 N95-60161
Aeroacoustic probe design for microphone to reduce flow-induced self-noise [AIAA PAPER 93-4343] p 19 N95-60163
An experimental investigation of wing tip turbulence with applications to aerosound [AIAA PAPER 86-1918] p 1 N95-60164
Oblique incidence sound absorption of porous materials covered by perforated metal and exposed to tangential airflow [HTN-94-00681] p 19 N95-60165
On the scaling of small-scale jet noise to large scale [AIAA PAPER 92-02109] p 27 N95-60166
Flight test development and evaluation of a Kalman filter state estimator for low-altitude flight [HTN-94-00684] p 16 N95-60167
Design of a model following, state variable feedback controller for the X-14 VTOL aircraft [HTN-94-00685] p 16 N95-60168
Recent advances in Euler and Navier-Stokes methods for calculating helicopter rotor aerodynamics and acoustics [HTN-94-00686] p 2 N95-60169
Simulation development of a forward sensor-enhanced low-altitude guidance system [HTN-94-00688] p 17 N95-60170
- Experimental and analytical investigations of wave enhanced supersonic combustors [AIAA PAPER 89-2787] p 14 N95-60172
Computation of nonequilibrium viscous flows in arc-jet wind tunnel nozzles [AIAA PAPER 94-0254] p 2 N95-60173
Jet to freestream velocity ratio computations for a jet in a crossflow [AIAA PAPER 93-4860] p 2 N95-60178
Numerical simulation of powered-lift flows [HTN-94-00700] p 3 N95-60179
Dryden lectureship in research, a perspective on CFD validation [AIAA PAPER 93-0002] p 3 N95-60180
Accuracy enhancements for overset grids using a defect correction approach [AIAA PAPER 94-0523] p 3 N95-60181
Interferometry and computational studies of an oscillating airfoil compressible dynamic stall flow field [HTN-94-00703] p 3 N95-60182
Dynamic stall of an oscillating wing. Part 1: Evaluation of turbulence models [AIAA PAPER 93-3403] p 3 N95-60184
A comparison of turbulence models in computing multi-element airfoil flows [AIAA PAPER 94-0291] p 4 N95-60185
A comparison of three-dimensional nonequilibrium solution algorithms applied to hypersonic flows with stiff chemical source terms [AIAA PAPER 93-2861] p 4 N95-60186
Numerical simulation of a complete STOVL aircraft in ground effect [AIAA PAPER 93-4880] p 4 N95-60187
Wing download reduction using vortex trapping plates [HTN-94-00710] p 4 N95-60188
An assessment of upper surface blowing for the reduction of tilt rotor download [HTN-94-00711] p 5 N95-60189
Study of noise on a small-scale hovering tilt rotor [HTN-94-00712] p 5 N95-60190
LDV measurements in dynamically separated flows [ISBN 0-8194-1311-9] p 5 N95-60191
Aerodynamic interactions between a rotor and wing in hover [HTN-94-00714] p 5 N95-60192
A study of compressibility effects on dynamic stall of rapidly pitching airfoils [HTN-94-00715] p 5 N95-60193
Three-dimensional model interpretation of NO(x) measurements from the lower stratosphere [HTN-95-90534] p 213 N95-67806
Review of numerical procedures for computational surface thermochemistry [BTN-94-EIX94441386682] p 205 N95-68191
Effect of ground and ceiling planes on shape of energized wakes [BTN-95-EIX95062487558] p 186 N95-68372
Trajectory-based heating analysis for the European Space Agency/Rosetta Earth Return Vehicle [BTN-95-EIX95041503787] p 205 N95-69218
Numerical simulation of incidence and sweep effects on delta wing vortex breakdown [BTN-95-EIX95062487526] p 186 N95-69234
Simulation and flight test evaluation of head-up-display guidance for harrier approach transitions [BTN-95-EIX95062487533] p 194 N95-69241
Flow resolution and domain influence in rarefied hypersonic blunt-body flows [BTN-95-EIX95082502729] p 220 N95-70136
Measurement and analysis of nitric oxide radiation in an arcjet flow [BTN-95-EIX95082502727] p 243 N95-71040
Rotorcraft control system design for uncertain vehicle dynamics using quantitative feedback theory [HTN-95-31012] p 236 N95-71182
Advance finite element modeling of rotor blade aeroelasticity [HTN-95-31013] p 221 N95-71183
Performance of a focused cavity aerosol spectrometer for measurements in the stratosphere of particle size in the 0.06-2.0-micrometer-diameter range [HTN-95-90914] p 253 N95-72423
High-order state space simulation models of helicopter flight mechanics [HTN-95-A0494] p 237 N95-72565
Flap-lag damping in hover and forward flight with a three-dimensional wake [HTN-95-A0496] p 221 N95-72567
Progress in high-lift aerodynamic calculations [BTN-95-EIX95152582315] p 264 N95-73518
Navier-Stokes prediction of large-amplitude delta-wing roll oscillations [BTN-95-EIX95152582329] p 281 N95-73531
Forebody flow control on a full-scale F/A-18 aircraft [BTN-95-EIX95152582333] p 281 N95-73535

Hypersonic nonequilibrium Navier-Stokes solutions over an ablating graphite nosetip
[BTN-95-EIX95152583252] p 305 A95-73553

Hypersonic convective heat transfer over 140-deg blunt cones in different gases
[BTN-95-EIX95152583253] p 306 A95-73554

Investigation of the effects of bandwidth and time delay on helicopter roll-axis handling qualities
[HTN-95-80853] p 290 A95-75095

Aeroacoustic model for weak shock waves based on Burgers equation
[BTN-95-EIX95182619076] p 269 A95-75761

Estimates of total organic and inorganic chlorine in the lower stratosphere from in situ and flask measurements during AASE 2
[HTN-95-A0861] p 317 A95-76265

In situ observations in aircraft exhaust plumes in the lower stratosphere at midlatitudes
[HTN-95-A0862] p 318 A95-76266

H-infinity helicopter flight control law design with and without rotor state feedback
[BTN-95-EIX95182619129] p 291 A95-76606

Automatic guidance and control for helicopter obstacle avoidance
[BTN-95-EIX95182619130] p 291 A95-76607

CFD optimization of a theoretical minimum-drag body
[BTN-95-EIX95182619234] p 308 A95-76660

Analysis of the physical state of one Arctic polar stratospheric cloud based on observations
[HTN-95-70917] p 351 A95-77982

The distribution of hydrogen, nitrogen, and chlorine radicals in the lower stratosphere: Implications for changes in O3 due to emission of NO(y) from supersonic aircraft
[HTN-95-70935] p 351 A95-78000

Vertical transport rates in the stratosphere in 1993 from observations of CO2, N2O, and CH4
[HTN-95-70941] p 351 A95-78006

Fine-scale, poleward transport of tropical air during AASE 2
[HTN-95-70949] p 352 A95-78014

Identification and simulation evaluation of a combat helicopter in hover
[BTN-95-EIX95242670749] p 335 A95-81098

SOFIA: Stratospheric Observatory for Infrared Astronomy
p 363 A95-81583

Education, training, and human engineering in aerospace; SAE Aerotech '93, Costa Mesa, CA, Sep. 27-30, 1993
[SAE SP-992] p 417 A95-84553

Optimal trajectories for hypersonic launch vehicles
[HTN-95-61120] p 415 A95-84884

Transition correlations in three-dimensional boundary layers
[HTN-95-51648] p 432 A95-85030

Practical formulation of a positively conservative scheme
[HTN-95-51668] p 433 A95-85050

Effect of Reynolds number and turbulence on airfoil aerodynamics at -90-degree incidence
[HTN-95-42320] p 370 A95-86149

Reduction of blade-vortex interaction noise through porous leading edge
[HTN-95-42324] p 371 A95-86153

Interferometric investigations of compressible dynamic stall over a transiently pitching airfoil
[HTN-95-42338] p 372 A95-86167

Head-on parallel blade-vortex interaction
[HTN-95-61197] p 491 A95-87570

Unsteady panel method for flows with multiple bodies moving along various paths
[HTN-95-61203] p 540 A95-87576

Heat-transfer measurements and computations of swept-shock-wave boundary-layer interactions
[HTN-95-81634] p 541 A95-87682

Dynamic-stall and structural-modeling effects on helicopter blade stability with experimental correlation
[HTN-95-81646] p 542 A95-87694

Laser interferometer skin-friction measurements of crossing-shock-wave/turbulent-boundary-layer
[HTN-95-20834] p 544 A95-88095

Equivalent plate structural modeling for wing shape optimization including transverse shear
[HTN-95-20839] p 492 A95-88100

Symposium on Aerodynamics & Aeroacoustics, Tucson, AZ, Mar. 1-2, 1993
[ISBN 981-02-1732-3] p 462 A95-88892

Adaptive-wall wind-tunnel research at Ames Research Center: A retrospective
p 519 A95-88902

Adaptive wall technology for minimization of wind tunnel boundary interferences - where are we now?
p 519 A95-88903

Supersonic and hypersonic shock/boundary-layer interaction database
[HTN-95-20930] p 463 A95-88969

Aerodynamic tailoring of the Learjet Model 60 wing
[SAE PAPER 932534] p 492 A95-89194

Boundary-layer transition and global skin friction measurement with an oil-fringe imaging technique
[SAE PAPER 932550] p 547 A95-90054

Accurate drag prediction: A prerequisite for drag reduction research
[SAE PAPER 932571] p 467 A95-90060

Flight-testing and frequency-domain analysis for rotorcraft handling qualities
[HTN-95-01083] p 515 A95-90269

Navier-Stokes calculations of rotor-airframe interaction in forward flight
[HTN-95-01087] p 468 A95-90273

Sensitivity of engine-integrated waverider performance to static margin constraint
[AIAA PAPER 95-6142] p 496 A95-90458

Research activity at the shock tube facility at NASA Ames
p 547 A95-90559

Parallel CFD design on network-based computer
[AIAA PAPER 95-0984] p 565 A95-90656

A computational environment for exhaust nozzle design
[AIAA PAPER 95-1016] p 566 A95-90688

Assessment of Russian VSTOL technology evaluating the YAK-38 'FORGER' and YAK-141 'FREESTYLE'
p 497 A95-90868

Parallel computational fluid dynamics '91; Conference Proceedings, Stuttgart, Germany, Jun. 10-12, 1991
[ISBN 0-444-89363-6] p 548 A95-91479

Aerodynamic simulation on massively parallel systems
p 549 A95-91487

Turbulence near thunderstorm tops
p 675 A95-93553

The application of potential CFD methods to helicopter hover flows
[ISBN 1-879921-01-4] p 587 A95-93747

Analytic solution of the thickness problem of a rectangular wing in steady subsonic flow
[ISBN 1-879921-01-4] p 588 A95-93758

Lift-enhancing tabs on multielement airfoils
[BTN-95-EIX0619952748187] p 591 A95-94479

EMS helicopter incidents reported to the NASA Aviation Safety Reporting System
p 596 A95-95201

Emergency medical service (EMS): A unique flight environment
p 596 A95-95203

Initial exploration of the ASRS database
p 681 A95-95204

Computational fluid dynamics '92; Proceedings of the European Computational Fluid Dynamics Conference, 1st, Brussels, Belgium, Sep. 7-11, 1992. Vols. 1 & 2
[ISBN 0-444-89793-3] p 638 A95-95357

Design and flight evaluation of an integrated navigation and near-terrain helicopter guidance system for night-time and adverse weather operations
[NASA-TM-108837] p 11 N95-10846

Computational fluid dynamics uses in fluid dynamics/aerodynamics education
[NASA-TM-108834] p 8 N95-10847

Dynamic response of NASA Rotor Test Apparatus and Sikorsky S-76 hub mounted in the 80- by 120-Foot Wind Tunnel
[NASA-TM-108847] p 25 N95-11389

Numerical analysis of tangential slot blowing on a generic chined forebody
[NASA-TM-108845] p 37 N95-11927

Test model designs for advanced refractory ceramic materials
p 55 N95-11968

Science objectives and performance of a radiometer and window design for atmospheric entry experiments
[NASA-TM-4637] p 63 N95-12190

Flight investigation of the use of a nose gear jump strut to reduce takeoff ground roll distance of STOL aircraft
[NASA-TM-108819] p 44 N95-12225

The selective use of functional optical variables in the control of forward speed
[NASA-TM-108849] p 35 N95-12227

Measurements of atmospheric turbulence effects on tail rotor acoustics
[NASA-TM-108843] p 38 N95-12360

Modification of the Ames 40- by 80-foot wind tunnel for component acoustic testing for the second generation supersonic transport
[NASA-TM-108850] p 65 N95-13642

User's guide for ENSAERO: A multidisciplinary program for fluid/structural/control interaction studies of aircraft (release 1)
[NASA-TM-108853] p 65 N95-13662

VUV shock layer radiation in an arc-jet wind tunnel experiment
p 67 N95-13719

Measured and calculated spectral radiation from a blunt body shock layer in an arc-jet wind tunnel
[AIAA PAPER 94-0086] p 67 N95-13720

Dynamics of the McDonnell-Douglas Large Scale Dynamic Rig and dynamic calibration of the rotor balance
[NASA-TM-108855] p 65 N95-13891

Simulation of Shuttle launch G forces and acoustic loads using the NASA Ames Research Center 20G centrifuge
p 86 N95-14089

Numerical simulation of the flow about an F-18 aircraft in the high-alpha regime
p 68 N95-14232

Free-to-roll tests of X-31 and F-18 subscale models with correlation to flight test results
p 69 N95-14237

Computational analysis of forebody tangential slot blowing
p 71 N95-14253

Comparison of full-scale, small-scale, and CFD results for F/A-18 forebody slot blowing
p 72 N95-14255

Higher harmonic control analysis for vibration reduction of helicopter rotor systems
[NASA-TM-103855] p 66 N95-14419

Aircraft maneuver envelope warning system
[NASA-CASE-ARC-11953-1] p 82 N95-14518

Experimental/analytical approach to understanding mistuning in a transonic wind tunnel compressor
[NASA-TM-108833] p 95 N95-14617

Air-breathing aerospace plane development essential: Hypersonic propulsion flight tests
[NASA-TM-108857] p 66 N95-14921

A supercritical airfoil experiment
p 111 N95-17858

Low aspect ratio wing experiment
p 113 N95-17865

STOVL CFD model test case
p 115 N95-17881

Parametric study on laminar flow for finite wings at supersonic speeds
[NASA-TM-108852] p 116 N95-18101

VSTOL Systems Research Aircraft (VSRA) Harrier
[NASA-TM-110117] p 126 N95-18347

NASA develops new digital flight control system
[NASA-NEWS-RELEASE-94-47] p 144 N95-19029

An assessment of the adaptive unstructured tetrahedral grid, Euler Flow Solver Code FELISA
[NASA-TP-3526] p 119 N95-19041

2-D and 3-D oscillating wing aerodynamics for a range of angles of attack including stall
[NASA-TM-4632] p 120 N95-19119

Wall interaction effects for a full-scale helicopter rotor in the NASA Ames 80- by 120-foot wind tunnel
p 121 N95-19270

Simulation of rotor blade element turbulence
[NASA-TM-108862] p 232 N95-21186

A three-dimensional orthogonal laser velocimeter for the NASA Ames 7- by 10-foot wind tunnel
[NASA-TM-108864] p 249 N95-21323

Flow visualization studies of VTOL aircraft models during Hover in ground effect
[NASA-TM-108860] p 272 N95-22666

Nonlinear system guidance in the presence of transmission zero dynamics
[NASA-TM-4661] p 309 N95-22804

Experimental results for a hypersonic nozzle/afterbody flow field
[NASA-TM-4638] p 274 N95-23250

System for determining aerodynamic imbalance
[NASA-CASE-ARC-11913-1] p 311 N95-23377

Engines-only flight control system
[NASA-CASE-ARC-11944-1] p 294 N95-23389

Aerodynamic surface distension system for high angle of attack forebody vortex control
[NASA-CASE-ARC-11979-1] p 286 N95-23390

Cueing light configuration for aircraft navigation
[NASA-CASE-ARC-11982-1] p 280 N95-23393

Lift enhancing tabs for airfoils
[NASA-CASE-ARC-11990-1] p 286 N95-23395

AVIRIS and TIMS data processing and distribution at the land processes distributed active archive center
p 325 N95-23872

TRISTAR 1: Evaluation methods for testing head-up display (HUD) flight symbology
[NASA-TM-4665] p 288 N95-24030

Geometric analysis of wing sections
[NASA-TM-110346] p 335 N95-24629

Aerodynamic shape optimization of wing and wing-body configurations using control theory
[NASA-CR-198024] p 335 N95-25334

Angular displacement measuring device
[NASA-CASE-ARC-11937-1] p 362 N95-26015

Aerodynamics model for a generic ASTOVL lift-fan aircraft
[NASA-TM-110347] p 332 N95-26302

Simulation model of the integrated flight/propulsion control system, displays, and propulsion system for ASTOVL lift-fan aircraft
[NASA-TM-108866] p 405 N95-26412

Flightpath synthesis and HUD scaling for V/STOL terminal area operations
[NASA-TM-110348] p 383 N95-26587

The lift-fan aircraft: Lessons learned
[NASA-CR-196694] p 392 N95-27143

- Calculation of three-dimensional (3-D) internal flow by means of the velocity-vorticity formulation on a staggered grid
[NASA-TM-110352] p 376 N95-27258
NAS Technical Summaries, March 1993 - February 1994
- [NASA-RP-1355] p 453 N95-27367
A procedure for automating CFD simulations of an inlet-bleed problem p 552 N95-28768
Investigation of wing upper surface flow-field disturbance due to NASA DC-8-72 in-flight inboard thrust-reverser deployment
[NASA-TM-110351] p 457 N95-28816
Bibliography of Doctor Chul Park
[NASA-TM-110353] p 527 N95-29351
Boundary-layer transition and global skin friction measurement with an oil-fringe imaging technique
[NASA-CR-198814] p 557 N95-30224
Numerical simulations of the flow in the HYPULSE expansion tube
[NASA-TM-110357] p 523 N95-30228
Telepresence media resource tape
[NASA-TM-110648] p 569 N95-30248
Moving base simulation of an integrated flight and propulsion control system for an ejector-augmentor-STOVL aircraft in hover
[NASA-TM-108867] p 606 N95-30646
Flight test evaluation of the Stanford University/United Airlines differential GPS Category 3 automatic landing system
[NASA-TM-110354] p 593 N95-30788
Stratospheric Observatory For Infrared Astronomy (SOFIA). Phase A: System concept description
[NASA-TM-110669] p 680 N95-32187
Numerical solution of the full potential equation using a chimera grid approach
[NASA-TM-110360] p 594 N95-32188
Flight test of a low-altitude helicopter guidance system with obstacle avoidance capability p 688 N95-32490
SOFIA: Aft cavities wind tunnel test
[NASA-TM-110673] p 683 N95-32682
Full-scale hingeless rotor performance and loads
[NASA-TM-110356] p 691 N95-32699
SOFIA 2 model telescope wind tunnel test report
[NASA-TM-110668] p 683 N95-32764
- National Aeronautics and Space Administration. Flight Research Center, Edwards, CA.**
Flight test of the X-29A at high angle of attack: Flight dynamics and controls
[NASA-TP-3537] p 284 N95-22806
Direct adaptive performance optimization of subsonic transports: A periodic perturbation technique
[NASA-TM-4676] p 284 N95-22829
NASA Dryden flow visualization facility
[NASA-TM-4631] p 449 N95-27914
- National Aeronautics and Space Administration. Goddard Space Flight Center, Greenbelt, MD.**
Using IRI for the computation of ionospheric corrections for altimeter data analysis p 212 A95-66949
Microwave and infrared simulations of an intense convective system and comparison with aircraft observations
[HTN-95-60511] p 214 A95-68762
Possible near-IR channels for remote sensing precipitable water vapor from geostationary satellite platforms
[HTN-95-70139] p 214 A95-69431
Behavior of an inversion-based precipitation retrieval algorithm with high-resolution AMPR measurements including a low-frequency 10.7-GHz channel
[HTN-95-70134] p 252 A95-70656
A survey of bidirectional greater than or equal to MeV ion flows during the Helios 1 and Helios 2 mission: Observations from the Goddard Space Flight Center instruments
[HTN-95-70542] p 237 A95-71656
Trajectory modeling of emissions from lower stratospheric aircraft
[HTN-95-41219] p 317 A95-75031
Sensitivity of two-dimensional model predictions of ozone response to stratospheric aircraft: An update
[HTN-95-A0863] p 318 A95-76267
The distribution of hydrogen, nitrogen, and chlorine radicals in the lower stratosphere: Implications for changes in O₃ due to emission of NO_x from supersonic aircraft
[HTN-95-70935] p 351 A95-78000
Comparison of column abundances from three infrared spectrometers during AASE 2
[HTN-95-70946] p 352 A95-78011
Chemical change in the arctic vortex during AASE 2
[HTN-95-70947] p 352 A95-78012
Fine-scale, poleward transport of tropical air during AASE 2
[HTN-95-70949] p 352 A95-78014
- Guidance and control, 1993; Annual Rocky Mountain Guidance and Control Conference, 16th, Keystone, CO, Feb. 6-10, 1993
[ISBN-0-87703-365-X] p 341 A95-80389
Effects of a polar stratosphere cloud parameterization on ozone depletion due to stratospheric aircraft in a two-dimensional model
[HTN-95-A1038] p 443 A95-84543
Reentry analysis for low Earth orbiting spacecraft
p 415 A95-85774
The effect of high lift to drag ratio on aerobraking
p 415 A95-85807
Low-dimensional description of the dynamics in separated flow past thick airfoils
[HTN-95-20832] p 544 A95-88093
Three dimensional model calculations of the global dispersion of high speed aircraft exhaust and implications for stratospheric ozone loss p 26 N95-10657
Flight Mechanics/Estimation Theory Symposium 1995
[NASA-CP-3299] p 416 N95-27763
Impact of Ada and object-oriented design in the flight dynamics division at Goddard Space Flight Center
[NASA-CR-189412] p 567 N95-28807
Correction of thin cirrus effects in AVIRIS images using the sensitive 1.375-micron cirrus detecting channel
p 708 N95-33748
Remote sensing of smoke, clouds, and radiation using AVIRIS during SCAR experiments p 708 N95-33749
- National Aeronautics and Space Administration. Hugh L. Dryden Flight Research Center, Edwards, CA.**
A flying qualities study of longitudinal long-term dynamics of hypersonic planes
[AIAA PAPER 95-6150] p 521 A95-90464
Propulsion controlled aircraft research
p 497 A95-90869
Development and flight testing of the HL-10 lifting body
p 498 A95-90872
Operational and research aspects of a radio-controlled model flight test program
[BTN-95-EIX0619952748177] p 606 A95-94471
Dryden and transonic research
[NASA-TM-104281] p 1 N95-10709
Dryden overview for schools
[NASA-TM-104282] p 21 N95-10710
F-18 HARV presentation for industry
[NASA-TM-104283] p 13 N95-10711
Dryden tour tape, 1994
[NASA-TM-104288] p 21 N95-10714
Research excitation system flight testing
[NASA-TM-104289] p 13 N95-10715
NASA and the SR-71: Back to the future
[NASA-TM-104290] p 13 N95-10716
Radio controlled for research
[NASA-TM-104292] p 17 N95-10717
The crash of Flight 232
[NASA-TM-104279] p 11 N95-10737
Building the Integrated Test Facility: A foundation for the future
[NASA-TM-104280] p 21 N95-10738
HL-10 dedication ceremony
[NASA-TM-104295] p 13 N95-10740
F-104 resource tape
[NASA-TM-104296] p 13 N95-10741
F-15 835 (HIDEC) resource tape
[NASA-TM-104297] p 13 N95-10742
F-16XL resource tape
[NASA-TM-104298] p 13 N95-10743
F-18 high alpha research vehicle resource tape
[NASA-TM-104299] p 13 N95-10744
X-31 resource tape
[NASA-TM-104300] p 13 N95-10745
The Western Aeronautical Test Range
[NASA-TM-104301] p 21 N95-10746
Dryden overview for schools
[NASA-TM-104302] p 21 N95-10747
F-15 Propulsion Controlled Aircraft (PCA)
[NASA-TM-104303] p 17 N95-10748
NACA/NASA: X-1 through X-31
[NASA-TM-104304] p 1 N95-10749
Dryden summer 1994 update
[NASA-TM-104305] p 33 N95-10750
X-31 tailless testing
[NASA-TM-104306] p 13 N95-10751
Effects of mass on aircraft sidearm controller characteristics
[NASA-TM-104277] p 51 N95-11868
Dynamic ground effects flight test of an F-15 aircraft
[NASA-TM-4604] p 38 N95-12191
Fourth High Alpha Conference, volume 1
[NASA-CP-10143-VOL-1] p 67 N95-14229
Flight and full-scale wind-tunnel comparison of pressure distributions from an F-18 aircraft at high angles of attack
p 68 N95-14231
Fourth High Alpha Conference, volume 2
[NASA-CP-10143-VOL-2] p 69 N95-14239
- F-18 high alpha research vehicle: Lessons learned
p 69 N95-14240
Design and development of an F/A-18 inlet distortion rake: A cost and time saving solution
p 69 N95-14241
X-31 high angle of attack control system performance
p 70 N95-14244
Multi-application controls: Robust nonlinear multivariable aerospace controls applications
p 71 N95-14249
Fourth High Alpha Conference, volume 3
[NASA-CP-10143-VOL-3] p 71 N95-14251
Development of a low-aspect ratio fin for flight research experiments
[NASA-TM-4596] p 108 N95-16858
Shear buckling analysis of a hat-stiffened panel
[NASA-TM-4644] p 158 N95-17490
F-15 resource tape
[NASA-TM-110502] p 230 N95-19994
F-16XL interview with Marta Bohn-Meyer
[NASA-TM-110505] p 223 N95-19996
Acoustic climb to cruise test
[NASA-TM-110504] p 230 N95-20155
Flight assessment of the onboard propulsion system model for the Performance Seeking Control algorithm on an F-15 aircraft
[NASA-TM-4705] p 617 N95-31425
Flight test validation of a frequency-controls flight identification method on an F-15 aircraft
[NASA-TM-4704] p 620 N95-31846
X-29 flight control system: Lessons learned
p 622 N95-32001
An Electronic Workshop on the Performance Seeking Control and Propulsion Controlled Aircraft Results of the F-15 Highly Integrated Digital Electronic Control Flight Research Program
[NASA-TM-104278] p 694 N95-33009
An overview of integrated flight-propulsion controls flight research on the NASA F-15 research airplane
p 694 N95-33010
Performance seeking control program overview
p 695 N95-33011
Minimum fuel mode evaluation
p 695 N95-33015
Minimum fan turbine inlet temperature mode evaluation
p 696 N95-33016
Maximum thrust mode evaluation
p 696 N95-33017
Rapid deceleration mode evaluation
p 696 N95-33018
Performance seeking control excitation mode
p 696 N95-33019
Performance seeking control (PSC) for the F-15 highly integrated digital electronic control (HIDEC) aircraft
p 697 N95-33020
Background and principles of throttles-only flight control
p 697 N95-33021
Flight test of a propulsion controlled aircraft system on the NASA F-15 airplane
p 691 N95-33023
Design challenges encountered in the F-15 PCA flight test program
p 692 N95-33025
- National Aeronautics and Space Administration. Hugh L. Dryden Flight Research Facility, Edwards, CA.**
Flight experience with lightweight, low-power miniaturized instrumentation systems
[BTN-95-EIX95062487522] p 180 A95-69230
Flow-visualization study of the X-29A aircraft at high angles of attack using a 1/48-scale model
[NASA-TM-104268] p 8 N95-10858
Transonic flight test of a laminar flow leading edge with surface excrescences
[NASA-TM-4597] p 9 N95-11158
On the use of controls for subsonic transport performance improvement: Overview and future directions
[NASA-TM-4605] p 10 N95-11408
Water tunnel flow visualization study of a 4.4 percent scale X-31 forebody
[NASA-TM-104276] p 36 N95-11898
Numerical modeling of a cryogenic fluid within a fuel tank
[NASA-TM-4651] p 89 N95-13892
In-flight lift-drag characteristics for a forward-swept wing aircraft and comparisons with contemporary aircraft
[NASA-TP-3414] p 117 N95-18565
Determination of stores pointing error due to wing flexibility under flight load
[NASA-TM-4646] p 134 N95-19044
PIO: A historical perspective
p 597 N95-31062
- National Aeronautics and Space Administration. John C. Stennis Space Center, Bay Saint Louis, MS.**
Evaluation of the Sparton light-tolerance AXBT
[HTN-95-40728] p 251 A95-70473
- National Aeronautics and Space Administration. John F. Kennedy Space Center, Cocoa Beach, FL.**
Application of airborne field mill data for use in launch support
[HTN-95-50054] p 98 A95-62279

- Development of a climatological data base to help forecast cloud cover conditions for shuttle landings at the Kennedy Space Center p 670 A95-93529
- Analysis of rapidly developing fog at the Kennedy Space Center p 671 A95-93531
- A review of falconry as a bird control technique with recommendations for use at the Shuttle Landing Facility, John F. Kennedy Space Center, Florida, USA [NASA-TM-110142] p 381 N95-27859
- National Aeronautics and Space Administration.**
- Lyndon B. Johnson Space Center, Houston, TX.**
- Guidance and control, 1993: Annual Rocky Mountain Guidance and Control Conference, 16th, Keystone, CO, Feb. 6-10, 1993 [ISBN-0-87703-365-X] p 341 A95-80389
- Education, training, and human engineering in aerospace; SAE Aerotech '93, Costa Mesa, CA, Sep. 27-30, 1993 [SAE SP-992] p 417 A95-84553
- Reentry analysis for low Earth orbiting spacecraft p 415 A95-85774
- Development of the NASA/FLAGRO computer program for analysis of airframe structures p 94 N95-14473
- Landing gear energy absorption system [NASA-CASE-MSC-22277-1] p 96 N95-15306
- Virtual environment application with partial gravity simulation p 169 N95-15988
- Documentation and archiving of the Space Shuttle wind tunnel test data base. Volume 1: Background and description [NASA-TM-104806-VOL-1] p 151 N95-19237
- Documentation and archiving of the Space Shuttle wind tunnel test data base. Volume 2: User's Guide to the Archived Data Base [NASA-TM-104806-VOL-2] p 205 N95-19624
- Preload release mechanism [NASA-CASE-MSC-22327-1] p 350 N95-25592
- National Aeronautics and Space Administration.**
- Langley Research Center, Hampton, VA.**
- A grid generation and flow solution method for the Euler equations on unstructured grids [HTN-95-20003] p 153 A95-63201
- Demonstration of an elastically coupled twist control concept for tilt rotor blade application [BTN-94-EIX94441386633] p 196 A95-68182
- Parallel implicit unstructured grid Euler solvers [BTN-95-EIX95042474393] p 217 A95-68307
- Coupling equivalent plate and finite element formulations in multiple-method structural analyses [BTN-95-EIX95062487548] p 192 A95-68362
- Passive porosity with free and fixed separation on a tangent-ogive forebody [BTN-95-EIX95062487554] p 185 A95-68368
- Approximate method for calculating heating rates on three-dimensional vehicles [BTN-95-EIX95041503778] p 210 A95-69209
- Navier-Stokes simulations of Orbiter aerodynamic characteristics including pitch trim and bodyflap [BTN-95-EIX95041503779] p 204 A95-69210
- Multiblock analysis for Shuttle Orbiter reentry heating from Mach 24 to Mach 12 [BTN-95-EIX95041503780] p 205 A95-69211
- Recent studies of rotorcraft blade-vortex interaction noise [BTN-95-EIX95062487521] p 218 A95-69229
- Interpretation of waverider performance data using computational fluid dynamics [BTN-95-EIX95062487534] p 193 A95-69242
- Numerical study of the performance of swept, curved compression surface scramjet inlets [BTN-95-EIX95112524198] p 197 A95-69310
- Subsidence of aircraft engine exhaust in the stratosphere: Implications for calculated ozone depletions [PAPER-93GL03426] p 251 A95-70297
- Effects of leading and trailing edge flaps on the aerodynamics of airfoil/vortex interactions [HTN-95-31011] p 221 A95-71181
- Air and ground resonance of helicopters with elastically tailored composite rotor blades [HTN-95-A0497] p 222 A95-72568
- Buckling and vibration analysis of laminated panels using VICONOPT [PAPER-1746] p 230 A95-72580
- Mach wave emission from a high-temperature supersonic jet [BTN-95-EIX95152577586] p 264 A95-73496
- Separation control on high-lift airfoils via micro-vortex generators [BTN-95-EIX95152582326] p 265 A95-73529
- Analysis of a higher harmonic control test to reduce blade vortex interaction noise [BTN-95-EIX95152582330] p 265 A95-73532
- Computational study of plume-induced separation on a hypersonic powered model [BTN-95-EIX95152582346] p 266 A95-73548
- Aerodynamic characteristics of a hypersonic viscous optimized waverider at high altitudes [BTN-95-EIX95152583251] p 266 A95-73552
- Application of the multigrid solution technique to hypersonic entry vehicles [BTN-95-EIX95152583254] p 306 A95-73555
- Higher-order viscous shock-layer solutions for high-altitude flows [BTN-95-EIX95152583255] p 306 A95-73556
- Optimization of contoured hypersonic scramjet inlets with a least-squares parabolized Navier-Stokes procedure [HTN-95-20976] p 261 A95-74042
- Sensitivity of acoustic predictions to variation of input parameters [HTN-95-80855] p 267 A95-75097
- An analytical and experimental investigation of the response of the curved, composite frame/skin specimens [HTN-95-80857] p 283 A95-75099
- Aerodynamics of the Shuttle Orbiter at high altitudes [BTN-95-EIX95182617454] p 298 A95-75725
- Zonally decoupled direct simulation Monte Carlo solutions of hypersonic blunt-body wake flows [BTN-95-EIX95182617458] p 268 A95-75729
- Multigrid solution of compressible turbulent flow on unstructured meshes using a two-equation model [BTN-94-EIX94401378794] p 307 A95-76484
- Summary of an active flexible wing program [BTN-95-EIX95182619209] p 283 A95-76635
- Application of transonic small disturbance theory to the active flexible wing model [BTN-95-EIX95182619210] p 270 A95-76636
- Simulation and model reduction for the active flexible wing program [BTN-95-EIX95182619211] p 295 A95-76637
- Multiple-function digital controller system for active flexible wing wind-tunnel model [BTN-95-EIX95182619212] p 322 A95-76638
- On-line analysis capabilities developed to support the active flexible wing wind-tunnel tests [BTN-95-EIX95182619213] p 296 A95-76639
- Flutter suppression control law design and testing for the active flexible wing [BTN-95-EIX95182619214] p 292 A95-76640
- Design and multifunction tests of a frequency domain-based active flutter suppression system [BTN-95-EIX95182619215] p 292 A95-76641
- Flutter suppression for the active flexible wing: A classical design [BTN-95-EIX95182619216] p 292 A95-76642
- Rolling maneuver load alleviation using active controls [BTN-95-EIX95182619217] p 270 A95-76643
- Viscoplastic response of structures for intense local heating [HTN-95-41540] p 346 A95-77921
- The distribution of hydrogen, nitrogen, and chlorine radicals in the lower stratosphere: Implications for changes in O₃ due to emission of NO(y) from supersonic aircraft [HTN-95-70935] p 351 A95-78000
- An analysis of aircraft exhaust plumes form accidental encounters [HTN-95-70943] p 351 A95-78008
- Meridional distributions of NO(X), NO(Y), and other species in the lower stratosphere and upper troposphere during AASE 2 [HTN-95-70944] p 352 A95-78009
- Guidance and control, 1993: Annual Rocky Mountain Guidance and Control Conference, 16th, Keystone, CO, Feb. 6-10, 1993 [ISBN-0-87703-365-X] p 341 A95-80389
- Effects on stratospheric ozone from high-speed civil transport: Sensitivity to stratospheric aerosol loading [HTN-95-91842] p 354 A95-80830
- An intercomparison of aircraft instrumentation for tropospheric measurements of sulfur dioxide [HTN-95-91855] p 354 A95-80843
- An intercomparison of aircraft instrumentation for tropospheric measurements of carbonyl sulfide, hydrogen sulfide, and carbon disulfide [HTN-95-91856] p 355 A95-80844
- An intercomparison of instrumentation for tropospheric measurements of dimethyl sulfide: Aircraft results for concentrations at the parts-per-trillion level [HTN-95-91857] p 355 A95-80845
- Load alleviation maneuvers for a launch vehicle p 342 A95-81360
- A higher harmonic control test in the DNW to reduce impulsive BVI noise [HTN-95-61071] p 385 A95-83655
- Computational/experimental investigation of staged injection into a Mach 2 flow [HTN-95-51646] p 432 A95-85028
- Screesh tones from free and ducted supersonic jets [HTN-95-51647] p 432 A95-85029
- Shear buckling response of tailored composite plates [HTN-95-51680] p 418 A95-85062
- Nonreflective boundary conditions for high-order methods [HTN-95-42328] p 371 A95-86157
- Quantitative investigation of compressible mixing: Staged transverse injection into Mach 2 flow [HTN-95-42330] p 404 A95-86159
- An overview of millimeter-wave spectroscopic measurements of chlorine monoxide at Thule, Greenland, February-March, 1992: Vertical profiles, diurnal variation, and longer-term trends [HTN-95-00722] p 444 A95-86292
- Mach wave emission from a high-temperature supersonic jet [HTN-95-42571] p 458 A95-87201
- Preconditioned domain decomposition scheme for three-dimensional aerodynamic sensitivity analysis [HTN-95-42597] p 459 A95-87227
- Thrust modeling for hypersonic engines [AIAA PAPER 95-6081] p 509 A95-87410
- Active control of fan noise from a turbofan engine [HTN-95-61198] p 570 A95-87571
- Improving the efficiency of aerodynamic shape optimization [HTN-95-61204] p 540 A95-87577
- Multipoint inverse design of an infinite cascade of airfoils [HTN-95-81640] p 541 A95-87688
- The detection and measurement of microburst wind shear by an airborne lidar system p 543 A95-87798
- Fluctuating wall pressures near separation in highly swept turbulent interactions [HTN-95-20823] p 543 A95-88084
- Aerodynamic investigation with focusing schlieren in a cryogenic wind tunnel [HTN-95-20835] p 544 A95-88096
- Chemical recombination in an expansion tube [HTN-95-20844] p 544 A95-88105
- Sensitivity derivatives for three dimensional supersonic Euler code using incremental iterative strategy [HTN-95-20845] p 545 A95-88106
- Symposium on Aerodynamics & Aeroacoustics, Tucson, AZ, Mar. 1-2, 1993 [ISBN 981-02-1732-3] p 462 A95-88892
- An introduction to generalized functions with some applications in aerodynamics and aeroacoustics p 565 A95-88895
- Lightning protection technology for small general aviation composite material aircraft [SAE PAPER 931241] p 483 A95-88964
- Computing unsteady shock waves for aeroacoustic applications [HTN-95-20928] p 463 A95-88967
- Control-nonlinear-nonstationary structural response and radiation near a supersonic jet [HTN-95-20929] p 463 A95-88968
- Demonstration of an elastically coupled twist control concept for tilt rotor blade application [HTN-95-20959] p 465 A95-88998
- Low-speed wind tunnel tests of two waverider configuration models [AIAA PAPER 95-6093] p 493 A95-89251
- NASA evaluation of Type 2 chemical depositions [SAE PAPER 932582] p 495 A95-90086
- Noise control in aeroacoustics; Proceedings of the 1993 National Conference on Noise Control Engineering, NOISE-CON 93, Williamsburg, VA, May 2-5, 1993 [ISBN 0-931784-26-3] p 573 A95-90088
- The high speed civil transport: A technology challenge p 496 A95-90089
- Studies of blade-vortex interaction noise reduction by rotor blade modification p 573 A95-90093
- A prediction method for broadband shock associated noise from supersonic rectangular jets p 574 A95-90100
- Progressive wave equations and algorithms for sonic boom propagation p 575 A95-90104
- A total variation diminishing finite difference algorithm for sonic boom propagation models p 575 A95-90105
- Recent laboratory studies of loudness and annoyance to sonic booms p 575 A95-90117
- Improvement of the predicted aural detection code ICHIN (I Can Hear It Now) p 576 A95-90123
- Numerical investigation of sound transmission through double wall cylinders with respect to active noise control p 577 A95-90134
- The influence of source acceleration on acoustic signals p 577 A95-90136
- Effects of signal analysis parameters and noise removal on measured aircraft spectra p 578 A95-90137
- Navier-Stokes calculations of rotor-airframe interaction in forward flight [HTN-95-01087] p 468 A95-90273

- Research and educational initiatives at the Syracuse University Center for Hypersonics
[AIAA PAPER 95-6107] p 520 A95-90439
- Characterization of a hot-film probe for hypersonic flow
[AIAA PAPER 95-6110] p 511 A95-90440
- Integrated performance and reliability specification for digital avionics systems
[AIAA PAPER 95-0953] p 506 A95-90632
- Buffeting tests in a cryogenic windtunnel
[HTN-95-92833] p 470 A95-90751
- Algorithmic trends in computational fluid dynamics; The Institute for Computer Applications in Science and Engineering (ICASE)/LaRC Workshop, NASA Langley Research Center, Hampton, VA, US, Sep. 15-17, 1991
[ISBN 0-387-94014-6] p 550 A95-91915
- Comparison of coordinate-invariant and coordinate-aligned upwinding for the Euler equations
[HTN-95-A1753] p 633 A95-93316
- Aircraft nose gear shimmy studies
[SAE PAPER 931401] p 628 A95-93671
- An electromechanically controlled semi-active landing gear
[SAE PAPER 931403] p 605 A95-93673
- Evaluation of a multigrid-based Navier-Stokes solver for aerothermodynamic computations
[BTN-95-EIX95302694459] p 583 A95-94056
- Quantifiable vortex features of F-106B aircraft at subsonic speeds
[BTN-95-EIX0619952748161] p 588 A95-94455
- Comparison of the predictive capabilities of several turbulence models
[BTN-95-EIX0619952748167] p 589 A95-94461
- In-flight pressure measurements on a subsonic transport high-lift wing section
[BTN-95-EIX0619952748170] p 589 A95-94464
- Actuated forebody strake controls for the F-18 High-Alpha Research Vehicle
[BTN-95-EIX0619952748173] p 619 A95-94467
- Implicit upwind-Euler solution algorithms for unstructured-grid applications
[NASA-TM-4549] p 641 A95-95454
- Effect of leading- and trailing-edge flaps on clipped delta wings with and without wing camber at supersonic speeds
[NASA-TM-4542] p 5 A95-10028
- Effect of passive venting on static pressure distributions in cavities at subsonic and transonic speeds
[NASA-TM-4549] p 6 A95-10029
- Two-dimensional converging-diverging rippled nozzles at transonic speeds
[NASA-TP-3440] p 6 A95-10129
- Extended cooperative control synthesis
[NASA-TM-4561] p 17 A95-10220
- Fly-By-Light/Power-By-Wire Requirements and Technology Workshop
[NASA-CP-10108] p 12 A95-10245
- Langley overview
[NASA-TM-109891] p 20 A95-10547
- Airborne Windshear Detection and Warning Systems. Fifth and Final Combined Manufacturers' and Technologists' Conference, part 1
[NASA-CP-10139-PT-1] p 10 A95-10566
- Vertical wind estimation from horizontal wind measurements
[NASA-TM-109157] p 26 A95-10567
- Characteristics of a dry, pulsating microburst at Denver Stapleton Airport
[NASA-TM-109157] p 26 A95-10568
- The NASA Langley 8-1001 Transonic Pressure Tunnel calibration
[NASA-TP-3437] p 8 A95-10739
- Computer-aided light sheet flow visualization using photogrammetry
[NASA-TP-3416] p 26 A95-10859
- High-Alpha Research Vehicle (HARV) longitudinal controller: Design, analyses, and simulation results
[NASA-TP-3446] p 17 A95-10860
- Formal design and verification of a reliable computing platform for real-time control (phase 3 results)
[NASA-TM-109140] p 33 A95-10873
- Design and evaluation of candidate pressure ports for the HYFLITE experiment
[NASA-TM-109146] p 22 A95-11003
- The use of the Regier number in the structural design with flutter constraints
[NASA-TM-109128] p 13 A95-11465
- Effects of vibration on inertial wind-tunnel model attitude measurement devices
[NASA-TM-109083] p 21 A95-11466
- Potential impacts of advanced aerodynamic technology on air transportation system productivity
[NASA-TM-109154] p 10 A95-11489
- Accurate interlaminar stress recovery from finite element analysis
[NASA-TM-109149] p 57 A95-11815
- Modeling and life prediction methodology for Titanium Matrix Composites subjected to mission profiles
[NASA-TM-109148] p 55 A95-11915
- Computer code for determination of thermally perfect gas properties
[NASA-TP-3447] p 37 A95-11995
- Application of two procedures for dual-point design of transonic airfoils
[NASA-TP-3466] p 38 A95-12176
- En route noise levels from propfan test assessment airplane
[NASA-TP-3451] p 62 A95-12341
- Ten-year ground exposure of composite materials used on the Bell Model 206L helicopter flight service program
[NASA-TP-3468] p 55 A95-12357
- Flight test of takeoff performance monitoring system
[NASA-TP-3403] p 51 A95-12664
- Experimental aerodynamic characteristics of a generic hypersonic accelerator configuration at Mach numbers 1.5 and 2.0
[NASA-TM-4413] p 39 A95-12770
- NASA's Hypersonic Research Engine Project: A review
[NASA-TM-107759] p 50 A95-12860
- Planar Rayleigh scattering and laser-induced fluorescence for visualization of a hot, Mach 2 annular air jet
[NASA-TM-4576] p 54 A95-13196
- Airborne Windshear Detection and Warning Systems. Fifth and Final Combined Manufacturers' and Technologists' Conference, part 2
[NASA-CP-10139-PT-2] p 41 A95-13203
- Windshear certification data base for forward-look detection systems
[NASA-TM-4576] p 41 A95-13204
- Certification methodology applied to the NASA experimental radar system
[NASA-CP-10139-PT-2] p 41 A95-13205
- Simultaneous three-dimensional velocity and mixing measurements by use of laser Doppler velocimetry and fluorescence probes in a water tunnel
[NASA-TP-3454] p 53 A95-13553
- A review of 50 years of aerodynamic research with NACA/NASA
[NASA-TM-109163] p 102 A95-13663
- Spiral microstrip antenna with resistance
[NASA-CASE-LAR-15088-1] p 91 A95-14139
- Base passive porosity for drag reduction
[NASA-CASE-LAR-15246-1] p 91 A95-14183
- High Alpha Technology Program (HATP) ground test to flight comparisons
[NASA-CP-3274-PT-2] p 68 A95-14230
- Comparison of X-31 flight, wind-tunnel, and water-tunnel yawing moment asymmetries at high angles of attack
[NASA-TP-3454] p 68 A95-14234
- Flight validation of ground-based assessment for control power requirements at high angles of attack
[NASA-CP-3274-PT-2] p 70 A95-14246
- High angle of attack flying qualities criteria for longitudinal rate command systems
[NASA-CP-3274-PT-2] p 70 A95-14247
- Preparations for flight research to evaluate actuated forebody strakes on the F-18 high-alpha research vehicle
[NASA-CP-3274-PT-2] p 72 A95-14257
- Airplane takeoff and landing performance monitoring system
[NASA-CASE-LAR-14745-2-SB] p 85 A95-14415
- FAA/NASA International Symposium on Advanced Structural Integrity Methods for Airframe Durability and Damage Tolerance
[NASA-CP-3274-PT-1] p 92 A95-14453
- Influence of crack history on the stable tearing behavior of a thin-sheet material with multiple cracks
[NASA-TM-4577] p 93 A95-14467
- Spatial awareness comparisons between large-screen, integrated pictorial displays and conventional EFIS displays during simulated landing approaches
[NASA-TP-3467] p 80 A95-14852
- High-Speed Research: 1994 Sonic Boom Workshop: Atmospheric Propagation and Acceptability Studies
[NASA-CP-3279] p 75 A95-14878
- An optical technique for examining aircraft shock wave structures in flight
[NASA-TM-109152] p 96 A95-14879
- Heavy rain effects
[NASA-TM-109152] p 78 A95-14899
- The characterization of widespread fatigue damage in fuselage structure
[NASA-TM-109142] p 88 A95-14920
- Research and technology highlights, 1993
[NASA-TM-4575] p 102 A95-15065
- Wind-tunnel blockage and actuation systems test of a two-dimensional scramjet inlet unstart model at Mach 6
[NASA-TM-109152] p 97 A95-15898
- Two-dimensional scramjet inlet unstart model: Wind-tunnel blockage and actuation systems test
[NASA-TM-109984] p 97 A95-15899
- Experimental study at low supersonic speeds of a missile concept having opposing wraparound tails
[NASA-TM-4582] p 106 A95-16069
- A study of software standards used in the avionics industry
[NASA-TM-4582] p 137 A95-16456
- Rapid solution of large-scale systems of equations
[NASA-TM-4582] p 169 A95-16458
- Applications of automatic differentiation in computational fluid dynamics
[NASA-TM-109948] p 156 A95-16461
- Matlab as a robust control design tool
[NASA-TM-109948] p 169 A95-16474
- Measurements of unsteady pressure and structural response for an elastic supercritical wing
[NASA-TP-3443] p 104 A95-16560
- Applications of automatic differentiation in CFD
[NASA-TM-109948] p 157 A95-16828
- Comparison of computational and experimental results for a supercritical airfoil
[NASA-TM-4601] p 108 A95-16908
- Modeling of Instrument Landing System (ILS) localizer signal on runway 25L at Los Angeles International Airport
[NASA-TM-4588] p 125 A95-17384
- Active load control during rolling maneuvers
[NASA-TP-3455] p 129 A95-17397
- Single-engine tail interference model
[NASA-TM-4588] p 115 A95-17879
- Twin engine afterbody model
[NASA-TM-4588] p 115 A95-17880
- Microburst vertical wind estimation from horizontal wind measurements
[NASA-TP-3460] p 131 A95-18198
- Special effects of gust loads on military aircraft
[NASA-TM-4588] p 133 A95-18605
- Dynamic Stability Instrumentation System (DSIS). Volume 1: Hardware description
[NASA-TM-109160-VOL-1] p 171 A95-18899
- Static investigation of two fluidic thrust-vectoring concepts on a two-dimensional convergent-divergent nozzle
[NASA-TM-4574] p 120 A95-19042
- Navier-Stokes, flight, and wind tunnel flow analysis for the F/A-18 aircraft
[NASA-TP-3478] p 120 A95-19114
- Impact of dynamic loads on propulsion integration
[NASA-TM-4574] p 174 A95-19148
- FAA/NASA International Symposium on Advanced Structural Integrity Methods for Airframe Durability and Damage Tolerance, part 2
[NASA-CP-3274-PT-2] p 124 A95-19468
- The characterization of widespread fatigue damage in fuselage structure
[NASA-TM-4574] p 166 A95-19472
- Nonlinear analysis of damaged stiffened fuselage shells subjected to combined loads
[NASA-TM-4574] p 137 A95-19499
- Static investigation of two fluidic thrust-vectoring concepts on a two-dimensional convergent-divergent nozzle
[NASA-TM-4574] p 222 A95-19913
- Vapor generator wand
[NASA-CASE-LAR-15058-1] p 238 A95-20080
- Parallel calculation of sensitivity derivatives for aircraft design using automatic differentiation
[NASA-TM-110103] p 231 A95-20370
- 16-foot transonic tunnel test section flowfield survey
[NASA-TM-109157] p 238 A95-20669
- The personal aircraft: Status and issues
[NASA-TM-109174] p 223 A95-20688
- Why do airlines want and use thrust reversers? A compilation of airline industry responses to a survey regarding the use of thrust reversers on commercial transport airplanes
[NASA-TM-109158] p 226 A95-20706
- Acoustic receptivity due to weak surface inhomogeneities in adverse pressure gradient boundary layers
[NASA-TM-4577] p 249 A95-21258
- Application of Navier-Stokes code PAB3D with kappa-epsilon turbulence model to attached and separated flows
[NASA-TP-3480] p 224 A95-21338
- Effects of yaw and pitch motion on model attitude measurements
[NASA-TM-4641] p 250 A95-22109
- Wing pressure distributions from subsonic tests of a high-wing transport model
[NASA-TM-4583] p 272 A95-22802
- Integrated aerodynamic/dynamic/structural optimization of helicopter rotor blades using multilevel decomposition
[NASA-TP-3465] p 285 A95-22953
- Compendium of NASA data base for the Global Tropospheric Experiment's Pacific Exploratory Mission West-A (PEM West-A)
[NASA-TM-109177] p 320 A95-23009
- Dynamic response tests of inertial and optical wind-tunnel model attitude measurement devices
[NASA-TM-109182] p 296 A95-23011
- Mach 10 computational study of a three-dimensional scramjet inlet flow field
[NASA-TM-4602] p 309 A95-23015
- Mach 10 computational study of a three-dimensional scramjet inlet flow field
[NASA-TM-4602] p 310 A95-23210

- New nondestructive techniques for the detection and quantification of corrosion in aircraft structures p 315 N95-23512
- DSMC calculations for 70-deg blunted cone at 3.2 km/s in nitrogen [NASA-TM-109181] p 348 N95-24396
- Performance of an aerodynamic yaw controller mounted on the space shuttle orbiter body flap at Mach 10 [NASA-TM-109179] p 330 N95-24397
- A crew-centered flight deck design philosophy for High-Speed Civil Transport (HSCT) aircraft [NASA-TM-109171] p 335 N95-24582
- Aviation system capacity improvements through technology [NASA-TM-109165] p 333 N95-24633
- Internal performance characteristics of thrust-vectoring axisymmetric ejector nozzles [NASA-TM-4610] p 331 N95-25338
- Design and evaluation of a foam-filled hat-stiffened panel concept for aircraft primary structural applications [NASA-TM-109175] p 346 N95-26251
- Flutter clearance flight tests of an OV-10A airplane modified for wake vortex flight experiments [NASA-TM-109168] p 366 N95-26381
- Airfoil modification effects on subsonic and transonic pressure distributions and performance for the EA-6B airplane [NASA-TP-3516] p 373 N95-26382
- Aircraft noise prediction program theoretical manual: Rotorcraft System Noise Prediction System (ROTONET), part 4 [NASA-TM-83199-PT-4] p 451 N95-26392
- Radiation safety aspects of commercial high-speed flight transportation [NASA-TP-3524] p 453 N95-26427
- Incorporating biplane wing theory into a large, subsonic, all-cargo transport p 391 N95-26956
- A study of workstation computational performance for real-time flight simulation [NASA-TM-109184] p 449 N95-27241
- Hardware cleanliness methodology and certification p 419 N95-27656
- Modeling of aircraft unsteady aerodynamic characteristics. Part 2: Parameters estimated from wind tunnel data [NASA-TM-110161] p 410 N95-27839
- A numerical study of fundamental shock noise mechanisms [NASA-TM-110608] p 451 N95-27908
- Measurements of store forces and moments and cavity pressures for a generic store in and near a box cavity at subsonic and transonic speeds [NASA-TM-4611] p 378 N95-28241
- Resin transfer molding of textile preforms for aircraft structural applications p 421 N95-28276
- Experimental investigation of inlet-combustor isolators for a dual-mode scramjet at a Mach number of 4 [NASA-TP-3502] p 407 N95-28343
- Effects of floor location on response of composite fuselage frames p 423 N95-28439
- Overview of the ACT program p 424 N95-28463
- Designers' unified cost model p 424 N95-28464
- Composite fuselage shell structures research at NASA Langley Research Center p 425 N95-28466
- Technology integration box beam failure study p 441 N95-28468
- Development of stitched/RTM composite primary structures p 425 N95-28469
- Test and analysis results for composite transport fuselage and wing structures p 398 N95-28470
- Tension fracture of laminates for transport fuselage. Part 1: Material screening p 398 N95-28471
- Recent progress in NASA Langley textile reinforced composites program p 425 N95-28475
- Effect of low-speed impact damage and damage location on behavior of composite panels p 426 N95-28481
- Damage tolerance of a geodesically stiffened advanced composite structural concept for aircraft structural applications p 399 N95-28487
- Study of potential aerodynamic benefits from spanwise blowing at wingtip [NASA-TP-3515] p 378 N95-28669
- Numerical study to assess sulfur hexafluoride as a medium for testing multielement airfoils [NASA-TP-3496] p 378 N95-28674
- Rapid Airplane Parametric Input Design (RAPID) p 501 N95-28730
- Algorithms for high aspect ratio oriented triangulations p 476 N95-28731
- Block-structured grids for complex aerodynamic configurations: Current status p 551 N95-28736
- An unstructured-grid software system for solving complex aerodynamic problems p 476 N95-28743
- An efficiency study of the simultaneous analysis and design of structures [NASA-TM-110168] p 501 N95-28820
- Third NASA Advanced Composites Technology Conference, volume 1, part 2 [NASA-CP-3178-VOL-1-PT-2] p 531 N95-28823
- Tension fracture of laminates for transport fuselage. Part 2: Large notches p 532 N95-28837
- Design and evaluation of a foam-filled hat-stiffened panel concept for aircraft primary structural applications p 502 N95-28841
- Buckling analysis of curved composite sandwich panels subjected to inplane loadings p 533 N95-28845
- Technology integration box beam failure study p 552 N95-28847
- A global/local analysis method for treating details in structural design p 552 N95-28848
- Third NASA Advanced Composites Technology Conference, volume 1, part 1 [NASA-CP-3178-VOL-1-PT-1] p 534 N95-29029
- Advanced composites technology program p 534 N95-29032
- Weavability of dry polymer powder towpreg p 535 N95-29036
- Mechanical characterization of 2D, 2D stitched, and 3D braided/RTM materials p 535 N95-29038
- Performance of resin transfer molded multiaxial warp knit composites p 535 N95-29039
- The effects of aircraft fuel and fluids on the strength properties of Resin Transfer Molded (RTM) composites p 536 N95-29047
- An extension of the Lighthill theory of jet noise to encompass refraction and shielding [NASA-TM-110163] p 580 N95-29452
- A hybrid electronically scanned pressure module for cryogenic environments [NASA-TM-110146] p 554 N95-29453
- Transport delays associated with NASA Langley Flight Simulation Facility [NASA-TM-110150] p 568 N95-29454
- Low-speed wind-tunnel investigation of the stability and control characteristics of a series of flying wings with sweep angles of 50 deg [NASA-TM-4640] p 505 N95-30226
- Manual for a workstation-based generic flight simulation program (LaRCsim), version 1.4 [NASA-TM-110164] p 518 N95-30327
- Structural design using equilibrium programming formulations [NASA-TM-110175] p 645 N95-30682
- Orbiter rarefied-flow reentry measurements from the OARE on STS-62 [NASA-TM-110182] p 646 N95-30783
- A wind tunnel investigation of the effects of micro-vortex generators and Gurney flaps on the high-lift characteristics of a business jet wing [NASA-TM-110626] p 607 N95-30827
- Patterns in the sky: Natural visualization of aircraft flow fields [NASA-SP-514] p 584 N95-31000
- Afterbody/nozzle pressure distributions of a twin-tail twin-engine fighter with axisymmetric nozzles at Mach numbers from 0.6 to 1.2 [NASA-TP-3509] p 594 N95-31984
- Computer model to simulate testing at the National Transonic Facility [NASA-TM-4664] p 627 N95-32217
- A highly reliable, high performance open avionics architecture for real time Nap-of-the-Earth operations p 693 N95-32497
- Drag measurements of an axisymmetric nacelle mounted on a flat plate at supersonic speeds [NASA-TM-4660] p 684 N95-32821
- National Aeronautics and Space Administration. Lewis Research Center, Cleveland, OH.**
- Effect of wind tunnel acoustic modes on linear oscillating cascade aerodynamics [HTN-94-00760] p 14 A95-60199
- Marangoni-Bernard convection in a low-aspect-ratio liquid layer p 56 A95-61544
- Repeatability of ice shapes in the NASA Lewis icing research tunnel [BTN-95-EIX95062487528] p 204 A95-69236
- Flow structure in the wake of a wishbone vortex generator [BTN-95-EIX95142553044] p 304 A95-73454
- Integrated flight/propulsion control for helicopters [HTN-95-80854] p 290 A95-75096
- Numerical analysis of hypersonic low-density scramjet inlet flow [BTN-95-EIX95212645694] p 272 A95-76746
- Structure of supersonic jet flow and its radiated sound [HTN-95-51645] p 431 A95-85027
- Practical formulation of a positively conservative scheme [HTN-95-51668] p 433 A95-85050
- Stationary premixed flames in spherical and cylindrical geometries [HTN-95-42336] p 418 A95-86165
- Enhanced mixing of multiple supersonic rectangular jets by synchronized screech [HTN-95-42592] p 459 A95-87222
- Airfoil pressure measurements during oblique shock-wave/vortex interaction in a Mach 3 stream [HTN-95-81641] p 542 A95-87689
- Numerical study of contaminant effects on combustion of hydrogen, ethane, and methane in air [AIAA PAPER 95-6097] p 510 A95-88005
- Symposium on Aerodynamics & Aeroacoustics, Tucson, AZ, Mar. 1-2, 1993 [ISBN 981-02-1732-3] p 462 A95-88892
- Unsteady aerodynamics of vortical flows: Early and recent developments p 462 A95-88896
- Design and operation of a supersonic annular flow facility [HTN-95-20941] p 465 A95-88980
- Noise control in aeroacoustics; Proceedings of the 1993 National Conference on Noise Control Engineering, NOISE-CON 93, Williamsburg, VA, May 2-5, 1993 [ISBN 0-931784-26-3] p 573 A95-90088
- A large hemi-anechoic enclosure for community-compatible aeroacoustic testing of aircraft propulsion systems p 577 A95-90132
- Operating capability and current status of the reactivated NASA Lewis Research Center hypersonic tunnel facility [AIAA PAPER 95-6146] p 521 A95-90461
- Parallel computational fluid dynamics '91; Conference Proceedings, Stuttgart, Germany, Jun. 10-12, 1991 [ISBN 0-444-89363-6] p 548 A95-91479
- Power system characteristics for more electric aircraft [SAE PAPER 931406] p 613 A95-93675
- Experimental performance of a ventral nozzle with pitch and yaw vectoring capability for SSTOVL aircraft [SAE PAPER 931412] p 614 A95-93678
- 3-D Navier-Stokes analysis of crossing glancing shocks/turbulent boundary layer interactions [BTN-95-EIX95302729768] p 636 A95-94130
- Computational fluid dynamics '92; Proceedings of the European Computational Fluid Dynamics Conference, 1st, Brussels, Belgium, Sep. 7-11, 1992. Vols. 1 & 2 [ISBN 0-444-89793-3] p 638 A95-95357
- Effects of a forward-swept front rotor on the flowfield of a counterrotation propeller [NASA-TM-106671] p 7 N95-10148
- An aerodynamic analysis of a mixed flow turbine [NASA-TM-106674] p 15 N95-10153
- Flutter analysis of supersonic axial flow cascades using a high resolution Euler solver. Part 1: Formulation and validation [NASA-TM-105798] p 23 N95-10244
- NASA Lewis Propulsion Systems Laboratory test article systems criteria [NASA-TM-106589] p 20 N95-10446
- A full Navier-Stokes analysis of subsonic diffuser of a bifurcated 70/30 supersonic inlet for high speed civil transport application [NASA-TM-106637] p 8 N95-10820
- NASA Lewis Propulsion Systems Laboratory customer guide manual [NASA-TM-106569] p 21 N95-10822
- Control of wind tunnel operations using neural net interpretation of flow visualization records [NASA-TM-106683] p 24 N95-10854
- Inlet flow test calibration for a small axial compressor facility. Part 1: Design and experimental results [NASA-TM-106719] p 16 N95-11005
- Application of an integrated methodology for propulsion and airframe control design to a STOVL aircraft [NASA-TM-106729] p 16 N95-11159
- Fan noise research at NASA p 28 N95-11260
- Radiant energy measurements from a scaled jet engine axisymmetric exhaust nozzle for a baseline code validation case [NASA-TM-106686] p 25 N95-11409
- Brush seal performance and durability issues based on T-700 engine test results [NASA-TM-106502] p 22 N95-11483
- Object-oriented technology for compressor simulation [NASA-TM-106723] p 49 N95-11864
- The development of a highly reliable power management and distribution system for civil transport aircraft [NASA-TM-106697] p 50 N95-11867
- Structure of a swirl-stabilized, combustor spray [NASA-TM-106724] p 50 N95-11890
- Modification of the two-equation turbulence model in NPARC to a Chien low Reynolds number k-epsilon formulation [NASA-TM-106710] p 37 N95-11917
- A new algorithm for five-hole probe calibration, data reduction, and uncertainty analysis [NASA-TM-106458] p 38 N95-12378
- Piloted evaluation of an integrated methodology for propulsion and airframe control design [AD-A290207] p 51 N95-12763

- Analytical and experimental vibration analysis of a faulty gear system
[NASA-TM-106689] p 58 N95-12843
- Validation of the RPLUS3D code for supersonic inlet applications involving three-dimensional shock wave-boundary layer interactions
[NASA-TM-106579] p 39 N95-13058
- Role of wind tunnels and computer codes in the certification and qualification of rotorcraft for flight in forecast icing
[NASA-TM-106747] p 39 N95-13197
- Activities of the Structures Division, Lewis Research Center
[NASA-TM-108081] p 59 N95-13235
- Hypersonic engine seal development at NASA Lewis Research Center
[NASA-TM-106742] p 60 N95-13602
- Computational analysis in support of the SSTO flowpath test
[NASA-TM-106757] p 89 N95-13665
- A Cartesian, cell-based approach for adaptively-refined solutions of the Euler and Navier-Stokes equations
[NASA-TM-106786] p 73 N95-14297
- Hypersonic engine leading edge experiments in a high heat flux, supersonic flow environment
[NASA-TM-106742] p 91 N95-14299
- Axis switching and spreading of an asymmetric jet: Role of vorticity dynamics
[NASA-TM-106385] p 73 N95-14418
- Characterization of annular two-phase gas-liquid flows in microgravity
[NASA-TM-106742] p 95 N95-14556
- Graphical user interface for the NASA FLOPS aircraft performance and sizing code
[NASA-TM-106649] p 80 N95-14604
- Noise radiation by instability waves in coaxial jets
[NASA-TM-106738] p 100 N95-14618
- Icing: Accretion, detection, protection
[NASA-TM-106782] p 77 N95-14897
- The aeroacoustics of supersonic coaxial jets
[NASA-TM-106782] p 101 N95-15059
- An approach for dynamic grids
[NASA-TM-106774] p 76 N95-15853
- Sensor fault detection and diagnosis simulation of a helicopter engine in an intelligent control framework [AD-A290223] p 137 N95-15970
- Numerical simulation of supersonic compression corners and hypersonic inlet flows using the RPLUS2D code
[NASA-TM-106580] p 105 N95-16038
- Airfoil optimization by the one-shot method
[NASA-TM-106799] p 128 N95-16569
- Static and dynamic friction behavior of candidate high temperature airframe seal materials
[NASA-TM-106571] p 152 N95-16905
- A workstation based simulator for teaching compressible aerodynamics
[NASA-TM-106799] p 170 N95-16906
- Optimization of adaptive intraply hybrid fiber composites with reliability considerations
[NASA-TM-106632] p 157 N95-16911
- Interactive computer graphics applications for compressible aerodynamics
[NASA-TM-106802] p 170 N95-17264
- Microgravity isolation system design: A case study
[NASA-TM-106804] p 104 N95-17657
- Background noise levels measured in the NASA Lewis 9- by 15-foot low-speed wind tunnel
[NASA-TM-106817] p 145 N95-18054
- Numerical mixing calculations of confined reacting jet flows in a cylindrical duct
[NASA-TM-106736] p 139 N95-18133
- Microgravity isolation system design: A modern control synthesis framework
[NASA-TM-106805] p 105 N95-18197
- Measurement of gust response on a turbine cascade
[NASA-TM-106776] p 117 N95-18457
- Microgravity isolation system design: A modern control analysis framework
[NASA-TM-106803] p 105 N95-18486
- Collection efficiency and ice accretion calculations for a sphere, a swept MS(1)-317 wing, a swept NACA-0012 wing tip, an axisymmetric inlet, and a Boeing 737-300
[NASA-TM-106831] p 123 N95-18582
- Users guide for NASA Lewis Research Center DC-9 Reduced-Gravity Aircraft Program
[NASA-TM-106755] p 146 N95-18586
- Enhanced capabilities and modified users manual for axial-flow compressor conceptual design code CSPAN
[NASA-TM-106833] p 119 N95-18933
- Detecting gear tooth fracture in a high contact ratio face gear mesh
[NASA-TM-106822] p 162 N95-19125
- Methods for scaling icing test conditions
[NASA-TM-106827] p 124 N95-19284
- Ice accretion with varying surface tension
[NASA-TM-106826] p 124 N95-19285
- Operating capability and current status of the reactivated NASA Lewis Research Center Hypersonic Tunnel Facility
[NASA-TM-106808] p 148 N95-19286
- NASA Lewis Research Center Workshop on Forced Response in Turbomachinery
[NASA-CP-10147] p 141 N95-19380
- Steady potential solver for unsteady aerodynamic analyses
[NASA-TM-106785] p 167 N95-19501
- Technology Benefit Estimator (T/BEST): User's manual
[NASA-TM-106785] p 167 N95-19501
- Ice-impact analysis of blades
[NASA-TM-106785] p 200 N95-19672
- Resistance of silicon nitride turbine components to erosion and hot corrosion/oxidation attack
[NASA-TM-106785] p 202 N95-19683
- Improved speed control system for the 87,000 HP wind tunnel drive
[NASA-TM-106840] p 211 N95-19794
- Flow coefficient behavior for boundary layer bleed holes and slots
[NASA-TM-106846] p 244 N95-19953
- Application of pressure sensitive paint in hypersonic flows
[NASA-TM-106824] p 223 N95-20794
- Two-dimensional imaging of OH in a lean burning high pressure combustor
[NASA-TM-106854] p 236 N95-21383
- Additional improvements to the NASA Lewis ice accretion code LEWICE
[NASA-TM-106849] p 309 N95-22669
- Stable H(infinity) controller design for the longitudinal dynamics of an aircraft
[NASA-TM-106847] p 293 N95-22954
- Supersonic jet noise reductions predicted with increased jet spreading rate
[NASA-TM-106872] p 323 N95-23178
- NASA low-speed axial compressor for fundamental research
[NASA-TM-4635] p 296 N95-23192
- Design of a GaAs/Ge solar array for unmanned aerial vehicles
[NASA-TM-106870] p 320 N95-23259
- A time-accurate finite volume method valid at all flow velocities
[NASA-TM-106872] p 314 N95-23447
- Sensitivity of combustion-acoustic instabilities to boundary conditions for premixed gas turbine combustors
[NASA-TM-106890] p 289 N95-23550
- Motor drive technologies for the power-by-wire (PBW) program: Options, trends and tradeoffs
[NASA-TM-106885] p 295 N95-23671
- Research and Technology, 1994
[NASA-TM-106764] p 262 N95-24025
- The 1994 Fiber Optic Sensors for Aerospace Technology (FOSAT) Workshop
[NASA-CP-10166] p 337 N95-24207
- Crossflow mixing of noncircular jets
[NASA-TM-106865] p 338 N95-24390
- The effect of altitude conditions on the particle emissions of a J85-GE-5L turbojet engine
[NASA-TM-106669] p 339 N95-24561
- Assessment of avionics technology in European aerospace organizations
[NASA-CR-189201] p 337 N95-24624
- Recent improvements to and validation of the one dimensional NASA wave rotor model
[NASA-TM-106913] p 332 N95-25962
- A combined geometric approach for solving the Navier-Stokes equations on dynamic grids
[NASA-TM-106919] p 332 N95-26075
- Thermal Barrier Coating Workshop
[NASA-CP-10170] p 344 N95-26119
- Thermal barrier coatings for aircraft engines: History and directions
[NASA-TM-106913] p 344 N95-26121
- Jet mixer noise suppressor using acoustic feedback
[NASA-CASE-LEW-15170-2] p 362 N95-26187
- Supersonic coaxial jet noise predictions
[NASA-TM-106917] p 451 N95-26801
- The high speed civil transport and NASA's High Speed Research (HSR) program
[NASA-TM-106917] p 390 N95-26945
- Visualization of the multiple supersonic jet oscillations by swept focused strobed schlieren technique
[NASA-TM-106917] p 367 N95-26952
- NASA Lewis Research Center's combustor test facilities and capabilities
[NASA-TM-106903] p 412 N95-27176
- Comparison of numerical results and multicavity purge and rim seal data with extensions to dynamics
[NASA-TM-106685] p 416 N95-27434
- Further investigations of icing effects on an advanced high-lift multi-element airfoil
[NASA-TM-106947] p 381 N95-27762
- Two-phase flow research using the learjet apparatus
[NASA-TM-106814] p 438 N95-27854
- Optimization of wave rotors for use as gas turbine engine topping cycles
[NASA-TM-106951] p 406 N95-27860
- Industry-Wide Workshop on Computational Turbulence Modeling
[NASA-CP-10165] p 439 N95-27882
- Analysis of aircraft engine blade subject to ice impact
[NASA-TM-106951] p 407 N95-28277
- Numerical analysis of intra-cavity and power-stream flow interaction in multiple gas-turbine disk-cavities
[NASA-TM-106886] p 407 N95-28344
- Probabilistic evaluation of fuselage-type composite structures
[NASA-TM-106886] p 398 N95-28444
- Influence of turbulence parameters, Reynolds number, and body shape on stagnation-region heat transfer
[NASA-TP-3487] p 550 N95-28719
- Surface Modeling, Grid Generation, and Related Issues in Computational Fluid Dynamic (CFD) Solutions
[NASA-CP-3291] p 476 N95-28723
- Surface modeling and grid generation for aeropropulsion CFD
[NASA-TM-106952] p 551 N95-28732
- IPACS (Integrated Probabilistic Assessment of Composite Structures): Code development and applications
[NASA-TM-106952] p 534 N95-28849
- Influence of tooth-profile modification on spur-gear dynamic tooth strain
[NASA-TM-106952] p 553 N95-29112
- Leading edge film cooling effects on turbine blade heat transfer
[NASA-TM-106955] p 513 N95-29115
- Grid orthogonality effects on predicted turbine midspan heat transfer and performance
[NASA-TM-106931] p 554 N95-29371
- Acoustic scattering from ellipses by the modal element method
[NASA-TM-106935] p 579 N95-29401
- Inlet flow test calibration for a small axial compressor rig. Part 2: CFD compared with experimental results
[NASA-TM-106999] p 514 N95-30007
- Use of the PARC code to estimate the off-design transonic performance of an over/under turboramjet nozzle
[NASA-TM-106924] p 482 N95-30091
- Laser doppler velocimeter system for subsonic jet mixer nozzle testing at the NASA Lewis Aeroacoustic Propulsion Lab
[NASA-TM-106984] p 457 N95-30229
- Grid resolution and turbulent inflow boundary condition recommendations for NPARC calculations
[NASA-TM-106959] p 482 N95-30253
- Wave rotor-enhanced gas turbine engines
[NASA-TM-106998] p 615 N95-30517
- The effect of adding roughness and thickness to a transonic axial compressor rotor
[NASA-TM-106958] p 645 N95-30524
- Fabry-Perot interferometer measurement of static temperature and velocity for ASTOVL model tests
[NASA-TM-107014] p 645 N95-30587
- Effects of initial conditions on a single jet in crossflow
[NASA-TM-107002] p 615 N95-30589
- NASA Lewis Research Center's preheated combustor and materials test facility
[NASA-TM-106676] p 626 N95-30592
- Object-oriented approach for gas turbine engine simulation
[NASA-TM-106970] p 615 N95-30594
- A numerical model for dynamic wave rotor analysis
[NASA-TM-106997] p 615 N95-30617
- Preliminary assessment of combustion modes for internal combustion wave rotors
[NASA-TM-107000] p 616 N95-30632
- Jet mixing and emission characteristics of transverse jets in annular and cylindrical confined crossflow
[NASA-TM-106976] p 616 N95-30698
- Effect of velocity and temperature distribution at the hole exit on film cooling of turbine blades
[NASA-TM-106954] p 616 N95-30702
- Validation of the NPARC code for nozzle afterbody flows at transonic speeds
[NASA-TM-106971] p 592 N95-30704
- A laser-based ice shape profilometer for use in icing wind tunnels
[NASA-TM-106936] p 646 N95-30851
- Jet mixing in a reacting cylindrical crossflow
[NASA-TM-106975] p 616 N95-30853
- Parametrics on 2D Navier-Stokes analysis of a Mach 2.68 bifurcated rectangular mixed-compression inlet
[NASA-TM-107003] p 617 N95-30861
- Experimental and computational investigation of the tip clearance flow in a transonic axial compressor rotor
[NASA-TM-106711] p 649 N95-31738
- Laser anemometer measurements of the three-dimensional rotor flow field in the NASA low-speed centrifugal compressor
[NASA-TP-3527] p 618 N95-31985

- A probabilistic design method applied to smart composite structures
[NASA-TM-106715] p 651 N95-32206
- Steady-state dynamic behavior of an auxiliary bearing supported rotor system p 703 N95-32690
- Investigation of water droplet trajectories within the NASA icing research tunnel
[NASA-TM-107023] p 684 N95-32769
- Low-order nonlinear dynamic model of IC engine-variable pitch propeller system for general aviation aircraft
[NASA-TM-107006] p 694 N95-32916
- Review of combustion-acoustic instabilities
[NASA-TM-107020] p 705 N95-32930
- Combustion-acoustic stability analysis for premixed gas turbine combustors
[NASA-TM-107024] p 694 N95-32931
- National Aeronautics and Space Administration.**
Marshall Space Flight Center, Huntsville, AL.
- Aircraft electric field measurements: Calibration and ambient field retrieval
[HTN-95-90508] p 213 A95-67780
- High-resolution imaging of rain systems with the advanced microwave precipitation radiometer
[HTN-95-70133] p 252 A95-70655
- Behavior of an inversion-based precipitation retrieval algorithm with high-resolution AMPR measurements including a low-frequency 10.7-GHz channel
[HTN-95-70134] p 252 A95-70656
- Guidance and control, 1993; Annual Rocky Mountain Guidance and Control Conference, 16th, Keystone, CO, Feb. 6-10, 1993
[ISBN-0-87703-365-X] p 341 A95-80389
- Parameters of Nocilla gas/surface interaction model from measured accommodation coefficients
[HTN-95-81639] p 541 A95-87687
- A programmable heater control circuit for spacecraft
[NASA-TM-108459] p 9 N95-11157
- A shadowgraph study of the National Launch System's 1 1/2 stage vehicle configuration and Heavy Lift Launch Vehicle configuration
[NASA-RP-1347] p 35 N95-11710
- Illustrated structural application of universal first-order reliability method
[NASA-TP-3501] p 54 N95-11870
- Building complex simulations rapidly using MATRIX(x): The Space Station redesign
[TABES PAPER 94-632] p 87 N95-14653
- Tuned mass damper for integrally bladed turbine rotor
[NASA-CASE-MFS-28697-1] p 159 N95-18325
- Validation of a Computational Fluid Dynamics (CFD) code for supersonic axisymmetric base flow
p 315 N95-23652
- Dynamically timed electric motor
[NASA-CASE-MFS-28958-1] p 437 N95-26890
- Bearing defect signature analysis using advanced nonlinear signal analysis in a controlled environment
[NASA-TM-108491] p 441 N95-28364
- Transonic aerodynamic characteristics of a proposed wing-body reusable launch vehicle concept
[NASA-TM-108489] p 592 N95-30712
- National Aeronautics and Space Administration.**
Pasadena Office, CA.
- Virtual reality flight control display with six-degree-of-freedom controller and spherical orientation overlay
[NASA-CASE-NPO-18733-1-CU] p 288 N95-22578
- National Aeronautics and Space Administration.**
Wallops Flight Center, Wallops Island, VA.
- A comparative study of internally and externally capped balloons using small scale test balloons
p 181 A95-66285
- Status of the NASA balloon program
p 181 A95-66296
- Overview of the NASA balloon R&D program
p 181 A95-66297
- National Aeronautics and Space Administration.**
Wallops Flight Facility, Wallops Island, VA.
- Orbital velocities induced by surface waves
[HTN-95-90902] p 253 A95-72411
- National Aerospace Lab., Amsterdam (Netherlands).**
- Reanalysis of European flight loads data
[AD-A282052] p 9 N95-11179
- Mach number control in the High Speed Wind Tunnel of NLR
[PB94-201670] p 53 N95-13243
- Residual-correction type and related computational methods for aerodynamic design. Part 1: Airfoil and wing design p 128 N95-16566
- Residual-correction type and related computational methods for aerodynamic design. Part 2: Multi-point airfoil design p 128 N95-16567
- Two-dimensional 16.5 percent thick supercritical airfoil NLR 7301 p 110 N95-17854
- Low-speed surface pressure and boundary layer measurement data for the NLR 7301 airfoil section with trailing edge flap p 111 N95-17855
- Wind tunnel test on a 65 deg delta wing with a sharp or rounded leading edge: The international vortex flow experiment p 114 N95-17872
- Sectional prediction of 3D effects for separated flow on rotating blades
[PB94-201696] p 117 N95-18503
- Results of uniaxial and biaxial tests on riveted fuselage lap joint specimens p 136 N95-19491
- Gas turbine compressor corrosion and erosion in Western Europe
[AD-B196178L] p 201 N95-19678
- Review of aeronautical fatigue investigation in the Netherlands during the period March 1991-March 1993
[PB95-139184] p 285 N95-23161
- Eddy current detection of pitting corrosion around fastener holes p 315 N95-23507
- Demonstration of an automated CFD system for three-dimensional flow simulations p 551 N95-28767
- Multigrid convergence acceleration for the 2D Euler equations applied to high-lift systems
[PB95-198081] p 593 N95-30814
- Development of advanced approach and departure procedures. Failure scenarios p 601 N95-30815
- Validation of the helicopter rotor code HERO
[PB95-198040] p 607 N95-30838
- National Aerospace Lab., Bangalore (India).**
- Experimental Aerodynamics Division
[NAL-SP-9404] p 35 N95-12166
- Ageing nuclear power plant management: An aeronautical viewpoint
[NAL-PD-SN-9306] p 105 N95-18606
- Solution of full potential equation on an airfoil by multigrid technique
[NAL-TM-CSS-9303] p 119 N95-18904
- CFD: Advances and Applications, part 1
[NAL-SP-9322-PT-1] p 165 N95-19444
- Computation of inviscid flows: Full potential method p 165 N95-19447
- Panel methods p 165 N95-19448
- Viscous flow past aerofoils axisymmetric bodies and wings p 123 N95-19457
- Computation of vortex breakdown p 165 N95-19462
- Parabolized Navier-Stokes solution of supersonic/hypersonic flows p 123 N95-19464
- National Aerospace Lab., Tokyo (Japan).**
- Aeroelastic tailoring research
[PB94-180031] p 6 N95-10135
- Computations of unsteady aerodynamic loads around oscillating wings. Part 1: Formulation
[PB94-180049] p 7 N95-10136
- Computations of unsteady aerodynamic loads around oscillating wings. Part 2: Computed results and discussions
[PB94-180056] p 7 N95-10137
- Study on tensile fatigue testing method of unidirectional fiber-resin matrix composites
[NAL-TR-1241] p 343 N95-24989
- Effect of film cooling/regenerative cooling on scramjet engine performances
[NAL-TR-1242] p 339 N95-24990
- Numerical and experimental study of drag characteristics of two-dimensional HLFC airfoils in high subsonic, high Reynolds number flow
[NAL-TR-1244T] p 331 N95-24998
- Preliminary experiments of an optical fiber display
[NAL-TR-1257] p 362 N95-25004
- Flight reference display for powered-lift STOL aircraft
[NAL-TR-1251] p 337 N95-25005
- Low speed aerodynamic characteristics of delta wings with vortex flaps: 60 deg and 70 deg delta wings
[NAL-TR-1245] p 331 N95-25105
- Aerodynamic characteristics of the orbital reentry vehicle experimental probe fins in a supersonic flow
[NAL-TR-1232] p 342 N95-25664
- Measurements of longitudinal static aerodynamic coefficients by the cable mount system
[NAL-TR-1226] p 331 N95-25761
- Fundamental wind tunnel experiments on low-speed flutter of a tip-fin configuration wing
[NAL-TR-1228] p 332 N95-25762
- Reentry guidance for hypersonic Flight Experiment (HYFLEX) vehicle
[NAL-TR-1235] p 334 N95-25764
- A quiet STOL Research Aircraft Development program
[NAL-TR-1223] p 336 N95-25862
- Numerical simulation of combustion flow around a flame holder with hydrogen injection
[NAL-TR-1233] p 419 N95-26523
- Experimental investigation of static and dynamic ground effect on HOPE ALFLEX vehicle
[NAL-TR-1238] p 388 N95-26525
- Flight evaluation of GPS/DGPS sensor systems installed in NAL Do228
[NAL-TR-1230] p 382 N95-26585
- Experiment on a rectangular cross section scramjet combustor. 2: Effects of fuel injector geometry
[NAL-TR-1220] p 405 N95-26600
- Effects of dust from storage heaters on ignition in scramjets
[NAL-TR-1234] p 405 N95-26706
- Effects of cavity bleed and its configuration on aerodynamic characteristics of supersonic internal flow
[NAL-TR-1247] p 594 N95-31715
- Special publication of National Aerospace Laboratory
[NAL-SP-27] p 684 N95-34505
- Numerical simulation of high enthalpy shock tunnel
p 700 N95-34514
- Hypersonic CFD analysis for the aerothermodynamic design of HOPE
p 684 N95-34520
- Direct numerical simulation of incompressible homogeneous isotropic turbulence using NWT
p 706 N95-34530
- Performance evaluation of the NWT with incompressible NS code p 707 N95-34533
- An unsteady simulation of a centrifugal compressor stage using the NWT p 707 N95-34536
- Application of CFD technique for HYFLEX aerodynamic design p 693 N95-34542
- Direct analysis of transonic rotor noise with CFD technique p 711 N95-34549
- National Center for Atmospheric Research, Boulder, CO.**
- Determining F-factor using ground-based Doppler radar: Validation and results p 11 N95-10571
- National Defence Research Establishment, Linköping (Sweden).**
- Interfacing a digital compass to a remote-controlled helicopter
[PB95-164927] p 340 N95-24260
- National Defence Research Establishment, Stockholm (Sweden).**
- Propulsion research concerning SFRJ-motors
[PB94-179520] p 14 N95-10083
- Military aviation maintenance industry in Western Europe: Concentration and internationalization
[PB94-189180] p 104 N95-17451
- Evaluation of an autopilot based multimodelling
[PB94-190725] p 142 N95-17454
- Computation of transonic flow on composite overlapping grids in 2 D
[PB95-131348] p 248 N95-21132
- National Inst. of Standards and Technology, Boulder, CO.**
- Measurements of shielding effectiveness and cavity characteristics of airplanes
[PB94-210051] p 244 N95-20191
- National Inst. of Standards and Technology, Gaithersburg, MD.**
- Overview of NASREM: The NASA/NBS standard reference model for telerobot control system architecture
[PB94-194560] p 58 N95-12854
- Evaluation of alternative in-flight fire suppressants for full-scale testing in simulated aircraft engine nacelles and dry bays
[PB94-203403] p 42 N95-13247
- Risk analysis for the fire safety of airline passengers
[PB94-194065] p 77 N95-14179
- Measurement methods and standards for processing and application of thermal barrier coatings
p 344 N95-26123
- STEP: A future revision, today
[NONP-NASA-VT-95-49121] p 452 N95-27209
- National Physical Lab., Teddington (England).**
- Effect of atmospheric pressure on measured aircraft noise levels
[PB95-130423] p 232 N95-21425
- National Renewable Energy Lab., Golden, CO.**
- Structural effects of unsteady aerodynamic forces on horizontal-axis wind turbines
[DE94-011863] p 157 N95-16939
- Wind turbine blade aerodynamics: The combined experiment
[DE94-011866] p 118 N95-18645
- Wind turbine blade aerodynamics: The analysis of field test data
[DE94-011867] p 118 N95-18646
- Evidence that aerodynamic effects, including dynamic stall, dictate HAWT structural loads and power generation in highly transient time frames
[DE94-011865] p 216 N95-19855
- Advanced wind turbine design studies: Advanced conceptual study
[DE93-000031] p 256 N95-20985
- Using digital filtering techniques as an aid in wind turbine data analysis
[DE94-011862] p 357 N95-24853

- NREL airfoil families for HAWTs
[DE95-000267] p 357 N95-24882
- Wind technology development: Large and small turbines
[DE95-000286] p 358 N95-26090
- A comparison of measured wind park load histories with the WISPER and WISPERX load spectra
[DE95-000295] p 446 N95-27459
- Wind-tunnel test of the S814 thick root airfoil
[DE95-000268] p 376 N95-27541
- Experimental investigation of aerodynamic devices for wind turbine rotational speed control, phase 1
[DE95-004034] p 564 N95-30016
- Wind turbine trailing edge aerodynamic brakes
[DE95-004061] p 683 N95-32548
- Techniques for the determination of local dynamic pressure and angle of attack on a horizontal axis wind turbine
[DE95-009204] p 707 N95-32685
- National Research Council of Canada, Ottawa (Ontario).**
- Surface pressure and wake drag measurements on the Boeing A4 airfoil in the IAR 1.5X1.5m Wind Tunnel Facility
p 110 N95-17850
- Noise transmission and reduction in turboprop aircraft
p 175 N95-19164
- Spectrogram diagnosis of aircraft disasters
p 124 N95-19167
- Erosion of T56 5th stage rotor blades due to bleed hole overtip flow
p 200 N95-19666
- Bonded composite repair of thin metallic materials: Variable load amplitude and temperature cycling effects
p 393 N95-27509
- Practical experiences in control systems design using the NCR Bell 205 Airborne Simulator
p 624 N95-32015
- National Science Foundation, Washington, DC.**
- Propulsion/airframe interference for ducted propfan engines with ground effect
[NASA-CR-197110] p 81 N95-14909
- National Technical Univ., Athens (Greece).**
- Single-pass method for the solution of inverse potential and rotational problems. Part 1: 2-D and quasi 3-D theory and application
p 107 N95-16563
- Single-pass method for the solution of inverse potential and rotational problems. Part 2: Fully 3-D potential theory and applications
p 107 N95-16564
- National Transportation Safety Board, Washington, DC.**
- Aircraft accident report: Overspeed and loss of power on both engines during descent and power-off emergency, landing Simmons Airlines, Inc., d/b/a, American Eagle Flight 3641, N349SB False River Air Park, New Roads, Louisiana, 1 February 1994
[PB94-910408] p 78 N95-14916
- Annual review of aircraft accident data: US air carrier operations, calendar year 1992
[PB95-100319] p 78 N95-15066
- Aircraft accident report: Stall and loss of control on final approach, Atlantic Coast Airlines, Inc./United Express Flight 6291 Jetstream 4101, N304UE Columbus, OH, 7 January 1994
[PB94-910409] p 123 N95-17646
- Annual review of aircraft accident data: US Air carrier operations, calendar year 1992
[PB95-100319] p 123 N95-17748
- Safety study: Commuter airline safety
[PB94-917004] p 124 N95-19132
- Special investigation report: Maintenance anomaly resulting in dragged engine during landing rollout, Northwest Airlines Flight 18, Boeing 747-251B, N637US, New Tokyo International Airport, Narita, Japan, 1 Mar. 1994
[PB94-917006] p 188 N95-19793
- Report of proceedings: Aviation Accident Investigation Symposium. Volume 2: Participant presentations
[PB94-917007] p 277 N95-23598
- Aircraft accident report: Runway overrun following rejected takeoff, Continental Airlines flight 795, McDonnell Douglas MD-82, N18835, LaGuardia Airport, Flushing, NY, 2 March 1994
[PB95-910401] p 277 N95-23609
- Aviation Accident Investigation Symposium. Volume 1: Industry recommendations and Safety Board responses
[PB94-917005] p 278 N95-24105
- Aircraft accident report: Impact with blast fence upon landing rollout Action Air Charters flight 990 Piper PA-31-350, N990RA, Stratford, Connecticut, 27 April 1994
[PB94-910410] p 333 N95-24206
- Aircraft accident report: Controlled collision with Terrain Transportes Aereos Ejecutivos, S.A. (TAE SA) Learjet 25D, XA-BBA Dulles International Airport Chantilly, Virginia, June 18, 1994
[NTSB/AAR-95/02] p 380 N95-26498
- Annual review of aircraft accident data: US general aviation calendar year 1993
[PB95-215828] p 599 N95-31712
- Native American Services, Huntsville, AL.**
- NLS Flight Simulation Laboratory (FSL) documentation
[NASA-CR-196564] p 363 N95-24439
- Naval Air Development Center, Warminster, PA.**
- Preliminary evaluation of the F/A-18 quantity/multiple envelope expansion
[AD-A284119] p 132 N95-18407
- Benefits and limitations of composites in carrier-based aircraft
p 422 N95-28422
- Navy composite maintenance and repair experience
p 424 N95-28446
- Naval Air Station, Norfolk, VA.**
- US Navy operating experience with new aircraft construction materials
p 303 N95-23517
- Naval Air Systems Command, Arlington, VA.**
- Naval Aviation System TEAM mapping, charting, and geodesy handbook
[AD-A288590] p 446 N95-26841
- Naval Air Test Center, Patuxent River, MD.**
- Evaluation of F-18A approach and landing flying qualities using an in-flight simulator
[CALSPAN-6241-F-1] p 12 N95-10442
- Naval Air Warfare Center, China Lake, CA.**
- A pulsed liquid fuel ramjet
p 617 N95-31201
- Naval Air Warfare Center, Indianapolis, IN.**
- Standard Hardware Acquisition and Reliability Program (SHARP) advanced SEM-E packaging
p 233 N95-20633
- Immersion/two phase cooling
p 246 N95-20648
- Naval Air Warfare Center, Patuxent River, MD.**
- Add a dimension to your analysis of the helicopter low airspeed environment
[AD-A283982] p 79 N95-14205
- X-31 post-stall envelope expansion and tactical utility testing
p 70 N95-14242
- Navy and the HARV: High angle of attack tactical utility issues
p 71 N95-14252
- Composite waveform generation for EMP and lightning direct-drive testing
[AD-A284159] p 92 N95-14405
- Flight testing high lateral asymmetries on highly augmented Fighter/Attack aircraft
[AD-A284206] p 130 N95-17953
- Comparison of frequency response and perturbation methods to extract linear models from a nonlinear simulation
[AD-A284115] p 146 N95-18405
- Tilt Rotor Unmanned Air Vehicle System (TRUS) demonstrator flight test program
[AD-A284151] p 132 N95-18415
- Application of photogrammetry of F-14D store separation
[AD-A284154] p 132 N95-18417
- The generic simulation executive at Manned Flight Simulator
[AD-A283997] p 146 N95-18724
- Helicopter in-flight simulation development and use in test pilot training
[AD-A283998] p 146 N95-18725
- Assessing aircraft survivability to high frequency transient threats
[AD-A283999] p 134 N95-18726
- Waveform bounding and combination techniques for direct drive testing
[AD-A284075] p 161 N95-19035
- E-6A hardness assurance, maintenance and surveillance program
[AD-A283994] p 134 N95-19067
- The use of genetic algorithms for flight test and evaluation of artificial intelligence and complex software systems
[AD-A284824] p 217 N95-19688
- Airship applications of modern flight test techniques
[AD-A284253] p 194 N95-19731
- Naval Air Warfare Center, Trenton, NJ.**
- Unmanned aerial vehicle heavy fuel engine test
[AD-A284332] p 139 N95-18383
- Navy foreign object damage and its impact on future gas turbine engine low pressure compression systems
p 198 N95-19658
- Testing considerations for military aircraft engines in corrosive environments (a Navy perspective)
p 202 N95-19684
- Naval Air Warfare Center, Warminster, PA.**
- Evaluation of alternate F-14 wing lug coating
[AD-A283207] p 129 N95-17631
- The Advanced Avionics Subsystem Technology Demonstration Program
p 234 N95-20636
- The IEEE scalable coherent interface: An approach for a unified avionics network
p 234 N95-20650
- Corrosion behavior of landing gear steels
[AD-A285862] p 242 N95-22132
- Corrosion of landing gear steels
p 302 N95-23500
- Corrosion detection and monitoring of aircraft structures: An overview
p 303 N95-23515
- An evaluation of the Software Through Pictures/T Tool (StP/T) for the Software Support Activity (SSA)
[AD-A288822] p 447 N95-26348
- Field repair materials for naval aircraft
p 394 N95-27514
- Evaluation of proposed agility metrics using X-31 vs. F/A-18 flight data
[AD-A292573] p 502 N95-28977
- A comparison of coating alternatives for US Coast Guard aircraft
[AD-A293270] p 629 N95-31124
- Naval Facilities Engineering Service Center, Port Hueneme, CA.**
- Moisture induced pressures in concrete airfield pavements
[AD-A281974] p 52 N95-11789
- Naval Postgraduate School, Monterey, CA.**
- Development of an experimental facility for analysis of rotordynamic phenomena
[AD-A281897] p 25 N95-11330
- An application of virtual prototyping to the flight test and evaluation of an unmanned air vehicle
[AD-A281749] p 14 N95-11595
- Flight dynamics of an unmanned aerial vehicle
[AD-A282259] p 45 N95-12410
- Spectral analysis of vortex/free-surface interaction
[AD-A283210] p 96 N95-14658
- Artificial neural network modeling of damaged aircraft
[AD-A283227] p 80 N95-14849
- Evaluation of energy-sink stability criteria for dual-spin spacecraft
[AD-A283228] p 87 N95-14850
- Low-speed wind tunnel testing of the NPS and NASA Ames Mach 6 optimized waverider
[AD-A283585] p 75 N95-15319
- Combustion efficiency in a dual-inlet side-dump ramjet combustor
[AD-A283564] p 83 N95-15329
- An investigation of the transonic pressure drag coefficient for axis-symmetric bodies
[AD-A280990] p 105 N95-15994
- A computational investigation of wake-induced airfoil flutter in incompressible flow and active flutter control
[AD-A281534] p 142 N95-16109
- Low rate initial production in Army Aviation systems development
[AD-A281871] p 127 N95-16356
- Spread spectrum applications in unmanned aerial vehicles
[AD-A281035] p 156 N95-16448
- Mach number, flow angle, and loss measurements downstream of a transonic fan-blade cascade
[AD-A280907] p 108 N95-16824
- Numerical optimization of synergetic maneuvers
[AD-A283398] p 109 N95-17435
- Wind tunnel performance comparative test results of a circular cylinder and 50 percent ellipse tailboom for circulation control antitorque applications
[AD-A283335] p 130 N95-18008
- A platform independent application of Lux illumination prediction algorithms
[AD-A283669] p 170 N95-18018
- Course module for AA201: Wing structural design project
[AD-A283618] p 133 N95-18616
- Plant and controller optimization by convex methods
[AD-A283700] p 133 N95-18621
- Interaction, bursting and control of vortices of a cropped double-delta wing at high angle of attack
[AD-A283656] p 119 N95-18669
- An analysis of the costs and benefits in improving F402-RR-406A High Pressure Turbine, second stage blades under the aircraft engine Component Improvement Program (CIP)
[AD-A285127] p 197 N95-19595
- Automation of hardware-in-the-loop testing of control systems for unmanned air vehicles
[AD-A284833] p 194 N95-19693
- Inband radar cross section of phased arrays with parallel feeds
[AD-A284249] p 210 N95-19730
- A computer code (SKINTEMP) for predicting transient missile and aircraft heat transfer characteristics
[AD-A286044] p 248 N95-21001
- A computer-based multimedia prototype for night vision goggles
[AD-A286208] p 258 N95-21882
- Effect of juncture fillets on double-delta wings undergoing sideslip at high angles of attack
[AD-A286165] p 232 N95-22039
- Evaluation of the Haworth-Newman avionics Display Readability Scale
[AD-A286127] p 235 N95-22232

- Forecasting aircraft mishaps using monthly maintenance reports
[AD-A286049] p 227 N95-22417
- Design and synthesis of a real-time controller for an unmanned air vehicle
[AD-A289134] p 408 N95-26555
- Comparison of fixed wing aircraft algorithms for JANUS
[AD-A288503] p 389 N95-26652
- Air cushioned landing craft (LCAC) based ship to shore movement simulation: A decision aid for the amphibious commander. A (SMMAT) application
[AD-A289635] p 436 N95-26722
- A mathematical analysis of the Janus combat simulation weather effects models and sensitivity analysis of sky-to-ground brightness ratio on target detection
[AD-A289629] p 446 N95-26858
- Construction and wind tunnel test of a 1/12th scale helicopter model
[AD-A288487] p 378 N95-28331
- Proof test methodology for composites
p 424 N95-28445
- Modeling helicopter blade dynamics using a modified Myklestad-Prohl transfer matrix method
[AD-A289891] p 400 N95-28626
- An analysis of the impact of ASPA on organizational and depot level maintenance
[AD-A292670] p 457 N95-29414
- Compressibility effects on and control of dynamic stall of oscillating airfoil
[AD-A291804] p 480 N95-29428
- Applications of digital video and synthetic environments to unmanned aerial vehicles
[AD-A291875] p 504 N95-29437
- Design and evaluation of a LQR controller for the bluebird unmanned air vehicle
[AD-A289769] p 504 N95-29457
- Probabilistic reliability modeling of fatigue on the H-46 tie bar
[AD-A289926] p 607 N95-30927
- An investigation of the side-dump dual in-line ramjet combustor
p 617 N95-31199
- A case study of the teaming concept in the procurement of the V-22 aircraft
[AD-A293770] p 608 N95-31578
- Modeling F/A-18 flight hour program costs using regression analysis
[AD-A293771] p 608 N95-31579
- An LDV investigation of support structure influence on the flow field near the wingtip of a STOVL configuration in hover
[AD-A294126] p 686 N95-34750
- Naval Research Lab., Monterey, CA.**
Environmental support of naval aviation
[AD-A292873] p 598 N95-31454
- Naval Research Lab., Washington, DC.**
Problems with aging wiring in Naval aircraft
p 154 N95-16048
- Wind tunnel tests of a 42 inch diameter self-starting autogyro rotor
[AD-A279922] p 188 N95-19863
- A review of water mist technology for fire suppression
[AD-A285738] p 225 N95-20071
- Statistics of multi-look AIRSAR imagery: A comparison of theory with measurements
p 320 N95-23947
- Speech analysis and synthesis based on pitch-synchronous segmentation of the speech waveform
[AD-A288824] p 435 N95-26349
- Naval Sea Systems Command, Washington, DC.**
A theoretical analysis of airborne sound transfer for a resiliently mounted machine to its foundation
p 30 N95-11304
- Naval Surface Warfare Center, Bethesda, MD.**
Laws of infrared similitude
[AD-A282209] p 62 N95-12426
- 175Hp contrarotating homopolar motor design report
[AD-A291138] p 557 N95-30122
- Naval Surface Warfare Center, Dahlgren, VA.**
Engineering Codes for aeroprediction: State-of-the-art and new methods
p 73 N95-14447
- Electromagnetic reverberation characteristics of a large transport aircraft
[AD-A282923] p 82 N95-15392
- Wavelet transformations for helicopter identification via acoustic signatures
[AD-A279980] p 257 N95-20963
- Parallel block implicit integration technique for trajectory parallelism
[AD-A288961] p 450 N95-28335
- Nonlinear calibration of an infrared radiometer
[AD-A292436] p 579 N95-28996
- The 1995 version of the NSWC aeroprediction code. Part 1: Summary of new theoretical methodology
[AD-A291518] p 481 N95-29853
- Naval Surface Warfare Center, Silver Spring, MD.**
Hypervelocity wind tunnel number 9, high Mach number development program
[AD-A289934] p 594 N95-30929
- Naval Test Pilot School, Patuxent River, MD.**
T-45A High Angle of Attack Testing: US Naval Test Pilot School 46th Annual Reunion and Symposium
[AD-A284000] p 231 N95-20466
- Naval War Coll., Newport, RI.**
Bomber force 2000: Operational concepts for long-range combat aircraft
[AD-A279378] p 230 N95-20181
- Naval Weapons Center, China Lake, CA.**
Composite flight-control actuator development
p 410 N95-28281
- Nevada Univ., Reno, NV.**
Application of CFD to the analysis and design of high-speed inlets
[NASA-CR-198574] p 438 N95-27240
- New Jersey Inst. of Tech., Newark, NJ.**
Design of a variable area diffuser for a 15-inch Mach 6 open-jet tunnel
p 297 N95-23309
- New Mexico State Univ., Las Cruces, NM.**
Demonstration study of hierarchical control of fluid-dynamic phenomena
[AD-A289341] p 437 N95-26751
- New South Wales Univ., Kensington (Australia).**
Efficient and effective handling of cycle slips in global positioning system data
p 43 N95-12230
- AIRSAR deployment in Australia, September 1993: Management and objectives
p 321 N95-23948
- New York Univ., New York, NY.**
Computational fluid dynamics and transonic flow
[AD-A288962] p 436 N95-26405
- Nielsen Engineering and Research, Inc., Mountain View, CA.**
Vorticity dynamics and control of dynamic stall
[AD-A288658] p 620 N95-31400
- Norfolk State Univ., VA.**
Proceedings of the 12th Annual National Conference on Ada Technology
[AD-A290693] p 569 N95-29644
- North Carolina State Univ., Raleigh, NC.**
Time accurate computation of unsteady inlet flows with a dynamic flow adaptive mesh
[AD-A285498] p 157 N95-16736
- Development of a model protection and dynamic response monitoring system for the national transonic facility
[NASA-CR-195041] p 340 N95-24388
- North Dakota Univ., Grand Forks, ND.**
Preliminary analysis of University of North Dakota aircraft data from the FIRE Cirrus IFO-2
[NASA-CR-198038] p 357 N95-24219
- Northern Research and Engineering Corp., Woburn, MA.**
Small gas turbine component evaluation study
[PB95-147542] p 338 N95-24293
- Northrop Corp., Hawthorne, CA.**
Analysis of composite structures with delaminations under combined bending and compression
p 422 N95-28429
- C-130 Advanced Technology Center wing box conceptual design/cost study
p 423 N95-28437
- Reliability analysis of composite structures
p 423 N95-28441
- A weight-efficient design strategy for cutouts in composite transport structures
p 533 N95-28843
- Northrop Corp., Pico Rivera, CA.**
Eddy current for detecting second layer cracks under installed fasteners
[AD-A282412] p 158 N95-17507
- Northrop Grumman Corp., Hawthorne, CA.**
Repair technology for thermoplastic aircraft structures
p 395 N95-27519
- Northrop Grumman Corp., Pico Rivera, CA.**
Environmentally regulated aerospace coatings
p 631 N95-31775
- Northwestern Univ., Evanston, IL.**
Fatigue reliability method with in-service inspections
p 94 N95-14475
- Norwegian Defence Research Establishment, Kjeller (Norway).**
Results from tests of the Kearsfott T16-B Inertial Measurement Unit
[PB95-212031] p 644 N95-30502
- Norwegian Inst. for Air Research, Kjeller (Norway).**
Results from tests of the Honeywell integrated flight management unit
[PB95-211355] p 601 N95-30597
- Notre Dame Univ., IN.**
The Elite: A high speed, low-cost general aviation aircraft for Aeroworld
[NASA-CR-197161] p 45 N95-12530
- Icarus Rewaxed: A high speed, low-cost general aviation aircraft for Aeroworld
[NASA-CR-197155] p 45 N95-12609
- The Balsa bullet: A high speed, low-cost general aviation aircraft for Aeroworld
[NASA-CR-197165] p 46 N95-12638
- Experiments on the flow field physics of confluent boundary layers for high-lift systems
[NASA-CR-197318] p 224 N95-21343
- Effects of three-dimensional imposed 3-D disturbances on bluff-body near wake flows
p 374 N95-26757
- The effects of three-dimensional imposed disturbances on bluff body near wake flows: Effects of taper and splitter plates on the near wake characteristics of a circular cylinder in uniform and shear flow
[AD-A292113] p 477 N95-28921
- The pressure field of a gust interacting with a flat plate
p 557 N95-30161
- Nottingham Univ. (England).**
A rose by any other name: Certification seen as process rather than content
p 688 N95-34766
- NYMA, Inc., Brook Park, OH.**
Resonant interaction of a linear array of supersonic rectangular jets: An experimental study
[NASA-CR-195398] p 76 N95-15852
- Prediction of wind tunnel effects on the installed F/A-18A inlet flow field at high angles-of-attack
[NASA-CR-195429] p 197 N95-19651
- Users manual for the improved NASA Lewis ice accretion code LEWICE 1.6
[NASA-CR-198355] p 485 N95-29132
- A PC program for estimating measurement uncertainty for aeronautics test instrumentation
[NASA-CR-198361] p 523 N95-30067
- Flow quality improvements in the NASA Lewis Research Center 9- by 15-foot Low Speed Wind Tunnel
[NASA-CR-195439] p 627 N95-31653
- Effects of civil titrotor service in the northeast corridor on en route airspace loads
[AD-A293586] p 599 N95-31687
- Computation of noise radiation from turbofans: A parametric study
[NASA-CR-198359] p 710 N95-32836
- Numerical simulation of supersonic flow using a new analytical bleed boundary condition
[NASA-CR-198368] p 697 N95-33208
- NYMA, Inc., Cleveland, OH.**
On supersonic-inlet boundary-layer bleed flow
[NASA-CR-195426] p 202 N95-19769
- Oak Ridge National Lab., TN.**
Scale-up and modeling of forced chemical vapor infiltration
[DE94-017769] p 247 N95-20781
- Evolution of oxidation and creep damage mechanisms in HIPed silicon nitride materials
[DE95-001360] p 300 N95-22689
- Cu deposition using a permanent magnet electron cyclotron resonance microwave plasma source
[DE94-017768] p 304 N95-23981
- Thermal conductivity of zirconia thermal barrier coatings
p 345 N95-26133
- Office National d'Etudes et de Recherches Aérospatiales, Modane (France).**
Calculation of wall effects of flow on a perforated wall with a code of surface singularities
p 165 N95-19277
- Office National d'Etudes et de Recherches Aérospatiales, Paris (France).**
Lateral jet control for tactical missiles
p 84 N95-14448
- High angle of attack aerodynamics
p 74 N95-14450
- Ellipsoid-cylinder model
p 158 N95-17869
- Supersonic vortex flow around a missile body
p 114 N95-17870
- Test data on a non-circular body for subsonic, transonic and supersonic Mach numbers
p 158 N95-17871
- Delta-wing model
p 114 N95-17873
- Office National d'Etudes et de Recherches Aérospatiales, Toulouse (France).**
Data from the GARTEUR (AD) Action Group 02 airfoil CAST 7/DOA1 experiments
p 111 N95-17856
- OAT15A airfoil data
p 111 N95-17857
- Evaluation of the techniques of fuzzy control for the piloting an aircraft
p 621 N95-31997
- Office of Naval Research, Arlington, VA.**
Fiber-optic rotary joint with bundle collimator assemblies
[AD-DO16504] p 258 N95-21673
- Ohio Aerospace Inst., Brook Park, OH.**
Optimization of aerospace structures
[NASA-CR-196763] p 48 N95-12787

Ohio State Univ., Columbus, OH.

- A users manual for the method of moments Aircraft Modeling Code (AMC), version 2
[NASA-CR-196445] p 24 N95-11252
- Electromagnetic on-aircraft antenna radiation in the presence of composite plates
[NASA-CR-196126] p 58 N95-12856
- Wing-body juncture flows
[AD-A281526] p 106 N95-16099
- Comparative wind tunnel test at high Reynolds numbers of NACA 64 621 airfoils with two aileron configurations
p 377 N95-27977
- A numerical study of the small scale wing-body junction problem
p 482 N95-30235

Ohio Univ., Athens, OH.

- Oscillating-flow regenerator test rig
[NASA-CR-196982] p 53 N95-13200
- An investigation into the use of satellite-based positioning systems for flight reference/autoland operations
p 489 N95-29542

Oklahoma City Air Logistics Center, Tinker AFB, OK.

- Proceedings of the 2d USAF Aging Aircraft Conference
[AD-A288217] p 336 N95-25578

Old Dominion Coll., Norfolk, VA.

- System identification of the Large-Angle Magnetic Suspension Test Fixture (LAMSTF)
p 296 N95-23299
- Optimized design of a hypersonic nozzle
p 297 N95-23304
- Inner loop flight control for the High-Speed Civil Transport
p 293 N95-23314

Old Dominion Univ., Norfolk, VA.

- Methodology for sensitivity analysis, approximate analysis, and design optimization in CFD for multidisciplinary applications
[NASA-CR-196981] p 58 N95-13201
- Aerodynamic shape optimization of a HSCT type configuration with improved surface definition
[NASA-CR-197011] p 67 N95-13701
- Automation of reverse engineering process in aircraft modeling and related optimization problems
[NASA-CR-197109] p 129 N95-16899
- A CFD study of complex missile and store configurations in relative motion
[NASA-CR-197912] p 285 N95-22949
- Aerodynamic design optimization with sensitivity analysis and computational fluid dynamics
[NASA-CR-197419] p 274 N95-23218
- Extension to the dynamic modeling of the large angle magnetic suspension test fixture
[NASA-CR-197801] p 411 N95-26768
- Unsteady flow simulations about moving boundary configurations using dynamic domain decomposition techniques
p 649 N95-31837
- Geometric modeling for computer aided design
[NASA-CR-198828] p 679 N95-31982
- Three-dimensional aerodynamic shape optimization using discrete sensitivity analysis
p 691 N95-32904

Oregon State Univ., Corvallis, OR.

- Preliminary analysis of dynamic stall effects on a 91-meter wind turbine rotor
p 376 N95-27975
- Nonlinear adaptive control of highly maneuverable high performance aircraft
p 710 N95-33712

Organisatie voor Toegepast Natuurwetenschappelijk Onderzoek, Delft (Netherlands).

- Partial camera automation in a simulated Unmanned Air Vehicle
[AD-A288786] p 337 N95-26190

Overset Methods, Inc., Los Altos, CA.

- Aerodynamic optimization studies on advanced architecture computers
[NASA-CR-198045] p 330 N95-24379
- The coupling of fluids, dynamics, and controls on advanced architecture computers
[NASA-CR-197727] p 360 N95-25797
- Global flowfield about the V-22 Tiltrotor Aircraft
[NASA-CR-198603] p 375 N95-27248

Oxford Univ., Oxford (England).

- Particle deposition in gas turbine blade film cooling holes
p 199 N95-19661
- Soft body impact on titanium fan blades
p 200 N95-19671

P**Pacific Northwest Lab., Richland, WA.**

- An artificial neural network system for diagnosing gas turbine engine fuel faults
[DE94-013960] p 138 N95-17371

Pacific-Sierra Research Corp., Santa Monica, CA.

- Hot jet/wake turbulent structure and laser propagation. Part 3: Laser propagation measurements and modeling
p 647 N95-30992

Palermo Univ. (Italy).

- An airborne monitoring system for FOD and erosion faults
p 200 N95-19668

Paragon Pacific, Inc., El Segundo, CA.

- Design of a real-time wind turbine simulator using a custom parallel architecture
p 449 N95-27979

Paris VI Univ. (France).

- Optimal shape design for aerodynamics
p 128 N95-16568

PDA Engineering, Costa Mesa, CA.

- Response of the B-1B air data sensor to simulated dust cloud environments
[AD-A286134] p 235 N95-22036

Pennsylvania State Univ., State College, PA.

- Empirical refinements to boundary layer transition noise models
p 28 N95-11262
- Active minimization of energy density in three-dimensional enclosures
[NASA-CR-197213] p 172 N95-16848
- Cavitation modeling in Euler and Navier-Stokes codes
p 315 N95-23630

Pennsylvania State Univ., University Park, PA.

- Flame-spreading phenomena in the fin-slot region of a solid rocket motor
p 23 N95-10296
- Achievements and tasks for active noise control
p 29 N95-11270
- The effect of aircraft speed on the penetration of sonic boom noise into a flat ocean
p 100 N95-14887
- Wake turbulence
p 75 N95-14894
- Anisotropic heat exchangers/stack configurations for thermoacoustic heat engines
[AD-A280974] p 168 N95-16506
- Numerical computation of aerodynamics and heat transfer in a turbine cascade and a turn-around duct using advanced turbulence models
p 313 N95-23444
- Convergence acceleration of implicit schemes in the presence of high aspect ratio grid cells
p 313 N95-23446

Physical Sciences, Inc., Andover, MA.

- Ultraviolet emissions occurring about hypersonic vehicles in rarefied flows
[AD-A281452] p 106 N95-16076

Planning Research Corp., Edwards, CA.

- High-angle-of-attack yawing moment asymmetry of the X-31 aircraft from flight test
[NASA-CR-186030] p 13 N95-11410
- Strain gage selection in loads equations using a genetic algorithm
[NASA-CR-4597] p 48 N95-12831
- Dynamic ground effects flight test of the NASA F-15 aircraft
p 692 N95-33024

Polish Academy of Sciences, Warsaw (Poland).

- Actuating signals in adaptive control systems
[IFTR-13/1994] p 361 N95-26330
- Photoacoustic chambers for studying solids and gases: Theory and practical examples
[IFTR-39/1994] p 412 N95-26837

Polytechnic Univ., Farmingdale, NY.

- Research instrumentation for polytechnic university's supersonic wind tunnel facility
[AD-A290232] p 523 N95-29468

Pratt and Whitney Aircraft, East Hartford, CT.

- Unsteady flows in turbines: Impact on design procedure
p 90 N95-14132
- Ultra-high bypass ratio jet noise
[NASA-CR-195394] p 100 N95-14610
- Thermal barrier coating experience in the gas turbine engine
p 345 N95-26125
- Thermal barrier coating life modeling in aircraft gas turbine engines
p 346 N95-26140

Pratt and Whitney Aircraft, West Palm Beach, FL.

- STOVL Control Integration Program
[NASA-CR-195358] p 18 N95-11487
- High temperature strain gage technology for gas turbine engines
[NASA-CR-191177] p 57 N95-11996
- Fatigue in single crystal nickel superalloys
[AD-A283459] p 56 N95-12546
- Fatigue in single crystal nickel superalloys
[AD-A282917] p 88 N95-15415
- Fatigue in single crystal nickel superalloys
[AD-A285727] p 152 N95-18068
- Aerodynamic design and analysis of a highly loaded turbine exhaust
p 312 N95-23435
- Phase 2: HGM air flow tests in support of HEX vane investigation
p 312 N95-23438
- A design perspective on thermal barrier coatings
p 344 N95-26120

- Jet engine applications for materials with nanometer-scale dimensions
p 345 N95-26131
- F-15 propulsion system
p 695 N95-33012

Pratt and Whitney Aircraft Group, West Palm Beach, FL.

- Composite intermediate case manufacturing scale-up for advanced engines
p 406 N95-28275

Praxair, Inc., Tonawanda, NY.

- Airborne rotary separator study
[NASA-CR-191045] p 150 N95-18743

Princeton Univ., NJ.

- Optimum aerodynamic design via boundary control
p 127 N95-16565
- Studies on high pressure and unsteady flame phenomena
[AD-A284126] p 152 N95-18410
- An investigation of helicopter dynamic coupling using an analytical model
[NASA-CR-197420] p 285 N95-23217
- Computational algorithms for aerodynamic analysis and design
[AD-A291084] p 482 N95-29972
- Requirements and trends of computational aerodynamics as a tool for aircraft design
p 692 N95-34506

Prins Maurits Lab. TNO, Rijswijk (Netherlands).

- Integral rocket ramjets
[AD-A285135] p 240 N95-20906

Purdue Univ., West Lafayette, IN.

- Active control of turbomachine discrete tones
p 29 N95-11275
- Design of a high capacity long range cargo aircraft
[NASA-CR-197176] p 45 N95-12363
- Bending effects of unsymmetric adhesively bonded composite repairs on cracked aluminum panels
p 92 N95-14456
- Gas turbine pre-diffuser-combustor performance during operation with air-water mixture
[DOT/FAA/CT-93/52] p 83 N95-15683
- Aero-thermodynamic distortion induced structured dynamic response
[AD-A279931] p 203 N95-19864
- Wake measurements in a strong adverse pressure gradient
[NASA-CR-197272] p 224 N95-21031
- Development of quiet-flow supersonic wind tunnels for laminar-turbulent transition research
[NASA-CR-197286] p 239 N95-21436
- Supersonic quiet-tunnel development for laminar-turbulent transition research
[NASA-CR-198040] p 340 N95-24302
- Thermal fracture mechanisms in ceramic thermal barrier coatings
p 346 N95-26138
- WINCLR: A computer code for heat transfer and clearance calculation in a compressor
[NASA-CR-195436] p 366 N95-26363
- Linear and nonlinear discrete-time state-space modeling of dynamic systems for control applications
p 567 N95-29251

Q**Queensland Univ., Saint Lucia (Australia).**

- Shock tunnel studies of scramjet phenomena 1993
[NASA-CR-195038] p 350 N95-25394
- Thrust measurements of a complete axisymmetric scramjet in an impulse facility
p 339 N95-25395
- Scramjet thrust measurement in a shock tunnel
p 339 N95-25396
- Thrust measurement in a 2-D scramjet nozzle
p 339 N95-25397
- The Supersonic Expansion Tube concept, experiment and analysis
p 341 N95-25399
- Balances for the measurement of multiple components of force in flows of a millisecond duration
p 350 N95-25400

R**Radian Corp., Austin, TX.**

- Community relations plan: Galena Airport and Camp ion Air Force Station, Alaska
[AD-A286722] p 446 N95-27234

Radian Corp., Research Triangle Park, NC.

- Nitrogen oxide emissions and their control from uninstalled aircraft engines in enclosed test cells: Joint report to Congress on the Environmental Protection Agency - Department of Transportation study
[PB95-166237] p 358 N95-26005

RAND Corp., Santa Monica, CA.

- Case study of risk management in the USAF B-1B bomber program
[AD-A282371] p 62 N95-11944
- The development of the F100-PW-220 and F110-GE-100 engines: A case study of risk assessment and risk management
[AD-A282467] p 51 N95-13289
- The F-16 multinational staged improvement program: A case study of risk assessment and risk management
[AD-A281706] p 81 N95-15451

- Remtech, Inc., Huntsville, AL.**
Rarefied gas effects on aerobraking/reentry vehicles with wakes [NASA-CR-196586] p 415 N95-27093
- Research Inst. for Advanced Computer Science, Moffett Field, CA.**
Optimum aerodynamic design via boundary control [NASA-CR-195882] p 36 N95-11877
Control theory based airfoil design using the Euler equations [NASA-CR-196360] p 36 N95-11884
Mesh quality control for multiply-refined tetrahedral grids [NASA-CR-197595] p 160 N95-18737
- Research Inst. of National Defence, Linköping (Sweden).**
Orientation determination of aircraft using visual 3D matching and radar. Case study 2 [PB95-165791] p 350 N95-25749
- Research Triangle Inst., Hampton, VA.**
Characteristics of civil aviation atmospheric hazards p 42 N95-13208
- Reticular Systems, Inc., San Diego, CA.**
PalymSys (TM): An extended version of CLIPS for construction and reasoning using blackboards p 217 N95-19767
- Rochester Univ., NY.**
Scientific and technical photography at NASA Langley Research Center p 310 N95-23290
- Rocket Research Corp., Redmond, WA.**
Arcjet thruster research and technology, phase 2 [NASA-CR-182276] p 105 N95-18044
- Rockwell International Corp., Canoga Park, CA.**
CFD analysis of turbopump volutes p 312 N95-23436
Impeller flow field characterization with a laser two-focus velocimeter p 313 N95-23440
- Rockwell International Corp., Downey, CA.**
Requirements report for SSTO vertical take-off and horizontal landing vehicle [NASA-CR-197029] p 80 N95-14794
Program test objectives milestone 3 [NASA-CR-197030] p 127 N95-15971
Strategic avionics technology definition studies. Subtask 3-1A3: Electrical Actuation (ELA) Systems Test Facility [NASA-CR-188360] p 143 N95-18567
Fatigue loads spectra derivation for the Space Shuttle: Second cycle p 166 N95-19470
- Rockwell International Corp., El Segundo, CA.**
Extracting a representative loading spectrum from recorded flight data p 80 N95-14469
- Rockwell International Corp., Golden, CO.**
Horizontal axis wind turbine post stall airfoil characteristics synthesis p 376 N95-27974
- Rockwell International Corp., Huntsville, AL.**
Automated test environment for a real-time control system [TABES PAPER 94-631] p 99 N95-14652
High frequency flow-structural interaction in dense subsonic fluids [NASA-CR-4652] p 330 N95-24217
- Rockwell International Science Center, Thousand Oaks, CA.**
Fundamental concepts in the suppression of delamination buckling by stitching p 426 N95-28486
- Rockwell Space Operations Co., Houston, TX.**
The navigation toolkit [NASA-CR-197290] p 229 N95-22161
- Rohde and Schwartz, Munich (Germany).**
Modular CNL avionics system p 234 N95-20659
- Rolls-Royce Ltd., Bristol (England).**
Out of area experiences with the RB199 in Toronto p 198 N95-19654
Future directions in helicopter protection system configuration p 198 N95-19657
- Rome Lab., Griffiss AFB, NY.**
Generic architectures for future flight systems p 99 N95-14159
A VHF/UHF antenna for the Precision Antenna Measurement System (PAMS) [AD-A285673] p 156 N95-16621
Reliability assessment of Multichip Module technologies via the Triservice/NASA RELTECH program p 245 N95-20643
Assuring Known Good Die (KGD) for reliable, cost effective MCMs p 246 N95-20644
- Rose Engineering and Research, Inc., Incline Village, NV.**
SOFIA: Aft cavities wind tunnel test [NASA-TM-110673] p 683 N95-32682
- Royal Air Force Inst. of Aviation Medicine, Farnborough (England).**
Quality assurance and risk management: Perspectives on Human Factors Certification of Advanced Aviation Systems p 690 N95-34771
- Royal Australian Air Force, Amberley (Australia).**
The development of an engineering standard for composite repairs p 396 N95-27528
- Royal Inst. of Tech., Stockholm (Sweden).**
Turbulence models in the Navier-Stokes simulation of airfoil stall [TRITA-NA-9312] p 705 N95-33059
- Royal Military Coll. of Saint-Jean, Richelein (Quebec).**
Transport aircraft loading and balancing system: A CLIPS expert system for military aircraft load planning p 217 N95-19751
- Royal Netherlands Meteorological Inst., De Bilt (Netherlands).**
Atmospheric effects of high-flying subsonic aircraft: A catalogue of perturbing influences [KNMI-SR-94-03] p 168 N95-18722
- Rutgers - The State Univ., New Brunswick, NJ.**
Modal identification and its applications to damage detection in vibrating structures p 704 N95-32920
- Rutgers Univ., Piscataway, NJ.**
Study of multiple cracks in airplane fuselage by micromechanics and complex variables p 94 N95-14468

S

- Saab-Scania, Linköping (Sweden).**
SAAB experience with PIO p 598 N95-31069
- Saint Cloud State Coll., MN.**
Differential GPS and system integration of the Low Visibility Landing and Surface Operations (LVLASO) demonstration p 280 N95-23318
- Saint Louis Univ., Cahokia, IL.**
Preliminary identification of buffet problems in high speed civil transport p 294 N95-23319
- Saint Petersburg Inst. of Aerospace Instrumentation, Saint Petersburg (Russia).**
Sea wave parameters, small altitudes and distances: measurers design for movement control systems of ships, wing-in-surface effect crafts and seaplanes p 708 N95-33141
- San Antonio Air Logistics Center, Kelly AFB, TX.**
Bicarbonate of soda paint stripping process validation and material characterization p 631 N95-31778
- Sandia National Labs., Albuquerque, NM.**
Navier-Stokes simulations of WECS airfoil flowfields [DE94-013341] p 7 N95-10226
Ceramic manufacturing: Optimizing a multivariable system [DE94-015016] p 56 N95-13184
Error propagation equations for estimating the uncertainty in high-speed wind tunnel test results [DE94-014136] p 145 N95-16509
Evaluation of scanners for C-scan imaging in nondestructive inspection of aircraft [DE94-012473] p 152 N95-19100
Environmental effects on composite airframes: A study conducted for the ARM UAV Program (Atmospheric Radiation Measurement Unmanned Aerospace Vehicle) [DE94-015351] p 206 N95-19579
SAR image registration in absolute coordinates using GPS carrier phase position and velocity information [DE94-018738] p 228 N95-20195
Assessment of a non-dedicated GPS receiver system for precise airborne attitude determination [DE94-019309] p 229 N95-21520
A user's guide to LUGSAN 1.1: A computer program to calculate and archive lug and sway brace loads for aircraft-carried stores [DE95-001919] p 232 N95-21730
Moving mass trim control for aerospace vehicles [DE95-002602] p 299 N95-23532
Verification of computational aerodynamic predictions for complex hypersonic vehicles using the INCA(trademark) code [DE95-004757] p 330 N95-24308
Emerging nondestructive inspection for aging aircraft [PB95-143053] p 328 N95-25401
A NASTRAN-based computer program for structural dynamic analysis of Horizontal Axis Wind Turbines p 439 N95-27980
High strain-rate testing of parachute materials [DE95-009577] p 648 N95-31614
- Scandinavian Airlines System, Oslo (Norway).**
Scandinavian Airlines Systems experience on erosion, corrosion and foreign object damage effects on gas turbines p 198 N95-19659
- Science Applications International Corp., Dayton, OH.**
Systems engineering design and technical analyses for Strategic Avionics Crew-station Design Evaluation Facility (SACDEF) [AD-A286239] p 235 N95-22024
Visual contrast detection thresholds for aircraft contrails [AD-A288618] p 328 N95-25607
- Science Univ. of Tokyo (Japan).**
Calculation for aerodynamic characteristics on delta wing with leading-edge separated vortex effect using boundary element method p 684 N95-34524
Grid generation around airfoil with a flap using boundary element method p 686 N95-34552
- Seagull Technology, Inc., Sunnysvale, CA.**
ACSynt inner loop flight control design study [NASA-CR-196316] p 17 N95-11223
- Selskapet for Industriell og Teknisk Forskning, Trondheim (Norway).**
Metascientific problems in safety science [PB95-196408] p 645 N95-30521
- Sextant Avionique, Saint Medard en Jalles (France).**
A helmet mounted display for night missions at low altitude p 693 N95-32503
- Sextant Avionique, Valence (France).**
Lightweight electronic enclosures using composite materials p 241 N95-20656
- Ship Research Inst., Tokyo (Japan).**
Numerical simulation of two-dimensional PAR-WIG p 685 N95-34548
- Sikorsky Aircraft, Stratford, CT.**
Static and fatigue testing of full-scale fuselage panels fabricated using a Therm-X(R) process p 420 N95-28270
- Simula, Inc., Phoenix, AZ.**
Rotorcraft crashworthy airframe and fuel system technology development program [AD-A289986] p 382 N95-28630
- Smith Advanced Technology, Inc., Huntsville, AL.**
HLLV avionics requirements study and electronic filing system database development [NASA-CR-193993] p 49 N95-13027
- Societe Nationale d'Etude et de Construction de Moteurs d'Aviation, Evry (France).**
New Trends in coatings developments for turbine blades: Materials processing and repair p 201 N95-19676
- Societe Nationale d'Etude et de Construction de Moteurs d'Aviation, Moissy-Cramayel (France).**
New methods, new methodology: Advanced CFD in the Snecma turbomachinery design process p 90 N95-14134
Design of fan blades subjected to bird impact p 200 N95-19669
- Solar Turbines, Inc. San Diego, CA.**
Perspective on thermal barrier coatings for industrial gas turbine applications p 345 N95-26128
- Sorbent Technologies Corp., Twinsburg, OH.**
Laboratory evaluation of a reactive baffle approach to NOx control [AD-A283802] p 255 N95-19921
- Southampton Univ. (England).**
Near field noise prediction requirements [ISVR-TR-234] p 27 N95-11166
- Southwest Research Inst., San Antonio, TX.**
A study of aircraft post-crash fuel fire mitigation [AD-A282208] p 40 N95-12499
Analysis of small crack behavior for airframe applications p 95 N95-14484
Aircraft stress sequence development: A complex engineering process made simple p 136 N95-19480
Eddy current for detecting second-layer cracks under installed fasteners [AD-A279871] p 244 N95-20414
Mechanism of deposit formation on fuel-wetted hot metal surfaces [AD-A289847] p 426 N95-28621
- Spectra Research Systems, Inc., Huntsville, AL.**
A graphical user interface for design and analysis of air breathing propulsion systems [TABES PAPER 94-616] p 83 N95-14645
- Spectrum Sciences and Software, Inc., Fort Walton Beach, FL.**
Integrating NOISEMAP with the Geographic Resource Analysis Support System (GRASS) to enhance environmental impact assessments and land use compatibility studies p 31 N95-11311
MOAMAP: A model that combines several different kinds of aircraft operations p 32 N95-11323
- SPEEL Ltd., Prague (Czechoslovakia).**
Solid-state data recorder, next development and use p 705 N95-33143
- SRI International Corp., Menlo Park, CA.**
Active control of complex noise problems using a broadband, multichannel controller p 29 N95-11271
Broadband, wide-area active control of sound radiated from vibrating structures using local surface-mounted radiation suppression devices p 30 N95-11283
Formal verification of an avionics microprocessor [NASA-CR-4682] p 710 N95-33396
- Stanford Univ., CA.**
High altitude hypersonic flowfield radiation [AD-A281386] p 106 N95-16160
Design and flight test of a simplified control system for a transport helicopter p 144 N95-18902

- Computing methods for the approximate solution of time dependent problems
[AD-A286007] p 256 N95-20719
- Unstructured-grid large-eddy simulation of flow over an airfoil p 225 N95-22448
- Large-eddy simulation of flow through a plane, asymmetric diffuser p 250 N95-22449
- Experimental investigations of on-demand vortex generators p 250 N95-22451
- Direct numerical simulations of on-demand vortex generators: Mathematical formulation p 251 N95-22452
- Acoustics of laminar boundary layers breakdown p 251 N95-22455
- Compressive strength of damaged and repaired composite plates p 442 N95-28484
- A study of fluid problems requiring a direct particle simulation [AD-A290212] p 567 N95-29074
- Wide Area Differential GPS (WADGPS) p 489 N95-29107
- Solution of the Navier-Stokes equations on locally refined Cartesian meshes using state-vector splitting p 553 N95-29197
- Linear matrix inequalities for the problem of absolute stability of control systems p 518 N95-29680
- DC electrostatic gyro suspension system for the Gravity Probe B experiment p 527 N95-29794
- A method for the modelling of porous and solid wind tunnel walls in computational fluid dynamics codes p 523 N95-29795
- Computation of high-altitude hypersonic flow-field radiation p 593 N95-30843
- Foundations of technology for constructing highly reliable distributed realtime systems [AD-A293254] p 678 N95-30892
- State Univ. of New York, Binghamton, NY.**
- Wormgear geometry adopted for implementing hydrostatic lubrication and formulation of the lubrication problem [AD-A290331] p 210 N95-19567
- State Univ. of New York, Farmingdale, NY.**
- Quality optimization of thermally sprayed coatings produced by the JP-5000 (HVOF) gun using mathematical modeling p 152 N95-19008
- State Univ. of New York, Oneonta, NY.**
- A CMC database for use in the next generation launch vehicles (rockets) p 150 N95-18993
- Stevens Inst. of Tech., Hoboken, NJ.**
- Computational predictive methods for fracture and fatigue p 93 N95-14466
- Stockholm Univ. (Sweden).**
- Turbulence models in the Navier-Stokes simulation of airfoil stall [TRITA-NA-9312] p 705 N95-33059
- Strathclyde Univ., Glasgow (Scotland).**
- SMART materials: Surfaces, transforms and interfaces. The commensurate engineering dimension [AD-A289598] p 442 N95-28649
- Sulzer Innotec A.G., Winterthur (Switzerland).**
- Computational methods for preliminary design and geometry definition in turbomachinery p 89 N95-14128
- The industrial use of CFD in the design of turbomachinery p 90 N95-14133
- Sundstrand Aviation-Rockford, IL.**
- In situ processing methods for composite fuselage sandwich structures p 531 N95-28826
- Sundstrand Power Systems, San Diego, CA.**
- Small turbojets: Designs and installations p 138 N95-16323
- Sverdrup Technology, Inc., Brook Park, OH.**
- An analysis code for the Rapid Engineering Estimation of Momentum and Energy Losses (REMEL) [NASA-CR-191178] p 108 N95-16887
- Three-dimensional Navier-Stokes analysis and redesign of an imbedded bellmouth nozzle in a turbine cascade inlet section p 311 N95-23423
- Sydney Univ. (Australia).**
- Six degree of freedom flight dynamic and performance simulation of a remotely-piloted vehicle [AERO-TN-9301] p 131 N95-18097
- Syracuse Univ., NY.**
- The noise reduction potential of dual-stream coaxial rectangular improperly expanded jet flows [NASA-CR-197820] p 437 N95-26995
- Systems and Electronics, Inc., Elk Grove Village, IL.**
- Flight parameters monitoring system for tracking structural integrity of rotary-wing aircraft p 135 N95-19469
- Systems Control Technology, Inc., Arlington, VA.**
- Vertical flight terminal operational procedures. A summary of FAA research and development [AD-A283550] p 85 N95-15328
- Helicopter/vertiport MLS precision approaches [AD-A283505] p 126 N95-18059
- Systems Technology, Inc., Hawthorne, CA.**
- Proposed incorporation of mission-oriented flying qualities into MIL-STD-1797A [AD-A294211] p 698 N95-34306
- Sytronics, Inc., Dayton, OH.**
- More supportable T-38A enhancement study [AD-A283671] p 66 N95-15331

T

- Technion - Israel Inst. of Tech., Haifa (Israel).**
- Review of some results of the author's fatigue investigations with applications in engineering and material science [TAE-698] p 316 N95-23662
- Technion Research and Development Foundation Ltd., Haifa (Israel).**
- Advanced interactive display formats for terminal area traffic control [NASA-CR-198576] p 384 N95-28188
- Technische Hochschule, Aachen (Germany).**
- Prediction of rotor-blade deformations due to unsteady airloads [AD-A284467] p 81 N95-15821
- Investigation of an NLF(1)-0416 airfoil in compressible subsonic flow p 110 N95-17852
- Prediction of rotor-blade deformations due to unsteady airloads [AD-A286593] p 231 N95-20860
- Technische Hogeschool, Delft (Netherlands).**
- Experiments in the trailing edge flow of an NLR 7702 airfoil p 110 N95-17853
- Experimental investigation of the vortex flow over a 76/60-deg double delta wing p 114 N95-17874
- Fatigue life until small cracks in aircraft structures: Durability and damage tolerance p 135 N95-19478
- Technische Univ., Brunswick (Germany).**
- Turbulence: Engineering models, aircraft response p 84 N95-14900
- Effects of the specific military aspects of satellite navigation on the civil use of GPS/GLONASS p 688 N95-33134
- Technische Univ., Delft (Netherlands).**
- Numerical time dependent sheet cavitation simulations using a higher order panel method [PB94-204435] p 59 N95-13249
- Studies on the flow induced by an oscillating airfoil in a uniform stream p 40 N95-13250
- A SIMULINK environment for flight dynamics and control analysis: Application to the DHC-2 Beaver. Part 1: Implementation of a model library in SIMULINK. Part 2: Nonlinear analysis of the Beaver autopilot [NONP-NASA-SUPPL-DK-94-2802] p 84 N95-14815
- The utilization of a high speed reflective visualization system in the study of transonic flow over a delta wing p 121 N95-19259
- Numerical simulation of crack growth in pressurized fuselages [PB95-192415] p 400 N95-28636
- PREDICHTAT: First order performance calculations of windturbine rotors using the method of the acceleration potential [PB95-206454] p 564 N95-30200
- Axial loads on yawed rotors [PB95-214193] p 592 N95-30638
- Numerical investigation into vortical flow about a delta-wing configuration up to incidences at which vortex breakdown occurs in experiment [PB95-198024] p 593 N95-30837
- Dynamical systems as models for flow-induced vibrations [PB95-206991] p 647 N95-30956
- Acceleration potential models [PB95-206991] p 647 N95-30956
- PREDICHTAT/PREDICDYN applied for calculation of axisymmetric dynamic inflow cases [PB95-207015] p 647 N95-30957
- Digital simulation of wind velocities for wind turbine rotors: General considerations [PB95-206447] p 677 N95-31157
- Robust control: A structured approach to solve aircraft flight control problems p 621 N95-31995
- Technische Univ., Munich (Germany).**
- Aero design of turbomachinery components: CFD in complex systems p 90 N95-14136
- Velocity measurements with hot-wires in a vortex-dominated flowfield p 121 N95-19261
- Technology Integration and Development Group, Inc., Bedford, MA.**
- Gearbox vibration diagnostic analyzer [NASA-CR-189141] p 316 N95-23792
- Tennessee Technological Univ., Cookeville, TN.**
- Fatigue and residual strength investigation of ARALL(R) -3 and GLARE(R) -2 panels with bonded stringers p 137 N95-19495
- Tennessee Univ., Tullahoma, TN.**
- A wall interference assessment/correction system [NASA-CR-197421] p 309 N95-23183
- Tennessee Univ. Space Inst., Tullahoma, TN.**
- A wall interference assessment and correction system [NASA-CR-196940] p 58 N95-12228
- Supersonic laminar flow control research [NASA-CR-196049] p 249 N95-21340
- Handling qualities of the High Speed Civil Transport p 294 N95-23325
- Test Devices, Inc., Hudson, MA.**
- Portable static test facility for small, expendable, turbojet engines, phase 1 [AD-A286337] p 239 N95-21719
- Texas A&M Univ., College Station, TX.**
- Knowledge-based processing for aircraft flight control [NASA-CR-194976] p 99 N95-13727
- Control of flow separation in airfoil/wing design applications p 274 N95-23294
- Thermohydrodynamic analysis of cryogenic liquid turbulent flow fluid film bearings, phase 2 [NASA-CR-197412] p 349 N95-24461
- Sailplane glide performance and control using fixed and articulating winglets [NASA-CR-198579] p 392 N95-27180
- A two element laminar flow airfoil optimized for cruise [NASA-CR-198580] p 479 N95-29338
- Texas Instruments, Inc., Dallas, TX.**
- Ultra-Reliable Digital Avionics (URDA) processor p 245 N95-20638
- Texas Technological Univ., Lubbock, TX.**
- A brief survey of constrained mechanics and variational problems in terms of differential forms p 360 N95-25803
- How to fly an aircraft with control theory and splines p 360 N95-25805
- Texas Univ., Austin, TX.**
- Precision orbit determination of altimetric satellites p 86 N95-14282
- Effect of stratification and geometrical spreading on sonic boom rise time p 75 N95-14880
- Unsteadiness of shock-induced turbulent boundary layer separation. An inherent feature of turbulent flow or solely a wind tunnel phenomenon [AD-A290367] p 554 N95-29228
- Texas Univ., San Antonio, TX.**
- Micro-measurements of mechanical properties for adhesives and composites using digital imaging technology [NASA-CR-196111] p 22 N95-10231
- Probabilistic material strength degradation model for Inconel 718 components subjected to high temperature, high-cycle and low-cycle mechanical fatigue, creep and thermal fatigue effects [NASA-CR-197832] p 419 N95-27167
- Textron Bell Helicopter, Fort Worth, TX.**
- Aircraft fatigue and crack growth considering loads by structural component p 137 N95-19497
- Bell Helicopter Advanced Rotocraft Transmission (ART) program [NASA-CR-195479] p 555 N95-29538
- Textron Specialty Materials, Lowell, MA.**
- Evaluation of bonded boron/epoxy doublers for commercial aircraft aluminum structures p 92 N95-14457
- Status of bonded boron/epoxy doublers for military and commercial aircraft structures p 393 N95-27506
- Thomson-CSF, Paris (France).**
- FASTPACK: Optimized solutions for modular avionics derived from a parametric study. Part 2: Avionics p 233 N95-20635
- Composite cases for airborne electronic equipment: A technology study and EMC p 241 N95-20655
- Modular supplies for a distributed architecture p 234 N95-20657
- Tica Technologies, Inc., Cambridge, MA.**
- Optimizing cockpit display configurations with a genetic algorithm system [AD-A289799] p 508 N95-29123
- Tokai Univ., Tokyo (Japan).**
- Numerical solutions of inviscid and viscous flows about airfoils by TVD method p 684 N95-34521
- Tokyo Noko Univ. (Japan).**
- Vector-parallel simulations of transonic wind tunnel flows about a fully configured model of aircraft p 685 N95-34538
- Tokyo Univ. (Japan).**
- Transonic, supersonic and hypersonic wind-tunnel tests on aerodynamic characteristics of reentry body with blunted cone configuration [ISAS-658] p 480 N95-29640
- Experimental studies on boundary-layer transition on a reentry vehicle at transonic and supersonic speeds [ISAS-659] p 555 N95-29712
- A study on the convergence of a 3-D Euler code for cascade flow calculations p 706 N95-34508

Sidewall-effect of the wind tunnel on the estimation of the aerodynamic characteristics of a delta wing
p 685 N95-34525

Static pressure drop by swirling flow of an internal cooling air system through a turbine shaft p 698 N95-34560

Tokyo Univ., Sagamihara (Japan).

Viscous shock-layer analysis on hypersonic flow over reentry capsule with nonequilibrium chemistry
[NASA-656] p 436 N95-26739

Wind tunnel experiments on wake flow field behind a reentry capsule from a viewpoint of parachute deployment at supersonic speeds
[ISAS-655] p 374 N95-26740

Toledo Univ., OH.

Modeling improvements and users manual for axial-flow turbine off-design computer code AXOD
[NASA-CR-195370] p 8 N95-10853

User's manual for the NASA Lewis ice accretion/heat transfer prediction code with electrothermal deicer input
[NASA-CR-195430] p 57 N95-11888

Enhanced capabilities and updated users manual for axial-flow turbine preliminary sizing code TURBAN
[NASA-CR-195405] p 76 N95-15912

FPCAS2D user's guide, version 1.0
[NASA-CR-195413] p 156 N95-16588

Enhanced analysis and users manual for radial-inflow turbine conceptual design code RTD
[NASA-CR-195454] p 275 N95-23462

User's guide for ECAP2D: An Euler unsteady aerodynamic and aeroelastic analysis program for two dimensional oscillating cascades, version 1.0
[NASA-CR-189146] p 316 N95-24189

FPCAS3D User's guide: A three dimensional full potential aeroelastic program, version 1
[NASA-CR-198367] p 651 N95-32205

Toronto Univ. (Ontario).

Activities of the Institute for Aerospace Studies of Toronto University p 63 N95-12699

Hailstone heat and mass transfer measurements
[ISBN-0-315-86304-8] p 563 N95-29797

Transportation Research Board, Washington, DC.
Public-sector aviation issues: Graduate research award papers, 1992-1993
[PB94-217478] p 219 N95-19967

TRW, Inc., Redondo Beach, CA.

Passive MMW camera for low visibility landings
p 59 N95-13215

Tsentralni Aerogidrodinamicheskii Inst., Moscow (USSR).

The traditional and new methods of accounting for the factors distorting the flow over a model in large transonic wind tunnels p 165 N95-19275

Tulsa Univ., OK.

Controller resource management: What can we learn from aircrews?
[DOT/FAA/AM-95/21] p 602 N95-32186

Turbine Support Europa, Tilburg (Netherlands).
High velocity oxygen fuel spraying of erosion and wear resistant coatings on jet engine parts
p 202 N95-19680

Turbomeca S.A. - Brevets Szydlowski, Bordes (France).
Multilayer anti-erosion coatings p 201 N95-19679

Turkish Land Forces Command, Ankara (Turkey).
Scarf joint technique with cocured and precured patches for composite repair p 396 N95-27524

U

Union Carbide Industrial Gases, Inc., Tonawanda, NY.
Airborne rotary air separator study
[NASA-CR-189099] p 290 N95-24053

United Technologies Corp., East Hartford, CT.
Method for extracting forward acoustic wave components from rotating microphone measurements in the inlets of turbofan engines
[NASA-CR-195457] p 616 N95-30779

United Technologies Research Center, East Hartford, CT.
Computational fluid dynamics study of the variable-pitch split-blade fan concept
[NASA-CR-189206] p 15 N95-10247

Hydrocarbon-fueled ramjet/scramjet technology program, phase 2 extension
[NASA-CR-189659] p 15 N95-10319

Small crack test program for helicopter materials
p 92 N95-14455

Unsteady aerodynamic analyses for turbomachinery aeroelastic predictions p 141 N95-19381

Evaluation of a doubly-swept blade tip for rotorcraft noise reduction
[NASA-CR-189677] p 452 N95-28264

Automatic blocking for complex three-dimensional configurations p 566 N95-28734

Development of a linearized unsteady Euler analysis for turbomachinery blade rows
[NASA-CR-4677] p 592 N95-30611

Universitaet der Bundeswehr Muenchen, Neubiberg (Germany).
The 4-D approach to visual control of autonomous systems
[AIAA PAPER 94-1243-CP] p 27 N95-11513

Universities Space Research Association, Columbia, MD.
The Elite: A high speed, low-cost general aviation aircraft for Aeroworld
[NASA-CR-197161] p 45 N95-12530

Icarus Rewaxed: A high speed, low-cost general aviation aircraft for Aeroworld
[NASA-CR-197155] p 45 N95-12609

The FC-1D: The profitable alternative Flying Circus Commercial Aviation Group
[NASA-CR-197152] p 46 N95-12628

Triton 2 (1B)
[NASA-CR-197188] p 46 N95-12636

The OFP-6M transport jet
[NASA-CR-197159] p 46 N95-12637

The Balsa bullet: A high speed, low-cost general aviation aircraft for Aeroworld
[NASA-CR-197165] p 46 N95-12638

Cabin fuselage structural design with engine installation and control system
[NASA-CR-197173] p 47 N95-12639

Central coast designs: The Eightball Express. Taking off with convention, cruising with improvements and landing with absolute success
[NASA-CR-197181] p 47 N95-12643

LCX: Proposal for a low-cost commercial transport
[NASA-CR-197186] p 47 N95-12645

A preliminary design proposal for a maritime patrol strike aircraft: MPS-2000 Condor
[NASA-CR-197182] p 47 N95-12689

Design and construction of a remote piloted flying wing
[NASA-CR-197195] p 47 N95-12695

Integrated design and manufacturing for the high speed civil transport
[NASA-CR-197183] p 48 N95-12700

Design of a vehicle based system to prevent ozone loss
[NASA-CR-197199] p 48 N95-12702

Cabin-fuselage-wing structural design concept with engine installation
[NASA-CR-197172] p 49 N95-12993

Viper
[NASA-CR-197191] p 79 N95-13703

The Aluminum Falcon: A low cost modern commercial transport
[NASA-CR-197180] p 81 N95-15742

Universities Space Research Association, Houston, TX.
Gemini: A long-range cargo transport
[NASA-CR-197149] p 45 N95-12626

University of Central Florida, Orlando, FL.
User type certification for advanced flight control systems p 699 N95-34772

University of Southern California, Los Angeles, CA.
Programmed ignition of metal compounds in a scramjet p 16 N95-10466

An extension of the continuum model by Grad's thirteen moment equations for hypersonic rarefied flows
p 478 N95-29118

Flow models for the design of a hypersonic iodine vapor wind tunnel nozzle with chemical and vibrational nonequilibrium effects p 592 N95-30448

Utah Univ., Salt Lake City, UT.
The role of fretting corrosion and fretting fatigue in aircraft rivet hole cracking p 94 N95-14470

The effects of pitting on fatigue crack nucleation in 7075-T6 aluminum alloy p 88 N95-14482

V

Vaerloese Air Base, Vaerloese (Denmark).
Flying ambulances: The approach of a small air force to long distance aeromedical evacuation of critically injured patients p 568 N95-29618

Veda, Inc., Dayton, OH.
Industry review of a crew-centered cockpit design process and toolset
[AD-A282966] p 130 N95-17661

Integrated mission precision attack cockpit technology (IMPACT). Phase 1: Identifying technologies for air-to-ground fighter integration
[AD-A289562] p 389 N95-26684

Vigyan Research Associates, Inc., Hampton, VA.
A simple analytical aerodynamic model of Langley Winged-Cone Aerospace Plane concept
[NASA-CR-194987] p 54 N95-12175

Transonic Navier-Stokes calculations about a 65 deg delta wing
[NASA-CR-4635] p 108 N95-17273

Performance of the 0.3-meter transonic cryogenic tunnel with air, nitrogen, and sulfur hexafluoride media under closed loop automatic control
[NASA-CR-195052] p 310 N95-23257

Virginia Polytechnic Inst., Blacksburg, VA.
Development and verification of a resin film infusion/resin transfer molding simulation model for fabrication of advanced textile composites
[NASA-CR-197439] p 301 N95-23179

Flow structure generated by perpendicular blade vortex interaction and implications for helicopter noise predictions
[NASA-CR-198590] p 377 N95-28193

A general inverse design procedure for aerodynamic bodies p 606 N95-30497

Virginia Polytechnic Inst. and State Univ., Blacksburg, VA.
Active control of interior noise in a business jet using piezoceramic actuators p 29 N95-11276

Analytical investigation of adaptive control of radiated inlet noise from turbofan engines p 30 N95-11277

Design of a vehicle based system to prevent ozone loss
[NASA-CR-197199] p 48 N95-12702

Compression strength of composite primary structural components
[NASA-CR-197554] p 160 N95-18388

Supersonic flow and shock formation in turbine tip gaps p 312 N95-23429

Load transfer in the stiffener-to-skin joints of a pressurized fuselage
[NASA-CR-198610] p 439 N95-27865

Vibrational behavior of adaptive aircraft wing structures modelled as composite thin-walled beams
p 423 N95-28435

Computational methods for control and optimal design of aerospace systems
[AD-A292861] p 608 N95-31451

Performance improvement of composite wings through aeroelastic tailoring and modern control
[AD-A293689] p 608 N95-31602

Virginia Univ., Charlottesville, VA.
NASA-UVa light aerospace alloy and structures technology program (LA2ST)
[NASA-CR-198041] p 343 N95-24220

Severe edge effects and simple complimentary interior solutions for thin-walled anisotropic and composite structures
[AD-A290645] p 555 N95-29562

Spatially-resolved velocity measurements in steady, high-speed, reacting flows using laser-induced OH fluorescence p 650 N95-32109

Virginia Univ. Hospital, Charlottesville, VA.
NASA-UVa light aerospace alloy and structures technology program supplement: Aluminum-based materials for high speed aircraft
[NASA-CR-4645] p 343 N95-24878

Von Karman Inst. for Fluid Dynamics, Rhode-Saint-Genese (Belgium).
Aerodynamic investigation of the flow field in a 180 deg turn channel with sharp bend p 163 N95-19257

Vought Corp., Dallas, TX.
Repair of high temperature composite aircraft structure p 395 N95-27520

W

Washington State Univ., Pullman, WA.
Interactions of spanwise and chordwise vorticity associated with three-dimensional dynamic stall over an oscillating wing
[AD-A290546] p 477 N95-29091

Washington Univ., Seattle, WA.
Visualization of one-dimensional flow processes in a dual-mode scramjet engine p 15 N95-10465

Axial crack propagation and arrest in pressurized fuselage p 94 N95-14479

Automatic multi-block grid generation for high-lift configuration wings p 567 N95-28764

Investigation of starting and ignition transients in the thermally choked ram accelerator p 698 N95-34805

Wayne State Univ., Detroit, MI.
Active control of panel vibrations induced by a boundary layer flow
[NASA-CR-197867] p 273 N95-23182

West Virginia Univ., Morgantown, VA.
Determination of stability and control derivatives from the NASA F/A-18 HARV from flight data using the maximum likelihood method
[NASA-CR-197320] p 204 N95-19576

- Westinghouse Electric Corp., Baltimore, MD.**
 Certification of windshear performance with RTCA class D radomes p 41 N95-13206
 High density monolithic packaging technology for digital/microwave avionics p 240 N95-20646
- Westinghouse Savannah River Co., Aiken, SC.**
 Residual Stress Measurements with Laser Speckle Correlation Interferometry and Local Heat Treating [DE95-060082] p 349 N95-24598
- Wichita State Univ., Wichita, KS.**
 Plastic hinge modeling of structures [NIAR-94-14] p 24 N95-11168
 The airline quality report, 1994 [NIAR-94-11] p 277 N95-24012
 A multibody/finite element analysis approach for modeling of crash dynamic responses [NIAR-94-3] p 277 N95-24050
 Analysis of warping effects on the static and dynamic response of a seat-type structure [NIAR-94-12] p 348 N95-24211
 AIAA Techfest 20 Proceedings [NIAR-94-1] p 367 N95-26941
 An exploratory application of neural networks for airfoil design p 448 N95-26943
 Creating an alternative parameter optimization method (APO) p 375 N95-26946
 The near-wake flow behavior of an oscillating airfoil with modified trailing edge p 375 N95-26953
 Full span flaperons for a biplane p 391 N95-26954
 An experimental investigation of helicopter downwash and tailboom interaction at the Wichita State University 7x10 foot wind tunnel p 375 N95-26955
 Comparative wind tunnel tests of NACA 23024 airfoils with several aileron and spoiler configurations p 376 N95-27976
- Wisconsin Univ., Madison, WI.**
 Modeling spatio-temporal databases to measure the performance of the GPS satellite constellation p 489 N95-29596
 Air/fuel ratio visualization in a diesel spray p 556 N95-29807
- Woodfield (Alan A.), Bedford (England).**
 Wind shear and its effects on aircraft p 77 N95-14898
- Woods Hole Oceanographic Inst., MA.**
 Assimilation of altimeter data in a quasi-geostrophic model of the Gulf Stream system: A dynamical perspective [NASA-CR-196313] p 320 N95-23766
- Worcester Polytechnic Inst., MA.**
 Design and construction of a remote piloted flying wing [NASA-CR-197195] p 47 N95-12695
- Wright Lab., Eglin AFB, FL.**
 Eglin Air Force Base Ram Accelerator Research Facility p 19 N95-10284
- Wright Lab., Wright-Patterson AFB, OH.**
 Numerical study of mixing in a high and low enthalpy supersonic test facility p 7 N95-10467
 Pressure measurements on an F/A-18 twin vertical tail in buffeting flow. Volume 3: Buffet power spectral densities [AD-A281444] p 36 N95-11829
 Draft standard for color active matrix liquid crystal displays (AMLCDs) in US Military aircraft. Recommended best practices [AD-A282950] p 49 N95-12591
 Air Force seal activities p 60 N95-13600
 Developments in laser-based diagnostics for wind tunnels in the Aeromechanics Division: 1987-1992 [AD-A283011] p 84 N95-13687
 Flight evaluation of pneumatic forebody vortex control in post-stall flight p 72 N95-14259
 Pressure measurements on an F/A-18 twin vertical tail in buffeting flow. Volume 2: Steady and unsteady RMS pressure data [AD-A281581] p 76 N95-15465
 Large amplitude nonlinear response of flat aluminum, and carbon fiber plastic beams and plates [AD-A282440] p 96 N95-15547
 An engineering code to analyze hypersonic thermal management systems p 155 N95-16322
 Numerical simulation of transient vortex breakdown above a pitching delta wing [AD-A281075] p 107 N95-16808
 Universal wind tunnel data acquisition and reduction software [AD-A283897] p 171 N95-18365
 Pressure measurements on an F/A-18 twin vertical tail in buffeting flow. Volume 4, part 2: Buffet cross spectral densities [AD-A285555] p 143 N95-18641
 Weapons bay acoustic environment p 173 N95-19146
 High-temperature acoustic test facilities and methods p 174 N95-19149
- Nonlinear dynamic response of aircraft structures to acoustic excitation p 135 N95-19151
 Modelling structurally damaging twin-jet screech p 135 N95-19154
 Thermo-acoustic fatigue design for hypersonic vehicle skin panels p 162 N95-19161
 Determination of solid/porous wall boundary conditions from wind tunnel data for computational fluid dynamics codes p 164 N95-19266
 Proceedings of the USAF Structural Integrity Program Conference [AD-A285684] p 194 N95-19517
 Summary of a joint program of research into aircraft flight control concepts [AD-A280012] p 237 N95-20004
 The impact of advanced packaging technology on modular avionics architectures p 233 N95-20632
 Pressure measurements on an F/A-18 twin vertical tail in buffeting flow. Volume 4, part 1: Buffet cross spectral densities [AD-A285593] p 237 N95-21214
 Pressure measurements on an F/A-18 twin vertical tail in buffeting flow. Volume 1: Wind tunnel test summary [AD-A279126] p 225 N95-21877
 Optical processing and control [AD-A279157] p 259 N95-21975
 Damage tolerant repair techniques for pressurized aircraft fuselages [AD-A286298] p 219 N95-22046
 Heat transfer measurements in small scale wind tunnels [AD-A288689] p 341 N95-26053
 A non-iterative grid deformation algorithm for computational fluid dynamics for aeroelasticity [AD-A288298] p 436 N95-26418
 Partial discharge testing of high voltage wiring harness for airborne displays [AD-A289150] p 401 N95-27003
 Structural design optimization with survivability dependent constraints application: Primary wing box of a multi-role fighter p 398 N95-28440
 Recirculating cavity casing treatment failure [AD-A289330] p 513 N95-28908
 Computational Fluid Dynamics (CFD) analysis of a C-135 aircraft with a side-mounted splitter plate (with comparison to wind tunnel data) [AD-A292029] p 553 N95-29187
 Survey of CFD applications for high speed inlets [AD-A291365] p 557 N95-30087
 The control system design methodology of the STOL and maneuver technology demonstrator p 621 N95-31998
 Flight evaluation of forebody vortex control in post-stall flight p 609 N95-32003
- Wright Research Development Center, Wright-Patterson AFB, OH.**
 Characterization of stall inception in high-speed single-stage compressors [AD-A291275] p 514 N95-29934
- Wyle Labs., Inc., Arlington, VA.**
 25 years of airport sound insulation programs p 31 N95-11307
 Noise modeling for MOAs and ranges p 32 N95-11322
 USAF single-event sonic boom prediction model: PCBooms3 p 101 N95-14889
 The acoustic characteristics of turbomachinery cavities [NASA-CR-4671] p 476 N95-28720

Y

Yale Univ., New Haven, CT.

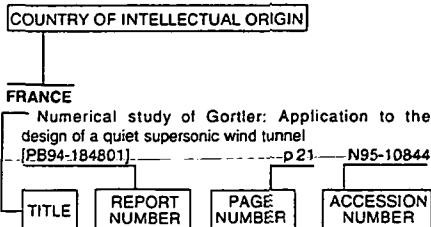
- Transport phenomena and interfacial kinetics in multiphase combustion systems [AD-A288297] p 418 N95-26417
 An analytic modeling and system identification study of helicopter dynamics p 505 N95-29787
- Yalif (Guy U.), MA.**
 The Computer Aided Aircraft-design Package (CAAP) p 217 N95-19759

FOREIGN TECHNOLOGY INDEX

AERONAUTICAL ENGINEERING / A Continuing Bibliography
1995 Cumulative Index

December 1995

Typical Foreign Technology Index Listing



Listings in this index are arranged alphabetically by country of intellectual origin. The title of the document is used to provide a brief description of the subject matter. The page number and accession number are included in each entry to assist the user in locating the abstract in the abstract section. If applicable, a report number is also included as an aid in identifying the document.

A

AUSTRALIA

- Fatigue resistance of peened 7050-T7451 aluminium alloy: Repair and re-treatment of a component surface [BTN-94-EIX94371347838] p 206 A95-69131
- Fatigue crack growth in nickel-based superalloys at 500-700 C. 1: Waspaloy [BTN-94-EIX94371347843] p 206 A95-69136
- Bonded composite repair of cracked load-bearing holes [BTN-94-EIX94401360553] p 243 A95-71867
- Electromagnetic backscattering from a helicopter rotor in the decametric wave band regime [BTN-94-EIX94381353130] p 243 A95-72648
- Time-of-flight mass spectrometer for impulse facilities [BTN-95-EIX95142553057] p 262 A95-73441
- Shock tunnel measurements of hypervelocity blunted cone drag [BTN-95-EIX95152577606] p 305 A95-73477
- Subharmonic and quasi-periodic motions of an eccentric squeeze film damper-mounted rigid rotor [BTN-94-EIX95011440601] p 429 A95-82982
- Effect of squeeze film damper land geometry on damper performance [HTN-95-92247] p 434 A95-85291
- Drag coefficients of spherical liquid droplets. Part 1: Quiescent gaseous fields [BTN-95-EIX95262697040] p 538 A95-86857
- Drag coefficients of spherical liquid droplets. Part 2: Turbulent gaseous fields [BTN-95-EIX95262697041] p 538 A95-86858
- Shock tunnel measurements of hypervelocity blunted cone drag [HTN-95-42591] p 459 A95-87221
- Period evolution of PSR B1259-63: Evidence for propeller-torque spin-down [HTN-95-B0194] p 581 A95-87903
- Chemical recombination in an expansion tube [HTN-95-20844] p 544 A95-88105

- Scramjet thrust measurement in a shock tunnel [HTN-95-C0008] p 586 A95-93396
- Residual strength of composites with multiple impact damage [BTN-94-EIX94511433967] p 701 A95-96664
- Efficient and effective handling of cycle slips in global positioning system data p 43 N95-12230
- Residual strength of composites with multiple impact damage [AD-A284230] p 87 N95-14409
- Development of a composite repair and the associated inspection intervals for the F-111C stiffener runout region p 66 N95-14477
- A PC-based interactive simulation of the F-111C Pavé Tack system and related sensor, avionics and aircraft aspects [AD-A285500] p 129 N95-16969
- Data acquisition and processing software for the Low Speed Wind Tunnel tests of the Jindivik auxiliary air intake [AD-A285455] p 108 N95-17178
- Six degree of freedom flight dynamic and performance simulation of a remotely-piloted vehicle [AERO-TN-9301] p 131 N95-18097
- Programmable cockpit research simulator [AD-A279219] p 204 N95-19848
- Variations observed in the AC generator signal period of a Sea King helicopter [AD-A284280] p 230 N95-19963
- A preliminary study of the airwake model used in an existing SH-60B/FFG-7 helicopter/ship simulation program [DSTO-TR-0015] p 224 N95-21659
- Derived gust spectra for the Macchi MB326H [ARL-TN-3] p 225 N95-21892
- Enhancement of F/A-18 operational flight measurements: Data report for phase 1 [DSTO-TR-0049] p 286 N95-23666
- AIR SAR deployment in Australia, September 1993: Management and objectives p 321 N95-23948
- An overview of Health and Usage Monitoring Systems (HUMS) for military helicopters [DSTO-TR-0061] p 327 N95-24200
- Helicopter life substantiation: Review of some USA and UK initiatives [DSTO-TR-0062] p 328 N95-24201
- A portable transmission vibration analysis system for the S-70A-9 Black Hawk helicopter [DSTO-TR-0072] p 348 N95-24203
- Shock tunnel studies of scramjet phenomena 1993 [NASA-CR-195038] p 350 N95-25394
- Thrust measurements of a complete axisymmetric scramjet in an impulse facility p 339 N95-25395
- Scramjet thrust measurement in a shock tunnel p 339 N95-25396
- Thrust measurement in a 2-D scramjet nozzle p 339 N95-25397
- The Superorbital Expansion Tube concept, experiment and analysis p 341 N95-25399
- Balances for the measurement of multiple components of force in flows of a millisecond duration p 350 N95-25400
- Configuration and other differences between Black Hawk and Seahawk helicopters in military service in the USA and Australia [AR-008-386] p 336 N95-25935
- Assessment of overhaul surge margin tests applied to the T53 engines in ADF Iroquois helicopters [AR-008-389] p 339 N95-25936
- Design and development of a test rig for the high frequency testing of rolling sleeve airsprings [DSTO-TN-0001] p 411 N95-26378
- F/A-18 IFOSTP Fatigue test airbag load determination on the vertical and horizontal tails [DSTO-TR-0135] p 388 N95-26389
- Characteristics of the turbine inlet temperature sensing circuit for the T56 turbo-prop engine [DSTO-TR-0095] p 405 N95-26424
- Bonded composite repair of metallic aircraft components: Overview of Australian activities p 392 N95-27505

- Scarf repairs to graphite/epoxy components p 396 N95-27523
- The development of an engineering standard for composite repairs p 396 N95-27528
- A review of Australian and New Zealand investigations on aeronautical fatigue during the period Apr. 1993 - Mar. 1995 [AR-009-202] p 397 N95-27918
- Tie-down trials involving a Sikorsky S-70B-2 helicopter [DSTO-TR-0132] p 400 N95-28567
- Helicopter life substantiation: Review of some USA and UK initiatives [AD-A290045] p 502 N95-28851
- Unmanned Aerial Vehicle technology [DSTO-GD-0044] p 503 N95-29362
- Estimation of aerodynamic load distributions on the F/A-18 aircraft using a CFD panel code [DSTO-TR-0147] p 504 N95-29445
- Preparation of S-70A-9 Black Hawk helicopter for flight tests to investigate cause of cracking of inner fuselage panel [AD-A293891] p 608 N95-31544
- Expert systems and artificial intelligence applications in engineering design and inspection p 710 N95-33008
- Water model tests on the Allison T56 series 3 combustion system [DSTO-TR-0139] p 697 N95-33250
- ### AUSTRIA
- Balloon technology and observations; Symposium P3 of the COSPAR Plenary Meeting, 29th, Washington, DC, Aug. 28-Sept. 5, 1992 [HTN-95-70250] p 181 A95-66276
- Multidimensional calculation of spark flame initiation by adopting a generic hydrocarbon kinetic scheme p 528 A95-87566
- A poor man's expert system for aviation VSRF in complex terrain p 869 A95-93524

B

BELGIUM

- Modeling resonance in waveguide-to-microstrip junctions by unilateral fin line resonators [BTN-94-EIX94381323445] p 242 A95-70844
- Experimental investigation of the flowfield about an upswept afterbody [BTN-95-EIX95152582321] p 265 A95-73524
- Quality estimates and stretched meshes based on Delaunay triangulations [HTN-95-42575] p 564 A95-87205
- Computational methods in applied sciences; European Computational Fluid Dynamics Conference, 1st, Brussels, Belgium, Sept. 7-11, 1992 [ISBN 0-444-89795-X] p 539 A95-87552
- In-flight interior sound field mapping in propeller aircraft p 572 A95-88472
- Aircraft interior sound field analysis in view of active control: Results from the ASANCA project p 575 A95-90109
- Computational fluid dynamics '92; Proceedings of the European Computational Fluid Dynamics Conference, 1st, Brussels, Belgium, Sep. 7-11, 1992. Vols. 1 & 2 [ISBN 0-444-89793-3] p 638 A95-95357
- Permeable wall boundary conditions for transonic airfoil design p 641 A95-95445
- A 2D parallel multiblock Navier-Stokes solver with applications on shared- and disturbed memory machines p 643 A95-95475
- Hypersonic Navier-Stokes computations about complex configurations p 644 A95-95497
- Aerodynamic investigation of the flow field in a 180 deg turn channel with sharp bend p 163 N95-19257
- In-situ detection of surface passivation or activation and of localized corrosion: Experiences and perspectives in aircraft p 302 N95-23508
- Test method and test results for environmental assessment of aircraft materials p 302 N95-23509
- ### BRAZIL
- The joint Russian-Brazil research on balloons p 182 A95-66303

- Regenerative cooling for liquid propellant rocket thrust chambers
[INPE-5565-TDI/540] p 150 N95-18720
- BULGARIA**
- A program for scientific and applied investigations using aerostat complexes p 182 A95-66304
- Thundercloud electric field modeling for the ionosphere-Earth region. 1: Dependence on cloud charge distribution
[HTN-95-41223] p 317 A95-75035

C

CANADA

- Geometrical acoustics approach for calculating the effects of flow on acoustics scattering
[BTN-94-EIX94321331207] p 61 A95-60790
- Lapunov exponents and stochastic stability of two-dimensional parametrically excited random systems
[BTN-94-EIX94361122401] p 207 A95-65897
- Vortical flow structure near the F/A-18 LEX at high incidence
[BTN-95-EIX95062487555] p 186 A95-68369
- Aircraft icing measurements in East Coast winter storms
[HTN-95-60505] p 214 A95-68756
- Flight control system mode transitions influence on handling qualities and task performance
[BTN-95-EIX95062487525] p 203 A95-69233
- Mesoscale structure of precipitation bands in a North Atlantic winter storm
[HTN-95-40659] p 215 A95-69803
- Ice accretion on aircraft wings
[BTN-95-EIX95082502224] p 225 A95-71021
- Numerical modelling of transverse impact on composite coupons
[BTN-95-EIX95082502225] p 240 A95-71022
- Modelling of pillowing due to corrosion in fuselage lap joints
[BTN-95-EIX95082502227] p 240 A95-71024
- Adaptive remeshing for convective heat transfer with variable fluid properties
[BTN-95-EIX95082502720] p 243 A95-71033
- Large-scale computational fluid dynamics by the finite element method
[BTN-94-EIX94381359154] p 243 A95-71744
- Adaptive finite element method for turbulent flow near a propeller
[BTN-95-EIX95142553038] p 305 A95-73460
- Coupled FEM-BEM approach for mean flow effects on vibro-acoustic behavior of planar structures
[BTN-95-EIX95152577587] p 263 A95-73495
- Postinstability behavior of a two-dimensional airfoil with a structural nonlinearity
[BTN-95-EIX95152582337] p 266 A95-73539
- Multiple site fatigue damage in fuselage skin splices: Experimental simulation and theoretical prediction
[BTN-95-EIX95152584676] p 276 A95-73588
- Validation of an effective flat cruciform-shaped specimen to study CFRP composite laminate under biaxial loading
[BTN-95-EIX95152584677] p 282 A95-73589
- Evaluation of advanced aerospace materials by depth sensing indentation and scratch methods
[BTN-95-EIX95152584678] p 282 A95-73590
- Improving prediction: The incorporation of simplified rotor dynamics in a mathematical model of the bell 412HP
[BTN-95-EIX95152584679] p 282 A95-73591
- Finite element model for a flexible non-symmetric rotor on distributed bearing: A stability study
[BTN-94-EIX94381352212] p 306 A95-74612
- Application of a control-volume-based finite-element formulation to the shock tube problem
[BTN-95-EIX95182619099] p 295 A95-76584
- A comparison of some aerodynamic resistance methods using measurements over cotton and grass from the 1991 California ozone deposition experiment
[HTN-95-11295] p 319 A95-77000
- Theoretical and experimental studies of fretting-initiated fatigue failure of aeroengine compressor discs
[BTN-94-EIX94421372285] p 343 A95-78467
- Study of heat transfer rates during quenching of a hot tube under microgravity p 428 A95-82641
- Experimental investigation of flow-boiling heat transfer under microgravity p 428 A95-82642
- Fractal properties of whitecaps
[HTN-95-92121] p 443 A95-83827
- Evolution of the concentrations of trace species in an aircraft plume: Trajectory study
[HTN-95-A1044] p 443 A95-84549
- The effects of surface modification on fretting fatigue in Ti alloy turbine components
[HTN-95-61145] p 404 A95-84909

- Explicit Kutta condition for an unsteady two-dimensional constant potential panel method
[HTN-95-51679] p 433 A95-85061
- Compressible Navier-Stokes computations of multielement airfoil flows using multiblock grids
[HTN-95-42327] p 371 A95-86156
- Development of a large-aspect-ratio rectangular turbulent free jet
[HTN-95-42333] p 372 A95-86162
- A flow pattern map for two-phase liquid-gas flow under reduced gravity conditions p 539 A95-87280
- Role of Kutta waves on oscillatory shock motion on an airfoil
[HTN-95-81642] p 542 A95-87690
- Inter-Noise 92: Noise control and the public; International Congress on Noise Control Engineering, Toronto, Ontario, Canada, July 20 - 22, 1992. Vols. 1 & 2
[ISBN 0-931784-25-5] p 559 A95-88457
- Development and validation of a numerical acoustic analysis program for aircraft interior noise prediction
p 572 A95-88471
- Aircraft noise at a West Coast airport in the next century p 560 A95-90095
- Viscous contribution to the high Mach number damping in pitch of blunt slender cones at small angles of attack
[HTN-95-01096] p 469 A95-90282
- Turbulent flow measurements with a triple-split hot-film probe
[HTN-95-A1774] p 634 A95-93337
- Stratus' tephigram as a training/forecasting tool
p 657 A95-93465
- Transport Canada proposed R&D program for the development of a multi-parameter dual X-Ka band Doppler radar for aviation meteorology applications
p 659 A95-93477
- The performance of forward scatter visibility sensors for application in autostations and runway visual range in snow and freezing precipitation events p 662 A95-93489
- Development of a climatology for possible microburst occurrence in Canada p 664 A95-93497
- FTGEN - An automated FT production system
p 668 A95-93519
- Aviation terminal forecasts based on automated observations (FTAUTO) p 668 A95-93520
- Propulsion education at Carlton University
[SAE PAPER 931391] p 613 A95-93667
- An educational introduction to transonic compressor stage design principles
[SAE PAPER 931393] p 613 A95-93668
- Modeling and analysis for the GPS pseudo-range observable
[BTN-95-EIX95302731227] p 600 A95-94046
- Depolarizing trihedral corner reflectors for radar navigation and remote sensing
[BTN-95-EIX9530272634] p 636 A95-94108
- An improved finite element method for the solution of the compressible Euler and Navier-Stokes equations
p 640 A95-95439
- New eigensolutions and modal analysis for gyroscopic/rotor systems, part 1: undamped systems
[BTN-94-EIX94522410219] p 702 A95-96373
- New eigensolutions and modal analysis for gyroscopic/rotor systems, part 2: perturbation analysis for damped systems
[BTN-94-EIX94522410220] p 702 A95-96374
- Modal parameters for cracked rotors: models and comparisons
[BTN-94-EIX94522410226] p 702 A95-96378
- Activities of the Institute for Aerospace Studies of Toronto University p 63 N95-12699
- Surface pressure and wake drag measurements on the Boeing A4 airfoil in the IAR 1.5X1.5m Wind Tunnel Facility p 110 N95-17850
- A review of gust load calculation methods at de Havilland p 118 N95-18604
- Noise transmission and reduction in turboprop aircraft
p 175 N95-19164
- Spectrogram diagnosis of aircraft disasters
p 124 N95-19167
- Applications of the five-hole probe technique for flow field surveys at the Institute for Aerospace Research
p 163 N95-19255
- Unsteady flow testing in a passive low-correction wind tunnel p 147 N95-19272
- Evaluation of combined wall- and support-interference on wind tunnel models p 122 N95-19278
- Interference corrections for a centre-line plate mount in a porous-walled transonic wind tunnel
p 122 N95-19280
- Erosion of T56 5th stage rotor blades due to bleed hole overtip flow p 200 N95-19666
- Protective coatings for compressor gas path components p 201 N95-19675
- Transport aircraft loading and balancing system: Using a CLIPS expert system for military aircraft load planning
p 217 N95-19751

- Double pass retroreflection for corrosion detection in aircraft structures p 323 N95-23503
- Characterization of corrosion and development of a breadboard of a D sight aircraft inspection system, phase 1
[AD-A288347] p 380 N95-26527
- Bonded composite repair of thin metallic materials: Variable load amplitude and temperature cycling effects
p 393 N95-27509
- Design and structural validation of CF116 upper wing skin boron doubler p 393 N95-27510
- Composite repair issues on the CF-18 aircraft
p 395 N95-27518
- Finite element vorticity-based methods for the solution of the incompressible and compressible Navier-Stokes equations p 553 N95-29119
- Hailstone heat and mass transfer measurements
[ISBN-0-315-86304-8] p 563 N95-29797
- Thermal-mechanical fatigue crack growth in aircraft engine materials
[ISBN-0-315-86543-1] p 647 N95-31098
- Practical experiences in control systems design using the NCR Bell 205 Airborne Simulator
p 624 N95-32015
- Water blasting paint removal methods
p 650 N95-32170
- Facilities used for plastic media blasting
p 627 N95-32176
- Operational parameters and material effects
p 651 N95-32179

CHILE

- Natural convection in central microcavities of vertical, finned enclosures of very high aspect ratios
[BTN-95-EIX95282711336] p 632 A95-92405

CHINA

- New strategy combining backward inference with forward inference in monitoring and diagnosing techniques for hydrodynamic bearing-rotor systems
[BTN-94-EIX94331336949] p 88 A95-61795
- Improved analytical solution for varying specific heat parallel stream mixing
[BTN-94-EIX94481415349] p 103 A95-65339
- Development and application of the double V type flame stabilizer
[BTN-94-EIX94481415355] p 154 A95-65345
- Direct splitting of coefficient matrix for numerical calculation of transonic nozzle flow
[BTN-94-EIX94481415356] p 103 A95-65346
- Aerodynamic design and calculation of flow around the plane cascade of turbine
[BTN-94-EIX94481415357] p 104 A95-65347
- Development of aeronautical mobile satellite services over the past thirty years
[BTN-95-EIX95152569458] p 305 A95-73498
- Effects of AMB parameters on the dynamic stability of the rotor
[BTN-94-EIX94381353450] p 323 A95-75494
- A new type of simulator for simulating the flow-field distortion of engine inlet
[BTN-95-EIX95202638963] p 289 A95-76673
- Simulation on the 3-D turbulent flow in the passages of finocyl grain
[BTN-95-EIX95202638962] p 279 A95-76674
- Aerodynamic parameters of crop canopies estimated with a center-of-pressure technique
[HTN-95-41901] p 356 A95-81648
- Numerical analysis of flow field around gas rudder
p 407 A95-82333
- Nonlinear observer and its application in flight control
p 447 A95-82449
- Study on a scheme for the prolongation of microgravity time of balloon-borne drop capsule p 414 A95-82515
- An inverse design method of transonic airfoil and wing
[HTN-95-71128] p 385 A95-83489
- Nonlinear decoupling control study for aircraft maneuvering flight
[HTN-95-71130] p 408 A95-83491
- Non-linear viscoelastic-plastic constitutive relations for an aeronautical PMMA
[HTN-95-71132] p 385 A95-83493
- The analysis of the processing increased weight for pilot production of F-X aircraft
[HTN-95-71133] p 385 A95-83494
- Analysis of backscattering from wing and fuselage joints
[HTN-95-71134] p 430 A95-83495
- Swirl control in an S-duct at high angle of attack
[HTN-95-20846] p 545 A95-88107
- Optimization of waverider configurations generated from inclined circular and elliptic cones
[AIAA PAPER 95-6089] p 492 A95-89198
- Numerical design methods for transonic NLF configurations p 471 A95-91498
- Multivariable adaptive control using only input and output measurements for turbojet engines
[BTN-95-EIX95292721165] p 677 A95-92597

- New experimental approach to determine initial fatigue quality with fastener holes
[BTN-94-EIX94522406136] p 701 A95-96273
- Joint Proceedings on Aeronautics and Astronautics (JPA) [ISBN-7-80-046602-7] p 104 N95-16249
- Investigation of dynamic inflow's influence on rotor control derivatives p 155 N95-16250
- An approach to aerodynamic characteristics of low radar cross-section fuselages p 106 N95-16251
- An improved method of airfoil design p 106 N95-16252
- Wall-signature methods for high speed wind tunnel wall interference corrections p 107 N95-16257
- An investigation of polynomial calibrations methods for wind tunnel balances p 144 N95-16258
- Linear prediction data extrapolation superresolution radar imaging p 155 N95-16268
- Application of GPS/SINS/RA integrated system to aircraft approach landing p 125 N95-16277
- The computer analysis of the prediction of aircraft electrical power supply system reliability p 155 N95-16278
- Simulation investigation on system identification of gas turbine [PB95-104238] p 139 N95-17749
- Assessment of a non-dedicated GPS receiver system for precise airborne attitude determination [DE94-019309] p 229 N95-21520
- Numerical investigation to S-inlet flows (Numerical simulation study of S-inlet flows) [AD-A289590] p 374 N95-26713
- Plate manipulators [AD-A289601] p 374 N95-26719
- A numerical method for unsteady transonic flow about wings with control surfaces [AD-A289631] p 375 N95-26859
- Thermal design of returnable satellites [AD-A294113] p 701 N95-34500
- CROATIA**
- Powerful bolide explosion over North Italy [HTN-95-80564] p 218 A95-69658
- CZECHOSLOVAKIA**
- Numerical solution of Euler and Navier-Stokes equations for 2D transonic problems p 638 A95-95366
- Solid-state data recorder, next development and use p 705 N95-33143
- D**
- DENMARK**
- Nordic Standards for measurement of aircraft noise immission in residential areas and noise reduction of dwellings p 570 A95-88463
- Viscous flow simulation using the discrete vortex diffusion velocity method p 639 A95-95421
- Flying ambulances: The approach of a small air force to long distance aeromedical evacuation of critically injured patients p 568 N95-29618
- E**
- EGYPT**
- Variations of perturbations in perigee height with eccentricity for artificial Earth's satellites due to air drag [HTN-95-40013] p 85 A95-62657
- Main features of overexpanded triple jets [BTN-95-EIX95142553040] p 304 A95-73458
- F**
- FINLAND**
- The combination of forecasts in an automated aviation weather forecasting system p 669 A95-93522
- Airborne imaging radiometer scan simulation [BTN-95-EIX95332753018] p 638 A95-94793
- TKKMOD: A computer simulation program for an integrated wind diesel system. Version 1.0: Document and user guide [PB94-179090] p 60 N95-11798
- Using landmarks for the vehicle location measurement [PB94-184512] p 43 N95-12582
- FRANCE**
- French contribution to new balloon designs and materials p 181 A95-66277
- Balloon flights in France and in Europe p 204 A95-66301
- Nonhydrostatic simulation of frontogenesis in a moist atmosphere. Part 3: Thermal wind imbalance and rainbands [HTN-95-90356] p 212 A95-66429
- Aspects of vortex breakdown [HTN-95-A0001] p 183 A95-67828
- Shock layers and boundary layers in hypersonic flows [HTN-95-A0003] p 183 A95-67830
- Experimental study of three-dimensional separation [BTN-94-EIX94441385752] p 179 A95-68216
- Prediction of ice accretion: Comparison between the 2D and 3D codes [BTN-94-EIX94441385753] p 213 A95-68217
- Phenomenological description and simplified modelling of the vortex wake issuing from a jet in a crossflow [BTN-94-EIX94441385754] p 184 A95-68218
- Tip vortex on a swept wing. Mean flow and unsteady phenomena [BTN-94-EIX94441385755] p 184 A95-68219
- Future SSTs a European approach [BTN-95-EIX95072419883] p 180 A95-68396
- Measurement by coherent anti-Stokes Raman scattering in the R5Ch hypersonic wind tunnel [BTN-95-EIX95112523811] p 188 A95-69322
- Side forces at high angles of attack. Why, when, how? [BTN-95-EIX95112523809] p 194 A95-69324
- Precise orbit determination with a short-arc technique p 240 A95-70543
- Secondary source locations in active noise control: Selection or optimization? [BTN-94-EIX94381352222] p 257 A95-71738
- Two-equation turbulence model for unsteady separated flows around airfoils [BTN-95-EIX95142553054] p 262 A95-73444
- Geoid lineations of 1000 km wavelength over the central Pacific [HTN-95-11304] p 319 A95-77009
- Impact of present aircraft emissions of nitrogen oxides on tropospheric ozone and climate forcing [HTN-95-21364] p 353 A95-78679
- Potential effects on ozone of future supersonic aircraft/2D simulation [HTN-95-51282] p 356 A95-80867
- International cooperation in standardization p 452 A95-82665
- Stochastic approach to noise modeling for free turbulent flows [HTN-95-42321] p 371 A95-86150
- Airborne lidar observation of mountain-wave-induced polar stratospheric clouds during EASOE [HTN-95-00738] p 444 A95-86308
- High pressure vaporization and burning of methanol droplets in reduced gravity p 527 A95-87285
- High temperature aspects of the European Hermes programs p 524 A95-87379
- Scramjet combustor design in France [AIAA PAPER 95-6094] p 510 A95-88002
- Injection studies in the French hypersonic technology program [AIAA PAPER 95-6096] p 510 A95-88004
- Integration of an hypersonic airbreathing vehicle: Assessment of overall aerodynamic performances and of uncertainties [AIAA PAPER 95-6100] p 492 A95-88007
- Separation of winged vehicles in supersonics [AIAA PAPER 95-6092] p 526 A95-88601
- Compressible Navier-Stokes calculations of the flow over airfoil sections. Comparisons of 1st and 2nd order turbulence models [SAE PAPER 932510] p 546 A95-89183
- Corrective term in wall slip equations for Knudsen layer [BTN-95-EIX95282705070] p 455 A95-89667
- High-frequency acoustic radiation from a curved duct of circular cross section p 573 A95-90098
- Noise and vibration control in aircraft: A global approach p 576 A95-90128
- ASTRYD: A new numerical tool for aircraft cabin and environmental noise prediction p 576 A95-90129
- Temperature diagnostics in the hypersonic flow regime: An application to develop a stagnation temperature probe [AIAA PAPER 95-6114] p 511 A95-90442
- Review of new French facilities for PREPHA program [AIAA PAPER 95-6128] p 520 A95-90449
- Intermetallic and titanium matrix composite materials for hypersonic applications [AIAA PAPER 95-6132] p 530 A95-90451
- Implicit multi-domain method for unsteady compressible inviscid fluid flows around 3D projectiles p 548 A95-91482
- Effects of free-stream turbulence intensity on a boundary layer recovering from concave curvature effects [BTN-95-EIX95282710058] p 632 A95-92471
- Optimal shape design in hypersonic aerodynamics and electromagnetics p 639 A95-95397
- Numerical simulation of the 3D turbulent flow around the combustor dome of an aircraft engine p 640 A95-95423
- Implicit multidomain calculation of viscous transonic flows without artificial viscosity or upwinding p 640 A95-95443
- A cartesian grid finite element method for aerodynamics of moving rigid bodies p 642 A95-95471
- High performance parallelized implicit Euler solver for the analysis of unsteady aerodynamic flows p 644 A95-95495
- Numerical study of Gortler instability: Application to the design of a quiet supersonic wind tunnel [PB94-184801] p 21 N95-10844
- Shock tube investigations of combustion phenomena in supersonic flows [PB94-175262] p 55 N95-11796
- Supersonic base flow investigation over axisymmetric afterbodies [PB94-180957] p 39 N95-12578
- AGARD highlights 94/2 [AGARD-HIGHLIGHTS-94/2] p 102 N95-13640
- Identification of dynamic systems. Volume 3: Applications to aircraft. Part 2: Nonlinear analysis and manoeuvre design [AGARD-AG-300-VOL-3-PT-2] p 79 N95-14102
- Scale effects on aircraft and weapon aerodynamics [AGARD-AG-323] p 67 N95-14103
- Turbomachinery Design Using CFD [AGARD-LS-195] p 89 N95-14127
- New methods, new methodology: Advanced CFD in the Snecma turbomachinery design process p 90 N95-14134
- Quality assessment for wind tunnel testing [AGARD-AR-304] p 67 N95-14197
- The principles of flight test assessment of flight-safety-critical systems in helicopters [AGARD-AG-300-VOL-12] p 77 N95-14199
- A selection of experimental test cases for the validation of CFD codes, volume 1 [AGARD-AR-303-VOL-1] p 91 N95-14201
- Computational aerodynamics based on the Euler equations [AGARD-AG-325] p 72 N95-14264
- Missile Aerodynamics [AGARD-R-804] p 73 N95-14445
- Lateral jet control for tactical missiles p 84 N95-14448
- High angle of attack aerodynamics p 74 N95-14450
- Computation of supersonic air-intakes p 74 N95-14452
- Flight in an Adverse Environment [AGARD-LS-197] p 77 N95-14893
- Optimum Design Methods for Aerodynamics [AGARD-R-803] p 127 N95-16562
- Optimal shape design for aerodynamics p 128 N95-16568
- Review of the EUROPT Project AERO-0026 p 129 N95-16573
- A processing centre for the CNES CE-GPS experimentation p 125 N95-17196
- Experimental and analytical methods for the determination of connected-pipe ramjet and ducted rocket internal performance [AGARD-AR-323] p 149 N95-17278
- Aircraft and sub-system certification by piloted simulation [AGARD-AR-278] p 145 N95-17388
- A selection of experimental test cases for the validation of CFD codes, volume 2 [AGARD-AR-303-VOL-2] p 109 N95-17846
- Data from the GARTEUR (AD) Action Group 02 airfoil CAST 7/DOA1 experiments p 111 N95-17856
- OAT15A airfoil data p 111 N95-17857
- Ellipsoid-cylinder model p 158 N95-17869
- Supersonic vortex flow around a missile body p 114 N95-17870
- Test data on a non-circular body for subsonic, transonic and supersonic Mach numbers p 158 N95-17871
- Delta-wing model p 114 N95-17873
- A selection of experimental test cases for the validation of CFD codes. Supplement: Datasets A-E [AGARD-AR-303-SUPPL] p 117 N95-18539
- Aircraft Loads due to Turbulence and their Impact on Design and Certification [AGARD-R-798] p 143 N95-18597
- Gyroscopic and propeller aerodynamic effects on engine mounts dynamic loads in turbulence conditions p 132 N95-18599
- On-line handling of air traffic: Management, guidance and control [AGARD-AG-321] p 126 N95-18927
- Mathematical Models of Gas Turbine Engines and their Components [AGARD-LS-198] p 139 N95-19017
- Impact of Acoustic Loads on Aircraft Structures [AGARD-CP-549] p 173 N95-19142
- Aeroacoustic qualification of HERMES shingles p 173 N95-19145
- Brite-Euram programme: ACOUFAT acoustic fatigue and related damage tolerance of advanced composite and metallic structures p 174 N95-19159

Wall Interference, Support Interference and Flow Field Measurements
 [AGARD-CP-535] p 162 N95-19251
 Experimental techniques for measuring transonic flow with a three dimensional laser velocimetry system. Application to determining the drag of a fuselage p 163 N95-19258
 Analysis of test section sidewall effects on a two dimensional airfoil: Experimental and numerical investigations p 165 N95-19276
 Calculation of wall effects of flow on a perforated wall with a code of surface singularities p 165 N95-19277
 Interaction of a three strut support on the aerodynamic characteristics of a civil aviation model p 122 N95-19279
 Erosion, Corrosion and Foreign Object Damage Effects in Gas Turbines
 [AGARD-CP-558] p 197 N95-19653
 Design of fan blades subjected to bird impact p 200 N95-19669
 New Trends in coatings developments for turbine blades: Materials processing and repair p 201 N95-19676
 Multi-layer anti-erosion coatings p 201 N95-19679
 Advanced Packaging Concepts for Digital Avionics [AGARD-CP-562] p 233 N95-20631
 FASTPACK: Optimized solutions for modular avionics derived from a parametric study. Part 1: Platform features p 233 N95-20634
 FASTPACK: Optimized solutions for modular avionics derived from a parametric study. Part 2: Avionics p 233 N95-20635
 Composite cases for airborne electronic equipment: A technology study and EMC p 241 N95-20655
 Lightweight electronic enclosures using composite materials p 241 N95-20656
 Modular supplies for a distributed architecture p 234 N95-20657
 Experimental study of the helicopter-mobile radioelectrical channel and possible extension to the satellite-mobile channel p 247 N95-20945
 Application of Direct and Large Eddy Simulation to Transition and Turbulence [AGARD-CP-551] p 248 N95-21061
 Data link terminal DLT document [PB95-110805] p 229 N95-21369
 Corrosion detection and management of advanced airframe materials [AGARD-CP-565] p 302 N95-23496
 Corrosion in service experience with aircraft in France p 303 N95-23518
 Composite Repair of Military Aircraft Structures [AGARD-CP-550] p 392 N95-27504
 Composite repair of metallic airframe: Twenty years of experience p 393 N95-27508
 Composite or metallic bolted repairs on self-stiffened carbon wing panel of the commuter ATR72 design criteria, analysis, verification by test p 396 N95-27525
 AGARD flight test techniques series. Volume 13: Reliability and maintainability [AGARD-AG-300-VOL-13] p 504 N95-29503
 Flight Vehicle Integration Panel Workshop on Pilot Induced Oscillations [AGARD-AR-335] p 597 N95-31061
 Active control technology: Applications and lessons learned [AGARD-CP-560] p 620 N95-31989
 Evaluation of the techniques of fuzzy control for the piloting an aircraft p 621 N95-31997
 Catapult-launching of the RAFALE design and experimentation p 609 N95-32008
 Flying qualities of civil transport aircraft with electrical flight control p 624 N95-32016
 Environmentally Safe and Effective Processes for Paint Removal [AGARD-LS-201] p 650 N95-32165
 Selective chemical stripping p 650 N95-32175
 Process evaluation p 651 N95-32180
 Standardization work p 651 N95-32181
 Low-Level and Nap-of-the-Earth (NOE) night operations [AGARD-CP-563] p 686 N95-32486
 A helmet mounted display for night missions at low altitude p 693 N95-32503
 Low-level data fusion for landing runways detection p 689 N95-33136
 AGARD index of publications: 1992-1994 [AGARD-INDEX-92-94] p 711 N95-33198

G

GERMANY

Time-optimal turn to a heading: An analytic solution [BTN-94-EIX94511433940] p 142 A95-64606

Planar air density measurements near model surfaces by ultraviolet Rayleigh/Raman scattering [BTN-94-EIX94441386614] p 213 A95-67345
 High accuracy navigation and landing system using GPS/IMU system integration [BTN-94-EIX94441386129] p 189 A95-68185
 GPS/GLONASS/INS test program [BTN-94-EIX94441386131] p 189 A95-68187
 On wave-front curvature in linear stability theory [BTN-94-EIX94441385756] p 184 A95-68220
 Using adaptive structures to attenuate rotary wing aeroelastic response [BTN-95-EIX95062487547] p 192 A95-68361
 On-the-fly carrier phase ambiguity resolution for precise aircraft landing [BTN-95-EIX95112522535] p 190 A95-69328
 Laplace interaction law for the computation of viscous airflow flow in low- and high-speed aerodynamics [BTN-95-EIX95142553037] p 263 A95-73461
 Analytical solution and parameter estimation of projectile dynamics [BTN-95-EIX95212645695] p 272 A95-76747
 Transport of exhaust products in the near trail of a jet engine under atmospheric conditions [HTN-95-91421] p 319 A95-77334
 Nitrous oxide and methane emissions from aero engines [HTN-95-21363] p 353 A95-78678
 North Atlantic air traffic within the lower stratosphere: Cruising times and corresponding emissions [HTN-95-91841] p 354 A95-80829
 Dynamics of aircraft exhaust plumes in the jet-regime [HTN-95-51275] p 355 A95-80860
 Modeling of aircraft exhaust emissions and infrared spectra for remote measurement of nitrogen oxides [HTN-95-51276] p 355 A95-80861
 Empirical corrections of the rigid rotor interaction potential of H₂-H₂ in the attractive region: Dimer features in the FIR absorption spectra [HTN-95-41943] p 361 A95-81690
 Mapping of forest fire damages using imaging spectroscopy
 A higher harmonic control test in the DNW to reduce impulsive BVI noise [HTN-95-61071] p 385 A95-83655
 On the influence of time-varying flow velocity on unsteady aerodynamics [HTN-95-61073] p 369 A95-83657
 Forming and bonding techniques for high-strength aluminum alloys [HTN-95-20605] p 418 A95-84786
 Automatic riveting cell for commercial aircraft floor grid assembly [HTN-95-92309] p 365 A95-85353
 Compressible inviscid vortex flow of a sharp edge delta wing [BTN-95-EIX95262694308] p 370 A95-85479
 Aeroelastic stability of cascades in turbomachinery [HTN-95-61156] p 405 A95-86255
 Aircraft measurements of CLO and HCL during EASOE 1991/92 [HTN-95-00721] p 444 A95-86291
 Two dimensional stratospheric aerosol distributions during EASOE [HTN-95-00726] p 444 A95-86296
 Airborne measurements during the European Arctic Stratospheric Ozone Experiment column amounts of HNO₃ and O₃ derived from FTIR emission sounding [HTN-95-00742] p 445 A95-86312
 Airborne measurements during the European Arctic Stratospheric Ozone Experiment: Observation of OCIO [HTN-95-00745] p 445 A95-86315
 Airborne measurements during the Arctic stratospheric experiment: Observation of O₃ and NO₂ [HTN-95-00748] p 445 A95-86318
 Orbital transport: Technical, meteorological and chemical aspects; Aerospace Symposium, 3rd, Braunschweig, Germany, Aug. 26-28, 1991 [ISBN 3-540-563180] p 524 A95-87373
 Environmental aspects of Orbital transport: Hypersonic technology experimental vehicles (The need for flight testing at hypersonic speed) p 559 A95-87377
 The aerothermodynamic validation reentry experiment HYPERBA p 524 A95-87380
 Design optimization of an airbreathing aerospaceplane p 524 A95-87382
 Integrated thermal and mechanical analysis of hypersonic vehicles by using adaptive finite element methods p 524 A95-87383
 Estimation of aerodynamic derivatives: Euler scheme validation and approximate methods for hypersonic configurations p 460 A95-87385
 Numerical modeling and simulation of chemically reacting reentry flows p 525 A95-87387

The high enthalpy shock tunnel in Goettingen (HEG) p 518 A95-87391
 Reentry trajectories and their optimization by an evolution algorithm p 525 A95-87394
 Optimal separation and ascent of lifting upper stages p 525 A95-87396
 Trim conditions for optimal flight performance of hypersonic aircraft p 514 A95-87397
 Handling qualities of hypersonic aircraft and related control requirements p 515 A95-87398
 Real time for the calculation of the aerodynamic of aircrafts with delta wings p 460 A95-87399
 Low-speed aerodynamic characteristics of a slender wing with vertical fins p 460 A95-87400
 Influence of the flight trajectory on the exhaust gas composition of a H₂-fueled air-breathing ramjet engine p 509 A95-87404
 Modeling of plume chemistry of high flying aircraft with H₂ combustion engines p 509 A95-87405
 Testing the hypersonic technology demonstration nozzle: Results from the test campaign 1993/94 [AIAA PAPER 95-6084] p 509 A95-87413
 Experimental and numerical analysis of a two-duct nozzle/afterbody model at supersonic Mach numbers [AIAA PAPER 95-6085] p 490 A95-87414
 Drag and lift in nonadiabatic transonic flow [HTN-95-61208] p 540 A95-87581
 Doppler lidar investigation of wake vortex transport between closely spaced parallel runways [HTN-95-81645] p 462 A95-87693
 Broadband noise characteristics of a model counter-rotating shrouded propfan p 572 A95-88470
 Planar air density measurements near model surfaces by ultraviolet Rayleigh/Raman scattering [HTN-95-20950] p 546 A95-88989
 Aerodynamic off-design behavior of integrated waveriders from take-off up to hypersonic flight [AIAA PAPER 95-6091] p 466 A95-89200
 Aircraft controller synthesis by solving a nonconvex optimization problem [BTN-95-EIX95282706672] p 515 A95-89636
 Experimental results of the European HELINOISE aeroacoustic rotor test [HTN-95-01080] p 578 A95-90266
 Chemically reacting non-equilibrium boundary layers in air breathing propulsion systems [AIAA PAPER 95-6139] p 512 A95-90456
 Ultrasonic imaging of damages in CRFT-laminates p 578 A95-90828
 Solution of the Navier-Stokes equations on a massively parallel transputer system p 549 A95-91490
 Autonomous helicopter hover positioning by optical tracking [HTN-95-C0006] p 585 A95-93394
 An in-situ system for warning of icing conditions p 660 A95-93481
 An innovative algorithm to accurately solve the Euler equations for rotary wing flow p 642 A95-95467
 The 4-D approach to visual control of autonomous systems [AIAA PAPER 94-1243-CP] p 27 N95-11513
 Thermoacoustic environments to simulate reentry conditions p 86 N95-14096
 Aero design of turbomachinery components: CFD in complex systems p 90 N95-14136
 Parameter identification for X-31A at high angles of attack p 69 N95-14235
 X-31 quasi-tailless flight demonstration p 70 N95-14243
 Aeromechanical design of modern missiles p 73 N95-14446
 Turbulence: Engineering models, aircraft response p 84 N95-14900
 Prediction of rotor-blade deformations due to unsteady airloads [AD-A284467] p 81 N95-15821
 Tools for applied engineering optimization p 128 N95-16570
 The global aircraft shape p 128 N95-16571
 Aerodynamic shape optimization p 128 N95-16572
 Safety aspects of spacecraft commanding p 149 N95-17248
 EURECA mission control experience and messages for the future p 149 N95-17252
 Packet utilisation definitions for the ESA XMM mission p 150 N95-17596
 2-D airfoil tests including side wall boundary layer measurements p 158 N95-17847
 Investigation of an NLF(1)-0416 airfoil in compressible subsonic flow p 110 N95-17852
 DLR-F4 wing body configuration p 130 N95-17863
 DLR-F5: Test wing for CFD and applied aerodynamics p 113 N95-17864
 Wind tunnel investigations of the appearance of shocks in the windward region of bodies with circular cross section at angle of attack p 113 N95-17866

- Three-dimensional boundary layer and flow field data of an inclined prolate spheroid p 158 N95-17867
- Force and pressure data of an ogive-nosed slender body at high angles of attack and different Reynolds numbers p 113 N95-17868
- Wind tunnel test on a 65 deg delta wing with rounded leading edges: The International Vortex Flow Experiment p 114 N95-17875
- Subsonic flow around US-orbiter model FALKE in the DNW p 115 N95-17877
- Pressure distribution measurements on an isolated TPS 441 nacelle p 115 N95-17878
- Treatment of non-linear systems by timeplane-transformed CT methods: The spectral gust method p 143 N95-18600
- Theoretical investigations of shock/boundary layer interactions on a $Ma(\infty) = 8$ waverider [DLR-FB-94-12] p 119 N95-18910
- Flow field investigation in a free jet - free jet core system for the generation of high intensity molecular beams [DLR-FB-94-11] p 172 N95-18912
- Helicopter internal noise p 173 N95-19144
- Design and operation of a thermoacoustic test facility p 147-N95-19150
- Acoustic fatigue testing on different materials and skin-stringer elements p 174 N95-19156
- Velocity measurements with hot-wires in a vortex-dominated flowfield p 121 N95-19261
- Wall correction method with measured boundary conditions for low speed wind tunnels p 164 N95-19263
- Development of load spectra for Airbus A330/A340 full scale fatigue tests p 135 N95-19479
- Performance deterioration of axial compressors due to blade defects p 199 N95-19665
- Impact loading of compressor stator vanes by hailstone ingestion p 200 N95-19670
- Damage of high temperature components by dust-laden air p 201 N95-19673
- Microchannel heat pipe cooling of modules p 246 N95-20649
- Optical backplane for modular avionics p 257 N95-20652
- Modular CNI avionics system p 234 N95-20659
- Prediction of rotor-blade deformations due to unsteady airloads [AD-A286593] p 231 N95-20860
- Corrosion protection measures for CFC/metal joints of fuel integral tank structures of advanced military aircraft p 303 N95-23510
- Experience of in-service corrosion on military aircraft p 303 N95-23516
- On aircraft repair verification of a fighter A/C integrally stiffened fuselage skin p 394 N95-27515
- Composite repair of a CF18: Vertical stabilizer leading edge p 395 N95-27517
- External patch repair of CFRP/honeycomb sandwich p 395 N95-27522
- Damage occurrence on composites during testing and fleet service: Repair of Airbus aircraft p 396 N95-27526
- Numerical simulation and analysis of the hypersonic turbulent flow past a blunt-fin/ramp configuration [DLR-FB-94-19] p 483 N95-30349
- SCARLET: DLR rate saturation flight experiment p 598 N95-31068
- Handling qualities analysis on rate limiting elements in flight control systems p 619 N95-31071
- Experimental investigation of turbulent particle dispersion in swirling flows [DLR-FB-94-20] p 647 N95-31355
- Experiences with ADS-33 helicopter specification testing and contributions to refinement research p 621 N95-31993
- Model following control for tailoring handling qualities: ACT experience with ATHeS p 622 N95-32000
- Advanced gust management systems: Lessons learned and perspectives p 622 N95-32002
- Automatic flight control system for an unmanned helicopter system design and flight test results p 622 N95-32004
- Structural aspects of active control technology p 623 N95-32006
- X-31: A program overview and flight test status p 609 N95-32013
- Laser based obstacle warning sensors for helicopters p 686 N95-32499
- A nonlinear vortex lattice method for unsteady flow with separated vortex [DLR-FB-94-32] p 704 N95-32787
- Effects of the specific military aspects of satellite navigation on the civil use of GPS/GLONASS p 688 N95-33134
- The DLR research programme on an integrated multi sensor system for surface movement guidance and control p 689 N95-33135
- HeliRadar: A rotating antenna synthetic aperture radar for helicopter allweather operations p 705 N95-33137
- Integrated special mission flight management for a flight inspection aircraft p 692 N95-33145
- GREECE**
- Adaptive modeling of jet engine performance with application to condition monitoring [BTN-95-EIX95112524205] p 196 A95-69303
- Meteorological impacts on airport noise prediction by the 'Integrated Noise Model' application based on Hamiltonian Ray-Tracing program and measurements p 571 A95-88467
- Enroute NASA/FAA low-frequency propfan test in Alabama (October 1987): A versatile atmospheric aircraft long-range noise prediction system p 573 A95-90099
- A robust inverse inviscid method for airfoil design p 640 A95-95431
- On the prediction of transonic unsteady flows using second order time accuracy p 641 A95-95448
- Multigrid solution for the compressible Euler equations by an implicit characteristic-flux-averaging p 642 A95-95459
- Single-pass method for the solution of inverse potential and-rotational problems. Part 1: 2-D and quasi-3-D theory and application p 107 N95-16563
- Single-pass method for the solution of inverse potential and rotational problems. Part 2: Fully 3-D potential theory and applications p 107 N95-16564
- Investigation of shear layer transition using various turbulence models p 248 N95-21096
- H**
- HONG KONG**
- Auxiliary power unit noise of Boeing B737 and B747 aircraft p 571 A95-88468
- I**
- INDIA**
- Field-consistent element applied to flutter analysis of circular cylindrical shells [BTN-94-EIX94341341971] p 56 A95-60871
- Unbalance response of a dual rotor system: Theory and experiment [BTN-94-EIX94351143320] p 195 A95-65854
- Recent trends in balloon flights from TIFR's National Balloon Facility, Hyderabad p 191 A95-66300
- Transient analysis of a cracked rotor passing through critical speed [BTN-94-EIX94401360022] p 306 A95-74702
- Some aspects of the aerodynamics of separating strap-ons [BTN-95-EIX95182617464] p 298 A95-75735
- Simple method of supersonic flow visualization using watertable [BTN-95-EIX95182619105] p 269 A95-76590
- Switched bias proportional navigation for homing guidance against highly maneuvering targets [BTN-95-EIX95182619145] p 279 A95-76622
- Flow past a symmetric wedge with forward splitter plate p 427 A95-82406
- Boundary layer studies over an S-blade [HTN-95-92261] p 434 A95-85305
- Mobile domes for TACTIC telescope p 453 A95-86113
- Failure behaviour of carbon fiber/epoxy composites in pin-ended buckling and bending tests [HTN-95-71388] p 528 A95-87606
- Automatic identification of modal damping from Floquet analysis [HTN-95-01084] p 506 A95-90270
- Low speed wind tunnel blockage corrections for airfoils at medium to large angles of attack p 474 A95-91557
- Use of partially open wind tunnel walls for blockage-free separated flows on bodies p 474 A95-91558
- Reaction-time response of aircraft crash [BTN-95-EIX95292721296] p 595 A95-92626
- Geodesic constant method: A novel approach to analytical surface-ray tracing on convex conducting bodies [BTN-95-EIX95302731054] p 637 A95-94205
- Experimental Aerodynamics Division [NAL-SP-9404] p 35 N95-12166
- Evaluation of the dynamic stability characteristics of the NAL Light Transport Aircraft [NAL-PD-CA-9217] p 142 N95-16392
- Ageing nuclear power plant management: An aeronautical viewpoint [NAL-PD-SN-9306] p 105 N95-18606
- Solution of full potential equation on an airfoil by multigrid technique [NAL-TM-CSS-9303] p 119 N95-18904
- CFD: Advances and Applications, part 1 [NAL-SP-9322-PT-1] p 165 N95-19444
- Computation of inviscid flows: Full potential method p 165 N95-19447
- Panel methods p 165 N95-19448
- Viscous flow past aerofoils axisymmetric bodies and wings p 123 N95-19457
- Computation of vortex breakdown p 165 N95-19462
- Parabolized Navier-Stokes solution of supersonic/hypersonic flows p 123 N95-19464
- INDONESIA**
- Prediction of fatigue crack growth under flight-simulation loading with the modified CORPUS model p 166 N95-19471
- IRELAND**
- The influence of alternate inter-blade connections on ground resonance [HTN-95-80859] p 267 A95-75101
- Safety in airport ground handling p 626 A95-95193
- ISRAEL**
- Continuous gust response and sensitivity derivatives using state-space models [BTN-95-EIX95062487551] p 203 A95-68365
- Grid refinement test of time-periodic flows over bluff bodies [BTN-94-EIX94401378822] p 307 A95-76491
- Dynamic investigation of the angular motion of a rotating body-parachute system [BTN-95-EIX95182619220] p 270 A95-76646
- Stress considerations in reduced-size aeroelastic optimization [BTN-95-EIX95262694313] p 366 A95-85484
- Effects of periodic spanwise blowing on Delta-wing configuration characteristics [HTN-95-81631] p 461 A95-87679
- Optimal design of composite helicopter power transmission shafts with axially varying fiber layup [HTN-95-01086] p 529 A95-90272
- Fundamentals of catastrophic failure prevention by thrust vectoring [BTN-95-EIX0619952748176] p 606 A95-94470
- Optimal trajectories for an unmanned air-vehicle in the horizontal plane [BTN-95-EIX0619952748191] p 606 A95-94480
- Probabilistic inspection strategies for minimizing service failures p 93 N95-14461
- Review of some results of the author's fatigue investigations with applications in engineering and material science [TAE-698] p 316 N95-23662
- Advanced interactive display formats for terminal area traffic control [NASA-CR-198576] p 384 N95-28188
- Prediction of fatigue crack growth under constant amplitude and random loading using specimens with multiple cracks [AD-A291614] p 397 N95-28409
- Lavi flight control system: Design requirements, development and flight test results p 621 N95-31994
- ITALY**
- Selecting and management of fire fighter aircraft [BTN-95-EIX95062487538] p 193 A95-69246
- Simulation of turbulent fluctuations [BTN-95-EIX95142553041] p 304 A95-73457
- Structural acoustic calculations in the low-frequency range [BTN-95-EIX95152582336] p 323 A95-73538
- Simulation of transverse gas injection in turbulent supersonic air flows [BTN-95-EIX95182619080] p 269 A95-75765
- Possible effects of CO2 increase on the high-speed civil transport impact on ozone [HTN-95-60779] p 317 A95-75976
- High-speed civil transport impact: Role of sulfate, nitric acid trihydrate, and ice aerosols studied with a two-dimensional model including aerosol physics [HTN-95-91843] p 354 A95-80831
- Impact on ozone of high-speed stratospheric aircraft: Effects of the emission scenario [HTN-95-51283] p 356 A95-80868
- Matrix fraction approach for finite-state aerodynamic modeling [BTN-95-EIX95262694311] p 365 A95-85482
- Aerodynamic design and optimization at Alenia D.V.D. p 491 A95-87564
- Numerical and flight measured interior noise characteristics of a twin-engine turboprop general aviation aircraft p 573 A95-90094
- Experimental active control of sound in the ATR 42 p 575 A95-90110
- Calculation of control laws for the digital fuel control unit of a small thrust turbojet [SAE PAPER 931411] p 614 A95-93677

Analysis of some interference effects in a transonic wind tunnel
 [BTN-95-EIX0619952748166] p 589 A95-94460
 Estimation of supersonic leading-edge thrust by a Euler flow model
 [BTN-95-EIX0619952748194] p 591 A95-94483
 Transonic vortical flow predicted with a structured multiblock Euler solver p 642 A95-95462
 An unstructured node centered scheme for the simulation of 3-D inviscid flows p 642 A95-95463
 Impact of noise environment on engine nacelle design p 173 N95-19147
 An overall approach of cockpit noise verification in a military aircraft p 175 N95-19163
 Adaptive wind tunnel walls versus wall interference correction methods in 2D flows at high blockage ratios p 147 N95-19267
 An airborne monitoring system for FOD and erosion faults p 200 N95-19668
 Thermal testing of high performance thermal barrier coatings for turbine blades p 202 N95-19681
 Electromagnetic compatibility effects of advanced packaging configurations p 247 N95-20658
 MAX-91: Polarimetric SAR results on Montepertoli site p 320 N95-23940
 Dynamics of phase ordering of nematics in a pore [DE95-607662] p 362 N95-25978
 Control law design using H-infinity and mu-synthesis short-period controller for a tail-airplane p 622 N95-31999
 Digital autopilot design for combat aircraft in ALENIA p 623 N95-32009
 An approach to sensor data fusion for flying and landing aid purpose p 686 N95-32488

J

JAPAN

Dynamic behavior of valves with pneumatic chamber for reciprocating compressors
 [BTN-94-EIX94351143311] p 207 A95-65845
 Three-dimensional analysis of scramjet nozzle flows [BTN-94-EIX94441380978] p 196 A95-68162
 Surface morphology and structure of carbon-carbon composites in high-energy sliding contact [BTN-94-EIX94371347996] p 206 A95-69164
 Preliminary assessment of tunnel wall interference in the NDA cryogenic wind tunnel [BTN-95-EIX95062487531] p 187 A95-69239
 Aerodynamic mechanism of galloping [BTN-94-EIX94371347709] p 219 A95-69968
 Ground effect calculation of two-dimensional airfoil [BTN-94-EIX94371347710] p 219 A95-69969
 Vortex shedding noise control in idling circular saws using air ejection at the teeth [BTN-94-EIX94371347214] p 257 A95-69970
 Thermochemical nonequilibrium viscous shock-layer analysis for a Mars aerocapture vehicle [BTN-95-EIX95082502732] p 239 A95-70139
 Flow visualization studies on sidewall effects in two-dimensional transonic airfoil testing [BTN-95-EIX95152582313] p 264 A95-73516
 Polar Patrol Balloon [BTN-95-EIX95152582318] p 316 A95-73521
 Derivation of system matrices from nonlinear dynamic simulation of jet engines [BTN-95-EIX95182619139] p 288 A95-76616
 Numerical investigation of supersonic flows around a spiked blunt body [BTN-95-EIX95212645690] p 271 A95-76742
 Similarity rule for jet-temperature effects on transonic base pressure [BTN-95-EIX95222650791] p 329 A95-79247
 Determination of piloting feedback structures for an altitude tracking task [BTN-95-EIX95242670770] p 327 A95-81077
 Ignition analysis of hydrogen/air mixture in supersonic mixing layer p 416 A95-82301
 Design features of the NAL ramjet engine test facility p 410 A95-82319
 Hypersonic wind tunnel test of sidewall compression type scramjet inlet p 410 A95-82320
 Evaluation of scramjet nozzle performance p 402 A95-82321
 An experimental investigation of scramjet nozzle flow p 402 A95-82322
 Prediction of pre-combustion shock in scramjet combustors: A new method p 402 A95-82323
 Experiment of rocket-ram annular combustor p 412 A95-82324
 An advanced scramjet propulsion concept for A 350 MG SSTO space plane p 402 A95-82325
 Test results on air turbo ramjet engine for a future space plane p 402 A95-82327

Life evaluation of a low power arcjet thruster p 403 A95-82337
 R & D on HOPE structure p 413 A95-82355
 Research and development of thermal protection system of HOPE re-entry vehicle p 413 A95-82358
 Hypersonic trajectory control of aerospace plane with integrated SCRAMJET engine p 413 A95-82384
 Rarefied gas numerical wind tunnel: OREX and HOPE p 427 A95-82391
 VSL analysis of hypersonic flows around a reentry vehicle with equilibrium air chemistry p 413 A95-82400
 The aerodynamic characteristics of cup-like body in supersonic flow p 427 A95-82407
 Air data sensors for atmospheric reentry flight test of winged space vehicle p 413 A95-82412
 NAL aerothermodynamic probing and CFD verification mission in OREX experiment p 368 A95-82413
 Hypersonic thermal protection with mass injection at angle of attack p 414 A95-82414
 Numerical simulation of unsteady aerodynamic heating induced by shock reflections p 428 A95-82418
 A study on aerodynamic heating phenomena in three-dimensional shock wave/turbulent boundary layer interaction induced by sweptback sharp fins at supersonic flow p 428 A95-82419
 Experiment and analysis on heat transfer of a scramjet leading edge model p 403 A95-82420
 An experimental study on radiation from strong shock layer p 368 A95-82421
 Flight evaluation of DGPS and DGPS-INS navigation systems p 382 A95-82462
 A concept of a hypersonic flight experiment of a winged vehicle p 414 A95-82477
 A conceptual design of hypersonic research vehicle with subscale scramjet engine p 384 A95-82482
 Atmospheric reentry flight test of winged space vehicle p 414 A95-82483
 Reentry technology experiment on the first mission of reentry capsule 'EXPRESS' p 414 A95-82499
 Development and flight results of fiber reinforced balloon p 384 A95-82511
 Polar Patrol Balloon system and preliminary experimental results p 368 A95-82513
 How 'HITEN's' aerobraking experiments were carried out p 415 A95-82553
 Aero-thermodynamic flight environment at HITEN aerobrake experiment p 415 A95-82554
 Experimental investigation of composite channel heat pipe operation in micro-gravity environment p 428 A95-82645
 Hypersonic flow simulation with thermoelectric effect p 368 A95-82669
 Studies on gain performance of a combustion driven CO₂ gas dynamic laser p 428 A95-82679
 Studies on plasma jet igniters p 403 A95-82680
 Development of 70MW class superconducting generators [BTN-94-EIX95011440854] p 429 A95-82905
 Multiple instabilities of three-dimensional boundary layers along a concave wall [HTN-95-71126] p 429 A95-83487
 Observation of traveling waves in the three-dimensional boundary layer along a yawed cylinder [HTN-95-61064] p 430 A95-83648
 Instability of three-dimensional boundary layers due to streamline curvature [HTN-95-61070] p 430 A95-83654
 Study on the turbine vane and blade for a 1500 C class industrial gas turbine [BTN-94-EIX95011441254] p 431 A95-84211
 Air truth validation of cloud albedo estimated from NOAA advanced very high resolution radiometer data [HTN-95-A1021] p 443 A95-84526
 Pulsed jet ignition modeling with a full chemistry p 538 A95-87184
 Prediction of NO(x) emission index of turbulent diffusion flame p 538 A95-87195
 Numerical simulation of real gas effects and aerodynamic heating of hypersonic space transportation vehicles p 540 A95-87558
 Prediction level of noise by a helicopter p 571 A95-88469
 A method for disbond detection in thermal tomography by domain decomposition method p 545 A95-88955
 Application of restructurable flight control system to large transport aircraft [BTN-95-EIX95282706666] p 515 A95-89639
 Preliminary study on the fixed transition technique for a shock tube transonic airfoil flow [BTN-95-EIX95282705928] p 455 A95-89663
 Nonlinear analysis of the Gortler instability [BTN-95-EIX95282705926] p 455 A95-89664
 Note on prediction of aerodynamic lift/drag ratio of WIG (Wing-In-Ground) at cruise [BTN-95-EIX95282705925] p 467 A95-89665

Turbulence characteristics of supersonic boundary layer past a backward facing step [AIAA PAPER 95-6126] p 470 A95-90447
 Numerical studies of Mach reflection with air chemistry Aircraft Symposium, 30th, Tsukuba, Japan, Sep. 30 - Oct. 2, 1992 p 498 A95-91491
 [HTN-95-A1609] p 498 A95-91491
 MIMO H infinity control design method combined with exact model matching p 506 A95-91492
 A gust alleviation method by the response feedback p 506 A95-91493
 Analysis of approach paths of two aircraft p 487 A95-91494
 Estimation of aerodynamic characteristics for the vortex flaps by the suction analogy p 471 A95-91496
 Numerical experiments on aerodynamic heating mechanism in shock reflection processes p 471 A95-91497
 Application of ACT to unstable motions of an airfoil in ground effect p 471 A95-91500
 Experience of aircraft manufacturer for paint removal using dry stripping method p 456 A95-91501
 Aero-engine R&D efforts for environmental protection p 512 A95-91502
 Flight testing of the composite material bearingless rotor system for the helicopter p 498 A95-91503
 Hubload responses of a rotor in forward flight due to multiple frequency blade pitch variations p 515 A95-91504
 Application of GPS and Fuzzy Theory to a helicopter p 516 A95-91505
 Development of Fly-By-Wire system for BK117 p 516 A95-91506
 Aerofoil characteristics at low Reynolds number p 472 A95-91507
 High subsonic and high Reynolds number wind tunnel tests of two-dimensional natural-laminar-flow airfoils with suction boundary layer control p 472 A95-91508
 Fixed transition for shock tube transonic flow p 472 A95-91509
 Experimental study of shock/shock interference heating on a swept cylinder p 472 A95-91510
 An experimental study on interacting flow between supersonic flow and secondary flow injected normally through circular nozzle p 472 A95-91511
 Aerodynamic characteristics of supersonic air-intake/aircraft integrated models p 472 A95-91512
 A singularity method for a two dimensional stratified shear flow p 473 A95-91513
 Optimum aerodynamic design of aircraft fuselage using boundary element method p 473 A95-91514
 A detailed Euler flow analysis of TPS and fanjet engine p 473 A95-91515
 Requirements for next generation supersonic transports p 498 A95-91516
 The concept of high speed commercial transporter structure p 498 A95-91517
 Overview of feasibility study on propulsion concepts for high speed civil transport p 498 A95-91518
 Research of the method for evaluating noise caused by sonic boom p 562 A95-91519
 A conceptual design of the SST without horizontal tail p 498 A95-91520
 Conceptual study of next generation high-speed civil transport: A candidate with horizontal tail p 499 A95-91521
 Some considerations on system design of the hypersonic transport and supersonic air-intakes p 473 A95-91522
 An experimental study on supersonic laminar flow control p 473 A95-91523
 Experimental study for improving the lift to drag ratio of next generation SST p 473 A95-91524
 Experimental investigation on aerothermodynamic characteristics of hypersonic transport p 473 A95-91525
 A design of a robust scheduled autopilot p 516 A95-91532
 A design of a self-learning robust scheduled autopilot p 516 A95-91533
 Design of a flight control system by a new way of pole placement in LQR p 516 A95-91534
 An intelligent tutoring system for civil aviation flight training p 521 A95-91535
 Introduction of the GPS to civil aviation field p 487 A95-91536
 Arrival traffic handling for a parallel runway airport p 487 A95-91537
 A shock tunnel test of a winged hypersonic research vehicle p 474 A95-91538
 Flight test of STS radio controlled scale model p 499 A95-91539
 CCLA operation on MLS p 487 A95-91540
 Aeronautical satellite communications using the ETS-5 satellite p 487 A95-91541

- State of Enhanced Vision System p 506 A95-91542
- Guidance and control of HOPE and its future technologies p 506 A95-91543
- Multiobjective trajectory optimization by goal programming with fuzzy decision p 526 A95-91544
- A guidance concept for hypersonic aerospacecrafts p 526 A95-91549
- Optimality of the steady-state flight for hypersonic aircraft p 526 A95-91550
- An application of TLS (Total Least Squares) method to estimation of aircraft aerodynamic derivatives p 517 A95-91551
- A method for calculating mean aerodynamic center and zero-lift moment coefficient of aircraft without tail by using measured flight loads p 474 A95-91552
- Determination of flight simulator time delay p 522 A95-91553
- A systems for flight data acquisition and analysis for a remotely-piloted research vehicle p 517 A95-91554
- Functions of NAL fixed base simulator for helicopter research p 522 A95-91555
- A simulator study about effects of visibility upon helicopter pilot performance p 522 A95-91556
- On the UF-104 system p 507 A95-91559
- On the flight control system for UF-104 p 507 A95-91560
- Aeroservoelastic coupling on the UF-104 aircraft p 517 A95-91561
- Experimental study of the aerodynamic characteristics of the counter-rotation propellers p 474 A95-91562
- Wake velocity measurement of counter-rotation propellers p 474 A95-91563
- Experiment of the large elastic deformation of biconvex wing sections in an air-flow p 475 A95-91564
- Simultaneous structure/aerodynamic design optimization for a flexible wing structure p 499 A95-91565
- Preliminary tests of a transonic flutter control wing model p 499 A95-91566
- Supersonic flutter analysis of cantilevered composite plate-wings p 499 A95-91567
- Neural network approach to identification of aerodynamic loads on a wing. 1: Application to cantilevered beam models p 475 A95-91568
- Mechanical properties of advanced toughened bismaleimide matrix composite p 530 A95-91570
- Some comments on current research and development of civil VTOL aircrafts p 499 A95-91572
- Ducted fan VTOL and its flight control system p 500 A95-91573
- Flight Test Monitoring System using X-window p 500 A95-91574
- Performance evaluation test of GPS/DGPS navigation system installed in the NAL Dornier 228: Preliminary ground test results p 487 A95-91575
- Analysis and scale-model experiment of propeller driving motor for microwave-powered airplane p 487 A95-91576
- Development of a pilot tube with multi-hole pyramidal head. 2: A five-hole yew probe of engineering model p 522 A95-91577
- Exact solution of stability margin for the MIMO control system p 507 A95-91582
- Effect of coupling term on stability for the two input control system p 507 A95-91583
- Comparison of the method of analyzing stability margin by using Minus Inverse Vector Locus with classical method p 507 A95-91584
- A study of computational difficulty of numerical method in optimal control p 507 A95-91585
- Flight control system design with Multiple Delay Model/Multiple Design Point Approach p 507 A95-91586
- Missile autopilot designs using full state feedback p 507 A95-91587
- Analysis of an MLS automatic landing control law for the NAL experimental research aircraft DO-228. 2: Curved approach and landing p 508 A95-91588
- Automatic grid generation procedure for complex aircraft configurations [BTN-95-EIX95302729765] p 605 A95-94127
- Performance variation of scramjet nozzle at various nozzle pressure ratios [BTN-95-EIX0616952745781] p 615 A95-94505
- Heat transfer on bent-noise biconic in hypersonic flow p 639 A95-95394
- A numerical investigation of flow around a square-section cylinder mounted with a splitter plate p 639 A95-95401
- 2-D and 3-D numerical simulation of a supersonic inlet flowfield p 641 A95-95457
- Arbitrary Lagrangian-Eulerian finite element analysis for flow-induced vibration of rigid body p 643 A95-95485
- Activities of Mitsubishi Heavy Industries Ltd. [PB94-179694] p 22 N95-10085
- Aeroelastic tailoring research [PB94-180031] p 6 N95-10135
- Computations of unsteady aerodynamic loads around oscillating wings. Part 1: Formulation [PB94-180049] p 7 N95-10136
- Computations of unsteady aerodynamic loads around oscillating wings. Part 2: Computed results and discussions [PB94-180056] p 7 N95-10137
- Study on tensile fatigue testing method of unidirectional fiber-resin matrix composites [NAL-TR-1241] p 343 N95-24989
- Effect of film cooling/regenerative cooling on scramjet engine performances [NAL-TR-1242] p 339 N95-24990
- Numerical and experimental study of drag characteristics of two-dimensional HLFC airfoils in high subsonic, high Reynolds number flow [NAL-TR-1244T] p 331 N95-24998
- Preliminary experiments of an optical fiber display [NAL-TR-1257] p 362 N95-25004
- Flight reference display for powered-lift STOL aircraft [NAL-TR-1251] p 337 N95-25005
- Low speed aerodynamic characteristics of delta wings with vortex flaps: 60 deg and 70 deg delta wings [NAL-TR-1245] p 331 N95-25105
- Aerodynamic characteristics of the orbital reentry vehicle experimental probe fins in a supersonic flow [NAL-TR-1232] p 342 N95-25664
- Measurements of longitudinal static aerodynamic coefficients by the cable mount system [NAL-TR-1226] p 331 N95-25761
- Fundamental wind tunnel experiments on low-speed flutter of a tip-fin configuration wing [NAL-TR-1228] p 332 N95-25762
- Reentry guidance for hypersonic Flight Experiment (HYFLEX) vehicle [NAL-TR-1235] p 334 N95-25764
- A quiet STOL Research Aircraft Development program [NAL-TR-1223] p 336 N95-25862
- Long endurance stratospheric solar powered airship [PB95-178729] p 336 N95-26009
- Numerical simulation of combustion flow around a flame holder with hydrogen injection [NAL-TR-1233] p 419 N95-26523
- Experimental investigation of static and dynamic ground effect on HOPE ALFLEX vehicle [NAL-TR-1236] p 388 N95-26525
- Flight evaluation of GPS/DGPS sensor systems installed in NAL Do228 [NAL-TR-1230] p 382 N95-26585
- Experiment on a rectangular cross section scramjet combustor. 2: Effects of fuel injector geometry [NAL-TR-1220] p 405 N95-26600
- Effects of dust from storage heaters on ignition in scramjets [NAL-TR-1234] p 405 N95-26706
- Viscous shock-layer analysis on hypersonic flow over reentry capsule with nonequilibrium chemistry [ISAS-656] p 436 N95-26739
- Wind tunnel experiments on wake flow field behind a reentry capsule from a viewpoint of parachute deployment at supersonic speeds [ISAS-655] p 374 N95-26740
- Transonic, supersonic and hypersonic wind-tunnel tests on aerodynamic characteristics of reentry body with blunted cone configuration [ISAS-658] p 480 N95-29640
- Experimental studies on boundary-layer transition on a reentry vehicle at transonic and supersonic speeds [ISAS-659] p 555 N95-29712
- Effects of cavity bleed and its configuration on aerodynamic characteristics of supersonic internal flow [NAL-TR-1247] p 594 N95-31715
- Special publication of National Aerospace Laboratory [NAL-SP-27] p 684 N95-34505
- Design of secondary flow control cascade using numerical simulation p 698 N95-34507
- A study on the convergence of a 3-D Euler code for cascade flow calculations p 706 N95-34508
- Verification of turbine cascade flow with tip clearance p 698 N95-34511
- A study of supersonic mixing flow field with ramp injector p 706 N95-34512
- Calculation of supersonic combustion in SCRAMJET engines p 698 N95-34513
- Numerical simulation of high enthalpy shock tunnel p 700 N95-34514
- Hypersonic CFD analysis for the aerothermodynamic design of HOPE p 684 N95-34520
- Numerical solutions of inviscid and viscous flows about airfoils by TVD method p 684 N95-34521
- Calculation for aerodynamic characteristics on delta wing with leading-edge separated vortex effect using boundary element method p 684 N95-34524
- Sidewall-effect of the wind tunnel on the estimation of the aerodynamic characteristics of a delta wing p 685 N95-34525
- Direct numerical simulation of incompressible homogeneous isotropic turbulence using NWT p 706 N95-34530
- Performance evaluation of the NWT with incompressible NS code p 707 N95-34533
- An unsteady simulation of a centrifugal compressor stage using the NWT p 707 N95-34536
- Parallel computation of transonic flows about an aircraft configuration using multi-block structured grids p 685 N95-34537
- Vector-parallel simulations of transonic wind tunnel flows about a fully configured model of aircraft p 685 N95-34538
- A large scale 3D Navier-Stokes analysis using NAL-NWT p 707 N95-34539
- Role of computational fluid dynamics in aeronautical engineering. Number 12: Formulation and verification of uni-particle upwind schemes for the Euler equations p 707 N95-34540
- Numerical analysis around the whole SST configuration p 693 N95-34541
- Application of CFD technique for HYFLEX aerodynamic design p 693 N95-34542
- Computations of low speed flow about space-plane p 685 N95-34544
- Numerical simulation of two-dimensional PAR-WIG p 685 N95-34548
- Direct analysis of transonic rotor noise with CFD technique p 711 N95-34549
- A simulation of damping process of pendulum motion due to aerodynamic forces p 711 N95-34551
- Grid generation around airfoil with a flap using boundary element method p 686 N95-34552
- Static pressure drop by swirling flow of an internal cooling air system through a turbine shaft p 698 N95-34560

K

KOREA, REPUBLIC OF

- Aeroelastic stability of hingeless rotor blade in hover using large deflection theory [BTN-94-EIX94441386616] p 183 A95-67347
- Comparison of parameter identification algorithms for flight vehicles [BTN-94-EIX94371347708] p 219 A95-69967
- Static aeroelastic characteristics of a composite wing [BTN-95-EIX95152582340] p 282 A95-73542
- Numerical study of sound generation due to a spinning vortex pair [BTN-95-EIX95182619075] p 307 A95-75760
- Covariance analysis of strapdown INS considering gyrocompass characteristics [BTN-95-EIX95202637592] p 279 A95-76697
- Two-dimensional viscous flow past a flat plate [HTN-95-42210] p 430 A95-84026
- Prediction of two-dimensional momentumless wake by k-epsilon-gamma model [BTN-95-EIX95262694299] p 434 A95-85470
- Aeroelastic response of composite rotor blades considering transverse shear and structural damping [HTN-95-81647] p 542 A95-87695
- Design of an effective controller via disturbance accommodating left eigenstructure assignment [BTN-95-EIX95282706663] p 565 A95-88178
- Aeroelastic stability of hingeless rotor blade in hover using large deflection theory [HTN-95-20952] p 546 A95-88991
- Effects of structural damping on aeroelastic stability of various shaped composite plate wing p 530 A95-91530
- Numerical calculations of the turbulent flow through a controlled diffusion compressor cascade [BTN-95-EIX95282710056] p 632 A95-92473

N

NETHERLANDS

- On the dynamics of aeroelastic oscillators with one degree of freedom [BTN-94-EIX94501431527] p 153 A95-64524
- The ICAO CNS/ATM system: New king, new law? [HTN-95-50218] p 175 A95-64855
- World trends in air transport policies. (Approaching the 21st century) [HTN-95-50220] p 176 A95-64857
- EC Aviation Scene [HTN-95-50223] p 176 A95-64860
- Optimal lateral-escape maneuvers for microburst encounters during final approach [BTN-95-EIX95182619127] p 276 A95-76604

- Quantitative comparison between interferometric measurements and Euler computations for supersonic cone flows
[BTN-95-EIX95222650782] p 358 A95-79238
- Flight simulation fatigue crack growth testing of aluminum alloys
[HTN-95-00652] p 418 A95-84731
- Fatigue of aircraft materials; Specialists' Conference, Delft, Netherlands, 1992
[HTN-95-B0076] p 387 A95-85892
- Status and prospects for aluminium-lithium alloys in aircraft structures
p 387 A95-85893
- Fatigue of aircraft materials and structures
p 387 A95-85894
- Fibre-Metal laminates
p 387 A95-85895
- A review of the hot-wire technique in 2-D compressible flow
[HTN-95-61157] p 373 A95-86256
- Pressure controlled surfaces - a 3D inverse panel method as a design tool
p 491 A95-87565
- Functional requirements of an aerospace Design Representation Programming Interface
[AIAA PAPER 95-0967] p 497 A95-90643
- Momentum and scalar transfer coefficients over aerodynamically smooth Antarctic surfaces
[HTN-95-92932] p 562 A95-91870
- Automation of observations in the Netherlands
p 661 A95-93485
- Discretization of the parabolised Navier-Stokes equations
p 638 A95-95362
- Grid adaptation for problems in computational fluid dynamics
p 643 A95-95472
- Surface grid generation for multi-block structured grids
p 643 A95-95478
- Reanalysis of European flight loads data
[AD-A282052] p 9 N95-11179
- Mach number control in the High Speed Wind Tunnel of NLR
[PB94-201670] p 53 N95-13243
- Numerical time dependent sheet cavitation simulations using a higher order panel method
[PB94-204435] p 59 N95-13249
- Studies on the flow induced by an oscillating airfoil in a uniform stream
[PB94-204450] p 40 N95-13250
- A SIMULINK environment for flight dynamics and control analysis: Application to the DHC-2 Beaver. Part 1: Implementation of a model library in SIMULINK. Part 2: Nonlinear analysis of the Beaver autopilot
[NONP-NASA-SUPPL-DK-94-2802] p 84 N95-14815
- Residual-correction type and related computational methods for aerodynamic design. Part 1: Airfoil and wing design
p 128 N95-16566
- Residual-correction type and related computational methods for aerodynamic design. Part 2: Multi-point airfoil design
p 128 N95-16567
- Experiments in the trailing edge flow of an NLR 7702 airfoil
p 110 N95-17853
- Two-dimensional 16.5 percent thick supercritical airfoil NLR 7301
p 110 N95-17854
- Low-speed surface pressure and boundary layer measurement data for the NLR 7301 airfoil section with trailing edge flap
p 111 N95-17855
- Wind tunnel test on a 65 deg delta wing with a sharp or rounded leading edge: The international vortex flow experiment
p 114 N95-17872
- Experimental investigation of the vortex flow over a 76/60-deg double delta wing
p 114 N95-17874
- Sectional prediction of 3D effects for separated flow on rotating blades
[PB94-201696] p 117 N95-18503
- Atmospheric effects of high-flying subsonic aircraft: A catalogue of perturbing influences
[KNMI-SR-94-03] p 168 N95-18722
- The utilization of a high speed reflective visualization system in the study of transonic flow over a delta wing
p 121 N95-19259
- Correction of support influences on measurements with sting mounted wind tunnel models
p 122 N95-19281
- Fatigue life until small cracks in aircraft structures: Durability and damage tolerance
p 135 N95-19478
- Results of uniaxial and biaxial tests on riveted fuselage lap joint specimens
p 136 N95-19491
- Braze repair possibilities for hot section gas turbine parts
p 201 N95-19677
- Gas turbine compressor corrosion and erosion in Western Europe
[AD-B196178L] p 201 N95-19678
- High velocity oxygen fuel spraying of erosion and wear resistant coatings on jet engine parts
p 202 N95-19680
- Integral rocket ramjets
[AD-A285135] p 240 N95-20906
- Review of aeronautical fatigue investigation in the Netherlands during the period March 1991-March 1993
[PB95-139184] p 285 N95-23161

- Eddy current detection of pitting corrosion around fastener holes
p 315 N95-23507
- Partial camera automation in a simulated Unmanned Air Vehicle
[AD-A288786] p 337 N95-26190
- Numerical simulation of crack growth in pressurized fuselages
[PB95-192415] p 400 N95-28636
- Demonstration of an automated CFD system for three-dimensional flow simulations
p 551 N95-28767
- PREDICAT: First order performance calculations of windturbine rotors using the method of the acceleration potential
[PB95-206454] p 564 N95-30200
- Axial loads on yawed rotors
[PB95-214193] p 592 N95-30638
- Multigrid convergence acceleration for the 2D Euler equations applied to high-lift systems
[PB95-198081] p 593 N95-30814
- Development of advanced approach and departure procedures. Failure scenarios
[PB95-198123] p 601 N95-30815
- Numerical investigation into vortical flow about a delta-wing configuration up to incidences at which vortex breakdown occurs in experiment
[PB95-198024] p 593 N95-30837
- Validation of the helicopter rotor code HERO
[PB95-198040] p 607 N95-30838
- Dynamical systems as models for flow-induced vibrations
[PB95-206991] p 647 N95-30956
- Acceleration potential models
PREDICAT/PREDICDYN applied for calculation of axisymmetric dynamic inflow cases
[PB95-207015] p 647 N95-30957
- Digital simulation of wind velocities for wind turbine rotors: General considerations
[PB95-206447] p 677 N95-31157
- Robust control: A structured approach to solve aircraft flight control problems
p 621 N95-31995

NEW ZEALAND

- An air-driven pressure booster pump for aircraft-based air sampling
[HTN-95-40689] p 216 A95-69833
- Verification of terminal forecasts
p 664 A95-93502

NORWAY

- Assessment of helicopter noise annoyance: A comparison between noise from helicopters and from jet aircraft
[BTN-94-EIX94341341967] p 62 A95-60867
- Aircraft noise zoning in Norway
p 581 A95-88476
- Assessment of helicopter noise annoyance: A comparison between helicopters and jet aircraft
p 560 A95-88480
- Implicit multiblock Euler and Navier-Stokes calculations
[HTN-95-A1755] p 634 A95-93318
- Response to noise around Vaernes and Bodoe airports
[PB94-207065] p 62 N95-13575
- Scandinavian Airlines Systems experience on erosion, corrosion and foreign object damage effects on gas turbines
p 198 N95-19659
- Results from tests of the Kearsott T16-B Inertial Measurement Unit
[PB95-212031] p 644 N95-30502
- Metascientific problems in safety science
[PB95-196408] p 645 N95-30521
- Results from tests of the Honeywell integrated flight management unit
[PB95-211355] p 601 N95-30597

O

OMAN

- Study of an airfoil with a flap and spoiler
[BTN-95-EIX95152582327] p 265 A95-73530

P

POLAND

- A tool for airframe shaping - idea and application
[SAE PAPER 931224] p 491 A95-87568
- Actuating signals in adaptive control systems
[IFTR-13/1994] p 361 N95-26330
- Photoacoustic chambers for studying solids and gases: Theory and practical examples
[IFTR-39/1994] p 412 N95-26837

Q

QATAR

- Criteria of forecasting low level wind shear over Qatar
p 663 A95-93493

R

ROMANIA

- Direct boundary integral equations method to subsonic flow with circulation past thin airfoils in ground effect
[BTN-95-EIX95242673940] p 365 A95-82224
- Free convection past a uniform flux surface inclined at a small angle to the horizontal
[HTN-95-42213] p 430 A95-84029

RUSSIA

- Soft landing on the slope surface of a landing vehicle with an air shock-absorber of forced pressurization
[BTN-94-EIX94461407941] p 85 A95-62259
- Stabilization of objects with unknown nonstationary parameters, using adaptive nonlinear continuous control systems
[BTN-94-EIX94461407944] p 98 A95-62262
- On profiling a cam of an axial aviation diesel engine by periodic splines
[BTN-94-EIX94461407946] p 82 A95-62264
- On calculated models for impellers of centrifugal compressors
[BTN-94-EIX94461407947] p 88 A95-62265
- Heat transfer in the flow-through part of axial compressors
[BTN-94-EIX94461407949] p 89 A95-62267
- Mechanism and technological particular features of thermomagnetic hardening
[BTN-94-EIX94461407953] p 89 A95-62627
- Local-optimal control of a flying vehicle, with final state optimized
[BTN-94-EIX94461407957] p 83 A95-62631
- The effect of rotating loads suspended under a helicopter on their amplitude-frequency characteristics
[BTN-94-EIX94461407959] p 78 A95-62633
- On introduction of artificial intelligence elements to heat power engineering
[BTN-94-EIX94461407961] p 100 A95-62635
- Profiling of the working surface of electrodes-tools for circle electrochemical dimensional treatment of compressor blades
[BTN-94-EIX94461407964] p 83 A95-62638
- Analytical description of and forecast for stress relaxation of aviation materials under the vibration conditions
[BTN-94-EIX94461408751] p 126 A95-63634
- Selection of optimal parameters for a system, controlling the flight height, when information about the state vector is incomplete
[BTN-94-EIX94461408753] p 168 A95-63636
- Gas-turbine engines with increased efficiency of two circuits, due to the use of the utilizing steam-turbine circuit
[BTN-94-EIX94461408755] p 153 A95-63638
- On the particular features of dynamic processes in solids with varying boundary during interaction with intensive heat flows
[BTN-94-EIX94461408756] p 171 A95-63639
- Ultimate characteristics of a rocket engine with a turbo-pump supply system
[BTN-94-EIX94461408757] p 148 A95-63640
- Mathematical modelling concerning the development of a system of similar installations, taking into account their operational intensity (an aircraft-helicopter fleet taken as an example)
[BTN-94-EIX94461408763] p 103 A95-63646
- A stationary flow of a viscous liquid in radial clearances of rotor bearings in the turbocompressor of an internal combustion engine
[BTN-94-EIX94461408765] p 153 A95-63648
- New approach to geometric profiling of the design elements of the passage part in turbo-machines
[BTN-94-EIX94461408769] p 153 A95-63652
- Calculation of geometry of stamps with small allowances for pieces of the aerodynamic profile
[BTN-94-EIX94461408772] p 103 A95-63655
- On a program-information system TDsoft
[BTN-94-EIX94461408773] p 175 A95-63656
- Modelling for optimal operations of line milling of aerodynamic surfaces
[BTN-94-EIX94461408774] p 138 A95-63657
- Two projects of V. M. Myasishchev
[HTN-95-50269] p 176 A95-65764
- The scientific ballooning in Russia
p 191 A95-66302
- Kinetic theory in aerothermodynamics
[HTN-95-A0002] p 183 A95-67829
- State-space representation of aerodynamic characteristics of an aircraft at high angles of attack
[BTN-95-EIX95062487536] p 187 A95-69244
- A new generation of instruments for flying laboratories
[BTN-94-EIX94401363947] p 317 A95-75532
- Laser device for measuring a vessel's speed
[HTN-95-60992] p 361 A95-80633

- Stability of viscoelastic plate in supersonic flow under random loading
[BTN-95-EIX95262694312] p 435 A95-85483
- Verification of engineering methods of aerodynamics for reentry vehicles by DSMC p 525 A95-87386
- Numerical simulation of three-dimensional hypersonic reacting flows over blunt bodies with catalytic surface [HTN-95-61184] p 539 A95-87557
- Operation of the adaptive-wall wind tunnel of TsAGI, Moscow p 519 A95-88901
- Disturbance generation in supersonic jets under acoustic excitation
[HTN-95-20926] p 463 A95-88965
- Aviation weather forecasting automated methods in the RAFC Moscow and the Airport Vnukovo p 669 A95-93523
- JPRS report: Science and technology, Central Eurasia: Engineering and equipment. Gas dynamics of supersonic shortened nozzles
[JPRS-UST-94-003-L] p 22 N95-10931
- Service and physical properties of liquid-jet fuels p 151 N95-16256
- Development of strength analysis methods and design model for aircraft constructions in Kazan Aviation Institute p 127 N95-16264
- Theoretical fundamentals of the aircraft GTE tests p 138 N95-16265
- Generalized method of solving topological optimization problems for electrical airplane equipment systems in computer-aided design p 169 N95-16272
- Development of processes, means, and theoretical principles of thin-walled detail plastic forming at Kazan Aviation Institute p 155 N95-16281
- Solution of Navier-Stokes equations using high accuracy monotone schemes p 161 N95-19019
- The mathematical models of flow passage for gas turbine engines and their components p 140 N95-19020
- Simulation of multidisciplinary problems for the thermostress state of cooled high temperature turbines p 140 N95-19021
- Application of multicomponent models to flow passage simulation in multistage turbomachines and whole gas turbine engines p 140 N95-19022
- Simulation of steady and unsteady viscous flows in turbomachinery p 140 N95-19023
- Application of multidisciplinary models to the cooled turbine rotor design p 140 N95-19024
- Verification of multidisciplinary models for turbomachines p 140 N95-19025
- Perspective problems of gas turbine engines simulation p 140 N95-19026
- Optical surface pressure measurements: Accuracy and application field evaluation p 175 N95-19274
- JPRS report: Science and technology, Central Eurasia [JPRS-UST-94-027] p 349 N95-24470
- JPRS report: Science and technology, Central Eurasia [JPRS-UST-94-018] p 349 N95-24472
- JPRS report: Science and technology, Central Eurasia [JPRS-UST-95-011] p 335 N95-24541
- JPRS Report: Science and technology, Central Eurasia [JPRS-UST-94-032] p 350 N95-24759
- JPRS report: Science and technology, Central Eurasia [JPRS-UST-94-022] p 438 N95-27699
- FBI report: Science and technology, Central Eurasia [FBIS-UST-95-029] p 649 N95-31728
- Navigational technology of dual usage p 688 N95-33131
- Sea wave parameters, small altitudes and distances measurers design for movement control systems of ships, wing-in-surface effect crafts and seaplanes p 708 N95-33141
- S**
- SAUDI ARABIA**
- Suppression of vortex asymmetry and side force on a circular cone
[BTN-95-EIX95042474413] p 209 A95-68287
- Analytical solution for controls, heats, and states of flight trajectories
[BTN-95-EIX95152583286] p 282 A95-73587
- Stability derivatives of a flapped plate in unsteady ground effect
[BTN-95-EIX95182619225] p 270 A95-76651
- Unsteady ground effects on aerodynamic coefficients of finite wings with camber
[BTN-95-EIX95182619233] p 271 A95-76659
- Modal characteristics of rotors using a conical shaft finite element
[BTN-94-EIX94401359745] p 346 A95-77379
- Similarity solutions for hypersonic flow past slender bodies of revolution at small incidence
[HTN-95-12195] p 475 A95-91895
- Cooling of aerospace plane using liquid hydrogen and methane
[BTN-95-EIX0619952748171] p 590 A95-94465
- SINGAPORE**
- Scheduling of local nonlinear control laws by exogenous signals - an application to flight control
[BTN-95-EIX95262694059] p 447 A95-85675
- Reduced-order nonlinear analysis of aircraft dynamics
[BTN-95-EIX95282706665] p 455 A95-89640
- Measurement in laminar and transitional boundary-layer flows on concave surface
[BTN-95-EIX95282711333] p 632 A95-92408
- Multi-block finite volume calculation of compressible flow past aerodynamic configurations p 643 A95-95473
- SOUTH AFRICA**
- Aerodynamic effects of delta planform tip sails on wing performance
[BTN-95-EIX95062487544] p 185 A95-68358
- Aerodynamic characteristics of strake vortex flaps on a strake-wing configuration
[BTN-95-EIX95062487537] p 187 A95-69245
- Static pressure distribution in the inlet of a helicopter turbine compressor
[BTN-95-EIX95152582339] p 266 A95-73541
- Analytic prediction of lift for delta wings with partial leading-edge thrust
[BTN-95-EIX95152582345] p 266 A95-73547
- Erosion of dust-filtered helicopter turbine engines. Part 1: Basic theoretical considerations
[BTN-95-EIX95182619222] p 288 A95-76648
- Erosion of dust-filtered helicopter turbine engines. Part 2: Erosion reduction
[BTN-95-EIX95182619223] p 289 A95-76649
- Life prediction of helicopter engines fitted with dust filters
[BTN-95-EIX95182619224] p 289 A95-76650
- Differencing of density in compressible flow for a pressure-based approach
[HTN-95-42349] p 373 A95-86178
- SPAIN**
- Design constraints in the payload-range diagram of ultrahigh capacity transport airplanes
[BTN-95-EIX95152582319] p 276 A95-73522
- A study of the effect of store unsteady aerodynamics on gust and turbulence loads p 133 N95-18601
- Repairs of CFC primary structures p 396 N95-27527
- SWEDEN**
- Turbulent transonic airfoil flow simulation using a pressure-based algorithm
[BTN-95-EIX95182619078] p 269 A95-75763
- Experimental investigation of the flow around a circular cylinder: Influence of aspect ratio
[BTN-94-EIX95011441120] p 347 A95-80044
- Ventilation of the damage tolerance of a fighter aircraft p 388 A95-85897
- Secondary power system study for the hytex RA3 flight test vehicle
[AIAA PAPER 95-6158] p 512 A95-90470
- The Saab-Scania approach to development simulators [CONGRESS PAPER C428-10-137] p 522 A95-91698
- Nortaf: Computer generated aerodome forecasts p 668 A95-93521
- Navier-Stokes computations around a realistic fighter configuration p 591 A95-95440
- High-lift calculations using Navier-Stokes methods p 641 A95-95444
- Multigrid/multiblock method for transonic potential flow around wing/body/nacelle configurations including a slipstream p 591 A95-95451
- Navier-Stokes simulation of turbulent vortex high-Re-number flows over a delta wing p 644 A95-95507
- Propulsion research concerning SFRJ-motors [PB94-179520] p 14 N95-10083
- Military aviation maintenance industry in Western Europe: Concentration and internationalization [PB94-189180] p 104 N95-17451
- Evaluation of an autopilot based multimodelling [PB94-190725] p 142 N95-17454
- Low speed propeller slipstream aerodynamic effects p 116 N95-17882
- Computational simulations for some tests in transonic wind tunnels p 164 N95-19264
- Calculation of low speed wind tunnel wall interference from static pressure pipe measurements p 164 N95-19273
- Computation of transonic flow on composite overlapping grids in 2 D [PB95-131348] p 248 N95-21132
- Interfacing a digital compass to a remote-controlled helicopter [PB95-164927] p 340 N95-24260
- Orientation determination of aircraft using visual 3D matching and radar. Case study 2 [PB95-165791] p 350 N95-25749
- Aspect estimation of an aircraft using library model silhouettes
[PB95-141834] p 360 N95-25894
- SAAB experience with PIO p 598 N95-31069
- Turbulence models in the Navier-Stokes simulation of airfoil stall [TRITA-NA-9312] p 705 N95-33059
- SWITZERLAND**
- Test bench for rotorcraft hover control
[BTN-94-EIX94511433919] p 169 A95-64585
- Data processing and mapping in airborne radiometric surveys
[HTN-95-51587] p 442 A95-83591
- Criticism of the Leq as an index for aircraft noise and other discontinuous noise sources p 559 A95-88477
- Broadband polarization-transfer experiments for rotating solids
[GTN-95-0009261494012091-58] p 579 A95-92319
- Experimental investigation of the flow in diffusers behind an axial flow compressor
[BTN-95-EIX95282710057] p 632 A95-92472
- Aviation and the environment p 657 A95-93464
- Computational methods for preliminary design and geometry definition in turbomachinery p 89 N95-14128
- The industrial use of CFD in the design of turbomachinery p 90 N95-14133
- T**
- TAIWAN, PROVINCE OF CHINA**
- Analysis of an oscillating Joukowski airfoil with surface suction and moving vortices
[BTN-95-EIX95062487527] p 186 A95-69235
- Sidewash on the vertical tail in subsonic and supersonic flows
[BTN-95-EIX95152582316] p 264 A95-73519
- Solutions of generalized proportional navigation with maneuvering and nonmaneuvering targets
[BTN-95-EIX95202637606] p 279 A95-76683
- Integrated design of hypersonic waveriders including inlets and tailfins
[BTN-95-EIX95212645692] p 271 A95-76744
- Impingement cooling of an isothermally heated surface with a confined slot jet
[BTN-94-EIX94421348950] p 347 A95-78494
- Ideal proportional navigation p 342 A95-81374
- Transonic flutter suppression using active acoustic excitations
[BTN-95-EIX95262694310] p 408 A95-85481
- High angle-of-attack airfoil performance improvement by internal acoustic excitation
[HTN-95-42347] p 372 A95-86176
- Nonlinear asymptotic theory of hypersonic flow past a circular cone
[HTN-95-92599] p 461 A95-87415
- Modeling three-dimensional gas-turbine combustor model flow using second-moment closure
[HTN-95-20935] p 464 A95-88974
- Controlling mechanisms of ignition of solid fuel in a sudden-expansion combustor
[BTN-95-EIX0616952745791] p 628 A95-94255
- Damage tolerance certification of a fighter horizontal stabilizer
[BTN-95-EIX0619952748186] p 637 A95-94478
- TURKEY**
- Aerodynamic characteristics of external store configurations at low speeds
[BTN-95-EIX95182619230] p 271 A95-76656
- Effect of spherical roughness elements upon transition of a 3-D boundary layer
[HTN-95-92835] p 471 A95-90753
- Vortex lattice method simulation of unsteady flow due to wing/external store combination p 471 A95-91499
- Computer aided static aeroelastic analysis of wing/pylon/store combination p 499 A95-91531
- Effects of splitter plate on wake formation from a circular cylinder: A discrete vortex simulation p 639 A95-95404
- At Istanbul-Ataturk Airport measurement and analysis of noise in due of take-off time p 31 N95-11319
- Scarf joint technique with cocured and precured patches for composite repair p 396 N95-27524
- U**
- UKRAINE**
- Investigation of heat transfer in a rotating ring gap with the axial flow of a coolant during the rotation of the central shaft
[BTN-94-EIX94461407951] p 89 A95-62625

Engineering methods for the evaluation of transonic flutter characteristics for aerodynamic control surfaces [BTN-94-EIX94461408589] p 141 A95-63064
 Investigation of heat transfer between rotating shafts of transmissions of turbojet engines [BTN-94-EIX94461408760] p 138 A95-63643
 Fatigue strength of high-temperature alloys under conditions of cyclic temperature variation. Communication 1: Experimental procedure and results [BTN-94-EIX94401363884] p 307 A95-75516

UNITED KINGDOM

Validation of empirical orbit error corrections using crossover difference differences [HTN-94-00912] p 25 A95-60227
 Construction of nearly orthogonal multiblock grids for compressible flow simulation [BTN-94-EIX94361133526] p 207 A95-65981
 Antarctic snow record of southern hemisphere lead pollution [HTN-95-40359] p 212 A95-66869
 Behavior of the Johnson-King turbulence model in axisymmetric supersonic flows [BTN-94-EIX94441386606] p 183 A95-67337
 Interference between tanker wing wake with roll-up and receiver aircraft [BTN-95-EIX95062487552] p 185 A95-68366
 Results and performance of multi-site reference station differential GPS [BTN-95-EIX95112522534] p 190 A95-69329
 Integrated GPS/Glonass navigation: Algorithms and results [BTN-95-EIX95112522531] p 190 A95-69332
 Water vapor continuum absorption in mid-latitudes: Aircraft measurements and model comparisons [HTN-95-40756] p 252 A95-71186
 Aircraft measurements of water vapour continuum absorption at millimetre wavelengths [HTN-95-90884] p 253 A95-72393
 Electro-optic characterization of ultrafast photodetectors using adiabatically compressed soliton pulses [BTN-94-EIX94381359637] p 257 A95-72675
 Microphysical and radiative properties of small cumulus clouds over the sea [HTN-95-A0526] p 255 A95-73180
 On the link between cloud-top radiative properties and sub-cloud aerosol concentrations [HTN-95-A0527] p 255 A95-73181
 Dynamical instability of the aerogravity assist maneuver [BTN-95-EIX95152583282] p 298 A95-73583
 Design of wide angle head up displays for synthetic vision [BTN-95-EIX95212641070] p 287 A95-76735
 Sensitivity of supersonic aircraft modelling studies to HNO3 photolysis rate [HTN-95-11475] p 353 A95-79453
 Unsteady lift on a swept blade tip [BTN-94-EIX95011441154] p 329 A95-80030
 Vibration measurements on rotating machinery using laser Doppler velocimetry [BTN-94-EIX95011440597] p 429 A95-82986
 The legal status and liability of the copilot, part 2 [HTN-95-A0578] p 452 A95-83158
 Considerations in the development of the coupled rotor fuselage model [HTN-95-61077] p 370 A95-83661
 The dynamic nature of rotor thermal bending due to unsteady lubricant shearing within a bearing [HTN-95-42091] p 430 A95-83857
 Control requirements for the RB 211 low-emission combustion system [BTN-94-EIX95011441244] p 416 A95-84201
 Computational analysis of buffet alleviation in viscous transonic flow over a porous airfoil [BTN-95-EIX95262694321] p 366 A95-85492
 An overview of the EASOE campaign [HTN-95-00702] p 443 A95-86272
 Mesh generation and adaptivity for the solution of compressible viscous high speed flows [BTN-95-EIX95262697157] p 538 A95-86893
 Active boundary-layer control in diffusers [HTN-95-42580] p 458 A95-87210
 Numerical model of boundary-layer control using air-jet generated vortices [HTN-95-42581] p 459 A95-87211
 Vorticity in an inviscid fluid at hypersonic speeds [HTN-95-42590] p 539 A95-87220
 Possible guidelines for helicopter noise assessment [HTN-95-92535] p 558 A95-87355
 The effects and prediction of rotary wing aircraft noise on the community [HTN-95-92536] p 558 A95-87356
 Environmental noise monitoring - source identification [HTN-95-92537] p 558 A95-87357
 Aircraft noise and sleep disturbance: A field study [HTN-95-92543] p 558 A95-87363

Noise levels of helicopters performing elevated pad take-off and landing procedures [HTN-95-92544] p 559 A95-87364
 Measurement of free-flight dynamic stability derivatives of cones in a hypersonic gun tunnel [AIAA PAPER 95-6082] p 519 A95-87411
 Experimental investigation of hypersonic flow over a wing-body combination [AIAA PAPER 95-6083] p 460 A95-87412
 Buckling and postbuckling of composite structures [HTN-95-71387] p 528 A95-87605
 A prediction model for noise from low-altitude military aircraft p 571 A95-88466
 Some aspects of the aerocoacustics of extreme-speed jets p 572 A95-88893
 Behavior of the Johnson-King turbulence model in axisymmetric supersonic flows [HTN-95-20932] p 464 A95-88971
 The effect of wing sweep back upon transition in hypersonic flow [AIAA PAPER 95-6090] p 466 A95-89199
 Polymer composite applications to aerospace equipment [HTN-95-B0257] p 529 A95-89201
 Structural composites in civil gas turbine aero engines [HTN-95-B0258] p 529 A95-89202
 Blade-by-blade tip clearance measurement system for gas turbine applications [BTN-95-EIX95292721167] p 546 A95-89899
 Past and present UK research on aircraft noise effects p 560 A95-90090
 Reduction of supersonic jet noise using swirl: A concept revisited p 574 A95-90101
 Evaluation of a model for boundary-layer induced noise in aircraft p 574 A95-90102
 Optimum design of composite stiffened wing panels - a parametric study [HTN-95-01088] p 496 A95-90274
 A note on the interpretation of mini-tuft photographs [HTN-95-01089] p 468 A95-90275
 Measurement of drag using a momentum balance [HTN-95-01090] p 468 A95-90276
 Drag reduction in a rectangular duct using riblets [HTN-95-01091] p 468 A95-90277
 Central-difference and upwind-biased schemes for steady and unsteady Euler aerofoil computations [HTN-95-01094] p 469 A95-90280
 Crack growth characteristics of integrally machined stringer-skin panels [HTN-95-01095] p 496 A95-90281
 Preliminary results from a particle image velocimetry study of blade-vortex interaction [HTN-95-01098] p 547 A95-90284
 Unsteady aerodynamic effects of trailing edge controls on delta wings [HTN-95-01099] p 469 A95-90285
 Predictive algorithms for the roll control autopilot of a jet fighter aircraft [HTN-95-21047] p 515 A95-90424
 The use of thermochromic liquid crystals for heat transfer measurements in short duration hypersonic wind tunnel facilities [AIAA PAPER 95-6115] p 520 A95-90443
 Buffeting tests in a cryogenic windtunnel [HTN-95-92833] p 470 A95-90751
 High angle of attack missile aerodynamics [CONGRESS PAPER C428-3-060] p 475 A95-91673
 Repairs to composite structure on military aircraft [CONGRESS PAPER C428-4-067] p 531 A95-91677
 The air systems controllerate initiatives and policies for the procurement of reliable and maintainable equipment [CONGRESS PAPER C428-6-113] p 549 A95-91682
 Air traffic management: The future challenge [CONGRESS PAPER C428-7-145] p 488 A95-91686
 Airbourne collision avoidance systems - The UK experience [CONGRESS PAPER C428-7-146] p 488 A95-91687
 Developments in airfield lighting [CONGRESS PAPER C428-7-147] p 488 A95-91688
 Explosive sabotage: The potential effects of explosive charges on aircraft [CONGRESS PAPER C428-11-034] p 484 A95-91702
 Fault Diagnosis for condition monitoring applied to hydraulic circuits [CONGRESS PAPER C428-12-165] p 456 A95-91703
 Health monitoring and cost implications for an airline operator [CONGRESS PAPER C428-12-166] p 457 A95-91704
 Gas path debris monitoring [CONGRESS PAPER C428-15-031] p 508 A95-91710

Developments in wear particle analysis using computerised procedures [CONGRESS PAPER C428-15-216] p 457 A95-91713
 RAF ejections - historical perspectives and future requirements [CONGRESS PAPER C428-18-168] p 484 A95-91717
 Novel implements of optical diagnostic techniques for aerospace applications [CONGRESS PAPER C428-21-081] p 550 A95-91726
 The use of structural optimisation within aerospace [CONGRESS PAPER C428-23-008] p 500 A95-91729
 Simulation of the unsteady interaction of a centrifugal impeller with its vaned diffuser: flow analysis [BTN-95-EIX95282710055] p 633 A95-92474
 Condensation in jet engine intake ducts during stationary operation [BTN-95-EIX95292721154] p 612 A95-92590
 Modelling 2D separation from a high lift aerofoil with a non-linear eddy-viscosity model and second-moment closure [HTN-95-C0005] p 585 A95-93393
 A three-dimensional moving mesh method for the calculation of unsteady transonic flows [HTN-95-C0007] p 585 A95-93395
 The improvement of meteorological data for air traffic management purposes p 668 A95-93518
 Dissemination of weather products p 670 A95-93526
 Weather products for aviation from WAFAC Bracknell p 670 A95-93527
 A study of the savings in time and fuel to aviation through the use of upper-air wind forecasts p 672 A95-93538
 Creating a global climatology of freezing rain using numerical model output p 673 A95-93541
 Dependable software - the state of the art [CONGRESS PAPER C428-24-212] p 678 A95-93596
 Development of an aircraft cabin water spray system [CONGRESS PAPER C428-25-030] p 595 A95-93599
 Aircraft cabin water spray systems - research and regulatory issues [CONGRESS PAPER C428-25-150] p 595 A95-93600
 The mini-business approach at Chadderton [CONGRESS PAPER C428-26-037] p 681 A95-93602
 Development of an intelligent tool-condition monitoring system for FMS [CONGRESS PAPER C428-32-012] p 583 A95-93617
 Non-contact calibration of a CNC rivetting machine [CONGRESS PAPER C428-32-075] p 583 A95-93618
 Variable camber geometry for transport aircraft wings [CONGRESS PAPER C428-35-061] p 603 A95-93626
 The basis of civil certification and continued airworthiness for composite aircraft structures [CONGRESS PAPER C428-37-173] p 628 A95-93632
 ASTRA - A safe, simplex, fly-by-wire aircraft control system [CONGRESS PAPER C428-37-218] p 610 A95-93634
 An efficient discrete vortex method for low Reynolds number incompressible flows p 639 A95-95407
 SAUNA: A system for grid generation and flow simulation using hybrid structured/unstructured grids p 642 A95-95470
 Partially implicit method for simulating viscous aerofoil flows [BTN-94-EIX94522406680] p 709 A95-96299
 Near field noise prediction requirements [ISVR-TR-234] p 27 N95-11166
 Symmetric steady manoeuvre loads on rigid aircraft of classical configuration at subsonic speeds [ESDU-94009] p 43 N95-11774
 Application of multivariate optimisation techniques to determination of optimum flight path trajectories [ESDU-94012] p 44 N95-11793
 Examples of flight path optimisation using a multivariate gradient-search method. Addendum A: Variation of optimum flight profile parameters with range [ESDU-94016-ADD-A] p 44 N95-11794
 Designing in three dimensions p 90 N95-14130
 A method of calculating the safe fatigue life of compact, highly-stressed components p 93 N95-14464
 Wind shear and its effects on aircraft p 77 N95-14898
 Measurements on a two-dimensional aerofoil with high-lift devices p 109 N95-17848

- Investigation of the flow over a series of 14 percent-thick supercritical aerofoils with significant rear camber p 109 N95-17849
- Measurements of the flow over a low aspect-ratio wing in the Mach number range 0.6 to 0.87 for the purpose of validation of computational methods. Part 1: Wing design, model construction, surface flow. Part 2: Mean flow in the boundary layer and wake, 4 test cases p 112 N95-17860
- Detailed study at supersonic speeds of the flow around delta wings p 112 N95-17861
- Pressure distributions on research wing W4 mounted on an axisymmetric body p 112 N95-17862
- Investigation of the flow development on a highly swept canard/wing research model with segmented leading- and trailing-edge flaps p 114 N95-17876
- Investigation into the aerodynamic characteristics of a combat aircraft research model fitted with a forward swept wing p 116 N95-17884
- Investigation of the influence of pylons and stores on the wing lower surface flow p 116 N95-17885
- The impact of non-linear flight control systems on the prediction of aircraft loads due to turbulence p 143 N95-18598
- Current and future problems in structural acoustic fatigue p 173 N95-19143
- Application of superplastically formed and diffusion bonded structures in high intensity noise environments p 174 N95-19162
- Transonic and supersonic flowfield measurements about axisymmetric afterbodies for validation of advanced CFD codes p 121 N95-19260
- Boundary-flow measurement methods for wall interference assessment and correction: Classification and review p 163 N95-19262
- Estimating wind tunnel interference due to vectored jet flows p 164 N95-19265
- Interference determination for wind tunnels with slotted walls p 147 N95-19269
- An investigation of drag repeatability in half model testing in the ARA Transonic Wind Tunnel [ARA-MEMO-392] p 188 N95-19546
- Out of area experiences with the RB199 in Toronto p 198 N95-19654
- The operation of gas turbine engines in hot and sandy conditions: Royal Air Force experiences in the Gulf conflict p 198 N95-19655
- Future directions in helicopter protection system configuration p 198 N95-19657
- Particle deposition in gas turbine blade film cooling holes p 199 N95-19661
- Particle trajectories in gas turbine engines p 199 N95-19663
- The calculation of erosion in a gas turbine compressor rotor p 199 N95-19664
- Soft body impact on titanium fan blades p 200 N95-19671
- Multipoint pressure measurements on continuously moving wind tunnel models [ARA-MEMO-391] p 188 N95-19772
- Validation and evaluation of the advanced aeronautical CFD system SAUNA: A method developer's view [ARA-MEMO-390] p 210 N95-19774
- Application of three-dimensional hybrid structured/unstructured grids to land, sea and air vehicles [ARA-MEMO-399] p 210 N95-19775
- Verification of the CFD simulation system SAUNA for complex aircraft configurations [ARA-MEMO-401] p 211 N95-19776
- Inviscid and viscous flow modelling of complex aircraft configurations using the CFD simulation system sauna [ARA-MEMO-403] p 211 N95-19777
- The aerodynamic design of an integrated wing lower surface and pylons for reduced drag [ARA-MEMO-406] p 194 N95-19789
- Investigation of a thermal buoyancy effect on the drag of half models tested in the ARA Transonic Wind Tunnel [ARA-MEMO-407] p 222 N95-19946
- MCMs for avionics: Technology selection and intermodule interconnection p 234 N95-20641
- High performance backplane components for modular avionics p 247 N95-20653
- The dynamic approach to rotor blade research: ARA's oscillatory test facility [ARA-MEMO-405] p 223 N95-20758
- Testing in the ARA Transonic Wind Tunnel [ARA-MEMO-395] p 239 N95-20799
- Effect of atmospheric pressure on measured aircraft noise levels [PB95-130423] p 232 N95-21425
- Collaborative research on aircraft icing and charging processes in ice [AD-A285102] p 276 N95-23201
- The corrosion and protection of advanced aluminium-lithium airframe alloys p 302 N95-23497
- Non-destructive detection of corrosion for life management p 314 N95-23505
- Health and usage monitoring systems: Corrosion surveillance p 262 N95-23506
- POD assessment of NDI procedures using a round robin test [AGARD-R-809] p 315 N95-23602
- Three-dimensional interaction of wake/boundary-layer and vortex/boundary-layer data report [CUED/A-AEREO/TR-23] p 329 N95-24210
- A theoretical and experimental investigation of the flow over supersonic leading edge wing/body configurations [DRA-TM-AERO-PROP-41] p 331 N95-25649
- Adhesively bonded composite patch repair of cracked aluminum alloy structures p 393 N95-27507
- Composite repair of composite structures p 395 N95-27521
- SMART materials: Surfaces, transforms and interfaces. The commensurate engineering dimension [AD-A269598] p 442 N95-28649
- Ejectors and jet pumps: Computer program for design and performance for steam/gas flow [ESDU-94046] p 500 N95-28704
- Effects of small changes on rate of climb [ESDU-94039] p 501 N95-28707
- Computer program for estimation of leading-edge suction distribution for plane thin wings at subsonic speeds [ESDU-94038] p 476 N95-28708
- Leading-edge suction distribution for plane thin wings at subsonic speeds [ESDU-94037] p 477 N95-28800
- Increments in aerofoil lift coefficient at zero angle of attack and in maximum lift coefficient due to deployment of a plain trailing-edge flap, with or without a leading-edge high-lift device, at low speeds [ESDU-94028] p 477 N95-28885
- Shear force, bending moment and torque of rigid aircraft in symmetric steady maneuvering flight [ESDU-94045] p 502 N95-28896
- Excrescence drag levels on aircraft [ESDU-94044] p 477 N95-28897
- Wave drag coefficient for axisymmetric forecows at zero incidence (M sub infinity less than or equal to 1.5) [ESDU-94014] p 552 N95-28903
- Surface pressure coefficient distributions for axisymmetric forecows at zero incidence (M sub infinity less than or equal to 1.5) [ESDU-94015] p 477 N95-28904
- Effects of cabin pressure on climb and descent rates [ESDU-94040] p 503 N95-29016
- Increments in aerofoil lift coefficient at zero angle of attack and in maximum lift coefficient due to deployment of a trailing-edge split flap, with or without a leading-edge high-lift device, at low speeds [ESDU-94029] p 479 N95-29129
- The effects of three dimensional imposed disturbances on bluff body near wake flows [AD-A290824] p 555 N95-29654
- Increments in aerofoil lift coefficient at zero angle of attack and in maximum lift coefficient due to deployment of various leading-edge high-lift devices at low speeds [ESDU-94027] p 481 N95-29898
- Introduction to the estimation of the lift coefficients at zero angle of attack and at maximum lift for aerofoils with high-lift devices at low speeds [ESDU-94026] p 481 N95-29899
- Looking for the simple PIO model p 597 N95-31066
- The prevention of PIO by design p 620 N95-31991
- The FCS-structural coupling problem and its solution p 623 N95-32005
- Experimental Aircraft Programme (EAP): Flight control system design and test p 623 N95-32010
- Flight demonstration of an advanced pitch control law in the VAAC Hamier aircraft p 623 N95-32012
- Pilot Induced Oscillation: A report on the AGARD Workshop on PIO p 624 N95-32017
- A tactical navigation and routing system for low-level flight p 709 N95-32494
- The application of helicopter mission simulation to Nap-of-the-Earth operations p 710 N95-32496
- The Anglo-French Compact Laser Radar demonstrator programme p 703 N95-32501
- The application of Ada and formal methods to a safety critical engine control system p 710 N95-33142
- A rose by any other name: Certification seen as process rather than content p 688 N95-34766
- Quality assurance and risk management: Perspectives on Human Factors Certification of Advanced Aviation Systems p 690 N95-34771
- UNKNOWN**
- Aircraft accident investigation and airworthiness - A practical example of the interaction of two disciplines with some reflections on possible legal consequences [HTN-95-50219] p 176 N95-64856
- Hypersonic model testing in a shock tunnel [BTN-95-EIX9522650789] p 329 A95-79245
- SR-71 may launch targets for missile defense tests [HTN-95-91872] p 335 A95-81974
- European firms team on supersonic studies [HTN-95-42215] p 386 A95-84031
- Maintenance programs [HTN-95-92310] p 365 A95-85354
- Aircraft stripping and painting [HTN-95-92311] p 365 A95-85355
- Condition monitoring and diagnostics [HTN-95-92312] p 387 A95-85356
- Artificial intelligence for turboprop engine maintenance [HTN-95-92313] p 404 A95-85357
- Techniques for tailoring aircraft stall and post-stall behavior [SAE PAPER 931226] p 458 A95-87199
- Concorde: Silver jubilee Mach 2 marks 25 years [HTN-95-42618] p 483 A95-87248
- Flight Simulators: Better than the real thing? [HTN-95-42619] p 518 A95-87249
- Euro-noise '92, London, UK, Sept. 14-18, 1992. Bks. 1-3 [ISBN 1-873082-39-8] p 558 A95-87354
- The use of the Equivalent Continuous Sound Level (L(sub eq)) as an aircraft noise index [HTN-95-92542] p 558 A95-87362
- Flyover noise reduction of piston-engine propeller aeroplanes using an active noise control technique [SAE PAPER 931218] p 509 A95-87466
- 'Global avionics in the future' report from the 10th annual battery conference [BTN-95-EIX95282706404] p 545 A95-88184
- Materials and structures for the HSCT [BTN-95-EIX95282711241] p 455 A95-89634
- The verification of a theoretical helicopter rotor blade sailing method by means of windtunnel testing [HTN-95-01093] p 468 A95-90279
- Aeronautical technology - recent advances and future prospects [HTN-95-01097] p 496 A95-90283
- A low fin height heat exchanger technology demonstrator for Hermes [SAE PAPER 932119] p 526 A95-90360
- AIAA Computing in Aerospace 10, San Antonio, TX, March 28-30, 1995 [ISBN 1-56347-119-1] p 565 A95-90629
- Dependability issues in the reuse of standard components in open architectures [AIAA PAPER 95-1006] p 566 A95-90678
- Accelerated application development for flight software [AIAA PAPER 95-1031] p 566 A95-90703
- An investigation of piloting strategies for engine failures during takeoff from offshore platforms [HTN-95-92834] p 497 A95-90752
- Collectively variable incidence wingtips for lift control and reduced gust sensitivity [HTN-95-92836] p 471 A95-90754
- Integrated aircraft thermal management and power generation [SAE PAPER 932055] p 500 A95-91636
- Condensing cycle air conditioning system [SAE PAPER 932056] p 513 A95-91637
- What's next in commercial aircraft environmental control systems? [SAE PAPER 932057] p 513 A95-91638
- Kinetic heating in hypersonic flight [CONGRESS PAPER C428-3-056] p 475 A95-91674
- Damage to composite aircraft structures from lightning strike attachment to unprotected CFC and internal sparking causing fuel injection [CONGRESS PAPER C428-4-026] p 531 A95-91675
- The rain erosion of PEEK (polyetheretherketone) [CONGRESS PAPER C428-4-039] p 531 A95-91676
- New computer delivered training systems to support technical crew training programmes [CONGRESS PAPER C428-5-036] p 522 A95-91678
- The advanced flight simulator complex [CONGRESS PAPER C428-5-025] p 522 A95-91679
- ASTOVL Aircraft: Some thoughts on new control strategies [CONGRESS PAPER C428-5-011] p 517 A95-91680
- General requirements for the electrohydraulic systems of the aircraft controls loading force on the simulators [CONGRESS PAPER C428-5-138] p 522 A95-91681
- The impact of new technology on reliability of avionic equipment [CONGRESS PAPER C428-6-114] p 549 A95-91683
- The avionics integrity programme (AVIP) [CONGRESS PAPER C428-6-115] p 549 A95-91684
- Automatic vehicle location and airfield ground movement [CONGRESS PAPER C428-7-148] p 488 A95-91689

- Evaluation and management of research and development in aeronautics
[CONGRESS PAPER C428-8-102] p 581 A95-91691
- Recent research in ASTOVL aircraft ground environment
[CONGRESS PAPER C428-9-040] p 475 A95-91694
- Cost effective small-scale experiments to aid the design of ASTOVL aircraft
[CONGRESS PAPER C428-9-098] p 475 A95-91695
- Pitot/static leak testing
[CONGRESS PAPER C428-9-035] p 508 A95-91696
- The use of hot film for the investigation of boundary-layer transition
[CONGRESS PAPER C428-9-199] p 475 A95-91697
- Universal electrohydraulic system for the steering gear loading
[CONGRESS PAPER C428-10-106] p 517 A95-91700
- Ageing aircraft after ALOHA
[CONGRESS PAPER C428-11-188] p 484 A95-91701
- Rolling bearing failure and wear debris detection
[CONGRESS PAPER C428-15-094] p 457 A95-91711
- Aircraft gear train diagnostics using the irregular rotation of the external shafts
[CONGRESS PAPER C428-15-097] p 508 A95-91712
- Intelligent skins development for future military aircraft
[CONGRESS PAPER C428-17-189] p 531 A95-91714
- Aerospace applications of new materials
[CONGRESS PAPER C428-17-135] p 531 A95-91716
- Computer simulation of ejection seat motion
[CONGRESS PAPER C428-18-169] p 484 A95-91718
- The use of math-dynamic models to aid the development of integrated health and usage monitoring systems
[CONGRESS PAPER C428-19-079] p 457 A95-91720
- Theory and evaluation of active control as a means of reducing helicopter vibration
[CONGRESS PAPER C428-19-124] p 517 A95-91721
- Passive and active vibration control activities in the German helicopter industry
[CONGRESS PAPER C428-19-126] p 517 A95-91722
- Simultaneous engineering in aero gas turbine design and manufacture
[CONGRESS PAPER C428-20-204] p 581 A95-91723
- An example of airborne vibration monitoring improving flight safety in the Soloviev D-30-KU engine
[CONGRESS PAPER C428-21-141] p 508 A95-91728
- A better than average stress model-photoelastic analysis for airbus design
[CONGRESS PAPER C428-23-005] p 500 A95-91730
- Impact finite element analysis, as an alternative to the testing of windscreens for bird impact
[CONGRESS PAPER C428-23-196] p 500 A95-91732
- The world of regional aircraft - challenges and opportunities
[HTN-95-C0002] p 595 A95-93390
- Modelling requirements in flight simulation
[HTN-95-C0004] p 585 A95-93392
- International Conference on Aviation Weather Systems, 5th, Vienna, VA, Aug. 2-6, 1993. Preprint Volume
[HTN-95-92940] p 652 A95-93441
- Evolving standards for safety critical software
[CONGRESS PAPER C428-24-142] p 678 A95-93595
- Development of software for safety critical applications for the EH101 Helicopter
[CONGRESS PAPER C428-24-160] p 678 A95-93597
- External viewing airborne CCTV system
[CONGRESS PAPER C428-25-172] p 595 A95-93598
- Civil aircraft performance - developments for improved safety
[CONGRESS PAPER C428-25-175] p 596 A95-93601
- Changing MRP Systems within the aerospace industry
[CONGRESS PAPER C428-26-051] p 681 A95-93603
- Manufacture technology
[CONGRESS PAPER C428-27-088] p 612 A95-93605

- The role of material behaviour modelling in stressing and life assessment of modern Aero-engine components
[CONGRESS PAPER C428-27-127] p 612 A95-93606
- Airborne integrated communications system
[CONGRESS PAPER C428-30-162] p 610 A95-93612
- The use of satellites for aeronautical communications, navigation and surveillance
[CONGRESS PAPER C428-30-159] p 600 A95-93613
- Progress and experience with helicopter health and usage monitoring
[CONGRESS PAPER C428-31-151] p 603 A95-93615
- Improving the fire resistance of aircraft structures
[CONGRESS PAPER C428-31-152] p 603 A95-93616
- Tooling - a source of productivity
[CONGRESS PAPER C428-32-017] p 583 A95-93619
- Design trends in propulsion control systems
[CONGRESS PAPER C428-33-123] p 610 A95-93620
- Chinook goes FADEC
[CONGRESS PAPER C428-33-078] p 610 A95-93621
- Surge recovery and compressor working line control using compressor exit mach number measurement
[CONGRESS PAPER C428-33-210] p 610 A95-93622
- Load alleviation for civil transport aircraft
[CONGRESS PAPER C428-35-057] p 604 A95-93627
- Flight control systems/structural coupling BAe Warton experience in aero-servo elasticity
[CONGRESS PAPER C428-35-059] p 610 A95-93628
- The A340 electrical power generation system
[CONGRESS PAPER C428-36-193] p 625 A95-93630
- The auxiliary and emergency power supply on the Saab JAS39 Gripen aircraft
[CONGRESS PAPER C428-36-192] p 612 A95-93631
- The certification of composite structures for military aircraft
[CONGRESS PAPER C428-37-198] p 628 A95-93633
- The development of a model specification for ground support equipment
[CONGRESS PAPER C428-38-095] p 625 A95-93636
- Electromagnetic compatibility - A general overview
[CONGRESS PAPER C428-38-084] p 634 A95-93637
- Laser processing aircraft and turbine engine parts
[SAE PAPER 931356] p 634 A95-93640
- Condition monitoring for helicopters: 3303 Airborne vibration monitoring system
[SAE PAPER 931360] p 610 A95-93642
- Laser velocimetry in the supersonic regime: Advancements, limitations, and outlook
[SAE PAPER 931365] p 634 A95-93646
- Primary and secondary vortex structures over accelerated-decelerated airfoils at high angles of attack
[SAE PAPER 931368] p 586 A95-93649
- An advanced vehicle management system
[SAE PAPER 931376] p 618 A95-93655
- Concepts for aircraft subsystem integration
[SAE PAPER 931377] p 604 A95-93656
- A subsystem integration technology concept
[SAE PAPER 931382] p 604 A95-93658
- A design trade study using CFD modeling of reaction jets for aerodynamic control
[SAE PAPER 931384] p 586 A95-93660
- Hybrid laminar flow over wings enhanced by continuous boundary layer suction
[SAE PAPER 931386] p 587 A95-93662
- A detailed power inverter design for a 250 kW switched reluctance aircraft engine starter/generator
[SAE PAPER 931388] p 613 A95-93664
- Detailed design of a 250-kW switched reluctance starter/generator for an aircraft engine
[SAE PAPER 931389] p 613 A95-93665
- Modelling and analysis of a dual-wheel nosegear: Shimmy instability and impact motions
[SAE PAPER 931402] p 605 A95-93672
- Dissolved gas - the hidden saboteur
[SAE PAPER 931404] p 628 A95-93674
- Modular avionics: Taking today's aircraft into tomorrow
[SAE PAPER 931416] p 610 A95-93681
- Integrated test system single point control of aircraft checkout
[SAE PAPER 931417] p 583 A95-93682

- Fiber optic hardware for transport aircraft
[SAE PAPER 931439] p 680 A95-93691
- Lightweight high-temperature fuel metering valves
[SAE PAPER 931444] p 635 A95-93693
- Lean manufacturing for lean times
[BTN-95-EIX95302730538] p 583 A95-94036
- Airfoil leading-edge suction and energy conservation for compressible flow
[BTN-95-EIX95302730589] p 637 A95-94197
- USSR**
- Advanced method and processing technology for complicated shape airframe part forming
p 80 N95-14486
- The traditional and new methods of accounting for the factors distorting the flow over a model in large transonic wind tunnels
p 165 N95-19275

V

VENEZUELA

- Contribution of thermal radiation to the temperature profile of ceramic composite materials
[BTN-94-EIX95011441252] p 417 A95-84209

Y

YUGOSLAVIA

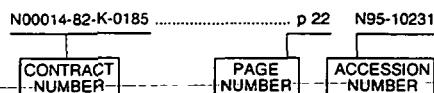
- Van der pol absorber for rotor vibrations
[BTN-94-EIX94441385106] p 702 A95-96579

CONTRACT NUMBER INDEX

AERONAUTICAL ENGINEERING / A Continuing Bibliography
1995 Cumulative Index

December 1995

Typical Contract Number Index Listing



Listings in this index are arranged alphanumerically by contract number. Under each contract number the accession numbers denoting documents that have been produced as a result of research done under the contract are shown. The accession number denotes the number by which the citation is identified in the abstract section. Preceding the accession number is the page number on which the citation may be found.

N00014-82-K-0185	p 22	N95-10231	CEC-STEP-CT91-0140	p 445	A95-86312	DE-AC04-76DP-03533	p 376	N95-27974
			CEC-STEP-CT91-040	p 445	A95-86315	DE-AC04-94AL-85000	p 7	N95-10226
			CR-4303-430220	p 445	A95-86318		p 56	N95-13184
			DA PROJ. 1L1-61102-AH-43	p 22	A95-86308		p 145	N95-16509
			DA PROJ. 1L1-61102-AH-45	p 44	N95-10231		p 152	N95-19100
			DA PROJ. 1L1-61102-AH-49	p 119	N95-18670		p 206	N95-19579
			DA PROJ. 1L1-62211-A-47-AB	p 137	N95-15970		p 228	N95-20195
			DA PROJ. 1L1-62211-A-47-A	p 210	N95-19567		p 229	N95-21520
			DA PROJ. 1L1-62211-A-47-A	p 618	N95-31985		p 232	N95-21730
			DA PROJ. 1L1-62211-A-47-A	p 117	N95-18340		p 299	N95-23532
			DA PROJ. 1L1-62211-A-47-A	p 555	N95-29538		p 330	N95-24308
			DA PROJ. 1L1-62211-A-47-AB	p 55	N95-12357	DE-AC05-84OR-21400	p 648	N95-31614
			DA PROJ. 1L1-62211-A-47-A	p 15	N95-10153		p 247	N95-20781
			DA PROJ. 1L1-6241-A-47-AB	p 58	N95-12843	DE-AC06-76RL-01830	p 300	N95-22689
			DA PROJ. 1L1-62618-AH-80	p 80	N95-14852	DE-AC06-76RL-01830	p 304	N95-23981
			DA PROJ. 1L1-62786-D-283	p 162	N95-19125	DE-AC08-93NV-11265	p 138	N95-17371
			DA PROJ. 3E1-62787-A-879	p 438	N95-27855	DE-AC09-89SR-18035	p 358	N95-25110
			DA PROJ. 3M1-62787-A-879	p 553	N95-29112	DE-AC21-93MC-29257	p 349	N95-24598
			DAA HQ4-93-G0019	p 285	N95-22953		p 650	N95-32163
			DAAE07-90-C-R030	p 131	N95-18381		p 694	N95-32636
			DAAE07-90-C-R059	p 118	N95-18611	DE-AC36-83CH-10093	p 157	N95-16939
			DAAG29-82-K-0093	p 284	N95-22510		p 118	N95-18646
			DAAH01-92-C-R097	p 117	N95-18340		p 216	N95-19855
			DAAH01-94-C-R032	p 172	N95-17334		p 256	N95-20985
			DAAH04-93-C-0015	p 259	N95-22044		p 357	N95-24853
			DAAH04-93-G-0001	p 391	N95-26993		p 357	N95-24882
			DAAH04-93-G-0500	p 212	N95-66315		p 358	N95-26090
			DAAH04-94-G-0038	p 211	N95-19809		p 446	N95-27459
			DAAH04-94-G-0039	p 126	N95-17706		p 376	N95-27541
			DAAH04-94-6-0351	p 529	N95-90272		p 564	N95-30016
			DAAJ02-93-C-0021	p 59	N95-13213		p 683	N95-32548
			DAAK70-87-C-0043	p 239	N95-21719	DE-AI01-76ET-20320	p 447	N95-27970
			DAAK70-92-C-0059	p 106	N95-16076	DE-AR21-93MC-30358	p 392	N95-27440
			DAAL-03-88-C-0004	p 369	N95-83659	DE-FC02-92CE-41000	p 235	N95-21243
			DAAL-03-91-G-0007	p 369	N95-83660	DE-FC05-85ER-250000	p 252	N95-70656
			DAAL-03-91-G-0096	p 169	N95-16864	DEN3-153	p 377	N95-27981
			DAAL03-88-C-0002	p 514	N95-29496		p 440	N95-27982
			DAAL03-88-C-0003	p 580	N95-30084		p 440	N95-27985
			DAAL03-88-C-0004	p 370	N95-83662		p 440	N95-27986
			DAAL03-88-C-002	p 648	N95-31475	DEN3-335	p 101	N95-15743
			DAAL03-89-K-0007	p 40	N95-12499	DNA-MIPR-92-501	p 509	N95-29950
			DAAL03-90-C-0013	p 426	N95-28621	DNA001-90-C-0127	p 86	N95-14639
			DAAL03-90-G-0008	p 40	N95-12499	DNA001-91-C-0021	p 235	N95-22036
			DAAL03-90-G-0031	p 541	N95-87685	DNA001-92-C-0076	p 676	N95-93556
			DAAL03-90-G-0138	p 542	N95-87694	DOT-FA4H2/A4044	p 328	N95-24295
			DAAL03-90-G-0186	p 461	N95-87676	DOT-SHRP-H-208A	p 78	N95-15439
			DAAL03-91-G-0007	p 222	N95-72568	DRET-88-520	p 644	N95-95495
			DAAL03-91-G-0022	p 236	N95-71184	DRET-90-34-162	p 640	N95-95443
			DAAL03-91-G-0023	p 221	N95-72566	DTFA03-89-C-00043	p 99	N95-13895
			DAAL03-91-G-0026	p 458	N95-87200	DTFA01-87-C-00014	p 85	N95-15328
			DAAL03-91-G-0308	p 635	N95-93703	DTFA01-90-Z-02069	p 55	N95-12131
			DAAL03-92-C-0013	p 2	N95-60169		p 53	N95-12216
			DAAL03-92-C-0016	p 3	N95-60184	DTFA01-90-25001	p 254	N95-72543
			DAAL03-92-C-0021	p 256	N95-20828	DTFA01-91-Z-02036	p 677	N95-31465
			DAAL03-92-G-0277	p 106	N95-16160		p 602	N95-31521
			DAAL03-93-G-002	p 155	N95-16163	DTFA01-93-C-00001	p 382	N95-26454
			DABT60-90-D-0010	p 106	N95-16099	DTFA01-93-C-0001	p 599	N95-31687
			DACA76-89-C-0014	p 106	N95-16099	DTFA01-93-P-02265	p 226	N95-21518
			DAJA45-83-C-0011	p 221	N95-72567	DTFA01-93-Z-02012	p 98	N95-15749
			DAJA45-83-C-0041	p 503	N95-29322		p 154	N95-16097
			DASG60-84-C-0117	p 555	N95-29562	DTFA02-91-C-91089	p 245	N95-20599
			DASG60-89-C-0147	p 554	N95-29228		p 689	N95-33480
			DE-AC02-76CH-00016	p 477	N95-29091		p 384	N95-28540
			DE-AC02-76CH-03000	p 400	N95-28504		p 488	N95-28790
			DE-AC02-83CH-10093	p 620	N95-31400	DTFA02-93-P-7913	p 602	N95-32186
			DE-AC04-76DP-00789	p 647	N95-31374	DTFA03-83-A-00328	p 366	N95-26363
				p 87	N95-14363	DTFA03-84-R-40032	p 382	N95-28630
				p 537	N95-29482	DTFA03-89-C-00043	p 189	N95-19805
				p 464	N95-88976		p 226	N95-20174
				p 554	N95-29387		p 226	N95-20275
				p 543	N95-88083		p 227	N95-22319
				p 370	N95-83662		p 448	N95-26638
				p 391	N95-27018		p 693	N95-34583
				p 126	N95-17706	DTFA03-89-C-0043	p 328	N95-25401
				p 302	N95-23509	DTFA03-91-A-00018	p 380	N95-26497
				p 302	N95-23509	DTFA03-92-C-00003	p 225	N95-20093
				p 98	N95-62279	DTFA03-92-C-0035	p 77	N95-14179
				p 98	N95-62279	DTFA03-92-Z-00018	p 690	N95-34562
				p 252	N95-71186	DTRSS7-88-C-00078	p 601	N95-31520
				p 629	N95-30765	DTRSS7-88-C-0078	p 643	N95-95472
				p 451	N95-27991	EEC-AERO-0018-C(H)	p 575	N95-90109
				p 439	N95-27980	EEC-AERO-0028-C		

CONTRACT

EG-77-C-01-4042	p 451	N95-27991	F49620-92-J-0399	p 372	A95-86160	NAG1-537	p 160	N95-18388
EPA-68-C0-0003	p 104	N95-17466	F49620-93-C-0050	p 237	N95-21122		p 439	N95-27865
EPA-68-C4-0020	p 343	N95-26004	F49620-93-1-0090	p 686	N95-34763	NAG1-745	p 343	N95-24220
EPA-68-D1-0177	p 358	N95-26005	F49620-93-1-0143	p 567	N95-29074		p 343	N95-24878
ESPRIT 3 PROJ. 6276	p 247	N95-20653	F49620-93-1-0338	p 250	N95-22212	NAG1-795	p 432	N95-85028
F-49620-93-1-0009	p 542	A95-87689	F49620-93-1-0444	p 245	N95-20484	NAG1-833	p 397	N95-28262
FAA-92-G-0004	p 94	N95-14470	F49620-93-1-0579	p 397	N95-28409	NAG1-922	p 526	N95-29339
FAA-92-G-0005	p 94	N95-14479	F49620-93-1-0588	p 523	N95-29468	NAG1-928	p 316	N95-23670
FAA-92-G-0006	p 87	N95-14465	F49620-93-1-0608	p 485	N95-29210	NAG2-1005	p 543	A95-88084
FAA-92-G-002	p 83	N95-15683	F49620-94-C-0040	p 241	N95-20299	NAG2-175	p 98	N95-13725
FAA-93-G-0068	p 94	N95-14470	F49620-94-C-0042	p 151	N95-16371	NAG2-458	p 253	A95-72423
F04701-90-C-0023	p 98	A95-62279		p 381	N95-27186	NAG2-462	p 221	A95-72567
F08630-93-C-0074	p 567	N95-28745		p 504	N95-29426	NAG2-477	p 37	N95-11911
F08635-82-C-0131	p 356	A95-80862	F49620-94-C-0043	p 241	N95-20481	NAG2-561	p 285	N95-23217
F08635-89-C-0208	p 404	A95-86158		p 241	N95-20716	NAG2-565	p 463	A95-88969
F08635-90-C-0053	p 255	N95-19921		p 556	N95-29946	NAG2-592	p 541	A95-87682
F08635-91-C-0189	p 341	N95-24424	F49620-94-C-0049	p 556	N95-29941	NAG2-663	p 445	N95-26669
F09603-89-G-0096	p 92	N95-14455	F49620-94-1-0275	p 601	N95-31433	NAG2-731	p 351	A95-78000
F09603-90-D-2217	p 241	N95-21687	F49620-94-1-0292	p 648	N95-31432	NAG2-733	p 588	A95-93758
	p 367	N95-26629	F49629-89-C-0014	p 462	A95-88898		p 58	N95-12228
F19628-90-C-0002	p 11	N95-10570	GRI-5089-291-2077	p 338	N95-24293		p 309	N95-23183
	p 98	N95-15749	IRAD PROJ. R-1056	p 423	N95-28441	NAG2-789	p 518	N95-30254
	p 245	N95-20599	JPL-958123	p 447	N95-27805	NAG2-794	p 52	N95-12791
	p 300	N95-23781	JPL-958208	p 320	N95-23766	NAG2-797	p 542	A95-87694
F19628-90-C-0003	p 450	N95-28627	MDA903-89-C-0003	p 248	N95-20966	NAG2-817	p 566	A95-90688
F19628-90-C-002	p 42	N95-13209	MDA903-92-C-0047	p 386	A95-84558	NAG2-847	p 462	A95-88892
F19628-93-C-0054	p 226	N95-21831	MDA972-90-C-0035	p 83	N95-14343	NAG2-854	p 224	N95-21031
F19628-93-K-0018	p 514	N95-29764	MIPR-ARO-132-90	p 432	A95-85042	NAG2-881	p 249	N95-21340
F19628-94-C-0001	p 60	N95-12805	MIPR-ARO-137-86	p 5	A95-60193	NAG2-882	p 43	N95-11699
F19628-95-C-0002	p 677	N95-31465	MIPR-114-91	p 5	A95-60191	NAG2-905	p 224	N95-21343
	p 689	N95-33480	MIPR-130-92	p 5	A95-60191	NAG2-908	p 691	N95-32928
F29601-89-C-0089	p 449	N95-27246	MIPR-91-0007	p 432	A95-85042	NAG3-1072	p 377	N95-28003
F29601-92-C-0109	p 247	N95-20772	MIPR-92-0004	p 5	A95-60191	NAG3-1137	p 316	N95-24189
	p 231	N95-20772	MOESC-05650154	p 470	A95-90447	NAG3-1165	p 8	N95-10853
	p 448	N95-26845	MOESC-06650186	p 470	A95-90447		p 76	N95-15912
F30602-89-D-0100	p 679	N95-31455	NAG-991	p 252	A95-70656		p 275	N95-23462
F30602-93-C-0040	p 489	N95-28887	NAGW-1230	p 351	A95-78000	NAG3-1177	p 290	A95-75096
F30602-93-C-0090	p 566	A95-90683	NAGW-1331	p 458	A95-87207	NAG3-1198	p 137	N95-15970
F30602-94-C-0013	p 12	N95-10442	NAGW-1727	p 352	A95-78014	NAG3-1203	p 48	N95-12787
F33615-78-C-3602	p 138	N95-18164	NAGW-2182	p 444	A95-86292	NAG3-1234	p 156	N95-16588
F33615-84-C-3627	p 406	N95-28275	NAGW-2183	p 351	A95-77982		p 651	N95-32205
F33615-85-C-5152	p 235	N95-22024	NAGW-3713	p 520	A95-90439	NAG3-1242	p 418	A95-86165
F33615-87-C-0531	p 242	N95-21969		p 511	A95-90440	NAG3-1269	p 53	N95-13200
F33615-88-C-2817	p 239	N95-20992	NAGW-3715	p 519	A95-88010	NAG3-1273	p 289	N95-23088
F33615-90-C-0005	p 700	N95-34344		p 470	A95-90455	NAG3-1316	p 210	N95-19567
	p 700	N95-34362	NAGW-674	p 496	A95-90458	NAG3-1378	p 542	A95-87689
F33615-90-C-0006	p 679	N95-31684		p 544	A95-88105	NAG3-1425	p 23	N95-10132
F33615-90-C-2052	p 613	A95-93664	NAG1-P1267	p 586	A95-93396	NAG3-1434	p 349	N95-24461
	p 613	A95-93665	NAG1-1056	p 350	N95-25394	NAG3-1436	p 462	A95-88892
F33615-90-C-3613	p 256	N95-21913	NAG1-1058	p 468	A95-90273	NAG3-1507	p 310	N95-23190
F33615-90-D-4013	p 446	N95-27234		p 411	N95-26768		p 338	N95-24213
F33615-91-C-1758	p 569	N95-29644		p 24	N95-11252		p 703	N95-32689
F33615-91-C-1788	p 566	A95-90693	NAG1-1065	p 58	N95-12856	NAG3-1523	p 418	A95-86165
F33615-91-C-2139	p 634	A95-93669	NAG1-1066	p 335	N95-24630	NAG3-1561	p 338	N95-24392
F33615-91-C-2142	p 160	N95-18660	NAG1-1067	p 99	N95-13727	NAG3-178	p 172	N95-16401
F33615-91-C-2169	p 155	N95-16322	NAG1-1088	p 535	N95-29036	NAG3-300	p 377	N95-27977
F33615-91-C-3407	p 493	A95-90065	NAG1-1133	p 293	N95-22908	NAG3-376	p 465	A95-88980
F33615-91-C-5563	p 530	A95-90477	NAG1-1135	p 239	N95-21436	NAG3-378	p 451	N95-27992
F33615-91-C-5660	p 158	N95-17507	NAG1-1141	p 462	A95-88892	NAG3-481	p 366	N95-26363
F33615-91-C-5661	p 244	N95-20414	NAG1-1150	p 418	A95-85062	NAG3-510	p 95	N95-14556
F33615-92-C-1028	p 647	N95-30992	NAG1-1170	p 285	N95-22949	NAG3-72	p 57	N95-11888
F33615-92-C-3400	p 131	N95-18162	NAG1-1175	p 10	N95-11582	NAG3-768	p 75	N95-14803
	p 133	N95-18677	NAG1-1184	p 273	N95-23182	NAG3-867	p 419	N95-27167
	p 485	N95-28811	NAG1-1188	p 166	N95-19473	NAG3-965	p 418	A95-86165
F33615-92-C-3405	p 630	N95-31471		p 459	A95-87227	NAG3-998	p 142	N95-17404
F33615-92-C-3601	p 612	N95-31655	NAG1-1189	p 540	A95-87577	NAGS-1440	p 150	N95-17493
	p 612	N95-31656	NAG1-1240	p 274	N95-23218	NAGS-1490	p 707	N95-32823
F33615-92-C-3604	p 698	N95-34306	NAG1-1253	p 509	A95-87410	NAGS-1602	p 252	A95-70656
F33615-92-C-5936	p 130	N95-17661	NAG1-1254	p 437	N95-26995	NAGS-2058	p 447	N95-27805
F33615-92-D-2293	p 328	N95-25607	NAG1-1257	p 222	A95-72568	NAGS-30552	p 214	A95-69431
F33615-93-C-2321	p 407	N95-28646	NAG1-1265	p 444	A95-86292	NAG9-622	p 92	N95-14454
F33615-93-D-3800	p 389	N95-26684		p 526	N95-29339	NAL PROJ. EA-9-000	p 35	N95-12166
F33615-94-C-3402	p 579	N95-28870	NAG1-1311	p 545	A95-88106	NAL PROJ. ID-8-117L	p 142	N95-16392
F33617-91-C-3004	p 132	N95-18483	NAG1-1329	p 58	N95-13201	NAS ASC 92-17394	p 23	N95-10132
F33657-84-C-0247	p 593	N95-30885	NAG1-1351	p 153	N95-19490	NASA ORDER L-40679-D	p 449	N95-27246
F33657-90-D-0027	p 423	N95-28437	NAG1-1365	p 86	N95-14639	NASW-4435	p 44	N95-12294
F33657-93-C-2440	p 66	N95-15331	NAG1-1380	p 357	N95-24219		p 45	N95-12305
F34601-90-C-1336	p 152	N95-19482	NAG1-1400	p 575	A95-90105		p 45	N95-12363
F41624-93-C-2002	p 379	A95-84560	NAG1-1410	p 295	N95-23410		p 45	N95-12530
F49620-88-C-0076	p 432	A95-85030	NAG1-1437	p 520	A95-90439		p 45	N95-12609
F49620-90-C-0027	p 643	A95-95477	NAG1-1478	p 605	A95-93673		p 45	N95-12626
F49620-91-C-0003	p 62	N95-11944		p 27	N95-11593		p 46	N95-12628
	p 81	N95-15451	NAG1-1522	p 704	N95-32822		p 46	N95-12636
F49620-91-C-0014	p 248	N95-21146		p 392	N95-27180		p 46	N95-12637
F49620-91-C-0037	p 539	A95-87220	NAG1-1539	p 479	N95-29338		p 46	N95-12638
F49620-91-C-0059	p 639	A95-95383	NAG1-1557	p 377	N95-28193		p 47	N95-12639
F49620-92-C-0070	p 479	N95-29316	NAG1-1571	p 172	N95-16848		p 47	N95-12643
F49620-92-J-0078	p 608	N95-31451	NAG1-1607	p 130	N95-18090		p 47	N95-12645
F49620-92-J-0097	p 707	N95-34597	NAG1-19317	p 340	N95-24302		p 47	N95-12689
F49620-92-J-0127	p 257	N95-22216	NAG1-226	p 283	A95-75099		p 47	N95-12695
	p 679	N95-30961	NAG1-230	p 81	N95-14909		p 48	N95-12700
F49620-92-J-0146	p 541	A95-87582	NAG1-343	p 30	N95-11277		p 48	N95-12702
F49620-92-J-0184	p 23	N95-10535		p 283	A95-75099		p 49	N95-12993
F49620-92-J-0189	p 157	N95-16736	NAG1-365	p 301	N95-23179		p 79	N95-13703
F49620-92-J-0227	p 152	N95-18410	NAG1-373	p 575	A95-90104		p 81	N95-15742
F49620-92-J-0386	p 619	N95-30937		p 432	A95-85028	NAS1-14101	p 61	N95-11932

CONTRACT NUMBER INDEX

W-7405-ENG-82

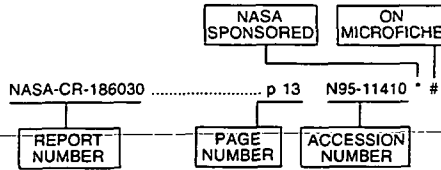
RTOP 505-64-36	p 11	N95-10846	RTOP 510-02-11-02	p 23	N95-10318	W-7405-ENG-48	p 249	N95-21478
	p 35	N95-12227	RTOP 510-02-11-08	p 630	N95-31421		p 256	N95-21552
	p 288	N95-24030	RTOP 510-02-13-01	p 11	N95-10240		p 250	N95-22299
RTOP 505-64-50-03	p 33	N95-10873		p 12	N95-10242		p 297	N95-24019
RTOP 505-64-52-01	p 17	N95-10220		p 12	N95-10316		p 441	N95-28029
	p 99	N95-13727		p 151	N95-16859		p 452	N95-28108
	p 335	N95-24630		p 531	N95-28823		p 441	N95-28139
	p 410	N95-27839		p 503	N95-29027		p 644	N95-30507
	p 518	N95-30327		p 534	N95-29029		p 584	N95-32164
RTOP 505-64-52	p 309	N95-22804	RTOP 532-05-37-63	p 55	N95-12357		p 701	N95-33408
RTOP 505-64-53-03	p 80	N95-14852	RTOP 532-06-37-01	p 451	N95-26392		p 708	N95-33642
RTOP 505-68-00	p 37	N95-11927	RTOP 533-02-00	p 13	N95-11410	W-7405-ENG-82	p 24	N95-11135
	p 108	N95-16858		p 36	N95-11898		p 436	N95-26445
	p 620	N95-31846	RTOP 533-02-03	p 617	N95-31425			
RTOP 505-68-10	p 57	N95-11888	RTOP 533-02-31	p 38	N95-12191			
	p 39	N95-13197	RTOP 533-02-38	p 8	N95-10858			
	p 123	N95-18582	RTOP 535-03-10	p 23	N95-10244			
	p 124	N95-19284		p 323	N95-22675			
	p 124	N95-19285	RTOP 535-03-11-02	p 62	N95-12341			
	p 309	N95-22669	RTOP 536-01-11	p 453	N95-27367			
	p 381	N95-27762	RTOP 537-02-00	p 592	N95-30704			
	p 485	N95-29132	RTOP 537-02-20	p 616	N95-30853			
RTOP 505-68-20	p 51	N95-11868	RTOP 537-02-21	p 139	N95-18133			
RTOP 505-68-30-01	p 330	N95-24443		p 236	N95-21383			
	p 505	N95-30226		p 289	N95-23550			
RTOP 505-68-30-03	p 120	N95-19114		p 615	N95-30589			
	p 273	N95-22917		p 616	N95-30698			
	p 273	N95-23095		p 705	N95-32930			
	p 273	N95-23185		p 694	N95-32931			
RTOP 505-68-30-05	p 17	N95-10860	RTOP 537-02-22	p 76	N95-15852			
RTOP 505-68-30	p 67	N95-14229		p 617	N95-30861			
	p 197	N95-19651	RTOP 537-02-23	p 8	N95-10820			
RTOP 505-68-32	p 18	N95-11487		p 37	N95-11917			
	p 49	N95-11864		p 39	N95-13058			
	p 272	N95-22666		p 105	N95-16038			
	p 332	N95-26302		p 482	N95-30253			
	p 405	N95-26412	RTOP 537-03-21-03	p 75	N95-14878			
	p 606	N95-30646	RTOP 537-03-23-03	p 249	N95-21258			
RTOP 505-68-50	p 117	N95-18565	RTOP 537-06-20-06	p 151	N95-16860			
RTOP 505-68-53	p 157	N95-17418		p 343	N95-24878			
RTOP 505-68-70-06	p 406	N95-28227	RTOP 537-06-21-09	p 645	N95-30682			
RTOP 505-68-70-08	p 6	N95-10029	RTOP 537-07-00	p 116	N95-18101			
RTOP 505-68-70-09	p 44	N95-11952	RTOP 537-07-20	p 273	N95-23193			
	p 378	N95-28241	RTOP 537-08-21-01	p 335	N95-24582			
RTOP 505-69-10	p 10	N95-11408	RTOP 537-09-21-05	p 453	N95-26427			
	p 284	N95-22829	RTOP 537-10-20	p 406	N95-27866			
RTOP 505-69-20-01	p 102	N95-13663	RTOP 538-01-11	p 50	N95-11867			
	p 333	N95-24633	RTOP 538-01-13-01	p 334	N95-25341			
RTOP 505-69-50	p 8	N95-10853	RTOP 538-02-10-01	p 92	N95-14453			
	p 80	N95-14604		p 88	N95-14920			
	p 76	N95-15912		p 124	N95-19468			
	p 108	N95-16887	RTOP 538-03-11-01	p 711	N95-33831			
	p 119	N95-18933	RTOP 538-03-11	p 7	N95-10148			
	p 275	N95-23462		p 50	N95-11901			
	p 615	N95-30594		p 50	N95-11951			
RTOP 505-70-59-03	p 37	N95-11995		p 100	N95-14610			
RTOP 505-70-59	p 89	N95-13665		p 156	N95-16588			
RTOP 505-70-62-01	p 407	N95-28343		p 145	N95-18054			
RTOP 505-70-62-03	p 50	N95-12860		p 258	N95-21888			
RTOP 505-70-62-04	p 350	N95-25394		p 580	N95-29641			
RTOP 505-70-62	p 148	N95-19286		p 457	N95-30229			
	p 274	N95-23250		p 616	N95-30779			
	p 482	N95-30091		p 710	N95-32836			
	p 523	N95-30228	RTOP 538-03-15-01	p 362	N95-26160			
RTOP 505-70-63	p 89	N95-13892		p 452	N95-28670			
RTOP 505-70-91-01	p 54	N95-13196	RTOP 538-04-13-01	p 292	N95-22674			
RTOP 505-90-21	p 377	N95-28003	RTOP 538-05-13-01	p 238	N95-20669			
RTOP 505-90-5K	p 439	N95-27882		p 226	N95-20706			
RTOP 505-90-52-01	p 8	N95-10848	RTOP 538-06-13	p 316	N95-24189			
	p 27	N95-11593	RTOP 538-06-14	p 651	N95-32205			
	p 57	N95-11812	RTOP 538-08-11	p 338	N95-24304			
	p 61	N95-11932	RTOP 550-00-00	p 416	N95-27763			
	p 170	N95-16897	RTOP 694-03-0C	p 146	N95-18586			
	p 170	N95-16898	RTOP 763-01-51-25	p 22	N95-11003			
	p 170	N95-18110	RTOP 763-23-35-08	p 97	N95-15898			
	p 159	N95-18190		p 97	N95-15899			
	p 159	N95-18191	RTOP 776-33-41	p 447	N95-27970			
	p 159	N95-18193	RTOP 778-32-21	p 101	N95-15743			
	p 314	N95-23466	RTOP 963-20-0C	p 438	N95-27854			
	p 361	N95-26085	RTOP 963-70-OH	p 104	N95-17657			
	p 438	N95-27179		p 105	N95-18197			
	p 442	N95-28673		p 105	N95-18486			
	p 569	N95-30353	RTOP-505-68-30	p 69	N95-14239			
RTOP 505-90-53-02	p 26	N95-10859		p 71	N95-14251			
	p 449	N95-27241	RTOP-509-10-11	p 23	N95-10132			
	p 568	N95-29454	SBIR-02.04-8581	p 415	N95-27093			
RTOP 505-90-58	p 406	N95-27860	S2-13534	p 1	A95-60160			
	p 615	N95-30517	T2-341085/8B03	p 22	N95-10231			
	p 616	N95-30632	W-31-109-ENG-38	p 52	N95-11752			
RTOP 506-40-41-02	p 309	N95-23015		p 157	N95-16828			
	p 310	N95-23210		p 231	N95-20370			
RTOP 506-42-31	p 105	N95-18044		p 258	N95-21388			
RTOP 506-43-11-01	p 537	N95-30252	W-7405-ENG-36	p 39	N95-12652			
RTOP 508-68-10	p 684	N95-32769		p 324	N95-24076			
RTOP 509-10-00	p 8	N95-10847		p 420	N95-27851			
RTOP 509-10-11	p 65	N95-13662						

REPORT NUMBER INDEX

AERONAUTICAL ENGINEERING / A Continuing Bibliography
1995 Cumulative Index

December 1995

Typical Report Number Index Listing



Listings in this index are arranged alphanumerically by report number. The page number indicates the page on which the citation is located. The accession number denotes the number by which the citation is identified. An asterisk (*) indicates that the item is a NASA report. A pound sign (#) indicates that the item is available on microfiche.

AD-A279602	p 238	N95-19955	#	AD-A283656	p 119	N95-18669	
AD-A279605	p 255	N95-20441		AD-A283669	p 170	N95-18018	
AD-A279692	p 341	N95-24424		AD-A283671	p 66	N95-15331	#
AD-A279717	p 239	N95-20992		AD-A283688	p 119	N95-18670	#
AD-A279871	p 244	N95-20414		AD-A283700	p 133	N95-18621	#
AD-A279922	p 188	N95-19863		AD-A283718	p 160	N95-18436	#
AD-A279931	p 203	N95-19864		AD-A283802	p 255	N95-19921	#
AD-A279965	p 237	N95-21122		AD-A283828	p 118	N95-18624	#
AD-A279980	p 257	N95-20963		AD-A283849	p 77	N95-14350	#
AD-A279981	p 257	N95-20966		AD-A283854	p 91	N95-14351	#
AD-A280012	p 237	N95-20004	#	AD-A283867	p 119	N95-18674	#
AD-A280037	p 245	N95-20599	#	AD-A283874	p 99	N95-14357	#
AD-A280063	p 238	N95-20624		AD-A283897	p 171	N95-18365	#
AD-A280074	p 412	N95-28151		AD-A283925	p 133	N95-18677	#
AD-A280075	p 420	N95-28152		AD-A283926	p 131	N95-18162	#
AD-A280100	p 228	N95-21020		AD-A283933	p 138	N95-18164	#
AD-A280237	p 19	N95-10349	#	AD-A283981	p 134	N95-18891	#
AD-A280238	p 20	N95-10350		AD-A283982	p 79	N95-14205	#
AD-A280239	p 20	N95-10351	#	AD-A283994	p 134	N95-19067	#
AD-A280432	p 20	N95-10352		AD-A283997	p 146	N95-18724	#
AD-A280433	p 20	N95-10353		AD-A283998	p 146	N95-18725	#
AD-A280434	p 20	N95-10354		AD-A283999	p 134	N95-18726	#
AD-A280824	p 79	N95-14306	#	AD-A284000	p 231	N95-20466	#
AD-A280860	p 21	N95-10919	#	AD-A284049	p 226	N95-21518	#
AD-A280907	p 108	N95-16824	#	AD-A284050	p 160	N95-18660	#
AD-A280933	p 23	N95-10535	#	AD-A284057	p 118	N95-18663	#
AD-A280974	p 168	N95-16506	#	AD-A284064	p 8	N95-10848	#
AD-A280990	p 105	N95-15994	#	AD-A284075	p 161	N95-19035	#
AD-A281035	p 156	N95-16448	#	AD-A284097	p 117	N95-18380	#
AD-A281075	p 107	N95-16808	#	AD-A284099	p 131	N95-18398	#
AD-A281380	p 87	N95-14363	#	AD-A284115	p 146	N95-18405	#
AD-A281386	p 106	N95-16160	#	AD-A284119	p 132	N95-18407	#
AD-A281399	p 169	N95-16884	#	AD-A284126	p 152	N95-18410	#
AD-A281412	p 155	N95-16163	#	AD-A284151	p 132	N95-18415	#
AD-A281444	p 36	N95-11829	#	AD-A284154	p 132	N95-18417	#
AD-A281452	p 106	N95-16076	#	AD-A284159	p 92	N95-14405	#
AD-A281520	p 154	N95-16097	#	AD-A284206	p 130	N95-17953	#
AD-A281526	p 106	N95-16099	#	AD-A284230	p 87	N95-14409	#
AD-A281534	p 142	N95-16109	#	AD-A284249	p 210	N95-19730	#
AD-A281580	p 127	N95-16171	#	AD-A284253	p 194	N95-19731	#
AD-A281581	p 76	N95-15465	#	AD-A284280	p 230	N95-19963	#
AD-A281706	p 81	N95-15451	#	AD-A284291	p 223	N95-20248	#
AD-A281749	p 14	N95-11595	#	AD-A284319	p 131	N95-18381	#
AD-A281871	p 127	N95-16356	#	AD-A284332	p 139	N95-18383	#
AD-A281897	p 25	N95-11330	#	AD-A284375	p 117	N95-18340	#
AD-A281974	p 52	N95-11789	#	AD-A284433	p 81	N95-15815	#
AD-A281982	p 65	N95-14144	#	AD-A284467	p 81	N95-15821	#
AD-A281985	p 145	N95-17444	#	AD-A284745	p 27	N95-11593	#
AD-A282052	p 9	N95-11179	#	AD-A284763	p 146	N95-18087	#
AD-A282208	p 40	N95-12499	#	AD-A284765	p 126	N95-18088	#
AD-A282209	p 62	N95-12426	#	AD-A284802	p 216	N95-19685	#
AD-A282259	p 45	N95-12410	#	AD-A284824	p 217	N95-19688	#
AD-A282371	p 62	N95-11944	#	AD-A284833	p 194	N95-19693	#
AD-A282412	p 158	N95-17507	#	AD-A284877	p 98	N95-15749	#
AD-A282440	p 96	N95-15547	#	AD-A284887	p 120	N95-19110	#
AD-A282467	p 51	N95-13289	#	AD-A284971	p 171	N95-16226	#
AD-A282479	p 125	N95-17373	#	AD-A284982	p 61	N95-11932	#
AD-A282664	p 60	N95-12805	#	AD-A284998	p 241	N95-20481	#
AD-A282729	p 54	N95-12507	#	AD-A285053	p 245	N95-20484	#
AD-A282787	p 126	N95-17706	#	AD-A285102	p 276	N95-23201	#
AD-A282839	p 83	N95-14343	#	AD-A285118	p 300	N95-23781	#
AD-A282917	p 88	N95-15415	#	AD-A285127	p 197	N95-19595	#
AD-A282923	p 82	N95-15392	#	AD-A285135	p 240	N95-20906	#
AD-A282950	p 49	N95-12591	#	AD-A285190	p 123	N95-16404	#
AD-A282966	p 130	N95-17661	#	AD-A285323	p 151	N95-16371	#
AD-A283011	p 84	N95-13687	#	AD-A285455	p 108	N95-17178	#
AD-A283052	p 61	N95-12996	#	AD-A285498	p 157	N95-16736	#
AD-A283081	p 172	N95-17334	#	AD-A285500	p 129	N95-16969	#
AD-A283207	p 129	N95-17631	#	AD-A285555	p 143	N95-18641	#
AD-A283210	p 96	N95-14658	#	AD-A285593	p 237	N95-21214	#
AD-A283227	p 80	N95-14849	#	AD-A285622	p 248	N95-21146	#
AD-A283228	p 87	N95-14850	#	AD-A285626	p 228	N95-21148	#
AD-A283335	p 130	N95-18008	#	AD-A285673	p 156	N95-16621	#
AD-A283398	p 109	N95-17435	#	AD-A285684	p 194	N95-19517	#
AD-A283450	p 62	N95-12512	#	AD-A285691	p 226	N95-20275	#
AD-A283459	p 56	N95-12546	#	AD-A285713	p 132	N95-18483	#
AD-A283464	p 38	N95-12548	#	AD-A285727	p 152	N95-18068	#
AD-A283500	p 40	N95-12623	#	AD-A285738	p 225	N95-20071	#
AD-A283505	p 126	N95-18059	#	AD-A285758	p 238	N95-19931	#
AD-A283550	p 85	N95-15328	#	AD-A285797	p 284	N95-22510	#
AD-A283564	p 83	N95-15329	#	AD-A285832	p 232	N95-20032	#
AD-A283585	p 75	N95-15319	#	AD-A285845	p 226	N95-21831	#
AD-A283618	p 133	N95-18616	#	AD-A285862	p 242	N95-22132	#
AD-A279089	p 256	N95-21913					
AD-A279126	p 225	N95-21877					
AD-A279144	p 242	N95-21969					
AD-A279157	p 259	N95-21975					
AD-A279164	p 189	N95-19805					
AD-A279176	p 211	N95-19809					
AD-A279188	p 191	N95-19810					
AD-A279219	p 204	N95-19848					
AD-A279220	p 176	N95-18578	#				
AD-A279378	p 230	N95-20181					
AD-A279436	p 320	N95-23766	*				
AD-A279527	p 241	N95-21687					

REPORT

AD-A285921	p 255	N95-19989	#	AD-A289540	p 390	N95-26873	AD-A292911	p 679	N95-31455	#
AD-A285928	p 223	N95-19991	#	AD-A289553	p 407	N95-28646	AD-A292973	p 626	N95-31468	#
AD-A285930	p 241	N95-20299	#	AD-A289556	p 374	N95-26757	AD-A292992	p 630	N95-31471	#
AD-A285998	p 241	N95-20716	#	AD-A289598	p 389	N95-26684	AD-A293012	p 648	N95-31475	#
AD-A286007	p 256	N95-20719	#	AD-A289601	p 374	N95-26713	AD-A293039	p 599	N95-31667	#
AD-A286032	p 248	N95-20998	#	AD-A289629	p 442	N95-28649	AD-A293056	p 392	N95-27504	#
AD-A286044	p 248	N95-21001	#	AD-A289631	p 374	N95-26719	AD-A293113	p 593	N95-30885	#
AD-A286049	p 227	N95-22417	#	AD-A289635	p 446	N95-26858	AD-A293223	p 646	N95-30902	#
AD-A286058	p 258	N95-21170	#	AD-A289758	p 375	N95-26859	AD-A293277	p 646	N95-30906	#
AD-A286077	p 247	N95-20849	#	AD-A289759	p 436	N95-26722	AD-A293254	p 678	N95-30892	#
AD-A286127	p 235	N95-22232	#	AD-A289760	p 170	N95-18110	AD-A293270	p 629	N95-31124	#
AD-A286134	p 235	N95-22036	#	AD-A289769	p 508	N95-28691	AD-A293277	p 617	N95-31191	#
AD-A286165	p 232	N95-22039	#	AD-A289771	p 508	N95-28692	AD-A293308	p 646	N95-30922	#
AD-A286190	p 231	N95-20329	#	AD-A289799	p 504	N95-29457	AD-A293309	p 607	N95-30923	#
AD-A286208	p 258	N95-21882	#	AD-A289800	p 410	N95-28598	AD-A293416	p 679	N95-31684	#
AD-A286239	p 235	N95-22024	#	AD-A289820	p 508	N95-29123	AD-A293442	p 630	N95-31368	#
AD-A286279	p 249	N95-22005	#	AD-A289838	p 552	N95-28948	AD-A293452	p 647	N95-31374	#
AD-A286287	p 259	N95-22044	#	AD-A289847	p 197	N95-19653	AD-A293586	p 599	N95-31687	#
AD-A286295	p 226	N95-22318	#	AD-A289891	p 368	N95-28610	AD-A293611	p 612	N95-31655	#
AD-A286298	p 219	N95-22046	#	AD-A289912	p 426	N95-28621	AD-A293612	p 612	N95-31656	#
AD-A286309	p 219	N95-20091	#	AD-A289926	p 400	N95-28626	AD-A293682	p 584	N95-31598	#
AD-A286312	p 225	N95-20093	#	AD-A289938	p 450	N95-28627	AD-A293689	p 608	N95-31602	#
AD-A286315	p 226	N95-20174	#	AD-A289986	p 607	N95-30927	AD-A293690	p 689	N95-33480	#
AD-A286319	p 223	N95-20177	#	AD-A290005	p 594	N95-30929	AD-A293691	p 602	N95-32022	#
AD-A286337	p 239	N95-21719	#	AD-A290045	p 382	N95-28630	AD-A293741	p 599	N95-31569	#
AD-A286338	p 231	N95-20212	#	AD-A290107	p 502	N95-28851	AD-A293753	p 602	N95-31572	#
AD-A286381	p 227	N95-22352	#	AD-A290136	p 485	N95-29210	AD-A293770	p 608	N95-31578	#
AD-A286382	p 227	N95-22319	#	AD-A290149	p 490	N95-30031	AD-A293771	p 608	N95-31579	#
AD-A286507	p 250	N95-22212	#	AD-A290196	p 479	N95-29316	AD-A293775	p 677	N95-31465	#
AD-A286515	p 257	N95-22216	#	AD-A290203	p 485	N95-29057	AD-A293782	p 602	N95-31581	#
AD-A286572	p 256	N95-20828	#	AD-A290207	p 553	N95-29060	AD-A293797	p 611	N95-31584	#
AD-A286593	p 231	N95-20860	#	AD-A290212	p 51	N95-12763	AD-A293808	p 677	N95-31587	#
AD-A286632	p 247	N95-20771	#	AD-A290223	p 567	N95-29074	AD-A293882	p 601	N95-31520	#
AD-A286633	p 231	N95-20772	#	AD-A290232	p 137	N95-15970	AD-A293891	p 608	N95-31544	#
AD-A286722	p 446	N95-27234	#	AD-A290249	p 523	N95-29468	AD-A293902	p 599	N95-31512	#
AD-A286825	p 630	N95-31268	#	AD-A290331	p 504	N95-29426	AD-A293932	p 602	N95-31521	#
AD-A288217	p 336	N95-25578	#	AD-A290358	p 210	N95-19567	AD-A293962	p 608	N95-31525	#
AD-A288280	p 445	N95-26453	#	AD-A290366	p 503	N95-29322	AD-A294113	p 701	N95-34500	#
AD-A288281	p 382	N95-26454	#	AD-A290421	p 554	N95-29228	AD-A294126	p 686	N95-34750	#
AD-A288284	p 366	N95-26455	#	AD-A290532	p 554	N95-29387	AD-A294167	p 686	N95-34763	#
AD-A288289	p 366	N95-26409	#	AD-A290542	p 514	N95-29496	AD-A294211	p 698	N95-34306	#
AD-A288297	p 418	N95-26417	#	AD-A290546	p 505	N95-29565	AD-A294369	p 700	N95-34362	#
AD-A288298	p 436	N95-26418	#	AD-A290645	p 477	N95-29091	AD-A294375	p 706	N95-34343	#
AD-A288347	p 380	N95-26527	#	AD-A290693	p 555	N95-29562	AD-A294385	p 700	N95-34344	#
AD-A288348	p 367	N95-26629	#	AD-A290720	p 569	N95-29644	AD-A294752	p 690	N95-34562	#
AD-A288395	p 350	N95-25606	#	AD-A290755	p 480	N95-29500	AD-A294878	p 690	N95-34570	#
AD-A288401	p 380	N95-26497	#	AD-A290824	p 537	N95-29482	AD-A294931	p 707	N95-34597	#
AD-A288487	p 378	N95-28331	#	AD-A290835	p 555	N95-29654	AD-A294968	p 707	N95-34818	#
AD-A288492	p 448	N95-26638	#	AD-A290856	p 490	N95-29880	AD-A295035	p 693	N95-34793	#
AD-A288503	p 389	N95-26652	#	AD-A290889	p 678	N95-30406	AD-A295108	p 691	N95-34797	#
AD-A288536	p 381	N95-27186	#	AD-A290920	p 537	N95-29842				
AD-A288590	p 446	N95-26841	#	AD-A290940	p 580	N95-30084				
AD-A288610	p 388	N95-26481	#	AD-A290952	p 514	N95-29764				
AD-A288618	p 328	N95-25607	#	AD-A290966	p 490	N95-29733				
AD-A288624	p 334	N95-25609	#	AD-A291058	p 485	N95-29873	AD-B167205L	p 15	N95-10319	#
AD-A288652	p 380	N95-26485	#	AD-A291065	p 509	N95-29950	AD-B196152L	p 139	N95-19017	#
AD-A288658	p 620	N95-31400	#	AD-A291084	p 523	N95-29967	AD-B196178L	p 201	N95-19678	#
AD-A288689	p 341	N95-26053	#	AD-A291138	p 482	N95-29972				
AD-A288696	p 601	N95-31013	#	AD-A291175	p 557	N95-30122	AD-D016222	p 258	N95-21100	#
AD-A288744	p 401	N95-28586	#	AD-A291315	p 514	N95-29934	AD-D016423	p 116	N95-18337	#
AD-A288786	p 337	N95-26190	#	AD-A291345	p 556	N95-29941	AD-D016457	p 151	N95-19073	#
AD-A288822	p 447	N95-26348	#	AD-A291365	p 556	N95-29946	AD-D016458	p 152	N95-19090	#
AD-A288824	p 435	N95-26349	#	AD-A291435	p 557	N95-30087	AD-D016475	p 160	N95-18461	#
AD-A288899	p 502	N95-28928	#	AD-A291518	p 556	N95-30072	AD-D016504	p 258	N95-21673	#
AD-A288961	p 450	N95-28335	#	AD-A291520	p 481	N95-29853	AD-D016522	p 224	N95-21864	#
AD-A288962	p 436	N95-26405	#	AD-A291566	p 485	N95-29855	AD-D016573	p 244	N95-20295	#
AD-A289015	p 384	N95-27903	#	AD-A291614	p 162	N95-19251	AD-D017251	p 389	N95-26537	#
AD-A289134	p 408	N95-26555	#	AD-A291628	p 397	N95-28409	AD-D017265	p 388	N95-26507	#
AD-A289145	p 437	N95-26998	#	AD-A291666	p 398	N95-28411	AD-D017360	p 611	N95-31180	#
AD-A289150	p 401	N95-27003	#	AD-A291714	p 381	N95-28454	AD-D017455	p 646	N95-30727	#
AD-A289174	p 411	N95-26556	#	AD-A291804	p 400	N95-28504	AD-D017462	p 629	N95-30749	#
AD-A289190	p 391	N95-27018	#	AD-A291875	p 480	N95-29428	AD-D017463	p 629	N95-30750	#
AD-A289215	p 449	N95-26990	#	AD-A291932	p 504	N95-29437	AD-D017476	p 706	N95-34449	#
AD-A289220	p 409	N95-26957	#	AD-A291964	p 488	N95-28790				
AD-A289221	p 409	N95-26958	#	AD-A292019	p 67	N95-14103	AD-E501787	p 248	N95-20966	#
AD-A289246	p 412	N95-26966	#	AD-A292113	p 315	N95-23602				
AD-A289263	p 383	N95-26978	#	AD-A292121	p 553	N95-29187	ADST/TR-94-003276-VOL-2	p 20	N95-10352	#
AD-A289271	p 409	N95-26981	#	AD-A292135	p 477	N95-28921	ADST/TR-94-003276-VOL-5	p 20	N95-10353	#
AD-A289280	p 383	N95-26985	#	AD-A292253	p 248	N95-21061	ADST/TR-94-003280	p 79	N95-14306	#
AD-A289288	p 410	N95-27036	#	AD-A292284	p 537	N95-29572	ADST/TR-94-003281	p 20	N95-10354	#
AD-A289301	p 391	N95-27042	#	AD-A292357	p 563	N95-29160				
AD-A289306	p 448	N95-26920	#	AD-A292436	p 489	N95-28887	ADST/TR94-003276-VOL-1	p 20	N95-10350	#
AD-A289325	p 448	N95-26895	#	AD-A292522	p 579	N95-28870	ADST/TR94-003276-VOL-3	p 20	N95-10351	#
AD-A289328	p 383	N95-26898	#	AD-A292573	p 302	N95-23496	ADST/TR94-003282	p 19	N95-10349	#
AD-A289330	p 513	N95-28908	#	AD-A292711	p 579	N95-28996				
AD-A289334	p 375	N95-26901	#	AD-A292758	p 485	N95-28811	ADST/WDL/TR-93-003274	p 127	N95-16171	#
AD-A289336	p 419	N95-26842	#	AD-A292777	p 502	N95-28977	ADST/WDL/TR-94-00325	p 99	N95-14357	#
AD-A289341	p 437	N95-26751	#	AD-A292781	p 457	N95-29414				
AD-A289376	p 390	N95-26876	#	AD-A292819	p 619	N95-30937	AEDC-TR-94-10	p 258	N95-21170	#
AD-A289378	p 437	N95-26877	#	AD-A292863	p 598	N95-31428	AEDC-TR-94-12	p 599	N95-31667	#
AD-A289379	p 406	N95-26878	#	AD-A292871	p 648	N95-31432	AEDC-TR-94-14	p 646	N95-30906	#
AD-A289457	p 391	N95-26993	#	AD-A292883	p 601	N95-31433	AEDC-TR-94-5	p 119	N95-18674	#
AD-A289458	p 391	N95-26994	#	AD-A292883	p 648	N95-31443	AEDC-TR-94-6	p 118	N95-18663	#
AD-A289503	p 390	N95-26844	#	AD-A292871	p 608					

AERO-TN-9301	p 131	N95-18097	#	AGARD-AR-278	p 145	N95-17388	#	AIAA PAPER 95-2470	p 694	N95-32931	#
AFCESA/ESL-TR-92-25	p 341	N95-24424		AGARD-AR-303-SUPPL	p 117	N95-18539		AIAA PAPER 95-2613	p 482	N95-30253	#
AFIT/CI-95-028	p 690	N95-34570	#	AGARD-AR-303-VOL-1	p 91	N95-14201	#	AIAA PAPER 95-2614	p 592	N95-30704	#
AFIT/CI/CIA-94-013D	p 145	N95-17444		AGARD-AR-303-VOL-2	p 109	N95-17846	#	AIAA PAPER 95-2616	p 482	N95-30091	#
AFIT/CI/CIA-94-030D	p 62	N95-12512		AGARD-AR-304	p 67	N95-14197	#	AIAA PAPER 95-2681	p 412	N95-27176	#
AFIT/CI/CIA-94-033D	p 91	N95-14351	#	AGARD-AR-323	p 149	N95-17278	#	AIAA PAPER 95-2787	p 457	N95-30229	#
AFIT/CI/CIA-94-095	p 65	N95-14144	#	AGARD-AR-335	p 597	N95-31061	#	AIAA PAPER 95-2799	p 615	N95-30517	#
AFIT/CI/CIA-94-118	p 38	N95-12548		AGARD-CP-535	p 162	N95-19251	#	AIAA PAPER 95-2800	p 615	N95-30617	#
AFIT/CI/CIA-94-158	p 508	N95-28692		AGARD-CP-549	p 173	N95-19142	#	AIAA PAPER 95-2801	p 616	N95-30632	#
AFIT/CI/CIA-94-166	p 508	N95-28691		AGARD-CP-550	p 392	N95-27504	#	AIAA PAPER 95-2985	p 616	N95-30698	#
AFIT/CI/CIA-94-170	p 552	N95-28948		AGARD-CP-551	p 248	N95-21061	#	AIAA PAPER 95-2998	p 615	N95-30589	#
AFIT/CI/CIA/94-136	p 388	N95-26481		AGARD-CP-558	p 197	N95-19653	#	AIAA PAPER 95-3037	p 514	N95-30007	#
AFIT/CI/CIA/94-159	p 410	N95-28598		AGARD-CP-560	p 620	N95-31989	#	AIAA PAPER 95-3048	p 438	N95-27855	#
AFIT/DS/AA/94-4	p 120	N95-19110		AGARD-CP-562	p 233	N95-20631	#	AIAA PAPER 95-3050	p 553	N95-29112	#
AFIT/DS/AA/94-7	p 480	N95-29500	#	AGARD-CP-563	p 686	N95-32486	#	AIAA PAPER 95-3072	p 523	N95-30067	#
AFIT/DS/ENS/95-01	p 678	N95-30406	#	AGARD-CP-565	p 302	N95-23496	#	AIAA PAPER 95-3109	p 616	N95-30853	#
AFIT/GA/ENY/94D-1	p 412	N95-26966		AGARD-HIGHLIGHTS-94/2	p 102	N95-13640	#	AIAA PAPER 95-6081	p 509	N95-87410	#
AFIT/GA/ENY/94D-8	p 410	N95-27036		AGARD-INDEX-92-94	p 711	N95-33198	#	AIAA PAPER 95-6082	p 519	N95-87411	#
AFIT/GAE/ENY/94D-11	p 390	N95-26844		AGARD-LS-195	p 89	N95-14127	#	AIAA PAPER 95-6083	p 460	N95-87412	#
AFIT/GAE/ENY/94D-13	p 406	N95-26878		AGARD-LS-197	p 77	N95-14893	#	AIAA PAPER 95-6084	p 509	N95-87413	#
AFIT/GAE/ENY/94D-14	p 375	N95-26901		AGARD-LS-198	p 139	N95-19017	#	AIAA PAPER 95-6085	p 490	N95-87414	#
AFIT/GAE/ENY/94D-3	p 448	N95-26920		AGARD-LS-201	p 650	N95-32165	#	AIAA PAPER 95-6089	p 492	N95-89198	#
AFIT/GAE/ENY/95M-01	p 611	N95-31584	#	AGARD-R-798	p 143	N95-18597	#	AIAA PAPER 95-6090	p 466	N95-89199	#
AFIT/GCS/ENC/94D-01	p 419	N95-26842		AGARD-R-803	p 127	N95-16562	#	AIAA PAPER 95-6091	p 466	N95-89200	#
AFIT/GCS/ENG/94D-02	p 390	N95-26876		AGARD-R-804	p 73	N95-14445	#	AIAA PAPER 95-6092	p 526	N95-88601	#
AFIT/GCS/ENG/94D-11	p 448	N95-26895		AGARD-R-809	p 315	N95-23602	#	AIAA PAPER 95-6093	p 493	N95-89251	#
AFIT/GE/ENG/94D-04	p 449	N95-26990		AIAA PAPER 86-0732	p 18	A95-60161	*	AIAA PAPER 95-6094	p 510	N95-88002	#
AFIT/GE/ENG/94D-06	p 391	N95-27042		AIAA PAPER 86-1918	p 1	A95-60164	*	AIAA PAPER 95-6095	p 510	N95-88003	#
AFIT/GE/ENG/94D-07	p 437	N95-26877		AIAA PAPER 89-2787	p 14	A95-60172	*	AIAA PAPER 95-6096	p 510	N95-88004	#
AFIT/GE/ENG/94D-09	p 383	N95-26898		AIAA PAPER 92-02109	p 27	A95-60166	*	AIAA PAPER 95-6097	p 510	N95-88005	#
AFIT/GE/ENG/94D-13	p 383	N95-26985		AIAA PAPER 93-0002	p 3	A95-60180	*	AIAA PAPER 95-6100	p 492	N95-88007	#
AFIT/GE/ENG/94D-18	p 409	N95-26957		AIAA PAPER 93-2861	p 4	A95-60186	*	AIAA PAPER 95-6105	p 519	N95-88010	#
AFIT/GE/ENG/94D-24	p 409	N95-26958		AIAA PAPER 93-3403	p 3	A95-60184	*	AIAA PAPER 95-6106	p 520	N95-90438	#
AFIT/GE/ENG/94D-30	p 409	N95-26981		AIAA PAPER 93-4343	p 19	A95-60163	*	AIAA PAPER 95-6107	p 520	N95-90439	#
AFIT/GEE/ENS/94S-26	p 216	N95-19685	#	AIAA PAPER 93-4860	p 2	A95-60178	*	AIAA PAPER 95-6110	p 511	N95-90440	#
AFIT/GOA/ENS/95M-02	p 602	N95-31581	#	AIAA PAPER 93-4880	p 4	A95-60187	*	AIAA PAPER 95-6114	p 511	N95-90442	#
AFIT/GOA/ENS/95M-04	p 599	N95-31512	#	AIAA PAPER 94-0086	p 67	N95-13720	#	AIAA PAPER 95-6115	p 520	N95-90443	#
AFIT/GSO/ENS/94D-06	p 390	N95-26873		AIAA PAPER 94-0254	p 2	A95-60173	*	AIAA PAPER 95-6125	p 469	N95-90446	#
AFIT/GSS/LAR/94D-3	p 401	N95-28586		AIAA PAPER 94-0291	p 4	A95-60185	*	AIAA PAPER 95-6126	p 470	N95-90447	#
AFOSSR-TR-94-0463	p 54	N95-12507	#	AIAA PAPER 94-0319	p 76	N95-15853	#	AIAA PAPER 95-6128	p 520	N95-90449	#
AFOSSR-0020TR	p 479	N95-29316	#	AIAA PAPER 94-0393	p 211	N95-19776	#	AIAA PAPER 95-6130	p 512	N95-90450	#
AFOSSR-94-0310TR	p 237	N95-21122		AIAA PAPER 94-0523	p 3	A95-60181	*	AIAA PAPER 95-6132	p 530	N95-90451	#
AFOSSR-94-0338TR	p 203	N95-19864	#	AIAA PAPER 94-1240-CP	p 18	N95-11510	*	AIAA PAPER 95-6133	p 547	N95-90452	#
AFOSSR-94-0375TR	p 23	N95-10535	#	AIAA PAPER 94-1243-CP	p 27	N95-11513	*	AIAA PAPER 95-6137	p 520	N95-90454	#
AFOSSR-94-0488TR	p 248	N95-21146	#	AIAA PAPER 94-1264-CP	p 27	N95-11529	*	AIAA PAPER 95-6138	p 470	N95-90455	#
AFOSSR-94-0501TR	p 152	N95-18410	#	AIAA PAPER 94-1803	p 13	N95-11410	#	AIAA PAPER 95-6139	p 512	N95-90456	#
AFOSSR-94-0559TR	p 245	N95-20484	#	AIAA PAPER 94-2112	p 134	N95-19044	#	AIAA PAPER 95-6140	p 581	N95-90457	#
AFOSSR-94-0608TR	p 241	N95-20481	#	AIAA PAPER 94-2133	p 108	N95-16858	#	AIAA PAPER 95-6142	p 496	N95-90458	#
AFOSSR-94-0625TR	p 157	N95-16736	#	AIAA PAPER 94-2142	p 9	N95-11158	#	AIAA PAPER 95-6146	p 148	N95-19286	#
AFOSSR-94-0640TR	p 151	N95-16371	#	AIAA PAPER 94-2190	p 100	N95-14618	#	AIAA PAPER 95-6148	p 512	N95-90462	#
AFOSSR-94-0673TR	p 241	N95-20716	#	AIAA PAPER 94-2613	p 224	N95-21031	#	AIAA PAPER 95-6150	p 521	N95-90464	#
AFOSSR-94-0674TR	p 241	N95-20299	#	AIAA PAPER 94-2690	p 16	N95-11005	#	AIAA PAPER 95-6151	p 521	N95-90465	#
AFOSSR-94-0687TR	p 381	N95-27186	#	AIAA PAPER 94-2694	p 7	N95-10148	#	AIAA PAPER 95-6157	p 470	N95-90469	#
AFOSSR-94-0691TR	p 418	N95-26417	#	AIAA PAPER 94-3095	p 49	N95-11864	#	AIAA PAPER 95-6158	p 512	N95-90470	#
AFOSSR-94-0727TR	p 250	N95-22212	#	AIAA PAPER 94-3515	p 10	N95-11408	#	AIAA PAPER 95-6160	p 470	N95-90472	#
AFOSSR-94-0741TR	p 257	N95-22216	#	AIAA PAPER 94-3611	p 16	N95-11159	#	AIAA PAPER 95-6162	p 496	N95-90473	#
AFOSSR-94-0756TR	p 336	N95-25578	#	AIAA PAPER 94-4107	p 50	N95-11867	#	AL-CF-TR-1994-0159	p 288	N95-24030	#
AFOSSR-94-0760TR	p 436	N95-26405	#	AIAA PAPER 94-4262	p 58	N95-13201	#	AL-TR-1994-0116	p 328	N95-25607	#
AFOSSR-95-0005TR	p 485	N95-29210	#	AIAA PAPER 95-0031	p 244	N95-19953	#	AL/CF-TR-1994-0063	p 130	N95-17661	#
AFOSSR-95-0048TR	p 523	N95-29468	#	AIAA PAPER 95-0038	p 202	N95-19769	#	AL/CF-TR-1994-0074	p 235	N95-22024	#
AFOSSR-95-0055TR	p 567	N95-29074	#	AIAA PAPER 95-0070	p 170	N95-16906	#	AL/EQ-TR-1993-0017	p 255	N95-19921	#
AFOSSR-95-0082TR	p 482	N95-29972	#	AIAA PAPER 95-0119	p 170	N95-17264	#	AL/HR-TR-1994-0024	p 239	N95-20992	#
AFOSSR-95-0099TR	p 556	N95-29941	#	AIAA PAPER 95-0173	p 236	N95-21383	#	AL/HR-TR-1994-0041	p 21	N95-10919	#
AFOSSR-95-0106TR	p 556	N95-29946	#	AIAA PAPER 95-0538	p 124	N95-19285	#	AL/HR-TR-1994-0106	p 679	N95-31684	#
AFOSSR-95-0174TR	p 619	N95-30937	#	AIAA PAPER 95-0540	p 124	N95-19284	#	AL/HR-TR-1994-0168	p 700	N95-34362	#
AFOSSR-95-0191TR	p 648	N95-31443	#	AIAA PAPER 95-0560	p 124	N95-19284	#	AL/HR-TR-1994-0170	p 700	N95-34344	#
AFOSSR-95-0192TR	p 648	N95-31432	#	AIAA PAPER 95-0566	p 314	N95-23466	#	AL/OE-TR-1994-0130	p 617	N95-31191	#
AFOSSR-95-0202TR	p 679	N95-30961	#	AIAA PAPER 95-0720	p 145	N95-18054	#	ANL/DIS/CP-81788	p 52	N95-11752	#
AFOSSR-95-0235TR	p 678	N95-30892	#	AIAA PAPER 95-0732	p 338	N95-24390	#	ANL/MCS/CP-82870	p 231	N95-20370	#
AFOSSR-95-0326TR	p 608	N95-31602	#	AIAA PAPER 95-0733	p 139	N95-18133	#	ANL/MCS/CP-82980	p 157	N95-16828	#
AFOSSR-95-0344TR	p 686	N95-34763	#	AIAA PAPER 95-0752	p 309	N95-22669	#	ANL/TD/CP-83462	p 300	N95-22764	#
AFOSSR-95-0382TR	p 707	N95-34597	#	AIAA PAPER 95-0755	p 123	N95-18582	#	ANL/TD/CP-83927	p 258	N95-21388	#
AGARD-AG-300-VOL-12	p 77	N95-14199	#	AIAA PAPER 95-0889	p 73	N95-14418	#	AR-007-124	p 225	N95-21892	#
AGARD-AG-300-VOL-13	p 504	N95-29503	#	AIAA PAPER 95-0952	p 565	A95-90631	#	AR-007-138	p 697	N95-33250	#
AGARD-AG-300-VOL-3-PT-2	p 79	N95-14102	#	AIAA PAPER 95-0953	p 506	A95-90632	#	AR-008-372	p 503	N95-29362	#
AGARD-AG-321	p 126	N95-18927	#	AIAA PAPER 95-0961	p 581	A95-90638	#	AR-008-374	p 405	N95-26424	#
AGARD-AG-323	p 67	N95-14103	#	AIAA PAPER 95-0967	p 497	A95-90643	#	AR-008-386	p 336	N95-25935	#
AGARD-AG-325	p 72	N95-14264	#	AIAA PAPER 95-0984	p 565	A95-90656	#	AR-008-389	p 339	N95-25936	#
				AIAA PAPER 95-1012	p 566	A95-90663	#	AR-008-418	p 400	N95-28567	#
				AIAA PAPER 95-1016	p 566	A95-90668	*	AR-008-420	p 504	N95-29445	#
				AIAA PAPER 95-1021	p 566	A95-90693	#	AR-008-644	p 224	N95-21659	#
				AIAA PAPER 95-1031	p 566	A95-90703	#	AR-008-910	p 286	N95-23666	#
				AIAA PAPER 95-1033	p 566	A95-90703	#	AR-008-923	p 327	N95-24200	#
				AIAA PAPER 95							

AR-009-193	p 388	N95-26389	B-256707	p 367	N95-26817	#	BTN-94-EIX94441386682	p 205	A95-68191	*
AR-009-201	p 411	N95-26378	B-256721	p 585	N95-32198	#	BTN-94-EIX94441386686	p 184	A95-68195	
AR-009-202	p 397	N95-27918	B-256709	p 699	N95-32786	#	BTN-94-EIX94451393721	p 88	A95-61720	
ARA-MEMO-390	p 210	N95-19774	B-257718	p 231	N95-20212	#	BTN-94-EIX94461047054	p 82	A95-61741	
ARA-MEMO-391	p 188	N95-19772	B-257854	p 603	N95-32199	#	BTN-94-EIX94461047055	p 78	A95-61740	
ARA-MEMO-392	p 188	N95-19546	B-257915	p 683	N95-32783	#	BTN-94-EIX94461047056	p 78	A95-61739	
ARA-MEMO-395	p 239	N95-20799	B-259097	p 687	N95-32705	#	BTN-94-EIX94461290240	p 82	A95-61737	
ARA-MEMO-399	p 210	N95-19775	B-259204	p 386	N95-26338	#	BTN-94-EIX94461290241	p 82	A95-61736	
ARA-MEMO-401	p 211	N95-19776	B-259256	p 236	N95-24091	#	BTN-94-EIX94461290242	p 84	A95-61735	
ARA-MEMO-403	p 211	N95-19777	B-259389	p 397	N95-27910	#	BTN-94-EIX94461290277	p 65	A95-61734	
ARA-MEMO-405	p 223	N95-20758	BFLRF-290	p 426	N95-28621		BTN-94-EIX94461290278	p 77	A95-61733	
ARA-MEMO-406	p 194	N95-19789	BFLRF-292	p 40	N95-12499	#	BTN-94-EIX94461290279	p 82	A95-61732	
ARA-MEMO-407	p 222	N95-19946	BFLRF-292	p 40	N95-12499	#	BTN-94-EIX94461290506	p 66	A95-61728	
ARAED-TR-95009	p 700	N95-34342	BRL-IMR-971	p 119	N95-18670		BTN-94-EIX94461290507	p 82	A95-61727	
ARB-R-94/534	p 216	N95-19582	BTN-94-EIX94321331207	p 61	A95-60790		BTN-94-EIX94461407944	p 98	A95-62269	
ARFSD-TR-94010	p 256	N95-20828	BTN-94-EIX94331336949	p 88	A95-61795		BTN-94-EIX94461407944	p 82	A95-62266	
ARI-RR-1666	p 238	N95-19931	BTN-94-EIX94341340068	p 103	A95-63520		BTN-94-EIX94461407947	p 88	A95-62265	
ARL-CR-219	p 210	N95-19567	BTN-94-EIX94341340070	p 171	A95-63522		BTN-94-EIX94461407949	p 89	A95-62267	
ARL-CR-238	p 555	N95-29538	BTN-94-EIX94341340316	p 35	A95-60852		BTN-94-EIX94461407951	p 89	A95-62625	
ARL-GD-43	p 336	N95-25935	BTN-94-EIX94341340329	p 61	A95-60865		BTN-94-EIX94461407953	p 89	A95-62627	
ARL-MR-184	p 118	N95-18611	BTN-94-EIX94341341967	p 62	A95-60867		BTN-94-EIX94461407957	p 83	A95-62631	
ARL-RR-13	p 87	N95-14409	BTN-94-EIX94341341971	p 56	A95-60871		BTN-94-EIX94461407959	p 78	A95-62633	
ARL-SR-18	p 350	N95-25606	BTN-94-EIX94341342286	p 56	A95-60872		BTN-94-EIX94461407961	p 100	A95-62635	
ARL-TN-3	p 225	N95-21892	BTN-94-EIX94351108100	p 56	A95-60842		BTN-94-EIX94461407964	p 83	A95-62638	
ARL-TN-48	p 339	N95-25936	BTN-94-EIX94351143311	p 191	A95-66500		BTN-94-EIX94461407964	p 83	A95-62638	
ARL-TN-49	p 204	N95-19848	BTN-94-EIX94351143320	p 207	A95-65845		BTN-94-EIX94461407969	p 141	A95-63064	
ARL-TR-333	p 618	N95-31985	BTN-94-EIX94351143320	p 195	A95-65854		BTN-94-EIX94461408751	p 126	A95-63634	
ARL-TR-438	p 119	N95-18670	BTN-94-EIX94351143328	p 195	A95-67298		BTN-94-EIX94461408753	p 168	A95-63636	
ARL-TR-480	p 55	N95-12357	BTN-94-EIX94351143331	p 207	A95-67301		BTN-94-EIX94461408755	p 153	A95-63638	
ARL-TR-489	p 131	N95-18381	BTN-94-EIX94361122401	p 207	A95-67304		BTN-94-EIX94461408756	p 171	A95-63639	
ARL-TR-518	p 285	N95-22953	BTN-94-EIX94361133526	p 207	A95-65897		BTN-94-EIX94461408757	p 148	A95-63640	
ARL-TR-519	p 51	N95-12763	BTN-94-EIX94361133526	p 207	A95-65898		BTN-94-EIX94461408760	p 138	A95-63643	
ARL-TR-572	p 15	N95-10153	BTN-94-EIX94371338964	p 207	A95-65969		BTN-94-EIX94461408763	p 103	A95-63646	
ARL-TR-574	p 58	N95-12843	BTN-94-EIX94371346933	p 257	A95-70797		BTN-94-EIX94461408765	p 153	A95-63648	
ARL-TR-581	p 284	N95-22510	BTN-94-EIX94371347126	p 300	A95-73345		BTN-94-EIX94461408769	p 153	A95-63652	
ARL-TR-600	p 162	N95-19125	BTN-94-EIX94371347126	p 242	A95-69976		BTN-94-EIX94461408772	p 103	A95-63655	
ARL-TR-603	p 255	N95-19989	BTN-94-EIX94371347708	p 257	A95-69970		BTN-94-EIX94461408772	p 175	A95-63656	
ARL-TR-614	p 248	N95-20998	BTN-94-EIX94371347708	p 219	A95-69967		BTN-94-EIX94481415349	p 103	A95-63339	
ARL-TR-637	p 137	N95-15970	BTN-94-EIX94371347709	p 219	A95-69968		BTN-94-EIX94481415355	p 154	A95-63345	
ARL-TR-723	p 438	N95-27855	BTN-94-EIX94371347838	p 206	A95-69969		BTN-94-EIX94481415356	p 103	A95-63346	
ARL-TR-778	p 553	N95-29112	BTN-94-EIX94371347843	p 206	A95-69131		BTN-94-EIX94481415356	p 103	A95-63346	
ARL-TR-806	p 615	N95-30517	BTN-94-EIX94371347843	p 206	A95-69136		BTN-94-EIX94481415357	p 104	A95-63347	
ARO-27480.6-EG-SDI	p 106	N95-16160	BTN-94-EIX94371347996	p 206	A95-69164		BTN-94-EIX94501431527	p 153	A95-64524	
ARO-27627.3-EG	p 155	N95-16163	BTN-94-EIX94381323445	p 242	A95-70844		BTN-94-EIX94511309932	p 103	A95-64608	
ARO-27894.27-EG	p 480	N95-29428	BTN-94-EIX94381351617	p 252	A95-70950		BTN-94-EIX94511309983	p 127	A95-64609	
ARO-28123.10-EG	p 503	N95-29322	BTN-94-EIX94381352212	p 306	A95-74612		BTN-94-EIX94511309984	p 103	A95-64610	
ARO-28159.9-EG	p 477	N95-29091	BTN-94-EIX94381352222	p 257	A95-71738		BTN-94-EIX94511433698	p 701	A95-66655	
ARO-28249.2-EG	p 106	N95-16099	BTN-94-EIX94381353130	p 243	A95-72648		BTN-94-EIX94511433914	p 168	A95-64580	
ARO-28293.4-EG	p 554	N95-29228	BTN-94-EIX94381353142	p 306	A95-74496		BTN-94-EIX94511433916	p 168	A95-64582	
ARO-28399.15-EG	p 555	N95-29562	BTN-94-EIX94381353450	p 323	A95-75494		BTN-94-EIX94511433918	p 141	A95-64584	
ARO-28493.1-EG	p 400	N95-28504	BTN-94-EIX94381359040	p 295	A95-74554		BTN-94-EIX94511433919	p 169	A95-64585	
ARO-29049.4-EG-S	p 620	N95-31400	BTN-94-EIX94381359041	p 295	A95-74629		BTN-94-EIX94511433920	p 141	A95-64586	
ARO-30357.1-MS	p 87	N95-14363	BTN-94-EIX94381359154	p 243	A95-71744		BTN-94-EIX94511433922	p 142	A95-64587	
ARO-30357.2-MS	p 537	N95-29482	BTN-94-EIX94381359637	p 257	A95-72675		BTN-94-EIX94511433922	p 169	A95-64588	
ARO-30443.1-CH-5	p 647	N95-31374	BTN-94-EIX94401359745	p 346	A95-77379		BTN-94-EIX94511433940	p 142	A95-64606	
ARO-30697.1-EG-H	p 554	N95-29387	BTN-94-EIX94401360022	p 306	A95-74702		BTN-94-EIX94511433967	p 701	A95-96664	
ARO-31210.2-EG-SDI	p 106	N95-16076	BTN-94-EIX94401360553	p 243	A95-71867		BTN-94-EIX94522406136	p 701	A95-96273	
ARO-32483.1-MA-CF	p 169	N95-16864	BTN-94-EIX94401363884	p 307	A95-75516		BTN-94-EIX94522406680	p 709	A95-96289	
ARO-32664.1-GS-CF	p 580	N95-30084	BTN-94-EIX94401363947	p 317	A95-75532		BTN-94-EIX94522407592	p 709	A95-96241	
ARO-3305.1-EG-CF	p 514	N95-29496	BTN-94-EIX94401378794	p 307	A95-76484	*	BTN-94-EIX94522410219	p 702	A95-96373	
ASC-TR-94-1022	p 375	N95-26854	BTN-94-EIX94401378820	p 307	A95-76489		BTN-94-EIX94522410220	p 702	A95-96374	
ASC-TR-94-5026-PHASE-1	p 131	N95-18398	BTN-94-EIX94401378822	p 307	A95-76491		BTN-94-EIX94522410226	p 702	A95-96378	
ASC-TR-94-5027	p 223	N95-19991	BTN-94-EIX94401348950	p 347	A95-78494		BTN-94-EIX950114400597	p 429	A95-82986	
ATC-214	p 245	N95-20599	BTN-94-EIX94401372285	p 343	A95-78467		BTN-94-EIX950114400601	p 429	A95-82982	
ATC-221	p 154	N95-16097	BTN-94-EIX94401380518	p 302	A95-96559		BTN-94-EIX950114400854	p 429	A95-82905	
ATC-222	p 98	N95-15749	BTN-94-EIX94401380856	p 125	A95-64288		BTN-94-EIX95011441063	p 429	A95-82798	
ATC-229	p 689	N95-33480	BTN-94-EIX94401380862	p 125	A95-64294		BTN-94-EIX95011441078	p 348	A95-81056	
ATC-233	p 677	N95-31465	BTN-94-EIX94401380977	p 195	A95-68158		BTN-94-EIX95011441120	p 347	A95-80044	
ATC-234	p 602	N95-31521	BTN-94-EIX94401380978	p 195	A95-68161		BTN-94-EIX95011441127	p 348	A95-81027	
ATCOM-TR-95-A-001	p 330	N95-24566	BTN-94-EIX94401380981	p 196	A95-68162		BTN-94-EIX95011441134	p 340	A95-81020	
B-229489	p 609	N95-32196	BTN-94-EIX94401380981	p 208	A95-68165		BTN-94-EIX95011441142	p 347	A95-81012	
B-247729	p 603	N95-32197	BTN-94-EIX94401380983	p 208	A95-68165		BTN-94-EIX95011441142	p 340	A95-81012	
B-253662	p 679	N95-31987	BTN-94-EIX94401380983	p 208	A95-67329		BTN-94-EIX95011441154	p 329	A95-80030	
B-254704	p 687	N95-32784	BTN-94-EIX94401385106	p 702	A95-96579		BTN-94-EIX95011441236	p 431	A95-84193	
B-255687	p 176	N95-18578	BTN-94-EIX94401385752	p 179	A95-68216		BTN-94-EIX95011441238	p 370	A95-84195	
B-255832	p 584	N95-32194	BTN-94-EIX94401385754	p 183	A95-68217		BTN-94-EIX95011441239	p 403	A95-84196	
B-256001	p 700	N95-32888	BTN-94-EIX94401385754	p 184	A95-68218		BTN-94-EIX95011441240	p 403	A95-84197	
B-256330	p 699	N95-32759	BTN-94-EIX94401385756	p 184	A95-68219		BTN-94-EIX95011441241	p 431	A95-84198	
B-256584	p 687	N95-32885	BTN-94-EIX94401385756	p 184	A95-68220		BTN-94-EIX95011441244	p 416	A95-84201	
B-256707	p 367	N95-26817	BTN-94-EIX944013861129	p 189	A95-68185		BTN-94-EIX95011441245	p 417	A95-84202	
B-256721	p 585	N95-32198	BTN-94-EIX94401386131	p 189	A95-68187		BTN-94-EIX95011441246	p 417	A95-84203	
B-256709	p 699	N95-32786	BTN-94-EIX94401386132	p 189	A95-68188		BTN-94-EIX95011441250	p 431	A95-84207	
B-257718	p 231	N95-20212	BTN-94-EIX94401386601	p 182	A95-67332		BTN-94-EIX95011441252	p 417	A95-84209	
B-257854	p 603	N95-32199	BTN-94-EIX94401386604	p 182	A95-67335		BTN-94-EIX95011441254	p 431	A95-84211	
B-257915	p 683	N95-32783	BTN-94-EIX94401386605	p 182	A95-67336		BTN-94-EIX95011441256	p 417	A95-84213	
B-259097	p 687	N95-32705	BTN-94-EIX94401386606	p 183	A95-67337		BTN-95-EIX0608952736485	p 678	A95-92708	
B-259204	p 386	N95-26338	BTN-94-EIX94401386606	p 208	A95-67342		BTN-95-EIX0616952745782	p 614	A95-94504	
B-259256	p 236	N95-24091	BTN-94-EIX94401386611	p 208	A95-67343		BTN-95-EIX0616952745783	p 614	A95-94505	
B-259389	p 397	N95-27910	BTN-94-EIX94401386612	p 208	A95-67343		BTN-95-EIX0616952745791	p 628	A95-94525	
BFLRF-290	p 426	N95-28621	BTN-94-EIX94401386612	p 213	A95-67345		BTN-95-EIX0616952745793	p 614	A95-94495	
BFLRF-292	p 40	N95-12499	BTN-94-EIX94401386619	p 183	A95-67347		BTN-95-EIX0616952745803	p 638	A95-94487	

BTN-95-EIX0619952748163	p 619	A95-94457	BTN-95-EIX95062487554	p 185	A95-68368	BTN-95-EIX95152583252	p 305	A95-73553
BTN-95-EIX0619952748164	p 605	A95-94458	BTN-95-EIX95062487555	p 186	A95-68369	BTN-95-EIX95152583253	p 306	A95-73554
BTN-95-EIX0619952748165	p 589	A95-94459	BTN-95-EIX95062487556	p 193	A95-68370	BTN-95-EIX95152583254	p 306	A95-73555
BTN-95-EIX0619952748166	p 589	A95-94460	BTN-95-EIX95062487557	p 203	A95-68371	BTN-95-EIX95152583255	p 306	A95-73556
BTN-95-EIX0619952748167	p 589	A95-94461	BTN-95-EIX95062487558	p 186	A95-68372	BTN-95-EIX95152583256	p 266	A95-73557
BTN-95-EIX0619952748168	p 625	A95-94462	BTN-95-EIX95072419881	p 180	A95-68398	BTN-95-EIX95152583257	p 267	A95-73558
BTN-95-EIX0619952748169	p 589	A95-94463	BTN-95-EIX95072419883	p 180	A95-68396	BTN-95-EIX95152583258	p 297	A95-73559
BTN-95-EIX0619952748170	p 589	A95-94464	BTN-95-EIX95072498877	p 210	A95-68393	BTN-95-EIX95152583259	p 267	A95-73560
BTN-95-EIX0619952748171	p 590	A95-94465	BTN-95-EIX95072498878	p 180	A95-68394	BTN-95-EIX95152583260	p 267	A95-73561
BTN-95-EIX0619952748172	p 590	A95-94466	BTN-95-EIX95072498879	p 180	A95-68395	BTN-95-EIX95152583261	p 298	A95-73562
BTN-95-EIX0619952748173	p 619	A95-94467	BTN-95-EIX95072499029	p 253	A95-71908	BTN-95-EIX95152583262	p 298	A95-73563
BTN-95-EIX0619952748174	p 584	A95-94468	BTN-95-EIX95082502224	p 225	A95-71021	BTN-95-EIX95152583267	p 278	A95-73571
BTN-95-EIX0619952748175	p 584	A95-94469	BTN-95-EIX95082502225	p 240	A95-71022	BTN-95-EIX95152583276	p 298	A95-73577
BTN-95-EIX0619952748176	p 606	A95-94470	BTN-95-EIX95082502227	p 240	A95-71024	BTN-95-EIX95152583282	p 298	A95-73583
BTN-95-EIX0619952748177	p 606	A95-94471	BTN-95-EIX95082502216	p 220	A95-71029	BTN-95-EIX95152583283	p 306	A95-73584
BTN-95-EIX0619952748178	p 680	A95-94478	BTN-95-EIX95082502270	p 243	A95-71033	BTN-95-EIX95152583286	p 282	A95-73587
BTN-95-EIX0619952748179	p 619	A95-94482	BTN-95-EIX95082502272	p 243	A95-71040	BTN-95-EIX95152584676	p 276	A95-73588
BTN-95-EIX0619952748180	p 590	A95-94473	BTN-95-EIX95082502279	p 220	A95-70136	BTN-95-EIX95152584677	p 282	A95-73589
BTN-95-EIX0619952748181	p 606	A95-94474	BTN-95-EIX95082502322	p 239	A95-70139	BTN-95-EIX95152584678	p 282	A95-73590
BTN-95-EIX0619952748182	p 590	A95-94475	BTN-95-EIX95112522529	p 190	A95-69334	BTN-95-EIX95152584679	p 282	A95-73591
BTN-95-EIX0619952748183	p 590	A95-94476	BTN-95-EIX95112522530	p 190	A95-69333	BTN-95-EIX95172595292	p 287	A95-75720
BTN-95-EIX0619952748184	p 606	A95-94477	BTN-95-EIX95112522531	p 190	A95-69332	BTN-95-EIX95172595294	p 287	A95-75718
BTN-95-EIX0619952748186	p 637	A95-94478	BTN-95-EIX95112522534	p 190	A95-69329	BTN-95-EIX95172595295	p 287	A95-75717
BTN-95-EIX0619952748187	p 591	A95-94479	BTN-95-EIX95112522535	p 190	A95-69328	BTN-95-EIX95172595296	p 287	A95-75716
BTN-95-EIX0619952748188	p 637	A95-94250	BTN-95-EIX95112523809	p 194	A95-69324	BTN-95-EIX95172595298	p 279	A95-75714
BTN-95-EIX0619952748190	p 637	A95-94252	BTN-95-EIX95112523811	p 188	A95-69322	BTN-95-EIX95182617454	p 298	A95-75725
BTN-95-EIX0619952748191	p 606	A95-94480	BTN-95-EIX95112524190	p 206	A95-69318	BTN-95-EIX95182617457	p 267	A95-75728
BTN-95-EIX0619952748192	p 591	A95-94481	BTN-95-EIX95112524198	p 197	A95-69310	BTN-95-EIX95182617458	p 268	A95-75729
BTN-95-EIX0619952748193	p 591	A95-94482	BTN-95-EIX95112524199	p 195	A95-69309	BTN-95-EIX95182617460	p 268	A95-75731
BTN-95-EIX0619952748194	p 591	A95-94483	BTN-95-EIX95112524200	p 210	A95-69308	BTN-95-EIX95182617462	p 268	A95-75733
BTN-95-EIX0619952748195	p 591	A95-94484	BTN-95-EIX95112524204	p 196	A95-69304	BTN-95-EIX95182617463	p 298	A95-75734
BTN-95-EIX95031502749	p 217	A95-68256	BTN-95-EIX95112524205	p 196	A95-69303	BTN-95-EIX95182617464	p 298	A95-75735
BTN-95-EIX95031502750	p 196	A95-68257	BTN-95-EIX95112524206	p 196	A95-69302	BTN-95-EIX95182617465	p 268	A95-75736
BTN-95-EIX95031502751	p 179	A95-68258	BTN-95-EIX95112530749	p 193	A95-69295	BTN-95-EIX95182617807	p 261	A95-75752
BTN-95-EIX95031502752	p 209	A95-68259	BTN-95-EIX95122538875	p 408	A95-83000	BTN-95-EIX95182617808	p 261	A95-75753
BTN-95-EIX95031502753	p 188	A95-68260	BTN-95-EIX95142553033	p 263	A95-73465	BTN-95-EIX95182617809	p 261	A95-75754
BTN-95-EIX95041503010	p 192	A95-68313	BTN-95-EIX95142553036	p 263	A95-73462	BTN-95-EIX95182617810	p 300	A95-75755
BTN-95-EIX95041503011	p 213	A95-68314	BTN-95-EIX95142553037	p 263	A95-73461	BTN-95-EIX95182617811	p 261	A95-75756
BTN-95-EIX95041503093	p 184	A95-68353	BTN-95-EIX95142553038	p 305	A95-73460	BTN-95-EIX95182617812	p 288	A95-75757
BTN-95-EIX95041503778	p 210	A95-69209	BTN-95-EIX95142553040	p 304	A95-73458	BTN-95-EIX95182619073	p 268	A95-75758
BTN-95-EIX95041503779	p 204	A95-69210	BTN-95-EIX95142553041	p 304	A95-73457	BTN-95-EIX95182619075	p 307	A95-75760
BTN-95-EIX95041503780	p 205	A95-69211	BTN-95-EIX95142553044	p 304	A95-73454	BTN-95-EIX95182619076	p 269	A95-75761
BTN-95-EIX95041503781	p 205	A95-69212	BTN-95-EIX95142553046	p 304	A95-73452	BTN-95-EIX95182619077	p 307	A95-75762
BTN-95-EIX95041503782	p 193	A95-69213	BTN-95-EIX95142553047	p 286	A95-73451	BTN-95-EIX95182619078	p 269	A95-75763
BTN-95-EIX95041503783	p 193	A95-69214	BTN-95-EIX95142553054	p 262	A95-73444	BTN-95-EIX95182619080	p 269	A95-75765
BTN-95-EIX95041503784	p 180	A95-69215	BTN-95-EIX95142553057	p 262	A95-73441	BTN-95-EIX95182619087	p 291	A95-75772
BTN-95-EIX95041503785	p 180	A95-69216	BTN-95-EIX95142555475	p 278	A95-73435	BTN-95-EIX95182619088	p 283	A95-75773
BTN-95-EIX95041503787	p 205	A95-69218	BTN-95-EIX95142555477	p 278	A95-73433	BTN-95-EIX95182619093	p 269	A95-75778
BTN-95-EIX95041503799	p 239	A95-70124	BTN-95-EIX95142555482	p 228	A95-72891	BTN-95-EIX95182619097	p 283	A95-75782
BTN-95-EIX95041503806	p 242	A95-70131	BTN-95-EIX95142555485	p 227	A95-72888	BTN-95-EIX95182619099	p 295	A95-75784
BTN-95-EIX95041505023	p 242	A95-70132	BTN-95-EIX95142555488	p 227	A95-72885	BTN-95-EIX95182619100	p 307	A95-75785
BTN-95-EIX95041505024	p 235	A95-70133	BTN-95-EIX95142556201	p 304	A95-73439	BTN-95-EIX95182619101	p 308	A95-75786
BTN-95-EIX95042474388	p 209	A95-68312	BTN-95-EIX95142556202	p 286	A95-73438	BTN-95-EIX95182619103	p 321	A95-75788
BTN-95-EIX95042474389	p 196	A95-68311	BTN-95-EIX95142556203	p 280	A95-73437	BTN-95-EIX95182619104	p 269	A95-75789
BTN-95-EIX95042474393	p 217	A95-68307	BTN-95-EIX95152569458	p 305	A95-73498	BTN-95-EIX95182619105	p 269	A95-75790
BTN-95-EIX95042474398	p 209	A95-68302	BTN-95-EIX95152577585	p 264	A95-73497	BTN-95-EIX95182619115	p 321	A95-75792
BTN-95-EIX95042474400	p 192	A95-68300	BTN-95-EIX95152577586	p 264	A95-73496	BTN-95-EIX95182619121	p 321	A95-75793
BTN-95-EIX95042474401	p 203	A95-68299	BTN-95-EIX95152577587	p 263	A95-73495	BTN-95-EIX95182619125	p 322	A95-75794
BTN-95-EIX95042474409	p 209	A95-68291	BTN-95-EIX95152577588	p 263	A95-73494	BTN-95-EIX95182619126	p 291	A95-75795
BTN-95-EIX95042474413	p 209	A95-68287	BTN-95-EIX95152577589	p 263	A95-73493	BTN-95-EIX95182619127	p 276	A95-75796
BTN-95-EIX95042474418	p 209	A95-68282	BTN-95-EIX95152577597	p 305	A95-73486	BTN-95-EIX95182619128	p 269	A95-75797
BTN-95-EIX95042474624	p 189	A95-68278	BTN-95-EIX95152577604	p 305	A95-73479	BTN-95-EIX95182619129	p 291	A95-75798
BTN-95-EIX95042474626	p 209	A95-68280	BTN-95-EIX95152577606	p 305	A95-73477	BTN-95-EIX95182619130	p 291	A95-75799
BTN-95-EIX95042477108	p 179	A95-68351	BTN-95-EIX95152577612	p 321	A95-73471	BTN-95-EIX95182619131	p 291	A95-75800
BTN-95-EIX95042477109	p 179	A95-68350	BTN-95-EIX95152582313	p 264	A95-73516	BTN-95-EIX95182619132	p 292	A95-75801
BTN-95-EIX95042477110	p 192	A95-68349	BTN-95-EIX95152582314	p 316	A95-73517	BTN-95-EIX95182619138	p 269	A95-75805
BTN-95-EIX95062487521	p 218	A95-69229	BTN-95-EIX95152582315	p 264	A95-73518	BTN-95-EIX95182619139	p 288	A95-75806
BTN-95-EIX95062487522	p 180	A95-69230	BTN-95-EIX95152582316	p 264	A95-73519	BTN-95-EIX95182619144	p 299	A95-75807
BTN-95-EIX95062487523	p 186	A95-69232	BTN-95-EIX95152582317	p 264	A95-73520	BTN-95-EIX95182619145	p 279	A95-75808
BTN-95-EIX95062487524	p 203	A95-69233	BTN-95-EIX95152582318	p 316	A95-73521	BTN-95-EIX95182619149	p 322	A95-75812
BTN-95-EIX95062487526	p 186	A95-69234	BTN-95-EIX95152582319	p 276	A95-73522	BTN-95-EIX95182619153	p 292	A95-75816
BTN-95-EIX95062487527	p 186	A95-69235	BTN-95-EIX95152582320	p 264	A95-73523	BTN-95-EIX95182619154	p 279	A95-75817
BTN-95-EIX95062487528	p 204	A95-69236	BTN-95-EIX95152582321	p 265	A95-73524	BTN-95-EIX95182619209	p 283	A95-75835
BTN-95-EIX95062487530	p 186	A95-69238	BTN-95-EIX95152582322	p 265	A95-73525	BTN-95-EIX95182619210	p 270	A95-75836
BTN-95-EIX95062487531	p 187	A95-69239	BTN-95-EIX95152582323	p 281	A95-73526	BTN-95-EIX95182619211	p 295	A95-75837
BTN-95-EIX95062487532	p 187	A95-69240	BTN-95-EIX95152582324	p 265	A95-73527	BTN-95-EIX95182619212	p 322	A95-75838
BTN-95-EIX95062487533	p 194	A95-69241	BTN-95-EIX95152582326	p 265	A95-73529	BTN-95-EIX95182619213	p 296	A95-75839
BTN-95-EIX95062487534	p 193	A95-69242	BTN-95-EIX95152582327	p 265	A95-73530	BTN-95-EIX95182619214	p 292	A95-75840
BTN-95-EIX95062487535	p 190	A95-69243	BTN-95-EIX95152582329	p 281	A95-73531	BTN-95-EIX95182619215	p 292	A95-75841
BTN-95-EIX95062487536	p 187	A95-69244	BTN-95-EIX95152582330	p 265	A95-73532	BTN-95-EIX95182619216	p 292	A95-75842
BTN-95-EIX95062487537	p 187	A95-69245	BTN-95-EIX95152582331	p 281	A95-73533	BTN-95-EIX95182619217	p 270	A95-75843
BTN-95-EIX95062487538	p 193	A95-69246	BTN-95-EIX95152582333	p 281	A95-73535	BTN-95-EIX95182619218	p 284	A95-75844
BTN-95-EIX95062487539	p 187	A95-69247	BTN-95-EIX951525					

BTN-95-EIX95182619233	p 271	A95-76659	BTN-95-EIX95292721153	p 612	A95-92589	CONF-950256-1	p 441	N95-28029	#
BTN-95-EIX95182619234	p 308	A95-76660	BTN-95-EIX95292721154	p 612	A95-92590	CONF-950309-2	p 683	N95-32548	#
BTN-95-EIX95182619235	p 271	A95-76661	BTN-95-EIX95292721155	p 572	A95-89894	CONF-950463-1	p 694	N95-32636	#
BTN-95-EIX95202637575	p 332	A95-78583	BTN-95-EIX95292721165	p 677	A95-92597	CONF-950550-2	p 648	N95-31614	#
BTN-95-EIX95202637582	p 347	A95-78576	BTN-95-EIX95292721167	p 546	A95-89899	CONF-9506126-2	p 584	N95-32164	#
BTN-95-EIX95202637592	p 279	A95-76697	BTN-95-EIX95292721173	p 546	A95-89904				
BTN-95-EIX95202637603	p 308	A95-76686	BTN-95-EIX95292721296	p 595	A95-92626	CONGRESS PAPER C428-10-106	p 517	A95-91700	
BTN-95-EIX95202637606	p 279	A95-76683	BTN-95-EIX95292721316	p 633	A95-92511	CONGRESS PAPER C428-10-137	p 522	A95-91698	
BTN-95-EIX95202637608	p 292	A95-76681	BTN-95-EIX95292721321	p 609	A95-92513	CONGRESS PAPER C428-11-034	p 484	A95-91702	
BTN-95-EIX95202637613	p 279	A95-76676	BTN-95-EIX95302679864	p 636	A95-94102	CONGRESS PAPER C428-11-188	p 484	A95-91701	
BTN-95-EIX95202638962	p 279	A95-76674	BTN-95-EIX95302694459	p 583	A95-94056	CONGRESS PAPER C428-12-165	p 456	A95-91703	
BTN-95-EIX95202638963	p 289	A95-76673	BTN-95-EIX95302694460	p 636	A95-94057	CONGRESS PAPER C428-12-166	p 457	A95-91704	
BTN-95-EIX95212641069	p 287	A95-76734	BTN-95-EIX95302694461	p 636	A95-94058	CONGRESS PAPER C428-15-031	p 508	A95-91710	
BTN-95-EIX95212641070	p 287	A95-76735	BTN-95-EIX95302694469	p 588	A95-94065	CONGRESS PAPER C428-15-094	p 457	A95-91711	
BTN-95-EIX95212641071	p 287	A95-76736	BTN-95-EIX95302694471	p 636	A95-94067	CONGRESS PAPER C428-15-097	p 508	A95-91712	
BTN-95-EIX95212641072	p 319	A95-76737	BTN-95-EIX95302727634	p 636	A95-94108	CONGRESS PAPER C428-15-216	p 457	A95-91713	
BTN-95-EIX95212645688	p 271	A95-76740	BTN-95-EIX95302729765	p 605	A95-94127	CONGRESS PAPER C428-17-135	p 531	A95-91714	
BTN-95-EIX95212645690	p 271	A95-76742	BTN-95-EIX95302729768	p 636	A95-94130	CONGRESS PAPER C428-17-189	p 531	A95-91716	
BTN-95-EIX95212645692	p 271	A95-76744	BTN-95-EIX95302729772	p 637	A95-94134	CONGRESS PAPER C428-18-168	p 484	A95-91717	
BTN-95-EIX95212645694	p 272	A95-76746	BTN-95-EIX95302730538	p 583	A95-94036	CONGRESS PAPER C428-18-169	p 484	A95-91718	
BTN-95-EIX95212645695	p 272	A95-76747	BTN-95-EIX95302730589	p 637	A95-94197	CONGRESS PAPER C428-19-079	p 457	A95-91720	
BTN-95-EIX95212645706	p 299	A95-76758	BTN-95-EIX95302731054	p 637	A95-94205	CONGRESS PAPER C428-19-124	p 517	A95-91721	
BTN-95-EIX95212645707	p 299	A95-76759	BTN-95-EIX95302731089	p 618	A95-94208	CONGRESS PAPER C428-19-126	p 517	A95-91722	
BTN-95-EIX95212645712	p 272	A95-76764	BTN-95-EIX95302731223	p 600	A95-94044	CONGRESS PAPER C428-20-204	p 581	A95-91723	
BTN-95-EIX95212645713	p 261	A95-76765	BTN-95-EIX95302731226	p 618	A95-94045	CONGRESS PAPER C428-21-081	p 550	A95-91726	
BTN-95-EIX95222650780	p 347	A95-79236	BTN-95-EIX95302731227	p 600	A95-94046	CONGRESS PAPER C428-21-141	p 508	A95-91728	
BTN-95-EIX95222650781	p 327	A95-79237	BTN-95-EIX95332750473	p 638	A95-94687	CONGRESS PAPER C428-23-005	p 500	A95-91730	
BTN-95-EIX95222650782	p 358	A95-79238	BTN-95-EIX95332753018	p 638	A95-94793	CONGRESS PAPER C428-23-008	p 500	A95-91729	
BTN-95-EIX95222650784	p 334	A95-79240	CALSPAN-6241-F-1	p 12	N95-10442	CONGRESS PAPER C428-23-196	p 500	A95-91732	
BTN-95-EIX95222650789	p 329	A95-79245	CARDIVNSWC-TR-81-94/25	p 557	N95-30122	CONGRESS PAPER C428-24-142	p 678	A95-93595	
BTN-95-EIX95222650790	p 329	A95-79246	CARDIVNSWC-TR-94/002	p 62	N95-12426	CONGRESS PAPER C428-24-160	p 678	A95-93597	
BTN-95-EIX95222650791	p 329	A95-79247	CARDIVNSWC-TR-94/024	p 579	N95-28996	CONGRESS PAPER C428-24-212	p 678	A95-93599	
BTN-95-EIX95222650792	p 329	A95-79248	CCMS-95-01	p 301	N95-23179	CONGRESS PAPER C428-25-030	p 595	A95-93599	
BTN-95-EIX95222650793	p 334	A95-79249	CCMS-95-04	p 439	N95-27865	CONGRESS PAPER C428-25-100	p 595	A95-93600	
BTN-95-EIX95222650795	p 340	A95-79251	CDI-95-03	p 607	N95-30923	CONGRESS PAPER C428-25-172	p 595	A95-93598	
BTN-95-EIX95242670746	p 327	A95-81101	CEAS/AIAA-95-171	p 451	N95-26801	CONGRESS PAPER C428-25-175	p 596	A95-93601	
BTN-95-EIX95242670747	p 359	A95-81100	CECOM-TR-94-E-1	p 80	N95-14852	CONGRESS PAPER C428-26-037	p 681	A95-93602	
BTN-95-EIX95242670748	p 327	A95-81099	CERL-SR-EC-94/15	p 255	N95-20441	CONGRESS PAPER C428-26-051	p 681	A95-93603	
BTN-95-EIX95242670749	p 335	A95-81098	CGR/DC-01/94	p 241	N95-21687	CONGRESS PAPER C428-27-088	p 612	A95-93605	
BTN-95-EIX95242670750	p 334	A95-81097	CMOTT-94-5	p 37	N95-11917	CONGRESS PAPER C428-27-127	p 612	A95-93606	
BTN-95-EIX95242670751	p 336	A95-81096	CMOTT-94-9	p 439	N95-27882	CONGRESS PAPER C428-27-182	p 612	A95-93608	
BTN-95-EIX95242670754	p 342	A95-81093	CMU-CS-94-134	p 238	N95-20624	CONGRESS PAPER C428-3-056	p 475	A95-91674	
BTN-95-EIX95242670755	p 327	A95-81092	CMU-CS-94-147	p 83	N95-14343	CONGRESS PAPER C428-3-060	p 475	A95-91673	
BTN-95-EIX95242670759	p 359	A95-81088	CMU-RI-TR-94-17	p 126	N95-17706	CONGRESS PAPER C428-30-159	p 600	A95-93613	
BTN-95-EIX95242670766	p 359	A95-81081	CMU-SEI-94-TR-22	p 450	N95-28627	CONGRESS PAPER C428-30-162	p 610	A95-93612	
BTN-95-EIX95242670768	p 359	A95-81079	CONF-9204294-1	p 157	N95-16939	CONGRESS PAPER C428-31-151	p 603	A95-93615	
BTN-95-EIX95242670770	p 327	A95-81077	CONF-9304280-1	p 357	N95-24853	CONGRESS PAPER C428-31-152	p 603	A95-93616	
BTN-95-EIX95242673665	p 427	A95-82259	CONF-930726-8	p 118	N95-18645	CONGRESS PAPER C428-32-017	p 583	A95-93619	
BTN-95-EIX95242673673	p 450	A95-82251	CONF-940113-11	p 118	N95-18646	CONGRESS PAPER C428-32-075	p 610	A95-93621	
BTN-95-EIX95242673940	p 365	A95-82224	CONF-940135-9	p 247	N95-20781	CONGRESS PAPER C428-33-123	p 610	A95-93620	
BTN-95-EIX95242674338	p 450	A95-82176	CONF-940416-20	p 56	N95-13184	CONGRESS PAPER C428-33-210	p 610	A95-93622	
BTN-95-EIX95242679097	p 359	A95-81253	CONF-9404162-10	p 250	N95-22299	CONGRESS PAPER C428-35-057	p 604	A95-93627	
BTN-95-EIX95262694059	p 447	A95-85675	CONF-9404162-12	p 256	N95-21552	CONGRESS PAPER C428-35-059	p 610	A95-93628	
BTN-95-EIX95262694295	p 434	A95-85466	CONF-9404162-14	p 297	N95-24019	CONGRESS PAPER C428-35-061	p 603	A95-93626	
BTN-95-EIX95262694297	p 435	A95-85468	CONF-9404179-1	p 138	N95-17371	CONGRESS PAPER C428-36-192	p 612	A95-93631	
BTN-95-EIX95262694298	p 434	A95-85469	CONF-940440-5	p 304	N95-23981	CONGRESS PAPER C428-36-193	p 625	A95-93630	
BTN-95-EIX95262694299	p 434	A95-85470	CONF-940548-3	p 7	N95-10226	CONGRESS PAPER C428-37-173	p 628	A95-93632	
BTN-95-EIX95262694303	p 435	A95-85474	CONF-940548-7	p 216	N95-19855	CONGRESS PAPER C428-37-198	p 628	A95-93633	
BTN-95-EIX95262694306	p 411	A95-85477	CONF-9406188-1	p 145	N95-16509	CONGRESS PAPER C428-37-218	p 610	A95-93634	
BTN-95-EIX95262694308	p 370	A95-85479	CONF-940625-7	p 39	N95-12652	CONGRESS PAPER C428-38-084	p 634	A95-93637	
BTN-95-EIX95262694309	p 408	A95-85480	CONF-940662-1	p 157	N95-16828	CONGRESS PAPER C428-38-095	p 625	A95-93636	
BTN-95-EIX95262694310	p 370	A95-85481	CONF-940664-29	p 258	N95-21388	CONGRESS PAPER C428-38-096	p 625	A95-93637	
BTN-95-EIX95262694311	p 365	A95-85482	CONF-940723-28	p 249	N95-21478	CONGRESS PAPER C428-39-026	p 531	A95-91675	
BTN-95-EIX95262694312	p 365	A95-85483	CONF-940723-36	p 644	N95-30507	CONGRESS PAPER C428-4-039	p 531	A95-91676	
BTN-95-EIX95262694313	p 366	A95-85484	CONF-940784-1	p 52	N95-11752	CONGRESS PAPER C428-4-067	p 531	A95-91677	
BTN-95-EIX95262694314	p 435	A95-85485	CONF-9408163-1	p 228	N95-20195	CONGRESS PAPER C428-5-011	p 517	A95-91680	
BTN-95-EIX95262694314	p 435	A95-85485	CONF-940865-4	p 300	N95-22689	CONGRESS PAPER C428-5-025	p 522	A95-91679	
BTN-95-EIX95262694320	p 387	A95-85491	CONF-9409185-2	p 229	N95-21520	CONGRESS PAPER C428-5-036	p 522	A95-91678	
BTN-95-EIX95262694321	p 366	A95-85492	CONF-9409187-1	p 231	N95-20370	CONGRESS PAPER C428-5-138	p 522	A95-91681	
BTN-95-EIX95262696444	p 435	A95-85519	CONF-9410259-1	p 358	N95-25110	CONGRESS PAPER C428-6-113	p 549	A95-91682	
BTN-95-EIX95262697040	p 538	A95-86857	CONF-941109-3	p 708	N95-33642	CONGRESS PAPER C428-6-114	p 549	A95-91683	
BTN-95-EIX95262697041	p 538	A95-86858	CONF-9411142-4	p 299	N95-23532	CONGRESS PAPER C428-6-115	p 549	A95-91684	
BTN-95-EIX95262697042	p 569	A95-86859	CONF-9411149-4	p 392	N95-27440	CONGRESS PAPER C428-7-145	p 488	A95-91686	
BTN-95-EIX95262697073	p 564	A95-86862	CONF-941118-3	p 436	N95-26445	CONGRESS PAPER C428-7-146	p 488	A95-91687	
BTN-95-EIX95262697157	p 538	A95-86893	CONF-941129-9	p 300	N95-22764	CONGRESS PAPER C428-7-147	p 488	A95-91688	
BTN-95-EIX95282705070	p 455	A95-89667	CONF-941144-14	p 324	N95-24076	CONGRESS PAPER C428-7-148	p 488	A95-91689	
BTN-95-EIX95282705925	p 467	A95-89665	CONF-941210-2	p 358	N95-26090	CONGRESS PAPER C428-8-102	p 581	A95-91691	
BTN-95-EIX95282705926	p 455	A95-89666	CONF-9501116-6	p 446	N95-27459	CONGRESS PAPER C428-8-103	p 508	A95-91696	
BTN-95-EIX95282705928	p 455	A95-89663	CONF-9501116-7	p 446	N95-27459	CONGRESS PAPER C428-9-040	p 475	A95-91694	
BTN-95-EIX95282706404	p 545	A95-88184	CONF-9501116-8	p 376	N95-27541	CONGRESS PAPER C428-9-098	p 475	A95-91695	
BTN-95-EIX95282706655	p 486	A95-89649	CONF-950130-3	p 330	N95-24308	CONGRESS PAPER C428-9-199	p 475	A95-91697	
BTN-95-EIX95282706656	p 486	A95-89648	CONF-950130-7	p 420	N95-27851				
BTN-95-EIX95282706663	p 565	A95-88178	CONF-950226-3	p 349	N95-24598	CPIA-PUBL-602-VOL-1	p 148	N95-16312	#
BTN-95-EIX95282706664	p 466	A95-89641	CONF-950256-1-REV-2	p 441	N95-28139	CRAD-9206-TR-8940	p 228	N95-19950	#
BTN-95-EIX95282706665	p 455	A95-8964							

REPORT NUMBER INDEX

E-9279

CSE-TR-207-94	p 238	N95-20624	DOT-VNTSC-FAA-94-11	p 160	N95-18436	DOT/FAA/RD-94/7	p 131	N95-18198	* #
CU-CAS-95-03	p 289	N95-23088	DOT-VNTSC-FAA-94-12	p 118	N95-18624	DOT/FAA/RD-95-7	p 602	N95-31572	#
CUED/A-AEREO/TR-23	p 329	N95-24210	DOT-VNTSC-FAA-94-29	p 602	N95-23022	DOT/FAA/RD-95/2	p 691	N95-34797	#
DAAP-LEW-137682	p 59	N95-13235	DOT-VNTSC-FAA-94-4	p 328	N95-24295	DOTVNTSC-FAA-95/2	p 601	N95-31520	#
DA9426923	p 481	N95-29965	DOT-VNTSC-FAA-95-7	p 602	N95-31572	DRA-TM-AERO-PROP-41	p 331	N95-25649	#
DE93-000031	p 256	N95-20985	DOT-VNTSC-FAA-95-9	p 691	N95-34797	DRA/AP/TM9341/1.0	p 331	N95-25649	#
DE94-011862	p 357	N95-24853	DOT/FAA/AAR-95/1	p 690	N95-34562	DSTO-GD-0004	p 230	N95-19963	#
DE94-011863	p 157	N95-16939	DOT/FAA/AM-94/19	p 40	N95-12146	DSTO-GD-0044	p 503	N95-29362	#
DE94-011865	p 216	N95-19855	DOT/FAA/AM-95/15	p 384	N95-28540	DSTO-TN-0001	p 411	N95-26378	#
DE94-011866	p 118	N95-18645	DOT/FAA/AM-95/16	p 488	N95-28819	DSTO-TN-0002	p 397	N95-27918	#
DE94-011867	p 118	N95-18646	DOT/FAA/AM-95/1	p 278	N95-24071	DSTO-TN-0004	p 608	N95-31544	#
DE94-012473	p 152	N95-19100	DOT/FAA/AM-95/21	p 602	N95-32186	DSTO-TR-0015	p 224	N95-21659	#
DE94-013330	p 52	N95-11752	DOT/FAA/AM-95/22	p 599	N95-31845	DSTO-TR-0043	p 108	N95-17178	#
DE94-013341	p 7	N95-10226	DOT/FAA/AM-95/2	p 333	N95-24384	DSTO-TR-0049	p 286	N95-23666	#
DE94-013400	p 157	N95-16828	DOT/FAA/AM-95/4	p 280	N95-23565	DSTO-TR-0061	p 327	N95-24200	#
DE94-013960	p 138	N95-17371	DOT/FAA/AM-95/6	p 323	N95-23603	DSTO-TR-0062	p 328	N95-24201	#
DE94-014136	p 145	N95-16509	DOT/FAA/AM-95/8	p 277	N95-24024	DSTO-TR-0062	p 502	N95-28851	#
DE94-014240	p 436	N95-26445	DOT/FAA/AM-95/9	p 488	N95-28790	DSTO-TR-0072	p 348	N95-24203	#
DE94-014242	p 24	N95-11135	DOT/FAA/AOR-100/94/008	p 599	N95-31687	DSTO-TR-0095	p 405	N95-26424	#
DE94-014468	p 39	N95-12652	DOT/FAA/AOR-100/95-01	p 602	N95-32022	DSTO-TR-0132	p 400	N95-28567	#
DE94-015016	p 56	N95-13184	DOT/FAA/ASC-94-1	p 598	N95-31428	DSTO-TR-0135	p 388	N95-26389	#
DE94-015351	p 206	N95-19579	DOT/FAA/AT-94/1	p 382	N95-26454	DSTO-TR-0139	p 697	N95-33250	#
DE94-016894	p 231	N95-20370	DOT/FAA/CT-TN92/33	p 57	N95-11888	DSTO-TR-0147	p 504	N95-29445	#
DE94-017768	p 304	N95-23981	DOT/FAA/CT-TN92/41-1	p 125	N95-17373	E-5666-Vol-1-3	p 236	N95-22341	* #
DE94-017769	p 247	N95-20781	DOT/FAA/CT-TN92/47	p 228	N95-21148	E-7229	p 23	N95-10244	* #
DE94-018328	p 250	N95-22299	DOT/FAA/CT-TN93/25	p 228	N95-21020	E-7267	p 377	N95-28003	* #
DE94-018370	p 258	N95-21388	DOT/FAA/CT-TN93/35	p 384	N95-27903	E-7680	p 57	N95-11888	* #
DE94-018738	p 228	N95-20195	DOT/FAA/CT-TN94-19	p 61	N95-12996	E-8079	p 108	N95-16887	* #
DE94-019103	p 256	N95-21552	DOT/FAA/CT-TN94-61	p 366	N95-26363	E-8151	p 162	N95-19236	* #
DE94-019309	p 229	N95-21520	DOT/FAA/CT-TN94/16	p 485	N95-29855	E-8319	p 38	N95-12378	* #
DE94-019310	p 249	N95-21478	DOT/FAA/CT-TN94/23	p 232	N95-20032	E-8520	p 22	N95-11483	* #
DE95-000088	p 650	N95-32163	DOT/FAA/CT-TN94/28	p 383	N95-26978	E-8725	p 154	N95-16072	* #
DE95-000267	p 357	N95-24882	DOT/FAA/CT-TN94/29	p 146	N95-18087	E-8769	p 21	N95-10822	* #
DE95-000268	p 376	N95-27541	DOT/FAA/CT-TN94/36	p 445	N95-26453	E-8774	p 152	N95-16905	* #
DE95-000286	p 358	N95-26090	DOT/FAA/CT-TN94/41	p 380	N95-26485	E-8839	p 39	N95-13058	* #
DE95-000295	p 446	N95-27459	DOT/FAA/CT-TN94/48	p 556	N95-30072	E-8840	p 105	N95-16038	* #
DE95-001360	p 300	N95-22689	DOT/FAA/CT-TN94/49	p 601	N95-31013	E-8856	p 20	N95-10446	* #
DE95-001919	p 232	N95-21730	DOT/FAA/CT-TN94/55	p 646	N95-30922	E-8882	p 550	N95-28719	* #
DE95-002602	p 299	N95-23532	DOT/FAA/CT-TN94/6	p 126	N95-18088	E-8933	p 157	N95-16911	* #
DE95-002851	p 235	N95-21243	DOT/FAA/CT-TN95/10	p 646	N95-30902	E-8939	p 8	N95-10820	* #
DE95-002988	p 300	N95-22764	DOT/FAA/CT-TN95/1	p 677	N95-31587	E-8957	p 80	N95-14604	* #
DE95-003625	p 358	N95-25110	DOT/FAA/CT-88/10-VOL-2	p 448	N95-26638	E-8994	p 7	N95-10148	* #
DE95-003630	p 297	N95-24019	DOT/FAA/CT-90-10	p 226	N95-22318	E-9007	p 23	N95-10132	* #
DE95-003703	p 324	N95-24076	DOT/FAA/CT-91/17	p 382	N95-28630	E-9008	p 15	N95-10153	* #
DE95-004034	p 564	N95-30016	DOT/FAA/CT-92-25-VOL-1	p 421	N95-28420	E-9012	p 626	N95-30592	* #
DE95-004061	p 683	N95-32548	DOT/FAA/CT-92-25-VOL-2	p 424	N95-28462	E-9016	p 296	N95-23192	* #
DE95-004757	p 330	N95-24308	DOT/FAA/CT-92-25-VOL-3	p 420	N95-28266	E-9023	p 18	N95-11487	* #
DE95-006347	p 420	N95-27851	DOT/FAA/CT-92/13	p 189	N95-19805	E-9024	p 50	N95-11901	* #
DE95-007566	p 392	N95-27440	DOT/FAA/CT-92/14	p 226	N95-20275	E-9025	p 50	N95-11951	* #
DE95-007948	p 452	N95-28108	DOT/FAA/CT-93/14	p 333	N95-24631	E-9034	p 24	N95-10854	* #
DE95-008053	p 441	N95-28029	DOT/FAA/CT-93/49	p 191	N95-19810	E-9039	p 416	N95-27434	* #
DE95-008060	p 441	N95-28139	DOT/FAA/CT-93/52	p 83	N95-15683	E-9042	p 25	N95-11409	* #
DE95-008829	p 644	N95-30507	DOT/FAA/CT-94/04	p 227	N95-22352	E-9045	p 58	N95-12843	* #
DE95-008956	p 629	N95-30765	DOT/FAA/CT-94/106	p 505	N95-29565	E-9052	p 8	N95-10853	* #
DE95-009204	p 707	N95-32685	DOT/FAA/CT-94/119	p 626	N95-31468	E-9058	p 50	N95-11867	* #
DE95-009577	p 648	N95-31614	DOT/FAA/CT-94/111	p 328	N95-25401	E-9072	p 37	N95-11917	* #
DE95-010308	p 694	N95-32636	DOT/FAA/CT-94/120	p 523	N95-29967	E-9076	p 649	N95-31738	* #
DE95-010684	p 708	N95-33642	DOT/FAA/CT-94/121	p 226	N95-21518	E-9081	p 651	N95-32206	* #
DE95-011531	p 584	N95-32164	DOT/FAA/CT-94/12	p 9	N95-11179	E-9085	p 16	N95-11005	* #
DE95-011532	p 701	N95-33408	DOT/FAA/CT-94/23-PHASE-1	p 40	N95-12623	E-9089	p 49	N95-11864	* #
DE95-060082	p 349	N95-24598	DOT/FAA/CT-94/41	p 99	N95-13895	E-9091	p 50	N95-11890	* #
DE95-607662	p 362	N95-25978	DOT/FAA/CT-94/56	p 380	N95-26527	E-9093	p 57	N95-11711	* #
DLR-FB-94-11	p 172	N95-18912	DOT/FAA/CT-94/58	p 380	N95-26527	E-9104	p 16	N95-11159	* #
DLR-FB-94-12	p 119	N95-18910	DOT/FAA/CT-94/58	p 53	N95-12216	E-9111	p 141	N95-19380	* #
DLR-FB-94-19	p 483	N95-30349	DOT/FAA/CT-94/62	p 490	N95-30031	E-9124-1	p 76	N95-15853	* #
DLR-FB-94-20	p 647	N95-31355	DOT/FAA/CT-94/63	p 368	N95-28610	E-9128	p 76	N95-15852	* #
DLR-FB-94-32	p 704	N95-32787	DOT/FAA/CT-94/64	p 77	N95-14350	E-9141	p 100	N95-14618	* #
DNA-TR-93-164	p 235	N95-22036	DOT/FAA/CT-94/74	p 380	N95-26497	E-9143	p 339	N95-24561	* #
DNA-TR-94-123	p 509	N95-29950	DOT/FAA/CT-94/75	p 226	N95-20174	E-9149	p 51	N95-12763	* #
DOC-0710-001	p 66	N95-15331	DOT/FAA/CT-94/78	p 55	N95-12131	E-9152	p 91	N95-14299	* #
DODA-AR-007-005	p 129	N95-16969	DOT/FAA/CT-94/86	p 225	N95-20093	E-9159	p 39	N95-13197	* #
DODA-AR-007-100	p 108	N95-17178	DOT/FAA/CT-94/87	p 227	N95-22319	E-9160	p 138	N95-17402	* #
DODA-AR-008-375	p 204	N95-19848	DOT/FAA/CT-94/89	p 693	N95-34583	E-9170-VOL-1	p 258	N95-21888	* #
DODA-AR-008-383	p 87	N95-14409	DOT/FAA/CT-94/90	p 328	N95-24295	E-9171	p 101	N95-15743	* #
DODA-AR-008-545	p 230	N95-19963	DOT/FAA/CT-95/9	p 599	N95-31569	E-9172	p 100	N95-14610	* #
DODA-AR-008-924	p 502	N95-28851	DOT/FAA/NR-94-1	p 249	N95-22005	E-9175	p 146	N95-18586	* #
DODA-AR-009-205	p 608	N95-31544	DOT/FAA/PP-94-1	p 412	N95-28151	E-9179	p 89	N95-13665	* #
DOE/CE-41000/2	p 235	N95-21243	DOT/FAA/RD-93/30	p 55	N95-12131	E-9203	p 244	N95-19912	* #
DOE/MC-29257/4018	p 650	N95-32163	DOT/FAA/RD-93/34	p 53	N95-12216	E-9207	p 262	N95-24025	* #
DOE/MC-29257/95/C0452	p 694	N95-32636	DOT/FAA/RD-94-25	p 118	N95-18624	E-9227	p 117	N95-18457	* #
DOE/MC-30358/95/C0432	p 392	N95-27440	DOT/FAA/RD-94/14-PT-1	p 10	N95-10566	E-9230	p 73	N95-14418	* #
DOE/NASA/5776-2	p 447	N95-27970	DOT/FAA/RD-94/14-PT-2	p 41	N95-13203	E-9235	p 101	N95-15059	* #
DOT-VNTSC-FAA-94-10	p 249	N95-22005	DOT/FAA/RD-94/15	p 160	N95-18436	E-9237	p 137	N95-15970	* #
			DOT/FAA/RD-94/17	p 14	N95-11684	E-9239	p 167	N95-19501	* #
			DOT/FAA/RD-94/23	p 126	N95-18059	E-9241	p 73	N95-14297	* #
			DOT/FAA/RD-94/24	p 85	N95-15328	E-9252	p 76	N95-15912	* #
						E-9265	p 161	N95-19538	* #
						E-9275	p 170	N95-16906	* #
						E-9279	p 170	N95-17264	* #

E-9281	p 105	N95-18486 * #	EEC/NOTE-12/94	p 229	N95-21369	H-1918	p 8	N95-10858 * #
E-9282	p 104	N95-17657 * #				H-1962	p 48	N95-12831 * #
E-9283	p 105	N95-18197 * #	EGG-11265-3011	p 358	N95-25110	H-1972	p 449	N95-27914 * #
E-9294	p 148	N95-19286 * #				H-1984	p 284	N95-22806 * #
E-9295	p 439	N95-27882 * #	EOARD-TR-94-07	p 276	N95-23201 #	H-1993	p 108	N95-16858 * #
E-9299	p 156	N95-16588 * #	EOARD-TR-95-06	p 397	N95-28409	H-1994	p 9	N95-11158 * #
E-9332	p 105	N95-18044 * #				H-1997	p 36	N95-11898 * #
E-9340	p 438	N95-27854 * #	EPA/453/R-94/068	p 358	N95-26005 #	H-1999	p 38	N95-12191 * #
E-9345	p 210	N95-19567 * #	EPA/600/R-94/127	p 104	N95-17466	H-2002	p 10	N95-11408 * #
E-9349	p 139	N95-18133 * #	EPA/600/R-95/006	p 343	N95-26004 #	H-2007-VOL-1	p 67	N95-14229 * #
E-9356	p 145	N95-18054 * #				H-2007-VOL-2	p 69	N95-14239 * #
E-9364	p 323	N95-22675 * #	ERL-0656-RR	p 129	N95-16969 #	H-2007-VOL-3	p 71	N95-14251 * #
E-9366	p 162	N95-19125 * #				H-2014	p 51	N95-11868 * #
E-9373	p 223	N95-20794 * #	ESC-TR-93-293	p 300	N95-23781 #	H-2015	p 13	N95-11410 * #
E-9375	p 124	N95-19285 * #	ESC-TR-94-022	p 450	N95-28627 *	H-2019	p 158	N95-17490 * #
E-9376	p 124	N95-19284 * #				H-2020	p 694	N95-33009 * #
E-9381	p 123	N95-18582 * #	ESDU-94009	p 43	N95-11774	H-2022	p 134	N95-19044 * #
E-9387	p 150	N95-18743 * #	ESDU-94012	p 44	N95-11793	H-2027	p 157	N95-17418 * #
E-9390	p 618	N95-31985 * #	ESDU-94014	p 552	N95-28903	H-2029	p 89	N95-13892 * #
E-9393	p 202	N95-19769 * #	ESDU-94015	p 477	N95-28904	H-2030-VOL-1	p 161	N95-18955 * #
E-9394	p 119	N95-18933 * #	ESDU-94016-ADD-A	p 44	N95-11794	H-2030-VOL-2	p 161	N95-18956 * #
E-9404	p 211	N95-19794 * #	ESDU-94026	p 481	N95-29899	H-2040	p 284	N95-22829 * #
E-9416	p 197	N95-19651 * #	ESDU-94027	p 481	N95-29898	H-2059	p 620	N95-31846 * #
E-9420	p 244	N95-19953 * #	ESDU-94028	p 477	N95-28885	H-2060	p 617	N95-31425 * #
E-9421	p 293	N95-22954 * #	ESDU-94029	p 479	N95-29129			
E-9425	p 309	N95-22669 * #	ESDU-94037	p 477	N95-28800	HTN-94-00663	p 18	A95-60155 *
E-9426	p 337	N95-24207 * #	ESDU-94038	p 476	N95-28708	HTN-94-00666	p 18	A95-60156 *
E-9439	p 447	N95-27970 * #	ESDU-94039	p 501	N95-28707	HTN-94-00673	p 1	A95-60160 *
E-9444	p 236	N95-21383 * #	ESDU-94040	p 503	N95-29016	HTN-94-00674	p 18	A95-60161 *
E-9458	p 476	N95-28723 * #	ESDU-94044	p 477	N95-28897	HTN-94-00677	p 19	A95-60163 *
E-9461	p 366	N95-26363 * #	ESDU-94045	p 502	N95-28896	HTN-94-00678	p 1	A95-60164 *
E-9465	p 627	N95-31653 * #	ESDU-94046	p 500	N95-28704	HTN-94-00681	p 19	A95-60165 *
E-9477	p 338	N95-24390 * #				HTN-94-00682	p 27	A95-60166 *
E-9488	p 338	N95-24304 * #	ESL-TR-722792-6	p 24	N95-11252 * #	HTN-94-00684	p 16	A95-60167 *
E-9489	p 320	N95-23259 * #				HTN-94-00685	p 16	A95-60168 *
E-9491	p 323	N95-23178 * #	F-632	p 211	N95-19809	HTN-94-00686	p 2	A95-60169 *
E-9493	p 289	N95-23222 * #				HTN-94-00688	p 17	A95-60170 *
E-9498	p 438	N95-27855 * #	FAA-AC-91-70	p 277	N95-24065 #	HTN-94-00692	p 14	A95-60172 *
E-9509	p 344	N95-26119 * #				HTN-94-00694	p 2	A95-60173 *
E-9521	p 295	N95-23671 * #	FAA-AFS-550	p 277	N95-24065 #	HTN-94-00699	p 2	A95-60174 *
E-9523	p 407	N95-28344 * #				HTN-94-00697	p 2	A95-60176 *
E-9530	p 289	N95-23550 * #	FAA-AOR-100-94-009	p 380	N95-26485	HTN-94-00698	p 2	A95-60177 *
E-9538	p 275	N95-23462 * #	FAA-AOR-100-94-012	p 601	N95-31013 #	HTN-94-00699	p 2	A95-60178 *
E-9552	p 316	N95-24189 * #				HTN-94-00700	p 3	A95-60179 *
E-9575	p 592	N95-30611 * #	FAA-APO-94-10	p 219	N95-20091	HTN-94-00701	p 3	A95-60180 *
E-9577	p 616	N95-30779 * #	FAA-APO-94-11	p 490	N95-29880 #	HTN-94-00702	p 3	A95-60181 *
E-9582	p 338	N95-24392 * #	FAA-APO-95-1	p 584	N95-31598 #	HTN-94-00703	p 3	A95-60182 *
E-9583	p 290	N95-24053 * #				HTN-94-00704	p 3	A95-60183 *
E-9584	p 451	N95-26801 * #	FAA/ACE-100-01	p 79	N95-13981	HTN-94-00705	p 3	A95-60184 *
E-9589	p 316	N95-23792 * #				HTN-94-00707	p 4	A95-60185 *
E-9592	p 337	N95-24624 * #	FBI-UST-95-029	p 649	N95-31728 #	HTN-94-00708	p 4	A95-60186 *
E-9599	p 412	N95-27176 * #				HTN-94-00709	p 4	A95-60187 *
E-9621	p 332	N95-25962 * #	FNAL-TM-1929	p 629	N95-30765 #	HTN-94-00710	p 4	A95-60188 *
E-9630	p 332	N95-26075 * #				HTN-94-00711	p 5	A95-60189 *
E-9638	p 482	N95-30091 * #	FOA-C-10358-1.3	p 104	N95-17451	HTN-94-00712	p 5	A95-60190 *
E-9652	p 554	N95-29371 * #	FOA-C-20957-2.1	p 142	N95-17454	HTN-94-00713	p 5	A95-60191 *
E-9653	p 406	N95-27866 * #	FOA-C-20963-2.1	p 14	N95-10083	HTN-94-00714	p 5	A95-60192 *
E-9663	p 579	N95-29401 * #	FOA-C-20972-2.5	p 248	N95-21132 #	HTN-94-00715	p 5	A95-60193 *
E-9664	p 646	N95-30851 * #	FOA-C-30763-8.4.3.4	p 360	N95-25894 #	HTN-94-00760	p 14	A95-60199 *
E-9683	p 381	N95-27762 * #	FOA-C-30768-3.6	p 340	N95-24260	HTN-94-00912	p 25	A95-60227
E-9689	p 406	N95-27860 * #				HTN-95-A0001	p 183	A95-67828
E-9691	p 553	N95-29112 * #	FR001	p 608	N95-31525 #	HTN-95-A0002	p 183	A95-67829
E-9704	p 616	N95-30702 * #	FR2198-20	p 88	N95-15415	HTN-95-A0003	p 183	A95-67830
E-9705	p 513	N95-29115 * #	FR7060-001	p 502	N95-28928 *	HTN-95-A0175	p 215	A95-69766
E-9708	p 555	N95-29538 * #				HTN-95-A0314	p 341	A95-80389 *
E-9709	p 645	N95-30524 * #	F93-2B-0R15	p 79	N95-13703 * #	HTN-95-A0330	p 251	A95-70297 *
E-9711	p 482	N95-30253 * #				HTN-95-A0493	p 236	A95-72564
E-9729	p 485	N95-29132 * #	GAO/AIMD-95-27	p 687	N95-32705 #	HTN-95-A0494	p 237	A95-72565 *
E-9730	p 480	N95-29402 * #				HTN-95-A0495	p 221	A95-72566 *
E-9731	p 615	N95-30594 * #	GAO/NSIAD-94-118	p 679	N95-31987 #	HTN-95-A0496	p 221	A95-72567 *
E-9732	p 592	N95-30704 * #	GAO/NSIAD-94-140	p 367	N95-26817 #	HTN-95-A0497	p 222	A95-72568 *
E-9736	p 616	N95-30853 * #	GAO/NSIAD-94-141	p 585	N95-32198 #	HTN-95-A0498	p 229	A95-72569
E-9737	p 616	N95-30698 * #	GAO/NSIAD-94-63	p 584	N95-32194 #	HTN-95-A0499	p 222	A95-72570
E-9740	p 580	N95-29641 * #	GAO/NSIAD-94-65	p 609	N95-32196 #	HTN-95-A0500	p 230	A95-72571 *
E-9747	p 710	N95-32836 * #	GAO/NSIAD-94-71	p 176	N95-18578 #	HTN-95-A0509	p 230	A95-72580 *
E-9748	p 648	N95-31423 * #	GAO/NSIAD-95-112	p 397	N95-27910 #	HTN-95-A0514	p 230	A95-72585
E-9753	p 457	N95-30229 * #	GAO/NSIAD-95-12	p 231	N95-20212 #	HTN-95-A0526	p 255	A95-73180
E-9759	p 523	N95-30067 * #	GAO/NSIAD-95-52	p 286	N95-24091 #	HTN-95-A0527	p 255	A95-73181
E-9769	p 629	N95-30787 * #	GAO/NSIAD-95-59	p 336	N95-26338 #	HTN-95-A0578	p 452	A95-83158
E-9776	p 615	N95-30617 * #	GAO/NSIAD-95-9	p 683	N95-32783 #	HTN-95-A0861	p 317	A95-76265 *
E-9777	p 615	N95-30517 * #				HTN-95-A0862	p 318	A95-76266 *
E-9778	p 514	N95-30007 * #	GAO/RCED-94-118FS	p 699	N95-32759 #	HTN-95-A0863	p 318	A95-76267 *
E-9779	p 616	N95-30632 * #	GAO/RCED-94-142	p 687	N95-32885 #	HTN-95-A1021	p 443	A95-84526 *
E-9782	p 615	N95-30589 * #	GAO/RCED-94-15	p 687	N95-32784 #	HTN-95-A1038	p 443	A95-84543 *
E-9784	p 617	N95-30861 * #	GAO/RCED-94-167FS	p 603	N95-32197 #	HTN-95-A1044	p 443	A95-84549 *
E-9789	p 694	N95-32916 * #	GAO/RCED-94-209	p 700	N95-32888 #	HTN-95-A1048	p 417	A95-84553 *
E-9796	p 651	N95-32205 * #	GAO/RCED-94-226	p 699	N95-32786 #	HTN-95-A1463	p 546	A95-89183
E-9799	p 645	N95-30587 * #	GAO/RCED-94-265	p 603	N95-32199 #	HTN-95-A1465	p 465	A95-89185
E-9807	p 697	N95-33208 * #				HTN-95-A1466	p 466	A95-89186
E-9825	p 705	N95-32930 * #	GRI-94/0350	p 338	N95-24293	HTN-95-A1467	p 466	A95-89187
E-9828	p 684	N95-32769 * #				HTN-95-A1468	p 466	A95-89188
E-9834	p 694	N95-32931 * #				HTN-95-A1469	p 486	A95-89189
ECU-8200-270	p 710	N95-33396 * #	GTN-95-0009261494012091-5879	p 579	A95-92319	HTN-95-A1470	p 492	A95-89190
EDR-17199	p 406	N95-27866 * #	GTN-95-00406090-4621	p 680	A95-93965	HTN-95-A1471	p 466	A95-89191
			GTN-95-0301010494002231-1662	p 578	A95-92210	HTN-95-A1472	p 466	A95-89192
						HTN-95-A1473	p 492	A95-89193
			H-1913	p 117	N95-18565 * #			

HTN-95-A1474	p 492	A95-89194	HTN-95-00742	p 445	A95-86312	HTN-95-21113	p 549	A95-91682
HTN-95-A1475	p 510	A95-89195	HTN-95-00745	p 445	A95-86315	HTN-95-21114	p 549	A95-91683
HTN-95-A1477	p 547	A95-90052	HTN-95-00748	p 445	A95-86318	HTN-95-21115	p 549	A95-91684
HTN-95-A1479	p 547	A95-90054	HTN-95-00877	p 509	A95-87466	HTN-95-21117	p 488	A95-91686
HTN-95-A1481	p 511	A95-90056	HTN-95-00891	p 526	A95-88601	HTN-95-21118	p 488	A95-91687
HTN-95-A1482	p 511	A95-90057	HTN-95-01080	p 578	A95-90266	HTN-95-21119	p 488	A95-91688
HTN-95-A1483	p 505	A95-90058	HTN-95-01081	p 547	A95-90267	HTN-95-21120	p 488	A95-91689
HTN-95-A1484	p 511	A95-90059	HTN-95-01082	p 468	A95-90268	HTN-95-21122	p 581	A95-91691
HTN-95-A1485	p 467	A95-90060	HTN-95-01083	p 515	A95-90269	HTN-95-21125	p 475	A95-91694
HTN-95-A1486	p 467	A95-90061	HTN-95-01084	p 506	A95-90270	HTN-95-21126	p 475	A95-91695
HTN-95-A1487	p 467	A95-90062	HTN-95-01086	p 529	A95-90272	HTN-95-21127	p 508	A95-91696
HTN-95-A1488	p 467	A95-90063	HTN-95-01087	p 468	A95-90273	HTN-95-21128	p 475	A95-91697
HTN-95-A1490	p 493	A95-90065	HTN-95-01088	p 496	A95-90274	HTN-95-21129	p 522	A95-91698
HTN-95-A1491	p 494	A95-90066	HTN-95-01089	p 468	A95-90275	HTN-95-21131	p 517	A95-91700
HTN-95-A1492	p 494	A95-90067	HTN-95-01090	p 468	A95-90276	HTN-95-21132	p 484	A95-91701
HTN-95-A1493	p 494	A95-90068	HTN-95-01091	p 468	A95-90277	HTN-95-21133	p 484	A95-91702
HTN-95-A1494	p 505	A95-90069	HTN-95-01092	p 468	A95-90278	HTN-95-21134	p 456	A95-91703
HTN-95-A1495	p 494	A95-90070	HTN-95-01093	p 468	A95-90279	HTN-95-21135	p 457	A95-91704
HTN-95-A1496	p 494	A95-90071	HTN-95-01094	p 469	A95-90280	HTN-95-21141	p 508	A95-91710
HTN-95-A1497	p 494	A95-90072	HTN-95-01095	p 496	A95-90281	HTN-95-21142	p 457	A95-91711
HTN-95-A1498	p 494	A95-90073	HTN-95-01096	p 469	A95-90282	HTN-95-21143	p 508	A95-91712
HTN-95-A1499	p 495	A95-90074	HTN-95-01097	p 496	A95-90283	HTN-95-21144	p 457	A95-91713
HTN-95-A1500	p 495	A95-90075	HTN-95-01098	p 547	A95-90284	HTN-95-21145	p 531	A95-91714
HTN-95-A1501	p 495	A95-90076	HTN-95-01099	p 469	A95-90285	HTN-95-21147	p 531	A95-91716
HTN-95-A1504	p 486	A95-90079	HTN-95-01218	p 484	A95-91450	HTN-95-21148	p 484	A95-91717
HTN-95-A1505	p 456	A95-90080	HTN-95-10686	p 214	A95-68845	HTN-95-21149	p 484	A95-91718
HTN-95-A1506	p 456	A95-90081	HTN-95-11295	p 319	A95-77000	HTN-95-21151	p 457	A95-91720
HTN-95-A1507	p 456	A95-90082	HTN-95-11304	p 319	A95-77009	HTN-95-21152	p 517	A95-91721
HTN-95-A1508	p 511	A95-90083	HTN-95-11475	p 353	A95-79453	HTN-95-21153	p 517	A95-91722
HTN-95-A1509	p 495	A95-90084	HTN-95-11909	p 404	A95-85990	HTN-95-21154	p 581	A95-91723
HTN-95-A1510	p 495	A95-90085	HTN-95-11969	p 543	A95-88011	HTN-95-21157	p 550	A95-91726
HTN-95-A1511	p 495	A95-90086	HTN-95-11994	p 559	A95-88457	HTN-95-21159	p 508	A95-91728
HTN-95-A1512	p 495	A95-90087	HTN-95-12033	p 528	A95-88496	HTN-95-21160	p 500	A95-91729
HTN-95-A1513	p 573	A95-90088	HTN-95-12142	p 497	A95-90866	HTN-95-21161	p 500	A95-91730
HTN-95-A1597	p 548	A95-91479	HTN-95-12195	p 475	A95-91895	HTN-95-21163	p 500	A95-91732
HTN-95-A1609	p 498	A95-91491	HTN-95-12213	p 485	A95-91913	HTN-95-21164	p 678	A95-93595
HTN-95-A1753	p 633	A95-93316	HTN-95-12215	p 550	A95-91915	HTN-95-21165	p 678	A95-93596
HTN-95-A1755	p 634	A95-93318	HTN-95-12417	p 611	A95-95210	HTN-95-21166	p 678	A95-93597
HTN-95-A1767	p 627	A95-93330	HTN-95-20003	p 153	A95-63201	HTN-95-21167	p 595	A95-93598
HTN-95-A1774	p 634	A95-93337	HTN-95-20602	p 443	A95-84783	HTN-95-21168	p 595	A95-93599
HTN-95-A1843	p 638	A95-95357	HTN-95-20603	p 404	A95-84784	HTN-95-21169	p 595	A95-93600
HTN-95-B0076	p 387	A95-85892	HTN-95-20605	p 418	A95-84786	HTN-95-21170	p 596	A95-93601
HTN-95-B0194	p 581	A95-87903	HTN-95-20631	p 215	A95-69574	HTN-95-21171	p 681	A95-93602
HTN-95-B0254	p 492	A95-89198	HTN-95-20713	p 435	A95-86603	HTN-95-21172	p 681	A95-93603
HTN-95-B0255	p 466	A95-89199	HTN-95-20731	p 435	A95-86621	HTN-95-21174	p 612	A95-93605
HTN-95-B0256	p 466	A95-89200	HTN-95-20822	p 543	A95-88083	HTN-95-21175	p 612	A95-93606
HTN-95-B0257	p 529	A95-89201	HTN-95-20823	p 543	A95-88084	HTN-95-21181	p 610	A95-93612
HTN-95-B0258	p 529	A95-89202	HTN-95-20825	p 543	A95-88086	HTN-95-21182	p 600	A95-93613
HTN-95-B0276	p 483	A95-89220	HTN-95-20829	p 544	A95-88090	HTN-95-21184	p 603	A95-93615
HTN-95-B0277	p 565	A95-89221	HTN-95-20832	p 544	A95-88093	HTN-95-21185	p 603	A95-93616
HTN-95-B0278	p 493	A95-89222	HTN-95-20834	p 544	A95-88095	HTN-95-21186	p 583	A95-93617
HTN-95-B0279	p 493	A95-89223	HTN-95-20835	p 544	A95-88096	HTN-95-21187	p 583	A95-93618
HTN-95-B0280	p 493	A95-89224	HTN-95-20839	p 492	A95-88100	HTN-95-21188	p 583	A95-93619
HTN-95-B0307	p 493	A95-89251	HTN-95-20844	p 544	A95-88105	HTN-95-21189	p 610	A95-93620
HTN-95-B0357	p 520	A95-90438	HTN-95-20845	p 545	A95-88106	HTN-95-21190	p 610	A95-93621
HTN-95-B0358	p 520	A95-90439	HTN-95-20846	p 545	A95-88107	HTN-95-21191	p 610	A95-93622
HTN-95-B0359	p 511	A95-90440	HTN-95-20853	p 462	A95-88892	HTN-95-21195	p 603	A95-93626
HTN-95-B0361	p 511	A95-90442	HTN-95-20921	p 463	A95-88960	HTN-95-21196	p 604	A95-93627
HTN-95-B0362	p 520	A95-90443	HTN-95-20922	p 528	A95-88961	HTN-95-21197	p 610	A95-93628
HTN-95-B0365	p 469	A95-90446	HTN-95-20923	p 529	A95-88962	HTN-95-21199	p 625	A95-93630
HTN-95-B0366	p 470	A95-90447	HTN-95-20924	p 529	A95-88963	HTN-95-21200	p 612	A95-93631
HTN-95-B0368	p 520	A95-90449	HTN-95-20925	p 483	A95-88964	HTN-95-21201	p 628	A95-93632
HTN-95-B0369	p 512	A95-90450	HTN-95-20926	p 463	A95-88965	HTN-95-21202	p 628	A95-93633
HTN-95-B0370	p 530	A95-90451	HTN-95-20927	p 463	A95-88966	HTN-95-21203	p 610	A95-93634
HTN-95-B0371	p 547	A95-90452	HTN-95-20928	p 463	A95-88967	HTN-95-21205	p 625	A95-93636
HTN-95-B0373	p 520	A95-90454	HTN-95-20929	p 463	A95-88968	HTN-95-21206	p 634	A95-93637
HTN-95-B0374	p 470	A95-90455	HTN-95-20930	p 463	A95-88969	HTN-95-21209	p 634	A95-93640
HTN-95-B0375	p 512	A95-90456	HTN-95-20931	p 464	A95-88970	HTN-95-21211	p 610	A95-93642
HTN-95-B0376	p 581	A95-90457	HTN-95-20932	p 464	A95-88971	HTN-95-21215	p 634	A95-93646
HTN-95-B0377	p 496	A95-90458	HTN-95-20935	p 464	A95-88974	HTN-95-21216	p 586	A95-93647
HTN-95-B0380	p 521	A95-90461	HTN-95-20937	p 464	A95-88976	HTN-95-21217	p 586	A95-93648
HTN-95-B0381	p 512	A95-90462	HTN-95-20938	p 464	A95-88977	HTN-95-21218	p 586	A95-93649
HTN-95-B0383	p 521	A95-90464	HTN-95-20940	p 545	A95-88979	HTN-95-21219	p 604	A95-93650
HTN-95-B0384	p 521	A95-90465	HTN-95-20941	p 465	A95-88980	HTN-95-21224	p 618	A95-93655
HTN-95-B0388	p 470	A95-90469	HTN-95-20948	p 465	A95-88987	HTN-95-21225	p 604	A95-93656
HTN-95-B0389	p 512	A95-90470	HTN-95-20949	p 546	A95-88988	HTN-95-21226	p 604	A95-93657
HTN-95-B0391	p 470	A95-90472	HTN-95-20950	p 546	A95-88989	HTN-95-21227	p 604	A95-93658
HTN-95-B0392	p 496	A95-90473	HTN-95-20952	p 546	A95-88991	HTN-95-21228	p 618	A95-93659
HTN-95-B0394	p 530	A95-90475	HTN-95-20955	p 465	A95-88994	HTN-95-21229	p 586	A95-93660
HTN-95-B0396	p 530	A95-90477	HTN-95-20959	p 465	A95-88998	HTN-95-21231	p 587	A95-93662
HTN-95-B0408	p 456	A95-90756	HTN-95-20976	p 261	A95-74042	HTN-95-21233	p 613	A95-93664
HTN-95-C0002	p 595	A95-93390	HTN-95-20983	p 526	A95-90360	HTN-95-21234	p 613	A95-93665
HTN-95-C0004	p 585	A95-93392	HTN-95-21047	p 515	A95-90424	HTN-95-21236	p 613	A95-93667
HTN-95-C0005	p 585	A95-93393	HTN-95-21067	p 500	A95-91636	HTN-95-21237	p 613	A95-93668
HTN-95-C0006	p 585	A95-93394	HTN-95-21068	p 513	A95-91637	HTN-95-21238	p 634	A95-93669
HTN-95-C0007	p 585	A95-93395	HTN-95-21069	p 513	A95-91638	HTN-95-21239	p 604	A95-93670
HTN-95-C0008	p 586	A95-93396	HTN-95-21090	p 530	A95-91659	HTN-95-21240	p 628	A95-93671
HTN-95-Z0621	p 578	A95-92210	HTN-95-21104	p 475	A95-91673	HTN-95-21241	p 605	A95-93672
HTN-95-Z0749	p 579	A95-92319	HTN-95-21105	p 475	A95-91674	HTN-95-21242	p 605	A95-93673
HTN-95-Z0863	p 680	A95-93965	HTN-95-21106	p 531	A95-91675	HTN-95-21243	p 628	A95-93674
HTN-95-Z0865	p 418	A95-84731	HTN-95-21107	p 531	A95-91676	HTN-95-21244	p 613	A95-93675
HTN-95-00702	p 443	A95-86272	HTN-95-21108	p 531	A95-91677	HTN-95-21245	p 625	A95-93676
HTN-95-00721	p 444	A95-86291	HTN-95-21109	p 522	A95-91678	HTN-95-21246	p 614	A95-93677
HTN-95-00722	p 444	A95-86292	HTN-95-21110	p 522	A95-91679	HTN-95-21247	p 614	A95-93678
HTN-95-00726	p 444	A95-86296	HTN-95-21111	p 517	A95-91680	HTN-95-21250	p 610	A95-93681

HTN-95-21260	p 680	A95-93691	HTN-95-51680	p 418	A95-85062	HTN-95-90694	p 215	A95-69721
HTN-95-21261	p 614	A95-93692	HTN-95-51845	p 525	A95-87483	HTN-95-90884	p 253	A95-72393
HTN-95-21262	p 635	A95-93693	HTN-95-51892	p 539	A95-87530	HTN-95-90902	p 253	A95-72411
HTN-95-21267	p 635	A95-93698	HTN-95-60505	p 214	A95-68756	HTN-95-90914	p 253	A95-72423
HTN-95-21363	p 353	A95-78678	HTN-95-60511	p 214	A95-68762	HTN-95-91363	p 318	A95-76394
HTN-95-21364	p 353	A95-78679	HTN-95-60545	p 205	A95-69854	HTN-95-91421	p 319	A95-77334
HTN-95-31007	p 220	A95-71177	HTN-95-60779	p 317	A95-75976	HTN-95-91841	p 354	A95-80829
HTN-95-31008	p 220	A95-71178	HTN-95-60992	p 361	A95-80633	HTN-95-91842	p 354	A95-80830
HTN-95-31009	p 220	A95-71179	HTN-95-61064	p 430	A95-83648	HTN-95-91843	p 354	A95-80831
HTN-95-31010	p 221	A95-71180	HTN-95-61070	p 430	A95-83654	HTN-95-91855	p 354	A95-80843
HTN-95-31011	p 221	A95-71181	HTN-95-61071	p 385	A95-83655	HTN-95-91856	p 355	A95-80844
HTN-95-31012	p 236	A95-71182	HTN-95-61072	p 369	A95-83656	HTN-95-91857	p 355	A95-80845
HTN-95-31013	p 221	A95-71183	HTN-95-61073	p 369	A95-83657	HTN-95-91872	p 335	A95-81974
HTN-95-31014	p 236	A95-71184	HTN-95-61074	p 369	A95-83658	HTN-95-92121	p 443	A95-83827
HTN-95-40013	p 85	A95-62657	HTN-95-61075	p 369	A95-83659	HTN-95-92246	p 433	A95-85290
HTN-95-40359	p 212	A95-66869	HTN-95-61076	p 369	A95-83660	HTN-95-92247	p 434	A95-85291
HTN-95-40659	p 215	A95-69803	HTN-95-61077	p 370	A95-83661	HTN-95-92255	p 434	A95-85299
HTN-95-40689	p 216	A95-69833	HTN-95-61078	p 370	A95-83662	HTN-95-92261	p 434	A95-85305
HTN-95-40728	p 251	A95-70473	HTN-95-61120	p 415	A95-84884	HTN-95-92309	p 365	A95-85353
HTN-95-40756	p 252	A95-71186	HTN-95-61145	p 404	A95-84909	HTN-95-92310	p 365	A95-85354
HTN-95-41219	p 317	A95-75031	HTN-95-61156	p 405	A95-86255	HTN-95-92311	p 365	A95-85355
HTN-95-41223	p 317	A95-75035	HTN-95-61157	p 373	A95-86256	HTN-95-92312	p 387	A95-85356
HTN-95-41393	p 288	A95-76389	HTN-95-61179	p 539	A95-87552	HTN-95-92313	p 404	A95-85357
HTN-95-41394	p 283	A95-76390	HTN-95-61184	p 539	A95-87557	HTN-95-92510	p 539	A95-87330
HTN-95-41540	p 346	A95-77921	HTN-95-61195	p 491	A95-87568	HTN-95-92534	p 558	A95-87354
HTN-95-41799	p 353	A95-80525	HTN-95-61196	p 491	A95-87569	HTN-95-92535	p 558	A95-87355
HTN-95-41833	p 353	A95-80559	HTN-95-61197	p 491	A95-87570	HTN-95-92536	p 558	A95-87356
HTN-95-41901	p 356	A95-81648	HTN-95-61198	p 570	A95-87571	HTN-95-92537	p 558	A95-87357
HTN-95-41943	p 361	A95-81690	HTN-95-61199	p 461	A95-87572	HTN-95-92542	p 558	A95-87362
HTN-95-42091	p 430	A95-83857	HTN-95-61203	p 540	A95-87576	HTN-95-92543	p 558	A95-87363
HTN-95-42210	p 430	A95-84026	HTN-95-61204	p 540	A95-87577	HTN-95-92544	p 559	A95-87364
HTN-95-42213	p 430	A95-84029	HTN-95-61208	p 540	A95-87581	HTN-95-92545	p 460	A95-87365
HTN-95-42215	p 386	A95-84031	HTN-95-61209	p 541	A95-87582	HTN-95-92557	p 524	A95-87373
HTN-95-42269	p 380	A95-84963	HTN-95-61210	p 541	A95-87583	HTN-95-92594	p 509	A95-87410
HTN-95-42298	p 418	A95-84992	HTN-95-61221	p 491	A95-87594	HTN-95-92595	p 519	A95-87411
HTN-95-42308	p 450	A95-85002	HTN-95-70133	p 252	A95-70655	HTN-95-92596	p 460	A95-87412
HTN-95-42320	p 370	A95-86149	HTN-95-70134	p 252	A95-70656	HTN-95-92597	p 509	A95-87413
HTN-95-42321	p 371	A95-86150	HTN-95-70139	p 214	A95-69431	HTN-95-92598	p 490	A95-87414
HTN-95-42322	p 371	A95-86151	HTN-95-70149	p 227	A95-70671	HTN-95-92599	p 461	A95-87415
HTN-95-42324	p 371	A95-86153	HTN-95-70250	p 181	A95-66276	HTN-95-92641	p 510	A95-88002
HTN-95-42327	p 371	A95-86156	HTN-95-70542	p 237	A95-71656	HTN-95-92642	p 510	A95-88003
HTN-95-42328	p 371	A95-86157	HTN-95-70917	p 351	A95-77982	HTN-95-92643	p 510	A95-88004
HTN-95-42329	p 404	A95-86158	HTN-95-70935	p 351	A95-78000	HTN-95-92644	p 510	A95-88005
HTN-95-42330	p 404	A95-86159	HTN-95-70941	p 351	A95-78006	HTN-95-92646	p 492	A95-88007
HTN-95-42331	p 372	A95-86160	HTN-95-70943	p 351	A95-78008	HTN-95-92649	p 519	A95-88010
HTN-95-42332	p 372	A95-86161	HTN-95-70944	p 352	A95-78009	HTN-95-92710	p 565	A95-90629
HTN-95-42333	p 372	A95-86162	HTN-95-70946	p 352	A95-78011	HTN-95-92833	p 470	A95-90751
HTN-95-42334	p 372	A95-86163	HTN-95-70947	p 352	A95-78012	HTN-95-92834	p 497	A95-90752
HTN-95-42336	p 418	A95-86165	HTN-95-70948	p 352	A95-78013	HTN-95-92835	p 471	A95-90753
HTN-95-42337	p 405	A95-86166	HTN-95-70949	p 352	A95-78014	HTN-95-92836	p 471	A95-90754
HTN-95-42338	p 372	A95-86167	HTN-95-71126	p 429	A95-83487	HTN-95-92908	p 484	A95-91846
HTN-95-42340	p 408	A95-86169	HTN-95-71128	p 385	A95-83489	HTN-95-92932	p 562	A95-91870
HTN-95-42347	p 372	A95-86176	HTN-95-71130	p 408	A95-83491	HTN-95-92940	p 652	A95-93441
HTN-95-42348	p 373	A95-86177	HTN-95-71132	p 385	A95-83493			
HTN-95-42349	p 373	A95-86178	HTN-95-71133	p 385	A95-83494	IC-94/138	p 362	N95-25978 #
HTN-95-42368	p 418	A95-86197	HTN-95-71134	p 430	A95-83495			
HTN-95-42549	p 458	A95-87199	HTN-95-71387	p 528	A95-87605	ICAM-94-06-03	p 608	N95-31451 #
HTN-95-42570	p 458	A95-87200	HTN-95-71388	p 528	A95-87606			
HTN-95-42571	p 458	A95-87201	HTN-95-71450	p 545	A95-88789	ICASE-94-45	p 27	N95-11593 #
HTN-95-42575	p 564	A95-87205	HTN-95-80258	p 212	A95-66315	ICASE-94-48	p 57	N95-11812 #
HTN-95-42577	p 458	A95-87207	HTN-95-80564	p 218	A95-69658	ICASE-94-62	p 8	N95-10848 #
HTN-95-42580	p 458	A95-87210	HTN-95-80651	p 254	A95-72495	ICASE-94-77	p 170	N95-16897 #
HTN-95-42581	p 459	A95-87211	HTN-95-80656	p 254	A95-72500	ICASE-94-86	p 159	N95-18190 #
HTN-95-42582	p 459	A95-87212	HTN-95-80699	p 254	A95-72543	ICASE-94-89	p 170	N95-18110 #
HTN-95-42589	p 459	A95-87219	HTN-95-80701	p 254	A95-72545	ICASE-94-92	p 159	N95-18191 #
HTN-95-42590	p 539	A95-87220	HTN-95-80702	p 254	A95-72546	ICASE-94-94	p 159	N95-18193 #
HTN-95-42591	p 459	A95-87221	HTN-95-80851	p 290	A95-75093	ICASE-95-39	p 438	N95-21719 #
HTN-95-42592	p 459	A95-87222	HTN-95-80852	p 290	A95-75094	ICASE-95-40	p 569	N95-30353 #
HTN-95-42597	p 459	A95-87227	HTN-95-80853	p 290	A95-75095	ICASE-95-41	p 442	N95-28673 #
HTN-95-42618	p 483	A95-87248	HTN-95-80854	p 290	A95-75096	ICASE-95-5	p 314	N95-23466 #
HTN-95-42619	p 518	A95-87249	HTN-95-80855	p 267	A95-75097			
HTN-95-50054	p 98	A95-62279	HTN-95-80856	p 283	A95-75098	ICOMP-94-20	p 37	N95-11917 #
HTN-95-50218	p 175	A95-64855	HTN-95-80857	p 283	A95-75099	ICOMP-94-30	p 439	N95-27882 #
HTN-95-50219	p 176	A95-64856	HTN-95-80858	p 283	A95-75100			
HTN-95-50220	p 176	A95-64857	HTN-95-80859	p 267	A95-75101	IDA-D-1490	p 248	N95-20966
HTN-95-50223	p 176	A95-64860	HTN-95-81498	p 386	A95-85212			
HTN-95-50269	p 176	A95-65764	HTN-95-81499	p 386	A95-85213	IDA-P-2982	p 411	N95-26556
HTN-95-51275	p 355	A95-80860	HTN-95-81628	p 461	A95-87676			
HTN-95-51276	p 355	A95-80861	HTN-95-81631	p 461	A95-87679	IDA/HQ-93-44599	p 248	N95-20966
HTN-95-51277	p 356	A95-80862	HTN-95-81632	p 461	A95-87680	IDA/HQ-94-45529	p 411	N95-26556
HTN-95-51282	p 356	A95-80867	HTN-95-81633	p 462	A95-87681			
HTN-95-51283	p 356	A95-80868	HTN-95-81634	p 541	A95-87682	IFTR-13/1994	p 361	N95-26330
HTN-95-51323	p 356	A95-80908	HTN-95-81637	p 541	A95-87685	IFTR-39/1994	p 412	N95-26637
HTN-95-51587	p 442	A95-83591	HTN-95-81639	p 541	A95-87687			
HTN-95-51645	p 431	A95-85027	HTN-95-81640	p 541	A95-87688	INPE-5565-TDI/540	p 150	N95-18720 #
HTN-95-51646	p 432	A95-85028	HTN-95-81641	p 542	A95-87689			
HTN-95-51647	p 432	A95-85029	HTN-95-81642	p 542	A95-87690	INT-PATENT-CLASS-B64C-11/00	p 311	N95-23377
HTN-95-51648	p 432	A95-85030	HTN-95-81643	p 542	A95-87691	INT-PATENT-CLASS-B64C-19/00	p 294	N95-23389
HTN-95-51660	p 432	A95-85042	HTN-95-81644	p 542	A95-87692	INT-PATENT-CLASS-B64C-25/58	p 96	N95-15306
HTN-95-51664	p 432	A95-85046	HTN-95-81645	p 462	A95-87693	INT-PATENT-CLASS-B64C-5/00	p 286	N95-23390
HTN-95-51666	p 433	A95-85048	HTN-95-81646	p 542	A95-87694	INT-PATENT-CLASS-B64C-9/16	p 286	N95-23395
HTN-95-51668	p 433	A95-85050	HTN-95-81647	p 542	A95-87695			
HTN-95-51669	p 433	A95-85051	HTN-95-90356	p 212	A95-66429	INT-PATENT-CLASS-F02C/7/00	p 362	N95-26187
HTN-95-51670	p 433	A95-85052	HTN-95-90508	p 213	A95-67780	INT-PATENT-CLASS-F16F-7/10	p 159	N95-18325
HTN-95-51678	p 404	A95-85060	HTN-95-90534	p 213	A95-67806			
HTN-95-51679	p 433	A95-85061	HTN-95-90690	p 215	A95-69717	INT-PATENT-CLASS-G01B-11/16	p 362	N95-26015

INT-PATENT-CLASS-G01C-21/00	p 82	N95-14518 *	ISBN-92-836-1006-7	p 77	N95-14893 #	LESC-31195	p 49	N95-11913 * #
INT-PATENT-CLASS-G08B-21/00	p 85	N95-14415 *	ISBN-92-836-1007-5	p 127	N95-16562 #	LG92ER0035	p 11	N95-10240 * #
INT-PATENT-CLASS-G08B-21/00	p 280	N95-23393 *	ISBN-92-836-1008-3	p 139	N95-19017 #	LG92ER0036	p 12	N95-10242 * #
INT-PATENT-CLASS-H01R-13/629	p 350	N95-25592 *	ISBN-92-836-1010-5	p 315	N95-23602 #	LG94ER0099	p 87	N95-14363 #
IS-M-790	p 436	N95-26445 #	ISBN-92-836-1011-3	p 302	N95-23496 #	LG94ER0129	p 537	N95-29482
IS-T-1681	p 24	N95-11135 #	ISBN-92-836-1013-X	p 597	N95-31061 #	LT-94-1067	p 380	N95-26497
ISAS-655	p 374	N95-26740 #	ISBN-92-836-1014-8	p 504	N95-29503 #	M-755	p 35	N95-11710 * #
ISAS-656	p 436	N95-26739 #	ISBN-92-836-1017-2	p 650	N95-32165 #	M-756	p 54	N95-11870 * #
ISAS-658	p 480	N95-29640 #	ISBN-92-836-1019-9	p 711	N95-33198 #	M-773	p 330	N95-24217 * #
ISAS-659	p 555	N95-29712 #	ISBN-951-22-1910-7	p 60	N95-11798 #	M-778	p 476	N95-28720 * #
ISBN 0-387-94014-6	p 550	A95-91915 *	ISBN-951-22-1994-8	p 43	N95-12582 #	M/FAA/002-93-1	p 83	N95-15683 #
ISBN 0-444-89363-6	p 548	A95-91479 *	ISI/SR-94-379	p 238	N95-20624	M/NAFA/94-1	p 366	N95-26363 * #
ISBN 0-444-89793-3	p 638	A95-95357 *	ISL-PU-347/93	p 39	N95-12578	MCAT-05-06	p 411	N95-26775 * #
ISBN 0-444-89795-X	p 539	A95-87552	ISTIC-TR-93123	p 139	N95-17749	MCAT-94-005	p 101	N95-13717 * #
ISBN 0-8194-1311-9	p 5	A95-60191 *	ISVR-TR-234	p 27	N95-11166	MCAT-94-01	p 9	N95-11366 * #
ISBN 0-931784-25-5	p 559	A95-88457	IW-93069R	p 564	N95-30200 #	MCAT-94-07	p 52	N95-11938 * #
ISBN 0-931784-26-3	p 573	A95-90088 *	IW-93070R	p 677	N95-31157 #	MCAT-94-08	p 36	N95-11766 * #
ISBN 1-56091-428-9	p 417	A95-84553	IW-93071R	p 647	N95-30957 #	MCAT-94-09	p 48	N95-12785 * #
ISBN 1-56347-119-1	p 565	A95-90629	IW-93073R	p 592	N95-30638 #	MCAT-94-10	p 28	N95-11192 * #
ISBN 1-873082-39-8	p 558	A95-87354	JILA-153-1236	p 245	N95-20484 #	MCAT-94-11	p 9	N95-10940 * #
ISBN 1-879921-01-4	p 635	A95-93703	JPRS-UST-94-003-L	p 22	N95-10931 #	MCAT-94-11	p 74	N95-14614 * #
ISBN 1-879921-01-4	p 628	A95-93716	JPRS-UST-94-018	p 349	N95-24472 #	MCAT-94-20	p 74	N95-14613 * #
ISBN 1-879921-01-4	p 635	A95-93723	JPRS-UST-94-022	p 438	N95-27699 #	MCAT-94-22	p 10	N95-11367 * #
ISBN 1-879921-01-4	p 635	A95-93728	JPRS-UST-94-027	p 349	N95-24470 #	MCAT-94-23	p 6	N95-10131 * #
ISBN 1-879921-01-4	p 605	A95-93731	JPRS-UST-94-032	p 350	N95-24759 #	MCAT-95-01	p 374	N95-26760 * #
ISBN 1-879921-01-4	p 635	A95-93735	JPRS-UST-95-011	p 335	N95-24541 #	MCAT-95-03	p 448	N95-26648 * #
ISBN 1-879921-01-4	p 587	A95-93736	KNMI-SR-94-03	p 168	N95-18722	MCAT-95-07	p 389	N95-26651 * #
ISBN 1-879921-01-4	p 625	A95-93744	L-16700-PT-4	p 451	N95-26392 * #	MCAT-95-08	p 436	N95-26589 * #
ISBN 1-879921-01-4	p 605	A95-93746	L-17053	p 129	N95-17397 * #	MCAT-95-08	p 594	N95-32193 * #
ISBN 1-879921-01-4	p 587	A95-93747 *	L-17073	p 104	N95-16560 #	MCAT-95-11	p 389	N95-26591 * #
ISBN 1-879921-01-4	p 587	A95-93748	L-17105	p 39	N95-12770 * #	MCAT-95-13	p 374	N95-26735 * #
ISBN 1-879921-01-4	p 587	A95-93749	L-17162	p 249	N95-21258 * #	MCAT-95-14	p 389	N95-26590 * #
ISBN 1-879921-01-4	p 587	A95-93750	L-17167A-VOL-1-PT-1	p 534	N95-29029 #	MCAT-95-18	p 406	N95-26777 * #
ISBN 1-879921-01-4	p 587	A95-93751	L-17167B-VOL-1-PT-2	p 531	N95-28823 * #	MCAT-95-18	p 373	N95-26649 * #
ISBN 1-879921-01-4	p 588	A95-93752	L-17212	p 17	N95-10220 * #	MDC-91K0418	p 441	N95-27999 * #
ISBN 1-879921-01-4	p 578	A95-93757	L-17233	p 285	N95-22953 * #	MDC-93K0265	p 630	N95-31421 * #
ISBN 1-879921-01-4	p 588	A95-93758 *	L-17265	p 6	N95-10129 * #	MIT-TR-998	p 300	N95-23781 #
ISBN 3-540-56318-0	p 524	A95-87373	L-17268	p 38	N95-12176 * #	MTR-90W00179	p 382	N95-26454
ISBN 981-02-1732-3	p 462	A95-88892 *	L-17272	p 5	N95-10028 * #	MTR-94B000071	p 60	N95-12805
ISBN-0-309-05045-6	p 381	N95-27907 #	L-17274	p 51	N95-12664 * #	MTR-94W0000110	p 382	N95-26454
ISBN-0-309-05183-5	p 446	N95-27156 #	L-17291	p 26	N95-10859 * #	MTR-94W0000150	p 599	N95-31687 #
ISBN-0-309-05506-7	p 219	N95-19967 #	L-17299	p 6	N95-10029 * #	NAIC-ID(RS)T-0558-93	p 701	N95-34500 #
ISBN-0-309-05761-2	p 78	N95-15439	L-17322	p 8	N95-10739 * #	NAIC-ID(RS)T-0918-92	p 374	N95-26719
ISBN-0-315-86304-8	p 563	N95-29797	L-17323	p 17	N95-10860 * #	NAIC-ID(RS)T-0920-90	p 375	N95-26859
ISBN-0-315-86543-1	p 647	N95-31098	L-17327	p 37	N95-11995 * #	NAIC-ID(RS)T-0922-92	p 374	N95-26713
ISBN-0-856-79925-4	p 476	N95-28708	L-17328	p 53	N95-13553 * #	NAL-PD-CA-9217	p 142	N95-16392 #
ISBN-0-856-79926-2	p 501	N95-28707	L-17330	p 108	N95-16908 * #	NAL-PD-SN-9306	p 105	N95-18606 #
ISBN-0-856-79927-0	p 503	N95-29016	L-17334	p 125	N95-17384 * #	NAL-SP-27	p 684	N95-34505 #
ISBN-0-856-79931-9	p 477	N95-28897	L-17336	p 120	N95-19114 * #	NAL-SP-9322-PT-1	p 165	N95-19444 #
ISBN-0-85678-914-9	p 481	N95-29898	L-17337	p 106	N95-16069 * #	NAL-SP-9404	p 35	N95-12166 #
ISBN-0-85679-896-7	p 43	N95-11774	L-17339	p 62	N95-12341 * #	NAL-TM-CSS-9303	p 119	N95-18904 #
ISBN-0-85679-899-1	p 44	N95-11793	L-17341	p 55	N95-12357 * #	NAL-TR-1200	p 405	N95-26600 #
ISBN-0-85679-901-7	p 552	N95-28903	L-17348	p 309	N95-23015 * #	NAL-TR-1223	p 336	N95-25862 #
ISBN-0-85679-902-5	p 477	N95-28904	L-17348	p 310	N95-23210 * #	NAL-TR-1226	p 331	N95-25761 #
ISBN-0-85679-903-3	p 44	N95-11794	L-17350	p 120	N95-19042 * #	NAL-TR-1228	p 332	N95-25762 #
ISBN-0-85679-913-0	p 481	N95-29899	L-17350	p 222	N95-19913 * #	NAL-TR-1230	p 382	N95-26585 #
ISBN-0-85679-915-7	p 477	N95-28885	L-17354	p 224	N95-21338 * #	NAL-TR-1232	p 342	N95-25664 #
ISBN-0-85679-916-5	p 479	N95-29129	L-17356	p 80	N95-14852 * #	NAL-TR-1233	p 419	N95-26523 #
ISBN-0-85679-924-6	p 477	N95-28800	L-17360	p 373	N95-26382 * #	NAL-TR-1234	p 405	N95-26706 #
ISBN-0-85679-932-7	p 502	N95-28896	L-17368	p 378	N95-28669 * #	NAL-TR-1235	p 334	N95-25764 #
ISBN-0-85679-933-5	p 500	N95-28704	L-17374	p 54	N95-13196 * #	NAL-TR-1236	p 388	N95-26525 #
ISBN-0-87703-365-X	p 341	A95-80389 *	L-17376	p 131	N95-18198 * #	NAL-TR-1241	p 343	N95-24989 #
ISBN-0-931784-27-1	p 28	N95-11259	L-17380	p 272	N95-22802 * #	NAL-TR-1242	p 339	N95-24990 #
ISBN-1-883-71231-9	p 454	N95-28038 #	L-17381	p 250	N95-22109 * #	NAL-TR-1244	p 331	N95-24998 #
ISBN-7-80-046602-7	p 104	N95-16249 #	L-17386	p 331	N95-25339 * #	NAL-TR-1245	p 331	N95-25105 #
ISBN-90-369-2054-X	p 168	N95-18722	L-17388	p 378	N95-28241 * #	NAL-TR-1247	p 594	N95-31715 #
ISBN-90-6275-963-7	p 40	N95-13250	L-17397	p 102	N95-15065 * #	NAL-TR-1251	p 337	N95-25005 #
ISBN-90-6275-965-3	p 59	N95-13249	L-17401	p 378	N95-28674 * #	NAL-TR-1251	p 362	N95-25004 #
ISBN-90-9007413-9	p 400	N95-28636 #	L-17409	p 330	N95-24566 * #	NAL/TR-1202-PT-1	p 7	N95-10136
ISBN-92-835-0748-7	p 79	N95-14102 #	L-17416	p 684	N95-32821 * #	NAL/TR-1203-PT-2	p 7	N95-10137
ISBN-92-835-0749-5	p 89	N95-14127 #	L-17422	p 407	N95-28343 * #	NAL/TR-1208	p 6	N95-10135
ISBN-92-835-0752-5	p 73	N95-14445 #	L-17427	p 505	N95-30226 * #	NAS 1.15:103855	p 66	N95-14419 * #
ISBN-92-835-0753-3	p 67	N95-14197 #	L-17432-PT-1	p 92	N95-14453 * #	NAS 1.15:104268	p 8	N95-10858 * #
ISBN-92-835-0754-1	p 67	N95-14103 #	L-17432-PT-2	p 124	N95-19468 * #	NAS 1.15:104276	p 36	N95-11898 * #
ISBN-92-835-0755-X	p 149	N95-17278 #	L-17434	p 75	N95-14878 * #	NAS 1.15:104277	p 51	N95-11868 * #
ISBN-92-835-0756-8	p 162	N95-19251 #	L-17438	p 594	N95-31984 * #	NAS 1.15:104278	p 694	N95-33009 * #
ISBN-92-835-0757-6	p 145	N95-17388 #	L-17450	p 453	N95-26427 * #	NAS 1.15:104806-VOL-1	p 151	N95-19237 * #
ISBN-92-835-0758-4	p 126	N95-18927 #	L-17459	p 627	N95-32217 * #	NAS 1.15:104806-VOL-2	p 205	N95-19624 * #
ISBN-92-836-0001-0	p 173	N95-19142 #	LA-UR-94-2080	p 39	N95-12652 #			
ISBN-92-836-0002-9	p 143	N95-18597 #	LA-UR-94-3872	p 324	N95-24076 #			
ISBN-92-836-0004-5	p 233	N95-20631 #	LA-UR-95-42	p 420	N95-27851 #			
ISBN-92-836-0005-3	p 197	N95-19653 #	LC-75-24750	p 28	N95-11259			
ISBN-92-836-0006-1	p 248	N95-21061 #	LC-94-65759	p 381	N95-27907 #			
ISBN-92-836-0007-X	p 620	N95-31989 #	LC-94-67487	p 236	N95-22341 * #			
ISBN-92-836-0009-6	p 686	N95-32486 #	LC-94-68678	p 446	N95-27156			
ISBN-92-836-0010-X	p 392	N95-27504 #						
ISBN-92-836-1001-6	p 77	N95-14199 #						
ISBN-92-836-1002-4	p 91	N95-14201 #						
ISBN-92-836-1003-2	p 109	N95-17846 #						
ISBN-92-836-1005-9	p 72	N95-14264 #						

NAS 1.15:105798	p 23	N95-10244 * #	NAS 1.15:107020	p 705	N95-32930 * #	NAS 1.15:4602	p 310	N95-23210 * #
NAS 1.15:106385	p 73	N95-14418 * #	NAS 1.15:107023	p 684	N95-32769 * #	NAS 1.15:4604	p 38	N95-12191 * #
NAS 1.15:106458	p 38	N95-12378 * #	NAS 1.15:107024	p 694	N95-32931 * #	NAS 1.15:4605	p 10	N95-11408 * #
NAS 1.15:106502	p 22	N95-11483 * #	NAS 1.15:107759	p 50	N95-12860 * #	NAS 1.15:4610	p 331	N95-25338 * #
NAS 1.15:106569	p 21	N95-10822 * #	NAS 1.15:108081	p 59	N95-13235 * #	NAS 1.15:4611	p 378	N95-28241 * #
NAS 1.15:106571	p 152	N95-16905 * #	NAS 1.15:108459	p 9	N95-11157 * #	NAS 1.15:4631	p 449	N95-27914 * #
NAS 1.15:106579	p 39	N95-13058 * #	NAS 1.15:108489	p 592	N95-30712 * #	NAS 1.15:4632	p 120	N95-19119 * #
NAS 1.15:106580	p 105	N95-16038 * #	NAS 1.15:108491	p 441	N95-28364 * #	NAS 1.15:4634	p 330	N95-24566 * #
NAS 1.15:106589	p 20	N95-10446 * #	NAS 1.15:108574	p 453	N95-28002 * #	NAS 1.15:4635	p 296	N95-23192 * #
NAS 1.15:106632	p 157	N95-16911 * #	NAS 1.15:108819	p 44	N95-12225 * #	NAS 1.15:4637	p 63	N95-12190 * #
NAS 1.15:106637	p 8	N95-10820 * #	NAS 1.15:108833	p 95	N95-14617 * #	NAS 1.15:4638	p 274	N95-23250 * #
NAS 1.15:106649	p 80	N95-14604 * #	NAS 1.15:108834	p 8	N95-10847 * #	NAS 1.15:4640	p 505	N95-30226 * #
NAS 1.15:106669	p 339	N95-24561 * #	NAS 1.15:108837	p 11	N95-10846 * #	NAS 1.15:4641	p 250	N95-22109 * #
NAS 1.15:106671	p 7	N95-10148 * #	NAS 1.15:108843	p 38	N95-12360 * #	NAS 1.15:4644	p 158	N95-17490 * #
NAS 1.15:106674	p 15	N95-10153 * #	NAS 1.15:108845	p 37	N95-11927 * #	NAS 1.15:4646	p 134	N95-19044 * #
NAS 1.15:106676	p 626	N95-30592 * #	NAS 1.15:108847	p 25	N95-11389 * #	NAS 1.15:4651	p 89	N95-13892 * #
NAS 1.15:106683	p 24	N95-10854 * #	NAS 1.15:108849	p 35	N95-12227 * #	NAS 1.15:4653	p 176	N95-18573 * #
NAS 1.15:106685	p 416	N95-27434 * #	NAS 1.15:108850	p 65	N95-13642 * #	NAS 1.15:4660	p 684	N95-32821 * #
NAS 1.15:106686	p 25	N95-11409 * #	NAS 1.15:108853	p 116	N95-18101 * #	NAS 1.15:4661	p 309	N95-22804 * #
NAS 1.15:106689	p 58	N95-12843 * #	NAS 1.15:108855	p 65	N95-13662 * #	NAS 1.15:4664	p 627	N95-32217 * #
NAS 1.15:106697	p 50	N95-11867 * #	NAS 1.15:108855	p 65	N95-13891 * #	NAS 1.15:4665	p 288	N95-24030 * #
NAS 1.15:106710	p 37	N95-11917 * #	NAS 1.15:108857	p 66	N95-14921 * #	NAS 1.15:4676	p 284	N95-22829 * #
NAS 1.15:106711	p 649	N95-31738 * #	NAS 1.15:108860	p 272	N95-22666 * #	NAS 1.15:4704	p 620	N95-31846 * #
NAS 1.15:106715	p 651	N95-32206 * #	NAS 1.15:108862	p 232	N95-21186 * #	NAS 1.15:4705	p 617	N95-31425 * #
NAS 1.15:106719	p 16	N95-11005 * #	NAS 1.15:108863	p 367	N95-26710 * #	NAS 1.15:83199-PT-4	p 451	N95-26392 * #
NAS 1.15:106723	p 49	N95-11864 * #	NAS 1.15:108864	p 249	N95-21323 * #	NAS 1.21:290-Vol-1-3	p 236	N95-22341 * #
NAS 1.15:106724	p 50	N95-11890 * #	NAS 1.15:108866	p 405	N95-26412 * #	NAS 1.21:514	p 584	N95-31000 * #
NAS 1.15:106729	p 16	N95-11159 * #	NAS 1.15:108867	p 606	N95-30646 * #	NAS 1.21:7037(315)	p 219	N95-21640 * #
NAS 1.15:106736	p 139	N95-18133 * #	NAS 1.15:109083	p 21	N95-11466 * #	NAS 1.21:7037(316)	p 328	N95-24465 * #
NAS 1.15:106738	p 100	N95-14618 * #	NAS 1.15:109128	p 13	N95-11465 * #	NAS 1.21:7037(317)	p 328	N95-25798 * #
NAS 1.15:106741	p 51	N95-12763 * #	NAS 1.15:109140	p 33	N95-10873 * #	NAS 1.21:7037(318)	p 367	N95-27543 * #
NAS 1.15:106742	p 91	N95-14299 * #	NAS 1.15:109142	p 88	N95-14920 * #	NAS 1.21:7109(01)	p 363	N95-24238 * #
NAS 1.15:106747	p 39	N95-13197 * #	NAS 1.15:109146	p 22	N95-11003 * #	NAS 1.26:182276	p 105	N95-18044 * #
NAS 1.15:106755	p 146	N95-18586 * #	NAS 1.15:109148	p 55	N95-11915 * #	NAS 1.26:186030	p 13	N95-11410 * #
NAS 1.15:106757	p 89	N95-13665 * #	NAS 1.15:109149	p 57	N95-11815 * #	NAS 1.26:186031	p 157	N95-17418 * #
NAS 1.15:106764	p 262	N95-24025 * #	NAS 1.15:109152	p 97	N95-15898 * #	NAS 1.26:188330	p 49	N95-11913 * #
NAS 1.15:106774	p 76	N95-15853 * #	NAS 1.15:109154	p 10	N95-11489 * #	NAS 1.26:188343	p 54	N95-11937 * #
NAS 1.15:106776	p 117	N95-18457 * #	NAS 1.15:109157	p 238	N95-20669 * #	NAS 1.26:188360	p 143	N95-18567 * #
NAS 1.15:106782	p 101	N95-15059 * #	NAS 1.15:109158	p 226	N95-20706 * #	NAS 1.26:188370	p 527	N95-29447 * #
NAS 1.15:106784	p 137	N95-15970 * #	NAS 1.15:109160-VOL-1	p 171	N95-18899 * #	NAS 1.26:189077	p 441	N95-27999 * #
NAS 1.15:106785	p 167	N95-19501 * #	NAS 1.15:109163	p 102	N95-13663 * #	NAS 1.26:189099	p 290	N95-24053 * #
NAS 1.15:106786	p 73	N95-14297 * #	NAS 1.15:109165	p 333	N95-24633 * #	NAS 1.26:189141	p 316	N95-23792 * #
NAS 1.15:106799	p 170	N95-16906 * #	NAS 1.15:109168	p 366	N95-26381 * #	NAS 1.26:189146	p 316	N95-24189 * #
NAS 1.15:106802	p 170	N95-17264 * #	NAS 1.15:109171	p 333	N95-24582 * #	NAS 1.26:189201	p 337	N95-24624 * #
NAS 1.15:106803	p 105	N95-18486 * #	NAS 1.15:109174	p 225	N95-20688 * #	NAS 1.26:189206	p 15	N95-10247 * #
NAS 1.15:106804	p 104	N95-17657 * #	NAS 1.15:109175	p 346	N95-26251 * #	NAS 1.26:189412	p 567	N95-28807 * #
NAS 1.15:106805	p 105	N95-18197 * #	NAS 1.15:109177	p 320	N95-23009 * #	NAS 1.26:189657	p 23	N95-10318 * #
NAS 1.15:106808	p 148	N95-19286 * #	NAS 1.15:109179	p 330	N95-24397 * #	NAS 1.26:189659	p 15	N95-10319 * #
NAS 1.15:106814	p 438	N95-27854 * #	NAS 1.15:109181	p 348	N95-24396 * #	NAS 1.26:189677	p 452	N95-28264 * #
NAS 1.15:106817	p 145	N95-18054 * #	NAS 1.15:109182	p 296	N95-23011 * #	NAS 1.26:189705-VOL-2	p 452	N95-28073 * #
NAS 1.15:106822	p 162	N95-19125 * #	NAS 1.15:109184	p 449	N95-27241 * #	NAS 1.26:189714	p 406	N95-28227 * #
NAS 1.15:106824	p 223	N95-20794 * #	NAS 1.15:109948	p 157	N95-16828 * #	NAS 1.26:191045	p 150	N95-18743 * #
NAS 1.15:106826	p 124	N95-19285 * #	NAS 1.15:109950	p 1	N95-11463 * #	NAS 1.26:191177	p 57	N95-11996 * #
NAS 1.15:106827	p 124	N95-19284 * #	NAS 1.15:110103	p 231	N95-20370 * #	NAS 1.26:191178	p 108	N95-16887 * #
NAS 1.15:106831	p 123	N95-18582 * #	NAS 1.15:110142	p 381	N95-27859 * #	NAS 1.26:191194	p 162	N95-19236 * #
NAS 1.15:106833	p 119	N95-18933 * #	NAS 1.15:110146	p 554	N95-29453 * #	NAS 1.26:191441	p 630	N95-31421 * #
NAS 1.15:106840	p 211	N95-19794 * #	NAS 1.15:110150	p 568	N95-29454 * #	NAS 1.26:193993	p 49	N95-13027 * #
NAS 1.15:106846	p 244	N95-19953 * #	NAS 1.15:110161	p 410	N95-27839 * #	NAS 1.26:194215	p 101	N95-13717 * #
NAS 1.15:106847	p 293	N95-22954 * #	NAS 1.15:110163	p 580	N95-29452 * #	NAS 1.26:194893	p 51	N95-11869 * #
NAS 1.15:106849	p 309	N95-22669 * #	NAS 1.15:110164	p 518	N95-30327 * #	NAS 1.26:194931	p 27	N95-11593 * #
NAS 1.15:106854	p 236	N95-21383 * #	NAS 1.15:110168	p 501	N95-28820 * #	NAS 1.26:194934	p 57	N95-11812 * #
NAS 1.15:106865	p 338	N95-24390 * #	NAS 1.15:110175	p 645	N95-30682 * #	NAS 1.26:194942	p 61	N95-11932 * #
NAS 1.15:106870	p 320	N95-23259 * #	NAS 1.15:110182	p 646	N95-30783 * #	NAS 1.26:194953	p 8	N95-10848 * #
NAS 1.15:106872	p 323	N95-23178 * #	NAS 1.15:110346	p 335	N95-24629 * #	NAS 1.26:194972	p 325	N95-23276 * #
NAS 1.15:106875	p 438	N95-27855 * #	NAS 1.15:110347	p 332	N95-26302 * #	NAS 1.26:194976	p 99	N95-13727 * #
NAS 1.15:106885	p 295	N95-23671 * #	NAS 1.15:110348	p 383	N95-26587 * #	NAS 1.26:194980	p 170	N95-16897 * #
NAS 1.15:106886	p 407	N95-28344 * #	NAS 1.15:110349	p 409	N95-26773 * #	NAS 1.26:194987	p 54	N95-12175 * #
NAS 1.15:106890	p 289	N95-23550 * #	NAS 1.15:110351	p 457	N95-28816 * #	NAS 1.26:194994	p 159	N95-18190 * #
NAS 1.15:106903	p 412	N95-27176 * #	NAS 1.15:110352	p 376	N95-27258 * #	NAS 1.26:194997	p 170	N95-18110 * #
NAS 1.15:106913	p 332	N95-25962 * #	NAS 1.15:110353	p 527	N95-29351 * #	NAS 1.26:195001	p 170	N95-16898 * #
NAS 1.15:106917	p 451	N95-26801 * #	NAS 1.15:110354	p 593	N95-30788 * #	NAS 1.26:195003	p 96	N95-14912 * #
NAS 1.15:106919	p 332	N95-26075 * #	NAS 1.15:110357	p 691	N95-32699 * #	NAS 1.26:195004	p 151	N95-16860 * #
NAS 1.15:106924	p 482	N95-30091 * #	NAS 1.15:110360	p 523	N95-30228 * #	NAS 1.26:195005	p 159	N95-18191 * #
NAS 1.15:106931	p 554	N95-29371 * #	NAS 1.15:110608	p 594	N95-32188 * #	NAS 1.26:195007	p 159	N95-18193 * #
NAS 1.15:106935	p 579	N95-29401 * #	NAS 1.15:110626	p 451	N95-27908 * #	NAS 1.26:195008	p 97	N95-15604 * #
NAS 1.15:106936	p 646	N95-30851 * #	NAS 1.15:110668	p 607	N95-30827 * #	NAS 1.26:195014	p 159	N95-18042 * #
NAS 1.15:106947	p 381	N95-27762 * #	NAS 1.15:110669	p 683	N95-32764 * #	NAS 1.26:195026	p 292	N95-22674 * #
NAS 1.15:106951	p 406	N95-27860 * #	NAS 1.15:110673	p 680	N95-32187 * #	NAS 1.26:195028	p 362	N95-28160 * #
NAS 1.15:106952	p 553	N95-29112 * #	NAS 1.15:110743	p 683	N95-32682 * #	NAS 1.26:195032	p 314	N95-23466 * #
NAS 1.15:106954	p 616	N95-30702 * #	NAS 1.15:14413	p 681	N95-31979 * #	NAS 1.26:195033	p 330	N95-24443 * #
NAS 1.15:106955	p 513	N95-29115 * #	NAS 1.15:4542	p 39	N95-12770 * #	NAS 1.26:195038	p 350	N95-25394 * #
NAS 1.15:106958	p 645	N95-30524 * #	NAS 1.15:4549	p 5	N95-10028 * #	NAS 1.26:195041	p 340	N95-24388 * #
NAS 1.15:106959	p 482	N95-30253 * #	NAS 1.15:4561	p 6	N95-10029 * #	NAS 1.26:195043	p 361	N95-26085 * #
NAS 1.15:106970	p 615	N95-30594 * #	NAS 1.15:4574	p 17	N95-10220 * #	NAS 1.26:195048	p 537	N95-30252 * #
NAS 1.15:106971	p 592	N95-30704 * #	NAS 1.15:4575	p 120	N95-19042 * #	NAS 1.26:195050	p 273	N95-23193 * #
NAS 1.15:106975	p 616	N95-30853 * #	NAS 1.15:4576	p 222	N95-19913 * #	NAS 1.26:195051	p 711	N95-33831 * #
NAS 1.15:106976	p 616	N95-30698 * #	NAS 1.15:4577	p 102	N95-15065 * #	NAS 1.26:195052	p 310	N95-23257 * #
NAS 1.15:106984	p 457							

NAS 1.26:195392-VOL-1	p 258	N95-21888 *	NAS 1.26:197420	p 285	N95-23217 *	NAS 1.26:4642-VOL-1	p 161	N95-18955 *
NAS 1.26:195393	p 101	N95-15743 *	NAS 1.26:197421	p 309	N95-23183 *	NAS 1.26:4642-VOL-2	p 161	N95-18956 *
NAS 1.26:195394	p 100	N95-14610 *	NAS 1.26:197438	p 310	N95-23190 *	NAS 1.26:4645	p 343	N95-24878 *
NAS 1.26:195398	p 76	N95-15852 *	NAS 1.26:197439	p 301	N95-23179 *	NAS 1.26:4649	p 273	N95-22917 *
NAS 1.26:195405	p 76	N95-15912 *	NAS 1.26:197440	p 289	N95-23088 *	NAS 1.26:4650	p 273	N95-23185 *
NAS 1.26:195408	p 161	N95-18938 *	NAS 1.26:197449	p 172	N95-16401 *	NAS 1.26:4651	p 273	N95-23095 *
NAS 1.26:195413	p 156	N95-16588 *	NAS 1.26:197488	p 107	N95-16589 *	NAS 1.26:4652	p 330	N95-24217 *
NAS 1.26:195416	p 210	N95-19567 *	NAS 1.26:197493	p 142	N95-17404 *	NAS 1.26:4653	p 361	N95-24879 *
NAS 1.26:195421	p 323	N95-22675 *	NAS 1.26:197516	p 134	N95-19130 *	NAS 1.26:4654	p 335	N95-24630 *
NAS 1.26:195426	p 202	N95-19769 *	NAS 1.26:197517	p 150	N95-17493 *	NAS 1.26:4660	p 338	N95-24392 *
NAS 1.26:195429	p 197	N95-19651 *	NAS 1.26:197523	p 130	N95-18090 *	NAS 1.26:4665	p 397	N95-28262 *
NAS 1.26:195432	p 447	N95-27970 *	NAS 1.26:197554	p 160	N95-18388 *	NAS 1.26:4671	p 476	N95-28720 *
NAS 1.26:195436	p 366	N95-26363 *	NAS 1.26:197574	p 150	N95-18196 *	NAS 1.26:4672	p 526	N95-29339 *
NAS 1.26:195439	p 627	N95-31653 *	NAS 1.26:197595	p 160	N95-18737 *	NAS 1.26:4675	p 392	N95-27371 *
NAS 1.26:195443	p 338	N95-24304 *	NAS 1.26:197638	p 258	N95-21170 *	NAS 1.26:4677	p 592	N95-30611 *
NAS 1.26:195445	p 289	N95-23222 *	NAS 1.26:197661	p 293	N95-22908 *	NAS 1.26:4679	p 648	N95-31423 *
NAS 1.26:195454	p 275	N95-23462 *	NAS 1.26:197697	p 333	N95-24391 *	NAS 1.26:4682	p 710	N95-33396 *
NAS 1.26:195457	p 616	N95-30779 *	NAS 1.26:197699	p 316	N95-23670 *	NAS 1.55:10108	p 12	N95-10245 *
NAS 1.26:195469	p 406	N95-27866 *	NAS 1.26:197727	p 360	N95-25797 *	NAS 1.55:10139-PT-1	p 10	N95-10566 *
NAS 1.26:195479	p 555	N95-29538 *	NAS 1.26:197744	p 389	N95-26651 *	NAS 1.55:10139-PT-2	p 41	N95-13203 *
NAS 1.26:195882	p 36	N95-11877 *	NAS 1.26:197745	p 390	N95-26813 *	NAS 1.55:10143-VOL-1	p 67	N95-14229 *
NAS 1.26:196049	p 249	N95-21340 *	NAS 1.26:197747	p 374	N95-26760 *	NAS 1.55:10143-VOL-2	p 69	N95-14239 *
NAS 1.26:196059	p 98	N95-13885 *	NAS 1.26:197748	p 373	N95-26649 *	NAS 1.55:10143-VOL-3	p 71	N95-14251 *
NAS 1.26:196111	p 22	N95-10231 *	NAS 1.26:197749	p 406	N95-26777 *	NAS 1.55:10147	p 141	N95-19380 *
NAS 1.26:196126	p 58	N95-12856 *	NAS 1.26:197750	p 411	N95-26775 *	NAS 1.55:10165	p 439	N95-27882 *
NAS 1.26:196192	p 52	N95-12791 *	NAS 1.26:197752	p 448	N95-26648 *	NAS 1.55:10166	p 337	N95-24207 *
NAS 1.26:196313	p 320	N95-23766 *	NAS 1.26:197754	p 389	N95-26591 *	NAS 1.55:10170	p 344	N95-26119 *
NAS 1.26:196316	p 17	N95-11223 *	NAS 1.26:197755	p 374	N95-26735 *	NAS 1.55:3178-VOL-1-PT-1	p 534	N95-29029 *
NAS 1.26:196360	p 36	N95-11884 *	NAS 1.26:197756	p 389	N95-26590 *	NAS 1.55:3178-VOL-1-PT-2	p 531	N95-28823 *
NAS 1.26:196394	p 48	N95-12785 *	NAS 1.26:197757	p 436	N95-26589 *	NAS 1.55:3274-PT-1	p 92	N95-14453 *
NAS 1.26:196395	p 6	N95-10131 *	NAS 1.26:197785	p 445	N95-26669 *	NAS 1.55:3274-PT-2	p 124	N95-19468 *
NAS 1.26:196396	p 9	N95-10940 *	NAS 1.26:197801	p 411	N95-26768 *	NAS 1.55:3279	p 75	N95-14878 *
NAS 1.26:196397	p 28	N95-11192 *	NAS 1.26:197820	p 437	N95-26995 *	NAS 1.55:3299	p 476	N95-28723 *
NAS 1.26:196445	p 24	N95-11252 *	NAS 1.26:197832	p 419	N95-27167 *	NAS 1.60:3451	p 416	N95-27763 *
NAS 1.26:196543	p 168	N95-18093 *	NAS 1.26:197850	p 502	N95-28928 *	NAS 1.60:3403	p 62	N95-12341 *
NAS 1.26:196560	p 300	N95-24032 *	NAS 1.26:197860	p 338	N95-24213 *	NAS 1.60:3414	p 51	N95-12664 *
NAS 1.26:196564	p 363	N95-24439 *	NAS 1.26:197867	p 273	N95-23182 *	NAS 1.60:3416	p 117	N95-18565 *
NAS 1.26:196586	p 415	N95-27093 *	NAS 1.26:197912	p 285	N95-22949 *	NAS 1.60:3437	p 26	N95-10859 *
NAS 1.26:196594	p 392	N95-27143 *	NAS 1.26:197931	p 294	N95-23392 *	NAS 1.60:3440	p 8	N95-10739 *
NAS 1.26:196749	p 9	N95-11366 *	NAS 1.26:197944	p 295	N95-23410 *	NAS 1.60:3446	p 6	N95-10129 *
NAS 1.26:196750	p 10	N95-11367 *	NAS 1.26:198024	p 335	N95-25334 *	NAS 1.60:3447	p 104	N95-16560 *
NAS 1.26:196759	p 61	N95-12832 *	NAS 1.26:198029	p 348	N95-24412 *	NAS 1.60:3448	p 17	N95-10860 *
NAS 1.26:196763	p 48	N95-12787 *	NAS 1.26:198030	p 349	N95-24413 *	NAS 1.60:3447	p 37	N95-11995 *
NAS 1.26:196777	p 10	N95-11582 *	NAS 1.26:198038	p 357	N95-24219 *	NAS 1.60:3454	p 53	N95-13553 *
NAS 1.26:196786	p 98	N95-13725 *	NAS 1.26:198040	p 340	N95-24302 *	NAS 1.60:3455	p 129	N95-17397 *
NAS 1.26:196813	p 43	N95-11699 *	NAS 1.26:198041	p 343	N95-24220 *	NAS 1.60:3460	p 131	N95-18198 *
NAS 1.26:196835	p 36	N95-11766 *	NAS 1.26:198045	p 330	N95-24379 *	NAS 1.60:3465	p 285	N95-22953 *
NAS 1.26:196836	p 52	N95-11938 *	NAS 1.26:198162	p 438	N95-27179 *	NAS 1.60:3466	p 38	N95-12176 *
NAS 1.26:196940	p 58	N95-12228 *	NAS 1.26:198163	p 569	N95-30353 *	NAS 1.60:3467	p 80	N95-14852 *
NAS 1.26:196960	p 38	N95-12389 *	NAS 1.26:198164	p 442	N95-28673 *	NAS 1.60:3468	p 55	N95-12357 *
NAS 1.26:196981	p 58	N95-13201 *	NAS 1.26:198165	p 449	N95-27246 *	NAS 1.60:3478	p 120	N95-19114 *
NAS 1.26:196982	p 53	N95-13200 *	NAS 1.26:198355	p 485	N95-29132 *	NAS 1.60:3480	p 224	N95-21338 *
NAS 1.26:197011	p 67	N95-13701 *	NAS 1.26:198356	p 480	N95-29402 *	NAS 1.60:3487	p 550	N95-28719 *
NAS 1.26:197023	p 74	N95-14614 *	NAS 1.26:198357	p 580	N95-29641 *	NAS 1.60:3496	p 378	N95-28674 *
NAS 1.26:197024	p 74	N95-14613 *	NAS 1.26:198359	p 710	N95-32836 *	NAS 1.60:3501	p 54	N95-11870 *
NAS 1.26:197025	p 74	N95-14612 *	NAS 1.26:198361	p 523	N95-30067 *	NAS 1.60:3502	p 407	N95-28343 *
NAS 1.26:197029	p 80	N95-14794 *	NAS 1.26:198363	p 629	N95-30787 *	NAS 1.60:3509	p 594	N95-31984 *
NAS 1.26:197030	p 127	N95-15971 *	NAS 1.26:198367	p 651	N95-32205 *	NAS 1.60:3515	p 378	N95-28669 *
NAS 1.26:197102	p 75	N95-14803 *	NAS 1.26:198368	p 697	N95-33208 *	NAS 1.60:3516	p 373	N95-26382 *
NAS 1.26:197109	p 129	N95-16899 *	NAS 1.26:198563	p 454	N95-28038 *	NAS 1.60:3524	p 453	N95-26427 *
NAS 1.26:197110	p 81	N95-14909 *	NAS 1.26:198574	p 438	N95-27240 *	NAS 1.60:3526	p 119	N95-19041 *
NAS 1.26:197135	p 76	N95-15762 *	NAS 1.26:198576	p 384	N95-28188 *	NAS 1.60:3527	p 618	N95-31985 *
NAS 1.26:197149	p 45	N95-12626 *	NAS 1.26:198579	p 392	N95-27180 *	NAS 1.60:3537	p 284	N95-22806 *
NAS 1.26:197152	p 46	N95-12628 *	NAS 1.26:198580	p 479	N95-29338 *	NAS 1.61:1347	p 35	N95-11710 *
NAS 1.26:197155	p 45	N95-12609 *	NAS 1.26:198590	p 377	N95-28193 *	NAS 1.61:1355	p 453	N95-27367 *
NAS 1.26:197159	p 46	N95-12637 *	NAS 1.26:198603	p 375	N95-27248 *	NAS 1.61:1359	p 357	N95-24274 *
NAS 1.26:197161	p 45	N95-12530 *	NAS 1.26:198609	p 401	N95-28203 *	NAS 1.71:LAR-15058-1	p 238	N95-20080 *
NAS 1.26:197162	p 45	N95-12305 *	NAS 1.26:198610	p 439	N95-27865 *	NAS 1.71:LAR-15088-1	p 91	N95-14139 *
NAS 1.26:197164	p 44	N95-12294 *	NAS 1.26:198621	p 447	N95-27805 *	NAS 1.71:LAR-15246-1	p 91	N95-14183 *
NAS 1.26:197165	p 46	N95-12638 *	NAS 1.26:198718	p 420	N95-28266 *	NAS 1.71:MFS-28958-1	p 437	N95-26890 *
NAS 1.26:197172	p 49	N95-12993 *	NAS 1.26:198722	p 424	N95-28462 *			
NAS 1.26:197173	p 47	N95-12639 *	NAS 1.26:198723	p 421	N95-28420 *	NAS-CR-196560	p 300	N95-24032 *
NAS 1.26:197176	p 45	N95-12363 *	NAS 1.26:198814	p 557	N95-30224 *			
NAS 1.26:197180	p 81	N95-15742 *	NAS 1.26:198828	p 679	N95-31982 *	NASA-AAV-1387	p 569	N95-30248 *
NAS 1.26:197181	p 47	N95-12643 *	NAS 1.26:198831	p 505	N95-30335 *			
NAS 1.26:197182	p 47	N95-12689 *	NAS 1.26:198858	p 518	N95-30254 *	NASA-ASR-268	p 129	N95-16982 *
NAS 1.26:197183	p 48	N95-12700 *	NAS 1.26:198972	p 594	N95-32193 *			
NAS 1.26:197186	p 47	N95-12645 *	NAS 1.26:198974	p 704	N95-32822 *	NASA-CASE-ARC-11913-1	p 311	N95-23377 *
NAS 1.26:197188	p 46	N95-12636 *	NAS 1.26:199080	p 703	N95-32689 *	NASA-CASE-ARC-11937-1	p 362	N95-26015 *
NAS 1.26:197191	p 79	N95-13703 *	NAS 1.26:199081	p 691	N95-32928 *	NASA-CASE-ARC-11944-1	p 294	N95-23389 *
NAS 1.26:197195	p 47	N95-12695 *	NAS 1.26:288367	p 488	N95-28716 *	NASA-CASE-ARC-11953-1	p 82	N95-14518 *
NAS 1.26:197199	p 48	N95-12702 *	NAS 1.26:4348	p 378	N95-28265 *	NASA-CASE-ARC-11979-1	p 286	N95-23390 *
NAS 1.26:197213	p 172	N95-16848 *	NAS 1.26:4349	p 377	N95-28230 *	NASA-CASE-ARC-11982-1	p 280	N95-23393 *
NAS 1.26:197223	p 97	N95-15785 *	NAS 1.26:4447	p 12	N95-10316 *	NASA-CASE-ARC-11990-1	p 286	N95-23395 *
NAS 1.26:197224	p 97	N95-15728 *	NAS 1.26:4448	p 11	N95-10240 *			
NAS 1.26:197229	p 96	N95-14922 *	NAS 1.26:4449	p 12	N95-10242 *	NASA-CASE-LAR-14745-2-SB	p 85	N95-14415 *
NAS 1.26:197272	p 224	N95-21031 *	NAS 1.26:4485	p 503	N95-29027 *	NASA-CASE-LAR-15058-1	p 238	N95-20080 *
NAS 1.26:197286	p 239	N95-21436 *	NAS 1.26:4496	p 377	N95-28003 *	NASA-CASE-LAR-15088-1	p 91	N95-14139 *
NAS 1.26:197288	p 707	N95-32823 *	NAS 1.26:4530	p 57	N95-11888 *	NASA-CASE-LAR-15246-1	p 91	N95-14183 *
NAS 1.26:197290	p 229	N95-22161 *	NAS 1.26:4597	p 48	N95-12831 *			
NAS 1.26:197318	p 224	N95-21343 *	NAS 1.26:4620	p 151	N95-16859 *	NASA-CASE-LEW-15170-2	p 362	N95-26187 *
NAS 1.26:197320	p 204	N95-19576 *	NAS 1.26:4623	p 37	N95-11911 *			
NAS 1.26:197383	p 309	N95-22481 *	NAS 1.26:4627	p 44	N95-11952 *	NASA-CASE-MFS-28697-1	p 159	N95-183

NASA-CASE-MSC-22327-1	p 350	N95-25592 *	NASA-CR-195421	p 323	N95-22675 #	NASA-CR-197517	p 150	N95-17493 #
NASA-CASE-NPO-18733-1-CU	p 288	N95-22578 *	NASA-CR-195426	p 202	N95-19769 #	NASA-CR-197523	p 130	N95-18090 #
NASA-CP-10108	p 12	N95-10245 #	NASA-CR-195429	p 197	N95-19651 #	NASA-CR-197554	p 160	N95-18388 #
NASA-CP-10139-PT-1	p 10	N95-10566 #	NASA-CR-195432	p 147	N95-27970 #	NASA-CR-197574	p 150	N95-18196 #
NASA-CP-10139-PT-2	p 41	N95-13203 #	NASA-CR-195436	p 366	N95-26363 #	NASA-CR-197595	p 160	N95-18737 #
NASA-CP-10143-VOL-1	p 67	N95-14229 #	NASA-CR-195439	p 627	N95-31653 #	NASA-CR-197638	p 258	N95-21170 #
NASA-CP-10143-VOL-2	p 69	N95-14239 #	NASA-CR-195443	p 338	N95-24304 #	NASA-CR-197661	p 293	N95-22908 #
NASA-CP-10143-VOL-3	p 71	N95-14251 #	NASA-CR-195445	p 289	N95-23222 #	NASA-CR-197697	p 333	N95-24391 #
NASA-CP-10147	p 141	N95-19380 #	NASA-CR-195454	p 275	N95-23462 #	NASA-CR-197699	p 316	N95-23670 #
NASA-CP-10165	p 439	N95-27882 #	NASA-CR-195457	p 616	N95-30779 #	NASA-CR-197727	p 360	N95-25797 #
NASA-CP-10166	p 337	N95-24207 #	NASA-CR-195469	p 406	N95-27866 #	NASA-CR-197744	p 389	N95-26651 #
NASA-CP-10170	p 344	N95-26119 #	NASA-CR-195479	p 555	N95-29538 #	NASA-CR-197745	p 390	N95-26813 #
NASA-CP-3178-VOL-1-PT-1	p 534	N95-29029 #	NASA-CR-195882	p 36	N95-11877 #	NASA-CR-197747	p 374	N95-26760 #
NASA-CP-3178-VOL-1-PT-2	p 531	N95-28823 #	NASA-CR-196049	p 249	N95-21340 #	NASA-CR-197748	p 373	N95-26649 #
NASA-CP-3274-PT-1	p 92	N95-14453 #	NASA-CR-196059	p 98	N95-13885 #	NASA-CR-197749	p 406	N95-26777 #
NASA-CP-3274-PT-2	p 124	N95-19468 #	NASA-CR-196111	p 22	N95-10231 #	NASA-CR-197750	p 411	N95-26775 #
NASA-CP-3279	p 75	N95-14878 #	NASA-CR-196126	p 58	N95-12856 #	NASA-CR-197752	p 448	N95-26648 #
NASA-CP-3291	p 476	N95-28723 #	NASA-CR-196192	p 52	N95-12791 #	NASA-CR-197754	p 389	N95-26591 #
NASA-CP-3299	p 416	N95-27763 #	NASA-CR-196313	p 320	N95-23766 #	NASA-CR-197755	p 374	N95-26735 #
NASA-CR-182276	p 105	N95-18044 #	NASA-CR-196316	p 17	N95-11223 #	NASA-CR-197756	p 389	N95-26590 #
NASA-CR-186030	p 13	N95-11410 #	NASA-CR-196360	p 36	N95-11884 #	NASA-CR-197757	p 436	N95-26589 #
NASA-CR-186031	p 157	N95-17418 #	NASA-CR-196394	p 48	N95-12785 #	NASA-CR-197785	p 445	N95-26669 #
NASA-CR-188330	p 49	N95-11913 #	NASA-CR-196395	p 6	N95-10131 #	NASA-CR-197801	p 411	N95-26768 #
NASA-CR-188343	p 54	N95-11937 #	NASA-CR-196396	p 9	N95-10940 #	NASA-CR-197820	p 437	N95-26995 #
NASA-CR-188360	p 143	N95-18567 #	NASA-CR-196397	p 28	N95-11192 #	NASA-CR-197832	p 419	N95-27167 #
NASA-CR-188367	p 488	N95-28716 #	NASA-CR-196445	p 24	N95-11252 #	NASA-CR-197850	p 502	N95-28928 #
NASA-CR-188370	p 527	N95-29447 #	NASA-CR-196543	p 168	N95-18093 #	NASA-CR-197860	p 338	N95-24213 #
NASA-CR-189077	p 441	N95-27999 #	NASA-CR-196564	p 363	N95-24439 #	NASA-CR-197867	p 273	N95-23182 #
NASA-CR-189099	p 290	N95-24053 #	NASA-CR-196586	p 415	N95-27093 #	NASA-CR-197912	p 285	N95-22949 #
NASA-CR-189141	p 316	N95-23792 #	NASA-CR-196694	p 392	N95-27143 #	NASA-CR-197931	p 294	N95-23392 #
NASA-CR-189146	p 316	N95-24189 #	NASA-CR-196749	p 9	N95-11366 #	NASA-CR-197944	p 295	N95-23410 #
NASA-CR-189201	p 337	N95-24624 #	NASA-CR-196750	p 10	N95-11367 #	NASA-CR-198024	p 335	N95-25334 #
NASA-CR-189206	p 15	N95-10247 #	NASA-CR-196759	p 61	N95-12832 #	NASA-CR-198029	p 348	N95-24412 #
NASA-CR-189412	p 567	N95-28807 #	NASA-CR-196763	p 48	N95-12787 #	NASA-CR-198030	p 349	N95-24413 #
NASA-CR-189657	p 23	N95-10318 #	NASA-CR-196777	p 10	N95-11582 #	NASA-CR-198038	p 357	N95-24219 #
NASA-CR-189659	p 15	N95-10319 #	NASA-CR-196786	p 98	N95-13725 #	NASA-CR-198040	p 340	N95-24302 #
NASA-CR-189677	p 452	N95-28264 #	NASA-CR-196813	p 43	N95-11699 #	NASA-CR-198041	p 343	N95-24220 #
NASA-CR-189705-VOL-2	p 452	N95-28073 #	NASA-CR-196835	p 36	N95-11766 #	NASA-CR-198045	p 330	N95-24379 #
NASA-CR-189714	p 406	N95-28227 #	NASA-CR-196836	p 52	N95-11938 #	NASA-CR-198162	p 438	N95-27179 #
NASA-CR-191045	p 150	N95-18743 #	NASA-CR-196940	p 58	N95-12228 #	NASA-CR-198163	p 569	N95-30353 #
NASA-CR-191177	p 57	N95-11996 #	NASA-CR-196960	p 38	N95-12389 #	NASA-CR-198164	p 442	N95-28673 #
NASA-CR-191178	p 108	N95-16887 #	NASA-CR-196961	p 58	N95-13201 #	NASA-CR-198165	p 449	N95-27246 #
NASA-CR-191194	p 162	N95-19236 #	NASA-CR-196982	p 53	N95-13200 #	NASA-CR-198355	p 485	N95-29132 #
NASA-CR-191441	p 630	N95-31421 #	NASA-CR-197011	p 67	N95-13701 #	NASA-CR-198356	p 480	N95-29402 #
NASA-CR-193993	p 49	N95-13027 #	NASA-CR-197023	p 74	N95-14614 #	NASA-CR-198357	p 580	N95-29641 #
NASA-CR-194215	p 101	N95-13717 #	NASA-CR-197024	p 74	N95-14613 #	NASA-CR-198359	p 710	N95-32836 #
NASA-CR-194893	p 51	N95-11869 #	NASA-CR-197025	p 74	N95-14612 #	NASA-CR-198361	p 523	N95-30067 #
NASA-CR-194931	p 27	N95-11593 #	NASA-CR-197029	p 80	N95-14794 #	NASA-CR-198363	p 629	N95-30787 #
NASA-CR-194934	p 57	N95-11812 #	NASA-CR-197030	p 127	N95-15971 #	NASA-CR-198367	p 651	N95-32205 #
NASA-CR-194942	p 61	N95-11932 #	NASA-CR-197102	p 75	N95-14803 #	NASA-CR-198368	p 697	N95-33208 #
NASA-CR-194943	p 8	N95-10848 #	NASA-CR-197109	p 129	N95-16899 #	NASA-CR-198563	p 454	N95-28038 #
NASA-CR-194944	p 159	N95-18190 #	NASA-CR-197110	p 81	N95-14909 #	NASA-CR-198574	p 438	N95-27240 #
NASA-CR-194947	p 170	N95-18110 #	NASA-CR-197135	p 76	N95-15762 #	NASA-CR-198576	p 384	N95-28188 #
NASA-CR-195001	p 170	N95-16898 #	NASA-CR-197149	p 45	N95-12626 #	NASA-CR-198579	p 392	N95-27180 #
NASA-CR-195003	p 96	N95-14912 #	NASA-CR-197152	p 46	N95-12628 #	NASA-CR-198580	p 479	N95-29338 #
NASA-CR-195004	p 151	N95-16860 #	NASA-CR-197155	p 45	N95-12609 #	NASA-CR-198590	p 377	N95-28193 #
NASA-CR-195005	p 159	N95-18191 #	NASA-CR-197159	p 46	N95-12637 #	NASA-CR-198603	p 375	N95-27248 #
NASA-CR-195007	p 159	N95-18193 #	NASA-CR-197161	p 45	N95-12530 #	NASA-CR-198609	p 401	N95-28203 #
NASA-CR-195008	p 97	N95-15604 #	NASA-CR-197162	p 45	N95-12305 #	NASA-CR-198610	p 439	N95-27865 #
NASA-CR-195014	p 159	N95-18042 #	NASA-CR-197164	p 44	N95-12294 #	NASA-CR-198621	p 447	N95-27805 #
NASA-CR-195026	p 292	N95-22674 #	NASA-CR-197165	p 46	N95-12638 #	NASA-CR-198718	p 420	N95-28266 #
NASA-CR-195028	p 362	N95-26160 #	NASA-CR-197172	p 49	N95-12993 #	NASA-CR-198719	p 424	N95-28462 #
NASA-CR-195032	p 314	N95-23466 #	NASA-CR-197173	p 47	N95-12639 #	NASA-CR-198723	p 421	N95-28420 #
NASA-CR-195033	p 330	N95-24443 #	NASA-CR-197176	p 45	N95-12363 #	NASA-CR-198724	p 421	N95-28420 #
NASA-CR-195038	p 350	N95-25394 #	NASA-CR-197177	p 45	N95-12363 #	NASA-CR-198814	p 557	N95-30224 #
NASA-CR-195041	p 340	N95-24388 #	NASA-CR-197180	p 81	N95-15742 #	NASA-CR-198828	p 679	N95-31982 #
NASA-CR-195043	p 361	N95-26085 #	NASA-CR-197181	p 47	N95-12643 #	NASA-CR-198831	p 505	N95-30335 #
NASA-CR-195048	p 537	N95-30252 #	NASA-CR-197182	p 47	N95-12689 #	NASA-CR-198958	p 518	N95-30254 #
NASA-CR-195050	p 273	N95-23193 #	NASA-CR-197183	p 48	N95-12700 #	NASA-CR-198972	p 594	N95-32193 #
NASA-CR-195051	p 711	N95-33831 #	NASA-CR-197186	p 47	N95-12645 #	NASA-CR-198974	p 704	N95-32822 #
NASA-CR-195052	p 310	N95-23257 #	NASA-CR-197188	p 46	N95-12636 #	NASA-CR-199080	p 703	N95-32689 #
NASA-CR-195067	p 334	N95-25341 #	NASA-CR-197191	p 79	N95-13703 #	NASA-CR-199081	p 691	N95-32928 #
NASA-CR-195077	p 452	N95-28670 #	NASA-CR-197195	p 47	N95-12695 #	NASA-CR-4348	p 378	N95-28265 #
NASA-CR-195312	p 154	N95-16072 #	NASA-CR-197199	p 48	N95-12702 #	NASA-CR-4349	p 377	N95-28230 #
NASA-CR-195355	p 23	N95-10132 #	NASA-CR-197213	p 172	N95-16848 #	NASA-CR-4447	p 12	N95-10316 #
NASA-CR-195358	p 18	N95-11487 #	NASA-CR-197223	p 97	N95-15785 #	NASA-CR-4448	p 11	N95-10240 #
NASA-CR-195359	p 50	N95-11901 #	NASA-CR-197224	p 97	N95-15728 #	NASA-CR-4449	p 12	N95-10242 #
NASA-CR-195360	p 50	N95-11951 #	NASA-CR-197229	p 96	N95-14922 #	NASA-CR-4485	p 503	N95-29027 #
NASA-CR-195370	p 8	N95-10853 #	NASA-CR-197272	p 224	N95-21031 #	NASA-CR-4496	p 377	N95-28003 #
NASA-CR-195378	p 57	N95-11711 #	NASA-CR-197286	p 239	N95-21436 #	NASA-CR-4530	p 57	N95-11888 #
NASA-CR-195390	p 138	N95-17402 #	NASA-CR-197288	p 707	N95-32823 #	NASA-CR-4597	p 48	N95-12831 #
NASA-CR-195392-VOL-1	p 258	N95-21888 #	NASA-CR-197290	p 229	N95-22161 #	NASA-CR-4620	p 151	N95-16859 #
NASA-CR-195393	p 101	N95-15743 #	NASA-CR-197318	p 224	N95-21343 #	NASA-CR-4623	p 37	N95-11911 #
NASA-CR-195394	p 100	N95-14610 #	NASA-CR-197320	p 204	N95-19576 #	NASA-CR-4627	p 44	N95-11952 #
NASA-CR-195398	p 76	N95-15852 #	NASA-CR-197383	p 309	N95-22481 #	NASA-CR-4631	p 228	N95-19950 #
NASA-CR-195405	p 76	N95-15912 #	NASA-CR-197409	p 229	N95-21891 #	NASA-CR-4633	p 244	N95-19912 #
NASA-CR-195408	p 161	N95-18938 #	NASA-CR-197412	p 349	N95-24461 #	NASA-CR-4635	p 108	N95-17273 #
NASA-CR-195413	p 156	N95-16588 #	NASA-CR-197419	p 274	N95-23218 #	NASA-CR-4642-VOL-1	p 161	N95-18955 #
NASA-CR-195416	p 210	N95-19567 #	NASA-CR-197420	p 285	N95-23217 #	NASA-CR-4642-VOL-2	p 161	N95-18956 #
			NASA-CR-197421	p 309	N95-23183 #		p 343	N95-24878 #
			NASA-CR-197438	p 310	N95-23190 #		p 273	N95-22917 #
			NASA-CR-197439	p 301	N95-23179 #		p 273	N95-23185 #
			NASA-CR-197440	p 289	N95-23088 #		p 273	N95-23095 #
			NASA-CR-197449	p 172	N95-16401 #		p 330	N95-24217 #
			NASA-CR-197488	p 107	N95-16589 #		p 361	N95-24879 #
			NASA-CR-197493	p 142	N95-17404 #		p 335	N95-24630 #
			NASA-CR-197516	p 134	N95-19130 #		p 338	N95-24392 #

NASA-CR-4665	p 397	N95-28262	#	NASA-TM-106805	p 105	N95-18197	#	NASA-TM-109177	p 320	N95-23009	#
NASA-CR-4671	p 476	N95-28720	#	NASA-TM-106808	p 148	N95-19286	#	NASA-TM-109179	p 330	N95-24397	#
NASA-CR-4672	p 526	N95-29339	#	NASA-TM-106814	p 438	N95-27854	#	NASA-TM-109181	p 348	N95-24396	#
NASA-CR-4675	p 392	N95-27371	#	NASA-TM-106817	p 145	N95-18054	#	NASA-TM-109182	p 296	N95-23011	#
NASA-CR-4677	p 592	N95-30611	#	NASA-TM-106822	p 162	N95-19125	#	NASA-TM-109184	p 449	N95-27241	#
NASA-CR-4679	p 648	N95-31423	#	NASA-TM-106824	p 223	N95-20794	#	NASA-TM-109869	p 10	N95-10548	#
NASA-CR-4682	p 710	N95-33396	#	NASA-TM-106826	p 124	N95-19285	#	NASA-TM-109891	p 20	N95-10547	#
				NASA-TM-106827	p 124	N95-19284	#	NASA-TM-109902	p 20	N95-10552	#
NASA-NEWS-RELEASE-94-47	p 144	N95-19029	*	NASA-TM-106831	p 123	N95-18582	#	NASA-TM-109904	p 22	N95-10553	#
				NASA-TM-106833	p 119	N95-18933	#	NASA-TM-109907	p 7	N95-10556	#
NASA-RP-1347	p 35	N95-11710	#	NASA-TM-106840	p 211	N95-19794	#	NASA-TM-109948	p 157	N95-16828	#
NASA-RP-1355	p 453	N95-27367	#	NASA-TM-106846	p 244	N95-19953	#	NASA-TM-109950	p 1	N95-11463	#
NASA-RP-1359	p 357	N95-24274	#	NASA-TM-106847	p 293	N95-22954	#	NASA-TM-109984	p 97	N95-15899	#
				NASA-TM-106849	p 309	N95-22669	#	NASA-TM-110098	p 157	N95-16828	#
NASA-SP-290-Vol-1-3	p 236	N95-22341	#	NASA-TM-106854	p 236	N95-21383	#	NASA-TM-110103	p 231	N95-20370	#
NASA-SP-514	p 584	N95-31000	#	NASA-TM-106855	p 338	N95-24390	#	NASA-TM-110113	p 129	N95-16982	#
NASA-SP-7037(315)	p 219	N95-21640	#	NASA-TM-106870	p 320	N95-23259	#	NASA-TM-110117	p 126	N95-18347	#
NASA-SP-7037(316)	p 328	N95-24465	#	NASA-TM-106872	p 323	N95-23178	#	NASA-TM-110142	p 381	N95-27859	#
NASA-SP-7037(317)	p 328	N95-25798	#	NASA-TM-106875	p 438	N95-27855	#	NASA-TM-110146	p 554	N95-29453	#
NASA-SP-7037(318)	p 367	N95-27543	#	NASA-TM-106885	p 295	N95-23671	#	NASA-TM-110150	p 568	N95-29454	#
NASA-SP-7109(01)	p 363	N95-24238	#	NASA-TM-106886	p 407	N95-28344	#	NASA-TM-110161	p 580	N95-29439	#
				NASA-TM-106890	p 289	N95-23550	#	NASA-TM-110163	p 410	N95-29452	#
NASA-TM-103855	p 66	N95-14419	#	NASA-TM-106903	p 412	N95-27176	#	NASA-TM-110166	p 518	N95-30327	#
NASA-TM-104268	p 8	N95-10858	#	NASA-TM-106913	p 332	N95-25962	#	NASA-TM-110168	p 501	N95-28820	#
NASA-TM-104276	p 36	N95-11898	#	NASA-TM-106917	p 451	N95-26801	#	NASA-TM-110175	p 645	N95-30682	#
NASA-TM-104277	p 51	N95-11868	#	NASA-TM-106919	p 332	N95-26075	#	NASA-TM-110182	p 646	N95-30783	#
NASA-TM-104278	p 694	N95-33009	#	NASA-TM-106924	p 482	N95-30091	#	NASA-TM-110346	p 335	N95-24629	#
NASA-TM-104279	p 11	N95-10737	#	NASA-TM-106931	p 482	N95-30091	#	NASA-TM-110347	p 332	N95-26302	#
NASA-TM-104280	p 21	N95-10738	#	NASA-TM-106935	p 554	N95-29371	#	NASA-TM-110348	p 383	N95-26587	#
NASA-TM-104281	p 1	N95-10709	#	NASA-TM-106936	p 579	N95-29401	#	NASA-TM-110349	p 409	N95-26773	#
NASA-TM-104282	p 21	N95-10710	#	NASA-TM-106947	p 646	N95-30851	#	NASA-TM-110351	p 457	N95-28816	#
NASA-TM-104283	p 13	N95-10711	#	NASA-TM-106951	p 381	N95-27762	#	NASA-TM-110352	p 376	N95-27258	#
NASA-TM-104288	p 21	N95-10714	#	NASA-TM-106952	p 406	N95-27860	#	NASA-TM-110353	p 527	N95-29351	#
NASA-TM-104289	p 13	N95-10715	#	NASA-TM-106955	p 553	N95-29112	#	NASA-TM-110354	p 593	N95-30788	#
NASA-TM-104290	p 13	N95-10716	#	NASA-TM-106958	p 616	N95-30702	#	NASA-TM-110356	p 691	N95-32699	#
NASA-TM-104292	p 17	N95-10717	#	NASA-TM-106959	p 513	N95-29115	#	NASA-TM-110357	p 523	N95-30228	#
NASA-TM-104295	p 13	N95-10740	#	NASA-TM-106970	p 645	N95-30524	#	NASA-TM-110360	p 594	N95-32188	#
NASA-TM-104296	p 13	N95-10741	#	NASA-TM-106971	p 482	N95-30253	#	NASA-TM-110502	p 230	N95-19994	#
NASA-TM-104297	p 13	N95-10742	#	NASA-TM-106972	p 615	N95-30594	#	NASA-TM-110504	p 230	N95-20155	#
NASA-TM-104298	p 13	N95-10743	#	NASA-TM-106976	p 592	N95-30704	#	NASA-TM-110505	p 223	N95-19996	#
NASA-TM-104299	p 13	N95-10744	#	NASA-TM-106984	p 616	N95-30853	#	NASA-TM-110608	p 451	N95-27908	#
NASA-TM-104300	p 13	N95-10745	#	NASA-TM-106987	p 616	N95-30698	#	NASA-TM-110626	p 607	N95-30827	#
NASA-TM-104301	p 21	N95-10746	#	NASA-TM-106989	p 457	N95-30229	#	NASA-TM-110648	p 569	N95-30248	#
NASA-TM-104302	p 21	N95-10747	#	NASA-TM-106997	p 615	N95-30617	#	NASA-TM-110668	p 683	N95-32764	#
NASA-TM-104303	p 17	N95-10748	#	NASA-TM-106998	p 615	N95-30517	#	NASA-TM-110669	p 680	N95-32187	#
NASA-TM-104304	p 1	N95-10749	#	NASA-TM-106999	p 514	N95-30007	#	NASA-TM-110673	p 683	N95-32682	#
NASA-TM-104305	p 33	N95-10750	#	NASA-TM-107000	p 616	N95-30632	#	NASA-TM-110674	p 681	N95-31979	#
NASA-TM-104306	p 13	N95-10751	#	NASA-TM-107002	p 615	N95-30589	#	NASA-TM-110743	p 389	N95-12770	#
NASA-TM-104806-VOL-1	p 151	N95-19237	#	NASA-TM-107003	p 617	N95-30861	#	NASA-TM-4413	p 61	N95-12770	#
NASA-TM-104806-VOL-2	p 205	N95-19624	#	NASA-TM-107006	p 694	N95-32916	#	NASA-TM-4542	p 5	N95-10028	#
NASA-TM-105798	p 23	N95-10244	#	NASA-TM-107014	p 645	N95-30587	#	NASA-TM-4549	p 6	N95-10029	#
NASA-TM-106385	p 73	N95-14418	#	NASA-TM-107020	p 705	N95-32930	#	NASA-TM-4561	p 17	N95-10220	#
NASA-TM-106458	p 38	N95-12378	#	NASA-TM-107023	p 684	N95-32769	#	NASA-TM-4574	p 120	N95-19042	#
NASA-TM-106502	p 22	N95-11483	#	NASA-TM-107024	p 694	N95-32931	#	NASA-TM-4574	p 222	N95-19913	#
NASA-TM-106569	p 21	N95-10822	#	NASA-TM-107025	p 50	N95-12860	#	NASA-TM-4575	p 102	N95-15065	#
NASA-TM-106571	p 152	N95-16905	#	NASA-TM-107026	p 59	N95-13235	#	NASA-TM-4576	p 54	N95-13196	#
NASA-TM-106579	p 39	N95-13058	#	NASA-TM-107027	p 9	N95-11157	#	NASA-TM-4577	p 249	N95-21258	#
NASA-TM-106580	p 105	N95-16038	#	NASA-TM-107028	p 592	N95-30712	#	NASA-TM-4582	p 106	N95-16069	#
NASA-TM-106589	p 20	N95-10446	#	NASA-TM-107029	p 441	N95-28364	#	NASA-TM-4583	p 272	N95-22802	#
NASA-TM-106632	p 157	N95-16911	#	NASA-TM-107030	p 453	N95-28002	#	NASA-TM-4588	p 125	N95-17384	#
NASA-TM-106637	p 8	N95-10820	#	NASA-TM-107031	p 44	N95-12225	#	NASA-TM-4596	p 108	N95-16858	#
NASA-TM-106649	p 80	N95-14604	#	NASA-TM-107032	p 95	N95-14617	#	NASA-TM-4597	p 9	N95-11158	#
NASA-TM-106669	p 339	N95-24561	#	NASA-TM-107033	p 8	N95-10847	#	NASA-TM-4601	p 108	N95-16908	#
NASA-TM-106671	p 7	N95-10148	#	NASA-TM-107034	p 11	N95-10846	#	NASA-TM-4602	p 309	N95-23015	#
NASA-TM-106674	p 15	N95-10153	#	NASA-TM-107035	p 38	N95-12360	#	NASA-TM-4603	p 310	N95-23210	#
NASA-TM-106676	p 626	N95-30592	#	NASA-TM-107036	p 11	N95-10846	#	NASA-TM-4604	p 38	N95-12191	#
NASA-TM-106683	p 24	N95-10854	#	NASA-TM-107037	p 37	N95-11927	#	NASA-TM-4605	p 10	N95-11408	#
NASA-TM-106685	p 416	N95-27434	#	NASA-TM-107038	p 25	N95-11389	#	NASA-TM-4606	p 331	N95-25338	#
NASA-TM-106686	p 25	N95-11409	#	NASA-TM-107039	p 35	N95-12227	#	NASA-TM-4610	p 378	N95-28241	#
NASA-TM-106689	p 58	N95-12843	#	NASA-TM-107040	p 65	N95-13642	#	NASA-TM-4611	p 449	N95-27914	#
NASA-TM-106697	p 50	N95-11867	#	NASA-TM-107041	p 116	N95-18101	#	NASA-TM-4632	p 120	N95-19119	#
NASA-TM-106710	p 37	N95-11917	#	NASA-TM-107042	p 65	N95-13662	#	NASA-TM-4634	p 330	N95-24566	#
NASA-TM-106711	p 649	N95-31738	#	NASA-TM-107043	p 65	N95-13891	#	NASA-TM-4635	p 296	N95-23192	#
NASA-TM-106715	p 651	N95-32206	#	NASA-TM-107044	p 66	N95-14921	#	NASA-TM-4637	p 63	N95-12190	#
NASA-TM-106719	p 16	N95-11005	#	NASA-TM-107045	p 272	N95-22666	#	NASA-TM-4638	p 274	N95-23250	#
NASA-TM-106723	p 49	N95-11864	#	NASA-TM-107046	p 232	N95-21186	#	NASA-TM-4640	p 505	N95-30226	#
NASA-TM-106724	p 50	N95-11890	#	NASA-TM-107047	p 367	N95-26710	#	NASA-TM-4641	p 250	N95-22109	#
NASA-TM-106729	p 16	N95-11159	#	NASA-TM-107048	p 249	N95-21323	#	NASA-TM-4644	p 158	N95-17490	#
NASA-TM-106736	p 139	N95-18133	#	NASA-TM-107049	p 405	N95-26412	#	NASA-TM-4646	p 134	N95-19044	#
NASA-TM-106738	p 100	N95-14618	#	NASA-TM-107050	p 606	N95-30646	#	NASA-TM-4651	p 89	N95-13892	#
NASA-TM-106741	p 51	N95-12763	#	NASA-TM-107051	p 21	N95-11466	#	NASA-TM-4653	p 176	N95-18573	#
NASA-TM-106742	p 91	N95-14299	#	NASA-TM-107052	p 13	N95-11465	#	NASA-TM-4660	p 684	N95-32821	#
NASA-TM-106747	p 39	N95-13197	#	NASA-TM-107053	p 33	N95-10873	#	NASA-TM-4661	p 309	N95-22804	#
NASA-TM-106755	p 146	N95-18586	#	NASA-TM-107054	p 88	N95-14920	#	NASA-TM-4664	p 627	N95-32217	#
NASA-TM-106757	p 89	N95-13665	#	NASA-TM-107055	p 22	N95-11003	#	NASA-TM-4665	p 288	N95-24030	#
NASA-TM-106764	p 262	N95-24025	#	NASA-TM-107056	p 55	N95-11915	#	NASA-TM-4676	p 284	N95-22829	#
NASA-TM-106774	p 76	N95-15853	#	NASA-TM-107057	p 57	N9					

NASA-TP-3451	p 62	N95-12341 *	#	NONP-NASA-VT-94-23646	p 21	N95-10746 *	PB94-204435	p 59	N95-13249
NASA-TP-3454	p 53	N95-13553 *	#	NONP-NASA-VT-94-23647	p 21	N95-10747 *	PB94-204450	p 40	N95-13250
NASA-TP-3455	p 129	N95-17397 *	#	NONP-NASA-VT-94-23648	p 17	N95-10748 *	PB94-207065	p 62	N95-13575
NASA-TP-3460	p 131	N95-18198 *	#	NONP-NASA-VT-94-23649	p 1	N95-10749 *	PB94-207610	p 216	N95-19582 #
NASA-TP-3465	p 285	N95-22953 *	#	NONP-NASA-VT-94-23650	p 33	N95-10750 *	PB94-210051	p 244	N95-20191 #
NASA-TP-3466	p 38	N95-12176 *	#	NONP-NASA-VT-94-23651	p 13	N95-10751 *	PB94-217445	p 188	N95-19720 #
NASA-TP-3467	p 80	N95-14852 *	#	NONP-NASA-VT-95-35013	p 129	N95-16982 *	PB94-217478	p 219	N95-19967 #
NASA-TP-3468	p 55	N95-12357 *	#	NONP-NASA-VT-95-37002	p 126	N95-18347 *	PB94-910408	p 78	N95-14916 #
NASA-TP-3478	p 120	N95-19114 *	#	NONP-NASA-VT-95-41114	p 230	N95-19994 *	PB94-910409	p 123	N95-17646 #
NASA-TP-3480	p 224	N95-21338 *	#	NONP-NASA-VT-95-41116	p 230	N95-20155 *	PB94-910410	p 333	N95-24206 #
NASA-TP-3487	p 550	N95-28719 *	#	NONP-NASA-VT-95-41117	p 223	N95-19996 *	PB94-917004	p 124	N95-19132 #
NASA-TP-3496	p 378	N95-28674 *	#	NONP-NASA-VT-95-49121	p 452	N95-27209 *	PB94-917005	p 278	N95-24105 #
NASA-TP-3501	p 54	N95-11870 *	#	NONP-NASA-VT-95-57872	p 569	N95-30248 *	PB94-917006	p 188	N95-19793 #
NASA-TP-3502	p 407	N95-28343 *	#				PB94-917007	p 277	N95-23598 #
NASA-TP-3509	p 594	N95-31984 *	#	NPL-RSA(EXT)0048	p 232	N95-21425	PB95-100319	p 78	N95-15066 #
NASA-TP-3515	p 378	N95-28669 *	#				PB95-100319	p 123	N95-17748 #
NASA-TP-3516	p 373	N95-26382 *	#	NREC-1762	p 338	N95-24293	PB95-104238	p 139	N95-17749 #
NASA-TP-3524	p 453	N95-26427 *	#				PB95-110805	p 229	N95-21369 #
NASA-TP-3526	p 119	N95-19041 *	#	NREL/TP-440-7224	p 358	N95-26090 #	PB95-130423	p 232	N95-21425 #
NASA-TP-3527	p 618	N95-31985 *	#	NREL/TP-441-6913	p 564	N95-30016 #	PB95-131348	p 248	N95-21132 #
NASA-TP-3537	p 284	N95-22806 *	#	NREL/TP-441-7077	p 357	N95-24853 #	PB95-136032	p 324	N95-23168 #
NATICK/TR-95/017	p 381	N95-28454		NREL/TP-441-7078	p 157	N95-16939 #	PB95-139184	p 285	N95-23161 #
NAVY-CASE-74885	p 160	N95-18461 #		NREL/TP-441-7080	p 216	N95-19855 #	PB95-141834	p 380	N95-25894 #
NAWCAD-SA80	p 132	N95-18407		NREL/TP-441-7107	p 118	N95-18645 #	PB95-143053	p 328	N95-25401 #
NAWCADPAX-95-10-RTR	p 288	N95-24030 *	#	NREL/TP-441-7108	p 118	N95-18646 #	PB95-147542	p 338	N95-24293 #
NAWCADTRN-PE-261	p 139	N95-18383		NREL/TP-441-7805	p 683	N95-32548 #	PB95-149381	p 328	N95-24295 #
NAWCADWAR-93082-60	p 129	N95-17631 #		NREL/TP-442-4740	p 256	N95-20985 #	PB95-164927	p 340	N95-24260 #
NAWCADWAR-94001-60	p 242	N95-22132 #		NREL/TP-442-7109	p 357	N95-24882 #	PB95-165791	p 350	N95-25749 #
NAWCADWAR-95012-4.3	p 502	N95-28977 #		NREL/TP-442-7226	p 446	N95-27459 #	PB95-166146	p 343	N95-26004 #
NAWCADWAR-95014-43	p 629	N95-31124 #		NREL/TP-442-7388	p 376	N95-27541 #	PB95-166237	p 358	N95-26005 #
NDU-ICAF-94-F2	p 366	N95-26409		NREL/TP-442-7393	p 707	N95-32685 #	PB95-178729	p 336	N95-26009 #
NDU-ICAF-94-F56	p 366	N95-26455		NRL/FR/5550-94-9743	p 435	N95-26349	PB95-192415	p 400	N95-28636 #
NEAR-TR-482	p 620	N95-31400					PB95-196408	p 645	N95-30521 #
NFESC-TR-2019-ENV	p 52	N95-11789		NRL/MR/5710-94-7485	p 188	N95-19863	PB95-198024	p 593	N95-30837 #
NIAR-94-11	p 277	N95-24012 #		NRL/MR/6180-94-7624	p 225	N95-20071 #	PB95-198040	p 607	N95-30838 #
NIAR-94-12	p 348	N95-24211 #		NRL/MR/7543-94-7218	p 598	N95-31454 #	PB95-198081	p 593	N95-30814 #
NIAR-94-14	p 24	N95-11168 #		NSWCDD/TR-93/169	p 257	N95-20963	PB95-198123	p 601	N95-30815 #
NIAR-94-1	p 367	N95-26941 #		NSWCDD/TR-93/339	p 82	N95-15392	PB95-206447	p 677	N95-31157 #
NIAR-94-3	p 277	N95-24050 #		NSWCDD/TR-94/217	p 450	N95-28335	PB95-206454	p 564	N95-30200 #
NIST/SP-861	p 42	N95-13247		NSWCDD/TR-94/379	p 481	N95-29853 #	PB95-206991	p 647	N95-30956 #
NISTIR-5023	p 244	N95-20191 #		NSWCDD/TR-94/96	p 594	N95-30929 #	PB95-207015	p 647	N95-30957 #
NISTIR-5412	p 58	N95-12854 #		NTSB/AAR-94/06	p 78	N95-14916 #	PB95-211355	p 601	N95-30597 #
NISTIR-5441	p 77	N95-14179 #		NTSB/AAR-94/07	p 123	N95-17646 #	PB95-212031	p 644	N95-30502 #
NLR-CR-93570L	p 593	N95-30885 #		NTSB/AAR-94/08	p 333	N95-24206 #	PB95-214193	p 592	N95-30638 #
NLR-TP-92371-U	p 53	N95-13243		NTSB/AAR-95/01	p 277	N95-23609 #	PB95-215828	p 599	N95-31712 #
NLR-TP-92409-U	p 117	N95-18503		NTSB/ARC-94/02	p 78	N95-15066 #	PB95-910401	p 277	N95-23609 #
NLR-TP-93109-U	p 285	N95-23161 #		NTSB/ARC-94/02	p 123	N95-17748 #	PB95-910402	p 380	N95-26498 #
NLR-TP-93301-U	p 593	N95-30814 #		NTSB/ARG-95/01	p 599	N95-31712 #	PDA-TR-1754-02-01	p 235	N95-22036 #
NLR-TP-93348-U	p 601	N95-30815 #		NTSB/RP-94/01-VOL-1	p 278	N95-24105 #	PL-TR-93-1110	p 231	N95-20772 #
NLR-TP-93418-U	p 607	N95-30838 #		NTSB/RP-94/02-VOL-2	p 277	N95-23598 #	PL-TR-93-1111	p 247	N95-20771 #
NLR-TP-93511-U	p 593	N95-30837 #		NTSB/SIR-94/02	p 188	N95-19793 #	PL-TR-94-2146	p 226	N95-21831 #
NLR-TP-93535-U	p 9	N95-11179 #		NTSB/SS-94/02	p 124	N95-19132 #	PL-TR-94-2253	p 514	N95-29764 #
NONP-AGARD-SUPPL-VT-95-3838	p 117	N95-18539		ODURF-124303	p 129	N95-16899 *	PSI-1177/TR-1305	p 106	N95-16076
NONP-NASA-DK-95-48301	p 383	N95-26587 *	#	OMI-01-92	p 375	N95-27248 *	PW/GESP-FR21998-23	p 56	N95-12546
NONP-NASA-SUPPL-DK-94-28027	p 84	N95-14815 #		OMI-02-93	p 330	N95-24379 *	R/D-7213-AN-01	p 81	N95-15821
NONP-NASA-SUPPL-VT-94-32020	p 97	N95-15899 *		PAPER C15	p 1	A95-60160 *	R/D-7213-AN-01	p 231	N95-20860 #
NONP-NASA-VT-94-23139	p 20	N95-10547 *	#	PAPER-1746	p 230	A95-72580 *	RAD-93-269-107-12-01	p 446	N95-27234 #
NONP-NASA-VT-94-23140	p 10	N95-10548 *	#	PAPER-4384	p 230	A95-72585 *	RAND/N-3616-AF	p 62	N95-11944
NONP-NASA-VT-94-23144	p 20	N95-10552 *	#	PAPER-93GL03426	p 251	A95-70297 *	RAND/N-3618-AF	p 51	N95-13289
NONP-NASA-VT-94-23146	p 22	N95-10553 *	#	PB94-155702	p 454	N95-28038 *	RAND/N-3619-AF	p 81	N95-15451
NONP-NASA-VT-94-23149	p 7	N95-10556 *	#	PB94-175262	p 55	N95-11796	REPT-030601-5-T	p 704	N95-32822 *
NONP-NASA-VT-94-23149	p 7	N95-10556 *	#	PB94-179090	p 60	N95-11798 #	REPT-10428A	p 98	N95-13885 *
NONP-NASA-VT-94-23267	p 11	N95-10737 *	#	PB94-179520	p 14	N95-10083	REPT-31-12089	p 101	N95-15743 *
NONP-NASA-VT-94-23628	p 21	N95-10738 *	#	PB94-179694	p 22	N95-10085	REPT-63193-94U/P60099	p 130	N95-17661 #
NONP-NASA-VT-94-23629	p 1	N95-10709 *	#	PB94-180031	p 6	N95-10135	REPT-722792-5	p 58	N95-12856 *
NONP-NASA-VT-94-23630	p 21	N95-10710 *	#	PB94-180049	p 7	N95-10136	REPT-73-C1	p 12	N95-10316 #
NONP-NASA-VT-94-23631	p 13	N95-10711 *	#	PB94-180056	p 7	N95-10137	REPT-91-R-1475	p 105	N95-18044 *
NONP-NASA-VT-94-23634	p 21	N95-10714 *	#	PB94-180957	p 39	N95-12578	REPT-92RR-28	p 126	N95-18059 #
NONP-NASA-VT-94-23635	p 13	N95-10715 *	#	PB94-184512	p 43	N95-12582 #	REPT-931122-01	p 17	N95-11223 *
NONP-NASA-VT-94-23636	p 13	N95-10716 *	#	PB94-184801	p 21	N95-10844	REPT-94-4	p 330	N95-24443 *
NONP-NASA-VT-94-23637	p 17	N95-10717 *	#	PB94-189180	p 104	N95-17451	REPT-95-C-SRA-001	p 556	N95-29941 #
NONP-NASA-VT-94-23640	p 13	N95-10740 *	#	PB94-190725	p 142	N95-17454	REPT-95B00075	p 416	N95-27763 *
NONP-NASA-VT-94-23641	p 13	N95-10741 *	#	PB94-193323	p 104	N95-17466	RIACS-TR-94-17	p 36	N95-11877 *
NONP-NASA-VT-94-23642	p 13	N95-10742 *	#	PB94-194065	p 77	N95-14179 #	RIACS-TR-94-18	p 36	N95-11884 *
NONP-NASA-VT-94-23643	p 13	N95-10743 *	#	PB94-194560	p 58	N95-12854 #	RIACS-TR-94-19	p 160	N95-18737 *
NONP-NASA-VT-94-23644	p 13	N95-10744 *	#	PB94-194594	p 61	N95-12855 #	RIACS-TR-95-01	p 335	N95-25334 *
NONP-NASA-VT-94-23645	p 13	N95-10745 *	#	PB94-194883	p 123	N95-17476 #	RL-TR-94-196	p 448	N95-26845
				PB94-195369	p 78	N95-15439	RL-TR-94-218	p 679	N95-31455 #
				PB94-196813	p 79	N95-13981	RL-TR-94-85	p 159	N95-16621 #
				PB94-201670	p 53	N95-13243	RL-TR-95-4	p 489	N95-28887 #
				PB94-201696	p 117	N95-18503			
				PB94-203403	p 42	N95-13247			

REPORT NUMBER INDEX

US-PATENT-CLASS-364-578

RTR-249-01	p 415	N95-27093 *	#	SAE PAPER 932582	p 495	A95-90086 *	TRB/TRR-1428	p 219	N95-19967 #
R93081	p 237	N95-21122		SAE PAPER 932584	p 494	A95-90068	TRITA-NA-9312	p 705	N95-33059 #
R95-970293	p 592	N95-30611 *	#	SAE PAPER 932585	p 505	A95-90069	UC-706	p 358	N95-25110
S-786-VOL-1	p 151	N95-19237 *	#	SAE PAPER 932586	p 494	A95-90070	UCLA ENG-93-43	p 150	N95-17493 * #
S-786-VOL-2	p 205	N95-19624 *	#	SAE PAPER 932596	p 379	A95-84568	UCRL-ID-118981	p 452	N95-28108 #
SAE PAPER 930485	p 386	A95-84554		SAE PAPER 932598	p 379	A95-84570	UCRL-ID-119964	p 701	N95-33408 #
SAE PAPER 931218	p 509	A95-87466		SAE PAPER 932599	p 380	A95-84571	UCRL-JC-117130	p 708	N95-33642 #
SAE PAPER 931219	p 539	A95-87530		SAE PAPER 932600	p 380	A95-84572	UCRL-JC-117918-REV-1	p 441	N95-28029 #
SAE PAPER 931221	p 543	A95-88011		SAE PAPER 932601	p 494	A95-90071	UCRL-JC-117918-REV-2	p 441	N95-28139 #
SAE PAPER 931223	p 545	A95-88789		SAE PAPER 932602	p 494	A95-90072	UCRL-JC-118149	p 256	N95-21552 #
SAE PAPER 931224	p 491	A95-87568		SAE PAPER 932603	p 494	A95-90073	UCRL-JC-118213	p 644	N95-30507 #
SAE PAPER 931226	p 458	A95-87199		SAE PAPER 932604	p 495	A95-90074	UCRL-JC-118226	p 249	N95-21478 #
SAE PAPER 931227	p 460	A95-87365		SAE PAPER 932605	p 495	A95-90075	UCRL-JC-118289	p 250	N95-22299 #
SAE PAPER 931228	p 463	A95-88960		SAE PAPER 932606	p 495	A95-90076	UCRL-JC-118476	p 297	N95-24019 #
SAE PAPER 931230	p 528	A95-88961		SAE PAPER 932610	p 486	A95-90079	UCRL-JC-120546	p 584	N95-32164 #
SAE PAPER 931233	p 529	A95-88962		SAE PAPER 932615	p 456	A95-90080	UDR-TR-93-81-2	p 242	N95-21969
SAE PAPER 931234	p 529	A95-88963		SAE PAPER 932616	p 456	A95-90081	UDR-TR-94-94	p 485	N95-28811 #
SAE PAPER 931241	p 483	A95-88964 *	*	SAE PAPER 932619	p 456	A95-90082	US-PATENT-APPL-SN-010986	p 389	N95-26537
SAE PAPER 931248	p 483	A95-89220		SAE PAPER 932622	p 511	A95-90083	US-PATENT-APPL-SN-014581	p 286	N95-23395 *
SAE PAPER 931249	p 565	A95-89221		SAE PAPER 932623	p 495	A95-90084	US-PATENT-APPL-SN-014584	p 286	N95-23397 *
SAE PAPER 931253	p 493	A95-89222		SAE PAPER 932624	p 495	A95-90085	US-PATENT-APPL-SN-020940	p 116	N95-18337
SAE PAPER 931258	p 493	A95-89224		SAE SP-992	p 417	A95-84553 *	US-PATENT-APPL-SN-032067	p 82	N95-14518 *
SAE PAPER 931356	p 634	A95-93640		SAE 931256	p 493	A95-89223	US-PATENT-APPL-SN-045337	p 85	N95-14415 *
SAE PAPER 931360	p 610	A95-93642		SAND-93-0208C	p 145	N95-16509 #	US-PATENT-APPL-SN-046256	p 362	N95-26187 *
SAE PAPER 931365	p 634	A95-93646		SAND-93-4037C	p 7	N95-10226 #	US-PATENT-APPL-SN-056503	p 288	N95-22578 *
SAE PAPER 931366	p 586	A95-93647		SAND-94-0945	p 152	N95-19100 #	US-PATENT-APPL-SN-067763	p 224	N95-21864
SAE PAPER 931367	p 586	A95-93648		SAND-94-1136C	p 229	N95-21520 #	US-PATENT-APPL-SN-082766	p 85	N95-14415 *
SAE PAPER 931368	p 586	A95-93649		SAND-94-1305C	p 56	N95-13184 #	US-PATENT-APPL-SN-083602	p 706	N95-34449
SAE PAPER 931370	p 604	A95-93650		SAND-94-1417C	p 228	N95-20195 #	US-PATENT-APPL-SN-094663	p 611	N95-31180
SAE PAPER 931376	p 618	A95-93655		SAND-94-1826	p 232	N95-21730 #	US-PATENT-APPL-SN-125715	p 629	N95-30749
SAE PAPER 931377	p 604	A95-93656		SAND-94-2302C	p 648	N95-31614 #	US-PATENT-APPL-SN-127567	p 244	N95-20295
SAE PAPER 931381	p 604	A95-93657		SAND-94-2746C	p 299	N95-23532 #	US-PATENT-APPL-SN-129499	p 646	N95-30727
SAE PAPER 931382	p 604	A95-93658		SAND-94-3190C	p 330	N95-24308 #	US-PATENT-APPL-SN-134443	p 159	N95-18325 *
SAE PAPER 931383	p 618	A95-93659		SAND-94-8210	p 206	N95-19579 #	US-PATENT-APPL-SN-159606	p 96	N95-15306 *
SAE PAPER 931384	p 586	A95-93660		SBI-AD-E501-856	p 411	N95-26556	US-PATENT-APPL-SN-192562	p 85	N95-14415 *
SAE PAPER 931386	p 587	A95-93662		SCT-92-RR-9	p 85	N95-15328 #	US-PATENT-APPL-SN-194854	p 362	N95-26187 *
SAE PAPER 931388	p 613	A95-93664		SEL-95-001	p 567	N95-28807 * #	US-PATENT-APPL-SN-230571	p 350	N95-25592
SAE PAPER 931389	p 613	A95-93665		SER-PK-001	p 683	N95-32764 * #	US-PATENT-APPL-SN-269268	p 91	N95-14139 * #
SAE PAPER 931391	p 613	A95-93667		SHRP-H-385	p 78	N95-15439	US-PATENT-APPL-SN-279037	p 160	N95-18461 #
SAE PAPER 931393	p 613	A95-93668		SKS/95/1	p 648	N95-31443 #	US-PATENT-APPL-SN-287027	p 258	N95-21673
SAE PAPER 931397	p 634	A95-93669		SR-1	p 226	N95-21831 #	US-PATENT-APPL-SN-327061	p 91	N95-14183 * #
SAE PAPER 931400	p 604	A95-93670		SR-1	p 514	N95-29764 #	US-PATENT-APPL-SN-329621	p 152	N95-19090
SAE PAPER 931401	p 628	A95-93671 *	*	SSD94D0217B	p 80	N95-14794 * #	US-PATENT-APPL-SN-359320	p 238	N95-20080 * #
SAE PAPER 931402	p 605	A95-93672		SSD94D0298	p 143	N95-18567 * #	US-PATENT-APPL-SN-365880	p 437	N95-26890 * #
SAE PAPER 931403	p 605	A95-93673 *	*	SSD94D0335	p 127	N95-15971 * #	US-PATENT-APPL-SN-666104	p 151	N95-19073
SAE PAPER 931404	p 628	A95-93674		STF40-A93136	p 62	N95-13575	US-PATENT-APPL-SN-755248	p 85	N95-14415 *
SAE PAPER 931406	p 613	A95-93675 *	*	STF75-S93041	p 645	N95-30521	US-PATENT-APPL-SN-774490	p 362	N95-26015 *
SAE PAPER 931410	p 625	A95-93676		SWRI-17-4665	p 244	N95-20414	US-PATENT-APPL-SN-839721	p 388	N95-26507
SAE PAPER 931411	p 614	A95-93677		TABES PAPER 94-604	p 100	N95-14638 #	US-PATENT-APPL-SN-874403	p 629	N95-30750
SAE PAPER 931412	p 614	A95-93678 *	*	TABES PAPER 94-605	p 86	N95-14639 * #	US-PATENT-APPL-SN-889347	p 294	N95-23389 *
SAE PAPER 931416	p 610	A95-93681		TABES PAPER 94-616	p 83	N95-14645 #	US-PATENT-APPL-SN-921863	p 258	N95-21100
SAE PAPER 931417	p 583	A95-93682		TABES PAPER 94-619	p 74	N95-14646 #	US-PATENT-APPL-SN-926117	p 311	N95-23377 *
SAE PAPER 931422	p 495	A95-90087		TABES PAPER 94-631	p 99	N95-14652 #	US-PATENT-APPL-SN-935939	p 280	N95-23393 *
SAE PAPER 931439	p 680	A95-93691		TABES PAPER 94-632	p 87	N95-14653 * #	US-PATENT-CLASS-149-19.9	p 152	N95-19090
SAE PAPER 931442	p 614	A95-93692		TACOM-13603	p 211	N95-19809	US-PATENT-CLASS-188-379	p 159	N95-18325 *
SAE PAPER 931444	p 635	A95-93693		TAE-698	p 316	N95-23662 #	US-PATENT-CLASS-188-381	p 96	N95-15306 *
SAE PAPER 931449	p 635	A95-93698		TARDEC-TR-13613	p 537	N95-29572 #	US-PATENT-CLASS-244-100R	p 96	N95-15306 *
SAE PAPER 932055	p 500	A95-91636		TARDEC-TR-13641	p 630	N95-31368 #	US-PATENT-CLASS-244-104R	p 96	N95-15306 *
SAE PAPER 932056	p 513	A95-91637		TDCK-93-2570	p 240	N95-20906 #	US-PATENT-CLASS-244-130	p 116	N95-18337
SAE PAPER 932057	p 513	A95-91638		TDCK-94-2179	p 337	N95-26190	US-PATENT-CLASS-244-138	p 706	N95-34449
SAE PAPER 932084	p 530	A95-91659		TII-R9201-001-RD	p 316	N95-23792 * #	US-PATENT-CLASS-244-182	p 294	N95-23389 *
SAE PAPER 932119	p 526	A95-90360		TKK-F-C155	p 60	N95-11798 #	US-PATENT-CLASS-244-199	p 286	N95-23390 *
SAE PAPER 932510	p 546	A95-89183		TNO-TM-1994-B-16	p 337	N95-26190	US-PATENT-CLASS-244-215	p 286	N95-23395 *
SAE PAPER 932512	p 465	A95-89185		TOP-7-3-531	p 81	N95-15815 #	US-PATENT-CLASS-244-216	p 286	N95-23395 *
SAE PAPER 932513	p 466	A95-89186		TOP-7-3-534	p 391	N95-26994 #	US-PATENT-CLASS-244-217	p 224	N95-21864
SAE PAPER 932514	p 466	A95-89187		TR-080594-4871F	p 333	N95-24391 * #	US-PATENT-CLASS-244-3.22	p 151	N95-19073
SAE PAPER 932515	p 466	A95-89188		TR-112894-3570P	p 316	N95-23670 * #	US-PATENT-CLASS-244-51	p 294	N95-23389 *
SAE PAPER 932517	p 386	A95-84555		TR-1291-1	p 698	N95-34306 #	US-PATENT-CLASS-244-7R	p 294	N95-23389 *
SAE PAPER 932521	p 486	A95-89189		TR-2-FSRC-93	p 171	N95-18564 #	US-PATENT-CLASS-244-75R	p 294	N95-23389 *
SAE PAPER 932527	p 386	A95-84556		TR-524727	p 397	N95-28409	US-PATENT-CLASS-244-75R	p 286	N95-23390 *
SAE PAPER 932530	p 492	A95-89190		TR-90425	p 382	N95-28630	US-PATENT-CLASS-250-225	p 362	N95-26015 *
SAE PAPER 932531	p 466	A95-89191		TR-94-A-019	p 288	N95-24030 * #	US-PATENT-CLASS-340-945	p 82	N95-14518 *
SAE PAPER 932532	p 466	A95-89192					US-PATENT-CLASS-340-946	p 280	N95-23393 *
SAE PAPER 932533	p 492	A95-89193					US-PATENT-CLASS-340-953	p 280	N95-23393 *
SAE PAPER 932534	p 492	A95-89194 *	*				US-PATENT-CLASS-340-959	p 85	N95-14415 *
SAE PAPER 932535	p 379	A95-84557					US-PATENT-CLASS-340-971	p 280	N95-23393 *
SAE PAPER 932536	p 386	A95-84558					US-PATENT-CLASS-340-978	p 82	N95-14518 *
SAE PAPER 932538	p 379	A95-84559					US-PATENT-CLASS-340-981	p 280	N95-23393 *
SAE PAPER 932541	p 510	A95-89195					US-PATENT-CLASS-342-25	p 646	N95-30727
SAE PAPER 932544	p 547	A95-90052					US-PATENT-CLASS-345-8	p 288	N95-22578 *
SAE PAPER 932550	p 547	A95-90054 *	*				US-PATENT-CLASS-348-117	p 611	N95-31180
SAE PAPER 932559	p 511	A95-90056					US-PATENT-CLASS-356-152	p 362	N95-26015 *
SAE PAPER 932560	p 511	A95-90057					US-PATENT-CLASS-356-34	p 362	N95-26015 *
SAE PAPER 932561	p 505	A95-90058					US-PATENT-CLASS-362-62	p 280	N95-23393 *
SAE PAPER 932562	p 511	A95-90059					US-PATENT-CLASS-364-427	p 85	N95-14415 *
SAE PAPER 932570	p 401	A95-84567					US-PATENT-CLASS-364-578	p 288	N95-22578 *
SAE PAPER 932571	p 467	A95-90060 *	*						
SAE PAPER 932572	p 467	A95-90061							
SAE PAPER 932573	p 467	A95-90062							
SAE PAPER 932574	p 467	A95-90063							
SAE PAPER 932577	p 493	A95-90065							
SAE PAPER 932579	p 494	A95-90066							
SAE PAPER 932580	p 494	A95-90067							

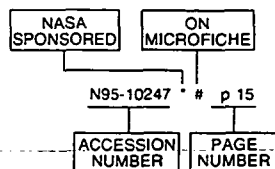
US-PATENT-CLASS-395-152	p 288	N95-22578 *	WL-TR-94-3039	p 237	N95-20004 #
US-PATENT-CLASS-416-144	p 159	N95-18325 *	WL-TR-94-3054	p 84	N95-13687 #
US-PATENT-CLASS-416-34	p 311	N95-23377 *	WL-TR-94-3063	p 171	N95-18365 #
US-PATENT-CLASS-416-61	p 311	N95-23377 *	WL-TR-94-3064	p 630	N95-31471 #
US-PATENT-CLASS-428-34	p 629	N95-30749	WL-TR-94-3089	p 553	N95-29187 #
US-PATENT-CLASS-430-324	p 629	N95-30750	WL-TR-94-3094	p 593	N95-30885 #
US-PATENT-CLASS-434-307R	p 288	N95-22578 *	WL-TR-94-3097	p 341	N95-26053
US-PATENT-CLASS-434-372	p 288	N95-22578 *	WL-TR-94-3129	p 485	N95-28811 #
US-PATENT-CLASS-434-38	p 288	N95-22578 *	WL-TR-94-3131	p 557	N95-30087 #
US-PATENT-CLASS-434-43	p 288	N95-22578 *	WL-TR-94-3134	p 219	N95-22046 #
US-PATENT-CLASS-439-248	p 350	N95-25592 *	WL-TR-94-3143	p 389	N95-26684
US-PATENT-CLASS-60-204	p 362	N95-26187 *	WL-TR-94-3162	p 698	N95-34306 #
US-PATENT-CLASS-60-271	p 362	N95-26187 *	WL-TR-94-4006	p 158	N95-17507
US-PATENT-CLASS-62-467	p 244	N95-20295	WL-TR-94-4079	p 194	N95-19517 #
US-PATENT-CLASS-73-178H	p 280	N95-23393 *	WL-TR-94-4083-VOL-1	p 133	N95-18677
US-PATENT-CLASS-73-178T	p 85	N95-14415 *	WL-TR-94-4084-VOL-2	p 131	N95-18162 #
US-PATENT-CLASS-74-573R	p 159	N95-18325 *	WL-TR-94-5005	p 259	N95-21975
US-PATENT-CLASS-74-574	p 159	N95-18325 *	WL-TR-95-2001	p 407	N95-28646
			WL-TR-95-3025	p 612	N95-31656 #
			WL-TR-95-3026	p 612	N95-31655 #
US-PATENT-5,137,353	p 362	N95-26015 *	WSRC-MS-94-0632	p 349	N95-24598 #
US-PATENT-5,294,080	p 286	N95-23395 *			
US-PATENT-5,303,882	p 116	N95-18337			
US-PATENT-5,315,296	p 280	N95-23393 *			
US-PATENT-5,320,304	p 151	N95-19073			
US-PATENT-5,320,692	p 152	N95-19090			
US-PATENT-5,326,050	p 286	N95-23390 *			
US-PATENT-5,327,745	p 244	N95-20295			
US-PATENT-5,330,131	p 294	N95-23389 *			
US-PATENT-5,335,886	p 224	N95-21864			
US-PATENT-5,340,054	p 388	N95-26507			
US-PATENT-5,342,737	p 629	N95-30750			
US-PATENT-5,352,090	p 311	N95-23377 *			
US-PATENT-5,353,022	p 85	N95-14415 *			
US-PATENT-5,359,326	p 82	N95-14518 *			
US-PATENT-5,366,181	p 96	N95-15306 *			
US-PATENT-5,373,318	p 611	N95-31180			
US-PATENT-5,373,922	p 159	N95-18325 *			
US-PATENT-5,388,990	p 288	N95-22578 *			
US-PATENT-5,389,411	p 629	N95-30749			
US-PATENT-5,392,597	p 362	N95-26187 *			
US-PATENT-5,393,016	p 706	N95-34449			
US-PATENT-5,394,151	p 646	N95-30727			
US-PATENT-5,397,244	p 350	N95-25592 *			
USAARL-94-29	p 172	N95-17334 #			
USAARL-94-37	p 171	N95-16226 #			
USAARL-94-42	p 123	N95-16404 #			
USAARL-94-47	p 259	N95-22044 #			
USAARL-95-19	p 693	N95-34793 #			
USAARL-95-3	p 485	N95-29057 #			
USAARL-95-4	p 391	N95-26993			
USAATCOM-TR-94-A-011	p 120	N95-19119 * #			
USAATCOM-TR-94-A-022	p 367	N95-26710 * #			
USAATCOM-TR-94-D-22	p 648	N95-31475 #			
USAATCOM-TR-95-A-003	p 409	N95-26773 * #			
USCG-D-05-94	p 241	N95-21687			
UTRC-R91-254576-20	p 15	N95-10247 * #			
UTSA-MM2-6274	p 22	N95-10231 * #			
UVA/528266/MSE94/117	p 343	N95-24220 * #			
VPI-E-94-09	p 301	N95-23179 * #			
VPI-E-95-01	p 439	N95-27865 * #			
WBE-228-001	p 341	N95-24424			
WES/TN/DRP-4-10	p 334	N95-25609			
WES/TR/GL-94-12	p 238	N95-19955 #			
WHOI-93-29	p 320	N95-23766 *			
WL-TM-94-3039-VOL-1	p 225	N95-21877			
WL-TM-94-3065-VOL-2	p 76	N95-15465			
WL-TM-94-3066-VOL-3	p 36	N95-11829			
WL-TM-94-3077	p 96	N95-15547			
WL-TM-94-3112-VOL-4-PT-1	p 237	N95-21214 #			
WL-TM-94-3130	p 436	N95-26418			
WL-TM-94-3132-VOL-4-PT-2	p 143	N95-18641 #			
WL-TR-91-7020	p 138	N95-18164 #			
WL-TR-93-1177	p 49	N95-12591 #			
WL-TR-93-2058	p 514	N95-29934 #			
WL-TR-93-2126-2	p 242	N95-21969			
WL-TR-93-3010-VOL-1	p 132	N95-18483 #			
WL-TR-93-3048	p 107	N95-16808 #			
WL-TR-93-4125	p 244	N95-20414			
WL-TR-94-2025	p 160	N95-18660			
WL-TR-94-2092	p 513	N95-28908			
WL-TR-94-2099	p 401	N95-27003			
WL-TR-94-3017	p 117	N95-18380			
WL-TR-94-3030	p 256	N95-21913			

ACCESSION NUMBER INDEX

AERONAUTICAL ENGINEERING / A Continuing Bibliography
1995 Cumulative Index

December 1995

Typical Accession Number Index Listing



Listings in this index are arranged alphanumerically by accession number. The page number indicates the page on which the citation is located. The accession number denotes the number by which the citation is identified. An asterisk (*) indicates that the item is a NASA report. A pound sign (#) indicates that the item is available on microfiche.

A95-60155 *	p 18	A95-62259	p 85	A95-65981	p 207	A95-68360	p 185	A95-70136 *	p 220
A95-60156 *	p 18	A95-62262	p 98	A95-66276	p 181	A95-68361	p 192	A95-70139	p 239
A95-60160 *	p 1	A95-62264	p 82	A95-66277	p 181	A95-68362 *	p 192	A95-70297 *	p 251
A95-60161 *	p 18	A95-62265	p 88	A95-66282	p 181	A95-68364	p 203	A95-70473	p 251
A95-60163 *	p 19	A95-62267	p 89	A95-66285 *	p 181	A95-68365	p 203	A95-70543	p 240
A95-60164 *	p 1	A95-62279 *	p 98	A95-66296 *	p 181	A95-68366	p 185	A95-70655 *	p 252
A95-60165 *	p 19	A95-62625	p 89	A95-66297 *	p 181	A95-68367	p 203	A95-70656 *	p 252
A95-60166 *	p 27	A95-62627	p 89	A95-66300	p 191	A95-68368 *	p 185	A95-70671	p 227
A95-60167 *	p 16	A95-62628	p 89	A95-66301	p 204	A95-68369	p 186	A95-70797	p 257
A95-60168 *	p 16	A95-62631	p 83	A95-66302	p 191	A95-68370	p 193	A95-70844	p 242
A95-60169 *	p 2	A95-62633	p 78	A95-66303	p 182	A95-68371	p 203	A95-70950	p 252
A95-60170 *	p 17	A95-62635	p 100	A95-66304	p 182	A95-68372	p 185	A95-71021	p 225
A95-60172 *	p 14	A95-62638	p 83	A95-66305	p 191	A95-68373	p 186	A95-71022	p 240
A95-60173 *	p 2	A95-62657	p 85	A95-66429	p 212	A95-68393	p 210	A95-71024	p 240
A95-60174 *	p 2	A95-63064	p 141	A95-66500	p 191	A95-68394	p 180	A95-71029	p 220
A95-60176 *	p 2	A95-63201 *	p 153	A95-66869	p 212	A95-68395	p 180	A95-71033	p 243
A95-60177 *	p 2	A95-63520	p 103	A95-67298	p 195	A95-68396	p 180	A95-71040 *	p 243
A95-60178 *	p 2	A95-63522	p 171	A95-67301	p 207	A95-68398	p 180	A95-71177	p 220
A95-60179 *	p 3	A95-63634	p 126	A95-67304	p 207	A95-68756	p 214	A95-71178	p 220
A95-60180 *	p 3	A95-63636	p 168	A95-67329	p 208	A95-68762 *	p 214	A95-71179	p 220
A95-60181 *	p 3	A95-63638	p 153	A95-67332	p 182	A95-68845	p 214	A95-71180	p 221
A95-60182 *	p 3	A95-63639	p 171	A95-67335	p 182	A95-69131	p 206	A95-71181 *	p 221
A95-60183	p 3	A95-63640	p 148	A95-67336	p 182	A95-69136	p 206	A95-71182 *	p 236
A95-60184 *	p 3	A95-63643	p 138	A95-67337	p 183	A95-69164	p 206	A95-71183 *	p 221
A95-60185 *	p 4	A95-63646	p 103	A95-67342	p 208	A95-69209	p 210	A95-71184	p 236
A95-60186 *	p 4	A95-63648	p 153	A95-67343	p 208	A95-69210 *	p 204	A95-71186	p 252
A95-60187 *	p 4	A95-63652	p 153	A95-67345	p 213	A95-69211 *	p 205	A95-71656 *	p 237
A95-60188 *	p 4	A95-63655	p 103	A95-67347 *	p 183	A95-69212	p 205	A95-71738	p 257
A95-60189 *	p 5	A95-63656	p 175	A95-67780 *	p 213	A95-69213	p 193	A95-71744	p 243
A95-60190 *	p 5	A95-63657	p 138	A95-67806 *	p 213	A95-69214	p 193	A95-71867	p 243
A95-60191 *	p 5	A95-64288	p 125	A95-67828	p 183	A95-69215	p 180	A95-71908	p 253
A95-60192 *	p 5	A95-64294	p 125	A95-67829	p 183	A95-69216	p 180	A95-72393	p 253
A95-60193 *	p 5	A95-64524	p 153	A95-67830	p 183	A95-69218 *	p 205	A95-72411 *	p 253
A95-60199 *	p 14	A95-64580	p 168	A95-68158	p 195	A95-69229 *	p 218	A95-72423 *	p 253
A95-60227	p 25	A95-64582	p 168	A95-68162	p 196	A95-69230 *	p 180	A95-72495	p 254
A95-60790	p 61	A95-64584	p 141	A95-68165	p 208	A95-69232	p 186	A95-72500	p 254
A95-60842	p 56	A95-64585	p 169	A95-68166	p 208	A95-69233	p 203	A95-72543	p 254
A95-60852	p 35	A95-64586	p 141	A95-68172	p 179	A95-69234 *	p 186	A95-72545	p 254
A95-60865	p 61	A95-64588	p 169	A95-68173	p 183	A95-69235	p 186	A95-72546	p 254
A95-60867	p 62	A95-64588	p 169	A95-68180	p 184	A95-69236 *	p 204	A95-72564	p 236
A95-60871	p 56	A95-64606	p 142	A95-68181	p 179	A95-69238	p 186	A95-72565 *	p 237
A95-61544 *	p 56	A95-64608	p 103	A95-68182	p 196	A95-69239	p 187	A95-72566	p 221
A95-61720	p 88	A95-64609	p 125	A95-68187	p 189	A95-69240	p 187	A95-72567 *	p 221
A95-61727	p 82	A95-64610	p 103	A95-68188	p 189	A95-69241 *	p 194	A95-72568 *	p 222
A95-61728	p 66	A95-64855	p 175	A95-68191 *	p 205	A95-69242 *	p 193	A95-72569	p 229
A95-61732	p 82	A95-64856	p 176	A95-68195	p 184	A95-69243 *	p 190	A95-72570	p 222
A95-61733	p 77	A95-64857	p 176	A95-68216	p 179	A95-69244	p 187	A95-72571	p 230
A95-61734	p 65	A95-64860	p 176	A95-68217	p 213	A95-69245	p 187	A95-72578 *	p 230
A95-61735	p 84	A95-64877	p 176	A95-68218	p 184	A95-69246	p 193	A95-72585	p 230
A95-61736	p 82	A95-64886	p 176	A95-68219	p 184	A95-69247	p 187	A95-72586	p 243
A95-61737	p 82	A95-64890	p 176	A95-68220	p 184	A95-69248	p 187	A95-72648	p 243
A95-61739	p 78	A95-65339	p 103	A95-68256	p 217	A95-69249	p 193	A95-72675	p 257
A95-61740	p 78	A95-65345	p 154	A95-68257	p 196	A95-69255	p 193	A95-72675	p 227
A95-61741	p 82	A95-65347	p 104	A95-68258	p 179	A95-69302	p 196	A95-72885	p 227
A95-61795	p 88	A95-65346	p 103	A95-68259	p 209	A95-69303	p 196	A95-72888	p 227
		A95-65374	p 176	A95-68260	p 188	A95-69304	p 196	A95-72891	p 228
		A95-65845	p 207	A95-68278	p 189	A95-69308	p 210	A95-73180	p 255
		A95-65845	p 195	A95-68280	p 209	A95-69309	p 195	A95-73181	p 255
		A95-65897	p 207	A95-68282	p 209	A95-69310 *	p 197	A95-73345	p 300
				A95-68287	p 209	A95-69318	p 206	A95-73345	p 278
				A95-68299	p 203	A95-69322	p 188	A95-73435	p 278
				A95-68300	p 192	A95-69324	p 194	A95-73437	p 280
				A95-68302	p 209	A95-69328	p 190	A95-73438	p 286
				A95-68307	p 217	A95-69329	p 190	A95-73439	p 304
				A95-68311	p 196	A95-69332	p 190	A95-73441	p 262
				A95-68312	p 209	A95-69333	p 190	A95-73444	p 262
				A95-68313	p 192	A95-69334	p 190	A95-73451	p 286
				A95-68314	p 213	A95-69431 *	p 214	A95-73452 *	p 304
				A95-68349	p 192	A95-69574	p 215	A95-73454 *	p 304
				A95-68350	p 179	A95-69658	p 218	A95-73457	p 304
				A95-68351	p 179	A95-69717	p 215	A95-73458	p 304
				A95-68353	p 184	A95-69721	p 215	A95-73460	p 305
				A95-68355	p 184	A95-69766	p 215	A95-73461	p 263
				A95-68356	p 192	A95-69803	p 215	A95-73462	p 263
				A95-68357	p 185	A95-69833	p 216	A95-73465	p 263
				A95-68358	p 185	A95-69854	p 205	A95-73471	p 321
				A95-68359	p 185	A95-69967	p 219	A95-73477	p 305
						A95-69968	p 219	A95-73479	p 305
						A95-69969	p 219	A95-73486	p 305
						A95-69970	p 257	A95-73493	p 263
						A95-69976	p 242	A95-73494	p 263
						A95-70124	p 239	A95-73495	p 263
						A95-70131	p 242	A95-73496 *	p 264
						A95-70132	p 242	A95-73497	p 264
						A95-70133	p 235	A95-73498	p 305

A95-73516

A95-73516 p 264
 A95-73517 p 316
 A95-73518 p 264
 A95-73519 p 264
 A95-73520 p 264
 A95-73521 p 316
 A95-73522 p 276
 A95-73523 p 264
 A95-73524 p 265
 A95-73525 p 265
 A95-73526 p 281
 A95-73527 p 265
 A95-73529 p 265
 A95-73530 p 265
 A95-73531 p 281
 A95-73532 p 265
 A95-73533 p 281
 A95-73535 p 281
 A95-73536 p 276
 A95-73537 p 281
 A95-73538 p 323
 A95-73539 p 266
 A95-73540 p 281
 A95-73541 p 266
 A95-73542 p 282
 A95-73544 p 282
 A95-73546 p 266
 A95-73547 p 266
 A95-73548 p 266
 A95-73549 p 282
 A95-73551 p 305
 A95-73552 p 266
 A95-73553 p 305
 A95-73554 p 306
 A95-73555 p 306
 A95-73556 p 306
 A95-73557 p 266
 A95-73558 p 267
 A95-73559 p 297
 A95-73560 p 267
 A95-73561 p 267
 A95-73564 p 298
 A95-73568 p 298
 A95-73571 p 278
 A95-73577 p 298
 A95-73583 p 298
 A95-73584 p 306
 A95-73587 p 282
 A95-73588 p 276
 A95-73589 p 282
 A95-73590 p 282
 A95-73591 p 282
 A95-74042 p 261
 A95-74496 p 306
 A95-74554 p 295
 A95-74612 p 306
 A95-74629 p 295
 A95-74702 p 306
 A95-75031 p 317
 A95-75035 p 317
 A95-75093 p 290
 A95-75094 p 290
 A95-75095 p 290
 A95-75096 p 290
 A95-75097 p 267
 A95-75098 p 283
 A95-75099 p 283
 A95-75100 p 283
 A95-75101 p 267
 A95-75494 p 323
 A95-75516 p 307
 A95-75532 p 317
 A95-75714 p 279
 A95-75716 p 287
 A95-75717 p 287
 A95-75718 p 287
 A95-75720 p 287
 A95-75725 p 298
 A95-75728 p 267
 A95-75729 p 268
 A95-75731 p 268
 A95-75733 p 268
 A95-75734 p 298
 A95-75735 p 298
 A95-75736 p 268
 A95-75752 p 261
 A95-75753 p 261
 A95-75754 p 261
 A95-75755 p 300
 A95-75756 p 261
 A95-75757 p 288
 A95-75758 p 268
 A95-75760 p 307
 A95-75761 p 269
 A95-75762 p 307
 A95-75763 p 269

A95-75765 p 269
 A95-75772 p 291
 A95-75773 p 283
 A95-75778 p 269
 A95-75976 p 317
 A95-76265 p 317
 A95-76266 p 318
 A95-76267 p 318
 A95-76389 p 288
 A95-76390 p 283
 A95-76394 p 318
 A95-76484 p 307
 A95-76489 p 307
 A95-76491 p 307
 A95-76582 p 283
 A95-76584 p 295
 A95-76585 p 307
 A95-76586 p 308
 A95-76588 p 321
 A95-76589 p 269
 A95-76590 p 269
 A95-76592 p 321
 A95-76598 p 321
 A95-76602 p 322
 A95-76603 p 291
 A95-76604 p 276
 A95-76605 p 269
 A95-76606 p 291
 A95-76607 p 291
 A95-76608 p 291
 A95-76609 p 292
 A95-76615 p 269
 A95-76616 p 288
 A95-76621 p 299
 A95-76622 p 279
 A95-76626 p 322
 A95-76630 p 292
 A95-76631 p 279
 A95-76635 p 283
 A95-76636 p 270
 A95-76637 p 295
 A95-76638 p 322
 A95-76639 p 296
 A95-76640 p 292
 A95-76641 p 292
 A95-76642 p 292
 A95-76643 p 270
 A95-76644 p 284
 A95-76645 p 276
 A95-76646 p 270
 A95-76648 p 308
 A95-76648 p 288
 A95-76649 p 289
 A95-76650 p 289
 A95-76651 p 270
 A95-76652 p 308
 A95-76653 p 270
 A95-76654 p 284
 A95-76655 p 284
 A95-76656 p 271
 A95-76657 p 319
 A95-76658 p 308
 A95-76659 p 271
 A95-76660 p 308
 A95-76661 p 271
 A95-76673 p 289
 A95-76674 p 279
 A95-76676 p 279
 A95-76681 p 292
 A95-76683 p 279
 A95-76686 p 308
 A95-76697 p 279
 A95-76734 p 287
 A95-76735 p 287
 A95-76736 p 287
 A95-76737 p 319
 A95-76740 p 271
 A95-76742 p 271
 A95-76744 p 271
 A95-76746 p 272
 A95-76747 p 272
 A95-76758 p 299
 A95-76759 p 299
 A95-76764 p 272
 A95-76765 p 261
 A95-77000 p 319
 A95-77009 p 319
 A95-77334 p 319
 A95-77379 p 346
 A95-77921 p 346
 A95-77982 p 351
 A95-78000 p 351
 A95-78006 p 351
 A95-78008 p 351
 A95-78009 p 352
 A95-78011 p 352

A95-78012 p 352
 A95-78013 p 352
 A95-78014 p 352
 A95-78467 p 343
 A95-78494 p 347
 A95-78576 p 347
 A95-78583 p 332
 A95-78678 p 353
 A95-78679 p 353
 A95-79236 p 347
 A95-79237 p 327
 A95-79238 p 358
 A95-79240 p 334
 A95-79245 p 329
 A95-79246 p 329
 A95-79247 p 329
 A95-79248 p 329
 A95-79249 p 334
 A95-79251 p 340
 A95-79453 p 353
 A95-79988 p 361
 A95-80030 p 329
 A95-80044 p 347
 A95-80389 p 341
 A95-80390 p 341
 A95-80405 p 359
 A95-80409 p 342
 A95-80427 p 342
 A95-80525 p 353
 A95-80559 p 353
 A95-80633 p 361
 A95-80829 p 354
 A95-80830 p 354
 A95-80831 p 354
 A95-80843 p 354
 A95-80844 p 355
 A95-80845 p 355
 A95-80860 p 355
 A95-80861 p 355
 A95-80862 p 356
 A95-80867 p 356
 A95-80868 p 356
 A95-80908 p 356
 A95-81012 p 347
 A95-81020 p 340
 A95-81027 p 348
 A95-81056 p 348
 A95-81077 p 327
 A95-81079 p 359
 A95-81081 p 359
 A95-81088 p 359
 A95-81092 p 327
 A95-81093 p 342
 A95-81096 p 336
 A95-81097 p 334
 A95-81098 p 335
 A95-81099 p 327
 A95-81100 p 359
 A95-81101 p 327
 A95-81253 p 359
 A95-81360 p 342
 A95-81374 p 342
 A95-81583 p 363
 A95-81648 p 356
 A95-81690 p 361
 A95-81974 p 335
 A95-82176 p 450
 A95-82224 p 365
 A95-82251 p 450
 A95-82259 p 427
 A95-82301 p 416
 A95-82319 p 410
 A95-82320 p 410
 A95-82321 p 402
 A95-82322 p 402
 A95-82324 p 412
 A95-82325 p 402
 A95-82327 p 402
 A95-82333 p 407
 A95-82337 p 403
 A95-82355 p 413
 A95-82358 p 413
 A95-82384 p 413
 A95-82391 p 427
 A95-82400 p 413
 A95-82406 p 427
 A95-82407 p 427
 A95-82412 p 413
 A95-82413 p 368
 A95-82414 p 414
 A95-82418 p 428
 A95-82419 p 428
 A95-82420 p 403
 A95-82421 p 368
 A95-82449 p 447

A95-82462 p 382
 A95-82477 p 414
 A95-82482 p 384
 A95-82483 p 414
 A95-82499 p 414
 A95-82511 p 384
 A95-82512 p 385
 A95-82513 p 368
 A95-82515 p 414
 A95-82553 p 415
 A95-82554 p 415
 A95-82641 p 428
 A95-82642 p 428
 A95-82645 p 428
 A95-82665 p 452
 A95-82669 p 368
 A95-82679 p 428
 A95-82680 p 403
 A95-82798 p 429
 A95-82905 p 429
 A95-82982 p 429
 A95-82986 p 429
 A95-83000 p 408
 A95-83158 p 452
 A95-83487 p 429
 A95-83489 p 385
 A95-83491 p 408
 A95-83493 p 385
 A95-83494 p 385
 A95-83495 p 430
 A95-83591 p 442
 A95-83627 p 442
 A95-83648 p 430
 A95-83654 p 430
 A95-83655 p 385
 A95-83656 p 369
 A95-83657 p 369
 A95-83658 p 369
 A95-83659 p 369
 A95-83660 p 369
 A95-83661 p 370
 A95-83662 p 370
 A95-83827 p 443
 A95-83857 p 430
 A95-84026 p 430
 A95-84029 p 430
 A95-84031 p 386
 A95-84193 p 431
 A95-84196 p 370
 A95-84196 p 403
 A95-84197 p 403
 A95-84198 p 431
 A95-84201 p 416
 A95-84202 p 417
 A95-84203 p 417
 A95-84207 p 431
 A95-84209 p 417
 A95-84211 p 431
 A95-84213 p 417
 A95-84526 p 443
 A95-84543 p 443
 A95-84554 p 417
 A95-84554 p 386
 A95-84555 p 386
 A95-84556 p 386
 A95-84557 p 379
 A95-84558 p 386
 A95-84559 p 379
 A95-84560 p 379
 A95-84567 p 401
 A95-84568 p 379
 A95-84571 p 380
 A95-84572 p 380
 A95-84731 p 418
 A95-84783 p 443
 A95-84784 p 404
 A95-84786 p 418
 A95-84884 p 415
 A95-84909 p 404
 A95-84963 p 380
 A95-84992 p 418
 A95-85002 p 450
 A95-85002 p 431
 A95-85028 p 432
 A95-85029 p 432
 A95-85030 p 432
 A95-85042 p 432
 A95-85046 p 432
 A95-85048 p 433
 A95-85050 p 433
 A95-85051 p 433
 A95-85052 p 433
 A95-85060 p 404
 A95-85061 p 433

A95-85062 p 418
 A95-85212 p 386
 A95-85213 p 386
 A95-85290 p 433
 A95-85291 p 434
 A95-85299 p 434
 A95-85305 p 434
 A95-85353 p 365
 A95-85354 p 365
 A95-85355 p 365
 A95-85356 p 387
 A95-85357 p 404
 A95-85466 p 434
 A95-85468 p 365
 A95-85469 p 434
 A95-85470 p 434
 A95-85474 p 435
 A95-85477 p 411
 A95-85479 p 370
 A95-85480 p 370
 A95-85481 p 408
 A95-85482 p 365
 A95-85483 p 435
 A95-85484 p 366
 A95-85485 p 435
 A95-85491 p 387
 A95-85492 p 366
 A95-85519 p 435
 A95-85565 p 447
 A95-85774 p 415
 A95-85807 p 415
 A95-85892 p 387
 A95-85893 p 387
 A95-85894 p 387
 A95-85895 p 387
 A95-85896 p 387
 A95-85897 p 388
 A95-85898 p 388
 A95-85990 p 404
 A95-86113 p 453
 A95-86149 p 370
 A95-86150 p 371
 A95-86151 p 371
 A95-86153 p 371
 A95-86156 p 371
 A95-86157 p 371
 A95-86158 p 404
 A95-86159 p 404
 A95-86160 p 372
 A95-86161 p 372
 A95-86162 p 372
 A95-86163 p 372
 A95-86165 p 418
 A95-86166 p 405
 A95-86167 p 372
 A95-86169 p 408
 A95-86176 p 372
 A95-86177 p 373
 A95-86178 p 373
 A95-86197 p 418
 A95-86255 p 405
 A95-86256 p 373
 A95-86272 p 443
 A95-86291 p 444
 A95-86292 p 444
 A95-86296 p 444
 A95-86308 p 444
 A95-86312 p 445
 A95-86315 p 445
 A95-86318 p 445
 A95-86603 p 435
 A95-86621 p 435
 A95-86657 p 538
 A95-86658 p 538
 A95-86659 p 569
 A95-86662 p 564
 A95-86693 p 538
 A95-87184 p 538
 A95-87191 p 538
 A95-87195 p 538
 A95-87199 p 458
 A95-87200 p 458
 A95-87201 p 458
 A95-87205 p 564
 A95-87207 p 458
 A95-87210 p 458
 A95-87211 p 459
 A95-87212 p 459
 A95-87219 p 459
 A95-87220 p 539
 A95-87221 p 459
 A95-87222 p 459
 A95-87227 p 459
 A95-87248 p 483
 A95-87249 p 518
 A95-87280 p 539

ACCESSION NUMBER INDEX

A95-87285	p 527	A95-88178	p 565	A95-89904	p 546	A95-90440	p 511	A95-91531	p 499
A95-87330	p 539	A95-88184	p 545	A95-90052	p 547	A95-90442	p 511	A95-91532	p 516
A95-87354	p 558	A95-88264	p 528	A95-90054	p 547	A95-90443	p 520	A95-91533	p 516
A95-87355	p 558	A95-88457	p 559	A95-90056	p 511	A95-90446	p 469	A95-91534	p 516
A95-87357	p 558	A95-88459	p 570	A95-90057	p 511	A95-90447	p 470	A95-91535	p 521
A95-87362	p 558	A95-88462	p 570	A95-90058	p 505	A95-90449	p 520	A95-91536	p 487
A95-87363	p 558	A95-88463	p 570	A95-90059	p 511	A95-90450	p 512	A95-91537	p 487
A95-87364	p 559	A95-88464	p 570	A95-90060	p 467	A95-90451	p 530	A95-91538	p 474
A95-87365	p 460	A95-88465	p 571	A95-90061	p 467	A95-90452	p 547	A95-91539	p 499
A95-87373	p 524	A95-88466	p 571	A95-90062	p 467	A95-90454	p 520	A95-91540	p 487
A95-87377	p 559	A95-88467	p 571	A95-90063	p 467	A95-90455	p 470	A95-91541	p 487
A95-87378	p 490	A95-88468	p 571	A95-90065	p 493	A95-90456	p 512	A95-91542	p 506
A95-87379	p 524	A95-88469	p 571	A95-90066	p 494	A95-90457	p 581	A95-91543	p 506
A95-87380	p 524	A95-88470	p 572	A95-90067	p 494	A95-90458	p 496	A95-91544	p 526
A95-87382	p 524	A95-88471	p 572	A95-90068	p 494	A95-90461	p 521	A95-91549	p 526
A95-87383	p 524	A95-88472	p 572	A95-90069	p 505	A95-90462	p 512	A95-91550	p 526
A95-87385	p 460	A95-88474	p 559	A95-90070	p 494	A95-90464	p 521	A95-91551	p 517
A95-87386	p 525	A95-88475	p 559	A95-90071	p 494	A95-90465	p 521	A95-91552	p 474
A95-87387	p 525	A95-88476	p 581	A95-90072	p 494	A95-90469	p 470	A95-91553	p 522
A95-87391	p 518	A95-88477	p 559	A95-90073	p 494	A95-90470	p 512	A95-91554	p 517
A95-87394	p 525	A95-88478	p 559	A95-90074	p 495	A95-90472	p 470	A95-91555	p 522
A95-87395	p 460	A95-88480	p 560	A95-90075	p 495	A95-90473	p 496	A95-91556	p 522
A95-87396	p 525	A95-88496	p 528	A95-90076	p 495	A95-90475	p 530	A95-91557	p 474
A95-87397	p 514	A95-88601	p 526	A95-90079	p 486	A95-90477	p 530	A95-91558	p 474
A95-87398	p 515	A95-88789	p 545	A95-90080	p 456	A95-90559	p 547	A95-91559	p 507
A95-87399	p 460	A95-88892	p 462	A95-90081	p 456	A95-90559	p 547	A95-91560	p 507
A95-87400	p 460	A95-88893	p 572	A95-90082	p 456	A95-90575	p 548	A95-91561	p 517
A95-87404	p 509	A95-88895	p 565	A95-90083	p 511	A95-90629	p 565	A95-91562	p 474
A95-87405	p 509	A95-88896	p 462	A95-90084	p 495	A95-90631	p 565	A95-91563	p 474
A95-87410	p 509	A95-88897	p 455	A95-90085	p 495	A95-90632	p 506	A95-91564	p 475
A95-87411	p 519	A95-88898	p 462	A95-90086	p 495	A95-90638	p 581	A95-91565	p 499
A95-87412	p 460	A95-88898	p 492	A95-90087	p 495	A95-90643	p 497	A95-91566	p 499
A95-87413	p 509	A95-88899	p 462	A95-90088	p 573	A95-90649	p 521	A95-91567	p 499
A95-87414	p 490	A95-88900	p 519	A95-90089	p 496	A95-90656	p 565	A95-91568	p 475
A95-87415	p 461	A95-88901	p 519	A95-90090	p 560	A95-90665	p 506	A95-91569	p 530
A95-87466	p 509	A95-88902	p 519	A95-90092	p 573	A95-90678	p 566	A95-91570	p 499
A95-87483	p 525	A95-88903	p 519	A95-90093	p 573	A95-90683	p 566	A95-91572	p 499
A95-87500	p 539	A95-88955	p 545	A95-90094	p 573	A95-90688	p 566	A95-91573	p 500
A95-87552	p 539	A95-88960	p 463	A95-90095	p 573	A95-90693	p 566	A95-91574	p 500
A95-87557	p 539	A95-88961	p 528	A95-90097	p 573	A95-90703	p 566	A95-91575	p 487
A95-87558	p 540	A95-88962	p 529	A95-90098	p 573	A95-90751	p 470	A95-91576	p 487
A95-87559	p 540	A95-88963	p 529	A95-90099	p 573	A95-90752	p 497	A95-91577	p 522
A95-87564	p 491	A95-88964	p 483	A95-90099	p 573	A95-90753	p 471	A95-91582	p 507
A95-87565	p 491	A95-88965	p 463	A95-90100	p 574	A95-90754	p 471	A95-91583	p 507
A95-87566	p 491	A95-88966	p 463	A95-90101	p 574	A95-90756	p 456	A95-91584	p 507
A95-87568	p 491	A95-88967	p 463	A95-90102	p 574	A95-90828	p 578	A95-91585	p 507
A95-87569	p 491	A95-88968	p 463	A95-90103	p 574	A95-90866	p 497	A95-91586	p 507
A95-87570	p 491	A95-88969	p 463	A95-90104	p 575	A95-90867	p 483	A95-91587	p 507
A95-87571	p 570	A95-88970	p 464	A95-90105	p 575	A95-90868	p 497	A95-91588	p 508
A95-87572	p 461	A95-88971	p 464	A95-90109	p 575	A95-90869	p 497	A95-91636	p 500
A95-87576	p 540	A95-88974	p 464	A95-90110	p 575	A95-90871	p 497	A95-91637	p 513
A95-87577	p 540	A95-88976	p 464	A95-90111	p 560	A95-90872	p 498	A95-91638	p 513
A95-87581	p 540	A95-88977	p 464	A95-90112	p 561	A95-90920	p 548	A95-91659	p 530
A95-87582	p 541	A95-88979	p 545	A95-90115	p 561	A95-90924	p 548	A95-91673	p 475
A95-87583	p 541	A95-88980	p 465	A95-90117	p 575	A95-90924	p 548	A95-91674	p 475
A95-87594	p 491	A95-88987	p 465	A95-90118	p 561	A95-90953	p 486	A95-91675	p 531
A95-87605	p 528	A95-88988	p 546	A95-90119	p 561	A95-90955	p 486	A95-91676	p 531
A95-87606	p 528	A95-88989	p 546	A95-90120	p 529	A95-91450	p 484	A95-91677	p 531
A95-87676	p 461	A95-88989	p 546	A95-90121	p 561	A95-91479	p 548	A95-91677	p 531
A95-87679	p 461	A95-88991	p 546	A95-90122	p 562	A95-91482	p 548	A95-91678	p 522
A95-87680	p 461	A95-88994	p 465	A95-90123	p 576	A95-91487	p 549	A95-91679	p 522
A95-87681	p 462	A95-88998	p 465	A95-90124	p 576	A95-91490	p 549	A95-91680	p 517
A95-87682	p 541	A95-89183	p 546	A95-90125	p 562	A95-91491	p 498	A95-91681	p 522
A95-87687	p 541	A95-89185	p 465	A95-90126	p 576	A95-91492	p 506	A95-91682	p 549
A95-87688	p 541	A95-89186	p 466	A95-90127	p 576	A95-91493	p 506	A95-91683	p 549
A95-87689	p 542	A95-89187	p 466	A95-90127	p 562	A95-91494	p 487	A95-91684	p 549
A95-87690	p 542	A95-89188	p 466	A95-90128	p 576	A95-91495	p 512	A95-91686	p 488
A95-87691	p 542	A95-89189	p 486	A95-90129	p 576	A95-91495	p 512	A95-91687	p 488
A95-87692	p 542	A95-89190	p 492	A95-90130	p 576	A95-91496	p 471	A95-91688	p 488
A95-87693	p 462	A95-89191	p 466	A95-90131	p 577	A95-91497	p 471	A95-91689	p 488
A95-87694	p 542	A95-89192	p 466	A95-90132	p 577	A95-91498	p 471	A95-91691	p 581
A95-87695	p 542	A95-89193	p 492	A95-90133	p 577	A95-91499	p 471	A95-91692	p 475
A95-87794	p 543	A95-89194	p 492	A95-90136	p 577	A95-91500	p 471	A95-91695	p 475
A95-87798	p 543	A95-89195	p 510	A95-90137	p 578	A95-91501	p 456	A95-91696	p 508
A95-87903	p 581	A95-89198	p 492	A95-90140	p 578	A95-91502	p 512	A95-91697	p 475
A95-88002	p 510	A95-89199	p 466	A95-90266	p 578	A95-91503	p 498	A95-91698	p 522
A95-88003	p 510	A95-89200	p 466	A95-90267	p 547	A95-91504	p 515	A95-91700	p 517
A95-88004	p 510	A95-89201	p 466	A95-90268	p 468	A95-91505	p 516	A95-91701	p 484
A95-88005	p 510	A95-89202	p 529	A95-90269	p 515	A95-91506	p 516	A95-91702	p 484
A95-88007	p 492	A95-89220	p 483	A95-90270	p 506	A95-91507	p 472	A95-91703	p 456
A95-88010	p 519	A95-89221	p 565	A95-90272	p 529	A95-91508	p 472	A95-91704	p 457
A95-88011	p 543	A95-89222	p 493	A95-90273	p 468	A95-91509	p 472	A95-91710	p 508
A95-88083	p 543	A95-89223	p 493	A95-90274	p 496	A95-91510	p 472	A95-91711	p 457
A95-88084	p 543	A95-89224	p 493	A95-90275	p 468	A95-91511	p 472	A95-91712	p 508
A95-88086	p 543	A95-89251	p 493	A95-90276	p 468	A95-91512	p 472	A95-91713	p 457
A95-88090	p 544	A95-89634	p 455	A95-90277	p 468	A95-91513	p 473	A95-91714	p 531
A95-88093	p 544	A95-89636	p 515	A95-90278	p 468	A95-91514	p 473	A95-91716	p 531
A95-88095	p 544	A95-89639	p 515	A95-90279	p 468	A95-91515	p 473	A95-91717	p 484
A95-88096	p 544	A95-89640	p 455	A95-90280	p 469	A95-91516	p 498	A95-91718	p 484
A95-88100	p 492	A95-89641	p 466	A95-90281	p 496	A95-91517	p 498	A95-91720	p 457
A95-88105	p 544	A95-89648	p 486	A95-90282	p 496	A95-91518	p 498	A95-91721	p 517
A95-88106	p 545	A95-89649	p 486	A95-90283	p 496	A95-91519	p 562	A95-91722	p 517
A95-88107	p 545	A95-89663	p 455	A95-90284	p 547	A95-91520	p 498	A95-91723	p 581
A95-88175	p 564	A95-89664	p 455	A95-90285	p 469	A95-91521	p 499	A95-91726	p 550
		A95-89665	p 467	A95-90360	p 526	A95-91522	p 473	A95-91728	p 508
		A95-89667	p 455	A95-90424	p 515	A95-91523	p 473	A95-91729	p 500
		A95-89894	p 542	A95-90438	p 520	A95-91524	p 473	A95-91730	p 500
		A95-89899	p 546	A95-90439	p 520	A95-91525	p 473	A95-91732	p 500
						A95-91530	p 530		

A95-91846	p 484	A95-93513	p 667	A95-93672	p 605	A95-95091	p 601	N95-10467	p 7
A95-91870	p 562	A95-93514	p 667	A95-93673	p 605	A95-95159	p 625	N95-10535	# p 23
A95-91895	p 475	A95-93515	p 667	A95-93674	p 628	A95-95161	p 626	N95-10547	* p 20
A95-91913	p 485	A95-93516	p 668	A95-93675	p 613	A95-95192	p 596	N95-10548	* p 10
A95-91915	p 550	A95-93517	p 668	A95-93676	p 625	A95-95193	p 626	N95-10552	* p 20
A95-91916	p 550	A95-93518	p 668	A95-93677	p 614	A95-95194	p 611	N95-10553	* p 22
A95-91917	p 550	A95-93519	p 668	A95-93678	p 614	A95-95198	p 596	N95-10556	* p 7
A95-91925	p 550	A95-93520	p 668	A95-93679	p 610	A95-95201	p 596	N95-10566	* # p 10
A95-92210	p 578	A95-93521	p 668	A95-93682	p 583	A95-95202	p 596	N95-10567	* # p 26
A95-92319	p 579	A95-93522	p 669	A95-93689	p 680	A95-95204	p 681	N95-10568	* # p 26
A95-92405	p 632	A95-93523	p 669	A95-93692	p 614	A95-95210	p 611	N95-10570	* # p 11
A95-92408	p 632	A95-93524	p 669	A95-93693	p 635	A95-95357	p 638	N95-10571	* # p 11
A95-92471	p 632	A95-93525	p 669	A95-93698	p 635	A95-95366	p 638	N95-10657	* # p 26
A95-92472	p 632	A95-93526	p 670	A95-93703	p 635	A95-95383	p 639	N95-10709	* # p 1
A95-92473	p 632	A95-93527	p 670	A95-93716	p 628	A95-95394	p 639	N95-10710	* # p 21
A95-92474	p 633	A95-93528	p 670	A95-93723	p 635	A95-95397	p 639	N95-10711	* # p 13
A95-92475	p 633	A95-93529	p 670	A95-93728	p 635	A95-95401	p 639	N95-10714	* # p 21
A95-92511	p 633	A95-93531	p 671	A95-93731	p 605	A95-95404	p 639	N95-10715	* # p 13
A95-92513	p 609	A95-93532	p 671	A95-93735	p 635	A95-95407	p 639	N95-10716	* # p 13
A95-92589	p 612	A95-93533	p 671	A95-93736	p 587	A95-95421	p 639	N95-10717	* # p 17
A95-92590	p 612	A95-93534	p 671	A95-93744	p 625	A95-95423	p 640	N95-10737	* # p 11
A95-92597	p 677	A95-93535	p 671	A95-93746	p 605	A95-95431	p 640	N95-10738	* # p 21
A95-92626	p 595	A95-93536	p 672	A95-93747	p 587	A95-95439	p 640	N95-10739	* # p 8
A95-92708	p 678	A95-93537	p 672	A95-93748	p 587	A95-95440	p 591	N95-10740	* # p 13
A95-92751	p 633	A95-93538	p 672	A95-93749	p 587	A95-95443	p 640	N95-10741	* # p 13
A95-93316	p 633	A95-93539	p 672	A95-93750	p 587	A95-95444	p 641	N95-10742	* # p 13
A95-93318	p 634	A95-93540	p 673	A95-93751	p 587	A95-95445	p 641	N95-10743	* # p 13
A95-93330	p 627	A95-93541	p 673	A95-93752	p 588	A95-95446	p 641	N95-10744	* # p 13
A95-93337	p 634	A95-93542	p 673	A95-93757	p 678	A95-95448	p 641	N95-10745	* # p 13
A95-93390	p 595	A95-93543	p 673	A95-93758	p 588	A95-95451	p 591	N95-10746	* # p 21
A95-93392	p 585	A95-93544	p 674	A95-93965	p 680	A95-95454	p 641	N95-10747	* # p 21
A95-93393	p 585	A95-93545	p 674	A95-94036	p 583	A95-95457	p 641	N95-10748	* # p 17
A95-93394	p 585	A95-93546	p 674	A95-94044	p 600	A95-95459	p 642	N95-10749	* # p 1
A95-93395	p 585	A95-93547	p 674	A95-94045	p 618	A95-95462	p 642	N95-10750	* # p 33
A95-93396	p 586	A95-93548	p 674	A95-94046	p 600	A95-95463	p 642	N95-10751	* # p 13
A95-93441	p 652	A95-93549	p 675	A95-94056	p 583	A95-95467	p 642	N95-10820	* # p 8
A95-93442	p 652	A95-93551	p 675	A95-94057	p 636	A95-95470	p 642	N95-10822	* # p 21
A95-93443	p 652	A95-93552	p 675	A95-94058	p 636	A95-95471	p 642	N95-10844	* # p 21
A95-93445	p 652	A95-93553	p 675	A95-94065	p 588	A95-95472	p 643	N95-10846	* # p 11
A95-93446	p 652	A95-93554	p 675	A95-94066	p 636	A95-95473	p 643	N95-10847	* # p 8
A95-93447	p 652	A95-93555	p 676	A95-94102	p 636	A95-95475	p 643	N95-10848	* # p 8
A95-93448	p 653	A95-93556	p 676	A95-94108	p 636	A95-95477	p 643	N95-10853	* # p 8
A95-93449	p 653	A95-93560	p 676	A95-94127	p 605	A95-95478	p 643	N95-10854	* # p 24
A95-93450	p 653	A95-93561	p 677	A95-94130	p 636	A95-95485	p 643	N95-10858	* # p 8
A95-93452	p 654	A95-93595	p 678	A95-94134	p 637	A95-95495	p 644	N95-10859	* # p 26
A95-93453	p 654	A95-93596	p 678	A95-94197	p 637	A95-95497	p 644	N95-10860	* # p 17
A95-93454	p 654	A95-93597	p 678	A95-94205	p 637	A95-95507	p 644	N95-10873	* # p 33
A95-93455	p 654	A95-93598	p 595	A95-94208	p 618	A95-96221	p 709	N95-10919	* # p 21
A95-93456	p 655	A95-93599	p 595	A95-94228	p 680	A95-96273	p 701	N95-10931	* # p 22
A95-93457	p 655	A95-93600	p 595	A95-94250	p 637	A95-96299	p 709	N95-10940	* # p 9
A95-93458	p 655	A95-93601	p 596	A95-94252	p 637	A95-96373	p 702	N95-11003	* # p 22
A95-93459	p 655	A95-93602	p 681	A95-94255	p 637	A95-96374	p 702	N95-11005	* # p 16
A95-93460	p 656	A95-93603	p 681	A95-94256	p 628	A95-96378	p 702	N95-11135	* # p 24
A95-93461	p 656	A95-93605	p 612	A95-94454	p 588	A95-96559	p 702	N95-11157	* # p 9
A95-93462	p 656	A95-93606	p 612	A95-94455	p 588	A95-96579	p 702	N95-11158	* # p 9
A95-93463	p 657	A95-93612	p 610	A95-94456	p 589	A95-96655	p 701	N95-11159	* # p 16
A95-93464	p 657	A95-93613	p 600	A95-94457	p 619	A95-96664	p 701	N95-11166	* # p 27
A95-93465	p 657	A95-93615	p 603	A95-94458	p 605			N95-11168	* # p 24
A95-93466	p 657	A95-93616	p 603	A95-94459	p 589			N95-11179	* # p 9
A95-93467	p 657	A95-93617	p 583	A95-94460	p 589	N95-10028	* # p 5	N95-11192	* # p 28
A95-93468	p 658	A95-93618	p 583	A95-94461	p 589	N95-10029	* # p 6	N95-11223	* # p 17
A95-93469	p 658	A95-93619	p 583	A95-94462	p 625	N95-10083	p 14	N95-11252	* # p 24
A95-93470	p 658	A95-93620	p 610	A95-94463	p 589	N95-10085	p 22	N95-11259	* # p 28
A95-93471	p 658	A95-93621	p 610	A95-94464	p 589	N95-10129	* # p 6	N95-11260	* # p 28
A95-93472	p 659	A95-93622	p 610	A95-94465	p 590	N95-10131	* # p 6	N95-11261	* # p 28
A95-93476	p 659	A95-93626	p 603	A95-94466	p 619	N95-10132	* # p 23	N95-11262	* # p 28
A95-93477	p 659	A95-93627	p 604	A95-94467	p 584	N95-10135	p 6	N95-11263	* # p 29
A95-93479	p 659	A95-93628	p 610	A95-94468	p 584	N95-10136	p 7	N95-11270	* # p 29
A95-93480	p 660	A95-93630	p 625	A95-94469	p 584	N95-10137	p 7	N95-11271	* # p 29
A95-93481	p 660	A95-93631	p 612	A95-94470	p 606	N95-10148	* # p 7	N95-11275	* # p 29
A95-93482	p 660	A95-93632	p 628	A95-94471	p 606	N95-10153	* # p 15	N95-11276	* # p 29
A95-93483	p 660	A95-93633	p 628	A95-94473	p 619	N95-10220	* # p 17	N95-11277	* # p 30
A95-93484	p 661	A95-93634	p 610	A95-94474	p 590	N95-10226	* # p 7	N95-11280	* # p 25
A95-93485	p 661	A95-93636	p 625	A95-94475	p 606	N95-10231	* # p 22	N95-11283	* # p 30
A95-93486	p 661	A95-93637	p 634	A95-94476	p 590	N95-10240	* # p 11	N95-11287	* # p 30
A95-93488	p 661	A95-93638	p 634	A95-94477	p 606	N95-10242	* # p 12	N95-11288	* # p 25
A95-93489	p 662	A95-93640	p 610	A95-94478	p 637	N95-10244	* # p 23	N95-11304	* # p 30
A95-93490	p 662	A95-93642	p 634	A95-94479	p 591	N95-10245	* # p 12	N95-11306	* # p 30
A95-93491	p 662	A95-93644	p 586	A95-94480	p 606	N95-10247	* # p 15	N95-11307	* # p 31
A95-93492	p 662	A95-93648	p 586	A95-94481	p 591	N95-10282	p 19	N95-11310	* # p 31
A95-93493	p 663	A95-93649	p 586	A95-94482	p 591	N95-10284	p 19	N95-11311	* # p 31
A95-93494	p 663	A95-93650	p 604	A95-94483	p 591	N95-10285	p 19	N95-11319	* # p 31
A95-93495	p 663	A95-93655	p 618	A95-94484	p 591	N95-10296	p 23	N95-11320	* # p 31
A95-93497	p 664	A95-93656	p 604	A95-94485	p 614	N95-10316	* # p 12	N95-11321	* # p 31
A95-93498	p 664	A95-93657	p 604	A95-94487	p 638	N95-10318	* # p 23	N95-11322	* # p 32
A95-93500	p 664	A95-93658	p 604	A95-94495	p 614	N95-10319	* # p 15	N95-11323	* # p 32
A95-93501	p 664	A95-93659	p 618	A95-94503	p 614	N95-10349	* # p 19	N95-11324	* # p 32
A95-93502	p 664	A95-93660	p 586	A95-94504	p 614	N95-10350	p 20	N95-11330	* # p 25
A95-93503	p 665	A95-93662	p 587	A95-94505	p 615	N95-10351	* # p 20	N95-11366	* # p 9
A95-93504	p 665	A95-93664	p 613	A95-94687	p 638	N95-10352	p 20	N95-11367	* # p 10
A95-93505	p 665	A95-93665	p 613	A95-94793	p 638	N95-10353	p 20	N95-11389	* # p 25
A95-93506	p 665	A95-93667	p 613	A95-95044	p 611	N95-10354	p 20	N95-11408	* # p 10
A95-93508	p 666	A95-93668	p 613	A95-95066	p 681	N95-10442	* # p 12	N95-11409	* # p 25
A95-93509	p 666	A95-93669	p 634	A95-95083	p 596	N95-10446	* # p 20	N95-11410	* # p 13
A95-93510	p 666	A95-93670	p 604	A95-95085	p 600			N95-11463	* # p 1
A95-93512	p 666	A95-93671	p 628	A95-95090	p 600			N95-11465	* # p 13

ACCESSION NUMBER INDEX

N95-17862

N95-11466 * #	p 21	N95-12695 * #	p 47	N95-14231 * #	p 68	N95-14849 #	p 80	N95-16404 #	p 123
N95-11483 * #	p 22	N95-12699 #	p 63	N95-14232 * #	p 68	N95-14850 #	p 87	N95-16448 #	p 156
N95-11487 * #	p 18	N95-12700 * #	p 48	N95-14233 * #	p 68	N95-14852 * #	p 80	N95-16456 * #	p 137
N95-11489 * #	p 10	N95-12702 * #	p 48	N95-14234 * #	p 68	N95-14878 * #	p 75	N95-16458 * #	p 169
N95-11510 * #	p 18	N95-12763 * #	p 51	N95-14235 * #	p 69	N95-14879 * #	p 96	N95-16461 * #	p 156
N95-11513 * #	p 27	N95-12770 * #	p 39	N95-14236 * #	p 69	N95-14880 * #	p 75	N95-16474 * #	p 169
N95-11529 * #	p 27	N95-12785 * #	p 48	N95-14237 * #	p 69	N95-14886 * #	p 100	N95-16506 #	p 168
N95-11582 * #	p 10	N95-12787 * #	p 48	N95-14238 * #	p 69	N95-14889 * #	p 101	N95-16509 #	p 145
N95-11593 * #	p 27	N95-12791 * #	p 52	N95-14239 * #	p 69	N95-14893 #	p 77	N95-16560 * #	p 104
N95-11595 * #	p 14	N95-12805 #	p 60	N95-14240 * #	p 69	N95-14894 #	p 75	N95-16562 #	p 127
N95-11684 #	p 14	N95-12831 * #	p 48	N95-14241 * #	p 69	N95-14897 * #	p 77	N95-16563 #	p 107
N95-11699 * #	p 43	N95-12832 * #	p 61	N95-14242 * #	p 70	N95-14898 #	p 77	N95-16564 #	p 107
N95-11710 * #	p 35	N95-12843 * #	p 58	N95-14243 * #	p 70	N95-14899 * #	p 78	N95-16565 #	p 127
N95-11711 * #	p 57	N95-12854 #	p 58	N95-14244 * #	p 70	N95-14900 #	p 84	N95-16566 #	p 128
N95-11752 * #	p 52	N95-12855 #	p 61	N95-14245 * #	p 70	N95-14909 * #	p 81	N95-16567 #	p 128
N95-11766 * #	p 36	N95-12856 * #	p 58	N95-14246 * #	p 70	N95-14912 * #	p 96	N95-16568 #	p 128
N95-11774 #	p 43	N95-12860 * #	p 50	N95-14247 * #	p 70	N95-14916 * #	p 78	N95-16569 * #	p 128
N95-11789 #	p 52	N95-12993 * #	p 49	N95-14248 * #	p 71	N95-14920 * #	p 88	N95-16570 #	p 128
N95-11793 #	p 44	N95-12996 #	p 61	N95-14249 * #	p 71	N95-14921 * #	p 66	N95-16571 #	p 128
N95-11794 #	p 44	N95-13027 * #	p 49	N95-14251 * #	p 71	N95-14922 * #	p 96	N95-16572 #	p 128
N95-11796 #	p 55	N95-13058 * #	p 39	N95-14252 * #	p 71	N95-15059 * #	p 101	N95-16573 #	p 129
N95-11798 #	p 60	N95-13184 #	p 56	N95-14253 * #	p 71	N95-15065 * #	p 102	N95-16588 * #	p 156
N95-11812 * #	p 57	N95-13196 * #	p 54	N95-14254 * #	p 72	N95-15066 #	p 78	N95-16589 * #	p 107
N95-11815 * #	p 57	N95-13197 * #	p 39	N95-14255 * #	p 72	N95-15306 #	p 96	N95-16621 #	p 156
N95-11829 - #	p 36	N95-13200 #	p 53	N95-14256 * #	p 72	N95-15319 #	p 75	N95-16736 - #	p 157
N95-11864 * #	p 49	N95-13201 * #	p 58	N95-14257 * #	p 72	N95-15328 #	p 85	N95-16776 * #	p 149
N95-11867 * #	p 50	N95-13203 * #	p 41	N95-14258 * #	p 72	N95-15329 #	p 83	N95-16808 #	p 107
N95-11868 * #	p 51	N95-13204 * #	p 41	N95-14259 * #	p 72	N95-15331 #	p 66	N95-16824 #	p 108
N95-11869 * #	p 51	N95-13205 * #	p 41	N95-14264 * #	p 72	N95-15392 #	p 82	N95-16828 * #	p 157
N95-11870 * #	p 54	N95-13206 * #	p 41	N95-14282 * #	p 86	N95-15415 #	p 88	N95-16848 * #	p 172
N95-11877 * #	p 36	N95-13207 * #	p 41	N95-14297 * #	p 73	N95-15439 #	p 78	N95-16858 * #	p 108
N95-11884 * #	p 36	N95-13208 * #	p 42	N95-14299 * #	p 91	N95-15451 #	p 81	N95-16859 * #	p 151
N95-11888 * #	p 57	N95-13209 * #	p 42	N95-14306 #	p 79	N95-15465 #	p 76	N95-16860 * #	p 151
N95-11890 * #	p 50	N95-13210 * #	p 59	N95-14343 #	p 83	N95-15547 #	p 96	N95-16864 #	p 169
N95-11892 #	p 35	N95-13211 * #	p 42	N95-14350 #	p 77	N95-15604 * #	p 97	N95-16887 * #	p 108
N95-11898 * #	p 36	N95-13212 * #	p 42	N95-14351 #	p 91	N95-15683 #	p 83	N95-16897 * #	p 170
N95-11901 * #	p 50	N95-13213 * #	p 59	N95-14357 #	p 99	N95-15728 * #	p 97	N95-16898 * #	p 170
N95-11911 * #	p 37	N95-13215 * #	p 59	N95-14363 #	p 87	N95-15742 * #	p 81	N95-16899 * #	p 129
N95-11913 * #	p 49	N95-13235 * #	p 59	N95-14405 #	p 92	N95-15743 * #	p 101	N95-16905 * #	p 152
N95-11915 * #	p 55	N95-13235 * #	p 59	N95-14409 #	p 87	N95-15749 * #	p 98	N95-16906 * #	p 170
N95-11917 * #	p 37	N95-13243 #	p 53	N95-14415 #	p 85	N95-15762 * #	p 76	N95-16908 #	p 108
N95-11927 * #	p 37	N95-13247 #	p 42	N95-14418 * #	p 73	N95-15785 * #	p 97	N95-16911 * #	p 157
N95-11932 * #	p 61	N95-13249 #	p 59	N95-14419 * #	p 66	N95-15815 #	p 81	N95-16939 #	p 129
N95-11937 * #	p 54	N95-13250 #	p 40	N95-14445 #	p 73	N95-15821 #	p 81	N95-16969 #	p 157
N95-11938 * #	p 52	N95-13289 #	p 51	N95-14446 #	p 73	N95-15852 * #	p 76	N95-16982 * #	p 129
N95-11944 #	p 62	N95-13553 * #	p 53	N95-14447 #	p 73	N95-15853 * #	p 76	N95-17178 #	p 108
N95-11951 * #	p 50	N95-13575 #	p 62	N95-14448 #	p 84	N95-15898 #	p 97	N95-17196 * #	p 125
N95-11952 * #	p 44	N95-13595 * #	p 59	N95-14448 #	p 84	N95-15899 * #	p 97	N95-17248 * #	p 149
N95-11967 * #	p 37	N95-13599 #	p 60	N95-14451 #	p 74	N95-15912 * #	p 76	N95-17252 * #	p 149
N95-11968 * #	p 55	N95-13600 #	p 60	N95-14452 #	p 74	N95-15970 * #	p 137	N95-17264 * #	p 170
N95-11968 * #	p 55	N95-13601 * #	p 53	N95-14453 * #	p 92	N95-15971 * #	p 127	N95-17273 * #	p 108
N95-11995 * #	p 37	N95-13602 * #	p 60	N95-14454 * #	p 92	N95-15988 * #	p 169	N95-17278 #	p 149
N95-11996 * #	p 57	N95-13640 #	p 102	N95-14455 * #	p 92	N95-16038 #	p 105	N95-17291 * #	p 109
N95-12131 #	p 55	N95-13642 * #	p 65	N95-14456 * #	p 92	N95-16048 * #	p 154	N95-17334 #	p 172
N95-12146 #	p 40	N95-13662 * #	p 65	N95-14457 * #	p 92	N95-16069 * #	p 106	N95-17371 #	p 138
N95-12166 #	p 35	N95-13663 * #	p 102	N95-14458 * #	p 93	N95-16072 * #	p 154	N95-17373 #	p 125
N95-12175 * #	p 54	N95-13665 * #	p 89	N95-14459 * #	p 93	N95-16076 #	p 106	N95-17384 * #	p 125
N95-12176 * #	p 38	N95-13665 * #	p 89	N95-14460 * #	p 93	N95-16097 #	p 154	N95-17388 * #	p 145
N95-12190 * #	p 63	N95-13687 #	p 84	N95-14461 * #	p 93	N95-16099 #	p 106	N95-17397 * #	p 129
N95-12191 * #	p 38	N95-13701 * #	p 67	N95-14464 * #	p 93	N95-16109 #	p 142	N95-17402 * #	p 138
N95-12191 * #	p 38	N95-13703 * #	p 79	N95-14465 * #	p 87	N95-16160 #	p 106	N95-17404 * #	p 142
N95-12216 #	p 53	N95-13717 * #	p 101	N95-14466 * #	p 93	N95-16163 #	p 155	N95-17418 * #	p 107
N95-12225 * #	p 44	N95-13718 * #	p 85	N95-14467 * #	p 93	N95-16226 #	p 151	N95-17435 #	p 159
N95-12227 * #	p 35	N95-13719 * #	p 67	N95-14468 * #	p 94	N95-16257 #	p 107	N95-17444 #	p 145
N95-12228 * #	p 58	N95-13720 * #	p 67	N95-14469 * #	p 80	N95-16258 #	p 144	N95-17451 #	p 104
N95-12230 #	p 43	N95-13725 * #	p 98	N95-14470 * #	p 94	N95-16264 #	p 127	N95-17454 #	p 142
N95-12294 * #	p 44	N95-13727 * #	p 99	N95-14471 * #	p 94	N95-16265 #	p 138	N95-17466 #	p 104
N95-12305 * #	p 45	N95-13885 * #	p 98	N95-14472 * #	p 94	N95-16268 #	p 155	N95-17476 #	p 123
N95-12341 * #	p 62	N95-13891 * #	p 65	N95-14473 * #	p 94	N95-16272 #	p 169	N95-17490 * #	p 158
N95-12357 * #	p 55	N95-13892 * #	p 89	N95-14475 * #	p 94	N95-16277 #	p 125	N95-17493 * #	p 150
N95-12360 * #	p 38	N95-13892 * #	p 89	N95-14476 * #	p 94	N95-16278 #	p 155	N95-17507 #	p 158
N95-12363 * #	p 45	N95-13895 #	p 99	N95-14477 * #	p 66	N95-16312 #	p 148	N95-17596 * #	p 150
N95-12363 * #	p 45	N95-13981 #	p 79	N95-14479 * #	p 94	N95-16316 #	p 148	N95-17646 #	p 123
N95-12378 * #	p 38	N95-14089 * #	p 86	N95-14480 * #	p 95	N95-16317 #	p 138	N95-17657 * #	p 104
N95-12389 * #	p 38	N95-14096 #	p 86	N95-14481 * #	p 80	N95-16318 #	p 144	N95-17661 #	p 130
N95-12410 #	p 45	N95-14102 #	p 79	N95-14482 * #	p 88	N95-16319 #	p 144	N95-17706 #	p 126
N95-12426 #	p 62	N95-14103 #	p 67	N95-14484 * #	p 95	N95-16320 * #	p 145	N95-17748 #	p 139
N95-12499 #	p 40	N95-14127 #	p 89	N95-14485 * #	p 95	N95-16321 #	p 148	N95-17846 #	p 109
N95-12507 #	p 54	N95-14128 #	p 89	N95-14486 * #	p 80	N95-16322 #	p 155	N95-17847 #	p 158
N95-12512 #	p 62	N95-14129 #	p 90	N95-14487 * #	p 80	N95-16323 #	p 138	N95-17848 #	p 109
N95-12530 * #	p 45	N95-14130 #	p 90	N95-14488 * #	p 82	N95-16324 #	p 149	N95-17849 #	p 109
N95-12546 #	p 56	N95-14132 #	p 90	N95-14489 * #	p 95	N95-16325 #	p 155	N95-17850 #	p 110
N95-12548 #	p 38	N95-14133 #	p 90	N95-14490 * #	p 80	N95-16326 #	p 148	N95-17851 #	p 110
N95-12578 #	p 39	N95-14134 #	p 90	N95-14556 * #	p 95	N95-16327 #	p 169	N95-17852 #	p 110
N95-12582 #	p 43	N95-14135 #	p 90	N95-14563 * #	p 95	N95-16328 #	p 125	N95-17853 #	p 110
N95-12591 #	p 49	N95-14136 #	p 90	N95-14604 * #	p 80	N95-16329 #	p 155	N95-17854 #	p 110
N95-12609 * #	p 45	N95-14137 * #	p 90	N95-14610 * #	p 100	N95-16330 #	p 148	N95-17855 #	p 111
N95-12623 #	p 40	N95-14138 #	p 90	N95-14611 * #	p 74	N95-16331 #	p 149	N95-17856 #	p 111
N95-12626 * #	p 45	N95-14139 #	p 91	N95-14612 * #	p 74	N95-16332 #	p 155	N95-17857 #	p 111
N95-12628 * #	p 46	N95-14140 #	p 65	N95-14613 * #	p 74	N95-16333 #	p 149	N95-17858 * #	p 111
N95-12636 * #	p 46	N95-14141 * #	p 99	N95-14614 * #	p 95	N95-16334 #	p 156	N95-17859 #	p 112
N95-12637 * #	p 46	N95-14142 * #	p 86	N95-14615 * #	p 100	N95-16335 #	p 127	N95-17860 #	p 112
N95-12638 * #	p 46	N95-14143 * #	p 99	N95-14616 * #	p 100	N95-16336 #	p 149	N95-17861 #	p 112
N95-12639 * #	p 47	N95-14144 * #	p 86	N95-14617 * #	p 83	N95-16337 #	p 151	N95-17862 #	p 112
N95-12643 * #	p 47	N95-14145 * #	p 86	N95-14618 * #	p 83	N95-16338 #	p 142		
N95-12645 * #	p 47	N95-14146 * #	p 77	N95-14619 * #	p 83	N95-16339 #	p 142		
N95-12652 #	p 39	N95-14147 * #	p 77	N95-14620 * #	p 74	N95-16340 #	p 149		
N95-12664 * #	p 51	N95-14148 * #	p 91	N95-14621 * #	p 87	N95-16341 #	p 149		
N95-12689 * #	p 47	N95-14149 * #	p 67	N95-14622 * #	p 99	N95-16342 #	p 156		
		N95-14199 #	p 77	N95-14623 * #	p 87	N95-16343 #	p 149		
		N95-14201 #	p 91	N95-14624 * #	p 99	N95-16344 #	p 127		
		N95-14205 #	p 79	N95-14625 * #	p 87	N95-16345 #	p 149		
		N95-14229 * #	p 67	N95-14626 * #	p 96	N95-16346 #	p 127		
		N95-14230 * #	p 68	N95-14627 * #	p 80	N95-16347 #	p 151		
				N95-14628 * #	p 80	N95-16348 #	p 142		

N95-17863 # p 130
 N95-17864 # p 113
 N95-17865 # p 113
 N95-17866 # p 113
 N95-17867 # p 158
 N95-17868 # p 113
 N95-17869 # p 158
 N95-17870 # p 114
 N95-17871 # p 158
 N95-17872 # p 114
 N95-17873 # p 114
 N95-17874 # p 114
 N95-17875 # p 114
 N95-17876 # p 114
 N95-17877 # p 115
 N95-17878 # p 115
 N95-17879 # p 115
 N95-17880 # p 115
 N95-17881 # p 115
 N95-17882 # p 116
 N95-17883 # p 116
 N95-17884 # p 116
 N95-17885 # p 116
 N95-17953 # p 130
 N95-18008 # p 130
 N95-18018 # p 170
 N95-18042 # p 159
 N95-18044 # p 105
 N95-18054 # p 145
 N95-18059 # p 126
 N95-18068 # p 152
 N95-18087 # p 146
 N95-18088 # p 126
 N95-18090 # p 130
 N95-18093 # p 168
 N95-18097 # p 131
 N95-18101 # p 116
 N95-18110 # p 170
 N95-18133 # p 139
 N95-18162 # p 131
 N95-18164 # p 138
 N95-18190 # p 159
 N95-18191 # p 159
 N95-18193 # p 159
 N95-18196 # p 150
 N95-18197 # p 105
 N95-18198 # p 131
 N95-18325 # p 159
 N95-18337 # p 116
 N95-18340 # p 117
 N95-18347 # p 126
 N95-18365 # p 171
 N95-18380 # p 117
 N95-18381 # p 131
 N95-18383 # p 139
 N95-18388 # p 160
 N95-18398 # p 131
 N95-18405 # p 146
 N95-18407 # p 132
 N95-18410 # p 152
 N95-18415 # p 132
 N95-18436 # p 160
 N95-18457 # p 117
 N95-18461 # p 160
 N95-18483 # p 132
 N95-18486 # p 105
 N95-18503 # p 117
 N95-18539 # p 117
 N95-18542 # p 172
 N95-18564 # p 171
 N95-18565 # p 117
 N95-18567 # p 143
 N95-18573 # p 176
 N95-18578 # p 176
 N95-18582 # p 123
 N95-18586 # p 146
 N95-18597 # p 143
 N95-18598 # p 143
 N95-18599 # p 132
 N95-18600 # p 143
 N95-18601 # p 133
 N95-18602 # p 133
 N95-18603 # p 133
 N95-18604 # p 118
 N95-18605 # p 133
 N95-18606 # p 105
 N95-18611 # p 118
 N95-18616 # p 133
 N95-18621 # p 133
 N95-18624 # p 118
 N95-18641 # p 143
 N95-18645 # p 118
 N95-18646 # p 118
 N95-18660 # p 160
 N95-18663 # p 118

N95-18669 # p 119
 N95-18670 # p 119
 N95-18674 # p 119
 N95-18677 # p 133
 N95-18720 # p 150
 N95-18722 # p 168
 N95-18724 # p 146
 N95-18725 # p 146
 N95-18726 # p 134
 N95-18737 # p 160
 N95-18743 # p 150
 N95-18891 # p 134
 N95-18899 # p 171
 N95-18901 # p 161
 N95-18902 # p 144
 N95-18903 # p 146
 N95-18904 # p 119
 N95-18910 # p 119
 N95-18912 # p 172
 N95-18927 # p 126
 N95-18933 # p 119
 N95-18938 # p 161
 N95-18955 # p 161
 N95-18956 # p 161
 N95-18993 # p 150
 N95-19008 # p 152
 N95-19017 # p 139
 N95-19019 # p 161
 N95-19020 # p 140
 N95-19021 # p 140
 N95-19022 # p 140
 N95-19023 # p 140
 N95-19024 # p 140
 N95-19025 # p 140
 N95-19026 # p 140
 N95-19029 # p 144
 N95-19035 # p 161
 N95-19041 # p 119
 N95-19042 # p 120
 N95-19044 # p 134
 N95-19067 # p 134
 N95-19073 # p 151
 N95-19090 # p 152
 N95-19100 # p 152
 N95-19110 # p 120
 N95-19114 # p 120
 N95-19119 # p 120
 N95-19125 # p 162
 N95-19130 # p 134
 N95-19132 # p 124
 N95-19142 # p 173
 N95-19143 # p 173
 N95-19144 # p 173
 N95-19145 # p 173
 N95-19146 # p 173
 N95-19147 # p 173
 N95-19148 # p 174
 N95-19149 # p 174
 N95-19150 # p 147
 N95-19151 # p 135
 N95-19154 # p 135
 N95-19156 # p 174
 N95-19157 # p 174
 N95-19159 # p 174
 N95-19161 # p 162
 N95-19162 # p 174
 N95-19163 # p 175
 N95-19164 # p 175
 N95-19167 # p 124
 N95-19236 # p 162
 N95-19237 # p 151
 N95-19251 # p 162
 N95-19252 # p 162
 N95-19255 # p 163
 N95-19257 # p 163
 N95-19258 # p 163
 N95-19259 # p 121
 N95-19260 # p 121
 N95-19261 # p 121
 N95-19262 # p 163
 N95-19263 # p 164
 N95-19264 # p 164
 N95-19265 # p 164
 N95-19266 # p 164
 N95-19267 # p 147
 N95-19268 # p 121
 N95-19269 # p 147
 N95-19270 # p 121
 N95-19271 # p 147
 N95-19272 # p 147
 N95-19273 # p 164
 N95-19274 # p 175
 N95-19275 # p 165
 N95-19276 # p 165
 N95-19277 # p 165
 N95-19278 # p 122

N95-19279 # p 122
 N95-19280 # p 122
 N95-19281 # p 122
 N95-19282 # p 122
 N95-19284 # p 124
 N95-19285 # p 124
 N95-19286 # p 148
 N95-19380 # p 141
 N95-19381 # p 141
 N95-19382 # p 141
 N95-19383 # p 141
 N95-19444 # p 165
 N95-19447 # p 165
 N95-19448 # p 165
 N95-19457 # p 123
 N95-19462 # p 165
 N95-19464 # p 123
 N95-19468 # p 124
 N95-19469 # p 135
 N95-19470 # p 166
 N95-19471 # p 166
 N95-19472 # p 166
 N95-19473 # p 166
 N95-19477 # p 166
 N95-19478 # p 135
 N95-19479 # p 135
 N95-19480 # p 136
 N95-19482 # p 152
 N95-19483 # p 167
 N95-19485 # p 136
 N95-19486 # p 136
 N95-19488 # p 136
 N95-19490 # p 153
 N95-19491 # p 136
 N95-19495 # p 137
 N95-19496 # p 167
 N95-19497 # p 137
 N95-19499 # p 137
 N95-19501 # p 167
 N95-19517 # p 194
 N95-19546 # p 188
 N95-19567 # p 210
 N95-19576 # p 204
 N95-19579 # p 206
 N95-19582 # p 216
 N95-19595 # p 197
 N95-19624 # p 205
 N95-19651 # p 197
 N95-19653 # p 197
 N95-19654 # p 198
 N95-19655 # p 198
 N95-19656 # p 198
 N95-19657 # p 198
 N95-19658 # p 198
 N95-19659 # p 198
 N95-19660 # p 199
 N95-19661 # p 199
 N95-19662 # p 199
 N95-19663 # p 199
 N95-19664 # p 199
 N95-19665 # p 199
 N95-19666 # p 200
 N95-19668 # p 200
 N95-19669 # p 200
 N95-19670 # p 200
 N95-19671 # p 200
 N95-19672 # p 200
 N95-19673 # p 201
 N95-19675 # p 201
 N95-19676 # p 201
 N95-19677 # p 201
 N95-19678 # p 201
 N95-19679 # p 201
 N95-19680 # p 202
 N95-19681 # p 202
 N95-19683 # p 202
 N95-19684 # p 202
 N95-19685 # p 216
 N95-19688 # p 217
 N95-19693 # p 194
 N95-19720 # p 188
 N95-19730 # p 210
 N95-19731 # p 194
 N95-19751 # p 217
 N95-19759 # p 217
 N95-19767 # p 217
 N95-19769 # p 202
 N95-19772 # p 188
 N95-19774 # p 210
 N95-19775 # p 210
 N95-19776 # p 211
 N95-19777 # p 211
 N95-19789 # p 194
 N95-19793 # p 188
 N95-19794 # p 211
 N95-19798 # p 211

N95-19805 # p 189
 N95-19809 # p 211
 N95-19810 # p 191
 N95-19848 # p 204
 N95-19855 # p 216
 N95-19863 # p 188
 N95-19864 # p 203
 N95-19912 # p 244
 N95-19913 # p 222
 N95-19921 # p 255
 N95-19931 # p 238
 N95-19946 # p 222
 N95-19950 # p 228
 N95-19953 # p 244
 N95-19955 # p 238
 N95-19963 # p 230
 N95-19967 # p 219
 N95-19989 # p 255
 N95-19991 # p 223
 N95-19994 # p 230
 N95-19996 # p 223
 N95-20004 # p 237
 N95-20032 # p 232
 N95-20071 # p 225
 N95-20080 # p 238
 N95-20091 # p 219
 N95-20093 # p 225
 N95-20155 # p 230
 N95-20174 # p 226
 N95-20177 # p 223
 N95-20181 # p 230
 N95-20191 # p 244
 N95-20195 # p 228
 N95-20212 # p 231
 N95-20248 # p 223
 N95-20275 # p 226
 N95-20295 # p 244
 N95-20299 # p 241
 N95-20329 # p 231
 N95-20370 # p 231
 N95-20414 # p 244
 N95-20441 # p 255
 N95-20466 # p 231
 N95-20481 # p 241
 N95-20484 # p 245
 N95-20530 # p 245
 N95-20599 # p 245
 N95-20624 # p 238
 N95-20631 # p 233
 N95-20632 # p 233
 N95-20633 # p 233
 N95-20634 # p 233
 N95-20635 # p 233
 N95-20636 # p 234
 N95-20638 # p 245
 N95-20641 # p 234
 N95-20643 # p 245
 N95-20644 # p 246
 N95-20646 # p 240
 N95-20647 # p 246
 N95-20648 # p 246
 N95-20649 # p 246
 N95-20650 # p 234
 N95-20652 # p 257
 N95-20653 # p 247
 N95-20655 # p 241
 N95-20656 # p 241
 N95-20657 # p 234
 N95-20658 # p 247
 N95-20659 # p 234
 N95-20669 # p 238
 N95-20688 # p 223
 N95-20706 # p 226
 N95-20716 # p 241
 N95-20719 # p 256
 N95-20758 # p 223
 N95-20771 # p 247
 N95-20772 # p 231
 N95-20781 # p 247
 N95-20794 # p 223
 N95-20799 # p 239
 N95-20828 # p 256
 N95-20849 # p 247
 N95-20860 # p 231
 N95-20906 # p 240
 N95-20945 # p 247
 N95-20963 # p 257
 N95-20966 # p 248
 N95-20985 # p 256
 N95-20992 # p 239
 N95-20998 # p 248
 N95-21001 # p 248
 N95-21020 # p 228
 N95-21031 # p 224
 N95-21061 # p 248
 N95-21096 # p 248

N95-21100 # p 258
 N95-21122 # p 237
 N95-21132 # p 248
 N95-21146 # p 248
 N95-21148 # p 228
 N95-21170 # p 258
 N95-21186 # p 232
 N95-21214 # p 237
 N95-21243 # p 235
 N95-21258 # p 249
 N95-21323 # p 249
 N95-21338 # p 224
 N95-21340 # p 249
 N95-21343 # p 224
 N95-21369 # p 229
 N95-21383 # p 236
 N95-21388 # p 258
 N95-21425 # p 232
 N95-21436 # p 239
 N95-21478 # p 249
 N95-21518 # p 226
 N95-21520 # p 229
 N95-21552 # p 256
 N95-21640 # p 219
 N95-21659 # p 224
 N95-21673 # p 258
 N95-21687 # p 241
 N95-21719 # p 239
 N95-21730 # p 232
 N95-21831 # p 226
 N95-21864 # p 224
 N95-21877 # p 225
 N95-21882 # p 258
 N95-21888 # p 258
 N95-21891 # p 229
 N95-21892 # p 225
 N95-21913 # p 256
 N95-21969 # p 242
 N95-21975 # p 259
 N95-22005 # p 249
 N95-22024 # p 235
 N95-22036 # p 235
 N95-22039 # p 232
 N95-22044 # p 259
 N95-22046 # p 219
 N95-22109 # p 250
 N95-22132 # p 242
 N95-22161 # p 229
 N95-22212 # p 250
 N95-22216 # p 257
 N95-22232 # p 235
 N95-22299 # p 250
 N95-22318 # p 226
 N95-22319 # p 227
 N95-22341 # p 236
 N95-22352 # p 227
 N95-22417 # p 227
 N95-22448 # p 225
 N95-22449 # p 250
 N95-22451 # p 250
 N95-22452 # p 251
 N95-22455 # p 251
 N95-22457 # p 251
 N95-22481 # p 309
 N95-22510 # p 284
 N95-22578 # p 288
 N95-22666 # p 272
 N95-22669 # p 309
 N95-22674 # p 292
 N95-22675 # p 323
 N95-22689 # p 300
 N95-22764 # p 300
 N95-22802 # p 272
 N95-22804 # p 309
 N95-22806 # p 284
 N95-22829 # p 293
 N95-22917 # p 273
 N95-22949 # p 285
 N95-22953 # p 285
 N95-22954 # p 293
 N95-23009 # p 320
 N95-23011 # p 296
 N95-23015 # p 309
 N95-23031 # p 301
 N95-23038 # p 301
 N95-23088 # p 289
 N95-23095 # p 273
 N95-23161 # p 285
 N95-23168 # p 324
 N95-23178 # p 323
 N95-23179 # p 301
 N95-23182 # p 273
 N95-23183 # p 309
 N95-23185 # p 273
 N95-23190 # p 310

ACCESSION NUMBER INDEX

N95-28462

N95-23192	#	p 296	N95-24050	#	p 277	N95-25936	p 339	N95-26844	p 390	N95-27791	#	p 383	
N95-23193	#	p 273	N95-24053	#	p 290	N95-25962	#	p 332	N95-26845	p 448	N95-27805	#	p 447
N95-23201	#	p 276	N95-24065	#	p 277	N95-25978	#	p 362	N95-26854	p 375	N95-27839	#	p 410
N95-23210	#	p 310	N95-24071	#	p 278	N95-26004	#	p 343	N95-26858	p 446	N95-27851	#	p 420
N95-23217	#	p 285	N95-24076	#	p 324	N95-26005	#	p 358	N95-26859	p 375	N95-27854	#	p 438
N95-23218	#	p 274	N95-24091	#	p 286	N95-26009	#	p 336	N95-26873	p 390	N95-27855	#	p 438
N95-23222	#	p 289	N95-24105	#	p 278	N95-26015	#	p 362	N95-26876	p 390	N95-27859	#	p 381
N95-23250	#	p 274	N95-24189	#	p 316	N95-26053	#	p 341	N95-26877	p 437	N95-27860	#	p 406
N95-23257	#	p 310	N95-24200	#	p 327	N95-26075	#	p 332	N95-26878	p 406	N95-27865	#	p 439
N95-23259	#	p 320	N95-24201	#	p 328	N95-26085	#	p 361	N95-26890	#	N95-27866	#	p 406
N95-23276	#	p 325	N95-24202	#	p 363	N95-26090	#	p 358	N95-26895	p 448	N95-27882	#	p 439
N95-23277	#	p 301	N95-24203	#	p 348	N95-26119	#	p 344	N95-26898	p 383	N95-27885	#	p 439
N95-23283	#	p 274	N95-24206	#	p 333	N95-26120	#	p 344	N95-26901	p 375	N95-27886	#	p 439
N95-23284	#	p 324	N95-24207	#	p 337	N95-26121	#	p 344	N95-26920	p 448	N95-27889	#	p 439
N95-23287	#	p 310	N95-24210	#	p 329	N95-26122	#	p 344	N95-26941	#	N95-27903	#	p 384
N95-23290	#	p 310	N95-24211	#	p 348	N95-26123	#	p 344	N95-26942	#	N95-27907	#	p 381
N95-23294	#	p 274	N95-24213	#	p 338	N95-26124	#	p 345	N95-26943	#	N95-27908	#	p 451
N95-23297	#	p 293	N95-24217	#	p 330	N95-26125	#	p 345	N95-26944	#	N95-27910	#	p 397
N95-23299	#	p 296	N95-24219	#	p 357	N95-26126	#	p 345	N95-26945	#	N95-27914	#	p 449
N95-23300	#	p 301	N95-24220	#	p 343	N95-26128	#	p 345	N95-26946	#	N95-27918	#	p 397
N95-23304	#	p 297	N95-24238	#	p 363	N95-26131	#	p 345	N95-26947	#	N95-27970	#	p 447
N95-23308	#	p 322	N95-24260	#	p 340	N95-26133	#	p 345	N95-26948	#	N95-27974	#	p 376
N95-23309	#	p 297	N95-24274	#	p 357	N95-26138	#	p 346	N95-26949	#	N95-27975	#	p 376
N95-23311	#	p 311	N95-24293	#	p 338	N95-26140	#	p 346	N95-26951	#	N95-27976	#	p 376
N95-23314	#	p 293	N95-24295	#	p 328	N95-26160	#	p 362	N95-26952	#	N95-27977	#	p 377
N95-23317	#	p 285	N95-24302	#	p 340	N95-26187	#	p 362	N95-26953	#	N95-27978	#	p 377
N95-23318	#	p 280	N95-24304	#	p 338	N95-26190	#	p 337	N95-26953	#	N95-27979	#	p 449
N95-23319	#	p 294	N95-24308	#	p 330	N95-26251	#	p 346	N95-26954	#	N95-27980	#	p 439
N95-23320	#	p 324	N95-24308	#	p 330	N95-26302	#	p 332	N95-26955	#	N95-27981	#	p 377
N95-23325	#	p 294	N95-24379	#	p 330	N95-26303	#	p 361	N95-26956	#	N95-27982	#	p 440
N95-23333	#	p 275	N95-24384	#	p 333	N95-26330	#	p 336	N95-26957	p 409	N95-27983	#	p 440
N95-23377	#	p 311	N95-24388	#	p 340	N95-26338	#	p 336	N95-26958	p 409	N95-27985	#	p 440
N95-23389	#	p 294	N95-24390	#	p 338	N95-26348	#	p 447	N95-26966	#	N95-27985	#	p 440
N95-23390	#	p 286	N95-24391	#	p 333	N95-26349	#	p 435	N95-26978	p 383	N95-27986	#	p 440
N95-23392	#	p 294	N95-24392	#	p 338	N95-26378	#	p 411	N95-26981	p 409	N95-27989	#	p 440
N95-23393	#	p 280	N95-24396	#	p 348	N95-26381	#	p 366	N95-26985	p 383	N95-27990	#	p 451
N95-23395	#	p 286	N95-24397	#	p 330	N95-26382	#	p 373	N95-26990	p 449	N95-27991	#	p 451
N95-23410	#	p 295	N95-24412	#	p 348	N95-26389	#	p 388	N95-26993	p 391	N95-27992	#	p 441
N95-23419	#	p 322	N95-24413	#	p 349	N95-26392	#	p 451	N95-26994	p 391	N95-27999	#	p 453
N95-23423	#	p 311	N95-24424	#	p 341	N95-26405	#	p 436	N95-26995	#	N95-28002	#	p 377
N95-23425	#	p 312	N95-24439	#	p 363	N95-26409	#	p 366	N95-26998	p 437	N95-28029	#	p 441
N95-23429	#	p 312	N95-24443	#	p 330	N95-26412	#	p 405	N95-27003	p 401	N95-28038	#	p 454
N95-23435	#	p 312	N95-24461	#	p 349	N95-26417	#	p 418	N95-27018	p 391	N95-28073	#	p 452
N95-23436	#	p 312	N95-24465	#	p 328	N95-26418	#	p 436	N95-27036	p 410	N95-28108	#	p 452
N95-23438	#	p 312	N95-24470	#	p 349	N95-26424	#	p 405	N95-27042	p 391	N95-28139	#	p 441
N95-23440	#	p 313	N95-24472	#	p 349	N95-26427	#	p 453	N95-27093	#	N95-28151	#	p 412
N95-23444	#	p 313	N95-24541	#	p 335	N95-26445	#	p 436	N95-27143	#	N95-28152	#	p 420
N95-23446	#	p 313	N95-24561	#	p 339	N95-26453	#	p 445	N95-27156	#	N95-28188	#	p 384
N95-23447	#	p 314	N95-24566	#	p 330	N95-26454	#	p 382	N95-27167	#	N95-28193	#	p 377
N95-23462	#	p 275	N95-24582	#	p 335	N95-26455	#	p 366	N95-27176	#	N95-28203	#	p 401
N95-23466	#	p 314	N95-24598	#	p 349	N95-26481	#	p 388	N95-27179	#	N95-28227	#	p 406
N95-23496	#	p 302	N95-24624	#	p 337	N95-26485	#	p 380	N95-27180	#	N95-28230	#	p 377
N95-23497	#	p 302	N95-24629	#	p 335	N95-26497	#	p 380	N95-27186	#	N95-28241	#	p 378
N95-23500	#	p 302	N95-24630	#	p 335	N95-26498	#	p 380	N95-27209	#	N95-28262	#	p 397
N95-23503	#	p 323	N95-24631	#	p 333	N95-26507	#	p 388	N95-27234	#	N95-28264	#	p 452
N95-23505	#	p 314	N95-24633	#	p 333	N95-26523	#	p 419	N95-27240	#	N95-28265	#	p 378
N95-23506	#	p 262	N95-24759	#	p 350	N95-26525	#	p 388	N95-27241	#	N95-28266	#	p 420
N95-23507	#	p 315	N95-24853	#	p 357	N95-26527	#	p 380	N95-27246	#	N95-28267	#	p 420
N95-23508	#	p 302	N95-24878	#	p 343	N95-26537	#	p 389	N95-27248	#	N95-28268	#	p 420
N95-23509	#	p 302	N95-24879	#	p 361	N95-26555	#	p 408	N95-27258	#	N95-28270	#	p 420
N95-23510	#	p 303	N95-24882	#	p 357	N95-26556	#	p 411	N95-27354	#	N95-28271	#	p 420
N95-23512	#	p 315	N95-24989	#	p 343	N95-26556	#	p 411	N95-27367	#	N95-28273	#	p 421
N95-23513	#	p 303	N95-24990	#	p 339	N95-26585	#	p 382	N95-27371	#	N95-28273	#	p 421
N95-23515	#	p 303	N95-24998	#	p 331	N95-26587	#	p 383	N95-27434	#	N95-28274	#	p 421
N95-23516	#	p 303	N95-25004	#	p 362	N95-26589	#	p 436	N95-27440	#	N95-28275	#	p 406
N95-23517	#	p 303	N95-25005	#	p 337	N95-26590	#	p 389	N95-27459	#	N95-28276	#	p 421
N95-23518	#	p 303	N95-25105	#	p 331	N95-26591	#	p 389	N95-27504	#	N95-28277	#	p 407
N95-23519	#	p 262	N95-25110	#	p 358	N95-26600	#	p 405	N95-27505	#	N95-28278	#	p 397
N95-23532	#	p 299	N95-25264	#	p 360	N95-26629	#	p 367	N95-27506	#	N95-28281	#	p 410
N95-23550	#	p 289	N95-25334	#	p 335	N95-26638	#	p 448	N95-27507	#	N95-28289	#	p 421
N95-23565	#	p 280	N95-25338	#	p 331	N95-26648	#	p 448	N95-27508	#	N95-28331	#	p 378
N95-23598	#	p 277	N95-25341	#	p 334	N95-26649	#	p 448	N95-27509	#	N95-28335	#	p 450
N95-23602	#	p 315	N95-25394	#	p 350	N95-26651	#	p 389	N95-27510	#	N95-28343	#	p 407
N95-23603	#	p 323	N95-25395	#	p 339	N95-26652	#	p 389	N95-27511	#	N95-28364	#	p 441
N95-23609	#	p 277	N95-25396	#	p 339	N95-26669	#	p 445	N95-27512	#	N95-28409	#	p 397
N95-23630	#	p 315	N95-25397	#	p 339	N95-26684	#	p 389	N95-27513	#	N95-28411	#	p 398
N95-23652	#	p 315	N95-25399	#	p 341	N95-26706	#	p 405	N95-27514	#	N95-28420	#	p 421
N95-23662	#	p 316	N95-25400	#	p 350	N95-26710	#	p 367	N95-27515	#	N95-28421	#	p 421
N95-23666	#	p 286	N95-25401	#	p 328	N95-26713	#	p 374	N95-27516	#	N95-28422	#	p 422
N95-23670	#	p 316	N95-25578	#	p 336	N95-26719	#	p 374	N95-27517	#	N95-28426	#	p 422
N95-23671	#	p 295	N95-25592	#	p 350	N95-26722	#	p 436	N95-27518	#	N95-28427	#	p 422
N95-23761	#	p 299	N95-25606	#	p 350	N95-26735	#	p 374	N95-27519	#	N95-28429	#	p 422
N95-23766	#	p 320	N95-25607	#	p 328	N95-26739	#	p 436	N95-27520	#	N95-28432	#	p 422
N95-23781	#	p 300	N95-25609	#	p 334	N95-26740	#	p 374	N95-27521	#	N95-28435	#	p 423
N95-23792	#	p 316	N95-25649	#	p 331	N95-26751	#	p 437	N95-27522	#	N95-28436	#	p 423
N95-23872	#	p 325	N95-25664	#	p 342	N95-26757	#	p 374	N95-27523	#	N95-28437	#	p 423
N95-23940	#	p 320	N95-25749	#	p 350	N95-26760	#	p 374	N95-27524	#	N95-28438	#	p 423
N95-23947	#	p 320	N95-25761	#	p 331	N95-26768	#	p 411	N95-27525	#	N95-28439	#	p 423
N95-23948	#	p 321	N95-25762	#	p 332	N95-26773	#	p 409	N95-27526	#	N95-28440	#	p 398
N95-23981	#	p 304	N95-25764	#	p 334	N95-26775	#	p 406	N95-27527	#	N95-28441	#	p 423
N95-24012	#	p 277	N95-25797	#	p 360	N95-26777	#	p 406	N95-27528	#	N95-28443	#	p 424
N95-24019	#	p 297	N95-25798	#	p 328	N95-26801	#	p 451	N95-27541	#	N95-28444	#	p 398
N95-24024	#	p 277	N95-25803	#	p 360	N95-26813	#	p 390	N95-27543	#	N95-28445		

N95-28463

N95-28463 * # p 424
 N95-28464 * # p 424
 N95-28465 * # p 453
 N95-28466 * # p 425
 N95-28467 * # p 441
 N95-28468 * # p 441
 N95-28469 * # p 425
 N95-28470 * # p 398
 N95-28471 * # p 398
 N95-28473 * # p 398
 N95-28474 * # p 399
 N95-28475 * # p 425
 N95-28476 * # p 399
 N95-28477 * # p 425
 N95-28478 * # p 426
 N95-28480 * # p 399
 N95-28481 * # p 426
 N95-28482 * # p 399
 N95-28483 * # p 426
 N95-28484 * # p 442
 N95-28486 * # p 426
 N95-28487 * # p 399
 N95-28488 * # p 400
 N95-28489 * # p 400
 N95-28504 # p 400
 N95-28540 # p 384
 N95-28567 # p 400
 N95-28586 # p 401
 N95-28598 # p 410
 N95-28610 # p 368
 N95-28621 # p 426
 N95-28626 # p 400
 N95-28627 # p 450
 N95-28630 # p 382
 N95-28636 # # p 400
 N95-28646 # p 407
 N95-28649 # p 442
 N95-28669 * # p 378
 N95-28670 * # p 452
 N95-28673 * # p 442
 N95-28674 * # p 378
 N95-28691 # p 508
 N95-28692 # p 508
 N95-28704 # p 500
 N95-28707 # p 501
 N95-28708 # p 476
 N95-28716 * # p 488
 N95-28719 * # p 550
 N95-28720 * # p 476
 N95-28723 * # p 476
 N95-28725 * # p 551
 N95-28726 * # p 551
 N95-28730 * # p 501
 N95-28731 * # p 476
 N95-28732 * # p 551
 N95-28734 * # p 566
 N95-28736 * # p 551
 N95-28743 * # p 476
 N95-28745 * # p 567
 N95-28763 * # p 567
 N95-28764 * # p 567
 N95-28767 * # p 551
 N95-28768 * # p 552
 N95-28790 # p 488
 N95-28800 # p 477
 N95-28807 * # p 567
 N95-28811 # p 485
 N95-28816 * # p 457
 N95-28819 # p 488
 N95-28820 * # p 501
 N95-28823 * # p 531
 N95-28826 * # p 531
 N95-28830 * # p 532
 N95-28831 * # p 501
 N95-28832 * # p 532
 N95-28835 * # p 532
 N95-28836 * # p 532
 N95-28837 * # p 532
 N95-28838 * # p 533
 N95-28839 * # p 533
 N95-28840 # p 501
 N95-28841 * # p 502
 N95-28843 * # p 533
 N95-28845 * # p 533
 N95-28846 * # p 533
 N95-28847 * # p 552
 N95-28848 * # p 552
 N95-28849 * # p 534
 N95-28851 # p 502
 N95-28870 # p 579
 N95-28885 # p 477
 N95-28887 # p 489
 N95-28896 # p 502
 N95-28897 # p 477
 N95-28903 # p 552
 N95-28904 # p 477

N95-28908 # p 513
 N95-28921 # # p 477
 N95-28928 * # p 502
 N95-28948 # p 552
 N95-28977 # # p 502
 N95-28996 # # p 579
 N95-29016 # p 503
 N95-29027 * # # p 503
 N95-29029 * # # p 534
 N95-29030 * # # p 534
 N95-29031 * # # p 534
 N95-29032 * # # p 534
 N95-29033 * # # p 534
 N95-29034 * # # p 534
 N95-29035 * # # p 535
 N95-29036 * # # p 535
 N95-29038 * # # p 535
 N95-29039 * # # p 535
 N95-29041 * # # p 536
 N95-29043 * # # p 536
 N95-29044 * # # p 536
 N95-29047 * # # p 536
 N95-29050 * # # p 537
 N95-29051 * # # p 537
 N95-29057 # # p 485
 N95-29060 # # p 553
 N95-29074 # # p 567
 N95-29091 # # p 477
 N95-29094 # p 478
 N95-29102 # p 478
 N95-29107 # p 489
 N95-29108 # p 478
 N95-29110 # p 562
 N95-29112 * # # p 553
 N95-29115 * # # p 513
 N95-29118 # # p 478
 N95-29119 # p 553
 N95-29121 # p 479
 N95-29122 # p 503
 N95-29123 * # p 508
 N95-29129 # p 479
 N95-29132 * # # p 485
 N95-29156 # p 517
 N95-29160 # # p 563
 N95-29187 # # p 553
 N95-29197 # # p 553
 N95-29210 # # p 485
 N95-29228 # # p 554
 N95-29242 # p 554
 N95-29243 # p 479
 N95-29244 # p 513
 N95-29251 # p 567
 N95-29316 # # p 479
 N95-29322 # # p 503
 N95-29338 * # # p 479
 N95-29339 # # p 526
 N95-29351 * # # p 527
 N95-29362 # p 503
 N95-29371 * # # p 554
 N95-29387 # # p 554
 N95-29401 * # # p 579
 N95-29402 * # # p 480
 N95-29414 # # p 457
 N95-29415 # p 579
 N95-29426 # # p 504
 N95-29428 # # p 480
 N95-29437 # # p 504
 N95-29445 # p 507
 N95-29447 * # # p 524
 N95-29452 * # # p 580
 N95-29453 * # # p 554
 N95-29454 * # # p 568
 N95-29457 # p 504
 N95-29468 # # p 523
 N95-29482 # p 537
 N95-29486 # # p 514
 N95-29496 # # p 480
 N95-29502 # p 580
 N95-29503 # # p 504
 N95-29538 * # # p 555
 N95-29542 # p 489
 N95-29562 # # p 555
 N95-29565 # # p 505
 N95-29572 # # p 537
 N95-29596 # p 489
 N95-29618 # # p 568
 N95-29619 # # p 568
 N95-29620 # # p 568
 N95-29622 # # p 569
 N95-29640 # # p 480
 N95-29641 * # # p 580
 N95-29644 # # p 569
 N95-29654 # # p 555
 N95-29679 # p 514
 N95-29680 # p 518
 N95-29712 # # p 555

N95-29729 # p 556
 N95-29733 # # p 490
 N95-29764 # # p 514
 N95-29771 # p 480
 N95-29787 # p 505
 N95-29788 # p 481
 N95-29794 # p 527
 N95-29795 # p 523
 N95-29797 # p 563
 N95-29807 # p 556
 N95-29830 # p 563
 N95-29842 # # p 537
 N95-29853 # # p 481
 N95-29855 # # p 485
 N95-29873 # # p 485
 N95-29880 # # p 490
 N95-29885 # p 563
 N95-29898 # p 481
 N95-29899 # p 481
 N95-29934 # # p 514
 N95-29941 # # p 556
 N95-29946 # # p 556
 N95-29950 # # p 509
 N95-29965 # # p 481
 N95-29967 # # p 523
 N95-29972 # # p 482
 N95-30007 * # # p 514
 N95-30016 # # p 564
 N95-30031 # # p 490
 N95-30067 * # # p 523
 N95-30072 # # p 556
 N95-30084 # # p 580
 N95-30087 # # p 557
 N95-30091 * # # p 482
 N95-30122 # # p 557
 N95-30158 * # # p 580
 N95-30161 * # # p 557
 N95-30200 # # p 564
 N95-30224 * # # p 557
 N95-30226 * # # p 505
 N95-30228 * # # p 523
 N95-30229 * # # p 457
 N95-30235 # p 482
 N95-30248 * # # p 569
 N95-30252 * # # p 537
 N95-30253 * # # p 482
 N95-30254 * # # p 518
 N95-30290 # p 557
 N95-30294 # p 482
 N95-30304 # p 557
 N95-30327 * # # p 518
 N95-30335 # # p 505
 N95-30349 # # p 483
 N95-30353 * # # p 569
 N95-30406 # # p 678
 N95-30448 # p 592
 N95-30486 # p 601
 N95-30493 # p 626
 N95-30497 # p 606
 N95-30502 # # p 644
 N95-30507 # # p 644
 N95-30517 * # # p 615
 N95-30521 # # p 645
 N95-30524 * # # p 645
 N95-30587 * # # p 645
 N95-30589 * # # p 615
 N95-30592 * # # p 626
 N95-30594 * # # p 615
 N95-30597 # # p 601
 N95-30611 * # # p 592
 N95-30617 # # p 615
 N95-30632 * # # p 616
 N95-30638 # # p 592
 N95-30646 # # p 606
 N95-30669 # # p 645
 N95-30682 * # # p 645
 N95-30698 # # p 616
 N95-30702 * # # p 616
 N95-30704 * # # p 592
 N95-30712 * # # p 592
 N95-30727 # p 646
 N95-30749 # p 629
 N95-30750 # p 629
 N95-30765 # # p 629
 N95-30779 # # p 616
 N95-30783 # # p 646
 N95-30787 * # # p 629
 N95-30788 # # p 593
 N95-30814 # # p 593
 N95-30815 # # p 601
 N95-30827 * # # p 607
 N95-30837 # # p 593
 N95-30838 # # p 607
 N95-30843 # p 593
 N95-30851 * # # p 646
 N95-30853 * # # p 616

N95-30861 * # # p 617
 N95-30885 # # p 593
 N95-30892 # # p 678
 N95-30902 # # p 646
 N95-30906 # # p 646
 N95-30922 # # p 646
 N95-30923 # # p 607
 N95-30927 # # p 607
 N95-30929 # # p 594
 N95-30937 # # p 619
 N95-30956 # # p 647
 N95-30957 # # p 647
 N95-30961 # # p 679
 N95-30992 # # p 647
 N95-31000 * # # p 584
 N95-31013 # # p 601
 N95-31061 # # p 597
 N95-31062 * # # p 597
 N95-31063 # # p 597
 N95-31064 # # p 597
 N95-31065 # # p 607
 N95-31066 # # p 597
 N95-31067 # # p 597
 N95-31068 # # p 598
 N95-31069 # # p 598
 N95-31070 # # p 598
 N95-31071 # # p 619
 N95-31072 # # p 598
 N95-31098 # # p 647
 N95-31124 # # p 629
 N95-31157 # # p 677
 N95-31180 # # p 611
 N95-31191 # # p 617
 N95-31199 # # p 617
 N95-31201 # p 617
 N95-31203 # p 629
 N95-31208 # p 629
 N95-31268 # p 630
 N95-31355 # # p 647
 N95-31368 # # p 630
 N95-31374 # # p 647
 N95-31400 # # p 620
 N95-31416 # # p 607
 N95-31421 * # # p 630
 N95-31423 * # # p 648
 N95-31425 # # p 617
 N95-31428 # # p 598
 N95-31432 # # p 648
 N95-31433 # # p 601
 N95-31443 # # p 648
 N95-31451 # # p 608
 N95-31454 # # p 598
 N95-31455 # # p 679
 N95-31465 # # p 677
 N95-31468 # # p 626
 N95-31471 # # p 630
 N95-31475 # # p 648
 N95-31512 # # p 599
 N95-31520 # # p 601
 N95-31521 # # p 602
 N95-31525 # # p 608
 N95-31544 # # p 608
 N95-31569 # # p 599
 N95-31572 # # p 602
 N95-31578 # # p 608
 N95-31579 # # p 608
 N95-31581 # # p 602
 N95-31584 # # p 611
 N95-31587 # # p 677
 N95-31598 # # p 584
 N95-31602 # # p 608
 N95-31614 # # p 648
 N95-31653 # # p 627
 N95-31655 # # p 612
 N95-31656 # # p 612
 N95-31667 # # p 599
 N95-31684 # # p 679
 N95-31687 # # p 599
 N95-31712 # # p 599
 N95-31715 # # p 594
 N95-31728 # # p 649
 N95-31738 * # # p 649
 N95-31767 # # p 630
 N95-31768 # # p 631
 N95-31773 * # # p 631
 N95-31775 * # # p 631
 N95-31778 * # # p 631
 N95-31798 * # # p 631
 N95-31837 # # p 649
 N95-31845 # # p 599
 N95-31846 * # # p 620
 N95-31948 # # p 649
 N95-31979 * # # p 681
 N95-31982 * # # p 679
 N95-31984 * # # p 594
 N95-31985 * # # p 618

N95-31987 # # p 679
 N95-31989 # # p 620
 N95-31990 # # p 620
 N95-31991 # # p 620
 N95-31992 # # p 621
 N95-31993 # # p 621
 N95-31994 # # p 621
 N95-31995 # # p 621
 N95-31996 # # p 621
 N95-31997 # # p 621
 N95-31998 # # p 621
 N95-31999 # # p 622
 N95-32000 # # p 622
 N95-32001 * # # p 622
 N95-32002 # # p 622
 N95-32003 # # p 609
 N95-32004 # # p 622
 N95-32005 # # p 623
 N95-32006 # # p 623
 N95-32007 # # p 609
 N95-32008 # # p 609
 N95-32009 # # p 623
 N95-32010 # # p 623
 N95-32011 # # p 623
 N95-32012 # # p 623
 N95-32013 # # p 609
 N95-32014 # # p 624
 N95-32015 # # p 624
 N95-32016 # # p 624
 N95-32017 # # p 624
 N95-32022 # # p 607
 N95-32109 # p 650
 N95-32111 # # p 624
 N95-32163 # # p 650
 N95-32164 # # p 584
 N95-32165 # # p 650
 N95-32170 # # p 650
 N95-32175 # # p 650
 N95-32176 # # p 627
 N95-32179 # # p 651
 N95-32180 # # p 651
 N95-32181 # # p 651
 N95-32186 # # p 602
 N95-32187 * # # p 680
 N95-32188 * # # p 594
 N95-32193 * # # p 594
 N95-32194 # # p 584
 N95-32196 # # p 609
 N95-32197 # # p 603
 N95-32198 # # p 585
 N95-32199 # # p 603
 N95-32205 * # # p 651
 N95-32217 * # # p 627
 N95-32486 # # p 686
 N95-32488 # # p 686
 N95-32490 # # p 688
 N95-32492 # # p 702
 N95-32494 # # p 709
 N95-32496 # # p 710
 N95-32497 * # # p 693
 N95-32499 # # p 686
 N95-32500 # # p 687
 N95-32501 # # p 703
 N95-32503 # # p 693
 N95-32548 # # p 683
 N95-32636 # # p 694
 N95-32682 * # # p 683
 N95-32685 # # p 707
 N95-32689 * # # p 703
 N95-32690 # # p 703
 N95-32691 # # p 703
 N95-32692 * # # p 703
 N95-32693 # # p 703
 N95-32699 * # # p 691
 N95-32705 # # p 687
 N95-32759 # # p 699
 N95-32764 * # # p 683
 N95-32769 * # # p 684
 N95-32783 # # p 683
 N95-32784 # # p 687
 N95-32786 # # p 699
 N95-32787 # # p 704
 N95-32821 * # # p 684
 N95-32822 * # # p 704
 N95-32823 * # # p 707
 N95-32836 * # # p 710
 N95-32885 # # p 687
 N95-32888 # # p 700
 N95-32902 # # p 704
 N95-32904 # # p 691
 N95-32916 * # # p 694
 N95-32920 # # p 704
 N95-32928 * # # p 691
 N95-32930 * # # p 705
 N95-32931 * # # p 694

ACCESSION NUMBER INDEX

ACCESSION NUMBER INDEX

N95-34818

N95-33008 # p 710
 N95-33009 * # p 694
 N95-33010 # p 694
 N95-33011 * # p 695
 N95-33012 * # p 695
 N95-33013 * # p 695
 N95-33014 * # p 695
 N95-33015 * # p 695
 N95-33016 * # p 696
 N95-33017 * # p 696
 N95-33018 * # p 696
 N95-33019 * # p 696
 N95-33020 * # p 697
 N95-33021 * # p 697
 N95-33022 * # p 697
 N95-33023 * # p 691
 N95-33024 * # p 692
 N95-33025 * # p 692
 N95-33059 # p 705
 N95-33131 # p 688
 N95-33134 # p 688
 N95-33135 # p 689
 N95-33136 # p 689
 N95-33137 # p 705
 N95-33140 # p 689
 N95-33141 # p 708
 N95-33142 # p 710
 N95-33143 # p 705
 N95-33145 # p 692
 N95-33198 # p 711
 N95-33208 # p 697
 N95-33250 # p 697
 N95-33278 * # p 701
 N95-33311 # p 692
 N95-33396 * # p 710
 N95-33408 # p 701
 N95-33480 # p 689
 N95-33642 # p 708
 N95-33712 # p 710
 N95-33748 * # p 708
 N95-33749 * # p 708
 N95-33754 * # p 705
 N95-33760 * # p 709
 N95-33799 * # p 709
 N95-33831 * # p 711
 N95-34236 * # p 711
 N95-34306 # p 698
 N95-34342 # p 700
 N95-34343 # p 706
 N95-34344 # p 700
 N95-34362 # p 700
 N95-34449 # p 706
 N95-34500 # p 701
 N95-34505 # p 684
 N95-34506 # p 692
 N95-34507 # p 698
 N95-34508 # p 706
 N95-34511 # p 698
 N95-34512 # p 706
 N95-34513 # p 698
 N95-34514 # p 700
 N95-34520 # p 684
 N95-34521 # p 684
 N95-34524 # p 684
 N95-34525 # p 685
 N95-34530 # p 706
 N95-34533 # p 707
 N95-34536 # p 707
 N95-34537 # p 685
 N95-34538 # p 685
 N95-34539 # p 707
 N95-34540 # p 707
 N95-34541 # p 693
 N95-34542 # p 693
 N95-34544 # p 685
 N95-34546 # p 685
 N95-34547 # p 685
 N95-34548 # p 685
 N95-34549 # p 711
 N95-34551 # p 711
 N95-34552 # p 686
 N95-34560 # p 698
 N95-34562 # p 690
 N95-34570 # p 690
 N95-34583 # p 693
 N95-34597 # p 707
 N95-34750 # p 686
 N95-34763 # p 686
 N95-34766 * # p 688
 N95-34770 * # p 690
 N95-34771 * # p 690
 N95-34772 * # p 699
 N95-34793 # p 693
 N95-34797 # p 691
 N95-34805 # p 698
 N95-34806 # p 699

N95-34818 # p 707

SPECIAL NOTICE

The abstract sections of the monthly supplements of *Aeronautical Engineering* can be bound separately. Individual abstracts can be located readily by means of the page numbers given at each entry, e.g., p 226 N95-22341. To assist the user in binding Supplements SP-7037 (313) through SP-7037 (324), a title page is included in this Cumulative Index.

AERONAUTICAL ENGINEERING

A CONTINUING BIBLIOGRAPHY

Abstracts

January – December 1995

TABLE OF CONTENTS

<i>SP-7037 Supplement</i>	<i>Page</i>
313	1
314	35
315	65
316	103
317	179
318	219
319	261
320	327
321	365
322	455
323	583
324	683

REPORT DOCUMENT PAGE

1. Report No. NASA SP-7037 (325)	2. Government Accession No.	3. Recipient's Catalog No.	
4. Title and Subtitle Aeronautical Engineering A Cumulative Index to the 1995 Issues		5. Report Date December 1995	
		6. Performing Organization Code JT	
7. Author(s)		8. Performing Organization Report No.	
		10. Work Unit No.	
9. Performing Organization Name and Address NASA Scientific and Technical Information Office		11. Contract or Grant No.	
		13. Type of Report and Period Covered Special Publication	
12. Sponsoring Agency Name and Address National Aeronautics and Space Administration Washington, DC 20546-0001		14. Sponsoring Agency Code	
		15. Supplementary Notes	
16. Abstract This is a cumulative index to the abstracts contained in NASA SP-7037 (313) through NASA SP-7037 (324) of <i>Aeronautical Engineering: A Continuing Bibliography</i> . NASA SP-7037 and its supplements have been compiled by the Center for AeroSpace Information of the National Aeronautics and Space Administration (NASA). This cumulative index includes subject, personal author, corporate source, foreign technology, contract number, report number, and accession number indexes.			
17. Key Words (Suggested by Author(s)) Aerodynamics Aeronautical Engineering Aeronautics Bibliographies			
19. Security Classif. (of this report) Unclassified		18. Distribution Statement Unclassified - Unlimited Subject Category - 01	
		20. Security Classif. (of this page) Unclassified	21. No. of Pages 466

FEDERAL REGIONAL DEPOSITORY LIBRARIES

ALABAMA

AUBURN UNIV. AT MONTGOMERY LIBRARY
Documents Dept.
7300 University Dr.
Montgomery, AL 36117-3596
(205) 244-3650 Fax: (205) 244-0678

UNIV. OF ALABAMA

Amelia Gayle Gorgas Library
Govt. Documents
P.O. Box 870266
Tuscaloosa, AL 35487-0266
(205) 348-6046 Fax: (205) 348-0760

ARIZONA

DEPT. OF LIBRARY, ARCHIVES, AND PUBLIC RECORDS
Research Division
Third Floor, State Capitol
1700 West Washington
Phoenix, AZ 85007
(602) 542-3701 Fax: (602) 542-4400

ARKANSAS

ARKANSAS STATE LIBRARY
State Library Service Section
Documents Service Section
One Capitol Mall
Little Rock, AR 72201-1014
(501) 682-2053 Fax: (501) 682-1529

CALIFORNIA

CALIFORNIA STATE LIBRARY
Govt. Publications Section
P.O. Box 942837 - 914 Capitol Mall
Sacramento, CA 94337-0091
(916) 654-0069 Fax: (916) 654-0241

COLORADO

UNIV. OF COLORADO - BOULDER
Libraries - Govt. Publications
Campus Box 184
Boulder, CO 80309-0184
(303) 492-8834 Fax: (303) 492-1881

DENVER PUBLIC LIBRARY

Govt. Publications Dept. BSG
1357 Broadway
Denver, CO 80203-2165
(303) 640-8846 Fax: (303) 640-8817

CONNECTICUT

CONNECTICUT STATE LIBRARY
231 Capitol Avenue
Hartford, CT 06106
(203) 566-4971 Fax: (203) 566-3322

FLORIDA

UNIV. OF FLORIDA LIBRARIES
Documents Dept.
240 Library West
Gainesville, FL 32611-2048
(904) 392-0366 Fax: (904) 392-7251

GEORGIA

UNIV. OF GEORGIA LIBRARIES
Govt. Documents Dept.
Jackson Street
Athens, GA 30602-1645
(706) 542-8949 Fax: (706) 542-4144

HAWAII

UNIV. OF HAWAII
Hamilton Library
Govt. Documents Collection
2550 The Mall
Honolulu, HI 96822
(808) 948-8230 Fax: (808) 956-5968

IDAHO

UNIV. OF IDAHO LIBRARY
Documents Section
Rayburn Street
Moscow, ID 83844-2353
(208) 885-6344 Fax: (208) 885-6817

ILLINOIS

ILLINOIS STATE LIBRARY
Federal Documents Dept.
300 South Second Street
Springfield, IL 62701-1796
(217) 782-7596 Fax: (217) 782-6437

INDIANA

INDIANA STATE LIBRARY
Serials/Documents Section
140 North Senate Avenue
Indianapolis, IN 46204-2296
(317) 232-3679 Fax: (317) 232-3728

IOWA

UNIV. OF IOWA LIBRARIES
Govt. Publications
Washington & Madison Streets
Iowa City, IA 52242-1166
(319) 335-5926 Fax: (319) 335-5900

KANSAS

UNIV. OF KANSAS
Govt. Documents & Maps Library
6001 Malott Hall
Lawrence, KS 66045-2800
(913) 864-4660 Fax: (913) 864-3855

KENTUCKY

UNIV. OF KENTUCKY
King Library South
Govt. Publications/Maps Dept.
Patterson Drive
Lexington, KY 40506-0039
(606) 257-3139 Fax: (606) 257-3139

LOUISIANA

LOUISIANA STATE UNIV.
Middleton Library
Govt. Documents Dept.
Baton Rouge, LA 70803-3312
(504) 388-2570 Fax: (504) 388-6992

LOUISIANA TECHNICAL UNIV.

Prescott Memorial Library
Govt. Documents Dept.
Ruston, LA 71272-0046
(318) 257-4962 Fax: (318) 257-2447

MAINE

UNIV. OF MAINE
Raymond H. Fogler Library
Govt. Documents Dept.
Orono, ME 04469-5729
(207) 581-1673 Fax: (207) 581-1653

MARYLAND

UNIV. OF MARYLAND - COLLEGE PARK
McKeldin Library
Govt. Documents/Maps Unit
College Park, MD 20742
(301) 405-9165 Fax: (301) 314-9416

MASSACHUSETTS

BOSTON PUBLIC LIBRARY
Govt. Documents
666 Boylston Street
Boston, MA 02117-0286
(617) 536-5400, ext. 226
Fax: (617) 536-7758

MICHIGAN

DETROIT PUBLIC LIBRARY
5201 Woodward Avenue
Detroit, MI 48202-4093
(313) 833-1025 Fax: (313) 833-0156

LIBRARY OF MICHIGAN

Govt. Documents Unit
P.O. Box 30007
717 West Allegan Street
Lansing, MI 48909
(517) 373-1300 Fax: (517) 373-3381

MINNESOTA

UNIV. OF MINNESOTA
Govt. Publications
409 Wilson Library
309 19th Avenue South
Minneapolis, MN 55455
(612) 624-5073 Fax: (612) 626-9353

MISSISSIPPI

UNIV. OF MISSISSIPPI
J.D. Williams Library
106 Old Gym Bldg.
University, MS 38677
(601) 232-5857 Fax: (601) 232-7465

MISSOURI

UNIV. OF MISSOURI - COLUMBIA
106B Ellis Library
Govt. Documents Sect.
Columbia, MO 65201-5149
(314) 882-6733 Fax: (314) 882-8044

MONTANA

UNIV. OF MONTANA
Mansfield Library
Documents Division
Missoula, MT 59812-1195
(406) 243-6700 Fax: (406) 243-2060

NEBRASKA

UNIV. OF NEBRASKA - LINCOLN
D.L. Love Memorial Library
Lincoln, NE 68588-0410
(402) 472-2562 Fax: (402) 472-5131

NEVADA

THE UNIV. OF NEVADA LIBRARIES
Business and Govt. Information Center
Reno, NV 89557-0044
(702) 784-6579 Fax: (702) 784-1751

NEW JERSEY

NEWARK PUBLIC LIBRARY
Science Div. - Public Access
P.O. Box 630
Five Washington Street
Newark, NJ 07101-7812
(201) 733-7782 Fax: (201) 733-5648

NEW MEXICO

UNIV. OF NEW MEXICO
General Library
Govt. Information Dept.
Albuquerque, NM 87131-1466
(505) 277-5441 Fax: (505) 277-6019

NEW MEXICO STATE LIBRARY

325 Don Gaspar Avenue
Santa Fe, NM 87503
(505) 827-3824 Fax: (505) 827-3888

NEW YORK

NEW YORK STATE LIBRARY
Cultural Education Center
Documents/Gift & Exchange Section
Empire State Plaza
Albany, NY 12230-0001
(518) 474-5355 Fax: (518) 474-5786

NORTH CAROLINA

UNIV. OF NORTH CAROLINA - CHAPEL HILL
Walter Royal Davis Library
CE 3912, Reference Dept.
Chapel Hill, NC 27514-8890
(919) 962-1151 Fax: (919) 962-4451

NORTH DAKOTA

NORTH DAKOTA STATE UNIV. LIB.
Documents
P.O. Box 5599
 Fargo, ND 58105-5599
(701) 237-8886 Fax: (701) 237-7138

UNIV. OF NORTH DAKOTA

Chester Fritz Library
University Station
P.O. Box 9000 - Centennial and University Avenue
Grand Forks, ND 58202-9000
(701) 777-4632 Fax: (701) 777-3319

OHIO

STATE LIBRARY OF OHIO
Documents Dept.
65 South Front Street
Columbus, OH 43215-4163
(614) 644-7051 Fax: (614) 752-9178

OKLAHOMA

OKLAHOMA DEPT. OF LIBRARIES
U.S. Govt. Information Division
200 Northeast 18th Street
Oklahoma City, OK 73105-3298
(405) 521-2502, ext. 253
Fax: (405) 525-7804

OKLAHOMA STATE UNIV.

Edmon Low Library
Stillwater, OK 74078-0375
(405) 744-6546 Fax: (405) 744-5183

OREGON

PORTLAND STATE UNIV.
Branford P. Millar Library
934 Southwest Harrison
Portland, OR 97207-1151
(503) 725-4123 Fax: (503) 725-4524

PENNSYLVANIA

STATE LIBRARY OF PENN.
Govt. Publications Section
116 Walnut & Commonwealth Ave.
Harrisburg, PA 17105-1601
(717) 787-3752 Fax: (717) 783-2070

SOUTH CAROLINA

CLEMSON UNIV.
Robert-Muldrow-Cooper Library
Public Documents Unit
P.O. Box 343001
Clemson, SC 29634-3001
(803) 656-5174 Fax: (803) 656-3025

UNIV. OF SOUTH CAROLINA

Thomas Cooper Library
Green and Sumter Streets
Columbia, SC 29208
(803) 777-4841 Fax: (803) 777-9503

TENNESSEE

UNIV. OF MEMPHIS LIBRARIES
Govt. Publications Dept.
Memphis, TN 38152-0001
(901) 678-2206 Fax: (901) 678-2511

TEXAS

TEXAS STATE LIBRARY
United States Documents
P.O. Box 12927 - 1201 Brazos
Austin, TX 78701-0001
(512) 463-5455 Fax: (512) 463-5436

TEXAS TECH. UNIV. LIBRARIES

Documents Dept.
Lubbock, TX 79409-0002
(806) 742-2282 Fax: (806) 742-1920

UTAH

UTAH STATE UNIV.
Merrill Library Documents Dept.
Logan, UT 84322-3000
(801) 797-2678 Fax: (801) 797-2677

VIRGINIA

UNIV. OF VIRGINIA
Alderman Library
Govt. Documents
University Ave. & McCormick Rd.
Charlottesville, VA 22903-2498
(804) 824-3133 Fax: (804) 924-4337

WASHINGTON

WASHINGTON STATE LIBRARY
Govt. Publications
P.O. Box 42478
16th and Water Streets
Olympia, WA 98504-2478
(206) 753-4027 Fax: (206) 586-7575

WEST VIRGINIA

WEST VIRGINIA UNIV. LIBRARY
Govt. Documents Section
P.O. Box 6069 - 1549 University Ave.
Morgantown, WV 26506-6069
(304) 293-3051 Fax: (304) 293-6638

WISCONSIN

ST. HIST. SOC. OF WISCONSIN LIBRARY
Govt. Publication Section
816 State Street
Madison, WI 53706
(608) 264-6525 Fax: (608) 264-6520

MILWAUKEE PUBLIC LIBRARY

Documents Division
814 West Wisconsin Avenue
Milwaukee, WI 53233
(414) 286-3073 Fax: (414) 286-8074

National Aeronautics and
Space Administration
Code JT
Washington, DC 20546-0001